NUCLEAR SCIENCE ABSTRACTS

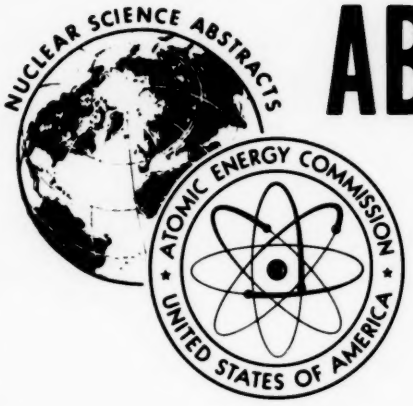

Volume 25 Number 18

Abstracts 41713-44310

September 30, 1971

UNITED STATES ATOMIC ENERGY COMMISSION
Division of Technical Information

REPORT COLLECTIONS IN THE UNITED STATES

The libraries listed below purchase and maintain microfiche collections of USAEC and foreign reports that are abstracted in *NSA*. Their collections also include *NSA* and its indexes, AEC's Technical Progress Reviews, AEC-sponsored translations, conference proceedings published by AEC, and various bibliographic tools. Most of these libraries have microfiche reader-printers or other photocopy facilities with which to reproduce enlarged copies from microfiche. Charges for reproduction services vary.

ALABAMA
Auburn, Auburn University
Tuskegee Institute, Tuskegee Institute

ALASKA
College, University of Alaska

ARIZONA
Tucson, University of Arizona

ARKANSAS
Fayetteville, University of Arkansas

CALIFORNIA
Davis, University of California
Los Angeles, University of California

COLORADO
Boulder, University of Colorado

DISTRICT OF COLUMBIA
Washington, Library of Congress (by deposit)

FLORIDA
Gainesville, University of Florida

GEORGIA
Atlanta, Georgia Institute of Technology

HAWAII
Honolulu, University of Hawaii

IDAHO
Pocatello, Idaho State University

ILLINOIS
Evanston, Northwestern University
Urbana, University of Illinois

INDIANA
Lafayette, Purdue University

IOWA
Ames, Iowa State University

KANSAS
Manhattan, Kansas State University

KENTUCKY
Lexington, University of Kentucky
Louisville, University of Louisville

LOUISIANA
Baton Rouge, Louisiana State University
New Orleans, Tulane University

MARYLAND
Baltimore, Johns Hopkins University
College Park, University of Maryland

MASSACHUSETTS
Cambridge, Massachusetts Institute of Technology
Worcester, Worcester Polytechnic Institute

MICHIGAN
Ann Arbor, University of Michigan

MISSISSIPPI
State College, Mississippi State University

MISSOURI
Kansas City, Linda Hall Library

NEVADA
Las Vegas, University of Nevada

NEW JERSEY
Princeton, Princeton University

NEW MEXICO
Albuquerque, University of New Mexico

NEW YORK
Albany, New York State Library
Albany, State University at Albany
Buffalo, State University of New York at Buffalo
Ithaca, Cornell University
New York, Columbia University
Rochester, University of Rochester
Syracuse, Syracuse University
Troy, Rensselaer Polytechnic Institute

NORTH CAROLINA
Raleigh, North Carolina State University

OHIO
Cincinnati, University of Cincinnati
Cleveland, Cleveland Public Library
Columbus, Ohio State University
Toledo, University of Toledo

OKLAHOMA
Norman, University of Oklahoma

PENNSYLVANIA
Philadelphia, University of Pennsylvania
Pittsburgh, Carnegie Library
University Park, Pennsylvania State University

PUERTO RICO
San Juan, University of Puerto Rico

SOUTH CAROLINA
Columbia, University of South Carolina

TENNESSEE
Knoxville, University of Tennessee
Nashville, Joint University Libraries
Oak Ridge, Oak Ridge Associated Universities

TEXAS
Austin, University of Texas
College Station, Texas A & M University
Houston, Rice University

UTAH
Salt Lake City, University of Utah

VIRGINIA
Blacksburg, Virginia Polytechnic Institute
Charlottesville, University of Virginia

WASHINGTON
Pullman, Washington State University
Seattle, University of Washington

WEST VIRGINIA
Morgantown, West Virginia University

WISCONSIN
Madison, University of Wisconsin

WYOMING
Laramie, University of Wyoming

The following governmental and international organizations offer for sale USAEC reports abstracted in *Nuclear Science Abstracts:*

National Technical Information Service, U. S. Department of Commerce
Springfield, Virginia 22151
International Atomic Energy Agency, Vienna, Austria
National Lending Library, Boston Spa, England

XUN

NOTICE

A title page for Volume 25, Numbers 13–18, is included at the back of this issue for use in binding those issues.

CORRECTIONS

NSA Vol. 24, No. 7, Abst. 13478, line 2 should read: 2]. Preliminary Safety Analysis Report, Amendment 6. (Con-

NSA Vol. 25, No. 3, Abst. 5285, line 1 should read: (RLO-2041-50) SCATTERING OF REAL PIONS ON

NSA Vol. 25, No. 3, Abst. 5426, line 1 should read: (NYO-2262-TA-226) CROSSED CHANNEL PARTIAL

NSA Vol. 25, No. 5, Abst. 10324, line 1 should read: (EURFNR-775) RESULTS OF ERROR ANALYSIS

NSA Vol. 25, No. 6, Abst. 10640, line 8 should read: 1-butene, neopentane, isopentane, and n-pentane. All these products

NSA Vol. 25, No. 6, Abst. 10640, line 10 should read: tion of nitric oxide. The formation of the pentenes results from the

NSA Vol. 25, No. 6, Abst. 10810, line 1 should read: (CEA-CONF-1668) STATIONARY GAS DETECTORS

NSA Vol. 25, No. 7, Abst. 13127, line 14 should read: ing and the production. Most mines evolved from a series of events

NSA Vol. 25, No. 8, Abst. 17047, line 2 should read: SPHERIC ELECTRONS. Catchpoole, J. R. (York Univ., Toronto).

NSA Vol. 25, No. 9, Abst. 20384, line 18 should read: 4.891, 4.921, 4.974, 5.070, 5.091, 5.163, 5.1876, 5.2540, 5.285, and

NSA Vol. 25, No. 9, Abst. 20425, line 5 should read: The relative intensities of γ rays following the decay of ^{152g}Eu

NSA Vol. 25, No. 9, Abst. 20489, line 4 should read: 48: 3016-20(15 Dec 1970).

NSA Vol. 25, No. 10, Abst. 23430, line 1 should read: (COO-1222-44) COMPUTER-CONTROLLED GAS

NSA Vol. 25, No. 11, Abst. 24662, line 4 should read: (U. S. Sales Only) AECL $1.00.

NSA Vol. 25, No. 11, Abst. 25055, line 5 should read: The anomalous scattering of Bogoliubov excitations at sharp

XUN

Volume 25, Number 18, September 30, 1971

NUCLEAR SCIENCE ABSTRACTS

A semimonthly publication of the USAEC Division of Technical Information, Edward J. Brunenkant, Director, Published by the USAEC Division of Technical Information Extension, Robert L. Shannon, Extension Manager.

Nuclear Science Abstracts provides the only comprehensive abstracting and indexing coverage of international nuclear science literature. *Nuclear Science Abstracts* covers scientific and technical reports of the U. S. Atomic Energy Commission and its contractors, other U. S. Government agencies, other governments, universities, and industrial and research organizations. In addition, books, conference proceedings, individual conference papers, patents, and journal literature on a worldwide basis are abstracted and indexed. Each issue of *Nuclear Science Abstracts* includes four indexes: subject, personal author, corporate author, and report number.

The following organizations scan and abstract the nuclear science literature in their respective countries:

Atomic Energy of Canada Limited
Australian Atomic Energy Commission
Danish Atomic Energy Commission
Finnish Atomic Energy Commission
French Atomic Energy Commission
Japan Atomic Energy Bureau–Atomic Energy Research Institute
Institutt for Atomenergi (Norway)
Aktiebolaget Atomenergi (Sweden)
United Kingdom Atomic Energy Authority

Numerous organizations, societies, and publishers throughout the world provide *Nuclear Science Abstracts* with advance page-proof copy of their publications, e.g., in the United States the American Institute of Physics provides page-proof copy of its publications.

A list of the journals scanned regularly and the abbreviations used appears in Issue 1 (January 15) of each volume of *Nuclear Science Abstracts* and is supplemented in Issues 7, 13, and 19. Issue 1 of each volume also describes the scope and arrangement of the subject matter covered in *Nuclear Science Abstracts*. The subject matter covered is also described in TID-4552, *Subject Scope of Nuclear Science Abstracts*, available free from the USAEC Division of Technical Information Extension, P.O. Box 62, Oak Ridge, Tennessee 37830. An outline of the subject categories appears in the Contents of each issue.

AVAILABILITY OF PUBLICATIONS ABSTRACTED

Public availability of all U. S. Atomic Energy Commission reports is indicated in the report number indexes. The availability of other reports, when known, is also indicated. The availability of some unnumbered reports is given in the abstract.

Dissertations abstracted in *Dissertation Abstracts* and included in *Nuclear Science Abstracts* are available from University Microfilms, Inc., 315 N. First Street, Ann Arbor, Michigan 48103.

Information on the availability of the published literature and unpublished conference papers abstracted in *Nuclear Science Abstracts* can be obtained from the USAEC Division of Technical Information Extension, P.O. Box 62, Oak Ridge, Tennessee 37830.

HOW TO OBTAIN NUCLEAR SCIENCE ABSTRACTS

Nuclear Science Abstracts is available to the public on a subscription basis from the Superintendent of Documents, U. S. Government Printing Office, Washington, D. C. 20402.

For the 24 regular issues, the yearly rate is $42.00 for domestic subscribers and $52.50 for foreign subscribers. A single issue costs $1.75, domestic rates, or $2.19, foreign rates. Domestic rates apply to the United States, Canada, Mexico, and Central and South American countries except Argentina, Brazil, Guyana, French Guiana, Surinam, and British Honduras.

For a yearly subscription to the cumulative indexes, the rates are $38.00 for domestic subscribers and $47.50 for foreign subscribers.

The following cumulative indexes are available:

From Johnson Reprint Corporation, 111 Fifth Avenue, New York, N. Y. 10003:

Vols. 1–4, Subjects and Authors (1948–1950), $30.00.

From Superintendent of Documents, U. S. Government Printing Office, Washington, D. C. 20402:

Vols. 5–10, Subjects and Authors (1951–1956), $5.25.

Vols. 11–15, Subjects (1957–1961), $19.00.
Vols. 11–15, Personal Authors (1957–1961), $14.25.
Vols. 11–15, Corporate Authors (1957–1961), $2.50.

Vols. 16–20, Subjects (1962–1966), $36.00.
Vols. 16–20, Personal Authors (1962–1966), $22.50.
Vols. 16–20, Corporate Authors (1962–1966), $3.75.

Vol. 21, Subjects and Authors (1967), $16.00.
Vol. 22, Subjects and Authors (1968), $26.00.
Vol. 23, Subjects and Authors (1969), $25.75.
Vol. 24, Subjects and Authors (1970), $22.50.

Cumulative Report Number Index, Vols. 1-15 Revised, $4.00.
Cumulative Report Number Index, Vols. 16-20 Revised, $5.50.
Cumulative Report Number Index, Vols. 21-24, $4.25.

Nuclear Science Abstracts is available on an exchange basis to universities, research institutions, industrial firms, and publishers of scientific information. Government agencies may obtain *NSA* free of charge. Inquiries should be directed to the USAEC Division of Technical Information Extension, P. O. Box 62, Oak Ridge, Tennessee 37830.

INDEXES TO NSA

Comprehensive indexes appear in each issue and are cumulated quarterly and annually. Multivolume cumulations have been issued as indicated above.

All documents abstracted are indexed by subjects and personal authors. Report literature is indexed also by corporate author and report number. Each of these indexes in every issue is preceded by an introduction explaining in detail the organization of the index and the principles by which it is compiled. The reader is referred to these explanations for information not found in the brief summary below.

Personal Authors

Each author's name is indexed in the form appearing on the document abstracted:

ISHIHARA, T., Accumulation of fallout ^{137}Cs in newborn infants, 23:50538
ISHIHARA, Toyokuki, Shielding effect of paraffin, water, soil, concrete, Fe, and Pb for high-energy neutrons, 23:51748

Subjects

The subject index consisting of specific materials, objects, and processes is arranged alphabetically. Modifying phrases specific to these subjects in turn are arranged alphabetically under the subjects.

MELPHALAN
effects on proliferation of cultured antigen-stimulated spleen cells from mice, dose-response curve for, 23:50820
MEMBRANE FILTERS
design for removal of cell-free Streptococcus faecalus from bacteria cultures in fermentation tank, 23:49996 (UCRL-18667, pp 322-9)
MENDELEVIUM
separation from einsteinium and fermium by electrolysis, 23:49772 (UCRL-18667, pp 277-312)
separation from sodium acetate solutions by solvent extraction using sodium amalgam, 23:49772 (UCRL-18667, pp 277-312)
stability of divalent state of, 23:49772 (UCRL-18667, pp 277-312)

Corporate Authors

Technical report literature is indexed from the name of the organization or institution responsible for the issuance of the report.

51093 (LA-4164) FABRICATION OF BORON CARBIDE RINGS AND DISKS. Sheinberg, H.; Herrera, T.; Kostacopoulos, J. **(Los Alamos Scientific Lab., N. Mex.).** Apr. 25, 1969. Contract W-7405-eng-36. 11p. Dep. CFSTI.

is indexed as:

LOS ALAMOS SCIENTIFIC LAB., N. MEX.
Fabrication of boron carbide rings and disks, 23:51093 (LA-4164)

Report Numbers

Technical report literature is also indexed by report numbers. This index includes information on where individual reports may be obtained. While not reports, patents and conference papers are indexed here as a matter of convenience.

JPRS-	**(Non-AEC)**	
46949	23-51587	CFSTI
48330	23-52305	CFSTI
48331	23-52451	CFSTI
48481	23-50889	CFSTI
48743	23-51034	CFSTI
49025	23-51706	CFSTI (U. S. Sales Only)
JUL-	**(German)**	
571-RG	23-52269	Dep
578-PP	23-51624	Dep. CFSTI (U. S. Sales Only)
581-FN	23-51079	Dep. CFSTI (U. S. Sales Only)
584-RG	23-52313	Dep
586-FN	23-51035	Dep. CFSTI (U. S. Sales Only)
K-		
1777	23-50987	Dep. CFSTI
1778	23-50988	Dep. CFSTI
KFK-	**(German)**	
743	23-52461	Dep
743	23-52447	For translation see EURFNR-613
781/I	23-52462	Dep
824	23-52397	Dep. CFSTI (U. S. Sales Only)

XUM

TABLE OF CONTENTS

Volume 25, Number 18, September 30, 1971

Category	Page
CHEMISTRY	4081
Analytical Chemistry	4081
Chemical and Spectral Procedures	4081
Isotope Dilution Procedures	4084
Radiometric and Radiochemical Procedures	4084
Activation Procedures	4085
Inorganic, Organic, and Physical Chemistry	4088
Chemical Properties	4088
Isotope Effects and Exchange	4088
Physical Chemistry	4093
Radiation and Nuclear Chemistry	4094
Radiation Effects	4095
Radiation Processes	4096
Radiolysis	4096
Radioisotope Production	4099
Recoil Production and Reactions	4100
Radiochemistry	4100
Separation Processes	4100
EARTH SCIENCES	4105
Geology and Hydrology	4105
Meteorology	4105
Mineralogy and Exploration	4106
Oceanography	4107
Seismology	4108
ENGINEERING	4109
Nuclear Explosions	4109
Facilities and Equipment	4109
Heat Transfer and Fluid Flow	4111
Isotope Technology	4112
Materials Testing	4115
Protective Structures	4117
Radioactive Material Handling	4117
Vacuum Engineering	4118
INSTRUMENTATION	4119
Radiation Detection Instruments	4119
General Detectors and Monitors	4119
Nuclear Spectroscopic Instrumentation	4124
High Energy Physics Instrumentation	4127
Radiation Dosimeters	4129
Radiometric Instruments	4130
Miscellaneous Instruments and Components	4130
Radiation Effects on Instruments and Instrument Components	4134
LIFE SCIENCES	4136
Biochemistry, Physiology, and Molecular Biology	4136
Basic Processes	4136
Metabolism, Physiology, and Toxicology	4136
Radiation Effects	4139
Immunology	4143
Ecology	4144
Genetics and Cytogenetics	4145
Health Physics and Safety	4151
Radioactive Contamination and Decontamination	4151
Dosimetry and Monitoring	4153
Radiation Protection	4159
Safety Procedures	4164

Category	Page
LIFE SCIENCES (Cont'd.)	
Civil Defense	4164
Legal Aspects	4164
Medicine	4165
Protective Substances	4165
Radiation Sickness and Injuries	4169
Radiodiagnosis	4169
Radiotherapy	4173
Blast and Thermal Effects	4174
Radiation Effects on Animals	4174
Invertebrates	4175
Vertebrates	4176
Man	4184
Radiation Effects on Plants	4189
Radiation Effects on Microorganisms	4190
Radiosterilization and Radiopreservation	4192
METALS, CERAMICS, AND OTHER MATERIALS	4195
Metals and Alloys	4195
Corrosion and Erosion	4197
Preparation and Fabrication	4199
Properties Evaluations	4201
Structure and Phase Studies	4206
Radiation Effects	4207
Ceramics and Cermets	4212
Corrosion and Erosion	4212
Preparation and Fabrication	4212
Properties Evaluations	4214
Structure and Phase Studies	4217
Radiation Effects	4219
Plastics and Other Materials	4220
PHYSICS (GENERAL)	4221
Astrophysics and Cosmology	4221
Stars	4221
Quasi-Stellar, Radio, and X-Ray Sources	4223
Solar Phenomena	4224
Galaxies	4226
Cosmology	4226
Planetary Phenomena	4227
Atomic and Molecular Physics	4228
Atomic, Electron, Ion, and Molecular Beams and Their Reactions	4228
Atomic and Molecular Properties	4229
Positronium, Muonium, and Mesic Atoms and Molecules	4230
Collision Phenomena	4230
Atomic Theory	4233
Cosmic Radiation	4234
Direct Energy Conversion	4235
Fluid Physics	4236
Geophysics (Upper Atmosphere)	4238
Low-Temperature Physics and Cryogenic Equipment	4246
Superfluidity	4246
Superconductivity	4247
Equipment and Devices	4251
Plasma and Thermonuclear Physics	4251
Confinement and Heating	4252
Diagnostics	4252

TABLE OF CONTENTS (continued)

Category	Page
PHYSICS (GENERAL) (Cont'd.)	
Kinetics (General)	4253
Kinetics (Experimental)	4253
Kinetics (Theoretical)	4254
Production	4256
Stability	4257
Thermonuclear Processes	4258
Wave Phenomena	4259
Shielding	4260
Solid-State Physics	4262
Radiation Effects	4262
Physical Properties	4265
Moessbauer Effects and NMR	4268
Theory	4269
Theoretical Physics	4269
PHYSICS (HIGH-ENERGY)	4272
Particle Interactions and Properties (Experimental)	4272
Electromagnetic	4272
Weak	4272
Strong (Baryon-Induced)	4272
Strong (Meson-Induced)	4274
Particle Interactions and Properties (Theoretical)	4276
General	4276
Electromagnetic	4278
Weak	4281
Strong (General)	4281
Strong (Baryon No. = 0)	4282
Strong (Baryon No. = 1)	4284
Strong (Baryon No. ≥ 2)	4285
Particle Invariance Principles and Symmetries	4286
General	4286
Applications (Electromagnetic and Weak)	4286
Applications (Strong)	4287
Field Theories	4287
General	4287
Quantum Field Theory	4288
Gravitation and General Relativity	4290
Scattering Theory	4292
Particle Accelerators	4293
PHYSICS (NUCLEAR)	4298
Neutron Interactions with Matter	4298
Nuclear Properties and Reactions, A ≤ 5	4298

Category	Page
PHYSICS (NUCLEAR) (Cont'd.)	
Nuclear Properties and Reactions, 6 ≤ A ≤ 19	4300
Nuclear Properties and Reactions, 20 ≤ A ≤ 89	4303
Nuclear Properties and Reactions, A ≥ 90	4309
Nuclear Theory	4316
REACTOR TECHNOLOGY	4321
Commercial Power Reactors	4321
Operation and Economics	4321
Safety and Siting	4322
Steam and Power Conversion Systems	4325
Power Reactor Development	4325
Kinetics and Dynamics	4326
Control Systems	4327
Shielding	4327
Cooling Systems	4328
Fuels	4329
Operation and Economics	4330
Safety and Siting	4331
Power Conversion Systems	4332
Research and Test Reactors	4332
Rocket and Space Reactors	4334
Process Heat and Desalination Reactors	4335
Marine and Portable Power Reactors	4335
Reactor Theory	4336
Kinetics	4337
Experimental Applications	4338
Reactor Components, Fuels, and Accessories	4338
GENERAL	4341
CORPORATE AUTHOR INDEX	INDEX-1
PERSONAL AUTHOR INDEX	INDEX-13
SUBJECT INDEX	INDEX-65
REPORT NUMBER INDEX	INDEX-169

STAFF OF NUCLEAR SCIENCE ABSTRACTS

John W. Norris
Managing Editor

Donald D. Davis
Assistant Managing Editor

David E. Bost
Production Manager

Sidney F. Lanier
Subject Heading Specialist

J. Paul Meredith
Descriptive Cataloging Specialist

Frederick E. Marsh, Jr.
Computer Index Coordinator

Clara L. Fox
Corporate Author Specialist

Helen W. White
Report Number Specialist

Section Editors

Everett J. Hoffman
Chemistry

Robert C. Kelly
Engineering; Earth Sciences; Metals, Ceramics, and Other Materials

Lee M. Thompson
General Physics

Charles E. Stuber
High Energy Physics; Instrumentation

Donald D. Davis
Life Sciences

Lawrence T. Whitehead
Nuclear Physics

James M. Jacobs
Reactor Technology

Evaluators

Thomas S. Chapman
John H. Mitchell
Mary H. Newman
Polly C. Summers

Abstractors

F. S. Armstrong*
Ellis R. Bedford
Mary M. Brown
Jane G. Buchanan
D. Lamar Cason
Gloria M. Caton
David C. Cunningham
James R. Dulaney
Helga B. Gerstner
Mary C. Grissom
Phyllis C. Hansen
Carolyn D. Houston
Elaine E. Huber
Rose V. Jermain
W. Hugh Kinser, Jr.
Lisbeth C. Lieberman
Betty L. McDowell
Patricia B. McEwen
Fay M. Martin
William D. Matheny
Dora H. Moneyhun
Jean F. Peckham
Henry D. Raleigh
Mona H. Raridon
Julia S. Redford
Jessie W. Rushing
Robert W. Rutkowski
Francis L. Sachs
Lila B. Smith
Anne G. Ward
Helen L. Ward
Kenneth S. Warren
Milton O. Whitson
Juanita Wilson

*Atomic Energy of Canada, Ltd.

Charles R. Bruce
Publishing Coordinator

Communication concerning the editorial policy and content of *Nuclear Science Abstracts* should be addressed to the Managing Editor, *Nuclear Science Abstracts*, USAEC Division of Technical Information Extension, P. O. Box 62, Oak Ridge, Tennessee 37830.

Use of funds for printing this publication approved by the Director of the Bureau of the Budget, June 26, 1969.

XUM

Volume 25, Number 18 September 30, 1971

NUCLEAR SCIENCE ABSTRACTS

CHEMISTRY

Analytical Chemistry

Refer also to abstract 41832.

41713 (AECL-3672) ORGANIC REACTOR COOLANT ANALYSIS: CANADIAN PRACTICE, 1970. Stewart, R. B. (Atomic Energy of Canada Ltd., Pinawa (Manitoba). Whiteshell Nuclear Research Establishment). Jun 1970. 30p. Dep. NTIS (U. S. Sales Only). AECL $1.00.

Methods used in current Canadian practice for analysis of hydrogenated terphenyl reactor coolant mixtures are briefly described. They deal with major constituents, physical properties, impurities, radioactivities, and coolant quality tests. Continuous in-system measurements are included. (auth)

41714 EVALUATION OF LUNAR ELEMENTAL ANALYSES. Morrison, George H. (Cornell Univ., Ithaca, N. Y.). Anal. Chem.; 43: No. 7. 22A-31A(Jun 1971).

A review is presented on the analytical techniques used by investigators of the major, minor, and trace element composition as well as isotopic composition of lunar materials returned by Apollo missions 11, 12, and 14. For the determination of elemental composition the techniques of activation analysis, atomic absorption, emission spectroscopy, flame photometry, inert gas fusion, mass spectrometry, spectrophotometry, wet chemistry, and x-ray fluorescence were used. For isotopic information, mass spectrometry and gamma spectrometry were used. Surface studies involved the use of Auger spectroscopy, and oxidation states were studied using Moessbauer spectroscopy, nuclear magnetic resonance, and electron spin resonance. Information on the distribution of elements in the lunar samples was obtained through the use of ion microprobe analysis and scanning electron microscopy. (J.G.B.)

41715 SEPARATION OF CALCIUM-STRONTIUM INVESTIGATED BY THE USE OF TRACERS. Baratta, Edmond J.; Knowles, Forrest E. Jr. (Northeastern Radiological Health Lab., Winchester, Mass.). Anal. Chem.; 43: No. 8, 1138-9(Jul 1971).

^{47}Ca and ^{85}Sr were used as tracers to verify the optimum HNO_3 concentration range for recovery of Sr. Data and results using one and two separations for 6 normalities are given. Approximately 15N (67%) was found to be the best nitric acid concentration. (M.C.G.)

Chemical and Spectral Procedures

Refer also to abstract 42217.

41716 (AECL-3676) DETERMINATION OF SULPHATE IN NITRIC ACID-SULPHURIC ACID MIXTURES. Boase, D. G.; Eisenzimmer, M.; Thomson, R. G. (Atomic Energy of Canada Ltd., Pinawa (Manitoba). Whiteshell Nuclear Research Establishment). Mar 1971. 12p. Dep. NTIS (U. S. Sales Only). AECL $0.50.

A method is described for the determination of the sulfate ion in the presence of nitric acid. The method may be applied to aqueous acid and aliphatic amine-xylene solutions. A preliminary ion-exchange separation to remove cations allows the method to be applied to solutions containing milligram amounts of plutonium, uranium, and iron. Microgram quantities of these elements do not interfere. The method is based on direct titration of sulfate ion by lead nitrate in an aqueous methanol medium at a controlled pH. 1-(2-pyridylazo)-2-naphthol is used as the indicator. A precision (2σ) of ±2% in the range 1 to 0.1 mmole sulfate is achieved. The detection limit is 0.002 mmole sulfate. (auth)

41717 (CEA-N-1446) RAPID DETECTION OF BERYLLIUM. Chuiton, Genevieve (Commissariat a l'Energie Atomique, Fontenay-aux-Roses (France). Centre d'Etudes Nucleaires). Jun 1971. 22p. (In French). Dep. NTIS (U. S. Sales Only).

The principal methods currently used for measuring beryllium concentrations in atmospheric control are recalled. The need for a rapid method is emphasized. The method chosen involves the formation of a beryllium-eriochrome-cyanine complex. The principal parameters involved in the formation of the complex were determined so that optimum experimental conditions could be chosen. (France)

41718 (CEA-R-4106) STUDY OF THE PRINCIPLE OF STANDARD SAMPLES REALISATION IN ANALYTICAL CHEMISTRY; TRACE ELEMENTS PROBLEMS IN PLUTONIUM: APPLICATIONS. Buffereau, Michel; Genty, Claude (Commissariat a l'Energie Atomique, Bruyeres-le-Chatel (France). Centre d'Etudes). Feb 1971. 43p. (In French). Dep. NTIS (U. S. Sales Only).

Problems associated with development of reference standards for the chemical analysis of various forms of plutonium for trace impurities were studied. Sampling techniques, composition of reference standards, and methods of analysis are discussed. (J.G.B.)

41719 (CONF-700303-(Absts.)) PITTSBURGH CONFERENCE ON ANALYTICAL CHEMISTRY AND APPLIED SPECTROSCOPY, CLEVELAND, OHIO, MARCH 1-6, 1970. (Spectroscopy Society of Pittsburgh, Pa. Society for Analytical Chemists of Pittsburgh, Pa.). 156p.

41720 (CONF-710207-(Absts.)) THE PITTSBURGH CONFERENCE ON ANALYTICAL CHEMISTRY AND APPLIED SPECTROSCOPY, INC., CLEVELAND, OHIO, FEBRUARY 28-MARCH 5, 1971. Exposition of Modern Laboratory Equipment. (Society for Analytical Chemistry of Pittsburgh, Pa. Spectroscopy Society of Pittsburgh, Pa.). 160p.

41721 (EUR-4352) SPECTROPHOTOMETRIC DETERMINATION OF TRACES OF AMERICIUM IN PLUTONIUM OXIDE. Buijs, K.; Maurice, M. J. (European Atomic Energy Community). 1969. 10p. NTIS (U. S. Sales Only).

The spectrophotometric determination of americium in the presence of plutonium is described. Plutonium is removed from the sample solution by an extraction with tributyl phosphate and americium is determined in the aqueous phase by an absorbance measurement at 504 nm. In the case of a determination in plutonium oxide the sample is dissolved in sulfuric acid-ammonium sulfate, americium and plutonium are precipitated as their hydroxides, redissolved in nitric acid, and plutonium is removed by extraction. (auth)

41722 (JAERI-13622) SOME CAUTIONARY PROBLEMS OF FLUOROMETRIC DETERMINATION OF URANIUM. Akaishi, Jun; Yabe, Akira (Japan Atomic Energy Research Inst., Tokai). Jun 1969. 21p. NTIS (U. S. Sales Only).

The fluorometric method is sensitive for determination of uranium and is suitable for low-level uranium determination. However, many kinds of substances interfere. Several important problems in the fluorometric method were surveyed: characteristics of the fluorescence, interference elements, composition of fusing flux, fusion temperature and time, fusion atmosphere, fluctuation of readings of the fluoresence, etc. Dilution and standard addition methods for determination of uranium under the co-existence of interference elements are also described. (auth) (Japan)

41723 (NIM-1077) DETERMINATION OF ACID-SOLUBLE, ACID-INSOLUBLE, AND TOTAL URANIUM IN SILICATE ORES. Gereghty, Anna M.; Cook, E. B. T. (National Inst. for Metallurgy, Johannesburg (South Africa)). 19 Oct 1970. 7p. Dep. NTIS (U. S. Sales Only).

A method for determination of acid-soluble, acid-insoluble, and total uranium in silicate ores is described. Acid-soluble uranium is leached from the ore with nitric acid, and total or insoluble uranium is fused with boric oxide followed by leaching with hydrofluoric and nitric acids. The uranium is extracted into a solution of trioctylphosphine oxide in cyclohexane and determined spectrophotometrically with the reagent 2-(2-pyridylazo)-5-diethylaminophenol (PADAP). The method is applicable to silicate ores for concentrations of U_3O_8 ranging from 1 to 2000 ppM as acid-soluble uranium and from 5 to 2000 ppM as acid-insoluble and total uranium. (auth)

41724 LITHIUM ISOTOPIC ANALYSIS BY NUCLEAR MAGNETIC RESONANCE SPECTROMETRY. Attalla, Albert; Eckstein, Ralph R. (Mound Lab., Miamisburg, Ohio). Contract AT(33-1)-Gen-53. Anal. Chem.; 43: No. 7, 949-50(Jun 1971).

Nuclear magnetic resonance spectrometry (NMR) was used for isotopic abundance ratio determinations as well as for quantitative analysis of ^6Li and ^7Li. The smallest amount of ^6Li detectable was about 0.7 mole/liter of solution. Approximately 0.2 mole/liter of ^7Li was necessary to produce a satisfactory spectrum. (J.G.B.)

41725 DETERMINATION OF URANYL AND THORIUM(IV) BY GAS CHROMATOGRAPHY OF VOLATILE MIXED-LIGAND COMPLEXES. Sieck, R. F.; Richard, J. J.; Iversen, Kay; Banks, C. V. (Ames Lab., Iowa). Anal. Chem.; 43: No. 7, 913-17(Jun 1971).

A gas chromatographic method is reported for the separation and determination of UO_2^{2+} and Th(IV) as mixed-ligand complexes. Several new volatile UO_2^{2+} and Th(IV) complexes are reported. By using the β-diketone hexafluoroacetylacetone, H(HFA), and the neutral donor di-n-butylsulfoxide, (DBSO), to form the mixed-ligand complexes, separation and quantitative determination of UO_2^{2+} and Th(IV) was possible in the range 1 mg metal/ml to 120 mg metal/ml with a relative error of less than 10%. Detection limits were 0.4 mg/ml for thorium and 0.6 mg/ml for uranium. The use of solvent extraction procedures to obtain the mixed-ligand complexes provides a method which is quick and highly selective. (auth)

41726 SPECTROPHOTOMETRIC DETERMINATION OF MOLYBDENUM WITH PHENYL-FLUORONE. Halasz, A.; Polyak, K.; Pungor, E. (Univ. of Chemical Engineering, Veszprem, Hungary). Hung. Sci. Instrum.; No. 18, 15-18(May 1970).

A spectrophotometric method is described for the rapid determination of molybdenum in an aqueous medium employing phenylfluorone or methylfluorone as the reagent. The optimum concentration of both the reagent and the acid was determined. Beer's law was found to be valid up to 4.8 γ/ml molybdenum concentration. The molar extinction coefficient of the molybdenum–phenylfluorone complex was 3.02×10^4. (auth)

41727 DETERMINATION OF THE ISOTOPIC COMPOSITION OF TIN AND INDIUM. Grudinkina, N. P.; Levin, E. M.; Pevzner, M. G. Tr. Metrol. Inst. SSSR: No. 96, 184-6(1968). (In Russian).

A Russian-made mass spectrometer was used to determine the isotopic composition of two samples of tin that were to be used in international comparison of melting points. The optimal conditions included an accelerating voltage of 3 kV, ionizing voltage 48 V, the preheater current 0.5 A, and emission current 1.8 A. Results are presented for the range of isotopic masses from 112 to 124. In the case of indium, the accelerating potential was 3 kV and the preheater current 4.3 A. The indium samples were also for international mp checking. The mass spectrometer yielded: 4.24% of isotope 113 and 96.76% of 115. (K.S.W.)

41728 SOME STUDIES INVOLVING THE DETERMINATION OF MOLYBDENUM BY ATOMIC ABSORPTION SPECTROSCOPY. Grosz, Fred A. Vermillion, S. Dak.; Univ. of South Dakota (1970). 175p. University Microfilms Order No. 71-12,644. Thesis.

The atomic absorption of molybdenum was studied in air–acetylene and nitrous oxide–acetylene flame systems. Atomic absorption of molybdenum was found to be greatly affected by the nature of the solvent, complexing agents used, and diverse ions present. A detailed study of these effects was made, and the results applied to the analysis of molybdenum in steel and other samples. The study of the interference effects of a number of diverse ions showed that their effect is dependent on the pH and on the nature of the mineral acid used. Aluminum and phosphate ions were investigated to evaluate their effectiveness as suppressing agents. The suppressing action of these ions is quite dependent on the mineral acid present. It was found that a mixture of aluminum and phosphate is more effective in eliminating interference due to diverse ions encountered in analyzing steel samples, than either ion alone. Results from analysis of steel samples and molybdenum carbonyl complexes are given. Several organic solvents were investigated as sample diluents for atomic absorption analysis. As expected, the addition of organic solvents such as methanol, ethanol, and isopropanol causes an enhancement of molybdenum absorption in both flame systems. The enhancement effect was considerably greater in the nitrous oxide–acetylene flame than in the air–acetylene flame. Several solvent extraction systems were investigated in conjunction with the atomic absorption determination of molybdenum. The extraction of molybdenum(V) thiocyanate into butyl acetate or methyl isobutyl ketone was successfully employed in removing interference from numerous ions and matrix effects. This extraction system was successfully applied to the simultaneous determination of molybdenum and tungsten. Mixtures of butyl acetate or methyl isobutyl ketone with tri-n-butyl phosphate were found to completely extract molybdenum from hydrochloric acid solutions. Results using this extraction method along with the atomic absorption determination of molybdenum are given for several samples. Investigations were also undertaken using butyl acetate–oxine and butyl acetate–α-benzoin oxime extraction systems with subsequent determination of molybdenum by atomic absorption. The results obtained from application of these methods to analysis of samples are included. (Diss. Abstr. Int., B)

41729 DETERMINATION OF MI-1305 MASS SPECTROMETER D/H RATIO BY USING MODULATED ACCELERATING VOLTAGE. Matus, L.; Opauszki, J. (Central Physics Research Inst., Budapest). Instrum. Exp. Tech. (USSR) (Engl. Transl.); No. 5, 1529-30(Sep-Oct 1970).

Translated from Prib. Tekh. Eksp.; No. 5, 241-2(Sep-Oct 1970).

A method for measuring H_2^+ and HD^+ ion beams simultaneously with a MI-1305 mass spectrometer is described in application to analysis of the isotope composition of hydrogen in atmospheric precipitation. A technique of modulating the accelerating voltage so that the current intensity of a beam of ions of mass 2 would be recorded at a voltage of 3 kV, and that of a beam of ions of mass 3 would be recorded at a voltage $\approx$2.5 kV, was worked out for this purpose. The D/H concentration ratio in the specimen measured was determined by comparison with a standard reference specimen. The error in the determination of the D/H ratio was $\pm$0.3%. (auth)

41730 SPECTROPHOTOMETRIC STUDY AND ANALYTICAL APPLICATION OF RARE-EARTH TIRON COMPLEXES. II. DETERMINATION OF EUROPIUM. Taketatsu, Tomitsugu; Yamauchi, Taeko (Kyushu Univ., Fukuoka). Talanta; 18: No. 6, 647-9(Jun 1971).

The absorption spectra of europium–Tiron complexes in aqueous solution were measured from 340 to 600 nm. The absorbance at 390 and 420 nm followed Beer's law up to 0.8 mg/ml (pH 6.2 to 6.6). Other rare earths, except for cerium(III), did not interfere. The interference of cerium could be removed by addition of ascorbic acid. The combining ratio of Tiron to europium was found to be 1:1. (auth) (UK)

41731 DETERMINATION OF THE ISOTOPIC COMPOSITION OF CADMIUM. Grudinkina, N. P.; Pevzner, M. G. Tr. Metrol. Inst. SSSR: No. 96, 181-3(1968). (In Russian).

The following optimum conditions were established for mass spectrometer operation with Cd isotopes: accelerating voltage, 3 kV, ionization voltage, 34 kV, and cathode emission, 1.5 A. The Cd samples had been prepared for ultimate international temperature comparisons. The following results were obtained for the average isotope composition of Canadian Cd: 106-1.28%, 108-0.88%, 110-12.49%, 111-12.89%, 112-24.25%, 113-12.23%, 114-28.64%, 116-7.34%. (K.S.W.)

41732 CONDUCTING GLASS ELECTRODE IN A THIN-LAYER ELECTROCHEMICAL CELL WITH APPLICATION TO THE ANALYSIS OF NEPTUNIUM. Propst, R. C. (E. I. du Pont de Nemours and Co., Aiken, S. C.). Contract AT(07-2)-1. Anal. Chem.; 43: No. 8, 994-9(Jul 1971).

XUM

A cylindrical cell for coulometry in thin layers of solution at a conducting glass electrode is described. Volumes were reproducible to ±0.3%. Techniques are recommended to reduce edge diffusion and iR gradient effects. Application of the method to determine neptunium in process samples is described. (auth)

41733 ANALYTICAL SIGNIFICANCE OF PEAKS AND PEAK RATIOS IN X-RAY FLUORESCENCE ANALYSIS USING A HIGH RESOLUTION SEMICONDUCTOR DETECTOR. ANALYSIS OF URANIUM SOLUTIONS BY X-RAY SPECTROMETRY. Shenberg, Cesia; Amiel, Saadia (Soreq Nuclear Research Centre, Yavne, Israel). Anal. Chem.; 43: No. 8, 1025-30(Jul 1971).

L x-ray peaks detected in the x-ray fluorescence spectrum of uranium in solution and the respective peak ratios were tested for proportionality to uranium content over a wide range of concentrations. The uranium L x rays were induced using an ^{241}Am-iodine source-target assembly. The direct comparison method of analysis was compared with the peak ratio method. Individual peaks of L_α, L_β, and L_γ lines were checked as well as their ratios to the backscattered I K_α and I K_β lines. It was found that the relative intensities of the U L_α x-ray lines vary with the U concentration in a nonlinear manner. The ratio U L_α/I $K_{\alpha\,\text{incoherent}}$ is the one least influenced by self-absorption, which makes it most suitable for the quantitative determination of uranium. The range of 0.12 to 500 mg U/ml was studied and satisfactory results were obtained. (auth)

41734 DETERMINATION OF IODINE AND FLUORINE IN SELENIUM. Westerlund-Helmerson, Ulla (Roennskaer Works, Skelleftehamn, Sweden). Anal. Chem.; 43: No. 8, 1120-2(Jul 1971).

The selenium to be analyzed was melted with an excess of sodium hydroxide. The halogens present were bound as sodium halides. To increase sensitivity, the halogens were concentrated using melting extraction. Bromine was determined by x-ray fluorescence and iodine and fluorine by using an ion-selective electrode. The limit of detection was 0.05 ppM for iodine and 0.1 ppM for fluorine. (M.C.G.)

41735 DETERMINATION OF STRONTIUM IN SILICATES, CARBONATES, AND SULFATES BY ATOMIC ABSORPTION SPECTROSCOPY. Moldan, B.; Miksovsky, M. (Geological Survey of Czechoslovakia, Prague). Collect. Czech. Chem. Commun.; 36: No. 4, 1673-7(Apr 1971).

Strontium was determined in silicates, carbonates, and sulfates by atomic absorption at 4607 Å using an air–acetylene flame. The effects of most other elements of low ionization energy on the ionization of Sr were negligible, since only relatively few of the Sr atoms ionize. However, it was necessary to suppress the effects of the condensed phase due to Al and Ti by the addition of La and oxine. When an acetylene–air flame was used, the sensitivity of the determination was 0.2 ppM, but a greater sensitivity (0.06 ppM) can be achieved with an acetylene–NO flame. However, this hotter flame introduced other interferences because of ionization. (B.L.M.)

41736 X-RAY SPECTROGRAPHIC DETERMINATION OF TELLURIUM AND PLATINUM. Verkhovodov, P. A.; Tolstopyatenko, L. I. (Scientific-Research Inst. of Non-Ferrous Metallurgy, Krasnoyarsk, USSR). Zh. Anal. Khim.; 26: No. 4, 791-5(Apr 1971). (In Russian).

A method was developed for the quantitative x ray spectrographic determination of tellurium and platinum in powdered materials of complex composition. The relationship between the relative mass coefficients of weakening the monochromatic x ray radiation with different wavelengths was derived. By this relationship the mutual effects of elements were taken into account. (auth)

41737 STUDY OF COMPLEX FORMATION BETWEEN ZIRCONIUM AND CERTAIN ORGANIC REAGENTS. Tataev, O. A.; Guseinov, V. K. (Daghestan State Univ., Makhach-Kala, USSR). Zh. Anal. Khim.; 26: No. 4, 829-32(Apr 1971). (In Russian).

Complex formation of zirconium with the reagents of the triphenylmethane series, glycinecresol red (GCR) and glycinethymol blue (GTB), and with trihydroxyfluorones 9-salicylfluorone (SF) and p-dimethylaminophenylfluorone (DAPF), was studied spectrophotometrically. Conditions for developing the complex color were found and their composition determined. GCR and GTB form complex compounds with zirconium in a moderately acid medium, whereas SF and DAPF do so in a strongly acid medium. The ratio of the components in all the complexes studied is 1 : 2. The molar extinction coefficients of the complexes, their strength, and selectivity of the reagents were determined. The chemistry of complex formation was studied. The method for determining zirconium by means of trihydroxyfluorones was tested on certain industrial samples. (auth)

41738 POLYHYDROXY FLAVONES AS EXTRACTION REAGENTS. COMMUNICATION 1. EXTRACTION OF METAL COMPLEXES WITH MORIN BY ISOAMYL ALCOHOL. Blank, A. B.; Mirenskaya, I. I.; Zolotovitskaya, E. S.; Yakovenko, E. I. (All-Union Scientific-Research Inst. of Monocrystals, Scintillation Materials, and Specially Pure Chemicals, Kharkov). Zh. Anal. Khim.; 26: No. 4, 656-63(Apr 1971). (In Russian).

It was shown, by studying the extraction of morin complexes of metals by isoamyl alcohol, that morin forms extracted compounds with many elements of the main subgroups of the II–V groups and of the odd subgroups of the I–VIII groups of the periodic system. Possibilities are discussed of using morin as a reagent for the group concentration of microimpurities, separation of certain elements with similar properties or different ions of the same element, and extraction-photometric or extraction-fluorometric determinations. (auth)

41739 APPLICATIONS OF RADIOISOTOPE X-RAY FLUORESCENCE ANALYSERS IN METALLIFEROUS MINERAL EXPLORATION AND IN MINING. Clayton, C. G. (United Kingdom Atomic Energy Authority, Wantage, Eng.). pp 27-35 of Nuclear Techniques for Mineral Exploration and Exploitation. Vienna; International Atomic Energy Agency (1971).

From Panel on nuclear techniques and mineral resources in developing countries; Krakow, Poland (8 Dec 1969). See STI/PUB-279; CONF-691229.

A review is made of current portable radioisotope x-ray fluorescence analyzers and their use in the exploration of localized regions and in mining operations. Examination of rock surfaces, analysis of drill cores and powdered samples with the portable analyzers, and borehole logging with XRF probes currently under development are discussed. Comments are made on the advantages and limitations of the instruments. (auth)

41740 USE OF NUCLEAR TECHNIQUES IN ON-STREAM ANALYSIS IN MINERAL PROCESSING PLANTS. Clayton, C. G. (United Kingdom Atomic Energy Authority, Wantage, Eng.). pp 59-72 of Nuclear Techniques for Mineral Exploration and Exploitation. Vienna; International Atomic Energy Agency (1971).

From Panel on nuclear techniques and mineral resources in developing countries; Krakow, Poland (8 Dec 1969). See STI/PUB-279; CONF-691229.

Radioisotope x-ray fluorescence was established as the most important nuclear technique for on-stream analysis in mineral processing plants because of operational advantages arising from the low cost, ruggedness, and instrumental simplicity associated with its use. Neutron activation analysis also has considerable potential for on-line applications, its most significant advantages being its insensitivity to variations in particle sizes, limited inter-elemental effects, and the ability to operate directly on process streams and conveyor belts. A review is made on the application of these two complementary techniques for on-stream analyses, and an indication is given of some specific applications for which the use of preferential absorption or x-ray scatter technique is preferred. (auth)

41741 USE OF MONOENERGETIC X-RAY SOURCES IN X-RAY FLUORESCENCE ANALYSIS. RECENT DEVELOPMENTS AND APPLICATIONS IN MINERAL INDUSTRIES. Kasemsanta, S. P. (International Atomic Energy Agency, Vienna). pp 81-101 of Nuclear Techniques for Mineral Exploration and Exploitation. Vienna; International Atomic Energy Agency (1971).

From Panel on nuclear techniques and mineral resources in developing countries; Krakow, Poland (8 Dec 1969). See STI/PUB-279; CONF-691229.

In radioisotope x-ray fluorescence analysis the accuracy that could be achieved is limited mainly by inter-element and particle-size effects. By using a monochromatic radiation having an appropriate energy for the excitation of the matrix under analysis, inter-element interferences could be minimized and, as an additional advantage, the need for balanced x-ray filters is also eliminated. A review is made of recent designs of monoenergetic x-ray sources for x-ray fluorescence analysis, their use and their potential. Brief descriptions are given of promising developments in the application of the technique for on-stream analyses in mineral processing plants and, to a limited extent, for field determination of heavy and medium-weight elements in minerals. (auth)

41742 QUANTITATIVE ANALYSIS BY SORPTION ON ION EXCHANGERS. Bobleter, O.; Dincler, G.; Sabau, C. (Oesterreichische Hochschule, Vienna). Mikrochim. Acta; No. 2, 310-16(1971). (In German).

In the case of the sorption of ions by a regenerated ion exchanger, the concentration of these ions increases logarithmically in the effluent over a wide range of the break-through curve. At constant flow rate and column dimensions the slope q of the logarithmically

plotted break-through curve is dependent on the concentration of the applied solution. At low flow-rates and concentrations, a direct proportionality between the q values and concentration was found. At higher concentration (or flow rates) a deviation from linearity was observed, which can be determined by a standard curve. In the case of strontium the determination of break-through curves and the standard curve is demonstrated. Using the standard curve the concentration of unknown solutions can be determined. Labelling the solution to be examined with radionuclides is desirable because it enables the determination of the slope q by measuring the radioactivity of the effluent. The method described is especially suitable for an automatic analytical procedure. (auth)

41743 QUERCETIN AS A SPRAY REAGENT IN INORGANIC THIN-LAYER CHROMATOGRAPHY AND EVALUATION OF THE CHROMATOGRAPHED SPECIES BY RING COLORIMETRY. Johri, K. N.; Mehra, Harish C. (Univ. of Delhi). Mikrochim. Acta; No. 2, 317-21(1971).

Clean and rapid micro analytical separations of various ions (including Zr, Th, U, Mo, and Ce) in their mixed solutions were made by ascending TLC using quercetin (3,5,7,3′,4′-pentahydroxyflavone) as a spray reagent. The visualized spots are scooped out with the help of a Mottier gadget and transferred to the paper set on the ring oven. Separate rings were obtained for individual metal ions and the computation of their amounts is made possible by ring colorimetry, using suitable chromogenic reagents. (auth)

41744 MICRODETERMINATION OF TELLURIUM AND ORGANO-TELLURIUM COMPOUNDS. Ma, T. S.; Zoellner, W. G. (City Univ., Brooklyn. New York Univ., N. Y.). Mikrochim. Acta; No. 2, 329-34(1971).

A method is described for conversion of elemental tellurium and organotellurium compounds quantitatively to Te(IV) by digestion with a mixture of nitric and sulfuric acids in the micro-Kjeldahl flask. After removal of nitrogen oxides by means of urea, exactly 5 ml of 0.02N potassium dichromate is added, whereupon Te(IV) is oxidized to Te(VI). The tellurium content of the sample is related to the amount of dichromate consumed, the latter being determined either spectrophotometrically or by back-titration with 0.02N ferrous sulfate. This method, applicable to 1 to 4 mg of tellurium, is amenable to automation and multi-element determinations. (auth)

41745 GAS CHROMATOGRAPHIC METHOD FOR THE MICRODETERMINATION OF IODINE. Hasty, R. A. (Montana State Univ., Bozeman). Mikrochim. Acta; No. 2, 348-52(1971).

Iodine was quantitatively converted by reaction with acetone to a form which was easily separated by gas chromatography and which was easily detected with an electron capture detector. Linear response of the detector was obtained for solutions which contained up to 1 μg/ml with an uncertainty of 8%. Milligram amounts of chloride or bromide and μg amounts of iodide do not interfere. Amplification of the amount of reaction product and the determination of both iodine and iodide were accomplished by the addition of KIO_3. (auth)

41746 QUANTITATIVE ANALYSIS OF GAS CHROMATOGRAMS OF PARTIALLY SEPARATED MATERIAL MIXTURES. Bosshard, Ch.; Piringer, O.; Gaeumann, T. (Eidgenoessiche Technische Hochschule, Lausanne, Switzerland). Helv. Chim. Acta; 54: No. 4, 1059-68(1971). (In German).

A method is described for the qualitative and quantitative analysis of gas chromatograms with considerably overlapping peaks, based on the assumption of known retention indices and peak shapes. Its application to mixtures of deuteriated hydrocarbons is indicated. The extent to which the results are reproducible is shown to be about the same as that of high-resolution gas chromatography or mass spectrometry. (auth)

Isotope Dilution Procedures

41747 (AAEC/TM-588) PRECISE DETERMINATION OF HYDROGEN IN METALS (WITH PARTICULAR REFERENCE TO ZIRCONIUM) BY THE ISOTOPIC EQUILIBRATION-MASS SPECTROMETRY PROCEDURE. Dale, L. S.; de Jong, S. (Australian Atomic Energy Commission Research Establishment, Lucas Heights). Mar 1971. 11p. Dep. NTIS (U. S. Sales Only).

A simple apparatus connected directly to a mass spectrometer makes possible the fairly rapid determination of hydrogen in metals by isotopic equilibration with deuterium. Equilibration conditions were established from kinetic studies of the exchange process as a function of heating time. Results for titanium metal standards are in excellent agreement with the certified values; relative standard deviations (1σ) range from 3.3% at 30 ppM hydrogen to 0.8% at 200 ppM. No standards are available for hydrogen in zirconium, Zircaloy, niobium, vanadium, and hafnium. For these metals the equipment was used to prepare samples with known hydrogen content. Analysis verified the reliability of the technique. The sample size requirements are 0.1 to 0.5 g (usually 0.25 g) for the range 1000 to 10 ppM hydrogen. (auth)

41748 DETERMINATION OF OXYGEN AND NITROGEN IN METALS USING FLUXES ENRICHED WITH ^{18}O AND ^{15}N ISOTOPES. Vitol, E. N.; Orlova, K. B.; Nikolaev, G. I.; Antipov, V. S. Zh. Anal. Khim.; 26: No. 4, 777-83(Apr 1971). (In Russian).

Fluxes enriched with ^{15}N and ^{18}O have been prepared and used for determining nitrogen and oxygen in refractory metals by the isotopedilution method. (auth)

41749 DETERMINATION OF BORON IN NUCLEAR MATERIALS BY ISOTOPE DILUTION TECHNIQUE. PART I. Marsel, J.; Millivojevic, D. (Josef Stefan Nuclear Inst., Ljubljana, Yugoslavia). Mikrochim. Acta; No. 2, 353-61 (1971).

The application of the mass-spectrometric stable-isotope dilution technique for the determination of microgram and submicrogram quantities of boron in nuclear materials is described. An adequate amount of spike solution (enriched in ^{10}B) is added to the sample and the mixture is treated chemically to ensure isotopic equilibration. Boron is then separated as methyl borate by distillation from phosphoric acid and converted into sodium tetraborate suitable for isotopic analysis by surface ionization in a mass spectrometer. The results for boron content in a standard boric acid solution, reagents, ammonium diuranate, uranium dioxide, sintered pellets of UO_2, and uranyl nitrate are given. Owing to the simplicity, accuracy, and high precision a possible application of the method would be its use for routine boron determinations in a natural uranium processing plant and/or as a standard method for intercomparison with other analytical methods. (auth)

Radiometric and Radiochemical Procedures

Refer also to abstracts 41945, 42058, 42102, 42113, 42118, and 42802.

41750 (AE-416) QUANTITATIVE ASSAY OF ^{239}Pu AND ^{240}Pu BY NEUTRON TRANSMISSION MEASUREMENTS. Johansson, Erik (Aktiebolaget Atomenergi, Studsvik (Sweden)). Apr 1971. 25p. Dep. NTIS (U. S. Sales Only).

A method for quantitative assay of ^{239}Pu and ^{240}Pu was tested at the reactor R1 in Stockholm. The method makes use of a fast chopper to measure the neutron transmission through a sample around the main resonances of these two isotopes, 0.296 eV in ^{239}Pu and 1.056 eV in ^{240}Pu. The transmission data measured are then combined with the known resonance cross sections to give the content of the isotopes. The method is nondestructive. A time-of-flight spectrometer of moderate capacity, like the fast chopper, is sufficient as the resonances are located at low energy. Five samples were used in the tests of the method. The results were compared with mass spectrometer values. This comparison came out quite well for ^{239}Pu, whereas the chopper results for ^{240}Pu were more than 10% higher than the mass spectrometer results. This large deviation might be due to errors in the resonance cross section for ^{240}Pu used in the analysis of the transmission data from the chopper. The best possible accuracy for a 15-hour run is ±1% for ^{239}Pu and ±2% for ^{240}Pu, obtained for thick samples—about 3×10^{20} atoms/cm^2 for each isotope. The accuracy corresponds to 68% confidence level and does not include any contribution from the uncertainty in the resonance cross section. (auth)

41751 STUDY OF SYNTHETIC INORGANIC ION EXCHANGE MATERIALS INCLUDING TWO APPLICATIONS OF AMMONIUM MOLYBDOPHOSPHATE ION EXCHANGER. McKay, James Brian. Detroit; Wayne State Univ. (1966). 62p. University Microfilms Order No. 71-12,051.

Thesis.

The development of synthetic inorganic ion exchangers is reviewed; and the major analytical applications of ion exchange with hydrous oxides, acid salts, complex ferrocyanides, and heteropoly acid salts are presented. A method for the analysis of milk for radiocesium is described, and a detailed procedure is given. The procedure consists of the isolation of cations from milk on lithium-form Dowex-50, elution of alkali metal ions from the resin, retention of radiocesium from this eluate by ion exchange on a small column of ammonium molybdophosphate, and direct counting of the gamma activity of this column. A method for the isolation of ^{137m}Ba from ^{137}Cs by elution from cesium-containing ammonium molybdophosphate exchanger is described. A procedure for the determination of the half life of ^{137m}Ba

XUM

based on this separation technique is presented in the form of a student experiment. (Diss. Abstr. Int., B)

41752 CHEMICAL ANALYSIS FROM ABSORPTION MEASUREMENTS ON COMPTON SCATTERED RADIATION. Martinelli, Pierre (to Commissariat a l'Energie Atomique). French Patent 2,038,756. 28 Dec 1970. Filed 28 Mar 1969. (In French).

A chemical analysis method is described in which a monoenergetic x ray or γ-ray beam is scattered by the Compton effect and the wavelength of the scattered beam measured. The scattered radiation is discontinuously absorbed according to its wavelength. The variation in the absorption coefficient near to an absorption discontinuity is measured with a detector and the energy of the scattered radiation determined from measurements of the scattering angle of the γ or x rays. The existence of certain rare earths was established using this method and a ^{241}Am source. (France)

41753 METHOD AND A DEVICE FOR MEASURING THE ACTIVITY OF RADIOISOTOPES FOUND IN A GAS. Fournier, Jacques; Gonnin, Rene; Villain, Paul (to Commissariat a l'-Energie Atomique). French Patent 2,034,347. 11 Dec 1970. Filed 19 Mar 1969. (In French).

A procedure for determining the activity of the isotopes of various elements present in a gas is described. A gas sample is carried away with a carrier gas across a chromatographic column where the various gaseous elements are successively eluted. The activities corresponding to each of these elements are measured at the outlet of the chromatographic column; activities corresponding to γ rays characteristic of different elements are distinguished. The procedure is applied to a cyclic analysis of the activity of the cover gas in a fast neutron reactor (argon). The γ activities of the isotopes ^{133}Xe, ^{135}Xe, ^{85m}Kr, and ^{88}Kr are measured. (France)

41754 DETERMINATION OF ^{90}Sr AND ^{89}Sr AND THE EFFECT OF FRACTIONATION PHENOMENA. Santholzer, Vilem. Sb. Ved. Pr. Lek. Fak. Karlovy Univ. Hradci Kralove, Suppl.; 13: No. 2, 197-207(1970). (In Czech).

A simple method of differentiation was tested on model mixtures of ^{90}Sr and ^{89}Sr by measurement of beta activity in a period of about 2 weeks. This method of differentiation of radionuclides of strontium can be used for samples of fresh atmospheric fallout after nuclear tests from which the strontium component was separated chemically. Fractionation phenomena, which may distort the results, should also be taken into account. For this reason, the question of fractionation of radionuclides is discussed in more detail on the basis of experimental results. (auth)

41755 NEUTROGRAPHIC HYDROGEN DETERMINATION IN ZIRCONIUM ALLOYS. Klepfer, H. H.; Kosanke, H. D.; Esch, E. L. (General Electric Co., San Jose, Calif.). pp 447-64 of Conference on the Use of Zirconium Alloys in Nuclear Reactors. Plzen, Czech.; Skoda Works (1968).

From Conference on the use of zirconium alloys in nuclear reactors; Marianske Lazne, Czech. (1 Oct 1968).

Qualitative studies of hydride detection in irradiated zirconium alloy cladding, as well as quantitative studies to determine the sensitivity and lower limit for hydrogen detection in zirconium alloy fuel tubing, are described. Tests indicated that the method is not sensitive below 500 ppM hydrogen. (J.G.B.)

41756 IMPROVED METHOD FOR AMERICIUM ANALYSIS IN URINE. Horm, I. E. (Univ. of Pittsburgh). Health Phys.; 20: No. 6, 641-3(Jun 1971).

Calcium in the urine was used as a carrier for americium; an oxalate precipitation of calcium carried americium, but left most other ions in solution. Ammonium oxalate was added to the calcium and other metal ions dissolved in the acid strip of the liquid ion exchanger HDEHP [bis(2-ethylhexyl) hydrogen phosphate]. The solution was neutralized until calcium oxalate was precipitated. The precipitate was dissolved in an ammonium chloride–hydrochloric acid solution and the americium electroplated by Mitchell's method. Alpha counting was then used to detect ^{241}Am. Comparisons were made for americium recovery using 1:3 nitric acid, concentrated nitric acid and 1M oxalic acid. (UK)

41757 NON-DESTRUCTIVE DETERMINATION OF REACTOR FUEL ELEMENT BURNUP BY MEASUREMENT OF FISSION NEUTRONS. Lin, Chia-shi; Tsai, Jensan (National Tsing Hua Univ., Hsinchu, Taiwan). J. Nucl. Sci. Technol. (Tokyo); 8: No. 5, 285-7(May 1971).

A narrow neutron beam was induced from the reactor and made incident on a fuel element vertically located at the center of a cylindrical water tank. The burnup was determined by comparing the fission neutrons generated by ^{235}U with those scattered by Al. A clean MTR-type fuel element containing 10 fuel plates was used in the experiment. In order to simulate spent fuel, the fuel plates in this clean fuel element were replaced by dummy Al plates. The burnup values obtained were smaller than expected values. (M.C.G.)

Activation Procedures

Refer also to abstracts 41877, 41878, 41920, 41941, and 43775.

41758 (AWRE-O-24/71) MULTI-ELEMENT ANALYSIS OF GLASS FRAGMENTS BY NEUTRON ACTIVATION AND THE APPLICATION TO FORENSIC SCIENCE. Goode, G. C.; Wood, G. A.; Brooke, N. M.; Coleman, R. F. (Atomic Weapons Research Establishment, Aldermaston (England)). May 1971. 32p. Dep. NTIS (U. S. Sales Only). UK 30p.

By the use of neutron activation techniques, the concentrations of 22 elements in approximately 540 samples of window glass from England and Wales were determined. An assessment of the discrimination of multielement analysis for the comparison of glass fragments in forensic examination was made statistically and compared objectively with existing physical methods. The method is illustrated by reference to a number of simulated forensic cases. (auth)

41759 SULFUR DIOXIDE MEASUREMENT SYSTEM. Cho, Boong Y.; Anderson, Larry B. (to United States Atomic Energy Commission). U. S. Patent 3,578,406. 11 May 1971. Filed 3 Mar 1969.

A quantitative determination of relatively small or trace amounts of gaseous sulfur dioxide involves a reaction between mercurous chloride and sulfurous acid, the latter formed when sulfur dioxide was dissolved in water. One of the reaction products is a water soluble bis-sulfitomercurate complex, the mercurate being easily removable from the remainder of the reaction mixture. The conversion of sulfur dioxide to the bis-sulfitomercurate complex is about 95% complete. By nucleonically detecting the amount of the bis-sulfitomercurate complex, which contains a metal having a high Z number (atomic number), using a monoenergetic source of nuclear radiation in the range of 15 to 25 keV, the amount of the complex is determinable and easily compared against a known standard sample either electronically or visually. The present system may be used on a continuously flowing gas such as stack gas, in which event it is unnecessary to scrub the gas, and permitting accurate determination of trace amounts of sulfur dioxide by monitoring or controlling the gas flow rate. (Offic. Gaz.)

41760 PREPARATION AND PROPERTIES OF ANTIMONY(V) AQUOXIDE FOR SEPARATION OF SODIUM IN ACTIVATION ANALYSIS. Toeroek, G.; Diehl, J. F. (Bundesforschungsanstalt fuer Lebensmittelfrischhaltung, Karlsruhe, Ger.). Radiochim. Acta; 15: 96-100(Mar 1971). (In German).

Hydrated antimony pentoxide (HAP) was used to remove sodium from biological samples prior to neutron activation analysis. Five different methods for the preparation of HAP were investigated. Superior results were obtained with the following procedure: hydrolysis with 10% NH_4OH, 12-hr maturation, and 5 hours of drying at 270°C. The procedure yielded a lemon yellow substance with good mechanical properties. Sorption experiments were performed with columns. Maximal load was 11 mg/g HAP. (H.B.G.)

41761 APPLICATION OF NEUTRON ACTIVATION ANALYSIS TO THE STUDY OF INTERSTITIAL SOLID SOLUTION OF OXYGEN IN NIOBIUM AND IN NIOBIUM–TITANIUM ALLOYS. Rodriguez-Gonzalez, Federico Angel. Austin, Tex.; Univ. of Texas (1970). 141p. University Microfilms Order No. 71-11,600.

Thesis.

The neutron activation analysis (NAA) technique was applied to the study of interstitial oxygen in niobium and in a 60 at. % niobium–40 at. % titanium solid solution alloy and to determine the effect of interstitial oxygen on the superconductive transition temperatures of these materials. A quantitative evaluation of impurities in the niobium and titanium raw materials is carried out, because these impurities affect the superconductivity properties. A completely nondestructive approach to the radioactivation analysis of niobium and titanium is described. This method is based on the development of a systematic irradiation-counting procedure and the use of computer techniques to "unfold" the complex gamma spectra. The samples of niobium and a library of high-purity standards were irradiated in the 250-kW TRIGA I Nuclear Reactor of The University of Texas at Austin. Gamma spectra for these activated samples were counted with a 3" × 3" NaI(Tl) crystal after 2 min, 1 hr and 1 day, following irradiation, and were recorded with a 256-channel pulse height analyzer. These complex spectra were then analyzed using the computer program ALPHA–M, which employs the method of linear least squares. Titanium was analyzed for hafnium and zirconium. Arc-melted Nb–O and Nb–Ti–O alloys were prepared, and oxygen contents were determined using fast

neutron activation analysis. It is found that interstitial oxygen lowers the superconductive transition temperatures of niobium (−0.94°K/at. % oxygen) and 60 at. % niobium−40 at. % titanium (−0.56°K/at. % oxygen). These results are discussed in terms of the electronic structure of these materials. (Diss. Abstr. Int., B)

41762 DISTRIBUTION AND HISTOPATHOLOGICAL EFFECTS OF CIS-PLATINUM(II)DIAMMINODICHLORIDE ON NONTUMORED AND TUMORED (SARCOMA 180) SWISS WHITE MICE. Toth-Allen, Jean Elizabeth. East Lansing, Mich.; Michigan State Univ. (1970). 130p. University Microfilms Order No. 71-11,774.

Thesis.

Cis-platinum(II)diamminodichloride (cis-$Pt(II)(NH_3)_2Cl_2$) has been shown to be an effective cancer chemotherapeutic agent in laboratory animals. As a first step toward understanding the metabolism and mode of action of this compound, studies were undertaken to determine the relative lifetime of platinum in the Swiss white mouse (both non-tumored and tumored), as well as its distribution, with time, in the major organs. Neutron activation analysis, with gamma spectrometry, was the analytical technique employed for this purpose. Three animals were sacrificed at 1, 6, 12, and 24 hr after injection of a therapeutic dose (8 mg/kg), and then every 12 hr for 144 hr. The major organs were removed and placed in pre-weighed polyethylene irradiation vials, which were then weighed and heat-sealed. (Blood samples were likewise collected, by heart puncture from 3 animals per time, at various intervals for 24 hr.) A fourth animal was simultaneously sacrificed at each time interval, for histopathological studies, and its major organs or representative sections thereof immediately placed in buffered formalin for fixation. The samples for platinum determination were irradiated for 8 hr in a Triga Mark I reactor at a flux of approximately 2×10^{12} neutrons/cm^2/sec. In a biological matrix, even qualitative detection of ^{199}Pt is practically impossible. However, ^{199}Pt decays to another radionuclide, ^{199}Au, whose half-life is 3.15 days. Its characteristic γ rays are of low energy, and high concentrations of ^{24}Na tend to interfere with accurate detection. Thus, after a lapse of approximately 60 hr after irradiation, for efficient formation of ^{199}Au and radioactive decay of matrix elements, a radiochemical separation was undertaken. Exchange on a Dowex 1-X8 resin from an HCl solution leaves the hexachloro salt of the gold bound to the surface of the resin, while most interfering ions passed through. After a suitable wash with 6N HCl, the column was placed in a 3″ by 3″ well-type NaI(Tl) crystal and the area under the 158-keV photopeak of ^{199}Au determined and compared with that of a control. Results were expressed as μg Pt/gm tissue and μg Pt/cc blood. Although a therapeutic dose was employed, the amount of platinum present in the tumor is relatively low. This eliminates the possibility that the potent antitumor properties result from specific uptake into neoplastic tissue. However, platinum is present as early as 1 hr following treatment, and a greater sensitivity of neoplastic, as compared to normal, tissue is a plausible alternative. The total absence of platinum from brain samples suggests that the original neutral molecule is rapidly metabolized to form a charged molecule, incapable of passing the blood-brain barrier. The fall and subsequent rise in the amount of platinum present in the major organs, during the first 24 hr following treatment, suggests a temporary storage elsewhere in the body. Blood studies revealed a similar pattern, ruling out combination with and retention in the blood elements. However, peripheral shunting, as a temporary edema, or merely temporary distribution into muscle, etc., are possible, and present data are insufficient to resolve the problem. Histopathological studies revealed little if any relation between platinum concentration and amount of damage. Although large amounts of platinum are consistently found in liver and kidney tissue, minimal damage is evidenced. Most pathological alterations are seen in rapidly proliferating tissue, gastrointestinal mucosa and lymphoid elements of thymus and spleen. Thus, as with most cancer chemotherapeutic drugs and x-radiation, tissues with high mitotic activity are primary targets. However, the general damage resulting from platinum, at least as evidenced in mice and rats, is considerably less than that found for other such agents. (Diss. Abstr. Int., B)

41763 NEUTRON ACTIVATION ANALYSIS OF SEDIMENTS FOR HALOGENS USING SZILARD-CHALMERS REACTIONS. Walters, L. J. Jr.; Winchester, J. W. (Massachusetts Inst. of Tech., Cambridge). Anal. Chem.; 43: No. 8, 1020-5(Jul 1971).

Nuclear recoil reactions following neutron capture are used to determine the character of binding of chlorine, bromine, and iodine in sedimentary minerals. After neutron irradiation of thoroughly-washed clays, a substantial fraction of induced iodine radioactivity is removed by a water leach, suggesting a predominantly water-insoluble surface binding of natural iodine to particle surfaces. A smaller fraction of bromine and very little chlorine appear to be surface-bound. Pre-irradiation removal of sedimentary interstitial water by squeezing and ion-exchange replacement by washing with aqueous ammonium nitrate operationally distinguish soluble from surface-adsorbed states; post-irradiation fusion and analysis following the water leach distinguish internally bound from surface-insoluble states. An analytical procedure for distinguishing the four degrees of association of halogens in sediments was tested by radiotracers and by activation analysis of standard samples, and was applied to studies of geological samples of recent marine sediments and ancient sedimentary rocks. (auth)

41764 PHOTON-ACTIVATION ANALYSIS FOR ZIRCONIUM WITH MOLYBDENUM USED AS THE INTERNAL-REFERENCE ELEMENT. Pung, Tong-chuin; Kato, Toyoaki; Oka, Yoshinaga (Tohoku Univ., Sendai). Bull. Chem. Soc. Jap.; 44: No. 4, 1031-4(Apr 1971).

A method for the determination of zirconium was studied by activation analysis with bremsstrahlung photons, with molybdenum used as the internal-reference element. This method is based on the γ spectrometric measurement of the ^{89}Zr activity produced by the $^{90}Zr(\gamma,n)$ reaction and on the comparison of this activity with the ^{88}Zr activity formed by the (γ,α) reaction on molybdenum. The reaction products and their rates of production in zirconium and molybdenum were examined as functions of bremsstrahlung maximum energies up to 60 MeV, and the best conditions for the determination of zirconium are proposed. When the maximum energy was set at 20 MeV, no interfering reactions occurred. Under the present experimental conditions, a zirconium content down to about 18 μg can be determined accurately. (auth)

41765 BEHAVIOR OF SURFACE CARBON DURING ITS DETERMINATION BY NUCLEAR REACTIONS. Quaglia, L.; Weber, G. (Univ., Liege). Bull. Soc. Roy. Sci. Liege; 40: No. 1-2, 54-67(1971). (In French).

In order to make possible the fast and precise determination of carbon at the surface of metallic targets by means of nuclear reactions, the variation of the carbon layer was investigated under several experimental conditions. The main cause of carbon pollution seems to be the presence of organic vapors in the vicinity of the target. It was determined that the best means to inhibit this interference is obtained by placing a trap containing liquid N_2 around the target. (auth)

41766 STUDY OF PHOTON ACTIVATION ANALYSIS. Sato, Nobuyoshi; Saito, Tatsuya; Tsai, Hui-tuh; Pung, Tong-chuin; Nomura, Koichi (Tohoku Univ., Sendai). Kakuriken Kenkyu Hokoku; 2: No. 2, 130-8(Dec 1969). (In Japanese).

Four studies on photon activation analysis are reported. The photon activation determination of I using Cs as an internal standard element is described. As an internal standard nuclide, ^{130}I with the photoelectric peak of 0.538 MeV was used, which resulted from the reaction $^{133}Cs(\gamma, 2pn)^{130}I$. Bremsstrahlung of 45-MeV maximum energy was chosen. To determine iodine, ^{123}I, ^{124}I, and ^{126}I were used. The determination of Rb using Sr as an internal standard element is reported. As an internal standard nuclide, ^{83}Rb with the photoelectric peak of 0.553 MeV was used, which resulted from the reaction $^{84}Sr(\gamma,p)^{83}Rb$. Bremsstrahlung of 17.6-MeV maximum energy was chosen. To determine rubidium, ^{84}Rb was used. The determination of Rb using Cs as an internal standard element is also reported. Bremsstrahlung of 30-MeV maximum energy was chosen. ^{132}Cs with the photoelectric peak of 0.667 MeV and ^{86}Rb with the photoelectric peak of 1.078 MeV were used, which resulted from the reactions $^{133}Cs(\gamma,n)^{132}Cs$ and $^{87}Rb(\gamma,n)^{86}Rb$ respectively. The determination of Zr using Mo as an internal standard element is described. Irradiation was carried out by the use of 20-MeV bremsstrahlung. ^{88}Zr and ^{89}Zr with the photoelectric peak of 0.91 MeV were used, which resulted from the reactions $^{92}Mo(\gamma,\alpha)^{88}Zr$ and $^{90}Zr(\gamma,n)^{89}Zr$, respectively. (TACHIYA, M) (Japan)

41767 ACTIVATION ANALYSIS IN MINERAL PROSPECTING. Winchester, J. W. (Univ. of Michigan, Ann Arbor). pp 1-5 of Nuclear Techniques for Mineral Exploration and Exploitation. Vienna; International Atomic Energy Agency (1971).

From Panel on nuclear techniques and mineral resources in developing countries; Krakow, Poland (8 Dec 1969). See STI/PUB-279; CONF-691229.

Neutron activation analysis was established as being one of the most sensitive and reliable methods for trace element determination in a wide variety of materials, including rocks and minerals. A review is made of current techniques and applications of activation analysis for obtaining high-quality geochemical data relevant to mineral prospecting. Guidance on selection of analytical procedures to meet some particular requirements is given. (auth)

41768 MOBILE EQUIPMENT FOR COMBINED NEUTRON ACTIVATION AND X-RAY FLUORESCENCE ANALYSIS. Tolmie,

XUM

R. W. (Atomic Energy of Canada Ltd., Ottawa). pp 7-26 of Nuclear Techniques for Mineral Exploration and Exploitation. Vienna; International Atomic Energy Agency (1971).

From Panel on nuclear techniques and mineral resources in developing countries; Krakow, Poland (8 Dec 1969). See STI/PUB-279; CONF-691229.

By one or other of the thermal neutron activation analysis and x-ray fluorescence techniques most of the elements having atomic numbers greater than 8 (oxygen) can be analyzed, with sensitivity limits that are determined by interelement interferences in most cases. Radioisotope sources can be used to excite the radiations and, if it is necessary to measure silicon, which is an important constituent of most rocks, a small radioisotope fast neutron source can be added to the system. Although each of the three means of excitation generally requires that a different kind of detection be used, the remainder of the system, comprising the data accumulation and computation facilities, can be shared. A mobile facility is described in which the data-handling facilities incorporate a small computer. Some details of the analytical techniques employed and the results obtained are given with brief comments on the economics of using such a facility in mineral resources exploitations. (auth)

41769 COMPUTER TECHNIQUES IN NEUTRON ACTIVATION ANALYSIS. Thompson, C. J. (Atomic Energy of Canada Ltd., Ottawa). pp 115-28 of Nuclear Techniques for Mineral Exploration and Exploitation. Vienna; International Atomic Energy Agency (1971).

From Panel on nuclear techniques and mineral resources in developing countries; Krakow, Poland (8 Dec 1969). See STI/PUB-279; CONF-691229.

The use of highly dispersive detectors and multi-channel pulse-height encoders in γ spectroscopy vastly increased the amount of information available in a spectrum. Spectra containing over 4000 channels of information are now quite common and spectra in neutron activation analysis may contain about 100 peaks. Correlating these peaks with the elements they represent and obtaining the concentration of each element detected can be performed more efficiently by a suitably programmed computer because of its speed in measuring the area and energy of peaks and its thoroughness in searching standard tables and correlating the peaks with standards. The advantages of computers in neutron activation analysis are described and off-line computers are compared with on-line systems where the entire analysis is controlled by the computer. Some experience and results from two years' operation of an on-line activation analysis computer system are discussed. (auth)

41770 CONTRIBUTION TO GEOBOTANICAL AND GEOCHEMICAL PROSPECTING FOR GOLD BY ACTIVATION ANALYSIS. Schiller, P.; Cook, G. B.; Beswick, C. K. (International Atomic Energy Agency, Seibersdorf, Austria). pp 129-35 of Nuclear Techniques for Mineral Exploration and Exploitation. Vienna; International Atomic Energy Agency (1971).

From Panel on nuclear techniques and mineral resources in developing countries; Krakow, Poland (8 Dec 1969). See STI/PUB-279; CONF-691229.

The use in geochemical and geobotanical prospecting of activation analysis is discussed. A study was undertaken on a few general methodological problems involved in this connection, e.g., those of sampling, homogenization of samples, and sensitivity of the detection with and without chemical separation. The first series of investigations was directed toward gold in rock, natural water, and plant samples. Details of the investigations and results are reported. (auth)

41771 DETERMINATION OF TRACE AMOUNTS OF GOLD IN NATURAL WATERS BY NON-DESTRUCTIVE ACTIVATION ANALYSIS USING PRECONCENTRATION BEFORE IRRADIATION. Schiller, P.; Cook, G. B. (International Atomic Energy Agency, Seibersdorf, Austria). pp 137-42 of Nuclear Techniques for Mineral Exploration and Exploitation. Vienna; International Atomic Energy Agency (1971).

From Panel on nuclear techniques and mineral resources in developing countries; Krakow, Poland (8 Dec 1969). See STI/PUB-279; CONF-691229.

A study was made to develop an optimum method for determining trace amounts of gold in natural waters by neutron activation analysis, with the emphasis on avoiding chemical separations after the irradiation. The method of choice is based on simple preconcentration of gold followed by nondestructive activation analysis of the carrier for the absorbed gold. The first step is to find a carrier with an optimum efficiency for gold absorption that would introduce no significant interfering effects to the subsequent measurement of absorbed gold by γ spectrometry. Details of the experiments and results are discussed with the conclusion that lead sulfide is the best carrier for the purpose and that the method developed is both satisfactory and practical for nondestructive activation analysis of gold in water. (auth)

41772 GOLD PROVINCES IN THE PHILIPPINES DEFINED BY ACTIVATION ANALYSIS. Santos, G. G. Jr.; Walters, L. J. Jr. (Philippine Atomic Energy Commission, Manila). pp 143-56 of Nuclear Techniques for Mineral Exploration and Exploitation. Vienna; International Atomic Energy Agency (1971).

From Panel on nuclear techniques and mineral resources in developing countries; Krakow, Poland (8 Dec 1969). See STI/PUB-279; CONF-691229.

Neutron activation analysis is being employed for analyses of mineral sulfides, chalcopyrite, pyrite, sphalerite, and marcasite from the Luzon area. The general aim of the program was to define and delineate high gold-bearing areas or regions in the light of the metallogenic provinces approach based on trace element distribution in the sulfides. The elements determined are Mn, Co, As, Cu, Cd, Zn, Au, Sb, and Fe. Emphasis is placed on the nature of the Au distribution in the sulfides. The broader relations of the other trace elements seem more noteworthy for copper rather than for gold. The gold-collector minerals, pyrite, chalcopyrite, and sphalerite, are useful in evaluating prospective gold mining regions, as shown in the present work in Luzon. A lower threshold limit of 1 ppM gold distinguished gold-producing mines from base-metal mines. (auth)

41773 NEUTRON ACTIVATION ANALYTICAL DETERMINATION OF A NUMBER OF TRACE ELEMENTS IN METEORITIC PHASES. Hermann, F.; Kiesl, W.; Kluger, F.; Hecht, F. (Univ., Vienna). Mikrochim. Acta; No. 2, 225-40(1971). (In German).

The distribution of trace elements over four main phases of iron meteorites (metallic, phosphidic, graphitic, sulfidic phases) was investigated by means of neutron activation. A strong chalcophilic behavior for selenium and chromium was deduced from the distribution circumstances, as opposed to strong siderophilic behavior for the elements antimony and arsenic. Most surprisingly, the main part of the molybdenum is present in the form of schreibersite. With the exception of chromium and molybdenum, all other elements are represented in those phases that also occur in chondrites. Hence certain consequences with regard to the affinity changes of these elements during the creation and genesis of the meteoritic material are disclosed by these comprehensive analyses. (auth)

41774 ACTIVATION ANALYTICAL STUDIES OF STANDARDIZED IRON ALLOYS. I. QUANTITATIVE VANADIUM DETERMINATION AND QUALITATIVE CERTIFICATE TESTING. Gruber, E.; Sorantin, H. (Univ., Vienna. Oesterreichische Studiengesellschaft fuer Atomenergie, Seibersdorf, Austria). Mikrochim. Acta; No. 2, 262-6(1971). (In German).

Vanadium was determined without interference by means of neutron activation analysis and gamma spectrometry in two standardized alloys (NBS-1138 Cast Steel 1 and NBS-1140 Ductile Iron 1). In the preliminary trials for determining the optimization of the measurement conditions the presence of arsenic and antimony was established qualitatively in addition to the elements stated provisionally in the certificate describing NBS-1138, and likewise antimony and lanthanum were found in the NBS-1140. (auth)

41775 COMPARISON OF PHYSICAL EVIDENCE BY MEANS OF TRACE ELEMENT ANALYSIS. Liebscher, Kurt (Univ. of Glasgow). Mikrochim. Acta; No. 2, 272-84(1971). (In German).

The trace element concentrations of small pieces of evidence (hair, car paint, and the like) can be determined nondestructively by thermal neutron activation followed by gamma spectrometry. The significance of the probability that two samples have different origin is calculated from the variations in the distribution of trace elements in two halves of each sample, so that the distribution in the total population need not be known. (auth)

41776 QUANTITATIVE DETERMINATION OF RARE EARTHS IN METEORITES BY MEANS OF HIGH VOLTAGE ELECTROPHORESIS. Grass, F.; Kittl, R. (Oesterreichische Hochschule, Vienna. Univ., Vienna). Mikrochim. Acta; No. 2, 371-9(1971). (In German).

A procedure was developed for the determination of rare earths in chondrites using neutron activation analysis followed by a separation by means of high-voltage electrophoresis. The distribution of the rare earth elements La, Ce, Pr, Sm, Eu, Dy, Ho, Er, Yb, and Lu was determined in 8 meteorites. The results are compared with previously published data. (auth)

XUM

Inorganic, Organic, and Physical Chemistry

Refer also to abstracts 41713 and 41832.

41777 (UCRL-20500) INORGANIC MATERIALS RESEARCH DIVISION ANNUAL REPORT, 1970. (California Univ., Berkeley. Lawrence Radiation Lab.). Apr 1971. Contract W-7405-eng-48. 254p. Dep. NTIS.

Research progress is reported in 4 sections: chemistry, metallurgy, ceramic science, and solid-state physics. An abstract was prepared for each section. (M.C.G.)

For abstracts of individual sections see: 41778, 42886, 42957, and 43470.

41778 (UCRL-20500, pp 1-85) CHEMISTRY. (California Univ., Berkeley. Lawrence Radiation Lab.).

In Inorganic Materials Research Division annual report, 1970.

Research progress is reported on: inorganic chemistry, chemical thermodynamics, solid-state chemistry and physics, electrochemistry, physical chemistry, and nuclear science. Abstracts of and references to published work are included. (M.C.G.)

Chemical Properties

Refer also to abstracts 41919, 42267, 42945, 42968, and 44166.

41779 (ORNL-TM-3358) KINETIC MODELS FOR THE SYNTHESIS OF $(U,Pu)O_{2-\gamma}$ BY HYDROGEN-REDUCTION AND CARBOTHERMIC TECHNIQUES. Lindemer, T. B.; Bradley, R. A. (Oak Ridge National Lab., Tenn.). Apr 1971. Contract W-7405-eng-26. 35p. (CONF-710415-2). Dep. NTIS.

From seventy-third annual meeting of the American Ceramics Society; Chicago, Ill. (26 Apr 1971).

Three models were developed that permit the calculation of the time necessary for the synthesis of hypostoichiometric oxide from $(U,Pu)O_2$. The models are based on the interrelation between oxygen potential, valence of plutonium, and temperature determined by Rand and Markin and on the experimental conditions for reduction. Two reduction techniques are considered: the flowing hydrogen system and the $C-CO-CO_2$ system. At the usual temperatures for reduction, the partial pressure of water, the hydrogen flow, and the total weight of oxide are the most important factors in the hydrogen system, while in the $C-CO-CO_2$ system the important factors are the weight of the oxide in each oxide pellet, the partial pressure of carbon monoxide, the proximity of the oxide and the carbon used for reduction, and the minimum oxygen-to-metal ratio possible at the oxygen potential of the $C-CO-CO_2$ equilibrium. (auth)

41780 (SC-T-713038) PHENOXIDES OF THE TRIAD ELEMENTS. Masthoff, Rolf; Koehler, Helmut; Boehland, Heinz; Schmeil, Franz. Translated for Sandia Labs., Albuquerque, N. Mex., from Z. Chem.; 4: 122-30(1965). 28p. Dep. NTIS.

The formation tendencies and the reactivities of phenoxides of the triad elements, including uranium, are reviewed. The various preparation methods are described. A particularly important method is the reaction of metal halides with phenols in anhydrous media under various conditions. The phenoxides and phenoxide halides of the triad elements described so far are discussed by groups in the periodic table. Complex derivatives and pyrocatecholates are also described. (auth)

41781 TREATMENT OF POLYPEPTIDE-CONTAINING HYDROPHILIC POLYMERIC CAPSULE WALL MATERIAL WITH URANIUM AND VANADIUM COMPOUNDS. Emrick, Donald D. (to National Cash Register Co.). U. S. Patent 3,576,758. 27 Apr 1971. Filed 17 Oct 1966.

A process is provided for manufacturing novel, minute, capsules en masse in which preformed capsules having walls of polypeptide-containing hydrophilic polymeric material are further treated by uranyl or vanadyl ions in an aqueous liquid vehicle. Capsules produced by practice of this process have walls that exhibit decreased water solubility, decreased swelling in water, and decreased sensitivity to high relative humidity. (Offic. Gaz.)

41782 METHOD AND APPARATUS FOR THE CONTINUOUS PRECIPITATION OF URANIUM. Delpech, Andre (to Commissariat a l'Energie Atomique). British Patent 1,230,937. 5 May 1971. Priority date 10 May 1968, France.

An apparatus and method are described for the continuous precipitation of U from uranyl nitrate solutions as uranyl formate. The apparatus comprises a vertical column, the bottom part of which consists of a bed of glass of poly(tetrafluoroethylene) balls resting on a grid. At least one propeller is included for keeping the balls in circulation along an ascending and descending path. An aqueous preheated uranyl nitrate solution (~400g/l) is fed into the top part of the column along with formic acid (0.35 g/g U). These reagents are mixed before being poured onto the balls. The formate is collected as a dry powder, which has passed through the grid, after contact with the balls in the lower portion of the column that is heated to 100°C to vaporize the water and liberate nitrogen vapors. (B.L.M.)

41783 KINETICS OF THE REACTION BETWEEN URANIUM (III) AND $Co(NH_3)_4(H_2O)_2^{3+}$ IN AQUEOUS PERCHLORATE SOLUTIONS. White, James D.; Newton, T. W. (Los Alamos Scientific Lab., N. Mex.). J. Phys. Chem.; 75: No. 14, 2117-22(8 Jul 1971).

The reaction $U^{3+} + cis\text{-}Co(NH_3)_4(H_2O)_2^{3+} + 4H^+ = U^{4+} + Co^{2+} + 4NH_4^+ + 2H_2O$ was studied in acid perchlorate solutions from 0.01 to 1.98 M $HClO_4$, from 0.8 to 45°C, and at ionic strengths from 0.12 to 3.6 M ($LiClO_4$). The predominant term in the rate law is $-d[U(III)]/dt = 1.64 + 10^3[U(III)][Co(III)][H^+]^0$ M sec^{-1} at 25° and $\mu = 2.0$ M. The activation parameters are $\Delta F^* = 13.06$ kcal/mole, $\Delta H^* = 3.67 \pm 0.04$ kcal/mole, and $\Delta S^* = -31.5 \pm 0.3$ cal/mole deg^{-1} for $\mu = 2.0$ M. Chloride ion causes a moderate increase in the rate, first power in $[Cl^-]$. The ionic strength dependence is in accord with an extended form of the Debye-Hückel equation with the distance of closest approach term equal to 9.3 Å. (auth)

41784 EFFECT OF SOLVENTS ON THE ADDUCT FORMATION OF URANYL THENOYLTRIFLUOROACETONATE WITH TRIBUTYL PHOSPHATE. Akiba, Kenichi; Suzuki, Nobuo (Tohoku Univ., Sendai). Bull. Chem. Soc. Jap.; 44: No. 4, 1043-7 (Apr 1971).

Addition compound formation between uranyl bis-thenoyltrifluoroacetonate (UO_2A_2) and tributyl phosphate(S) was studied by a partition method, using uranium-237 as the tracer. The formula of the adduct complex was shown to be $UO_2A_2 \cdot S$. The solvent effect on the adduct formation constant was taken into account in connection with the activity; the activity coefficients of each species in various solutions were calculated from the molar volume and the solubility parameter. The formation constants based on the molar fraction, K_x, in a number of solvents were pre-estimated, employing $\log K_x = 7.08$ in carbon tetrachloride as a reference. They are in agreement with the observed values. The formation constant in terms of activity was found to be constant $\log K_s^0 = 5.77 \pm 0.30$. A correlation between the formation constants of the two adducts, $UO_2A_2 \cdot S$ and $ZnA_2 \cdot S$, was demonstrated. (auth)

41785 KINETIC STUDIES ON THE OXIDATION OF Am(III) WITH AMMONIUM PEROXYDISULPHATE. Ohyoshi, A.; Jyo, A.; Kanaya, T.; Shinohara, T. (Kumamoto Univ., Japan). Radiochem. Radioanal. Lett.; 7: No. 1, 7-14(15 Jun 1971).

Kinetics of the reaction between Am(III) and ammonium peroxydisulfate in the presence of silver (I) ions were studied by a coprecipitation method. The apparent rate constants were found to be 2.33×10^{-3} min^{-1} ($[Ag^+] = 0$) and 7.20×10^{-2} min^{-1} ($[Ag^+] = 0.01M$) at 50°C with 0.02M ammonium peroxydisulfate and 3.3×10^{-7}M Am(III) solution at an ionic strength of 0.5. An induction period depending on the silver ion concentration and reaction temperature was observed. The enthalpy and entropy of activation were 18.9 kcal $mole^{-1}$ and 2.2 eu, respectively. (auth)

41786 SOME OBSERVATIONS ON THE BEHAVIOR OF PROTACTINIUM(V) ON AN INDICATOR SCALE IN ALKALINE AQUEOUS SOLUTION. Cazaussus, A.; Arapaki-Strapelias, H.; Muxart, R. (Institut du Radium, Arcueil, France). Radiochem. Radioanal. Lett.; 6: No. 5, 297-306(19 May 1971). (In French).

Pa(V) shows a very low solubility in strongly alkaline solutions. The existence of at least one anionic species in these solutions was demonstrated by paper chromatography, electrophoresis, and ion exchange. (auth)

Isotope Effects and Exchange

Refer also to abstracts 41897, 41921, and 41923.

41787 HYDROLYSIS OF PYRYLIUM SALTS. KINETIC EVIDENCE FOR HEMIACETAL INTERMEDIATES. Williams, A. (Univ. of Kent, Canterbury, Eng.). J. Amer. Chem. Soc.; 93: No. 11, 2733-7(2 Jun 1971).

The hydrolyses of 2,4,6-triphenylpyrylium tetrafluoroborate, 2,4,6-trimethylpyrylium perchlorate, and 2-methyl-4,6-diphenylpyrylium chloride (to yield diketones) were measured over a range of pH, buffer concentration, and in deuterium oxide solvent.

XUM

The rate constant for the forward reaction in each case obeyed the empirical equation $k_f = k_{H_2O}/(1 + a_H/K_a) + k_{OH}[OH] + k_B[B]$. The titration term is judged to arise from the pH-dependent partitioning of a cyclic hemiacetal intermediate formed by reaction of water at the C_2 position. The attack of water on the 2-methyl-4,6-diphenylpyrylium cation proceeds at the 2 position and the product is shown to be the 1,3-diphenyl-2-hexene-1,5-dione. (auth)

41788 PHOTOCHEMICAL DEGRADATION OF FLAVINS. VI. A NEW PHOTOPRODUCT AND ITS USE IN STUDYING THE PHOTOLYTIC MECHANISM. Cairns, William L.; Metzler, David E. (Iowa State Univ., Ames). J. Amer. Chem. Soc.; 93: No. 11, 2772-7(2 Jun 1971).

Two new products were isolated from riboflavin (RF) photolysates. The first is the 2′-ketoflavin 7,8-dimethyl-10-(1′-deoxy-D-erythro-2′-pentulosyl)isoalloxazine. It is formed over the pH range 4 to 10 and its production, like that of formylmethylflavin (FMF), is very sensitive to quenching by KI. The other product, believed to be the 4′-ketoflavin, is not produced under alkaline conditions and its formation under neutral conditions (like that of lumichrome, LC) is not easily quenched by KI. The ketones are suggested to result from abstraction of the 2′- and 4′-α hydrogens by the excited ring. Reduction of the 2′-ketoflavin with NaB^3H_4 yielded 2′-^{3}H-RF, which upon photolysis generated ^{3}H-FMF. This proves that the 2′-α hydrogen is not abstracted during FMF production. Possible mechanisms for production of FMF are discussed; the observation of an isotope effect when RF is photolyzed in D_2O under alkaline conditions suggests abstraction of the 2′-hydroxyl hydrogen. The rate of photolysis increases 30-fold at pH 8 and 2.5-fold at pH 3 relative to the rate at pH 5. The existence of bent triplet and a planar excited singlet differing in the center for hydrogen abstraction and protonation could explain the dependence of rate and product distribution on pH. (auth)

41789 DEMONSTRATION OF INTERMEDIATES IN THE HYDROLYSIS OF 4-ETHOXYPYRYLIUM SALTS. Salvadori, G.; Williams, A. (Univ. of Kent, Canterbury, Eng.). J. Amer. Chem. Soc.; 93: No. 11, 2727-33(2 Jun 1971).

The formation of open chain diketone intermediates was demonstrated during the hydrolysis of 4-ethoxypyrylium salts. Reaction occurs at both $C_{2(6)}$ and C_4 positions to yield open chain diketone and 4-pyrone, respectively; the diketone (a vinyl ether) hydrolyzes and cyclizes to give the 4-pyrone. The yield of 4-pyrone is stoichiometric and oxygen-18 and deuterium isotope experiments show that at low pH the direct mechanism (attack at C_4) predominates but at high pH the diketone intermediate ($C_{2(6)}$ attack) is predominantly involved. The maximal concentration of intermediate varies with pH according to an equation derived from the proposed theoretical mechanism and can be accurately predicted using rate constants reported here. The rate constant for decomposition of pyrylium salt is given by the equation $k_a = k_0 + k_B[B] + k_{OH}[OH^-] + k_{H_2O}/(1 + a_H/K_a)$. The ionization term in the equation can arise from the pH-dependent partitioning of a cyclic hemiacetal intermediate between pyrylium salt and diketone intermediate. Decomposition of the diketone intermediate to give 4-pyrone is specific acid catalyzed (the existence of a preequilibrium protonation is supported by an inverse deuterium isotope effect) and is rate determining at high pH, but as the pH decreases the formation of diketone becomes rate determining. However, the latter rate constant decreases with decreasing pH and a pH-independent direct attack of water at C_4 becomes predominant (k_0); the rate constant for 4-pyrone production (k_b) therefore exhibits a plateau region at low pH. The diketone intermediate is shown to yield 2,6-dimethyl-4-pyrone via a pathway not including diacetylacetone. (auth)

41790 VIBRATIONAL SPECTRA OF AND ISOTOPE EFFECT IN HYDROGEN BONDED POTASSIUM HYDROGEN OXALATE. de Villepin, J.; Novak, A. (CNRS, Thiais, France). Spectrosc. Lett.; 4: No. 1-2. 1-8(Jan-Feb 1971).

The crystal structure of potassium hydrogen oxalate, KHC_2O_4, was determined by Pedersen. There are infinite chains of hydrogen oxalate ions held together by short (2.534 Å) hydrogen bonds. The O–D. . .O distance of KDC_2O_4 derived from lattice constant changes was estimated to be about 0.005 Å larger than the O-H. . .O distance, which means that the isotope effect is small. The infrared and Raman spectra of KHC_2O_4 and KDC_2O_4 reported show that the isotope effect in these crystals is much larger. (auth)

41791 VIBRATIONAL NORMAL COORDINATE ANALYSIS OF H(D)NCO AND H(D)NCS. Orel, B.; Peterman, B.; Obradovic, M.; Hadzi, D.; Azman, A. (Univ., Ljubljana, Yugoslavia). Spectrosc. Lett.; 4: No. 3-4, 39-41(Mar-Apr 1971).

Experimental and calculated results of the normal coordinate analysis of H(D)NCO and H(D)NCS are given in support of proposed infrared band assignments. (D.P.O.)

41792 SULFONYL CHLORIDE KINETICS. PART III. NUCLEOPHILIC INTERACTION ON THE TRANSITION STATE FOR 4-X-BENZENESULFONYL CHLORIDE SOLVOLYSES. Rossall, B.; Robertson, R. E. (Univ. of Calgary, Alberta). Can. J. Chem.; 49: 1451-5(1 May 1971).

The kinetic solvent isotope effect (k.s.i.e.) = k_{H_2O}/k_{D_2O}, was measured for 4-X-benzenesulfonyl chlorides (where X = MeO, Me, H, Br, and NO_2) and shown to vary systematically, giving linear correlations with Hammett σ values and with k_{OH^-}/k_{H_2O} ratios. These results contrast with the lack of sensitivity in k.s.i.e. to structural changes for displacement from a saturated carbon atom. This behavior is attributed to a greater degree of bond making required to achieve a critical charge on the chloride of the sulfonyl chloride at the transition state. (auth) (Canada)

41793 THERMAL DENATURATION OF RIBONUCLEASE DISSOLVED IN HEAVY WATER. Gerasimov, V. V.; Getashvili, G. R.; Melitauri, T. G.; Mikhailov, V. S. (Inst. of Physiology, Tbilisi, USSR). Soobshch. Akad. Nauk Gruz. SSR; 62; No. 1. 173-6(Apr 1971). (In Russian).

The enthalpy of the thermal denaturation of ribonuclease solutions in ordinary and heavy water was measured. The curves of heat capacity and free energy changes in the range of transition are given. On the basis of the experimental data it is suggested that the isotopic interchange in ribonuclease occurs without changes in the macromolecular conformation. (auth)

41794 THERMOCHEMICAL HYDROGEN–DEUTERIUM ISOTOPE EFFECTS. Duer, Wayne Carlton. Rolla, Mo.; Univ. of Missouri (1970). 117p. University Microfilms Order No. 71-12,314.

Thesis.

The heats of solution at 25.0 ± 0.1°C for each member of hydrogen–deuterium isotopic pairs (chloroform–chloroform-d, acetone–acetone-d_6, methanol–methanol-d_1, ethanol–ethanol-d_1, and water–heavy water) were determined as a function of molality in a variety of solvents. The heats for most of the systems could be described as a linear function of average molality with an average deviation in fit of less than one percent. Using these linear equations, heats of solution at infinite dilution were obtained by extrapolation to zero molality. The heats of solution at infinite dilution of the hydrogen-containing compounds were subtracted from those of the corresponding deuterium-containing compounds to yield isotope effects on heats of solution. These isotope effects were interpreted in terms of hydrogen bonding and an empirical equation for the prediction of enthalpies of formation of hydrogen bonds. It was concluded that for a given isotopic pair the deuterium isomer is both more strongly and more extensively hydrogen bonded to bases than the hydrogen isomer. Heats of solution of water and heavy water were determined in each other as solvents and in the equimolar mixture as solvent. Considering the formation of HOD to be entirely responsible for the heat effect and using $K = 3.8 = X_{HOD}^2/(X_{H_2O}X_{D_2O})$ where X represents mole fraction gave 7.88 ± 0.05 cal/mole for the heat of formation of HOD in mixtures of water and heavy water at 25°C. With the experimental results at 25°C for the mixing of different pairs in the set (methanol, methanol-d_1, water, heavy water), near infinite dilution of one component, the enthalpy change for the complete hydrogen–deuterium transfer between methanol (one mole) and heavy water (one-half mole) has been calculated. Values of -95 and -97 cal/mole were obtained for this transfer by two independent schemes. These studies have yielded some of the first definitive data concerning the effect of deuterium versus hydrogen on intermolecular interactions. The results not only demonstrated that isotope effects on heats of solution are measurable but also that they are amenable to meaningful interpretation. (Diss. Abstr. Int., B)

41795 CHLORINE KINETIC ISOTOPE EFFECTS IN NUCLEOPHILIC DISPLACEMENT REACTIONS. Grimsrud, Eric Paul. Madison, Wis.; Univ. of Wisconsin (1971). 217p. University Microfilms Order No. 71-5640.

Thesis.

The leaving group kinetic isotope effects of chlorine for a series of nucleophilic displacement reactions at a saturated carbon atom were measured. Once the techniques for measuring these values to an accuracy of ±0.01% were developed, it was found that these isotope effects provided a valid probe of the transition-state structure and could be used to gain insight into the S_N2 mechanism. Where changes in the nucleophile were made, a decreased chlorine kinetic isotope effect resulted from an increase in the basicity of the nucleophile even when the attacking atom of the nucleophile was altered. This correlation was not obtained with the reaction rates when the attacking atom was changed, and this was interpreted to indicate that the relative rates are determined largely by solvation effects of the nucleophile. The factor of increased polarizability of the larger attacking atoms was not reflected in the isotope effects, suggesting its lack of importance in these reactions. Changes in

XUM

the substrate were made by changing the para substituent of benzyl chloride. The most subtle of these changes, the change from unsubstituted to p-methyl, yielded isotope effects consistent with the theoretical predictions supporting the thesis that chlorine kinetic isotope effects are a valid probe for changes in the transition-state structure. The other substituent changes, to p-chloro or p-nitro, were not always consistent with the predictions. However, these substituents would be most susceptible to anomalous resonance and solvation effects and may not provide a valid test only of electron supply to the center carbon atom. The use of chlorine kinetic isotope effects may prove to be useful in defining these additional factors which comprise the overall effect of a sub-stituent on a reaction. When the solvent was changed from methanol to dimethylformamide, the chlorine isotope effects for a displacement reaction were increased. This observation was opposite to that predicted from the resulting increase in basicity of the nucleophile and was taken to indicate the importance of solvation of the leaving group in the isotope effects determined in methanol. The temperature dependence of the chlorine kinetic isotope effects of a displacement reaction in methanol was found to be consistent with the S_N2 model of this reaction. The form of the temperature dependence was that of an Arrhenius equation, the slope of which was consistent with the bonding and solvation changes thought to be occurring in the transition-state. By this technique it is anticipated that the changes in transition-state structure caused by a change in the reaction conditions will be determined more precisely. The methanolysis isotope effects of the same substrates in the absence of added nucleophiles also were studied, and were found to be the same as those observed for the reactions of these substrates with the methoxide anion. This was taken as strong evidence that the solvolysis mechanism is S_N2 involving strong participation from the conjugate base of the solvent in the transition-state. (Diss. Abstr. Int., B)

41796 INFRARED SPECTRA OF PENTACYANONITROSYL-MANGANESE (^{14}NO AND ^{15}NO) COMPLEXES. Miki, Eiichi; Kubo, Soto-o; Mizumachi, Kunihiko; Ishimori, Tatsujiro; Okuno, Hisateru (Rikkyo Univ., Tokyo). Bull. Chem. Soc. Jap.; 44: No. 4, 1024-7(Apr 1971).

The ^{15}NO-complexes for $K_3[Mn(CN)_5(NO)] \cdot 2H_2O$, $K_3[Mn(CN)_5(NO)]$, and $Ag_2[Mn(CN)_5(NO)]$ were prepared. By measuring and calculating the effect of the nitrogen isotope ^{15}N on the infrared spectra, the Mn−N−O arrangement was found in all the complexes, and the absorption bands due to the skeletal vibrations between the manganese and the NO group were clearly assigned. (auth)

41797 EFFECT OF PRESSURE ON THE KINETICS OF THE EXCHANGE OF ^{18}O BETWEEN HEXAAQUOCHROMIUM(III) ION AND SOLVENT WATER. EVIDENCE FOR AN ASSOCIATIVE INTERCHANGE MECHANISM. Stranks, D. R. (Univ. of Adelaide); Swaddle, T. W. J. Amer. Chem. Soc.; 93: No. 11, 2783-4(2 Jun 1971).

The pressure dependence of the first-order rate coefficient for the ^{18}O exchange of the six water molecules of $Cr(H_2O)_6^{3+}$ was determined at seven different pressures ranging from 1.0 bar to 2.48 kbars using a high pressure steel bomb. An observed $\Delta V^* = -9.3 \pm 0.3$ cm^3 mole^{-1} and a $|(\partial \Delta V^*/\partial P)_T|$ less than 2.0×10^{-4} cm^3 bar^{-1} mole^{-1} are consistent with an associative interchange mechanism. The main contribution to ΔV^* in the chromium(III)-water exchange originates in the vacancy created when the incoming water molecule is transferred to the first coordination sphere. (D.P.O.)

41798 PROTON TRANSFER FROM CYANOCARBON ACIDS. II. GENERAL-BASE-CATALYZED DETRITIATION AND BROMINATION OF MALONONITRILES. RATES OF THE REVERSE REACTIONS. Hibbert, F.; Long, F. A.; Walters, E. A. (Cornell Univ., Ithaca, N. Y.). J. Amer. Chem. Soc.; 93: No. 12, 2829-35(16 Jun 1971).

The detritiation of malononitrile-1-t and tert-butylmalononitrile-1-t in aqueous acid and in buffer solutions is a general-base-catalyzed reaction whose slow step is a proton transfer from the cyanocarbon acid. Catalytic coefficients for carboxylate anions conform to the Brønsted relation with an exponent $\beta = 0.98 \pm 0.02$. The bases, hydroxide ion and solvent water, show sizable deviations from the Brønsted plot. Bromination of the two malononitriles and of their 1-D derivatives in aqueous solution is also general base catalyzed and gives rates which are independent of bromine concentration and closely comparable to the detritiation rates, indicating that these rates are also determined by a slow proton transfer from the carbon acids. The primary hydrogen isotope effects are very low for reactions of the malononitriles with the bases water and acetate ion. This fact and also the Brønsted coefficient of almost unity indicate a transition state in which the proton is almost fully transferred from the cyanocarbon acid to the attacking base. Dissociation constants for the acids ($pK^0 = 11.19$ for malononitrile and 13.10 for the tert-butyl derivative) permit a calculation of the rates of the reverse reactions of their carbanions with general acids, and also hydronium ion. Typical rate coefficients at 25° are 4.0×10^9 and 1.0×10^8 M^{-1} sec^{-1} for reaction of the anion of tert-butylmalononitrile with hydronium ion and chloroacetic acid, respectively. These rates as well as their calculated isotope effects and energies of activation indicate the reverse reactions to be virtually diffusion controlled. This is plausible for the indicated transition state but is a considerably different behavior from the "slow" proton transfers exhibited by other important categories of carbon acids. (auth)

41799 PROTON TRANSFER FROM CYANOCARBON ACIDS. III. PRIMARY AND SOLVENT KINETIC ISOTOPE EFFECTS IN THE IONIZATION OF MALONONITRILES. Hibbert, F.; Long, F. A. (Cornell Univ., Ithaca, N. Y.). J. Amer. Chem. Soc.; 93: No. 12, 2836-40(16 Jun 1971).

The slow proton-transfer reactions involved in the detritiation of malononitrile-1-t and tert-butylmalononitrile-1-t and in the bromination of the 1-H and 1-D malononitriles in the solvents H_2O and D_2O are characterized by unusual isotope effects. The primary isotope effects are $k^H/k^D = 1.49 \pm 0.03$ for reaction of both malononitriles with the catalyst H_2O and $k^H/k^D = 1.47$ for reaction of the tert-butyl derivative with acetate ion. Primary isotope effects can be calculated for the reverse reactions of the carbanions and are found to be very small. Both results are consistent with a transition state having the structure $RC^-\text{---}HB^+$. In the water-catalyzed detritiation of tert-butylmalononitrile, the solvent isotope effect k_{H_2O}/k_{D_2O} has the value 3.48. When allowance is made for the second isotope effect on the base water, using fractionation factor theory, the large solvent isotope effect is shown to include an unusually large medium effect, which, however, can be understood in terms of the known structure of the transition state. The overall solvent isotope effect obtained when the malononitriles are allowed to exchange prior to bromination has the value $k^H_{H_2O}/k^D_{D_2O} = 5.4$. This more or less normal value results from the joint contributions of the very low primary kinetic isotope effect and the high solvent isotope effect. (auth)

41800 EFFECTS OF α-DEUTERIUM SUBSTITUTION, POLAR SUBSTITUENTS, TEMPERATURE, AND SALTS ON THE KINETICS OF HYDROLYSIS OF ACETALS AND ORTHO ESTERS. Bull, H. G.; Koehler, K.; Pletcher, T. C.; Ortiz, J. J.; Cordes, E. H. (Indiana Univ., Bloomington. Univ. Central, Caracas). J. Amer. Chem. Soc.; 93: No. 12, 3002-11(16 Jun 1971).

Kinetic secondary deuterium isotope effects for the hydrolysis of ethyl orthoformate, 1.05, and propionaldehyde diethyl acetal, 1.17, reveal that the transition state for ortho ester hydrolysis resembles the substrate, although that for hydrolysis of acetals derived from aliphatic aldehydes resembles the intermediate carbonium ion. Secondary deuterium isotope effects for hydrolysis of substituted benzaldehyde diethyl acetals increase from 1.04 to 1.09 to 1.15 as the nature of the polar substituent changes from methoxy to hydrogen to nitro. Thus, the transition state structure for hydrolysis of these substrates increasingly resembles the carbonium ion intermediates as the electron-withdrawing power of the substituent in the aldehyde moiety increases and the substrate reactivity, hence, decreases. Corresponding isotope effects for hydrolysis of (2-para-substituted phenoxy)tetrahydropyrans decrease from 1.10 to 1.06 as the polar substituent is changed from methoxy to nitro. Thus, the transition state for these reactions increasingly resembles the carbonium ion intermediates as the electron-donating power of the polar substituent in the leaving group (and the substrate reactivity) increases. Second-order rate constants for the hydrolysis of para-substituted methyl orthobenzoates in aqueous solution are well correlated by the Hammett substituent constants, $\rho = -1.16$. This value accords with the conclusion that little carbon−oxygen bond cleavage has occurred at the transition state for ortho ester hydrolysis. General acid catalysis for orthobenzoate hydrolysis in water is not detectable. Activation parameters have been determined for the hydrolysis of substituted methyl orthobenzoates. Values of entropy of activation for hydrolysis are near zero and show no systematic trend as the nature of the polar substituent is varied. Rate constants for hydrolysis of p-nitrobenzaldehyde diethyl acetal increase severalfold as the concentration of alkali and alkaline earth halides is increased from zero to 1 to 3 M. The rate changes principally reflect the increased activity of the hydrated proton with increasing salt concentration. (auth)

41801 SECONDARY β-DEUTERIUM EFFECTS ON THE RATES OF SOLVOLYSES OF BENZONORBORNEN-2(exo)- AND -2(endo)-YL p-BROMOBENZENESULFONATES. Tanida, Hiroshi; Tsushima, Tadahiko (Shionogi and Co., Ltd., Osaka). J. Amer. Chem. Soc.; 93: No. 12, 3011-16(16 Jun 1971).

C_3-Deuterated benzonorbornen-2(exo)- and -2(endo)-yl brosyl-

XUM

ates and their aromatic nitrated derivatives were synthesized and solvolyzed in acetic and formic acids to measure the β-deuterium effects on the rates of solvolysis. Benzonorbornen-2(exo)-yl-3(exo)-d and -3,3-d_2 brosylates (1-d_1e-OBs and 1-d_2e-OBs) showed markedly small deuterium effects in both acetolysis (1.03 for 1-d_1e-OBs and 1.05 for 1-d_2e-OBs) and formolysis (1.04 for 1-d_2e-OBs) compared to the values for the corresponding endo epimers, which were, in acetolysis, 1.16 for the 3(exo)-d and 1.28 for the 3,3-d_2 and, in formolysis, 1.15 for the 3(exo)-d and 1.24 for the 3,3-d_2 compound. When two nitro groups were introduced into the C_6 and C_7 positions of the benzene ring, the magnitudes of the deuterium effects were raised with the exo-brosylates (in acetolysis, 1.10 for the dinitro-3(exo)-d and 1.12 for the dinitro-3,3-d_2), but decreased with the endo-brosylates (in acetolysis, 1.13 for the dinitro-3(exo)-d and 1.22 for the dinitro-3,3-d_2). A geometric dependence of the β-deuterium effects was observed in the solvolyses of the dinitro exo-brosylates; the increment of the effects on conversion of the dinitro-3(exo)-d into the dinitro-3,3-d_2 compound was very small, from 1.10 to 1.12 (in acetolysis). In the case of the dinitro endo-brosylates, such conversion raised the effects substantially, from 1.13 to 1.22. Results with the exo system are discussed in terms of competing aryl participation and hyperconjugative electron release mainly due to the exo proton at C_3, and release of steric compression at the reaction site; those with the endo system are discussed in terms of competing solvent participation and hyperconjugation due to both the exo and endo protons at C_3, as well as the release of steric compression. (auth)

41802 NUCLEOPHILIC SUBSTITUTION AT TETRAHEDRAL BORON. TRIMETHYL- AND TRIETHYLAMINE–BORANE SUBSTRATES. Budde, William L.; Hawthorne, M. Frederick (Univ. of California, Riverside). J. Amer. Chem. Soc.; 93: No. 13, 3147-50(30 Jun 1971).

Both trimethylamine–borane and triethylamine–borane react with tri-n-butylphosphine in o-dichlorobenzene solution to produce tri-n-butylphosphine–borane and the corresponding amine. Both reactions are second order overall and an SN2-B mechanism is proposed to account for this fact. A secondary kinetic α-deuterium isotope effect was not observed with $Me_3N^+-BD_3^-$ substrate, and this observation is in agreement with the proposed SN2 mechanism. Thermodynamic activation parameters obtained with the $Me_3N^+-BH_3^-$ reaction give $\Delta H^{\ddagger} = 23.4$ kcal/mol and $\Delta S^{\ddagger} = -5 \pm 3$ eu, values, which again support an SN2 mechanism. (auth)

41803 NUCLEOPHILIC SUBSTITUTION AT TETRAHEDRAL BORON. TRIMETHYLAMINE–ALKYL- AND -ARYLBORANE SUBSTRATES. Walmsley, Donald E.; Budde, William L.; Hawthorne, M. Frederick (Univ. of California, Riverside). J. Amer. Chem. Soc.; 93: No. 13, 3150-5(30 Jun 1971).

The four isomeric trimethylamine–butylboranes and six para- and ortho-substituted trimethylamine–arylboranes were examined as substrates in displacement reactions with tri-n-butylphosphine as the nucleophile. Kinetic data gave good evidence for second-order SN2-B displacement reactions in all cases except that of trimethylamine-tert-butylborane, which gave a predominant first-order SN1-B displacement reaction. The aryl systems gave second-order, SN2-B terms, which in the p-anisyl- and mesitylborane cases had small first-order terms superimposed on them. Secondary deuterium kinetic isotope effects were observed with the sec-butyl system. Activation parameters, solvent effects, and other associated data point to the simultaneous operation of SN1-B and SN2-B displacement processes when moderately bulky groups are attached to the boron atom of the amine–borane substrate. (auth)

41804 NUCLEOPHILIC SUBSTITUTION AT TETRAHEDRAL BORON. METHYLAMINE–DIARYLBORANE SUBSTRATES. Lalor, Fergus J.; Paxson, Timm; Hawthorne, M. Frederick (Univ. of California, Riverside). J. Amer. Chem. Soc.; 93: No. 13, 3156-60(30 Jun 1971).

Six methylamine-di(para-substituted phenyl)boranes were synthesized and subjected to nucleophilic displacement reactions with 2,2-diphenylethylamine in diglyme solution. All reactions were strictly first order in amine–borane and suggestive of an SN1-B mechanism involving the rate-determining dissociation of amine–borane. The effect of nucleophile identity, the effect of leaving group bulk, thermodynamic activation parameters, α-deuterium secondary kinetic isotope effect, and a Hammett treatment ($\log k/k_0 = \rho\Sigma\sigma$; $\rho = -3.25$) satisfactorily support the proposed SN1-B mechanism. (auth)

41805 CONFIGURATIONAL STABILITIES OF STRAINED α-SULFONYL CARBANIONS. KINETICS OF BASE-CATALYZED RACEMIZATION AND DEUTERIUM EXCHANGE OF REPRESENTATIVE THIETE AND THIETANE DIOXIDES. Paquette, Leo A.; Freeman, John P.; Wyvratt, Matthew J. (Ohio State Univ., Columbus). J. Amer. Chem. Soc.; 93: No. 13, 3216-21 (30 Jun 1971).

Rate constants and activation parameters for racemization and hydrogen–deuterium exchange were measured for optically active (R)-(+)-2-methyl-3,8-diphenyl-2H-naphtho[2,3-b]thiete 1,1-dioxide (10), a representative thiete dioxide, and (R)-(–)-2-methylthietane 1,1-dioxide (11), a typical saturated four-membered cyclic sulfone. Because these two molecules represent the smallest sulfone systems yet examined, knowledge of the stereochemical fate of the derived α-sulfonyl carbanions was of considerable interest. In the case of 10, k_e/k_α values were essentially unity in tert-butyl alcohol-d_1-benzene (70 : 30), denoting complete racemization. In methanol-d_1-benzene (70 : 30), the rate constants for racemization were consistently somewhat larger than those for exchange ($k_e/k_\alpha \approx 0.90$). The isotopic exchange and racemization rates for 11 in methanol-d_1 were too slow to measure. In tert-butyl alcohol-d_1 (neat or admixed with benzene), 11 was seen to react approximately 10^5 times more slowly than 10 in both processes. Also, the k_e/k_α ratios were notably smaller (0.60 to 0.67). These results are discussed in terms of configurational and conformational considerations and proton transfer phenomena, and a comparison with open-chain α-sulfonyl carbanions is made. (auth)

41806 REACTION OF p-PHENYLENEBISDIAZONIUM ION WITH ALCOHOLS. Lewis, Edward S.; Chalmers, David J. (Rice Univ., Houston, Tex.). J. Amer. Chem. Soc.; 93: No. 13, 3267-72(30 Jun 1971).

In acidic aqueous solution, p-phenylenebisdiazonium ion (I, tetrazotized p-phenylenediamine) reacts with alcohols more rapidly than it does with water. A first-order course for the disappearance of the uv absorption of I describes only about the first half of the reaction. Deviations are ascribed to both chemical and analytical problems. The initial rate with 2-propanol and ethanol is $-d[I]/dt = k[I][ROH]/[H^+]$; the identified products were benzene and a smaller amount of benzenediazonium ion. The products are different and not identified in the presence of oxygen. Benezenediazonium ion is reduced extensively by this system. When 2-propanol-d is used, $k_H/k_D = 6$. A free-radical chain, initiated by the electron transfer from diazotate to diazonium ion or homolysis of a diazoanhydride, is proposed. With allyl alcohol, the product appears to be a p-alkylbenzenediazonium ion, the rate law is $-d[I]/dt = k[I][C_3H_5OH]/[H^+]^{1/2}$, and there is an inverse isotope effect using $CH_2=CH-CD_2OH$. Different initiation and chain-carrying steps are proposed. As predicted earlier, the iodide ion promoted conversion of I to p-hydroxybenzenediazonium ion involves oxygen; when oxygen is carefully excluded, this reaction is not observed. (auth)

41807 CONFORMATION OF POLY-β-ALANINE IN AQUEOUS SOLUTION FROM PROTON MAGNETIC RESONANCE AND DEUTERIUM EXCHANGE STUDIES. Glickson, J. D.; Applequist, Jon (Iowa State Univ., Ames). J. Amer. Chem. Soc.; 93: No. 13, 3276-81(30 Jun 1971).

Studies of poly-β-alanine (PBA) in D_2O solution were carried out on a highly branched, high-molecular-weight (>58,000) sample and a linear low-molecular-weight (18,000) sample using proton magnetic resonance (PMR) to observe the spin–spin coupling between α and β protons and deuterium exchange kinetics to test for conformational concealment of NH groups. PMR spectra of PBA, β-alanine, N-acetyl-β-alanine ethyl ester (ABAEE), and N-acetyl-β-alanine-N′-methylamide (ABAMA) imply rapid internal rotation about the $C^\alpha-C^\beta$ bond with equal populations of the three staggered conformations. The pD dependence of the deuterium exchange rate of PBA is very similar to that of ABAEE and ABAMA, suggesting an absence of appreciable intramolecular hydrogen bonding in PBA, consistent with the random structure indicated by the PMR spectrum. The absence of hypochromism in the $\pi-\pi^*$ band at 190 nm in a linear PBA (mol wt 58,000) is likewise consistent with the absence of ordered secondary structure. (auth)

41808 SPONTANEOUS DISSOLUTION OF METALS IN AQUEOUS ELECTROLYTES. I. KINETIC ISOTOPE EFFECTS IN THE REACTION OF IRON WITH HYDROCHLORIC ACID SOLUTIONS IN PROTIUM AND IN DEUTERIUM OXIDE. Bellobono, I. R.; Mazza, F. (Univ., Milan). J. Phys. Chem.; 75: No. 14, 2112-16(8 Jul 1971).

First-order rate coefficients for hydrogen ion disappearance during the dissolution of pure polycrystalline iron at temperatures from 18 to 65°C were measured in H_2O and in D_2O solutions containing 10^{-3} to 1 M HCl or DCl, at constant ionic strength (1.0 M). Kinetic coefficients showed an appreciable dependence on pH [(7.1 to 63) $\times 10^{-5}$ sec^{-1} at 25°C, for 1 to 10^{-3} M HCl, respectively]. Experimental activation energies resulted: 11.3 kcal/g mole (in H_2O) and 13.1 kcal/g mole (in D_2O). The ratios of rate coefficients (in H_2O and D_2O) varied accordingly from

about 3 at 18°C to about 2 at 65°C. Rates of dissolution in H_2O were employed to evaluate corrosion current densities as a function of hydrogen ion activity in the range 0 to 3.5 pH. Their values were favorably compared with those predicted using a model that considers the reaction of a hydroxide film, formed at the metal–electrolyte interface, with hydrogen ions, as the rate-determining step for the dissolution process. The good agreement between calculated and experimental isotope effects constitutes another argument in favor of this reaction being responsible for the rate of dissolution. (auth)

41809 INTRAMOLECULAR ENERGY RELAXATION. NONRANDOM DECOMPOSITION OF HEXAFLUOROBICYCLOPROPYL. Rynbrandt, J. D.; Rabinovitch, B. S. (Univ. of Washington, Seattle). J. Phys. Chem.; 75: No. 14, 2164-71(8 Jul 1971).

Nonrandom decomposition of vibrationally excited hexafluorobicyclopropyl-d_2 (HBC) was observed. HBC* was chemically activated at room temperature to ~111 kcal mol^{-1} by the addition of $^1CD_2$ or $^1CH_2$ to hexafluorovinylcyclopropane (HVC) or HVC-d_2, respectively. HBC* decomposes to tetrafluorovinylcyclopropane-d_2 (TVC) with a specific rate of 2.3×10^9 sec^{-1}. Mass spectral analysis of TVC products indicates that ~3.5% was formed via a nonrandom decomposition of the newly formed ring of HBC*; this nonrandom decomposition is substantially noninterceptible at the highest pressure (4 atm) to which studies were carried. A rate of intramolecular energy relaxation of 1.1×10^{12} sec^{-1} was obtained for HBC* by consideration of the rate of nonrandom decomposition of the newly formed ring whose initial value was calculated to be ~3.5×10^{11} sec^{-1}. (auth)

41810 ISOTOPIC EXCHANGE BETWEEN GLASSES AND NONAQUEOUS LIQUIDS. Levi, H. W.; Lutze, W.; Malow, G.; Sedighi, N. (Hahn-Meitner Inst., Berlin). Phys. Status Solidi (a); 5: No. 3, 617-25(16 Jun 1971).

A new technique was established for determining self-diffusion coefficients by heterogeneous isotopic exchange in solids with low ion mobility. The efficiency of this method is demonstrated using a standard Na/Ca-silicate glass for which the temperature dependence of the Na self-diffusion coefficient is measured with high accuracy in the range of 230 to 880°C. Furthermore, some measurements with a Na/Al-phosphate glass are presented. (auth)

41811 PURIFICATION AND SOME PROPERTIES OF MOLYBDOFERREDOXIN, A COMPONENT OF NITROGENASE FROM CLOSTRIDIUM PASTEURIANUM. Dalton, H.; Morris, J. A.; Ward, M. A.; Mortenson, L. E. (Purdue Univ., Lafayette, Ind.). Biochemistry; 10: No. 11, 2066-72(25 May 1971).

A method for the purification of molybdoferredoxin (Mo–Fe protein), a component of the nitrogenase complex from Clostridium pasteurianum, is presented. This method yields about 2 g of pure protein and can be prepared within 2 days from 1 kg of dried cells (170 g of crude protein). The molecular weight of the protein is 168,000 and has a partial specific volume based on sedimentation equilibrium studies of 0.72 ml/g. The protein contained the following metals and sulfur groups (moles/mole of protein): Mo, 1.0; Fe, 14.0; SH, 23; S^{2-}, 16. The protein showed a tendency to aggregate if oxidized or stored for several months in liquid nitrogen. Significant changes in both the visible and paramagnetic resonance spectra occurred as well as a 70% loss in acetylene reduction activity after 1-hr exposure to air. Less loss of activity resulted from short-term exposure to air even though the spectral change was optimal. (auth)

41812 INFLUENCE OF VACANCIES AND IMPURITIES ON THE ORDER–DISORDER TRANSITION IN HEXAGONAL ICE Ih. Sesselmann, I.; Helmreich, D. (Technical Univ., Munich). Z. Naturforsch.; 26a: No. 5, 803-9(May 1971). (In German).

The temperature dependence of the longitudinal elastic constants of pure and HF-doped heavy ice was measured in the region between 80 and 200°K with a phase-comparison method. A positive anomaly was found for the HF-doped ice-d_2 below 150°K. Pure ice-d_2 remained normal in the measured temperature range. The results could be explained by seeds of the low-temperature phase stable in the high-temperature region, which were cooled centers of the new phase. (tr-auth)

41813 DELAYED FLUORESCENCE AND PHOSPHORESCENCE IN PURE NAPHTHALENE CRYSTALS. Benz, K. W.; Port, H.; Wolf, H. C. (Univ., Stuttgart). Z. Naturforsch.; 26a: No. 5, 787-93(May 1971). (In German).

In purified naphthalene crystals triplet exciton lifetimes up to 500 msec at room temperature were measured. The triplet annihilation coefficient was measured from an analysis of the light intensity dependence of delayed fluorescence as $\gamma = 3.5 \cdot 10^{-12}$ cm^3 sec^{-1} at 300 and 135°K. The quantum yields in the weak excitation limit at room temperature are $\eta DF = (3 \pm 0.6) \cdot 10^{-3}$ for delayed fluorescence and $\eta p = (1.2 \pm 0.3) \cdot 10^{-3}$ for prompt phosphorescence, both after triplet excitation. The phosphorescence spectra of naphthalene and perdeuteronaphthalene crystals were analyzed between 300 and 50°K. The line width decreased from 270 cm^{-1} at 300°K to 42 cm^{-1} at 60°K. (auth)

41814 GENERALIZED MEAN SQUARE AMPLITUDES OF VIBRATION FOR SUBSTITUTED ETHYLENE: VINYLIDENE HALIDES AND THEIR DEUTERATES. Jeyapandian, S.; Savari Raj, G. A. (Univ. of Madras). Z. Naturforsch.; 26a: No. 4, 778-80(Apr 1971).

For six vinylidene halides the generalized mean square amplitudes of displacements parallel and perpendicular to the bond for both bonded and non-bonded atom distances were calculated from spectroscopic data using the method of Morino and Hirato. The results are discussed and the mean amplitudes of these molecules ($H_2C = CX_2$) are compared with those from electron diffraction data for the similar molecules of the type C_2X_4. (auth)

41815 MODIFICATION OF THE INTENSITY OF OPTICAL SPECTRA OF ORGANIC DYES THROUGH DEUTERIUM LABELING. Trauzeddel, R.; Huebner, H. (Zentralinstitut fuer Isotopen- und Strahlentechnik, Leipzig). Isotopenpraxis; 7: No. 3, 106-7(Mar 1971). (In German).

41816 REVERSED ISOTOPE DEPENDENCE FOR HYDROGEN DIFFUSION IN PALLADIUM. Voelkl, J.; Wollenweber, G.; Klatt, H.-H.; Alefeld, G. (Kernforschungsanlage, Juelich, Ger.). Z. Naturforsch.; 26a: No. 5, 922-3(May 1971).

Gorsky-effect measurements applied to H and D in Pd show that D diffuses faster than H in the temperature range from about –60 to 200°C. The diagonal components of the dipole moment tensor were estimated as 3.5 eV. (auth)

41817 IODINE-CATALYZED IODINE EXCHANGE REACTIONS. Koroes, E.; Orban, M. (Lorand Eoetvoes Univ., Budapest). Radiochem. Radioanal. Lett.; 6: No. 5, 319-25 (19 May 1971).

Some iodine exchange reactions occurring between molecular iodine and organic iodides (e.g., benzoyl iodides, benzhydryl iodides, iodopyrazolone derivatives) exhibit polar mechanisms. In these cases the activated complexes contain more than one iodine molecule. These reactions can be regarded as iodine-catalyzed processes. The quantitative measure of iodine catalysis is the difference in free energy of activation between the n-molecular and (n-1)-molecular transition states ($-\Delta\Delta F^{\ddagger}$). This value is between 2-5 kcal.$mole^{-1}$ for the systems studied so far and depends strongly on the coordinating ability of the solvent toward iodine. (auth)

41818 REARRANGEMENT–FRAGMENTATION IN AROMATIC NITRATION. Myhre, P. C.; Beug, M.; Brown, K. S.; Oestman, B. (Harvey Mudd Coll., Claremont, Calif. Research Inst. of National Defense, Sundbyberg, Sweden). J. Amer. Chem. Soc.; 93: No. 14, 3452-7(14 Jul 1971).

Two toluene derivatives, 2,4-dinitro-3,5-di-tert-butyltoluene and 2,6-dinitro-3,5-di-tert-butyltoluene, are formed in 32 and 2% yields, respectively, by nitration of 2,4,6-tri-tert-butylnitrobenzene with fuming nitric acid. The paths leading to these compounds are characterized as molecular rearrangements of the intermediate cyclohexadienyl cation followed by alkyl fragmentation. Deuterium labeling studies established the intramolecular character of the methyl migration. Nitrogen-15 labeling studies permitted identification of the tert-butyl group undergoing rearrangement-fragmentation. These data, coupled with kinetic isotope effect data, serve as the basis for discussion of the detailed mechanism of rearrangement–fragmentation. (auth)

41819 ISOTOPE SHIFTS AND HYPERFINE STRUCTURE IN THE ATOMIC SPECTRUM OF PLATINUM. Stacey, Virginia; Kuhn, H. G. (Oxford Univ.). Proc. Roy. Soc. (London), Ser. A; 322: No. 1550, 301-11(4 May 1971).

Two lines in the arc spectrum of platinum were studied by high-resolution interferometry, and results were obtained for the isotope shifts in both lines. No evidence was found for large specific mass effects and, after allowance for normal mass effects, the results for the two lines give the following relative field isotope shifts: 192 – 194 : 194 – 196 : 196 – 198 = 0.895 ± 0.009 : 0.919 ± 0.004 : 1 and 194 – 195 : 194 – 196 = 0.458 ± 0.003. These values are compared with the relative isotope shifts in mercury and thallium. Differences in the mean square radius of the proton distribution for the platinum isotopes are calculated from the field isotope shifts. The contribution of changes in nuclear deformation to the shifts is discussed. (auth) (UK)

41820 β-SECONDARY DEUTERIUM ISOTOPE EFFECTS AS A MEASURE OF CHARGE LOCALIZATION IN CARBONIUM ION

XUM

REACTIONS: THE EXISTENCE OF A MAJOR INCONSISTENCY IN INTERPRETATION. Scheppele, Stuart E. (Oklahoma State Univ., Stillwater). J. Chem. Soc., D; No. 11, 592-3(9 Jun 1971).

In contrast to published interpretations, the solvolytic β-deuterium isotope effects for secondary and tertiary norborn-2-yl derivatives are qualitatively inconsistent with anchimerically assisted solvolysis for exo-secondary substrates. (auth) (UK)

41821 C-H VALENCE VIBRATIONS IN HYDROCARBONS AND BUTYL HALIDES. Avanessoff, M.; Gaeumann, T. (Ecole Polytechnique Federale, Lausanne, Switzerland). Helv. Chim. Acta; 54: No. 4, 995-1012(1971). (In French).

The valence vibrations, C-H and C-D, of a number of alkanes and of $(CH_3)_3CX$ are studied using compounds deuterated in specific positions. For the methyl and the methylene groups an experimental model of group frequencies is proposed, which allows some general conclusions to be drawn concerning the assignation of the frequencies. The methyl group always shows a Fermi resonance between ν_s and $2\delta_{as}$ in the region of 2930 to 2870 cm^{-1}. In consequence the unperturbed $\nu_s CH_3$ frequency may be situated at ~2915 cm^{-1} and the absence of a coupling with other groups can be checked. The vibrations of the methylene group adjacent to a methyl group have higher frequencies than those of CH_2 groups further removed. The coupling of the methylene group with other groups is always strong and may amount to 10 cm^{-1}. For a chain of methylene groups, the coupling is larger the longer the chain; being relatively small for symmetrical modes (~3 cm^{-1}), its value can be as large as 15 cm^{-1} for the antisymmetric mode. A correlation was found between protonated and deuterated groups which leads to isotope effects comparing well with recorded values. (auth)

41822 FUNDAMENTAL AND HARMONIC C-H/C-D VALENCE VIBRATIONS OF HALOGEN DERIVATIVES OF METHANE AND OF DEUTERIOMETHANE. Avanessoff, M.; Ho Dac Thang; Gaeumann, T. (Ecole Polytechnique Federale, Lausanne, Switzerland). Helv. Chim. Acta; 54: No. 4, 1013-29(1971). (In French).

The fundamentals and overtones of the C-H stretching vibrations of a number of halogenated methanes and deuteriomethanes were compared with a hypothetical model consisting of isolated groups. The anharmonicity constants were evaluated and they lie between -20 cm^{-1} and -130 cm^{-1} for the C-H and C-D stretching vibrations. The value of the anharmonicity constant for a coupling between two different modes of vibration is always greater (in absolute numbers) than its value for an overtone of one frequency. The constant is larger for a symmetric mode than for an asymmetric mode in the case of a C-H vibration; the contrary is true for a C-D bond. Complex interactions between different vibrations often strongly modify the spectra of the overtones. It is shown, however, that the conception of an isolated group is helpful for evaluating the spectra of these substances. (auth)

Physical Chemistry

Refer also to abstracts 42934 and 44206.

41823 (ANL-7802) SOLUBILITY OF HELIUM AND ARGON IN LIQUID SODIUM. Veleckis, E.; Dhar, S. K.; Cafasso, F. A.; Feder, H. M. (Argonne National Lab., Ill.). Apr 1971. Contract W-31-109-eng-38. 10p. Dep. NTIS.

The solubilities of helium and argon in liquid sodium were determined as functions of pressure and temperature. The data obeyed Henry's law to at least 9 atm. In the temperature range 330 to 550°C, the solubilities may be represented by the following linear equations: helium, $\log \lambda = 0.516 - 3078T^{-1}$; argon, $\log \lambda = 1.08 - 4462T^{-1}$; where λ is the Ostwald coefficient. The 95% confidence limits of the mean value of λ predicted by these equations are ±4% for helium and ±16% for argon. For the standard state defined as one gram-atom of ideal gas confined to a volume equal to the molar volume of sodium, the heats of solution are 14.1 ± 0.6 kcal/mole for helium and 20.4 ± 2.1 kcal/mole for argon. The results are compared with experimental data of others and with calculations based on existing theoretical models. (auth)

41824 (CEA-R-4089) STUDY OF THE STRUCTURE OF PHYSISORBED PHASES BY THERMODYNAMIC ANALYSIS OF STEPWISE ISOTHERMS OF KRYPTON, XENON, ARGON, AND METHANE ON THE CLEAVAGE FACE OF HALIDES HAVING A LAYER-LIKE STRUCTURE. Larher, Yves (Commissariat a l'Energie Atomique, Saclay (France). Centre d'Etudes Nucleaires). Mar 1971. 203p. (In French). Dep. NTIS (U. S. Sales Only).

Thesis. Submitted to Univ. of Paris, Orsay, France.

Adsorption isotherms of argon, krypton, xenon, and methane on the cleavage plane of halides having a layer-like structure ($NiCl_2$, $CoCl_2$, $FeCl_2$, $CdCl_2$, $CdBr_2$, CdI_2, and PbI_2) were determined at various temperatures. In most cases, it is possible to prepare, by sublimation in a rapid current of inert gas, adsorbing powders of these halides, of which the grains have highly developed cleavage faces. The isotherms show steps corresponding to the formation of successive monomolecular layers by two-dimensional condensation. Derivation of formulas enabled a comparison to be made of the structure of the successively adsorbed monolayers and of the compact layer of the solid adsorbate((111) plane of its fcc crystal) in terms of their internal energies and their entropies. It is concluded that the first adsorbed layer is the (111) plane of solid adsorbate which becomes more loosely packed as the dimensional compatibility of the lattices of the adsorbent and adsorbate becomes poorer. This conclusion is supported by the study of the two dimensional critical temperatures. The study of the second and third adsorbed layers makes possible a test of the inverse cube law for the diminution of the interaction energy between the adsorbed atoms and the adsorbing surfaces. (auth)

41825 (LA-DC-12348) SEGREGATION OF IMPURITIES ON SURFACES OF THORIUM: THERMODYNAMICS AND KINETICS. Ellis, Walton P. (Los Alamos Scientific Lab., N. Mex.). [1970]. 7p. (CONF-710426-1). Dep. NTIS.

From seventh annual symposium on vacuum science, Albuquerque, N. Mex. (21 Apr 1971).

LEED and secondary-electron spectroscopic studies are being made on thorium for a comparison with previous ThO_2 work. Three features of thorium metal are discussed: the thermodynamics of impurity segregation on Th surfaces as determined by the Auger method, segregation kinetics and electron desorption, and alteration of the metal valence-band Auger spectrum by surface impurities. (M.C.G.)

41826 (NBS-TN-270-5) SELECTED VALUES OF CHEMICAL THERMODYNAMIC PROPERTIES. Tables for Elements 54 Through 61 in the Standard Order of Arrangement. Wagman, D. D.; Evans, W. H.; Parker, V. B.; Halow, I.; Bailey, S. M.; Schumm, R. H.; Churney, K. L. (National Bureau of Standards, Washington, D. C.). Mar 1971. 49p. GPO $0,55.

Tables of values are presented for the standard heats and Gibbs (free) energies of formation, entropies, and enthalpies at 298.15°K and heats of formation at 0°K for compounds of vanadium, niobium, tantalum, titanium, zirconium, hafnium, scandium, and yttrium (elements 54 to 61 in the Standard Order of Arrangement). These tables are a continuation of the comprehensive revision of NBS Circular 500. (auth)

41827 PROTECTION AGAINST INTENSE LIGHT. I. DISCUSSION OF THE USUAL MECHANISMS OF ENERGY DISSIPATION. Prosser, R. A. (Army Natick Labs., Mass.). J. Appl. Polym. Sci.; 15: No. 5, 1041-51(May 1971).

The relative thermal protection offered by a series of halogenated vinyl polymers is discussed in terms of the usual modes of energy attenuation and dissipation, such as reflection, endothermic decomposition, etc. It is shown that none of these modes is so overwhelming that it alone can account for the relative thermal protection offered by these polymers. (auth)

41828 SPECTROSCOPIC STUDY OF OUTER-SPHERE INTERACTION IN $M_3UO_2F_5$ COMPLEXES. Sergienko, V. I.; Davidovich, R. L.; Kostin, V. I.; Matsutsin, A. A. Spectrosc. Lett.; 4: No. 1-2, 19-27(Jan-Feb 1971).

Results are given for the influence of outer sphere cations on the spectral characteristics of complex uranyl fluorides with the composition $M_3UO_2F_5$. The methods used were ir spectroscopy, luminescence, and NMR. (D.P.O.)

41829 DILUENT EFFECTS ON DIFFUSION FOR THE SYSTEM URANYL NITRATE-TRIBUTYL PHOSPHATE-n-HEPTANE. Hortacsu, Amable Dorotan. Stillwater, Okla.; Oklahoma State Univ. (1970). 137p. University Microfilms Order No. 71-11,170. Thesis.

Diffusion rates for the system uranyl nitrate-tributyl phosphate-n-heptane were studied with respect to two variables: the degree of dilution of tributyl phosphate and the concentration of uranyl nitrate. Experimental diffusion coefficients at 25°C were obtained for uranyl nitrate in 30 V/V % tributyl phosphate-n-heptane, in 50 V/V % tributyl phosphate-n-heptane and in 70 V/V % tributyl phosphate-n-heptane, using a one Savart plate birefringent interferometer. The uranyl nitrate concentration covered the range from 0.01 M to near saturation for each solvent system. Diffusion coefficients for the binary systems uranyl nitrate-tributyl phosphate and uranyl nitrate-tributyl phosphate complex-n-heptane at 0.01 M uranyl nitrate were also obtained. In addition, density and viscosity data for all the systems studied were also determined. The diffusion coefficients decreased with an increase in uranyl nitrate concentration and increased with dilution of tri-

butyl phosphate by n-heptane. The diffusion coefficients exhibit similar uranyl nitrate concentration dependence for all the tributyl phosphate dilutions used. In the dilute uranyl nitrate concentration region, the system may be considered a pseudo-binary, with solvent properties calculated from mole fraction averages of tributyl phosphate and n-heptane. Semi-empirical theories of diffusion based on the linear additivity of the free energies of activation of the pure components show good agreement with the experimental diffusion data. Viscosity data of the separate binary pairs qualitatively indicate no strong interaction effects present in the system. An empirical correlation which expresses the ratio of the viscosity product $D\mu/D_0\mu_0$ as a linear function of the mole fraction uranyl nitrate may be used to represent the data for all systems studied with an uncertainty of ±.07. (Diss. Abstr. Int., B)

41830 COMPOSITION AND STABILITY OF THE COMPLEX BETWEEN URANYL IONS AND 2,4-DIHYDROXYBENZOIC ACID IN AQUEOUS MEDIUM. Soni, R. N. (Birla Inst. of Tech. and Science, Pilani, India). Collect. Czech. Chem. Commun.; 36: No. 4, 1650-3(Apr 1971).

2,4-Dihydroxybenzoic acid was found to form an orange water-soluble complex with uranyl ions having an absorption maximum at 450 nm and a flat region thereafter. The stability constant of the uranyl-2,4-dihydroxybenzoate complex was determined at various ionic strengths and temperatures to obtain thermodynamic functions such as change in free energy, enthalpy, and entropy of the complex formation. The straight line method of Asmus was also used for determination of molecular composition of the complex. (B.L.M.)

41831 POTENTIAL-pH DIAGRAM FOR PLUTONIUM. Silver, G. L. (Monsanto Research Corp., Miamisburg, Ohio). Contract AT(33-1)-GEN-53. Radiochem. Radioanal. Lett.; 7: No. 1, 1-5(15 Jun 1971).

A method for solving the general plutonium equilibrium problem is presented, and a potential-pH diagram for plutonium is constructed with the aid of this method. Four conditions of acidity and oxidation number calculated to result in equal concentrations of three plutonium species are suggested, and the locus of each "triple point" is indicated in the potential –pH diagram. (auth)

Radiation and Nuclear Chemistry

Refer also to abstracts 42271 and 42721.

41832 (AECL-3851) CHEMISTRY AND MATERIALS DIVISION PROGRESS REPORT, OCTOBER 1–DECEMBER 30, 1970. (Atomic Energy of Canada Ltd., Chalk River (Ontario). Chalk River Nuclear Labs.). 143p. (PR-CMa-15). Dep. NTIS (U. S. Sales Only). AECL $3.00.

ALKANES — radiolysis in adamantane matrix, ESR studies on
ALKENES — radiolysis in adamantane matrix, ESR studies on
ALUMINUM — determination in aluminum silicon–uranium alloys by atomic absorption spectrometry
ALUMINUM ALLOYS — Al–Si–U, analysis for aluminum by atomic absorption spectroscopy
ALUMINUM A & S — Al–Zr-base, precipitation in, effects of vacancies on
AMINES — radiolysis of, ESR studies on
AMMONIA — radiolysis of, electron pulse
AMMONIUM NITRATES — corrosive effects on zirconium alloys
ANALYTICAL CHEMISTRY — research progress on
ARGON IONS — effects of implanted, on stripping rates of tantalum oxide films
— implantation in silicon at 300, 400, and 500 keV, technique for
AUTORADIOGRAPHY — method for tritiated Zircaloy-2
CALCIUM FLUORIDES — analysis for yttrium by x-ray fluorescence spectroscopy
CALCIUM FLUORIDES — diffusion of calcium in CaF_2
CARBON DIOXIDES — radiolysis of, electron pulse
DEUTERIUM — determination in water by mass or ir spectrometry
— separation from hydrogen, electrochemical
— exchange between hydrogen and water-d or methylamines
ELECTRON MICROSCOPES — resolution of, techniques for improvement of
ELECTRONS — effects of pulsed, on water–heavy water systems
— effects of pulsed, on ammonia, carbon dioxide, hydrogen sulfide, and nitrous oxide
FILMS — mounting of thin, for channeling studies, technique for
FLUORINE — determination in Zircaloy by proton (p,αγ) reactions using 1.188-MeV resonance
FURNACES — design for destruction of graphite-coated uranium dioxide microspheres using replaceable combustion tube
FUSED SALTS — corrosive effects of chloride–nitrate, on zirconium alloys
GALLIUM ARSENIDES — radiation effects on structure of, 1.5-MeV electron
— radiation effects on, infrared absorption spectra of electron- and neutron-, (E)
GAMMA SOURCES — determination in organic coolant
GERMANIUM — analysis of detector-grade monocrystals of, for trace impurities
HELIUM IONS — channeling in sodium chloride at 1 MeV, (E)
HYDROGEN — separation from deuterium, electrochemical
HYDROGEN SULFIDES — radiolysis of, electron pulse
INDIUM — deformation at 4°K, recovery after
LEAD — deformation at low temperature, recovery of normal and superconducting
MAGNESIUM OXIDES — diffusion in monocrystals of
NEUTRONS — effects on zirconium and zirconium alloys, annealing of damaging
NIOBIUM A & S — Nb–Zr-base, corrosion by fused chloride–nitrate salts, stress
NITROGEN — determination simultaneously with oxygen in silicon nitride films by deuteron activation
NITROGEN OXIDES N_2O — radiolysis of, electron pulse
OXYGEN — determination simultaneously with nitrogen in silicon nitride films by deuteron activation
PHOSPHORIC ACID — corrosive effects on zirconium alloys
REACTOR COOLANTS — analysis of organic, for gamma emitters
SILICON — ion implantation with 300-, 400-, and 500-keV Ar^+ ions, technique for
SILICON NITRIDES — analysis of films of, for nitrogen and oxygen by deuteron activation
SILICON SYSTEMS — Al–Si–U, analysis for aluminum by atomic absorption spectroscopy
SODIUM CHLORIDES — ion channeling in, 1-MeV He^+, (E)
TANTALUM OXIDES — removal from tantalum surfaces, effects of ion implantation on
THORIUM OXIDES ThO_2 — spectra of, effects of impurities on optical absorption
— thermoluminescence of
— fluorescence of, under uv
URANIUM ALLOYS — Al–Si–U, analysis for aluminum by atomic absorption spectroscopy
URANIUM-234 — half-life of
WATER — analysis for deuterium by ir or mass spectrometry
— D_2O–H_2O, radiolysis of, electron pulse
WATER-d_2 — D_2O–H_2O, radiolysis of, electron pulse
YTTRIUM — determination in calcium fluoride by x-ray fluorescence spectrometry
ZIRCALOY — analysis for fluorine by proton (p,αγ) reactions using 1.188-MeV resonance
ZIRCALOY-2 — corrosion by fused chloride–nitrate salts, stress
— oxide film formation on, model of electric switching in anodic
— crystal structure of oxide films on
ZIRCONIUM — oxide film formation on morphology of ammonium nitrate induced
— oxide film formation on, morphology of phosphoric acid induced
— radiation damage in, annealing of neutron
ZIRCONIUM A & S — Nb–Zr-base, corrosion by fused chloride–nitrate salts, stress
— radiation damage in, annealing of neutron
— Al–Zr-base, precipitation in, effects of vacancies on
ZIRCONIUM OXIDES — electric conductivity of crystalline and powdered (L.M.T.)

41833 (IA-1218) RESEARCH LABORATORIES ANNUAL REPORT, JANUARY–DECEMBER 1969. (Israel Atomic Energy Commission, Tel Aviv). 268p. Dep. NTIS (U. S. Sales Only).

Short summaries are given that illustrate some aspects of work done in the fields of: neutron and reactor physics; nuclear physics; solid state physics and metallurgy; pure and applied mathematics; high energy and nuclear chemistry; radiation chemistry; physical and inorganic chemistry; spectroscopy and spectrochemical analysis; geochemistry; food irradiation and applications of tracer techniques; radiobiology and medicine; health physics; nuclear safety; instrumentation and methods; production of radioisotopes and labeled compounds; and information exchange and retrieval. (P.C.H.)

41834 MONOLAYER STUDIES WITH NORMAL AND γ IRRADIATED POLY-L-SERINE. Joshis, V.; Korgaonkar, K. S. (CRI, Bombay). Indian J. Biochem.; 6: No. 3, 138-41(1969).

XUM

Dilute aqueous solutions of poly-L-serine (45 μg/ml) were irradiated with ^{60}Co γ rays at a dose rate of 1.26×10^5 rad/hr. The film properties of the nonirradiated and irradiated samples were studied using Langmuir-type trough and float system and plotting pressure (P) versus area (A), PA versus P, and coefficient of area-compressibility (δ) versus A curves. The effect of irradiation on pH and uv absorption in the peptide band region of the aqueous peptide solution was also studied. The observed marked reduction in various film characteristic areas, viz. limiting area, packing area, and actual area, was attributed to increased solubility of this polypeptide due to radiation action on the side group. The steep rise in molecular weight on irradiation was explained as possibly due to crosslinking action. The data do not indicate the peptide bond as the major target of radiation attack. (10 ref.) (Indian Sci. Abstr.)

Radiation Effects

Refer also to abstract 43443.

41835 BUBBLE NUCLEATION INDUCED IN LIQUID FILMS BY IRRADIATION. Kato, Ryuhei (Ritumeikan Univ., Kyoto). J. Appl. Phys.; 42: 2014-23(Apr 1971).

An attempt is made to explain the mechanism of rupture by irradiation for thin liquid films using a visualized model for the rupture. When liquid films, whose main component is water, are irradiated, first the microbubble formation occurs as in bubble chambers and second, if the diameter is more than about 0.3 times the film thickness, the film is broken. If the diameter is less than this, the microbubble will immediately disappear without any change in the film. Calculations for the radius and for the probability of rupture of a film are given. Various experiments to affirm this picture were attempted, and some experimental evidence available for this model is also shown. Moreover, it was found that the agent responsible for film rupture consists of recoil oxygen nuclei rather than delta rays or recoil hydrogen nuclei. The threshold energy for film rupture slightly exceeds $\sim 1.1 \times 10^5$ eV. (auth)

41836 ESR STUDY OF INTRAMOLECULAR ENERGY TRANSFER IN THE RADIOLYSIS OF CELLULOSE THENOATES. Singh, Sujan; Hinojosa, Oscar; Arthur, Jett C. Jr. (Dept. of Agriculture, New Orleans). J. Appl. Polym. Sci.; 15: No. 5, 1129-37(May 1971).

The substitution of 2-thenoyl, 5-methyl-2-thenoyl, 2-thiopheneacryloyl, 5-bromo-2-thenoyl, and 5-bromo-2-thiopheneacryloyl groups on fibrous cotton cellulose increased the radiation resistance of cellulose, as indicated by the retention of the breaking strengths of the modified fibrous celluloses at high dosages of γ radiation, as compared with that of irradiated, unmodified fibrous cellulose. The presence of electropositive or electronegative substituents on the thiophene groups did not reduce the radioprotective effects of these groups for cellulose. Crosslinking of the cellulose thenoates in 1,3-di(4-pyridyl)-propane did not significantly reduce the radiation resistance of the thenoates. Examination of the ESR spectra of irradiated cellulose and cellulose thenoates indicated that the site of the long-lived free radicals on the irradiated cellulose molecules was not changed by the chemical modification. However, the concentration of long-lived free radicals in irradiated cellulose thenoates, at a given radiation dosage, was less than that in irradiated cellulose. The localization of energy on carbon C_1 or C_4 of the cellulose molecule, which leads to depolymerization and loss in breaking strength of fibrous cellulose, was decreased. The radioprotective effects of thiophene groups for cellulose were similar to those of furan and benzenoid groups. (auth)

41837 RADIATION-INDUCED HYDROGEN TRANSFER IN NUCLEIC ACIDS, PROTEINS, AND RELATED SUBSTANCES: EFFECTS OF TEMPERATURE AND SCAVENGERS. Smitherman, Thomas C.; Moss, Harold M.; Riesz, Peter (National Cancer Inst., Bethesda, Md.). Radiat. Res.; 46: No. 2, 251-67 (May 1971).

G values for γ-induced hydrogen transfer from exchangeable to carbon-bound sites in dry salmon sperm DNA, D-glucose, ribonuclease, and poly-DL-alanine were measured and compared with the initial radical yields previously determined by ESR. The effects of temperature, of hydrogen atom scavengers (formate and cupric ions and glucose), and of electron scavengers (cupric and cadmium ions and sulfur hexafluoride) were investigated. Of the scavengers, only cupric ions had a significant effect on the G values, with a decrease of about 90% for DNA and of about 70% for ribonuclease and glucose. Cupric ions may act as scavengers of electrons and/or hydrogen atoms or by quenching triplet states, thus reducing the initial yield of secondary radicals, whose subsequent radioinduced destruction appears to be responsible for the tritium incorporation. The relationship between radioinduced hydrogen transfer, the mechanism of radical saturation and the hypothesis that either primary or secondary free radicals are involved in the chain of events that leads to loss of biological activity is discussed for the case of ribonuclease. (auth)

41838 ELECTRON SPIN RESONANCE OF X- AND γ-IRRADIATED POTASSIUM DIFLUOROMALONATE AND ELECTRON PARAMAGNETIC RESONANCE OF COPPER(II) COMPLEX WITH TRIFLUOROACETATE LIGANDS. Mustafa, Mohammed Rafti. Vancouver, British Columbia; Univ. of British Columbia (1970). National Library of Canada, Ottawa.

Thesis.

An irradiated single crystal of dipotassium difluoromalonate monohydrate was studied by ESR. On x-irradiation the crystal yields $\dot{C}F(COO^-)_2$ radical with a highly anisotropic hyperfine tensor, characteristic of a ^{19}F nucleus. In addition, some other lines were also observed that were too weak to be analyzed. On γ irradiation, the crystal yields mainly the same radical in addition to two types of $\dot{C}F_2COO^-$ radicals. In one type, the carboxyl group was found to be nearly coplanar with the CF_2 fragment while in the other, it was nearly perpendicular. A broad central line in each spectrum indicated also the possibility of the presence of the CO_2^- radical. An unrestricted Hartree–Fock calculation, using the approximation of Intermediate Neglect of Differential Overlap was carried out on a number of fluorinated radicals to correlate the ^{19}F hyperfine tensors obtained in the present study with those obtained previously. The theory was used to calculate the theoretical hyperfine tensors for various radicals and gave a reasonably good agreement with the experimental results. On this basis the hyperfine tensor for $\dot{C}HFCOO^-$ radical was predicted. The calculation also showed that one of the carboxyl groups in $\dot{C}F(COO^-)_2$ radicals is coplanar with the radical plane while the other makes an angle of 85°. A crystal of zinc trifluoroacetate dihydrate, containing small amounts of Cu^{2+} was studied at 77°K and it was found that the Cu^{2+} ion resides in an approximately tetragonal environment with the ground state consisting of mainly d_{z^2} orbital, which is coupled to $d_{x^2-y^2}$ orbital, perhaps through vibronic interactions. Also a solution of copper trifluoroacetate in trifluoroacetic acid was studied at room temperature and at 77°K, and the results were interpreted by assuming a tetragonal symmetry with the ground state being pure $d_{x^2-y^2}$. (Diss. Abstr. Int., B)

41839 EFFECT OF GAMMA-RADIATION ON THE PROPERTIES OF EXTRACTED COTTONSEED OIL FOR THE PREPARATION OF K-5 DRYING OIL. Muminova, S. N.; Ibragimov, A. P.; Mirzakarimov, R. M.; Rizaev, N. U. (Tashkent Polytechnic Inst.). Uzb. Khim. Zh.; No. 1, 38-40(1971). (In Russian).

The effects of γ radiation on the physicochemical properties of extracted cottonseed oil were studied, and, in addition, of oil obtained from irradiated cake made from a low grade of cottonseed. In general, the oil lost color, the iodine number decreased, and the viscosity rose as a result of irradiation. These three factors were used to judge the optimal dose of radiation for oil from a given source. For the manufacture of K-5 drying oil it was judged more expedient to use low-grade irradiated cottonseed oil (3×10^8 R) than oil expelled from irradiated cake. (K.S.W.)

41840 QUENCHING OF LUMINESCENCE OF ORGANIC CRYSTALS BY X RAYS. Krisch, O. (Univ., Giessen, Ger.). Z. Phys.; 244: No. 5, 468-81(1971). (In German).

Quenching of luminescence upon irradiation with x rays is investigated on the systems anthracene–tetracene, 2,3-dimethylnaphthalene–anthracene, and 2,3-benzdiphenylene oxide (Brasan)–tetracene. An annealing process is observed at the system anthracene–tetracene by tempering the samples at temperatures above 100°C. From the temperature dependence of luminescence, some conclusions can be drawn concerning the irradiation defects. It is possible to interpret the nonlinearity between quenching effect and irradiated dose as a consequence of exciton diffusion to the surface. (auth)

41841 ELECTRON SPIN RESONANCE EVIDENCE FOR POSITIVE HOLES PRODUCED IN IRRADIATED SINGLE CRYSTALS OF CARBOXYLIC ACIDS. Iwasaki, Machio; Minakata, Kayoko; Toriyama, Kazumi (Government Industrial Research Inst., Nagoya, Japan). J. Amer. Chem. Soc.; 93: No. 14, 3533-4(14 Jul 1971)

Single crystals of potassium hydrogen fumarate and its deuterium analog were irradiated in the dark at 77°K. Two kinds of carboxyl radicals, $O_O(I)$ and $O_O(II)$, are obtained. Data indicated that $O_O(I)$ is formed by removal of the acidic proton from the COOH group and $O_O(II)$ by ejection of an electron from the COO^- group. It was concluded that the positive hole can be trapped in the oxygen nonbonding orbital in irradiated carboxylic acid salts having no acidic proton. (M.C.G.)

XUM

Radiation Processes

41842 (CONF-690977-(Absts.)) ABSTRACTS OF PAPERS TO BE PRESENTED AT THE FIFTEENTH CANADIAN HIGH POLYMER FORUM, KINGSTON, ONTARIO, CANADA, SEPTEMBER 3-5, 1969. (Queen's Univ., Kingston (Ontario)). 17p.

Abstracts of 27 papers are presented. Topics covered include: structure of oligomers of isoprene, preparation of block copolymers, electropolymerization, properties of aqueous systems containing salts of acidic random copolymers, gas chromatographic studies of polymers, deformation in polymer films and fibers, sequence distribution in copolymers, elasticity of rubbers and polymers, thermodynamics of plasticized PVC compounds, thermal degradation of poly(1,4-cyclohexylenedimethylene terephthalate), surface reactions in polypropylene, radioinduced polymerization, solid-state polymerization, catalyzed polymerization, and free-radical polymerization. (M.C.G.)

41843 (ORO-2945-10) PREPARATION OF WOOD-PLASTIC COMBINATIONS USING GAMMA RADIATION TO INDUCE POLYMERIZATION. Final Report, November 1, 1961-June 30, 1968. Boyle, William R.; Winston, Anthony; Loos, Wesley E. (West Virginia Univ., Morgantown. Engineering Experiment Station). 10 May 1971. Contract AT(40-1)-2945. 249p. Dep. NTIS.

A study is presented that includes evaluations of various wood-plastic combinations (WPC), kinetic data on the radiation-induced polymerization of vinyl monomers in wood and with certain dyes incorporated, results obtained with other additives, results obtained using ^{60}Co and high energy electrons as the radiation source, results using NMR to study polymerization, and the use of DTA to study certain properties of WPC. Results of studies on the manufacture of WPC are presented including impregnation, polymer distribution studies, thermal problems during polymerization, veneers and the use of vinyl chloride (a gas) as a monomer. Results of studies on the properties of WPC including data on physical properties, techniques for moisture determination, dimensional changes during manufacture, dimensional stability, results of biological exposure, and data on flame resistance are presented. (auth)

41844 IMPROVEMENTS IN OR RELATING TO COATING PROCESSES. (to Kansai Paint Co., Ltd.). British Patent 1,234,684. 9 Jun 1971. Priority date 1 Mar 1968, Japan.

A coating for articles curable by ionizing radiation is prepared by reacting a methacrylic acid ester having one functional group capable of combining with an isocyanate group and a polyisocyanate compound having at least two isocyanate groups in its molecule to obtain a partially blocked polyisocyanate compound having one equivalent or less of free isocyanate groups per molecule of the polyisocyanate compound and then causing a reaction between the partially blocked polyisocyanate compound and a polyester having at least one hydroxyl group to produce a urethanated unsaturated polyester product. (B.L.M.)

41845 REACTIVITY RATIOS AND MICROSTRUCTURE FOR THE RADIATION INDUCED COPOLYMERS OF STYRENE AND METHYL METHACRYLATE. Ramig, Alexander Jr. Louisville, Ky.; Univ. of Louisville (1970). 136p. University Microfilms Order No. 71-12,477.

Thesis.

The γ-induced copolymerization of the low-temperature liquid state of styrene and methyl methacrylate was studied to determine the dependence of copolymer microstructure on the temperature of polymerization. Copolymer composition was determined from the NMR spectra of five to ten percent copolymer solution in chloroform-d. Reactivity ratios were determined by the Fineman-Ross method in conjunction with a Fortran program. At polymerization temperatures of 22, 0, and -20°C, the reactivity ratios for styrene were 0.480 +/- 0.056, 0.399 +/- 0.071, and 0.206 +/- 0.021, respectively. Results for methyl methacrylate were 0.450 +/- 0.026, 0.403 +/- 0.072, and 0.298 +/- 0.015. These values were compared to those found in the literature and it was concluded that the mechanism of polymerization was predominately free radical. Activation energies for copolymerization propagation were calculated. For steps involving homopolymerization, activation energies already reported were employed and then activation energies for cross addition were determined. Sequence distributions for all copolymers used to determine reactivity ratios were calculated using a method developed by Harwood. Of particular interest were methyl methacrylate centered triads as they could be related to multiple methoxy resonance observed in the NMR spectra. The relationships between methyl methacrylate centered triads and methoxy resonance were calculated for copolymerization at 22, 0, and -20°C. For SMS triads, percent resonance contribution to total methoxy resonance moved upfield as temperature of polymerization decreased. An opposite effect was observed for SMM triads. As temperature of polymerization decreased, SMM resonance moved downfield. To explain the results, the ten possible configurations for methyl methacrylate centered triads were considered. Each structure was determined to contribute to one of the three intensities observed for methoxy resonance. A treatment of triad tacticity is included that relates copolymer microstructure to temperature of polymerization. The 10 possible configurations are illustrated, and the percentages of various structures present at different temperatures are shown in tabular form. (Diss. Abstr. Int., B)

41846 RADIOCHEMICAL ADHESION PROCESS. Balestic, Francis; Bex, Guy; Mardon, Yves (to Commissariat a l'Energie Atomique). French Patent 2,029,939. 12 Oct 1970. Filed 31 Jan 1969. (In French).

This sticking process consists of reacting a reactive radiosensitive monomer with an epoxy resin, spreading the subsequently modified resin over the surfaces to be stuck, contacting the surfaces, and hardening the modified resin by subjecting it to ionizing radiation. (France)

41847 PROCESS OF PRODUCING MOULDED MASSES AND COATED SUBSTRATES. Metzner, Wolfgang; Rudolph, Hans; Deninger, Wolfgang; Patheiger, Manfred (to Farbenfabriken Bayer Aktiengesellschaft). British Patent 1,235,990. 16 Jun 1971. Priority date 10 Aug 1968, Germany.

A process is described for curing a coating or a molding mass by means of electron radiation in the presence of a polymerization initiator, such as mono-, di-, or trialkylphosphines, arsines, or stibines. The coating or molding mass is made up of an unsaturated polyester, such as polycondensation products obtained from α, β-unsaturated carboxylic acids with polyhydric alcohols and monomeric unsaturated compounds, such as styrene, vinyltoluene, divinylbenzene, and vinyl esters. (B.L.M.)

41848 GAMMA-INDUCED POLYMERIZATION OF FLUORINE-CONTAINING PENTADIENE. Ito, Katsukiyo; Muramatsu, Hiroshige; Matsuda, Tatsuo (Government Industrial Research Inst., Nagoya, Japan). Kobunshi Kagaku; 27: No. 308, 938-42 (Dec 1970). (In Japanese).

The γ-radioinduced bulk polymerizations of 3,4,5,5,5-pentafluoro-1,3-pentadiene (PFP) and 3,4,5,5,5-pentafluoro-2-methyl-1,3-pentadiene (MPFP) were investigated in the temperature range from +25 to -196°C. PFP was polymerized both in the liquid and solid states and the structures of the resulting polymers was found to be 1,4-units. The intrinsic viscosity of the polymer obtained in the liquid state polymerization was considerably higher than that in the solid state polymerization. Poly-MPFP having 1,4-structure was obtained only in the liquid state polymerization and its rate was about one-tenth of PFP. These results suggest that 2-substituted methyl group in pentafluoropentadiene presumably reduces reactivity due to the steric effect. (auth) (Japan)

Radiolysis

Refer also to abstracts 42268, 42291, 42294, 42753, and 43451.

41849 (AECL-3853) PULSE RADIOLYSIS FACILITIES AT CHALK RIVER. Seddon, W. A.; Willis, C.; Young, M. J.; Selkirk, E. B. (Atomic Energy of Canada Ltd., Chalk River (Ontario). Chalk River Nuclear Labs.). Mar 1971. 66p. Dep. NTIS (U. S. Sales Only). AECL $1.50.

The facilities presently available for pulse radiolysis studies at the Chalk River Nuclear Laboratories of Atomic Energy of Canada Limited are described. A 2.5-MeV Van de Graaff accelerator with microsecond pulsing is used to investigate condensed systems and a Febetron 705 (2-MeV) or 706 (600-keV) is used for gases. Detailed descriptions of the electronics including photomultiplier, remote sample handling, and pulsed Xenon lamp circuitry are given. Design of the optical detection systems together with safety features and general experimental layouts are also included. (auth)

41850 (CEA-N-1438) PHYSICAL CHEMISTRY SERVICE. Semiannual Progress Report, July-December 1970. (Commissariat a l'Energie Atomique, Saclay (France). Centre d'Etudes Nucleaires). Apr 1971. 59p. (In French). Dep. NTIS (U. S. Sales Only).

The following fields are covered: flash photolysis and pulsed radiolysis of gases (study of He afterglow, radiolysis of N_2) and liquids (development of a Febetron 707 gun, study in aqueous KIO_4 solutions); classical radiolysis of gases and liquids (study of the atomic H yield in concentrated aqueous solutions); the study by ESR and NMR of radicals produced in solid undecafluoro(trifluoromethyl)cyclohexane; the radioinduced polymerization in the solid phase of vinylic monomers; and the desorption of the oxygen chemisorbed by a natural graphite. (France)

41851 (JAERI-13780) CHEMICAL REACTIONS BY REACTOR RADIATION. 4. Nitrous Oxide Dosimeter. Ikezoe, Yasu-

XUM

masa; Tokunaga, Okihiro; (and others) (Japan Atomic Energy Research Inst., Takasaki. Takasaki Radiation Chemistry Research Establishment). Nov 1969. 26p. NTIS (U. S. Sales Only).

The decomposition of nitrous oxide induced by ^{60}Co γ rays was examined. The dependences of the decomposition on irradiation temperature and pressure are: $G(N_2) = 10.1$ at 25°C and 1 atm, $G(N_2) = 12.6$ at 150°C, $G(N_2) = 10.7$ at 25°C and 0.2 atm, and $G(N_2) = 9.0$ at 2.4 atm. When glass wool, with a surface area of nearly 10 m^2, is in contact with the gas, $G(N_2)$ becomes about 14. The decomposition mixture of gases, such as N_2O-NH_3, $N_2O-C_2H_4$, and $N_2O-C_2H_6$ induced by ^{60}Co γ rays and reactor radiation was examined. It is found that different radiation has different effect on the mixture gases. (auth) (Japan)

41852 (LA–4657) RADIOLYSIS OF MIXTURES OF CARBON DIOXIDE AND HYDROGEN. Beattie, W. H. (Los Alamos Scientific Lab., N. Mex.). Oct 1969. Contract W-7405-eng-36. 14p. Dep. NTIS.

The self radiolysis of mixtures of carbon dioxide (CO_2) and tritium ($^3H_2$) was studied at pressures of 0.1 to 1.0 atmospheres, temperatures of –80 to +100°C, and in the presence of added H_2O, He, or Ar. The products of decomposition are CO, C^3H_4, $C_2{}^3H_4$, ^3H_2O, and a white polymer. The initial rates and G values were measured and the rates were compared with the rates of ion pair formation. A mechanism of decomposition of CO_2 and formation of products is presented. The initial rates are consistent with a mechanism involving ionization of CO_2 followed by dissociative recombination forming CO and O. Back reactions forming CO_2 by recombination of products and by ion transfer are shown to exist. The computed net decomposition of CO_2 is in general agreement with the measured disappearance of CO_2. (auth)

41853 (NP–18817) RADIOLYSIS OF PETROLEUM PRODUCTS: RESIDUE AFTER DISTILLATION. Peralta, Jose Antonio (Universidad Nacional Autonoma de Mexico, Mexico City. Facultad de Ciencias). 1971. 51p. (In Spanish). Dep. NTIS (U. S. Sales Only).

Thesis.

The radiolysis of heavy residues in order to obtain light hydrocarbons was investigated using the residue after distillation and electron irradiation from a Van de Graaff accelerator. Experimental conditions and chromatographic analysis of the radiolysis products are described in detail. The results show that, although some light previously unknown hydrocarbons are obtained in the radiolysis, the yield is not great enough under the conditions used to warrant industrial application. (J.S.R.)

41854 ELECTRON SPIN RESONANCE OF γ-IRRADIATED TRIGLYCINE SELENATE. Suzuki, Ikuo; Abe, Ryuji (Nagoya Univ., Japan). J. Phys. Soc. Jap.; 31: No. 1, 179-83 (Jul 1971).

The ESR spectra of γ-irradiated TGSe single crystals were studied. The dominant stable damage center was identified as SeO_3^-. The additional splitting and the change of intensity of the spectrum were observed below the Curie point. The infrared spectra showed that the absorption intensity of SeO_4^{2-} band was changed by γ-irradiation. (auth)

41855 SUPRAMOLECULAR BONDING ORBITALS FROM MOLECULAR ANTIBONDING ORBITALS. STRUCTURE OF THE RADICAL ANION OF SULFURYL CHLORIDE. Kerr, Carolyn M. L.; Williams, Ffrancon (Univ. of Tennessee, Knoxville). Contract AT(40-1)-2968. J. Amer. Chem. Soc.; 93: No. 11, 2805-7 (2 Jun 1971). (ORO–2968-60).

The ESR spectrum of γ-irradiated polycrystalline sulfuryl chloride at 77°K is given and interpreted to give a supramolecular bonding orbital representation. The unpaired electron resides in a supramolecular bonding orbital derived from a combination of the lowest unoccupied antibonding orbitals of individual sulfur dioxide and chlorine molecules. (D.P.O.)

41856 ELECTRON SPIN RESONANCE STUDIES OF THE RADIOLYSIS OF ALIPHATIC AMINES ADSORBED ON SILICA GEL. Wardman, P.; Smith, D. R. (Atomic Energy of Canada Ltd., Chalk River, Ont.). Can. J. Chem.; 49: 1880-7 (1 Jun 1971). (AECL–3871).

Several aliphatic amines were adsorbed in sub-monolayer amounts on silica gel and γ-irradiated at 77°K. The electron spin resonance (ESR) spectra of the radicals trapped on the surface at 77°K were similar, in most cases, to the spectra obtained after irradiating the corresponding polycrystalline solid amine at 77°K. Methyl-, ethyl-, n-propyl, and n-butylamines all gave $\dot{R}NH$ radicals, and dimethylamine gave $(CH_3)_2\dot{N}$ radicals. The radical cation ($(CH_3)_3\dot{N}$) was observed in the case of trimethylamine. Adsorbed methoxy-amine and t-butyl amine were also studied and the cation-radical of the latter tentatively identified. The results are discussed in terms of reaction of the adsorbed amine with a surface active site. (auth) (Canada)

41857 ELECTRON SPIN RESONANCE STUDIES OF THE RADIOLYSIS OF ALIPHATIC AMINES AT 77°K. Wardman, P.; Smith, D. R. (Atomic Energy of Canada Ltd., Chalk River, Ont.). Can. J. Chem.; 49: 1869-79 (1 Jun 1971). (AECL–3872).

Several frozen aliphatic amines were γ-irradiated at 77°K and the electron spin resonance (ESR) spectra of the trapped radicals obtained at 77°K and on warming. Radiolysis of methyl, ethyl and isopropyl amines produces predominantly alkylamino ($\dot{R}NH$) radicals. The proton hyperfine (h.f.) couplings of $\dot{R}NH$ radicals are 10 to 30% larger than those in the corresponding isoelectronic alkyl radicals and the parallel component of the ^{14}N coupling is about 35 G. Restricted rotation of alkyl groups occurs at 77°K in some cases. On warming from 77°K, the $\dot{R}NH$ radicals generally abstract from the solvent or isomerize to produce radicals of the aminoalkyl type (e.g. $R\dot{C}HNH_2$). The alkyl proton h.f. splittings of these latter radicals are 20 to 40% lower than in the corresponding alkyl radicals, and the observed ^{14}N coupling was $A_{^{14}N||} = 12 \pm 3$ G in $\dot{C}H_2NR_2$ and $A_{^{14}N,iso} \simeq 4$ G in $(CH_3)_2\dot{C}NH_2$ and $CH_3\dot{C}HNH_2$. The amino proton couplings in the aminoalkyl radicals were not resolved. Irradiated dimethylamine produces both $(CH_3)_2\dot{N}$ and $\dot{C}H_2N(CH_3)$ radicals, but $(CH_3)_2\dot{N}$ disappears on warming. Only $\dot{C}H_2N(CH_3)_2$ was observed after irradiation of $(CH_3)_3N$ at 77°K. Solid methoxyamine (giving CH_3ONH) and tert-butylamine were also studied. (auth) (Canada)

41858 RADIATION CHEMICAL STUDIES OF WATER AND AQUEOUS SOLUTIONS OF AROMATIC COMPOUNDS. Christensen, Hilbert. Stockholm; Kungliga Tekniska Hogskolan (1971). 15p.

Thesis.

Radiation chemical studies published in ten earlier papers are summarized. Aqueous solutions of aromatic compounds were irradiated with ^{60}Co gamma rays and with pulsed electrons from a 11–MeV, 250-mA peak current accelerator. The effects of oxygen, Fe(II), and Fe(III) ions on the yields of phenol from irradiated aqueous benzene solutions and the effect of increased temperature, 150° to 200°C, were investigated. Cresol isomers and dimers were found in irradiated aqueous toluene solutions, and the effects of air and Fe(III) ions on the yields were observed. By means of pulse radiolysis, the absorption of the OH radical at 300 nm and the absorption spectrum of hydrogen atoms in aqueous solution were determined. Aqueous aniline solutions were examined after gamma radiolysis and during pulse radiolysis. (Sweden)

41859 EVALUATION OF THE CONTRIBUTION OF EXCITATION TO THE FORMATION OF FREE RADICALS IN THE RADIOLYSIS OF ALKANES. Bichiashvili, A. D. (Inst. of Inorganic and Electrical Chemistry, Tbilisi, USSR). Soobshch. Akad. Nauk Gruz. SSR; 62: No. 1, 73-6 (Apr 1971). (In Russian).

The dependence of the yields of free radicals formed at 77°K via the electronic excitation state of the molecules is discussed for n-alkanethiols, n-alkylbenzenes, and n-alkyl disulfides. Transfer of the excitation energy takes place only on the 4σ-bonds. The yield of radicals formed via excitation in the alkanes was estimated to be 1.2 to 1.45 per 100 eV. (auth)

41860 RADIOLYSIS OF HYDROGEN SULFIDE AT VERY HIGH DOSE RATES. THE EFFECT OF SF_6. Willis, C.; Boyd, A. W.; Miller, O. A. (Atomic Energy of Canada Ltd., Chalk River, Ont.). Can. J. Chem.; 49: 1677-81 (15 May 1971). (AECL–3848).

Gaseous H_2S was irradiated with electron pulses from a Febetron 705 at a dose rate of $\sim 2 \times 10^{27}$ eV $g^{-1}s^{-1}$. For single pulse experiments, the yield of hydrogen is $G(H_2) = 12.0 \pm 0.5$, independent of pressure from at least 350 to 1600 Torr. Addition of SF_6 reduces the yield to $G(H_2) = 7.9 \pm 0.3$, which is fairly close to that observed for pure H_2S at low dose rates. The reduction, $\Delta G(H_2) = 4.1 \pm 0.3$, agrees very well with the ion pair yield based on a W value of 25.3 eV. In multi-pulse irradiations, for pure H_2S, the yield falls off with dose giving a limiting yield close to $G(H_2) = 8.0$. No similar fall-off is observed for H_2S-SF_6 mixtures. It is proposed that at high absorbed doses and at low dose rates, there is no contribution to the hydrogen yield from neutralization processes; and that this is due to neutralization of H_3S^+ by an ion of the type S_n^- rather than a free electron. (auth) (Canada)

41861 RADIOLYSIS OF FATS. Kopecky, A. Prum. Potravin; 21: No. 5, 150-3 (May 1970). (In Czech).

Prevailing opinions on the mechanism of fat radiolysis are reviewed. Principal forms of the radical splitting of saturated and nonsaturated fatty acids and subsequent reactions of free radicals both in the presence and in the absence of oxygen are discussed.

XUM

Irradiation of fats reduces their stability and also affects their chemical and physical properties. (INIS)

41862 PULSE RADIOLYSIS: AN OXIDATIVE–REDUCTIVE PROBE IN GENERAL BIOCHEMICAL AND ENZYME STUDIES. Adams, G. E.; Cundall, R. B.; Willson, R. L. (Mount Vernon Hospital, Northwood, Eng. Univ. of Nottingham, Eng.). Biochem. Soc. Symp.; 31: 171-82(1970).

The application of pulse radiolysis to the study of functional groups in enzymes is described. Although the free radicals produced in an irradiated system are formed and react simultaneously, they can be studied in isolation by carrying out the experiments in the presence of suitable concentrations of selective radical scavengers. The use of a system with one reactive species to study reductive attacks at the disulfide bond by e^-_{aq} and CO_2^- and oxidative free radical attack of specific amino acids by the hydroxyl radical and the thiocyanate radical ion are discussed. (D.P.O.)

41863 SOLVATED ELECTRON YIELD IN THE RADIOLYSIS OF FORMAMIDE. Head, David Alan. Vancouver, British Columbia; Univ. of British Columbia (1970). National Library of Canada, Ottawa.

Thesis.

The e^-_{solv} yield in formamide was found to be only slightly greater than its yield in water. A modified correlation that, in addition to the dielectric constant, included the solvating ability and the stopping power of the solvent was shown to give a better fit for the data for a number of liquids (resolving, for instance, the ammonia anomaly), indicating that these factors also govern the yield of e^-_{solv}. The yields of hydrogen, carbon monoxide, and nitrogen formed when formamide and its nitrous oxide solutions were irradiated with ^{60}Co γ rays gave information concerning the e^-_{solv} yield. Using the electron scavenger N_2O and the scavenger pairs N_2O/Cd^{2+}, N_2O/Ag^+, and N_2O/acid, the number of e^-_{solv} formed per 100 eV of energy absorbed was found to be 2.9 ± 0.1. This yield corresponds fairly closely with the value that can be calculated using Freeman's nonhomogeneous model. The primary yields of H_2, $HCONH_2^*$, CO, and HCO were evaluated as 0.75 ± 0.05, 0.4 ± 0.1, ≤0.55 ± 0.07, and ≥1.15 ± 0.20 molecules/100 eV respectively. At low doses (up to ~5 × 10^{19} eV/ml) the yields of H_2, N_2, and CO were dose independent for the dose rate of ~4 × 10^{17} eV/ml-minute used. In two types of pulse radiolysis experiments light absorption was not observed in the 4500 to 8500 Å wavelength region contrary to expectations. A comparison of these results with those from other work may be interpreted as suggesting that the half-life of formation of e^-_{solv} in formamide is between 0.36 and 1.9 microseconds. This tentative conclusion, if correct, would mean that e^-_{solv} was a secondary, not a primary, product in formamide and this would be of general significance to the primary processes of radiation chemistry. (Diss. Abstr. Int., B)

41864 EFFECT OF PHASE ON EXCITATION TRANSFER IN THE RADIOLYSIS OF ISOBUTANE. Miyazaki, Tetsuo; Yamada, Takahisa; Wakayama, Terunobu; Fueki, Kenji; Kuri, Zen-ichiro (Nagoya Univ., Japan). Bull. Chem. Soc. Jap.; 44: No. 4, 934-7(Apr 1971).

The effects of CCl_4 on the formation of H_2 and C_4H_8 radicals in the radiolysis of i-C_4H_{10} were studied in glass at 77°K and the liquid at 195°K. The yield of H_2, which is not affected by the addition of N_2O or SF_6, decreases sharply on the addition of CCl_4 in the glass, as in the crystal. It does not decrease so sharply in the liquid as in the solid. The effects of CCl_4 on the yields of H_2 correspond fairly well to the yields of the C_4H_8 radicals. The effects of CCl_4 in the glass are explained by the excitation transfer from the excited butane molecule to CCl_4, as in the radiolysis of crystalline i-C_4H_{10}. A kinetic treatment suggests that its mechanism may be the exciton transfer. Some remarks on the primary process of ionization in the radiolysis of solid hydrocarbons are given from the viewpoint of exciton transfer. (auth)

41865 ROLE OF REACTION SITES IN THE RADIOLYSIS OF SOLID SUCCINIC ACID. Miyazaki, Tetsuo; Fujitani, Yoshiteru; Wakayama, Terunobu; Fueki, Kenji; Kuri, Zen-ichiro (Nagoya Univ., Japan). Bull. Chem. Soc. Jap.; 44: No. 4, 984-8 (Apr 1971).

The main gaseous products in the radiolysis of solid succinic acid are CO_2, CO, and H_2. The G(CO + H_2) from the powder is much higher than that from the single crystal, while there is no difference in G(CO_2) between the powder and the single crystal, indicating that CO_2 is produced homogeneously in the solid. The difference in G(CO + H_2) between the powder and the single crystal cannot be attributed to the analytical procedure, the secondary reaction of CO, or the presence of H_2O as an impurity. It may be due to the difference in the primary process of the radiolysis. It is conceivable that the mobile active entity formed by the γ irradiation of the crystal migrates to the special reaction sites and produces CO and H_2. The difference in G(CO + H_2) may also be due to the different number of sites between the powder and the single crystal. (auth)

41866 FORMATION OF HYPOPHOSPHATE IN THE RADIOLYSIS OF PHOSPHITE SOLUTION. Matsuura, Niro (Tokyo Univ.); Yoshimura, Masahito; Takizawa, Masao; Sakaki, Yukio. Bull. Chem. Soc. Jap.; 44: No. 4, 1027-30(Apr 1971).

The formation of hypophosphate and phosphate in the radiolysis of a phosphite solution was established by the anion-exchange chromatographic technique. The quantitative determination of their yields was made by colorimetry of the phosphate and hypophosphate with the Mo(V) + Mo(VI) reagent. The G values in an aerated condition are 0.01 molecule/100 eV in acid and 0.1 molecule/100 eV in neutral pH with respect to the hypophosphate formation, independent of the phosphite concentration. In a deaerated system much higher values are obtained, amounting to around 0.5 molecule/100 eV at a phosphite concentration of 10^{-3} M. The G values of hypophosphate plus phosphate are around 3.0; this is in agreement with the half-value of the primary radical yields, $\frac{1}{2} \cdot (g_{red} + g_{OH})$, reported in the data derived from the radiation-chemical studies in the aqueous system. The hypothesis that the hypophosphate (IV) ion radical is a transient species in the oxidation of phosphite to phosphate is supported by these results. (auth)

41867 EXCITED STATE AND CYCLOBUTADIENE INTERMEDIATES IN THE RADIATION CHEMISTRY OF ALKYNES. γ RADIOLYSIS OF 2-BUTYNE. Whitten, David G.; Berngruber, Walter (Univ. of North Carolina, Chapel Hill). J. Amer. Chem. Soc.; 93: No. 13, 3204-8(30 Jun 1971).

Gamma radiolysis of liquid 2-butyne gives rise to 3-methyl-2-hepten-5-yne, 2,6-octadiyne, cis- and trans-2-butene, hexamethylbenzene, and syn-octamethyltricyclo[4.2.0.$0^{2,5}$]octadiene as major products. These products account for approximately 72% of the reacted alkyne. The first four products arise from radicals; scavenging experiments suggest that either ions or excited states (or both) could be immediate precursors to the "radical products." These four products are formed also in the photolysis of 2-butyne with a low-pressure mercury lamp. The latter two products of radiolysis, hexamethylbenzene and the tricyclooctadiene, appear to arise from a cyclobutadiene precursor. Formation of the cyclobutadiene precursor can be suppressed by scavengers only at very high scavenger concentration. (auth)

41868 RADIOLYTIC DECOMPOSITION OF SOLID OXALIC ACID. Gal, O.; Baugh, P. J.; Phillips, G. O. (Univ. of Salford, Eng.). Int. J. Appl. Radiat. Isotop.; 22: No. 6, 321-4(Jun 1971).

It was shown that there is no significant difference in the γ radiolytic decomposition of the following forms of oxalic acid: dihydrate, anhydrous, and freeze-dried. A definite difference in the resistance to mixed pile radiation between the dihydrate and anhydrous form of oxalic acid was, however, noted. (auth) (UK)

41869 PULSE RADIOLYSIS OF AMMONIA GAS. II. RATE OF DISAPPEARANCE OF THE $NH_2(X^2B_1)$ RADICAL. Gordon, Sheffield; Mulac, W.; Nangia, P. (Argonne National Lab., Ill.). J. Phys. Chem. 75: No. 14, 2087-93(8 Jul 1971).

The free-radical species NH_2 and NH were produced by irradiating NH_3 vapor at pressures ranging from 250 to 1520 torr with pulses of 2-MV electrons. The rate of disappearance of these radicals was followed by measuring the decrease in absorption at 597.6 (NH_2) and 336.0 nm (NH). Rate constants for the following reactions were determined: in the pressure range 250 to 1520 torr NH_3, $k_{NH_2+NH_2} = 6.2 \times 10^{10}$ M^{-1} sec^{-1}; between 250 and 1000 torr NH_3, $k_{NH_2+H_2M} = 2.2 \times 10^{12}$ M^{-2} sec^{-1}, and appears to approach a second-order limit beyond this pressure; $k_{NH_2+NO} = 1.6 \times 10^{10}$ M^{-1} sec^{-1}; and $k_{NH+NO} = 2.3 \times 10^{10}$ M^{-1} sec^{-1}. (auth)

41870 RADIOLYSIS OF LIQUID 1,1,2-TRICHLOROTRIFLUOROETHANE. Kazanjian, A. R.; Horrell, D. R. (Dow Chemical Co., Golden, Colo.). Contract AT(29-1)-1106. J. Phys. Chem.; 75: No. 14, 2217-19(8 Jul 1971).

The relative proportions of carbon–carbon, carbon–fluorine, and carbon–chlorine bond scissions in γ radiolysis of 1,1,2-trichloro-1,2,2-trifluoroethane were studied. The material balance, C : F : Cl, obtained for the radiolytic products was 2 : 3 : 3.2. It was concluded that only C–Cl and C–C bonds were broken. (M.C.G.)

41871 GAS-PHASE ACIDITIES OF ALCOHOLS. McAdams, Mary Jane; Bone, Larry I. (East Texas State Univ., Commerce). J. Phys. Chem.; 75: No. 14, 2226-8(8 Jul 1971).

XUM

Equimolar mixtures of two alcohols were irradiated with 50-keV x rays and an electric field was applied. At a pressure from 50 to 100 torr these field strengths were insufficient to contribute substantially to the kinetic energy of the ions but were sufficient to collect 80 to 100% of the ions produced. From a series of 14 experiments with methanol and ethanol, the equilibrium constant that can probably be best considered as the equilibrium for replacement of a methanol with an ethanol in the solvation sphere was found to be 4.3 ± 1.4. (M.C.G.)

41872 RADIOLYSIS OF 2,2'-AZO-BIS-ISOBUTYRONITRILE IN BENZENE SOLUTION. II. EFFECTS OF ADDITIVES. Hirano, Katsuhiko (Tokyo Metropolitan Univ.). J. Nucl. Sci. Technol. (Tokyo); 8: 226-9(Apr 1971).

The effect of additives on the radiolytic yield of nitrogen from the radiolysis of 2,2'-azobis(isobutyronitrile) (AIBN) in benzene solution was examined. These additives quench excited benzene very effectively. Diacetyl, naphthalene, 2,5-diphenyloxazole (PPO), and anthracene with excitation energies lower than that of AIBN in the lowest triplet state decrease the nitrogen yield. The rate constants of these compounds in quenching the excited benzene are equal for both singlet and triplet states. An anomalously high quenching rate constant was seen for anthracene, which could be attributed to the quenching of high-lying excited state benzene. Certain ketones with excitation energies higher than that of AIBN in the lowest triplet state also decrease the nitrogen yield with the exception of benzophenone, these compounds all provide about the same degree of reduction in nitrogen yield in the range of concentration studied. The rate constants of self-quenching and the average life of acetone and acetophenone were determined from kinetic studies, and the results agree with that by other investigators. The effect of several charge scavengers on the nitrogen yield is also reported. (auth)

41873 STUDIES ON THE MANUFACTURE OF LOW DP PULPS BY IRRADIATION. I. IRRADIATION OF DISSOLVING PULPS BY GAMMA RAYS AND ELECTRON BEAMS. Imamura, Rikizo (Kyoto Univ.); Ueno, Takeo. Kami Pa Gikyoshi; 25: No. 3, 121-7(Mar 1971). (In Japanese).

Studies were made to determine whether there are any differences between γ rays and electron beams for the radiation effect on cellulose. As to the depolymerization and the formation of oxidized groups (carbonyl, and carboxyl groups), for irradiation of same dosage (absorbed dose), no difference between two radiations was observed. From the consideration of the action of radiation on cellulose, that is, reaction processes consisting of the excitation of molecules, the formation of free radicals in them, and the reaction of free radicals with other reactants, it was concluded that there is no difference between the effect by two radiations. (auth) (Japan)

41874 GAMMA IRRADIATION OF THYMINE IN DEAERATED AQUEOUS SOLUTION: CIS AND TRANS 6-HYDROXY-5,6-DIHYDROTHYMINE. Cadet, J.; Teoule, R. (CEN, Grenoble, France). Int. J. Appl. Radiat. Isotop.; 22: No. 5, 273-80(May 1971). (In French).

Both isomers of the 6-hydroxy-5,6-dihydrothymine were obtained from ^{60}Co gamma irradiation of thymine in deaerated aqueous solution (2×10^{-3} M). Their chemical and chromatographic behaviours, IR and NMR spectra, and their synthesis are described. The quantities of these thymine hydrates and other radiolysis products were measured from 9000 rads to 10^6 rads. In deaerated conditions G formation of hydrogenated compounds, especially 5,6-dihydrothymine, was important. Thymine hydrates may play a part in thermoradiorestauration of living cells. (auth) (UK)

41875 SOLID PHASE PHOTOLYSIS AND RADIOLYSIS OF ETHYLENE AT 20 TO 77 K. Gorden, R. Jr.; Ausloos, P. (National Bureau of Standards, Washington, D. C.). J. Res. Nat. Bur. Stand.; 75A: No. 3, 141-6(May-Jun 1971).

Films of ethylene condensed on a cold finger maintained at 20°K were irradiated with photons whose energy ranged from 8.4 to 21.2 eV. At the higher photon energies the relative yields of products compare well with those seen in the radiolysis of solid ethylene. Experiments on CH_2CD_2 demonstrate that in the photolysis hydrogen is mainly formed by the elimination processes $CH_2CD_2^* \rightarrow H_2(D_2) + C_2D_2(C_2H_2)$ and $CH_2CD_2^* \rightarrow HD + C_2HD$. The relative probabilities of these three processes are independent of the energy of the incident photons from 8.4 to 11.6 eV and are within experimental error identical to those observed in earlier gas phase photolysis experiments. Relative to acetylene, cyclobutane is a minor product at 8.4 eV but increases by an order of magnitude at higher energies where ions play a role. Cyclobutane, 1-butene, and methylcyclopropane formed on irradiation of frozen $C_2H_4-C_2D_4$ mixtures consisted mainly of C_4D_8, $C_4D_6H_4$, and C_4H_8. Plausible mechanisms that may account for the formation of the latter products are examined. In the solid phase as in the gas phase the relative importance of H-atom production increased with increasing photon energy. Cyclopropane, apparently formed by insertion of CH_2 into C_2H_4, is a product at all wavelengths in the photolysis and in the radiolysis. (auth)

Radioisotope Production

41876 (CONF-680986-2) PREPARATION AND SEPARATION OF CARRIER-FREE ^{131}Cs FROM IRRADIATED $BaCO_3$. Wassilopulos, Miltiades (Kernforschungszentrum, Karlsruhe (West Germany). Institut fuer Radiochemie). [nd]. 7p. (In German). Dep. NTIS (U. S. Sales Only).

From Meeting on preparative radiochemistry production of radionuclides and labelled compounds; Lindau Im Bodensee, Germany (5 Sep 1968).

Cesium-131 was prepared from reactor-irradiated $BaCO_3$ by the reaction $^{130}Ba(n,\gamma)^{131}Ba \xrightarrow{12d} {}^{131}Cs \xrightarrow{9.7d} {}^{131}Xe$ (stable) and chemically isolated from the target. Dipicrylamine in nitrobenzene was used as the extraction agent. Parameters affecting the extraction of chemically and radiologically pure ^{131}Cs were studied. (J.S.R.)

41877 (JAERI-13545) IMPURITIES IN RADIOISOTOPES PRODUCED BY (n,γ) REACTION. Purities of ^{153}Sm and ^{90}Y. Kubota, Masumitsu; Amano, Hiroshi; (and others) (Japan Atomic Energy Research Inst., Tokai. Tokai Research Establishment). May 1969. 12p. NTIS (U.S. Sales Only).

Impurities in samarium and yttrium oxides were determined in order to estimate the radiochemical purity of ^{153}Sm and ^{90}Y radioisotopes produced by neutron irradiation of these materials. An impurity of 85 ppM Eu was found in the samarium oxide, and 30 ppM Dy and 24 ppM Tb in the yttrium oxide by radioactivation analysis. From these results the radiochemical purity at the time immediately after irradiation for 15 hours in a neutron flux of 1×10^{11} n/cm^2/sec is calculated to be 99.7% for ^{153}Sm and 94% for ^{90}Y because of the formation of ^{152}Eu in samarium and of ^{165}Dy in yttrium, respectively. After 24 hours, however, the radiochemical purity will become higher than 99.9% by disintegration of the short-lived impurities, and the specific activity is estimated to be 38 mCi/g Sm and 2.1 mCi/g Y. (auth) (Japan)

41878 (JAERI-13579) DETERMINATION OF RADIOACTIVE IMPURITIES IN THE ^{45}Ca SAMPLE PRODUCED BY THE (n,γ) REACTION. Takahashi, Satoko; Amano, Hiroshi (Japan Atomic Energy Research Inst., Tokai). Jun 1969. 19p. NTIS (U.S. Sales Only).

For the production of ^{45}Ca by the (n,γ) reaction, calcium carbonate was selected as the target material. The targets were tested from two origins and analyzed by the radioactivation method. Their radioactive impurities were estimated by comparison of the γ spectrum from sources irradiated in the vertical hole of JRR-2 for 130 hr. × 5 cycles. The average thermal neutron flux was 7×10^{13} n/cm^2·s. The results were the amounts obtained for 7 days after irradiation. To keep the radiochemical purity of the product higher than 99.9%, the sample should be cooled for more than 24 days after irradiation. The specific activity of the product was estimated 32.6 mCi/g Ca at this time. (auth) (Euratom)

41879 (JAERI-13726) INORGANIC ION EXCHANGER. A Literature Search. Tachimori, Shoichi; Amano, Hiroshi (Japan Atomic Energy Research Inst., Tokai). Sep 1969. 36p. NTIS (U. S. Sales Only).

Information on inorganic ion exchangers found in the literature till now is summarized in order to apply it to the field of the radioisotope production. Individual reports are mainly collected from "Journal of Inorganic and Nuclear Chemistry", and "Inorganic Ion Exchangers" by C. B. Amphlett is used as a reference book with a view to systematize the collected informations. (auth) (Japan)

41880 LARGE SCALE PRODUCTION OF CARRIER-FREE ^{131}I BY AN ADSORPTION METHOD USING Mg_3TeO_6 AS TARGET MATERIAL. Toth, G. (Isotope Inst., Budapest). Radiochem. Radioanal. Lett.; 7: No. 1, 57-60(15 Jun 1971).

Mg_3TeO_6 was applied as target material for producing carrier-free ^{131}I, utilizing the adsorption of iodine on platinum black. The thermal and radiation stability of Mg_3TeO_6 permits irradiation even in high-flux reactors. The large specific surface area of platinum black permits the separation of ^{131}I in multicurie amounts. (auth)

41881 PRODUCTION OF IRON-FREE AND CARRIER-FREE ^{67}Ga. Neirinckx, R. D.; van der Merwe, M. J. (CSIR, Pretoria). Radiochem. Radioanal. Lett.; 7: No. 1, 31-5(15 Jun 1971).

A cation exchange procedure for the preparation of iron-free

and carrier-free ^{67}Ga is described. It is based on the reduction of Fe(III) with iodide ions and the subsequent elution of Zn(II) and Fe(II) by means of hydrochloric acid from a cation exchange column. ^{67}Ga is desorbed by 3.5N HCl. The procedure is used for the production of ^{67}Ga for medical purposes. (auth)

41882 CONTINUOUS ISOLATION OF ISOTOPICALLY PURE ^{249}Cf FROM ^{248}Bk. Myasoedov, B. F.; Barsukova, K. V. (Inst. of Geochemistry and Analytical Chemistry, Moscow). Radiochem. Radioanal. Lett.; 6: No. 5, 275-9(19 May 1971).

A simple method is described for the continuous isolation of isotopically pure ^{249}Cf from ^{249}Bk. On a column, filled with a mixture of zirconium phosphate silicate sorbent and lead(IV) oxide, a nitric acid solution of berkelium is oxidized to Bk(IV), and sorbed on the zirconium phosphate silicate sorbent. The Cf(III) accumulated in ^{249}Bk is periodically eluted from the column with 1M HNO_3. (auth)

41883 RAPID RADIOCHEMICAL PURIFICATION AND CONTINUOUS MILKING OF ^{144}Pr FROM ^{144}Ce USING A MnO_2 COLUMN. Shukla, J. P.; Chandrasekharan, E. S.; Rengan, K. (Bhabha Atomic Research Centre, Bombay). Radiochem. Radioanal. Lett.; 6: No. 5, 307-11(19 May 1971).

A rapid single-step procedure for carrier-free separation and continuous milking of ^{144}Pr from ^{144}Ce employing a MnO_2 column is described. Radiochemical purity of the product was checked both by half-life determination and spectrometry. Decontamination factors for praseodymium from cerium were found to be of the order of 10^5. (auth)

Recoil Production and Reactions

Refer also to abstracts 41763 and 41920.

41884 INORGANIC YIELDS OF ^{38}Cl IN SZILARD–CHALMERS REACTIONS OF α-, β-, γ-, AND δ-BENZENE HEXACHLORIDES. Shimojima, Hikaru, Kawasaki, Japan) Nuclear Research Lab., Lin, Tsing-ko. J. Nucl. Sci. Technol. (Tokyo); 8: No. 4, 179-83 (Apr 1971).

The four isomers α-, β-, γ- and δ-benzene hexachloride (1,2,3, 4,5,6-hexachlorocyclohexane) were used as target materials to study the effect of structure isomerism in the Szilard-Chalmers reaction. They were irradiated in the solid state and also in benzene solution and frozen states, after which the recoil ^{38}Cl retained therein was stripped into 0.1 M K_2SO_3 solution. In the case of solid state, the radioactivity yields of the isomers decreased rapidly in the early stage of irradiation and a corresponding diminution was also seen in the difference in yield between the four isomers. The greatest yield was registered by the δ-isomer, followed by α-, γ- and β-forms in that order, but the difference dwindled down with progress of irradiation until it became insignificant. When the four isomers were irradiated in benzene solution, nearly the same yield was obtained for all four isomers, and the yield did not appear to vary significantly with progress of irradiation. This value was higher than either the solid or frozen states. In the case of frozen state, the yield characteristics were intermediate between solid and liquid targets, both in absolute value and in the difference according to structure. (auth)

41885 DIFFUSION EFFECTS DURING DETERMINATION OF RANGES OF RECOIL ATOMS IN GASES. Boos, A. H.; Herrmann, G. (Univ., Mainz). Radiochim. Acta; 15: 54-6(Jan 1971). (In German).

A thin layer of ^{235}U on beryllium bronze was irradiated for 3 to 5 hours at 8×10^{10} neutron flux. Fission products traversed a 30 mm long aluminum collimator and entered a condenser with 2 aluminum foils. Hydrogen served as breaking gas. Following irradiation, the aluminum foils were cut into strips and these were analyzed for fission products. It was concluded that electrostatic collection is not generally applicable for the determination of ranges because of considerable diffusion of noble gases, especially krypton and xenon. (H.B.G.)

41886 FATE OF ^{13}N FORMED BY THE $^{12}C(d,n)^{13}N$ REACTION IN INORGANIC CARBIDES. Welch, Michael J.; Lifton, Judith F. (Washington Univ., St. Louis). J. Amer. Chem. Soc.; 93: No. 14, 3385-8(14 Jul 1971).

The behavior of nitrogen atoms in the inorganic matrices Al_4C_3, CaC_2, Li_2C_2, and Na_2C_2 was studied by inducing 10-min half-lived nitrogen-13 in the carbides by the $^{12}C(d,n)^{13}N$ nuclear reaction. On dissolution in acid solution the methanide (Al_4C_3) gave $^{13}NH_3$ and $CH_3{}^{13}NH_2$ as the major products while the acetylides gave $^{13}NH_3$, $C^{13}N^-$, and $CH_3C^{13}N$. The variation in product yield with varying cyclotron beam current, total irradiation dose, and postirradiation thermal annealing was studied. The products formed and their yields are correlated with the structures of the various carbides in the solid phase. (auth)

Radiochemistry

Refer also to abstract 41891.

Separation Processes

Refer also to abstracts 41715, 41738, 41740, 41742, 41743, 41757, 41762, 41829, 41882, 41883, 42037, 42384, and 44219.

41887 (ARH-SA-25) TREATMENT OF LIQUID WASTES BY EVAPORATION TO SALT CAKES. Kirkman, M. J.; Godfrey, W. L. (Atlantic Richfield Hanford Co., Richland, Wash.). 4 Aug 1969. Contract AT(45-1)-2130. 17p. (CONF-690819-3). Dep. NTIS.

From 66. national meeting of the American Institute of Chemical Engineers; Portland, Ore. (24 Aug 1969).

Methods for in-tank solidification by evaporating radioactive waste solutions to a minimum volume as salt cakes are outlined. Wastes are continuously concentrated and then cooled in a nearby underground tank where salt crystallized and deposited. The cooled, clarified supernatant was pumped from the crystallizer tank, mixed with fresh feed, and recycled back to the evaporator for further concentration. The process was continued until the crystallizer tank filled with salt cake. (M.C.G.)

41888 (ARH-SA-78) PLUTONIUM–URANIUM PARTITIONING BY A REFLUX EXTRACTION FLOWSHEET. Bruns, L. E. (Atlantic Richfield Hanford Co., Richland, Wash.). 18 Aug 1970. Contract AT(45-1)-2130. 17p. (CONF-710417-3). Dep. NTIS.

From International solvent extraction conference; The Hague, Netherlands (19 Apr 1971).

A solvent extraction flowsheet was devised for the separation and purification of plutonium from systems containing uranium. The flowsheet permits purification and concentration of plutonium in a single solvent extraction cycle. This concept was developed in the Plutonium Reclamation Facility. The development of the flowsheet and the parameters pertinent to process performance are described. After the plutonium–uranium scrap is dissolved or leached, the resulting solution is adjusted for salting strength and the plutonium is adjusted to the extractable (IV) and (VI) states. Uranium and plutonium are coextracted in a multistage extractor, using 20% TBP in CCl_4 as the solvent. In the same extractor, the loaded solvent is scrubbed for impurity removal. In a second multistage unit, plutonium is reduced to Pu(III) with hydroxylamine nitrate. The purified Pu(III) leaving the concentrated end of this second multistage unit is split into a product stream and a reflux stream, which flows to a hold-up tank where it is oxidized to the extractable Pu(IV) state by merely adding nitric acid. This Pu(IV) stream is reintroduced as a scrub stream in the first extractor. Plutonium(III) product is withdrawn from the system when a 30 to 60 g Pu/liter concentration is attained. Uranium is removed from the Pu(III) by a 20% TBP–CCl_4 scrub in the initial stages of this second extractor. The uranium quantitatively leaves the second extractor via the organic stream. The plutonium impurity (about 1%) in this uranium stream is removed by a hydrofluoric strip in a third extractor. Further conventional extractors remove the uranium and organic impurities from the organic stream. The flowsheet was tested to identify and correct process difficulties. (M.C.G.)

41889 (BNWL-1573) IMPROVED ZIRCONIUM DECONTAMINATION IN PUREX PROCESS. Swanson, J. L. (Battelle-Northwest, Richland, Wash. Pacific Northwest Lab.). May 1971. Contract AT(45-1)-1830. 22p. Dep. NTIS.

Studies showed that the improved zirconium decontamination observed in the Hanford Purex Plant when processing Zircaloy-clad fuel elements (which were declad in ammonium fluoride solutions–The Zirflex Process) was due to the presence of fluoride in the feed solutions. Related studies identified uranium carbide as a source of material that forms highly extractable zirconium complexes that limit the attainable decontamination. The effects of complexants other than fluoride were also evaluated. (auth)

41890 (CEA-N-1450) INVESTIGATION OF SOME NONLINEAR EFFECTS IN EXTRACTION EQUIPMENT USING COMPUTER SIMULATION. Rouyer, Hubert; Demarthe, Jean-Michel (Commissariat a l'Energie Atomique, Fontenay-aux-Roses (France). Centre d'Etudes Nucleaires). Jun 1971. 21p. (In French). Dep. NTIS (U. S. Sales Only).

Automatic control of liquid–liquid extraction units requires precise knowledge of the dynamic behavior of the installations. Results from experiments and computer simulation of mixer–settler behavior are reported. The example of the uranium extraction from nitric acid medium using TBP was considered. The importance of the settlers is discussed and the physicochemical parameters underlined. A model describing the hydrodynamic phenomena occurring in transient operation is developed for the settler. This model changes with the nature of the perturbation involved. The results and the conclusions of the work

XUM

demonstrate that differences observed between the behavior of industrial units and theoretical equilibrium operation can be explained in terms of the superposition of the effects of perturbations. (France)

41891 (DOCKET-50201-74) WEST VALLEY REPROCESSING PLANT. Proposed Change in Technical Specifications for Operating License CSF-1. (Nuclear Fuel Services, Inc., West Valley, N. Y.). 12 Jul 1971. 2p. Dep. NTIS.

Proposed technical specification changes for receipt and storage of $Pu(NO_3)_4$ and depleted $UO_2(NO_3)_2$ solutions at the plant are listed. (M.C.G.)

41892 (EUR-4353) STUDY OF THE "HEAD-END" PROBLEM IN NUCLEAR FUEL REPROCESSING. Final Report. (Societe Belge pour Nucleaire, Brussels). 1969. 284p. (In French). NTIS (U. S. Sales Only).

A wide range of reference works was compiled concerning nuclear fuels (especially fast reactor fuels) and their head-end reprocessing after irradiation. The head-end was studied from reception of the irradiated assemblies down to preparation of the charges for reprocessing, by way of storage, disassembling, and decanning, including the equipment. In the light of this study, exchanges of information, study trips, and full-scale trial tests on mockup fuel elements, a comprehensive synthesis was attempted. It was concluded that a certain number of studies still need to be done before final conclusions can be drawn. (Euratom)

41893 (IN-1474) THIRD PROCESSING CAMPAIGN IN THE WASTE CALCINING FACILITY. Bendixsen, C. L.; Lohse, G. E.; Hales, M. P. (Idaho Nuclear Corp., Idaho Falls). May 1971. Contract AT(10-1)-1230. 50p. Dep. NTIS.

The third processing campaign in the Waste Calcining Facility was devoted solely to processing radioactive, zirconium fluoride waste stored at the Idaho Chemical Processing Plant. During the campaign, extending from August 1968 to June 1969, 312,000 gallons of zirconium fluoride waste were calcined in an air-fluidized bed heated to 400°C by means of a liquid metal heat-transfer system. A minor amount, 17,000 gallons, of aluminum nitrate waste also was calcined. Decontamination of off-gas from the fluidized-bed was excellent; an overall operating on-stream time of 88.9% was achieved during the campaign. (auth)

41894 (INR-1297) OPTIMUM START-UP OF THE FUEL REPROCESSING INDUSTRY. Frankovski, V. (Institute of Nuclear Research, Warsaw (Poland)). 1971. 14p. (In Russian). Dep. NTIS (U. S. Sales Only).

The investment costs of a fuel reprocessing plant depend very strongly on its size. The choice of an optimum fuel reprocessing plant construction program becomes a nonlinear optimization problem. This was investigated using the dynamic programming method with special reference to the situation of smaller states. The results show that in this case substantial savings can be gained when there are some possibilities of cooperation with existing and not fully loaded large plants abroad. (auth)

41895 (INR-1309) LABORATORY MIXER-SETTLER EXTRACTOR LMOM2. Goffmann, Pshemyslav M.; Gavlovska, Vatslava; Pochinailo, Andzhei; Vonsovich, Stanislav; Charnodolya, Galina (Institute of Nuclear Research, Warsaw (Poland)). 1971. 26p. (In Russian). Dep. NTIS (U. S. Sales Only).

Construction, hydrodynamic characteristics, and principle of operation of a small mixer-settler laboratory extractor are described. Extraction of $UO_2(NO_3)_2$ from 0.5M nitric acid into the 30% TBP-mepasine organic phase shows an example of applications of this 16-stage extractor. The results of U extraction indicate that the extraction efficiency is independent of phase flow velocity in the range 0.7 to 11 ml/min. Efficiency of a single stage of the extractor is 89 to 95%. For the organic to water phase ratio 1.59 only 5 stages are needed to extract 99.6% of the U into the organic phase. The output of the laboratory mixer-settler is about 0.6 kg U/day. (auth)

41896 (NP-18878) REPROCESSING OF NUCLEAR FUEL. (Arbetsgrupp Inom Industri-, Jordbruks- Och Civildepartementen (Sweden)). Mar 1971. 69p. (In Swedish). Dep. NTIS (U. S. Sales Only).

The role of reprocessing spent fuel and ultimate disposal of radioactive waste in the fuel cycle for nuclear power stations is described. A picture is given of the situation in Europe, the United States, and Sweden as to plans and forecasts for the nuclear power expansion and the related reprocessing requirements. Where Sweden is concerned, the reprocessing problem is assessed mainly from three points of view: industry and energy policy, safety, and physical planning. It is estimated that a reprocessing plant based exclusively on the Swedish requirement may be economically justified around 1990 at a 900 tons/year capacity. Before this time it should be possible to satisfy the reprocessing requirements by the utilization of foreign installations, provided these are available for Swedish enterprises on nondiscriminatory conditions. The factors governing the siting of reprocessing plants are discussed as well as their application in Sweden. It is proposed that the possibility of joint siting of nuclear power stations and reprocessing plants is considered in the future planning. (auth) (Sweden)

41897 (ORNL-tr-2512) ISOTOPE EFFECT AND ISOTOPE SEPARATION. Kakihana, Hidetake. Translated for Oak Ridge National Lab., Tenn., from Nippon Kagaku Zasshi; 89: 743-5 (1968). 37p. Dep. NTIS.

An abstract of this paper, prepared from the original language, appeared as NSA 22: 51058.

41898 (TRG-Report-2135) TRAPPING OF METHYL IODIDE AT HIGH PRESSURE AND HIGH TEMPERATURE. Taylor, R.; Yuille, W. D. (United Kingdom Atomic Energy Authority, Sellafield (England). Reactor Group). 1971. 13p. (CONF-691104-6). Dep. NTIS (U. S. Sales Only).

From International congress on the diffusion of fission products; Saclay, France (4 Nov 1969).

The trapping of methyl iodide by impregnated charcoal in carbon dioxide-carbon monoxide-methane atmospheres was investigated at pressures in the range 15 lbf/in^2 to 400 lbf/in^2 and temperatures from 20 to 300°C. The relative humidity of the gas, at pressure and temperature, varied between <1 and 100%. The effectiveness of the material is described by a parameter obtained by dividing the product of the logarithm of the decontamination factor and the volume flow rate by the volume of the packed bed. This parameter is appropriate for operation for several hours up to ~230°C but above this temperature desorption becomes appreciable. At high pressures performance is sensitive to water content below 100°C. For coolant containing 700 v.p.m. water the boundary of the region in which the parameter exceeds 10 passes through 100 lbf/in^2 20°C and 400 lbf/in^2 104°C. Beyond this boundary the performance falls quite sharply. Within the region defined by these limits it is possible to design a trapping plant which is much smaller than would be required for equal performance at atmospheric pressure. (auth) (UK)

41899 DISTRIBUTION COEFFICIENTS AND CATION EXCHANGE BEHAVIOR OF ELEMENTS IN HYDROCHLORIC ACID-ACETONE. Strelow, F. W. E.; Victor, A. H.; van Zyl, C. R.; Eloff, Cynthia (National Chemical Research Lab., Pretoria). Anal. Chem.; 43: No. 7, 870-6(Jun 1971).

Cation exchange distribution coefficients with Bio-Rad AG 50W-X8, a sulfonated polystyrene cross-linked with divinylbenzene are presented for 54 cations in hydrochloric acid-acetone media, covering the acid concentration range 0.1 to 3.0M and the acetone concentration range 0 to 95%. The elements are arbitrarily arranged in tables according to their coefficients in aqueous hydrochloric acid. A number of the possibilities of this system for separations are pointed out and some aspects of the elution behavior of various elements are discussed. The versatility of hydrochloric acid-acetone mixtures as eluting agent for cation exchange separations is demonstrated by sequential elution of the mixtures Ti(III), In, Ga, Al, Yb; Cd, Zn, Fe(III), Cu(II), Co(II), Mn(II); and V(V), Fe(III), U(VI), Ti(IV), Ca, Ba. (auth)

41900 EXTRACTION OF METALS BY AMINES. II. EXTRACTION OF URANYL CHLORIDE BY TRI-n-OCTYLAMINE. Mrnka, Miroslav; Celeda, J. (Inst. of Chemical Tech., Prague). Jad. Energ.; 17: 81-7(1971). (In Czech).

The extraction of UO_2Cl_2 by trioctylamine was experimentally studied. Cryoscopic and viscometric measurements showed that uranium extraction increased with increasing concentration of hydrochloric acid in the aqueous phase and was accompanied by a marked decrease in the concentration of water in the organic phase. The law of simple additivity was found not to apply to the viscosity of the organic phase, and variations were also observed in the cryoscopic constant with changes in the UO_2Cl_2 content of the extract (the value of the constant did not exceed 5). Polymerization of the resulting complex in the organic phase was thus demonstrated. (auth)

41901 FRACTIONAL EXTRACTION OF ZIRCONIUM, NIOBIUM, AND NEPTUNIUM WITH TRI-n-BUTYL PHOSPHATE. Aratono, Yasuyuki; Ueno, Kaoru; Ishimori, Tomitaro (Japan Atomic Energy Research Inst., Tokai). J. Nucl. Sci. Technol. (Tokyo); 8: No. 5, 241-3(May 1971).

Radioactive Zr, Nb, and Np were separated from each other by a continuous fractional extraction method. The extraction of Zr and Nb was carried out with 1% TBP in chloroform from the 10 N hydrochloric acid solution of irradiated U. Under these conditions, Zr, Nb, and Np could be extracted continuously with the organic

solution, while U and fission products remained in the aqueous solution. Finally, Zr in the organic solution was back-extracted with concentrated hydrochloric acid containing 1 to 2 drops of hydrofluoric acid. The method is convenient for the separation of Zr, Nb, and Np from the fission products. The distribution ratios in the extraction system were also obtained for a number of radioactive nuclides. (auth)

41902 MULTISTAGE PROCESS FOR EXTRACTING U AND Pu WITH SOLVENT COMPRISING TRIBUTYLPHOSPHATE. Grieneisen, Andre (to Commissariat a l'Energie Atomique). U. S. Patent 3,523,765. 11 Aug 1970. Priority date 8 Mar 1966, France.

A process is described for the extraction of uranium and plutonium ions from an aqueous solution, derived from the reprocessing of irradiated nuclear fuels, and comprises successively a primary stage in which the ions are extracted into a first organic solvent containing tributyl phosphate, followed by washing the loaded solvent thus obtained with an aqueous washing solution. In a secondary stage the ions, which are carried over with the aqueous washing solution, are extracted into a second organic solvent stream prior to recycling. (Offic. Gaz.)

41903 METHOD FOR SEPARATING URANIUM, PROTACTINIUM, AND RARE EARTH FISSION PRODUCTS FROM SPENT MOLTEN FLUORIDE SALTS REACTOR FUELS. Shaffer, James H.; Moulton, David M.; Grimes, Warren R. (to United States Atomic Energy Commission). U. S. Patent 3,577,225. 4 May 1971. Filed 15 May 1969.

A method for reprocessing spent molten metallic fluoride salt mixtures suitable as molten salt breeder reactor fuels is described in which uranium and bred-in protactinium values as well as certain fission products of the lanthanide series are selectively and consecutively extracted from the salt phase into an immiscible molten bismuth solution by controlling the reduction potential between the metal and salt phases. Uranium values, which are extracted first, are oxidized and transferred from the bismuth solution into a barren salt mixture for ultimate recycle to the reactor prior to extracting the contaminants. The protactinium values are then extracted at a slightly higher reduction potential into the bismuth solution, oxidized, and transferred to a molten salt outside the reactor environment to await decay of the protactinium-233 to uranium-233. Finally, the lanthanide elements are extracted at a yet higher reduction potential into the bismuth solution, oxidized, and transferred to a separate salt mixture for their recovery or disposal. (Offic. Gaz.)

41904 PROCESS FOR THE PRODUCTION OF DEUTERIUM-ENRICHED WATER. Mandel, Heinrich (to Rheinisch-Westfalisches Elektrizitatswerk Aktiengesellschaft). British Patent 1,234,906. 9 Jun 1971. Priority date 12 Oct 1968, Germany.

A process for the production of D-enriched water comprises operating a number of cooling towers connected in series in such a manner that a bleed-off of cooling water circulating in one tower is added to the water circulating in the next tower in an amount to make up the bleed-off and evaporation losses to the next tower. Successive bleed-off passes water with a higher D content due to evaporation enrichment to each successive tower to the final tower where the enriched water is withdrawn. (B.L.M.)

41905 STATUS OF THE WASTE SOLIDIFICATION DEMONSTRATION PROGRAM. McElroy, Jack L.; Blasewitz, Albert G.; Schneider, Kenneth J. (Battelle-Northwest, Richland, Wash.). Nucl. Technol.; 12: No. 1, 69-82(Sep 1971).

Solidification of high-level radioactive waste by the pot, spray, and phosphate glass solidification processes was successfully demonstrated. More than 50 million curies of radionuclides were processed and collected in 6-, 8-, and 12-inch-diameter containers during thirty-three engineering-scale demonstration runs in the Waste Solidification Engineering Prototypes (WSEP). The maximum self-generating heat rate values in the solidified wastes for an 8-inch-diameter pot ranged from 205 W/liter for the spray solid to 85 W/liter for the pot calcine. Wastes equivalent to those from thermal power reactors with exposures as high as 45,000 MWd/tonne at 30 MW/tonne were demonstrated. The WSEP auxiliary equipment consisting of an evaporator, an acid fractionator, filters, and a caustic scrubber reduced radionuclides in the stack gas to well below government release limits. The final liquid effluent from WSEP contains radioruthenium that is 10^4 to 10^6 times allowable government release values. Strontium and other nonvolatile materials are present to a much smaller extent. Initial studies indicated that the effluent water and acid streams from the waste solidification processes are sufficiently low in volume and radioactivity that they can be reasonably recycled into the fuel reprocessing plant's operations. The pots of solidified wastes from the WSEP runs are undergoing testing to determine the effects of storage temperature (air or water), radiation, and feed type on the physical and chemical properties of the solidified wastes. (auth)

41906 HEAD-END SEPARATION OF TRISO-COATED FISSILE AND FERTILE PARTICLES FOR HIGH-TEMPERATURE GAS-COOLED REACTORS. Langer, S.; Baldwin, N. L.; Phillips, H. R. (Gulf General Atomic Co., San Diego, Calif.). Nucl. Technol.; 12: No. 1, 26-30(Sep 1971).

Recycle fuel for HTGRs uses TRISO-coated particles containing two fissile materials, ^{233}U and ^{235}U. The economics of the fuel cycle makes separation of these materials before reprocessing desirable. Laboratory scale head-end studies have demonstrated that the silicon carbide layer has adequate integrity after irradiation to permit separation of the two types of fissile material by size. (auth)

41907 HEAD-END SEPARATION OF BISO-COATED FISSILE AND FERTILE PARTICLES FOR HIGH-TEMPERATURE GAS-COOLED REACTORS. Langer, S.; Phillips, H. R.; Baldwin, N. L. (Gulf General Atomic Co., San Diego, Calif.). Nucl. Technol.; 12: No. 1, 31-5(Sep 1971).

An attractive recycle fuel for Advanced HTGRs uses bonded fuel beds containing BISO-coated fissile and fertile particles (i.e., those having buffer and isotropic pyrolytic carbon coatings surrounding the fuel kernel). Two types of fissile material are used, ^{233}U and ^{235}U. The economics of the fuel cycle makes separation of these materials prior to reprocessing desirable. Laboratory-scale studies have shown that a conceptual separation process, based on the stability of $(Th,U)O_2$ kernels in contrast to $(Th,U)C_2$, UC_2, or UO_2 kernels under oxidizing conditions, is feasible on unirradiated fuel. However, damage to the oxide microspheres during irradiation is sufficient to result in fragmentation of the kernels on removal of the pyrolytic carbon coating. Other head-end separation processes will be required in order to utilize bonded BISO-recycle fuel in advanced HTGRs. (auth)

41908 CONTINUOUS SEPARATION OF URANIUM AND PLUTONIUM WITH THE HELP OF COUNTERCURRENT ION MIGRATION. Bilal, B. A.; Metscher, K. (Hahn-Meitner Institut fuer Kernforschung, Berlin). Atomwirt., Atomtech.; 16: 79-80(Feb 1971). (In German).

To separate uranium from plutonium ions through high voltage ionophoresis, various complexing media were studied. Most suitable were: 0.1N HNO_3 + 0.1N HF + 0.2N NaF and 2N CH_3COOH + 0.05N HNO_3. Mixtures of uranium and plutonium were subjected to countercurrent electrolysis in which the fluid flowed from cathode to anode. The separated elements were withdrawn continuously. The separation procedure, yielding high purity, might be applied for the reprocessing of burned nuclear fuel. (H.B.G.)

41909 SEPARATION OF METAL IONS ON INORGANIC ION-EXCHANGE PAPERS. Qureshi, M.; Husain, W.; Khan, F. (Aligarh Muslim Univ., India). Experientia; 27: No. 5, 607-8 (15 May 1971).

The chromatographic separation of metal ions in nine solvent systems using paper impregnated with titanic tungstate or titanic molybdate is reported. (D.P.O.)

41910 ION EXCHANGE CHROMATOGRAPHY OF RARE EARTHS IN AQUEOUS ORGANIC MEDIA. VIII. THE DISTRIBUTION OF SOLVENTS IN THE ION EXCHANGER PHASE IN MIXED MEDIA SYSTEM. Alexa, J. (Inst. of Nuclear Research, Prague). Collect. Czech. Chem. Commun.; 36: No. 4, 1670-3 (Apr 1971).

The existence and probable composition of intra-solutions (solutions surrounding active groups of the resin) were studied in elution chromatography of water–organic systems. Studies were made of this in separation of europium from yttrium using α-hydroxyisobutyric acid in ethanol–water mixtures as eluting solution. (M.C.G.)

41911 PROCESS FOR DECONTAMINATING RADIOACTIVE EFFLUENTS. Auchapt, Jacqueline; Gaudier, Jean-Francois (to Commissariat a l'Energie Atomique). French Patent 2,031,844. 9 Nov 1970. Filed 10 Feb 1969. (In French).

A decontamination process for effluent of high or intermediate activity arising from irradiated fuel reprocessing is presented. A pH of about 12 is obtained by adding a suitable base to the effluent to be decontaminated, then an oxidizing reagent and a soluble manganese salt are successively added to the solution. The manganese dioxide precipitate obtained is separated from the solution. Some examples of the decontamination of effluents with various compositions are given. The decontamination factors for Sr, Ru, Zr, Nb, Ce, Cs and the corresponding α, β, and γ activities are given. (France)

XUM

41912 SELECTIVE STRIPPING OF PLUTONIUM FROM ORGANIC EXTRACTS. Coleman, Charles; Weaver, Boyd S. (to United States Atomic Energy Commission). U. S. Patent 3,580,705. 25 May 1971. Filed 2 Oct 1968.

Dialkyl substituted hydroquinones, such as 2,5-di-tert-butylhydroquinone, dissolved in an organic solvent were found effective in reducing plutonium in the 4^+ and 6^+ oxidation states dissolved in diesters of orthophosphoric acids, such as bis(2-ethylhexyl) phosphatic, to the 3^+ oxidation state. This enables quantitative stripping of the plutonium with aqueous solutions of hydrochloric acid. (Offic. Gaz.)

41913 PROCESS FOR DECONTAMINATION OF RADIOACTIVE EFFLUENTS. (to Ugine Kuhlmann). British Patent 1,235,567. 16 Jun 1971. Priority date 4 Dec 1967, France.

A process for decontaminating liquid radioactive effluents, particularly those containing Ru, comprises adjusting the pH value to 1 to 3, causing the effluent to percolate over activated Fe of large specific surface at a temperature not exceeding 70°C, then raising the pH to a value of 8 to 10, and treating the effluent with a zeolite or zeolites. (B.L.M.)

41914 PROCESS AND DEVICE FOR PURIFYING GASES CONTAINING OXIDIZABLE IMPURITIES SUCH AS THE COOLING GASES OF A GRAPHITE MODERATED NUCLEAR REACTOR. Dirian, Gregoire; Zermizoglou, Roger (to Commissariat a l'-Energie Atomique). French Patent 2,038,559. 28 Dec 1970. Filed 19 Mar 1969. (In French).

A process for purifying gases containing oxidizable impurities, such as the cooling gases of a graphite-moderated reactor, is described. The gases are contaminated by mercury. Some of this gas is burned on a catalytic mass maintained at a temperature sufficiently high to eliminate oxygen and hydrogen, and the water vapor produced. The active element of the catalytic mass may be platinum or palladium, the nature and content of the second metal being such that the adsorption of mercury by the active element does not appreciably reduce its efficiency. (France)

41915 USE OF ZIRCONIUM TELLURATE IN ION EXCHANGE SEPARATION TECHNIQUE. Szirtes, L.; Zsinka, L. (Isotope Inst., Budapest). Radiochem. Radioanal. Lett.; 7: No. 1, 61-5(15 Jun 1971).

Distribution coefficients were determined for 45 ions in hydrochloric acid and ammonium chloride solutions on zirconium tellurate. The measurements were carried out at room temperature under stationary conditions using a tracer technique. (auth)

41916 EXPERIMENTAL APPROACH TO THE OPTIMIZATION OF SOLVENT EXTRACTION PROCESSES. Ikuta, A.; Costa, E. C. (Instituto de Energia Atomica, Sao Paulo, Brazil). pp 175-84 of Materials Technology. I. New York; American Society of Mechanical Engineers (1970).

From second inter-american conference on materials technology; Mexico City, Mex. (24 Aug 1970). See CONF-700812.

The application of an optimization factor defined from fundamental reasoning is described in the determination of optimal choices of operating levels of process variables, and in the comparison of the performance of different experimental assemblies. The factor was defined for an extraction process as being directly proportional to the rate of transfer of the extractable species into the organic stream, inversely proportional to the rate of loss of the species in the raffinate stream, and directly proportional to the rate of production. The use of this factor permitted the extrapolation of conclusions from simple one-stage lab-scale batch experiments, to multi-stage pilot-scale units. (auth)

41917 METALS PURIFICATION BY SOLVENT EXTRACTION. Beyer, G. H. (Virginia Polytechnic Inst., Blacksburg). pp 185-9 of Materials Technology. I. New York; American Society of Mechanical Engineers (1970).

From second inter-american conference on materials technology; Mexico City, Mex. (24 Aug 1970). See CONF-700812.

The ideal-stage requirements for the separation of hafnium from zirconium are discussed. Fractional solvent extraction uses a center-feed column, with a scrubbing section above the feed to ensure zirconium quality and an extraction section below the feed to ensure zirconium recovery. The results of computer calculations are presented as response surfaces which graphically display the recovery and quality for 100 combinations of scrubbing section and extraction section stages. Operational limits are represented as specification planes intersecting the response surfaces. (auth)

41918 CHEMICAL EXTRACTION OF LOW-GRADE RESOURCES. Deju, Raul A. (Univ. Nacional Autonoma de Mexico, Mexico City). pp 190-4 of Materials Technology. I.. New York; American Society of Mechanical Engineers (1970).

From second inter-american conference on materials technology; Mexico City, Mex. (24 Aug 1970). See CONF-700812.

Extraction of ores from low-grade deposits is discussed. Fracturing techniques include detonating a nuclear explosive. Leaching of Cu, Ce, K, Ni, Th, and Mo is considered. (M.C.G.)

41919 ION-EXCHANGE PILOT PLANT FOR THE PREPARATION OF NUCLEAR PURE URANIUM COMPOUNDS. Abrao, Alcidio; Franca, J. M. Jr.; de Araujo, J. A.; (and others) (Instituto de Energia Atomica, Sao Paulo, Brazil). pp 195-202 of Materials Technology. I. New York; American Society of Mechanical Engineers (1970).

From second inter-american conference on materials technology; Mexico City, Mex. (24 Aug 1970). See CONF-700812.

The installation and operation of a pilot plant for uranium purification based on an ion-exchange process is described. The preparation of uranyl nitrate solution used to feed the ion-exchanger columns is performed by fractional dissolution of raw sodium diuranate. The decontamination of thorium plus rare earth elements is achieved by oxalic acid precipitation directly in the bulk of uranyl nitrate. The decontamination of various impurities is enhanced by an EDTA complex formation before the uranyl load on the strong cationic resin bed. The uranyl sulfate obtained by eluting the resin column with ammonium sulfate is reverse precipitated to avoid sulfate coprecipitation in the nuclear grade ammonium diuranate obtained. (auth)

41920 RADIOACTIVATION OF PLATINUM BY THERMAL NEUTRONS AND HALF-LIFE OF ^{195m}Pt. Bussiere, P. (CNRS, Villeurbanne, France). Radiochem. Radioanal. Lett.; 7: No. 1, 23-9(15 Jun 1971). (In French).

Pure platinum was radioactivated by thermal neutrons and separated by paper chromatography from the radioisotopes of gold and iridium formed simultaneously. The platinum spots exhibited a half-life of 4.0 days from the 13th to the 30th day after the end of the irradiation, with a maximum sensitivity of 50 imp m^{-1} μg^{-1}. A half-life of 3.75 ± 0.25 days is ascribed to ^{195m}Pt from the theoretical comparison of the activities due to ^{193m}Pt and ^{195m}Pt. (auth)

41921 FRACTIONATING OF ^{18}O BETWEEN ICE AND WATER VAPOR. Majoube, Michel (CEA, Saclay, France). J. Chim. Phys.; 68: No. 4, 625-36(Apr 1971). (In French).

The fractionating factors of ^{18}O between water vapor and ice were measured between 0 and 33.4°C. The experimental results can be represented by the relation $\ln \alpha = 11.839/T - 28.224.10^{-3}$. The difference between the heats of sublimation of $H_2{}^{18}O$ (H') and $H_2{}^{16}O$ (H) deduced from this relation is given by: $\Delta H' - \Delta H = 23.5 \simeq 0.5$ Cal/mole. The experimental method used enabled the diffusion coefficients for $H_2{}^{18}O$ molecules in $H_2{}^{16}O$ molecules to be determined in the vapor phase, (25 ± 1°C) at pressures between 0.60 and 4.58 mmHg. Fractionating factors were calculated from spectroscopic data between 0 and −40°C and are in perfect agreement with the experimental results. (France)

41922 RETENTION OF TANTALUM BY HYDRATED ANTIMONY(V) OXIDE IN STRONGLY ACID MEDIA. Pueschel, Sonia M. P.; Lima, F. W. (Inst. of Atomic Energy, Sao Paulo, Brazil). Radiochem. Radioanal. Lett.; 6: No. 5, 313-18(19 May 1971).

The retention of tantalum by hydrated antimony(V) oxide, HAP, was studied in nitric, hydrochloric, and perchloric acids at various concentrations. The tantalum capacity of HAP 1M nitric acid was determined and the kinetics of the retention was studied at 25°C. (auth)

41923 ISOTOPE SEPARATION OF RADIOACTIVE SODIUM ISOTOPES BY ISOTACHOPHORESIS. Wiedemann, B. (Technische Hochschule, Stockholm); Vestermark, A. Radiochem. Radioanal. Lett.; 6: No. 5, 287-96(19 May 1971). (In German).

Measurements of the isotope effects for ^{22}Na and ^{24}Na in the isotachophoresis technique were carried out using ^{23}Na as a "spacer". From the variation in the isotopic ratios ^{22}Na/^{23}Na; ^{24}Na/^{23}Na within the sodium band the relative mobilities of ^{22}Na and ^{24}Na relative to ^{23}Na were calculated. The height of a theoretical plate and the number of plates are given. (auth)

41924 SEPARATION OF URANIUM(VI) BY EXTRACTION CHROMATOGRAPHY FROM THE SOLUTIONS RESULTING FROM NUCLEAR TECHNOLOGY. Schmid, E. R.; Pfannhauser, W. (Univ., Vienna). Mikrochim. Acta; No. 2, 250-61(1971). (In German).

The extraction-chromatographic separation of uranium(VI) from nitric acid solutions is described. Columns were employed containing bis(2-ethylhexyl)phosphoric acid (HDEHP) in xylene as stationary phase. If only uranium(IV) and uranium(VI) are present,

it is sufficient to elute with nitric acid–0.1M hydrazine. From solutions of more complex composition, which in addition to uranium(IV) and uranium(VI) also contain longer-lived fission products (^{144}Ce, ^{106}Ru, ^{95}Nb, and ^{137}Cs), plutonium(III) and corrosion products of steel [Fe(III), Co(II), Ni(II), and Cr(III)], the uranium(IV) was separated by two methods. In the first variant it was retained on the column by 5% HDEHP in xylene and all accompanying ions were removed with 2N nitric acid–0.1M hydrazine. In the second variant, in addition to the uranium(IV), the uranium(VI) also was captured in a separate fraction. 30% HDEHP was employed as stationary phase, while the elution agent was 11.7N nitric acid–0.1M hydrazine. In both variants, the uranium(IV) could be eluted from the column by a mixture of 15% sulfuric acid–5% phosphoric acid. In the first variant, the uranium(IV) could also be eluted by means of 11.7N nitric acid/0.1M hydrazine in case it was planned to have it present after the separation in nitric acid solution. The stability of the columns and of the uranium(IV) and the influence of the HDEHP concentration in xylene and the nitric acid concentration as well as the behavior of several ions under the separation conditions are discussed. (auth)

EARTH SCIENCES

Geology and Hydrology

Refer also to abstracts 41770, 41771, 41941, 41945, 41953, 42117, 42176, 42319, and 42427.

41925 (CEA-tr-R-1979) PHYSICOCHEMICAL CONDITIONS FOR BURIAL OF RADIOACTIVE WASTE. Spitsyn, V. I.; Balukova, V. D.; Bagretsov, N. F. Translated from Bureau Central d'Informations Technico-Scientifiques, Moscow, 1967. 11p. (In French). Dep. NTIS (U. S. Sales Only).

Fundamental physicochemical studies necessary for the evaluation of the burial of radioactive wastes are described. Conditions for the burial of deactivated solutions were determined. Technological processes have been established to assure the stability of the liquid phase at the time of contact of the waste with the geological medium. General conditions were examined for the sorption of the radioisotopes from waste waters in a closed pocket of heavily mineralized water at the time of burial. (tr-auth)

41926 (UCLA-12-819) SOME PHYSICAL AND CHEMICAL CHARACTERISTICS OF HEATED SOILS. Nishita, H.; Haug, R. M. (California Univ., Los Angeles. Lab. of Nuclear Medicine and Radiation Biology). [1971]. Contract AT(04-1)-Gen-12. 31p. Dep. NTIS.

The physical and chemical characteristics of five different heated soils were examined. The properties examined include particle size distribution, pH, cation exchange capacity, electrical conductivity, water and ammonium acetate extractable Na, K, Mg, Ca, and Sr, and total N, lime and organic C contents. (auth)

41927 (USGS-474-75(Rev.1)) TECTONIC SETTING OF AMCHITKA ISLAND, ALASKA. Anderson, R. Ernest (Geological Survey, Denver, Colo.). 1971. Contract AT(29-2)-474. 46p. Dep. NTIS.

A review of published and unpublished geologic and geophysical data pertaining to the problem of defining the tectonic setting of Amchitka Island indicates that known and inferred structures affecting the upper crust reflect predominantly tensional strain of diverse orientations, whereas evidence from natural seismicity suggests oblique compressional strain across the Aleutian arc in the vicinity of Amchitka. Features of probable tensional origin on the Aleutian Ridge are inferred to have formed from igneous-related tectonism including distension of the surficial skin over rising and spreading epizonal plutons, volcano-tectonic subsidence, and rifting; those features on the Aleutian Terrace and landward wall of the Aleutian Trench are inferred to have formed from distension of a decoupled surficial skin above a prolongated zone of imbrication and uplift; and those in the trench and on the seaward wall are formed from dynamic loading of the Pacific lithospheric plate by overthrusting and southward migration of the Aleutian tectogene. The plutonism, imbrication, and dynamic loading are considered to be the result of a first-order process of crustal foreshortening across the arc. The features of tensional origin along the Aleutian Ridge are, according to this view, second-order structures that are inactive in areas where the plutonism has ceased; that is, in all areas except possibly along the volcanic arc. Judged from unpublished information, Bowers Ridge appears to be part of a structural arc. Amchitka Island is, therefore, located near an arc-arc intersection. Judged from physiographic considerations, the structure of the Aleutian arc in the vicinity of Amchitka is inferred to be strongly modified by superposition of the now-inactive Bowers arc structure. An important, though highly speculative, result of the arc-arc intersection would be a low-angle fault that dips away from the leading edge of Bowers arc beneath Amchitka Island. This hypothetical fault could serve as an effective zone of tectonic and seismic decoupling of the Rat block from the Aleutian Ridge east of Amchitka Pass. (auth)

41928 STUDIES ON THE ENVIRONMENTAL RADIOACTIVITY AT THE CLUJ BRANCH OF THE INSTITUTE OF ATOMIC PHYSICS DURING 1964 TO 1968. Szabo, A.; Chereji, I. (Inst. of Atomic Physics, Cluj). Stud. Cercet. Fiz.; 22: No. 6, 671-5(1970). (In Rumanian).

Studies and techniques for measuring the radioactivity of the environment, developed at the Laboratory of Radioactivity are described. Radon was determined by a novel portable instrument which combines the principles of an electrometer, ionization chamber, a drying tube, and a voltage stabilizer; field experiments were carried out for the same purpose also with an alpha scintillation counter. The radium was determined on the basis of the accumulated radon; a visual fluorescence method was used for uranium measurements. Thorium in the waters was analyzed spectrophotometrically on the basis of thoron, while measurement of ^{40}K involved precipitation with Kalignost reagent, determining the boron spectrophotometrically in the tetraphenyl borate precipitate in which the two elements are in stoichiometric equilibrium. Radiolead was determined indirectly on the basis of the beta radiation of the daughter ^{210}Bi. For measuring the total activity of the medium, an anticoincidence device with a proportional counter was developed; tests were carried out with plastic scintillators which are expected to reach a sensitivity of 1 pCi/l. A liquid chromatograph with radioactive control was developed for measuring the radioactivity of environmental samples. The water supply is protected against radioactive contamination by an automatic warning device placed at the reservoirs which give a visual and audible remote alarm and close valves and stop pumps when the preset threshold is exceeded. The Th/Ra ratio was found to be higher for soils with a high humus content, revealing that the humus adsorbs thorium preferentially. A close correlation was found between the radioisotopic abundance in waters and the geological structure of the rocks through which the water passes. The data are used for the protection of the population. (TTT)

41929 ON RADON CONTENT IN THE WATERS OF THE UPPER VOLGA. Khristianov, V. K.; Korchuganov, B. N. (Inst. of Geochemistry and Analytical Chemistry, Moscow). Geokhimiya; No. 4, 492-6(Apr 1971). (In Russian).

Water sampling was conducted in 1969 from seven Russian rivers: Volga, Oka, Protva, Moscow, Ruza, Vazuza, and the Tvertsa. Radon determinations yielded a concentration range from 5 to 69×10^{-12} Ci/l, but from one underground seepage an analysis showed 210×10^{-2} Ci/l. Radium determinations were made in four of these samples, yielding a range of concentrations 0.04 to 0.72×10^{-12} Ci/l. The sensitivity of the method was 1.4×10^{-14} Ci Ra/l. Of interest are the corresponding Rn/Ra ratios: 31, 42, 96, and 420, the latter being peculiar to the Moscow River, and in all four cases the Rn concentration was higher than the equilibrium value by a factor of 10 or 100. Underground waters apparently contain 5 to 10 times as much Rn as nearby river water. For underground rivers and for flat country rivers conditions must prevail which encourage prolonged retention of higher concentrations of Rn. (K.S.W.)

41930 PHYSICOCHEMICAL CHARACTERISTICS OF THE LAND SURROUNDING C.S.N. AT CASACCIA WITH REFERENCE TO THE PROBLEM OF SAFETY AND MEDICAL PROTECTION. Lenzi, Giuseppe (CNEN, Rome). Minerva Fisiconucl.; 13: 105-8(Jan-Mar 1969). (In Italian).

A study was made of the physicochemical characteristics of the soil and subsoil surrounding the C.S.N. The results showed that the subsoil has optimum characteristics for the absorption of Cs, but the inverse for Sr. (J.S.R.)

41931 NUCLEAR METHODS FOR PROSPECTING AND EXPLOITING NON-PETROLEUM MINERAL RESOURCES. Peteu, G. I. (Ministere du Petrole, Ploiesti, Rumania). pp 37-57 of Nuclear Techniques for Mineral Exploration and Exploitation. Vienna; International Atomic Energy Agency (1971). (In French).

From Panel on nuclear techniques and mineral resources in developing countries; Krakow, Poland (8 Dec 1969). See STI/PUB-279; CONF-691229.

The applicability of nuclear borehole methods for non-petroleum mineral resources prospecting is now being recognized. The information obtained through these methods is an aid to geological studies for the discovery and evaluation of ore and mineral salt deposits. In general, the borehole methods for these types of investigation could be adapted from those most commonly employed in the petroleum industry. Nuclear borehole methods are based on one or more of the following techniques or disciplines: measurement of natural radioactivity, gamma-ray scattering, photoneutron reactions, radioisotope x-ray fluorescence, thermal and fast neutron activation, fast neutron inelastic scattering, thermal neutron capture, and cyclic activation. An analysis is given on the performance and limitations of the methods and their applicability for deposit prospecting of potash salt; coal; and ores of low, medium, and high atomic mass elements. (auth)

Meteorology

Refer also to abstracts 41754, 42314, and 42377.

41932 (AD-719619) FINAL REPORT ON HIGH-ALTITUDE NUCLEAR DETECTION STUDIES. VOLUME I. THE HANDS SYSTEM. Hornback, C. E. (Space Disturbances Lab., Boulder, Colo.). Nov 1970. 92p. (SDL-18; ERL-188).

A summary of the engineering aspects of the High Altitude Nuclear Detection Studies (HANDS) project is presented. The system was oriented around a computer that performed control functions and recorded and processed data from a number of geophysical sensors. Brief descriptions of the facility and various sensor equipment are presented. The system operation is described, and some recommendations are given. (USGRDR)

41933 (AD-719620) FINAL REPORT ON HIGH-ALTITUDE NUCLEAR DETECTION STUDIES. VOLUME II. RESULTS AND RECOMMENDATIONS. Jean, A. G.; Hornback, C. E.; Doherty, R. H.; Lewis, L. D.; Lerfald, G. M. (Space Disturbances Lab., Boulder, Colo.). Nov 1970. 139p. (SDL-18-2; ERL-188-2).

The results produced by the HANDS program are of three general types: developments in automatic processing and handling of geophysical data collected from a large number of sensors, and findings bearing on the capabilities of nuclear detection systems, and conclusions of rather broad scientific interest. Descriptions and/or examples of some of the more important of these results are given. An appraisal is made of the HANDS program, including some shortcomings, and some recommendations for future similar systems are given. (auth) (USGRDR)

41934 SEASONAL VARIATIONS OF THE CONCENTRATION OF ^{7}Be, ^{54}Mn AND THEIR DECAY PRODUCTS IN GROUND-LEVEL AIR. Kolb, W. (Physikalisch-Technische Bundesanstalt, Brunswick). Tellus: 22: No. 4, 443-50(1970). (In German).

Manganese-54, antimony-125 and cesium-137 were measured in ground-level air in Brunswick (52°18′N, 10°28′E) since the end of 1963. Until 1967 the activity concentrations decreased with a stratospheric half-life of 11 months superimposed by seasonal variations, the ratio between maximum in May and minimum in late fall being 10. Against this the corresponding ratio for ^{7}Be, produced by cosmic rays, is only 2.6. The reason for this difference is due to the fact that the nuclear bomb debris during that time are of stratospheric origin exclusively whereas averaged over one year about 50% of beryllium-7 stems from tropospheric production. From 1964 through 1968 the mean activity concentration of ^{7}Be in ground level air was between 65 and 69 fCi/m^3. (auth) (Sweden)

41935 ASSESSMENT OF MECHANICAL TURBULENCE UNDER CONDITIONS OF THERMAL INVERSION ON THE BASIS OF RICHARDSON'S NUMBER. Pagliari, M. (ENEL, Rome). Minerva Fisiconucl.: 14: 120-3(Jul-Sep 1970). (In Italian). (CONF-690929-11).

From fifteenth national congress of the Italian Association for Health Physics and Protection Against Radiation; Cagliari, Italy (Sep-Oct 1969).

The evaluation of atmospheric turbulence under conditions of nocturnal thermal inversion was considered by making use of the Richardson number Ri. When Ri = 1 a relation exists between the temperature profiles and of the wind velocity. On the basis of some hypotheses on the distribution with the velocity contribution, the existence of a thermal gradient as a function of the wind velocity is assumed. (tr-auth)

41936 FREQUENCY OF THE CATEGORIES OF STABILITY, ACCORDING TO THE CRITERIA OF PASQUILL, FOR THE VARIOUS REGIONS OF ITALY. Cagnetti, P.; Giudici, G.; Rosini, E. (CNEN, Rome). Minerva Fisiconucl.; 13: 46-60 (Jan-Mar 1969). (In Italian). (CONF-680535-6).

From fourteenth national conference of the Italian Association for Health Physics and Protection from Radiation; Formia, Italy (29 May 1968).

The frequency of various stability conditions in the lower atmospheric layers was calculated, according to the Pasquill criteria, for all the 1st and 2nd class Italian meteorological stations. The calculations were made with the IBM 1401 on the basis of the cloudiness wind data obtained from weather balloons at the principal synoptic hours from 1951 to 1963. The results were taken in relation with the possibility of evaluating the diffusion characteristic of gaseous effluents for all Italian regions. A critical study was made of the values obtained at the various stations, either with respect to the variations of the stability in relation to the various hours of the day or with respect to the variations of the stability itself in relation to the climatic characteristics of the various regions. (tr-auth)

41937 STATISTICAL CONSIDERATIONS IN THE ITALIAN ATMOSPHERIC RADIOACTIVITY SURVEILLANCE NETWORK. Mastinu, G. G.; Zuccaro Labellarte, G. (CNEN, Rome). Minerva Fisiconucl.; 14: 17-23(Jan-Mar 1970). (In Italian). (CONF-690929-6).

From fifteenth national congress of the Italian Association for Health Physics and Protection Against Radiation; Cagliari, Italy (Sep-Oct 1969).

The increase of the concentration of radioactive aerosols measured in 1962 to 64 was analyzed as a function of the geographic positions and the seasonal characteristics. The linear correlation coefficient was higher in winter than in summer. In the periods immediately following a nuclear test there was a greater dispersion of this coefficient. Some stations in the network deviated systematically from the general increase. Isoactivity curves were drawn. (J.S.R.)

41938 MODIFICATION OF ATMOSPHERIC TRITIUM AND WATER VAPOR BY LAKE TAHOE. Oestlund, H. Goete (Univ. of Miami, Fla.): Berry, Edwin X. Tellus; 22: No. 4, 463-5 (1970).

Changes in humidity and tritium concentration in the air over Lake Tahoe are described by two derived equations. These equations were experimentally tested and good agreement was found between the two. (Sweden)

41939 SPACE-TIME VARIATIONS IN RADIOACTIVITY FOR SURFACE LAYERS OF AIR IN TASHKENT. Kulagin, D. I. (Tashkent General Army Command School). Izv. Akad. Nauk Uzb. SSR, Ser. Fiz.-Mat. Nauk; No. 6, 22-5(1970). (In Russian).

The radioactive background in surface air at Tashkent was measured during the interval April 1966 to July 1967. Sampling was performed twice every 24 hr at heights 0.1 m, 1.1 m, and 1.6 m, and typical meteorological data were recorded, as temperature, humidity, wind velocity, etc. The results of the investigation showed that the daily gamma background was apparently a very stable component of the total radioactivity, to a lesser degree associated with the aerosol phase of the air, and less subject to 24-hr fluctuations. (K.S.W.)

41940 DETERMINATION OF ENVIRONMENTAL RADIOACTIVITY. Parra Gil, F. Rev. Ecuator. Hig. Med. Trop.; 25: No. 1, 31-60(Jan-Apr 1968). (In Spanish).

The results of measurements of the particulate radioactivity of the air and milk during the period from June 1966 to May 1967 are reported. A comparative study was also made of the radioactive rains falling in the same period in Colombia, Ecuador, Peru, and Chile. The results are given in tables and graphs. They show an appreciable increase in the radioactive particulate concentration in the air of the city of Guayaquil. The decay indices indicate that the increased radioactivity could be attributed to the French nuclear tests in July, September, and October of 1966. After December 1966 the total β activity decreased. The milk samples showed an increase in radioactivity, especially during October. (J.S.R.)

Mineralogy and Exploration

Refer also to abstracts 41739, 41741, 41767, 41768, 41772, and 41931.

41941 (STI/PUB-279) NUCLEAR TECHNIQUES FOR MINERAL EXPLORATION AND EXPLOITATION. Panel Proceedings Series. Proceedings of a Panel on Nuclear Techniques and Mineral Resources in Developing Countries Held in Krakow, 8-12 December 1969. (International Atomic Energy Agency, Vienna (Austria)). Feb 1971. 194p. (In French and English). (CONF-691229). IAEA $5.00.

The proceedings of this conference review the present status of nuclear techniques in the oil industry and in mineral exploration and identifies those techniques most suitable for adoption by developing countries. A summary of the findings of the panel members is presented as well as individual papers. Fifteen separate papers are presented. Abstracts were prepared for 14 of these papers. The remaining paper deals with field experience in complex geochemical research in Czechoslovakia. (B.L.M.)

For abstracts of individual papers see: 41739-41741, 41767-41772, 41931, 41945-41947, and 42133.

41942 URANIUM PROSPECTION OF THE EISENWERK-GESELLSCHAFT MAXIMILIANSHUETTE IN NORDOSTBAYERN. Gudden, H.; Eckmann, W. Glueckauf; 106: 380-7(1970). (In German).

In 1950 the Eisenwerk-Gesellschaft Maximilianshuette, Sulzbach-Rosenberg, started with uranium ore prospecting in the Federal Republic of Germany. In the beginning there were mining studies of a uranium deposit at the Rudolfstein near Weissenstadt. Sixty to 70 tons of uranium were detected and this deposit was developed to the stage of possible exploitation but in 1957 it was stopped because it was unprofitable. At the same time uranium mineralization at the Fuchsbau near Leopoldsdorf was studied

XUM

but considerable uranium concentrations were not detected. During the same years the gradually developed surface prospecting which was at first restricted to the Fichtelgebirge was extended to crystalline and paleozoic formations of the Frankenwald, Steinwald, the northern Oberpfaelzer Wald and the mesozoic foreland. The prospecting was done in a more intensive way beginning in 1957. The total prospecting area extends over about 5000 square kilometers. The following methods were used: carborne and airborne radioactivity measurements, radioactivity measurements by walking, geochemical prospecting and prospecting by digging and in boreholes. The most profitable deposit was found in the Falkenberger Granit near Tirschenreuth, an area of hardly 50 square kilometers. The uranium reserves yielded 150 to 350 tons. Higher reserves probably exist. The prospecting of this area and some others with probable profitable deposits are continuing. (INIS)

41943 FIELD DETERMINATION OF URANIUM AND THORIUM BY GAMMA-RAY SPECTROMETRY, EXEMPLIFIED BY MEASUREMENTS IN THE ILIMAUSSAQ ALKALINE INTRUSION, SOUTH GREENLAND. Loevborg, Leif; Wollenberg, Harold; Soerensen, Poul; Hansen, John (Danish Atomic Energy Commission Research Establishment, Risoe). Econ. Geol.; 66: 368-84 (May 1971).

Gamma-ray spectrometry in the field was used in connection with an intensive study of the abundance and distribution of U and Th in peralkaline rocks of the Ilímaussaq intrusion, south Greenland. U and Th were determined from counts accumulated in the 1.76 and 2.62 MeV intervals of a portable γ spectrometer. In order to permit a direct comparison with conventional surface sampling, an effective sample in field γ spectrometry is defined as the volume of rock in which the variance of a particular radioelement (U, Th, or K) is equal to the estimation variance of a γ-spectrometric determination of this radioelement. This volume contributes about 60% of the measured γ rays. It is roughly one-tenth the volume which contributes 90% the sample size which until now has been widely accepted. The mass of the effective sample for a NaI(Tl) detector whose sides are surrounded by 5 cm of lead, placed on a rock surface, is ~20 kg and ~15 kg for 2.62 and 1.76 MeV γ rays, respectively. Calibrations for U and Th were achieved by use of large concrete standards of known radioelement content, and having a γ-ray mass absorption nearly equal to that of the rock to be measured. The calibration for U based on the concrete standards was more accurate than a calibration based on rock samples collected from measurement localities. The accuracy of the field γ spectrometer, depending on standard errors associated with calibration equations, was about 2.5% for Th, and ranged from 2.5 to 7.5% for U, as Th/U varied from 1 to 5. Analytical precision for single measurements, combining the effects of counting statistics and instrument instability, ranged between 1 and 8% for Th and between 1 and 12% for U. As many as 100 measurements per day with a lead-collimated detector were made along grids with 1-meter spacings in rock with a rough surface and an uneven distribution of radioelements. Results confirmed that specific rock types have characteristic U and Th contents. The measurement system was accurate enough so that where adequate radioelement contrasts existed, contours of U and Th corresponded closely to rock type and followed structural trends in the rock. (auth)

41944 PROBABILISTIC APPRAISAL OF MINERAL RESOURCES IN A PORTION OF THE GRENVILLE PROVINCE OF THE CANADIAN SHIELD. De Geoffroy, J.; Wignall, T. K. Econ. Geol.; 66: 466-79(May 1971).

A probabilistic method of appraisal of mineral resources is applied to a 17,000 square mile portion of the Grenville Province of the Canadian Shield. Regression and Bayesian classification models are formulated from geological data obtained in well prospected 100 square mile cells including known commercial deposits. These models provide predictions of ore values and probabilities of success for the cells of the study area. The expected dollar payoff is used to rate the exploration potential of these cells. As a result of the application of this procedure eleven cells with a total predicted ore value of $425 million are selected for exploration by airborne and ground reconnaissance surveys. (auth)

41945 RADON MEASUREMENT IN SOIL IN THE EXPLORATION FOR URANIUM IN INDIA. Bhatnagar, A. S. (Dept. of Atomic Energy, New Delhi). pp 157-62 of Nuclear Techniques for Mineral Exploration and Exploitation. Vienna; International Atomic Energy Agency (1971).

From Panel on nuclear techniques and mineral resources in developing countries; Krakow, Poland (8 Dec 1969). See STI/PUB-279; CONF-691229.

Radon distribution in soil is influenced by many factors and present knowledge on these factors is incomplete. Daily variation in the results of radon measurement made at the same station has been noted. This indicates that the measurement is subject to unknown influences and any interpretation based on a single observation can be very misleading. The radon content of the soil is derived not only from the parent material diffused in the soil, but also from the migration of radon from another source containing a higher concentration of the parent. In interpreting a radon anomaly it is necessary to distinguish between the contributions made by these two types of sources. Because of the influence of the unknown factors, the problems of interpretation become very entangled. Since the migration of radon from a distant source with a large concentration of its parent is highly subject to meteorological factors, it is suggested that the unaccounted fluctuations in observed radon values may be themselves taken as an indication of the presence of a distant large source, such as a uranium deposit, in the area. (auth)

41946 USE OF NUCLEAR TECHNIQUES IN SPAIN'S PROGRAM FOR THE DEVELOPMENT OF MINERAL RESOURCES. del Val Cob, M. (Junta de Energia Nuclear, Madrid). pp 163-7 of Nuclear Techniques for Mineral Exploration and Exploitation. Vienna; International Atomic Energy Agency (1971).

From Panel on nuclear techniques and mineral resources in developing countries; Krakow, Poland (8 Dec 1969). See STI/PUB-279; CONF-691229.

A brief but complete summary is made of nuclear techniques, which are used throughout the world for various applications in mineral resources development. Comments are given on the exploitation of these techniques in Spain. (auth)

41947 STATUS OF NUCLEAR METHODS IN THE PROGRAM FOR MINERAL RESOURCES DEVELOPMENT IN INDIA. Bhatnagar, A. S. (Dept. of Atomic Energy, New Delhi). pp 169-78 of Nuclear Techniques for Mineral Exploration and Exploitation. Vienna; International Atomic Energy Agency (1971).

From Panel on nuclear techniques and mineral resources in developing countries; Krakow, Poland (8 Dec 1969). See STI/PUB-279; CONF-691229.

A wide variety of nuclear techniques have been investigated in India's attempt to exploit its mineral resources. Techniques applicable to uranium and thorium exploration are more developed than the others and are now in routine use. Methods based on the measurement of natural γ radioactivities are also being employed in the exploitation of lignite deposits and in phosphorite prospecting. In the exploration for beryl the γ-neutron method is used both in the field and in laboratory. In oil exploration the neutron-neutron logging, employed in combination with resistivity logging, is found to be helpful in providing a qualitative discrimination between water and oil content of the formation. The methods and equipment used are described and some typical results are given. (auth)

Oceanography

41948 (CEA-CONF-1733) SOCIO-PSYCHOLOGICAL FACTORS LIMITING THE EMISSION OF RADIOACTIVE EFFLUENTS. Bovard, P. (Commissariat a l'Energie Atomique, Fontenay-aux-Roses (France). Centre d'Etudes Nucleaires). [nd]. 7p. (In French). (CONF-701127-1). Dep. NTIS (U. S. Sales Only).

From Panel on procedures for establishing limits for radionuclides in the sea; Vienna, Austria (9 Nov 1970).

The psychological factors limiting the release of radioactive effluents into the ocean are considered from the viewpoint of three social groups: the general population, people directly concerned (particularly seamen), and specialized scientific populations. An attempt was made to relate regional differences in attitudes regarding marine disposal of radioactive wastes to the difference in the mentality of these populations, the social situation, and the political regime. (J.S.R.)

41949 RESEARCH ON THE VERTICAL DISTRIBUTION OF RADIOACTIVITY IN SEDIMENT FROM THE LIGURIAN SEA. Schreiber, B. (Univ., Parma, Italy); Cerrai, E.; Triulzi, C.; Tassi Pelati, L.; Mezzadri, M. G. Minerva Fisiconucl.; 13: 1-19(Jan-Mar 1969). (In Italian). (CONF-680535-3).

From fourteenth national conference of the Italian Association for Health Physics and Protection from Radiation; Formia, Italy (29 May 1968).

The total β activity of 30 bores made from 1964 to 1968 in the sediment of the Ligurian Sea is reported. Typical vertical distributions of the radioactivity are shown. Radiochemical analysis was used for the determination of the principal natural and artificial radioisotopes. These include Th, U, ^{230}Th, ^{226}Ra, radioactive rare earths, and ^{90}Sr. (J.S.R.)

Seismology

Refer also to abstract 41952.

41950 (AD–718388) THEORETICAL GROUND MOTION PREDICTIONS SUPPORTING THE HEST PROGRAM. Leahy, J.; Maxwell, D.; Lange, R.; Christensen, D. (Physics International Co., San Leandro, Calif.). Dec 1970. Contract DASA01-67-C-0076. 85p. (PIFR–82; DASA–2575). NTIS.

The computations done to predict, design, or support the experimental program are described. MINIDIHEST 1 and 2, and PLANEWAVE 1 are computations done to predict ground motion resulting from relatively simple arrays of alluvium (MINIDIHEST) and layered limestone-shale (PLANEWAVE), PLANEWAVE 2 are computations done to design an experimental explosives array which would produce a plane wave in the ground having a specified intensity and rate of attenuation at a particular range. Another computation predicted the actual ground motion resulting from this experimental array. Merry-Go-Round presents computationally predicted ground motion in Cedar City granite. The parametric studies relate a series of computations which predicted the effect of variation of the explosives array on resulting ground motion as a function of range. (auth) (USGRDR)

41951 (NVO–87) SEISMOLOGY, AFTERSHOCKS, AND RELATED PHENOMENA ASSOCIATED WITH UNDERGROUND NUCLEAR EXPLOSIONS. A BIBLIOGRAPHY OF SELECTED PAPERS WITH ABSTRACTS. (Nevada Operations Office (AEC), Las Vegas. Office of Effects Evaluation). May 1971. 36p. Dep. NTIS.

A bibliography of selected papers with abstracts on the seismology, aftershocks, and related phenomena associated with underground nuclear explosions is presented that includes 81 references. (D.H.M.)

XUM

ENGINEERING

Nuclear Explosions

Refer also to abstracts 41918, 41932, 41933, 41951, and 42318.

41952 (AD–838894) SEISMIC ANALYSIS OF THE GASBUGGY EXPLOSION AND AN EARTHQUAKE OF SIMILAR MAGNITUDE AND EPICENTER. Rasmussen, Darrell C.; Lande, Larry C. (Geotech, Garland, Tex.). 1 Aug 1968. Contracts F33657-67-C-1457; F33657-68-C-0734. 55p. (TR–68-15). NTIS.

Seismic comparisons are made between the Gasbuggy explosion and an earthquake which had a nearly identical epicenter. Utilizing travel time residuals derived from the Gasbuggy arrival data, the earthquake epicenter is relocated 35 km NNE of the Gasbuggy shotpoint. The corrected epicenter of the earthquake and the true Gasbuggy location are located approximately 5 km WNW of their respective uncorrected epicenters, which indicates that the travel time anomalies are consistent for the region between and including the two sources. (auth) (USGRDR)

41953 (CEA-R–4099) DISTRIBUTION OF RADIOACTIVITY IN THE LAVA ISSUING FROM THE CAVITY OF A NUCLEAR EXPLOSION. Audidiere, Pierre; Balard, Francois; Dupouy, Jean-Pierre; Van Kote, Francis (Commissariat a l'Energie Atomique, Bruyeres-le-Chatel (France). Centre d'Etudes). Mar 1971. 25p. (In French). Dep. NTIS (U. S. Sales Only).

In the framework of a general experimental and theoretical study on the distribution of radioactivity in the vicinity of contained nuclear explosions, photographs and α and β autoradiographs of granite lava fragments issuing from an old Sahara cavity were compared. The negatives obtained indicated a relatively homogeneous distribution of α emitters and a definitely heterogeneous distribution of β and γ emitters tending to accumulate at the surface of the bubbles. An explanation of the phenomena was proposed. (auth) (France)

41954 (CEA-R–4128(1)) RADIOACTIVITY DISTRIBUTION IN THE ENVIRONMENT OF A CONTAINED NUCLEAR EXPLOSION. PART 1. THEORETICAL STUDY: ACCOUNT OF THE RESEARCH METHOD FORESEEN FOR THE PROBLEM AS A WHOLE; BEHAVIOR OF MACRO COMPONENTS OF A GRANITE BETWEEN 3000 AND 6000°K AT PRESSURES BETWEEN 10 AND 1000 BARS. Audidiere, Pierre; Balard, Francois; Dupouy, Jean-Pierre; Lavollee, Philippe; Van Kote, Francis (Commissariat a l'Energie Atomique, Bruyeres-le-Chatel (France). Centre d'Etudes). Mar 1971. 47p. (In French). Dep. NTIS (U. S. Sales Only).

A plan of theoretical research on the distribution of fission products and activation in the environment of a contained nuclear explosion is proposed. Results are presented concerning the change in chemical composition of the gas phase filling the cavity created by the explosion. A program for automatic calculation of simultaneous chemical equilibria was used to study the special case of a granite (Tan Affela range) in the temperature region 3000 to 6000°K for pressures ranging from 10 to 1000 bars. (auth)

41955 SOME COMMENTS ON THE POSSIBILITY OF THERMODYNAMICALLY EQUILIBRATING WASTE ORGANIC MATERIALS WITH NUCLEAR DEVICES. Safrany, David R. (Bechtel Corp. Lab., Belmont, Calif.). Nucl. Technol.; 12: No. 1, 119-26(Sep 1971).

Nuclear explosions contained underground may be a way to produce hydrogen commercially from common waste organic materials. The idea is to use the explosion to heat the wastes to 2000°C or higher, at which temperatures hydrogen and carbon monoxide are produced. Carbon monoxide can subsequently be converted to tritium-free additional hydrogen by oxidizing it with steam. The pertinent thermodynamic equilibria, kinetics and energy requirements are discussed. (auth)

Facilities and Equipment

Refer also to abstracts 42858, 43330, 43425, and 44158.

41956 (BM-RI–7019) POWER REQUIRED TO CIRCULATE GAS-SOLIDS SUSPENSIONS. Rosenecker, C. N.; Coates, N. H.; Lucas, H. G. (Bureau of Mines, Morgantown, W. Va. Morgantown Coal Research Center). Sep 1967. 10p. Dep. NTIS.

The power required to circulate a gas-solids suspension was determined using a centrifugal compressor and a closed system. The suspension consisted of 18- to 40-micron glass beads in a mixture of 89 percent N_2 and 11 percent CO_2 at 20 psig. Solids-to-gas (S/G) ratios were 0 to 2.2 lb/lb; gas flow rates were 1.2 to 2.5 lb/min. Power requirement was found to follow the relationship $hp_t = hp_g [(S/G) + 1]$, where hp_t = the total power, and hp_g = the power required for pure gas. (auth)

41957 (BNL–50147(Rev.)) TABULATED DOSE DISTRIBUTION DATA FOR GAMMA IRRADIATOR DESIGN. Rizzo, F. X.; Galanter, L.; Krishnamurthy, K. (Brookhaven National Lab., Upton, N. Y.). Dec 1970. 66p. Dep. NTIS.

Revised data are tabulated that make available to the designer of package irradiators the dose distribution information necessary to perform quick, easy, and reasonably accurate calculations of the dose distribution characteristics of irradiators when using either ^{60}Co or ^{137}Cs plaque sources. The data should find its greatest use in performing dose distribution calculations necessary for plant and product feasibility studies, cost estimates for bid purposes, and for most preliminary design calculations. Those who are especially knowledgeable in the fields of radiation physics and irradiator design will find that these data, when properly operated upon, can be put to an even wider range of usefulness. The data presented in the tables are the depth dose distributions in semi-infinite homogeneous media over a range of target densities from both ^{60}Co and ^{137}Cs source plaques of various sizes. These targets were assumed to be bounded only at the front surfaces, by the source, air gap, and the absorbers. (J.R.D.)

41958 (CONF-700307–8) PUMPS FOR CIRCULATING LIQUID METALS. Rineiskii, A. A.; Aristarkhov, N. N.; Karpov, A. V.; Nikulin, M. P.; Tymow, B. S.; Yarovitsyn, V. V. (Gosudarstvennyi Komitet po Ispol'zovaniyu Atominoi Energii SSSR, Obninsk. Fiziko-Energeticheskii Institut). Translated from Symposium on Progress in Sodium-Cooled Fast Reactor Engineering, Monaco, (23 Mar 1970). 29p. Dep. NTIS.

Pump performance requirements for reactor application are discussed and centrifugal and electromagnetic pumps are compared for this service. Performance data for pumps used in Soviet fast reactor plants are summarized. Chapter 1 is a survey which considers the: main requirements from the reactor standpoint; operating conditions in reactor (coolant) circuits and peculiarities of construction; and types and applications and operating data on mechanical and electromagnetic pumps used in Soviet fast reactors. Ten years' operating experience with sodium pumps in the BR-5 Reactor are reviewed in Chapter 2. In Chapter 3, experimental programs for development of hydrostatic bearings for sodium pumps are described. Performance data for a 12-pocket hydrostatic bearing equipped with a bushing and flow-controlling clearances are presented. (auth)

41959 (CONF-710512–15) EFFECT OF FILLETS ON STRESS CONCENTRATIONS IN CYLINDRICAL SHELLS WITH STEP CHANGES IN OUTSIDE DIAMETER. Gwaltney, R. C.; Corum, J. M.; Greenstreet, W. L. (Oak Ridge National Lab., Tenn.). 10 Feb 1971. 7p. (71-PVP-27). Dep. NTIS.

From 1. national congress on pressure vessels and piping; San Francisco, Calif. (10 May 1971).

The effect of varying the radii of circumferential fillets in the transition region of cylindrical shells with a step change in outside diameter and loaded with internal pressure was examined by means of finite element analyses for 27 models. Parameters studied were ratios of the thickness of the thicker section to the thickness of the thinner section, ratios of the fillet radius to thickness of the thinner section, and ratios of the inside radius of the cylindrical shell to the thickness of the thinner section. Comparisons are presented between experimental and theoretical results for two experimental models, and duplicate analyses for two cases were made with different computer programs for comparison purposes. (auth)

41960 (EUR–4512) "DDO" COMPUTER PROCEDURE FOR THE INVENTORY CONTROL OF A SUPPLY OF DEUTERIUM. Schweitzer, A. L. M. (European Atomic Energy Community, Ispra (Italy). Joint Nuclear Research Center). 1970. 32p. NTIS (U. S. Sales Only).

The DDØ computer procedure for the inventory control of a supply of deuterium is designed in such a way as to produce a minimum of work for laboratory personnel in the compilation of input data. The procedure can handle a great variety of laboratory operations and the consequent computations. The three computer programs performing these tasks, as well as the codings and the input cards, are described in detail. (auth)

41961 (NBS-SPEC. PUBL-329) AN INDEX OF U. S. VOLUNTARY ENGINEERING STANDARDS. Covering those Standards, Specifications, Test Methods, and Recommended Practices Issued by National Standardization Organizations in the United States. Slattery, William J. (ed.) (National Bureau of Standards, Washington, D. C.). Mar 1971. 1000p. GPO $9.00.

A computer-produced Index is presented that contains the permuted titles of more than 19,000 voluntary engineering and related standards, specifications, test methods, and recommended practices, in effect as of December 31, 1969, published by some 360 U. S. technical societies, professional organizations, and trade associations. The title of each standard can be found under all the significant key words which it contains. These key words are arranged alphabetically down the center of each page together with their surrounding context. The date of publication or last revision, the standard number, and an acronym designating the standards-issuing organization appear as part of each entry. A list of these acronyms and the names and addresses of the organizations which they represent are found at the beginning of the Index. (auth)

41962 (ORNL-TM-3236) PERFORMANCE CHARACTERISTICS OF A SHORT REENTRY TUBE STEAM GENERATOR AT LOW STEAM OUTPUT. Holcomb, R. S.; Lackey, M. E. (Oak Ridge National Lab., Tenn.). Jun 1971. Contract W-7405-eng-26. 38p. Dep. NTIS.

The performance of a short reentry tube steam generator was investigated for steam flow rates of 1 to 7 lb/hr and pressures from atmospheric to 200 psia for possible application in a radioisotope power plant. The outer boiler tube had an OD of $\frac{3}{4}$ in. and a length of 50 in. Six combinations of internal geometry were tested to determine the configuration that would yield the highest exit steam temperature at 200 psia with an outer tube wall temperature of 1000°F. An exit steam temperature of 720°F at a flow rate of 5.2 lb/hr was achieved with Model 2, which had a 12-in.-long insulating sleeve in the lower end of the central tube. A boiler tube having this configuration should operate in a stable manner for flow rates up to 6 lb/hr if a pressure drop of about 100 psi is provided between the feed pump discharge and the boiler. (auth)

41963 (RDT-C-4-1-T) ORIFICE PLATE FOR ORIFICE FLANGE UNION. (Division of Reactor Development and Technology (AEC), Washington, D. C.). Jan 1971. 8p. RSO.

A standard prescribing requirements for orifice plate for orifice flange union for use in nuclear and associated applications is presented. (TSS)

41964 (RDT-C-4-4-T) VENTURI FLOW TUBE FOR LIQUID SODIUM. (Division of Reactor Development and Technology (AEC), Washington, D. C.). Jan 1971. 19p. LMEC.

A standard prescribing requirements for Venturi flow tube for liquid sodium for use in nuclear and associated applications is presented. (auth)

41965 (RDT-E-1-18-T) CLASS I VALVES FOR LIQUID METAL SERVICE. (Division of Reactor Development and Technology (AEC), Washington, D. C.). Feb 1971. 60p. LMEC.

A standard prescribing requirements for Class I valves for liquid metal service for nuclear and associated applications is presented. (TSS)

41966 (RDT-E-1-19-T) SMALL, CLASS II, LIQUID METAL VALVES. (Division of Reactor Development and Technology (AEC), Washington, D. C.). Sep 1970. 35p. LMEC.

A standard prescribing requirements for small, Class II, liquid metal valves for nuclear and associated applications is presented. (TSS)

41967 (RDT-E-3-9-T) ELECTROMAGNETIC PUMP FOR LIQUID METAL SERVICE. (Division of Reactor Development and Technology (AEC), Washington, D. C.). Mar 1971. 46p. LMEC.

A standard prescribing requirements for electromagnetic pump for liquid metal service for nuclear and associated applications is presented. (TSS)

41968 (RDT-E-4-13-T) FREEZE VENT FOR SODIUM SERVICE. (Division of Reactor Development and Technology (AEC), Washington, D. C.). Feb 1971. 32p. LMEC.

A standard prescribing requirements for freeze vent for sodium service for nuclear and associated applications is presented. (TSS)

41969 (RDT-E-10-2-T) GUARD VESSEL FOR PRIMARY SODIUM CONTAINING COMPONENTS. (Division of Reactor Development and Technology (AEC), Washington, D. C.). Nov 1970. 28p. LMEC.

A standard prescribing requirements for guard vessel for primary sodium containing components for nuclear and associated applications is presented. (TSS)

41970 (RDT-F-7-2-T) PREPARATIONS FOR SEALING, PACKAGING, PACKING, AND MARKING OF COMPONENTS FOR SHIPMENT AND STORAGE. (Division of Reactor Development and Technology (AEC), Washington, D. C.). 14 Feb 1969. 29p. RSO.

A standard prescribing requirements for preparations for sealing packaging, packing, and marking of components for shipment and storage for nuclear and associated applications is presented. (TSS)

41971 (RDT-F-8-1-T) PRELOADING THREADED FASTENERS AND CLOSURES. (Division of Reactor Development and Technology (AEC), Washington, D. C.). 9 Feb 1969. 39p. RSO.

A standard prescribing requirements for preloading threaded fasteners and closures for nuclear and associated applications is presented. (TSS)

41972 (RDT-M-1-1-T) CORROSION RESISTING CHROMIUM AND CHROMIUM-NICKEL STEEL COVERED WELDING ELECTRODES (MODIFIED ASTM A298). (Division of Reactor Development and Technology (AEC), Washington, D. C.). 14 Feb 1969. 8p. RSO.

A standard prescribing requirements for corrosion-resisting chromium and chromium-nickel steel covered welding electrodes (modified ASTM A298) for nuclear and associated applications is presented. (TSS)

41973 (RDT-M-6-2-T) MECHANICAL LOCKING DEVICES. (Division of Reactor Development and Technology (AEC), Washington, D. C.). Mar 1969. 21p. RSO.

A standard prescribing requirements for mechanical locking devices for fasteners for use in nuclear and associated applications is presented. (auth)

41974 (RDT-M-9-2-T) EXAMINATION REQUIREMENTS AND ACCEPTANCE STANDARDS FOR SEAL MEMBRANES. (Division of Reactor Development and Technology (AEC), Washington, D. C.). 14 Feb 1969. 4p. RSO.

A standard prescribing requirements for examination requirements and acceptance standards for seal membranes for use in nuclear and associated applications is presented. (auth)

41975 (RDT-M-11-1-T) NONMETALLIC SEAL MATERIALS. (Division of Reactor Development and Technology (AEC), Washington, D. C.). Feb 1969. 9p. RSO.

A standard prescribing requirements for nonmetallic seal materials for nuclear and associated applications is presented. (TSS)

41976 HEAT PIPE THERMIONIC CONVERTER RESEARCH IN EUROPE. Busse, C. A. (EURATOM CCR, Ispra, Italy). pp 861-72 of Proceedings of the Fourth Intersociety Energy Conversion Engineering Conference, September 22-26, 1969, Washington, D. C. New York; American Inst. of Chemical Engineers (1969).

From fourth intersociety energy conversion engineering conference; Washington, D. C. (21 Sep 1969). See CONF-690905.

Heat pipe research performed in West European laboratories is described. Three questions are discussed: how much heat can be transported with a heat pipe? what is the maximum heating rate? and what is the lifetime of a heat pipe? Thermionic energy conversion devices which use heat pipes for heating emitters and cooling collectors are discussed. (auth)

41977 HEAT PIPE DEVELOPMENT FOR THERMIONIC APPLICATIONS. Shefsiek, P. K.; Ernst, D. M. (Thermo Electron Corp., Waltham, Mass.). pp 879-87 of Proceedings of the Fourth Intersociety Energy Conversion Engineering Conference, September 22-26, 1969, Washington, D. C. New York; American Inst. of Chemical Engineers (1969).

From fourth intersociety energy conversion engineering conference; Washington, D. C. (21 Sep 1969). See CONF-690905.

Heat pipe development is discussed which has been specifically oriented for applications to thermionic conversion devices and related systems. High temperature lithium heat pipes for emitter applications and low temperature sodium and potassium heat pipes for collector applications were investigated. Test results are presented for the following heat pipes: unalloyed tungsten-lithium; TZM-lithium at 1560°C; nickel-sodium; and nickel-potassium at 500 to 550°C. The results of a metallurgical examination of the TZM-lithium heat pipe are presented. The heat transfer capability of the nickel-sodium, the nickel-potassium, and the tungsten-lithium heat pipes are discussed with respect to analytical predictions. (auth)

XUM

41978 DEVELOPMENT OF AN ADVANCED SPACE RADIATION SYSTEM. Peters, J. T.; Hannah, R. G. (Teledyne Co., Baltimore). pp 1010-15 of Proceedings of the Fourth Intersociety Energy Conversion Engineering Conference, September 22-26, 1969, Washington, D. C. New York; American Inst. of Chemical Engineers (1969).

From fourth intersociety energy conversion engineering conference; Washington, D. C. (21 Sep 1969). See CONF-690905.

An advanced space radiator system was developed which employs the use of hybrid, water heat pipes to transport waste heat from a radioisotopic thermoelectric generator. The heat rejection system was shown to be capable of transporting and rejecting all module design and off-design heat loads. Practical, production-oriented, fabrication techniques have been developed for large length-to-dia ratio heat pipe assemblies incorporating one or more radii of curvature in a single pipe. Structurally-adequate, curved, radiator panels employing multiple heat pipes were successfully fabricated utilizing adhesive bonding techniques and have successfully passed thermal performance and thermal cycle testing. The results of the development program on this subsystem proved that a lightweight, highly reliable, space radiator system can be evolved utilizing heat pipes. (auth)

41979 PROCEDURE FOR AUTHORIZATION OF NUCLEAR INSTALLATIONS IN VIEW OF THE EXPERIENCE ACQUIRED IN THE FIRST THREE YEARS. Nocera, F.; Di Loreto, A. (CNEN, Rome). Minerva Fisiconucl.; 13: 160-4(Apr-Jun 1969). (In Italian). (CONF-680535-18).

From 14. national conference of the Italian Association for Health Physics and Protection from Radiation; Formia, Italy (29 May 1968).

A statistical and illustrative review is made of the last three years of authorization of nuclear installation under the D.P.R. Number 185 of February 13, 1964. (J.S.R.)

41980 CHOUCA FURNACES. Bull. Inform. Sci. Tech. (Paris); No. 153-154, 88-90(Nov-Dec 1970). (In French).

The Chouca furnaces are used to irradiate structural materials or fuel samples between 150 and 1250°C, in Melusine, Siloe, Triton, Osiris, BR_2, HFR, Avogadro, Safari, and VVRS. The temperature is controlled to ±1°C by 6 independent heating elements. The Chouca furnaces operate in intense nuclear fluxes. The design and fabrication of the sample holders for Chouca furnaces are particular to each case. (France)

41981 AUTOMATED WELDER (17 Mar 1971) (Engineering Materials). (Oak Ridge National Lab., Tenn.). (CAPE-2086). 141 drawings.

This programmer-controlled tungsten arc-welding system, which is used to join pipes, is light-weight, portable, and compact. Reproducible high quality, defect-free welds are produced either semi-directly or remotely. The system consists of a horseshoe-shaped drive assembly that moves interchangeable welding or milling heads around a pipe, a welding programmer-controller, a conventional weld power source, and a portable recorder. The drive assembly rotates at preset reproducible speeds and keeps the head inserts at a constant distance from the pipe surface and the pipejoint. The welding torch is self-adjusting, arc-voltage regulated with adaptive depth control. The programmer-controller regulates weld current, current pulsing, voltage, drive-assembly speed, wire-feed rate and torch oscillation. Carriages of the following sizes are included: 3 to 6, 6 to 9, and 12 to 16 inches. (For details see TID-4100 Suppl. 64) (F.S.)

41982 SURFACE HEAT FLUX FOR INCIPIENT BOILING IN LIQUID METAL HEAT PIPES. Silverstein, Calvin C. Nucl. Technol.; 12: No. 1, 56-62(Sep 1971).

Conditions required for incipient boiling in liquid metal heat pipes are examined. It is shown that the heat flux for boiling in heat pipes can be larger than for pool boiling if thin capillary wicks are used with low frictional resistance to liquid flow in the axial direction. Methods for calculating the heat flux for incipient boiling in heat pipes are derived. Data on nucleation site radii and interface heat transfer coefficients, which are needed for heat flux calculations, are available. An upper limit of 3 to 7 microns is determined for the nucleation site radius in sodium heat pipes. (auth)

Heat Transfer and Fluid Flow

Refer also to abstracts 41962, 41976–41978, 41982, 42017, 42849, and 42962.

41983 (ANL-ETD-71-7) TENTATIVE DESIGN GUIDE FOR CALCULATING THE VIBRATION RESPONSE OF FLEXIBLE CYLINDRICAL ELEMENTS IN AXIAL FLOW. Wambsganss, M. W.; Chen, S. S. (Argonne National Lab., Ill.). Apr 1971. Contract W-31-109-eng-38. 26p. Dep. NTIS.

Many reactor and plant equipment components, such as fuel pins, control rods, and heat exchanger tubes, are long, slender, beam-like members which are exposed to nominally axial coolant flow. The flowing coolant represents a source of energy which can induce vibratory motion of these components. This design guide presents a relationship for calculating the root-mean-square (rms) displacement of a flexible rod or tube in axial flow. The relationship is based on the results of a parameter study and is valid for components that can be approximated as beams with either simply-supported or fixed-fixed ends. It is given in terms of beam natural frequency, damping factor, and intensity of the mean-square spectral density of the pressure field in the low-frequency range; all three are functions of mean axial flow velocity. Empirical expressions are developed for damping factor and intensity of the mean-square pressure spectrum. With these, an empirical equation for rms displacement is written which is in terms of known quantities and, therefore, provides a tool which can be used by designers. Since the equation is based on experiments involving a smooth rod in flow with minimal entrance effects, the predicted displacements should be interpreted and used with care. They are not conservative and, at best, will represent the minimum response to be expected. (auth)

41984 (INIS-mf-26) EXPERIMENTAL INVESTIGATION OF TEMPERATURE FIELDS IN ANNULAR SODIUM CHANNEL WITH EXCENTRICALLY MOUNTED INNER HEATING ELEMENT (e = %). Sulc, V. (Ceskoslovenska Komise pro Atomovou Energii, Prague). [nd]. 23p. (In Czech). NTIS (U. S. Sales Only).

An experimental sodium circuit equipped with electrical preheating and capable of attaining a maximum sodium temperature of 500°C and a maximum flow volume of 7000 liters per hour was used to measure the temperature distribution in an annular channel with an excentrically mounted inner heating element. The measurements were carried out at various channel outputs (1.5 kW, 1.7 kW). At an output of 2.4 kW the spread of measured values was too great, and also two of the thermocouples failed and a sodium leak occurred. Some of the data obtained are presented in graphs. (INIS)

41985 (ORNL-TM-3324) ORTHIS, ORTHAT: TWO COMPUTER PROGRAMS FOR SOLVING TWO-DIMENSIONAL STEADY-STATE AND TRANSIENT HEAT CONDUCTION PROBLEMS. Durfee, R. C.; Nestor, C. W. Jr. (Oak Ridge National Lab., Tenn.). Jul 1971. Contract W-7405-eng-26. 173p. Dep. NTIS.

The two programs, ORTHIS and ORTHAT, are designed to solve steady-state and transient heat conduction problems, respectively, in two-dimensional geometries. Either Cartesian (x-y) or cylindrical (r-z, r-θ) coordinate systems may be used. Thermal properties, heat generation rates, and boundary conditions may be functions of position, time, or temperature. The first program uses the iterative method of successive overrelaxation (SOR) to solve the steady-state problem. In addition to overrelaxation it also uses a dominant-error-mode extrapolation procedure to increase the rate of convergence. The second program uses a modified alternating-direction implicit method (ADI) to solve the transient problem. The input for both programs has been designed in an easily usable free-form style. (auth)

41986 TEPLO-I MASSOPERENOS. TOM II. MATERIALY DISKUSSII NA III VSESOYUZNOM SOVESHCHANII PO TEPLO-I MASSOOBMENU, MINSK, 1969. (Heat and Mass Transfer. Volume II. 3rd All-Union Conference on Heat and Mass Transfer, Minsk, May 14-18, 1968). Lykov, A. V. (ed.). Minsk; Institute of Heat and Mass Transfer (1969). 1974p. (CONF-680563).

This collection of over 200 papers deals with heat and mass transfer problems under a wide variety of conditions such as during interaction of bodies with liquid and gaseous systems, and heat exchange at high turbulence. Fluid flow in tubes, in the presence of natural convection, in the presence of radiation, and during evaporation, fusion, and condensation, represents one group of papers. Heat and mass transfer in dispersed systems is the general topic for another group of papers, with specialized sub-topics such as: non-stationary heat transfer, gas movement and intermixing, mathematical models and methods of measurement of local characteristics, heat transfer by radiation, and the use of a boiling layer for heat treatment of metals. Heat and mass transfer in capillary-porous systems became the focal point for another group of papers, including: drying processes, transfer of moisture in porous bodies, physicochemical methods of investigating wet materials, and problems in industrial drying. Heat and mass transfer is dealt with in technical processes and the equipment of the chemical industry, and also in what the authors call "rheological systems." The book concludes with

papers on the physical parameters of heat and mass transfer, and mathematical treatments of the theory. (K.S.W.)

41987 HEAT AND MASS TRANSFER IN TURBULENT BOUNDARY LAYERS. VOLUME I. International Summer School on Heat and Mass Transfer, 9–21 September 1968, Herceg-Novi, Yugoslavia. Jovic, B. (ed.). Belgrade, Boris Kidric Institute of Nuclear Sciences (1970). 372p.

The invited lectures and communications presented at the First International Summer School on Heat and Mass Transfer are presented. Twenty-six lectures are included in Volume I. The lectures review various theories of heat and mass transfer in turbulent boundary layers. Methods for investigating heat and mass transfer in turbulent boundary layers on various surfaces and configurations are presented. (R.C.K.)

41988 HEAT AND MASS TRANSFER IN TURBULENT BOUNDARY LAYERS. VOLUME II. International Summer School on Heat and Mass Transfer, 9–21 September 1968, Herceg-Novi, Yugoslavia. Jovic, B. (ed.). Belgrade; Boris Kidric Institute of Nuclear Sciences (1970). 408p.

The invited lectures and communications presented at the First International Summer School on Heat and Mass Transfer are presented. Thirty-four lectures are included in Volume II. Theories of fully-developed and vortex flow are presented. Various methods for calculation and measurement of flow, turbulent mixing, temperature, critical heat fluxes, and boiling are discussed. (R.C.K.)

41989 HEAT TRANSFER WITH WATER AND FREON-113 BOILING ON A NONISOTHERMAL SURFACE. Dul'kin, I. N.; Rakushina, N. I.; Royzen, L. I.; Fastovskii, V. G. (All-Union Electrical Engineering Inst., Moscow). Heat Transfer-Sov. Res.; 3: No. 3, 61-9(May-Jun 1971).

An analytical and experimental study is described of heat transfer modes with boiling water and Freon-113 on a nonisothermal surface of a cylindrical rod. The heat was supplied through the rod end and was dissipated from its surface at which different pool boiling modes coexisted simultaneously. The experiments were carried out with 1.4 cm diameter copper rods with lengths of 1.25, 2.65, 4.4 and 6.6 cm. The experimental data are compared with theory. (auth)

Isotope Technology

Refer also to abstracts 41741, 41904, 41957, 41962, 42027, 42590, and 43184.

41990 (JAERI–13617) APPLICATION TEST FOR RADIOISOTOPES DEVELOPED IN THE FISCAL YEARS OF 1965, 1966, AND 1967. (Japan Atomic Energy Research Inst., Tokai). Jun 1969. 17p. NTIS (U. S. Sales Only).

In the fiscal year of 1965, 28 products that included eight nuclides (^{18}F, ^{28}Mg, ^{32}P, ^{35}S, ^{54}Mn, ^{86}Rb, ^{131}I, and ^{192}Ir) were sent to users in order to test their reliabilities for actual use. The total activity was 112,219.3 mCi. In the fiscal years of 1966 and 1967, products of high specific activity ^{64}Cu that had been produced by using hot atom reactions were sent out for application tests. This three year's period was the second half in the first five year program that started in October 1962 in the radioisotope production plan of the Division of Radioisotope Production, JAERI. (auth)

41991 (JAERI–13778) STUDIES ON FUNDAMENTAL PROPERTIES OF ALUMINA ADSORBENT FOR RADIOISOTOPE PRODUCTION. Amano, Hiroshi; Nakamura, Haruto; (and others) (Japan Atomic Energy Research Inst., Tokai). Nov 1969. 20p. NTIS (U. S. Sales Only).

Fundamental properties of chromatographic alumina, which is being used for the preparation of radioisotope generators and the separation of the fission products, were examined in connection with pretreatment procedures, dissolution, adsorption capacity for ions, and the effects of various storage modes. A commercial chromatographic alumina used in this work showed an increase in its absorption capacity and a decrease in the dissolution rate, when it was ignited for ten hours at 400°C and treated with boiling dilute hydrochloric acid. The dissolution rate and the adsorption capacity of alumina treated in this manner were not affected during the course of the storage under normal operation conditions. The pretreated alumina was loaded in a column. The dissolution of alumina by various eluants and the adsorption capacity for chloride, sulfate, fluoride, tellurite, tellurate, and molybdate ions were examined. The dissolution of alumina decreased in sodium hydroxide, hydrochloric acid, nitric acid, ammonium hydroxide, and sodium chloride respectively. It was also observed that the adsorption capacity and the elution conditions for tellurium and molybdenum were greatly affected by pH of the solution and their valency state. (auth)

41992 (ORNL–4640) REVIEW OF ORNL ELECTROMAGNETIC SEPARATIONS PROGRAM, 1968–69. Love, L. O.; Bell, W. A. (Oak Ridge National Lab., Tenn.). Apr 1971. Contract W-7405-eng-26. 65p. Dep. NTIS.

Information is reviewed on stable isotopes, methods and equipment development, enrichment of ^{85}Kr, ion implantation, development of 180° sector isotope separator, development of two-stage separator with magnetic field, performance of 540° multistage isotope separator, heavy-element separations, and contamination control in separation processes. (J.R.D.)

41993 (ORNL–4692) ORNL ISOTOPIC POWER FUELS QUARTERLY REPORT FOR PERIOD ENDING MARCH 31, 1971. Lamb, Eugene (Oak Ridge National Lab., Tenn.). Jun 1971. Contract W-7405-eng-26. 24p. Dep. NTIS.

The series of tests on $^{244}Cm_2O_3$ solubility was completed, and the results indicate a low solubility in both distilled and sea water. A new series of tests to identify the dissolution reaction(s) will be started. A process for manufacturing microspheres using ion-exchange resins is being investigated. Cermet fuel forms of nominally 20 and 40 vol % oxide fuel contents are being developed with ThO_2 as a stand-in for $^{244}Cm_2O_3$. Parametric studies of both cold pressing and sintering, and hot pressing fabrication processes are underway. The curium source test completed one year of operation on February 19, 1971. Thulium sesquioxide powders originally introduced into a Knudsen cell to obtain weight-loss data sintered into a pellet after two 48-hr runs. Two $Tm_2O_3-Yb_2O_3$ mixtures were prepared by the coprecipitation method. Experiments to obtain vapor pressure data, as well as correction factors for the observed weighing data, will be continued. The Pt–Rh–W alloy is being more fully characterized because of its potential as an improved heat source container material. Properties being evaluated include fabricability, weldability, recrystallization and grain growth behavior, mechanical properties, air oxidation behavior, and compatibility with other heat source materials. A composition of Pt-26% Rh-8% W was found to be readily fabricable and weldable while exhibiting tensile strengths comparable to T-111 at 1100°C. A proposed phase diagram of the Ta–O system was constructed from available information. Potential melting at temperatures as low as ~1840°C is indicated for tantalum with oxygen contents above 0.46 wt %. Production of 112 ThO_2–Mo cermet fuel simulant disks was completed, and shipments were made to Mound Laboratory and LASL. All disks were >96% of theoretical density. (auth)

41994 ULTRACENTRIFUGE SEPARATION OF HEAVY ISOTOPES. Theyse, F. H. (UC Project, Amsterdam). J. Mech. Eng. Sci.; 13: No. 3, 168-72(Jun 1971).

The fundamental equations describing the physical principles that underly the ultracentrifuge isotope separation process are outlined leading to a description of the engineering problems encountered. (auth) (UK)

41995 PROCEEDINGS OF THE FOURTH INTERSOCIETY ENERGY CONVERSION ENGINEERING CONFERENCE, SEPTEMBER 22–26, 1969, WASHINGTON, D. C. New York; American Institute of Chemical Engineers (1969). 1186p. $45.70. (CONF-690905).

One-hundred-thirty-five unclassified papers on energy conversion engineering were presented at the conference and are included in this issue. A separate abstract was prepared for each of 29 papers. One paper appeared previously in NSA. For an abstract of this paper see 23: 39499. 107 papers were not within the scope of NSA. (L.C.L.)

For abstracts of individual papers see: 41976–41978, 41996–42010, 42962, 43187, 44145, 44169–44173, 44175, 44179, and 44180.

41996 NUCLEAR ELECTRIC POWER SOURCES FOR BIOMEDICAL APPLICATION. Knapp, D. E.; Bennett, A. B.; DeSteese, J. G.; (and others) (McDonnell Douglas Corp., Richland, Wash.). pp 101-6 of Proceedings of the Fourth Intersociety Energy Conversion Engineering Conference, September 22–26, 1969, Washington, D. C. New York; American Inst. of Chemical Engineers (1969).

From fourth intersociety energy conversion engineering conference; Washington, D. C. (21 Sep 1969). See CONF-690905.

Development of small nuclear electric power sources has concentrated on two approaches: thermionic and betavoltaic energy conversion. These approaches have produced devices known as Isomite cells in the case of thermionics and Betacel in the case of betavoltaics. Isomite and Betacel nuclear power cells find greatest utility when a remoteness criterion exists.

XUM

Examples of remote applications are satellite power sources, undersea power supplies, and power supplies for in vivo telemetry units or functional requirements such as cardiac pacemaking. (auth)

41997 FRENCH THERMIONIC PROGRAM AND ACCOMPLISHMENTS. Devin, B. (CEN, Saclay, France). pp 137-45 of Proceedings of the Fourth Intersociety Energy Conversion Engineering Conference, September 22–26, 1969, Washington, D. C. New York; American Inst. of Chemical Engineers (1969).

From fourth intersociety energy conversion engineering conference; Washington, D. C. (21 Sep 1969). See CONF-690905.

The French program for the development of thermionic converters is reviewed. General converter technology and converter performance and life testing are discussed. Thermionic fuels and materials, advanced research, and converter production and cast reduction are described. It is concluded that the complete design of simplified systems where the requirements are not as severe as for space missions is of great importance for the orientation of present thermionic technology and for the establishment of realistic operational costs. (R.C.K.)

41998 SNAP-21 10-WATT THERMOELECTRIC POWER SYSTEM. Fox, F. K. (3M Company, St. Paul); Niendorf, L. R. pp 146-52 of Proceedings of the Fourth Intersociety Energy Conversion Engineering Conference, September 22–26, 1969, Washington, D. C. New York; American Inst. of Chemical Engineers (1969).

From fourth intersociety energy conversion engineering conference; Washington, D. C. (21 Sep 1969). See CONF-690905.

Development of 10-watt radioisotope-powered thermoelectric generators for deep-sea applications is described. The system has a five-year design life and is composed of the following components: thermoelectric generator, high temperature vacuum insulation system, fuel capsule, biological shield, power conditioner, and pressure vessel. The thermoelectric generator and vacuum insulation system required extensive development effort. The thermoelectric generator is a 48-couple lead-tin-telluride/bismuth-antimony-telluride flat plate configuration. Technical accomplishments achieved include overall performance improvement relating to: fabrication techniques to provide strong thermoelectric element (leg) segment to segment bond; leg bonding techniques resulting in minimum cross contamination between segments; reduction of P-type leg hot junction electrical contact resistance; and reduction of thermal impedance from the leg cold end to the cold frame. The high temperature vacuum insulation system has the dual purpose of supporting the 265-pound biological shield while allowing minimum heat loss from the fuel. It is hermetically sealed and incorporates chemical getters to maintain a hard vacuum for five years. The biological radiation shield is supported by a thin walled neck tube at the generator end and three ball joint tension support rods at the other end. Two systems are presently on long-term test in the ocean off San Clemente Island. These systems were implanted in June 1969 and are expected to remain in shallow water from three to five years. One additional system will be implanted in the ocean off San Clemente Island in August 1969. (auth)

41999 SNAP-27 PROGRAM REVIEW. Pitrolo, A. A. (General Electric Co., Cincinnati); Rock, B. J.; Remini, W.; Leonard, J. A. Contract AT(29-2)2581. pp 153-70 of Proceedings of the Fourth Intersociety Energy Conversion Engineering Conference, September 22–26, 1969, Washington, D. C. New York; American Inst. of Chemical Engineers (1969).

From fourth intersociety energy conversion engineering conference; Washington, D. C. (21 Sep 1969). See CONF-690905.

The SNAP-27 Radioisotope Thermoelectric Generator (RTG) System was designed, developed, and fabricated for the Apollo Lunar Surface Experiment Package (ALSEP). The program began in late 1965 and the first electrically heated generators were on test in late 1966. Initial power requirements of 56 watts were exceeded and each of the five flight units is expected to produce more than 67 watts after one year of lunar surface operation. The last flight hardware was delivered in May of 1969. The SNAP-27 Program was successfully concluded and the AEC has provided NASA with a $^{238}PuO_2$ isotopic power system of proven performance and reliability. (auth)

42000 COMPACT ^{60}Co KERNEL FOR SPACE POWER. Ruehle, W.; Forrest, D. L. (Aerojet-General Corp., San Ramon, Calif.). pp 321-38 of Proceedings of the Fourth Intersociety Energy Conversion Engineering Conference, September 22–26, 1969, Washington, D. C. New York; American Inst. of Chemical Engineers (1969).

From fourth intersociety energy conversion engineering conference; Washington, D. C. (21 Sep 1969). See CONF-690905.

The compact ^{60}Co kernel shows promise of becoming a leading heat source concept for multikilowatt power in space. It includes shielding and will prevent loss of radioactive material by diffusion or chemical attack. Its weight is comparable to a ^{238}Pu heat source, and costs are substantially lower. A program was recently started to analyze and evaluate the safety of a 30 kW(t) ^{60}Co kernel in a manned Earth orbit application of 1 year duration. The design definition and introduction to the safety study are presented. (auth)

42001 MODEL TO DESCRIBE LONG-TERM PERFORMANCE CHARACTERISTICS OF PRESSURE-CONTACTED LEAD-TELLURIDE THERMOELECTRIC GENERATORS. Field, D. R.; Bunde, G. W. (3M Company, St. Paul). pp 425-35 of Proceedings of the Fourth Intersociety Energy Conversion Engineering Conference, September 22–26, 1969, Washington, D. C. New York; American Inst. of Chemical Engineers (1969).

From fourth intersociety energy conversion engineering conference; Washington, D. C. (21 Sep 1969). See CONF-690905.

A model is presented which describes observed long-term performance behavior of thermoelectric generators utilizing hot-junction pressure-contacted lead–telluride technology. The model, based on degradation due to thermoelectric material sublimation, describes thermal and electrical changes as influenced by electrode temperatures, temperature gradient, cover-gas type and pressure, and thermoelement geometry. Performance predictions based on this model agree well with test data from devices containing N-type lead–telluride and P-type lead–tin–telluride thermoelectric materials. The devices have thermoelement diameters ranging from 0.188 to 0.250 in., hot junction temperatures ranging from 1050 to 1200°F, temperature gradients ranging from 1300 to 1800°F/in., and xenon and argon cover gasses ranging in pressure from 2.5 to 25 psia. Post-test analyses data, and over 50 million couple hours of supporting life test data, have been obtained from the SNAP-21, -23, -23A, and -27 programs. A portion of this data is derived from devices which have logged nearly five years of continuous test time. (auth)

42002 PERFORMANCE EVALUATION AND LIFE TESTING OF THERMOELECTRIC GENERATORS AT THE JET PROPULSION LABORATORY. Rouklove, Peter; Truscello, Vincent (Jet Peopulsion Lab., Pasadena, Calif.). pp 436-46 of Proceedings of the Fourth Intersociety Energy Conversion Engineering Conference, September 22–26, 1969, Washington, D. C. New York; American Inst. of Chemical Engineers (1969).

From fourth intersociety energy conversion engineering conference; Washington, D. C. (21 Sep 1969). See CONF-690905.

Ten generators have been, or are being, evaluated. Generators tested have included those of the SNAP-11 and SNAP-19-type, as well as a cylindrical thermoelectric module generator mounted on a heat pipe. Results of testing show that thermoelectric generators are capable of reliable long-time operation and are well suited for long-term space missions. (auth)

42003 ORGANIC RANKINE CYCLE FOR MANNED SPACE APPLICATIONS. Diamond, S. D.; Taylor, A. M. (McDonnell Douglas Astronautics Co., Santa Monica, Calif.). pp 447-55 of Proceedings of the Fourth Intersociety Energy Conversion Engineering Conference, September 22–26, 1969, Washington, D. C. New York; American Inst. of Chemical Engineers (1969).

From fourth intersociety energy conversion engineering conference; Washington, D. C. (21 Sep 1969). See CONF-690905.

The results of an analysis of the isotope organic Rankine cycle system for a 1 year or greater manned space station are presented. The analysis was performed using a modified version of the H-521 space power computer program. A baseline power system was selected to meet the manned earth orbiting mission requirements; parametric tradeoff studies were performed to determine system operating parameters; and design information in the form of weight, volume, area, reliability, and internal design parameters is presented for the organic Rankine power system. The baseline system for the study is a ^{238}Pu isotope organic Rankine cycle suitable for a manned space station which can be launched during the 1975 to 1985 time period. Operation is at an orbital altitude of 464 km for 1 year (baseline) with variations in duration up to 10 years. The average power level is 6.4 kW(e) at the user load with peak loads to 10.8 kW(e). The resulting power system has a cycle efficiency of 19.5%, an overall system efficiency of 11%, and a specific mass of 390 kg/kW(e) based on peak power output. The system has a mass of 4,204 kg and a radiator area of 92 m^2. (auth)

42004 RADIOISOTOPE THERMAL ENERGY SOURCES FOR SPACE STATION LIFE-SUPPORT SYSTEMS. Elms, R. V. Jr.; Greenfield, H. H. (Lockheed Missiles and Space Co., Sunnyvale, Calif.). pp 494-504 of Proceedings of the Fourth Intersociety Energy Conversion Engineering Conference, September 22–26,

1969, Washington, D. C. New York; American Inst. of Chemical Engineers (1969).

From fourth intersociety energy conversion engineering conference; Washington, D. C. (21 Sep 1969). See CONF-690905.

Candidate life support system approaches to perform life support functions for a two-man, 180-day mission were evaluated to identify an optimum integrated LSS and to determine the optimum energy source after considering radioisotopes for direct thermal energy. The heating requirements for each component were established and seven integrated life support system concepts were generated utilizing electrical and radioisotope thermal energy (RITE) sources. Eight candidate radioisotopes were selected and evaluated from an initial screening of isotope heat sources. PuO_2 and Pm_2O_3 capsules were selected for detailed evaluation. The integrated LSS concepts were compared on the basis of power, weight, volume, maintainability, reliability, crew safety, cost, thermal control, and development problems. The selected integrated concept utilized three RITE sources as follows: an individual 355-W(t), 1900°F RITE source, located inside the space cabin radiating to a combined urine vapor pyrolysis unit/waste incinerator and using an active thermal control system; an individual 75-W(t) 600°F RITE source, located inside the space cabin heating a catalytic oxidizer and using passive thermal control; and a central 1500-W(t) 800°F RITE source, with a heat exchanger and heat transfer loop providing the intermediate and low temperature thermal requirements of the ISS. The central RITE unit is located outside the cabin, and thermal control is obtained with a louver system. The design and operation of the combined incinerator/RITE/urine pyrolysis unit are described. (auth)

42005 ELECTRICAL/THERMAL INTEGRATION OF DYNAMIC POWER AND LIFE-SUPPORT SYSTEMS FOR MANNED SPACECRAFT. Shinbrot, C. H.; Coggi, J. V. (McDonnell Douglas Astronautics Co., Santa Monica, Calif.). pp 505-14 of Proceedings of the Fourth Intersociety Energy Conversion Engineering Conference, September 22–26, 1969, Washington, D. C. New York; American Inst. of Chemical Engineers (1969).

From fourth intersociety energy conversion engineering conference; Washington, D. C. (21 Sep 1969). See CONF-690905.

Design studies of the thermal integration of environmental control and life support systems (EC/LS) with Brayton cycle and low-temperature Rankine cycle power systems are currently in progress for manned spacecraft. The studies are based on empirical life support thermal data obtained during a manned test of a closed regenerative life support system and analyses of the effects of thermal transients on the design of the dynamic power conversion systems. The Brayton and organic Rankine cycle systems are both under evaluation for a possible future 30 day test with space cabin simulator regenerative EC/LS systems within the next several years. An organic Rankine cycle simulated loop will be integrated and used to obtain the first real test data to help prove the feasibility of integrating regenerative life support systems with power systems using both waste heat and electrical energy. The analyses of the thermal integration of an organic Rankine cycle system is sufficiently advanced to permit publication of the study results. Additional work is continuing on the analyses of thermally integrated isotope Brayton cycle and EC/LS systems. The thermally integrated Brayton cycle power system analyses is in progress and will be published at a later date. The baseline power system investigated consists of a 6.4-kW(e) dynamic power conversion system with a cobalt-60 heat source for a six-man space station. The waste thermal energy of the power system is supplied to both the EC/LS water recovery system and the regenerable molecular sieve carbon dioxide control system. The baseline integrated 6.4-kW(e) power system is compared with a nonintegrated 8.9-kW(e) dynamic power system. The EC/LS system in the nonintegrated design utilizes electrical heaters for the supply of thermal energy. (auth)

42006 ISOTEC THERMOELECTRIC GENERATOR FOR SPACE POWER. Steeger, E. J.; Cruver, J. E. (Gulf General Atomic Inc., San Diego, Calif.). pp 515-21 of Proceedings of the Fourth Intersociety Energy Conversion Engineering Conference, September 22–26, 1969, Washington, D. C. New York; American Inst. of Chemical Engineers (1969).

From fourth intersociety energy conversion engineering conference; Washington, D. C. (21 Sep 1969). See CONF-690905.

The design features of the ISOTEC thermoelectric generators are summarized. The generators employ small bonded lead telluride elements operating at low hot junction temperatures to give long-life operation and stable performance. Thermoelectric elements are incorporated in a lightweight panel structure which is coupled thermally by radiation to a radioisotope heat source. Radiative heat transfer coupling allows wide variation of the heat source design without performance penalty. The modular concept of the ISOTEC generator permits a wide range of power output using the already developed lightweight panels as building blocks. The quantity of thermoelectric panels or the number of couples per panel can be varied in a straightforward manner. Thus, generators of a wide range of power levels can be constructed with the present panel and structure technology. Reliability of the generator is enhanced by a large series-parallel matrix electrical circuit of the thermoelectric couples and by low temperature vacuum operation. The latter eliminates the need for, and hence, reliability limitations resulting from, a pressure vessel and a gas overpressure around the thermoelectric couples. (auth)

42007 CLOSED BRAYTON CYCLE POWER SYSTEM APPLICATIONS. Pietsch, Anthony (Garrett Corp., Phoenix, Ariz.). pp 642-51 of Proceedings of the Fourth Intersociety Energy Conversion Engineering Conference, September 22–26, 1969, Washington, D. C. New York; American Inst. of Chemical Engineers (1969).

From fourth intersociety energy conversion engineering conference; Washington, D. C. (21 Sep 1969). See CONF-690905.

The closed Brayton cycle power system satisfies many unique applications where the special environmental conditions of space, lunar, terrestrial and undersea must be met for both manned and unmanned missions. A number of such systems are described. The closed Brayton cycle has been developed to a state where overall performance of the system is accurately predictable. Both components and complete systems have been operated over a wide range of power, pressure, temperature, and speed conditions, and this data has been accurately measured and mapped. In general, the measured performance has exceeded that which was predicted. This has proven that high performance can be achieved with a single system over a wide power range and with large variations in heat input and heat rejection temperatures. Thus a wide variety of heat sources including radioisotopes, reactors, solar and chemical, are suitable to power the closed Brayton cycle. The range of power investigated where high efficiency was attained is from 0.5 kilowatt to more than 100 kilowatts. The progress made in the development of hardware for these systems will be presented to substantiate the performance calculations. (auth)

42008 BRAYTON-B POWER SYSTEMS: A PROGRESS REPORT. Brown, William J. (Lewis Research Center, Cleveland). pp 652-8 of Proceedings of the Fourth Intersociety Energy Conversion Engineering Conference, September 22–26, 1969, Washington, D. C. New York; American Inst. of Chemical Engineers (1969).

From fourth intersociety energy conversion engineering conference; Washington, D. C. (21 Sep 1969). See CONF-690905.

Progress and current status of the 2-to-10 kW Brayton-B power system are reported. All power conversion component hardware has been built and initial component testing has begun. A Brayton-B power system with an electric heat source is ready for test at Plum Brook Space Power Facility. Analysis, based on preliminary test data, shows that the power conversion unit can provide 2-to-15 kW(e) at high system efficiencies from 0.17 to 0.30. (auth)

42009 ANALOG COMPUTER STUDIES OF A 2 TO 10 KILOWATTS ELECTRIC BRAYTON CYCLE SPACE POWER SYSTEM INCLUDING STARTUP AND SHUTDOWN. Cantoni, Dennis A.; Thomas, Ronald L. (Lewis Research Center, Cleveland). pp 668-78 of Proceedings of the Fourth Intersociety Energy Conversion Engineering Conference, September 22–26, 1969, Washington, D. C. New York; American Inst. of Chemical Engineers (1969).

From fourth intersociety energy conversion engineering conference; Washington, D. C. (21 Sep 1969). See CONF-690905.

An analog computer was used to simulate the dynamics of a single-shaft Brayton cycle power system. Investigations were made of startup and shutdown transients. Startup studies were made to size the injection and vent valves, determine self-sustaining speed, and devise a startup procedure. Shutdown studies were used to determine a shutdown procedure. Presented are results of these studies, their impact on the Brayton power system and a description of the analog simulation. (auth)

42010 RADIOISOTOPE-ENERGIZED STIRLING ENGINE FOR SPACECRAFT AUXILIARY ELECTRIC POWER IN THE 250- TO 500-W(e) POWER RANGE. Leach, C. E.; Fryer, B. C. (Pacific Northwest Lab., Richland, Wash.). pp 679-91 of Proceedings of the Fourth Intersociety Energy Conversion Engineering Conference, September 22–26, 1969, Washington, D. C. New York; American Inst. of Chemical Engineers (1969).

From fourth intersociety energy conversion engineering conference; Washington, D. C. (21 Sep 1969). See CONF-690905.

XUM

A variety of spacecraft experiments are projected in the 1970's on which radioisotope devices could provide electrical power. This study was performed to identify likely system configurations, estimate weight and fueling requirements of the Stirling engine cycle in the middle and low end of the 100 to 1000 W(e) power range. (auth)

42011 ELEMENTARY DETERMINATION OF DISTRIBUTION IN SEPARATION TUBES. I. Zieger, K. (Zentralinstitut fuer Isotopen- und Strahlentechnik, Leipzig). Isotopenpraxis; 7: No. 3, 95-8(Mar 1971). (In German).

The prototype system of transport equations describing the steady distribution of an isotopic multicomponent mixture renders possible elementary integration. A summary of the results previously published in this connection is presented. An equivalent system of transcendental equations in a particularly simple and lucid form that makes it accessible even to graphic solution is described. (tr-auth)

42012 NUCLEAR PACEMAKERS AND THE PRODUCTION OF ^{238}Pu SOURCES. Casa, Anna F. Com. Naz. Energ. Nucl., Notiz.; 17: No. 4, 84-9(Apr 1971). (In Italian).

A review of nuclear-powered heart stimulators (pacemakers) and their recent implants in men and animals, and of the production of plutonium sources is presented. (auth)

42013 USE OF RADIOISOTOPES IN INDUSTRIAL PLANTS IN RELATION TO ARTICLE 55 OF THE D.P.R. NUMBER 185 OF FEBRUARY 13, 1964: OBSERVATIONS ON THE THEME OF AUTHORIZATIONS. Nocera, F. (CNEN, Rome). Minerva Fisiconucl.; 13: 154-9(Apr-Jun 1969). (In Italian). (CONF-680535-17).

From 14. national conference of the Italian Association for Health Physics and Protection from Radiation; Formia, Italy (29 May 1968).

An interpretative and critical examination is made of the procedural aspects of the use of radioactive sources in industrial pl[illegible]. Nuclear security and health safety in various types of plants are discussed. The authorizing procedures for the industrial use of radioisotopes are outlined. (J.S.R.)

42014 ISOTOPIC POWER SOURCES. Penn, A. W. (Atomic Energy Research Establishment, Harwell, Eng.). Phys. Bull. (London); 22: 207-10(Apr 1971).

The concept of isotopic power generators is explained. The criteria for choice of isotope fuels are given and the properties of suitable isotopes (^{238}Pu, ^{244}Cm, ^{242}Cm, ^{210}Po, ^{228}Th, ^{90}Sr, ^{137}Cs, ^{144}Ce, ^{60}Co, ^{227}Ac, ^{232}U) listed. Thermal insulation requirements are disucssed and the problem of thermoelectric materials considered. The UKAEA RIPPLE (radioisotope-powered prolonged life equipment) generator is described and the specification of other terrestrial thermoelectric generators tabulated. The heart pacemaker batteries and space generators are described. Finally the power to weight ratio and generator costs for such applications are considered. (UK)

42015 RADIATION UNIT RCH-GAMMA-30. Jokel, Jozef; Pullmann, Michal (State Forest Products Research Inst., Bratislava). Jad. Energ.; 17: No. 7, 238-40(1971). (In Czech).

A self-shielded Soviet-made radiation unit was installed at State Forest Products Research Institute in Bratislava in 1969. The capacity of the unit is 30,000 to 100,000 Ci of ^{60}Co. Because of insufficient homogeneity of the dose rate, the unit was reconstructed in 1970. The activity of the source was 7730 Ci. The capacity of the cylindrical radiation chamber is 4.4 dm^3. The dose rate ranges from 373 krad h^{-1} to 482 krad h^{-1}. (auth)

42016 RADIATION SAFETY IN THE DESIGN AND OPERATION OF POWERFUL BETA-INSTALLATIONS. Mamin, E. B.; Terman, A. B.; Chistov, E. D. (Physical-Chemical Research Inst., Moscow. Central Inst. of Medical Advance, Moscow. All-Union Central Science-Research Inst. of Workers Protection, Moscow. All-Union Central Council of Trade Unions, Moscow). Gig. Sanit.; No. 4, 39-44(Apr 1971). (In Russian).

A method of calculating biological shield parameters is presented for high-intensity beta sources, with sufficient accuracy for solving practical problems of attenuation of accompanying radiation. A simple apparatus is described for testing the integrity of a hermetically sealed radiation source and the presence of surface contamination. The system incorporates an experimental source, pump, and an end-window counter. The leakage of beta radiation through openings and cracks is discussed and suggestions are made for preventing such leakage by means of magnetic traps or labyrinths. (K.S.W.)

42017 SUBLIMING NUCLEAR MICROTHRUSTER AND ITS SPACE APPLICATIONS. Choong, Philip T.; Mason, Edward A. (Massachusetts Inst. of Tech., Cambridge). Nucl. Technol.; 12: No. 1, 127-36(Sep 1971).

A conceptual two-stage microthruster employing sublimed molecules as the propellant of the first stage and alpha particles as the propellant of the second stage is analyzed. Transient thermal analysis is developed as a tool to provide design information on material compositions. The numerical result suggests that the radioisotope-heating of the nozzle wall could help to flatten the subliming surface temperature. The modified Monte Carlo technique for analyzing the vapor flow through the nozzle is shown to be very accurate and flexible. The result clearly points the direction to optimize the performance. Applications of this device are particularly suited in the spin-stabilization and the precession-damping of small scientific probes. (auth)

42018 METHOD FOR ACTIVATING CHROMED SURFACES FOR RADIOINDICATOR INVESTIGATION OF THEIR WEAR (EXCHANGE OF EXPERIENCE). Magarik, K. N.; Bogdanov, V. A. Ind. Lab. (USSR) (Engl. Transl.); 36: No. 11, 1747(Nov 1970). Translated from Zavod. Lab.; 36: No. 11. 1369-70(Nov 1970).

The best method for activating chromed rubbing surfaces is the direct introduction of an isotope during the electrolysis of the chrome. This method has not received wide use, however, due to the high radioactivity of the electrolyte when using the ^{51}Cr isotope and due to the lack of success in depositing chromium along with isotopes of other elements. In order to obviate this difficulty, a method of activating the chromium with the selenium isotope ^{75}Se during electrolysis was developed. The total activity of the electrolyte containing ^{75}Se was reduced from 10 to Ci to μCi, and the duration of the experiments is increased. Tests conducted with an engine having a radioactive piston ring (due to ^{75}Se) and a radioactive upper cylinder sleeve (due to ^{60}Cr) for 200 hr showed that the use of the isotope ^{75}Se as a wear indicator for the chrome plating of a ring has no effect on its wear resistance. The ring activity is sufficient for making tests for an extended period of time. The proposed method for activating not only permits a sharp reduction of the electrolyte activity, but is also more economical (40 times cheaper) than when activating with ^{51}Cr. (R.C.K.)

42019 NUCLEAR POWER SOURCE. Round, K. J. Canadian Patent 870,188. 4 May 1971.

A means is described for utilizing radioactive emission from a radioisotope to generate relatively high voltages at small current. The device consists of a hollow metallic body, vacuum-tight closure means, a high voltage insulator, a mounting post, several isotope bearing plates containing ^{147}Pm and collector plates interspaced with, and insulated from, the isotope bearing plates. (F.S.A.)

Materials Testing

Refer also to abstracts 41961, 42761, 42817, 42835, 42840, 42849, 42850, 44080, 44084, 44110–44113, and 44148.

42020 (BNWL-B-103) DEVELOPMENT AND DESIGN OF AN ULTRASONIC INSPECTION SYSTEM FOR RADIOACTIVE WASTE CONTAINERS. (Battelle-Northwest, Richland, Wash. Pacific Northwest Lab.). 8 Jun 1971. Contract AT(45-1)-1830. 31p. Dep. NTIS.

Waste storage containers must exhibit a high degree of structural integrity. The results of a project to develop and define a nondestructive test system capable of performing ultrasonic inspection of the waste containers to assure container integrity is presented. The basic design of the inspection system is outlined including detailed circuit drawings, functional specification design drawings for the inspection tanks, and appropriate interconnection diagrams. In addition, some examples of the results obtained with a laboratory prototype inspection system are presented which illustrate the performance of the system design. (auth)

42021 (CONF-710512-2) FRACTURE MECHANICS AND NONDESTRUCTIVE TESTING OF BRITTLE MATERIALS. Clark, W. G. Jr. (Westinghouse Research Labs., Pittsburgh, Pa.). 21 Jan 1971. 7p. (71-PVP-4). ASME, New York $2.00.

From first national congress on pressure vessels and piping; San Francisco, Calif. (10 May 1971).

The fracture mechanics approach to the development of meaningful nondestructive inspection requirements is presented. The basic concepts underlying the technology are reviewed, and the practical engineering aspects of this approach to the prevention of structural failure are demonstrated. Particular emphasis is placed on evaluating the influence of defect morphology (size, shape, orientation, distribution) on fracture behavior. A hypothetical inspection problem is included and the pertinent con-

siderations associated with the development of a realistic nondestructive inspection specification are discussed in detail. (auth)

42022 (RDT-F-2-4-T) QUALITY VERIFICATION PROGRAM REQUIREMENTS. (Division of Reactor Development and Technology (AEC), Washington, D. C.). Oct 1969. 7p. RSO.

A standard prescribing requirements for quality verification program requirements for nuclear and associated applications is presented. (auth)

42023 (RDT-F-3-4-T) ULTRASONIC SHEAR-WAVE EXAMINATION OF PLATES (MODIFIED ASTM A577). (Division of Reactor Development and Technology (AEC), Washington, D. C.). Feb 1969. 5p. RSO.

A standard prescribing requirements for ultrasonic shear-wave examination of plates (modified ASTM A577) for nuclear and associated applications is presented. (auth)

42024 (RDT-F-3-5-T) LONGITUDINAL-WAVE ULTRASONIC EXAMINATION OF PLAIN AND CLAD STEEL PLATES (MODIFIED ASTM A578). (Division of Reactor Development and Technology (AEC), Washington, D. C.). Feb 1969. 8p. RSO.

A standard prescribing requirements for longitudinal-wave ultrasonic examination of plain and clad steel plates (modified ASTM A578) for nuclear and associated applications is presented. (auth)

42025 (RDT-F-3-6-T) NONDESTRUCTIVE EXAMINATION. (Division of Reactor Development and Technology (AEC), Washington, D. C.). Mar 1969. 29p. RSO.

A standard prescribing requirements for nondestructive examination for nuclear and associated applications is presented. (auth)

42026 (RDT-F-3-8-T) ULTRASONIC EXAMINATION OF METAL PIPE AND TUBING FOR LONGITUDINAL DISCONTINUITIES (MODIFIED ASTM E213). (Division of Reactor Development and Technology (AEC), Washington, D. C.). Feb 1969. 5p. RSO.

A standard prescribing requirements for ultrasonic examination of metal pipe and tubing for longitudinal discontinuities (modified ASTM E213) for nuclear and associated applications is presented. (auth)

42027 (RFP-1706) NEUTRON RADIOGRAPHY WITH A SEALED-TUBE NEUTRON GENERATOR AND GRAPHITE MODERATED SYSTEM. Vasilik, Dennis; Murri, Richard (Dow Chemical Co., Golden, Colo. Rocky Flats Div.). 30 Jun 1971. Contract AT(29-1)-1106. 25p. Dep. NTIS.

Neutron radiographs of good quality were produced by using a sealed-tube neutron generator and a graphite moderator system. The graphite moderator is a right-cylinder 76.2 cm in diameter and 76.2-cm high. A thermal neutron flux at the object of 1.1×10^5 n/cm^2-sec and a cadmium ratio of 3.5 was measured. The collimator ratio was 7.25; the x-ray intensity was 0.50 mR/sec; and the resolution was measured to be 0.025 cm. Experimental techniques for determining fast and thermal neutron fluences are also described. (auth)

42028 NONDESTRUCTIVE TESTING AS A FACTOR OF TECHNICAL AND INDUSTRIAL DEVELOPMENT. Sabato, Jorge A.; Baez, Juan N. (National Atomic Energy Commission, Buenos Aires). pp 622-7 of Materials Technology. I. New York; American Society of Mechanical Engineers (1970).

From second inter-american conference on materials technology; Mexico City, Mex. (24 Aug 1970). See CONF-700812.

Nondestructive testing (NDT) plays a critical and well recognized role in almost every branch of industry, especially in quality control, but it is also an important tool in the improvement of materials, in the development and design of better and improved processes. These facts are examined and the significant changes introduced in the concepts and philosophy of NDT are reviewed. The important role of NDT in the developed countries is considered and it is compared with the existing conditions of developing countries. The situation of NDT in Argentina is described, and the need for a center for NDT and quality control methods is defined. Details about its philosophy and organization are given, together with an estimated budget for an initial five year period. (auth)

42029 ^{85}Kr PRINCIPLES OF APPLICATION IN MATERIALS SURFACE STUDIES. Walker, E. Dean (Kelly AFB, San Antonio). pp 650-5 of Materials Technology. I. New York; American Society of Mechanical Engineers (1970).

From second inter-american conference on materials technology; Mexico City, Mex. (24 Aug 1970). See CONF-700812.

Studies of surface adsorbed and absorbed radioactive krypton-85 gas offer a new and extremely sensitive means of displaying microdefects in materials. The process takes advantage of the extremely small krypton-85 atom which has demonstrated preferential adsorption in areas of material distress. The ability with which the lattice structure can either adsorb or absorb the gas is a function of the material integrity, microcracking and stress concentrations. Stress concentrations were correlated with patterns found in stress corrosion of materials studied. This technique offers a potential detection system well in advance of the present day state-of-the-art production inspection methods. (auth)

42030 ANNUAL TECHNICAL CONFERENCE TRANSACTIONS, 1969. Twenty-Third Annual Technical Conference, May 5-7, 1969, Los Angeles, California. Milwaukee; American Society for Quality Control, Inc. (1969). 831p. $13.00. (CONF-690524).

One-hundred-two papers on quality control were presented at the conference. A separate abstract was prepared for each of four. Ninety-eight papers were not within the scope of NSA. (L.C.L.)

For abstracts of individual papers see: 42031—42033 and 42835.

42031 X-RAY ATTENUATION SCANNING OF NUCLEAR FUEL PLATES. Foster, B. E.; Snyder, S. D.; Knight, R. W. (Oak Ridge National Lab., Tenn.). pp 459-66 of Annual Technical Conference Transactions, 1969. Milwaukee; American Society for Quality Control, Inc. (1969).

From twenty-third annual technical conference of the American Society for Quality Control; Los Angeles, Calif. (5 May 1969). See CONF-690524.

A technique was developed and successfully used for high-speed homogeneity evaluation of reactor fuel plates. Specially designed x-ray equipment is used as the irradiation source, while a NaI(Tl) crystal optically coupled to a photomultiplier tube serves as the radiation detector. Careful control of the operating conditions produces very accurate and reproducible results. The method uses the x-ray attenuation principle, and on recent applications the area of evaluation has been as small as 0.0048 in.^{2} Precise mechanical x-y scanning of the fuel plate is accomplished with longitudinal speeds of 0 to 250 in./min and horizontal indices of 0 to 5 in. in 0.001 in. increments. The system is provided with recording capabilities for continuous quantitative data or automatic readout for a go no-go operation. Tolerance limits are set by a series of programmed equivalent attenuation standards at the beginning of each longitudinal pass of the fuel plate through the x-ray beam. The advantages and capabilities of the system are discussed relative to its use in industry. (auth)

42032 STRICT COMPLIANCE TO PRODUCT QUALITY STANDARDS: AIDED BY NONDESTRUCTIVE TESTS. Spencer, Winthrop W. (General Electric Co., New York). pp 467-71 of Annual Technical Conference Transactions, 1969. Milwaukee; American Society for Quality Control, Inc. (1969).

From twenty-third annual technical conference of the American Society for Quality Control; Los Angeles, Calif. (5 May 1969). See CONF-690524.

The development of nondestructive materials testing methods for determining that manufactured products meet strict quality standards for product safety and product reliability is discussed. These methods include x-radiography, ultrasonic testing, penetrant inspection, and eddy current testing. Cost factors to be considered in selecting the best method for a specific application are discussed. Examples are presented of nondestructive testing methods used to provide quality assurance during the production of commercial, industrial, and military products. (L.C.L.)

42033 USE OF STATISTICAL TOLERANCE LIMITS IN THE NUCLEAR INDUSTRY. Willner, O. (Bettis Atomic Power Lab., Pittsburgh). pp 669-74 of Annual Technical Conference Transactions, 1969. Milwaukee; American Society for Quality Control, Inc. (1969).

From twenty-third annual technical conference of the American Society for Quality Control; Los Angeles, Calif. (5 May 1969). See CONF-690524.

Nuclear and space industries specifications frequently require that the final product be subjected to a sampling procedure which shall demonstrate product conformance by use of statistical tolerance limits. Variable sampling plans and attribute sampling plans are discussed. It is concluded that the choice of sample size in meeting statistical tolerance limits for both variable and attribute sampling plans should be based on the operating characteristic curves applicable to these plans rather than choosing the minimum sample size. Since the statistical tolerance limit specifies the consumer's risk and the associated error, the vendor is left free to optimize his choice of sample sizes to maximize the probability of lot acceptance and to mini-

XUM

mize his total inspection cost. The vendor should also investigate the possibility of increasing his lot size where a lower percentage sampling rate is considered desirable. (auth)

Protective Structures

42034 (JPRS–53498) PROTECTION FROM PENETRATING RADIATION OF A NUCLEAR EXPLOSION. Kukhtevich, V. I.; Goryachev, I. V.; Trykov, L. A. Translation of Zashchita ot Pronikayushchey Radiatsii Yadernogo Vzryva, Moscow, Atomizdat Press, 1970. 217p. NTIS.

An engineering method for design of above-ground protective structures to provide shielding from the penetrating radiation of a nuclear explosion is presented. Since the nuclear explosion as a source of penetrating radiation has been discussed in considerable detail in the literature, only its most important characteristics are presented. Primary attention is given to the field of neutrons and γ radiation, formed in air at the division boundary between air and ground, and the transmission of penetrating radiation through typical shielding media for the geometry of shielding structures. (auth)

Radioactive Material Handling

Refer also to abstracts 41925, 42020, 42456, 42457, and 44189.

42035 (BHO–68–6) INTEGRATED SAFEGUARDS EXPERIMENT. Third Quarterly Report, December 1970–March 1971. Wadekamper, D. C.; Hagie, L. T. (comps.) (General Electric Co., Sunnyvale, Calif. Breeder Reactor Development Operation). Apr 1971. Contract AT(30-1)-68. 19p. (GEAP–12114-6). Dep. NTIS.

A data reduction and limit of error model was developed for the first Integrated Safeguards Experiment (ISE Campaign 1) material which was measured by passive neutron counting. Additional refinements to the model for future applications are suggested. Fuel processing associated with the second experiment (ISE Campaign 2) was completed. A nested experimental design which makes a direct comparison between analytical chemistry and nondestructive assay measurements was incorporated in ISE Campaign 2. A summary of the measurement and process data applicable to material balance accounting is included. Mechanized Accountability and Criticality System modifications accomplished during the reporting period are summarized. (auth)

42036 (DP–1242) FIRE PREVENTION AND PROTECTION IN HOT CELLS AND CANYONS. Hill, A. J. (Du Pont de Nemours (E. I.) and Co., Aiken, S. C. Savannah River Lab.). Apr 1971. Contract AT(07-2)-1. 140p. Dep. NTIS.

In a comprehensive study of fires and explosions that have occurred in shielded facilities and glove boxes at atomic energy sites, the modes of initiation and propagation were identified. Some measures were defined to prevent fires and explosions in hot cells and canyons and to prevent propagation of fires into ventilation exhaust systems. To provide guides for selecting automatic fire extinguishing systems for hot cells, the characteristics and performance data of commercially available detectors and the suitability of various extinguishing agents were studied. (auth)

42037 (JAERI–13666) RI LIQUID WASTES CARRIED FROM JAPAN RADIOISOTOPE ASSOCIATION TO JAPAN ATOMIC ENERGY RESEARCH INSTITUTE. Wadachi, Yoshiki; Nagaoka, Yukio; (and others) (Japan Atomic Energy Research Inst., Tokai). Aug 1969. 6p. NTIS (U. S. Sales Only).

Data are presented of radioactive liquid wastes that were shipped from Japan Radioisotope Association to Japan Atomic Energy Research Institute during the 6 years from April 1963 to March 1969. Information is included on kind, quality, quantity, and present methods of treatment and disposal. (TSS)

42038 (ORNL-TM-3426) THERMAL ANALYSIS OF NATIONAL RADIOACTIVE WASTE REPOSITORY: BRIEF SUMMARY OF RESULTS OBTAINED THROUGH APRIL 1971. Cheverton, R. D.; Turner, W. D. (Oak Ridge National Lab., Tenn.). Jun 1971. Contract W-7405-eng-26. 27p. Dep. NTIS.

At the proposed National Radioactive Waste Repository at Lyons, Kansas, solidified high-level waste will be placed in thick salt formations 1000 ft below the earth's surface. Heat release from the waste will result in temperature increases throughout the immediate geologic formations. The following factors influence the permissible temperature rises: thermal instability of the solidified waste; migration of brine; integrity of the mine during operation; integrity of the overlying formations; temperature in freshwater aquifers; temperature of earth's surface; and temperatures beyond the boundaries of the mine. Preliminary thermal calculations indicated the technical feasibility of the repository. More recent analyses have considered the repository in greater detail and have employed updated thermal property and stratigraphy data. The results indicate that all of the criteria can be satisfied, and that a heat load of about 130 kW per acre can be tolerated. (auth)

42039 (RFP–1286) DRYBOX GLOVES: EVALUATION AND PROCUREMENT. Giebel, Ray E.; Riegel, Robert L. (Dow Chemical Co., Golden, Colo. Rocky Flats Div.). 23 Jun 1971. Contract AT(29-1)-1106. 30p. Dep. NTIS.

A comprehensive testing program for drybox gloves is described. Criteria are outlined for selecting the proper glove for a given application. Desirable qualities of gloves such as protection of the worker or glovebox contents, longevity, comfort, dexterity, reasonable cost, and adaptability to the operation, are discussed. Appendices include a data sheet for glove tests, specifications for seven types of gloves, and inspection acceptance procedures. (auth)

42040 AMENDMENT TO THE ACT OF DECEMBER 31, 1962, NUMBER 1860 ON THE PEACEFUL USES OF NUCLEAR ENERGY. Minerva Fisiconucl.; 14: 49–50(Jan-Mar 1970). (In Italian).

The amendment to the act of December 31, 1962, extends the provisions of Act 1860 on the storage, sale, and transportation of radioactive materials to radiation levels of any quantity, however low it may be. (J.S.R.)

42041 RADIOPROTECTION AND THE PROBLEMS ASSOCIATED WITH NUCLEAR DESIGN. Paggi, A. (Progettazioni Meccaniche Nucleari, Genoa). Minerva Fisiconucl.; 14: 44–8 (Jan-Mar 1970). (In Italian).

In order to illustrate the criteria which must be used in nuclear design, contamination and decontamination tests were made on 15 varnishes of Italian production. In one series, varnished samples were contaminated and decontaminated 24 hrs later. In the second series the samples were contaminated and decontaminated after a year's exposure to a controlled atmosphere. In the third series the varnished samples were exposed to inclement weather for a year before decontamination. The significant feature of the tests is the change in the decontamination under the various conditions. Samples which behaved in an optimum manner in the first series failed completely in the second or third. The implication of such changes in the radioprotective behavior was applied to the design of any nuclear facility in a brief discussion. (J.S.R.)

42042 HEALTH SAFETY CONSIDERATIONS IN THE TRANSPORT OF RADIOACTIVE MATERIALS ON RAILROAD CAR FERRIES. Cagnetti, P.; Susanna, A. (CNEN, Rome). Minerva Fisiconucl.; 13: 145–53(Apr-Jun 1969). (In Italian). (CONF-680535–16; RT/PROT–70(4)).

From fourteenth national conference of the Italian Association for Health Physics and Protection from Radiation; Formia, Italy (29 May 1968).

A study was made of the transport conditions for radioactive material on railroad car ferries with particular regard to the health protection of people from the risk of ionizing radiation. The study was made on ferries in the Straits of Messina and on the Czechoslovakian Gulf route. It was concluded that the limitation of 10 mR/hr for the sum of the transportation indices of radioactive packages will guarantee the protection of both travelers and seamen. (J.S.R.)

42043 SAFE DISTANCES FOR DOSE-EVALUATION IN THE CARRIAGE OF GAMMA-EMITTING RADIOACTIVE MATERIALS IN SHIPS. Cagnetti, P.; Susanna, A. (CNEN, Rome). Minerva Fisiconucl.; 13: 61–71(Jan-Mar 1969). (CONF-680535–7).

From fourteenth national conference of the Italian Association for Health Physics and Protection from Radiation; Formia, Italy (29 May 1968).

A method was studied for calculating safe distances between packages containing radioactive materials and persons (passengers and crew) or undeveloped photographic and x-ray films. The international regulations for the carriage of radioactive materials by ship were used as a basis for achieving a more accurate determination of such distances. An expression was obtained which supplies the safe distances as a function of the transport index, duration of the voyage, and the product of the thickness of the cargo by its density. From this expression it is possible to plot a nomogram which can be used to determine graphically the safe distances between the radioactive packages and the persons or undeveloped film, whatever the transport index, the duration of the voyage and the product of the thickness by the density of the interposed cargo. (auth)

42044 HANDLING FACILITIES AND METHODS. Lloyd, Christopher George (to United Kingdom Atomic Energy Authority). British Patent 1,225,921. 24 Mar 1971. Filed 21 Mar 1969.

Reference is made to methods of handling irradiated nuclear reactor fuel elements of elongate form, and an object of the method described is to provide a remote handling facility that will assist in the transfer of fuel from a water-submerged trough to a pond rack without subjection to high tensile loading which might cause disintegration. The handling facility comprises a sling for cradling the fuel assembly, supported within a trough, with means for varying the relative heights of the ends of the sling so that the trough and fuel assembly are caused to roll along the sling to an inverted attitude; the sling has a number of spaced, parallel, flexible straps arranged side-by-side. In operation the fuel assembly is transferred from the supporting trough to a lifting member by placing the combination of trough and fuel assembly in the sling, varying the relative heights of the ends of the sling to invert the combination by rolling it along the sling, lifting the trough from the inverted combination and engaging the underside of the fuel assembly with the lifting member at positions between the straps. The lifting member may comprise hooks or clamping arms. At all stages of the operation the fuel member is supported horizontally from beneath. (UK)

42045 OPTIMIZATION OF NUCLEAR MATERIALS SAFEGUARDS SAMPLING SYSTEMS BY DYNAMIC PROGRAMMING. Bouchey, G. D.; Koen, B. V.; Beightler, C. S. (Univ. of Texas, Austin). Nucl. Technol.; 12: No. 1, 18-25(Sep 1971).

The dynamic programming algorithm is used to determine the optimal allocation of effort (measured in dollars or other appropriate units) in order to minimize the variance on the measurement of Material Unaccounted For (MUF) in a nuclear materials safeguards system. A multistage model of a hypothetical safeguards sampling system is formulated and optimized. The dynamic programming approach for optimization of a safeguards system allows more exact treatment of the model than is possible with classical optimization techniques and can easily be extended to handle large problems of the type that might be encountered in a real-world safeguards sampling system. (auth)

42046 GLASS AMPOULE SEALER. Pokorny, G. J.; Paulsen, A. D. (Argonne National Lab., Ill.). Nucl. Technol.; 12: No. 1, 141-5(Sep 1971).

A semiautomatic device for hermetically sealing radioactive samples in glass ampoules by a flameless method has been developed for use within an inert atmosphere glovebox. Sealing is performed by heating the open end of the ampoule with an electrical resistance heater, elevating the heated portion of the ampoule to the sealing position, and sealing off the end with mechanically operated, electrically heated jaws. The method is rapid, automatic, and consistently forms helium mass-spectrometer-tight seals. (auth)

Vacuum Engineering

42047 ULTRAHIGH VACUUM METROLOGY: DESCRIPTION OF A CALIBRATION UNIT AND THE MEANS OF MEASUREMENT EMPLOYED. Lefevre (Laboratoire Central de l'Armement, Arcueil, France). Bull. Inform. Bur. Nat. Metrol.; 2: No. 3, 8-10(Jan 1971). (In French).

The work done in the ultrahigh vacuum laboratory of the Laboratoire Central de l'Armement in the field of metrology at low pressures is described. The test bench, based on a method of variable conductance, permits manometers to be calibrated down to 10^{-5} Pa with an accuracy of 3%. Diamagnetic suspension-type manometers were studied. Graphical methods were developed for measuring the pressure; the parasites were treated statistically. In this way, the precision available with this type of manometer was improved. A molecular manometer was connected to the test bench in order to verify its absolute characteristics, and to check the working of the bench. The calibration of a thermomolecular manometer by comparison with the molecular manometer completed the domain of pressures measurable with the assembly. (auth) (France)

XUM

INSTRUMENTATION

Radiation Detection Instruments

Refer also to abstracts 41833 and 41932.

General Detectors and Monitors

Refer also to abstracts 42231, 42436, 42443, 42564, 42565, 43175, 43452 and 44190.

42048 (ANL–7710, pp 263-364) EXPERIMENTAL TECHNIQUES AND FACILITIES. (Argonne National Lab., Ill.).

ARGONNE BIOLOGICAL RESEARCH REACTOR — gamma spectra measurements for, Compton recoil spectroscopy methods for
— neutron spectra measurements for, use of proton-recoil proportional detectors for
CALIFORNIUM-252 — neutron fission yield measurements using manganese bath, leakage correction factor for
CRITICAL ASSEMBLIES — gamma dose distribution in, thermoluminescent dosimmetry methods for
— fission rate distribution measurements in, non-perturbing fission counter for
— reactivity for ZPPR, data acquisition systems for measurement of
FISSION FRAGMENTS — energy distribution measurements using silicon detectors
GAMMA SPECTROMETERS — time resolution of lithium-drifted germanium, for (n,n′γ) experiments
HODOSCOPES — development of fast neutron
NEUTRON SOURCES — description of Dynamitron
— beam buncher for Dynamitron, klystron
RADIATION DETECTORS — dead time corrections for counting rapidly decaying sources
RADIATION DETECTORS, PROPORTIONAL — development of proton-recoil, for neutron spectroscopy
RADIATION DETECTORS, SCINTILLATION — development of helium-3 gas, for time-of-flight neutron measurements
RADIATION DETECTORS, SEMICONDUCTOR (GERMANIUM) — efficiency of lithium-drifted, effects of source distance on
— efficiency calibration of lithium-drifted
RADIOISOTOPES — determination of small amounts of, using lithium-drifted germanium spectrometers
REACTOR CONTROL SYSTEMS — instrumentation for, statistics of fluctuations in
SODIUM — monitoring of vapors of, system based on atomic absorption of sodium light for (W.H.K.)

42049 (EUR–4513) INDIRECT EXPERIMENTAL DETERMINATION OF THE PHOTOPEAK EFFICIENCIES OF NaI(Tl) DETECTORS FOR CYLINDRICAL GASEOUS SOURCES. Busca, G.; Drago, A. (European Atomic Energy Community, Petten (Netherlands). Joint Nuclear Research Center). 1970. 10p. NTIS (U. S. Sales Only).

An experimental approach for the photopeak efficiencies evaluation of a 3″ × 3″ NaI(Tl) detector, when gaseous sources are employed, is presented. The experimental approach consists of utilizing a thin paper disc imbued with a standard solution, having the same diameter as the counting chamber which is used for the gas sampling. The variation of the photopeak efficiency with the energy is given for gaseous sources contained in two stainless steel cylinder boxes of 6.2 cm diameter and a height of respectively 10 and 6 cm; the bottom side of both cylinders is 0.5 mm thick. The validity of the method was checked by determining the absolute activity of a calibrated ^{133}Xe source. (auth)

42050 (JAERI–13546) FULL ENERGY PEAK EFFICIENCY OF THE NaI CRYSTAL. Baba, Sumiko; Tanaka, Kichizo (Japan Atomic Energy Research Inst., Tokai). May 1969. 23p. NTIS (U. S. Sales Only).

Full energy peak efficiencies for gamma-rays incident on a 7.5 cm × 7.5 cmϕ NaI(Tl) crystal in a lead-shielding box have been measured. The measurement has been carried out with the sources whose absolute disintegration rates were determined by the $\beta-\gamma$ coincidence method. The errors involved in the absolute measurements are discussed. It was found that they were able to be reduced by using radiochemically pure sources with simple decay schemes. It is concluded that the absolute disintegration rates of the nuclides emitting γ-rays could be determined with satisfactorily good accuracy by the present method without the use of such an absolute measurement as the $4\pi\gamma_{-4}$ coincidence counting. (auth) (Japan)

42051 (JAERI–13718) TECHNIQUE FOR DETERMINING THE ACTIVITY AND SIZE DISTRIBUTION OF β EMITTING PARTICLES BY AUTORADIOGRAPHY. Matsui, Hiroshi; Serizawa, Masahiko (Japan Atomic Energy Research Inst., Tokai). Sep 1969. 18p. NTIS (U. S. Sales Only).

Sakura-R film was more sensitive to β-rays and more useful than the nuclear emulsion "Fuji ET-2E" in the β-ray autoradiography. Variation of the black spot diameter with the development time and temperature was a few percent for ±0.1 min and ±0.5°C respectively. A fifty micron thick separator did not give rise to variation of the spot for β-rays from fission product nuclides. Error in estimating the activity and size distribution of β emitting particles by autoradiography is discussed. The application of the technique investigated to aerosol analysis is described and an example is shown. (auth) (Japan)

42052 (JAERI–13725) COUNTING CHANNEL FOR USE WITH GAS FLOW PROPORTIONAL COUNTER. Mizuho, Mitsuru (Japan Atomic Energy Research Inst., Tokyo). Sep 1969. 18p. NTIS (U. S. Sales Only).

A counting channel for use with gas flow proportional counters was investigated and advantages of the use of a specially developed preamplifier of the current-to-voltage conversion type are pointed out. Advantages of the current mode signals from a flow counter are retained through the channel in this system. Also, conventional voltage amplifiers may be used as the main amplifier. Good plateau characteristics were obtained for α and β from a RaDEF source with double or triple differentiation pulse shaping. The β slope of less than 0.1%/100 V was also obtained with a ^{32}P source at the counting rate of 2000 cps. A noise level of 0.03 μ A peak to peak was realized with no selection of transistors, enabling the detection of 2–3 ion pairs of ionization. (auth)

42053 (JINR–P13-5782) ON NEW METHODS OF DETECTING THE PARTICLE TRACKS IN LIQUID AND SOLID MEDIA. Nikanorov, V. I.; Pisarev, A. F.; Selivanov, G. I. (Joint Inst. for Nuclear Research, Dubna (USSR). Lab. of Nuclear Problems). 1971. 14p. (In Russian). Dep. NTIS (U. S. Sales Only).

A possibility is considered of designing solid detectors containing thin wires frozen or polymerized in a media. Near these wires the gas bubbles are created artificially where primary electrons produced in the particle tracks are multiplied. Discrete particle counters are also considered which are a combination of scintillating threads, tunnel photodiodes, or channel electron multipliers (CEM). The possibility of using separate CEM for fast particle detection is studied. (auth)

42054 (LPN-UM–53) GEOMETRICAL CORRECTION FACTORS FOR ANGULAR CORRELATION MEASUREMENTS WITH Ge(Li) DETECTORS. Barrette, J.; Lamoureux, G.; Monaro, S. (Montreal Univ. (Quebec). Laboratoire de Physique Nucleaire). Nov 1970. 41p. Dep. NTIS (U. S. Sales Only).

A computer program calculation for the determination of the finite solid-angle corrections for truly coaxial Ge(Li) detectors is presented. The basis of these calculations is an exact knowledge of the differential efficiency of the detectors, i.e., the efficiency versus the position of irradiation on the detector surface. In order to calculate the differential efficiency of the Ge(Li) detectors two approaches were employed. The first is based on the probability of a direct photoelectric interaction of the γ-ray impinging on the crystal whereas the second is a Monte Carlo simulation method. These calculations were carried out on four truly coaxial Ge(Li) detectors. These counters have active volume of 5.3, 32, 36 and 45 cm^3 respectively. The finite solid-angle corrections were calculated for source–detector distances of 3.0, 5.0, 7.0, 10.0 and 14.0 cm and for an energy range from 60 keV to 2.0 MeV. (auth) (Canada)

42055 (ORNL-TM–3465) CALIBRATION OF THE BONNER BALL NEUTRON DETECTORS USED AT THE TOWER SHIELDING FACILITY. Maerker, R. E.; Muckenthaler, F. J.; Manning, J. J.; Hull, J. L.; Money, J. N.; Henry, K. M.; Freestone, R. M. Jr. (Oak Ridge National Lab., Tenn.). 30 Jun 1971. 16p. Dep. NTIS.

Efficiencies of the Bonner balls using BF_3 detectors in use at the Tower Shielding Facility were determined from measurements performed with a calibrated ^{252}Cf source. Additional measurements with a monoenergetic ~30-keV source indicate that the efficiencies are spectrum independent down to ~10 keV. Further measurements in a soft spectrum indicate that upscattering effects in the thermalization process rendered by the polyethylene may be spectrum dependent below incident energies of ~10 keV. (auth)

42056 (RT/PROT–(71)1) ELECTROCHEMICAL ETCHING OF DAMAGED TRACK DETECTORS BY H. V. PULSE AND SINUSOIDAL WAVEFORMS. Tommasino, L. (Comitato Nazionale per l'Energia Nucleare, Rome (Italy)). 13 Jan 1971. 18p. Dep. NTIS (U. S. Sales Only).

It is known that the etching reagents rapidly diffuse in the fine channels produced in insulators by the passage of the charged particles. Conductive paths are thus produced, which penetrate the insulating foils. By applying H. V. square or sinusoidal waveforms through the irradiated insulator, currents are produced in the conductive paths, delivering energy mostly along the tracks. This type of etching enables us to increase the sensitivity of alpha particle registration on cellulose Acetate-Butyrate, to produce well defined and elongated alpha particle tracks and to enlarge the damaged tracks at will. (auth)

42057 AMERICAN NATIONAL STANDARD AND IEEE STANDARD TEST PROCEDURE FOR GEIGER–MUELLER COUNTERS. ANSI N42.3 1969, IEEE No. 309 1969. New York: Institute of Electrical and Electronics Engineers, Inc. (1969). 8p. Available from Institute of Electrical and Electronics Engineers, New York.

Standard test procedures for Geiger–Mueller counters are presented. Specifications for the test conditions, counter parameters, and test equipment are given, and pulse characteristics are defined. (W.H.K).

42058 PROGRAMMING APPARATUS FOR AN AUTOMATIC LIQUID SCINTILLATION COUNTING SYSTEM. Frank, Richard B.; Hanz, George J. (to Nuclear-Chicago Corp.). U. S. Patent 3,571,596. 23 Mar 1971. Filed 8 Jan 1969.

A sample group programming apparatus comprising a program indicating plug mounted on a sample conveyor and reading apparatus adjacent the conveyor is described. The program indicating plug includes a support member carrying a vertically disposed optical structure, and a code cylinder rotatably mounted thereon. Five circumferential rows of apertures exist on the code cylinder, one for admitting light to the optical structure and four for providing 16 separate binary coded vertical arrays. The reading apparatus comprises a light source and four light responsive elements appropriately mounted on a support structure adjacent the conveyor to read the operative array of apertures on a plug in a reading position. (auth)

42059 DIGITAL SUBTRACTION TECHNIQUE FOR DUAL ISOTOPE SCINTIGRAPHY. Kemplay, J. R. (Westminster Hospital, London); Aspinall, J. A. Phys. Med. Biol.; 16: No. 2, 243-8(Apr 1971).

A technique for the subtraction of one random pulse train from another is described. The technique uses digital methods and operates at count-rates up to 5000 per second. It is particularly suited to dual isotope investigations in nuclear medicine where techniques employing analog methods may introduce errors because of inherent integrating time-constants. (auth) (UK)

42060 SMALL FISSION CHAMBER, OF THE PULSE TYPE, OPERATING AT HIGH TEMPERATURE. Guery, Marcel (to Commissariat a l'Energie Atomique). French Patent 2,031,672. 9 Nov 1970. Filed 3 Feb 1969. (In French).

A small fission chamber, of the pulse type, is described. Its principal characteristics are its envelope, used as the cathode, and its end plug. The two parts are made of a metal capable of being welded with titanium. The anode is made of titanium and the sealed electrical penetration consists of at least one insulator made of alumina brazed with Ag–Cu eutectics. This fission chamber is robust and does not significantly absorb neutrons. (France)

42061 ENERGY PARTITION OF HEAVY IONS OF INTERMEDIATE ENERGIES IN SILICON SURFACE-BARRIER DETECTORS. Petrilak, Michael Jr. Madison, Wis.; Univ. of Wisconsin (1970). 194p. University Microfilms Order No. 71-5660.

Thesis.

The partition of energy of heavy ions of intermediate energy in solid state detectors leads to a pulse-height defect. Using the theory of Lindhard, Scharff, and Schiott as well as the recoil correction due to Haines and Whitehead, theoretical predictions of pulse-height defect are made for ions of mass 1 to 238 amu with incident energies of 0.5 to 6.0 MeV. Account is also taken for the energy loss in the entrance gold window of the detector by Lindhard theory. Predictions for the pulse-height defects for molecular ions are made for the first time. Reasonably good theoretical agreement of about 10 to 20% is found for the partition of energy for masses from mass 10 to 70 amu. With increasing mass and decreasing energy the agreement becomes worse. The disagreement at mass 132 and energy 0.5 MeV is as great as a factor of 2. The pulse-height defect is reasonably independent of the particular silicon surface barrier detector employed provided that the reverse bias is sufficient to insure efficient charge collection. At 1.0 MeV the difference in performance between two similar detectors is a few percent and the difference between two similar detectors with window thicknesses of 20 $\mu gm/cm^2$ and 40 $\mu gm/cm^2$ cannot be attributed to the different window thicknesses. Molecular ions, in general, have significantly lower defects compared to atomic ions of the same total mass and energy. Agreement with Lindhard theory is sufficient to substantiate the hypothesis that the molecular ions break up immediately upon entering the detector and that the total pulse height is the sum of the pulse heights of the individual breakup components. (Diss. Abstr. Int., B)

42062 DECAY AND THERMOLUMINESCENCE OF ZIRCONIUM-ACTIVATED STRONTIUM SULPHIDE PHOSPHORS. Sharma, D.; Singh, Amar (Univ. of Gorakhpur, India). Indian J. Pure Appl. Phys.; 6: 346-9(1968).

Forty-five samples of SrS: Zr phosphors were prepared. The concentration of zirconium was varied from 0.0105 to 0.882 wt %. The phosphorescence and thermoluminescence were studied by exciting the phosphors with a 200-W, 250-V tungsten filament lamp, the intensity having been measured with the help of a photomultiplier tube. It is concluded that the decay is of the form $I_t = I_0 t^{-b}$, where the values of b vary from 0.75 to 0.80 for different samples. By peeling off the curves into three exponentials, it is estimated that at room temperature (31°C) traps having depths of 0.65 ± 0.06 eV are effective. By measuring the thermal glow intensity of 10 samples at two different warming rates, the trap depth and the constant s (a frequency factor called the "attempt to escape frequency") were calculated and these values agree with those obtained by phosphorescence studies. The results are satisfactorily explained on the basis of the superposition theory, the kinetics being monomolecular. (auth)

42063 VARIABLE DELAY GATE GENERATOR FOR TWO-CHANNEL COUNTING SYSTEMS. Burgess, D. A.; Kwei, G. H. (State Univ. of New York, Stony Brook). Rev. Sci. Instrum.; 42: No. 7, 1081-2(Jul 1971).

The design and operation of an inexpensive but versatile variable-width, variable-delay gating circuit, which can be used for modulated pulse counting and time-of-flight velocity analysis, are described. (R.W.R.)

42064 MASS ATTENUATION COEFFICIENTS FOR PLASTIC PILOT-B SCINTILLATOR. Hayn, Carl H.; Carroll, Daniel E. (Univ. of Santa Clara, Calif.). Rev. Sci. Instrum.; 42: No. 7, 1059-60(Jul 1971).

Mass attenuation coefficients of the commercial plastic Pilot-B scintillator were determined as a function of energy. Sources emitting gamma rays with energies of 0.36, 0.66, 0.80, and 1.33 MeV were used. The results indicate strong absorption in the low-energy region and a smooth nonlinear decrease in the mass attenuation coefficients with increasing gamma-ray energy. The experimental procedure and apparatus are described. (auth)

42065 LIGHT COLLECTION FROM LARGE CYLINDRICAL SCINTILLATORS. Friesenhahn, S. J. (Gulf Radiation Tech., San Diego, Calif.). Rev. Sci. Instrum.; 42: No. 7, 1016-30(Jul 1971).

The parameters determining the light collection efficiency from large cylindrical scintillators are experimentally determined, and the effects of varying these parameters are examined by means of a theoretical model of the scintillator. The temporal behavior of the scintillator is calculated, and methods of improving both the light collection and time response are suggested. (auth)

42066 HEAVY PARTICLE IDENTIFICATION WITH A T.O.F. METHOD IN NUCLEAR REACTIONS. Yasue, Masaharu; Fujiwara, Noboru; Ohsawa, Takao; Izutsu, Norihiko (Kyoto Univ.). Bull. Inst. Chem. Res., Kyoto Univ.; 48: No. 6, 223-35(Dec 1970).

A particle-identification system with a time-of-flight (TOF) method is developed to accommodate the high repetition rate of a cyclotron beam of 13 MHz. Starting signals of the TOF system are obtained from a tantalum plate in the path of a bunched beam from the Kyoto University cyclotron. Stop and energy signals are obtained from a solid-state detector. An experiment on p–d scattering at E_p = 7.3 MeV shows that protons and deuterons are identified clearly with each other. The time resolution was estimated to be 2.6 nsec, but finally was improved to be 1.5 nsec by adding a diode limiter circuit to the TOF system. (auth)

42067 SATURATION IN CONTINUOUS CHANNEL ELECTRON MULTIPLIERS. Harris, L. A. (General Electric Co., Schenectady, N. Y.). Rev. Sci. Instrum.; 42: No. 7, 987-92(Jul 1971).

XUM

The steady-state gain of electron space current in straight continuous channel electron multipliers is calculated. Ion-feedback and space-charge effects are neglected, but variation of secondary yield with primary energy and increased wall conductivity due to electron bombardment are considered. Saturation occurs when enough wall current is converted to space current so that the reduced electric field diminishes the effective secondary yield to unity. Predicted results are in good qualitative agreement with reported observations. (auth)

42068 PROPERTIES OF FEU-79 PHOTOMULTIPLIERS USED AS PHOTON COUNTERS IN ASTRONOMICAL OBSERVATIONS. Gutkevich, S. M.; Shulov, O. S.; Konshin, V. M.; Skripko, N. S. Uch. Zap. Leningrad. Gos. Univ., No. 353, Ser. Mat. Nauk; No. 45, 64-80(1970). (In Russian).

The amplitude distribution of photoelectronic and thermionic anode pulses is measured for several photomultipliers of the FEU-79 type. Using these data, the optimum regimes for these PM's used as photon counters are calculated and the accuracy of the astronomical photometric and polarimetric observations with the 20″ reflector (of AT-14 type) of Leningrad University Bjurakan Station are determined. The pulse-counting method of photometric observations is compared with the dc method and is found to have some advantage in accuracy. The necessity of taking into consideration the real observational conditions to optimize the use of PM's is emphasized. The best FEU-79 photomultipliers have the quantum outputs of approximately 10% in the V-band of the UBV-system and thermemissions of about 10 to 30 pulses per second at the temperature +22°C. (auth)

42069 LIQUID SCINTILLATOR COMPOSITIONS FOR COUNTING THERMAL NEUTRONS. Benson, Royal H. (to Monsanto Co.). U. S. Patent 3,573,220. 30 Mar 1971. Filed 4 Feb 1969.

A scintillator composition for liquid scintillation counting and detection of thermal neutrons comprising (1) a scintillator solution comprised of an aromatic hydrocarbon solvent, a scintillation solute, and an ethoxylated alkyl phenol, and (2) a loading agent comprised of an aqueous solution of a compound of an element having high thermal-neutron-capture efficiency. The element interacts with thermal neutrons resulting in the production of an exo-ergic nuclear reaction. (Office. Gaz.)

42070 MECHANISM AND APPLICATIONS OF NUCLEAR TRACK FORMATION IN POLYMERS. Johnson, Dennis Ray. Lawrence, Kan.; Univ. of Kansas (1970). 86p. University Microfilms Order No. 71-13,321.

Thesis.

A radiolytic damage mechanism for nuclear track formation in polymers was corroborated by studies that utilized a radical scavenger technique. The work was considerably simplified, both experimentally and statistically, by the successful adaptation of a spark counting technique for automatically counting etched alpha particle tracks in thin polymer films. In addition, a combination of the track etching and spark counting techniques resulted in several new dosimetric and imaging applications of charged particle detection that included (1) a highly sensitive dosimeter for radon progeny in the uranium mining industry. (2) an improved method for the ultrasensitive determination of the quantity and distribution of fissile elements in liquids and solids; (3) a new, more sensitive method of alpha particle autoradiography, which permits automatic track counting and provides replicas as well as direct images; and (4) a new method of personnel neutron dosimetry, which utilizes automatic readout. (Diss. Abstr. Int., B)

42071 METHOD OF TREATING A LIQUID SCINTILLATOR COMPOSITION. Benson, Royal H. (to Monsanto Co.). U. S. Patent 3,573,219. 30 Mar 1971. Filed 7 May 1969.

A method is described for treating a scintillator composition composed of an aromatic hydrocarbon solvent, a scintillation solute, and an ethoxylated alkyl phenol by contacting the composition with an effective amount of basic ion-exchange resins, alkali metal carbonates, alkali metal bicarbonates, ammonium hydroxide, or mixtures of these for a period of time sufficient to reduce the chemiluminescence to an acceptable background level when a basic material is added to the composition. (B.L.M.)

42072 LIQUID SCINTILLATION COUNTING COMPOSITION AND PROCESS. Benson, Royal H. (to Monsanto Co.). U. S. Patent 3,573,218. 30 Mar 1971. Filed 11 Apr 1968.

A liquid scintillation counting composition comprises an aromatic hydrocarbon solvent, a scintillation solute and an ethoxylated alkyl phenol having from 7 to 16 carbon atoms in the alkyl substituent and a ratio of carbon atoms in the alkyl substituent to the average number of ethoxy groups of from 0.83 to 1.67. This composition was developed for counting samples having a relatively large percentage of water. (Office. Gaz.)

42073 RULES FOR PORTABLE MONITORS. NEN 2384 1962. The Hague; Nederlands Normalisatie-Instituut (1962). 2p. (In Dutch). Available from Nederlands Normalisatie-Instituut, The Hague.

42074 RULES FOR POCKET ELECTROSCOPES FOR PERSONNEL MONITORING. NEN 2386 1962. The Hague; Nederlands Normalisatie-Instituut (1962). 2p. (In Dutch). Available from Nederlands Normalisatie-Instituut, The Hague.

42075 RULES FOR CONDENSOR TYPE IONIZATION CHAMBERS AND ACCESSORY ELECTROMETERS FOR PERSONNEL MONITORING. NEN 2387 1962. The Hague; Nederlands Normalisatie-Instituut (1962). 2p. (In Dutch). Available from Nederlands Normalisatie-Instituut, The Hague.

42076 GAS SCINTILLATOR AS A KINETIC ENERGY SPECTROMETER FOR FISSION FRAGMENTS. Pagano, Roberto. Gainesville, Fla.; Univ. of Florida (1970). 125p. University Microfilms Order No. 71-13,446.

Thesis.

Several gases and gas mixtures were examined as scintillators for fission fragment kinetic energy spectrometry. Carbon tetrafluoride was found to be the most satisfactory because of its high scintillation efficiency at pressures above one atmosphere and its insensitivity to impurities. A study of the radiation chemistry of CF_4 revealed that the chemiluminescent formation of C_2F_4 could be considered as a mechanism contributing to the light emitted by CF_4. A measure of the instrumental broadening of the gas scintillation spectrometer was obtained by simulating the scintillations produced in the gas; a NaI(Tl) crystal which was doped with ^{241}Am and a set of neutral density optical filters were used for this purpose. From the simulation measurements, an estimate of the absolute intensity of the scintillations produced in the gas by fission fragments could be derived also; for CF_4 at a pressure of 760 mm, the G-value for photon production was found to be 0.026 photons per 100 eV. A mathematical model was developed to predict the response of the gas scintillation spectrometer to the input generated by fission fragments with kinetic energies distributed over a wide range. The assumption that a linear relationship existed between scintillation response and particle energy was incorporated in the model. A second mathematical model was developed to account for the contamination caused by fission fragments with degraded kinetic energies in the pulse-height spectrum obtained with a gas scintillation spectrometer and a source of fission fragments. The two models were combined to analyze the pulse-height spectrum obtained with the CF_4 scintillation spectrometer and the fission fragments arising from the spontaneous fission of ^{252}Cf. The existence of a fine structure in the kinetic energy distribution of the fission fragments of ^{252}Cf was established. (Diss. Abstr. Int., B)

42077 PLASTICS MATERIALS FOR INDICATING A RADIATION DOSAGE. (to Nitto Electric Industrial Co. Ltd.). British Patent 1,235,970. 16 Jun 1971. Priority date 9 Jul 1968, Japan.

A plastics composition for indicating a radiation dosage is described. The composition comprises a chlorine-containing polymer, 5 to 80 parts per 100 parts by weight of the polymer; a plasticizer for the polymer, which plasticizer is a phosphoric acid ester, a polyester, a chlorinated paraffin, or a trimellitic ester of an aliphatic alcohol; and at least one acid-sensitive colorant. (W.H.K.)

42078 RADIATION DOSE INDICATOR PAINT. (to Medimpex Gyrogyszerkulkereskedelmi Vallalat). British Patent 1,234,172. 3 Jun 1971. Priority date 18 Jan 1968, Hungary.

A dose indicator paint for assessing the irradiation of polyethylene and other hydrophobic target materials is described. The paint comprises an aqueous emulsion of a vinyl chloride copolymer, 0.5 to 10% by weight (based on the weight of the aqueous emulsion); 4′-anilino-azobenzene-m-sulfonic acid; and if desired additives. (W.H.K.)

42079 ELECTRON MULTIPLIER DETECTION OF FAST POTASSIUM ATOM BEAMS. Cuderman, J. F. (Sandia Labs., Albuquerque, N. Mex.). Rev. Sci. Instrum.; 42: No. 7, 1094-5 (Jul 1971).

The characteristics of an electron multiplier for detecting fast K atoms in the energy range from 5 to 500 eV are described. The sensitivity is given as a function of the energy of the incident atoms. (R.W.R.)

42080 SUPERCONDUCTING THIN-FILM DETECTOR OF NUCLEAR PARTICLES. Crittenden, E. C. Jr.; Spiel, Donald E. (Naval Postgraduate School, Monterey, Calif.). J. Appl. Phys.; 42: No. 8, 3182-8(Jul 1971).

Superconducting films of tin and indium on supporting sub-

strates have functioned successfully as detectors of individual nuclear particles. The films are sufficiently thin and narrow that individual α-particle impacts initiate superconducting-to-normal transitions that spread, in the presence of a transport current, to span a full film cross section. The transitions are observed by means of the ir drop produced by a transport current. For low current densities, self-terminating voltage pulses of a few nsec duration are observed. At higher current densities, the boundaries of a normal region initiated by an α particle propagate by Joule heating to the ends of the film. The range of the 5.3-MeV α particles utilized for these experiments greatly exceeds the 0.1 μm thickness of the films, and the resulting deposition of energy in the substrate affects the response of any film that is in direct contact with its substrate. The introduction of a thin thermally insulating layer of varnish between the film and its substrate, which in these experiments was either glass or crystalline quartz, increases the thermal decay constant to the extent that the film is thermally isolated from its substrate for a period comparable to that of pulse formation. The variation of count rate with film current is shown to be consistent with the variation of critical current density along the length of the film. This model, coupled with classical heat diffusion within the film, accounts for the observed behavior of the thermally isolated films. (auth)

42081 WHOLE-BODY COUNTER AT THE E.N.E.L. NUCLEAR ELECTRIC CENTER AT GARIGLIANO. Farulla, A. (Univ., Sassari, Italy); Antonucci, L.; Naro, G. Minerva Fisiconucl.; 14: 104-8(Jul-Sep 1970). (In Italian). (CONF-680535-32).

From 14. national conference of the Italian Association for Health Physics and Protection from Radiation; Formia, Italy (29 May 1968).

The technical characteristics of the Garigliano nuclear power plant whole body counter are summarized. The methods for its use and calibration are described. The counting technique used is selected so as to give rapidity and ease of operation, shortness of counting time, good sensitivity, ease of calibration, and independence of the location of the radioisotope in the body and of the physical constitution of the person counted. (tr-auth)

42082 USE OF CHERENKOV INSERTS FOR COUNTING HIGH ENERGY β AND γ CONTAMINATION SAMPLES. Ballance, P. E.; Johnson, Shirley (Univ. of East Anglia, Eng.). Health Phys.; 20: 447-8(Apr 1971).

A Cherenkov insert was developed which eliminates count-rate variations caused by pigments in radioactive solutions of biological origin. Cheap throw-away inserts are used to eliminate contamination and, as a further economy, the Cherenkov liquid in which the insert is immersed can remain in the vial and be reused. Fifty-seven liquids in addition to water were examined for increased count-rate efficiencies. Results are tabulated. The most practicable, giving marked increase in counting efficiency, were found to be toluene and L-chloronaphthalene. It is concluded that the results indicate that counting in Cherenkov inserts is an effective technique for the routine evaluation of coloured contamination. Samples contained high-energy β- and γ-emitting radionuclides. (UK)

42083 ABSOLUTE CALIBRATION OF BREMSSTRAHLUNG BEAM MONITORS. Kusumegi, Asao; Miyachi, Takashi; Narushima, Katsuya; Sato, Isamu; Watanabe, Shin-ichi (Tokyo Univ.). Jap. J. Appl. Phys.; 10: No. 6, 766-73(Jun 1971).

The absolute calibration of the bremsstrahlung beam monitors of the INS electron synchrotron is made by using a Faraday cup and converters of known thicknesses with external electrons. The results show that the calibration constant of the quantameter is independent of the maximum photon energies from 302 MeV to 1102 MeV; the average value is $(4.69 \pm 0.14) \times 10^{18}$ MeV/C. The calibration constant of the thick-walled ionization chamber varies slowly with the maximum photon energy, and the results are consistent with the previous measurement. At the same time, the effects of saturation were investigated for these bremsstrahlung beam monitors at a maximum photon energy 1000 MeV by varying the intensity, the beam spill length, and the bias voltage to the monitor as parameters. The results of the measurements are given and discussed in connection with the ion recombination effect. (auth)

42084 CRYOSTAT FOR A Ge(Li) DETECTOR. Donde, A. L.; L'vov, A. N. (Physical-Technical Inst., Kharkov). Instrum. Exp. Tech. (USSR) (Engl. Transl.); No. 5, 1491-2(Sep-Oct 1970).

Translated from Prib. Tekh. Eksp.; No. 5, 213-14(Sep-Oct 1970).

A cryostat for a Ge(Li) detector, based on a carbon adsorption pump cooled by liquid N_2 is described. The capacity of the liquid-N_2 container is 5 liters. Under stationary conditions, 0.5 liter of liquid N_2 is consumed in 24 h. During 15 months of use, without additional pumping and heating to room temperature, the pressure in the cryostat changed from $2 \cdot 10^{-7}$ to $3 \cdot 10^{-6}$ torr. It is estimated that the pressure will rise to 10^{-5} torr in several years. In 15 months, the detector located in the cryostat did not change its characteristics. (auth)

42085 MEAN MASS STOPPING POWER RATIOS FOR γ AND X-RAYS FOR USE WITH CAVITY IONIZATION CHAMBER. Tomimasu, Takio; Sugiyama, Suguru. Denki Shikensho Iho; 35: No. 1, 68-80(1971). (In Japanese).

The mean mass stopping power ratio of water/air for γ- and x-rays is calculated and presented with the mean mass stopping power ratios of C/air, Al/air, Cu/air and Cu/Ar published in 1967. The calculated values of water/air and C/air are compared with the ones presented in ICRU report 14 (1969). In contrast to the calculating method in the ICRU report, which is applicable only to materials of low atomic numbers such as water or carbon in the range of energy below 30 MeV, and which needs primary electron, spectra induced by incident γ- and X-rays, completely neglecting secondary electrons induced by bremsstrahlung, Compton scattered photons and 0.511 MeV annihilation photons, the authors' method published in 1967 is applicable to any kind of materials in any energy range without requiring any primary electron spectra induced by incident radiations. Absorption of the secondary electrons induced by bremsstrahlung, etc., is taken into consideration. Accordingly the calculated values of water/air and C/air for X-rays are about 1% larger than the ones by the ICRU's. The values of Cu/air and Cu/Ar calculated are given for the energy range from 0.1 to 1000 MeV, and are used to determine the calibration constants of ETL type quantameters. The calibration of NBS P2 chamber given by the calibration of ETL-quantameter-I through intercomparison experiment agrees with other calibrations determined by the calorimetric method. (auth)

42086 METHOD FOR PRODUCING A CHROMIUM ACTIVATED ALUMINUM OXIDE SCINTILLATOR. Allison, Robert W. Jr.; Brokloff, Robert W.; Woodyard, John R. (to United States Atomic Energy Commission). U. S. Patent 3,580,822. 25 May 1971. Filed 7 Jul 1969.

A method of preparing a radiation resistant chromium activated aluminum oxide scintillator by immersing an aluminum anode and lead cathode in an anodic bath and gradually increasing an applied potential until bright flashes or "anodic scintillation" occurs whereby Cr ions from the solution are injected into the Al_2O_3 base lattice is described. The scintillators produced by this process may be readily utilized to visually aid in the control and transport of high intensity beams without radiation damage thereto. (auth)

42087 FEEDBACK-TYPE DETECTION SYSTEM FOR PULSED RADIATION MEASUREMENT. Narita, Masakuni; Tanida, Hiroaki; Ozawa, Yasutomo (Hokkaido Univ., Sapporo). Nippon Genshiryoku Gakkaishi; 13: No. 5, 248-53(May 1971). (In Japanese).

The dynamic response of a feedback-type detection device for pulsed radiation measurements has been theoretically and experimentally investigated, and an estimation made of the error incurred. The device is analyzed approximately as a linear second order lag system. A feed-back system is embodied, which consists of a side-window GM counter covered with a movable shielding lead plate whose displacement from the origin indicates the output of the device. Experimental results and theoretical expressions both indicate that the mean value and the relative error of the output are proportional respectively to the intensity of radiation and to the square root there-of. (auth)

42088 IONIZATION CHAMBER RESPONSE FOR PULSED RADIATION AND THE DRIFT VELOCITY DISTRIBUTION OF FILLING GAS. Mikado, Tomohisa; Tomimasu, Takio; Tsuchiya, Yoshio. Denki Shikensho Iho; 35: No. 1, 81-91(1971). (In Japanese).

The saturation current of an ionization chamber exposed to a pulsed radiation beam degrades slightly with increasing repetition rate of radiation pulse even though the radiation intensity per pulse and the applied voltage to the chamber are kept constant. The repetition rate dependence of the saturation characteristic varies with each filling gas. This phenomenon is commonly seen in ten kinds of gases including air, Ar, N_2, CO_2, He, 95% Ar + 5% Co_2, 90% Ar + 10% Co_2, 80% Ne + 20% He, CCl_2F_2, and SF_6. In order to explain the experimental results mentioned above, it has been assumed that the drift velocity of ions produced by the radiation has a certain distribution and that the deviation from the mean velocity depends upon the kind of gases. To confirm the above-mentioned hypotheses, the ionization chamber is operated as an ion pulse chamber and its output pulses are directly observed with an oscilloscope and photographed for each filling gas with varying applied voltages. The fwhm of the output pulses

XUM

was measured and compared to ideal pulses for the various filling gases. (auth)

42089 CALCULATION OF THE SENSITIVITY FUNCTION OF A DETECTING SYSTEM WITH A MULTICHANNEL RING COLLIMATOR. Kostylev, V. A.; Fishman, L. Ya.; Narkevich, B. Ya. (Moscow Inst. of Experimental and Clinical Oncology). Med. Radiol.; 14: No. 4, 71-6(Apr 1971). (In Russian).

A method of calculating the function of sensitivity of the detecting system with a multicanal ring-focusing collimator is described. Calculations were made of the function of sensitivity of the system with NaI(Tl) detector measuring 150 × 80 mm and with a collimator from a pseudoalloy of tungsten and copper to the isotropic ^{198}Au gamma emitter. The calculated characteristics correlate well with experimental results. This method enables the optimization of parameters of collimator detecting systems for medical radioisotope diagnosis. (auth)

42090 COMPUTER PROCESSING OF CEREBRAL SCINTILLATION CAMERA STUDIES. Silfverskioeld, B. P.; Soederborg, B.; Kiibus, A. (Soedersjukhuset, Stockholm). Acta Neurol. Scand.; 47: 209-26(1971).

A technique is described which employs a scintillation camera and a construction for on-line computer processing in cerebral isotope studies. After intravenous injection, sequential imaging, optimal timing of short exposures, and selection of appropriate fields allowed assessment of tracer flow through precerebral and cerebral areas. The same construction could conveniently be used for contrast enhancement and quantitative studies of local uptake of radioisotopes. (auth)

42091 MEASURING OF THE STANDARD IONIC DOSE IN SOLID AND LIQUID MEDIA DURING X-RAY AND GAMMA IRRADIATION AT ENERGIES BETWEEN 50 keV AND 3 MeV. V. INVESTIGATIONS ON AIR EQUIVALENCE OF IONIZATION CHAMBER MATERIALS. Will, Wolfram; Rakow, Adalbert (Institut fuer Biophysik, Berlin). Strahlentherapie; 141: No. 2, 166-75(Feb 1971). (In German).

Ionization chambers must be constructed of homogeneous air-equivalent materials if there is a need for limited energy, air-density, and volume dependence of chamber sensitivity. Mistakes in dose measuring may particularly arise within solid or liquid media, if different influences on the chamber sensitivity and non-air-equivalent chamber materials are combined in order to obtain, by measuring freely in air, a chamber indication that is not dependent on energy factors. The known air-equivalence criteria, consisting in the comparison of the effective electron numbers and the electron concentration, can only be considered as equivalent for the calculation of material compositions that require, owing especially to the great influence of contamination, an experimental examination of the materials with regard to air equivalence. The air-equivalence examination of several chamber materials was effected, under alteration of air pressure in the chamber, by shifting the relation of wall ionization to gas ionization. As far as the developed materials (epoxide resin serving as fundamental substance) are concerned, air equivalence is nearly fulfilled over a large energy range, whereas combinations of non-air-equivalent materials in general only lead to an air-equivalent reciprocal action if there is a narrow energy range and a special chamber construction. The application of the cavity ionization theory according to Burlin [Brit. J. Radiol., 39: 727(1966)], for the calculation of the energy dependence of the sensitivity of non-air-equivalent chambers, offers difficulties for conventional energies of x-ray irradiations. (auth)

42092 THERMAL STABILITY AND ITS RELATION TO SCINTILLATION DETECTOR PARAMETERS WITH DOMESTIC NaI(Tl) CRYSTALS 40 x 40 mm AND PHOTOMULTIPLIERS 61 PK 413 THROUGH 415 AT ELEVATED TEMPERATURES. Silar, J.; Lomberska, L. (Inst. for the Study of Nuclear Tech., Premysleni, Czech.). Jad. Energ. 17: No. 7, 227-35(1971). (In Czech).

Measurements with photomultipliers 61 PK 413–415 in combination with domestic NaI(Tl) crystals 40 × 40 mm show promise for the use of these instruments at temperatures up to 70°C. Stabilization of the detector system is proposed as a requirement for spectrometric measurements. For radiometric measurements at extreme temperatures it is advantageous to select a detector voltage in the overheating interval of the horizontal portion of the characteristic. (tr-auth)

42093 ALPHA RADIOGRAPHY WITH PLASTIC TRACK DETECTORS. Somogyi, G.; Srivastava, D. S. (Inst. of Nuclear Research, Debrecen, Hungary). Int. J. Appl. Radiat. Isotop.; 22: No. 5, 289-99(May 1971).

Systematic investigations were made on the features of translucency observed on etched irradiated surfaces of plastics having a high density of α-tracks (>10^5 alphas/cm^2). Quantitative data are presented for the correlation between the optical density and the etching time and track density for three plastic track detectors of different sensitivities (namely cellulose nitrate, cellulose acetate and polycarbonate) under different irradiation conditions. The role of some parameters (irradiation geometry, particle energy, environmental conditions etc.) in the observed α-ray patterns was investigated. The effect of irradiation in vacuum on the optical density curves of the plastics was also studied. A possibility for making energy-selective α-radiography by using the less sensitive plastics such as polycarbonate was shown. (auth) (UK)

42094 ENVIRONMENTAL RADIATION MONITORING SYSTEM. Ishihara, Toyohide (Japan Atomic Energy Research Inst., Tokai). Keisoku To Seigyo; 9: No. 12, 981-9(Dec 1970). (In Japanese).

Environmental radiation monitoring systems are indispensable to nuclear power facilities. Optimum design of the systems is expected to be possible by elucidation of influencing factors and analyses of relations of how radioactive gases and dusts diffuse in air, deposit on the ground surface and other surfaces, shift to animals and vegetables, and give damage to man. System design is performed by combining the results analyzed above with required measuring range, measuring period, arrangement of detectors, background survey and others. If more precise data on the diffusion into the air, deposition and accompanying exposure is obtained in the future, the environmental radiation monitoring will be replaced with monitoring in release sources. The monitoring systems must be, of course, rechecked periodically and corrected so as to be able to respond to changes in facilities and conditions under which radioactive material is released, and to environmental situations. (Japan)

42095 METHOD FOR DETERMINING DEAD TIMES OF A G.M. DETECTOR AS A FUNCTION OF THE COUNT RATE. Ro, Seung Gy. J. Korean Nucl. Soc.; 3: No. 1, 3-7(Mar 1971).

A method for determining dead times of a G–M detector as a function of the count rate was investigated using ^{56}Mn radioactive sample. The formula $T(N_1) = (N_t - N_1 e^{-\lambda t})/(N_1 N_t)$ seems to be useful for determining a relation between the dead time and the count rate. Here $T(N_1)$ is the dead time for the count rate N_1, N_1 is the count rate at time zero, N_t is the count rate at time t, λ is the radioactive decay constant of the sample used, and t is the time between the first and second runs. When all the counting data were corrected for the dead times evaluated with this formula and then a variation of these corrected counting data with time was observed, the results showed quite a good agreement with the published data for the radioactive decay of ^{56}Mn. Besides, it appears that the dead time decreases as the count rate increases in a dead time-to-count rate relation obtained by the same formula. (auth)

42096 DETERMINATION OF THE EFFICIENCY OF SCINTILLATION CRYSTALS IMMERSED IN A HOMOGENEOUS MEDIUM CONTAMINATED BY γ-EMITTERS. De Franceschi, L.; Pagni, F. (CAMEN, Pisa, Italy). Minerva Fisiconucl.; 13: 165-72(Apr-Jun 1969). (In Italian). (CONF-680535-19).

From fourteenth national conference of the Italian Association for Health Physics and Protection from Radiation; Formia, Italy (29 May 1968).

The experimental technique for the measurement of the efficiency of a 2″ × 2″ scintillator immersed in water contaminated with various isotopes (^{131}I, ^{137}Cs, ^{60}Co, or ^{24}Na) is described. The calculation method used is described, and the theoretical and experimental results are compared. (tr-auth)

42097 SUPERCONDUCTING PARTICLE DETECTORS. Hesse, K. (AEG-Telefunken, Heilbronn, Ger.). Nucl. Instrum. Methods; 94: No. 2, 385-6(1971).

The application of superconductors as energy discriminators or spectrometers in nuclear spectroscopy is discussed. A proposal is made for a position-sensitive counter for highly ionizing particles. The advantage of the (in principle) very high resolution of a superconducting spectrometer may be exploited by using the kinetic inductance effect in superconductors. (auth)

42098 SIMPLE BEAM SCANNING METHODS FOR LOW CURRENTS. Arnold, H. (Inst. for Nuclear Physics Research, Amsterdam). Nucl. Instrum. Methods; 94: No. 2, 315-18(1971).

An instrument for direct registration of the position, the intensity, and the energy distribution of low-intensity beams for nuclear experiments is described. The equipment was tested for a charged-particle and a gamma-ray beam. It may even be used to scan the intensity distribution of neutron beams. The distribu-

tions are determined with respect to the symmetry axis of the instrument, which normally will be aligned with the optical axis of the beam transport system. (auth)

42099 PRESSURE DEPENDENCE OF GAIN AND BACKGROUND FOR PARALLEL PLATE CHANNEL MULTIPLIERS. Nilsson, Oe. (Uppsala Univ.). Nucl. Instrum. Methods; 94: No. 2, 311-13(1971).

A pressure dependence of the amplification and spontaneous pulse count rate of parallel-plate channel multipliers is established. The variation in gain is quite small and does not cause any problems for the practical use of the multipliers. At pressures below 10^{-6} torr the pressure dependence of the background can be neglected also. (auth)

42100 METHODS OF DETERMINATION OF FAST-NEUTRON SPECTRA FROM THRESHOLD–FOIL ACTIVATION DATA. Hrabovcova, Alojzia; Nikodemova, Denisa (Inst. of Industrial Hygiene and Occupational Medicine, Bratislava). Jad. Energ.; 17: No. 7, 241-5(1971). (In Czech).

Three methods of determination of fast neutron spectra by foil activation measurements are compared. Five detectors were selected: Np, Th, Ni, Al and In. Examined were the expansion method using the Gram-Schmidt method of orthonormalization for cross section functions, the orthonormal expansion method which employs Laguerr polynomials, and a polynomial method. The comparison and evaluation were made by investigation of six trial fluxes. Good agreement was obtained with the cross section method. The approximate representations of neutron spectra in the form of orthonormal expansion with Laguerr polynomials were the best except in one case. The utilization of two independent methods can give the most reliable results. (auth)

42101 RADIOMETRIC AND RADIATION MONITORING EQUIPMENT OF THE NEAR FUTURE. Matveev, V. V. Tr. Soyuznogo Nauch.-Issled. Inst. Priborostr.; No. 12, 3-14 (1970). In Russian).

The status and trends in development of radiometric and radiation monitoring equipment are reviewed. Basic assumptions are made on the development of a modular system of instruments in the field of measuring physical quantities which characterize ionizing radiation. New types of radiometric and radiation monitoring equipment which have been recently developed and made ready for series production are described. (JPRS)

42102 OPTIMIZING THE PARAMETERS OF RADIOMETRIC EQUIPMENT WHEN DETERMINING LOW LEVELS OF RADIATION. Konstantinov, D. I.; Matveev, V. V.; Yuzvuk, Yu. A. Tr. Soyuznogo Nauch.-Issled. Inst. Priborostr.; No. 12, 15-20(1970). (In Russian).

The possibility of using the method of verifying statistical hypotheses to derive working formulas for determining the threshold of sensitivity of radiometric equipment for measuring vanishingly small concentrations of radioactive isotopes is considered. It is shown that the Gaussian distribution can be used to approximate the Poisson probability distribution of readings up to unity. A working formula is given for the sensitivity threshold of a radiometric unit with a known photon flux. (JPRS)

42103 RADIATION DETECTION SYSTEM WITH AUTOMATIC SAMPLE COUNTING RATE DETERMINATION. Georgi, Heinz W.; Nather, Roy E. (to Beckman Instruments, Inc.). U. S. Patent 3,578,960. 18 May 1971. Filed 6 Apr 1966.

A radiation detection system with automatic and continuous on-line computation of sample count rate is disclosed. Logic circuitry is provided by which count pulses are added to a X register and subtracted from a dividend register. A comparator circuit is provided to detect the condition of identical tally in the X register and a timer register. Upon comparison and tally coincidence of the X register with the timer register, a means to increment a quotient register is provided. Such incrementation is continued until the dividend register is reduced to zero as indicated by the negative detection circuit provided therefor. The quotient register thereby contains the number of times the timer register can be divided into the dividend register. Other circuitry is provided to transfer the counts from a sample radiation detector into the dividend register. Therefore, at the end of computation the quotient register contains the sample count rate desired. Further logic circuitry and a cycle phase counter circuit are provided to accomplish division in a time substantially less than the elapsed measurement time period. By this logic means the various registers are incremented or decremented, as the case may be, at higher decade levels in the register progressing to lower decade levels as the logic circuitry and cycle phase counter direct, thereby providing a short computational time approaching a continuous presentation of sample count rate. Automatic compensation for undesired background counts is provided by means of digital circuits for subtraction of such count from the quotient register. (auth)

Nuclear Spectroscopic Instrumentation

Refer also to abstracts 43823 and 44205.

42104 (FEI–208) LIQUID BORON NEUTRON DETECTOR FOR A TIME-OF-FLIGHT SPECTROMETER. Kitaev, V. Ya. (Gosudarstvennyi Komitet po Ispol'zovaniyu Atomnoi Energii SSSR, Obninsk. Fiziko-Energeticheskii Institut). 1970. 11p. (In Russian). Dep. NTIS (U. S. Sales Only).

A study is made of the problems of building a liquid boron slow neutron detector with the application of low-noise photomultipliers type FEU-42. The counter container is installed with one photomultiplier. The cross sectional area of the container (80 cm^2) is much greater than the photocathode area of the photomultiplier (12 cm^2). The operation of the detector is illustrated by spectral-amplitude measurements during irradiation by neutrons and γ-rays and also by time-of-flight measurements with a sample of copper for a resolution of 7 nanoseconds/m. (JPRS)

42105 (JAERI–13561) GAMMA-RAY DISCRIMINATING SYSTEM FOR A PROTON-RECOIL COUNTER. Obu, Makoto; Ichimori, Toshihiro; (and others) (Japan Atomic Energy Research Inst., Tokai. Tokai Research Establishment). May 1969. 39p. NTIS (U. S. Sales Only).

Studies have been made on the characteristics of proton-recoil counters and a gamma-ray pulse-shape discriminating circuit, prepared for neutron spectroscopy in a fast reactor system. Using the neutrons from the $T(p,n)^3He$ reaction and a ^{60}Co gamma source, and applying the method to the fast reactor core system, the distributions of ionization vs. specific ionization were obtained with the two-dimensional dot-on method. The condition of gamma-ray discrimination was studied by the analysis of the dot-on distributions. The discrimination with the hydrogen-filled counter is satisfactory in the neutron energy range above ~10 keV; but, below ~10 keV, gamma-ray events occur in the neutron channels, and below ~5 keV, discrimination is not sufficient. The discrimination with the methane counter is not good, compared with that of the hydrogen counter, which should further be studied. The gamma-ray pulse-shape discrimination, using a "Rise time to pulse height converter," is also discussed. (auth) (Japan)

42106 (JAERI–13580) CHARACTERISTICS OF THE PROTON RECOIL PROPORTIONAL COUNTER GD-A FOR NEUTRON AND GAMMA-RAY. Ichimori, Toshiro; Obu, Makoto; (and others) (Japan Atomic Energy Research Inst., Tokai). Jun 1969. 44p. NTIS (U. S. Sales Only).

A proton recoil proportional counter was designed and constructed to measure fast neutron spectra over the energy range from 1 keV to 1 MeV in FCA. There are two types; one is hydrogen and the other is methane filled. The counter was tested on the characteristics of gas multiplication, resolution, proportionality and $n-\gamma$ discrimination with exposure of monochromatic neutrons, thermal neutrons and γ-rays by using the Van de Graaff, JRR-1 and a ^{60}Co source. The results indicate that the counter has the possibility for $n-\gamma$ discrimination, and will be adequate for a neutron energy spectrometer. In addition, significant information is obtained for further improvements in the counter and electronic instruments. (auth) (Japan)

42107 (JAERI–13771) JAERI PULSED TYPE NEUTRON SPECTROMETER. Motohashi, Haruhiko; Hamaguchi, Yoshikazu; (and others) (Japan Atomic Energy Research Inst., Tokai). Oct 1969. 60p. NTIS (U. S. Sales Only).

During the several years since the TOF neutron spectrometer (PTNS-1) was constructed, troubles with the long time operation and with the measurement of weakly scattered neutrons have been experienced. For the elimination of the causes of such troubles several improvements have been made including 1) replacement of the inpile plug, 2) improvement of the neutron filter, 3) adaptation of the chopper system, 4) adoption of a new detector system, and 5) improvement of neutron shielding. By such improvements, both the intensity of incoming monochromatic neutrons and the resolution of the detection system increased by a factor of two. (auth) (Japan)

42108 (UUIP–701) AN ITERATIVE COMPUTER METHOD FOR CORRECTION OF SPECTRAL DATA. Ekstig, B. (Uppsala Univ. (Sweden). Inst. of Physics). Apr 1970. 6p. NTIS (U. S. Sales Only).

An iterative computer method for correction of smearing distortions on spectral data is presented. It is shown that the method can be used for complex forms of distortion functions.

XUM

The method is applied to x-ray and ESCA-spectra, where ESCA stands for Electron spectroscopy for Chemical Analysis. (INIS)

42109 (UUIP-737) REDUCTION OF THE BACKGROUND IN A NaI(Tl) SCINTILLATION SPECTROMETER BY THE USE OF GEIGER ANTICOINCIDENCE AND MASSIVE SHIELDING. Stenberg, Allan (Uppsala Univ. (Sweden). Inst. of Physics). Mar 1971. 31p. Dep. NTIS (U. S. Sales Only).

The background of a NaI(Tl) detector 3" long and 3" in diameter was reduced from 84 to 55 cpm, totally above 200 keV, by adding a 6-cm-thick layer of boric acid, 1 mm of cadmium, and 5 cm of lead in the cavity of the used shield originally built up of a good 10 tons of lead, 160 kg of borated paraffin, and 45 Geiger counters as an anticoincidence screen. This reduction mainly refers to the decreased contributions from airborne activities and from the secondary cosmic radiation. The reduced and the remaining source of the background are discussed. (auth) (Sweden)

42110 BETA-SPEKTROGRAFY S POSTOYANNYMI MAGNITAMI. (Beta-Spectrographs with Permanent Magnets). Abdurazakov, A. A.; Gromov, K. Ya.; Umarov, G. Ya. Tashkent; Izdatel'stvo FAN Uzbekskoi SSR (1970). 188p.

The principles of operation of a beta-spectrograph with a fixed uniform field are explored. Structural features of existing instruments are discussed, including magnet parameters, field characteristics within magnet gaps, and vacuum chambers. Various methods of determination of the energies of lines of conversion electrons and their relative intensities are explained. The use of the beta-spectrograph at the Joint Institute for Nuclear Research for studying radioactive decay of isotopes is discussed, in particular when such work was performed in conjunction with the Institute's synchrocyclotron. The book's appendix presents in detail an investigation of decay schemes for ^{158}Ho and ^{159}Ho as examples of techniques and treatment of results. (141 references) (K.S.W.)

42111 EXPERIENCES CONCERNING THE POSSIBILITIES OF LOW LEVEL MEASUREMENTS IN THE ATOMKI. Bornemisza-Paupertl, P. ATOMKI (At. Kut. Intez.) Kozlem.; 12: No. 4, 179-90(Dec 1970). (In Hungarian).

In addition to ordinary lead caves, the facilities available in the ATOMKI for the reduction of background radiation are lead and limestone chambers with respective wall thicknesses of 5 and 50 cm, and with internal dimensions of 70 × 70 × 80 and 80 × 80 × 80 cm, respectively. Measurements for background spectra and deformation of spectra due to backscattering were performed in the above chambers and, for comparison, in a lead cave, as well as without any shielding, with a NaI(Tl) crystal-photomultiplier low-level assembly. The background spectra in the limestone chamber are compared with the ones reported in the literature. (auth)

42112 SILICON SEMICONDUCTOR SPECTROMETER. Varga, D.; Lakatos, T.; Nagy, J.; Novak, D. ATOMKI (At. Kut. Intez.) Koslem.; 12: No. 4, 239-42(Dec 1970). (In Hungarian).

A cryostat, vacuum chamber, and electronics used for beta-spectrometric measurements with a silicon semiconductor detector are described. (auth)

42113 RADIOANALYTICAL APPLICATIONS OF GAMMA-GAMMA COINCIDENCE TECHNIQUES WITH LITHIUM-DRIFTED GERMANIUM DETECTORS. Cooper, John A. (Battelle-Northwest, Richland, Wash.). Contract AT(45-1)-1830. Anal. Chem.; 43: No. 7, 838-45(Jun 1971).

The radioanalytical applications of gamma-gamma coincidence techniques with Ge(Li) detectors were examined with and without anticoincidence shielding. The Compton interference was reduced about 20 times more with the anticoincidence shield than without it when the interference was due to a radionuclide such as ^{60}Co which emits coincident gamma rays but showed little difference when the interference was a single gamma-ray emitting radionuclide such as ^{54}Mn. Background reductions of about 4 orders of magnitude and sensitivity improvements of about a factor of 5 were shown to be possible for radionuclides such as ^{75}Se which emit low energy coincident gamma rays. The application of this technique to the general problem of radioanalytical chemistry is discussed. (auth)

42114 VINCA NOVA: AN AUTOMATIC UNIT FOR NEUTRON SPECTROMETER CONTROL. Brankowski, Jerzy; Olejarczyk, Wiktor; Sarga, Tadeusz; Sciesinski, Jan; Zaleski, Tadeusz (Inst. of Nuclear Physics, Krakow). Nukleonika; 15: No. 11-12, 749-59(1970).

A neutron spectrometer control unit is described whose operational programming may be accomplished manually or automatically by means of punched tape. The unit is constructed of solid state elements. The logical structure and coordination of blocks are described. The technical parameters of the Vinča Nova unit are given. The neutron spectrometer is a triple table type. (auth)

42115 GRADIENT-FREE OVEN FOR EXAMINING THE MOESSBAUER EFFECT. Lyubutin, I. S.; Vishnyakov, Yu. S. (Inst. of Crystallography, Moscow). Instrum. Exp. Tech. (USSR) (Engl. Transl.); No. 5, 1500-1(Sep-Oct 1970).

Translated from Prib. Tekh. Eksp.; No. 5, 221-2(Sep-Oct 1970).

An oven for use in Moessbauer and x-ray spectroscopy, which has the heater wound as a two-layer grid, is described. This provides nearly zero gradient at the specimen up to 1000°C. (auth)

42116 PROCESSING OF SPECTRA FROM Ge-Li DETECTORS ON DIGITAL COMPUTERS (KATOK PROGRAM). Gadzhkov, V. (Joint Inst. for Nuclear Research, Dubna, USSR). Instrum. Exp. Tech. (USSR) (Engl. Transl.); No. 5, 1338-41(Sep-Oct 1970).

Translated from Prib. Tekh. Eksp.; No. 5, 82-5(Sep-Oct 1970).

The problem of processing spectra from Ge-Li-detectors is formulated. The mathematical model of the spectrum is described, and methods are considered for the solution of the resultant system of nonlinear equations. A description is given for a program solving the postulated problem, using the algorithm of the regular Newton-Kantorovich computational process. (auth)

42117 NEW METHOD FOR DETECTING GAMMA RADIATION FROM DRILLED GEOLOGICAL FORMATIONS AND A DEVICE UTILIZING THIS METHOD. Pelet, Regis; Douzon, Jean (to Institut Francais du Petrole). French Patent 2,036,754. 31 Dec 1970. Filed 21 Mar 1969. (In French).

A process for the γ ray analysis of the geological formations traversed by a probe is described. The probe developed is provided with a means of sorting out the signals corresponding to different gamma energies. A transmission cable links the probe to a measuring station. An elongated rectangular signal whose height depends upon the pulse amplitude is formed from each pulse. At the measuring station the height of the rectangular signal is determined during an interval of time in which it remains sensibly constant. (France)

42118 METHOD FOR DETERMINING THE CONCENTRATION OF A HIGHLY ACTIVE ELEMENT BY alpha SPECTROMETRY OF A THICK RADIATION SOURCE AND THE CORRESPONDING DEVICE. Guery, Marcel (to Commissariat a l'Energie Atomique). French Patent 2,029,146. 5 Oct 1970. Filed 14 Jan 1969. (In French).

A process is described for measuring the quantity of highly α active plutonium in a U-Pu alloy of low activity by α spectrometry with a source whose thickness is at least equal to the path of the alphas. A spectral curve formed by the superposition of several spectra is produced; this curve has an almost rectilinear portion. The concentration of this element in the source is determined from measurements of the area beneath the curve bounded by the two fixed energies corresponding to the linear portion. The counting equipment which incorporates a cylinder for receiving the samples is described. The Pu content was measured with an accuracy greater than 0.5%. (France)

42119 MEASUREMENT OF FAST NEUTRON SPECTRUM OUTSIDE BEAM PORT BY ^{6}Li SEMICONDUCTOR SPECTROMETER. Yang, Teh-li; Yen, Chen-shyong (National Tsinghua Univ., Hsinchu, Taiwan). J. Nucl. Sci. Technol. (Tokyo); 8: No. 5, 262-6(May 1971).

The neutron spectrum outside a beam port of the Tsing Hau Open-pool Reactor (THOR) has been obtained by using a ^{6}LiF sandwich-type semiconductor neutron spectrometer. Only those neutrons between 0.5 and 8 MeV have been shown. The spectrum falls off exponentially above 4.5 MeV. The valley in the spectra at about 3.5 MeV may be due to the elastic scattering resonance of oxygen at that energy. (auth)

42120 DUAL-MOTION MOESSBAUER ABSORBER SYSTEM WITH EXTRA-WIDE BLACK REGION AND ITS APPLICATIONS FOR PRECISION f-MEASUREMENTS. Kolk, B.; Harwig, B. (Natuurkundig Laboratorium, Groningen, Netherlands). Nucl. Instrum. Methods; 94: No. 2, 211-19(1971).

A system is described in which the width of the black region of a ^{57}Fe black absorber is tripled by moving two absorbers with opposite velocities while keeping a third absorber stationary. In this way, recoilless fractions of quadrupole split sources can be measured. Other applications of the system are discussed. An accurate correction is obtained for the residual transmission of black absorbers. (auth)

42121 DIGITAL NUCLEAR SPECTROMETER. Goldsworthy, W. W. (Univ. of California, Berkeley). Nucl. Instrum. Methods; 94: No. 2, 221-4(1971).

Charge developed at the output of a nuclear event detector, as a result of event occurrence and leakage, is digitally extracted

from the detector's output to maintain balance and to serve as a means of conversion of event-liberated charge to a digital number. The quantity of charge extracted to maintain balance is metered and converted to a train of pulses, each of which represents the extraction of a discrete amount of charge. By processing these pulses, information can be derived relating to real-event energies, rate of occurrence of events, time relationships of event occurrences, and background. Early numerical conversion of event-liberated charge, elimination of the need for processing of analog signals, the digital nature of the converted information (which lends itself to more efficient transmission and processing), and the greater spectrometer simplicity achieved are all advantages. (auth)

42122 SOME STATISTICAL CONSIDERATIONS IN THE LOCATION OF MOESSBAUER LINES. Wilson, A. J. C. (Univ. of Birmingham, Eng.). Nucl. Instrum. Methods; 94: No. 2, 225-7 (1971).

The low counting rates often encountered in investigations of or with the Moessbauer effect make it important to ensure the best possible use of the counting time available, and measures of location involving only three or four intensity observations are desirable. The counting times required to produce minimum variance of the mid-chord based on three observations, the mid-chord based on four observations, and the parabola minimum based on three observations are derived, together with expressions for the corresponding minimum variances. Translational velocity variations increase the variance of the measure of location by approximately one-half of the variance of the velocity. (auth)

42123 Si(Li) SPECTROMETERS FOR ELECTRONS AND LOW-ENERGY PHOTONS. Wood, R. E.; Rao, P. Venugopala; Puckett, O. H.; Palms, J. M. (Emory Univ., Atlanta). Nucl. Instrum. Methods; 94: No. 2, 245-52(1971).

The determination, using calibrated radioactive sources, of the photopeak efficiency is described for a Si(Li) spectrometer over an energy range of 5 keV to 170 keV. The nature of the silicon dead layer and the active detector volume is investigated. The probability of Si K-X-ray escape from the front surface of the detector is measured as a function of energy and compared to theory. A simple design for converting a Si(Li) photon detector to an efficient and good-resolution electron detector suitable for singles and coincidence spectrometry is described. (auth)

42124 192-DETECTOR SYSTEM FOR THE STUDY OF 3-BODY REACTIONS. Saylor, D. P.; McIntyre, J. A.; Bronson, J. D.; (and others) (Texas A and M Univ., College Station). Nucl. Instrum. Methods; 94: No. 2, 253-69(1971).

A system of 192 scintillation detectors was mounted on a spherical scattering chamber so that all portions of the sphere were equally covered. An electronics system, interfaced to an IBM 7094 computer, was constructed so that particle energies and detector locations are recorded when two particles are detected in coincidence. Such a measurement is sufficient to define completely the kinematics of a 3-body reaction. The apparatus is designed particularly for the study of reactions such as $p + d \rightarrow p + p + n$, $n + d \rightarrow n + n + p$, $p + p \rightarrow p + p + \gamma$, and $n + p \rightarrow n + p + \gamma$ between 10 MeV and 60 MeV. (auth)

42125 METHOD FOR ABSOLUTE CALIBRATION OF Ge(Li) DETECTORS USING EFFECTIVE INTERACTION DEPTH. Crisler, D. F.; Jarmer, J. J.; Eldridge, H. B. (Univ. of Wyoming, Laramie). Nucl. Instrum. Methods; 94: No. 2, 285-8(1971).

The measured full-energy-peak efficiencies of two coaxial Ge(Li) detectors that are nearly equal in sensitive volume but differ appreciably in measured γ-ray efficiency due mainly to differences in mounting characteristics are compared. The effective interaction depth of γ rays in these crystals was measured for the two detectors. Knowledge of this depth results in being able to calculate the absolute efficiency for any source-to-detector distance if the efficiency has been measured at one known distance. Curves are presented for the measured absolute efficiencies, the effective interaction depths, and γ-ray activities that have been adjusted correctly by using the effective interaction depth. (auth)

42126 FIGURE-OF-MERIT MEASUREMENTS FOR Ge(Li) DETECTORS. Cooper, J. A. (Battelle-Northwest, Richland, Wash.). Nucl. Instrum. Methods; 94: No. 2, 289-96(1971).

The sensitivities of a large number of Ge(Li) gamma-ray detectors under a variety of conditions are evaluated with figure-of-merit measurements and discussed in terms of their application. (auth)

42127 FAST COUNTING WITH NaI SPECTROMETERS. Brassard, C. (Yale Univ., New Haven). Nucl. Instrum. Methods; 94: No. 2, 301-6(1971).

A fast counting system designed for large NaI(Tl) scintillator detectors allows counting rates forty times higher than conventional double-delay-line amplifiers, without utilizing pile-up rejection. The operation of the system is based upon a rational compromise between energy resolution and permissible counting rates. (auth)

42128 TOTAL ABSORPTION OF 100 MeV PROTONS WITH A Ge(Li) DETECTOR. Sundqvist, B.; Hagberg, E.; Grafstroem, P. (Uppsala Univ.). Nucl. Instrum. Methods; 94: No. 2, 343-7(1971).

A test of a Ge(Li) detector used for total absorption of protons in the energy region 20 to 100 MeV is described. The detector showed good linearity, and the best energy resolution obtained was 270 keV (fwhm). A large contribution to the width probably came from energy straggling in an insensitive entrance window of the Ge crystal. A small part of the crystal was found to be not fully compensated. (auth)

42129 CALIBRATION OF Ge(Li) DETECTORS FOR LEVEL STRUCTURE STUDY IN PROTON AND NEUTRON CAPTURE REACTIONS. Haque, A. K. M. M. (Polytechnic of the South Bank, London). Nucl. Instrum. Methods; 94: No. 2, 349-56(1971).

The performance of a 5-cm^3 Ge(Li) detector in the gamma energy range of 100 keV to 12 MeV is described; readily available radioactive sources and resonance reactions were used. The detector resolution (fwhm) varied from 4.7 keV at 122 keV to 16 keV at 9 MeV; a considerable low-energy tailing was observed for high-energy gammas. The Fano factor measured with 661-keV gammas was found to be 0.25. To obtain the absolute photopeak efficiency, a radium source in equilibrium with its daughter products was used; an empirical fit was then obtained in the region 200 to 1500 keV. In order to evaluate the double escape efficiency, Fe(n,γ), Ti(n,γ), and Ni(n,γ) reactions with thermal neutrons (Am–Be neutrons moderated in paraffin wax) were employed. The combined methods are suitable for calibration for energy and efficiency for Ge(Li) detectors of different sizes. Finally, the detector was used to study the yield of (p,γ) resonances in Al by using an unstabilized proton beam with E_p = 200 to 500 keV; preliminary results show that the method is promising for γ-yield measurements as well as for locating the resonances accurately. (auth)

42130 HIGH-PURITY GERMANIUM CRYSTAL GROWING. Hansen, W. L. (Univ. of California, Berkeley). Nucl. Instrum. Methods; 94: No. 2, 377-80(1971).

It is shown that high-purity germanium can be grown with rather simple precautions against airborne contamination. Several crystals were grown with net impurity concentrations less than $5 \times 10^{10}/cm^3$ over more than half the crystal length. Some initial results with detectors made from this material are presented. (auth)

42131 COINCIDENCE SYSTEM FOR ELECTRODISINTEGRATION STUDIES. Shin, Y. M.; Skopik, D. M.; Wait, G. D. (Univ. of Saskatchewan, Saskatoon). Nucl. Instrum. Methods; 94: No. 2, 381-4(1971).

A method of observing coincidence pairs from the reaction X(e,e'p)Y is described. The method utilizes kinematic relations of the reaction. A heavy-particle coincidence spectrum from the disintegration of ^4He is presented. (auth)

42132 DUAL CHAMBER VACUUM CRYOSTAT FOR GERMANIUM LITHIUM DRIFTED DIODES. Detko, J. F. (Sloan-Kettering Inst. for Cancer Research, New York). Nucl. Instrum. Methods; 94: No. 2, 395-6(1971).

A dual-chamber cryostat, which has a permanent charge of cryosorption material that can be isolated from the diode chamber when it is opened to air, is described. (auth)

42133 SOLID-STATE DETECTORS AND ELECTRONICS IN GAMMA AND X-RAY SPECTROMETRY. REVIEW OF PRESENT KNOWLEDGE AND TECHNIQUES. Gorski, L. (Inst. of Nuclear Techniques, Krakow). pp 103-14 of Nuclear Techniques for Mineral Exploration and Exploitation. Vienna; International Atomic Energy Agency (1971).

From Panel on nuclear techniques and mineral resources in developing countries; Krakow, Poland (8 Dec 1969). See STI/PUB-279; CONF-691229.

The superior energy resolution of solid-state detectors offers an excellent advantage for gamma and x-ray spectrometry. At present only two types of solid-state detectors are generally available, namely the lithium-drifted germanium and lithium-drifted silicon semiconductors, and both require cryogenic cooling. The high-resolution potential of these detectors is being realized more fully through recent improvements in the design of the associated electronic circuitry and cooling devices. The need for cryogenic cooling of the present detectors and the first amplifier stage is not considered as a significant practical draw-

XUM

back, although it imposes a certain degree of limitation on field applications. Some basic knowledge of the techniques is reviewed. (auth)

42134 NEUTRON SPECTROMETER EMPLOYING TWO SEMICONDUCTOR COUNTERS IN COMBINATION WITH A COINCIDENCE CIRCUIT FOR ELIMINATING BACKGROUND. Meijer, Albertus Cornelis (to Philips Corp.). U. S. Patent 3,581,091. 25 May 1971. Priority date 15 Sep 1968, Netherlands.

A hydrogen rich foil is arranged at right angles to a beam of neutrons to be measured and emits protons which are interrupted and counted by a semiconductor barrier layer transmission counter (dE/dx−counter) and a semiconductor absorption or output counter (E−counter which counts the protons and measures the energy, background being eliminated by a coincidence counter. Both the transmission counter and absorption counter consists of a checkerboard counter and the scattering foil is arranged substantially immediately against the transmission counter, the scattered protons being measured by means of the coincidence circuit not only according to their number and energy, but also according to their direction. (auth)

High Energy Physics Instrumentation

Refer also to abstract 43735.

42135 (CERN-Trans-71-8) FILTERING OF TRACKS MEASURED ON THE SMP. Kokoulin, R. P.; Mikheev, V. P.; Protasov, V. P. (Gosudarstvennyi Komitet po Ispol'zovaniyu Atomnoi Energii SSSR, Moscow. Institut Teoreticheskoi i Eksperimental'noi Fiziki). Translated by R. Luther (CERN, Geneva, Switzerland), from report ITEF-784. 20p. Dep. NTIS (U. S. Sales Only).

A computer program for analysis of particle-track-photographs is described. The program discards background points and averages the remaining track points so that 5 to 20 mean points are obtained. Test runs resulted in errors of 14.2% from film with a 70% background and 1.8% from a film with a 40% background. The average processing time for one track is 1.5 sec on an M-20 machine. A block diagram of the program is included. (R.W.R.)

42136 (JINR-P13-5828) TIME PROPERTIES OF A SPARK CHAMBER FILLED WITH HELIUM AND HELIUM-HYDROGEN MIXTURE. Zaimidoroga, O. A.; Ivan'shin, Yu. I.; Chernenko, L. P. (Joint Inst. for Nuclear Research, Dubna (USSR). Lab. of Nuclear Problems). 1971. 13p. (In Russian). Dep. NTIS (U. S. Sales Only).

The time characteristics and efficiency of a spark chamber filled with helium and helium-hydrogen mixtures were determined. It is shown that the mechanism of remembrance of the charged particle tracks acts in helium due to the transition of atoms to metastable levels. (auth)

42137 APPLICATIONS OF CRYOGENICS TO NUCLEAR PHYSICS: LOW TEMPERATURE BUBBLE CHAMBERS. Newport, R. W. (Rutherford High Energy Lab., Chilton, Eng.). pp 415-37 of Advanced Cryogenics. /Bailey, C. A. (ed.). London; Plenum Press (1971).

Topics include operating conditions of bubble chambers, expansion systems, refrigeration, particular problems, present chambers, and future developments. (11 references) (UK)

42138 SPARK CHAMBERS IN HIGH ENERGY PHYSICS. PART III. FILMLESS SPARK CHAMBERS. Waligorski, Michal (Inst. Nuclear Tech., Krakow). Postepy Fiz.; 22: No. 2, 163-79(1971). (In Polish).

Filmless methods of data collection from spark chambers are described. The principles of recording tracks in the spark chamber using the vidicon, and using other methods based on acoustic and electromagnetic effects connected with the electrical discharge in the chamber, are given. The application of computers in filmless data collection is also briefly discussed. (auth)

42139 CONTRIBUTION TO THE MEASUREMENT OF SMALL ANGLES OF SCATTERED PARTICLES IN A PHOTOGRAPHIC EMULSION. Karabova, M.; Tucek, J. (Safarik Univ., Kosice, Czech.). Fyz. Cas.; 20: No. 2, 75-82(1970).

Accurate measurements are described of the angular distribution of secondary fast particles in nuclear emulsions, especially in the region of small angles. Special attention is paid to the evaluation of statistical and geometrical errors. (NSA of Czech)

42140 DESCRIPTION OF AN IONIZATION CALORIMETER SUPPLEMENTED WITH PROPORTIONAL COUNTERS. Babayan, Kh. P.; Boyadzhyan, N. G.; Vasil'tsov, V. V.; Mamidzhanyan, E. A. (Inst. of Physics, Erevan. Moscow State Univ.). Izv. Akad. Nauk Arm. SSR, Ser. Fiz.; 5: No. 6, 458-60(1970). (In Russian).

An arrangement, consisting of an ionization calorimeter and a system of proportional counters, allowing the determination of the sign and the energy of the nuclear active particle producing interaction in the target is described. (auth)

42141 COUNTER TELESCOPE MEASUREMENTS OF A BEAM OF NEGATIVE π MESONS. Tisljar-Lentulis, G. M.; Bond, V. P.; Robertson, J. S.; Moore, W. H. Jr. (Brookhaven National Lab., Upton, N. Y.). Radiat. Res.; 46: 16-27(Apr 1971).

Data are presented on negative π mesons from measurements in a low-intensity beam of the Cosmotron. Analogous data for protons and positive π mesons are discussed for comparison. The energies of the particles were selected to give a range in water of 15 cm. A Cherenkov counter used in the negative beam reduced the background of muons to 15% and electrons to 20% of the registered particles. Pulse-height spectra from scintillation detectors permitted a determination of the depth dose in polyethylene relative to the dose without absorber. The relative heights of the ionization peaks measured with a CsI(Tl) crystal were 3.1, 2.4, and 2.1 for protons, π^- mesons and π^+ mesons, respectively. Subtraction of the muon−electron beam contamination results in a peak height for π^- mesons of 3.0 relative to the plateau of the ionization curve. Plotting the counts registered in the high-amplitude channels of the pulse-height analyzer vs absorber depth shows, at greater depth, the contribution by π^- capture processes. (auth)

42142 SEMIAUTOMATIC TELEVISION DEVICE FOR MEASURING IONIZATION LOSSES. Ovsov, Yu. V.; Magonov, G. M.; Evseenko, A. K.; Rudenchenko, E. V. (Inst. of Nuclear Physics, Alma-Ata, USSR). Instrum. Exp. Tech. (USSR) (Engl. Transl.); No. 5, 1342-4(Sep-Oct 1970).

Translated from Prib. Tekh. Eksp.; No. 5, 85-8(Sep-Oct 1970).

A device which is intended for automatically measuring the parameters which characterize particle ionization losses, and which permits identifying particles up to 2 GeV/c with a film trace length of 2 cm and up to 2.5 GeV/c with a film trace length of 10 cm is described. The measurement speed attained in experimental operation is 30 cm/h. The computed measurement speed is 60 to 80 cm/h. The technical characteristics of the automatic television device are close to the characteristics of the known foreign instruments and, in some respects, surpass them. (auth)

42143 POWER SUPPLY SYSTEM FOR THE 100-cm LIQUID HYDROGEN BUBBLE CHAMBER ELECTROMAGNET. Omel'chenko, B. D. (Joint Inst. for Nuclear Research, Dubna, USSR). Instrum. Exp. Tech. (USSR) (Engl. Transl.); No. 5, 1409-13(Sep-Oct 1970).

Translated from Prib. Tekh. Eksp.; No. 5, 142-6(Sep-Oct 1970).

An automatic regulation system for the power supply of a 15-kA MS-12 electromagnet, used in a 100-cm liquid hydrogen bubble chamber, is described. Increase and decrease of the supply current is accomplished at a set rate by a voltage regulator. The supply current is maintained constant within ±0.05%. (auth)

42144 DETERMINATION OF γ-RAY ENERGY IN A XENON BUBBLE CHAMBER BY MEANS OF INTEGRAL CASCADE CURVES. Ogrzeval'skii, Z. (Joint Inst. for Nuclear Research, Dubna, USSR). Instrum. Exp. Tech. (USSR) (Engl. Transl.); No. 5, 1302-5(Sep-Oct 1970).

Translated from Prib. Tekh. Eksp.; No. 5, 51-4(Sep-Oct 1970).

A method for determining γ-ray energy is described which is convenient for automatic treatment of the photographs from bubble chambers filled with heavy liquids. A set of calibration curves for γ-ray energies from 20 to 2000 MeV is given for determining the energies of the γ rays on photographs from a xenon bubble chamber. (auth)

42145 SOME ASPECTS OF THE CONSTRUCTION OF THE 2-m LIQUID-HYDROGEN BUBBLE CHAMBER. Stepanov, A. M. (Inst. of Theoretical and Experimental Physics, Moscow). Instrum. Exp. Tech. (USSR) (Engl. Transl.); No. 5, 1306-9(Sep-Oct 1970).

Translated from Prib. Tekh. Eksp.; No. 5, 54-7(Sep-Oct 1970).

The construction of the 2-m liquid-hydrogen bubble chamber of the Institute of Theoretical and Experimental Physics and its basic components—the frame, the expansion system, and the vacuum housing—are described. (auth)

42146 TELESCOPE OF SPARK CHAMBERS WITH A MAGNETIC SPECTROMETER FOR POLARIZATION EXPERIMENTS. Tonapetyan, S. G.; Konovalov, O. G.; Derebchinskii, A. I.; (and

others) (Physical-Technical Inst., Kharkov). Instrum. Exp. Tech. (USSR) (Engl. Transl.); No. 5, 1310-12(Sep-Oct 1970).

Translated from Prib. Tekh. Eksp.; No. 5, 58-60(Sep-Oct 1970).

The mode of operation of a spark-chamber telescope in conjunction with a magnetic spectrometer is described in connection with experiments relating to the polarization of secondary protons formed by the interaction between high-energy photons and atomic nuclei. A method of calibrating the focal line of the spectrometer with respect to energy is developed. The range of momenta embraced by the telescope is 7%, and the accuracy of determining the proton energies ±2.5 MeV or better. (auth)

42147 NEW METHOD OF TAKING INFORMATION FROM SPARK CHAMBERS. Karzhavin, Yu. A.; Matyushin, A. T.; Matyushin, V. T.; Khachaturyan, M. N. (Joint Inst. for Nuclear Research, Dubna, USSR). Instrum. Exp. Tech. (USSR) (Engl. Transl.); No. 5, 1313-16(Sep-Oct 1970).

Translated from Prib. Tekh. Eksp.; No. 5, 60-3(Sep-Oct 1970).

Some experimental results associated with a new method of taking information from spark chambers with continuous (solid) electrodes are presented. The signals excited by the spark in the electrodes of the chamber are recorded by pressure-sensitive detectors. The possibility of creating a spherical chamber is discussed, and the amount of electronic apparatus required for coupling to a computer is considered. The realization of the technique and the associated chamber should lead to the creation of a highly-efficient "focusing" apparatus with a target situated inside the chamber for recording both charged particles and γ quanta. (auth)

42148 EFFECT OF A MAGNETIC FIELD ON THE ACCURACY WITH WHICH PARTICLE MOMENTUM IS DETERMINED IN A STREAMER OR SPARK CHAMBER. Daion, M. I.; Egorov, O. K.; Krylov, S. A.; (and others) (Inst. of Physics, Moscow). Instrum. Exp. Tech. (USSR) (Engl. Transl.); No. 5, 1317-21(Sep-Oct 1970).

Translated from Prib. Tekh. Eksp.; No. 5, 64-8(Sep-Oct 1970).

When streamer chambers are placed in magnetic fields, the scatter of the streamers decreases significantly, so the accuracy of the particle-momentum measurements improves. The rms deviations of streamers from the trajectories have been measured for various magnetic fields and delay times of the high-voltage pulses. The experimental results are compared with the electron-diffusion equations in a magnetic field. Measurement of the thermalization time for δ-electrons which arise in the gas in the chamber along a particle track is discussed. (auth)

42149 STUDY OF A STREAMER CHAMBER CONTAINING XENON. Avakyan, K. M.; Matevosyan, E. M. (Erevan Physics Inst.). Instrum. Exp. Tech. (USSR) (Engl. Transl.); No. 5, 1322-4(Sep-Oct 1970).

Translated from Prib. Tekh. Eksp.; No. 5, 68-70(Sep-Oct 1970).

A streamer chamber having a high γ-efficiency because of a Xe admixture is described. The experimental dependences of the memory time, the parameters of the high-voltage pulse, and the number of "bright" streamers on the Xe concentration are reported. The streamer velocity has been determined for a chamber containing 10% Xe. (auth)

42150 CIRCUIT PARAMETERS OF A SPARK CHAMBER WITH A DECOUPLED HIGH-VOLTAGE ELECTRODE. Barabash, L. S. (Joint Inst. for Nuclear Research, Dubna, USSR). Instrum. Exp. Tech. (USSR) (Engl. Transl.); No. 5, 1325-7(Sep-Oct 1970).

Translated from Prib. Tekh. Eksp.; No. 5, 71-2(Sep-Oct 1970).

A method of calculating the circuit of a spark chamber with a resistance-decoupled high-voltage electrode is proposed. Factors determining the magnitude of the decoupling resistances and the internal resistance of the high-voltage generator are discussed. (auth)

42151 CONSTRUCTION AND PERFORMANCE OF A CURRENT SPARK CHAMBER. Sugiyama, Suguru; Tomimasu, Takio. Denki Shikensho Iho; 35: No. 1, 55-63(1971).

A current spark chamber was constructed and its characteristics were measured. Positions of the tracks produced by charged particles were determined by the magnitude of the spark current flowing through the path between the spark position and the contact point of ground lead to the earth. The method was simpler than in other types of spark chambers. A precision of 3 mm in the localization of the sparks was obtained. The relation between the output signal and the spark position was linear within ±1% over the range of distance between 1 and 17 cm from the edge of the spark chamber. (auth)

42152 APPARATUS FOR CONTINUOUS OBSERVATION OF COSMIC RAY INTENSITY AT A SHALLOW UNDERGROUND STATION. Murakami, Kazuaki (Inst. of Physical and Chemical Research, Yamato, Japan); Miyagawa, Tadayoshi; Miyazaki, Tadakuni; Mishima, Yasushi; Ukigaya, Fumio. Rikagaku Kenkyusho Hokoku; 47: No. 1, 1-12(Jan 1971). (In Japanese).

A cosmic ray telescope with two layers of plastic scintillators was settled underground at Takeyama (Geographic 35°13′12″N, 139°37′22″E, 6 m above sea level). One layer consists of 9 arrays, 1 m^2 each. The depth of the tunnel is estimated to be 54 mwe. Counting rates are 4×10^4/h for 9 m^2 of vertical component, 1.5×10^4/h for each of 6 m^2 of geographical N, S, E, W components inclined at 30° from the zenith, and 2×10^3/h for each of 3 m^2 of four components inclined at 50°. Continuous observation started in August 1967. Details of the apparatus and the tunnel are presented. (auth) (Japan)

42153 BUBBLE DENSITY MEASUREMENTS WITH HPD 2 AT CERN. Duinker, P.; Quercigh, E. (CERN, Geneva). Nucl. Instrum. Methods; 94: No. 2, 333-41(1971).

Measurement of ionization on bubble chamber events by the flying spot digitizer (HPD 2) at CERN is discussed. The technique of analyzing the measurements is described, and results showing that this method compares favorably with visual estimates are presented. (auth)

42154 TOTAL ABSORPTION TYPE LEAD GLASS CHERENKOV COUNTER WITH HIGH RESOLUTION. Hayashi, M.; Homma, S.; Kajiura, N.; Kondo, T.; Yamada, S. (Tokyo Univ.). Nucl. Instrum. Methods; 94: No. 2, 297-9(1971).

A total absorption-type lead-glass Cherenkov counter that had a thickness of 11 radiation lengths was constructed and tested by using monochromatic electron beams with energies from 200 MeV to 900 MeV. Cherenkov light was viewed by four photomultipliers (RCA 8575) with high quantum efficiencies. The peak of the pulse-height distribution as a function of the incident energy was found to be linear in the energy region investigated. The energy resolution, defined by the full-width of the distribution at the half-maximum, ΔE over E, is less than 12% at 900 MeV and proportional to $E^{-\frac{1}{2}}$.

42155 RATE OF ENERGY LOSS AND INTRINSIC RESOLUTION OF SILICON DETECTORS. Paul, J. M. (Louisiana State Univ., Baton Rouge). Nucl. Instrum. Methods; 94: No. 2, 275-83 (1971).

The rate of energy loss in silicon is calculated with both shell correction and density effect for various particles taken into account. The values of fwhm as percentage of the most probable energy loss in silicon detectors of four different thicknesses are calculated and presented graphically; energy ranges of interest in both high-energy physics and cosmic-ray studies are covered. (auth

42156 SYSTEM OF PROPORTIONAL WIRE CHAMBERS ON-LINE WITH A COMPUTER. Zanevskii, Yu. V.; Nigmanov, T. S.; Peshekhonov, V. D.; Pugachevich, V. P.; Turala, M. (Joint Inst. for Nuclear Research, Dubna, USSR). Nucl. Instrum. Methods; 94: No. 2, 233-5(1971).

A system of two proportional wire chambers on-line with a computer or analyzer is described. Results obtained by operating the system in the 4.03-GeV/c beam are presented. (auth)

42157 EFFECT OF THE RADIUS OF THE APPARATUS ON THE MEAN DISTANCE OF THE SHOWER AXIS FROM ITS CENTER. Jatczak, Jerzy (Univ. of Lodz, Poland). Nukleonika; 15: No. 11-12, 707-15(1970). (In Polish).

The effect of the radius a of the apparatus on the mean distance $\bar{r}$ of the registered shower axis from its center is described. The distance $\bar{r}$ is related linearly to the radius a of the apparatus by the expression: $\bar{r} = p + qa$, where p and q are dependent on the configuration of the detectors. (auth)

42158 SPARK CHAMBER AS AN ELEMENT OF THE HODOSCOPIC DETECTOR OF EXTENSIVE AIR SHOWERS. Firkowski, Ryszard (Instytut Badan Jadrowych, Lodz, Poland); Glowacki, Jerzy; Knapik, Jerzy; Olejniczak, Wielislaw; Rachowski, Jan. Nukleonika; 16: No. 1-2, 65-84(Feb 1970). (In Polish).

An experimental neon spark chamber system (500 × 500 × 100 mm) whose electrodes are covered with glass is presented. The characteristics of the high voltage supply system are investigated, and the possibility of using this system for supplying simultaneously more than one chamber is analyzed. The detection properties of the spark chamber were evaluated, and their dependence on the parameters of the high voltage pulse was assessed. The use of spark chambers of this type as detection elements of a hodoscope system for the investigation of extensive air showers in cosmic radiation is discussed. (auth)

42159 BALLOON-BORNE INSTRUMENT FOR LOW-ENERGY PRIMARY COSMIC-RAY MEASUREMENTS. Tamai, Eiji; Sakai, Takasuke; Kogami, Shinichi; Narita, Nobuo; Ogura, Koichi (Nihon Univ., Chiba, Japan). Nihon Daigaku Seisan Kogakubu Hokoku; 3: No. 2, 61-5(Sep 1970). (In Japanese).

XUM

Observation of cosmic-ray protons and alpha particles, originating in the sun or galaxy, near the top of the atmosphere over Showa base, South Pole, has been planned to obtain qualitative information about the acceleration mechanisms and nuclear interaction processes of solar particles during a solar flare, and also solar modulation of the solar and galactic cosmic rays. In this paper, a counter telescope and its electronics for observing those particles are described in detail. (auth) (Japan)

Radiation Dosimeters

Refer also to abstracts 42411 and 42442.

42160 (N-71-14602) APOLLO HELMET DOSIMETRY EXPERIMENTS. Final Report. Comstock, G M.; Fleischer, R. L.; Hart, H. R. Jr. (General Electric Co., Schenectady, N. Y. Research and Development Center). Nov 1970. Contract NAS9-9828. 29p. (NASA-CR-114804). NTIS.

Recent reports by Apollo astronauts of lines of light apparently seen with the eyes closed have caused concern for the possible biological effects of heavily ionizing particles that penetrate the shielding of the spacecraft or space suit. A dosimetry experiment consists of using plastic Apollo helmets as recorders of heavy cosmic ray particles directly incident on the face and heads of the astronauts. Particle tracks are revealed by chemically etching the interior of the Lexan polycarbonate helmet to produce cone-shaped holes, which are later counted. (STAR)

42161 (NP-18892) MATHEMATICAL METHOD FOR THE COMPUTER PROCESSING OF DOSIMETRIC FILMS. Callonnec, Jean-Pierre (Laboratoire Central de l'Armement, Arcueil (France)). Apr 1970. 45p. (In French). Dep. NTIS (U. S. Sales Only).

A mathematical formulation of the problem associated with the computer processing of dosimetric films is presented. Many methods are proposed and discussed which take into account the difficulties inherent in badly posed problems leading to a theoretical infinity of possible solutions (doses having the same darkening effect on photographic films). (France)

42162 (NYO-3409-10) ROLE OF TRAPPING PROCESSES IN SOLID STATE RADIATION DOSIMETRY. Final Report. Henisch, H. K. (Pennsylvania State Univ., University Park. Materials Research Lab.). May 1971. Contract AT(30-1)-3409. 40p. Dep. NTIS.

Research progress on new ideas in solid state dosimetry including field enhancement of thermoluminescence, photo-stimulated radiation dosimetry, current glow methods, pyroelectric method, and dosimetry by electric depolarization is reported. Polymer electset dosimetry and a technique for the measurement of pyroelectric coefficients are discussed in detail. (W.H.K.)

42163 RADIATION YIELD OF Mn^{+3} IN DOSIMETRIC GLASSES. Trofimov, V. M.; Galimov, D. G.; Dobretsova, I. N.; Orlov, N. F.; Yudin, D. M. At. Energ. (USSR); 30: 63-4(Jan 1971). (In Russian).

Phosphate glasses containing various activators which create a band of induced absorption under the effect of ionizing radiation are promising materials in recording a dose up to 3×10^8 r at temperatures from -200 to 200°C. The gamma and electron dose is measured from the change in intensity of the band of induced absorption. Divalent manganese which is converted to trivalent manganese ion under the effect of radiation is the most suitable activator for phosphate glasses. A study of the radiation yield of Mn^{3+} was carried out in order to select the optimal initial concentration of manganese in phosphate glasses that creates a stable band of induced absorption. EPR data showed a maximum radiation yield of Mn^{3+} at an initial manganese concentration of about 0.8 mole %. These studies have shown that Mn^{3+} ions are responsible for the formation of a band of induced absorption in phosphate glass, and the intensity of this band is maximum at an initial manganese concentration of about 0.8 mol %. (TTT)

42164 RULES FOR FILM BADGES FOR PERSONNEL MONITORING. NEN 2388 1962. The Hague; Nederlands Normalisatie-Instituut (1962). 2p. (In Dutch). Available from Nederlands Normalisatie-Instituut, The Hague.

42165 FILM BADGE SERVICES. NSF Standard No. 16 1966. Ann Arbor, Mich.; National Sanitation Foundation (1966). 27p. Available from National Sanitation Foundation, Ann Arbor, Mich.

A standard prescribing minimum requirements for film badge services is presented. (W.H.K.)

42166 REMARKS ON THE THEORY OF ENERGY DEPOSITION IN CAVITIES. Spencer, L. V. (National Bureau of Standards, Washington, D. C.). Acta Radiol., Ther., Phys., Biol.; 10: 1-20(1971).

The contributions of Gray and Bragg to the theory of energy deposition in cavities are reviewed in connection with a mathematical formulation of the problem. The two principal contributors to the Bragg-Gray theory apparently used approaches that were equivalent but dual in the sense of involving adjoint expressions of the energy deposition. Burch has later attempted an extension of Gray's ideas and Spencer-Attix have extended the theory by applying Bragg's point of view. Some comments on future cavity theory research are included. (auth) (Sweden)

42167 USE OF THERMOLUMINESCENT DETECTORS IN THE DOSIMETRY OF HIGH ENERGY ELECTRON BEAMS FROM THE BETATRON. Tosi, G.; Pedrinazzi, G.; Scielzo, G.; Botturi, M. (Ospedale Maggiore Ca' Granda, Milan). Minerva Fisiconucl.; 14: 65-9(Apr-Jun 1970). (In Italian). (CONF-690929-8).

From fifteenth national congress of the Italian Association for Health Physics and Protection Against Radiation; Cagliari, Italy (Sep-Oct 1969).

The possibility of using thermoluminescent detectors in the relative dosimetry of intense betatron beams was investigated in the energy range from 5 to 43 MeV. Cylinders of LiF, mm in diameter and 7 mm in height, were used in the study. The results showed that in the energy range studied the response of the LiF detectors to absorbed dose is independent of the energy and the dose intensity for doses between 1 and 300 rad. This characteristic, in addition to the reproducibility of the response of better than ±1%, makes this thermoluminescent detector useful in miniaturized dosimeter of electron beams and especially in the field of radiotherapy. (tr-auth)

42168 IONIZATION CHAMBER FOR DOSIMETRY OF MIXED GAMMA-FAST NEUTRON RADIATION. Daddi, L.; D'Angelo, V.; Musumeci, L. (CAMEN, Pisa, Italy). Minerva Fisiconucl.; 13: 141-4(Apr-Jun 1969). (In Italian). (CONF-680535-15).

From fourteenth national conference of the Italian Association for Health Physics and Protection from Radiation; Formia, Italy (29 May 1968).

The construction and calibration of a pair of ionization chamber dosimeters for the measurement of mixed γ-fast neutron doses are described. One of the dosimeters was constructed in tissue-equivalent material, and the other was constructed of a material that was little sensitive to neutrons. The calibration of the pair, carried out in a γ field, deviated from the fast neutron measurement. The calibration was carried out in the mixed γ-fast neutron field of a 160-kV Crockroft-Walton accelerator. (tr-auth)

42169 DOSIMETRY OF HIGH ENERGY (12 TO 32 MeV) ELECTRON BEAMS USING PHOTOLUMINESCENT GLASS. Tosi, G.; Turchi, L.; Maffi, A. (Clinica S. Ambrogio, Milan). Minerva Fisiconucl.; 13: 135-40(Apr-Jun 1969). (In Italian). (CONF-680535-14).

From fourteenth national conference of the Italian Association for Health Physics and Protection from Radiation; Formia, Italy (29 May 1968).

The possiblity of using photoluminescent glass in the relative dosimetry of intense accelerated electron beams from a betatron in the energy range from 12 to 32 MeV was studied. Ag-activated metaphosphate glass in the form of cylinders 1 mm in diameter per 6 mm of height was used in the study. The studies showed that in the energy interval examined, the response of the glass was independent of the energy and of the dose rate. The response is proportional to the absorbed dose for doses between 15 to 20 rad and about 15 krad. This characteristic led to the conclusion that the photoluminescent glasses examined could be used as miniaturized dosimeters in the study of the radiation fields produced by high energy electrons. The limitations of the method and the possible error sources are discussed. Some improvements to reduce these errors to the minimum are described. (tr-auth)

42170 POLYTETRAFLUOROETHYLENE: DOSIMETER FOR GAMMA DOSE MEASUREMENTS TO ABOUT 10^{11} RAD. Jeltsch, E.; Graf, W. (Kernforschungsanlage, Juelich, Ger.). Atomkernenergie; 17: 218-22(May 1971). (In German).

At about 2×10^9 rad, the colorless PTFE powder changes into a weakly brown liquid of which both coloration and viscosity intensify with increasing γ dose. At about 10^{10} rad, a brown fine crystalline powder forms, which changes into a liquid at higher temperatures. Two methods of dosimetry between 10^{10} and 10^{11} rad are developed. One is based on the measurement of the melting temperature, and the other one on measurement of viscosity. (H.B.G.)

42171 USE OF PHOTOGRAPHIC FILMS FOR INDIVIDUAL RADIOMETRY OF THE DAUGHTER PRODUCTS OF RADON.

Markov, K. P.; Ryabov, N. V.; Stas, K. N. Tr. Soyuznogo Nauch.-Issled. Inst. Priborostr.; No. 12, 184-91(1970). (In Russian).

The possibility of personnel monitoring for the atmospheric con tent of radon decay products according to the "latent" energy by pumping air through a filtering cloth while simultaneously using a ZnS(Ag) scintillator and a photographic film to register the α-activity of the specimen is considered. The results of theoretical and experimental studies on determining the sensitivity of the method and the measurement range are given. (JPRS)

42172 INTERCOMPARISONS OF ABSORBED DOSE IN ^{60}Co TELETHERAPY USING MAILED LiF DOSIMETERS. II. RESULTS FOR CANADA AND SIX ASIAN COUNTRIES. Pfalzner, Paul M.; Jayarman, S. (Ottawa Clinic. International Atomic Energy Agency, Vienna). Acta Radiol., Ther., Phys., Biol.; 9: 501-12(1970).

A series of dosimeter capsules containing LiF phosphor were distributed by the International Atomic Energy Agency to 14 Canadian radiotherapy centers and to 15 centers in six countries in Asia. The dosimeters were irradiated with a cobalt-60 beam at a depth of 5 cm in water to an absorbed dose calculated by the participants to be 500 rad, and returned to IAEA by mail for read-out. The maximum difference in absorbed dose between participating centers was found to be 11.6% for Canada and 31.7% for the Asian countries, with percent standard deviations of 3.3% and 8.7% for the respective overall mean doses. The lack of uniformity in the dosimetric methods and in the factors used by participants to convert exposure to absorbed dose indicates a need for closer international collaboration and standardization in medical radiation dosimetry. (auth) (Sweden)

Radiometric Instruments

42173 BETA BACKSCATTER THICKNESS MEASURING APPARATUS FOR APERTURES IN PRINTED CIRCUIT BOARDS AND THE LIKE. (to Unit Process Assemblies, Inc.). British Patent 1,231,484. 12 May 1971. Priority date 1 Apr 1968, United States.

The beta source and radiation detector design for measuring the thickness of coatings on the side walls of apertures in printed circuit board workpieces and for other uses is described. (W.H.K.)

42174 PROBE ASSEMBLY FOR USE IN BETA RAY BACKSCATTER THICKNESS MEASURING APPARATUS. (to Unit Process Assemblies Inc.). British Patent 1,231,485. 12 May 1971. Priority date 1 Apr 1968, United States.

A beta source and radiation detector configuration is described for beta backscatter thickness measurements. (W.H.K.)

42175 SEMICONDUCTOR SYSTEM FOR ANALOG PROCESSING OF RADIOMETRIC SIGNALS OBTAINED FROM A CONTROL SET USED FOR DETERMINATION OF THE CALCIUM CONTENT IN THE CEMENT FEEDING. Korbel, Kazimierz (Inst. of Nuclear Physic, Krakow); Lacki, Eugeniusz. Nukleonika; 15: No. 11-12, 761-70(1970). (In Polish).

When using the radiometric method for continuous control of the chemical composition of the cement feed in the continuous technological process, the determination of the calcium content reduces to the processing of the results obtained according to the content-function $Y(X_1,X_2)$. The analog information processing system described operates on the basis of a slide rule, where the function of units taking logarithms as well as antilogarithms is performed by the transistor junctions. The principles of operation of this analog calculator as well as its accuracy and thermal stability are discussed. (auth)

42176 REKOMENDATSII PO ISPOL'ZOVANIYU RADIOIZOTOPNYKH METODOV DLYA OPREDELENIYA FIZIKO-MEKHANICHESKIKH SVOISTV GRUNTOV. (Recommendations on the use of Radioisotopic Methods for Determining the Physico-Mechanical Properties of Soils). Moscow; Izdatel'stvo Literatury po Stroitel'stvu (1971). 49p.

The careful organization of material on radioisotopic methods and the conciseness of presentation combine to make this small volume a handbook of rules for conducting radiometric determinations of density, moisture, and abrasiveness of soils. For gamma source probes for density measurements to depths of 1.5 m, Co-60, Cs-137, and Ra-226 are recommended. Fast neutron sources for moisture determinations may contain Be and one of the following: Pu, Po, Ra, or Am. The direction and speed of movement of underground water are also subject to radiometric techniques. Indicators listed are H-3, Na-24, S-35, Fe-59, Br-82, Rb-80, and I-131, and proper choice and application are outlined. How to handle the results of continuous monitoring, and suggestions for assembling recording equipment are subjects of separate sections. No references. (K.S.W.)

42177 ACCURACY OF THE NEUTRON METHOD OF MOISTURE MEASUREMENT. Sciesinska, Ewa (Jagiellonian Univ., Krakow). Nukleonika; 15: 593-612(1970).

A discussion is given of the influence of density and chemical composition of the medium, as well as the measurement geometry, on the accuracy of the neutron method of the moisture measurement. Experimental and theoretical calibration curves obtained for foundry mass in finite 4 π-geometry were compared for this purpose. The influence of density was investigated for all variants of the 4 π-geometry employed, whereas the influence of absorbents of thermal neutrons was studied only for the simplest geometry. The incompatibility of the obtained results with the Fermi age theory is interpreted. The accuracies of the epithermal and thermal variant of the neutron method are compared. (auth)

42178 QUANTITATIVE ESTIMATION OF THE URANIUM DISTRIBUTION IN MTR FUEL PLATES USING A SCINTILLATION DETECTOR. Cotterell, K. (Atomic Energy Research Establishment, Harwell, Eng.). Brit. J. Non-Destruct. Test.; 13: 46-52 (Mar 1971).

An apparatus was developed to provide quantitative information on uranium distribution in MTR fuel plates. Details of the apparatus, setting-up procedure, and the calibration methods are given. The relationship between accuracy and rate of inspection is discussed together with possible methods of increasing the latter. (auth) (UK)

42179 RADIOACTIVE FORCE INDICATING DEVICE. Woodburn, Charles R. U. S. Patent 3,584,217. 8 Jun 1971. Filed 31 Dec 1968.

The invention relates to a means for determining the force applied between related parts comprising a resilient, compressible body of radioactive material having a predetermined, substantially constant emission rate, force transmitting structure between said body and parts whereby forces exerted through the construction are transmitted onto and through the body so as to compress the body and reduce or increase its volumetric extent in direct predetermined relationship to the force exerted thereon, an emission shield related to the body with an emission port therein, the cross section of which is less than the normal cross section of the body and substantially equal to the cross section of the body when it is in its fully compressed condition and an emission counter spaced from and in alignment with the port and adapted to count the volume of emission flowing through the part and translate it into force units. (auth)

42180 UTILIZING PENETRATING RADIATION. Brown, Leonard Carlton (to United States Atomic Energy Commission). U. S. Patent 3,581,090. 25 May 1971. Filed 20 Oct 1966.

A system for determining the position of a plurality of objects carrying sources of radiation relative to a detector for said radiation includes means for modulating each of the radiation sources at a different frequency. The modulated radiation is received by an array including a plurality of mutually shielded detectors. Each detector feeds a voltage indicative of the amount of penetrating radiation impinging thereon to a computing network which derives visual signals indicative of the angular location and range of each object carrying a radiation source. Provision is made for eliminating background radiation from the signal derived from each of the detectors. Use of the system on helicoptors for maintaining a flight formation is described. (auth)

Miscellaneous Instruments and Components

Refer also to abstracts 42048, 43221, 43343, 43474, and 44115.

42181 (CERN-Trans-71-18) MODULAR PROGRAMMING SYSTEM FOR PROGRAMMING EXPERIMENTS ON THE PDP-9. Degenhardt, K. H.; Frevert, L.; Woletz, W. (Hahn-Meitner-Institut fuer Kerforschung, Berlin (West Germany)). Translated by J. Nicholls (CERN, Geneva, Switzerland), from report HMI-B-96. 114p. Dep. NTIS (U. S. Sales Only).

An abstract of this paper, prepared from the original language, appeared as NSA 25: 8572. (W.H.K.)

42182 (COO-1140-194) COMPUTER CONTROL OF A HIGH-TEMPERATURE QUADRUPOLE MASS SPECTROMETER. Fast, Peter M.; Castles, Jeffrey R.; Gilles, Paul W. (Kansas Univ., Lawrence, Dept. of Chemistry). 13 May 1971. 8p. (CONF-710704-2). Dep. NTIS.

From Conference on computers in chemical education and research; DeKalb, Ill. (19 Jul 1971).

The University of Kansas is developing, under a National Science Foundation grant, an automatic data acquisition and equipment con-

XUM

trol system for experiments in high-temperature chemistry. A quadrupole mass spectrometer is one of several laboratory devices joined to this system. The heart of the system is a small general-purpose digital computer. Programs for this computer have been written at the University which allow automatic operation of the quadrupole mass spectrometer. The mass-to-charge ratio is selected by the computer, intensities are measured and displayed, and the data are recorded permanently in a retrievable fashion. (auth)

42183 (CTO–756) DIELECTRIC WAVEGUIDES AND AERIALS FOR 2 mm MICROWAVE INTERFEROMETERS WITH HIGH SPATIAL RESOLUTION FOR PLASMA DENSITY MEASUREMENTS. Hartwig, H. (Kernforschungsanlage, Juelich (West Germany)). Translated by J. B. Sykes (Culham Lab., Abingdon, Eng.), from report JUL–473-PP. 11p. Dep. NTIS (U. S. Sales Only).

An abstract of this paper, prepared from the original language, appeared as NSA 21: 46316. (W.H.K.)

42184 (JAERI–13536) THEORIES AND THEIR APPLICATIONS OF ELECTROMAGNETIC METHOD IN LIQUID FLOW RATE-MEASUREMENT. Hayashi, Toshikazu (Japan Atomic Energy Research Inst., Tokai). May 1969. 86p. NTIS (U. S. Sales Only).

Theories and applications of the electromagnetic method concerning flow rate-measurement of electrically conducting fluids are considered. Various factors which influence the electric potential difference between the electrodes including asymmetry of the velocity profile, the electric contact resistance between the fluid and the pipe walls, and the shorting effect of the electrically conducting walls, and end effects due to non-uniformity of the magnetic flux density are discussed. Magnetohydrodynamic effect on the liquid metal and its pressure loss are also estimated. Nonlinear relations between the electric potential difference and the flow rate of the electromagnetic flowmeter for a large diameter pipe are discussed, and some problems in designing a large flowmeter are pointed out according to some data from the flow calibration tests. Furthermore the design problems of an electromagnetic flowmeter for the in-core instrumented fuel assembly are made clear, and a method of design and selection of the permanent magnet for the flowmeter is shown. The theory and design of an implantable electromagnetic blood flowmeter are described and their applications for measurement of the liquid metal flow rate in a small channel are discussed. (auth) (France)

42185 (JAERI–13605) JAERI NUCLEAR INSTRUMENT MODULE SYSTEM. 5. (Japan Atomic Energy Research Inst., Tokai). Jun 1969. 87p. NTIS (U. S. Sales Only).

Eight kinds of the JAERI Nuclear Instrument modules are described. General description, specifications, circuit description and performances for each unit are summarized. These units are Model 121 B preamplifier, Model 133 A timing single-channel analyzer, Model 142 A sum/delay amplifier, Model 154 risetime to height converter, Model 156 spectroscopy amplifier, Model 157 baseline restorer, Model 158 fast amplifier, and Model 159 fast discriminator. (auth) (Japan)

42186 (JAERI–13768) JAERI NUCLEAR INSTRUMENT MODULE SYSTEM. Standardized Part, Revision 1. (Japan Atomic Energy Research Inst., Tokai). Oct 1969. 39p. NTIS (U. S. Sales Only).

This is the first revised copy for the "JAERI nuclear instrument module system-standardized part" which was presented in 1967. (auth) (Japan)

42187 (JINR–P13-5801) NANOSECOND LIFETIME MEASUREMENTS OF EXCITED NUCLEAR STATES AT THE HEAVY ION CYCLOTRON, U-300. PART I. ELECTRONIC APPARATUS. Hagemann, U.; Neubert, W.; Stary, F.; Schulze, W. (Joint Inst. for Nuclear Research, Dubna (USSR). Lab. of Nuclear Reactions). 1971. 16p. (In Russian). Dep. NTIS (U. S. Sales Only).

The microscopic time characteristic of the U-300 heavy-ion beam enables lifetime measurements on excited nuclear states in the time range 10 ns $\lesssim T_{1/2} \lesssim$ 300 ns. By making use of two-fold leading-edge triggering, a resolving time $2\tau_0 < 10$ ns was obtained for gamma energies above 50 keV. A Ge(Li) planar detector and two parameter time–energy analysis of the gamma spectra were used for these measurements. (auth)

42188 (MATT–845) BROADBAND POWER DENSITY MONITOR FOR PULSED MICROWAVE SOURCES. Ernst, W. P. (Princeton Univ., N. J. Plasma Physics Lab.). May 1971. Contract AT(30-1)-1238. 11p. (CONF-710418–17). Dep. NTIS.

From 4. symposium on engineering problems of fusion research; Washington, D. C. (20 Apr 1971).

In recent years there has been an increase in the use of high power microwave sources for plasma heating, and their multikilowatt peak powers are potentially a hazard to operating personnel. Existing instrumentation has been found unsuitable for monitoring the peak power density of the single rf pulse output required for transient plasma heating. An instrument was developed to satisfy the following requirements: (1) Broadband frequency operation from 2 to 12 GHz. (2) Respond to a single pulse of milliseconds pulse width or to continuous wave conditions. (3) Be multi-range; have meter readout; be portable. (4) Provide a calibration method for checking detector sensitivity. (auth)

42189 (NYO–3906-6) ULTRASONIC THERMOMETRY IN LMFBR SYSTEMS. Sixth Quarterly Progress Report Covering the Period Ending March 1969. Fam, S.; Lynnworth, L. C.; Carnevale, E. H. (Panametrics, Inc., Waltham, Mass.). Contract AT(30-1)-3906. 8p. Dep. NTIS.

Two composite W–Re thermocouple/ultrasonic composite probes were tested, and the results are presented. (W.H.K.)

42190 (RDT-C-2-1-T) DETERMINATION OF INSULATION COMPACTION IN CERAMIC INSULATED CONDUCTORS. (Division of Reactor Development and Technology (AEC), Washington, D. C.). Aug 1970. 6p. RSO.

A standard prescribing requirements for determination of insulation compaction in ceramic insulated conductors for use in nuclear and associated applications is presented. (W.H.K.)

42191 (RDT-C-4-5-T) SMALL PERMANENT MAGNET FLOWMETER FOR LIQUID METAL SERVICE. (Division of Reactor Development and Technology (AEC), Washington, D. C.). Nov 1970. 20p. LMEC.

A standard prescribing requirements for the design, fabrication, testing and inspection of a permanent magnet flowmeter for liquid metal service to be used in a gas environment is presented. (W.H.K.)

42192 (RDT-C-5-1-T) INDUCTIVE LEVEL MEASUREMENT SENSOR FOR USE IN LIQUID METAL. (Division of Reactor Development and Technology (AEC), Washington, D. C.). Apr 1970. 30p. LMEC.

A standard prescribing requirements for the design, material selection, fabrication, and examination of inductive level measurement sensors for use in liquid metals is presented. (W.H.K.)

42193 (RDT-C-5-2-T) RESISTIVE LEVEL MEASUREMENT SENSOR FOR USE IN LIQUID METAL. (Division of Reactor Development and Technology (AEC), Washington, D. C.). Apr 1970. 30p. LMEC.

A standard prescribing requirements for the design, material selection, fabrication, examination, and shipping of resistive level measurement sensors for use in liquid metals is presented. (W.H.K.)

42194 (RDT-C-6-1-T) NaK-TRANSMISSION HIGH-TEMPERATURE PRESSURE TRANSMITTER FOR LIQUID METAL SERVICE. (Division of Reactor Development and Technology (AEC), Washington, D. C.). Mar 1971. 31p. LMEC.

A standard prescribing requirements for the design, materials, fabrication, quality assurance, shipping, and performance of pressure transmitters for use in sodium or sodium–potassium alloy liquid metal systems at temperatures up to 1200°F is presented. (W.H.K.)

42195 (RDT-C-6-3-T) LIQUID METAL PRESSURE MEASUREMENT SYSTEM, FLUSH-MOUNTED, EDDY CURRENT TYPE, INDUCTIVE, ABSOLUTE OR GAGE. (Division of Reactor Development and Technology (AEC), Washington, D. C.). Oct 1970. 19p. LMEC.

A standard prescribing requirements for the material selection, fabrication, examination, and installation of eddy current pressure gages for use in liquid metals is presented. (W.H.K.)

42196 (RDT-C-7-1-T) THERMOCOUPLE MATERIAL, IRON AND CONSTANTAN, SOLID CONDUCTOR (BARE, FIBERGLASS INSULATED, AND SHEATHED OVER FIBERGLASS INSULATION). (Division of Reactor Development and Technology (AEC), Washington, D. C.). Apr 1970. 11p. RSO.

A standard prescribing requirements for solid conductor iron and Constantan thermocouple material of four types, bare, fiberglass insulated, and sheathed over fiberglass insulation for use in nuclear and associated applications is presented. (auth)

42197 (RDT-C-7-2-T) THERMOCOUPLE MATERIAL, IRON-CONSTANTAN, MAGNESIUM-OXIDE INSULATED AND

SHEATHED. (Division of Reactor Development and Technology (AEC), Washington, D. C.). Apr 1970. 10p. RSO.

A standard prescribing requirements for thermocouple material consisting of iron and Constantan conductors magnesium oxide insulation, and a sheath of seamless stainless steel tubing for use in nuclear and associated applications is presented. (auth)

42198 (RDT-C-7-3-T) THERMOCOUPLE MATERIAL, COPPER AND CONSTANTAN, SOLID CONDUCTOR (BARE, FIBERGLASS INSULATED, AND SHEATHED OVER FIBERGLASS INSULATION). (Division of Reactor Development and Technology (AEC), Washington, D. C.). Apr 1970. 10p. RSO.

A standard prescribing requirements for solid conductor copper and Constantan thermocouple materials of four types, bare, fiberglass insulated, and sheathed over fiberglass insulation for use in nuclear and associated applications is presented. (auth)

42199 (RDT-C-7-4-T) THERMOCOUPLE MATERIAL, COPPER-CONSTANTAN, MAGNESIUM-OXIDE INSULATED AND SHEATHED. (Division of Reactor Development and Technology (AEC), Washington, D. C.). Apr 1970. 9p. RSO.

A standard prescribing requirements for thermocouple material consisting of copper and Constantan, magnesium insulation, and a sheath of seamless stainless steel tubing for use in nuclear and associated applications is presented. (W.H.K.)

42200 (RDT-C-7-6-T) THERMOCOUPLE ASSEMBLY, NUCLEAR GRADE, CHROMEL-P VS. ALUMEL, STAINLESS STEEL SHEATHED, MAGNESIUM OXIDE INSULATED. (Division of Reactor Development and Technology (AEC), Washington, D. C.). Jul 1970. 21p. RSO.

A standard prescribing material and assembly requirements for seamless stainless steel sheathed, magnesium oxide insulated, Chromel-P/Alumel thermocouple assemblies for use in direct contact with flowing high-temperature liquid sodium fluid in nuclear reactor systems is presented. (W.H.K.)

42201 (RDT-C-8-2-T) LIQUID SODIUM BEARING FILM THICKNESS, VARIABLE RELUCTANCE TRANSDUCER, PROXIMITY MEASUREMENT SYSTEM. (Division of Reactor Development and Technology (AEC), Washington, D. C.). Oct 1970. 19p. LMEC.

A standard prescribing requirements for the material selection, fabrication, and examination of displacement gages for use in liquid sodium systems is presented. (W.H.K.)

42202 (RDT-C-9-1-T) SINGLE-POINT STRIP-CHART RECORDING POTENTIOMETER. (Division of Reactor Development and Technology (AEC), Washington, D. C.). Aug 1970. 8p. RSO.

A standard prescribing requirements for single-point strip-chart recording potentiometers for use in nuclear and associated applications is presented. (W.H.K.)

42203 (RDT-C-9-2-T) MULTIPOINT STRIP-CHART RECORDING POTENTIOMETER. (Division of Reactor Development and Technology (AEC), Washington, D. C.). Sep 1970. 10p. RSO.

A standard prescribing requirements for multipoint strip-chart recording potentiometers for use in nuclear and associated applications is presented. (W.H.K.)

42204 (RDT-C-18-1-T) CERAMIC ELECTRICAL INSULATORS. (Division of Reactor Development and Technology (AEC), Washington, D. C.). Jul 1970. 9p. LMEC.

A standard prescribing requirements for ceramic electrical insulators for use in high-temperature nuclear and associated applications is presented. (W.H.K.)

42205 (RDT-F-3-2-T) CALIBRATION SYSTEM REQUIREMENTS. (Division of Reactor Development and Technology (AEC), Washington, D. C.). Feb 1969. 5p. RSO.

A standard prescribing requirements for the calibration of measuring and test equipment for use in nuclear and associated applications is presented. (W.H.K.)

42206 (RISO-M-1357) ELECTRONICS DEPARTMENT SEMIANNUAL REPORT FOR THE PERIOD 1 APRIL–30 SEPTEMBER 1970. (Danish Atomic Energy Commission, Risoe. Research Establishment). Mar 1971. 28p. Dep. NTIS (U. S. Sales Only).

The computer–computer link interface in the computer system for the DR 2 reactor was installed; the complete system is expected to be on line during the next period. The programming of the data handling system for the Isotope Laboratory is making good progress, and the two-way transfer between the magnetic tape stations and the PDP-8/I computer is described as is a new triple-axis spectrometer, TAS-6, controlled by a PDP-8/e computer for which the instrumentation will be built from NIM and CAMAC modules. The PDP-8 programming system was extended with a DEC-tape station and a link to the hybrid computer; a debugging program for users' programs was developed. Work on control system structure for instrumentations led to the definition of a framework for future discussions, while the reactor safety studies involved investigations of a computer program and of cause/consequence diagrams. Work in Greenland involved airborne and field gamma-spectrometry as well as x-ray fluorescence analysis; bore hole heat flow studies were undertaken in cooperation with the Greenland Geological Survey and the U. S. Geological Survey. The work on laser measurements of two-phase flows led to a study of the detection and processing of Doppler-signals and determination of a velocity vector. A tilt angle indicator for the remote control of platforms and the stabilizing system for a high-resolution laser interferometer are described, and publications during the period are listed. (Denmark)

42207 (UNC-5258) A CONTINUOUS ELECTROCHEMICAL METER FOR MEASUREMENT OF HYDROGEN IN SODIUM. Phase II. Development of a Laboratory Meter. Progress Report, October 1, 1969–December 31, 1969. (United Nuclear Corp., Elmsford, N. Y. Research and Engineering Center). 6 May 1970. Contract AT(30-1)-3908. 22p. Dep. NTIS.

The electrochemical hydrogen sensor design was established for Phase II of the program — Laboratory Meter Development. Based on the Phase I sensor performance data and other selection criteria, the design incorporates a liquid electrolyte, 1.2 m/o CaO in LiCl–KCl eutectic, and nickel electrodes. To withstand the external pressures expected in sodium service, the design incorporates a hemispherical dish sensing septum. Three Phase I sensors were recalibrated in gas after extended sodium tests and good agreement with the original gas calibration was found in those sensors having the reference design electrolyte. (auth)

42208 DEVICE WITH A LARGE DYNAMIC RANGE FOR MEASURING DIRECT CURRENTS AND VOLTAGES. Burkhart, Andre; Guillot, Francois; Vitez, Andre (to Commissariat a l'Energie Atomique). French Patent 1,602,171. 19 Oct 1970. Filed 15 Mar 1968. (In French).

A device which has a large dynamic range suitable for measuring small direct currents (10^{-14} A) and voltages is described; it is compact and low priced. The temperature compensation is excellent and high peaks of current and voltage may be measured with a great accuracy without any manual switching or discontinuity. A symmetrical high impedance input adaptor is used. The amplifier circuit is coupled to the adaptor output and involves a linear feedback circuit and a logarithmic feedback circuit. A logarithmic unit for the temperature compensation is associated with the amplifier circuitry. A threshold circuit is coupled to the amplifier circuit output and to the input of a circuit actuating the band switch. Units for testing and shifting the reader system are associated with the amplifier circuitry. (France)

42209 MATHEMATICAL MODEL OF THE ARC PIONEER 6/7 PLASMA PROBE. Smith, Zdenka K. (Ames Research Center, Moffett Field, Calif.); Day, John R. Rev. Sci, Instrum.; 42: No. 7, 968-76(Jul 1971).

A mathematical model of a quadrispherical electrostatic analyzer is formulated to give the response of such an instrument to a monoenergetic, unidirectional charged-particle beam. The model is developed by taking into account the aperture and collector geometry — it does not rely on the usual simplifying assumptions that the ratio of the analyzer plate separation to the mean radius is small or that any of the angular or energy acceptance windows are negligible. The model is compared to calibration data and is found to agree well. It is also readily adaptable to the determination of the response function of electrostatic analyzers with other partial spherical geometries utilizing an arbitrary charged particle distribution input function. (auth)

42210 X-RAY DETECTOR FOR DYNAMIC DIFFRACTION STUDIES. Johnson, Quintin; Mitchell, Arthur; Evans, L. (Univ. of California, Livermore). Rev. Sci. Instrum.; 42: No. 7, 999-1001(Jul 1971).

A scintillation detector system, which can be used for dynamic diffraction studies, is described. This system contains several individual channels with each channel (consisting of a scintillator, light pipe, and photomultiplier tube) positioned at a unique 2θ position; thus, measurement of diffracted intensity vs 2θ can be made. Signal-to-background ratio for the (200) reflection of powdered LiF was measured to be 3.0 by using copper radiation. Angular resolution depends upon the scintillator size and proximity to the x-ray source. For a four-channel system used in x-ray diffraction studies of material undergoing shock-wave compression [Q. Johnson et al., 25: 1099 (1970)], angular resolution

XUM

was about 1° in 2θ. This resolution can be increased by methods that increase signal strength. (auth)

42211 MASS AND CHARGE DEPENDENT ION DISCRIMINATION IN A LINEAR PULSED TIME-OF-FLIGHT MASS SPECTROMETER. Van Brunt, R. J.; Lightner, G. S.; Whitehead, W. D. (Univ. of Virginia, Charlottesville). Rev. Sci. Instrum.; 42: No. 7, 1052-9(Jul 1971).

Two potential sources of mass and charge discrimination in a linear pulsed time-of-flight mass spectrometer are analyzed in detail. The first is a well-known effect due to spreading of the ion beam in the drift tube. The ion-flux-density distribution at the detector is calculated as a function of the ion source dimensions, initial ion kinetic energy, and drift-tube length and voltage. The second effect results from motion of the ions in the ion source region prior to being accelerated into the drift tube. It is shown that, by appropriate choice of the source parameters and operating conditions, it is possible to store ions in the source region prior to extraction and thereby to enhance ion count without introducing severe discrimination effects. (auth)

42212 SIMPLE POSITIONER FOR QUADRUPOLE MASS SPECTROMETER. Lin, Sin-shong (Materials Research Lab., Watertown, Mass.). Rev. Sci. Instrum.; 42: No. 7, 1083-4(Jul 1971).

A simple, compact support for positioning a quadrupole mass spectrometer in vacuum is described. The device can manipulate the spectrometer in x, y, and z directions to permit alignment of the entrance hole of the ionizer with the molecular beam. The fixed wiring in this arrangement assures minimum disturbance of the applied rf to the poles. (R.W.R.)

42213 TIME-TO-AMPLITUDE CONVERTER. Kadar, Imre. ATOMKI (At. Kut. Intez.) Kozlem.; 12: No. 4, 233-7(Dec 1970). (In Hungarian).

A time-to-amplitude converter, working in the nanosecond range, is described. The circuit is based on the start–stop principle. Its time range is adjusted to 50 to 80 nsec, and it is adjustable by changing a capacitance and an inductance. The intrinsic resolution of the circuit is 66 picosec. Differential nonlinearity is ±3.5%, integral nonlinearity is better than 1%. Internal gating ensures that an output signal is generated only if a start and a stop signal arrive in the proper time sequence in the working range. (auth)

42214 AMERICAN NATIONAL STANDARD FOR HIGH VOLTAGE CONNECTORS FOR NUCLEAR INSTRUMENTS. ANSI N42.4 1971. New York; Institute of Electrical and Electronics Engineers, Inc. (1971). 8p. Available from Institute of Electrical and Electronics Engineers, Inc., New York.

A specification standard for coaxial high voltage connectors for nuclear instruments for dc applications up to 5000 V and ac applications up to 3500 V rms at 60 Hz is presented. (W.H.K.)

42215 ELECTROSTATIC SPECTROMETER FOR BEAMS OF CHARGED PARTICLES. Zashkvara, V. V.; Korsunskii, M. I.; Red'kin, V. S.; Lavrov, V. P. (Inst. of Nuclear Physics, Alma-Ata, USSR). Instrum. Exp. Tech. (USSR) (Engl. Transl.); No. 5, 1295-6(Sep-Oct 1970).

Translated from Prib. Tekh. Eksp.; No. 5, 44-5(Sep-Oct 1970).

An electrostatic spectrometer of the cylindrical-mirror type is described; this has an ion-optical beam-focusing system of the "ring-axis" type. The spectrometer has no quadratic angular aberration; it has a very high transmission. (auth)

42216 PULSE PILE-UP MONITOR FOR A PRECISION PULSE-HEIGHT SPECTROMETER WITH RC FILTERS. Antyukhov, V. A.; Semenov, B. Yu. (Joint Inst. for Nuclear Research, Dubna, USSR). Instrum. Exp. Tech. (USSR) (Engl. Transl.); No. 5, 1297-1301(Sep-Oct 1970).

Translated from Prib. Tekh. Eksp.; No. 5, 46-50(Sep-Oct 1970).

A device that gates a pulse-height analyzer when events overlap (tail pile-up monitor) is described. The characteristics are examined, the functional and theoretical circuits are given, and tests are discussed. The monitor gives high performance in a precision spectrometer with RC filters for the following reasons: (1) the gating pulse has a logarithmic dependence on the input amplitude; (2) the monitor has no inherent dead time; (3) the dynamic range on input signals is over 1000; (4) the system remains operational at high rates. (auth)

42217 USE OF AN X-RAY ANALYZER WITH A SEMICONDUCTOR DETECTOR FOR ELEMENTAL ANALYSIS. Baldin, S. A.; Egiazarov, B. G.; Ioannesyants, L. M.; Sel'dyakov, Yu. P. (All-Union Instrument Construction Research Inst., Moscow). Instrum. Exp. Tech. (USSR) (Engl. Transl.); No. 5, 1475-7(Sep-Oct 1970).

Translated from Prib. Tekh. Eksp.; No. 5, 198-200(Sep-Oct 1970).

The analyzer has a Si(Li) detector. The block diagram of the apparatus is given. The total energy resolution is 1.0 keV. The sensitivity and linearity have been determined in analyses for Sn and Mo. ^{109}Cd, ^{147}Pm, and ^{153}Gd sources are used for excitation. The method is compared with other methods of analysis. (auth)

42218 CAMAC: A SYSTEM OF COMPUTER-DIRECTED ELECTRONICS. Tradowsky, K. (Gesellschaft fuer Kernforschung mbH, Karlsruhe, Ger.). Atomwirt., Atomtech.; 15: No. 8, 394-5(Aug 1970). (In German).

Computer application to measurement and control (CAMAC) represents a system of computer-directed electronics which was elaborated by the European standard of nuclear electronics (ESONE) committee of the European nuclear research laboratories. CAMAC specifies the data exchange between an experimental station and a computer; therefore, it is more than a new standard of equipment, such as ESONE and nuclear instrument modules (NIM). CAMAC is a modular system that also determines mechanical dimensions, power supply, and digital as well as analog signals in such a way that a compatible system of computer-directed electronics can be designed. Practical applications are discussed with respect to counters and timers, gamma spectrometry, and nuclear fission. (H.B.G.)

42219 TUNNELING CONDUCTANCE ANOMALY AND SWITCHING EFFECT FOR NORMAL MIM STRUCTURES. Ignat'ev, O. M.; Tarenkov, V. Yu. (Physical-Technical Inst., Donetsk, USSR). Phys. Status Solidi (a); 5: No. 3, 559-62(16 Jun 1971).

It was shown experimentally that in MIM tunnelling structures containing paramagnetic impurities, a conductance anomaly takes place both at low and high biases applied to the electrodes of the junction. The peculiarities of the i(U) characteristic in the case of the switching effect are in agreement with the assumption of the tunnelling conductance anomaly at $U > U_c$ and with the hypothesis of induced local or surface superconductivity in the electrode material. (auth)

42220 SYSTEM FOR DIGITALIZATION OF FAST NON-RECURRENT ANALOGUE SIGNALS. Van Ramele, H. J. F.; De Stigter, J.; Van Ingen, A. M. (EURATOM-FOM, Jutphaas, Netherlands). Nucl. Instrum. Methods; 94: No. 2, 307-10(1971).

A digitalizing system is described for analog signals in the microseconds region, with a time resolution of nsec. This system is developed to be used in plasma physics for data acquisition in fast single-shot experiments (e.g. pulsed gas discharges). The signals, written on a scope screen, are scanned by a TV camera, digitized, and stored into a core memory. Both single and double-beam scopes can be used. Time resolution and accuracy are mainly determined by the scope (for a TEKTRONIX 551, 4 nsec at 100 nsec/div and 2%). The stored signals can be displayed in analog form or punched on paper tape. (auth)

42221 USE OF MAGNETIC SECTOR FIELDS WITH CYLINDRICAL SYMMETRY AS ONE-GAP BROAD-RANGE SPECTROGRAPHS. Bister, M. (Univ. of Helsinki). Nucl. Instrum. Methods; 94: No. 2, 271-3(1971).

The suitability of cylindrically-symmetric magnetic sector fields for one-gap broad-range heavy-particle spectrographs is investigated. If the desired energy range is not large ($E_{max}/E_{min} \leq 2$), the focusing properties are good. The biggest advantages, compared to homogeneous field analyzers, are a wider opening angle (≈2 msr) and a larger dispersion. The usable energy range (E_{max}/E_{min}) can be increased by curving the entrance and exit edges of the analyzer, which partly eliminates the aberration. (auth)

42222 MEASUREMENT OF NUCLEAR HALF-LIVES UP TO 100 s BY THE DELAYED COINCIDENCE METHOD. Glatz, J.; Loebner, K. E. G. (Technische Univ., Munich). Nucl. Instrum. Methods; 94: No. 2, 237-43(1971).

To extend the applicability of the delayed-coincidence method to the determination of half-lives up to 100 s, a small on-line computer was programmed to work as a time-analyzing system with negligible dead time. The feasibility of measurements of such long half-lives is discussed in detail and compared to that of conventional time analyzers. The half-lives of the 1315.2-keV level in ^{177}Hf ($T_{½}$ = 1.08 ± 0.06 s), of the 1663.1-keV level in ^{207}Pb ($T_{½}$ = 0.77 ± 0.03 s), and of the ground state of ^{144}In ($T_{½}$ = 73 ± 16 s) were remeasured using this new method. (auth)

42223 OPTIMIZATION TECHNIQUE APPLIED TO EXPERIMENTS MEASURING REACTION GAMMA-RAY ANGULAR DISTRIBUTIONS. Walraven, R. L.; McCauley, D. G. (Univ. of California, Davis). Nucl. Instrum. Methods; 94: No. 2, 205-9 (1971).

A general mathematical technique is presented for optimization of any experiment whose data is fit with a model. As an example, this technique is applied to the optimization of experiments measuring the angular distribution of reaction gamma rays. (auth)

42224 ENERGY SELECTIVE ION BEAM INTENSITY MEASURING APPARATUS AND METHOD UTILIZING A SCINTILLATOR TO DETECT ELECTRONS GENERATED BY THE BEAM. Daly, Norman Richard; Powell, Royal Edward (to United Kingdom Atomic Energy Authority). U. S. Patent 3,579,270. 18 May 1971. Priority date 31 Oct 1967, Great Britain.

The apparatus is primarily intended for use with ion beams from mass spectrometers, and has one application in determining metastable ion spectra. It comprises a retarding electrode carrying a scintillator detector and preceded by an apertured electrode. When the retarding electrode voltage equals or exceeds the source accelerating voltage, all ions are repelled to the apertured electrode where secondary electrons are produced which are accelerated to the scintillator and an output is obtained from a photomultiplier located beyond the retarding electrode. When the retarding electrode voltage is less than the source accelerating voltage only ions resulting from metastable fragmentations (which have less energy) are so repelled. The parent ions strike the scintillator but produce no output because the latter is coated with an ion-opaque layer. A second, apertured, retarding electrode can precede the above-described arrangement, to which a lower voltage is applied, thus setting a lower as well as an upper limit to the ion energy detected and making the apparatus of more general application as an energy range selector. (auth)

42225 RADIATION SAFETY FOR X-RAY DIFFRACTION AND FLUORESCENCE ANALYSIS EQUIPMENT. ANSI N43.2 1967. New York: American National Standards Institute ([1967]). 34p. Available from American National Standards Institute, New York.

Standard guidelines for the radiation safety aspects of the design and operation of x-ray diffraction and fluorescence analysis equipment are presented. (W.H.K.)

Radiation Effects on Instruments and Instrument Components

Refer also to abstracts 43008 and 43439.

42226 (AD-715261) LOW-ENERGY PROTON DAMAGE TO SILICON/SOLAR CELLS. Report for January 1969-January 1970. Stofel, Edwin J.; Joslin, David E. (Aerospace Corp., El Segundo, Calif.). 15 Oct 1970. Contract F04701-70-C-0059. 37p. (TR-59(6250-20)-8; SAMSO-TR-70-47). NTIS.

The effect of low-energy (<2 MeV) proton irradiation upon the junction properties of silicon solar cells has been measured. These measurements are used to explain the large power loss observed on the ATS-1 and Intelsat II-4 satellites. (auth) (USGRDR)

42227 (N-71-12257) DEVELOPMENT OF LITHIUM-DIFFUSED RADIATION-RESISTANT SOLAR CELLS. Quarterly Report. Payne, P. A.; Somberg, H. (Heliotek, Sylmar, Calif.). Oct 1970. Contract JPL-952547. 31p. (NASA-CR-111581). NTIS.

The problems associated with diffusion using a BBr3 source in an inert ambient are reviewed. The problems included: 1) inconsistent results with respect to both the visual appearance and sheet resistance measurements of cell blanks from one diffusion to the next; 2) nonuniformity in the electrical characteristics as the number of cells per diffusion was increased above ten; and 3) rapid depletion of the liquid source in the bubbler and, consequently, increased cost for the source. Typical efficiencies of 10.5% to 11.0% can be obtained with cells lithium diffused eight hours at 325 C; however, two problems have become apparent which cause lower efficiencies. One of the problems, a soft knee, can be eliminated by etching the cell edges. The other problem, tunneling or internal field emission, was found to occur not only in cells lithium diffused eight hours at 325 C, but also in varying degrees in cells with other lithium diffusion parameters and 1 ohm cm P/N cells with no lithium. However, only cells lithium diffused eight hours at 325 C exhibited the excessive current between 0 and 0.1 volt in reverse bias and the shunted characteristics in the forward direction when illuminated. (auth) (STAR)

42228 (N-71-17325) PERFORMANCE OF CERAMIC INSULATOR SEALS AT HIGH NEUTRON AND GAMMA FLUENCE LEVELS. Rohal, Robert G.; Tambling, Thomas N.; Smith, Roger L. (National Aeronautics and Space Administration, Cleveland, Ohio. Lewis Research Center). Feb 1971. 15p. (NASA-TM-X-2180; E-5683). NTIS.

An experimental program to evaluate the in-pile performance of a group of commercially available ceramic insulator seals is described. The ceramic insulator seals were irradiated to thermal neutron fluence levels greater than 10 to the 20th power neutrons/cm squared and gamma dose rates greater than 10 to the 14th power ergs/g of H_2O. During the irradiation the seals were thermally cycled several times. Neutron radiographic investigation showed that all 24 seals investigated were leaktight to reactor cooling water at 150 F (339 K) and 150 psia (103.4 N/cm squared) throughout the irradiation. (auth)

42229 ENHANCEMENT OF CO_2 LASER POWER AND EFFICIENCY BY NEUTRON IRRADIATION. Ganley, T.; Verdeyen, J. T.; Miley, G. H. (Univ. of Illinois, Urbana). Appl. Phys. Lett.; 18: No. 12, 568-9(15 Jun 1971).

Experiments have been performed which show that it is possible to increase the efficiency and power of a CO_2 laser by irradiating the discharge with energetic α and Li ions produced by the (n,α) reaction with ^{10}B. This effect is explained by a tailoring of the electron-energy distribution towards optimum pumping of the laser. (auth)

42230 LIGHT CONDUCTORS. Bret, Antoine (to Commissariat a l'Energie Atomique). British Patent 1,234,958. 9 Jun 1971. Priority date 23 Jun 1967, France.

A light conductor for use in optical apparatus such as periscopes or endiscopes in a neutron field at temperatures up to 500°C is described. (W.H.K.)

42231 EFFECT OF ULTRAVIOLET RADIATION ON PLASTIC SCINTILLATORS WITH p-TERPHENYL. Matveeva, E. N.; Stoletova, I. M.; Shafranov, M. D. (Joint Inst. for Nuclear Research, Dubna, USSR). Instrum. Exp. Tech. (USSR) (Engl. Transl.); No. 5, 1332-7(Sep-Oct 1970).

Translated from Prib. Tekh. Eksp.; No. 5, 76-8(Sep-Oct 1970).

The effects of UV radiation on the polymer base and activator in plastic scintillators containing polystyrene and p-terphenyl have been studied. The polyphenyl activators are shown to be better able to withstand the effects of ionizing radiation than the oxazole activators. A plastic scintillator which resists aging under the influence of UV radiation contains 2 wt. % p-terphenyl and 0.2 wt. % quaterphenyl. (auth)

42232 OBSERVATION OF DAMAGE REGIONS PRODUCED IN SILICON SOLAR CELLS BY NEUTRON IRRADIATION. Ghosh, S.; Sargent, G. A. (Univ. of Kentucky, Lexington). Mater. Res. Bull.; 6: No. 6, 441-9(Jun 1971).

Defect regions produced in float-zone melted N/P-type silicon solar cells by irradiation with mono-energetic neutrons at doses from 10^{10} to 10^{13} n/cm^2 have been studied. The regions were revealed by using a chemical etch and observing carbon replicas of the surface with an electron microscope. It was found that the density of defect regions increased with increasing dose, whereas the average size was found to decrease. Results of thermal annealing experiments carried out on the irradiated specimens over the temperature range 300 to 1200°K revealed that for those samples subjected to the highest dose there was no change in either the defect density or defect size. At the lowest dose, however, the defect size was found to decrease with increasing temperature and the defect density was found to increase. The defect structures were found to be similar to those observed by Bertolotti and predicted theoretically by Gossick. (auth)

42233 RADIATION DAMAGE OF MOS FETs BY X-RAY AND ELECTRON IRRADIATIONS. Chiwaki, Mitsukuni; Tomimasu, Takio. Denki Shikensho Iho; 35: No. 1, 47-54(1971). (In Japanese).

N-channel MOS FETs (NEC 3SK 14) were irradiated at various bias voltages ($V_S = V_G = V_D = 0V$; $V_G = 3V$, $V_D = 10V$; $V_G = 0V$, $V_D = 10V$; $V_G = -3V$, $V_D = 10V$) by continuous X-rays of 40 to 190 kV_p and 24 MeV electrons. The changes in the drain current and conductance were observed by exposure to more than 10^3 R of low energy continuous X-rays, and also to fluence of more than 4×10^{11} electrons/cm^2 of 24 MeV electrons. The X-ray energy dependence of the changes in the drain current was found when the source, the gate, and the drain were earthed. The drain current decreased with increasing exposure to X-rays lower than 160 kV_p in energy, while increased by irradiations of X-rays higher than 170 kV_p in energy and of 24 MeV electrons. The drain current also increased under other bias conditions, and features of the increase were similar to other experimental results that had been published. (auth)

42234 EFFECTS OF X RADIATION ON MOS DEVICES AT T = 79K. Kreutz, E. W.; Pagnia, H.; Waidelich, W. (Technische Hochschule, Darmstadt, Ger.). Phys. Status Solidi (a); 5: No. 3, 691-9(16 Jun 1971).

XUM

Changes of drain current and of transfer characteristics have been measured during x-irradiation in commercially available n-channel field-effect transistors of the metal/oxide/semiconductor configuration. The drain current increases with irradiation time at liquid nitrogen temperature. The partial relaxation and the thermal annealing characteristics of x-ray-induced changes are presented. During x-irradiation, the inversion in the surface layer becomes stronger. The resulting positive insulator charge is trapped in oxide states which are characteristically distributed in energy dependent from the states occupancy. (auth)

LIFE SCIENCES

Biochemistry, Physiology, and Molecular Biology

Refer also to abstract 42606.

Basic Processes

Refer also to abstract 42563.

42235 VISUALIZATION OF THE HUMAN SPLEEN WITH ^{99m}Tc-LABELED RED BLOOD CELLS. Eckelman, W.; Richards, P.; Atkins, H. L.; Hauser, W.; Klopper, J. F. (Brookhaven National Lab., Upton, N. Y.). J. Nucl. Med.; 12: No. 6, 310-11(Jun 1971).

A method is described for the preparation of ^{99m}Tc-labeled human erythrocytes for use in spleen visualization by scintillation scanning following reinjection into the patient. The use of stannous chloride instead of heat treatment of the cells resulted in a shorter and more sterile labeling procedure. (C.H.)

42236 RADIOIMMUNOASSAY: A SIMPLIFIED PROCEDURE FOR DOSE INTERPOLATION. Weaver, C. Kenneth; Cargille, Charles M. (National Inst. of Child Health and Human Development, Bethesda, Md.). J. Lab. Clin. Med.; 77: 661-4(Apr 1971).

A procedure for radioimmunoassay dose interpolation of sufficient simplicity to be automated on a programmable desk-top calculator was developed. The procedure is based on approximating the functional relationship between the dose potency and the radioimmunoassay response variable as an algebraic series. (auth)

42237 RADIOIMMUNOASSAY FOR RHESUS MONKEY LUTEINIZING HORMONE (LH) WITH ANTI-OVINE LH SERUM AND OVINE LH-^{131}I. Niswender, G. D.; Monroe, S. E.; Peckham, W. D.; (and others) (Univ. of Michigan, Ann Arbor. Univ. of Pittsburgh. Emory Univ., Atlanta). Endocrinology; 88: No. 6, 1327-31(Jun 1971).

A sensitive and specific radioimmunoassay was developed for luteinizing hormone (LH) in serum from rhesus monkeys using a unique anti-ovine LH serum (GDN-15) and ovine LH for radioiodination. It did not appear that high levels of follicle-stimulating hormone (FSH) or thyroid-stimulating hormone (TSH) influenced the measurement of LH in this assay. The good agreement between the estimates of LH by radioimmunoassay and by bioassay for a crude pituitary extract suggested that other pituitary factors did not influence the measurement of LH. (auth)

42238 ACCURATE AND RAPID MEASUREMENT OF PLASMA RENIN ACTIVITY BY RADIOIMMUNOASSAY. RESULTS IN NORMAL AND HYPERTENSIVE PEOPLE. Cohen, E. L.; Grim, C. E.; Conn, J. W.; (and others) (Univ. of Michigan, Ann Arbor). J. Lab. Clin. Med.; 77: No. 6, 1025-38(Jun 1971).

A sensitive and accurate radioimmunoassay for angiotensin I is described that requires 10 μl of incubated plasma for determination of plasma renin activity. Outlined are the methods that were employed for producing antiserum from angiotensin I, for radioiodination of angiotensin I, and for separation of iodinated products. A protocol is presented for performing plasma renin activity determinations on small volumes of plasma with the use of a short (15 to 30 min) incubation time. Normal ranges for this method are tabulated. Patients with primary aldosteronism or idiopathic aldosteronism have significantly lower, yet easily measurable, values for plasma renin activity. Elevations induced by operation or preoperatively by Aldactone are recorded. Elevations of renal venous plasma renin activity in patients with renal artery stenosis are also recorded, and their functional significance is supported. In 4 of 21 patients with essential hypertension, subnormal values were found by this method. (auth)

42239 RADIOISOTOPES IN PESTICIDE RESEARCH. IV [AND] V. Dedek, W. (Deutsche Akademie der Wissenschaften zu Berlin, Leipzig). Isotopenpraxis; 6: 204-14(Jul 1970). (In German).

The preceding reviews of literature from 1964 and 1967 are continued. Mainly papers from 1967 to 1969 are reported. Investigations about labeled substrata are not referred to. Part IV: Reviews, general methods of analysis, insecticides; 271 references. Part V: Fungicides, herbicides, other pesticides; 360 references. (auth)

42240 AUTORADIOGRAPHIC STUDY OF THE NORMAL LYMPHOID CELL DECAY IN THE MESENTERIC LYMPH NODE OF THE MOUSE. Claesson, Mogens Helweg (Univ. of Copenhagen). Acta Pathol. Microbiol. Scand., Sect. A; 79: 293-7 (1971).

The cellular decay in mesenteric lymph node cell suspensions was studied by combining nigrosin dye exclusion and ^{3}H-thymidine autoradiography. The labeling pattern of nonviable cells was followed during a period of 14 days after injection of a single dose of ^{3}H-thymidine into NMRI-mice 30 to 45 days of age. The decaying cells were divided into DNA-synthesizing and non-DNA-synthesizing cells. The decay of DNA-synthesizing cells partly reflects a decay of blast cells proliferating in situ, i.e., germinal center cells with a decay rate of 20 per cent. The majority of cells decaying in the lymph node seemed to be carried to the organ by the blood or lymph stream. The results are discussed on the basis of knowledge of lymphoid cell migration streams between the various lymphoid organs and the existence of short-lived lymphocyte populations. (auth)

42241 ^{125}I-LABELLING OF ANGIOTENSIN I AND II. Nielsen, Meta Damkjaer; Joergensen, Mogens; Giese, Joern (Glostrup Hospital, Copenhagen). Acta Endocrinol.; 67: 104-16(1971).

A simple procedure for a reproducible preparation of radioiodinated angiotensin analogues is described. The iodination is performed at a low level of radioactivity — 200 μCi per 10 μg peptide — with low concentrations of chloramine-T and sodium metabisulphite. No destruction of the peptide occurs during the iodination. The yield is high, and the only purification step needed is a separation of iodinated peptide from non-labeled peptide. This separation is performed by means of column chromatography on DEAE-Sephadex A 25. The specific activity of labeled angiotensin I or II prepared by this method was about 500 μCi/μg. The homogeneity of the radioiodinated angiotensin analogues was established by means of paper chromatography and enzymatic degradation studies, including experiments on the enzymatic conversion of ^{125}I-angiotensin I to ^{125}I-angiotensin II. Radiochromatograms obtained after storage for various periods showed perfect stability of the labeled compounds. Immunological characteristics, as evaluated by standard displacement curves with selected antisera and maximal binding to excess antibody, were reproducible from batch to batch. (auth)

42242 FEEDING BY CAECULID MITES ON FUNGUS DEMONSTRATED WITH RADIOACTIVE TRACERS. Crossley, D. A. Jr.; Merchant, Virginia A. (Univ. of Georgia, Athens). Contract AT(40-1)-3859. Ann. Entomol. Soc. Amer.; 64: No. 4, 760-2(Jul 1971).

Caeculid mites (Caeculus sp., Acarina: Caeculidae) have been thought to be predaceous, but laboratory experiments demonstrated successful feeding and reproduction in cultures containing fungal hyphae. Mites that fed upon fungi tagged with ^{134}Cs exhibited bioelimination patterns characteristic of cryptozoan arthropods. (auth)

42243 NEW TECHNIQUE FOR THE QUANTITATIVE ESTIMATION OF FIBRINOLYSIS USING IN VIVO [^{125}I]FIBRINOGEN. Hickman, J. A. (Middlesex Hospital, London). Brit. J. Haematol.: 20: No. 6, 611-21(Jun 1971).

A technique for the quantitative measurement of the fibrinolytic activity of blood is described, based on the rate of release of radioactivity in vitro from clotted blood obtained from patients previously receiving ^{125}I-fibrinogen. The accuracy of the technique was assessed by comparison of the release of radioactivity with the appearance of fibrin degradation products, by observation of the effects of fibrinolytic inhibitors and by comparison of the initial fibrin content of the clot with the measurement of radioactivity released after total lysis. The measurement of fibrinolysis with this technique correlated well with the dilute blood clot lysis time in samples with a normal fibrinogen concentration, but the correlation was poor when the fibrinogen concentration was elevated. Since the measurement of fibrinolysis by this new technique is likely to be largely unaffected by the fibrinogen concentration, it is suggested that this technique is of particular value when the fibrinogen concentration is outside the normal range and, further, will allow significant comparison of fibrinolytic activity between blood samples of differing fibrinogen concentration. (auth) (UK)

Metabolism, Physiology, and Toxicology

Refer also to abstracts 41762, 41833, 42315, 42317, 42322, 42378, 42382, and 42671.

42244 (GAT-Z-5047) STUDY AND RESULTS OF EXAMINATION MADE AS A RESULT OF AN INHALATION OF SO-CALLED

XUM

SOLUBLE COMPOUNDS OF NATURAL URANIUM. PART 1. Chalabreysee, J. Translated for Goodyear Atomic Corp., Piketon, Ohio, from Radioprotection; 5: 1-17(1970). 23p. Dep. NTIS.

Results of examinations performed on approximately 800 personnel after the accidental inhalation of UF_6 in May 1965 in the pilot plant of the Pierrelatte Center are presented. Introduction of the so-called soluble compounds of natural uranium (such as UF_6 or UO_2F_2, a product of UF_6 decomposition in water or moisture in the air) is of a purely chemical nature, with the kidneys as the critical organ, whatever the path of entry. Thus, the internal contamination can be evaluated only by measurement of the amounts eliminated in the excreta. In the organism, uranium behaves like a foreign element; it is not metabolized. An indirect method of determining the amount of natural uranium in the biological media was used based on the fluorescence of uranium salts when exposed to ultraviolet radiation. This fluorescence has a considerable sensitivity when the uranyl salts are fused with sodium fluoride and sodium carbonate. Three values were appraised for each individual: amount inhaled, amount retained after the initial purification processes, and amount remaining in the organism the day of the examination. Excretion in the urine starts very rapidly: during the first 24 hours following absorption, about 70% of the absorbed compound is excreted for the soluble U^{+6} compounds. However, the rate of urinary elimination then decreases. Therefore, it was necessary to analyze excreta from directly exposed personnel for as long as 22 days. A total of 2654 urine analyses were performed. Of those examined, only three of the directly exposed personnel had a calculated initial bodily charge greater than 625 micrograms, the maximum admissible limit of absorption for natural uranium in the form of soluble compounds. No organic lesion, phenomenon of poisoning, or biological manifestation was found among the individuals examined. (auth)

42245 (NYO-3086-10(Vol.1)) RADIOACTIVITY STUDIES. VOLUME I. THE RETENTION AND DISTRIBUTION OF ^{210}Pb IN THE ADULT BABOON. Annual Progress Report, September 1, 1969-August 31, 1970. Cohen, Norman; Eisenbud, Merril; Wrenn, McDonald E. (New York Univ., N. Y. Inst. of Environmental Medicine). 1 Sep 1970. Contract AT(30-1)-3086. 235p. Dep. NTIS.

The metabolic behavior of non-pathogenic amounts of lead in the primate was studied by in vivo and bioassay techniques using ^{210}Pb as the isotopic tracer. Studies were made at periods of 24 hours, one, two, and twelve months. Retention of lead in the skeleton and in the body was determined from in vivo measurements over the skull and thorax. The detector used for this purpose consisted of a NaI-CsI(Tl) crystal pair operated in the anti-coincidence mode. The longest effective half life calculated from in vivo measurements of ^{210}Pb in the skull bones was 0.96 years for two animals studied for over 12 months post-injection. The maximum contribution to the ^{210}Pb spectrum from bremsstrahlung radiation arising from ^{210}Bi beta decay in the skull was determined to be less than 5% in the region of from 30 to 60 keV. The contribution to the spectrum from ^{210}Bi beta particles themselves was negligible. Counting efficiencies for the skull measurement were determined after autopsies at one and two months post-injection. The results of analysis of urine and fecal samples definitely established that fecal excretion is an important mode of lead loss from the body with 24 hour urine to fecal concentrations approximately equal to 1.25 to 1.70 for as long as two months after injection. The results obtained are considered with respect to radiation exposures of uranium mining personnel. The most important result obtained in this respect is the relatively short half time calculated for whole-body retention and the corresponding sensitivity of the model relating ^{210}Pb body burden to the manner in which a radon daughter exposure is sustained with respect to time. (auth)

42246 (PRNC-148) PROGRAM FOR FASCIOLA HEPATICA IN PUERTO RICO. Initial Report, January 1970-April 1971. de Leon, Delfin D.; Ritchie, Lawrence S.; Chiriboga, Jorge (Puerto Rico Nuclear Center, [Mayaguez]). Contract AT(40-1)-1833. 18p. (In Spanish). Dep. NTIS.

Investigations leading to the control of fasciolasis are being conducted. A survey of 19 farms in the Dorado area for infections among dairy herds has been completed and periodic observations on the snail population and the occurrence of the infection therein have been started. The snail vectors, Lymnaea cubensis and L. columella, and all stages of the life cycle are maintained under laboratory conditions. Fasciola was not found on two farms, while the rate of occurrence in the other 17 herds ranged from 5 to 90%. A paramphistomid was found to occur with greater frequency and higher egg counts than Fasciola. It uses the same snail vectors and its identity requires critical attention as does its egg. On the farms surveyed, L. cubensis was the dominant vector. Its life cycle can be as brief as 3 weeks thus, it can repopulate relatively soon after a dry period. An enormous snail population occurred in 1970-71 in correlation with a near-record rainfall. This was noted also in the Loiza area where the infection rate of F. hepatica approached 100% in cattle and 46% in one collection of snails. Whether irradiated metacercariae can serve as a vaccine for cattle will be determined. In the meantime, rats are being infected with irradiated metacercariae for evidence of acquired resistance. (auth)

42247 (SFL-A-16) STUDIES ON THE ELIMINATION RATE AND THE RADIATION EXPOSURE FOLLOWING INGESTION OF ^{222}Rn RICH WATER. Kahlos, H.; Suomela, M. (Institute of Radiation Physics, Helsinki (Finland)). Dec 1970. 51p. Dep. NTIS (U. S. Sales Only).

Radon-222 and its daughters in drinking water cause a significant radiation dose to the stomach when water containing more than 100 nCi/l ^{222}Rn is used regularly. To evaluate the radiation dose in real conditions two types of experiment were performed with a whole body counter. In the first series of measurements the elimination of ^{222}Rn from the body was followed in subject who had ingested radon rich water as a single intake. A one-component exponential function with a biological half-life varying from 30 to 50 min was found to describe the elimination of radon. In the second series of measurements a group of persons who had used radon rich water daily was studied. The daily intake of ^{222}Rn for these persons was estimated and some calculations on the radiation dose to the stomach were performed. A special attention was given to the escape of radon from water and its effect on the state of disequilibrium between radon and its daughters after intake. From the results of the experiments the $(MPC)_w$-value of 10^{-4} μCi/ml for ^{222}Rn in drinking water was proposed. (auth)

42248 ABSORBED DOSES DURING RADON INHALATION PROCEDURES. Andreev, S. V. (Inst. of Health and Physiotherapy, Moscow). Med. Radiol.; 16: No. 6, 58-63(Jun 1971). (In Russian).

The distribution of Rn, RaA, RaB, RaC, and absorbed doses in organs and tissues of albino rats during the inhalation of filtered air containing ^{222}Rn was investigated. The level of irradiation of organs and tissues of a patient during radon procedures was also determined. The greatest loading in this form of alpha therapy, along with the respiratory tract, was on the kidneys, skin, fatty tissues, and liver. (auth)

42249 ACCUMULATION OF RADIONUCLIDES BY FISHES. Ettenhuber, E. (Staatliche Zentrale fuer Strahlenschutz, Berlin). Isotopenpraxis; 7: No. 3, 75-84(Mar 1971). (In German).

A review is given on investigations on the accumulation of radionuclides by fishes in relation to radiation protection. Biochemical and physiological relationships, especially the relationship between the accumulation factors and environmental parameters are discussed only as far as they are necessary to evaluate the compiled factors. A tabular compilation is given of accumulation factors fish/water for different species of fishes and a number of radionuclides. (76 references). (auth)

42250 AGE-SPECIFIC PECULIARITIES OF ^{137}Cs ELIMINATION FROM THE HUMAN ORGANISM. Drichko, V. F.; Popov, D. K. (Inst. of Radiation and Health Physics, Leningrad). Med. Radiol.; 16: No. 6, 55-7(Jun 1971). (In Russian).

The period of ^{137}Cs semi-elimination from the human organism and the cross size of the muscle fiber are functionally related which, during the period of the organism's growth, may be expressed by a straight line equation. (auth)

42251 TOXICITY OF TRITIATED THYMIDINE IN P388F LYMPHOMA CELLS. I. INCORPORATION INTO DNA AND CELL SURVIVAL. Peterson, A. R.; Fox, B. W.; Fox, Margaret (Christie Hospital and Holt Radium Inst., Manchester, Eng.). Int. J. Radiat. Biol.; 19: 123-32(1971).

The incorporation of thymidine into the newly-synthesized DNA of P388F lymphoma cells, increased non-linearly with respect to an increasing concentration of ^3H-thymidine (TdR) of constant specific activity. As the external TdR concentration rose, in the presence of a constant low level of tritium a progressively greater proportion of the incorporation was hydroxyurea-resistant. These effects were attributed to negative-feedback actions of TdR metabolites on nucleotide biosynthesis. Thymidine incorporation was stimulated at high specific activities of ^3H-TdR, largely owing to enhanced hydroxyurea-sensitive DNA synthesis, resulting from DNA damage produced by the incorporated tritium. For concentrations of ^3H-TdR up to 8.4 mμM, reduced survival of P388F cells was solely the result of effects of tritium incorporated into newly-synthesized DNA. (auth)

42252 INCREASED ELIMINATION OF RADIOSTRONTIUM DURING LACTATION, IN RELATION TO THE AGE OF THE

ANIMALS. Kollmer, W. E. (Gesellschaft fuer Strahlenforschung mbH, Munich). Int. J. Radiat. Biol.; 19: 183-6(1971). (In German).

Lactating rats aged 2 and 12 months were compared with nonlactating controls. Three μCi ^{85}Sr was injected on the day after littering and its retention measured daily for 10 days with a whole-body counter in both mother and infant rats (the latter receiving ^{85}Sr in the milk). Results for the litter were independent of the mother's age, rising to a constant level after 2 days; as they are known to excrete no strontium, there can be none in the milk after 2 days. The younger adult rats show a higher retention than the older ones, confirming previous results. Lactating animals showed less retention than the corresponding controls for both ages; the difference is greater for the younger animals, and exceeds the amount found in the litter, so that more must be eliminated in feces and urine. For the older animals the difference from the controls is less than the amount in the litter, and therefore a smaller quantity is thus eliminated by the lactating animals. The effects found are ascribed to age-dependent bone metabolism and mineral metabolism. (UK)

42253 BIOLOGICAL ACTION OF ^{237}Np NITRATE. Moskalev, Y. I.; Rudnitskaya, E. I.; Zalikin, G. A.; Petrovich, I. K. Gig. Sanit.; No. 2, 42-7(Feb 1971). (In Russian).

Biological effects of neptunium nitrate on rats were studied using concentrations of 0.0001 to 0.005. Neptunium was found to be of high chemical toxicity causing the animal's death within 3 to 6 days due to insufficiency of the liver and kidneys. Neptunium nitrate was more toxic than other transuranium elements, ^{241}Am and ^{239}Pu. A single dose of ^{237}Np caused development of pronounced neutrophil leukocytosis. Animals that died later showed nephrosclerosis, sclerotic changes in the liver, and bone tumors. (auth)

42254 EFFECT OF ALGINATES FROM ALGAE GROWING IN THE ADRIATIC ON STRONTIUM TRANSPORT THROUGH RAT'S DUODENUM. Gruden, Nevenka; Kostial, Krista; Turjak-Zebic, V.; Skaric, V. (Inst. for Medical Research and Occupational Health, Zagreb. Ruder Boskovic Inst., Zagreb). Arh. Hig. Rada Toksikol.; 21: No. 2, 137-41(1970). (In Serbo-Croatian).

Regarding the significance of alginates in the prevention of internal radiostrontium contamination it was considered useful to study the effect of some alginates isolated from the algae growing in the Adriatic sea on strontium transport through the duodenal wall of the rat. The effect of alginates was compared to that of sodium alginate known as O.G. 1 which proved most efficient in the selective reduction of radiostrontium absorption. The results show that the alginates isolated from four species of algae in the Adriatic (out of the five species studied) reduce strontium transport equally efficiently as O. G. 1. As a rule, domestic alginates also lowered duodenal calcium absorption the more so the stronger was their effect on strontium. The effect on calcium, however, was always weaker than on strontium. (auth)

42255 COMPARATIVE STRONTIUM AND CALCIUM METABOLISM IN LACTATION. Blanusa, Maja; Harmut, Magda; Kostial, Krista (Inst. for Medical Research and Occupational Hygiene, Zagreb). Arh. Hig. Rada Toksikol.; 21: No. 2, 125-7 (1970).

The strontium-85 to calcium-47 ratio in the body of lactating non-lactating and control rats and in the litter was determined at several time intervals after an intraperitoneal application of radioactive isotopes (0–120 hours). The body ratio was slightly higher in lactating animals during the early phase of lactation (0–5 day) and much higher during the late phase of lactation (12–17 day) indicating a greatly reduced discrimination against strontium. (auth)

42256 ROLE OF MICROORGANISMS IN THE BIOGENIC MIGRATION OF URANIUM. Koval'skii, V. V.; Letunova, S. V. (Inst. of Geochemistry and Analytical Chemistry, Moscow). Biol. Nauki; 13: No. 6, 81-7(1970). (In Russian).

The majority of the microorganisms (74 strains) isolated from uranium enriched silts (1.5×10^{-3} %) of Issyk-Kul Lake and from diluted silts (5.0×10^{-5} %) of the Moscow Pond were adapted to the natural uranium content of the silt deposits. The number of nonadapted strains amounted to about 10% of the total number of isolates. The degree to which uranium was concentrated by the cells and the quantity of biomass accumulated depended on the extent to which the microorganisms adapted to the natural uranium content of the silts. Adapted strains played a more active role in the biogenic migration of uranium than did nonadapted strains. (tr-auth)

42257 KINETICS OF DOSE DISTRIBUTION IN SKIN CONTAMINATED WITH RADIOACTIVE SUBSTANCES. Osanov, D. P.; Ershov, E. B.; Klykov, O. V.; Rakova, V. A. Med. Radiol.; 16: No. 5, 44-50(May 1971). (In Russian).

The results of experimental investigation of the kinetics of microdistribution in the skin of tritium oxide, ^{137}Cs, and nitrates of ^{89}Sr, ^{239}Pu, and ^{241}Am are given. The dose distributions in structural layers of the skin from these isotopes are also given and the correlation of doses, surface contamination, and penetration into the skin of the activity is discussed. (auth)

42258 AUTORADIOGRAPHIC LOCALIZATION OF RADIOACTIVITY IN FEMALE RAT NEOCORTEX AFTER INJECTION OF TRITIATED ESTRADIOL. Presl, J.; Pospisil, J.; Horsky, J. (Inst. for the Care of Mother and Child, Prague). Experientia; 27: No. 4, 465-7(15 Apr 1971).

Female rats aged 5, 10, 15, 20, 25, 30, and 50 days were injected intraperitoneally with tritium-labeled estradiol. Two hours later the animals were killed and the brains were prepared for autoradiography. In all age groups an uptake of radioactivity by a clear-cut demarcated area of neocortex was found. Labeled cells were dispersed diffusely through the whole thickness of the neocortex in the circumscribed area. It is suggested that there is a relationship between the preferential localization of tritiated estradiol in the neocortex and the efferent corticohypothalamic connections. (H.L.W.)

42259 METHOD FOR DETERMINING SPERM PRECEDENCE IN INSECTS. Retnakaran, Arthur (Canadian Forestry Service, Sault Ste. Marie, Ont.). J. Econ. Entomol.; 64: No. 3, 578-80 (Jun 1971).

A reliable method for assaying mating success in the spruce budworm, Choristoneura fumiferana (Clemens), as indicated by actual insemination using ^{3}H or ^{14}C-leucine labeled sperms was developed. The use of this technique in establishing whether or not sperm precedence exists in multiple mating species by sequential mating of a female with a sterile male followed by a fertile male is described. Sperm precedence was observed in the spruce budworm when γ-radiation from a ^{60}Co source was used as the sterilant. Metepa-sterilized sperms were unable to compete with untreated sperms. (auth)

42260 UPTAKE OF ^{144}Ce, ^{147}Pm, AND ^{238}Pu BY OAT PLANTS FROM SOILS. Cummings, S. L.; Bankert, L. (Southeastern Radiological Health Lab., Montgomery, Ala.). Radiol. Health Data Rep.; 12: No. 2, 83-5(Feb 1971).

The uptakes of cerium-144, promethium-147, and plutonium-238 by oat plants were determined for nine soils, and promethium-147 and plutonium-238 uptakes compared with cerium-144 uptake. The percentage uptake values for all three radionuclides were very low, ranging from 10^{-6} to 10^{-3} percent. Nitrogen and potassium fertilizers increased the uptake of promethium-147 by oat plants from an Amite soil. Because the amount of cerium-144, promethium-147, and plutonium-238 taken up by plants from soils is very small, the health hazards to man by the soil-plant-man pathway from these radionuclides will probably be negligible at the levels used in this study. (auth)

42261 UPTAKE AND DISTRIBUTION OF STRONTIUM IN OAT AS INFLUENCED BY THE TIME OF SUPPLY. Andersen, A. J. (Danish Atomic Energy Commission, Risoe). Soil Sci.; 111: No. 6, 379-81(Jun 1971).

Oats were grown in culture solution and were allowed to adsorb ^{90}Sr at a precisely determined period during development. The results indicate that absorbed ^{90}Sr is immediately transported to the developing part of the plant and remains at the site of deposition without being redistributed. The ^{90}Sr found in the mature grain was absorbed at a relatively late period of the development. (auth)

42262 INCORPORATION OF TRITIUM INTO MOUSE TISSUES AFTER ORAL ADMINISTRATION OF TRITIATED THYMIDINE. Van de Reit, William G. Lawrence, Kan.; Univ. of Kansas (1970). 96p. University Microfilms Order No. 71-13,376.

Thesis.

Studies were conducted to measure the uptake, distribution, and retention of tritium in the mouse following a single ingestion of ^{3}HTdR. The excretion curves of nonvolatile activity had two components: one with a fast rate of decrease and one with a much slower rate of decrease of the tritium label. A radiation effect characterized by an accelerated rate of removal of the tritium label from the slowly diminishing component with increasing radioactivity of ^{3}HTdR was observed. In order to further evaluate earlier findings, a radiochemical determination of the fate of the tritium label following ingestion of ^{3}HTdR was carried out. In one experiment, male albino mice were given one microcurie ^{3}HTdR by stomach intubation and sacrificed after one day. Six organs were removed for assay. A portion of each organ was weighed, freeze-dried, and digested for determination of total nonvolatile tritium activity. The biochemical components of a second portion

XUM

of each organ were extracted. Each fraction was assayed for tritium activity; the acid-soluble fraction was assayed for total radioactivity and nonvolatile radioactivity. Another study was performed to determine the elimination pattern of the label from the various biochemical components of the small intestine and liver. A third study was carried out to follow the elimination of the label from the DNA fractions of the small intestine, testis, liver, and kidney. The data in this study led to the following conclusions: there is significant incorporation of tritium into all the tissues of the mouse after ingestion of tritiated thymidine; a large part of this incorporation represents nonvolatile tritium-labeled materials that are acid-soluble; a significant part of this incorporation occurs into acid-insoluble materials other than DNA; the quantity of tritium labeling of DNA reflects the amount of proliferative activity of the tissue; and a radiation effect occurs in the DNA characterized by an accelerated rate of removal of tritium label with increasing radioactivity of tritiated thymidine. (Diss. Abstr. Int., B)

42263 PREVENTION OF INTESTINAL ABSORPTION OF RADIOCESIUM AND RADIOSTRONTIUM WITH THE HELP OF INDIGENOUS IONIC RESINS. Bergheanu, S.; Gheorghe, N.; Koerner, O.; Cirstoiu, I. (Centrul de Radiobiologie si Biologie Moleculara, Bucharest). Fiziol. Norm. Patol. (Bucharest); 15: No. 4, 349-59(1969). (In Rumanian).

A method for preventing the absorption of radioisotopes with Romanian ion exchange resins is described. The results obtained with ^{134}Cs and ^{89}Sr are reported, the efficiency of the method being determined by comparing the radioactivity of the organs collected from the treated animals at 2, 24, 48 and 72 hours with the control lot. The ion exchange resins (kelatic cationite and sulfocationite) were analyzed by physicochemical and biological methods. The experiments showed that the Romanian resins are well tolerated by the animals and possess a good exchange capacity. (auth)

42264 SOME ASPECTS OF THE METABOLISM OF ^{35}S-SELENOMETHIONINE IN RATS. II. COMPARATIVE STUDY OF ^{35}S-METHIONINE AND ^{75}Se-SELENOMETHIONINE UPTAKE AND INCORPORATION IN X-IRRADIATED WHITE RATS. Kovacs, V. Stud. Cercet. Biochim.; 13: No. 4, 381-7(1970). (In Rumanian).

The uptake and incorporation of ^{35}S-methionine and ^{75}Se-selenomethionine into the liver, spleen, kidney, and proteins of these organs were investigated in x-irradiated (200, 500 and 800 R) white rats. It was found that 24 hours after irradiation an increase of ^{35}S uptake and incorporation took place both in the whole liver and in its proteins. Under the same conditions a decrease of these processes occurred in the case of ^{75}Se. In the spleen of irradiated animals a decrease in ^{35}S and ^{75}Se uptake and incorporation was observed, both in the whole organ and in its proteins. In the case of the kidneys, the irradiation effect was dose dependent. The hypothesis of enzyme liberation is discussed in view of an explanation of the observed anabolic modifications. (Rom. Sci. Abstr.)

42265 ASPECTS OF ^{35}S-METHIONINE AND ^{75}Se-SELENOMETHIONINE METABOLISM IN RATS. III. RADIOCHROMATOGRAPHIC STUDY OF ^{35}S-AMINOACID UPTAKE IN THE LIVER, SPLEEN, AND KINDNEY PROTEINS FOLLOWING X-IRRADIATION. Kovacs, V. Rev. Roum. Biochim.; 7: No. 4, 281-6(1970). (In German).

The qualitative changes of in vivo ^{35}S-methionine metabolism in Albino rats subjected to 200, 500, and 800 R of x radiation were investigated. The ^{35}S-methionine, ^{35}S-cystine, and cysteine contents of liver, spleen and kidney proteins were assessed chromatographically. 24 hours after irradiation, the amount of sulfur-containing amino acids in liver and kidney proteins increased whereas the spleen proteins decreased. These qualitative and quantitative changes in sulfur-containing amino acids in the proteins of irradiated animals may be assigned to the qualitative changes of the DNA molecules subsequent to irradiation. (auth) (Rom. Sci. Abstr.)

Radiation Effects

Refer also to abstracts 41788, 41837, 41862, 42535, 42586, 42726–42729, 42731, and 42756.

42266 (AEC-tr-7225) RADIOBIOLOGY. Translation of Radiobiologiya; 10: No. 6, 803-960(1970). 223p. Dep. NTIS.

Of the 30 papers in this issue, 29 author abstracts of papers were translated and appeared in NSA, volume 25, issue 13 as abstract numbers 29440, 29458, 29484-7, 29546-8, 29609-10, 29612, 29637-48, 29714-6, and 29725-6. The paper not included in NSA discussed the permutation index as an information source on radiogiological literature. (E.R.B.)

42267 (RLO-2225-T-15-3) PHOTOBIOLOGY AND PHOTOCHEMISTRY OF RIBONUCLEIC ACIDS. Progress Report, January 1970–December 1970. Gordon, Milton P. (Washington Univ., Seattle). Contract AT(45-1)-2212. 8p. Dep. NTIS.

The acetone–sensitized irradiation of highly labeled E. coli ribosomal RNA at 313 nm led to the formation of uracil dimer as the only detectable lesion. The acetone-sensitized irradiation of tobacco mosaic virus-RNA(TMV-RNA) and potato virus X-RNA(PVX-RNA) caused loss of biological activity, part of which could be restored by in vivo photoreactivation. The photoreactivable sectors were approximately equal to the sectors observed upon irradiation of these RNA's at 253.7 nm. It was concluded that the introduction of only pyrimidine dimers is sufficient for both inactivation and photoreactivation to occur. The role of cyclobutane pyrimidine dimer formation in photoreactivation following uv irradiation, the effects of D_2O on pyrimidine hydrate formation, in vivo and in vitro photoreactivation studies, and the in vitro labeling of DNA and RNA are discussed. (D.P.O.)

42268 REGENERATION OF γ-RADIATION-INDUCED SINGLE RUPTURES OF DNA STRANDS BY POLYNUCLEOTIDE LIGASES IN VITRO. Gaziev, A. I.; Fomenko, L. A.; Zakrzhevskaya, D. T. (Inst. of Biological Physics, Pushchino, USSR). Dokl. Akad. Nauk SSSR; 195: 479-82(11 Nov 1970). (In Russian).

The role of various polynucleotide (PN) ligases in the regeneration of breaks in the DNA strands induced by γ radiation was investigated by using transforming DNA from Bac. subtilis SHGW and 2 PN ligases, a DNA dependent one of the same strain and an ATP dependent one from Escherichia coli B, infected by the T4-phage. The formation and regeneration of the breaks were evaluated on the basis of the transforming activity of the DNA. The Bac. subtilis 168 (Try) served as the recipient culture. The culture was irradiated by a ^{137}Cs source at doses ranging from 0.5 to 10.0 krad. The results indicated that the irradiated preparations were regenerated to the same extent by the 2 ligases. The PN ligase completely regenerated the transforming ability of DNA irradiated by a 500-rad dose, indicating that at low dose levels PN ligase-specific 3-OH ~ 5'-phosphate type breaks are formed. Increasing the γ radiation dose resulted in the reduction of the regenerative effect. (TTT)

42269 DARK REPAIR OF ULTRAVIOLET-IRRADIATED DEOXYRIBONUCLEIC ACID BY BACTERIOPHAGE T4: PURIFICATION AND CHARACTERIZATION OF A DIMER-SPECIFIC PHAGE-INDUCED ENDONULCEASE. Freidberg, Errol C.; King, John J. (Walter Reed Army Inst. of Research, Washington, D. C.). J. Bacteriol.; 106: 500-7(May 1971).

The purification and properties of an uv repair endonuclease are described. The enzyme is induced by infection of cells of Escherichia coli with phage T4 and is missing from extracts of cells infected with the uv-sensitive and excision-defective mutant $T4V_1$. The enzyme attacks uv-irradiated DNA containing either hydroxymethylcytosine or cytosine, but does not affect native DNA. The specific substrate in uv-irradiated DNA appears to be pyrimidine dimer sites. The purified enzyme alone does not excise pyrimidine dimers from uv-irradiated DNA. However, dimer excision does occur in the presence of the purified endonuclease plus crude extract of cells infected with the mutant $T4V_1$. (auth)

42270 SULFHYDRYL GROUPS AS INDEXES OF REMOTE SEQUELAE OF RADIOTHERAPY OF BREAST CANCER. Vishnevetskaya, E. M.; Ivanitskaya, V. I.; Semenov, V. D. (Kharkov Scientific Research Inst for Medical Radiology). Klin. Khir.; 4: 57-9(Apr 1970). (In Russian).

Because of the known role of -SH groups in preventing radiation sickness and the effect of radiation in decreasing the content of these groups in the body, the -SH content was determined in the blood serum of cancer patients who had undergone radical mastectomy followed by radiation treatment. The average serum -SH content was about 30% lower in the albumin and about 30% higher in the globulin and non-protein fractions for the 15 patients than in the 52 controls, but the total serum -SH values were about the same for the two groups. Possibly the increase in the -SH globulin content is a protective reaction against both cancer and radiation damage. The results should permit improving treatment procedures. (TTT)

42271 EFFECTS OF γ-RADIATION ON DILUTE SOLUTIONS OF TRYPSIN. Lynn, K. R. (National Research Council of Canada, Ottawa). Radiat. Res.; 46: No. 2,268-78(May 1971).

Trypsin (5×10^{-6} M) was irradiated in 10^{-3} M HCl solution under atmospheres of air and nitrogen. Oxygen was found to be protective for esterolytic and proteolytic functions of the enzyme. Reactivity for synthetic esters and amides was lost by trypsin in an exponential manner but at rates which varied with the nature of the substrate. Proteolytic ability for casein, but

not for hemoglobin or bovine plasma albumin declined in a non-exponential manner on γ irradiation. High voltage electrophoresis experiments demonstrated that the nonexponential loss of proteolytic activity resulted from tryptic digestions yielding peptides whose characters changed with the extent of radiation delivered to the enzyme. Changes in the tryptophan content and the difference spectra of irradiated trypsin were interpreted as indicating an inactivating alteration in the conformation of the enzyme. (auth)

42272 DEOXYRIBONUCLEASE ACTIVITY OF HeLa CELLS SPECIFIC FOR UV-IRRADIATED DNA. Burt, David H.; Brent, T. P. (McGill Univ., Montreal). Biochem. Biophys. Res. Commun.: 43: No. 6, 1382-7(18 Jun 1971).

A deoxyribonuclease activity which is specific for ultraviolet light irradiated DNA has been demonstrated in extracts of a mammalian cell (HeLa). The release of acid-soluble products from tritium labeled DNA shows a maximum at elevated pH's and at Mg concentrations of 3–6 mM. Further results are reported. (auth)

42273 INFECTION OF SPHEROPLASTS OF PSEUDOMONAS WITH DNA OF BACTERIOPHAGE PM2. van der Schans, G. P.; Weyermans, J. P.; Bleichrodt, J. F. (National Defence Research Organization TNO, Rijswijk, Netherlands). Mol. Gen. Genet.; 110: No. 3, 263-71(2 Apr 1971).

Spheroplasts of Pseudomonas BAL-31/PM2, obtained by treatment of the bacteria with lysozyme, can be infected with purified DNA from bacteriophage PM2. After 4 h of incubation the yield of progeny phage reaches a value of $10^7 - 6 \times 10^7$ plaque forming units/μg PM2 DNA. The yield increases linearly with the concentration of DNA over at least 3 orders of magnitude. The biological activity of double-stranded circular PM2 DNA containing one or more single-strand breaks per molecule (component II) does not differ significantly from that of intact PM2 DNA (component I). Single-stranded PM2 DNA obtained by irradiation of component II, and the irreversibly alkali-denatured form of component I are also infective. (auth)

42274 RADIATSIONNAYA BIOFIZIKA NUKLEOPROTEIDA. (Radiobiophysics of the Nucleoproteins). Spitkovskii, D. M.; Andrianov, V. T.; Pisarevskii, A. N. Moscow; Atomizdat (1969). 176p.

The book represents the first attempt to systematically explore the current state of the question of the radiation biophysics of deoxyribonucleoproteins (DNP) – the most vital macromolecule in the structure of living things. The main biophysical characteristics of DNP and its behavior under the effects of ionizing radiation (changes in the supramolecular and molecular characteristics, structural bonds and function within the cell, protection, and the role of the radiation insult to DNP in the general mechanism of radiation effects) are examined. Comparison of diapason to doses of ionizing radiation, resulting in changes in the individual molecules of DNA, DNP, and in DNP-systems, allowed the conclusion to be drawn that at biological doses of irradiation, structural changes in the chromosomes were not, in the majority of cases, related to disturbances in the DNA macromolecules. In this connection, the possible mechanisms of the action of radioprotective substances on the level of so-called structural protection are presented. The current methodology of physico-chemical experimentation with DNP is also examined in detail. (tr-auth)

42275 ISSLEDOVANIE PARAMAGNITNYKH TSENTROV OBLUCHENNYKH BELKOV. (Investigation of the Paramagnetic Centers of Irradiated Proteins). Kayushin, L. P.; L'vov, K. M.; Pulatova, M. K. Moscow; Izdatel'stvo Nauka (1970). 264p.

Experimental information concerning paramagnetic centers, which emerge in biologically important substances following the action of radiation, is systematized. A significant portion of the book is devoted to an analysis of the EPR spectra of free radicals that are formed by the γ irradiation of amino acids and peptides. The results of investigations of paramagnetic resonance in irradiated proteins are given. The study of paramagnetic centers in irradiated biopolymers with different steric structures and under different physical conditions permitted the determination of the way in which the transfer and exchange of the energy of absorbed radiation takes place in biological systems thus obtaining information concerning unusual structures in biopolymers. The book is of interest to people working in the field of biophysics, biochemistry, radiation chemistry, solid state physics, and also for the student and post-graduate in related fields. (tr-auth)

42276 SEGREGATION FOLLOWING INTERCHANGE INDUCED BY IRRADIATING MATURE OOCYTES OF DROSOPHILA MELANOGASTER. Busby, Nancy (Univ. of California, Riverside). Mutat. Res.; 11: No. 4, 391-6(Apr 1971).

Induced C(1)-4 interchange in mature oocytes does not alter the normal segregation pattern by directing disjunction of centromeres of the involved chromosomes to opposite poles as it does in immature oocytes. Thus, one would predict that the sister of 4 is recovered in the same oocyte with the C(I)-4 detachment much more frequently than is the homolog or no free 4, which are recovered most frequently with C(I)-4 detachments when immature oocytes are irradiated. It was found that the sister free 4 is recovered with the C(I)-4 detachment in 15 of 23 cases. (auth)

42277 ACTIVITY OF PYROPHOSPHATASE AND CATALASE AFTER A LONG IRRADIATION WITH SMALL DOSES OF ^{60}Co. Benetata, Gr.; Capalna, S.; Ghizari, Eugenia; Stefan, Maria. Stud. Cercet. Fiziol.; 15: No. 4, 291-5(1970). (In Rumanian).

The activity of the pyrophosphatase of the brain and liver and the catalase of the blood of rats exposed for 24 and 48 hrs to a continuous irradiation of about 0.5 R/min. from a ^{60}Co source was analyzed. The activity of the enzymes was determined at 24, 48, and 72 hrs after the irradiation and compared with that of unirradiated controls. (tr-auth)

42278 MODIFICATIONS OF THE SYNTHESIS OF THE HEPATIC CATALASE IN MICE EXPOSED TO THE EFFECT OF IONIZING RADIATION. Stefan, Maria. Stud. Cercet. Fiziol.; 15: No. 4, 327-31(1970). (In Rumanian).

It has been assumed by many investigators that the majority of modifications occurring in the activity of an enzyme under various physiological and pathological conditions are due to the changes of the degree of synthesis or degradation of the system studied. By use of an experimental model accepted in the literature for the in vivo study of the degree of synthesis of catalase, the present study attempts to establish to what degree the modifications induced by ionizing radiation in the activity of hepatic catalase are the expression of its degree of synthesis. (tr-auth)

42279 ACTIVITY OF REDOX ENZYMES IN THE LIVER IN INTERNAL USE OF RADON WATER. Gornak, K. A.; Ryumshina, T. A. (Inst. of Human Morphology, Moscow). Byull. Eksp. Biol. Med.; 71: No. 4, 115-19(Apr 1971). (In Russian).

In internal employment of radon (0.18, 3.64, 36.4, and 364 μC/l) water there occurs an intensification of the activity of redox enzymes in the hepatic tissue of experimental animals (rats) and changes in the content of fat and glycogen. The authors used the method of quantitative determination of the activity of redox enzymes in the hepatic tissue. The changes observed were in direct relation with the content of radon in the water, duration of its introduction, and the absorbed dose of radiation in the liver. (auth)

42280 INVESTIGATION OF HETEROGENEITY OF THE LIVER NUCLEAR RNA OF IRRADIATED RATS EMPLOYING THE METHOD OF DNA–RNA HYBRIDIZATION. Saenko, A. S.; Zharkov, Yu. A. (Inst. of Medical Radiology, Obninsk, USSR). Biokhimiya; 36: No. 3, 545-50(May-Jun 1971). (In Russian).

The method of RNA – RNA hybridization on nitrocellulose filters in competitive conditions was employed to compare identity of the composition of the total nuclear RNA synthetized by the liver of the intact Wistar rats and the rats exposed to the whole-body γ irradiation at a dose of 5000 R. Preliminary saturation of DNA by nonlabelled RNA from the liver of intact animals markedly, yet to the same extent, inhibited complementation of nuclear RNAs labeled with ^{32}P isolated from the liver of intact and irradiated animals. The data obtained evidence that stimulation of incorporation of precursors into RNA by the liver of irradiated animals apparently is due to change in the rate of nuclear RNA turnover rather than to a depression of DNA in the liver. (auth)

42281 EFFECT OF WHOLE-BODY X-RADIATION ON THE LIPOLYTIC ACTIVITY OF RAT HEART EXTRACTS. Szabo, Rezso; Soevenyi, Ervin; Lehotai, Lajos. Kiserl. Orvostud.; 20: No. 6, 651-4(1968). (In Hungarian).

Following whole-body irradiation of rats at 800 R, the lipolytic activity of the heart at different intervals was evaluated. Twenty-four hours after irradiation the activity showed a temporary increase, then later decreased. Five days later the activity again increased. When cysteamine is administered prior to the irradiation, these fluctuations are enhanced, although by itself cysteamine shows no such effects. These observations are correlated with the known reduction of the heparin content of tissues. (tr-auth)

42282 BROMINE METABOLISM AFTER LETHAL X-RAY IRRADIATION OF THE ABDOMEN IN RATS. Bouckaert, A. (Univ., Louvain, Belgium). Atomkernenergie; 17: No. 4, 297-8 (Jul 1971).

Radiobromine excretion is consistently slower in lethally irradiated rats than in normal controls. The reduction of radiobromine excretion rate appears to be correlated with the severity

XUM

of the radiation syndrome. The origin of the radiobromine metabolism disturbances is thought to be similar to that of radiosodium metabolism disturbances. Both seem to be a part of a generalized imbalance of electrolyte distribution caused by lethal doses of x-rays. (auth)

42283 INFLUENCE OF METHYLENE BLUE ON LIVER GLYCOGEN, BLOOD GLUCOSE, AND ELECTROLYTES IN SERUM OF RATS EXPOSED TO X RAYS. Chang, Seung Han; Nam, Sang Yul. Tongmul Hakhoe Ji; 11: No. 2, 48-54(1968).

Male rats of the Albino strain received methylene blue in the dose of 40 mg/kg by subcutaneous injection and were subjected to total body x-irradiation, 300 roentgen, at 30 minutes after the injection. The protective effect of methylene blue against the single total body x-irradiation was studied for 24 days after x-irradiation with regard to the levels of liver glycogen, blood glucose, and electrolytes in serum. (Korean Sci. Abstr.)

42284 RADIOPROTECTIVE EFFECT OF METHYLENE BLUE. 1. EFFECT OF METHYLENE BLUE ON LACTIC DEHYDROGENASE LEVEL AND LACTIC DEHYDROGENASE ISOENZYMES OF RATS EXPOSED TO GAMMA IRRADIATION. Nam, Sang Yul; Chang, Seung Han. Tongmul Hakhoe Ji; 12: No. 3, 94-102(1969).

The protective action of methylene blue against gamma-irradiation was studied with rats. Albino rats were given 360 rads of whole-body gamma-irradiation following an intraperitoneal injection of physiological saline or methylene blue. Male rats given methylene blue (38 mg/kg) and the control rats given saline were alive following gamma-irradiation. Serum lactic dehydrogenase (LDH) activity, and LDH isoenzyme patterns in serum and various organs were determined at various time intervals after the exposure. (Korean Sci. Abstr.)

42285 RECOGNITION OF PYRIMIDINE DIMERS IN DNA BY THE INCISION ENZYME FROM MICROCOCCUS LYSODEIKTICUS. Paribok, V. P.; Tomilin, M. V. (Inst. of Cytology, Leningrad). Nature (London) New Biol.; 230: 210-11(14 Apr 1971).

DNA hybrids containing pyrimidine dimers were prepared from Bacillus subtilis by irradiation with 8,500 ergs/mm^2 of ultraviolet radiation (254nm). They were then labeled with ^{14}C thymine and tested for breaks in the labeled strand after incubation with ultraviolet-endonuclease from Micrococcus lysodeikticus. The enzyme activity for the non-irradiated strands was lower than that for the strands containing dimers, suggesting that ultraviolet-endonuclease recognized specific chemical modifications of the DNA, rather than the local melting of the DNA double helix. Further sedimentation patterns showed that ultraviolet-endonuclease did not break the hydroxylamine-treated DNA of Escherichia coli. It was concluded that there was no reason to predict errors in the incision step of repair of ultraviolet irradiated DNA. (UK)

42286 ENZYME ACTIVITY IN IRRADIATED SKIN. CYTOCHROME OXIDASE AND MONOAMINE OXIDASE. Csrmely, E.; De Panfilis, G.; Marcheselli, W.; Santini, R. G. Ital. Dermatol.; 45: 151-3(Mar 1970). (In Italian).

Modifications of the cytochrome oxidase and monoamine oxidase activity in normal human skin exposed to x-ray doses of 500, 1000, and 1500 R were studied. The 500 and 1000 R doses had no effect on the cytochrome oxidase, but the 1500 R dose caused a decrease in its activity in the epidermis. No change was found in the monoamine oxidase activity. The significance of these results is discussed. (J.S.R.)

42287 EFFECT OF X RAYS ON THE MOUSE THYMUS GLAND. Gibertini, Giancarlo (Univ., Rome). Riv. Biol.; 61: 273-83(Apr-Sep 1968). (In Italian).

The localization of acid phosphatase at the level of Hassall corpuscles in the thymus following a whole-body single irradiation of 450 R was conducted. The variations of the dimensions and modifications in the formation and evolution of the Hassall corpuscles were followed histologically and a correlation between charge changes and percent of lymphocytes was made. The location of the acid phosphatase in the thymus of irradiated animals was studied. The active participation of Hassall corpuscles in the phagocytosis process was discussed on the basis of the results obtained. (tr-auth)

42288 TEMPERATURE-DEPENDENCE OF RADIATION SENSITIVITY IN THE DRY STATE: A MODEL DERIVED FROM EXPERIMENTS USING ATOMIC HYDROGEN. II. Kuerzinger, Klaus (Kernforschungszentrum, Karlsruhe, Ger.). Int. J. Radiat. Biol.; 19: 45-50(1971).

Diffusible and reactive species were liberated by proton bombardment of thin foils of organic material and allowed to react with bacteriophage T1. Whereas in earlier experiments the temperature of either the samples alone (method A), or both foil and samples (method B), were varied, a third mode of exposure was used (method C), allowing the temperature of the bombarded foil alone to be varied (down to 88°K), while the phage samples were kept at room temperature. The rate of phage-inactivation by radical attack in dependence on temperature led to activation energies of 0.65 ± 0.1 kcal/mole for method A, 0.95 ± 0.1 kcal/mole for method B, and 0.34 ± 0.05 kcal/mole for method C. It is suggested that H radicals separated from macromolecules by ionizing radiation need an activation energy to leave the site of their production and be liberated for good, and that experimental evidence that this activation energy for liberation accounts for the difference of roughly 0.3 kcal/mole between the activation energies found in methods A and B. (auth)

42289 METABOLISM OF p-NITROPHENOL IN WHOLE-BODY IRRADIATED RATS. Scoppa, P.; Marafante, E. (CCR-EURATOM, Ispra, Italy). Boll. Soc. Ital. Biol. Sper.; 45: No. 24, 1623-6(31 Dec 1969). (In Italian).

Rats were administered p-nitrophenol 24 hrs. after whole-body irradiation with x rays. The urinary excretion of the p-nitrophenol was determined for the 0 to 24 and 24 to 48 hr. period. In the irradiated rats there is a smaller excretion of p-nitrophenyl-glucuronide than in the unirradiated rat. The irradiated rats excrete almost 20% of the administered dose of p-nitrophenol in the second 24 hrs. This is attributed to a secondary effect of the irradiation. (J.S.R.)

42290 DEOXYRIBONUCLEIC ACID REPLICATION IN UV-DAMAGED BACTERIA REVISITED. Doudney, C. O. (Albert Einstein Medical Center, Philadelphia). Mutat. Res.; 12: No. 2, 121-8(Jun 1971).

Exposure of Escherichia coli strain B/r thy$^-$ to uv doses below a critical dose of about 200 erg/mm^2 induced short, dose-dependent delays in DNA replication. DNA replication then resumed. The maximum delay after the critical dose was about 45 min. With uv doses above this critical dose, little or no further delay in initiation of DNA replication was induced but the rate of DNA replication was decreased with higher doses indicating inactivation of the DNA synthetic mechanism. Thus after an exposure of about 560 erg/mm^2 DNA replication was almost completely suppressed in the culture. After doses up to the critical dose, little DNA breakdown was seen with post-irradiation incubation. Even after the dose inducing complete inactivation of DNA replication, at least 85% of the DNA was stable with prolonged incubation. The results of a labeled thymine incorporation method of measuring DNA replication were compared with the results of the Burton diphenylamine method with good agreement. (auth)

42291 RADIATION EFFECTS ON AN ALLOSTERIC ENZYME WITH TWO CATALYTIC ACTIVITIES. X-RAY INACTIVATION OF THE THREONINE-SENSITIVE ASPARTO-KINASE-HOMOSERINE DEHYDROGENASE FROM ESCHERICHIA COLI. DiMarco, Giorgio; Sanner, Tore; Pihl, Alexander (Norwegian Radium Hospital, Oslo). Biochim. Biophys. Acta; 220: 1-9 (Oct 1970).

The threonine-sensitive aspartokinase–homoserine dehydrogenase (ATP: L-aspartate 4-phosphotransferase, EC 2.7.2.4; L-homoserine: NAD oxidoreductase, EC 1.1.1.3) from Escherichia coli was irradiated in dilute aqueous solution in the presence of air with x rays at 25°C. The two enzyme activities were destroyed as exponential functions of the radiation dose, the G values being 0.006 and 0.015 for the dehydrogenase and the kinase activities, respectively. The sensitivity of the dehydrogenase activity to inhibition by threonine was inactivated with a G-value of 0.015, whereas the corresponding sensitivity of the kinase activity was unaffected by irradiation. The enzyme sulfhydryl groups were destroyed with a G-value of 0.25. The radioinduced loss of the sensitivity of the dehydrogenase activity to threonine was effectively protected by the presence of threonine during irradiation, whereas the dehydrogenase activity as such was protected only to a limited extent. Kinetic studies indicated that the radio-induced loss of the allosteric dehydrogenase function is an all-or-none process. The results indicated that destruction of sulfhydryl groups plays an important role in the radioinduced loss of the allosteric dehydrogenase function and the catalytic kinase function. The mechanisms probably involve dissociation of the enzyme. (auth)

42292 PROBLEMS IN EXPERIMENTAL AND CLINICAL RADIOLOGY. Shantyr, V. I. (ed.). Vop. Eksp. Klin. Radiol., Khar'kov. Inst. Med. Radiol.; No. 5, 1-243(1970). (In Russian).

Fifty-one separate papers by different authors comprise this book and treat the biological effects of radiation on animals under controlled experimental conditions. Subjects of the articles include high-energy electron effects on the mucoprotein of rat liver; electrolyte exchange in rats treated with 45 MeV electrons;

thyroid glands of rats irradiated with fast neutrons; irradiation of animal liver and spleen; and the resistance of animals to botulin toxin during radiation sickness. Experiments with radio-phosphorus, ^{131}I, ^{67}Ga, ^{59}Fe, ^{51}Cr, and radio-xenon are described, and the effects on the blood, urine, thyroid gland, and liver are noted. The diagnostic uses of various radioisotopes are referred to in a number of papers. (K.S.W.)

42293 THROMBELASTOGRAPHY OF ANTIFIBRINOLYTICA BEFORE AND AFTER IRRADIATION WITH GAMMA RAYS. Stamm, H. (Univ., Basel); Berkarda, B.; Szirmai, E. J. Int. Nucl. Eng.; 12: 13-15(Jan-Feb 1971).

The effect of epsilon-aminocaproic-acid (EACA) and protaminsulphate on blood clotting was examined. Different concentrations of EACA and protaminsulphate were added to blood and clotting was measured in a thrombelastograph (TEG). The blood of a woman patient suffering from carcinoma was used because the blood clotting system of carcinoma patients is specially labile. The irradiation of EACA with 2000 R gamma rays did not change the intensity of the effect. (auth)

42294 PULSE- AND X-RADIOLYSIS OF 2-MERCAPTOETHANOL IN AQUEOUS SOLUTION. Jayson, G. G. (Liverpool Polytechnic); Stirling, D. A.; Swallow, A. J. Int. J. Radiat. Biol.; 19: 143-56(1971).

Aqueous solutions of 2-mercaptoethanol were irradiated with pulses of 4 MeV electrons and with 240 kVp x rays. The specific rate-constants for reactions of hydroxyl radicals, hydrated electrons, and hydrogen atoms with the thiol were found to be 6.5×10^9, 1.2×10^{10}, and 2×10^9 M^{-1} sec^{-1}, respectively. Reaction products were identified by gas chromatography and functional group analysis as hydrogen peroxide, hydrogen sulphide, acetaldehyde, ethanol, and dithiodiglycol. Yields were determined quantitatively by spectrophotometric means. Radical scavengers such as acetone were used to isolate effects due to the various primary species. In the absence of oxygen, dithiodiglycol was formed with G up to 5 while hydrogen peroxide was formed in very small yield. In oxygenated solutions, dithiodiglycol and hydrogen peroxide were formed in equal yields with G values up to about 30, while hydrogen sulphide and ethanol had yields up to G about 1. A reaction mechanism was proposed, involving 2-hydroxyethyl, thiyl, and organosulphur-peroxy radicals, and a role for thiols as radiation protectors was suggested. (auth)

42295 EFFECTS OF X IRRADIATION ON THE OXYGEN CONSUMPTION AND LYSINE UPTAKE OF HeLa CELLS IN THE PRESENCE OF METABOLIC SUBSTRATES AND INHIBITORS. Kang, Yung Sun: Ha, Doo Bong: Ahn, Kyung Ja. Tongmul Hakhoe Ji; 11: No. 3, 75-82(1968).

The effects of x-irradiation on the utilization of glucose, succinate, citrate and α-ketoglutarate, on the response of the cell metabolism to NaN_3 and DNP, and on the uptake of lysine in the presence or absence of the metabolites or the inhibitors were studied using HeLa cells. (Korean Sci. Abstr.)

42296 EFFECT OF HYDRATION ON THE DECAY OF RADIATION-INDUCED RADICALS AND OXYGEN-SENSITIVE CENTERS IN BARLEY SEEDS. Ahnstroem, G. (Univ. of Stockholm); Sanner, T. Radiat. Bot.; 11: 27-32(1971).

Barley seeds were adjusted to a water content of 6 percent and irradiated under anoxic conditions. The reduction of seedling growth was taken as a measure of the radiation effect. At the moisture content of 6 percent, radiation damage was potentiated by the presence of oxygen in the soaking water. The oxygen-sensitive centers decayed if the seeds are soaked under anoxic conditions prior to the exposure to oxygen, and this decay process was strongly temperature dependent. The radiation-induced free radicals were measured in whole seeds and in different parts of the seeds after soaking in oxygen-free water. All electron spin resonance measurements were carried out at 77°K. The stability of unpaired spins decreased with increasing soaking temperature and differed greatly in various parts of the seeds. While no correlation was found between the lifetime of the oxygen-sensitive centers and the free radicals, the rate of disappearance of the radicals could well be correlated with the water uptake of the embryo. (auth)

42297 T4 DNA REPLICATION AND REPAIR. Soll, Helen Jean Newman. Stanford, Calif.; Stanford Univ. (1970). 150p. University Microfilms Order No. 71-12,994.

Thesis.

Bacteriophage T4 DNA replication and uv repair synthesis have been investigated utilizing physical measurements and analysis of incorporation of radioactive tracers. Newly synthesized T4 DNA can be isolated as fragments of low molecular weight. These newly synthesized fragments accumulate in the absence of an enzyme (polynucleotide ligase) which repairs single strand breaks in double stranded DNA. Rates of T4 DNA replication decrease upon inactivation of polynucleotide ligase after a short lag (2 minutes at 43°C). However, newly synthesized DNA accumulates as fragments of low molecular weight after ligase inactivation when rates of DNA synthesis are still essentially normal. The fragments of newly synthesized DNA accumulated in the absence of polynucleotide ligase are converted into high molecular weight DNA in vivo. It is concluded that newly replicated T4 DNA contains single strand breaks which polynucleotide ligase normally joins to yield high molecular weight DNA. It was found that the study of repair synthesis of irradiated T4 DNA was hindered by continued normal replication and large intracellular pools of thymine. Nonetheless it was possible to demonstrate uv stimulated repair synthesis at least part of which is related to a phage directed recovery mechanism which involves excision of uv photoproducts (pyrimidine dimers) from irradiated virus DNA. (Diss. Abstr.)

42298 VARIATIONS OF SGOT AND SGPT IN RATS FED A DIET OF DIFFERENT UNSATURATED FATTY ACID CONTENT FOLLOWING X IRRADIATION. Nemec, R. Cesk. Gastroenterol. Vyz.; 25: No. 1, 34-9(Jan 1971). (In Czech).

The influence of two types of semisynthetic diets with an extremely differing content of unsaturated fatty acids, administered to the animals by different routes, on the GO and GP transaminase serum levels of white rats irradiated by a single whole-body dose of 600 R was investigated. Marked changes were found in GOT and GPT in animals fed a diet with a high unsaturated fatty acid content (linseed oil acid) as compared with animals with a diet with a low unsaturated fatty acid content (coco nut oil). The authors assume that the diet containing a higher percentage of saturated fatty acids influences by some so far unknown mechanism the passage of transaminases from cells into blood. A more marked influence — inhibition — of this passage observed after coconut oil and after both routes of administration than when linseed oil was administered. The authors found that intragastric administration of half the daily fat allowance (the daily allowance being 15 g of diet per rat per day, which amounted to 0.5 ml of the oil) directly into the stomach suffices, independently on the unsaturated fatty acid content, to meet the basic energy needs of the organism on the first days after irradiation and thus the animals do not develop postirradiation symptoms, contrary to animals who received the fat in the diet only. (auth)

42299 EFFECTS OF X IRRADIATION ON THE VARIOUS ENZYMIC FUNCTIONS OF $NADP^+$-LINKED ISOCITRATE DEHYDROGENASE. Holland, P.; Little, C. (Memorial Univ. of Newfoundland, St. John's). Can. J. Biochem.; 49: 510-15(May 1971).

Highly purified $NADP^+$-linked isocitrate dehydrogenase was x-irradiated in dilute aqueous solution and proved to be very radiosensitive, being inactivated with a G value of 0.5. The catalytic functions of the enzyme were destroyed at the same rate. However, unlike most allosteric enzymes, the allosteric properties were not more radiosensitive than the catalytic properties. X-ray inactivation was associated with the destruction of seven to eight sulfhydryl groups. The first four sulfhydryls destroyed were extremely radiosensitive, having G values for destruction of almost 2. Comparison with several reagents known to attack sulfhydryl groups suggested that sulfhydryl destruction was sufficient to account for the X-ray response of the enzyme. Destruction of the single essential methionine did not seem significant in the inactivation. X-ray inactivation was also associated with increases in the K_m values for isocitrate and manganese. (auth) (Canada)

42300 TARGET SIZE OF DNA IN ULTRAVIOLET IRRADIATION. Radman, M. (Centre National de la Recherche Scientifique, Gif-sur-Yvette, France). Nature (London) New Biol.; 230: 277-8(28 Apr 1971).

The surviving fraction of plaque forming units of bacteriophages λ+ and λ62, (assayed on Escherichia coli), was plotted as a function of ultraviolet dose. Assuming the correspondence between DNA content and ultraviolet sensitivity, the rate of inactivation of phages appeared to be proportional to the quantity of DNA, the cause of inactivation being mainly interference with DNA replication, rather than an effect on transcription. (UK)

42301 INTESTINAL ENZYME ACTIVITIES FOLLOWING WHOLE-BODY IRRADIATION IN HAMSTERS. Sayeed, M. M.; Musacchia, X. J.; Barr, R. E. (Washington Univ., St. Louis. Jewish Hospital, St. Louis. Univ. of Missouri, Columbia). Proc. Soc. Exp. Biol. Med.; 137: No. 2, 709-13(Jun 1971).

The phosphomonoesterase and Mg-(Na + K)-adenosine triphosphatase (ATPase) activities were measured in the mucosa of the small intestine of hamsters (Mesocricetus auratus) exposed to 1,000 rads ^{60}Co whole-body γ irradiation. The enzyme assays were made in irradiated and sham-irradiated hamsters sacrificed at intervals through day 4 postirradiation. The two enzymic ac-

XUM

tivities expressed per unit of tissue weight were significantly higher in the irradiated animals as compared to the sham-irradiated group at day 2 postirradiation. No changes were found in the protein contents of jejunal mucosa between irradiated and sham-irradiated animals. While the ATPase activity was significantly lowered at day 4, the phosphomonoesterase activity was observed to be higher at that time. The increase in enzyme activities may represent increased synthesis of these enzymes in the crypt cells that gave origin to the mature cells of the intestinal villi of animals sacrificed at day 2 postirradiation. The increase in ATPase activity at day 2 followed by a decrease at day 4 corresponds to the previously observed alterations in the intestinal glucose absorption by irradiated hamsters. (auth)

42302 PREPARATION AND ULTRAVIOLET LIGHT-INDUCED TRANSFORMATION OF AN ANTIFUNGAL MIXTURE OF HEPTAENE ANTIBIOTICS OF STREPTOMYCES SURINAM. Siewert, Gerhard; Kieslich, Klaus (Schering AG, Berlin). Appl. Microbiol.; 21: No. 6, 1007-10(Jun 1971).

Conditions for the production and isolation of an antifungal antibiotic mixture (DJ400) were investigated. Different preparations of DJ400 may contain at least 12 different heptaenes, which were characterized by partition chromatography (peak number) and ultraviolet (uv) spectra (types A, B, C). Irradiation with uv light transformed the predominant uv spectrum of type B into A. Comparison of untreated and uv-irradiated products indicated that the main components may exist in two forms with identical structures except for an all trans-heptaene system in A compounds and one internal cis double bond in B compounds. The ratio of the major components 6B and 8B depended on the media composition. Component 4B is probably a precursor of 6B; 10B and 12 may be precursors of 8B. (auth)

42303 SPECIFIC PROTEIN–PROTEIN INTERACTION AND ITS APPLICATION IN STUDIES ON RADIATION-INDUCED PROTEIN MODIFICATION. Kasche, Volker. Uppsala; Uppsala Univ. (1971). 132p.

Thesis.

Expressions for the initial yields in protein modification, G_{mod}, and activity change, G_{deact}, are derived. These are functions of molecular properties (activity change for a specified modification, rate constants for reactions with ·H, ·OH and e^-_{aq}) and G-values for the formation of ·H, ·OH, e^-_{aq} or G-values for excitation and ionization. Protons of 185 MeV and γ-rays from ^{60}Co were used. In the protein concentration interval, $6 \times 10^{-6} - 4 \times 10^{-4}$ M, G_{deact} was determined in the interval pH 2-7. It was found to decrease with protein content at high pH, but decreased only slightly at low pH. Gel exclusion chromatography in the presence and absence of urea showed that all irradiation products with measurable activities are monomers. It was found that the majority of the radioinduced changes in native α-chymotrypsin result in products with activities in the interval $(0.1\ \alpha_0 - \alpha_0)$, where α_0 is the activity of native α-chymotrypsin. The decrease in activity is accompanied by an increase in the Michaelis–Menten constant. The average activity change per radiation-induced protein modification was found to be $0.1\ \alpha_0$ for the indirect and $0.45\ \alpha_0$ for the direct effect. The radiobiological implications of the results, including radiation-induced labelling of proteins with ^{11}C and ^{13}N, are discussed. (auth) (Sweden)

Immunology

Refer also to abstract 42740.

42304 CHANGES OF THE TESTES OF IRRADIATED MICE IN BONE MARROW TRANSPLANTATION. Zaitseva, K. K.; Fomina, G. S. Med. Radiol.; 16: No. 6, 63-8(Jun 1971). (In Russian).

Morphological changes in the epithelium of seminiferous tubules in CC57W sexually mature mice were investigated after total irradiation with a dose of 750 r ^{60}Co and transplantation of syngenous and allogenous bone marrow. The testes of mice with a diverse degree of markedness of the reaction of tissue incompatibility were investigated. It was found that bone marrow transplantation, prolonging the life of lethally irradiated animals, enables dynamic studies of processes of affection and restoration of the spermatogenous epithelium. The graft-against-host reaction developing after transplantation of allogenous bone marrow did not exert a negative effect on the restorative processes in the testes. (auth)

42305 PREVENTION OF TUMOR GROWTH BY IMMUNIZING HAMSTERS WITH X-IRRADIATED, SV_{40}-TRANSFORMED CELLS. Ashkenazi, A. Harefuah; 77: 376-9(1969). (In Hebrew).

Properties of unaltered cells and those of derived lines were compared. The study was based on the immunization of hamsters inoculated with irradiated transformed cells. Kidney cells of hamsters were transformed by the SV_{40} virus; transfers and choice of tumors with and without metastasis made it possible to derive three separate lines. Tumors caused by two of these lines grew more rapidly and metastasized sooner and in a higher percentage of the animals than those due to the third line, which grew at a relatively reduced speed; the tumors caused by the original species grew very slowly. Both the original cells and the derived lines were found to contain the same amount of neoantigen of SV_{40}. Morphological testing and transplantation immunization study of the original HK7 and of one of its derivatives HK7T1 revealed differences in the growth rate in a cell culture; the first ones tended to grow close to each other and looked like epithelial cells while the latter spread and resembled fibroblasts. Their appearance and growth characteristics remained constant through many transfers. The HK7T1 was found to possess a more powerful antigen and to be better suited for immunization. These findings may be of importance for studies on immunization against tumors. (TTT)

42306 FREQUENCY OF ANTIBODY TO HEPATITIS-ASSOCIATED ANTIGEN AS MEASURED BY A NEW RADIOIMMUNOASSAY TECHNIQUE. Lander, Jerrold J.; Alter, Harvey J.; Purcell, Robert H. (National Inst. of Allergy and Infectious Diseases, Bethesda, Md. National Institutes of Health, Bethesda, Md.). J. Immunol.; 106: No. 5, 1166-71(May 1971).

A modification of the radioimmunoassay procedure for measuring antibody to hepatitis-associated antigen (HAA) using a double antibody precipitation method in a microtiter system is described. The test is 2,000 to 500,000 times more sensitive than complement fixation and is reproducible and specific for anti-HAA. The frequency of anti-HAA was 14.4% in voluntary blood donors, 22.6% in commercial blood donors, 14.8% in blood bank personnel, 11.4% in laboratory personnel and 82.6% in persons given multiple transfusions. The high frequency anti-HAA in persons with no history of hepatitis or parenteral exposure to blood suggests that HAA-positive hepatitis is endemic in the United States and that it is transmitted by a non-parenteral route. (auth)

42307 EFFECT OF ACUTE RADIATION EXPOSURE RATES ON FORMATION OF HEMAGGLUTINATING ANTIBODY IN MICE. Carlson, Donald E.; Gengozian, Nazareth (Oak Ridge Associated Universities, Inc., Tenn.). J. Immunol.; 106: No. 5, 1353-62(May 1971).

The acute radiation exposure rate is a critical determinant for suppression of the hemagglutinin response in irradiated mice. It was found that this exposure-rate dependence of the immune response varied with: the total radiation dose, the time of radiation exposure relative to antigen injection, and the antigenic challenge, either as antigen dosage or species (red blood cell) of antigen. Maximum radiation-rate antibody sensitivity occurred 12 hr after antigen injection. Under these conditions, 700 R at either 40 R/min or 72 R/min suppressed the response by a factor of 68 below the same total dose at 8 R/min. This highly significant difference in the exposure-rate-dependent period together with the kinetics of killing curves for transferred spleen cells suggested that one or more populations of immunocytes may be differentially inactivated. The absence of a correlation between mortality rate and the hemagglutinin response as a function of exposure rate suggested that radiation-death itself is not a measure of immune incompetence. (auth)

42308 DETECTION OF AUSTRALIA ANTIGEN BY RADIOIMMUNOASSAY. Aach, Richard D.; Grisham, Joe W.; Parker, Charles W. (Washington Univ., St. Louis). Proc. Nat. Acad. Sci. U. S. A.; 68: No. 5, 1056-60(May 1971).

A double-antibody radioimmunoassay has been developed for the detection of Australia antigen and antibodies to Australia antigen in human sera. The assay is simple to perform, and can be completed in 18 hr. Based on parallel studies of human sera, it is approximately 2000 times more sensitive than agar gel diffusion and 200 times more sensitive than quantitative complement fixation. Australia antigen or antibody to Australia antigen was demonstrated in 22 of 23 single serum samples obtained from patients acutely ill with the long-incubation form of hepatitis; eight of the sera were negative when evaluated by less sensitive techniques. (auth)

42309 IN VITRO DETECTION OF CYTOTOXIC CELLULAR IMMUNITY AGAINST TUMOR-SPECIFIC ANTIGENS BY A RADIOISOTOPIC TECHNIQUE. Jagarlamoody, S. M.; Aust, J. C.; Tew, R. H.; McKhann, C. F. (Univ. of Minnesota, Minneapolis). Proc. Nat. Acad. Sci. U. S. A.; 68: No. 6, 1346-50(Jun 1971).

[^{3}H]Thymidine-labeled tumor cells are used to evaluate the cytotoxic cellular immune response against tumor-specific antigens; the loss of label due to destruction and detachment of target cells from the surface of the culture vessel is measured.

Spleen cells from mice immunized against Moloney virus-induced rhabdomyosarcoma specifically destroyed the sarcoma cells, while cells from normal syngeneic mice did not. Peripheral blood lymphocytes from patients with malignant tumors were specifically cytotoxic to autologous tumor cells and to allogeneic tumor cells histopathologically identical to the autologous tumor, but not to autologous nonmalignant fibroblasts, or to allogeneic tumor cells from a histologically dissimilar tumor. Serum from the same patients specifically protected autologous tumor cells from lymphocyte cytotoxicity. This serum-mediated protection of tumor cells against autologous cellular immunocytotoxicity also extended to histologically identical allogeneic tumor cells. Cross-reactivity of anti-tumor cellular immunocytotoxicity in vitro, and its "blocking" by autologous serum, strongly suggest the presence of common tumor antigens. The antagonism demonstrated in vitro between serum and cellular immunity may explain the continued growth of malignant tumors in the face of demonstrable cellular immunity. (auth)

42310 RADIATSIONNAYA IMMUNOLOGIYA I TRANSPLANTATSIYA. (Radiation Immunology and Transplantation). Petrov, R. V.; Zaretskaya, Yu. M. Moscow; Atomizdat (1970). 544p.

The characteristics and basis of radiation immunology as an individual scientific discipline at its present stage of development are given. The effects of radiation on antibody production and antimicrobial immunity and on noninfectious immunity (at the cellular and subcellular levels) are considered. Special attention is given to the effects of radiation on transplantation immunity, immunity, immunological tolerance, and the interrelations of the donor and recipient. The book is designed for a wide range of investigators working in the fields of radiobiology, immunology, or related areas associated with the application of radiological and immunological methods. It is also designed for investigators and practical workers associated with the transplantation of tissues and organs, as well as for students, postgraduate biologists, and doctors. (73 tables, 1372 references, and 106 illustrations.) (tr-auth)

42311 TRANSFER OF IMMUNITY TO HYMENOLEPIS NANA IN MICE WITH SPLEEN CELLS OR SPLEEN CELL FRACTIONS. Liu, Ching Lung. Norman, Okla.; Univ. of Oklahoma (1970). 62p. University Microfilms Order No. 71-12,591.

Thesis.

Transfer of immunity to Hymenolepis nana was investigated in laboratory mice. Donor mice were immunized by various routes. Spleen cells or spleen cell fractions from immunized donors were injected into normal syngeneic recipients which were pre-irradiated (950R) or untreated. All mice were challenged with approximately 5,000 H. nana eggs orally 20 days after injection of the cells or the cell fractions. The degree of immunity induced in the recipient animals was determined by comparison of infection rates in these mice with those in controls. Mice could be immunized to H. nana by administration of eggs via the intraperitoneal, intravenous, or oral route, or by several combinations of oral and intraperitoneal egg doses. The effect of pre-irradiation of the recipients on adoptive transfer of immunity was studied. A higher level of adoptive immunity to H. nana was transferred to x-irradiated spleen-cell recipients than to non-irradiated cell recipients. In mice challenged three weeks after 950R irradiation and spleen cell implantation, the susceptibility to H. nana infection was the same as in normal mice. Thus, either 950R x-radiation had no effect on the natural immunity or if there was some loss of natural immunity it was regained by the time of the egg challenge 20 days after spleen cell implantation. Normal spleen cells and spleen cells from donors given intraperitoneally injected eggs were both effective in the restoration of immune capacity in otherwise lethally irradiated recipients, and in promoting persistence of pre-irradiation-acquired immunity. The results of an experiment in which spleen cells were transferred from immunized donors to irradiated, allogeneic recipients indicate that, if immunizing antigen was transferred with the spleen cells in the adoptive immunity experiments, the amount was insufficient to actively immunize non-irradiated recipients. Resistence to H. nana was induced in non-immunized mice by the injection of spleen-cell fractions from immunized donors. Unlike adoptive transfer of immunity with intact spleen cells, irradiation of the recipients and injection of normal spleen cells did enhance the induced immunity. (Diss. Abstr.)

42312 PREPARATION AND EVALUATION OF VARIOUS RADIOACTIVE METALLOPORPHYRINS FOR SELECTIVE LYMPHATIC ABLATION. Fawwaz, Rashid Adib. (Berkeley, Calif.; Univ. of California (1970). 148p. University Microfilms Order No. 71-9809.

Thesis.

The present experiments demonstrate a selective deposition of certain metallo-hematoporphyrins in lymph nodes with lesser concentration in thymus and other radiosensitive structures as bone marrow and intestinal mucosa. The kinetics and in vivo distribution of a variety of radioisotopic metallo-hematoporphyrins were studied and it was determined that ^{109}Pd, a predominantly beta-emitting radioisotope, chelated to hematoporphyrin or protoporphyrin IX showed the greatest promise for selective lymphatic ablation. The effect of metallo-hematoporphyrin was studied. It was found that within limits, the localization of ^{109}Pd-hematoporphyrin in lymph nodes increased with the administration of increased carrier doses of hematoporphyrin or metallo-hematoporphyrin. This result suggested that maximum lymph node irradiation can be obtained if the subject is initially given a loading dose of hematoporphyrin or metallo-hematoporphyrin prior to the administration of ^{109}Pd-hematoporphyrin chelate. As an initial test for the efficacy of lymphatic ablation using this material, dogs were given a sufficient amount of ^{109}Pd-hematoporphyrin to deliver an average dose of 1000 rads to mesenteric lymph nodes, 400 rads to popliteal lymph nodes, 200 rads to bone marrow, 100 rads to intestinal mucosa, and 10 rads to the thymus. Subsequent to such irradiation there was massive destruction of mesenteric lymph nodes. However, minimal histologic changes were noted in the remaining tissues of the body. The results described in this work suggest the usefulness of the ^{109}Pd-hemato or protoporphyrin complexes in selective irradiation of lymphatic tissues and possibly in control of homograft rejection response. (Diss. Abstr. Int., B)

42313 EFFECT OF TRANSPLANTED LYMPHOID CELLS, IRRADIATION, AND DRUG THERAPY ON PERMANENT IMMUNOLOGIC TOLERANCE. Larsen, Joergen Hannover (Copenhagen County Hospital. Univ. of Copenhagen). J. Immunol.; 107: No. 1, 185-94(Jul 1971).

Abolition of the permanent and constant tolerance to lymphocytic choriomeningitis (LCM) virus in inbred mice has hitherto only been possible by transplantation of syngeneic, sensitized or unsensitized lymphoid cells to the tolerant virus-carriers. A series of experiments showed that no essential difference exists between lymphoid cells isolated from the spleens, lymph nodes, or buffy coat of hyperimmune, syngeneic mice in their ability to abolish the tolerance of virus-carrier recipients after transplantation. Large numbers of unsensitized thymus cells were without effect. Sensitized bone marrow cells only had a slight effect. Fetal liver cells were without effect. Using the same system with transplantation of lymphoid cells an Eichwald-Silmser effect was found in the highly inbred strain of C3H mice that was used. Large doses of transplanted, killed, syngeneic or living xenogeneic cells had no effect on the tolerance, nor did x irradiation or treatment with cortisone or methotrexate. Syngeneic, sensitized lymphoid cells in Millipore chambers implanted into tolerant virus-carriers conferred the ability to produce antibody, but the viremia was not essentially affected. (auth)

Ecology

Refer also to abstracts 42245, 42249, 42256, 42260, 42370, 42373, 42377, 42378, 42380, 42381, 42383, 42388, 42393, 42394, 42691–42693, 42717, 42718, 44138, 44143, and 44147.

42314 (CONF-710511-3) PRELIMINARY ECOLOGICAL STUDIES AT JERVIS BAY. Giles, M. S. (Australian Atomic Energy Commission Research Establishment, Lucas Heights). 1971. 22p. Dep. NTIS (U. S. Sales Only).

From forty-third congress of the Australian and New Zealand association for the advancement of science; Brisbane, Australia (24 May 1971).

The philosophy behind and the present status of the preliminary biological studies connected with the proposed installation of a 500 MW nuclear power station at Jervis Bay are presented. Results are included of studies on terrestrial and marine ingestion routes, population statistics for weedbeds and littoral communities, plankton productivity, chlorophyll "a" content of seawater, and zooplankton biomass. (auth)

42315 (ORNL-NSIC-89) BIOLOGICAL CONCENTRATION AND TURNOVER OF RADIONUCLIDES IN FOOD CHAINS: A BIBLIOGRAPHY. Reichle, D. E.; Nelson, D. J.; Dunaway, P. B. (Oak Ridge National Lab., Tenn.). Jul 1971. Contract W-7405-eng-26. 42p. (ORNL-TM-2492). Dep. NTIS.

One-hundred and ninety-six references are presented to literature published through 1970 on radioisotope transport through food chains and concentration by fish, invertebrates, and mammals. (C.H.)

42316 (ORO-3299-107) EFFECTS OF IONIZING RADIATION ON PLANT SPECIES, POPULATIONS AND ECOSYSTEMS. Progress Report, September 1, 1970–August 31, 1971. McCormick,

XUM

J. Frank (North Carolina Univ., Chapel Hill). Contract AT(40-1)-3299. 18p. Dep. NTIS.

Objectives of the research were to analyze the effects of gamma and beta radiation on the physiology, morphology, growth, and survival of plant species and to analyze effects on natural ecosystems. Results are reported for the following projects: effects of gamma radiation and ozone on pine seedlings and trees; field investigations of dominant plant species; effects of beta radiation from simulated fallout on the reproductive potential of a dominant plant species (Viguiera porteri) in a natural community; population dynamics of Viguiera porteri and Euterpe globosa; quantitative descriptions of a northern hardwood forest ecosystem in Wisconsin; growth rates of pioneer species in rain forest at El Verde; and effects of beta radiation from simulated fallout on a natural ecosystem. (H.L.W.)

42317 (PRNC-147) THE RAIN FOREST PROJECT. Annual Report. Clements, Richard G.; Drewry, George E.; Lavigne, Robert J. (Puerto Rico Nuclear Center, Mayaguez). Jun 1970. Contract AT(40-1)-1833. 142p. Dep. NTIS.

Forest ecology studies included a determination of the quantitative relationships between gross rainfall as measured above the canopy and the parameters of throughfall and stemflow yield, litter interception and evaporation, and soil moisture changes. Information obtained from these studies will be used for designing radioisotope cycling studies. A versatile stemflow collar for interception studies on large scale rainfall is described. Studies on forest recovery following gamma irradiation included a census of all plants growing in a sample plot inside the area of damage from a 1965 ^{137}Cs gamma irradiation. Graphs are presented to show composite ratios of vines and old trees in the irradiated area for 1969 and composite ratios of new vegetation in the irradiated area for 1966, 1967, and 1969. Studies on the role of amphibians in the ecology of the Puerto Rican rain forest included classification and geographic distribution, microhabitat, reproductive behavior, vocal organization, and evolutionary relationships. Studies on niche definition and energy flow included monitoring of frogs for uptake of ^{134}Cs, ^{54}Mn, and ^{85}Sr. In other experiments lichens, algae, and bryophytes associated with tree trunks were labeled with ^{65}Zn and uptake by frogs, lizards, and snails was monitored. Large canopy trees were injected with ^{137}Cs, ^{54}Mn, ^{86}Rb, and ^{85}Sr; frogs and lizards foraging on the trees were monitored and lizards showed measurable uptake of ^{85}Sr. Progress is also reported on feeding behavior of frogs and lizards in the tropical wet forest; ecology of ants in the Luquillo Forest; the role of insects in the food web of the tropical wet forest; properties of aquatic communities in container habitats; studies on the chemistry of the tropical maritime atmosphere; karyotypic studies of bats of the family Phyllostomatidae; arrested succession in tropical, terrestrial ecosystems; field studies on the Puerto Rican tody; the termites at El Verde, polyethism in workers of Nasutitermes costalis; occurrence and distribution of aquatic fungi in the El Verde forest; and radiotracer studies on nutrient cycling. (H.L.W.)

42318 (TID-25735) ENVIRONMENTAL STATEMENT CANNIKIN. (Atomic Energy Commission, Washington, D. C.). Jun 1971. 111p. Dep. NTIS.

Cannikin is a proposed underground nuclear test of less than five megatons to be fired about 6,000 feet underground in a fully stemmed hole on Amchitka Island, Alaska, in the autumn of 1971. Preparatory to Cannikin, a test called Milrow, which had a yield of about one megaton, was conducted on Amchitka on October 2, 1969. Its sole purpose was to obtain data concerning the physical and biological effects of a high-yield underground explosion upon the Amchitka environment, and to provide an experimental basis for prediction of Cannikin effects. Milrow behaved about as predicted and did not have any important long-term impact on the environment. The observed Milrow effects provided valued evidence that Cannikin can also be fired without important detrimental impact. The principal environmental effects expected from Cannikin are those resulting from occupation of Amchitka by a work force of some hundreds of men. The most probable effects of the Cannikin explosion itself should be localized, with little alteration to the surface conditions or any long-term damage to biological populations. Both the most probable effects and the worst conceivable effects of Cannikin are postulated. (C.H.)

42319 BEHAVIOR OF RADIOACTIVE FISSION PRODUCTS IN SOME SOILS OF THE SIEROZEM ZONE OF UZBEKISTAN. Gulyakin, I. V.; Dergunov, I. D.; Moroz, V. D. Izv. Timiryazev. Sel'skokhoz. Akad.; No. 1, 84-93(1968). (In Russian).

Samples of sierozem and meadow soils (0.5 g) were treated with solutions (10 ml) containing 5×10^{-4} mCi of ^{90}Sr, ^{137}Cs, and ^{144}Ce. Following determination of the residual activity of the samples, they were leached with solutions of $CaCl_2$, KCl, NaCl, NH_4Cl, and NaOAc, and with water (control). The salt solutions leached very little ^{144}Ce and practically all of the ^{90}Sr. Large amounts of ^{137}Cs were leached with KCl and NH_4OAc. The adsorption of ^{90}Sr and ^{137}Cs was independent of the soil type and its salinity. They were most effectively removed from the soil by NH_4OAc. The addition of Sr in amounts up to 1000 mg/kg of soil had no effect on the adsorption of ^{90}Sr, but large amounts increased ^{90}Sr desorption. Cotton plants grown on previously leached typical sierozem developed normally. The ^{90}Sr uptake by these plants was half that of plants grown on water leached soils. (E.R.B.)

42320 ECOLOGICAL EFFECTS OF ACUTE BETA IRRADIATION FROM SIMULATED FALLOUT PARTICLES UPON A NATURAL PLANT COMMUNITY. Murphy, Peter George. Chapel Hill, N. C.; Univ. of North Carolina (1970). 165p. University Microfilms Order No. 71-11,732.

Thesis.

Simulated fallout particles overcoated with yttrium-90 were applied at two levels of radioactivity to granite outcrop plant communities. The experiment resembled conditions expected at a site 170 miles downwind of a 2.5 megaton detonation with a wind velocity of 15 mph. Mean community dose levels were 7,000 and 4,000 rads. In the 7,000 rad communities the ratio of mean ground surface dose (8,770 rads) to mean canopy dose (5,092 rads) was 1.7. In the 4,000 rad communities the mean ground surface dose (4,824 rads) was 1.6 times higher than the mean canopy dose (2,996 rads). In the 7,000 rad communities the death of 46% of all terminal buds in the dominant Viguiera porteri (A. Gray) Blake resulted in a 37% height growth reduction, a compensatory lateral branch development, a 24% reduction in community biomass (585.0 g/m^2), and a lower, more clumped, vertical distribution of leaves in the canopy. In the same communities 46.6% of the V. porteri flower heats were aberrant and 35.9% produced fewer and less vigorous seed. Comparison with earlier studies indicated that acute beta irradiation is two to three times more effective than gamma irradiation, at equivalent doses, in causing height growth reduction in V. porteri. No radiation induced change in the metabolism of the outcrop ecosystem was detected through measurements of CO_2 exchange rates 43 days following fallout dispersal. The mean rate of net production on clear days in both July and September, between the hours of 9:30 AM and 4:40 PM, was 1.2 gC/m^2hr. Early nighttime rates of respiration (9:30 PM to 10:10 PM, shown to be the period of maximum nighttime respiration rates in a previous study) averaged 2.9 gC/m^2hr in July and 2.2 gC/m^2hr in September. (Diss. Abstr.)

Genetics and Cytogenetics

Refer also to abstracts 42266, 42395, 42405, 42406, 42512, 42534, 42611, 42614, 42629, 42656, 42659, 42722, 42723, and 42755.

42321 (COO-697-23) GENETIC EFFECTS OF IRRADIATION IN THE RAT. (Wisconsin Univ., Madison). [1971]. Contract AT(11-1)-697. 23p. Dep. NTIS.

Male and female rats were given 450 R x radiation in doses of 100, 150, and 200 R at 10, 12, and 14 weeks of age and irradiation was repeated for nine generations. Random mating and full-sib mating experiments are outlined and effects of the various types of mutations are discussed as follows: dominant and recessive autosomal lethals; sex-linked recessive lethals; visible mutations; mutations affecting quantitative traits; and fertility. Other experiments using irradiated rats were conducted as follows: genetic effects of cumulative irradiation in the female rat on prenatal survival and development to the twelfth day of gestation; linkage relationships of irradiated induced mutants, spontaneous mutants, and marker genes; and effects of radiation on avoidance learning. Experiments were initiated to study the frequency of occurrence of different classes of mutants induced by a single dose of acute spermatogonial irradiation. (H.L.W.)

42322 (COO-1097-46) GENETIC CONTROL OF PHYSIOLOGICAL PROCESSES IN HIGHER PLANTS. Final Report, 1961-70. (Minnesota Univ., Minneapolis). Contract AT(11-1)-1097. 19p. Dep. NTIS.

Genotypic differences in accumulation of ^{89}Sr and ^{90}Sr were investigated using wheat (Triticum aestivum), barley (Hordeum vulgare), and soybeans (Glycine max). Results showed that entry of ^{90}Sr into the food chain could be reduced by growing varieties that are low in accumulation or that accumulate reduced amounts in edible plant parts. Experiments on wheat and barley showed that ^{89}Sr accumulation was influenced by environment and by several genes; thus the inheritance pattern is of a quantitative character. Varietal differences in concentrations of 11 mineral elements were observed in wheat, barley, and soybeans; the differences

were found in grain, in leaves of green and mature plants, and in leaves of seedling plants. Studies on wheat and barley showed that there were no varietal differences in efficiency of utilization of phosphorus or potassium. Studies were conducted on physiological and morphological bases for genotypic differences in accumulation of ^{89}Sr with emphasis on root absorption of ^{89}Sr, accumulation of ^{89}Sr in grain, translocation, and deposition. Distribution of ^{89}Sr, P, Ca, Mg, and K during growth and development was studied in wheat, barley, and soybeans. Plant-soil studies focused on establishing relative amounts and variability of ten essential mineral elements plus Sr in two soils formed in different parent materials under different climatic conditions in Minnesota. (H.L.W.)

42323 RADIATION-INDUCED HOODED EYE MUTANTS IN POTATO. Singh, Udai (Indian Agricultural Research Inst., New Delhi). Sci. Cult. (Calcutta); 36: 609-10(Nov 1970).

Induced mutagenesis is being increasingly attempted in the vegetatively propagated plants. Report is given on the hooded eyed mutants induced by γ irradiation in Kufri Kuber, a commercially important variety of potato. Healthy tubers were cut into three pieces with equal number of eyes; two pieces were treated with 6 and 10 kR, and the third served as control. The treated tubers, along with the control ones, were planted in the field; 250 tubers were treated in this way. Normally, Kufri Kuber has smooth tubers with fleet eyes. In SM_2, the second clonal generation following mutagenic treatment, a tuber line with hooded eyes instead of the normal eyes was discovered. In the tubers of the mutant, a hood or fleshy sheath developed over the eyes. (P.B.M.)

42324 MUTANTS OF GOLDEN DELICIOUS APPLE INDUCED BY IONIZING RADIATION. Lapins, K. O. (Canada Dept. of Agriculture, Summerland, B. C.). Can. J. Plant Sci.; 51: 123-31(Mar 1971).

The study of 300 selections of Golden Delicious apple from plant material irradiated with gamma rays from a ^{60}Co source resulted in the final selection of two clones that represent an improvement of the original cultivar in reduced russetting in fruit stem cavity, greatly reduced tendency to biennial bearing, and slightly lowered fertility, an advantage in Golden Delicious which tends to overset. In a single tree first trial, about 50% of the examined clones showed reduced pollen stainability; the majority of the semi fertile mutants had 51 to 55% stainable pollen. The number of seeds per fruit was very closely related to pollen fertility. A close relationship was found among indicators of fruit maturity, that is, skin color, flesh color, soluble solids, and titratable acidity of fruit at harvest. (auth) (Canada)

42325 PROBLEMS OF PROTECTION AGAINST THE GENETIC EFFECT OF RADIATION. Tazimo, Yataro (National Inst. of Genetics, Misima, Japan). pp 7-15 of Biological Aspects of Radiation Protection. /Sugahara, Tsutomu (ed). Tokyo; Igaku Shoin Ltd, (1971).

From International symposium on biological aspects of radiation protection; Kyoto, Japan (13 Oct 1969). See CONF-691041.

Based on recent advances in radiation genetics, several possible means for protection against harmful radioinduced genetic consequences to man are discussed. At present, the best methods for the protection of the genetic system are to avoid exposure or to decrease the exposure dose rate as much as possible. The effects of fractionated irradiation appear to resemble those of a decreased dose rate. However, experimental data indicate that it is dangerous from a genetic point of view unless administered with long enough intervals between doses. This reduces the opportunity for interaction of effects and allows repair of sublethal damage. Anoxia shows marked effects of dose reduction but cannot be directly applied to man. Chemical compounds may some day offer good protection against genetic damage but further work must be done. (E.E.H.)

42326 DNA POLYMERASE REQUIRED FOR RAPID REPAIR OF X-RAY-INDUCED DNA STRAND BREAKS IN VIVO. Town, Christopher D.; Smith, Kendric C.; Kaplan, Henry S. (Stanford Univ., Calif.). Science; 172: No. 3985, 851-4(21 May 1971).

A much higher yield of DNA single-strand breaks was obtained in the DNA polymerase-deficient mutant Escherichia coli K-12 pol A1 after a given dose of x-rays than had been found before in Escherichia coli. The increased yield of single-strand breaks was due to the absence of a rapid repair system, which had not been described in Escherichia coli K-12. This absence probably accounts for the x-ray sensitivity of the pol A1 mutant. The rapid repair system can be reversibly inhibited in pol$^+$ cells. (auth)

42327 OBTAINING NEW TYPES OF DAHLIA BY INDUCED MUTATIONS. Lantin, B.; Decourtye, L. Pepinieristes, Hort., Maraichers; No. 99, 5875-8(Aug-Sep 1969). (In French).

Irradiation techniques have been used for several years on a number of ornamental and fruit species for the purpose of inducing mutations while maintaining the essential qualities of the plant treated. Following an experiment on fruit trees, an attempt was made to utilize the method for research on new coloring of a flower species such as the dahlia (D. variabilis). The growing of this species does not present any particular difficulties. Its abundant flowering makes possible the detection of mutants from the first year, and the possibilities of vegetative multiplication assure the isolation and conservation of these new types. (tr-auth)

42328 GENETIC LOCATIONS OF uvrD AND pol GENES OF E. COLI. Ogawa, Hideyuki (Osaka Univ.). Mol. Gen. Genet.; 108: 378-81(23 Nov 1970).

Two mutants, Escherichia coli K12 N214 and N611, with similar properties were found in a stock of radiosensitive mutants that were isolated from survivors of W3623 after infection with γ-irradiated T1 phages. Some properties of these pol mutants are described in comparison to those of the wild type and uvrD bacteria. The pol mutant lacks uv reactivation ability for uv-irradiated λ phage. Precise locations of uvrD and pol genes were clarified by P1 transduction. Co-transduction frequencies of various markers with metE were determined and results are tabulated. Radiosensitivity of E. coli mutants is discussed. It was established that uvrD is located between metE and ilv genes, and pol is located near metE between metE and rha genes. (H.L.W.)

42329 ON SOME MORPHOLOGICAL AND PHYSIOLOGO-BIOCHEMICAL CHANGES IN M_1 OF THREE PEA VARIETIES AS AFFECTED BY GAMMA RAYS ^{60}Co. Petkov, V.; Georgiev, Z.; Topchieva, A. (Forage Research Inst., Pleven, Bulgaria). Genet. Selek.; 2: No. 6, 491-502(1969). (In Bulgarian).

Results obtained from investigations of the influence of ^{60}Co gamma rays on some morphological and biochemical changes in F_1 of the pea varieties Hödinger (Pisum arvense), Funduleci and Volodman Gunduleci (P. sativum) are discussed. The following inferences are drawn: Pea varieties differing in origin and morphological peculiarities have different radiosensitivity to ^{60}Co gamma rays. The critical dose (after Gustavson) for the varieties Funduleci and Hödinger is about 7.5 kR and for the varieties Volodman Gunduleci about 10 kR. Greatest radiosensitivity (after Hangildin) at dose of 10 kR is shown with regard to Volodman Gunduleci (50.44 per cent), followed by Hödinger (46.75 per cent) and Funduleci (33.52 per cent). The chromosome aberration frequency is different in different varieties and at irradiation in different doses. As the doses of irradiation increase the frequency of normal anaphases becomes greater. Greatest frequency of chromosome aberrations was found in Funduleci variety followed by Volodman Gunduleci while lowest frequency was found in Hödinger variety. The results in relation to field germination, plant height at full maturity, yield elements as well as in relation to stems and roots of plants grown in nutrient medium are related to those of the cytological analysis. An enhanced frequency of chromosome disturbances is accompanied by a decrease in the values of the observed characteristics. Irradiation causes considerable changes in the nitrogen exchange of plants. They are expressed by an increased total and protein nitrogen content of irradiated plants. At the same time radiation enhances the intensity of the oxidizing processes as a result of which the intensity of respiration increases in irradiated seeds and in plants grown from them. (auth)

42330 INCREASE IN THE RADIORESISTANCE OF A THYMINE-DEPENDENT STRAIN OF E. COLI K-12 (THY-) UNDER THE INFLUENCE OF GAMMA IRRADIATION. Pershina, Z. G.; Tumanyan, M. A.; Samoilenko, I. I.; Molchanova, E. I. (Inst. of Epidemiology and Microbiology, Moscow). Zh. Mikrobiol., Epidemiol. Immunobiol.; 46: 101-6(Oct 1969). (In Russian).

As a result of γ-irradiation there were revealed mutants of Escherichia coli K-12 (thy$^-$) with increased radioresistance. Bacterial cultures obtained differed from the initial strain by a number of morphological and physiological characteristics. The strain obtained tolerated radiation in a dose of 1 mrad., stained indefinitely by Gram, lost the capacity to ferment glucose, mannite and maltose, and acquired the capacity to ferment saccharose. Radioresistant mutants agglutinated in a high titre by immune sera against the initial strain of bacteria. Immune sera against the radioresistant mutants agglutinated both the radioresistant strain and the initial culture. The mutants with increased radioresistance acquired a higher sensitivity to penicillin. Mutants with increased radioresistance retained their capacity to recombinations with a radiosensitive recipient culture. (auth)

42331 X-IRRADIATION SENSITIVITY IN ESCHERICHIA COLI DEFECTIVE IN DNA REPLICATION. Fangman, Walton L.; Russel, Marjorie (Univ. of Washington, Seattle). Mol. Gen. Genet.; 110: No. 4, 332-47(11 May 1971).

XUM

A mutant of Escherichia coli with a temperature sensitive defect in DNA replication is sensitive to x-irradiation but not to uv-irradiation. After uv-irradiation, dark-repair processes—dimer excision, DNA breakdown, repair synthesis and DNA strand joining—appear normal at the restrictive temperature. After x-irradiation, DNA degradation exceeds that in the wild type, and irradiation-dependent DNA synthesis does not occur. Single-strand breaks introduced into the DNA by the irradiation are not repaired. The data indicate that the mutation results in a defect in repair of x-ray induced single-strand breaks as well as a defect in DNA replication. They provide evidence for the existence of a repair pathway for x-irradiated DNA similar to, but at least partially independent from, that postulated for the dark-repair of uv-irradiated DNA, viz., degradation at the site of the lesion, resynthesis of the degraded DNA complement and ligation of the DNA strand. (auth)

42332 EFFECT OF CAFFEINE ON MUTATION AND RECOMBINATION IN SCHIZOSACCHAROMYCES POMBE. Loprieno, Nicola (Univ., Pisa, Italy. CNR, Pisa, Italy); Schuepbach, Martin. Mol. Gen. Genet.; 110: No. 4, 348-54(11 May 1971).

In Schizosaccharomyces pombe the experiments performed in order to assess some possible influence of caffeine on biological processes related to the induced or spontaneous mutations and meiotic recombinations have shown that caffeine decreases uv- and NG-induced forward mutations at ad-6 and ad-7 loci and uv-induced reverse-mutations of his^- mutants whereas spontaneous mutations to adenine or histidine independence were not affected; intergenic meiotic recombinations in the MT chromosomal region were also decreased when caffeine was present in the crossing medium. (auth)

42333 INDUCTION OF TRANSLOCATIONS IN MATURE DROSOPHILA OOCYTES OVER A DOSE RANGE OF 10 TO 500 ROENTGENS OF X RAYS (STAGE-14 OOCYTE/RADIATION DAMAGE). Abrahamson, S.; Gullifor, P.; Sabol, E.; Voigtlander, J. (Univ. of Wisconsin, Madison). Proc. Nat. Acad. Sci. U. S. A.; 68: No. 6, 1095-7(Jun 1971).

Data are presented that demonstrate that a dose of 10 R of x rays to mature oocytes in Drosophila causes a significant increase, more than double the spontaneous frequency, of inherited translocations. The dose-frequency relationship appears to fit best a linear response between 10 and 50 R. From 50 to 500 R, the frequency of rearrangements increases at the conventional dose 3/2 relationship. (auth)

42334 COMPARATIVE RADIOMIMETIC EFFECT OF EMULSIN, CYCASIN, METHYLAZOXYMETHANOL, AND X RAYS IN ZAMIA INTEGRIFOLIA. Porter, E. D.; Teas, H. J. (West Georgia Coll., Carrollton. Univ. of Miami, Coral Gables, Fla.). Radiat. Bot.; 11: 21-6(1971).

Root tips of Zamia integrifolia were treated with cycasin (an azoxyglycoside), emulsin (β-glucosidase), an incubated mixture of cycasin and emulsin, methylazoxymethanol (the aglycone of cycasin) and x rays (100, 200, 300 and 500 R at 80 R/min). Tissues of Zamia contain both azoxyglycosides and emulsin. Allium cepa roots were treated and used as a non-cycad control. The incidence of anaphase bridges was used as an index for comparisons. Chemical and radiation treatments resulted in significant increases in the incidence of chromosome bridges in both Zamia and Allium. Differences in results between treatments and between Allium and Zamia indicated that in the intact Zamia the emulsin and cycasin were not active radiomimetically. However, cycasin and emulsin as well as MAM produced significant damage in the intact root cells when treated, indicating some protective mechanism, either compartmentalization or chemical inhibition, in the intact plant in normal conditions. (auth) (UK)

42335 INHERITED SEMISTERILITY FOR CONTROL OF HARMFUL INSECTS. I. PRODUCTIONS OF SEMISTERILITY DUE TO TRANSLOCATION IN THE MOSQUITO, CULEX PIPIENS L., BY X RAYS. Laven, H.; Jost, E. (Johannes-Gutenberg Univ., Mainz). Experientia; 27: No. 4, 471-3(15 Apr 1971).

Chromosome translocations were induced in male Culex pipiens by x radiation. These mosquitoes were used for outcrossing and backcrossing experiments and dose-response curves were determined for dominant lethality and semisterility in the F_1 generation. Semisterility occurred with doses from 3500 to 5000 R. Data are compared with results of similar experiments on Drosophila. Possible mechanisms for translocation production in mosquitoes are discussed. (H.L.W.)

42336 SOMATIC RECOMBINATION IN THE COMMON-AB DIPLOID OF SCHIZOPHYLLUM COMMUNE. Mills, Dallice I. Ellingboe, Albert H. (Michigan State Univ., East Lansing). Contract AT(11-1)-1301. Mol. Gen. Genet.; 110: No. 1, 67-76(2 Mar 1971).

A recessive suppressor, su-1, of arg-2 was used to detect somatic recombination in common-AB diploids of S. commune. Recombinants were recovered from dense, fast-growing sectors on arginine-deficient medium. The majority of spontaneous recombinants (129/154) recovered in this study were apparently haploid. Strains which scored as aneuploid and diploid were also recovered and analyzed. Genetic analysis of spontaneous recombinants indicated that crossing over is rare and that haploidization very likely proceeds via stages of aneuploidy. No increase in the frequency of crossing over was detected in recombinants derived following treatment with UV light. The preliminary results favor a parasexual mechanism of recombination in common-AB diploids. (auth)

42337 UV-SUPERSENSITIVE MUTANT IN THE YEAST SCHIZOSACCHAROMYCES POMBE. EVIDENCE FOR TWO REPAIR PATHWAYS. Fabre, F. (Institut du Radium-Biologie, Orsay, France). Mol. Gen. Genet.; 110: No. 2, 134-43(29 Mar 1971).

A highly uv-sensitive mutant was obtained from a uv-sensitive strain of the yeast Schizosaccharomyces pombe after a mutagenic treatment. By genetic analysis, it was possible to distinguish two independent loci. The double mutant is supersensitive, that is more uv-sensitive than either of the two single mutants. This suggests that the mutations involved interfere with two repair pathways that are, at least partially, independent of each other. Some properties of the two single mutants were studied. These mutants differ notably in their response to caffeine, to liquid-holding, to exposure to visible light after uv irradiation, and in their uv-sensitivity during the logarithmic growth phase. Comparison of the properties of the wild-type strain and of the different uv sensitive mutants leads to the conclusion that one repair pathway is used preferentially in the wild-type strain. (auth)

42338 RESPIRATION DEFICIENT MUTANTS OF SCHIZOSACCHAROMYCES POMBE I. Wolf, K.; Sebald-Althaus, M.; Schweyen, R. J.; Kaudewitz, F. (Univ., Munich). Mol. Gen. Genet.; 110: No. 2, 101-9(29 Mar 1971).

By use of N-methyl-N′-nitro-N-nitrosoguanidin (NG) respiration deficient (RD) mutants were induced. They could be selected by replica-plating on glycerol medium. RD mutants were also induced by uv irradiation, enriched by use of 2,3,5-triphenyltetrazolium chloride (TTC) and tested for their inability to grow on glycerol medium. The RD mutants were characterized enzymatically for their decrease or loss in cytochrome c oxidase activity and in succinate- cytochrome c reductase activity. These assays allowed the localization of the mutational blocks in complexes II, III and IV of the respiratory chain. Tetrad analysis and random spore analysis demonstrated that all mutants contained chromosomal defects. (auth)

42339 REPAIR OF UV-INDUCED MUTATIONS IN PHAGE T4. Azizbekyan, R. R.; Pogosov, V. Z. (Inst. of Genetics and Selection of Industrial Microorganisms, Moscow). Biochem. Biophys. Res. Commun.; 43: No. 6, 1402-7(18 Jun 1971).

Introduction of mutations in V and X genes into genome of T4 rII phage remarkably increased uv-induced mutability. Mutator alleles of gene 43 increased the number of spontaneous rII^+-reversions, but did not affect the frequency of uv-induced reversions. (auth)

42340 INDUCTION OF PROPHAGE λ IN A MUTANT OF E. COLI K12 DEFECTIVE IN INITIATION OF DNA REPLICATION AT HIGH TEMPERATURE. Monk, Marilyn; Gross, Julian (Univ. of Edinburgh). Mol. Gen. Genet.; 110: No. 4, 299-306 (11 May 1971).

Prophage λ is not induced when DNA synthesis ceases at 42°C in a mutant of Escherichia coli which is unable to initiate rounds of DNA replication at high temperature. However, induction occurs when the cells are uv irradiated after completion of rounds of replication at 42°C. Evidence is presented that the uvr functions, necessary for dimer excision, are not required for this induction, and that the uv irradiation itself does not provoke net host DNA synthesis under these conditions. We conclude that prophage induction can result from irradiation damage in chromosomes that are unable to replicate. (auth)

42341 IDENTIFICATION OF THE GENETIC ALTERATION AT THE MOLECULAR LEVEL OF ULTRAVIOLET LIGHT-INDUCED ad-3B MUTANTS IN NEUROSPORA CRASSA. Kilbey, B. J.; de Serres, F. J.; Malling, H. V. (Oak Ridge National Lab., Tenn.). Mutat. Res.; 12: No. 1, 47-56(May 1971).

The genetic alterations in uv-induced ad-3B mutants of Neurospora crassa were identified by tests for specific revertibility

after treatment with nitrous acid (NA), ethyl methanesulfonate (EMS), hydroxylamine (HA), and a monofunctional nitrogen mustard derivative of acridine, ICR-170. On the basis of their reactions with these chemicals, mutants were classified as base-pair transitions, base-pair transversions, base-pair insertions or deletions, or nonrevertible. A random sample of 151 uv-induced ad-3B mutants were analyzed: 46 with nonpolarized and 49 with polarized complementation patterns and 56 that are noncomplementing. The mutants were characterized as to reversion mechanism as follows: base-pair transitions AT → GC, 27.7%; GC → AT, 8.0%; base-pair transversions, 6.6%; base-pair insertions or deletions, 27.0%; nonrevertible, 8.6%; and mutants that revert only spontaneously, 22.1%. The correlation between complementation pattern and genetic alteration at the molecular level found previously by Malling and De Serres among Na- and EMS-induced ad-3B mutants, was also found among uv-induced mutants. Mutants with nonpolarized patterns resulted mainly from base-pair substitutions, whereas mutants with polarized complementation patterns and noncomplementing mutants are derived from a variety of genetic alterations. (auth)

42342 LIFETIME REPRODUCTIVE CAPACITY IN OFFSPRING OF AN IRRADIATED MOUSE POPULATION. Sheridan, William (Lab. of Radiation Genetics, Stockholm). Mutat. Res.; 12: No. 1, 81-90(May 1971).

Unirradiated offspring of the 14th generation of an irradiated mouse population in which the males of each generation had received 276 R to the spermatogonia, and offspring of the parallel control population were tested in single pair matings for lifetime reproductive performance. The offspring of the irradiated population showed a significant tendency towards lower age at 1st litter that was interpreted as a sign of earlier sexual maturity. This group also exhibited an overall mean litter size lower than that of the control that was attributable to the presence of semi-sterile animals among the pairs tested. An examination of the sex proportion based on the total material showed a significant downward shift for the irradiated population offspring when compared with the control. However, pedigree studies and analysis of sex proportion in relation to litter size led to the conclusion that the observed change was not due to the presence of sex-linked recessive lethals. The overall effects of ancestral irradiation on reproduction were found to be exceedingly small, which was in keeping with results obtained from other studies of irradiated populations. It was therefore concluded that a reduction of reproductive capacity may not play any great role as a selective factor in the removal of induced genetic damage from an irradiated population. (auth)

42343 VISUALIZATION OF ACHROMATIC LESIONS (GAPS) INDUCED BY X-RAYS IN CHROMOSOMES OF VICIA FABA BY STAINING OF CHROMOSOMAL PROTEINS. Scheid, W.; Traut, H. (Univ., Muenster, Ger.). Mutat. Res.; 12: No. 1, 97-9 (May 1971).

A method is described for the visualization of x-radioinduced achromatic lesions (gaps) in chromosomes of Vicia faba by staining of the chromosomal proteins with protein-specific dyes. Ten-day old seedlings of V. faba were irradiated and the chromosomes isolated. Most of the gaps observed were induced in late interphase or early prophase. The isolated chromosomes were then stained with the protein-specific dyes Fast Green or Naphthol Yellow S or with the DNA-specific Feulgen Reagent. For each staining series, the ratio of the number of chromosomes without gaps, with gaps, and with semi-gaps was determined and the X^2 test was performed to determine the significance of the correlation between the ratios of the three staining series. It was concluded that x-radioinduced gaps can be visualized by the use of protein-specific dyes because not only local DNA loss, but also local protein loss is involved in the production of a gap. (E.R.B.)

42344 INDUCTION BY X-RAYS OF DOUBLE MOSAICS INVOLVING THE Y-CHROMOSOME, SUPPORTING FIRST CLEAVAGE SEGREGATION IN DROSOPHILA MELANOGASTER. Sobels, F. H.; Leigh, B. (Univ., Leiden. Cohen Inst. for Radiopathology and Radiation Protection, Leiden). Mutat. Res.; 12: No. 1, 100-1(May 1971).

New isochromosomes (compound reversed metacentrics) were induced following x irradiation of spermatozoa of Drosophila melanogaster in a previous experiment. At that time, it was concluded that chromosomal rearrangement products could segregate during the first cleavage division. To verify this, one-day-old male flies carrying a doubly marked Y-chromosome were irradiated and attempts made to recover mosaics derived from both of the segregation nuclei. The evidence obtained here, along with other phenotypic, cytological, and genetic segregation evidence, indicates not only that rearrangements do segregate during the first cleavage division, but also that both division products are involved in the development of the adult fly. (E.R.B.)

42345 5-BU SENSITIZATION TO UV-INDUCED KILLING AND MUTABILITY IN hcr^+ AND hcr^- STRAINS OF ESCHERICHIA COLI. Kondratev, Yu. S.; Skavronskaya, A. G. (Inst. for Epidemiology and Microbiology, Moscow). Mutat. Res.; 12: No. 1, 105-8(May 1971).

Escherichia coli B/r hcr^+ and hcr^- cells containing 5-BU showed increased sensitivity to uv irradiation. Sensitivity to the mutagenic effects was less pronounced compared to the lethal effects. The effects of 5-BU substitution seem to be mainly due to the enhanced number of uv-radioinduced damages in 5-BU-containing DNA. Increased uv mutability in 5-BU-containing cells may be due to the formation of some kind of 5-BU photoproducts that are not lethal and that can not be eliminated by repair enzymes although they can cause mutations (mistakes in the course of DNA replication or repair resynthesis). In the latter case, the source of such mistakes could be both 5-BU and its photoproducts located in the complementary DNA strand serving as a template for the reconstruction of the degraded region of DNA. (E.R.B.)

42346 INDUCTION OF CHLOROPHYLL MUTATIONS BY DEUTERIUM OXIDE (D_2O) IN ORYZA SATIVA L. Rao, D. M.; Reddy, T. P.; Reddy, G. M. (Osmania Univ., Hyderabad, India). Mutat. Res.; 12: No. 1, 109-11(May 1971).

The mutagenic effects of deuterium oxide (D_2O) on rice based on the criteria of M_1 seedling growth rate and M_2 chlorophyll mutation frequency were studied. A highly significant growth depression of seedlings in D_2O treatment was observed as compared to an H_2O control. Similarly, seeds presoaked in D_2O and treated with EMS showed significant growth depression compared to H_2O-presoaked seeds. Both the chlorophyll mutation and mutant frequencies were significantly higher in seeds presoaked in D_2O than in H_2O-presoaked seeds. Likewise, seeds treated with EMS showed higher frequencies following D_2O presoaking compared to H_2O presoaking. (E.R.B.)

42347 HAPLOID CELLS IN RAT KANGAROO CORNEAL ENDOTHELIUM CULTURES AND X-RAY-INDUCED CHROMOSOME ABERRATIONS. Yao, Kenneth T. S. (Dept. of Health, Education, and Welfare, Rockville, Md.). Genetics; 67: No. 3, 399-409(Mar 1971).

Many haploid cells were observed among the mitotic figures of rat kangaroo corneal endothelial cell cultures. The cultures were exposed to 250 kVcp x rays. The percentages of haploid cells in cultures varied from 18 to 32, and increased with culture age but not with x-ray dose until the x-ray dose exceeded 100 R. The number of haploid cells was inversely related to mitotic index with a negative correlation coefficient of −0.70. The percentages of x-ray-damaged haploid cells (0 to 14%) and diploid cells (6 to 30%) decreased with the culture age but increased with x-ray dose. The results also showed that larger x-ray doses produced a greater average number of chromosome breaks per cell, but larger doses were less efficient in inducing chromosome aberrations. In all cases, x-ray damage to chromosomes in haploid cells appeared to be three times less than that in diploid cells. (auth)

42348 DIFFERENCES IN RADIOSENSITIVITY OF THE CHROMOSOMES OF RAT KANGAROO (POTOROUS TRIDACTYLIS) CELLS IN VITRO. van Steenis, H. (Univ., Leiden). Mutat. Res.; 11: No. 4, 445-7(Apr 1971).

The x-radiosensitivity of mammalian chromosomes in vitro was studied in cultured cells derived from the Tasmanian rat kangaroo. Synchronized (S-phase) and unsynchronized populations were irradiated with a dose of 600 R. In the unsynchronized cultures, nearly 30% of the breaks were observed in the X chromosome as opposed to the expected 15% on the basis of length. In the synchronized cultures, 40% of the breaks were observed in chromosome-2 as opposed to the expected 24%. Both deviations were highly significant ($P < 0.01$). (E.R.B.)

42349 APPLIED ASPECTS OF MICROBIAL GENETICS. Alikhanyan, S. (Inst. of Genetics and Selection of Industrial Microorganisms, Moscow). Curr. Top. Microbiol. Immunol.; 53: 91-148(1970).

A review is presented of the literature on various aspects of microbial genetics. Selection of microorganisms by induced mutagenesis is discussed with regard to antibiotic-producing microorganisms. Studies on the effects of fast neutrons, ultraviolet radiation, x radiation, and chemical mutagens on actinomycetes are described and tables are presented to show frequency of plus and minus variants following treatment with various agents. A review of the literature on hybridization in the selection of microorganisms showed that the use of genetic recombination in selection offers the opportunity of using hybridization methods for the breeding of strains with new and valuable properties. A summary of the practical use of auxotrophic mutants

XUM

is presented with emphasis on studies on Micrococcus glutamicus. Biochemical mutants of this organism were obtained following treatment with ultraviolet light, gamma radiation, fast neutrons, and sarcolysine. (H.L.W.)

42350 GENETIC EFFECTS OF CHRONIC GAMMA-IRRADIATION OF DROSOPHILA MELANOGASTER MALES. Glembotskii, Ya. L.; Kamshilova, E. M.; Ovakimov, V. G. (Inst. of General Genetics, Moscow. Inst. of Hygiene of Labor and Professional Diseases, Moscow). Genetika; 7: No. 6, 94-104(Jun 1971). (In Russian).

The procedure developed by the authors allowed a more exact determination of the frequency of sex-linked recessive lethals induced in male gametes of Drosophila melanogaster by chronic γ radiation with a total dose of 60 R and rate of 0.042 R/min. It was shown that in Drosophila, the dose rate does not affect the frequency of point mutations. During postmeiotic stages of spermatogenesis, the acute and split-dose irradiation with doses of 20 R of ^{60}Co γ rays, 20 rads of 126 to 130 MeV protons, and 20 or 8 rads of fast neutrons induced 2 to 6 times as many point mutations per 1 R or rad/10^7 gametes than that by acute irradiation with the same rays at a dose of 1000 R or rads. At the same stages of spermatogenesis, a chronic irradiation with γ rays of ^{60}Co with a dose of 60 R and rate of 0.042 R/min produced an effect that was very near to the effects of total and split-dose irradiation by γ rays of ^{60}Co at a total dose of 20 R and rate of 0.9 R/min. The chronic, acute, and split-dose irradiations at low doses are most effective in spermatogonia. These cells are highly radiosensitive and the most mutable. They have a high lethality upon γ irradiation at massive doses notwithstanding the dose rate. The comparison of genetic effects of chronic and split-dose irradiations of Drosophila and mouse spermatogonia reveals a complexity and species-specificity. (auth)

42351 DOSE-DEPENDENT FREQUENCY OF ENCIRCLED RING CHROMOSOMES. Dubinin, N. P.; Nemtseva, L. S.; Yurgelaitite, K.-N. V. (Inst. of General Genetics, Moscow). Genetika; 7: No. 6, 5-10(Jun 1971). (In Russian).

Among the chromosome aberrations induced by ^{137}Cs gamma rays (1 and 2 kR) in soaked Crepis capillaris seeds there were ring chromosomes vesting ordinary rod-shaped chromosomes. A 2-fold increase of the dose resulted in a 3-fold increase of the frequency of all the chromosome aberrations including rings whereas an increase of the frequency of the vested rings was 30-fold. (auth)

42352 MUTAGEN SPECIFICITY IN NEUROSPORA CRASSA. de Serres, F. J.; Brockman, H. E.; Barnett, W. E.; Koelmark, H. G. (Oak Ridge National Lab., Tenn.). Mutat. Res.; 12: No. 2, 129-42(Jun 1971).

Tests for mutagen specificity were made on spontaneous and by x-ray, uv, 2-aminopurine (AP), nitrous-acid (NA), ethyl methanesulfonate (EMS), and mesodiepoxybutane (DEB) induced ad-3 mutants of Neurospora crassa induced in wild-type strains OR 74A and 74-OR23-1A. Differences were found between the percentages of leaky ad-3A mutants and leaky ad-3B mutants as a function of mutagenic origin as well as the ratios of ad-3A mutants to ad-3B mutants. Ad-3B mutants were further characterized by means of tests for allelic complementation with a tester set of 17 strains that define a linear complementation map consisting of 17 complons. Complementation tests were made on a total of 564 ad-3B mutants. Of the 107 different complementation patterns detectable with this tester set, 52 different patterns were detected among the 530 ad-3B mutants that could be mapped. Marked differences were found in the percentages of mutants with nonpolarized or polarized complementation patterns and non-complementing mutants as well as the average complon coverage for all of the complementing mutants in each sample. Mutants with nonpolarized patterns have an average complon coverage of 4.9 and mutants with polarized patterns of 13.4. Evidence for "hot spotting" was found in the NA- and EMS-induced samples where many of the mutants had the same type of nonpolarized complementation patterns. The highest percentage of mutants with different nonpolarized complementation patterns was found among DEB- and uv-induced mutants. The striking difference between the characteristics of the ad-3 mutants in each of the 7 samples was interpreted as evidence for mutagen specificity. (auth)

42353 INFLUENCE OF SELECTION, NON-UNIFORM CELL POPULATION, AND REPAIR ON DOSE-EFFECT CURVES OF GENETIC EFFECTS. Gerber, G. B.; Leonard, A. (CEN/SCK, Mol, Belgium). Mutat. Res.; 12: No. 2, 175-82(Jun 1971).

Dose-effect curves of chromosomal aberrations can be modified after irradiation by selection, presence of a non-uniform cell population and/or repair. In order to affect not only the scale but also the shape of dose curves, these factors must depend on radiation dose. Selection either by interphase death, early elimination of severe abnormalities or delayed elimination of small genetic detriments can result in modifying a square law curve into a pseudolinear one or into one showing saturation at high doses. If the irradiated population is not uniform, conditions are conceivable under which aberrations are retained for a long time and then disappear rapidly. Repair, if dose dependent, can only result in a dose–effect curve following a law with a higher dose exponent than that induced by the exposure. (auth)

42354 INTERACTION OF CHROMOSOME BREAKS IN SPERMATIDS AND SPERMATOCYTES OF DROSOPHILA MELANOGASTER. Leigh, B. (Univ., Leiden). Mutat. Res.; 12: No. 2, 211-13(Jun 1971).

Male pre-pupae were collected and exposed to 650 R x radiation after 4, 24, and 48 hrs. Mating experiments were conducted and the F_2 offspring were scored for translocations between the X chromosome and chromosomes II and III. A table is presented to show detailed results. The data within each germ cell sample were pooled and the total frequencies of translocations and F_2 male sterility are tabulated together with proportions of translocations which involve the X chromosome. The data show that there is an asynchrony of the availability of chromosome breaks for the formation of translocations. (H.L.W.)

42355 EVIDENCE AGAINST A CYTOGENETICALLY RADIORESISTANT SPERMATOGONIAL POPULATION IN MALE MICE. Searle, A. G.; Evans, E. P.; Beechey, C. V. (Medical Research Council, Harwell, Eng.). Mutat. Res.; 12: No. 2, 219-20(Jun 1971).

Adult male mice were exposed to three doses of fast neutrons at intervals of eight weeks. The mice were killed and meiotic preparations of the testes were made. Spermatocytes were scored for multivalent configurations indicative of translocation heterozygosity. Results did not indicate increased radioresistance to translocation induction after a large initial dose of radiation when there was a long interval between doses. This suggests that there are no radioresistant cell lines or that such lines are present and initially predominant after a large radiation dose, but tend to disappear after further cell generations unless selected for by repeated irradiation. (H.L.W.)

42356 RECOVERY OF CHROMOSOMAL BREAKS INDUCED BY X RADIATION IN SEEDS OF CREPIS CAPILLARIS L. Batikyan, G. G.; Martirosyan, S. N. (Erevan State Univ.). Biol. Zh. Arm.; 23: No. 9, 98-101(Sep 1970). (In Russian).

An investigation was made of the possible restorative action of DNA on irradiated cells of Crepis capillaris L. seeds. After being subjected to a 4000 R dose of x radiation, the seeds were immersed in 0.001% DNA solution for 3, 6, and 9 hrs. Controls were soaked in water for the same periods. Structural chromosomal changes were noted during the metaphase of the first mitosis. The data showed that DNA was effective in decreasing radiation damage in the nuclear structure of cells of C. capillaris. The mechanism of the action is not yet apparent, but damaged chromosomes are apparently restored by stimulating the cell's metabolic processes. (K.S.W.)

42357 PRODUCTION AND REPAIR OF X-RAY INDUCED STRAND BREAKS IN DNA: IN VITRO AND IN VIVO STUDIES. Kapp, Daniel Stuart. Stanford, Calif.; Stanford Univ. (1970). 152p. University Microfilms Order No. 71-71-12,932. Thesis.

Initial studies employing the polynucleotide-joining enzyme and alkaline sucrose gradient centrifugation techniques have demonstrated that x-ray induced strand breakage in aqueous solutions of DNA did not result in a simple rupture of the phosphodiester bonds in polynucleotide chains to produce 3'-hydroxyl and 5'-phosphoryl groups in juxtaposition. Analytical studies employing enzymological and spectrophotometric methods quantitated the chemical aspects of chain breakage and emphasized the role of deoxyribose damage in this process. It was found that for each single-strand break produced in 0.15 M NaCl solutions of calf thymus DNA by x-irradiation, 0.60 molecules of malonic-aldehyde-like product were formed; 0.33 molecules of inorganic phosphate were liberated and 1.35 molecules of phosphomonoester groups were produced (29% of which were 5'-phosphoryl groups). The ratio of newly formed 5'-phosphoryl termini to 5'-hydroxyl termini was 32:1. The presence of the radical scavenger 1-histidine (0.001 M) reduced the number of single-strand breaks by a factor of 0.39, the yield of inorganic phosphate by 0.24, the formation of phosphomonester groups by 0.42, and the deoxyribose damage by 0.41. The relationship between radiosensitivity and the production and repair of x-ray induced single-strand breaks in bacterial DNA was investigated employing strains of E. coli K-12 mutant in the genes controlling excision repair (uvr) and genetic recombination (rec). Mutations in the rec genes were demonstrated to appreciably increase the radiosensitivity of the

cells, while a uvr mutation produced little change in radiosensitivity. Alkaline sucrose gradient studies, employing techniques for isolating DNA from bacteria with minimal shearing, were utilized to quantitate the in vivo production and rejoining of single-strand breaks. The initial yield of single-strand breaks (for a given dose of x-rays) was found to be largely independent of the presence of rec or uvr mutations. The rec^+ cells (including those carrying the uvrB5 mutation) were able to rejoin efficiently x-ray induced single-strand breaks in their DNA while the radiosensitive recA56 mutant was unable to repair these breaks to any great extent. The recB21 and recC22 mutants showed some indication of repair capacity and an intermediate sensitivity to killing. A correlation was therefore established between inability to repair single-strand breaks and the radiosensitivity of the rec mutants of E. coli K-12 suggesting that unrepaired single-strand breaks may be lethal lesions in E. coli. Further evidence supporting hypothesis that unrepaired single-strand breaks may lead to cell death was obtained from investigations on the effects of postirradiation treatment of bacteria with an impure preparation of hydroxyurea (Nutritional Biochemicals Corporation). The drug actively potentiated radiation induced killing when added immediately after irradiation and had a diminishing effect as the rec^+ cells were first permitted to repair; it irreversibly prevented the repair of x-ray induced single-strand breaks in the DNA of the rec^+ cells; and it produced no detectable sensitization of irradiated recA mutants (which lack the ability to repair single-strand breaks). Additional studies have demonstrated that a similar postirradiation potentiation of x-ray induced killing and inhibition of strand-break repair is produced by acriflavine. In summary, quantitative determinations of the yields of x-ray induced single-strand breaks in DNA have been performed in vitro and in vivo. The chemical nature of the chain breaks induced in aqueous solutions of DNA by x-irradiation has been characterized and mechanisms for chain breakage have been proposed. Investigations on the role of the production and repair of x-ray induced single-strand breaks in cellular lethality have shown that: single-strand breakage can account to a considerable degree for the lethality in radiosensitive, repair-deficient rec mutants of E. coli K-12, and x-ray induced single-strand breaks can be lethal to bacteria when the repair of these lesions is irreversibly blocked. (Diss. Abstr.)

42358 CHLOROPHYLL AND MORPHOLOGICAL MUTANTS OF COTYLEDONS INDUCED BY ^{60}Co γ IRRADIATION IN ARABIDOPSIS THALIANA (L.) HEYNK. Bianu-Morea, M. Stud. Cercet. Biol., Ser. Bot.; 22: No. 6, 523-9(1970). (In Rumanian).

After a γ-ray treatment of the dry Arabidopsis thaliana seeds, Dijon species, X_3 the generation, significant changes in chlorophyll morphology and pigmentation of the cotyledons resulted. Compared to the spontaneous appearance of the morphological mutants (10^{-5}–10^{-6}) by γ-ray induction, the frequency of some specific types increases by 1000–10,000 times. From the analysis of chlorophyll mutants (early indicators of the mutagenic phenomenon) it has been observed that the lability of the genes controlling chlorophyll pigmentation is significantly different. In Arabidopsis thaliana, doses ranging between 15 and 50 Kg induce the most different types of chlorophyll mutants, and the 40 and 45 Kg the highest frequency. (Rom. Sci. Abstr.)

42359 COMBINED EFFECT OF NITROGEN YPERITE (HN2) AND GAMMA RADIATION ON DRY SEEDS OF CREPIS CAPILLARIS L. Azatyan, R. A. (Inst. of General Genetics, Moscow). Biol. Zh. Arm.; 23: No. 10, 99-100(Oct 1970). (In Russian).

The combined action of two mutagenic agents upon dry seeds of Crepis capillaris L. was studied: gamma radiation at dosages of 15 kR, and nitrogen yperite (HN_2). The mutation level of cells was observed to be 1.5 to 2 times lower than the added cell aberrations resulting from independent action of the two mutagenic agents. The spectrum of the structural mutations indicates that both chromatid and chromosomal aberrations are induced by combinations of the two mutagens. (K.S.W.)

42360 MUTAGENESIS OF HYBRIDS OF WHEAT. II. THE ACTION OF X-RAYS ON THE F_1M_2 GENERATION OF HYBRIDS. Avakyan, V. A. (Lab. of Induced Mutagenesis of Plants, Erevan). Biol. Zh. Arm.; 23: No. 10, 42-7(Oct 1970). (In Russian).

The influence of x rays on the hybridization of plants was studied for intraspecies hybridization of two varieties of soft wheat and one variety of hard wheat. The dose rate was 515 R/min for total doses of 10 and 15 kR. Irradiation of the maternal form in interspecies hybridization led to an increase in the percent of setting of grain on the hybrid plant of the second generation; in the first generation, however, there appeared abnormal plants with pubescent white and red heads. The data permit the conclusion that when the maternal component of wheat hybrids is given x-ray exposures, different radiosensitivities are manifested depending upon the hybrid combinations. In the manifestation of radiosensitivity of hybrid plants in the F_1M_2 generation, a definite role belongs to the paternal component. (K.S.W.)

42361 X-RAYS INFLUENCE ON CHROMOSOME ABERRATIONS IN HELIANTHUS ANNUUS L. Georgieva-Todorova, Iordanka (Inst. of Genetics and Plant Breeding, Sofia). Genet. Selek.; 2: No. 6, 469-76(1969). (In Bulgarian).

Results are reported of a study of the effects of x rays on seeds of the Peredovik variety of sunflowers. It was found that seeds germinate normally when irradiated in doses of 8, 12, 16, 32, and 40 kR. In cells of rootlets developed from dry sunflower seeds microdensitometer measurements of DNA demonstrated the presence of 2C nuclei corresponding to G_1. Analysis of chromosome aberrations showed a considerable deviation from the normal course of mitotic division. A substantial percentage of anaphase aberrations were chromosome breaks. Occurrence of chromatid breaks regardless of the presence of cells in G_1 points to the relation of this type of aberration to other factors independent of DNA synthesis in the cell. (auth)

42362 CHROMOSOMAL DISTURBANCES FOLLOWING X-RAY EXAMINATIONS. Konstantinova, Bl. P.; Kasabov, L. L. Rentgenol. Radiol.; 7: No. 1, 4-10(1968). (In Bulgarian).

A report is made of somatic mutations occurring in a newborn in connection with x-ray examination. The child was born with severe malformations — inferior coelosomia, hermaphroditism, prolapse of the anus and rectum, ectopy of the urinary bladder, and teratoma of the sacrococcigeal area. Urography was performed soon after birth to specify the state of the urogenital system. The child received 7 ml. opacuran and a total irradiation dose of 300 m R in three roentgenograms. The child was delivered from first normal pregnancy; the parents were young — 21 and 26 years of age, with good housing conditions, and free of familial overburdening. During the third and fourth month of pregnancy the mother had received a single dose of 2 coffenal tablets and after birth 2,300,000 U. of penicillin, 3 g of streptomycin, and 9 dragees of metergin. The chromosomal analysis performed by the authors with peripheral blood of the child and the parents showed somatic mutations — 21.2% in the child and 4% in the mother. The urographic examination is held responsible for the occurrence of somatic mutations in the child and the antibiotic treatment — in the mother. This communication is of interest being the first one of somatic mutations in a newborn child. (auth)

42363 STUDY OF THE BIOCHEMICAL ACTIVITY OF ANASTOMOSE ASPERGILLUS NIGER STRAINS INFLUENCED BY X RAYS. Pashev, Il.; Kibarska, T.; Parchev, N. Izv. Mikrobiol. Inst., Bulg. Akad. Nauk.; 15-20(1969). (In Bulgarian).

A study was made of the effect resulting from the influence of x rays on anastomose cultures obtained through anastomosis between two single cells from various Aspergillus niger strains. The numerous mutants thus produced were investigated morphologically, physiologically, and biochemically as well as with regard to their capacity of synthetizing an acid. Use was even made of x rays — 7000 R by means of which, according to preliminary studies, the authors obtained the most favorable mutant effect. The conducted investigations resulted in physiological mutants with changed physiological and biochemical qualities and properties. The anastomose strains have an increased sensitivity towards roentgen influences. Irradiation with 7000 R results in mutants and a 10 to 20% increased productivity. One of the mutants obtained forms about 90% of citric acid as compared with fermenting sugar. (auth)

42364 RADIOGENETIC EFFECTS OF GAMMA- AND FAST NEUTRON IRRADIATION ON DIFFERENT ONTOGENETIC STAGES OF THE TOMATO. Contant, R. B.; Devreux, M.; Ecochard, R. M.; (and others) (EURATOM–ITAL, Wageningen, Netherlands. CNEN, Rome. Wageningen Univ., Netherlands). Radiat. Bot.; 11: No. 2, 119-36(Apr 1971).

A comparison was made of radiation effects (γ rays and fast neutrons) on premeiotic pollen mother cells (PMC), dry pollen, gametes after pollination but before fusion, and dry seeds of tomato. PMC and pollen irradiations produced only very low frequencies of recessive visible mutations transmissible to the M_2 generation. The elimination of deleterious genetic side-effects was more efficient after PMC than after pollen irradiation. Pollen, which has advantages for radiogenetical studies, seems to hold little promise for mutation breeding purposes. With irradiation of gametes after pollination, much higher mutation frequencies were obtained than with treatment of PMC or pollen; these frequencies, however, were considerably lower than those resulting from seed irradiation. When expressed per rad, the mutation frequencies were higher after irradiation of gametes. At comparable degrees of radiation-induced M_1 sterility, the mutation frequencies obtained after gamete irradiation were probably equal to or somewhat higher than after seed irradiation. The visible

XUM

mutations induced by treatment of gametes were associated with much disturbance in the genetic background. The fast neutron RBE values were much higher with irradiation of dry pollen or seeds than with irradiation of gametes after pollination. The likelihood of the presence of recessive mutations in M_2 was, within a given treatment, hardly (fast neutrons) or not all (γ rays) related to the fertility of the M_2 plants. Chimerism was not completely avoided by irradiation of prezygotic stages. (auth) (UK)

42365 IN VITRO STUDY OF THE EFFECT OF γ RAYS ON HUMAN CHROMOSOMES. Mouriquand, C.; Gilly, C.; Wolff, C.; Patet, J. (CEN, Grenoble, France). Int. J. Radiat. Biol.; 19: No. 3, 263-79(1971). (In French).

Aberrations in human chromosome induced by γ radiation were studied in vitro with doses ranging from 25 to 500 rads. The investigation of 1841 karyotypes showed a dose–effect relationship for numerical and structural aberrations. For dicentrics, the power exponent in the function $y = aD^n$ was found to be 1.20, and for fragments 1.55. (auth) (UK)

Health Physics and Safety

Refer also to abstracts 42012, 42034, 42036, 42039, 42042, 42043, and 42605.

42366 EVALUATION OF TELEVISION CONTRIBUTION TO THE ANNUAL GENETICALLY SIGNIFICANT RADIATION DOSE OF THE POPULATION. Broyles, Morris; Neely, Orville; Slinkman, Roger; Thierfelder, Charles. IEEE (Inst. Elec. Electron. Eng.), Trans. Broadcast Telev. Receivers; BTR-16: No. 3, 157-64(1 Aug 1970).

United States Public Health Service data are used to estimate the annual significant dose to the U. S. population from television usage. This study indicated that the dose due to television usage in early 1968 was about 0.5 mrem or less than 0.5% of the average dose from natural background radiation. The study methods are reviewed along with a current appraisal of steps which have been taken or will be taken to limit further x radiation from TV sets. (E.E.H.)

Radioactive Contamination and Decontamination

Refer also to abstracts 42245, 42315, and 42691.

42367 (AWTSC–1) FALLOUT OVER AUSTRALIA FROM NUCLEAR WEAPONS TESTED BY FRANCE IN POLYNESIA FROM MAY–AUGUST 1970. (Atomic Weapons Tests Committee, Victoria (Australia)). Feb 1971. 40p. Dep. NTIS (U. S. Sales Only).

In this paper measurements on fallout in Australia from May to November 1970 following nuclear weapons tests by France in Polynesia are reported. The measurements were made for 26 stations and nine major centers of population to determine radiation doses to whole body and to thyroid. The data show that radiation doses from the fallout are small. The whole body doses range from 0.2 to 1.8% of the average annual background radiation, and the thyroid doses range from 1.2 to 8.1% of the dose, over a year, equivalent to the guide level adopted by the National Radiation Advisory Committee. The radiation doses for 1970 are lower than those for the major series of nuclear weapons tests in Polynesia in 1966 and comparable to those for 1968. The National Radiation Advisory Committee considers that radiation doses of this magnitude are of no significance as a hazard to health. As this report is the first of a new series, some detailed information is included in Chapter 1 which, it is hoped, will be of general interest in relation to the monitoring programs. (auth)

42368 (LF-tr–53) EFFECTS OF PULMONARY LAVAGE ON THE RETENTION OF PARTICLES OF PLUTONIUM OXIDE. Kunzle-Lutz, M.; Metivier, H.; Molibe, D.; Simon-Vermot, A.; Gimbert, J.-L.; Jockey, P. Translated by A. A. Horvath for Lovelace Foundation for Medical Education and Research, Albuquerque, N. Mex., from Arch. Mal. Prof. Med. Trav. Secur. Sociale; 31: 513-16(Sep 1970). 5p. Dep. NTIS.

Pulmonary lavage, using isotonic saline solution, removed approximately 50% of inhaled insoluble PuO particles from the lungs of baboons. The technique used is described and applications for the decontamination of personnel are discussed. (C.H.)

42369 (NP–18905) RADIATION HEALTH AND SAFETY. Annual Report for the Year Ended 31st December 1970. (New South Wales Univ., Kensington (Australia)). 15p. Dep. NTIS (U. S. Sales Only).

All aspects of the work which concerned the University's radiation officer during 1970 are reviewed. Procedures involving the purchase and transfer of radiation sources are discussed and quantities of radioisotopes concerned are tabulated on a basis of allocation to research or teaching project. Brief evaluations of personnel monitoring and associated services are made. (Australia)

42370 (SWRHL–43–r) ^{131}I TRANSPORT THROUGH THE AIR–FORAGE–COW–MILK SYSTEM USING AN AEROSOL MIST (PROJECT RAINOUT). Douglas, Richard L.; Black, Stuart C.; Barth, Delbert S. (Southwestern Radiological Health Lab., Las Vegas, Nev.). Jun 1971. 38p. Dep. NTIS.

Project Rainout was an experiment conducted to determine the transfer of ^{131}I from forage to dairy cow milk when the radioiodine was sprayed on the forage as an aqueous solution. Growing alfalfa, cut as green chop, and spread hay were used as forage. The peak activity in milk from cows consuming both types of forage occurred about one day after the start of feeding. The peak milk-to-peak forage ratio was 0.013 for the cows fed hay and 0.041 for the cows fed green chop. The hay fed cows secreted in milk an average of 4.5% of the amount of ^{131}I they ingested, while the green chop fed cows secreted 6.1%. (auth)

42371 DISTRIBUTION OF RADIONUCLIDE IN THE SKIN RESULTING FROM SURFACE CONTAMINATION BY ^{89}Sr. Zaichik, V. E. Med. Radiol.; 16: No. 6, 73-5(Jun 1971). (In Russian).

In the presence of surface contamination by ^{89}Sr of the integument, the dose rate received by the skin at various depths as a function of the penetrability of several layers of the skin itself is of interest. The diurnal radiation dose received in the basal layer at a depth of 70μ is of particular importance in medicine. Calculations were made on hypothetical models of isotope distribution in the skin as well as on experimental data. It was found that penetration of the skin by ^{89}Sr does not substantially affect the magnitude of the dose rate at the depth of the basal layer. The dose rate received in the basal layer may to a significant degree depend upon the amount of residual contamination. (K.S.W.)

42372 FALLOUT RADIOACTIVITY IN KOREAN FOODSTUFFS. PART 4. ^{90}Sr IN LIQUID WHOLE MILK PRODUCED IN KOREA. Yang, Kyun Rin. Daehan Hwahak Hwoejee; 13: No. 2, 181-6(1969).

The concentration of ^{90}Sr in liquid whole milk produced in Korea was measured during the past four years. The samples of milk were purchased from dairies in Seoul. ^{90}Sr was analyzed radiochemically and the amount of stable calcium was also determined. Radioactivity of ^{90}Y was counted. The concentrations of ^{90}Sr in the milk were 25.1 PCi ^{90}Sr/g Ca in 1965, 26.8 PCi ^{90}Sr/g Ca in 1966, 13.7 PCi ^{90}Sr/g Ca in 1967 and 18.2 PCi ^{90}Sr/g Ca in 1968 in annual average. The concentrations of ^{90}Sr in the milk during 1967 and 1968 were decreased as compared with the values for 1965 and 1966. From the results it was concluded that ^{90}Sr concentrations in milk vary roughly proportionally with the specific activity of fallout. Considering the safety problems, the ^{90}Sr levels in milk produced in Korea were far below the maximum permissible level recommended by ICRP. (Korean Sci. Abstr.)

42373 BIOLOGICAL EFFECTS OF RADIOACTIVE WASTE. Woodhead, D. S. (Ministry of Agriculture, Fisheries, and Food, Lowestoft, Eng.). Proc. Roy. Soc. (London), Ser. B; 177: 423-37(1971).

The discharge of radioactive waste into the marine environment is, in general, limited by the requirement that the resulting increments of dose to members of the general public are within internationally agreed limits. The implicit assumption is made that when this requirement is met the fauna and flora of the marine ecosystem, which are generally less radiosensitive than man, are not at risk. The data relating to the effects of both acute and chronic irradiation on marine species are reviewed and the dose rates which can occur in contaminated environments due to the reconcentration of activity, either by the animals themselves or by some component of their habitat, e.g., silt, are indicated. From this it is possible to predict that present waste disposal practices are unlikely to have any observable effect in the natural environment. Nevertheless, further research is necessary to find more sensitive indicators of damage at both the individual and population levels. (auth) (UK)

42374 RESIDUAL β ACTIVITY AND γ-SPECTROMETRIC NUCLIDE DETERMINATIONS IN BEES AND HONEYS. Herrmann, H. (Demoll–Hofer Institut, Munich). Z. Wasser-Abwasserforsch.; 3: 152-3(1970). (In German).

The results of tests on the radioactivity of honey since 1965 and honeybees since 1961 from the environment of VAK (Kahl), KRB (Gundremmingen), and of the planned KKN (Niederaichbach) are reported. It was confirmed that most of the radioactivity originated from fallout. (INIS)

42375 PROBLEMS OF THE RADIOCONTAMINATION OF MAN: LEVELS OF ^{137}Cs AND ^{90}Sr IN THE DIET AND URINE OF ITALIAN POPULATION GROUPS OF DIFFERENT AGES. Tomassi, G. (Univ., Rome); Cigna, A.; Mariani, A.; Migliaccio, P. A.; Spadoni, M. A. Quad. Nutr.; No. 6, 397-408(1968). (In Italian). (RT/PROT-(71)6).

Research was carried out on the influence of some physiological factors on ^{137}Cs and ^{90}Sr contamination in the body of Italian population groups of different ages. The ^{137}Cs and ^{90}Sr content of a 3-day diet and of the urine eliminated during the 24 hr corresponding to the last day of the diet collection were measured. The results, compared with those of previous research, showed that the SU diet/SU urine ratio varied according to age, whereas no significant variation seemed to occur with age in the CU diet/CU urine ratio. The meaning of these variations is discussed and their practical utility is underlined in reporting rapidly from urinary radiocontamination back to that of diet in population groups. (auth)

42376 CONTENT OF ^{137}Cs IN THE POPULATION OF DIFFERENT REGIONS OF THE SOVIET UNION. Dzyubenko, I. I.; Krisyuk, E. M.; Prokofev, O. N.; Shapiro, E. L.; Chumakov, V. V. (Leningrad Research Inst. of Radiation Protection). Med. Radiol.; 16: No. 5, 36-44(May 1971). (In Russian).

Data on the dynamics of ^{137}Cs accumulation in the population of the Soviet Union are presented. The period between 1967 and 1968 is characterized by a decelerated rate of reduction of ^{137}Cs content, this testifying to the increased role of root passage of ^{137}Cs into food products of plant origin. Between 1966 and 1968, a total of 2240 residents of different towns were examined to determine the mean content of ^{137}Cs in different regions of the country. These studies enabled to reveal a significant difference of ^{137}Cs content in inhabitants of northern, central, and southern zones. The mean content of ^{137}Cs in inhabitants of these zones differs by a factor of 1.5 to 2. The distribution of ^{137}Cs content in inhabitants of each zone does not contradict the log normal law. On the basis of these data, the number of persons who received an irradiation dose from incorporated ^{137}Cs that was five times greater than the mean dose for each zone was determined. The genetically significant dose from incorporated ^{137}Cs that comprised 12.8 mrad for 1962 to 1968 and 52 mrad for the next 30 yr if nuclear weapons would not be tested is calculated. (auth)

42377 ^{108m}Ag IN BIOTA SEDIMENTS AT BIKINI AND ENIWETOK ATOLLS. Beasley, T. M.; Held, E. E. (Univ. of Washington, Seattle). Nature (London); 230: 450-1(16 Apr 1971).

Large amounts of ^{108m}Ag and ^{110m}Ag were not produced during the 1958 nuclear test series, or earlier, and the production activity ratio $^{110m}Ag/^{108m}Ag$ was about 162. These observations may, however, require reconsideration. The present authors found ^{108m}Ag in biota and sediments collected at previous nuclear testing sites in the Pacific, including the hepatopancreases of spiny lobsters, collected from Bikini and Eniwetok Atolls. The concentrations in the Bikini samples were two to three times higher than in those from Eniwetok. The time between cessation of tests and collection of specimens ranged from 6 to 12 years, and it is reasonable to conclude that higher concentrations of both ^{108m}Ag and ^{110m}Ag were present at earlier times. The sediment investigated was taken from the site of a large thermonuclear detonation in 1954, the crater being exposed to both lagoon and sea water and therefore a source of ^{108m}Ag for the biota of the area (the ^{110m}Ag would have largely decayed since 1954). It is concluded that the amount of ^{108m}Ag present in the Pacific Ocean and elsewhere as a result of pre-1959 testing may be significant. The observation about the initial production activity ratio of $^{110m}Ag/^{108m}Ag$ may be conservative in its estimate of ^{108m}Ag production. The results obtained assumed production only by thermal neutron activation of stable Ag, but there are other production mechanisms for these two nuclides, which are under investigation. Production pathways are important since different types and designs of nuclear devices can generate different ratios of fast and thermal neutron fluxes. The absence of definite knowledge of the rates at which Ag is removed from the layers of the ocean makes it impossible to decide whether ^{108m}Ag from pre-1961 to 62 testing confuses subsequent dating. (UK)

42378 ESTIMATION OF FUTURE RADIOSTRONTIUM LEVEL IN THE SYSTEM FALLOUT, FODDER PLANT, MILK. Csupka, St. (Hygiene-Epidemiology Inst., Bratislava). Kernenergie; 13: No.12, 391-4(Dec 1970). (In German).

Results of ^{90}Sr concentration measurements in fallout, fodder plants, and milk during 1964 through 1969 have been evaluated and proportional factors have been estimated by regression analysis. These factors have been used in the regression equation for estimating ^{90}Sr content to be expected in the milk. The estimations were based on two models: model A implying constant annual fallout, and model B implying decreasing annual fallout, starting from its value in 1969 (1 nCi $^{90}Sr/m^2$). (auth)

42379 PROBLEMS OF RADIATION SAFETY AND EFFICACY OF PREVENTIVE MEASURES IN WORK WITH URANIUM ENRICHED WITH ^{235}U ISOTOPE. Andreeva, O. S.; Parkhomenko, G. M. Gig. Sanit.; No. 4, 36-9(Apr 1971). (In Russian).

The authors revealed and assessed the sources of air pollution with γ-active aerosols. The isotope ^{235}U was found to be the main factor responsible for the air pollution. The γ-quanti with an energy of 30 to 60 GeV makes the greater part of the total intensity of the radiation dose. The authors demonstrated the efficacy of the protective measures introduced. (auth)

42380 SOME ANALYTICAL ASPECTS OF RADIOACTIVE EFFLUENT DISPOSAL. Dutton, J. W. R. (Ministry of Agriculture, Fisheries, and Food, Lowestoft, Eng.). Proc. Soc. Anal. Chem.; 8: 594(Apr 1971).

Control of the discharge of radioactive wastes to the environment in England and Wales is the responsibility of the Department of the Environment and the Ministry of Agriculture, Fisheries, and Food. As a result of operations at the United Kingdom Atomic Energy Authority's (U.K.A.E.A.) nuclear fuel reprocessing plants and at the Central Electricity Generating Board's (C.E.G.B.) nuclear-powered electricity-generating stations, large volumes of low-level radioactive liquid waste are produced. The effect of discharging these wastes to the marine environment is assessed by calculating the dilution and dispersion of the radionuclides and their subsequent reconcentration in biological materials and on sediments; a survey is then carried out to assess the various habits of the public that could result in exposure to the radiation, e.g., the consumption of seafood (fish, crustacea, mollusca, edible seaweed, etc.), handling of fishing gear, the time spent on the beaches, etc. By compounding these various factors, a critical pathway is defined in which the radionuclide, the material, and the group of the population most at risk are identified. If necessary, the discharge is limited so that the exposure of this group to radiation is kept well below the maximum permissible levels laid down by the International Commission on Radiological Protection. (auth)

42381 ^{90}Sr AND ^{137}Cs CONTENT IN SOME BULGARIAN FOODSTUFFS. Keslev, D.; Boyadzhiev, A.; Novakova, E.; Kerteva, A; Nikolova, M. Rentgenol. Radiol.; 7: No. 1, 10-13 (1968). (In Bulgarian).

From 10 representative areas within Bulgaria samples of 16 agricultural products were drawn and subjected to analysis. The products were: butter, milk, rice, wheat, potatoes, maize, beans, (green and dried), cabbage, tomatoes, onions, peppers, blue plums, apples, pears, and grapes. The highest ^{90}Sr contents were found in wheat, dried beans, and milk, whereas the highest ^{137}Cs contents existed in wheat, dried beans, butter, blue plums, apples, and milk, in that order. (K.S.W.)

42382 RESEARCH ON THE BONE DEPOSITION OF $^{210}Pb(^{210}Po)$ AND ^{90}Sr. Lanzola, E. (Univ., Pavia, Italy); Allegrini, M.; Breuer, F.; D'Arca Simonetti, A. Minerva Fisiconucl.; 14: 132-6(Jul-Sep 1970). (In Italian). (CONF-690929-13).

From fifteenth national congress of the Italian Association for Health Physics and Protection Against Radiation; Cagliari, Italy (Sep-Oct 1969).

Measurements of ^{210}Po in the center of bones of cattle bred in the same zone of Marche and divided into five groups by their age were reported. The ages of the cattle were 5 months, 8 months, 20 months, 4 years, and 10 years and they were slaughtered in 1962, 1964, 1966, 1967, and 1968. Measurements were made of the ^{90}Sr, and for those slaughtered in 1962 also ^{89}Sr, in the ashes. For all ages a comparison was made on the increase with time between the values of ^{90}Sr and ^{210}Po. These latter values are independent of the nuclear explosions in the atmosphere and show a continuous increase with time, expressible as a power function. The increase is similar to the increase announced by Loutit for stable Sr in human bone. Some conclusions on the metabolism of bone increase were made from this behavior analogy. (tr-auth)

42383 POLLUTION IN OUR ENVIRONMENT. Baxter, Philip. Aust. Chem. Process. Eng.; 24: No. 4, 18-23(Apr 1971).

A comparison is made between emanation of pollution from fossil-fueled power stations and nuclear power stations. Safety precautions taken to limit escape of fission products to levels below the permissible levels of discharge from nuclear power reactors are outlined, and these levels are compared with natural background exposures. (Australia)

42384 PROCESS FOR DECONTAMINATING RADIOACTIVE WATERS IN VIEW OF RETURNING THEM BACK TO THE NATURAL ENVIRONMENT OR RENDERING THEM DRINKABLE.

XUM

Lion, Philippe French Patent 2,031,748. 9 Nov 1970. Filed 6 Feb 1969. (In French).

A process for removal of radioisotopes (^{137}Cs, ^{106}Ru, and ^{90}Sr) from waters and rendering them drinkable is described. The waters are treated with bentonite at concentrations of between 200 g and 5000 g per cubic meter. The bentonite is used in a very fine powder form and remains in suspension in the water which is slowly agitated. After fifteen minutes contact the water and the bentonite are separated by filtration. This treatment reduces the activity to a hundredth of its initial value. (France)

42385 CONTENT OF RADIOACTIVE STRONTIUM IN MILK [IN CZECHOSLOVAKIA]. Papezova, A. (Inst. of Biophysics, Brno). Cesk. Hyg.; 13: No. 6, 348-50(1968). (In Czech).

The ^{90}Sr content of milk in Czechoslovakia was at its highest point in 1963 (16.5 pCi/gCa), dropping to 8.4 pCi/gCa during 1964 to 1966. (E.R.B.)

42386 DETERMINATION OF ^{90}Sr IN MILK AND COTTAGE CHEESE IN THE NORTH-MORAVIAN REGION. Hillova, J. (Krajska Hygienicka Stanice, Ostrava, Czech.). Cesk. Hyg.; 15: No. 6, 208-12(1970). (In Czech).

The ^{90}Sr content in milk and cottage cheese was determined at the Regional Hygienic Station for the North-Moravian Region. Results for the period 1965 to 1968 are presented and a comparison was made with results obtained by other Czechoslovakian and by some foreign authors. In the North-Moravian Region, higher concentrations of ^{90}Sr were observed than the ^{90}Sr concentrations in powdered milk reported in previous years. The results correspond to similar data reported by foreign authors. (auth) (INIS)

42387 INVESTIGATIONS ON ^{210}Pb CONCENTRATIONS IN VARIOUS REGIONS OF INDIA. Joshi, L. U.; Rangarajan, C.; Gopalakrishnan, S. S. (Bhabha Atomic Research Centre, Trombay, India). Health Phys.; 20: No. 6, 665-8(Jun 1971).

Seasonal measurements of ^{210}Pb were carried out to explore the possibility of increased ^{210}Pb levels resulting from high uranium or ^{224}Ra activity of the soil. Seasonal variations of ^{210}Pb were measured at Srinagar, Delhi, and at Nainital where results did not show a pronounced variation. The radon daughter activity was compared with that of ^{210}Pb at Bombay and the latitudinal variation of ^{210}Pb was plotted in surface air and rainfall. At Gangtok the results were higher than a factor of 2, than those of the other stations, the increase occuring mainly in the winter months, and not apparently due to a significant increase in ^{226}Ra in the soil. (UK)

42388 ^{131}I DISCHARGES FROM AN OPERATING BOILING WATER REACTOR NUCLEAR POWER STATION. Stigall, G. E.; Fowler, T. W.; Krieger, H. L. (Bureau of Radiological Health, Rockville, Md.). Health Phys.; 20: No. 6, 593-9(Jun 1971).

A series of radiological surveillance studies was conducted at Dresden Nuclear Power Station by the Radiological Engineering Laboratory of the Division of Environmental Radiation which provided data on ^{131}I concentrations observed in the plant, the plant's effluent, and the environment. Based on the Dresden study data, an evaluation is made in this paper of the public health significance of ^{131}I discharges from BWR nuclear power plants. The in-plant barriers to the transport of ^{131}I through a BWR nuclear power plant to the site environs were found to function at a high efficiency. As a result, the critical phase of the environmental surveillance program for Dresden, a BWR without gaseous holdup, was concluded to be the submersion dose from noble gases, not ^{131}I in milk. For a BWR nuclear power plant employing gaseous holdup, it was concluded that the ingestion ^{131}I dose may be more limiting than the submersion dose from noble gases. (auth) (UK)

42389 RESULTS OF 3 YEARS (1964–1966) OF MEASURING THE RADIOACTIVITY OF FOODS SAMPLED IN THE CITY AND PROVINCE OF PAVIA. Lanzola, E.; Meloni, C.; Marcheti, R. (Univ., Pavia, Italy). Ann. Sanita Pubblica; 29: 61-83(Jan-Feb 1968). (In Italian).

The results of a three-year (1964 to 1966) measurement of ^{90}Sr and ^{137}Cs made in various foods sampled in the province of Pavia and the city, with emphasis on the results obtained for milk, are presented. The mean of the values for ^{90}Sr and ^{137}Cs found in milk, sampled weekly in the centrals of Pavia, Mede, Voghera, and Vigevano and measured monthly, were compared with those of the monitoring network of the CNEN for Italy, of the PHS of the United States, and of the ARCRL of Great Britain. It was found that the disappearance half-life for ^{137}Cs in milk was 12 months and for ^{90}Sr varied from 17 to 26 months. This difference was attributed to the different behavior in the soil of ^{90}Sr with respect to that of ^{137}Cs and, in the absence of atmospheric nuclear explosions, to a prevalence of indirect absorption rather than direct absorption

It was found that the ^{90}Sr values calculated with the Russell and Bartlett equation (based on the deposition of fallout on the soil) were in good agreement with the measured values. By taking into consideration the exponential trends of ^{90}Sr and ^{137}Cs in milk, the quantity of the two nuclides probably to be found in milk in 1970, in the absence of new atmospheric nuclear explosions, was deduced. (tr-auth)

42390 TRITIUM CONTENT IN URINE OF NEUTRON GENERATOR OPERATORS. Studena, Olga; Stojanov, Milan (Krajska Hygienicka Stanice, Brno). Jad. Energ.; 17: 125-7(1971). (In Czech).

The risk of internal contamination from tritium to neutron generator operators and a method of investigation by analysis of urine samples for tritium content are described. Equations for calculating dose equivalents in cases of a single and chronic incorporation, and results of measurements on two neutron generator facilities are presented. (auth)

42391 NOTES ON MEDICAL PROCEDURE FOR RADIATION ACCIDENTS AND RADIOACTIVE CONTAMINATION. AAEC A-7 1968. Canberra, Australia; National Health and Medical Research Council (1969). 7p. Available from National Health and Medical Research Council, Curtin, Australia.

Procedures are outlined for the care of personnel following accidents resulting in external exposure to radiations, skin contamination with radioactive materials, or internal contamination following the intake of radioactive materials. Both health physics and medical procedures are included. (C.H.)

Dosimetry and Monitoring

Refer also to abstracts 42081, 42094, 42171, 42247, 42257, 42512, 42549, 42594, 42600, 42622–42624, 42626, 42627, 42646, 42685, 42707, and 44135.

42392 (AE-423) PERSONNEL DOSIMETRY AT AB ATOMENERGI DURING 1969. Carlsson, J.; Wahlberg, T. (Aktiebolaget Atomenergi, Studsvik (Sweden)). May 1971. 10p. Dep. NTIS (U. S. Sales Only).

This report presents the results of personnel dosimetry at AB Atomenergi during 1969. A total of 24,200 gamma films and 3,300 neutron films were evaluated, and 770 urine analyses and 1,150 measurements of body activity were made. The external total-body gamma dose for all employees (quarterly doses <100 mrem are not reported) corresponds to 136 manrem. The highest external total body gamma dose during 1969 to one person was 4,800 mrem. (auth) (Sweden)

42393 (BNWL-B-69) RACER: A COMPUTER PROGRAM FOR CALCULATING POTENTIAL EXTERNAL DOSE FROM AIRBORNE FISSION PRODUCTS FOLLOWING POSTULATED REACTOR ACCIDENTS. Strenge, D. L.; Hendrickson, M. M.; Watson, E. C. (Battelle-Northwest, Richland, Wash. Pacific Northwest Lab.). Jun 1971. Contract AT(45-1)-1830. 78p. Dep. NTIS.

Mathematical methods were developed or adopted and corresponding computer programs completed to calculate the whole-body tissue dose from airborne radioisotopes following accidental release to the atmosphere. These programs permit rapid and consistent estimates of whole-body dose resulting from exposure to a plume of airborne radionuclides accidentally released from a nuclear reactor. The method and computer program incorporate the desirable features of existing methods and programs into a single efficient program. The desirability of the incorporated features was determined after analysis of the results of a survey made by investigators experienced in the field of environmental radiation dose calculations. (C.H.)

42394 (NYU-4256-1) SPATIAL DISTRIBUTION OF RADON DAUGHTER AND ^{239}Pu ALPHA LUNG DOSE BASED ON EXPERIMENTAL ENERGY ABSORPTION MEASUREMENTS. Progress Report, December 1, 1970–June 1, 1971. Pasternack, Bernard (New York Univ., N. Y. Inst. of Environmental Medicine). 1 Jun 1971. Contract AT(30-1)-4256. 152p. Dep. NTIS.

Alpha attenuation data were obtained in polycarbonate which is essentially identical to tissue in ionization potential. Alpha transmission and stopping power data are shown for the ^{222}Rn daughters ^{218}Po and ^{214}Po, and for ^{239}Pu, ^{244}Cm, and ^{210}Po. The experimental stopping power measurements are in agreement with values calculated using the Bethe–Bloch equation and the Bragg additivity rule. Experimental α attenuation data were also obtained in a gas with the same composition as ICRP tissue and compared with the attenuation in polycarbonate. The stopping power in the gas was found to be identical with that in the solid tissue equivalent (poly-

carbonate). The experimental data were then applied to determine the spatial distribution of α dose in bronchial epithelium when α activity is present in mucus on the tracheobronchial surfaces. Alpha dose curves as a function of depth into the bronchial epithelium were developed for two different airway diameters. The dose curves are shown in rads/min per dpm/cm^2, so that realistic α dose may be computed if the activity on the bronchial surfaces is known. The α dose from exposure to ^{214}Po and ^{218}Po radon daughters and ^{239}Pu were computed as specific examples. The radon daughter dose was computed using the bronchial activities derived by Altshuler for a radon concentration of 100 pCi/liter. A comparison with Altshuler's original dose calculation indicates differences arising solely from the new dosimetry. At the depth in bronchial epithelium of carcinogenic interest (22 microns) the new dosimetry yields results which are lower by about 20%. An independent dose calculation for radon daughters was also performed incorporating more recent data on uranium mine atmospheres which has appeared in the literature. These newer data include factors which characterize the atmosphere, such as particle size, the daughter ratios, the fraction of the daughters which are not attached to inert aerosol, and factors which determine overall lung deposition such as nasal retention. The α dose to bronchial epithelium using these factors is considerably lower than any calculated previously for the same radon concentration. A few α doses were also computed in terms of working level units. It was found that the α dose for one working level may be widely different depending upon the ratios of the radon daughters. (auth)

42395 (STI/PUB-280). BIOCHEMICAL INDICATORS OF RADIATION INJURY IN MAN. Panel Proceedings Series. Proceedings of a Scientific Meeting Held in Paris, France, 22-26 June 1970. (International Atomic Energy Agency, Vienna (Austria)). Mar 1971. 327p. (In several languages). (CONF-700650). IAEA $9.00.

Separate abstracts were prepared for all 20 of the papers included. (E.E.H.)

For abstracts of individual papers see: 42400-42409, 42622-42628, and 42683-42685.

42396 CONTRIBUTION TO THE FILM DOSIMETRY OF HIGH-ENERGY RAYS. IV. ENERGY- AND PHANTOM-DEPTH DEPENDENCY OF FILM SENSITIVITY FOR HIGH-ENERGY PHOTON- AND ELECTRON RAYS DURING VERTICAL EXPOSURE TO THE DIRECTION OF INCIDENCE. Strueter, Horst-Dieter; Rassow, Juergen; Erdmann, Ute; Lambers, Rolf (Ruhr Univ., Essen). Strahlentherapie; 141: No. 2, 176-84(Feb 1971). (In German).

The dependence of film-density for x rays of 60 to 300 kV, cesium and cobalt γ rays as well as for betatron bremsstrahlung (43 MV) and betatron electron rays (5 to 43 MeV) was examined in films that were exposed vertically to the direction of incidence; the film-blackening was achieved under equal energy doses or ion doses in different depths of water-equivalent materials. The measurements were carried out for various film developing combinations; reproduction possibilities were checked as well. (auth)

42397 DETERMINATION OF THE OPTIMAL CANAL OF REGISTRATION OF GAMMA-RADIATION IN RADIOISOTOPE DIAGNOSIS. Kostylev, V. A.; Rzhevskii, V. E.; Simonov, B. L.; Narkevich, B. Ya. Med. Radiol.; 16: No. 6, 69-72(Jun 1971). (In Russian).

The spectra of impulses caused by radiation scattered on the phantom were calculated and then, using the statistical parameter of the accuracy of measurements, optimization of the canal of registration of gamma radiation of the phantom with ^{131}I, ^{198}Au, and ^{75}Se was performed. (auth)

42398 RADIATION-INDUCED CHROMOSOME ABERRATIONS IN LYMPHOCYTES: POSSIBLE BIOLOGICAL DOSIMETER IN MAN. Sasaki, Masao S. (Tokyo Medical and Dental Univ.). pp 81-91 of Biological Aspects of Radiation Protection. /Sugahara, Tsutomu (ed.). Tokyo; Igaku Shoin Ltd. (1971).

From International symposium on biological aspects of radiation protection; Kyoto, Japan (13 Oct 1969). See CONF-691041.

Chromosome aberrations in blood lymphocytes have been demonstrated in several population groups exposed to ionizing radiation. These findings stimulated interest in the possibility of using the yield of chromosome aberrations in the circulating lymphocytes as a biological indicator of absorbed dose. In theory, dose estimates may be obtained through the yield in exposed persons and directly extrapolated to an equivalent yield obtained in vitro. In practical application, however, many uncertainties exist such as the lack of homogeneity of the radiation dose, time lapse after exposure, chromosomal radiosensitivity, etc. The effects of these factors on the yield of chromosome aberrations are presented and some techniques that allow use of the aberration yield in the lymphocytes of exposed persons to estimate the absorbed dose are described. (E.E.H.)

42399 FEASIBILITY OF CYTOGENETIC ASSAY IN RADIOPHOSPHORUS DOSE ASSESSMENT. Holmes, Howard; Ilbery, Peter (Univ. of Sydney). pp 98-101 of Biological Aspects of Radiation Protection. /Sugahara, Tsutomu (ed.). Tokyo; Igaku Shoin Ltd. (1971).

From International symposium on biological aspects of radiation protection; Kyoto, Japan (13 Oct 1969). See CONF-691041.

Blood cultures from polycythemic patients receiving ^{32}P treatments were examined cytogenetically to determine the feasibility of using lymphocyte chromosome aberrations as an indicator of dose. The cytogenetic results were arranged so that each type of damage was recorded as a percentage of the total number of cells observed for each of 56 cultures and these figures became the dependent variables submitted to multiple regression analysis. The dose increments of ^{32}P were 4 mCi and these dose data together with the time lapse between doses became the independent variables. Increasing C type damage correlated with increasing dosage over a range 4 to 12 mCi. Dicentric yield appeared to be the best cytogenetic parameter. There were many disadvantages to this method, such as the time involved in the examination, unknown factors in variation in lymphocyte kinetics, age, stress, disease, repair of chromosome damage, and elimination of cells with chromosome damage. (E.E.H.)

42400 CRITERIA FOR THE EVALUATION AND SELECTION OF RADIATION-INDUCED METABOLIC CHANGES AS BIOCHEMICAL INDICATORS OF RADIATIN DAMAGE. Altman, K. I. (Univ. of Rochester, N. Y.). pp 1-9 of Biochemical Indicators of Radiation Injury in Man. Vienna; International Atomic Energy Agency (1970). (UR-49-1333).

From Meeting on biochemical indicators of radiation injury in man; Paris, France (22 Jun 1970). See STI/PUB-280; CONF-700650.

In evaluating the suitability of radioinduced metabolic changes for application as biochemical indicators of radiation damage, the following general criteria may be set forth: the biochemical response to radiation must be dose-dependent within a certain, sufficiently wide range; the sensitivity of the indicator should be high in terms of units of response per R exposure; the detectability of the biochemical response in relation to the time of exposure should be maximal at a single time point during the post-irradiation period and should not vary with the radiation dose; the biochemical procedure for detecting the radiation response should be rapid, simple, and should not require sophisticated apparatus; the sample should be easily biopsied without endangering the recovery of the patient; and the indicator should not be affected by interference from metabolic changes related to disease processes that are not related to radiation exposure. Thus, multiple biochemical indicators will be needed that are applicable at various dose levels and times after exposure, and the ideal indicator system should be applicable after total- as well as partial-body irradiation. (E.E.H.)

42401 BIOCHEMICAL POST-IRRADIATION CHANGES AND RADIATION INDICATORS: A REVIEW. Streffer, C. (Univ., Freiburg i. B.). pp 11-32 of Biochemical Indicators of Radiation Injury in Man. Vienna; International Atomic Energy Agency (1970).

From Meeting on biochemical indicators of radiation injury in man; Paris, France (22 Jun 1970). See STI/PUB-280; CONF-700650.

Investigations into radioinduced biochemical changes in mammals and man for use in diagnosing radiation damage or for biological dosimetry are reviewed. An explanation for the limited success that has been obtained in finding useful indicators is given and some ideas are suggested for future investigations. (E.E.H.)

42402 SOME BIOCHEMICAL CHANGES IN BODY FLUIDS AS INDICATORS OF RADIATION DAMAGE. Dienstbier, Z.; Arient, M.; Zicha, B.; Pospisil, J. (Charles Univ., Prague). pp 33-59 of Biochemical Indicators of Radiation Injury in Man. Vienna; International Atomic Energy Agency (1970).

From Meeting on biochemical indicators of radiation injury in man; Paris, France (22 Jun 1970). See STI/PUB-280; CONF-700650.

Some results of several biochemical studies after external irradiation from reports of working groups and laboratories of the radiobiological centre of Prague are presented. In the peripheral blood of irradiated dogs (exposure 600 R) a significant increase of serum α_{3-4} globulins occurs. Simultaneously the content of bound hexoses and seromucoids is significantly increased as well as the polarographical reaction according to

XUM

Brdicka. It is assumed that the height of the level of the glycoproteins observed is caused by the functional state of the organism and contributes to individual radiosensitivity. In irradiated dogs (exposure 600 R) an increased activity of the transaminases of glutamo–oxalacetic and glutamo–pyruvic acid was observed in the first 24 hr and a statistically significant increase of phosphorus in the first six hours. The activity of the total dehydrogenase of lactic acid appeared to have a variable decrease which was also observable in individual fractions. Some of the changes indicated show an apparent gradation after administration of AET and after whole-body irradiation. The activity of serum pepsin in rats after irradiation (200 and 800 rad) was decreased within 24 hours. Early biochemical changes studied in vitro in the liver of irradiated rats are described. A two-phase drop in the ATP level accompanied by an AMP increase during an unchanged ADP level was observed. The dehydrogenation ability of irradiated liver was temporarily regressed. Up to 24 hours, a significant increase of GSH occurs and the activity of glutathion reductase is decreased. The regulation ability of liver was further observed by estimating the steady-state concentration of some metabolites, their steady-state constant and by comparing values of thermodynamic equilibrium. The importance of excretion of deoxynucleosides by urine after irradiation in animals and also in healthy and irradiated humans is reviewed. Special attention was paid to deoxycytidine-uria as a specific reaction after whole-body irradiation. During the elucidation of the mechanism of increased excretion of deoxycytidine in man after ^{60}Co γ irradiation, the results obtained after comparative estimation of the activity of deoxycytidine-deminase are presented. The practical aspects of utilizing biochemical changes to gain further knowledge of post-irradiation disturbance and also for clinical application during an evaluation of radiation hazard are discussed. (auth)

42403 POST-RADIATIONAL CHANGES IN DNA METABOLISM AS INDICATORS OF RADIATION INJURY. Fedorova, T. A. (Inst. of Biophysics, Moscow). pp 61-74 of Biochemical Indicators of Radiation Injury in Man. Vienna; International Atomic Energy Agency (1970). (In Russian).

From Meeting on biochemical indicators of radiation injury in man; Paris, France (22 Jun 1970). See STI/PUB-280; CONF-700650.

To serve as indicators of radiation effects, post-radiation metabolic reactions must be highly radiosensitive with a quantitative dependence on irradiation dose: they must possess the property of specificity, i.e. they must respond to irradiation in the biological dose range much more strongly than to any extreme non-radiational influence; and they must be correlated with the main post-radiational pathogenetic mechanisms. An analysis of the published research on post-radiation disturbances of DNA metabolism in the organism led to the conclusion that the above-mentioned criteria are largely met by the following phenomena: hyperexcretion of deoxynucleosides in the urine caused by irradiation (deoxynucleosiduria), and an increased amount of polydeoxyribonucleotides in the bone marrow of an irradiated organism. Deoxynucleosiduria has the following characteristics: quantitative dependence on the irradiation dose rate in animals; maximum radiosensitivity occurring during the period 6–12 hours after irradiation; specificity; phasing, the hyperexcretion of deoxycytidine during the first two days after irradiation reflects the destruction of cells in the radiosensitive tissues; a new wave of restorative activity, which reflects the hyperproduction of DNA precursors in the post-radiational recovery phase. This indicator can be used for quantitative and time estimation of both pathogenetic effects of irradiation, i.e. damage and recovery. The fact that post-radiational nucleosiduria in man has not yet been adequately studied limits its clinical use as a test for radiation damage. Determining the amount of polydeoxyribonucleotides in bone-marrow punctures from an irradiated organism is to some extent inferior to the use of deoxynucleosiduria as a test for radiation damage. With this indicator the injury caused by irradiation at doses above 300 R cannot be evaluated or be estimated. Before use can be made of the hyperexcretion of β-aminoisobutyric acid in the urine or the DNase activity of the blood and urine as tests for radiation damage, further data on the specificity of these phenomena are required. (auth)

42404 BIOCHEMICAL AND RADIOBIOLOGICAL FACTORS IN THE EARLY DETECTION OF RADIATION INJURY IN MAMMALS. Cole, L. J. (Stanford Research Inst., Menlo Park, Calif.). pp 135-47 of Biochemical Indicators of Radiation Injury in Man. Vienna; International Atomic Energy Agency (1970).

From Meeting on biochemical indicators of radiation injury in man; Paris, France (22 Jun 1970). See STI/PUB-280; CONF-700650.

In considering the body of radiobiological knowledge upon which the present possibilities for the development of an objective quantitative laboratory procedure for early detection of radiation injury depend, it is evident that there are at least three general categories of radiation effects which are relevant to this objective: products of the enzymatic-chemical breakdown of macromolecules, and lysis of killed or dying cells from radiosensitive tissues, for example deoxypolynucleotides from lymphoid tissues and bone marrow; radioinduced inhibition of synthesis of deoxyribonucleic acid (DNA) and/or other macromolecules, eliciting alterations in tissue and blood concentrations and pool size of metabolic intermediates in the synthesis; and radioinduced alterations, suppression, or cessation of specialized cell function. Of particular interest are the immunological functions of lymphocytes, including those in the circulating blood. A modified colony-formation technique for dog bone marrow cells x irradiated in vitro and in vivo gave D_0 values of ~100 R. Thus, on the basis of radiosensitivity and the time-relationships for interphase cell death for lymphocytes, it appears that this cell class is probably the best candidate for an early radiation injury detection system. Biochemical and immunological tests on peripheral blood lymphocytes removed within hours after x radiation exposure may afford a sensitive approach to early detection of radiation injury. Thus, DNA synthesis as measured by the incorporation of tritiated thymidine into the DNA fraction is drastically inhibited in irradiated rat lymphocytes incubated in vitro, in response to the addition of phytohamagglutinin. Theoretically, the responses of these easily accessible cells to phytohamagglutinin and to other selected antigens in vitro should be amenable to quantitation after radiation-dose levels which elicit only minimal lymphopenic effects. Further studies on the molecular basis of these radiation effects on lymphocytes, together with deeper insights into the mechanism by which ionizing radiations initiate the sequence of events leading to the breakdown of DNA and the release of histones from nucleoproteins of these cells, are required for the implementation of practical methods for biochemical detection of radiation injury in man. (auth)

42405 CYTOGENETIC INDICATORS OF RADIATION (AND OTHER) DAMAGE–CALIBRATION: PRESENT AND FUTURE PRACTICAL APPLICATIONS. Abbatt, J. D. (Dept. of National Health and Welfare, Ottawa). pp 149-80 of Biochemical Indicators of Radiation Injury in Man. Vienna; International Atomic Energy Agency (1970).

From Meeting on biochemical indicators of radiation injury in man; Paris, France (22 Jun 1970). See STI/PUB-280; CONF-700650.

An international collaborative study for the identification of human chromosome aberrations that is currently underway is described to indicate some of the main requirements for the experimental design of such studies. The use of quantitative chromosome breakage by ionizing radiation as an indicator of damage or dose is now accepted. The degree of this acceptance varies and a large number of qualifications must be applied depending upon the circumstances of use and exposure. Some of the main indications for the use of this tool and the pros and cons of the main method currently used are given. Within the perspective provided by this framework a brief description of the present limitations and requirements for this method of assay are given. The potential importance of the method as a tool is briefly presented together with some comments on its present and future general applicability. (auth)

42406 CYTOLOGIC-BIOCHEMICAL RADIATION DOSIMETERS IN MAN. Silberstein, E. B.; Chen, I-wen; Saenger, E. L.; Kereiakes, J. G. (Univ. of Cincinnati). pp 181-214 of Biochemical Indicators of Radiation Injury in Man. Vienna; International Atomic Energy Agency (1970).

From Meeting on biochemical indicators of radiation injury in man; Paris, France (22 Jun 1970). See STI/PUB-280; CONF-700650.

The result of radiation interacting with living tissue is the deposition of energy therein. This energy triggers numerous chemical reactions within the molecules of the target tissues. The results of some of these reactions in man were measured at doses up to 300 rads. There were chromosome aberrations, alterations in the kinetics of specific human cell populations and changes in 37 biochemical constituents of serum and/or urine. The utilization of chromosomes as a biological dosimeter is partially perfected but there are numerous discrepancies in data between different laboratories. Etiocholanolone can be used to evaluate marrow injury before the white-cell count falls below 5000/mm^3. Most biochemical dosimeters evaluated gave negative or inconsistent results. However, salivary amylase is a promising indicator of human radiation injury from doses as low as 100 rads. (92 references) (auth)

42407 SOME PROBLEMS ON THE EVALUATION OF BIOCHEMICAL INDICATORS OF RADIATION INJURY. Szabo, L. D.; Antoni, F.; Ferencz, A.; Varteresz, V. (National Research Inst.

for Radiobiology and Radiohygiene, Budapest). pp 215-21 of Biochemical Indicators of Radiation Injury in Man. Vienna; International Atomic Energy Agency (1970).

From Meeting on biochemical indicators of radiation injury in man; Paris, France (22 Jun 1970). See STI/PUB-280; CONF-700650.

The basic principle of loading tests consists of introducing into the organism a certain amount of biological molecules or their intermediary products. It is suggested that combining loading by some normal metabolic product with a low-level tracer may have some value as a biochemical indicator of radiation injury. Male rats were whole-body irradiated with 1200 R ^{60}Co γ rays and injected with ^{131}I-labeled albumin to determine the amount of isotope excreted in the urine and its distribution in the liver, lungs, muscles, blood, and spleen. The results indicated that irradiation reduces the half-life of ^{131}I-albumin in the blood and increases the relative ^{131}I activity in the various organs. A similar test, at a lower dose performed with ^{14}C-labeled orotic acid showed that essential differences may be demonstrated in ^{14}C activity excreted in urine. (E.E.H.)

42408 VALUE OF BIOCHEMICAL INDICATORS. Jammet, H. (CEN, Fontenay-aux-Roses, France). pp 223-58 of Biochemical Indicators of Radiation Injury in Man. Vienna; International Atomic Energy Agency (1970). (In French).

From Meeting on biochemical indicators of radiation injury in man; Paris, France (22 Jun 1970). See STI/PUB-280; CONF-700650.

The biochemical effects of irradiation seem likely to provide extremely interesting information which will help in obtaining a quantitative evaluation of the biological damage suffered by exposed persons. Biochemical dosimetry is based, in particular, on the changes that occur in certain aspects of metabolism (the metabolism of amino acids and fatty acids for example) and on alterations of enzymatic activity. The value of biochemical indicators is illustrated by an accident that resulted in heterogenous whole-body irradiation, and the results obtained by biochemical dosimetry. It is reasonable to suppose that biochemical methods, used in conjunction with other biological techniques and with physical dosimetry, will soon make it possible to assess radiological damage with great precision. (auth)

42409 ENZYMOLOGICAL EXAMINATIONS: AN INDICATION OF RADIATION EFFECTS IN EXPERIMENTS AND CLINICAL PRACTICE. Kaercher, K. H. (Univ., Vienna). pp 277-84 of Biochemical Indicators of Radiation Injury in Man. Vienna; International Atomic Energy Agency (1970).

From Meeting on biochemical indicators of radiation injury in man; Paris, France (22 Jun 1970). See STI/PUB-280; CONF-700650.

Both experiments and clinical practice have proved that the estimation of enzyme activities, in particular those of glycolysis and of the citrate cycle as well as of the hydrolytic enzymes such as peptidase, is a useful indicator of the effects of ionizing radiation on cells and tissues. Such experiments are able to indicate cell damage, i.e. increased permeability of the cell membrane, should it be both reversible and deleterious damage. The enzymes detach after irradiation from the organelles and the cells, respectively, and are then found in the intercellular fluid or in the serum. This phenomenon can be morphologically corroborated by histological examinations. Biocytocultures or tissue homogenates help to determine the quantitative decrease in enzymes, thus rendering conclusions as to dose and duration of therapy. In clinical practice, information on the radiosensitivity of tumors or normal organs can be obtained, even after a single radiotherapeutical dose, provided that an examination of the enzymes is carried out immediately after the first irradiation. Demonstration of post-irradiation changes in the isoenzyme pattern of lactate-dehydrogenase has been successful. The functional damage to the kidney is best characterized by increased excretion of leucineaminopeptidase, whereas immediate radiation damage to the kidney is best demonstrated by changes in the malate-dehydrogenase level. (auth)

42410 NUCLEAR POLLUTION. Bovard, Pierre (CEA, Cadarache, France). Cah. Ing. Agron.; No. 247, 1-5(Jun-Jul 1970). (In French).

The pollution risk resulting from the accumulation of radioactive wastes has been examined. A study was made of the natural radioactivity level previous to any artificial contamination. Since the artificial radioactivity from nuclear explosions is negligible, only that due to industrial radioactive wastes is studied; fuel preparation plants, energy-producing reactors, spent fuel processing plants, research centers and laboratories. To protect the environment of these plants it was necessary to carry out radioecological research. (France)

42411 COMPARISON OF IONIZATION AND PHOTOGRAPHIC MEASUREMENTS IN BEAMS OF FAST ELECTRONS. Vatnitskii, S. M.; Mikhailov, V. A.; Sinitsyna, A. P. (Leningrad Neuro-Surgical Inst.). Med. Radiol.; 16: No. 5, 53-6(May 1971). (In Russian).

A comparison of ionization and photographic measurements of the dose along the axis of an electron beam (23 MeV) has shown that upon corrections the results of both measurements are in good coincidence. (auth)

42412 DETERMINATION OF THE RADIATION DOSE TO CHILDREN DURING X-RAY DIAGNOSTIC PROCEDURES. Bergmanis, I. A.; Gubatova, D. Ya.; Nemiro, E. A. (Riga Medical Inst.). Med. Radiol.; 16: No. 5, 25-30(May 1971). (In Russian).

A thermofluorescent dosimeter was used on the basis of lithium fluoride (LiF) for the determination of radiation doses in children during different x-ray diagnostic procedures. In 184 patients (89 boys and 95 girls) aged from 2 months to 14 yr, the skin exposure doses were measured during roentgenological examination of thoracic organs, esophagus, stomach, intestine, bile-excreting system, and kidneys. The gonad and skin-gonad doses in the same type of examination were measured in 60 children. The skin exposure doses fluctuated significantly depending on the type and region of examination. Maximal doses were noted in subanesthetic bronchography and x-ray investigation of the gastrointestinal tract. Gonad doses reached maximal values in investigation of abdominal organs associated with the use of roentgenoscopic control of diverse duration. In such cases gonad doses were significantly greater in girls than in boys. (auth)

42413 CRITICAL LOOK AT THE RET. Liversage, W. E. (Charing Cross Group Hospitals, London). Brit. J. Radiol.; 44: 91-100(Feb 1971).

The Ellis formulae (and modifications) for a unit of biologically effective dose are criticized. It is proposed that a biological unit should be defined in terms of an equivalent single dose for skin and a new formula is proposed, based on the data of Fowler, corrected for variation in over-all time by the method of Cohen. It is claimed that the new formula is more accurate, easier to use, and should form a sounder basis for a unit of biologically effective dose than the ret. (auth)

42414 EXPERIMENTAL ANIMAL RESULTS RELATING TO TIME-DOSE RELATIONSHIPS IN RADIOTHERAPY AND THE RET CONCEPT. Fowler, J. F. (Mount Vernon Hospital, Northwood, Eng.). Brit. J. Radiol.; 44: 81-90(Feb 1971).

The experimental animal results for late and early normal tissue injury are considered in relation to the roentgen equivalent therapeutic (ret) concept. The relevance of skin reaction results to clinical situations is discussed. The variation of total dose required to produce a given degree of injury with a number of fractions only and over-all time only is examined. It is concluded that Ellis's proposed time exponent of 0.11 (or slightly less) together with a fraction-number exponent of 0.24 (or slightly more) is a reasonable approximation for radiotherapeutic injury to certain normal tissues. This approach is compared and contrasted with Liversage's proposal to use a curve relating dose to fraction-number together with a time correction of 20 (or 30) rads/day. (auth)

42415 AUTOMATION OF DOSE ANALYSIS IN RADIOTHERAPY. da Rocha, A. F. Goncalves; Borges, M. Aranha (Scuola di Medicina e Chirugia, Rio de Janeiro. Univ. Federale, Rio de Janeiro). Minerva Radiol.; 15: 77-85(Mar 1970). (In Italian).

A computer method for the calculation of the integral dose and for tracing isodose curves is presented. (J.S.R.)

42416 DATA. SECTION IV. OTHER DATA. Radiol. Health Data Rep.; 12: No. 2, 113-18(Feb 1971).

Data are presented on the environmental levels of radioactivity at Atomics International in Canoga Park, California and at the Neutron Devices Department of General Electric in St. Petersburg, Florida. Onsite and offsite monitoring data are given for air, surface waters, effluents, soils, and vegetation during January to June 1970 at both sites. It is also reported that no nuclear detonations or seismic signals were detected by the Atomic Energy Commission during January 1971. (E.R.B.)

42417 DATA. SECTION I. MILK AND FOOD. Radiol. Health Data Rep.; 12: No. 2, 87-99(Feb 1971).

Data are presented on the average ^{90}Sr, ^{131}I, and ^{137}Cs contents of raw and pasteurized milk samples in Canada, the United States, and Central and South America during October 1970 and for the 12-month period ending on that date. Data are also presented on the stable calcium and potassium and the ^{89}Sr, ^{90}Sr, and ^{137}Cs contents of diet samples from institutions in the United States during July to September 1970. All data are presented in tabular form. (E.R.B.)

XUM

42418 DATA. SECTION III. AIR AND DEPOSITION. Radiol. Health Data Rep.; 12: No. 2, 107-12(Feb 1971).

Data are presented on the radioactivity in airborne particulates and precipitation during October 1970. Reports from the Radiation Alert Network, Canadian Air and Precipitation Monitoring Program, and Pan American Air Sampling Program are included. The data include gross β radioactivity in surface air and precipitation in the United States and its territories; in Canada; and in surface air in Central and South America. These data are presented in tabular form. The monthly and yearly profiles of β radioactivity in surface air samples from selected cities in the United States and its territories during 1964 to October 1970 are also presented in graphic form. (E.R.B.)

42419 DATA. SECTION II. WATER. Radiol. Health Data Rep.; 12: No. 2, 100-6(Feb 1971).

Data are presented on the radioactivity in Washington surface waters during July 1968 to June 1969. Included in the data are monthly averages of the β and γ radioactivity in the Columbia River; average, minimum, and maximum β radioactivity in surface waters (except Columbia River) in the state; tritium content of Washington surface waters; ^{32}P, ^{51}Cr, and ^{65}Zn contents of the Columbia River; and gross β radioactivity in the Columbia River. All data are for the time period indicated, and all are presented in tabular and graphic forms. (E.R.B.)

42420 DATA. SECTION IV. OTHER DATA. ENVIRONMENTAL LEVELS OF RADIOACTIVITY. Radiol. Health Data Rep.; 12: 159-168(Mar 1971).

The environmental levels of radioactivity at the Feed Materials Production Center in Fernald, Ohio and at the Paducah Plant in Kentucky are given for the period of January to June 1970. The data include onsite and offsite air and water samples. A chart and accompanying map are presented showing the locations and capacities (net kilowatts) of current and proposed nuclear power plants in the United States. No nuclear tests were conducted nor seismic signals detected by the AEC during February 1971. (E.R.B.)

42421 DATA. SECTION I. MILK AND FOOD. Radiol. Health Data Rep.; 12: 141-50(Mar 1971).

Data on the ^{90}Sr, ^{131}I, and ^{137}Cs content of raw and pasteurized milk samples from network sampling stations in Canada, USA, and Central and South America are presented. The data, presented in tabular form, represents samples collected in November 1970. An average value for the 12-month period ending in November 1970 is also given. No data are presented from the food and diet surveillance networks. (E.R.B.)

42422 ^{90}Sr AND ^{137}Cs LEVELS IN THE DIET OF CHILDREN ON A SCHOOL LUNCH PROGRAM. Weng, P. S.; Hsu, C. N. (National Tsing Hua Univ., Hsinchu, Taiwan). Radiol. Health Data Rep.; 12: 139-40(Mar 1971).

The ^{90}Sr and ^{137}Cs contents of the diet of children on a school lunch program in Taiwan are compared with the content of these radioisotopes in the lunch diet of Taiwan adults. The basic constituent of the children's UN-supported school lunch program is imported flour products while the adults rely primarily on rice and soup. All data are presented in tabular and graphic forms. (E.R.B.)

42423 RELATIONSHIP BETWEEN SIGNAL AND BODY BACKGROUND IN THE EXTERNAL MEASUREMENT OF RADIOACTIVITY: EXPERIMENTS ON A PHANTOM. Meldolesi, U.; Roncari, G. (Univ., Milan). Radiol. Med.; 56: 656-69(Aug 1970). (In Italian).

Conditions applicable to the external determination of radioisotope data concerning dynamic phenomena were reproduced in experiments on the phantom. A separate assessment was made for each condition of the radioactivity contained in the simulated organ and in its surroundings. These data were then normalized against radioactivity concentration values and a signal/body background ratio was determined; this ratio is taken as having general significance as a parameter of measurement sensitivity with respect to the organ under study. Ratio values under different conditions were then reproduced graphically in the form of readily consultable families of curves. This permits easy estimation of the changes in selectivity that will result from alteration of various physical and geometrical detection parameters. (auth)

42424 RADIATION MEASUREMENTS IN BRASOV DURING THE PERIOD AUGUST 1961 TO AUGUST 1968. Munteanu, G.; Parpala, V.; Sisak, St.; (and others). Bul. Inst. Politeh. Brasov, Ser. B; 11: 35-43(1969). (In Rumanian).

The results obtained from the measurement of the radioactivity in the environment surrounding the RMA stations of the Institute of Atomic Physics of the Academy of Rumania at Brasov over a 7-yr period are given. The main conclusions were obtained in the course of the analysis of the experimental data and are an indication of the prospects of the future. (E.R.B.)

42425 DOZIMETRIYA I ZASHCHITA OT IONIZIRUYUSHCHIKH IZLUCHENII. (Dosimetry and Protection Against Ionizing Radiation). Golubev, B. P. Moscow; Atomizdat (1971). 400p.

The subjects of dosimetry and radiation protection are surveyed in some depth. The first several chapters deal with the biological action of ionizing radiation, the interaction of alpha and beta particles as well as x and gamma radiation with matter, the attenuation of radiation, and the absorption and scattering of neutrons. The subject of dosimetry is next presented: units of activity, radiation dose units, equivalent dosage, flux, and flux density. Crystal and semiconductor counters, ionization chambers, gas counters, and scintillation techniques are the basis for two chapters. Four chapters deal with photographic, calorimetric, and chemical methods of dosimetry, together with techniques of measuring and recording neutron dosages. Other equipment for measuring ionizing radiation include electroscopes, electrometers, detection by charge or discharge, and scalers. Dosimetric control at nuclear station sites, decontamination of radioactive gases, aerosols, and liquids, radiation safety, and protection from ionizing radiation constitute the closing chapters. Extensive tables are included for the calculation of dose factors for various geometries, attenuation coefficients for shielding, penetration of α- and β-particles, data on selected radioisotopes, and a special table of biological interest: for each isotope there is given the annual maximum permissable intake, an annual average permissible concentration for workers handling radiation sources, and the maximum permissible body exposure for personnel. (166 figures, 62 tables, and 152 references.) (K.S.W.)

42426 DATA. SECTION III. AIR AND DEPOSITION. Radiol. Health Data Rep.; 12: 152-8(Mar 1971).

Data are presented on the radioactivity in airborne particulates and precipitation in Canada, the United States and its territories, and Central and South America during November 1970. Included among the data are the gross β radioactivity in the surface atmosphere and atmospheric precipitation in the United States and its territories; in Canada; and in the surface atmosphere of Central and South America. The ^{238}Pu and ^{239}Pu contents of airborne particulates in selected cities on the Radiation Alert Network during January to June 1970 are also given. Monthly and Yearly profiles are presented of the β radioactivity in the atmosphere of eight cities on the Radiation Alert Network during 1964 to November 1970. (E.R.B.)

42427 ALPHA-ACTIVITY OF WESTERN AUSTRALIAN SOILS AND WHEATS. Chute, J. H.; Clapp, R. A.; Quirk, J. P. (Univ. of Western Australia, Nedlands). J. Roy. Soc. West. Aust.; 53: 37- (1970).

Lateritic soils formed on the Precambrian shield of southwestern Australia have measured α activities in the range of 40 to 100 pCi/g from naturally occurring isotopes; whereas in soils formed on Mesozoic and Cainozoic coastal sediments the α activity seldom exceeds 20 pCi/g. The ash activity of wheat growing on the more active soils can be as high as 90 pCi/g. However, there is at least a three-fold variation in uptake of active isotopes depending on wheat variety. For the lateritic soils, there is a correlation between total α activity and both ironstone gravel content and the total Fe + Al in the soil. There is also some evidence for an activity dependence on present climate and rainfall. Although applied superphosphate fertilizer is high in natural radioactivity, it is not believed to have made a significant contribution to the measured α activity of the soil. (auth) (Australia)

42428 COMPUTERISED STUDY OF DOSE DISTRIBUTIONS AROUND LINEAR ^{192}Ir SOURCES. Botturi, M.; Jucker, C.; Tosi, G.; Pedrinazzi, G.; Scielzo, G. (Ospedale Maggiore, Milan. Univ., Pavia, Italy). Radiol. Med.; 56: 670-84(Aug 1970). (In Italian).

A computerized mathematical model giving very high dosimetric accuracy at a large number of points at various distances from differently combined ^{192}Ir needles is reported. Detailed assessment of theoretical dose distributions around ideally arranged sources and of the dose actually absorbed in practice is described. The method gives rad/hr tables for different source types so that isodose curves can be determined. It can also be employed in dose intensity evaluation around multi-source systems with well-defined geometry. (auth)

42429 STUDY OF ^{210}Po CONTENT IN THE ENVIRONMENT AND THE HUMAN BODY. Kozlova, M. V.; Korenkov, I. P.; Novikov, Yu. V.; Korzunova, R. A.; Pedchenko, V. I. Gig. Sanit.; No. 4, 44-7(Apr 1971). (In Russian).

Polonium-210 makes up a considerable part of the radioactive background of man. The concentration of this substance in the at-

mosphere makes 7.1 ± 1.10^{-18} Ci/l and in certain kinds of plants—from 530 to 7250 · 10^{-12} Ci/kg. The highest concentrations of ^{210}Po were detected in the reindeer moss from Anadyr (7250 · 10^{-12} Ci/kg). Its concentration in the drinking water is at the level of 0.03 · 10^{-12} Ci/l and in the rainwater—at the level of 0.39 · 10^{-12} Ci/l. The smallest concentrations of ^{210}Po were found in the potatoes of the central zone of the Soviet Union (2.2 · 10^{-12} Ci/kg) and the highest concentrations were in the liver of cattle (90 · 10^{-12} Ci/kg). In the deer's meat of the Yakutskaya ASSR and the Murmansk district, the ^{210}Po content amounted to 260 · 10^{-12} and 957 10^{-12} Ci/kg accordingly. In case of daily average consumption of this meat by man in an amount of 230 g, the irradiation dose of the skeleton would make 0.35 to 1.8 rad/yr. High concentrations of ^{210}Po were found in the deer's bones in the Murmansk district (1057 · 10^{-12} Ci/kg) and the Arkhangelsk district (4923 · 10^{-12} Ci/kg). The dose of internal irradiation in the first case equals 5 rad/yr and in the second case amounts to 25 rad/yr. Taking into account the concentration of ^{210}Po in the reindeer moss and that in the skeleton, its accumulation may be from 2.5 to 4.5 fold. The ^{210}Po content in the bone tissues amounts to 0.032 to 0.078 Ci/g, in the teeth—$0.17 \pm 0.06 \cdot 10^{-12}$ and that in the hair—0.1 ± 0.014 10^{-12} Ci/g. No correlation was found to exist between the concentrations of ^{210}Po in the hair and those in the bones. The concentrations of ^{210}Po in the liver and the kidneys were at the level of 0.048 · 10^{-12} and 0.041 · 10^{-12} Ci/g. (auth)

42430 ATTENUATION OF X RAYS IN THE HUMAN BODY. Cohen, M. (London Hospital). Radiography; 37: 88-90(Apr 1971).

The choice of x ray energies for diagnostic radiography and radiotherapy is discussed in relation to energy attenuation by photoelectric absorption and the Compton effect. White-Grodstein attenuation data are presented for calcium phosphate and water, to show how the percentage of the total photoelectric attenuation varies with the photon energy of the radiation. Fifty percent or more of the attenuation in bone in the diagnostic range was due to photoelectric absorption, but in other tissues, this was so only for photons below 25 keV, or x rays generated below 60 kV. It was concluded that for most diagnosis, the Compton effect predominates, but the differentiation between bone and other tissues would be better in the absence of the effect, especially at the upper end of the diagnostic range. For radiotherapy, where the beam has to pass through a considerable thickness of bone, attenuation throughout by the Compton effect would be an advantage, being independent of the atomic number of the absorber. (UK)

42431 EXPOSURE RATES FROM DIAGNOSTIC X RAY UNITS. McCullough, Edwin C.; Cameron, John R. (Univ. of Wisconsin, Madison). Health Phys.; 20: 443-4(Apr 1971).

The exposure rates from diagnostic x-ray units operated at 40 to 150 kVp and with 1 to 4.5 mm of Al filtration were calculated using Kramer's rule for the differential bremsstrahlung spectra produced by a tungsten target. The results for a focus-to-skin distance of 40 in. are tabulated. It was found possible to estimate the exposure rate with an accuracy of ±20%. (auth)

42432 COMPARISON OF TWO RADIATION THERAPY-TREATMENT PLANS FOR CARCINOMA OF THE CERVIX. I PERSONNEL RADIATION EXPOSURE. Boronow, Richard C.; Hickman, Bernard T. (Univ. of Mississippi, Jackson). Amer. J. Obstet. Gynecol.; 110: No. 5, 693-5(1 Jul 1971).

Patients receiving radiation therapy for invasive carcinoma of the cervix were put in a randomized study to evaluate two different modalities (on a stage-for-stage basis) in terms of survival data, early and late complications, and physician radiation exposure. The traditional treatment plan employed at this institution and utilization of a loaded radium applicator (Ernst) were compared in a random fashion with another treatment plan with the use of an after-loading radium system (Fletcher-Suit). Radiation exposure to the operator and assistant were measured by utilizing film badges in the operating room when the loaded system was employed and at the bedside when the after-loading was used. In this manner, it was possible to document the marked quantitative difference in physician radiation exposure with the two systems. In addition, qualitative benefits are discussed. Our institution has discontinued the use of the loaded system. (auth)

42433 MATHEMATICS OF RADIOLOGY AND NUCLEAR MEDICINE. Jackson, Herbert L. A Monograph in Modern Concepts of Radiology, Nuclear Medicine, and Ultrasound. St. Louis; Warren H. Green, Inc. (1971). 178p. $12.00.

The specific quantitative techniques required by the radiologist are explained and examples and problems for drill are provided. Arithmetic facility and graphical methods are stressed. The book is designed primarily for the radiologist, but will also be of value to x-ray technicians. (E.R.B.)

42434 DOSE COMMITMENT. Barry, P. J. (Atomic Energy of Canada Ltd., Chalk River, Ont.); Shleien, Bernard. Health Phys.; 20: 451-2(Apr 1971).

Comments are made on a paper by Shleien (Health Phys: 18: 267 (1970)) in which doses to adult bone from ^{90}Sr in food ingested between 1961 and 1968 were reported. It is stated that these could be misleading unless the restricted portion of the adult population to which they apply is realized. Computations of the necessary life span of those individuals used to estimate the dose commitment of the population are given to emphasize the point. In his reply Shleien redefines dose commitment as that dose delivered to an individual in a population group over a 50-yr period within the context of the individual's dietary intake, life span, organ size, and radiobiological facts and states that it was presented as a tool for evaluation of environmental surveillance data. Although it is believed that the limitations are not as severe as indicated by Barry it is not proposed that the technique be employed to estimate dose commitments to world wide populations. (UK)

42435 MEASUREMENT OF INTERNAL CONTAMINATION IN THE VICINITY OF THE E.N.E.L. NUCLEAR ELECTRIC CENTER AT GARIGLIANO. Antonucci, L. (ENEL, Garigliano, Italy); Farulla, A.; Naro, G. Minerva Fisiconucl.; 14: 101-3 (Jul-Sep 1970). (In Italian). (CONF-680535-33).

From fourteenth national conference of the Italian Association for Health Physics and Protection from Radiation; Formia, Italy (29 May 1968).

The results of whole-body counting done from 1964 to 1967 at the Garigliano nuclear electric system were reported. Of the 992 cases studied, only 11 had contamination levels higher than the significant value, corresponding to 1/100 of the maximum permissible body accumulation. Some of the implications of the radioprotection connected with the detection of an internal radiocontamination were discussed. Emphasis was placed on the identification of the critical organ for the most frequently found radioisotopes. (tr-auth)

42436 DOSIMETRY OF A FLAT CIRCULAR ^{210}Po α SOURCE. Scarpa, Giorgio (CNEN, Rome). Minerva Fisiconucl.; 13: 109-20(Jan-Mar 1969). (In Italian).

The results of a theoretical and experimental study on the problem of the evaluation of the particle flux and of the absorbed dose for a biological sample irradiated with a flat circular α source of ^{210}Po were reported. The experimental methods included measurements with surface-barrier semiconductor detector and measurements with extrapolation ionization chamber. These methods were shown to be useful in giving data on absolute values and on the spatial distribution of dosimetric magnitudes. The method that appears to be most convenient in practical use is the extrapolation ionization chamber. The results of a study on the spatial distribution of the flux and dose at the surface and the interior of samples are reported. Some objective criteria for the selection of technical irradiation parameters are given. (tr-auth)

42437 MATHEMATICAL SIMULATION OF RADIATION THERAPY OF SOLID TUMORS. I. CALCULATIONS. Fischer, James J. (Yale Univ., New Haven). Acta Radiol., Ther., Phys., Biol.; 10: 73-85(1971).

A mathematical model has been developed to simulate the treatment of solid tumors with radiation therapy. It is sufficiently detailed to take into account differences in sensitivity of hypoxic and well oxygenated cells, radiation induced mitotic delay, reproduction of viable cells between treatments, delayed dissolution of sterilized cells, and re-oxygenation of hypoxic cells as the tumor decreases in size. Any desired treatment regimen may be specified. The results obtained in using this model agree exceptionally well with known clinical and experimental data. A sample calculation is presented in detail. (auth) (Sweden)

42438 INHERENT DOSIMETER FOR IRRADIATED FOODS: PAPAYAS. Boshard, J. P.; Holmes, D. E.; Piette, L. H. (Univ. of Hawaii, Honolulu). Int. J. Appl. Radiat. Isotop.; 22: No. 5, 316-18(May 1971).

The variation of the average fractional increase in papaya seed free radical content with gamma irradiation dose was used as an indicator of dose received. Papaya fruit age and pre-irradiation storage temperature did not have a large effect on the dosimetry values determined by the electron spin resonance technique. (UK)

42439 MONITORING FOR INTERNAL EXPOSURE. 2. EXPERIENCE IN THE CONTROL OF PERSONAL EXPOSURE AT JAERI AND PROBLEMS FOR SOLUTION. Yabe, Akira (Japan Atomic Energy Research Inst., Tokai). Hoken Butsuri; 5: No. 3, 145-9(Sep 1970). (In Japanese).

The present state of monitoring for internal exposure at the Japan Atomic Energy Research Institute is reported. At JAERI,

XUM

both periodical and occasional monitorings are adopted. The former is to check personal internal contamination periodically, and is conducted four times a year. Although it is desirable that all members be monitored, only selected members are monitored because of the investigation staff and economics. The latter is carried out at every completion of work in which some contamination is inevitable, in cases of accident, or as a supplement to the periodical one. For monitoring, both whole-body counting and sample (urine, feces, and blood) analyses have been adopted. Each has its advantages and disadvantages, and the combined use of both for γ emitters makes it possible to obtain more accurate information about contamination. Calculation of exposure dose by urinalysis is possible in case of single ingestion of one nuclide, but impossible or inaccurate in case of repeated ingestion or of single ingestion of many nuclides. (Japan)

42440 COMMENTS ON RADIATION QUANTITIES AND THEIR SIGNIFICANCE IN HEALTH PHYSICS. PARTS 1 AND 2. Wyckoff, H. O. Health Phys.; 20: No. 6, 669(Jun 1971).

Brief comments are presented on the relation between linear energy transfer and quality factor and definitions of generalised dose equivalent, reference dose, and standard increment of reference dose. The definitions of the ICRP and ICRU in this field are noted. (UK)

42441 QUALITY FACTOR: A SOUND CONCEPT. Dunster, H. J. (United Kingdom Atomic Energy Authority, Harwell, Eng.). Health Phys.; 20: No. 5, 529-31(May 1971).

Includes reply by W. H. Patterson; R. H. Thomas; and J. Neufield.

Dunster states that in interpreting the term quality factor (QF) the present position is logically unassailable although of more limited practical use than had originally been expected and that QF is not a special case of relative biological effectiveness (RBE) but an altogether different quantity. It is considered that the difficulty is not a conceptual one but only the practical one of providing the arithmetical rules for obtaining the product $D \times QF$ (D absorbed dose). The need for an average value of QF, or modifying factor, is doubted. Patterson and Thomas agree with Dunster about the limited use of QF and in the difficulty in providing arithmetical rules. However the difficulties of selection of an appropriate average value of QF from a LET spectrum are stressed and official and authoritative guidance is called for. Neufeld disagrees with the statement that the present position is logically unassailable and foresees difficulties in obtaining the true estimate of QF. The arguments for recognizing two different concepts to which different numerical values would be assigned are reiterated; $^{(QF)}$LET being the quality factor which is LET dependent and $(QF)_{DE}$ being defined as DE/D where D is absorbed dose and DE dose equivalent. (UK)

42442 POSITIONING OF FILM BADGES. Farmer, F. T.; Langmead, W. A. (British Inst. of Radiology, London). Brit. J. Radiol.; 44: No. 522, 480-1(Jun 1971).

A statement is made of the views of the Radiation Protection Committee of the British Institute of Radiology on the Draft Code of Practise to be followed when wearing film badges for individual monitoring. A primary film badge should be worn in a constant position, preferably at the waist, under the protective apron if worn. Additional ones should be worn if it is possible that unprotected parts may receive maximum permitted doses. The position of film badges worn for monitoring the working environment may be different. Note is made of the dangers to radioisotope workers and the wearing of LiFl-teflon discs instead of film badges. (UK)

42443 WHAT QUALITY FACTOR. Patterson, H. Wade; Routti, Jorma T.; Thomas, Ralph H. (Univ. of California, Berkeley). Health Phys.; 20: No. 5, 517-27(May 1971).

The evaluation of dose-equivalent rates in mixed radiation environments such as are found, for example, around a high energy particle accelerator is discussed. It is shown that it is not possible to evaluate absorbed dose and dose-equivalent rates by any single measurement, in such complicated environments, with sufficient accuracy for purposes of radiation protection. The problems of evaluating dose equivalent from measurements of absorbed dose made with a tissue-equivalent ionization chamber are discussed. The potential errors in estimating dose equivalent when making absorbed dose measurements and assuming a single value of quality factor are indicated. Knowledge of such errors is a valuable guide to operational health physicists. (auth) (UK)

42444 PERSONAL MONITORING OF WORKERS DURING THE TRANSLOCATION OF A ^{90}Sr–^{90}Y BETA SOURCE BY THE AID OF TLD. Spurny, Z. (Nuclear Research Inst., Prague); Koci, J.; Jerabek, J.; Novotny, J. Jad. Energ.; 17: No. 5, 168-70(May 1971). (In Czech).

For the personal monitoring of workers during the transport of a 2 Ci $^{90}Sr-^{90}Y$ beta source, thermoluminescent dosimeters (TLDs) were successfully used. Exposures of the whole body as well as the hands, head, and gonads were assessed during the whole operation. The couple $LiF-CaF_2$ served for rough estimation of the bremsstrahlung-energy that is necessary for the absorbed dose calculation. Estimated exposures were strongly unhomogeneous. The results of the experiment may be successfully applied to safe monitoring of radiation sources. (auth)

42445 NEUTRON DOSE DISTRIBUTIONS FOR ^{252}Cf SOURCES. Nagarajan, P. S.; Dayashankar; Venkataraman, G. (Bhabha Atomic Research Centre, Trombay, India). Int. J. Appl. Radiat. Isotop.; 22: No. 6, 325-9(Jun 1971).

The neutron dose distribution in tissue-equivalent material for a ^{252}Cf point source was calculated by the Monte Carlo method. Using these data, the dose-rate distribution for an implantable ^{252}Cf line source was obtained, and the results are compared with available experimental data. Calculated neutron isodose curves for line sources of length 1.35 and 2 cm are presented. (auth) (UK)

42446 NOMINAL STANDARD DOSE AND THE RET. Liversage, W. E. (Charing Cross Hospital, London). Brit. J. Radiol.; 44: No. 522, 477-8(Jun 1971).

The Ellis formula for establishing a unit of biologically effective dose (the RET) is criticised and reviewed, with reference to tumors which do not fit the formula, including squamous cell carcinomas of the skin. Emphasis is made on the need to define the specific biological effect being measured. (UK)

Radiation Protection

Refer also to abstracts 42680, 42692, and 42693.

42447 REDUCTION OF DOSAGE IN X RAYS OF THE PELVIS. Smith, A. R. B. (Dept. of Public Health, New South Wales, Australia). Radiographer; 17: No. 3, 6-8(Mar 1971).

The use of filters to reduce patient dose during diagnostic radiographic procedures in the pelvic region is discussed. Codes of practice in New South Wales and Western Australia are compared with requirements in the rest of Australia. A series of radiographs of a phantom pelvis taken with aluminum filters from 0 to 3 mm thick showed little discernible difference in radiographic quality while the dose was substantially reduced. Scattered radiation in the theatre of operation was also significantly reduced. (Australia)

42448 VOPROSY ZASHCHITY OT IONIZIRUYUSHCHIKH IZLUCHENII V RADIATSIONNOI KHIMII. (Problems of Protection from Ionizing Radiations in Radiation Chemistry). Bykhovskii, A. V.; Larichev, A. V.; Chistov, E. D. Moscow; Atomizdat (1970). 280p.

The characteristics of the main concepts of radiation chemistry, radiation protection, and dosimetry are given, and the factors regarding radiation dangers attendant to the use of research apparatus are briefly clarified. Conditions for protection against external radiation and methods of averting the penetration of radioactive substances into the body during work with radiochemical apparatus are described. The services of radiation safety organizations are also recommended. The book is designed for a wide range of readers; technicians, engineers, radiation chemistry personnel, and workers in the field of personnel protection. The bibliography contains 378 titles. (tr-auth)

42449 NOTES FOR THE GUIDANCE OF PERSONS CONCERNED IN THE CARRIAGE OF RADIOACTIVE SUBSTANCES BY SEA. Australia; Department of Shipping and Transport (1969). 44p. Available from Atomic Energy Attache, Australian Embassy, Washington, D. C.

Standards of Australia governing the transportation of radioactive materials on ships are presented. The standards are based on IAEA regulations. Requirements for the packaging, labeling, stowage, and monitoring of radioactive materials are summarized. Radiation sources and radioisotopes are classified in groups for shipment purposes. Instructions for special arrangements for shipment when the package or packaging does not meet all relevant parts of the IAEA regulations are included. (C.H.)

42450 ATOMIC ENERGY AND RADIOACTIVE SUBSTANCES. THE RADIOACTIVE SUBSTANCES (CARRIAGE BY ROAD) (GREAT BRITAIN) REGULATIONS, 1970. Statutory Instruments, No. 1826 1970. London; Her Majesty's Stationery Office (1970). 19p. Available from British Information Service, New York.

Regulations in Great Britain concerning the transportation on

roads of radioactive materials are summarized. Regulations for labeling packages and the marking of vehicles are included. (C.H.)

42451 ATOMIC ENERGY AND RADIOACTIVE SUBSTANCES. THE RADIOACTIVE SUBSTANCES (ROAD TRANSPORT WORKERS) (GREAT BRITAIN) REGULATIONS, 1970. Statutory Instruments, No. 1827 1970. London: Her Majesty's Stationery Office (1970). 14p. Available from British Information Service, New York.

Regulations in Great Britain governing the radiation protection of transportation personnel hauling radioactive materials on roads are summarized. Provisions for maintaining records of radiation dose are summarized. (C.H.)

42452 RADIATION PROTECTION STANDARDS. Taylor, Lauriston S. (National Academy of Sciences, Washington, D. C.). CRC Crit. Rev. Environ. Contr.; 2: No. 1, 81-124(Apr 1971).

The evolution of radiation protection standards is reviewed with emphasis on the role of the National Council on Radiation Protection (NCRP) in the U.S.A., the International Commission on Radiation Units (ICRU), and the International Commission on Radiation Protection (ICRP). The contributions of other organizations in the development of radiation protection standards are reported. The contents of a number of reports covering various aspects of radiation protection issued by the NCRP are summarized briefly. (C.H.)

42453 PROTECTION OF THE PATIENT IN X-RAY DIAGNOSIS. A REPORT PREPARED BY A TASK GROUP OF COMMITTEE 3 OF THE INTERNATIONAL COMMISSION ON RADIOLOGICAL PROTECTION. RADIATION PROTECTION. ICRP Publication 16 1969. New York; Pergamon Press (1970). 46p. Available from Pergamon Press, Inc., Elmsford, N. Y.

Basic physical and biological concepts pertinent to the protection of patients from x radiation during diagnostic radiography are reviewed. The long-term genetic and somatic effects of radiation on human populations as a function of energy absorbed in the body, dose rate, the tissue exposed, the cumulative radiation dose, and the age and sex of the patient are considered. Data on the annual frequencies of diagnostic radiographic examinations in 12 representative countries and data on the radiation dose to the bone marrow and gonads during various radiographic examinations are presented. General recommendations applicable to radiation protection of the patient and specific recommendations for protection during fluoroscopic examinations of the chest; during heart catheterization; during pregnancy; during mammography; and during dental radiography are included. (C.H.)

42454 RADIOSENSITIVITY AND SPATIAL DISTRIBUTION OF DOSE. RADIATION PROTECTION. ICRP Publication 14 1969. New York; Pergamon Press (1969). 118p. Available from Pergamon Press, Inc., Elmsford, N. Y.

Data pertinent to the establishment of radiation dose limits for the occupational exposure of personnel and for the exposure of the human population are presented. The data represent the contributions of two task groups, one of which considered the spatial distribution of radiation dose in tissues and the other the relative radiosensitivity of different tissues. The limitations of various methods for deriving dose limits for exposure are discussed. It was concluded that somatic radiation effects that should be considered when setting dose limits for occupational exposure include induction of cataracts and tumors, impaired fertility, and defective development of the fetus. (C.H.)

42455 PROTECTION AGAINST IONIZING RADIATION FROM EXTERNAL SOURCES. A REPORT BY COMMITTEE 3 OF THE INTERNATIONAL COMMISSION ON RADIOLOGICAL PROTECTION. RADIATION PROTECTION. ICRP Publication 15 1969. New York; Pergamon Press (1970). 32p. Available from Pergamon Press, Inc., Elmsford, N. Y.

Recommendations for the protection of personnel from external sources of radiation are presented. Emphasis is placed on the protection of medical personnel using radioisotopes and radiation sources for diagnosis and therapy. It is pointed out that the same basic precautions will apply during the use of radioisotopes and radiation sources in industry, veterinary medicine, and research establishments. (C.H.)

42456 IATA RESTRICTED ARTICLES REGULATIONS. 14th EDITION EFFECTIVE 1st JUNE 1971. Montreal; International Air Transport Association (1971). 164p. Available from International Air Transport Association, Montreal.

Regulations of the International Air Transport Association, effective June 1, 1971, governing the air transport of restricted articles, including combustible liquids, compressed gases, corrosive liquids, explosives, flammable liquids, flammable solids, magnetized materials, oxidizing materials, poisons, polymerizable materials, noxious or irritating substances, and radioactive materials are presented. Labeling and packaging requirements, including container standards, for transport by passenger and cargo aircraft and recommendations and mandatory regulations for the handling and loading of restricted materials are included. Regulations concerning the air transport of radioactive materials are detailed. The regulations are based on the International Atomic Energy Agency (IAEA) Recommendations for the Safe Transport of Radioactive Materials (1967 ed.) now in effect in many countries. (C.H.)

42457 QUICK REFERENCE GUIDE FOR CARRIAGE OF RADIOACTIVE MATERIALS BY AIR. THIRD EDITION, 1st JUNE, 1970. Montreal; International Air Transport Association (1970). 11p. Available from International Air Transport Association, Montreal.

A quick reference guide to regulations concerning the shipment of radioactive materials by aircraft is presented. The guide is based on 1970 standards of the International Air Transport Association. (C.H.)

42458 MANUAL OF INDUSTRIAL RADIATION PROTECTION. PART I. CONVENTION AND RECOMMENDATION CONCERNING THE PROTECTION OF WORKERS AGAINST IONISING RADIATIONS. Geneva; International Labour Office (1963). 24p. Available from International Labour Office, Geneva.

The Convention adopted in 1960 lays down the basic principles of radiation protection based on universally accepted scientific knowledge. The Recommendations presented expand these principles as they apply to the protection of personnel against ionizing radiations. (C.H.)

42459 MANUAL OF INDUSTRIAL RADIATION PROTECTION. PART II. MODEL CODE OF SAFETY REGULATIONS (IONISING RADIATIONS). Geneva; International Labour Office (1959). 54p. Available from International Labour Office, Geneva.

A model code of safety regulations is presented for industrial establishments using unsealed radioactive materials having a specific activity above 0.002 μCi/gm, sealed radiation sources exposure to which would exceed mrems/hr, and apparatus producing electron beams that might give rise to stray x rays during use. The provisions of the Code are also applicable to industrial establishments where such radioactive materials are stored. This code does not apply to chemical and metallurgical plants processing natural radioactive materials or nuclear fuels, facilities for the bulk storage of radioactive materials, nuclear reactors, or high-energy accelerators for the production of radioisotopes. (C.H.)

42460 MANUAL OF INDUSTRIAL RADIATION PROTECTION. PART III. GENERAL GUIDE ON PROTECTION AGAINST IONISING RADIATIONS. Geneva; International Labour Office (1963). 95p. Available from International Labour Office, Geneva.

The basic fundamentals of nuclear physics are reviewed for the guidance of industrial administrators and others in industry in acquiring an understanding of the principles of radiation protection. Radiation dose units and limits are defined, radiation measuring instruments are described, and the principles of radiation protection and monitoring are reviewed. (C.H.)

42461 MANUAL OF INDUSTRIAL RADIATION PROTECTION. PART IV. GUIDE ON PROTECTION AGAINST IONISING RADIATIONS IN INDUSTRIAL RADIOGRAPHY AND FLUOROSCOPY. Geneva; International Labour Office (1964). 62p. Available from International Labour Office, Geneva.

Radiation protection methods applicable to control of radiation exposures of personnel in industrial radiography and fluoroscopy are presented. The use of both γ and x ray sources is considered. Shielding calculations and operating procedures to ensure safety are included. (C.H.)

42462 MANUAL OF INDUSTRIAL RADIATION PROTECTION. PART V. GUIDE ON PROTECTION AGAINST IONISING RADIATIONS IN THE APPLICATION OF LUMINOUS COMPOUNDS. Geneva; International Labour Office (1964). 48p. Available from International Labour Office, Geneva.

A guide to radiation protection practices for personnel applying luminescent paints or other substances containing radioactive materials is presented. The hazards from external or internal exposure to the α, β, and γ radiations emitted by various radioactive substances used for the activation of luminescent materials are reviewed. (C.H.)

42463 MANUAL OF INDUSTRIAL RADIATION PROTECTION. PART VI. RADIATION PROTECTION IN THE MINING AND MILLING OF RADIOACTIVE ORES. IAEA Safety Series No. 26

XUM

1968. Geneva; International Labour Office and International Atomic Energy Agency (1968). 108p. Available from International Labour Office, Geneva.

A code of practice for the radiation protection of personnel mining and milling radioactive ores is presented. General radiation protection methods, monitoring methods for personnel and the environment, protective methods and equipment for the control of radioactive dust and gases, and technical information that may be useful in the application of control measures are included. (C.H.)

42464 REPORT OF COMMITTEE IV ON PROTECTION AGAINST ELECTROMAGNETIC RADIATION ABOVE 3 MeV AND ELECTRONS, NEUTRONS, AND PROTONS. RECOMMENDATIONS OF THE INTERNATIONAL COMMISSION ON RADIOLOGICAL PROTECTION. RADIATION PROTECTION. ICRP Publication 4 1962. New York; Pergamon Press (1964). 44p. Available from Pergamon Press, Inc., Elmsford, N. Y.

Recommendations are presented for the protection of personnel working with electromagnetic radiations above 3 MeV, electrons, protons, and neutrons with energies up to 1000 MeV. The special risks involved in working with high-energy radiation and heavy particles are reviewed. Recommendations for monitoring the area around generators and general recommendations as to the installation and shielding of sources of high-energy radiation and heavy particles are included. (C.H.)

42465 PRINCIPLES OF ENVIRONMENTAL MONITORING RELATED TO THE HANDLING OF RADIOACTIVE MATERIALS. A REPORT BY COMMITTEE 4 OF THE INTERNATIONAL COMMISSION ON RADIOLOGICAL PROTECTION. RADIATION PROTECTION. ICRP Publication 7 1965. New York; Pergamon Press ([1966]). 11p. Available from Pergamon Press, Inc., Elmsford, N. Y.

Environmental radiation monitoring is defined as the measurement of radiation and radioactivity outside the boundaries of installations handling radioactive materials or radiation sources, and is restricted to measurements made necessary by the operation of these installations. Monitoring of the release of wastes is closely connected with environmental monitoring and provide sufficient information to make environmental monitoring unnecessary in the great majority of cases although emergency surveys may be necessary. The object of environmental monitoring programs is protection of the public against the inhalation or ingestion of radioactive materials. (C.H.)

42466 RECOMMENDATIONS OF THE INTERNATIONAL COMMISSION ON RADIOLOGICAL PROTECTION. RADIATION PROTECTION. ICRP Publication 9 1965. New York; Pergamon Press (1966). 27p. Available from Pergamon Press, Inc., Elmsford, N. Y.

The basic principles underlying the ICRP radiation protection recommendations for personnel and the general public are reviewed. It is pointed out that, since any exposure may involve a degree of risk, it is recommended that all doses be kept as low as is readily achievable while taking economic and social considerations into account. Recommendations for radiation dose limits are intended for planning the design and operation of facilities leading to foreseeable conditions of radiation exposure. When the source of radiation exposure is uncontrolled, as in the case of nuclear weapon explosions or reactor accidents, the exposure can only be controlled by remedial measure, which in themselves may be more hazardous than the risks from the unplanned exposure. The decision to take remedial action will have to take account of the particular circumstances that prevail, the risks involved, and the social consequences of the remedial action. The setting of standards for radiation dose levels at which various countermeasures should be considered would be the responsibility of the health physics department in the case of reactor accidents and of national authorities in the case of nuclear weapon explosions. (C.H.)

42467 REPORT OF COMMITTEE IV ON EVALUATION OF RADIATION DOSES TO BODY TISSUES FROM INTERNAL CONTAMINATION DUE TO OCCUPATIONAL EXPOSURE. RECOMMENDATIONS OF THE INTERNATIONAL COMMISSION ON RADIOLOGICAL PROTECTION. RADIATION PROTECTION. ICRP Publication 10 1968. New York; Pergamon Press (1968). 94p. Available from Pergamon Press, Inc., Elmsford, N. Y.

Methods for the calculation of radiation doses to various human organs and tissues following the intake and deposition of some 30 radioisotopes and naturally radioactive materials frequently encountered by atomic energy personnel are described. The chemical and physical form of the radioisotopes and the method of intake (inhalation, ingestion, or through wounds) are considered. Mathematical models of radioisotope distribution in tissues and supplemental data from animal studies are included. Metabolic information is presented on ^{22}Na, ^{32}P, ^{35}S, ^{36}Cl, ^{45}Ca, ^{59}Fe, ^{60}Co; ^{65}Zn, ^{86}Rb, ^{85}Sr, ^{89}Sr, ^{90}Sr, ^{132}Te, ^{131}I, ^{132}I, ^{137}Cs, ^{140}Ba, ^{144}Ce, ^{198}Au, ^{210}Po, ^{226}Ra, ^{233}U, ^{234}U, ^{235}U, ^{238}U, ^{239}Np, ^{239}Pu, ^{241}Pu, natural thorium, natural uranium, tritium oxide, and ^{14}C-labeled CO_2. (C.H.)

42468 FACTORIES: THE IONISING RADIATIONS (UNSEALED RADIOACTIVE SUBSTANCES) REGULATIONS, 1968. Statutory Instruments, No. 780 1968. London; Her Majesty's Stationery Office (1968). 32p. Available from British Information Service, New York.

Regulations adopted in Great Britain in 1968 governing the radiation protection of persons employed by industries using unsealed radioactive substances are presented. Data are included on maximum permissible levels of contamination on surfaces for some 250 radioisotopes, which are grouped in four classes according to their toxic effects on man. (C.H.)

42469 FACTORIES: THE IONISING RADIATIONS (SEALED SOURCES) REGULATIONS, 1969. Statutory Instruments, No. 808 1969. London; Her Majesty's Stationery Office (1969). 20p. Available from British Information Service, New York.

Regulations adopted in Great Britain in 1969 governing the radiation protection of persons employed by industrial establishments using sealed sources of ionizing radiation or x-ray generating apparatus are presented. Data are included on the maximum permissible radiation dose for industrial uses of radiations. (C.H.)

42470 PUBLIC HEALTH SERVICE DRINKING WATER STANDARDS. Public Health Service Publication No. 956 1962. Washington, D. C.; Department of Health, Education, and Welfare (1969). 61p. Available from Superintendent of Documents, GPO, Washington, D. C.

Standards for drinking water supplies in the U.S.A. are presented. Data are included on maximum permissible concentrations of ^{131}I, ^{226}Ra, ^{89}Sr, and ^{90}Sr acceptable in water for human consumption. (C.H.)

42471 PREVENTIVE ORAL CARE FOR THE IRRADIATED CANCER PATIENT. Daly, Thomas E.; Drane, Joe B. (Texas Medical Center, Houston). Dent. Surv.; 46: 36-8(Nov 1970).

Preventive dentistry has much to offer for the head and neck cancer patient who is to undergo radiation therapy or surgery. The proper use of all diagnostic tools and the experiences of all practitioners will greatly reduce the need for rehabilitation of these patients and improve the overall quality of survival. The significance of this hopeful prognosis is not universally known. For years the various aspects of oral care for the head and neck cancer patient have been grossly misunderstood, with the main objective limited only to eradication of the disease. For many years, too, the high incidence of bone necrosis after irradiation and the subsequent breakdown of tooth surfaces by a rampant type of decay were considered to be a by-product of aggressive radiation therapy. Consider, then, current knowledge which gives rise to the improved prognosis set forth. (auth)

42472 REVIEW OF THE RADIOSENSITIVITY OF THE TISSUES IN BONE. RADIATION PROTECTION. ICRP Publication 11 1968. New York; Pergamon Press (1968). 36p. Available from Pergamon Press, Inc., Elmsford, N. Y.

Data are summarized from human and animal studies on: the radiosensitivity of the various cells comprising bone and bone marrow; the localization of bone-seeking radioisotopes (^{226}Ra, ^{228}Ra, ^{228}Th, ^{239}Pu, ^{90}Sr, ^{90}Y, ^{241}Am, ^{32}P) in bones; the ionization patterns resulting from the deposition of various radioisotopes in bone; changes in these patterns resulting from the growth and remodeling of bone; and pathological effects of external and internal irradiation on bone, with emphasis on tumorigenic effects. (C.H.)

42473 RADIATION PROTECTION IN SCHOOLS FOR PUPILS UP TO THE AGE OF 18 YEARS. RADIATION PROTECTION. ICRP Publication 13 1968. New York; Pergamon Press (1970). 7p. Available from Pergamon Press, Inc., Elmsford, N. Y.

Science courses in schools often include demonstrations and experiments involving the use of sources of ionizing radiations. The radiation dose limits recommended for exposure of children up to 18 years of age are: gonads and red bone marrow 50 mrems/yr; skin, bones, and thyroid gland 300 mrems/yr; hands, forearms, feet, and ankles 750 mrems/yr; and other single organs 150 mrems/yr. It is recommended that compliance with these dose limits be assured by the design and operation of equipment for school demonstrations. A radiation safety plan for the guidance of school administrators and teachers is included. (C.H.)

42474 GENERAL PRINCIPLES OF MONITORING FOR RADIATION PROTECTION OF WORKERS. A REPORT BY COMMITTEE 4 OF THE INTERNATIONAL COMMISSION ON RADIO-

LOGICAL PROTECTION. RADIATION PROTECTION. ICRP Publication 12 1968. New York; Pergamon Press (1969). 24p. Available from Pergamon Press, Inc., Elmsford, N. Y.

Recommendations for the radiation monitoring of work areas for external radiation, surface contamination, and air contamination are presented. Criteria and programs for the radiation monitoring of personnel for external exposure, skin contamination, and internal contamination during normal work procedures, and in the event of accidents resulting in the release of radioactivity, are included. (C.H.)

42475 EVALUATION OF RISKS FROM RADIATION. RADIATION PROTECTION. ICRP Publication 8 1965. New York; Pergamon Press (1966). 60p. Available from Pergamon Press, Inc., Elmsford, N. Y.

Data on the genetic and somatic effects of exposure of man to small doses of ionizing radiations, and related animal studies, are reviewed. A small dose is defined as less than 50 rads received acutely at high intensity, or multiple doses totaling less than 10 rads/yr irrespective of dose rate. At these doses the only effects that appear likely to be of interest are the induction of cancer, the production of developmental anomalies in the fetus, and a nonspecific reduction in the life span. It was concluded that the sum of the evidence was inconclusive as to the biological effects of small radiation doses. (C.H.)

42476 REPORT OF COMMITTEE V ON THE HANDLING AND DISPOSAL OF RADIOACTIVE MATERIALS IN HOSPITALS AND MEDICAL RESEARCH ESTABLISHMENTS. RECOMMENDATIONS OF THE INTERNATIONAL COMMISSION ON RADIOLOGICAL PROTECTION. RADIATION PROTECTION. ICRP Publication 5 1964. New York; Pergamon Press (1965). 50p. Available from Pergamon Press, Inc., Elmsford, N. Y.

Recommendations are presented for the handling, storage, and transportation of radioactive materials in hospitals and medical research establishments to ensure protection to personnel, patients, and the public. Both sealed and unsealed radiation sources are considered. Radiation monitoring of personnel and surfaces; decontamination of personnel, clothing, equipment, and surfaces; and emergency procedures in the event of minor or major spills or fires are covered. The disposal of liquid and solid radioactive wastes is discussed. The discharge of hospital patients during treatment with radioactive materials and precautions to be taken during autopsy, embalming, or cremation of radioactive corpses are considered. (C.H.)

42477 PROTECTIVE CONSIDERATIONS IN THE USE OF ^{192}Ir SOURCES FOR INTERSTITIAL RADIOTHERAPY. Botturi, M.; Pedrinazzi, G.; Scielzo, G.; Tosi, G. (Ospedale Maggiore Ca' Granda, Milan). Minerva Fisiconucl.; 14: 70-3(Apr-Jun 1970). (In Italian). (CONF-690929-9).

From fifteenth national congress of the Italian Association for Health Physics and Protection Against Radiation; Cagliari, Italy (Sep-Oct 1969).

The problems of radioprotection connected with the use of ^{192}Ir in interstitial radiotherapy were considered. Because of its clinical advantages, the exposure dose to the operator and the environment around the patient carrying the ^{192}Ir were measured and the values obtained were compared with those for Ra. The conditions to minimize the exposure dose to the operator, with particular attention to the technical considerations of afterloading, were analyzed. A series of ambient dose measurements were made around a patient. The results showed that with the higher dose the beds should be spaced 3 m apart or a protective barrier of 4 mm of Pb at the maximum be inserted to reduce the exposure dose to the other patients and to the hospital personnel. (tr-auth)

42478 HEALTH PHYSICS OPERATING EXPERIENCES IN THE VICINITY OF E.N.E.L. NUCLEAR ELECTRIC CENTERS. Antonucci, L. (ENEL, Garigliano, Italy); Bramati, L.; Fiorentino, F.; Malossi, S. Minerva Fisiconucl.; 14: 74-8(Apr-Jun 1970). (In Italian). (CONF-680535-31).

From fourteenth national conference of the Italian Association for Health Physics and Protection from Radiation; Formia, Italy (29 May 1968).

The health physics experiences acquired during the operation of the E.N.E.L. nuclear electric centers are summarized. The guidelines followed in the application of protection standards for personnel, in the treatment of the liquid and gaseous effluents, in the maintenance and refueling operations, and in the transport of radioactive materials are emphasized. (tr-auth)

42479 MONITORING FOR INTERNAL EXPOSURE. 3. PROBLEMS EXPERIENCED AT A NUCLEAR POWER UTILITY. Higashi, Aritsune (Japan Atomic Power Co., Tokai). Hoken Butsuri; 5: No. 3, 151-4(Sep 1970). (In Japanese).

At Tokai Nuclear Power Station the total dose of external and internal radiation exposure for personnel is controlled not to exceed the maximum permissible dose. Attention is paid to keep the internal exposure as low as possible, and in areas of high-level radioactivity workers must change clothing totally and wear filter masks or air masks. Periodic monitoring is conducted for both environment and personnel, on whom urinalysis is carried out four times a year. Besides the periodic monitoring, additional studies are made in the case of accidents. The urinalysis has the advantage that it can detect clearly individual ingestion, that workers are unrestrained, and that it can measure α- and β-emitters, but it requires much time for the analysis to be performed. Therefore, it is desirable that whole-body counting also be used. In estimating exposure dose, it is necessary to know the contribution of the individual nuclides, process of ingestion (temporary or continuous), time of ingestion, effective half-life, and distribution of the nuclides in various organs. Therefore, sufficient records of labor in various areas are important. (Japan)

42480 RADIATION HAZARD CONTROL SYSTEM. Miki, Ryota; Morishima, Hiroshige; Koga, Taeko, Uchida, Kumao; Mizumoto, Yoshihiko (Kinki Univ., Fuse, Japan). Kinki Daigaku Genshiryoku Kenkyusho Nenpo; 7: 13-20(1968). (In Japanese).

The radiation protection program of the Atomic Energy Research Institute of Kinki University during fiscal 1968 is described. Blood tests were made twice annually on personnel. No abnormality due to radiation injury was observed. The maximum permissible cumulative radiation dose was not exceeded. The highest whole-body exposure during a three-months period was 420 mR. Laboratory monitoring was carried out to detect the escape of radioactivity and to measure personnel exposure. Environmental radioactivity was measured at 1 m above ground. Radioactivity in vegetation and ground water was also measured. (Japan)

42481 MONITORING FOR INTERNAL EXPOSURE. 1. PHILOSOPHY AND STANDARDS OF INDIVIDUAL INTERNAL EXPOSURE MONITORING. Fujita, Minoru (Japan Atomic Energy Research Inst., Tokai). Hoken Butsuri; 5: No. 3, 141-4(Sep 1970). (In Japanese).

Philosophy and standards for monitoring internal radiation exposure of personnel described in ICRP Publications 10 and 12 are reviewed. The aim of this monitoring is to calculate the exposure dose, to protect workers against excessive exposure as occasion demands, and to record information on radiation doses. The monitoring program includes ordinary monitoring which is periodically carried out, and occasional monitoring which is conducted in case of unavoidable contamination or of accident. Ordinary monitoring is scarcely necessary except when volatile elements such as ^{3}H and ^{131}I are manipulated in large quantity, or when uranium or transuranic elements are handled. The frequency of ordinary monitoring should be determined according to effective half-life and limit of detection of monitored nuclides. Direct whole-body counting is suitable for γ-emitters, and urinalysis for α- and β-emitters. When data obtained from the ordinary monitoring show that contamination exceeds a certain level, the cause of this contamination must be investigated. At the Atomic Energy Research Institute it was decided to start an investigation when the dose by contamination was estimated to exceed 10 mrem. (Japan)

42482 AUTHORIZED PROTECTION STANDARDS OR CRITERIA ON THE RADIOACTIVE CONTAMINATION OF FOOD AND DRINKING WATER IN JAPAN. Urakubo, Goro; Kido, Yasumasa (National Inst. of Hygienic Sciences, Tokyo). Shokuhin Eiseigaku Zasshi; 11: No. 5, 396-404(Oct 1970). (In Japanese).

The need for standards for the maximum permissible concentration of radioactivity in food and water supplies in Japan is discussed. Values based on standards of the USA and Great Britain have been used in the past. (TSS) (Japan)

42483 INSTRUCTIONS FOR THE WORK IN RADIOLOGICAL LABORATORIES. pp 17-21 of Skyddsfoereskrifter foer Kemiskt Laboratoriearbete. /Ehrner-Samuel, Harriet. Stockholm; Arbetsmedicinska Institutet. (In Swedish).

The meanings of radiological work and of exposure are clarified. The difference between external and internal irradiation is explained. General rules for the radiation protection of personnel in Sweden are given with some advice about practical measures. (Sweden)

42484 RADIATION HAZARDS AND PROTECTION IN DENTAL RADIOGRAPHY. Singhal, N. C.; Chaddha, S. K. (S.M.S. Medical Coll. and Hospital, Jaipur, India). J. Indian Dent. Ass.; 42: 239-42(Sep 1970).

XUM

Although the doses received by the patient, operator, and general public during routine dental radiography are of low level, they may be significantly effective somatically and genetically if not used with correct techniques. Proper collimation and filtration of the beam, use of long focal distances, lead shield, fast film, high kilovoltage and taking proper precautions in handling of the film during exposure reduces the dental exposure to the patient, operator, and general public well below the maximum permissible limits of radiation exposure. (auth)

42485 RADIATION PROTECTION IN A VETERINARY PRACTICE. Unwin, D. D. (Wheel House, Chesham, Eng.). J. Small Anim. Pract.; 11: 523-32(Aug 1970).

The risk to the health of Veterinary Surgeons using x-ray equipment in general practice is reviewed. The publication "Radiation Safety in Veterinary Practice" has recently been published. Some of the points in it are considered and an attempt is made to show how its suggestions can be carried out in a small veterinary practice. (auth)

42486 INVESTIGATION OF RADIATION HAZARD IN X-RAY WORKERS. Ishizaka, Masatsuna; Endo, Kouichi (Inst. of Public Health, Tokyo). Nippon Hoshasen Gijutsu Gakkai Zasshi; 26: No. 3, 280-90(Nov 1970). (In Japanese).

A questionnaire survey was made in order to collect information on the actual condition of exposure and protection for radiation workers (total number of 1779) in 1260 facilities in Japan, including local health centers, national hospitals, and sanatoria. Results are compared with results of a 1967 survey conducted by the ministry of Health and Welfare. (TSS) (Japan)

42487 RADIATION PROTECTION TRENDS IN THE UNITED STATES. Taylor, Lauriston S. (National Council on Radiation, Protection, and Measurements, Washington, D. C.). Health Phys.; 20: No. 5, 499-504(May 1971).

Following the last major change in radiation protection standards introduced by the National Council on Radiation Protection and Measurements (NCRP) in 1957, the basic protection criteria have been under continuous review. During the ensuing period no breakthrough has occurred in our fundamental knowledge that justifies any significant changes in protection standards. New data tend to show that standards adopted two decades ago were overly conservative although not sufficiently to warrant upward revisions now. The 1970 report on Basic Radiation Protection Criteria will show some minor adjustments, mainly in the direction of numerical simplification. In spite of the fairly well stabilized position of radiation protection philosophy, especially in comparison with other environmental pollutants, radiation hazard as a headline catcher continues to flourish in the U. S. This caused undue alarm and concern among patients reading death-calculating stories about radiation and fosters an undesirable and even dangerous public fear of radiation. Improvement in the efficiency of radiation usage is nevertheless progressing in an orderly manner, but vast numbers of professional man-hours are being wasted fighting radiation hazard windmills instead of performing useful work. An important trend in the U. S. is toward governmental control of all uses of radiation. Applied rationally, this promises to be useful, but radiation control is already better than for most pollutants and there is dubious need for continued frenetic attacks on the problem. (auth) (UK)

42488 BIOLOGICAL PROBLEMS IN THE RADIOLOGICAL PROTECTION OF WORKERS EXPOSED TO ^{239}Pu. Dolphin, G. W. (United Kingdom Atomic Energy Authority, Harwell, Eng.). Health Phys.: 20: No. 6, 549-57(Jun 1971).

Some of the biological problems associated with the protection of workers exposed to ^{239}Pu are reviewed. The present knowledge on Pu metabolism and the gross pathology produced by its incorporation in the body are discussed. Most of this knowledge comes from animal experiments, but there are some pathological findings in humans, particularly chromosome aberrations in workers with a long history of Pu exposure. An important biological problem concerns the choice of critical organ and the appropriate MPC for control of the environment. Soluble and insoluble Pu is considered and a single value of MPC, 10^{-11} $\mu Ci/cm^3$, is suggested for all compounds. A discussion is given of the biological problems associated with estimating, by means of urinary excretion measurements, the amount of Pu transferred from the site of entry to the body. A short comment is made on the treatment of exposure cases. (auth) (UK)

42489 CODE OF PRACTICE FOR THE USE OF IONIZING RADIATIONS IN SECONDARY SCHOOLS. AAEC A-10 1965. Canberra, Australia; National Health and Medical Research Council (1965). 4p. Available from National Health and Medical Research Council, Curtin, Australia.

A Code of Practice to ensure the protection of children against ionizing radiations used for demonstrations in schools is presented. The use of x-ray generators in general schools is forbidden in Australia. (C.H.)

42490 CODE OF PRACTICE FOR THE CONTROL AND SAFE HANDLING OF SEALED RADIOACTIVE SOURCES USED IN INDUSTRIAL RADIOGRAPHY. AAEC A-6 1968. Canberra, Australia; National Health and Medical Research Council (1969). 28p. Available from National Health and Medical Research Council, Curtin, Australia.

A Code of Practice for the safe handling of sealed γ sources used in industrial radiography is presented. Design criteria for sources and holders are summarized. The requirements for transport and storage of sources to ensure the protection of personnel and the public are outlined, methods for radiation monitoring of the sources are described, and working rules and emergency procedures for personnel using the sources are included. (C.H.)

42491 CODE OF PRACTICE FOR THE CONTROL AND SAFE HANDLING OF SEALED RADIOACTIVE SOURCES USED IN RADIATION THERAPY (OTHER THAN TELETHERAPY). AAEC A-8 1962. Canberra, Australia; National Health and Medical Research Council (1962). 15p. Available from National Health and Medical Research Council, Curtin, Australia.

A Code of Practice for the safe handling of sealed radiation sources used for therapy is presented. Such sources may emit β or γ radiations singly or in combination to give a prescribed dose of radiation to tissues within a prescribed time. Procedures to ensure the radiation protection of the patient, medical personnel, and the public are included. (C.H.)

42492 NURSING STAFF EXPOSED TO IONISING RADIATIONS. AAEC A-9 1969. Canberra, Australia; National Health and Medical Research Council (1969). 13p. Available from National Health and Medical Research Council, Curtin, Australia.

A Code for the radiation protection of medical personnel during the insertion of sealed radiation sources in patients and during the subsequent care of the patients is presented. Such sources may emit β or γ radiations singly or in combination and may be used singly or in combination to give a prescribed dose of radiation to tissue in a prescribed time. (C.H.)

42493 MINIMISING RADIOLOGICAL HAZARDS TO PATIENTS. AAEC A-3 1966. Canberra, Australia; National Health and Medical Research Council (1969). 5p. Available from National Health and Medical Research Council, Curtin, Australia.

Radiation protection procedures for the protection of patients and medical personnel against x radiation during diagnostic radiography are summarized. Data on the radiation dose to critical tissues of the patient during various radiographic procedures are included. (C.H.)

42494 CONDITIONS CONCERNING THE TRANSMISSION OF RADIOACTIVE MATERIAL BY POST. Australia; Postmaster-General's Department ([1970]). 15p. Available from Atomic Energy Attache, Australian Embassy, Washington, D. C.

Radiation protection standards for the shipment of radioisotopes by mail in Australia are presented. Radioisotopes are classified into groups for transport purposes. Requirements for packaging and labeling for each group are discussed. (C.H.)

42495 REVISED RADIATION PROTECTION STANDARDS FOR INDIVIDUALS EXPOSED TO IONISING RADIATION. AAEC A-5 1967. Canberra, Australia; National Health and Medical Research Council (1967). 10p. Available from National Health and Medical Research Council, Curtin, Australia.

A Code of Practice for the radiation protection of personnel in Australia using radiation sources or radioactive substances is presented. The Code is based on recommendations of the International Commission on Radiological Protection and was revised in 1967 to incorporate the most recent recommendations. (C.H.)

42496 CODE OF PRACTICE FOR RADIATION HYGIENE IN DENTISTRY. AAEC A-4 1967. Canberra, Australia; National Health and Medical Research Council (1967). 9p. Available from National Health and Medical Research Council, Curtin, Australia.

A Code of Practice for the radiation protection of patients and personnel during dental radiography is presented. The responsibility of dentists in Australia for radiation protection during the use of x-ray equipment for diagnostic dental studies is discussed. (C.H.)

42497 SAFE HANDLING OF CORPSES CONTAINING RADIOACTIVE SUBSTANCES. AAEC A-2 1966. Canberra, Australia; National Health and Medical Research Council (1969). 3p. Available from National Health and Medical Research Council, Curtin, Australia.

A Code of Practice is presented as a guide to the safe handling of radioactive cadavers following therapy using sealed or unsealed radioactive substances. It is recommended that hospitals and other relevant institutions prepare detailed administrative procedures, based on this Code, to ensure the protection of pathologists, morticians, and others who may be exposed to radiation while handling the cadaver. (C.H.)

Safety Procedures

Refer also to abstract 42225.

42498 (NP–18858) WORK INJURIES IN ATOMIC ENERGY, 1968. A SURVEY OF PRIVATELY-OWNED AND -OPERATED ESTABLISHMENTS. (Bureau of Labor Statistics, Washington, D. C.). 1970. 14p.

The frequency of work injuries in 1968 was virtually the same as in 1967 in privately owned and operated establishments in the atomic energy field in the USA. The number of establishments with very high injury-frequency rates increased in 1968. However, such firms still constitute a small percent of the total. The frequency of injury increased for employees spending at least half their time working in the atomic energy field. Injuries in 1968 were more severe, on the average, than those in the previous year. No injuries resulting from exposure to radiations were reported. Work-injury rates of AE establishments compare favorably with rates in manufacturing establishments reporting to the Bureau of Labor Statistics for its 1968 nationwide survey of work injuries (BLS national survey). Atomic energy establishment rates were comparable also with rates reflecting the group experience of manufacturing companies reporting to the National Safety Council (NSC). (auth)

42499 LES RADIOELEMENTS ET L'INCENDIE. (Radioelements and the Outbreak of Fire.). Paris; Institut National de Recherche et de Securite (1970). 166p.

Radiation shielding is discussed in general terms. The different forms in which radioelements can be present, their probable behavior in a fire, the dangers resulting from a break in shielding, and the risk of criticality are examined. The extent to which the presence of radioelements affects fire protection is estimated (fire fighting preparation, intervention). Documentary information on the subject is presented. (France)

42500 EXPERIENCE IN THE ORGANIZATION OF A PHYSICO-TECHNICAL LABORATORY OF THE KRASNODAR REGIONAL ONCOLOGICAL DISPENSARY. Akatkina, N. V.; Akatkin, O. A. Med. Radiol.; 14: No. 4, 59-63(Apr 1971). (In Russian).

The radiation apparatus for radiological laboratories determines the necessity of setting up specialized services in order to operate the apparatus and conduct clinical dosimetry and radiometry. The paper analyzes the experience gained with the organization of a physico-technical laboratory and gives recommendations on the planning of radiation safety and training of personnel. (auth)

42501 COLOR TELEVISION SURVEY IN PENNSYLVANIA. Lane, Richard A. (Pennsylvania Dept. of Health, Harrisburg). Radiol. Health Data Rep.; 12: 137-8(Mar 1971).

During 1968 to 1970, 322 color television sets in Pennsylvania were surveyed for emissions of x radiation. Eighty-seven percent were found to emit radiation less than or equal to 0.1 mR/hr. Two percent emitted radiation in excess of 0.5 mR/hr. It was determined from the survey that the primary cause for leakage from color television sets is related to high voltage adjustments. It was found that two of the sets emitting radiation in excess of 0.5 mR/hr were serviced shortly before the investigation. Voltage readings as high as 39 kV were observed. (auth)

42502 RESULTS OF RADIATION SAFETY SURVEYS OF X-RAY FACILITIES WITHIN THE BUREAU OF PRISONS AND FEDERAL HEALTH PROGRAMS SERVICE. Miller, Lois A.; Seabron, LaVert C. (Public Health Service, Rockville, Md.). Radiol. Health Data Rep.; 12: 129-35(Mar 1971).

This report presents the results of comprehensive surveys of x-ray facilities in 26 Bureau of Prison installations and in 11 hospitals and 20 outpatient clinics of the Public Health Service throughout the United States. Facility workloads, types of equipment, operator training, and equipment deficiencies are discussed. (auth)

42503 ESTABLISHMENT OF A UNIVERSITY RADIATION SAFETY OFFICE. Ice, Rodney D. (Temple Univ., Philadelphia). Health Phys.; 20: 444-6(Apr 1971).

The necessity for a radiation safety officer at Temple University, necessary due to increased use of radioactive materials, is outlined. The establishment of a university safety program is detailed, and the organizational objectives and responsibilities of the radiation safety officer are given. The many duties of the officer are outlined, and the necessary administrative organization is shown. (UK)

42504 HEALTH EDUCATION IN CZECHOSLOVAK URANIUM INDUSTRY. Nedvidek, A. (Inst. of National Health in Uranium Industry, Pribram, Czech.). Cesk. Zdrav.; 18: No. 1, 40-3(Jan 1970). (In Czech).

Health education in the Czechoslovakian uranium industry is described and the problems resulting from the specific character of work in mines and chemical plants are analyzed. In addition to general hazards, the hazard of ionizing radiation must be considered. Health education is directed at these specific hazards and instructions for physicians were drawn up to this effect. The importance of cooperation with senior workers and trade union authorities in the plants is emphasized. In the future, attention must be focused on the hygiene and safety of work, the elimination of dust, the prevention of injuries, diet, and other specific conditions. Ways of improving health education in the future should be sought based on sociological surveys. (NSA of Czech.)

Civil Defense

Refer also to abstract 41827.

42505 (BARC/BIB–1) CIVIL DEFENCE: AN ANNOTATED BIBLIOGRAPHY 1960-1968. Malwad, N. M. (Bhabha Atomic Research Centre, Bombay (India)). Jan 1970. 250p. NTIS (U. S. Sales Only).

A selective bibliography is presented including 393 documents with abstracts on civil defence against nuclear war, its effects on men and materials, preparations needed to face nuclear war such as construction of shelters, medical problems, food storage and supply, sanitation, ventilation, and possible recovery after nuclear war. It is based on Nuclear Science Abstracts 1960 to August 1969 and the report collection of the Depository Library, Bhabha Atomic Research Centre, Trombay, Bombay-85 (India) and covers technical reports, periodicals, papers presented at conferences, symposia, and books published during the period 1960 to 1968. Cumulative author, subject, and report number indexes are provided. (INIS)

42506 (ORNL–4566(Pt.1)) CIVIL DEFENSE RESEARCH PROJECT ANNUAL PROGRESS REPORT, MARCH 1969–MARCH 1970. (Oak Ridge National Lab., Tenn.). Apr 1971. Contract W-7405-eng-26. 100p. Dep. NTIS.

Results are reported from research in 14 areas related to urban problems and civil defense. Urban problems discussed include methods for the processing of solid wastes, the underground location of utility systems, the economic aspects of urban decentralization, and the effects of urban environments on child development. Civil defense research included: cost estimates for blast shelters in relation to their protective value; a comparison of civil defense programs in the USA and Soviet Union; an analysis of the effects of shock waves from a nuclear weapon detonation on an operating large sodium-cooled fast breeder reactor and the possibility of the release of reactor fission products to the environment; the response of elasto-plastic membranes to shock loading; the possible effects of electromagnetic pulses released during nuclear weapons detonations on the performance of electrical and electronic equipment in civilian power and communication systems; an analysis of the shelter potential of 98 cities in the USA; the design of high-protective-factor shelters that can be built hastily in rural areas; the development of a simple, inexpensive electrostatic detector for monitoring the γ dose rate around shelters; a survey of the national food supply; the development of a plan for relocation of a portion of the wheat supply for national security; and studies related to the salvage of wholesome meat from lethally-irradiated livestock. (C.H.)

Legal Aspects

Refer also to abstract 42544.

42507 DIE KANALISIERUNG DER HAFTUNG UNTER BESONDERER BERUECKSICHTIGUNG DES ATOMRECHTES. (The Channelization of Liability with Special Regard for Atomic Law). Mohr, Peter Conrad. Hamburger Rechtsstudien, Heft 64. Berlin; Walter de Gruyter and Company (1970). 140p. DM 30.-.

Legal liability with respect to civil disturbances and labor is discussed with emphasis on liability in the event of a radiation accident in Germany. Recent changes in the German laws regarding legal responsibility of personnel and industry are sum-

XUM

marized. The legal systems of various nations are compared. (H.B.G.)

42508 PLUTONIUM INHALATION: THE BURDEN OF NEGLIGIBLE CONSEQUENCE. Long, A. B. (Argonne National Lab., Ill.). Nucl. News; 14: No. 6, 69-73(Jun 1971).

The determination of the maximum permissible lung burden of $^{239}PuO_2$ and the related maximum permissible air concentration is based upon the choice of two crucial factors: the model of the lung and the effective mass of the critical organ. The data presently available, which relates to these two factors, is certainly more reliable than what was used in 1959 to calculate the present limits. However, there are still uncertainties in the human lung model in the long term effects of highly localized radiation damage; these uncertainties may be resolved only through experience with humans. Nevertheless, there is the well-documented experimental evidence of Bair that lung cancer has resulted consistently in dogs that inhaled $^{239}PuO_2$ and had terminal lung burdens greater than 0.05 μCi. In the light of these facts, it would seem appropriate for the federal government, the NCRP, or the ICRP to recommend a decrease in the maximum permissible burden and the maximum permissible air concentration of PuO_2 based upon the best available lung models and the most recent experimental data. Until sufficient experimental data become available to allow an accurate assessment of the risks involved in plutonium inhalation, there is an urgent need to dispel the sense of security and certainty that the present limits for the maximum permissible lung burden and the maximum permissible air concentration bring. The public should be informed of the uncertainties that exist in these limits, and as new data from dogs or humans becomes available, the levels should be reassessed. For these reasons personnel who run the risk of PuO_2 inhalation should be aware of the total scope of the problem. With the present levels of detection sensitivity, one must rely on the understanding of the individuals to keep exposures down in the expanding nuclear industry. (E.R.B.)

42509 ENFORCEMENT DECREE ON ARTICLE 1 OF THE D.P.R. NUMBER 185. Minerva Fisiconucl.; 14: 88-91(Apr-Jun 1970). (In Italian).

The quantity of radioactivity, the specific activity or concentration, and the intensity of exposure dose subject to the provision of Article I of the D.P.R. No. 185 are tabulated in D.P.R. 1303. (J.S.R.)

Medicine

Protective Substances

Refer also to abstracts 42266, 42281, 42283, 42295, 42325, 42332, 42614, 42617, 42618, 42620, 42625, 42632, 42672, and 42737.

42510 PROBLEM OF THE EFFECT OF SOME FOODS, NUTRITIVE AND PROTECTIVE SUBSTANCES UPON THE COURSE OF AN EXPERIMENTAL URANIUM INTOXICATION. Markova, M. Khig. Zdraveopayvane; 13: No. 3, 280-94(1970). (In Bulgarian).

Experimental investigations were carried out on animals for establishing the effects of some nutritive and protective substances upon uranium intoxication produced by low doses of uranyl nitrate (0.10 to 1.0 mg/kg body weight), with the purpose of their use in the prevention of intoxications. Those substances were: vitamins C, P, and B_{12}, the protective substances tryptophan, lysine, calcium fluoride, liver hydrolysate, egg shell powder applied in different combinations, as well as some vitaminized milk products and vitaminized milk-pectin foods. They had a favorable effect on the course of uranium intoxication and are recommended for preventive application in the nutrition of workers in the uranium industry. (Abstr. Bulg. Sci. Med. Lit.)

42511 OXIDATION-REDUCTION POTENTIAL IN TISSUES EXPOSED TO RADIOPROTECTIVE AGENTS AND HYPOXIA. Seryakov, V. N.; Deev, L. I. (Moscow State Univ.). Vestn. Mosk. Univ., Ser. VI, Biol. Pochvoved.; No. 5, 87-9(Sep-Oct 1970). (In Russian).

Changes in redox potential were studied in rat spleen, liver, and subcutaneous tissues after exposure to S-β-aminoethylisothiuronium bromide (AET), β-mercaptoethylamine bitartrate (MEA), and serotonin creatinine sulfate combined with hypoxic hypoxia (HH). Exposure to HH (6% oxygen, 94% nitrogen) 15 to 17 minutes after injection of AET or MEA decreased the redox potential in all of the tissues studied more than after injection of the radioprotector alone. The decrease was greatest 5 to 7 minutes after the start of HH. The shifts were reversible. In animals that were x irradiated after receiving AET or MEA combined with HH, the radioprotective additive effect was significantly less when serotonin was combined with HH. (JPRS)

42512 BIOLOGICAL ASPECTS OF RADIATION PROTECTION. Proceedings of the International Symposium, Kyoto, October 13–15, 1969. Sugahara, Tsutomu; Hug, Otto (eds.). Tokyo; Igaku Shoin Ltd. (1971). 279p. $18.00. (CONF-691041).

Separate abstracts were prepared for each of 28 papers included in the symposium. (E.E.H.)

For abstracts of individual papers see: 42325, 42398, 42399, 42513–42523, 42599, 42600, 42629–42637, and 42680–42682.

42513 RADIATION PROTECTION OF NON-SPECIFIC BODY DEFENCE: RETICULOENDOTHELIAL SYSTEM AND ADRENAL CORTEX. Flemming, Kurt (Univ., Freiburg i. B. Heiligenberg Inst., Baden, Ger.). pp 107-16 of Biological Aspects of Radiation Protection. /Sugahara, Tsutomu (ed). Tokyo; Igaku Shoin Ltd. (1971).

From International symposium on biological aspects of radiation protection; Kyoto, Japan (13 Oct 1969). See CONF-691041.

Experiments were conducted to determine the interrelation between radioprotection and the reticulo-endothelial and adrenal-cortical systems. Mice were given whole-body lethal x radiation and the phagocyte index, K, was calculated from blood samples. Cysteamine, serotonin, and Pyrexal®, a bacterial lipopolysaccharide, were given to three series of mice. The results showed that after whole-body irradiation, the reticulo-endothelial system was impaired and the phagocytic efficiency and capacity of the RES cells were decreased. The manifestation of the radiation injury was inhibited by radioprotective agents. The protective effects of the substances with respect to RES injury and the mortality of the animals were in good agreement. The specific influence of radioprotective agents on the reaction of the adrenal cortex following whole-body x irradiation of mice was also investigated. It was found that the first corticosteroid increase, 2.5 hrs post-radiation, and the second corticosteriod increase, 72 hrs post-radiation, were inhibited. This protective effect was found in both the adrenals and the peripheral blood. In the investigation of the first reaction, cysteamine showed a stronger effect than serotonin using doses of 750 and 1000 R, while the effects of Pyrexal® were quantitatively inconsistent. Investigations on the second reaction after administration of a midline lethal dose of 750 R showed that serotonin was not as effective as cysteamine and the effects of Pyrexal® were still weaker than that of serotonin. When lethal doses of 1000 R were applied Pyrexal® had no protective effects. These results show that radioprotective agents not only influence the molecular and submolecular effects of radiation but also affect changes in the activity of the adrenocortical system. (E.E.H.)

42514 MODE OF RADIOPROTECTIVE ACTION OF AMINOTHIOLS IN HeLa S_3 CELLS. Shikita, Mikio; Sato, Fumiko; Akaboshi, Sanya (National Inst. of Radiological Sciences, Chiba, Japan). pp 117-23 of Biological Aspects of Radiation Protection. /Sugahara, Tsutomu (ed). Tokyo; Igaku Shoin Ltd. (1971).

From International symposium on biological aspects of radiation protection; Kyoto, Japan (13 Oct 1969). See CONF-691041.

Experiments were conducted to determine the radioprotective action of β-mercaptoethylguanidine (MEG) and cysteamine (MEA) on HeLa S_3 cells. Treatment of the cells with MEA of MEG prior to x radiation reduced the loss of reproductive integrity of the cells. The dose reduction factor was approximately 2 with MEG and greater than 3 with MEA. It was found that the maximum radioprotective action of MEG on the cells developed much slower than that of MEA. However, it lasted longer after washing with fresh medium and subsequent incubation of the cells. When the cells were incubated with MEG at 5°C, development of protection was incomplete after 60 min incubation. It was demonstrated that MEA and MEG had a synergistic action and resulted in better protection than either compound alone. The cellular uptake of ^{14}C-labeled MEG was measured, and it was found that the radioactivity accumulated in the cells progressively with time and approached a plateau after 60 min incubation. Five derivatives of MEG, which were also tested for protective potency all proved to be less potent than MEG. To determine the relation between the cytotoxic effects of radioprotective substances and their protective action, the inhibitory effects of MEG and its derivatives on the cell proliferation rate were studied. It was observed that all the derivatives of MEG were less inhibitory than MEG on cell proliferation. (E.E.H.)

42515 RADIOPROTECTIVE EFFECT OF METHYLENE BLUE IN MICE AND RATS. Nam, Sang Yul (Kyung Hee Univ., Seoul). pp 124-31 of Biological Aspects of Radiation Protection. /Sugahara, Tsutomu (ed.). Tokyo; Igaku Shoin Ltd. (1971).

From International symposium on biological aspects of radiation protection; Kyoto, Japan (13 Oct 1969). See CONF-691041.

The radioprotective effects of methylene blue on mice and rats following whole-body γ or x radiation were studied. In order to achieve maximum protection, methylene blue must be given im-

mediately prior to exposure. Injection immediately after exposure gave no protection effect towards survival of the animals. Methylene blue delayed the radioinduced increase in liver glycogen and blood glucose and the radioinduced decrease in serum proteins but did not affect serum electrolytes. Subcutaneous injection of methylene blue into male rats prior to whole-body x radiation delayed the radioinduced increase in serum cholesterol. Albino rats were given 360 rads whole-body γ radiation following intraperitoneal injection of methylene blue. The agent slightly retarded the rise in serum lactate dehydrogenase (LDH) in the initial phase after exposure. No differences in isoenzyme patterns of the serum, liver, and testes were observed between the control and the methylene blue treated rats after exposure. The methylene blue did cause a slight delay in the radioinduced change in heart tissue LDH. (E.E.H.)

42516 RADIOPROTECTIVE EFFECTS OF ADENOSINE DERIVATIVES. Asakura, Hideo (Tokyo Univ.). pp 132-7 of Biological Aspects of Radiation Protection. /Sugahara, Tsutomu (ed.). Tokyo; Igaku Shoin Ltd. (1971).

From International symposium on biological aspects of radiation protection; Kyoto, Japan (13 Oct 1969). See CONF-691041.

Some derivatives of adenosine, which were obtained by introducing different kinds of side-chains into position-6 of adenosine, were synthesized and studied to determine their radioprotective effects on the 30 day survival of mice lethally irradiated with ^{60}Co γ rays with a dose of 780 R. The substances were injected 5 to 15 min before radiation. Three of the samples had no radioprotective effect. Two samples had a hypotensive and muscle relaxant action as well as a radioprotective effect. These effects were maintained for hours but their action was reversible. Results showed that the adenosine derivatives have a potent radioprotective effect almost comparable to that of cysteamine and serotonin. (E.E.H.)

42517 CHEMICAL RADIOPROTECTION WITH N- AND S-CONTAINING POLYMERS. Ringsdorf, H.; Heisler, A. G.; Mueller, F. H.; Graul, E. H.; Ruether, W. (Univ., Marburg, Ger.). pp 138-47 of Biological Aspects of Radiation Protection. /Sugahara, Tsutomu (ed.). Tokyo; Igaku Shoin Ltd. (1971).

From International symposium on biological aspects of radiation protection; Kyoto, Japan (13 Oct 1969). See CONF-691041.

Macromolecular radioprotective agents were synthesized from monomers by copolymerization. N-vinylpyrrolidinone was built into the molecules as a comonomer, since it makes the polymers water soluble and increases their tolerance in the organism. Polyelectrolytes with adjustable pH were produced by the additional introduction of 3% acrylic acid. The effects of these copolymerizates on the mortality of x-irradiated rats and mice were tested quantitatively and qualitatively. Macromolecular radioprotective agents, depending on their composition, proved to be effective against a lethal radiation dose. The DRF vlaues obtained from dose-effect curves were between 1.2 and 1.4. A long-term radioprotective effect was found with maintenance of efficiency for hours and, in the case of one polymer, (S_3), even for days. The toxicity of all the polymers tested was very low. Comparative examinations with micromolecular model compounds showed that the mechanism of macromolecular substances could be explained by the delayed hydrolysis of micromolecular protective groupings (depot effect) and by special properties resulting from their macromolecular structure. Polymeric protective substances with molecular weights from 3,000 to 8,000 showed a strong protective effect with no significant difference in results. (E.E.H.)

42518 NEW POTENTIALITIES OF COMBINATION OF RADIOPROTECTION AND CYCLOPHOSPHAMIDE. Bozduganov, Athanas (Higher Medical Inst., Plovdiv, Bulgaria). pp 148-56 of Biological Aspects of Radiation Protection. /Sugahara, Tsutomu (ed.). Tokyo; Igaku Shoin Ltd. (1971).

From International symposium on biological aspects of radiation protection; Kyoto, Japan (13 Oct 1969). See CONF-691041.

The possibility of decreasing an organism's radiosensitivity by a combination of several radioprotectors was examined. Mice were divided into three groups. Group I mice were injected once prior to x radiation with 1 ml of a solution containing 0.02 mg monarsine, 0.0006 mg dehydroergotamine, and 0.2 ml of 25% magnesium sulfate solution. Group II mice were subcutaneously injected three times after irradiation with 1 ml of a solution containing 0.0015 g cytisine, 0.015 g apitonine, and 0.04 ml of 24% solution of neophylline. Group III served as irradiated controls. Lethality in group I proved to be 82% lower than in the control group on the seventh day. Group II showed an 80% survival rate on the seventh day. Forty-eight guinea pigs were divided into two groups. Group I guinea pigs were given a solution containing 0.05 mg dehydroergotamine, 5 mg monarsine, and 1.5 ml of a 25% magnesium sulfate solution prior to x irradiation. The second group was used as an irradiated control. The 30 day survival rate in the protected pigs was 75% and only 37.5% in the controls. Further experiments were carried out on rats to determine the effects of cyclophosphamide injected prior to whole-body x radiation and external ^{90}Sr β radiation. The results showed that small doses of cyclophosphamide injected prior to irradiation decreased the radiosensitivity of the animals by approximately a factor of 3 when applied at weekly intervals. Variations in cyclophosphamide dose had no effect on its protective action. (E.E.H.)

42519 HISTOPATHOLOGICAL ACTION OF SEROTONIN ON CERTAIN TISSUES IN MICE. Srivastava, Pratap Narain (Univ. of Rajasthan, Jaipur, India). pp 157-63 of Biological Aspects of Radiation Protection. /Sugahara, Tsutomu (ed.). Tokyo; Igaku Shoin Ltd. (1971).

From International symposium on biological aspects of radiation protection; Kyoto, Japan (13 Oct 1969). See CONF-691041.

Mice of C57 inbred strain were injected with serotonin at a dose of 75 mg/kg body weight. The animals were autopsied 1, 2, 4, and 7 days after serotonin administration. Pronounced histopathological damage was noted in the ovaries, liver, and adrenal glands while no apparent damage was seen in the thyroid. In the ovaries all the stages of oocytes were affected. The liver showed vacuolation, depletion of granular cytoplasm, and pyknosis of nuclei. The adrenal displayed severe hemorrhage and penetration of cortical cells into medullary region. (auth)

42520 CHEMICAL PROTECTION AND CELL STRUCTURE. Braun, Hildegard (Univ., Freiburg i. B.) pp 173-84 of Biological Aspects of Radiation Protection. /Sugahara, Tsutomu (ed.). Tokyo; Igaku Shoin Ltd. (1971).

From International symposium on biological aspects of radiation protection; Kyoto, Japan (13 Oct 1969). See CONF-691041.

Investigations were carried out on the crypt cells of the duodenum of mice to compare the ultrastructural changes induced by SH-protectors, cysteine, cysteamine, and 5-mercaptopyridoxine, with the alterations that occur in the cell after injection of thiol-blocking agents, such as iodoacetamide, N-ethylmaleimide, and iodoacetic acid. Studies were also made to show how thiol-blocking agents influence the cellular lesions induced by pretreatment with protective SH-compounds. The results showed that SH-compounds produce a swelling of the mitochondria with degradation of their cristae and an increase in the agranular endoplasmic reticulum. Thiol-blocking agents induced an increase in the mitochondrial granula and pycnotic mitochondria. The agranular reticulum was greatly increased. The subcellular architecture of the altered stem cells was quantitatively analyzed. The mitochondrial swelling induced by SH-compounds was eliminated by subsequent injection of a thiol-blocking agent. (E.E.H.)

42521 CHEMICAL PROTECTION OF THE RECOVERY PROCESS. Revesz, Laszlo; Littbrand, Bo (Karolinska Inst., Stockholm). pp 195-200 of Biological Aspects of Radiation Protection. /Sugahara, Tsutomu (ed.). Tokyo; Igaku Shoin Ltd. (1971).

From International symposium on biological aspects of radiation protection; Kyoto, Japan (13 Oct 1969). See CONF-691041.

Experiments were conducted to determine the possible action of radioprotective substances on the repair processes that ensue following radiation with divided doses and result in recovery of the cells. In four series of 6 to 10 repeated experiments, the effects of cysteamine in 20 mM concentrations on the survival parameters of Chinese hamster cells exposed to x radiation in the presence or absence of oxygen were determined. The survival regression decreased by a factor of 2.3 and the extrapolation number of the survival curve was raised from unity to 1.6 under anoxic conditions. In the presence of oxygen, the survival regression changed by a factor of 4.1 without a change in the extrapolation number. Cysteamine increased the ratio between the surviving fraction after single or split dose exposures to the same total dose when irradiated under anoxic conditions. In the presence of oxygen, the split dose ratio did not change. The data strongly supports the idea that radioprotection by cysteamine is due to a reduction in the amount of damage inflicted and to its interaction with the physiological protective mechanisms. (E.E.H.)

42522 CYSTEAMINE AND RADIATION-INDUCED SINGLE STRAND BREAKS OF DNA IN CULTURED MAMMALIAN CELLS. Okada, Shigefumi; Sawada, S. (Univ. of Rochester, N. Y. Tokyo Univ.). pp 201-3 of Biological Aspects of Radiation Protection. /Sugahara, Tsutomu (ed.). Tokyo; Igaku Shoin Ltd. (1971).

From International symposium on biological aspects of radiation protection; Kyoto, Japan (13 Oct 1969). See CONF-691041.

The toxicity and protective action against radiation injury and, inhibition of DNA synthesis and rejoining process by cysteamine and cystamine were studied in cultured mammalian cells. Al-

XUM

though cysteamine in high concentrations was non-toxic, it was toxic in relatively low concentrations (0.5 mM). In low concentrations, it induced single strand breaks of DNA both in the x-irradiated and non-irradiated cells, depressed DNA synthesis in non-irradiated cells, and depressed the rate of rejoining of radioinduced single strand breaks of DNA in irradiated cells. Cysteamine (over 5 mM) protected DNA molecules from radioinduced single strand breaks and double strand cuts. The degree of protection by cysteamine increased with increasing cysteamine concentrations. Cysteamine in high concentrations (over 5 mM) inhibited normal DNA synthesis of the non-irradiated cells and slowed the rejoining of radioinduced single strand breaks in irradiated cells. Cystamine showed no toxic effect and afforded little protection for DNA molecules from radioinduced single strand breaks. However, cystamine inhibited both DNA synthesis of non-irradiated cells and the rejoining process of irradiated cells. (auth)

42523 MECHANISMS OF CHEMICAL RADIOPROTECTION. Birzu, I.; Grigorescu, St.; Nedelcu, C. (Clinics of Radiology, Bucharest). pp 244-8 of Biological Aspects of Radiation Protection. /Sugahara, Tsutomu (ed.). Tokyo; Igaku Shoin Ltd. (1971).

From International symposium on biological aspects of radiation protection; Kyoto, Japan (13 Oct 1969). See CONF-691041.

To determine the mechanisms of chemical protection, the uptake of adrenalin-^{14}C, AET-^{35}S, and cysteine-^{35}S by various organs in rats was studied. The amount of stored radioprotective substances was compared with the degree of radioprotection estimated by histological examination. No agreement was observed between the stored amount and histological protection. Protection provided by cysteine against lethal toxic action of monoiodoacetic acid was also studied. The in vitro studies indicated that a dose of 100 mg cysteine was sufficient to counteract the toxic effects of 100 mg monoiodoacetic acid. However, 1,100 mg cysteine was necessary to protect against the in vivo toxic effect. The results suggest that the mechanism of chemical radioprotection is not the total amount of protective molecules stored by cells but the number of free molecules present that can interact with radioinduced radicals. (E.E.H.)

42524 MECHANISM OF RADIOPROTECTIVE ACTION OF DIMETHYL SULFOXIDE. Lappenbusch, William L. (Illinois State Univ., Normal). Radiat. Res.; 46: No. 2, 279-89(May 1971).

More than 1000 Holtzman female rats, weighing 138 to 144 g each, were used to examine the radioprotective action of dimethyl sulfoxide (DMSO). One hundred and ten rats were injected intraperitoneally with 2.5 to 25 g undiluted DMSO/kg body weight. The maximum sublethal concentration of DMSO was found to be approximately 10 g/kg while the LD_{50} ranged between 15 and 16 g/kg. Five hundred and eight rats were administered x ray exposures ranging between 250 and 1200 R following an injection with 0, 5, 7.5, or 10 g DMSO/kg. Radiosensitization occurred in some animals administered 10 g/kg, others experienced some radioprotection. Animals injected with 5 or 7.5 g/kg had dose reduction factors of 1.27 and 1.31, respectively. Animals administered 7.5 g/kg appeared to have received the optimal amount of DMSO. The degree of protection or sensitization was found to be dependent on the DMSO concentration and the radiation exposures, concentration being less important with higher exposures. Three hundred and eighty two rats were injected with 7.5 g/kg and irradiated with 400 or 700 R in order to determine if DMSO reduced those manifestations commonly observed in the peripheral blood in the hematopoietic syndrome. Furthermore, an ^{59}Fe study was completed in order to determine the effects of DMSO and/or irradiation on red blood cell production. This chemical appeared to partially protect the animals by partially opposing the typical primary acute reactions commonly found in the hematopoietic syndrome, notably anemia and leukopenia. The fact that DMSO initiated polycythemia may explain the lower mortality rates in DMSO treated, irradiated animals. However, this observation does not rule out the hypothesis that DMSO may also protect the animals by altering physicochemical reactions immediately after irradiation. (auth)

42525 RADIOBIOLOGICAL AND BIOCHEMICAL STUDIES OF THIOPHOSPHATE RADIOPROTECTIVE COMPOUNDS RELATED TO CYSTEAMINE. Harris, John W.; Phillips, Theodore L. (Univ. of California, San Francisco). Radiat. Res.; 46: No. 2, 362-79(May 1971).

The radioprotective efficacy and the cellular metabolism of several phosphorylated derivatives of cysteamine, with particular reference to comparison of normal and malignant cells, were investigated. Two compounds were studied in detail: S-2-(3-aminopropylamino) ethyl phosphorothioic acid (WR2721) and sodium hydrogen S-(2-aminoethyl) phosphorothioate (WR638). Both agents protected euoxic marrow-colony forming units (CFUs) in vivo better than cysteamine when the cells were treated with both drug and x radiation prior to transplantation. Under these conditions, the DMF for WR2721 was 3.0 and for WR638, 2.3. Hypoxic CFUs were protected only slightly, the net result being to lower the oxygen enhancement ratio (OER) to 1.1 with WR2721 and 1.3 with WR638. Both compounds also protected euoxic tumor cells (Ehrlich carcinoma and P388 leukemia growing as ascites tumors) with a DMF of approximately 2; anoxic tumors were not protected. Biochemical studies disclosed that the thiophosphates enter cells by passive diffusion and are then enzymatically dephosphorylated to the protective free-SH form. The rate of dephosphorylation varied from tissue to tissue but the tumor cells studied appeared to fall within the normal range. Tissue distribution data and preliminary biochemical characterization of the dephosphorylating enzyme(s) (pH optima, inhibitor data, and kinetic analysis) are presented and analyzed with reference to the radiobiologic protection which they afford. It was concluded that the thiophosphates, and particularly WR2721, are prime candidates for eventual clinical use. (auth)

42526 EFFECT OF SOME RADIOPROTECTIVE SUBSTANCES ON THE REDOX EQUILIBRIUM IN THE SPLEEN. Mustea, I.; Uray, Z. (Oncological Inst., Cluj). Int. J. Radiat. Biol.; 19: No. 3, 281-6(1971).

The redox potential of spleen tissue in vivo was measured, and changes were observed after the administration of radioprotective drugs with reducing properties (aminothiols, dimercaptans, hydrazine derivatives, glucose, sulphites). The redox potential can be regarded as an indicator of the level of the energy metabolism of a tissue. The depression of the energy metabolism could be correlated with the potency of radioprotective drugs. The time-course of this depression on administration of AET follows that of its radioprotective property. (auth)

42527 RECOVERY EFFECT OF SEROTONIN-CREATININE SULFATE COMPLEX ON X-IRRADIATED PLANARIANS. Villalobos-Pietrini, R.; Laguarda-Figueras, A. (Univ. Nacional Autonoma de Mexico, Mexico City. Comision Nacional de Energia Nuclear, Mexico City). Experientia; 27: No. 4, 441-2 (15 Apr 1971).

Planarians (Dugesia dorotocephala) were x-irradiated in petri dishes containing electro-purified water. Following irradiation one group of planarians were submerged for one h in a solution of serotonin-creatinine sulfate complex. Mortality data were recorded daily for 60 days. Results demonstrated that serotonin was effective in restoration of the recovery mechanism altered by x rays. (H.L.W.)

42528 OKISLITEL'NOE RAVNOVESIE I RADIOCHUVSTVITEL'NOST' ORGANIZMOV. (Oxidation Equilibrium and the Radiosensitivity of Organisms). Sumarukov, G. V. Moscow; Atomizdat (1970). 104p.

The book is devoted to the vital issues of radiobiology—to the study of the initial mechanisms of the biological action of ionizing radiation and to antiradiation prophylaxis. On the basis of original research and the latest literature available, it is shown that the radiosensitivity of different organisms, not being a constant quantity, depends on the disturbances of the steady state of the organism. Such disturbances can be stipulated by different actions (by the introduction of different substances, hypoxia) before irradiation. The protective effect is proportional to the reduction of the oxidation-reduction potential in the tissues. The equilibrium shifts are recorded directly in the living organism by means of electrodes or spectrophotometrically. Using the indicated methods, it is possible to predetermine in the unirradiated organism, the antiradiation efficiency of a certain action. This is significant in the search for new protective substances. The book is of interest to radiobiologists, doctors (radiotherapists), and biophysicists. (tr-auth)

42529 PHAGE-INDUCED RADIORESISTANCE OF LYSOGENIC BACTERIA. Trgovcevic, Zeljko; Petranovic, Drago; Zgaga, Vera (Ruder Boskovic Inst., Zagreb). Biochem. Biophys. Res. Commun.; 43: 688-93(7 May 1971).

Lysogen that contains heat-inducible prophage was subjected to an appropriate heat treatment to allow only early events following phage induction. Using this system, it can be shown that early steps of phage development are responsible for increased radioresistance of the bacterial host in terms of survival and post-irradiation DNA breakdown. (auth)

42530 EFFECT OF DIRECT CURRENT AND X RADIATION ON THE MITOTIC ACTIVITY OF BONE MARROW CELLS, THE PHAGOCYTIC CAPACITY OF RETICULOENDOTHELIAL CELLS, AND THE RADIOSENSITIVITY OF WHITE RATS. Stepanyan, E. D.; Zakharyan, E. G.; Petrosyan, R. A.; Grigorenko, L. P. (Inst. of Zoology, Erevan). Biol. Zh. Arm.; 23: No. 9, 39-44 (Sep 1970). (In Russian).

White rats were subjected to a small direct current and/or radiation and their bone marrow was tested for mitotic activity. Lead electrodes with 2 to 6 mA of dc for 20 min were employed; the irradiation consisted of a 700 R dose of x radiation. The criterion was the survivor count among the rats after 30 days. Three hours after the joint action of both dc and x radiation, the mitotic activity and in part the phagocytosis were suppressed, but more weakly by far than after radiation alone. The dc treatment of animals not only reduced the depressing effect of ionizing radiation on the mitotic activity of bone marrow cells and on the phagocytosis of the reticuloendothelial cells, but to a significant measure raised the resistance of the organism toward radiation. Evidently, the radiation protection effect of the electrical treatment predetermines, in many respects, an increase in the phagocytic and reparative capacity of the elements of the reticuloendothelial system. (K.S.W.)

42531 POTENTIAL RADIOPROTECTIVE AGENTS: DERIVATIVES OF α-ALKYLOXIMINOMERCAPTANS. Hines, Norman Leroy. Urbana, Ill.; Univ. of Illinois (1970). 108 p. University Microfilms Order No. 71-6736.

Thesis.

In this work, the N–C–C–S skeleton of MEA was taken as the active pharmacophoric grouping and molecular modifications were executed with the hope that a decrease in the undesirable properties of the prototype would accompany an increase in potency. Modifications were considered where the basic amino group of MEA is replaced by an O-alkyloximino group. The S-ethyl 2-alkyloximinoalkanethioates and the di- and trithiocarbonate derivatives of the O-alkyl ethers of ketoximes were submitted for biological testing. Though all the compounds have not yet been screened for radioprotective activity, the preliminary data indicate no significant activity for any of the derivatives. (Diss. Abstr. Int., B)

42532 DERIVATIVES OF 2-ALKOXYIMINOMERCAPTANS AS RADIOPROTECTIVE AGENTS. Chu, Sou-yie. Urbana, Ill.; Univ. of Illinois (1970). 124p. University Microfilms Order No. 71-6725.

Thesis.

Radioprotective activity is usually found in compounds related to cysteamine where two carbons separate a nitrogen from a sulfur atom. Methods were investigated for the synthesis of derivatives of 2-alkoxyiminomercaptans, namely, S-(2-alkoxyiminoalkyl) isothiuronium salts and the S-(2-alkoxyiminoalkyl) thiosulfates that contain the same arrangement of atoms with the nature of the nitrogen atom changed from amine to alkyloxime. The S-(2-alkoxyiminoalkyl) thiosulfates were prepared in 24 to 97% yield by reacting 2-alkoxyiminoalkyl bromides with sodium thiosulfate in aqueous ethanol. By this procedure, 2-alkoxyiminoalkyl halides were prepared in yields up to 80%. Although α-haloketones are known to be reactive in S_N2 displacements, but unreactive by the S_N1 mechanism, the 2-alkoxyiminoalkyl bromides (O-alkyl ethers of α-haloketoximes and α-haloaldoximes) prepared in this study were found to be active in both S_N1 and S_N2 displacements. Treatment of the 2-alkoxyiminoalkyl bromides with thiourea yielded derivatives of 2-aminothiazoles as when thiourea reacts with an α-halo carbonyl compound in the well-known Hantzsch thiazole synthesis. When O-alkyl ethers of 3-bromo-2-butanone oxime were treated with ethylenethiourea, under no conditions could an uncyclized product be obtained. (Diss. Abstr. Int., B)

42533 MODIFICATION BY ACRIDINE ANALOGS OF THE SURVIVAL OF ULTRAVIOLET IRRADIATED ESCHERICHIA COLI B. Lankford, John C.; Yielding, K. Lemone (Univ. of Alabama, Birmingham). Biochem. Biophys. Res. Commun.; 44: No. 1, 224-8(2 Jul 1971).

A comparison was made of the effects of mutagenic and non-mutagenic acridines on the survival of Escherichia coli B following uv irradiation. Organisms were plated after various levels of uv exposure on both minimal and Brain Heart Infusion (Difco) agar either with no added drug or with 10^{-6} M 9-aminoacridinium chloride, acridine orange, or 10-methylacridine hydrochloride. The non-mutagenic acridine (10-methylacridinium chloride) caused no modification of uv survival. The most potent mutagen, 9-aminoacridine hydrochloride was a strong inhibitor; while acridine orange, which is less mutagenic was less effective in decreasing post-irradiation survival. Thus, with these three acridine analogs, mutagenic effects could be correlated with the ability to inhibit post uv survival. (auth)

42534 EFFECT OF CHEMICAL PROTECTION AGAINST RADIATION AS INDICATED BY THE CHROMOSOME ABERRATIONS IN THE BONE MARROW OF MICE AFTER EXPOSURE TO X RADIATION. Padeh, B. Harefuah; 77: 392-5(1969). (In Hebrew).

Radioprotective agents were investigated to determine their effectiveness and to establish whether aberrations in the bone marrow may serve to indicate the level of radiation damage and the protective ability of the agents. The compounds tested included 2-mercaptoethylamine, 2-aminoethyl thiosulfuric acid, and dimethyl aminoethyl thiosulfuric acid. Mice exposed to a whole-body irradiation of 400 R were used in the study, analyzing their chromosomes 24 hrs after exposure. Three groups were treated with the agents only, one was only irradiated and three other groups were injected 10 min prior to the irradiation. The radiation injury of the protected groups was determined on the basis of the chromosome aberrations. The results revealed that the first two chemicals have superior protective properties in comparison with the third one. (TTT)

42535 BIOCHEMICAL MECHANISMS INVOLVED IN THE SENSITIZATION OF LIVING ORGANISMS BY CHEMICAL AGENTS TOWARDS THE ACTIVITY OF RADIATIONS AND CYTOSTATICS. I. THE EFFECT OF IRRADIATION OF HYDROXYMERCURO-BENZOIC ACID-INJECTED RATS ON DNA CHROMATOGRAPHIC ASPECT. Furnica, M.; Spiridon, M.; Ganea, A. Rev. Roum. Biochim.; 7: No. 4, 265-73(1970). (In French).

p-Hydroxymercurobenzoic acid induces the sensitization of rats consecutive to 800 R irradiation, i.e., significantly reduces lifetime. The DNA extracted from the liver of radiosensitized rats three days later is chromatographically different following methylated albumin column fractionation—from the DNA extracted from the irradiated animals. These changes are not obvious immediately after irradiation and seem to be related to the recovery stage of DNA radiolesions. (Rom. Sci. Abstr.)

42536 THERAPEUTIC EFFECT OF GLUTATHIONE ON IMPAIRED LEUCOPOIESIS OF IRRADIATED BONE MARROW. EXPERIMENT BY SIMPLIFIED BONE MARROW CULTURE. Sonezaki, Shozo (Kyushu Univ., Beppu, Japan). Rinsho Hoshasen; 15: No. 11, 867-70(Nov 1970). (In Japanese).

Glutathione was injected intravenously into rabbits for ten days following exposure of thighs to 1000 R doses of ^{137}Cs gamma radiation. Fourteen days after irradiation cultures of bone marrow from irradiated and unirradiated femurs were prepared, and the growth coefficient of leukocytes was determined. Results indicated that glutathione was effective in promoting recovery of leukopoiesis in irradiated bone marrow; no side effects of glutathione were observed. (Japan)

42537 HEMORRHAGIC SYNDROME IN RADIATION DISEASE. II. EXPERIMENTAL STUDY ON THE RADIOPROTECTIVE EFFECTS OF CYSTAMINE AND TREATMENT WITH HOMOLOGOUS BONE MARROW NUCLEIC ACIDS ON COAGULATION AND FIBRINOLYSIS IN RATS EXPOSED TO LETHAL X-RAY DOSES. Cutcudache, Caliopi; Boldescu, Gabriela; Popa, Rodica; (and others). Fiziol. Norm. Patol. (Bucharest); 16: No. 2, 169-77 (Mar-Apr 1970). (In Rumanian).

The radioprotective effect of cystamine and homologous marrow nucleic acids on coagulation and fibrinolysis alterations was determined by biologic tests in rats exposed to lethal x-ray doses (700 R). The results obtained 2, 5, 10 and 15 days after irradiation, processed statistically, showed that cystamine administered by mouth has in general a favorable effect upon coagulability of the blood. Differential coagulation tests showed that, on the one hand, cystamine protects proaccelerin and stimulates thrombocytic recovery in the irradiated animal and, on the other, does not exercise an inhibitory effect on prothrombin. The decrease of antithrombin III is discussed, as well as the possible mechanism of action of cystamine on blood coagulation in vivo, under conditions of irradiation with lethal doses. Homologous marrow nucleic acids, with the molecular weight and dose administered, do not confer a satisfactory protection, either from the biological or the clinical point of view. (auth)

42538 STUDY OF THE RELATIONS BETWEEN GLUTATHIONE AND X-RAY CATARACT. Hoshi, Yoshio (Nippon Medical School, Tokyo). Nippon Ganka Gakkai Zasshi; 74: No. 3, 211-34(Mar 1970). (In Japanese).

Young rats were irradiated with 200 kvp x rays (1500 R) after they were given various radioprotective agents (glutathione), mercaptoethylamine(MEA), salivary hormone(Parotin) and 1-hydroxy-pyrido-(3-2-a)-5-phenoxazone-carboxylic acid(Catalin). Mature cataract was observed in 100% of the irradiated subjects after 11 weeks, epilation occurred in all cases after two weeks, and cornea injuries were seen in 95% of the cases after one week. In the group of subjects injected with glutathione before x-ray-treatment, mature cataract was observed in 60% after 14 weeks, epilation occurred in 80% after two weeks, and cornea injuries in 60% after two weeks. In the group of MEA-treated subjects, mature cataract was observed in 60% after 15 weeks, epilation in 83% after three weeks, and cornea injuries in 50% after one week. In

XUM

the group of Parotin-treated subjects, mature cataract was observed in 100% of the subjects after 12 weeks, epilation in 100% after two weeks, and cornea injuries in 92.3% after one week. In the group of Catalin-treated subjects, mature cataract was observed in 100% after 11 weeks, epilation in 90% after three weeks, and cornea injuries in 90% after one week. In the group of cysteine-treated subjects, mature cataract was not observed, but 90% of the subjects died after one week. Thus glutathione and MEA were determined to be effective (the latter more effective than the former) in checking the occurance and development of mature cataract. (Japan)

Radiation Sickness and Injuries

Refer also to abstracts 42391, 42395, 42401–42407, 42622–42624 42626, 42627, and 42685.

42539 EFFECT OF PETROLEUM GROWTH SUBSTANCE ON THE HEALING OF RADIATION WOUNDS OF THE SKIN. Taratukhin, V. R.; Rappoport, I. A.; Murav'ev, V. N.; Sudakova, V. O. Med. Radiol.; 16: No. 6, 53-5(Jun 1971). (In Russian).

The influence of petroleum growth substance (PGS) on the healing of radiation wounds on the skin was investigated. It was found that the use of a 0.5% and 10% emulsion of PGS produces a stimulating effect on restoration of the skin affected with β radiation: the area of skin affection was less by an average of 24%, the time of complete regeneration of the skin was 19 days shorter. A 10% emulsion of PGS had a statistically significantly greater effectiveness in comparison with a 0.5% PGS emulsion. (auth)

42540 INFLUENCE OF TRANSFUSION OF XIII FACTOR ON THE ULTRASTRUCTURE OF FIBRIN IN ACUTE RADIATION SICKNESS. Baluda, V. P.; Aladatov, A. G.; Ponomarev, Yu. T. (Obninsk Research Inst. of Medical Radiology, USSR). Med. Radiol.; 16: No. 5, 51-2(May 1971). (In Russian).

In acute radiation sickness the ultrastructure of fibrin becomes disturbed: transverse striation of fibrin characteristic for physiological fibrin disappears, fibrin fibers are shortened, and their contours are indistinct. Intravenous injection of XIII factor (40 mg of protein per kg of weight), obtained by means of gel filtration of the plasma of healthy animals through Sephadex G-200, to Wistar rats at the peak of acute radiation sickness restored the ultrastructure of fibrin and reduced the hemorrhage. The use of other plasma components of healthy rats without XIII factor activity did not exert any effect on disturbances of fibrin ultrastructure and did not reduce hemorrhage. (auth)

42541 HEALING OF RADIATION ULCERS OF THE SKIN UNDER THE INFLUENCE OF METACYL AND DIBUNOL (EXPERIMENTAL RESEARCH). Disvetova, V. V.; Bunto, T. V.; Vasilev, P. N. Med. Radiol.; 14: No. 4, 68-71(Apr 1971). (In Russian).

Extensive radiation ulcers of the skin were obtained in 29 rats in local x irradiation to a dose of 10,000 rad without a filter. The local application of a 1% emulsion of metacyl and dibunol reduced the intoxication associated with the development of radiation ulcers (decrease of the number of perished animals) and stimulated the healing of the ulcers. Histological investigations of areas of the skin from the healed ulcers have shown that the use of the preparations reduced the degenerative changes in the skin healing on a radiation ulcer. (auth)

42542 LUCHEVAYA BOLEZN' CHELOVEKA. (Radiation Sickness in Man). Gus'kova, A. K.; Baĭsogolov, G. D. Moscow: Izdatel'stvo Meditsina (1971). 384p.

Twenty papers discuss the clinical, pathological, and therapeutic aspects of radiation sickness in man. (950 references.) (TSS)

42543 MANDIBULAR OSTEORADIONECROSIS. Cachin, Y.; Vandenbrouck, C. (Institut Gustave Roussy, Villejuif, France). Probl. Actuels Oto-Rhino-Laryngol.; 189-201(1969). (In French).

Mandibular osteoradionecrosis is defined. A clinical description and its pathological anatomy are given. The etiological factors are discussed. The treatment, consisting of surveillance, antibiotics, and surgery, is described. (J.S.R.)

42544 PROBLEMS POSED BY RADIODERMATITIS. Bertaud, J.; Delplace, Y.; Cabasson, G. B.; Cavigneaux, A. Arch. Mal. Prof. Med. Trav. Secur. Sociale; 32: No. 3, 299-302(Mar 1971). (In French).

Thirty-six cases of radiodermatitis occurred between 1960 and 1970 and were treated under the Social Security. In two cases, compensation was required for more than 10 years following exposure. The 10 year after-care period envisaged by the social security appears to be insufficient. Legally, since the 15th of March 1967, medical records should be kept during the whole life of the exposed person or for at least thirty years after the exposure. The possible need for excision-graft must be considered in all the cases of localized radiodermatitis. All light lesions should be treated, as soon as they appear, by electrocoagulation. (France)

42545 BERYLLIUM WINDOW TUBES FOR MAMMOGRAPHIC EXAMINATIONS. Wright, D. J.; Nichini, F. M.; Stauffer, H. M. (Temple Univ., Philadelphia). Brit. J. Radiol.; 44: No. 522, 480(Jun 1971).

A case of radiation reaction is reported after use of a beryllium window x ray tube without added filtration for routine mammographic examination. Two weeks after radiography, there was tanning of both breasts and blistering and moist desquamation of one. It was not appreciated that the tube output included tungsten L radiation, rapidly absorbed into the skin, but of sufficient intensity to produce skin changes. The N.C.R.P. requirement was emphasized for .5mm Al as a total minimum filtration for diagnostic equipment operated below 50 kVp. (UK)

42546 CASES OF ATOMIC BOMB RADIATION CATARACT IN THE LAST 10 YEARS. Fujinaga, Yutaka (Hiroshima Red Cross Hospital). Nippon Ganka Kiyo; 21: No. 3, 233-6(Mar 1970). (In Japanese).

Thirty cases of cataract were seen in Hiroshima atomic bomb survivors during 1959 to 1969. They were examined for progressiveness, combined diseases, and tissue image of the crystalline lens obtained by surgery. The cases were classified as to: progressive opacity of atomic bomb-induced cataract; no progression of opacity of atomic bomb-induced cataract; no progression of atomic bomb cataract but senile cataract in progress; and combined disease. There were no cases in which the radioinduced cataract had progressed. Two cases were found in those aged below 40, indicating their exposure at a young age, and two cases of primary cataract were observed suggesting the possibility that exposure to the atomic bomb radiation might lower the age for senile cataract to appear. Cases of senile cataract were all aged above 40 and showed no change in opacity characteristic of radioinduced cataract. The tissue of incised crystalline lens showed characteristic findings for radiation cataract, such as pseudoepithelial and foaming cells seen in the posterior cortex. The occurrence of simple glaucoma was observed in several cases, and this responded well to surgical operation and drug therapy. There was no change in the state of radioinduced cataract in these cases. Progression in the development of radioinduced cataract occurs after some latency, and appears as spotty opacity below the posterior capsula and cement-like opacity, and forms the opacity characteristic to this disease. Radioinduced cataract developed about 12 years following radiation exposure, and after the initial symptoms seemed to stop without any further progress. (Japan)

Radiodiagnosis

Refer also to abstracts 42059, 42089, 42090, 42243, 42292, 42362, 42397, 42412, 42430, 42431, 42433, 42447, 42476, 42493, 42496, 42502, 42696, 42702, and 42711.

42547 (ACRH-1000-248) CORRELATION BETWEEN BRAIN TUMOR DETECTABILITY ON BRAIN SCAN AND PROTEIN LEVELS OF THE SPINAL FLUID. Pinsky, Steven M.; Hoffer, Paul B.; Flom, Richard; Quinn III, James L.; Gottschalk, Alexander (Chicago Wesley Memorial Hospital, Ill. Nuclear Medicine Lab.). [Feb 1970]. Contract AT(11-1)-69. 11p. (CONF-701129-2). Dep. NTIS.

From 56. annual meeting of the radiological society of America; Chicago, Ill. (29 Nov 1970).

The clinical records of fifty-eight patients with proven primary brain tumors were reviewed. Each patient had spinal fluid protein determinations and ^{99}Tc-pertechnetate brain scans before surgery. Twenty-five patients had elevated spinal fluid protein levels. Of this group, 22 had positive scans. Thirty-three had normal protein levels and 17 had positive brain scans. In patients with brain tumors and elevated spinal fluid protein levels 88% had positive scans, if the protein level was normal, only 52% had positive scans. The differences are statistically significant. Thus, there is a positive correlation between brain tumor detectability on brain scans and spinal fluid protein levels. (auth)

42548 (CONF-710204-4) POTENTIAL USE OF FLUORESCENT SCANNING FOR BRAIN TUMOR IDENTIFICATION. Patton, James A.; Brill, A. B.; Johnston, R. E. (Vanderbilt Univ., Nashville, Tenn. School of Medicine). [1970]. 31p. Dep. NTIS.

From Symposium on the role of semiconductor detectors in the future of nuclear medicine; Chicago, Ill. (12 Feb 1971).

The feasibility of imaging fluorescence radiation from stable Bi for the localization of brain tumors was investigated using vials of Bi suspended in a water phantom. Preliminary studies using 200 mCi of ^{99m}Tc as the γ excitation source and a scanning device consisting of eight 1.5-in. × 0.5 NaI detectors in a cylindrical array are reported. It was concluded that this method would require the administration of an excessive amount of Bi to the patient. An experiment was conducted using a 3 Ci encapsulated ^{153}Gd source for excitation and a Ge(Li) semiconductor detector for scanning. Results indicated that this system will provide an increase in photoelectric absorption and improve the scan resolution. (C.H.)

42549 (ORAU-113) 1970 RESEARCH REPORT FOR THE YEAR ENDING DECEMBER 31, 1970. (Oak Ridge Associated Universities, Inc., Tenn. Medical Div.). 216p. Dep. NTIS.

The effectiveness of radioisotope scanning of ^{67}Ga for the localization of neoplasms in lymphatic tissues was evaluated. The uptake of ^{67}Ga in human tissues obtained at autopsy and in 22 different types of rat, hamster, and mouse tumors was studied. The radiation dose to human spleen, kidneys, adrenal glands, bone marrow, and liver at various times following the administration of tracer doses of ^{67}Ga was measured. The development of computer data analysis and recording systems for the analysis and storage of information on effects of whole-body irradiation on man and for the analysis of data from clinical radioisotope diagnostic tests is discussed. (C.H.)

42550 (ORNL-TM-2091(Suppl.2)) ^{99m}Tc AND GALLIUM IN MEDICINE: A SUPPLEMENTARY BIBLIOGRAPHY. Stemple, Ruth M. (comp.) (Oak Ridge National Lab., Tenn.). Jul 1971. Contract W-7405-eng-26. 29p. Dep. NTIS.

A list is presented of approximately 500 publications during 1969 and the first three quarters of 1970 on scintigraphy using ^{99m}Tc. Forty-one publications during the same period of time on scintigraphy using ^{67}Ga or ^{68}Ga are listed. (C.H.)

42551 DIAGNOSTIC FINDINGS IN HYPOPLASIA OF THE PULMONARY ARTERY. Schawohl, P.; Hennig, K.; Thomas, E. (Medizinische Akademie Carl Gustav Carus, Dresden. Bezirkskrankenhaus fuer Tbk und Lungenkrankheiten, Dresden). Deut. Gesundheitsw.; 26: No. 9, 384-90(25 Feb 1971). (In German).

Apart from the typical radiological characteristics a combination with a bronchopulmonary dysplasia could very frequently be identified in 13 patients suffering from a one-sided hypoplasia of the pulmonary artery. The results of perfusion and ventilation scintigraphy enlarge the knowledge with regard to morphology and functional diagnostics, and are a valuable supplement of cardiorespiratory diagnostics, where obstructive restrictions and functional insufficiency are considered typical characteristics. For an early diagnosis fluorography proved suitable. An essential prerequisite for avoiding late damages is dispensary care. (auth)

42552 PERMISSIBLE LEVELS OF IRRADIATION OF THE ORGANISM IN RADIOISOTOPE DIAGNOSIS. Agranat, V. Z.; Knizhnikov, V. A.; Lyass, F. M. (Inst. of Oncology, Moscow. Inst. of Biophysics, Moscow. Inst. of Neurosurgary, Moscow). Med. Radiol.; 16: No. 6, 3-10(Jun 1971). (In Russian).

Radiation burdens to the organism during the use of radioisotopes for diagnostic purposes are, as a rule, associated with an extremely low but definite risk. The maximal permissible levels in diagnostic investigations should be such that the hazard of the examination would be essentially less than the possible consequences of delay in diagnostic information. In determining the maximum permissible doses it is assumed that the degree of justified risk for different persons varies. Doses for different persons depend on age, sex, and nature of the medical investigation. Criteria for evaluating the risk from the diagnostic procedure are: immediate somatic effects; remote sequelae; therapeutic effects; and genetic sequelae. When determining the maximum permissible dose, the critical organ for the radioactive preparation should be considered. On the basis of these principles and concepts maximum permissible doses for different groups of persons with due consideration of the tasks of the medical investigation are proposed. (auth)

42553 SCANNING OF THE LIVER IN THE DIAGNOSIS OF CHRONIC HEPATITIS AND CIRRHOSIS. Loginov, A S.; Petrova, O. P. (Inst. of Gastroenterology, Moscow). Med. Radiol.: 16: No. 6, 10-15(Jun 1971). (In Russian).

The possibility of scanning in the diagnosis of chronic hepatitis and cirrhosis of the liver is discussed. Characteristic changes of the form of the liver and the character of distribution of the radioisotope in cirrhosis of the liver at different stages of the disease were noted. The relation of changes in the structure of the liver on scintigrams in cirrhosis with alterations of the architectonics of the portal channel of the liver was revealed. Also discussed are the causes of augmented accumulation of ^{198}Au in the spleen and its diagnostic importance. (auth)

42554 EXTERNAL MEASUREMENTS OF PULMONARY PRESSURES BY MEANS OF RADIOISOTOPIC DILUTION CURVES. Di Matteo, J.; Vacheron, A.; De Vernejoul, P.; (and others) (Hospital Necker, Paris. CEA, Orsay, France). Ann. Med. Interne; 121: 889-94(Nov 1970). (In French).

The use of computer analysis of radioisotope scan data enabled correlations to be established between certain heart parameters and pulmonary blood pressures. It is now possible to evaluate the mean pulmonary arterial and capillary pressures by simple external detection. A hundred cases of various heart diseases were studied. Comparison of the results obtained by radioisotope scanning with those supplied by cardiac catheterization proved the validity of the equations used for the pulmonary pressure calculations. The easy repetition of the radioisotope method makes it an ideal exploratory tool for the haemodynamic supervision of heart diseases. (auth)

42555 BASIC MEDICAL RADIATION PHYSICS. Stanton, Leonard. New York; Appleton-Century-Crofts (1969). 655p. $12.75.

The basic concepts and tools of medical radiation physics of interest to physicians working in radiology and nuclear medicine are presented. Emphasis is placed on uses of x radiation for diagnosis and therapy. Methods used for the dosimetry of external and internal radiation sources commonly used for therapy, clinical radioisotope dosimetry, and basic concepts and specific methods for radiation protection are covered. (C.H.)

42556 SCINTIPHOTOGRAPHIC EVALUATION OF RESPONSE OF BRAIN NEOPLASMS TO SYSTEMIC CHEMOTHERAPY. Handel, Stanley F.; Powell, Malcolm R.; Wilson, Charles B.; Enot, K. Jean (Univ. of California, San Francisco). J. Nucl. Med.; 12: No. 6, 292-6(Jun 1971).

Serial scintiphotographic examinations of the brain were performed to follow responses of brain tumors in 29 patients given chemotherapy. Scintiphotographic changes were consistent with clinical changes in 64% of the serial scintiphotographic studies. In 15% of the studies correlation was inverse and in 21% it was intermediate. (auth)

42557 COMPUTER PROCESSING OF SCANS USING FOURIER AND OTHER TRANSFORMATIONS. Brown, Donald W.; Kirch, Dennis L.; Ryerson, Thomas W.; (and others) (Univ. of Colorado, Denver. Veterans Administration Hospital, Denver). J. Nucl. Med.; 12: No. 6, 287-91(Jun 1971).

Methods of achieving resolution enhancement of radionuclide scans by computer processing were investigated. A digital array of scan data was transformed from the spatial to the frequency domain using a two-dimensional Fast Fourier Transform algorithm. A frequency domain filter which combines smoothing and deconvolution with the modulation transfer function of the scanning system was then applied, followed by inversion back to the spatial domain. Differential, homomorphic, and other filtering techniques, as well as Hadamard transforms, were also studied. Resolution enhancement of phantom and patient scans was achieved, but the degree of improvement has not yet been quantitated. (auth)

42558 DETERMINATION OF IN VIVO PERSISTENCE OF TANTALUM DUST FOLLOWING BRONCHOGRAPHY USING REACTOR-ACTIVATED TANTALUM AND TOTAL BODY COUNTING. Upham, T.; Graham, L. S.; Steckel, R. J.; Poe, N. (Univ. of California, Los Angeles). Amer. J. Roentgenol., Radium Ther. Nucl. Med.; 111: 690-4(Apr 1971).

Tantalum dust, administered as an aerosol has been proposed for use as a radioopaque agent for bronchial radiography. A convenient experimental method for the in vivo estimation of retained metallic substances, using neutron activation of ^{182}Ta prior to administration and subsequent total-body counting, was applied in a study of thallium dust retention in the respiratory tract. Unexpectedly long persistence of tantalum dust suggests caution in the use of this agent. (auth)

42559 PRIMARY CONGENITAL LYMPHEDEMA IN INFANCY EVALUATED BY ISOTOPE LYMPHANGIOGRAPHY. Gates, Gary F.; Dore, Earl K. (Memorial Hospital Medical Center, Long Beach, Calif.). J. Nucl. Med.; 12: No. 6, 315-17(Jun 1971).

A 15-week-old infant with primary congenital lymphedema was evaluated by isotope lymphangiography. The scan showed absence of ^{198}Au in the right inguinal and femoral lymph node groups at both 24 and 96 hr after injection. This is a safe, relatively easy, nontraumatic method for studying the lymphatic system of the infant. (auth)

42560 SOCIETY OF NUCLEAR MEDICINE, 18th ANNUAL MEETING, LOS ANGELES, CALIFORNIA, JUNE 28–JULY 2, 1971. ABSTRACTS FOR SCIENTIFIC PROGRAM. J. Nucl. Med.; 12: No. 6, 334-483(Jun 1971). (CONF-710605(Absts.)).

Abstracts are included for approximately 300 papers presented

XUM

at the 1971 annual meeting of the Society of Nuclear medicine. (C.H.)

42561 STUDY OF THE ABSORPTION OF GASES IN THE LUNGS WITH THE AID OF ^{133}Xe. Vorobeva, Z. V. Med. Radiol.; 16: No. 5, 7-13(May 1971). (In Russian).

A technique for determining mass exchange in the lungs using ^{133}Xe, that characterizes the absorption (elimination) of gases in the lungs, is substantiated. A mathematical model of mass exchange in the lungs and the initial data for it are given. The results of investigations of mass exchange in the lungs of healthy people and patients using ^{133}Xe are demonstrated. (auth)

42562 EFFECTIVENESS OF SCANNING BONE TUMORS WITH ^{85}Sr AND ^{87m}Sr. Zubovskii, G. A.; Gleizer, Yu. Ya.; Gilyazutdinov, I. A. (Moscow Inst. of X-Ray Radiology. Kazan Inst. for Medical Graduate Work, USSR). Med. Radiol.; 16: No. 5, 3-7(May 1971). (In Russian).

Twenty-five patients with primary and secondary tumors of the bones were examined. All the patients were subjected to roentgenological investigation and scanning with ^{87m}Sr and ^{85}Sr. The X-ray and radioisotope data were compared. A conclusion is made on the higher diagnostic efficacy of ^{85m}Sr in comparison with ^{87m}Sr, especially for the detection of lesions of the lumbar region of the spine and pelvic bones. (auth)

42563 USE OF A NEW VECTOR IN THE DIAGNOSIS OF MELANOMAS. Blanquet, P.; Moretti, J. L.; Safi, N.; Verin, Ph. (Hopital Saint-Andre, Bordeaux. Institut National de la Sante et de la Recherche Medicale, Bordeaux). J. Biol. Med. Nucl.; 5: No. 22, 17-20(1970). (In French).

A new method of ocular scintigraphy was recently developed, using a new iodine-containing tracer: ^{131}I-labeled 7-iodoquine. This vector proved of interest for the diagnosis of melanomas, whatever their topography, and that of the residual disease. The preparation of the tracer, its testing, and the results obtained are presented. The mechanism of fixation of this substance seems to be linked with the β-glycuronidase concentration in the tumor, which explains the rare cases when the method is not effective. (France)

42564 POSITRON CAMERA IN HOSPITAL PRACTICE. PRELIMINARY CONSIDERATIONS. Beck, C.; Blanquet, P.; Basse-Cathalinat, B.; Ducassou, D.; Dupuy, J. C. (Hopital Saint-Andre, Bordeaux. Institut National de la Sante et de la Recherche Medicale, Bordeaux). J. Biol. Med. Nucl.; 5: No. 22, 10-16(1970). (In French).

The positron camera permits the use of short-lived radioisotopes in diagnostic studies. Its value was proved for routine use for bone scintigraphy using ^{18}F, and for spleen scintigraphy after injection of ^{64}Cu-labeled fragmented erthyrocytes. It offers invaluable assistance when it is desirable, after a standard examination, to define the true outline of a poorly defined area or its actual extension, an application which is especially useful in bone scintigraphy. (France)

42565 DETECTION OF HYPERFIXING ZONES BY MEANS OF A POSITRON CAMERA TYPE POSITRON. III. TOMAGRAPHIC PROPERTIES. Bard, J. J. (INSERM, Clermont-Ferrand, France); Meyniel, G.; Isabelle, D. B. J. Biol. Med. Nucl.; 5: No. 22, 5-9 (1970). (In French).

The results described show the advantages of a scintigraphic positron camera for the tomographic study of brain tumors. A particular study was made of hot nodule detection in a transparent plastic model corresponding to the skull of a human adult. The experiments were carried out with ^{22}Na as β^+ emitter, showing that a positron camera of the Positron III type gives an accurate localization of brain tumors by a series of simple measurements. This method of examination is nevertheless limited by the use of β^+ emitters which are generally very short-lived, the result being that the isotopes must be produced near the hospital service where they are used. (France)

42566 RADIOISOTOPIC EVALUATION OF SALIVARY GLAND DYSFUNCTION IN SJOEGREN'S SYNDROME. Alarcon-Segovia, Donato; Gonzalez-Jimenez, Yolanda; Garza, Luis Rene; Maisterrena, Jorge (Instituto Nacional de la Nutricion, Mexico City). Amer. J. Roentgenol., Radium Ther. Nucl. Med.; 112: No. 2, 373-9(Jun 1971).

The capability of the salivary glands to selectively concentrate elements of Periodic Group VII and secrete them in saliva was utilized to assess salivary gland function in 28 patients with Sjögren's syndrome by means of radioisotopic studies following the intravenous administration of ^{99m}Tc pertechnetate. The findings were compared with those obtained in 10 normal controls. Scintiscans and direct counts over parotid glands showed lower uptake in patients than in controls. The counts were similar over both parotid glands in all controls, while there was significant difference of uptake between the two glands in many patients. Ratios of thyroid/parotid uptake were thus higher in most patients than in controls. Concentration of the isotope in saliva diminished from the 15 to the 60 minute postinjection samples in all normal controls, while it increased in all but three of the patients. All three had extreme xerostomia and low salivary gland uptake. Repeat studies in five patients revealed changing patterns of dysfunction and gland involvement which occurred either spontaneously or under corticosteroid treatment. Abnormalities in salivary gland function could be detected by these studies in patients with Sjögren's syndrome without clinical xerostomia. (auth)

42567 SCINTICISTERNOGRAPHY IN INDIVIDUALS WITHOUT KNOWN NEUROLOGICAL DISEASE. Kieffer, Stephen A.; Wolff, John M.; Prentice, Walter B.; Loken, Merle K. (Univ. of Minnesota, Minneapolis). Amer. J. Roentgenol., Radium Ther. Nucl. Med.; 112: No. 2, 225-36(Jun 1971).

Quantitative scinticisternographic studies in a group of 54 presumably normal individuals, using ^{99m}Tc-labeled human serum albumin as the tracer, established both a mean and a range of normal for this examination. Significant variations from what has heretofore been accepted as normal have been found in this group. These include variations in the rate of ascent and absorption of the labelled albumin, frequent lateralization of flow to one or the other side intracranially, and occasional transient backflow into the cerebral ventricles. Leakage outside the subarachnoid space at the site of lumbar puncture was frequent, preventing quantitative studies in 13 patients (24% of the total group). Scinticisternography, including both pictorial and quantitative examinations, is a valid diagnostic test in the evaluation of cerebrospinal fluid dynamics in normal and hydrocephalic patients. The range of normal varies from rapid ascent with early absorption of the labeled albumin to slower ascent and absorption. Transient ventricular reflux appears to lie at the lower end of this spectrum. (auth)

42568 RADIONUCLIDE EVALUATION OF THE DANDY-WALKER MALFORMATION AND CONGENITAL ARACHNOID CYST OF THE POSTERIOR FOSSA. Conway, James J. (Children's Memorial Hospital, Chicago. Northwestern Univ., Chicago); Yarzagaray, Luis; Welch, Dennis. Amer. J. Roentgenol., Radium Ther. Nucl. Med.; 112: No. 2, 306-14(Jun 1971).

The cyclops sign or the isogonal sign noted in the posterior view of a brain scintigram, along with a high midline position of the torcular, has been found to be associated with congenital cystic malformations in the posterior fossa. Differentiation between the Dandy–Walker malformation and congenital arachnoid cyst of the posterior fossa cannot be achieved on the brain scintigram. Filling of the cyst from a radionuclide ventricular injection (^{131}I-human serum albumin) without visualization of the subarachnoid spaces supports the diagnosis of Dandy–Walker malformation. Filling of the cyst from a radionuclide subarachnoid injection would more likely suggest an arachnoid cyst than the Dandy–Walker malformation. The angle produced by the transverse sinuses of the torcular (torcular angle) provides a ready index for the detection of congenital or acquired malformations of the brain. A standard of normalcy in children is established with a mean angle of 162° and a standard deviation of 8°, whereas the cystic malformations had a mean angle of 110° with a standard deviation of 10°. An abnormal torcular angle requires further definitive studies such as angiography or pneumoencephalography. (auth)

42569 QUANTITATIVE GAMMAGRAPHY OF THE THYROID GLAND WITH ^{99m}Tc and ^{131}I. A COMPARATIVE STUDY. Baptista, A. M.; Clode, W. H. (Centro de Estudos de Medicina Nuclear, Lisbon). Arq. Patol. (Lisbon); 42: No. 1-3, 47-54(1970).

From this study it is concluded that gammagraphy with ^{99m}Tc gave essentially the same clinical information as the one obtained with ^{131}I. In only two cases, about 9% of the total, we could not arrive at any conclusion from the technetium gammagraphy but also, in two of the cases, the 50 μCi of ^{131}I was clearly insufficient to give a useful image. However, in 60% of the cases, the radioiodine image was clearly superior to the technetium one, as far as the topographic details are concerned. In 30% of the cases, on the contrary, the technetium gammagraphy was superior. No appreciable difference was noticed in about 10% of the cases betweer the two images with the two radionuclides. Therefore, from the point of view of the clinical information, ^{99m}Tc gammagraphy can give useful indications in 90% of the cases that are sent to a Nuclear Medicine laboratory. This is important, for in the case of children where only the thyroid image is required, the use of ^{99m}Tc is imperative. The radioactivity necessary for a thyroid function study, from 1 μCi to 5 μCi, is clearly insufficient to obtain a useful thyroid image. (auth)

42570 SUITABILITY OF TECHNETIUM-LABELED ERYTHROCYTES FOR THE EXAMINATIONS OF THE SPLENIC FUNCTION. Franke, W.-G.; Hennig, K.; Woller, P. (Carl Gustav Carus Mediznische Akademie, Dresden). Radiol. Diagn.; 11: 783-9(1970). (In German).

For 31 persons, the behavior of simultaneously technetium- and radiochrome-labeled erythroyctes was compared with erythrocytes being usually exclusively radiochrome-labeled and thermally altered. It could be shown that those erythrocytes that were prepared by the method of double labeling differed from those that were radiochrome-labeled with respect to their kinetics. The differences are discussed in detail. On the premises that the behavior of the double-labeled erythrocytes and of those being exclusively labeled by technetium may be considered as identical, the conclusion may be drawn from the given results that also technetium-labeled erythrocytes are suitable for the functional diagnosis of the lienal reticulohistiocyte system. (auth)

42571 XEROSTOMIA IN SJOEGREN'S SYNDROME. EVALUATION BY SEQUENTIAL SALIVARY SCINTIGRAPHY. Schall, Gerald L.; Anderson, Larry G.; Wolf, Robert O.; (and others) (National Institutes of Health, Bethesda, Md.). J. Amer. Med. Ass.; 216: No. 13, 2109-16(28 Jun 1971).

Sequential salivary scintigraphy, or the visual recording with a gamma scintillation camera of the uptake, concentration, and excretion of ^{99m}Tc pertechnetate by the major salivary glands after the administration of ^{99m}Tc–sodium pertechnetate, was performed on 20 female patients with Sjögren's syndrome. The results were compared with those of other procedures currently used to evaluate xerostomia. The scintigraphic findings closely paralleled the results of the salivary flow-rate determinations and contrast sialography and the patients' clinical symptoms, but did not correlate with the finding of lymphocytic infiltration in lip biopsy specimens or the detection of the anti-salivary-duct antibody. The scintigraphic examination proved to be extremely sensitive in depicting small asymmetric differences in parotid gland activity and in monitoring the improvement in salivary gland function with immunosuppressive therapy. Sequential salivary scintigraphy appears to be an easy, safe, and objective means of evaluating xerostomia in patients with Sjögen's syndrome. (auth)

42572 RADIOISOTOPE SCANNING FOR PAROTID ONCOCYTOMA. Ausband, John R.; Kittrell, Bill J.; Cowan, Robert J. (Wake Forest Univ., Winston-Salem, N. C.). Arch. Otolaryngol.; 93: No. 6, 628-9(Jun 1971).

This is the first report of radioisotope scanning in parotid oncocytoma. This tumor showed increased concentration of ^{99m}Tc-labeled sodium pertechnetate. Review of the recent literature indicates that benign tumors are hot, while intermediate and malignant tumors are either normal, or cold on radioisotope scanning. (auth)

42573 RADIOISOTOPES AS APPLIED TO DIAGNOSTIC HEMATOLOGY. Masouredis, S. P. (Univ. of California, San Diego). CRC Crit. Rev. Clin. Lab. Sci.; 2: No. 1, 139-71(Jan 1971).

Radioisotopes have found diagnostic applications in almost all areas of hematology. The major applications and their contributions to the study of blood are reviewed. Included are those that because of cost, technical considerations, or radiation hazard are primarily investigative studies, and those that are readily applicable to routine diagnostic use. In this latter category, probably the most useful has been the use of ^{51}Cr to label erythrocytes for survival and sequestration studies, the use of ^{51}Cr to study platelet survival in the thrombocytopenias, the use of ^{59}Fe for the study of iron metabolism, and the use of ^{58}Co-labeled vitamin B-12 for absorption studies. (C.H.)

42574 MEASUREMENT OF GLOMERULAR FILTRATION RATE. Materson, Barry J. (Univ. of Miami, Fla. Veterans Administration Hospital, Miami, Fla.). CRC Crit. Rev. Clin. Lab. Sci.; 2: No. 1, 1-43(Jan 1971).

The clinical importance of accurate measurements of the rate at which renal glomeruli filter plasma during the initial step of urine formation is discussed. Various methods used for the measurement of glomerular filtration rate are reviewed, with emphasis on radioisotope methods using external scintillation scanning and radiography using radioisotope-labeled contrast media. It is pointed out that inulin remains the standard reference index substance for the measurement of the glomeruli filtration rate and that there are many radioisotope-labeled inulins and substitutes for inulin. The advantages and disadvantages of 17 radioisotopes incorporated into a number of compounds are evaluated for use for kidney scanning. (C.H.)

42575 NEUTRON RADIOGRAPHY OF OSSEOUS TUMOURS. Boyne, P. J. (Univ. of California, Los Angeles); Whittemore, W. L. Nature (London); 230: 461-2(16 Apr 1971).

A description is given of what is believed to be the first effective neutron radiographic technique for detecting pathological tissue within unsectioned biopsied bone specimens. The neutron source used in the studies was a nuclear reactor with thermal neutrons collimated to form a beam of $\sim 1/100$ radian angular divergence. After penetration of the specimens a 0.001 inch Gd screen was used to convert the neutrons to 70 keV electrons which created the photographic image on the x-ray film. The case of a large cyst of the mandible containing a ameloblastoma was investigated. X-radiographic and neutron radiographic results are shown photographically. In other cases of tumors involving the facial bones, significant invasion by the tumor which had not produced sufficient bone destruction to be visible by routine x-radiography was revealed by the neutron radiography. It is considered that future development of the techniques may make possible in vivo imaging of tissue if the required radiation dose can be reduced to permissible ranges. (UK)

42576 RADIO-MERCURY DIAGNOSIS OF THE TUMOR. Vandor, Ferenc; Szabo, Imre. Magy. Radiol.; 23: No. 2, 118-21(Apr 1971). (In Hungarian).

In the diagnosis of tumors of the oral cavity, the pharynx, and the mamma, the applicability of $^{197}HgCl_2$, $^{203}HgCl_2$, and ^{203}Hg-neohydrin (chlormerodrin) was examined. In the case of rapidly growing and radiosensitive tumors, considerable accumulation of radiomercury was observed. The detection is not impeded by the blood-background. In the case of more slowly growing tumors with mature cells, the use of $^{203}HgCl_2$ is a safer method. The examination may be performed also after the elimination of the nuclide from the circulation and in this case, the background is less disturbing. (auth)

42577 DIFFERENCES BETWEEN LESIONS IN CEREBRAL SCANNING. Sephton, R. G. (Cancer Inst., Melbourne); Morley, J. Barrie; Steven, L. W.; Andrews, J. T.; Cornell, F. N. Australas. Radiol.; 13: No. 4, 337-41(Nov 1969).

An account is given of attempts to differentiate between varieties of cerebral lesions by using brain scanning. The differences between vascular uptake of isotope in a lesion, and permeation of an isotope into it or into surrounding material, were the criteria for differentiation. Technetium-99m was used to indicate vascularity on the early post-injection scan (5 to 10 mins). Permeation effects were used for late scans (one hour or more). Indium-113m was used as a blood-pool marker. (Australia)

42578 OPTIMUM MEASUREMENT OF ^{75}Se FOR PANCREAS SCANNING. Steven, L. W.; Andrews, J. T.; Arkles, L. B. (Royal Melbourne Hospital). Australas. Radiol.; 13: No. 4, 418-20(Nov 1969).

It is proposed that the most accurate scanning method for the pancreas using ^{75}Se is that of using two separate pulse height analyzers (one set to measure 140 keV radiations and the other to measure 270 keV radiations). This is the case provided the pancreas scan is planned to be done in as long a pre-set time as is possible. (Australia)

42579 SCINTIPHOTOGRAPHY AND RECTILINEAR SCANNING OF THE LUNG USING ^{99m}Tc-MAFH (MACROAGGREGATED FERROUS HYDROXIDE). Cook, David J.; Lander, Harry (Univ. of Adelaide. Inst. of Medical and Veterinary Science, Adelaide). Australas. Radiol.; 15: No. 1, 32-7(Feb 1971).

Comparative lung perfusion studies of multiple view rectilinear scanning and scintillation camera photos were made on 123 occasions using 100 subjects. Correlation was found to be good, however scintiphotography was faster, with consequent reduction of artificialities due to movement, and less variation in quality. Differences in focusing characteristics of the two systems produced slight differences in appearance. Lateral projection was of great value in delineation of perfusion defects. Changes in scan defects were rarely parallel in all views and the lateral projection was valuable for assessing defect resolution. (Australia)

42580 NEW DOUBLE-TRACER TECHNIQUE (COLLOIDAL ^{198}Au + ^{75}Se-LABELLED SODIUM SELENITE) IN THE DIAGNOSIS OF LIVER NEOPLASIA. Mombelli, L.; Favaro, L.; Meldolesi, U. (Univ., Milan). Radiol. Med.; 56: No. 10, 913-23(Oct 1970). (In Italian).

A new scintiscan method for the detection of neoplastic lesions of the liver is described. ^{75}Se-labeled sodium selenite is employed. Since this tracer is also taken up by healthy tissue, conventional scanning would not suffice to display neoplastic processes as positive images. Healthy parenchyma suppression was obtained by the addition of colloidal radiogold and scanning was carried out with a pulse subtraction circuit. The neoplastic area

XUM

was unable to take up radiogold and was therefore displayed as a positive image. The new method is considered useful in the differential diagnosis of uptake deficiencies revealed by ^{198}Au liver scintiscans. (auth)

42581 RADIOISOTOPE INVESTIGATION OF LYMPH SYSTEM FUNCTION AND MORPHOLOGY. Spreafico, G. L.; Lualdi, M.; Puricelli, G. (Ospedale Generale Provinciale, Busto Arsizio, Italy). Radiol. Med.; 56: No. 10, 924-38(Oct 1970). (In Italian).

A radioisotope scintiscan of the iliac and lumbo-aortic inguinal lymph node chains is reported. Comparison was made between the results achieved with this method and with radiological lymphadenography in 62 cases in a series that included healthy subjects and patients with genital tumors or systemic neoplasia of the lymphatic system. Though less accurate by comparison with radiological lymphography, the new method is recommended as a routine test in the detection of organic, inflammatory or tumoral lesions of these lymph nodes, particularly since it is completely harmless and easily repeatable. (auth)

42582 NUCLEAR MEDICINE. SECOND EDITION. Blahd, William H. New York; McGraw-Hill Book Company (1971). 873p. $33.50.

The field of nuclear medicine is presented as an integrated discipline. Various facets of the field are considered including fundamentals, clinical applications, and new developments. Although the primary approach is clinical, major topics are presented in sufficient depth to be of interest and value to both the medical investigator and instructor. Each chapter contains an extensive bibliography. The chapters of the book are arranged into three sections: fundamentals (1 through 8); diagnosis (9 through 25); and therapeutics (26 through 32). An extensive subject index is also included. (E.R.B.)

42583 USE AND INTERPRETATION OF THE LUNG SCAN. Mishkin, Fred S.; Brashear, Richard E. Springfield, Ill.; Charles C Thomas, Publisher (1971). 129p. $12.25.

An anatomically grounded physiologic approach to lung scan interpretation is presented, stressing practical points of technique that aid in appropriate recording of data with instruments widely used today. The five chapters in the book discuss: anatomy and physiology; technology; pulmonary bronchial and parenchymal diseases; pulmonary vascular diseases; and pleural and chest wall abnormalities. (E.R.B.)

42584 RADIOBIOLOGICKA KONFERENCIA, TATRANSKA LOMNICA, CZECHOSLOVAKIA, 30.IX.-3.X.1969. SUHRNY REFERATOV. (Radiobiological Conference, Tatranska Lomnica, Czechoslovakia, September 30-October 3, 1969. Abstracts). Kosice, Czech.; P. J. Safarik University ([1969]). 91p. (CONF-690978-(Absts.)).

Seventy-eight abstracts, by Czechoslovakian authors, on radiation-biological and nuclear medical subjects are presented. One hundred and forty-nine persons participated in the conference, which was sponsored by the Biophysical Section of the Czechoslovak Biological Society, the Czechoslovak Medical Association, the Slovene Biological Society, and the Department of Natural Sciences of Kosice University. (TTT)

42585 LIVER AND SPLEEN SCINTIGRAPHY IN STAGING HODGKIN'S DISEASE. Hardin, Virgil M.; Johnston, Gerald S. (Letterman General Hospital, San Francisco). J. Surg. Oncol.; 3: No. 2, 109-15(1971).

Liver-spleen scintigraphy is a useful adjunctive procedure in the diagnosis and staging of Hodgkin's disease. Scintigraphy is easily obtained for both the patient and the physician. It usually directs attention to a liver or spleen involved with the disease by revealing organomegaly with or without defects in concentration of radioactive colloid. The information may be diagnostic. Patients are presented who were studied with lymphangiography, diagnostic laparotomy with splenectomy, and liver-spleen scintigraphy using ^{99m}Tc-sulfur colloid among other tests for staging. The routine use of liver-spleen scintigraphy is recommended in the diagnosis and management of Hodgkin's disease. (auth)

Radiotherapy

Refer also to abstracts 42141, 42172, 42270, 42409, 42413, 42414, 42428, 42432, 42437, 42446, 42471, 42477, 42491, 42492, 42603, 42678, 42679, 42683, 42687, 42689, 42695, 42699, 42700, 42701, 42704, 42705, 42709, 42713, 43753, 43754, and 43768.

42586 (ORAU-113, pp 4-77) RADIATION EFFECTS AND RELATED TOPICS. (Oak Ridge Associated Universities, Inc., Tenn. Medical Div.).

In 1970 research report for the year ending December 31, 1970.

Thirteen patients with various hematologic disorders, (chronic granulocytic leukemia, chronic lymphocytic leukemia, polycythemia vera, and lymphosarcoma), were treated with low-dose-rate (1.5 R/hr or 1.5 R/min) low-dose (up to 250 R) whole-body γ irradiation with distinct benefits, but no evidence of remarkable advantages over other forms of treatment. An adult patient with acute leukemia was given a successful graft of allogenic bone marrow following preparation with 500 R whole-body γ irradiation and antilymphocyte globulin. Results are reported from studies on: the effects of low-dose-rate whole-body γ irradiation on leukocyte survival time and platelet count in peripheral blood samples; the radioresistance of the gonads in man and monkeys; the time sequence of the onset of anorexia, nausea, and vomiting associated with radiation sickness; the effects of low-dose whole-body γ irradiation on levels of proteins, immunoglobulins, and transferrin in the blood serum of patients; and the effects of whole-body low-dose γ irradiation on physiological responses in man as determined by measurements of respiratory function with and without exercise stress. Mice exposed to daily whole-body γ irradiation at different dose rates over long periods of time showed changes in the chemical composition of hemoglobin. (C.H.)

42587 (ORAU-113, pp 78-133) RESEARCH IN NUCLEAR MEDICINE. (Oak Ridge Associated Universities, Inc., Tenn. Medical Div.).

In 1970 research report for the year ending December 31, 1970.

Separate abstracts were prepared on two sections of this report. The third section reports the results of basic studies related to neoplasia and metabolism. A list of 101 publications during the period covered by this report is included. (C.H.)

For abstracts of individual sections see: 42549 and 42586.

42588 COMBINATION OF PREOPERATIVE IRRADIATION AND SURGERY IN THE TREATMENT OF CANCER OF THE OROPHARYNX, HYPOPHARYNX, AND LARYNX. Levitt, S. H.; Beachley, M. C.; Zimberg, Y.; (and others) (Medical Coll. of Virginia, Richmond). Cancer; 27: 759-67(Apr 1971).

Sixty-eight patients with carcinoma of the oropharynx, hypopharynx, and larynx were treated with combinations of preoperative γ or x irradiation and surgery. Fifty-six had low-dose preoperative irradiation, and 12 had high-dose preoperative irradiation. This report evaluates the 2-year survival, morbidity, wound healing, and local recurrence in relation to the type of surgery and to radiation dose and timing in these groups where applicable. These findings are compared to those in a similar group of 29 patients receiving surgery alone. (auth)

42589 PRE-IRRADIATION 5-FLUOROURACIL INFUSION IN ADVANCED HEAD AND NECK CARCINOMAS. Gollin, Frank F.; Johnson, Robert O. (Univ. of Wisconsin, Madison). Cancer; 27: 768-70(Apr 1971).

Results of therapy of one hundred and eight patients with advanced head and neck carcinomas are reviewed. Half of the patients were treated with intra-arterial 5-fluorouracil infusion prior to external γ or x irradiation; the other half were irradiated without prior infusion. In spite of good regression with intra-arterial infusion, no increase in survival or cure rates was noted in the combined therapy group. (auth)

42590 RADIOACTIVE NEEDLE WITH LINEAR ACTIVITY INCREASING GRADUALLY TOWARDS THE ENDS. Mihailov, M.; Majkarov, S.; Moutaftchiev, K.; (and others) (Inst. of Physics, Sofia). J. Radiol., Electrol., Med. Nucl.; 52: 43-5(Jan-Feb 1971). (In French).

A new type of ^{226}Ra applicator was developed for interstitial curietherapy that emits a linear γ activity that increases uniformly from the center towards the ends. The fundamental advantage of these needles lies in the more favorable dose distribution and in the elimination of the need to close or extend the implantation tips. (France)

42591 RENAL ADENOCARCINOMA: REGRESSION OF PULMONARY METASTASES FOLLOWING IRRADIATION OF PRIMARY TUMOR. Ridings, G. Ray (St. Paul Hospital, Dallas). Cancer; 27: 936-8(Apr 1971).

A case is presented of an adult male with an advanced right renal adenocarcinoma demonstrated by angiography and bilateral pulmonary metastases demonstrated by chest roentgenograms and laminography. Approximately five months after completion of γ irradiation of the primary tumor, before nephrectomy was performed, the pulmonary metastases had disappeared and have remained so for over two years, or approximately three years after diagnosis of the tumor. The patient remains clinically free of tumor and is well enough to work regularly. This case appears to add evidence that palliative treatment, including irradiation, to far-advanced primary renal adenocarcinoma may be of value to more patients than formerly realized. (auth)

42592 EFFECT OF IRRADIATION ON THE MATURATION OF WILMS' TUMOR. Bannayan, George A.; Huvos, Andrew G.; D'Angio, Giulio J. (Memorial Sloan-Kettering Cancer Center, New York). Cancer; 27: 812-18(Apr 1971).

A study was undertaken to ascertain the morphological differences that exist between the primary tumor and the metastatic deposits of 55 selected cases of Wilms' tumors in children. The observations in this study point towards a greater degree of non-epithelial differentiation and a decrease in the tubular and glomerular differentiation in the metastases as compared to the primary tumors. The study also suggests that irradiation accelerates and possibly induces non-epithelial differentiation. (auth)

42593 CONCEPTS IN THE NATURAL HISTORY AND TREATMENT OF MEDULLOBLASOMA IN CHILDREN: INCREASING SURVIVAL RATES AND POSSIBLE RISKS WITH CURRENT RADIOTHERAPY TECHNIQUES. Bloom, H. J. G. (Royal Marsden Hospital, London). CRC Crit. Rev. Radiol. Sci.; 2: No. 1, 89-143(Jan 1971).

There is general agreement that the initial treatment for medulloblastoma should be surgical, i.e., excision of as much tumor as possible without adding unduly to the operative risk and morbidity, the chief aim of which is to establish the diagnosis and create a decompression to preserve vision. The operative mortality is about 20%. Until quite recently treatment results reported by most authors were very poor, the tumor being widely regarded as incurable. Over the past five years some greatly improved results have been published, and it now appears that approximately 40% of children surviving operation and completing a course of cerebrospinal axis irradiation by modern techniques will be alive at five years, and 25% to 30% at ten years. All recurrences of medulloblastoma develop within a period of time defined as the patient's age when treated plus a period of nine months for gestation: this is a useful guide to prognosis for the individual case. The importance of irradiating the entire brain and spinal theca is emphasized and the problem of optimum dosage, especially in relation to age, is considered. Although the doses recommended are probably safe in terms of avoiding gross morphological damage to the central nervous system, the possibility of more subtle functional changes developing, especially in the youngest children, must remain in question. It seems that a maximum dose of 4,500 to 5,000 R to the posterior fossa in not less than six weeks and 3,000 to 3,500 R in five weeks to the remaining part of the brain and spinal cord is safe. For the youngest children of less than two or three years a reduced maximum brain dose of 4,000 to 4,500 R is advised. The chief danger to brain and spinal cord from irradiation is the administration of high doses in too short an overall time. (auth)

42594 MANTLE TREATMENT OF HODGKIN'S DISEASE WITH ^{60}Co. TECHNIQUE AND DOSIMETRY. Svahn-Tapper, Gudrun; Landberg, Torsten (Univ. Hospital, Lund, Sweden). Acta Radiol., Ther., Phys., Biol.; 10: 33-55(1971).

Patients with Hodgkin's disease were given mantle treatment with cobalt 60. The treatment arrangement, dose planning and dose measurements are described. Methods for diminishing the variation in the absorbed dose in different parts of the target are discussed. (auth) (Sweden)

42595 RADIOTHERAPY OF CANCER OF UTERINE CERVIX. Arai, Tatsuo (National Inst. of Radiological Sciences, Chiba, Japan). Hoshasen Kagaku; 13: No. 10, 1-8(Oct 1970). (In Japanese).

Results are reported for 268 patients with cervical carcinomas treated by combined intracavitary ^{226}Ra γ (4,000 to 5,000 R total dose) and external γ irradiation (4,000 to 6,000 R total dose). All primary lymph nodes were included in the field for external exposure. The incidence of radioinduced injuries of the bladder and rectum was less than 5%. Data on the three-year survival rate showed the method was effective in 92% of the patients with stage I carcinoma and in 14.5% of the patients with stage IV carcinoma. (TSS) (Japan)

42596 RADIOTHERAPY OF EYE DISEASES. Andersen, S. Ry. Trans. Pac. Coast Oto-Ophthalmol. Soc.; 50: 237-63(1969).

Radiotherapy of diseases of the eye and orbit is an excellent aid in selected cases, but never devoid of risk. The principles and indications for radiotherapy of neoplastic eye diseases and of tumors in the eye and its adnexa are described. (F.M.M.)

42597 NEW CLINICAL AND EXPERIMENTAL TESTS USING IRRADIATION. Stamm, H.; Lopez Gonzalez, J. M.; Szirmai, E. (Univ., Stuttgart). Acta Oncol.; 7: 91-2(1968). (In Spanish).

Reports are given on satisfactory results obtained by radiotherapy of secondary anemia, radioinduced secondary effects caused by prior exposure, treatment of hepatic injuries, hepatitis, and other diseases difficult to cure. (tr-auth)

42598 PRIMARY HIGH-DOSAGE ^{60}Co IRRADIATION IN ADVANCED UTERINE CERVIX AND VAGINAL CANCER. Martin, K. (Univ., Mainz). Geburtsh. Frauenheilk.; 31: 50-61(Jan 1971). (In German).

A report is given of the therapeutic results with high dose homogeneous pelvic telecobalt irradiation on 67 advanced cases of uterine cervix cancer, six advanced cases of vaginal cancer, and complications of the irradiation at the site of adjacent organs. The relatively good palliative results with regression of the neoplasm and the prolongation of the survival time shows the practicability of this method. The less advanced cases are treated surgically or by combination of radium- and telecobalt-therapy. Interpretation of the prognosis or the sensitivity to irradiation on the grounds of histological findings on continuous tissue biopsies were possible only in some cases. (auth)

Blast and Thermal Effects

Refer also to abstract 42367.

Radiation Effects on Animals

Refer also to abstracts 42266, 42347, 42348, 42353, 42395, 42402, 42404, 42405, 42512, 42727, and 43754.

42599 HEMATOLOGICAL EFFECTS OF PARTIAL BODY IRRADIATION: CLINICAL AND EXPERIMENTAL DATA. Tubiana, Maurice; Frindel, Emilia; Croizat, Helene (Inst. Gustave-Roussy, Villejuif, France). pp 53-63 of Biological Aspects of Radiation Protection. /Sugahara, Tsutomu (ed.). Tokyo; Igaku Shoin Ltd. (1971).

From International symposium on biological aspects of radiation protection; Kyoto, Japan (13 Oct 1969). See CONF-691041.

The variation in the number of blood leukocytes as a function of the integral absorbed dose administered to a series of patients treated for cancer of the esophagus, bronchus, or bladder with a 24-MeV Betatron was compared. The leukopenia induced by partial-body radiation in patients did not correlate with the dose received by the bone marrow or with the proportion of the bone marrow that was irradiated. Experiments were also conducted to determine the effects of partial-body irradiation on the hematology of mice. The results showed that during sublethal fractionated irradiation the number of leukocytes reached a plateau at a level that was lower than the proportion of shielded bone marrow in spite of compensatory mechanisms that stimulated the hematopoietic activity. This was explained by a progressive depletion of the protected bone marrow caused by the migration of cells from the protected zones into the irradiated area. (E.E.H.)

42600 SOME HEMATOLOGIC CHANGES DUE TO IONIZING RADIATIONS. Chisleag, Gheorghe; Baran, Traian; Baran, Elena (Inst. of Medicine and Pharmaceutics, Iasi). pp 92-7 of Biological Aspects of Radiation Protection. /Sugahara, Tsutomu (ed.). Tokyo; Igaku Shoin Ltd. (1971).

From International symposium on biological aspects of radiation protection; Kyoto, Japan (13 Oct 1969). See CONF-691041.

Quantative and qualitative hematological examination of 62 hospital staff members revealed hematological changes or clinical symptoms that could be attributed to working in the x-ray department. It was found that similar conditions of work did not bring about similar changes in the blood. Important blood changes were found in a group of eight personnel who had worked in the department for only 18 months to 3 yrs. Leukopenia with neutropenia and lymphocytosis, eosinophilia, immature cells, and thrombocytopenia were found. The changes were reversible within two to eight months, but they reappeared when work was resumed and the subjects had to change their profession. The leukocyte changes must be attributed to the general action of the x rays. Coagulation changes were investigated by thromboelastography in dogs that received small doses of internal ^{131}I β and external ^{60}Co γ radiation. Constant and early changes beginning within the first hours post-radiation were found. The intensity of the changes varied in relation to the dose employed. Assuming high sensitivity of the thromboelastographic method, investigations are in progress to determine the usefulness of this method as a biological indicator for man. (E.E.H.)

42601 SURVIVAL OF COLONY-FORMING UNITS IN MOUSE BONE MARROW AFTER IN VIVO IRRADIATION WITH D–T NEUTRONS, X-, AND GAMMA RADIATION. Broerse, J. J. (Radiobiological Inst TNO, Rijswijk, Netherlands); Engels, A. C.; Lelieveld, P.; (and others). Int. J. Radiat. Biol.; 19: 101-10(1971).

The CFU survival in mouse bone-marrow was investigated after

XUM

in vivo irradiation with D–T neutrons, 300 kV x-rays and ^{60}Co and ^{137}Cs gamma-rays. All the survival curves for x- and gamma-radiation showed the same extrapolation number (2.47 ± 0.28), whereas D_0 values of 72.2 ± 1.7 rads and 90.7 ± 2.4 rads, respectively, were found for the two types of radiation. With D–T neutrons, the Manchester group found a D_0 value of 62.5 ± 2.2 rads; the Rijswijk group found a D_0 value of 78.3 ± 2.1 rads. A common extrapolation number of 1.34 ± 0.16 could be calculated for the neutron survival curves. Owing to the difference in extrapolation numbers for x-rays and neutrons, the RBE depended on the level of survival. From the combined results of both groups a mean RBE of 1.1 was derived for low surviving fractions. The 25 percent difference in the effectiveness of D–T neutrons, as measured by the two groups, was not due to dose-rate nor to the strain of mice, and could only in part be attributed to the 8 percent difference in dosimetry revealed by intercomparative measurements. It was probably due mainly to a difference in quality of the two neutron beams resulting from the collimation of the Manchester beam with consequent degradation of neutron energy. (auth)

42602 EFFECT OF IONIZING RADIATIONS ON LYMPHOCYTES FROM ADULTS AND NEWBORN INFANTS, CULTURED IN VITRO IN PRESENCE OF PHYTOHEMAGGLUTININ. Marchese, G. S.; Franceschini, P.; Zanetti, P.; de Sanctis, C. (Ospedale Infantile Regina Margherita, Turin). Univ., Turin). Minerva Pediat.; 20: 2018-23(Sep 1968). (In Italian).

Lymphocytes from adults and newborn infants, cultivated in the presence of phytohemagglutinin, were exposed to single doses of 50, 150, and 300 R. The number of mitoses and blastizations (significant increase of the cell diameter and cytoplasmic vacuolization) was determined after 48, 72, and 96 hrs. The results are graphed and show a mitotic delay in the irradiated cultures from the newborn infants but no mitotic delay in the cultures from adults. (J.S.R.)

42603 EXPERIMENTAL AND CLINICAL STUDIES OF TISSUE DAMAGE IN COMBINATION NECK DISSECTION AND RADIOTHERAPY. Weiss, Peter (Medizinsche Univ., Erlangen, Ger.). Fortschr. Kiefer- Gesichtschir.; 13: 177-84 (1968). (In German).

Animal experiments using rabbits are described. Irradiation of the neck was carried out after a surgical procedure had been performed. An inappropriate incision and an extensive operation was followed by a more severe skin reaction. Following extensive operations and post-operative irradiation, there was histological evidence of the formation of granulation tissue with a reduction of epithelialization and marked tissue edema. Two patients who developed necrosis after combined neck dissection and radiotherapy with fast electrons are described. Operative and radiological considerations for the prevention of this type of damage are discussed. (auth)

42604 FIRST ESLER. Proceedings of the First European Symposium on Late Effects of Radiation Held at Casaccia, Italy, April 22–23, 1969. Serie Simposi. Rome; Comitato Nazionale Energia Nucleare (1970). 215p. (CONF-690414).

Twelve papers are included; separate abstracts were prepared for 10. The remaining two papers on epidemiological and cellular effects of chronic radiation exposure and the role of mutations in the development of radioinduced aging were previously included in NSA as 24: 23309 and 23: 29732, respectively. (F.M.M.)

For abstracts of individual papers see: 42605, 42663–42670, and 42714.

42605 LATE EFFECTS OF EXPOSURE TO IONIZING RADIATION: ANIMAL EXPERIMENTATION AND HUMAN PROTECTION. Mole, R. H. (Medical Research Council, Harwell, Eng.). pp 179-99 of First ESLER. Rome; Comitato Nazionale Energia Nucleare (1970).

From first European symposium on late effects of radiation; Rome, Italy (22 Apr 1969). See CONF-690414.

The relation of animal experimentation to recommendations for radiation exposure limits for man is discussed. The effects of ionizing radiation on leukemia induction, genetics, aging, carcinogenesis, and teratogenesis are reviewed. (F.M.M.)

42606 LOW RADIATION DOSES AND THE CONTROL OF METABOLIC PATHWAYS. Pana, I.; Murgoci, P. Oncol. Radiol.; 9: No. 4, 331-8(1970). (In Rumanian).

Some aspects in the destruction of cells by radiation are discussed. The effects of radiation on the control of the metabolic pathways are described on the basis of a metabolic control model that takes into consideration the oscillatory behavior of enzymatic activity. Two important aspects are emphasized, namely the consumption and production only of a given type of metabolite during and immediately after irradiation, and the change of the phase factor in enzymatic activity and its consequences. (auth)

Invertebrates

Refer also to abstracts 42246, 42276, 42333, 42335, 42344, 42350, 42354, 42527, and 42751.

42607 HISTOPATHOLOGICAL EFFECTS OF IONIZING RADIATION ON THE PACIFIC OYSTER, CRASSOSTREA GIGAS. AN EXAMINATION OF DEGENERATIVE SYNDROMES, CELLULAR REPARATIVE MECHANISMS, AND THEIR RELATION TO NORMAL CELL RENEWAL SYSTEMS. Mix, Michael Cary. Seattle; Univ. of Washington (1970). 183p. University Microfilms Order No. 71-8518.

Thesis.

Two studies were conducted in the spring of 1968 and 1970. Oysters were irradiated with 1, 5, 10, 20, 50, 100, 200, and 400 Krads in the first experiment, to determine approximate lethal doses and a sublethal dose which causes maximum tissue damage without subsequent death. All but one oyster irradiated with 200 and 400 Krads died by nine days post-irradiation. The digestive tissues, especially the stomach, and the gills showed severe degeneration in oysters irradiated with lethal doses. There were few mortalities in the other dose groups during the 90 day experimental period. The second experiment involved irradiation of oysters with 75 Krads. The purpose of the second study was to explore in greater detail reactions to sublethal doses, and demonstrate that results obtained in the first study could be reproduced under a similar set of experimental conditions. Tissues in oysters irradiated with sublethal doses showed degeneration which could be classified as acute or chronic depending on the dose and whether or not the tissue possessed undifferentiated, or stem, cells. The gut, stomach, and gills underwent chronic degeneration. The gonads contain the most active cell population with regard to mitotic cell division. This tissue showed rapid degeneration after irradiation. Complete denudation occurred in all, except the 1-Krad, dose groups. Some germinal cells survived in these oysters, but production of ova was severely retarded and only a few of these cells were observed 76 days post-irradiation. Only one tissue, the digestive tubules, showed repopulation of destroyed or injured tissue. Complete denudation is the ultimate observable manifestation in the digestive tubule degenerative syndrome. All normal epithelial cells associated with this structure disappeared and only an abnormal squamous cell lining remained. Mechanisms of cell repopulation include formation of cell nests through mitotic division of crypt cells, migration of the cells from the nests and finally reepithelization of the tubule. This sequence of repopulation was observed in all dose groups, but at 50, 75, and 100 Krad doses, less than 50% of the tubles were able to undergo repair. One oyster irradiated with 75 Krads was observed, 120 days post-irradiation, with no digestive tubules. The fact that many invertebrates are thought to be resistant to ionizing radiation may be an artifact and explained by the phenomenon of chronic degeneration. Low initial mortality rates, even after high doses of radiation, may reflect slow cell turnover times. Thus, mitotic inhibition does not cause immediate death but may induce chronic degeneration and, unless this process is reversible, death of the organism. (Diss. Abstr.)

42608 HISTOMONAS MELEAGRIDIS: EFFECT OF GAMMA RADIATION ON IN VITRO GROWTH. Ruff, M. D.; Hansen, M. F. (Kansas State Univ., Manhattan). Contract AT(11-1)-1209. Exp. Parasitol.; 28: 450-64(Dec 1970). (COO–1209-8).

Histomonas meleagridis in DeVolt's alkaline serum medium were exposed to various dosages of gamma rays. No immediate effect of the radiation was observed. The LD_{50} for the organism grown 28 to 54 days in vitro was 400 kr, and the LD_{50} after 209 days of growth was 80 kR, demonstrating a definite age effect on radiosensitivity. In the experiments, an exposure of 50 kR did not influence the growth of Histomonas, when compared with the controls. Intermediate dosages (150 and 200 kR) reduced growth. A relationship was found between an extended lag phase and the level of exposure. In some irradiated groups there was an extension of the number of days during which logarithmic growth occurred. An exposure of 100 kR stimulated growth, but apparently the stimulation range was narrow; for example, exposures of 75 and 125 kR retarded growth, compared with the controls. Growth changes were transmitted to subsequent generations. Data from the subculture of exposed cultures indicated that more organisms were produced in the 100 and 150 kR groups than in the control group. Growth in the 200 kR group was comparable with that in the control group. Organisms in the 150 and 200 kR groups decreased significantly in size by 7 days after radiation. Adding nonirradiated cecal bacteria to nutrient medium increased survival of irradiated histomonads. These treated cultures could survive more than 400 kR, and many of the effects of exposure also were eliminated. DeVolt's medium was exposed

to 0, 50, 100, 200, and 300 kR to determine whether irradiated media affected growth. No effect was observed with exposure to 50 kR. Growth was retarded by exposures of 100 and 200 kR and greatly retarded by 300 kR. Histomonas grown for 7 days in the medium exposed to 300 kR were significantly larger than those in the control group. (auth)

42609 COMPARISON OF THE STAGE SENSITIVITY TO X RAYS DURING MEIOSIS IN THE EGG OF THE SILKWORM, BOMBYX MORI. Murakami, Akio (National Inst. of Genetics, Misima, Japan). Int. J. Radiat. Biol.; 19: 167-76(1971).

Oocytes of the silkworm, Bombyx mori, were irradiated with x-rays ranging up to 5000 R at various phases of the meiotic stage. The radiosensitivity was determined by scoring the hatchability of irradiated eggs in comparison with unirradiated control eggs. Cells in the dividing phase were more sensitive to x-rays than those in any other phases in both the first and the second meioses, and cells in the first meiosis were more resistant than those in the second meiosis. Furthermore, the sensitivity of the second meiotic cells almost corresponded to that of early mitotic cells. These differences in radiosensitivity were interpreted as being due to whether or not cells were associated with DNA synthesis or chromosome duplication, and/or the difference in the chromosomal structure at the time of irradiation. It was concluded that the radiosensitivity in cell-killing during meiosis of silkworm oocytes shows the same pattern as in other insect orders, although there are some differences in the degree of sensitivity. (auth)

42610 CHANGES IN THE RATIO OF THE SEXES IN F_1 AFTER IRRADIATION WITH GAMMA RAYS OF FEMALE AND MALE IMAGOS OF SITOTRAGA CEREALELLA OLIVIER. Glavanakova, S. I.; Dryanovska, O. A.; Kalkanova, E. V. (Dept. of Cytogenetics, Sofia). Compt. Rend. Acad. Bulg. Sci.; 23: 1529-32(1970).

Mature male and female insects of Sitotraga cerealella were γ-irradiated with doses of 1, 5, 10, 25, 50, and 60 kR. A survey was then conducted of the dynamics and the percentage of flying-off of imago from the F_1 generation, related to the number of eggs hatched, as well as the change in the correlation of the sexes of the grain moth following irradiation of the parents. Irradiation of the male specimens resulted in: reduction of the population from F_1 at all doses except at 1 kR (slight stimulation); reduction in the percentage of female progeny; and induction of visible mutations in the moths. Irradiation of the female specimens resulted in: reduction in the percentage of progeny flying-off and a delay in flying-off; reduction in the percentage of female moths in the progeny; and insignificant induction of visible mutations in the moths. (E.R.B.)

42611 GENETIC COLLAPSE OF INSECT POPULATIONS. 1. EXTINCTION OF INBRED AND OUTBRED LINES IN LABORATORY POPULATIONS OF THE SUGARCANE BORER. Walker, David W.; Quintana, Victor; Torres, Josefa (Univ. of Puerto Rico, Mayaguez). J. Econ. Entomol.; 64: No. 3, 660-7 (Jun 1971).

Inherited partial sterility patterns believed to be caused by chromosomal translocations can be induced by gamma-irradiation in Diatraea saccharalis (F.). Even at low dose levels where dominant lethality was minimal, the population collapsed in a few generations in a laboratory population recently taken from nature. The swift collapse even in outbred lines appeared to be from an interaction of the induced inherited partial sterility with debilitating genetic factors already present in the population, and to deficient diet, and possibly pathogens. (auth)

42612 AGING AND IONIZING RADIATION: A STUDY OF LIFE-SPAN AND FINE-STRUCTURAL ALTERATIONS IN THE DROSOPHILA MELANOGASTER. Gartner, Leslie Paul. New Brunswick, N. J.; Rutgers–The State Univ. (1970). 216p. University Microfilms Order No. 71-12,246.

Thesis.

A Canton-S wild type strain of Drosophila melanogaster (Meigen) was exposed to 0, 33, 66, and 93 kilo-Roentgens of ^{60}Co gamma irradiation at a dose rate of 9000 R/minute. The irradiation procedures took place within the first few days post eclosion. The flies were subsequently maintained at 19 ± 0.5°C. They were checked nearly every day, and all deaths were recorded by age and sex. Great care was taken to eliminate most environmental hazards in order to decrease the chances of accidental deaths. It was noted that the males were consistently more radiosensitive than the females, and that the average life-span of the fruit fly was an inverse function of the radiation dose. Drosophila was also exposed to 99 kR of ^{60}Co gamma radiation at a dose rate of 25 R/minute. They were subsequently maintained as above. This population and its control were used to investigate the fine-structural alterations that occur with the passing of time. For the electron microscopic observations, the midgut of the fly was removed and prepared in accord with the standard electron microscopic techniques. The time-related, ultra-structural changes in the cells of the midgut of the Drosophila were as follows: the appearance of lamellar lipid deposits, the appearance of virus-like particles in the nuclei, the appearance of nuclear inclusions, the disruption of the regular arrangement of the cristae mitochondriales, the appearance of virus-like particles in the cytoplasm, and a moderate swelling of the mitochondria. A theory of radiation-induced, life-span shortening, based on loss of cellular function, was suggested. (Diss. Abstr.)

42613 RELATIVE RADIO-SENSITIVITY OF DIFFERENT CELL-TYPES IN HYDRA. Mitra, Jaganmay (Presidency Coll., Calcutta). Gegenbaurs Morphol. Jahrb.; 114: 258-68 (1969).

Relative radiosensitivity of the different cell-types in the body of Hydra has been worked out by employing the suitable lethal dose of x rays (25,000 r). Interstitial cells which are found to be highly sensitive to x rays exhibit certain degree of regional difference as regards the rapidity of cell mortality. Interstitial cell populations at the anterior portion of the stem die earlier than those of the posterior portion. Cnidoblast cells of tentacles and hypostome exhibit greater sensitivity to x rays than those of the body column. Epitheliomuscular cells are found to be conspicuously radio-resistant and their quantitative increase has been noted on the 12th and the 18th day. Similarly, the radio-resistivity of both the cell-types of endoderm is also striking. Increase of both the cell-types of endoderm has been encountered on the 12th day. The probable reasons for the increase of epithelio-muscular cells of ectoderm and nutritive muscular and gland cells of endoderm have been suggested. (auth)

Vertebrates

Refer also to abstracts 42262, 42264, 42265, 42277–42284, 42287, 42289, 42292, 42298, 42301, 42304, 42311, 42312, 42313, 42321, 42325, 42342, 42355, 42403, 42407, 42472, 42520–42522, 42524, 42525, 42528, 42530, 42534, and 42535–42538.

42614 (AEC-tr-7215) RADIOBIOLOGY. Translation of Radiobiologiya; 10: 643-800(1970). 247p. Dep. NTIS.

Translations of the author abstracts from the Russian journal appeared previously in NSA. The abstracts (38) appeared in Vol 25: issue 13 as abstract numbers 29452, 29489-91, 29551-6, 29657-77, 29709, 29710, 29717-20, and 29733. (E.R.B.)

42615 (COO-1201-30) EFFECTS OF RADIATION AND OTHER FACTORS ON THE DEVELOPING FORM AND FUNCTION OF THE NERVOUS SYSTEM. Comprehensive Review and Progress Report, 1962–1971. Hicks, Samuel P. (Michigan Univ., Ann Arbor. Dept. of Pathology). May 1971. Contract AT(11-1)-1201. 21p. Dep. NTIS.

Effects of radiation on the development of motor-sensory and visual systems in the rat were investigated. Hemispherectomy was carried out in newborn and mature rats in order to establish baselines for understanding abnormal development. Comparative studies of effects of ablation and irradiation on frontal regions in infant and mature rats were made; similar motor abnormalities resulted from both kinds of treatment. Studies on the origin and course of the corticospinal tract in rats included exposing the frontal regions of the brain of newborn rats to 50, 200, and 400 R radiation and measuring the level in the cord to which the corticospinal axones had extended by the fifth day; no impairment of axonal growth was observed. Effects of irradiation and ablation of the cerebellum in infant or mature rats were compared. Ablation of the cerebellum in early infancy was severely incapacitating. Incoordination following irradiation was dose dependent. Experiments on ablation of the visual cortex and superior colliculi of rats showed that the animals were not deprived of their ability to discriminate a series of visual patterns. Effects of radiation on the histology and function of the retina of newborn rats were studied; it was found that the animals had useful detail vision in spite of severe injury to the retina. The role of visual cues in jumping behavior was studied by depriving rats of their eyes at birth. (H.L.W.)

42616 (RLO-2225-T-2-2) LOW LEVEL CHRONIC IRRADIATION OF SALMON. Annual Progress Report. Donaldson, Lauren R. (Washington Univ., Seattle. Coll. of Fisheries). 24 Jun 1971. Contract AT(45-1)-2225. 19p. Dep. NTIS.

During a five-year period (1965 through 1969) eggs and alveins of chinook salmon (Onchorhynchus tschawtscha) were exposed to chronic γ irradiation at a dose rate varying from 1.3 R/day (1965) to 20.0 R/day (1969) for periods of time ranging from 72 to 84 days and released to the sea as fingerlings. Data are presented

XUM

on the number that returned to the home pond as adults in 1970 and on the average length and weight of the fish in comparison to controls. A total of 111 irradiated fish and 577 control fish returned in 1970. Data are included on the number of abnormalities and mortalities observed during the spring of 1971 in fingerlings from eggs exposed during the fall of 1970 to a total dose of 4,100 to 4,300 R given at a dose rate of 50 R/day for 82 to 89 days. (C.H.)

42617 (UR-49-1462) EFFECTS OF EPSILON-AMINO-n-CAPROIC ACID ON RADIATION-INDUCED INCREASE IN CAPILLARY PERMEABILITY AND SUBSEQUENT PATHOLOGY IN SKIN. Eassa, Eassa-Helmy M. (Rochester Univ., N. Y. Dept. of Radiation Biology and Biophysics). 1971. 199p. Dep. NTIS.

Thesis.

The temporal patterns and degrees of initial (within hours) and delayed (within 21 days) radiation-induced increases in capillary permeability in rabbit skin (blue dye flush in irradiated skin after I.V. injection of the vital dye Pontamine Sky-Blue 6 BX) have been investigated after localized x-irradiation with various single exposures ranging from 100 to 4000 R. The effect of single intravenous doses of epsilon-amino-n-caproic acid (EACA), administered at various times before and after exposure, on the temporal patterns and degrees of the radiation-induced increases in capillary permeability were studied. These experiments were followed by a multiparameter investigation of the consequences of reduction of the radiation-induced increase in capillary permeability in skin by a single intravenous dose of EACA 15 minutes prior to irradiation (2500 R), in terms of the degree of development, of the subsequent radiation-induced changes in connective tissue, vasculature, circulation, and epithelial structures in skin, leading to the permanent and delayed skin lesions during a 6-month period following irradiation. The studies included macroscopic, histopathological, biochemical (hydroxyproline and hexosamine determinations), and a new radioactive isotope technique, using ^{99m}Tc pertechnetate, for assessing microcirculatory capability of skin in terms of clearance time for intradermally injected isotope. Background literature was reviewed and the results discussed. The following conclusions were drawn: the minimal single x-ray exposure to induce visibly detectable dye leakage (increased capillary permeability) in locally irradiated rabbit skin within 3 hours (initial period), is 450 R; the average time elapsing between irradiation and the first visible sign (blue flush) of increased capillary permeability, and also the duration of this initial period of increased capillary permeability, are inversely dose-dependent. The peak intensity of this effect was directly dose-dependent; epsilon-amino-n-caproic acid, injected intravenously (0.30 g/kg body weight) at various times within the period from an hour before to an hour after irradiation, markedly decreased or completely abolished the initial (within hours) radiation-induced increase in capillary permeability; the effectiveness of the EACA was inversely related to the size of the radiation exposure and was most marked when given in the interval from 15 minutes before to 15 minutes after irradiation; intravenous injection of EACA 15 minutes before irradiation (1000 R) eliminated the second period (2 to 3 days) and reduced the degree and shortened the duration of the 3rd period (10 to 17 days) of increased capillary permeability; intravenous injection of EACA just before irradiation (2500 R), in markedly reducing the degree of radiation-induced increase in capillary permeability, markedly reduced also the degrees of subsequent connective tissue changes, vascular damage, circulatory impairment, acute skin lesions (dry and moist desquamation, ulceration, necrosis), and permanent or delayed skin lesions (atrophy of epidermis and adnexal structures, and fibrosis). The effects on epithelial structures are discussed in terms of direct versus indirect (mediated by vasculoconnective tissue changes) mechanisms. (auth)

42618 CONTENT OF PROTEIN SH-GROUP IN TUMORS OF DIFFERENT RADIOSENSITIVITY IN THE NORM AND AFTER IRRADIATION. Ismailov, B. I.; Imangalieva, N. T.; Efimov, M. L. (Scientific Research Inst. of Oncology and Radiology, Alma-Ata, USSR). Med. Radiol.; 16: No. 6, 76-8(Jun 1971). (In Russian).

A comparison was made between the sulfhydryl group concentration in protein and the enhanced radiosensitivity of neoplasms resulting from x irradiation. Experiments were conducted with 220 unrelated white rats, weight 100 to 110 g, which were injected subcutaneously with C-45, LSP, and their radio-stable variants obtained by repeated exposure to 300 R of radiation before each transplantation. The results of cytochemical determination of SH-groups in C-45 and LSP tumors and their radiostable variants showed that both the concentration and total quantity of SH-groups in the radiostable variants of both neoplasms significantly increased the corresponding characteristics of the original stocks from 21 to 45% for the C-45, and from 44 to 67% for the LSP. For a single dose of 2000 R, x irradiation of radiostable variants of C-45 and LSP, in contrast to the original tumors, led to a decrease in the protein SH-group level at all stages of investigation. (K.S.W.)

42619 BIOCHEMICAL DISEQUILIBRIA INDUCED IN THE BRAIN OF THE RAT BY IRRADIATION AND THE PROTECTIVE EFFECT OF CYSTEINE. I. Gheorghe, N.; Tanase, Ioana. Rev. Roum. Physiol.; 7: No. 2, 145-54(1970). (In French).

The metabolic equilibrium of the cellular elements in the brain of the rat is disturbed by x irradiation. The existence of selective and specific metabolic alterations was established. By chemical fractionation at pH 8.5 a ribonucleic acid rich in 2-thiouracil was isolated in the brain. A structural role was assumed for this nucleic acid. The intervention of a mechanism capable of easily disturbing or making rigid the hydrogen bonds between the purine and pyrimidine bases of the polynucleotides of the nucleic acids induced by irradiation and the formation of a durable bond between the proteic SH groups and the SH group of 2-thiouracil was assumed. Cysteine restores these metabolic disequilibria only partially. (tr-auth)

42620 EFFECT OF IONIZING RADIATIONS ON THE COMPLEX LIPIDS OF THE BRAIN AND THE PROTECTIVE EFFECT OF CYSTEINE. II. Tanase, Ioana; Gheorghe, N.; Ciontescu, Lelia. Rev. Roum. Physiol.; 7: No. 2, 155-61(1970). (In French).

The phospholipids and cerebrosides of the brain of animals x irradiated present qualitative and quantitative modifications rigidly bound to the chemical nature of the lipid constituents. By beginning with the lipid fractions, such as neutral fats, glycerophosphatides, and cholinephosphatides, the nonsaturated fatty acids were separated into oleic, linoleic, and linolenic acids which are labile easily oxidizable compounds whose presence was detected partially in the brain of irradiated animals. The administration of cysteine before and after the irradiation contributes to the restoration of the lipid disequilibrium induced by ionizing radiation. (tr-auth)

42621 STEROID 7α-HYDROXYLASE OF RAT TESTES. Inano, Hiroshi; Tamaoki, Bun-ichi (National Inst. of Radiological Sciences, Chiba, Japan). Biochemistry; 10: 1503-9 (13 Apr 1971).

Previous identification of 7α-hydroxyandrostenedione as a testicular metabolite of androstenedione suggested the presence of 7α-hydroxylase activity in the testicular tissue of rat. Inter- and intracellular distribution of this enzyme, substrate specificity pH and temperature dependence of the enzyme activity, and the effects of certain inhibitors on this enzyme are reported. The specific activity per protein of the 7α-hydroxylase in the locally x irradiated testes of rat was found higher than in the intact testes, indicating the localization of the 7α-hydroxylase activity in the relatively radioresistant cells of the testicular tissue, or most likely the interstitial cells which contained the enzyme systems related to testosterone formation from pregnenolone. Intracellularly the enzyme activity was concentrated in the microsomal fraction (10,000 to 105,000g precipitate), and furthermore, was found to be relatively concentrated in the smooth-surfaced microsomal fraction. Among C-19 steroids such as androstenedione, testosterone, and dehydroepiandrosterone, the testicular 7α-hydroxylase exhibited a substrate preference for androstenedione. The optimal temperature and pH for the 7α-hydroxylase were 40° and pH 7.0, being different from the 17β-hydroxysteroid dehydrogenase which shared androstenedione as the common substrate. In the time-course study of the transformation of androstenedione with the testicular microsomal fraction, exponential consumption of the substrate was observed, and amount of 7α-hydroxyandrostenedione increased and reached a plateau 20 min after incubation, while testosterone was produced continuously during the elapsed time of incubation up to the 4th hr. Since atmospheric carbon monoxide was found to inhibit 7α-hydroxylase activity, the cytochrome P-450 was demonstrated to be involved in the testicular 7α-hydroxylation system. The 7α-hydroxylase activity in the microsomal fraction was inhibited in vitro by addition of the following compounds to the incubation medium: sodium p-chloromercuribenzoate, disodium EDTA, 3-(chloro-3-methyl-2-indenyl)pyridine, 3-(1,2,3,4-tetrahydro-4-oxo-7-chloro-2-naphthyl)pyridine, 2-methyl-1,2-dipyridyl-(3)-1-oxopropane, 3,3-bis(p-aminophenyl)-2-butane dihydrochloride, and 2-diethylaminoethyl-2,2-diphenylvalerate hydrochloride. The results on testicular 7α-hydroxylase were compared to those on hepatic 7α-hydroxylase. (auth)

42622 EXCRETION OF DEOXYRIBOSYL COMPOUNDS IN URINE FROM RATS AND MICE AFTER IRRADIATION. Soerbo, B.; Bouveng, R. (Research Inst. of National Defence, Sundbyberg, Sweden). pp 75-7 of Biochemical Indicators of Radiation Injury in Man. Vienna; International Atomic Energy Agency (1970).

From Meeting on biochemical indicators of radiation injury in

man; Paris, France (22 Jun 1970). See STI/PUB-280; CONF-700650.

Acid-labile deoxyribosyl compounds were measured in rat urine by the periodate-thiobarbituric acid method and found to increase after irradiation. Rat and mouse urine also gave a direct reaction with periodate-thiobarbituric acid, but the values thus obtained did not increase after irradiation of the animals. The compound responsible for this direct reaction behaved on chromatography as free deoxyribose. (auth)

42623 STUDIES INTO THE MECHANISM OF EXCESS EXCRETION OF NUCLEIC-ACID AND NICOTINAMIDE-ADENINE-DINUCLEOTIDE (NAD) METABOLITES AFTER IRRADIATION. Gerber, G. B. (EURATON-CEN, Mol, Belgium). pp 79-94 of Biochemical Indicators of Radiation Injury in Man. Vienna; International Atomic Energy Agency (1970).

From Meeting on biochemical indicators of radiation injury in man; Paris, France (22 Jun 1970). See STI/PUB-280; CONF-700650.

The application of, and the search for biochemical indicators of radiation injury must be based on an understanding of the mechanisms causing the metabolic alterations involved. The possibilities of elucidating these mechanisms with the aid of isotope experiments are discussed and their application is demonstrated by means of studies on the metabolism of nucleic acids and NAD in rats and mice after irradiation. These studies were carried out, in part, by means of techniques of isolated organ perfusion. It appears that metabolites of nucleic acid are mainly derived from cells dying from interphase death shortly after irradiation. A similar mechanism may also be responsible for excretion of NAD metabolites, but these substances are probably not very suitable biochemical indicators because they are influenced also by starvation. A method for measuring deoxycytidine, deoxyuridine, thymidine, and pseudouridine in human urine is reported. (auth)

42624 SOME ASPECTS ON THE DEGRADATION OF MACROMOLECULES IN LYMPHOID AND HAEMOPOIETIC TISSUES OF IRRADIATED ANIMALS. Skalka, M. (International Atomic Energy Agency, Vienna). pp 95-103 of Biochemical Indicators of Radiation Injury in Man. Vienna; International Atomic Energy Agency (1970).

From Meeting on biochemical indicators of radiation injury in man; Paris, France (22 Jun 1970). See STI/PUB-280; CONF-700650.

The irradiated cells of lymphoid and hematopoietic tissues undergo an early, pyknotic death. Their macromolecules, especially the deoxyribonucleoprotein complex, are degraded and thus provide metabolites, used as biochemical indicators of radiation injury. The first steps in the degradation of deoxyribonucleoprotein molecules have been extensively studied, namely the release of salt-soluble polydeoxyribonucleotides from deoxyribonucleoprotein and the labilization of deoxyribonucleoprotein, as revealed by the increased sensitivity to heparin and other strong polyanions. Both these changes appear very soon after irradiation in vivo, reaching their maximum about 6 hours after irradiation. They are almost linearly dose-dependent in the range of whole-body exposures of 0 to 300 R, the lowest provable exposure being 20 to 30 R. Data are presented on the possible mechanisms of these changes and the question is discussed whether this early post-irradiation damage to deoxyribonucleoprotein could be used as an indicator of radiation injury. Furthermore, the relation of the deoxyribonucleoprotein changes described to the appearance of low-molecular DNA degradation products in body fluids and their significance for biochemical diagnosis is considered. Finally, some proposals are discussed on the improvement of the sensitivity of biochemical indicators based on testing the amount of degradation products and low-molecular metabolites. (auth)

42625 EFFECT OF MODIFYING FACTORS ON RADIOSENSITIVE BIOCHEMICAL REACTIONS. Romantsev, E. F.; Filippovich, I. V.; Zhulanova, Z. I.; (and others) (Inst. of Biophysics, Moscow). pp 105-12 of Biochemical Indicators of Radiation Injury in Man. Vienna; International Atomic Energy Agency (1970).

From Meeting on biochemical indicators of radiation injury in man; Paris, France (22 Jun 1970). See STI/PUB-280; CONF-700650.

Some of the radioprotective aminothiols are used in clinics to decrease the radiation reaction which appears as a side effect during the radiotherapy of cancer. The action of effective modifying agents on radiosensitive biochemical reactions in the organisms of mammals, in principle, cannot be different from the same effects of the protectors on biochemical systems of the human organism. The effects of modifying agents are mediated by biochemical systems. The administration of radioprotective doses of MEA to rats before γ irradiation results in a significant normalization of the excretion in urine of degradation products of nucleic acids (so-called Dische-positive compounds), the excretion of which sharply rises after irradiation. The curve of the radioprotective effect of MEA (survival rate after administration of radioprotectors at different intervals of time) completely corresponds to curves of the accumulation of MEA which is bound (by mixed disulphide links) to the proteins of liver mitochondria, to proteins of the nuclear-sap, to the hyaloplasm of rat thymus and to the nuclear ribosomes of the spleen. After MEA administration the curve of the biosynthesis of deoxycytidine represents a mirror reflection of the curve of MEA bound to proteins of the thymus hyaloplasm by means of mixed disulphide links. The mechanism of action of such modifying factors as MEA in experiments on mammals is mediated to a great degree through the temporary formation of mixed disulphide links between the aminothiol and the protein component of enzymes in different biochemical systems. (auth)

42626 EARLY POST-IRRADIATION CHANGES IN THE METABOLISM OF BIOGENIC AMINES. Deanovic, Z. (Inst. Rudjer Boskovic, Zagreb). pp 113-23 of Biochemical Indicators of Radiation Injury in Man. Vienna; International Atomic Energy Agency (1970). (In French).

From Meeting on biochemical indicators of radiation injury in man; Paris, France (22 Jun 1970). See STI/PUB-280; CONF-700650.

There is accumulating evidence for the radioinduced release of biogenic amines from their body stores. Having in mind the high patho-physiological activity of these local hormones and neurohormones, it is reasonable to assume that they play an important role in the pathogenesis of the acute radiation syndrome. Under these pathological conditions the possible synergic and antagonistic effects of biogenic amines due to their complex interactions must be taken into consideration. The extent and dose-dependence of post-irradiation changes in the metabolism of histamine, serotonin, catecholamines, and acetylcholine were examined regarding the search for biochemical indicators of radiation injury. The determination of bio-amines and their metabolites in urine seems to be a suitable method for following up those metabolic changes which could be of a biodosimetrical and/or prognostical value. Data published on this subject, obtained in experimental animals as well as in man, are reviewed and the applicability of these tests is discussed. (auth)

42627 SIGNIFICANCE OF BIOGENIC AMINES AS RADIO-INDICATORS IN EXPERIMENTAL ANIMALS WITH REFERENCE TO MAN. Veninga, T. S. (Univ., Groningen, Netherlands). pp 125-34 of Biochemical Indicators of Radiation Injury in Man. Vienna; International Atomic Energy Agency (1970).

From Meeting on biochemical indicators of radiation injury in man; Paris, France (22 Jun 1970). See STI/PUB-280; CONF-700650.

Although variable results have been obtained by various investigators, radioinduced release of biogenic amines from several tissues in a variety of animals appears to be well established. Such a release will lead to enhanced blood levels and subsequently give rise to an increase in the urinary excretion of the native compounds. To a certain extent the released bio-amines are broken down thus causing an increase in the urinary level of bio-amine metabolites. Apart from these two possibilities a minute quantity of the released amines seems to be trapped by adequate receptor sites introducing responses either of physiological or, by disturbing physiolgical processes based upon the normal delicately balanced release of bio-amines of a pathological nature. As such, the erythemal response, radiation sickness, and a rise in body temperature may be mentioned. Recently, by employing pharmacological techniques, the x radioinduced rise in body temperature was found to be based upon the release of catecholamines in the rabbit and of serotonin in the cat. It is believed that this temperature response, which is maximal 2 to 3 hours following a radiation insult, might be evaluated as a simple, additional factor for indicating radiation injury, perhaps rather than the bio-amine compounds in urine. As such, biogenic amines might be worth studying more extensively in regard to recovery from radiation injury. (auth)

42628 LABILIZATION OF HYDROLYTIC ENZYMES IN LIVER AND SPLEEN CELLS FOLLOWING WHOLE-BODY X-IRRADIATION OF RATS. Chapman, I. V. (Univ. of Dundee, Eng.). pp 285-9 of Biochemical Indicators of Radiation Injury in Man. Vienna; International Atomic Energy Agency (1970).

From Meeting on biochemical indicators of radiation injury in man; Paris, France (22 Jun 1970). See STI/PUB-280; CONF-700650.

Initially the relative distribution of typical lysosomal enzymes (acid phosphatase and β-glucuronidase) was investigated in cells of spleen from rats exposed to 800 R whole-body x irradiation.

XUM

The investigation was carried out between one hour and 140 hours post-irradiation. No changes directly attributable to radiation effects were observed. An alternative approach involved estimations of the same enzymes in liver and spleen homogenates of rats. Total and labile enzyme specific activities were determined at varying time periods post-irradiation and compared with controls. Total-to-labile ratios showed a progressive decrease reaching a minimum at 24 hours followed by a period of recovery. Proposals are made regarding the investigation of the existence and dose dependency of this effect in the mammalian circulating lymphocyte. The application of such an effect to dosimetry in man is considered. (auth)

42629 RADIATION EFFECT ON PRENATAL DEVELOPMENT. Murakami, Ujihiro; Kameyama, Yoshiro; Hoshino, Kiyoshi (Nagoya Univ., Japan). pp 28-37 of Biological Aspects of Radiation Protection. /Sugahara, Tsutomu (ed.). Tokyo; Igaku Shoin Ltd. (1971).

From International symposium on biological aspects of radiation protection; Kyoto, Japan (13 Oct 1969). See CONF-691041.

The dangers involved with human fetal exposure to therapeutic or atomic explosion radiation are discussed. The gross malformations seem to be those of the central nervous system. The ICRP has recommended that all x-ray examinations or treatments involving the uterus should be done during the 10 day interval following the onset of the menstral period to avoid possible embryo exposure. A comparative study was made of rats and mice to determine species or strain differences in fetal sensitivity. Microcephalus was found in both strains of mice and rats, although the morphology was different from that observed in mice. The incidence of eye malformations in rats was similar to that of CF#1 mice. Generally, the effects of x radiation with 200 R were much greater in the rats than in either strain of mice exposed to 300 R. Experiments on the effects of low dose x radiation on the development and growth of the brain of ddN mice irradiated in utero showed that histological changes caused by 25 R presented a spectrum of changes from normal to abnormal cytoarchitecture of the dorsal cortex such as a sparsity of neurons. In cases exposed to 50 R, disturbances of the laminal organization of the cortex were apparent. (E.E.H.)

42630 COMPARATIVE LATE EFFECTS IN MICE FOLLOWING FAST NEUTRON OR ^{60}Co EXTERNAL IRRADIATION VERSUS TRITIATED THYMIDINE INTERNAL IRRADIATION. Mewissen, Dieudonne J. (Univ. of Chicago). pp 38-47 of Biological Aspects of Radiation Protection. /Sugahara, Tsutomu (ed.). Tokyo; Igaku Shoin Ltd. (1971).

From International symposium on biological aspects of radiation protection; Kyoto, Japan (13 Oct 1969). See CONF-691041.

Experiments were conducted on mice to investigate the late effects of radiation in differing situations regarding exposure and quality factors after single exposure from external ^{60}Co γ or fast neutron irradiation and after single injection of tritiated thymidine. Preliminary results indicated that tumor incidence in C57 BL mice amounts to more than 50% throughout the life span. The mechanism of carcinogenesis in mice may merely reduce the mean latent period of spontaneous tumor development rather than actually induce tumors. At specific low doses, radiation may possibly inhibit or delay tumor development. Although the overall tumor incidence was about equivalent in both sexes, the specific latent period of each tumor type contributed to differences in life span. It was found that a dose of 13 rems of fast neutrons approximates the effects of 0.3 μCi of tritiated thymidine given at birth. (E.E.H.)

42631 CELL POPULATION KINETICS IN THYMUS LYMPHOCYTES UNDER CONTINUOUS IRRADIATION. Fabrikant, Jacob I. (Johns Hopkins Univ., Baltimore). pp 74-80 of Biological Aspects of Radiation Protection. /Sugahara, Tsutomu (ed.). Tokyo; Igaku Shoin Ltd. (1971).

From International symposium on biological aspects of radiation protection; Kyoto, Japan (13 Oct 1969). See CONF-691041.

Experiments were conducted on C57 BL male mice to investigate the cellular response and cell population kinetics during lymphopoiesis in the mouse thymus. Mice were given whole-body ^{137}Cs γ radiation continuously at 45 rads/day. After 14 days exposure, the mice were removed from the chamber, labeled with ^{3}H-TdR, and returned to the chamber until sacrificed. After an initial decrease in weight, the thymus maintained a steady level of cell population for at least two weeks or more. There was a progressive shift in the cell size distribution to a greater proportion of primitive cells, increased labeling in all lymphoid cell compartments, and an increased rate of accumulation of labeled small lymphocytes. These changes were associated with the narrowing of the distribution of lymphoid cell cycle time, but with little change in the duration of the DNA synthesis period or the overall mean generation time. Thus, under the additional stress of continuous irradiation, compensatory mechanisms can occur in the thymus to maintain the cell population. (E.E.H.)

42632 METABOLISM OF EHRLICH ASCITES TUMOR CELLS UNDER ANOXIA AND ITS IMPLICATION IN THE REJOINING OF X-RAY-INDUCED DNA STRAND BREAKS. Matsudaira, Hiromichi; Furuno, Ikuko; Otsuka, Haruki (National Cancer Center Research Inst., Tokyo). pp 183-94 of Biological Aspects of Radiation Protection. /Sugahara, Tsutomu (ed.). Tokyo; Igaku Shoin Ltd. (1971).

From International symposium on biological aspects of radiation protection; Kyoto, Japan (13 Oct 1969). See CONF-691041.

Studies were made on the factors involved in the rejoining of x-radioinduced breaks in the DNA of Ehrlich ascites tumor cells in vivo and in vitro. Female albino mice ddN strain were used for the in vivo studies. It was found that DNA breaks were rejoined shortly after irradiation of living mice, but they did not rejoin after irradiation of recently sacrificed mice. In in vitro experiments, the radioinduced DNA breaks rejoined when incubated in a phosphate buffered saline medium in air but not in a nitrogen atmosphere. In a phosphate buffered saline medium supplemented with glucose, rejoining could be detected even after incubation under nitrogen. A marked reduction in the incorporation of radioactive precursors into DNA, RNA, protein, and thymidine triphosphate (TTP) was observed after incubation of the cells under nitrogen without glucose as compared with incubation in air. The reduction was partly or completely eliminated by the addition of glucose to the medium. After incubation under nitrogen without glucose, the intracellular content of ATP was greatly decreased. This decrease was also partly prevented by the addition of glucose. It was concluded that ATP is necessary for the rejoining of x-radioinduced breaks in the DNA of ascites tumor cells. (E.E.H.)

42633 ANIMAL SURVIVAL AND CELL SURVIVAL SEEN IN DOSE RATE EFFECTS ON MOUSE INTESTINAL DAMAGE. Hornsey, Shirley (Hammersmith Hospital, London). pp 207-12 of Biological Aspects of Radiation Protection. /Sugahara, Tsutomu (ed.). Tokyo; Igaku Shoin Ltd. (1971).

From International symposium on biological aspects of radiation protection; Kyoto, Japan (13 Oct 1969). See CONF-691041.

Studies on the effects of a change in dose rate on animal survival curves 4 to 5 days after whole-body irradiation and on cell survival curves obtained using a clonal technique on the intestine were made to obtain evidence for a relation between cell survival and animal survival. In a series of experiments on mice, differences in LD_{50} and slope of animal survival curves were observed when electron doses were delivered at 6 krad/min as compared to 100 rad/min with 7 MeV electrons. The animals proved to be less sensitive to the lower dose. The survival of stem cells in mice jejunum after irradiation with 1.8 MeV electrons at 500 rad/min or 6 krad/min was measured. The results indicated that acute intestinal death following irradiation of the intestine is predominantly due to the loss of proliferative capacity of the stem cells of the small intestine and the animal survival curves should follow qualitatively and quantitatively changes predictable from cell survival data. (E.E.H.)

42634 MORTALITY OF FISH UNDER CONTINUOUS IRRADIATION CONDITIONS. Etoh, Hisami; Hyodo-Taguchi, Yasuko; Egami, Nobuo (National Inst. of Radiological Sciences, Chiba, Japan). pp 213-18 of Biological Aspects of Radiation Protection. /Sugahara, Tsutomu (ed.). Tokyo; Igaku Shoin Ltd. (1971).

From International symposium on biological aspects of radiation protection; Kyoto, Japan (13 Oct 1969). See CONF-691041.

Experiments were conducted in order to compare the response of fish to continuous irradiation at a low dose rate with the response to repeated radiation at a high dose rate. A small freshwater fish, Oryzias latipes, and the common goldfish, Carassius auratus, were given repeated daily x radiation with doses of 50, 100, 200, 500, or 1000 R. A second series of tests were conducted in which fish were continuously irradiated with a ^{137}Cs γ source. The Oryzias given daily x radiation showed a median mortality of 42 days in the 50 R/day group, 36 days in the 100 R group, and 19 days in the 200 R group with accumulated doses for LD_{50} of 1800, 3200, and 3600 R, respectively. All fish died about ten days after acute single irradiation with 4000 R at 25°C. Goldfish given repeated daily x radiation showed a median survival time of 10 days at 25°C with dose rates of 500 and 1000 R/day but at 15 and 18 days at 15°C. It was concluded that fish can survive higher accumulated doses at lower temperatures. Goldfish given continuous γ radiation at a dose rate of 0.14 R/min showed an LD_{50} at 27,800 R. No dead fish were observed for 200 days during continuous irradiation at a dose rate of 0.03 R/min. The data on continuous irradiation are in good agreement with results reported for rodents. (E.E.H.)

42635 RELATIONSHIP BETWEEN METABOLISM AND RADIOSENSITIVITY. Taketa, S. Tom (Ames Research Center, Moffet Field, Calif.). pp 217-32 of Biological Aspects of Radiation Protection. /Sugahara, Tsutomu (ed.). Tokyo; Igaku Shoin Ltd. (1971).

From International symposium on biological aspects of radiation protection; Kyoto, Japan (13 Oct 1969). See CONF-691041.

Experiments were conducted to show the influence of the metabolic or physiologic state at time of irradiation on radiation response. Male and female rats, Sprague–Dawley strain, were age grouped and animals of several age groups were given whole-body x irradiation with exposure doses of from 625 to 1050 R. The intestinal radiation response as measured by 3 to 5 day acute intestinal death was greatest in the 30 to 45 day old males and decreased with increasing age in both sexes. The only exception seemed to be in females in which the radiosensitivity appeared to be greater in 300 day old animals than in 150 to 180 day old animals. The effects of pre-exposure fasting on mortality in animals given 825 R whole-body irradiation were also studied. It was observed that a 24 hr pre-exposure fasting protected against acute 3 to 5 day intestinal radiation death but not against hematopoietic death. This protective effect was nullified by feeding the rats 1 and ½ hrs before exposure but remained when fed immediately after exposure. Radiosensitivity is known to vary among individuals in a given species or strain, but results showed that the relative radiosensitivity of animals can be distinguished on the basis of pre-exposure metabolic activity. It is postulated that the mechanism whereby metabolism modifies radiation response is through its influence on cellular rhythm. The literature data concerning the use of metabolic indices in predicting individual or group radiosensitivity is reviewed and a bibliography of 57 is given. (E.E.H.)

42636 MEDICAL ASPECT OF CHRONIC HYPOXIA IN RADIATION EXPOSED GLOMERULUS IN HAMSTERS TREATED WITH INJECTED OZONE GAS. Sang, James B.; Imamoto, K.; Ogawa, M. (Pan American Inst. of Oncology, Seoul). pp 233-6 of Biological Aspects of Radiation Protection. /Sugahara, Tsutomu (ed.). Tokyo; Igaku Shoin Ltd. (1971).

From International symposium on biological aspects of radiation protection; Kyoto, Japan (13 Oct 1969). See CONF-691041.

Experiments were conducted to determine whether hypoxia influences glomerular enlargement in the kidneys. Golden hamsters were exposed to ionizing radiation at a dose of 0.1 roentgen per day and divided into three groups. Group A was exposed to hypoxia for 50 days, Group B acted as a control, and hypoxia exposed Group C animals were given 2cc of ozone intragluteally one a day for a week. The results showed development of erythremia and polycythemia, and erythrocyte counts and hemoglobin and hematocrit indexes increased 45 to 50% but returned to normal after oxone administration. Oxygen content in arterial blood was 21% vol in Group A as compared to 14.5% in Group B. The diameter and area of glomeruli were definitely enlarged after exposure to hypoxia and hypercellularity and capillary ectasia were found. The enlarged glomeruli returned to normal size after ozone injections. The results indicate that ozone therapy will be useful for air sickness and decompression sickness. (E.E.H.)

42637 COMPARATIVE RADIOSENSITIVITY OF ASCITES OVARIAN TUMORS AND ASCITES LYMPHOSARCOMA OF RATS. Balmukhanov, S. B.; Efimov, M. L.; Ismailov, B. I.; Arkhipova, L. D.; Yakovleva, S. S. (Kazakh Inst. of Oncology and Radiology, Alma-Ata, USSR). pp 249-57 of Biological Aspects of Radiation Protection. /Sugahara, Tsutomu (ed.). Tokyo; Igaku Shoin Ltd. (1971).

From International symposium on biological aspects of radiation protection; Kyoto, Japan (13 Oct 1969). See CONF-691041.

A comparative analysis of the radiosensitivities of ascites ovarian tumors and ascites Pliss' lymphosarcoma in rats was made. Cells were transplanted intraperitoneally into white rats. X irradiation of the tumors was performed in vivo with a dose of 1,400 R. The mitotic indexes, chromosome aberrations, and number of viable cells of the tumors were compared. The data showed a relatively low radiation damage in ovarian tumors. The mitotic index was not fully inhibited and the number of nonviable cells increased only slightly. The ovarian tumors also had a pronounced capacity to recover from cell depletion. The number of nonviable cells in the lymphosarcoma during the absence of mitotic activity increased significantly. This increase was not connected with the mitotic death of the cells but was caused by cell death in the interphase. The number of nonviable cells increased after 24 to 48 hrs when the first peak of mitoses was observed. It was also found that in the radioresistant ovarian tumor the concentration of cellular basic amino acids of histadine, arginine, and basic proteins increased and the concentration of acid proteins was low as compared to lymphosarcoma cells. It is possible that the basic amino acids perform a radioprotective function regarding the radiosensitive substances in the cells similar to the sulfhydryl groups. (E.E.H.)

42638 EXPERIMENTAL STUDIES ON TOOTH ERUPTION. Grivu, Ov.; Mihalceanu, I.; Bratu, Elisabeta; Theiss, Erika; Mecher, E. Stomatologia (Bucharest); 17: 481-8(Nov-Dec 1970). (In Rumanian).

Pregnant female rats were given the following agents: barbitone, thyroid extract, hydrocortisone, vitamin A. They also applied x-ray procedures in a study of the dental eruption in the offspring as compared to a control group of animals. In cases when barbitone, hydrocortisone and x-ray procedures were administered there was retardation of the dental eruption, up to 7 days. In the case of vitamin A there was an acceleration of the dental eruption and in the case of thyroid extract there was retardation as well as acceleration of the eruption. The possible mechanisms of these changes in dental eruption are discussed. (auth)

42639 SPECIES DIFFERENCES OF THE EFFECTS OF X-IRRADIATION UPON THE RAT AND MOUSE EMBRYO. Hoshino, Kiyoshi; Kameyama, Yoshiro; Murakami, Ujihiro (Nagoya Univ., Japan). Annu. Rep. Res. Inst. Environ. Med., Nagoya Univ.; 17: 25-34(1969)

The experiment was designed to examine species differences of radiosensitivity of the embryos of the rat and mouse during the period of organogenesis. Pregnant Wistar rats were treated with a single exposure of x-irradiation of 200 R, and ddN mice were treated with a single exposure or 200 R or 300 R during the period of organogenesis. Fetuses were removed from the mothers on day 20 in rats and on day 18 in mice for gross observations. The mortality of the rat embryo was higher than that of the mouse in the groups exposed in the early stages of organogenesis, while there was no apparent difference of mortality between the two species in those treated in the later periods. The incidence of malformations in the rat fetus treated with 200 R was higher than that in the mouse treated with the same dose, and in some malformations, it was higher than in the mouse exposed to 300 R. Arrhinencephalia was found only in the mouse fetus, while malformations of the hindlimbs accompanied by hypoplasia of the lower part of the trunk were found only in the rat fetus. Anal atresia was frequently found in the rat fetus, while rarely found in the mouse fetus. (Japan)

42640 OPEN-FIELD BEHAVIOR AND HEART RATE IN PRENATALLY X-IRRADIATED RATS. Furchtgott, Ernest; Tacker, R. Stephen; Draper, Douglas O. (Univ. of Tennessee, Knoxville). Teratology; 1: 201-6(May 1968).

Albino rats were exposed to x irradiation in utero on day 16 of gestation. In two separate experiments, animals that received 200 R, but not those that received 100 R, showed increased locomotor activity in an open-field on three successive daily 3-minute test sessions. In contrast to this hyperactivity, exploration measured by the duration of sniffing at novel objects was lower in irradiated animals on the first test day, but reached the level of the controls on the second test day. Animals with previous testing experience did not show increased locomotor activity at the age of one year. Measures of defecation did not discriminate as reliably as did locomotor activity. Animals that received 200 R also had a higher heart rate than a control group, with the difference decreasing over a 60-minute testing period. The data would indicate that prenatally x-irradiated rats show fearfulness when exposed to novel situations but with increased exposure to the testing situation or experience the animals' responses tend to approximate those of unexposed animals. (auth)

42641 ACTION OF FAST NEUTRONS ON THE NERVOUS SYSTEM. Panov, A. G.; Ulitovskaya, I. I.; Ulitovskii, D. A. Zh. Nevropatol. Psikhiat.; 70: No. 11, 1601-5(1970). (In Russian).

One hundred and fourteen rats were irradiated in the channel of a VVR–M reactor where neutrons constituted 92% of the dose. A histological study of the nervous system was performed following administration of 150 to 300 rad doses. A degeneration of the neutrons and filaments was observed. Changes in the glia and blood vessels were phasic and protracted. In comparison to the effects of γ radiation, the effects were more severe, more diverse, and at certain doses there were more frequent associations with gastro-intestinal than with marrow syndromes. The RBE of neutrons was 3 to 10 for neuromorphological effects. Studies on molecular, cellular, tissue, and whole-body levels revealed different mechanisms of radioinduced changes. (auth)

42642 MONKEY PERFORMANCE AFTER PARTIAL BODY IRRADIATION. Thorp, J. W.; Young, R. W. (Armed Forces

XUM

Radiobiology Research Inst., Bethesda, Md.). Aerosp. Med.: 42: 503-7(May 1971).

Forty-one male and 30 female monkeys (Macaca mulatta) were trained by shock avoidance conditioning to work a simultaneous visual discrimination problem. Trained subjects received either 2500, 4500, or 10,000 rads (midline tissue doses) of pulsed mixed gamma-neutron radiation. Within each dose group some animals were head shielded, some were trunk shielded, and some were not shielded. The midline tissue dose behind the shield (at the middle of the head or chest) was less than 8% of the midline tissue dose to the same point without the shield in place. All unshielded monkeys and many shielded monkeys suffered early incapacitation after irradiation. Within dose groups at 2500 rads and at 10,000 rads, the incapacitation was about equally severe for unshielded, head-shielded, and trunk-shielded subjects; however, it generally was more severe at 10,000 rads than in similarly irradiated monkeys that received 2500 rads. At 4500 rads, early incapacitation did not occur in all shielded subjects, and, if it did occur in a shielded monkey, recovery occurred sooner than in most unshielded subjects at 4500 rads. There was some indication that, generally, males could perform better than females after irradiation. (auth)

42643 ORGANOTYPICAL CULTURE OF IRRADIATED AND NON-IRRADIATED CHICK MESONEPHROS. de Ridder, L.; Mareel, M.; Vakaet, L. (Univ.,, Ghent. Rijksuniversitair Centrum, Antwerp). Experientia; 27: No. 4, 428-30(15 Apr 1971).

The mesonephros was dissected from 9-day old chick embryos and irradiated in doses of 500, 1000, and 2000 rad; unirradiated controls were kept in Tyrode's solution. At intervals up to seven days tissues were removed and prepared for histological examination. It was found that the organized structures of the mesonephros were less radiosensitive than the interstitial cell compartment. The radioinduced changes were dose dependent. (H.L.W.)

42644 EFFECT OF NORMAL AND IRRADIATED MARROW GRAFTS ON THE HEMOPOIETIC RECOVERY AFTER A SUBLETHAL IRRADIATION. Delrez, M.; Haot, J.; Betz, E. H. (Univ., Liege). Experientia; 27: No. 4, 453-4(15 Apr 1971).

Three groups of mice were given 500 R x radiation. The first group was transplanted with isogenic bone marrow; the second was given bone marrow from irradiated donors; the third, or control group, received no transplants. The variations of the haematocrit, the leukocyte counts, and the total number of marrow nucleated cells are shown by means of graphs; results are similar in the three groups. A transitory accumulation of lymphoid cells occurred in the second and third groups. Mechanisms to explain the absence of lymphoid accumulation in animals given transplants of normal bone marrow are discussed. (H.L.W.)

42645 COMPARATIVE EVALUATION OF THE EFFECTS OF URANIUM NITRATE AND RADIOACTIVE IODINE ON AUTOANTIBODY FORMATION. Malenchanka, A. F.; Bakhanovich, U. I.; Radzyuk, K. A. (Inst. of Nuclear Engineering, Minsk). Vesti. Akad. Navuk BSSR, Ser. Biyal. Navuk; No. 2, 95-7(1971). (In Belorussian).

The formation and development of autoantibodies with respect to the thyroid gland were investigated following administration of uranium nitrate and ^{131}I. Uranium nitrate produces more regular development of the autoimmunizing processes than ^{131}I. (tr-auth)

42646 BIOLOGICHESKOE DEISTVIE VNESHNEGO BETAOBLUCHENIYA. (Biological Effects of External Beta Irradiation). Sebrant, Yu. V. Moscow; Atomizdat (1970). 112p.

On the basis of generalizations made from the current literature and original research, the reaction of organisms to both local and general external β irradiation is considered. Special attention is given to the questions of the specific nature of the dosimetry and metrology of β irradiation. The radiobiological effects on small and large laboratory animals, and also the physical basis and experimental technology are described. The principal differences between clinical β injuries and radiation sickness caused by the other forms of penetrating radiation are established. The book is designed for a wide range of biologists and doctors. (tr-auth)

42647 EFFECTS OF LIMBIC LESIONS ON IRRADIATION CONTINGENT SACCHARIN PREFERENCE SHIFTS. Elkins, Ralph Leroy Jr. Athens, Ga.; Univ. of Georgia (1970). 79p. University Microfilms Order No. 71-13,053.

Thesis.

This experiment investigated the effects of olfactory bulb, amygdaloid, and septal lesions on irradiation-contingent shifts in saccharin preference that can be observed when rats consume a novel saccharin solution in conjunction with x irradiation. Amygdaloid and septal lesions were produced with a radio frequency lesion maker and olfactory bulb damage was effected by aspiration. Following surgical recovery, groups of lesioned, sham operated, and normal water deprived Ss were given their first exposure to saccharin solution while being subjected to 60 R of x irradiation or to a sham irradiation. This treatment was followed by seven days of two-bottle preference testing during which Ss had continuous access to saccharin solution and tap water. Daily saccharin preference scores were obtained for each S by computing the percentage of total daily fluid intake accounted for by saccharin consumption. All operated subjects were sacrificed at the conclusion of behavioral testing and the brains were prepared to permit the verification of lesion placements. In accord with prior findings, olfactory bulb lesions disrupted the development of irradiation produced saccharin aversion. This disruption was not complete, however, since bulbectomized subjects did show a significant decrease in post-irradiation preference scores. A similar pattern of results was also produced by corticomedial amygdaloid lesions. These findings suggest that the olfactory bulbs and amygdala are important mediators of the motivational consequences of x-ray exposure but raise the possibility that other mechanisms may also be involved. Different explanations of the olfactory bulb and amygdala lesion effects were discussed and it was concluded that available data provide no clear cut basis for selecting between alternatives. Both septal lesioned and septal control subjects displayed post-irradiation saccharin aversion. This aversion was less permanent than that obtained in normal exposed subjects, but the similarity of results obtained from the septal lesioned and sham septal subjects led to the conclusion that septal lesions per se had no effect on the development of post-irradiation saccharin aversion. Irradiated normal subjects in this experiment displayed much lower post-irradiation saccharin preference scores than sham exposed subjects. It was concluded that the high level of aversion obtained was probably a function of pairing x irradiation and saccharin as novel stimuli. (Diss. Abstr. Int., B)

42648 SERUM LYSOZYME, TRYPSIN INHIBITORS, AND LEUCOCYTES NUMBER LEVEL AFTER X-RAY IRRADIATION OF RABBITS. Stefanovic, J.; Absolonova, O. (Univ. Komenskeho, Bratislava). Bratislav. Lek. Listy; 54: No. 5, 618-25 (Nov 1970). (In Czech).

Levels of lysozyme and trypsin inhibitors in serum and changes in leucocyte number in rabbits after whole-body x irradiation in doses of 150, 500, and 1000 R were observed. In rabbits irradiated by a dose of 150 R, an increase of serum lysozyme and trypsin inhibitors in serum in first days after the irradiation was stated. However, the changes were not significant. In the leucocyte number, no marked changes were observed at these doses. In rabbits irradiated at a dose of 500 R, the lysozyme level oscillated. In most cases a decrease in comparison to initial value was observed lasting up to the 21st day of observation and followed by a rapid, significant increase. Dynamics of trypsin-inhibitor activity in serum was different. It was increasing rapidly after irradiation with a maximum on the 4th day, staying at the same level up to the 7th day, and then showed an oscillating and decreasing tendency with return to initial value on the 29th day. Number of leucocytes decreased significantly after these doses with a minimum on the 4th day and staying at this level up to the 14th day. Further, a progressive increase was observed, however it did not reach the initial value up to the 29th day. All parameters observed had a decreasing tendency to zero values after 1000 R. Animals perished on the 5th day after this irradiation. (auth)

42649 EFFECT OF X IRRADIATION ON TOOTH PRIMORDIA IN THE GOLDEN HAMSTER IN EARLY STAGES OF DEVELOPMENT. Piekos, Boleslaw. Folia Med. Cracov.; 11: No. 4, 471-514(1969). (In Polish).

The influence of x irradiation (70 R) on the teeth in golden hamsters during intrauterine development was studied. The results showed: a higher number of developmental anomalies of the teeth occurred in irradiated animals compared with the control group; deep defects (usuration, niches) in the tooth enamel and dentin occurred; disorders of structure of various dental tissues (enamel, dentin, tooth papilla, organ enamel); hyperaemia and cicatrization of the pulp; delayed developmental stages of the teeth; macroscopic changes in the teeth such as thinning, curving, or bifurcation of the roots and small dimensions of the crowns; abnormalities in the mesoblastic component of teeth such as different character of reactions and accumulation of paS-positive material in the dilated blood vessels and other layers of the tooth; displacement and intensification of diffuse and diffuse-granular reactions in the tooth papilla, steilate cells, and intermediate layer for alkaline and acid phosphatase. (auth)

42650 EFFECT OF TRITIATED THYMIDINE ON THE OOCYTES OF FOETAL RATS FOLLOWING MATERNAL INFU-

SION IN PREGNANCY. Haas, R. J.; Fliedmer, T. M. (Univ., Ulm, Ger.). Int. J. Radiat. Biol.; 19: 197-200(1971).

Tritiated thymidine (^{3}H−TdR) at a specific activity of 2Ci/mM and at doses of 290μCi/day was given to rats by continuous infusion from the ninth day of pregnancy till term, oocyte survival was scored in the offspring killed at ages from 0 to 70 days. The ovarian tissue was found to be abnormal, with a marked reduction in oocyte numbers, and evidence pointing to accelerated maturation to stage III in surviving oocytes. (UK)

42651 EFFECT OF SOLAR OVERHEATING ON THE CARDIOVASCULAR SYSTEM DURING EXPERIMENTAL RADIATION SICKNESS. Mustafin, K. S. (Kirghiz State Medical Inst., USSR. Oshskaya Oblast Hospital, USSR). Sov. Zdravookhr. Kirg.; No. 3, 10-13(May-Jun 1970). (In Russian).

A series of experiments was conducted in which 15 rabbits were exposed to the sun (28 to 33°C) for 30 to 45 min daily for 20 days. Electrocardiographic and histological studies revealed symptoms of hypoxia and myocardial degeneration (focal swelling and basophilia of individual groups of fibers, histiocytic micronecroses, and cardiosclerotic areas). In another series of experiments, 15 additional rabbits received whole-body x irradiation. Exposure to the sun immediately afterward resulted in acute disturbance of the coronary circulation and calcinosis of myocardial fibers. In a third series, 15 more rabbits were irradiated but not exposed to the sun until 7 days later, i.e., at the height of radiation sickness. Dyspnea set in quickly, and the EKG showed signs of acute coronary insufficiency. (JPRS)

42652 ELECTROMYOGRAPHIC EXAMINATION OF STRIATED MUSCLE IN THE GUINEA PIG AFTER ^{60}Co IRRADIATION. Faes, M. G. (CEN, Mol, Belg.); Rosselle, N.; Sonck, W. Electromyography; 9: 229-35(May-Jul 1969). (In French).

The right hind leg of each of 24 guinea pigs was γ-irradiated in doses of 200 to 6400 R. Ten unirradiated animals served as controls. Electromyographic examinations of the muscle were made after 15 days and after three weeks. The muscular potentials detected during relaxation or contraction were classified according to their form, amplitude, or frequency as electric fibrillations, fibrillar excitations, fasciculations, fascicular excitations, myotonic excitations, prolonged insertions, and polyphasic potentials. The appearance of a group of higher potentials was noted, and a relatively simple quantitative expression was derived for their intensity and frequency. A graph is presented to show effects of radiation dose on myotonic responses and the significance of the results is discussed. (H.L.W.)

42653 BIOELECTRICAL ACTIVITY OF CEREBRAL STRUCTURES OF THE RABBIT RESULTING FROM THE COMBINED ACTION OF RADIAL ACCELERATION AND IRRADIATION. Akopyan, S. A.; Baklavadzhyan, O. G.; Grigoryan, S. S. (Erevan State Univ.). Biol. Zh. Arm.; 23: No. 10, 3-12(Oct 1970). (In Russian).

The bioelectric activity of the central nervous system of experimental animals was studied under the combined influences of several g's of acceleration and sub-lethal dose of x radiation. Rabbits were subjected to radial acceleration of 3 to 5 g on a home-made apparatus (radius 35 cm) for periods of from 3 to 5 min. The animals were subsequently given an x-ray dose of 700 to 800 R. A simultaneous recording of the animals' EEG, EKG, and respiration was made. Electrodes with a diameter of 100 μ and an inter-electrode distance of 1 mm were placed in various areas of the brain to monitor the hypothalmus, the reticular formation, sensomotor cortex, and other cortical regions. All brain areas studied responded to acceleration with changes in electrical activity. Fifteen min after irradiation, biopotential activity was inhibited; 2 hrs later it was partially restored, and on the third day, EEG activity was completely normal. It was found, however, that the irradiated animals became very sensitive to radial acceleration and death frequently resulted from acceleration testing at this stage. In 30 to 50 min after irradiation, an increase in amplitude of slow EEG waves was observed; particularly in the cortex. The observed changes in electrical activity were linked with the effect of radiation on the cortex, the hypothalmus, and the reticular formation. The electrical disturbances observed during the first few hours after irradiation, however, were not the result of profound injury to nerve elements, since regeneration occurs comparatively fast. (K.S.W.)

42654 PATHOLOGIC EFFECTS OF DIFFERENT DOSES OF RADIOSTRONTIUM IN MICE. DEVELOPMENT AND INCIDENCE OF LEUKAEMIA. Nilsson, Agnar (Forsvarets Forskningsanstalt, Stockholm). Acta Radiol., Ther., Phys., Biol.; 10: 115-28 (1971).

Varying doses of ^{90}Sr were administered to 1430 CBA mice, about 75 days old, to investigate the site of origin, development and relation between the dose and incidence of leukemia. The significance of the bone marrow, particularly of the thoracic vertebrae, as the site of origin of leukemia, and its relationship to the thymus and spleen in this respect as well as following irradiation, are considered in turn. (auth)

42655 NEONATAL CRANIAL IRRADIATION AND ITS DELAYED EFFECTS ON LEARNING. Elam, LeRoy Harry. St. Louis; Washington Univ. (1970). 128p. University Microfilms Order No. 71-11,033.

Thesis.

One day old rats were given a single exposure to either 200, 400, or 600R of x-irradiation to the head, while the rest of their bodies were shielded with lead. Littermate controls were also shielded and received only background radiation. At 60 days of age half of the experimental rats, Group I Experimental, and their respective controls, Group I Controls, were given their first light-dark discrimination task in a water escape Y-maze. The other half of experimentals, Group II Experimentals, and Group II Controls were given the same light-dark discrimination task at 130 days of age. Both groups I Experimental and Control and groups II Experimental and Control were tested for habit reversal learning at 200 days of age. This constitutes a delay for groups I Experimental and Control of 70 days between original learning and habit reversal, while groups II Experimental and Control had no delay. The results of an unweighted means analysis of variance show that the control rats were significantly better on trials to criterion and had significantly fewer discrimination errors than the experimental groups. These results were consistent for groups I and II, which learned the original discrimination learning task at ages 60 and 130 days respectively. The blood serum proteins were analyzed by electrophoresis and revealed a shift in the relative percents. The results showed that the controls and 200R were significantly different from the 400R and 600R groups in the protein. This increase in gamma globulin is characteristic of antibody production and is relatively common in the autoimmune reactions that increase with age. The histopathological changes that were found were loss of superficial neurons and subsequent cortical atrophy, retinal atrophic changes, periventricular gliosis, glial plaques and lymphocytic infiltration of the central nervous system. The endocrine glands were analyzed for frequency of lesions that are aging related phenomena. For example, pancreatic hyperplasia was relatively high in frequency for the irradiated animals, while the controls and the radiated animals had a similar incidence of thyroid follicle distention. The formation of cysts of the thyroid and pituitary and the atrophy of the testes of irradiated rats are definite signs of age-related changes. The marked enlargement of the Islets of Langerhans in the irradiated group is also a common manifestation of aging. Grain irradiation of neonatal rats appears to be a technique applicable to the study of accelerated aging effects similar to mental retardation. (Diss. Abstr.)

42656 LIFE-SPAN OF DIVIDING MAMMALIAN CELLS IN VIVO. Curtis, Howard J.; Tilley, John (Brookhaven National Lab., Upton, N. Y.). J. Gerontol.; 26: No. 1, 1-7(Jan 1971).

Experiments were designed to test the hypothesis that differentiated mammalian somatic cells are capable of only about 50 divisions before they lose viability and die and that this contributes to the aging process. Bone marrow cells in mice and rats were scored for aberrations in anaphase and early telophase figures. It was found that for normal rats and mice of several inbred strains, there is no change in aberration frequency even into extreme old age. A large dose of radiation given to animals when young increases the aberration frequency throughout life with no increase in old age. An anemic strain of mice has a considerably higher aberration frequency than its normal siblings, but this does not increase with age. The radiation sensitivity of bone marrow cells does not change with age. Finally, for 42 weeks, mice were given large weekly doses of vinblastine, each of which virtually destroyed the bone marrow, and no increase in aberration frequency with age was found. All these experiments indicate that repeated cell division does not lead to chromosomal deterioration, and thus does not support the limited division hypothesis. If such a limitation exists it apparently plays no part in normal aging. (auth)

42657 EFFECTS OF X-RADIATION ON THE CEREBELLAR GRANULE CELL AND THE RESULTANT EFFECTS ON SOME VESTIBULAR AND SPINAL REFLEXES. Olson, Karin Emily. Bloomington, Ind.; Indiana Univ. (1970). 190p. University Microfilms Order No. 71-12,462.

Thesis.

Cerebellar evoked field potentials from peripheral stimulation have been analyzed and the cells responsible for individual components identified by previous investigators. These potentials were monitored with an intracortical glass microelectrode and a silver ball surface electrode. The part of the potential caused

XUM

by the granule cell was noted to be depressed consistently and predictably with radiation. The other components were changed in complex, unpredictable ways. The consequences of this radiosensitivity were monitored at the level of the spinal reflexes. These responses were consistently but unpredictably changed by 200 R of radiation to the brain stem and cerebellum. If the cerebellum were removed and the brain stem alone radiated there was no effect of radiation. Lesions established that most of the cerebellar effects were transmitted via tracts passing through the midline at the level of the obex. The vestibular nerve was stimulated and the reflexes through the medial and lateral vestibular nucleus into the tracts leading to the cord and upper brain stem were monitored. Radiation had little effect on these reflexes. Cats irradiated at birth were shown to have unusual cerebellar evoked potential patterns which showed minimal effects from low acute radiation exposures. The conclusions of this study were that the cerebellar granule cell is sensitive to acute radiation exposures as compared to other nervous system elements. The effect of varying granule cell response acts at the level of the spinal reflex as an off balance control system might be expected to perform: the changes being definite but unpredictable. The major pathways carrying the cerebellar effect descend in the midline. The chronic effects of neonatal radiation can be seen in the cerebellar potential fields of the mature animal. The neonatally radiated granule cell seems to be more resistant to acute radiation than the non-previously exposed granule cell. This resistance is demonstrated physiologically by a lack of change with radiation in the cerebellar evoked potentials and the lumbar cord spinal reflexes. (Diss. Abstr.)

42658 ABSCOPAL RADIATION DAMAGE TO CHICK THYMUS AND BURSA OF FABRICIUS. Montour, James L. (Medical Coll. of Virginia, Richmond). Acta Radiol., Ther., Phys., Biol.; 10: 150-7(1971).

Ten-day old white leghorn cockerels were exposed to 200 R, 400 R, or 600 R of x rays delivered to the cephalic half, the caudal half, or to the whole-body. Thymic and bursal weights were obtained 2, 5, and 8 days after exposure. Partial body exposures indicate that 20 to 30% of the post-irradiation weight loss in the lymphatic organs may be the result of abscopal processes and that, in the chicken, this damage is evident as early as two days after exposure. (auth) (Sweden)

42659 IMMEDIATE AND DELAYED EFFECTS OF 1000 R X-RAYS ON THE RODENT TESTIS. Rugh, Roberts; Skaredoff, L. (Columbia Univ., New York). Contract AT(30-1)-2740. Fert. Steril.; 22: No. 2, 73-82(Feb 1971).

A total of 64 control, 198 immediate, and 191 second generation implantations were examined for the effects of x radiation on the testes of the male mouse, including CF1-S and C57BL/6 strains. The study dealt with the effects of 1000 R coned to the testes only, as revealed in matings with normal females of the same strain as well as with females of the C57BL/6 strain. The criteria of interest were: duration of successful pregnancies on days following radiation exposure; average number of implants per pregnancy; and percentage normals, dead, resorptions, and anomalies. X radiation of the mouse testes to 1000 R had no effect on the mating endeavors of the males, nor on plug production found in the vaginae of exposed females, even after full sterility occurred. There was no immediate effect of such radiation on the fertilizing ability of mature spermatazoa. Resorption percentages were greater when the exposed male involved females of the same strain, and least when there was a heterozygous cross. The average number of implants was least affected when the CF1-S × CF1-S crosses were made, and most when C57BL/6 mice were used. There was no evidence of any differential radiosensitivity of the sex dimorphic mature spermatozoa, since there was no statistical alteration of the sex ratios of delivered litters following testes exposure to 1000 R. The major anomaly effect was stunting. Normality of offspring of x-irradiated fathers was always greater when heterozygous matings were involved. (auth)

42660 HEMATOLOGICAL AND ELECTROCARDIOGRAPHICAL CHANGES DURING RADIATION SICKNESS INDUCED DURING REAR HYPOTHALAMUS MALFUNCTION. Arutyunyan, R. K.; Tokhiyan, S. R. (Dept. of Radiobiology, Erevan). Biol. Zh. Arm.; 23: No. 10, 84-7(Oct 1970). (In Russian).

This investigation was conducted with the purpose of studying peripheral blood and EKG of animals when subjected to radiation at the climax of the clinical manifestation of diencephalic pathology, i.e., 16 days after disturbance of the rear hypothalamus. The mammillary bodies of the hypothalamus of 17 male rabbits were destroyed by 2 mA of dc for 1 min while under Nembutal narcosis, then were subsequently exposed to a radiation dose of 600 R. Six controls were given identical treatment except for the coagulation of the rear hypothalamus. It was concluded that radiation sickness, in the case of the hypothalamus-altered rabbits, was more lingering in character, accompanied by prolonged anemia, acute leukopenia and lymphopenia, and occasionally caused death. (K.S.W.)

42661 X-RAY AND ALKYLATING AGENTS ALTER DIFFERENTIATION OF SURVIVING HEMATOPOIETIC STEM CELLS. Hellman, Samuel; Grate, Helen E. (Harvard Medical School, Boston). Blood; 38: No. 2, 174-83(Aug 1971).

Repopulation assays indicate that erythrocyte differentiation is preferentially impaired in the progeny of progenitor cells surviving radiation or alkylating agents. This was confirmed by study of the iron incorporation into spleen colonies produced by survivors of such treatments. These colonies were characterized by a reduced size and decreased radioactive iron incorporation. Thus, it appears that radiation and alkylating agents not only affect survival of stem cells, but also alter the differentation capacities of such surviving cells. (auth)

42662 EXPERIMENTAL STUDIES ON THE CHANGE OF MAXILLO-ORAL LYMPHATIC SYSTEM AFTER TELECOBALT IRRADIATION ON THE NECK. 2. HISTOPATHOLOGICAL CHANGE OF CERVICAL LYMPH NODES AFTER TELECOBALT IRRADIATION OF THE NECK. Matsui, Sumio (Kagoshima Univ., Japan). Kagoshima Daigaku Igaku Zasshi; 21: No. 3, 519-31(Jan 1970). (In Japanese).

Telecobalt γ irradiation (2000 R, 4000 R, 6000 R) was applied on one side of the neck of adult dogs and for three months after irradiation the lymph nodes on both the irradiated and the unirradiated sides were extirpated at regular intervals and examined histopathologically. A marked fibrosis was observed in the irradiated lymph nodes and degeneration and disappearance of lymph node endothelial cells and reticulum cells at the peripheral sinus and the medulla were observed. From the above findings, as well as from the observed hyperplasia of the capsule and the remarkable increase of connective tissue in the medulla, it was concluded that lymphatic flow and the function of lymph nodes were affected to a considerable degree. (Japan)

42663 LIFE SHORTENING AND CAUSE OF DEATH IN IRRADIATED GERMFREE MICE. Walburg, H. E. Jr.; Cosgrove, G. E. (Oak Ridge National Lab., Tenn.). pp 49-67 of First ESLER. Rome; Comitato Nazionale Energia Nucleare (1970).

From first European symposium on late effects of radiation; Rome, Italy (22 Apr 1969). See CONF-690414.

To determine whether a decline in the effectiveness of defense mechanisms of the animal and a resultant increase in susceptibility to infectious diseases play a role in radioinduced life shortening, life span, and diseases present at death were studied in germfree (GF) as compared with conventional (CONV) mice. GF and CONV RFM mice of both sexes were exposed to 300 R of whole-body x radiation at 5 to 6 weeks of age or were examined as unirradiated controls. RFM GF mice had an increased mean life span but did not show maximum longevity in excess of that expected for the species. It was also found that infectious diseases play little or no role in the decreased mean life span of CONV mice, in the development of senescent lesions, or in the maximum life span of RFM mice. Life-shortening effects of radiation were found in both GF and CONV mice and no influence of the microbial flora on shortening of the mean life span or on age distribution of the effect was noted. Principal causes of death in this strain were neoplasms of the reticular tissues and severe glomerulosclerosis. Radiation caused an increase in myeloid leukemia and thymic lymphoma with a resultant decrease in life span. Nonleukemic life shortening occurred early in males, but no effect of radiation was found in older males. Females, on the other hand, showed the typical upward displacement of the Gompertz plot with little change in slope, possibly because of an increase in ovarian tumors and earlier onset of severe glomerulosclerosis in irradiated mice of this sex. (auth)

42664 COMPARATIVE LATE EFFECTS IN MICE FOLLOWING FAST NEUTRON EXTERNAL IRRADIATION VERSUS TRITIATED THYMIDINE INTERNAL IRRADIATION. Mewissen, D. J. (Univ. of Chicago). pp 69-87 of First ESLER. Rome; Comitato Nazionale Energia Nucleare (1970).

From first European symposium on late effects of radiation; Rome, Italy (22 Apr 1969). See CONF-690414.

The late effects of single, low-dose exposures to radiations of various linear energy transfers (LET) were assessed comparatively. A total of 8,229 mice were assigned to four groups namely: nonirradiated control mice; fast-neutron irradiated mice; mice irradiated with ^{60}Co γ rays; and mice treated with tritiated thymidine. The doses used were 9, 13, 18, 25, 36, 51, 71, 100, and 141 rems for fast neutrons or ^{60}Co radiation (quality factor neutron/Cobalt = 1.8). Tritiated thymidine was injected at birth at the following dose levels: 0.3, 0.4, 0.6, 0.9, and 1.5 μC per gram. It was

concluded that although C57BL mice are classically considered to be tumor free, tumor incidence amounts to more than 50 percent during the animal's life span. Radiation exposure causes a change in the tumor incidence pattern by possibly shortening the mean latent period for tumor development. There is a questionable inhibitory effect on tumor incidence or development after a single whole-body exposure to 9 rems of fast neutrons. (auth)

42665 PATHOLOGY OF THE LATE SYNDROME IN MICE LETHALLY IRRADIATED AND TREATED WITH ISOLOGOUS BONE MARROW TRANSPLANTATION. Hollander, C. F.; Van Bekkum, D. W. (Inst. of the Organization for Health Research TNO, Rijswijk, Netherlands). pp 89-101 of First ESLER. Rome; Comitato Nazionale Energia Nucleare (1970).

From first European symposium on late effects of radiation; Rome, Italy (22 Apr 1969). See CONF-690414.

Adult, thymectomized and non-thymectomized CBA/Rij mice were irradiated with 960 rad x rays (250 kVp) and treated with 2 to 5×10^6 isologous bone marrow cells. In both groups some earlier deaths occurred due to acute pneumonitis, probably of viral origin. Late death started around 4 to 6 months after irradiation and in a large number of these mice hydrothorax and partial or complete collapse of the lungs was found at autopsy. Contrary to the conclusion of Barnes, Bungay, and Mole (1966), the results of this study point to a definite pathology of the late syndrome in mice lethally irradiated and treated with isologous bone marrow transplantation. The morphological picture is that of late radiation fibrosis and is the same as was described to occur in man, rabbits, and dogs after higher doses of localized irradiation. A similar late syndrome was observed after partial irradiation of the thoracic region in mice. (auth)

42666 LATE SOMATIC EFFECTS IN SYNGENEIC RADIATION CHIMAERAS. I. PRELIMINARY DATA ON THE PATHOLOGY OF (C57B1 x C3H)F_1 MICE. Covelli, V.; Silini, G.; Metalli, P.; Bassani, B. (CNEN, Rome). pp 103-23 of First ESLER. Rome; Comitato Nazionale Energia Nucleare (1970).

From first European symposium on late effects of radiation; Rome, Italy (22 Apr 1969). See CONF-690414.

Late radiation effects were investigated in syngeneic chimeras in order to elucidate the role of the hemopoietic stem cells in the long term survival of whole-body irradiated mice. The pathological findings at death are reported. Emphasis is given to qualitative data rather than to incidence rates of specific diseases. Experimental data indicated a very low incidence of leukemia in the transplanted mice while the unirradiated controls dying at comparable ages showed a high incidence of leukemic syndromes, including reticulum cell sarcoma, non-thymic generalized lymphocitic leukemia, and other types. Tumors were found with a very high incidence in all treated animals, although specific patterns with regard to the numbers of cells injected were not immediately apparent. A large spectrum of non-neoplastic and degenerative diseases was found in all experimental groups. Glomerulo- and nephrosclerosis were among the most frequent syndromes, often associated with fibrosis, arteritis, and pleural effusion at death. (auth)

42667 INFLUENCE OF HYPERTENSION ON LATENT CEREBRAL IRRADIATION DAMAGE. Hopewell, J. W. (St. Mary's Hospital Medical School, London); Wright, E. A. pp 125-35 of First ESLER. Rome; Comitato Nazionale Energia Nucleare (1970).

From first European symposium on late effects of radiation; Rome, Italy (22 Apr 1969). See CONF-690414.

The effects of hypertension and x irradiation on the cerebral hemispheres of rats were studied. The results suggest that radiation acts on the brain by two modes, one vascular that is most effective with doses of 2000 to 3000 R for normotensive animals and the other affecting white matter, through damage to the supporting glia. This type of damage is found with doses of 3000 to 4000 R. Thus hypertension will accelerate the onset of vascular damage with doses of 2000 to 3000 R but not with 4000 R when delayed vascular damage is of less importance. It would appear that the effects of hypertension and radiation on blood vessels are in many ways supplementary. Radiation will sensitize blood vessels to hypertensive damage and hypertension will facilitate vascular irradiation lesions. Thus, it was concluded that radiation acts on the brain by two modes and both of these can be explained by the general theory that radiation damage is revealed when cells attempt mitosis. In the brain there is an exceptionally slow mitotic replacement of both vascular and glial cells and this accounts for the extremely long latent periods observed. (auth) (F.M.M.)

42668 LATE FUNCTIONAL CHANGES IN IRRADIATED RATS. Dunjic, A.; Keyeux, A.; Ditu, S. (Univ., Louvain, Belg.). pp 137-50 of First ESLER. Rome; Comitato Nazionale Energia Nucleare (1970).

From first European symposium on late effects of radiation; Rome, Italy (22 Apr 1969). See CONF-690414.

It has been suggested that functional changes play a role in the shortening of life span in irradiated animals. To test this theoretical approach, several projects have been initiated. In vivo techniques with appropriate isotopes or labeled compounds, that can be carried out on the rat, were considered, and the results are discussed. (auth)

42669 LIFE SPAN AND TUMOR INCIDENCE IN RATS SUBJECTED TO SEVERE STRESS BEFORE WHOLE BODY X-IRRADIATION. Reincke, U.; Stutz, E.; Hunstein, W. (Univ., Freiburg i. B. Medizinische Univ., Goettingen, Ger.). pp 151-72 of First ESLER. Rome; Comitato Nazionale Energia Nucleare (1970).

From first European symposium on late effects of radiation; Rome, Italy (22 Apr 1969). See CONF-690414.

The influence on life shortening and tumor incidence of acute severe stress additional to whole-body irradiation was studied in Wistar rats of both sexes. One of three types of stress was administered to separate groups prior to irradiation with 280 R: starvation for 9 days; withdrawal of water for 6 days; or forced swimming for 11 to 13 minutes. No additional influence of stress was seen on the radioinduced tumor incidence. The radioinduced shortening, however, was less in stressed and irradiated rats than in animals receiving irradiation only. (auth)

42670 COMBINATION OF RADIATION AND CHRONIC PHYSICAL TRAUMA IN CARCINOGENESIS OF THE ENAMEL ORGAN IN MICE. Eulderink, F. (Univ., Leiden). pp 173-7 of First ESLER. Rome; Comitato Nazionale Energia Nucleare (1970).

From first European symposium on late effects of radiation; Rome, Italy (22 Apr 1969). See CONF-690414.

Mice were exposed to x irradiation at doses of 500 or 1000 R. Some were also treated by thread implantation into the enamel forming organ of the incisor. It was found that irradiation alone did not induce carcinomas of the enamel organ but irradiation combined with thread implantation enhanced carcinogenesis. The higher dose did not show a stronger co-carcinogenic effect. (F.M.M.)

42671 EFFECT OF IONIZING RADIATION ON THE EXCRETION OF RADIOPROTECTORS IN RATS' URINE. Golubentsev, D. A.; Merkina, T. N.; Mordikhovich, V. V.; Titov, A. V. Farmakol. Toksikol.; 35: No. 5, 607-10(Sep-Oct 1970). (In Russian).

The administration of sulfur-containing radioprotectors such as β-mercaptoethylamine (MEA), cystamine, or cystophos in optimal doses to nonirradiated rats produced a sharp rise in nonprotein thiols in the urine due to excretion of MEA. When cystamine was administered, the amount of MEA excreted in urine was twice as low as when MEA itself was used. Administration of sulfur-containing protectors in combination with serotonin lowered considerably the excretion of non-protein thiols in urine. Whole-body irradiation of rats at a dose of 700 R (LD 100/30) 5 to 10 min after administration of the radioprotector resulted in a drastic drop in the excretion of MEA. This indicates a change in metabolism due to the effect of radiation. (J PRS)

42672 SYNERGISM IN IMMUNOSUPPRESSION. I. EFFECT OF METHYLPREDNISOLONE, AZATHIOPRINE, CHLORAMBUCIL, AND RADIATION ON TETANUS ANTITOXIN PRODUCTION. Friedman, Eli A.; Gelfand, Michael; Bernheimer, Harriet P. (State Univ. of New York, Brooklyn). Transplantation; 11: No. 5, 479-86(May 1971).

The relative efficacy of azathioprine, chlorambucil, methylprednisolone, and total body γ radiation, alone and as combined therapy, in suppressing tetanus antitoxin production in mice was determined. An in vivo assay for serum antitoxin titer was developed. Increasing the number of drugs in the treatment regimen to two or three caused greater depression of the primary immune response than did only one drug. The most profound immunosuppression was produced when sublethal radiation and three drugs were used together. (auth)

42673 EFFECTS OF ACTINOMYCIN D ON ENDOGENOUS ERYTHROPOIETIC RECOVERY OF IRRADIATED MICE. Scaro, J. L.; Carrera, M. A.; De Tombolesi, R. A. P. ((Univ. Nacional, Tucuman, Argentina). Tex. Rep. Biol. Med.; 29: No. 1, 125-31 (Spring 1971).

Administration of various doses of actinomycin D to x-irradiated mice with a shielded limb resulted in a decreased repopulating capacity of endogenous stem cells. Repopulating capacity was measured through the spleen weight, number of colonies, and uptake of ^{59}Fe by the spleen. The effect proved to be dose-dependent. (auth)

Man

Refer also to abstracts 42286, 42362, 42365, 42366, 42394, 42399, 42400, 42406, 42408, 42409, 42430, 42431, 42453–42455, 42473–42475, 42484, 42542, 42544–42546, 42586, 42591, 42592, 42597, and 42598.

XUM

42674 (RLO-1780-32) EFFECTS OF IONIZING RADIATION ON THE TESTICULAR FUNCTION OF MAN. Progress Report, August 1, 1970-July 31, 1971. Heller, Carl G. (Pacific Northwest Research Foundation, Seattle, Wash.). Contract AT-(45-1)-1780. 67p. Dep. NTIS.

Samples of human testicular tissues obtained by biopsy at various time intervals following local exposure of the testis to doses of x radiation ranging from 20 to 600 R were examined histologically for evidence of radiation injury and repair processes. Preliminary findings on samples obtained 22 hours and 24 days following exposure to 600 R are reported. (C.H.)

42675 ETIOLOGIC RELATION BETWEEN RADIATION CASTRATION AND MALIGNANT GYNECOLOGIC NEOPLASMS. Grossmann, H. (Bezirkskrankenhauses, Karl-Marx-Stadt, Ger.). Zentralbl. Gynaekol.; 92: No. 3, 1415-16(Oct 1970). (In German).

Malignancies in the genital area developed in 8 of 1360 women who underwent radiation castration. Of the 8 malignancies, 6 occurred within 3 years following irradiation. Since they were located in the uterus and tubes, they probably existed prior to radiation and escaped detection. It is emphasized that an etiological connection should not be assumed between radiation and malignancies when only a few cases are available. (H.B.G.)

42676 VARIANTS OF THE SYNDROME OF NEUROVASCULAR DYSTONIA IN CHRONIC RADIATION EFFECT. Denisova, E. A.; Gorbarenko, N. I. (Inst. of Hygiene, Moscow). Med. Radiol.; 16: No. 6, 43-8(Jun 1971). (In Russian).

A complex study on the state of the cardiovascular, nervous, and endocrine systems in 178 persons exposed to ionizing radiation was carried out. By the character of clinico-physiological reactions three forms of the syndrome of neurovascular dystonia were singled out: hypotensive, hypertensive, and cardiac. Clinical manifestations were determined by the form of the syndrome and were not specific for persons occupationally exposed to ionizing radiation. However, a hypotensive form of the syndrome of neurovascular dystonia was characteristic for chronic radiation effect. (auth)

42677 BIOELECTRIC POTENTIALS OF THE BRAIN IN PERSONS SUBJECTED TO SINGLE WHOLE-BODY AND LOCAL IRRADIATION. Sosnovskaya, F. M. (Inst. of Hygiene, Moscow). Med. Radiol.; 16: No. 6, 35-43(Jun 1971). (In Russian).

A study on the bioelectric activity in the brain in 8 persons subjected to massive irradiation of diverse localization demonstrated that in whole-body irradiation the electroencephalogram is characterized more commonly by reduction in the alpha-rhythm, dysrhythmia, and intensified quick-frequency rhythmics. Irradiation of the head along with a well marked alpha-activity an increase in the number of slow components of the electroencephalogram was observed. Shifts in the cerebral electric activity depend on functional or organic changes of the central nervous system. (auth)

42678 ALTERATION OF THE BIOELECTRIC ACTIVITY OF THE BRAIN IN PATIENTS WITH ARACHNOIDITIS UNDER THE INFLUENCE OF RADIATION TREATMENT. Pil, B. N.; Iovlev, B. V. (Histoneurological Inst., Leningrad). Med. Radiol.; 16: No. 6, 29-34(Jun 1971). (In Russian).

Comparison of the initial electroencephalographic pictures with investigations carried out after radiation treatment in 120 patients with arachnoiditis made it possible to assume that the therapeutic effect sums up as the result of the effect on the hypothalamic region and pathologically changed cerebral membranes by the chronic inflammatory process. (auth)

42679 MORPHOLOGICAL CHANGES OF THYROID CANCER IN TELEGAMMATHERAPY. Gel'bshtein, M. I.; Kiseleva, E. S. (Inst. of Oncology, Moscow). Med. Radiol.; 16: No. 6, 20-6 (Jun 1971). (In Russian).

Morphological changes in thyroid cancer were studied in 130 patients who underwent telegammatherapy before the operation. The radiation doses varied from 2000 to 5000 rad in a period of 2 to 4 weeks, the interval between the end of radiation treatment and the operation ranging from 7 days to 6 weeks. In the irradiated tumors of the thyroid gland there were dystrophic changes, the markedness of which depended upon the morphological structure of the tumor, its differentiation, and radiation dose. The most distinct lesions were observed in solid and microcellular cancer. In papillary and follicular structures morphological changes were slight. In the irradiation dose comprising 2000 to 3000 rad, changes were observed only in low-differentiated tumors; increase of the dose up to 3500 to 5000 rad resulted in the appearance of morphological changes of the tumors in the majority of cases. No complete morphological regression of the tumor was observed. In 9 patients in whom the operation was performed 5 to 6 weeks after radiation treatment a repeated growth of the tumor was noted. (auth)

42680 RADIATION RISK AND PROTECTION WITH REFERENCE TO RECENT ICRP REPORTS. Hug, Otto (Univ., Munich). pp 16-27 of Biological Aspects of Radiation Protection. /Sugahara, Tsutomu (ed.). Tokyo; Igaku Shoin Ltd. (1971).

From International symposium on biological aspects of radiation protection; Kyoto, Japan (13 Oct 1969). See CONF-691041.

The ICRP recommendations for maximum permissible radiation dose to man are discussed. Background on the research and hypotheses on which these are based is examined. The methods for calculation of the MPD from radioactive substances to the irradiated fraction of an organ or tissue are given. Attempts have been made to consider the different situations involved when particular regions and tissue fractions are exposed by the introduction of a distribution factor into the calculations. The MPD of bone seeking nuclides are based on 0.1 μCi or less of ^{226}Ra and it has been established that the tolerance between this value and the critical dose is not as large as was earlier believed. Newer ICRP reports are based on attempts to determine the MPD for critical tissue fractions and cells and to determine the MPC of bone seeking nuclides by taking into consideration chemical, biological, and physical properties. Three types have been distinguished: alkaline earths, plutonium and thorium; and americium, and transuranium, and rare earth elements. At present all available data on the retention of radioactive nuclides is being collected in order to further evaluate their effects. The aim of the ICRP work is to utilize the improving knowledge of biological radiation effects to radiation protection. This may lead to restriction or relaxation of the recommendations. (E.E.H.)

42681 HEMTOLOGICAL EFFECTS ON HEAVILY IRRADIATED JAPANESE FISHERMEN. Kumatori, Toshiyuki (National Inst. of Radiological Sciences, Chiba, Japan). pp 64-73 of Biological Aspects of Radiation Protection. /Sugahara, Tsutomu (ed.). Tokyo; Igaku Shoin Ltd. (1971).

From International symposium on biological aspects of radiation protection; Kyoto, Japan (13 Oct 1969). See CONF-691041.

The hematological changes in Japanese fishermen exposed to fallout in 1954 are reported. Follow-up studies have been conducted annually on 16 to 18 of the fishermen. These studies are summarized as graphs in order to show the cumulative distribution curves of leukocytes and the changes in the number of leukocytes, neutrophils, and lymphocytes over the past 15 yrs. Chromosome abnormalities in the peripheral leukocytes and bone marrow were analyzed and reported. The number of spermatozoa decreased and minimum numbers were obtained in 16 cases about eight months after exposure. Indications of recovery were observed in some cases after a year, but in most cases signs of regeneration did not appear until two yrs. after exposure, with subsequent production of children. (E.E.H.)

42682 LOW DOSE EFFECTS OF X-RAYS ON ELECTROPHORETIC MOBILITY OF HUMAN ERYTHROCYTES. Sundaram, K.; Phondke, G. P.; Sadarangani, S. H. (Bhabha Atomic Research Center, Bombay). pp 237-43 of Biological Aspects of Radiation Protection. /Sugahara, Tsutomu (ed.). Tokyo; Igaku Shoin Ltd. (1971).

From International symposium on biological aspects of radiation protection; Kyoto, Japan (13 Oct 1969). See CONF-691041.

Comparative investigations were made on human erythrocytes irradiated in vitro with low doses of x rays at a dose rate of 100 R/min. The electrophoretic mobility (EPM) in standard saline was measured with a cylindrical cell microelectrophoresis apparatus. The dose response relation displayed an oscillatory behavior. In order to determine whether the oscillatory pattern correlated with the amount of sialic acid at the cell surface, the cells were treated with neuraminidase. The EPM of enzyme treated RBC also exhibited an oscillatory behavior with respect to radiation dose. It was found that when the EPM of cells increased as a result of irradiation, there was a concomitant increment in the sialic acid content and with decrease in EPM there was a reduction in the amount of sialic acid present. Fixation of cells at pH 7.2 with $KMnO_4$ abolished the oscillatory behavior of the EPM and a continuously increasing dose response was observed. This phenomenon could possibly be developed into a biological dosimeter, however, the dose response to in vivo irradiation must be determined before proposing this system for dosimetric purposes. (E.E.H.)

42683 ALKALINE RIBONUCLEASE ACTIVITY IN RESPONSE TO THERAPEUTIC RADIATION IN THE HUMAN FEMALE. Goldberg, D. M. (Royal Hospital, Sheffield, Eng.). pp 259-75 of Biochemical Indicators of Radiation Injury in Man. Vienna; International Atomic Energy Agency (1970).

From Meeting on biochemical indicators of radiation injury in man; Paris, France (22 Jun 1970). See STI/PUB-280; CONF-700650.

Radium treatment of Stage-2 uterine cervical cancers in the human female at a dose rate of 3,000 rads over 48 hours produced significant increases in the activity of ribonuclease (RNase) measured at pH 7.4 in all cytoplasmic fractions of tumor tissue removed 7 days later. Of 24 patients studied, 13 have survived 5 years and three have died within this period. Similar treatment given to another group of patients with cervical cancer increased the RNase activity of exfoliated cells and extracellular fluid obtained by vaginal irrigation. No change in the RNase activity of blood serum was observed in patients with cervical cancer studied over a 6-week period of radium treatment and supervoltage therapy involving administration of 5,000 to 8,500 rads. However, this treatment led to a significant increase in the urinary output of RNase per ml of urine and per mg creatinine during the last week of therapy although the total daily excretion was only moderately raised. The response shown by Stage-3 subjects tended to be greater than that shown by Stage-2 subjects. Major surgery failed to produce any alteration in the RNase activity of urine or vaginal fluid, indicating that these changes were not simply the result of stress. The effects of supervoltage therapy on urine and vaginal fluid RNase activity were studied in two further groups of patients. One group consisted of patients after simple mastectomy given prophylactic radiation to axillary nodes, skin flaps, and mediastinum, presumed to be free of cancer. The second comprised patients with mediastinal tumors. Whereas no change in vaginal-fluid activity was observed, urine activity was considerably raised in the second group and moderately raised in the first. It was concluded that changes in urine-RNase activity are specifically related to irradiation, and are due to changes in both non-malignant and malignant tissues, although the response was greater when a higher proportion of the latter was included in the field. Preliminary data failed to demonstrate consistent change in RNase-inhibitor levels of tumor tissue and vaginal fluid after irradiation of patients with cancer of the uterine cervix. (auth)

42684 URINARY EXCRETION OF β-AMINOISOBUTYRIC ACID AFTER EXPOSURE TO RADIATION. Smith, H. (United Kingdom Atomic Energy Authority, Chapelcross, Eng.); Langlands, A. O. pp 291-301 of Biochemical Indicators of Radiation Injury in Man. Vienna; International Atomic Energy Agency (1970).

From Meeting on biochemical indicators of radiation injury in man; Paris, France (22 Jun 1970). See STI/PUB-280; CONF-700650.

The excretion of β-aminoisobutyric acid (BAIBA) was measured in the urine of a group of males who were exposed to 150 rads of 4-MeV X rays to the abdomen. No consistent pattern in the excretion of endogenous BAIBA was observed although most patients did show some small increase after exposure. Feeding thymine and thus introducing an exogenous source of BAIBA produced a definite increase in BAIBA excretion on the day before irradiation. A further consistent and significant increase was observed in the 8 hour period following exposure. This was a transient effect which was not demonstrable on the second day after irradiation. The implication of these findings in terms of the use of BAIBA excretion as a biological indicator of absorbed dose is briefly discussed. Because of the wide individual variation in BAIBA excretion, it would be necessary to obtain pre-irradiation control data. This would be possible only in special circumstances. (auth)

42685 THOUGHTS CONCERNING THE FURTHER DEVELOPMENT OF BIOCHEMICAL INDICATORS. Gerber, G. B. (EURATOM-CEN, Mol, Belgium). pp 303-15 of Biochemical Indicators of Radiation Injury in Man. Vienna; International Atomic Energy Agency (1970).

From Meeting on biochemical indicators of radiation injury in man; Paris, France (22 Jun 1970).. See STI/PUB-280; CONF-700650.

The following questions with respect to biochemical indicators of radiation injury are discussed: Whether biological indicators are needed, which requirements they should fulfil, and under which conditions they may be useful? Which place can biochemical techniques occupy among the different types of indicators hematological, cytogenetic, etc.? Under which conditions of exposure may biochemical indicators of radiation injury be most useful? What could be done to develop biochemical indicators to practical application? Suggestions are made for a cooperative investigation of this subject. (auth)

42686 EPITHELIOMA DEVELOPING ON AN ANGIOMA TREATED WITH CURIETHERAPY 33 YEARS PREVIOUSLY. Dollfus, M. A.; Halimi. Bull. Soc. Belge Ophthalmol.; 146: 227-9(1967). (In French).

The case history is reported for a patient with epithelioma that developed in the skin area exposed to an undetermined dose of γ radiation from a radium applicator used to treat an angioma 33 years previously. Data are reviewed from two groups of adults, aged 20 to 40 years, who were treated for angioma during infancy with fractionated doses of ionizing radiations (with a total dose of 600 R in some cases) in whom no sign of a skin malignancy was observed. (C.H.)

42687 SUBCUTANEOUS INDURATION FOLLOWING TELECOBALT THERAPY. Stepanek, J.; Maly, Vl. Cesk. Radiol.; 25: No. 1, 35-9(Jan 1971). (In Czech).

The occurrence of 11 cases of postirradiational subcutaneous indurations (fibrosis) from a total number of 227 irradiated patients after telecobalt therapy as well as their characteristic features has been discussed. Subcutaneous indurations may cause serious diagnostic difficulties due to blastomatous infiltration. (auth)

42688 VISUAL PHENOMENA NOTED BY HUMAN SUBJECTS ON EXPOSURE TO NEUTRONS OF ENERGIES LESS THAN 25 MILLION ELECTRON VOLTS. Budinger, Thomas F. (Univ. of California, Berkeley); Bichsel, Hans; Tobias, Cornelius A. Science; 172: No. 3985, 868-70(21 May 1971).

Six subjects reported multiple starlike flashes and short streaks on exposure to neutrons of energies up to 25 million electron volts. The probable mechanism is interaction with the retinal rods by proton recoils and by alpha particles released from neutron reactions with carbon and oxygen. These observations are similar to light flashes and streaks seen by astronauts who are exposed to high-energy cosmic rays on translunar flight. (auth)

42689 LOCAL RECURRENCE OF GENERALIZED HERPES ZOSTER FOLLOWING X IRRADIATION. Guss, Stephen B.; Sober, Arthur J.; Rosenberg, Gary L.; Arndt, Kenneth A. (Harvard Medical School, Boston. Beth Israel Hospital, Boston). Arch. Dermatol.; 103: 513-14(May 1971).

In a patient with chronic lymphatic leukemia and disseminated herpes zoster, an exacerbation of herpetic vesicles developed on the skin corresponding to a portal of irradiation, despite clearing of other lesions. A similar case has not been previously reported. Attention is called to the possible morbidity of radiotherapy in such a patient. (auth)

42690 CHANGES IN PROLIFERATIVE ACTIVITY OF MARROW LEUKEMIC CELLS DURING AND AFTER EXTRACORPOREAL IRRADIATION OF BLOOD. Chan, B. W. B.; Hayhoe, F. G. J. (Cambridge Univ., Eng.). Blood; 37: No. 6, 657-63(Jun 1971).

Proliferation activity of bone marrow cells was studied in six patients with acute myeloid leukemia treated by extra-corporeal irradiation of the blood (ECIB). One patient with acute lymphoblastic leukemia in full remission was also studied and one patient received splenic irradiation in addition to ECIB. The observations support the hypothesis that ECIB may alter feedback mechanisms of growth control within the leukemic tissue, resulting in an increased proliferative fraction. It is suggested that the nonproliferative leukemic blast cell is not an end cell but is capable of being recalled into cell cycle by an appropriate stimulus such as ECIB. (auth)

42691 REPORT OF THE UNITED NATIONS SCIENTIFIC COMMITTEE ON THE EFFECTS OF ATOMIC RADIATION. Supplement No. 13 (A/7613) 1969. New York; United Nations (1969). 165p. Available from United Nations, Sales Section, New York.

Radiation dose estimates for human populations in the temperate zones of the northern and southern hemispheres from fallout present in the environment in 1969 are presented. The dose commitments to the year 2000 were calculated. The increased dose received by populations in subarctic regions from ^{137}Cs transported through food chains is discussed. Data are summarized from studies on the effects of ionizing radiation on the human nervous system during development and in adults and from studies on radioinduced aberrations of chromosomes in human cells in vivo and in vitro. (1065 references) (C.H.)

42692 REPORT OF THE UNITED NATIONS SCIENTIFIC COMMITTEE ON THE EFFECTS OF ATOMIC RADIATION. Supplement No. 16 (A/5216) 1962. New York; United Nations (1962). 442p. Available from United Nations, Sales Section, New York.

Current knowledge (1962) on the effects of ionizing radiations on man and his environment are reviewed. Background information relevant to fundamental radiobiology is summarized. The genetic and somatic effects of radiation on man, the sources of radiations to which man may be exposed, and the estimated radiation dose to the human population from natural background radiations, fallout, medical exposures, and occupational exposures are discussed. (2968 references) (C.H.)

XUM

42693 REPORT OF THE UNITED NATIONS SCIENTIFIC COMMITTEE ON THE EFFECTS OF ATOMIC RADIATION. Supplement No. 17 (A/3838) 1958. New York; United Nations (1958). 228p. Available from United Nations, Sales Section, New York.

Data available in 1958 on the genetic and somatic effects of various doses of ionizing radiations on man are reviewed. The sources of radiations to which man may be exposed, including natural background radiation, medical uses, industrial uses, and environmental contamination caused by nuclear explosions, are discussed. It is pointed out that knowledge as to the nature and extent of the effects of radiation on man is still meager, particularly for the effects of low doses received over long periods of time. It is concluded that: at present it must be assumed that even small radiation doses may cause deleterious genetic, and perhaps also somatic, effects; both natural radiation and radiation from fallout result in the exposure of the whole world population, whereas only a fraction of the population receives medical or occupational exposure; and that the time delay for the manifestation of genetic and somatic effects of radiations in man makes estimation of the consequences of radiation received by the world population from various sources uncertain. The need for basic research in radiation biology to identify the harmful effects of radiation and relate them to radiation dose is stressed. (897 references) (C.H.)

42694 RADIATION THRESHOLDS. Brues, Austin M. (Argonne National Lab., Ill.). Arch. Environ. Health; 22: No. 6, 690-1(Jun 1971).

Two general types of response to noxious agents, are identified that may be called physiological and statistical. The physiological type exists when all of the persons exposed at a certain level receive more or less the same degree of injury; following low exposures there may be complete recovery or no injury, thus defining a threshold. Carbon monoxide or alcohol might fall into such a category. In the case of the statistical type, the end result, while fatal or very serious, is sporadic and fully affects only a proportion of those exposed, and it is this statistical proportion that is related to the level of exposure. Here, as in the case of malignant tumors induced by radiation, it is more difficult to envision a true threshold. However, if the relation is not a linear or proportional one, as appears often to be the case, the result may be very close to that of a threshold effect. (auth)

42695 ALTERATIONS IN SERUM THYROTROPIN (TSH) AND THYROID FUNCTION FOLLOWING RADIOTHERAPY IN PATIENTS WITH MALIGNANT LYMPHOMA. Glatstein, Eli; McHardy-Young, Stuart; Brast, Neil; Eltringham, James R.; Kriss, Joseph P. (Stanford Univ., Calif.). J. Clin. Endocrinol. Metab.; 32: No. 6, 833-41(Jun 1971).

Seventy-seven of 174 patients (44%) with lymphomas who had lymphangiography and who received high-dose bilateral neck irradiation developed elevated serum TSH concentrations. Many of the elevations were recorded during the first post-treatment year. Elevated serum TSH values were observed with a higher frequency in treated patients under 20 yr of age. In untreated (x-irradiation) Hodgkin's disease, serum TSH levels were normal. Similarly, normal values were seen in patients whose field of irradiation did not include the neck. Nineteen patients developed radiation-induced pericarditis; 16 of the 19 had elevated serum TSH levels and 9 were clinically hypothyroid. Twenty-five patients (11%) developed clinical hypothyroidism and/or showed evidence of thyroid hypofunction by laboratory test other than serum TSH. The post-treatment incidence of abnormally high serum TSH levels was lower in a group of patients with tumors involving the neck region who received irradiation without prior lymphangiography, suggesting that an expanded extrathyroidal iodide pool may increase the susceptibility to hypothyroidism in the irradiated subject. The present data suggest that the concept of relative radioresistance of normal thyroid tissue should be revised. It is recommended that all patients undergoing high-dose bilateral neck irradiation for treatment of neoplasm be evaluated at least quarterly thereafter for laboratory and clinical evidence of hypothyroidism. Determination of immunoassayable serum TSH appears to be a sensitive means of detecting impaired thyroid function in such patients. The finding of an elevated serum TSH level is by itself probably sufficient evidence to indicate that thyroid dysfunction is present; prompt and adequate replacement thyroid therapy not only may give the patient great symptomatic relief, but may also resolve a question of recurrence or extension of the neoplastic process and/or forestall the development or lessen the severity of post-radiation pericarditis with effusion. (auth)

42696 PRENATAL RADIATION EXPOSURE AND CHILDHOOD CANCER. Stewart, A. (Oxford Univ.). Lancet; 1: 751-2(10 Apr 1971).

The British theories of the origins of juvenile cancers are criticized, with reference to the Oxford Survey. Data are given showing numbers of films used in various obstetric x ray examinations in different types of hospitals, and age specific death rates from various causes, malignant and otherwise, in England and Wales in 1968. (UK)

42697 RADIOSENSITIVITY OF MAMMALIAN OOCYTES WITH PARTICULAR REFERENCE TO THE HUMAN FEMALE. Baker, T. G. (Univ. of Edinburgh). Amer. J. Obstet. Gynecol.; 110: No. 5, 746-61(1 Jul 1971).

The results of experiments on laboratory mammals clearly demonstrate that the response of oocytes to x irradiation varies considerably according to: age; species; strain; physical factors (dose, dose rate, etc.); and according to the criterion chosen to assess the effect. The duration of the postirradiation interval is also important, however, the first three litters born to irradiated mice may appear normal except for a slightly increased load of mutations and stillbirths. Thereafter, the number of offspring per litter, and also the mutation frequency, reduces considerably. Perhaps the most important conclusions to be drawn from this review are that one must state exactly the conditions of irradiation, age, and reproductive history of the patient, and interspecies comparisons are rarely, if ever, justified. In many respects the prospects for radiotherapy of the human ovary are fraught with difficulties. First, there is no reliable empirical information on dose response, and second there is no doubt that some women, especially those under 35 years, may become pregnant following exposure to doses that may well induce a high mutation load. Fortunately, few of the human oocytes are likely to undergo ovulation, and consequently germinal selection may permit the exclusion of a large number of the affected cells. The effects of irradiation upon the early embryo are most serious in that they almost always induce severe congenital abnormalities. Extreme caution must be exercised in deducing the so-called doubling dose (that which doubles the mutation frequency in man). The fact is that we have little information on the genetic effects of radiation in man and at best can only assume that it is of the same order of magnitude to that in the mouse. The studies of atomic bomb casualties and those of groups exposed to nuclear fallout and radiotherapy were designed mainly to assess dominant traits: the fact that none was found is reassuring but gives no indication of the incidence of recessive mutations about which we may never have reliable information. (E.R.B.)

42698 STUDY OF APLASTIC ANEMIA IN AN AUTOPSY SERIES WITH SPECIAL REFERENCE TO ATOMIC BOMB SURVIVORS IN HIROSHIMA AND NAGASAKI. Kirshbaum, Jack D.; Matsuo, Takeshi; Sato, Kazuo; (and others) (Atomic Bomb Casualty Commission, Seattle. Nagasaki Univ., Japan. Hiroshima Univ. Japanese National Inst. of Health, Hiroshima). Blood; 38: No. 1, 17-26(Jul 1971).

A study of the occurrence of aplastic anemia among atomic bomb survivors in Nagasaki and Hiroshima, Japan was made from a review of a series of 6327 autopsies from 1949 to June 1967 and the late effects of ionizing radiation were evaluated. There were 340 cases reviewed independently by a team of hematologists and pathologists. Of the 45 cases documented as aplastic anemia, 42 were definite and three were probable. Six additional cases were classified as probable. The cases were grouped into four categories depending upon the distance of the subject from the hypocenter at the time of the bomb (ATB). All patients fulfilled the requirement clinically of having pancytopenia. Bone marrow findings at autopsy from various sites revealed aplastic or hypocellular changes in 77.3%. The etiology in 42 cases was idiopathic, one case was drug-induced, one case received radiation for carcinoma of the cervix, and one case was congenital in origin. No difference was noted in the exposed cases from the nonexposed. Of those who were exposed to 10 or more rad, the majority (four of five) died prior to 1955. On the basis of the data presented, there is no definite morphologic evidence that implicates ionizing radiation in the pathogenesis of aplastic anemia as a delayed complication of exposure in the A-bomb survivors. (auth)

42699 EFFECT OF IRRADIATION IN HIGH DOSES ON PAROTID GLANDS. Eneroth, C. M.; Henrikson, C. O.; Jakobsson, P. Aa. (Karolinska Sjukhuset, Stockholm. Tandlaerkarhoegskolan, Stockholm). Acta Oto-Laryngol.; 71: 349-56(1971).

On radiation therapy of malignant tumours in the head and neck region, the salivary glands are often situated in the radiation field. Ten patients undergoing radiation therapy with high doses for tumours in the region of nasopharynx, lingua and bucca have been examined with respect to the function of the parotid glands. The glands received doses of 4,400–7,200 rad, and the function has been investigated by sialographic and sialometric methods.

The sialograms show that one year or more after irradiation the parotid glands have a significantly smaller projected area than the non-irradiated glands. The irradiated glands had a sparser duct system than the non-irradiated ones. The sialometric examinations showed that all the irradiated glands stimulated with 1% citric acid produced very little saliva. The secretion was in all cases remarkably lower than in a normal material, and in most cases only a few drops were collected during 10 min. In spite of a marked decrease in secretion at the end of the irradiation treatment the size of the glands was still unchanged. Only a certain time after irradiation was the decrease in size observed. The reason for this is discussed. (auth)

42700 FIVE CASES SUSPECTED OF RADIATION MYELITIS. Egawa, Jun; Watari, Tsutomu; Takenaka, Eiichi; Asakura, Hideo (Tokyo Univ.). Rinsho Hoshasen; 15: No. 10, 758-63 (Oct 1970). (In Japanese).

Five cases diagnosed as radioinduced myelitis are described that occurred in a total of 87 patients with malignant tumors of the head and neck treated with radiotherapy. The patients who developed symptoms of myelitis all received radiation doses above 6000 rad over a six-week period, with an average single dose above 1500 ret delivered to a field above 10 cm in length. The difficulties encountered in diagnosing radioinduced myelitis in the patients are discussed. (TSS) (Japan)

42701 RADIOTHERAPY OF INTRACEREBRAL ASTROCYTOMAS. Stenberg, B.; Moberg, A. (Karolinska Sjukhuset, Stockholm). Acta Radiol., Ther., Phys., Biol.; 10: 27-32(1971).

The survival rate of 49 patients with intracerebral astrocytoma of all grades of malignancy was reviewed. It became apparent that a comparison and assessment of different therapeutic measures require knowledge of the neurologic state of the patient following surgery and before and after radiotherapy. The potential hazards of radiation effects on brain tissue outside the tumor must be duly considered when planning the latter. (auth) (Sweden)

42702 LONG TERM FOLLOW-UP OF PATIENTS WITH MENORRHAGIA TREATED BY IRRADIATION. Alderson, M. R. (Univ. of Manchester, Eng.); Jackson, S. M. Brit. J. Radiol.: 44: 295-8(Apr 1971).

Two thousand and forty-nine patients treated for menorrhagia by ovarian irradiation at the Christie Hospital during 1946 to 1960 were followed-up for an average of 14.6 yrs. The number of deaths occurring from different causes were compared with the expected number, taking age, calendar period, and region of residence into account. There was a slight excess of deaths from all causes, an excess of deaths from leukaemia, pelvic cancer, and coronary artery disease, (not significant at the 5% level); the number of deaths from breast cancer was significantly below that expected. When examined by interval since irradiation, there were three deaths from leukaemia five to nine years after treatment compared with an expected figure of 0.37 (significant at the 1% level). (auth) (UK)

42703 REAL IMPORTANCE OF RISKS FROM SMALL DOSES OF RADIATIONS. Pacelli, M. Ann. Med. Nav.; 75: 426-7(Jul-Aug 1970). (In Italian).

The Gofman and Tamplin hypothesis and the Pauling calculations on the risks of small doses of radiation are summarized and briefly analyzed. It is the conclusion that the pollution of the biosphere is much more important. (J.S.R.)

42704 RADIATION-INDUCED CARDIOPATHY. Dusi, U.; Ferri, G. G. (Ospedale Civile, Belluno, Italy). Cardiol. Prat.; 20: 389-96(Oct 1969). (In Italian).

The damage to various structures of the heart that may arise in the course of antineoplastic radiation treatment of thoracic organs is outlined. Radiogenic pericarditis and myocardiopathy are emphasized and their clinical, anatomo-pathological, electrocardiographical aspects and prognosis are discussed. The pathogenesis of the radiogenic cardiac lesion, and its frequency, prevention, and cure are also mentioned. (auth)

42705 RADIOINDUCED SARCOMAS. CONSIDERATIONS WITH REFERENCE TO TWO CASES. Iancu, I.; Dobrescu, G.; Timofte, D.; Clement, C. Oncol. Radiol.; 8: No. 5, 443-6(1969). (In Rumanian).

With reference to two cases of radioinduced sarcomas, the problem is reviewed in detail and the artificial aspect of the rare occurrence of radioinduced sarcomas is demonstrated. Particular stress is given to several elementary measures of prevention and a more detailed treatment of the cases, with repeated biopsies, in order to make a more substantial progress in this field that still presents many unknown factors. (auth)

42706 RADIATION INDUCED CHANGES IN RED CELL FILTERABILITY. Karle, Hans; Hansen, Niels Ebbe (Rigshospitalet, Copenhagen). Scand. J. Haematol.; 8: 72-4(1971).

A decrease in filterability of human red blood cells was demonstrated after in vitro irradiation. The importance of this finding is discussed in relation to the reduced survival of red blood cells during extracorporeal irradiation. (auth)

42707 LIMITATIONS OF CHROMOSOME ANALYSIS AS A METHOD FOR BIOLOGICAL DOSIMETRY OF CHRONIC EXTERNAL RADIATION AND OF INTERNAL EXPOSURE TO THERAPEUTIC RADIOPHOSPHORUS. Visfeldt, Jakob (Kommunehospitalet, Copenhagen). Acta Pathol. Microbiol. Scand., Sect. A; 79: 233-42(1971).

A comparison between the results of chromosome analyses from persons exposed to chronic external irradiation and chromosome analyses from patients having received treatment with radiophosphorus showed that chromosome aberrations in the peripheral blood are found in both cases, and that the aberrations are similar. A quantitative correlation between the radiation dose from chronic external exposure and the aberration yield will involve so many unknown parameters that it seems irrelevant. A quantitative determination of the chromosome aberrations can however, when sufficient data have been collected, probably be used for biological dosimetry, provided that the exposure is approximately uniform. A correlation between the amount of radiophosphorus administered and the aberration yield cannot be used for biological dosimetry, at least if the treatment, as is the case in practice, is given discontinuously. (auth)

42708 LIVER DAMAGE FOLLOWING COLLOIDAL THORIUM DIOXIDE. Madsen, Stig Nistrup; Volck, Erling. Ugeskr. Laeger; 133: No. 18, 883-6(1971).

A brief review is given of liver damage caused by intravascular injection of ThO. Cirrhosis and hemangiotheliomata of the liver were particularly concerned but hepatomata and cholangiocarcinomata have also been described. The latent period varies from 20 to 30 years. A case of cirrhosis of the liver induced by Thorotrast with a latent period of 33 years before manifestation of clinical symptoms and 34 years until death ensued is reported. The incidence of liver damage induced by ThO_2 will probably increase with tissue. Liver biopsy in patients in whom ThO_2-induced liver tumors are suspected is not advised because there is a risk of fatal intraperitoneal hemorrhage. (auth)

42709 CHLOROMA FOLLOWING IRRADIATION IN ANKYLOSING SPONDYLITIS. Gardner-Thorpe, Christopher; Neophytou, Michael (City General Hospital, Newcastle, Eng.). Med. J. Aust.; 1: No. 21, 1121-2(22 May 1971).

Chloroma (granulocytic sarcoma) developed in a patient previously treated with spinal γ irradiation and phenylbutazone for ankylosing spondylitis. The tumors were situated in the sites of maximal irradiation. The significance of this is discussed and the literature on this rare disease is surveyed. (auth)

42710 NERVOUS SYSTEM AND RADIATION. CHIEFLY ON PARTICULAR PROBLEMS. Tsuya, Akira (Japanese Foundation for Cancer Research, Tokyo). Rinsho Hoshasen; 15: No. 10, 717-26(Oct 1970). (In Japanese).

The human central nervous system (CNS) during prenatal and postnatal development is divided into four phases; cell division phase (until 210 days after conception); cell growth and differentiation phase (from 210 days after conception to delivery); early myelin sheath formation phase (from delivery to 120 days after birth); and late myelin sheath formation phase (from 5 to 10 years old). During all these phases even a small dose of 50 rad ionizing radiation can cause radiation injury. Especially during the cell division phase doses above 100 rad cause marked malformation, such as microcephalus, hydrocephalus, and brain hernia with severe dysfunction. On the other hand, it is reported that the earlier the stage of the fetus, the more complete the recovery of the CNS from radiation injury. Repeated irradiation accumulates the radiation effect and causes severe damage. Radiation myelopathy is characterized by chronic vascular changes, including thickening of the tunica and fibrinoid or hyaline degeneration of the wall. The tolerance dose for the radiation myelopathy decreases for patients with hypertension and during radiotherapy under hyperbaric oxygen inhalation. New experimental methods of studying radiation effect on the CNS are discussed. (Japan)

42711 PROFESSIONAL RESPONSIBILITIES OF THE HEALTH PHYSICIST IN RELATION TO THE MEDICAL PROFESSION. Lindell, Bo (National Inst. of Radiation Protection, Stockholm). Health Phys.; 20: No. 5, 475-83(May 1971).

From the genetic point of view, the medical uses of ionizing radiation cause the highest dose contribution in addition to the ex-

XUM

posure to natural radiation. In consequence, it is natural and appropriate that health physicists are particularly interested in these exposures and that the profession as a whole has a certain responsibility with regard to promulgating information on dose levels and protection measures. The various sources of medical exposures are reviewed and their relative importance is discussed with regard to the resulting radiation doses to the patients and to the staff members. Reference is made to new international recommendations which it is hoped that health physicists and hospital physicists will disseminate and support. (auth) (UK)

42712 RADIATION EFFECTS IN MAN: CURRENT VIEWS AND PROSPECTS. Mole, R. H. (Medical Research Council, Harwell, Eng.). Health Phys.; 20: No. 5, 485-90(May 1971).

Radiation protection is concerned with only a small number of possible kinds of late somatic damage and of these malignant disease is the most important. Non-specific ageing is probably irrelevant. Accumulated information suggests that after uniform whole-body exposure cancers will be an order of magnitude more frequent than leukemias. A linear dose-response relationship is compatible with the data on leukemia induction in Japanese atomic bomb survivors and on thyroid cancer in Americans irradiated in childhood. Cancers following external exposure to penetrating radiation have not yet occurred frequently enough for examination from this point of view. Two observations support a simple linear hypothesis: the exponential increase in susceptibility of ankylosing spondylitis to leukemia with linear increase in age at the time of exposure and the synergistic action of cigarette smoking and uranium mining. The dose-response relationship for lens opacification is highly sigmoid and definitely non-linear. There is no general answer to practically important questions about the existence of a threshold, the form of the dose-response relationship, or the effect of dose rate. These questions have to be considered separately for each different kind of late somatic damage. (auth) (UK)

42713 CHROMOSOME ABERRATION FOLLOWING RADIOPHOSPHORUS TREATMENT OF POLYCYTHAEMIA. Barnes, C. A.; Holmes, H. L.; Ilbery, P. L. T. (Univ. of Sydney). Australas. Radiol.; 13: No. 4, 396-417(Nov. 1969).

Cultured leukocytes and bone marrow cells from 51 patients with polycythemia were examined for chromosome aberrations. Therapeutic ^{32}P in accumulated doses of 3.2 to 32.5 mCi was present in 56 patients. The remaining 18 had been treated by venesection only. Variation in all types of cytogenetic damage in the first two months following administration of the isotope did not allow early recognition of trends in dose response. After this period an increase in breaks (and possibly all rearrangements) was recognizable. Multiple regression analysis showed that the Cu type of chromosome damage is likely to be the most reliable index of absorbed dose. In vivo studies showed that small radiation dose increments of the order of several mCi ^{32}P are detectable in radiation treated polycythemics by an increase in the yield of dicentrics and rings as compared with untreated polycythemics. Lymphopoietic stem cells may retain β induced injuries for periods longer than 20 half lives of ^{32}P. Changes similar to those induced by radiation were seen in a small number of cases treated by radiomimetic therapy. Aneuploidy was a consistent finding in the treated cases. Two clearly defined hypomodal clones with the absence of one or two C group chromosomes were seen in the only case of acute leukemia in the series (the patient had received 28.5 mCi ^{32}P). Cytogenetic damage was randomly distributed throughout the chromosome groups of all patients. (auth) (Australia)

42714 PROBLEMS INVOLVED IN ASSESSING LATE EFFECTS OF RADIATION IN MAN. Clemente, G. (CNEN, Rome). pp 201-14 of First ESLER. Rome; Comitato Nazionale Energia Nucleare (1970).

From first European symposium on late effects of radiation; Rome, Italy (22 Apr 1969). See CONF-690414.

Estimates of radiation doses causing late effects in man are necessarily based on accidental or therapeutical exposures, rather than calculated from properly planned experiments on animals. The clinical course of an irradiated human may be defined accurately by medical observations, but the accidents have been too few and the dosages to the patients too variable to allow any statistical study of time-dose relationships in man. For these reasons, difficulties are met in relating dose and effect in man, concerning: the validity of the extrapolations from animals to humans; the influence of other external factors; the calculation of doses and the validity of extrapolations from high to lower doses. Studies were conducted in 1930 to 1940 on patients contaminated with ^{226}Ra or ThO_2 (Thorotrast) in order to assess the late effects produced by internal irradiation by various doses of the contaminants. Problems connected with the calculations of these doses were examined. (auth)

42715 CREDIBILITY AND INFERENCE IN EXPERIMENTATION. Kastenbaum, Marvin A. (Tobacco Inst., Washington, D. C.). Newslett. Environ. Mutagen Soc.; No. 4, 9-11(Mar 1971).

Important business and governmental decisions concerning alleged low-dose radiation hazards in the environment are being made from statistical analyses based on inadequate observations of relevant material. These errors in inference lie in the realm of conceptual error regarding sample size and the power of a given test. Examples of such errors in inference are given. (E.R.B.)

Radiation Effects on Plants

Refer also to abstracts 42266, 42296, 42316, 42317, 42323, 42324, 42329, 42334, 42341, 42343, 42346, 42349, 42351, 42352, 42356, 42358–42360, 42363, 42364, 42614, 42727, and 42742.

42716 (COO–1313-29) EFFECTS OF GAMMA-IRRADIATION ON DNA TRANSCRIPTION AND RNA TRANSLATION IN PLANTS. Progress Report. Cherry, Joe H. (Purdue Univ., Lafayette, Ind. Dept. of Horticulture). Apr 1971. 14p. Dep. NTIS.

Chromatin associated RNA polymerase activity increased during washing of sugar beet tissue to a maximum in 20 hours. This increase was inhibited by γ irradiation but had no effect on enzyme activity when chromatin was extracted from unwashed tissue following exposure. Enzyme activity was most severely inhibited by irradiation during the early stages of washing. The data suggest that γ irradiation inhibits RNA synthesis and subsequent protein synthesis at the transcription level by altering RNA polymerase and/or the DNA template. Changes in specific tRNA as a function of tissue washing were also investigated and it was found that leucyl–tRNA synthetase activity more than doubled during the first six hours of tissue aeration while the leucine tRNA acceptor activity did not change during tissue aeration. This data does not substantiate the idea that translation control mechanisms are involved in the biosynthesis of proteins during aeration of sugar beet. (D.P.O.)

42717 (EGG–1183-2272) ARTEMISIA SHRUB SIZE AND RADIATION DAMAGE TO ARTEMISIA FROM LOCAL FALLOUT FROM PROJECT SCHOONER. Rhoads, W. A.; Ragsdale, H. L. (EG and G, Inc., Santa Barbara, Calif.). May 1971. Contracts AT(29-1)-1183; AT(40-1)-2412. 25p. (S–64-TP; CONF-710501–23). Dep. NTIS.

From third national symposium on radioecology; Oak Ridge, Tenn. (10 May 1971).

Project Schooner was a nuclear cratering experiment in the Plowshare Program for peaceful applications of nuclear explosives. The 31 kt device produced a crater about 260 meters across and 63 meters deep on Pahute Mesa in the northwest corner of the Nevada Test Site. At distances of 1.7 kilometers the accumulated γ doses on dosimeters removed from the field 12 days post-event ranged from background to more than 900 rads; the β doses reached maximums of 10,650 rads. At these highest doses all Artemisia shrubs were killed. At dosimeter stations with less than total mortality, samples of 100 shrubs were measured, and estimates were made of the extent of their damage. Analysis of these data showed that shrubs with smaller volumes were more likely to be killed or severely damaged than were larger shrubs. The results are in accord with conclusions that shrub damage in local fallout patterns is primarily attributable to β radiation. The diminution of β doses by air shielding and shrub self-shielding protects larger shrubs more than the smaller ones. (auth)

42718 (ORO–3299-110) EFFECTS OF BETA RADIATION FROM SIMULATED FALLOUT ON THE REPRODUCTIVE POTENTIAL OF A DOMINANT PLANT SPECIES IN A NATURAL COMMUNITY. Murphy, Peter G. (Michigan State Univ., East Lansing. Dept. of Botany and Plant Pathology); McCormick, J. Frank (North Carolina Univ., Chapel Hill. Dept. of Botany). [1971]. Contract AT(40-1)-3299. 19p. (CONF-710501–22). Dep. NTIS.

From 3, national symposium on radioecology; Oak Ridge, Tenn. (10 May 1971).

The effects of acute β irradiation from simulated fresh fallout particles (albite particles coated with ^{90}Y) on the reproductive potential of Viguiera porteri (Asteraceae), a typical plant of granite outcrop communities, were studied in a natural ecosystem. Certain plant structures, such as leaf axils and terminal buds, captured and retained fallout particles and consequently received higher than average doses. The average radiation doses to the plant community ranged from a mean canopy dose of 3000 rads to 13,000 rads. On the basis of particle size, mass loading, and radiation dose, the experimental conditions resembled those expected at a site 170 miles downwind from a 2.5 megaton nuclear detonation. The rate of anthesis and percentage of aberrant Viguiera flower heads observed during the month of September

was recorded. The quantity and weight of seed produced by normal and aberrant flower heads were also determined. The following April the germination rates of 1700 seed from irradiated and normal flower heads were compared. Results showed that radiation had no effect on the time of initiation or rate of anthesis but did induce a variety of aberrant flower head forms. No differences in the total percent germination or rate of germination of seeds from normal or irradiated plants were seen. It was concluded that acute β irradiation from simulated fallout particles is capable of altering the morphology of reproductive structures in Viguiera porteri under field conditions. (C.H.)

42719 EFFECT OF GAMMA RADIATION ON SEEDLING EMERGENCE OF CUCUMIS SATIVUS. Whelan, E. D. P. (Canada Dept. of Agriculture, Morden, Manitoba). Can. J. Plant Sci.; 50: 606-7(Sep 1970).

The effects of high levels of radiation on seedling emergence in 8 cucumber cultivars are reported. Air-dried seeds of the cultivars were exposed to radiation doses of 10,000 to 80,000 rads, and sown 24 hr later. Emergence counts were taken 5, 7, 9, and 12 days after seeding. There were highly significant differences in emergence both among cultivars and radiation treatments. The cultivar, Early Fortune, showed the most drastic reduction of emergence. Tablegreen 65 showed significantly less emergence at the three higher doses than 6 other cultivars. The radiation treatments had little effect on the emergence of Burpless Hybrid, Marketmore, SMR 58, and the gynoecious hybrid NK 805. The two remaining cultivars, Snappy and SMR 18, showed some loss of seed viability at the highest dose. (Canada)

42720 EFFECTS OF VARIOUS γ-RADIATION DOSES ON THE SIZE OF SAFFRON POLLEN. Muzaferova, R. Sh. (Inst. of Botany, Baku). Dokl. Akad. Nauk Azerb. SSR; 26: No. 8, 62-5(1970). (In Russian).

Gamma irradiation of the bulbo-tubers of Saffron Crocus sativus before planting strongly affected the pollen and flowers of the plant. Irradiation with 250, 500, and 1000 R resulted in enlarged pollen grains and increased the number of colored fertile pollen which was of high importance considering the high sterility of saffron. (R.V.J.)

42721 EFFECT OF IONIZING RADIATION ON THE QUANTITATIVE CONTENT OF CARBOHYDRATES IN WHEAT RADICLES. Gamkrelidze, L. M. Soobshch. Akad. Nauk Gruz. SSR; 62: No. 1, 149-52(Apr 1971). (In Georgian).

Six-day radicles of durum and soft wheat were x irradiated at different doses. Accumulation of carbohydrates increased proportionally to the dose. This phenomenon was more pronounced in soft wheat than in durum, pointing to radioresistance of the durum wheat. (auth)

42722 RADIATION RESISTANCE OF HYBRID PLANTS. Gardzei, I. A.; Valodzin, U. G.; Gardzei, G. M. (Inst. of Genetics and Cytology, Minsk). Vestsi Akad. Navuk BSSR, Ser. Biyal. Navuk; No. 2, 56-61(1971). (In Belorussian).

The effect of radiation on 12 plant characters was investigated in 9 hybrid and 20 non-hybrid forms of corn. The highly productive hybrids exhibited greater resistance to ^{60}Co radiation than their parent strains and hybrids manifesting a lesser degree of heterosis. Analysis of radiation depression in the development of morphological characters of 20 self-pollinated strains of corn of different inbreeding periods showed no direct correlation between radiation resistance and the degree of heterozygosity. Hybrids apparently possessed more highly active mechanisms for post-radiation recovery from cytogenetic damage, and thus enhanced resistance to radiation injury. (tr-auth)

42723 ISOLATION AND GENETIC CLASSIFICATION OF UV-SENSITIVE MUTANTS OF SCHIZOSACCHAROMYCES POMBE. Schuepbach, M. (Univ., Bern). Mutat. Res.; 11: No. 4, 361-71 (Apr 1971).

Sixteen mutants of Schizosaccharomyces pombe, induced by N-methyl-N′-nitro-N-nitrosoguanidine (NNG), were isolated that are more sensitive to uv irradiation than the wild-type. Genetic analysis shows that they occupy 10 different loci. The higher spontaneous lethality observed in 13 of these strains suggests that the mechanisms of radiation repair affected in these mutants, are also involved in normal DNA replication or in the repair of spontaneously occurring DNA lesions. A method for distinguishing between uv-sensitive and insensitive colonies is described that is based on the higher spontaneous lethality of the cells of uv-sensitive mutants. (auth)

42724 RESPONSE OF SOME VARIETIES OF HEXAPLOID WHEAT AND A TWO-ROWED BARLEY VARIETY TO CHRONIC GAMMA-IRRADIATION. Kapoor, M. L.; Natarajan, A. T. (Indian Agricultural Research Inst., New Delhi). Indian J. Genet. Plant Breed.; 30: No. 2, 335-46(Jul 1970).

Information is presented on the response of different varieties of bread wheat (Triticum aestivum, 2n = 42) and one variety of 2-rowed barley (Hordeum distichon, 2n = 14) to varying doses of chronic gamma irradiation. The observations were confined to general gross morphological changes in wheat and the differential stage-sensitivity of barley. After completion of these studies, reports have appeared on differential radiosensitivity of wheat using chronic gamma irradiation at pre- and post-meiotic stages and the results are in agreement with those recorded in this paper. (auth)

42725 EFFECTS OF MEDIA, TEMPERATURE, AND DELAYED PLATING ON THE DARK REPAIR OF UV-IRRADIATED HAPLOID SACCHAROMYCES CARLSBERGENSIS. Azad, Ahmed A.; Hannan, M. A. (Atomic Energy Centre, Dacca, Pakistan). Nucleus (Karachi); 7: No. 4, 273-80(Oct 1970).

The effects of different types of media, temperature, and delayed plating on the repair of uv-induced lesions were studied in the haploid yeast cells, Saccharomyces carlsbergensis. Post-irradiation dark-holding in non-nutrient medium (distilled water) at 4°C was found to result in the recovery of cells from radiation damage in 4 to 24 hr while holding in nutrient liquid medium and storage on agar medium at 4°C, and incubation in non-nutrient medium at 28°C did not give similar results. The effects of post-irradiation environmental factors on the dark-repair of radiation damage are discussed in relation to the results presented. (auth)

42726 INFLUENCE OF ^{60}Co γ IRRADIATION OF WHEAT SEEDS ON THE ASCORBIC ACID CONTENT IN THE DIFFERENT PERIODS OF PLANT GROWTH. Kulesza, J.; Kroh, J ; Rajchert, A. (Technical Univ., Lodz, Poland). Zesz. Nauk. Politech. Lodz., No. Chem. Spozyw.; No. 14, 49–53(1968). (In Polish).

The content of ascorbic acid in 4, 8, 12 and 15 day plants of Ostka Chlopicka wheat grown from irradiated seeds has been determined. The seeds were subjected to the following doses of ^{60}Co γ-radiation: 1, 5 and 10 krads. The doses of 5 and 10 krads increased the content of ascorbic acid not only in 4 days, but also in 8, 12 and 15 day plants. Thus the positive radiation effect in respect to vitamin C was prolonged over later stages of wheat vegetation. (auth)

Radiation Effects on Microorganisms

Refer also to abstracts 42266, 42288, 42300, 42326, 42328, 42330, 42331, 42345, 42357, 42529, 42533, and 42755.

42727 (NYO–2804-38) ACTION OF IONIZING RADIATION ON THE MOLECULAR BIOLOGY OF E. COLI. Pollard, Ernest C. (Pennsylvania State Univ., University Park. Dept. of Biophysics). [1970]. 37p. Dep. NTIS.

The effects of ionizing radiations on molecular biological functions in living cells are discussed. Results are reviewed from a series of studies on γ-radioinduced degradation of DNA in Escherichia coli and the rate of repair of DNA breaks. Suggestions are presented that may explain the molecular events involved in radio-induced injuries of living cells. The possibility of the involvement of various molecular biological processes is discussed. (C.H.)

42728 (NYO–2804-39) ACTION OF IONIZING RADIATION ON SENSITIVE STRAINS OF ESCHERICHIA COLI B. Pollard, Ernest C.; Tilberg, Anna (Pennsylvania State Univ., University Park. Dept. of Biophysics). [1970]. 48p. Dep. NTIS.

The effects of anoxia and genetic strain on the γ-radiosensitivity of DNA degradation and repair in Escherichia coli were investigated. Possible molecular reactions involved are discussed. (C.H.)

42729 (NYO–2804-40) STRAIN OF ESCHERICHIA COLI RESISTANT TO DNA DEGRADATION INDUCED BY IONIZING RADIATION. Horan, Paul; Hird, Kathryn; Pollard, Ernest C. (Pennsylvania State Univ., University Park. Dept. of Biophysics). [1970]. 21p. Dep. NTIS.

The effects of a dose of 20 kR γ radiation on the degradation of DNA were studied in Escherichia coli strains PHH1 and Bs-1. The DNA in strain PHH1 did not degrade, while that of strain Bs-1 was degraded. The effects of a dose of 10 kR, 20 kR, or 40 kR γ radiation on the synthesis of DNA and RNA in Escherichia coli strain PHH1 were studied using ^{14}C-thymidine as a tracer for DNA synthesis and ^{14}C-uracil as a tracer for RNA synthesis. A dose of 40 kR was required to depress the synthesis of both DNA and RNA significantly. (C.H.)

42730 (NYO–2804-41) EFFECTS OF IONIZING RADIATION ON THE CAPACITY OF ESCHERICHIA COLI TO SUPPORT BACTERIOPHAGE GROWTH. Marsden, Howard; Ginoza, William; Pollard, Ernest C. (Pennsylvania State Univ., University Park. Dept. of Biophysics). [1970]. 33p. Dep. NTIS.

The loss in capacity of γ-irradiated bacteria to support the

XUM

growth of T4 phage was studied for two strains, E. coli B and E. coli B_{s-1}. Following a dose of 25 krads, the capacity was quite rapidly lost during postirradiation incubation so that after two hours of such incubation only 12% remains in strain B and 3% in B_{s-1}. Evidence that capacity is lost in an all-or-none fashion was provided by two types of experiments: a single-burst analysis of those cells which survived to give a burst; and an analysis of the regulation of an early phage enzyme. Several processes were examined to try to determine the cause of the loss in capacity. These were the ability of the irradiated and postirradiation incubated cells to respire, to allow phage adsorption and injection of phage DNA, to support the transcription and translation of an early gene and to support replication of phage DNA. Of these processes, transcription and translation appeared to be the most closely associated with the capacity loss, although respiration was reduced to 50% after two hours. (auth)

42731 (NYO-2804-42) SUCROSE GRADIENT ANALYSIS OF DNA IN IRRADIATED CELLS OF PHH1. Horan, Paul; Pollard, Ernest C. (Pennsylvania State Univ., University Park. Dept. of Biophysics). [1970]. 9p. Dep. NTIS.

The effects of a dose of 20 kR γ radiation on the degradation of DNA in Escherichia coli strains PHH1 and Bs-1 were studied using the technique of sucrose gradient analysis for the identification of single-strand breaks in DNA. Minimum degradation was observed in strain PHH1. The rate of repair of single-strand DNA breaks in E. coli at temperatures ranging from 0°C to 45°C was studied using ^{3}H-thymidine as a tracer. (C.H.)

42732 EFFECT OF NEAR-ULTRAVIOLET LIGHT ON THE RESPIRATORY CHAIN OF ESCHERICHIA COLI. Bragg, P. D. (Univ. of British Columbia, Vancouver). Can. J. Biochem.; 49: 492-5(May 1971).

Irradiation of a particulate fraction from Escherichia coli with near uv light destroyed NADH oxidase activity. This treatment did not affect the levels of cytochromes b_1 and o, and ubiquinone in this preparation. Cytochrome a_2 was destroyed by irradiation. A progressive increase in the aerobic steady state level of cytochrome b_1 reduction during irradiation confirmed that irradiation affected the cytochrome oxidase region of the respiratory chain. There was a second site of inactivation between substrate and cytochrome b_1. This was indicated by lowered NADH: cytochrome b_1 reductase activity. Partial reactivation of this activity was obtained by addition of ubiquinone-2 but not ubiquinone-8. (auth) (Canada)

42733 DIFFERENTIAL SENSITIVITY TO UV-IRRADIATION OF VIRUS AND CELL GENOME EXPRESSION IN SV40 TRANSFORMED CELLS (LINE PM3). Monti-Bragadin, C.; Conventi, L.; Meloni, G. A. (Univ., Padua). Boll. Soc. Ital. Biol. Sper.; 46: 565-9(30 Jun 1970). (In Italian).

The production of SV40 in heterokaryons of sensitive cells fused with transformed cells exposed to various doses of uv radiation was studied. The fusion of the PM3 cells (transformed from the SV40 virus) with the sensitive cells (AGMK) by means of the Senaai virus and the determination of the infectious centers were determined by the Dubbs and Kit technique. The suspension of PM3 cells was irradiated with various doses of uv and determinations were made on the fraction of cells capable of producing virus after fusion with AGMK cells, the eventual production of virus in non-fused cells, the synthesis of RNA 8 hrs after irradiation, and the number of living cells present 48 hrs after irradiation. The results are tabulated and shown graphically for uv doses from 0 to 1,200 erg/mm^2. These results showed that uv irradiation can not induce the activation of the viral genome with production of infectious SV40. The lethal effect of uv irradiation on the cells is more intense than the effect inhibiting the synthesis of RNA and this inhibiting effect is clearer than that exercised on the capacity of producing infectious centers after fusion with the sensitive cells. The maximum resistance to uv inactivation was found in the case of the infectivity of the complete virus. (J.S.R.)

42734 DIFFERENT PHOTODYNAMIC ACTION OF PROFLAVINE AND METHYLENE BLUE ON BACTERIOPHAGE. I. HOST CELL REACTIVATION OF SERRATIAPHAGE KAPPA. Brendel, Martin (Goethe-Univ., Frankfurt am Main. York Univ., Toronto). Mol. Gen. Genet.; 108: 303-11(23 Nov 1970).

Photodynamically induced DNA damage in Serratiaphage κ may be repaired by the host cell. The extent of this host cell reactivation (HCR) depends on the photosensitizing dye used: HCR of proflavine + visible light induced DNA damage appears to be more efficient than the one of DNA damage induced by methylene blue + visible light. This significant difference in HCR is not due to a preferential inhibition of the enzymes of DNA dark repair by either one of the dyes injected into the host cell along with the phage's genome. (auth)

42735 MEMBRANE ASSOCIATION OF CONJUGALLY TRANSFERRED DEOXYRIBONUCLEIC ACID IN ESCHERICHIA COLI MINICELLS. Shull, Fred W. Jr.; Fralick, Joe A.; Stratton, Lewis P.; Fisher, William D. (Oak Ridge National Lab., Tenn. Univ. of Tennessee, Knoxville. Furman Univ., Greenville, S. C.). J. Bacteriol.; 106: 626-33(May 1971).

The conjugally acquired deoxyribonucleic acid (DNA) of small, anucleate cells (minicells) of a mutant strain of Escherichia coli K-12 was found to be predominantly associated with the bacterial membrane. Evidence from x-irradiation studies in vivo showed that there was no decrease in DNA-membrane association under conditions that reduce the DNA to one-sixth its original size and suggests the possibility of multiple DNA-membrane association sites. Preliminary enzymatic studies indicated the involvement of protein, DNA, and lipids in the membrane association of the DNA. (auth)

42736 X-RAY STUDY OF COMPETENCE DEVELOPMENT IN BACILLUS SUBTILIS. Epstein, H. T. (Brandeis Univ., Waltham, Mass.). Mol. Gen. Genet.; 110: No. 4, 327-31(11 May 1971).

Pre-competent and competent cultures of Bacillus subtilis were x-irradiated before and after centrifugal separation of cells in a Renografin density gradient. Pre-competent cultures have no cells at the radiosensitivity of the cells in the bulk competent culture, but there is a substantial fraction of cells in a multi-target state, with heterogeneous target numbers. On reaching maximal competence, the survival becomes entirely linear in radiosensitivity. Irradiation of the separated competent cells shows that competence development correlates with disappearance of multi-target cells from the non-competent band of cells and the appearance of single-target cells in the competent band at a radiosensitivity equal to that of the bulk competent culture. Thus the multi-target state may be a required stage in the development of competence in this system. (auth)

42737 PROTECTION OF IRRADIATED LAMBDA PHAGE BY METHYLATED PROFLAVINE. Jaffe-Brachet, A. (Univ., Brussels). Mol. Gen. Genet.; 110: No. 4, 374-7(11 May 1971).

The lethal action of uv on λ bacteriophage is diminished by pretreatment with methylated proflavine. The effective distance over which each dye molecule inhibits dimer formation is calculated to be 5 to 7.5 base pairs. (auth)

42738 DIFFERENCES IN HOST CONTROLLED REACTIVATION OF LAMBDOID AND T PHAGES. Geissler, Erhard (Univ., Rostock, Ger.). Mol. Gen. Genet.; 109: 257-63(22 Dec 1970).

Phages 434, T4, T5, and T7 were studied with regard to host controlled reactivation of damage produced by uv or photodynamic action sensitized by thiopyronine. Repair of 434 phages proceeded under control of both hcr and rec genes. UV irradiated T5 and T7 phages were reactivated under control of the host's hcr genes only. If these phages were inactivated by photodynamic action they were not reactivated at all. T4 phages inactivated by both treatments were also refractory to host controlled reactivation. These differences might reflect different degrees of autarchy and different abilities of phage DNAs to serve as substrate for recombination enzymes of the host. (auth)

42739 BACTERIOLOGICAL PROCEEDINGS, 1971. Abstracts of the 71st Annual Meeting, Minneapolis, Minn., 2-7 May 1971. Washington, D. C.; American Society for Microbiology (1971). 283p. (CONF-710516-(Absts.)).

Abstracts of 1,351 papers presented at the 71st Annual Meeting of the American Society for Microbiology (May 1971) are presented. Several papers discuss the radiosensitivity of microorganisms. (C.H.)

42740 ACTION OF GAMMA RADIATION ON ENTEROCOCCAL BACTERIOPHAGE 341. Ciuca, M.; Pleceas, M.; Pleceas, Paula; Petrovici, A.; Constantinesco, S. P. (Inst. Dr. I. Cantacuzino, Bucharest. Inst. of Hygiene, Bucharest). Arch. Roum. Pathol. Exp. Microbiol.; 28: No. 1, 219-24(Mar 1969). (In French).

Inactivation of enterococcal bacteriophage was achieved by irradiation with 2,500,000 r/γ for fluid bacteriophage and 3,000,000 r/γ for lyophilized bacteriophage. Irradiation with γ rays did not induce morphological changes in the bacteriophage; no lesions could be demonstrated by the methods used in this investigation. Immunogenicity was not altered by irradiation with γ rays. (auth)

42741 STABILIZATION OF POLIOVIRUS TO ^{32}P DECAY. Hughes, H. G.; Tershak, D. R. (Pennsylvania State Univ., University Park). Can. J. Microbiol.; 17: 725-30(May 1971).

Suicide experiments with ^{32}P-labeled poliovirus were performed with HeLa S_3 cells. The results showed that virus-cell complexes become increasingly refractory to ^{32}P decay during

the eclipse period, i.e., stabilization to ^{32}P decay occurs during the first 3 hr of infection. The data suggest that stabilization is probably due in part to the production of early RNA during the eclipse period because the presence of ^{32}P in the medium during the first 2 hr of growth sensitizes infective centers. (auth) (Canada)

42742 STUDIES ON THE INFLUENCE OF IONIZING (GAMMA) IRRADIATION ON THE MILK MICROFLORA. Niewolak, S. (Coll. of Agriculture, Olsztyn, Poland). Rocz. Nauk. Roln., Ser. B; 89: No. 3, 419-40(1967). (In Polish).

Studies were carried out on the influence of ionizing irradiation on milk microflora to obtain information on what radiation doses would destroy various groups of microorganisms. Raw milk was irradiated with γ rays from a ^{60}Co source type Gammacel, with activity of about 4000 Ci. Four series of milk samples were irradiated with doses varying from 1 to 500 kR. The irradiation time was from 19 sec to 155 min, respectively, depending on irradiation doses. In the milk samples tested the following determinations were made: total number of bacteria; lactic acid bacteria; bacteria of coli-aerogenes group; proteolytic bacteria; spore-forming aerobic bacteria; spore-forming anaerobic bacteria; and yeasts and molds. In the case of total bacterial counts a remarkable destruction of microorganisms was still observed in raw milk at doses of the order of 1 to 3 kR. In order to obtain commercial sterility of milk, doses of 90 to 100 kR were required, while 99.99% of bacteria were destroyed at a dose of 500 kR. A slightly higher resistance by lactic acid bacteria was found, especially at low doses. The coli-aerogenes bacteria appeared to be the most sensitive to γ radiation. Their complete destruction was reached at doses of 10 to 20 kR. The survival of proteolytic bacteria was more or less of the same order as that of lactic acid bacteria. Spore forming aerobic bacteria showed the highest survival numbers, as compared with other groups of microorganisms studied. At 500 kR 0.790% of them were still alive. The complete destruction of yeasts in milk required radiation doses of more than 500 kR. No spore-forming anaerobic bacteria were found both in control samples and in irradiated ones. (NSA of Poland)

42743 ACTION OF GAMMA RAYS ON BACTERIA USED AS SANITARY INDICATORS. Pleceas, M.; Arizan, D. (Inst. of Hygiene, Bucharest). Arch. Roum. Pathol. Exp. Microbiol.; 28: No. 2-3, 587-90(Jun-Sep 1969). (In French).

Resistance to irradiation with γ rays was investigated in several bacterial species including Escherichia coli, Streptococcus faecalis, Proteus vulgaris (sanitary indicators), and Salmonella typhi. Proteus vulgaris was found to be more sensitive and Streptococcus faecalis to be more resistant to γ rays than Salmonella typhi. The resistance of E. coli was closely similar to that of Salmonella typhi. It is inferred that Escherichia coli maintains its value as a bacteriological sanitary indicator for products exposed to ionizing radiations. (auth)

Radiosterilization and Radiopreservation

Refer also to abstracts 41833, 42438, 42610, and 42614.

42744 (COO-2038-2) STUDY OF CONTROL OF PUBLIC HEALTH PROBLEMS USING IRRADIATION. Annual Report, May 1, 1969-April 30, 1970. Maxcy, R. B.; Tiwari, N. P.; Anagnostis, C. C. (Nebraska Univ., Lincoln. Dept. of Food Science and Technology). May 1971. Contract AT(11-1)-2038. 38p. Dep. NTIS.

Red meat, as exemplified by ground beef and pork, is subject to numerous opportunities for contamination and harborage of pathogenic organisms with the present commercial system of processing and distribution. A study was made to determine the usefulness of γ irradiation for public health protection when applied to red meat. Results indicated that retail products are commonly heavily contaminated with bacteria. The contamination can be reduced somewhat through central processing as shown by the data obtained from ground beef. Considerable numbers of the contaminants can be destroyed by irradiation at a 68 Krad level. This work indicates that commercial ground red meat contained a great diversity of contaminants, many of which belong to the family Enterobacteriaceae. Of most interest are Salmonella species and other pathogens of lesser pathogenicity. Many of these organisms are quite sensitive to γ radiation. While a 68 Krad level of radiation likely will not destroy all these pathogens, a substantial reduction in numbers is possible. Future use of higher dosage should destroy more microorganisms and add further to public health protection. (auth)

42745 (RISO-238) STUDIES ON THE EFFECTS OF IONIZING RADIATION FOR EXTENDING THE STORAGE LIVES OF ONIONS. Skou, J. P. (Danish Atomic Energy Commission, Risoe. Research Establishment). Feb 1971. 46p. Dep. NTIS (U. S. Sales Only).

Experiments with ionizing radiation for extending the storage lives of onions are described and compared with the available literature on the subject. The aim was to form a general picture of the effects of ionizing radiation applied to onions on the basis of the multitudinous environmental and physiological conditions influencing the results. All that contributes to optimal growth, uniform maturation, and good storage conditions will improve the results. Only first-class market onions should be used for irradiation as even apparently negligible deviation from that category will increase the rot during storage. It was found very important to use strains of cultivars with a specially good storability. The best results were obtained with irradiation shortly after lifting when the onions are in the deepest state of rest. At that time only 6 to 12 krads were necessary to inhibit, but not to prevent, the onions from sprouting. At the above conditions the effect on the incidence of rot will be small, but all deviations from them may result in an increase in both sprouting and rot. Doses above the optimal for sprout inhibition cause an increase in storage rot and may promote a transitory, relatively high sprouting rate within 1 to 2 months after the application. Small bulbs sprout faster than larger ones. Discoloration of the growth center of irradiated onions may often occur, but with great variation between strains of cultivars and from one bulb to another. The cause has not been elucidated, but some explanations are given. Generally the discoloration should not make the onions objectionable for most kinds of use. The total loss by respiration and transpiration in the whole storage period was greatest in the non-irradiated, but in the first months of storage, until the sprouting accelerates, the loss was greatest in the irradiated onions. The culinary value was practically unchanged. (auth) (Denmark)

42746 (STI/DOC-10/124) RADURIZATION OF SCAMPI, SHRIMP, AND COD. Hannesson, G.; Dagbjartsson, B. (International Atomic Energy Agency, Vienna (Austria)). Apr 1971. 93p. IAEA $3.00.

The feasibility of γ processing for extension of the storage life of lobster tails (scampi), shrimp, and cod fish during export from Iceland was investigated. Results showed that irradiation alone gave a three-fold increase in the storage life of lobster (Nephros norvegicus) tails. The storage life of lobster tails blanched for two minutes before irradiation at a dose level of 2×10^5 to 3×10^5 rad was found to be about six to seven weeks. The storage life of shrimp (Pandolus borealis) was found to be about seven weeks following processing using 5-min blanching and irradiation at a dose level of 1×10^5 rad. Cod (Gadus callarias) fillets irradiated at a dose level of 2.0×10^5 rad had a storage life of 24 days at 0 to 1°C. Only cod caught by line or trawl and landed daily were found suitable for radiation processing. Whole eviscerated cod irradiated at 0.5×10^5 rad had a shorter storage life than the irradiated fillets. The economic aspects of exporting radiation-processed sea foods from Iceland are discussed. (C.H.)

42747 RADIATION FOR FRESHER FOOD. Shea, K. G. (International Atomic Energy Agency, Vienna). New Sci. Sci. J.; 49: 108-10(21 Jan 1971).

The idea of preserving food with atomic radiation has met a suspicious, even hostile, reception in many quarters, particularly within the U.S.A. But for certain foods and food products irradiation offers unique advantages. Results of a survey on irradiated food products cleared for human consumption are reported and research programs on the wholesomeness of irradiated foods are discussed, covering Canada, Israel, Netherlands, Spain, U.K., U.S.A., and U.S.S.R. A new international project, involving 19 nations, to study the wholesomeness of irradiated foods was recently launched. (UK)

42748 EFFECTS OF GAMMA RADIATION ON THE REFRIGERATION STORAGE OF GOLDEN DELICIOUS APPLES. STUDIES OF 1968 AND 1969. Paulin, A. (CNRS, Bellevue, France). Rev. Gen. Froid; 61: 587-98(May 1970). (In French).

The use of nitrogen during irradiation makes it possible to reduce the changes in organoleptic character produced by ionizing radiation. This favorable effect is obtained only if a clearance, prior to irradiation, of sufficient duration eliminates most of the internal oxygen. The irradiated fruits are then placed in a sealed polyethylene packing case. Because of the increased respiration and the vigorous chemical transformations following the action of γ rays there is produced in the center of the packing case an atmosphere characterized by a decrease in oxygen pressure (with

XUM

an increase in the ratio of CO_2) and by an increase in the volatile products, such as acetaldehyde, ethyl acetate, methanol, and methyl propionate. The changes in CO_2 and O_2 in the atmosphere are not sufficient to explain the appearance of fermentation browning observed in the sealed package. This change seems to be due either to the toxic action of the volatile products present around the fruit (this hypothesis seems the most plausible) or the combined action of the decrease in oxygen and the accumulation of volatile products. (tr-auth)

42749 STERILIZATION OF INSECT DIET BY GAMMA IRRADIATION. Spencer, Neal R. (Dept. of Agriculture, Gainesville, Fla.). J. Econ. Entomol.; 64: No. 3, 753-4(Jun 1971).

Effects of low doses of gamma radiation on a diet prepared for larvae of the cabbage looper, Trichoplusia ni, were studied. The diet was poured into 1 oz cups and all cups of medium were infested with T. ni. Irradiation was not effective with 150 krad; some cups were sterilized with 530 krad and the maximum effect was reached at 795 krad. A test was designed to demonstrate the degree of control when different methods of handling the cups were used. It was found that contamination of insect diet could be greatly reduced by using gamma radiation. (H.L.W.)

42750 APPLICATION OF THE STERILE-INSECT-RELEASE TECHNIQUE IN MEDITERRANEAN FRUIT FLY SUPPRESSION. Rhode, R. H.; Simon, J.; Perdomo, A.; (and others) (International Atomic Energy Agency, San Jose, Costa Rica). J. Econ. Entomol.; 64: No. 3, 708-13(Jun 1971).

Populations of wild Ceratitis capitata (Wiedemann) were suppressed by gamma-irradiated flies in a 48-km^2 coffee and citrus area in Nicaragua. From September 1968 to May 1969, approximately 40 million sterile flies were released by air each week. Wild Mediterranean fruit flies in a 2-km-wide border area around the nonisolated sterile-fly-release area were depressed by aerial applications of bait sprays. Average deposition of viable Mediterranean fruit fly eggs, larval infestation in coffee fruits, and recoveries of pupae from mandarin oranges were at least 90.1% less in the release area than in the checks. During the experimental period, wild fly populations increased only 4-fold in the release area compared with 15- and 28-fold increases in the respective check areas. (auth)

42751 RADIATION-STERILIZATION OF THE MEDITERRANEAN FRUIT FLY (DIPTERA: TEPHRITIDAE): COMPARISON OF SPERMATOGENESIS IN FLIES TREATED AS PUPAE OR ADULTS. Anwar, Mahmood; Chambers, D. L.; Ohinata, K.; Kobayashi, R. M. (Univ. of Hawaii, Honolulu). Ann. Entomol. Soc. Amer.; 64: No. 3, 627-33(17 May 1971).

Ceratitis capitata (Wiedemann) were irradiated with 10 kilorad (krad) of gamma radiation from a cobalt-60 source 2 days prior to and after pupal ecdysis to determine the effects of radiation when administered at these two different stages. Testes were removed from adult flies at intervals of 1, 2, 4, 6, and 8 days after emergence, stained with Feulgen, and whole-mounted for microscopic examination. The radiation dose of 10 krad completely stopped spermatogenesis. In irradiated flies, the sperm in the existing sperm bundles completed their maturation, but no additional sperm were produced. The spermatogonial cells, primary and secondary spermatocytes, and the spermatids were completely aborted. The cytological effects of radiation were manifested in full 4 days after treatment. The radiation dose of 10 krad produced dominant lethality in the fully differentiated sperm. Irradiation of adult fruit flies is recommended, since these flies have a higher total number of sperm (carrying dominant lethality) available as compared with the flies that were irradiated as pupae. (auth)

42752 ACUTE TOXICITY (LD_{50}) AND ANALGESIC ACTIVITY OF MORPHINE HYDROCHLORIDE IRRADIATED BY ^{60}Co GAMMA RAYS. Tanasijevic, D.; Radovic, G.; Milosevic, V. (Boris Kidric Inst. of Nuclear Sciences, Vinca, Yugoslavia). Bull. Boris Kidric Inst. Nucl. Sci., Chem.; 21: No. 1, 1-5(May 1970).

The work was carried out in order to estimate to what extent the degradation products of irradiated Morphine hydrochloride are toxic and to show the increase of toxicity with increasing gamma radiation dose. It was found that injection solutions are much more sensitive to radiation than the Morphine hydrochloride powder. The mutual dependence between the damaging effect, the absorbed dose, and the concentration of the solution was also shown; dilute solutions are more sensitive to radiation than concentrated ones. The analgesic activity of irradiated Morphine hydrochloride is saved even at relatively high irradiation doses. (auth)

42753 VOLATILE RADIOLYTIC COMPOUNDS IN IRRADIATED FISH. Barrera, R. (Junta de Energia Nuclear, Madrid); Gasco, L. Energ. Nucl. (Madrid); 15: No. 69, 21-33(Jan-Feb 1971). (In Spanish).

After a bibliographic review of the subject, in which there are classified by functional groups the characteristic volatile constituents in fish and seafood as a function of the methods of preservation, both conventional and by radiation, the results of investigations on the hake (Merlucius merlucius) are given. The experimental part consists of the following parts: (a) Gamma irradiation of fillets of 200 g of raw hake in a dose range between 0.1 and 5 Mrads. (b) Concentration of volatiles by a method of distillation at room temperature, under reduced pressure, and in a current of nitrogen. (c) Direct analysis of the aqueous concentrates of volatiles by gas chromatography and the method of "vapor in equilibrium." (d) Gas chromatographic analysis of derivatives of functional groups: carbonyl compounds such as 2,4-dinitrophenylhydrazones; primary and secondary amines such as N-alkylbenzamides; and mercaptans such as 2,4-dinitrophenylalkyl thioethers. An increase of the total fraction of carbonyl constituents as a linear function of the radiation dose is observed. The radiolytic yield of the principal components is: G(acetaldehyde) = 0.04; G(propionaldehyde) = 0.005; G(formaldehyde) = 0.002. Very slight variations with dose of traces of ammonia, methylamine, trimethylamine, ethylamine, diethylamine, propylamine, butylamine, and pentylamine are found in the samples of fresh fish. The concentrations of methyl mercaptan and dimethyl disulfide increase as a linear function of the radiation dose. (tr-auth)

42754 EFFECT OF HIGH-ENERGY RADIATION ON THE HYDROLYTIC RESISTANCE OF GLASS CONTAINERS. Huettenrauch, R. (Wissenschaftliche Laboratorien, Jena, Ger.). Pharmazie; 25: 270-1(Apr 1970). (In German).

To simulate sterilization conditions, three types of glass for manufacture of ampoules were exposed to 2.5 Mrad γ radiation. Following irradiation, release of alkali was determined. Results showed that radiation does not increase alkali release but, frequently, even improves the glass quality as judged by hydrolytic resistance. Therefore, sterilization of clinical ampules by high dose γ radiation appeared promising. (H.B.G.)

42755 DETERMINATION OF MUTAGENIC EFFECT OF IRRADIATED MEDIA ON ESCHERICHIA COLI. Islam, Fakhrul; Khan, S. U.; Munir, M.; Muhammed, Amir (Radiation Genetics Inst., Lyallpur, Pakistan). Nucleus (Karachi); 7: No. 4, 281-9 (Oct 1970).

The following effects of γ-irradiated growth media were tested on Escherichia coli K12: effect on growth rate, lethal effect, and mutagenic effect. It was found that in irradiated liquid minimal medium, log phase cells went into lag and growth rate was slowed down. Synthetic agar media irradiated with 80 to 300 kRads had significant lethal effect on the survival of E. coli when the cells were grown for 36 to 48 hr on agar plates. In the irradiated nutrient agar, however, no such effect was observed. Growth media both minimal and nutrient, irradiated at 50 and 300 kRads doses had no mutagenic effect on E. coli cells, for mutation from streptomycin sensitivity to streptomycin resistance. (auth)

42756 LOW DOSE GAMMA IRRADIATION OF BOVINE METMYOGLOBIN. Satterlee, L. D.; Wilhelm, Mari S.; Barnhart, H. M. (Univ. of Nebraska, Lincoln). J. Food Sci.; 36: No. 4, 549-51(May-Jun 1971).

Bovine metmyoglobin (MetMb) in a pure state, in several differing states of purity, and in meat was γ-irradiated. Irradiation caused the brown MetMb to convert to a red myoglobin pigment that is similar but not identical to oxymyoglobin (MbO_2). The formation of red pigment was accelerated at slightly basic pHs and under nitrogen atmospheres. Rate of red pigment formation was not dependent upon MetMb purity. Rate of red pigment formation in meat was identical to the rate of formation in buffered MetMb solutions. This study also demonstrated that gamma irradiation does alter MetMb structure. This alteration may be the loss of amide nitrogen from the protein. (auth)

42757 FOOD PRESERVATION BY IRRADIATION. Sreenivasan, A. (Bhabha Atomic Research Centre, Bombay). Vigyan Pragati; 19: No. 12, 501-6(Dec 1970). (In Hindi).

Preservation of food by γ irradiation and storage is described. Bhabha Atomic Research Centre, Trombay, is actively engaged in the irradiation of perishable food material which is of economic importance to the country. Specially designed cobalt-60 radiation sources are used for this purpose. The techniques developed are now being examined by the expert scientists in other fields in order to be made available on a large industrial scale. Experiments have been carried out on onions, potatoes, mangoes, bananas, fish, bread, etc. Recently, a ^{137}Cs irradiator was procured from the United States Atomic Energy Commission which will be installed after its initial testing. There are at present 76 countries in the world engaged in research on preservation of food by irradiation. (INIS)

42758 GAMMA RAY STERILISATION OF HOMOGRAFT VALVES. Gibbons, J. R. P.; Alladine, F. Bull. Soc. Int. Chir.; 28: No. 3, 353-8(May-Jun 1969).

Gamma-irradiated homograft valves were found to be sterile, and there was no change on histological examination of the tissue or change in tensile strength when irradiated at 2.5 to 3.0 megarads. They were best stored at 4°C. The homografts were inserted into 110 patients suffering from severe aortic and mitral valve disease, with good results. (auth)

42759 PROCESS FOR RADIATION STERLIZING A PACKAGED PRECOOKED MEAT AND GRAVY PRODUCT. Shults, Gary W. (to Secretary of the Army). U. S. Patent 3,573,067. 30 Mar 1971. Filed 8 Oct 1968.

An improved process for sterilizing a precooked-meat and gravy product with high energy ionizing radiation is described. The meat and gravy are each frozen separately and kept frozen and apart during the sterilization step and subsequently allowed to thaw and mix within the container. (Official Gazette)

XUM

METALS, CERAMICS, AND OTHER MATERIALS

Metals and Alloys

Refer also to abstracts 41832, 41969, and 44219.

42760 (COO–2069-7) STUDY OF THE MECHANISMS OF STRESS CORROSION CRACKING IN THE IRON–NICKEL–CHROMIUM ALLOY SYSTEM IN CHLORIDE ENVIRONMENTS. Quarterly Report, April 1–June 30, 1970. Slater, J. E.; Staehle, R. W. (Ohio State Univ., Columbus. Dept. of Metallurgical Engineering). 18 Feb 1971. Contract AT(11-1)-2069. 66p. Dep. NTIS.

Studies in circulating autoclave tests, studies of corrosion topology in $MgCl_2$ solutions, passivation studies on pure iron, and studies of Fe–Ni alloy dissolution are reported. Circulating autoclave studies were conducted at 200°C in 2 ppM Cl^- plus nominally O ppM O_2. Specimens showed more resistance to attack than in higher concentration tests. Scanning electron microscopic studies of corrosion of stressed Fe, Ni, and Type 304 stainless steel maintained at various potentials $MgCl_2$ are included and interpreted. Finally, the effect of solution analysis vs. direct current read-out techniques on the results from potentiostatic dissolution studies of Fe–Ni alloys in H_2SO_4 was determined. (auth)

42761 (RDT-F-3-3-T) ULTRASONIC EXAMINATION OF HEAVY STEEL FORGINGS (MODIFIED ASTM A388). (Division of Reactor Development and Technology (AEC), Washington, D. C.). Feb 1969. 7p. RSO.

A standard prescribing requirements for ultrasonic examination of heavy steel forgings (modified ASTM A388) for nuclear and associated applications is presented. (TSS)

42762 (RDT-F-7-1-T) CONTINUOUS IDENTIFICATION MARKING OF WROUGHT METAL PRODUCTS. (Division of Reactor Development and Technology (AEC), Washington, D. C.). 7 Sep 1967. 6p. RSO.

A standard prescribing requirements for continuous identification marking of wrought metal products for nuclear and associated applications is presented. (TSS)

42763 (RDT-M-1-2-T) STAINLESS STEEL WELDING RODS AND BARE ELECTRODES (ASME SFA-5.9 WITH ADDITIONAL REQUIREMENTS). (Division of Reactor Development and Technology (AEC), Washington, D. C.). Jul 1971. 11p. RSO.

A standard prescribing requirements for stainless steel welding rods and bare electrodes (ASTE SFA–5.9 with additional requirements) for nuclear and associated applications is presented. (TSS)

42764 (RDT-M-1-3-T) MILD STEEL COVERED ARC-WELDING ELECTRODES (MODIFIED ASTM A233). (Division of Reactor Development and Technology (AEC), Washington, D. C.). 14 Feb 1969. 4p. RSO.

A standard prescribing requirements for mild steel-covered welding electrodes (modified ASTM A233) for use in nuclear and associated applications is presented. (TSS)

42765 (RDT-M-1-4-T) LOW ALLOY STEEL COVERED ARC-WELDING ELECTRODES (MODIFIED ASTM A316). (Division of Reactor Development and Technology (AEC), Washington, D. C.). Feb 1969. 7p. RSO.

A standard prescribing requirements for low alloy steel covered arc welding electrodes (modified ASTM A316) for use in nuclear and associated applications is presented. (auth)

42766 (RDT-M-1-6-T) MILD STEEL ELECTRODES AND WELDING RODS FOR GAS–METAL–ARC WELDING (MODIFIED ASTM A559). (Division of Reactor Development and Technology (AEC), Washington, D. C.). 14 Feb 1969. 5p. RSO.

A standard prescribing requirements for mild steel electrodes and welding rods for gas-metal-arc welding (modified ASTM A55t for use in nuclear and associated applications is presented. (auth)

42767 (RDT-M-1-7-T) COPPER AND COPPER ALLOY ARC-WELDING ELECTRODES (MODIFIED ASTM B225). (Division of Reactor Development and Technology (AEC), Washington, D. C.). Feb 1969. 3p. RSO.

A standard prescribing requirements for copper and copper alloy arc-welding electrodes (modified ASTM B225) for nuclear and associated applications is presented. (TSS)

42768 (RDT-M-1-8-T) COPPER AND COPPER ALLOY WELDING RODS (MODIFIED ASTM B259). (Division of Reactor Development and Technology (AEC), Washington, D. C.). Feb 1969. 4p. RSO.

A standard prescribing requirements for copper and copper alloy welding rods (modified ASTM B259) for use in nuclear and associated applications is presented. (TSS)

42769 (RDT-M-1-9-T) BRAZING FILLER METAL (MODIFIED ASTM B260). (Division of Reactor Development and Technology (AEC), Washington, D. C.). Feb 1969. 2p. RSO.

A standard prescribing requirements for brazing filler metal (modified ASTM B260) for use in nuclear and associated applications is presented. (auth)

42770 (RDT-M-1-10-T) NICKEL AND NICKEL ALLOY COVERED WELDING ELECTRODES (MODIFIED ASTM B295). (Division of Reactor Development and Technology (AEC), Washington, D. C.). 14 Feb 1969. 4p. RSO.

A standard prescribing requirements for nickel and nickel alloy covered welding electrodes (modified ASTM B295) for use in nuclear and associated applications is presented. (auth)

42771 (RDT-M-1-11-T) NICKEL AND NICKEL-ALLOY BARE WELDING RODS AND ELECTRODES (MODIFIED ASTM B304). (Division of Reactor Development and Technology (AEC), Washington, D. C.). 14 Feb 1969. 4p. RSO.

A standard prescribing requirements for nickel and nickel alloy bare welding rods and electrodes (modified ASTM B304) for use in nuclear and associated applications is presented. (auth)

42772 (RDT-M-1-16-T) ZIRCONIUM AND ZIRCONIUM ALLOY BARE WELDING RODS (ASTM B351 WITH ADDITIONAL REQUIREMENTS). (Division of Reactor Development and Technology (AEC), Washington, D. C.). May 1970. 7p. RSO.

A standard prescribing requirements for zirconium and zirconium alloy bare welding rods (ASTM B351) for nuclear and associated applications is presented. (TSS)

42773 (RDT-M-2-1-T) CARBON STEEL FORGINGS (MODIFIED ASTM A105). (Division of Reactor Development and Technology (AEC), Washington, D. C.). Feb 1969. 17p. RSO.

A standard prescribing requirements for carbon steel forgings (modified ASTM A105) for nuclear and associated applications is presented. (TSS)

42774 (RDT-M-2-3-T) WROUGHT SEAMLESS CARBON STEEL WELDING FITTINGS (MODIFIED ASTM A234). (Division of Reactor Development and Technology (AEC), Washington, D. C.). 14 Feb 1969. 11p. RSO.

A standard prescribing requirements for wrought seamless carbon steel welding fittings (modified ASTM A234) for nuclear and associated applications is presented. (TSS)

42775 (RDT-M-2-4-T) ALLOY STEEL FORGINGS (MODIFIED ASTM A336). (Division of Reactor Development and Technology (AEC), Washington, D. C.). Feb 1969. 13p. RSO.

A standard prescribing requirements for alloy steel forgings (modified ASTM A336) for nuclear and associated applications is presented. (TSS)

42776 (RDT-M-2-5-T) FACTORY MADE WROUGHT AUSTENITIC STEEL WELDING FITTINGS (MODIFIED ASTM A403). (Division of Reactor Development and Technology (AEC), Washington, D. C.). 10 Feb 1969. 11p. RSO.

A standard prescribing requirements for factory-made wrought austenitic steel welding fittings (modified ASTM A403) for nuclear and associated applications is presented. (TSS)

42777 (RDT-M-2-6-T) LOW CARBON CHROMIUM STEEL FORGINGS (MODIFIED ASTM A473). (Division of Reactor Development and Technology (AEC), Washington, D. C.). Feb 1969. 8p. RSO.

A standard prescribing requirements for low carbon chromium steel forgings (modified ASTM A473) for nuclear and associated applications is presented. (TSS)

42778 (RDT-M-2-7-T) QUENCHED AND TEMPERED VACUUM TREATED CARBON AND ALLOY STEEL FORGINGS FOR PRESSURE VESSELS (MODIFIED ASTM A508). (Division of Reactor Development and Technology (AEC), Washington, D. C.). Feb 1969. 7p. RSO.

A standard prescribing requirements for quenched and tempered vacuum treated carbon and alloy steel forgings for pressure vessels (modified ASTM A508) for nuclear and associated applications is presented. (TSS)

42779 (RDT-M-3-1-T) SEAMLESS CARBON STEEL PIPE FOR HIGH-TEMPERATURE SERVICE (MODIFIED ASTM A106). (Division of Reactor Development and Technology (AEC), Washington, D. C.). 14 Feb 1969. 6p. RSO.

A standard prescribing requirements for seamless carbon steel pipe for high-temperature service (modified ASTM A106) for nuclear and associated applications is presented. (TSS)

42780 (RDT-M-3-2-T) STAINLESS AND ALLOY STEEL SEAMLESS TUBES (ASME SA-213 WITH ADDITIONAL REQUIREMENTS). (Division of Reactor Development and Technology (AEC), Washington, D. C.). Jul 1971. 11p. RSO.

A standard prescribing requirements for stainless and alloy steel seamless tubes (ASME SA-213 with additional requirements) for nuclear and associated applications is presented. (TSS)

42781 (RDT-M-3-3-T) SEAMLESS AUSTENITIC STAINLESS STEEL PIPE (MODIFIED ASTM A376). (Division of Reactor Development and Technology (AEC), Washington, D. C.). 13 Feb 1969. 12p. RSO.

A standard prescribing requirements for seamless austenitic stainless steel pipe (modified ASTM A376) for use in nuclear and associated applications is presented. (TSS)

42782 (RDT-M-3-4-T) SEAMLESS ANNEALED NICKEL–CHROMIUM–IRON AND NICKEL–IRON–CHROMIUM ALLOY CONDENSER AND HEAT EXCHANGER TUBES (MODIFIED ASTM B163). (Division of Reactor Development and Technology (AEC), Washington, D. C.). Feb 1969. 6p. RSO.

A standard prescribing requirements for seamless annealed nickel–chromium–iron and nickel–iron–chromium alloy condenser and heat exchanger tubes for nuclear and associated applications is presented. (auth)

42783 (RDT-M-3-5-T) WELDED AUSTENITIC STAINLESS STEEL TUBING (MODIFIED ASTM A249). (Division of Reactor Development and Technology (AEC), Washington, D. C.). May 1969. 11p. RSO.

A standard prescribing requirements for welded austenitic stainless steel tubing (modified ASTM A249) for nuclear and associated applications is presented. (TSS)

42784 (RDT-M-3-6-T) SEAMLESS AND WELDED AUSTENITIC STAINLESS STEEL PIPE (MODIFIED ASTM A312). (Division of Reactor Development and Technology (AEC), Washington, D. C.). May 1969. 11p. RSO.

A standard prescribing requirements for seamless and welded austenitic stainless steel pipe (modified ASTM A312) for nuclear and associated applications is presented. (TSS)

42785 (RDT-M-3-7-T) WELDED LARGE DIAMETER STAINLESS STEEL PIPE (MODIFIED ASTM A358). (Division of Reactor Development and Technology (AEC), Washington, D. C.). May 1969. 11p. RSO.

A standard prescribing requirements for welded large diameter stainless steel pipe (modified ASTM A358) for nuclear and associated applications is presented. (TSS)

42786 (RDT-M-3-8-T) ZIRCONIUM AND ZIRCONIUM ALLOY TUBES (ASTM B353 WITH ADDITIONAL REQUIREMENTS). (Division of Reactor Development and Technology (AEC), Washington, D. C.). May 1970. 9p. RSO.

A standard prescribing requirements for zirconium and zirconium alloy tubes (ASTM B353 with additional requirements) for nuclear and associated applications is presented. (TSS)

42787 (RDT-M-3-12-T) SEAMLESS FERRITIC ALLOY STEEL PIPE (MODIFIED ASTM A335). (Division of Reactor Development and Technology (AEC), Washington, D. C.). Feb 1969. 14p. RSO.

A standard prescribing requirements for seamless ferritic alloy steel pipe (modified ASTM A335) for nuclear and associated applications is presented. (TSS)

42788 (RDT-M-4-1-T) CARBON-STEEL CASTINGS SUITABLE FOR FUSION WELDING FOR HIGH-TEMPERATURE SERVICE (MODIFIED ASTM A216). (Division of Reactor Development and Technology (AEC), Washington, D. C.). 14 Feb 1969. 11p. RSO.

A standard prescribing requirements for carbon-steel castings suitable for fusion welding for high-temperature service (modified ASTM A216) for use in nuclear and associated applications is presented. (auth)

42789 (RDT-M-4-2-T) AUSTENITIC STAINLESS STEEL CASTINGS FOR HIGH-TEMPERATURE SERVICE (MODIFIED ASTM A351). (Division of Reactor Development and Technology (AEC), Washington, D. C.). 14 Feb 1969. 10p. RSO.

A standard prescribing requirements for austenitic stainless steel castings for high-temperature service (modified ASTM A351) for use in nuclear and associated applications is presented. (auth)

42790 (RDT-M-4-3-T) COBALT–CHROMIUM ALLOY CASTINGS, WEAR AND CORROSION RESISTANT. (Division of Reactor Development and Technology (AEC), Washington, D. C.). Feb 1969. 7p. RSO.

A standard prescribing requirements for wear and corrosion-resistant cobalt-chromium alloy castings for use in nuclear and associated applications is presented. (auth)

42791 (RDT-M-5-1-T) CHROMIUM AND CHROMIUM–NICKEL STAINLESS STEEL PLATE, SHEET, AND STRIP (MODIFIED ASTM A240). (Division of Reactor Development and Technology (AEC), Washington, D. C.). Feb 1969. 14p. RSO.

A standard prescribing requirements for chromium and chromium–nickel stainless steel plate, sheet, and strip (modified ASTM A240) for use in nuclear and associated applications is presented. (TSS)

42792 (RDT-M-5-2-T) CARBON STEEL PLATES FOR PRESSURE VESSELS FOR MODERATE AND LOWER-TEMPERATURE SERVICE (MODIFIED ASTM A516). (Division of Reactor Development and Technology (AEC), Washington, D. C.). 10 Jan 1968. 8p. RSO.

A standard prescribing requirements for carbon steel plates for pressure vessels for moderate and lower-temperature service (modified ASTM A516) for use in nuclear and associated applications is presented. (auth)

42793 (RDT-M-5-3-T) MANGANESE–MOLYBDENUM AND MANGANESE–MOLYBDENUM–NICKEL ALLOY STEEL PLATES, QUENCHED AND TEMPERED, FOR PRESSURE VESSELS (MODIFIED ASTM A533). (Division of Reactor Development and Technology (AEC), Washington, D. C.). 14 Feb 1969. 7p. RSO.

A standard prescribing requirements for manganese–molybdenum and manganese–molybdenum–nickel alloy steel plates for pressure vessels (modified ASTM A533) for use in nuclear and associated applications is presented. (TSS)

42794 (RDT-M-5-4-T) NICKEL–CHROMIUM–IRON ALLOY PLATE, SHEET, AND STRIP (MODIFIED ASTM B168). (Division of Reactor Development and Technology (AEC), Washington, D. C.). Feb 1969. 11p. RSO.

A standard prescribing requirements for nickel–chromium–iron alloy plates, sheets, and strips (modified ASTM B168) for nuclear and associated applications is presented. (TSS)

42795 (RDT-M-5-5-T) CHROMIUM–MOLYBDENUM ALLOY STEEL PLATES (MODIFIED ASTM A387). (Division of Reactor Development and Technology (AEC), Washington, D. C.). Feb 1969. 14p. RSO.

A standard prescribing requirements for chromium–molybdenum alloy steel plates (modified ASTM A387) for nuclear and associated applications is presented. (TSS)

42796 (RDT-M-5-6-T) ZIRCONIUM AND ZIRCONIUM ALLOY PLATE, SHEET, AND STRIP (ASTM B352 WITH ADDITIONAL REQUIREMENTS). (Division of Reactor Development and Technology (AEC), Washington, D. C.). May 1970. 8p. RSO.

A standard prescribing requirements for zirconium and zirconium alloy plate, sheet, and strip (ASTM B352 with additional requirements) for use in nuclear and associated applications is presented. (auth)

42797 (RDT-M-6-1-T) ALLOY STEEL BOLTING MATERIALS FOR LOW-TEMPERATURE SERVICE (MODIFIED ASTM A320). (Division of Reactor Development and Technology (AEC), Washington, D. C.). 14 Feb 1969. 10p. RSO.

A standard prescribing requirements for alloy steel bolting materials for low-temperature service (modified ASTM A320) for use in nuclear and associated applications is presented. (auth)

42798 (RDT-M-6-3-T) ALLOY STEEL BOLTING MATERIALS FOR HIGH-TEMPERATURE SERVICE (MODIFIED ASTM A193. (Division of Reactor Development and Technology (AEC), Washington, D. C.). 14 Feb 1969. 14p. RSO.

A standard prescribing requirements for alloy steel bolting material for high-temperature service (modified ASTM A193) for use in nuclear and associated applications is presented. (auth)

42799 (RDT-M-7-1-T) LOW CARBON CHROMIUM STEEL BARS (MODIFIED ASTM A276). (Division of Reactor Development and Technology (AEC), Washington, D. C.). Feb 1969. 8p. RSO.

XUM

A standard prescribing requirements for low carbon chromium steel bars (modified ASTM A276) for nuclear and associated applications is presented. (TSS)

42800 (RDT-M-10-1-T) ZIRCONIUM AND ZIRCONIUM ALLOY INGOTS (ASTM B350 WITH ADDITIONAL REQUIREMENTS). (Division of Reactor Development and Technology (AEC), Washington, D. C.). May 1970. 7p. RSO.

A standard prescribing requirements for zirconium and zirconium alloy ingots (ASTM B350 with additional requirements) for nuclear and associated applications is presented. (TSS)

42801 (RDT-M-13-1-T) REACTOR GRADE SODIUM-PURCHASE SPECIFICATIONS. (Division of Reactor Development and Technology (AEC), Washington, D. C.). Jun 1970. 7p. LMEC.

A standard prescribing requirements for reactor grade sodium-purchase specifications for use in nuclear and associated applications is presented. (TSS)

42802 CONFERENCE ON THE USE OF ZIRCONIUM ALLOYS IN NUCLEAR REACTORS, MARIANSKE LAZNE, CZECHOSLOVAKIA, OCTOBER 1–3, 1968. GENERAL PROCEEDINGS. Plzen, Czech.; Skoda Works (1968). 512p. (In several languages). (CONF-681086).

Twenty-six papers are included. A separate abstract was prepared for each. (J.G.B.)

For abstracts of individual papers see: 41755, 42807–42815, 42830, 42831, 42875–42882, 42897, 42898, 42927–42929, and 43010.

Corrosion and Erosion

Refer also to abstracts 41825 and 42930.

42803 (CEA-R-4103) STUDY OF OXIDATION RESISTANT ZIRCONIUM ALLOYS IN CARBON DIOXIDE AT HIGH TEMPERATURES. Darras, Raymond (Commissariat a l'Energie Atomique, Fontenay-aux-Roses (France). Centre d'Etudes Nucleaires). Mar 1971. 121p. (In French). Dep. NTIS (U. S. Sales Only).

Thesis. Submitted to Univ. of Paris, France.

A systematic investigation of zirconium alloys more resistant to oxidation than the base metal was performed by gravimetric and metallographic methods. Carbon dioxide under pressure was chosen as the corroding medium. Corrosion tests were performed during several thousand hours. Very few alloying elements were found to be effective in this respect, at least with the relatively low contents imposed. Only alloys with calcium, chromium, nickel, and especially copper were found to have good corrosion-resistant properties under the conditions considered. Zirconium–copper alloys were studied in more detail. Their optimum content in copper lies between 1.6 and 3 percent by weight. Oxide scales developed by those alloys were much more compact and less prone to cracking than in the case of pure zirconium or other alloys; consequently, oxidation kinetics remain nearly parabolic for long durations. Moreover, in the presence of moisture, these scales restrict largely the hydridation of the metal. (auth)

42804 (LMEC-71-1) LIQUID METAL ENGINEERING CENTER (LMEC) SEMIANNUAL TECHNICAL PROGRESS REPORT, JULY–DECEMBER 1970. (Atomics International, Canoga Park, Calif. Liquid Metal Engineering Center). Contract AT(04-3)-700. 113p. Dep. NTIS.

Results of research and test work are reported on Na-water reactions, operation of Na components test installation, operation of precision control and handling equipment in liquid Na, materials compatibility in Na, instrumentation, chemistry and metallurgy of materials used in Na, operation of Na-heated boilers, operation of intermediate heat exchangers, and operation of Na test loops. (J.R.D.)

42805 (N-71-20390) HYPERVELOCITY OXIDATION TESTS OF THORIA DISPERSED NICKEL–CHROMIUM ALLOYS. Centolanzi, Frank J. (National Aeronautics and Space Administration, Moffett Field, Calif. Ames Research Center). 11 Feb 1971. 52p. (NASA-TM-X-62015). NTIS.

Hypervelocity oxidation tests of thoria dispersed nickel–chromium alloys are described which are being considered for use on the space shuttle vehicle. Measurements of mass loss in both stagnation and wedge flows are presented, together with estimates of emissivity derived from radiometric measurements. The results of detailed metallurgical examination of the specimens are also shown. The results show that thoria dispersed nichrome (TD-NiCr) loses weight steadily with time in a hypervelocity environment. This loss of weight results in internal depletion of chromium accompanied by porosity. A modified alloy, containing aluminum and yttrium (TD-NiCrAlY), has superior oxidation resistance. Its emissivity, however, is considerably lower. (auth) (STAR)

42806 OXIDATION OF TANTALUM–NIOBIUM SINGLE CRYSTALS AND POLYCRYSTALS IN THE TEMPERATURE RANGE 850° TO 1050°C. Dooley, R. B.; stringer, J. (Univ. of Liverpool). J. Less-Common Metals; 24: No. 2, 139-57(Jun 1971).

Single crystals and polycrystals of three dilute tantalum–niobium alloys were oxidized in dry oxygen at approximately 740 torr in the temperature range 850 to 1050°C. Niobium reduces the linear oxidation rate at all temperatures. It appears to increase the thermal stability of the suboxide platelet phase, but also increases the scale plasticity, which leads to a decrease in the scale porosity associated with the suboxide platelets, thus decreasing the oxidation anisotropy of single crystals. The exfoliation failure over $\{100\}_{Ta}$ faces observed in pure tantalum at temperatures close to 1025°C is also eliminated. The scale exhibits a preferred orientation in the niobium-containing specimens, whereas the scale formed on pure tantalum appears to be random. The scale growing on pure tantalum consists of large columnar crystals at temperatures above 950°C, but on the alloys it appears to be fine-grained. A new failure mode is observed over the {100} faces at 950°C in the alloys, apparently due to decohesion at the metal/oxide interface. The effect increases with increasing niobium content and it is considered to be related to the preferred orientation in the scale. At higher temperatures the effect diminishes, probably due to the increasing scale plasticity. (auth)

42807 MEASURING OF THE SPEED OF CORROSION IN ZIRCONIUM ALLOYS USING THE METHOD OF POLARIZING RESISTANCE IN WATER PRESSURE LOOPS OF THE REACTOR. Beran, J.; Sulc, J.; Zajic, V. (Skoda Works, Plzen, Czech.). pp 25-36 of Conference on the Use of Zirconium Alloys in Nuclear Reactors. Plzen, Czech.; Skoda Works (1968).

From Conference on the use of zirconium alloys in nuclear reactors; Marianske Lazne, Czech. (1 Oct 1968).

Results of experiments are described which show that remote measurements of Zr-2.5% Nb alloy corrosion by polarization resistance may be applicable to in-pile water loops using parameters comparable to those found in the A1 reactor heavy water loop. In a loop test lasting 66½ hr, important data were acquired on corrosion behavior of Zr-2.5% Nb in flowing water. (J.R.D.)

42808 CORROSION OF ZIRCONIUM ALLOY SAMPLES IN 340°C CIRCULATING WATER BEFORE AND AFTER THE PERFORMANCE OF A DECONTAMINATION TREATMENT. Van Der Linde, A. (Reactor Centrum Nederland, Petten). pp 69-92 of Conference on the Use of Zirconium Alloys in Nuclear Reactors. Plzen, Czech.; Skoda Works (1968).

From Conference on the use of zirconium alloys in nuclear reactors; Marianske Lazne, Czech. (1 Oct 1968).

Results of out-of-pile corrosion testing of zirconium alloys are presented. It was found that the weight gain rates of Zircaloy-2 and Zircaloy-4 in 340°C, 0.1 to 0.2 ppM oxygen, circulating water show a +5% deviation for Zircaloy-4, but are in agreement with the weight gain rates as calculated using the oxidation relations derived from autoclave experiments. The influence of an alkaline-permanganate/oxalate-citrate two step decontamination treatment on post-transition weight gain rates is negligible. (auth)

42809 OXIDATION OF Zr–0.8 PERCENT Cu–0.8 PERCENT Mo ALLOY IN CARBON DIOXIDE. Mrkous, P.; Staif, M.; Benda, K. (Skoda Works, Plzen, Czech.). pp 151-72 of Conference on the Use of Zirconium Alloys in Nuclear Reactors. Plzen, Czech.; Skoda Works (1968).

From Conference on the use of zirconium alloys in nuclear reactors; Marianske Lazne, Czech. (1 Oct 1968).

Results of corrosion tests show that the oxidation of Zr–0.8 Cu–0.8 Mo alloy in CO_2 + 0.001% by weight of H_2O, p = 1 atm is controlled until film breakaway according to the parabolic hypothesis (n = 2 – 3). The stated activation power of oxidation Q_1 = 25.690 cal/mol corresponds to the activation power of diffusion oxygen by nonstoichiometric zirconium oxide Q_{D1} = 29.300 cal/mol. In temperature ranges used for corrosion tests there was a breakaway at t = 580 in 450 hours, at t = 650 in 220 hours, and at t = 700°C for 50 hours. The critical value of the weight increase varies in the limits of 3.2 to 4.2 mg/cm². The increased moisture CO_2 (0.1 weight percent of H_2O) has no substantial effect on oxidation rate. The penetration of oxygen into the basic material under the oxide layer is controlled by diffusion. At t = 650°C, a delay on a ternary curve at Hm = 625 was identified as corresponding to a phase of oxygen solid solution in Zr (alpha). Results of x-radiographic analyses and electron microscope diffraction studies proved that oxide layer is primarily monoclinic ZrO_2. The Cu and Mo content in oxide layer is lower than in basic material in which copper is not fully homogenously subdivided. At a distance of about 100 microns from the oxide layer (t = 650°)

a copper-enriched zone could be identified. The carbon content in oxide layer varies from 0.1 to 0.7%. The cracks in oxide layer are filled with carbon. (auth)

42810 INFLUENCE OF IMPURITIES AND STRUCTURE ON THE CORROSION OF ZIRCONIUM ALLOYS IN WATER AND STEAM AT HIGH TEMPERATURE. Blanchet, J.; Coriou, H.; Grall, L.; Olivier, P.; Pelras, M. (Centre d'Etudes Nucleaires de Saclay, Gif-sur-Yvette, France). pp 173-97 of Conference on the Use of Zirconium Alloys in Nuclear Reactors. Plzen, Czech.; Skoda Works (1968). (In French).

From Conference on the use of zirconium alloys in nuclear reactors; Marianske Lazne, Czech. (1 Oct 1968).

The ternary alloy Zr–1% Fe–1% Cu shows a satisfactory resistance to oxidation in steam at 500°C. Among the four experimental metallurgical states, the behavior of the annealed β state after tempering is unique. It has been shown that this treatment leads to an almost total solubility of the precipitates of the second phase; maintenance at 500°C during the steam exposure is equivalent to annealing, and produces a fine well-distributed precipitate. The structure thus obtained gives the alloy not only an excellent resistance to oxidation but also a relatively low ratio of hydridation. The diffusion of oxygen in the metal, although not negligible at 500°C, is still very low. It appears that the mechanisms of oxidation in steam at 500°C, in water at 360°C, and in steam at 400°C, are different, as is shown by results of a comparative study of the alloys under study with Zircaloy-2 in different media. It was shown that additions of niobium (0.2 to 1%) or of chromium (1%) to the ternary alloy Zr–1%Fe–1%Cu have deleterious effects on the resistance to oxidation of this alloy in superheated steam at 500°C. (tr-auth)

42811 CERTAIN CONCEPTS ON THE CORROSION MECHANISM OF ZIRCONIUM AND ITS ALLOYS. Parfenov, B. G.; Lupakov, I. S. (Kurchatov Inst. of Nuclear Energy, Moscow). pp 199-213 of Conference on the Use of Zirconium Alloys in Nuclear Reactors. Plzen, Czech.; Skoda Works (1968). (In Russian).

From Conference on the use of zirconium alloys in nuclear reactors; Marianske Lazne, Czech. (1 Oct 1968).

The oxidation of zirconium can be represented as the growth of a new oxide phase on an initial zirconium matrix. The crystal lattice of the new oxide is interlocked with the crystal lattice of the zirconium matrix. The protective deformed oxide film is deformed, and tends to go over into a stable, nondeformed modification. X-ray studies show that a black protective oxide film is monoclinic with lattice parameters a = 5.09, b = 5.24, and c = 5.34. After 830 hours the parameters are a = 5.11, b = 5.25, and c = 5.34; after 2500 hours the parameters have changed to a = 5.14, b = 5.25, and c = 5.32. The more brittle, friable oxide film has a white or grey color, and is nonprotective. Corrosion stability is noticeably enhanced by the use of cold plastic deformation which assures the presence of texture. Sharp edges or protuberances should be removed by etching. Addition of alloying elements can also increase the corrosion stability. It is necessary that the alloying element be completely soluble in the oxide, and form a solid substitution solution with the oxide. The formation of two independent oxides would lead to a decrease in protective properties. A study of ionic radii and lattice structures of the oxides shows that zirconium alloys containing niobium, iron, molybdenum, copper, vanadium, and chromium appear to be the most suitable for use at high temperatures. (TTT)

42812 ZIRCONIUM ALLOYS USED IN CARBON DIOXIDE AT HIGH TEMPERATURES. Darras, R.; Loriers, H.; Baque, P.; Berry, J. L. (Centre d'Etude de l'Energie Nucleaire de Saclay, Gif-sur-Yvette, France). pp 285-309 of Conference on the Use of Zirconium Alloys in Nuclear Reactors. Plzen, Czech.; Skoda Works (1968). (In French).

From Conference on the use of zirconium alloys in nuclear reactors; Marianske Lazne, Czech. (1 Oct 1968).

Zirconium–copper alloys containing 1.6 to 3% of copper are less oxidizable than unalloyed zirconium or all other experimental zirconium alloys previously studied. The role of copper seems to be based on three principal factors. Of the copper in the zirconia formed, 0.15% is in a soluble form (solubility limits determined by specific experiments) resulting in a decrease in the coefficient of diffusion of oxygen in the zirconia. The remainder is in an insoluble form resulting in an improvement in the properties of the zirconia such as coefficient of expansion, plasticity, and sinterability. There is a boundary enriched in copper and oxygen at the metal–oxide interface which reduces the discontinuity, and thus the mechanical stresses, at this interface. The accumulation of copper at this interface is dependent on a decrease in the concentration of zirconium causing a slowing up of oxidation (which is produced at this level by the penetration of oxygen ions), the copper playing the role of an inert diluent. When the copper content of these alloys exceeds about 3%, the large excess in the zirconia cannot be distributed uniformly, and the continuity and homogeneity of the oxide layer is impaired weakening its protective character. Zirconium–copper alloys constitute an interesting solution for the cladding of uranium oxide fuel elements, functioning in the presence of carbon dioxide up to a surface temperature of about 600°C. Their performance can be further improved either by the addition of a third element or by suitable protective cladding. (tr-auth)

42813 CORROSION AND MECHANICAL PROPERTIES OF ZIRCONIUM ALLOYS IN CARBON DIOXIDE. Zaimovskii, A. S.; Tsuprun, L. I.; Khaikovskii, A. A. (Kurchatov Inst. for Nuclear Power, Moscow). pp 351-68 of Conference on the Use of Zirconium Alloys in Nuclear Reactors. Plzen, Czech.; Skoda Works (1968). (In Russian).

From Conference on the use of zirconium alloys in nuclear reactors; Marianske Lazne, Czech. (1 Oct 1968).

Studies of a large group of ternary and multi-component zirconium alloys showed that Zr–Mo–Cu alloys (0.5 to 0.8 wt % copper, and 0.7 to 1.0 wt % molybdenum) possessed the best combination of corrosion resistance and required mechanical properties at 450 to 500°C in a carbon dioxide atmosphere. The thickness of the ZrO_2 film was 28 microns after 5000 hours exposure. The increase in alloy weight Δm as a function of temperature T(°K) at 300 to 500°C is given empirically as follows: $\lg \Delta m = 5.3 - (3030/T)$. Neutron irradiation leads to an increase in strength, and to a decrease in the plasticity of the alloy. The maximum decrease in plasticity (51%) and increase in strength (24%) is observed in annealed samples; the minimum decrease is noted in previously deformed samples. However, the absolute value of the residual plasticity after irradiation is lower, while the strength is higher in the deformed alloy. The change in mechanical properties depends to a small extent on the irradiation temperature from 100 to 300°C. The greatest changes in mechanical properties are observed at an integral dose of 2×10^{19} fast neutrons/cm^2. Radiation strengthening can be removed by annealing at 350 to 400°C for 3 hours. The plasticity in the alloy is also restored almost completely. This Zr–Mo–Cu alloy is suitable for use in a reactor cooled by carbon dioxide at temperatures up to 500°C. (TTT)

42814 CORROSION AND ELECTROCHEMICAL BEHAVIOR OF ZIRCONIUM ALLOY. Gerasimov, V. V.; Gromovoa, A. I.; Morozova, I. K.; Belous, V. A.; Ilyukhin, A. S. (Kurchatov Inst. for Nuclear Power, Moscow). pp 417-27 of Conference on the Use of Zirconium Alloys in Nuclear Reactors. Plzen, Czech.; Skoda Works (1968). (In Russian).

From Conference on the use of zirconium alloys in nuclear reactors; Marianske Lazne, Czech. (1 Oct 1968).

The corrosion rate from the gain in weight (g/m^2·hr) for a 1% Nb–Zr alloy at 300°C was found to be 0.012 for deaerated, deionized water at a pH of 7, 0.013 at a pH of 3 (HNO_3), 0.011 at a pH of 10 (NH_4OH), and 0.02 for deaerated deionized water containing 10 mg/l of fluoride ion. The passivation of zirconium or its alloys in water at high temperatures is ordinarily associated with the formation of an oxide film on the surface. A black film is protective, while a white friable film is non-protective. Hence the rates of the anode process in these two cases should be different. The anodic polarization rate increases with increasing rate of corrosion. An increase in anodic polarization was also noted while irradiating a zirconium alloy with thermal neutrons in a flux of 10^{12} neutrons/cm^2·sec. (TTT)

42815 INFLUENCE OF SURFACE TREATMENT ON THE CORROSION OF BINARY ZIRCONIUM ALLOYS IN HEAVY WATER UNDER PRESSURE AND IN SUPERHEATED STEAM AT TEMPERATURES. Warzee, M. (Serai, Brussels); Sonnen, C.; Vanleugenhaghe, C.; Berge, Ph. pp 485-512 of Conference on the Use of Zirconium Alloys in Nuclear Reactors. Plzen, Czech.; Skoda Works (1968). (In French).

From Conference on the use of zirconium alloys in nuclear reactors; Marianske Lazne, Czech. (1 Oct 1968).

This is a revised version of EURAEC–1894.

In the case of Zircaloy-2, the surface treatment can be considered as a factor of very secondary influence on its behavior in water or steam at high temperature. When this alloy is exposed to water or to superheated steam between 300 and 400°C, it is observed that the initial speed of oxidation is particularly sensitive to the chemical state of the surfaces. It appears, however, that an initial increase in the oxide layer, accelerated by certain surface treatments, is accompanied by a reduction in the rate of long-term corrosion in the pretransition period. These conclusions agree with those of Demant and Wanklyn (Corrosion 22: 60 (1966)). In the posttransition period the influence of the initial surface treatment is negligible. When the oxidation is carried out in superheated steam at 450°C, the effects of the chemical state of the surfaces is not involved under ordinary

XUM

conditions. Superficial cold-hammering has, in this case, minor effects on the kinetics of oxidation that can be neglected since the scaling of the oxide layers at the same time for all states of the surface. As for the parallel phenomenon of hydridation, it appears that electrolytic polishing would permit reduction of the quantity of hydrogen fixed in the water under pressure or in the superheated steam at 360°C. When the temperature of the superheated steam is raised to 450°C, this advantage disappears. The zirconium–2% chromium–0.16% iron alloy is oxidized considerably less than Zircaloy-2 in superheated steam at 450°C. For this alloy there is a definite advantage in electrolytic polishing over other methods of surface preparation. This advantage is not found in the rate of hydridation. The quantities of fixed hydrogen do not appear to be sensitive to the structural condition of the surface layers of the alloy, a strongly cold-hammered state favoring the capture of hydrogen. (tr-auth)

Preparation and Fabrication

Refer also to abstracts 42951 and 43467.

42816 (LA–4644) FABRICATION OF OWR GAMMA SHIELD ASSEMBLIES. Kirby, R. S.; Hanks, G. S. (Los Alamos Scientific Lab., N. Mex.). Jan 1971. Contract W-7405-eng-36. 12p. Dep. NTIS.

A procedure was developed for metallurgically bonding lead to 6061-T6 aluminum plates for use as gamma shields in the Omega West Reactor (OWR). The procedure used was to plate the 6061-T6 aluminum component with approximately 0.002 in. of silver then bake the assembly to remove volatiles and to diffusion bond the silver plating to the aluminum plates. The plated aluminum component and the lead component were then plated with approximately 0.002 in. of tin. The plates were assembled with the tin plated faces together then pressed at a temperature of 200°C and a load of 0.5 t/in.^{2}. Ultrasonic inspection of the bonded assemblies has indicated that nominally 95% of the surface area was bonded. (auth)

42817 (RDT-F-3-37-T) SPECIAL REQUIREMENTS FOR METAL PRODUCTS. (Division of Reactor Development and Technology (AEC), Washington, D. C.). Jul 1971. 44p. RSO.

This standard provides requirements for the manufacture, examination or test of metal products which, when specified by a referencing standard, this standard, or other ordering document, must be satisfied in addition to all other requirements for the material. Some of these must be performed due to requirements of the ASME Boiler and Pressure Vessel Code, Section III, Nuclear Power Plant Components (hereafter called the Code) or other RDT standard requirements. Others are stated for the convenience of the designer or user who may specify them for reasons not related to the Code. Information is included on: ductile-brittle transition and other mechanical test requirements; specimen and temperature condition standards for Charpy V-notch impact transition testing; nondestructive examination requirements; high neutron field applications; steel manufacturing process; P and S limitations; Co content limitations; grain size; extra low carbon grades, austenitic stainless steel; and welding materials qualification requirements. 13 referenced documents are listed. (L.C.L.)

42818 SINTERING OF INTERMETALLIC COMPOUNDS IN THE SYSTEMS Fe–Mo AND Fe–Cr. Pollanz, Herwig; Thuemmler, Fritz (Univ., Karlsruhe, Ger.). Phys. Sintering; 3: No. 2, 85-107(May 1971).

Homogeneous and well-characterized powders were prepared from intermetallic phases and other compositions in the binary systems iron-molybdenum and iron-chromium. Isothermal sintering experiments with coarse powders resulted in a sintering behavior according to an exponential law with n = 0.43, in a temperature range between 1300 and 1500°C, for which a mechanism of volume diffusion played a dominant part. At lower temperatures lower exponents were observed. Fine powders sinter according to a logarithmic time law which appears in connection with grain growth occurring continuously. With decreasing particle size of the powders and depending on the material it becomes valid for the entire course of sintering. The intermetallic phases, which are stable during sintering conditions, show much less sinterability and higher activation energies than solid solutions and two phase compositions in the same binary system. This seems to be a consequence of their bonding state especially of the influence of directional, covalent bonding. From sintered material, strength values were determined which resulted in a minimum in the case of intermetallic phases. (auth)

42819 PROCESS TO OBTAIN OXIDE LAYERS ON ZIRCONIUM, HAFNIUM, AND THEIR ALLOYS. Loriers, Henri; Tissier, Jean-Claude (to Commissariat a l'Energie Atomique). French Patent 1,597,725. 29 Jun 1970. Filed 5 Dec 1968. (In French).

A method of obtaining oxide layers on pieces in zirconium, hafnium or their alloys is described. These oxide layers are obtained by heating the pieces in a carbon dioxide atmosphere at a temperature between 500 and 800°C for periods of 30 minutes to 100 hours. The oxide layer is between 1 and 50 microns thick. (auth) (France)

42820 FUNDAMENTAL INVESTIGATIONS ON SOLIDIFICATION STRUCTURE IN WELD METAL. Senda, Tomio; Matsuda, Fukuhisa; Kato, Mitsuaki (Osaka Univ.). Technol. Rep. Osaka Univ.; 20: No. 932-972, 527-58(Oct 1970).

Fundamental observations on the change in the weld structure and discussions on the mechanism of weld metal solidification are presented from the viewpoint of modern solidification theory. Bead-on-plate welding, in which the bead width at the back side of the sheet is almost the same as on the top side, was carried out with a tungsten arc under pure argon of one atmosphere in a chamber which was initially evacuated to 10^{-3} torr vacuum with 1-mm-thick electron beam-melted pure and commercially pure niobium, commercially pure tantalum, zirconium, titanium, nickel, copper and aluminum, and stainless steel, carbon steel and Monel alloy metals. Investigations were made on the epitaxial growth and grain size of columnar crystal at the fusion boundary. Moreover, the structural changes in the weld bead were observed on unpolished and polished surfaces macro- and microscopically. Also, the crystallization rate of columnar grains in weld bead of each metal was measured for the different welding speeds and the concept of the maximum crystallization rate (MCR) was also introduced. Lastly, an example of the extent of constitutional supercooling was calculated and discussed for actual weld bead using the modern solidification theory. (auth)

42821 POLARIZATION OF A ZINC CATHODE DURING THORIUM PRECIPITATION FROM MOLTEN HALIDE SALTS. Kanashin, Yu. P.; Lebedev, V. A.; Nichkov, I. F.; Raspopin, S. P. (Ural Polytechnic Inst., Sverdlovsk, USSR). Izv. Vyssh. Ucheb. Zaved., Tsvet. Met.; No. 6, 101-5(1970). (In Russian).

The polarization of a liquid zinc cathode was studied in thorium-containing molten halide salts. Temperature and concentration were investigated as functions of limiting diffusion currents of Th^{4+} ions and also of limiting currents of melt-formation. Experiment showed that addition of fluoride ion to the NaCl/KCl melt shifted the discharge potential of Th^{4+} ions toward the negative. Thorium precipitation proceeded with greater polarization than in the pure chloride melts. (tr-auth)

42822 CONTROL ROD FABRICATION EXPERIMENTS. Dalmastri, B.; Fizzotti, C.; Lo Tenero, B. (CNEN, Rome). Com. Naz. Energ. Nucl., Notiz.; 16: No. 12, 61-7(Dec 1970). (In Italian).

Techniques were developed for the fabrication of two types of control rods: boron carbide rods and Ag–In–Cd rods. The techniques were described. (J.S.R.)

42823 MANUFACTURING OF VAPOR DEPOSITED REFRACTORY MATERIALS. Lorel, Roland (Societe Generale du Vide, Paris). Entropie; No. 37, 18-34(Jan-Feb 1971). (In French).

Equipment used in the experiments is described and the results obtained on the mechanical, physical, and thermal properties of the coatings are presented. The effects of the substrate temperature, and the total and partial gas pressures on the morphology of the deposit were investigated. An original method of obtaining W (110) layers is described; this method is particularly interesting for the manufacture of thermionic conversion emitters. (auth) (France)

42824 PREPARATION OF HIGH PURITY THORIUM AND THORIUM SINGLE CRYSTALS. Peterson, D. T.; Schmidt, F. A. (Ames Lab., Iowa). J. Less-Common Metals; 24: No. 2, 223-8(Jun 1971).

Ultrahigh purity thorium was prepared using electrotransport as the refining method. This metal has a total impurity content of less than 50 ppM and a resistance ratio of greater than 1000. A procedure was also developed by which single crystals of the high purity thorium could be prepared by repeated heating of the specimen through its alpha to beta phase transformation followed by prolonged heating just below the transformation temperature. (auth)

42825 PRODUCTION OF HIGH-QUALITY ZIRCONIUM CONCENTRATE. Doronin, N. A.; Komarov, O. K.; Ziv, E. F.; (and others) Tsvetn. Metal.; No. 1, 51-3(Jan 1971). (In Russian).

A method of reducing calcination in a flow of natural gas, followed by a magnetic separation step, is recommended for removing Ti and Fe oxides from a zirconium concentrate. The TiO_2 content was decreased from 8.4 to 1.2%, and the total Fe

dropped from 0.61 to 0.2%. A description of the bench-scale apparatus is given, and a flow sheet is suggested. (K.S.W.)

42826 INFLUENCE OF SILICON AND OTHER ELEMENTS IN CONTROLLING INTERPARTICLE FRICTION AND SINTERING OF BERYLLIUM POWDER. Butcher, J. W. (International Nickel Ltd., Birmingham, Eng.); Scott, V. D. Powder Met.; 14: No. 27, 1-21(Spring 1971).

The effect of small additions of activating elements such as silicon on the consolidation behavior of beryllium powder was investigated. Evidence was obtained that compacts of activated powder have more uniform high density than those produced from non-activated material. Studies carried out on prepared beryllium discs showed that silicon modifies the micro-structure of the surface layer of beryllium oxide and, in consequence, affects its sliding behavior and bonding characteristics. From these results a model is proposed to account for the observations made on both sintered and hot-pressed beryllium leading to the conclusion that, in addition to interparticle bonding, some measure of metal particle rearrangement is necessary for maximum densification. Activating elements may, in modifying the surface characteristics of the individual powder particles, assist in achieving an improved balance between particle sliding on the one hand and interparticle bonding on the other. In taking into account the bulk consolidation characteristics as well as the micromechanics of the process, the model also explains the observed influence of particle-size distribution on porosity in the compact. The extent to which friction and sliding can influence compaction was demonstrated by using a system of colored Plasticine balls to simulate individual powder particles. Analysis of the behavior of the Plasticine compacts substantiates the proposed model of the hot pressing of beryllium powder. (auth) (UK)

42827 FORM ROLLING COMPLEX CLOSE TOLERANCE SHAPES. Wassil, G. N.; Kelman, D. M.; Grider, E. E. (Engelhard Minerals and Chemicals Corp., Attleboro, Mass.). pp 221-32 of Materials Technology. I. New York; American Society of Mechanical Engineers (1970).

From second inter-american conference on materials technology; Mexico City, Mex. (24 Aug 1970). See CONF-700812.

Form rolling, a high yield, precision cold forming operation was successfully applied to the production of a myriad of material-shape combinations to close tolerance net shapes without machining. Design concepts using form rolled shapes benefited from the characteristics of the process. Long lengths are produced with metallurgically sound surfaces of aircraft quality finish. Dimensional accuracy and control of contour both within and between lengths are exceptional. Tooling surfaces are moving in conjunction with the workpiece, thereby reducing problems of tool wear and lubrication. The grain flow pattern is similar to that of a forging, eliminating end grain at the surface and yielding superior fatigue and impact properties. The process is applicable to most wrought metals and alloys including tool steels and the high strength high temperature superalloys; even titanium alloys exhibited a promising potential during development studies. Although a wide variety of shapes in a broad range of dimensions can be form rolled, material handling and equipment capacity are limiting factors. (auth)

42828 COMPARISON OF CONVENTIONAL AND HYDROSTATIC PRESSING OF METAL POWDERS. Gripshover, Paul J. (Battelle Memorial Inst., Columbus, Ohio). pp 520-4 of Materials Technology. I. New York; American Society of Mechanical Engineers (1970).

From second inter-american conference on materials technology; Mexico City, Mex. (24 Aug 1970). See CONF-700812.

The utilization of powder metallurgy as a fabrication and manufacturing technique is rapidly increasing. Powder metallurgy offers the opportunity to produce almost any configuration from any material with little or no subsequent machining. For conventional uniaxial die pressing, highly accurate powder preforms can be made. Gear, teeth, internal splines, and multilevel geometries can be made to exacting tolerances requiring no machining. However, uniaxial die pressing has several limitations for the process engineer: the geometry of the piece in question must be such that closed die pressing is possible; the length-to-diameter ratio of the component is very limited, normally to a maximum value of 1.5 to 1; the density of die pressings is not uniform; and die cost may be excessive for certain geometries and short runs of parts. The limitation of conventional die pressing can often be overcome by applying hydrostatic pressing techniques. Illustrations are provided which graphically demonstrate the basic differences between die and hydrostatic-pressing methods as well as their relative effects on the resulting microstructures, dimensional tolerances, and properties. The significant differences are that no die is required in hydrostatic pressing and pressure application is omnidirectional. Because of these two basic differences, any geometry can be prepared by hydrostatic pressing. Since die friction is eliminated, large length-to-diameter ratios can be pressed without failure, and uniform density can be achieved throughout the pressing. Hydrostatic pressing is particularly well suited for large components and those having high surface area-to-volume ratios such as hollow cylinders, cones. In such components, substantial, input-materials savings can be achieved when compared with many other fabrication approaches. Hydrostatic pressing has limitations. In general, only one surface can be pressed to finish size in complex pressings; some finish machining will be required on the other surfaces. Further, the production rates of components made by hydrostatic pressings are generally lower than those for conventional pressing and that naturally implies increased cost. (auth)

42829 FORGING OF POWDER METALLURGY PREFORMS. Hirschhorn, Joel S.; Bargainnier, Roger B. (Univ. of Wisconsin, Madison). pp 525-34 of Materials Technology. I. New York; American Society of Mechanical Engineers (1970).

From second inter-american conference on materials technology; Mexico City, Mex. (24 Aug 1970). See CONF-700812.

The forging of powder metallurgy preforms in closed dies is a relatively new technology, especially for ferrous materials. The best features of two established technologies are melded into a manufacturing process that offers increased design freedom and improved properties at reduced costs for a variety of engineering components. This review emphasizes a discussion of the unique technical and economic aspects of the process, the latitude of possible process variations, and the need for development work in potential problem areas. (auth)

42830 ELECTRON BEAM WELDING OF ZIRCALOY-2. Milosavljevic, D. (Boris Kidric Inst. of Nuclear Sciences, Belgrade). pp 369-90 of Conference on the Use of Zirconium Alloys in Nuclear Reactors. Plzen, Czech.; Skoda Works (1968).

From Conference on the use of zirconium alloys in nuclear reactors; Marianske Lazne, Czech. (1 Oct 1968).

Results of electron beam welding experiments are presented. It was found that the power used at a given moment and the welding rate have an effect on Zircaloy-2 weld depth, width of heat affected zone, and grain size. Optimum power and welding rates are given. (J.R.D.)

42831 ZIRCONIUM–NIOBIUM ALLOY WELDMENTS. Marquiardt, E. (Central Welding Inst., Halle, Ger.). pp 429-45 of Conference on the Use of Zirconium Alloys in Nuclear Reactors. Plzen, Czech.; Skoda Works (1968).

From Conference on the use of zirconium alloys in nuclear reactors; Marianske Lazne, Czech. (1 Oct 1968).

Optimum methods for welding Zr–Nb alloys are described. Information is included on choice of welding processes, welding technology and equipment, preweld treatments, use of spacing grids in welding, fuel element welding, and corrosion control. (J.R.D.)

42832 SPREADING OF ZIRCONIUM BETWEEN PARALLEL GRAPHITE PLATES. Kostikov, V. I.; Summ, B. D. Fiz. Khim. Obrab. Mater.; No. 2, 149-51(Mar-Apr 1971). (In Russian).

The kinetics of spreading of liquid Zr between parallel graphite plates was investigated. The temperature of the liquid Zr was maintained 20° above its mp (2060°C). The graphite plates were fine-grained with a porosity of about 20% of total volume and the gap between pores about 20 μ in all of the tests. It was found by experiment that the fused zirconium metal flowed in the form of two 5 μ-thick films, the radius of the wetted surface increasing as the square root of the time. (K.S.W.)

42833 INFLUENCE OF THE DEFORMATION RATE ON THE DEFORMABILITY OF Mo–0.5% Ti ALLOY. Sogrishin, Yu. P.; Mat'yazh, V. A.; Vitorskii, Ya. M.; Kuznetsova, A. S. Kuznechno–Shtampovochnoe Proizvod.; No. 11-12: 1-4(1969). (In Russian).

Results of studies are described which show that recrystallized Mo–0.5 Ti has a high degree of ductility at high temperatures and high deformation rates. An increase in the deformation rate from 0.2 to 20 m/sec is accompanied by deformation resistance during precipitation in the alloy at deformation rates of less than 1.2 m/sec. A decrease in deformation resistance is found in extruded cylindrical samples of precipitated alloy at deformation rates greater than 1.2 m/sec. The optimum temperature for high-speed deformation of the alloy in the temperature range examined is 900°C. Turbine blades of satisfactory quality were stamped from the alloy. (tr-auth)

42834 PREPARATION OF LANTHANIDE SINGLE CRYSTALS: PRASEODYMIUM, NEODYMIUM, AND LUTETIUM. Tonnies, J. J.;

XUM

Gschneider, K. A. Jr. (Ames Lab., Iowa). J. Cryst. Growth; 10: No. 1, 1-5(Jun 1971).

An experimental study has been made on three methods that could be used in preparing large single crystals, approximately 1.25 cm in diameter and length, of praseodymium, neodymium, and lutetium. The strain-anneal process with its variations has been successfully applied in preparing lutetium crystals. The electron-beam floating-zone technique and the crystallographic transformation method have shown the greatest promise for growing large praseodymium and neodymium single crystals. (auth)

42835 LOT CONTROL IN THE PRODUCTION OF URANIUM FUEL CORES. McCreery, Paul N. (National Lead Co. of Ohio, Cincinnati). pp 421-5 of Annual Technical Conference Transactions, 1969. Milwaukee; American Society for Quality Control, Inc. (1969).

From twenty-third annual technical conference of the American Society for Quality Control; Los Angeles, Calif. (5 May 1969). See CONF-690524.

The quality control program used in the production of uranium fuel cores at National Lead Company is described. Since the implementation of the controls described the identification and certification problems have been reduced to a very low level. (D.H.M.)

Properties Evaluations

Refer also to abstracts 41761, 41816, 41823, 41833, 42962, 42967, 42970, 42980, 43473, 43476, 43484, 43490, and 44087.

42836 (AD-715877) MECHANICAL-PROPERTY DATA, 38-6-44 TITANIUM ALLOY: AGED FORGING. (Battelle Memorial Inst., Columbus, Ohio). Sep 1970. Contract F33615-69-C-1115. 9p. NTIS.

38-6-44 alloy (3Al-8V-6Cr-4Mo-4Zr) is a new deep-hardening beta composition alloy. The large amount of beta stabilizing elements in this composition results in sluggish transformation characteristics that give deep hardening. The metallurgy of 38-6-44 alloy is similar to other beta alloys such that solution annealing retains the more ductile body-center-cubic beta phase at room temperature. The 6-inch by 6-inch billet used in this property survey was solution annealed at 1500°F for 15 minutes and air cooled, plus aging at 1050°F for four hours. (auth) (USGRDR)

42837 (AERE-R-6745) COMPARISON TESTS FOR EXTINGUISHING MEDIA ON METAL FIRES. Smith, A. J.; Lunney, A. J. (Atomic Energy Research Establishment, Harwell (England)). Apr 1971. 82p. Dep. NTIS (U. S. Sales Only). UK 60p.

A series of tests carried out to compare the effectiveness of various dry powders used in combating fires of magnesium, misch metal, sodium, and uranium is described. (auth) (UK)

42838 (CONF-710512-1) INVESTIGATION OF CRACKING IN NUCLEAR REACTOR PRIMARY PIPING SYSTEM. Burghard, H. C. Jr.; Lyle, F. F. Jr. (Southwest Research Inst., San Antonio, Tex. Dept. of Materials Engineering). 8 Feb 1971. Contract AT(11-1)-1228. 9p. (71-PVP-33).

From first national congress on pressure vessels and piping; San Francisco, Calif. (10 May 1971).

In October 1969 a leak occurred in a Type 304 stainless steel safe-end attached to a feedwater inlet nozzle on the primary piping system of the LaCrosse Boiling Water Reactor (LACBWR). A metallurgical investigation conducted on the failed safe-end and ten other stainless steel components removed from LACBWR is described. Nondestructive tests, a metallographic examination, accelerated corrosion tests, and chemical analyses were performed to determine the cause of the failure. The results of the investigation indicate that the failure was caused by intergranular stress-corrosion cracking resulting from a combination of: sensitization of the safe-end resulting from stress relieving the safe-end-to-nozzle weld; a corrosion reaction possibly sustained by reduction of cupric ions in the primary water; and tensile stresses in excess of the yield strength of Type 304 stainless steel imposed by a piping support failure early in the operation of the reactor. (auth)

42839 (CONF-710512-3) EXPERIMENTAL AND FINITE ELEMENT STRESS ANALYSIS OF A THIN-SHELL CYLINDER-TO-CYLINDER MODEL. Corum, J. M.; Bolt, S. E.; Greenstreet, W. L.; Gwaltney, R. C. (Oak Ridge National Lab., Tenn.). 10 Feb 1971. 15p. (71-PVP-36). ASME, New York $2.00.

From first national congress on pressure vessels and piping; San Francisco, Calif. (10 May 1971).

The first in a series of four thin-shell cylinder-to-cylinder models was tested and the experimentally determined elastic stress distributions were compared with theoretical predictions obtained from a thin-shell finite element analysis. The models in the series are idealized thin-shell structures consisting of two circular cylindrical shells intersecting at right angles. The cylinder of the model tested had an outside diameter of 10 in. and the nozzle had an outside diameter of 5 in. giving a d_0/D_0 ratio of $\frac{1}{2}$. For both cylinder and nozzle the outside diameter-to-thickness ratio was 100. Thirteen separate loading cases were analyzed. The experimental stress distributions for each loading were obtained using 322 three-gage strain rosettes located on the inner and outer surfaces. Comparisons of theory and experiment for all 13 loadings show reasonably good general agreement, and it is felt that the analysis would be satisfactory for most engineering purposes. (auth)

42840 (CONF-710512-4) FRACTURE OF STRUCTURAL METALS AS RELATED TO PRESSURE-VESSEL INTEGRITY AND IN-SERVICE MONITORING. Hartblower, C. E.; Crimmins, P. P. (Aerojet-General Corp., Sacramento, Calif.). 12 Feb 1971. 19p. (71-PVP-60). ASME, New York $2.00.

From first national congress on pressure vessels and piping; San Francisco, Calif. (10 May 1971).

Elastic waves emanating from a propagating crack are the basis for a new technique which is being used both in research on the mechanisms of subcritical crack growth and as a supplementary nondestructive test method for detection and location of growing cracks. If, during proof test or the first in-service application of load a system is used which is capable of detecting the elastic waves and incorporates a digital computer for quick analysis of the data, flaws that grow during a given load application can be both detected and located. Conventional NDI methods are then employed to determine the size and orientation of each flaw. If the defect appears innocuous in terms of the fracture toughness (critical crack size) of the host material, further proof testing or an additional period of service is allowed under surveillance of the monitoring system. Then, should the rate of crack growth increase or the characteristics of the elastic-wave emissions indicate the crack to be approaching critical dimensions the load is removed and the defect repaired. (auth)

42841 (CONF-710512-8) ANALYSIS OF RADIATION-INDUCED EMBRITTLEMENT GRADIENTS ON FRACTURE CHARACTERISTICS OF THICK-WALLED PRESSURE VESSEL STEELS. Loss, F. J.; Hawthorne, J. R.; Serpan, C. Z. Jr.; Puzak, P. P. (Naval Research Lab., Washington, D. C.). 28 Jan 1971. 9p. (71-PVP-7). ASME, New York $2.00.

From first national congress on pressure vessels and piping; San Francisco, Calif. (10 May 1971).

The fracture behavior of thick-walled nuclear vessels is considered for the case of a radiation-induced toughness gradient through the wall which characteristically results from neutron attenuation by the wall material itself. Fracture-safe design analyses based on linear elastic formulations or extrapolations of these formulations to the elastic-plastic regime are not sufficiently developed to characterize the integrated behavior of a wall whose toughness can range from brittle at the inner surface to highly ductile at the outer surface. Solutions to the problem in the foreseeable future will be obtained only by experimental means. The present approach uses the Fracture Analysis Diagram (FAD) together with a new interpretative method for fracture extension resistance based on modified dynamic tear specimens as the tools for gradient assessments. With these techniques the significance of the toughness gradient through the wall is assessed in terms of thick section mechanical constraint, and fracture characteristics of the complete wall are predicted. Characterization of a hypothetical 8-in. vessel wall is based on measured through-thickness fluence levels; this behavior is correlated with fracture toughness degradation for steels of varying sensitivity to irradiation using the FAD. This analysis indicates that major portions of the vessel wall remain above the FTE temperature, which dictates yield stress loading requirements for fracture, when the wall temperature is maintained at the limiting value, NDT + 60°F, for the inside surface. Fracture extension resistance measurements based on data from a 3-in. thick plate having a metallurgically induced toughness gradient suggest that nuclear vessels with analogous gradients will not fracture in an unstable fashion and will not generate missiles capable of breaching the containment system. Additional research is necessary to fully develop the approach for application to the individual reactor vessel. (auth)

42842 (CONF-710512-9) CREEP STRESS DISTRIBUTION IN LONG, CYLINDRICAL REACTOR PRESSURE VESSELS. Ma, B. M. (Ames Lab., Iowa). 4 Feb 1971. 10p. (71-PVP-29). ASME, New York $2.00.

From first national congress on pressure vessels and piping; San Francisco, Calif. (10 May 1971).

The stress, strain, and strain rate distributions in long, cylindrical pressure vessels of nuclear reactors under internal pressure and irradiation creep conditions are determined analytically. Equations for the creep strains, strain rates, and stresses of the pres-

sure vessel are derived. These equations obtained are based on the basic assumptions of isotropic, homogeneous, and constant-density material, zero axial strain and the distortion-energy principle. For purposes of comparison, the following computed results vary with the pressure vessel wall thickness and are shown by curves: elastic and plastic tangential stresses at the inside surface of the vessels; elastic and creep radial, tangential and axial stress distributions in the vessels; and creep strain and strain rate. In addition, the creep tangential stresses that vary with creep rate at the inside surface of the pressure vessels are also shown. In the creep analysis the power-function creep law was used. (auth)

42843 (CONF-710512-10) ANALYTICAL BASIS FOR NOTCH SHARPENING BY FATIGUE. Merkle, J. G. (Oak Ridge National Lab., Tenn.). 16 Feb 1971. 14p. (71-PVP-46). ASME, New York $2.00.

From first national congress on pressure vessels and piping; San Francisco, Calif. (10 May 1971).

An important problem in the design of large fracture test specimens is the development of a practical and reliable method for sharpening the machined notches that are used to cause fracture. While gross load cycling does not appear to be a feasible method for notch sharpening by fatigue, for large specimens, local load cycling does appear to be a feasible method. Local compressive stresses, applied to the notch faces only, for example by hydraulic pressure, can produce the same crack tip stress intensity factor that would be produced by an overall tensile stress of the same magnitude. Calculations are made to estimate the number of load cycles required to initiate flaw growth by fatigue at the base of a machined notch and the number of load cycles required to grow the flaw a given distance by fatigue. Experimental data were obtained which tend to verify the analysis and to support the feasibility of notch sharpening by fatigue using locally applied loads. (auth)

42844 (EURFNR-922) ROOM TEMPERATURE MECHANICAL PROPERTIES AND PRECIPITATION BEHAVIOUR OF STEEL X8CrNiMoVNb 1613 (4988), INCOLOY 800 AND INCONEL 718 AFTER ANNEALING IN CONTACT WITH UC AT 600°C TO 800°C. Stumpf, W. E.; Goetzmann, O. (Kernforschungszentrum, Karlsruhe (West Germany). Institut fuer Material- und Festkoerperforschung). Mar 1971. 66p. (KFK-1384). Dep. NTIS (U. S. Sales Only).

Work performed under United States–Euratom Fast Reactor Exchange Program.

The room temperature mechanical properties and the precipitation behavior was studied in tensile test specimens that had been annealed in UC powder (4.84% equivalent C) and in vacuum respectively, for times up to 1100 hours at 600, 700, and 800°C. An electron microscope technique was developed that made possible the examination of the reaction products in the alloys at the reaction interface. Steel 4988 showed a considerable decrease in mechanical strength, after annealing in UC, at all three temperatures. No carburization of the specimens was found, however, and the ductility remained unaffected. This behavior is caused by the partial dissolution of the NbC and V(CN) precipitates in the steel near the reaction interface. The room temperature strength properties of Incoloy 800 in the millannealed condition, after annealing in UC at 600°C, are decreased but the ductility is unaffected. At 700 and 800°C, in both the millannealed and in the solution treated condition, however, the strength properties were unaffected but the ductility was reduced by the UC. For both initial conditions, extensive precipitation of $M_{23}C_6$ is found near the reaction interface and in the solution treated condition enhanced precipitation of TiC also occurs after annealing in UC. After Inconel 718 was annealed in UC at 600°C no effect was found on the strength properties but the ductility was decreased to only a few percent elongation after 1100 hours. After annealing at 700°C the strength and ductility are decreased by the UC and at 800°C practically no effect on the yield strength, a decrease in tensile strength and a very small increase in ductility was found. At all three temperatures a M_6C phase is formed in the alloy at the reaction interface while, at the same time, the niobium-containing precipitates Ni_3(NbAlTi) and Ni_3Nb are dissolved, causing the observed effects on the mechanical properties. (auth)

42845 (GEAP-10236) FAILURE BEHAVIOR OF FLAWED CARBON STEEL PIPES AND FITTINGS. Reynolds, M. B. (General Electric Co., San Jose, Calif. Atomic Power Equipment Dept.). Oct 1970. Contract AT(04-3)-189. 36p. Dep. NTIS.

The pressure load limit for a cylindrical shell containing a flaw is a function of cylinder radius and wall thickness, flaw dimensions, and properties of the material. The strength of large diameter thin-wall cylinders of brittle material containing axial through-wall flaws can be predicted by linear elastic fracture mechanics if corrections for effect of curvature are made. Expressions to predict pressure load limits in more ductile materials become more empirical. Such expressions have been developed by several investigators. Pressure load limits for cylinders containing full-length, axial, part-through flaws can be predicted by equating the effective stress in the ligament at the base of the flaw to the plastic instability stress for the material. Load limits for cylinders having short part-through flaws are predicted from a failure diagram in which relative burst pressure is plotted against the reciprocal of flaw length. Results of hydrostatic tests at 60°F on flawed ASTM A 106B pipes in nominal diameters ranging from 4 to 12 inches are presented. Results of tests on pipes with axial through-wall flaws are compared with empirical equations. Results of burst tests on flawed tees and elbows are presented. (auth)

42846 (JAERI-13578) EVALUATION OF STAINLESS STEEL PIPE FOR CLADDING MATERIAL OF FAST REACTOR. Nagasaki, Ryukichi; Kawasaki, Satoru; (and others) (Japan Atomic Energy Research Inst., Tokai). May 1969. 44p. NTIS (U. S. Sales Only).

Mechanical and microstructural changes of AISI Type 316 stainless steel tubes by prolonged heating were studied. In highly cold-worked specimens, carbide precipitated on grain boundaries and in grains by heating increasing the tensile strength. Carbide preferentially precipitated on grain boundaries in less cold-worked specimens, and did not increase strength. Formation of δ phase by heating did not decrease tensile elongation behavior. Considerable decrease of elongation was observed when as-received specimens were tested at about 350°C, but it was increased by heating at 650°C for one day. This phenomenon is considered to be strain aging by interstitial solute atoms. (auth) (Japan)

42847 (ORNL-TM-3247) INTERPRETATIONS OF THE DROP WEIGHT TEST IN TERMS OF STRAIN TOLERANCE (GROSS STRAIN) AND FRACTURE MECHANICS. Merkle, J. G.; Kooistra, L. F.; Derby, R. W. (Oak Ridge National Lab., Tenn.). Jun 1971. Contract W-7405-eng-26. 57p. Dep. NTIS.

The NDT temperature of a material is defined as the test temperature above which a crack does not propagate completely across the tension face of a drop weight specimen from a notch in a brittle weld. For purposes of safety analysis, it is desirable to know the actual strain in a drop weight specimen that corresponds to NDT conditions. By means of an inelastic bending analysis it is shown that the maximum bending strain in a drop weight specimen loaded statically at the stop distance deflection, depends on the stress-strain curve of the material. The strain corresponding to NDT conditions increases as the strain hardening exponent decreases. For a mild steel the strain corresponding to NDT conditions is about 3.5%. For A533-B steel in its original condition the strain corresponding to NDT conditions is about 4.8%. An equation recently proposed by the Martin Marietta Corporation for estimating strain tolerance above the yield strain is examined. It is shown that this equation leads to the prediction that the transition temperature should vary linearly with the reciprocal square root of flaw size. (auth)

42848 (ORNL-TM-3313) DISCUSSION OF SwRI MODEL PARAMETRIC TESTS. Robinson, G. C. (Oak Ridge National Lab., Tenn.). Jun 1971. Contract W-7405-eng-26. 21p. Dep. NTIS.

One of the activities of the Heavy Section Steel Technology Program is the testing of large, flawed, 6-in.-thick specimens in tension, preferably representative of ordinary tensile specimen testing. The tests are being performed on a special, large, 15,000,000-lb capacity, wide, thin-plate, tensile testing machine. Although this machine is not ideally suited for testing of thick-plate specimens, the considerations of adaptability, availability, and economics dictated its employment, however, with some penalties. Adapting the machine for the testing of thick plates imposed a nonideal length confinement on the large, thick-plate specimen. Being forced to use a specimen with a shorter gage length than was deemed desirable created a distinct possibility that the data obtained in the test region could be biased by restraints from the nearby reinforced grip ends. A model parametric study of the effect of the specimen geometry on failure load was conducted to evaluate the degree of error introduced by this lack of gage length and to insure that the data from the full-scale series would be useful without more extensive investigations of the shape of the specimen, its length-to-width, and width-to-thickness ratios. The model parametric tests have substantiated the validity of the data from the full-scale tests now underway, but have also indicated that testing of specimens with larger width-to-thickness ratios will give nonrepresentative data. (auth)

42849 (RDT-F-6-1-T) WELDING. (Division of Reactor Development and Technology (AEC), Washington, D. C.). 10 Feb 1969. 127p. RSO.

XUM

A standard prescribing requirements for welding, examining, and testing of watercooled reactor coolant systems and liquid metal heat transfer systems for nuclear and associated applications is presented. (TSS)

42850 (RDT-F-6-5-T) WELDING QUALIFICATIONS (SUPPLEMENT TO ASME BOILER AND PRESSURE VESSEL CODE SECTION IX). (Division of Reactor Development and Technology (AEC), Washington, D. C.). Jul 1971. 41p. RSO.

A standard prescribing requirements for welding qualifications (supplement to ASME boiler and pressure vessel code Section IX) for nuclear and associated applications is presented. (TSS)

42851 (RFP-1703) MECHANICAL PROPERTIES OF URANIUM-BASE NIOBIUM ALLOYS. Jackson, Ross J.; Boland, Joseph F. (Dow Chemical Co., Golden, Colo. Rocky Flats Div.). 17 Jun 1971. Contract AT(29-1)-1106. 32p. Dep. NTIS.

Tensile properties of gamma-quenched and aged binary U-2, U-4, U-5, U-6, and U-8 wt % Nb alloys, and the ternary U-7.5 wt %-2.5 wt % Zr alloy are presented. Two hundred sixty-four different combinations of composition-time-temperature representing 527 tests are included. Impact properties of gamma-quenched and aged binary U-4 and U-6 wt % Nb alloys, and the ternary U-7.5 Nb-2.5 Zr alloy are presented. Thirty-six different combinations of composition-time-temperature representing 106 tests are included. (auth)

42852 EVALUATION OF RATE-CONTROLLING OBSTACLES FOR LOW-TEMPERATURE DEFORMATION OF ZIRCONIUM. Sastry, D. H.; Prasad, Y. V. R. K.; Vasu, K. I. (Indian Inst. of Science, Bangalore). J. Mater. Sci.; 6: No. 4, 332-41(Apr 1971).

The low-temperature plastic flow of alpha-zirconium was studied by employing constant-rate tensile tests and differential-stress creep experiments. The activation parameters, enthalpy and area, were obtained as a function of stress for pure, as well as commercial zirconium. The activation area is independent of grain size and purity and falls to about $9b^2$ at high stresses. The deformation mechanism below about 700°K is found to be controlled by a single thermally activated process, and not a two-stage activation mechanism. Several dislocation mechanisms are examined and it is concluded that overcoming the Peierls energy humps by the formation of kink pairs in a length of dislocation is the rate-controlling mechanism. The total energy needed to nucleate a double kink is about 0.8 eV in pure zirconium and 1 eV in commercial zirconium. (auth) (UK)

42853 HIGH-TEMPERATURE MATERIALS. Marmer, E. N.; Gurvich, O. S.; Mal'tseva, L. F. Holon, Israel; Freund Publishing House (1971). 293p.

Data are given on the high-temperature chemical, electrical, electronic, mechanical, optical, thermal, and vacuum properties of the major refractory metals, oxides, carbides, and graphite including; molybdenum, tungsten, rhenium, tantalum, niobium, refractory alloys, aluminum oxide, zirconium dioxide, magnesium oxide, beryllium oxide, and thorium oxide. The accurate measurement of high temperatures is described. (G.M.C.)

42854 INTERACTION OF CARBON WITH BORIDE COATINGS ON HIGH-MELTING METALS. Samsonov, G. V.; Zhunkovskii, G. L.; Evtushok, T. M. (Inst. of Problems of Materials Science, Kiev). Inorg. Mater. (USSR) (Engl. Transl.); 6: 1426-9 (Sep 1970).

Translated from Izv. Akad. Nauk SSSR, Neorg. Mater.; 6: 1617-21(Sep 1970).

The possibility of using diffusion boride layers on Nb, Ta, Mo, and W as barriers against carburization of the latter was investigated. The limiting temperatures of stability of the boride layers in contact with different carbon-containing media were found. The kinetics of interaction and the phase compositions of the reaction products of boride layers with metal substrates were studied. During annealing, the phase composition of the boride layers changes, and lower boride phases appear which are unstable with respect to carbon; the formation and rate of growth of these layers, respectively, determine the onset and rate of the process of interaction of a boride barrier layer with a carbon-containing medium. The use of boride layers as barriers is limited by the temperature at which they begin to interact with the metal substrate, as well as the temperature of onset of the interaction; the process kinetics are also crucial. The relation between the stabilities of boride barrier layers and the physical states of the substances with which they are in contact and the media in which the interaction takes place was established. (J.R.D.)

42855 PRECIPITATION AND INFLUENCE OF HYDRIDES IN ZIRCONIUM ALLOYS. Castaldelli, L.; Fizzotti, C.; Tinti, F. (CNEN, Rome). Com. Naz. Energ. Nucl., Notiz.; 16: No. 12, 53-60(Dec 1970). (In Italian).

The precipitation of zirconium hydride platelets in supersaturated solutions occurs preferentially along the grain boundaries; the orientation of the platelet is affected by the internal pressures, external stresses, and the texture of the matrix. The mechanical properties of the Zr alloys are altered according to the orientation and concentration of the platelets. Generally an embrittlement of the alloy occurs. (J.S.R.)

42856 PLASTIC DEFORMATION OF ZIRCONIUM SINGLE CRYSTALS. Akhtar, A.; Teghtsoonian, A. (Univ. of British Columbia, Vancouver). Acta Met.; 19: No. 7, 655-63(Jul 1971).

Single crystals of Zr up to 20 cm in length and containing as little as 120 ppM interstitial oxygen were grown from the melt. The deformation modes operative at various crystal orientations and the effect of purity, temperature, orientation, and strain rate, on the work hardening parameters were investigated. In prismatic slip, three stages of work hardening similar to those in the fcc crystals were identified. Stages I and II are associated with single and conjugate slip respectively, while dynamic recovery in stage III occurs due to cross slip from the prism to the basal plane. From the temperature and strain rate sensitivity of the stress at the onset of cross slip the stacking fault energy of Zr on the prism planes is calculated to be 56 ergs/cm^2. Transmission electron microscopy of deformed crystals was used to examine the dislocation structures. (auth)

42857 ANNEALING KINETICS OF SHOCK HARDENED PLUTONIUM-1 WT. PERCENT GALLIUM. Rafalski, A. L. (Dow Chemical Co., Golden, Colo.). Contract AT(29-1)-1106. J. Less-Common Metals; 24: No. 3, 328-32(Jul 1971).

Sheets of Pu-1% Ga were subjected to explosive shocks of ~90 ± 20 kbav, annealed at up to 425°C, and the hardness measured. The shock loading increased the hardness from 38.7 to 51.4 DPH, and a hardness traverse showed constant shock intensity through the sample. Annealing at 425°C did not remove all of the residual hardening; the fractional term $(1-r) = (H-H_0)/(H_s-H_0)$ leveled off at 0.2. Recrystallization did not occur. The annealing behavior is compared with that of rolled material and shocked iron. (D.L.C.)

42858 SEALED CONTAINER HAVING A ZIRCONIUM-TIN ALLOY GETTER. (to Westinghouse Electric Corp.). British Patent 1,224,152. 3 Mar 1971. Priority date 8 Jan 1968, United States.

A getter arrangement for use in adsorbing residual gases in hermetically sealed containers is described. The getter material is a binary Zr-Sn alloy containing 10 to 30 wt % Sn. A means of heating the alloy to temperatures ranging from 300 to 700°C and a method for maintaining a temperature gradient in the alloy are provided. (J.R.D.)

42859 ZIRCALOY FUEL CLADDING TUBES FOR NUCLEAR POWER GENERATION. THE COLLECTION OF DATA SHEET. Sumitomo Kinzoku; 22: No. 4, 581-8(Oct 1970). (In Japanese).

Information is presented on manufacturing processes and quality control methods, dimension of Zircaloy fuel cladding tubes, chemical composition of Zircaloy, properties of Zircaloy fuel cladding tubes, relations between oxygen content and tensile properties of Zircaloy fuel cladding tubes, and precipitation state of metal hydrides. A photograph taken using an electron microscope of hydride precipitated at a crystal grain boundary is included along with (0002) reflection pole figures of a cladding tube after working and annealing. (Japan)

42860 EFFECTS OF FABRICATION CONDITIONS ON MECHANICAL PROPERTIES OF ZIRCALOY TUBES FOR NUCLEAR FUEL CLADDING. Konishi, Takao; Matsuda, Katsuhiko (Sumitomo Metal Industries, Ltd., Amagasaki, Japan). Sumitomo Kinzoku; 23: No. 1, 40-8(Jan 1971). (In Japanese).

The effects of fabrication conditions on mechanical properties and related features of Zircaloy tubes for nuclear fuel cladding are discussed. Mechanical properties and related features of Zircaloy tubes are variable in wide range by controlling the fabrication conditions. In general, choice of the reducing process which would give large final reduction, large final Q value and large total Q value in cold working stage will yield versatile material that can meet varieties of specifications by varying the subsequent finishing process. An R_T value is newly defined. This value (analogous to the r value used in deep drawing of sheet) is considered to be an effective measure in discussing the mechanical properties and related features of Zircaloy tubes. (auth) (Japan)

42861 KILOCYCLE ACOUSTIC EMISSION DURING CREEP IN LEAD, ALUMINUM, AND CADMIUM. II. THEORETICAL. Siegel, E. J. (Michigan State Univ., East Lansing). Phys. Status Solidi (a); 5: No. 3, 607-15(16 Jun 1971).

The general mechanism-independent features of the Sedgwick theory of acoustic emission and the Gilman approach to microplasticity are used to analyze acoustic emission creep results. (auth)

42862 KILOCYCLE ACOUSTIC EMISSION DURING CREEP IN LEAD, ALUMINUM, AND CADMIUM. I. EXPERIMENTAL. Siegel, E. J. (Michigan State Univ., East Lansing). Phys. Status Solidi (a); 5: No. 3, 601-6(16 Jun 1971).

Acoustic emission in the 100- to 200-kHz frequency band during simple, axial tensile loading of polycrystalline lead, aluminum, and cadmium has been observed and a general correspondence and mirroring of the usual strain–time creep curve in the total cumulative counts–time curve at room temperature were found, both at constant load and during loading increments. Stress was not a constant in these experiments. (auth)

42863 MEASUREMENT OF CESIUM SORPTION ISOTHERMS IN LIQUID SODIUM. Cooper, M. H.; Taylor, G. R. (Westinghouse Electric Corp., Madison, Pa.). Nucl. Technol.; 12: No. 1, 83-92(Sep 1971).

Sorption isotherms at 300, 500, 750, and 1000°F for Cs in Na were measured on polished Ni, as-received Type 304 stainless steel, polished Type 304 stainless steel, oxidized Zr, and single crystal Al_2O_3 over Cs concentrations from 46 apM (atom parts per million) to 0.03 apM. Cs concentrations on specimen surfaces that had been equilibrated with the Na–Cs solution were determined using ^{137}Cs tracer. Cs sorption was reversible, increased with rising Cs concentrations, and decreased with higher temperatures. Ni and Al_2O_3 are superior as packing materials for Cs cold traps because of their higher sorption capacities at low Cs concentrations. (auth)

42864 THERMAL DIFFUSION OF OXYGEN IN Ta–O AND Nb–O SOLID SOLUTIONS. Lohnert, Wolfgang; Fromm, Eckehard (Max-Planck-Institut fuer Metallforschung, Stuttgart). Z. Metallk.; 62: No. 6, 457-63(Jun 1971). (In German).

Experiments on thermal migration of oxygen in tantalum and niobium, performed in a wide temperature and concentration range (800 to 1500°C, 0.3 to 2.5 at. % O) show that in the Ta–O system the heat of transport Q^+ changes from –2 to –20 kcal/mole O and depends strongly on temperature and concentration. In contrast to this, in the system Nb–O the heat of transport Q^+ is very small (about 0.1 kcal/mole O). (auth)

42865 SOME THEORETICAL ASPECTS OF THERMAL DIFFUSION IN INTERSTITIAL SOLID SOLUTIONS. Fromm, Eckehard; Lohnert, Wolfgang (Max-Planck-Institut fuer Metallforschung, Stuttgart). Z. Metallk.; 62: No. 6, 463-8(Jun 1971). (In German).

New results in the Ta–O system have proved that the heat of transport, Q^+, depends strongly on temperature and concentration. Therefore the interpretation of this term as a characteristic energy of the system, for example as part of the activation energy of diffusion, seems to be no longer reasonable and is discussed within the framework of the phenomenological theory. It can be shown that Q^+ can also be defined as the most important factor of material coefficients such as the electrical conductivity. In addition the experimental data on thermal diffusion in transition metals were discussed on the basis of a model assuming the interaction of dissolved atoms and electrons as driving force for thermal diffusion. (auth)

42866 COMPARATIVE CREEP-RUPTURE PROPERTIES OF TUNGSTEN–25 PERCENT RHENIUM CONSOLIDATED BY ARC-MELTING AND POWDER-METALLURGY TECHNIQUES. Stephenson, R. L. (Oak Ridge National Lab., Tenn.). J. Less-Common Metals; 24: No. 2, 173-82(Jun 1971).

The creep–rupture properties of W–25% Re materials consolidated by arc-melting and powder-metallurgy techniques were compared at 1650 and 2200°C for rupture times up to 1000 hr. At comparable stresses, powder-metallurgy material has a shorter rupture life and lower rupture ductility than arc-melted material. On the basis of secondary creep rate, powder-metallurgy material is weaker than arc-melted material at 1650°C but stronger at 2200°C. Optical and electron metallography showed that voids form at grain boundaries in both materials. In the powder-metallurgy material, grain boundaries appear to be immobile, and massive growth of voids initiates fracture with very little deformation. In the arc-melted material, grain boundaries appear to be mobile, and fracture seems to be forestalled by their ability to move. The relative creep rates can be explained on the basis of void growth and grain size. (auth)

42867 WELDING DEFECTS, THEIR ORIGIN AND EFFECT. Lundin, Carl D. (Univ. of Tennessee, Knoxville). pp 381-8 of Materials Technology. I. New York; American Society of Mechanical Engineers (1970).

From second inter-american conference on materials technology; Mexico City, Mex. (24 Aug 1970). See CONF-700812.

The results of investigations into discontinuity formation revealed that both liquation related hot cracking mechanisms and solid state hot cracking mechanisms may be operable depending upon the alloy system in question. A relationship between hot cracking and subsequent initiation of cold cracks from the hot cracks was confirmed in TZM alloy by fractographic techniques. A method of introducing discontinuities of known orientation into the fusion zone of electron beam welds was developed and the effect of the discontinuities produced was evaluated by tensile and short-time stress rupture testing. The materials studied included Inconel 600, Ni-200, Inconel X-750, 310 stainless steel, TZM, and CVD tungsten. (auth)

42868 DEVELOPING METAL: COBALT. Morral, F. R. (Cobalt Information Center, Columbus, Ohio). pp 472-9 of Materials Technology. I. New York; American Society of Mechanical Engineers (1970).

From second inter-american conference on materials technology; Mexico City, Mex. (24 Aug 1970). See CONF-700812.

The engineering properties of cobalt and cobalt alloys of particular concern to developing nations are presented. Cobalt additions that are made to many alloys and steels to impart specific properties are enumerated, with examples. Magnetic materials, hard-facing, wear-resistant, and cutting alloys, as well as alloys used in human implants (dental and surgical, among others) are discussed, in addition to steels. (auth)

42869 Ti–Be COMPOSITES PRODUCED BY THE CO-EXTRUSION OF POWDERS. Dull, Dennis L.; Kendall, E. George; Raymond, Louis (Aerospace Corp., El Segundo, Calif.). pp 535-40 of Materials Technology. I. New York; American Society of Mechanical Engineers (1970).

From second inter-american conference on materials technology; Mexico City, Mex. (24 Aug 1970). See CONF-700812.

A new family of Ti-Be co-extruded powder metal composites can be added to the inventory of high specific strength/modulus fracture resistant materials for weight-critical design applications. Preliminary experimental data show that these two highly reactive metals can be consolidated into a composite with a microstructure that cannot be developed by conventional melting practices. Microprobe analysis and x-ray diffraction showed that no detrimental beryllides were formed during processing. Potentially, this new system could compare to the Al-50 vol % B composites. Currently, a composite with the modulus of steel (28.7×10^6 lb/in.^{2}) and the density of aluminum (0.10 lb/in.^{3}) is commercially available. These composites are stable to 1000°F. (auth)

42870 X-RAY STUDY OF COLD-WORK AND RECOVERY IN TUNGSTEN. Gupta, R. K.; Anantharaman, T. R. (Banaras Hindu Univ., India). Curr. Sci. (India); 40: No. 12, 307-9(20 Jun 1971).

X-ray line broadening in freshly cold-worked and partially annealed tungsten filings was subjected to Fourier analysis. Values of small domain size, microstrains and dislocation densities were estimated. Annealing for an hour at 300°C was shown to reduce the dislocation density in the filings from 3.30×10^{11} to 1.68×10^{11} cm/cm^3. The flow stresses estimated from dislocation densities at different temperatures were found to approximate the measured yield stress values for an annealed sample extrapolated to an extremely high strain rate. (auth)

42871 EFFECT OF HYDROGEN ON THE DUCTILE PROPERTIES OF IRRADIATED PRESSURE VESSEL STEELS. Brinkman, C. R.; Beeston, J. M. (Idaho Nuclear Corp., Idaho Falls). Contract AT(10-1)-1230. ASTM (Amer. Soc. Test. Mater.) Spec. Tech. Publ.; No. 484, 42-72(1970).

From Symposium on irradiation effects on structural alloys for nuclear reactor applications; Niagara Falls, Canada (Jun-Jul 1970). See ASTM-STP-484; CONF-700630.

The influence of hydrogen on the mechanical properties (ductility, fracture strength, and tendency towards delayed failure) was investigated for several irradiated pressure vessel steels. Included were ASTM A302B, A542, and HY-80 steel irradiated at fluences from 8×10^{18} to 4×10^{20} n/cm^2, E > 1 MeV. Specimens from plate sections of these steels which had been quenched and tempered and some from A542 which were given prestrain and heat treatment modifications were prepared and tested. The effects of strength level from irradiation, heat treatment, and microstructure were thus determined. Reductions in ductility and true fracture strength occurred with increasing hydrogen content but were not extensive at strength levels less than 180 ksi in specimens containing 1 to 2 ppM hydrogen. This concentration, however, produced a marked effect on the ductile properties when the strength level was increased by irradiation hardening or heat treatment beyond this threshold range. Irradiation hardening increased the

XUM

magnitude of the decrease in notched strength resulting from a given hydrogen content in all of the steels and conditions tested. Hydrogen induced delayed failure, however, did not occur to any large extent in HY-80, A302B, and A542 steel in the normal quenched and tempered condition even after irradiation to fluences in excess of 10^{20} n/cm^2, E > 1 MeV, and hydrogen concentrations of up to 4 ppM. (auth)

42872 EFFECTS OF HELIUM ON THE HIGH-TEMPERATURE DUCTILITY OF SANDVIK 12R72HV AND INCO IN-744X. Kramer, D. (Atomics International, Canoga Park, Calif.); Garr, K. R.; Rhodes, C. G.; Pard, A. G. Contract AT(04-3)-701. ASTM (Amer. Soc. Test. Mater.) Spec. Tech. Publ.; No. 484, 509-20(1970).

From Symposium on irradiation effects on structural alloys for nuclear reactor applications; Niagara Falls, Canada (Jun-Jul 1970). See ASTM-STP-484; CONF-700630.

Small tension specimens of Sandvik 12R72HV and Inco IN-744X were injected with helium by means of α particle irradiation from a cyclotron to produce approximately uniform concentrations of from 1×10^{-6} to 2.5×10^{-5} atom fraction. The specimens subsequently were tension tested in vacuum between 500 and 800°C. Sandvik 12R72HV is significantly more resistant to helium embrittlement than Type 304 or 316 stainless steel. Helium in Inco IN-744X has little effect on the superplastic behavior of this alloy. (auth)

42873 THERMAL EXPANSION OF A COPPER–TUNGSTEN COMPOSITE. Savchenko, B. I.; Ozhigov, L. S. Fiz. Khim. Obrab. Mater.; No. 2, 19-25(Mar-Apr 1971). (In Russian).

The effective coefficient of thermal expansion of a composite cylinder was investigated. An equation was developed which describes the strained state of the components of the system "cylindrical rod–jacket" possessing a durable adherence between the two. The system Cu–W is characterized by no mutual solubility nor chemical interaction; however, Cu does have the ability to wet W metal. The experimental unit was prepared by casting Cu at 1250°C in a Mo mold about a W wire in a vacuum and allowing it to cool slowly. Measurements made in a special dilatometer showed that the experimental coefficient of thermal expansion of the Cu–W system agreed with that calculated. Some discrepancy exists, however, between the calculated and measured temperatures of the elastic-plastic transition which is associated with the previously strained state of the components of the system. (K.S.W.)

42874 EXAMINATION OF WELDED JOINTS OF THE MOLYBDENUM ALLOY TZM-2A. Kantor, M. M.; Chernyshova, T. A.; Ignatov, D. V.; Shorshorov, M. Kh. Fiz. Khim. Obrab. Mater.; No. 2, 97-100(Mar-Apr 1971). (In Russian).

The TZM-2A alloy under investigation consisted primarily of Mo plus 0.015% Zr, 0.11% Ti, and 0.003% C. Electron microscope examination of an electric arc (continuous) weld revealed disintegration of the solid solution with separation of Mo_2C along the grain boundaries. The formation of a second phase depends upon the thermal cycle of the welding program. It is possible to inhibit the formation of this second phase by decreasing the chemical inhomogeneity of the weld metal by means of temperature cycle control or by aging at temperatures above that of phase separation. (K.S.W.)

42875 STUDIES OF THE INFLUENCE OF NITROGEN ON ALLOYS OF Zr–Cr–Fe TYPE. Delafosse, J.; Poeydomenge, P. (Commissariat a l'Energie Atomique, Saclay, France). pp 93-119 of Conference on the Use of Zirconium Alloys in Nuclear Reactors. Plzen, Czech.; Skoda Works (1968). (In French).

From Conference on the use of zirconium alloys in nuclear reactors; Marianske Lazne, Czech. (1 Oct 1968).

Alloys of the zirconium–chromium type are of interest for use in water-cooled nuclear reactors. The most advanced formula for alloys of this family (zirconium with additions of 1% chromium, 0.1% iron, and 0.5% tin) presents a group of properties which are superior to those of alloys of the Zircaloy-type (Zircaloy-2 and Zircaloy-4). These include greater resistance to oxidation than that of Zircaloy-2, lower ratio of absorption of hydrogen than that of Zircaloy-4 (greater resistance to hydridation), resistance to contamination by nitrogen analogous to that of Zircaloy-2, capability of transformation analogous to that of the Zircaloys, good weldability, good resistance to oxidation at the welds, and good mechanical properties. Furthermore, it appears that the addition of tin to the zirconium–1.15% chromium–0.1% tin alloy (Valoy) improves the resistance of this alloy to hydridation which would place the zirconium–chromium–iron–tin alloy at the head of all the alloys studied in France from this point of view. These qualities are such that these alloys are worth preparing in industrial quantities for the fabrication of parts going into a reactor. (tr-auth)

42876 STUDIES OF THE INFLUENCE OF SILICON ON THE ZIRCALOY-2 AND ZIRCALOY-4 ALLOYS. Delafosse, J.; Poeydomenge, P. (Commissariat a l'Energie Atomique, Saclay, France). pp 121-50 of Conference on the Use of Zirconium Alloys in Nuclear Reactors. Plzen, Czech.; Skoda Works (1968). (In French).

From Conference on the use of zirconium alloys in nuclear reactors; Marianske Lazne, Czech. (1 Oct 1968).

The addition of silicon to Zircaloy-2 and Zircaloy-4 in amounts up to 1200 ppM does not greatly change the characteristics of the material. The rates of oxidation in water at 310, 345, and 360°C are the same for Zircaloy-2 and Zircaloy-4 whatever the amounts of silicon from 400 to 1200 ppM; the rates of oxidation in steam at 400°C have a tendency to increase with the silicon content in Zircaloy-2 while they are less sensitive to the silicon content in Zircaloy-4; for Zircaloy-2 the absorption of hydrogen decreases when the silicon content increases (the absorption decreases from 59 to 43 ppM which corresponds to absorption ratios of 42 to 19%, respectively, when the silicon content increases from 400 to 1200 ppM), a phenomenon that is especially sensitive to steam and exists to a much less marked degree in water; and for Zircaloy-4 hydrogen remains at a low level and changes very little if the silicon content is between 0 and 1200 ppM while it has a tendency to increase for silicon contents greater than 800 ppM. (tr-auth)

42877 STUDIES OF THERMALLY-ACTIVATED DEFORMATION IN ZIRCONIUM. Craig, T.; Higgins, G. T. (Univ. of Liverpool). pp 215-28 of Conference on the Use of Zirconium Alloys in Nuclear Reactors. Plzen, Czech.; Skoda Works (1968).

From Conference on the use of zirconium alloys in nuclear reactors; Marianske Lazne, Czech. (1 Oct 1968).

Results of the studies show that polycrystalline zirconium alloys exhibit a discontinuity in the deformation behavior consistent with the operation of two rate controlling mechanisms, one below 300°K and the second above that temperature. The grain size contribution to the flow stress is oxygen dependent. Zircaloy 2 follows the behavior of a zirconium-1400 ppM oxygen alloy. The results are consistent with a model in which oxygen atoms are the rate controlling obstacles at low temperatures. At high temperatures the nonconservative movement of jogs on screw dislocations appears to be the most probable mechanism, but further work is required to resolve this point. After irradiation a discontinuous yield effect is evident. Activation volumes determined at strains beyond this range are identical to those found in unirradiated materials suggesting that the damage may be swept up by a channeling process during the early stages of deformation. (auth)

42878 STUDY OF THE PROPERTIES OF THE Zr–Cu–Mo ALLOYS. Filip, R.; Staif, M.; Velkoborsky, J. (Skoda Works, Plzen, Czech.). pp 229-54 of Conference on the Use of Zirconium Alloys in Nuclear Reactors. Plzen, Czech.; Skoda Works (1968).

From Conference on the use of zirconium alloys in nuclear reactors; Marianske Lazne, Czech. (1 Oct 1968).

A zirconium alloy of the Zr–Cu–Mo type selected for fabrication of the fuel elements for the Czechoslovak gas-cooled reactor was investigated. Fundamental studies were carried out to determine the behavior of the alloy under working conditions in connection with the fuel element fabrication. Information is included on alloy composition, microstructure, and effects of heat treatment. (J.R.D.)

42879 STUDIES OF STRUCTURE OF Zr–Cr ALLOYS. Demars, H.; Givord, J. P. (Ugine-Kuhlmann, Venthon, France). pp 255-76 of Conference on the Use of Zirconium Alloys in Nuclear Reactors. Plzen, Czech.; Skoda Works (1968). (In French).

From Conference on the use of zirconium alloys in nuclear reactors; Marianske Lazne, Czech. (1 Oct 1968).

Experiments are reported which constitute a contribution to the study of the behavior of Zr–Cr alloys that have been the object of considerable work already by Klepper and his associates. The experiments were conducted to show the effects of the oxygen and chromium contents on the choice of temperatures of treatment. These are not simple binary alloys, and the addition of a few hundred ppM of oxygen is sufficient to produce a transformation interval of 50 to 100°C even in the neighborhood of the eutectoid composition if it is about 1% Cr. Beyond this content the solubility limit, which already has increased very rapidly in the case of alloys that do not contain oxygen, is again raised by the presence of this element. The thermal treatments, associated with mechanical deformation or not, of hypereutectoid alloys in the region $\beta + ZrCr_2$ involves a rapid coalescence of the insoluble phase. It seems that a fairly large quantity of particles of $ZrCr_2$ thus coalesced would be very unfavorable to corrosion

by water or steam. The Zr–Cr alloys have, with respect to Zircaloy or Zr–Cu alloy, the important advantage of a much lower diffusion of Cr in the α region. If solution formation and tempering are properly controlled, it is possible to preserve fine-grain through the final stage of the transformation. It is under these conditions that the corrosion experiments give the best results. The small number of corrosion experiments carried out do not permit any conclusions on the effects of the addition of iron; many more experiments would be necessary to determine the optimum concentration. It appears that the corrosion results obtained on these alloys are more affected by variations in transformation conditions than by modifications in composition. (tr-auth)

42880 VARIATIONS OF THE MODULUS OF ELASTICITY FOR ZIRCALOY-2 AS A FUNCTION OF TEMPERATURE. Spasic, Z.; Pavlovic, M.; Simic, G. (Boris Kidric Inst. of Nuclear Sciences, Vinca, Yugoslavia). pp 277-84 of Conference on the Use of Zirconium Alloys in Nuclear Reactors. Plzen, Czech.; Skoda Works (1968). (In French).

From Conference on the use of zirconium alloys in nuclear reactors; Marianske Lazne, Czech. (1 Oct 1968).

A contribution to the systematic investigation of Zircaloy-2 is presented. It is a part of the studies that are required to complete a preliminary project on fuel elements. According to the results obtained it was verified that the curve $E = f(T)$ can be best expressed by an exponential relation of the form $E = 8.25\ E_0 T^{-0.369}$ (where E = modulus of elasticity and E_0 = modulus of elasticity at ambient temperature) for the temperature range $27°C \leq t \leq 400°C$. (tr-auth)

42881 ZIRCONIUM–COPPER ALLOYS USED IN FUEL ELEMENT CLADDING FOR GAS-COOLED HEAVY-WATER REACTORS. (Centre d'Etudes Nucleaires, Saclay, France). pp 329-43 of Conference on the Use of Zirconium Alloys in Nuclear Reactors. Plzen, Czech.; Skoda Works (1968). (In French).

From Conference on the use of zirconium alloys in nuclear reactors; Marianske Lazne, Czech. (1 Oct 1968).

Results of experiments carried out, especially in a reactor, show that it can be reasonably expected that zirconium–copper alloy can be used as a cladding material in CO_2 provided that the temperature does not exceed 600°C. Since the experiments in Pegase were not statistical in character, it was decided to start a larger program in the EL-4 reactor. One hundred zirconium–copper sheaths are being fabricated for the EL-4, two hundred will be made later, and, on the basis of the results of irradiation, it will eventually be possible to consider charging the whole reactor with elements clad with zirconium–copper instead of with stainless steel. (tr-auth)

42882 OBSERVATIONS ON THE ROLE OF HYDRIDE EMBRITTLEMENT IN A FAILURE OF A ZIRCALOY-2 CLAD FUEL ELEMENT. Estberg, Gustaf (Aktiebolaget Atomenergi, Stockholm). pp 345-9 of Conference on the Use of Zirconium Alloys in Nuclear Reactors. Plzen, Czech.; Skoda Works (1968).

From Conference on the use of zirconium alloys in nuclear reactors; Marianske Lazne, Czech. (1 Oct 1968).

A preliminary description of Zircaloy-2 fuel cladding failure in Halden BHWR is presented. It is thought that racheting occurred between the cladding and the fuel. Cracks that inevitably develop in the fuel imposed a heavy strain on the adjacent cladding resulting in failure. (J.R.D.)

Structure and Phase Studies

Refer also to abstracts 41777, 41778, 43475, and 43485.

42883 (IS-T-425) X-RAY DIFFRACTION STUDY OF THE YTTRIA–HAFNIA SYSTEM. Stacy, Denzil Wayne (Ames Lab., Iowa). Jun 1971. Contract W-7405-eng-82. 84p. Dep. NTIS.

Thesis.

Phase equilibria in the yttria–hafnia system were investigated by high temperature x-ray diffraction and by room temperature x-ray diffraction after fixed temperature anneals. The monoclinic-to-tetragonal phase transformation in hafnia was found to occur over the temperature interval 1750 to 1850°C on heating. The reverse reaction occurred from 1800 to 1550°C on cooling. At 1750°C, the tetragonal unit cell was found to be 2.7% smaller than the monoclinic unit cell. Under 2000°C, the solubility of yttria in hafnia is below 1 mole %. The fluorite domain extends from 7 to 53 mole % yttria at 1600°C and from 5 to 55 mole % yttria at 2000°C. A single phase domain of yttria solid solution exists above 73 mole % yttria at 1600 and 2000°C. The fluorite and yttria solid solution domains are separated by a two phase domain. The liquidus curve remains nearly at the melting point of hafnia (2825°C) up to 40 mole % yttria. Beyond, the liquidus decreases to a minimum of 2340°C at 85 mole % yttria and then increases to the melting point of yttria (2410°C). A tentative phase diagram of the yttria–hafnia system was proposed. The thermal expansion of yttria and several fluorite compositions was measured by high temperature x-ray diffraction. The mean thermal expansion coefficients of the fluorite compositions from 25 to 2000°C were found to be about 1.1×10^{-5} in./in.°C. The mean thermal expansion coefficient for yttria over the same temperature interval was found to be 9.3×10^{-6} in./in.°C. (auth)

42884 (JAERI-13731) RECRYSTALLIZATION OF VANADIUM-20 WT % TITANIUM ALLOY. Ogawa, Yutaka; Nagasaki, Ryukichi (Japan Atomic Energy Research Inst., Tokai). Sep 1969. 19p. NTIS (U.S. Sales Only).

The recrystallization of vanadium and its alloy containing 20% titanium was studied by hardness, x-ray diffraction, and optical and electron microscope. The materials were cold rolled 20 and 50% in reduction and annealed for 1 hr at temperatures from 500 to 1100°C. A decrease in hardness of the vanadium-20% titanium alloy occurred at temperatures from 600 to 700°C upon heating after the cold work and the hardness increased again at temperatures above 900°C, while in the pure vanadium the hardness decreased gradually in the temperature range from 600 to 1000°C. It was revealed from microscopic observations that recrystallization was complete at 900°C in both materials, only the pure vanadium began to recrystallize at 800°C. The dislocations in the vanadium-20% titanium alloy disappeared almost completely after the heating at 900°C, whereas in the pure vanadium retained locally in the form of stable networks. The dislocations structure was thought to result in the different softening behavior of the pure vanadium from that of the alloy on annealing at temperatures up to 900°C. Using an electron microscope, a banded structure that might arise from ordered state was observed in the pure vanadium specimen heated at 600°C and stacking fault appeared in the specimen heated at 1100°C. In the vanadium-20% titanium alloy precipitates were observed in the specimen heated at temperatures above 900°C; the increase in hardness in the alloy with heating at temperatures above 900°C was thought to be due to the precipitates. (auth)

42885 (JAERI-13764) RECRYSTALLIZATION OF Zr-2.5 WT % Nb ALLOY. Ogawa, Yutaka; Nagasaki, Ryukichi (Japan Atomic Energy Research Inst., Tokai). Oct. 1969. 21p. NTIS (U.S. Sales Only).

Recrystallization of Zr-2.5 % Nb alloy was studied by using hardness measurement, x-ray diffraction, specific heat measurement, and optical and electron microscopic techniques. After slow-cooling from 800°C, the alloy was cold-rolled 20, 60, and 80% in reduction and heated for 2 hr at 300 to 800°C. Recrystallization of water-quenched Zr-2.5% Nb alloy, Zr and Zircaloy-2 was also studied in relation to that of the slow-cooled Zr-2.5% Nb alloy. The recrystallization of the slow-cooled Zr-2.5% Nb alloy started at 550 and almost completed at 600°C. Grain growth was not observed in the slow-cooled Zr-2.5% Nb alloy on heating at 800°C, while grain growth occurred in Zr and Zircaloy-2 on heating at 800°C. In the slow-cooled Zr-2.5% Nb alloy, an increase in hardness occurred with heating at about 400°C and the hardness recovered at temperatures of 400 to 600°C. The increment of the hardness at about 400°C increased with the amount of reduction in cold-rolling. In the water-quenched Zr-2.5% Nb alloy, softening on heating appeared to be inhibited by cold-rolling. (auth)

42886 (UCRL–20500, pp 86-146) METALLURGY. (California Univ., Berkeley. Lawrence Radiation Lab.).

In Inorganic Materials Research Division annual report, 1970.

Activities in research programs are reported on crystal imperfections, kinetics of crystal dislocation mechanisms, relations of crystal structure with material properties, electron microscopy, properties of high-strength materials, high-field superconductivity, electric properties of solids, thermodynamics of metal systems, and properties of advanced materials. (J.R.D.)

42887 (Y-1785) IRON–NICKEL–TUNGSTEN PHASE DIAGRAM. Winslow, F. R. (Union Carbide Corp., Oak Ridge, Tenn. Y-12 Plant). 15 Jun 1971. Contract W-7405-eng-26. 21p. Dep. NTIS.

In a study of the properties of liquid-phase-sintered iron-nickel-tungsten alloys, the most probable phase diagram was drawn. The space diagram is shown as a series of isothermal sections between 1,650 and 800°C and a liquidus and solidus projection. (auth)

42888 CRYSTALLIZATION OF Ni–Ta AND Ni–Nb ALLOYS AT SUPERHIGH RATES OF COOLING. Varich, N. I.; Petrunina, A. N. (Daepropetrovsk State Univ., USSR). Fiz. Metal. Metalloved.; 31: No. 2, 447-8(Feb 1971). (In Russian).

The peculiarities of crystallization of the systems Ni–Ta and Ni–Nb were investigated at cooling rates of 10^7 to 10^8 degrees/sec. The latter effect was achieved by blowing a drop of the melt onto a rotating (8,000 rpm) Cu cylinder with a jet of helium gas. The composition ranges studied for the two systems

were 14.9 to 23.8 at. % Ta and 6.89 to 24.84 at. % Nb, respectively. In cooling melts representing the upper ranges of the two binary systems, intermetallic compounds separated out: the melt with 21.6 at. % Ta produced $TaNi_3$ and the melt with 24.84 at. % Nb produced $NbNi_3$. In the Ni–Ta system the region of α-solid solution extended to 17.3 or 19.5 at. % Ta, depending upon the initial temperature of the melt immediately before cooling. Crystal lattice constants, grain size, and the microstructure of the quenched alloy films were studied. (K.S.W.)

42889 TERNARY SYSTEM MOLYBDENUM–IRON–CARBON. Savitskii, E. M.; Zakharov, A. M.; Burkhanov, G. S.; Kataev, R. S. (Inst. of Metallurgy, Moscow). Izv. Vyssh. Ucheb. Zaved., Tsvet. Met.; No. 6, 113-15(1970). (In Russian).

Melting points and microhardness were determined and microscopic and x-ray phase analysis were made in a study of the molybdenum corner of the phase diagram for Mo–Fe–C at the temperature 1200 and 1800°C. Complex carbides were not detected in this corner which extended to 12% Fe and 0.6% C. Additions of Fe proved to have a noticeable effect on the solubility of C in Mo in the solid state by increasing that solubility as well as increasing the ductility of Mo. (K.S.W.)

42890 TERNARY SYSTEM MOLYBDENUM–TITANIUM–CARBON. Zakharov, A. M.; Novikov, I. I.; Parshikov, V. G. (Inst. of Steel and Alloys, Moscow). Izv. Vyssh. Ucheb. Zaved., Tsvet. Met.; No. 6, 106-12(1970). (In Russian).

The Mo corner of the phase diagram for Mo–Ti–C was studied up to 7% Ti and 0.86% C and at the isothermal cross sections 2100, 1800, 1500, and 1200°C. Over this range of temperatures Mo_2C is found in equilibrium with Mo and the δ-solid solution of chiefly TiC. The Mo–TiC section is characterized as quasibinary, a eutectic α + TiC melts at 2290°C. The carbide, TiC, exhibits a variable solubility in Mo in solid solution, decreasing with a decrease in temperature. At 2290°C the maximum solubility of TiC in Mo is about 3 wt %; this value decreases to 0.3 at 1200°C. (tr-auth)

42891 SYSTEMS Y–Al–Si (Ge,Sb) IN THE RANGE 0 TO 33.3 at. PERCENT Y. Murav'eva, A. A.; Zarechnyuk, O. S.; Gladyshevskii, E. I. (Lvov State Univ.). Inorg. Mater. (USSR) (Engl. Transl.); 7: No. 1, 34-6(Jan 1971).

Translated from Izv. Akad. Nauk SSSR, Neorg. Mater.; 7: No. 1, 38-40(Jan 1971).

Using x-ray phase analysis the systems Y–Al–Si and Y–Al–Ge were investigated in the concentration range 0 to 33.3 at. % Y, and the Al-rich alloys of the system Y–Al–Sb were studied. (auth)

42892 CRYSTAL STRUCTURE OF YbPt. Johnson, Quintin; Bedford, R. G.; Catalano, E. (Univ. of California, Livermore). J. Less-Common Metals; 24: No. 3, 335-6(Jul 1971).

YbPt was formed when YbF_2 and Pt were heated at 1230°C. X-ray diffraction powder patterns were indexed as orthorhombic with a = 6.805 ± 0.005, b = 4.416 ± 0.004, c = 5.492 ± 0.005 Å, and calculated density of 14.8 g/cm³. The structure is of the FeB type. (D.L.C.)

42893 CRYSTAL STRUCTURE OF PROMETHIUM. Pallmer, P. G.; Chikalla, T. D. (Battelle-Northwest, Richland, Wash.). Contract AT(45-1)-1830. J. Less-Common Metals; 24: No. 3, 233-6(Jul 1971).

The crystal structure of promethium was determined to be double hexagonal close packed with a = 3.65 ± 0.01 Å and c = 11.65 ± 0.09 Å. This leads to a calculated density of 7.26 g/cm³. No systematic effect of the ingrowth of the daughter samarium was noted on the cell parameters up to 15% Sm. The hardness of as-cast promethium metal was found to be 63 kg/mm². (auth)

42894 STRUCTURAL AND HIGH TEMPERATURE MAGNETIC STUDIES OF THE SYSTEMS $PrMn_2$–$GdMn_2$ AND $PrMn_2$–$TbMn_2$. Nair, Chitra; Oesterreicher, Hans (Oregon Graduate Center, Portland). J. Less-Common Metals; 24: No. 3, 237-42(Jul 1971).

Induction-melted and annealed specimens crystallize with a cubic-face-centered structure isotypical with Th_6Mn_{23}(G phase) from $PrMn_2$ to $Pr_{0.178}Gd_{0.155}Mn_{0.667}$ and $Pr_{0.173}Tb_{0.16}Mn_{0.667}$. $C_{15}GdMn_2$ and $TbMn_2$ dissolve about 2 mole % $PrMn_2$. The G-phase compounds are ferrimagnets at room temperature with saturation moments of about 1 μ_B per mole. Curie temperatures in the order of 450°K are followed by complex magnetic behavior up to 1000°K. (auth)

42895 RARE-EARTH SILICIDES AND GERMANIDES OF THE Mn_5Si_3 TYPE SUBSTITUTED BY EUROPIUM. Mayer, I.; Felner, I. (Hebrew Univ., Jerusalem). J. Less-Common Metals; 24: No. 3, 243-6(Jul 1971).

The substitution of europium atoms for other rare-earth metals in Ce_5Ge_3, Pr_5Ge_3, Gd_5Ge_3, and Gd_5Si_3 was studied. Results show that a maximum of one europium atom can be substituted in the above compounds without destroying their crystal structure. Crystal and ^{155}Gd Moessbauer measurements were used to study the effect of europium. (auth)

42896 QUANTITATIVE TRANSMISSION ELECTRON MICROSCOPY OF BUBBLES IN Al AND Al–Al_2O_3 ALLOYS. Ruedl, E. (CCR-EURATOM, Ispra, Italy). ASTM (Amer. Soc. Test. Mater.) Spec. Tech. Publ.; No. 484, 300-16(1970).

From Symposium on irradiation effects on structural alloys for nuclear reactor applications; Niagara Falls, Canada (Jun-Jul 1970). See ASTM-STP-484; CONF-700630.

The density and size distribution of small helium bubbles, present in thin foils of Al and Al–Al_2O_3 after alpha particle bombardment and postbombardment annealing, were measured by means of transmission electron microscopy. For making these measurements the conditions for visibility were first established by theoretical calculations of contrast for void sizes similar to those of the observed bubbles. Micrographs were then taken in suitable contrast conditions and the number and size of the bubbles measured on the micrographs. It was found that the density of small bubbles, present in the matrix, can be measured accurately. The density of small bubbles attached to particles, on the other hand, is difficult to measure. Furthermore, the size of very small bubbles is hard to determine with precision since it depends on different parameters. The size and shape of larger bubbles can be established by tilting and stereomicroscopy. (auth)

42897 CONTRIBUTION TO THE STUDY OF STRUCTURES AND PHASES OF ZIRCONIUM ALLOYS. Chmelo, P.; Pazitny, J. pp 391-400 of Conference on the Use of Zirconium Alloys in Nuclear Reactors. Plzen, Czech.; Skoda Works (1968).

From Conference on the use of zirconium alloys in nuclear reactors; Marianske Lazne, Czech. (1 Oct 1968).

Results of structural studies of Zr-base alloys containing 0.5% Mo and Cu are presented. Information is included on unequilibrated structure of Zr alloys, methods of establishing Zr alloy structures, identification of intermediate phases, and electrolytic isolation. (J.R.D.)

42898 CONTRIBUTION TO THE STUDY OF STRUCTURE AND PHASE OF ZIRCONIUM ALLOYS WITH Zu AND Mo. Bren, J. (State Research Inst. for the Protection of Material, Prague); Hodul, P. pp 401-16 of Conference on the Use of Zirconium Alloys in Nuclear Reactors. Plzen, Czech.; Skoda Works (1968).

From Conference on the use of zirconium alloys in nuclear reactors; Marianske Lazne, Czech. (1 Oct 1968).

The microstructure of Zr-base alloys containing 0.5% of Cu and Mo was examined. Information is included on use of these alloys in reactors, oxidation behavior, and alloy phases. (J.R.D.)

42899 EFFECT OF CARBON ON THE MECHANICAL PROPERTIES AND STRUCTURE OF MOLYBDENUM CRYSTALS. Kopetskii, Ch. V.; Orzhekhovskii, V. L.; Pashkovskii, A. I.; (and others). Fiz. Khim. Obrab. Mater.; No. 2, 67-74(Mar-Apr 1971). (In Russian).

The effect of carbon over the range 0.003 to 0.02 wt % on the mechanical properties and structure of Mo crystals was investigated. Mo crystals were purified by zone-melting, obtaining axial alignment of [110] and [100]. Annealing of the crystals was performed at 2100°C for 2 hr before they were subjected to elongation tests at 77 to 293°K. A decrease of the C content increased the plasticity of the Mo crystals, and decreased the yield limits notably at low temperatures. Decrease of the C content also resulted in more perfect Mo crystals and in a more uniform distribution of dislocations. It was confirmed that orientation of the axis of elongation strongly influenced the yield limits, the relative elongation, the relative constriction, and the character of disintegration of the Mo crystals. (K.S.W.)

Radiation Effects

Refer also to abstracts 41980, 43758, 44086, 44093, and 44116.

42900 (AD-719905) RADIATION-ENHANCED CREEP. Ashby, M. F. (Harvard Univ., Cambridge, Mass. Div. of Engineering and Applied Physics). Feb 1971. Contract N00014-67-A-0298-0020. 16p. (TR-4). NTIS.

A physical model for a mechanism by which a flux of neutrons can enhance the creep rate of a material leads to a creep rate which is linear in stress. The radiation-induced climb of dislocations or dislocation loops is biased by a small applied stress. At steady state, the density of climbing dislocations depends on the generation rate of point defects. The model leads to a creep rate which may be almost independent of temperature. (auth) (USGRDR)

42901 (HEDL-TME-71-76) FRACTURE AND TENSILE BEHAVIOR OF NEUTRON-IRRADIATED A533-B PRESSURE VESSEL STEEL. Hunter, C. W.; Williams, J. A. (Hanford

Engineering Development Lab., Richland, Wash.). 5 Feb 1971. Contract AT(45-1)-1830. 49p. Dep. NTIS.

The fracture potential of reactor pressure vessel materials can be evaluated in terms of critical fracture load-flaw size relationships by determining the linear elastic fracture mechanics K_{Ic} toughness properties. Irradiation of one-inch thick fracture mechanics specimens of A533 Grade B Class 1 steel to a fluence of 2×10^{19} n/cm^2 (E > 1 MeV) at 540°F produced a shift of 230°F in the 50,000 psi$\sqrt{\text{in.}}$ K_{Ic} level. The measurement capability of small fracture mechanics specimens is limited to regions of lower toughness. The difficulty of irradiating large specimens will normally preclude K_{Ic} determinations at higher toughness levels. Therefore, experimental correlations are needed between K_{Ic} and impact energy behavior of materials that exhibits a degraded upper shelf toughness. Irradiation at fluence levels of 2×10^{19} and 4.3×10^{19} produced a 45 and 54% increase, respectively, in the room temperature yield strength. Post-irradiation annealing of tensile specimens revealed that reduction of irradiation hardening commenced above 540°F and was 70% complete at 650°F. (auth)

42902 (JAERI-13692) EFFECT OF NEUTRON IRRADIATION ON THE PRECIPITATION-HARDENING OF Al–3.8% Cu ALLOY. Nagasaki, Ryukichi; Murata, Tomomi; (and others) (Japan Atomic Energy Research Inst., Tokai). Aug 1969. 23p. NTIS (U. S. Sales Only).

Hardness measurements and the transmission electron microscope were employed to study the effects of neutron irradiation on the precipitation-hardening in Al–3.8% Cu alloy. Specimens were irradiated at –130 and 130°C in JRR-2 to a total fluence of 1×10^{19} nvt (thermal) and 1×10^{17} nvt (fast), after different thermal treatments as-quenched and as-aged. It is concluded that vacancies generated by irradiation with neutrons can aid Guinier–Preston zone formation and formation of an Al–Cu intermetallic compound, but the defect distribution as obtained by quenching and cold working is different from that resulting from neutron irradiation. For the case of the present alloy, neutron irradiation gives rise to enhanced nucleation. (auth)

42903 (N–71-14040) EFFECT OF REACTOR IRRADIATION ON PROPERTIES OF A NONGALLING ALLOY. Hasse, Robert A. (National Aeronautics and Space Administration, Cleveland, Ohio. Lewis Research Center). Dec 1970. 33p. (NASA-TM-X–2144; E–5704). NTIS.

The effect of reactor irradiation on Waukesha Metal 88, a nongalling alloy, was determined at fast neutron fluences up to 1×10^{21} n/cm^2 (neutron energy > 1.0 MeV). Average specimen bulk temperature during irradiation was 355°K. The ultimate tensile strength increased by 120% and the 0.2% offset yield strength increased by 220%. The coefficient of sliding friction against Type 304 stainless steel was unaffected. The alloy swelled slightly during irradiation. Corrosion resistance of the alloy in contact with deionized water in-pile was good, although a slight susceptibility to crevice corrosion when mated with Type 304 stainless steel was noted. (auth) (STAR)

42904 INFLUENCE OF NEUTRON IRRADIATION ON THE GRAPHITIZATION OF UNALLOYED AND ALLOYED MALLEABLE CAST IRON. Mitter, Werner; Koss, Peter (Oesterreichische Studiengesellschaft fuer Atomenergie, Seibersdorf, Austria). Z. Metallk.; 62: No. 6, 482-7(Jun 1971). (In German).

The influence of fast neutron irradiation prior to heat treatment on the graphitization of unannealed malleable cast iron was investigated. Malleable cast iron of normal composition was investigated as well as material alloyed with manganese or chromium. In all cases the number of graphite precipitates in the irradiated samples was found to be higher than that in the samples that had not undergone the irradiation treatment. The only plausible explanation for this effect is the existence of depleted zones (Seeger zones), which are formed on irradiating the samples and which may act as graphitization centers. From this follows, among other things, the considerable importance of cavities on the atomic scale for the graphitization of white cast iron. (auth)

42905 RADIATION EFFECTS ON THE METALLURGICAL FRACTURE PARAMETERS AND FRACTURE TOUGHNESS OF PRESSURE VESSEL STEELS. Wullaert, R. A. (Effects Tech., Inc., Santa Barbara, Calif.); Ireland, D. R.; Tetelman, A. S. ASTM (Amer. Soc. Test. Mater.) Spec. Tech. Publ.; No. 484, 20-41(1970).

From Symposium on irradiation effects on structural alloys for nuclear reactor applications; Niagara Falls, Canada (Jun-Jul 1970). See ASTM-STP-484; CONF-700630.

The effect of radiation on tensile properties, notch bend properties, and fracture toughness was determined on A212B and A533B steel. Impact tests were performed on an instrumented Charpy machine which provided load-deflection data in addition to energy absorption data. Valid fracture toughness values were obtained from precracked Charpy specimens. The results of the notch bend tests on the irradiated steels indicated that the radiation induced increase in the ductile-brittle transition temperature was mainly due to the large radiation induced increase in the friction stress. Radiation reduced the strain rate sensitivity of the yield stress but did not change the temperature dependence of the yield stress. The microscopic cleavage strength was essentially unaffected by irradiation. The relationships between the metallurgical fracture parameters (Cottrell–Petch) and the ductile-brittle transition temperature and fracture toughness were established. These relationships were used to predict the radiation induced change in fracture toughness from a knowledge of the effect of radiation on metallurgical fracture parameters. (auth)

42906 EVALUATION OF THE EMBRITTLEMENT OF PRESSURE VESSEL STEELS IRRADIATED IN JPDR. Kawasaki, Masayuki (Japan Atomic Energy Research Inst., Tokyo); Fujimura, T.; Suzuki, K.; Namatame, H.; Kawasaki, Minoru ASTM (Amer. Soc. Test. Mater.) Spec. Tech. Publ.; No. 484, 74-95(1970).

From Symposium on irradiation effects on structural alloys for nuclear reactor applications; Niagara Falls, Canada (Jun-Jul 1970). See ASTM-STP-484; CONF-700630.

Three surveillance programs of the JPDR pressure vessel was performed to date. From the assessment of both the shift of NDT temperature and the reduction of upper shelf energy in the pressure vessel steel due to irradiation, it was concluded that the pressure vessel could be used with safety for about ten years at equivalent full power (45 MWt) operation. A reference test was also performed on two potential steels for pressure vessel use, namely a Mn–Mo–0.4 to 0.7 Ni steel (A533B Class 1) and a 2¼ Cr–1 Mo (A542 Class 1) steel, following the completion of the surveillance test. The latter steel was found to be much less sensitive to irradiation than the former. The weld metal and heat affected zone are somewhat more sensitive to irradiation than the base metal for the 2¼ Cr–1 Mo steel submerged arc weldment. (auth)

42907 DEMONSTRATION OF IMPROVED RADIATION EMBRITTLEMENT RESISTANCE OF A533B STEEL THROUGH CONTROL OF SELECTED RESIDUAL ELEMENTS. Hawthorne, J. R. (Naval Research Lab., Washington, D. C.). ASTM (Amer. Soc. Test. Mater.) Spec. Tech. Publ.; No. 484, 96-127(1970).

From Symposium on irradiation effects on structural alloys for nuclear reactor applications; Niagara Falls, Canada (Jun-Jul 1970). See ASTM-STP-484; CONF-700630.

A successful demonstration test of metallurgically controlled radiation embrittlement sensitivity was conducted with a large commercial melt of A533B steel. The 30-ton melt represents a scaleup from 300-lb laboratory melts which provided the first evidence of the potential for very low sensitivity to radiation embrittlement at power reactor pressure vessel service temperatures (~550°F). The primary objective of special melt specifications and melt planning was the reduction of copper and phosphorus contents to the lowest possible level. Restrictions were also imposed on the content of other residual impurity elements with known or suspected influences on radiation embrittlement resistance. For a broad experimental analysis, the melt was split to provide material representing the primary melt analysis (0.03% copper) and a melt modification (0.13% copper). Plates representing each analysis were also split and sections individually heat-treated to Class 1 or Class 2 strength conditions. All procedures used were standard mill practices. Radiation assessments showed the primary melt analysis to have very low sensitivity to radiation embrittlement at 550°F, thereby validating the composition specification approach for future melts. Transition temperature increases measured independently by Charpy V (Cv) and dynamic tear (DT) test methods were 70°F or less for fluences up to 3.1×10^{19} n/cm^2, E > 1 MeV. Based upon DT results, the nil ductility transition (NDT) temperature of the Class 1 plate remained below 75°F after 550°F irradiation. Results for the 0.13% copper melt modification provided direct confirmation of the primary, highly detrimental influence of copper content on radiation embrittlement resistance. The Cv 30 ft · lb transition temperature increases for the Class 1 and Class 2 plates were 140 and 125°F, respectively, for a fluence of 2.8×10^{19} n/cm^2, E > 1 MeV. The enhancement of radiation sensitivity by copper content appeared independent of the strength class. Postirradiation DT characteristics of the primary melt analysis (Class 1 plate) were indicative of excellent fracture resistance at shelf level temperatures. The A533B scaleup demonstration test fully supports the principles for control of radiation embrittlement sensitivity developed in laboratory research. A summary of 550°F radiation data for the ASTM A302B reference plate and A533 standard production plate and weld metals places the results for the special melt in full perspective. The radiation embrittlement sensitivity of the primary melt analysis is shown to be only one-third

XUM

that of the reference plate and significantly less than that of A533 production materials. (auth)

42908 NEUTRON IRRADIATION EFFECTS ON IRON CONTAINING ALUMINUM AND NITROGEN. Igata, N. (Tokyo Univ.); Hasiguti, R. R.; Yagi, E.; Nishiike, U.; Watanabe, K. ASTM (Amer. Soc. Test. Mater.) Spec. Tech. Publ.; No. 484, 128-41 (1970).

From Symposium on irradiation effects on structural alloys for nuclear reactor applications; Niagara Falls, Canada (Jun-Jul 1970). See ASTM-STP-484; CONF-700630.

Several authors have emphasized that aluminum nitride in iron and iron alloys not only lowers the transition temperature but also suppresses the rise of the transition temperature due to irradiation. To clarify the mechanism of the effect of aluminum nitride, structural changes after irradiation and annealing are observed by means of internal friction and electron microscopy. Materials investigated are iron, containing 0.05 wt % Al, 0.01 wt % N, <1 ppM C, and a few ppM O, and iron, containing 0.02 wt % Al, 0.005 wt % N, 10 ppM C and 20 ppM O. The materials are annealed at 750°C before irradiation and irradiated in the JRR-2 at temperatures of 60°C and up to 1.2×10^{19} n/cm^2, E > 1 MeV. Two new peaks in internal friction are found at ~125°C and ~155°C after irradiation. Besides these changes a new type of precipitate is observed by electron microscopy. These precipitates are thin, doughnut shaped disks with a diameter of 0.3 μm and are considered to be complex defects of irradiation induced point defects, nitrogen, and aluminum atoms. The 125°C peak of internal friction disappears after annealing at 250°C for 30 min; the 150°C peak disappears after annealing at 150°C for 30 min or aging at room temperature for about half a year. Resolution of free nitrogen is observed, but precipitates do not disappear even after annealing at 350°C for 30 min. The precipitates suppress the formation of irradiation induced complex nitrogen defects and irradiation hardening because of the strong effect of aluminum on nitrogen atoms. (auth)

42909 EFFECT OF FAST NEUTRON IRRADIATION ON THE MECHANICAL PROPERTIES OF SOME QUENCHED AND TEMPERED STEELS. Hosbons, R. R.; Wotton, B. L. (Chalk River Nuclear Labs., Ont.). ASTM (Amer. Soc. Test. Mater.) Spec. Tech. Publ.; No. 484, 142-63(1970).

From Symposium on irradiation effects on structural alloys for nuclear reactor applications; Niagara Falls, Canada (Jun-Jul 1970). See ASTM-STP-484; CONF-700630.

Specimens from seven heats of AISI 403, five heats of A542, and one heat of AISI 431 were irradiated at 300°C in pressurized water to find the effect of chemical composition on their irradiated properties. The change in ductile-brittle transition temperature ΔT after the maximum integrated fast neutron flux of 1×10^{20} n/cm^2, E > 1 MeV, was similar for these steels. Some of the heats were also tested after an integrated flux of 6×10^{19} n/cm^2, E > 1 MeV, and the results showed that the latter flux caused saturation of damage in AISI 403. The total impurity concentration of AISI 403 appeared to control the size of ΔT at saturation, but there was no such correlation in the other steels. Obversely, the nitrogen concentration of A542 did affect its change of transition temperature for a given flux; a titanium concentration of 0.1 wt % increased the unirradiated transition temperature but not ΔT. AISI 431 is unsuitable for use at 300°C as it is thermally embrittled. Although the ΔT values for AISI 403 and A542 were the same, the latter had a lower initial transition temperature. (auth)

42910 STRUCTURE AND COMPOSITION EFFECTS ON IRRADIATION SENSITIVITY OF PRESSURE VESSEL STEELS. Steele, L. E. (Naval Research Lab., Washington, D. C.). ASTM (Amer. Soc. Test. Mater.) Spec. Tech. Publ.; No. 484, 164-75(1970).

From Symposium on irradiation effects on structural alloys for nuclear reactor applications; Niagara Falls, Canada (Jun-Jul 1970). See ASTM-STP-484; CONF-700630.

Engineering implications of the effects of structure and composition on the irradiation sensitivity of steels are emphasized. Theoretical considerations are discussed and reviewed as they relate to possible explanations for observations on the subject. The structural aspects include primarily the type of metallurgical microstructure and the grain size and also the steel condition, that is, plate, forging, weld metal, or weld heat affected zone. The compositional factors are never quite separable from structural factors in a microscopic sense. Several interstitial elements, primarily nitrogen, carbon, oxygen, and hydrogen, were investigated for their relationship to neutron radiation sensitivity. Substitutional elements, including nickel, copper, phosphorus, vanadium, sulfur, and boron, as constituents in steels were also included. Copper and phosphorus are found particularly detrimental to radiation resistance when present in quantities above certain levels. (auth)

42911 EFFECTS OF IRRADIATION IN A THERMAL REACTOR ON THE TENSILE PROPERTIES OF ZIRCALOY 2 AND 4 AND BORATED STAINLESS STEEL. Baroch, C. J. (Babcock and Wilcox Co., Lynchburg, Va.); Munim, A. V.; Harbinson, E. N. ASTM (Amer. Soc. Test. Mater.) Spec. Tech. Publ.; No. 484, 176-93(1970).

From Symposium on irradiation effects on structural alloys for nuclear reactor applications; Niagara Falls, Canada (Jun-Jul 1970). See ASTM-STP-484; CONF-700630.

A series of tests were conducted to determine the effects of irradiation and thermal aging on the tensile properties of core structural materials used in a PWR. Type 304 stainless steel (containing about 250 ppM boron) and Zircaloy 2 specimens were obtained from the first core of the Consolidated Edison Indian Point reactor, and Zircaloy 4 specimens were irradiated in the Babcock & Wilcox test reactor. The Type 304 stainless steel cladding and the Zircaloy 2 channel from the Indian Point reactor had operated at about 600 and 525°F, respectively, and had achieved peak fluences of about 3×10^{21} n/cm^2, E > 1 MeV. The Zircaloy 4 specimens were irradiated at 130, 650, and 725°F to peak fluences of about 9×10^{20} n/cm^2, E > 1 MeV. The borated stainless steel specimens were tested at 70 to 1450°F. Some of the specimens were annealed at 1832°F for 1 hr to eliminate all displacement-type defects. Irradiation increased the strength of the cladding at test temperatures below 900°F, but it had little effect on the strength at higher test temperatures. At all test temperatures the ductility of the cladding was quite low—often less than 0.5%. Postirradiation annealing for 1 hr at 1832°F returned the strength to the unirradiated condition but had little effect on the ductility. Specimens obtained from both the longitudinal and transverse directions of the Zircaloy 2 channel were tested at 70, 525, and 750°F. At all test temperatures the ultimate and yield strengths increased with fluence up to the peak fluence achieved in the program. The uniform elongations were all 1% or less, regardless of fast fluence or specimen orientation. Zircaloy 4 ring specimens were tested at 900 to 1600°F. About half of the tension specimens were in the mill-annealed condition, and the remainder were cold-worked. At 1100°F and above the tensile properties of cold-worked and mill-annealed Zircaloy 4 were identical. At a test temperature of 900°F, irradiation caused some changes in the tensile properties of both materials. The extent of the effect of irradiation was dependent on the level of cold work and fluence. (auth)

42912 INFLUENCE OF IRRADIATION TEMPERATURE ON THE TENSILE PROPERTIES OF STAINLESS STEEL. Kangilaski, M. (Battelle Memorial Inst., Columbus, Ohio); Spretnak, J. W.; Bauer, A. A.; Wullaert, R. A. Contract W-7405-eng-92. ASTM (Amer. Soc. Test. Mater.) Spec. Tech. Publ.; No. 484, 194-214(1970).

From Symposium on irradiation effects on structural alloys for nuclear reactor applications; Niagara Falls, Canada (Jun-Jul 1970). See ASTM-STP-484; CONF-700630.

As an initial step in comparing the effects of irradiation in neutron spectrums characteristic of thermal and fast reactors, irradiations to establish the role of temperature on tensile property changes in the thermal reactor spectrum were undertaken. For this purpose specimens of Type 347 stainless steel were irradiated in the ETR at 400 and 650°C to a target fluence of 5×10^{21} n/cm^2. The results of this irradiation are reported and are compared with previous results for specimens irradiated to the same fluence at 50°C. (auth)

42913 EFFECT OF NEUTRON IRRADIATION ON THE MECHANICAL PROPERTIES OF ZIRCONIUM ALLOY FUEL CLADDING IN UNIAXIAL AND BIAXIAL TESTS. Hardy, D. G. (Chalk River Nuclear Labs., Ont.). ASTM (Amer. Soc. Test. Mater.) Spec. Tech. Publ.; No. 484, 215-58(1970).

From Symposium on irradiation effects on structural alloys for nuclear reactor applications; Niagara Falls, Canada (Jun-Jul 1970). See ASTM-STP-484; CONF-700630.

Short-time axial tension, transverse ring tension, and biaxial closed end burst tests were conducted on sections of fuel cladding from 17 different batches and heat treatments of Zircaloy 2, Zircaloy 4, and Zr-2.5 Nb alloy. Specimens were irradiated at 2 to 3×10^{20} n/cm^2, E > 1 MeV, at temperatures of 125 to 250°C and tested at temperatures of 20 and 300°C. The level of residual cold work was found to have the greatest effect on the mechanical properties of the Zircaloys prior to irradiation, and, although irradiation altered the general level of each property, the effect of cold work was preserved after irradiation for all properties except the uniform elongation. Very low values of uniform elongation (<1%) were obtained in the burst test after irradiation at all levels of cold work. In the instances where the texture and grain size influenced the properties, the effect was also preserved after irradiation. For the Zircaloys, the increment in the strength properties due to irradiation was constant at this fluence, independent of

cold work, texture, and grain size. The decrements in the uniform and total elongations due to irradiation decreased with increasing cold work. The irradiation hardening of the Zr–2.5 Nb alloy was greater than that experienced by the Zircaloys. Beta heat-treated Zircaloy had higher strength and lower ductility than alpha annealed material in the tension test. Grain size was found to have a much more significant effect on the strength and ductility in the burst and ring tests than in the axial tension test. (auth)

42914 METALLURGICAL PROPERTIES OF COLD-WORKED ZIRCALOY 2 PRESSURE TUBES IRRADIATED UNDER CANDU-PHW POWER REACTOR CONDITIONS. Langford, W. J. (Chalk River Nuclear Labs., Ont.). ASTM (Amer. Soc. Test. Mater.) Spec. Tech. Publ.; No. 484, 259-86(1970).

From Symposium on irradiation effects on structural alloys for nuclear reactor applications; Niagara Falls, Canada (Jun-Jul 1970). See ASTM-STP-484; CONF-700630.

The performance of cold-worked Zircaloy 2 reactor pressure tubes was assessed by destructive tests of tubes irradiated under CANDU-PHW power reactor conditions of temperature (240 to 280°C), stress (10,500 to 17,200 psi), and neutron irradiation. Reactor service increases biaxial burst strength, accompanied by a change in deformation mode that leads to reduced ductility after irradiation. Crack tolerance of the tubing is virtually unaffected by reactor service, and the critical crack length exceeds 3 in. (75 mm) at 16,000 psi (11.3 kg/mm^2) hoop stress and 300°C. Uniaxial tension tests indicate that operating stress reduces the transverse tensile strength of unirradiated tubing. Irradiation strengthening appears to be direction dependent, suggesting a possible influence of operating stress on the distribution of irradiation damage. Transmission electron microscopy shows the damage to be in the form of discrete dislocation loops. Oxidation rate in water is enhanced by neutron irradiation but is acceptably low, as is hydrogen/deuterium pickup. Diameter measurements support the evidence from in-pile creep investigations that creep rate partly depends on fast neutron flux. (auth)

42915 TEMPERATURE AND NEUTRON DOSE DEPENDENCE OF IRRADIATION GROWTH IN ZIRCALOY 2. Harbottle, J. E. (Central Electricity Generating Board, Berkeley, Eng.). ASTM (Amer. Soc. Test. Mater.) Spec. Tech. Publ.; No. 484, 287-99 (1970).

From Symposium on irradiation effects on structural alloys for nuclear reactor applications; Niagara Falls, Canada (Jun-Jul 1970). See ASTM-STP-484; CONF-700630.

Irradiation growth due to fast neutron bombardment was measured in textured Zircaloy 2 as a function of neutron dose (ϕt) and irradiation temperature. The growth strain ϵ obeys a relationship $\epsilon \propto (\phi t)^n$ over a temperature range −196 to 280°C and for doses up to 10^{21} n/cm^2. For irradiation temperatures up to 80°C, n = 0.4; but at 280°C, n = 0.7. The temperature dependence of irradiation growth in Zircaloy 2 is small, and in the temperature and dose ranges considered the growth strains do not differ by more than a factor of four. The growth rate $G \propto d\epsilon/d(\phi t)$ is initially large at low doses but approaches 1 at high doses (~10^{21} n/cm^2). (auth)

42916 MECHANISM AND KINETICS OF VOID GROWTH DURING NEUTRON IRRADIATION. Bullough, R.; Perrin, R. C. (Atomic Energy Research Establishment, Harwell, Eng.). ASTM (Amer. Soc. Test. Mater.) Spec. Tech. Publ.; No. 484, 317-31 (1970).

From Symposium on irradiation effects on structural alloys for nuclear reactor applications; Niagara Falls, Canada (Jun-Jul 1970). See ASTM-STP-484; CONF-700630.

A theoretical model is presented that is particularly appropriate for a study of void growth kinetics at high neutron doses. These kinetics are presented for peak swelling temperatures where recombination effects can be neglected; their dependence on dislocation density, void density, and dose rate is discussed. (auth)

42917 VOID FORMATION IN PROTON IRRADIATED STAINLESS STEEL. Keefer, D. W.; Neely, H. H.; Robinson, J. C.; Pard, A. G.; Kramer, D. (Atomics International, Canoga Park, Calif.). Contract AT(04-3)-701. ASTM (Amer. Soc. Test. Mater.) Spec. Tech. Publ.; No. 484, 332-46(1970).

From Symposium on irradiation effects on structural alloys for nuclear reactor applications; Niagara Falls, Canada (Jun-Jul 1970). See ASTM-STP-484; CONF-700630.

Voids were produced by 1.2-MeV proton irradiation at 500°C in Type 316 stainless steel containing 2 appM helium. The proton fluence was 6×10^{18} p/cm^2. Observations of electron microscope foils obtained at various positions along the proton path length showed that the volume swelling increased with increasing number of atom displacements. Calculated volume swelling ranged from 0.2 to 5%. In addition to voids, irradiation produced dislocation loops and small precipitate particles on dislocations were observed. (auth)

42918 CONSIDERATIONS OF METAL SWELLING AND RELATED PHENOMENA CAUSED BY FAST NEUTRON IRRADIATION. Li, Che-yu; Franklin, D. G.; Harkness, S. D. (Argonne National Lab., Ill.). ASTM (Amer. Soc. Test. Mater.) Spec. Tech. Publ.; No. 484, 347-61(1970).

From Symposium on irradiation effects on structural alloys for nuclear reactor applications; Niagara Falls, Canada (Jun-Jul 1970). See ASTM-STP-484; CONF-700630.

The existing analytical model that describes metal swelling under fast neutron irradiation is reviewed. The assumption of quasi-steady state and uniform point defect generation used in the present model is partially justified. Possible effects, due to microstructural defect interactions, that may occur at high fluences are discussed. The effect of stress field on point defect migration and its consequences on metal swelling and creep are considered. (auth)

42919 SOME OBSERVATIONS ON THE STRUCTURE AND TENSILE PROPERTIES OF AISI TYPE 316 STEEL AS A FUNCTION OF FAST REACTOR IRRADIATION TEMPERATURE. Barton, P. J.; Higgins, P. R. E. (Atomic Energy Research Establishment, Harwell, Eng.). ASTM (Amer. Soc. Test. Mater.) Spec. Tech. Publ.; No. 484, 362-74(1970).

From Symposium on irradiation effects on structural alloys for nuclear reactor applications; Niagara Falls, Canada (Jun-Jul 1970). See ASTM-STP-484; CONF-700630.

Solution treated AISI Type 316 steel strip specimens were irradiated in the Dounreay fast reactor to doses of 1.0 to 1.3×10^{22} n/cm^2 (total), 1.7 to 2.6×10^{21} n/cm^2 (fission) within the following measured temperature ranges: 420 to 440, 500 to 513, 520 to 533, 560 to 570, and 645 to 650°C. Transmission electron microscopy reveals the presence of voids after irradiation at all these temperatures. Distribution is uniform after irradiation at 420 to 440, 500 to 513, and 520 to 533°C. At higher temperatures it is uneven and concentration is so low that probably helium bubbles and not voids are being observed. From the temperature dependence of void concentration and average diameter it is deduced that the consequent density decrease is maximal after irradiation at 500 to 513°C. Dislocation loops are present for irradiation at all but the highest temperature. They are interstitial and lie on {111} planes with Burgers vectors of the type a/3 ⟨111⟩. At 420 to 440°C all loops are faulted. As irradiation temperature increases, loop concentration decreases, and at 520 to 533°C a few unfaulted loops are observed. Yield stress increases estimated from loop and void concentrations are found to be in fair agreement with measured values. (auth)

42920 HOW DO WE SOLVE THE VOID PROBLEMS? ASTM (Amer. Soc. Test. Mater.) Spec. Tech. Publ.; No. 484, 400-8(1970).

From Symposium on irradiation effects on structural alloys for nuclear reactor applications; Niagara Falls, Canada (Jun-Jul 1970). See ASTM-STP-484; CONF-700630.

A four-part discussion was conducted on how to solve the void problem. Swelling in irradiated metals and alloys is influenced by impurity content, cold work, temperature, fluence, and metallurgical structure. One solution to the problem may involve alloy composition modifications, heat treatment, mechanical working, or a combination of them, all of which are within present commercial capability. Theories on void formation are still in a state of flux. With more understanding of the phenomenon, a more realistic assessment of the consequences of the various simplifying assumptions will be possible and appropriate modifications will be made. The production of voids in stainless steel by charged particle irradiation has been demonstrated. (G.M.C.)

42921 AXIAL FATIGUE OF IRRADIATED STAINLESS STEELS TESTED AT ELEVATED TEMPERATURES. Beeston, J. M.; Brinkman, C. R. (Idaho Nuclear Corp., Idaho Falls). Contract AT(10-1)-1230. ASTM (Amer. Soc. Test. Mater.) Spec. Tech. Publ.; No. 484, 419-50(1970).

From Symposium on irradiation effects on structural alloys for nuclear reactor applications; Niagara Falls, Canada (Jun-Jul 1970). See ASTM-STP-484; CONF-700630.

Uniaxial fatigue properties from tests at 400 to 700°C on Type 304, 304L (Ti modified), and 316 stainless steel specimens irradiated at 450°C in sodium and 750°C in argon at fluences of 0.03 to 9.3×10^{21} n/cm^2, E > 0.1 MeV, are given and compared with control specimens. Material was tested in the annealed, cold-worked, and chilled-swaged-tempered condition, while primary controls received a pretest anneal of 1500 hr at 750°C. The data at 400, 500, and 600°C are compared with proposed design curves for 18-8 steels. Some data on microstructural changes due to irradiation are given. A reduction in the fatigue life by a factor of less than 2.5 was found in the annealed material, which was attributed to irradiation damage. A beneficial effect on fatigue life of pretreatment by swaging was found after irradiation at 450 and 750°C for 2550 hr. (auth)

XUM

42922 EFFECT OF FAST NEUTRON IRRADIATION ON THE CREEP RUPTURE PROPERTIES OF TYPE 304 STAINLESS STEEL AT 600 C. Bloom, E. E.; Stiegler, J. O. (Oak Ridge National Lab., Tenn.). ASTM (Amer. Soc. Test. Mater.) Spec. Tech. Publ.; No. 484, 451-67(1970).

From Symposium on irradiation effects on structural alloys for nuclear reactor applications; Niagara Falls, Canada (Jun-Jul 1970). See ASTM-STP-484; CONF-700630.

The creep rupture properties of Type 304 stainless steel were determined at 600°C after irradiation at temperatures in the range from 370 to 600°C to fast neutron fluences of 1×10^{21} to 6.7×10^{22} n/cm², E > 0.1 MeV. The microstructure were characterized by electron microscopy. Irradiation at 370 to 470°C caused a decrease in ductility and rupture life which became larger with increasing fast neutron fluence. The irradiated specimens fractured along the grain boundaries with no evidence of deformation within the matrix. A specimen irradiated at 410°C to 6.7×10^{22} n/cm² ruptured in 0.5 hr with 0.1% elongation, as compared to a rupture life of 185 hr and elongation of 19.7% for the unirradiated material tested at the same stress. Specimens irradiated at 600°C to fluences from 2.5 to 3.5×10^{22} n/cm² exhibited decreased ductilities and creep rates and essentially the same rupture lives as unirradiated specimens. The increased tendency for grain boundary fracture, and thus reduced ductility and rupture life, appears to result from the effects of the irradiation produced voids and dislocations upon deformation processes, which effects would be inoperative in an unirradiated specimen. The voids and dislocations prevent dislocation motion within the matrix. Regions along grain boundaries are denuded of these defects and grain boundary sliding occurs, leading to stress concentrations and the initiation of grain boundary cracks. The presence of helium at the boundaries may increase the rate of crack propagation. (auth)

42923 EFFECT OF IRRADIATION ON THE MECHANICAL PROPERTIES OF 19-9DL ALLOY. Lowe, A. L. Jr.; Baroch, C. J. (Babcock and Wilcox Co., Lynchburg, Va.). ASTM (Amer. Soc. Test. Mater.) Spec. Tech. Publ.; No. 484, 484-94 (1970).

From Symposium on irradiation effects on structural alloys for nuclear reactor applications; Niagara Falls, Canada (Jun-Jul 1970). See ASTM-STP-484; CONF-700630.

Austenitic stainless steels, which are used extensively in water cooled nuclear reactors, are presently being considered for use in fast reactors; however, these steels are susceptible to irradiation embrittlement and irradiation induced swelling. The modified austenitic stainless steel 19-9DL alloy, on the other hand, exhibits good creep strength at high temperatures. An exploratory program was conducted to determine the effects of irradiation on 19-9DL alloy at temperatures of 55, 343, and 413°C. The maximum fluence in this program (9.2×10^{20} n/cm², E > 1 MeV) was too low to prove the suitability of the alloy's potential for fast reactor applications but did show that additional evaluation of the alloy for fast reactors was warranted. The results indicate that the alloy is suitable for use in thermal reactors, since the ductility at 413°C was greater than 10% at a fluence approaching 1×10^{21} n/cm², E > 1 MeV. (auth)

42924 INFLUENCE OF NEUTRON IRRADIATION ON THE CREEP RUPTURE PROPERTIES OF A 16Cr-13Ni STEEL. Ehrlich, K.; Boehm, H.; Wassilew, C. (Kernforschungszentrum, Karlsruhe, Ger.). ASTM (Amer. Soc. Test. Mater.) Spec. Tech. Publ.; No. 484, 495-508(1970).

From Symposium on irradiation effects on structural alloys for nuclear reactor applications; Niagara Falls, Canada (Jun-Jul 1970). See ASTM-STP-484; CONF-700630.

The influence of neutron irradiation (up to 1.1×10^{22} n/cm², E > 0.1 MeV) on the creep rupture properties of a Nb stabilized 16Cr-13Ni steel was studied. Different heat treatments and cold work conditions and several irradiation temperatures were investigated. Low-temperature irradiation causes an increase in time to rupture at 650 and 750°C, whereas creep rate is reduced by more than a factor of ten. The creep ductility decreased to less than 1%. High-temperature irradiation does not cause a substantial change in rupture time at 650°C for the aged condition and the 50% cold work and 50% cold work + 1 hr 850°C conditions. The rupture life of specimens which were cold-worked 10% is strongly decreased by irradiation. Only slight changes in creep rate could be observed after high-temperature irradiation. Electron microscopy investigations indicate that the increase in rupture life and reduction in creep rate after low-temperature irradiation is due to a large number of dislocation loops. In the specimens irradiated at 650°C and above only He bubbles could be detected. (auth)

42925 CORRELATION BETWEEN THE MECHANICAL PROPERTIES AND MICROSTRUCTURE OF IRRADIATED IRON AND LOW-CARBON STEEL. Stefanovic, V. M.; Milasin, N. Lj. (Boris Kidric Inst. of Nuclear Sciences, Vinca, Yugoslavia). ASTM (Amer. Soc. Test. Mater.) Spec. Tech. Publ.; No. 484, 521-36(1970).

From Symposium on irradiation effects on structural alloys for nuclear reactor applications; Niagara Falls, Canada (Jun-Jul 1970). See ASTM-STP-484; CONF-700630.

The radiation hardening of iron and low-carbon steel was studied on the basis of transmission electron microscopy and tension test data. No visible defects were observed in the iron specimens after irradiation to 3.5×10^{19} n/cm², E > 1 MeV, at 35°C, as well as after postirradiation annealing at 150°C. Marked microstructural changes occurred in steel irradiated to 2.5×10^{18} n/cm² both at 320 and 450°C. In the former case a 5.1×10^{9} cm^{-2} increase in dislocation density was found, while in the latter the presence of small dislocation loops of average diameter 200 Å and density 2.4×10^{14} cm^{-3} was observed. The approximative theoretical values of yield stress increment were calculated using the models for hardening by small dislocation loops and by a dislocation forest and were compared with the experimental values of the yield stress increment. A satisfactory agreement was obtained. (auth)

42926 IRRADIATION EFFECTS AT CRYOGENIC TEMPERATURE ON TENSILE PROPERTIES OF TITANIUM AND TITANIUM-BASE ALLOYS. Younger, C. L.; Haley, F. A. (Lewis Research Center, Cleveland). ASTM (Amer. Soc. Test. Mater.) Spec. Tech. Publ.; No. 484, 537-63(1970).

From Symposium on irradiation effects on structural alloys for nuclear reactor applications; Niagara Falls, Canada (Jun-Jul 1970). See ASTM-STP-484; CONF-700630.

Significant increases in tensile strength and slight decreases in ductility occur when titanium and titanium-base alloys are irradiated at 17°K to 1 to 10×10^{17} fast neutrons per square centimeter. The magnitude of the irradiation effect appears to depend on total alloy content and, over the fluence range investigated, does not reveal a significant dependence on impurity content or initial heat treat condition. These results were obtained using commercially pure titanium, Ti-5Al-2.5Sn, Ti-6Al-4V (annealed and age hardened conditions), and Ti-8Al-1Mo-1V alloys. Test specimens were exposed to irradiations at 17°K and then tension tested at 17°K without intervening warmup using test loops specially designed and fabricated for cryogenic irradiation testing. Additional results, using commercially pure titanium, show recovery of about 50% of the irradiation induced increase in yield strength following heat treatment at 178°K. For the ultimate strength, 50% recovery occurred following heat treatment at 78°K. (auth)

42927 EFFECTS OF ALLOYING AND IRRADIATION ON THE OXIDATION BEHAVIOUR OF ZIRCONIUM ALLOYS. Campbell, C. S.; Tyzack, C. (United Kingdom Atomic Energy Authority, Culcheth, Eng.). pp 7-24 of Conference on the Use of Zirconium Alloys in Nuclear Reactors. Plzen, Czech.; Skoda Works (1968).

From Conference on the use of zirconium alloys in nuclear reactors; Marianske Lazne, Czech. (1 Oct 1968).

Theories of radioinduced corrosion of Zircaloy-2 and other Zr alloys are discussed. It is suggested that irradiation produces an oxide film sensitive to the partial pressure of molecular oxygen, in which the radiation displaced oxygen ions are equivalent to the population of interstitial oxygen ions created by niobium doping in films on zirconium–2½% niobium alloys under oxidizing conditions. By analogy with hyperstoichiometric UO_2 it is suggested that the interstitial population induces a higher effective oxygen mobility and hence flux through the film than is the case with stoichiometric or slightly sub-stoichiometric oxide. It is further suggested that the lower in-pile oxidation rates observed with the zirconium–niobium alloys under oxidizing conditions may be due to higher oxidation rates which would give less time for the accumulation of any given level of damage. If the defect (interstitial oxygen in the outer p-type film oxygen vacancies in the inner n-type film) concentrations are high, a greater radiation dose is required to give the same relative increase in rate. (J.R.D.)

42928 STUDIES OF DEFORMATION AND CRACKING EFFECTS IN ZIRCONIUM–COPPER CLADDING IN CARBON DIOXIDE. Frenkel, J. M.; Weisz, M. (Centre d'Etude de l'Energie Nucleaire de Saclay, Gif-sur-Yvette, France). pp 311-27 of Conference on the Use of Zirconium Alloys in Nuclear Reactors. Plzen, Czech.; Skoda Works (1968). (In French).

From Conference on the use of zirconium alloys in nuclear reactors; Marianske Lazne, Czech. (1 Oct 1968).

Laboratory studies show that a Zr–Cu cladding makes it possible to obtain valuable data on fuel burnups at maximum temperatures of the cladding of the order of 600°C. A very important improvement is produced by the use of β-treated cladding. (tr-auth)

42929 STRUCTURES OF ZIRCONIUM ALLOYS IN HEAVY-WATER REACTORS: OPERATION OF EL-4 AND FUTURE

ASPECTS. Foulquier, H. (Commissariat a l'Energie Atomique, Saclay, France). pp 465-83 of Conference on the Use of Zirconium Alloys in Nuclear Reactors. Plzen, Czech.; Skoda Works (1968). (In French).

From Conference on the use of zirconium alloys in nuclear reactors; Marianske Lazne, Czech. (1 Oct 1968).

The French program for the development of zirconium alloy pressure tubes for the EL-4 Reactor is discussed. The effects of neutron irradiation on swelling of annealed and unannealed as-drawn Zircaloy-2 tubes were evaluated. Methods for welding pressure tubes are discussed. Tensile tests of the welded joints showed that rupture occurred outside the weld. Destructive and nondestructive testing of the tubes were carried out. Methods for improving the corrosion-resistant and mechanical properties of the tubes are described. It was found that these properties partially depend upon the fabrication methods used. (R.C.K.)

Ceramics and Cermets

Refer also to abstracts 41832, 42204, and 44219.

Corrosion and Erosion

Refer also to abstract 44123.

42930 OXIDATION OF Ni–20 WT. PERCENT Cr–2ThO_2. Wallwork, G. R.; Hed, A. Z. (Battelle Memorial Inst., Columbus). Oxidation Metals; 3: No. 3, 229-41(May 1971).

The oxidation of TD NiCr(Ni–20 wt % Cr–2ThO_2) was investigated between 900 and 1200°C, and the oxidation behavior is compared with Ni–30 wt % Cr and Co–35 wt % Cr alloys. All alloys develop Cr_2O_3 scales but the weight changes obtained for the NiCr and CoCr alloys show an increase with time whereas above 1000°C the TD NiCr shows a progressive loss in weight from the evaporation of CrO_3 from the scale, and the reaction products appear to be formed mainly at the alloy–scale interface. However, no mechanism for its formation was established. (auth)

42931 COMPARISON OF THE CATALYTIC EFFECTS OF VARIOUS METALS IN THE GRAPHITE–OXYGEN AND GRAPHITE–NITROUS OXIDE REACTIONS. Magne, Pierre; Duval, Xavier (Univ., Nancy). Bull. Soc. Chim. Fr.; No. 5, 1593-7(May 1971). (In French).

The catalytic effect of metals (such as Ba, Pb, Cd, Cr, and U) is different in the reactions graphite–oxygen and graphite–nitrous oxide. The activation energy and reaction rates are similar in both reactions and sometimes lower with N_2O. A factor which differs in the two reactions is the possibility of the catalyst metal causing dissociation with N_2O. However, this factor does not appear to play the most important role. (auth) (France)

42932 KINETICS OF GRAPHITE OXIDATION IN N_2O: COMPARISON WITH OXIDATION IN OXYGEN. Magne, Pierre; Duval, Xavier (Univ., Nancy). Bull. Soc. Chim. Fr.; No. 5, 1585-92(May 1971). (In French).

The kinetics of the oxidation reaction of graphite in N_2O is difficult to obtain, because of secondary and parallel reactions. When parallel reactions are eliminated, it is found that the oxidation reaction of graphite in N_2O is not fundamentally different from oxidation O_2, having the same activation energy and CO/CO_2 ratio. However, in N_2O the order of the reaction is twice as high and the rate five times slower than in O_2. (auth) (France)

42933 KINETICS OF MOLYBDENUM DIOXIDE OXIDATION. Ramadorai, Gopalan. Salt Lake City; Univ. of Utah (1971). 175p. University Microfilms Order No. 71-14,565. Thesis.

Pressed cylinders and powder molybdenum dioxide samples were oxidized in the temperature range of 390 to 620°C and oxygen partial pressures of 0.009 to 0.18 atmosphere. The oxidation was followed by a continuous weight change method. Parabolic oxidation kinetics was observed with the powder in the temperature range 390 to 460°C and oxygen partial pressures in the range 0.009 to 0.18 atm. The reaction was controlled by the diffusion of oxygen. An activation enthalpy of 38.2 ± 2 kcal/mole was observed. The partial pressure dependence at 407°C and 455°C was found to be approximately 1/5. The oxidation was explained in terms of mono- and divalent oxygen interstitials. Above 465°C, at oxygen partial pressure of 0.009 atm, after correcting for area change linear oxidation kinetics was observed with MoO_2 powder. The pressure dependence of the linear oxidation was not obtained since excessive superheating of samples occurred. An activation enthalpy of 24.8 kcal/mole was observed for the linear oxidation in the temperature range 465 to 530°C. X-ray studies on the oxidation products of the powder indicated the presence of only MoO_2. An infrared study of the oxidation products in the diffusion range indicated a new band at 650 cm^{-1}. This band at 650 cm^{-1} was found to shift as the temperature was increased in the linear oxidation region. This band is shown to shift to 570 cm^{-1} which compares with the value in the literature. The shifting of the band with temperature in the linear oxidation region was attributed to a decreasing concentration of oxygen interstitials. With pressed pellets, the oxidation rate per unit surface area of residual molybdenum dioxide was linear. The reaction was shown to be highly exothermic by means of thermograms. Inconsistencies were observed in the data with pressed pellets. An infrared pattern of the oxidation product using pressed pellets indicated the lack of the 650 cm^{-1} band observed in the diffusion region. (Diss. Abstr. Int., B)

Preparation and Fabrication

Refer also to abstracts 41779, 42130, 42819, and 42822.

42934 (COO–1109-60) HYDROTHERMAL EQUILIBRIA AND CRYSTAL GROWTH OF RARE EARTH OXIDES, HYDROXIDES, HYDROXYNITRATES, AND HYDROXYCARBONATES. Haschke, John M.; Eyring, LeRoy (Arizona State Univ., Tempe. Dept. of Chemistry). [1969]. 39p. Dep. NTIS.

The equilibria of praseodymium, neodymium, and terbium oxides with water were examined at temperatures up to 900°C and 1360 atm by hydrothermal techniques. In the trivalent Pr and Nd systems, only hexagonal trihydroxide and oxyhydroxide were observed with the phase boundary near 800°C. In the presence of oxygen or an oxidizing agent, fcc PrO_2 was found to be stable in water at temperatures above 600°C, under similar conditions diphasic mixtures of rhombohedral $TbO_{1.714}$ and monoclinic $TbO_{1.818}$ were obtained. The equilibria of praseodymium hydroxynitrate and hydroxycarbonate systems were explored, and monoclinic $Pr(OH)_2NO_3$, hexagonal $Pr_2(OH)_5NO_3$, hexagonal $PrOHCO_3$, and hexagonal $Pr_2O_2CO_3$ were characterized. Single crystals of trihydroxide, hydroxynitrate, and hydroxycarbonate phases were prepared and examined by Weissenberg techniques; small crystals of the higher oxides were also obtained. The use of nitrate ion as an oxidizing agent under high temperature conditions and as an effective mineralizer at lower temperatures is described and discussed. TGA data for the hydroxy-anion phases are presented, and discrepancies between the present hydrothermal results and those of previous reports are discussed. (auth)

42935 (EURFNR–859) SEPARATION OF VANADIUM ON UO_2 SPHERES FROM THE GASEOUS PHASE. Schneider, H.; Schoenwald, D. (Kernforschungszentrum, Karlsruhe (West Germany). Institut fuer Material- und Festkoerperforschung). Translation of KFK–1292. 21p. Dep. NTIS.

Work Performed under United States–Euratom Fast Reactor Exchange Program.

An abstract of this paper, prepared from the original language, appeared as NSA 25: 13737.

42936 (JUL–728-RW) FORMATION OF U_2C_3 BY DECOMPOSITION OF URANIUM DICARBIDE. Schneider, Felix H. (Kernforschungsanlage, Juelich (West Germany). Institut fuer Reaktorwerkstoffe). Feb 1971. 17p. (In German). Dep. NTIS (U. S. Sales Only).

For the operation of gas-cooled high-temperature reactors with dicarbide particle fuel, the question of phase stability is of interest. The literature data on the dicarbide decomposition to U_2C_3 + C are very variant. In a series of studies this reaction was detected along with simultaneous reaction-inhibiting and reaction-accelerating factors. The acceleration of the dicarbide decomposition because of the admitted mechanical energy was studied on the basis of kinetic investigations on UC_2 granulates. A semiquantitative relation between the surface changes during crushing and the experimental activation energy was developed. A U_2C_3 formation was observed in the heat treatment around 1400°C of irradiated coated particles. This shows the necessity of stabilizing dicarbide fuel. A contamination of the UC_2 with approximately 1500 ppM of dissolved nitrogen was determined to be an essential stabilizing factor. Comparative studies of characteristic phenomena in UC_2 and U_2C_3 formation using synthetic reactions in over-stoichiometric monocarbide were reported. An effect of the nitrogen surpressing the reaction was not established. The U_2C_3 formation mechanism was discussed on the basis of lattice-geometric relations and the diffusion effect. (tr-auth)

42937 (ORNL–4544) ENGINEERING-SCALE DEMONSTRATION OF THE SOL-GEL PROCESS: PREPARATION OF 100 kg OF ThO_2–UO_2 MICROSPHERES AT THE RATE OF 10 kg/day. Haws, C. C.; Finney, B. C.; Bond, W. D. (Oak Ridge National Lab., Tenn.). May 1971. Contract W-7405-eng-26. 90p. Dep. NTIS.

XUM

Microspheres of the composition 81% ThO_2–19% UO_2 were prepared in a near-continuous, engineering-scale demonstration at the rate of 10 kg (Th + U)/day. Approximately 120 kg of ThO_2–UO_3 gel microspheres were produced. Sol preparation by the amine extraction process was routine and reproducible, and a 99.5% yield of 1.6 M ThO_2–UO_3 sol was obtained based on the metal nitrate feed. A material balance of 100.2% was achieved. No significant problems are anticipated in adapting this sol preparation process to fully remote operations. Microsphere-forming results showed that yields of up to 95% (based on sol fed to the system and product-grade microspheres) are attainable when 250- to 450-μ-dia spheres (calcined) are produced using multiple two-fluid nozzles and the sol droplets are gelled in 2-ethyl-1-hexanol (2EH). The material balance was 99.5%. Addition rates of surfactants required to maintain sustained operation of the sphere-forming column demonstrated the need for a cleanup and recycle process for the 2EH in long-term operations. The operation of batch, fixed-bed dryers of 20-kg capacity, previously used for drying ThO_2 gel microspheres, proved to be unsuccessful for drying ThO_2–UO_3 microspheres because of uncontrollable, deleterious temperature excursions. The method of heat input to the bed by external heating and the instrumentation provided for measuring bed temperatures made it impossible to carry out the drying step in the required turnaround time (i.e., 48 hr). After an adequately designed dryer was installed 20-kg batches of the ThO_2–UO_3 gel microspheres were successfully dried in the specified time. No problems were encountered in firing 10-kg batches of dried gel microspheres in a fixed-bed calciner. The product microspheres met High-Temperature Gas-Cooled Reactor specifications with regard to size, Th/U atom ratio, roundness, O/U atom ratio, gas release, density, and carbon content. (auth)

42938 PROCESS AND APPARATUS FOR PRODUCING UO_2 POWDER. McCoy, John J. (to General Electric Co.). U. S. Patent 3,579,311. 18 May 1971. Filed 25 Apr 1968.

An improved process and apparatus for preparing uranium dioxide powder suitable for use in the fabrication of fuel for nuclear reactors are described. The process consists of hydrolyzing uranium hexafluoride to form an aqueous uranyl fluoride solution, treating with ammonia to precipitate ammonium diuranate, dehydrating and drying the precipitate, and finally calcining the precipitate to form uranium dioxide. The precipitate is dehydrated to about 40% to about 60% by weight, preferably about 50% by weight water and is thereafter directly calcined. (Official Gazette)

42939 PROCESS FOR FABRICATION OF STOICHIOMETRIC URANIUM MONOCARBIDE. Johnson, Bruce M.; De Crescenti, Michael A.; Darrah, James G. (to United Aircraft Corp.). U. S. Patent 3,578,610. 11 May 1971. Filed 30 Nov 1960.

An improved process of fabricating stoichiometric uranium monocarbide for use as nuclear reactor fuel is described. (Official Gazette)

42940 KINETICS OF SOLID-PHASE SYNTHESIS OF ZIRCON DURING SINTERING UNDER PRESSURE. Dyban, Yu. P.; Merkulov, A. G. (Inst. of Physicochemical Principles of Processing of Crude Mineral, Novosibirsk, USSR). Inorg. Mater. (USSR) (Engl. Transl.); 6: 1261-4(Aug 1970).

Translated from Izv. Akad. Nauk SSSR, Neorg. Mater.; 6: 1432-6(Aug 1970).

The kinetics of diffusion-chemical processes during solid-phase reaction of ZrO_2 and SiO_2 were investigated. The optimal temperature of zircon synthesis is 1400 ± 20°C. Under optimal conditions, the yield of $ZrSiO_4$ can be increased by using the method of sintering under pressure, with intermediate crushing of the sinter. The activation energy of zircon synthesis in the regions of chemical and diffusion kinetics is 83 and 38 kcal/mole, respectively. (auth)

42941 SYNTHESIS AND PROPERTIES OF MOLYBDENUM BOROCARBIDE. Salibekov, S. E.; Levinskii, Yu. V.; Lobankov, V. V. Inorg. Mater. (USSR) (Engl. Transl.); 6: 1430-2(Sep 1970).

Translated from Izv. Akad. Nauk SSSR, Neorg. Mater.; 6: 1622-4(Sep 1970).

Molybdenum borocarbide of the composition Mo_2BC was synthesized by two methods. Properties of this compound which were determined include melting point, specific gravity, electrical and thermal conductivity, thermal-emf, coefficient of thermal expansion, modulus of elasticity, microhardness and resistance to heat. (auth)

42942 PRODUCTION OF ZIRCONIUM DIOXIDE FROM BADDELEYITE CONCENTRATE. Kolenkova, M. A.; Shumenko, V. N.; Rybachuk, N. T.; Mikhnevich, V. I.; Bolotich, E. G. (Inst. of Steel and Alloys, Moscow). Izv. Vyssh. Ucheb. Zaved., Tsvet. Met.; No. 6, 87-90(1970). (In Russian).

Baddeleyite concentrate represents a higher grade raw material for technical grade production of ZrO_2 than does zircon. The ZrO_2 content in baddeleyite concentrate approaches 90%, but that of zircon only reaches 65. Processing of the concentrate should include HCl lixiviation which removes only impurities but for improved removal of foreign substances an oxidative calcination is also necessary. Industrial testing showed that electromagnetic cleaning followed by acid treatment of the nonmagnetic fraction produced ZrO_2 of acceptable quality, low in Fe and Ti. (tr-auth)

42943 HYDROTHERMAL SYNTHESIS OF $V_2O_{4-x}F_x$ DERIVATIVES. Chamberland, B. L. (E. I. du Pont de Nemours and Co., Wilmington, Del.). Mater. Res. Bull.; 6: No. 6, 425-32(Jun 1971).

Several members of the $V_2O_{4-x}F_x$ series, ($0.01 \leq x \leq 0.85$) have been prepared by the hydrothermal reaction of V_2O_5, V_2O_3, and VF_3 in sealed gold tubes. At low fluorine concentrations, crystalline, monoclinic-type products are formed while higher fluorine substitutions yielded microcrystalline rutile-type derivatives. The crystallographic transitions (monoclinic to tetragonal) were determined by differential thermal analysis. The transition temperature decreased rapidly as fluorine substitution in the V_2O_4 cell increased. Crystallographic and electrical properties were determined. (auth)

42944 NEW METHOD FOR PREPARING METAL BORIDES. Cueilleron, J.; Lahet, G.; Thevenot, F.; Paris, R. A. (Faculte des Sciences de Lyon, Villeurbanne, France). J. Less-Common Metals; 24: No. 3, 317-22(Jul 1971). (In French).

The preparation of vanadium, chromium, iron, cobalt, and nickel borides is by reaction between the mixture of boron trichloride–hydrogen and metallic sulfides in the temperature range 500 to 1000°C. The boride CrB_4 is formed between 800 and 1000°C. Titanium, vanadium, and chromium diborides are synthesized by reaction of elementary boron with metallic sulfides in the temperature range 700 to 1000°C. (auth)

42945 METHOD OF PREPARING A STABLE MIXED SOL OF HEXAVALENT URANIUM AND TETRAVALENT THORIUM BY PEPTIZATION. van der Plas, Theo; Kanij, Johannes B. W.; Noothout, Arend J.; Hermans, Marie E. A. U. S. Patent 3,573,217. 30 Mar 1971. Filed 30 Jun 1969.

A method of preparing a mixed sol containing U(VI) oxide and Th(IV) oxide comprises very quickly precipitating a hydroxide coprecipitate of the mixed hydroxides with a very low content of ammonium diuranate with a large excess of base, separating the coprecipitate, washing the precipitate with an aqueous solution of the base, and peptizing the precipitate by heating with an aqueous solution of a peptizing agent selected from the group consisting of HNO_3, HCl, $UO_2(NO_3)_2$, UO_2Cl_2, $ThCl_4$, $Th(NO_3)_2$, or mixtures of these. The molar ratio of nitrate or chloride to total metal present is at least 0.25. (B.L.M.)

42946 FORMATION OF CARBONITRIDES AND OXYCARBONITRIDES OF NIOBIUM CRYSTALLIZING IN THE CUBIC SYSTEM. Roubin, M.; Paris, J. M. (Faculte des Sciences, Lyon). J. Less-Common Metals; 24: No. 2, 195-200(Jun 1971). (In French).

Niobium carbonitrides and oxycarbonitrides were prepared by treatment of niobium nitrided compounds with suitable proportions of hydrogen, methane, and nitrogen according to the method which has been described for vanadium, at temperatures between 800 and 1000°C. (auth)

42947 GROWTH AND PROPERTIES OF SINGLE CRYSTAL LaB_4. Deacon, J. A.; Hiscocks, S. E. R. (Royal Radar Establishment, Great Malvern, Eng.). J. Mater. Sci.; 6: No. 4, 309-12(Apr 1971).

A technique was developed for the growth of single crystals of lanthanum tetraboride, LaB_4, from solution in La. Under optimum conditions, crystal size is limited by the size of the crucible. Lattice parameters, thermal expansion coefficient and microhardness are reported and the growth facets were identified. An initial check on the electron emitting properties showed them to be comparable with those of LaB_6. (auth) (UK)

42948 CHARACTERISTICS OF POROUS GRAPHITE IMPREGNATED WITH FUSED ZIRCONIUM. Elyutin, V. P.; Kostikov, V. I.; Dergunova, V. S.; (and others). Tsvetn. Metal.; No. 1, 46-50(Jan 1971). (In Russian).

The process of graphite impregnation has many metalloceramic applications. The testing of two industrial graphites impregnated with molten zirconium over the temperature range 1860 to 2550°C and in a vacuum of 2×10^{-2} mm Hg is described. The zirconium spreads itself along the pore walls, and the time dependence of advance of the impregnating front under isothermal conditions resembles a square parabola. The apparent activation energy for the impregnation process in the two graphites studied was 22 and 24 kcal/mole over the temperature range 1860 to 2100°C. Soaking

time of the graphite samples in the liquid metal was varied from 5 to 240 seconds. The specimens were cylindrical with a diameter of 60 mm and a height of 110 mm. (K.S.W.)

42949 IMPORTANCE OF STEARATES IN THE FABRICATION OF UO_2 AND $(U,Pu)O_2$ PELLETS. Flipot, A. J.; Gilissen, R.; Smolders, A. (CEN, Mol, Belgium). Powder Met.; 14: No. 27, 93-109(Spring 1971).

Eighteen qualities of metallic soaps were studied, either as lubricants or as additives, for the fabrication of UO_2 and $(U,Pu)O_2$ pellets. Compounds of the same family, such as stearates, differ in their effectiveness as lubricants. This property is strongly dependent on the particle size of the powder and its purity. The behavior of the dry lubricants when used as admixtures in UO_2 and also when employed for the direct lubrication of the pelletizing tools is discussed. The efficiency of metallic soaps as additives to lower the density of the sintered pellets is related to the nature of the metallic ion. Thus, zinc stearate has little influence on the fired density of UO_2, whereas barium stearate and other barium compounds are very effective. Barium inhibits sintering, but zinc, which is eliminated at low temperature, does not diminish the sinterability of the oxide powders. In the latter case, the decrease in density is caused by thermal decomposition of the organic molecule. (auth) (UK)

42950 SINTERING OF URANIUM DIOXIDE: INFLUENCE OF THE CHARACTERISTICS OF THE POWDERS. Haydt, H. M.; Capocchi, J. D. T.; Nishioka, I.; (and others) (Instituto de Energia Atomica, Sao Paulo, Brazil). pp 203-12 of Materials Technology. I. New York; American Society of Mechanical Engineers (1970).

From second inter-american conference on materials technology; Mexico City, Mex. (24 Aug 1970). See CONF-700812.

The UO_2 powder produced from ammonium diuranate of different conditions of precipitation is characterized. The UO_2 characterization includes the determination of the physical and chemical properties of the material affected largely by the preparation methods and thus, have a marked influence on the characteristics of pressing and sintering capability of the pellets and its performance as solid fuel. Emphasis is given to the importance of the differential thermal analysis, surface area measurements, and O/U ratio. The shape and texture of the particles and porosity of the sintered pellets are also considered. Sintering operations realized at 1400°C in argon atmosphere for 4 hours, corroborated the data established by the characterization tests of the uranium dioxide. (auth)

42951 COMPOSITE MATERIALS. Weinstein, Martin; Speirs, K. K. (Chromalloy American Corp., San Antonio). pp 550-8 of Materials Technology. I. New York; American Society of Mechanical Engineers (1970).

From second inter-american conference on materials technology; Mexico City, Mex. (24 Aug 1970). See CONF-700812.

A general review is presented of the new metallurgical technologies utilized in the new class of multicomponent materials-composite materials. This active area of materials science is classified for purposes of clarity into three major subdivisions; fiber-reinforced structures, utilizing oriented high modulus-high strength refractory filaments or whiskers in a ductile matrix; clad-metals, utilizing various laminates of copper-stainless steel produced by rolling technologies producing atomic bonding; and bulk materials with extraordinary surface properties produced by the formation of high hardness-oxidation resistant intermetallic compounds through surface diffusion. Some of the new metallurgical processes employed in the production of these composites include chemical vapor deposition, eutectic solidification, dendritic growth, diffusion bonding, fused salt metallizing, and pack cementation diffusion coating. Some general aspects of these new metallurgical processes are discussed. (auth)

Properties Evaluations

Refer also to abstracts 41777, 41810, 41850, 41898, 41956, 41991, 41993, 42001, 42190, 42853, 43481, and 43482.

42952 (GEAP-12188) FISSION GAS RE-SOLUTION RATES. Quarterly Report No. 2, October 1-December 31, 1970. Marlowe, M. O. (General Electric Co., Pleasanton, Calif. Nucleonics Lab.). Jan 1971. Contract AT(04-3)-189. 5p. Dep. NTIS.

Progress in experimental programs and studies to determine the re-solution rates of fission gases in oxide nuclear fuels under irradiation is described. The furnace and associated inert atmosphere control system for in-cell annealing of the irradiated specimens was assembled and tested. The first dummy unirradiated specimens for transmission electron microscopy was thinned in-cell. A topical report (GEAP-12148) describing the limitations of fission gas bubble growth by the re-solution process was written. (auth)

42953 (GEAP-12189) FISSION GAS RE-SOLUTION RATES. Quarterly Report No. 3, January 1-March 31, 1971. Marlowe, M. O. (General Electric Co., Pleasanton, Calif. Nucleonics Lab.). Apr 1971. Contract AT(04-3)-189. 7p. Dep. NTIS.

Progress in experimental programs and studies to determine the re-solution rates of fission gases in oxide nuclear fuels under irradiation is described. An abrasive blasting technique was developed out-of-pile for thinning of the disk specimens to approximately 10 micrometers. Accurate determination of the current radioactivity of the specimens indicated that thinning before handling will be required. The capability of the Nucleonics Laboratory JEOLCO electron microscope to reveal fission gas bubbles to 30Å and less in diameter was demonstrated. A copy of the LIFE computer code for fuel performance prediction was received from Argonne National Laboratory and will be used for development of a compatible subroutine for incorporation of the results of this study into such models. (auth)

42954 (HEDL-SA-131) DISSOLUTION OF UNIRRADIATED MECHANICALLY BLENDED MIXED OXIDE FAST REACTOR FUEL. Lerch, R. E.; Schiefelbein, G. F. (WADCO Corp., Richland, Wash.). Apr 1971. Contracts AT(45-1)-1830; AT(45-1)-2170. 22p. (CONF-710606-1). Dep. NTIS.

From seventeenth annual meeting of the American nuclear society; Boston, Mass. (13 Jun 1971).

A statistical, fractional factorial experiment was performed to determine the effect of six fuel fabrication variables on the dissolubility of unirradiated, mechanically blended PuO_2-UO_2 fuels. The six fabrication variables were source of PuO_2, PuO_2 content, sintering temperature, sintering time, rate of temperature rise during sintering, and pellet pressing pressure. All six fabrication variables had some effect on pellet dissolubility with source of PuO_2, PuO_2 content, and sintering temperature having major effects. (auth)

42955 (IS-T-446) ANOMALOUS ELASTIC BEHAVIOR OF POLYCRYSTALLINE Nb_2O_5. Manning, William Roger (Ames Lab., Iowa). Jun 1971. Contract W-7405-eng-82. 150p. Dep. NTIS.

Thesis.

The Young's modulus of polycrystalline niobium pentoxide was investigated as a function of temperature using the sonic resonance technique. For samples fabricated by sintering, the modulus increased three times in value over the range 600 to 1000°C, changed with time at constant temperatures in this interval, and showed a large hysteresis between heating and cooling data. For similar samples the room-temperature values for the Young's and shear moduli showed no correlation with sample density. For samples fabricated by hot-pressing, a small decrease in modulus with temperature, no variation in modulus with time, no hysteresis effects, and a linear relationship between room-temperature moduli and sample density were observed. Internal friction measurements revealed similar discrepancies between the two types of samples. In addition, the bulk linear thermal expansion of both sintered and hot-pressed samples of niobium pentoxide was determined with a dilatometer from room temperature to 1000°C. The over-all linear expansion of the sintered samples was found to be unusually small and a hysteresis between heating and cooling data was observed. The over-all linear expansion of the hot-pressed sample was three times that of the sintered sample and no hysteresis was observed. The observed phenomena are attributed to the occurrence and recombination of internal microcracks in the sintered samples arising from thermal stresses introduced when the solid is cooled from its fabrication temperature. The internal stresses are a result of the anisotropic lattice expansion of niobium pentoxide as revealed by high-temperature x-ray measurements. Microcracks are apparently absent from the hot-pressed material because of smaller grain size. Scanning electron micrographs of the sintered samples reveal that cracking occurs along the grain boundaries. (auth)

42956 (JAERI-13517) PHYSICAL PROPERTIES OF CARBIDE FUELS AND THEIR EVALUATION. Kikuchi, Takeo (Japan Atomic Energy Research Inst., Tokai). Apr 1969. 26p. NTIS (U. S. Sales Only).

Physical properties of carbide, nitride and similar compounds having a NaCl-type crystal structure are reviewed, and some problems associated with power and burnup of a fast breeder reactor are pointed out. Thermal conductivity and swelling of these compounds are discussed. Chemical bonding, growth of fission gas bubbles, and creep are also discussed. (auth)

42957 (UCRL-20500, pp 147-73) CERAMIC SCIENCE. (California Univ., Berkeley. Lawrence Radiation Lab.).

In Inorganic Materials Research Division annual report, 1970.

XUM

Activities in research programs are reported on high-temperature reactions in ceramic materials, microstructure of ceramics and cermets, reactions and properties of glass and cermets, and relations of microstructure with properties of ceramics. (J.R.D.)

42958 (WAPD-TM-850) GAS RELEASE FROM THORIA-BASE OXIDE FUEL PELLETS. (LWBR Development Program). Smid, R. J. (Bettis Atomic Power Lab., Pittsburgh, Pa.). Apr 1971. Contract AT(11-1)-Gen-14. 33p. Dep. NTIS.

The gas release from unirradiated thoria-base oxide fuel pellets was investigated over the temperature range of 90 to 2000°C using mass-spectrographic techniques. Approximately 75 percent of the released hydrogen gas from ThO_2-UO_2 samples was extracted at 1000°C and below; thermal exposure to approximately 1200°C was necessary to release the remaining hydrogen gas. Temperature had a similar effect on the total gas; complete release was not attained until a temperature of 1200°C was reached. Pure ThO_2 samples released more than 90 percent of the hydrogen gas at 1000°C; however, only about 30 percent of the total gas was released at this temperature. Diffusion coefficients for hydrogen in ThO_2-UO_2 were estimated from release data, and an activation energy for hydrogen diffusion was estimated to be in the range of 44 to 67 kcal/mole. Increase in the carbon content of the sintered oxide increased the solubility limits of hydrogen in both ThO_2 and ThO_2-UO_2. It was proposed that the presence of carbon in the ThO_2 or ThO_2-UO_2 lattice promoted an anion-deficient structure having an increased solubility for hydrogen. The effects of density and porosity on gas release were minor providing the carbon content of the low-density, high-porosity samples was very low (<10 ppM). Exposure of the sintered oxides to various relative humidities prior to vacuum extraction had little effect on the total gas release except at the higher relative humidities. Gas adsorbed during storage under high-humidity conditions was almost completely desorbed by exposure to a 90°C vacuum treatment. (auth)

42959 INFLUENCE OF FIBROUS ALUMINIUM NITRIDE ON THE STRENGTH OF SINTERED AlN–Y_2O_3. Komeya, K.; Inoue, H. (Tokyo Shibaura Electric Co. Ltd., Kawasaki, Japan). Trans. J. Brit. Ceram. Soc.; 70: No. 3, 107-14(May 1971).

Dense and fiber-reinforced bodies were produced by sintering pressed powders composed of AlN and Y_2O_3. The system AlN–Y_2O_3 was studied in detail with a view to developing structural material with high strength. Densification, mechanical properties, phases present, and microstructures of sintered masses were examined. Heat treatment over 1400°C formed two kinds of crystal phases, which resembled $Y_3Al_5O_{12}$ and $Al_2Y_4O_9$ respectively in the x-ray diffraction pattern. The specimens containing up to 25 wt % Y_2O_3 and sintered at temperatures above 1700°C consisted of AlN and $Y_3Al_5O_{12}$, or of AlN, $Y_3Al_5O_{12}$ and $Al_2Y_4O_9$ phases, and showed well developed and randomly orientated fibrous texture. The strength of the specimens exceeded 30 kg/mm^2. The high strength is considered to be due to the fibers formed during sintering. Although the specimens contained more than 30 wt % Y_2O_3 and had high density, the structures were not fibrous and the strengths were quite low: the specimen with 40 wt % Y_2O_3 sintered at 1700°C consisted of granular crystals of AlN, $Y_3Al_5O_{12}$, and $Al_2Y_4O_9$ phases and the density was about 96% of the weighed mean of the densities of the end-members. The strength, however, was only about 30% of that of fiber-reinforced specimen containing 25 wt % Y_2O_3. The fibrous crystals were provisionally identified as AlN by x-ray diffraction and a polarizing microscope. (auth) (UK)

42960 TEMPERATURE DEPENDENCE OF FRACTURE EFFECTS IN SELF-BONDED SiC. Stevens, R. (Atomic Energy of Canada Ltd., Pinawa, Manitoba). J. Mater. Sci.; 6: No. 4, 324-31(Apr 1971).

The effect of temperature on the fracture strength and work of fracture of a self-bonded SiC was measured from room temperature to 1100°C. Over the same temperature range the work of fracture was observed to increase twofold. These phenomena were accounted for in terms of the behavior of the free-silicon phase. In addition, electron microscopy of the fractured surface was undertaken. Fracture chips showed that dislocations were generated during the failure process in both the secondary SiC and silicon phases. Stacking faults were observed in the SiC phases, and some of these were shown to have formed during the fracture process. (auth)

42961 ENTHALPY AND HEAT CAPACITY OF EUROPIUM, NEODYMIUM, AND SAMARIUM HEXABORIDES AT 300 TO 1300°K. Prilepskii, V. N.; Timofeeva, E. N.; Timofeev, V. A.; Trubitsyn, A. Ya. Inorg. Mater. (USSR) (Engl. Transl.); 6: 1816-17(Nov 1970).

Translated from Izv. Akad. Nauk SSSR, Neorg. Mater.; 6: 2069-70(Nov 1970).

The enthalpy measurements were performed in a high-temperature calorimetric apparatus by the mixing method. Values for enthalpies of Eu, Nb, and Sm hexaborides are tabulated. (J.R.D.)

42962 MULTI-FOIL THERMAL INSULATION DEVELOPMENT PROGRAM. A STATUS REPORT. Paquin, Michael L. (Thermo Electron Corp., Waltham, Mass.). pp 408-15 of Proceedings of the Fourth Intersociety Energy Conversion Engineering Conference, September 22-26, 1969, Washington, D. C. New York; American Inst. of Chemical Engineers (1969).

From fourth intersociety energy conversion engineering conference; Washington, D. C. (21 Sep 1969). See CONF-690905.

An up-to-date status report is presented on the multi-foil thermal insulation development program. Particular emphasis is placed on the most recent test results. The recently completed reproducibility tests are discussed and data is presented illustrating the importance of properly optimizing the oxide coatings. The first results obtained by testing lower temperature types of multi-foil are presented. Also included are a discussion of the layer variation tests which have studied the variation in heat flux with the number of layers of insulation and a new series of measurements relating performance to applied pressure. Three years of development have resulted in a significant reduction in the thermal conductivity of multi-foil insulation to between 8×10^{-5} BTU in/hr ft^2 °F and 7×10^{-3} BTU in/hr ft^2 °F, depending upon the materials and the temperatures involved. Although originally intended for application at temperatures above 1000°C, less costly forms of multi-foil insulation are proving highly efficient and useful at lower temperatures. (auth)

42963 CONSIDERATIONS OF PuC AND SiC COATED OXIDE PARTICLES FOR GAS COOLED FAST REACTOR APPLICATION. Donne, M. Dalle; Schumacher, G. (Gesellschaft fuer Kernforschung mbH., Karlsruhe, Ger.). J. Nucl. Mater.; 40: No. 1, 27-40(Jul 1971).

Recently, coated particles with a SiC outer coating layer have been proposed for Gas Cooled Fast Reactor application. SiC is a very fragile material. Although under fast irradiation it can creep at relatively low temperatures, a very low strain (>0.3%) can produce hairline cracks. A SiC coating layer can, therefore, withstand only moderate overpressures when subjected to large fast neutron exposures. The pressure inside the particle due to gaseous fission products and CO–CO_2 was calculated. The operation temperature of the particle due to the condition strain ≤0.3% is given as a function of SiC layer thickness in conditions typical for GCFR's application. (auth)

42964 STABILITIES OF SOLID SOLUTIONS OF THE SYSTEM EuO–CaO WHEN HEATED IN AIR. Ignat'eva, N. I.; Bamburov, V. G. (Inst. of Chemistry, Moscow). Inorg. Mater. (USSR) (Engl. Transl.); 7: No. 1, 94-7(Jan 1971).

Translated from Izv. Akad. Nauk SSSR, Neorg. Mater.; 7: No. 1, 103-7(Jan 1971).

Using derivatographic analysis, the thermal behavior of solid solutions in the system EuO–CaO was studied during heating from 20 to 900°C. For solutions containing less than 50 mole % europium oxide, it was found that one of the solid solution components (CaO) has a disintegrating effect owing to its tendency to absorb atmospheric moisture and carbon dioxide. A solid-solution region with a higher resistance to oxidation by atmospheric oxygen during heating was found and the dependence of this property on the composition of the solid solution was established. (auth)

42965 REPORT ON THE URANIUM–NITROGEN SYSTEM. Katsura, Masahiro; Sano, Tadao (Osaka Univ.). Technol. Rep. Osaka Univ.; 20: No. 932-972, 451-9(Oct 1970). (In German).

The formation enthalpy of U_2N_{3+x} as a function of the x value was calculated again with the aid of new thermodynamic data. At present, the recommended equation is $\Delta H_f^\circ(U_2N_{3+x}) = -167.6 - 51.4x + 25.4x^2$ (kcal/mol). The formation entropy of U_2N_3 in equilibrium with UN was also calculated tentatively. (auth)

42966 THERMAL EXPANSION OF NIOBIUM CARBIDE, HAFNIUM CARBIDE, AND TANTALUM CARBIDE AT HIGH TEMPERATURES. Jun, C. K.; Shaffer, P. T. B. (Carborundum Co., Niagara Falls, N. Y.). J. Less-Common Metals; 24: No. 3, 323-7(Jul 1971).

The thermal expansions of hot-pressed $NbC_{0.95}$, $HfC_{0.98}$, and $TaC_{0.99}$ were measured over the temperature range 700 to 2600°C. The data are shown in graphs with literature data for comparison, and average thermal expansion coefficients are tabulated for various temperature ranges. (D.L.C.)

42967 NITROGEN DIFFUSION IN ZIRCONIUM. Levinskii, Yu. V.; Kiparisov, S. S.; Strogonov, Yu. D. (Inst. of Steel and Alloys, Moscow). Izv. Vyssh. Ucheb. Zaved., Tsvet. Met.; No. 6, 91-6(1970). (In Russian).

The diffusion of N in Zr at 1260 to 1720°C was investigated by means of metallographic and gravimetric analysis, and diffusion coefficients for N were measured in the nitride, ZrN, and in the α-solid solution of Zr. The values of diffusion coefficients thus obtained agreed satisfactorily with extrapolated data from other workers. (tr-auth)

42968 REDUCTION CYCLE $MO_2 \rightarrow M_2O_3$ FOR CERIUM, PRASEODYMIUM, AND TERBIUM OXIDES. Rudenko, V. S.; Boganov, A. G. (Inst. of Silicate Chemistry, Moscow). Inorg. Mater. (USSR) (Engl. Transl.); 7: No. 1, 98-103(Jan 1971).

Translated from Izv. Akad. Nauk SSSR, Neorg. Mater.; 7: No. 1, 108-15(Jan 1971).

The reduction of cerium dioxide, praseodymium dioxide, and terbium dioxide was studied. The crystallochemical theory of superstructure formation by ordering of defect positions in the matrix dioxide lattice is discussed; the compositions of the discrete phases in the range $MO_2-M_2O_3$ are predicted and are realized in experiment. The C $\rightarrow$ A transition in praseodymium oxide is the last stage in the reduction of the higher oxides in the transition to the composition M_2O_3. For the oxides of terbium, the reversible C $\rightarrow$ B transition is also due to reduction processes in the transition to the composition M_2O_{3-x}. (auth)

42969 HOW THE PARTIAL VAPOR PRESSURE OF OXYGEN AND THE TEMPERATURE AFFECT THE ELECTRICAL PROPERTIES OF LIQUID V_2O_5. Musikhin, V. I.; Pastukhov, E. A.; Batolin, N. A.; Lepinskikh, B. M. (Inst. of Metallurgy, Moscow). Inorg. Mater. (USSR) (Engl. Transl.); 7: No. 1, 91-3(Jan 1971).

Translated from Izv. Akad. Nauk SSSR, Neorg. Mater.; 7: No. 1, 99-102(Jan 1971).

The character of the conductivity of fused V_2O_5 is not changed by the addition of up to 20% CaO. Dissociation of V_2O_5 with increasing temperature or falling P_{O_2} leads to rearrangement of the structure; this is reflected as extrema and inflections on the resistance and thermo-emf curves. (auth)

42970 ENERGIES OF MIXING IN SYSTEMS CONTAINING GERMANIUM AND SILICON WITH ELEMENTS OF GROUPS III AND V. Nikitina, G. V.; Romanenko, V. N.; Ishutinova, L. N. (Higher Engineering Marine Coll., Leningrad). Inorg. Mater. (USSR) (Engl. Transl.); 7: No. 1, 41-4(Jan 1971).

Translated from Izv. Akad. Nauk SSSR, Neorg. Mater.; 7: No. 1, 45-9(Jan 1971).

The theory of regular solutions accounts for the eutectic diagrams of the semiconductor-impurity type in the case of impurity elements of Groups III and V dissolved in germanium and silicon. The energies of mixing in the solid and liquid phases were determined for the systems Ge–Sb, Ge–In, Ge–Ga, Ge–Al, Si–Al, Si–Sb, and Si–Ga. The predicted solubility curves of silicon and germanium in aluminum and of germanium in antimony were constructed. (auth)

42971 CARBON–CARBON MATERIALS FOR ABLATIVE ENVIRONMENTS. Frye, E. R. (Sandia Labs., Albuquerque, N. Mex.). Nucl. Technol.; 12: No. 1, 93-107(Sep 1971). (SC-DC-70-5157).

A family of carbon-fiber-reinforced carbon (and graphite) composites was developed for high-temperature applications. The method of screening for ablation resistance is described. The effects of filament orientation, matrix composition, and heat treatment are related to ablation performance. Between the angles of 15 and 75° a general insensitiveness to filament orientation is reported. Usually, but not always, materials having a chemical vapor deposited matrix performed better than a carbonized organic counterpart. Graphitized materials are more effective than less ordered forms. Process control may be more important than specific composite constituents. (auth)

42972 INFLUENCE OF SOME SALTS ON THE DOUBLE DECOMPOSITION OF ZIRCON WITH CALCIUM CARBONATE. Galkin, Yu. M.; Chukhlantsev, V. G.; Levakov, E. N. Tsvetn. Metal.; No. 1, 54-6(Jan 1971). (In Russian).

Sintering of zircon with chalk at 1150 to 1300°C results in monoclinic zirconia and calcium metasilicate: $ZrSiO_4 + CaCO_3 = ZrO_2 + CaSiO_3 + CO_2$. In order to increase the reaction rate and lower the sintering temperature, various additives were tried: $CaCl_2$, CaF_2, $CaSO_4$, Na_2CO_3, and NaF. The testing procedure included grinding the zircon to –0.05 mm, mixing with the chalk and additive, and pelletizing under pressure before firing. Chemical analyses and x-ray diffraction patterns indicated that the most effective additive among those tested was $CaCl_2$, the quantity used corresponding to the eutectic composition for the system $CaCl_2-CaCO_3$. (K.S.W.)

42973 STRESS RELAXATION IN BERYLLIA. Walker, D. G.; Rotsey, W. B.; Wood, B. R. A. (Australia Atomic Energy Commission Research Establishment, Sutherland, New South Wales). J. Mater. Sci.; 6: No. 4, 281-8(Apr 1971).

Beryllia beams were loaded at temperature in four-point bending to a deflection of 0.001 in. or 0.002 in. and the decrease in load necessary to maintain the deflection constant was measured as a function of time. The beryllia was fine-grained, in the range ~1 to 7 μm, and the porosity varied between 3 and 21%. The test conditions covered a temperature range of 850 to 1240°C, experiments took from 10 min to 8 hr: the loads used produced initial maximum outer fibre stresses of the order 3000 to 6000 psi. A method was developed for calculating the stress distribution in a beam at any time and this was used to analyse the results. The stress relaxation process was found to be stress-activated, and the conversion of elastic to plastic strain could be expressed as a creep law having the form $\dot{\epsilon} = k_0 \exp(-Q/RT) \exp(C\nu\sigma/RT)$. The activation energy was 100 ± 2 kcal mole^{-1} and the activation volume was large, probably of the order of 10^3 atoms. The rate constant k_0 was approximately proportional to the fraction of intergranular porosity and inversely proportional to the cube of the grain diameter. It is suggested that the mechanism of grain boundary sliding is consistent with the observations. (auth) (UK)

42974 LOW-TEMPERATURE HEAT CAPACITIES OF TRANSITION METAL BORIDES. Hanson, B. D.; Mahnig, M.; Toth, Louis E. (Univ. of Minnesota, Minneapolis). Z. Naturforsch.; 26a: No. 4, 739-47(Apr 1971).

Low-temperature heat capacities from 1.5 to 15°K were measured for a number of transition-metal borides with the compositions Me_2B, MeB and MeB_2, and their solid solutions. The measurements show that the borides are characterized by a narrow d-band with a relatively large density of electron states. The variation of γ with position of the transition metal in the periodic table for the borides is considerably different from that of the transition metals and solid solutions. This result suggests considerable differences in the shapes of the respective band structures. There is evidence for an electron transfer from the boron atoms to the d-bands of the transition metal. (auth)

42975 SIMULTANEOUS OXIDE EVAPORATION AND THERMAL DIFFUSION IN TANTALUM–OXYGEN SOLID SOLUTIONS. Lohnert, Wolfgang; Fromm, Eckehard (Max-Planck-Institut fuer Metallforschung, Stuttgart). Z. Metallk.; 62: No. 6, 469-71(Jun 1971). (In German).

In specimens, containing oxygen, annealed in a temperature gradient a superposition of diffusion, thermal diffusion, and oxide evaporation is observed when the maximum temperature lies between 1600 and 2000°C. For maximum temperatures below 1700°C the O-concentration is decreased mainly in the cooler part of the specimen, whereas for maximum temperatures higher than 1700°C the degassing process in the hot zone is predominant. (auth)

42976 HEAVY CONCRETES FOR GAMMA RADIATION PROTECTION: THE USE OF ZIRCON AS AGGREGATES. da Costa, Jose Ribeiro (Instituto de Engenharia Nuclear, Rio de Janeiro). pp 55-61 of Materials Technology. I. New York; American Society of Mechanical Engineers (1970).

From second inter-american conference on materials technology; Mexico City, Mex. (24 Aug 1970). See CONF-700812.

Hematite and limonite are good materials for use as aggregates in heavy concretes for gamma radiation protection; however, such concretes present many variations in several mechanical and physical parameters as: weight loss, shrinkage, density, tensile and compressive strength. The change in these properties is not good behavior for materials used to shield against radiation. The addition of a zircon sand, as fine aggregate (about 12% of the concrete weight) can provide a good improvement in such a concrete and also, avoid the difficulty in obtaining fine aggregate from limonite. The behavior of such concretes is discussed, including a comparison with baryte and limonite + baryte concretes. (auth)

42977 ALLOTROPES OF CARBON (AMORPHOUS, GRAPHITE, DIAMOND) AS ENGINEERING MATERIALS. Fagan, A. Wayne (Poco Graphite, Inc., Decatur, Tex.); Wehrmann, R. F.; Tait, R. D. pp 467-71 of Materials Technology. I. New York; American Society of Mechanical Engineers (1970).

From second inter-american conference on materials technology; Mexico City, Mex. (24 Aug 1970). See CONF-700812.

Carbon, in the form of its various allotropes and modifications (amorphous, graphite, diamond), is well established as an engineering material in a diversity of applications. Usage of carbonaceous substances as component and constituent materials in engineering and structural applications can be expected to increase as materials specialists and design engineers become better acquainted with the properties of these materials and acquire a more profound understanding of their capabilities and potentials.

XUM

Research, development, and production efforts to provide improved synthetic carbonaceous materials most certainly will continue, and probably at an accelerating rate. The properties of several modifications of carbon are described and compared with other engineering materials, and the prospects for improved carbon materials are discussed. (auth)

42978 DEVELOPMENT OF CERAMIC FIBER REINFORCED METALS. Hahn, Henry (American Standard Inc., Falls Church, Va.); Kershaw, John P. pp 559-82 of Materials Technology. I. New York; American Society of Mechanical Engineers (1970).

From second inter-american conference on materials technology; Mexico City, Mex. (24 Aug 1970). See CONF-700812.

The reinforcement of metals with ceramic whiskers and continuous filaments is shown to have progressed far from their initial status as laboratory curiosities. A spectrum of reinforcements were developed possessing outstanding properties. Consolidation techniques were developed which result in the production of viable and competitive engineering materials. The characterization of these materials has included establishing their tensile, fatigue, creep, stress rupture, and fracture behavior. Many of the properties of reinforced metals are found to be superior to their monolithic counterparts, especially when a given property is normalized on a weight basis. (auth)

42979 SINTERING OF UN AS A FUNCTION OF TEMPERATURE AND N_2 PRESSURE. Tennery, V. J.; Godfrey, T. G.; Potter, R. A. (Oak Ridge National Lab., Tenn.). J. Amer. Ceram. Soc.; 54: No. 7, 327-31(Jul 1971).

The sintering of uranium mononitride (UN) depends on temperature and the N_2 pressure maintained over the nitride during heat treatment. At a given temperature, an N_2 pressure that maintained the UN in the single-phase region slightly above the phase boundary where the reaction $UN \rightarrow U + \frac{1}{2} N_2(g)$ occurred was most effective in accelerating the sintering of single-phase UN. For example, specimens sintered at 1600°C under N_2 pressures of either 1140 or 1.7×10^{-4} torr had essentially identical compositions, but the density of the former was 10.78 g/cm^3 (75% of theoretical), whereas that of the latter was 12.20 g/cm^3 (85% of theoretical). Results were similar at temperatures up to 2100°C. The x-ray lattice constant of UN sintered at reduced N_2 pressures was slightly larger than that of UN sintered in 1140 torr of N_2. The observed constants ranged from 4.88904 to 4.88991 Å; the combined O + C content varied from 400 to 900 ppM. (auth)

42980 WETTING OF CERAMICS BY LIQUID METALS. Rhee, S. K. (Bendix Corp., Southfield, Mich.). J. Amer. Ceram. Soc.; 54: No. 7, 332-4(Jul 1971).

A linear relation is established between the cosine of the contact angle and the temperature of a liquid metal sessile drop resting on a ceramic substrate. This relation is demonstrated for many liquid metal/ceramic systems. The work of adhesion and the effects of surface roughness, porosity, chemical reactions, and structural transformations in the substrate surface are also discussed. (auth)

Structure and Phase Studies

Refer also to abstracts 42891 and 42896.

42981 (JAERI-13635) ELECTRON MICROSCOPE OBSERVATION OF THE ZIRCONIUM HYDRIDE. Katano, Yoshio; Ogawa, Yutakai; (and others) (Japan Atomic Energy Research Inst., Tokai). Jul 1969. 21p. NTIS (U. S. Sales Only).

An electron microscopic study was carried out on the hydride precipitation behavior in zirconium. Previous studies of this type have employed comparatively high cooling rates following the homogenization heat treatment, while in the described study, precipitation after slow cooling has been observed. Marked difference in the shape of the hydride precipitates was noted depending on the cooling condition. In contrast to the needle shaped hydride precipitation under rapid cooling conditions, hexagonal and/or rhombic plates were formed parallel to the {0001} planes of the matrix when cooled slowly, i.e., at 15 to 55°C/hr. Selected-area diffraction patterns from the latter precipitates were identified as those from zirconium hydride with fct structure. (auth) (Japan)

42982 (JAERI-13650) REVIEW OF THE PHASE RELATIONS AND THE STRUCTURES OF THE NaCl TYPE COMPOUNDS IN THE SYSTEM U-Pu-C-N. Tagawa, Hiroaki (Japan Atomic Energy Research Inst., Tokai). Jul 1969. 29p. NTIS (U. S. Sales Only).

The present state of knowledge of the phase relations and the structures of the NaCl-type compounds in the system U-Pu-C-N are reviewed, and further works in these areas are pointed out. (auth)

42983 (MIT-3773-103) BASIC RESEARCH IN CRYSTALLINE AND NONCRYSTALLINE CERAMIC SYSTEMS. Annual Report. Kingery, W. D.; Coble, R. L. (Massachusetts Inst. of Tech., Cambridge. Dept. of Metallurgy and Materials Science). Apr 1971. Contract AT(30-1)-3773. 44p. Dep. NTIS.

The major areas of investigation of ceramic systems included: studies of kinetics of phase changes, diffusion, and the development of microstructure; relations of properties to composition, crystal structure, and microstructure; and materials synthesis and preparation. Defect structures and their mobilities in crystals and atomic transport of grain boundaries were studied in several materials for application to the myriad of processes governed by diffuson—notably sintering, high temperature reactions, creep. The effects of thermal gradients on nonstoichiometric oxides have delineated the effects of trace impurities on resulting properties. Further modelling for microstructure development in hot pressing was carried out, as were sintering studies which showed the mechanisms of the process and the importance of fabrication procedures prior to heat treatment. Strength and microstructural effects were studied briefly. Dislocation dynamics in fluorite structures remain a continuing program. Chemical vapor deposition apparatus was assembled and process variables studied for the preparation of a variety of crystals, both pure and doped. Studies of solid solutions and defect compensation in single crystals are underway. Crystals for general studies by x-ray techniques, electrical, mechanical, and optical property characterization are also provided. From the results, several prominent areas are identified where further emphasis will be rewarding and for which new work is proposed. In particular, there is need for improved procedures to make higher purity ceramics and a need to learn more about solute effects in saturated systems. Further, it is proposed to measure grain boundary sliding characteristics directly in order to contribute to an understanding of high temperature deformation behavior in oxides. (auth)

42984 (ORNL-tr-2483) PHASE EQUILIBRIA IN THE SYSTEMS ThO_2-UO_{2+x}, CeO_2-UO_{2+x}, AND NpO_2-UO_{2+x}. Paul, Robert (Kernforschungszentrum, Karlsruhe (West Germany). Institut fuer Radiochemie). Translated for Oak Ridge National Lab., Tenn., from report KFK-1297. 64p. Dep. NTIS.

An abstract of this paper, prepared from the original language, appeared as NSA 25: 24645.

42985 PHASE EQUILIBRIA IN THE HIGH-ALUMINA REGION OF THE SYSTEM Al_2O_3-Nb_2O_5. Toropov, N. A.; Fedorov, N. F.; Andreev, I. F.; Kasparyan, R. M. (Leningrad Technological Inst.). Inorg. Mater. (USSR) (Engl. Transl.); 6: 1515-16(Sep 1970).

Translated from Izv. Akad. Nauk SSSR, Neorg. Mater.; 6: 1718-19(Sep 1970).

The overall results of crystallooptical, x-ray, and differential-thermal analysis are reflected in an included phase diagram; the investigated part of the Al_2O_3-Nb_2O_5 system contains a chemical compound which melts with decomposition. Above 1100°C Nb_2O_5 begins to dissociate in accordance with the equation $Nb_2O_5 = 2NbO_2 + \frac{1}{2}O_2$. Bearing this in mind, and beginning from the calculated K_e of the reaction, a series of calcinations in a specially designed furnace under a pressure $P_{O_2} = 4 - 5$ atm was performed. From a comparison of the x-ray diffraction patterns and ir spectrograms of compositions roasted in air in a Silit furnace and in oxygen under pressure, it can be inferred that niobium pentoxide undergoes no changes under these conditions, so that the phase interrelationships remain the same as in air. (auth)

42986 PHASE DIAGRAM OF THE SYSTEM Pr-Te. Yarembash, E. I.; Vigileva, E. S. (Inst. of General and Inorganic Chemistry, Moscow). Inorg. Mater. (USSR) (Engl. Transl.); 6: 1388-93(Sep 1970).

Translated from Izv. Akad. Nauk SSSR, Neorg. Mater.; 6: 1572-8(Sep 1970).

Studies of the Pr-Te system revealed the following compounds: PrTe, Pr_3Te_4, Pr_2Te_3, $PrTe_{1.9}$, (Pr_4Te_9), Pr_3Te_7, Pr_2Te_5, Pr_4Te_{11}, $PrTe_3$. Most of the praseodymium tellurides exist in phases of variable composition, the range of homogeneity of which decreases with increasing relative tellurium content. The similarity of the main features of the laminated structures of Pr polytellurides was observed to be Te-Te-two-layer network. The relative weakness of the Te interatomic bonds adjoining different layers is due to the possibility of a change in the degree of population of these layers, while the main shell of the structure is retained on the whole. This process is equivalent to formation of periodic packing defects, and may be considered as the cause of the usual polytypic character, which is called a concentration polytype. As regards their physical properties, Pr_2Te_3, Pr_4Te_7 and $PrTe_{1.9}$ may be classed as semiconductors; the properties of the other compounds display much in common with those of metals and semimetals. (auth)

42987 POSSIBILITY OF THE EXISTENCE OF STABLE ZIRCONIUM MONOXIDE. Zainulin, Yu. G.; Alyamovskii, S. I.; Shveikin, G. P.; Gel'd, P. V. (Inst. of Chemistry, Sverdlovsk, USSR). Inorg. Mater. (USSR) (Engl. Transl.); 6: 1192-4(Jul 1970).

Translated from Izv. Akad. Nauk SSSR, Neorg. Mater.; 6: 1356-7(Jul 1970).

The materials used in the investigation were synthesized from ZrO_2 and Zr metal powder. Results of the investigation showed that neither stable ZrO or Zr_2O_3 is formed in solid phase below 1700°C. The cubic phase found previously apparently was not a binary product but a multicomponent product containing elements with atomic radii greater than that of oxygen. (J.R.D.)

42988 PHASE EQUILIBRIA IN THE SYSTEM Er_2O_3–GeO_2. Bondar, I. A.; Petrova, M. A. (Inst. of Silicate Chemistry, Moscow). Inorg. Mater. (USSR) (Engl. Transl.); 6: 1127-9(Jul 1970).

Translated from Izv. Akad. Nauk SSSR, Neorg. Mater.; 6: 1285-7(Jul 1970).

Phase equilibria in the $Er_2O_3-GeO_2$ system were studied. The existence of compounds such as $2Er_2O_3 \cdot GeO_2$, $Er_2O_3 \cdot GeO_2$, and $Er_2O_3 \cdot 2GeO_2$ was established. The physicochemical and crystallooptical properties of these oxides were studied. (J.R.D.)

42989 PHASE DIAGRAM OF THE SYSTEM Cd–As. Gukov, O. Ya.; Ugai, Ya. A.; Pshestanchik, V. R.; Goncharov, E. G.; Pakhomova, N. V. (Voronezh State Univ., USSR). Inorg. Mater. (USSR) (Engl. Transl.); 6: 1693-5(Nov 1970).

Translated from Izv. Akad. Nauk SSSR, Neorg. Mater.; 6: 1926-9(Nov 1970).

Stable and unstable partial $CdAs_2-As$ phase diagrams were constructed from thermal, microstructural, and x-ray phase analysis data. The stable diagram is a system with a simple eutectic, the melting point and composition of which are 620°C and 58.3 wt % As, respectively. (auth)

42990 FORMATION OF SUBOXIDES IN THE SYSTEM NIOBIUM–OXYGEN. Dekanenko, V. M.; Vavilova, V. V. (Inst. of Metallurgy, Moscow). Inorg. Mater. (USSR) (Engl. Transl.); 7: No. 1, 88-90(Jan 1971).

Translated from Izv. Akad. Nauk SSSR, Neorg. Mater.; 7: No. 1, 96-8(Jan 1971).

The suboxide, Nb_6O, was discovered in an alloy of niobium with 6 at. % oxygen, obtained by fusing niobium with Nb_2O_5, after the alloy was annealed at 300°C. After annealing at 500°C, alloys of niobium and oxygen to which 2 at. % titanium was added displayed acicular segregations. X-ray phase analysis showed that these segregations are the suboxide Nb_2O. (auth)

42991 METAL SUBOXIDES. Kornilov, I. I. (Inst. of Metallurgy, Moscow). Inorg. Mater. (USSR) (Engl. Transl.); 7: No. 1, 83-7(Jan 1971).

Translated from Izv. Akad. Nauk SSSR, Neorg. Mater.; 7: No. 1, 91-5(Jan 1971).

Recent investigations have revealed many suboxides. Metals of Groups IV to VIA, which have many vacant sites in the d-electron shell, have a particular tendency for formation of these suboxides. These suboxides have ordered structures and an ordered location of the oxygen atoms in the octahedral cavities of the lattice of the metal-base. On the basis of the existence of binary suboxides the existence of ternary and more complex suboxides of transition metals is assumed, the compositions of which are located in ternary diagrams in quasibinary cross sections joining the binary suboxides. Both theoretical and practical interest are attached to study of this class of compounds located at the boundary of typical inorganic compounds and metallides. (auth)

42992 STRUCTURE OF ALLOYS IN THE SYSTEM Ta–C–Re. Ordan'yan, S. S.; Kosterova, N. V.; Avgustinik, A. I. (Leningrad Technological Inst.). Inorg. Mater. (USSR) (Engl. Transl.); 7: No. 1, 57-9(Jan 1971).

Translated from Izv. Akad. Nauk SSSR, Neorg. Mater.; 7: No. 1, 64-6(Jan 1971).

The isothermal cross section of the ternary system Ta–C–Re at 2100°C was constructed from chemical, metallographic, and x-ray analyses. No ternary compounds were observed in the system Ta–C–Re. Equilibrium of phases based on the ξ-phase and tantalum monocarbide with the solid solution of rhenium in tantalum was not observed. X-ray analysis revealed that the solid solution (Ta, Re) coexists with the Ta_2C-based phase. (auth)

42993 SYSTEM YTTRIUM–CHROMIUM–SILICON. Sobolev, A. S.; Bodak, O. I.; Gladyshevskii, E. I. (Lvov State Univ.). Inorg. Mater. (USSR) (Engl. Transl.); 7: No. 1, 37-40(Jan 1971).

Translated from Izv. Akad. Nauk SSSR, Neorg. Mater.; 7: No. 1, 41-4(Jan 1971).

Using x-ray and microstructural phase analysis, the phase equilibrium diagram of the system Y–Cr–Si was studied at 800°C. The existence of the compound YCr_2Si_2 with a tetragonal structure of the $CeGa_2Al_2$ type (a = 3.916 Å and c = 10.631 Å) was established. (auth)

42994 MECHANISM OF THE PHASE TRANSITION IN BORON NITRIDE. Neshpor, V. S.; Samsonov, G. V.; Fel'dgun, L. I.; Khusidman, M. B. (Inst. of Applied Chemistry, Leningrad. Inst. of Problems in Materials Science, Kiev). Inorg. Mater. (USSR) (Engl. Transl.); 7: No. 1, 155-6(Jan 1971).

Translated from Izv. Akad. Nauk SSSR, Neorg. Mater.; 7: No. 1, 173-4(Jan 1971).

The mechanism for the α-BN to β-BN transition was investigated by using the EPR method to observe the behavior of stable atomic structural defects during the phase transition. The experimental results point toward a direct transformation of the graphite-like lattice of α-BN to the cubic one of β-BN. The role of the catalyst (alkali or alkaline-earth metal), which is an effective electron donor, in the transition probably consists in giving the more electropositive boron atom the stable sp^3 electron configuration necessary for the formation of the system of tetrahedral hybridized bonds characteristic of the β-BN lattice. (G.M.C.)

42995 STUDY OF THREE CROSS SECTIONS IN THE SYSTEM CaO–Nd_2O_3–Al_2O_3. le Flem, J.; Bondar, I. A.; Udalov, Yu. P. (Inst. of Silicate Chemistry, Moscow). Inorg. Mater. (USSR) (Engl. Transl.); 7: No. 1, 104-7(Jan 1971).

Translated from Izv. Akad. Nauk SSSR, Neorg. Mater.; 7: No. 1, 116-19(Jan 1971).

Fusion of the melilite-like compound $CaNdAl_3O_7$ had an incongruent character. New ternary compounds were discovered: $CaNdAlO_4$, isostructural with K_2NiF_4, and $Ca_3Nd_5Al_5O_{18}$, isostructural with $8CaO \cdot 5SiO_2$. The binary cross sections $CaAl_2O_3-CaNdAl_3O_7$, $CaNdAl_3O_7-Nd_2O_3$, and $CaNdAlO_4-NdAlO_3$ were investigated, and information is given on the liquidus surface in the system $CaO-Nd_2O_3-Al_2O_3$. (auth)

42996 MIXED CRYSTAL PHASES IN THE SYSTEM ThO_2-PrO_x. Brauer, G.; Willaredt, B. (Univ., Freiburg i. B.). J. Less-Common Metals; 24: No. 3, 311-16(Jul 1971).

Praseodymia and thoria form homogeneous crystalline phases when mixed and heated to 1300°C. The oxygen content of these phases depends on the pressure of molecular oxygen maintained during the cooling of the samples from 500°C down to room temperature. It is noteworthy that the addition of thoria does not promote the uptake of oxygen to form more Pr(IV) compared with the case of pure praseodymia. The lattice parameters of the mixed crystal series $(Pr,Th)O_2$ and $(Pr,Th)O_{2-x}$ show appreciable deviations from Vegard's Rule. An attempt is made to explain this phenomenon by the ionic size effect. (auth)

42997 ELECTROPHYSICAL PROPERTIES AND CHEMICAL BOND TYPES IN COMPOUNDS OF BERYLLIUM WITH BORON AND CARBON. Neshpor, V. S.; Samsonov, G. V. (Inst. of Problems in Materials Science, Kiev). Inorg. Mater. (USSR) (Engl. Transl.); 7: No. 1, 45-9(Jan 1971).

Translated from Izv. Akad. Nauk SSSR, Neorg. Mater.; 7: No. 1, 50-5(Jan 1971).

The electrical resistivity of the borides of beryllium increases with the relative boron content, from values characteristic of metallic conductors for the lower borides to values characteristic of insulators for the higher ones. The structures and electrophysical properties of the lower borides of beryllium are governed by the pattern of bonds of beryllium, mainly of the metallic type, with little localization of the s-electrons of beryllium. In these compounds there is equilibrium between the electron configurations $(s^2 \rightleftharpoons sp)Be \rightleftharpoons (sp^2 \rightleftharpoons sp^3)B$, with similar energies and mutually overlapping, which gives rise to metallic conductivity. The structures and electrophysical properties of the higher borides of beryllium are governed by the pattern of covalent boron bonds. The beryllium atoms in these compounds are electron donors, which stabilize the sp^3 electron configurations of boron, and in turn they acquire stable s^0 configurations. Between the higher-energy electron configurations of beryllium and the electron configurations of boron there is an energy gap, which is responsible for their insulating properties. As the boron content of the beryllium borides is increased, there is a gradual increase in the pattern of boron bonds in the structures; the sp^3 electron configurations of the boron atoms and the s^0 configurations of beryllium become stabilized, and the energy difference between them increases. In structure, hardness, and electrical properties, the higher borocarbide of beryllium, BeC_2B_{12}, resembles B_4C, owing to the opposing influences of the beryllium valence electrons on the valence electron configurations of boron and carbon. The lower borocarbide of beryllium, BeC_2B_2, has submetallic properties like those of the lower borides of beryllium and is com-

XUM

paratively soft, owing to the fairly strong disturbance of the stable sp^3 configurations of boron by the valence electrons of beryllium. (auth)

42998 THERMODYNAMIC CALCULATIONS ON THE QUINARY SYSTEM U–Pu–C–O–N. Imoto, Shosuke (Osaka Univ.). Technol. Rep. Osaka Univ.: 20: No. 943, 473-87(Oct 1970).

The equilibrium partial pressures of N_2 and CO for the quinary U–Pu–C–O–N system at 1800°K were calculated using an ideal solution model, except for the monoxycarbonitride solid solution for which the model was modified to involve a non-ideal term. According to the calculation, the maximum solubility of oxygen in hypostoichiometric mixed carbide showed a marked minimum at a cationic composition of about $U_{0.8}Pu_{0.2}C$, which falls within the composition range of a possible breeder fuel. The possible maximum contents of oxygen in mixed oxycarbonitride were also calculated which showed always higher values for the hypostoichiometric solutions than for the hyperstoichiometric solutions. The topology of the volume phase field in the M–C–O–N tetrahedron was studied and the result agreed with that experimentally found by Henry et al. The carbon activity of the mixed carbonitride at 1400°K was also estimated. (auth) (Japan)

42999 ANALYSIS OF EVAPORATED SILICON OXIDE FILMS BY MEANS OF (d,p) NUCLEAR REACTIONS AND INFRARED SPECTROPHOTOMETRY. Cachard, A.; Roger, J. A.; Pivot, J.; Dupuy, C. H. S. (Univ. Claude Bernard, Lyon). Phys. Status Solidi (a); 5: No. 3, 637-44(16 Jun 1971).

An analysis was made of SiO_x thin films evaporated either by electronic bombardment (SiO_B) or by Joule effect (SiO_J). Stoichiometry was studied by nuclear microanalysis and bondings by infrared spectrophotometry. It is found that SiO_B, which never involves a negative resistance phenomenon in M–SiO_B–M sandwiches, is a SiO stable pseudophase. But SiO_J should be a mixture of a SiO_2 phase and SiO and Si_2O_3 pseudophases; in this case the negative differential resistance phenomena are related to this "Si_2O_3" pseudo-phase. (auth)

43000 CRYSTAL STRUCTURE OF CURIENITE, $Pb(UO_2)_2(VO_4)_2.5H_2O$. Borene, Jacques; Cesbron, Fabien (Univ., Paris). Bull. Soc. Fr. Miner. Crist.; 94: No. 1, 8-14 (Jan-Feb 1971). (In French).

The crystal structure of curienite, natural lead uranyl vanadate, has been solved using three-dimensional x-ray diffraction data obtained using an automatic diffractometer. The space group is Pcan and the final R factor is 0.118 with anisotropic thermal parameters for the cations and isotropic factors for the oxygen atoms. The crystal is built up by $[(UO_2)\ V_2O_8]_n^{2n-}$ slabs parallel to (001) which contain symmetry centers. Lead atoms, lying between these slabs, are surrounded by four water molecules, two oxygen atoms belonging to two VO_5 pyramids and two oxygen atoms belonging to two uranyl groups. The fifth water molecule seems to be interstitial. A comparison is made between the stacking modes of the uranyl vanadate slabs in the various known structures. (auth)

43001 COMBINATIONS BETWEEN THE URANIUM CHALCOGENIDES UX AND U_3X_4 (X = S, Se, Te), AND THE SULFIDES, SELENIDES, AND TELLURIDES OF LANTHANIDES, YTTRIUM, AND SCANDIUM. Demoncy, Philippe; Khodadad, Parviz (Univ., Paris). Ann. Chim. (Paris); 5: 341-56(Sep-Oct 1970). (In French).

A systematic survey of combinations between the chalcogenides of uranium, UX and U_3X_4 (X = S, Se, Te), and the L_2X_3–L_3X_4 compounds (L = lanthanides, Y, Sc) was made. A number of solid solutions of the Th_3P_4 and Y_5S_7 types were identified. The crystallographic parameters of U_3S_4 were determined (a = 8.44 Å). (France)

43002 PHASE RELATIONSHIPS AND CRYSTAL CHEMISTRY IN THE SYSTEMS US–CaS, US–SrS, AND US–BaS. Komac, M.; Golic, L.; Kolar, D.; Brcic, B. S. (Jozef Stefan Nuclear Inst., Ljubljana, Yugoslavia. Univ. of Ljubljana, Yugoslavia). J. Less-Common Metals; 24: No. 2, 121-8(Jun 1971).

Phase equilibria in the systems US–CaS, US–SrS and US–BaS were investigated by x-ray diffraction, metallography and electron-probe microanalysis. New ternary sulphides, $CaUS_2$, $SrUS_2$, and $BaUS_2$, which appeared in the corresponding systems, formed eutectic mixtures with primary solid solutions. Eutectic melting temperatures were determined for the systems US–CaS and US–SrS and tentative phase diagrams constructed. Detailed crystal structure analyses of $CaUS_2$ and $SrUS_2$ were carried out. (auth)

43003 NONSTOICHIOMETRIC HEXABORIDE OF THORIUM $Th_{1-x}B_6$. Etourneau, J. (Faculte des Sciences, Bordeaux); Naslain, R.; La Placa, S. J. Less-Common Metals; 24: No. 2, 183-93(Jun 1971). (In French).

Nonstoichiometric thorium hexaboride was obtained by heating high purity boron–thorium mixtures ($6 \leq B/Th \leq 24$) at 1300°C under high vacuum. The limit of homogeneity range is x = 0.22 as shown by x-ray diffraction, neutron diffraction, and density studies. Neutron diffraction requires the use of 98.05% ^{11}B, thorium hexaboride phases have the CaB_6-type structure. The cell parameters increase from a = 4.1105 Å (x = 0) to a = 4.1125 Å (x = 0.22). The B–B interoctahedral bonds (1.612 Å) are shorter than B–B intraoctahedral bonds (1.767 Å). (auth)

43004 ERBIUM DISELENIDE. Haneveld, A. J. Klein; Jellinek, F. (Univ., Groningen, Netherlands). J. Less-Common Metals; 24: No. 2, 229-31(Jun 1971).

The preparation of β–$ErSe_2$ is described. The diffraction pattern of β–$ErSe_2$, observed at 940°C, was indexed by a body-centered orthorhombic cell of dimensions: a = 4.12, b = 5.64, and c = 13.25 Å. Beta–$ErSe_2$ retained at room temperature was found to have undergone a slight monoclinic deformation. The dimensions of the monoclinic C-centered cell were: a = 6.862, b = 13.15, c = 4.073 Å, β = 125.44°. (G.M.C.)

43005 PHASE RELATIONS IN THE SrO–IrO_2–Ir SYSTEM IN AIR. McDaniel, C. L.; Schneider, S. J. (National Bureau of Standards, Washington, D. C.). J. Res. Nat. Bur. Stand.; 75A: No. 3, 185-96(May-Jun 1971).

The equilibrium phase relations for the SrO–IrO_2–Ir system were determined in an air environment at atmospheric pressure. A ternary equilibrium phase diagram was constructed indicating selected oxygen reaction lines and tie lines. A binary representation is given for the ternary system in air. Of the nine phases detected in this study, three are stable and six are probably metastable under atmospheric conditions. The stable compounds, $4SrO \cdot IrO_2$, $2SrO \cdot IrO_2$, and $SrO \cdot IrO_2$ dissociate at 1540, 1445, and 1205°C, respectively. The metastable phases include low-$4SrO \cdot IrO_2$, $2SrO \cdot 3IrO_2$, $xSrO \cdot IrO_2 (x > 2)$, $ySrO \cdot IrO_2 (4 > y > 2)$, $zSrO \cdot IrO_2 (2 > z > 1)$, and $3SrO \cdot 2IrO_2$. The specific composition of the metastable phases could not be ascertained with certainty. The x-ray patterns of all phases detected in this study were indexed with the exception of that of the $zSrO \cdot IrO_2 (2 > z > 1)$ compound. A summary of x-ray data is given for all known phases occurring in the system. (auth)

43006 PHASE RELATIONS IN THE SYSTEM PbO–WO_3. Chang, Luke L. Y. (Miami Univ., Oxford, Ohio). J. Amer. Ceram. Soc.; 54: No. 7, 357-8(Jul 1971).

The system PbO–WO_3 was investigated as a part of a study of the stability relations of tungstates. The starting materials used in the study were highly purified WO_3 and reagent-grade PbO. Mixtures of proper proportions of the constituent oxides were blended under acetone for 2 hr. Samples were pelletized, sealed in a Pt container, and treated at the desired temperatures in muffle and SiC furnaces. Phases were identified microscopically using reflected light and by x-ray diffraction methods using Ni-filtered Cu radiation. Phase relations in the system from 600 to 1200°C are shown. (R.C.K.)

43007 SUPERSTRUCTURE OF VO_x IN THE RANGE, x = 1.15 TO 1.25, AND ITS STABILITY. Saeki, Masanobu; Nakahira, Mitsuoki (National Inst. for Research in Organic Materials, Tokyo). Mater. Res. Bull.; 6: No. 7, 603-11(Jul 1971).

X-ray and electron-diffraction studies of VO_x in the range, x = 1.15 to 1.25, revealed a superstructure at 700°C with the space group $I4_1/amd$ in its idealized form. The tetragonal cell is related to the original cubic cell in terms of $a = 2\sqrt{2}a_c$ and $c = 2a_c$. The major features of the structure involve the formation of the cation–vacancy clusters and their symmetrical arrangement. The stability of the superstructure is also discussed. (auth)

Radiation Effects

Refer also to abstracts 42928, 44093, 44118, and 44125.

43008 (N-71-12278) EFFECT OF RADIATION ON CERIUM-DOPED SOLAR-CELL COVER GLASS. Haynes, Gilbert A. (National Aeronautics and Space Administration, Langley Station, Va. Langley Research Center). Dec 1970. 14p. (NASA-TN-D-6024; L-7323). NTIS.

The results of an investigation to determine the feasibility of using an inexpensive, radiation-resistant solar-cell cover glass to replace synthetic fused quartz are reported. Several samples of a frequently used solar-cell cover glass were doped with various amounts of cerium. These samples were irradiated with 1-MeV electrons to a maximum fluence of 5×10^{14} e/cm^2 and with 22-MeV protons to a maximum fluence of 10^{13} protons/cm^2. The effects of the electrons and protons used in this investigation are representative of those of the corpuscular radiation found in space. Cerium doping of the cover glass improves its radiation resis-

tance. The optimum level of cerium doping appears to be between 1 and 2% by weight. (auth) (STAR)

43009 VALENCE STATE OF TIN AND THE STRUCTURE OF RADIATION DEFECTS IN SILICATE GLASSES CONTAINING TIN. Brekhovskikh, S. M.; Tyul'kin, V. A. Inorg. Mater. (USSR) (Engl. Transl.); 6: 1324-6(Aug 1970).

Translated from Izv. Akad. Nauk SSSR, Neorg. Mater.; 6: 1503-6(Aug 1970).

The EPR spectra and optical absorption spectra of gamma-irradiated silicate glasses containing tin were investigated. The presence of tin atoms in the glass gives a specific EPR signal with $g_{eff} = 1.990$, the complicated shape of which is due to two largely overlapping lines. The two-component structure of the contour is due to the existence of two valence states of tin atoms in glasses 2 and 4. Analysis of the EPR and optical spectra of glasses with various SnO_2 contents reveals that one of the lines of the complicated contour is due to $Sn^{2+}\oplus$ hole centers at divalent tin atoms in tetrahedral coordination. The other line is attributed to $Sn^{4+}e$ electron centers at tetravalent tin atoms in octahedral coordination. (auth)

43010 RESULTS OF LOOP TESTS ON Zr-CLAD EXPERIMENTAL FUEL RODS IN THE MR REACTOR. Amaev, A. D.; Goncharov, V. V.; Ivanov, E. G.; (and others) (Kurchatov Inst. of Nuclear Power, Moscow). pp 37-67 of Conference on the Use of Zirconium Alloys in Nuclear Reactors. Plzen, Czech.; Skoda Works (1968). (In Russian).

From Conference on the use of zirconium alloys in nuclear reactors; Marianske Lazne, Czech. (1 Oct 1968).

Fuel rod testing was carried out on calcined uranium dioxide clad with Zr–Nb or Zr–Fe–Ni alloys. The gap between fuel and cladding was 0.05, 0.075, 0.10 or 0.15 mm. The density of UO_2 was 90 and 95% theoretical (9.9 and 10.6 g/cm^3). The thermal flux was varied from 0.3 to 1.7×10^6 kcal/m^2·hr. The integral fast neutron dose was 1.5 and 5.0×10^{20} neutrons/cm^2. The fuel burnup was 13,000 to 22,000 megawatt-days/ton. Microstructural studies and mechanical tests showed the presence of hydrides in the Zr–Fe–Ni alloy to a much greater extent than in the Zr–Nb alloy which showed a sufficient reserve of plasticity (a relative elongation of 7 to 11%) and a breaking strength of 50 and 32 kg/mm^2 (at 20° and 300°C). The hydrogen content in the Zr–Nb alloy was moderate (0.002 to 0.37 wt %). The hydrides were distributed in a ring, that is, without a dangerous radial orientation, and the grain size did not exceed 0.06 mm. High thermal fluxes up to 1.75×10^6 kcal/m^2·hr did not lead to corrosion of the Zr–Nb cladding. Zr-clad fuel rods assemblies operated 4447 hours in channel 4 at a maximum thermal flux of 1.7×10^6 kcal/m^2·hr with a fuel burnup of 24,193 megawatt-days per ton, and in channel 2 at a maximum thermal flux of 1.3×10^6 kcal/m^2·hr with a fuel burnup of 19,973 megawatt-days/ton. (TTT)

Plastics and Other Materials

Refer also to abstracts 41843, 43446, and 44219.

43011 (N-71-16499) EVALUATION OF LINEAR POLYETHYLENE AND FIBER GLASS REINFORCED EPOXY FOR USE AS IRRADIATION CAPSULES. Mittendorf, Richard J. (National Aeronautics and Space Administration, Cleveland, Ohio. Lewis Research Center). Feb 1971. 24p. (NASA-TM-X-52957). NTIS.

Sealed plastic capsules were irradiated in unsealed metal rabbits (irradiation containers). The purpose was to determine the operating limits for the irradiation of experiments in these capsules. Both linear polyethylene and fiberglass reinforced epoxy capsules were tested. The operating limits for the irradiation of experiments in polyethylene capsules are defined. The epoxy capsules became highly radioactive when irradiated and failed at lower levels of exposure than the polyethylene capsules. (auth) (STAR)

43012 (RDT-M-11-2-T) IMPREGNATED ASBESTOS PACKING MATERIAL. (Division of Reactor Development and Technology (AEC), Washington, D. C.). Feb 1969. 7p. RSO.

A standard prescribing requirements for impregnated asbestos packing material for nuclear associated applications is presented. (auth)

43013 (RDT-M-12-1-T) TEST REQUIREMENTS FOR THERMAL INSULATING MATERIALS FOR USE ON AUSTENITIC STAINLESS STEELS. (Division of Reactor Development and Technology (AEC), Washington, D. C.). Feb 1969. 19p. RSO.

A standard prescribing requirement for test requirements for thermal insulating materials for use on austenitic stainless steels for nuclear and associated applications is presented. (auth)

43014 (RDT-M-12-2-T) CALCIUM SILICATE BLOCK AND PIPE THERMAL INSULATION (ASTM C533 WITH ADDITIONAL REQUIREMENTS). (Division of Reactor Development and Technology (AEC), Washington, D. C.). Jun 1971. 6p. RSO.

A standard prescribing requirements for calcium silicate block and pipe thermal insulation (ASTM C533 with additional requirements) for nuclear and associated applications is presented. (auth)

43015 STRESS WAVE EMISSION AND FRACTURE OF PRESTRESSED CONCRETE REACTOR VESSEL MATERIALS. Green, Allen T. (Aerojet-General Corp., Sacramento, Calif.). pp 635-49 of Materials Technology. I. New York; American Society of Mechanical Engineers (1970).

From second inter-american conference on materials technology; Mexico City, Mex. (24 Aug 1970). See CONF-700812.

Applicability of using stress-wave emissions to detect the failure and progression of failure in cylindrical concrete specimens and a model prestressed concrete pressure vessel is presented. Stress-wave-emission data obtained during structural tests have provided a description of the time relations between the onset and continuing failure process. Three concrete aggregates, one mortar model of prestressed pressure vessel material and a model prestressed pressure vessel were tested in the course of the investigation. Findings of the study showed that variations in the stress-wave-emission data can determine impending failure and previous structural loading extremes. A limited correlation between stress-wave-emission data and modulus is shown, as is a potential means of observing long-term structural changes in prestressed concrete structures. Variations in the time of stress-wave arrival and emission data can be used to determine anomalous structural responses and maximum cracking locations. Stress-wave-emission data are also shown as being an extremely fine measurement of deviation from elastic response of the mortar model material. (auth)

43016 FLUORINATED POLYMERS AND THE NUCLEAR INDUSTRY: PTFE AND PTFCE. Monnet, A.; Bensa, R. (Ugine-Kuhlmann, Paris). Energ. Nucl. (Paris); 13: No. 2, 123-32(Mar-Apr 1971). (In French).

Whereas fluorinated polymers react rather badly in the presence of radiations, they behave very well in the presence of UF_6 and the various reagents used either for its fabrication or for the passivation of the installations used for its handling. It is therefore, in this field that the fluorinated polymers find their principal applications. After giving a summary on the general properties of these polymers, their behavior in the presence of the aggressive fluorinated reagents and also certain applications arising are described. The effect of the radiations on the properties of these polymers was investigated. (auth) (France)

XUM

PHYSICS (GENERAL)

Astrophysics and Cosmology

43017 PROSPECT FOR THE USE OF ORBITAL STATIONS AND SPACE SHUTTLES IN THE NEXT TEN YEARS. Eleventh International Technical and Scientific Conference on Space, Rome, Italy, April 1–3, 1971. Rome; XVIII Rassegna Internazionale Elettronica e Nucleare (1971). 375p. (In several languages). (CONF-710430).

Twenty-seven papers, five titles, and one abstract are included here. Separate abstracts were prepared for two of the papers. (M.O.W.)

For abstracts of individual papers see: 43191 and 43351.

Stars

43018 (N–71–19301) STUDY OF ABUNDANCE ANALYSIS OF STARS IN THE SPECTRAL RANGE B5 THROUGH G2. Final Report. Strom, Stephen E. (Smithsonian Astrophysical Observatory, Cambridge, Mass.). Oct 1970. 26p. (NASA-CR–116862). NTIS.

The progress in the photometric and spectroscopic study of the blue stragglers and the evolution of stars in clusters is summarized. Also included is a brief analysis of the super-metal-rich K-giant phenomena. (STAR)

43019 (NBS-MON–119) A HIGH-DISPERSION SPECTRAL ANALYSIS OF THE Ba II STAR HD 204075 (ξ CAPRICORNI). Tech, Jack L. (National Bureau of Standards, Washington, D. C.). Mar. 1971. 174p. GPO $3.25.

A double differential curve of growth analysis, using the Sun and ϵ Vir as comparison stars, was performed for the Ba II star ξ Capricorni. The observational material consisted of equivalent widths, central depths, and half-widths for 1100 spectral lines measured on direct-intensity tracings of plates obtained at the coudé focus of the 200-inch telescope. Atmospheric abundances were derived for 37 elements. (W.D.M.)

43020 PROGRAMMING ATTEMPTS OF THE ORBITAL ELEMENT DETERMINATIONS FOR THE ECLIPSING VARIABLE STARS. Minti, Hari (Astronomical Observatory, Bucharest). Stud. Cercet. Astron.; 16: No. 1, 45-54(1971). (In Rumanian).

The two programs of the Bucharest Astronomical Observatory related to the orbital element determinations are discussed. The first program, used for light curve rectification, starts from the individual observations and calculates the rectification normals. The second program, used for the theoretical light curve calculation, is based upon both the polynomial approximating functions ${}^{10}\alpha^{oc}$ and ${}^{10}\alpha^{tr}$ proposed by Fliegel and Wilson (1968) and polynomial approximating functions ${}^{10}\alpha^{ann}$ proposed by the author (1970). The two programs were verified for the orbital element determination of the Z Vul. (auth)

43021 PERIOD DETERMINATION OF THE VARIABLE STAR DP AQUARII. Todoran, Ioan (Astronomical Observatory, Cluj). Stud. Cercet. Astron.; 16: No. 1, 19-23(1971).

Sixty-nine maxima were used in order to obtain the following elements: Max. hel. = JD2437884.4543 + 0.4448946d.E. (auth)

43022 NONLINEAR PULSATIONS AND STABILITY OF RAPIDLY ROTATING COLUMNS. Tassoul, Jean-Louis (Univ. of Montreal). Bull. Cl. Sci., Acad. Roy. Belg.; 56: No. 11, 1231-7(1970).

The influence of a large angular momentum on nonlinear axisymmetric motions of centrally condensed bodies is discussed. In order to illustrate the problem finite-amplitude pulsations of rapidly rotating columns are considered. An analysis involving the virial theorem gives an approximate description of adiabatic radial motions. It is shown that nonlinearity lessens the stabilizing influence of angular momentum predicted in a linear stability analysis. (auth)

43023 DEVIATION FROM A MAXWELLIAN VELOCITY DISTRIBUTION IN LOW-DENSITY PLASMAS. Gould, R. J.; Thakur, R. K. (Univ. of California, San Diego, La Jolla). Phys. Fluids; 14: No. 8, 1701-7(Aug 1971).

The problem of the electron velocity distribution for a plasma in a steady state is investigated. The principal deviation from Maxwellian results from inelastic collisions of electrons with atoms and ions wherein the excited level depopulates predominantly by radiating a photon. A simple analytic solution to the Boltzmann equation is obtained for the case where we are in the tail of the distribution (this allows simplification of the Fokker–Planck Coulomb operator) and for the case where the inelastic cross section varies as 1/E, where E is the kinetic energy of the incident electron. A generalization is made to the case where many atomic levels can be excited, if the cross section for each varies as 1/E. In applying the results to astrophysical plasmas it is found that the non-Maxwellian corrections are always small. For example, the relative corrections to inelastic collision rates for the primordial hydrogen–helium plasma are less than 10^{-3}. In gaseous nebulae the typical corrections are even smaller (about 10^{-6}). For some cosmic x-ray sources and for stellar coronae the corrections are also of this order (10^{-6}). (auth)

43024 OBSERVATIONS OF THE VARIABILITY OF THE POLARIZATION OF RADIATION OF THE HIGH LUMINOSITY RED VARIABLES. Dombrovskii, V. A.; Polyakova, T. A.; Yakovleva, V. A. Uch. Zap. Leningrad. Gos. Univ., No. 353, Ser. Mat. Nauk; No. 45, 3-18(1970). (In Russian).

Results of polarimetric and photometric observations of high-luminosity red variables are given. The time variation of polarization was found for μ Cep, VCVn, R Sct, Z UMa, and X Her. Within the accuracy of observations the polarization of UX Dra and YCVn in 1967–1968 was constant. (auth)

43025 POLARIMETRIC STUDY OF THE NEBULA NEAR FU ORI. Yakovleva, V. A. Uch. Zap. Leningrad. Gos. Univ., No. 353, Ser. Mat. Nauk; No. 45, 49-54(1970). (In Russian).

The method of polarimetric observations with the polarigraph is described. The photographic observations showed that the radiation of the nebula near FU Ori is radially polarized. (auth)

43026 EMPIRICAL STUDY OF THE PULSATIONS OF THE UPPER LAYERS OF CEPHEIDS. Latyshev, I. N. Uch. Zap. Leningrad. Gos. Univ., No. 353, Ser. Mat. Nauk; No. 45, 80-7 (1970). (In Russian).

Properties of pulsations in those layers of Cepheids that are accessible to direct observations were studied using the data on brightness, color indices, and radial velocities. It was found that in the deeper layers there exists a wave that propagates in the outward direction. In the course of its propagation the wave changes its shape and increases its amplitude, and this may explain the increase of asymmetry of the light curves of Cepheids with the increase of the amplitude of light variations. In the highest layers the propagating wave is transformed into a shock wave. Some reasons are given in favor of the assumption that at each pulsation cycle some part of matter is ejected from the Cepheid into space. (auth)

43027 STAR STREAMS IN THE SOLAR NEIGHBORHOOD. Ogorodnikov, K. F.; Latyshev, I. N. Uch. Zap. Leningrad. Gos. Univ., No. 353, Ser. Mat. Nauk; No. 45, 88-93(1970). (In Russian).

Space velocities of near-by stars corrected for the effect of local solar motion were studied. It appears that stars of the Ursa Major stream form a more compact cluster in the velocity space than those of the Hyades stream. This confirms a previously known fact that the U Ma-stream stars are younger than those of the Hyades one. Using the V_r catalog of Wilson, a search was made of the hypothetical star stream containing the Sun. It was found that this stream, if it exists at all, has a partial star density not exceeding 0.0003 stars per ps^3. (auth)

43028 CATALOGUE OF RIGHT ASCENSIONS OF 231 PAIRS OF STARS. Pyshnenko, V. N. Uch. Zap. Leningrad. Gos. Univ., No. 353, Ser. Mat. Nauk; No. 45, 128-37(1970). (In Russian).

The catalog contains 231 pairs of stars. Observations were made with the photoelectric transit instrument and are independent of the figure of the pivots and of the azimuth of the instrument. As regards the $\Delta\alpha_z$ and $\Delta\alpha_\alpha$ errors, the system of the catalog is closest to those of CK and FK4. (auth)

43029 SYSTEMS OF THE PROPER MOTIONS OF THE STARS OF PZT PROGRAM. Dobretsova, K. V. Uch. Zap. Leningrad. Gos. Univ., No. 353, Ser. Mat. Nauk; No. 45, 149-58(1970). (In Russian).

The proper motion systems of star programs PZT (photographic zenith tubes) were investigated, and their comparison with the various fundamental catalog is given. (auth)

43030 SPECTRA OF NONSTATIONARY STARS. SOME CHARACTERISTIC SPECTRA OF WR STARS. Nikitin, A. A. Uch. Zap. Leningrad. Gos. Univ., No. 353, Ser. Mat. Nauk; No. 45, 44-8(1970). (In Russian).

Some peculiarities in the spectra of WR stars as compared with the spectra of novae are considered qualitatively. The possible presence of N III and Ne I lines in the infrared region of the spectra of WN and WC stars is discussed. (auth)

43031 ULTRAVIOLET STELLAR SPECTRA AND RELATED GROUND-BASED OBSERVATIONS. International Astronomical Union Symposium No. 36 Held in Lunteren, Netherlands, 24-27 June, 1969. Houziaux, L.; Butler, H. E. (eds.). New York; Springer-Verlag New York Inc. (1970). 373p. $19.80. (CONF-690659).

Fifty papers were presented on absolute calibration, interstellar extinction, theoretical models for stellar fluxes, observed stellar fluxes, rocket and satellite observations of ultraviolet spectra, ground-based observations of spectra relevant to the ultraviolet, theory relevant to uv spectra, the Sun, absorption lines, and emission. Discussions following the talks are included. (W.D.M.)

43032 LONG-RANGE NEUTRINO FORCES EXERTED BY KERR BLACK HOLES. Hartle, James B. (Univ. of California, Santa Barbara). Phys. Rev., D; 3: No. 12, 2938-40(15 Jun 1971).

In flat space there is a long-range $1/r^5$ potential between two collections of matter arising from the exchange of neutrino pairs between them. It is shown that a Kerr black hole cannot exert a weak-interaction force of this kind. A Kerr black hole has no exterior neutrino field with classical effects. (auth)

43033 THERMONUCLEAR DETONATIONS IN EVOLVED STELLAR CORES. Buchler, Jean-Robert; Wheeler, J. Craig; Barkat, Zalman (California Inst. of Tech., Pasadena). Astrophys. J.; 167: No. 3, 465-78(1 Aug 1971).

The nature of detonations in evolved stellar cores is an important factor in determining whether or not a star explodes and whether it leaves a remnant. An investigation was made of the local effects of the propagation of a Chapman–Jouguet detonation (CJD) fueled by ^{12}C or ^{16}O burning under conditions of high electron degeneracy, the type of CJD of most immediate astrophysical interest. If the initial matter is composed entirely of carbon and oxygen in any ratio, a CJD will be a self-consistent phenomenon for any reasonable initial temperatures and for initial densities greater than $\sim 10^7$ g cm^{-3}. The temperature, density, and pressure behind the detonation front are tabulated as a function of the initial density and the energy released in the front. The astrophysical significance of the results is discussed. (auth)

43034 GUM NEBULA: FURTHER EVIDENCE FROM SPACECRAFT AND GROUND-BASED INSTRUMENTS. Alexander, Joseph K.; Brandt, John C.; Maran, Stephen P.; Stecher, Theodore P. (Goddard Space Flight Center, Greenbelt, Md.). Astrophys. J.; 167: No. 3, 487-90(1 Aug 1971).

Measurements by the RAE-1 and OGO-5 satellites were combined with data from ground-based telescopes to yield more accurate parameters for the Gum Nebula, including a somewhat smaller size and an estimate of the electron temperature. The supernova that ionized the nebula must have been observed at the Earth, and it is possible that records exist. (auth)

43035 PHOTOMETRIC STUDY OF THE METAL-RICH GLOBULAR CLUSTER M71. Arp, H. C. (Carnegie Institution of Washington D. C. California Inst. of Tech., Pasadena); Hartwick, F. D. A. Astrophys. J.; 167: No. 3, 499-509(1 Aug 1971).

M71, alternatively designated NGC 6838, is classified by Morgan as metal richness VI. Photoelectric and photographic observations on the UBV system yield a color–magnitude diagram typical of a metal-rich cluster with only a short, red horizontal branch and a gently sloping giant branch. The color–magnitude diagram reaches stars as faint as the unevolved main sequence at $M_V = +4.5$ mag. The following parameters are derived: (a) $E_{B-V} = 0.31 \pm 0.02$, (b) $(m - M)_0 = 13.07 \pm 0.21$, (c) [Fe/H] = −0.30 ± 0.2, and (d) age = $7.6\ (+3.1, -2.3) \times 10^9$ years, on the assumption that Y = 0.29. This age is younger than that customarily derived for globular clusters in the halo but does not lie outside the present range of uncertainty of those determinations. A relatively strong extension of the main sequence beyond the turnoff point is observed. The close-binary explanation for these stars is consistent with the present limited knowledge of the difference in the frequency of spectroscopic binaries among different stellar populations. (auth)

43036 LITHIUM CONTENT OF CAPELLA. Boesgaard, Ann Merchant (Univ. of Hawaii, Honolulu). Astrophys. J.; 167: No. 3, 511-19(1 Aug 1971).

The lithium content of the two components of the spectroscopic binary α Aur was determined from seven spectrograms of 2 Å mm^{-1} dispersion widened to 2 mm. A Li I line of 22 mÅ was detected in the G star in addition to the Li I line previously found in the F star by Wallerstein. An abundance analysis gave the result that the Li content of the F star is 15 times greater than in the G star. It was concluded that the G star need not have evolved to or past the red-giant tip, as was previously thought on the basis of Wallerstein's lower-dispersion work. Measurements made to determine the Li isotope ratio indicated that there is little or no ^6Li in either star, but the probable errors are fairly large due to the weakness of the Li line in the G star and the rotational broadening of the lines in the F star. (auth)

43037 SOME INTRINSIC PROPERTIES OF CARBON STARS. Richer, Harvey B. (Univ. of Rochester, N. Y.) Astrophys. J.; 167: No. 3, 521-35(1 Aug 1971).

Near-infrared spectrograms of moderate dispersion were employed to establish a new two-dimensional classification scheme for carbon stars which involves temperature and luminosity. Intrinsic colors of the spectral subtypes were determined, and these were employed to construct a color–color diagram which clearly separated out the early- and late-type stars. A galactic-rotation solution, using radial velocities and intrinsic colors, yielded a mean absolute magnitude of −2.7 for the middle carbon stars. This value was employed to construct the (M_{bol}, log T_e)-diagram for these stars which were found to form an extension of the normal giant branch to cooler temperature. (auth)

43038 EXPANSION OF THE ORION-NEBULA CLUSTER. Vasilevskis, S. (Univ. of California, Santa Cruz). Astrophys. J.; 167: No. 3, 537-9(1 Aug 1971).

Expansion of the Orion Nebula cluster was derived by Strand under an assumption that the scale of the Yerkes 40-inch refractor did not change during a 50-year interval. It is shown that the scale did actually change due to the use of various filters, to readjustments, and to the variable thermal condition of the lens. Consequently, there is now no observational evidence for expansion of the cluster. (auth)

43039 BLAST-WAVE MODEL FOR THE VELA X SUPERNOVA REMNANT AND THE ORIGIN OF THE GUM NEBULA. Tucker, Wallace H. (American Science and Engineering, Cambridge, Mass.). Astrophys. J.; 167: No. 3, L85-7(1 Aug 1971).

The origin of the radio and x-ray emission from Vela X is discussed. The x-ray observations can be interpreted in terms of thermal radiation from a blast wave produced by the supernova explosion that formed Vela X. For an appropriate choice of parameters, the total power radiated by the shock wave is sufficient to explain the ionization in the Gum Nebula. The radio emission can be explained in terms of synchrotron radiation from relativistic electrons interacting with the region of high magnetic field behind the shock front. The pulsar in Vela X must have been about 100 times more active in the past in order to explain the energy content in relativistic electrons. A synchrotron origin for the x-ray emission is also possible. It should be possible to prove or disprove the thermal model by means of high-resolution x-ray observations and perhaps by the observation of coronal iron-line emission. (auth)

43040 ORIGIN OF THE REPORTED MILLIMETER CONTINUUM IN IRC +10216. Woolf, N. J. (Univ. of Minnesota, Minneapolis); Solomon, P. M.; Penzias, A. A. Astrophys. J.; 167: No. 2, L65(15 Jul 1971).

It is suggested that the reported 3.5-mm continuum in IRC + 10216 is due to one or more emission lines within the receiver bandpass. (auth)

43041 RAPID VARIATIONS IN THE SPECTRUM OF ZETA TAURI. Bahng, J. D. R. (Northwestern Univ., Evanston, Ill.). Astrophys. J.; 167: L75-7(15 Jul 1971).

Photoelectric spectrum scans of ζ Tau show an indication of extremely rapid variations in the equivalent widths of Hβ and Hγ in the time scale of about 10 minutes. (auth)

43042 WAVELENGTH DEPENDENCE OF POLARIZATION. XXIV. INFRARED OBJECTS. Kruszewski, A. (Univ. of Arizona, Tucson. Inst. of Astronomy, Warsaw). Astron. J.; 76: No. 6, 576-80(Aug 1971).

Polarimetric observations of 11 infrared objects are presented. All observed stars show intrinsic polarization or large interstellar polarization. The interstellar origin is evident for CIT 11. For NML Cygnus, in addition to a large interstellar polarization,

XUM

there is also a variable intrinsic polarization component. NML Taurus and CIT 6 both show large-amplitude variations of the polarization with maximum polarization at light minimum. (auth)

43043 Hβ PHOTOMETRY OF A-TYPE STARS NEAR THE NORTH GALACTIC POLE. Philip, A. G. Davis; Tifft, Linda E. (State Univ. of New York, Albany). Astron. J.; 76: No. 6, 567-70 (Aug 1971).

Hβ measures were obtained for 52 B- and A-type stars in an area near the North Galactic Pole, for which Strömgren four-color photometry had been obtained by Philip. The color excesses of the Population I stars in the sample indicated a color excess of E_{b-y} = 0.00 in areas close to the pole, and a color excess of E_{b-y} = 0.05 in an area just north (in declination) of the pole. The intrinsic color indices of 14 field horizontal-branch stars found in the area were calculated. (auth)

43044 RADIOFREQUENCY OBSERVATIONS OF SYMMETRIC NEBULAE AROUND WOLF–RAYET STARS AND AN O7f STAR. Johnson, Hugh M. (Lockheed Missiles and Space Co., Palo Alto, Calif.). Astrophys. J.; 167: No. 3, 491-8(1 Aug 1971).

New observations were made of the symmetric nebulae around the Population I Wolf–Rayet stars HD50896 and HD 192163 and around the O7f star BD + 60°2522. Nine more Wolf–Rayet stars not centered in symmetric nebulae were scanned at 7795 MHz, and one of them, HD 211853, coincides with a source in the telescope beam. Existing optical data were used to estimate some physical characteristics of the objects. The peculiar nebula NGC 7635 and the star observed in it, BD + 60°2522, are discussed in some detail. NGC 7635 is probably a planetary nebula, and not a diffuse nebula as it has been classified lately. (auth)

43045 TEMPERATURE AND GRAVITY VARIATIONS OF THE CLASSICAL CEPHEID BETA DORADUS. Parsons, Sidney B. (Case Western Reserve Univ., East Cleveland). Astron. J.; 76: No. 6, 562-6(Aug 1971).

Large differences exist in reported values of the range in effective temperature and of the mean radius for β Dor. Comparing these with results from analysis of six-color photometry in the Stebbins and Kron system, it is concluded that the range in T_e is probably about 950 ± 70°K, the mean radius 77 ± 10 $R_\odot$, and the mean visual absolute magnitude −4.7 ± 0.4. This star may be pulsating in the first-overtone mode. Evidence is now strong, from the variation in surface gravity as obtained from the Balmer jump and from the phase lag of the Hα core radial velocity, that the outer envelope of β Dor is characterized by running-wave pulsation. (auth)

43046 LIGHT CURVE AND APSIDAL MOTION OF AR Cas. Catalano, S.; Rodono, M. (Univ., Catania, Italy). Astron. J.; 76: No. 6, 557-61(Aug 1971).

The photoelectric observations of AR Cas carried out at the Catania Astrophysical Observatory during the 1968 international campaign organized by Herczeg are presented. A rediscussion of the apsidal motion, which is based upon the ω advancing obtained from photometric data alone, leads to an apsidal motion period of about 10^3 yr. The value of the orbital eccentricity e = 0.21, deduced from the relative durations of photometric eclipses, is utilized. (auth)

43047 SPECTROSCOPIC BINARIES WITH CIRCULAR ORBITS. Lucy, L. B.; Sweeney, M. A. (Columbia Univ., New York). Astron. J.; 76: No. 6, 544-56(Aug 1971).

Because of observational errors, a spectroscopic binary with a truly circular orbit will be found to have an elliptical orbit of small, but nonzero, eccentricity. This effect is analyzed and shown to lead to spurious eccentricities comparable with those assigned to a great many binaries. It is then argued, following Luyten, that such elliptical orbits should be rejected in favor of circular orbits. In order to eliminate these spurious eccentricities, an extensive program of orbit recomputation was carried out for single-lined systems hitherto assigned orbits of small eccentricity ($e \lesssim 0.1$). Adopting the 5% level of significance for accepting an elliptical orbit, 103 systems were found whose elliptical orbits should be rejected. As a result of these calculations, most single-lined systems with periods less than 5 days now have circular orbits. It was also found that many long-period binaries with late-type giant components now have circular orbits. (auth)

43048 DETERMINATION OF CORRECTION TO PRECESSION FROM STELLAR PROPER MOTIONS. Vasilevskis, S.; Klemola, A. R. (Univ. of California, Santa Cruz). Astron. J.; 76: No. 6, 508-12(Aug 1971).

Recent values for correction to centennial precession, with their mean errors, derived by Fricke (1967) from fundamental proper motions are: Δp_l = +1.10 ± 0.15″ and Δλ + Δe = +1.20 ± 0.16″, as a consequence of the directly determined Δn = +0.44 ± 0.06″ and Δk = −0.19 ± 0.07″. Proper motions with reference to galaxies, derived at Lick and compared with those in AGK3, yield Δn = +0.31 ± 0.07″ and Δk = −0.78 ± 0.09″. The disagreement between both sets, particularly for Δk, can be explained either by systematic errors in the Lick proper motions or by local star streamings that vitiate the correction to precession derived from the fundamental proper motions. Although at present there is no evidence of systematic errors in proper motions measured at Lick, a more definite conclusion must await the future progress of the Lick program, only 7% of which has been completed up to date. (auth)

Quasi-Stellar, Radio, and X-Ray Sources

Refer also to abstracts 43039, 43094, and 43701.

43049 QUASARS REVISITED: RAPID TIME VARIATIONS OBSERVED VIA VERY-LONG-BASELINE INTERFEROMETRY. Whitney, Alan R. (Massachusetts Inst. of Tech., Cambridge); Shapiro, Irwin I.; Rogers, Alan E. E.; (and others). Science; 173: No. 3993, 225-30(16 Jul 1971).

Recent Goldstone–Haystack radio-interferometric observations of the quasars 3C 279 and 3C 273 reveal rapid variations in their fine structure. Most notably, the data for 3C 279, interpreted in terms of a symmetric double-source model and the accepted redshift distance, indicate differential proper motion corresponding to an apparent speed about ten times that of light. A number of possible mechanisms that might give rise to such an apparent speed are considered; although several may be plausible, no definitive choice can be made on the basis of present evidence. More interferometric observations of quasars are clearly needed to clarify their structure and internal kinematics. (auth)

43050 DETECTION OF H137α RECOMBINATION-LINE EMISSION FROM AN H I REGION IN THE DIRECTION OF NGC 2024. Cesarsky, Diego A. (Harvard Coll. Observatory, Cambridge, Mass.). Astrophys. J.; 167: L89-92(1 Aug 1971).

The H137α recombination-line emission from an H I region was observed in the spectrum of NGC 2024 (Orion B). This observation confirms a previous detection of the same feature at the frequency of H157α. The fraction of ionized hydrogen in the H I region is $n_{HII}/n_H = (2.5 \pm 2) \times 10^{-4}$, in good agreement with the earlier determination. (auth)

43051 OBSERVATIONS OF 1.35-CENTIMETER H_2O EMISSION IN THE SOUTHERN HEMISPHERE. Johnston, K. J.; Knowles, S. H.; Sullivan III, W. T. (Naval Research Lab., Washington, D. C.). Astrophys. J.; 167: No. 3, L93-6(1 Aug 1971).

Results of a search for 1.35-cm H_2O sources with $\delta < -38°$ are presented. H_2O emission at the positions of the 18-cm OH emission sources G331.5−0.1 and G285.2−0.0 was discovered. Thirteen other OH emission sources exhibited no H_2O line radiation of intensity greater than ~200 f.u. (1 f.u. = 10^{-26} W m^{-2} Hz^{-1}). G331.5−0.1 had a maximum intensity of ~900 f.u. with 1.3 km s^{-1} resolution and a spread in radial velocity of ~25 km s^{-1} while the intensity of G285.2−0.0 was ~200 f.u. (auth)

43052 DISCOVERY OF INTERSTELLAR SILICON MONOXIDE. Wilson, R. W. (Bell Telephone Labs., Holmdel, N. J.); Penzias, A. A.; Jefferts, K. B.; Kutner, M.; Thaddeus, P. Astrophys. J.; 167: No. 3, L-97-100(1 Aug 1971).

Line emission attributed to the J = 3 → 2 rotational transition of SiO was detected in Sgr B2, at a radial velocity comparable to that of other molecules; the estimated column number density of SiO was 4×10^{13} cm^{-2}. The line was not found in Ori A, IRC + 10216, Sgr A, W51, DR 21, or NML Cyg. (auth)

43053 PROPERTIES OF PSR 0525 + 21. Manchester, R. N. (National Radio Astronomy Observatory, Green Bank, W. Va.). Astrophys. J.; 167: No. 3, L101-5(1 Aug 1971).

Observations at frequencies between 250 and 450 MHz have shown that the pulsar PSR 0525 + 21 is highly linearly polarized with position angle varying continuously through the pulse by almost 180°. The pulse profile and its variation with frequency are discussed. Dispersion and rotation measures for the pulsar were determined from measurements of pulse arrival times and position angle at six frequencies. (auth)

43054 DETECTION OF AN UNIDENTIFIED EMISSION FEATURE IN THE MICROWAVE SPECTRUM OF W3. Chaisson, Eric J. (Harvard Coll. Observatory, Cambridge, Mass.). Astrophys. J.; 167: L61-4(15 Jul 1971).

An anomalous emission line reported in the 10.5-GHz microwave spectrum of W3A was detected at 7.8 GHz. It was determined to be a recombination line, and is probably an additional carbon emission. (auth)

43055 DISCOVERY OF PERIODIC X-RAY PULSATIONS IN CENTAURUS X-3 FROM UHURU. Giacconi, R.; Gursky, H.; Kellogg, E.; Schreier, E.; Tananbaum, H. (American Science and Engineering, Inc., Cambridge, Mass.). Astrophys. J.; 167: L67-73(15 Jul 1971).

A search for x-ray sources exhibiting pulsating characteristics similar to the ones recently discovered in Cyg X-1 by Oda et al., and confirmed by Holt et al., has revealed the existence of periodic pulsations in the x-ray emission from Cen X-3. The pulsations are of large amplitude, comprising at least 70% of the total flux from the source. The period is approximately 5 s. Due to the amplitude of the effect and the long period, it is established that the period and phase of the pulsations are maintained for several hours. In addition, two very remarkable events are observed to occur during a 1-day interval. The first is a change in the intensity of the source by a factor of 10 occurring in approximately 1 hour. The second is a decrease and then an increase in the period of the pulsations, corresponding to about 0.02 and 0.04%, each change of period occurring in a time of about 1 hour. The magnitude of the changes, and the short time interval in which they take place, are quite different from any observed in radio pulsars. In addition, evidence is seen for changes of the period by about 1% occurring over a time span of 3 months. Present data are inconclusive about the presence of faster pulsations from the source. The x-ray spectrum shows evidence of substantial absorption below 3.8 keV. (auth)

43056 STRONG X-RAY SOURCE IN THE COMA CLUSTER OBSERVED BY UHURU. Gursky, H.; Kellogg, E.; Murray, S.; (and others) (American Science and Engineering, Inc., Cambridge, Mass.). Astrophys. J.; 167: No. 3, L81-4(1 Aug 1971).

X rays were observed from a source in the Coma cluster of galaxies. The source is extended, with a size of about 45′. Its x-ray luminosity is 2.6×10^{44} ergs s^{-1}, and its spectrum is consistent with thermal bremsstrahlung at 7.3×10^{7} °K or a power law. If the source is hot gas, its mass is 3×10^{13} $M_{\odot}$, which is about 1% of the mass required to stabilize the cluster. (auth)

43057 WEAK X-RAY SOURCES IN THE SOUTHERN HEMISPHERE. Davison, P. J. N.; Buselli, G.; Clancy, M. C.; Thomas, R. M. (Univ. of Adelaide). Astrophys. J.; 167: No. 3, 479-86 (1 Aug 1971).

The first statistically significant observation of hard x rays (energy > 27 keV) from the source Nor X-1 is reported. Measurements of the flux and energy spectrum of the source Ara X-1 are also given. A statistically marginal observation of the variable x-ray source Cen X-2 is reported and compared with observations made several months earlier by Lewin et al. Upper limits to the flux above 27 keV are reported for Lup X-1, Nor X-2, Sco X-4, and the quiet Sun. (auth)

43058 DYNAMICS OF EXTENDED EXTRAGALACTIC RADIO SOURCES. De Young, D. S. (National Radio Astronomy Observatory, Green Bank, W. Va.). Astrophys. J.; 167: No. 3, 541-51 (1 Aug 1971).

The propagation of extended radio sources into an intergalactic medium was examined through a series of time-dependent, axisymmetric calculations. The sources considered ranged in mass from 10^{6} to 10^{8} $M_{\odot}$ and in energy from 10^{57} to 10^{59} ergs. Sources are ejected in a narrow cone at $v \sim 0.1c$ into an intergalactic medium of various densities and temperatures. It was found that confinement by the medium produces results in agreement with observations only for ambient densities $\gtrsim 10^{-29}$ g cm^{-3}. Implications of this result are discussed, together with the dominant dynamical processes and time scales revealed by the calculations. (auth)

43059 COMPARATIVE STUDY OF RADIO AND OPTICAL PHOTOMETRY OF SEVERAL H II REGIONS. Schmitter, E. F. (Univ. Nacional Autonoma de Mexico, Mexico City). Astron. J.; 76: No. 6, 571-5(Aug 1971).

Values of optical depth for NGC 896, NGC 1976, NGC 2024, NGC 2237-46, and IC 1795 were calculated at different points of each object. The H II regions were observed at Hα with the 26–31-inch Schmidt telescope at the Observatory of Tonantzintla in Mexico. Expected values of the Hα intensity were calculated from radio data obtained by other observers. The differences between the observed and calculated Hα intensity values were assumed to be due to interstellar extinction produced by material far away from the nebulae. The reddening measurements of some stars made by other observers were found to be systematically higher than those obtained in this work. The results can be explained if the material responsible for the nebular extinction is partially mixed with the gas. (auth)

43060 RADIO SOURCES: 3.3-mm FLUX AND VARIABILITY MEASUREMENTS. Fogarty, William G.; Epstein, Eugene E.; Montgomery, John W.; Dworetsky, Michael M. (Aerospace Corp., Los Angeles). Astron. J.; 76: No. 6, 537-43(Aug 1971).

Graphical and tabular summaries of 3.3-mm (90-GHz) flux measurements of 35 discrete galactic and extragalactic sources are presented, including results of extensive monitoring of nine sources. Variability at 3.3 mm is certain for NGC 1068, NGC 1275, 3C 120, 3C 273, 3C 279, VRO 42.22.01, and 3C 454.3; repeated outbursts with time scales ranging from a week to several months were observed for all of these except NGC 1068 and 3C 454.3. The 3-mm flux of Vir A agrees with the value obtained by extrapolating longer-wavelength data, but the flux of Cyg A seems to be significantly less than the extrapolated value. No evidence was found at 3 mm of the strong infrared flux that has been observed for some extragalactic objects (the infrared galaxy phenomenon) and for the planetary nebula NGC 7027; this absence indicates that there is a sharp drop in the spectra from the infrared to the millimeter region for all these objects. The 3-mm fluxes of K3-50 and NGC 7027 are consistent with thermal spectra. (auth)

43061 TWO-DIMENSIONAL STRUCTURES OF 76 EXTRAGALACTIC RADIO SOURCES AT 1425 MHz. Fomalont, E. B. (California Inst. of Tech., Pasadena). Astron. J.; 76: No. 6, 513-24(Aug 1971).

The two-dimensional structures of 76 extragalactic radio sources at a frequency of 1425 MHz are given. All of the observations were made using the Owens Valley Radio Observatory twin-element interferometer with a resolution of 45 arc sec in the east–west direction and $45'' \cdot \sec(\delta - 37°)$ in the north–south direction. The inversion of the interferometric data was obtained using a model-fitting technique. The structure for each source and the optical identification are given in tabular and graphical form. (auth)

43062 OBSERVATIONS OF EXTRAGALACTIC RADIO SOURCES AT CENTIMETER WAVELENGTHS. Bell, M. B. (National Research Council of Canada, Ottawa); Seaquist, E. R.; Braun, L. D. Astron. J.; 76: No. 6, 524-9(Aug 1971).

Flux-density data at 6,630 and 10,700 MHz are presented for 101 presumably extragalactic radio sources. The results of this investigation provide data at high frequencies for approximately 30 sources whose spectra are very flat or show concave spectral curvature. The remaining sources were found to have straight spectra and for each of these a spectral index is given. Three sources were found to be variable. (auth)

43063 FLUX DENSITY MEASUREMENTS OPTICALLY IDENTIFIED B2 RADIO SOURCES AT 5 GHz. Grueff, Gavril (California Inst. of Tech., Pasadena). Astron. J.; 76: No. 6, 530-6(Aug 1971).

Observations of 224 optically identified B2 radio sources at 5 GHz are reported. The mean spectral index between 408 and 5000 MHz was computed; according to the source's optical identification, an indication of a correlation between the spectrum shape and the absolute power (or cosmological epoch) was found for radio galaxies. (auth)

43064 STUDY OF THE STRUCTURE OF RADIO SOURCES. Kardashev, N. S.; Matveenko, L. I. Zemlya Vselennaya; 36-41 (Jan-Feb 1971). (In Russian).

The resolving power of radio telescopes is discussed, and the principle of radio interferometry is explained. Different radio interferometric systems are reviewed. Three different radio emission regions associated with a solar flare are examined. The measurement of the angular diameter of a Jovian radio source, using 16-m radio waves, is described. This diameter was found to be equal to or below 430 km. Radio images of the Andromeda Galaxy and Crab Nebula are described. (IAA)

Solar Phenomena

43065 (AD-715257) OBSERVATION OF AUTOIONIZING STATES IN THE SOLAR CORONA. Report for June–August 1970. Walker, Arthur B. C. Jr.; Rugge, Hugo R. (Aerospace Corp.,

XUM

El Segundo, Calif.). 20 Nov 1970. Contract F04701-70-C-0059. 33p. (TR-59(9260-02)-2; SAMSO-TR-70-391). NTIS.

Weak satellites to the lines of the principal series of the helium- and hydrogen-like ions of magnesium, aluminum, silicon, and sulfur in the solar spectrum were observed. These lines coincide in wavelength with the extrapolated positions of transitions from the autoionizing levels in helium-like ions, and the autoionizing levels in lithium-like ions. The observations provide direct evidence of dielectric recombination in the corona. (auth) (USGRDR)

43066 (LA-4454(Vol.5)) VELA V AND VI SOLAR X-RAY ATLAS. V. SEPTEMBER 1, 1970 TO JANUARY 1, 1971. Blocker, N. K.; Chambers, W. H.; Fehlau, P. E.; Fuller, J. C.; Kunz, W. E.; Milkey, R. W. (Los Alamos Scientific Lab., N. Mex.). Jun 1971. Contract W-7405-eng-36. 124p. Dep. NTIS.

Data obtained from the solar radiation monitors on the Vela VI Satellites are presented. Equivalent graybody flux in three bands (0.3 to 3, 1 to 8, and 1 to 16Å) is plotted as a function of universal time, one day per page. (auth)

43067 (N-71-16749) TOPICS IN SOLAR COSMIC RAY AND X-RAY PRODUCTION. Cline, Thomas L. (National Aeronautics and Space Administration, Greenbelt, Md. Goddard Space Flight Center). Dec 1970. 50p. (NASA-TM-X-65439; X-661-71-33). NTIS.

Topics related to energetic interplanetary particle and x-ray production by the Sun are presented. They are based upon certain observations of solar protons, electrons, and x rays resulting from some experiments using the IMP, OGO, and OSO series of satellites. These observations help to provide a basic phenomenology needed for the theorizing of an accurate and complete picture of particle acceleration at the Sun. These results contrast to the solar-particle data available a decade ago in that these were gathered using instruments with lower-energy sensitivity flown outside the Earth's atmosphere and magnetosphere and exposed throughout much of the solar cycle. These data show that solar energetic particles are produced more often than only in the larger flares and suggest that they are produced in more than one manner. (auth) (STAR)

43068 (N-71-19294) STRUCTURE OF THE CHROMOSPHERE-CORONA TRANSITION REGION. Moore, R. L.; Fung, P. C. W. (Stanford Univ., Calif. Inst. for Plasma Research). Jan 1971. Contract F4462-69-C-0008. 49p. (NASA-CR-116872; SUIPR-377). NTIS.

The structure and energy balance of the chromosphere-corona transition region was investigated using a static, planar model which was compared with the results of xuv-resonance line observations. In this model, the transition region is heated by thermal conduction from the corona and cooled by radiative losses. Comparison of the model with observational results implied that this is the dominant process in the energy balance of the transition region and that the base of the transition region is inherently nonstatic and/or nonplanar. The implications of results are discussed with regard to spicules. (auth) (STAR)

43069 (N-71-20535) AVERAGE ENERGIES OF GROUND AND SINGLY AND DOUBLY EXCITED CONFIGURATIONS IN HIGHLY IONIZED ATOMS: ELECTRON NUMBERS N = 3 TO N = 20. Shadmi, Yehuda; Kastner, Sidney O. (National Aeronautics and Space Administration, Greenbelt, Md. Goddard Space Flight Center). 1971. 258p. (NASA-SP-3056). NTIS.

Calculations are presented of the average energies for many configurations of spectroscopic interest, using a basis of orthogonalized screened hydrogenic radial functions. The energy of a core is calculated in a zeroth-order approximation (electronic interactions included implicitly through the screening parameters) and the energy of all other electrons is calculated in a first-order approximation (electronic interactions included explicitly as a perturbation). Results are presented for the ground configurations and for many singly and doubly excited configurations. A discussion of their accuracy is included. (auth) (STAR)

43070 (N-71-21564) U-TYPE SOLAR RADIO BURST ORIGINATING IN THE OUTER CORONA. Stone, R. G.; Fainberg, Joseph (National Aeronautics and Space Administration, Greenbelt, Md. Goddard Space Flight Center). Mar 1971. 14p. (NASA-TM-X-65484; X-693-71-107). NTIS.

A discussion is presented of the very rare occurrence of a U-type burst observed between 5 and 0.7 MHz by RAE-1. A possible model is developed from the data. In terms of the model, in which the exciter moves along a magnetic loop, the observations suggest that such loops or magnetic bottles can extend out to the order of 35 solar radii. (auth) (STAR)

43071 RADIOMETER STUDIES OF ATMOSPHERIC ATTENUATION OF SOLAR EMISSION AT 19 GHz. Davies, P. G. (Radio and Space Research Station, Slough, Eng.). Proc. Inst. Elec. Eng. (London); 118: No. 6, 737-41(Jun 1971).

Frequencies above 10 GHz are proposed for Earth-satellite communication links, and the planning and operation of such links require a knowledge of the total attenuation produced by the troposphere under various meteorological conditions. A statistical analysis on the attenuation of solar radio emission measured at Slough, Bucks., England, at 19GHz was carried out for the period June 1968 to May 1970. Data covering this period are presented to show the percentage time for which the attenuation exceeds various values for three cases: measured data covering the range of zenith angles between 28 and 90; the same data normalised to zenith and to a zenith angle of 70° using a cosine normalisation; and the measured data obtained within 10° ranges of zenith angle. The longest duration of any fade exceeding 10 dB was 17 min, recorded in September 1968. (auth) (UK)

43072 ASPECTS OF NORTH-SOUTH ASYMMETRY OF CHROMOSPHERIC ERUPTIONS IN CORRELATION WITH GEOPHYSICAL PHENOMENA. Maris, Georgeta (Astronomical Observatory, Bucharest). Stud. Cercet. Astron.; 15: 219-23 (1970). (In Rumanian).

In the study of the Sun-Earth relationships, the efficiency of chromospheric eruptions on the two solar hemispheres in the generation of geophysical phenomena is of great interest. There are occasionally relatively short time periods during which the northern and southern hemispheres of the Sun, are in different positions with respect to the Sun. During such a period, from 1957 to 1961, the effect of solar eruptions of the order of ≥ 1 in the two hemispheres on geophysical phenomena was studied. The ranges examined were $-7.25° < B_0 < -5°$ and $+5° < B_0 < +7.25°$; the study involved the calculation of the correlation indices (r) of the radio flux density at 2800 MHz, and of the planetary index A_p with respect to the daily eruption index E for each of the solar hemispheres. The values obtained for r indicated that the two positions of the Sun on the ecliptic do not affect the transmission of the electromagnetic radiation emitted by eruptions in the two hemispheres. In the case of corpuscular radiation, the correlation favored the northern hemisphere in the $+5° < B_0 < +7.25°$ range and the southern hemisphere in the $-7.25° < B_0 < -5°$ range. (TTT)

43073 ARBITRARY AMPLITUDE MAGNETO-ACOUSTIC WAVES UNDER GRAVITY: AN EXACT SOLUTION. Chiu, Y. T. (Aerospace Corp., Los Angeles). Phys. Fluids; 14: No. 8, 1717-24(Aug 1971).

Exact Riemann wave solutions to the magnetohydrodynamic equations for a compressible medium under the influence of a gravitational field are obtained. The method of solution consists of an application of Hamburger's subsidiary equations previously found useful in the analysis of such three-dimensional waves in compressible hydrodynamics under gravity. The resultant magneto-acoustic waves cannot be classified as slow and fast modes, and their propagation characteristics are found to be quite different from those in a uniform medium. In particular, the phenomenon of large-amplitude wave ducting is examined. Certain wave properties correspond exceedingly well with the observed fine structure of waves propagating away from solar flares. (auth)

43074 SYSTEMS OF FRAUHOFER WAVELENGTHS IN SOLAR SPECTRA: DIFFERENTIAL LINE SHIFTS IN THE CENTER AND AT THE LIMB. Mel'nikov, O. A.; Salman-Zade, R. Kh.; Pakhomov, V. P. Uch. Zap. Leningrad. Gos. Univ., No. 353, Ser. Mat. Nauk; No. 45, 18-31(1970). (In Russian).

The residual shifts of Fe Fraunhofer lines in the spectra of the center and the limb of the solar disk were studied in a wide range. Differences of limb center shifts were determined. These differences being added to the center line shifts show that the shifts at the limb are absent for all of the visual photographic region studied. Therefore, one has a "center effect" and not a "limb effect," as was previously supposed. To study the influence of line asymmetry on the measured residual shifts, a special "mark" imitating real Fraunhofer spectra with asymmetric lines was used. A hypothesis is proposed on possible causes of the observed residual shifts of Fraunhofer lines at the center of the solar disk. (auth)

43075 MONITORING OF THE LYMAN ALPHA EMISSION LINE OF THE SUN DURING THE YEAR 1969. Blamont, J. E.; Madjar, A. Vidal (CNRS, Verrieres le Buisson, France). J. Geophys. Res.; 76: No. 19, 4311-24(1 Jul 1971).

The shape of the Lyman-α line emitted by the whole solar disk was measured with an experiment on board the Oso 5 satellite during the year 1969. The intensity of the line in a 100-Å band-

pass was measured, and the use of two resonance cells, one filled with hydrogen and the other one with deuterium, gave the intensity of the line at the center and on the blue wing with a resolution better than 0.02 A. These measurements showed that the shape of the line changes considerably with solar activity owing to variations in intensity at the center of the line, which are much greater than on the blue wing or averaged over the whole line. (auth)

43076 ACTIVE CAVITY RADIOMETRIC SCALE, INTERNATIONAL PYRHELIOMETRIC SCALE, AND SOLAR CONSTANT. Willson, Richard C. (Jet Propulsion Lab., Pasadena, Calif.). J. Geophys. Res.; 76: No. 19, 4325-40(1 Jul 1971).

The active cavity radiometer type II, a new and accurate standard detector, was developed for the absolute measurement of optical radiant flux. The active cavity radiometric scale (ACRS), defined by the active cavity radiometer (ACR), and the international pyrheliometric scale (IPS), defined by a U.S. standard angstrom pyrheliometer, have been compared in recent experiments. Simultaneous measurements of solar irradiance demonstrated an average systematic difference between the two scales of 2.2%, the measurements on the ACRS exceeding those on the IPS. An analytical study of the sensitivity of the ACR to sources of experimental error is presented. The uncertainty in the ACRS is found to be less than ±0.5% at the one solar constant level relative to the absolute scale based on fundamental physical principles. In August 1968 two ACR's measured the solar irradiance at an altitude of 25 km in a balloon-flight experiment. The solar-constant value derived from this measurement was $H_0 = 137.0$ mW/cm². (auth)

For abstract of individual chapter see: 43078.

43077 ADVANCES IN SPACE SCIENCE AND TECHNOLOGY, VOLUME 9. Ordway III, Frederick I. (ed.). New York; Academic Press Inc. (1967). 481p. $21.00.

Six subjects dealing with the science and technology of space flight are treated. Two articles consider technological aspects of astronautics, one chemistry, two astrobiology, and one space exploration and mission planning. A separate abstract was prepared for the chapter on chemical composition of the solar system. (W.D.M.)

43078 CHEMICAL COMPOSITION OF THE SOLAR SYSTEM. Briggs, Michael H. (Schering Chemicals Ltd., Burgess Hill, Eng.). Advan. Space Sci. Technol.; 9: 197-274(1967).

Topics covered include masses and densities of the constituents of the solar system, composition of the Sun, geochemistry, interiors of the planets, Mars, Venus, the major planets, meteorites, comets, and interplanetary dust. (W.D.M.)

Galaxies

43079 (N-71-20472) CONTRIBUTIONS TO X-RAY PHYSICS IN SPACE. Schocken, Klaus (National Aeronautics and Space Administration, Huntsville, Ala. George C. Marshall Space Flight Center). 27 Jan 1971. 62p. (NASA-TM-X-64571). NTIS.

Continuous x radiation in space that originates as blackbody radiation, deceleration radiation, and by inverse Compton processes is discussed. It is shown that the radiation Tau X-1 originates as synchrotron radiation, in Cyg X-2 and Sco X-1 as deceleration radiation, and the diffuse background radiation by inverse Compton processes. The hypothesis is made that the background x-ray flux in the Galaxy consists partly of synchrotron x rays generated in a galactic dynamo. Synchrotron radiation from the Galaxy was observed at radio frequencies. The radio emission of the Galaxy provides evidence that magnetic fields extend far beyond the boundaries of the Galaxy proper into a corona, which is called the halo. Maintenance of the synchrotron radiation of the Crab Nebula by magnetic fields is attributed to the dynamo theory. The radio and optical pulsar NP 0532 is also an x-ray pulsar close to the center of the Crab Nebula. It is shown that pulsar properties can be explained if the falling core of a collapsing star rebounds as assumed in an oscillating model of the Universe. (auth) (STAR)

43080 (N-71-21563) THREE INVESTIGATIONS OF THE INTERSTELLAR MEDIUM. Schocken, Klaus (National Aeronautics and Space Administration, Huntsville, Ala. George C. Marshall Space Flight Center). 11 Feb 1971. 30p. (NASA-TM-X-64577). NTIS.

A study of the attenuation of x rays in space is presented, with mathematical determinations of the absorption and scattering coefficients, the distribution of interstellar matter, and the radiative transfer in an absorbing–scattering cloud. The attenuation of x rays in the interstellar medium and in intergalactic space is analyzed, and numerical computations of the attenuation, along with approximate characteristic values of the interstellar medium, are given. The physical state of a hydrogen cloud is reviewed, and a model for obtaining the diffusion velocity is presented. (STAR)

43081 WHAT IS THE EXPLANATION FOR THE SPIRAL STRUCTURE OF GALAXIES? Marochnik, L. S.; Suchkov, A. A. Zemlya Vselennaya; 25-9(Jan-Feb 1971). (In Russian).

The "material" and "wave" theories that attempt to explain the spiral structure of galaxies are reviewed, and the drawbacks of these theories are indicated. A new "wave" theory is proposed that explains the formation and stability of spiral structure in terms of an interaction of different stellar subsystems in the galaxy. (IAA)

43082 OPTICALLY VARIABLE RADIO SOURCE PKS 1514-24 = AP LIBRAE. Bond, Howard E. (Louisiana State Univ., Baton Rouge). Astrophys. J.; 167: No. 2, L79(15 Jul 1971).

The optically variable object AP Librae is identified with the radio source PKS 1514-24, an N-type galaxy whose variations were previously unknown. (auth)

43083 DETECTION OF INTERSTELLAR OH IN TWO EXTERNAL GALAXIES. Weliachew, L. (California Inst. of Tech., Pasadena). Astrophys. J.; 167: No. 2, L47-52(15 Jul 1971).

Molecular OH lines at 1665 and 1667 MHz were detected in absorption in the spiral galaxy NGC 253 and the irregular galaxy M82. This is the first time that interstellar molecular lines, either radio or optical, have been observed outside the Galaxy. Observations were made with the Owens Valley interferometer; thus the amplitude and phase of the absorption features could both be measured. The run of phase versus velocity agrees with the sense of rotation of both galaxies. Abundances close to those found in the Galaxy are derived; however, this comparison is not very meaningful because of possible differences in excitation conditions. (auth)

43084 EXTRAORDINARY RED OBJECT IN SAGITTARIUS. Warner, John W.; Wing, Robert F. (Ohio State Univ., Columbus. Ohio Wesleyan Univ., Delaware). Astrophys. J.; 167: No. 2, L53-4(15 Jul 1971).

The infrared source IRC–20385 has been found to coincide with an extended object, at least 2 arc min in diameter, which is conspicuous on red plates but invisible in the blue. Its location in Sagittarius, within 5° of the direction to the galactic center, sets an upper limit to its distance. If it lies in the Sagittarius arm, its linear dimensions are on the order of 1 pc. (auth)

Cosmology

43085 (ITF-71-16-P) CONFORMALLY PLANE COSMOLOGICAL SOLUTIONS OF THE AXIAL SYMMETRY. Bondarenko, N. P. (Akademiya Nauk Ukrainskoi SSR, Kiev. Institut Teoreticheskoi Fiziki). 1971. 20p. (In Russian). Dep. NTIS (U. S. Sales Only).

The exact solutions for the axial generalization of Friedmann–Lemaitre's solutions are found and their physical interpretation as cosmological solutions is given. The cosmological models described by these solutions are anisotropic and nonhomogeneous in the sense of the Zelmanov criteria and allow the regular minimum of the gauge factor. Redshift and distortion of galaxies are investigated. (auth)

43086 RELATIVISTIC QUANTUM THEORY. Berestetskii, V. B.; Lifshitz, E. M.; Pitaevskii, L. P. Course on Theoretical Physics, Volume 4, Part 1. Oxford; Pergamon Press (1971). 390p. £6.

Translated by J. B. Sykes and J. S. Bell.

The relativistic quantum theory is dealt with in the broad sense, i.e., the theory of all phenomena that depend on the finite velocity of light, including the whole of the theory of radiation. Most of the book is devoted to quantum electrodynamics. Section headings are as follows: introduction; photons; bosons; fermions; particles in an external field; radiation; scattering of radiation; the scattering matrix; invariant perturbation theory; interaction of electrons; and interactions of electrons with photons. (UK)

43087 COSMOLOGICAL CONSTANT AND FUNDAMENTAL LENGTH. Anderson, James L. (Stevens Inst. of Tech., Hoboken, N. J.); Finkelstein, David. Amer. J. Phys.; 39: No. 8, 901-4 (Aug 1971).

In usual formulations of general relativity, the cosmological constant Λ appears as an inelegant ambiguity in the fundamental

XUM

action principle. With a slight reformulation, Λ appears as an unavoidable Lagrange multiplier, belonging to a constraint. The constraint expresses the existence of a fundamental element of space-time hypervolume at every point. The fundamental scale of length in atomic physics provides such a hypervolume element. In this sense, the presence in relativity of an undetermined cosmological length is a direct consequence of the existence of a fundamental atomic length. (auth)

43088 SHEAR IN A PERTURBED FRIEDMANN UNIVERSE. Stoermer, Olaf (Univ., Hamburg). Gen. Relativity Gravitation; 1: No. 2, 103-15(1970).

For perturbed Friedmann models of vanishing and positive curvature the time development of shear is computed by means of a linear perturbation theory. Mathematically exact and physically meaningful conditions are stated for the perturbation functions. The shear is computed for different stages of the Universe. (auth) (UK)

43089 DOES A VACUUM GRAVITATE. Novikov, I. D. Zemlya Vselennaya; 36-41(Sep-Oct 1969). (In Russian).

A possible gravitational-repulsion property of the interstellar vacuum is discussed. The theoretical and observed relations between the magnitudes and redshift of galactic objects and quasars are examined. The significance of the cosmic constant lambda characterizing the gravitational-repulsion forces is discussed as a possible explanation for the random relation between the magnitude and redshift of quasars. (IAA)

43090 POST-NEWTONIAN EFFECTS OF GENERAL RELATIVITY ON THE EQUILIBRIUM OF UNIFORMLY ROTATING BODIES. VI. THE DEFORMED FIGURES OF THE JACOBI ELLIPSOIDS. Chandrasekhar, S. (Univ. of Chicago). Astrophys. J.; 167: No. 3, 455-63(1 Aug 1971).

The theory of the (deformed) post-Newtonian Jacobi ellipsoid developed in an earlier paper is specialized suitably to make a comparison with the Newtonian ellipsoid having the same angular momentum and baryon number. (auth)

43091 POST-NEWTONIAN EFFECTS OF GENERAL RELATIVITY ON THE EQUILIBRIUM OF UNIFORMLY ROTATING BODIES. V. THE DEFORMED FIGURES OF THE MACLAURIN SPHEROIDS. Chandrasekhar, S. (Univ. of Chicago). Astrophys. J.; 167: No. 3, 447-53(1 Aug 1971).

The theory of the (deformed) post-Newtonian Maclaurin spheroid developed in an earlier paper is specialized suitably to make a comparison with the Newtonian spheroid having the same angular momentum and baryon number. (auth)

43092 RELATIVISTIC DISKS. I. UNIFORM ROTATION. Bardeen, James M. (Univ. of Washington, Seattle); Wagoner, Robert V. Astrophys. J.; 167: No. 3, 359-423(1 Aug 1971).

The structure and gravitational field of uniformly rotating, infinitesimally thin disks is calculated numerically within the framework of general relativity. The methods of calculation are described in some detail, since they can easily be extended to differentially rotating disks. Most results are quite accurate, even in the extreme relativistic limit in which the redshift from the center of the disk to infinity becomes infinite. An example is the fractional binding energy, which is calculated to reach 37.3% in this limit. The geometry of space–time exterior to the disk is found to approach that of the Kerr metric with $cJ = GM^2$ in the extreme relativistic limit, if the limit is taken in the appropriate way. A substantial fraction of the photons emitted even by highly relativistic disks can escape to infinity with blueshifts, while other photons are trapped into bound orbits if the disk is highly relativistic. An investigation of the local instability to fragmentation indicates that a large amount of differential rotation and/or thickness is necessary to stabilize the disks. The behavior of rotating disks when their gravitational fields become strong is very different from the behavior of spherical or slowly rotating configurations, and offers intriguing possibilities in astrophysics if the stability problem can be solved. (auth)

43093 REEXAMINATION OF THE POST-NEWTONIAN MACLAURIN SPHEROIDS. Bardeen, James M. (Univ. of Washington, Seattle). Astrophys. J.; 167: No. 3, 425-46(1 Aug 1971).

The post-Newtonian corrections to Maclaurin spheroids are calculated in such a way that the Newtonian and relativistic configurations being compared have the same energy density, rest mass, and angular momentum. The singularity found by Chandrasekhar is interpreted as a splitting of the Maclaurin sequence into a spherelike sequence and a disklike to ringlike sequence. The post-Newtonian corrections are calculated to several quantities of physical interest, including the binding energy. (auth)

43094 MEASUREMENT OF THE GRAVITATIONAL DEFLECTION OF MICROWAVE RADIATION NEAR THE SUN, OCTOBER 1970. Sramek, R. A. (National Radio Astronomy Observatory, Green Bank, W. Va.). Astrophys. J.; 167: L55-60(15 Jul 1971).

The position of the radio source 3C 279 was monitored during an occultation by the Sun using a 2.7-km-baseline radio interferometer. Observations were made simultaneously at wavelengths of 11.1 and 3.7 cm. The two-wavelength observations gave a measurement of the refraction in the solar corona independent of the gravitational deflection. After correcting for this refraction, the gravitational bending was found to be $1.57 \pm 0.08''$ at the limb of the Sun. This is 0.90 ± 0.05 of the deflection predicted by Einstein's general theory of relativity. (auth)

43095 HAMILTONIAN COSMOLOGY. Estabrook, F. B.; Wahlquist, H. D. (California Inst. of Tech., Pasadena). Phys. Lett.; 35A: No. 6, 453-4(12 Jul 1971).

A simple polynomial Hamiltonian is given for Type VIII and IX vacuum cosmologies. This Hamiltonian also describes solutions with time-like homogeneous 3-surfaces, and so suggests quantized versions that include fluctuations of 3-space signature and topology. (auth)

43096 PERTURBATIONS IN ANISOTROPIC EUCLIDEAN-HOMOGENEOUS COSMOLOGIES. Matzner, R. A.; Perko, T. E.; Shepley, L. C. (Univ. of Texas, Austin). Phys. Lett.; 35A: No. 6, 467-8(12 Jul 1971).

The role of anisotropy in the galaxy formulation process is considered. It is found that the growth rate of a density perturbation does not appreciably differ from the isotropic growth rate. (auth)

43097 PULSATING UNIVERSE OF SENGUPTA. Maccallum, M. A. H. (Cambridge Univ., Eng.). Phys. Lett.; 35A: No. 6, 474(12 Jul 1971).

It is pointed out that the recently announced pulsating universe of Sengupta does not satisfy Einstein's field equations. A discussion of the possibility of pulsating solutions is given. (auth)

43098 COSMOLOGY AS A SCIENCE. Bergmann, Peter G. (Syracuse Univ., N. Y.). Found. Phys.; 1: No. 1, 17-22(1970).

In recent years, observational techniques at cosmological distances have been sufficiently improved that cosmology has become an empirical science, rather than a field for unchecked speculation. There remains the fact that its object, the whole universe, exists only once; hence, one is unable to separate "general" features from particular aspects of the universe. This might not be a serious drawback if one was justified in the belief that presently accepted laws of nature remain valid on the cosmological scale. However, there are grounds for doubting that belief. The three arguments presented are the possibility that apparent constants of nature may, during cosmological times, turn out to vary (Dirac conjecture); the effective breakdown of the principle of relativity caused by the effects of the cosmological environment on local experiments; and the fact that present theory leads to field singularities at the early stages of the expanding universe, which might be a signal that currently accepted theoretical concepts are inadequate for an understanding of highly condensed matter. (auth)

Planetary Phenomena

Refer also to abstracts 43272 and 43446.

43099 DISTRIBUTION AND ORIGIN OF HELIUM, NEON, AND ARGON ISOTOPES IN APOLLO 12 SAMPLES MEASURED BY IN SITU ANALYSIS WITH A LASER-PROBE MASS SPECTROMETER. Megrue, G. H. (Smithsonian Astrophysical Observatory, Cambridge, Mass.). J. Geophys. Res.; 76: No. 20, 4956-68(10 Jul 1971).

Distributions of the relative isotopic abundances of helium, neon, and argon were measured in situ by laser-probe mass spectrometric analysis of Apollo samples 12070,67 (fines and individual gabbro, basalt, feldspar, and glass fragments); 12018,24 gabbro (interior and exterior surface); and 12010,13 breccia (interior and exterior of matrix and vein of fine-grained material). On a scale of 10^{-3} to 10^{-5} gram, the distributions of helium, neon, and argon isotopes in these samples are highly variable. The maximum abundances of these gases are located (1) in rocks within $<30\ \mu$ of the pitted "top" surface (that surface exposed to solar irradiation), (2) in loose fines from the lunar surface, or (3) in veins of fine-grained material within rock breccias. The relative abundances of the helium,

neon, and argon isotopes from the "top" surface (<30 μ) of 12018,24 are similar to the isotopic abundances measured in the lunar fines of 12070,67 and are consistent with an origin by solar-wind implantation, having $^3He/^4He = 5.5$ and $4.4 \pm 0.3 \times 10^{-4}$, $^4He/^{20}Ne = 97 \pm 14$, $^4He/^{36}Ar = 1050 \pm 150$, $^{20}Ne/^{22}Ne = 11.2 \pm 0.4$, and $^{21}Ne/^{22}Ne = 0.035 \pm 0.006$. A comparison of the ratios of helium, neon, and argon isotopes from these samples with the ratios determined on the fine-grained vein material of Fayetteville and Kapoeta meteorites shows that the $^3He/^4He$ is 30% less in the meteorites than in the lunar samples. Furthermore, although the $^4He/^{20}Ne$ from Kapoeta is consistent with the lunar results, the $^4He/^{36}Ar$ is a factor of 3 higher, whereas the relative abundances of isotopic helium, neon, and argon from Fayetteville are not equivalent to the lunar results. Cosmogenic gases, isotopically similar to the gases produced in achondritic meteorites by galactic cosmic-ray bombardment, as well as ^{40}Ar, which is believed to be radiogenic in origin, are distributed in the interior and occasionally on the exterior of the lunar samples. (auth)

Atomic and Molecular Physics

43100 EXISTENCE OF SMALL NEGATIVE RADIOACTIVE IONS COMING FROM A ^{228}Th SOURCE. Wajsfelner, Rene; Bricard, Jean; Madelaine, Guy J. (Univ., Paris. CEA, Fontenay-aux-Roses, France). Compt. Rend., Ser. B; 272: No. 11, 664-7 (15 Mar 1971). (In French).

The results from measurements by three different methods on the distribution of the mobility spectrum of small negative radioactive ions from ^{228}Th are given. The methods used involved Zélény tubes, the Erikson spectrograph or a parallel-plate capacitor; each apparatus was used with a convenient counting device. (auth) (France)

Atomic, Electron, Ion, and Molecular Beams and Their Reactions

Refer also to abstracts 42079, 43135, 43474, 43736, and 43756.

43101 (SCL-T-69-256) SECONDARY-ELECTRON EMISSION PRODUCED BY RELATIVISTIC PRIMARY ELECTRONS IN STRONG ELECTRIC FIELDS. Bartasius, J.; Pranevicius, O. Translated by T. Watt for Sandia Labs., Albuquerque, N. Mex., from Liet. Fiz. Rinkinys.; 8: No. 1-2, 293-9(1968). 10p. Dep. NTIS.

An abstract of this paper, prepared from the original language, appeared as NSA 23: 18413.

43102 AUGER TRANSITION AND SUPPLEMENTARY ELECTRON EJECTION IN THE IONIZATION OF ALUMINUM BY ELECTRON IMPACT. Abouaf, R. (Faculte des Sciences, Orsay, France). Phys. Lett.; 35A: No. 5, 319-20(28 Jun 1971).

It is shown that the Auger transitions $L_{2,3}$-MM(Al^{2+}), $L_{2,3}$MMM and $L_{2,3}$M-MMM(Al^{3+}) are predominant in the Al^{2+} and Al^{3+} production. (auth)

43103 POSSIBILITY OF PRODUCING INVERTED POPULATION IN ATOMIC BEAMS BY CHARGE EXCHANGE OF PROTONS WITH ATOMS. Presnyakov, L. P.; Shevel'ko, V. P. (Lebedev Inst. of Physics, Moscow). JETP Lett. (USSR) (Engl. Transl.); 13: No. 6, 203-4(20 Mar 1971).

Translated from Zh. Eksp. Teor. Fiz., Pis'ma Red.; 13: No. 6, 286-8(20 Mar 1971).

An inverted medium (H atoms in a state with n = 2) can be produced when a beam of atomic cesium is intersected by a beam of protons having an energy less than or equal to 10 keV. The charge exchange cross sections of protons with cesium atoms are shown graphically, for proton energies up to 40 keV. It was found that, with increasing proton energy, charge exchange with capture of an electron from an inner shell of the Cs atom becomes effective. (J.C.W.)

43104 CLASSICAL MODEL FOR GAS–SURFACE INTERACTION. Busby, M. R.; Haygood, J. D.; Link, C. H. Jr. (Arnold Engineering Development Center, Arnold Air Force Station, Tenn.) J. Chem. Phys.; 54: No. 11, 4642-7(1 Jun 1971).

A three-dimensional classical theoretical model for the interaction of a monatomic gas impinging as a monoenergetic atomic beam on its own solid phase was formulated and tested using the experimental data for the argon gas–solid system. The theoretical interaction is modeled as the collision of hard spheres with the inclusion of an attractive surface field energy, the only adjustable parameter in the model, and surface temperature. The theoretical results from this exceedingly simple model exhibit nearly every characteristic of the available experimental data for argon. (auth)

43105 CROSS-SECTION ENHANCEMENT BY SCATTERING WITH CORRELATED NONSTATIONARY STATES. Favro, L. D.; Kuo, P. K. (Wayne State Univ., Detroit). Phys. Rev., D; 3: No. 12, 2931-4(15 Jun 1971).

It is shown that the successive scattering of particles in correlated nonstationary states produces a cross section which is enhanced by a factor that depends on the flux, the range of interaction, and the relaxation time of the target. (auth)

43106 ENERGY TRANSFER VIA SCATTERING OF A COHERENT MODULATED ELECTRON BEAM. Favro, L. D.; Fradkin, D. M.; Kuo, P. K. (Wayne State Univ., Detroit). Phys. Rev., D; 3: No. 12, 2934-7(15 Jun 1971).

The total inelastic cross section for the scattering of a coherent modulated electron beam, viewed as a single quantum state, is calculated. In addition to the conventional one-electron contribution, there is a many-electron interference contribution which, under proper conditions, can lead to a greatly enhanced cross section. Furthermore, the interference term has the property of selectively exciting the target at a sharply defined frequency which is determined by the modulator. The possible relevance of this interference effect to the Schwarz–Hora experiment and potential applications, such as in electron microscopy, are discussed. (auth)

43107 PRODUCTION OF CARBON K X RAYS BY HEAVY-ION BOMBARDMENT. Der, R. C.; Fortner, R. J.; Kavanagh, T. M.; Khan, J. M. (Univ. of California, Livermore). Phys. Rev., A; 4: No. 2, 556-62(Aug 1971).

Cross sections for K x-ray production in carbon are presented for collisions involving incident C^+, N^+, O^+, Ne^+, Ar^+, Kr^+, and Xe^+ in the energy range 20 to 1.5 MeV. Thick-target x-ray-yield data are also included. The cross-section measurements are in excellent agreement with a simple theoretical model based on the Landau–Zener theory of level crossing. (auth)

43108 K-SHELL-FLUORESCENCE YIELD FOR CARBON AND OTHER LIGHT ELEMENTS. Hink, W.; Paschke, H. (Univ., Wuerzburg, Ger.). Phys. Rev., A; 4: No. 2, 507-11(Aug 1971).

By recording the absolute number of K x-ray quanta emitted from a thin graphite target bombarded with electrons of energy E between 2 and 30 keV, the quantity $\omega_K \cdot Q_K$ (E) for carbon was measured, where ω_K is the K-shell-fluorescence yield and Q_K (E) the ionization cross section for the K shell. Q_K(E) was calculated with the formula of Gryzinski, and the fluorescence yield of carbon was obtained as $\omega_K = 0.0035$. This value is much higher than the two other experimental values, but it is in agreement with a semiempirical formula of Byrne and Howarth and in near agreement with a recent calculation of McGuire. It is shown that this formula and this calculation seem to be valid for elements with atomic numbers down to $Z \approx 6$. (auth)

43109 FAST HYDROGEN-ATOM INJECTOR. II. PRODUCTION AND FORMATION OF PROTON BEAMS AND NEUTRAL BEAMS. Panasenkov, A. A.; Semashko, N. N. Sov. Phys.-Tech. Phys. (Engl. Transl.); 15: No. 12, 1979-85(Jun 1971).

Translated from Zh. Tekh. Fiz.; 40: No. 12, 2525-33(Dec 1970).

An injector is described, which creates an atomic-hydrogen flux having energies from 15 to 30 keV and an intensity greater than 0.5 equivalent amperes. The proton beam is produced and shaped in a gas-discharge source operating in a transverse magnetic field, which is at the same time the focusing element for the ion beam. The flux of neutrals is formed by proton charge exchange in a gas target consisting of magnesium vapor. Experiments are described, which involve the production and formation of proton and neutral beams as well as an investigation of beam characteristics. (auth)

43110 RESOLVED STRUCTURE IN Fe Kα X RAYS PRODUCED BY 30-MeV OXYGEN IONS. Burch, D. (Univ. of Texas, Austin); Richard, Patrick; Blake, R. L. Phys. Rev. Lett.; 26: No. 22, 1355-9(31 May 1971).

The Fe Kα x-ray spectrum produced by 30-MeV O^{5+} bombardment is found to consist of two major components, which have been identified as 1s → 2p transitions shifted 38 and 68 eV above the $K\alpha_{1,2}$ energy primarily because of one and two additional vacancies, respectively, in the 2p shell. (auth)

43111 SURFACE AND VACUUM PHYSICS INDEX. VOLUME 6, NO. 5, 1971. Bibliography, Author Index, Subject Index in Alphabetical Order, Cumulative Subject Index in Logical Order. Frankfurt am Main: Zentralstelle fuer Atomkernenergie-Dokumentation (1971). 51p.

XUM

This listing includes 148 references on various aspects of surface and vacuum physics. (M.O.W.)

Atomic and Molecular Properties

Refer also to abstracts 41778, 43069, 43207, and 43469.

43112 RAISING OF DISCRETE LEVELS INTO THE FAR CONTINUUM. Dehmer, J. L. (Univ. of Chicago); Starace, A. F.; Fano, U.; Sugar, J.; Cooper, J. W. Phys. Rev. Lett.; 26: No. 25, 1521-5(21 Jun 1971).

Broad peaks observed in the photoabsorption spectra of rare earths ~10 to 20 eV above the 4d edge are attributed to transitions $4d^{10}4f^N \rightarrow 4d^9 4f^{N+1}$. Exchange interaction splits the $4d^9 4f^{N+1}$ configuration and raises some multiplets by ~20 eV. Autoionization to $4d^9 - 4f^N \epsilon f$ broadens the high levels. The interpretation extends to p → d processes observed in the absorption of synchrotron light by transition elements. (auth)

43113 EMISSION SPECTRUM OF THORIUM IN THE 5400 TO 6400 cm^{-1} REGION. Bernage, P.; Houdart, R.; Niay, P. (Faculte des Sciences, Lille). Spectrochim. Acta, Part B; 26: No. 5, 261-70(May 1971). (In French).

Investigation of the Th spectrum between 5400 and 6400 cm^{-1} was undertaken to test the qualities of the S.I.S.A.M. spectrometer recently built in the authors' laboratory. This spectrum is rich and intense and could possibly provide wavelength standards for high-resolution measurements in the infrared region. A comparison is made with the results of other experimenters. (auth) (UK)

43114 GRAPHICAL PRESENTATIONS OF SYSTEMATIC TRENDS OF ATOMIC OSCILLATOR STRENGTHS ALONG ISOELECTRONIC SEQUENCES AND NEW OSCILLATOR STRENGTHS DERIVED BY INTERPOLATION. Smith, M. W.; Wiese, W. L. (National Bureau of Standards, Washington, D. C.). Astrophys. J., Suppl. Ser.; 23: No. 196, 103-92(Jun 1971).

Recently detected systematic trends of atomic oscillator strengths along isoelectronic sequences are utilized for the determination of new numerical data and for the evaluation of the reliability of existing material. All well-established systematic trends, which number about 100, are presented graphically. New oscillator strengths are interpolated from the graphs, mainly for the higher ions with wavelengths located principally in the vacuum ultraviolet, and are tabulated with their estimated uncertainties. The graphs are ordered according to isoelectronic sequences and are given with full grids to allow the addition of future data. (auth)

43115 S AND P STATES OF THE HELIUM ISOELECTRONIC SEQUENCE UP TO Z = 10. Accad. Y. (Weizmann Inst. of Science, Rehovot, Israel); Pekeris, C. L.; Schiff, B. Phys. Rev., A; 4: No. 2, 516-36(Aug 1971).

Calculations were made of the energy levels and other properties of the states n^1S, n^3S, n^1P, and n^3P, n = 2 to 5, for atoms belonging to the helium isoelectronic sequence up to Z = 10, and also for the higher excited S states of helium. The theoretical term values, including the contributions from the mass-polarization correction and the relativistic effects of order α^2 are listed. A detailed comparison with the experimentally determined energy differences between S and P states for He I up to F VIII shows a satisfactory agreement in almost every case, provided that an estimate of the Lamb-shift correction to the S-state energy level is included when considering transitions involving the 1^1S, 2^1S, or 2^3S states. (auth)

43116 MANY-BODY CALCULATIONS FOR THE HEAVY ATOMS. Morrison, J. C.; Rajnak, K. (Argonne National Lab., Ill.). Phys. Rev., A; 4: No. 2, 536-42(Aug 1971).

Corrections to the Hartree–Fock (HF) theory which arise as a result of electrostatic configuration interaction are calculated for a heavy ion Pr^{3+}. The effect of configuration interaction upon the $4f^2$ configuration is represented by effective two-body operators of the form $\Sigma_k a_k C_1^{(k)} C_2^{(k)}$. These operators are evaluated using perturbation theory and graphical methods. The effect of the operators of even rank is to depress the values of the Slater F^k integrals below their HF values. The two-body operators of odd rank do not appear within the ordinary HF theory. The Trees parameter α is the coefficient of an operator of this kind. It is found that the corrections to the Slater integrals converge slowly. The contributions to the operators of odd rank converge properly, however, and the values $\alpha = 28$, $\beta = -616$, and $\gamma = 1611$ are obtained. This may be compared with the empirical values $\alpha = 24$, $\beta = -586$, and $\gamma = 728$. The value of γ is determined empirically by the position of a single level, ^1S. It is suggested that the free-ion ^1S level has not been properly identified. (auth)

43117 PERTURBATION CALCULATION OF ATOMIC POLARIZABILITIES. Hameed, S. (Yeshiva Univ., New York). Phys. Rev., A; 4: No. 2, 543-9(Aug 1971).

A procedure is presented that uses perturbation theory to calculate correlation corrections for atomic polarizability when the atom is described by a local potential in the starting approximation. Zeroth-order polarizabilities and first-order correlation corrections for them were calculated for Mg, Na, Ne, Be, Li, and He atoms using the Hartree–Fock–Slater potential and another local potential. For most of the atoms, the corrections are found to be significantly large. Implications are discussed. (auth)

43118 g_J VALUE FOR THE ATOMIC GROUND STATE OF FERMIUM. Goodman, L. S.; Diamond, H.; Stanton, H. E.; Fred, M. S. (Argonne National Lab., Ill.). Phys. Rev., A; 4: No. 2, 473-5(Aug 1971).

The atomic-beam magnetic-resonance method was used to measure $g_J = 1.16052 \pm 0.00014$ for the atomic ground state of fermium I. An intermediate-coupling calculation with parameters extrapolated from lower actinides, and with corrections for diamagnetic and relativistic effects, yielded the value $g_J = 1.1606$. The agreement between the measured and calculated values of g_J establishes the fermium ground state as the $^3H_6$ level of the $5f^{12}7s^2$ configuration. The neutral fermium atoms were obtained by heating FmF_3 and its HoF_3 carrier in the presence of ZrC and tungsten. (auth)

43119 IDENTIFICATION OF THE $4f^{10}5d$, $4f^95d6s$, AND $4f^96s^2$ CONFIGURATIONS IN THE SPECTRUM OF Dy II. Wyart, Jean-Francois (CNRS, Orsay, France). Compt. Rend., Ser. B; 272: No. 16, 933-6(19 Apr 1971). (In French).

The identification of the spectral lines of Dy II led to the discovery of the first excited even configuration $4f^{10}5d$ and that of two odd configurations of lower energy: $4f^95d6s$ and $4f^96s^2$. The interpretation of these levels is based on Landé-factor measurements and parametric calculations of the configuration. (France)

43120 STUDY OF THE FIELD-INDUCED SPECTRUM OF HYDROGEN AT HIGH RESOLUTION. Buijs, Hendricus Leonardus. Vancouver; Univ. of British Columbia (1970). National Library of Canada, Ottawa.

Thesis.

The static-field-induced absorption spectrum of hydrogen was investigated at high resolution and with reliable frequency calibration over the density range from 1.5 to 28 amagat. Frequencies were extrapolated to zero density in order to obtain molecular constants for the isolated molecule. Line profiles were compared with various functions and the simple dispersion profile seems to fit the data best over the density range studied. The linewidth, however, decreases with density until it reaches a minimum at about 2.5 amagat below which it starts to increase again. The minimum width is about 4 times less than the width of the classical doppler line. This behavior of the line width is consistent with the phenomena of "collision narrowing" in the infrared. From the intensities of the lines one obtains the isotropic polarizability $(\alpha)_{1-0} = 1.21\ cm^3$. (Diss. Abstr. Int., B)

43121 HYPERFINE STRUCTURE MEASUREMENTS IN THE GROUND STATES $^4F_{\frac{3}{2}}$, $^4F_{\frac{5}{2}}$, AND $^4F_{\frac{7}{2}}$ OF ^{181}Ta WITH THE ATOMIC BEAM MAGNETIC RESONANCE METHOD. Buettgenbach, S.; Meisel, G. (Univ., Bonn). Z. Phys.; 244: No. 2, 149-62(1971).

Applying a recently developed evaporation technique for refractory elements, results were obtained for ^{181}Ta in an atomic beam magnetic resonance experiment studying the hyperfine structure of 3 levels of the ground state multiplet ^4F. From these measurements, constants of the magnetic dipole interaction and the electric quadrupole interaction were derived. (M.O.W.)

43122 PRECISE MEASUREMENT OF THE 2^3P_0–2^3P_1 FINE-STRUCTURE INTERVAL OF HELIUM. Kponou, A.; Hughes, V. W.; Johnson, C. E.; Lewis, S. A.; Pichanick, F. M. J. (Yale Univ., New Haven). Phys. Rev. Lett.; 26: No. 26, 1613-16(28 Jun 1971).

The $2^3P_0 - 2^3P_1$ fine-structure interval ν_{01} of helium was measured by the atomic-beam optical-microwave magnetic-resonance method. The result is $\nu_{01} = 29\ 616.864(36)$ MHz (1.2 ppM), in which the error is 1 standard deviation. This precision is more than a factor of 10 better than that obtained by any other method. Comparison with the present theoretical value of ν_{01} is given, and the possibility of obtaining a value for the fine-structure constant α accurate to better than 1 ppM from this experimental result is emphasized. (auth)

43123 EIGENVALUES AND CERTAIN EXPECTATION VALUES FOR ALL BOUND AND QUASI-BOUND LEVELS OF GROUND-STATE $(X^1\Sigma_g^+)H_2$, HD, AND D_2. LeRoy, Robert J.

(Univ. of Wisconsin, Madison). J. Chem. Phys.; 54: No. 12, 5433-4(15 Jun 1971).

The Kolos–Wolniewicz potential with its relativistic and adiabatic corrections and with the nuclear reduced mass was used to calculate the eigenvalues and the expectation values of R, R^2, R^{-2}, and kinetic energy for all the bound and quasi-bound levels of H_2, HD, and D_2. The level widths Γ were computed for all quasi-bound levels for which $0.05 < \Gamma \lesssim 100$ cm^{-1}. The heights and positions of the centrifugal barrier maxima were also determined. The calculations are described briefly here; tables of the results are available in a separate report. (A.G.W.)

43124 SHAPE RESONANCES AND ROTATIONALLY PREDISSOCIATING LEVELS: THE ATOMIC COLLISION TIME-DELAY FUNCTIONS AND QUASI-BOUND LEVEL PROPERTIES OF $H_2(X^1\Sigma_g^+)$. Le Roy, Robert J.; Bernstein, Richard B. (Univ. of Wisconsin, Madison). J. Chem. Phys.; 54: No. 12, 5114-26 (15 Jun 1971).

The energy dependence of the collisional time-delay function was computed for H(1S) atoms interacting via the ab initio H_2 $(X^1\Sigma_g^+)$ potential. Peaks in this function determine the scattering resonance energies E_r and widths Γ and the lifetimes for each of the corresponding quasi-bound vibrational–rotational levels. Small differences are found between these values of E_r and Γ and the values obtained by a "maximum internal amplitude" approach (intended to characterize the spectroscopically observable predissociating levels). Approximate procedures for rapid, accurate numerical evaluation of E_r are appraised; a new outer-boundary-condition criterion for resonances leads to the best agreement with the exact results. Also, a primitive WKB procedure yields Γ's of usable accuracy. For ground-state H_2, HD, and D_2 the onset of line broadening due to centrifugal barrier penetration is found to occur at energies some hundreds of cm^{-1} below the locus of barrier maxima. The predissociation method of estimating long-range interatomic forces therefore cannot be expected to yield valid results for hydridic diatomics. (auth)

Positronium, Muonium, and Mesic Atoms and Molecules

Refer also to abstracts 43453, 43482, 43806, 43821, 43904, 43913, and 43949.

43125 X-RAY YIELDS IN MUONIC HYDROGEN. Leon, M. (Rensselaer Polytechnic Inst., Troy, N. Y.). Phys. Lett.; 35B: No. 5, 413-14(21 Jun 1971).

The relative yields for K x rays from muonic hydrogen as functions of the hydrogen density are calculated. The experimental data agree with the analysis. (auth)

43126 POSITRON ANNIHILATION IN RARE EARTH HYDRIDES. Chouinard, M. P.; Gustafson, D. R. (Wayne State Univ., Detroit). J. Chem. Phys.; 54: No. 12, 5082-4(15 Jun 1971).

Analysis of the angular correlations of positron-annihilation radiation from erbium, gadolinium, holmium, and ytterbium hydrides indicates that the electronic structure of these materials is basically metallic in nature. As was previously found in the case of cerium hydride, the angular correlations were found to be broader than those from their parent metals by amounts that were consistent with the assumption that the rare-earth-metal valence electrons and the electrons of the hydrogen atoms are all contributing to metallic bonding. (auth)

Collision Phenomena

Refer also to abstract 43930.

43127 (BNL-tr-429) EXCITATION OF THE AROMATIC MOLECULES BY ELECTRON IMPACT. I. MOLECULES WITH D_{2h} SYMMETRY. Lyash, A. V.; Poshyunaite, N. P.; Bolotin, A. B. Translated by S. J. Amoretty (Brookhaven National Lab., Upton, N. Y.), from Liet. Fiz. Rinkinys; 8: Nos. 1 and 2, 762-8(1968). 12p. Dep. NTIS.

Total effective cross sections for excitation of pyrene and naphthacene molecules by fast electrons are calculated in the Born approximation using molecular orbitals obtained in the LCAO approximation. Excitation from the ground state to the first three excited states is considered. Results are tabulated for incident-electron energies of 50 eV to 10 keV. The excitation cross sections for the pyrene molecule are seen to be, on the average, twice as large as those for the naphthacene molecule. (A.G.W.)

43128 ABSTRACT EXCITATION CROSS SECTIONS OF He^+ IN 20 TO 100 keV He^+–He COLLISIONS USING ENERGY-LOSS SPECTROMETRY. Schoonover, Donald Roy. Rolla, Mo.; Univ. of Missouri (1970). 68p. University Microfilms Order No. 71-12,326.

Thesis.

Application of positive-ion energy-loss spectrometry was extended to include experimental determination of absolute excitation cross sections of ground-state helium ions. Helium ion–atom collisions were studied for impact energies ranging between 20 and 100 keV, in 10 keV intervals. The data were taken with an apparatus resolution between 0.6 and 0.8 eV fwhm. Cross sections for transitions from the ground state to the second and third principal quantum levels of the ion, plotted as a function of impact energy, were still rapidly increasing at 100 keV. The cross sections at this energy were $1.64\ (\pm 0.28) \times 10^{-18}$ cm^2 for $He^+(1^2s_{\frac{1}{2}}) \rightarrow He^+$ $(n = 2)$ and $3.46(\pm 0.45) \times 10^{-19}$ cm^2 for $He^+(1^2s_{\frac{1}{2}}) \rightarrow He^+(n = 3)$. (Diss. Abstr. Int., B)

43129 STUDY OF THE $3\,^1P$–$2\,^1S$ LINE OF HELIUM EXCITED BY A HYDROGEN ION BEAM AT AVERAGE ENERGY. Grouard, Jean-Pierre; Hirszowski, Julien; Lefebure, Patrice; De Palmas, Henri (Univ., Paris). Compt. Rend., Ser. B; 272: No. 16, 937-40(19 Apr 1971). (In French).

The polarization of the 3^1P-2^1S line of helium excited by H^+ and H_2^+ ions in the energy range 15 to 40 keV was measured. (France)

43130 SIMPLE MODEL FOR SCATTERING OF ELECTRONS BY A ROTATING DIPOLE. Bottcher, C. (Harvard College Observatory, Cambridge, Mass.). Chem. Phys. Lett.; 9: No. 1, 57-61(1 Apr 1971).

The coupled equations describing the interaction of one electron with a dipole and hard sphere are shown to be exactly soluble, even when the energy levels of the dipole are taken into account. This model is used to discuss the critical moment for binding the electron in the dipole field. The condition for the existence of Feshbach resonances is similarly discussed. When the model is applied to calculate scattering phase shifts, shape resonances are found. (auth)

43131 CROSSED-MOLECULAR-BEAM STUDY OF COLLISION-INDUCED DISSOCIATION OF ALKALI HALIDES. Tully, F. P.; Lee, Y. T.; Berry, R. S. (Univ. of Chicago). Chem. Phys. Lett.; 9: No. 1, 80-4(1 Apr 1971).

The dissociation of alkali metal halides to ion pairs induced by collisions with high-energy Xe was studied by a crossed-molecular-beam method. The dependence of the dissociation cross section on relative kinetic energy and on alkali metal halide internal energy was investigated. (auth)

43132 FRACTIONAL-ORDER BESSEL FUNCTION APPROXIMATIONS TO BOTH ATTRACTIVE AND REPULSIVE COULOMB SCATTERING. Lu, P. (Arizona State Univ., Tempe). Chem. Phys. Lett.; 9: No. 3, 207-9(1 May 1971).

Using the $L + \frac{1}{2}$ order Bessel function as the solved part, much improved results are obtained for the scattering cross section to the order of $\hbar^2$ by using Miller and Good's modified WKB method. (auth)

43133 EXCITATION TRANSFER IN COLLISIONS OF HIGHLY EXCITED ALKALI ATOMS. CESIUM–CESIUM COLLISIONS. Zembekov, A. A.; Nikitin, E. E. (Inst. of Chemical Physics, Moscow). Chem. Phys. Lett.; 9: No. 3, 213-16(1 May 1971).

Possible mechanisms of the resonance and near-resonance excitation transfer in collisions of $Cs^{**}(8^2P)$ with $Cs(6^2S)$ are discussed. The estimated cross section for the intramultiplet mixing is in close agreement with experimental results. (auth)

43134 CROSS SECTIONS FOR Ar L-SHELL X-RAY EMISSION IN COLLISIONS OF He^+, C^+, N^+, O^+, Al^+, Ti^+, Fe^+, Cu^+ ON Ar. Saris, F. W. (FOM, Instituut voor Atoom- en Molecuulfysica, Amsterdam). Physica; 52: No. 2, 290-8(31 Mar 1971).

Observation of Ar L-shell x-ray emission in collisions of He^+, C^+, N^+, O^+, Al^+, Cl^+, Ti^+, Fe^+, and Cu^+ with Ar indicates that inner-shell vacancies are produced during these heavy-ion–atom collisions. The cross sections for Ar L-shell x-ray emission are shown to be strongly dependent on the atomic number of the projectile. The data are discussed in the framework of the Fano–Lichten model for inner-shell excitations. Critical internuclear distances for inner-shell excitation are deduced from the threshold of the cross sections and compared with data from other investigators. These critical internuclear distances present a characteristic oscillation, which is correlated with the Z dependence of the geometrical sizes of the inner shells involved. (auth)

XUM

43135 METHOD FOR PRODUCING IONS UTILIZING A CHARGE-TRANSFER COLLISION. Haeberli, Willy (to United States Atomic Energy Commission). U. S. Patent 3,577,026. 4 May 1971. Filed 24 Jun 1969.

The method comprises effecting a charge-transfer collision between a first beam of polarized neutral atoms to be ionized and a generated second beam of atoms whereby the polarized atoms in the first beam are ionized. (auth)

43136 DISPERSION DIPOLE BETWEEN S-STATE ATOMS. Whisnant, David Melvin. Madison, Wis.; Univ. of Wisconsin (1971). 95p. University Microfilms Order No. 71-5671. Thesis.

When two unlike atoms collide, a dipole moment may be induced because of different distortions of their charge clouds. The long-range contribution to this interaction dipole was investigated. This contribution can be expanded in a series in R^{-n} in a manner analogous to the long-range interaction energy. An approximation to the first term in this series, D_7, is developed. This coefficient is first expressed in a convenient form involving integrals of frequency-dependent properties of the isolated atoms, and then an approximate method that involves fairly simple properties of the individual atoms is developed making use of this form. The approximation is tested with accurate variation-perturbation values of D_7 for a model system, for helium-hydrogen, and for helium-helium and is found to be accurate to within 10% or less for these three cases. It is finally used to calculate D_7 for interactions of the rare gas atoms. (Diss. Abstr. Int., B)

43137 EXCITATION OF ATOMIC HYDROGEN. Walker, James D. Norman, Okla.; Univ. of Oklahoma (1970). 134p. University Microfilms Order No. 71-12,623. Thesis.

The Balmer optical-excitation cross sections of atomic hydrogen were measured for the n = 3 to 13 states. In order to make these measurements an apparatus utilizing crossed beams of electrons and hydrogen atoms was constructed. The hydrogen atoms were obtained by the dissociation of hydrogen molecules in a Wood's-type glow discharge tube. Measurements of cross sections were made in the range 100 to 450 eV. For the measurement of an absolute optical excitation cross section of a state, absolute measurements must be made of the photon emission rate from the state by a given radiation channel, the electron beam current, and the ground-state atom density in the electron beam. The absolute atomic hydrogen density in the electron beam in this work could not be measured. However, by holding the mass flow rate constant it was possible to measure the ratio of the hydrogen atom density to the hydrogen molecule density in the electron beam with the Wood's tube on and off, respectively. The measurement of this ratio and the measurements of the Balmer radiation from the crossed beams and the electron beam current with the Wood's tube on and off gave the ratios of the atomic to molecular Balmer optical excitation cross sections. Absolute Balmer optical excitation cross sections of molecular hydrogen, which were measured in a static system, were combined with these ratios to give the absolute Balmer optical excitation cross sections of atomic hydrogen. The measured Balmer optical excitation cross sections of atomic hydrogen at 200 eV in units of 10^{-20} cm^2 for n = 3 to 13 were 697.4, 165.9, 62.9, 21.9, 14.0, 4.6, 5.2, 3.2, 1.9, 1.1, and 0.55. (TSS) (Diss. Abstr. Int., B)

43138 IMPORTANCE OF POLARIZATION FOR ELECTRON SCATTERING IN THE INTERMEDIATE-ENERGY REGION. Truhlar, D. G. (Univ. of Minnesota, Minneapolis); Rice, J. K.; Trajmar, S.; Cartwright, D. C. Chem. Phys. Lett.; 9: No. 4, 299-305(15 May 1971).

The angular dependence of electron scattering from the helium atom and the hydrogen molecule for small scattering angles in the 34- to 100-eV impact energy range is explained in terms of the first Born approximation and the polarized Born approximation. The theoretical results compare favorably with the experimental data for both elastic and inelastic scattering. New experimental and theoretical results are presented. 105 references. (auth)

43139 NATURAL LINE SHAPES RESOLVED IN THE IONIZATION YIELD OF He^+ BELOW THE n = 2 THRESHOLD. Quemener, J. J.; Paquet, C.; Marmet, P. (Univ., Laval, Quebec). Phys. Rev., A; 4: No. 2, 494-8(Aug 1971).

Natural line shapes of the states $(2s^22p)^2P$ and $(2s2p^2)^2D$ of He^- are observed in the ionization-efficiency curve of He. The shape factor q and bandwidth Γ are determined. The energies of those states are measured, respectively, as 57.15 ± 0.04 and 58.23 ± 0.04 eV. Furthermore, doubly excited levels of He are detected in the ionization-efficiency curve of He as they autoionize and add a contribution to the He^+ continuum. All nine energy states measured are in very good agreement with values reported using other techniques. (auth)

43140 CHOOSING PSEUDOSTATES IN THE CLOSE-COUPLING FORMALISM FOR THE ELECTRON–ATOMIC-HYDROGEN SYSTEM. Matese, John J.; Oberoi, R. S. (Louisiana State Univ., Baton Rouge). Phys. Rev., A; 4: No. 2, 569-79(Aug 1971).

A modified close-coupling formalism was applied to the electron–atomic-hydrogen system. Various possible choices of pseudostates used to augment the eigenfunction expansion were investigated. As a test of the appropriateness of these choices various bound and scattering properties of the electron–atomic-hydrogen system were evaluated, and photodetachment cross sections for H^- were computed. It was found that pseudostates that emphasize short-range interactions are superior to those that incorporate long-range polarization effects when elastic scattering phase shifts are computed in the nonresonant region below the n = 2 threshold. Excellent photodetachment cross sections for H^- are also obtained using initial and final states obtained from a modified close-coupling formalism that includes these short-range pseudostates. (auth)

43141 VIBROROTATIONAL EXCITATIONS OF H_2^+ BY e^+ IMPACT. I. Faisal, F. H. M. (Goddard Space Flight Center, Greenbelt, Md.). Phys. Rev., A; 4: No. 2, 596-601(Aug 1971).

Analogies between Coulomb excitations of nuclei and ionic molecules by charged projectiles are utilized to calculate vibrorotational excitations of H_2^+ ions by e^+ impact by a semiclassical method developed in the nuclear case. The coupling between vibrational and rotational states of target molecules can very significantly affect the scattering cross sections for either kind of excitation. It is shown that the effect of such coupling may be included very conveniently, under the present model, whenever applicable. In a subsequent paper results for the experimentally more accessible systems, including the $H^+ + H_2^+$ system, are to be published. (auth)

43142 MULTIPLE IONIZATION OF Ne, Ar, AND Kr PRODUCED BY X RAYS IN THE ENERGY RANGE 0.28 TO 8.03 keV. Lightner, G. S.; Van Brunt, R. J.; Whitehead, W. D. (Univ. of Virginia, Charlottesville). Phys. Rev., A; 4: No. 2, 602-9(Aug 1971).

Relative abundances of multiply charged neon, argon, and krypton ions produced by x rays of energies 0.28, 1.5, 5.4, and 8.0 keV were measured with a time-of-flight mass spectrometer. Effectively monoenergetic x rays were obtained by a filtering technique whereby two filters with transmissions matching at all energies except at the K characteristic line of the x-ray tube target material were alternately placed in the x-ray beam. The data when corrected for charge-dependent discrimination effects are consistent with previous measurements and, except for neon, with calculations that include the electron shakeoff mechanism in addition to Auger transitions. The results for neon at 0.28 keV confirm the need for including electron correlation effects in the description of the ionization process. Other discrepancies between theory and experiment can be explained by considering the energy dependence of partial photoionization cross sections calculated by Rakavy and Ron. (auth)

43143 EXCITATION OF THE O I(^{3}S) AND N I(^{4}P) RESONANCE STATES BY ELECTRON IMPACT ON O AND N. Stone, E. J.; Zipf, E. C. (Univ. of Pittsburgh). Phys. Rev., A; 4: No. 2, 610-13(Aug 1971).

The absolute cross sections for the excitation of the OI(^{3}S) and NI(^{4}P) resonance states by electron impact on atomic oxygen and nitrogen were measured over the aeronomically important energy range from threshold to 150 eV. The peak excitation cross sections for these states were found to be 1.2×10^{-16} and 6.2×10^{-16} cm^2, respectively. At low energies, the total OI(^{3}S) and NI(^{4}P) cross sections exhibited well-developed peaks near 15 and 25 eV, respectively, indicating that cascade processes probably play an important role in exciting the OI(^{3}S) and NI(^{4}P) states. (auth)

43144 EULER–LAGRANGE OPTIMIZATION OF PLANE-WAVE FACTORS. Riley, Merle E.; Green, Thomas A. (Sandia Labs., Albuquerque, N. Mex.). Phys. Rev., A; 4: No. 2, 619-24 (Aug 1971).

The Euler–Lagrange variational method is applied to plane-wave factors as they appear in the parametric time-dependent Schrödinger-equation model for atom–atom scattering. The resulting Euler–Lagrange equations provide a prescription for determining a general plane-wave-factor function of the electron coordinates and time. (auth)

43145 CALCULATION OF IONIZATION AMPLITUDES BY THE COMPLEX-ENERGY METHOD. McCartor, G. D. (Manned

Spacecraft Center, Houston, Tex.); Nuttall, J. Phys. Rev., A; 4: No. 2, 625-30(Aug 1971).

It is shown that, as the complex energy approaches its real physical value, the dominant part of the amplitude for ionization derived from the Faddeev equations is a product of a known singular factor and the physical scattering amplitude. This information suggests a method of calculating ionization amplitudes from the Faddeev equations. Corrections to the dominant term for this and another amplitude are discussed. Some numerical tests of the method as applied to a simple model are given. (auth)

43146 QUANTUM-MECHANICAL TRANSITION PROBABILITIES FOR ATOM–ATOMIC-OSCILLATOR COLLISIONS WITH MORSE POTENTIAL INTERACTION. Diestler, D. J.; Feuer, P. (Purdue Univ., Lafayette, Ind.). J. Chem. Phys.; 54: No. 11, 4626-30(1 Jun 1971).

Exact quantum-mechanical transition probabilities for the collision of an atom with an atomic oscillator for the case in which the interaction has the form of a Morse potential are obtained by numerical integration of the relevant close-coupled scattering equations. These transition probabilities are compared with approximate ones calculated from distorted-wave theory over a range of parameters that have been of interest in examining the collision of helium atoms with a tungsten surface. Some information is obtained concerning the range of validity of the first-order theory, and certain suggestions that have appeared in the literature for correcting the distorted-wave results are found to be inadequate. (auth)

43147 CALCULATION OF ENERGIES AND WIDTHS OF COMPOUND-STATE RESONANCES IN ELASTIC SCATTERING: STABILIZATION METHOD. Fels, Margaret Fulton; Hazi, Andrew U. (Univ. of California, Los Angeles). Phys. Rev., A; 4: No. 2, 662-74(Aug 1971).

In a previous paper, the stabilization method of calculating resonance parameters was applied to a one-dimensional model problem of potential scattering. The method is here extended to compound-state resonances in elastic scattering, and its application to a model problem for a target with two bound states is examined. The resonance parameters are calculated by two methods that use information obtained in the diagonalization of the exact Hamiltonian in appropriately chosen sets of square-integrable basis functions: One is presented for the first time here; the other is similar to the procedure used in the potential-scattering problem. In addition to the stabilization method, some other techniques previously proposed for the calculation of resonance parameters are applied to the model problem. The availability of the exact solutions makes possible some preliminary assessments of the reliability and the difficulty that might be expected from these approximation methods. (auth)

43148 CENTRAL POTENTIAL FROM A VARIATIONAL POLARIZED-ORBITAL METHOD. Decoster, Alain (CEA, Villeneuve-Saint-Georges, France). Phys. Rev., A; 4: No. 2, 800-2(Aug 1971).

Drachman's and Oberoi and Callaway's variational polarized-orbital equations for low-energy particle–atom scattering can be rewritten without any approximation in a central-potential form. (auth)

43149 ELECTRON CAPTURE AND LOSS BY ATOMS, PROTONS, AND NEGATIVE HYDROGEN IONS IN COLLISIONS WITH ATOMS AND MOLECULES. EXPERIMENTAL CROSS-SECTION DATA. Fedorenko, N. V. (Ioffe Inst. of Physics and Tech., Leningrad). Sov. Phys.-Tech. Phys. (Engl. Transl.); 15: No. 12, 1947-59(Jun 1971).

Translated from Zh. Tekh. Fiz.; 40: No. 12, 2481-97(Dec 1970).

The experimental data on the cross sections for electron loss by hydrogen atoms and negative hydrogen ions (01, $1\bar{1}$, $\bar{1}0$) and electron capture by protons and hydrogen atoms (10, $1\bar{1}$, $0\bar{1}$) in gas collisions are reviewed. The experimental data are presented as curves showing the cross section as a function of the energy of the incident particle for each of the six processes. The cross sections are expressed in cm^2 and are normalized to the gas-target molecule, and the energy is given in electron volts in the laboratory system. The survey includes the whole range of energies for which there are published experimental data, viz., from several tens of electron volts to 20 MeV. The cross-section data are discussed on the basis of the existing qualitative ideas about inelastic atomic collisions. The interpretation of the values obtained directly by two of the most widely used methods of measuring electron capture and loss cross sections, namely, the magnet method and the capacitor method, is considered. 70 references. (auth)

43150 CHARACTERISTIC ENERGY LOSSES IN Ne^+–Ne COLLISIONS. Kishinevskii, L. M. (Inst. of Electronics, Tashkent). Sov. Phys.-Tech. Phys. (Engl. Transl.); 15: No. 12, 2027-9(Jun 1971).

Translated from Zh. Tekh. Fiz.; 40: No. 12, 2585-8(Dec 1970).

Calculations of characteristic energy losses for the following process are presented: $Ne^+ + Ne \rightarrow Ne^{m+} + Ne^{n+} + (m + n - 1)e$. It is assumed in the calculation that the electrons are excited into the nearest shell. Comparison shows that in most cases the calculated losses are comparable in magnitude with experimental values, but for large multiplicities of ionization the theoretical estimates of losses exceed the experimental values. Agreement between theory and experiment is improved by taking into account the contribution of slow electrons in multiple ionization. (A.G.W.)

43151 I. EXCITATION OF 3914-A N_2^+ RADIATION IN COLLISIONS OF HEAVY IONS WITH N_2. II. OBSERVATION OF FINE STRUCTURE EFFECTS IN HYDROGEN LYMAN-ALPHA USING THE BEAM–FOIL METHOD. Kurzweg, Lutz. Pittsburgh; Univ. of Pittsburgh (1970). 216p. University Microfilms Order No. 71-13,220.

Thesis.

Cross sections for the production of N_2^+ 3914-Å radiation by the impact of 30-keV to 2-MeV heavy ions on N_2 are given. Metallic ion (Ba^+, Ba^{++}, Al^+, and K^+) and gaseous ion (Ne^+, Kr^+, Xe^+, N_2^+, H_2^+, N^+, and O^+) beams are produced in electron-bombardment ion sources and are mass selected using an rf quadrupole mass filter before being accelerated in a Van de Graaff accelerator. Using a thin film interference filter and a photomultiplier, the 3914-Å excitation is observed as these beams traverse an N_2-filled gas cell. Where possible, the results are compared to other measurements of production of 3914 Å as well as some rudimentary theories for such processes. A measurement of the absolute cross section for the production of 3914-Å radiation by electron bombardment is also discussed. In a second set of experiments, H_2^+ beams with energies in the .2- to 2-MeV range are dissociated and excited in a beam–foil interaction. The subsequent decay of the n = 2 states of the hydrogen atoms is observed as a function of distance from the excitation foil. A field-free decay of n = 2 excited states in which the polarization of the Ly-α photons was measured as a function of distance from the foil was also observed. This experiment was because of a suggestion by Macek that if the fine structure states of an atom are excited coherently, then quantum beats in the intensity of each polarized component of the total intensity would be present even in a field-free region with a frequency given by the field-free energy separation of the two states. Macek emphasizes that the total intensity would not oscillate but that the polarization of the photons would oscillate as a function of distance downstream. Zero-field oscillations in the polarization of (10.5 ± .6) GHz with an amplitude in the polarization of somewhat less than 5% were observed and believed to be due to the coherent excitation of the $2P_{\frac{1}{2}}$ and $2P_{\frac{3}{2}}$ fine structure states. Experimental difficulties such as foil changes in time coupled with the necessity for taking long periods of time to gather statistics for one intensity measurement have resulted in some difficulties in fitting these results to all the expected results derived from the theory. (TSS) (Diss. Abstr. Int., B)

43152 ANGULAR DISTRIBUTION OF H^+ OR D^+ FROM ELECTRON IMPACT DISSOCIATION OF HD^+ ION. Dastidar, T. K. Rai; Barua, A. K. (Indian Association for the Cultivation of Science, Calcutta). J. Phys. Soc. Jap.; 31: No. 1, 230-5(Jul 1971).

The dissociation of the HD^+ ion induced by electron impact was considered by applying the Born approximation to the transition from the ground to the first excited repulsive state. The angular distribution of the proton or deuteron produced as dissociation fragments was considered in detail. Because of the heteronuclear nature of HD^+ ion some interesting deviations from the results obtained for protons from the dissociation of the homonuclear H_2^+ ion were observed. (auth)

43153 ELECTRON STRIPPING OF GROUND- AND METASTABLE-STATE HELIUM ATOMS IN HELIUM, NEON, AND ARGON. Tawara, Hiroyuki (Kyushu Univ., Fukuoka). J. Phys. Soc. Jap.; 31: No. 1, 236-41(Jul 1971).

The cross sections for one-electron stripping from ground-state (σ_{01}) and metastable (σ_{0*1}) helium atoms in helium, nitrogen, neon, and argon were measured by a beam-attenuation technique in the energy range from 13 to 50 keV. The cross sections σ_{0*1} are larger than the cross sections σ_{01} by a factor ranging from 10 in the higher-energy region to 20 in the lower-energy region in helium, nitrogen, and argon. The corresponding factor in neon is about three. The present values of σ_{0*1} are generally consistent with the results of Miers and Anderson for all gases investigated and with those of Gilbody et al. or their extrapolation except for

XUM

neon. These are also in agreement with the results predicted theoretically by Bates et al. for neon and argon but differ by a factor of about three from those of Bastien et al. for neon. (auth)

43154 MANIFESTATION OF AUTOIONIZING STATES IN THE IONIZATION OF KRYPTON BY ELECTRON IMPACT. Lossing, F. P. (National Research Council of Canada, Ottawa); Emmel, R. H.; Giessner, B. G.; Meisels, G. G. J. Chem. Phys.; 54: No. 12, 5431-3(15 Jun 1971).

Ionization efficiency curves of Kr were obtained; points were taken at 0.02-eV intervals. Data were smoothed and differentiated numerically, and the resultant curve was differentiated again. It is concluded that derivative ionization efficiencies clearly reveal the spacing of autoionizing levels but that the derivative curve neither greatly resembles the photoionization efficiency curve nor supports the notion of a sharp transition to a linear curve at the onset of ionization. (A.G.W.)

43155 EFFECT OF ROTATIONAL EXCITATION ON DISSOCIATIVE ELECTRON ATTACHMENT IN H_2. Spence, D.; Schulz, G. J. (Yale Univ., New Haven). J. Chem. Phys.; 54: No. 12, 5424-5(15 Jun 1971).

Dissociative electron attachment in H_2 at 3.75 eV was measured at several gas temperatures between 300 and 1300°K. The cross section for H^- production was found to be independent of temperature in this range; the peak value obtained was $1.98 \pm 0.05 \times 10^{-21}$ cm^2. It is concluded that rotational excitation of H_2 plays no role in the dissociative attachment process at this energy and in this temperature range. (A.G.W.)

43156 CLASSICAL S MATRIX FOR ROTATIONAL EXCITATION: QUENCHING OF QUANTUM EFFECTS IN MOLECULAR COLLISIONS. Miller, William H. (Univ. of California, Berkeley). J. Chem. Phys.; 54: No. 12, 5386-97(15 Jun 1971).

A previously developed theory in which exact solutions of the classical equations of motion for a complex collision system (i.e., numerically computed trajectories) can be used to generate the classical limit of the quantum mechanical S matrix (the "classical S matrix") for the scattering process is applied to rigid-rotor–atom collisions (rotational excitation). Comparison with essentially exact quantum results shows that transition probabilities (the square modulus of an S-matrix element) between individual quantum states are given reasonably accurate by classical dynamics provided the interference terms are properly accounted for; a strictly classical approach (neglect of interference) gives poor agreement with the quantum values. For averaged collision properties, however, it is found that interference and tunneling effects are rapidly quenched. The linear atom–diatom system (vibrational excitation) and the rigid-rotor–atom system are both investigated with regard to this question, namely, how much averaging is necessary to quench these quantum effects. Results indicate that even summation over a few quantum states is often sufficient to make a completely classical treatment appropriate. (auth)

43157 CHARGE-EXCHANGE CALCULATIONS WITH HARTREE WAVE-FUNCTIONS. Nebenzahl, I. (Cornell Univ., Ithaca, N. Y.). J. Chem. Phys.; 54: No. 12, 5254-6(15 Jun 1971).

Symmetric resonance charge-exchange cross sections are calculated, in the quasi-classical approximation. Previous calculations of the same type, due to Rapp and Francis, give systematically lower cross sections than the experimental ones. It is suggested that this is a result of the rough form of the atomic wave functions used by Rapp and Francis. Here, Hartree–Fock–Slater wave functions are used. The necessary integrations are done numerically. On the average, much better agreement with experimental results is achieved. The calculations were performed for He, K, Cs, and Hg. (auth)

43158 STATISTICAL PHASE-SPACE MODEL OF THE COLLISION-INDUCED DISSOCIATION OF EXCITED O_2^+ AND NO^+ IONS. Moran, T. F.; Fullerton, D. C. (Georgia Inst. of Tech., Atlanta). J. Chem. Phys.; 54: No. 12, 5231-6(15 Jun 1971).

Cross sections for the collision-induced dissociation of O_2^+ and NO^+ ions were calculated as a function of reactant-ion kinetic energy. The dissociative cross sections for individual reactant-ion electronic and vibrational states, weighted to account for the internal state distributions of reactant ions produced in electron-impact ionization processes, were compared with recent measurements. The magnitudes of the cross sections estimated by the statistical model are larger than those observed in the laboratory; however, the variations of the calculated cross sections with both ion internal energy and ion kinetic energy are in good agreement with experiment. (auth)

43159 APPLICATION OF THE STATISTICAL PHASE-SPACE THEORY TO THE REACTIONS OF RARE GAS IONS WITH NITROGEN MOLECULES. Fullerton, D. C.; Moran, T. F. (Georgia Inst. of Tech., Atlanta). J. Chem. Phys.; 54: No. 12, 5221-30 (15 Jun 1971).

The statistical phase-space theory of chemical reactions was applied to molecular and dissociative charge-transfer reactions of He^+, Ne^+, Ar^+, and Kr^+ with neutral N_2 molecules in the 0.05- to 200-eV energy range. Comparison between calculated and experimental cross sections for the molecular charge-transfer channels indicated an incomplete mixing of statistically available N_2^+ product-ion electronic states. Cross sections computed for endoergic dissociative channels of reaction are in good agreement with experiment. Calculated product-ion vibrational distributions are compared with those inferred from product N_2^+ kinetic energies and with vibrational distributions obtained from spontaneous radiative transitions of excited N_2^+ ions produced in the respective ion–molecule reactions. (auth)

Atomic Theory

Refer also to abstracts 43417, 43506, 43515, and 43953.

43160 (IS-T-456) EVEN-TEMPERED ATOMIC ORBITALS IN QUANTUM CHEMICAL AB INITIO CALCULATIONS: LIGHT ATOMS, HEAVY ATOMS, TRIATOMIC ALKALI IONS. Raffenetti, Richard Charles (Ames Lab., Iowa). Jun 1971. Contract W-7405-eng-82. 291p. Dep. NTIS.

Thesis.

A new concept for the selection of large bases for accurate ab initio quantum chemical calculations is introduced. The self-consistent-field (SCF) matrix Hartree–Fock technique is used to test the basis in application. The even-tempered basis primitive function is $X(klm) = N_l(\zeta_k)\, r^l S_l^m(\theta,\phi) \exp(-\zeta_k r^p)$ where $r^l S_l^m$ is a real, solid harmonic, p is taken equal to either 1 (exponential form) or 2 (Gaussian form), and $N_l(\zeta_k)$ is the appropriate normalization factor. No additional power of r is used. Also essential to the new basis is the selection of the exponents of the M primitives in a geometric sequence depending on just two independent parameters: $\zeta_k = \alpha \cdot \beta^k$, $\alpha, \beta > 0$, $\beta \neq 1$, $k = 1,2, \ldots M$. Advantages and disadvantages of this basis are discussed. Application is made first to atoms using primitives of exponential form where the exponent parameters are optimized separately for each value of the quantum number l. Each primitive is considered an independent basis function for the SCF process. In comparison to Slater-type bases employing "mixed" powers of r in each symmetry, the present basis does very well energetically. Several atomic properties are tabulated. In order to test the basis for molecular work, primitives of Gaussian form are employed. No nonlinear optimization is carried out in the molecular calculation and the exponent parameters are the same for all symmetries of the atom. A new scheme for forming contracted or linear combination of primitive functions for use as the SCF basis is introduced and compared to the present popular method. A significant energy advantage is found where fewer contracted functions are used. Molecular SCF results are given for the series of triatomic ions: H_3^+, LiH_2^+, Li_2H^+, Li_3^+, NaH_2^+, $NaLi_2^+$, Na_2H^+, Na_2Li^+, Na_3^+; the diatomics, H_2, LiH, Li_2, NaH, NaLi, Na_2; and the atomic ions: Li^+, Na^+. All triatomic ions except LiH_2^+ and NaH_2^+ are predicted to be stable through examination of the SCF energies, bond distances, electron population analyses, and dissociation reaction energies. (auth)

43161 PERTURBATION THEORY FOR CONFIGURATION-INTERACTION WAVE FUNCTIONS. Adams, W. H. (Technische Univ., Munich. Rutgers–The State Univ., New Brunswick, N. J.). Chem. Phys. Lett.; 9: No. 3, 199-202(1 May 1971).

A zeroth-order Hamiltonian is given for configuration-interaction wave functions constructed from orbitals that may be open-shell Hartree–Fock orbitals, multiconfiguration self-consistent-field orbitals, or some other kind of orbitals that are eigenfunctions of a common one-electron Hamiltonian. The perturbation expansion for the wave function in each order may be decoupled into equations for internal, single, pair, etc., excitations. (auth)

43162 EFFECTIVE NUCLEAR CHARGES IN MANY-ELECTRON ATOMS. Dautov, L. M. Izv. Akad. Nauk Kaz. SSR, Ser. Fiz.-Mat.; No. 6, 84-8(Nov-Dec 1970). (In Russian).

The author demonstrates that, in the helium isoelectronic sequence, a modification of the electron–electron interaction must not be the basis of disregarding the Kohlrausch constants. In many cases the latter appears to be comparable with a single-electron energy. The Kohlrausch constants and single-electron energy were found to be dependent upon ionization potentials and single-particle-component energy of the electron. Correlation

and relativistic effects are taken into account. The results obtained permit a nonempirical approach to the problem of effective nuclear charges and electron quantum numbers in non-hydrogen-like atoms. (tr-auth)

43163 SPIN-FREE QUANTUM CHEMISTRY. IX. THE AGGREGATE THEORY OF POLYELECTRONIC SYSTEMS. Matsen, F. A.; Klein, D. J. (Univ. of Texas, Austin). J. Phys. Chem.; 75: No. 12, 1860-6(10 Jun 1971).

The aggregate theory of polyelectronic systems is applicable to interactions between shells, between atoms, and between molecules. The aggregate theory of an N-electron system consists of the following steps: (1) the construction of a zero-order Hamiltonian by partitioning N electrons among "aggregates"; (2) the construction of a vector space for the full Hamiltonian by induction on the zero-order spaces by S_N, the symmetric group on N objects; (3) the construction of kets symmetry-adapted to S_N; (4) the application of the Wigner–Eckart theorem for S_N; and (5) a reduction in the number of primary matrix elements by the double coset decomposition of S_N with respect to the group of the zero-order Hamiltonian. The double coset generators are permutations of electrons among aggregates, which permit ready identification of exchange types. (auth)

43164 SPIN-FREE QUANTUM CHEMISTRY. X. THE EFFECTIVE SPIN HAMILTONIAN. Matsen, F. A.; Klein, D. J.; Foyt, D. C. (Univ. of Texas, Austin). J. Phys. Chem.; 75: No. 12, 1866-73(10 Jun 1971).

An effective spin Hamiltonian for coarse structure states is constructed, which when employed with the appropriate spin space yields a representation identical with that obtained with a spin-free Hamiltonian operating on spin-free space. Application of the aggregate theory of polyelectronic systems (paper IX), together with the Dirac identity, yields a rigorous effective spin Hamiltonian to which the Heisenberg effective spin Hamiltonian is an approximation. These Hamiltonians contain both single and multiple exchange terms. (auth)

43165 SPLIT HAMILTONIAN MATRIX METHOD AND THE INTERACTION BETWEEN TWO HYDROGEN ATOMS. Pecul, K. (Univ., Warsaw). Chem. Phys. Lett.; 9: No. 4, 316-18(15 May 1971).

The Hamiltonian matrix in the Ritz variational equation is split into "unperturbed" and "perturbed" parts, and new matrix equations are derived. The Pauli principle and symmetry are properly taken into account. The calculated energies of the interaction between the two hydrogen atoms are in good agreement with the variational results. (auth)

43166 ONSET OF ATOMIC-SUBSHELL FILLING IN ORDINARY AND SUPERHEAVY ELEMENTS. Abrahamson, Adolf A. (City Coll., New York). Phys. Rev., A; 4: No. 2, 454-6(Aug 1971).

Energy considerations in the central-field approximation to the one-electron problem are used to derive a theoretical expression, namely, $Z_1(l) \geq (1/\phi)\ (2l + 1)^3$, for the atomic number $Z_1(l)$ at which a given atomic l subshell first begins to become occupied. The lowest integral values of $Z_1(l)$ satisfying this relation for l = 0, 1, 2, and 3 are found to be in exact agreement with the corresponding empirical values, i.e., Z_1 = 1, 5, 21, and 58, respectively. In the domain of the superheavy elements ($100 \lesssim Z \lesssim 200$) and beyond, this relation gives $Z_1(l)$ = 122, 222, and 367 for l = 4, 5, and 6, respectively. The first member of this latter triad is in close accord with a recent estimate of $Z_1(4)$ = 125, cited by Seaborg. Comparison is made with the work of others in this field. To the writer's knowledge, this is the first calculation, without arbitrary introduction or adjustment of parameters, to yield results in complete accord with experiment. (auth)

43167 SOLUTION OF THE THOMAS–FERMI MODEL WITH QUANTUM CORRECTIONS. Enstrom, James E. (Rand Corp., Santa Monica, Calif.). Phys. Rev., A; 4: No. 2, 460-4(Aug 1971).

A new and more accurate numerical solution was obtained to the differential equation that determines the first-order quantum-mechanical corrections to the Thomas–Fermi model of the atom. When used to calculate the diamagnetic susceptibility and atomic polarizability of the inert gases, it leads to a substantial improvement over the Thomas–Fermi model alone and hence lends support to the validity of the quantum-mechanical corrections. (auth)

43168 VARIATIONAL-BOUND METHODS FOR AUTOIONIZATION STATES. II. THREE-ELECTRON ATOMS. Perkins, J. F. (Army Missile Command, Redstone Arsenal, Ala.). Phys. Rev., A; 4: No. 2, 489-93(Aug 1971).

Singly auto-ionizing (SAI) states of three-electron atoms below the first core excitation threshold are defined as eigenfunctions of an operator QHQ. It is shown that a particular type of multiconfiguration calculation provides upper-energy-bound estimates of such states, subject to a certain definition of Q (and the assumption that a certain set of equations has a solution). For SAI states with $L \neq 0$, Q is the proper Feshbach operator, which projects out all wave-function components that overlap the exact ground state of the two-electron core. For SAI states with L = 0, the bound is only established by adopting a modified, approximate Q, which projects out only those wave-function components that overlap the angle-independent part of the core ground state. It is proposed that doubly auto-ionizing (DAI) states be defined as eigenfunctions of Q′HQ′, where Q′ is the projection operator that eliminates all wave-function components that overlap the known 1s hydrogenic ground state of the one-electron system. The explicit form of P′ and Q′ is given, and a brief summary is given of various upper-energy-bound computational methods for DAI states; these closely parallel methods were discussed previously for SAI states of two-electron atoms. (auth)

43169 RESONANT INTERACTION BETWEEN TWO NEUTRAL ATOMS. Chang, C. S.; Stehle, P. (Univ. of Pittsburgh). Phys. Rev., A; 4: No. 2, 630-40(Aug 1971).

A standard formalism of quantum electrodynamics is used to investigate the interaction between two neutral atoms. The study is based on an approximate solution of the two-particle Green's function. The frequency distribution of the photon scattering is obtained. The self-stimulation effect when both atoms are in excited states is also considered. (auth)

43170 QUANTUM ELECTRODYNAMICAL THEORY OF ATOMS INTERACTING WITH HIGH-INTENSITY RADIATION FIELDS. Chang, C. S.; Stehle, P. (Univ. of Pittsburgh). Phys. Rev., A; 4: No. 2, 641-61(Aug 1971).

The interaction of a bound electron with external radiation fields of finite intensity is treated with the standard quantum electrodynamical (QED) formalism of Feynman and Dyson. An equation for a bound electron in finite-intensity radiation fields, such as those encountered in early molecular-beam experiments and in recent masers and lasers, is first constructed. The Green's function for the equation so obtained makes possible computation of the induced transition probabilities for various systems of interest. In this paper, the calculations on the two-level and three-level systems are carried out explicitly, and it is found that, to order e^4, the QED method based on forward scattering and the semiclassical treatment differ. As only the interaction of electrons with low-energy photons is considered, the virtual photon processes may be ignored, in accordance with the low-energy theorem. As a result, this treatment contains only finite calculations. It is demonstrated explicitly that the results are in qualitative agreement with the molecular-beam experiments of Kusch, for which the semiclassical treatment of Salwen fails to predict the results. Consequently, an intensity-dependent effect that can be properly explained only by QED and not by the semiclassical treatment is expected. The effect of nonelectromagnetic relaxation on the induced transition probability of a two-level system is also included for which an expression slightly different from that used by Ramsey for the hydrogen maser is obtained. Finally, some expressions of interest in experiments related to lasers and masers are derived. (auth)

43171 GENERALIZED NONRELATIVISTIC LAMB-SHIFT THEORY. Bullough, R. K.; Caudrey, P. J. (Univ. of Manchester, Eng.). J. Phys., A (London); 4: No. 3, L41-5(May 1971).

A natural all-order decorrelation procedure is reported for the interaction of a single two-level atom with all modes of the radiation field which replaces the semiclassical boson approximation for the atom by an exact fermion treatment. In consequence, the spontaneous emission of the semiclassical theory is extended to include stimulated emission, a semiclassical Lamb-type shift is explicitly replaced by a shift satisfying the Bethe formula manifestly due to vacuum fluctuations, and there can be two intensity-dependent terms, one of which generalizes the Bethe formula. (auth) (UK)

Cosmic Radiation

Refer also to abstracts 42157–42159, 43540, 43567, 43621, and 43647.

43172 FORBUSH MICRODECREASES IN THE COSMIC-RAY INTENSITY. Blanariu, D. (Univ., Iasi); Moldovanu, A.; Bradu, E.-B. Gerlands Beitr. Geophys.; 79: No. 5, 321-6(1970).

The two-year registration of the neutron supermonitor at Alert revealed a great number of short-lived Forbush decreases. The

XUM

detailed study of these Forbush microdecreases (FMD events) in connection with the geomagnetic perturbations at Surlari, Rumania was undertaken. The main statistical features of the FMD events are discussed in terms of their influence on the daily variation of the cosmic-ray intensity, as well as of the geoefficiency of the geomagnetic perturbations. (auth)

43173 ISOTOPIC COMPOSITION OF LOW-ENERGY HELIUM NUCLEI IN PRIMARY COSMIC RAYS. Tamai, Eiji; Narita, Nobuo; Sakai, Takasuke (Nihon Univ., Chiba, Japan). Nihon Daigaku Seisan Kogakubu Hokoku; 4: No. 1, 105-10(Feb 1971). (In Japanese).

The isotopic composition of low-energy helium nuclei in primary cosmic radiation was analyzed, using a nuclear emulsion stack flown from Fort Churchill, Canada, on July 11, 1965. The ratio of ^{3}He to total He at the top of the atmosphere was determined to be 11.8 ± 3.8%, in the kinetic energy interval of 100 to 260 MeV/nucleon. Assuming that the ^{3}He nuclei are produced in fragmentation of heavier nuclei in collisions with interstellar matter, it is concluded that low-energy primary cosmic rays have traversed about 3.7 gr/cm^2 of this medium from the cosmic-ray source. (auth) (Japan)

43174 DETECTION OF HIGH-ENERGY NEUTRINOS. Jatczak, J. (Univ. of Lodz, Poland). Postepy Astron.; 4: No. 2, 33-57(1970). (In Polish).

Cosmic rays produce in the atmosphere a flux of high-energy neutrinos. The detection techniques for high-energy neutrinos were worked out during the Brookhaven Laboratory and CERN experiments. The first proofs of underground registration of the neutrinos produced by cosmic rays have been obtained. (auth) (NSA of Poland)

43175 CALCULATION OF THE MULTIPLICITY YIELD FUNCTION OF THE IGY NEUTRON MONITOR. Debrunner, H.; Flueckiger, E. (Univ., Bern). Helv. Phys. Acta; 44: No. 2, 241-51(1 Apr 1971).

Calculations to determine the multiplicity response function for IGY neutron monitors are reported for vertically incident primary cosmic-ray protons of the rigidity range 2.2 GV < R_0 < 100 GV. A Monte Carlo method is used to calculate the secondary nucleon flux intensities in the atmosphere. Empirical and theoretical data on neutron monitor response are employed to relate the calculated flux data to the counting rates of the various multiplicities. A direct comparison of the multiplicity response function and other related quantities with experimental data is at present not yet possible. But indirect comparisons show fairly good agreement. (auth)

43176 INTERPLANETARY HYDROGEN AND HELIUM FROM COSMIC DUST AND THE SOLAR WIND. Banks, P. M. (Max-Planck-Institut fuer Kernphysik, Heidelberg). J. Geophys. Res.; 76: No. 19, 4341-8(1 Jul 1971).

Interplanetary dust grains saturated with solar-wind gases may act as sources of H and He in the inner solar system. Calculations for the density and fluxes of these gases are given in terms of the basic dust size distribution function. Owing to the lack of agreement between the different experimental data, it is not possible to fully assess the importance of this process. By using the data available, H and He densities in the ranges 8×10^{-7} to 6×10^{-3} cm^{-3} and 6×10^{-8} to 5×10^{-4} cm^{-3} can be predicted at 1 AU. Depending on the true effective area of the dust particles, the higher He densities could be adequate to explain the presence of ^{4}He$^+$ in the solar wind. (auth)

43177 SOLAR MODULATION ORIGIN OF SIDEREAL COSMIC-RAY ANISOTROPIES. Swinson, Derek B. (Univ. of New Mexico, Albuquerque). J. Geophys. Res.; 76: No. 19, 4217-23(1 Jul 1971).

It has been suggested that the sidereal diurnal variation in cosmic-ray intensity could be due to the cooperative effects of the interplanetary magnetic field and a radial heliocentric cosmic-ray density gradient. A more comprehensive data analysis was made to test the model. Data from underground μ-meson telescopes in the northern and southern hemispheres have been analyzed in sidereal time as a function of the direction of the interplanetary magnetic field. The observed anisotropy is shown to be dependent on the magnetic-field direction. Sidereal cosmic-ray data from several underground detectors are displayed as a function of the threshold rigidity of the detectors, and the results appear to indicate that the mechanism responsible for the sidereal anisotropy has an upper cutoff rigidity below 100 GV. Other observed sidereal cosmic-ray anisotropies are reviewed in the light of these results, and the likelihood of observing a true sidereal anisotropy above and below 100 GV is discussed. (auth)

43178 CHARGED-PARTICLE OBSERVATIONS FROM OSO 3. Badhwar, G. D.; Kaplon, M. F.; Valentine, D. A. (Univ. of Rochester, N. Y.). J. Geophys. Res.; 76: No. 19, 4224-9(1 Jul 1971).

The results on the nucleonic component of the primary cosmic rays obtained from the analysis of 5800 orbits of data (March 8, 1968, to May 10, 1969) from the University of Rochester telescope on Oso-3 satellite are presented. The results indicate that the slopes of the integral rigidity spectrum $J(>R) = AR^{-\gamma}$ particles/m^2 sec ster of helium, medium ($6 \leq Z \leq 9$), and heavy ($Z \geq 10$) nuclei above a rigidity R of about 8 BV are the same ($\gamma = +1.47 \pm 0.05$). The heavy-to-medium ratio is found to be 0.32 ± 0.06 constant with rigidity in the region 2.5–31.0 BV. (auth)

43179 MAGNETIC CUTOFF VARIATIONS DURING THE MAIN PHASE OF A GEOMAGNETIC STORM. Louis, Serge (CNRS, Verrieres-le-Buisson, France). Compt. Rend., Ser. B: 272: No. 18, 1089-92(3 May 1971). (In French).

The variations of the counting-rate ratio of neutron monitors at two stations (Pic du Midi and Kerguelen Island) were studied. The sudden increase of this ratio during a magnetic activity led to the evaluation of the magnetic cutoff variations during these periods. (auth)

Direct Energy Conversion

Refer also to abstracts 41995, 41996, 41998–42002, and 44172.

43180 (AD–715809) EFFECT OF SIMULATED FISSION PRODUCTS IN THE INTERELECTRODE SPACING OF A THERMIONIC DIODE. Final Report, November 1, 1968–May 31, 1970. Davis, Monte V. (Arizona Univ., Tucson. Engineering Experiment Station). 1 Nov 1970. Contract Nonr-2173(13). 24p. NTIS.

The development of experimental diodes to operate at extremely high temperatures with mixed vapors in the interelectrode spaces is discussed. Attempts at calculating the operational effects of multiple adsorbates on refractory substrates are presented. The theoretical discussion of dielectric breakdown in the environment such as would be found in a nuclear thermionic system is discussed. (auth) (USGRDR)

43181 (AD–715883) VOLUME IONIZATION BY MEANS OF LASER RADIATION IN A CESIUM PLASMA DIODE. Oettinger, Peter E.; Dewey, C. Forbes Jr. (Aerospace Corp., El Segundo, Calif.). 30 Sep 1970. Contract F04701-70-C-0059. 43p. (TR-59(6220-50)-6; SAMSO-TR-70-397). NTIS.

The possibility of enhancing neutralization of the interelectrode space charge in a cesium diode by the use of line radiation is considered. Ionization results from a two-step process. The neutral cesium atoms are first raised to be an excited electronic level by line radiation (typically from a solid-state laser). The excited neutrals, being within a few kT of the continuum, are then collisionally ionized by plasma electrons. A detailed consideration of the optical excitation cross sections and electron–neutral collision cross sections for the highly excited states suggests that plasma densities of 10^{15} cm^{-3} can be produced. The thermal economics of this system appear to be attractive when compared to contact ionization and collisional ionization, as well as previously proposed schemes employing radiation. (auth) (USGRDR)

43182 (JUL–742-TP) APPLIED MAGNETOHYDRODYNAMICS. NO. 7. ELECTRICAL LOSSES IN THE MHD GENERATOR. Holzapfel, Christian (Kernforschungsanlage, Juelich (West Germany). Institut fuer Technische Physik). Mar 1971. 65p. (In German). Dep. NTIS (U. S. Sales Only).

By separation of the flow system in an MHD generator into boundary layer and bulk, a simple model of the electrical conditions in the bulk flow of the generator is set up. With this model, the influence of the reductions of the Hall field on the other parameters in the generator is described by use of a generalized characteristic. With increasing magnetic field, a saturation of the Faraday voltage appears, which is also found experimentally by other authors. The calculation shows that this saturation appears in the lower region of the magnetic field where no electrothermal instabilities appear. At higher magnetic fields with electrothermal instabilities, the Faraday voltage increases again with increasing magnetic field. Moreover, there exists a lower limit of the velocity below which no nonequilibrium ionization appears if the resistance in the diffusor due to which the Hall field is reduced is too low. On the other hand, there exists an upper limit of the velocity in the subsonic case in a generator with constant cross section above which the Mach number increases to the value 1 due to the energy conversion in the generator. This leads to the existence of a critical length of the subsonic constant-cross-section generator above which it is not possible to get nonequilibrium conditions without

increasing the Mach number to the value 1 in the channel. The nonlinearity of the current–voltage characteristic is not always caused by nonequilibrium ionization. Due to electrothermal instabilities, the Faraday component of the current is increased also in the case of higher electron temperature without increased electron density due to relaxation effects. (auth)

43183 (N-71-15856) HOT ELECTRODE DROPS IN AN UNSEEDED SUPERSONIC ARGON MAGNETOHYDRODYNAMIC GENERATOR. Mantenieks, Maris A. (National Aeronautics and Space Administration, Cleveland, Ohio. Lewis Research Center). Jan 1971. 23p. (NASA-TN-D-7041; E-5926). NTIS.

Experiments were performed in an unseeded, supersonic argon generator. Floating potential profiles, electrode drops, and electrode temperatures were measured. The following conclusions were reached: (1) electrode drops are independent of the magnetic field; (2) the discharge is not symmetrical in the presence of a magnetic field; (3) it is possible to go from a self-sustaining arc discharge mode to a non-self-sustaining mode by increasing the initial cathode temperature; (4) there is a cathode temperature (about 2250°K) for which a minimum cathode drop is found; and (5) a cooling effect for low-discharge current is observed at the cathode in the non-self-sustaining mode; this cooling depends on the magnetic field. (auth) (STAR)

43184 (N-71-16776) THERMOELECTRIC GENERATORS FOR DEEP SPACE APPLICATION. Rouklove, P.; Truscello, V. (Jet Propulsion Lab., Pasadena, Calif.). 15 Jan 1971. Contract NAS7-100. 27p. (NASA-CR-116246; JPL-TR-32-1495). NTIS.

To provide a source of electrical energy independent of the Sun for the use of unmanned spacecraft investigation of the outer planets, radioisotope thermoelectric generators are evaluated. Criteria for the selection of the thermoelectric materials, the design of the generator, and its integration with the spacecraft are discussed. Results of the tests of ten generators that have been, or are presently, under test are also presented. (auth) (STAR)

43185 (N-71-17252) ELECTRICAL PERFORMANCE OF THREE SOLAR THERMOELECTRIC TEST SECTIONS. Bifano, William J.; Kroeger, Erich W.; Ruch, Robert B. (National Aeronautics and Space Administration, Cleveland, Ohio. Lewis Research Center). Feb 1971. 24p. (NASA-TM-X-2175; E-5925). NTIS.

Current–voltage characteristics were measured for three planar test sections of a solar thermoelectric generator designed to operate at 0.25 au from the Sun. Each test section consisted of nine silicon–germanium thermocouples mechanically attached to a beryllium radiator plate. Measurements were made at average hot junction temperatures in the range of 640 to 940°C. All three test sections produced the design power output of 2.8 watts at 1.0 volt; however, junction temperatures approximately 50°C higher than predicted were required to achieve this power because of poor thermal contact between the thermocouple stud and the radiator plate. One of the test sections, life-tested for 3000 hours, exhibited an increase in internal resistance of about 14%, corresponding to a decrease in power output of about 6%. (auth) (STAR)

43186 ADVANCED POWER SYSTEMS: WHERE DOES THEIR POTENTIAL LIE? Evans, R. K. Des. Eng.; 48-51(Apr 1971).

The economics, size, and power of various direct energy conversion systems in the form of magnetohydrodynamics, electrogasdynamics, thermionic, and thermoelectric systems and small nuclear reactor and radioisotope systems are considered. Advantages and drawbacks are discussed. (UK)

43187 USE OF ION SPUTTERING IN MAKING ELECTRODES FOR THERMIONIC ENERGY CONVERTERS. Kramar, Jaroslav (Research Inst. of Electrical Engineering, Bechovice, Czech.). pp 383-5 of Proceedings of the Fourth Intersociety Energy Conversion Engineering Conference, September 22–26, 1969, Washington, D. C. New York; American Inst. of Chemical Engineers (1969).

From 4. intersociety energy conversion engineering conference; Washington, D. C. (21 Sep 1969). See CONF-690905.

The sputtering method selected is analyzed and a brief description of the apparatus is given. Experience obtained in preparing samples of ceramic (alumina) and metal (tungsten) layers is outlined. The properties of these layers are also discussed. (auth)

43188 THERMODYNAMIC DRIVE. (to Licentia Patent-Verwaltungs-GmbH). British Patent 1,236,052. 16 Jun 1971. Priority date 10 Nov 1967, Germany.

The thermodynamic drive described consists of a heat source, a combined disintegration and expansion nozzle connected thereafter, a working medium that is liquid or droplets and vapor, and a condensation path. (M.H.R.)

43189 THERMIONIC CONVERTER WITH CONCENTRIC COLLECTOR AND EMITTER. Gross, Franz; Krapf, Rudolf (to Brown, Boveri and Cie AG). U. S. Patent 3,578,991. 18 May 1971. Priority 27 Sep 1966, Germany.

A thermionic converter for converting heat energy directly into electrical energy is described, the heat being derived from the use in the device of nuclear fuel. The emitter is so disposed as to extend into the mass of nuclear fuel, and has a chamber formed therewithin in which there is disposed the collector electrode element, but spaced from the emitter so as to form a sealed interspace chamber that is filled with a gaseous vapor, e.g., cesium. Electric terminals are provided for carrying outwardly to an electric line the electrical energy from the coupled emitter and collector, and coolant means are provided for conducting coolant fluid into the interior of the collector. (auth)

43190 OPTIMUM MAGNETIC FIELD DISTRIBUTION ALONG THE CHANNEL OF AN MHD GENERATOR WITH ELECTRODES FINITE LENGTH. Lur'e, K. A. (Ioffe Inst. of Physics and Tech., Leningrad). Sov. Phys.-Tech. Phys. (Eng. Transl.); 15: No. 12, 2025-6(Jun 1971).

Translated from Zh. Tekh. Fiz.; 40: No. 12, 2583-5(Dec 1970).

The magnetic field strength corresponding to the maximum current along an MHD channel with finite electrodes is sought, and the optimum electrode length is determined. The field strength is assumed to be a bounded, positive definite function, and the magnetic flux through the channel is assumed to be known. It is shown that, under optimum conditions, the field is nonvanishing only near the electrodes of the channel. (auth)

43191 ENERGY FOR SPACEFLIGHT IN THE FUTURE. Peschka, W. (Deutsche Forschungs- und Versuchsanstalt fuer Luft- und Raumfahrt, Stuttgart). pp 285-95 of Prospects for the Use of Orbital Stations and Space Shuttles in the Next Ten Years. Rome; XVIII Rassegna Internazionale Elettronica e Nucleare (1971).

From eleventh international technical and scientific conference on space; Rome, Italy (1 Apr 1971). See CONF-710430.

Space missions are restricted mainly by energy storage and energy conversion limitations. Therefore, basic work on high-power nuclear energy systems becomes important for the future. In connection with the continuous increase of the temperature range of energy-generation systems, all such investigations are of interest for earth-bound and space-flight applications. For spacecraft, energy is required for on-board and propulsion systems. The former systems mainly require electrical energy. For electrical propulsive systems, ion propulsion requires electrostatic fields and plasma propulsion requires electromagnetic fields. Because of the high power consumption, no practical possibility exists for utilizing electrical propulsion with high thrust. Nuclear thermal propulsion, using a solid-core high-temperature reactor system, may be more convenient for high thrust, but also for obtaining considerably small thrust. The application of high thrusts with electrical propulsion systems depends on the development of power systems with high power-to-mass ratio, which are currently not available. The use of high-temperature reactors in a temperature range where the nuclear fuel is in the plasma state offers the possibility of obtaining energy systems with high power density for future spacecraft and also earth-bound power plants. Furthermore, a nuclear system with nuclear fuel in the plasma state cannot be used without an electrical energy system used for plasma confinement, heat flux reduction by magnetic fields, etc. This energy can be generated through use of Magnetoplasmadynamic (MPD) Converters using a propulsive electrical conducting jet. (auth)

Fluid Physics

43192 STEADY SUPERSONIC SOURCE OF NONEQUILIBRIUM PLASMA. Luk'yanov, G. A. Zk. Prikl. Mekh. Tekh. Fiz.; No. 6, 13-19(Nov-Dec 1968). (In Russian).

The recombination of electrons in the scattering of a monoatomic-gas plasma in a vacuum is examined. It was assumed that the main elementary process is collisional–radiative recombination. Under certain conditions, scattering with infinite residual ionization of the gas is possible. Steady flow in the supersonic spherical source of nonequilibrium plasma of monatomic gas, consisting of electrons, monovalent ions, and atoms is considered. Flows of this type are realized in such important cases as the motion of gas along a nozzle or steady-state discharge in a vacuum. (tr-auth)

43193 DETERMINATION OF JOULE DISSIPATION IN MOTION OF FLUID WITH VARIABLE CONDUCTIVITY IN NON-

XUM

HOMOGENEOUS MAGNETIC FIELD. Buchin, V. A. Zh. Prikl. Mekh. Tekh. Fiz.; No. 6, 107-10(Nov-Dec 1968). (In Russian).

The problem is examined with the premise that the conductivity depends weakly on the current. In addition, a formula is obtained that gives the first approximation according to ϵ, for these losses, in the expression of which only the zero approximation for the current enters. In the case of conductivity, which depends weakly on the current, the electrodynamic equations are always elliptic. A numerical calculation is presented according to the obtained formula for the specific form of the conductivity $\tau = \tau_0 + \epsilon\tau_1(j)$, τ_0 = const. (where $\sigma(j)$ is a differentiable function, and ϵ is a certain small parameter), that is, $\sigma_1(j) = \sigma$, j^2/j_*^2, σ_1 = const. Here j_* is a certain characteristic value of current. (tr-auth)

43194 INVESTIGATION OF GROUP PROPERTIES OF MHD EQUATIONS AND THEIR INVARIANT SOLUTION. Gridnev, N. P. Zh. Prikl. Mekh. Tekh. Fiz.; No. 6, 103-7(Nov-Dec 1968). (In Russian).

Group analysis of a system of MHD equations is conducted. In contrast to earlier works, the group properties of the equations of motion of a confined fluid, with calculation of finite conductivity, are studied. A possible invariant solution of a system of MHD equations is written for the one-dimensional case. Examples of analytical and numerical equations of problems concerning the interaction of streams of conducting gas with a magnetic field are given. Equations describing, in the hydrodynamic approach, the unsteady flow of electroconductive gas in a magnetic field are studied. (tr-auth)

43195 ACCELERATION OF CONDUCTING GAS IN STRONG NONSTATIONARY ELECTROMAGNETIC FIELDS. Bam-Zelikovich, G. M. Zh. Prikl. Mekh. Tekh. Fiz.; No. 6, 36-40 (Nov-Dec 1968). (In Russian).

A problem concerning the nonstationary acceleration of a conducting gas in a channel is resolved, together with the problem of discharge in an electric circuit. In contrast to previous work, where a thin cluster is accelerated, the case is considered where the moving gas fills the channel. The motion of the gas in the channel is considered, in addition to that in the one-dimensional formulation, on the premises that the transit time of a particle along the channel is small in comparison with the discharge time and that the electromagnetic force is great in comparison with the pressure gradient. (M.H.R.)

43196 ANNUAL REVIEW OF FLUID MECHANICS. VOLUME 3. Van Dyke, Milton; Vincenti, Walter G.; Wehausen, J. V. (eds.). Palo Alto, Calif.; Annual Reviews Inc. (1971). 413p.

Separate abstracts were prepared for 3 of the included chapters. The remaining chapters were not in scope for NSA and hence omitted. (M.O.W.)

For abstracts of individual papers see: 43197, 43347, and 43348.

43197 MAGNETOHYDRODYNAMICS AT HIGH HARTMANN NUMBER. Hunt, J. C. R.; Shercliff, J. A. (Trinity Coll., Cambridge, Eng. Univ. of Warwick, Coventry, Eng.). Annu. Rev. Fluid Mech.; 3: 37-62(1971).

The various phenomena that occur and the various mathematical methods that apply when the Hartmann number is large are surveyed. Rectilinear, two-dimensional flow problems, invariant in the flow direction, are discussed. A brief indication is given of how the treatment may be extended to three-dimensional problems, when the magnetic forces also outweigh inertia forces and the magnetic field is negligibly perturbed by currents in the fluid. The work is concentrated mainly on the case of a uniform imposed magnetic field. Some remarks on the general mathematical aspects of the problems encountered and on their practical implications conclude the review. 45 references. (M.H.R.)

43198 HEAT TRANSFER IN MAGNETO-HYDRODYNAMIC COUETTE FLOW AS AFFECTED BY WALL ELECTRICAL CONDUCTANCES AND SUCTION. Rao, S. V. Seshagiri (NB Science Coll., Hyderabad, India); Jain, M. K. Arch. Mech. Stosow.; 21: No. 4, 435-47(1969).

Heat transfer in an MHD Couette flow influenced by wall electrical conductances with suction and bound by two moving walls infinite in both x and y directions is investigated. Topics analyzed include: (1) the flow problem with suction, (2) heat transfer when the wall temperature varies along the wall and with allowance for the presence of a constant heat source, and (3) the case of variable heat sources with constant wall temperature. (IAA)

43199 MAGNITOGIDRODINAMICHESKOE OBTEKANIE TEL. (Magnetohydrodynamic Flow Around Bodies). Tsinober, A. B. Riga; Izdatel'stvo Zinatne (1970). 292p.

Mathematical problems of magnetohydrodynamics (MHD) of incompressible fluids are described in both the steady and the unsteady cases. A chapter entitled "Some Precise Solutions" includes flow in rectilinear current lines, MHD flow in a diffusor, and layer-type flow. MHD flow of the Stokes type, boundary layer flow, and flow around bodies are handled mathematically, and only in the closing chapter are the experimental aspects of flow around bodies examined. Coefficients of flow resistance of various shapes, pressure distribution about the surface of an object, and flow in the presence of a longitudinal magnetic field, are each graphically analyzed. (K.S.W.)

43200 PROPAGATION OF MFD WAVES IN A HEAT-CONDUCTING COMPRESSIBLE FLUID IN THE PRESENCE OF THE HALL EFFECT. Mattei, Giulio (Univ., Pisa, Italy). Ann. Sci. Norm. Super. Pisa, Sci. Fis. Mat.; 24: 555-70(Jul-Sep 1970). (In Italian).

Wave propagation in a compressible, viscous, heat-conducting fluid of finite electrical conductivity was studied, taking the Hall effect into account. The perturbations of plane waves are first considered, using linearized equations. The investigation is then extended to cylindrical perturbations and, in particular, to torsional oscillations. The cases when the magnetic field is normal and parallel to the propagation direction are considered. The case in which the Hall effect is negligible is also considered. (IAA)

43201 BOUNDARY-LAYER DEVELOPMENT IN AN MHD DUCT. Merck, W. F. H. (Eindhoven Univ. of Tech., Netherlands). Appl. Sci. Res. (The Hague); 24: No. 1, 21-43(Apr 1971).

A method of calculation for two-dimensional, steady-state, laminar flow in the entrance region of an MHD duct is presented. The electrically conducting fluid in the free stream is compressible, whereas the medium in the boundary layer itself is taken to be incompressible. Thus, the density is variable in the axial direction of the duct only, and the momentum and energy equations for the boundary layer are uncoupled. These equations are solved using an extended Von Kármán–Pohlhausen method as described by U. P. Hwang for a compressible MHD flow with zero electric field. In this study, however, the electric field is essentially not zero, and the MHD duct can work as a generator. The equations of the insulator boundary layer are solved in the assumption that the displacement thickness of the electrode boundary layer equals that of the insulator boundary layer, so the total influence of the varying effective cross section on the free stream is taken into account. In this way a quick method of calculating the MHD flow in the entrance region of a duct is obtained. (auth)

43202 LONGITUDINAL BOUNDARY PROBLEMS CONCERNING THE DISTRIBUTION OF ELECTRIC FIELDS IN MHD CHANNEL WITH CONDUCTING WALLS. Vasil'ev, V. F.; Lavrent'ev, I. V. Magn. Gidrodin., Akad. Nauk Lat. SSR; No. 2, 83-9(Apr-Jun 1970). (In Russian).

A solution of the two-dimensional problem of the distribution of an electric current in an MHD channel with thin conducting walls is presented. An expression for Joule losses and distribution of electric potential along the channel wall with arbitrary velocity profile and magnetic field distribution along the channel is derived. (tr-auth)

43203 EHD FLOW IN CHANNELS WITH SMALL INTERACTION PARAMETERS. Semenova, I. P.; Yakubenko, A. E. (Inst. of Mechanics, Moscow). Izv. Akad. Nauk SSSR, Mekh. Zhidk. Gaza; No. 1, 38-45(Jan-Feb 1971). (In Russian).

Equations of the quasi-one-dimensional approach in electrohydrodynamics are derived, considering two-dimensional effects associated with the presence of crossed electric fields and current leakages through the channel walls. Experimental data for flow in channels with small interaction parameters are compared with numerical estimates obtained by means of the method above. The problem of obtaining multipurpose volt–ampere characteristics for channels with various width/length ratios is discussed. (tr-auth)

43204 RAYLEIGH–TAYLOR INSTABILITY IN MAGNETO-HYDRODYNAMICS IN THE GALVANIC APPROXIMATION. Zimin, E. P.; Eismont, O. A. Zh. Prikl. Mekh. Tekh. Fiz.; No. 5, 31-8(Sep-Oct 1970). (In Russian).

In previous studies of the Rayleigh–Taylor stability, the external magnetic field was assumed to be constant. The problem was further investigated by examining the stability of the boundary between viscous, conducting media when a current and a magnetic field were applied to the system at a magnetic Reynolds number much less than 1. The calculation method used for determining the magnetic field was found to yield good results. The dependence of the maximum increase increment of the instability on various parameters was determined. The stability of the fluid layer in the solid walls was examined for the case of linearly

distributed conductance and density. The results indicated that increasing Hartmann numbers exert a stabilizing influence although the effect is not very strong. (TTT)

43205 THREE-DIMENSIONAL MAGNETOHYDRODYNAMIC FLOW IN DIVERGING RECTANGULAR DUCTS UNDER STRONG TRANSVERSE MAGNETIC FIELDS. Walker, John Scott. Ithaca, N. Y.; Cornell Univ. (1970). 196p. University Microfilms Order No. 71-12,143.

Thesis.

Several steady MHD duct flows are treated for an electrically conducting liquid with uniform properties and for a uniform applied magnetic field B_0. If the duct's centerline (in the flow direction) is taken as the x-axis, B_0 lies in the x-sections, parallel to one pair of walls (side walls). Both pairs of walls diverge (or converge) smoothly and symmetrically along the x-axis. The side walls are either perfectly conducting or insulating, while the other walls (top and bottom walls) are always insulating. If the magnetic Reynolds number is small, while the interaction parameter and the Hartmann number (M) are large, the induced magnetic field and the inertial forces are negligible everywhere, while the viscous forces are only significant in thin boundary layers adjacent to the walls. The inviscid core solution is found in terms of several functions of x, which are determined by the matching between this solution and that for the boundary layers on the side walls. The structure of these $O(M^{-\frac{1}{2}})$ layers is found by using Fourier sine and cosine transforms to solve a boundary-value problem on a pair of stream-functions defined in a semi-infinite strip. (TSS) (Diss. Abstr. Int., B)

43206 MERCIER'S CRITERION FOR A CLASS OF MHD EQUILIBRIA. Kueppers, G.; Tasso, H. (Max-Planck-Institut fuer Plasmaphysik, Garching, Ger.). Phys. Lett.; 35A: No. 6, 410-12(12 Jul 1971).

For a class of axially symmetric equilibria, the terms in Mercier's criterion can be reduced to complete elliptic integrals with certain arguments and coefficients. For one particular choice of the equilibrium parameters the latter quantities can be evaluated explicitly without using any expansion. This case corresponds to "vertical" elliptic magnetic surfaces near the magnetic axis. (auth)

Geophysics (Upper Atmosphere)

Refer also to abstracts 43176, 43179, and 43403.

43207 (AD–706130) PHYSICS OF THE UPPER ATMOSPHERE. Final Scientific Report, August 1, 1964–July 31, 1969. Bates, David R. (Queen's Univ., Belfast (Northern Ireland). Dept. of Applied Mathematics and Theoretical Physics). 30 Sep 1969. Contract AF61(052)-780. 18p. (AFCRL–70-204). NTIS.

Quantal investigations were carried out on the following: the average excitation energy of an atom or molecule appropriate to the slowing down of a beam of charged particles in a gas; the long-range interactions between pairs of atoms and also between three hydrogen atoms; various atomic-structural problems including the polarization of a closed-shell core by an outer electron; relativistic corrections to the eigenenergies for the helium sequence; correlation energies of the lithium sequence; and isotope shifts in Li and B (2+). Theoretical studies were made of the following upper atmospheric problems: the source, abundance and distribution of hydrogen, metastable helium and nitrous oxide; the electron temperature in the D region; the diurnal variation of the temperature and density (assuming solar ultraviolet heating); the Doppler profiles of the 5577-A airglow. (auth) (USGRDR)

43208 (AD–714365) ELECTRICAL STRUCTURE OF THE D AND E REGION. Webb, Willis L. (Army Electronics Command, White Sands Missile Range, N. Mex. Atmospheric Sciences Lab.). Jul 1970. 28p. (ECOM–5313). NTIS.

Based on the stratopause tidal circulation model of dynamo-current motivation through low-latitude vertical charge separation and the Hall effect, a sectional model illustrating the low-latitude global D- and E-region electrical structure is presented. Model conductivity structures are derived from mean electron density and collision-frequency profiles and are applied to delineate atmospheric sources and sinks of electromotive energy and the resulting electric current and potential fields. These models indicate that the lower ionosphere rather than being electrically neutral is the site of important electrical structure which must be joined with the observed lower atmosphere and exospheric structures to obtain the complete global electrical structure. The lower ionospheric dynamo current is by far the largest atmospheric current and, therefore, dominates the global electrical structure, with tropospheric and exospheric electrical phenomena resulting principally from relaxation currents below and above the lower ionospheric region. (auth) (USGRDR)

43209 (AD–714993) STUDIES OF WAVELIKE VARIATIONS IN THE IONOSPHERE. Research and Development Technical Report. Arendt, P. R.; Gorman, F. J. Jr.; Soicher, H. (Army Electronics Command, Fort Monmouth, N. J.). Sep 1970. 24p. (ECOM–3332). NTIS.

Determination of the true height of specific ionospheric plasma frequencies was used for finding actual motions within the ionospheric plasma. The reported vertical soundings reveal a periodic variation in time at all bottomside altitudes. Spatial variations of this periodic structure were observed at points separated by about 50 km. Daytime and nighttime periodic structures are different. Periodic variations of angle-of-arrival data of an oblique propagation experiment on a 1330-km circuit were observed. The periodicities are related to spatial periodic electron-density structure in the bottomside ionosphere. The oblique reflections had dominant azimuth periods in the order of ¼, ½, and 1 hour. (auth) (USGRDR)

43210 (AD–715260) TURBULENT LOSS OF RING CURRENT PROTONS. Report for July 1969–June 1970. Cornwall, John M.; Coroniti, F. V.; Thorne, Richard M. (Aerospace Corp., El Segundo, Calif.). 1 Nov 1970. Contract F04701-70-C-0059. 38p. (TR–59(6260-20)-10; SAMSO-TR–70-406). NTIS.

Ring-current protons (<50 keV), which are unaffected by ion-cyclotron waves outside the plasmapause, undergo strong turbulent diffusion just inside the plasmapause. Lifetimes from ion-cyclotron turbulence are predicted to be of the order of one hour, as observed by Frank for $3 \leq L \leq 5$. During the main phase of a geomagnetic storm, the protons rapidly diffuse across the plasmapause (probably at the Bohm rate), and are lost before reaching the noon meridian, giving rise to the asymmetric part of the ring current. During the recovery phase the ring current decays on a time scale of a day or less as the turbulent region moves outward with the expansion of the plasmapause. Further decay takes place on a charge-exchange time scale. One consequence of the dissipation of ring-current energy at the plasmapause should be the formation of midlatitude red arcs, probably by the conversion of this energy into heat as the ion-cyclotron waves are absorbed by electrons. (USGRDR)

43211 (AD–715266) OUTER-ZONE ELECTRON PRECIPITATION. Vampola, Alfred L.; Koons, Harry C.; McPherson, Donald A. (Aerospace Corp., El Segundo, Calif.). 15 Aug 1970. Contract F04701-70-C-0059. 32p. (TR–59(9220-02)-5; SAMSO-TR–70-395). NTIS.

Measurements of energetic electrons (300 keV to 2.3 MeV) within the drift loss cone, of elf emissions, and of the plasmapause location obtained with instruments aboard the low-altitude, polar satellite OV3-3 (1966-70A) are compared. It is found that there is a knee in the L-shell profile of the precipitated fluxes of outer-zone electrons with the flux decreasing toward lower latitudes. The location of this knee strongly correlates with the morning location of the plasmapause but does not correlate with the evening location of the plasmapause. It is also found that, for $3.3 \leq L \leq 4.3$, electrons are preferentially precipitated in the morning hours after 6:00 local time. This corresponds to the strong morning maximum in the occurrence of whistler-mode elf emissions. Electromagnetic elf emissions are often observed just outside of the plasmapause where the maximum flux of precipitated electrons is observed. The experimental data suggest that the morning location of the plasmapause is the controlling factor in the low-latitude decrease of outer-zone electron precipitation. (USGRDR)

43212 (AD–715893) IONOSPHERIC MODEL FOR THE ARCTIC. Environmental Research Papers. Gassmann, G. J. (Air Force Cambridge Research Labs., L. G. Hanscom Field, Mass.). 9 Oct 1970. 17p. (AFCRL–70-562; AFCRL-ERP–332). NTIS.

A first-order approximation model of the Arctic ionosphere is described, based on published observations and concepts. The location of the phenomena is specified in corrected geomagnetic latitude and local time. Various input parameters are included whenever some of their influences are known, such as UT, seasons, sunspot number, magnetic variations. The Arctic ionospheric features are specified as "quasi-instant" deviations from routine predictions whereby the deviations represent probabilities of occurrence during periods that may range from 20 min to 3 hr. Ionospheric features covered are auroral E (or night-E), auroral E_s (or Esr), hf absorption, Arctic F. Necessary improvements to the model are indicated, including the inclusion of storm time of individual substorms and the requirement that routine observations be maintained in the midnight sector of the auroral oval. (auth) (USGRDR)

43213 (AD–715898) ELECTROSTATIC VLF WAVES OBSERVED IN THE POLAR MAGNETOSPHERE. Report for August

XUM

1969–July 1970. McPherson, Donald A.; Koons, Harry C. (Aerospace Corp., El Segundo, Calif.). 15 Aug 1970. Contract F04701-70-C-0059. 37p. (TR–59(9220-02)-4; SAMSO-TR–70-393). NTIS.

Broadband electrostatic emissions are detected by a vlf receiver aboard the satellite OV3-3 (1966-70A). Enhancements of the electric-field intensity in ten bandpass channels at frequencies between 400 Hz and 14.5 kHz are observed when the spacecraft passes over the south polar region at altitudes between 2500 and 4500 km (satellite apogee). The power spectral density of these emissions decreases approximately as the inverse fourth power of the observed frequency. The most interesting feature of these emissions is the range of invariant magnetic latitudes (INVL) over which they are observed. The low-latitude limit at which they are detected is typically 72 to 76° INVL in local morning and 68° INVL near midnight. This dependence suggests that these emissions occur on magnetic-field lines along which the polar wind flows. During geomagnetically active periods, electrostatic waves with a high-frequency cutoff between 1.3 and 3.9 kHz are also observed in this altitude range. These emissions occur at latitudes below the low-latitude limit of the polar-electrostatic waves and above the latitude of the plasmapause. (auth) (USGRDR)

43214 (N–71-16589) DIFFERENTIAL ELECTRON FLUX AS DETERMINED BY AURORAL OBSERVATIONS OF THE N_2^+ AND N_2^+ SYSTEMS. Shemansky, D. E.; Donahue, T. M.; Zipf, E. C. (Pittsburgh Univ., Pa. Space Research Coordination Center). Jan 1971. 20p. (NASA-CR–116240; SRCC–146). NTIS.

The relative emission rates of the auroral N^{2+} and N_2^+ systems can be used as measures of the differential electron-flux distribution function, due to the remarkable differences in electron excitation functions. Observations of aurora over the years have suggested that the four major systems are excited mainly by electrons. Calculations of relative emission rates using recently measured electron cross sections are entirely consistent with the ground-based and rocket-borne measurements. (auth) (STAR)

43215 (N–71-17052) INVESTIGATION OF THE D AND E REGIONS OF THE IONOSPHERE. Final Report. Smith, L. G. (GCA Corp., Bedford, Mass. GCA Technology Div.). Jan 1971. Contract NASw-1402. 90p. (NASA-CR–116441; GCA-TR–70-11-N). NTIS.

An experimental investigation of the ionosphere using sounding rockets is presented. The payload instrumentation and objectives are described for each of the twenty-one launches, covering the period June 14, 1966 to September 11, 1969. The experimental program includes: four launches in Brazil during and following the total solar eclipse of November 12, 1966; three in Puerto Rico in September 1967 in cooperation with the Arecibo Ionospheric Observatory; and fourteen launches at Wallops Island including investigations of the ionosphere at sunrise and of anomalous winter absorption. (auth) (STAR)

43216 (N–71-18405) DOUBLE PROBE MEASUREMENTS OF DC ELECTRIC FIELDS WITH THE INJUN 5 SATELLITE. Cauffmann, David P.; Gurnett, Donald A. (Iowa Univ., Iowa City. Dept. of Physics and Astronomy). Jan 1971. Contracts NAS5-10625; NAS1-8141; NAS1-8144(f); NAS1-8150(f); N00014-68-A-0196-0003. 75p. (NASA-CR–116791). NTIS.

At high latitudes, convection electric fields >30 mV/meter, and sometimes >100 mV/meter, are frequently observed in the auroral zone. A common feature is the occurrence of abrupt reversals in the east–west convection velocity at auroral-zone latitudes. For dusk–dawn local times, these reversals generally correspond to an east–west flow away from the Sun on the high-latitude side of the reversal and toward the Sun on the low-latitude side. Over the polar region above the auroral zone, the convection velocity is usually 10 to 20 mV/meter, electric-field perturbations are sometimes observed, corresponding to generally westward convection outside the plasmasphere. At high altitudes, above about 1500 km, over the auroral-zone/polar-cap regions, irregular electric-field noise with amplitudes from 10 to 30 mV/meter is consistently observed. (auth) (STAR)

43217 (N–71-18502) STUDY OF POLAR SUBSTORM RELATED TRAVELING IONOSPHERIC DISTURBANCES BASED ON COLUMNAR ELECTRON CONTENT MEASUREMENTS. Davis, Michael J. (Stanford Univ., Calif. Radioscience Lab.). Aug 1970. Contract NAS5-10102. 147p. (NASA-CR–116784; SU-SEL–70-51; TR–12). NTIS.

The disturbances exhibit a diurnal variation in their direction of arrival at a midlatitude observing site, explained by an average source location in the evening sector of the auroral oval. It is possible to relate their occurrence to the occurrence of polar substorms and to determine the location of the source of individual disturbances. These disturbances are not generally observed to travel across the equator, explained on the basis of the high rate of damping of the disturbances in the neutral atmosphere that produced them. A possible source related to the westward traveling surges observed in auroras is discussed. Numerical results are obtained for the height range 200 to 600 km considered. The effects of perturbations in loss and diffusion are shown to produce considerable changes in the perturbation in the ionization caused by internal atmospheric gravity waves; in particular, it results in a large depression of the perturbed electron concentration at high levels. The effect of atmospheric gravity waves on electron content is also considered. (auth) (STAR)

43218 (N–71-18997) MASS SPECTROMETER OBSERVATION OF NO IN AN AURORAL ARC. Zipe, E. C.; Borst, W. L.; Donahue, T. M. (Pittsburgh Univ., Pa. Dept. of Physics). 27 Jul 1970. 34p. (NASA-CR–116877; SRCC–133). NTIS.

The neutral and ion data obtained by mass spectrometer are discussed. The mass spectrometer observed remarkably large concentrations of NO and NO^+ within the auroral form. The molecular ions O_2^+ and N_2^+ were conspicuously absent and comparatively large densities of O^+ ions were detected. In the altitude range 110 to 130 km the neutral NO concentration exceeded the ambient O_2 concentration. (auth) (STAR)

43219 (N–71-20708) ON THE DISTRIBUTIONS OF PLASMAS AND ELECTRIC FIELDS OVER THE AURORAL ZONES AND POLAR CAPS. Frank, L A.; Gurnett, D. A. (Iowa Univ., Iowa City. Dept. of Physics and Astronomy). Feb 1971. Contracts NAS5-10625; NAS1-8141; NAS1-2973; N00014-68-A-0196-003. 56p. (NASA-CR–117403). NTIS.

Simultaneous observations of dc electric fields and low-energy charged particles at low altitudes over the Earth's auroral zones and polar caps were obtained with the satellite Injun 5. These observations are interpreted in terms of a magnetospheric model as deduced from plasma observations in the distant magnetosphere and in terms of essential elements for any credible theory of auroral arcs, in particular, those associated with inverted-V precipitation bands. Several of the principal results for the evening and dawn local-time sectors are summarized. (auth) (STAR)

43220 (N–71-20853) MOTION AND STRUCTURE OF THE MAGNETOPAUSE. Aubry, Michel P.; Kivelson, Margaret G.; Russell, Christopher T. (California Univ., Los Angeles. Inst. of Geophysics and Planetary Physics). [1970]. Contract NAS5-9098. 70p. (NASA-CR–117741). NTIS.

On March 27, 1968, following a reversal of the interplanetary magnetic field from northward to southward, some large-amplitude oscillatory motions developed on the magnetosphere boundary; at the same time the very structure of this boundary was very variable and this variability increased with the southward component of the interplanetary field. Associated with these phenomena, variable components of the magnetic field normal to the boundary were recorded and produced a large transfer of momentum across the magnetopause leading to the erosion of the dayside magnetosphere. It must be emphasized that, during this time, the observed local characteristics of the boundary, including the amplitude and orientation of the normal component as well as the counting rate of energetic electrons on either side of the boundary, were extremely variable and thus did not fit with any steady open or closed model of the magnetosphere. (auth) (STAR)

43221 (N–71-21469) SOLAR-WIND MASS SPECTROGRAPH. Final Report, August 12, 1969–August 12, 1970. Taylor, Lawnie (Electro-Optical Systems, Inc., Pasadena, Calif.). 31 Dec 1970. Contract NAS9-9909. 79p. (NASA-CR–114948; EOS–4044). NTIS.

The engineering and performance specifications obtained for a solar-wind mass/charge spectrograph and a solar-wind direction indicator are presented. The spectrograph developed in this program is a miniaturized double-focusing instrument designed to demonstrate the feasibility of measuring photographically the mass/charge number composition of the solar wind with a high degree of resolution and sensitivity. The unit is primarily designed to measure mass/charge numbers in the range 1.5 to 4.7; however, it is not limited to this range. The direction indicator is a self-contained instrument which has been designed to demonstrate the feasibility of determining attitude with respect to the flow direction of an incident ion beam over a range of angles from 15 deg to 0.25° within an accuracy of 5%. The instrument can provide an Apollo astronaut with the capability of adjusting the roll and pitch of the spacecraft within ±0.5° of the solar-wind mean direction. (auth) (STAR)

43222 SIMPLE MODEL FOR AN ION EXOSPHERE IN AN OPEN MAGNETIC FIELD. Lemaire, J.; Scherer, M. (Belgain Inst. for Space Aeronomy, Brussels). Phys. Fluids; 14: No. 8, 1683-94(Aug 1971).

A simple model for an ion-exosphere with an open magnetic

field is set up. The ions move under the influence of (1) the gravitational field, (2) the monotonic decreasing static magnetic field, and (3) the electrostatic potential due to a small charge separation. Neglecting collisions and particle drift across the magnetic field lines the particles can be classified into four classes: ballistic, escaping, trapped, and incoming particles. For each class the number density, the particle flux, the momentum fluxes, and the energy flux are calculated as a function of the electrostatic potential. Finally, it is shown how this potential can easily be computed by considering two basic physical conditions: (1) the quasi neutrality, and (2) the zero current condition. (auth)

43223 OBSERVATIONS SUGGESTING PARTICLE PRECIPITATION AT LATITUDES BELOW 40°N. Doherty, Robert H. (Inst. for Telecommunication Sciences, Boulder, Colo.). Radio Sci.; 6: No. 6, 639-46(Jun 1971).

Low-frequency pulse transmissions are received over reciprocal paths after being reflected once from the ionospheric D region. The daytime reflection height is near 70 km and the nighttime height is near 90 km. Over an 1830-km path between Nantucket, Massachusetts, and Jupiter Inlet, Florida, rapid simultaneous phase and amplitude fluctuations are frequently observed at night, occurring more frequently near the equinox and near dawn. They seem to occur more frequently on the path indicated above than on higher-latitude paths at quite different geomagnetic longitudes; the events have not appeared at all on paths at geomagnetic latitudes below 30°N. A possible explanation for the more-frequent occurrence on the Nantucket–Jupiter path is the fact that the midpoint lies slightly west of the magnetic conjugate to the South Atlantic anomaly. Detailed correlation of both phase and amplitude at both ends of reciprocal propagation paths tends to rule out gradients, offpath reflections, or instrumentation as causes of these events. Paths with similar geomagnetic latitudes can be similarly affected when they are separated by more than 100° in geomagnetic longitude. These lf phase measurements over oblique paths may prove to be an excellent method for detecting leakage or dumping of charged particles from the radiation belts into the lower ionosphere. (J.C.W.)

43224 OBSERVATION OF F-REGION VERTICAL VELOCITIES AT MILLSTONE HILL. I. EVIDENCE FOR DRIFTS DUE TO EXPANSION, CONTRACTION, AND WINDS. Evans, J. V. (Massachusetts Inst. of Tech., Lexington). Radio Sci.; 6: No. 6, 609-26(Jun 1971).

The theory for the drift of ions in the F region is briefly reviewed, and it is shown that, for the restricted case of no external electric fields or neutral air motion, the velocity of the ions along the magnetic-field lines in the upper part of the F2 region can be derived from the continuity equation. Experimental results for the electron density, electron and ion temperatures, and O^+ vertical velocity obtained by the incoherent (Thomson) scatter technique at Millstone Hill are presented, for two 24-hour periods taken a year apart in March 1969 and 1970. The largest vertical velocities encountered occur around sunrise and sunset and give rise to vertical fluxes of the order of 5×10^8 ions/cm^2/sec through 600-km altitude. These fluxes are a result primarily of the growth or decay of the layer. The difference between the observed and computed velocities is attributed to thermospheric neutral winds that have diurnal behavior similar to those determined by Vasseur (1969a, b) from incoherent-scatter observations in France. (auth)

43225 APPROXIMATE PICTURE OF THE DISTRIBUTION OF PLASMA DRIFT IN THE F2 REGION. Muradov, A. (Inst. of Terretrial Magnetism, Ionosphere, and Radio-Wave Propagation, Ashkhabad, USSR). Inst. of Physics of the Earth and Atmosphere, Ashkhabad, USSR). Izv. Akad. Nauk Turkm. SSR, Ser. Fiz.-Tekh., Khim. Geol.; No. 1, 113-15(1970). (In Russian).

Calculations are made of the planetary distribution of drifts in the F2 region taking into consideration the effects of winds in the upper atmosphere. The latitudinal distributions of the vertical and the meridional velocity components of the drift are presented in graphs. The complex interaction effects of the motions of the neutral atmosphere and the ionospheric plasma are considered. (IAA)

43226 POLAR IONOSPHERE AND MAGNETOSPHERIC PROCESSES. Skovli, Gunnar (ed.). New York; Gordon and Breach, Science Publishers, Inc. (1970). 352p. $19.50.

The eighteen papers included are the review papers from the sixth NATO Advanced Study Institute arranged in Norway by the Norwegian Defence Research Establishment, April 9–18, 1969, and devoted to the subject of "production and maintenance of the polar ionosphere." The papers were taken from sessions entitled: Magnetospheric Processes; Particle Observations in the Earth's Magnetic Tail; Low-Altitude Particle Observations; Particle Trajectories in the Magnetosphere; Particle Impact on the Polar Ionosphere; The Upper Polar Atmosphere; The Polar Ionosphere Theoretical Considerations; The Polar F1 Layer; The Polar F2 Layer; Irregularities in the Polar F-Layer Electron Density; the Polar E- and D-Layers; and the Optical Emission over the Polar Cap. (J.C.W.)

43227 GEOMAGNETIC CONTROL OF THE GEOGRAPHIC DISTRIBUTION OF NOON IONIZATION OF F2 LAYER. Besprozvannaya, A. S. Ionos. Issled.; No. 16, 52-67(1968). (In Russian).

Analytical results are given of the geographical distribution of F2-layer noon ionization according to the world network data of the vertical ionosphere sounding. The P. Rothwell hypothesis is the basis of the analysis of the equilibrium state of ionosphere at the extreme ends of the magnetic-force line. The analytical expression is given of F2-layer noon ionization on the given i latitude and k longitude as the function of cos χ, with an additional coefficient M allowing for a geomagnetic control of the F2-layer ionization: $f_0F2 = A_0 (\cos \chi)^n M$. The noon critical frequencies of the F2 layer of the Northern Hemisphere in March, June, Sept., and Dec. of 1958 were calculated using the values of A_0 and of the power indicator n and calculated values of the M-factor for the geographic network with sides equal to 5° latitude and 10° longitude. The calculation maps of the geographical distribution of noon ionization of the F2 layer and regions of anomalies in high latitudes were determined on the basis of comparisons of calculated and experimental data. (Meteorol. Geoastrophys. Abstr.)

43228 INFLUENCE OF SOLAR ACTIVITY ON THE POST-SUNSET PEAK OF HEIGHTS OF THE EQUATORIAL F REGION. Anufrieva, T. A.; Shapiro, V. S. Ionos. Issled.; No. 16, 68-75 (1968). (In Russian).

The annual variations of the post-sunset peak, $(h_{max})_{peak}$ of the equatorial ionosphere are considered. The variations of the height of the top and the width of the equatorial anomaly were calculated according to the variations of the $(h_{max})_{peak}$. (Meteorol. Geoastrophys. Abstr.)

43229 INTERRELATION BETWEEN ELECTRON AND ION TEMPERATURE. Breus, T. K. Ionos. Issled.; No. 16, 39-51 (1968). (In Russian).

Theoretical concepts are discussed on the interrelations between electron and ion temperatures and electron concentration in the ionosphere. On the basis of a number of theoretical works, in which the thermal balance for electronic gas was studied and the height distribution of the electron and ion temperature was obtained, the lower ionosphere can be roughly divided into regions characterized by certain peculiarities depending on temperatures and concentration of charged particles. In the F1 region the temperature and concentration of electrons are connected by approximately inverse dependence. In the F2-region, T_e is approximately inversely proportional to ^2N. At large heights where the temperature is determined by thermal conductivity and N by diffusion, T_e, and N are not controlled by the local contribution of heat. In the upper ionosphere, higher than 500 to 1000 km, where the distribution of the electron concentration is subject to the laws of diffusion equilibrium, the electron and ion temperatures determine the rate of decrease of electron concentration with height for regions where the ion content changes slightly. Results of experiments on rockets and satellites are given that illustrate the conclusions drawn on the basis of the analysis of theoretical works. The influence of solar activity on the character of dependence of electron concentration on temperatures T_e and T_i is discussed. (Meteorol. Geoastrophys. Abstr.)

43230 THEORY OF THE UNDISTURBED F2 LAYER. Poliakov, V. M. Ionos. Issled.; No. 16, 6-29(1968). (In Russian).

Electron concentration in the ionosphere is studied with an unstationary model with consideration of changes in time and height of electron concentration, concentration of ions of atomic oxygen, and intermediate molecular ions formed by ion-change reactions and diffusion of the electron–ion gas in a homogeneous geomagnetic field. A system of equations was solved by computer. Kinetic coefficients of photochemical reactions in the first approximation were determined on analog computers. Periodic solutions are given, describing diurnal changes at different heights of the electron and ion concentration, as well as the values of diffusion and the recombination term. It is shown that a simple model including photoionization, neutralization, and diffusion considered in unstationary conditions well describes the major peculiarities of diurnal and seasonal changes of the electron concentration in the F region of the ionosphere in middle latitudes. (Meteorol. Geoastrophys. Abstr.)

XUM

43231 STATISTICAL STUDY OF SOLAR PROTONS, ALPHA PARTICLES, AND Z ≥ 3 NUCLEI IN 1967–1968. Armstrong, T. P. (Univ. of Kansas, Lawrence); Krimigis, S. M. J. Geophys. Res.; 76: No. 19, 4230-44(1 Jul 1971).

Comprehensive measurements of protons, α particles, and Z ≥ 3 nuclei of E ≳ 0.5 MeV/nucleon obtained with the lunar-orbiting Explorer-35 spacecraft for the period July 20, 1967, to May 14, 1968, are reported. The major results of this study are the following: (a) protons of E ≥ 0.5 MeV are present (exceeding 1.3 (cm^2 sec sr^{-1}) in the interplanetary medium at least 63% of the time; (b) protons, α particles, and Z ≥ 3 (medium) nuclei always appear together although in variable mixtures; (c) events with harder proton spectrums have smaller p/α ratios; (d) the α/M nuclei ratio of 20 ± 10 characterizes most events; (e) the event-integrated p/α ratio varies from 10 to 150; (f) a directional anisotropy exists in the p/α ratio, believed to be observed for the first time; and (g) by combining spectroscopic data of Lambert (1967) with the observed α/M ratio, a value of ~50 for the p/α ratio at the Sun is obtained. The data are discussed in the context of particle propagation and properties of the solar source region. (auth)

43232 PENETRATION OF SOLAR PROTONS OVER THE POLAR CAP DURING THE FEBRUARY 25, 1969, EVENT. Engelmann, J. (CEN, Saclay, France); Hynds, R. J.; Morfill, G.; (and others). J. Geophys. Res.; 76: No. 19, 4245-61(1 Jul 1971).

During the February 25, 1969 solar-proton event, particle measurements from the close-orbiting satellite Esro 2, and particle and magnetic-field measurements outside the magnetosphere from the Heos A1 satellite are available. The Esro 2 data for proton energies from E > 27 to E > 90 MeV show intensity enhancements in the auroral-zone region and in the central polar region relative to the rest of the polar cap. At energies of a few million electron volts such enhancements are significantly less marked. By comparison of observations inside and outside the magnetosphere and by suitable trajectory computations inside the magnetosphere, the auroral-zone enhancements at energies >27 MeV in terms of a form of impact-zone effect allied to a particle anisotropy outside the magnetosphere are explained. It is suggested that the enhancements observed over the polar region may be due to the particle anisotropy outside the magnetosphere plus coupling between the central polar-cap lines of force and the interplanetary-field lines. (auth)

43233 ASYMMETRIC ACCESS OF ENERGETIC SOLAR PROTONS TO THE EARTH'S NORTH AND SOUTH POLAR CAPS. Van Allen, J. A. (Univ. of Iowa, Iowa City); Fennell, J. F.; Ness, N. F. J. Geophys. Res.; 76: No. 19, 4262-75(1 Jul 1971).

During the energetic solar-particle event that began on January 24, 1969, the ratio N/S of the intensity of protons E_p > 0.3 MeV over the Earth's north (N) polar cap (Λ > 80°) to that over its south (S) polar cap ($-\Lambda$ > 80°) varied from a value greater than 20 to about 1, as observed with satellite Injun 5 in a low-altitude polar orbit. The interplanetary intensity of protons was measured simultaneously with similar detectors on Explorer 33 and 35 in two nearly orthogonal planes and in eight different directions on the unit sphere (some overlap). High values of the N/S ratio early in the event corresponded to an extraordinarily strong anisotropy of intensity in interplanetary space with the anisotropy vector pointing dominantly southward. The N/S ratio dropped toward 1 as the interplanetary beam relaxed toward isotropy. Similar, although less-well-determined, findings applied to protons E_p > 3.4 MeV and α particles E_α > 1.18 MeV. The directions of interplanetary-field lines that connect with the respective polar caps are uniquely identified by intensity considerations. The interplanetary magnetic vector was measured on Explorer 35 also. Early in the event, the Earth was in a solar positive (B outward from the sun) magnetic sector ($\varphi_{SE} \approx 140°$), with a dominantly southward direction ($\theta_{SE} \approx -40°$ to $-70°$). The anisotropy vector was approximately parallel to the magnetic vector and in the same sense. The composite evidence favors the direct access of energetic particles to the Earth's polar caps via magnetic-field lines interconnected between the terrestrial field and the interplanetary medium; it strongly contradicts models that contemplate diffusion across the magnetospheric tail as an important feature of particle access. (auth)

43234 SOLAR PARTICLE CUTOFFS AS OBSERVED AT LOW ALTITUDES. Imhof, W. L.; Reagan, J. B.; Gaines, E. E. (Lockheed Palo Alto Research Lab., Calif.). J. Geophys. Res.; 76: No. 19, 4276-90(1 Jul 1971).

Differential energy measurements were made on board the low-altitude (~500 km) polar-orbiting satellite OV1-18 of protons (1.4 to 46 MeV) and α particles (7 to 22 MeV) during several solar-particle events in 1969 and 1970. The measured 1/e cutoffs for ~2-MeV protons show the same general variation with local time as those calculated by Smart et al. (1969) but are displaced to somewhat lower latitudes, even at times of low magnetic activity. The rate of change of cutoff latitude with rigidity is generally less on the nightside than on the dayside, with the α particle 1/e cutoffs being consistent with the cutoffs for protons of the same rigidity. At a given particle energy the curves of flux versus latitude are nearly always steeper on the nightside than on the dayside, with large variations from one pass to the next sometimes occurring in the slopes of the flux profiles near cutoff. The profiles of counting rate versus latitude are often smooth near the boundary, but sometimes pronounced flux and spectral variations with time and/or latitude are observed. (auth)

43235 SECONDARY ELECTRONS AND PHOTONS IN THE UPPER ATMOSPHERE. Beuermann, Klaus P. (California Inst. of Tech., Pasadena). J. Geophys. Res.; 76: No. 19, 4291-4310 (1 Jul 1971).

Theoretical and experimental results of the production and propagation of atmospheric secondary negatrons, positrons, and photons moving in the vertical direction are presented. The one-dimensional transport equations were solved numerically to obtain energy spectra and intensity-versus-depth for energies as low as 4 MeV and for atmospheric depths up to 400 g/cm^2. The calculations are performed for the solar modulation level of 1968 and geomagnetic cutoff values of zero and 4.5 GV. Also presented are experimental data on negatrons and positrons in the energy range from 6.5 to 200 MeV obtained from balloon observations near Ft. Churchill, Canada, in 1968. The comparisons with measurements confirm the calculated energy spectra and intensity-versus-depth. The spectral shapes of secondary negatrons and positrons are found to be very dependent upon the atmospheric depth. In the high atmosphere, the photon spectrum below ~70 MeV is dominated by bremsstrahlung from primary and reentrant albedo electrons rather than by π^0 decays. The derived intensity-versus-depth deviates distinctly from the commonly assumed linear growth of the secondary flux with increasing depth. Results on the functional depth dependence are useful for determining the contribution from atmospheric secondaries to measurements of the electron (and photon) flux at balloon altitudes. (auth)

43236 SINGLE SPACECRAFT METHOD OF ESTIMATING SHOCK NORMALS. Lepping, R. P.; Argentiero, P. D. (Goddard Space Flight Center, Greenbelt, Md.). J. Geophys. Res.; 76: No. 19, 4349-59(1 Jul 1971).

By assuming the validity of the Rankine–Hugoniot conservation relations for interplanetary shocks in an isotropic medium, it is demonstrated that improved shock normals can be calculated by employing a least-squares technique to combined magnetic field and plasma data from a single spacecraft. The scheme uses only the conservation relations (six in number) that are devoid of pressure and temperature terms. Transformation of these equations into an arbitrary frame of reference reduces the system to three independent overdetermination equations. These three equations constitute a 3-parameter redundancy among the 11 measured parameters of the system: B_1, B_2, W (= $V_2 - V_1$), ρ_1, and ρ_2, where subscripts 1 and 2 refer to before and after the shock, respectively. By exploiting this redundancy in the cases of simulated shocks, whose basic noiseless characteristics are known exactly, it has been shown for many realistic examples, through the minimization of a least-squares loss function, that the normals are calculated with error improvements of factors of about three or so over calculations made using the magnetic field alone. As an example of the method a corrected normal and improved shock parameters are then obtained for a real case: the August 29, 1966, shock observed by the Pioneer-7 spacecraft. The scheme should prove useful in examining the shape of a shock surface whenever data for a shock event are available from two or more spacecraft widely separated in solar longitude. (auth)

43237 NATURE AND ORIGIN OF DIRECTIONAL DISCONTINUITIES IN THE SOLAR WIND. Burlaga, Leonard F. (Goddard Space Flight Center, Greenbelt, Md.). J. Geophys. Res.; 76: No. 19, 4360-5(1 Jul 1971).

Less than 25% of the directional discontinuities (directional changes >30° in less than 30 sec) identified by Burlaga in Ness's interplanetary magnetic-field data for the period December 18 to 25, 1965, are rotational discontinuities. Thus it is inferred that most of these directional discontinuities are tangential. The Pioneer-6 magnetic-field and plasma data are not consistent with the hypothesis that directional discontinuities originate primarily by the collision of fast streams with slower plasma, since the rate of occurrence of discontinuities in regions of increasing bulk speed is only a little higher than the rate elsewhere. The rate at which discontinuities are seen at 0.82 AU is somewhat lower than at 1 AU,

but the difference may be due to the lower data quality and increase in the number of data gaps when the spacecraft is far from the Earth. The distributions of the change in direction of the field across the discontinuity and of the normals' ($B_1 \times B_2/|B_1 \times B_2|$) are very similar at ≈0.8, ≈0.9, and ≈1.0 AU. This suggests that most discontinuities originate within 0.8 AU and do not evolve appreciably between 0.8 and 1.0 AU. (auth)

43238 CORRELATED OBSERVATIONS OF ELECTRONS AND MAGNETIC FIELDS AT THE EARTH'S BOW SHOCK. Neugebauer, M. (California Inst. of Tech., Pasadena); Russell, C. T.; Olson, J. V. J. Geophys. Res.; 76: No. 19, 4366-80(1 Jul 1971).

The internal structure of the Earth's bow shock has been studied by using simultaneous observations made on board the Ogo-5 satellite of the magnetic field (0 to 3 Hz), the elf magnetic fluctuations (10 to 1000 Hz), and the suprathermal electrons (100 to 800 eV). The initial acceleration of electrons from ~10 to 100 eV could not be observed, but electrons with energy ≥100 eV were already present near the foot of the field gradient. These hot electrons were then compressed as they moved up the field strength gradient. In two of the six shock crossings studied, further acceleration accompanied the compression. The profiles of the flux of electrons with energies >100 eV were similar to the field strength profiles, with the exception that increased fluxes of accelerated electrons were also associated with steep field gradients. For all shock crossings observed, there was a high positive correlation of the flux of both 100- and 200-eV electrons with field strength. Both electron flux and field magnitude reached peak values in the shock front greater than the values found further downstream in the magnetosheath. For the two shock crossings for which directional electron data were available, the solar-oriented instrument observed equal or greater fluxes of accelerated electrons than did the instrument pointing away from the center of the Earth. There was a positive correlation between the fluxes of these two instruments even though they were observing different-energy electrons. (auth)

43239 MAGNETOTAIL CHANGES IN RELATION TO THE SOLAR-WIND MAGNETIC FIELD AND MAGNETOSPHERIC SUBSTORMS. Aubry, Michel P.; McPherron, Robert L. (Univ. of California, Los Angeles). J. Geophys. Res.; 76: No. 19, 4381-4401(1 Jul 1971).

Substorm activity is known to be associated with changes in the solar-wind parameters and the magnetotail configuration. It is investigated whether the magnetotail changes occur only as a consequence of substorms or also as a direct consequence of changes in the solar-wind parameters. Using data from several satellites (Ogo 5, ATS 1, Imp 4, Explorer 33 and 35) and 17 ground magnetic observatories, it is concluded that the tail responds to both changes in the north–south orientation of the interplanetary field and substorm activity. A change from a northward to a southward interplanetary field causes a slow increase of the field to be recorded by a satellite within the lobe of the tail, and a thinning of the plasma sheet. A change from a southward to a northward interplanetary field causes the plasma sheet to expand. In contrast, it seems that in the inner magnetosphere the distortion of the magnetic field due to a period of southward interplanetary field is not relieved by an interval of northward field but only through the occurrence of a substorm expansion. A substorm expansion causes a slow decrease of the field within the lobe of the tail and an expansion of the plasma sheet. (auth)

43240 TIME VARIATIONS OF THE MAGNETOTAIL PLASMA SHEET AT 18 R_E DETERMINED FROM CONCURRENT OBSERVATIONS BY A PAIR OF VELA SATELLITES. Hones, E. W. Jr., Asbridge, J. R.; Bame, S. J. (Los Alamos Scientific Lab., N. Mex.). J. Geophys. Res.; 76: No. 19, 4402-19(1 Jul 1971).

Energy spectral measurements of electrons (~100 eV < $E_e \gtrsim$ 18 keV) taken concurrently by hemispherical-plate electrostatic analyzers on Vela satellites 3A and 4A on several passes through the magnetotail plasma sheet during August and September 1967 are reported. The satellites were within the plasma sheet simultaneously for several hours during each pass. The measurements showed that the plasma sheet is quite symmetrical about a midplane whose location usually matches, within ~1 R_E, the location of the neutral sheet. Both satellites detected a plasma decrease associated with nearly every one of the magnetospheric substorms that occurred during the passes. It is shown that these substorm-related plasma decreases result from thinning of the plasma sheet, as has been suggested earlier, and not from a flapping motion of it. The thinning process seems to involve (at 18 R_E) not a squeezing or compression of the plasma into a more intense plasma sheet, but a net loss of plasma from that region of the tail. The data suggest that the plasma sheet (at 18 R_E) never disappears completely during these events. During quiet periods between substorms, the plasma sheet's boundaries are rather diffuse. However, during the plasma sheet's expansion after a substorm, its boundary is only 2000 to 3000 km thick. A phenomenon that is interpreted as a long-period (~4 hours) large-amplitude (several R_E) flapping motion of the plasma sheet was observed in a pass during a magnetically very quiet period. The flapping motion ceased when a magnetospheric substorm started about midway through the pass. (auth)

43241 ASYMMETRIC RING CURRENT AT TWILIGHT LOCAL TIME. Langel, Robert A.; Sweeney, Ronald E. (Goddard Space Flight Center, Greenbelt, Md.). J. Geophys. Res.; 76: No. 19, 4420-7(1 Jul 1971).

Ogo-2 rubidium vapor magnetometer measurements were compared with surface magnetic observatory data collected during three magnetic storms, March 13–15, 22–25, and 28–29, 1966. These comparisons were made at local times near the dawn–dusk meridian for dip latitudes less than 45°. The sources of low-latitude and midlatitude field depressions (Dst and Ds) are not in the ionosphere, but are located beyond the altitude of the satellite (413 to 1510 km). The resulting disturbance is longitudinally nonsymmetric; the disturbance at dusk is greater than the disturbance at dawn. (auth)

43242 UNIFIED THEORY OF SAR ARC FORMATION AT THE PLASMAPAUSE. Cornwall, John M. (Univ. of California, Los Angeles. Aerospace Corp., El Segundo, Calif.); Coroniti, F. V.; Thorne, R. M. J. Geophys. Res.; 76: No. 19, 4428-45(1 Jul 1971).

It is proposed that SAR arcs are generated at the plasmapause as a consequence of the turbulent dissipation of ring current energy. During the recovery phase of a geomagnetic storm, the plasmapause expands outward into the symmetric ring current. When the cold plasma densities reach about 100 cm^{-3}, ring current protons ($E_p \sim 20$ keV) become unstable and generate intense ion cyclotron wave turbulence in a narrow region $\frac{1}{2}$ R_E wide (just inside the plasmapause). Approximately one-half of the ring current energy is dissipated into wave turbulence, which in turn is absorbed through a Landau resonant interaction with plasmaspheric electrons. The combined thermal heat flux to the ionosphere due to Landau absorption of the wave energy and proton–electron Coulomb dissipation is sufficient to drive SAR arcs at the observed intensities. It is predicted that the arcs should be localized to a narrow latitudinal range just within the stormtime plasmapause. They should occur at all local times and persist for the 10- to 20-hour duration of the plasmapause expansion. Expected proton precipitation fluxes will not contaminate the spectral purity of SAR arcs. (auth)

43243 RELATIVISTIC ELECTRON PRECIPITATION DURING MAGNETIC STORM MAIN PHASE. Thorne, R. M.; Kennel, C. F. (Univ. of California, Los Angeles). J. Geophys. Res.; 76: No. 19, 4446-53(1 Jul 1971).

Relativistic electrons can have cyclotron resonances with electromagnetic ion-cyclotron waves. The resonant energy is generally well above 1 MeV throughout the magnetosphere, but it can fall to near 1 MeV just within the plasmapause. This also corresponds to the region where ring current (10 to 50 keV) protons are expected to be strongly unstable. The resulting ion-cyclotron wave amplitude necessary to precipitate ring current protons leads to electron lifetimes near the strong diffusion limit. Thus, >1-MeV electrons whose drift orbits intersect the stormtime plasmapause should rapidly be precipitated in the region $3 < L < 5$ during the initial phase of a magnetic storm. (auth)

43244 MAGNETIC DRIFT WAVE INSTABILITIES IN PLASMAS WITH TEMPERATURE GRADIENT. Wu, C. S. (Univ. of Maryland, College Park). J. Geophys. Res.; 76: No. 19, 4454-62(1 Jul 1971).

A plasma instability believed to be important in space plasma is discussed. The instability may occur in various regions where plasma density, magnetic field, and temperature are nonuniform. In some cases electron and proton temperature gradients can give rise to a new instability that is much stronger than the magnetic drift-wave instability known in existing theory. Furthermore, temperature gradients can produce either stabilizing or destabilizing effect under different conditions. The present work is motivated by a recent study of magnetic field and plasma data obtained by the OGO-5 satellite. (auth)

43245 THEORY OF TRIGGERED vlf EMISSIONS. Sudan, R. N.; Ott, E. (Cornell Univ., Ithaca, N. Y.). J. Geophys. Res.; 76: No. 19, 4463-76(1 Jul 1971).

The theory presented to explain the origin of triggered discrete vlf emissions is more complete than earlier theories in that it is not restricted to discussion of kinematical relations but evaluates the dynamics of the problem. Resonant electrons are phase-correlated with the wave magnetic field by a finite-length whistler

XUM

train moving in the opposite direction. The time for phase correlation is of the order of the period of oscillation of a particle in the effective potential well of the wave. It is recognized that the wave acceleration due to the inhomogeneous magnetic field of the Earth must be small enough for the particle to stay trapped in the potential well. The phase-correlated electrons are subject to an instability in the form of an emitted whistler with a growth rate $\gamma/\omega \sim (n/n_0)^{1/4}(v_\perp / c)^{1/2}(\omega_p / \Omega)^{1/4}$, where (n/n_0) is the fractional density of the resonant particles, $v_\perp$ is their mean transverse velocity, and ω_p and Ω are local cold plasma and gyrofrequencies. The emitted frequency varies according to $\omega = k(\omega)v_{||} - \Omega$, where $v_{||}$ is the zero-order longitudinal velocity of the resonant electron and the wave vector k is a function of frequency ω through the whistler dispersion relation. The theory is in good agreement with observation. (auth)

43246 OBSERVATIONS OF AURORAL HISS, LHR NOISE, AND OTHER PHENOMENA IN THE FREQUENCY RANGE 20 Hz TO 540 kHz ON OGO 6. Laaspere, T.; Johnson, W. C.; Semprebon, L. C. (Dartmouth College, Hanover, N. H.). J. Geophys. Res.; 76: No. 19, 4477-93(1 Jul 1971).

The payload of the polar-orbiting Ogo 6 spacecraft includes an experiment with four broadband receivers, two narrowband receivers at 200 and 540 kHz, and a broadband intensity detector. The receivers respond not only to electromagnetic but also to electrostatic waves, such as lower hybrid resonance (LHR) noise observed below auroral latitudes in the range from a few to about 20 kHz. The broadband intensities of the signals often exceed the full-scale reading of about 3 mV/m of the broadband detector. The intense signals are usually contained in a bandwidth of only a few kHz. Full-scale readings are also exceeded by auroral hiss, but its bandwidth often extends from a lower cutoff near the LHR frequency to the highest frequency monitored by the experiment (540 kHz). The intensity and spectral shape of auroral hiss vary both within an event and from event to event. Under geomagnetically quiet conditions the center of the auroral hiss zone extends from about 70° invariant at magnetic midnight, through 75° invariant at 0600 and 1800 MLT, to about 78° invariant at magnetic noon. In subpolar and polar latitudes very intense signals are observed in a narrow band near the low-frequency cutoff of the experiment, suggesting the presence of dc electric fields. Intense vlf hiss was observed near the equator with the dipole antenna nearly parallel to the geomagnetic field. These signals may result from some type of interaction between the spacecraft and the local plasma. (J.C.W.)

43247 SPATIAL AND TEMPORAL RELATIONS BETWEEN Pi BURSTS AND IPDP MICROPULSATION EVENTS. Heacock, R. R. (Univ. of Alaska College, College). J. Geophys. Res.; 76: No. 19, 4494-4504(1 Jul 1971).

Temporal and spatial relationships are found between impulsive Pi bursts occurring near local midnight and IPDP events occurring in the afternoon–evening side. The Pi burst occurring at the onset of a polar substorm is followed immediately by the IPDP event in the late evening sector. The IPDP is registered most clearly equatorward and westward of the center of the Pi-burst event. This morphology is consistent with the IPDP's generation by protons drifting westward from the midnight precipitation region. The IPDP's appear most clearly at sites in the 60 to 65° geomagnetic latitude range, whereas the Pi bursts are usually more prominent at 70°. Unstructured Pc 1 and 2 activity often precedes IPDP's and is most prominent near 70° latitude. If the midnight precipitation region spans both open and closed field lines, the westward drift of quasi-trapped protons on the innermost L shells may account for the IPDP events. (auth)

43248 ROCKET MEASUREMENTS OF LOW-ENERGY AURORAL ELECTRONS. Rearwin, Stephen (Univ. of California, San Diego, La Jolla). J. Geophys. Res.; 76: No. 19, 4505-17 (1 Jul 1971).

A Nike–Tomahawk flown from Fort Churchill into a widespread, diffuse (~2 kR at 3914 A), stable aurora detected thermal (kT ~ 3.2 keV) electron fluxes from 1 to 30 keV at 60 to 120° pitch angles. Peak fluxes were ~10^7 el/cm^2 sec sr keV. The total electron flux in this energy range was very nearly a linearly decreasing function of pitch angle; the temperature was roughly constant for $\alpha \lesssim 90°$ and decreased steadily with increasing pitch angle for $\alpha \gtrsim 90°$. Analysis of 230 sec of data from altitudes above 200 km revealed no coherent time variations with periods 3 sec $\lesssim \tau \lesssim$ 100 sec. It is suggested that the electrons measured in this experiment had been convected toward the Earth from the magnetospheric tail region. (auth)

43249 PULSATING AURORAL PATCHES EXHIBITING SUDDEN INTENSITY-DEPENDENT SPATIAL EXPANSION. Scourfield, M. W. J.; Parsons, N. R. (Univ. of Calgary, Alberta). J. Geophys. Res.; 76: No. 19, 4518-24(1 Jul 1971).

A class of pulsating aurora has been observed in which the repeated spatial expansion of a patch from a small persistent core region is evidently dependent on the attainment of a critical intensity level in this core region. Characteristics of patches exhibiting this behavior are summarized, and the phenomenon is discussed in relation to possible triggered instabilities of the precipitating electron beam. (auth)

43250 POLAR SUBSTORMS AS THE SOURCE OF LARGE-SCALE TRAVELING IONOSPHERIC DISTURBANCES. Davis, M. J. (Stanford Univ., Calif.). J. Geophys. Res.; 76: No. 19, 4525-33(1 Jul 1971).

It is shown that it is possible to relate the occurrence of large-scale traveling ionospheric disturbances (TID's) observed at midlatitudes with polar substorms on a statistical basis. In addition, under favorable conditions (relatively low geomagnetic activity) it is possible to show a connection between the occurrence of the TID's and substorms on a one-to-one basis. Columnar electron-content measurements were used to detect the TID's, and magnetograms from several high-latitude geomagnetic observatories were used to study the substorms. The results strongly support the theory that large-scale TID's originate during polar substorms. It was also possible to determine the location of the source of a number of individual TID's. These locations lie primarily in the evening sector of the auroral oval. (auth)

43251 EQUATORIAL ION TEMPERATURE: A COMPARISON OF CONFLICTING INCOHERENT SCATTER AND OGO 4 RETARDING POTENTIAL ANALYZER VALUES. McClure, J. P. (Univ. of Texas, Dallas); Troy, B. E. Jr. J. Geophys. Res.; 76: No. 19, 4534-40(1 Jul 1971).

During October and November 1967, the satellite Ogo 4 crossed the geomagnetic equator near the Jicamarca Radar Observatory at approximately 400- to 650-km altitude at night. For this period comparisons are made between radar values of the ion temperature T_i and those from the retarding-potential analyzer (RPA) on Ogo 4. There is generally disagreement, with T_i (RPA) > T_i (radar) by as much as 40%. Although nothing is obviously wrong with either set of data, this discrepancy cannot be accommodated within the error bars placed on each data set. Typical examples of the conflicting data are presented. The conflicting geophysical implications of these data regarding the heating of the equatorial ionosphere at night are discussed. (auth)

43252 STRIATIONS IN IONOSPHERIC ION CLOUDS. I. Voelk, Heinrich J.; Haerendel, Gerhard (Max-Planck-Institut fuer Physik and Astrophysik, Garching, Ger.). J. Geophys. Res.; 76: No. 19, 4541-59(1 Jul 1971).

The occurrence of striated irregularities in ionospheric ion clouds is discussed. Striations can either be impressed on the cloud from the ambient medium or generated by the cloud itself. If they are impressed on the cloud, the striations are simply tracers of small-scale electric fields in their environment. To ascertain whether this is indeed the case, the stability of the cloud is investigated. It is pointed out that the cloud cannot be considered an isolated object and that its interaction with the ionosphere is essential if striation formation by the cloud itself is considered. The short-circuiting effect on cloud-generated polarization fields is considered in detail. The effect of the simultaneously generated image striations is discussed for a homogeneous ionosphere. This effect is very strong, but for its final evaluation a more realistic model of the ionosphere is needed. (auth)

43253 WESTWARD ELECTRIC FIELDS AS THE CAUSE OF NIGHTTIME ENHANCEMENTS IN ELECTRON CONCENTRATIONS IN MIDLATITUDE F REGION. Park, Chung G. (Stanford Univ., Calif.). J. Geophys. Res.; 76: No. 19, 4560-8(1 Jul 1971).

Large enhancements in electron concentrations are frequently observed in the midlatitude nighttime F region. These enhancements are explained in terms of enhanced downward diffusion flux from the protonosphere induced by substorm-associated electric fields in the ionosphere. A mechanism is proposed by which a westward electric field enhances downward flux from the protonosphere while lowering the F layer. (An eastward electric field has opposite effects). This mechanism plus height variations of recombination loss can explain the observed behavior of the nighttime F layer during substorms. Crude estimates of electric fields and protonospheric fluxes are made from ionospheric parameters observed during a substorm. Under favorable conditions ground-based ionosonde records may be used to infer spatial and temporal variations of electric fields in the ionosphere during substorms. The results of this study suggest that in middle latitudes the nighttime ionosphere is controlled by vertical drifts and fluxes from the protonosphere. (auth)

43254 FARADAY ROTATION OF SATELLITE SIGNALS ACROSS THE TRANSVERSE REGION. Titheridge, J. E. (Univ. of Auckland, New Zealand). J. Geophys. Res.; 76: No. 19, 4569-77(1 Jul 1971).

The plane of polarization of a high-frequency radio wave rotates on passing through the ionosphere. The rotation is in one direction above the transverse point, and in the opposite direction below. In general, however, the rotation angle is reflected across the transverse region, giving a change of sign. The total rotation is then equal to the sum of the absolute rotations in each section. This does not pass through zero during a satellite transit, but has a minimum value (of several rotations) when the transverse point is near the center of the ionosphere. The sign of the total rotation undergoes a sudden jump when the transverse point is in the lower ionosphere, at a height of 110 to 220 km (day) or 200 to 300 km (night). A second jump occurs when the transverse point is in the topside ionosphere. Between these two times, a clockwise rotation of the transmitting antenna appears as an anticlockwise rotation at the ground, and the measured Faraday rotation differs from the expected value by 90° (for the Beacon satellites). (auth)

43255 ENHANCEMENT OF SPORADIC E BY HORIZONTAL TRANSPORT WITHIN THE LAYER. Chimonas G. (Univ. of Colorado, Boulder). J. Geophys. Res.; 76: No. 19, 4578-86 (1 Jul 1971).

The tidal winds in the E region, acting through the wind-shear mechanism, produce thin horizontal layers of metallic ions, which descend in time as the phases of the winds change. Gravity waves generated below the E region also have a downward-directed phase velocity and, if this is of the same order of magnitude (but greater than) the descent velocity of the layer, the wave seen by the ions in the layer can be almost stationary in time. The interaction of the wave with the layer then produces a very strong horizontal redistribution of the ion density, although hardly affecting the height of the layer. It is suggested that this process is responsible for enhancing the ion density at certain locations and producing experimentally observable E_s. The sporadic nature of the phenomenon then arises from the variable presence of suitable waves, while the horizontal scale of the enhanced-layer region is controlled by the horizontal wave length of the gravity wave. (auth)

43256 MEASUREMENT OF THE EFFECTIVE ELECTRON LOSS RATES IN THE D REGION DURING POLAR CAP ABSORPTION EVENTS. Megill, L. R.; Adams, G. W.; Haslett, J. C.; Whipple, E. C. (Environmental Research Labs., Boulder, Colo.). J. Geophys. Res.; 76: No. 19, 4587-95(1 Jul 1971).

The effective electron-loss rates from 64 to 100 km have been measured for daytime and nighttime conditions during polar-cap absorption events by using rocket-borne proton spectrometers and Faraday-rotation experiments. The daytime results agree within a factor of 2 with the Adams and Masley (1965) profiles in the 64- to 80-km region where they overlap. The nighttime loss rates coincide with the daytime loss rates down to ~75 km and then increase rapidly below that altitude. The loss rates above 90 km imply a dissociative recombination coefficient of 4.1 (±1.3) $\times 10^{-7}$ cm^3/sec. The coincidence of the day and night profiles down to 75 km suggests that no photodetachment processes are of significance during the daytime. (auth)

43257 SUNLIGHT PHOTODETACHMENT OF O_3^-. Byerly, Radford Jr.; Beaty, Earl C. (National Bureau of Standards, Boulder, Colo. Univ. of Colorado, Boulder). J. Geophys. Res.; 76: No. 19, 4596-4601(1 Jul 1971).

The rate of photodetachment of O_3^- by sunlight has been determined. The O_3^- ions were identified by their mobility as they drifted in a weak field in 1 torr of O_2 buffer gas. This allowed the ions to lose any vibrational or electronic excitation through collisions with the buffer gas. Energy dependence of the cross section was estimated by the use of colored filters in the photon beam. The sunlight photodetachment rate measured was 0.2 ± 0.1 sec^{-1}. (auth)

43258 SEMIANNUAL VARIATION IN THE HETEROSPHERE: A REAPPRAISAL. Jacchia, L. G. (Smithsonian Astrophysical Observatory, Cambridge, Mass.). J. Geophys. Res.; 76: No. 19, 4602-7(1 Jul 1971).

Past attempts to represent the semiannual density variation in the heterosphere as a consequence of temperature variation have run into difficulties in two height regions: below 200 and above 1000 km. The main argument in favor of the temperature variations was the dependence of their amplitude on the solar cycle; it can be shown, however, that this dependence is spurious, being caused by the variation of the density change $d\rho/dT$ with the temperature T. An analysis of the semiannual density variations at different height levels fails to show a dependence of the amplitude with the sunspot cycle. All difficulties are removed if it is assumed that the semiannual density variation is not a direct consequence of temperature variations. (auth)

43259 OBSERVATIONS OF THE O I 1304-A AIRGLOW FROM OGO 4. Meier, R. R.; Prinz, D. K. (Naval Research Lab., Washington, D. C.). J. Geophys. Res.; 76: No. 19, 4608-20(1 Jul 1971).

The atomic oxygen 1304-A day airglow was observed from the Ogo-4 spacecraft. The subsolar emission rates from the nadir lie in the range 10 to 17 kR for August 1967 and vary approximately as the cosine of the solar zenith angle. Day-to-day variations (for observations fixed relative to the Sun) can typically be of the order of 10 to 20% and occasionally as much as 40% over a several day period. Long-term variations (of the order of weeks) correlate with solar activity. Photoelectron impact excitation of atomic oxygen is apparently the only process sufficient to account for the observed emission rates. Resonant scattering of sunlight is too small to account for the observations. (auth)

43260 IONOSPHERIC ESTIMATES OF ATOMIC OXYGEN CONCENTRATION FROM CHARGED PARTICLE MEASUREMENTS. Mahajan, K. K. (National Physical Lab., New Delhi). J. Geophys. Res.; 76: No. 19, 4621-9(1 Jul 1971).

Radar-backscatter and the rocket-probe measurements of electron and ion temperatures and electron concentration are used to solve the thermal energy equation for the O^+ ions. By equating the heat gained by the O^+ ions from the hotter thermal electrons to the heat lost to the cooler neutrals, the concentration of the oxygen atoms n(O) is deduced. Significant seasonal changes in n(O) are identified. The calculated values of oxygen concentration are found to be consistently smaller than the Cira (1965) values throughout the latest rising phase (1964–1967) of solar activity. This disagreement is greatest at low solar activity and reduces with the increase in activity. There is, however, general agreement on the time of diurnal maximum of n(O) between the calculated and model values. (auth)

43261 MOLECULAR OXYGEN DENSITY MEASUREMENTS FROM 80 TO 140 KILOMETERS. Brannon, P. J.; Hoffman, J. M. (Sandia Labs., Albuquerque, N. Mex.). J. Geophys. Res.; 76: No. 19, 4630-3(1 Jul 1971).

Molecular oxygen densities were measured from a rocket by observing the absorption of the solar Lyman-α line and the C–IV doublet at 1550 A. Densities were obtained by taking the derivative of an analytic function best fitted to the logarithm of the ion-chamber current. The expression for the density (particles/cm^3) from 80 to 95 km was given by $N(Z) = 6{,}77 \times 10^{13}$ exp $[-0{,}20176(Z-80)]$, where Z is the altitude in km and is limited to the range 80 to 95 km. Owing to the large variation of the intensity of the C–IV line with the position being observed on the solar disc, there is a large amount of scatter in the data, and accurate densities in the altitude region 115 to 140 km could not be obtained. A comparison with the Cira 1965 standard atmosphere indicates that the densities in this altitude region are about a factor of 2 lower than the standard. (auth)

43262 ROCKET-BORNE ULTRAVIOLET SPECTROMETER MEASUREMENT OF OH RESONANCE FLUORESCENCE WITH A DIFFUSIVE TRANSPORT MODEL FOR MESOSPHERIC PHOTOCHEMISTRY. Anderson, James G. (Univ. of Colorado, Boulder). J. Geophys. Res.; 76: No. 19, 4634-52(1 Jul 1971).

An upper limit on the column density of the hydroxyl radical in the Earth's upper atmosphere was determined with a rocket-borne scanning spectrometer using resonance fluorescence techniques in the near uv. The (0 – 0) band of the $A^2\Sigma - X^2\Pi$ transition at 3064 A was studied between 60 and 108 km under evening twilight conditions from Wallops Island, Virginia, on June 27, 1969. The solar zenith angle was 92°. The Rayleigh scattered background was used to determine the column emission rate from the OH molecule. An emission rate factor calculation for OH is presented that considers the rotational structure of the molecule and the effect of absorption by OH in the solar atmosphere. The dissociation rate for water vapor was calculated by using a high-resolution analysis of the O_2 absorption cross section. A significant amount of H_2O dissociation was found to occur throughout the mesosphere down to the stratopause. A mesospheric oxygen–hydrogen model that includes diffusive transport of water vapor and the recalculated H_2O dissociation rate is considered in order to interpret the experimental results. A model for the concentration of H, OH, HO_2, and H_2O in the mesosphere is presented that uses a water vapor mixing ratio of 5×10^{-6} at 50 km and an eddy diffusion coefficient of 1×10^{-6} cm^2/sec. (auth)

43263 ABLATION AND BREAKUP OF LARGE METEOROIDS DURING ATMOSPHERIC ENTRY. Baldwin, Barrett; Sheaffer,

XUM

Yvonne (Ames Research Center, Moffett Field, Calif.). J. Geophys. Res.; 76: No. 19, 4653-68(1 Jul 1971).

An ablation model is described that can be used to estimate the effect on a large meteoroid of passage through a planetary atmosphere. The effect on ablation and deceleration of breakup due to aerodynamic pressure is investigated. Results from arc-jet wind-tunnel tests and strength measurements of meteorite samples have been used to help determine the material properties needed in the calculations. Results are given from a series of calculations of the ablation and breakup of bronzite and carbonaceous chondrite meteoroids in the Earth's atmosphere. It is shown that evidence from meteor observations and meteorite falls can be interpreted in terms of a preponderance in space of meteoroids of density comparable to that of meteorites rather than low density. Carbonaceous chondrite is a likely candidate as the most common type of meteoroid in space. (auth)

43264 POSITION OF THE PLASMAPAUSE DURING A STORM-TIME INCREASE IN TRAPPED ENERGETIC (E gt 280 keV) ELECTRONS. Carpenter, D. L. (Stanford Univ., Calif.); Park, C. G.; Arens, J. F.; Williams, D. J. J. Geophys. Res.; 76: No. 19, 4669-73(1 Jul 1971).

The position of the plasmapause relative to the region of appearance of enhanced fluxes of energetic (E > 280 keV) electrons is reported during the magnetic storm of June 15, 1965. The plasmapause was measured near the prime geomagnetic meridian by whistler techniques; the trapped energetic electrons were detected by the satellite 1963-38C in polar orbit at 1100-km altitude. As the stormtime reduction in plasmasphere radius occurred, the electron fluxes increased in a region that was apparently exterior to the diminishing plasmasphere. The plasmapause position appears to have been adjacent to the region of inflation of the magnetosphere reported by Cahill from Explorer-26 magnetometer data. This relationship is similar to that deduced from the Ogo-3 measurements of Frank (ring-current particles) and Taylor and his colleagues (thermal ion density). (auth)

43265 SOLAR CYCLE VARIATION IN DAYTIME IONOSPHERIC E_s PARAMETERS IN THE SOUTH PACIFIC AREA. Baggaley, W. J. (Univ. of Canterbury, Christchurch, New Zeland). J. Geophys. Res.; 76: No. 19, 4674-8(1 Jul 1971).

Daytime occurrence frequencies of f_0E_s and f_bE_s are presented for stations Rarotonga and Christchurch for a period of two solar cycles and for Scott Base for a period of one cycle. Although f_0E_s shows little association with sunspot activity, f_bE_s shows a strong positive correlation with both sunspot number and with noon f_0E. The data also indicate the presence of a 4-month time lag of f_bE_s peaks after sunspot maximums. (auth)

43266 MAGNETOSPHERIC SUBSTORM OBSERVATIONS NEAR THE NEUTRAL SHEET. Meng, C.-I. (Univ. of California, Berkeley); Akasofu, S.-I. J. Geophys. Res.; 76: No. 19, 4679-84(1 Jul 1971).

Six magnetospheric substorm events near the neutral sheet in March and April 1966 are studied to examine the variations of energetic electrons in the plasma sheet and magnetotail field. The IMP-3 data for each event include the magnitude, latitude and longitude angles of the tail magnetic field in solar ecliptic coordinate, and fluxes of energetic electrons greater than 40 and 45 keV. The study shows that the enhancements of energetic electrons do not appear at or very near the neutral sheet soon after the onset of magnetospheric substorms. The observed delay of the energetic electron events after the onset of substorms cannot be due only to a slow expansion speed of the plasma sheet. It is theorized that at a certain epoch of a substorm, the plasma sheet, which contains energetic electrons, begins to expand rapidly along the neutral sheet and perpendicular to it, the perpendicular expansion being much slower. (J.C.W.)

43267 ELECTRON PITCH ANGLE SCATTERING IN THE OUTER ZONE DURING MAGNETICALLY DISTURBED TIMES. Vampola, A. L. (Aerospace Corp., El Segundo, Calif.). J. Geophys. Res.; 76: No. 19, 4685-8(1 Jul 1971).

Thorne and Kennel have recently proposed that the rapid loss of energetic electrons in the outer zone observed during magnetic storms is due to pitch-angle scattering arising from a resonant interaction with Doppler-shifted ion cyclotron waves generated by ring-current protons. Examination of energetic electron flux pitch-angle distributions obtained by instrumentation of OV3-3 (1966-70A) reveals a number of events that meet most of the requirements of the Thorne-Kennel precipitation mechanism. Primary among these are: narrow ($\Delta L \approx 0.5$) spatial distribution of precipitation at and just inside the plasmapause; more rapid scattering of energetic electrons (E > 1.5 MeV) than of low-energy electrons (E ≈ 300 keV); and occurrence of the precipitation predominantly at local evening. (auth)

43268 SIGNIFICANCE OF ELECTROSTATIC PROBE OBSERVATIONS OF ELECTRON DENSITY IRREGULARITIES. Dyson, P. L. (La Trobe Univ., Bundoora, Australia). J. Geophys. Res.; 76: No. 19, 4689-90(1 Jul 1971).

Observations of electron-density irregularities by the electrostatic probe aboard the Alouette-2 satellite were previously presented in (NSA 24: 6431) a paper by Dyson. Latitudinal and diurnal occurrences of these irregularities were compared with observations of spread F, and results indicate that the percentage amplitude of the irregularities decreases at lower latitudes. It is desirous to know the latitudinal and diurnal behavior of the absolute amplitude of the irregularities so that, for techniques whose threshold sensitivity depends on the percentage deviation of the irregularities from the ambient density, the occurrence statistics may reflect changes in the ambient density rather than properties of the physical processes causing the irregularities. The extent of the occurrence characteristics being dependent on the ambient electron density is examined from the data in Dyson's paper. It is concluded that the observed diurnal behavior of fine-structure occurrence does in fact result from properties of the physical mechanisms causing the irregularities. (J.C.W.)

43269 ELECTRON LOSS DURING A NIGHTTIME PCA EVENT. Swider, W.; Narcisi, R. S.; Keneshea, T. J.; Ulwick, J. C. (Air Force Cambridge Research Labs., Bedford, Mass.). J. Geophys. Res.; 76: No. 19, 4691-4(1 Jul 1971).

Electron concentrations and the precipitating proton flux were measured with rocket-borne instruments over Fort Churchill, Canada, on Nov. 18, 1968, at nighttime. It is inferred that electrons are irretrievably lost below 75 km by means of a three-body attachment process producing O_2^- ions. Simple expressions for the electron concentration, the ratio of negative ions to electrons, and the effective recombination coefficient are deduced. The proton flux appeared to have a negligible cutoff and the role of atomic oxygen, the only available nighttime detachment agent, is discussed. An electron-concentration profile of a nighttime 1962 nuclear event is presented for purposes of comparison. (J.C.W.)

43270 IONOSPHERE-GRAVITY WAVE INTERACTIONS DURING THE MARCH 7, 1970, SOLAR ECLIPSE. Arendt, P. R. (Inst. for Exploratory Research, Fort Monmouth, N. J.). J. Geophys. Res.; 76: No. 19, 4695-7(1 Jul 1971).

Results are given from some observational data to study the origin of and the resulting atmospheric perturbation from the occurrence of TID during the solar eclipse of Mar. 7, 1970. Chimonas and Hines (Geophys. Res., 75: 875(1970)) predicted that observable TID effects would be generated during a solar eclipse by the thermospheric bow wave according to the concept that gravity waves produce TID. The ionosphere was suffering from various magnetic storms from Mar. 6-9, 1970. After studying the results from some observing stations, it is concluded that eclipse effects, not magnetic-storm effects, produced the electron-content variations measured during the initial phase of the eclipse. It is not evident that the reported perturbations are a part of the bow-wave spectrum. (J.C.W.)

43271 HARNESSING THE ENERGY IN THE RADIATION BELTS. Brice, Neil (National Science Foundation, Washington, D. C.). J. Geophys. Res.; 76: No. 19, 4698-4701(1 Jul 1971).

The feasibility of exerting a large measure of control over the loss of energy from the Van Allen belts and plasma sheet or cusp regions by cold plasma injection is discussed. Calculations indicate that about a kg-mole, properly distributed through the outer belt, plasma sheet, and ring current regions, could remove much of the trapped energy in a few hours. The significance of the cold-plasma density in the energetic particle precipitation process is described. By comparing whistler and other measurements of the total plasma density beyond the plasmapause with the energetic particle and magnetic-field measurements, it appears that the bulk of the energy in the radiation belt resides in the large fluxes of particles whose energies are less than the characteristic energy, defined by parameters of magnetic-field strength, permeability of free space, and plasma density. The role of the cold plasma is to reduce the characteristic energy in the equatorial plane and thereby make the stable trapping limit applicable to the bulk of the energetic particles. An experimental test of this technique should also include some injection of wave energy at suitable frequencies. (J.C.W.)

43272 INTERACTION OF SOLAR WIND AND PLANETARY ATMOSPHERES. Shimizu, Mikio (Tokyo Univ.). Kagaku (Tokyo); 40: No. 12, 655-62(Dec 1970). (In Japanese).

The effects of solar wind on planetary atmospheres were discussed. Various data from the planet-explorers Venera 4 and Mariner 5 have revealed in some detail the composition, pressure, temperature, outer-zone data, the state of motion of the Venusian atmosphere, and some data on the upper ionosphere. The data from Mariner 4, 6, and 7 concerning the Mars atmosphere are not as sufficient as those from the Mariner 5, because of their unfavorable flight courses. From scant data, some speculation for those subjects is presented. In conclusion, the effects of solar wind on both the Venus and Mars atmospheres are supposed to cease within several hundred kilometers above the planetary surfaces. Supposition about electromagnetic waves emitted by Jupiter and its magnetosphere vary, but no sufficient observations concerning them are expected before the coming exploration in 1972 by Pioneer F/G which will be equipped with magnetometer, plasmameter, ultraviolet spectrometer, etc. (Japan)

Low-Temperature Physics and Cryogenic Equipment

Superfluidity

Refer also to abstract 43512.

43273 IMPURITIES IN AN IMPERFECT BOSE GAS. I. THE CONDENSATE. Padmore, Timothy C.; Fetter, Alexander L. (Stanford Univ., Calif.). Contract F44620-68-C-0075. Ann. Phys. (N. Y.); 62: 293-319(Feb 1971).

A variational principle is used to evaluate the change in the condensate energy of an imperfect Bose gas arising from the introduction of stationary impurities. Moving impurities are incorporated by performing a Galilean transformation from a frame with bulk flow at infinity to one with asymptotically stationary fluid. The corresponding effective mass is calculated numerically and compared with that of ^{3}He impurities in He II. A generalization to charged impurities exhibits the anomalous flow pattern suggested by Gross and allows a model calculation of the effective mass of positive ions in He II. (auth)

43274 POINT TRANSFORM THEORY OF LIQUID HELIUM. Gross, Eugene P. (Brandeis Univ., Waltham, Mass.). Ann. Phys. (N. Y.); 62: 320-42(Feb 1971).

The method of point transformations is used to obtain a microscopically based theory of the excitations of a system of interacting bosons. The theory is governed by a transformed Hamiltonian whose ground state is a noninteracting state and which is quadratic in the new momenta. The form of Hamiltonian is compatible with translational, rotational, and Galilean invariance. If the assumption is made that two-body interactions between the dressed particles predominate, two well-behaved functions remain undetermined. In the absence of a microscopic calculation these functions may be fitted using experimental data for liquid helium. The thermal properties of the system can be calculated as with the less rigorously based Landau–Khalatnikov Hamiltonian. The present theory retains the possibility of describing the Bose–Einstein condensation and quantized circulation. (auth)

43275 ON A POSSIBLE MECHANISM FOR THE NORMAL-FLUID CRITICAL VELOCITY IN LIQUID He II. Goodman, S. E. (Univ. of Virginia, Charlottesville). Phys. Lett.; 35A: No. 5, 356(28 Jun 1971).

It is suggested that normal fluid turbulence may not be as "ordinary" as is generally thought, and that its origin may depend on the nature of the rotons in the excitation gas. (auth)

43276 EFFECT OF ION DRAG ON QUANTIZED VORTEX RING DYNAMICS. Steingart, M.; Glaberson, W. I. (Rutgers–The State Univ., New Brunswick, N. J.). Phys. Lett.; 35A: No. 5, 311-12(28 Jun 1971).

Differences in the motion of positively and negatively charged vortex rings were observed at moderate temperatures above 0.3°K. These can be explained in a simple way by incorporating the frictional drag associated with the bare ion into the equations of motion. (auth)

43277 LIQUID ^{4}He. II. THREE-BODY CORRELATIONS AND THEIR CONTRIBUTION TO THE BINDING ENERGY AND THE DEPLETION. Oestgaard, E. (Institut Max von Laue–Paul Langevin, Garching, Ger.). J. Low Temp. Phys.; 4: No. 6, 585-604(Jun 1971).

The three-body contribution to the binding energy of liquid ^{4}He is calculated. The methods applied are those developed mainly by Bethe and collaborators for nuclear-matter calculations, and later modified for liquid ^{3}He. Various two-body wave functions and reaction-matrix elements are calculated, as is the effective interaction or representation of the reaction matrix in coordinate space. Three-body wave functions and three-body energy contributions are then calculated or estimated. The calculations are repeated for several values of the density and for several values of the intermediate-state relative momentum between the two interacting particles. The three-body contribution to the binding energy is found to be approximately −1.3 to −1.6 K per particle. This is, however, a rather uncertain value because the results are very sensitive to the values chosen for the average relative momentum in the calculations of the effective interaction off the energy shell. Also, in parts of the calculations only the S wave is included, and it is taken to represent the effect of the total wave function. The total binding energy of liquid ^{4}He is estimated by adding the contributions from separate calculations of the two-body and the three-body interaction. A self-consistent solution is obtained through the depletion of the zero-momentum state, which is also estimated. The calculations are done for two different two-body potentials, an Yntema–Schneider potential given by Brueckner and Gammel and a Frost–Musulin potential given by Bruch and McGee. The theoretical results are −4.0 to −5.0 K for the binding energy and 44 to 50% for the depletion. The corresponding experimental results are −7°K and 83%, respectively, i.e., the difference is generally within a factor of 1.5 to 2. The agreement with experimental results is probably reasonably good (or bad) since four-body and higher-order cluster terms are not included. (auth)

43278 HIGH-ENERGY NEUTRON SCATTERING FROM LIQUID HELIUM IN THE IMPULSE APPROXIMATION. Gersch, H. A.; Smith, Phil N. (Georgia Inst. of Tech., Atlanta). Phys. Rev., A; 4: No. 1, 281-90(Jul 1971).

The impulse approximation is used to describe the inelastic cross section for high-energy neutron scattering from superfluid helium in terms of a ground-state momentum distribution of the helium atoms as given by existing variational calculations. The predicted shape of the cross section is compared with recent experimental data and with a previous theory that approximated the noncondensate contribution to the dynamic structure factor by a single-Gaussian function. In contrast to conclusions obtained using the single-Gaussian approximation, the predicted inelastic cross section, omitting a condensate contribution, provides an acceptable fit to the experimental data. This fit is worsened by introducing a contribution from a condensate fraction in the amount consistent with the variational calculations, namely 11%. If the condensate fraction is arbitrarily reduced from this value, it is found that a much smaller value, with an upper limit of about 3%, is consistent with the available experimental data. It appears that unique assignments of condensate-fraction contributions to inelastic neutron scattering, for the range of neutron energies presently available, will require an improved theory of final-state effects on the shape of the condensate contribution. (auth)

43279 SECOND SOUND REFLECTION ON A LIQUID He II SURFACE. Buchholz, F. I.; Brandt, D.; Wiechert, H. (Institut fuer Physik, Mainz). Phys. Lett.; 35A: No. 6, 471-2(12 Jul 1971).

The reflection coefficient of second sound waves at the free surface of liquid He-II was measured for vertical incidence between 1.26K and T_λ. (auth)

43280 POSSIBLE NMR EXPERIMENT TO OBSERVE SPIN WAVES IN DILUTE SOLUTIONS OF ^{3}He IN ^{4}He AND IN PURE ^{3}He. Tan, H.-T.; Halley, J. Woods (Univ. of Minnesota, Minneapolis). Contract AT(11-1)-1569. Phys. Lett.; 35A: No. 6, 443-4(12 Jul 1971).

A C-W NMR experiment to observe the spin waves in ^{3}He–^{4}He dilute solutions or pure liquid ^{3}He is suggested. Spin waves in He solutions should be detectable at a temperature of about 20 mK and an external field of about 20 kG. (auth)

43281 MODIFICATION OF THE DISSIPATIVE TERMS IN THE THERMOHYDRODYNAMICAL EQUATIONS OF HELIUM II. Schmidt, R. (Institut fuer Physik, Mainz). Phys. Lett.; 35A: No. 6, 439-40(12 Jul 1971).

The rate of production of ρ_n is proposed to be introduced in the dissipative terms of the linearized thermohydrodynamical equations given by Khalatnikov. From these equations the existence of some different types of wave modes in He II may be inferred. (M.H.R.)

43282 STUDY OF HEAT TRANSFER FROM HORIZONTAL WIRES TO HELIUM II AT HIGH HEAT-FLUX VALUES. Leon-

XUM

ard, Albert Clark. Ann Arbor, Mich.; Univ. of Michigan (1970). 236p. University Microfilms Order No. 71-15,217.
Thesis.

The transfer of heat from a solid to He-II at high heat fluxes was investigated using a conventional dewar system with horizontal wire heaters of various sizes. Maximum heat flux data are reported for specimen diameters of 25, 76, 254 and 635 μm, as a function of the He-II bath temperature, for depths of immersion up to 70 cm. Data presented indicated that, contrary to previous suppositions, q_{max} is not influenced strongly, if at all, by the dewar system type of specimen holder, or method of obtaining the data. An analysis of the vapor film growth along the specimen indicated that the discrepancy in q_{max} data from similar diameters which have been reported may be caused by local hot spots resulting from wire defects. Evidence is presented which indicates that the diameter effect on q^*_{max} diminishes as the depth of immersion is reduced and may disappear altogether at zero depth of immersion. Some comments on the physics of the heat transfer mechanism have been made. (TSS) (Diss. Abstr. Int., B)

43283 SOME EXPERIMENTS REGARDING DISSIPATION IN HELIUM SUPERFLOW. Williams, D. R.; Chester, Marvin (Univ. of California, Los Angeles). Phys. Rev., A; 4: No. 2, 707-18(Aug 1971).

Experiments are reported on the dissipative steady-state flow regime of liquid helium II. These were done with a view to examining the theoretical assertion that the chemical potential gradient $\nabla\mu$ is related to the superfluid-flow speed v_s, by the equation $-\nabla\mu = G \exp(1 - v_c(T)/v_s)$. The experiments showed good qualitative agreement with this equation. Other assertions about the magnitude of the parameters in this equation and their dependence upon the superfluid fraction ρ_s/ρ and temperature T were also explored experimentally. (auth)

43284 ORDER-PARAMETER FLUCTUATIONS IN A WEAKLY INTERACTING BOSE GAS NEAR THE SUPERFLUID TRANSITION. Gould, Harvey; Wong, Victor K. (Univ. of Michigan, Ann Arbor). Phys. Rev., A; 4: No. 2, 719-33(Aug 1971).

The contribution of order-parameter fluctuations to the static and dynamic properties of a weakly interacting Bose gas near the Bose–Einstein condensation temperature T_c is investigated via a novel approach. Self-consistent approximations for the propagator of order-parameter fluctuations G are generated in successive temperature ranges closer and closer to T_c. Mean-field theory corresponds to assuming that the correlation of fluctuations G_2 is given by $G_2^{(1)} = GG$. This first approximation is valid in the range $\tau_1 < \tau = (T - T_c)/T_c < 1$, where at $\tau = \tau_1$ the neglected terms are comparable to those included. The second approximation $G_2^{(2)} = GGVGG$ is considered, which involves the first-order interaction between the fluctuations. Two independent criteria for the range of validity $\tau_2 < \tau < \tau_1$ of the second approximation are established. It is conjectured that the qualitative results of the present model calculation are applicable to liquid helium in the presently accessible temperature range. The predicted temperature dependences of the specific heat, superfluid density, and fourth sound are in agreement with the scaling hypothesis and available experiments in helium. The condensate density is predicted to vanish linearly with τ. It is shown that the contribution of order-parameter fluctuations to the thermal conductivity diverges as $\tau^{-\frac{1}{2}}$ above T_c, and it is suggested that the absence of logarithmic factors is due to the inconsistent treatment of entropy fluctuations. (auth)

43285 THEORY OF SUPERFLUIDITY. Mann, A. (Indiana Univ., Bloomington). Phys. Rev., A; 4: No. 2, 750-3(Aug 1971).

The generator-coordinate method, well known in nuclear physics, is employed to derive the Bogolyubov theory of superfluidity of a boson system. The treatment is fully number conserving. Analogies to a normal Fermi system (especially to the random-phase approximation for that system) are pointed out, and some further insight into the nature of superfluidity is gained. Possible generalizations are mentioned. (auth)

43286 DEPRESSION OF THE SUPERFLUID TRANSITION TEMPERATURE IN ^{4}He BY A HEAT CURRENT. Ahlers, Guenter; Evenson, Alan; Kornblit, Avinoam (Bell Telephone Labs., Murray Hill, N. J.). Phys. Rev., A; 4: No. 2, 804-6(Aug 1971).

An attempt is made to measure the depression of the superfluid transition temperature T_λ in liquid helium by a heat current Q, and found that within our precision, T_λ is independent of Q for $0.2 \le Q \le 2$ W/cm^2. An effect of the size $\Delta T_\lambda/Q \cong 3 \times 10^{-3}$ K cm^2/W would have been observable. This upper limit is inconsistent with the value 59×10^{-3} K cm^2/W reported recently by Bhagat and Lasken for $10^{-3} \le Q \le 10^{-1}$ W/cm^2. (auth)

43287 SUPERFLUID DENSITY OF He II IN RESTRICTED GEOMETRIES. Henkel, Raymond Paul. Ithaca, N. Y.; Cornell Univ. (1971). 93p. University Microfilms Order No. 71-15,630.
Thesis.

The reduction of the superfluid density of He-II below its bulk value when confined to narrow pores and unsaturated films was studied as a function of temperature from .056K to $T_\lambda - T = 1$mK. The reduction is observed by measuring the superfluid density of a persistent current with a superfluid gyroscope. A new type of experiment shows that for a sufficiently thick unsaturated helium film the reduction in superfluid density is essentially a surface effect independent of film thickness. The reduction near the lambda transition is discussed in terms of a simplified Ginzburg–Pitaevskii superfluid healing length model. A superfluid healing length, ξ_s, is defined by setting the product, $\rho_{s,b}\xi_s$ equal to the reduction of superfluid mass per unit area, where $\rho_{s,b}$ is the bulk superfluid density. Near T_λ, the healing length can be described by a power law $\xi_s = \xi_{s,o}(1 - T/T_\lambda)^{-\nu}$, where $\nu = .63 \pm .05$. (Diss. Abstr. Int., B)

Superconductivity

Refer also to abstracts 41761, 42219, and 43483.

43288 (INR–1294) Nb_3Sn SUPERCONDUCTING PHASE IDENTIFICATION IN THE Nb–Sn ALLOYS BY THE CRITICAL TEMPERATURE MEASUREMENT METHOD. Horubala, Zenon; Jedrzejec, Henryk; Bukat, Andrzej (Institute of Nuclear Research, Warsaw (Poland)). 1971. 22p. (In Polish). Dep. NTIS (U. S. Sales Only).

The critical temperature measurement method and scheme for the superconducting transition are given. The method was applied to the Nb_3Sn superconducting phase identification in the Nb–Sn alloys. The critical temperature value for the samples containing the Nb_3Sn phase is 18 ± 2°K. (auth)

43289 (NYO–2150-71) THERMOMAGNETIC EFFECTS IN NORMAL AND SUPERCONDUCTING INDIUM AND NIOBIUM. Report No. 1545. Stephan, Craig Hamman (Cornell Univ., Ithaca, N. Y. Materials Science Center). Jun 1971. 109p. Dep. NTIS.
Thesis.

Measurements of the Hall effect, its thermal analogue the Righi–Leduc effect, and thermal magnetoresistance were made in In and Nb. The Hall and Righi–Leduc effects in large magnetic fields in polycrystalline In at 2.5 to 8°K followed a generalized Wiedemann–Franz law. The Righi–Leduc coefficient in oriented In single crystals at low magnetic fields changes sign as the field is increased from zero. The ratio of relaxation times of the third-zone electron-like carriers to the second-zone holes is calculated to be ~1.2. In the mixed state of Nb, the thermal resistance has a maximum near H_{c1}, decreasing sharply at H_{c2}, The ratio of the transverse-to-longitudinal temperature gradient is nearly constant for fields of 0.2 to 0.8 H_{c2}, but is much smaller than the normal-state value at H_{c2}. No unusual behavior is observed in the normal state. The thermal resistance follows the expected behavior in the intermediate state of polycrystalline In. The Righi–Leduc also coefficient changes sign. (D.L.C.)

43290 (ORNL–4703) EFFECT OF HEAT TREATMENT AND IMPURITIES ON THE CURRENT DENSITY OF TRANSITION METAL SUPERCONDUCTORS. Easton, D. S.; Scarbrough, J. O.; Betterton, J. O. Jr. (Oak Ridge National Lab., Tenn.). Jun 1971. Contract W-7405-eng-26. 35p. Dep. NTIS.

The critical current densities of alloys of Zr–Nb, Ti–Nb, and Hf–Nb were increased by the addition of interstitial impurities and by heat treatments to produce precipitation. The alloy Zr–50% Ta was found to be a good high-tield superconductor. Differences in the preparation and heat treatment of the alloys greatly affected the final critical current density. High-purity alloys prepared in an ultrahigh-vacuum zone refiner had lower critical current densities than those prepared by the usual arc-melting techniques. Electrical resistivity measurements made at 300 and 77°K are included in the Appendix along with critical current density values of the alloys prepared for this work. (auth)

43291 (ORNL-tr-2461) SUPERCONDUCTIVITY AND RANGE OF EXISTENCE OF THE A 15 PHASE IN THE SYSTEM Nb–Al–Ge. Mueller, A. Translated by R. Gregg Mansfield (Oak Ridge National Lab., Tenn.), from Z. Naturforsch.; 25A: 1659-69(1970). 21p. Dep. NTIS.

The isothermal section at 1840°C in the system Nb–Al–Ge with more than 60 at. % Nb was investigated and the range of existence of the A15 phase delimited. Critical temperatures, lattice constants and hardness are shown as a function of the composition of the A15 phase. The values T_c of single-phase specimens with

≈75 at. % Nb can be arranged according to valence electrons as well as according to ratios between calculated and measured lattice constants. Both correlations indicate that the upper limit of the critical temperature in the ternary system even for the metastable A15 phase is not higher than 22°K. (auth)

43292 SUPERCONDUCTING PROPERTIES OF MULTIFILAMENTARY V_3Ga WIRES. Suenaga, M.; Sampson, W. B. (Brookhaven National Lab., Upton, N. Y.). Appl. Phys. Lett.; 18: No. 12, 584-6(15 Jun 1971).

Multifilamentary superconducting V_3Ga wires in a Cu–Ga solid-solution matrix were prepared. The superconducting critical temperature T_c and the critical current density $J_c(H)$ are presented for wires with various heat treatments. (auth)

43293 MACROSCOPIC QUANTUM INTERFERENCE EFFECTS IN SUPERCONDUCTING SLUG-TYPE JUNCTIONS. Rose-Innes, A. C.; Niewodniczanska-Zawadzka, J. (Inst. of Physics, Warsaw). Acta Phys. Pol.; A39: No. 6, 725-6(1971).

The phenomenon of Josephson tunneling has been used in the construction of superconducting quantum interferometers based on Clarke-type junctions. A periodic structure of sinusoidal shape is observed in the dc voltage measured across the junctions as a function of the applied magnetic field. (auth)

43294 ANISOTROPY IN CUBIC SUPERCONDUCTORS. II. FLUX DISTRIBUTION IN LEAD–THALLIUM AND LEAD–INDIUM SINGLE CRYSTALS WITH $\kappa > 2^{-\frac{1}{2}}$. Obst, B. (Univ., Stuttgart). Phys. Status Solidi (b); 45: No. 2, 467-82(1 Jun 1971). (In German).

Lead–thallium alloys with Ginzburg–Landau parameters $\kappa > 2^{-\frac{1}{2}}$ (containing more than 1.5 wt.% Tl) show an anisotropy of the flux-line pattern. The orientations of the flux-line lattice and the crystal lattice are correlated. It is assumed that an interaction energy of the London type exists between the flux lines. The microscopic quantities are substituted into the corresponding expression and the anisotropy is attributed entirely to that of the energy gap Δ. The same angular dependence of the energy gap is obtained as from the analysis of the anisotropic flux distribution in the intermediate state of type-I superconductors. In the intermediate state in PbTl and PbIn alloys with $\kappa > 2^{-\frac{1}{2}}$ isolated diamagnetic regions embedded in the Shubnikov phase form a kind of "superlattice". The latter has the symmetry of the crystal lattice in the direction of the field and is rotated in a characteristic manner with respect to the flux-line lattice. (auth)

43295 ANISOTROPY IN CUBIC SUPERCONDUCTORS. I. FLUX DISTRIBUTION IN LEAD AND LEAD–THALLIUM SINGLE CRYSTALS WITH $\kappa > 2^{-\frac{1}{2}}$. Obst, B. (Univ., Stuttgart). Phys. Status Solidi (b); 45: No. 2, 453-65(1 Jun 1971). (In German).

Magnetic structures in cubic superconductors were investigated using the decoration technique developed by Träuble and Essmann. In the intermediate state in lead, the phase boundaries are preferentially oriented in certain directions. In lead–thallium alloys, the anisotropy phenomena are studied as a function of the Ginzburg–Landau parameter κ. The observed anisotropy of the specific surface energy σ_{NM} cannot be interpreted in terms of the phenomenological theory of Ginzburg and Landau. Tentatively, the microscopic quantities are substituted into the expression for σ_{NM} for the isotropic case, and the anisotropy is described merely by the parameter of the energy gap Δ. The resulting orientation dependence of Δ is compared with theoretical predictions. (auth)

43296 SUPERCONDUCTIVITY, LATTICE STABILITY, AND PHONON FREQUENCIES. Froehlich, H. (Univ. of Liverpool). Phys. Lett.; 35A: No. 5, 325-6(28 Jun 1971).

The interaction that leads to superconductivity may also cause anomalies in the phonon spectrum. (auth)

43297 RESPONSE OF SUPERCONDUCTING POINT CONTACTS TO HIGH-FREQUENCY RADIATION. Kanter, H.; Vernon, F. L. Jr. (Aerospace Corp., El Segundo, Calif.). Phys. Lett.; 35A: No. 5, 349-50(28 Jun 1971).

The high-frequency response predicted by a perturbation approach for a highly damped current-driven Josephson junction agrees in its parameter dependence remarkably well with observations on point contacts used as video-type detectors of microwave radiation. (auth)

43298 BEHAVIOR OF SUPERCONDUCTIVE THIN-FILM BRIDGES IN SHF FIELDS. Dmitriev, V. M.; Khristenko, E. V.; Trubitsyn, A. V.; Mende, F. F. (Inst. of Physics and Tech. of Low Temperatures, Kharkov). Ukr. Fiz. Zh.; 15: 1611-14 (Oct 1970). (In Russian).

Results are presented of experimental investigations of volt–ampere characteristics in short thin-film superconductive tin bridges 3 to 4 μm wide and ~2000 Å thick with shf irradiation (λ = 3 cm). Shf irradiation of the bridge at temperatures higher, but close to the critical T_c, is shown to cause an anomalous decrease in its resistivity and transition to a superconductive state at definite power levels. At $T < T_c$ an increase in critical current I_c is observed under the shf-irradiation effect. The constant magnetic field H perpendicular to the bridge plane, decreasing the value of the critical current of the bridge in practice, does not influence the effect of I_c increase under the action of the shf irradiation. It is shown that, being at a normal state with H greater, but close to H_c, the bridge can also be converted into a superconductive state by shf irradiation. The results obtained do not depend on whether shf current is parallel or perpendicular to the constant current through the bridge. (auth)

43299 RESISTIVE PHENOMENA IN THE INTERMEDIATE STATE. Shukhman, V. A.; Kano, L. M. (Inst. of Physics, Tbilisi, USSR). JETP Lett. (USSR) (Engl. Transl.); 13: No. 6, 197-9(20 Mar 1971).

Translated from Zh. Eksp. Teor. Fiz., Pis'ma Red.; 13: No. 6, 277-80(20 Mar 1971).

The possible existence of resistive effects in type-I superconductors in the initial stage of the intermediate state is examined. The current was measured in a closed superconducting circuit, one section of which was the investigated sample in the intermediate state. Polycrystalline tin samples of cold-rolled foils and annealed plates were used and the control samples were made of type-II superconducting In + Bi alloy in the form of annealed plates. It is concluded that the intermediate state begins with the appearance of isolated normal regions in the superconducting matrix, and assumes a layered character only in stronger fields. It is noted that the resistive state in tin samples was observed up to external field values of $H \simeq 0.7\ H_c$, and the field values did not vary noticeably with either the sample thickness or temperature. (J.C.W.)

43300 EFFECT OF PLASTIC DEFORMATION ON CRYSTAL CURRENT DENSITY IN Pb–In CRYSTAL. Kawai, Hisao; Okada, Touichi; Suita, Tokuo; Kamata, Kohji (Osaka Univ.). Technol. Rep. Osaka Univ.; 20: No. 932-972, 437-50(Oct 1970).

The effect of plastic deformation on the critical current density, J_c, of PbIn single crystals containing 2 at. % In was studied. It was found that the J_c is sensitively influenced by plastic deformation. The lattice defects that were introduced by plastic deformation are able to pin the motion of quantized flux line. The anisotropy in pinning force was also observed. (auth)

43301 SUPERCONDUCTIVITY AND SUPERCONDUCTING DEVICES. Mendelssohn, K. (Oxford Univ.). pp 261-91 of Advanced Cryogenics. /Bailey, C. A. (ed.). London; Plenum Press (1971).

After an introductory section, the following are discussed: superconductivity and the periodic table; critical current and critical field; the Meissner effect; theory of superconductivity; type-II superconductors; and applications of superconductivity. 15 references. (UK)

43302 SENSITIVITY OF THE SUPERCONDUCTING TRANSITION TEMPERATURE TO RESIDUAL STRESS IN HIGH-T_c INTERMETALLIC COMPOUNDS. McCarthy, S. L. (Univ. of California, San Diego, La Jolla). J. Low Temp. Phys.; 4: No. 6, 669-78(Jun 1971).

Residual-stress-induced superconductivity is reported to occur only in the high-T_c members of the C14 and C16 crystal systems. Second transitions are also seen in $ThIr_2$(C15) and $MoRe_3$(A12). The change in T_c, as a result of introducing large residual stresses, increases with the bulk T_c. (auth)

43303 SUPERCONDUCTIVITY OF COLD-DEPOSITED BERYLLIUM FILMS. Alekseevskii, N. E.; Tsebro, V. I. (Inst. for Physical Problems, Moscow). J. Low Temp. Phys.; 4: No. 6, 679-96(Jun 1971).

The results are presented from an investigation of the transition temperature T_c and energy gap $2\Delta(0)$ as a function of the thickness of superconducting cold-deposited beryllium films. The transition temperature increases exponentially as the film thickness is decreased. In the interval of very small thicknesses a drop in T_c is observed. The thickness dependence of $2\Delta(0)$ is analogous to the independence of T_c. In the investigated interval of thicknesses the ratio $2\Delta(0)/kT = 3.6 \pm 0.1$, indicating that the cold-deposited modification of beryllium is a superconductor with weak electron–phonon coupling. Superconducting beryllium films could only be produced up to thicknesses $d_{cr} \sim 200$ Å. At thicknesses close to d_{cr} a transition to the nonsuperconducting α phase is observed. The growth of the transition temperature

XUM

with decreasing thickness is attributable to the influence of dimensional quantization of the transverse motion of electrons in the film. The drop in T_c for very small thicknesses (~30 Å) is regarded as due to the influence of fluctuations. The functions $T_c(d)$ obtained by various authors for thin films of other superconductors, such as Al, Sn, Bi, Ga, and Pb, are discussed. (auth)

43304 RECTIFICATION EFFECT IN THIN-FILM SUPERCONDUCTORS IN SMALL, OSCILLATORY MAGNETIC FIELDS. Huebener, R. P.; Perkins, H. S. (Argonne National Lab., Ill.). J. Low Temp. Phys.; 4: No. 6, 697-707(Jun 1971).

The generation of dc voltages across superconducting films of lead and tin was observed due to the presence of a static magnetic field H_0 upon which a small, oscillatory magnetic field component is superimposed. The voltages are created without an external current passing through the samples. They change sign with a reversal of the static field H_0. The voltages are related to superconductivity and seem to be caused by a nonsymmetric penetration into the specimen of the magnetic field variation. During one cycle of the magnetic field oscillation a small fraction of the total flux entering and leaving the sample appears to be "pumped across" the specimen in a preferential direction. The thickness of the films ranged between 0.16 and 2.5 μm. The frequency ω and the amplitude H_1 of the oscillatory field were varied from 5 to 120 kHz and from 0 to 2 G rms, respectively. The rectified voltage varies between the different samples and depends upon H_0, ω, H_1, and the orientation of the film relative to the magnetic field. It generally shows a sharp peak near the critical magnetic field. Small rectified voltages caused by the oscillatory field were observed far above the nominal, critical magnetic fields of the films. Apparently, these voltages were associated with the film edges and the enhancement of the critical field at the edges. (auth)

43305 SUPERCONDUCTING STATE PARAMETERS FOR NONTRANSITION METALS USING EXACT OPW FORM FACTORS. Rajput, J. S. (Banaras Hindu Univ., India); Gupta, Ashok Kumar. pp 16-19 of Proceedings of the Nuclear Physics and Solid State Physics Symposium, Roorkee, December 28-31, 1969. Vol. III. Bombay; Dept. of Atomic Energy (1969).

From Nuclear physics and solid state physics symposium; Roorkee, India (28 Dec 1969). See CONF-691208-(Vol.3).

A method is given for the calculation of $\langle V_{ph} \rangle$, phonon-mediated attractive electron-electron interaction parameter; $\langle V_c \rangle$, the Coulomb pseudopotential; and Z_0, the quasi-particle renormalization parameter. The matrix elements between Bloch electron states were used, and for the e-e attractive matrix elements, the exact OPW forms were used. Estimated parameters are tabulated for the metals Na, K, Be, Ca, Al, In, Sn, Pb, Hg, and Tl. (D.L.C.)

43306 LOW TEMPERATURE PROPERTIES OF DILUTE SUPERCONDUCTING ALLOYS. Upadhyaya, U. N. (Univ. of Udaipur, India). pp 20-2 of Proceedings of the Nuclear Physics and Solid State Physics Symposium, Roorkee, December 28-31, 1969. Vol. III. Bombay; Dept. of Atomic Energy (1969).

From Nuclear physics and solid state physics symposium; Roorkee, India (28 Dec 1969). See CONF-691208-(Vol.3).

The effects of magnetic-element impurities in a virtual nonmagnetic state on the energy gap and density of states of superconductors are examined. Only two-body interactions between s and d electrons involving virtual transitions of d electrons are considered. (D.L.C.)

43307 FLUCTUATION CONDUCTIVITY OF TUNNEL JUNCTIONS. Cheishvili, O. D. (Inst. of Physics, Tbilissi, USSR). J. Low Temp. Phys.; 4: No. 6, 577-83(Jun 1971).

Tunneling of electrons is studied at joints between two metals separated by a thin dielectric layer. The conductivity of electrons in the case of the same metals at temperatures higher close to the temperature of superconducting transitions has a strong temperature dependence. Tunneling of electrons between a superconductor and a normal metal separated by a thin dielectric layer at temperatures higher than that of the superconducting transition of the normal metal is also considered. The fluctuation correction to the current increases strongly when the temperature approaches the transition temperature and the voltage applied to the barrier becomes of the order of magnitude of that of the energy gap of the superconductor. (auth)

43308 STUDY OF THE SUPERCONDUCTING PROXIMITY EFFECTS OF JOSEPHSON TUNNELING. Greenspoon, S.; Smith, H. J. T. (Univ. of Waterloo, Ont.). Can. J. Phys.; 49: No. 10, 1350-60(15 May 1971).

Josephson tunneling in lead/lead oxide/copper/lead junctions was studied with the intent of investigating the proximity effects between normal (Cu) and superconducting (Pb) metals. Zero-voltage tunneling currents of the order of milliamps was observed in junctions with varying copper thicknesses and electron mean free paths. Measurements of the temperature dependence of the maximum Josephson current were interpreted in terms of a model based on the de Gennes-Werthamer theory of the proximity effects. It is concluded that the de Gennes-Werthamer theory has considerable usefulness outside the strict limits of validity in which it was derived. (auth) (Canada)

43309 INFLUENCE OF ADDITIONS OF A THIRD ELEMENT ON THE CRITICAL MAGNETIC FIELD OF TITANIUM-NIOBIUM ALLOYS. Heller, W. (Univ., Erlangen, Ger.); Loehberg, R.; Babiskin, J. J. Less-Common Metals; 24: No. 3, 265-76(Jul 1971). (In German).

Additions of germanium or copper to β-TiNb solid solutions with about 50 wt % Nb (wires 1 mm in diameter) reduce the critical magnetic field H_c of the binary alloy to an amount of 10 kG/% Ge or 4 kG/% Cu. By measurements of H_c it is assumed that at 700°C less than 0.5% Ge and more than 1% Cu are in solid solution. The maximum critical field H_c of 117.7 kG in TiNb49Ge2.3 of 97% cold-worked samples after heat treatment 250 hr at 400°C is increased to 119.4 kG in TiNb48Ge4.5 of 97% cold worked and 16 hr in 500°C-annealed samples. The highest H_c value of the investigated binary alloys (TiNb55 with 117.5 kG) is exceeded because of the enrichment of niobium in the matrix. The solubility of germanium in the β-solid solution at 400°C is very low and the intermetallic compound Ti_5Ge_3 is precipitated. H_c of the alloys with copper additions reaches, in spite of the enrichment of niobium in the matrix after the heat treatment, not the H_c values of the alloys containing germanium, because the solubility of copper in the β-solid solution is higher than that of germanium. Additions of 2 at. % Sn, Ga, In, Fe, Mn, Cr, Al, Zr, Ag, or Ge to 97% cold-worked and 10 hr at 400°C aged wires with 50 wt. % Nb decrease H_c, while an addition of 2 at. % Cu does not change the value of TiNb50(114 kG) and an addition of 2 at. % Nb raises H_c to 116.1 kG. The change of H_c by aging between 300 and 700°C is explained by the dissolution of microsegregations in the β-solid solution, by precipitations of the pre-stage of the ω-phase, the ω- and α-phase, Ti_5Ge_3 or Ti_2Cu or other intermetallic compounds. (auth)

43310 INFLUENCE OF POINT DEFECTS ON MAGNETIC PROPERTIES OF TYPE II SUPERCONDUCTORS. Ullmaier, Hans (Kernforschungsanlage, Juelich, Ger.). pp 367-86 of Advances in Solid State Physics. /Madelung, O. (ed.). Elmsford, N. Y.; Pergamon Publishing Co. (1970). (In German).

Following a short introduction dealing with different types and properties of point defects in metals, a review is given on the influence of point defects on magnetic properties of Type-II superconductors. It is convenient to distinguish between reversible and irreversible effects. The former involve changes of the Ginsburg-Landau parameter κ (and therefore of the critical fields) of the superconductor due to the introduction of scattering centers. It is shown that κ not only depends on the transport mean free path but also on the specific scattering behavior of the defect type considered. Irreversible effects are due to pinning forces on flux lines in the mixed state. Pinning forces arise when structural defects cause a spatial variation of the free energy. In the case of point defect cascades or clusters, the observed pinning forces are very large in contrast to the action of statistically distributed defects. In the latter case it is proposed that fluctuations of the defect density are responsible for the irreversible behavior observed. (auth)

43311 PHOTOELECTRIC OBSERVATION OF THE SUPERCONDUCTING ENERGY GAP IN LEAD. Kunz, Louis W. (Stanford Univ., Calif.). Phys. Rev. Lett.; 26: No. 21, 1311-14 (24 May 1971).
1971).

The photoelectric yield of a thin lead film was measured between 2.5 and 12°K. There is a difference in temperature dependence between the normal and superconducting states that is in reasonable agreement with the BCS-based theory of Slezov. A value for the energy gap is obtained that is consistent with infrared and tunneling measurements of other observers. The size of the change in yield, however, is more than an order of magnitude larger than that predicted and is presently not understood. (auth)

43312 MEASUREMENT OF THE SUPERCONDUCTING ENERGY GAP AND FERMI VELOCITY IN SINGLE-CRYSTAL LEAD FILMS BY ELECTRON TUNNELING. Lykken, G. I.; Geiger, A. L.; Dy, K. S.; Mitchell, E. N. (Univ. of North Carolina, Chapel Hill). Phys. Rev. B; 4: No. 5, 1523-30(1 Sep 1971).

The superconducting energy gap and reduced Fermi velocity were measured as a function of crystallographic orientation by

tunneling experiments using single-crystal thin films of Pb. Double gaps were observed in all directions except [100] in which a triple gap was found. Except in this last direction, the values measured agree with those of earlier experiments on bulk single crystals of Pb. Fermi velocities due to electrons from the second and third Brillouin zones are evaluated from a study of Tomasch oscillations in these films. Data are reported for the following orientations: [100], [110], [111], [211], and 5° off [100]. (auth)

43313 PROPAGATION OF THE PHASE SURFACE IN SUPERCONDUCTING THIN FILMS. Volkov, R. A.: Skobelkin, V. I. (Inst. of Electron Tech., Moscow). Dokl. Akad. Nauk SSSR: 195: 807-10(1 Dec 1970). (In Russian).

The Maxwell–London equations and the authors' previously derived current function may be applied to Type-II superconductors, such as thin films, the thickness of which is less than the depth of penetration of the magnetic field. Assuming that the field is quasi-stationary and the problem is one-dimensional, these equations were applied to the layer separating the superconducting and the normally conducting regions. The derivations indicated that the rate of propagation of the normal phase does not exceed the velocity of the propagation of phonon excitations. The negative sign of the surface energy makes impossible the establishment of an equilibrium between the superconducting and normal phases when there is a phase transition of a Type-II superconductor from the superconducting to the normal state. The phase transition time τ needed to determine the rate of propagation of the normal phase was found to be $\tau \simeq 10^{-7}$ sec. The propagation of excitation in the form of the normal phase in a second-order superconductor must be taken into account in the design of thin-film cryotrons; the value of τ limits the fast action of these devices. (TTT)

43314 PLASMA WAVES AND SUPERCONDUCTIVITY IN QUANTIZING SEMICONDUCTOR (SEMIMENTAL) FILMS AND LAMELLAR MEDIA. Pashitskii, E. A.; Romanov, Yu. A. (Inst. of Physics, Kiev). Ukr. Fiz. Zh.: 15: 1594-1606(Oct 1970). (In Russian).

It is shown that a specific mechanism of coupling degenerate conduction electrons due to virtual acoustic plasmon exchange occurs in quantizing semiconductor (semimetal) films and lamellar media with a reasonably high mobility of free carriers. As a result, the critical temperature of the superconductive transition in such systems may be noticeably higher than in massive samples. (auth)

43315 ACOUSTIC SURFACE WAVE STUDY OF PERPENDICULAR FIELD SUPERCONDUCTING PROXIMITY EFFECT IN Cu/Pb/Cu SANDWICHES. Jain, M. C.; Tilley, D. R. (Univ. of Essex, Eng.). Phys. Lett.: 35A: No. 4, 217-8(14 Jun 1971).

A study was made of perpendicular critical field versus temperature of various Cu/Pb/Cu sandwiches. The critical field was determined from acoustic surface wave attenuation. The experimental points were compared with a theoretical expression given previously, using one disposable parameter, and found to be in satisfactory agreement. (auth)

43316 MICROWAVE-PHONON-INDUCED EXTRA CURRENTS IN SUPERCONDUCTIVE TUNNELING. Heidam, N. Z. (Technical Univ. of Denmark, Lyngby). Phys. Status Solidi (a); 5: No. 3, 645-50(16 Jun 1971).

The change ΔI of the tunneling current I(U) in superconducting $Sn/SnO_x/Pb$ diodes due to 2.5-GHz longitudinal sound waves was measured as functions of bias and acoustic power in the temperature range from 2.0 to 3.8°K. At low power levels, ΔI was found to be proportional to the second derivative of the characteristic, in agreement with theory. The dependence on the relative power also agrees with theory, but the magnitude of ΔI is larger than expected. The temperature dependence agrees with theory when both metals are superconducting, but seemingly not when one metal is normal. (auth)

43317 OFF-DIAGONAL LONG-RANGE ORDER AND THE MOMENTUM DISTRIBUTION OF ELECTRON PAIRS IN SUPERCONDUCTORS AND HELIUM ATOMS IN LIQUID ^{4}He. Girardeau, M. D. (Univ. of Oregon, Eugene). Phys. Rev., A; 4: No. 2, 777-88(Aug 1971).

The momentum distributions of electron pairs in superconductors and of helium atoms in liquid ^{4}He are defined by summing the pair or atomic state occupation probability over all internal states of the pair or ^{4}He atom corresponding to a given value of total translational momentum. By use of the closure relation for internal wave functions, the momentum distribution of electron pairs is expressed in terms of the two-electron density matrix $\rho_2(x_1x_2,\ x_1'x_2')$ of the 2n-electron system. Similarly, for ^{4}He atoms, the momentum distribution is expressed in terms of the single-atom density matrix $\rho_3(x_1x_2\,\vec{R},\ x_1'x_2'\,\vec{R}')$ of the n-atom system, where x_1, x_2, and $\vec{R}$ are the coordinates of two electrons and an α particle. The equivalence of this definition of the momentum distribution with two other plausible definitions is demonstrated. It is shown that exchange and the exclusion principle produce a strong spreading of the momentum distribution both for a superconductor and for liquid ^{4}He, completely suppressing Bose–Einstein condensation in the strong sense of macroscopic occupation of the zero-momentum state. However, a much weaker singularity at zero momentum, characteristic of the off-diagonal long-range order (ODLRO) of ρ_2 for a superconductor and of ρ_3 for liquid ^{4}He, does occur. By comparison with the hypothetical case of pairs of bosons, it is shown that the exclusion principle (not merely exchange) plays an essential role in broadening the momentum distribution in superconductors and liquid ^{4}He. (auth)

43318 SUPERCONDUCTING ALLOY. Fedotov, L. N.: Sokolov, V. I.; Mikhailov, N. N.; (and others) (to Central Scientific-Research Inst. of Ferrous Metallurgy). Russian Patent 243,841. 14 May 1969. Filed 22 Dec 1967. (In Russian).

A superconducting titanium-base alloy is described. It contains 31 to 35% niobium, 6 to 8% zirconium, 0.5 to 1.5% tantalum, and 0.3 to 0.7% iron. The iron is included to increase the electric resistance and to improve the superconducting properties. (TSS)

43319 SUPERCONDUCTING AND EXISTENCE REGIONS OF THE A15 PHASE IN THE SYSTEM Nb–Al–Ge. Mueller, A. (Siemens AG, Erlangen, Ger.). Z. Naturforsch.: 25a: 1659-69 (Nov 1970). (In German).

At 1840°C the isothermal section of the system Nb–Al–Ge was studied with more than 60 at. % of niobium and the existence region of the A15 phase was delineated. Critical temperatures, lattice constants, and hardness were determined in their dependency on composition of the A15 phase. T_c values of single-phase samples with more than 75 at. % niobium can be arranged in accordance with valence electrons or quotients either calculated or measured from lattice constants. The two correlations signify that the upper limit of critical temperature for the ternary system, even for the metastable A15 phase, does not exceed 22°K. (tr-auth)

43320 STOCHASTIC PROCESSES AND THERMAL FLUCTUATIONS IN SUPERCONDUCTORS. Leung, Man-chiu. Vancouver, British Columbia; Univ. of British Columbia (1970). National Library of Canada, Ottawa.

Thesis.

The generalized Langevin equation, derived by H. Mori, as a general, microscopic formulation of the stochastic theory of Brownian motions, is applied to evaluate the longitudinal attenuation rate of sound in weak-coupling, pure superconductors. In order to qualify the ultrasonic absorption as stochastic processes, the relaxation time of the random interactions on the phonon must be much shorter than the relaxation time of the phonon. It is shown that this is indeed the case by showing that the former is of the order of the relaxation time of the distribution function of the excitations from the BCS condensate. As compared with the earlier result derived by first order perturbation theory, the inclusion of the life-time effect has improved the agreement with experimental data. When $\tau^{-1} \gtrsim \Delta,\ \omega$, it is shown that Cooper pairs participate in the absorption processes even when $\omega < 2\Delta$. A sum rule for the longitudinal ultrasonic absorption rate is also derived. The Langevin approach is also employed to evaluate the spectra, variances and covariances of the magnetic flux, the currents and the magnetization in a long, thin, hollow, superconducting cylinder. When the wall thickness of a cylinder is arbitrary, the Langevin approach becomes inconvenient. In the above two approaches, the fluctuation of the electron density n_s in the BCS condensate is assumed to be negligible. To take care of the fluctuation of pair density, use is made of the fact that the probability density of n_s and Φ is proportional to $\exp\{-\beta G_s(n_s,\Phi)\}$ where Φ is the magnetic flux and G_s is the Gibbs free energy. To avoid mathematical complications, attention is restricted to the case of a long, thin, hollow cylinder in the Landau–Ginzburg temperature domain. The responses of magnetic flux and currents to an external magnetic field that changes stepwise at time $t = 0$ are also discussed. (TSS) (Diss. Abstr. Int., B)

43321 FLUCTUATION CONTRIBUTIONS TO THE HEAT CAPACITY OF SUPERCONDUCTING THIN FILMS. Zally, George Daniel. Urbana, Ill.; Univ. of Illinois (1970). 114p. University Microfilms Order No. 71-15,012.

Thesis.

Experimental investigations into the nature of the phase transi-

XUM

tion of a two-dimensional superconductor between its normal and superconducting states are reported. The heat capacity and electrical resistivity were measured for a series of amorphous bismuth–antimony films of various thicknesses. For the amorphous thin films examined in this experiment, the electrical conductivity measured was in agreement with theory and with other experiments. The heat capacity measurements showed an extra contribution that was consistent with the $(T - T_c)^{-1}$ behavior predicted. The width in temperature of the heat capacity transition was approximately the same as for the resistive transition. A recent calculation by Masker, Marcelja, and Parks, treating fluctuations to second order, predicts a sharp peak in heat capacity just below T_c. Such an effect should have been observable with the resolution of the present experiment, but no such peak was seen. (TSS) (Diss. Abstr. Int., B)

43322 MAGNETIC FLUX FLOW AND FLUCTUATION EFFECTS IN THIN FILM SUPERCONDUCTORS. Escher, John Stuart. Urbana, Ill.; Univ. of Illinois (1970). 109p. University Microfilms Order No. 71-14,741.

Thesis.

Critical-state measurements of single and binary thin film systems have been measured as a function of transport current density, magnetic field, temperature, and degree of annealing. Results are interpreted in terms of the present understanding of the mixed state in thin films. Studies of vortex guiding, the Hall angle in the mixed state, and ac versus dc measurement methods are reported. An unusual fluctuation effect in the resistive superconducting transition in many of the films is reported. The failure of the Aslamazov–Larkin theory to fit the resistive transition data is noted and compared with other recent experimental data on thin films. (Diss. Abstr. Int., B)

43323 NEW RESULTS ON THE DC TRANSPORT PROPERTIES IN A TYPE-II SUPERCONDUCTOR. Simon, Y.; Thorel, P. (CNRS, Paris). Phys. Lett.; 35A: No. 6, 450-2(12 Jul 1971).

Direct investigations of the current distribution and studies of the vortex lattice by neutron diffraction contribute in two different ways to reveal basic dc transport properties in the mixed state. Principal experimental conclusions are presented for niobium. (auth)

43324 THERMAL CONDUCTIVITIES OF NORMAL AND SUPERCONDUCTING INDIUM–LEAD ALLOYS AT LOW TEMPERATURES. Gledd, Ronald Elroy. Storrs, Conn.; Univ. of Connecticut (1970). 163p. University Microfilms Order No. 71-15,984.

Thesis.

Twelve indium–lead alloy samples with 3.00 at.% to 8.00 at.% lead concentrations were studied. These were divided into two sets, each consisting of six samples, one set with their c-axes oriented approximately at 81° with respect to the sample axis and the other set oriented at approximately 14° with respect to the sample axis. The electrical resistivities at 4.2, 77, and 273°K were measured, yielding the electrical anisotropies a(4.2), a(77) and a(273) where $a = \rho_\perp/\rho_\parallel$. These verified the earlier findings of Carriker. For pure indium a(77) = 0.986 ± .003 and a(273) = 1.041 ± .003, showing the same shift in maximum resistivity from the c to the a direction as the temperature is increased from 77°K to 273°K. Also the anomalies at 3.50 at.% and 7.00 at.% lead were again seen. The thermal conductivities were measured for all samples in both the normal and superconducting states. An anisotropy was evident in both, in the normal thermal conductivities at 3°K the anisotropy was a = 1.077 for the 3.00 at.% lead samples and a = 1.054 for the 8.00 at.% lead samples where $a = K_{11}/K_\perp$. The anomalies at 3.50 at.% and 7.00 at.% lead were evident. It is shown that this anisotropy is mainly due to the anisotropy in the electrical resistivity plus an unexplained anisotropy in the lattice thermal conductivity. This lattice anisotropy ranged around a value of 1.45 for all the samples, where $a = K_{g\perp}/K_{g11}$. However it did show a variation as a function of lead content that showed a rather general correlation with the c/a ratio for indium–lead alloys. A temperature minimum existed in the superconducting thermal conductivity for all samples and was a linear function of lead concentration for both sets, slowly increasing with increasing concentration from a temperature of 1.66°K to 2.1°K. This is due to the stronger electron scattering by mass defects that allows the phonon conduction to become predominate sooner in high lead concentration samples. The normal lattice thermal conductivity was never more than 10% of the total thermal conductivity and is composed of phonon–electron interaction scattering, mass defect scattering, and scattering due to distortion of the lattice around the mass defect. These last two scattering mechanisms are of approximately equal strength. The theoretical expression for mass defect and distortion scattering generally overestimated the strength but not by more than 10% of the experimental values. It was found that adding the squares of the strengths was more accurate than adding the mean square root values and then squaring since the phases of the scattering mechanisms were not known. The ratio K_{g_s}/K_{g_n} was plotted as a function of the reduced temperature and compared to the Klemens, Tewordt theoretical expression. While the general shape of the theoretical curves agrees with experimental results there was some disagreement in the values, probably caused by the absence of distortion scattering in the theoretical expression. (Diss. Abstr. Int., B)

Equipment and Devices

Refer also to abstracts 42080 and 42084.

43325 (CONF-700341–6) COOLING OF SUPERCONDUCTING MAGNETS, PRINCIPLES AND USES. Solente, P. (Air Liquide, Sassenage (France). Centre d'Etudes Cryogeniques). 1970. 9p. (In French). Dep. NTIS (U. S. Sales Only).

From Panel on superconductors; Paris, France (17 Mar 1970).

The problems of heat exchange in liquid or supercritical helium are briefly surveyed. The importance of correctly choosing the dimensions of the stabilizer for the superconductor with regard to the cooling loops provided within the magnet is emphasized. The principle of an installation intended for the cooling down and maintenance at low temperatures of a superconducting magnet is exposed. Some installations recently developed are described. (France)

43326 ADVANCED CRYOGENICS. Bailey, C. A. (ed.). London; Plenum Press (1971). 527p. £ 8.

This book is based on a course of lectures given in Oxford. It contains 20 chapters. Separate abstracts are included for five of these chapters. (UK).

For abstracts of individual chapters see: 42137, 43301, 43327, 43328, and 43735.

43327 ^{3}He DILUTION REFRIGERATOR. Wood, M. F. (Oxford Instrument Co. Ltd.). pp 245-60 of Advanced Cryogenics. /Bailey, C. A. (ed.). London; Plenum Press (1971).

It is stated that practical refrigerators using the ^{3}He-dilution refrigeration cycle make it possible to maintain temperatures down to ~0.01°K with heat extraction rates of the order of microwatts. The general principles are described first, followed by details of the still, the mixing chamber, the heat exchanger, and the instrumentation. 6 references. (UK)

43328 SUPERCONDUCTIVE MAGNETS. Wood, M. F. (Oxford Instrument Co. Ltd.). pp 293-315 of Advanced Cryogenics. /Bailey, C. A. (ed.). London; Plenum Press (1971).

After a brief introductory section, the following are discussed: the place of superconductive magnets; magnet design; practical materials; and cryogenic considerations. 23 references. (UK)

43329 ^{54}Mn IN Fe FOR ULTRALOW-TEMPERATURE THERMOMETRY. Sites, James R.; Smith, H. A.; Steyert, W. A. (Los Alamos Scientific Lab., N. Mex.). J. Low Temp. Phys.; 4: No. 6, 605-14(Jun 1971).

Experimental investigations into the accuracy of nuclear orientation thermometry are reported. ^{54}Mn in iron, a primary thermometer useful from 2 to 40 mK, gives consistent thermometry using both scintillation (3 × 3 in. NaI) and solid-state (40-cm^3 Ge) detectors. ^{60}Co-in-iron temperatures are consistent with the ^{54}Mn temperatures above 10 mK, but are about 10% higher at 4 mK. ^{125}Sb in iron registers a temperature that is perhaps 2 or 3% lower over the 4 to 15 mK region. Some of the techniques required for the utilization of this type of thermometry are discussed. (auth)

43330 SHAPING OF MAGNETIC FIELDS IN CYLINDRICAL CAVITIES WITH CIRCULAR AND ELLIPTICAL CROSS SECTIONS WITH HIGH CURRENT DENSITIES. Doinikov, N. I. Sov. Phys.-Tech. Phys. (Engl. Transl.); 15: No. 12, 2030-2 (Jun 1971).

Translated from Zh. Tekh. Fiz.; 40: No. 12, 2588-91(Dec 1970).

A procedure is described for designing coils that carry a constant current density and produce a desired field in circular or elliptical gaps; the method takes account of the saturation of the iron. Results for $\mu = \infty$ are presented. (auth)

Plasma and Thermonuclear Physics

Refer also to abstract 42220.

43331 (AD-715615) EQUILIBRIUM COMPOSITION AND NORMAL SHOCK PARAMETERS FOR NITROGEN UP THROUGH DOUBLE IONIZATION. Reprint-281. Sherman, M. P. (General Electric Co., Philadelphia, Pa. Missile and Space Div.). Sep 1964. Contract Nonr-4188(00). 36p. (R-64-SD-68). NTIS.

The equilibrium composition of nitrogen is computed up through double ionization. Equilibrium normal shock properties are shown to 100,000 ft/sec. Use is made of several simplifying assumptions: the perfect gas law, the strong shock approximation, no reduction in ionization potential due to multiple particle effects, and use of a limited number of states in the electronic partition function. (auth) (USGRDR)

Confinement and Heating

43332 (EUR-CEA-FC-595) PARAMETER STUDY FOR A TRANSIT TIME MAGNETIC PUMPING EXPERIMENT IN A TORUS. Brambilla, M.; Giuffre, S. (European Atomic Energy Community. Commissariat a l'Energie Atomique, Fontenay-aux-Roses (France). Centre d'Etudes Nucleaires). Apr 1971. 48p. Dep. NTIS (U. S. Sales Only).

The balance equations for the density, ion temperature, and electron temperature in a toroidal plasma, including TTMP heating, are written and solved numerically. The loss terms appropriate either to a Stellarator or to a Tokamak are carefully discussed. The feasibility of a TTMP heating experiment on a machine comparable with already existing ones is proved in principle, and its performance is evaluated. (auth) (France)

43333 (MATT-803) CONSIDERATION OF POWER REQUIREMENT IN FUSION FEASIBILITY EXPERIMENT. Yoshikawa, S. (Princeton Univ., N. J. Plasma Physics Lab.). Jun 1971. Contract AT(30-1)-1238. 17p. Dep. NTIS.

Assuming that pseudoclassical diffusion theory holds to the reactor condition, the estimate of power requirement of plasma heating in self-sustaining toroidal fusion devices is made. It is found that various heating methods such as neutral beam injection, rf heating, etc., are reasonably competitive from the power requirement except for the relativistic electron beam injection, which may be financially too difficult. The advantage of the astronspherator combination was noted. (auth)

43334 ELECTRON CYCLOTRON HEATING IN TOROIDAL OCTUPOLES. Sprott, J. C. (Univ. of Wisconsin, Madison). Phys. Fluids; 14: No. 8, 1795-1803(Aug 1971).

Microwave frequencies of 0.4 to 24 GHz at powers up to 100 kW were used to heat electrons in regions of cyclotron resonance in a supported and in a levitated toroidal octupole magnetic field. A theoretical model was developed to predict the heating rate of a cold, tenuous plasma in an arbitrary, nonuniform, magnetic field. The model predicts strong heating at places where $\nabla_{\parallel} B = 0$ at resonance, and heating efficiencies approaching 100% for sufficiently high densities ($\omega_p^2 > \omega^2/Q$). Scintillator probes were used to verify the predicted localized heating and to measure the density at which total absorption occurs. Gun injected plasmas and microwave-produced plasmas with $n \sim 10^9$ cm^{-3} and $kT_e \sim 5$ eV are heated to $\lesssim 1$ keV in the supported octupole and to $\lesssim 10$ keV in the levitated octupole. Upper off-resonance heating is also observed. (auth)

43335 EFFECT OF A TOROIDAL FIELD ON PLASMA TRANSPORT IN A MAGNETICALLY PERTURBED MULTIPOLE. Jernigan, T.; Rudmin, J.; Meade, D. M. (Univ. of Wisconsin, Madison). Phys. Rev. Lett.; 26: No. 21, 1298-1301(24 May 1971).

Field errors were observed to cause anomalous loss to an internal hoop and produce convection patterns that have potentials $\sim kT_e/e$. A simple model of plasma flowing along field lines accounts semiquantitatively for the observed anomalous loss and the production of convection patterns. The addition of a small (5%) toroidal field reduces the anomalous loss by a factor of 60 to the level given by classical ion-neutral diffusion across the field. (auth)

43336 EXPERIMENTS ON TOROIDAL CONFINEMENT OF HIGH-BETA PLASMAS WITH HELICAL MULTIPOLE FIELDS. Franzel, Ruediger (Max-Planck-Institut fuer Plasmaphysik, Garching, Ger.). Z. Phys.; 245: No. 2, 174-83(1971). (In German).

Helical multipole fields with multiplicities of 1 to 3 and up to 16 field cycles around the circumference of the torus are superposed on a toroidal theta pinch. The vacuum fields of the configurations are calculated and regions of closed flux surfaces are found. The experimental results are: (1) Equilibria of high-β plasmas also exist, if the vacuum field has no absolute minimum, provided that the region of closed flux surfaces in the vacuum field has a greater diameter than the plasma and that the helical multipole fields do not periodically increase and decrease the gradient of the toroidal main field. These equilibria are possibly unstable. (2) If the helical multipole fields periodically increase and decrease the gradient of the theta-pinch field along the circumference of the torus there is no equilibrium, even if the helical curvature of the field lines is great. (3) The main cause of the losses is the escape of particles along the field lines. (auth)

43337 OPTIMIZATION PROBLEMS IN THERMONUCLEAR PLASMA CONFINEMENT. Wang, P. K. C. (Univ. of California, Los Angeles). pp 336-50 of Symposium on Optimization, Held in Nice, June 29th-July 5th, 1969. /Balakrishnan, A. V. (ed.). Berlin; Springer-Verlag (1970).

From Symposium on optimization; Nice, France (Jun-Jul 1969). See CONF-690660.

A formal development of the basic equations governing the plasma motion is given. Then, various physical meaningful mathematical formulations of the confinement problem are discussed. Specific results in the form of necessary conditions for optimality are obtained for the cases where confinement is achieved by using (a) a spatially uniform time-varying magnetic field and (b) a spatially uniform time-varying electric field in the presence of a strong static magnetic field. The restriction to spatially uniform confining fields is motivated from the difficulties in the physical realization of nonuniform time-varying electromagnetic fields. (M.O.W.)

Diagnostics

Refer also to abstract 43402.

43338 (AD-715265) MEASUREMENT OF THE RF MAGNETIC FIELD DISTRIBUTION IN A THERMAL INDUCTION PLASMA. Eckert, Hans U. (Aerospace Corp., El Segundo, Calif.). 30 Oct 1970. Contract F04701-70-C-0059. 26p. (TR-59(9220-02)-2; SAMSO-TR-70-396). NTIS.

The radial distribution of the rf magnetic field is measured with a water-cooled search coil of 3-mm diam in the midsection of an argon induction plasma flame maintained at 2.6 MHz in a 150-mm-wide tube. Over most of the flame section, the field is reduced to ~0.5 A/cm. The skin depth is about 1 cm. In the annular space between the flame and the inductor coil, the field is increased by 10%. The resultant magnetic pressure gradients may cause a substantial radial flow of plasma toward the axis. The effects of signal averaging, current obstruction, and plasma cooling by the probe are discussed and found to be of minor consequence. (auth) (USGRDR)

43339 (IYAF-7-70) STUDIES OF PLASMA TURBULENCE BY MEANS OF CHARGED PARTICLE BEAM. Koidan, V. S.; Ponomarenko, A. G.; Rogozin, A. I.; Kyutov, D. D. (Akademiya Nauk SSSR, Novosibirsk. Institut Yadernoi Fiziki). 1970. 22p. (In Russian). Dep. NTIS (U. S. Sales Only).

Calculations were carried out on the interaction of a beam of charged particles with the turbulent oscillations of a plasma, and it was found that for given conditions there may be observed both spatial broadening and spread of the particles of the beam longitudinally according to energy after passage through the turbulent plasma. A relationship was obtained that links the energy density of the turbulent oscillations with the amount of beam broadening and its energy dispersal. An experiment is described for probing the turbulent plasma of a direct discharge with a 50-kV proton beam. The radial broadening of the beam is detected as that associated with ion beam scattering by turbulent plasma oscillations. The amount of beam broadening is determined by the energy density of the oscillating plasma. The possibility of applying this method to the investigation of a turbulent plasma is discussed. (tr-auth)

43340 (N-71-17594) ION-CURRENT RESPONSE OF LANGMUIR PROBES IN THE PRESENCE OF ION-ATOM COLLISIONS. Szuszczewicz, Edward P. (National Aeronautics and Space Administration, Greenbelt, Md. Goddard Space Flight Center). Jan 1971. 13p. (NASA-TM-X-65445; X-625-71-34). NTIS.

A previous analysis of the Langmuir-probe experiments is extended to present a more quantitative description of the effects of ion-atom collisions on the ion saturation current of a probe characteristic. The experiments were conducted with cylindrical probes of length-to-diameter ratios in the range $30 < l/d < 120$. The probes were studied in a weakly ionized argon plasma. The experimental results show that the ion-saturation current is an increasing function of the ratio of the ion-atom mean free path to the probe radius. The level at a ratio value of 4 approximately

XUM

equal 50% of that observed in the collision-free limit, and the absolute collision-free behavior is not achieved until the ratio is approximately 400. A comparison of experimental results with approximate theoretical analysis shows good agreement. (auth) (STAR)

43341 MEASUREMENT OF ION TEMPERATURE IN A SHORT-LIVED PLASMA BY MEANS OF A MULTICHANNEL FABRAY–PEROT INTERFEROMETER. Berney, A. (Centre de Recherches en Physique des Plasmas, Lausanne, Switzerland). Helv. Phys. Acta; 44: No. 2, 213-37(1 Apr 1971). (In French).

Ion temperature measurements made by means of Doppler line broadening in a rotating magnetic field pinch experiment are described. A 12-channel Fabry–Perot interferometer was constructed and profiles of various helium and impurity lines were measured as functions of time and position in the discharge tube. The theoretical standard deviation of the results was computed by a statistical analysis using a Monte Carlo simulation program. This allowed one to separate the real variations of the plasma from the fluctuations of the measurements. The main limitations of the accuracy of the results were due to lack of light intensity and parasitic broadening mechanisms (Stark and reabsorption effects). Nevertheless, reasonable values of the temperatures of ionized nitrogen, oxygen, and helium were obtained for three different filling pressures (20, 60, and 180 mtorr He). (auth)

43342 LANGMUIR PROBE AND MICROWAVE MEASUREMENTS OF THE PROPERTIES OF STREAMING PLASMAS GENERATED BY FOCUSED LASER PULSES. Koopman, David W. (Univ. of Maryland, College Park). Phys. Fluids; 14: No. 8, 1707-16(Aug 1971).

Measurements were made on density, velocity, electron temperature, and ion temperature in streaming plasmas generated by allowing the high-density, high-temperature material formed by a Q-switched laser pulse focused on a solid target to expand into vacuum. Langmuir probe and Lecher-wire microwave systems for this application were developed and their reliable operation was verified. Typical conditions at distances 15 to 50 cm from the target are found to be: $T_e \simeq 1$ to 12 eV, $n_e = \Sigma n_i Z_i \simeq 10^{10}$ to $10^{12}/cm^3$, $T_i < 10$ eV, peak flow velocity $U \simeq 10$ to 20 cm/μsec, the exact values depending on target materials, laser power, and position. Photoionization and charge exchange in a low-density background gas were observed. (auth)

43343 MULTICHANNEL SYSTEM FOR DETERMINATION OF TIME-VARYING SPECTRAL LINE PROFILES. Okazaki, Kiyohiko; Ando, Kozo; Mori, Kazuo; Okamoto, Kosuke (Inst. of Physical and Chemical Research, Tokyo). Jap. J. Appl. Phys.; 10: No. 7, 886-90(Jul 1971).

An instrument that can display time-resolved profiles of a spectral line emitted from a transient plasma directly on an oscilloscope is discussed. It has 17 closely spaced optical channels, and the wavelength coverage between the outermost channels can be varied from 10.4 to about 0.8Å by the proper choice of a grating and a magnifying cylindrical lens. Profile measurements can automatically be repeated with time resolution from 0.1 to 2 μsec. The display of these time-resolved line profiles is accomplished by means of electronic circuit. An application to a transient plasma is shown as an example. (auth)

43344 OBSERVATION OF ASYMMETRY OF THE DISTRIBUTION OF TURBULENT ELECTRIC FIELDS IN A DIRECT-DISCHARGE PLASMA BY MEANS OF THE POLARIZATION IN THE STARK PROFILE OF THE Hα LINE. Zavoiskii, E. K.; Kalinin, Yu. G.; Skoryupin, V. A.; Shapkin, V. V.; Sholin, G. V. JETP Lett. (USSR) (Engl. Transl.); 13: No. 1, 12-14(5 Jan 1971).

Translated from Zh. Eksp. Teor. Fiz., Pis'ma Red.; 13: No. 1, 19-23(5 Jan 1971).

The existence of anisotropy of the spectrum of ion acoustic oscillations in a direct discharge was established, and its magnitude was measured. To measure the degree of asymmetry, a new method based on the polarization in the Stark profile of the Hα line was used. The data are discussed. (M.O.W.)

43345 DEVICE FOR DIAGNOSTICS OF PLASMA. Vaganov, R. B.; Meriakri, V. V. (to Inst. of Radio Engineering and Electronics). Russian Patent 204,393. 22 Jun 1970. Filed 18 Mar 1965. (In Russian).

A device is described for diagnostics of plasma with the aid of a microwave quasi-optical beam formed by lenses, which contains an analyzer consisting of a receiving waveguide, transitional section, a matching adapter, and a number of microwave radiation detectors. The microwave radiation detectors are made in the form of directional couplers, each of which is tuned to one wave of higher order. (JPRS)

Kinetics (General)

Refer also to abstracts 43023 and 43756.

43346 (JINR–P9-5753) SOME SPECIFIC FEATURES OF THE COLD CATHODE OPERATING AT LOW PRESSURES. Dolbilov, G. V.; Sarantsev, V. P.; Sumbaev, A. P. (Joint Inst. for Nuclear Research, Dubna (USSR)). 1971. 24p. (In Russian). Dep. NTIS (U. S. Sales Only).

The conditions of forming an intense gas-focusing electron beam from the cold cathode at pressures of 10^{-3} to 10^{-2} torr are investigated. The behavior of the beam near the metal surfaces is examined. The energetic structure of the current carriers is studied by the method of corpuscular diagnostics. (auth)

43347 COLLISIONLESS SHOCKS IN PLASMAS. Friedman, Herbert W.; Linson, Lewis M.; Patrick, Richard M.; Petschek, Harry E. (Avco Everett Research Lab., Everett, Mass.). Annu. Rev. Fluid Mech.; 3: 63-88(1971).

The current state of experimental and theoretical understanding of the structure of collisionless shocks is reviewed. Theoretical discussions are included on nonlinear wave theory, anomalous dissipation in a collisionless plasma, and critical Mach numbers. A brief description is given of the principal laboratory experiments and their limitations. (80 references) (M.O.W.)

43348 GAS DYNAMICS OF EXPLOSIONS. Korobeinikov, V. P. (Mathematical Inst., Moscow). Annu. Rev. Fluid Mech.; 3: 317-46(1971).

The theory of explosions includes two main topics: (a) the propagation of blast waves in unbounded media; (b) the interaction of blast waves with different obstacles and shocks. The problems of reflection and diffraction of shock waves are not considered. (78 references) (M.O.W.)

43349 ATOMNYE STOLKNOVENIYA I ELEMENTARNYE PROTSESSY V PLAZME. (Atomic Collisions and Elementary Processes in Plasma). Smirnov, B. M. Moscow; Atomizdat (1968). 364p.

The elemental processes that occur in plasmas of gas discharges, lasers, magnetohydrodynamic generators, thermionic converters, and in the upper layers of the atmosphere, were investigated. Elastic and inelastic collisions of electrons with atoms and molecules were studied in particular. The properties of negative ions and the processes that occur upon their collision with atoms are described. Auto-ionization states and recombination processes are also discussed. (tr-auth)

43350 CONVERGING-BARREL PLASMA ACCELERATOR. Cheng, Dah Yu. (to National Aeronautics and Space Administration). U. S. Patent 3,579,028. 18 May 1971. Filed 23 Oct 1968.

A device is described for generating and accelerating plasma to extremely high velocity, while focusing the plasma to a decreasing cross section for attaining a very dense high-velocity plasma burst capable of causing nuclear fusion reactions. A converging,coaxial accelerator–electrode configuration is employed with "high-pressure" gas injection in controlled amounts to achieve acceleration by deflagration and focusing by the shaped electromagnetic fields. (auth)

43351 INVESTIGATION OF AN INDUCTIVE PLASMA ACCELERATOR FOR PROPULSION PURPOSES. Stampa, A.; Bieger, W.; Richter, F.; Tuczek, H. (Kernforschungsanlage, Juelich, Ger.). pp 311-17 of Prospect for the Use of Orbital Stations and Space Shuttles in the Next Ten Years. Rome; XVIII Rassegna Internazionale Elettronica e Nucleare (1971).

From eleventh international technical and scientific conference on space; Rome, Italy (1 Apr 1971). See CONF-710430.

A traveling wave plasma accelerator is described. Its potentialities to lead to a high-thrust high-specific impulse thruster has been demonstrated. Experiments show that the physics of the device may be much more complicated than expected by simple theory. Typical plasma effects e.g., the development of a micro-instability, are observed. By careful choice of the initial conditions, however, it is possible to obtain effective plasma acceleration. The measured thrust ranges between 3 and 30 newton, the exhaust velocity between 3×10^6 and 4×10^7 cm/s. (auth)

Kinetics (Experimental)

43352 (AD–715272) IONIZATIONAL AND THERMAL NON-EQUILIBRIUM IN MHD BOUNDARY LAYERS. Final Report, July 1, 1968–June 30, 1969. Cott, Donald W. (Arnold Engineering Development Center, Arnold Air Force Station, Tenn.

ARO, Inc., Arnold Air Force Station, Tenn.). Nov 1970. Contract F40600-70-C-0002. 71p. (AEDC-TR-70-231; ARO-PWT-TR-70-155). NTIS.

The effects of thermal nonequilibrium (elevated electron temperature) and ionizational nonequilibrium (finite-rate recombination) are studied in the insulator boundary layer of a potassium-seeded nitrogen MHD accelerator flow. The nonsimilar, compressible boundary layer is assumed steady, laminar, and two-dimensional. A collisionless sheath is assumed and matched with the boundary layer equations, which are solved numerically for a core-flow Hall-neutralized Faraday accelerator. The relative importance of the various terms in the electron energy equation is assessed, and the overall effect of the nonequilibrium phenomena on the boundary-layer parameters is described. It is concluded that thermal nonequilibrium can lead to significant B-wall shorting in long channels and that Hall effects should not be neglected but that operation is not noticeably affected by ionizational nonequilibrium or the physics of the electrostatic sheath. (auth) (USGRDR)

43353 (N-71-19984) CATHODE REGION OF A QUASI-STEADY MAGNETOPLASMADYNAMIC ARCJET. SUPPLEMENT 8. Turchi, Peter J.; Jahn, R. G. (Princeton Univ., N. J. Guggenheim Labs. for the Aerospace Propulsion Sciences). Oct 1970. 151p. (NASA-CR-117040). NTIS.

A magnetoplasmadynamic discharge is examined near the cathode of a 2.5-MW, quasi-steady, self-field arcjet. High-speed photography shows a concentration of arc luminosity in the cathode region, while detailed measurements with electric and magnetic field probes indicate that 85% of the total arc power is deposited within one base diameter of the cathode surface. Ion energies are shown to be proportional to the voltage drop in the cathode region even though current conduction is accomplished primarily by electrons in a tensor manner. It is found that a high-speed plasma flow is delivered to the cathode where it is converted into a useful exhaust jet in a thin, high-density layer at the cathode surface. Local measurements of electron temperature and estimates of electron density, made within the discharge and exhaust jet using a twin Langmuir probe technique, indicate a nearly uniform electron temperature of about 1.5 eV throughout the quasi-steady arcjet flow. (auth) (STAR)

43354 RADIATION TEMPERATURE OF A BOUNDED NON-THERMAL PLASMA. II. EXPERIMENT. Wright, B. L.; Bekefi, G. (Massachusetts Inst. of Tech., Cambridge). Phys. Fluids; 14: No. 8, 1773-81(Aug 1971).

Time-resolved measurements of the radiation temperature T_r in a weakly ionized plasma column subjected to an axial magnetic field are reported. The experiments are made at frequencies near the electron cyclotron frequency during and in the early afterglow of a pulsed argon discharge. The observed departures of T_r from the kinetic temperature are used in the determination of the distribution of electron velocities f(v). A comparison of the steady-state distribution with computations based on an appropriate kinetic model shows good agreement and establishes the validity of this experimental method of measuring f(v). In addition, the measured time dependence of f(v) allows the inference of the rates of electron-atom cooling and electron-electron relaxation during the early afterglow of the pulsed discharge. (auth)

43355 INTERACTION OF A HELIUM PLASMA WITH AN INHOMOGENEOUS TRANSVERSE MAGNETIC FIELD. Markovic, P. D.; Scott, F. R. (Univ. of Tennessee, Knoxville). Phys. Fluids; 14: No. 8, 1742-7(Aug 1971).

A dynamic helium plasma, produced by a conical z-pinch gun, was used to study interactions with an inhomogeneous transverse magnetic field. Magnetic probe measurements show that, up to a critical value of the field B_c, the plasma penetrates the region occupied by the field by completely removing it. An increase in the plasma electron temperature and density is seen. For fields higher than the critical value B_c, plasma penetrates in the form of thin sheets oriented along the magnetic field lines. The observed effects are compatible with the available theory if resistive effects are taken into account. (auth)

43356 STRUCTURE OF THE PLASMA BOUNDARY LAYER AT A CONDUCTING SPHERE. Ekbote, D. D.; Schott, L. (Univ. of Saskatchewan, Saskatoon). Phys. Fluids; 14: No. 8, 1695-1701(Aug 1971).

The spatial distributions of the ion density and the space potential in the boundary layer at a conducting sphere of 2.5-cm radius were measured with a small movable cylindrical probe. The measured density distributions are in good agreement with the theory of Lam in the collisionless case and with the diffusion model in the collision-dominated limit. The existence of a near-Boltzmann distribution of the electrons in the collisionless quasineutral layer is demonstrated by a plot of the logarithm of the ion density versus space potential. The electron temperature obtained from this plot, from the floating potential of the sphere, and from the characteristic of the small probe differ from each other by at most 12%. A new method to detect deviations from the Boltzmann distribution in the transitional layer is tested. The ion densities measured by using the sphere as a probe agree within 13% with those obtained with the small cylindrical probe in the collisionless case. (auth)

43357 POLARIZATION OF THE FREE-FREE BREMSSTRAHLUNG IN AN ANISOTROPIC HOT-ELECTRON PLASMA. Greene, D. G. S.; Shohet, J. L.; Raimbault, P. A. (Univ. of Wisconsin, Madison). Phys. Rev. Lett.; 27: No. 2, 90-2 (12 Jul 1971).

The polarization of the free-free bremsstrahlung emitted radially for an anisotropic hot-electron plasma in a magnetic mirror was measured by means of Compton scattering. The degree of polarization was found to be exceptionally sensitive to changes in system parameters. A quantum-mechanical nonrelativistic theory was found to agree well with the experimental results. (auth)

43358 PLASMA ACCELERATION UNDER VARIOUS OPERATING CONDITIONS IN A PULSED COAXIAL PLASMA ACCELERATOR. Kalmykov, A. A.; Timofeev, A. D.; Shevchuk, B. A. Sov. Phys.-Tech. Phys. (Engl. Transl.); 15: No. 12, 2002-19 (Jun 1971).

Translated from Zh. Tekh. Fiz.; 40: No. 12, 2553-62(Dec 1970).

The features of plasma acceleration under various operating conditions in a pulsed coaxial accelerator are discussed. It is shown that an important characteristic of the accelerator operation is the gas-pressure distribution along the system, which governs the slow and fast regimes of accelerator operation. The slow regime is characterized by a current sheath and by gas combustion. In the fast regime, most of the plasma acceleration occurs in the density gradient as the current front leaves the gas. (auth)

43359 INTERACTION OF A STREAMING PLASMA WITH A MAGNETIC MIRROR. Kramer, William Robert. Pittsburgh; Carnegie-Mellon Univ. (1970). 134p. University Microfilms Order No. 71-16,472.

Thesis.

The interaction between a supersonically streaming plasma and a spatially increasing longitudinal magnetic field was investigated experimentally. The object of the experiment was to obtain qualitative and quantitative data on this interaction and in particular, the transition from supersonic to subsonic flow and the attendant shock wave formation. It was shown that for distances in excess of 20 inches from the gun, where the plasma beam is formed, to the peak of the mirror field and for values of peak mirror field exceeding 3 kilogauss, a supersonic-subsonic flow transition does occur and a shock wave is formed. The helium plasma was produced by a conical theta pinch gun driven by a capacitor bank with a stored energy of 2.5 kilojoules. The density range is 10^{14} to 2×10^{15} particles per cubic centimeter. Parallel electron temperatures range from 3 to 30 electron volts while transverse temperatures range from 3 to 10 electron volts. The streaming velocity ranges from 0.1 to 3×10^5 meters per second with Mach numbers from 0.8 to 20. Beta ranges from 0.01 to 0.3. The experimental results are compared to and found in good agreement with an existing theory which predicts the parameter values for the formation of a shock wave. (Diss. Abstr. Int., B)

Kinetics (Theoretical)

43360 (CU-3954-9) NUMERICAL SIMULATION OF STRONG PLASMA SHOCK WAVES PRODUCED IN AN ELECTROMAGNETIC SHOCK TUBE. Report No. 55. Schneider, Stephen Henry (Columbia Univ., New York. Plasma Lab.). 1971. Contract AT(30-1)-3954. 112p. Dep. NTIS.

Thesis.

Two different continuum fluid models were used to study numerically plasma shock-wave formation and structure in an electromagnetic shock tube. Magnetohydrodynamic equations with numerical dissipation were first used to study qualitatively the important effects of diffusion and dissipation. Considerable physical insight was gained, particularly concerning the early-time evolution of the shock and its separation from the drive-current layer. A set of two-fluid Navier-Stokes equations with physical transport coefficients was then used to compute the detailed evolution and structure of these waves in a strong transverse bias magnetic field. The field significantly reduces the thermal conductivity so that the upstream diffusion of electron temperature is entirely suppressed. The whole structure is different from that of a two-fluid gasdynamic shock without transverse magnetic field. Espe-

XUM

cially significant is the effect of the small ion Larmor radius in reducing the gasdynamic shock thickness by at least an order of magnitude in the transverse shock, which permits collisional shocks with thickness much smaller than a mean free path to be produced in a laboratory-sized device. (auth)

43361 (N-71-12679) NONEQUILIBRIUM PLASMA BOUNDARY LAYER OVER A CATHODE. Seals, Robert Kincaid Jr. (North Carolina State Univ., Raleigh. Dept. of Mechanical and Aerospace Engineering). 1970. 68p. (NASA-CR-111611). NTIS.
Thesis.

An analysis of the nonequilibrium plasma boundary layer over a cathode in the presence of a magnetic field is presented. The cases considered are those where the Debye length is less than the mean free paths and the Larmor radii and where the thermal and nonequilibrium effects are important. The solution is obtained by matching the sheath solution and the solution of the conservation equations of the plasma constituents. The transport properties for a partially ionized gas in the presence of nonequilibrium ionization and magnetic fields are obtained from appropriate equations derived by the thirteen-moment method. Local similarity is assumed, and the problem is solved numerically, using an integral method on an IBM Model 360-75 digital computer. Results are presented for a range of values of magnetic fields and axial distance and for two values of wall temperature. The results indicate that the heat flux at the wall, the current density, and the electron temperature all tend to increase with increasing magnetic induction. (auth) (STAR)

43362 (N-71-18715) EXTENSION OF FROST'S MIXTURE RULE TO INCLUDE THE EFFECTS OF MULTIPLE IONIZATION ON ELECTRICAL CONDUCTIVITY: APPLICATION TO EQUILIBRIUM AIR AT 3000 TO 28000 K. Viegas, John R. (National Aeronautics and Space Administration, Moffett Field, Calif. Ames Research Center). Mar 1971. 30p. (NASA-TN-D-5977; A-3653). NTIS.

An extension of previously developed expressions for the electrical conductivity of a plasma is presented. This extension includes an accurate accounting for the effects of ionic charge in the Coulombic collision frequency and a correction factor that extends the range of temperatures and pressures. It is applied to the problem of obtaining accurate values for the electrical conductivity of equilibrium air. The temperatures and density ratios (based on standard atmospheric density) range from 3,000 to 28,000 K and 0.000001 to 100. The results, presented primarily in tabular form, include other useful plasma dynamic parameters for equilibrium air. Comparisons are also made with various other methods of calculating the electrical conductivity of air. (auth) (STAR)

43363 (NP-18805) CONDUCTIVITY AT HIGH FREQUENCIES OF A COMPLETELY IONIZED PLASMA WITH ION-ION CORRELATIONS. Alvarado, Fray de Landa Castillo (Instituto Politecnico Nacional, Mexico City. Escuela Superior de Fisica y Matematicas). 1970. 64p. (In Spanish). Dep. NTIS (U. S. Sales Only).
Thesis.

The frequency dependence on the resistance for frequencies higher than $\omega_c = 2\pi/t_D$ (where ω_c is the cyclotron frequency and t_D is the accumulated dispersion time at 90°) was studied. The approximation formulations describing the processes occurring in the plasma are discussed. The validity of the Vlasov equation for the conductivity is discussed. The Dawson-Oberman model (NSA 16: 18581) is established. The conductivity of a completely ionized plasma with ion-ion correlation is developed mathematically. The impedance is calculated analytically for the asymptotic forms. Graphs of the resistivity are presented as a function of ω/ω_p, where ω_p is the plasma frequency. (J.S.R.)

43364 PARTITION FUNCTION AND EFFECTIVE IONIZATION POTENTIAL OF AN ATOM IN A PLASMA AND POSSIBILITIES OF THEIR EXPERIMENTAL EXAMINATION. I. Guendel, H. (Zentralinstitut fuer Elektronenphysik, Berlin). Beitr. Plasmaphys.; 10: 455-67(1970). (In German).

From the behavior of term densities near the ionization boundary, the effective reduction of the ionization potential in the Saha equation as well as the atomic partition function were derived. For the calculation of density term, a statistical procedure was used that took into account microfield alterations. (tr-auth)

43365 NONLINEAR INTERACTION OF ELECTRON BEAMS WITH PLASMA. Kovtun, R. I.; Rukhadze, A. A. Radio Eng. Electron. Phys. (USSR) (Engl. Transl.); 15: No. 10, 1852-6(Oct 1970).

Translated from Radiotekh. Elektron.; 15: No. 10, 1852-6(Oct 1970).

Propagation of a finite-amplitude electrostatic wave through a plasma-beam system is discussed. A nonlinear dispersion relation is obtained which, in the limit of infinitely small amplitudes, approaches a linear dispersion relation and as such contains the well-known beam instability. The nonlinear dispersion relation contains the amplitude of vibrations and permits determination of its limiting value corresponding to the trapping of the beam by a wave and stabilizing the instability. From the stabilization condition, the energy of electrostatic oscillations in the plasma (which appear together with the beam instability) is determined. (auth)

43366 EQUATIONS OF MOTION OF PLASMA IN AXIALLY SYMMETRIC COORDINATE SYSTEM. Krzywoblocki, M. Z. E. (Michigan State Univ., East Lansing). Arch. Mech. Stosow.; 22: No. 3, 323-54(1970).

The hydrodynamic equations of motion, continuity, and energy of a moving plasma in the axially symmetric coordinate system are derived. The Maxwell equations, which constitute the second system of equations, are considered. They are treated separately, but in the functional correlation with the hydrodynamic system. The methods of solution of the resultant system of equations are outlined. (IAA)

43367 PROBLEM OF TRANSITION RADIATION FOR A PLASMA PLATE. Khachatryan, B. V.; Elbakyan, S. S. Izv. Akad. Nauk Arm. SSR, Ser. Fiz.; 5: No. 6, 409-17(1970). (In Russian).

The problem of transition radiation in a plasma plate in vacuum is solved, assuming that the reflection of plasma electrons from the plasma-vacuum boundary is a diffuse one. The limiting case of strong spatial dispersion is considered for both nonrelativistic and relativistic plasma. (auth)

43368 COMPARISON OF NUMERICAL SOLUTIONS OF THE VLASOV EQUATION WITH PARTICLE SIMULATIONS OF COLLISIONLESS PLASMAS. Denavit, J. (Naval Research Lab., Washington, D. C.). Phys. Fluids; 14: No. 8, 1782-91(Aug 1971).

Numerical solutions of the Vlasov and Poisson equations for several physically significant problems are presented and compared with the results of particle simulations. The numerical solutions of the Vlasov equation are based on the Fourier-Fourier transform method. The spatial representation includes up to 85 modes and is capable of representing strong nonlinear effects. The particle simulations are based on a multipole expansion of finite-size particles about their nearest grid point location. Special techniques are used to suppress the noise and to accurately control the initial conditions of the plasmas so that quantitative comparisons with Vlasov solutions can be made. Close quantitative agreement between the results of the two simulation techniques is observed. The problems considered are one-dimensional, with periodic boundary conditions, and involve (1) two-stream instabilities, with equal and unequal electron beams, and (2) large-amplitude electron oscillations, with sideband instabilities. (auth)

43369 SIMULATION OF PSEUDOWAVES AND OF PLASMA SHEATH FORMATION ABOUT A GRID BY COMPUTER SOLUTION OF THE ION VLASOV EQUATION. Estabrook, K.; Widner, M.; Alexeff, I.; Jones, W. D. (Oak Ridge National Lab., Tenn). Phys. Fluids; 14: No. 8, 1792-4(Aug 1971).

The time evolution of an ion distribution function is computed in the sheath about a negatively pulsed transparent grid. The algorithm details the ion flow in the potential well when the pulse is on and the burst of ions ejected after the pulse potential is removed. (auth)

43370 DISPERSAL OF A LOCALIZED DENSITY FLUCTUATION IN A UNIFORM MAGNETOPLASMA. Greenwald, R. A.; Shea, D. W. J. (National Oceanic and Atmospheric Administration, Boulder, Colo.). Phys. Fluids; 14: No. 8, 1753-8(Aug 1971).

The dispersal of a localized density fluctuation in a uniform magnetoplasma is studied using the macroscopic fluid equations. Expressions are obtained for the Fourier-Laplace transforms of the perturbed density, potential field, and flux distributions. These expressions are inverse-transformed, using a combination of analytic and numeric techniques. The resulting curves, which display the real space and time development of the system, are then compared with magnetic-field-free ambipolar diffusion. One finds that diffusion along the magnetic field, $\theta = 0°$, is much more rapid than ambipolar diffusion, that when the ion motion is not affected by the magnetic field, diffusion at $\theta = 90°$ proceeds at approximately the ambipolar rate, and that the electron and ion fluxes are not ambipolar. (auth)

43371 RADIATION TEMPERATURE OF A BOUNDED NONTHERMAL PLASMA. I. THEORY. Wright, B. L.; Bekefi, G. (Massachusetts Inst. of Tech., Cambridge). Phys. Fluids; 14: No. 8, 1764-72(Aug 1971).

The departure of the radiation temperature T_r from the kinetic temperature of the emitting electrons can be used as a measure of the distribution of electron velocities f(v). This relationship between T_r and f(v), using the theory of fluctuations of random currents, is explored theoretically. The method is particularly suited to radiation from relatively small, bounded plasmas of laboratory size where the traditional theory of radiative transport of wave packets becomes questionable. (auth)

43372 THERMAL EXPLOSION INDUCED IN A COLLISIONLESS PLASMA BY A RELATIVISTIC ELECTRON BEAM. Altyntsev, A. T.; Es'kov, A. G.; Zolotovskii, O. A.; (and others) (Nuclear Physics Inst., Novosibirsk, USSR). JETP Lett. (USSR) (Engl. Transl.); 13: No. 4, 139-41(20 Feb 1971).

Translated from Zh. Eksp. Teor. Fiz., Pis'ma Red.; 13: No. 4, 197-201(20 Feb 1971).

A diagram is shown of results of an experimental investigation of the interaction between a relativistic electron beam and a plasma. A hydrogen plasma was produced in a cylindrical glass tube by discharging low-inductance capacitors through six surge turns surrounding the outer diameter of the tube. The quasistatic magnetic field was varied from 0 to 2.5 kOe. The main effects were determined by comparing the initial and perturbed states of the plasma and the beam parameters after passage through the plasma and through vacuum. The experiments point to the consideration that collisionless plasma can develop anomalous scattering properties with respect to a relativistic electron beam. The phenomenon has the character of a thermal explosion ($T \sim 10$ to 100 keV) followed by secondary relaxation processes such as an electronic thermal wave and rapid equalization of the heat in the entire plasma volume. (J.C.W.)

43373 STRAIGHT-LINE ORBIT APPROXIMATION IN PERIODIC SYSTEMS. Berk, H. L.; Pearlstein, L. D. (Univ. of California, Livermore). Phys. Fluids; 14: No. 8, 1810-12(Aug 1971).

It is shown that the plasma response function, in a system whose particle orbits are periodic, is accurately approximated by the infinite medium response function for real frequencies when the bounce time is sufficiently spread. (auth)

43374 DIFFUSION OF PLASMA IN A TOROIDAL STELLARATOR. Galeev, A. A.; Sagdeev, R. Z.; Fyurs, G. P. Zh. Prikl. Mekh. Tekh. Fiz.; No. 6, 3-12(Nov-Dec 1968). (In Russian).

Particle trajectories in a small toroidal stellarator were studied. The particle distribution function was determined in the absence of collisions. In magnetic traps with rotational transformation the magnetic field lines of force form surfaces. The trajectories of plasma-drift particles in such traps, as a rule, form essentially magnetic surfaces. However, the particle drift surfaces, which move with small velocities along the lines of force, can display rather strong divergences from magnetic surfaces. This mixing can lead to an essential increase of particle streams and heat. The streams were found for the case of toroidal systems with axial symmetry [Zh. Eksp. Teoret. Fiz., 53: No. 7(1967)]. Toroidal stellarators do not possess axial symmetry. The particle orbits, which develop rather complex precession in such traps, can still be rather far removed from magnetic surfaces. Here are the most critical particles with low longitudinal velocities, especially particles restrained in their movement along the minimum lines of force in the magnetic field. The picture of such a particle movement is very confused because of the fact that they are in a field, which is the superposition of two potential dips, the first connected with the toroidal system (as axially asymmetric case), and the second emerging from the helical magnetic field. The limiting case of small toroidal stellarators was studied where it is possible to find the integrals of drift equations of particle motion. By this, the particle distribution function is automatically known in the absence of collisions. The collision influence is then considered according to perturbation theory. (tr-auth)

43375 IMPEDANCES OF WARM PLASMAS NEAR THE LOWER HYBRID RESONANCE. Babu, R.; Schlueter, H. (Ruhr Univ., Bochum, Ger.). Z. Naturforsch.; 26a: No. 5, 856-63 (May 1971).

With full electromagnetic treatment, electron pressure effects are included in the calculation of plasma impedances and power transfer to a plasma cylinder in the domain of the lower hybrid resonance. The general results are applied to cases of interest in radio-frequency discharges with azimuthally symmetric excitation and zero coil plasma-gap. For these specific situations the effects of electron pressure are found to be small. (auth)

43376 KINETIC THEORY OF FULLY IONIZED PLASMAS. I. THE KINETIC REGIME. Diener, Gerhard (Technische Univ., Dresden). Beitr. Plasmaphys.; 9: 405-24(1969).

The Bogolyubov method for the solution of the BBGKY hierarchy is generalized for plasma in such a way that oscillations are included. Thus, the method becomes applicable for unstable, weakly stable, and weakly inhomogenous plasmas. All entities describing the properties of plasmas are taken as functional single-particle distributions and as amplitudes of plasma oscillations. Oscillations with defined phase (coherent) and those with statistically distributed phase (incoherent) are considered separately. By means of the Vlasov equation, the method is first explained and then applied to the BBGKY hierarchy. (tr-auth)

43377 METHOD OF NORMAL MODES FOR VLASOV–BGK EQUATIONS. Vojta, G. (Arbeitsstelle fuer Statistiche Physik, Leipzig); Mocker, M. Ann. Phys. (Leipzig); 25: No. 2, 168-78 (1970). (In German).

The linearized Vlasov equation with collision damping is solved by the method of normal modes of Van Kampen and Case. The system considered is an infinitely extended nonrelativistic nondegenerate electron gas with neutralizing ion background and neutral particles. There is no magnetic field. Collision damping is taken into account by complete Bhatnagar–Gross–Krook collision integrals for electron–electron collisions and electron–ion collisions; in the case of a partially ionized gas, elastic collisions between electrons and neutrals can be included likewise. The Vlasov–BGK operator is transformed into an integral operator yielding complex singular normal modes even if the equilibrium distribution is Maxwellian. The adjoint integral equation belongs to a more complicated type than that of a collision-free system. Its solutions must be orthogonalized. The set of all normal modes is complete rendering the exact solution of the initial-value problem possible. The completeness is shown by transformations and regularization of the singular integral equation of the initial-value problem, the techniques of Case not being applicable because of the complicated type of this equation. (auth)

43378 KINETIC DESCRIPTION OF PLASMA CONFIGURATIONS. Korshakov, N. G. Sov. Phys.-Tech. Phys. (Engl. Transl.); 15: No. 12, 1960-5(Jun 1971).

Translated from Zh. Tekh. Fiz.; 40: No. 12, 2498-2506(Dec 1970).

A system of ordinary differential equations describing the structure of a plane sheath between a Maxwellian plasma and a magnetic field, and the equilibrium of a cylindrical plasma column in an axial magnetic field are obtained in the kinetic self-consistent field approximation on the basis of the Vlasov–Maxwell equations. The distributions of the characteristic sheath parameters over the entire sheath width were calculated on a computer and analyzed. Asymptotic solutions are given. (auth)

43379 EXACT SOLUTIONS FOR A TENUOUS PLASMA IN A MAGNETIC FIELD. Veselovskii, I. S. Sov. Phys.-Tech. Phys. (Engl. Transl.); 15: No. 12, 1966-9(Jun 1971).

Translated from Zh. Tekh. Fiz.; 40: No. 12, 2507-12(Dec 1970).

The existence of one-dimensional equilibrium configurations in a tenuous plasma with a magnetic field is discussed. A steady-state isothermal discontinuity cannot exist in a Maxwell–Boltzmann plasma with a magnetic field. The system of Vlasov equations reduces to two second-order, nonlinear, ordinary differential equations. A periodic solution of these equations is found for interpenetrating plasma streams in a magnetic field. (auth)

Production

Refer also to abstract 43192.

43380 (IPP-4/9) SURVEY OF STUDIES OF LASER PRODUCED PLASMAS AT THE IPP GARCHING. Sigel, R.; Witkowski, S.; Baumhacker, H.; Buechl, K.; Eidmann, K.; Hora, H.; Mennicke, H.; Mulser, P.; Pfirsch, D.; Salzmann, H. (Institut fuer Plasmaphysik, G.m.b.H., Garching (West Germany)). Jan 1971. 26p. Dep. NTIS (U. S. Sales Only).

A status report as of November 1970 on experimental and theoretical studies of laser-produced plasmas at the IPP is given. Experimental investigations of plasma production by nanosecond laser pulses from targets of solid hydrogen and deuterium, of Raman scattering from these materials, and of plasma production by picosecond laser pulses are described. The theoretical part comprises numerical studies of the expansion of a two-temperature plasma ($T_e \neq T_i$) and of a multicomponent plasma and also calculations of the fusion rate of an inertially confined plasma. (auth)

43381 (LGI-68/16) CONTRIBUTION TO THE STUDY OF DENSE PLASMAS. Haegi, Marcel (Comitato Nazionale per

XUM

l'Energia Nucleare, Frascati (Italy). Laboratorio Gas Ionizzati). 1968. 118p. (In French). Dep. CFSTI (U. S. Sales Only).

Thesis. Submitted to Univ. of Geneva, Switzerland.

This thesis is divided into two main parts, the first part including an introductory chapter that discusses the basic fusion reactions and processes. The second chapter of Part I includes discussions of dense and slightly dense plasmas; filled and hollow pinches; and zero-energy criteria with and without confinement. Part II also includes two chapters, the first chapter dealing with machines for dense plasma and including: peripheral injection of powders; peripheral volatilization of exploding wires; peripheral injection with hypersonic jets; peripheral injection at Mach ≥ 1; initial confinement of gas by the thermal gradient; cylindrical and spherical cases of filled pinches of heavy gas with supersonic central injection of deuterium; and Filippov and Mather focuses. The second chapter of Part II first discusses compression of a hypersonic jet of deuterium and describes the experimental setup; then experimental results are given that include electrical measurements, plasma images, time resolution of x rays, neutron measurements, and parameters and properties of plasmoids; finally, a model for plasmoids is given. 71 references. (L.M.T.)

43382 IGNITING AID FOR HIGH-EFFICIENCY PLASMA PRODUCERS. Pater, Maximilian (to Gebr. Bohler and Co.). U. S. Patent 3,579,027. 18 May 1971. Priority date 3 Mar 1967, Austria.

An ignition device is described for high-efficiency plasma producers. The device precludes the necessity for extremely high voltages to produce the initial ignition of the plasma producer by providing high specific ionic densities between the electrodes. The ignition device consists of an annular passage surrounding a rod electrode and through which ionizable gas is passed. The cylindrical wall that defines the outer periphery of the annulus continues axially beyond the end of the rod electrode to form a first tubular passage. A further cylindrical wall forms a second larger-diametered tubular passage beyond the first tubular passage. An arc is struck between the rod electrode and the cylindrical wall forming the second tubular passage, the arc having electric lines of force in the form of a cone with the apex pointing upstream the direction of the flow of the ionizable gas. The cone-shaped arc has an azimuthal magnetic field on the inside and outside thereof, and as the gas goes through the arc it is partially ionized and the opposite charge carriers are radially separated by the azimuthal magnetic field. By virtue of the separation, there is less tendency for the opposite charge carriers to recombine, and consequently there is a higher specific ionic density when the gas is introduced between the electrodes of the high-efficiency plasma producer. (auth)

43383 ACCELERATION OF IONS OF CATHODE MATERIAL IN VACUUM BREAKDOWN. Korop, E. D.; Plyutto, A. A. Sov. Phys.-Tech. Phys. (Engl. Transl.); 15: No. 12, 1986-9(Jun 1971).

Translated from Zh. Tekh. Fiz.; 40: No. 12, 2534-7(Dec 1970).

The process by which ions of cathode materials are accelerated in the pulsed breakdown of a vacuum gap 1 to 2 cm in length is described. In the high-voltage stage the ions are accelerated towards the anode at times that coincide with sharp bursts of electron current. This is accompanied by constriction of the electron beam towards the axis with resulting current densities of approximately 10 kA/cm^2. The maximum ion energies reach 10 to 15 MeV for a breakdown voltage of 300 kV. Conclusions are drawn as to the various current flow and ion acceleration processes in vacuum breakdown and in the formation of electron beams from plasma emitters under unstable conditions. (auth)

Stability

Refer also to abstract 43244.

43384 (CTO-759) POSSIBILITY OF SUPPRESSING SCREW MODES OF HYDROMAGNETIC INSTABILITY OF A PLASMA COLUMN CARRYING A CURRENT, BY MEANS OF A FEEDBACK SYSTEM. Arsenin, V. V. Translated by J. B. Sykes (Culham Lab., Abingdon, Eng.), from At. Energ. (USSR); 28: 141-2(1970). 6p. Dep. NTIS (U. S. Sales Only).

An abstract of this paper, prepared from the original language, appeared as NSA 25: 7400. (M.O.W.)

43385 (N-71-12892) INSTABILITIES AND TURBULENCE IN HIGHLY IONIZED PLASMAS IN A MAGNETIC FIELD. Semiannual Status Report, March 1-August 31, 1970. Noon, J. H.; Huchital, G.; Jennings, W. C. (Rensselaer Polytechnic Inst., Troy, N. Y. Plasma Dynamics Lab.). Oct 1970. 40p. (NASA-CR-111514; TR-70-2). NTIS.

Correlation studies show that some degree of coherence exists throughout the whole of the observed plasma turbulence spectrum, although time and length scales of coherence decrease markedly with increasing frequency. Propagation characteristics and energy-dissipation mechanisms of these turbulent eddies are being investigated. The growth of a strongly coherent drift wave instability is associated with an increase in amplitude of the high-frequency end of the turbulence spectrum. On the other hand, growth of another type of coherent oscillation (an ion acoustic wave) reduces the amplitude of the turbulent spectrum, but only in the frequency regions adjacent to that of the strong coherent oscillation. (auth) (STAR)

43386 (ORNL-tr-2434) NONLINEAR STAGE OF HYDROMAGNETIC CURRENT INSTABILITY OF PLASMA IN A STRONG ELECTRICAL FIELD. Sizonenko, V. L.; Stepanov, K. H. ([Akademiya Nauk Ukrainskoi SSR, Kharkov. Fiziko-Tekhnicheskii Institut]). Translated for Oak Ridge National Lab., Tenn., from report KHFTI-70-45. 24p. Dep. NTIS.

The development of hydromagnetic "Bunemanovsk" current instability of plasma in a strong electrical field $\vec{E}_0$, in which electrons acquire a velocity u_e significantly greater than their thermal velocity v_{te}, is studied. The electrical field is assumed to be more powerful than a Dreiser field and a certain critical field $E_0 > E_{Dr} = me/e\, v_{re}\nu_c$, $E_0 > E_{Cr} = me/e\, v_{te}\omega_{pi}$, where ν_c is the frequency of Coulomb collisions, and ω_{pi} is the ionic Langmuir frequency. The yield for the nonlinear stage of current instability in the one-dimensional case is examined when the electrons move only along the external magnetic field $\vec{H}_0$ parallel to $\vec{E}_0$. (M.O.W.)

43387 PLASMONS AND THE LINEAR AND NONLINEAR TWO-STREAM INSTABILITIES. Fukai, J. (Univ. of Tennessee, Knoxville); Harris, E. G. Phys. Fluids; 14: No. 8, 1748-52(Aug 1971).

For an infinite cold plasma consisting of several species in relative motion, a Hamiltonian is derived in terms of creation and annihilation operators for plasmons. From a quantum-mechanical point of view, the two-stream instability may be described as the creation of pairs of plasmons, one with positive and the other with negative energy. The Hamiltonian derived includes both the linear and nonlinear interactions. In order to discuss the nonlinear instability a canonical (Bogolyubov) transformation is performed to diagonalize the linear part of the Hamiltonian. It is shown that the nonlinear interactions may cause the explosive instabilities, even though the plasma is stable for the linear instability. (auth)

43388 FINITE-β STABILIZATION OF THE COLLISIONLESS TRAPPED-PARTICLE INSTABILITY. Rosenbluth, M.; Sloan, M. L. (Inst. for Advanced Study, Princeton, N. J.). Phys. Fluids; 14: No. 8, 1725-41(Aug 1971).

A particularly dangerous mode of instability in confined plasmas is the trapped-particle mode, which is highly insensitive to magnetic shear and average favorable curvature. The study of the collisionless trapped particle mode is extended to include the effects of finite $\beta = 8\pi nT/B^2$. It is found that the "magnetic well" dug by plasma diamagnetism is highly effective in stabilizing the collisionless trapped-particle mode. It is found that for magnetohydrodynamically stable systems the collisionless trapped-particle mode becomes stable when the diamagnetic well is sufficient to give all particles average favorable drift. It would appear from this result that, in general, the diamagnetic well should be an effective stabilizing agent against all nonflutelike microinstabilities. (auth)

43389 STABILIZATION OF PLASMA FILAMENTS WITH VARIABLE CURRENT BY QUADRUPOLE MAGNETIC FIELD. Nikulin, M. G. Zh. Prikl. Mekh. Tekh. Fiz.; No. 6, 20-7(Nov-Dec 1968). (In Russian).

The dynamic stabilization of straight or toroidal plasma filaments with current by a high-frequency quadrupole magnetic field was proposed by S. M. Osovets [Zh. Eksp. Teoret. Fiz., 39: No. 2, (1960)]. A more strict theoretical consideration of the question was conducted by M. L. Levin and M. S. Rabinovich [Zh. Tekh. Fiz., 33: No. 2, (1963)], where for thin filaments, undergoing long-wave perturbation of the spiral type and constriction, the Routh function was obtained, making it possible to study dynamics of filaments in different magnetic fields. The stabilization of a plasma filament was examined by means of the Levin method. A variable current proceeds along the filament and the quadrupole field is constant or is changed with high frequency. (tr-auth)

43390 TOROIDAL CONTRIBUTIONS TO THE SHEAR AND THE $j_\parallel$-KINK INSTABILITY IN THE TOKAMAK AND SCREW PINCH. Ware, A. A. (Univ. of Texas, Austin). Phys. Rev. Lett.; 26: No. 21, 1304-7(24 May 1971).

It is shown that, for a tokamak plasma with fixed boundary, the toroidal contributions to the shear are sufficiently important to modify the $j_{||}$-kink instability. Assuming that β is small and using the energy principle, δW is calculated to order $(r/R)^6$ and the toroidal corrections are shown to change the sign of the destabilizing term. One consequence is that the range of rotational transform angles for which the $m = 1$, $\nu = 1$ instability will occur, when the shear is weak, is below the Kruskal–Shafranov limit and not above it. Also, the new terms have an important stabilizing effect for the screw pinch. (auth)

43391 RADIAL DEPENDENCE OF TRAPPED-PARTICLE INSTABILITIES. Jablon, C. (CNRS, Orsay, France); Laval, G.; Pellat, R. Phys. Rev. Lett.; 27: No. 2, 83-5(12 Jul 1971).

The radial localization of trapped-particle instabilities is studied for a peaked diamagnetic-frequency profile and for a realistic profile. In the latter case it is shown that modes can be excited only with a high radial wave number. The correspondingly reduced coefficient of turbulent diffusion is computed for the collisionless instability. (auth)

43392 STABILITY OF AN INCOMPRESSIBLE EQUILIBRIUM PLASMA ELLIPSOID IN THE FIELD OF A TRAVELING ELECTROMAGNETIC WAVE. Khizhnyak, N. A.; Lysenko, O. E. Sov. Phys.-Tech. Phys. (Engl. Transl.); 15: No. 12, 2023-4(Jun 1971).

Translated from Zh. Tekh. Fiz.; 40: No. 12, 2581-2(Dec 1970).

The stability of the boundaries of the equilibrium ellipsoid against small perturbations of its surface, when immersed in hf fields, is theoretically studied. The analysis considers the stability of this configuration against the lowest deformation modes. (M.O.W.)

43393 NONLINEAR STABILIZATION OF IONIZATION WAVES. Sato, M. (Yamagata Univ., Yonezawa, Japan). Phys. Lett.; 35A: No. 6, 431-2(12 Jul 1971).

Nonlinear stabilization of self-excited ionization waves (moving striations) is observed in a column plasma. In the nonlinear regime the spatial growth rate and saturated amplitude of the waves decrease after passing their peaks. (auth)

43394 ELECTROMAGNETIC AND FINITE β_e EFFECTS ON COUNTERSTREAMING ION INSTABILITY. Wagner, C. E.; Papadopoulos, K.; Haber, I. (Naval Research Lab., Washington, D. C.). Phys. Lett.; 35A: No. 6, 440-2(12 Jul 1971).

It was found theoretically and by computer simulation that finite electron β_e simply enlarges the region of instability of ions counterstreaming across a magnetic field, while the rest of the linear and nonlinear theory remains unchanged. (auth)

43395 TRANSVERSE VELOCITY SHEAR INSTABILITIES IN A MAGNETOPLASMA COLUMN. Jassby, Daniel Lewis. Princeton, N. J.; Princeton Univ. (1970). 134p. University Microfilms Order No. 71-14,383.

Thesis.

An experimental and theoretical study was made of the transverse Kelvin–Helmholtz instability driven by nonuniform $E \times B$ rotation of a plasma column immersed in a uniform axial magnetic field and externally controlled radial electric field. Strong shear in the plasma rotation, whose magnitude is readily varied, is produced in the interior of a Q-machine plasma column (1×10^9 to 3×10^{10} cm^{-3}, 0.2 eV) with a specially developed segmented end plate heated by electron bombardment. The velocity shear layer contains up to seven ion gyroradii. Coherent low-frequency oscillations are observed localized in the region of large shear. The radial wave equation for the low-frequency transverse Kelvin–Helmholtz instability, derived from the finite-Larmor-radius fluid equations including resistive electron motion along the magnetic field, is analyzed with both quadratic forms and numerical techniques. The observed oscillations are demonstrated to be Kelvin–Helmholtz waves by the good agreement with theory for the mode frequencies, radial variation of amplitudes and phases of the potential and density fluctuations, and the multimode structure at large magnetic field and small rotation. The instability onset electric field agrees qualitatively with the results of an approximate dispersion relation obtained from the quadratic form. The mode evolution of the Kelvin–Helmholtz instability is studied as the magnitude of the electric field (directed inward) is increased. Onset occurs at $V_{EM} \sim 0.2\ V_T$, where V_T is the ion thermal velocity and V_{EM} the maximum rotation velocity. For $V_{EM} \gtrsim 0.6\ V_T$ there is a multimode spectrum peaked at the mode whose half-wavelength approximately equals the width of the velocity shear layer. When $V_{EM} \gtrsim 0.6\ V_T$ the multimode spectrum gives way to a succession of strong single modes. At large electric fields the Kelvin–Helmholtz modes are completely suppressed when the Doppler-shifted wave frequency, for the central layer of ions, is 0.5 to 0.65 times the ion cyclotron frequency, ω_c. This suppression occurs at the resonant condition for nonlinear Landau damping. Concomitant with low-frequency stabilization, there appear oscillations with $\omega \gtrsim \omega_c$. A second radial wave equation is derived for large rotation and arbitrary oscillation frequency, in which the zero-order ion polarization drift is retained. Two sets of solutions are found, the low-frequency Kelvin–Helmholtz waves, and a set of higher frequency, velocity-shear driven modes whose properties agree with the observed cyclotron oscillations. Finally, the Q-machine edge oscillation is examined in the light of the experiments in the plasma interior, and further evidence is presented that this instability is in fact of the transverse Kelvin–Helmholtz type. (Diss. Abstr. Int., B)

Thermonuclear Processes

Refer also to abstracts 42183 and 42188.

43396 (MATT–804) STEAM CONDITIONS IN A CATALYZED D REACTOR. Bonanos, P.; Citrolo, J. C. (Princeton Univ., N. J. Plasma Physics Lab.). Jun 1971. Contract AT(30-1)-1238. 10p. (CONF-710418–13). Dep. NTIS.

From fourth symposium on engineering problems of fusion research; Washington, D. C. (20 Apr 1971).

The nature of the steam cycle and boiler design for a fusion power plant using a catalyzed D reaction is discussed. A preliminary appraisal indicates that, with a superheated steam cycle, the materials and technology of conventional fossil-fueled steam generators may be directly applied. The severe metallurgical stress, heat transfer and tritium breeding problems associated with D–T reactors are, to a great extent, avoided by the use of this scheme. (auth)

43397 (MATT–848) LARGE SUPERCONDUCTING MAGNET DESIGNS FOR FUSION REACTORS. File, J.; Mills, R. G.; Sheffield, G. V. (Princeton Univ., N. J. Plasma Physics Lab.). Jun 1971. Contract AT(30-1)-1238. 8p. (CONF-710418–14). Dep. NTIS.

From fourth symposium on engineering problems of fusion research; Washington, D. C. (20 Apr 1971).

Fusion technology will require superconducting fields of larger working volume and higher field strengths than heretofore designed. The forces that will result are so large that novel approaches to magnet design must be developed. This paper describes two complementary approaches that may be combined to yield a satisfactory design for very-high-field toroidal magnets. The first provides a cylindrical load-bearing element in compression combined with return conductors in pure tension. The second follows the design techniques that have been developed in the studies of force-free toroidal magnets. (auth)

43398 (ORNL-TM–3231) THE BLASCON: AN EXPLODING PELLET FUSION REACTOR. Fraas, A. P. (Oak Ridge National Lab., Tenn.). Jul 1971. Contract W-7405-eng-26. 45p. Dep. NTIS.

A fusion reaction can be initiated by directing an intense laser beam with a short pulse duration at a pellet of a frozen deuterium–tritium mixture. A study of the application of this approach to a series of conceptual designs has yielded some surprisingly attractive systems. Analyses and tests indicate that the explosion can be contained in a pressure vessel, and that, if pellets can be exploded at about 10 sec intervals, a reactor and pressure vessel assembly can be obtained at a modest unit cost for central stations or ship power plants having outputs as low as 100 MW(t). A reactor of this type would require no large magnets, activation of the structure would be negligible thus easing afterheat and hazards problems, and the problems of fast neutron damage to the reactor structure would be avoided. The exploding-pellet concept might also be applied to give a spacecraft propulsion system that might reduce the propellant weight requirements for an Earth-Mars-Earth mission to about 10% of that for a Rover-type nuclear rocket. An examination of the principal problems of these systems indicates that the major uncertainty in each case is the feasibility of obtaining a practical laser that will ignite D–T pellets of the required size to yield a much greater energy output than the laser energy input. An analysis of the problem of laser ignition indicates that there is a reasonably good chance that this problem can be solved, and that analysis has been supported by an experiment that appears to have given 10^4 neutrons from a 130-μ-diameter D–D pellet heated with a 40-joule laser beam. The report concludes that, in view of the tremendous potential payoff and the relatively low cost of some definitive experiments, a small experimental program to investigate this type of reactor deserves a high priority. (auth)

XUM

43399 (UCRL–73076) LIVERMORE SUPERCONDUCTING LEVITRON. Taylor, Clyde E.; Duffy, Thomas J.; Rossow, Terry L.; Branum, David R.; Sexton, James H.; Leber, Robert L. (California Univ., Livermore. Lawrence Radiation Lab.). 13 May 1971. 18p. (CONF-710418–15). Dep. NTIS.

From fourth symposium on engineering problems of fusion research; Washington, D. C. (20 Apr 1971).

The Livermore Superconducting Levitron contains an 80-cm-diam superconducting ring as well as three pairs of superconducting coils that produce a poloidal field, that are 50, 112, and 160 cm in diameter, respectively, and that are located 40 cm above and below the midplane of the ring. Twelve control coils and optical position sensors form a feedback system for maintaining the ring's position. Magnetic damping plates above and below the ring prevent it from making accidental but dangerously violent movements. The ring was successfully tested about a year ago, and the entire system is now undergoing its first operating tests. Construction details and the initial operating results are presented. (auth)

43400 ABSORPTION OF LIGHT BY AN INHOMOGENEOUS LASER PLASMA. Vinogradov, A. V.; Pustovalov, V. V. (Lebedev Inst. of Physics, Moscow). JETP Lett. (USSR) (Engl. Transl.); 13: No. 6, 226-8(20 Mar 1971).

Translated from Zh. Eksp. Teor. Fiz., Pis'ma Red.; 13: No. 6, 317-20(20 Mar 1971).

High temperatures are obtained by focusing laser radiation on solid targets, high reflectivity of the radiation back to the focusing device being a problem. The possibility of increasing the coefficient of absorption of light by an inhomogeneous laser plasma is discussed, using linear theory. The phenomenon of transformation of a surface p-polarized wave with frequency close to the plasma wave into potential electronic Langmuir oscillations is applied. The absorption mechanism discussed differs in principle from the nonlinear anomalous absorption. The transformation of light into a Langmuir oscillation increases the light absorption by the inhomogeneous plasma at a field intensity below threshold, i.e. when there is no nonlinear anomalous absorption. (J.C.W.)

43401 PRODUCTION OF HIGH CURRENT, HIGH QUALITY BEAMS OF IONS, AND NEUTRAL PARTICLES. Coupland, J. R.; Thompson, E. (United Kingdom Atomic Energy Authority, Abingdon, Eng.). Rev. Sci. Instrum.; 42: No. 7, 1034-7(Jul 1971).

Results obtained with a hot-cathode constricted-arc plasma source and a single-aperture three-electrode accel–decel extraction system are described. The energy range covered is 5 to 25 keV for positive ions and 1.7 to 2.5 keV for neutral beams. Ion currents of the order of 80 mA H_3^+ and 100 mA He^+ at the higher energies were obtained through a 3.8-cm-diam aperture at a distance of 180 cm from the source. The performance as a neutral injector was evaluated by using the present PHOENIX II experiment. Finally, the relation between experiment and theory and the limitations of this type of source are discussed. (auth)

Wave Phenomena

Refer also to abstracts 43073 and 43377.

43402 (AD–715277) INTERACTION OF A QTX WAVE WITH DENSITY FLUCTUATIONS IN AN INHOMOGENEOUS MAGNETIZED PLASMA. Weyl, Guy M. (Avco-Everett Research Lab., Everett, Mass.). Oct 1970. Contract F44620-70-C-0023. 17p. (AERL-RR–361). NTIS.

Propagation of a QTX wave through an inhomogeneous magnetized plasma is studied. Modulation of the reflection coefficient of the plasma is predicted due to density fluctuations in the region of evanescence of the wave. A measurement of the modulation is proposed as a diagnostic of certain plasma instabilities. (auth) (USGRDR)

43403 (AD–715636) SOME ALGEBRAIC SOLUTIONS OF THE CYCLOTRON RESONANCE INTERACTION. Ho, H. S.; Liemohn, H. B. (Boeing Scientific Research Labs., Seattle, Wash.). Sep 1970. 40p. (D–1–82–1010). NTIS.

The cyclotron-resonance interaction between electromagnetic waves and nonthermal plasmas was investigated for Cauchy (resonance) velocity distributions that yield algebraic dispersion equations. Combinations of anisotropic and streaming distributions were considered for ions and electrons to ascertain the relative importance of the interaction at different frequencies. Distribution forms and parameter ranges were chosen that would simulate possible conditions in the magnetosphere and solar wind. Because the equations are algebraic, the valid characteristic roots are readily identified, and their unstable nature is determined by conventional convective/nonconvective criteria. Parameter regimes of spatial amplification (convective instability) and temporal growth (nonconvective instability) were identified. Amplitude exponents are presented as a function of frequency for several cases of interest, and algebraic expansions are derived. On the basis of the cases studied, it is concluded that the cyclotron-resonance interaction is a convective instability for parameter values appropriate for the undisturbed magnetosphere and solar wind. Nonconvective instabilities are only obtained for relatively large streaming conditions which may be encountered in laboratory or stellar applications (auth) (USGRDR)

43404 (AD–715910) COUPLED ELECTROMAGNETIC AND ELECTRON ACOUSTIC WAVE PROPAGATION IN AN INHOMOGENEOUS LOSSY PLASMA LAYER. Technical Report, November 1969–August 1970. Southall, Hugh L. (Air Force Weapons Lab., Kirtland AFB, N. Mex.). Sep 1970. 171p. (AFWL-TR–70-110). NTIS.

A hydrodynamic treatment is used to derive the coupled wave equations for wave propagation in a compressible plasma. Electron acoustic waves in the plasma are assumed to be excited by a vertically polarized electromagnetic wave obliquely incident upon a plane dielectric/plasma interface. Finite-difference numerical solutions for the electromagnetic field and the scalar pressure field are obtained in a reentry-type plasma layer surrounding high-performance hypersonic reentry vehicles. An inhomogeneous plasma layer (or sheath) is modeled with a linearly increasing electron density profile. The coupling of acoustic waves to electromagnetic waves in this inhomogeneous region is investigated. Numerical results are obtained for the conversion of electromagnetic energy to plasma wave energy and vice versa. (auth) (USGRDR)

43405 (CERN–71-4) STUDY OF HYBRID ELECTROMAGNETIC WAVES IN CYLINDRICAL STRUCTURES: APPLICATION OF RESULTS TO DEFLECTOR MODES. Vaghin, V. (European Organization for Nuclear Research, Geneva (Switzerland)). 28 Jan 1971. 132p. (In French). Dep. NTIS (U. S. Sales Only).

Theoretical and experimental studies were made of the properties of hybrid waves in different cylindrical structures. The general theory of hybrid waves is given first. The deflecting and focusing properties of hybrid waves are considered. It is shown that hybrid waves being propagated in a plasma column exposed to an infinite external magnetic field have the same deflecting and focusing properties as in a vacuum. In order to study the hybrid waves, a general structure model was chosen: cylindrical guide filled by two coaxial layers of anisotropic dielectrics. This model contains a large number of possible deflecting and focusing structures. The criterion of existence of the inverse waves for this model is proved rigorously. The problem of complex waves is discussed, and the method of obtaining the dispersion relation is presented. Hybrid waves in wave guides with a metallic iris are studied for three cases: normal, partially filled with dielectric, and with a magnetoplasma column. The fundamental parameters of the deflecting structure are presented. The effect of the dielectric and the plasma on the properties of the deflector mode is discussed. The results of the calculation of all the basic deflector parameters are presented systematically. The properties of complex waves are studied. Cylindrical deflector structures partially filled with dielectric are studied for three cases: wave guide with dielectric tube, wave guide with dielectric tube and plasma column, and charged wave guide with dielectric iris. For the first model, all the parameters calculated, including E_p/E_0, are presented. The effect of the magnetoplasma on the deflecting properties is discussed. Deflector cavities with iris are experimentally studied. The configuration of the fields on the surface of the cavities and the parameters were measured. The measurements are presented systematically. The application of the results is discussed. (J.S.R.)

43406 (JINR–P9-5846) ON THE ION–SOUND TURBULENCE IN DENSE PLASMA. Makhan'kov, V. G.; Khakimov, F. Kh. (Joint Inst. for Nuclear Research, Dubna (USSR). Lab. of Computing Techniques and Automation). 1971. 13p. (In Russian). Dep. NTIS (U. S. Sales Only).

Instability of acoustic vibrations with frequency $\omega \ll \nu_e, \nu_i$ was studied in dense completely ionized plasma. The interaction is of "quasi-decay" character. Unstable branches of vibration of the second-sound type appear in the region $\omega < \nu_e, \nu_i$ at the level of turbulence $u = w/nT$ exceeding the threshold value u_t. As a result, the s-wave energy is transferred on the spectrum to the side of smaller "k." This process can compete at certain conditions with the known transfer process due to induced scattering of s waves on the plasma ions. The increment of instability and the threshold value are found. (auth)

43407 (N–71–18696) THREE-WAVE INTERACTION IN A BEAM–PLASMA SYSTEM. Hopman, H. J. (Stanford Univ.,

Calif. Inst. for Plasma Research). Dec 1970. 48p. (NASA-CR-116783; SU-IPR-402). NTIS.

The coupling coefficient for a nonlinear three-wave interaction is derived for the case of a cylindrical plasma column penetrated by an electron beam. The parametric growth rate of two plasma waves is calculated, assuming that a negative energy wave on the beam satisfies appropriate synchronism conditions with them and acts as a pump wave. A beam–plasma experiment is described in which three-wave coupling was observed between two beam waves and a low frequency plasma wave. All three waves grow in space, with a growth rate of the order of one tenth of the wave number of the beam waves. (auth) (STAR)

43408 RADIATION DAMPING OF ELECTROMAGNETIC WAVES IN PLASMAS. Burman, R. (Univ. of Western Australia, Nedlands). Indian J. Phys.; 43: No. 10, 625-7(Oct 1969).

An outline is presented for derivation of the equation for Landau damping in plasmas. (M.O.W.)

43409 NOISE BROADENING OF TRAPPED-PARTICLE ECHOES. Williams, E. A.; Oberman, C. (Princeton Univ., N. J.). Phys. Fluids; 14: No. 8, 1759-63(Aug 1971).

The effects of noise (caused by collisions or weak turbulence) on the production of echoes in magnetically trapped particles are discussed using a propagator formalism. Provided the effective collision time is long compared with a typical bounce time, the echoes are found to be broadened but not destroyed. (auth)

43410 ASYMMETRY OF THE COMBINATION-FREQUENCY SPECTRUM IN A PLASMA. Rutkevich, B. N.; Fedorchenko, V. D.; Muratov, V. I. (Physical-Technical Inst., Kharkov). Sov. Phys.-Tech. Phys. (Engl. Transl.); 15: No. 12, 1974-8(Jun 1971). Translated from Zh. Tekh. Fiz.; 40: No. 12, 2518-24(Dec 1970).

Possible causes for the asymmetry of the spectrum of combination frequencies in the interaction of high-frequency and low-frequency plasma oscillations are examined. The asymmetry is due to amplitude and phase modulations of the high-frequency oscillations if the amplitude oscillations are shifted in a certain way with respect to the phase oscillations. This condition is satisfied by the phase oscillations caused by the Doppler effect in low-frequency plasma motion and by amplitude oscillations due to the change in the damping coefficient or to transverse plasma motion. (auth)

43411 COMMENTS ON THE PHYSICAL MECHANISM CAUSING THE NONLINEAR BEHAVIOR IN TONKS–DATTNER RESONANCE EXPERIMENTS. Hsuan, H. C. S.; Demokan, O.; Lonngren, K. E. (Univ. of Iowa, Iowa City). Phys. Lett.; 35A: No. 6, 390-1(12 Jul 1971).

Two possible mechanisms thought to be responsible for the nonlinear behavior that develops as a function of increasing external electric field in Tonks–Dattner resonance experiments are compared. (auth)

43412 OBSERVATION OF A NONLINEAR ELECTRON-WAVE INTERACTION AT THE DOPPLER-SHIFTED CYCLOTRON FREQUENCY. Christiansen, P. J.; Christopoulos, C.; Martelli, G. E. G. (Univ. of Sussex, Eng.). Phys. Lett.; 35A: No. 6, 447-8(12 Jul 1971).

Some preliminary observations of an electron beam–whistler resonance interaction, and nonlinear pitch-angle modulation are presented. The experimental results are in satisfactory agreement with some theoretical calculations. (auth)

Shielding

Refer also to abstracts 42016, 42085, 42141, 42155, 42430, 43613, 44108, and 44161.

43413 (BMBW-FBK-71-2) NEW MONTE CARLO TECHNIQUE FOR RADIATION TRANSPORT PROBLEMS; CALCULATION OF THE COMBINED SPATIAL, ANGULAR, AND ENERGY DISTRIBUTIONS OF MULTIPLY SCATTERED GAMMA RAYS. Stehfest, H. (Frankfurt Univ. (West Germany). Institut fuer Angewandte Physik). Mar 1971. 111p. (In German). Dep. NTIS (U. S. Sales Only).

A new Monte Carlo technique for radiation transport problems is described and applied to γ quanta. The fundamental idea of the technique is that in computing the radiation field at distance r_0 from the source one considers right from the start only such quanta which have already traveled a path of the length $t_0 = r_0$. Position and direction of the quanta after the path length t_0 are determined by a Monte Carlo calculation in which the quanta are traced back from t_0 to the source. The new technique appeared to be so efficient that it became possible to calculate the angular energy distribution of the γ radiation at penetration depths up to 20 mfp. Some results of the numerous calculations are presented. (auth)

43414 (BNWL-SA-3705) ANALYSIS OF DISTRIBUTIONS PRODUCED BY CHARGED PARTICLES (AND OTHER COMPOUND-POISSON PROCESSES). Roesch, W. C. (Battelle-Northwest, Richland, Wash. Pacific Northwest Lab.). 16 Apr 1971. Contract AT(45-1)-1830. 9p. (CONF-710508-1). Dep. NTIS.

From 19. annual meeting of the radiation research society; Boston, Mass. (9 May 1971).

The transformation of certain charged-particle distributions into what they would have been under somewhat different circumstances is discussed. A technique useful in analyzing certain experimental data is discussed. The distributions that can be transformed are those known as compound-Poisson distributions. (auth)

43415 (JUL-711-MA) INVESTIGATION OF THE PROBLEM OF CHARACTERISTIC VALUE AND NONNEGATIVE SOLUTION OF A GENERAL STATIONARY TRANSPORT EQUATION. Ebersoldt, Franz (Kernforschungsanlage, Juelich (West Germany). Zentralinstitut fuer Angewandte Mathematik). Nov 1970. 54p. (In German). Dep. NTIS (U. S. Sales Only).

The time-independent problem associated with the homogeneous stationary transport equation $(A - B)\Phi = \lambda C\Phi$ is considered. A convex body surrounded by a perfect absorber is considered as the reactor. The problem is reduced to the study of the eigenvalues and functions of the operator $(A - B)^{-1}C$. It is shown that under a physically rational condition of this operator, defined on the complex L_2, a completely constant representation of the space in it is represented. On the basis of the Riesz–Schauder theory of compact operators it follows that only discrete characteristic values, which can not be accumulated in the finite, are given. The existence of a positive fundamental solution with a pertinent positive extreme characteristic value is proved. (J.S.R.)

43416 (NP-18863) COMPUTATION OF THE SHIELDING THICKNESS REQUIRED TO REDUCE A NEUTRON FLUX OR A DOSE RATE TO A GIVEN VALUE. Nurdin, Guy (Laboratoire Central de l'Armement, Arcueil (France)). 5 Nov 1969. 18p. (In French). Dep. NTIS (U. S. Sales Only).

A computational method is described that uses Monte Carlo techniques to calculate the thickness of a given material required to attenuate a neutron flux such that the dose rate corresponds to a predetermined value in a spherical geometry. An example using lead is presented. (France)

43417 (NYO-3829-71) EXACT SCREENED CALCULATIONS OF ATOMIC-FIELD PAIR PRODUCTION AND LOW ENERGY SCREENING. Tseng, H. K.; Pratt, R. H. (Pittsburgh Univ., Pa. Dept. of Physics). May 1971. Contract AT(30-1)-3829. 38p. Dep. NTIS.

A discussion of relativistic pair production cross sections is given for incident-photon energies in the range 1.073 to 2.615 MeV. Cross sections are obtained numerically in a screened potential, using an exact partial-wave formulation. Comparisons are made with previous work. For low photon energies, the effect of atomic electron screening on pair production cross sections is significant. The screening increases the cross section since the atomic electrons decrease the nuclear Coulomb repulsion of the positron. Comparisons of screened with unscreened results show that angular distributions are essentially unaffected in shape by the screening; cross sections are simply renormalized by replacing $|N_+N_-|^2$ in the point-Coulomb field by $|N_+N_-|^2$ in the screened field, where N_i are the normalizations of the positron and electron wave functions at the origin. (auth)

43418 (ORNL-RSIC-32) RECENT DEVELOPMENTS IN THE SHIELDING OF NEUTRON SOURCES. Claiborne, H. Clyde (Oak Ridge National Lab., Tenn.). Jun 1971. Contract W-7405-eng-26. 54p. Dep. NTIS.

The impact of ^{252}Cf on shielding of neutron sources is discussed, the newer methods used for coupled neutron–gamma-ray shielding calculations and shield weight optimization are reviewed, and some shipping cask designs for ^{252}Cf and other transplutonium elements are discussed. The six papers on neutron source shielding that were contributed to the American Nuclear Society Topical Meeting on Neutron Sources and Applications at Augusta, Ga., 1971, are summarized and discussed. Two papers are about the attenuation properties of various materials for the neutrons from ^{252}Cf and other neutron sources; one compares measurements and calculations for ten different shielded containers for ^{252}Cf; two involve the

XUM

design of portable neutron source facilities; and one the use of tissue equivalent proportional counters for thin shield studies. (auth)

43419 (ORNL-TM-3269) STUDY OF THE OVERLAP CONDITIONS REQUIRED IN SEQUENTIAL DISCRETE ORDINATES TRANSPORT CALCULATIONS FOR A 14-MeV NEUTRON SOURCE IN A 5000-m RADIUS CYLINDER OF AIR. Pace III, J. V.; Mynatt, F. R.; Abbott, Lorraine S. (Oak Ridge National Lab., Tenn.). 9 Jun 1971. 13p. (CTC-40). Dep. NTIS.

Because of computer-storage limitations, the two-dimensional discrete ordinates code DOT cannot be applied to the calculation of the transport of radiation over large distances in an air-over-ground geometry unless the problem is divided in space and run in series so that the results of one run are used as the source in the succeeding one. With this technique the runs must be sufficiently overlapped to remove the effects caused by the assumption in each run that the outer boundary of the region being calculated is followed by a vacuum. The overlap conditions have been studied in a series of calculations with the one-dimensional code ANISN for the case of an infinitely long cylinder of air and a 14-MeV neutron source on the cylinder axis. Radial distances out to 5000 m were covered both in a single ANISN run and in a series of runs for a central cylindrical core and several successive cylindrical annuli. The results showed that for this problem a 500-m overlap is required unless boundary albedos are introduced in the runs, in which case the overlap is reduced to 30 m. The boundary albedos are based on the incoming and outgoing currents determined for the boundary locations in the single ANISN run. For a large DOT calculation involving a source spectrum, using the albedos would substantially reduce the number of runs required to complete the calculation. (auth)

43420 (ORNL-TM-3429) PREPARATION OF DATA SETS IN ENDF FORMAT FOR Na, Mg, Cl, AND K FOR USE IN SHIELDING CALCULATIONS. Roussin, R. W.; Penny, S. K.; Singletary, V. A.; Wright, J. B. (Oak Ridge National Lab., Tenn.). 27 May 1971. 11p. (ENDF-151). Dep. NTIS.

Neutron interaction and gamma-ray production cross sections for sodium, magnesium, potassium, and chlorine, which were originally evaluated by Drake et al., have been placed in the currently approved ENDF/B formats. This involved a format change for the neutron files and two format changes for the gamma-ray production files. Gamma-ray interaction cross sections were then added to the neutron interaction and gamma-ray production data to obtain a reasonably complete set of data for use in shielding calculations. (auth)

43421 (ORNL-tr-2476) SPECTRAL-ANGULAR CHARACTERISTICS OF AN ELECTRON BEAM IN IRRADIATION OF A TISSUE-EQUIVALENT MEDIUM. Lyubomirov, A. M.; Pozdneev, D. B. Translated for Oak Ridge National Lab., Tenn., from Med. Radiol.; 15: No. 7, 63-9(1970). 9p. Dep. NTIS.

An abstract of this paper, prepared from the original language, appeared as NSA 25: 523.

43422 (ORNL-tr-2488) BURN-OUT OF CADMIUM SHIELDS. Goerner, W. Translated by J. J. Pinajian (Oak Ridge National Lab., Tenn.), from Kernenergie; 11: 249-52(1968). 11p. Dep. NTIS.

An abstract of this paper, prepared from the original language, appeared as NSA 23: 17286.

43423 VECTOR EQUATIONS OF TRANSFER WITH PLANE AND SPHERICAL SYMMETRY. Schnatz, Thomas Wilbur. Raleigh, N. C.; North Carolina State Univ. (1970). 105p. University Microfilms Order No. 71-12,098.

Thesis.

The singular-eigenfunction-expansion technique, often employed for studies in neutron transport theory, is used to obtain a general solution to the azimuth-independent equation of transfer describing the transport of arbitrarily polarized light in a Rayleigh-scattering atmosphere with true absorption (imperfect scattering). The normal modes for the considered nonconservative vector equation of transfer are established; two discrete eigenvectors and two linearly independent, degenerate, continuum solutions are thus derived. Further, the necessary full-range completeness and orthogonality theorems are proved, so that all expansion coefficients can be determined explicitly, and in order to illustrate the technique, an exact analytical solution for the infinite-medium Green's function is developed. These eigenvectors form the basis for subsequent analysis, which is directed primarily toward the construction of solutions to typical half-space problems. The eigenvectors are used to establish a singular integral equation and linear integral constraint necessary and sufficient to specify the required $\underset{\sim}{H}$-matrix, a generalization of Chandrasekhar's H-function. Further, the analysis yields the nonlinear integral equation, previously derived from the classical principles of invariance; this nonlinear equation and the linear constraint are also shown to be sufficient to specify the $\underset{\sim}{H}$-matrix and are used for computational purposes. After the general formalism is established, the method is used to construct complete solutions (valid at any optical depth) to the half-space albedo problem and the classical Milne problem. These solutions are written explicitly in terms of the normal modes, and all unknown expansion coefficients are then expressed in terms of the $\underset{\sim}{H}$-matrix. To illustrate the computational merits of the analysis, highly accurate numerical results for the half-space albedo and the Milne-problem extrapolated endpoint, law of darkening and degree of polarization are presented for a representative set of values of the single-scatter albedo. Finally, the analysis of vector transport equations is extended by considering the two-group, steady-state neutron transport equation with isotropic scattering in spherical geometry. A set of normal modes is constructed and the singular-eigenfunction-expansion technique is then used to develop a rigorous solution to the isotropically emitting spherical shell-source problem in an infinite medium. (Diss. Abstr. Int., B)

43424 INVESTIGATION OF ELECTRON TRANSPORT UTILIZING THE PHASE-SPACE TIME EVOLUTION METHOD. Cordaro, Matthew C. New York; Cooper Union for the Advancement of Science and Art (1970). 315p. University Microfilms Order No. 71-12,808.

Thesis.

A computer-based method of analyzing the motion of electrons in phase space, called the "Phase-Space Time Evolution" method ("P-STE"), is developed. This technique is used to study the time-dependent transport of electrons through matter. "P-STE" results for 1-MeV electrons normally incident on a semi-infinite slab of aluminum are compared with reported Monte Carlo and experimental values. The agreement in both cases is very good. The effects of varying the polar angle of incidence and the initial energy of electrons impinging on a semi-infinite slab of aluminum are investigated utilizing the "P-STE" method. Results indicate that, as the angle of incidence is increased, both the number and energy transmission decrease with increasing penetration given in terms of fraction of the mean range traversed. These functions show little dependence on energy below 1 MeV but start to change appreciably in character at 2 MeV. Increasing the angle of incidence shifts the most probable energy of the transmitted energy spectrum toward lower energy and produces a broader energy spectrum. The angular distribution of transmitted electrons becomes almost independent of incident angle at large penetrations. There is almost no difference in the angular distributions for electrons incident at 0.5 and 1 MeV after they have traveled the same fraction of their mean range. In contrast, the angular distribution for 2-MeV electrons is more sharply peaked in the incident direction for small penetrations. The maximum time-dependent transmitted current at each penetration decreases as the angle of incidence increases. An increase in the angle of incidence also causes the transmitted current to vary less rapidly with time. The shape of the curve of transmitted current as a function of time becomes almost independent of the angle of incidence at large penetrations. The behavior of a pulse of electrons having an energy distribution similar to that of ^{90}Sr isotropically incident on a semi-infinite slab of aluminum is also examined using the "P-STE" method. The number transmission curve produced is exponential in shape, characteristic of experimentally determined beta-source range curves. (Diss. Abstr. Int., B)

43425 ACTIVE RADIATION SHIELD FOR CYLINDRICALLY SHAPED VEHICLES. Levine, S. H.; Lepper, R. (Northrop Corporate Labs., Hawthorne, Calif.). Contract AF 33(615)3831. J. Spacecraft Rockets; 8: No. 7, 773-7(Jul 1971).

An effective magnetic shield design was developed for protecting a cylindrical space vehicle from space electron radiation. It employs a few coils of equal diameter (and approximately twice the vehicle diameter) located coaxially about the vehicle. The magnetic shield simulator (MAGSIM) has been used to develop engineering data for designing this shield. The data are presented nondimensionally and can be used to design a cylindrical shield of any size; as an example, an active shield for a 10-ft-dia, 30-ft-long vehicle is designed, assuming a current density in the superconductor of 2.5×10^5 A/cm^2 at 10°K. This shield protects against electrons with a 7-MeV cutoff energy, produces ~500 gauss inside the vehicle, and weighs 525 lb. (auth)

43426 PARAMETERS DETERMINING THE GAMMA DISTRIBUTION IN A MEDIUM OF ARBITRARY ELEMENTAL COMPOSITION. Khaikovich, I. M. This paper was summarized in At. Energ. (USSR); 28: 140-1(Feb 1970) as paper No. 367/5209. (In Russian).

The rules of gamma distributions in complex media are es-

tablished from the principles of similitude developed in problems of borehole radiometry by Sh. A. Guberman (Theory of Similitude and Borehole Radiometry, Gostoptekhizdat, Moscow (1962)) and used by others. Relations are developed for point, line, and plane sources and for a uniform source density in an infinite medium. (L.M.T.)

43427 RANGE OF FISSION FRAGMENTS IN AIR DETERMINED BY FISSION-TRACK DETECTOR. Su, Ching-shen; Wu, Wei-kuo (National Tsing Hua Univ., Hsinchu, Taiwan). Jap. J. Appl. Phys.; 10: No. 6, 762-5(Jun 1971).

A fission-track detector was used to determine the range of fission fragments in air. A linear transmission curve was obtained for the number of fission tracks registered on the glass detector as a function of fission source to detector separation. The extrapolated range of fission fragments of ^{235}U in air was determined to be 2.16 ± 0.11 cm. (auth)

43428 SOME REGULARITIES OF FORMING GAMMA RADIATION DOSE FIELDS IN SHIELDING STRUCTURES AND SHELTERS. Bulatov, B. P.; Stoicheva, T. A. Izotopy SSSR; No. 17, 23-9(1970). (In Russian).

Theoretical problems are examined that pertain to the physical characteristics of a field of scattered radiation within a different type of shielding construction. The parameters of such construction are discussed as they relate to the potential to predict radiation levels in a variety of cases. (tr-INIS)

43429 INVESTIGATION OF CHERENKOV RADIATION BY 50 keV ELECTRONS IN THIN SILICON FOILS. Heitmann, D. (Univ., Hamburg). Z. Phys.; 245: No. 2, 154-73(1971). (In German).

For wavelengths near 5,000Å the index of light refraction in silicon is so large, that a considerable amount of Cherenkov radiation is generated by 50-keV electrons. The experimental radiation pattern of transition radiation, including Cherenkov radiation, emitted from 50 keV electrons traversing thin silicon foils of 2,000-Å thickness at different angles of electron incidence is discussed. There is good agreement of the experimental results with theory. (auth)

43430 INTERNAL VALUES IN PARTICLE TRANSPORT BY THE METHOD OF INVARIANT IMBEDDING. Nelson, Paul Jr. (Oak Ridge National Lab., Tenn.); Scott, Melvin R. J. Math. Anal. Appl.; 34: No. 3, 628-43(Jun 1971).

A method is presented that permits boundary conditions that are any linear combination of given incident particle fluxes and albedo conditions, and also permits more-or-less arbitrary internal particle sources. The fundamental imbedding relationships for the rod model are discussed. How the internal particle distributions can be obtained from the functions determined by the relationships is shown, and some numerical examples are given. The extension of the method to transport of monoenergetic particles in a slab is briefly indicated. A summary of the basic results and an outline of further possible extensions of the method are presented. (M.H.R.)

43431 AVERAGE ENERGIES OF BACK SCATTERED X-RAYS FROM Pb, Cu, AND DURALUMIN. Sugiyama, Suguru; Tomimasu, Takio. Denki Shikensho Iho; 35: No. 1, 64-7(1971). (In Japanese).

The measurement of the average energies of backscattered X-rays from Pb, Cu and Duralumin irradiated by X-rays with maximum energy from 11.3 to 23.2 MeV has been carried out with a plastic scintillation detector. The average energy of backscattered X-rays is determined by the use of the absorption method using aluminum and Lucite filters. Broad beam attenuation coefficients of aluminum are measured with the ETL quantameter at the energies of 0.66 and 1.25 MeV. It is found that the average energies of backscattered X-rays from Pb, Cu and Duralumin are 0.6, 0.72 and 0.7 MeV, respectively, at the incident X-ray energy of 23.2 MeV. The result suggests that positron annihilation in the flight and the bremsstrahlung of secondary electrons and positrons in the scatterer mainly contribute to the energy albedo of high energy X-rays. (auth)

43432 STOPPING POWER AND ENERGY STRAGGLING FOR SWIFT PROTONS. Bonderup, E.; Hvelplund, P. (Univ. of Aarhus, Denmark). Phys. Rev., A; 4: No. 2, 562-9(Aug 1971).

Calculations and measurements of energy dissipation by protons at energies above ~100 keV are presented. The calculations, which make use of a statistical model of the atom, are based on a refinement of a procedure suggested by Lindhard and Scharff. The theoretical section of the present paper is concerned with energy straggling, as stopping powers were dealt with in an earlier publication. Measurements of stopping power and energy straggling for 100- to 500-keV protons were made in various gases, viz., hydrogen, helium, air, neon, argon, and krypton. The stopping-power data are in good agreement with theory and earlier experimental work. For the heavy gases, the experimental straggling values are seen to be an increasing function of energy, as expected from theory. In a more quantitative comparison, however, some discrepancy between theory and experiment is observed. (auth)

43433 COMPARISON OF MASS ABSORPTION COEFFICIENTS OF POSITIVE AND NEGATIVE BETA PARTICLES IN ALUMINUM AND TIN. Thontadarya, S. R.; Umakantha, N. (Karnatak Univ., Dharwar, India). Phys. Rev. B; 4: No. 5, 1632-4(1 Sep 1971).

Mass absorption coefficients for six negative and three positive β-particle sources were determined for aluminum and tin absorbers. Most of the large difference in the μ/ρ values relevant to ^{86}Rb and ^{68}Ga reported for aluminum by Takhar is shown to be due to the difference in their end-point energies; however, a significant difference in μ/ρ values for tin remains. (auth)

43434 CRITICISM OF EXISTING TABULATIONS OF MASS ENERGY TRANSFER AND MASS ENERGY ABSORPTION COEFFICIENTS. Carlsson, G. A. (Linkoepings Hoegskola, Sweden). Health Phys.; 20: No. 6, 653-5(Jun 1971).

The following corrections were made to tabulations of the mass energy transfer coefficient ($f_\tau \cdot \tau/\rho$) and mass energy absorption coefficient: (1) For the neglected escape of L-, M-, etc., fluorescence radiation emitted upon photoelectric absorption in the L, M, etc., shells above the K-edge: in the case of lead, 3% overestimation of $f_\tau \cdot \tau/\rho$ was found for photon energies just above the K edge. (2) For the neglected escape of L fluorescence radiation emitted upon photoelectric absorption in the K-shell: using both corrections reduced $f_\tau \cdot \tau/\rho$ by 12% from tabulated values, just above the K-edge. Refinements of the calculations, taking into account the escape of M, N, etc., fluorescence radiations, yielded corrections at least a factor of 10 smaller than those due to the escape of L-fluorescence radiation. (UK)

Solid-State Physics

Refer also to abstracts 41832 and 43728.

Radiation Effects

Refer also to abstracts 41854, 42163, 43740, and 43747.

43435 (RISO–237) PHYSICS DEPARTMENT ANNUAL PROGRESS REPORT, 1 JANUARY–31 DECEMBER 1970. Moeller, H. Bjerrum; Lindgard, Per-Anker (Danish Atomic Energy Commission, Risoe. Research Establishment). Jan 1971. 46p. Dep. NTIS (U. S. Sales Only).

Research during the period Jan. through Dec. 1970 is reported on the five following main fields: (1) solid-state physics, (2) plasma physics, (3) nuclear spectroscopy, (4) radiation damage, and (5) meteorology. Only (1) has yet-unpublished worthwhile information. (M.O.W.)

43436 CHARGING OF POLYMER FOILS WITH MONOENERGETIC LOW-ENERGY ELECTRON BEAMS. Sessler, G. M.; West, J. E. (Bell Telephone Labs., Murray Hill, N. J.). Appl. Phys. Lett.; 17: 507-9(15 Dec 1970).

Results of charge deposition on 12.7 and 25.4-μm polymer foils with 10- to 40-keV monoenergetic electron beams are reported. The trapped charges have densities of about 10^{-7} C/cm^2, with a uniformity of ±5% over the bombarded area. The time constants of the charge decay are typically of the order of tens of years. Thermally stimulated currents show a more densely populated high-temperature portion than for foils charged with other methods. (auth)

43437 CHANGES IN ENERGY SPECTRUM OF CAPTURE CENTERS (TRAPS) IN ELECTRON-BOMBARDED CdS CRYSTALS. Grigor'ev, R. V.; Novikov, B. V.; Shestakova, T. V. Uch. Zap. Leningrad. Gos. Univ., No. 354, Ser. Fiz. Nauk; No. 16, 91-6(1970). (In Russian).

Energy spectra of captured centers in cadmium sulfide subjected to 3-keV electron bombardment in a vacuum of 10^{-6} torr at 80°K were studied. The spectral distribution of photoconductivity and temperature distribution of thermostimulated conductivity (TSC) changed considerably following 2 min of bombardment. Following 20 min of bombardment, a new level of capture distributed about 0.36 eV from the bottom conduction zone appeared in the TSC spectrum. It was also observed that the current in the maximums corresponding 0.15- and 0.2-eV levels from

XUM

the bottom conduction zone increased by a factor of 10^5. The chemisorption of oxygen increased with temperature; however, the adsorption begins at −80°C. (R.V.J.)

43438 CHARGED-PARTICLE RADIATION DAMAGE OBSERVED AS DIMPLING OF THIN SILICON TARGETS. Meek, R. L.; Gibson, W. M.; Sellschop, J. P. F. (Bell Telephone Labs., Murray Hill, N. J.). Appl. Phys. Lett.; 18: No. 12, 535-8 (15 Jun 1971).

When thin uniform silicon targets are bombarded with energetic ions, macroscopic deformation of the target occurs in the irradiated region. This deformation, which is euphemistically termed a "dimple", may be interpreted as a radiation-induced lattice expansion. Measurement of the amount of deformation allows lattice expansion to be determined with a sensitivity comparable to or better than the most sensitive existing methods. Measurements on silicon irradiated at room temperature by 1.8-MeV He ions show that the lattice expansion at low flux increases essentially linearly with fluence below about 5×10^{16} He ion/cm^{-2}, whereupon it increases more rapidly until saturation starts to occur at an order-of-magnitude higher fluence. Isochronal annealing results are discussed. (auth)

43439 RESIDUAL ELECTRICALLY ACTIVE DEFECTS AFTER LATTICE REORDERING IN ION-IMPLANTED SILICON. Davies, D. Eirug; Roosild, S. (Air Force Cambridge Research Labs., Bedford, Mass.). Appl. Phys. Lett.; 18: No. 12, 548-50(15 Jun 1971).

Thermally stimulated current measurements were conducted on low-dose carbon-implanted silicon. After annealing for lattice reordering, five defect levels were found still present, at energies ranging from 0.27 to 0.40 eV. Since they all showed similar annealing to above 500°C, they reveal a major annealing stage in low-dose ion-implanted silicon that occurs at considerably higher temperatures than what is generally ascribed to lattice reordering. (auth)

43440 RAMAN SCATTERING OF ION-IMPLANTED GaAs. Peercy, P. S. (Sandia Labs., Albuquèrque, N. Mex.). Appl. Phys. Lett.; 18: No. 12, 574-6(15 Jun 1971).

Measurements of Raman scattering in ion-implanted semiconductors are reported. The broadening of the phonon modes produced by lattice strains on Xe ion implantation was measured for GaAs. The measurements show pronounced effects on the line width at moderate fluence levels and demonstrate that Raman scattering can provide a sensitive technique for probing stresses introduced by ion implantation. At higher-fluence levels where the material begins to transform from crystalline to amorphous, the line width is found to increase rapidly with fluence. (auth)

43441 SENSITIVE TECHNIQUE FOR STUDYING ION-IMPLANTATION DAMAGE. EerNisse, E. P. (Sandia Labs., Albuquerque, N. Mex.). Appl. Phys. Lett.; 18: No. 12, 581-3 (15 Jun 1971).

The lattice damage created by ion implantation was investigated by measuring the stresses lateral to the implanted surface caused by the specific volume expansion inherent with lattice damage. A cantilever beam-shaped sample is implanted on one side, and the position of the free end is monitored by measuring the capacitance between it and a fixed electrode. Results are presented for various 220-keV noble-gas-ion implants into Si. A new region is observed at very low fluences (10^{11} cm^{-2} of ^{20}Ne), where damage is introduced linearly with fluence. The distinct maximum in the stress that appears at higher fluences is attributed to an elastic–plastic transformation. (auth)

43442 RADIATION PHYSICS OF FERROELECTRICS OF BARIUM TITANATE TYPE. Solov'ev, S. P.; Kuz'min, I. I. Izv. Akad. Nauk SSSR, Ser. Fiz.; 34: 2604-11(Dec 1970). (In Russian).

A short description is given on the composition of ferroelectrics and the radiophysical methods for studying the crystals. Radiation effects of fast (0.1 to 1.3 MeV) electrons, γ rays, and fast (1 to 2 MeV) neutrons on barium titanates and other binary oxides of ABO_3 composition with perovskite-type structure were evaluated. The concept of crystals of $A^{2+} + B^{4+} + O_3^{2-}$, which conserve the independence of molecules AO and BO_2, is considered. The inverse and irreversible radiation effects in $BaTiO_3$ and $PbTiO_3$ were studied. (tr-auth)

43443 DIELECTRIC PROPERTIES OF γ-IRRADIATED CRYSTALS OF KH_2PO_4. Kamysheva, L. N.; Burdanina, N. A.; Zhurkov, O. K.; Darinskii, B. M.; Sizova, L. N. (Voronezh State Univ., USSR). Izv. Akad. Nauk SSSR, Ser. Fiz.; 34: 2612-16 (Dec 1970). (In Russian).

The influence of small doses of γ radiation on the dielectric properties of KH_2PO_4 was studied. The radiation changed the shape of the curve $\epsilon(T)$ (the temperature dependence of the dielectric constant). The property most sensitive to γ irradiation was tan δ. With increased dose, the maximum losses in solidified region, the ferromagnetic domain, were reduced and a second maximum appeared. Irradiation with over 1-kR doses resulted in the presence of only the second maximum losses, clearly expressed by the relaxation character. The experimental data are interpreted, considering the role of moving dielectric boundaries. (tr-auth)

43444 PERMANENT DEFECTS IN ELECTRON BOMBARDED n-TYPE GERMANIUM. Hiraki, Akio (Osaka Univ.). Technol. Rep. Osaka Univ.; 20: No. 932-972, 415-25(Oct 1970).

Klontz and MacKay classified defects introduced in n-type Ge by electron bombardment at low temperature into two groups: (i) vacancy–interstitial closed pair defects, and (ii) permanent defects. Since the exact nature and origin of the permanent defects have remained almost unknown, a consistent model of these defects is proposed, mainly on the basis of recent experimental works done by Hiraki, Cleland, and Crawford. (auth)

43445 RADIATION-INDUCED CHANGES IN THE ELECTRICAL PROPERTIES OF LiF MONOCRYSTALS ALLOYED WITH Na. Lobanov, E. M.; Balbakov, Dzh.; Chubarov, L. B.; Shalpykov, A. Sh. (Inst. of Mathematical Physics, Frunze, USSR). Izv. Akad. Nauk Kirg. SSR; No. 4, 27-9(Jul 1970). (In Russian).

The effect of adding Na to LiF monocrystals on their electrical properties was investigated. The Na was inserted into the LiF crystals during growing of the latter, and monitoring of the Na content was accomplished by neutron activation analysis with an error of 5 to 6%. For this test, 3- to 5-mg samples were irradiated in a thermal neutron flux (10^{12} n/sec) for 10 min, and then analyzed in a gamma spectrometer with NaI scintillation crystal and photomultiplier. The Na content in two selected samples was 0.0082% and 0.0166%, respectively. (tr-auth) (INIS)

43446 RADIATION EFFECTS ON SILICATES (5-keV H^+, D^+, He^+, N_2^+. Dybwad, Jens Peter (Air Force Cambridge Research Labs., Bedford, Mass.). J. Geophys. Res.; 76: No. 17, 4023-9(10 Jun 1971).

Selected silicates were exposed to 5-keV, 10-μA cm^{-2} ion irradiation, and their mid-infrared spectra were monitored during the exposure. Irradiation with H^+, D^+, and He^+, and N_2^+ did not significantly alter the spectral signature of the minerals. A slight shift of the 10-μ Si–O band to longer wavelength was observed, however, in reflection spectra of single crystals when they were irradiated with any of the three smaller ions. The bandshift reached its maximum after exposure to about 10^{19} ions cm^{-2}. It is shown that the maximum represents a steady state of ion penetration and surface sputtering, and it is concluded, from comparison of irradiations with different ions, that the 10-μ bandshift is caused by gas retention within the samples rather than by lattice breakdown or chemical reactions. Implications for the lunar surface are that changes within silicates exposed to the low-energy solar wind remain small and will not increase after exposure of about 100,000 years. No darkening was observed on these surfaces as a result of ion irradiation. Sputtered deposits on recipient NaCl surfaces appear to be composed of silicate glass. (auth)

43447 DEPTH DISTRIBUTION OF IMPLANTED OXYGEN IN GALLIUM PHOSPHIDE MEASURED BY NUCLEAR REACTION TECHNIQUES. Whitton, J. L.; Mitchell, I. V.; Winterbon, K. B. (Atomic Energy of Canada Ltd., Chalk River, Ont.). Can. J. Phys.; 49: No. 10, 1225-32(15 May 1971). (AECL-3839).

The depth distribution of ion-implanted ^{18}O in gallium phosphide was measured by use of the nuclear reaction $^{18}O(p,\alpha)^{15}N$, which has a sharp resonance at a proton energy of 639 keV. Implantation energies of 20, 40, and 60 keV were used and average concentrations were achieved of as high as 3×10^{21} ions/cm^3 over the implanted depths. Post-annealing of the 20-keV implant at 600°C caused a slight broadening of the distribution. A mathematical treatment is given whereby the ^{18}O depth distribution can be derived from the experimental observation of the α-particle counting rate as a function of proton energy. This treatment involves a novel method of obtaining a smooth fit for the depth profile. Comparison of the smoothed experimentally measured distribution profiles with theoretical range distributions shows a reasonable fit, indicating that the projected ranges and distributions of oxygen implanted into GaP may be calculated with a fair degree of accuracy. (auth) (Canada)

43448 INFLUENCE OF ELECTRIC FIELDS ON THE SCINTILLATION PROCESS IN CsI(Tl). Scharmann, A.; Traunfelder, H. (Univ., Giessen, Ger.). Z. Naturforsch.; 26a: No. 5, 828-32(May 1971). (In German).

The luminescence yield of CsI/Tl crystals under the influence of electric fields is investigated. Following excitation with ionizing radiation, the intensity depends on the incident particles and their differential energy loss. The Tl centers are not influenced by the electric field during uv irradiation, while for β and γ excitation a decrease of luminescence intensity is observed, depending on the Tl concentration. When α-irradiated, the intensity of the Tl band remains unaffected. The possible mechanisms of the energy transfer are discussed in terms of the excitation density and Tl concentration. (auth)

43449 DETERMINATION OF DISPLACEMENT ENERGY OF TUNGSTEN ATOMS BY IRRADIATING FIM SPECIMEN WITH INERT GAS IONS. Tamaki, Shozo; Sugata, Eizi (Osaka Univ.). Oyo Butsuri; 40: No. 4, 380-90(Apr 1971). (In Japanese).

Tips of FIM tungsten specimens were irradiated with 0.5- to 9-keV inert-gas ions, which were emitted from a field-ion gun attached to a side of the FIM tube. The threshold voltage of ion acceleration at which surface damage appeared was determined through a direct observation of FIM images. This determination made it possible to estimate the displacement energy of surface atoms on tungsten to be about 22 eV. From this value, the displacement energy of bulk atoms of the same material was estimated to be 30 to 35 eV. By examining FIM images with particular attention to the stability of surface atoms on the field-evaporated specimen tips, some information was obtained concerning the process of formation of surface damage. The flight range of penetrating inert-gas ions in tungsten was also calculated by the LSS theory. The result indicated that surface damage which appeared on the side of the tip apex counter to the ion-injected one might be ascribed to the channeling of gas ions to the ⟨110⟩ direction in tungsten. (auth) (Japan)

43450 IMPURITY-CONTROLLED PROCESSES IN THE PRODUCTION OF F CENTERS IN ALKALI HALIDES. Sastry, E. V. R.; Srinivasan, T. M. (Indian Inst. of Tech., Kanpur). pp 61-5 of Proceedings of the Nuclear Physics and Solid State Physics Symposium, Roorkee, December 28-31, 1969. Vol. III. Bombay; Dept. of Atomic Energy (1969).

From Nuclear physics and solid state physics symposium; Roorkee, India (28 Dec 1969). See CONF-691208-(Vol.3).

F-center growth curves were measured during x irradiation of undoped and Co-, Ba-, and Cd-doped KCl crystals. The curves were fitted to the equation $\alpha_F = A_2(1 - e^{-a_2 t}) + A_3(1 - e^{-a_3 t}) + a_1 t$, where α_F is the absorption coefficient of the F-band peak, t is the time of x irradiation, and the first and second terms on right are the first and second substages and the last term is the linear growth that continues after saturation of the first two substages. The first substage is relatively insensitive to impurities, while the a_3 values are less for the doped crystals than for the undoped crystals. It is concluded that impurities reduce the rate of coloration in the second substage, while at the same time increasing its saturation level. Several possible explanations for the decrease in a_3 are considered. (D.L.C.)

43451 ESR ABSORPTION OF X-IRRADIATED $NaClO_3$ CRYSTAL THERMALLY BLEACHED AT 200°C. Ramasastry, C.; Sastry, S. B. S.; Murty, V. S. (Indian Inst. of Tech., Madras). pp 179-82 of Proceedings of the Nuclear Physics and Solid State Physics Symposium, Roorkee, December 28-31, 1969. Vol. III. Bombay; Dept. of Atomic Energy (1969).

From Nuclear physics and solid state physics symposium; Roorkee, India (28 Dec 1969). See CONF-691208-(Vol.3).

After bleaching for 2 hr at 200°C, only one peak was left in the originally complex ESR spectrum. The anisotropy of this peak was studied, and the g value was found to vary from 2.0104 to 2.0110, with the maximum value occurring at the 45° orientation of the magnetic field with [100]. There is no hyperfine splitting, and the absorption is not symmetric about the center and does not fit into a single gaussian shape, indicating overlapping absorptions of different widths. It is suggested that the peak is an unresolved pair due to the paramagnetic species O_3^- with g-anisotropy and half width variation. (D.L.C.)

43452 USE OF A CONTROLLED-GRID MULTIPLIER FOR FLUORESCENCE INVESTIGATIONS IN THE NANO- AND SUB-NANOSECOND REGION. Fiedler, O. (Univ., Giessen, Ger.). Z. Naturforsch.; 26a: No. 5, 888-96(May 1971). (In German).

A gated image converter was developed for measurements of fast-electron (50 keV) excited fluorescence rise and decay times. Crystals of pure anthracene, p-terphenyl, and p-terphenyl doped with tetracene give simple exponential decays (24 nsec and 3.5 nsec for pure anthracene and p-terphenyl, respectively) but the rise has more than one exponential component. That may be interpreted as a many-stage excitation process. (auth)

43453 INTERACTIONS OF POSITRONS WITH DEFECTS IN SODIUM CHLORIDE CRYSTALS. Tumosa, Charles S.; Nicholas, J. Blair; Ache, Hans J. (Virginia Polytechnic Inst., Blacksburg, Va.). J. Phys. Chem.; 75: No. 3, 2030-5(24 Jun 1971).

The positron lifetime spectra of nearly perfect NaCl crystals were decomposed into two components with the lifetimes $\tau_A = 4.0 \times 10^{-10}$ sec and $\tau_B \simeq 1.0 \times 10^{-9}$ sec and corresponding intensities of $I_A \simeq 96$ and $I_B \simeq 4\%$. Upon proton-, γ-, or x-irradiation or doping with Al metal a significant decrease in the lifetimes and a marked increase in the intensity of the long-lived component was observed, approaching "saturation values" of $\tau_A \simeq 2.8 \times 10^{-10}$ sec, $\tau_B \simeq 5.6 \times 10^{-10}$ sec and $I_B \simeq 40\%$ with increasing radiation doses. The results were explained in terms of a simple model that involves the trapping of positrons in cation vacancies. On the basis of this model, a maximum rate of 7.6×10^8 sec^{-1} was found for the capture of positrons in these vacancies, which corresponds to a defect fraction of about 2.6×10^{-7}. A mechanism is proposed to account for the observed saturation values in the positron lifetime spectra. (auth)

43454 ENERGY-LOSS SPECTRA OF CHANNELED IODINE AND OXYGEN IONS IN GOLD. Appleton, B. R.; Datz, Sheldon; Moak, C. D.; Robinson, Mark T. (Oak Ridge National Lab., Tenn.). Phys. Rev. B; 4: No. 5, 1452-7(1 Sep 1971).

Energy-loss spectra are reported for 15- and 21.6-MeV ^{127}I ions and for 10-MeV ^{16}O ions transmitted through the {111} and {100} planar channels of thin gold crystals. In agreement with earlier observations on 60-MeV ^{127}I and 3-MeV ^4He ions, the stopping power in each case is accurately proportional to the frequency with which the ions oscillate in traversing the channel. From the results of these experiments, it is concluded that the ^4He and ^{16}O ions behave in gold planar channels as test charges which sample the electron distribution of the medium. The ^{127}I ions behave nearly as test charges, but for them there is some evidence that the screening of the nuclear charge changes with the position of the ion in the channel. (auth)

43455 OSCILLATION FREQUENCIES OF PROTONS IN PLANAR CHANNELS OF SILICON. Eisen, F. H. (North American Rockwell Science Center, Thousand Oaks, Calif.); Robinson; Mark T. Phys. Rev. B; 4: No. 5, 1457-61(1 Sep 1971).

Measurements of the angular distributions and energy losses of 0.4-MeV protons transmitted through planar channels in thin silicon crystals were used to relate the stopping power of the ions to the frequencies with which they oscillate in traversing the channels. In agreement with analogous experiments for several ions in gold, the stopping power is found to be accurately proportional to the channel oscillation frequency. The interaction between the proton and the silicon atoms is in reasonable agreement with expectations based on a Thomas–Fermi model. (auth)

43456 DEDUCTION OF INTERACTION POTENTIALS FROM PLANAR-CHANNELING EXPERIMENTS. Robinson, Mark T. (Oak Ridge National Lab., Tenn.). Phys. Rev. B; 4: No. 5, 1461-70(1 Sep 1971).

A model is presented that allows planar-channeling data to be used to deduce the parameters of the interaction potential between the channeled ions and the atoms of the solid and which relates the stopping power of channeled ions to that of randomly directed ones. The analysis is based on the experimental observation of the proportionality between the stopping power and the transverse oscillation frequency of ions traversing the planar channels of thin crystal targets. It is applied to data on He, O, and I ions transmitted through the {111} and {100} channels of Au crystals and on H ions transmitted through the {111} and {110} channels of Si crystals. For both targets, the screening constants of the interaction potentials are in excellent agreement with recent Hartree calculations. The same potentials allow the calculation of random stopping powers from the channeling data, which are in good agreement with observation, especially when account is taken of thermal vibrations of the lattice atoms. (auth)

43457 IN SITU FIELD ION MICROSCOPE STUDY OF IRRADIATED TUNGSTEN. I. EXPERIMENTAL RESULTS. Scanlan, R. M.; Styris, D. L.; Seidman, D. N. (Cornell Univ., Ithaca, N. Y.). Phil. Mag.; 23: No. 186, 1439-57(Jun 1971).

The mobility of single self-interstitial atoms was studied in a series of in situ field ion microscope (FIM) experiments. High-purity ($\lesssim 1.5 \times 10^{-6}$ at. fr. impurity level) W specimens were irradiated with 20 keV W^+ ions under ultra-high vacuum ($\sim 10^{-10}$ torr) conditions at temperatures between 8 and 18°K. The specimens were examined directly at the irradiation temperature employing the pulse-field evaporation technique. The initial state of damage at 15°K consisted of depleted zones within 100 Å of the

irradiated surface, and a distribution of immobile self-interstitial atoms which were distributed throughout the bulk of the specimen, and which originated at the depleted zones. Direct observation of the FIM specimens during subsequent annealing experiments between 15 and 120°K showed that these self-interstitial atoms underwent long-range migration (i.e. distances of ~200 Å) in Stage I, and were mobile at temperatures as low as ~28°K. Warming these same specimens to 298°K (~ middle of Stage II) followed by post-anneal pulse-field evaporation experiments at 15°K showed that the initial concentration of self-interstitial atoms, which were distributed throughout the volume of the specimen, decreased by at least an order of magnitude as a result of this annealing treatment. (auth) (UK)

43458 IN SITU FIELD ION MICROSCOPE STUDY OF IRRADIATED TUNGSTEN. II. ANALYSIS AND INTERPRETATION. Scanlan, R. M.; Styris, D. L.; Seidman, D. N. (Cornell Univ., Ithaca, N. Y.). Contract AT(30-1)-3504. Phil. Mag.; 23: No. 186, 1459-78(Jun 1971).

The results of a series of experiments described previously (Phil. Mag. 23: 1439(1971)) demonstrated that self-interstitial atoms (SIAs) were immobile at an irradiation temperature of 15°K, and that these same SIAs subsequently underwent long-range migration at temperatures as low as ~28°K. These results are analysed quantitatively, and approximate values obtained of the diffusion coefficient [$\simeq 0.22 \exp(-0.085\ \mathrm{eV}/kT)\ \mathrm{cm}^2\ \mathrm{sec}^{-1}$], and the enthalpy change of migration of the SIA (~0.085 eV). The effect of the electric field on the diffusivity of a single SIA was considered, and it was shown that the volume change of migration for a SIA must have been $\lesssim 0.1$ atomic volume. The problems of SIA clustering and the formation of SIA-impurity atom clusters were considered and were shown to be possible sources of the broad annealing spectrum already reported. In addition the relationship of the post-anneal field-evaporation experiments to the 2-interstitial recovery model was discussed. Finally, the present experiments were compared with other Stage I recovery data on irradiated tungsten. (auth) (UK)

43459 HIGH-ENERGY HUMPS IN THE SPECTRA OF BACK-SCATTERED PROTONS FROM Si SINGLE CRYSTALS. Sone, K. (Kyoto Univ.); Teramoto, M.; Fukuzawa, F. Phys. Lett.; 35A: No. 6, 445-6(12 Jul 1971).

Conspicuous high-energy humps have been found in backscattering energy spectra for fast protons whose angle of incidence corresponds to the shoulder part of the channeling dip-shoulder pattern. A concept of compensation is insufficient to explain this phenomenon. (auth)

43460 DAMAGE-SENSITIVE CATHODOLUMINESCENCE OF ZINC TELLURIDE. Bryant, F. J.; Baker, A. T. J. (Univ. of Hull, Eng.). Phys. Lett.; 35A: No. 6, 457-8(12 Jul 1971).

Before and after bombardment with monoenergetic electrons in the range 100 to 400 keV, electrons of 100-keV energy were used to study the cathodoluminescence spectrum of zinc telluride at 10°K. At 235 ± 10 keV a threshold energy was found for the marked enhancement of a weak emission occurring at 2.360 eV. (auth)

43461 EFFECTS OF CRYSTAL SURFACE AND IMPERFECTIONS ON CHANNELING PHENOMENA OF PROTONS. Fujimoto, F. (Tokyo Univ.); Komaki, K.; Nakayama, H. Phys. Status Solidi (a); 5: No. 3, 725-35(16 Jun 1971).

The aligned spectra of protons backscattered from perfect and imperfect crystals of silicon and KCl are compared with the theory considering the beam divergence due to multiple scattering. The results show that the observed spectra agree with the theory at the high-energy side and in the region where the beam divergence is smaller than the critical angle, if the beam divergence at the surface is taken into account. The beam divergence at the surface is of the order of 10^{-3} rad, which coincides with the calculated value, and is affected by contamination adhered on the surface, but not by crystal imperfections. From the comparison between the aligned spectra from perfect and imperfect crystals, a method for estimating the degree of imperfection is presented and applied to crystals with dislocations and damaged by charged particles. (auth)

43462 PHOTOLUMINESCENCE IN GaP RESULTING FROM NITROGEN ION IMPLANTATION. Kennedy, D. I. (Bowmar Canada Ltd., Ottawa); Adolph, J. B. Phys. Status Solidi (a); 5: No. 3, K205-9(16 Jun 1971).

GaP crystals were implanted with N^+ and N_2^+ ions at doses from 2×10^{14} to $10^{16}\ \mathrm{cm}^{-2}$ at room temperature and 250°C. Annealing at 400 to 600°C in P vapor was used to alleviate the radiation damage, and a near-band edge luminescence was produced which is characteristic of the exciton recombination of the isoelectronic nitrogen center in GaP and which is not observed in annealed as-grown crystals. The optically active N concentration in crystals implanted at the $10^{16}\ \mathrm{cm}^{-2}$ dose level is on the order of $10^{20}\ \mathrm{cm}^{-3}$, higher than with conventional doping methods. (D.L.C.)

43463 DISTRIBUTION OF RADIATION DEFECTS IN SILICON IRRADIATED WITH FAST CHARGED PARTICLES. Bulgakov, Yu. V.; Kolomenskaya, T. I.; Kumakhov, M. A. (Moscow State Univ.). Phys. Status Solidi (a); 5: No. 3, 591-6(16 Jun 1971).

The profile of the radiation defect distribution in crystalline silicon irradiated with protons, deuterons, and α particles with the energy 6.3 MeV per amu was investigated. The incident direction of an ion beam corresponded to the case of an isotropic target. After irradiation the profile of the radiation defect concentration was studied by analyzing the local conductivity. For the interpretation of these results, the energy levels of defects and carrier mobility were determined from measurements of the Hall effect and photoconductivity. In all cases under investigation a sharp peak of the defect concentration was observed at the end of the particle path. The half-width of this peak was especially small for α particles, being about 2% of their path. The results obtained are discussed in terms of a radiation cascade model. The effect of ionization loss fluctuations, multiple scattering of incident particles in the crystal, and migration of primary radiation defects on the half-width of the peak was considered. It is shown that the half-width of the peak is mainly a function of the ionization loss fluctuations of stopping particles and of the original energy spread of a particle beam. The theoretical treatment is in good agreement with experiment. (auth)

43464 DETERMINATION BY CHANNELOGRAPHY OF ORIENTATION OF MICROCRYSTALS. Delsarte, G.; Desarmot, G.; Mory, J. (CEN, Fontenay-aux-Roses, France). Phys. Status Solidi (a); 5: No. 3, 683-90(16 Jun 1971). (In French).

If a crystalline thin foil is irradiated by means of an isotropic source of charged particles, the particles channeled in the sample leave on a detector an image called channelography. Channelographic projection consists in removing the detector to some distance from the crystal, and in observing the image obtained from a small portion of the sample. This image is always formed by continuous lines, and it is deduced that essentially planar (not axial) channeling is observed. These lines form a pattern the geometry of which is specific of the orientation of the crystal studied. It is then possible to orient easily, and with a good precision, microcrystals as small as a few tens of microns. (auth)

43465 THERMAL SPIKING IN HIGH-ENERGY BOMBARDED SILICON. Brack, K.; Schwuttke, G. H. (International Business Machines Corp., Hopewell Junction, N. Y.). Phys. Status Solidi (a); 5: No. 3, 711-17(16 Jun 1971).

Thermal spiking in 2-MeV N^+ bombarded silicon is reported. In areas of most intense irradiation the amorphous silicon, as a result of the ion bombardment, can melt locally and subsequently crystallize. The crystallized silicon has the same crystallinity and orientation as the surrounding lattice. In these areas the matrix lattice becomes strained. The strained lattice is visible in x-ray topographs through the presence of moiré fringes. The strained area around the crystallized silicon is soluble in HF. (auth)

Physical Properties

Refer also to abstracts 41777, 41778, 42062, 42886, 42892–42894, 42957, 42969, 42997, 43126, and 43289.

43466 (CONF-691208-(Vol.3)) PROCEEDINGS OF THE NUCLEAR PHYSICS AND SOLID STATE PHYSICS SYMPOSIUM, ROORKEE, DECEMBER 28–31, 1969. VOLUME III. SOLID STATE PHYSICS. (Department of Atomic Energy, Bombay (India). Physics Committee). 1969. 546p.

A total of 123 papers and 2 abstracts are included. Separate abstracts were prepared for 8 of the papers. (D.L.C.)

For abstracts of individual papers see: 43305, 43306, 43450, 43451, 43481, 43482, 43499, and 43500.

43467 (IPPJ-DT-20) EFFECT OF WORKING ON THE CHANGE OF PERMEABILITY (μ) OF AUSTENITIC STAINLESS STEELS. Fujiwaka, Setsuya (Nagoya Univ. (Japan). Inst. of Plasma Physics). Mar 1970. 27p. (In Japanese). Dep. NTIS (U. S. Sales Only).

The change of permeability (μ) by partial machining and welding was measured. The measurement is based on change of magnetic resistance caused by μ of samples. The change of magnetic flux was measured with a fluxmeter of electron tube type. Conventional SUS-27, SUS-32, SUS-41 and SUS-42 were used as samples. The

following treatments were applied to these samples; cold working, silver soldering and welding, use of different filler rods and solid solution treatment. Results showed that μ of the welded samples decreased in the order of argon arc welding (one layer), argon arc welding (two layers) and alternating current arc welding. This is due to difference in welding time among them and degree of fracture of austenite phase. (Japan)

43468 (NP-18657) ANNUAL REPORT, 1969-70. (Commonwealth Scientific and Industrial Research Organization, Melbourne (Australia). Div. of Chemical Physics). 52p. Dep. NTIS (U. S. Sales Only).

The Division's research activities have been carried out in eight main areas, namely: spectroscopy, mass spectroscopy, electron diffraction, electron microscopy, x-ray diffraction, solid-state chemistry, theoretical chemistry, instruments, and engineering services. (W.D.M.)

43469 (UCRL-20411) TABLE OF HYPERFINE FIELDS. Koster, Thomas A.; Shirley, David A. (California Univ., Berkeley). Nov 1970. Contract W-7405-eng-48. 17p. (CONF-700933-5). Dep. NTIS.

From Conference on Hyperfine Interactions Detected by Nuclear Radiation, Rehovot and Jerusalem, Israel.

Fields are tabulated for substitutional impurities in ferromagnetic iron, cobalt, nickel, and gadolinium. Data are given in columns listing elements, host material, temperature, hyperfine field, method of measurement, and reference. (M.O.W.)

43470 (UCRL-20500, pp 175-204) SOLID STATE PHYSICS. (California Univ., Berkeley. Lawrence Radiation Lab.).

In Inorganic Materials Research Division annual report, 1970.

Very brief summaries of individual items of research are included under the following broad categories: theoretical solid-state physics; magnetic properties of solids; far-infrared properties of solids; superconductivity; experimental solid-state physics and quantum electronics; and solid-state spin resonance and coherent laser pulse studies. References citing publication of the research, either as reports or in the open literature, are included at the end of each broad category. (L.M.T.)

43471 (YALE-3227-71) ANISOTROPIC INTERACTIONS BETWEEN MAGNETIC IONS. Wolf, W. P. (Yale Univ., New Haven, Conn.). [1970]. 28p. Dep. NTIS.

The conditions under which effective spin-spin interactions may be highly anisotropic are reviewed in the light of recent experimental results. It is shown that anisotropy may result from various orbital effects and also from restrictions imposed by certain types of single ion states. The most general situation is shown to be very complex but drastic simplifications are possible in some cases. For these, the interactions may be characterized by a few parameters which can be determined empirically. (auth)

43472 (YALE-3227-74) RADIO FREQUENCY MEASUREMENTS OF INTERACTIONS IN MAGNETIC INSULATORS. Skjeltorp, Arne T. (Yale Univ., New Haven, Conn.). 1971. 308p. Dep. NTIS.

Thesis.

A tunnel diode oscillator with an improved design used to carry out ac susceptibility experiments at radio frequencies is described. The real part of the susceptibility could be measured at frequencies from 0.4 to 100 MHz, at temperatures from 1 to 100°K, and in magnetic fields up to 25 kG. From such measurements one can obtain information on relaxation processes directly, and also the magnetic specific heat from the known thermodynamic relationship between the adiabatic susceptibility and the specific heat. A series of measurements were performed on three rare earth insulators having a hexagonal lattice structure. The magnetic specific heat was derived for $Tb(OH)_3$ and $Gd(OH)_3$ well above the ferromagnetic and antiferromagnetic ordering temperatures at 3.7 and 0.9°K, respectively. These specific heat data and data from the measurements of the isothermal susceptibilities were used, together with high-temperature expansions, to estimate the effective interactions between 1st, 2nd, and 3rd nearest neighbors. Rigorous calculations were performed on the 2 or 3 first coefficients in these expansions expressed in the dipolar and nondipolar interactions, leaving only nondipolar interactions for the three nearest neighbors as unknowns. The identification of these theoretical coefficients with the experimental values, gave consistent solutions of the nondipolar interactions. The second type of information one can obtain using this apparatus concerns relaxation processes. A series of measurements on neodymium ethyl sulfate $Nd(C_2H_5SO_4)_3 \cdot 9H_2O$ showed a temperature-independent but frequency-dependent change in the field dependence of the ac susceptibility. This is interpreted in terms of relatively slow electron spin-spin relaxation processes due to single-ion electron-nuclear hyperfine interaction in 20% of the Nd^{3+} ions. A reasonable phenomenological explanation of the experimental results is given, but a rigorous calculation of the ac susceptibility is shown to be prohibitively difficult. (auth)

43473 BERYLLIUM ADSORPTION ON TUNGSTEN. Zubenko, Yu. V.; Marinova, Ts. S. Uch. Zap. Leningrad. Gos. Univ., No. 354, Ser. Fiz. Nauk; No. 16, 3-7(1970). (In Russian).

Emission properties of beryllium film deposited on tungsten monocrystals in a 10^{-9} torr vacuum were studied at high temperatures using a field-emission microscope. Results showed that the beryllium emission was higher than in tungsten. The work function obtained for a thick layer of Be on W was ~4.8 ± 0.05 eV. At the (011) face where the work function was ~6 eV, Be reduced the work function, while at the other faces where the emission range was from 4.3 to 4.7 eV, it increased it. Data obtained are in good agreement with published data. (R.V.J.)

43474 FARADAY CUP LEED APPARATUS WITH FACILITY FOR INVESTIGATING THE ENERGY AND ANGULAR DISTRIBUTIONS OF INELASTICALLY SCATTERED OR PHOTOEMITTED ELECTRONS. Seah, M. P.; Forty, A. J. (Univ. of Warwick, Eng.). J. Phys., E (London); 3: 833-41(Nov 1970).

A relatively simple apparatus was developed for the direct measurement of the intensities of low-energy electron diffraction (LEED) beams from the surface of a single-crystal target. The energy and angular distributions of all the electrons inelastically scattered or emitted from a single crystal or polycrystalline target surface, monitored by LEED, can also be measured in this apparatus. LEED and electron or ultraviolet-light-induced electron emission measurements may be observed over a solid angle of emission of 3 π sterad. The apparatus includes a service area, for preparing crystal surfaces under uhv conditions, and manipulation devices for transferring the specimen and orienting its surface for a wide range of angles of incidence of the primary electron beam. (auth) (UK)

43475 LITHIUM DIHYDROGEN FLUORIDE: AN APPROACH TO METALLIC HYDROGEN. Gilman, J. J. (Allied Chemical Corp., Morristown, N. J.). Phys. Rev. Lett.; 26: 546-8(8 Mar 1971).

The possibility of making a new form of hydrogen in the metallic state through preparation of the compound LiH_2F is discussed. A proposed structure is specified which is believed to be nearly stable under ambient conditions. The pressures needed to stabilize this compound and to convert it to a metal are estimated. It may have an exceptionally high hydrogen density, high electrical conductivity, high Debye temperatures in the hydrogen sublattice, and perhaps a high superconducting transition temperature. (auth)

43476 INVESTIGATION OF SOME MAGNETO-ELECTRIC PROPERTIES OF NICKEL-MOLYBDENUM ALLOYS. Durdymuradova, R. Izv. Akad. Nauk Turkm. SSR, Ser. Fiz.-Tekh., Khim. Geol. Nauk.; No. 1, 109-13(1970). (In Russian).

A system of Ni-Mo alloys was investigated for which the ferromagnetic properties are lacking for the Mo/Ni composition 6/94 at.%. The chief goals of the investigation were: (1) a study of the longitudinal thermomagnetic Thompson-Bakhmet'ev effect on a system of Ni-Mo alloys over the temperature range from room temperature to the Curie point, and (2) a study of the specific electrical resistance of Ni-Mo alloys as a function of temperature. (tr-INIS)

43477 GENERALIZED SUSCEPTIBILITY FUNCTION FOR RARE EARTHS AND THORIUM AND THEIR ALLOYS. Liu, S. H.; Gupta, R. P.; Sinha, S. K. (Iowa State Univ., Ames). Phys. Rev., B; 4: No. 4, 1100-11(15 Aug 1971).

The results of calculations of the generalized susceptibility function $\chi(\vec{q})$ for the rare-earth metals and thorium and its alloys with rare earths are presented. For the heavy rare earths Gd, Tb, Dy, Er, and Lu, the calculation was confined to the ΓA direction, and a mesh of 450,000 points in the Brillouin zone was used. For the double-hexagonal close-packed crystals Nd and Pr, a mesh of 400,000 points in the Brillouin zone was chosen, while for thorium and its fcc alloys with rare earths, a mesh of 2,048,000 points in the Brillouin zone was used. The results of calculations on Sc and Y are also included for the sake of comparison with the heavy rare earths. The matrix elements, which couple the f electron and the conduction electron, appearing in the expression for the generalized susceptibility function, were taken to be constant. The calculations show that the $\chi(\vec{q})$ curves obtained in this way are reasonably smooth and the scatter of points along the curves is less than 3%. The results are compared with the experimental data on turn angles, spin-wave dispersion curves, and phonon spectra where available. (auth)

XUM

43478 LATTICE-DYNAMICAL CALCULATIONS FOR ZINC AND BERYLLIUM. Bezdek, H. F.; Finegold, Leonard (Univ. of Colorado, Boulder). Phys. Rev., B; 4: No. 4, 1390-3(15 Aug 1971).

Phonon dispersion curves for zinc and beryllium, measured by neutron-inelastic-scattering techniques, were used to determine the atomic force constants for the modified axially symmetric model developed by DeWames, Wolfram, and Lehman. However, calculations revealed that statistically equivalent fits to the experimental data may be obtained from more than one set of parameters. (auth)

43479 KONDO EFFECT IN SINGLE CRYSTALS OF DILUTE Y–Ce ALLOYS. Sugawara, T.; Yoshida, S. (Tokyo Univ.). J. Low Temp. Phys.; 4: No. 6, 657-67(Jun 1971).

The magnetic susceptibility and electrical resistivity of Ce impurities in single crystals of Y–Ce alloys were measured at temperatures down to 1.5°K in the directions parallel and perpendicular to the c axis of the crystal. The experimental results were interpreted in terms of the Kondo effect and the crystal-field effect. The data show that the crystal field of Y splits the $^2F_{5/2}$ ground state of the Ce^{3+} ion into three doublets, the lowest doublet specified by $j_z = \pm 1/2$. The susceptibility, resistivity, and specific heat results at low temperatures show evidence for the existence of a bound state due to the anisotropic Kondo interaction. Analysis of the low-temperature resistivity data yields a Kondo temperature of 40°K, which is independent of the current direction and the Ce concentration. The susceptibility and the resistivity at 0°K are nearly isotropic. (auth)

43480 MAGNETIC CHARACTERISTICS OF THE ALUMINUM-RICH TERNARY LAVES PHASES CONTAINING RARE EARTHS, NICKEL, AND ALUMINUM. Leon, B.; Rao, V. U. S.; Wallace, W. E. (Univ. of Pittsburgh). J. Less-Common Metals; 24: No. 3, 247-51(Jul 1971).

Weiss constants, Curie temperatures, saturation moments, and paramagnetic moments are reported for the four ternary systems $RAl_{2-x}Ni_x$ with R = Gd, Tb, Ho, and Er. The measurements apply to the primary solid-solution phase (C15 structure) based on RAl_2. For $TbAl_{2-x}Ni_x$, the magnetic properties decrease monotonically with increasing x. When R = Gd, Ho, or Er with increasing x the magnetic properties pass through a maximum at about x = 0.1. The results are discussed in terms of the RKKY interaction. Results for the Gd-, Ho- and Er-containing ternaries suggest $k_F \approx 1.4 \times 10^8$ cm^{-1} whereas $k_F \approx 1.3 \times 10^8$ cm^{-1} is required to account for the behavior of the $TbAl_2$-based ternaries. (auth)

43481 SEMICONDUCTOR-METAL TRANSITIONS IN VO_2, NbO_2, $V_{1-x}Ti_xO_2$ AND $V_{1-x}Nb_xO_2$. Subba Rao, G. V.; Natarajan, M.; Rao, C. N. R. (Indian Inst. of Tech., Kanpur). pp 301-2 of Proceedings of the Nuclear Physics and Solid State Physics Symposium, Roorkee, December 28–31, 1969. Vol. III. Bombay; Dept. of Atomic Energy (1969).

From Nuclear physics and solid state physics symposium; Roorkee, India (28 Dec 1969). See CONF-691208-(Vol. 3).

A study was made of the electric conductivity–temperature behavior of pure VO_2, NbO_2, and the solid solutions $V_{1-x}Ti_xO_2$ ($0 \le x \le 0.4$) and $V_{1-x}Nb_xO_2$ ($0.1 \le x \le 1.0$). Crystal structures before and after the transitions were examined, and differential thermal analysis was used to study the transition. The monoclinic structure of VO_2 is retained in $V_{1-x}Ti_xO_2$, and the high-temperature rutile structure is stabilized at room temperature in $V_{1-x}Nb_xO_2$. $V_{1-x}Nb_xO_2$ do not show the transition characteristics of VO_2 or NbO_2, while in $V_{1-x}Ti_xO_2$, the VO_2 transformation temperature and enthalpy decreases with x. The room-temperature conductivity of the solid solutions is higher than that of pure VO_2. A change from extrinsic to intrinsic conduction occurs in $V_{1-x}Nb_xO_2$ at x = 0.9 at 253° and 0.5 at 210°C. The transition in $V_{1-x}Ti_xO_2$ can be explained only on the basis of the localized model. (D.L.C.)

43482 POSITRON ANNIHILATION IN SOME TRANSITION AND ALKALINE EARTH OXIDES. Sishodia, Y. S.; Garg, J. C.; Chandra, R.; Sharma, B. K.; Saraf, B. L. (Univ. of Rajasthan, Jaipur, India). pp 414-16 of Proceedings of the Nuclear Physics and Solid State Physics Symposium, Roorkee, December 28–31, 1969. Vol. III. Bombay; Dept. of Atomic Energy (1969).

From Nuclear physics and solid state physics symposium; Roorkee, India (28 Dec 1969). See CONF-691208-(Vol.3).

Two-photon angular correlations and relative three-quantum yields of positrons were measured in NiO, ZrO_2, Nb_2O_5, and BeO pellets and powders. A single broad component was observed in the angular correlation curve, and a 10-kG field changed the peak rate of only BeO by 7%. The three-quantum yields did not differ from that of Al by more than two standard deviations. The results suggest that positronium is not formed in NiO, ZrO_2, and Nb_2O_5. (D.L.C.)

43483 ADVANCES IN SOLID STATE PHYSICS. Madelung, O. (ed.). Festkoerper Probleme X. Elmsford, N. Y.; Pergamon Publishing Company (1970). 442p. $23.00. (In German and English).

Thirteen papers are included. A separate abstract was prepared for the one paper in scope of NSA (on Type-II superconductors). The twelve papers not in scope include: narrow band gap in semiconductors; acousto-electric effects in picoelectric semiconductors; modulation spectroscopy of semiconductors; photoemission investigations of band structure in semiconductors; semiconductor properties of boron; 2-photon spectroscopy in solid state; theory of exciton spectra with consideration of exchange interaction; pseudopotential in semiconductor theory; determination of optical constants of solids from energy losses of medium-fast electrons; laser light—a new example of a phase transition; quantum and quasi-quantum crystals; and point defect arrangements in metal oxides. (M.H.R.)

For abstract of individual paper see: 43310.

43484 CROWDION MECHANISM OF PLASTIC DEFORMATION. Dranova, Zh. I.; D'yachenko, A. M.; Mikhailovskii, I. M. (Odessa State Univ.). JETP Lett. (USSR) (Engl. Transl.); 13: No. 1, 27-8(5 Jan 1971).

Translated from Zh. Eksp. Teor. Fiz., Pis'ma Red.; 13: No. 1, 40-3(5 Jan 1971).

It is shown that plastic deformation of tungsten at mechanical stresses close to the theoretical ultimate strength and at low temperatures may be associated with the formation and diffusion displacement of interstitial atoms with a mobility that is characteristic of metastable crowdion configurations. (auth)

43485 LATTICE CONSTANTS AND CURIE TEMPERATURES OF $CaCu_5$-TYPE THORIUM–COBALT COMPOUNDS. van der Goot, A. S.; Buschow, K. H. J. (Philips Research Labs., Eindhoven, Netherlands). Phys. Status Solidi (a); 5: No. 3, 665-8 (16 Jun 1971).

The homogeneity region of the compound $ThCo_5$ was studied by x-ray-diffraction and magnetic measurements. The increase in Co concentration corresponds to a substitution of a pair of Co atoms for each Th atom. An increase of the Co concentration of less than 2 at. % brings about approximately a doubling of the Curie temperature. (auth)

43486 PORTEVIN–Le CHATELIER EFFECT IN VANADIUM. Yoshinaga, H.; Toma, K.; Abe, K.; Morozumi, S. (Tohoku Univ., Sendai). Phil. Mag.; 23: No. 186, 1387-1403(Jun 1971).

In order to examine the temperature and strain-rate dependences of the Portevin–Le Chatelier (P–L) effect, tensile tests were carried out, using vanadium containing 170 ppm of carbon and 42 ppm of oxygen. The P–L effect was observed in the temperature range from about 200 to 500°C for a strain rate of 3.3×10^{-5}/sec. The serrations observed after the initial Lüders strain were classified into two types, relatively fine serrations (Type A) and coarser serrations (Type B) which appear intermittently and were observed clearly in the higher temperature region. Type A serration was associated with a very high work-hardening rate, while the rate was smaller with Type B serration. In the lower-temperature region, the P–L effect was observed only when the deformation proceeds beyond some critical strain, and the serration increased in stress amplitude with strain, while in the higher temperature region. Type A serration disappeared abruptly at some critical strain. Type B serration remained for some time after Type A serration had disappeared. The apparent activation energy was determined to be 27.9 kcal/mole from the critical conditions for the initiation of the P–L effect. The results as to Type A serration agree with the mechanism of jerky motion of dislocations dragged by solute atmospheres while those of Type B serration are understandable with the unlocking mechanism. (auth) (UK)

43487 SLOPE CHANGE IN TEMPERATURE DEPENDENCE OF ELECTRICAL RESISTIVITY OF THULIUM NEAR 22 K. Janos, S.; Mlynek, R. (Safarik Univ., Kosice, Czech. Inst. of Experimental Physics, Kosice, Czech.). Phys. Status Solidi (a); 5: No. 3, K211-12(16 Jun 1971).

A detailed study was made of the electric resistivity of 99.9%-pure thulium in the range 18 to 26°K. In the vicinity of 22°K (curie temperature of Tm), there was a marked change in the slope of the R vs T curve, in agreement with anticipations. (D.L.C.)

43488 5f MAGNETISM IN PALLADIUM–ACTINIDE SOLID SOLUTIONS. Nellis, W. J.; Brodsky, M. B. (Argonne National Lab., Ill.). Phys. Rev. B; 4: No. 5, 1594-1601(1 Sep 1971).

The electrical resistivities of palladium alloys containing 2.0 at.% or less neptunium or plutonium were measured in the range 1.3 to 300°K. The magnetic susceptibilities of these alloys were also measured in the range 2.5 to 300°K. Resistivity minima are observed for the Pd–Np alloys, but the resistivities of the Pd–Pu alloys have positive slopes at low temperatures. The magnetic susceptibilities of the alloys can be fitted to $\chi = \chi_0 + C/(T - \Theta)$ at low temperatures. For Pd–Np, $\Theta \simeq -13$°K and $\mu_{eff} = 2.0\mu_B$/Np atom. For Pd–Pu, $\Theta \simeq -3$°K and μ_{eff} increases from 0.55 to 1.3 μ_B/Pu atom with decreasing plutonium concentration. Apparently the 5f level is sufficiently localized to form a magnetic moment in Pd–Np, and is spin compensated at low temperatures. The Kondo temperature is estimated to be $T_K \simeq 15$°K. The Pd–Pu system is discussed in terms of localized spin fluctuations of the 5f electrons, with a spin-fluctuation temperature $T_S \simeq 1$°K. The Pd–U system was discussed earlier. It is suggested that in these alloys, indirect interactions between uranium impurities via the palladium conduction electrons and the modification of the 4d subband in the vicinity of uranium atoms cause the 5f level to narrow and lower to the Fermi level. (auth)

43489 PHYSICS OF EXOELECTRON EMISSION ON IONIC CRYSTALS. Bohun, A. PTB Mitt.; 80: 320-9(Oct 1970). (CONF-700715-1).

From 3rd International Symposium on Exoelectrons, Brunswick, West Germany (6 Jul 1970).

Exoelectron emission as well as related effects (luminescence, conductivity, optical absorption) are used to study ionic crystals. They are strongly influenced by internal and external factors e.g. lattice imperfections, impurities, irradiation, heat treatment, pressure. Results are given from "pure" and doped alkali halides mainly and from some more complicated substances. The different mechanisms of thermally and optically stimulated exoemission are discussed. Direct emission from traps as well as emission from the conduction band (Maxwell-tail theory) and recombination-induced emission (Auger-effect) are taken into account. (auth)

43490 VIBRATION SPECTRA AND DEBYE TEMPERATURES OF SOME TRANSITION METALS. Sharma, P. K.; Semwal, B. S.; Mehrotra, K. N. (Univ. of Allahabad, India). Z. Naturforsch.; 26a: No. 4, 747-52(Apr 1971).

The lattice vibration spectra and the associated constant-volume specific heats of the transition metals niobium, tantalum, chromium, and palladium were determined by using Sharma and Joshi's three-force constant model which includes the effect of electrons on lattice vibrations in metals. The calculated values of the specific heats and the equivalent Debye temperatures are compared with available calorimetric data. The frequency-versus-wave vector dispersion relations along the three major symmetry directions of chromium and palladium are determined and compared with curves deduced from recent neutron scattering experiments. Reasonably satisfactory agreement between theory and experiment is obtained. (auth)

43491 NATURE OF THE BOND AND ELECTRICAL CONDUCTIVITY OF CUBIC ZIRCONIUM CARBIDES AND OXYCARBIDES. Borukhovich, A. S.; Matveenko, I. I.; Zainulin, Yu. G.; Alyamovskii, S. I.; Gel'd, P. V. (Inst. of Chemistry, Sverdlovsk, USSR). Inorg. Mater. (USSR) (Engl. Transl.); 6: No. 12, 1866-70(Dec 1970).

Translated from Izv. Akad. Nauk SSSR, Neorg. Mater.; 6: No. 12, 2126-31(Dec 1970).

The temperature dependences of the electrical resistance of the temperature coefficient of the resistance of cubic ZrC_x and ZrC_xO_y in the homogeneous regions were studied. It is shown that the mechanism of transfer in ZrC_x can be explained only by taking account of s–d activation of the carriers and by using a two-tone model. It is concluded that the conductivity band of cubic ZrC_x must have the character of an "open" zone. Measurements of the coefficient of thermal expansion confirm the conclusion that polar interactions play a greater part in ZrC_xO_y than in ZrC_x. (auth)

43492 PROCEEDINGS OF THE FOURTH INTERNATIONAL COLLOQUIUM ON MAGNETIC THIN FILMS, PRAGUE, CZECHOSLOVAKIA, 21–23 SEPTEMBER 1970. Czech. J. Phys.; 21: No. 4-5, 329-587(1971). (CONF-700963).

Thirteen invited papers and 60 special papers were originally accepted for presentation; published here are 10 invited papers and 43 special papers, the others not submitted because of publication elsewhere or for other reasons. The 43 special papers are separated under the following categories: Theory of Magnetism, Spin Waves; Magnetization Reversal, Wall Creeping; Resonances; Anisotropy and Effects of Strain; Multilayered Films; Domains, Walls, Ripple; Composition, Structure, Magnetization; Mostly Oxides; and Miscellaneous. (L.M.T.)

Moessbauer Effects and NMR

Refer also to abstracts 42115, 42120, 42122, 42895, and 43894.

43493 NUCLEAR GAMMA-ACOUSTIC RESONANCE. Pokazan'ev, V. G. (Ural Polytechnic Inst., Sverdlovsk, USSR). Fiz. Metal. Metalloved.; 29: 496-501(Mar 1970). (In Russian).

It is shown that the intensity of gamma-radiation absorption is resonance-dependent on the ultrasonic frequency and on the degree of polarization of the nuclei. The resonance signal for ^{57}Fe nuclei was estimated. If the ultrasonic frequency is equal to the Larmor frequency of nuclei in the excited state, then the acoustic resonance of nuclei in this state develops according to the appearance of additional γ-radiation lines. Analogous results are anticipated for the case in which spin transitions are induced by a radio-frequency field. (tr-auth)

43494 HYPERFINE MAGNETIC FIELD FOR ^{119}Sn IMPURITY ATOMS IN FERROMAGNETIC TERBIUM. Kuchma, A. S.; Parfenova, V. I.; Shpinel, V. S. (Moscow State Univ.). JETP Lett. (USSR) (Engl. Transl.); 13: No. 4, 135-7(20 Feb 1971).

Translated from Zh. Eksp. Teor. Fiz., Pis'ma Red.: 13: No. 4, 192-4(20 Feb 1971).

Hyperfine magnetic fields for Sn impurity atoms in Tb and Gd matrices were measured with the aid of the Moessbauer effect on ^{119}Sn nuclei. Solid solutions of Sn(0.6 at.%), enriched to 86.9% with ^{119}Sn, in Tb and Gd were obtained by melting in an arc furnace in an argon atmosphere, followed by quenching. For the Sn–Tb alloy, the Mossbauer absorption spectra were measured at 4.2, 78, 85, 207, and 217°K. Similar measurements were made for the Gd–Sn system, and results agree with those made earlier on this system by Gotthardt et al. (Phys. Lett., 28A: 480(1969)). At a temperature close to 0°K the hyperfine fields are equal to 329 and 341 kOe, for the Sn–Tb and Gd–Sn systems, respectively. (J.C.W.)

43495 MAGNETIC SUSCEPTIBILITY OF URANIUM MONOPHOSPHIDE. Gulick, J. M.; Moulton, W. G. (Florida State Univ., Tallahassee). Phys. Lett.; 35A: No. 6, 429-30(12 Jul 1971).

The magnetic susceptibility of uranium monophosphide was measured from 300 to 1.3°K. The measurements above 77°K are in agreement with previous reported measurements. From 26 to 21°K the susceptibility decreases, levels off at a plateau from 23 to 22°K, and then decreases sharply until the temperature reaches 21°K. (auth)

43496 NUCLEAR QUADRUPOLAR RELAXATION IN SOLID AND LIQUID $AuGa_2$, $Au_{0.95}Pd_{0.05}Ga_2$, AND $AuIn_2$. Warren, William W. Jr.; Wernick, J. H. (Bell Telephone Labs., Murray Hill, N. J.). Phys. Rev. B; 4: No. 5, 1401-5(1 Sep 1971).

Nuclear quadrupolar relaxation rates were measured in the solid and liquid states of $AuGa_2$, $Au_{0.95}Pd_{0.05}Ga_2$, and $AuIn_2$ in order to investigate the effect of melting on quadrupolar relaxation processes. The quadrupolar relaxation rates are found to increase by factors of 3 and 5, respectively, when $AuGa_2$ and $AuIn_2$ are heated through their melting points. For $Au_{0.95}Pd_{0.05}Ga_2$, the relaxation rate decreases by about 35%. The relaxation rates observed in the solids have been identified by their temperature dependences as arising from interactions between the nuclei and lattice vibrations. Comparison of these rates with the rates in the liquids suggests that vibrational motions may make appreciable contributions to quadrupolar relaxation above the melting point as well. (auth)

43497 ^{17}O NMR STUDIES OF URANIUM OXIDES. Eastman, Michael P.; Hecht, Harry G.; Lewis, W. Burton (Los Alamos Stientific Lab., N. Mex.). J. Chem. Phys.; 54: No. 10, 4141-6 (15 May 1971).

The ^{17}O NMR of ^{17}O-enriched UO_2, $BiUO_4$, and KUO_3 was observed. A paramagnetic NMR shift was observed for UO_2 at 192.5, 299.5, and 405.2°K. The average isotropic coupling constant, A_s, calculated from these shifts is 2.84×10^{-5} cm^{-1}. In this calculation of A_s the magnitude of $\langle S_z \rangle$ on the uranium atom in UO_2 is determined assuming a $^3H_4$ ground state for the U^{4+}. Paramagnetic shifts were also observed for $BiUO_4$ and KUO_3 at 299.5°K. The value of A_s for $BiUO_4$ was determined to be 3.79×10^{-4} cm^{-1}. This value was calculated after assuming a $^2F_{\frac{5}{2}}$ ground state for U^{5+}. The same assumption in the case of KUO_3 yielded a value of 1.08×10^{-3} cm^{-1} for A_s. The validity of the assumption of pure Russell–Saunders ground states for these compounds is discussed. For KUO_3 the previously published spin–orbit coupling constant and crystal field terms are used to calculate a more reliable value of $\langle S_z \rangle$ on the central uranium atom. These calculations lead to a value of 7.01×10^{-4} cm^{-1} for A_s. The important

XUM

conclusions of this study are that the fractional s character in these compounds is small and that there is a negative spin density on the ^{17}O nuclei. Apparently the major contribution to the hyperfine interaction arises from the involvement of excited metal orbitals and/or from exchange polarization of core electrons. The NMR spectra of KUO_3 and $BiUO_4$ show the effect of anisotropic hyperfine interactions. The anisotropic interactions in $BiUO_4$ are shown to be predominantly π in character. An analysis of the KUO_3 spectrum indicates that anisotropic interactions are predominantly π in character and that $A_\pi \sim -6 \times 10^{-5}$ cm^{-1}. The linewidth of the isotropic UO_2 resonance is interpreted in terms of the Moriya spin-exchange mechanism and the value of ω_e is found to be $1.2 \times 10^{+13}$ sec^{-1}. (auth)

43498 NUCLEAR MAGNETIC RESONANCE AND RELAXATION OF ^{163}Dy IN FERROMAGNETIC DYSPROSIUM METAL AT LOW TEMPERATURE. Sano, Naokatsu; Kobayashi, Shun-ichi; Itoh, Junkichi (Osaka Univ.). Progr. Theor. Phys. (Kyoto), Suppl.; No. 46, 84-112(1970).

Nuclear magnetic resonance and relaxation of ^{163}Dy in ferromagnetic dysprosium metal were investigated at liquid helium temperatures. The NMR spectrum consists of five equally spaced lines in the frequency range from 300 MHz to 2000 MHz. Both spin–lattice and spin–spin relaxations were measured. It is concluded that a process in which the nuclear energy relaxes to the kinetic energy of the conduction electrons via spin waves (the Weger process) is predominant in the spin–lattice relaxation, and the spin–spin relaxation time is solely determined by the spin–lattice relaxation (the Walstedt mechanism). (auth)

Theory

Refer also to abstract 43505.

43499 ELECTRONIC ENERGY LEVELS OF U^{4+} AND U^{3+} IN UO_2 AND UI_3 CRYSTALS. Erdos, P.; Rudra, P. (Forida State Univ., Tallahassee. Saha Inst. of Nuclear Physics, Calcutta). pp 375-80 of Proceedings of the Nuclear Physics and Solid State Physics Symposium, Roorkee, December 28–31, 1969. Vol. III. Bombay; Dept. of Atomic Energy (1969).

From Nuclear physics and solid state physics symposium; Roorkee, India (28 Dec 1969). See CONF-691208-(Vol.3).

The energy levels were calculated in four parts: (1) electrostatic potential at the site of the U 5f electron, (2) the effect of crystal field (Sternheimer's shielding factor), (3) the matrix elements of the modified crystal-field potential, and (4) matrix diagonalization for eigenstates and eigenvalues. (D.L.C.)

43500 FERMI SURFACE AND ENERGY BANDS OF LANTHANUM. Ghosh, Aparna; Kumar, Santosh (Saha Inst. of Nuclear Physics, Calcutta). pp 435-8 of Proceedings of the Nuclear Physics and Solid State Physics Symposium, Roorkee, December 28–31, 1969. Vol. III. Bombay; Dept. of Atomic Energy (1969).

From Nuclear physics and solid state physics symposium; Roorkee, India (28 Dec 1969). See CONF-691208-(Vol.3).

Energy band calculations were carried out for La, using the symmetrized augmented plane wave method and the muffin-tin potential. Graphs are given for the energy band structure along all the symmetry lines and for the intersections of the Fermi surface with the boundary planes of $\frac{1}{24}$ Brillouin zone. A histogram is presented for the density of states. The electronic specific heat coefficient suggests that the electron–phonon interaction should be taken into account. (D.L.C.)

43501 METHOD OF CONSTRUCTING IRREDUCIBLE MULTIPLIER REPRESENTATIONS. Sahni, V. C.; Venkataraman, G. (Bhabha Atomic Research Centre, Bombay). Phys. Kondens. Mater.; 11: 199-211(1970).

A systematic method is presented for constructing the irreducible multiplier representations (ray representations) of a class of finite groups corresponding to a given factor system. The method consists in first identifying a normal subgroup of prime index, classifying its irreducible multiplier representations into orbits and then inducing the required representations from these orbits. The proposed technique finds useful application in solid state physics where irreducible multiplier representations of the point group underlying the group of the wave vector are frequently required. (auth)

43502 ANNIHILATION OF EXCITONS AND EXCITON–PHONON INTERACTION. Gross, E. F.; Permogorov, S. A.; Razbirin, B. S. Usp. Fiz. Nauk; 103: No. 3, 431-46(Mar 1971). (In Russian).

The motion of free excitons in crystals was examined from the emission spectra. Characteristic of the emission of free excitons is a mutual annihilation of an electron and a hole, forming the exciton. In accordance with the laws of conservation of energy and wave vectors, phonon-free emissive annihilation becomes possible only for excitons, possessing a very small quasi-impulse (in comparison to thermal) and kinetic energy. Excitons with a given value of kinetic energy may annihilate with the simultaneous release of one or two visual phonons, whereupon the form of the excited radiation line directly reflects the dispersion of excitons in the kinetic energy region. On the bases of the laws of conservation of energy and the quasi-impulse, a study was made of the form of the radiation spectra that arises as a result of single-phonon or double-phonon annihilation of excitons, and such a study of exciton–phonon annihilation is reported for crystals of Cd, CdSe, Cu_2O, and Si in the temperature range of 4.2 to 77°K. The results of the study showed that in a number of cases of free excitons it was possible to observe free quasi particles in thermal equilibrium with the crystal lattice. Analogous processes are discussed as well as the possibility of utilizing exciton–phonon annihilation for obtaining stimulated emission. (tr-auth)

43503 INTRODUCTION TO THE THEORY OF SOLID STATE PHYSICS. Patterson, James D. Addison-Wesley Series in Solid State Sciences. Reading, Mass.; Addison-Wesley Publishing Company (1971). 396p.

The purpose of this course in solid state physics for graduate students is to present a logical development of the ideas of this branch of physics. The book emphasizes fundamentals and offers a greater exposition of much of the mathematics than is usual. The text covers crystalline structure, electrons in crystals, phonons, magnetism in solids, the interactions of phonons and electrons, a brief introduction to the Fermi surface, semiconductors, optical properties of solids, defects in solids, dielectrics, and superconductivity. (auth)

Theoretical Physics

Refer also to abstracts 43367, 43590, 43668, and 43724.

43504 (BMBW-FBK-70-32) MONTE CARLO MODEL FOR LINEAR PARAMETER VARIATION. Schmid, E. W. (Tuebingen Univ. (West Germany). Institut fuer Theoretische Physik). Dec 1970. 26p. (In German). Dep. NTIS (U. S. Sales Only).

A variational principle for scattering problems is presented which minimizes the length of a vector in a given test function space by variation of linear parameters. For its practical use a model is suggested in which configuration space is represented by a discrete set of random variables. As an example, a way of solving the three-particle reaction problem with breakup is discussed. (auth)

43505 (EUR-4349) DETERMINATION OF THE EIGENVALUES OF THE MATHIEU EQUATION. Gloden, R. F. (European Atomic Energy Community, Ispra (Italy). Joint Nuclear Research Center). 1969. 37p. (In French). NTIS (U. S. Sales Only).

Eigenvalues were determined for the Mathieu equation $d^2\psi/d\varphi^2 + (\Lambda - 2\alpha \cos n\varphi)\psi = 0$, concerning the potential $V = V_n/2(1 + \cos n\varphi)$, in the cases $n = 3$ and $n = 6$, in order to extend to small values of α the table established by E. O. Stejskal and H. S. Gutowski for $n = 3$ and to construct an analogous table in the case $n = 6$. This work takes its origin from a nuclear relaxation problem and concerns hindered reorientations in certain orgainic substances, where the observed phenomena cannot be explained in a classical manner. The resolution of a Mathieu equation corresponding to a potential with n-fold symmetry is studied; the eigenvalues are determined either by the method of infinite determinants or by the method of continued fractions. Some simple procedures (linear change of the variable, limited series expansions) for checking the results obtained are outlined. (auth)

43506 (JINR-P4-5786) NOTE ON INTERFERENCE AT THE INTERSECTION OF LEVELS. Baryshevskii, V. G.; Podgoretskii, M. I. (Joint Inst. for Nuclear Research, Dubna (USSR). Lab. of High Energy). 1971. 7p. (In Russian). Dep. NTIS (U. S. Sales Only).

The effect of the inhomogeneous broadening on the form of the extension curve of intersecting levels is considered. It is shown that the area under the extension curve does not depend on the statistical field properties inducing the mentioned spread. It gives the possibility of separating inhomogeneous broadening from that connected with the decay of atoms and nuclei. (auth)

43507 (JPRS-52839, pp 3-16) MOTION OF CHARGED PARTICLES IN MAGNETIC FIELDS WITH MODEL EXPERIMENTS. Hsu Jung-lan; Chou Kuo-ch'eng. Translated from Ti Ch'iu Wu Li Hsueh Pao; 12: No. 2, 121-9(1963). NTIS.

It is assumed that the magnetic field is under potential and the

potential function is separately considered as having axial symmetry and as a plane function. As found from calculation results, when the magnetic field is strong enough the boundary of the region of charged-particle motion is similar to that of magnetic lines. This result shows that one can use the graphs of a magnetic coil to determine the region of charged-particle motion. Further, these results are compared with model experiments. In glow-discharge experiments in a magnetic field, part of the glow region in the discharge corresponds to the region of particle motion, and part of the dark region corresponds to the forbidden-particle region. Comparison of results reveals that the boundary of the glow region is similar to magnetic lines. (auth)

43508 BOUNDARY CONDITIONS FOR AN INFINITE SQUARE-WELL POTENTIAL IN QUANTUM MECHANICS. Seki, Ryoichi (San Fernando Valley State Coll., Northridge, Calif.). Amer. J. Phys.; 39: No. 8, 929-31(Aug 1971).

A well-known problem of an infinite square-well potential in quantum mechanics furnishes an interesting boundary condition. This was investigated in detail by considering the infinite square-well potential as a limiting case of a finite square-well potential. (auth)

43509 EXACTLY SOLUBLE QUANTUM-MECHANICAL THREE-BODY PROBLEM. Lim, T. K. (Florida State Univ., Tallahassee). Amer. J. Phys.; 39: No. 8, 932-4(Aug 1971).

An exact solution is obtained for a model three-body system in which the particles interact through pairwise, harmonic oscillator, and spin-dependent potentials, the solution being achieved by a simple transformation to an appropriate coordinate system. In particular, it is shown that the S-state wave functions of the ground state of the triton span the two-dimensional representation of the symmetric group S_3, are orthogonal, and resemble closely the Irving wave forms found so successful in variational calculations. (auth)

43510 HELLMANN–FEYNMAN THEOREMS IN CLASSICAL AND QUANTUM MECHANICS. McKinley, William A. (Rensselaer Polytechnic Inst., Troy, N. Y.). Amer. J. Phys.; 39: No. 8, 905-10(Aug 1971).

Theorems giving exact expressions for the derivative of the energy with respect to a parameter in the Hamiltonian for cyclic classical mechanical problems in both the relativistic and nonrelativistic cases are derived. Comparison is made with similar well-known theorems in the quantum mechanical case. Applications of both classical and quantum derivative relations are made to deduction of parametric dependence of the energy in simple cases, deduction of a meaning to the expectation value of the Dirac operator β, and construction of a test of consistency for a well posed problem in the theory of a Dirac particle in a bound state. (auth)

43511 STATISTICAL QUASIPARTICLES, EFFECTIVE GREEN'S FUNCTIONS, AND LANDAU DESCRIPTIONS OF QUANTUM LIQUIDS. I. IMPURITY SYSTEMS AT EQUILIBRIUM. Balian, Roger; de Dominicis, Cyrano (Centre d'Etudes Nucleaires, Saclay, France). Ann. Phys. (N. Y.); 62: 229-92(Feb 1971).

Landau descriptions of quantum liquids are dealt with, which are exact, in the sense that their derivation appeals to no approximation, and relies only on the convergence of the expansions involved. An extension of the validity of Landau's results is obtained, together with diagrammatic expansions for Landau's parameters. It is restricted to noninteracting particles in a random external field describing impurities. The impurities are distributed either homogeneously or at lattice sites. Such a system, though not a Landau–Fermi liquid in the usual sense, retains several features of the general system of interacting fermions. The method used is straightforward, the only delicate point being raised by the need for a regularization procedure whenever integrands with vanishing denominators show up. The final result expresses thermodynamic observables in terms of an effective Green's function $G_k^{eff}(y)$, defined on the real axis. G_k^{eff} has a single real pole at $y = \epsilon_k$ with a real residue Z_k, and describes a "statistical quasiparticle." The energy ϵ_k replaces here the complex pole of the causal Green's function usually associated with elementary excitations and bears a simple relation with the single-particle level density. The Gibbs potential itself turns out to be exactly the same as for noninteracting particles of energies ϵ_k. Alternatively, it may be obtained as the stationary value of a functional of the statistical quasiparticle energies ϵ_k (in a way reminiscent of Brillouin–Wigner expansions), of the wavefunction renormalization constants Z_k, and of the quasiparticle occupation numbers F_k. The validity of this formulation is tested by a study of the convergence of a typical subseries. Self-contained appendices are devoted to a discussion of the general regularization problem and to the extension of Lagrange expansions to matrices, respectively. (auth)

43512 APPLICATIONS OF THE COHERENT STATE REPRESENTATION IN THE THEORY OF MAGNETISM. I. THE HEISENBERG MODEL. Douglass, Kenneth H. (Pennsylvania State Univ., Schuylkill Haven). Ann. Phys. (N. Y.); 62: 383-421 (Feb 1971).

By transforming the Heisenberg model Hamiltonian to Bose operators it becomes possible to define a coherent state representation for the spin system. This representation proves to be a useful basis for evaluating the partition function in a manner similar to that used previously for a superfluid. A hard-core repulsive interaction is used to include the effects of the spin commutators exactly. The scattering of two spin waves is solved to all orders of perturbation theory in this formalism and used to rederive the low-temperature series expansions due to Dyson. The results using the hard-core interaction are compared with those using Dyson's dynamical interaction alone. The method is extended to give some results for the case of an anisotropic exchange interaction. (auth)

43513 DAMPED DEGENERATE-LEVEL ATOM. Aharony, Amnon (Tel Aviv Univ., Israel). Ann. Phys. (N. Y.); 62: 343-60 (Feb 1971).

Equations are derived for the time evolution of the reduced density operator for an (N + 1)-state atom which is damped by its coupling to a finite-temperature boson bath. General formal solutions are discussed in the limit of low temperature. Exact solutions are given for the decay of a p level in an electric field. The effects of a driving field and of transitions between the excited states on the equations are discussed. The application for the decay of elementary particles is mentioned. (auth)

43514 NOTE CONCERNING PROPOSITIONS IN QUANTUM MECHANICS. Schroeter, J. (Univ., Marburg, Ger.). Ann. Phys. (Leipzig); 25: No. 3, 243-5(1970).

It is shown that the interpretation of quantum mechanics as a theory describing systems for which their propositions are always valid or not leads to a contradiction within the theory. The proof does not depend on any specific property of measurements, but only the usual description of ensembles of quantum objects by statistical operators is used. (auth)

43515 SPECTRAL INTENSITY DISTRIBUTION OF COMPTON RADIATION BY THE THOMAS–FERMI MODEL. Weick, Dietrich (Fritz-Haber Inst., Berlin). Ann. Phys. (Leipzig); 25: No. 2, 143-67(1970). (In German).

It is shown that the results obtained by Heisenberg (Phys. Z., 32: 737(1931)) and Bewilogua (Phys. Z., 32: 740 (1931)) for the total intensity of incoherent scattering of x rays (at a fixed scattering angle) on the basis of the Thomas–Fermi model contain information also with respect to the spectral distribution of the scattered radiation. A remarkable consequence is an asymmetry of the Compton line profile, which is increasing with the influence of electron binding. This gives rise to some modifications of current views concerning: (1) the application of the Breit–Dirac correction factor to the Waller–Hartree formula, and (2) the relation between the Compton line profile and the electron momentum–density distribution. (auth)

43516 CERTAIN DISPERSION EFFECTS IN MOLECULAR GASES IN PARALLEL CONSTANT AND ALTERNATING MAGNETIC FIELDS. Borman, V. D.; Nikolaev, B. I.; Troyan, V. I. (Inst. of Engineering Physics, Moscow). JETP Lett. (USSR) (Engl. Transl.); 13: No. 6, 221-4(20 Mar 1971).

Translated from Zh. Eksp. Teor. Fiz., Pis'ma Red.; 13: No. 6, 311-14(20 Mar 1971).

A heated cylinder in a molecular gas rotates when a magnetic field directed along the axis is turned on (observed by Scott et al., 1967). It has also been shown by other authors that the dependence of the angle of rotation of the cylinder on the ratio of field intensity to gas pressure is determined by the kinetic coefficient that connects the tensor of the viscous stresses with the second derivative of the temperature in the second Chapman–Enskog approximation. The behavior of the transport coefficients of nonparamagnetic molecular gases in parallel constant and alternating magnetic fields is considered, and the explanation of the singularities of the Scott effect is given. It is shown that the number of maxima in the frequency dependence of this effect is connected with the form of the anisotropy of the distribution function in the space of the velocities and moments of the molecules. (J.C.W.)

43517 SCHROEDINGER PARTICLE IN A GRAVITATIONAL WELL. Langhoff, P. W. (Indiana Univ., Bloomington). Amer. J. Phys.; 39: No. 8, 954-7(Aug 1971).

It is suggested that a suitably designed experiment can discriminate mass in a bounded uniform gravitational field. To investigate this possibility, the closely related problem of one-

XUM

dimensional scattering from a gravitational barrier (or well), embedded in a region of otherwise constant potential, was considered and it was found that the transmission coefficient is indeed mass-dependent. (W.D.M.)

43518 FORCED LEVEL SHIFTS AND ENERGY RENORMALIZATION. Eldyshev, Yu. N. Vestn. Mosk. Univ., Ser. III. Fiz. Astron.; No. 1, 26-31(Jan-Feb 1969). (In Russian).

A Furry concept of energy renormalization was used for determining interactions of atomic electrons with incoming photons (the Stark effect in a variable field). The specific induced shift of energy levels produced by this interaction was investigated by Welton (Phys. Rev., 74: 1157(1948)) semiclassical model, and subsequently within the framework of quantum electrodynamics as illustrated with two-level models. (tr-auth)

43519 FOLDED DIAGRAMS. Johnson, Mikkel B.; Baranger, Michel (Massachusetts Inst. of Tech., Cambridge. Carnegie-Mellon Univ., Pittsburgh). Contract AT(30-1)-2098. Ann. Phys. (N. Y.); 62: 172-226(Jan 1971).

The Morita–Brandow folded diagrams are derived from a time-dependent point of view. The effective interaction in the model space is energy-independent, contains only linked clusters, and can easily be made Hermitian. Even then, it is still highly arbitrary. For each choice of effective interaction, rules are given for the calculation of effective operators, such that the matrix element of any effective operator between any two model states equals the matrix element of the true operator between the corresponding true states. Examples of folded diagrams are given and methods for calculating them are explained. Examples of effective operators are also given, including the effective spectroscopic amplitude, whose square is the spectroscopic factor of one-nucleon transfer reactions. (auth)

43520 INTERCHANGE THEOREMS FOR TRIPLE PERTURBATION THEORY. Tuan, Debbie Fu-tai (Harvard Univ., Cambridge, Mass. Kent State Univ., Ohio). J. Chem. Phys.; 54: No. 11, 4631-7(1 Jun 1971).

Based on Rayleigh–Schrödinger perturbation theory, eight general expressions of the triple perturbation energy $\epsilon^{a,m,t}$ are derived. The relationships among them give several general interchange theorems in a compact fashion. These interchange theorems exchange the integrals involving higher-order perturbed wave functions related to a complicated perturbation λV for integrals involving higher-order perturbed wave functions related to the simpler perturbations. From the perturbed wave function corrected to the nth order of λV, (1) in general, the interchange theorems make it possible to obtain the perturbation energy to the (n + 1)th order; (2) when H^0 and λV are Hermitian, the interchange theorems make it possible to obtain the perturbation energy to the (2n + 1)th order; (3) when H^0, λV, and other perturbations are Hermitian, the interchange theorems reduce the required total order of wave functions related to the Hermitian perturbations to almost half. These interchange theorems can be applied to any triple perturbation problem when the unperturbed state is nondegenerate. They are valid to all orders with respect to the three perturbations. The application of these interchange theorems to calculation of certain kinds of second-order physical properties, F, such as electric shielding factors, chemical shifts, and nuclear spin–spin coupling constants, is discussed. It is shown that if (1) the two perturbations associated with the properties are one-electron operators and (2) the zeroth-order wave function of a closed-shell system is obtained by the SCF method, then the first-order correction of F is determined solely by the first-order orbitals, $i^{0,1,0}$ and $i^{0,0,1}$, related separately to the two perturbations but does not depend on any "cross" second-order orbitals, $i^{0,1,1}$. This result will greatly simplify the calculation. (auth)

43521 VARIATION OF NONLINEAR PARAMETERS TO COMPUTE DECAY-CONSTANTS AND THEIR STANDARD DEVIATION. Klenk, R.; Grass, F.; Girsig, F.; Brandstaedter, O. (Oesterreichische Hochschule, Vienna). Nucl. Instrum. Methods; 94: No. 2, 357-63(1971).

A computer method, which does not require good initial estimates for the nonlinear parameters, was developed for fitting a decay curve. It is necessary only to declare intervals in which the values of the parameters are included. For a net of half-life combinations, taken from the intervals, the best linear parameters and a "goodness of fit" quantity are computed. This quantity, as a function of the nonlinear parameters, is used to compute the values of the "best" parameters and their standard deviation by means of parabolic interpolation. The sharpness of a chi-square test, depending on the number of data points, is investigated; and a general, semi-empirical formula for the relative error of the half-life of a single component with background using equidistant data points is deduced by analyzing suitable synthetic data. Under certain conditions the computer method can be generalized to any nonlinear curve fit. (auth)

43522 DENSITY FLUCTUATIONS IN AN INTERACTING BOSE GAS. Cheung, T. H.; Griffin, Allan (Univ. of Toronto). Phys. Rev., A; 4: No. 1, 237-45(Jul 1971).

The density fluctuation in a Bose gas interacting via a strong short-range repulsive potential and a weak long-range attractive potential is studied by the methods of quantum-field theory. The density-density correlation function is generated by taking the functional derivative of the single-particle matrix Green's function $G_2(1,2)$ with respect to an auxiliary scalar field. For $G_1(1,2)$, one uses the Hartree approximation for the attractive potential and the Hartree–Fock approximation for the short-range repulsive potential. It is shown that the density fluctuation spectrum is identical to the Beliaev approximation for the single-particle excitation spectrum. (auth)

43523 INTERPRETATION OF MEASUREMENT IN QUANTUM THEORY. Zeh, H. D. (Univ., Heidelberg). Found. Phys.; 1: No. 1, 69-76(1970).

It is demonstrated that neither the arguments leading to inconsistencies in the description of quantum-mechanical measurement nor those "explaining" the process of measurement by means of thermodynamical statistics are valid. Instead, it is argued that the probability interpretation is compatible with an objective interpretation of the wave function. (auth)

43524 DISTINGUISHABLE EQUIVALENT PARTICLES WITH SYMMETRIZED WAVE FUNCTIONS. Siegel, Armand (Boston Univ.). Found. Phys.; 1: No. 1, 57-68(1970).

The quantum formalism of distinguishable, yet equivalent particles (with symmetric or antisymmetric wave functions) is worked out. The result is an entirely explicit formulation of the way in which classical mechanics emerges from quantum mechanics for such particles. Distinguishability is achieved at the cost of dynamical precision; the two are, in fact, complementary. (auth)

43525 CONCEPT OF TRANSITION IN QUANTUM MECHANICS. Park, James L. (Washington State Univ., Pullman). Found. Phys.; 1: No. 1, 23-33(1970).

The concept of quantum transition is critically examined from the perspective of the modern quantum theory of measurement. Historically rooted in the famous quantum jump of the old quantum theory, the transition idea survives today in experimental jargon due to (1) the notion of uncontrollable disturbance of a system by measurement operations and (2) the wave-packet reduction hypothesis in several forms. Explicit counterexamples to both (1) and (2) are presented in terms of quantum measurement theory. It is concluded that the idea of transition, or quantum jump, can no longer be rationally comprehended within the framework of contemporary physical theory. (auth)

43526 SYMPOSIUM ON OPTIMIZATION, HELD IN NICE, JUNE 29th–JULY 5th, 1969. Balakrishnan, A. V.; Contensou, M.; de Veubeke, B. F.; Kree, P.; Lions, J. L.; Moiseev, N. N. (eds.). Lecture Notes in Mathematics. Volume 132. Berlin; Springer-Verlag (1970). 355p. $6.10. (In French and English). (CONF-690660).

Twenty-three papers are included. An abstract was prepared for one of these papers. (M.O.W.)

For abstract of individual paper see: 43337.

PHYSICS (HIGH ENERGY)

Particle Interactions and Properties (Experimental)

Refer also to abstract 43566.

Electromagnetic

Refer also to abstract 43583.

43527 (DESY–71/21) INELASTIC ELECTRON–PROTON SCATTERING IN THE REGION OF THE Δ (1236) RESONANCE. Bartel, W.; Buesser, F.-W.; Dix, W.-R.; Felst, R.; Harms, D.; Krehbiel, H.; Kuhlmann, P. E.; McElroy, J.; Meyer, J.; Weber, G. (Deutsches Elektronen-Synchrotron, Hamburg (West Germany)). May 1971. 10p. Dep. NTIS (U. S. Sales Only).

Electron–proton inelastic scattering cross sections were measured at four momentum transfers q^2 between 0.4 and 0.8 $(GeV/c)^2$ by detecting electrons scattered at 86°. The range of invariant mass W of the hadronic final state was 1.10 to 1.35 GeV. The data were combined with the results of an earlier experiment performed at small electron scattering angles and analyzed in terms of the cross sections G_T and G_L for the absorption of transverse and longitudinal photons. (auth)

43528 (LAL–1250) BACKWARD ELECTRON DEUTERON SCATTERING BELOW 280 MeV. Ganichot, D.; Grossetete, B.; Isabelle, D. B. (Paris Univ., Orsay (France). Laboratoire de l'Accelerateur Lineaire). Apr 1971. 35p. Dep. NTIS (U. S. Sales Only).

The elastic and inelastic scattering of electrons on deuterium at 180° was measured for four incident energies (70, 140, 210 and 280 MeV). The data were analyzed with a technique allowing an accurate comparison between experiment and theory. A good agreement was observed for the inelastic data with the Jankus–Durand predictions. But the experimental elastic cross section is systematically larger than the cross section expected using the presently available deuteron models and nucleon form factors. (auth)

43529 NEUTRAL PION AND ETA PHOTOPRODUCTION FROM HYDROGEN AT HIGH ENERGIES. Johnson, James Russel. Stanford, Calif.; Stanford Univ. (1970). 101p. University Microfilms Order No. 71-12,927.

Thesis.

Measurements were made of the process $\gamma p \rightarrow \pi^0 p$ for photon energies from 4 to 18 GeV and four-momentum transfers t between −0.1 and −1.4 $(GeV/c)^2$. The reaction $\gamma p \rightarrow \eta p$ was studied between 4 and 9 GeV for t-values from −0.3 to −1.4 $(GeV/c)^2$. The experiment was carried out at the Stanford Linear Accelerator Center (SLAC) by passing the SLAC photon beam through a target containing gaseous hydrogen for small momentum transfers and liquid hydrogen for higher t-values. The recoil protons were analyzed and detected in the SLCA 1.6 GeV/c spectrometer, and the "missing mass" of the neutral product was calculated from kinematics. The π^0 photoproduction cross sections decrease rapidly with increasing |t| beyond |t| = 0.1, show a local minimum or "dip" around |t| = 0.5 and a secondary maximum for |t| ≈ 0.85, then fall off smoothly out to |t| = 1.4. The energy dependence appears close to E_0^{-2}, becoming only gradually steeper with increasing |t|, contrary to some theoretical predictions. The energy dependence of η production is consistent with E_0^{-2}, but the t-dependence shows only a smooth decrease with |t| and no sign of a dip at t = −0.5 $(GeV/c)^2$. A simple t-channel exchange model cannot then explain both processes with the same assumptions, even though the quantum numbers of the two mesons are the same except for isospin. (Diss. Abstr. Int., B)

43530 NEUTRAL DECAYS OF THE η^0 MESON. Risser, Thomas Bard. Berkeley, Calif.; Univ. of California (1970). 150p. University Microfilms Order No. 71-15, 874.

Thesis.

Eta mesons were produced by the reaction $\pi^- p \rightarrow \eta^0 n$. Veto counters surrounding the hydrogen target in which this interaction takes place eliminate all reactions involving charged particles. The neutral decays of the eta meson are studied with a cubical array of lead plate spark chambers for the conversion of gamma rays. The eta producing reaction is identified by the time of flight of the neutron from the hydrogen target. The neutron is detected by one of twenty large scintillation counters. It is found that the data are consistent with zero decays of the type $\eta^0 \rightarrow \pi^0\gamma\gamma$. With the assumption that only the neutral decays $\eta^0 \rightarrow \gamma\gamma$ and $\eta^0 \rightarrow 3\pi^0$ are present, $R[(\eta^0 \rightarrow \gamma\gamma)/(\eta^0 \rightarrow \text{all neutrals})] = 0.580 \pm 0.013$ and $R[(\eta^0 \rightarrow 3\pi^0)/(\eta^0 \rightarrow \text{all neutrals})] = 0.420 \pm 0.015$ are found. Furthermore, it is found that, with 95% confidence $R[(\eta^0 \rightarrow \pi^0\gamma\gamma)/(\eta^0 \rightarrow \text{all neutrals})] < 0.061$. (Diss. Abstr. Int., B)

Weak

43531 MEASUREMENT OF THE TWO PHOTON DECAY OF THE K_1^0 MESON. Enstrom, James Eugene. Stanford, Calif.; Stanford Univ. (1970). 117p. University Microfilms Order No. 71-12,893.

Thesis.

A measurement of the rate $\Gamma(K_1^0 \rightarrow 2\gamma)$ was made relative to the rates $\Gamma(K_L^0 \rightarrow 3\pi^0)$, $\Gamma(K_L^0 \rightarrow \pi^\pm\mu^\mp\nu_\mu)$, and $\Gamma(K_L^0 \rightarrow \pi^\pm e^\mp \nu_e)$ using a spark chamber scintillation counter experiment. Using published branching ratios of the three body decays relative to the rate $\Gamma(K_L^0 \rightarrow \text{all})$, the branching ratio $\Gamma(K_L^0 \rightarrow 2\gamma)/\Gamma(K_L^0 \rightarrow \text{all})$ was found to be $(4.5 \pm 1.0) \times 10^{-4}$, based on 23 valid decays, which were separated from a small background. The result is compared with theoretical predictions and other experimental measurements. (Diss. Abstr. Int., B)

43532 MEASUREMENT OF THE ANGULAR CORRELATION BETWEEN THE NEUTRON SPIN AND THE ELECTRON MOMENTUM IN THE DECAY OF POLARIZED NEUTRONS. Erozolimskii, B. F.; Bondarenko, L. N.; Mostovoi, Yu. A.; (and others). JETP Lett. (USSR) (Engl. Transl.); 13: No. 7, 252-5(5 Apr 1971).

Translated from Zh. Eksp. Teor. Fiz., Pis'ma Red.; 13: No. 7, 356-9(5 Apr 1971).

A precision measurement of the coefficient of angular correlations in the β-decay of polarized neutrons is described. The result $A = -0.118 \pm 0.010$ is found in good agreement with other data. (L.B.S.)

Strong (Baryon-Induced)

43533 (CEA-R-4150) STUDY OF NUCLEON–NUCLEON INTERACTION FROM THE 3 NUCLEON INTERACTION D(n,nnp) AT 14 MeV. Gondrand, Jean-Claude (Commissariat a l'Energie Atomique, Grenoble (France). Centre d'Etudes Nucleaires). Jun 1971. 74p. (In French). Dep. NTIS (U. S. Sales Only).

Thesis. Submitted to Univ. of Grenoble, France.

The n-p spectrum for the neutron-proton final state interaction in a complete D(n,nnp) experiment at 14 MeV was measured with a two-dimensional time of flight spectrometer. A previously measured n-n spectrum, and the n-p spectrum are compared with theoretical convoluted spectra obtained from Faddeev equations (AMADO Model) for three nucleon-nucleon potentials. The cross sections $\sigma(E_1,\Omega_1,\Omega_2)$ are extracted from the two experimental spectra by a simulation method. (France)

43534 (NP–18814) SCATTERING LENGTH OF THE n–n REACTION. Maldonado, Javier Flores (Instituto Politecnico Nacional, Mexico City. Escuela Superior de Fisica y Matematicas). Oct 1970. 52p. (In Spanish). Dep. NTIS (U. S. Sales Only).

Thesis.

An experiment to measure the scattering length of the n–n direct reaction using the pulsed neutron source from the CNEN reactor is described. From the equations derived and the numerical calculations it was concluded that the effect is detectable. The problem of neutron background is null. A large number of measurements of n should be made in order to obtain good statistics. A good vacuum is necessary within the duct. N (the number of scattered neutrons) is determined and from it the corresponding value of σ_{nn}. From the calculated σ_{nn} the corresponding scattering length will be calculated. Data on the nuclear interaction potential between neutrons will be obtained in order to determine the scattering length. By comparison of the theoretical and experimental values of the scattering length, the validity of the hypothesis of symmetry of the nuclear forces with respect to the charge will be tested. (tr-auth)

43535 STUDY OF PROTON–PROTON INTERACTIONS AT 25 GeV/c IN THE FOUR-PRONG FINAL STATE. Nieporent, Richard Joel. New Brunswick, N. J.; Rutgers–The State Univ. (1970). 131p. University Microfilms Order No. 71-12,265.

Thesis.

Two aspects of proton–proton interactions in the four-prong final state are examined. The first aspect looked at was the production of isobars, especially the enhancements seen in the $p\pi^+\pi^-$

XUM

invariant mass spectrum from the $pp\pi^+\pi^-$ final state. The second aspect examined was a comparison of the theoretical model for the production of multi-particle final states with the experimental data. The data for the experiment was obtained from an 87,000 picture exposure of 25 GeV/c protons incident on the Brookhaven National Laboratory 80 inch hydrogen filled bubble chamber. The following reactions were investigated: (a) $p + p \rightarrow p + p + \pi^+ + \pi^-$; (b) $p + p \rightarrow p + n + \pi^+ + \pi^+ + \pi^-$; and (c) $p + p \rightarrow p + p + \pi^+ + \pi^- + \pi^0$. The Δ^{++} resonance production was found to account for 54% of reaction "a." Also, a small amount of f^0, with a cross section of 30 ± 10 μb, was produced in this reaction. Significant resonance production in reaction "b" was found only in the $p\pi^+$ and $n\pi^-$ invariant mass distributions, with cross sections of 0.41 ± 0.1 mb and 0.29 ± 0.1 mb, respectively. Two resonances were found in the $p\pi^+\pi^-$ mass spectrum obtained from reaction "a," one with a mass of 1426 ± 28 MeV and a width of 147 ± 62 MeV, and the other with a mass of 1692 ± 24 MeV and a width of 122 ± 48 MeV. The value of the branching ratio for the decay of the 1692 MeV resonance into a $\Delta^{++}\pi^-$ was determined to be 0.17 ± 0.06. In addition, evidence was found that the spin and parity of the 1692 MeV resonance can be assigned the value $J^P = 5/2^-$. The predictions of the multi-Regge model were found to be consistent with the momentum transfer, invariant mass, and Treiman–Yang angle distributions obtained from reaction "a." The fit to the Treiman–Yang angle distribution using a one-pion-exchange model was completely inconsistent with the experimental data. (Diss. Abstr. Int., B)

43536 ANTIPROTON–DEUTERON ANNIHILATIONS INTO KAONS AND PIONS AT 2.2 GeV/c. Redeker, Maynard S. Lawrence, Kan.; Univ. of Kansas (1970). 199p. University Microfilms Order No. 71-13,353.

Thesis.

The results presented were obtained from a bubble chamber analysis of $\bar{p}d$ and $\bar{p}p$ interactions at incident $\bar{p}$ momenta of 2.2 GeV/c. The KK, KKKK, $KK\pi$ and $KK\pi\pi$ final states were studied extensively and the most prominent feature of these is the production of the K*(890) resonance. The percentage production rates of the various resonances are given and comparisons are made with the multi-Regge model and previous experiments. A brief survey of the present experimental knowledge and theoretical understanding of K*(890) production as well as the possible $K\bar{K}$, $KK\pi$ and $K\pi\pi$ resonance production is discussed. The experimental details of the analysis are also discussed, including description of the high momentum separated beam to the 31″ hydrogen/deuterium bubble chamber at the Brookhaven National Laboratory AGS. The data processing system used for this analysis at the University of Kansas is also presented. Comparison of 2.2 GeV/c partial cross sections with data at 2.7, 3.0, 3.7 GeV/c indicates that the partial cross sections are relatively constant or slowly decreasing with energy. An enhancement at low $K\bar{K}$ effective mass in the four-kaon final state, with possible assignment I = 1, was observed. However, without better statistics or a better model for a production mechanism one cannot make a decisive interpretation of the data. The angular distribution of kaons for three-body final states shows striking anisotropy but the effect diminishes with increasing multiplicity. Another enhancement at low $K\bar{K}$ effective mass with I = 1 in the $KK\pi$ and $KK\pi\pi$ final states was observed, and this is compared with the same effect noted previously by several other groups. The K*(890) production are prominent in several channels, but the data are consistent with no production of $\phi(1019)$. K*(890) production and decay angular distributions are analyzed in terms of the multi-Regge model with the Ranft parameters. Baryon exchange is dominant in all resonance production. The results are in reasonable agreement with the multiperipheral production mechanism. A search for resonances in the $K\pi\pi$ at 1175, 1215, and 1270 MeV, as well as the $K\bar{K}\pi$ at 1280, 1410, and 1700 MeV, has yielded negative results. There was very little evidence for K*K* production in the $KK\pi\pi$ final states. (Diss. Abstr. Int., B)

43537 SINGLE- AND DOUBLE-PION PRODUCTION IN PROTON–ANTIPROTON NON-ANNIHILATIONS AT 2.2 GeV/c. Stringer, Thomas Arthur. Lawrence, Kan.; Univ. of Kansas (1970). 122p. University Microfilms Order No. 71-13,365.

Thesis.

The reactions $\bar{p}p \rightarrow p\bar{p}\pi^0$, (1), $\bar{p}p \rightarrow p\bar{n}\pi^-$, (2), and $\bar{p}p \rightarrow p\bar{p}\pi^+\pi^-$, (3), are considered at an incident antiproton momentum of 2.2 GeV/c. The exposure was taken in the Brookhaven National Laboratory 31″ bubble chamber and consisted of 100,000 frames, part of which were used for this study. The cross sections are found to be 2.16 ± 0.20 mb for (1) (349 events), 1.56 ± 0.22 mb for (2) (242 events), and 0.83 ± 0.06 events for (3) (235 events). A discussion of the experimental procedure is given. Also the possibility of a C-violating bias in the data is examined. The single-pion production reactions (1) and (2) are considered. An attempt is made to understand the data on the basis of a quasi-two body process involving production of the $\Delta(1236)$. Reaction (1) appears to be dominated (about 100%) by single-isobar production, but reaction (2) does not. The one pion exchange model, assuming isobar production fails to fit the highly peripheral momentum transfer distribution in (1). The Benecke–Dürr model also gives a poor fit to the data. An absorption model, which assumes a sharp cutoff on angular momentum, can be made to fit the momentum transfer distribution, but does not fit the isobar decay distribution. Reaction (2) appears to have large contributions from a diffraction process of some type, which favors the charged system $(n\pi^-)$ going forward. The double-pion production reaction is dealt with. It is found to be dominated (100%) by double-isobar $(\Delta^{++}\Delta^{--})$ production. The mass of the isobar, however, is found to be about 1200 MeV, and the width is about 100 MeV. The Benecke–Dürr model and the one pion exchange model in the Born approximation fail to fit the momentum transfer distribution. The Dürr–Pilkuhn form factors give a slightly better fit. The density matrices are determined and do not fit the predictions of either pion or vector meson exchange. No correlation between the polar decay angles is found. It is concluded that a one pion exchange model which does not include absorption effects is inadequate to explain the data. (Diss. Abstr. Int., B)

43538 COMPARISON OF PRINCETON–PENNSYLVANIA n–p SCATTERING DATA BY PHASE-SHIFT ANALYSES. Arndt, Richard A.; Roper, L. David (Virginia Polytechnic Inst., Blacksburg). Phys. Rev. Lett.; 26: No. 20, 1260-2(17 May 1971).

Recent Princeton-Pennsylvania n-p differential cross sections are combined with existing n-p data at 210 and 330 MeV in order to obtain partial-wave representations of the T = 0 N–N scattering matrix. The new data differ significantly from the existing large-angle cross sections at these energies, being more sharply peaked at the back angle and differing by as much as 30% in the midrange (near 90°). The new data are found inconsistent through phase-shift analyses with the older data, particularly at 330 MeV, even with a variety of renormalization methods. If the older data are eliminated, it is found that the resultant solutions differ greatly from the expected one-pion exchange contribution values at 330 MeV, the best of these solutions requiring $g_\pi^2 = 18.9 \pm 1.2$. (auth)

43539 LARGE ANGLE PROTON–PROTON ELASTIC SCATTERING AT INTERMEDIATE MOMENTA. Kammerud, Ronald Claire. Bloomington, Ind., Indiana Univ. (1970). 149p. University Microfilms Order No. 71-13,549.

Thesis.

Differential cross sections for proton–proton elastic scattering are presented at thirteen incident proton momenta between 1.5 and 5.5 GeV/c. The data cover the center of mass angular region from 30 to 90° with data point spacing of 2°. Typical statistical errors of ±4% were obtained. The experiment was performed at the Argonne National Laboratory Zero Gradient Synchrotron. The particle detection system consisted of a combination of wire spark chambers and scintillation counters. The results of the experiment indicate that the angular distributions in this intermediate energy region are quite smooth, varying monotonically with both momentum and angle. No strong evidence is observed in this momentum region for secondary diffraction-like behavior which has been observed at higher momenta. Among the more interesting results of the experiment is the determination of the location of a suspected discontinuity in the fixed angle cross section as a function of the four momentum transfer. Also, evidence is presented for an additional discontinuity. A calculation which predicts the masses at which di-baryon resonances might be expected to occur is outlined and a possible interpretation of the discontinuities in terms of these resonances is offered. Attempts to interpret the data in terms of several models are described. These include both diffractive models and a simple Regge pole model. In the latter case, an effective Regge trajectory was extracted from the data. Finally, strong evidence is found for rapid changes in the nature of the large-angle differential cross section in the region of 1.5 and 4.0 GeV/c. This conclusion is based on the observed discontinuities in the fixed-angle cross section and on the momentum dependence of parameters used in fitting the large-angle data. (Diss. Abstr. Int., B)

43540 OBSERVATIONS ON THE NUCLEAR INTERACTION OF COSMIC-RAY PIONS AND NUCLEONS OF ENERGIES > 20 GeV. PART I. EXPERIMENTAL DETAILS AND RESULTS RELATING TO FLUCTUATIONS IN THE ANGULAR DISTRIBUTION OF THE SECONDARY PARTICLES PRODUCED IN INTERACTIONS IN CARBON. Lal, S.; Raghavan, R.; Rangaswamy, T. N.; (and others) (Tata Inst. of Fundamental Research, Bombay). Proc. Indian Acad. Sci., Sect. A; 73: No. 3, 119-33(Mar 1971).

A description is given of the experimental arrangement, the

types of data collected and the methods employed to analyze and classify the data. Results on the fluctuations in the angular distribution of the secondary particles produced in interactions in carbon are also presented, and it is shown that these fluctuations are considerably larger in certain cases than what can be accounted for purely from statistical fluctuations in the isotropic and uncorrelated emission of secondaries in the c.m. system of the collision with a target nucleon and in others difficult to be understood on this basis if additional features of these interactions are also considered. It is suggested that "correlated emission" of secondaries possibly due to final state interactions or multiparticle resonances with different "Q-values" and other properties are perhaps the cause of the observed fluctuations; this is in contrast to the explanation in terms of simple motion of "fire balls" in the c.m. system as has been generally discussed. (auth)

43541 MESON SPECTRUM IN THE REACTION pp → d MM. Wicklund, Arthur Barry. (Berkeley, Calif.; Univ. of California (1970)). 191p. University Microfilms Order No. 71-9955.

Thesis.

The differential cross section for deuteron production in the reaction pp → dMM at 180° in the c.m. system was measured at 3.8, 4.5, and 6.3 GeV incident momenta. The experiment was carried out in the external proton beam of the Bevatron with a high-resolution wire-chamber spectrometer. At 1 GeV in the missing mass, the mass resolution (fwhm) is 8, 12, and 23 MeV respectively at the three energies 3.8, 4.5, and 6.3 GeV. Deuteron identification was accomplished by time of flight and Cerenkov radiation criteria. At 1 GeV in the mass, target full to empty rates range from five at 3.8 GeV to two at 6.3 GeV. After fiducial cuts, a total of 600,000 events are used in cross section analysis. Production rates for the π and ρ meson are determined; the former are in agreement with other measurements, provided the production angular dependence is taken into account. The π cross section exceeds the ρ cross section by a factor of five in this energy region. Evidence is presented for an enhancement at 975 MeV in the mass with full width 60 ± 12 MeV. This object may be identified with the $\pi_n(980)$ observed in the $\eta\pi$ spectrum, and possibly with the $\pi_n(1016)$ seen in the $K\bar{K}$ channel. It is shown that at 3.8 GeV incident momentum, the resonant contribution cannot be separated effectively from the rapidly varying phase space background; it is necessary to search at higher energies to obtain a clean signal. Thus, results at 3.8 GeV are consistent with the negative findings of the second Saclay experiment. Also upper limits were set for the production of the narrow $\delta(963)$. If this object has width less than 5 MeV as reported by the C.E.R.N. M.M.S. experiment, then identification with the enhancement seen in the present experiment is ruled out. (Diss. Abstr. Int., B)

Strong (Meson-Induced)

Refer also to abstracts 42141, 43640, and 43642.

43542 (COO-1195-215) SOME RECENT EXPERIMENTAL RESULTS FOR A_1, A_3, Q, AND L MESONS. Kruse, U. E. (Illinois Univ., Urbana. Dept. of Physics). [1971]. Contract AT-(11-1)-1195. 18p. Dep. NTIS.

The experimental production and properties of the A_1, A_3, Q, and L mesons are reviewed. The methods of analysis are summarized, and some of the new results are discussed. The discussion also includes the polarization in production, that is the s versus t channel helicity conservation. (J.F.P.)

43543 (COO-1428-274) NEW EVIDENCE FOR SPLITTING IN THE Q REGION OF $K^+\pi^+\pi^-$ MASS. Garfinkel, A. F.; Holland, R. F.; Carmony, D. D.; Clopp, H. W.; Cords, D.; Loeffler, F. J.; Rangan, L. K. (Purdue Univ., Lafayette, Ind.); Lander, R. L.; Pellett, D. E.; Yager, P. M. (California Univ., Davis). [nd]. 3p. (CONF-710421-2). Dep. NTIS.

From International conference on meson resonances and related electromagnetic phenomena; Bologna, Italy (14 Apr 1971).

A splitting of the Q region was observed in the reactions $K^+ + d \rightarrow K^+ + \pi^+ + \pi^- + d(p+n)$ at 9.04 GeV/c. The $K^+\pi^-$ mass spectrum was found to be dominated by K(890), and the $K^+\pi^+\pi^-$ spectrum has double peaks K(1243) with a width of 70 MeV/c^2 and K(1344) with a width below 40 MeV/c^2. (J.F.P.)

43544 (COO-1428-275) EVIDENCE FOR SPLITTING IN THE Q REGION OF $K^+\pi^+\pi^-$ MASS. Garfinkel, A. F.; Holland, R. F.; Carmony, D. D.; Clopp, H. W.; Cords, D.; Loeffler, F. J.; Rangan, L. K. (Purdue Univ., Lafayette, Ind.); Lander, R. L.; Pellett, D. E.; Yager, P. M. (California Univ., Davis.). [1970]. 10p. (CONF-710609-3). Dep. NTIS.

From International conference on elementary particles; Amsterdam, Netherlands (30 Jun 1971).

A splitting in the $K^+\pi^+\pi^-$ mass spectrum in K^+d interactions at 9 GeV/c is observed. A mass of 1243 ± 8 MeV/c^2 and a width of $70 \pm {}^{26}_{18}$ for the lower mass state, and a mass of 1344 ± 4 and a width of less than 40 MeV/c^2 for the higher mass state are found. The isospin of both states is determined to be ½. The results can be interpreted as evidence for the mixing of two $J^P = 1^+$ K* states. (auth)

43545 (COO-1428-277) R REGION IN 13 GeV/c π^+ NUCLEON INTERACTIONS. Miller, D. H.; Paler, K.; Baderwitz, R. C.; Barton, H. R. Jr.; Palfrey, T. R. Jr.; Tebes, J. (Purdue Univ., Lafayette, Ind.). [1971]. 9p. (CONF-710421-3). Dep. NTIS.

From International conference on meson resonances and related electromagnetic phenomena; Bologna, Italy (14 Apr 1971).

The π^+ + d interactions at 13 GeV/c in a bubble chamber are studied and compared with previous work on the π^+ + p interactions. The R region from 1.6 to 1.8 GeV in the meson system is considered. The $A_3(1640)$, f^0, ρ, and even G-parity states are discussed. From the preliminary analysis it is concluded that one pion exchange is not large in the R region and that I = O exchange, presumably ω, dominates in the π^+ + p data. It is also found that all of the 4π enhancement is not associated with the 2π enhancement. (J.F.P.)

43546 (COO-1428-279) EVIDENCE FOR A Kπ RESONANCE NEAR 1750 MeV/c^2. Carmony, D. D.; Clopp, H. W.; Cords, D.; (and others) (Purdue Univ., Lafayette, Ind.). [1971]. 6p. (CONF-710609-1). Dep. NTIS.

From International conference on elementary particles; Amsterdam, Netherlands (30 Jun 1971).

An analysis of the Kπ system in the final states of the reactions: $K^+d \rightarrow (p\,)pK^+\pi^-$ and $K^+d \rightarrow (p_s)nK^0\pi^+$ at 9.0 GeV/c indicates a resonance structure at ≈1750 MeV/c^2 which cannot be identified as the L-meson (1775). (auth)

43547 (COO-1428-281) K*(890) PRODUCTION IN THE CHARGE EXCHANGE REACTION $K^+n \rightarrow K^+\pi^-p$ AT 9.1 GeV. Cords, D.; Carmony, D. D.; Clopp, H. W.; (and others) (Purdue Univ., Lafayatte, Ind.). [1971]. Contract AT(11-1)-1428. 14p. (CONF-710609-2). Dep. NTIS.

From International conference on elementary particles; Amsterdam, Netherlands(30 Jun 1971).

Cross sections are presented for K*(890) and K*(1420) production in $K^+n \rightarrow K^+\pi^-p$ at 9.1 GeV. The K*(890) production mechanism is investigated by means of its energy dependence and decay correlations. The asymmetry in the decay angular distribution is discussed. (auth)

43548 (COO-1428-283) K*(890) PRODUCTION IN THE CHARGE EXCHANGE REACTION $K^+n \rightarrow K^+\pi^-p$ AT 9 GeV/c. Cords, D.; Carmony, D. D.; Clopp, H. W.; (and others) (Purdue Univ., Lafayatte, Ind.). [1971]. 11p. Dep. NTIS.

The dominant production mechanism for the reaction $K^+n \rightarrow pK^*(890)$ is π-exchange and the energy dependence of the cross section is found to be proportional to $P_{lab}^{-2.2}$. The conventional absorption model does not reproduce the rapid decrease of ρ_{00} as a function of the four momentum transfer. The Reggeized π-A_2 model of Dass and Froggatt reproduces the t-dependence of ρ_{00} and Re ρ_{10} but there is serious disagreement for ρ_{1-1} which may indicate the need to include A_1 exchange. The asymmetry in the decay angular distribution is interpreted as S-P wave interference. (auth)

43549 (COO-1428-286) FINAL STATES WITH THREE CHARGED PARTICLES AND A VISIBLE K^0 FROM K^-d INTERACTIONS AT 4.5 GeV/c. Yen, W. L. (Indiana-Purdue Univ., Indianapolis. Dept. of Physics); Ammann, A. C.; Carmony, D. D.; Garfinkel, A. F.; Gutay, L. J.; Miller, D. H.; Paler, K. (Purdue Univ., Lafayette, Ind. Dept. of Physics). [1971]. 40p. Dep. NTIS.

A study of the interactions of 4.48 GeV/c K^- mesons on neutrons is reported. The 372000-picture exposure was taken in the Argonne National Laboratory 30-in. deuterium-filled bubble chamber. $\bar{K}^0$ final states from the three-or four-prong-plus-vee topologies are discussed. The final states investigated include (1) $K^-n \rightarrow p\pi^-\pi^-\bar{K}^0$, (2) $K^-n \rightarrow p\pi^-\pi^-\bar{K}^0\pi^0$, (3) $K^-n \rightarrow \pi^+\pi^-\pi^-\bar{K}^0n$, (4) $K^-n \rightarrow p\pi^-\pi^-\bar{K}^0$ (missing mass), (5) $K^-n \rightarrow \pi^+\pi^-\pi^-\bar{K}^0$ (missing mass). These reactions are dominated by K*(890) and $\Delta(1236)$ production, and the quasi-two-body reaction $K^-n \rightarrow K^{*-}\Delta^0$ has been studied. A search for exotic resonances found no evidence for their production. A Reggeized multiperipheral model of Plahte and Roberts has been applied to reactions (1)–(3). Good agreement with our data is obtained for distributions in p_L^*, p_T, $\cos\theta^*$, effective mass. The model also gives the correct energy dependence between 3 and 4.5 GeV/c. (auth)

43550 (COO-1428-290) COHERENT PRODUCTION OF HIGH MASS MESON STATES IN π^+d COLLISIONS AT 13 GeV/c. Paler, K.; Badewitz, R. C.; Barton, H. R. Jr.; Miller, D. H.; Pal-

XUM

frey, T. R. Jr.; Tebes, J. (Purdue Univ., Lafayette, Ind.). [1971]. Contract AT(11-1)-1428. 11p. Dep. NTIS.

Evidence is found for the coherent production of high mass meson states in the 1.6- and 1.9-GeV mass regions. These states are observed, respectively, in the 3π and 5π systems produced in the reactions $\pi^+d \rightarrow d\pi^+\pi^+\pi^-$ and $\pi^+d \rightarrow d\pi^+\pi^+\pi^+\pi^-\pi^-$ at 13 GeV/c. The spin-parity of the 3π state, identified as the A_3 meson, is determined to be in the series 2^-, 3^+ ..... with a dominant $f\pi$ decay. (auth)

43551 (UCR-34-P-107-B-108) $\pi^+ + p \rightarrow \Delta^{++}(1236) + \pi^0$ AT 1.85 TO 2.09 GeV: A STUDY OF s- AND t-CHANNEL EFFECTS. Mehtani, U.; Fung, S. Y.; Kernan, A.; Williamson, Y. (California Univ., Riverside); Birge, R. W.; Kalmus, G. E.; Michael, W. (California Univ., Berkeley. Lawrence Radiation Lab.); Shepard, H. K. (New Hampshire Univ., Durham). [1970]. 20p. (CONF-700806-63). Dep. NTIS.

From 15th international conference on high energy physics; Kiev, USSR(26 Aug 1970).

In a large statistics bubble chamber experiment the differential cross section for $\pi^+ + p \rightarrow \Delta^{++}\pi^0$ was determined at six points in the c.m. energy interval 1.85 to 2.09 GeV. The rapid variation with energy of the shape of the angular distribution indicates that s-channel resonances are strongly coupled to $\Delta\pi$ in this energy region. At the same time it was observed that dips at $t = t_{min}$ and $t \simeq -0.5$ (GeV/c^2, characteristic of ρ exchange with dominant helicity flip coupling, are present at all energies. The angular distributions were fitted with (1) s-channel resonances as given by elastic partial wave analyses, and (2) s-channel resonances plus a Regge ρ amplitude. The latter fit was in better agreement with the data. By projecting out the partial wave amplitudes contained in the ρ amplitude, it was established that the resonances plus ρ fit does not involve double counting. The fact that a better fit to the data was obtained with resonances plus ρ, rather than resonances alone, does not necessarily invalidate the duality picture. It may simply indicate that some resonances are missing from the elastic phase shift analysis solutions. It is emphasized that the results presented are preliminary in nature. (auth)

43552 (UCR-34-P-107-B-110) STUDY OF $\pi^+p \rightarrow \rho^+p$ AT 1.85 TO 2.09 GeV. Williamson, Y.; Fung, S. Y.; Kernan, A.; Mehtani, U.; Poe, R. T.; Schalk, T.; Shen, B. C. (California Univ., Riverside); Birge, R. W.; Kalmus, G. E.; Michael, W. (California Univ., Berkeley. Lawrence Radiation Lab.). [1970]. 12p. (CONF-700806-64). Dep. NTIS.

From 15th international conference on high energy physics; Kiev, USSR(26 Aug 1970).

A systematic study of nucleon resonances in the π^+p inelastic reactions between 1.1 and 1.95 GeV/c is carried out in a large statistics bubble chamber experiment. Preliminary results of the reaction $\pi^+p \rightarrow \rho^+p$ are presented for six c.m. energies between 1.85 and 2.09 GeV. (auth)

43553 (UCR-34-P-107-B-120) REACTION $\pi^+p \rightarrow \rho^+p$ IN THE C.M. ENERGY REGION 1780 TO 2140 MeV. Note No. 206. Willamson, Yvonne (California Univ., Riverside). 6 May 1971. 9p. (CONF-710413-3). Dep. NTIS.

From American Physical Society meeting; Washington, D. C. (26 Apr 1971).

The reaction $\pi^+ + p \rightarrow \rho^+ + p$ in the channel $\pi^+ + p \rightarrow \pi^+ + \pi^0 + p$ at 1.780 to 2.140 GeV in a hydrogen bubble chamber is studied. The differential cross sections and density matrix elements of the ρ^+ are shown. The angular distributions are also studied. (J.F.P.)

43554 (UR-875-340) SINGLE-PARTICLE DISTRIBUTIONS OF π-MESONS PRODUCED IN π^+p, K^+p, pp, AND π^-p COLLISIONS AT HIGH ENERGIES. Chen, M. S.; Kinsey, R. R.; Morris, T. W.; (and others) (Rochester Univ., N. Y. Dept. of Physics and Astronomy). May 1971. Contract AT(30-1)-875. 13p. (CONF-710609-5). Dep. NTIS.

From International conference on elementary particles; Amsterdam, Netherlands (30 Jun 1971).

A comparison is made of single-particle momentum distributions of π-mesons produced in 7.0-GeV/c π^+p, 12.7-GeV/c K^+p, 28.5-GeV/c pp, and 24.8-GeV/c π^-p interactions. It is observed that the momentum distributions of target fragments in π^+p, K^+p, and pp interactions agree with each other when normalized by their respective total cross sections. This result is interpreted as providing evidence for factorization in inclusive processes. (auth)

43555 STUDY OF DIPIONS IN THE MASS RANGE 400 TO 1000 MeV PRODUCED IN π^-p COLLISIONS. Rangaswamy, Thambu Narayanaiyengar. Berkeley, Calif.; Univ. of California (1970). 161p. University Microfilms Order No. 71-9900.

Thesis.

A counter-spark chamber experiment was performed at the Bevatron to study the finer details of the $\pi\pi$ (dipion) interaction exhibited in the reaction $\pi^- + p \rightarrow \pi^+ + \pi^- + n$ at incident π^- momenta of 3, 4, 4.5, 5 GeV/c. The momenta of the secondaries were measured by a large aperture magnet spectrometer. The track segments were sampled by a set of optical spark chambers imbedded in the magnet. The design of the scintillation counter array and the triggering scheme vetoed a considerable fraction of πp elastic events, events with one or more π^0, s and events with more than two charged secondaries. A total of 1.9 million pictures was collected all of which were scanned and measured by SASS (Spark Chamber Automatic Scanning System). Of these, 1.6×10^5 events satisfied the above reaction hypothesis. The results from the 3 and 5 GeV/c data for the forward-backward ratio in the dipion decay and the S-wave phase shifts for iso-spin I = 0 agree well with published results from previous experiments. The density matrix elements of the dipion angular distribution particularly at 3 GeV/c incident π^- momentum disagree with published results at 2.7 BeV/c. It is not believed that systematic errors in the experiment can account for this large difference. The values for the density matrix elements are in better agreement with published results at 11.2 GeV/c incident π^- momentum. The shapes of the differential cross section at 3 and 5 GeV/c predicted by the one pion exchange model with absorption as put forth previously agree well with the results. This model is unable to explain quantitatively the observed variation of the density matrix elements as a function of t, the square of the 4-momentum transfer from the target proton to the outgoing neutron. The fits to the dipion mass distribution at 3 and 5 GeV/c lead to consistent values for the mass of ρ^0 the resonance; the widths are significantly different. For the 3 GeV/c data the fits necessitate an additional enhancement at a dipion mass ~645 MeV with a full width $\Gamma \sim 304$ MeV. This enhancement could arise from an improper knowledge of the background and πN cross channel effects. The 5 GeV/c data do not have a perceptible contribution from this enhancement; however there is evidence of two other enhancements in these data — one at a mass ~936 MeV with a full width $\Gamma \sim 47$ MeV, and another at a mass ~1029 MeV with a full width $\Gamma \sim 27$ MeV. The peak at 936 MeV is ~5 standard deviations away from the rest of the contribution and hence statistically significant. It is unlikely that this enhancement could arise from the decay of η' (958) $\rightarrow \pi^+\pi^-\gamma$. The peak at 1029 MeV being ~3 standard deviations away, is on the border line of being significant. The estimated resolution of 22.5 MeV at the ω^0 mass leads to a negligible contribution from $\omega \rightarrow \pi^+\pi^-$. The unweighted data however indicate a nonnegligible contribution from this decay for large values of t. (Diss. Abstr. Int., B)

43556 BARYON EXCHANGE PROCESSES IN THREE AND FOUR PRONG EVENTS FROM POSITIVE PIONS INCIDENT ON DEUTERIUM AT MOMENTA OF 1.83, 2.01, 2.14, AND 2.33 GeV/c. Terrell, Robert Edward. Madison, Wis.; Univ. of Wisconsin (1970). 71p. University Microfilms Order No. 71-2251.

Thesis.

Using the Princeton-Pennsylvania Accelerator rapid cycling bubble chamber and a combination of Cherenkov and scintillation counters backward $(\pi^+\pi^-)$ and $(\pi^+\pi^-\pi^0)$ multipion production in the reaction $\pi^+n \rightarrow p\,m(\pi)$ at 1.83, 2.01, 2.14, and 2.33 GeV/c were investigated. More than 5 million chamber expansions and over 24 million incident pions yielded about 150,000 pictures in which a high-momentum charged particle of $\beta < 0.98$ (a proton or kaon) was detected by the counter array. In order to study baryon exchange processes backward events were selected with production angles θ^* for the mesons such that $\cos\theta^* \leq -0.70$. There were 621 backward $\pi^+\pi^-$ events and 726 backward $\pi^+\pi^-\pi^0$ events. A single example of backward K^+K^- production was found. The $\pi^+\pi^-$ data are characterized by a dip in the ρ^0 production angular distribution at 180°. Backward $\pi^+\pi^-\pi^0$ production is dominated by ω^0 production, very sharply peaked near 180°. A small amount of η^0 production is observed, not sharply backward peaked. Suggestive but not conclusive evidence is presented for a $\pi^+\pi^-\pi^0$ resonance near 1050 MeV/c^2 produced only near 180°. (Diss. Abstr. Int., B)

43557 SYMMETRIC π^- PRODUCTION FROM $K^+p \rightarrow \pi^- +$ ANYTHING AT 12 GeV/c. Ko, Winston; Lander, Richard L. (Univ. of California, Davis). Phys. Rev. Lett.; 26: No. 20, 1284-7(17 May 1971).

The longitudinal momentum distribution of π^- meson from the reaction $K^+ + p \rightarrow \pi^-$ + anything at 11.8 GeV/c is examined in various reference frames. A forward-backward symmetry is found in that frame corresponding to a simple quark model. The frame of symmetry is dependent on the charged-particle multiplicity, however, which reduces the appeal of that model in explaining the present data. (auth)

43558 STUDY OF K^+ FORWARD SCATTERING FROM THE REACTION $\pi^-p \rightarrow K^+\Sigma(1375)^-$ AT 4.5 AND 6 GeV/c. Crennell, David J.; Gordon, Howard A.; Lai, Kwan-wu; (and others). (Brookhaven National Lab., Upton, N. Y.). Phys. Rev. Lett.; 26: No. 20, 1280-3(17 May 1971).

Experimental data are presented for the forward scattering of K^+ from the reaction $\pi^-p \rightarrow K^+\Sigma(1385)^-$. This "forbidden" peripheral scattering can not be explained by any simple kinematic effects in the $\Lambda K^+\pi^-$ final state. s-channel resonances, two-particle exchange, or a single "exotic"-meson exchange in the t channel are examined as possible explanations of this effect. (auth)

43559 LARGE-ANGLE DIFFERENTIAL CROSS SECTION K^+p ELASTIC SCATTERING AT 4.0 AND 5.0 GeV/c. Akerlof, C. W. (Univ. of Michigan, Ann Arbor); Han, K. S.; Meyer, D. I.; (and others). Phys. Rev. Lett.; 26: No. 20, 1278-9(17 May 1971).

Data on the reaction $K^+p \rightarrow K^+p$ at large angles are presented. Between the forward diffraction peak and the backward peak the cross section is independent of four-momentum transfer but varies with incident momentum. (auth)

43560 MEASURING np-COINCIDENCES IN PROCESSES OF THE INELASTIC INTERACTION OF NEUTRONS WITH HYDROGEN AND DEUTERIUM. Furich, M.; Milyanich, D.; Tomash, P.; Antolkovich, B.; Valkovich, V. Izv. Akad. Nauk SSSR, Ser. Fiz.: 35: No. 1, 211-4(1971). (In Russian).

Nucleon–nucleon bremsstrahlung radiation is the simplest of all processes giving information on the behavior of the nucleon–nucleon t matrix off the energy shell. The cross section for neutron–proton bremsstrahlung should significantly exceed the cross section for the proton–proton bremsstrahlung process. The experimental technique involved the production of a collimated beam of neutrons from a Cockcroft–Walton generator, directed to a hydrogenated or deuterated target of organic material. A counter telescope consisting of two gas-filled proportional counters for measuring ΔE_1 and ΔE_2 and of one counter for measuring the total energy E were used to identify the protons and measure their energies. Two pulses, one fast and one slow, were taken with this E counter. A liquid scintillator was used as a neutron detector. The slow E pulse and the ΔE_2 pulse served to identify the protons and to determine their energies, while the fast E pulse and the pulse from the neutron detector were used to measure the time shift T between the proton and neutron pulses. Three pulses (T, ΔE_2, and E) were sent to a $100 \times 100 \times 100$ channel analyzer. The equipment was calibrated by measuring np coincidences during elastic np scattering. True np coincidences appeared as a narrow peak on the T spectrum. The neutron–proton bremsstrahlung radiation was counted at an angle of 30° with respect to the neutron beam. The upper limit for the cross section for production of neutron–proton bremsstrahlung radiation was found to be greater than various calculated values in the literature. The proton spectrum from the breakup of deuterium by neutrons is presented. (TTT)

43561 STRANGE PARTICLE PRODUCTION IN π^+ DEUTERON INTERACTIONS AT 2.05, 2.19, AND 2.35 GeV/c. Moore, Craig Damon. Madison, Wis.; Univ. of Wisconsin (1970). 127p. University Microfilms Order No. 71-2229.

Thesis.

Strange particle production was studied in the region about $\sqrt{s} = 2.2$ GeV using a deuterium-filled bubble chamber exposed to a π^+ beam of 2.05, 2.19, and 2.35 GeV/c. When the number of events warranted a cut, production cross sections were presented for three equiflux partitions of the data. Angular distribution and polarization are presented for two-body and quasi-two-body reactions. Resonance production is studied and the amounts and parameters are presented. Furthermore, the decay angular correlations are given for these resonances. In particular, the following resonances: $Y^*(1385)$, $Y^*(1405)$, $Y^*(1520)$, $K^*(890)$, and the $\phi(1020)$ were observed and studied. The data are compared with those of other experiments and a sharp decrease in the production of the $Y^{*+}(1385)$ in the energy region examined in this experiment was observed. In the same energy region an apparent minimum in the ϕ production cross section was also observed. (Diss. Abstr. Int., B)

43562 BUBBLE CHAMBER STUDY OF THE $2\pi^0$ FINAL STATE AND NEUTRAL DECAYS OF THE η, ω, AND η' MESONS IN THE REACTION $\pi^+ + n \rightarrow p + \gamma$ RAYS AT 2.15 GeV/C. Bensinger, James Robert. Madison, Wis.; Univ. of Wisconsin 1971). 219p. University Microfilms Order No. 71-12,677.

Thesis.

The reaction $\pi^+ + d \rightarrow p + (p) + k\gamma$ where k is an integer between 2 and 6 at a beam energy of 2.15 GeV/c was studied. For this experiment the 15" PPA rapid cycling deuterium bubble chamber was used. Two $\frac{1}{8}$" tantalum plates were added to the chamber to convert γ rays. Counters were used to reduce the background. There were 2 million pictures taken, events with 2 or more γ rays and a recoil proton momentum ≤ 1 GeV/c were measured. The γ ray direction and energies were constrained in the kinematic fits to various η and π^0 hypothesis. Single π^0 and η production was found to be in good agreement with other measurements of the cross sections and angular distribution. Two π^0 production is observed to saturate s-wave unitarity in the $\pi\pi$ mass region between .6 and .9 GeV/c^2. This clearly favors the "up-down" solution for s-wave $\pi\pi$ scattering. Branching ratios for neutral decays of several mesons were measured. In addition cross sections and comparisons with other data are presented. (TSS) (Diss. Abstr. Int., B)

43563 BACKWARD ETA MESON PRODUCTION AT 5.9 GeV/c. Pawlicki, Anthony Joseph. Ithaca, N. Y.; (Cornell Univ. (1970). 114p. University Microfilms Order No. 71-7373.

Thesis.

Backward eta meson production, $\pi^- + p \rightarrow n + \eta$, was observed for 5.9 GeV/c negative pions incident on a liquid hydrogen target. The target was surrounded by an array of lead plate optical spark chambers and lead-scintillator sandwich shower veto counters. The chambers detected the electromagnetic showers from the two decay gamma rays from the eta meson. Backward charge exchange, $\pi^- + p \rightarrow n + \pi^0$, was simultaneously observed with the apparatus. The differential cross section shape for backward eta production was roughly measured over the momentum transfer range $-2.0 < u < u_{max} = +0.038$ (GeV)^2. The cross section integrated over this range, is (0.91 ± 0.27) μbarn. The ratio of eta production to charge exchange, with both cross sections averaged over the above given u range, is 0.45 ± 0.11. (Diss. Abstr. Int., B)

43564 EXPERIMENTAL STUDY OF LOW-ENERGY PION–NUCLEON CHARGE-EXCHANGE SCATTERING AND THRESHOLD NEUTRAL PION PRODUCTION. Crean, Peter Aidan. Princeton, N. J.; Princeton Univ. (1970). 170p. University Microfilms Order No. 71-14,367.

Thesis.

The differential cross section for pion-proton charge-exchange scattering was measured at six center-of-mass pion scattering angles from 60 to 170 degrees for twelve incident pion energies between 150 and 600 MeV. Events were identified by requiring a neutral final state and the detection of a neutron in one of eight two-foot cubical scintillation counters. The neutron time-of-flight from the target to the counter was measured and used to differentiate gamma rays, neutrons produced in change-exchange scattering, inelastically produced neutrons, and background events. The data, with the inclusion of a zero degree point calculated from dispersion theory, were fitted to a Legendre series, and the coefficients were compared with several phase-shift solutions. Total cross sections for neutral pion-production (i.e., final state containing two neutral pions and a neutron) were measured for five incident pion energies from 291 to 407 MeV. The cross sections were found to be considerably greater than current algebra predictions. (Diss. Abstr. Int., B)

Particle Interactions and Properties (Theoretical)

General

43565 (CALT–68-305) QUANTUM NUMBERS OF CROSS-CHANNEL EXCHANGES. Mandula, J.; Weyers, J.; Zweig, G. (California Inst. of Tech., Pasadena); Halzen, F. (European Organization for Nuclear Research, Geneva (Switzerland)). [1971]. Contract AT(11-1)-68. 11p. (CONF-710316–2). Dep. NTIS.

From Workshop on particle physics at intermediate energies; Pasadena, Calif. (29 Mar 1971).

A study of the quantum numbers of crossed-channel exchanges is made for high-energy interactions. All relations following from the absence of exotic exchanges which have the property that their violation is proportional to the interference between an exotic and a nonexotic exchange rather than to the square of an exotic exchange are cataloged. (J.F.P.)

43566 (COO–1545-99) HIGH ENERGY PHYSICS STUDIES PROGRESS REPORT. PART I AND II. (Ohio State Univ. Research Foundation, Columbus). 1 Jul 1971. Contract AT-(11-1)-1545. 34p. Dep. NTIS.

A summary of experimental research on leptonic decays of hyperons and neutron–proton charge exchange, and theoretical research on symmetry and dynamical calculations is presented. A list of publications is included. (J.F.P.)

XUM

43567 (INR-1280) POSSIBILITY OF EXISTENCE OF A NEW PROCESS AT INTERACTIONS WITH ENERGIES ABOVE 10^{12} eV. Gawin, J.; Maze, R.; Wdowczyk, J. (Institute of Nuclear Research, Warsaw (Poland)). 1971. 15p. Dep. NTIS (U. S. Sales Only).

Investigation of cosmic rays during last decade gave discovery of some phenomena which are difficult to explain within the generally accepted model of high-energy interactions. Among these phenomena one can quote such as the so-called X-process, the horizontal air showers and the mu-poor showers. It is shown that the three rather strange phenomena can be explained simultaneously if existence of a new process in interactions above 10^{12} eV is assumed. An essential feature of the process is production of a massive particle with relatively long life time and some small activity. The cross section of the process should be approximately by 2 to 3 orders of magnitude smaller than that of nuclear interactions. (auth)

43568 (JINR-P2-5765) APPLICATION OF THE PADE APPROXIMATION TO THE PROBLEM FOR BOUND STATES IN QUASIPOTENTIAL APPROACH. Atanasov, A. (Joint Inst. for Nuclear Research, Dubna (USSR). Lab. of Theoretical Physics). 1971. 13p. (In Russian). Dep. NTIS (U. S. Sales Only).

In the quasipotential approach the bound-state energy of the two spinless-particle system is determined by approximate method. It is shown that definition of the Pade-fraction poles is reduced to determination of the eigenvalues of corresponding homogeneous equation by the nucleus traces. (auth)

43569 (NYO-2262-TA-245) PROGRESS REPORT FOR A RESEARCH PROGRAM IN THEORETICAL HIGH-ENERGY PHYSICS. Feldman, David (Brown Univ., Providence, R. I. Dept. of Physics). 1 Jun 1971. Contract AT(30-1)-2262. 9p. Dep. NTIS.

Research on theoretical high-energy physics is summarized. A list of publications is included. (J.F.P.)

43570 (NYO-2262-TA-247) TRIPLE REGGE LIMITS AND DUALITY SUM RULE. Jen, Chian-li; Kang, Kyungsik; Shen, Pu; Tan, Chung-I (Brown Univ., Providence, R. I. Dept. of Physics). [1971]. 11p. Dep. NTIS.

Based on the dual amplitude analysis of the "di-triple" Regge limits in the inclusive hadronic reactions, the general properties of the Reggeon-Reggeon amplitude are conjectured and a duality sum rule is suggested. Predictions are made on the two-Reggeon-particle and triple Reggeon couplings from this sum rule. (auth)

43571 OPTICAL MODEL FOR HIGH ENERGY SCATTERING AT ALL ANGLES. Carroll, James Patrick. Bloomington, Ind.; Indiana Univ. (1970). 88p. University Microfilms Order No. 71-12,445.

Thesis.

An infinite number of scattering amplitudes are obtained which are Regge behaved and do not violate unitarity. All of these amplitudes have the same Regge pole dependence in the forward direction while at large angles they have essentially the same exponential dependence on the momentum transfer. This behavior is in qualitative agreement with experimental results. Unitarity is imposed on the scattering amplitude by means of the impact parameter representation. The mathematical properties of this integral representation are discussed. Approximate methods are shown for deriving this representation for the scattering of spinless particles and for the scattering of spin-zero with spin-one-half particles. Exact methods for obtaining these same representations are also shown. For the case of spinless particles, the unitarity constraint is derived on the spectral function of this integral representation. This spectral function is usually called the profile function. The corresponding constraint on the profile function for the scattering of spin zero and spin one-half is stated. From the unitarity constraint, a generalized form of the profile function is obtained. This generalized form contains a parameter p which can vary from one to infinity. The Glauber form and the Blankenbecler and Baker form are special cases of this generalized form. The convergence of these representations is also discussed. A review is made of recent models which use the impact parameter representation. These models fall into two classes depending on whether the scattering amplitude is assumed to be dominated by the Pomeranchuk Regge pole or diffractive effect at very high energies. Within the limit of current experimental information, it is difficult to distinguish between these two general groups. Also the application of these models to the scattering of particles with spin is limited. Scattering of spinless particles is examined. If the generalized profile function is expanded in a series and each term of the series is integrated, then an infinite series representation of the scattering amplitude is obtained. If the first term in this series is defined to be a Regge pole, it is shown that the nth term can be interpreted as the exchange of n Regge poles. The coefficient of each term in the series can range from a constant to $1/n!$ depending on the value of the parameter p. The scattering in the forward region is dominated by the first two terms of this series which are independent of p. An alternate series form for the amplitude is obtained for the case of $p = 1$ by performing a contour integral. The first term of this series is the asymptotic value of the scattering amplitude for large Δ. By using previous results it is concluded that the form of the scattering amplitude at large momentum transfer is insensitive to p and has an exponential dependence on Δ. An application is made to pion-nucleon scattering. It is assumed that the helicity nonflip amplitude is dominated by t-channel poles while the helicity flip amplitude is dominated by u-channel poles. Although it is realized that this assumption may be unphysical, this calculation is carried out as an illustration of how u-channel poles may be incorporated into this type of model. This was not done in any of the models reviewed. (Diss. Abstr. Int., B)

43572 PARTICLES OF ARBITRARY MASS AND SPIN. Hajj, Jack Philip. Medford, Mass.; Tufts Univ. (1970). 85p. University Microfilms Order No. 71-13,750.

Thesis.

Free particles of arbitrary mass and spin are studied. Primarily, the angular momentum, and the corresponding multipole states of such particles are obtained. The transition from the massive to the massless case is worked out. Finally, the theory is second-quantized in an angular-momentum representation. (Diss. Abstr. Int., B)

43573 EXAMPLE OF A CONSISTENT RELATIVISTIC MECHANICS OF POINT PARTICLES. Staruszkiewicz, A. (Jagellonian Univ., Krakow). Ann. Phys. (Leipzig); 25: No. 4, 362-7(1970).

An example of a relativistic mechanics of n particles in the two-dimensional Minkowski space is constructed. The essential feature of the theory is the occurrence of two histories for every physical system. (auth)

43574 INCLUSIVE CROSS SECTIONS ARE DISCONTINUITIES. Stapp, Henry P. (Univ. of California, Berkeley). Phys. Rev., D; 3: No. 12, 3177-84(15 Jun 1971).

Inclusive cross sections are discontinuities across certain cuts in the connected parts of appropriate multiparticle scattering amplitudes. This relationship, which is shown here to follow formally from field theory, is analogous to the well-known connection between total cross sections and total discontinuities. It has been used in recent work on the theory of high-energy reactions. (auth)

43575 TIME-LONGITUDINAL DILATIONS AND SCALING BEHAVIOR OF HIGH-ENERGY COLLISIONS. Bander, Myron (Univ. of California, Irvine). Phys. Rev., D; 3: No. 12, 3173-6(15 Jun 1971).

The assumption that a dilation transformation in time and one space direction is implementable for matrix elements of certain operators between states with constituent particles moving mainly along that direction with large momenta, leads to scaling of inclusive processes in the high-energy limit. Without further restriction, certain exclusive processes likewise survive this limit. A nonzero limit for some of these processes, namely, those involving a transfer of quantum numbers, is unacceptable. This difficulty is overcome by postulating that conserved quantities may be broken up into right- and left-moving ones, and each is separately conserved. (auth)

43576 VIOLATION OF THE POMERANCHUK THEOREM AND ZEROS OF THE SCATTERING AMPLITUDES. Auberson, G. (Rockefeller Univ., New York); Kinoshita, T.; Martin, A. Phys. Rev., D; 3: NO. 12, 3185-94(15 Jun 1971).

Assuming constant but unequal asymptotic total cross sections for particle-particle and particle-antiparticle collisions, it is proved within axiomatic field theory that the scattering amplitude must have infinitely many zeros in a certain narrow angular region of the t plane containing the physical region $t \leq 0$. It is shown further that this region cannot be made narrower without additional assumptions. These results are also valid for a more general class of scattering amplitudes, including those saturating the Froissart bound. (auth)

43577 LORENTZ-INVARIANT LOCALIZATION FOR ELEMENTARY SYSTEMS. IV. THE NONRELATIVISTIC LIMIT. Kalnay, A. J.; Torres, P. L. (Univ. Central de Venezuela, Caracas). Phys. Rev., D; 3: No. 12, 2977-81(15 Jun 1971).

In parts II and III of the present series of papers, the localization problem was studied for the relativistic nonzero-mass (spin

0 and ½) and zero-mass (spin 0, ½, and 1) cases. With a set of postulates of which the basic one was the imposition of Lorentz invariance of localization (which is a self-consistency requirement), it was possible to define the position operator uniquely (except for a constant for spin ½, nonzero mass). However, the position operator has unusual properties, e.g., non-Hermiticity. This does not preclude its having physical meaning, but is such a strange result that in the present paper the validity of the postulates is tested in the nonrelativistic case (spin 0 and ½) where the position operator is well known. The same set of postulates, except that here the Galilean invariance of localization is imposed. The result of the test is positive; the position operator found is the usual one. Moreover, with the set of postulates, the notion of localization is restated in a more physical basis, giving a precise definition of it without imposing avoidable requirements. (auth)

43578 OPERATOR APPROACH TO DUAL MULTIPARTICLE THEORY. Alessandrini, V. (CERN, Geneva. Univ., Geneva); Amati, D.; Le Bellac, M.; Olive, D. Phys. Rep.; 1C: No. 6, 269-46(Jul 1971).

The multi-particle dual model is analyzed by making use of the operatorial approach. A new technique is introduced, which allows a comprehensive and simple treatment of operatorial manipulations, and is based on the underlying 0(2; 1) symmetry of the dual resonance model. The multiloop unitarization program is sketched, and explicit results for the one-loop amplitudes, including their renormalization, are given. (auth)

43579 PARTICLE PRODUCTION IN HIGH ENERGY HADRON COLLISIONS. Van Hove, L. (CERN, Geneva). Phys. Rep.; 1C: No. 7, 347-79(Jul 1971).

Empirical facts and problems concerning multiparticle hadron collisions at high energy are reviewed in the light of recent experimental data and theoretical ideas. The emphasis lies on general, qualitative properties and on their extraction from the data rather than on success or failure of particular models. Single particle distributions and multiparticle properties, i.e. correlation effects are treated in succession. The latter are considered in inclusive as well as exclusive experiments. The final remarks are devoted to the central problem of identifying and describing the main particle production mechanisms, for which only tentative guesses can be made at present. (auth)

43580 MODEL ANALYSES OF ELEMENTARY PARTICLE SCATTERING AMPLITUDES. Coleman, Thomas Patrick. Ames, Iowa; Iowa State Univ. (1970). 85p. University Microfilms Order No. 71-14,214.

Thesis.

Several models of high energy scattering reaction are examined. First, the s-wave S-matrix of the double δ-function potential barrier does not contain a second-order pole, in contrast to an earlier analysis of the same potential. This suggests that the crossing of resonance levels with the same symmetry does not occur. Second, a model in which the $A_2(1300)$ meson consists of two coupled mesons of the same spin and parity is used to explain the variations of the mass structure of the A_2 in several experiments. The roles of these two mesons in group classifications of elementary particles and in S-matrix theory are discussed. Third, the double-Regge pole models are compared with data from the reaction $pp \rightarrow p\pi^-\Delta^{++}$ at 22 GeV/c. Berger's model is most consistent with the data and with earlier analyses. The relative merits of the three models are discussed. (Diss. Abstr. Int., B)

43581 DETERMINATION OF SPIN PARITY BY MEANS OF MULTIPOLE MOMENTS. Krasznovszky, Sandor; Pinter, Gyorgy; Telbisz, Ferenc (Central Research Inst. for Physics, Budapest). Magy. Fiz. Foly.; 19: No. 1, 13-29(1971). (In Hungarian).

To facilitate the determination of quantum numbers, the currently employed methods for the determination of the spin and parity of particles were examined, analyzing in greater detail the technique described previously which makes use of all available angle and energy information. Its relativistic approach renders the method more understandable than the conventional nonrelativistic calculation, especially for polarization measurements, as in the case of fermion decays; it may apply also for the study of boson resonances Decay into 2 or 3 particles, as in case of $\gamma \rightarrow \alpha + \beta$, under conservation of parity were examined, taking into account the effect of the nonresonant background which may distort the form of the resonance peak and the angular distribution. Decay into 3 particles, such as that of an ω meson into 3π mesons, were studied on the basis of the final state in the Dalitz diagram and the momentum distribution of the decay products. The baryon polarization was examined on the baryon + 2π final state, in which the multipoles obtained from the angular distribution yield enough information to define the multipole parameters. (TTT)

Electromagnetic

Refer also to abstracts 43658 and 43659.

43582 (DESY–71/20) FINITE-ENERGY SUM RULES AND THE REACTIONS e e → e e ϵ (750), e e → e e f (1260). Schrempp-Otto, B.; Schrempp, F.; Walsh, T. F. (Deutsches Elektronen-Synchrotron, Hamburg (West Germany)). Apr 1971. 9p. Dep. NTIS (U. S. Sales Only).

The $\epsilon\gamma\gamma$ and $f\gamma\gamma$ coupling constants are calculated from finite-energy sum rules for $\gamma\pi \rightarrow \gamma\pi$. The cross sections for ϵ and f production in colliding electron beam reactions are found to be significant. There is reasonable agreement with the tensor meson dominance estimated for the $f\gamma\gamma$ couplings. (auth)

43583 (DESY–71/22) ELECTROPRODUCTION OF PIONS BEYOND THE RESONANCE REGION AND THE PION FORM FACTOR. Schmidt, Winfried (Deutsches Elektronen-Synchrotron, Hamburg (West Germany)). May 1971. 25p. Dep. NTIS (U. S. Sales Only).

A model for the electroproduction of pions at high energies is discussed and applied to the recent data from DESY. With respect to the isovector amplitudes the model represents the electric Born term model, which includes the pion exchange and the pion form factor. The model is supplemented by absorption effects, which are partly derived from fixed-t-dispersion relations or fitted to the data. The isoscalar amplitudes are calculated under the assumption of ρ-exchange. The pion form factor is determined by a fit to the data. According to this fit the pion form factor is larger than predicted by ρ-dominance for photon masses in the range of the DESY experiment. This is a consequence of the unexpected large values for the longitudinal cross sections. A comparison is also made with the recent results from CEA and NINA. (auth)

43584 (ITF–71–27–E) SCALING, POMERANCHUK TRAJECTORY AND J = 1 FIXED POLES IN VIRTUAL COMPTON AMPLITUDE. Miranskii, V. A.; Shelest, V. P.; Zinov'ev, G. M. (Akademiya Nauk Ukrainskoi SSR, Kiev. Institut Teoreticheskoi Fiziki). 1971. 7p. Dep. NTIS (U. S. Sales Only).

Analyzing the "wrong" FESR for the virtual Compton amplitude $t_2(\partial,q^2)$ one comes to the conclusion that the Pomeranchukon residue decreases as $1/\ln Q^2$ or faster, with $Q^2 = q^2 \rightarrow \infty$, and that in t_2, irrespective of the Pomeranchukon, there are J = 1 fixed poles with isospin I = 0 and I = 1. (auth)

43585 (SU–1206–246) NOTE ON THE MOST PROBABLE NUMBER OF PARTONS IN PARTON MODELS. Gardiner, C. W. (Waikato Univ., Hamilton (New Zealand). Dept. of Physics); Majumdar, D. P. (Syracuse Univ., N. Y. Dept. of Physics). Feb 1971. 11p. (NYO–3399–246). Dep. NTIS.

From analysis of the inelastic e-p scattering data it is found that an important feature of the parton probability function P(N) is that it should be peaked around some small number of partons. The most probable number of partons is prognosticated to be around 4.5. Contrary to the usually accepted forms of P(N), where it decreases uniformly from a maximum, it is found that the data also allow a behavior of P(N) where it rises to a maximum first and then decreases with increase of N. (auth)

43586 (SU–1206–250) INELASTIC COMPTON SCATTERING INEQUALITIES IN QUARK-PARTON MODEL. Goswami, D. N.; Majumdar, D. P. (Syracuse Univ., N. Y. Dept. of Physics). Apr 1971. 16p. (NYO–3399–250) Dep. NTIS.

On the assumption that partons are quarks several constraint relations are derived (in the form of inequalities) for the structure functions of inelastic Compton scattering. Bounds on the structure functions of the inelastic Compton scattering with respect to those of inelastic electron-proton scattering are also discussed. All these inequalities must be true for any quark-parton model and, thus, furnish some means of testing the hypothesis of individual quark-parton identification. These are also very useful for obtaining information about the parton distribution function P(N) and about the minimum number of partons N_0 in a nucleon. The constraint relations derived can be made much stronger if one uses a detailed quark-parton model. Assuming $\langle 1/N \rangle = 0.1$, which is consistent with the presently available data on both inelastic electron and inelastic neutrino scatterings, some quantitative analysis of the structure functions is made. (auth)

43587 ASYMPTOTIC BEHAVIOR OF THE ELASTIC FORM FACTOR IN FIELD THEORY. Primack, Joel Robert. Stan-

XUM

ford, Calif.; Stanford Univ. (1970). 127p. University Microfilms Order No. 71-12,977.

Thesis.

The question whether local relativistic quantum field theory can account for the observed asymptotic behavior of the electromagnetic form factor of the proton is examined. Particular attention is devoted to the theory of pions and nucleons interacting via isospin symmetric pseudoscalar coupling with minimal coupling to the electromagnetic field, and to the theory of uncharged massive vector mesons interacting with nucleons through the vector (γ,μ) coupling, as in quantum electrodynamics. New techniques are developed for calculating and summing all asymptotically dominant contributions to vertex functions from all orders of perturbation theory. In renormalizable theories—as distinct from super-renormalizable and unrenormalizable theories—the leading terms in each order of perturbation theory when an external leg of a graph has very large ("asymptotic") momentum are proportional to logarithms of the appropriate asymptotic variable. Such logarithms arise in Feynman integrals either from logarithmic ultraviolet divergences, or else from the near-vanishing of sets of denominators. The former logarithmic terms are called "ultraviolet" and the latter "infrared." In the pseudoscalar theory there are no infrared logarithms because of the p-wave coupling. For this theory, it is found that the sums of all asymptotically leading logarithmic contributions to propagators and vertex functions from each order of perturbation theory have forms with incorrect analytic and unphysical asymptotic behavior. The findings extend and clarify results previously obtained using the renormalization group and other methods. In the vector theory, the form factor receives both infrared and ultraviolet logarithmic contributions, with the former dominant in each order of perturbation theory. Traditional soft-photon techniques are used to show that the leading infrared logarithms can be summed up to a rapidly decreasing expression with asymptotic behavior in rough agreement with the data. The leading ultraviolet logarithms from graphs for the form factor in this theory are not affected by the pathology seen in the pseudoscalar theory; however, one cannot regard the problems associated with these ultraviolet logarithms as being completely under control. It is consequently uncertain whether summing leading contributions from Feynman graphs in local quantum field theory can provide an explanation for the observed rapid decrease of the form factor for increasing momentum transfer. The greatest hope for success in this direction appears to lie with theories in which the infrared logarithms dominate, as in the vector theory. (Diss. Abstr. Int., B)

43588 NEW MODEL FOR THE INTERACTION BETWEEN A MOVING CHARGED PARTICLE AND A DIELECTRIC, AND THE CHERENKOV EFFECT. Lalor, Eamon; Wolf, Emil (Univ. of Rochester, N. Y.). Phys. Rev. Lett.; 26: No. 20, 1274-7(17 May 1971).

A new model is described for the interaction between a moving charged particle executing any two-dimensional motion and an infinite, homogeneous, linear dielectric. The model is based on the exact solution of the self-consistent integro-differential equation of molecular optics. The main results are illustrated by application to the Cherenkov effect. (auth)

43589 MAGNETIC MONOPOLES AND QUARKS. Westenholz, C. v. (Rhodes Univ., Grahamstown, S. Afr.). Ann. Phys. (Leipzig); 25: No. 4, 337-46(1970). (In German).

The concept of Schwinger is discussed, which starts with the hypothesis of the existence of magnetical monopoles and results in a baryon model with magnetically charged constituents. Especially the mathematical consistency of such a theory is analyzed, which admits a connection between some magnetically charged "quarks" and the homogeneous Maxwell-equations $\partial_\mu {}^*F^{\mu\nu}(x^\mu) = 0$, which, displaying a lack of symmetry with respect to the inhomogeneous one, $\partial_\mu F^{\mu\nu}(x^\mu) = 4\pi j^\mu$, are replaced by $\partial_\mu {}^*F^{\mu\nu} = 4\pi {}^*j^\mu$. Here ${}^*j^\mu(x^\mu)$ means a conserved magnetic current which provides a monopole source for the magnetic field. (auth)

43590 EFFECT OF COHERENCE ON INTENSITY-DEPENDENT FREQUENCY SHIFT IN COMPTON SCATTERING. Prakash, H.; Goyal, R.; Vachaspati (Univ. of Allahabad, India). Lett. Nuovo Cim.; 1: No. 19, 771-4(8 May 1971).

The intensity-dependent frequency shift in the scattering of radiation of a general nature (partially coherent) by a free electron is studied. The frequency is determined by considering a diffraction grating and interference experiments of the Fresnel double-mirror type. It is shown that, if the radiation is detected by a device that measures $\langle I^n \rangle$, where I is the intensity in one realization of the field and $\langle\ \rangle$ denotes ensemble average, the intensity-dependent frequency shift is found to depend on $\langle I^{n+1} \rangle / \langle I^n \rangle$. With the conventional detectors, e.g., photographic plates and photoelectric detectors (giving one-photon photoelectric emission), which measure $\langle I \rangle$, the observed intensity-dependent frequency shift is proportional to $\langle I^2 \rangle / \langle I \rangle$. Sufficiently intense photon beams are available that the intensity-dependent frequency shift should be detectable. (R.W.R.)

43591 HOW DOES THE MUON DIFFER FROM THE ELECTRON? Perl, Martin L. (Stanford Univ., Calif.). Phys. Today; 24: No. 7, 234-5; 38-44(Jul 1971).

A review is given on the properties of muons and electrons and speculations are made concerning the differences between them. Experimental studies at SLAC on muon-proton deep inelastic scattering are described. (L.B.S.)

43592 DUAL AMPLITUDE FOR PROCESSES WITH PARTICIPATION OF PHOTONS. Kobushkin, A. P. (Inst. of Theoretical Physics, Kiev). JETP Lett. (USSR) (Engl. Transl.); 13: No. 7, 277-9(5 Apr 1971).

Translated from Zh. Eksp. Teor. Fiz., Pis'ma Red.; 13: No. 7, 387-91(5 Apr 1971).

The parton model is used to construct a dual amplitude for processes involving mesons and photons. The obtained amplitude is compared with the Veneziano amplitude for the $\gamma\pi \to 2\pi$ process. (L.B.S.)

43593 ELECTROMAGNETIC FORM FACTOR FOR THE PION IN THE DUAL RESONANT MODEL. Iroshnikov, G. S.; Chernov, A. S. (Moscow Engineering-Physics Inst.). JETP Lett. (USSR) (Engl. Transl.); 13: No. 7, 265-8(5 Apr 1971).

Translated from Zh. Eksp. Teor. Fiz., Pis'ma Red.; 13: No. 7, 372-6(5 Apr 1971).

It is shown that the electromagnetic form factor for the pion can be obtained from the unitarity relation for the matrix element of the electromagnetic current, using the Veneziano form for the partial wave amplitude of $\pi\pi$ scattering and the Omnes function. (L.B.S.)

43594 SIXTH-ORDER RADIATIVE CORRECTIONS TO THE ANOMALOUS MAGNETIC MOMENT OF THE ELECTRON. Calmet, J. (Univ. of Utah, Salt Lake City. CNRS, Marseille); Perrottet, M. Phys. Rev., D; 3: No. 12, 3101-7(15 Jun 1971).

In order to evaluate the contributions to the anomalous magnetic moment of the electron (a_e), a method entirely based on computer techniques is developed. This method is embedded in the framework of the functional formalism. As a first result, the contributions to the α^3 part of a_3 from diagrams with vacuum polarization insertions are derived. (auth)

43595 DETERMINATION OF THE RADIUS OF STRONG INTERACTION OF Pb AND THE MEAN FREE PATH OF THE π^0 MESON IN NUCLEAR MATTER. Kryshkin, V. I.; Potashov, A. G.; Sterligov, A. G.; Usov, Yu. P. (Tomsk Polytechnic Inst., USSR). JETP Lett. (USSR) (Engl. Transl.); 13: No. 7, 242-3 (5 Apr 1971).

Translated from Zh. Eksp. Teor. Fiz., Pis'ma Red.; 13: No. 7, 341-3(5 Apr 1971).

The results of previous investigations of the photoproduction of π^0 on lead at a primary photon energy of 1.1 GeV are analyzed in order to obtain the parameters of the nucleon distribution in the nucleus and to determine the mean free path of π^0 in nuclear matter. The density distribution functions of the nucleons in the nucleus were chosen in accord with the uniform model and the Woods–Saxon model. It is found that both models agree equally well with the experimental data. (L.B.S.)

43596 REACTION OF PRODUCTION OF TWO SLOW PIONS IN ee AND ep COLLISIONS. Terent'ev, M. V. JETP Lett. (USSR) (Engl. Transl.); 13: No. 8, 318-20(20 Apr 1971).

Translated from Zh. Eksp. Teor. Fiz., Pis'ma Red.; 13: No. 8, 446-9(20 Apr 1971).

Expressions for the amplitude for production of two soft pions in ee and ep interactions are studied. It is pointed out that an experimental study of the process is of particular interest in connection with the verification of current algebra and PCAC. (L.B.S.)

43597 PHOTONS AS HADRONS. Murphy, Frederick V.; Yount, David E. Sci. Amer.; 225: No. 1, 94-104(Jul 1971).

A review is given on the hadronic character of high-energy photons undergoing interactions with hadrons. Following a brief history on the wave-particle duality of light, the methods for producing real or virtual photons are discussed. The vector dominance model of photon-hadron interactions is also discussed. (L.B.S.)

43598 HIGH-ENERGY ASYMPTOTIC CROSS SECTIONS FOR THE PRODUCTION OF e^+e^- PAIRS IN COLLISIONS OF HEAVY CHARGED PARTICLES. Kuraev, E. A.; Lazurik-El'tsufin, V. T.

(Physical-Technical Inst., Kiev). JETP Lett. (USSR) (Engl. Transl.); 13: No. 7, 280-2(5 Apr 1971).

Translated from Zh. Eksp. Teor. Fiz., Pis'ma Red.: 13: No. 7, 391-4(5 Apr 1971).

It was previously shown by Landau that the cross section for e^+e^- pair production in collisions between two fast charged particles, in the limit of high cms energies, is proportional to $\ln^3 E$. The limits of applicability of this formula are examined. The cross section is obtained, accurate to terms $\sim\ln^2 E$. It is found that the term $\sim\ln^2 E$ enters the cross section with a large negative coefficient; thus at energies $E \lesssim (6-7)$ GeV the cross section becomes negative if only these two terms are taken into account. (L.B.S.)

43599 COULOMB CORRECTIONS TO LOW-ENERGY ELASTIC AND CHARGE-EXCHANGE πN SCATTERING. Oades, G. C.; Rasche, G. (Univ., Zurich). Helv. Phys. Acta; 44: No. 1, 5-32 (15 Feb 1971).

The problem of πN scattering in the simultaneous presence of the short range nuclear potential and the long range Coulomb potential is considered. The existing treatment of π^+p scattering is outlined and similar methods are then used to derive the corresponding results for the coupled channel processes $\pi^-p \to \pi^-p$ and $\pi^-p \to \pi^0n$. Finally it is shown how the Coulomb corrections so obtained can be calculated to first order in the Coulomb parameter. (auth)

43600 RADIATIVE CORRECTIONS FOR MUON DECAY IN AN INTERMEDIATE VECTOR BOSON THEORY. Veghte, Richard Clark. Storrs, Conn.; Univ. of Connecticut (1970). 176p. University Microfilms Order No. 71-16,054.

Thesis.

The radiative corrections to the beta decay spectrum of the muon are evaluated. The calculation is based on a theory of the intermediate vector boson in which the mass of the boson is required to be very large ($\geq 10^3$ proton masses). The results of the calculation are that the decay spectrum is exceedingly insensitive to the intermediate vector boson mass and that the present data is entirely consistent with boson masses required by the theory. (Diss. Abstr. Int., B)

43601 NUMERICAL STUDY OF REGGE CUTS DUE TO ABSORPTION IN NEUTRAL PION PHOTOPRODUCTION. Miller, Robert Alan. Urbana, Ill.; Univ. of Illinois (1970). 72p. University Microfilms Order No. 71-14,874.

Thesis.

The numerical features of some absorptive Regge models of neutral pion photoproduction are examined in some detail. One starts by reviewing the formalism in a consistent notation. The formalism contains derivations of the two expressions commonly used to calculate absorbed scattering amplitudes and their relation to Regge cut parametrizations. The physical picture behind the derivations is that absorbed Regge scattering is the result of secondary scattering of the products of the pure Regge exchange so that particles are scattered into inelastic channels. The scattering of the particles which remain in the channel of interest is taken to be elastic scattering as measured experimentally. The oldest of the two absorptive expressions is the Gottfried–Jackson partial wave form; the newer expression involves an integral over the intermediate scattering angle. The integral absorption expression is used for most of the calculations. Unitarity and factorization are discussed briefly regarding their relation to the calculations presented. Numerical results are obtained by choosing a specific parametrization for the Regge exchange and performing the required numerical integrations. Graphs of the discontinuities across the Regge cut which is generated, the contribution to the s- and t-channel scattering amplitudes due to the cut, and the fit to the data which is obtained are presented. The s dependence of the absorptive corrections is discussed. It is found that the straightforward absorptive Regge model does not fit the data well. For this reason the effects produced by the modifications of the straightforward model which have been used in several published fits are examined. It is found that the omission of the nonsense wrong-signature zero has a beneficial effect. It is argued that, independent of the presence or absence of a nonsense wrong-signature zero, the effects of the cut calculated in the manner presented are too small, and that an arbitrary multiplication of the cut amplitude by a factor of about 2 is necessary in the types of absorptive Regge fits which were tried. (Diss. Abstr. Int., B)

43602 MULTIPERIPHERAL MODELS IN HIGH ENERGY SCATTERING. Jones, Stanley Tanner. Urbana, Ill.; Univ. of Illinois (1970). 109p. University Microfilms Order No. 71-14,816.

Thesis.

Phenomenological studies are made of two multiperipheral models. First an application of the multi-Regge model to the process $\pi^-p \to \pi^+\pi^-\pi^-p$ at 5 GeV/c is made. A good description of the data is obtained, including fits to numerous multi-particle distributions. It is found that predicted diffractive slopes are systematically high. Comments on duality and on the Treiman–Yang angle distribution, as they apply to this model, are made. Secondly, an application of the multiperipheral model to inelastic electron–proton scattering is made. The form factor νW_2 for this process is numerically evaluated in a multiperipheral model with scalar couplings, and in a generalization of this model which allows form factors to accompany the pion exchange. It is found that although the models are theoretically scale invariant in the sense that νW_2 approaches a finite limit as $q^2 \to -\infty$, this limit is approached very slowly; for values of $|q^2| \sim 1-7$ $(\text{GeV/c})^2$, experimentally attainable at SLAC, the models have not reached their scale invariant limits. (Diss. Abstr. Int., B)

43603 PRODUCTION OF W MESONS IN CHARGED LEPTON–PION COLLISIONS. Dominguez, Arnulfo Zepeda. Mexico City; Instituto Politecnico Nacional (1970). 89p. University Microfilms Order No. 71-15,059. (In Spanish).

Thesis.

The previous calculations of W producing processes are critically reviewed, and then the reaction $e^- + \pi \to W^- + \nu + \pi$ is computed to lowest order in the electromagnetic and the semi-weak couplings. The pion electromagnetic vertex is described by the ρ-dominance type form factor with mass parameter determined from experimental data. Numerical results for the total cross section were obtained for electron energies in the laboratory system from 30 to 300 GeV and for W masses of 2, 3, 4, and 5 GeV. A typical value of the W production cross section is 2.97×10^{-37} cm^2 when the mass of W is 3 GeV and the energy in the center of mass system of the incident particles is 7 GeV. It is concluded that the calculated process is an important source of W production. (Diss. Abstr. Int., B)

43604 DYNAMICAL EFFECTS OF INSTABILITY IN ρ^0 MESON PHOTOPRODUCTION AND ELASTIC SCATTERING. Bauer, Theodore Henry. Ithaca, N. Y.; Cornell Univ. (1970). 111p. University Microfilms Order No. 71-12,118.

Thesis.

Concentrating on the ρ^0 meson, simple mechanisms are proposed to illustrate that an unstable particle, while exhibiting many properties of a stable particle, derives some of its behavior from being a dynamical composite of its principal decay products (p wave $\pi^+\pi^-$ pairs in the case of the ρ^0). "Anomalous," possibly large real parts in the T matrices for high energy scattering of unstable particles are shown to be such a dynamical consequence of instability. This effect is estimated to be quite large in the case of the photoproduction and elastic scattering of ρ^0 mesons from nucleons and can be interpreted as a breakdown of the simple "ρ^0-photon analogy." Generalizing to nuclei, a theory is presented for the high energy photoproduction of nonresonant $\pi^+\pi^-$ pairs which takes into account the scattering of both pions from the nucleus. The amplitudes turn out to be significantly smaller than those calculated using the conventional Drell–Söding theory of this process, which allows for the scattering of only one pion. The above results are combined in an approximate theory of $\pi^+\pi^-$ pair photoproduction from nuclei that takes into account that $\pi^+\pi^-$ pairs can either be nonresonant or come from a ρ^0 and that ρ^0 mesons can be produced and scatter with "anomalous" amplitudes not only from individual nucleons but also from the nucleus as a whole. (Diss. Abstr. Int., B)

43605 NEUTRINO PAIR PRODUCTION BY PHOTONS. Schreiber, William Michael. New York; Yeshiva Univ. (1970). 105p. University Microfilms Order No. 71-14,309.

Thesis.

The neutrino pair production process $\gamma + \gamma \to V + \overline{V}$ is considered. Using an intermediate boson theory, the cross section for V_e, $\overline{V}_e$ and for V_μ, $\overline{V}_\mu$ production is evaluated to lowest order by dispersion relation techniques. The result is found to be essentially the same whether one uses the Haller, Landovitz, and Goldberg intermediate boson theory or the Lee and Yang intermediate boson theory. The lowest order nonvanishing matrix element is of the order ω^3, and hence the lowest order cross section is of the order ω^3. For electron-type neutrinos and a boson mass of 2 GeV, one obtains $\sigma = (4.8)\ (10^{-46})\ (\omega/\text{Mp})^6\ \text{cm}^2$ where Mp is the proton mass. The corresponding black body neutrino luminosity is $L = (2.4)\ (10^{-7})\ (T/10^9)^{13}$ ergs/cm^3-sec. For muon-type neutrinos, both of the above formulas are reduced by a factor of ten. (Diss. Abstr. Int., B)

43606 THEORY OF PHOTOPRODUCTION OF ELECTRONS IN A STRONG ELECTROMAGNETIC FIELD WITH ALLOWANCE

XUM

FOR INTERACTION IN THE FINAL STATE. Brodskii, A. M.; Gurevich, Yu. Ya. Zh. Eksp. Teor. Fiz.; 60: No. 4, 1452-64 (Apr 1971). (In Russian).

Interaction in the final state with a time-dependent field of a strong electromagnetic wave is considered for photoproduction of charged particles. The approach is based on an extension of the well known method for taking into account interaction in the final state. It is shown that in the threshold approximation allowance for the interaction defines the dependence of photoproduction on field strength. In the one-dimensional case, when additional external fields in the final state are absent, a nonsingular integral equation is obtained which can be solved by standard methods and the limit of a weak electromagnetic field is considered. Perturbation theory is developed for the more general case of presence of additional stationary fields and in particular of a Coulomb field. The results are compared with the experimental cruves for photo-emission from the surface of metals and with earlier calculations. (auth)

43607 INTERFERENCE BETWEEN COULOMB AND STRONG INTERACTIONS AT HIGH ENERGIES. Gorshkov, V. G.; Kuraev, E. A.; Lipatov, L. N.; Nesterov, M. M. (Ioffe Inst. of Physics and Tech., Leningrad). Zh. Eksp. Teor. Fiz.; 60: No. 4, 1211-15(Apr 1971). (In Russian).

It is demonstrated that the Bethe formula for the relative phase shifts of the Coulomb and hadron parts of scattering amplitudes for charged particles is valid at high energies and fixed transferred momenta. The proof is based on factorization of the electromagnetic correction to the strongly interacting amplitude in the region $k_\perp^2 \ll m^2$. The existence of factorization is a consequence of gauge invariance. The Bethe formula is invalidated by contribution from large values of $k_\perp$. However such contributions arise only in hadron theories with small coupling constants. (auth)

Weak

43608 EFFECT OF THE τ-t-Λ CLUSTER STRUCTURE OF $^7_\Lambda$Li ON THE ANGULAR DISTRIBUTION IN THE $^7_\Lambda$Li $\rightarrow$ ^{4}He + ^{3}He + π^- DECAY. Chlebowska, D. (Inst. for Nuclear Research, Warsaw). Phys. Lett.; 35B: No. 5, 393-4(21 Jun 1971).

The angular and energy distributions in the Λ-Li^7 $\rightarrow$ ^{4}He + ^{3}He + π^- decay are calculated with the use of the initial wave function: $\phi(\tau\text{-t-}\Lambda)$. The significant sensibility of the angular distribution on the $^7_\Lambda$Li cluster structure is demonstrated. (auth)

43609 DETERMINATION OF THE MASS OF THE MUONIC NEUTRINO IN RADIATIVE PION DECAYS. Bardin, D. Yu.; Mitsel'makher, G. V.; Shumeiko, N. M. (Joint Inst. for Nuclear Research, Dubna, USSR). JETP Lett. (USSR) (Engl. Transl.): 13: No. 7, 273-7(5 Apr 1971).

Translated from Zh. Eksp. Teor. Fiz., Pis'ma Red.: 13: No. 7, 383-7(5 Apr 1971).

Two experiments were previously proposed for determining the mass of ν_μ from the decay $\pi^+ \rightarrow \mu^+ + \nu_\mu + \gamma$: the first determines m_ν from the position of the end point of the γ-quantum spectrum, and the second measures in addition the muon momentum with high accuracy. The γ spectra is investigated in detail for the two experiments. (L.B.S.)

43610 ENERGY DECAY FOR THE NEUTRINO EQUATION IN THE EXTERIOR OF A TORUS. Phillips, Ralph; Sarason, Leonard (Stanford Univ., Calif. Univ. of Washington, Seattle). Arch. Ration. Mech. Anal.; 41: No. 1, 1-17(1971).

Local energy decay is established for the solutions of the neutrino equation in the exterior G of a torus for a class of boundary conditions, described as follows: To each energy-conserving boundary condition at a point x on ∂G there corresponds a vector in the tangent plane to ∂G at x. The result has been proved when the torus and boundary conditions are axially symmetric and when the paths generated by this vector field are closed. What is novel about this problem is the fact that the boundary conditions are nowhere coercive. (auth)

43611 PCAC AND THE $\pi\rho$ CONTRIBUTION TO THE ERROR IN THE GOLDBERGER–TREIMAN RELATION. Feigenbaum, Joel. Ithaca, N. Y.; Cornell Univ. (1970). 113p. University Microfilms Order No. 71-14,630.

Thesis.

The problem of accounting for the discrepancy between the experimental value of the pion decay constant, f_π, and the theoretical value predicted by the Goldberger–Treiman relation is considered. Of the possible contributions to the error, that of the $\pi\rho$ intermediate states has not previously been properly considered. The PCAC hypothesis is used to calculate the $\pi\rho$ contribution to the unsubtracted dispersion relation associated with the matrix element, $\langle P\bar{N}|\partial_\mu A^\mu(0)|0\rangle$. When evaluated at $s = 0$, this gives a correction to the Goldberger–Treiman relation. In the calculation special attention is paid to the effects of the ρ instability. These effects are of two kinds: the two-body phase space factor is altered; the treatment of the final state interaction needs to be handled quite differently from what is conventional for stable particles. The theory of unitary scattering amplitudes and form factors is developed from considerations of three pion processes. The contribution found is too small to account for the discrepancy in the Goldberger–Treiman relation. This suggests that some modification is required in the PCAC hypothesis. (Diss. Abstr. Int., B)

43612 STUDY OF THE SELF-COUPLING OF WEAK LEPTON CURRENTS AT HIGH ENERGIES. Fujikawa, Kazuo. Princeton, N. J.; Princeton Univ. (1970). 180p. University Microfilms Order No. 71-14,374.

Thesis.

The self-coupling of the weak lepton currents, $(e\nu_e)(e\nu_e)$ and $(\mu\nu_\mu)(\mu\nu_\mu)$, is interesting as a test of the universal Fermi coupling scheme and also in connection with astrophysical implications. Two special consequences of the self-coupling of the leptonic weak currents are studied: muon pair radiation from the neutrino and neutrino pair radiation from the muon in nuclear Coulomb fields. A numerical analysis is carried out by the computer to get detailed information for the various distributions of the kinematical variables in these processes. The energy, angular and invariant mass distributions of the muon pair produced by the neutrino were calculated. The following interesting features of these distributions were found: The energy and angular distributions of the muon and the antimuon are quite different from each other due to the charge conjugation violation of the weak currents. The muon appears more in the forward direction and is more energetic compared with the antimuon. The invariant mass of the muon pair was found to favor extremely small values, less than 1 GeV for 10 GeV incident neutrinos on a proton or ^{56}Fe target, although the energy loss of the incident neutrino is substantial. These characteristic features of the muon pair distributions may make it possible to discriminate these rare events from dominant background processes. The total cross section integrated over these distributions is in good agreement with previously known values. The calculation of the energy and angular distributions of the muon after neutrino pair radiation in a Coulomb field also shows several interesting features. In particular, the energy loss of the muon in this process is quite different from that due to bremsstrahlung, in spite of the close resemblance of the analytical expressions for these two processes. The muon loses more than 80 percent of its energy in the neutrino pair radiation process. It is interesting to remember that the energy loss of the leptons in bremsstrahlung is peaked at small energy values and is infrared divergent. Naturally the angular distribution of the scattered muon is less forwardly distributed in the present process as compared with bremsstrahlung. Yet the rate of the present process is smaller than that of bremsstrahlung by a factor of 10^{-9}, even in this enormous energy loss region. The total cross section of the neutrino radiation is 1.5×10^{-42} cm^2 for the proton target and 2.8×10^{-40} cm^2 for the ^{56}Fe target with incident energy of the muon at 150 GeV. The energy dependence of the total cross section is approximately what is expected from the asymptotic formula. The dependence on the polarization of the muon is also substantial; the spin flipping part is smaller than the spin nonflipping part by a factor of 100. Also the same calculation was repeated for the electron induced neutrino pair radiation process. The total cross section for the electron is approximately twice as large as that for the muon. The polarization dependence is, however, stronger for the electron case, and the spin flipping process is negligible. A brief discussion of the background processes expected in the actual experiments on these processes, the effects of the "weak bosons" and radiative corrections is presented. Astrophysical implications of these weak processes are also discussed. (Diss. Abstr. Int., B)

Strong (General)

43613 (CERN–71-13) SYSTEMATICS OF EXTRA-NUCLEAR HADRON CASCADES IN SHIELDS. Barbier, M.; Hunter, R. (European Organization for Nuclear Research, Geneva (Switzerland)). 21 Jun 1971. 35p. Dep. NTIS (U. S. Sales Only).

An attempt is made to find a mathematical model for the build-up and decay of cascades produced in the shield by very high-energy incident particles. It is found that a first approximation can be given for the lateral spread of such cascades. Simplification of the model, numbers and energy spectra of the various generations of secondaries, the development of the hadron shower

along an axis, the lateral spread of the cascade, the first generation, and muons are considered. (J.F.P.)

43614 (JINR-P2-5829) MODEL OF THE MULTIPLE PARTICLE PRODUCTION. Dushutin, N. K.; Mal'tsev, V. M. (Joint Inst. for Nuclear Research, Dubna (USSR). Lab. of Theoretical Physics). 1971. 17p. (In Russian). Dep. NTIS (U. S. Sales Only).

A model for the multiple particle production at high energies is suggested. In this model, as compared to statistical ones, the secondary particles do not reach the thermodynamical equilibrium during the collision time and the whole interaction is considered to be a random process. (auth)

43615 MULTIPLE QUARK SCATTERING ANALYSIS AND ITS APPLICATION TO THE HADRON CHARGE EXCHANGE SCATTERING PROCESSES. Cho, Dong Won. Seattle; Washington, Univ. (1970). 94p. University Microfilms Order No. 71-11,029.

Thesis.

The main objective is to investigate the hadron charge exchange (CEX) scattering processes in terms of multiple scattering formalism. Adopting the view that hadrons are composed of subparticles, one was previously able to explain the high-energy behavior of the pp, $\bar{p}p$ and πp elastic differential cross sections. Especially the explanation of the break structures of the differential cross sections in terms of multiple scattering picture, and the prediction concerning the pion form factor were satisfactory results. In order to explain the CEX scattering processes, one must consider the spin and isospin effects of the constituent particles. The nucleons and mesons are assumed to belong to 56- and 35- dimensional representations of the nonrelativistic SU(6) group. The Glauber formalism is extended to include the spin and isospin effects. As for the quark scattering amplitudes, the view is adopted that these fundamental scattering amplitudes can be expressed in terms of Regge pole exchange amplitudes. This leads one to the interesting aspect that the multiple scattering correction term provides an explicit way of calculating Regge cut contributions. By doing explicit calculations of these multiple scattering correction terms the energy and momentum transfer square dependencies of the π^-p, np and $\bar{p}p$ CEX scattering differential cross sections and polarization data of π^-p CEX scattering are explained. Thus it is shown that the multiple scattering picture provides natural explanations of the π^-p CEX scattering polarization effect and the forward peak in np CEX scattering differential cross section which, in standard Regge pole theory, would require the extra ξ' trajectory and pion conspirator trajectory. Finally the connection between the multiple scattering model and the absorptive correction model is discussed. (Diss. Abstr. Int., B)

43616 ELECTROMAGNETIC CONTRIBUTIONS TO THE TOTAL CROSS SECTION OF HADRON SCATTERING. Budnev, V. M.; Ginzburg, I. F. (Mathematics Inst., Novosibirsk, USSR). JETP Lett. (USSR) (Engl. Transl.): 13: No. 9, 370-3(5 May 1971).

Translated from Zh. Eksp. Teor. Fiz., Pis'ma Red.: 13: No. 9, 519-22(5 May 1971).

It is shown that contributions from electromagnetic processes to the total cross section of hadron scattering can reach 1 mb at 60 GeV, which accounts for the large deviation of the experimental cross section from the extrapolated hadronic cross section above 30 GeV. Two significant mechanisms discussed are bremsstrahlung and peripheral single-photon processes. (L.B.S.)

43617 ELASTIC HADRONIC PROCESSES, DUALITY, AND ABSORPTION. Harari, Haim (Weizmann Inst. of Science, Rehovot, Israel. Stanford Univ., Calif.). Ann. Phys. (N. Y.); 63: No. 2, 432-42(Apr 1971).

A simple qualitative model for hadronic two-body amplitudes is proposed. The model combines the two-component theory of duality with the main idea of the absorption model. The qualitative predictions of the model for elastic differential cross sections and polarizations correctly reproduce several interesting regularities of the data. In particular, the presence of dips in nonexotic elastic processes and their absence in exotic reactions is explained. (auth)

43618 PERSISTENCE OF THE PHOTON IN CONFORMAL-DUAL MODELS. Halpern, M. B. (Univ. of California, Berkeley). Phys. Rev., D; 3: No. 12, 3068-71(15 Jun 1971).

The spin-1 zero-mass "photon" of the (conformal) Veneziano model persists in the spectra of all "new" (conformal) dual models of the Bradakci-Halpern type. In these generalized models, however, the "photon" does not, in general, decouple through statistics. (auth)

43619 TOPICS IN DUAL RESONANCE MODELS. TOTAL WIDTHS ON THE LEADING TRAJECTORY. Galli, Eduardo Jorge. New York; Yeshiva Univ. (1970). 118p. University Microfilms Order No. 71-14,306.

Thesis.

The physically meaningful concept of "duality" in strong interactions is discussed, and its connections with chiral symmetry breaking are investigated. Also the generalized Veneziano model is reviewed stressing its factorization properties. Later on, the dual oscillator model of hadrons is presented in which factorization is achieved by construction. In the context of this formalism the first step toward unitarization of the theory can be worked out. It also provides a picture in which nonplanarity emerges in a natural way. Then factorization on the leading trajectory is discussed as a way to obtain amplitudes for spinning parent particles. One can also translate this into the language of the dual oscillator model. In possession of these tools attention is devoted to the problem of total widths along the leading trajectory. This is an essential test of the whole theory because it analyses the physical significance of the large number of degenerate states found after factorization. The numerical computation of the widths in the low energy region seems to show that the presence of daughters is for that purpose no source of difficulties, even though there was a priori the fear of completely unphysical outcomes. (Diss. Abstr. Int., B)

43620 MOMENTUM SPECTRUM OF HADRONIC SECONDARIES IN THE MULTIPERIPHERAL MODEL. DeTar, Carleton Edward. Berkeley, Calif.; Univ. of California (1970). 82p. University Microfilms Order No. 71-15,751.

Thesis.

Motivated by a simplified multiperipheral model, a general qualitative description of the momentum spectrum of secondaries, resulting from a collision of two hadrons at high energies is formulated. Arguing from two fundamental multiperipheral concepts, that transverse momenta are limited and that distant particles on the multiperipheral chain are uncorrelated, it is predicted that at sufficiently high incident energies, the momentum spectrum of particle X in the reaction $a + b \rightarrow X + \text{anything}$, when presented in the variables $p_\perp$ and $y = \sinh^{-1}[p_{||}/(p_\perp^2 + m^2)^{1/2}]$, develops a central plateau in the y dependence, which elongates and flattens to a value that is normalized by the total cross section as the incident energy increases. Moreover, it is shown that the resultant particle density distribution is consistent with the hypothesis of limiting fragmentation. This description is contrasted with the predictions of the two-fireball model, the isobar-pionization model, and the statistical thermodynamical model. (Diss. Abstr. Int., B)

43621 RATIO OF NEUTRAL-TO-CHARGED HADRONS IN COSMIC RADIATION AT AN ATMOSPHERIC DEPTH OF 976 g cm^{-2}. Le Coultre, Pierre (Univ., Bern). Helv. Phys. Acta; 44: No. 1, 115-132(15 Feb 1971). (In German).

The ratio of neutral to charged hadrons in the cosmic rays at an atmospheric depth of 976 gcm^{-2} is measured with a spark chamber set-up. A value of 0.73 ± 0.03 was found for incoming particles with a weighted average energy larger than or equal to 12 GeV. At a minimum value of 15 GeV approximately the ratio is 0.64 ± 0.04. Provided that the neutron to proton ratio equals unity at the atmospheric depth of 976 gcm^{-2}, the π-meson to nucleon ratios for energies larger or equal to 12 GeV and 15 GeV are 0.18 ± 0.03 and 0.28 ± 0.05 respectively. (auth)

43622 THEORY OF CURRENTS DESCRIBING A SYSTEM OF INTERACTING PSEUDOSCALAR MESONS AND BARYONS. Beckerman, Martin. Coral Gables, Fla.; Univ. of Miami (1970). 85p. University Microfilms Order No. 71-10,656.

Thesis.

A locally gauge-invariant chiral Lagrangian, describing interacting pseudoscalar mesons and baryons, without invoking higher spin fields is constructed. Higher spin particles are regarded as semi-bound states of basic ones. As an example, the Yang-Mills fields are exhibited. Then Sugawara's energy-momentum tensor is introduced, and a current algebra is obtained consistent with the Schwinger covariance condition. The model does not exhibit parity doubling. In addition, the model avoids the difficulties which arise in the sum rules for the nucleon form factor when the space-space current commutators vanish. It is found that a simple set of relations holds between the various space-space equal-time current commutators and the operator Schwinger terms which occur in the time-space equal-time current commutators. (Diss. Abstr. Int., B)

Strong (Baryon No. = 0)

Refer also to abstracts 43692 and 43711.

XUM

43623 (ITF-71-28-E) DUAL AMPLITUDE WITH MANDELSTAM ANALYTICITY. Bugrii, A. I.; Enkovskii, L. L.; Kobylinskii, N. A. (Akademiya Nauk Ukrainskoi SSR, Kiev. Institut Teoreticheskoi Fiziki). 1971. 9p. Dep. NTIS (U. S. Sales Only).

A dual crossing symmetric amplitude satisfying a Mandelstam representation with correct spectral function boundaries, second sheet poles and Regge asymptotic behavior is suggested. The explicit form of the amplitude for elastic $\pi\pi$-scattering is given. Possible applications are indicated. (auth)

43624 (UCR-34-P-107-B-112) ARE THERE TWO A_2 MESONS? Poe, R. T.; Shen, B. C. (California Univ., Riverside. Dept. of Physics). [1970]. Contract AT(04-3)-34. 13p. (CONF-700806-61). Dep. NTIS.

From 15th International conference on high energy physics; Kiev, USSR (26 Aug 1970).

A model for the A_2 phenomenon is described. The A_2 splitting and other seemingly conflicting data can be understood within the framework of this model which assumes different mass shifts in the A_2 production amplitude from ρ and f^0 exchanges. (auth)

43625 INEQUALITIES ON DOUBLE PARTIAL-WAVE AMPLITUDES FROM POSITIVITY, ANALYTICITY, AND CROSSING SYMMETRY. Griss, Martin L. (Univ. of Illinois, Urbana). Phys. Rev., D; 3: No. 12, 3124-33(15 Jun 1971).

Using "geometrical" inequalities similar to those of Martin for the partial waves $f_l(s)$ of the $\pi^0-\pi^0$ amplitude in the Mandelstam triangle, sets of inequalities are derived, following from positivity and analyticity alone, and involving only a finite number of the Balachandran double partial-wave amplitudes a_{nl}. Application of crossing symmetry gives further inequalities. Similar inequalities are obtained from the more constraining positivity and analyticity inequalities for $f_l(s)$, given by Yndurain. (auth)

43626 INEQUALITIES FOR THE s- AND p-WAVE $\pi\pi$ PARTIAL-WAVE AMPLITUDES. Balachandran, A. P. (Syracuse Univ., N. Y. Tata Inst. of Fundamental Research, Bombay); Blackmon, Maurice L. Phys. Rev., D; 3: No. 12, 3133-41 (15 Jun 1971).

An infinite number of inequalities are derived for integrals over the s- and p-wave $\pi\pi$ amplitudes in the interval $0 \le s \le 4m_\pi^2$ in terms of the $\pi\pi$ total cross sections and other experimentally accessible data. The main ingredients in the derivations are crossing symmetry, the positivity of the even $l \ge 2$ partial waves of the reactions $\pi^0\pi^0 \to \pi^0\pi^0$ and $\pi^0\pi^0 \to \pi^+\pi^-$ in the interval $0 \le s \le 4m_\pi^2$, and some known bounds on the crossed-channel absorptive parts of these reactions. It is shown that if the partial-wave sum over any subset of $\pi^0\pi^0 \to \pi^0\pi^0$ partial waves is itself invariant under permutations of s, t, and u, and this subset contains the s wave, then the entire $\pi^0\pi^0 \to \pi^0\pi^0$ amplitude has to vanish identically. (Actually, a somewhat stronger result is proved for the amplitudes of both the processes $\pi^0\pi^0 \to \pi^0\pi^0$ and $\pi^0\pi^0 \to \pi^+\pi^-$ or for any linear combination of these amplitudes with positive coefficients.) (auth)

43627 UNITARY SYMMETRY AND DUALITY IN MESON-MESON SCATTERING. Roy, T.; Chowdhury, A. Roy (Jadavpur Univ., Calcutta). Phys. Rev., D; 3: No. 12, 3213-17(15 Jun 1971).

Construction of Veneziano-type amplitudes for the general pseudoscalar meson-meson (PP) scattering incorporating unitary symmetry is considered. Emphasis is given to the use of the crossing matrix, both in the SU(3) and in the lower symmetry group SU(2). All the essential features of the quark-model calculations are reproduced. Eigenvalues of the crossing matrix are seen to correspond to the symmetry properties of the amplitudes, which in turn produce the different signatures of Regge trajectories. Incidentally it may be mentioned that the unwieldy tensorial decomposition in the internal symmetry space has been done away with. (auth)

43628 GHOST-ELIMINATING MODIFICATIONS IN MULTIPION AMPLITUDES: FACTORIZATION ON LEADING TRAJECTORIES. Jacobs, Mathew A. (Tel-Aviv Univ., Israel). Phys. Rev., D; 3: No. 12, 3220-7(15 Jun 1971).

The modification of B_n to eliminate the ghost at $\alpha_\rho = 0$ is investigated. The $J_1J_2J_3$ leading three-particle vertex in B_n is calculated. Using this form, it is shown that no finite number of term modification of B_n without trajectory depression satisfies consistent factorization in all multipion amplitudes. Allowing trajectory depression, although daughter levels still presumably do not factorize, a solution is found in which (a) all leading trajectories factorize, (b) are nondegenerate, and (c) the $\rho\rho\rho$ vertex need not be zero. This is believed to be the suitable generalization of the Lovelace 4-π amplitude. (auth)

43629 COMMENTS ON THE $A_1\pi \to A_1\pi$ AMPLITUDES IN THE VENEZIANO MODEL. Csikor, F. (Roland Eoetvoes Univ., Budapest). Phys. Rev., D; 3: No. 12, 3237-9(15 Jun 1971).

It is shown that one of the two solutions for the $A_1\pi \to A_1\pi$ amplitude of Carruthers and Lasley can be eliminated. The connection of this solution to that of Whippman is also established. (auth)

43630 CURRENT ALGEBRA AND THE TRACE OF THE ENERG-MOMENTUM TENSOR. Golowich, E.; Lasley, Eric (Univ. of Massachusetts, Amherst). Phys. Rev., D; 3: No. 12, 3114-24(15 Jun 1971).

A model is considered in which the trace of the energy-momentum tensor, $\Theta \equiv \Theta^\mu_\mu$, contains both SU(3) × SU(3)-invariant and -breaking terms. The latter are assumed to be proportional to S_0 and S_8, the $T = 0, J^P = 0^+$ members of $(3,3^*)\oplus(3^*,3)$. Each contribution to the trace is weighted by four minus the dimension of the associated local-field operator. Using Jacobi identity relations, it is proved that the dimensions of S_0 and S_8 are equal. In order to investigate the consequences of the assumed chiral properties of the energy-momentum trace, the $\pi\pi$, πA_1, and A_1A_1 matrix elements of Θ are examined. Ward-identity relations are employed to constrain the off-shell extensions of these matrix elements. In our model, the dimension d of S_0 and S_8 is found to equal two in the SU(2) × SU(2) limit of massless pions. A more general relation is derived for d that is valid even when SU(2) × SU(2) is only an approximate symmetry. Scalar-dominance and smoothness assumptions enable additional information from this model to be extracted. $\Gamma(A_1 \to \epsilon\pi)/\Gamma(\epsilon \to \pi\pi) = 0.07$ is predicted for the $A_1(1070)$ and $\epsilon(700)$ partial widths. The model also leads to tentative conclusions concerning two subjects of current interest: the possibility that scalar mesons couple to Θ with a universal strength, and the existence of chiral-invariant contributions to Θ. (auth)

43631 IS THE VENEZIANO MODEL CONSISTENT WITH THE YANG-MILLS COUPLING OF VECTOR-MESON FIELDS. Gounaris, G. J. (Democritus Nuclear Research Center, Athens). Phys. Rev., D; 3: No. 12, 3025-7(15 Jun 1971).

It is shown that the assumption that vector-mesons couple like Yang-Mills fields in a chiral Lagrangian model is consistent, in the tree approximation, with the simplest Veneziano model for the amplitudes $\omega \to 3\pi$, $\eta \to \pi^+\pi^-\gamma$, and $X \to \pi^+\pi^-\gamma$. (auth)

43632 BARYON ANNIHILATION AND EXOTIC EXCHANGE. Chiu, Charles B. (California Inst. of Tech., Pasadena. State Univ. of New York, Stony Brook); Hwa, Rudolph C. Phys. Rev., D; 3: No. 12, 3078-86(15 Jun 1971).

Within the framework of duality and quark diagrams, the importance of connecting the annihilation processes in $B\bar{B}$ collisions to the exchange of an (ϵ) trajectory with $q\bar{q}q\bar{q}$ quark content is suggested. It is argued that this ϵ should be an exchange-degenerate pair with natural parity and I = 0. It is coupled strongly to the $B\bar{B}$ system at t = 0. For the positive-t region, it is expected to be manifest as a physical vector meson with G = −1 at around 1 GeV. Available data do not rule out its existence. (auth)

43633 INEQUALITIES FOR THE $\pi\pi$ PARTIAL WAVES FROM THE PROPERTIES OF A CLASS OF ORTHOGONAL POLYNOMIALS. Balachandran, A. P. (Syracuse Univ., N. Y. Tata Inst. of Fundamental Research, Bombay): Blackmon, Maurice L. Phys. Rev., D; 3: No. 12, 3142-51(15 Jun 1971).

The $\pi\pi$ partial-wave amplitudes are the projections of the corresponding scattering amplitudes with respect to the Legendre polynomials with appropriate arguments. In the past few years, several inequalities for the $\pi\pi$ partial-wave amplitudes were obtained by using analyticity and unitarity. It is shown that many of these inequalities may be generalized into inequalities for the projections of the $\pi\pi$ scattering amplitudes with respect to suitable classes of orthogonal polynomials. The generalization yields several new inequalities for the $\pi\pi$ partial waves in the region $0 \le s \le 4m_\pi^2$. In particular, such inequalities involving only s, p, and d waves are derived. (auth)

43634 ASYMPTOTIC BEHAVIOR AND THE POSSIBILITY OF DUALITY WITHOUT GHOSTS IN FEYNMAN-DIAGRAM MODELS. Coon, D. D. (Univ. of Minnesota, Minneapolis). Phys. Rev., D; 3: No. 12, 3071-6(15 Jun 1971).

Elastic scattering of two spinless particles with equal or unequal masses is considered in Feynman-diagram models of the Van Hove type with the usual couplings and with arbitrary spectra of masses, spins, and coupling constants, including infinitely large masses and spins. It is shown that if the amplitude defined by analytic continuation of the sum of all lowest-order diagrams with s-channel poles has no unphysical or u-channel singularities, then for fixed t this amplitude is not bounded by any power of s as

$|s| \to \infty$ in any infinitely multiply connected domain which excludes only neighborhoods of the poles. Since a dual Born term with no u-channel poles can be represented entirely by the sum of s-channel pole diagrams (or by the sum of t-channel pole diagrams), this bad asymptotic behavior cannot be canceled in the Born approximation in a dual multiparticle theory. Regge asymptotic behavior is also supposed to be associated with duality, and consequently one sees that Feynman-diagram models of the Van Hove type cannot exhibit duality. The result is independent of the order of summation of diagrams. It depends crucially on the requirement that coupling constants be real. (auth)

43635 ALGEBRAIC STRUCTURE OF PION–HADRON TRANSITION AMPLITUDES AND HADRON MASS SPECTRA. Noga, Milan (Purdue Univ., Lafayette, Ind.). Phys. Rev., D; 3: No. 12, 3047-58(15 Jun 1971).

Making use of generally accepted assumptions about the equal-time commutator algebra of axial charges and axial divergences, the spin and helicity dependence of Weinberg's algebraic relations is entirely determined for pions in arbitrary partial waves. It is shown that the algebraic structure of axial-vector coupling matrices may be given by the Lie algebra of the group SO(4,3), and so hadron states must be assigned to unitary representations of this group. Furthermore it is proved that the mass-spectrum operator is given as a sum of a scalar and a component of a 35-dimensional totally antisymmetric irreducible tensor of the group SO(4,3). The general form of the mass spectrum is exhibited as a linear combination of the Clebsch–Gordan coefficients of the group SO(4,3). Application to hadron states of fixed intrinsic quantum numbers leads to the conclusion that mass-squared values of hadrons must be a linear function of spin. This result is a unique and exact consequence of the structure of certain algebraic relations. (auth)

43636 APPLICATION OF CONTINUOUS MOMENT SUM RULES TO $\pi\pi$ SCATTERING. Kaiser, Gerald Yurek. Madison, Wis.; Univ. of Wisconsin (1970). 97p. University Microfilms Order No. 71-304.

Thesis.

Continuous moment sum rules are applied to $\pi\pi$ scattering using phase shifts obtained from π-production data by OPE analysis. The calculation indicates that P, P′ and ρ Regge pole exchanges offer an adequate and consistent description of the available data. The fits suggest that P′–ρ exchange degeneracy is violated, with P′ choosing no compensation and ρ choosing nonsense. The P residue is found to have a linear zero at $t \sim -.6$ GeV^2. A crossing symmetric pole approximation to the Reggeized absorption model is formulated which lends itself to a continuous moment sum rule analysis, introducing small first-order corrections to the residues. Consistency with πN and NN Regge analyses is checked by employing factorization, and it is found that while the results for P′ and ρ agree, the P residue of this analysis appears to be too small. (Diss. Abstr. Int., B)

Strong (Baryon No. = 1)

43637 (DESY–71/24) UNITARIZED FINITE ENERGY SUM RULES AND THEIR APPLICATION TO πN-CHARGE EXCHANGE. Schrempp, F. (Deutsches Elektronen-Synchrotron, Hamburg (West Germany)). May 1971. 47p. Dep. NTIS (U. S. Sales Only).

The problem of "unitarizing" finite energy sum rules (FESR) by the inclusion of Regge cuts is investigated. Instead of considering Regge cuts in FESR for the full scattering amplitude T_{fi}, new FESR are proposed for that part of T_{fi}, which has just pure Regge pole asymptotic behavior if the Regge cuts are included in T_{fi}. The Regge cuts in the high-energy region are evaluated according to the "weak-cut" version of the reggeized K-matrix model. The new FESR then look like the conventional ones, however, with T_{fi} replaced by the corresponding two-particle K-matrix element. With these K-matrix FESR the serious difficulties arising in conventional approaches to the problem disappear. With the new K-matrix FESR a detailed analysis of πN-charge exchange is performed. The K-matrix FESR turn out to be satisfied with only the ρ pole on the high energy side much better and more locally than the corresponding conventional FESR. The ρ residues in the K-matrix are predicted to choose "nonsense" at $\alpha_\rho = 0$. If reduced ρ residues are defined as in the Regge limit of a πN-Veneziano formula, they are found to be practically constant between $t = m_\rho^2$ and $t \approx -0.4$ (GeV/c)^2. The values agree well with those known at $t = m_\rho^2$ and with results from high-energy fits. (auth)

43638 (ITF–71-9-P) PROBLEM OF THE TWO-NUCLEON MOTION FOR THE GAUSS POTENTIALS. Petrov, N. M. (Akademiya Nauk Ukrainskoi SSR, Kiev. Institut Teoreticheskoi Fiziki). 1971. 19p. (In Russian). Dep. NTIS (U. S. Sales Only).

The problem of the two-nucleon motion is considered on the basis of the Gauss potential approximated by a series with separable terms. The convergence of the separable expansion of the two-particle t-matrix off the energy shell is investigated. (auth)

43639 (JINR–P1-5849) THERMODYNAMICAL DESCRIPTION OF THE MOMENTUM DISTRIBUTIONS OF PIONS IN A π^-p INTERACTIONS AT p = 4 GeV/c. Grishin, V. G.; Inogamov, Sh. V.; Yuldashev, B. S.; Jancso, G. (Joint Inst. for Nuclear Research, Dubna (USSR). Lab. of High Energy). 1971. 16p. (In Russian). Dep. NTIS (U. S. Sales Only).

It is shown that the momentum distributions of secondary pions produced in the reactions π^- + p at p = 4 GeV/c can be well described by simple functions which were received from the Bose-statistic $dN/dP_\perp = A_\perp P_\perp^{\frac{1}{2}} e^{-A_\perp P_\perp} dN/dP_{||} = A_{||} e^{-A_{||} P_{||}}$. The results of the fit are presented for transverse and longitudinal momentum distributions, respectively. While introducing the cut-off $P_\perp \geq 0.2$ GeV/c and $P_{||} \geq 0.1$ GeV/c, the distributions $dN/dP_\perp$ and $dN/dP_{||}$ are described significantly better than without it. A very simple explanation of the difference of the slopes in the $dN/dP_{||}$ distributions for left- and right-moving pions in the c.m.s. is also given on the basis of the phenomenological quasi-two-body model for high multiplicity interactions. (auth)

43640 (LYCEN–7110) RECONSTRUCTION OF AMPLITUDES FOR PION–NUCLEON SCATTERING FROM EXPERIMENTAL DATA. Giffon, M.; Joseph, J.; Meyer, J. (Lyon Univ. (France). Institut de Physique Nucleaire). 9 Mar 1971. 22p. Dep. NTIS (U. S. Sales Only).

The possibility of using experimental data to reconstruct the energy and angular dependence of the amplitudes in pion-nucleon scattering without using any specific model was investigated. It was shown that this problem could be solved for near forward scattering. (France)

43641 (SU–1206-249) INEQUALITIES FOR THE PION–NUCLEON PARTIAL WAVES. Balachandran, A. P. (Syracuse Univ., N. Y. Dept. of Physics, Istituto Nazionale di Fisica Nucleare, Naples (Italy)); Case, W. (Syracuse Univ., N. Y. Dept. of Physics); Della Selva, A.; Saito, S. (Istituto Nazionale di Fisica Nucleare, Naples (Italy). Naples Univ. (Italy). Istituto di Fisica Teorica). [1971]. 9p. (NYO–3399-249). Dep. NTIS.

Two inequalities for the pion-nucleon partial waves with angular moments $l \leq 4$ are derived. (auth)

43642 (UCR–34-P-107-B-106) STUDY OF DUALITY FOR INELASTIC KN SCATTERING AT INTERMEDIATE ENERGIES. Ferro-Luzzi, M.; Shepard, H. K.; Kernan, A.; Poe, R. T.; Shen, B. C. (California Univ., Riverside. Dept. of Physics). [1970]. Contract AT(04-3)-34. 27p. (CONF-700806–62). Dep. NTIS.

From 15th international conference on high energy physics; Kiev, USSR(26 Aug 1970).

The duality diagram predictions for the reactions $\overline{K}N \to \pi\Sigma$ and $\overline{K}N \to \pi\Lambda$ were tested using the CERN-Heidelberg-Saclay energy independent partial wave analysis in the center-of-mass energy region 1500 < Ecm < 1900 MeV. It is found that the (imaginary part of the) $\pi\Lambda$ amplitudes show significantly better local averaging to zero than do the $\pi\Sigma$ amplitudes. In the $\pi\Sigma$ channel the $I_s = 1$ and $I_t = \frac{1}{2}$ amplitudes generally oscillate closer to zero than the $I_s = 0$ and $I_t = \frac{3}{2}$ components, and in all cases the helicity nonflip amplitudes are clearly superior to the helicity flip amplitudes. In general, however, it is concluded that the evidence for duality in these reactions is not convincing, at least for the somewhat low energies and limited energy interval examined. (auth)

43643 THEORETICAL STUDY OF PION NUCLEON INTERACTIONS. Ross, William Alexander. Stanford, Calif.; Stanford Univ. (1970). 117p. University Microfilms Order No. 71-12,984.

Thesis.

A study is made of pion nucleon interactions. Elastic scattering and pion production at low energies are treated. A simple model of π^-p elastic scattering which is shown to be in excellent agreement with the experimental data is presented. In this model the amplitude consists of s-channel resonances plus a diffraction, or Pomeron exchange term. A fit was made to the π^-p elastic differential cross section data from 0.55 to 1.3 GeV/c. At these energies the diffractive term is taken from the experimental data to be exponential in the invariant momentum transfer, although more structure may be present at higher energies. The resonant amplitudes were parametrized as Breit–Wigner line shapes. A fit is made to the data by varying, as parameters, the masses, widths and elasticities of the resonances as well as the parameters associated with the Pomeron exchange. A satisfactory fit to the data is obtained and the resonance and diffraction parameters so obtained are presented. Pion production in low energy pion nucleon interactions is studied. The approach taken is to treat the reaction

XUM

($\pi N \rightarrow \pi\pi N$) as a nonrelativistic three-body problem and to employ the Faddeev–Lovelace equations to study the reaction. The pion production process is dealt with specifically, and the main objective is to examine final state mass spectra. Specific methods of solving the Faddeev–Lovelace equations are studied. In addition one will also see how the features of two body dynamics are manifested in the three body system. Specifically, an attempt is made to relate the final state mass spectra to the two body forces which were used to generate these results. (Diss. Abstr. Int., B)

43644 BARYON CURRENTS AND FIELDS. Vasholz, David Paul. Madison, Wis.; Univ. of Wisconsin (1971). 118p. University Microfilms Order No. 71-5668.

Thesis.

Ways in which interpolating fields may be used to describe baryons are examined. Emphasis is placed on relations and analogies with vector and axial-vector currents. Possible baryon currents are constructed in the Fermi–Yang model and compared with currents obtained using the quark model. Asymptotic chiral symmetry is formulated in a way applicable to two-point functions of baryon currents. Three Weinberg-like sum rules are derived on the basis of asymptotic chiral symmetry, one of which also follows from a property abstracted from the constructed currents. These sum rules are compared qualitatively with experiment in the single particle approximation, with fair agreement. A simple model based on virtual transitions analogous to the ρ-meson-photon interaction is proposed. This model, applying to baryons of any spin, reproduces properties suggested by the sum rules. Relations between a number of electromagnetic mass differences are derived, assuming these also are dominated by virtual transitions. The relevance of the model to effective Lagrangians is examined. (Diss. Abstr. Int., B)

43645 MASS DIFFERENCES AS ADDITIONAL ELECTROMAGNETIC CORRECTIONS IN LOW-ENERGY ELASTIC AND CHARGE-EXCHANGE πN SCATTERING. Oades, G. C.; Rasche, G. (Univ., Zurich). Helv. Phys. Acta; 44: No. 2, 160-71(1 Apr 1971).

A treatment of low energy $\pi^-p \rightarrow \pi^-p$ and $\pi^-p \rightarrow \pi^0n$ scattering is presented, which includes non-relativistically both mass difference effects and the effect of the long range Coulomb potential. Using this formalism it is shown how the corrections to the usual charge independent expressions can be calculated in a first order perturbation treatment. (auth)

Strong (Baryon No. ≥ 2)

Refer also to abstracts 43534, 43726, 43799, and 43960.

43646 (JINR–P1-5775) SOME CHARACTERISTICS OF COHERENT INTERACTIONS AT 17 AND 45 GeV. Azimov, S. A.; Beter, E. V.; Grishin, V. G.; Gulyamov, U. G.; Gulamov, K. G.; Levin, A. Ya.; Chernov, G. M. (Joint Inst. for Nuclear Research, Dubna (USSR). Lab. of High Energy). 1971. 16p. (In Russian). Dep. NTIS (U. S. Sales Only).

It is shown that the main experimental characteristics of the reactions of diffraction coherent generation of pions by pions on complex nuclei in the region of accelerated energies can be satisfactorily described by the Deck model. (auth)

43647 (ORO–3992-61) MORE SIMULATED EXTENSIVE AIR SHOWERS WITH A MEDIUM-STRONG INTERACTION. Campbell, J. A. (Texas Univ., Austin). Jun 1971. 8p. (CPT–111). Dep. NTIS.

An improved version of a previous simulation of extensive air showers above 10^{13} eV is discussed. In the simulation, the central assumption of a medium-strong contact interaction between protons is retained, but a model is used in which secondary pions are produced during pp collisions rather than through isobar decay. The influence of several different expressions for the multiplicity of pions and for the magnetic form factor of the proton is examined. While these expressions have noticeable quantitative effects on the behavior of the showers, the previous qualitative observation that the medium-strong interaction leads to a gradual increase in a measure of transverse momentum above a primary energy of 10^{14} eV is unchanged. (auth)

43648 $\Lambda N - \Sigma N$ COUPLING FOR ΛN SCATTERING AND FOR THE Λ-PARTICLE BINDING IN NUCLEAR MATTER. Bodmer, A. R. (Univ. of Illinois, Chicago. Argonne National Lab., Ill.); Rote, D. M. Nucl. Phys.; A169: No. 1, 1-48(1971).

The effect of coupling of the ΛN to the (virtual) ΣN channel on the Λ-particle binding in nuclear matter (the Λ-well depth) is studied with perturbation theory and especially in the reaction-matrix approach with use of the g-matrix approximation. The g-matrix is calculated self-consistently by use of the Kallio-Day version of the reference-spectrum method, the free kinetic energies being assumed for the unoccupied single-particle states. A large variety of interactions is considered including in particular, hard-core interactions with (static) one-pion exchange (OPE) and ρ-meson exchange coupling potentials. The couplings have both central and tensor components. A meaningful measure of the suppression of the coupling in nuclear matter is obtained in perturbation theory by considering the effective nonlocal central potentials that represent the (s-state) effect of the coupling for nuclear matter and for ΛN scattering. For hard-core interactions one-channel ΛN potentials are used with the same hard core and the same low-energy scattering characteristics as the coupled-channel interactions to define the "unsuppressed" well depths appropriate to the effect of the coupling for scattering. The suppression δD of the well depth arises from the effect of the exclusion principle and of the spectrum gaps (binding-energy effects) on the coupling. δD depends strongly on the details of the interaction and is relatively much larger for central than for tensor couplings and is less for shorter ranges of the same type of coupling potential. Furthermore, δD depends on the "unsuppressed" (i.e., intrinsic) strength of the coupling. For the OPE coupling the tensor component is dominant and the central components contribute only very slightly; reasonable $\Lambda\Sigma\pi$ coupling constants can give large values of δD (as much as 15 MeV). For the ρ-exchange coupling the central components for both spin states, S = 0 and 1, can give quite large δD (possibly as much as 5 MeV for S = 0) in spite of the short range. Interesting possibilities arise from possible destructive interference between the OPE and ρ-exchange tensor couplings because the interference for nuclear matter differs from that for scattering, since the OPE coupling is more strongly suppressed than the ρ-exchange one. The possibility of 15 MeV suppression implies that agreement of the calculated with the phenomenological depth ($\approx$30 MeV) can be obtained for reasonable hard-core radii ($\approx$0.4 fm) and for an appreciable p-state interaction of about half the strength of the s-state one. (auth)

43649 DUALITY IN THE TRIPLE REGGE LIMIT. Edelstein, R. M.; Rittenberg, V.; Rubinstein, H. R. (Weizmann Inst. of Science, Rehovot, Israel). Phys. Lett.; 35B: No. 5, 408-12 (21 Jun 1971).

The Regge formula for inclusive processes, with duality applied to the missing-mass channel, is compared to existing high-energy, low- and intermediate-missing-mass data on $pp \rightarrow pX$ and $\pi^-p \rightarrow \pi^-X$. The formula is found to be valid to a good approximation, and conclusions are reached as to which trajectory contributions are indicated by the data. (auth)

43650 MATHEMATICAL QUARKS FROM A BOOTSTRAP PRINCIPLE. Capps, Richard H. (Weizmann Inst. of Science, Rehovot, Israel). Phys. Rev., D; 3: No. 12, 3059-68(15 Jun 1971).

A simple bootstrap hypothesis was previously applied to the meson–meson and meson–baryon scattering amplitudes of a hypothetical set of arbitrary numbers of even- and odd-parity mesons and baryons. A set of self-consistency relations for the trilinear interaction constants of the hadrons was obtained. This set is reexamined and extended by considering baryon–baryon scattering. The most striking new predictions are that the mesons must interact with the symmetry of quark–antiquark composites, while the baryons behave as quark–quark composites. The meson Regge trajectories must be parity-doubled, while the baryon parity depends on the symmetry with respect to the interchange of the two (mathematical) quarks. Particles of baryon number more than 1 are forbidden. (auth)

43651 Λ–d SCATTERING AS A PROBE OF THE Λ–N CORE POTENTIAL. Kashef, Bayesteh Ghaffary. Los Angeles; Univ. of Southern California (1970). 128p. University Microfilms Order No. 71-12,396.

Thesis.

A nonrelativistic quantum mechanical system of three hadrons, interacting via a sum of two-body potentials is studied. The three-body system studied consists of a Λ-hyperon and two nucleons (a neutron and a proton). The theoretical investigation of such a multiparticle system may provide a tool for probing the two-body ΛN potential; i.e., it may yield information which cannot be obtained from two body calculations and experiments directly. Low energy Λ-deuteron scattering was investigated to determine whether Λd scattering cross sections are sensitive to the details of the ΛN interactions. The Λd scattering problem, both in quartet and doublet spin state, was solved exactly using nonlocal separable S-wave, spin dependent, central potentials and a multiple-scattering formalism of the Faddeev type. The two-body potentials needed were the NN potential in the triplet spin state and the ΛN potential in both the singlet and the triplet spin states. The former was represented by an attractive separable potential, while each of the

latter was represented as a spin of an attractive and a repulsive nonlocal potential. The shape of the attractive part of the potentials was always of the Yamaguchi type, while the short range repulsion (core) was taken to be of various shapes (Yamaguchi, Tabakin and exponential). For a given ΛN spin channel, a set of two body nonlocal separable potentials (with various core shapes) were obtained, all of which produced the same low energy parameters as the phenomenological local potential and were equivalent to the local potential in that they produced the same phase shift over a wide energy range. No free potential parameters were left in this fit. Conclusions based on the behavior of the two-body wave functions, transition matrix and their singularities for the various core shapes are presented. It was determined that in the incident Λ laboratory momentum range of 100 to 300 MeV/c, the Λd cross sections are sensitive to the short range behavior of the two-body ΛN potentials. The reduction in the cross section was (13 to 25)%, being larger for higher energies and being dependent on the Λd spin state. Also, it was determined that Λd scattering cross section does depend on the two-body off-shell t-matrix elements. Comparisons of the S-wave cross sections with the case where all the necessary partial waves were included showed that almost the entire effect of the ΛN core appears in the S-wave Λd cross section. Finally, it was concluded that the sensitivity of Λd scattering to the ΛN potentials is strong enough to warrant further investigations with more realistic models. (Diss. Abstr. Int., B)

43652 CALCULATIONS OF HYPERNUCLEI BY MEANS OF THE K-HARMONICS METHOD. Khrylin, B. A. (Inst. of Atomic Energy, Moscow). Yadern. Fiz.; 13: 492-4(Mar 1971). (In Russian).

General formulas are obtained for calculations of hypernuclei by means of the K-harmonics method in the minimal K approximation. Results are presented on fitting the ΛN potential to the B_Λ values for Λ-He^4 and Λ-He^5, the question of the degree of closeness of the singlet and triplet ΛN potentials is discussed. (auth)

43653 NON-RELATIVISTIC HARD PION PRODUCTION AND THE TWO NUCLEON INTERACTION. Zollman, Dean Alvin. College Park, Md.; Univ. of Maryland (1970). 94p. University Microfilms Order No. 71-12,182.

Thesis.

The two-nucleon interaction is studied by analyzing single-pion production in nucleon–nucleon collisions. To obtain a theory of pion production the mass dispersion approach of Fubini and Furlan is applied to the production process. By considering the leading singularity in the mass dispersion relation, it is shown that, in the nonrelativistic approximation, this approach leads directly to a distorted wave Born approximation for the physical amplitude. The transition operator is determined from current-field algebra and is given by the usual Chew–Low operator generalized to be Galilean invariant. Using this transition amplitude the off-energy-shell two-nucleon interaction is studied. It is shown that, for suitably selected experiments, the production amplitude depends significantly on the phenomenological potential used to describe the nucleon–nucleon interaction. (Diss. Abstr. Int., B)

Particle Invariance Principles and Symmetries

General

Refer also to abstracts 43676 and 43721.

43654 (ITF-70-89-E) THE RELATIVISTIC EQUATIONS OF MOTION WITHOUT "REDUNDANT" COMPONENTS. Fushchick, V. I.; Grishchenko, A. L.; Nikitin, A. G. (Akademiya Nauk Ukrainskoi SSR, Kiev. Institut Teoreticheskoi Fiziki). 1970. 27p. Dep. NTIS (U. S. Sales Only).

Starting from the certain representation for the generators of the proper Poincaré group all the operator functions $\mathscr{N}$ at which the equation is invariant under the total Poincaré group (including the space-time reflection) are described (with accuracy to the unitary equivalence). The unitary operator for arbitrary spin is obtained. It connects the Poincaré representation with the canonical Foldy–Shirokov representation. The explicit forms of the operators of coordinate, velocity and spin in the Poincaré representation for arbitrary spin s are obtained. (auth)

43655 GENERAL PROPERTIES OF DUAL MODELS: CONFORMAL INVARIANCE. Galli, Alicia J. Couto. New York; Yeshiva Univ. (1970). 150p. University Microfilms Order No. 71-14,305.

Thesis.

The concept of duality is introduced and the Veneziano model presented. Some algebraic implications of duality and its connections with chiral symmetry are analyzed. The factorization of Veneziano amplitudes is briefly discussed and the so-called dual oscillator model presented. A further interpretation of the variables entering such a model provides a new framework where conformal invariance plays an important role. A class of conformal mappings proves to be useful in the search for relations which can cure some anomalies found in factorization. Generators are found in a Lagrangian scheme. More general relations lead also to conformal mappings which could have a new physical interpretation. (Diss. Abstr. Int., B)

Applications (Electromagnetic and Weak)

43656 (PITHA-44) ON THE POSSIBILITY OF CPT VIOLATION IN NEUTRAL KAON DECAY. Faissner, H.; Koepp, G.; Zerwas, P. (Technische Hochschule, Aachen (West Germany). Physikalisches Institut (III)). 1971. 19p. Dep. NTIS (U. S. Sales Only).

T and CPT breaking are indistinguishable if one observes K_L^0 decays only. Of one infers from existing experimental data that T is violated, but not CPT, one relies in addition on the unitary relation. This relation is generalized such as to include nonclosed systems with a nonhermitean, CPT violating Hamiltonian. An interaction of this type which couples only to neutral kaons is essentially equivalent to the superweak interaction of Wolfenstein. However, there is a sign difference between ϵ_S and ϵ_L, which is measurable in leptonic and 3π decays. (auth)

43657 CP VIOLATING DECAY OF THE NEUTRAL KAON INTO TWO NEUTRAL PIONS. Raymond, David James. Stanford, Calif.; Stanford Univ. (1970). 73p. University Microfilms Order No. 71-12,979.

Thesis.

The CP violating decay rate of the long lived neutral kaon into two neutral pions was measured in a spark chamber experiment at the Stanford Linear Accelerator Center. This yielded a value of $9.5 \pm 5 \times 10^{-6}$ for the parameter $|\eta_\infty|^2$, where the quoted error is statistical. (Diss. Abstr. Int., B)

43658 CHIRAL SU(3) × SU(3) AND THE DECAY $\eta \to 3\pi$. II. Cantor, Arnold J. (MITRE Corp., Bedford, Mass.). Phys. Rev., D; 3: No. 12, 3205-12(15 Jun 1971).

The decay $\eta \to 3\pi$ was previously examined in a very general way based on the current algebra of SU(3) × SU(3) and partial conservation of axial-vector current, but making use of nonlinear chiral Lagrangian techniques. The results restated the failure of this approach to η decay which was already known from the work of Sutherland, but in a new, quantitative form which we referred to as the "scale difficulty." The same approach, the same techniques, and the same symmetry-breaking model is applied to the same problem. In order to alleviate the scale difficulty, an extension of the theory is investigated in which η decay is mainly due to a new term which is also contained in the symmetry-breaking $(3,\bar{3}) + (\bar{3},3)$ representation. Firstly, it is found that the new contribution to η decay does not alter the good value for the slope. Secondly, using the soft-pion result for $m_{\pi^+}^2 - m_{\pi^0}^2$ the phenomenological Lagrangian can be uniquely determined and it is found that the scale difficulty disappears. Thirdly, a simple condition on the symmetry-breaking Lagrangian is presented, plus a speculative test of that condition that agrees with the new solution. A modification of the tadpole theory of Coleman and Glashow, in which the octet of tadpole mesons belongs to a nonlinear realization of SU(3) × SU(3), is explored in the light of the new theory of η decay. This new tadpole theory, unlike the old, has no difficulty in explaining octet dominance in the weak nonleptonic decays. It also explains why the non- $(3,\bar{3}) + (\bar{3},3)$ part of the pseudoscalar-meson Lagrangian is small compared to the $(3,\bar{3}) + (\bar{3},3)$ part, as well as why it is predominantly octet. A new numerical fit to the tadpole theory is presented, which shows that the baryon Lagrangian must also be predominantly $(3,\bar{3}) + (\bar{3},3)$. (auth)

43659 CHIRAL SU(3) × SU(3) AND THE DECAY $\eta \to 3\pi$. I. Cantor, Arnold J. (MITRE Corp., Bedford, Mass.). Phys. Rev., D; 3: No. 12, 3195-3205(15 Jun 1971).

The difficulties with the current-algebra treatment of the decay of the η meson into three π mesons are analyzed within the framework of a nonlinear Lagrangian calculation based on the chiral group SU(3) × SU(3). The most general η-decay Lagrangian with the symmetry properties of the effective second-order electromagnetic interaction, and containing no more than two derivatives, is constructed and is shown to involve only one arbitrary parameter, the coupling constant g. The energy dependence, or slope, of the $\eta \to \pi^+\pi^-\pi^0$ matrix element depends only on the choice of rep-

XUM

resentation for the SU(3) and SU(3) × SU(3) (collectively called medium-strong) symmetry-breaking terms. The simplest choice for these terms in a theory containing explicit partial conservation of axial-vector current—namely, a common $(3,\bar{3}) + (\bar{3},3)$ representation for both—gives good agreement with experiment. Furthermore, exactly three parameters exist for adjusting the coupling constant and the electromagnetic mass differences $m^2_{\pi^+} - m^2_{\pi^0}$ and $m^2_{k^+} - m^2_{k^0}$ to their measured values. However, the coefficients of terms in the resulting phenomenological Lagrangian are unnaturally large; they give rise to the small mass differences only because of extensive cancellations (a condition which we refer to as a "scale difficulty"). The same techniques used for η decay are also applied to the nonleptonic weak decays of the K mesons. The usual current-algebra results are obtained as a check that our methods are exactly equivalent to the conventional ones. (auth)

43660 ELECTROMAGNETIC FINAL-STATE INTERACTION CORRECTIONS TO SOME SEMILEPTONIC WEAK INTERACTIONS WITH REFERENCE TO TESTS OF TIME-REVERSAL INVARIANCE. Brodine, John Charles. Pittsburgh; Carnegie-Mellon Univ. (1971). 212p. University Microfilms Order No. 71-14,058.

Thesis.

Some quantities needed in the experimental determination of the existence of time-reversal-violating terms in the semileptonic weak interaction Hamiltonian are calculated. Expressions are given for the electromagnetic final-state interaction contribution to D, the triple-product correlation coefficient, in the nuclear beta decay transitions $\frac{1}{2} \to \frac{1}{2}$, $\frac{3}{2} \to \frac{3}{2}$, $\frac{3}{2}^{\pm} \to \frac{1}{2}^{\pm}$, $\frac{5}{2}^{\pm} \to \frac{3}{2}^{\pm}$, $\frac{7}{2}^{\pm} \to \frac{5}{2}^{\pm}$, $1^+ \to 0^+$, $\frac{1}{2}^{\pm} \to \frac{3}{2}^{\pm}$, $\frac{3}{2}^{\pm} \to \frac{5}{2}^{\pm}$, and $\frac{5}{2}^{\pm} \to \frac{7}{2}^{\pm}$ to all orders of $Z\alpha/v_e$ in the Coulomb interaction. The effect of the finite nuclear size is investigated. The contribution to D for the above transitions from the final-state magnetic scattering is investigated to order α. A calculation of the Coulomb final-state interaction effects in the neutral Kaon ($K^0_{l_3}$) decays $K_L \to \pi^{\pm} + l^{\pm} + \nu_e$ is presented. Specifically, the charge asymmetry for $l = e,\mu$ and the transverse polarization of the muon are investigated. The effects of possible $\Delta Q = -\Delta S$ amplitudes and the q^2 dependence of the form factors are considered. The results of an extensive numerical survey are given. The variation of the effects over the Dalitz plot is discussed. Finally, the Coulomb final-state interaction effects in some tests of time-reversal invariance are discussed using the K^0_{4} decays $K_L \to \pi^0 + \pi^{\pm} + l^{\pm} + \nu_e$. The electromagnetic scattering corrections to the Pais–Treiman equations (I-function) are found, and their value estimated. (Diss. Abstr. Int., B)

Applications (Strong)

43661 SUPERCONVERGENCE AND ALGEBRAIC REALIZATIONS OF CHIRAL SYMMETRY. McDonald, A.; Ram Mohan, L. R. (Purdue Univ., Lafayette, Ind.). Phys. Rev., D; 3: No. 12, 3076-8(15 Jun 1971).

The consequences of assuming that there is no isospin T = 2 part in the commutator $[\dot{Q}^a_5, \dot{Q}^b_5]$ of time derivatives of the axial charges Q^a_5 and Q^b_5 were investigated. The superconvergence condition derived from this assumption provides constraints on Weinberg's mass matrix. The mixing angles introduced by Weinberg for the π-A_1-ρ-σ system of mesons and for the nucleon resonances belonging to the $(1,\frac{1}{2})$ and $(\frac{1}{2},0)$ representations of the chiral group are now determined. When only p-wave pion interactions are considered, it is shown that the new constraints on the mass matrix lead to mass degeneracy for the symmetric representations of SU(2) ⊗ SU(4). The constraints on the spin spectrum derivable from the superconvergence conditions are briefly mentioned. (auth)

43662 SPONTANEOUS BREAKDOWN OF CONFORMAL AND CHIRAL INVARIANCE. Crewther, R. J. (California Inst. of Tech., Pasadena). Phys. Rev., D; 3: No. 12, 3152-65(15 Jun 1971).

The implications of a theory in which scale and chiral invariance are spontaneously broken, and the dilaton appears as a mixture of the two isoscalar members of the scalar nonet is discussed. The usual assumptions for the conformal properties of the axial-vector current constrain the low-energy behavior of the spin-2 form factor, $F_1(t)$, of the pionic matrix element of the stress-energy tensor. In the limit of scale invariance, $F'_1(0) = F'_{\sigma\pi}(0)/F_{\sigma\pi}(0)$ is found, where $F_{\sigma\pi}(t)$ is the axial-vector form factor obtained from the coupling of the dilaton to a pion via the axial-vector current, and the prime denotes differentiation. This relation connects the assumptions of f dominance of $F_1(t)$ and A_1 dominance of $F_{\sigma\pi}(t)$. Using the method of collinear dispersion relations, the effects of violation of scale invariance are estimated. A result previously obtained in the limit of scale invariance becomes $F_\sigma F_{\sigma\pi}(m^2_\sigma) f_\pi \simeq \frac{1}{2}$, where f_π is the decay constant of the pion, and F_σ couples the dilaton to the vacuum via the stress-energy tensor. Similar corrections to the scale-invariant prediction for $F'_1(0)$ are calculated. The magnitudes of the corrections are controlled by the $A_1\sigma\pi$ coupling constant. According to the usual estimates of this constant, the predicted width of the dilaton is compatible with the Adler–Weisberger sum rule for $\pi\pi$ scattering and phenomenological estimates of the σNN coupling constant. While the relation for $F'_1(0)$ obtained in the limit of scale invariance is compatible with the assumption of f dominance, the effects of symmetry breaking are large. In the real world, it is found that f dominance is a poor approximation, a conclusion which is supported by recent estimates of the fNN coupling constants. The relation of our work to the magnitude of parameters measuring symmetry violation in the energy density is discussed. The interpretation of a recent result of Cheng and Dashen is that scale invariance is spontaneously broken, and chiral SU(2) × SU(2) is a much better symmetry than SU(3). (auth)

43663 MULTIPLE PRODUCTION OF MASSLESS PIONS AS A CONSISTENCY TEST IN THE ALGEBRAIC REALIZATION OF CHIRAL SYMMETRY. Rockmore, Ronald (Rutgers–The State Univ., New Brunswick, N. J.). Phys. Rev., D; 3: No. 12, 3039-47(15 Jun 1971).

The symmetric amplitude for the multiple production of massless pions in the collinear frame is studied as a consistency test in the algebraic realization of chiral symmetry due to Weinberg. A revision of Ahmed's recent calculation of collinear pion production (the three-pion amplitude) together with a simplified approach to the four-pion amplitude form the basis for the plausible conjecture that the asymptotic symmetric amplitudes are alternately sums of T = 0 (for pion-target scattering and 2n-pion production with n = 1, . . .) and T = 1 [for (2n − 1)-pion production with n = 1, . . .] terms. Several corroborative calculations in higher order are adduced which indicate that this conjecture rests on a solid basis. It is concluded that Weinberg's hypotheses and procedure prove consistent in the case of multiple meson production; however, this extension does not appear to yield any additional algebraic restrictions on the axial-vector coupling matrix $\bar{X}(\lambda)$ or the mass matrix m^2. (auth)

Field Theories

General

Refer also to abstract 43513.

43664 (COO-1195-204) FAILURE OF S-CHANNEL HELICITY CONSERVATION IN A_1^- PRODUCTION. Ascoli, G.; Brockway, D. V.; Eisenstein, L.; (and others) (Illinois Univ., Urbana. Dept. of Physics). Jan 1971. 11p. Dep. NTIS.

A study of the A_1^- density matrix elements shows that s-channel helicity is not conserved in the process $\pi^- p \to A_1^- p$ between 5 and 25 GeV/c. Instead the A_1^- density matrix elements have simple behavior in the t-channel helicity frame. A new analysis of the A_1^- cross section as a function of the incident π^- momentum is also presented. (auth)

43665 (NP-18831) NEW CLASSICAL FIELD THEORY. Heberlein, Fermin Viniegra (Universidad Nacional Autonoma de Mexico, Mexico City. Facultad de Ciencias). 1970. 29p. (In Spanish). Dep. NTIS (U. S. Sales Only).

Thesis.

A Lorentz-invariant field theory in a Minkowki space-time E_4 is proposed. (J.S.R.)

43666 HELMHOLTZ AND RELATIVISTIC ELECTRODYNAMICS. Treder, H.-J. (Zentralinstitut fuer Astrophysik, Babelsberg, Ger.). Gerlands Beitr. Geophys.; 79: No. 6, 401-20 (1970). (In German).

Einstein has pointed out that the principle of relativity, far from being a logical necessity, is only an empirical fact. According to Einstein the principle of relativity is a principle of selection to find out the true form of the physical laws from the multiplicity of mathematically possible formulas. The most general form of the interaction potential in electrodynamics (without radiation terms) is the "kinetic potential". The Helmholtz potential depends explicitly on the absolute velocities of the charges. All electrodynamic interaction laws which agree with Coulomb's and Ampère's laws are able to be set up from the Helmholtz potential by special choice of a dimensionless constant k in Helmholtz's expression. For nonchoice of k there follows a Galilei-invariant electrodynamics. (A Galilei-invariant electrodynamics is not realizable but by way of a physically strange hypothesis about the nature of the electric currents,

as proposed previously.). Therefore, a Galilei-covariant electrodynamics cannot exist. However, postulating the Lorentz invariance of the kinetic potential allows Helmholtz's constant to be determined as k = 0. In this case, the Helmholtz interaction potential becomes identical with the relativistic electrodynamic potential of Darwin and Breit. So, the Darwin–Breit potential is the only interaction potential leading to a Lorentz-covariant electrodynamics (including terms up to $\sim v^2/c^2$). (auth)

Quantum Field Theory

Refer also to abstracts 43587 and 43594.

43667 (ITF-71-12-P) ASYMPTOTIC FIELDS FOR THE APPROXIMATED, RENORMALIZED, TWO DIMENSIONAL YUKAWA MODEL AND :P(φ_2): MODEL. Yakymiv, Ya. M. (Akademiya Nauk Ukrainskoi SSR, Kiev. Institut Teoreticheskoi Fiziki). 1971. 22p. (In Russian). Dep. NTIS (U. S. Sales Only).

The renormalized Yukawa theory in space–time of two dimensions and the boson field $\varphi(x)$ with interaction of the form :P(φ_2(x)): are considered. Asymptotic limits of the annihilation-creation operators are proved to exist. It is also shown that the commutation relation between these asymptotic operators and the total Hamiltonian are of the same form as those between free operators and the free Hamiltonian. In this way some information on the total Hamiltonian is obtained. (auth)

43668 SOLVABLE MODEL IN QUANTUM FIELD THEORY. Eachus, W. James. Syracuse, N. Y.; Syracuse Univ. (1970). 165p. University Microfilms Order No. 71-10,908.

Thesis.

The exact solution of a quantum field theory model is developed in detail and used to test some of the techniques of constructive quantum field theory. The model which is considered is determined by a Hamiltonian describing neutral spinless particles with an interaction term which is quadratic in the field. The interaction term contains a space cutoff but no momentum cutoff. One may interpret the model either as representing particles interacting with an external field, or as a finite mass renormalization with a spatial cutoff. If the number of space dimensions is no greater than three and the cutoff function is sufficiently well behaved, the Hamiltonian is found to have a ground state in Fock space and to be related to the free Hamiltonian by an isometric transformation. The ground state is constructed in a form suitable for comparison with the results of approximation techniques. The Wightman functions are constructed and used to define the theory in cases where the ground state is not in Fock space. For the case of four space dimensions, the approximate and exact ground states are shown to be in the same non-Fock Hilbert space. Perturbation theory is shown to predict correctly the extent of singularity of the Hamiltonian for each dimensionality of space, but a highly artificial example is constructed for which perturbation theory incorrectly predicts a non-Fock ground state. The analysis of the intertwining operator depends on the norm convergence of an operator series representing the positive square root of a related Schrödinger operator. This analysis reveals a great deal about analyticity in the coupling constant for the field theory problem. The radius of convergence is found to be limited by the appearance of a bound state at a depth greater than the mass energy of the particle. A method is found for continuing beyond this radius of convergence for positive coupling constant. A second type of singularity occurs which has no physical significance and which apparently can take the ground state out of Fock space even for small values of the coupling constant, if the cutoff function is negative and has a large enough volume of support. The Møller operators do not exist as strong limits, but a multiple of the unitary operator relating free and total Hamiltonians can be obtained as a related weak limit. The S operator is constructed by means of the LSZ asymptotic limits, and the scattering is shown to be given exactly by that of a Schrödinger Hamiltonian. As an incidental application of the techniques developed while analyzing the mass shift model, the Araki–Woods formulation of statistical mechanics is examined. For particles in a strongly binding external potential, the unitary equivalence of the Araki–Woods representation and the ensemble representation is constructed and is shown to break down when the partition function diverges. (Diss. Abstr. Int., B)

43669 ORTHOGONALITY RELATIONS OF MANY TIME GENERATING FUNCTIONALS OF HARMONIC OSCILLATORS. Weber, R. (Univ., Tuebingen, Ger.). Z. Naturforsch.; 26a: 220-3(Feb 1971). (In German).

The one-dimensional harmonic oscillator is treated completely in the field theoretic calculus of many time generating functionals. Without the results of common quantum mechanics eigenvalues and functionals of the energy are computed preparing all information of the harmonic oscillator. As an example of functional integration and for applications in scattering theory, orthogonality relations of these functionals are proven. (auth)

43670 SOME ESTIMATES FOR GENERATING FUNCTIONALS WITH AN APPLICATION TO QUANTUM FIELD THEORY. Rzewuski, J. (Univ., Wroclaw). Bull. Acad. Pol. Sci., Ser. Sci., Math., Astron. Phys.; 19: No. 3, 235-41(1971).

Estimates are given for functional power series and their derivatives in certain multiplets consisting of topological spaces invariant with respect to differentiation on certain domains. The results are applied to quantum field theory yielding an estimation of the convergence domain and asymptotic behavior of the generating functionals for the S-matrix on and off mass shell, for the field and for the derivatives of these quantities with respect to elements of the basic space. (auth)

43671 LEE MODEL WITH V PARTICLE HAVING CONTINUOUS MASS SPECTRUM AND ENERGY-CONSERVING V–NΘ VERTEX. Lukierski, J.; Oziewicz, M. (Univ., Wroclaw). Bull. Acad. Pol. Sci., Ser. Sci., Math., Astron. Phys.; 19: No. 3, 243-8 (1971).

The Lee model is considered where V-particle is replaced by the object described by the field operator having continuous mass spectrum. It is assumed that the vertex function conserves not only the three-momentum, but also the energy. The complete calculations of NΘ sector are given. It appears that the renormalization of the continuous mass is finite, but the amplitude of NΘ–NΘ scattering vanishes. The last result is further discussed and explained. (auth)

43672 TRANSFORMATION OF STABLE ELEMENTARY PARTICLES ON REGGE TRAJECTORIES BY MEANS OF FIELD-THEORETICAL BOUNDARY TRANSITIONS. Ebert, D. (Univ., Berlin); Wieczorek, E. Ann. Phys. (Leipzig); 25: No. 3, 269-79 (1970). (In German).

A dynamical limit for Reggeization of elementary particles is studied. For this purpose renormalization constants of elementary particles and Regge poles are discussed whose vanishing leads to a continuous transition from elementary to composite poles with finite vertex function. (auth)

43673 LEHMANN–SYMANZIK–ZIMMERMANN FORMALISM IN THE (n,2) SECTOR OF THE LEE MODEL. Uliu, F. S. (Univ. of Craiova, Rumania). Ann. Phys. (Leipzig); 25: No. 4, 347-61 (1970).

The Lehmann-Symanzik-Zimmermann treatment of the (n,2) sector of the Lee model is given. All physical quantities are expressed by means of the τ-functions. It is found that the solutions of two singular integral equations solve the entire sector. (auth)

43674 THREE-DIMENSIONAL COVARIANT FORMULATION OF TWO-BODY PROBLEM IN QUANTUM FIELD THEORY. Vinogradov, V. M. (Joint Inst. for Nuclear Research, Dubna, USSR). Teor. Mat. Fiz.; 7: No. 3, 289-97(Jun 1971). (In Russian).

Relativistic two-body problem is considered in arbitrary system of reference on the basis of the three-dimensional formulation of quantum field theory. It is shown that the corner of mass motion can be separated by means of transition to relative momenta, which are introduced by means of addition operation in Lobachevsky space, and the problem is formulated in the one-particle form. As a consequence, the covariant formulation of quasipotential approach is given and relativistic configuration space is introduced. The comparison with analogous formulation of non-relativistic problem is carried out. (auth)

43675 GENERALIZED COULOMB GREEN FUNCTION FOR BOUND STATES OF NON-RELATIVISTIC SCHROEDINGER EQUATION. Sherstyuk, A. I. Teor. Mat. Fiz.; 7: No. 3, 342-7(Jun 1971). (In Russian).

The well-known closed expression for Coulomb Green function in configuration space in terms of Whittaker functions is used to obtain an explicit formula of generalized Coulomb Green function for arbitrary bound state of non-relativistic three-dimension Schroedinger equation. The formulas are given which express the perturbation theory corrections of the higher orders in terms of generalized Green functions. (auth)

43676 EXTENSION OF THE ALGEBRA OF POINCARE GROUP GENERATORS AND VIOLATION OF P INVARIANCE. Gol'fand, Yu. A.; Likhtman, E. P. (Inst. of Physics, Moscow). JETP Lett. (USSR) (Engl. Transl.); 13: No. 8, 323-6(20 Apr 1971).

Translated from Zh. Eksp. Teor. Fiz., Pis'ma Red.; 13: No. 8, 452-5(20 Apr 1971).

The possibility of using a special algebra R, which is an ex-

XUM

tension of the algebra of the Poincare group, as a basis in constructing the Hamiltonian formulation of quantum field theory is examined. A realization of the algebra is found in which the Hamiltonian operator describes the interaction of quantized fields with parity nonconservation. (L.B.S.)

43677 NEW IMPROVED GENERATOR APPLIED TO CONFORMAL LAGRANGIANS. Longo, Stephen A. (Univ. of Notre Dame, Ind.). Phys. Rev., D; 3: No. 12, 2951-5 (15 Jun 1971).

Using the calculus of variations, a general expression for a conserved generator is obtained which includes the usual Noether form but with additional freedom. This freedom allows one to write geometric generators which depend only on the coordinate variation and not on the total field variation. The resultant energy-momentum tensor is then the tensor proposed by Callan, Coleman, and Jackiw. Also, a general condition is derived under which a generator can be expressed in terms of the coordinate variation only. (auth)

43678 FUNCTIONAL-EQUATION APPROACH TO CANONICAL THEORIES. Grodnik, Jesse (Univ. of Maryland, College Park). Phys. Rev., D; 3: No. 12, 2955-61(15 Jun 1971).

A possible formulation of canonical models is considered in terms of a system of functional differential equations that the ground-state expectation functionals of exponentiated fields satisfy. These equations are obtained for the anharmonic oscillator in one-dimensional quantum mechanics and in a $\lambda\phi^4$ theory of self-interacting mesons in quantum field theory. The implication of symmetries of the ground state on these functionals is considered. The system of functional equations is solved for a free theory of scalar mesons, the case $\lambda = 0$. (auth)

43679 SPACE–TIME SYMMETRIES AND THE SPONTANEOUS BREAKDOWN OF DILATION INVARIANCE. Bose, S. K.; McGlinn, W. D. (Univ. of Notre Dame, Ind.). Phys. Rev., D; 3: No. 12, 2962-9(15 Jun 1971).

The assumption that the Poincaré generators are the space integrals of local conserved currents is used to derive restrictions on the spectral function of certain vacuum expectation values. Then an argument is given that these restrictions and the vanishing of the trace of the stress-energy tensor (conservation of dilation current) imply that all single-particle states have zero mass, even when the conservation of the current is implemented by a Goldstone boson. (auth)

43680 PROPAGATOR GAUGE TRANSFORMATIONS FOR NON-ABELIAN GAUGE FIELDS. Mills, Robert (Ohio State Univ., Columbus). Phys. Rev., D; 3: No. 12, 2969-77(15 Jun 1971).

An explicit demonstration is given of the invariance under propagator gauge transformations of the Feynman-graph prescription obtained by several authors for a non-Abelian gauge field; the role of the anomalous closed-loop vertices of that prescription is thereby clarified. This invariance property permits a derivation of the covariant prescription starting with canonical quantization in a noncovariant gauge without unphysical degrees of freedom. (auth)

43681 SIMPLE DERIVATION OF SEAGULL TERMS FOR PROPAGATOR FUNCTIONS. Nutbrown, D. A. (Univ. of Rochester, N. Y.). Phys. Rev., D; 3: No. 12, 2981-5(15 Jun 1971).

It is demonstrated how a careful derivation of the Lehmann–Källén representation for the propagator function of any two operators, each with an arbitrary number of Lorentz indices, naturally gives rise to frame-dependent pieces. It is verified (a) that the Bjorken limit is satisfied, (b) that a previously proposed partial differential equation connecting the seagull and Schwinger terms is also satisfied, and (c) that covariantized propagator functions may be defined such that Feynman's hypothesis is satisfied. Finally, some concrete examples are given. (auth)

43682 SINGULARITY STRUCTURE OF EQUAL-TIME COMMUTATORS. Rawls, John M. (Yale Univ., New Haven). Phys. Rev., D; 3: No. 12, 2985-91(15 Jun 1971).

On the basis of simple dimensional considerations, it is argued that equal-time commutators as calculated canonically are, in general, not sufficiently singular. This general result is then verified in a number of examples of interest by computing the vacuum expectation values of the commutators in perturbation theory. Specific cases discussed are the electromagnetic current in spinor, scalar, and Pauli electrodynamics and the "new, improved" stress-energy tensor for a free scalar field. (auth)

43683 NUMERICAL STUDIES OF THE BETHE–SALPETER EQUATION AND THE MULTIPERIPHERAL INTEGRAL EQUATION OF AMATI, BERTOCCHI, FUBINI, STANGHELLINI, AND TONIN. Wyld, H. W. Jr. (Univ. of Illinois, Urbana). Phys. Rev., D; 3: No. 12, 3090-3101(15 Jun 1971).

Some numerical results are presented for Regge poles determined from the Bethe–Salpeter equation with scalar couplings. Both the trajectories and residue functions are determined. It is found that it is a good approximation to ignore the coupling between different O(4) states. The effect of a second-order correction to the potential (the crossed-box graph) is studied and evaluated numerically. The relation of the Bethe–Salpeter equation with the multiperipheral integral equation is reviewed, and it is shown how to solve the latter equation by numerical iteration. Some results are given which do not exhibit any oscillations in the total cross section. (auth)

43684 TWO-LOOP APPROXIMATIONS TO PROPAGATORS IN THE σ MODEL. Wong, T. F. (Brookhaven National Lab., Upton, N. Y.); Guralnik, G. S. Phys. Rev., D; 3: No. 12, 3028-38 (15 Jun 1971).

A simple and systematic procedure is established for directly generating perturbation theory for the σ model order by order in the number of loops rather than in powers of the bare coupling constant. This self-consistent Green's-function method is demonstrated by deriving the already known tree and one-loop approximations, and then is applied to the much more complex problem of the two-loop approximations to the propagators. The explicit form is displayed for these, and it is demonstrated that in the limit of no symmetry breaking and zero pion bare mass, the renormalized pion mass remains at zero as is required by the Goldstone theorem. These are the essential first steps toward calculating a unitary pion-pion scattering amplitude with this model to the two-loop order. (auth)

43685 EQUAL-TIME COMMUTATORS OF T^{ij}. Katzin, J. C.; Rolnick, William B. (Wayne State Univ., Detroit). Phys. Rev., D; 3: No. 12, 3240-2(15 Jun 1971).

The point-local criterion for the behavior of quantum fields under the variation of an external gravitation field yields canonical momenta which vary with g_{ij}. (Point locality thus produces a variation which differs from those usually considered.) A general expression for equal-time commutators was derived by Schwinger, which is valid only when the canonical momenta do not change with the variation. It is shown that no general expression of that type may be obtained for these variations, since the implicit interchange of the order of taking commutators and variations violates canonical quantum field theory. Thus no general expression for commutators with T^{ij} may be obtained within the framework of the point-local criterion. (auth)

43686 REMARKS ON THE COMPLEX-GHOST RELATIVISTIC FIELD THEORY. Nakanishi, Noboru (Brookhaven National Lab., Upton, N. Y.). Phys. Rev., D; 3: No. 12, 3235-7(15 Jun 1971).

Contrary to a recent comment of Lee and Wick, it is argued that the complex-ghost relativistic field theory with real space momenta should be regarded as a field theory, while the prescription of Cutkosky, Landshoff, Olive, and Polkinghorne should not. (auth)

43687 RECALCULATION OF THE CROSSED-GRAPH CONTRIBUTION TO THE FOURTH-ORDER LAMB SHIFT. Fox, J. A. (Cornell Univ., Ithaca, N. Y.). Phys. Rev., D; 3: No. 12, 3228-31(15 Jun 1971).

An analytic calculation of the "crossed"-graph contribution to the fourth-order radiative correction of the slope of the Dirac form factor of the free-electron vertex at zero momentum transfer is reported. The result confirms the result of Appelquist and Brodsky. (auth)

43688 SELF-CONSISTENCY IN THE THEORY OF QUANTIZED FIELDS. Aurilia, Antonio. Milwaukee; Univ. of Wisconsin (1970). 249p. University Microfilms Order No. 71-9344.

Thesis.

A method is proposed to construct the Hilbert space for physical states, by defining the physical field operator $\phi(x)$ associated with an observed particle of mass m and spin s. The entire formalism of free fields has been cast in a compact form by use of projection operators constructed by means of the principal invariant W. The method avoids the introduction of unwanted auxiliary fields as well as noncovariant concepts as "boost" transformation, and gives an interpretation of the intrinsic ambiguity of free field equations as due to the freedom in the choice of a basic representation of the Lorentz group and to the nonirreducibility of such representation, explaining in this way the appearance of arbitrary parameters in the equations themselves. The method applies however to any representation and in the multispinor formalism leads to a single matrix form of the Bargmann–Wigner equations. The

connection between dynamics and observation was exploited in the theory of Nambu and Jona–Lasinio, taking into account the existence of pseudovector gauge fields among the basic fields. The center of interest is in the question as to how the introduction of long-range interactions affects the dynamical mapping and the energy spectrum of physical states. By first coupling the helicity current to a massive vector field, one is naturally led, by the internal consistency of the theory, to a noncovariant solution of the problem which takes explicitly into account the surface effects through the introduction in the theory of a linear dimension L, or equivalently, of a finite volume $V = L^3$. It is found that a main part of the original massless Goldstone boson becomes massive and provides the longitudinal component of a physical massive vector field. The remainder of the Goldstone state stays at the vanishing energy-momentum ($q = 0$). This state plays the important role of preserving the invariance of the equations for physical fields. (TSS) (Diss. Abstr. Int., B)

43689 DIVERGENCE CONDITIONS AND PCAC RELATIONS IN PERTURBATION THEORY. Maurer, Richard Hornsby. Pittsburgh; Univ. of Pittsburgh (1970). 180p. University Microfilms Order No. 71-12,365.

Thesis.

The hypotheses of a conserved isotopic vector current (CVC) and a partially conserved axial vector current (PCAC) is investigated in Källén, Yang–Feldman perturbation theory. Gell–Mann and Lévy's "sigma" model is chosen for the investigation in which only the bosons, a pion-like particle (pseudoscalar with respect to parity, isovector triplet) and a "sigma" meson (scalar with respect to parity and an isoscalar) are included. To renormalize the equations of motion obtained from the canonical Lagrangian for the "sigma" model mass counter terms, a vertex renormalization constant, and wave function renormalization constants are introduced. The chiral symmetric theory where the axial vector and vector currents are both conserved, the untranslated case of the broken symmetry theory where the vacuum expectation value of the "sigma" meson is not zero, and the translated case of the broken symmetry theory where the vacuum expectation value of the "sigma" meson is zero are examined. It is concluded that the investigation of the boson sigma model does not support the proposition, based on formal properties of the classical Lagrangian, that the divergence of the axial vector current is proportional to the canonical pion field operator and that this formulation of the PCAC condition is too restrictive. (Diss. Abstr. Int., B)

43690 HISTORY OF RELATIVITY: THE ROLE OF HENRI POINCARE AND PAUL LANGEVIN. Cavaj, Camillo. New York; Yeshiva Univ. (1970). 423p. University Microfilms Order No. 71-14,304. (In several languages).

Thesis.

The presentation of the work of Poincaré and Langevin leads to a close view of the landmarks of special relativity in general. A detailed section on Einstein, Lorentz, and others such as Larmor, Voigt and Planck, is also included for thoroughness and enables one to discuss the history of special relativity according to ones viewpoint, stressing neglected contributions, misconceptions, priorities, the mathematical formalism of relativity, semantics, and unusual events. (TSS) (Diss. Abstr. Int., B)

43691 REINTERPRETATION OF WAVE MECHANICS. de Broglie, Louis (Institut de France, Paris). Found. Phys.; 1: No. 1, 5-15(1970).

The ideas of wave mechanics in generalizing the ideas of Einstein's theory of light quanta are recalled. A concrete physical picture was made of the coexistence of waves and particles and, in 1927 an attempt was made to give them precise form in "theory of the double solution." As other ideas prevailed at the time, the development of the conception was abandoned. But for the past twenty years, once again convinced, like Einstein, that present-day quantum mechanics is only a statistical theory and does not give a true picture of physical reality, one has again taken up the old ideas and developed them considerably. In particular an element of randomness was introduced into the theory and thus a "hidden thermodynamics of particles" was attained, the results of which appear to be very interesting. (auth)

43692 IDEALIZED MEASUREMENTS IN QUANTUM FIELD THEORY. Potupa, A. S. (Inst. of Physics, Minsk). Dokl. Akad. Nauk BSSR; 15: No. 2, 120-2(Feb 1971). (In Russian).

Problems of measurability were analyzed for massive meson fields. It was shown that basic difficulties arise during attempts to determine a test body. This is the consequence of short-range nuclear forces and leads to the absence of a physical model of a carrier of the test function, whereby massive quantum fields are determined as operator-significant functions. The problem of separability of electrodynamics among quantum field models was discussed. (K.S.W.)

43693 RELATIVISTIC INVARIANCE AND CAUSALITY IN THE THEORY OF CONTINUOUS MEDIA. Kurlandzki, J.; Rogula, D. (Inst. of Fundamental Technical Problems, Warsaw). Bull. Acad. Pol. Sci., Ser. Sci. Tech.; 19: No. 2, 91-9(Apr 1971).

Based on the variational formalism, the necessary and sufficient condition that the relativistic invariance theory of a continuous medium be causal was formulated. The hyperelastic, one-dimensional, nonlinear medium was considered. It was proved that the relativistic invariance does not bring about automatically causality in the local theory. (auth)

Gravitation and General Relativity

Refer also to abstracts 43032, 43086, and 43090–43092.

43694 VELOCITY OF LIGHT IN NEWTON AND EINSTEIN GRAVITATIONAL THEORIES. Treder, H.-J. (Zentralinstitut fuer Astrophysik, Potsdam, Ger.). Ann. Phys. (Leipzig); 25: No. 3, 315-20(1970). (In German).

The gravity theories of Newton and Einstein are giving opposite sentences about the velocity of light in gravitational field. According to the Newtonian theory the velocity v in gravitational field is greater than the velocity c in a field-free space: $v > c$. According to general relativity theory we have a smaller velocity: $v < c$. For a spherical symmetric gravitational field Newton's theory gives $v \approx c(1 + fM/c^2r)$ but Einstein's theory of 1911 gives $v \approx c(1 - fM/c^2r)$ and general relativity gives $v \approx c(1 - 2fM/rc^2$. Therefore, the radar-echo-measurements of Shapiro are the experimentum crucis for Einstein's against Newton's theory. (auth)

43695 SINGULARITIES IN GENERAL RELATIVITY. Pachner, J. (Univ. of Saskatchewan, Regina, Can.). Gen. Relativity Gravitation: 1: No. 3, 281-303(1971).

The problem of singularities is examined from the standpoint of a local observer. A singularity is defined as a state with an infinite proper rest mass density. The approach consists of three steps: The complete system of equations describing a nonsymmetric motion of a perfect fluid under assumption of adiabatic thermodynamic processes and of no release of nuclear energy is reduced to six Einstein field equations and their four first integrals for six remaining unknown components g_{ik}. A differential relation for the behavior of the rest mass density is deduced. It shows that any inhomogeneity and anisotropy in the distribution and motion of a nonrotating ideal fluid accelerates collapse to a singularity which will be reached in a finite proper time. Collapse is also inevitable in a rotating fluid in the case of extremely high pressure when the relativistic limit of the equation of state must be applied. In the case of a lower or zero pressure the relation does not give an unambiguous answer if the matter is rotating. The influence of rotation on the motion of incoherent matter is investigated. Some qualitative arguments are given for a possible existence of a narrow class of singularity-free solutions of Einstein equations. Assuming rotational symmetry the Einstein partial differential equations, together with their first integrals, are reduced to a system of simultaneous ordinary differential equations suitable for numerical integration. Without integrating this system the existence of the class of singularity-free solutions is confirmed and exactly delimited. These solutions, representing a new general relativistic effect, are, however, of no importance for application in cosmology or astrophysics. It is proved that in all the other cases interesting from the point of view of application the occurrence of a point singularity in incoherent matter with a rotational symmetry is inevitable even if the rotation is present. (auth) (UK)

43696 STABLE AND GENERIC PROPERTIES IN GENERAL RELATIVITY. Hawkins, S. W. (Cambridge Univ.). Gen. Relativity Gravitation: 1: No. 4, 393-400(1971).

Some aspects of the space of Lorentz metrics are discussed; in particular it is considered what it implies to say that a certain property is stable or generic, and some examples are given, including that of stable causality and the Cauchy problem. (UK)

43697 ORIGINS OF THE SCHWARZSCHILD AND CURZON STATIC SOLUTIONS. Bel, L. (Laboratoire de Mecanique Analytique, Paris). Gen. Relativity Gravitation: 1: No. 4, 337-47(1971). (In French).

The theory of stationary space-time and that of metric spaces is briefly reviewed. It is considered that the space provided by a metric conforms to the metric quotient, and two arguments are presented in favor of the interpretation of the first as metric space.

XUM

The implications of this interpretation for the problem of the origin of the static solutions of Schwarzschild and Curzon are discussed, and it is shown that these two solutions have an origin proportional to the Dirac distribution. (UK)

43698 NEW DEFINITION OF SINGULAR POINTS IN GENERAL RELATIVITY. Schmidt, B. G. (Univ., Hamburg). Gen. Relativity Gravitation; 1: No. 3, 269-80(1971).

To any space-time a boundary is attached on which incomplete geodesics terminate, as well as inextensible timelike curves of finite length and bounded acceleration. The construction is free of ad hoc assumptions concerning the topology of the boundary and the identification of curves defining the same boundary point. Moreover, it is a direct generalization of the Cauchy completion of positive definite Riemannian spaces. (auth) (UK)

43699 CAUSAL STRUCTURE IN SPACE–TIME. Carter, B. (Cambridge Univ.). Gen. Relativity Gravitation; 1: No. 4, 349-91(1971).

The adoption of a coherent and concise terminology for use in this field is discussed, and some of the most important elementary propositions are considered as the necessary terminology is built up. The terminology suggested represents the results of an attempt to improve on previous work by certain modifications designed to make it rather more systematic. Among matters considered are: time ordering relations, time symmetric relations, internal connectivity properties and theorems, Cauchy developments, unions and intersections, topology and higher degree causality, "imprisonment," axioms in etiological spaces, covering spaces, horizons, causality and chronology horizons, normal spacetime manifolds, and consequences of normalizability. (UK)

43700 FOCUSING OF GRAVITATIONAL RADIATION BY THE GALACTIC CORE. Lawrence, J. K. (Univ., Vienna). Phys. Rev., D; 3: No. 12, 3239-40(15 Jun 1971).

The possibility is considered that the gravitational radiation observed by Weber has an extragalactic origin and is focused by the galactic core acting as a gravitational lens. While sufficient intensification is possible, too few sources are correctly located for the effect to be important. (auth)

43701 SOME GENERAL RELATIONS IN RELATIVISTIC MAGNETOHYDRODYNAMICS. Yodzis, P. (Dublin Inst. for Advanced Studies). Phys. Rev., D; 3: No. 12, 2941-5(15 Jun 1971).

A method is outlined for obtaining general relations governing the behavior of magnetofluids in general relativity. Several such relations are obtained for the case of infinite conductivity, and their possible relevance to galactic cosmogony, gravitational collapse, and pulsar theory is briefly discussed. (auth)

43702 BRANS–DICKE THEORY UNDER A TRANSFORMATION OF UNITS AND THE THREE TESTS. Morganstern, R. E. (Lunar Science Inst., Houston, Tex.). Phys. Rev., D; 3: No. 12, 2946-50(15 Jun 1971).

The Brans–Dicke (BD) gravitational field equations are written down in arbitrary units by taking $\varphi = \varphi_0\lambda$ in the original equations, and then scaling length, time, and reciprocal mass by $\lambda^{(1-\alpha)/2}(x)$. This is a generalization of Dicke's units transformation (UT). It is found that the Machian requirement that matter makes a positive contribution to $\bar{\varphi}(= \varphi_0\lambda^\alpha)$ cannot be maintained under a UT. Mach's principle finds its expression, instead, in terms of matter making a positive contribution to the dimensionless scalar field λ. A solution is found to the spherically symmetric field equations in arbitrary units and generalize Schild's formula for perihelion precession to include nongeodesic equations of motion. These results are used to show that the BD field equations lead to the same predictions for the three tests in all units. This fact is consistent with the dimensionless character of the angular measurements and the interpretation of the alternate BD formalisms as being the same theory cast in different units. (auth)

43703 STATIC SOLUTIONS OF THE COMBINED DIRAC–ELECTROMAGNETIC–GRAVITATIONAL FIELD EQUATIONS. O'Hanlon, John David. Vancouver, British Columbia; Univ. of British Columbia (1970). National Library of Canada, Ottawa.

Thesis.

It is assumed that charged, spin-½, matter distributions can be described in terms of a Dirac spinor field interacting with the electromagnetic field and a scalar gravitational field. The field equations and the energy-momentum tensor are found from an action principle. The fields are not quantized. The field equations are examined and various limiting forms discussed. Particularly the time-independent spherically-symmetric case is considered. Solutions are found for the exterior region of a charged gravitating sphere. The behavior of these solutions depends on the value of the charge-mass ratio. When this ratio has the value $(4\pi G)^{\frac{1}{2}}$, where G is the gravitational constant, the entire system can be solved analytically. The ensuing solution, called the Weyl–Majumdar solution, is obtained and discussed. When the charge-mass ratio is smaller than $(4\pi G)^{\frac{1}{2}}$, normalized solutions are found which yield electrostatic and gravitational potentials singular at the origin. The matter density is well-behaved everywhere. Normalized solutions were not found for larger charge-mass ratios. The significance of the solutions, and the accuracy of the numerical technique are discussed. Alternative Lagrangian densities are considered which may yield nonsingular solutions. (Diss. Abstr. Int., B)

43704 CONSERVATION LAWS IN GENERAL RELATIVITY BASED UPON THE EXISTENCE OF PREFERRED COLLINEATIONS. Collinson, C. D. (Univ. of Hull, Eng.). Gen. Relativity Gravitation; 1: No. 2, 137-42(1970).

The conservation laws based upon the existence of curvature and Ricci collineations are investigated, and the previous results (J. Natk. Phys. 10: 617(1969)) are reinterpreted and generalized. The concept of a "Maxwell collineation" is introduced and corresponding conservation laws are found. (auth) (UK)

43705 SELF-COUPLED SCALAR GRAVITATION. Deser, S. (Brandeis Univ., Waltham, Mass.); Halpern, L. Gen. Relativity Gravitation; 1: No. 2, 131-6(1970).

The requirement in scalar theories of gravitation that the source of the field includes the trace of its own stress tensor is investigated in two models: the geometrical Nordstrøm (1913) theory, which is the conformally flat metric analog of Einstein's theory, and the ostensibly nongeometrical flat space system of Freund and Nambu (1968). Both are derived in closed form as cubic self-interacting systems and shown to be equivalent. (auth) (UK)

43706 CROSS SECTIONS FOR THE GRAVITATIONAL SCATTERING OF MASSLESS PARTICLES. Peet, Frederick Gordon. Vancouver, British Columbia; (Univ. of British Columbia (1970). National Library of Canada, Ottawa.

Thesis.

The gravitational scattering of massless scalar particles, photons, four component neutrinos, and two component neutrinos by one another is examined. A modification of the quantum theory of the weak gravitational field developed by Gupta is used as a basis for the considerations. Cross sections are given for the gravitational scattering of scalar particles by: scalar particles, photons, four component neutrinos, and two component neutrinos; of photons by: photons, four component neutrinos, and two component neutrinos; of four component neutrinos by four component neutrinos, and of two component neutrinos by two component neutrinos. The cross section given previously for the scattering of photons by photons is confirmed. Other previous cross sections for the scattering of massive scalar particles by massive scalar particles and the cross section for the scattering of photons by massive scalar particles are found to be in error and are corrected. (Diss. Abstr. Int., B)

43707 GLOBAL AND LOCAL PRINCIPLES OF RELATIVITY. Treder, Hans-J. (Zentral Institut fuer Astrophysik, Babelsberg, Ger.). Found. Phys.; 1: No. 1, 77-94(1970).

The principles of relativity are assertions about the structure of physical laws, whose validity or nonvalidity can only be empirically confirmed or denied. The weakest forms of those principles are the so-called global propositions. They furnish statements as to which operations—to be performed simultaneously throughout the whole universe—have no influence upon the physical events. Much stronger principles are those of a local nature. These assert that the physical properties of a system do not change, when the relation of the system is altered vis-a-vis the universe at large. On formulating these local principles it is presupposed either that it is possible to eliminate any influence of the environment or that the influence can be compensated as in the case of universal forces (e.g. gravitation) which can principally not be removed. Still weaker, however, are those formulations of the relativity principles which postulate relativity only for infinitesimally small space-time domains or regions. This distinction yields clarification of all discussions about existence and meaning of a general relativity principle. Such an analysis was already performed by Einstein and Abraham in 1912. (auth)

43708 GRAVITATION THEORY AS THEORY OF NON-LORENTZIAN TRANSFORMATIONS OF THE SYSTEMS OF REFERENCE. Liebscher, D.-E.; Treder, H.-J. (Zentralinstitut fuer Astrophysik, Berlin). Gen. Relativity Gravitation; 1: No. 2, 117-25(1970).

According to the program of Einstein as discussed with Abraham, gravitation can be described by the bending of the systems of inertia in special relativity. This bending means non-Lorentzian

transformations of the systems of reference, depending on the point in space-time. Einstein's equations for the metric imply equations for the transformation matrix, which are also of the same structure. The non-Lorentzian transformations of the reference systems of a manifold can lead to a general map of the set of metrics into the set of vacuum metrics on the same manifold. Resulting new aspects in problems of gravitation theory are discussed. (auth) (UK)

43709 GRAVITATIONAL POTENTIAL TENSOR AND EQUATIONS OF MOTION IN RELATIVISTIC MECHANICS. Fikhtengol'ts, I. G. (Inst. of Precision Mechanics and Optics, Leningrad). Zh. Eksp. Teor. Fiz.; 60: No. 4, 1206-10(Apr 1971). (In Russian).

The concept of gravitational potential tensor is introduced. Equations are established which define the gravitational potential tensor. An approximate solution of the equations is obtained for the astronomical problem of an isolated mass system. The equations of motion in relativistic mechanics are considered. General expressions are derived for the force acting on a body and for the momentum of the body. It is shown that the force and momentum depend not only on the mass tensor but also on the gravitational potential tensor. (auth)

43710 SPHERICALLY SYMMETRIC RADIATION OF CHARGE IN EINSTEIN-MAXWELL THEORY. Bonnor, W. B. (Queen Elizabeth Coll., London); Vaidya, P. C. Gen. Relativity Gravitation; 1: No. 2, 127-30(1970).

Solutions of the Einstein–Maxwell equations describing the emission of charged null fluid from a spherically symmetric body are given. The electromagnetic field is parallel to the direction of energy propagation, is of order r^{-2} at infinity, and is not null. (auth) (UK)

Scattering Theory

43711 (SU-1206-243) CROSSING AND POSITIVITY PROPERTIES OF PARTIAL WAVES. A Review. Balachandran, A. P. (Syracuse Univ., N. Y. Dept. of Physics. Indian Inst. of Tech., Kanpur. Dept. of Physics). [1970]. 18p. (NYO-3399-243; CONF-701212-1). Dep. NTIS.

From Symposium on particles and fields; Madras, India (30 Dec 1970).

Crossing symmetry of the scattering amplitude is used to derive an infinite number of sum rules each of which involves a finite number of partial waves. Such sum rules exist for four-body processes where the particles have arbitrary mass and spin and for N-body processes ($N \geq 5$) where the particles have arbitrary mass and no spin. These sum rules lead to an infinite number of inequalities involving the s- and p- $\pi\pi$ partial waves when certain positivity properties of the $\pi\pi$ partial waves proved previously are used. The generalization of such positivity statements to certain processes which involve particles with spin and unequal mass (for example, the process $\pi N \rightarrow \pi N$) is also possible. The use of these results in the construction of theoretical models for partial waves is discussed. (auth)

43712 PHYSICAL STATES ON DAUGHTER TRAJECTORIES IN THE DUAL AMPLITUDE UNDER THE CONDITION $\alpha(0) = 1$. Kudryavtsev, V. A.; Levin, E. M. (Ioffe Physical-Technical Inst., Moscow). JETP Lett. (USSR) (Engl. Transl.); 13: No. 9, 360-3 (5 May 1971).

Translated from Zh. Eksp. Teor. Fiz., Pis'ma Red.; 13: No. 9, 507-11(5 May 1971).

The physical states on the first three daughter trajectories are considered in the generalized Veneziano model, and it is shown that ghost states with negative norm are present on the third daughter trajectory at large masses. (L.B.S.)

43713 THRESHOLD ZEROS AND THE N/D METHOD IN YUKAWA-POTENTIAL SCATTERING. Nemanic, E. B. (Indiana State Univ., Terre Haute); Auvil, P. R. Phys. Rev., D; 3: No. 12, 3108-13(15 Jun 1971).

The various methods which have been used to enforce the existence of the threshold zeros in the solutions of the partial-wave dispersion relations are compared. It is found that these methods are very closely related and are in fact equivalent under the proper conditions. The above are then studied in detail for the case of the potential scattering of equal-mass particles under the influence of a Yukawa interaction. (auth)

43714 NEW DUAL N-POINT FUNCTIONS. Clavelli, L. (National Accelerator Lab., Batavia, Ill.). Phys. Rev., D; 3: No. 12, 3166-72(15 June 1971).

As an example of the group-theoretical approach to the construction of new dual amplitudes, a model pion N-point function is discussed in which the π trajectory lies $\frac{1}{2}$ unit below the leading (ρ) trajectory. The model is completely factorizable, contains a natural G parity, and obeys the Adler condition approximately. The degeneracy of the spectrum and the ghost problem are essentially the same as in the conventional Veneziano N-point function. In a separate section, a dual interaction of an SU(3) nonet of scalar mesons with mass splitting is discussed. (auth)

43715 COMPLEX NEGATIVE-SIGNATURE TRAJECTORIES AND THE POMERANCHUK THEOREM. Oehme, Reinhard (Univ. of Chicago). Phys. Rev., D; 3: No. 12, 3217-20(15 Jun 1971).

Within the framework of complex-angular-momentum methods, it is shown that amplitudes which violate the Pomeranchuk theorem require negative-signature trajectories which are of the form $\alpha(t) = 1 \pm \text{const}\sqrt{t} + O(t)$ near $t = 0$. There must be corresponding positive-signature trajectories. The character of the singular surfaces with negative signature is discussed briefly. (auth)

43716 THREE-BODY PROBLEMS IN THE AMADO MODEL. Avishai, Y. (Argonne National Lab., Ill.). Phys. Rev., D; 3: No. 12, 3232-5(15 Jun 1971).

The problems discussed here appear in the course of solving the three-particle scattering equations in the Amado model. A different contour of integration is suggested and, as an alternative, the equations are transformed into new ones with a finite domain of integration. (auth)

43717 UNITARIZATION OF THE DUAL-RESONANCE AMPLITUDE. III. GENERAL RULES FOR THE ORIENTABLE AND NONORIENTABLE MULTILOOP AMPLITUDES. Kaku, Michio; Yu, Loh-ping (Univ. of California, Berkeley). Phys. Rev., D; 3: No. 12, 3020-4(15 Jun 1971).

The Kikkawa–Sakita–Virasoro unitarization scheme for the dual-resonance amplitude is completed by presenting the nonorientable and overlapping multiloop amplitudes. Rules for writing down arbitrarily mixed planar, nonplanar, nonorientable, and overlapping multiloop amplitudes by inspection are also presented. (auth)

43718 UNITARIZATION OF THE DUAL-RESONANCE AMPLITUDE. I. PLANAR N-LOOP AMPLITUDE. Kaku, Michio; Yu, Loh-ping (Univ. of California, Berkeley). Phys. Rev., D; 3: No. 12, 2992-3007(15 Jun 1971).

The planar multiloop formula in the dual-resonance model is presented. Both the multiple-factorization formulation and the Sciuto three-Reggeon formulation are given. (auth)

43719 UNITARIZATION OF THE DUAL-RESONANCE AMPLITUDE. II. THE NONPLANAR N-LOOP AMPLITUDE. Kaku, Michio; Yu, Loh-ping (Univ. of California, Berkeley). Phys. Rev., D; 3: No. 12, 3007-38(15 Jun 1971).

Following a previous paper on the planar N-loop Veneziano amplitude, the non-planar N-loop formula is derived. The calculation is performed by tracing over both the multiply factorized tree and the Sciuto three-Reggeon vertex functions. (auth)

43720 PARTIAL WAVE ANALYSIS ON THE BASIS OF COMPLEX VECTOR PARAMETRIZATION. Tkharev, E. E.; Fedorov, F. I. (Minsk Radiotechnical Inst.). Teor. Mat. Fiz.; 7: No. 3, 322-31(Jun 1971). (In Russian).

Analysis of partial decompositions of one- and two-particle states is performed on the basis of complex vector parametrization of the Lorentz group. In this approach the interpretation of the little group transformations as the rotations in corresponding complex three-dimensional space of the group parameters makes it possible to construct in a convenient way the states of two-particle system with definite values of the total angular momentum and its projection. With the aid of such construction the partial wave decomposition of scattering matrix is carried out. (auth)

43721 DUALITAET. LOKALKOMPAKTER GRUPPEN. (Duality. Local Compact Groups). Heyer, Herbert. Lecture Notes in Mathematics. Volume 150. Berlin; Springer-Verlag (1970). 388p. $5.80.

Duality is treated with the method of group theory. The Alfsen proof for the existence of the Haar unit is given. The postulates of Gelfand–Raikow are proven. The postulate of Peter–Weyl as well as the duality statement of Tannaka and Krein are included. The duality postulate of Pontryagin is proven. The duality postulates of Takahashi and Tatsuuma are treated. Finally, the Chu duality is presented. (H.B.G.)

43722 FUNCTIONAL INTEGRAL FORMULATION OF DUAL RESONANCE AMPLITUDES. Hsue, Chen-shiung. Madison,

XUM

Wis.; Univ. of Wisconsin (1970). 87p. University Microfilms Order No. 71-3131.

Thesis.

The known dual resonance amplitudes such as the N-particle Veneziano amplitude and both the planar and nonplanar one-loop amplitudes are formulated in terms of functional integrals. This formulation may be derived from the corresponding formula in terms of the harmonic oscillator formulation by expressing the matrix elements of the harmonic oscillator operators in terms of functional integrals in a way similar to Feynman's space-time approach to quantum mechanics. The domain on which the functional integral is defined is closely related to the topological structure characterizing the given Feynman-like diagram. The integral can be evaluated by the familiar Green's function method in the Neuman boundary value problems. Explicit expressions for the N-particle Veneziano amplitudes as well as the one loop amplitudes are correctly reproduced. A study of the high-energy behavior of one-loop amplitudes is made. Both planar and nonplanar one-loop amplitudes exhibit the Gribov–Pomeranchuk phenomena of accumulation of Regge trajectories at the elastic threshold. Also the nonplanar amplitude exhibits a cut in the complex angular momentum plane. (Diss. Abstr. Int., B)

43723 TRIPLE-REGGE VERTEX. Misheloff, Michael Norman. Berkeley, Calif.; Univ. of California (1970). 57p. University Microfilms Order No. 71-9873.

Thesis.

A Reggeized model is developed for the 3-to-3 amplitude using group theoretical variables. The triple-Regge vertex is defined by the asymptotic form of the amplitude. It is defined entirely in terms of physical region quantities and therefore is, in principle, directly measurable. (Diss. Abstr. Int., B)

43724 CONJUGATE VARIABLES IN TWO-BODY COLLISIONS. Razavy, M.; Krebes, E. S. (Univ. of Alberta, Edmonton). Phys. Lett.; 35A: No. 6, 463-4(12 Jul 1971).

Using conjugate variables of classical dynamics, incompatible observables in elementary scattering theory are briefly discussed. (auth)

Particle Accelerators

Refer also to abstract 43401.

43725 (AERE-R-6812) NOTE ON THE ENERGY SPREAD VERSUS RADIAL OSCILLATION AMPLITUDE FOR THE SYNCHROCYCLOTRON REGENERATIVE BEAM EXTRACTOR. West, D. (Atomic Energy Research Establishment, Harwell (England)). May 1971. 8p. Dep. NTIS (U. S. Sales Only). UK 9p.

The magnetic field surveys taken during the installation of the extractor are used, in conjunction with orbit tracking computer programs to derive the relation between the amplitude of radial oscillations and energy spread in the extracted beam. (auth) (UK)

43726 (BNL-15893) PION FLUXES FROM 10-500 GeV PROTON SYNCHROTRONS. Wang, C. L. (Brookhaven National Lab., Upton, N. Y.). 18 May 1971. 26p. Dep. NTIS.

Meson (π^-) fluxes from 10 to 500 GeV proton synchrotrons are calculated by an empirical formula which well represents the data between 10 and 70 GeV. The formula has two scaling laws built in it and should be reasonably valid for extrapolation by a factor of 7, namely up to 500 GeV. Comparisons are made with the predictions of Cocconi–Koester–Perkins, Trilling, Hagedorn–Ranft, Liland–Pilkuhn and the hypothesis of limiting fragmentation. The validity of each prediction is discussed. Predictions are for beryllium targets. (auth)

43727 (BNL-tr-431) ACCELERATION AND EXTRACTION OF DEUTERONS FROM THE JINR PROTON SYNCHROTRON. Baldin, A. M.; (and others) (Joint Inst. for Nuclear Research, Dubna (USSR)). Translated by S. J. Amoretty (Brookhaven National Lab., Upton, N. Y.), from report JINR-P9-5442. 8p. Dep. NTIS.

An abstract of this paper, prepared from the original language, appeared as NSA 25: 12303. (W.H.K.)

43728 (CEA-CONF-1767) MULTI MICRO BEAMS FOR ION IMPLANTATION. Guernet, G.; Glotin, Ph. (Commissariat a l'Energie Atomique, Grenoble (France). Centre d'Etudes Nucleaires). 26 Oct 1970. 10p. (CONF-700945-2). Dep. NTIS (U. S. Sales Only).

From Conference on ion implantation; Reading, England (7 Sep 1970).

Equipment for the fabrication of integrated circuits in a batch process using multi micro beams of charged particles is described. Several methods, commonly used, to produce ion implanted integrated circuits of given configurations are presented: the traditional batch process (masking), an individual method (using a fine beam), a new batch process using multi micro beams, many beams being controlled simultaneously and in an identical manner. The accelerator used in these experiments was developed at LETI; it is described together with the way in which the microbeams are obtained. A double micro quadrupolar lens with filiform electrodes, the dimensions of which had been determined by computer simulation, was designed. A large number of spots (1000) of 1 μ diameter are obtained, the distance between two beams corresponding to the elementary cell length of the circuit (2 mm). The x y manipulation of the microscope is described. The applications of this new technique to the sensitization of the silicon dioxide and the metallic layer are discussed. (auth)

43729 (CERN-Trans-71-16) HIGH-INTENSITY (10-16) GeV/c NEGATIVE PARTICLE BEAM. Golovnya, N. I.; Grachev, M. I.; Gubrienko, K. I.; Eremenko, E. V.; Kotov, V. I.; Seleznev, V. S.; Khodyrev, Yu. S. (Gosudarstvennyi Komitet po Ispol'zovaniyu Atomnoi Energii SSSR, Serpukhov. Institut Fiziki Vysokikh Energii). Translated by R. Luther (CERN, Geneva, Switzerland), from report IFVE-OP-70-28. 8p. Dep. NTIS (U. S. Sales Only).

An abstract of this paper, prepared from the original language, appeared as NSA 25: 25555. (W.H.K.)

43730 (JAERI-13567) POWER INCREASING PLAN OF JAERI LINAC. (Japan Atomic Energy Research Inst., Tokai). May 1969. 58p. NTIS (U. S. Sales Only).

The reasons for a renewal of the JAERI Linac with an increase of the power are summarized as follows: (1) to obtain nuclear data required for the development of nuclear reactors, and (2) to make researches in the associated fields including nuclear physics, solid state physics, radiation chemistry and engineering of shielding. All of these researches give the basis for nuclear reactor studies. Necessity for the nuclear data with high accuracy is increasing more and more, which is connected with progress in studies on economy and safety of the power reactors. However, the accuracy of nuclear data strongly depends on the neutron intensity to be used in the measurements of these data. The proposed plan to meet this necessity is to raise the neutron intensity considerably by improving the present 20 MeV Linac to a 120 MeV Linac. With this proposed machine, measurements with high accuracy will be made on various neutron cross sections especially in the keV region, which have been most urgently required for the fast breeder reactor development. In addition, the proposed Linac will be able to produce not only high intensity neutrons, but also much stronger electron beams and x-rays than any other instruments, so that the Linac will be used in the studies of nuclear physics, reactor physics, solid state physics, radiation chemistry, engineering of shielding, etc. (auth)

43731 (JINR-P7-5177) SOURCES OF MULTICHARGED IONS. Summary of the 14th All-Union Conference on Emission Electronics, Tashkent, May 1970. Vorob'ev, E. D.; Pasyuk, A. S. (Joint Inst. for Nuclear Research, Dubna (USSR). Lab. of Nuclear Reactions). 1970. 32p. (In Russian). Dep. NTIS (U. S. Sales Only).

At the present time there are four known methods for obtaining multicharged ions: (1) in arc discharges at pressures ~10^{-3} torr, (2) with electron beams in vacuum of 10^{-8} to 10^{-10} torr, (3) interaction of powerful laser beams with gases or solid surfaces, and (4) powerful spark discharges. With arc-type sources, heavy ions up to 12^+ charge state can be obtained. In the first experiments with electron radiation sources, gold ions (Au^{19+}) were produced. Using lasers, optical spectra of ions up to 18^+ were observed. In condensation vacuum sparks, spectra of ions up to 20^+ were noted. (tr-auth)

43732 (OU-LNS-71-2) ANNUAL REPORT, JANUARY–DECEMBER 1970. (Osaka Univ. (Japan). Lab. of Nuclear Studies). 49p. Dep. NTIS (U. S. Sales Only).

Progress and research topics of the cyclotron division, high voltage accelerator division, mass spectroscopy division, AVF cyclotron division, radioisotope division, and theoretical physics division are summarized. (W.H.K.)

43733 (TID-25751) FINAL REPORT, PRELIMINARY FOUNDATION ANALYSIS, ATOMIC ENERGY COMMISSION 200 GeV ACCELERATOR, WESTON SITE, ILLINOIS. (Corps of Engineers, Chicago, Ill. Chicago District). Dec 1967. 435p. Dep. NTIS.

Results of the soil investigation program at the Weston accelerator site are presented. The geology and ground water are described, results of laboratory soil tests are given; and an analysis

of the settlement of the accelerator ring tunnel is discussed. (W.H.K.)

43734 (UCRL-20664) MONITORING OF POSITIVELY CHARGED PARTICLES IN THE ELECTRON RING ACCELERATOR. Goebel, J.; McCaslin, J. B.; Patterson, H. W.; Smith, A. R. (California Univ., Berkeley. Lawrence Radiation Lab.). Apr 1971. Contract W-7405-eng-48. 11p. Dep. NTIS.

Some methods for beam monitoring of protons and heavy ions at the ERA are discussed in terms of sensitivity and susceptibility to interference from competing reactions. Results presented of a pilot exposure at the 88-inch cyclotron compare calculated and measured production rates of ^{149}Tb and ^{151}Tb from bombardment of a cerium target with 55.48-MeV nitrogen ions. From this work it is concluded that at least 10^{11} ions (@ 5 MeV/amu) are needed to produce a measurable amount of alpha activity. (auth)

43735 APPLICATIONS OF CRYOGENICS TO HIGH ENERGY NUCLEAR PHYSICS. Atkinson, H. H. (Rutherford High Energy Lab., Chilton, Eng.). pp 345-413 of Advanced Cryogenics. /Bailey, C. A. (ed.). London; Plenum Press (1971).

The following are discussed: Applications to particle accelerators (accelerator vacuum systems, superconductive linear accelerators, superconductive synchrotrons, and energy storage for synchrotrons); application to beam handling and analysis (quadrupoles and bending magnets and superconducting rf separators); applications to equipment for experiments (cryogenic liquid targets, bubble chambers using cryogenic liquids, spark chamber magnets, Cerenkov counters, very high magnetic fields, reduction of electrical noise in detectors, and hydrogen moderators for reactors); and polarised nuclear targets. (15 references) (UK).

43736 STRUCTURE OF ELECTRON BEAMS. Karashokov, K. E.; Ostroverkhov, N. T.; Popov, V. K. Fiz. Khim. Obrab. Mater.; No. 2, 9-14(Mar-Apr 1971). (In Russian).

It was shown that within a broad range of specific power (10^5 to 10^8 volts/cm^2) the distribution of the current density in the transverse cross section of the electron beam, focused by a strong magnetic lens, obeys Gauss's law. In an electron-optical system with a triple electron beam the radial change of the beam and the current distribution in its transverse cross section depends upon the dimensions and the crossover position of the beam. A block diagram of the circuitry used in this investigation is given. (tr-auth)

43737 COMPTON BACK-SCATTERED HIGH-ENERGY PHOTON BEAM. Sauer, Jon Robert. Medford, Mass.; Tufts Univ. (1970). 106p. University Microfilms Order No. 71-13,757.

Thesis.

The theory applicable to laser photons back-scattered from multi-GeV electrons is treated in greater detail and generality than can be found previously. The feasibility of such "laser beams" at high-energy electron synchrotrons was demonstrated by achieving an intensity of 10^4/sec, adequate for those high-energy experiments in which relatively low intensities can be compensated by a high and controllable polarization and a harder energy spectrum. The measured energy spectrum and yield are in reasonable accord with theoretical expectations. The applicability of the laser beam as a nondestructive beam probe for relativistic beam studies was demonstrated by measuring the horizontal phase space parameters of the internal CEA beam. The laser beam technique offers a new and direct method of obtaining these parameters. (Diss. Abstr. Int., B)

43738 PROBLEMS OF RADIOPROTECTION FOLLOWING THE INCREASING OF THE INTENSITY OF THE ELECTRO-SYNCHROTRON AT FRASCATI. Ladu, M.; Lucci, F.; Pelliccioni, M.; Roccella, M. (CNEN, Rome). Minerva Fisiconucl.; 14: 1-6(Jan-Mar 1970). (In Italian). (CONF-690929-4).

From fifteenth national congress of the Italian Association for Health Physics and Protection Against Radiation; Cagliari, Italy (Sep-Oct 1969).

The most important problem in radioprotection following the increase of the electro-synchrotron intensity was solved by recovering the magnets with a 50-cm thick cement housing. The shielding of the experimentation posts and the control room was also discussed. (J.S.R.)

43739 COLLECTIVE ACCELERATION OF PARTICLES. Bartke, Jerzy (Inst. of Nuclear Physics, Krakow). Postepy Fiz.; 22: No. 2, 131-45(1971). (In Polish).

Physical principles of the collective acceleration of particles are presented and the present status of the development of the so-called electron ring accelerator (ERA) is reviewed. Future prospects of this method for the acceleration of heavy ions and construction of very high energy proton accelerators are discussed. (auth)

43740 ACCELERATION SYSTEM FOR IMPLANTING IONS IN SPECIMEN. Brewer, George R.; Buckey, Charles R. (to Hughes Aircraft Co.). U. S. Patent 3,569,757. 9 Mar 1971. Filed 4 Oct 1968.

A two-dimensional double-deflection system for ion implantation of semiconductor devices comprises means for deflecting an ion beam in orthogonal directions such that the ion incidence angle is always constant with respect to a target. The beam is first deflected in a direction away from a reference axis, and thereafter is redeflected along a path which lies parallel to the reference axis. The second double deflection is similarly performed but orthogonal to the first double deflection. The beam can thus be swept over the entire target for uniform device implantation characteristics. (auth)

43741 ELECTROMAGNET OF A TRANSPORTABLE BETATRON EXCITED BY CURRENT AT INCREASED FREQUENCY. Kim, M. V.; Loginov, V. S.; Shilin, G. F.; Chakhlov, V. L.; Yarushkin, Yu. P. (Tomsk Polytechnic Inst., USSR). Instrum. Exp. Tech. (USSR) (Engl. Transl.); No. 5, 1270-2(Sep-Oct 1970).

Translated from Prib. Tekh. Eksp.; No. 5, 23-5(Sep-Oct 1970).

The design of the electromagnet of a transportable betatron designed for excitation by a current having a frequency of 150 to 200 Hz is described. Effective cooling of the electromagnet is attained by through holes of triangular shape in the pole body. Temperature conditions in the magnetic path are investigated. (auth)

43742 DECREASING ION CLUSTER REPETITION FREQUENCY IN AN FEI CYCLOTRON. Biryukov, N. S.; Zhuravlev, B. V.; Krasnov, N. N.; (and others) (Physics and Power Inst., Obninsk, USSR). Instrum. Exp. Tech. (USSR) (Engl. Transl.); No. 5, 1273-7(Sep-Oct 1970).

Translated from Prib. Tekh. Eksp.; No. 5, 26-30(Sep-Oct 1970).

A system for a fourfold decrease in ion cluster repetition frequency in a cyclotron (a pulsing system) is described. Ion deflection is produced by using a high-frequency sinusoidal voltage which is applied to the cyclotron's deflection plate. The block-schematic, the principal circuit, and a description of the technical apparatus are cited. (auth)

43743 INSTRUMENT FOR MEASURING AND MONITORING THE ENERGIES OF PARTICLES ACCELERATED IN A CYCLOTRON. Gonchar, V. Yu.; Zheltonog, K. S.; Ivanov, G. N.; Rybin, S. N. (Inst. of Nuclear Physics, Alma-Ata, USSR). Instrum. Exp. Tech. (USSR) (Engl. Transl.); No. 5, 1278-80(Sep-Oct 1970).

Translated from Prib. Tekh. Eksp.; No. 5, 30-3(Sep-Oct 1970).

A description is given of an instrument for monitoring the energies of particles accelerated in a 150-cm cyclotron via comparison of the α-particle spectrum from a radioactive source with the spectrum of the particles scattered through 13° by a thin target. The energy can be measured to 0.55% for 38-MeV α-particles and 9.5-MeV protons. (auth)

43744 COMPENSATION OF THE STRAY FIELD OF MAGNETIC DEFLECTORS. Kireiko, P. A.; Shorin, K. N. (Inst. of Physics, Moscow). Instrum. Exp. Tech. (USSR) (Engl. Transl.); No. 5, 1281-2(Sep-Oct 1970).

Translated from Prib. Tekh. Eksp.; No. 5, 33-4(Sep-Oct 1970).

It is shown that the stray field throughout the external region can be reduced to $2 \cdot 10^{-3}$ of the field in the operating region by using a suitable arrangement and shape of the basic outside winding of the deflector and employing an additional compensating winding. (auth)

43745 MONOENERGETIC NATURE AND STABILITY OF THE BEAM CURRENT IN LINEAR INDUCTION ACCELERATORS. Grishin, V. K. (Moscow State Univ.). Instrum. Exp. Tech. (USSR) (Engl. Transl.); No. 5, 1283-5(Sep-Oct 1970).

Translated from Prib. Tekh. Eksp.; No. 5, 35-6(Sep-Oct 1970).

Linear induction accelerators are devices intended for accelerating currents of hundreds of amperes; the instabilities of the accelerated currents in these produce an additional statistical spread of the energy in the beam. The limitations imposed on the amplitude and frequency by various perturbations in the homogeneity of the particle beams are analyzed. (auth)

43746 UNIVERSAL APPARATUS FOR MEASURING THE PARAMETERS OF STRONG ION BEAMS. Bezverkhov, B. M.; Matveenko, O. G.; Pleshivtsev, N. V. (Inst. of Atomic Energy, Moscow). Instrum. Exp. Tech. (USSR) (Engl. Transl.); No. 5, 1286-9(Sep-Oct 1970).

Translated from Prib. Tekh. Eksp.; No. 5, 37-40(Sep-Oct 1970).

A universal apparatus for measuring the following parameters of strong ion beams is developed: distribution of current density over the cross section of a strong beam of hydrogen ions (40 keV,

XUM

0.4 A), inclination of the ion trajectories to the beam axis, percentage content of H_1^+, H_2^+ and H_3^+ ions at various beam radii, integral mass composition of the beam, and reduced beam admittance. (auth)

43747 ION-BEAM APPARATUS. Komarov, V. L.; Nalivaiko, G. A.; Razgulyaev, I. I.; Solnyshkov, A. I.; Tsepakin, S. G. Instrum. Exp. Tech. (USSR) (Engl. Transl.); No. 5, 1422-4(Sep-Oct 1970).

Translated from Prib. Tekh. Eksp.; No. 5, 154-6(Sep-Oct 1970).

An ion-beam apparatus for making semiconductor devices is described, and its basic characteristics are reported. The apparatus has been used to produce accelerated beams of the ions of various elements at controllable energies in the range 20 to 200 keV and at currents up to 300 μA. (auth)

43748 SUPERCONDUCTIVE SHIELDED MAGNETIC LENS. Goncharenko, I. I.; Sidorenko, I. S.; Skoromnyi, G. M. (Physical Technical Inst., Kharkov). Instrum. Exp. Tech. (USSR) (Engl. Transl.); No. 5, 1466-7(Sep-Oct 1970).

Translated from Prib. Tekh. Eksp.; No. 5, 191-2(Sep-Oct 1970).

A magnetic lens having windings of superconductive Nb + Zr + Ti wire and a magnetic path of steel St. 3 is described. The outer diameter of the lens is 70 mm; the aperture is 20 mm; and the maximum field in the axis is H = 24.6 kOe at T = 4.2°K. (auth)

43749 ENERGY CALIBRATION OF LINAC ANALYZING SYSTEM BY MEANS OF PHOTONUCLEAR REACTION. Mikado, Tomohisa; Tomimasu, Takio; Tsuchiya, Yoshio. Denki Shikensho Iho; 35: No. 1, 27-34(1971). (In Japanese).

The analyzing system of the ETL electron linear accelerator has been calibrated by means of measurements of several photoneutron threshold energies and magnetic fields. This system consists of a 60° bending magnet (M-A, $\rho_A \approx 200$ mm), a 60° analyzing magnet (M-B, $\rho_B \approx 200$ mm), X- and Y-slits, and so on. Isotopes used are ^{207}Pb (6.73 MeV), ^{208}Pb (7.38 MeV), ^{109}Ag (9.18 MeV), ^{65}Cu (9.91 MeV) and ^{12}C (18.72 MeV) for (γ,n) reaction and ^{16}O (28.89 MeV) for (γ,2n) reaction. The magnetic field is measured at the pole gap of the M-B, though it is subsidiary. From the field measurement, a relative calibration curve is obtained and then its absolute energy is evaluated by making use of results of the threshold measurements. With the calibration curve, the electron beam energy can be determined within a ±0.5% accuracy ranging from about 6 to about 35 MeV. (auth)

43750 ABSOLUTE MEASUREMENT OF LINAC X-RAY ENERGY FLUENCE BY THE USE OF ETL TYPE QUANTAMETER (ETL Q-II). Tsuchiya, Yoshio; Tomimasu, Takio; Mikado, Tomohisa; Chiwaki, Mitsukuni. Denki Shikensho Iho; 35: No. 1, 35-40 (1971). (In Japanese).

Energy fluence of micro-sec pulse high intensity x-rays from the 33 MeV ETL Linac has been measured by the use of the ETL type quantameter. The diameter of the x-ray source is 4 mm, and a Pb collimator having a conical hole is used in the energy fluence measurement. A filling gas difference (air, Ar, and Ar + CO_2) in the V-I saturation curve of the quantameter is studied for 50 pps and 300 pps x-ray bursts and for different electron beam currents. It has been shown that Ar is superior to the others in the measurement of high repetition rate x-ray bursts and high intensity x-rays. The V-I saturation curve of Ar + CO_2 mixture is similar to that of air, and is not suitable for the measurement of high repetition rate x-ray bursts. The measurable upper limit of energy fluence by the use of the ETL Q-II is shown to be 0.2 W/cm^2. (auth)

43751 DEPENDENCE OF ELECTRON BREMSSTRAHLUNG GENERATION ON TARGET THICKNESS AND FORWARD ANGLE. Tomimasu, Takio; Mikado, Tomohisa; Tsuchiya, Yoshio. Denki Shikensho Iho; 35: No. 1, 41-6(1971). (In Japanese).

Electrons from the 33 MeV ETL Linac are used to strike Pb foils and produce x-rays. Energy fluence of the x-rays is measured with the ETL type quantameter. The angular distribution of x-rays produced by high energy electrons has a sharp forward angle dependence, and also depends on the target thickness as the quantity of x-rays does. The range of experimental electron energy is from 16.5 to 28.0 MeV. The diameter of the x-ray source is 4 mm, and three kinds of Pb collimators, each having a conical hole whose vertical angle is $^1/_{40}$, $^2/_{40}$ or $^3/_{40}$, respectively, are used. The energy fluence of generated x-rays is almost proportional to the target thickness of less than 0.04 in radiation length (R.L.), and begins to saturate for 0.1 R.L. since the electron multiple scattering increases in thick targets. In the energy fluence measurement under the above-mentioned experimental conditions, it is found that the difference in the size of the conical hole causes a difference of several % in the energy fluence. The larger the vertical angle of the conical hole, the smaller the quantity of energy fluence is because of the sharp dependence on the forward angle. (auth)

43752 33 MeV ETL ELECTRON LINEAR ACCELERATOR. Tomimasu, Takio; Mikado, Tomohisa; Tsuchiya, Yoshio. Denki Shikensho Iho; 35: No. 1, 2-6(1971).

The 33 MeV electron linac of the Electrochemical Laboratory is in full operation. The accelerator consists of an injector, a prebuncher and three accelerator sections (each 1.15 m long), and the rf power is provided by two klystrons (each of 7.5 MW peak power). Unloaded energy is 35 MeV for 15 MW rf peak power, and loaded energy is 25 MeV at a 203 mA peak current. Energy spread of the accelerated beams is about 7% in the energy range of 10 to 31 MeV and the beam currents are of the order of 100 mA peak. Analyzed beam currents for 0.5% energy spread are about 5% of the accelerated beam currents, and are very stable. (auth)

43753 13 MeV LINEAR ACCELERATOR AT KURUME UNIVERSITY. Noda, Hiroji (Kurume Univ., Fukuoka). Nippon Igaku Hoshasen Gakkai Zasshi; 30: No. 8, 701-7(Nov 1970). (In Japanese).

The performance and maintenance for the LMR-13 linear accelerator are reported. The installation is operated at a fairly good controlled output of 6 to 12 MeV. However, daily adjustments of the linac for the dose distribution across the beam (beam flatness) and the indicated value of output monitor dosimeter (calibration by Radocon dosimeter) are required. (auth) (Japan)

43754 CHARACTERISTICS OF THE LINEAR ACCELERATOR AT HIROSHIMA UNIVERSITY. Takeshita, Kenji (Hiroshima Univ.); Antoku, Shigetoshi; Sunayashiki, Tadashi; Otani, Shiro; Kazusa, Chudo. Nippon Igaku Hoshasen Gakkai Zasshi; 30: No. 8, 687-97(Nov 1970). (In Japanese).

The NEC-Varian linear accelerator installed at Hiroshima University in February 1969 is used for studies on the biological effects of radiation and for radiation therapy of malignant tumors. In order to obtain an extremely high dose rate for radiobiological studies to simulate the radiation released by the atomic bomb and also a low dose rate for radiation therapy, the operation of the unit is divided into two systems: research mode and therapy mode. In the research mode, electron energy can be changed continuously between 5 and 39 MeV. Beam current is 320 mA at peak with an average of 90 μA and beam power is 2.25 kW at nominal operation (25 MeV). At this level of operation the x-ray output is 14,500 rad/min at a distance of 100 cm from the x-ray target. Radiation output is adjustable by changing the pulse repetition rate (15, 60, 120 pps) and the beam current. In the therapy mode, the attachments and accessories necessary for radiation therapy are connected to the unit. For electrons, six specific energies are programmed over the range of 5 to 30 MeV at 5 MeV intervals. For x-rays, an energy of 8 MeV is programmed. Radiation output in the therapy mode is less than 500 rad/min and dose distribution in the exposure field can be made very uniform by the use of appropriate scatterers and flattening filters. To shield high energy x-rays and neutrons, the room housing the linear accelerator was built below ground level. The stray radiations outside the building are well within the maximum permissible dose prescribed by Japanese Government regulations. (auth) (Japan)

43755 RECONSTRUCTION AND PERFORMANCE OF THE ETL ELECTRON LINEAR ACCELERATOR. Tomimasu, Takio; Tsuchiya, Yoshio; Watanabe, Hiroshi; Mikado, Tomoshisa. Denki Shikensho Iho; 35: No. 1, 7-19(1971). (In Japanese).

The accelerator designed in 1964 to be of E_0 = 25 MeV (unloaded energy) for 8 MW rf peak power became unable to give the designed energy due to some defects in vacuum and rf systems so it was decided in 1968 to replace the vacuum system and rf guide, and to seal up vacuum leakages in the three accelerator sections (each 1.15 m long). After leakage sealing and the renewing of the vacuum system and the guide, 14 MW rf peak power could be easily put into the accelerator because the vacuum in the accelerator became to the order of 1×10^{-7} torr. Consequently the beam energy reached 33 MeV, exceeding the former designed energy E_0 = 25 MeV. Unloaded energy was 35 MeV for 15 MW rf peak power, and loaded energy was 25 MeV at 203 mA peak current. Energy spread of the accelerated beam was about 7% in the energy range from 10 to 31 MeV and beam currents were of the order of 100 mA peak. Analyzed beam currents for 0.5% energy spread were about 5% of the accelerated beam currents, and were very stable. (auth)

43756 HYDRODYNAMIC STABILITY OF ELECTRON STREAMS IN VACUUM. Gladun, A. D.; Leiman, V. G. (Physical-Technical Inst., Moscow). Sov. Phys.-Tech. Phys. (Engl. Transl.); 15: No. 12, 1970-3(Jun 1971).

Translated from Zh. Tekh. Fiz.; 40: No. 12, 2513-17(Dec 1970).

It is shown that electron flow without slip between electron layers is stable. Slip of electron layers along the lines of force of the magnetic field (or in the direction of the flow axis in the case of centrifugal electrostatic focusing) causes a buildup of electron oscillations, as in the case of the current-convective instability in inhomogeneous plasma flow; electron layer slip perpendicular to the lines of force of the magnetic field (or in the direction of the flow axis in the case of centrifugal electrostatic focusing) leads to an instability analogous to the usual Rayleigh–Taylor instability. The growth rates for the two cases are estimated. (auth)

43757 SEMI-ANALYTICAL CALCULATIONS FOR CIRCULAR QUADRUPOLES. Lee-Whiting, G. E.; Yamazaki, L. (Chalk River Nuclear Labs., Ont.). Nucl. Instrum. Methods; 94: No. 2, 319-32(1971).

By expanding in appropriate series of singular harmonic functions, a solution is found to the equipotential problem for four circular poles (or electrodes) with quadrupole symmetry. The duodecapole term in the potential is found to be absent when the ratio of pole diameter to throat diameter is 1.14511; the contributions from multipoles of higher order are found to be small. The method is extended to permit the calculation of the effects of placing the exciting coils near the poles, of allowing the permeability to be finite (but uniform), and of adding a yoke. The distribution of flux density on a pole surface is calculated. It is recommended that circular arcs replace hyperbolic arcs as the basis for the design of quadrupole lenses. (auth)

43758 USE OF HEAVY IONS FROM A TANDEM ACCELERATOR TO SIMULATE HIGH FLUENCE, FAST NEUTRON DAMAGE IN METALS. Kulcinski, G. L. (Battelle-Northwest, Richland, Wash.). Nucl. Instrum. Methods; 94: No. 2, 365-75(1971).

The philosophy behind the use of high-energy heavy ions to simulate high-fluence, fast-neutron damage is discussed in some detail. The major advantage of this technique is that the rate at which atoms are displaced can be increased by a factor of 1 to 10,000 over that presently available in the core of fast test reactors. It is shown that the effects of the bombarding ion on the chemical composition of the sample and the inhomogeneity of the damage must be carefully assessed when interpreting results from ion-bombardment studies. The experimental techniques used to bombard samples with heavy ions are also described, with particular emphasis on the use of a tandem accelerator to attain ion energies in the 1 to 14 MeV range. The various sources used to inject ions into the accelerator are briefly described, and typical transmission data are presented for I, Cl, Al, and Ni ions. The effect of the stripping gases H_2, He, and O_2 on the equilibrium charge fraction of Ni ions is given. Finally, typical examples of pure Ni and 316 stainless steel that have been bombarded by both neutrons and ions are compared. (auth)

43759 METHOD FOR PREPARING THIN FILMS OF DEUTERATED POLYETHYLENE. Matsuki, S.; Yasue, M.; Yamashita, S. (Kyoto Univ.). Nucl. Instrum. Methods; 94: No. 2, 387-8(1971).

A simple method for preparing thin, uniform films of deuterated polyethylene is described. (auth)

43760 TIME SHAPING OF BEAM PULSES FROM THE HAMBURG ISOCHRONOUS CYCLOTRON BY DIFFERENT CENTRAL DIAPHRAGMS. Klages, H. O.; Krause, H.; Langkau, R. (Univ., Hamburg). Nucl. Instrum. Methods; 94: No. 2, 391-3(1971). (In German).

Time shaping of the beam pulses from the Hamburg isochronous cyclotron by central diaphragms of different configuration was investigated. (auth)

43761 ION-OPTICAL PROPERTIES OF AN ELECTROSTATIC CHARGED-PARTICLE ENERGY ANALYZER WITH RING-AXIS FOCUSING. Zashkvara, V. V.; Korsunskii, M. I.; Red'kin, V. S.; Lavron, V. P. (Inst. of Nuclear Physics, Alma-Ata, USSR). Sov. Phys.-Tech. Phys. (Eng. Transl.); 15: No. 12, 2033-4(Jun 1971).

Translated from Zh. Tekh. Fiz.; 40: No. 12, 2591-2(Dec 1970).

Equations are given for the relative focal distance, the relative linear energy dispersion, the quadratic angular aberration coefficient, and the cubic angular aberration coefficient for a cylindrical electrostatic analyzer with ring-axis focusing for various beam-entrance angles into the field region. (W.H.K.)

43762 EXTRACTION OF THE PROTON BEAM OF THE 1-GeV SYNCHROCYCLOTRON OF THE PHYSICOTECHNICAL INSTITUTE OF THE ACADEMY OF SCIENCES OF THE USSR. Abrosimov, N. K.; Volchenkov, V. A.; Eliseev, V. A.; Ryabov, G. A.; Chernov, N. N. Sov. Phys.-Tech. Phys. (Engl. Transl.); 15: No. 12, 2035-7(Jun 1971).

Translated from Zh. Tekh. Fiz.; 40: No. 12, 2593-6(Dec 1970).

The regenerative buildup of particle oscillations in the 1-GeV synchrocyclotron has been calculated, taking account of the synchrotron-oscillation spectrum for the magnetic field, and the beam passage through various types of focusing channels has been analyzed. Several recommendations for increasing extraction efficiency are offered on the basis of these calculations: an optimum inclination of the channel entrance should be chosen; the channel aperture should be enlarged; and all sections of the focusing channel and the magnitude and sign of the gradients should be chosen to match the radial and vertical beam emittances with the channel acceptance. (W.H.K.)

43763 LONGITUDINAL SECOND-ORDER ABBERRATIONS IN SYMMETRIC DEFLECTING MAGNETO-OPTICAL SYSTEMS. Basargin, Yu. G. Sov. Phys.-Tech. Phys. (Engl. Transl.); 15: No. 12, 2038-40(Jun 1971).

Translated from Zh. Tekh. Fiz.; 40: No. 12, 2596-8(Dec 1970).

Longitudinal motion in an individual bunch of charged particles is considered in the second approximation. A general expression for the aberration variation of the bunch length is obtained. Results for achromatic deflecting systems are discussed. (auth)

43764 BEAM TRANSPORT SYSTEM OF THE ETL LINAC. Tsuchiya, Yoshio; Tomimasu, Takio; Watanabe, Hiroshi; Mikado, Tomohisa; Sugiyama, Suguru. Denki Shikensho Iho; 35: No. 1, 20-6(1971). (In Japanese).

The beam transport system of the ETL Linac and its performance are described. The system consists of two 60° magnets, two X Y slits, two quadrupole (doublet) magnets, an X-ray converter inserting system and an ion vacuum pump. The system transports an analysed beam from the Linac to the electron scattering facility and allows research to be carried out with a purified beam of 0.2% energy spread whose cross section is 2mm × 5mm at the scattering chamber. Analysed beam currents for 0.5% energy spread are about 5% of the accelerated beam currents. (auth)

43765 ECONOMICAL SOURCE OF MULTIPLY-CHARGED CALCIUM AND ZINC IONS. Tret'yakov, Yu. P.; Kul'kina, L. P.; Kuznetsov, V. I.; Pasyuk, A. S. (Joint Inst. for Nuclear Research, Dubna, USSR). Instrum. Exp. Tech. (USSR) (Engl. Transl.); No. 5, 1290-4(Sep-Oct 1970).

Translated from Prib. Tekh. Eksp.; No. 5, 40-4(Sep-Oct 1970).

The construction of a cyclotron source with a hot discharge chamber is described. Cathodic sputtering of the working substance takes place in this source. Multiply-charged Ca and Zn ions are obtained. The heating of the discharge chamber reduces the consumption of Ca and Zn by an order of magnitude as compared with sources having a cooled discharge chamber. The distribution of Ca atoms and ions along the discharge chamber is measured. (auth)

43766 INCREASING THE ENERGY OF AN ELECTROSTATIC ACCELERATOR WITH CHARGE EXCHANGE FROM 10.5 TO 14 MeV. Almazov, A. V.; Myntsov, F. F.; Serov, Yu. A. Instrum. Exp. Tech. (USSR) (Engl. Transl.); No. 5, 1266-9(Sep-Oct 1970).

Translated from Prib. Tekh. Eksp.; No. 5, 20-3(Sep-Oct 1970).

A modernized version of an EGP-10 electrostatic accelerator with charge exchange [1] is considered; the maximum energy of the accelerated singly-charged particles is accordingly increased from 10.5 to 14 MeV. (auth)

43767 COLLIMATOR AND SCATTERING FOIL FOR 10 TO 20 MeV ELECTRONS. Lindskoug, B.; Johansson, K. A. (Univ., Goteborg). Acta Radiol., Ther., Phys., Biol.; 10: 21-6(1971).

A new electron collimator design in which scattered electrons increase the dose rate and the flatness of the beam is described. The original scattering foil of a BBC Asklepitron 35 betatron has been changed to produce less absorption and thus an improved dose rate. (auth) (Sweden)

43768 NEW RESEARCH OPPORTUNITIES WITH 25-MeV BETATRON. Bozoky, Laszlo (Oncological Inst., Budapest). Fiz. Szemle; 21: No. 2, 59-60(Feb 1971). (In Hungarian).

A 25-MeV betatron of Soviet manufacture has been installed at the Oncological Institute during December 1970. Its main purpose is to provide an ultrahigh voltage source for tumor irradiation but it is planned to carry out studies in cooperation with other radiobiological, biophysical and industrial research institutes. The betatron allows to create a several 100 million-volt x or electron radiation without encountering serious insulation problems. The ultrahard radiation exhibits a greatly modified depth dose curve: instead of decreasing with depth, the dose increases as the result of the build-up effect before it starts to decrease exponentially. The betatron may also be used as a source for an

XUM

accelerated electron beam which affects primarily the tumor itself, reducing exposure to the healthy tissue to a minimum. The probability of (γ,n) reactions must be taken into account. The new installation has a 60-cm diameter accelerating tube; the electrons are injected at 60 kV. The x-ray dose rate at 100 cm is about 50 R/min at an energy of 24 MeV; under identical conditions, the electron radiation dose rate is about 300 rads/min. (TTT)

43769 INCREASE OF THE GAMMA RADIATION WITH NEUTRAL FLUX AROUND A 1-MV VAN DE GRAAFF ACCELERATOR. Bodizs, Denes. ATOMKI (At. Kut. Intez.) Kozlem.; 12: No. 4, 175-8(Dec 1970). (In Hungarian).

The effect of the neutral component of the ion beam on the current loading of the acceleration tube is investigated by measuring the intensity of the gamma radiation of a 1 MV Van de Graaff accelerator. (auth)

43770 DYNAMICS OF PARTICLE POLARIZATION NEAR SPIN RESONANCES. Derbenev, Ya. S.; Kondratenko, A. M.; Skrinskii, A. N. (Inst. of Nuclear Physics, Novosibirsk, USSR). Zh. Eksp. Teor. Fiz.; 60: No. 4, 1216-27(Apr 1971). (In Russian).

The motion of particle spins in storage rings (accelerators) is investigated. The methods and results of investigations on spin resonances are extended to the case of an arbitrary closed orbit. Besides first approximation resonances, those of higher order are considered for which selection rules of resonating harmonics are obtained. The major part of the work is dedicated to passage of resonances. The concept of an effective and adiabatic band is introduced. A complete solution of the single passage problem is presented which embraces the particular solutions. On this basis the problem of periodic passage of resonance is solved by employing the general nature of motion of a spin in a periodic field. (auth)

PHYSICS (NUCLEAR)

Neutron Interactions with Matter

Refer also to abstracts 42048, 43278, 43423, 43789, 43834, and 43930.

43771 (EIR–189) INTEGRAL TRANSPORT EQUATION IN ONE-DIMENSIONAL CYLINDRICAL GEOMETRY. POLYNOMIAL APPROXIMATION AND LINEAR ANISOTROPIC SCATTERING. PART II. CHARACTERISTICS AND NUMERICAL APPLICATIONS OF THE SHADOK CODE: POSSIBLE EXTENSION OF THE METHOD. Ligou, J.; Thomi, P. A. (Eidgenoessisches Institut fuer Reaktorforschung, Wuerenlingen (Switzerland)). Dec 1970. 85p. (In French). Dep. NTIS (U. S. Sales Only).

The study of the utilization of a three-term polynomial approximation for the solution of the integral transport equation led to the development of the multigroup code SHADOK, written for the CDC 6500 computer. With this code problems of neutron scattering can be treated in one-dimensional cylindrical or spherical geometry. Some numerical peculiarities of the code, which are not evident, are first discussed. The numerical application of the method is given for three very different regions: calculation of one-group cells (thermal neutrons), shielding calculations with penetration of 2.5-MeV neutrons into light water, and calculation of critical assemblies with fast or mixed neutrons. The results obtained are compared with those given by other methods. A theoretical development for taking into account a higher order of anisotropy is presented. (J.S.R.)

43772 APPLICATION OF VARIATIONAL SYNTHESIS TO SOLUTIONS OF MULTIDIMENSIONAL NEUTRON TRANSPORT PROBLEMS. Cobb, William Ronald. Atlanta; Georgia Inst. of Tech. (1970). 168p. University Microfilms Order No. 71-13,779.

Thesis.

The variational synthesis method was applied to the steady-state Boltzmann neutron transport equation in two- and three-dimensional rectangular geometry. In this application the energy dependence is treated in the standard multigroup energy approximation, the dependence along all but a single remaining spatial variable was treated by a multichannel discontinuous spatial synthesis approximation and the angular dependence was treated by a discrete ordinates approximation. All approximate treatments of these variables were developed consistently from a variational principle by the standard trial function reduction procedure, applied sequentially to the energy variable, the spatial variables and the angular variable. The approximate method as developed in this application allows the user to obtain approximate solutions to the transport equation by combination of the solutions to related problems of lower dimensionality. An experimental computer code was written for use in obtaining approximate solution to the two-dimensional, one energy group problem with isotropic scattering. The experimental computer code was used to obtain approximate solutions to several test problems of the type encountered in the reactor field and the accuracy and comparative cost of these approximate solutions was determined by comparison to consistently obtained direct solutions to the same problems. Both fixed source and eigenvalue problems, as well as problems with both vacuum and reflected boundary conditions, were investigated. Results of the test problems indicated that the method, as developed, is capable of producing accurate approximate transport solutions at a fraction of the cost of the direct solutions, and with accuracy superior to the diffusion approximation. (Diss. Abstr. Int., B)

43773 NUMERICAL SOLUTIONS OF THE NEUTRON TRANSPORT EQUATION. Skeen, David Roy. Corvallis, Oreg.; Oregon State Univ. (1970). 101p. University Microfilms Order No. 71-12,670.

Thesis.

Because of the high cost of fuel for nuclear reactors, fuel cycle costs must be predicted accurately. This leads to the high cost computer computations and a search for cheaper yet still accurate methods. An alternate method for calculating thermal neutron cell averaged cross sections was studied. The method developed involves an expansion of the slab geometry transport equation by means of eigenfunctions. It utilizes moments matching boundary conditions similar to P_N methods. Theory and calculations are given in slab and cylindrical geometry. The method is extended to multigroup methods. Results indicate that this method can be used as an alternative to more standard methods such as integral transport and Monte Carlo theories. Accuracy of this method is quite good, better than P_3 theory in most cases. Computer calculation time is at least 50% faster than integral transport theory and, of course, only a small fraction of Monte Carlo theory. (Diss. Abstr. Int., B)

43774 MECHANICAL GENERATOR FOR ULTRACOLD NEUTRONS. Kashukeev, N. T. Compt. Rend. Acad. Bulg. Sci.; 23: 1473-6(1970). (In Russian).

Descriptions are given of the design and performance of a mechanical generator of ultracold neutrons. The generator consists of a rotor with four blades made of duralumin covered with a thin layer of nickel. A beam of thermal neutrons is incident on the rotor blades at an angle of 45°. Equations illustrating the relationship between rotor parameters and velocity of the transmittal neutrons are presented. (C.E.S.)

43775 NEUTRONEN-PHYSIKALISCHES PRAKTIKUM. ERSTER BAND. PHYSIK UND TECHNIK DER AKTIVIERUNGS-SONDEN. (Neutron Physics Practices. Volume I. Physics and Technology of Activation Probes). Bensch, Friedrich; Fleck, Carl M. B.I-Hochschultaschenbuecher, 170/170a. Mannheim, Ger.; Bibliographisches Institut AG (1968). 240p.

The technology of activation probes is discussed comprehensively from a fundamental standpoint as well as from its practical application for reactors and neutron physics. After discussion of the connection between neutron field and saturation activity, the measurement of thermal, epithermal, and fast neutrons is treated. Numerous practical examples are elaborated. A large number of figures and tables are included. (H.B.G.)

43776 FAST SWITCHING PULSED NEUTRON POLARIZATION INVERTER. Forgacs, R. L. (Ford Motor Co., Dearborn, Mich.). Rev. Sci. Instrum.; 42: No. 7, 1007-15(Jul 1971).

A system was developed for producing repetitive short bursts of preferentially oriented spin-polarized neutrons for magnetic investigations utilizing neutron spectroscopy. A continuous stream of polarized neutrons from a reactor–monochromator combination is passed through a region in which periodic inversion of polarization is effected by continuous application of an rf field at the Larmor frequency perpendicular to a pulse-modulated dc magnetic field. A novel circuit for fast transition modulation of the dc field permits currents as high as 1 A to be switched in less than 2 μsec in the 6 mH dc coil. The maximum burst repetition rate is approximately 83,300 pulses/sec. (auth)

43777 FURTHER REMARKS ON THE COHERENCE PROPERTIES OF A THERMAL NEUTRON BEAM. Boffi, S. (Univ., Pavia, Italy. Istituto Nazionale di Fisica Nucleare, Pavia, Italy); Caglioti, G. Nuovo Cim., 3B: No. 2, 262-8(11 Jun 1971).

The possibility of obtaining experimental evidence for antibunching effects due to the Fermi–Dirac statistics of the neutron is discussed and anticipated. (auth)

43778 DC OPERATED POSITIVE ION ACCELERATOR AND NEUTRON GENERATOR HAVING AN EXTERNALLY AVAILABLE GROUND POTENTIAL TARGET. Carr, Barney J. (to Kaman Sciences Corp.). U. S. Patent 3,581,093. 25 May 1971. Filed 23 Apr 1968.

A sealed neutron generator containing an isotope of hydrogen having an ion source, an accelerator, and a target containing a substance which reacts with impinging ions to produce neutrons maintained at ground potential and located to be available at the exterior of the generator is described. (auth)

Nuclear Properties and Reactions, A≤ 5

Refer also to abstracts 42131, 43533, 43538, 43560, 43966, and 43971.

43779 (CEA-N–1327) SAPRISTI CODE: NUCLEAR REACTIONS BETWEEN LIGHT NUCLEI. REACTION TABLE (2250 TO 2500). (Commissariat a l'Energie Atomique, Paris (France)). 7 May 1971. 64p. (In French). Dep. NTIS (U. S. Sales Only).

A list of nuclear reactions between light nuclei and the references of the corresponding article abstracts to be found in the Sapristi-code bibliography (Volume 4) are given. (France)

43780 (CEA-N–1327(Vol.4)) SAPRISTI CODE: NUCLEAR REACTIONS BETWEEN LIGHT NUCLEI. BIBLIOGRAPHY. VOLUME IV. (Commissariat a l'Energie Atomique, Paris

XUM

(France)). 7 May 1971. 84p. (In French). Dep. NTIS (U. S. Sales Only).

A list of 250 abstracts relative to nuclear reactions between light nuclei is given. The number of each summary refers to the list of the corresponding nuclear reactions given in the Sapristi-code reaction table. (France)

43781 ANALYSES OF ELASTIC PROTON-ALPHA SCATTERING. Arndt, Richard A.; Roper, L. David; Shotwell, Robert L. (Virginia Polytechnic Inst., Blacksburg). Phys. Rev., C; 3: No. 6, 2100-13(Jun 1971).

An energy-dependent solution to $p-\alpha$ scattering between 0 and 23 MeV is obtained from reported single-energy analyses of $p-\alpha$ elastic scattering. Single-energy analyses, starting from the energy-dependent solution, were also done at energies where both differential-cross-section and polarization data are available. The single-energy results are rather erratic, but tend to lie near the energy-dependent result. (auth)

43782 SEARCH FOR A NARROW STATE AT 23.9 MeV IN ^{4}He IN THE ^{3}H + p CHANNEL. Paetzgen Schieck, H. (Ohio State Univ., Columbus); Donoghue, T. R.; Prior, R. M.; Darden, S. E. Nucl. Phys.; A169: No. 1, 71-5(1971).

Some previous polarization and asymmetry measurements in the ^{2}H(d,n) and ^{2}H(d,p) reactions, when initiated with either unpolarized or polarized deuterons, have shown an anomaly in the excitation curves near $E_d \approx 100$ keV. A state at an excitation energy of 23.9 MeV in ^{4}He was proposed to account for this anomaly. In the present work, a search for this state was made by measuring ^{3}H + p elastic scattering in a proton energy range centered at about 5.45 MeV. The measurements were made using both an unpolarized as well as a polarized proton beam incident on a very thin ($\Delta E \approx 5$ keV) titanium–tritium target. No evidence for this state was found. (auth)

43783 EFFECT OF TENSOR FORCES ON THE CHARGE FORM FACTOR OF THE α-PARTICLE. Mahanti, D.; Yadav, H. L.; Srivastava, B. K. (Indian Inst. of Tech., Kharagpur). Nucl. Phys.; A169: No. 1, 76-80(1971).

The charge form factor of the α-particle was calculated using Irving and Gaussian forms for the radial wave functions. The ground state is assumed to be a mixture of the principal $^1S_0$ and the principal $^5D_0$ states. The parameters in the wave functions were determined from the variational calculations of the binding energy. Calculations using the Irving wave function show good agreement with electron-helium scattering experiments and with calculations using hard-core potentials up to 10 fm^{-2} transfer of the square of the momentum. The agreement is comparatively poor for the Gaussian wave function. (auth)

43784 TWO-CHANNEL CALCULATION FOR ELASTIC α-α SCATTERING. Le-Chi-Niem; Heiss, P.; Hackenbroich, H. H. (Univ., Cologne). Z. Phys.; 244: 346-51(1971).

Starting with a realistic nucleon–nucleon soft core potential the $\alpha-\alpha$ phase shifts were calculated in the refined cluster model framework. It is shown that the inclusion of inelastic $\alpha^*-\alpha$ channels yields considerable improvement in the results. Below inelastic thresholds, calculated and experimental values are in quantitative agreement. (auth)

43785 BRUECKNER–HARTREE–FOCK THEORY FOR THE ^{4}He NUCLEUS. Vashakidze, I. Sh.; Meboniya, J. V.; Dzhalaganiya, T. R.; Eliava, A. T. (Tbilisi State Univ., USSR). Yadern. Fiz.; 13: No. 4, 688-93(Apr 1971). (In Russian).

The Hartree–Fock method is used to study the ground state and one-particle states of the ^{4}He nucleus. In the total Hamiltonian of the system, the motion of the nuclear center of inertia is excluded. The self consistency of the problem can be achieved using the expansion of one-particle states in a series over the oscillator functions. As a nucleon–nucleon interaction the real potential describing the scattering of free nucleons is used. The Brueckner method is used to take into account the nucleon–nucleon correlation. Concrete results are obtained in the second approximation in the G matrix. The inclusion of the pair correlations essentially improves the agreement with experiment. (auth)

43786 SHELL INTERPRETATION OF THE SEPARABLE INTERACTIONS BETWEEN LIGHTEST NUCLEI. Kuznetsova, L. M.; Kukulin, V. I.; Neudachin, V. G. (Inst. of Nuclear Physics, Moscow). Yadern. Fiz.; 13: No. 4, 694-706(Apr 1971). (In Russian).

A new class of factorizable interaction potentials between the lightest nuclei is proposed. The functional form and the values of the parameters of the potential formfactors are taken directly from the oscillator wave functions of light nuclei with account of the Pauli principle. The phase shifts and the radial wave functions are explicitly calculated for the following nuclear pairs: ^{4}He–^{4}He, d–^{4}He, ^{4}He–t(^{3}He) for different partial waves. Simple general considerations are derived relating the positions of the phase shift zeroes for different nuclei and different orbital momenta. A good agreement between theoretical and experimental phases and a correct form of the radial functions show that the interactions proposed are reasonable. (auth)

43787 SATURATION FOR INTERACTION WITH A HARD CORE. Maksimenko, V. N.; Steshenko, A. I. (Inst. of Theoretical Physics, Kiev). Yadern. Fiz.; 13: No. 4, 707-11(Apr 1971). (In Russian).

Taking light double-magic nuclei ^{4}He, ^{16}O, and ^{40}Ca as examples, the possibility of getting stability in view of a collapse for some pair exchange central potentials with a hard core is investigated. The calculation was done by means of the variational method with oscillator functions. The hard core is taken into account in the gas approximation. The result is found to be negative. (auth)

43788 STUDY OF THE NEUTRON CONTINUUM FROM THE INTERACTION OF ^{7}Li WITH ^{3}He. Lin, Jung. Athens, Ga.; Univ. of Georgia (1970). 71p. University Microfilms Order No. 71-13,081.

Thesis.

Neutron continuous energy distributions resulting from the bombardment of ^{7}Li by ^{3}He were measured at ^{3}He energy range of 1 to 2 MeV. Time-of-flight spectra were taken with a liquid scintillator mounted on a space charge saturated photomultiplier tube. Relative differential cross sections were measured at laboratory angles from 0 to 130° in 10° steps. The results were used to search for a possible level of 7 MeV in ^{9}B and also analyzed by a PWBA calculation with a p-n pair final state interaction to determine the dominant reaction process which produced the observed neutron continua. Both the direct, ^{7}Li(^{3}He,pn)^{8}Be, and the sequential, ^{7}Li(^{3}He,p)^{9}Be(n)^{8}Be and ^{7}Li(^{3}He,n)^{9}B(p)^{8}Be, processes are possible to produce the observed neutron continuum. As the result of this investigation, the existence of a level of 7 MeV in ^{9}B is negative and the observed neutron continuous spectra very likely result from a direct three particle breakup process through the first excited state of ^{8}Be. (Diss. Abstr. Int., B)

43789 REACTION D(d,n)^{3}He AT 0^0 WITH POLARIZED BEAM: A NEW SOURCE OF POLARIZED NEUTRONS FROM 7 TO 18 MeV. Simmons, J. E.; Broste, W. B.; Lawrence, George P.; McKibben, Joseph L.; Ohlsen, Gerald G. (Los Alamos Scientific Lab., N. Mex.). Phys. Rev. Lett.; 27: No. 2, 113-17(12 Jul 1971).

Experimental results are reported for the neutron polarization from the reaction D(d,n)^{3}He at 0° with the incoming beam polarized to the extent $p_3 = p_{33} \approx 0.82$ perpendicular to the direction of motion, where p_3 and p_{33} are components of vector and tensor polarizations, respectively. The measured neutron polarization varies in the range 0.65 to 0.72 for E_d in the range 4.1 to 15.1 MeV. The measurements are consistent with a process in which the neutron spin suffers little interaction. The influence of the deuteron D state is noted. Comparison is made to several other sources of polarized neutrons, with the conclusion that near $E_n = 10$ MeV this process is outstanding. (auth)

43790 CALCULATION OF THE MEAN NEUTRON ENERGY FROM D(d,n)^{3}He REACTION BY USE OF THICK DEUTERIUM TARGETS. Haensgen, H.; Nitzsche, M. (Technische Univ., Dresden). Kernenergie; 14: No. 1, 26-7(Jan 1971). (In German).

If thick deuterium targets are used in the nuclear reaction D(d,n)^{3}He, the mean energy of the neutrons emitted is of interest. A method is given for obtaining this mean energy from the integral yield of neutrons per deuteron determined experimentally. (auth)

43791 THREE-NEUTRON RESONANCE IN THE REACTION ^{3}He(π^-,π^+)3n. Reitan, A. (Univ., Trondheim, Norway). Phys. Lett.; 35B: No. 5, 368-70(21 Jun 1971).

The cross section for the reaction ^{3}He(π^-,π^+)3n, leading to a possible low-energy resonance in the three-neutron system, is estimated. (auth)

43792 TRITON CALCULATIONS IN A HARMONIC OSCILLATOR BASIS WITH REALISTIC POTENTIALS. Jackson, A. D. (State Univ. of New York, Stony Brook). Phys. Lett.; 35B: No. 5, 365-7(21 Jun 1971).

By using the Reid potential and a basis of translationally invariant harmonic oscillator states of good particle permutation symmetry, the binding energy of the triton is calculated to be 6.30 MeV. (auth)

43793 DETERMINATION OF THE ABSOLUTE CROSS SECTION FOR THE ^{3}He(d,p)^{4}He REACTION. Carlton, Robert Free-

man. Athens, Ga.; Univ. of Georgia (1970). 61p. University Microfilms Order No. 71-13,034.

Thesis.

The angular distribution of the protons from the reaction was found to be isotropic at deuteron energies of 250, 450, 650 and 850 keV. The yield of the reaction at resonance (E_d = 450 keV was 770 ± 39 mb. Resonance parameters for the 16.6 MeV level of ^{5}Li were obtained using the Breit–Wigner single level formalism. These parameters are seen to be dependent on the choice of interaction radius. (Diss. Abstr. Int., B)

43794 BRUECKNER CALCULATIONS FOR LIGHT NUCLEI. Tripathi, Ram Kishore. Lawrence, Kan.; Univ. of Kansas (1970). 86p. University Microfilms Order No. 71-13,373.

Thesis.

The Brueckner theory is applied to calculate the binding energy for ^{3}H, ^{4}He, and ^{16}O using Hamada–Johnston, Yale and Reid (h.c.) potentials. To test the accuracy of the calculation and to investigate if a shift of the spectrum is needed, the Goldhammer potential is used. The agreement between the variational and Brueckner calculations for ^{3}H and the agreement with perturbation calculations for all nuclei considered show that the Brueckner method is quite accurate. The results further testify that no shift of the particle spectrum is warranted. All the three realistic forces underbind the finite nuclei. (Diss. Abstr. Int., B)

43795 BINDING ENERGY OF THE TRITON WITH THE HAMADA–JOHNSTON POTENTIAL. Hu, Chi-yu (California State Coll., Long Beach). Phys. Rev., C; 3: No. 6, 2151-5(Jun 1971).

A variational method that involves solution of inhomogeneous linear equations is used to calculate the wave function and binding energy of the triton. Cohen and Willis's classification of the triton wave function [Nucl. Phys., 32: 114(1962)] is employed. Internal wave functions are expanded in terms of polynomials of the interparticle distances up to 170 terms. A binding energy of −6.7 MeV is obtained for the unmodified Hamada–Johnston potential. Due to the simplicity of the variational wave function, all the matrix elements are evaluated analytically in terms of the exponential integrals. With the aid of recurrence relations, computing time is reduced to a minimum. (auth)

43796 CROSS-SECTION AND POLARIZATION MEASUREMENTS FOR THE ^{3}H(^{3}He,n)^{5}Li REACTION. Klopcic, J. T.; Darden, S. E. (Univ. of Notre Dame, Ind.). Phys. Rev., C; 3: No. 6, 2171-9(Jun 1971).

Measurements of the angular distribution and polarization of neutrons from the reaction ^{3}H(^{3}He,n)^{5}Li were made for mean ^{3}He bombarding energies of 2.70 and 3.55 MeV. Polarizations were measured using a ^{4}He gas scintillator, and cross sections were determined using a liquid scintillator employing pulse-shape discrimination. Contributions from the three-body breakup channel ^{3}H(^{3}He,np)^{4}He were removed by assuming these neutrons to be unpolarized and to have a statistical energy distribution in the high-energy portion of the neutron spectrum. The angular distribution of neutrons from the reaction ^{3}H(^{3}He,n)^{5}Li exhibits a broad peak in the vicinity of $\theta_{c.m.}$ = 45°. The neutron polarization was found to be negative at all angles investigated, and reaches a minimum value of −0.30 at $\theta_{c.m.}$ = 125°, $E_{^3He}$ = 2.7 MeV. Excitation functions for the cross section were measured at laboratory angles of 0 and 40° for ^{3}He energies between 0.7 and 3.8 MeV. The reaction data can be reproduced qualitatively by a simple two-nucleon-transfer distorted-wave Born-approximation calculation, but the ^{3}He–^{3}H potential parameters used do not reproduce published elastic scattering data at somewhat higher energy. (auth)

43797 STUDY OF p + ^{3}He AND n + ^{3}H SYSTEMS WITH THE RESONATING-GROUP METHOD. Reichstein, I.; Thompson, D. R.; Tang, Y. C. (Univ. of Minnesota, Minneapolis). Phys. Rev., C; 3: No. 6, 2139-48(Jun 1971).

The p + ^{3}He and n + ^{3}H systems are considered with the resonating-group method in the one-channel approximation. A purely central nucleon–nucleon potential that has different ranges in the singlet and triplet states is employed. The internal wave function of the three-nucleon cluster is a sum of two Gaussian functions, with its parameters adjusted to reproduce quite well the properties of the cluster. From the results obtained it is found that the agreement with experiment is quite satisfactory, although in the very low-energy region, detailed fit is not obtained; this lack of agreement is most probably due to the omission of the specific distortion effect in the calculation. An effective interaction between the clusters is also constructed. From this effective interaction it is concluded that the requirement of antisymmetry for the total wave function is very important; in particular, it creates an odd–even feature, wherein the effective potentials in the odd-l and even-l states are quite different. (auth)

43798 ^{1}H(n,n)^{1}H SCATTERING OBSERVABLES REQUIRED FOR HIGH-PRECISION FAST-NEUTRON MEASUREMENTS. Hopkins, J. C. (Los Alamos Scientific Lab., N. Mex.); Breit, G. Nucl. Data, Sect. A; 9: 137-45(Mar 1971).

Values of the free n–p scattering total cross sections, differential cross sections, and polarization for neutron energies between 100 keV and 30 MeV are given. These are important numbers because they are used as standards for most fast-neutron cross-section measurements above 2 MeV and are frequently used at much lower energies. The relevant n–p and p–p data, much of which has not been used in previous evaluations of the n–p cross sections, is discussed. It is shown that the differential cross sections below 10 MeV do not possess the isotropy frequently assumed; in fact, the cross-section ratios $\sigma(180°)/\sigma(90°)$ are approximately 1.023 at 7 MeV, 1.011 at 3 MeV, and 1.004 at 1 MeV. These ratios, minus 1.000, are higher than the values predicted by the Gammel formula by factors of about 2 at 7 MeV, 5 at 3 MeV, 8 at 2 MeV, and 18 at 1 MeV. In addition, it is shown that the shape of the differential cross section is far from symmetric about 90°, the 0° cross section, in fact, being less than the 180° cross section for all energies below 30 MeV. The cross sections given here differ significantly from previous estimates based only upon n–p data up to 30 MeV. The present results are derived from calculations using phase shifts obtained by the Yale N–N Interaction Group. Comparisons are made with the results obtained from calculations employing the Lawrence Radiation Laboratory (LRL) and Dubna phase shifts. In all cases, the general features of large anisotropy and nonsymmetry are verified. (auth)

43799 PHASE PARAMETERS FOR NUCLEON–DEUTERON SCATTERING. Sloan, I. H. (Univ. of New South Wales, Kensington, Australia). Nucl. Phys.; A168: No. 1, 211-24(1971).

Phase shifts and inelastic parameters (both unsplit) are calculated for nucleon–deuteron scattering below 40 MeV, using central, separable, spin-dependent two-nucleon interactions. The results are compared with those obtained by van Oers and Brockman from phase-shift analyses of experiments. The agreement is fair for the real parts of the phase shifts, but rather poor for the inelastic parameters. It is argued that there may be substantial errors in the inelastic parameters from the phase-shift analyses. In particular, one of the assumptions in that work, that the ^{4}S and ^{2}S inelastic parameters are equal, is strongly contradicted by the theoretical results. The theoretical results are also used in calculations of differential and total break-up cross sections, and in a discussion of recent N/D calculations of nucleon–deuteron scattering. (auth)

Nuclear Properties and Reactions, 6 ≤ A ≤ 19

Refer also to abstracts 42131, 43779, 43780, 43787, 43794, 43832, 43884, 43889, 43916, 43956, 43967, 43978, and 43979.

43800 (NP-18880) STUDY OF THE (p,px) REACTION WITH LIGHT NUCLEI AT 156 MeV. Bachelier, Daniel (Paris Univ., Orsay (France). Faculte des Sciences). [1970]. 74p. (In French). Dep. NTIS (U. S. Sales Only).

Thesis.

The angular correlations of the quasi-elastic scattering reactions ^{6}Li(p,pd)^{4}He, ^{6}Li(p,p^{3}He)^{3}H, ^{7}Li(p,pt)^{4}He and ^{12}C(p,pd)^{10}B and the energy spectra of the residual nucleus in the ^{12}C(p,pd)^{10}B reaction were studied. Improvements in thick semiconductor detector technology and on-line computers led to a new experimental technique. The results show that the ratio of the probabilities of finding the ^{6}Li nucleus in the form (^{4}He + ^{2}H) to the form (^{3}He + ^{3}H) is 0.43 and the probabilities of finding ^{6}Li in the form (^{4}He + ^{2}H) and ^{7}Li in the form (^{4}He + ^{3}H) are equal. In the ^{12}C(p,pd)^{10}B reaction, when the flip-spin is negligible, the nuclear levels excited are at 0.72 MeV, 2.15 MeV, and, to a lesser degree, around 15 MeV. The spectrum obtained is in good agreement with the theoretical prediction of Balashov et al. made from the intermediate-coupling shell model. (France)

43801 (UCLA-10-P-18-31) MEDIUM ENERGY STUDIES OF THE (p,pα) REACTION ON LIGHT NUCLEI. Quinn, James R. (California Univ., Los Angeles. Dept. of Physics). Apr 1970. 118p. Dep. NTIS.

The coplanar energy and angular correlations of the protons and alpha particles emitted from the (p,pα) reactions with ^{9}Be, ^{16}O, and ^{20}Ne were observed at 46.8 MeV. The ^{9}Be(p,pα) reaction was also observed at 35.0 and 26.0 MeV. The interaction is viewed in the Impulse Approximation, in which the incident

XUM

proton interacts only with an alpha cluster in the target nucleus. The momentum distribution of the alpha cluster is calculated from the measured cross sections by using this simple model of the interaction. The ^{9}Be data are well fitted by this model at 46.8 MeV. At lower incident energies, the quasi-elastic yield is reduced—the reaction proceeds primarily by a sequential mechanism at 26.0 MeV. The cluster-model parameters resulting from the Impulse Approximation analysis of these data reflect the effects of absorption of the quasi-elastically scattered particles and/or the effects of the increased de Broglie wavelength when compared to results obtained at higher energy. The ^{20}Ne and ^{16}O data also show possible evidence of absorption. The ^{16}O results give no indication of a quasi-elastic scattering mechanism. Some indication of quasi-elastic p–α scattering is, however, observed in Ne. (R.W.R.)

43802 (UCRL-20480) ISOSPIN PURITY AND VIOLATIONS OF MIRROR SYMMETRY: THE BETA-DELAYED PROTON DECAY OF ^{9}C, ^{13}O, ^{17}Ne, AND ^{33}Ar. Esterl, John Edward (California Univ., Berkeley. Lawrence Radiation Lab.). Mar 1971. Contract W-7405-eng-48. 111p. Dep. NTIS.

Thesis.

Beta-delayed proton studies of some light A = 4n + 1, $T_z = -3/2$ nuclei were made, with supplementary γ-ray measurements where necessary. A fast gas-transport system and particle-identification techniques combined to produce proton spectra in which the resolution was limited by the momentum spread of the preceding beta-ray. The half-lives measured are as follows: ^{9}C, 126.5 ± 1.0 ms; ^{13}O, 8.95 ± 0.20 ms; ^{17}Ne, 109.0 ± 1.0 ms; and ^{33}Ar, 173.0 ± 2.0 ms. Precise level energies in ^{17}F and ^{33}Cl were measured, and a discrepancy concerning levels in ^{17}F was resolved. Absolute log-ft values for the β-decay branches of ^{13}O, ^{17}Ne, and ^{33}Ar were obtained; these measurements indicate violations of mirror symmetry in beta decay. They also indicate that the lowest T = 3/2 state in ^{17}F has an isospin purity of ≥95%, in contrast to the lowest T = 3/2 state in ^{33}Cl, for which an impurity of ~10% is suggested. Circumstantial evidence indicates that four T = 1/2 states within 350 keV of the analog state cause the impurity observed in ^{33}Cl. (auth)

43803 ^{6}Li(α,2α) REACTION AS A TEST OF THE EXISTENCE OF α PARTICLES IN ^{6}Li. Deconninck, G. (Univ., Louvain, Belgium); Giorni, A.; Longequeue, J. P.; Maillard, J. P.; Chan, Tsan Ung. Phys. Rev., C; 3: No. 6, 2085-91 (Jun 1971).

The presence of a strong discontinuity in the free $\alpha-\alpha$ scattering amplitude at 40 MeV is used as a probe for the identification of α clusters in nuclei. The ^{6}Li(α,2α) reaction is investigated at 37.5 and 43.5 MeV with the deuteron as spectator in order to produce quasi-free scattering conditions. The distributions measured at these two energies are found to be very different in magnitude as well as in structure, and this phenomenon is attributed to the presence of $\alpha-\alpha$ scattering in the $\alpha-^{6}$Li collision. Calculations based on the plane-wave impulse approximation are unable to reproduce the distributions even qualitatively. A calculation based on the graph formalism that takes into account the exact phase-shift amplitude of the free $\alpha-\alpha$ collision fits the two distributions with the same set of parameters. One may conclude that these observations are in favor of the existence of α particles inside the ^{6}Li nucleus. (auth)

43804 OPTICAL MODEL ANALYSIS OF ^{9}Be(p,p$_0$)^{9}Be CROSS SECTIONS AND POLARIZATIONS FROM 6 MeV TO 30 MeV. Werby, Michael F. (Florida State Univ., Tallahassee); Edwards, Steve; Thompson, William J. Nucl. Phys.; A169: No. 1, 81-94(1971).

Cross-section and polarization data for proton elastic scattering from ^{9}Be in the lab energy range 6 to 30 MeV and in the angular range 20° to 160° were analyzed using an optical model potential. Good quality fits are obtained with potential parameters which vary smoothly with energy. The effects of energy-averaged compound-nucleus resonances and of quadrupole coupling on the elastic scattering are investigated. The reaction is suggested for use as a polarization monitor since it compares favorably with α(p,p)α for this purpose. Contour maps of polarization, P, and cross section times ^{2}P are given as a function of angle and energy. (auth)

43805 ^{7}Li(p,n)^{7}Be NEUTRON POLARIZATION MEASUREMENTS FOR E_p = 3.0 TO 5.5 MeV. Thornton, S. T.; Morris, C. L.; Smith, J. R.; Fogel, R. P. (Univ. of Virginia, Charlottesville). Nucl. Phys.; A169: No. 1, 131-44(1971).

Angular distributions of neutron polarization were measured for ^{7}Li(p,n$_0$)^{7}Be and ^{7}Li(p,n$_1$)^{7}Be* at proton energies 3.0, 3.5, 4.0, 4.5, 5.0 and 5.5 MeV. From Legendre polynomial fits of $\sigma(\theta)$ and associated Legendre polynomial fits of $P(\theta)\sigma(\theta)$, contour maps of $P(\theta)$ and $P^{2}(\theta)\sigma(\theta)$ were produced. Levels in the compound nucleus ^{8}Be and the reaction mechanism are discussed. (auth)

43806 PIONIC COMPLEX LEVEL SHIFTS AND OPTICAL POTENTIAL PARAMETERS IN TERMS OF THE π–N SCATTERING LENGTH. Konishi, Yozo; Narumi, Hajime (Hiroshima Univ.). Progr. Theor. Phys. (Kyoto); 45: No. 4, 1351-2(Apr 1971).

The optical potential parameters are determined through the pionic complex level shifts for carbon-12 and oxygen-16 in terms of the π-N scattering length. The pionic 2p-1s transition rate for carbon-12 is also evaluated. (L.B.S.)

43807 ELASTIC SCATTERING OF ELECTRONS FROM THE OXYGEN ISOTOPES. Singhal, Ravi Prakash. Saskatoon, Saskatchewan; Univ. of Saskatchewan (1970). 128p. University Microfilms Order No. 71-13,775.

Thesis.

Elastic scattering of electrons was used to measure the root mean square charge radii of the oxygen isotopes (^{16,17,18}O). The momentum transfer range covered was from 0.392 fm^{-1} to 0.993 fm^{-1} and the oxygen isotopes were in gaseous form. A gas target was designed for these experiments. It is an all welded assembly in the form of a vertical cylinder. The gas target system allows the cooling of the gas target cell through a cryostat mounted inside the scattering chamber. An efficient isotope recovery system makes possible the repeated use of the enriched isotope samples. The data were analyzed to extract the RMS radii of ^{17,18}O relative to ^{16}O. The absolute value of the ^{16}O RMS radius was obtained by comparing the electron scattering from ^{16}O with that from the proton. A χ^2-fit was used to obtain the values and the uncertainties in the RMS radii. The results show that the RMS radius of ^{16}O is bigger than that of ^{17}O. ^{18}O is seen to be larger than ^{16}O, but only by about half the amount required by the $A^{1/3}$ law. The absolute value of the RMS radius of ^{16}O is in very good agreement with previous measurements. A comparison of the ^{16}O charge distribution is made with the predictions of Hartree–Fock theory. (Diss. Abstr. Int., B)

43808 EXPERIMENTAL TEST OF THE ISOBARIC MULTIPLET MASS EQUATION. Trentelman, George Frederick. East Lansing, Mich.; Michigan State Univ. (1970). 82p. University Microfilms Order No. 71-11,993.

Thesis.

The ground state mass excesses of ^{9}C, ^{13}O, and ^{21}Mg were determined through measurement of the Q-values of the ^{12}C(^{3}He,^{6}He) ^{9}C, ^{16}O(^{3}He,^{6}He)^{13}O, ^{24}Mg(^{3}He,^{6}He)^{21}Mg reactions. These mass excesses represent the $T_z = -3/2$ members of the T = 3/2 quartets for A = 9, 13, and 21 respectively, and for ^{13}O and ^{21}Mg represent measurements of improved accuracy. These experimental values for the quartet members are used to test the isobaric multiplet mass equation (IMME) $M(\alpha,T,T_z) = a(\alpha,T) + b(\alpha,T)T_z + c(\alpha,T)T_z^2$. The measurements were made using 68–70 MeV ^{3}He beams, and a split pole magnetic spectrograph as an energy analyzer. An energy calibration procedure for the spectrograph and beam analysis system with proton and ^{3}He beams was developed, and was proven valuable in making precision Q-value measurements at high bombarding energies. The mass excess of ^{9}C was measured as 28.911 ± 0.009 MeV, that of ^{13}O as 23.103 ± 0.014 MeV, and that of ^{21}Mg as 10.912 ± 0.018 MeV. In addition, Coulomb radii for a uniformly charged sphere model for A = 9, 13, 17, 21, 25, and 37 were extracted from the coefficients of the IMME. (Diss. Abstr. Int., B)

43809 STUDY OF THE REACTIONS ^{7}Li(d,t)^{6}Li AND ^{7}Li(h,α) ^{6}Li. Zander, Arlen Ray. Tallahassee; Florida State Univ. (1970). 127p. University Microfilms Order No. 71-13,522.

Thesis.

Yield curves for the elastic scattering process ^{7}Li(d,d)^{7}Li and for the reaction ^{7}Li(d,t)^{6}Li were measured at bombarding energies ranging from 10 to 12 MeV. Detailed angular distributions for both processes were measured at 12 MeV incident energy. The elastic scattering process was analyzed with a standard optical model calculation, and the results were utilized in a conventional distorted-wave Born-approximation (DWBA) analysis of the reaction data. Absolute spectroscopic factors were extracted for the reaction. For the reaction ^{7}Li(^{3}He,α)^{6}Li, excitation functions were obtained at selected angles with bombarding energies ranging from 16 to 18 MeV. Detailed angular distributions, measured at 16, 17 and 18 MeV, were analyzed with conventional zero-range DWBA calculations and with finite-range DWBA calculations. The zero-range results are compared to the finite-range results, and absolute spectroscopic factors are extracted in both cases. (Diss. Abstr. Int., B)

43810 ELASTIC SCATTERING OF DEUTERONS AND ALPHA PARTICLES BY ^{6}Li AND ^{7}Li. Bingham, Hans Gabers Jr. Tallahassee; Florida State Univ. (1970). 124p. University Microfilms Order No. 71-13,486.

Thesis.

Angular distributions and absolute cross section measurements for the reactions ^{6}Li(α,α_0)^{6}Li and ^{7}Li(α,α_0)^{7}Li were obtained for

incident energies of from 12–18 MeV over an angular range of $\theta_{c.m.} \sim 20–160°$. Yield curves for the scattering show resonance structure corresponding to the 14.0 MeV level in the compound system ^{10}B and the 16.9 MeV and 18.3 MeV levels in the compound system ^{11}B. Tentative values of l = 3, l = 2 and l = 1, respectively, are assigned to the relative orbital angular momentum involved in the formation of these compound levels. The optical model with an I · l interaction term in the optical potential was used to describe the elastic scattering. For the lower energies the best parameter sets are for $^6Li(\alpha,\alpha_0)^6Li$, V = 189.5 MeV, W' = 7.1 MeV, $V_{l\text{-}l}$ = 10.8 MeV, R = 3.51 fm, a = 0.60 fm and for $^7Li(\alpha,\alpha_0)^7Li$, V = 143.6 MeV, W' = 4.5 MeV, $V_{l\text{-}l}$ = 5.1 MeV, R = 3.27 fm and a = 0.73 fm. The optical model was used to describe scattering from the reaction $^6Li(d,d_0)^6Li$ with best parameters for the 8.0 MeV data being V = 92.6 MeV, W' = 18.6 MeV, V_{s0} = 8.6 MeV, R = 3.93 fm and a = 0.61 fm. The effects of exchange elastic scattering for the three reactions were investigated using the finite-range, three-potential, DWBA computer code FANLU2. No absolute exchange magnitude could be determined. (Diss. Abstr. Int., B)

43811 ISOSPIN NONCONSERVATION IN REACTION $^{12}C(d,\alpha_0)^{10}B(1.74,T = 1)$. von Ehrenstein, D. (Argonne National Lab., Ill. Northern Illinois Univ., DeKalb); Meyer-Schuetzmeister, L.; Monahan, J. E.; Richter, A.; Stoltzfus, J. C. Phys. Rev. Lett.; 27: No. 2, 107-9(12 Jul 1971).

The isospin-forbidden reaction $^{12}C(d,\alpha_0)^{10}B(1.74,T = 1)$ was investigated for E_d = 14.0 to 17.0 MeV. Several full angular distributions were obtained and the excitation function from E_d = 16.0 to 17.0 MeV was measured at $\theta_{lab} = 152°$. In the light of these new data, it is clearly not sufficient to interpret the reaction in terms of simple compound-nucleus formation, as seemed to be indicated in previous investigations. (auth)

43812 PROTON CAPTURE BY ^{17}O. Zaremba, Loren Andrew. College Park, Md.; Univ. of Maryland (1970). 145p. University Microfilms Order No. 71-12,181.

Thesis.

A search for states in ^{18}F having excitation energies between 5.8 and 7.1 MeV was conducted using the $^{17}O(p,\gamma)^{18}F$ reaction. Resonances in the gamma-ray yield were observed at proton energies of 519, 561, 588, 674, 716, 748, 827, 932, 1098, 1242, 1273 and 1345 keV. Of these, the resonances at 561, 588 and 716 keV, corresponding to ^{18}F levels at 6.138, 6.165 and 6.286 MeV have not been reported in previous studies of this region using the $^{14}N + \alpha$ and $^{17}O(p,\alpha_0)$ reactions. Branching ratios and (p,γ) cross sections were measured for these three states and these data were used to determine radiative and reduced proton widths. Spectra used in the determination of the branching ratios were also used to obtain a direct determination of the Q-value of the $^{17}O(p,\gamma)^{18}F$ reaction. The $^{17}O(p,\alpha_0)$ reaction was investigated in a specific effort to observe these three levels. The 588 and 716 keV resonances were observed to be extremely weak and the 561 keV resonance was not observed. The differential cross sections of these resonances in the (p,α_0) reaction were determined at a laboratory angle of 120° and these data were used to obtain reduced alpha widths. Angular correlation and distribution measurements were made to determine the spins of the 6.138, 6.165 and 6.286 MeV levels. On the basis of these data and reduced width considerations, most probably assignments are $J^\pi = 0^+$, 3^+ and 2^+, respectively. The gamma-ray decay properties of the 6.138, 6.165 and 6.286 MeV levels were compared with theoretical decay schemes for the ^{18}F analogs of the 5.33, 5.37 and 5.25 MeV levels of ^{18}O using the wave functions of Benson and Flowers. The results support identification of the 6.138 and 6.165 MeV levels as the analogs of the 5.33 and 5.37 MeV states of ^{18}O. However, agreement between the observed gamma decay properties of the 6.286 MeV level and those calculated for the analog of the 5.25 MeV state of ^{18}O is poor. (Diss. Abstr. Int., B)

43813 RADIATIVE PROTON CAPTURE STUDIES IN THE GIANT RESONANCE REGION OF LOWER 1_p SHELL NUCLEI. Fisher, Gerald Allen. Stanford, Calif.; Stanford Univ. (1970). 113p. University Microfilms Order No. 71-12,899.

Thesis.

The giant resonance regions of the nuclei ^9Be and ^{10}B were investigated by means of the inverse (p,γ) reaction. The yields and angular distributions were measured for both the ground and first excited state transitions in both nuclei. The angular distributions expressed as a series of Legendre polynomials, are interpreted in terms of the contributing negative parity dipole states formed from the principal 1p-1h excitations. The characteristics of both the (p,γ) yields and angular distributions of ^9Be and ^{10}B are compared to the well-documented properties that have come to be regarded as "typical" of the giant resonances of nuclei. Of particular interest is the strength of the reaction in terms of the classical dipole sum. The gamma decays of the low lying resonances (E_x < 20 MeV) in these nuclei were also studied. The M1 transition strengths of the known levels in ^8Be at E_x = 18.15 MeV and E_x = 19.05 MeV are presented and compared to the predictions of Kurath; evidence for a possible parity assignment of the latter state is given. Similar positive parity energy levels which decay to the low lying bound states of ^{10}B are also suggested; the predictions of an intermediate coupling calculation are utilized in making possible J^π assignments to some of these states. (Diss. Abstr. Int., B)

43814 BROAD ENERGY PROTONS FROM THE REACTION $^{12}C + d \rightarrow p + {}^{13}C$ (7.64 MeV AND 8.33 MeV). Hosono, Kazuhiko (Osaka Univ.); Kakigi, Shigeru; Nakamura, Hitoshi; (and others). Bull. Inst. Chem. Res., Kyoto Univ.; 48: No. 6, 269-75(Dec 1970).

Broad energy spectra of protons leading to the resonance states of ^{13}C were observed in the $^{12}C(d,p)^{13}C$ reaction as a deuteron energy of 14.60 MeV. These proton spectra are compared with cross sections based on the phase shifts of neutron–^{12}C scattering. Peak positions agree with those predicted from the phase shifts, but the relative heights of the peaks disagree with the theoretical prediction. The phase shifts that can fit the proton spectra are obtained inversely from the experimental results, and an anomalous behavior of the phase shifts obtained is discussed. (auth)

43815 RESIDUAL POTENTIAL AND NUCLEON CORRELATION IN THE SHELL MODEL. I. E2 TRANSITION IN ^6Li. Lodhi, M. A. K. (Texas Tech. Univ., Lubbock). Phys. Rev., C; 3: No. 6, 2116-32(Jun 1971).

The effect of a class of residual potentials in the Hamiltonian and nucleon–nucleon correlation on calculations in the independent-particle shell-model wave function of ^6Li is investigated. A method is developed to give minimum energies of various states of a nuclear system with a somewhat realistic Hamiltonian and wave function. The results on energy calculations are in good agreement with the observed data. The E2 transition rate and other relevant observables pertaining to this transition are calculated by using this wave function and several others. Comparison of the results of these calculations with experimental data and other theoretical predictions shows a definite preference for the correlated wave function of ^6Li developed here. The method is convenient for application to other nuclear systems. (auth)

43816 $^6Li + {}^6Li$ SCATTERING AT $E_{c.m.}$ = 5 TO 17 MeV. Fortune, H. T.; Morrison, G. C.; Siemssen, R. H. (Argonne National Lab., Ill.). Phys. Rev., C; 3: No. 6, 2133-9(Jun 1971).

For the elastic scattering of ^6Li by ^6Li, excitation functions at cm angles of 60, 70, 80, and 90° were studied in the cm energy range 5 to 17 MeV; and angular distributions were measured at cm energies of 6, 10, and 14 MeV. The excitation functions are relatively featureless, with a broad gross-structure peak at 90° centered around 13 MeV. Good fits to individual angular distributions are obtained with the optical model and, except for the highest energies studied, parametrized phase-shift calculations. These calculations, however, do not correctly reproduce the energy dependence of the data. The single most outstanding conclusion from the present analysis is that $^6Li + {}^6Li$ scattering is dominated by absorption, and that this dominance leads to scattering behavior very different from that found for other heavy ions. (auth)

43817 ^{13}B NUCLEAR MAGNETIC DIPOLE MOMENT. Williams, R. L. Jr. (Johns Hopkins Univ., Baltimore. Brookhaven National Lab., Upton, N. Y.); Madansky, L. Phys. Rev., C; 3: No. 6, 2149-50(Jun 1971).

Polarized ^{13}B nuclei were produced through the $^{11}B(t,p)^{13}B$ reaction by using a 3.5-MeV Van de Graaff accelerator. The recoiling nuclei were stopped in Au, Pd, and Pt foils, and the effective dipole moments of ^{13}B in these metals were measured by a resonant depolarization technique. From earlier measurements of the spin-lattice relaxation times of ^{12}B in the same metals, the magnetic effects of the stopping foils were estimated. If a common enhancement factor is used for the three metals, the ^{13}B magnetic dipole moment is found to be $\mu(^{13}B) = +3.17712(51)\mu_N$, the plus sign being inferred from the Schmidt limits for odd-proton spin-$\frac{3}{2}$ nuclei. (auth)

43818 EXCITATION FUNCTIONS OF ^7Be AND ^{11}C PRODUCED IN NITROGEN BY LOW-ENERGY PROTONS. Epherre, M.; Seide, C. (CNRS, Orsay, France). Phys. Rev., C; 3: No. 6, 2167-71 (Jun 1971).

The cross sections for the production of ^{11}C and ^7Be by protons from a ^{14}N target was measured at energies from 5 to 24 MeV for ^{11}C and 13 to 42 MeV for ^7Be. A sharp rise above the thresholds for the $^{14}N(p,\alpha)$ and $^{14}N(p,2\alpha)$ reactions was observed, with maxima around 200 and 45 mb, respectively. (auth)

XUM

43819 T = 1 STATES IN THE A = 12 SYSTEM. Monahan, J. E. (Argonne National Lab., Ill.); Fortune, H. T.; Vincent, C. M.; Segel, R. E. Phys. Rev., C; 3: No. 6, 2192-7(Jun 1971).

An analysis of available data, with emphasis on the ^{11}B(d,p) and ^{11}B(p,x) reactions, indicates that the analogs of the first seven ^{12}B states can be identified in ^{12}C. Neutron reduced widths $\gamma^2_{\lambda n}$ for the first six states in ^{12}B are calculated from spectroscopic factors, which were extracted from the ^{11}B(d,p) data by use of a distorted-wave Born-approximation analysis. Proton reduced widths $\gamma^2_{\lambda p}$ of the ^{12}C analog states are deduced from observed widths by use of an R-matrix formulation. It is found that the analog relationship $\gamma^2_{\lambda n}/2\gamma^2_{\lambda p} = 1$ is satisfied to within ~30% for all of the observed pairs of states, except for the pair corresponding to the ^{12}B first excited state. The possibility that this discrepancy is due to experimental error is discussed. (auth)

43820 LIFETIME OF THE FIRST EXCITED STATES OF ^{11}Be. Hanna, S. S.; Nagatani, K.; Harris, W. R.; Olness, J. W. (Brookhaven National Lab., Upton, N. Y.). Phys. Rev., C; 3: No. 6, 2198-2204(Jun 1971).

The mean lifetime of the first excited state of ^{11}Be at 0.32 MeV was measured by the Doppler-shift-attenuation method. The result, 0.18 ± 0.06 psec, corresponds to a very strong E1 transition, 0.33 W.u. This value is in very good agreement with a simple harmonic-oscillator picture of the $2s_{\frac{1}{2}} \rightarrow 1p_{\frac{1}{2}}$ transition, which gives 0.32 W.u. However, the agreement is probably fortuitous, since the same model fails for the analogous transition in ^{13}C, which is an order of magnitude too slow. No simple model relieves this discrepancy. The energy of the state in ^{11}Be is found to be 319.8 ± 0.2 keV. (auth)

43821 MUON CAPTURE IN ^{6}Li IN THE DITRITON CHANNEL. Wienke, B. R.; Meyer, S. L. (Northwestern Univ., Evanston, Ill.). Phys. Rev., C; 3: No. 6, 2179-85(Jun 1971).

The reaction $\mu^- + {}^6\text{Li} \rightarrow {}^3\text{H} + {}^3\text{H} + \nu$ is analyzed within the context of the impulse approximation by using the current-current theory of weak interactions and an α-d model of ^{6}Li fitted to the binding energy and charge radius of ^{6}Li. The model is tested by considering the channel $\mu^- + {}^6\text{Li} \rightarrow {}^6\text{He} + \nu$. Within the limitations of the stated approximations, total rates are estimated for these two modes, and the combined triton distribution is given for the ditriton channel. (auth)

43822 YIELD CURVES FOR Li + Li AND Li + Be NUCLEAR REACTIONS. Wyborny, H. W.; Carlson, R. R. (Univ. of Iowa, Iowa City). Phys. Rev., C; 3: No. 6, 2185-91(Jun 1971).

Differential cross sections for ^{6,7}Li + ^{6,7}Li and ^{6,7}Li + ^{9}Be nuclear reactions leading to low-lying residual-nucleus states were measured over the energy range from 4 to 14 MeV. In the ^{7}Li(^{7}Li,α)^{10}Be (3.37) case, the energy range was extended to 2.1 and 21 MeV. Striking enhancement and weakening of cross sections for formation of the 0.72-MeV state in ^{10}B can be attributed to cluster structure of lithium nuclei. Resonance-like peaks are observed in some yields. Their general character is consistent with an extended-structure interpretation of the reaction mechanism. (auth)

43823 PRECISION MASS MEASUREMENT OF ^{9}C, ^{13}O, AND ^{21}Mg AND THE ISOBARIC-MULTIPLET MASS EQUATION. Trentelman, G. F.; Preedom, B. M.; Kashy, E. (Michigan State Univ., East Lansing). Phys. Rev., C; 3: No. 6, 2205-13(Jun 1971).

The ground-state masses of ^{9}C, ^{13}O, and ^{21}Mg were determined through measurement of the Q values of the ^{12}C(^{3}He,^{6}He)^{9}C, ^{16}O(^{3}He,^{6}He)^{13}O, and ^{24}Mg(^{3}He,^{6}He)^{21}Mg reactions. The measurements were made with 68- to 70-MeV ^{3}He beams by using a split-pole magnetic spectrograph. A new method for obtaining a precise calibration for the beam analyzer and magnetic spectrograph at these high bombarding energies is presented. The mass excess of ^{9}C was measured as 28.911 ± 0.009 MeV; that of ^{13}O, as 23.103 ± 0.014 MeV; and that of ^{21}Mg, as 10.912 ± 0.018 MeV. These nuclei represent the $T_z = -\frac{3}{2}$ members of the $T = \frac{3}{2}$ quartets for A = 9, 13, and 21, respectively. The present results show excellent agreement with a quadratic isobaric-multiplet mass equation for A = 13 and A = 21, but there is some indication that a small cubic term is required for the A = 9 multiplet. (auth)

43824 CALCULATION OF ELECTROEXCITATION OF CARBON IN THE REGION OF GIANT RESONANCE BY THE METHOD OF STRONG COUPLING OF CHANNELS. Grishanova, S. I.; Titarenko, N. N. (Inst. of Nuclear Physics, Moscow). Yadern. Fiz.; 13: No. 4, 712-18(Apr 1971). (In Russian).

The form factors of 1- and 2-C levels in the region of the giant resonance (19 to 27 MeV) are calculated by the method of strong coupling of channels in a framework for which the quasistationary nature of levels may be calculated in the most consistent way. The results are compared with the calculations by means of the Tamm-Dankoff method and with the experimental data. (auth)

43825 EQUIVALENCE OF ^{3}He-t AND d-α CLUSTER DESCRIPTION OF ^{6}Li. Amado, R. D.; Noble, J. V. (Univ. of Pennsylvania, Philadelphia). Phys. Rev., C; 3: No. 6, 2494(Jun 1971).

In response to a letter by Young, Blatt, and Seyler [Phys. Rev. Lett., 25: 1764(1970)], the equivalence rather than the mutual exclusion of the ^{3}He−t and d−α descriptions of ^{6}Li is pointed out. (auth)

43826 ENERGY SPECTRA OF SINGLE-PARTICLE STATES IN NUCLEI. Koehler, H. S.; Lin, Y. C. (Univ. of Arizona, Tucson). Nucl. Phys.; A167: 305-25(1971).

The single-particle spectra of ^{16}O, ^{40}Ca, ^{48}Ca and ^{56}Ni were studied using self-consistent field methods and a quadratically velocity-dependent two-nucleon effective (reaction-matrix) interaction. The self-consistent field equations are derived in some detail for the spin-independent interaction which is used. A one-body spin-orbit interaction of the Thomas form is added. The applicability of Koopmans' theorem to nuclear removal energies is discussed at some length. It is concluded that this theorem should be applied with caution. Orbital rearrangement energies are calculated and are found to be less than or about 0.2 MeV for states at the Fermi surface and 1−2 MeV for the deepest states. (auth)

43827 STRUCTURE OF ^{12}C. Takigawa, N.; Arima, A. (Tokyo Univ.). Nucl. Phys.; A168: No. 3, 593-624(1971).

The low-lying states of ^{12}C are investigated with the Heitler-London approximation of the clustering wave functions. The distances between α-clusters are determined to make the total energy minimum; they are relatively small in the ground state band but large in the excited band. The $\mathbf{l} \cdot \mathbf{s}$ force is taken into account in the ground-state band by hybridizing the shell model and the cluster model and is found important to raise the excitation energies of the 2^+ and 4^+ states. Even though the clusterization is small in the ground-state band, it has an important effect on the enhanced transition probabilities and the form factors for electron scattering. The clusterization is essential to explain the observed properties of the excited band such as the low excitation energy and the large α-decay width. (auth)

43828 TRUNCATION OF ROTATIONAL STATES IN THE SHELL MODEL. Das Gupta, S.; Hocquenghem, J. C.; Giraud, B. (Centre d'Etudes Nucleaires de Saclay, Gif-sur-Yvette, France). Nucl. Phys.; A168: No. 3, 625-9(1971).

The α-cluster model is used for ^{12}C to investigate the possibility of an extension of rotational levels beyond the SU(3) limit. The role of the kinetic energy in this rotation is studied. (auth)

43829 STATES OF ^{8}Be FROM ANALYSIS OF ^{7}Li(p,α)^{4}He REACTION DATA. Kumar, N. (Australian National Univ., Canberra); Barker, F. C. Nucl. Phys.; A167: 434-48(1971).

In order to obtain information about the α-emitting states of ^{8}Be lying in the region of 20 MeV excitation energy, an attempt was made to analyze experimental data from the ^{7}Li(p,α)^{4}He reaction up to 7 MeV proton energies, using many-level R-matrix theory. Data obtained with both polarized protons are included. The properties of ^{8}Be levels thus obtained are in reasonable agreement with the predictions of recent shell-model calculations. (auth)

43830 THEORETICAL STUDY OF ELASTIC AND INELASTIC PION-^{12}C SCATTERING AT INTERMEDIATE ENERGIES. Lee, H. K. (California State Coll., Dominguez Hills); McManus, H. Nucl. Phys.; A167: 257-70(1971).

Elastic and inelastic cross sections are computed using DWIA. The diffraction-approximation method and a modified distorted-wave code are compared. As input, pion-nucleon phase shifts, the nucleon density from electron scattering, and microscopic inelastic form factors are used. It is found that the interaction given by the impulse approximation gives a fair fit to the elastic data and that the diffraction approximation compares remarkably well with the distorted-wave calculation at all but the lowest energies. The microscopic form factors of the 2^+ level at 4.4 MeV and 3^- level at 9.6 MeV give a good account of the inelastic scattering. Discrepancies in the elastic scattering are similar to those observed in 1 GeV proton scattering from carbon. (auth)

Nuclear Properties and Reactions, 20 ≤ A ≤ 89

Refer also to abstracts 41764, 43787, 43801, 43802, 43823, 43826, 43884, 43889, 43891, 43908, 43916, 43929, 43931, 43932, 43950, 43951, 43963, 43964, 43967, and 43978.

43831 (INR–1262) CIRCULAR POLARIZATION OF GAMMA RAYS. Ratynski, W. (Institute of Nuclear Research, Warsaw (Poland)). 1971. 85p. (In Polish). Dep. NTIS (U. S. Sales Only).

Methods of thermal-neutron polarization are reviewed, and procedures for the analysis of polarized-neutron capture gamma rays are given. The results of some spin measurements in excited nuclei of ^{28}Al, ^{70}Ga, ^{72}Ga, ^{183}W, and ^{187}W are included. (auth)

43832 (NP–18920) MEASURED DIFFERENTIAL CROSS SECTIONS FOR ELASTIC AND INELASTIC SCATTERING OF 104-MeV α PARTICLES. Habs, D.; Hauser, G.; Hoffmann, Gudrun; Klewe-Nebenius, H.; Loehken, R.; Martens, Uta; Rebel, H.; Schatz, G.; Schweimer, G. W.; Specht, J. (Kernforschungszentrum, Karlsruhe (West Germany). Zyklotron-Laboratorium). Oct 1970. 69p. Dep. NTIS (U. S. Sales Only).

Measured differential cross sections for elastic and inelastic scattering of 104-MeV α particles are presented in numerical tables. (auth)

43833 (ORNL–4698) DIFFERENTIAL CROSS SECTIONS AT FORWARD ANGLES FOR HYDROGEN AND HELIUM PARTICLES FROM 62-MeV PROTONS INCIDENT ON ^{60}Ni. Peelle, R. W.; Bertrand, F. E. (Oak Ridge National Lab., Tenn.). Jun 1971. Contract W-7405-eng-26. 23p. Dep. NTIS.

Tabulated differential cross sections are presented for the production, at angles of 15, 20, 25, and 40 deg, of proton, deuteron, triton, helium-3, and alpha particles from ^{60}Ni bombarded by 62-MeV protons. Continuum cross sections are listed in ~1-MeV bins for energies above lower cutoffs, which range from 4 to 15 MeV for the different types of exit particles. For a considerable energy range within each spectrum, only the integral cross section is known. The proton, deuteron, and alpha-particle cross sections are the same in the continuum region above the evaporation peak as those cross sections previously observed for ^{54}Fe and ^{56}Fe, but the corresponding yield of tritons is higher from ^{60}Ni and ^{56}Fe than from ^{54}Fe. (auth)

43834 (RPI–328–209) LINEAR ACCELERATOR PROJECT. Progress Report, October 1–December 31, 1970. (Rensselaer Polytechnic Inst., Troy, N. Y.). Contract AT(30-1)-328. 47p. Dep. NTIS.

Research at the Linear Accelerator Project of Rensselaer Polytechnic Institute in the period Oct. 1 through Dec. 31, 1970 is briefly described. The work included neutron cross section measurements and experimental and theoretical reactor physics and engineering. (J.W.R.)

43835 THERMAL NEUTRON CAPTURE CROSS SECTIONS IN CALCIUM. Cranston, F. P.; White, D. H. (Univ. of California, Livermore). Nucl. Phys.; A169: No. 1, 95-100(1971).

Neutron capture γ-ray spectroscopy studies of calcium isotopes were analyzed to yield relative thermal neutron cross sections. These results were combined with direct measurements using a Moxon–Rae type detector in order to obtain absolute values of all the stable calcium isotope cross sections. The cross sections for the stable isotopes of calcium are (in b): $\sigma_{40} = 0.40 \pm 0.04$, $\sigma_{42} = 0.65 \pm 0.07$, $\sigma_{43} = 6.2 \pm 0.6$, $\sigma_{44} = 1.03 \pm 0.09$, $\sigma_{46} = 0.70 \pm 0.11$, $\sigma_{48} = 1.09 \pm 0.14$, $\sigma_{nat.} = 0.43 \pm 0.04$. (auth)

43836 DETERMINATION OF THE MASS OF ^{87}Y. Umbarger, C. J. (Univ. of Kansas, Lawrence); Robinson, J. A.; Reece, R. R.; Bearse, R. C.; Ahlen, M. C. Nucl. Phys.; A169: No. 1, 109-12(1971).

The mass excess of ^{87}Y was determined to be $-83,001.4 \pm 1.5$ keV by measuring the Q-values of the reactions ^{86}Sr(p,γ)^{87}Y and ^{87}Sr(p,n)^{87}Y, which were found to be 5785.4 ± 3.3 keV and -2643.5 ± 1.5 keV, respectively. The mass of ^{87}Y given in the 1970 mass tables appears to be in error, although the ^{87}Sr–^{86}Sr mass excess difference given in that compilation is in agreement with the present work. (auth)

43837 COINCIDENCE STUDIES OF THE ^{52}Cr(p,γ)^{53}Mn REACTION. Sparks, R. J. (Dept. of Scientific and Industrial Research, Lower Hutt, N. Z.). Nucl. Phys.; A169: No. 1, 113-21(1971).

A decay scheme for ^{53}Mn was obtained from a study of the ^{52}Cr(p,γ)^{53}Mn reaction at six resonances. Branching ratios were determined, and coincidence spectra were measured at the $E_p = 1006$ keV resonance. There is evidence that the level at 2405 keV may be a doublet. (auth)

43838 LIFETIMES AND OTHER PROPERTIES OF SOME LEVELS IN ^{23}Na. Rasmussen, V. K. (Franklin Inst., Swarthmore, Pa.). Nucl. Phys.; A169: No. 1, 166-76(1971).

Resonant elastic and inelastic scattering of 2 to 4 MeV bremsstrahlung by ^{23}Na was studied. Level widths are determined by a self-absorption measurement or by comparing the scattered intensity with that observed for levels of known width in ^{27}Al or ^{55}Mn. For the 2.08 MeV, $\frac{7}{2}^+$ level $\Gamma_0 = 1.11 \pm 0.10$ MeV and $\Gamma = 15 \pm 3$ MeV. For the 2.64 MeV, $\frac{1}{2}^-$ level, $\Gamma = 4.8 \pm 0.7$ MeV and for the 2.98 MeV, $\frac{3}{2}^+$ level, $\Gamma_0 = 74 \pm 6$ MeV, $\Gamma = 123 \pm 12$ MeV. Scattering and self-absorption measurements for the 3.92 MeV level are inconsistent, suggesting strongly that the level is a doublet. Observation of the scattered spectrum from a composite Na–Al scatterer with a Ge(Li) detector indicates a doublet separation <5 keV. An incidental self-absorption measurement gives $g\Gamma_0 = 112 \pm 9$ MeV for the 3.96 MeV level of ^{27}Al. (auth)

43839 STUDY OF THE ^{61}Cu NUCLEUS BY THE ^{58}Ni(α,pγ)^{61}Cu REACTION. Heusch, B.; Cujec, B.; Dayras, R.; Mo, J. N.; Szoeghy, I. M. (Univ. Laval, Quebec). Nucl. Phys.; A169: No. 1, 145-65(1971). (In French).

Gamma-ray spectroscopy of ^{61}Cu nucleus was undertaken up to 2.5 MeV excitation by the ^{58}Ni(α,pγ) reaction at $E_\alpha = 10.0$ MeV. Using a Ge(Li) detector, accurate values for energy levels and branching ratios were obtained. For most of the levels, up to 2.1 MeV excitation, spin assignments and γ-ray mixing ratios were obtained by using the Litherland–Ferguson angular correlation measurements method. The experimental results are compared to a recent shell-model calculation, based on intermediate coupling of a proton to the ^{60}Ni core. (auth)

43840 SPIN ASSIGNMENTS TO EXCITED STATES OF ^{58}Fe USING INELASTIC SCATTERING OF 50 MeV PROTONS. Mani, G. S. (Univ. of Manchester, Eng.). Nucl. Phys.; A169: No. 1, 194-200(1971).

Inelastic scattering of 49.35 MeV protons by ^{58}Fe was studied. The angular distribution has been measured for fourteen excited states. Spin and parity assignments to most of the states were made using DWBA analysis with first-order collective form factors. (auth)

43841 MAGNETIC MOMENTS OF ISOMERIC LEVELS IN THE Br ISOTOPES MEASURED WITH IN-BEAM NMR–PAC. Braeuer, N.; Focke, B.; Lehmann, B.; Nishiyama, K.; Riegel, D. (Freie Univ., Berlin). Z. Phys.; 244: No. 4, 375-82(1971).

The γ-ray angular correlation of the $\frac{9}{2}^+$, 37 μs state in ^{81}Br and of the 181 keV, 120 μs state in ^{78}Br was disturbed by nuclear magnetic resonance. The g-factors were determined to be $|g| = 1.297 \pm 0.015$ for the 37 μs level in ^{81}Br and $|g| = 1.025 \pm 0.003$ for the 120 μs state in ^{78}Br. (auth)

43842 SHAPES OF ANGULAR DISTRIBUTIONS OF (^{3}He,t) AND (p,n) TRANSITIONS TO 0^+ ANTIANALOG STATES. Rost, E. (Univ. of Colorado, Boulder); Schaeffer, R. Phys. Rev., C; 3: No. 6, 2491-3(Jun 1971).

This comment on a recent Physical Review Letter by Noble [Phys. Rev. Lett., 25: 1458(1970)] points out that the assumptions used by Noble are not valid for the reaction considered; hence, the anomaly in the angular distributions remains to be explained. (auth)

43843 DECAY OF ^{77}Kr. Borchert, I. (Univ., Goettingen, Ger.). Z. Phys.; 244: No. 4, 338-45(1971). (In German).

^{77}Kr ($T_{\frac{1}{2}} = 1.2$ h) was produced by bombarding ^{76}Se with 48 MeV-α-particles. After irradiation the radioactive ^{77}Kr gas was collected in glass ampoules filled with charcoal and cooled by liquid air. The decay of ^{77}Kr was investigated using Ge(Li)-counters and a Ge(Li)-Ge(Li)-coincidence circuit. 27 γ-transitions, 13 of them unknown up to the present, were found and their relative intensities determined. A level scheme for ^{77}Kr → ^{77}Br having 14 levels is proposed. This accounts for all the observed γ-transitions. (auth)

43844 EXPERIMENTAL STUDY OF THE DECAY OF ^{81g}Se AND ^{81m}Se. Dorikens, M.; Demuynck, J.; Dorikens-Vanpraet, L. (Univ., Ghent). Z. Phys.; 244: No. 4, 321-31 (1971).

The decay of ^{81g}Se and ^{81m}Se was investigated with Ge(Li) spectrometers and Ge(Li) gamma–gamma coincidences. Accurate energies, intensities and half-lives were measured for 11 gamma-rays. These gamma-rays fit into a ^{81}Br level scheme with levels at: 275.9, 535.9, 538.2, 565.9, 649.7 and 828.2 keV. Beta component intensities were deduced from measured gamma intensities. The half-life is found to be (17.9 ± 0.5) min for ^{81g}Se, and (57.28 ± 0.05) min for ^{81m}Se. (auth)

43845 LEVEL STRUCTURE OF ^{41}K AS DEDUCED FROM THE ^{40}K(n,γ)^{41}K AND ^{39}K(t,p)^{41}K REACTIONS. Beckstrand, Dale Ferrin. Provo, Utah; Brigham Young Univ. (1970). 113p. University Microfilms Order No. 71-12,103.

Thesis.

The low-lying level structure of ^{41}K was studied using the thermal-neutron capture reaction, ^{40}K(n,γ)^{41}K on an isotopically

enriched target of ^{40}K, and using the two nucleon transfer reaction ^{39}K(t,p)^{41}K at an incident triton energy of 7.5 MeV. The γ-ray spectrum from the ^{40}K(n,γ)^{41}K reaction was studied using a Li-drafted Ge spectrometer system. γ-γ coincidence measurements using Ge(Li) detectors were also made. Spin and parity assignments for the excited states below 2450 keV are proposed, primarily on the basis of γ-ray branching to levels with established spin and parity. The proposed level energy spin and parity values, E(I$^\pi$), are 0($\frac{3}{2}^+$), 980.4($\frac{1}{2}^+$), 1293.4($\frac{1}{2}^-$), 1559.9($\frac{1}{2}^+$), 1582.0($\frac{5}{2}^+$), 1677.5($\frac{5}{2}^+$,$\frac{1}{2}^+$), 1698.1($\frac{5}{2}^+$), 2144.1($\frac{5}{2}^+$), 2166.0($\frac{1}{2}^\pm$,$\frac{3}{2}^\pm$), 2316.5 ($\frac{5}{2}^+$,$\frac{1}{2}^+$), and 2447.9($\frac{1}{2}^+$,$\frac{3}{2}^+$). In addition, levels were observed at 2494.7, 2507.9, 2527.9, 2599.8, 2681.5, 2712.2, 2756.5, 2760.7, 3042.1, 3142.1, 3164.5, 3213.4, 3235.6, and 3281.1 keV. Proton angular distributions from the ^{39}K(t,p)^{41}K reaction were compared with distorted-wave calculations at laboratory angles between 12 and 85°. Levels populated in the charged particle reaction include the ground state and states at 980, 1560, 1582, 1678, 1698, 2144, and 2448 keV. The low-lying excited states of ^{41}K are discussed in terms of two-particle, one-hole configurations of the form $p(d_{\frac{3}{2}})^{-1}$-$n(f_{\frac{7}{2}})^2$. (Diss. Abstr. Int., B)

43846 STUDY OF THE VECTOR ANALYZING POWER AND CROSS SECTION FOR (d,p) STRIPPING REACTIONS ON INTERMEDIATE WEIGHT NUCLEI. Kocher, David Charles. Madison, Wis.; Univ. of Wisconsin (1970). 435p. University Microfilms Order No. 71-3136.

Thesis.

Angular distributions of the vector analyzing power $iT_{11}(\theta)$ and of the absolute cross section were measured for (d,p) stripping reactions on the even-A nuclei ^{28}Si, ^{40}Ca, ^{46}Ti, ^{48}Ti, ^{50}Ti, ^{52}Cr, and ^{54}Fe, and on the odd-A nuclei ^{53}Cr, ^{57}Fe, ^{117}Sn, and ^{119}Sn for deuteron energies between 5 and 12 MeV. Measurements for most of the target nuclei were made with an energy resolution of 40–80 keV so that many energy levels in the residual nucleus below about 5 MeV excitation energy could be observed. Transitions with orbital angular momentum transfer l_n = 1, 2, 3, 4 were studied in the reactions on even-A target nuclei. The observed dependence of the vector analyzing power angular distributions upon the total angular momentum transfer, $j_n = l_n + \frac{1}{2}$ or $j_n = l_n - \frac{1}{2}$, allowed unambiguous spin assignments to be made for states in the odd-A residual nuclei. In particular, the j-dependence of the vector analyzing power for l_n = 1 transitions was found to be pronounced for all target masses and reaction Q-values. Spectroscopic factors were obtained for the final states by normalizing the single-particle cross section obtained from a distorted-wave Born approximation (DWBA) calculation to the measured absolute cross section at the stripping peak. From the j_n-values and spectroscopic factors the energies of the $2p_{\frac{3}{2}}$ and $2p_{\frac{1}{2}}$ neutron single-particle states were calculated for odd-A nuclei between ^{41}Ca and ^{55}Fe. The strength of the nuclear spin-orbit interaction was then determined from the energy difference between the $2p_{\frac{3}{2}}$ and $2p_{\frac{1}{2}}$ single-particle states. The strength of the spin-orbit interaction for neutron bound states was found to be in good agreement with the strength obtained from analyses of neutron polarization in elastic scattering. For transitions on odd-A target nuclei, two or more j_n-values are generally allowed by conservation of angular momentum. An analysis of the data had shown that the j-dependence of the vector analyzing power can be used to quantitatively determine the mixing of $j_n = l_n + \frac{1}{2}$ and $j_n = l_n - \frac{1}{2}$ transitions. Vector analyzing power and cross section angular distributions for transitions on even-A and odd-A target nuclei were compared with DWBA calculations. The calculations qualitatively reproduce the measured angular distributions. In particular, the calculations show the same j-dependence of the vector analyzing power as is observed in the data for all j_n-values. The calculations employed deuteron and proton optical model parameters obtained from analyses of elastic cross sections and polarizations. The deuteron parameters for the odd-A target nuclei were obtained from an optical model analysis performed in the present work. (Diss. Abstr. Int., B)

43847 LIFETIME MEASUREMENTS ON E2 ISOMERS IN N = 48 NUCLEI AND E2 EFFECTIVE CHARGES OF $1g_{\frac{9}{2}}$ NUCLEONS. Ishihara, M. (Tokyo Univ.); Kawakami, H.; Yoshikawa, N.; Sakai, M.; Ishii, K. Phys. Lett.; 35B: No. 5, 398-400(21 Jun 1971).

New E2 isomeric $8^+ \rightarrow 6^+$ transitions were identified in three N = 48 nuclei, ^{86}Sr, ^{88}Zr, and ^{90}Mo. The half-lives were determined to be 0.46, 1.75, and 1.05 μsec, respectively. Comparison of the B(E2, $8^+ \rightarrow 6^+$) values in ^{86}Sr and ^{90}Zr indicates that the E2 polarization charge for the neutron is somewhat larger than that for the proton. (auth)

43848 ANOMALY IN THE ANGULAR DISTRIBUTIONS FOR (^{3}He,t) REACTIONS. Comfort, J. R. (Argonne National Lab., Ill. Princeton Univ., N. J.); Schiffer, J. P.; Richter, A.; Stautberg, M. M. Phys. Rev. Lett.; 26: No. 21, 1338-41(24 May 1971).

A systematic angular shift is noted between distorted-wave calculations and measured angular distributions for (^{3}He,t) reactions on even–even targets. The shift is apparent for final states whose isospin is one unit lower than that of the target state. (auth)

43849 NEW 0^+ STATES IN ^{50}Cr OBSERVED VIA THE (p,t) REACTION. Baer, H. W.; Kraushaar, J. J.; Shepard, J. R.; Ridley, B. W. (Univ. of Colorado, Boulder). Phys. Lett.; 35B: No. 5, 395-7(21 Jun 1971).

Measurements of differential cross sections in the ^{52}Cr(p,t) reaction at 27 MeV provide identification of four previously unreported 0^+ states in the 3.8- to 4.8-MeV excitation region of the stable nucleus ^{50}Cr. Additional spin–parity information is provided through observation of L = 2, 3, and 4 transitions. (auth)

43850 HINDRANCE OF M1 TRANSITIONS FROM ANALOG TO ANTIANALOG STATES IN f-p SHELL NUCLEI AS AN EFFECT OF THE f/sub 7/2/ PROTON SHELL. Klapdor, H. V. (Max- Planck Institut fuer Kernphysik, Heidelberg. Institut fuer Experimentalphysik, Hamburg). Phys. Lett.; 35B: No. 5, 405-7 (21 Jun 1971).

The hindrance of M1 transitions from the analog to the antianalog state is found in further f–p shell nuclei, and is shown to be an effect of the unclosed $f_{\frac{7}{2}}$ proton shell. (auth)

43851 EVIDENCE FOR INTERMEDIATE STRUCTURE NEAR AN ISOBARIC ANALOG RESONANCE. Temmer, G. M.; Maruyama, M.; Mingay, D. W.; Petrascu, M.; Van Bree, R. (Rutgers–The State Univ., New Brunswick, N. J.). Phys. Rev. Lett.; 26: No. 21, 1341-4(24 May 1971).

A particular $J = \frac{1}{2}^+$ analog resonance in ^{71}As, observed in elastic and inelastic scattering of protons by ^{70}Ge and corresponding to a single l = 0 state at 2.22 MeV excitation in ^{71}Ge, is found to contain significant substructure encompassing many ultimate fine-structure levels. (auth)

43852 COULOMB EXCITATION OF THE FIRST EXCITED STATE OF ^{24}Mg. Vitoux, Dominique. Pittsburgh; Univ. of Pittsburgh (1970). 52p. University Microfilms Order No. 71-12,367.

Thesis.

Coulomb excitation of the first excited state of ^{24}Mg was investigated by means of a coincidence experiment using a position sensitive detector. Interpreting the data according to the semiclassical theory and correcting for quantal effects, a reduced transition probability of B(E2; $0^+ \rightarrow 2^+$) = 0.042 ± 0.002 e^2b^2 and a static quadrupole moment of $Q_{2+} = -0.305 \pm 0.064$ e · b were obtained. (Diss. Abstr. Int., B)

43853 EXPERIMENTAL INVESTIGATION OF RADIATIVE PROTON CAPTURE INTO THE GIANT DIPOLE RESONANCES IN ^{40}Ca, ^{42}Ca, AND ^{60}Ni. Diener, Edward Moses. Stony Brook; N. Y.; State Univ. of New York (1971). 136p. University Microfilms Order No. 71-13,256.

Thesis.

The giant dipole resonances in ^{40}Ca, ^{42}Ca and ^{60}Ni were investigated by the radiative capture reactions ^{39}K(p,γ)^{40}Ca, ^{41}K(p,γ)^{42}Ca and ^{59}Co(p,γ)^{60}Ni. Cross sections and angular distributions were measured with a 25 cm × 25 cm anticoincidence-shielded NaI(Tl) detector. In ^{40}Ca, the giant dipole resonance is observed at 19.3 MeV excitation energy. Strongly anisotropic angular distributions consistent with dominant f-wave capture are obtained, in qualitative agreement with theory. Fine structure ≤50 keV wide and intermediate structure peaks of width 150 keV to 400 keV are superimposed on the 3-MeV wide envelope of the giant dipole resonance. In ^{42}Ca, two broad peaks, at 20.4 MeV and 17.4 MeV excitation, are interpreted as the T> and T< components of the giant dipole resonance. Angular distributions are less anisotropic than in ^{40}Ca. Intermediate structure peaks are observed at approximately the same excitation energies as in ^{40}Ca. The ground state transition in ^{60}Ni exhibits two broad peaks at excitation energies 19.6 MeV and 16.6 MeV; these are interpreted as the T> and T< components of the giant dipole resonance. The results of a detailed calculation ignoring isospin effects do not adequately explain all of the observations; a simple 1p–1h calculation using eigenfunctions of isospin describes the results quite well. The first excited state capture yield curve is similar to the ground state curve, shifted in energy by ~300 keV. The data suggest that most of the observed strength in the giant dipole resonance based on the first excited state of ^{60}Ni is concentrated in 2^- states. (Diss. Abstr. Int., B)

43854 LIFETIMES OF SOME NUCLEAR STATES IN ^{24}Mg, ^{26}Mg, ^{27}Al, AND ^{28}Si. Haskett, James Albert. Bloomington, Ind.; Indiana Univ. (1970). 135p. University Microfilms Order No. 71-13,547.

Thesis.

Lifetimes of several low lying levels in ^{24}Mg, ^{26}Mg, ^{27}Al and ^{28}Si were measured using the Doppler Shift Attenuation Method. The levels were populated by the X(α,α')X* reaction using 22 MeV alpha particles. The backscattered alpha particles were detected in annular surface barrier particle detectors and gamma rays resulting from the decay of the nuclear states were detected in coincidence by a 16.7 cm^3 lithium drifted germanium detector. The Doppler shifts were determined by fitting Gaussian (normal) curves to the gamma ray spectra. The lifetime of the excited state can be directly determined from the measured Doppler shift if the stopping time of the recoil ion is known. The recoil velocity problem was considered in great detail. A new form for the velocity of the recoiling ion as a function of time was used which seems preferable to other forms when heavy target backings and high initial recoil velocities are used. The results for the mean lifetimes, in units of 10^{-15} sec, for the excited states in parenthesis (MeV) are the following: ^{24}Mg(1.37) 2030, (4.12) 140, (4.23) 105, (5.23) 173, (6.01) 124, ^{26}Mg (2.94) 60, ^{27}Al (2.21) 110, ^{28}Si (4.61) 83. The results are compared with previously reported values and best averages are suggested. (Diss. Abstr. Int., B)

43855 EXPERIMENTAL INELASTIC SCATTERING OF 61 MeV PROTONS FROM ^{89}Y AND ^{90}Zr. Whiten, Morris Lewis. Athens, Ga.; Univ. of Georgia (1970). 186p. University Microfilms Order No. 71-13,146.

Thesis.

The differential cross sections for the excitation of the first seven resolved excited levels in ^{89}Y and ^{90}Zr by 61.2 MeV protons were measured over the angular range 17 to 120 degrees. The scattered protons were magnetically analyzed and recorded with 50 μm thick Ilford G5 emulsions. The weakly excited state at 2.62 MeV in ^{89}Y was observed but the 0^+ state at 1.75 MeV in ^{90}Zr was not. The differential cross sections for the 0.908 MeV ^{89}Y state and the corresponding 5^- ^{90}Zr state are quite different, both in shape and magnitude. The experimental data for the 0.908 MeV state in ^{89}Y are compared with four different microscopic-model calculations. The data for other states in ^{89}Y are compared with a microscopic-model including core polarization or a collective-model calculation, whichever is appropriate. The data for the 5^- state in ^{90}Zr are compared with two different antisymmetrized microscopic-model calculations, one using a Yukawa interaction and the other using a Hamada–Johnston interaction. Calculations for the 2^+, 4^+, 6^+, and 8^+ states in ^{90}Zr used a microscopic-model description with a Hamada–Johnston interaction. A microscopic-model description for the excitation of the strongly collective 3^- state in ^{90}Zr is also shown. The experimental differential cross sections for the excitation of the levels in ^{89}Y and ^{90}Zr by 61 MeV protons have much more structure than those at lower proton energies, so these data provide a more stringent constraint on current and future models of the reaction mechanisms involved in inelastic scattering of nucleons. (Diss. Abstr. Int., B)

43856 LIFETIME MEASUREMENTS OF EXCITED STATES IN ^{39}K BY THE DOPPLER SHIFT ATTENUATION METHOD. Tapphorn, Ralph M. Manhattan, Kan.; Kansas State Univ. (1970) 142p. University Microfilms Order No. 71-11,337.

Thesis.

The mean lifetimes of excited states up to 4.12 MeV in ^{39}K were measured by the Doppler shift attenuation method. The agreement between lifetimes measured in this work and previous lifetime measurements for the first three excited states of ^{39}K is very good. The Blaugrund method of calculating the attenuation factor for the case of the recoil ion slowing down in a compound target is presented. The calculation employs the Lindhard, Scharff and Schiott stopping cross sections and the Blaugrund large angle scattering correction. Transition strengths calculated for the first four excited states of ^{39}K are compared with predictions of the core-coupling model and the phonon-hole coupling model. The phonon-hole coupling model is shown to be in better agreement with experiment than the core-coupling model. (Diss. Abstr. Int., B)

43857 keV NEUTRON CAPTURE AND TRANSMISSION MEASUREMENTS ON ^{50}Cr, ^{52}Cr, ^{53}Cr, ^{54}Cr, ^{60}Ni, AND V. Stieglitz, Richard Gwydir. Troy, N. Y.; Rensselaer Polytechnic Inst. (1970). 231p. University Microfilms Order No. 71-12,829.

Thesis.

Neutron capture and transmission measurements were performed on vanadium and the separated nuclei of ^{60}Ni, ^{50}Cr, ^{52}Cr, ^{53}Cr, and ^{54}Cr with an experimental resolution of 0.6 nanoseconds per meter. The capture measurements cover the energy range 0.1 to 200 keV while the transmission measurements extend to over 300 keV. Parameters are extracted for both s-wave and p-wave resonances and s-wave and p-wave strength functions, potential scattering radii and resonance absorption integrals are determined. The radiation width is found to vary widely among the s-wave resonances of each nuclide. Average capture cross sections in the energy range 10 to 200 keV are also presented. (Diss. Abstr. Int., B)

43858 STUDY OF ELECTROMAGNETIC TRANSITIONS IN THE ^{55}Co NUCLEUS. Shoup, Robert Lynn. Tallahassee; Florida State Univ. (1970). 127p. University Microfilms Order No. 71-13,512.

Thesis.

The electromagnetic transitions between T> and T< states and between T< states and the ground state of ^{55}Co were investigated. The gamma ray decay of the $J^\pi = 3/2^-$ bound analog state at 4.72 MeV excitation is of particular interest. The gamma ray deexcitation of this state is used to test the fast $\Delta T = 1$ M1 transition predictions for $J_f = J_i = j = l + 1/2$. The gamma ray decays of the T> and T< states of the ^{55}Co nucleus were studied via the ^{54}Fe(^{3}He,dγ)^{55}Co reaction. Multi-parameter coincidence data consisting of a deuteron energy pulse, a gamma ray energy pulse and a time relationship pulse were accumulated by use of an 6130 EMR on-line computer. A new gamma ray decay scheme and energy level diagram were constructed by analyzing one level at a time starting with the first excited state and continuing to 5.7 MeV excitation energy. Calculations of reduced transition probabilities for $\Delta T = 1$ M1 transitions are performed. When mixed shell-model configurations are used to describe the initial and final states of the ^{55}Co nucleus, multiple branchings of the T> states are predicted. Only two or three branches are possible when pure configurations are used. By combining the results of the data from the ^{54}Fe(^{3}He,d)^{55}Co experiment with this study, a new energy level scheme is proposed for ^{55}Co and more conclusive spin and parity assignments are made for the excited levels. The multiple branching of the 4.72 MeV analog state decay suggests that the excited levels of ^{55}Co are best described by mixed nuclear configurations are used to represent the initial and the final states, the fast $\Delta T = 1$ M1 $J = j = l + 1/2$ transition predictions break down. (Diss. Abstr. Int., B)

43859 ISOBARIC SPIN SPLITTING OF SINGLE NUCLEON STATES IN ^{89}Y AND PARTICLE-HOLE EXCITATIONS OF THE CORE. Parish, Leslie Joe. Tallahasse; Florida State Univ. (1970). 94p. University Microfilms Order No. 71-13,510.

Thesis.

The role of collective core excitations in the T< single-proton strength distributions in ^{89}Y was investigated both experimentally and theoretically. Shell model calculations including approximately 80 two-particle one-hole and three-particle two-hole configurations were carried through for the $1/2^+$, $3/2^+$, $5/2^+$ and $7/2^+$ states in ^{89}Y. Both $T = 1/2$ and $T = 3/2$ states were considered. A second shell model calculation was executed with a configuration space limited to the core-polarization states. The results of both calculations are compared to the measured proton strength distribution and it is concluded that the larger configuration space is essential to a complete understanding of the fine structure in the T< giant resonances. The inelastic scattering of 26-MeV alpha particles from ^{89}Y was measured to locate the odd-parity collective core strength in ^{89}Y. The measured inelastic strength distribution is compared to that predicted by the shell model calculation and to the single-proton strength distribution. There is strong evidence that the mixing of collective core states with the single-proton strength is of major importance in producing the observed fine structure. (Diss. Abstr. Int., B)

43860 DISCUSSION OF A PARTICULAR FORM OF CLUSTER WAVE FUNCTIONS. Chang, F. C. (St. John's Univ., Jamaica, N. Y.). Phys. Rev., C; 3: No. 6, 2113-15(Jun 1971).

The meaning of a particular form of cluster wave functions, which have been used in a previous paper to describe the ground-state rotational band of ^{20}Ne, is discussed. (auth)

43861 LIFETIMES OF ^{39}K EXCITED STATES. Tapphorn, R. M.; Kregar, M.; Seaman, G. G. (Kansas State Univ, Manhattan). Phys. Rev., C; 3: No. 6, 2232-7(Jun 1971).

The mean lifetimes of nine levels in ^{39}K up to 4.12 MeV in excitation were measured by the Doppler-shift-attenuation method. The levels were populated by the ^{39}K(p,p'γ)^{39}K reaction at proton energies of 6.47 and 6.67 MeV. Gamma rays were detected in a 30-cm^3 coaxial Ge(Li) detector at 30 and 135° to the beam direction in coincidence with protons scattered into the range 164 to 174°. Transition strengths are calculated for the first four excited states, and the results are

XUM

compared with predictions of the weak-coupling model and a phonon–hole coupling model. The weak-coupling model is shown to underestimate E2, M2, and E3 strengths, while the phonon–hole coupling model predicts enhanced E3 strengths. (auth)

43862 SHELL-MODEL CALCULATIONS FOR ^{51}V AND ^{52}Cr. Rustgi, M. L.; Singh, R. P.; Roy, B. Barman; Raj, R.; Fu, C. C. (State Univ. of New York, Buffalo). Phys. Rev., C; 3: No. 6, 2238-45(Jun 1971).

By employing ^{48}Ca as the core and the reaction matrix elements of Kuo and Brown for the residual interaction among the three valence protons, the nuclear energy levels of ^{51}V are calculated within the spherical shell-model framework. All the 0f–1p configurations are included. The wave functions obtained on diagonalizing the Hamiltonian matrices are used to calculate the transition rates and spectroscopic factors for the reaction ^{50}Ti(^{3}He,d)^{51}V. Good agreement with experiments is found; it thus appears that it is not necessary to include deformation in ^{51}V as in the papers of Scholz and Malik [Phys. Rev., 147: 836(1966); ibid., 150: 919(1966); ibid., 153: 1971(1967)]. The consequences of mixing effective interaction matrix elements of Lips and McEllistrem [Phys. Rev. C, 1: 1009(1970)] and realistic Kuo–Brown matrix elements are studied, and it is pointed out that such a mixture does not yield a successful effective-interaction model. The results are further supported by similar calculations on ^{52}Cr. (auth)

43863 SPIN OF THE 937-keV LEVEL IN ^{54}Co. Sankey, R. R.; Kemper, K. W.; Plendl, H. S.; Nelson, J. W. (Florida State Univ., Tallahassee). Phys. Rev., C; 3: No. 6, 2273-7(Jun 1971).

The spin of the (937 ± 1)-keV level in ^{54}Co was determined by exciting that level with the reaction ^{54}Fe(p,n)^{54}Co and measuring the angular distributions of the neutrons that populate this level and of the subsequent γ-ray decay. A spin of 1 is assigned to this level. (auth)

43864 BETA–GAMMA CIRCULAR-POLARIZATION CORRELATION AND NUCLEAR MATRIX ELEMENTS OF ^{76}As. Smith, H. A.; Simms, P. C. (Purdue Univ., Lafayette, Ind.). Phys. Rev., C; 3: No. 6, 2278-85(Jun 1971).

The $\beta-\gamma$ circular-polarization correlation P_γ for the 2.41-MeV β transition of ^{76}As was measured as an average value over the energy interval E_β = 1.4 to 2.0 MeV at an average angle $\theta_{\beta\gamma}$ = 158°. Previous experimental data, this new value for P_γ, and theoretical arguments are used to set limits on the nuclear matrix elements and to investigate the diagonality of the Coulomb Hamiltonian. The analysis shows that matrix elements that change the angular momentum by 0, 1, and 2 units all contribute with approximately equal strength to the transition. The matrix-element analysis indicates that the A_3 term in P_γ is negligible compared to the A_1 term. When A_3 is set equal to zero, the experimental data give the following value for P_γ: P_γ (1.4 MeV < E_β < 2.0 MeV, $\theta_{\beta\gamma}$ = 180°) = 0.105 ± 0.02. (auth)

43865 OUTER-SHELL INTERNAL CONVERSION OF THE 14.4-keV TRANSITION IN ^{57}Fe: CHEMICAL EFFECTS AND LINE-SHAPE DIFFERENCES. Porter, F. T.; Freedman, M. S. (Argonne National Lab., Ill.). Phys. Rev., C; 3: No. 6, 2285-92(Jun 1971).

Internal conversion of the 14.4-keV transition in the outer shells of ^{57}Fe following the decay of ^{57}Co was examined at 0.05% momentum resolution. The intensity of the conversion in the outermost shell, N_1 in the free atom, relative to that of the M_1 shell shows a dependence on the chemical environment of the decaying ^{57}Co atom. ^{57}Co ions from an electromagnetic isotope separator were deposited at <25 eV on the surface ("oxide state") or were allowed at 500 eV to penetrate a natural graphite crystal lattice ("metallic state") where oxidation could not occur. The intensity ratio N_1/M_1 ("oxide") is 0.024 ± 0.002, and N_1/M_1 ("metal") is 0.034 ± 0.003. The N_1-shell line shapes show less low-energy tail than the M_1 lines (which are only ~0.7% lower in energy), an effect probably due to less outer-shell electron shakeoff in the case of the N_1 lines. This result throws doubt on the accuracy of the analyses of previous experiments in which the outermost-shell conversion lines were not well enough resolved to observe this effect and in which the assumption of similar line shapes was used. (auth)

43866 STRUCTURE OF ^{44}Ti AND THE ROLE OF SINGLE-PARTICLE ENERGIES AND THE T = 0 TWO-BODY INTERACTION IN THE DEVELOPMENT OF ROTATIONAL PROPERTIES IN NUCLEI. Bhatt, K. H.; McGrory, J. B. (Oak Ridge National Lab., Tenn.). Phys. Rev., C; 3: No. 6, 2293-2302(Jun 1971).

The structure of low-lying states in ^{44}Ti is studied in terms of a conventional shell model. The calculated spectrum is in reasonable agreement with available experimental information. The results of the "exact" shell-model calculation are compared with calculations of the ^{44}Ti spectrum in terms of the stretch scheme and the deformed Hartree–Fock scheme with projection. These two approximations are not in good agreement with the exact calculation. The effects on the calculated spectrum of varying the single-particle energy spectrum are studied. The "rotational" character of the calculated spectrum is sensitive to the single-particle energies. The sensitivity can be accounted for by assuming that the wave functions of the members of a rotational band are projections from an intrinsic state with a strong quadrupole deformation. The effect of the T = 0 part of the residual interaction, and of the Pauli principle, on the rotational character of the calculated spectrum of low-lying states is discussed. (auth)

43867 ISOSPIN SPLITTING OF THE GIANT DIPOLE RESONANCE IN ^{60}Ni. Diener, E. M. (State Univ. of New York, Stony Brook); Amann, J. F.; Paul, P.; Blatt, S. L. Phys. Rev., C; 3: No. 6, 2303-14(Jun 1971).

The radiative-capture reaction ^{59}Co(p,γ)^{60}Ni was studied for proton energies from 4.40 to 13.60 MeV. Cross-section and angular-distribution data were measured with a large anti-coincidence-shielded NaI(Tl) detector. The yield curve for ground-state capture shows two broad peaks, at ^{60}Ni excitations of 16.6 and 19.6 MeV; these are interpreted as the T< and T> components of the giant dipole resonance. The results of a detailed calculation ignoring isospin effects do not adequately explain all of the observations; a simple 1p–1h calculation using eigenfunctions of T describes the results quite well. The first-excited-state-capture yield curve is similar to the ground-state curve, shifted in energy by ~300 keV. The data suggest that most of the observed strength in the giant dipole resonance based on the first excited state of ^{60}Ni is concentrated in 2^- states. (auth)

43868 REACTION ^{36}Ar(d,p)^{37}Ar. Sen, S.; Hollas, C. L.; Riley, P. J. (Univ. of Texas, Austin). Phys. Rev., C; 3: No. 6, 2314-22(Jun 1971).

The level structure of ^{37}Ar was investigated via the reaction ^{36}Ar(d,p)^{37}Ar at an incident deuteron energy of 9.162 MeV and with an over-all energy resolution of approximately 30 keV. A total of 53 states of ^{37}Ar with excitation energies up to 9.012 MeV were observed. The orbital-angular-momentum-transfer values and the spectroscopic factors for 29 of the observed states are extracted by using finite-range distorted-wave Born-approximation calculations corrected for nonlocality of the optical potential. One l = 0, two l = 2, three l = 3, and twenty-three l = 1 transfer values are assigned. Spin assignments are made on the basis of the conventional shell-model ordering of states, by comparison of the states of ^{37}Ar with those of the mirror nucleus ^{37}K, and on the basis of the Lee–Schiffer effect. The spin, parity, excitation energies, and spectroscopic factors obtained for the lowest few states in ^{37}Ar are in fair agreement with those predicted through recent shell-model calculations. (auth)

43869 LEVELS OF ^{36}S FROM ^{34}S(t,p)^{36}S. Olness, J. W. (Brookhaven National Lab., Upton, N. Y.); Harris, W. R.; Gallmann, A.; (and others). Phys. Rev., C; 3: No. 6, 2323-44(Jun 1971).

Levels of ^{36}S were investigated via the ^{34}S(t,p)^{36}S reaction by using targets of Sb_2S_3 with the sulfur content enriched to 86% in the isotope ^{34}S. The excitation energies (given in MeV) of the levels observed, together with the restrictions on spins and parities resulting from this investigation and also previous work, are as follows: 3.29, 2^+; 3.34, 0^+; 4.19, 3^-; 4.52, 1^+; 4.57, 2^+; 5.26, 1, 2, 3; 5.38, 1, 2, or (3); 5.50, 2, (3), 4; 5.57, 1, (2), 3; 6.20, 2, 3; 6.51, 4^+; and 7.12, 1^+ or 2^+. Information on the γ-ray branching of these levels and on the angular-correlation patterns of major branches was obtained from two-parameter p–γ coincidence studies utilizing collinear detection of the reaction protons. The 3.29-MeV level decays by E2 radiation directly to the ^{36}S $J^\pi = 0^+$ ground state. An intermediate-image pair spectrometer was used to determine that the 3.34-MeV level has $J^\pi = 0^+$, since it decays by an E0 transition to the ground state. With the exception of the 4.52-, 5.38-, and 7.12-MeV levels, which decay mainly to the ground state, the higher-lying levels were observed to deexcite primarily by cascade transitions through the 3.29-MeV level. Ge(Li) studies of γ-ray Doppler shifts determined the following mean-lifetime restrictions for the indicated levels (excitations in MeV): 3.29, τ = 0.20 ± 0.03 psec; 4.19, τ > 2 psec; and 4.57, τ < 0.1 psec. Additional but less restrictive limitations are given for several of the remaining levels. The lifetime of the 0^+ 3.34-MeV state was measured by electronic techniques, which determine a mean life τ = 12.7 ± 0.3 nsec. The spin–parity limitations deduced herein

are from a combination of the results of the angular-correlation analysis and these lifetime limitations. No evidence was obtained for the existence of states at 2.00 and 2.85 MeV previously reported from the $^{34}S(t,p)^{36}S$ reaction. Finally, the observed level structure as deduced from this and previous experiments is compared with relevant shell-model calculations on the even- and odd-parity states of this $T_z = 2$ nucleus. (auth)

43870 LIFETIME OF THE $\frac{1}{2}^-$ 2791-keV ^{21}Ne LEVEL. Warburton, E. K.; Olness, J. W.; Engelbertink, G. A. P.; Jones, K. W. (Brookhaven National Lab., Upton, N. Y.). Phys. Rev., C; 3: No. 6, 2344-8(Jun 1971).

The mean lifetime of the $J^\pi = \frac{1}{2}^-$ ^{21}Ne level at an excitation energy of 2791 keV was measured by the gas-target variant of the recoil-distance technique. The result of 84 ± 10 psec is discussed in terms of the structure of mass-21 states. (auth)

43871 IONIZATION (SHAKEOFF) ACCOMPANYING K-SHELL INTERNAL CONVERSION. Porter, F. T.; Freedman, M. S.; Wagner, F. Jr. (Argonne National Lab., Ill.). Phys. Rev., C; 3: No. 6, 2246-59(Jun 1971).

Studies using a β-ray magnetic spectrometer at 0.05% momentum resolution with isotope-separator-prepared samples revealed structure below the K conversion lines of the 122- and 136-keV (^{57}Fe) and the 661-keV (^{137}Ba) transitions. This structure consists of an abrupt rise below the K conversion line (in atomic number Z) at an energy displacement approximately equal to the L_3 binding in the (Z + 1) neutral atom and a continuum extending to lower energies. These continua are interpreted as the spectra complementary to the (unobserved; energy near zero) L-shakeoff spectra; i.e., the sum or ejected K- and L-electron energies equals a constant. The double-vacancy binding energy for KL_3 is 7905^{+20}_{-10} eV for Fe and 43.01 ± 0.03 keV for Ba. The sum of KL shakeoff from all three L subshells compared with the K line is $\Sigma KL/K = 9 \times 10^{-3}$ for Fe and 1×10^{-3} for Ba (both with uncertainties estimated at ~50%), in good agreement with self-consistent-field overlap integrals for shakeoff in β^- decay if one takes the effective charge change for L electrons during K conversion as ~0.85 times that for β^- decay. The spectrum shape of the KL continua, in the main, confirms the predictions of the nonrelativistic calculations that have been made for β-decay processes, but some discrepancies are suggested. For the less probable K shakeoff accompanying K conversion, preliminary values for intensities of the continua with respect to the K line are KK/K between $(0.4 - 2) \times 10^{-4}$ for Fe, and $KK/K < 2 \times 10^{-4}$ for Ba. No M_1 or $M_{2,3}$ shakeoff was obvious on the K line of the 14-keV transition in ^{57}Fe. (auth)

43872 LOW-LYING LEVELS OF ^{40}Ar. Place, R. L.; Buerger, K. H. Jr., Wakatsuki, T.; Kern, B. D. (Univ. of Kentucky, Lexington). Phys. Rev., C; 3: No. 6, 2259-68(Jun 1971).

Seven excited levels of ^{40}Ar were populated by the $^{40}Ar(p,p')$ reaction and studied with $\gamma-\gamma$ and $p'-\gamma$ angular-correlation techniques. Spin–parity assignments are made as follows: 1461 keV, 2^+; 2121 keV, 0^+; 2524 keV, 2^+; 2892 keV, $(4)^+$; 3207 keV, 2^+ or 1^+; 3507 keV, 2^+ or 1^+; 3681 keV, 3^-. Multipole amplitude mixing ratios are as follows: 2524 → 1461-keV transition, $\delta(E2/M1) = +0.24$; and 3207 → 1461-keV transition, if $2^+ \rightarrow 2^+$, $\delta(E2/M1) = -0.20$, and if $1^+ \rightarrow 2^+$, $\delta = 0$. Gamma branching ratios for the second to seventh excited levels were measured. These results, together with lifetimes previously determined by others, are used to calculate B(E2) and B(M1) values, which are compared with those of similar levels in ^{42}Ca. (auth)

43873 NEW OBSERVATIONS IN THE A = 49 DECAY CHAIN; LEVELS IN ^{49}Sc AND ^{49}Ti. Eichler, Eugene; Raman, Subramanian (Oak Ridge National Lab., Tenn.). Phys. Rev., C; 3: No. 6, 2268-73(Jun 1971).

The γ rays from 8.7-min ^{49}Ca and from 57.4-min ^{49}Sc were measured with a 40-cm^3 Ge(Li) detector. It is proposed that ^{49}Ca decay populates levels in ^{49}Sc at 2228.6, 2371.8, 3084.4, 3516.6, 4071.9, 4493.3, and 4738.2 keV. The ^{49}Sc decay populates levels in ^{49}Ti at 1622.6 and 1761.9 keV. Limits on probable spin and parity values for these levels are established. Mixing ratios for the 1408.9-keV γ ray were obtained from angular-correlation measurements. Weak transitions observed in this study provide further insights into the structure of ^{49}Sc levels, in particular, the $\frac{1}{2}^+$ and $\frac{5}{2}^+$ hole states. (auth)

43874 NEUTRON RESONANCE SPECTROSCOPY. VII. Ti, Fe, AND Ni. Garg, J. B. (State Univ. of New York, Albany); Rainwater, J.; Havens, W. W. Jr. Phys. Rev., C; 3: No. 6, 2447-63(Jun 1971).

High-resolution neutron total cross-section measurements were performed on natural samples of titanium, iron, and nickel from 200 eV to a few MeV by using the Nevis synchrocyclotron neutron velocity spectrometer with a 200-m flight path. The energy resolution was adequate only up to 200 keV to perform a detailed R-matrix multilevel analysis of the data. The resonance energies, isotopic and l-value assignments, neutron widths, etc., up to this energy are determined. From these the mean level spacings $\langle D \rangle$ and the s-wave strength functions (S_0) are calculated. Information about the resonance parameters of the bound level in iron and nickel was also obtained. Values of $\Gamma_\gamma = 8.2$ eV for the ^{48}Ti (17.8-keV) resonance, $\Gamma_\gamma = 0.64$ for the bound level at −2 keV in ^{56}Fe, and $\Gamma_\gamma = 9.0$ eV for the bound level at −28.5 keV in ^{58}Ni are determined by requiring an agreement with the measured thermal-neutron-capture cross section in these nuclei. (auth)

43875 MASS AND HALF-LIFE OF ^{36}K. Jaffe, A. A. (Univ. of North Carolina, Chapel Hill. Triangle Universities Nuclear Lab., Durham, N. C.); Bissinger, G. A.; Shafroth, S. M.; (and others). Phys. Rev., C; 3: No. 6, 2489-91(Jun 1971).

The threshold for the $^{36}Ar(p,n)^{36}K$ reaction was found at E_p = 14.002 ± 0.024 MeV (lab). This leads to a mass excess of ^{36}K of −17.396 ± 0.023 MeV. The half-life of positron activity for ^{36}K was found to be 345 ± 5 msec. (auth)

43876 HEXADECAPOLE MOMENTS OF ^{20}Ne AND ^{28}Si FROM SCATTERING OF 104-MeV α PARTICLES. Rebel, H. (Kernforschungszentrum Karlsruhe, Ger.); Schweimer, G. W.; Specht, J.; (and others). Phys. Rev. Lett.; 26: No. 19, 1190-4(10 May 1971).

Cross sections were measured for the inelastic scattering of 104-MeV α particles by ^{20}Ne and ^{28}Si. The experimental results for the ground-state band are analyzed in terms of a coupled-channel calculation on the basis of the rotational model. This technique proves to be quite sensitive to contributions of hexadecapole deformations. Quadrupole and hexadecapole deformation lengths and their signs are determined for both nuclei. (auth)

43877 GAMMA RAYS FOLLOWING THE DECAY OF ^{85}Sr AND ^{85m}Sr. Bubb, I. F.; Naqvi, S. I. H.; Wolfson, J. L. (Univ. of Sasketchewan, Regina). Nucl. Phys.; A167: 252-6(1971).

Gamma rays resulting from the decay of the ground state and 237 keV isomeric state of ^{85}Sr have been studied using Ge(Li) detectors. A Ge(Li)-NaI coincidence system has been used to search for coincident γ-rays. Gamma rays of energy 151.2 keV, 231.2 keV, 238.0 keV and 514.0 keV were observed. A previously reported 880 keV γ-ray and a 356 keV−514 keV γ-ray cascade were not observed. An upper limit of 0.006% is placed on the intensity of any γ-ray near 880 keV relative to the intensity of the 514 keV γ-ray. A further γ-ray of 388.9 keV was due to the decay of ^{87m}Sr. (auth)

43878 OPTICAL-MODEL ANALYSIS OF 38 MeV ^{3}He ELASTIC SCATTERING EXTENDED INTO THE BACKWARD HEMISPHERE. Urone, P. P.; Put, L. W.; Ridley, B. W.; Jones, G. D. (Univ. of Colorado, Boulder). Nucl. Phys.; A167: 383-400(1971).

Angular distributions for ^{3}He elastic scattering, have been measured to 155° at 37.7 MeV on ^{48}Ti, ^{58}Fe and ^{90}Zr, and at 36.8, 37.4, 37.5 and 38.1 MeV on ^{58}Ni. These have been analyzed in terms of the optical model. Ambiguities in the real well depth and in the geometrical form of the imaginary potential have been studied. The usefulness of a surface-peaked imaginary potential, particularly in fitting the backward angle data, is indicated by these analyses. The utility of a spin-orbit term in fitting large angle data was investigated. Multiset fits were performed to the data. No conclusions concerning the necessity of either an isospin or asymmetry term in the optical potential at these energies could be drawn. Other information gained from extending ^{3}He elastic scattering measurements into the backward hemisphere is discussed. (auth)

43879 LIFETIMES AND DECAYS OF ENERGY LEVELS IN ^{30}Si AND ^{30}P. Sharpey-Schafer, J. F.; Alderson, P. R.; Bailey, D. C.; (and others) (Univ. of Liverpool). Nucl. Phys.; A167: No. 3, 602-24(1971).

The mean lifetimes of 15 levels in ^{30}Si and of 7 levels in ^{30}P have been measured by the Doppler-shift attenuation method. Limits on the lifetimes of further 8 levels in ^{30}Si and of the 3018 keV level in ^{30}P have been obtained. Branching ratios and excitation energies have been measured in both nuclei. The levels were populated by the reactions $^{27}Al(\alpha,p)^{30}Si$ and $^{27}Al(\alpha,n)^{30}P$ at α-particle bombarding energies of 5.0, 6.3 and 8.0 MeV. The γ-rays were detected with a Ge(Li)−NaI(Tl) escape suppressed and pair escape spectrometer. (auth)

43880 STATES OF ^{23}Na BELOW 5.4 MeV. da Silva, M. F.; Kossionides, S.; Lisle, J. C. (Univ. of Manchester, Eng.). Nucl. Phys.; A168: No. 3, 663-72(1971).

States of ^{23}Na below 5.4 MeV were excited by the reaction ^{24}Mg

XUM

$(t,\alpha)^{23}Na$ and their decay modes were observed. Branching ratios are presented. Particle-γ angular correlation measurements lead to a spin assignment of $\frac{3}{2}$ for the 3.68 MeV state providing that $J = \frac{1}{2}$ is assumed for the 2.64 MeV level. Odd parity is favored for both these states. A value of $J^\pi = \frac{3}{2}^+$ is tentatively assigned to the 2.98 MeV state and $J^\pi = \frac{5}{2}^+$ to the 5.38 MeV state. (auth)

43881 DECAY OF ^{78}As. Morcos, N. A.; Ward, T. E.; Kuroda, P. K. (Univ. of Arkansas, Fayetteville). Contract AT(40-1)-3235. Nucl. Phys.; A168: No. 3, 561-74(1971).

The decay of 91 min ^{78}As was studied using a Ge(Li) spectrometer and scintillation detectors. Fifty-four γ-rays were assigned to ^{78}As and several coincidence measurements were performed. A decay scheme incorporating 44 of the γ-rays is tentatively proposed. From singles β-spectra and $\beta\gamma$ coincidence measurements, a γ-decay Q-value of 4.35 ± 0.10 MeV was determined. Levels in ^{78}Se were established at energies (in keV) of: 613.7, 1308.5, 1499.2, 1502.0, 1693.4, 1721.7, 1854.0, 1997.1, 2327.6, 2508.0, 2681.2, 2798.0, 2839.2, 3144.8, 3227.1, 3232.5 and 3984.0. Spin and parity assignments were deduced for several levels. (auth)

43882 INTENSITIES OF γ-RAYS IN THE ^{57}Co DECAY. Konijn, J.; Lingeman, E. W. A. (Inst. for Nuclear Physics Research, Amsterdam). Nucl. Instrum. Methods; 94: No. 2, 389-90(1971).

New absolute values of γ-ray intensities in the decay of ^{57}Co are given as well as more accurate values for the γ-ray energies. (auth)

43883 COULOMB DISPLACEMENT ENERGIES FOR 1f-2p SHELL NUCLEI. Becchetti, F. D. (Univ. of Minnesota, St. Paul. Univ. of Copenhagen); Dehnhard, D.; Dzubay, T. G. Contracts AT(11-1)-1265; AT(30-1)-937. Nucl. Phys.; A168: No. 1, 151-76(1971). (COO-1265-96).

Coulomb displacement energies for 29 stable isotopes between A = 42 and A = 70 have been measured to an accuracy of ±6 keV using the (^{3}He, t) reaction at 24.6 MeV incident ^{3}He energy. Coulomb energy shifts between members of an isotopic sequence have been determined to an accuracy of ±3 keV. Triton spectra were obtained at 18° using a calibrated position-sensitive detector in the focal plane of an Enge split-pole magnetic spectrometer. In most of the spectra a single, strong transition could be identified as the transition to the isobaric analog of the target nucleus ground state and an unambiguous Coulomb displacement energy was calculated from the measured Q-value. The triton spectra for the residual nuclei ^{56}Co, ^{58}Co and ^{64}Cu showed two strong transitions in the energy region expected for the analog state. In these nuclei, the (^{3}He, t) cross sections to any single state were lower than those expected from the systematics obtained from neighboring isotopes. This indicates a fragmentation of the analog strength. Off-diagonal Coulomb matrix elements in the range 5 to 35 keV can account for the observed energy splittings and (^{3}He, t) cross-section ratios. The experimental Coulomb displacement energies were analyzed using various models. The experimental isotopic shifts in Coulomb displacement energies were used together with measured shifts in charge radii to extract isotopic shifts in the radii of the neutron excess distribution. (auth)

Nuclear Properties and Reactions, A ≥ 90

Refer also to abstracts 41833, 41885, 42110, 42187, 42222, 43831, 43832, 43846, 43847, 43848, 43855, 43871, 43921, 43953, 43955, 43964, 43967, 43970, 43974, 43976, 44190, and 44203.

43884 (ANL-7710, pp 1-52) FISSION PROPERTIES AND CROSS SECTION DATA. (Argonne National Lab., Ill.).

ARSENIC-75—neutron inelastic scattering up to 1.5 MeV, γ spectra from
CARBON—neutron inelastic scattering up to 1.5 MeV, γ spectra from
COPPER—neutron inelastic scattering up to 1.5 MeV, γ spectra from
—neutron total cross section up to 1.5 MeV, (E)
HOLMIUM-165—neutron capture by, resonance spin assignments for, (E)
LITHIUM-6—neutron total cross section up to 1.5 MeV, (E)
MOLYBDENUM-98—neutron total cross section up to 1.5 MeV, (E)
—neutron elastic and inelastic scattering up to 1.5 MeV, cross sections for, (E)
PALLADIUM—neutron total cross section up to 1.5 MeV, (E)
PLUTONIUM-240—neutron total cross section up to 1.5 MeV, (E)
—neutron elastic and inelastic scattering up to 1.5 MeV, cross sections for, (E)
SODIUM-23—neutron inelastic scattering up to 1.5 MeV, γ spectra from
THORIUM-232—neutron total cross section up to 1.5 MeV, (E)
TITANIUM—neutron total cross section up to 1.5 MeV, (E)
—neutron elastic and inelastic scattering up to 1.5 MeV, cross sections for, (E)
URANIUM-233—neutron fission at 0.5 to 1.5 MeV, cross-section rates to uranium-235, (E)
URANIUM-235—neutron fission at 0.5 to 1.5 MeV, cross-section rates to uranium-233, (E)
URANIUM-238—neutron inelastic scattering up to 1.5 MeV, γ spectra from
—neutron total cross section up to 10 MeV, optical-model analyses of, (E/T)
—neutron elastic and inelastic scattering up to 10 MeV, optical-model analyses of, (E/T)
—energy-level scheme from neutron inelastic scattering, (E) (J.W.R.)

43885 (ANL-7748) CRITICAL REVIEW OF THE ENERGY RELEASED IN NUCLEAR FISSION. Unik, J. P.; Gindler, J. E. (Argonne National Lab., Ill.). Mar 1971. Contract W-31-109-eng-38. 54p. Dep. NTIS.

Calculations of the total energy released during and following the fission of ^{232}Th, ^{233}U, ^{235}U, ^{238}U, ^{239}Pu, ^{240}Pu, ^{241}Pu, and ^{242}Pu by neutrons of various energies are presented. Two independent methods of calculation are used. The first method is based on the fact that the total energy released in fission is equal to the difference in energy-equivalent masses of the reactants (target nuclide plus neutron) and the stable fission products. The second method involves the summation of all individual contributions to the total energy release. The total energy absorbed in a reactor (the total energy released as a result of fission minus the antineutrino energy plus the energy released by capture of the fission neutrons in the reactor materials and the subsequent decay of the capture products) is estimated for a particular EBR-II-type reactor. Estimates are also made for the dependence of the total energy releases as a function of neutron energy. The limitations of these calculations and estimates as well as deficiencies in available data are discussed in detail. (auth)

43886 (INR-1268) (n,α) REACTIONS ON HEAVY NUCLEI INDUCED BY 14.2-MeV NEUTRONS. Jaskola, M.; Osakiewicz, W.; Turkiewicz, J.; Zemlo, L. (Institute of Nuclear Research, Warsaw (Poland)). 1971. 10p. Dep. NTIS (U. S. Sales Only).

The energy spectra of alpha particles from the (n,α) reaction with ^{122}Te, ^{139}La, ^{159}Tb, ^{160}Dy, ^{161}Dy, ^{163}Dy, ^{164}Dy, ^{166}Er, ^{168}Er, and ^{169}Tm, induced by 14.2-MeV neutrons, were measured using the semiconductor-detector technique. The analysis of the energy spectra leads to results that the evaporation theory is inadequate to describe the investigated reactions. The shapes of the experimental spectra suggest the presence of strong direct effects. (auth)

43887 (JINR-P6-5791) α DECAY OF NEUTRON-DEFICIENT RADON ISOTOPES. Golovkov, N. A.; Ivanov, R. B.; Kolachkovski, A.; Norseev, Yu. V.; Chumin, V. G. (Joint Inst. for Nuclear Research, Dubna (USSR). Lab. of Nuclear Problems). 1971. 21p. (In Russian). Dep. NTIS (U. S. Sales Only).

The α decay of the Ra isotopes with A = 206 to 212, separated on mass separator, was studied with the help of magnetic α spectrograph. New α transitions to levels of the daughter nuclei were obtained. (auth)

43888 (LA-4648) FISSION FRAGMENT ANGULAR DISTRIBUTIONS FOR ^{230}Th, ^{232}Th, ^{231}Pa, AND ^{239}Pu. Muir, D. W. (Los Alamos Scientific Lab., N. Mex.). Jun 1971. Contract W-7405-eng-36. 10p. Dep. NTIS.

Recently published experimental data on the angular distribution of fragments from the neutron-induced fission of ^{230}Th, ^{232}Th, ^{231}Pa, and ^{239}Pu are fitted with a power series in $\cos\theta$. The data, fitting coefficients, and values calculated at 15 and 80° are presented at neutron energies up to 3.0 MeV. (auth)

43889 (LA-4708) DCHAIN: A PDP-9/PDP-15 COMPUTER PROGRAM FOR RADIOACTIVE DECAY AND CAPTURE CHAIN CALCULATIONS. East, Larry V. (Los Alamos Scientific Lab., N. Mex.). Jun 1971. Contract W-7405-eng-36. 10p. Dep. NTIS.

A program written to calculate the time-dependent populations of radioactive decay and neutron capture chains is described. The program is written in FORTRAN IV, and intended for use on a DEC PDP-9 or PDP-15 computer. A complete program listing and sample calculations are included. (auth)

43890 (ORNL-TM-3436) NEUTRON ENERGY-DEPENDENT CAPTURE GAMMA-RAY YIELDS IN TANTALUM AND TUNGSTEN. Yost, K. J.; White, J. E.; Fu, C. Y.; Ford III, W. E. (Oak Ridge National Lab., Tenn.). 7 Jun 1971. Contract W-7405-eng-26. 36p. Dep. NTIS.

Gamma-ray yields as a function of neutron energy for tantalum and tungsten are calculated with the cascade code DUCAL. The results are presented in a format that would facilitate use in coupled neutron–gamma-ray transport calculations. In the case of tungsten, pronounced variations in the capture yield spectra were noticed above 3.0 MeV; on the other hand, only slight variations in the yield spectra were evident for tantalum. The results are compared with integral gamma-ray yield measurements, and the agreement is favorable. (auth)

43891 (RFP-Trans-78) DETERMINATION OF THE ACTIVATION CROSS-SECTION OF SHORT LIVED NUCLEAR ISOMERS FOR THERMAL NEUTRONS. Alexander, K. F.; Brinkmann, H. F. Translated from Ann. Phys. (Leipzig); (7) 12: 225-62(1963). 41p. Dep. NTIS.

An abstract of this paper, prepared from the original language, appeared as NSA 18: 15219. (R.W.R.)

43892 γ-RAY SPECTRUM FROM REACTION (n,γ) ON ^{150}Sm AND ^{151}Sm SAMPLES. Groshev, L. V.; Demidov, A. M.; Leonov, V. F.; Sokolovskii, L. L. (Inst. of Atomic Energy, Moscow). Yadern. Fiz.; 13: No. 4, 681-7(Apr 1971). (In Russian).

The γ-ray spectra from radiative capture of thermal neutrons by ^{150}Sm and radioactive ^{151}Sm were measured using a one-crystal Ge(Li) γ spectrometer. The necessary purity of a sample relative to ^{149}Sm was achieved by burning out the ^{149}Sm in the integral neutron flux, 2.2×10^{20} neutron/cm^2. The neutron binding energies were found to be (5596 ± 1 keV) in ^{151}Sm and (8258 ± 1 keV) in ^{152}Sm. Schemes of γ transitions for ^{151}Sm and ^{152}Sm are presented. (auth)

43893 INFORMATION ON EXCITATION MECHANISM OF THE ISOBARIC ANALOG STATES FROM ANALYSIS OF RESONANCE (p,n) REACTIONS. Guzhovskii, B. Ya.; Zaretskii, D. F.; Zvenigorodskii, A. G.; Urin, M. G. (Moscow Engineering-Physics Inst.). Yadern. Fiz.; 13: No. 4, 719-26(Apr 1971). (In Russian).

The effect of compound nucleus levels on excitation of isobaric analog resonances (IAR) is investigated. The formula for the cross section of resonance (p,n) reactions, obtained with account of the "inner" and "external" mixings of the analog and compound nuclear states, is used to analyze the experimental data. On basis of this analysis it is shown that the inner mixing is essential in formation of the IAR in the (p,n) reaction and dominates in a number of cases. (auth)

43894 RELAXATION PHENOMENA AND NUCLEAR MAGNETIC RESONANCE OF ^{116}In($T_{\frac{1}{2}}$ = 14s) PRODUCED BY CAPTURE OF POLARIZED NEUTRONS IN THE INDIUM III–V COMPOUNDS. Winnacker, A. (Univ., Heidelberg); Ackermann, H.; Dubbers, D.; Mertens, J.; von Blanckenhagen, P. Z. Phys.; 244: No. 4, 289-311(1971).

Polarized ^{116}In nuclei were produced by capture of polarized thermal neutrons in several In compounds. At temperatures T below 77°K and magnetic field strengths H_0 of several kOe, asymmetries of a few percent of the β^- decay of the ^{116}In ground state could be observed in polycrystalline InP, InAs and InSb, thus indicating the nuclear polarization. Nuclear magnetic resonance signals were measured with the result for the magnetic moment $\mu_I(^{116}\text{In}) = 2.7723\ (10)$ nm (uncorrected). β^- decay asymmetry and spin lattice relaxation time T_1 were studied as a function of H_0 and T. The effect of H_0 is to decouple the hyperfine interaction caused by the capture-γ recoil process. However, H_0 has no influence upon T_1, which demonstrates the absence of nuclear relaxation due to paramagnetic impurities. T_1 is determined by quadrupolar relaxation. A quadrupole moment Q (^{116}In) = 0.09 (2) b was calculated by comparison of the ^{116}In relaxation rates with those of the stable ^{115}In isotope in the same compounds. Above 30°K the temperature dependence of $1/T_1$ agrees with a recent theoretical investigation. Below 30°K the relaxation rate shows an anomalous behaviour, which can be explained by resonance modes due to recoil lattice defects. (auth)

43895 HALF-LIFE MEASUREMENTS OF 86.6-keV LEVEL IN ^{233}Pa AND 59.6-keV LEVEL IN ^{237}Np. Garg, R. K.; Chauhan, S. D.; Gupta, S. L.; Saha, N. K. (Univ. of Delhi). Z. Phys.; 244: No. 4, 312-20(1971).

The half-lives of the 86.6 keV level in ^{233}Pa and the 59.6 keV level in ^{237}Np were measured. A silicon surface barrier alpha detector and a NaI(Tl) gamma-detector were used. The decay time spectrum of alpha-gamma coincidences obtained from a start-stop type of time-to-pulse height converter was recorded on a 2048-channel analyser. Using the experimental level $T_{\frac{1}{2}}$'s, partial gamma-ray half-lives were calculated for the 86.6- and the 29.6-keV transitions (from the 86.6 keV level) in ^{233}Pa and the 59.6- and the 26.36-keV transitions (from the 59.6 keV level) in ^{237}Np. The results are compared with the single particle and the Nilsson estimates. (auth)

43896 ANGULAR CORRELATION STUDIES ON THE 326- AND 177-keV CASCADE IN ^{131}Xe. Gfirtner, H.; Kreisel, W. (Liebig Univ., Giessen, Ger.). Z. Phys.; 244: No. 4, 332-7(1971). (In German).

The angular correlation of the 326–177 keV gamma-gamma cascade in ^{131}Xe was measured with 2 Ge(Li)-detectors. For the corrected correlation coefficients we obtained $A_2 = 0.002 \pm 0.011$ and $A_4 = 0.097 \pm 0.012$. Estimating possible spins of $^7/_2$, $^9/_2$ and $^7/_2$, $^9/_2$, $^{11}/_2$, $^{13}/_2$ for the 667.0 and 341.2 keV states respectively, experimental value agrees with the following spin sequences: $^7/_2^- \rightarrow {}^9/_2^- \rightarrow {}^{11}/_2^-$, $^7/_2^- \rightarrow {}^{11}/_2^- \rightarrow {}^{11}/_2^-$ and $^9/_2^- \rightarrow {}^{13}/_2^- \rightarrow {}^{11}/_2^-$. (auth)

43897 DIRECT MEASUREMENT OF THE (n,2n) CROSS SECTION OF ^{93}Nb. Haering, M.; Vonach, H.; Feicht, E. J. (Technische Univ., Munich). Z. Phys.; 244: No. 4, 352-7(1971). (In German).

Using the watertank-method for natural niobium $\sigma_{n,2n} = 1.35 \pm 0.25$ barn was found. This value agrees with statistical model calculations and fits the systematics of the (n,2n) cross-sections. (auth)7

43898 SCATTERING OF FAST NEUTRONS ON ^{238}U: AVERAGE ENERGY AND ANGULAR DISTRIBUTIONS OF FISSION NEUTRONS. Knitter, H.-H.; Coppola, M.; Ahmed, N.; Jay, B. (EURATOM, Geel, Belgium). Z. Phys.; 244: No. 4, 358-70 (1970).

Angular distributions of neutrons elastically and inelastically scattered from ^{238}U were measured with a time-of-flight spectrometer at seven incident neutron energies between 1.5 and 5.5 MeV. Inelastic angular distributions for groups of unresolved levels are given for incoming neutron energies of 1.5, 1.9 and 2.3 MeV. The corresponding neutron cross sections were obtained relative to the n-p scattering cross sections. The average energies and angular distributions of the fission neutrons were extracted from the measured fission neutron spectra at 1.5, 1.9 and 2.3 MeV. Cross-section calculations based on a spherical optical model have shown to be inadequate to describe the neutron-nucleus interaction in case of strong nuclear deformation. The experimental reality may be better approached, instead, if the calculations are made using a potential which takes into account the deformation of the target nucleus. Some of the present measurements are interpreted in this theoretical perspective. (auth)

43899 LEVELS IN ^{101}Ru POPULATED BY THE DECAY OF ^{101}Tc. Aras, Namik K. (Oak Ridge National Lab., Tenn. Middle East Technical Univ., Ankara); Fettweis, P.; Chilosi, G.; O'Kelley, G. Davis. Nucl. Phys.; A169: No. 1, 209-24(1971).

The decay properties of 14 min ^{101}Tc were investigated by the use of Ge(Li) and NaI(Tl) γ-ray and anthracene β-ray detectors. Coincidence relationships between the γ-rays were determined with the aid of a multiparameter analyzer. Numerous γ-rays (33) could be identified. Two strong β-groups with end-point energies of 1.32 and 1.07 MeV were shown to be in coincidence with 306.7 and 544.7 keV γ-rays, respectively. A decay scheme consistent with the coincidence data is presented, with levels at 127.1, 306.7, 311.2, 422.4, 544.7, 616.1, 720.0, 842.6, 911.1, 928.2 and 918.1 keV. Spin assignments for the excited levels in ^{101}Ru are proposed. (auth)

43900 ^{142}Nd(d,t)^{141}Nd REACTION. Foster, J. L. Jr. (Univ. of Montreal. Univ. of Pittsburgh); Dietzsch, O.; Spalding, D. Nucl. Phys.; A169: No. 1, 187-93(1971).

The level structure of ^{141}Nd up to 2 MeV excitation was investigated by the reaction ^{142}Nd(d,t) with 17 MeV incident deuterons and with 6–8 keV resolution. The angular distributions were analyzed with both a standard zero-range distorted-wave Born approximation (DWBA) and with finite-range and non-local potential corrections, using the program DWUCK. (auth)

43901 ELASTIC AND INELASTIC PROTON SCATTERING FROM HEAVY COLLECTIVE NUCLEI. Kruse, T. (Rutgers–The State Univ., New Brunswick, N. J.); Makofske, W.; Ogata, H.; (and others). Nucl. Phys.; A169: No. 1, 177-86(1971).

Elastic and inelastic differential cross sections were measured for 16 MeV protons on nuclei with $148 \leq A \leq 198$. Optical model, DWBA and coupled-channel analyses were performed. Results show systematic dependence on deformations. (auth)

XUM

43902 LEVELS IN ^{191}Ir. Baecklin, A. (Swedish Research Councils' Lab., Studsvik); Hedin, G.; Malmskog, S. G. Nucl. Phys.; A169: No. 1, 122-30(1971).

The decay of ^{191}Pt → ^{191}Ir was studied with Ge(Li)–Ge(Li) coincidence systems as well as magnetic and Si(Li) conversion electron spectrometers. A new transition at 141.4 ± 0.5 keV was observed. Evidence was found for three new levels in ^{191}Ir at 588.1 ± 0.3, 747.97 ± 0.09 and 800.5 ± 0.5 keV. The two former levels have positive parity while the latter most probably has a negative parity and spin $^{5}/_{2}$. From measurements of K conversion coefficients multipolarities were determined for about eleven transitions. The 576.6 and 659.2 keV transitions were found to be E1, thus confirming the earlier observed negative parity of the 659.01 keV level. (auth)

43903 ABSOLUTE TRANSITION RATES IN ^{182}W. Hoeglund, A. (Univ. of Stockholm, Aktiebolaget Atomenergi, Studsvik, Sweden); Malmskog, S. G.; Marelius, A.; Vaelivaara, K. G.; Kozyczkowski, J. Nucl. Phys.; A169: No. 1, 49-61(1971).

Earlier measurements on half-lives of excited states in ^{182}W have shown remarkable disagreements. The main object of this investigation was to remeasure these half-lives and to find the reason for the discrepancies. The results are in agreement with the findings of Meiling and Stary but in disagreement with Bashandy et al. The half-life of the 453-keV level in ^{183}W was found to be $T_{½}$ = 19.5 ± 0.3 ns in agreement with earlier results. (auth)

43904 ISOTONE SHIFT IN MUONIC X-RAYS IN THE TIN REGION. Kast, J. W.; Bernow, S.; Cheng, S. C.; (and others) (Columbia Univ., New York). Nucl. Phys.; A169: No. 1, 62-70(1971).

The energies of the K and L muonic X-rays of six isotones in the region of tin (Z = 50) were measured, and the change in nuclear size on adding protons was calculated. The effect of nuclear shell closing at Z = 50 is substantial. (auth)

43905 DECAY SCHEME OF ^{121m}Sn AND MOESSBAUER EFFECT IN ^{121}Sb. Snyder, Richard E. Detroit; Wayne State Univ. (1966). 119p. University Microfilms Order No. 71-12,067.

Thesis.

The decays of ^{121m}Sn (76.3 yr) and ^{121}Sn (25.53 hr) were investigated with the use of a 4π scintillation beta spectrometer and gamma-ray spectrometers. The β^- spectra of both ^{121m}Sn and ^{121}Sn were measured; ^{121m}Sn was found to decay to the 37-keV level of ^{121}Sb and ^{121}Sn was found to decay, with a half-life of 25.53 ± 0.25 hours, to the ground state of ^{121}Sb. The beta spectrum of ^{121m}Sn yielded an end-point energy of 354 ± 4 keV and a linear Fermi–Kurie plot when a first forbidden unique shape factor was applied. The beta spectrum of ^{121}Sn was observed to have an end-point of 383 ± 3 keV and an allowed shape. Spins and parities of $^{3}/_{2}^{+}$ and $^{11}/_{2}^{-}$ were assigned to the ^{121}Sn and ^{121m}Sn states respectively. The transition from the first excited state to the ground state in ^{121}Sb was measured with a lithium-drifted silicon detector. An energy of 37.149 keV and a K internal conversion coefficient of 9.32 ± 0.37 were obtained. Based on the observed energies of the beta spectra and gamma ray, the $^{11}/_{2}^{-}$ ^{121m}Sn state was calculated to lie at 8 ± 5 keV above the $^{3}/_{2}^{+}$ ^{121}Sn ground state. The Moessbauer effect was used to study the quadrupole interaction of the 37-keV ^{121}Sb level. The ratio of the first excited ($^{1}/_{2}^{+}$) to ground state ($^{5}/_{2}^{+}$) quadrupole moments of ^{121}Sb was measured to be 1.38 ± 0.02. The ground state quadrupole interaction constant for Sb_2O_3 was found to be e^2qQ_{gnd} = +557 ± 20 MHz. (Diss. Abstr. Int., B)

43906 ELECTRON CAPTURE DECAY SCHEMES OF ^{203}Bi AND ^{204}Bi. Cross, James Burke. East Lansing, Mich.; Michigan State Univ. (1970). 332p. University Microfilms Order No. 71-11,811.

Thesis.

The electron capture decay schemes of ^{203}Bi and ^{204}Bi were investigated by high-resolution γ-ray spectroscopy in an effort to acquire information about their nuclear structure and properties. Such γ-ray spectroscopic techniques as Ge(Li) singles, Ge(Li)–NaI(Tl) coincidence, and Ge(Li)–Ge(Li) multiparameter, 2-dimensional coincidence techniques were utilized to identify the many new γ rays in ^{203,204}Bi and to determine the coincidence (cascade) relationships of these γ rays. Several computer programs which are useful in handling data from complex decay schemes are presented. Two hundred and ten (210) γ rays have been assigned to the electron capture decay of 11.2-hour ^{204}Bi. A secondary decay scheme was proposed; γ-ray transitions in this scheme are placed solely on the basis of precise energy sums and weak coincidence data. One hundred and forty seven (147) γ rays were associated with the electron capture decay of 11.7-hour ^{203}Bi. A secondary decay scheme with transitions placed solely on the basis of energy sums and weak coincidence data was also proposed. Limits on the spin and parity assignments of the nuclear states investigated are made on the basis of log ft values, relative γ intensities to states of known spin and parity, and transition multipolarities (for those transitions where internal conversion-electron intensities were available). A brief survey of and comparison with previously reported scattering reaction data is presented for ^{203}Pb and ^{204}Pb. Nuclear shell-model level spacings in the vicinity of Z = 82 and N = 121 are discussed. Possible shell-model transitions associated with the electron capture decay of ^{203,204}Bi are suggested. Probable dominant configurations of 8 low-lying levels in ^{203}Pb are offered in simple shell- and collective-model terminology. Finally, a summary of the previous theoretical calculations of ^{204}Pb is made along with suggestions for a theoretical re-evaluation of these lead isotopes. (Diss. Abstr. Int., B)

43907 NEUTRON PARTICLE HOLE STRUCTURE IN ^{208}Pb THROUGH ISOBARIC ANALOG RESONANCES. Kulleck, James Gerard. Austin, Tex.; Univ. of Texas (1970). 113p. University Microfilms Order No. 71-11,571.

Thesis.

Neutron neutron-hole states in ^{208}Pb were investigated by proton elastic and inelastic scattering through isobaric analog resonances. The elastic scattering data were analyzed to obtain parameters for the $g_{9/2}$, $d_{3/2}$, $s_{1/2}$, $g_{7/2}$, and $d_{5/2}$ analog resonances in the compound nucleus ^{209}Bi. With these parameters, spectroscopic factors were calculated. Excitation functions were measured for seven low-lying states and their particle hole character is discussed. Excitation energies for 71 states up to 7 MeV were determined along with quantitative information concerning their structure. Angular distributions were taken for those levels possessing an observable $d_{5/2}$ particle configuration. Inelastic proton partial widths were extracted from these data and final state spins and parities are specified based on these results and the findings of other experimental observations. The expression used in the analysis of the inelastic scattering cross sections is presented. This relation is generalized to include the derivation of the polarization cross section. (Diss. Abstr. Int., B)

43908 AVERAGE NEUTRON TOTAL CROSS SECTIONS AND THE OPTICAL MODEL. Pineo, Evans William Fletcher. Durham, N. C.; Duke Univ. (1970). 119p. University Microfilms Order No. 71-10,412.

Thesis.

Average neutron total cross sections were measured for samples of potassium chloride, scandium, zinc, arsenic, selenium, rubidium bromide, cesium iodide, cerium, neodymium, samarium, gadolinium, terbium, dysprosium, holmium, mercury, and the separated isotopes ^{144}Nd, ^{146}Nd, ^{148}Nd, ^{149}Sm and ^{152}Sm. These measurements were made with an improved geometry designed to minimize the inscattered and extraneous neutron background. Cross sections averaged over the energy ranges of 100–650 keV and 350–650 keV were compared with optical model calculations made using both spherical and deformed potentials. The agreement between the spherical optical model calculations and the averaged cross section data are only fair below A = 140, where the nuclei are not statically deformed, and fail completely above A = 140 where the nuclei are known to exhibit large static deformations. The agreement between the deformed optical model calculations and the averaged cross sections is somewhat better but descrepancies are still apparent near A = 100 and above A = 140. The effects of the simplified coupling schemes and of the known limits of error in the quadrupole deformation parameters which were used in the calculations are discussed at length. S-, p-, and d-wave strength functions, the s-wave scattering length, and the p-wave phase shift ratio were extracted from the average neutron total cross sections data using the Duke low resolution method. These parameters are compared with optical model calculations made using deformed potentials. The measurements of the s-wave strength functions add to the overwhelming evidence that the 4s giant resonance is split, and the measurements of the s-wave scattering length R′ add considerably to the details of its variation in the 4s giant resonance region. (Diss. Abstr. Int., B)

43909 NUCLEAR SPECTROSCOPIC STUDIES OF NEUTRON-DEFICIENT, ODD-MASS RARE EARTHS NEAR THE N = 82 CLOSED SHELL. Eppley, Richard Earl. East Lansing, Mich.; Michigan State Univ. (1970). 309p. University Microfilms Order No. 71-11,829.

Thesis.

The decay schemes of ^{149}Gd, Gd^{145g+m} and Sm^{141g+m} were studied by γ- and β-ray spectroscopy in an effort to elucidate their nuclear properties. Also, a search for Dy^{147g+m} was conducted, although no decay scheme can be proposed. γ-ray spectroscopic techniques including Ge(Li) singles, Ge(Li)–NaI(Tl) coincidence, and Ge(Li)–Ge(Li) megachannel, 2-dimensional coincidence tech-

niques have been employed. Where appropriate, electron spectra were obtained by use of Si(Li) surface barrier detectors. Spin and parity assignments for the nuclear levels encountered are based on log ft values, relative γ intensities, and transition multipolarities (where internal-conversion-electron intensities were available). Two intense transitions in ^{145}Eu, which account for ≈72% of the β decay from ^{145}Gd, are interpreted as being three-quasiparticle states. Also, there are 6 states in ^{141}Pm, lying between the energies of 1414.8 and 2702.4 keV, which appear to be three-quasiparticle states analogous to those reported recently for ^{139}Pr. Mechanisms are suggested for these three-quasiparticle types of decay in terms of simple shell-model transitions and nucleon rearrangements. Several families of nuclear isomers are compared with each other in terms of their level energies and reduced M4 transition probabilities. These include the Z = 82, N = 81, N = 79, Z − 50, Z = 49, and N = 49 families. High multipolarity electromagnetic transitions from these isomers are considered to be quite "pure" single-particle transitions. The experimentally measured transition probabilities are compared to these single particle predictions in an effort to determine the degree to which this is true. Finally, levels in the odd-mass N = 82 and Z = 63 nuclides are traced as far as possible in an effort to understand nuclear behavior in this region better. (Diss. Abstr. Int., B)

43910 COLLECTIVE VIBRATIONS OF THE STATISTICAL NUCLEAR MODEL. Balazs, E. (Research Group for Theoretical Physics, Budapest). Acta Phys. Acad. Sci. Hung.; 29: No. 2-3, 193-202(1970).

The collective vibrations of ^{90}Zr are calculated by applying the statistical nuclear model and the Bloch–Jensen theory. The results allow a theoretical interpretation of the experimentally observed resonances in the quasi-elastic photon scattering on ^{90}Zr. (auth)

43911 EVIDENCE FOR VIOLATION OF THE PORTER–THOMAS POSTULATE IN ^{232}Th. Forman, L.; Schelberg, A. D.; Warren, J. H.; Glass, N. W. (Los Alamos Scientific Lab., N. Mex.). Phys. Rev. Lett.; 27: No. 2, 117-20(12 Jul 1971).

The ^{232}Th neutron-capture cross section has been measured from 20 to 30 keV on the Physics-8 underground explosion. Resonance parameters and systematics for s-wave and p-wave levels that were obtained in the resolvable region, to 2000 eV, were used directly to calculate the average cross sections in the unresolved region. These calculations were in good agreement with the measured cross section. Our results do not support the Porter–Thomas postulate for single-channel reactions. (auth)

43912 HIGH-SPIN ISOMER IN ^{211}At. Maier, K. H.; Leigh, J. R.; Puehlhofer, F.; Diamond, R. M. (Univ. of California, Berkeley). Phys. Lett.; 35B: No. 5, 401-4(21 Jun 1971).

A 4-μsec isomer was observed in ^{211}At at an excitation energy of 4.816 MeV. The multipolarities of the de-excitation γ rays suggest a very high spin. The excitation energy, g-factor, and strongly enhanced E3 decay may be described by a 4p–1h configuration with $J^{\pi} = {}^{39}/_{2}{}^{-}$. (auth)

43913 NUCLEAR EXCITATION BY THE BOUND MUON. Konishi, Teruaki; Narumi, Hajime (Hiroshima Univ.). Progr. Theor. Phys. (Kyoto); 45: No. 4, 1348-9(Apr 1971).

The theory of nuclear rotational excitation by the mu meson is extended to nuclei in the transition region, such as Os. Since different models give somewhat different predictions for transitions in such nuclei, it is possible to evaluate the different models by precisely measuring the mesonic x rays for pure isotopic nuclei. (R.W.R.)

43914 ANALYSIS OF ^{127}I(n,n'γ) REACTION DATA. Sharma, H. C.; Nath, N. (Kurukshetra Univ., India). Progr. Theor. Phys. (Kyoto); 45: No. 4, 1337-40(Apr 1971).

The measured elastic angular distribution and total neutron cross-section data for ^{127}I at 4 MeV are used to obtain the optical-model potential parameters. The inelastic neutron scattering yields for only the low-lying excited states in ^{127}I are calculated using both the statistical and the resonance theory of average reaction cross-sections and compared with the experimental data. Conclusions are drawn concerning the applicability of the two theoretical approaches and spin–parity assignments for individual states. (R.W.R.)

43915 EVIDENCE FOR THE IMPORTANCE OF THE NUCLEON–NUCLEON SPIN-ORBIT INTERACTION IN THE INELASTIC EXCITATION OF HIGH SPIN STATES IN ^{90}Zr. Love, W. G. (Univ. of Georgia, Athens). Phys. Lett.; 35B: No. 5, 371-4(21 Jun 1971).

A microscopic calculation of the inelastic scattering of 61.2-MeV protons to the 6^+ and 8^+ states in ^{90}Zr is carried out; central, tensor, and spin–orbit parts of the nucleon–nucleon interaction are included. The two-body spin–orbit force is found to play an important role in exciting these high-spin states. (auth)

43916 β-STABILITY LINE AND LIQUID-DROP MASS FORMULAS. Kodama, Takeshi (Waseda Univ., Tokyo). Progr. Theor. Phys. (Kyoto); 45: No. 4, 1112-22(Apr 1971).

An empirical analysis of the masses of odd-mass nuclei is made, with emphasis on the gross structure of the nuclear mass surface, especially on the β-stability line. As a consequence of the analysis, three macroscopic (liquid-drop) mass formulas are derived. It is pointed out that large volume and surface symmetry-energies are necessary for the reproduction of the experimental β-stability line. (auth)

43917 DIRECTIONAL CORRELATION AND DECAY SCHEME STUDIES OF ^{178}Hf AND ^{156}Gd. Little, Paul Edward. Nashville; Vanderbilt Univ. (1970). 220p. University Microfilms Order No. 71-10,455.

Thesis.

Levels in ^{178}Hf, populated from the decay of ^{178}Ta, were studied. Five new levels at 1174.64 (KπI = 2 + 2), 1309.91 ($I\pi = 1^{\pm}$, 2^{+}), 1362.36 ($I\pi = 2^{\pm}$), 1566.45 ($I\pi = 1^{\pm}$, $2^{\pm}$, 3^{-}) and 1771.95 ($I\pi = 0^{+}$) keV and thirteen transitions were added to the decay scheme. Nine new transitions are reported. Accurate branching ratios were obtained for transitions from the 2^+ level at 1276 keV in ^{178}Hf. They have been used to calculate a Z_B parameter. Agreement between the theoretical ratios for a beta-vibrational band and experimental branching ratios is observed when a (73.0 ± 1.3)% M1 component is assumed in the 1183 keV, $\Delta I = 0$ transition from the 1276 keV level. The $\gamma-\gamma(\theta)$ measurements indicate an (85.6)% M1 component. Thus the branching ratios from this level are not in agreement with theoretical predictions for a beta band. The M1 component in the 1403 keV, $2^+ \rightarrow 2^+$ transition from the 1496 keV level is measured to be (61.0)% which compares favorably with the 62.5 ± 1.0)% M1 admixture predicted by the branching ratios. Neither of these levels has all the properties predicted for a beta-vibrational level, however. Further, $\gamma-\gamma(\theta)$ studies were also performed on the transitions in ^{156}Gd whose levels were populated from the decay of ^{156}Eu. A (97.9)% E2 component measured in the 1041 keV, $2_{\beta}^{+} \rightarrow 2^{+}$ transition is in clear disagreement with the (37.5 ± 5)% E2 predicted by the branching ratios. Fourteen other correlations were also measured including four one-three correlations. In particular, the E2 component in the 1063 keV $2_{\gamma}^{+} \rightarrow 2^{+}$ transition was measured to be (99.7 ± 0.1)%. (Diss. Abstr. Int., B)

43918 ISOBARIC ANALOG RESONANCES IN PROTON ELASTIC AND INELASTIC SCATTERING FROM ^{130}Te. Hiddleston, Hoyt Rodney. Austin, Tex.; Univ. of Texas (1970). 118p. University Microfilms Order No. 71-11,552.

Thesis.

Proton elastic scattering data are analyzed in the framework of a single-particle theory to obtain energies, partial widths, total widths, and spectroscopic factors for 14 isobaric analog resonances in ^{131}I. The compound nuclear states in ^{131}I are analogs of states in ^{131}Te formed by the addition of a neutron to the ^{130}Te core. Excitation functions and fits are presented and the results are compared with similar elastic analyses as well as with the related (d,p) investigation. A total of 42 excited states in ^{130}Te were identified from the inelastic spectra at the various resonances. Groups of states at the $d_{\frac{3}{2}}$, $f_{\frac{7}{2}}$, and $p_{\frac{3}{2}}$ resonances were analyzed as neutron particle-neutron hole states, and fits to the angular distribution data for these states are presented. The analysis provides proton partial widths, spectroscopic factors, and assignment of possible spins and parities for these states. Analysis of on-resonance angular distribution data for decay to the 2^+ first excited state has provided additional proton partial widths and spectroscopic factors. The ^{130}Te inelastic results are compared with those of other nuclei in the N = 82 mass region. (Diss. Abstr. Int., B)

43919 STABILITY OF SUPERHEAVY NUCLEI AGAINST FISSION, ALPHA DECAY, AND ELECTRON CAPTURE. Grumann, Jens; Morovic, Tihomir; Greiner, Walter (Univ., Frankfurt am Main). Z. Naturforsch.; 26a: No. 4, 643-52(Apr 1971).

The potential-energy surface is calculated by two methods, which are compared with respect to spontaneous fission. In the first one the sum of the single-particle energies is computed essentially as was done in a previous paper [Z. Phys., 228: 371 (1969)], while the second one the Strutinsky technique of renormalizing to a liquid-drop model is applied. The half-lives for electron capture are also investigated, together with the pre-

XUM

dictions of the half-lives for spontaneous fission and α decay. The results support the existence of superheavy nuclei in the regions around Z = 114 and Z = 164. (auth)

43920 SYMMETRIC FISSION OBSERVED IN THERMAL-NEUTRON-INDUCED AND SPONTANEOUS FISSION OF ^{257}Fm. John, W.; Hulet, E. K.; Lougheed, R. W.; Wesolowski, J. J. (Univ. of California, Livermore). Phys. Rev. Lett.; 27: No. 1, 45-8(5 Jul 1971).

The observed mass distribution for the thermal-neutron-induced fission of ^{257}Fm is strongly symmetric, whereas that for spontaneous fission of ^{257}Fm is found to be predominantly asymmetric with, however, some symmetric fission present. The mass distributions were derived from energy measurements on coincident fission fragments. The onset of symmetric fission at ^{257}Fm supports theories relating asymmetric fission to the second hump of the fission barrier. (auth)

43921 LEVEL STRUCTURE OF ^{143}Pr FROM γ DECAY. Bashandy, E. (Atomic Energy Establishment, Cairo). Z. Naturforsch.; 26a: No. 4, 683-9(Apr 1971).

The γ decay of ^{143}Ce was investigated using both a Ge(Li) γ-ray detector and a high-resolution iron-free double-focusing β-ray spectrometer. In addition to γ rays previously reported, more γ rays could be observed. Internal conversion coefficients and multipolarities of γ transitions were determined. Ten excited nuclear energy states were established in ^{143}Pr at 57, 351, 491, 722, 939, 1045, 1061, 1161, 1382, and 1452 keV. Possible spin values are assigned to all these states on the basis of conversion coefficients of γ rays. The level structure of ^{143}Pr is discussed in terms of existing nuclear models. (auth)

43922 INTERNAL-CONVERSION ELECTRONS EMITTED BY DIFFERENT ELEMENTS IN THE FISSION OF ^{252}Cf. Shapiro, N. L.; Wehring, B. W.; Wyman, M. E. (Univ. of Illinois, Urbana). Phys. Rev., C; 3: No. 6, 2464-74(Jun 1971).

Coincidence measurements of the internal-conversion electrons and x rays emitted by the fragments and products of the spontaneous fission of ^{252}Cf are reported. Two-parameter data were recorded event by event and stored sequentially on magnetic tape. The first parameter contained information on the energy of the x ray as measured by a high-resolution semiconductor detector and was used to determine the atomic number of the deexciting nucleus. The second parameter contained information on the energy of the internal-conversion electrons. Two measurements were performed. The first measurement recorded only electrons emitted from the pre-β-decay fission fragments, while the second measured events from both the fragments and products of fission. In general, it was found that the x rays from an element are produced by numerous internal-conversion transitions. The energies of these transitions are tabulated for each element produced in fission. A greater number of these transitions was observed to occur for odd-Z elements than for even-Z elements; this result suggests that the even–even nuclides contribute little to the x-ray spectrum. This even–odd effect was more pronounced in the measurement of events from both fragments and products of fission than in the measurement of events from the fission fragments alone. (auth)

43923 EFFECT OF THE MULTIPOLE PAIRING AND PARTICLE-HOLE FIELDS IN THE PARTICLE-VIBRATION COUPLING OF ^{209}Pb. II. THE ^{207}Pb(t,p)^{209}Pb REACTION AT 20 MeV. Flynn, E. R. (Los Alamos Scientific Lab., N. Mex.); Igo, G.; Barnes, P. D.; (and others). Phys. Rev., C; 3: No. 6, 2371-89 (Jun 1971).

The ^{207}Pb(t,p)^{209}Pb reaction was performed at 20 MeV. The excitation of the single-particle states is used as a normalization for the distorted-wave code of Bayman and Kallio [Phys. Rev., 156: 1121(1967)]. A large number of two-particle–one-hole states are seen in the excitation region examined, the first (the $\frac{1}{2}^-$) being at 2.152 MeV. The remaining states are interpreted as being multiplets of the $[p_{\frac{1}{2}}^{-1}|^{210}\mathrm{Pb}(J)\rangle]$ configurations. The magnitudes and energy centroids of the observed states are compared with those observed in the ^{208}Pb(t,p)^{210}Pb experiment and also with the theoretical treatment of a particle coupling to multipole pairing and particle–hole fields. (auth)

43924 DECAY OF ^{126}Sn AND OF THE 19-MIN AND 12.4-DAY ISOMERS OF ^{126}Sb. Orth, C. J. (Los Alamos Scientific Lab., N. Mex.); Dropesky, B. J.; Freeman, N. J. Phys. Rev., C; 3: No. 6, 2402-11(Jun 1971).

The γ radiations of $\approx 10^5$-yr ^{126}Sn and of the ^{126}Sb isomers were studied with NaI(Tl) scintillation spectrometers and Ge(Li) detectors. β-ray spectra were measured with a trans-stilbene scintillation unit, and conversion electrons were examined with Si(Li) detectors. The decay of ^{126}Sn involves a (0.25 ± 0.03)-MeV β transition followed by 21.6-, 23.4-, 42.7-, 64.4-γ and 87.7-keV γ transitions in ^{126}Sb. The 23.4- and 87.7-keV transitions are in prompt coincidence with the β rays; the 64.4-keV and either the 21.6- or 42.7-keV transition deexcite an intermediate delayed level with $t_{\frac{1}{2}} = 0.5 \pm 0.1\,\mu$sec. Both the 19-min and the 12.4-day isomers of ^{126}Sb have essentially the same (1.90 ± 0.15)-MeV maximum β-ray endpoint energy; however, the β spectrum of the latter is more complex (intense inner groups). The 19-min isomer decays by β emission (86%) to excited levels in ^{126}Te and by ≤31-keV isomeric transition (14%) to the 12.4-day ground state. The ^{126}Te excited levels involved in the decay of both ^{126}Sb isomers are at 665(2^+), 1359(4^+), 1774(6^+), 2215, 2395, 2494, 2514, 2702, 2761, 2834, 3086, 3187, and 3413 keV. Spin and parity assignments of 5^+ and 8^- are proposed for the 19-min and 12.4-day isomers, respectively. The total β-disintegration energy of the ^{126}Sb ground state is 3.67 ± 0.15 MeV. (auth)

43925 SELF-CONSISTENT THEORY OF NUCLEAR SPECTRA: THE PAIRING-PLUS-QUADRUPOLE INTERATION MODEL APPLIED TO THE TIN ISOTOPES. Dreiss, Gerard J. (Univ. of Pennsylvania, Philadelphia); Dreizler, R. M.; Klein, Abraham; Dang, G. Do. Phys. Rev., C; 3: No. 6, 2412-21(Jun 1971).

The equations of the self-consistent core–particle coupling method, or generalized Hartree–Fock approximation, are derived for the special case of the pairing-plus-quadrupole–quadrupole interaction model. The bases of the approximations of this method are discussed along with the resolution of certain associated technical difficulties. Results of calculations for the tin isotopes, which are completely self-consistent and satisfy all relevant physical constraints, are presented and compared with experiment. These results include the static quadrupole moments of the first 2^+ states of the even tin isotopes, energies of low-lying states of the odd tin isotopes, and relative spectroscopic factors for (p,d) reactions on even targets. (auth)

43926 NEGATIVE-PARITY STATES IN ^{208}Pb. True, William W. (Univ. of California, Davis); Ma, Chin W.; Pinkston, William T. Phys. Rev., C; 3: No. 6, 2421-41(Jun 1971).

The energies and the detailed structure of the excited states of ^{208}Pb with negative parity are well described by a conventional shell-model calculation that uses a "simple" phenomenological residual force. The calculated position of the analog of the ground state of ^{208}Pb in ^{208}Bi is also in agreement with the experimental results. (auth)

43927 γ-γ DIRECTIONAL CORRELATIONS IN THE DECAY OF ^{125}Sb. II. Wyly, L. D.; Salzberg, J. B.; Patronis, E. T. Jr.; Kendrick, N. S.; Braden, C. H. (Georgia Inst. of Tech., Atlanta). Phys. Rev., C; 3: No. 6, 2442-6(Jun 1971).

A proportional counter being used to resolve the 35.5-keV γ ray from Te x rays, the following directional correlations were measured: $(601 + 606) - 35.5A_2 = -0.060 \pm 0.020$, $427 - 35.5A_2 = 0.230 \pm 0.030$, and $636 - 35.5A_2 = -0.065 \pm 0.030$. The first correlation is consistent with L-subshell measurements that have given $|f(35.5)| \leq 0.03$, where $f = \delta/(1 + \delta^2)^{\frac{1}{2}}$ with δ defined according to Rose and Brink [Rev. Mod. Phys., 39: 306(1967)]. The present best mixing-parameter values, as determined by this and other work, are $f(427) \approx 0.4$ and $f(636) \approx -0.3$; but the results may be influenced by reorientation while in the 35.5-keV level. (auth)

43928 THREE-QUASIPARTICLE $15/2^-$ ISOMER IN ^{127}Sb. Apt, K. E. (Massachusetts Inst. of Tech., Cambridge. Univ. of Maryland, College Park); Walters, W. B. Phys. Rev. Lett.; 26: No. 19, 1189-90(10 May 1971).

The β decay of 2.2-h, $11/2^-$ ^{127g}Sn was found to populate an 11-μsec isomer of ^{127}Sb at 1920 keV. The spin and parity of the isomer are $15/2^-$, and it is believed to arise from the coupling of the $g_{\frac{7}{2}}$ proton to the two-neutron 5^- state observed in ^{128}Sn at 2054 keV. (auth)

43929 EVIDENCE FOR DOORWAY STATES IN ^{207}Pb, ^{209}Pb, AND ^{57}Fe FROM THRESHOLD PHOTONEUTRON CROSS-SECTION MEASUREMENTS. Baglan, R. J.; Bowman, C. D.; Berman, B. L. (Univ. of California, Livermore). Phys. Rev., C; 3: No. 6, 2475-88(Jun 1971).

The proposed doorway state in ^{207}Pb seen by neutron total cross-section measurements on ^{208}Pb was observed in the (γ,n) reaction. Both the envelope of the strength and the correlation between fine structure in the two channels support the doorway-state interpretation. The width for γ-ray decay of the doorway state to the ground state, $\Gamma_{\gamma 0}^{D}$, is found to be 36.5 ± 3.5 eV. Other possible doorway states in the γ-ray channel in ^{208}Pb at 500 keV, ^{207}Pb at 125 keV, and ^{57}Fe at 50 and 250 keV above threshold are discussed. An attempt is made to produce a correlation neutron and γ-ray widths; no significant correlation is observed for these nuclei. (auth)

43930 INFLUENCE OF CHEMICAL BINDING ON THE NEUTRON CROSS SECTION IN SOME URANIUM COMPOUNDS. Saad, Masoud (Univ., Kiel). Atomkernenergie; 17: No. 4, 281-5 (Jul 1971). (In German).

Total cross sections of powdered polycrystalline samples of uranium compounds were measured in the thermal-neutron energy region with a crystal spectrometer, whose energy resolution was 1 to 3%. Excited levels at neutron energies of 0.112, and 0.258 eV were observed for the proton oscillation in $UH_{2.67}$, and at 0.092 and 0.190 eV for the deuteron oscillation in $UD_{2.67}$. For the C atom bound in UC at room temperature three excited levels were observed at 0.044, 0.086, and 0.137 eV. Moreover, the cross-section curves at 250°C and 510°C confirm the existence of only one isolated harmonic oscillation in the optical range. The cross-section curve of UO_2 shows two distinct minima at 0.035 and 0.049 eV and a weak one at 0.072 eV, which correspond to the maxima of Dolling's frequency distribution at 0.035, 0.05, and 0.08 eV. (auth)

43931 CONTRIBUTION OF OUTER ATOMIC SHELLS TO TOTAL INTERNAL CONVERSION COEFFICIENTS. Dragoun, O. (Nuclear Research Inst., Rez, Czech.); Plajner, Z.; Schmutzler, F. Nucl. Data, Sect. A; 9: 119-35(Mar 1971).

The sums of approximate internal conversion coefficients for the (N + O + ...) shells are presented. All values of atomic number from Z = 37 to Z = 100 are treated. The conversion coefficients are tabulated for the E1, ..., E4, M1, ..., M4 multipolarities and for transition energies from 50 to 500 keV. Internal-conversion-coefficient ratios (N + O + ...)/(K + L + M) and (N + O + ...)/M are given for atomic numbers Z = 40, 50, ..., 100. (auth)

43932 DETECTION OF DOUBLE BETA DECAY. Kirsten, T. (Max Planck Institut fuer Kernphysik, Heidelberg). Fortschr. Phys.; 18: 449-78(1970). (In German).

An extremely uranium-poor tellurium ore from the precambrium of Colorado was studied. This sample showed a significant excess of ^{130}Xe that was not accompanied by anomalies of other xenon isotopes. The excess of ^{130}Xe could be explained only as double β decay. Thus, double β decay could be demonstrated for the first time. Similar experiments were performed with selenium ores from Sweden. In five samples, a ^{82}Kr excess was demonstrated. Additional practical and theoretical aspects of double β decay were presented. (H.B.G.)

43933 ISOBARIC ANALOGUE RESONANCES IN ^{127}I, ^{125}I, AND ^{123}I. Burde, J.; Engler, A.; Ginsburg, A.; (and others) (Hebrew Univ., Jerusalem). Nucl. Phys.; A167: No. 3, 583-601(1971).

Isobaric analog resonances in ^{127}I, ^{125}I and ^{123}I have been studied by (p,p) and (p,p') scattering in the range of incident energies 7.54 to 12.50 MeV, 7.30 to 11.04 MeV from ^{126}Te and ^{124}Te, respectively, and in the ranges of 6.70 to 7.76 MeV and 8.51 to 11.20 MeV from ^{122}Te. The energy differences between the resonances and the orbital angular momenta transferred in their formation agree very well with the corresponding analog states which have been previously observed by the (d,p) reaction on the same target nuclei. There is fairly good agreement between the corresponding spectroscopic factors. The Coulomb displacement energies were found to be 13.996 ± 0.02, 14.060 ± 0.02 and 14.109 ± 0.02 MeV for the pairs of isotopes $^{127}Te-^{127}I$, $^{125}Te-^{125}I$ and $^{123}Te-^{123}I$ respectively. Spins of some prominent resonances have been deduced from the angular distributions of the inelastic protons. The strong inelastic scattering observed through some odd-parity resonances is discussed in terms of the core excitation model. (auth)

43934 CORIOLIS COUPLING IN DOUBLY ODD DEFORMED NUCLEI: THE $\frac{1}{2}^-[510]$ AND $\frac{3}{2}^-[512]$ NEUTRON STATES IN ^{182}Ta. Reich, C. W.; Helmer, R. G.; Greenwood, R. C. (Idaho Nuclear Corp., Idaho Falls). Nucl. Phys.; A168: No. 3, 487-508(1971).

A Coriolis-mixing analysis was made of the energies, (d,p) cross sections and γ-ray transition probabilities of the members of the rotational bands built on the four intrinsic states which arise from the coupling of the $\frac{1}{2}^+[404]$ proton orbital and the $\frac{1}{2}^-[510]$ and $\frac{3}{2}^-[512]$ neutron orbitals in ^{182}Ta. The treatment considers doubly odd ^{182}Ta as an axially-symmetric rotator, and Nilsson wave functions are chosen to describe the unperturbed states. Explicit expressions are given for the (d,p) cross sections and M1 and E2 γ-ray transition probabilities involving the Coriolis-coupled states. While it has been found possible to fit the data for a fairly wide range of parameter values, the discussion is arbitrarily restricted to the case of "pure" I(I + 1) unperturbed rotational bands. With this restriction, the results are presented for two different assumed values of the matrix element $\langle\frac{3}{2}^-[512]|j_+|\frac{1}{2}^-[510]\rangle$. For a value of this matrix element ≈1.4 times as large as the Nilsson-model prediction, it is found that all four unperturbed rotational bands have $\hbar^2/2$ J values which are essentially equal (≈14.1 keV). This factor of 1.4 agrees well with that found to be necessary in the well-studied odd-A nucleus ^{183}W. A value of +0.21 is inferred for the decoupling parameter of the $\frac{1}{2}^-[510]$ neutron state. (auth)

43935 LEVEL STRUCTURE OF ^{182}Ta. Helmer, R. G.; Greenwood, R. C.; Reich, C. W. (Idaho Nuclear Corp., Idaho Falls). Nucl. Phys.; A168: No. 3, 449-86(1971).

The level structure of ^{182}Ta was studied from the decay of ^{182}Hf and ^{182m}Ta and from the prompt γ-rays emitted following the capture of both thermal and 2 keV neutrons in ^{181}Ta. These data establish the existence of 46 excited states below 1 MeV in ^{182}Ta. Excited states are populated at 97, 114 and 270 keV in the decay of ^{182}Hf and at 16, 163, 334 and 519 keV in the decay of ^{182m}Ta. Thirty-seven of these observed states were assigned as members of 15 rotational bands. The following levels were interpreted as members of the bands with $K^\pi = 2^-, 3^-, 4^-$ and 5^- which result from the coupling of the proton orbital $\frac{7}{2}^+[404]_p$ with the neutron orbitals $\frac{1}{2}^-[510]_n$ and $\frac{3}{2}^-[512]_n$: $0(I^\pi = 3^-)$, 97.80 (4^-), 114.33 (4^-), 173.4 (5^-), 237.27 (5^-), 270.41 (2^-), 292.97 (5^-), 317 (6^-), 360.53 (3^-), 479.8 (4^-), 488 (6^-) and 628.4 keV (5^-). States interpreted as members of the bands resulting from coupling of $\frac{9}{2}^-[514]_p$ to the neutron orbitals $\frac{1}{2}^-[510]_n$ and $\frac{3}{2}^-[512]_n$ are: 16.5 (5^+), 150.4 (4^+), 163.3 (6^+), 250.2 (3^+), 331.3 (5^+), 334.8 (7^+), 397.3 (6^+) and 505.4 keV (5^+). Other observed levels were assigned to bands with configurations involving the orbitals $\frac{5}{2}^+[402]_p$, $\frac{11}{2}^+[615]_p$ and $\frac{7}{2}^-[503]_n$. Four levels were assigned as members of the $\{\frac{7}{2}^+[404]_p, \frac{7}{2}^-[503]_n\}$, $K^\pi = 0^-$ band; the odd-even shift in this band is 54 keV. In all cases where the band heads from the two possible orientations of the intrinsic spins of the odd particles have been identified, the band corresponding to $\Sigma = 1$ lies lower by ≈100 keV than that for which $\Sigma = 0$. The absolute transition probabilities for the K forbidden E3 and M4 transitions from ^{182m}Ta are in reasonable agreement with those predicted from a Coriolis mixing calculation. No difference is observed in the strength of the primary capture γ-rays populating excited neutron and excited proton states in ^{182}Ta. The neutron binding energy in ^{182}Ta was determined to be 6062.9 ± 0.5 keV. (auth)

43936 CLOSED SHELLS FOR VERY HEAVY NUCLEI. Sobiczewski, A.; Krogulski, T.; Blocki, J.; Szymanski, Z. (Inst. for Nuclear Research, Warsaw). Nucl. Phys.; A168: No. 3, 519-38 (1971).

Neutron and proton single-particle energies in the Woods–Saxon potential are calculated for a wide region of the mass number A ≈ 200–600. Considerable energy gaps at neutron numbers N = 228, 308 and 406 (besides the gaps at N = 126 and 184) and at proton number Z = 164 (besides the gaps at Z = 82 and 114) are found. Smaller gaps or low level densities are observed at Z = 154 and 204. The sensitivity of the obtained gaps to the variations of the potential parameters is discussed. (auth)

43937 LIFETIMES OF EXCITED STATES IN THE 89-NEUTRON NUCLEUS ^{151}Sm. Andrejtscheff, W.; Schilling, K.-D.; Stary, F.; Dubbers, F. (Zentralinstitut fuer Kernforschung, Rossendorf, Ger.). Nucl. Phys.; A168: No. 3, 513-18(1971).

In ^{151}Pm decay, the half-lives of the excited states at 104.8 keV and 167.7 keV in ^{151}Sm were determined as $T_{\frac{1}{2}}(104.8\text{ keV}) = 0.48 \pm 0.06$ ns and $T_{\frac{1}{2}}(167.7\text{ keV}) = 0.38 \pm 0.04$ ns. Upper limits for the half-lives of the levels at 344.9, 445.8, 743 and 823 keV were found: $T_{\frac{1}{2}}(344.9\text{ keV}) \leq 0.09$ ns; and $T_{\frac{1}{2}}(445.8, 743, 823\text{ keV}) \leq 0.1$ ns. Comparisons with single-particle estimates are made. (auth)

43938 UNIFIED-MODEL CALCULATIONS IN SOME Zr ISOTOPES. Paradellis, Th.; Hontzeas, S.; Blok, H. (Univ. of Saskatchewan, Regina). Nucl. Phys.; A168: No. 3, 539-60(1971).

The excited states of the Zr isotopes with $91 \leq A \leq 95$ are investigated in the framework of the intermediate coupling approach of the unified model. The odd Zr isotopes are assumed to consist of a doubly even Zr core to which one or two extra core neutrons are coupled. The assumption is also made that the extra core neutrons may "feel" the vibrations of the doubly even core. The effect is not observed in the experimental spectra of the ^{96}Zr and ^{96}Zr nuclei, due to their closed shell structure. A good description of the observed energy levels, and their (d,p) spectroscopic factors is obtained. In addition it is possible to identify states which are tentatively assigned to the coupling of the extra core neutron to two proton excitations from the core. (auth)

43939 QUASI-K QUANTIUM NUMBER IN ^{152}Gd. Sakai, Mitsuo (Tokyo Univ.); Ishii, Kameo; Aoki, Takayoshi. Nucl. Phys.; A167: No. 3, 541-4(1971).

Evidence is discussed for the persistence of the K quantum number in a transitional nucleus ^{152}Gd in the form of a quasi-K quantum number K_q. It plays an important role for β-transitions in a similar way to the K quantum number in deformed nuclei. (auth)

XUM

43940 EXPERIMENTAL INVESTIGATION OF THE PERTURBED β-VIBRATIONAL BANDS IN ^{152}Sm, ^{154}Gd, AND ^{156}Gd. Rud, Niels; Nielsen, H. L.; Wilsky, K. (Univ. of Aarhus, Denmark). Nucl. Phys.; A167: 401-20(1971).

New measurements of ^{152,154,156}Eu γ-ray intensities, ^{154}Eu conversion electron intensities, and ^{152,154}Eu $\gamma\gamma$ directional correlations are presented. Analysis of these data and reevaluation of previous measurements lead to a consistent description of the E2 decay of the β-band in terms of coupling to the ground state and the γ-band for the three nuclei ^{152}Sm, ^{154}Gd and ^{156}Gd. The observed rate of E0 decay of the ^{154}Gd γ-band agrees with the rate predicted from the $\beta\gamma$ coupling strength. The new value of z_0 accounts well for the isomer shifts and also for the deviations of $B(E2)_0$ values within the ground state band from the adiabatic values. (auth)

43941 BETA–GAMMA CIRCULAR POLARIZATION CORRELATION MEASUREMENTS ON THE DECAYS OF ^{203}Hg, ^{199}Au, AND ^{141}Ce. van Rooijen, J. J.; Gues, J.; Helms, H. A.; Blok, J. (Vrije Univ., Amsterdam). Nucl. Phys.; A167: 421-33(1971).

Circular polarization correlations in the β-decay of ^{203}Hg, ^{199}Au and ^{141}Ce were measured. Both forward Compton scattering from magnetized iron and transmission through magnetized iron were used for the detection of circular polarization. Accurate polarimeter efficiencies were calculated for the involved forward scattering arrangement. The results can be summarized as follows: ^{203}Hg, cascade $\frac{5}{2} \rightarrow \frac{3}{2} \rightarrow \frac{1}{2}$, $\bar{\omega} = -0.170 \pm 0.020$ ($E_\beta \geq 45$ keV), ^{199}Au, cascade $\frac{3}{2} \rightarrow \frac{3}{2} \rightarrow \frac{1}{2}$, $\bar{\omega} = +0.45 \pm 0.20$ ($E_\beta \geq 55$ keV), ^{141}Ce, cascade $\frac{7}{2} \rightarrow \frac{7}{2} \rightarrow \frac{5}{2}$, $\bar{\omega} = -0.180 \pm 0.026$ ($E_\beta \geq 85$ keV). The result in the mercury case seems to deviate somewhat from the ξ-approximation value (-0.203). As far as the decay of ^{141}Ce is concerned, previous measurements of the shape factor of the 435 keV β-transition could be explained by assuming a $f_{\frac{5}{2}}$ neutron to $d_{\frac{5}{2}}$ proton single-particle transition; in this case a rather strong energy dependence of the circular polarization correlation of the 435 keV–145 keV cascade is predicted, the presence of which was found with a confidence limit of about 80%. As far as possible the experimental data were analyzed in terms of nuclear matrix element ratios. (auth)

43942 STUDIES OF PROTON STATES IN ^{173}Lu, ^{175}Lu, AND ^{177}Lu WITH (^{3}He,d) AND (α,t) REACTIONS. O'Neil, R. A. (McMaster Univ., Hamilton, Ont.); Burke, D. G.; Alford, W. P. Nucl. Phys.; A167: No. 3, 481-510(1971).

Proton particle states in the odd lutetium isotopes ^{173}Lu, ^{175}Lu and ^{177}Lu have been studied using the (^{3}He,d) and (α,t) reactions. The beams of 28 MeV ^{3}He and 30 MeV α-particles were provided by the University of Rochester model MP tandem Van de Graaff accelerator. The reaction products were analyzed with an Enge-type broad-range magnetic spectrograph and detected with photographic emulsions. The experimental peak widths (FWHM) were 15 to 20 keV and the spectra were studied up to excitation energies of 2 MeV in each final nucleus. The present results confirm earlier assignments for the low-lying $\frac{1}{2}^+$[404], $\frac{5}{2}^+$[402], $\frac{1}{2}^-$[541] and $\frac{9}{2}^+$[514] bands. Higher spin rotational members have been observed for several of these previously known bands. A number of new intrinsic states have been found and interpreted in terms of the Nilsson model. These include the $\frac{9}{2}^-$[514] orbital in ^{173}Lu and the $\frac{1}{2}^-$[541] orbital in ^{177}Lu. The $\frac{1}{2}^-$[530] band, and probably the $\frac{3}{2}^-$[532] band have been identified at excitation energies above 1 MeV in all three isotopes. Relative spectroscopic factors were extracted with the aid of DWBA calculations. These spectroscopic factors showed evidence for appreciable Coriolis mixing in some cases, particularly between the $\frac{1}{2}^-$[541] and $\frac{3}{2}^-$[532] orbitals. (auth)

43943 DECAY OF ^{96,96m}Rh AND LEVELS OF ^{96}Ru. Doron, T. A.; Blann, M. (Univ. of Rochester, N. Y.). Nucl. Phys.; A167: No. 3, 577-82(1971).

The γ-ray spectrum following the decay of ^{96,96m}Rh was investigated with a Ge(Li) spectrometer. Many unreported γ-rays were seen. The half-lives of ^{96}Rh and ^{96m}Rh have been measured and found to be 9.5 ± 0.3 and 1.45 ± 0.2 min respectively. Energy levels of ^{96}Ru were also studied by α-particle inelastic scattering. Levels at 0.83, 1.52, 2.15, 2.86 and 3.10 MeV were observed. A decay scheme is proposed based on these observations. (auth)

43944 LEVELS OF ^{159}Dy OBTAINED BY DECAY OF ^{159}Ho. Boutet, J. (Institut des Sciences Nucleaires, Grenoble, France); Torres, J. P.; Paris, P. Nucl. Phys.; A167: 326-36(1971). (In French).

The energy levels of ^{159}Dy were investigated from the decay of ^{159}Ho with Ge(Li), Si(Li) detectors and a β-spectrograph having homogeneous magnetic field. With the help of γ-γ multidimensional coincidence techniques a consistent scheme was obtained. Multipolarities of several transitions are determined. Properties of the levels are discussed in terms of the Bohr and Mottelson unified model and the single-particle Nilsson model. (auth)

43945 DECAY OF ^{104}Cd AND LEVELS OF ^{104}Ag. Doron, T. A.; Blann, M. (Univ. of Rochester, N. Y.). Nucl. Phys.; A167: 247-51(1971).

The γ-ray spectrum following the decay of ^{104}Cd was investigated with Ge(Li) spectrometers. Two unreported γ-rays with energies of 625.2 and 709.2 keV were observed and placed in the proposed decay scheme. (auth)

43946 FISSION OF U AND Th BY GAMMA RAYS FROM 200 TO 1150 MeV. Wakuta, Yoshihisa (Kyushu Univ., Fukuoka). J. Phys. Soc. Jap.; 31: No. 1, 12-22(Jul 1971).

Measurements of the photofission cross section, fragment angular distributions and fragment single kinetic energy distributions for ^{238}U and ^{232}Th over an energy range from 200 MeV to 1150 MeV are described. Semiconductor detectors were used for the measurements. It is found from a photon difference method that the photofission cross section shows a resonance at a photon energy of about 330 MeV and 350 MeV with a peak value of ~120 mb and ~40 mb for U and Th respectively. It is evident that this resonance can be attributed to the well known (3,3) resonance in the pion photoproduction from a free nucleon. Furthermore, the results of the photofission cross section measurements were analyzed by assuming that nuclear excitation resulting from the reabsorption of the created pions and the quasi-deuteron absorption within a nucleus induces the photofission in the heavy nucleus. From this analysis it is shown that these assumptions explain qualitatively the general properties of the photofission in the energy region studied. The fragment single kinetic energy distribution seems to be consistent with this conclusion. A preliminary result for the fragment angular distribution is shown. (auth)

43947 BETA DECAY TO THE SECOND 2^+ EXCITED STATE OF ^{122}Te. Yamada, Shigeru; Hayashi, Takeo (Kyoto Univ.). J. Phys. Soc. Jap.; 31: No. 1, 23-9(Jul 1971).

Beta-gamma angular correlations and beta spectra of the first forbidden beta transitions of ^{122}Sb were studied. The result of the angular correlation measurement of the (734 keV β, 1256 keV γ) cascade indicates deviation from the ξ approximation for the 734 keV β transition. The analysis using exact electron radial wave functions which include finite nuclear size corrections shows that cancellation exists among the matrix elements. Thus, the ξ approximation is not fulfilled. The nuclear matrix parameters fitted to the angular correlation data are $x = 0.34 \pm 0.44$, $u = 2.03 \pm 0.96$, $y' = 25.0 \pm 13.8$, $w = 1.63 \pm 4.94$ and $v' = -18.4 \pm 53.5$. These parameters describe well the measured spectrum of the 734 keV β transition which shows deviation from the allowed shape. A comparison between the experimental results and the theoretical prediction based on the CVC theory is given. (auth)

43948 DETERMINATION OF HEXADECAPOLE TRANSITION MOMENTS BY COULOMB EXCITATION. Winkler, P. (Univ., Erlangen, Ger.). Nucl. Phys.; A168: No. 1, 139-50(1971).

For one even-A rotational nucleus (^{152}Sm) the influence of the hexadecapole interaction on multiple Coulomb excitation has been calculated for a variety of bombarding conditions and different assumptions with regard to E4 transition moments. An experimental method is outlined by which the determination of E4 transition strengths is feasible. Extensive numerical results are presented which may be helpful in planning Coulomb excitation experiments. (auth)

43949 RESONANCE PROCESS AND THE INTENSITY ANOMALY IN MUONIC ^{127}I. Lee, W. Y.; Bernow, S.; Chen, M. Y.; (and others) (Columbia Univ., New York). Nucl. Phys.; A167: No. 3, 652-66(1971).

The muonic N, M, L and K X-rays of ^{127}I have been measured and analyzed. A resonance process involving the muonic 2p levels and the nuclear ground and first excited states was included in the analysis. A satisfactory fit to the experimental spectra was achieved, at the same time, the parameters of the Fermi charge distribution, the M1 and the E2 hyperfine structure constants and the M1 and the E2 transition moments were determined. The M1 hyperfine structure constants and the M1 transition moment showed the effects of the finite distribution of the static and the transition M1 moments, while the E2 hyperfine structure constants offered an independent determination of the electric quadrupole moment. (auth)

43950 STUDY OF THE ISOSPIN SPLITTING OF DIPOLE EXCITATIONS IN INTERMEDIATE MASS NUCLEI. Hasinoff, Michael David. Stanford, Calif.; Stanford Univ. (1970). 133p. University Microfilms Order No. 71-12,913.

Thesis.

The E1 strengths built upon the 0^+ ground states of ^{90}Zr and ^{88}Sr as well as the 2^+ first excited state of ^{88}Sr were studied by means of the reactions $^{89}Y(p,\gamma_0)^{90}Zr$, $^{87}Rb(p,\gamma_0)^{88}Sr$, $^{87}Rb(p,\gamma_1)^{88}Sr^*$, $^{89}Y(p,p_0)^{89}Y$ and $^{87}Rb(p,p_0)^{87}Rb$. In ^{90}Zr this study extended from E_x = 13.6 to 25.2 MeV and in ^{88}Sr the region investigated was E_x = 14.6 to 22.5 MeV. In each case the T < giant resonance is characterized by an approximately constant angular distribution with $a_2 = -0.50$. The T > dipole strength resides in many analogous levels situated in the vicinity of and above the T < giant resonance because of the large Coulomb displacement energy. These analog dipole states are superimposed on and interfere with the underlying broad T < giant resonance. They are found to exhibit the characteristic electric dipole spectrum; namely, the presence of a coherent state or states at the upper end of the spectrum which carries most of the strength. Their measured angular distributions are typical of E1 distributions observed in the giant resonance region of many nuclei. The positions and strengths of the T > levels are compared to the theoretical calculations of Fallieros, Goulard and Hughes which include the contribution of the mutliparticle, multihole (2p–2h) excitations to the dipole spectrum. The energy splitting between the T > and T < excitations is found to be only about 4.5 MeV for the giant resonance states. For ^{88}Sr this is considerably less than the predicted energy splitting. Considerable fine structure is observed in the high-lying analog levels. The width of the T > giant resonance is found to be much larger in ^{90}Zr than in ^{88}Sr. This is discussed in terms of an isospin allowed neutron decay channel which is energetically available for the ^{90}Zr state but not for the ^{88}Sr state. The reaction $^{87}Rb(p,\gamma_1)^{88}Sr^*(2^+, 1.84\ MeV)$ has revealed a separate T <, γ_1 giant resonance which is displaced upwards from the γ_0 giant resonance by an amount approximately equal to the excitation energy of the first excited state. Several other analog states ($J^\pi > 1^-$) were also observed superimposed on the T < giant resonance. The positions and spins of the low-lying levels of the parent nucleus, ^{89}Rb, are compared to those obtained from the $^{87}Rb(d,p)^{88}Rb$ experiments. The reactions $^{141}Pr(p,\gamma_0)^{142}Nd$ and $^{141}Pr(p,\gamma_1 + \gamma_2)^{142}Nd^*$ were investigated from E_x = 18.0 to 23.6 MeV. A sharp resonance is observed in the γ_0 yield curve at E_x = 19.7 MeV and a broad resonance is found in both the γ_0 and the $\gamma_1 + \gamma_2$ yield curves near E_x = 22.0 MeV. The latter corresponds to the T > giant resonance seen by other investigators in the inverse reaction $^{142}Nd(e,e'p)^{141}Pr$. (Diss. Abstr. Int., B)

43951 NEUTRON ACTIVATION CROSS SECTIONS OF MEDIUM-Z NUCLEI AT 14.4 MeV. Lu, Winston Wen-deh. Atlanta; Georgia Inst. of Tech. (1970). 123p. University Microfilms Order No. 71-12,358.

Thesis.

Cross sections were measured by using the mixed powder method with Ge(Li) gamma detection first developed by Rao and Fink, giving results of much improved accuracy. Many of the cross sections were measured for the first time. From the measured (n,2n) cross sections an empirical formula as a function of only Z and A of the target nucleus is obtained. This formula reproduces the (n,2n) cross sections from the present work to within about ±20% with a few exceptions. The predictions of Pearlstein and Gardner with some modifications generally give good agreement with experiment, i.e., within about ±20%, for (n,2n) cross sections. For (n,p) cross sections the predictions from Levkovskii's empirical formula give much better agreement than those of Gardner and Rosenblum. However, there are several cases in which the values from Levkovskii's formula are too small by factors up to 2.5 compared with experimental values. For (n,α) cross sections, the statistical model calculations for Facchini et al., using energy independent level density parameter a are generally an order of magnitude too small compared with experiment. Rather large [(n,np) + (n,pn) + (n,d)] cross sections of ^{58}Ni, ^{96}Ru, ^{106}Cd, and ^{112}Sn were observed. The cross sections were seen to be linearly related to both Z and A of the target nuclei. Empirical equations were obtained to predict the [(n,np) + (n,pn) + (n,d)] cross sections for target nuclei of the lightest stable isotopes of even-Z elements. From the statistical model with the constant nuclear temperature approximation for level densities and other approximations, equations were derived in the present work to calculate (n,2n), (n,np), (n,pn), (n,p), (n,α), and (n,d) cross sections. The predictions from these equations generally give better agreement with experiment compared with other predictions for all (n,2n), (n,p), and (n,α) cross sections measured in the present work. In all the calculations an average nuclear temperature of 1.5 MeV taken to be constant for all types of 14 MeV neutron reactions and for all nuclei as suggested by Cuzzocrea et al., was used. No normalization procedure is involved in the present calculations. However, when neutron emissions following a first particle emission are involved, effective thresholds obtained by adding to ground state thresholds 0.5 MeV and 1 MeV, respectively, for the second and third neutron emissions appeared necessary to get good agreement with experiment. The agreements with experiment are generally within about ±15%, ±20%, and ±30%, respectively, for (n,2n), (n,p), and (n,α) cross sections measured in the present work. For the [(n,np) + (n,pn) + (n,d)] cross sections the calculated value agrees with the measured cross section for ^{58}Ni which is known from the angular and energy distribution measurements of Glover and Weigold to go mainly through compound nucleus formation. For the cases of ^{96}Ru, ^{106}Cd, and ^{112}Sn the calculated values are far too small compared with measured cross sections suggesting that they likely go by some kind of direct interactions. No odd-even effects in Z and no shell effects at Z = 28, 50, and at N = 50, 82 were observed in (n,2n) cross sections. Moreover, no shell effects for proton shell closures at Z = 28 and 50 in (n,p) cross sections were seen. For (n,α) reactions the cross sections of ^{92}Mo and ^{138}Ba, which have neutron shell closures at N = 50 and 82, respectively, appeared to be greatly enhanced. However, the enhancement may also be due to direct interactions. (Diss. Abstr. Int., B)

Nuclear Theory

Refer also to abstracts 43534, 43660, 43842, 43919, and 43948.

43952 (BNL-tr-424) PARAMETRIC METHOD FOR CALCULATING THE COULOMB ENERGY OF CERTAIN SHAPES OF FISSIONABLE NUCLEI. Adeev, G. D.; Cherdantsev, P. A. Translated by S. J. Amoretty (Brookhaven National Lab., Upton, N. Y.), from Izv. Vyssh. Ucheb. Zaved, Fiz.; No. 12, 127-9(1969). 8p. Dep. NTIS.

An abstract of this paper, prepared from the original language, appeared as NSA 24: 26680. (R.W.R.)

43953 (BNL-tr-427) INFLUENCE OF THE VALENCE-SHELL STRUCTURE ON THE INTERNAL CONVERSION COEFFICIENTS OF γ-RADIATION AND ON THE ELECTRON DENSITY NEAR THE NUCLEUS. Anderson, E. M.; Listengarten, M. A.; Khanonkind, M A. Translated by S. J. Amoretty (Brookhaven National Lab., Upton, N Y.), from Izv. Akad. Nauk SSSR, Ser. Fiz.; 34: No. 4, 850-5(1971). 13p. Dep. NTIS.

An abstract of this paper, prepared from the original language, appeared as NSA 25: 31343. (R.W.R.)

43954 (INP-746) DISTORTED WAVE BORN APPROXIMATION PROGRAMMES FOR INELASTIC SCATTERING OF CHARGED PARTICLES "MIS-0," "MIS-2," "MIS-3," "MIS-4," AND "MIS-5." Kobos, Andrzej (Institute of Nuclear Physics, Krakow (Poland)). Feb 1971. 49p. Dep. NTIS (U. S. Sales Only).

The MIŚ-0, MIŚ-2, MIŚ-3, MIŚ-4, and MIS-5 programs, written in the MAT-4 autocode language for the Soviet MINSK-22 computer, are presented. The programs calculate, in the distorted-wave Born approximation, the reduced differential cross section for inelastic scattering of charged particles, for excitations with orbital-angular-momentum-transfer values of 0, 2, 3, 4, and 5, respectively. (auth)

43955 (INR-1270) CLOSED SHELLS FOR VERY HEAVY NUCLEI. Sobiczewski, A.; Krogulski, T.; Blocki, J.; Szymanski, Z. (Institute of Nuclear Research, Warsaw (Poland)). 1970. 36p. Dep. NTIS (U. S. Sales Only).

Neutron and proton single-particle energies in the Woods-Saxon potential are calculated for a wide region of the mass number number A ≈ 200 to 600. Considerable energy gaps at neutron numbers N = 228, 308, and 406 (besides the gaps at N = 126 and 184) and at proton number Z = 164 (besides the gaps at Z = 82 and 114) are found. Smaller gaps or low level densities are observed at Z = 154 and 204. The sensitivity of the gaps obtained to the variations of the potential parameters is discussed. (auth)

43956 (ORO-3765-30) BETHE GOLDSTONE EQUATION IN FINITE NUCLEI. Technical Report No. 71-115. Demos, Joslyn R.; Banerjee, Manoj K. (Maryland Univ., College Park, Dept. of Physics and Astronomy). May 1971. 42p. Dep. NTIS.

If one sets QUQ = 0[Brandow, Phys. Rev., 152: 863(1966)] where U is the single-particle potential, the Bethe-Goldstone equation becomes $\Psi = \Phi - (Q/QTQ-\omega)v\Psi$. This equation is approximated by replacing Q with the Eden-Emergy Pauli operator and by neglecting $\hat{T}\chi$, where $\hat{T}$ is the off-diagonal part of the c.m. kinetic-energy operator in the oscillator representation. Care is taken to retain $\hat{T}\Phi$, which is a large term. The approximate equation is solved iteratively. It yields defect functions with the bulk of the effect of Q built in. Correction terms to the approximate results are estimated. The biggest correction term is $\langle\chi|\hat{T}|\chi\rangle$, which can be as large as 0.5 MeV in the triplet-even case. (auth)

43957 (UCRL-73152) PRE-EQUILIBRIUM DECAYS OF THE COMPOUND NUCLEUS. Grimes, S. M. (California Univ., Liver-

XUM

more, Lawrence Radiation Lab.). 23 Apr 1971. 36p. (CONF-710413-2). Dep. NTIS.

From American physical society meeting; Washington, D. C. (26 Apr 1971).

The characteristics of the current model for pre-equilibrium decays of the compound nucleus are summarized. Comparison of the calculations with experimental results for nucleon- and alpha-induced reactions shows basic agreement, although uncertainties remain as to the role of shell effects. Pre-equilibrium reactions are found to comprise a relatively small fraction of the reaction cross sections for bombarding energies of 20 MeV or less, but to become quite large at energies of 40 MeV and up. The types of reactions expected to show particularly large and particularly small pre-equilibrium contributions are also discussed. (auth)

43958 PROBABLE SIGNIFICANCE OF EXCITATION QUANTUM NUMBERS IN NUCLEI. Dutta, A. K. (Calcutta Univ.). Phys. Rev., C; 3: No. 6, 2095-2100(Jun 1971).

It has been found that analytic expressions for binding energies of nuclei in the isobaric form and for their excitation energies together with their superposed irregular deviations determine the binding and excitation energies of nuclei. The irregular deviations of the excited-state energies from the associated analytic expression for a particular (A,Z) combination are determined by the corresponding irregular deviations of binding energy from its associated analytic expression. These deviations of binding energy are expected to be dependent on other irregular physical characteristics of nuclei and control, through their variations, the irregular deviations of excitation energies from the analytic part. The analytic part of the excitation energies for all nuclei consists of factors of which the first part is a function of A and the second part is dependent on integral quantum numbers n_i^* for different stages of excitations, with associated constants for all the even- or for the odd-nucleon numbers. The quantum numbers for nuclear excitation are thus independent of the characteristics of motion or of configurational changes and must, therefore, depend on some other purely nuclear characteristic of a general nature. From a study of the method of evaluating excitation energies of nuclei by the β-decay procedure and also from the study of nuclear reactions in small nuclei, it is considered that the mechanism causing excitations and that for isobaric changes in the ground state are very much alike. To conform to this allied character the analytic expression measuring isobaric energy change is brought into a form similar to the expression for excitation-energy change by replacing the parabolic factor $(Z^0 - Z)^2$ for isobaric change in energy by the exponential factor $[\sigma^+ n^+ - 1]$, where $n^+ = |Z^0 - Z|$ measures the number of replacements of protons by neutrons or vice versa externally. The values obtained by the exponential and the parabolic forms are close to each other in the effective region of isobaric parabolas when $\sigma^+ = 0.78$. As a result of comparing the expressions for energy change due to excitation and that due to isobaric change, it is concluded that the excitation quantum numbers n_i^* measure the number of replacements internally of neutrons by protons or vice versa at successively higher levels. (auth)

43959 EFFECTIVE s-WAVE INTERACTION IN FINITE NUCLEI. Muthukrishnan, R. (North Texas State Univ., Denton). Phys. Rev., C; 3: No. 6, 2091-5(Jun 1971).

It is shown that a simple s-wave separable interaction whose parameters are determined by a fit to the binding energy and density of nuclear matter, when modified by making the strength a smooth function of the mass number A (such that the strength approaches that for nuclear matter as $A \to \infty$), gives the binding energy and radii of spherical nuclei throughout the Periodic Table in excellent agreement with experimental values. This behavior of the strength as a function of A is discussed in the light of the results of calculations that use realistic interactions. (auth)

43960 CHARGE-DEPENDENT EFFECTS AND LOW-ENERGY NUCLEON–NUCLEON SCATTERING. Yalcin, C. (Univ. of Sussex, Eng.). Nucl. Phys.; A169: No. 1, 201-8(1971).

The observed discrepancy between the neutron–proton and proton–proton scattering lengths in the singlet state is examined in terms of short-range electromagnetic corrections to the two-nucleon potential. The finite size of nucleons, the magnetic interactions of neutron–proton, proton–proton systems, the electromagnetic mass difference of pions, $\Delta m(\pi) = m(\pi^\pm) - m(\pi^0)$, and the isospin mixing of various mesons contribute to the observed difference at most 50%. The remaining part is attributed to the very short-range charge-dependent potential stemming from the ρ-meson exchange. In order to eliminate the discrepancy between neutron–proton and proton–proton scattering lengths $\Delta m(\rho) = m(\rho^\pm) - m(\rho^0) = -1.4$ to -3.1 MeV was obtained. (auth)

43961 EFFECT OF TETRAGONAL GRAPH IN HEAVY ION STRIPPING (PICK-UP) REACTIONS. Zelenskaya, N. S. (Inst. of Nuclear Physics, Moscow). Yadern. Fiz.; 13: No. 4, 734-42(Apr 1971). (In Russian).

A stepped mechanism for the reaction A(x,y)B with transfer of several nucleons on light nuclei is considered: it is assumed that in the first stage only z nucleons from the total number $(x - y)$ of the transferred nucleons take part in the process, and then other nucleons are transfered. The simplest graph describing such a process is the tetragonal graph. It is pointed out at what values of the bound energies of the participating particles the tetragonal mechanism may be realized. The account of complicated graphs results in essential anomalies in angular distributions for the A(x,y)B reaction: $d\sigma/d\Omega$ is not determined by the value of the total transferred angular momentum L. The reaction ^{3}Be(^{3}He, ^{6}Li)^{6}Li is considered concretely in the work: the experimental $d\sigma/d\Omega$ has a maximum at $\theta \simeq 90°$ although L = 1. The theoretical angular distribution, calculated for the tetragonal graph with plane waves, is in qualitative agreement with the experiment. It is shown that an account of distortions does not change the general picture of $d\sigma/d\Omega$ but makes the agreement with experiment better, "filling" deep minima on the theoretical curve. (auth)

43962 PROCESSES LIKE DOUBLE CHARGE EXCHANGE ON LIGHT NUCLEI. Tarasov, A. V.; Tseren, Ch. (Joint Inst. for Nuclear Research, Dubna, USSR). Yadern. Fiz.; 13: No. 4, 727-33(Apr 1971). (In Russian).

Reactions like double charge exchange are considered that proceed effectively on two nucleons. The obtained expressions for the cross sections depend on an important physical quantity characterizing the nucleon distribution in the nucleus, the mean value of the inverse separation between the nucleon. (auth)

43963 DEFORMED SPIN–ORBIT POTENTIAL IN NUCLEAR SCATTERING AND STRUCTURE. Van Rij, Willem Idaniel. Tallahassee; Florida State Univ. (1970). 211p. University Microfilms Order No. 71-13,517.

Thesis.

An investigation was made of the collective-model generalization of the spin-orbit potential of the nuclear optical and shell models. A non-rigorous formulation of the generalized potential in terms of the matter density of the nucleus and the nucleon–nucleon interaction was derived. In particular, it was shown how the nucleon–nucleon spin-orbit interaction can give rise to the nucleon–nucleus deformed spin-orbit potential. Distorted waves Born approximation calculations were made for the proton inelastic-scattering excitation of collective states of deformed, even-A nuclei. At high proton energies the data on inelastic polarization definitely requires the spin-orbit potential to be deformed, and at intermediate energies the description of the inelastic asymmetry data improves substantially with spin-orbit deformation. Calculations of the excitation of the 1.78 MeV, 2^+ level of ^{28}Si with 40 MeV protons are presented to illustrate the effects of spin-orbit deformation for proton inelastic scattering. The different contributions arising from the spin-orbit distortion and spin-orbit deformation were considered separately in order to more clearly define the spin dependence of the distorted waves Born approximation. The proton inelastic-scattering investigation was complemented with its bound-state counterpart, an investigation of the role of the deformed spin-orbit potential in the description of the structure properties of deformed, odd-A nuclei. Nilsson-model calculations were made and it was found that the spin-orbit deformation affects the single-particle wave function appreciably in all mass regions. Its effect on the single-particle energies is more important for heavier nuclei. Decoupling parameters for rare-earth nuclei were calculated and the improved agreement with the experimental values substantiates the importance of the spin-orbit deformation. It was also shown that the spin-orbit contribution to the magnetic moment is significant for odd-proton nuclei. A more acceptable form than the harmonic oscillator potential, namely the Woods–Saxon potential, was investigated in calculations of single-particle states for odd-A actinide nuclei. It was found that the effect of the spin-orbit deformation using the Woods–Saxon potential is very similar to its effect in the Nilsson-model calculations, showing that the role of the deformed spin-orbit potential is determined primarily by its angular momentum properties, and not its radial dependence. Decoupling parameters for actinide nuclei were calculated and the improved agreement with the data gives evidence of the importance of the spin-orbit deformation. Simple calculations were made for super-heavy nuclei and the results indicate that deformation of the spin-orbit potential would be unimportant in determining the potential energy of such nuclei. (Diss. Abstr. Int., B)

43964 CLUSTER TRANSFER REACTIONS AT LOW ENERGIES. El-Nadi, M. (Univ. of Cairo); Osman, A.; Rihan, T. H. Acta Phys. Acad. Sci. Hung.; 29: No. 2-3, 143-58(1970).

The cluster transfer processes below the Coulomb barrier are investigated for arbitrary charges and angular momentum transfer, taking into account the finite range effects. An analytical expression for the differential cross section is obtained and calculations are carried out for the $^{90}Zr(d,p)^{91}Zr$ reaction. An analytical expression is also obtained for the differential cross section for two cluster transfer reactions, and the results are compared with the data on the $^{27}Al(^3He,p)^{29}Si$ reaction. (auth)

43965 FINITE-RANGE COULOMB STRIPPING IN (t,p) AND (^{3}He,n) REACTIONS. El-Nadi, M. (Univ. of Cairo); Osman, A.; Rihan, T. H. Acta Phys. Acad. Sci. Hung.; 29: No. 2-3, 127-41(1970).

The theory of two-nucleon stripping reactions is considered, taking into account the Coulomb distortion and the finite-range effects at projectile energies below the Coulomb barrier. Applying the results to the reactions $^{14}N(t,p)^{16}N$ and $^9Be(^3He,n)^{11}C$ reliable agreement is observed with the experimental data especially in the forward direction. (auth)

43966 APPLICATION OF THE NONRELATIVISTIC PERIPHERAL MODEL TO REACTIONS BETWEEN LIGHT PARTICLES. Borbely, I. (Central Research Inst. for Physics, Budapest). Phys. Lett.; 35B: No. 5, 388-90(21 Jun 1971).

It is shown that, in the case of transfer reactions between light particles, it is possible to get reliable information about the structure of the particles involved by taking into account only the peripheral part of the reaction amplitude. (auth)

43967 EVIDENCE FOR A REAL SAXON WOODS DERIVATIVE TERM IN THE PROTON OPTICAL POTENTIAL. Sinha, B. C.; Edwards, V. R. W. (Kings Coll., London). Phys. Lett.; 35B: No. 5, 391-2(21 Jun 1971).

It is shown that incorporating a real Saxon–Woods derivative term in the optical potential consistently improves the fits to a wide range of proton elastic scattering data. The origin of the term is briefly discussed. (auth)

43968 SPACING AND INDIVIDUAL EIGENVALUE DISTRIBUTIONS OF TWO-BODY RANDOM HAMILTONIANS. Bohigas, O.; Flores, J. (Institut de Physique Nucleaire, Orsay, France). Phys. Lett.; 35B: No. 5, 383-7(21 Jun 1971).

Comparison is made of the results of the Gaussian orthogonal ensemble with the ones produced with an ensemble in which the two-body character of the Hamiltonian and the Pauli principle are taken into account. Significant differences arise between the two ensembles of random matrices. (auth)

43969 PAIRING CORRELATION IN EXCITED NUCLEI WITH NON-ZERO ANGULAR MOMENTUM. Moretto, L. G. (Univ., Pavia, Italy). Phys. Lett.; 35B: No. 5, 379-82(21 Jun 1971).

The statistical properties of a paired nucleus are studied as a function of angular momentum, and the relevant thermodynamical expressions are derived. (auth)

43970 INFLUENCE OF NUCLEAR FORCES ON COULOMB FISSION. Holm, Hartmut; Greiner, Walter (Univ., Frankfurt am Main). Phys. Rev. Lett.; 26: No. 26, 1647-50(28 Jun 1971).

The Coulomb-fission cross sections for ^{132}Xe and ^{148}Nd incident on ^{238}U are calculated in a dynamical classical model; in particular, the influence of nuclear forces on the cross sections is studied. Since they are counteracting the Coulomb force, they diminish the cross sections for Coulomb fission significantly and shift the Coulomb barrier toward lower energies. (auth)

43971 EFFECT OF APPROXIMATE WAVE FUNCTIONS IN COMPOSITE-PARTICLE SCATTERING. Lavan, M. J.; Payne, G. L. (Univ. of Iowa, Iowa City). Phys. Rev., C; 3: No. 6, 2156-67(Jun 1971).

Many investigators have studied the scattering of low-energy nucleons by light nuclei by using a single-particle effective potential that is derived from a many-nucleon Hamiltonian under the assumption that the contribution to the scattering by virtual excitations of the target nucleus can be neglected. In addition, they have approximated the ground-state wave functions of the target nuclei by crude variational wave functions, this approximation introducing an unknown error into the results of the scattering calculation. That error is investigated for the specific case of neutron–triton scattering. Three approximate effective potentials that differ from each other and from the exact single-particle effective potential by the same order in the error of the approximate triton wave function are derived. The differences among the phase shifts calculated with the approximate potentials give an indication of the uncertainty in the calculations; and, as the approximate triton wave function is improved, the differences decrease. It is shown that previous calculations involve large errors, which may be reduced by improving the approximate target wave function. (auth)

43972 MIXING OF COLLECTIVE STATES IN AN EXACTLY SOLUBLE THREE-LEVEL MODEL. Meshkov, N. (Catholic Univ. of America, Washington, D. C.). Phys. Rev., C; 3: No. 6, 2214-28(Jun 1971).

A general class of exactly soluble three-level models is presented for an N-fermion system. Assuming a monopole–monopole interaction among the fermions allows one to express the model Hamiltonian in terms of the generators of the SU_3 group. A specialized version of this class of models is adapted for the study of mixing two collective states of opposite parity, in a way analogous to the mixing of giant-dipole-resonance vibrations and surface quadrupole vibrations in nuclei. Exact results of the model are studied as a function of interaction parameters and compared with approximations including up to three-particle–three-hole excitations. It is shown that, in the model, many-particle–many-hole states play an important role in the mixing of collective states and cannot be properly neglected. The implications of this result for the study of actual nuclei are discussed. (auth)

43973 REAL PART OF THE ALPHA-NUCLEUS POTENTIAL. Lilley, J. S. (Univ. of Minnesota, Minneapolis). Phys. Rev., C; 3: No. 6, 2229-31(Jun 1971).

The various phenomenological potential form factors that describe the elastic scattering of α particles from a given target nucleus are similar at large radii. It is shown that reasonably accurate limits can be placed on both the magnitude and falloff rate of the potential in this surface region close to the maximum of the Coulomb barrier. This surface-region potential is found to be well reproduced by a simple folding of the nuclear-matter distribution with a two-body potential that fits free nucleon–α scattering. (auth)

43974 EFFECT OF THE MULTIPOLE PAIRING AND PARTICLE-HOLE FIELDS IN THE PARTICLE-VIBRATION COUPLING OF ^{209}Pb. I. Bes, D. R.; Broglia, R. A. (Los Alamos Scientific Lab., N. Mex. Univ. of Minnesota, Minneapolis). Phys. Rev., C; 3: No. 6, 2349-71(Jun 1971).

The particle–vibration-coupling formalism for nuclei around closed shells is studied, and a microscopic description is given. Both particle–hole excitations and excitations that change the number of particles by 2 (pairing mode) are considered as collective modes of excitation of the closed-shell-system (N_0) ground state. To describe the pairing modes, multipole pairing residual interactions are used. The odd particle is allowed to couple to both types of vibrations. The coupling Hamiltonian is linear in the collective phonons and the particle variables. The effective Hamiltonian is constructed by a perturbative method. Explicit expressions are given for the spectroscopic amplitudes and spectroscopic factors associated with the $(N_0 - 1)(t,p)(N_0 + 1)$ and $(N_0 + 2)(p,d)(N_0 + 1)$ reactions, respectively. The concept of an effective transfer operator is used. Special attention is paid to the $^{207}Pb(t,p)$ and $^{210}Pb(p,d)$ reactions. (auth)

43975 INTERNAL IONIZATION OF THE K SHELL. Stephas, Paul. (Eastern Oregon Coll., La Grande); Crasemann, Bernd. Phys. Rev., C; 3: No. 6, 2495-7(Jun 1971).

A continuum wave function, improperly normalized in previous work, is corrected. Expressions for the probability of internal ionization of the atomic K shell, accompanying β decay and electron capture, are given explicitly including all factors. (auth)

43976 EFFECTIVE OPERATORS AND THE ANALYSIS OF SINGLE-NUCLEON TRANSFER REACTIONS ON CLOSED-SHELL NUCLEI. Bes, D. R.; Broglia, R. A. (Univ. of Minnesota, Minneapolis. Los Alamos Scientific Lab., N. Mex.). Phys. Rev., C; 3: No. 6, 2389-2401(Jun 1971).

Spectroscopic factors for the one-body stripping and pickup reactions on ^{208}Pb are analyzed within the particle–vibration-coupling model [Bes and Broglia, Phys. Rev., C, 3: 2349(1971)]. The calculation of the transfer amplitudes is performed up to third-order perturbation theory. A comparison with recent experimental data is carried out. (auth)

43977 HIGHER MULTIPOLE DEFORMATION OF THE PAIRING DENSITY IN DEFORMED NUCLEI AND THEIR EFFECTS ON THE (p,t) AND (t,p) REACTIONS. Udagawa, T. (Univ. of Texas, Austin). Nucl. Phys.; A164: 484-96(1971).

XUM

The Y_4 and Y_6 deformations of the nuclear pairing density of deformed nuclei are investigated both phenomenologically and microscopically. In the phenomenological study, the deformation parameters δ_λ; $\lambda = 4$ and 6, are introduced as unknowns whose values are to be fixed by fitting the theoretical DWBA cross sections to (p,t) reaction data. In the microscopic study, the values of δ_λ are calculated self-consistently. For this purpose, the expression for δ_λ is derived, taking into account the presence of both the deformed Hartree and pairing potentials and also assuming that the residual nuclear forces associated with these potentials are approximated by simple multipole-multipole and multipole-pairing forces. (auth)

43978 THEORY OF PION INTERACTIONS WITH ATOMIC NUCLEI AND OF HEAVY ION SCATTERING. Chatwin, Robert Antony. Tallahassee; Florida State Univ. (1970). 134p. University Microfilms Order No. 71-13,489.

Thesis.

Pion charge-exchange reactions on nuclei near resonance are discussed in a semi-classical model. It is shown that absorption of the pion wave into other channels ought to decrease the cross sections by at least an order of magnitude. Hence the success of theories which neglect absorption is surprising. Double-charge-exchange reactions to the analog state are shown to be so sensitive to absorption, that the resonance energy of 200 MeV is the worst energy at which to make an experimental study. Semi-classical attenuation factors are given for such processes. The ratio between π^+- and π^-- induced, nucleon knock-out reactions is shown to depend on the coherence between states of the outgoing nucleon plus core that are coupled to different isospins. The existing data on ^{4}He, ^{9}Be, and ^{12}C are studied in terms of a model of this process, and a prediction is given for the ratio on ^{64}Zn. In a theory of wave propagation in a random medium of discrete scatterers, it is shown that an infinite medium of uniform distribution is transparent to the propagation of a resonance with $l > 0$, if that resonance completely dominates the interaction with one scatterer. The result is different from that given by the effective field approximations. A theory of Foldy and Walecka for multiple scattering from a finite distribution of separable potentials is developed, and a bound on the form factor gl (t) is derived. A solution for scattering on two p-wave potentials is found analytically; the result is expressed in terms only of the physical amplitude for single scattering, the wave-number k, and the separation d. A calculation, using the πN amplitude as data, gives a vanishing total cross section as $d \to 0$, and a double humped curve as a function of k for a larger range of d. The absorptive part of the optical potential is considered as a function of conserved quantum numbers such as the total angular momentum J. This investigation results in the introduction of a smooth cutoff in the strength of the absorptive potential as J gets larger than a certain critical value. This value is typical of non-elastic channels, and the cutoff reflects poor matching between the angular momenta in the elastic channel and those in the nonelastic channels. Calculations in this model of ^{16}O–^{16}O and ^{40}Ca–^{16}O elastic scattering are presented and compared with data. In particular, the resonant contributions to those cross sections are discussed in terms of J-dependence. Discussions are given of the shallowness of the ^{16}O–^{16}O potential, of backward angle scattering, and of the terms "orbiting" and "glory". (Diss. Abstr. Int., B)

43979 RADIATIVE CORRECTIONS IN ee'N COINCIDENCE EXPERIMENTS. Borie, E.; Drechsel, D. (Univ., Frankfurt am Main). Nucl. Phys.; A167: 369-75(1971).

The cross-section differential in the energies and angles of all final particles for bremsstrahlung accompanying nucleon emission is derived in first Born approximation, in terms of the four form factors introduced by de Forest. This cross section is integrated over photon angles, using the peaking approximation, to give an expression for the radiative tail in nucleon emission processes. A numerical example for the case of ee'p coincidence experiments in ^{12}C is given, using the quasi-elastic model to describe the nuclear excitation. (auth)

43980 SEPARABLE APPROXIMATION TO THE TWO-BODY t-MATRIX FOR SHORT-RANGE CENTRAL LOCAL POTENTIALS. Purkayastha, Gita; Banerjee, S. N.; Sil, N. C. (Indian Association for the Cultivation of Science, Jadavpur). Nucl. Phys.; A167: 376-82(1971).

The S-wave potential in momentum space, $V_0(p,p')$, corresponding to a local two-body central short-range potential may be expanded in separable form with the help of suitable quadrature formulas. With a two-term separable expansion for a variety of nuclear potentials, the resulting t-matrix is found to be in close agreement with the corresponding result with a six-term expansion for small values of p and p' which are important in the calculation of the trinucleon binding energy. (auth)

43981 ONE-PARTICLE, j-j COEFFICIENTS OF FRACTIONAL PARENTAGE IN THE ISOSPIN REPRESENTATION FOR $n \leq 5$ IN THE $j = 7/2$ SHELL. Hubbard, L. B. (Oak Ridge National Lab., Tenn. Knoxville Coll., Tenn.). Nucl. Data, Sect. A; 9: 85-117 (Mar 1971).

Values for the one-particle, j–j coefficients of fractional parentage are calculated for a portion of the $j = 7/2$ shell. These coefficients join states that contain less than 5 particles and that are eigenfunctions of seniority, isospin, and total spin. (auth)

43982 TABLES OF SINGLE-PARTICLE REDUCED MATRIX ELEMENTS OF SPHERICAL TENSORS. Bell, W. K.; Satchler, G. R. (Oak Ridge National Lab., Tenn.). Nucl. Data, Sect. A; 9: 147-68(Mar 1971).

All allowed reduced matrix elements of the spherical tensor operators $T_{LSJ,M}(\theta,\phi;o)$ and $T_{J-1,1J,M}(\theta,\phi;L)$ are computed between all pairs of single-particle states from $S_{1/2}$ to $j_{15/2}$. (auth)

43983 HALL–POST LOWER BOUND CALCULATIONS FOR THE THREE-NUCLEON SYSTEM. Brady, T.; Harms, E.; Laroze, L.; Levinger, J. S. (Rensselaer Polytechnic Inst., Troy, N. Y.). Nucl. Phys.; A168: No. 3, 509-12(1971).

The usefulness of a method, due to Hall and Post, for obtaining a lower bound for the ground state energy of the trinucleon is explored. The numerical values of bounds obtained for various two-body potentials are compared with the exact trinucleon energies. It is found that the Hall-Post bound works moderately well for central potentials, which may include soft cores or weak tensor forces; but the bound is far from the true energy when hard cores or strong tensor forces are included. (auth)

43984 STUDY OF INELASTIC PROCESSES ON (d,p) REACTIONS IN DEFORMED NUCLEI. Glendenning, Norman K.; Mackintosh, Raymond S. (Univ. of California, Berkeley). Nucl. Phys.; A168: No. 3, 575-92(1971).

The stripping reaction (d,p) in deformed nuclei is usually treated as a single-step process leading directly from the ground to the product state. This paper adds to the usual direct amplitude those others that proceed through intermediate rotational states in the target and final nucleus. These higher-order processes introduce large corrections for the weaker states that sometimes alter the angular distribution and change the magnitude of the cross section by up to a factor of ten or more. In using these reactions to determine the amplitudes in the Nilsson wave functions for the single-particle states in odd nuclei, it is therefore essential that these processes be taken into account. (auth)

43985 COMPARISON BETWEEN THE BCS AND THE FBCS FORMALISMS AS APPROXIMATIONS TO THE LOW-SENIORITY SHELL MODEL. Allaart, K.; Boeker, E. (Vrije Univ., Amsterdam). Nucl. Phys.; A168: No. 3, 630-62(1971).

A discussion is given of the discrepancies between the wave functions of single-closed-shell nuclei as obtained from the BCS formalism and those from the FBCS formalism. Sources of these discrepancies for the ground states are made clear and demonstrated by simple examples. The difference between the BCS and FBCS two-quasiparticle spectra may especially become large when the number of particles corresponds to a closed subshell structure and if subshells of low degeneracy occur near the Fermi level. As an illustration the states of the even $N = 50$ nuclei are calculated in both approximations and compared to those of the exact $V \leqq 2$ shell model. Particle number projection is the main effect in improving spectra. The parameters u_a, v_a which minimize the ground state energy were found to be not the most suitable to calculate excited states. (auth)

43986 HARTREE–FOCK CALCULATIONS OF LIGHT DEFORMED NUCLEI USING DENSITY-DEPENDENT EFFECTIVE INTERACTIONS. Zofka, J.; Ripka, G. (CEN de Saclay, Gif-sur-Yvette, France). Nucl. Phys.; A168: No. 1, 65-96 (1971).

The Hartree–Fock states of the doubly even $N = Z$ nuclei from ^{12}C to ^{40}Ca were calculated using the density-dependent effective interaction of Negele. The results are compared with those obtained with the density-independent B1 interaction of Brink and Boeker as well as with those of calculations using other interactions. A detailed comparison of quadrupole moments, radii, separation and binding energies is made between the various calculations and experimental data. The HF wave functions are also compared to the equilibrium α-particle configurations and the structure of 2s–1d shell nuclei is analyzed. (auth)

43987 (d,^{6}Li) REACTION. Dragun, O.; Dussel, G. G.; Maqueda, E.; Perazzo, R. P. J. (Comision Nacional de Energia Atomica, Buenos Aires). Nucl. Phys.; A167: No. 3, 529-40(1971).

General features of the (d,^{6}Li) reaction are discussed in con-

nections with some residual forces. An enhancement of ground state transitions among superconducting nuclei is found. Some examples in the 1p shell are also worked out and coherence is found between the T = 0 and T = 1 channels of the residual force. (auth)

43988 SPECTROSCOPY OF UNBOUND LEVELS WITH THE AID OF WEINBERG'S QUASIPARTICLES. Huby, R. (Univ. of Liverpool). Nucl. Phys.; A167: 271-88(1971).

The resonant scattering of a neutron by a nucleus A is calculated using the method of Weinberg quasiparticles in a way modified from that of previous authors, with the object of obtaining fairly simple and explicit schematic formulas for both the scattering amplitude and the wave function that satisfy certain requirements of physical correctness. This is directed towards study of the unbound level both in n-A scattering and in its production as a final state by a stripping reaction. The level concerned involves the mixing of a single-particle resonance with other configurations. The structure aspect of the level is characterized, as for a bound level, by a spectroscopic amplitude Θ. The formula obtained for the wave function, while not requiring all the details of the nuclear model to be specified, should be rather accurate at all distances. (auth)

43989 SHELL-MODEL CALCULATIONS ON THE N = 82 ODD-PROTON NUCLEI. II. Heyde, K.; Waroquier, M. (Univ., Ghent). Nucl. Phys.; A167: No. 3, 545-76(1971).

The quasiparticle Tamm–Dancoff approximation was applied to a calculation of the low-lying states in single-closed-shell nuclei with N = 82 neutrons. A central force of Gaussian shape with spin exchange is taken as the residual nucleon-nucleon interaction. An extensive study is made of the resemblance with the realistic Elliott interaction. The single-particle energies are determined by the iterative inverse-gap-equation method. The Hamiltonian matrix is diagonalized in a one- and three-quasiparticle space after elimination of spurious states. Transition rates, half-lifes, magnetic dipole moments and electric quadrupole moments are calculated, discussed in detail and compared with results obtained with the realistic Elliott interaction and the experimental data. The evaluated spectroscopic factors are studied and compared with the experimental one-nucleon transfer data with good quantitative agreement. (auth)

43990 DIE RAUMSTRUKTUR DER ENERGETISCH ANGEREGTEN ATOMKERNE. (Space Structure of Energetically Excited Atomic Nuclei). Weckering, Rudolf. Stereophysik. Die Atomphysik auf Neuer Grundlage. Raeumliche Wellen- und Quantenmechanik. Band VII. Luxemburg; Buchdruckerei Hermann s.e.n.c. (1970). 169p.

A new theory is proposed according to which each atomic nucleus and each atomic shell possess an electromagnetic field of standing waves with central symmetry. Discussed are the spacial arrangements of nuclides in their ground state, excitation of nuclides, origin of γ quanta, nature of nuclear binding forces, nuclear isomery, radioactive decay processes, and nuclear isomery periods. Properties of special nuclides are presented in numerous tables and figures. (H.B.G.)

43991 STATISTICAL CALCULATION OF THE DENSITY OF DOORWAY STATES AND ON THE PROBLEMS OF THEIR EXPERIMENTAL DETECTION. Breunlich, W. H. Oesterr. Akad. Wiss., Math.-Naturwiss. Kl., Sitzungsber., Abt. II; 176: 245-52(1967). (In German).

The level density of doorway states in which both excited nucleons possess bound states was calculated. The calculations show that the assumption that only nucleons around the Fermi limit can play a roll could not be maintained. Possible methods for their experimental detection are proposed. (J.S.R.)

43992 FINITE NUCLEAR SIZE AND RADIATIVE CORRECTIONS IN THE CONSTRUCTION AND ASSESSMENT OF KURIE PLOTS FOR ALLOWED BETA-DECAY. Wilkinson, D. H. (Univ. of Washington, Seattle). Nucl. Instrum. Methods; 94: No. 2, 229-32(1971).

If only a small fraction of a beta spectrum is available for Kurie-plot analysis because of the existence of strong branches of lower energy, it may become important to take into account finite-nuclear-size and radiative effects in the construction and assessment of the Kurie plot. Failure to do this may result in errors of many percent in the extraction of the intensity of the high-energy beta branch. These effects are analyzed, and numerical estimates are made of the possible errors. (auth)

XUM

REACTOR TECHNOLOGY

Commercial Power Reactors

Refer also to abstracts 42388 and 42506.

43993 (RDT-E-15-2-T) REQUIREMENTS FOR NUCLEAR COMPONENTS. (SUPPLEMENT TO ASME BOILER AND PRESSURE VESSEL CODE, SECTION III). (Division of Reactor Development and Technology (AEC), Washington, D. C.). Jul 1971. 25p. RSO.

Supplemental requirements for the construction of pressure-containing components of water cooled power reactors are presented. (H.D.R.)

43994 (WASH-1139) FORECAST OF GROWTH OF NUCLEAR POWER. (Division of Operations Analysis and Forecasting (AEC), Washington, D. C.). Jan 1971. 187p. GPO $1.50.

The 1970 forecast of the growth of nuclear power at home and abroad is presented. The method used is extrapolation of data on nuclear and conventional power plants installed after 1959, currently being constructed, or definitely planned for future construction in various areas of the United States and in foreign countries of the Free World. After projecting the growth of nuclear power, estimates are made of requirements for nuclear fuel based on data and assumptions about the design and operating characteristics of nuclear power plants. (auth)

43995 FUEL ASSEMBLY IDENTIFICATION. ANS 13.8 1971. Hinsdale, Ill.; American Nuclear Society (1971). 6p. Available from American Nuclear Society, Hinsdale, Ill.

Requirements for the identification of fuel assemblies used in nuclear power plants are described. The characters and sequence to be used in assigning a facility identification prefix and a serial number are defined. (H.D.R.)

43996 BEGEHBARE SCHLEUSEN IN KERNKEAFTWERKEN: ANFORDERUNGEN. (Access Locks in Nuclear Power Plants: Requirements). DIN 25 406 1971. Berlin; Normblatter durch Beuth-Vertrieb GmbH (1971). 4p. Available from Normblatter durch Beuth-Vertrieb GmbH, Berlin.

In accordance with the present status of operational experience, standards are summarized for access locks in nuclear power plants. Under normal operations, the locks should permit easy recognition and accident free utilization. In emergencies, they should permit safe exit for personnel. For these standards, the case is considered in which a person using the lock is disabled during an emergency. Self-evident design aspects, such as tightness and pressure resistance of the lock are treated only cursorily. Compiled are: definitions, general requirements, special requirements, manual activation, motor activation, control panels, energy supply, and additional equipment. (H.B.G.)

43997 BORSSELE PLANT AND THE ENERGY PICTURE IN THE NETHERLANDS. Com. Naz. Energ. Nucl., Notiz.; 16: No. 12, 81-5(Dec 1970). (In Italian).

The energy needs of the Netherlands are briefly outlined. The Borssele power plant will use a PWR reactor with 450 MW(e) net. The principal data are tabulated. The safety and protection are briefly considered. (J.S.R.)

Operation and Economics

Refer also to abstract 44175.

43998 (DOCKET-1155-123) LA CROSSE BOILING WATER REACTOR. Failure of Reactor Safety System Pressure Channel No. 1 to Trip During the Performance of a Technical Specification Test. (Dairyland Power Cooperative, La Crosse, Wis.). 23 Jun 1971. 4p. (DPC-71-11). Dep. NTIS.

43999 (DOCKET-1155-124) LA CROSSE BOILING WATER REACTOR. Unplanned Reactor Shutdown Caused by Closure of the 1A Forced Circulation Pump (FCP) Discharge Valve. (Dairyland Power Cooperative, La Crosse, Wis.). 8 Jul 1971. 3p. (DPC-71-12). Dep. NTIS.

44000 (DOCKET-1155-125) LA CROSSE BOILING WATER REACTOR. Failure of Reactor Building Main Steam Isolation Valve to Close. (Dairyland Power Cooperative, La Crosse, Wis.). 9 Jul 1971. 5p. (DPC-71-13). Dep. NTIS.

44001 (DOCKET-50016-121) ENRICO FERMI ATOMIC POWER PLANT, UNIT 1. [Operations] Report, February 1971. (Power Reactor Development Co., Detroit, Mich.). 20 Jul 1971. 12p. (PRDC-EF-90). Dep. NTIS.

44002 (DOCKET-50016-122) ENRICO FERMI ATOMIC POWER PLANT, UNIT 1. [Operations] Report, March 1971. (Power Reactor Development Co., Detroit, Mich.). 20 Jul 1971. 13p. (PRDC-EF-91). Dep. NTIS.

44003 (DOCKET-50133-58) HUMBOLDT BAY POWER PLANT, UNIT NO. 3. Annual Average Offsite Exposures Below Limits Defined in 10 CFR 20. (Pacific Gas and Electric Co., San Francisco, Calif.). 8 Jun 1971. 2p. Dep. NTIS.

44004 (DOCKET-50171-90) PEACH BOTTOM ATOMIC POWER STATION, UNIT 1. Monthly Operations Report No. 63, May 1971. (Philadelphia Electric Co., Pa.). 20 Jul 1971. 15p. Dep. NTIS.

44005 (DOCKET-50206-114) SAN ONOFRE NUCLEAR GENERATING STATION, UNIT 1. Semiannual Operating Report No. 8, January 1-June 30, 1971. (Southern California Edison Co., Los Angeles, San Diego Gas and Electric Co., Calif.). 12 Jul 1971. 7p. Dep. NTIS.

44006 (DOCKET-50213-115) CONNECTICUT YANKEE ATOMIC POWER PLANT. Operation Report No. 71-5, May 1971. (Connecticut Yankee Atomic Power Co., Haddam). 24 Jun 1971. Contract AT(30-1)-3250. 22p. (NYO-3250-60). Dep. NTIS.

44007 (DOCKET-50219-142) OYSTER CREEK NUCLEAR POWER PLANT, UNIT NO. 1. Surveillance Testing Failures. (Jersey Central Power and Light Co., Morristown, N. J.). 21 Jul 1971. 4p. Dep. NTIS.

Surveillance test failures described include: absorption chamber spray header valve tripped on overload while opening on June 3, 1971; isolation condenser system time delay relay failure on June 11, 1971; and standby gas treatment system train inlet valve failure to open on June 15, 1971. Corrective actions for each incident are presented. (D.C.C.)

44008 (DOCKET-50237-183) DRESDEN NUCLEAR POWER STATION, UNIT 2. Primary Containment Local Leak Rates Outside Technical Specifications Limits. (Commonwealth Edison Co., Chicago, Ill.). 28 Jun 1971. 2p. Dep. NTIS.

44009 (DOCKET-50237-184) DRESDEN NUCLEAR POWER STATION, UNITS 2 AND 3. Failure of Diesel Generator to Start. (Commonwealth Edison Co., Chicago, Ill.). 14 Jul 1971. 2p. (DOCKET-50249-78). Dep. NTIS.

44010 (DOCKET-50237-185) DRESDEN NUCLEAR POWER STATION, UNIT 2. Current Plan for Operation. (Commonwealth Edison Co., Chicago, Ill.). 16 Jul 1971. 2p. Dep. NTIS.

44011 (DOCKET-50244-73) ROBERT EMMETT GINNA NUCLEAR POWER PLANT, UNIT NO. 1. Failure of Main Steam Isolation Valve to Close. (Rochester Gas and Electric Corp., N. Y.). 9 Jul 1971. 2p. Dep. NTIS.

44012 (DOCKET-50245-85) MILLSTONE NUCLEAR POWER STATION, UNIT 1. Generator Load Rejects on June 24-25, 1971. (Millstone Point Co., Hartford, Conn.). 12 Jul 1971. 3p. Dep. NTIS.

44013 (DOCKET-50249-79) DRESDEN NUCLEAR POWER STATION, UNIT 3. Level and Temperature Limits of Primary Containment Suppression Chamber Exceeded. (Commonwealth Edison Co., Chicago, Ill.). 14 Jul 1971. 2p. Dep. NTIS.

44014 (DOCKET-50249-80) DRESDEN NUCLEAR POWER STATION, UNIT 3. Failure of Steam Admission Control Valves to Open. (Commonwealth Edison Co., Chicago, Ill.). 14 Jul 1971. 2p. Dep. NTIS.

During a high pressure coolant injection system test, the steam admission control valves failed to open. The failure was caused by a sticking oil-actuated interlock valve in the flow-sensing feedback loop that controls the turbine motor gear unit and control valves during the high pressure coolant injection operation. Revised surveillance testing procedures for the valves is proposed. (D.C.C.)

44015 (DOCKET-50249-81) DRESDEN NUCLEAR POWER STATION, UNIT 3. Failure of High Pressure Coolant Injection System Auto-Isolation Signal Reset. (Commonwealth Edison Co., Chicago, Ill.). 14 Jul 1971. 2p. Dep. NTIS.

44016 (DOCKET-50249–83) DRESDEN NUCLEAR POWER STATION, UNIT 3. Failure of High Pressure Coolant Injection Turbine Stop Valve to Reset. (Commonwealth Edison Co., Chicago, Ill.). 18 Jul 1971. 3p. Dep. NTIS.

44017 (DOCKET-50261–63) H. B. ROBINSON UNIT NO. 2. Failure of Liquid Radioactive Waste Evaporator to Meet Specifications. (Carolina Power and Light Co., Raleigh, N. C.). 28 Jun 1971. 1p. Dep. NTIS.

44018 (DOCKET-50261–64) H. B. ROBINSON UNIT NO. 2. Clad Failure on Primary Side of Steam Generators. (Carolina Power and Light Co., Raleigh, N. C.). 28 Jun 1971. 1p. Dep. NTIS.

44019 (DOCKET-50263–75) MONTICELLO NUCLEAR GENERATING PLANT, UNIT 1. Report of Occurrences. (Northern States Power Co., Minneapolis, Minn.). 16 Jul 1971. 8p. Dep. NTIS.

Operations incidents for June 18, June 19, and July 9, 1971 are described. On June 18 while performing a heatup rate test in conjunction with the startup test procedure, the reactor coolant temperature was increased by 115°F during a one hour period. Revised test monitoring requirements to prevent such a rapid temperature change in the reactor vessel are indicated. On June 19 there was a failure of the standby gas treatment system air heater control circuitry. Corrective maintenance is described. On July 9 while performing a regularly scheduled surveillance test, two of the four reactor high pressure scram trip switches were found to trip outside of allowable deviation in technical specifications. The failed switches were replaced. (D.C.C.)

44020 (TID–25737) LA CROSSE BOILING WATER REACTOR MONTHLY OPERATING REPORT FOR APRIL 1971. (Dairyland Power Cooperative, La Crosse, Wis.). Contract AT(11-1)-851. 30p. (DPC–851-26). Dep. NTIS.

The plant was on the line connected to the grid for 628 hours. The reactor availability was 95%, turbine generation 87% and a plant availability of 84%. The plant capacity and plant efficiency were affected by the turbine steam reheater tube failures. One reactor scram occurred at power during a test on a safety system power/flow channel. Two shutdowns were scheduled for turbine steam reheater tube plugging. The purification system cation and mixed bed resins were replaced and resins were drummed for shipment. Class B and C containment building leak tests were performed. (auth)

44021 ANALYSIS OF RATED PARAMETERS AT THE ELECTRIC POWER STATION A-1. Bis, Jiri; Leitner, Zbynek; Kotyza, Vojtech; Toufar, Pavel (Skoda Works, Plzen, Czech.). Jad. Energ.; 17: No. 7, 222-7(1971). (In Czech).

Procedures and methods in use at the electric power station A-1 are critically examined, with tables and graphs illustrating typical operating parameters. At the maximum cladding temperature of 500°, the maximum thermal power developed is given as 566 MW(t), with generated electrical power of 49,432 kW. The project is a part of a design program MARCOS (Model Analysis of Reactor Cooling Systems) which entered into the documentation of the start-up of the power reactor A-1 at Joslovske Bohunice, Czechoslovakia. (K.S.W.)

44022 HOW TO MAKE A PROFIT ON WASTE HEAT. Beall, Sam E. Jr.; Samuels, G. (Oak Ridge National Lab., Tenn.). Nucl. Technol.; 12: No. 1, 12-17(Sep 1971).

The possibility of using warm water from power stations to control the temperature of plant and animal enclosures is examined. With the heat from a nuclear station, such as the 330-MW(e) gas-cooled reactor being built near Denver, Colorado, it appears that a good fraction of the fresh vegetable, poultry, and pork needs of a large city could be produced in a growing area near the power station, and that the profit incentive is high to both the grower and the utility. 9 references. (auth)

Safety and Siting

Refer also to abstract 42393.

44023 (DOCKET-1151–44) ELK RIVER REACTOR. Revised Technical Specifications (Dismantling and Maintenance). (Rural Cooperative Power Association, Elk River, Minn.). 1 Jul 1971. Contract AT(11-1)-651. 12p. Dep. NTIS.

44024 (DOCKET-50003–80) INDIAN POINT STATION, UNIT NO. 1. Analysis of Make-Up Water 4 Inch Nozzle Sleeve Modified Design). (Franklin Inst. Research Labs., Philadelphia, Pa.). 24 May 1971. 208p. Dep. NTIS.

For Consolidated Edison Co. of New York, Inc., New York.

44025 (DOCKET-50029–152) YANKEE NUCLEAR POWER STATION. Quality Assurance Program. (Yankee Atomic Electric Co., Westboro, Mass.). 14 Jun 1971. 16p. Dep. NTIS.

44026 (DOCKET-50133–59) HUMBOLDT BAY POWER PLANT, UNIT NO. 3. Final Safety Analysis Report, Suppl. (Pacific Gas and Electric Co., San Francisco, Calif.). 23 Jun 1971. 10p. Dep. NTIS.

The quality assurance program related to the operation, maintenance, repair, refueling, and modifications of Humboldt Bay Power Reactor is presented. (D.C.C.)

44027 (DOCKET-50146–82) SAXTON REACTOR. Quality Assurance Program. (Saxton Nuclear Experimental Corp., Pa.). 15 Jul 1971. 4p. Dep. NTIS.

44028 (DOCKET-50146–84) SAXTON REACTOR. License No. DPR-4; Technical Specifications Change Request No. 47. (Saxton Nuclear Experimental Corp., Pa.). 21 Jul 1971. 3p. Dep. NTIS.

Revised technical specifications are presented concerning the insertion of a solid Zircaloy 4 rod in a PuO_2–UO_2 fuel assembly. (D.C.C.)

44029 (DOCKET-50146–85) SAXTON REACTOR. License No. DPR-4; Technical Specifications Change Request No. 48. (Saxton Nuclear Experimental Corp., Pa.). 21 Jul 1971. 3p. Dep. NTIS.

Revised technical specifications are presented concerning operations with 2 previously irradiated test fuel rods of Zircaloy 4-clad PuO_2–UO_2 pellets. (D.C.C.)

44030 (DOCKET-50155–84) BIG ROCK POINT NUCLEAR PLANT. Final Safety Summary Report, Suppl. (Includes Quality Assurance Program). (Consumers Power Co., Jackson, Mich.). 24 Jun 1971. 5p. Dep. NTIS.

44031 (DOCKET-50155–85) BIG ROCK POINT NUCLEAR PLANT. Report of Inspection. (Division of Compliance (AEC), Glen Ellyn, Ill. Region III.). 16 Jul 1971. 2p. Dep. NTIS.

Inspection results for liquid effluent radioactive waste system operations, gaseous effluent radioactive waste system operations, effluent monitor calibrations and sensitivities, laboratory procedures for analysis of gaseous and liquid effluent samples, radioactive effluent releases to the environment, and malfunction of control rod drive C-3 are described. (D.C.C.)

44032 (DOCKET-50171–89) PEACH BOTTOM ATOMIC POWER STATION, UNIT 1. Emergency Rod Batteries: Status Report. (Philadelphia Electric Co., Pa.). 24 Jun 1971. 5p. Dep. NTIS.

44033 (DOCKET-50171–91) PEACH BOTTOM ATOMIC POWER STATION, UNIT 1. Thermally Released Shutdown Absorber Rods. (Philadelphia Electric Co., Pa.). 22 Jul 1971. 3p. Dep. NTIS.

44034 (DOCKET-50206–115) SAN ONOFRE NUCLEAR GENERATING STATION, UNIT 1. Provisional Operating License No. DPR-13, Amendment 24. Quality Assurance Program. (Southern California Edison Co., Los Angeles). 15 Jul 1971. 30p. Dep. NTIS.

44035 (DOCKET-50220–65) NINE MILE POINT NUCLEAR STATION, UNIT NO. 1. Technical Specifications and Bases for Operation at 1850 Thermal Megawatts. (Niagara Mohawk Power Corp., Syracuse, N. Y.). May 1971. 142p. Dep. NTIS.

44036 (DOCKET-50237–186) DRESDEN NUCLEAR POWER STATION, UNITS 2 AND 3. Additional Information Concerning Special Report No. 3, Unit 2; and Special Report No. 15, Unit 3. (Commonwealth Edison Co., Chicago, Ill.). 20 Jul 1971. 5p. (DOCKET-50249–82). Dep. NTIS.

A process flow diagram for the liquid rodwaste system is presented. Information concerning possible release rates due to damaged fuel elements from missing hardware of a purge dam is included. (D.C.C.)

44037 (DOCKET-50244–72) ROBERT EMMETT GINNA NUCLEAR POWER PLANT, UNIT NO. 1. Final Facility Description and Safety Analysis Report, Suppl. 14. (Rochester Gas and Electric Corp., N. Y.). 28 Jun 1971. 8p. Dep. NTIS.

The quality assurance program for the Robert E. Ginna Power Reactor Unit 1 is presented. (D.C.C.)

XUM

44038 (DOCKET-50244-74) ROBERT EMMETT GINNA NUCLEAR POWER PLANT, UNIT NO. 1. Citation Alleging Noncompliance with Action of the Technical Specifications. (Rochester Gas and Electric Corp., N. Y.). 15 Jun 1971. 17p. Dep. NTIS.

Information concerning radioactive and thermal effluents from the reactor is presented. Revised monitoring procedures are described. (D.C.C.)

44039 (DOCKET-50247-46) INDIAN POINT NUCLEAR GENERATING UNIT NO. 2. AEC Regulatory Staff Safety Evaluation, Suppl. 2. (Division of Compliance (AEC), Washington, D. C.). Jul 1971. 14p. Dep. NTIS.

44040 (DOCKET-50254-42) QUAD-CITIES STATION, UNITS 1 AND 2. Final Detailed Statement on Environmental Considerations. (Division of Radiological and Environmental Protection (AEC), Washington, D. C.). 2 Jul 1971. 108p. (DOCKET-50265-38). Dep. NTIS.

Information concerning chemical, radioactive, and thermal discharges from the reactor is presented. The effects of reactor operations on the environment are analyzed. (D.C.C.)

44041 (DOCKET-50254-44) QUAD-CITIES STATION, UNITS 1 AND 2. Preliminary Safety Analysis Report, Amendment 27 (Includes Additional Information to Final Safety Analysis Report). (Commonwealth Edison Co., Chicago, Ill. Iowa-Illinois Gas and Electric Co., Davenport, Iowa). 19 Jul 1971. 41p. (DOCKET-50265-39). Dep. NTIS.

Additional information is presented concerning fuel cask drop accident, pipe whip protection requirements, and emergency core cooling system performance requirements. (D.C.C.)

44042 (DOCKET-50254-45) QUAD-CITIES STATION, UNITS 1 AND 2. Preliminary Safety Analysis Report, Amendment 28 (Includes Additions and Revisions to Final Safety Analysis Report). (Commonwealth Edison Co., Chicago, Ill. Iowa-Illinois Gas and Electric Co., Davenport, Iowa). 26 Jul 1971. 4p. (DOCKET-50265-40). Dep. NTIS.

Additional information concerning the emergency core cooling system is presented. Graphs are included that illustrate the time that effective core cooling is initiated, the time that the fuel channel becomes wetted, and the time that temperature transient is terminated. (D.C.C.)

44043 (DOCKET-50255-48) PALISADES PLANT. Palisades Interim Loss of Coolant Analysis. (Consumers Power Co., Jackson, Mich.). 19 Jul 1971. 103p. (CENPD-22). Dep. NTIS.

44044 (DOCKET-50255-49) PALISADES PLANT. Safety Evaluation, Supplement No. 4. (Division of Reactor Licensing (AEC), Washington, D. C.). 22 Jul 1971. 18p. Dep. NTIS.

44045 (DOCKET-50261-65) H. B. ROBINSON UNIT NO. 2. Preoperational Flow Test on Safety Injection System. (Carolina Power and Light Co., Raleigh, N. C.). 1 Jul 1971. 3p. Dep. NTIS.

44046 (DOCKET-50261-66) H. B. ROBINSON UNIT NO. 2. Reply Regarding Operation of Emergency Diesel Generators. (Carolina Power and Light Co., Raleigh, N. C.). 6 Jul 1971. 23p. Dep. NTIS.

44047 (DOCKET-50267-32) FORT ST. VRAIN NUCLEAR GENERATING STATION, [UNIT 1]. Preliminary Safety Analysis Report, Amendment 22 (Includes Additions and Revisions to Final Safety Analysis Report). (Public Service Co. of Colorado, Denver). 15 Jul 1971. 114p. Dep. NTIS.

Revised design parameters and operations aspects of the Fort St. Vrain Power Reactor Unit 1 are presented. Data for the environmental radiation survey during January to March 1971 are included. (D.C.C.)

44048 (DOCKET-50271-55) VERMONT YANKEE NUCLEAR POWER STATION. Conformance of BWR ECCS to AEC Interim Acceptance Criteria for Light Water Reactors. (Vermont Yankee Nuclear Power Corp., Rutland). 19 Jun 1971. 17p. Dep. NTIS.

44049 (DOCKET-50271-56) VERMONT YANKEE NUCLEAR POWER STATION. Preliminary Safety Analysis Report, Amendment 28 (Includes Additions and Revisions to Final Safety Analysis Report). (Vermont Yankee Nuclear Power Corp., Rutland). 20 Jul 1971. 48p. Dep. NTIS.

Qualifications of personnel for pre-operation and power operation testing are presented. Performance requirements for the emergency core cooling system are described. (D.C.C.)

44050 (DOCKET-50271-57) VERMONT YANKEE NUCLEAR POWER STATION. Safety Evaluation, Supplement No. 1. (Division of Reactor Licensing (AEC), Washington, D. C.). 23 Jul 1971. 42p. Dep. NTIS.

44051 (DOCKET-50280-43) SURRY POWER STATION, UNITS 1 AND 2. Preliminary Safety Analysis Report, Amendment 23. (Virginia Electric and Power Co., Richmond). 2 Jul 1971. 169p. (DOCKET-50281-42). Dep. NTIS.

Revised design parameters and operation aspects of the Surry Power Reactor Units 1 and 2 are presented. Included also are meteorological data for the site, seismic design requirements for structures and piping systems, and testing of engineered safeguards. (D.C.C.)

44052 (DOCKET-50286-37) INDIAN POINT NUCLEAR GENERATING UNIT NO. 3. Preliminary Safety Analysis Report, Amendment 14 (Includes Report: Effect of Tornado Missiles on Stored Spent Fuel). (Westinghouse Electric Corp., Pittsburgh, Pa. Nuclear Energy Systems [Div.]). 30 Jun 1971. 42p. (WCAP-7572). Dep. NTIS.

For Consolidated Edison Co. of New York, Inc., New York.

The potential for tornado missile damage to spent fuel assemblies stored beneath water in the spent fuel storage pit is examined. Based on the strength of the tornado wind forces which could originate a missile and carry it into the pool, a spectrum of missiles is selected for analysis. A parameter study for the vertical deceleration of these missiles when they enter a partially dewatered spent fuel storage pit shows that few missiles would retain sufficient energy to distort the fuel storage racks and damage fuel assemblies. For the study, the conservative assumption was made that the missile penetrates the water vertically, with minimum drag orientation. However, missiles generated by tornado winds would be expected to be randomly orientated upon impact with the surface of the pool. Therefore, a more realistic analysis of the slab missile case was made to incorporate the rotational effects which would result from imperfect alignment of a missile as it enters the pool. This analysis demonstrates that deceleration would be much faster under these conditions because of the resultant increase in effective drag area. It is concluded that spent fuel damage by tornado-driven missiles is very unlikely. Furthermore, it is shown that if damage to a spent fuel assembly were to occur as the consequence of a tornado missile, the resultant site boundary dose would be orders of magnitude below the siting guideline. 6 references. (auth)

44053 (DOCKET-50286-38) INDIAN POINT NUCLEAR GENERATING UNIT NO. 3. Preliminary Safety Analysis Report, Amendment 15 (Includes Final Facility Description and Safety Analysis Report, Suppl. No. 1). (Consolidated Edison Co. of New York, Inc., New York). 8 Jul 1971. 170p. Dep. NTIS.

Revised design parameters and operations aspects for the Indian Point Power Reactor Unit 3 are presented. Meteorological data for the reactor site are included. (D.C.C.)

44054 (DOCKET-50301-35) POINT BEACH NUCLEAR PLANT, UNIT NO. 2. Report of Inspection. (Division of Compliance (AEC), Glen Ellyn, Ill. Region III.). 15 Jul 1971. 2p. Dep. NTIS.

Inspection results are presented for pre-operation testing program and repairs performed on Unit 2-B steam generator. (D.C.C.)

44055 (DOCKET-50315-38) DONALD C. COOK NUCLEAR PLANT, UNITS 1 AND 2. Benton Harbor Power Plant Limnological Studies. VI. (American Electric Power Service Corp., New York). 9 Jul 1971. 86p. (DOCKET-50316-38). Dep. NTIS.

44056 (DOCKET-50315-39) DONALD C. COOK NUCLEAR PLANT, UNITS 1 AND 2. Underwater Gamma Radiation Detection System. (American Electric Power Service Corp., New York). 9 Jul 1971. 54p. (DOCKET-50316-39). Dep. NTIS.

44057 (DOCKET-50315-40) DONALD C. COOK NUCLEAR PLANT, UNITS 1 AND 2. Lake Michigan Environmental Survey. (American Electric Power Service Corp., New York). 9 Jul 1971. 119p. (DOCKET-50316-40). Dep. NTIS.

44058 (DOCKET-50315-41) DONALD C. COOK NUCLEAR PLANT, UNITS 1 AND 2. Benton Harbor Power Plant Limnological Studies. VII. (American Electric Power Service Corp., New York). 9 Jul 1971. 90p. (DOCKET-50316-41). Dep. NTIS.

44059 (DOCKET-50317-26) CALVERT CLIFFS NUCLEAR POWER PLANT, UNITS 1 AND 2. Preliminary Safety Analysis Report, Amendment 12 (Includes Final Safety Analysis Report).

(Baltimore Gas and Electric Co., Md.). 16 Jul 1971. 85p. (DOCKET-50318-26). Dep. NTIS.

Information concerning mislocated vertical tendons in the prestressed, post-tensioned concrete containment structure is presented. Corrective actions are described. Changes made in the quality control program to minimize future occurrences are presented. (D.C.C.)

44060 (DOCKET-50342-7) VERPLANCK NUCLEAR FACILITY, UNITS 1 AND 2. Preliminary Safety Analysis Report, Amendment 1 (Suppl.1-Pt.A): Revised Pages. (Consolidated Edison Co. of New York, Inc., New York). 9 Apr 1971. 660p. (DOCKET-50343-7). Dep. NTIS.

Revised design parameters of the Verplanck Power Reactor Units 1 and 2 are presented. Included also are additional data on the reactor requested by the Division of Reactor Licensing. (D.C.C.)

44061 (DOCKET-50352-15) LIMERICK GENERATING STATION, UNITS 1 AND 2. Preliminary Safety Analysis Report, Amendment 9. (Philadelphia Electric Co., Pa.). 22 Jul 1971. 411p. (DOCKET-50353-15). Dep. NTIS.

Revised and additional data concerning design parameters and operations aspects of the Limerick Power Reactor Units 1 and 2 are presented. (D.C.C.)

44062 (DOCKET-50354-15) NEWBOLD ISLAND NUCLEAR GENERATING STATION, UNITS 1 AND 2. Preliminary Safety Analysis Report, Amendment 8. (Public Service Electric and Gas Co., Newark, N. J.). 2 Jul 1971. 190p. (DOCKET-50355-15). Dep. NTIS.

Revised design parameters and operations aspects for Newbold Island Power Reactor Units 1 and 2 are presented. (D.C.C.)

44063 (DOCKET-50358-19) WM. H. ZIMMER NUCLEAR POWER STATION, UNIT 1. Preliminary Safety Analysis Report, Amendment 13. (Cincinnati Gas and Electric Co., Ohio. Columbus and Southern Ohio Electric Co., Columbus, Ohio. Dayton Power and Light Co., Ohio). 12 Jul 1971. 207p. Dep. NTIS.

Revised design parameters and operations aspects of the William H. Zimmer Power Reactor Unit 1 are presented. (D.C.C.)

44064 (DOCKET-50358-20) WM. H. ZIMMER NUCLEAR POWER STATION, UNIT 1. Preliminary Safety Analysis Report, Amendment 14. (Cincinnati Gas and Electric Co., Ohio. Columbus and Southern Ohio Electric Co., Columbus, Ohio. Dayton Power and Light Co., Ohio). 19 Jul 1971. 51p. Dep. NTIS.

Revised design parameters of the William H. Zimmer Power Reactor Unit 1 are presented. Included also are additional data on the reactor requested by the Division of Reactor Licensing. (D.C.C.)

44065 (DOCKET-50368-14) ARKANSAS NUCLEAR ONE, UNIT 2. Preliminary Safety Analysis Report, Amendment 10. (Arkansas Power and Light Co., Little Rock). 14 Jul 1971. 43p. Dep. NTIS.

Revised design parameters of the Arkansas Nuclear One Power Reactor Unit 2 are presented. Included also are additional data on the reactor requested by the Division of Reactor Licensing. (D.C.C.)

44066 (DOCKET-50368-15) ARKANSAS NUCLEAR ONE, UNIT 2. Preliminary Safety Analysis Report, Amendment 11. (Arkansas Power and Light Co., Little Rock). 21 Jul 1971. 54p. Dep. NTIS.

Revised design parameters of the Arkansas Nuclear One Power Reactor Unit 2 are presented. Additional data on the reactor requested by the Division of Reactor Licensing are included. Also included are personnel qualifications, quality assurance program, and surface water hydrology for the site. (D.C.C.)

44067 (DOCKET-50369-12) McGUIRE NUCLEAR STATION, UNITS 1 AND 2. Preliminary Safety Analysis Report, Amendment 8. (Duke Power Co., Charlotte, N. C.). 12 Jul 1971. 79p. (DOCKET-50370-11). Dep. NTIS.

Revised design parameters of the McGuire Power Reactor Units 1 and 2 are presented. Included also are additional data on the reactor requested by the Division of Reactor Licensing. (D.C.C.)

44068 (DOCKET-50376-16) AGUIRRE NUCLEAR PLANT, UNIT NO. 1. Criteria Previously Adopted are Responsive to General Design Criterion 2. (Puerto Rico Water Resources Authority, San Juan). 9 Jul 1971. 2p. Dep. NTIS.

The possibility of tornadoes occurring in the reactor site area is discussed. (D.C.C.)

44069 (DOCKET-50376-18) AGUIRRE NUCLEAR PLANT, UNIT NO. 1. Preliminary Facility Description and Safety Analysis Report, Amendment 7. (Puerto Rico Water Resources Authority, San Juan). 16 Jul 1971. 81p. Dep. NTIS.

Geological data for the reactor site and surrounding area are presented. (D.C.C.)

44070 (DOCKET-50382-7) WATERFORD STEAM ELECTRIC STATION, UNITS 3 AND 4. Preliminary Safety Analysis Report, Amendment 3. (Louisiana Power and Light Co., New Orleans). 16 Jul 1971. 8p. (DOCKET-50383-7). Dep. NTIS.

Additional information concerning quality assurance requirements for the Waterford Power Reactor Units 3 and 4 is presented. (D.C.C.)

44071 (DOCKET-50395-1) VIRGIL C. SUMMER NUCLEAR STATION, UNIT 1. Application for License. (South Carolina Electric and Gas Co., Columbia). 30 Jun 1971. 33p. Dep. NTIS.

Financial data on the owners of the Virgil C. Summer Power Reactor Unit 1 are presented in support of the application for construction permit and operating license. The 1970 Annual Report for the South Carolina Electric and Gas Company is included. (D.C.C.)

44072 (DOCKET-50395-2) VIRGIL C. SUMMER NUCLEAR STATION, UNIT 1. Environmental Report. (South Carolina Electric and Gas Co., Columbia). 30 Jun 1971. 186p. Dep. NTIS.

Information concerning chemical, radioactive, and thermal discharges from the reactor is presented. The effects of reactor operations on the environment are analyzed. (D.C.C.)

44073 (DOCKET-50395-3) VIRGIL C. SUMMER NUCLEAR STATION, UNIT 1. Preliminary Safety Analysis Report, Vol. 1. (South Carolina Electric and Gas Co., Columbia). 30 Jun 1971. 300p. Dep. NTIS.

Overall design parameters and operations aspects of the Virgil C. Summer Power Reactor Unit 1 are presented. (D.C.C.)

44074 (DOCKET-50395-4) VIRGIL C. SUMMER NUCLEAR STATION, UNIT 1. Preliminary Safety Analysis Report, Vol. 2. (South Carolina Electric and Gas Co., Columbia). 30 Jun 1971. 379p. Dep. NTIS.

Information on the site for the Virgil C. Summer Power Reactor Unit 1 is presented. Meteorological and hydrological data for the site are included. (D.C.C.)

44075 (DOCKET-50395-5) VIRGIL C. SUMMER NUCLEAR STATION, UNIT 1. Preliminary Safety Analysis Report, Vol. 3. (South Carolina Electric and Gas Co., Columbia). 30 Jun 1971. 421p. Dep. NTIS.

Information on the cooling system and general design parameters for the Virgil C. Summer Power Reactor Unit 1 is presented. (D.C.C.)

44076 (DOCKET-50395-6) VIRGIL C. SUMMER NUCLEAR STATION, UNIT 1. Preliminary Safety Analysis Report, Vol. 4. (South Carolina Electric and Gas Co., Columbia). 30 Jun 1971. 749p. Dep. NTIS.

Information on the Virgil C. Summer Power Reactor Unit 1 is presented under the following broad topics: containment; engineered safety features; and instrumentation and control. (D.C.C.)

44077 (DOCKET-50395-7) VIRGIL C. SUMMER NUCLEAR STATION, UNIT 1. Preliminary Safety Analysis Report, Vol. 5. (South Carolina Electric and Gas Co., Columbia). 30 Jun 1971. 400p. Dep. NTIS.

Information on the Virgil C. Summer Power Reactor Unit 1 is presented under the following broad topics: electrical systems; auxiliary systems; steam and power conversion; waste disposal and radiation protection; conduct of operations; and initial tests and operations. (D.C.C.)

44078 (DOCKET-50395-8) VIRGIL C. SUMMER NUCLEAR STATION, UNIT 1. Preliminary Safety Analysis Report, Vol. 6. (South Carolina Electric and Gas Co., Columbia). 30 Jun 1971. 514p. Dep. NTIS.

Information on the Virgil C. Summer Power Reactor Unit 1 is presented under the following broad topics: safety analysis; and technical specifications. (D.C.C.)

44079 (UCLA-ENG-7037) SAN ONOFRE NUCLEAR GENERATING STATION VIBRATION TESTS. Smith, C. B.; Ibanez, P.; Wang, G. S. C.; Matthiesen, R. B. (California Univ., Los Angeles. School of Engineering and Applied Science). Aug 1970. 118p.

A series of forced vibration tests were conducted at the San Onofre Nuclear Generating Station. During the tests, the reactor was shut down for maintenance, so it was not possible to study the effects of vibration on the operation of the reactor. Tests were

XUM

made on the reactor building and the primary coolant system. Coolant Loop "B", consisting of a pressurizer, steam generator, and primary pump, was selected for detailed testing. Other tests were performed to compare the response of loops "A" and "C" to "B". The experimental data were analyzed, using a computer program and a linear, viscously damped, lumped parameter model which assumes that orthogonal modes exist. An iterative procedure is used to fit the analytical steady-state responses to the experimental test results. The resulting mode shapes are an excellent fit to experimental data but are not perfectly orthogonal. A gradient search on the orthogonality error, followed by a least mean square fitting routine, is then used to get orthogonal modes which reproduce the experimental response within a few percent over the frequency range of interest. The analytical model was then used to study the response of San Onofre to digitized earthquake-like records obtained by seismographs during the El Centro and Taft earthquakes. Preliminary results using a linear model indicate that the earthquake response of the plant was not excessive. The system responds nonlinearly to strong motion earthquake forces. Experimental data indicate that the linear model provides a conservative upper limit to the equipment response. Present research is directed at developing models to represent the nonlinearities associated with high force levels. 10 references. (auth)

44080 DEVELOPMENT OF AN INSPECTION SYSTEM FOR THE ATUCHA NUCLEAR REACTOR. Wylie, Robert D. (Southwest Research Inst., San Antonio); Lautzenheiser, Clarence E.; Wortman, Oscar. pp 628-34 of Materials Technology. I. New York; American Society of Mechanical Engineers (1970).

From second inter-american conference on materials technology; Mexico City, Mex. (24 Aug 1970). See CONF-700812.

The first nuclear reactor for the generation of electric power in Latin America is in the process of construction at Atucha about 150 kilometers from Buenos Aires, Argentina. The nuclear steam supply system is a heavy-water-moderated pressurized-water reactor of 319 megawatt electric. To assure the continued operational safety of the reactor vessel, there will be a planned inservice inspection program. This will cover all of the welds in the core region of the vessel and the areas of geometrical stress concentration such as at the primary coolant nozzles. The inspection system will be based on ultrasonic scanning from the outside of the pressure vessel. The development of techniques and equipment to accomplish this inspection is described. (auth)

Steam and Power Conversion Systems

44081 (RDT-E-4-1-T) STEAM GENERATOR FOR PRESSURIZED WATER REACTORS. (Division of Reactor Development and Technology (AEC), Washington, D. C.). Oct 1969. 45p. RSO.

Requirements for the design, fabrication, testing, and inspection of steam generators for pressurized water power reactors are presented. (H.D.R.)

44082 (SWRI-1228-9-10) ULTRASONIC INSPECTION OF SELECTED WELDS IN STAINLESS STEEL PRIMARY STEAM PIPING IN ELK RIVER POWER PLANT, JUNE 1-2, 1966. Lautzenheiser, C. E.; Viaclovsky, S. A. (Southwest Research Inst., San Antonio, Tex.). 28 Jun 1966. Contract AT(11-1)-1228. 9p. Dep. NTIS.

The program objective was to utilize an ultrasonic technique for the inspection of selected stainless steel piping weldments in the primary steam system of the Elk River Nuclear Plant at Elk River, Minnesota. The inspection was based on stress corrosion cracking that had been observed in stainless steel specimens exposed in the primary side of the heat exchangers. Weldments representative of the locations of maximum stress in the primary steam stainless steel piping and, consequently, highest potential areas for stress corrosion cracking were selected. A total of ten welds were chosen for an ultrasonic inspection. A 45-degree ultrasonic shear wave was propagated into the material being inspected at a frequency of 2.25 mHz. Reference standards were made from stainless steel plate for each size pipe wall thickness inspected and contained a slot $1/16$ inch deep and $1/32$ inch wide. The inspection revealed no defects in the welds inspected. Although the reference standard was reasonably large, no indications were observed of defects which were even a quarter of the standard size. (auth)

Power Reactor Development

Refer also to abstract 42929.

44083 (BNWL-SA-2738) MULTIPLE PURPOSE USE OF THERMAL CONDENSER DISCHARGES FROM LARGE NUCLEAR SYSTEMS TO SUPPLEMENT INTERREGIONAL WATER SUPPLY. Jaske, R. T.; Karr, M. H.; Touhill, C. J. (Battelle-Northwest, Richland, Wash. Pacific Northwest Lab.). Feb 1970. Contract AT(45-1)-1830. 17p. (CONF-700212-2). Dep. NTIS.

From sixty-seventh national meeting of the American Institute of Chemical Engineers; Atlanta, Ga. (17 Feb 1970).

As a partial solution to some of the technical, economic, and environmental problems of large nuclear power plant siting, a system of canals over regional areas is proposed. The canals, with flows up to 15,000 cfs, would serve as elongated cooling ponds for large nuplex stations and the warmed water would be used for irrigation of staple crops. The canal-lake cooling system concept is applied to a potential area in the Pacific Northwest, and the basic technical, economic, and sociological features of such systems are discussed. (H.D.R.)

44084 (CONF-700224) PROCEEDINGS OF THE INTERNATIONAL SYMPOSIUM ON NON-DESTRUCTIVE TESTING OF NUCLEAR POWER REACTOR COMPONENTS, ROTTERDAM, 26-27 FEBRUARY 1970. (Nederlands Atoomforum, The Hague. Roentgen Technische Dienst N. V., Rotterdam (Netherlands)). (Rotterdamsche Droogdok Maatschappij N. V. (Netherlands)). 191p.

Included are 8 papers on equipment and techniques for nondestructive testing of component material and joints in nuclear reactor construction. A separate abstract was prepared for each of the papers. (H.D.R.)

For abstracts of individual papers see: 44109-44113, 44136, 44137, and 44148.

44085 (CONF-710427-1) U. S. EXPERIENCE WITH FAST POWER REACTORS: EBR-II. Koch, L. J. (Argonne National Lab., Ill.). [1971]. 24p. Dep. NTIS.

From American power conference; Chicago, Ill. (20 Apr 1971).

The loop-type and pool-type concepts for liquid metal fast breeder reactors (LMFBR) are described. The design, construction, and operation of the 20 MW(e) Experimental Breeder Reactor-II are discussed with emphasis on those aspects of the design which relate to the pool concept. (H.D.R.)

44086 (EURFNR-853) IN-PILE EQUIPMENT FOR STRAIN MEASUREMENTS ON NUCLEAR FUELS AND STRUCTURAL MATERIALS. Will, H. (Kernforschungszentrum, Karlsruhe (Weatst Germany). Institut fuer Reaktorentwicklung). Translation of report KFK-1281. 33p. Dep. NTIS.

Work Performed under United States-Euratom Fast Reactor Exchange Program.

The design criteria of a creep capsule are presented. The possible methods of measurement for in-pile expansion measurements are discussed in detail with respect to suitability and applicability in an irradiation rig. A description of finished models of irradiation rigs is included. (auth)

44087 (EURFNR-854) STUDIES ON WEAR AND FRICTIONAL BEHAVIOR BETWEEN FUEL ROD BUNDLES AND SPACER GRIDS IN SODIUM. Kleefeldt, K. (Kernforschungszentrum, Karlsruhe (West Germany). Institut fuer Reaktorentwicklung). Translation of report KFK-1290. 24p. Dep. NTIS.

Work Performed under United States-Euratom Fast Reactor Exchange Program.

Results of experiments in sodium in which the friction between fuel element bundle and spacer grids were investigated up to temperatures of 680°C are described. The relative axial movement between the fuel pins and the spacers, which results from different heat expansion in the fuel element, was simulated mechanically using an eccentric drive. The frictional forces produced during this process were 5 to 20 kg per spacer grid in sodium and higher in air and argon. For two different spacer designs a critical frictional force $R_{crit} \approx 55$ kg and 60 to 80 kg, respectively, was determined. If the frictional force exceeds this critical value due to a lack of clearance, the bowing of the grid leads to a clamping effect and to plastic deformation. Repetitive movement of the bundle causes the spacer grid to rupture. The increase in clearance by wear is less than 0.02 mm. This means it is much below the tolerance level required in fabrication and operation. Diffusion welding of joints in sodium was not detectable after seven days of shutdown period at 600°C. Discussions are included on the advantages and drawbacks of the selected methods of spacer grid fastening. (auth)

44088 (RDT-F-2-2-T) QUALITY ASSURANCE PROGRAM REQUIREMENTS. (Division of Reactor Development and Technology (AEC), Washington, D. C.). Jun 1969. 44p. RSO.

General requirements are presented for planning, managing,

conducting, and evaluating quality assurance programs for reactor development and test facility projects and associated processes, structures, components, and systems. These quality assurance requirements are based on proven practices and provide the means of control and verification whereby those responsible for project management can assure that the quality required for safe, reliable, and economical operation will be achieved. The objective of the programs covered by the standard is to assure that structures, components, systems, and facilities are designed, developed, manufactured, constructed, operated, and maintained in compliance with established engineering criteria. To achieve this objective, controls are to be established and implemented at predetermined points, and necessary action taken to prevent, detect, and correct any deficiencies. (auth)

44089 (RDT-F-5-1-T) CLEANING AND CLEANLINESS REQUIREMENTS FOR NUCLEAR REACTOR COMPONENTS. (Division of Reactor Development and Technology (AEC), Washington, D. C.). Mar 1969. 26p. RSO.

Minimum requirements for cleaning and cleanliness of vessels, heat exchangers, pumps, piping, valves and other fabricated components for nuclear service are presented. (auth)

44090 (WAPD-T-2358) COMPUTER UTILIZATION IN NUCLEAR REACTOR DESIGN. Marlowe, O. J. (Bettis Atomic Power Lab., Pittsburgh, Pa.). Apr 1970. Contract AT(11-1)-Gen-14. 14p. (CONF-700443-1). Dep. NTIS.

From AEC computer information meeting; Washington, D. C. (30 Apr 1970).

The digital computer plays an important role in support of various engineering disciplines in nuclear reactor design. The special requirements of these computations are in the area of raw computing capability, task control and file management, and engineer support. These requirements are discussed in terms of present usage and indications are given as to the future need. (auth)

44091 EXPERIMENTAL FAST REACTOR JOYO. OUTLINE OF JOYO. Hirayama, Shoichi (Power Reactor and Nuclear Fuel Development Corp., Tokyo). Genshiryoku Kogyo; 17: No. 2, 4-8(Feb 1970). (In Japanese).

Construction of an experimental fast reactor "Joyo" is described. The Joyo with output of 100 MW(e) is a precursor to a prototype "Monju"; and after technical experience for the prototype is obtained, it will be used for irradiation of materials for fuel, etc. It is expected to be complete by about 1974. Concerning the construction of Joyo in Japan, the following are described. (1) Reactor development leading to the Joyo. History of nuclear power research and development in Japan in past years is reviewed: research reactors in JAERI; introduction of imported reactors; and power reactors by the nation's own technology, including the Joyo. (2) Various phases of the domestic, independent development of nuclear reactors. (Japan)

44092 BENELUX SURVEY. Nucl. Eng. Int.; 16: 395-419 (May 1971).

A review of nuclear energy in Belgium is presented which includes descriptions of the organization and activities of the nuclear power industry, activities of Belgian companies and utilities and a description of the CEN-SCK research center at Mol. Other topics include research and development in the Netherlands, activities of the Netherlands electricity supply undertakings, and the work of the Netherlands Atoomforum. Descriptions are given of the Luxembourg Na test facility and of the Finnish power station at Loviisa. A pull-out chart of the organization of the nuclear industry in the Benelux countries is included. (UK)

44093 IRRADIATION EFFECTS ON STRUCTURAL ALLOYS FOR NUCLEAR REACTOR APPLICATIONS. Symposium Held in Toronto, Ontario, 29 June–1 July 1970. ASTM Special Technical Publication 484. Philadelphia; American Society for Testing and Materials (1970). 569p. $49.25. (ASTM-STP-484; CONF-700630).

Information concerning radiation effects on structural materials and components of nuclear reactors is presented. Separate abstracts are included for 28 of the 29 papers presented. One paper has previously been abstracted and included in NSA and may be located under CONF-700630 in the Report Number Index. (D.C.C.)

For abstracts of individual papers see: 42871, 42872, 42896, 42905–42926, 44102, 44117, and 44167.

Kinetics and Dynamics

Refer also to abstracts 43885, 44190, and 44191.

44094 (AI-AEC-12991) LMFBR PHYSICS PROGRAMS. Quarterly Technical Progress Report, January–March 1971. (Atomics International, Canoga Park, Calif.). 31 May 1971. Contracts AT(04-3)-701; AT(04-3)-824. 30p. Dep. NTIS.

BORON — reactivity worth in fast reactor spectra, specific, (E/T)
BORON-10 — reactivity worth in fast reactor spectra, specific, (E/T)
EUROPIUM — reactivity worth in fast reactor spectra, specific, (E/T)
GRAPHITE — neutron slowing down density distribution in, evaluation of ENDF/B data for, (E/T)
LIQUID METAL FAST BREEDER REACTOR — physics measurement programs during January to March 1971
NEUTRON CROSS SECTIONS — calculations for fast assemblies, evaluation of ENDF/B data for, (E/T)
PLUTONIUM-239 — neutron fission cross section for, evaluation of ENDF/B data for microscopic, (E/T)
— neutron fission of, central reaction ratio of uranium-235 fission to, (E/T)
REACTOR CONTROL ELEMENTS — materials for fast, reactivity worths of, (E/T)
REACTORS, FAST — physics calculations for, development of VIM computer program for
— Doppler coefficient measurements for, review and evaluation of, (E/T)
TANTALUM — reactivity worth in fast reactor spectra, specific, (E/T)
TANTALUM-181 — neutron capture cross sections for, evaluation of data for calculation of, (T)
URANIUM-235 — neutron fission of, central reaction ratios of plutonium-239 and uranium-238 fission and uranium-238 capture to, (E/T)
URANIUM-238 — neutron fission of, central reaction ratio of uranium-235 fission to, (E/T)
— neutron capture by, central reaction ratio of uranium-235 fission to, (E/T)
WATER — neutron slowing down density distribution in, evaluation of ENDF/B data for, (E/T)
WATER-d_2 — neutron slowing down density distribution in, evaluation of ENDF/B data for, (E/T) (H.D.R.)

44095 (AI-CE-Memo-12) HEAVY WATER ORGANIC COOLED REACTOR. CLIP: A PROGRAM TO CONSTRUCT, UPDATE, AND LIST THE FORM OR THREDES MASTER DATA TAPE. Berland, R. F.; Blaine, R. A. (Atomics International, Canoga Park, Calif.). [nd]. Contract AT(38-1)-430. 26p. Dep. NTIS.

CLIP is the library tape manipulation program for THREDES and the FORTRAN 4 version of FORM. This program performs the following tasks: (1) convert a FORTRAN 2 FORM tape to FORTRAN 4 and construct a new FORM or THREDES tape; (2) create a master FORM or THREDES tape from cards; (3) update the FORM cross-sections on either a FORM or THREDES tape; (4) list the FORM or THREDES tape; and (5) duplicate the FORM or THREDES tape. The TEMPEST cross-sections (for a THREDES tape) may come from the Decimal or Binary library cards or from an existing THREDES tape. The FORM cross-sections may come from cards, an existing FORTRAN 2 or 4 FORM tape, or an existing THREDES tape. (auth)

44096 (ANL-7710, pp 53-262) FAST REACTOR PHYSICS. (Argonne National Lab., Ill.).

The analyses and measurements of liquid metal fast breeder reactor characteristics and parameters are presented. The measurements were made on the critical facilities ZPPR (Zero Power Plutonium Reactor), ZPR-3, ZPR-6 and ZPR-9, and were often performed to check calculated results and hence to evaluate the analytical methods and the nuclear constants used in the calculations. Again, the critical assemblies were constructed to permit measurements on mockups of liquid metal fast breeder power reactors. The results may possibly be extrapolated to aid in the design of the originally conceived reactor. The measurements are of value in understanding the fundamentals of the liquid metal fast breeder and in developing analytic methods for predicting with accuracy the performance of such reactors. (auth)

44097 (COO-2109-5) DYNAMICS OF A FAST REACTOR WITH IN-CORE THERMIONIC CONVERTERS. Fourth Annual Report, September 1, 1969–August 31, 1970. Brehm, R. L.; Ferg, D. A.; Guppy, J. G.; Kearns, K. D.; Kendall, J. M. (Arizona Univ., Tucson. Dept. of Nuclear Engineering). Feb 1971. Contract AT(04-3)-670. 14p. Dep. NTIS.

Brief summaries of research results in various areas of thermionic reactor system dynamics and control activities are presented. (H.D.R.)

44098 (EACRP-A-135, pp 30-7) FAST REACTORS: THE FLOTRAN MODULAR SCHEME. Brissenden, R. J. (Atomic Energy Establishment, Winfrith (England)).

XUM

In Modular coding system for reactor calculations.

The Flotran scheme was devised to provide an advanced system framework for complex computations. It is based on the assertion that there must be a databank which is to act as a base for methods and data for all modular working. The Flotran approach is illustrated by the example of describing the geometrical interface for reactor calculations. (H.D.R.)

44099 (EUR–4364) ORGEL PROTOTYPE PRELIMINARY DESIGN: FINE FLUX DISTRIBUTIONS IN THE FUEL ELEMENT. Decressin, A.; Haytink, B.; Realini, G. C. (European Communities, Brussels (Belgium). Commission). 1970. 21p. NTIS (U. S. Sales Only).

Radial flux and power distributions are investigated in the ORGEL prototype fuel element, a 18-rod cluster grouped around a Zircaloy-2 bar. Axial flux and power peaking arising at its bundle ends are described. In this context, the problem is studied whether fuel pellets of small thickness and of less enrichment than the fuel of the element are efficient to suppress power peaking at bundle ends. (auth) (EURATOM)

44100 (EUR–4365) ORGEL PROTOTYPE PRELIMINARY DESIGN: REACTIVITY COEFFICIENTS. Decressin, A.; Haytink, B.; Realini, G. C. (European Communities, Brussels (Belgium). Commission). 1970. 44p. NTIS (U. S. Sales Only).

Reactivity coefficients of the ORGEL Prototype core were calculated by means of the Equipoise code on the basis of group constants obtained using two different codes (Plutharco and Pinocchio). These coefficients were calculated for the equilibrium and initial core. The results obtained were analyzed separating the various effects contributing to the temperature coefficients. (auth) (EURATOM)

44101 (TRG-Report–2133) CALCULATIONS FOR A LARGE FAST REACTOR. A COMPARISON OF RESULTS ORGANISED BY THE INTERNATIONAL WORKING GROUP ON FAST REACTORS OF THE INTERNATIONAL ATOMIC ENERGY AGENCY. Baker, A. R.; Hammond, A. D. (United Kingdom Atomic Energy Authority, Risley (England). Reactor Group). 1971. 105p. Dep. NTIS (U. S. Sales Only). UK 70p.

The prime purpose of the comparison was to investigate the uncertainty in critical mass and breeding gain due to the current uncertainty in alpha for ^{239}Pu. The simple model chosen for the calculation had a spherical core of volume 2.5 m^3 with a blanket 0.457 m thick surrounded by void. The principal contributor to the root mean square (RMS) deviation about the mean of 0.012 in k_{eff} for Case A, in whose core the only heavy nuclides were ^{239}Pu and ^{238}U, was the calculated value of $\sigma_{c_8}/\sigma_{f_9}$, due to differing choices of group constants. The principal contributor to the RMS deviation about the mean of 0.04 in internal breeding gain, G_I, was the calculated value of α_9, due to differing choices of group constants. The uncertainty in external breeding was less important. Case B enabled the effect of fission products to be assessed: fission products representing 10% burn-up negligibly altered the RMS deviation. From Case C and from equivalent worths quoted, it was shown that the data for ^{240}Pu and ^{241}Pu may appreciably increase the uncertainty in k_{eff} if plutonium containing a high proportion of higher isotopes than ^{239}Pu were to be used in the core. It is shown that approximations in the recommended method of calculation do not invalidate the conclusions concerning nuclear data. The features studied were: different methods of producing a coarse-group data set from a fine-group library; a doubled space mesh; a double-thickness blanket; and the use of transport theory instead of diffusion theory. (auth) (UK)

44102 NEUTRON DOSIMETRY FOR FAST REACTOR APPLICATIONS. McElroy, W. N.; Dahl, R. E. Jr. (Battelle-Northwest, Richland, Wash.). Contract AT(45-1)-1830. ASTM (Amer. Soc. Test. Mater.) Spec. Tech. Publ.; No. 484, 375-99(1970).

From Symposium on irradiation effects on structural alloys for nuclear reactor applications; Niagara Falls, Canada (Jun-Jul 1970). See ASTM-STP-484; CONF-700630.

The status of fast reactor dosimetry is reviewed in terms of the results of recent studies in fast test reactors. Fast reactor dosimetry must provide proper spectral, flux, and fluence information for material and fuel irradiation effects programs and surveillance studies. Consideration is given to monitor materials in current use and information needed in the data reduction of reaction product measurements to neutron interaction rates, neutron flux-spectral definition from multiple foil interaction rates and comparison with results based on other methods of analysis, and application of the flux-spectral data to determination of flux levels and fluences. These dosimetry techniques are applied to determine flux spectra and fluence for material irradiation programs. Such information is needed in the determination of damage functions, which relate the damage producing effectiveness of neutrons to their energy. These damage functions permit correlation of irradiation effects data in different thermal and fast reactor irradiation facilities and therefore provide a basis for setting dosimetry accuracy requirements. 66 references. (auth)

44103 EFFECT OF GAMMA RADIATION ON LMFBR SUBCRITICALITY MEASUREMENTS USING NOISE ANALYSIS. Roux, D. P.; Buhl, A. R. (Oak Ridge National Lab., Tenn.). Nucl. Technol.; 12: No. 1, 137-40(Sep 1971).

As a result of the effect of residual gamma radiation on neutron detectors in shutdown reactors, the precision of subcriticality measurements by noise analysis is degraded. An equation for this gamma degradation effect was developed for application to fast reactors. The gamma degradation factor D and the detection efficiency W_a were evaluated for ^{10}B, ^{3}He, and ^{235}U detectors for application in the Fast Flux Test Facility (FFTF), and it was concluded that the ^{235}U, the least sensitive of the three detectors, is the best choice. The ^{235}U detector is 40 times less efficient than the ^{3}He detector, but it should experience only a slight degradation in the FFTF. By contrast, degradation factors varying between 100 and a few thousand are anticipated for the ^{3}He detector through the shutdown range of –1 to –10 dollars. Furthermore, D is unity up to 10^6 r/hr and is independent of ρ for the fission chamber when used as a counter. (auth)

Control Systems

Refer also to abstract 42189.

44104 (COO–2109-4) MULTIPLE INPUT-OUTPUT FEEDBACK SYNTHESIS INCORPORATING CROSS-COUPLING. Ferg, David A. (Arizona Univ., Tucson. Dept. of Nuclear Engineering). Jan 1971. Contract AT(04-3)-670. 187p. Dep. NTIS.

Thesis.

A computational procedure is formulated for the feedback synthesis of a linear multivariable control system with input, output cross-coupling. The feedback synthesis technique which is developed results in a closed-loop interacting transfer matrix containing the desired transfer functions between all permutations of the system outputs and the external control inputs. The technique depends on previously established decoupling techniques for the state-variable feedback design of noninteracting multivariable control systems. (auth)

44105 (RDT-E-6-5-T) COLLAPSIBLE-ROTOR, ROLLER-NUT CONTROL ROD DRIVE MECHANISM FOR SODIUM SERVICE. (Division of Reactor Development and Technology (AEC), Washington, D. C.). Mar 1971. 55p. LMEC.

Requirements for the design, fabrication, assembly, and quality assurance for the procurement of the electro-mechanical devices intended to move and position control elements within the core of a liquid sodium cooled nuclear reactor are presented. Only those drive mechanisms based upon a collapsible-rotor, roller-nut mechanical motor, energized by a magnetic field generated by an electrical coil are included. These control rod drive mechanisms may be connected to control rods having specific functions such as power regulation, power shimming, or safety shutdown, or any sequence or combination of these functions. (auth)

44106 APPLICATION OF OPTIMUM CONTROL TO 600 MWe PRESSURIZED WATER REACTOR. Koh, Byung Joon; Shin, Jae In (Atomic Energy Research Inst., Seoul). J. Korean Nucl. Soc.; 3: No. 2, 59-64(Jun 1971).

An approach to control that is a result of modern control theory and is based on the control philosophy of feeding back all the state variables through constant gain frequency independent elements is presented. The values of these elements or feedback coefficients are determined by equating like coefficients of the desired system transfer function to the transfer function of the system containing the unspecified coefficients. This application of modern control law is a simple design method depending on feeding back all the system variables for reactor control and it is particularly amenable to the control of pressurized water reactors. (8 references) (auth)

Shielding

44107 (EACRP-A–135, pp 15-20) SHIELDING. Bendall, D. E. (Atomic Energy Establishment, Winfrith (England)).

In Modular coding system for reactor calculations.

Many programs written for shielding calculations have large sections in common. It is clear that great savings in effort may be achieved by having those frequently-used sections written in a standard form and by providing the means for them to be used in

any program environment without alteration. The provision of such facilities in a FORTRAN IV environment is the main aim of WSRPG modular programming system. This entails the development of a set of coding rules for the modules and furnishing a number of system routines which are loaded at execution time and control the dynamic transfer of data between modules. (auth)

44108 DAS STRAHLUNGSFELD DES REAKTORS. BERECHNUNGEN DES NEUTRONEN-, GAMMA- UND WAERMEHAUSHALTS FUER EINE REAKTORABSCHIRMUNG. (Radiation Field of the Reactor. Calculations of Neutron-, Gamma-, and Heat Balance for Reactor Shielding). Hehn, Gerfried. Thiemig-Taschenbuecher, Band 22. Muenchen; Verlag Karl Thiemig KG (1964). 119p. DM 9,80.

For calculating neutron and γ radiation fields, common mathematical methods are summarized and supplemented by new methods. The mathematical procedures are utilized for optimization of reactor shielding. As a practical example, a pressurized water power reactor of 450 MW(t) is treated. With respect to neutron and γ balance, transmission is calculated for the solid shield as well as for cooling tubes that penetrate the shielding. Also calculated are temperature distribution and heat tension in various shielding layers. Finally, a reactor incident within the containment is considered with melting of the core and evaporation of the primary cooling water. Dose values are calculated for the outside of the secondary shielding. 15 references. (H.B.G.)

Cooling Systems

Refer also to abstracts 42048, 42184, 42191–42195, 42201, and 42207.

44109 (CONF-700224–, Paper 2) IN-SERVICE INSPECTION OF NUCLEAR PLANTS. Wylie, Robert D. (Southwest Research Inst., San Antonio, Tex.). 20p.

From International symposium on non-destructive testing of nuclear power reactor components; Rotterdam, The Netherlands (26 Feb 1970).

In Proceedings of the international symposium on non-destructive testing of nuclear power reactor components (1970).

Some of the problems encountered in pre-service and in-service ultrasonic inspection of heavy section steel pressure vessels are reviewed. Forecasts are made of the requirements for trained inspection personnel in the nuclear field. (H.D.R.)

44110 (CONF-700224–, Paper 5) INFLUENCE OF ENGINEERING INSPECTION STANDARDS ON THE MANUFACTURE OF NUCLEAR REACTOR PRESSURE VESSELS. van Veen, M. C. (Rotterdamsche Droogdok Maatschappij N. V. (Netherlands)). 12p.

From International symposium on non-destructive testing of nuclear power reactor components; Rotterdam, The Netherlands (26 Feb 1970).

In Proceedings of the international symposium on non-destructive testing of nuclear power reactor components (1970).

The effects of inspection standards on the cost and construction time of nuclear pressure vessels are examined. Both destructive and nondestructive tests necessary to comply with the required inspection standards represent 7 to 10% of the vessel cost and account for 15% of the total construction time. (H.D.R.)

44111 (CONF-700224–, Paper 6) ULTRASONIC INSPECTION OF WELDS IN NUCLEAR REACTOR PRESSURE VESSELS. (NEW DEVELOPED EQUIPMENT FOR AUTOMATIC SCANNING AND RECORDING OF BUTT WELDS). de Sterke, A. (Roentgen Technische Dienst N. V., Rotterdam (Netherlands)). 18p.

From International symposium on non-destructive testing of nuclear power reactor components; Rotterdam, The Netherlands (26 Feb 1970).

In Proceedings of the international symposium on non-destructive testing of nuclear power reactor components (1970).

The development of equipment for automatic ultrasonic scanning of thick welds is described. The system design and performance capabilities are discussed. (H.D.R.)

44112 (CONF-700224–, Paper 7) RADIOGRAPHIC EXAMINATION OF HEAVY-WALL PRESSURE VESSELS: CHOICE OF SOURCE OF RADIATION. Halmshaw, R. (Royal Armament Research and Development Establishment, Fort Halstead (England)). 14p.

From International symposium on non-destructive testing of nuclear power reactor components; Rotterdam, The Netherlands (26 Feb 1970).

In Proceedings of the international symposium on non-destructive testing of nuclear power reactor components (1970).

The types of equipment available for x-ray examination of thick-walled pressure vessels are described and evaluated. The equipment includes resonance-transformer generators, van de Graaff generators, linear accelerators, and betatrons. Output, field size, sensitivity, reliability, ease of control, costs, maintenance, and safety of the various types of systems are examined. (H.D.R.)

44113 (CONF-700224–, Paper 8) RADIOGRAPHIC CAPACITIES OF THE RTD-LINAC 8 MeV LINEAR ACCELERATOR. Eering, J. Th. (Roentgen Technische Dienst N. V., Rotterdam (Netherlands)). 15p.

From International symposium on non-destructive testing of nuclear power reactor components; Rotterdam, The Netherlands (26 Feb 1970).

In Proceedings of the international symposium on non-destructive testing of nuclear power reactor components (1970).

The design parameters, control, maintenance, application, and safety of a linear accelerator for x-ray inspection of thick-walled pressure vessels are described. (H.D.R.)

44114 METHOD OF OPERATING LIQUID METAL COOLED NUCLEAR REACTOR. Campbell, John W. E.; Peters, Martin C.; Perrin, Alfred J. U. S. Patent 3,568,781. 9 Mar 1971. Priority date 29 Sep 1966, Great Britain.

The invention relates to a nuclear reactor which utilizes liquid metal as a coolant medium in the primary coolant circuit to transfer heat from the core region of the reactor to a tubulous vapor generating unit. A recirculation branch is connected around a portion of the primary coolant circuit which contains the vapor generating tubes and means are provided to recirculate the primary coolant through the recirculation branch at a rate sufficient to ensure that the heat flux at the vapor generating tubes is less than the heat flux at which a departure from nucleate boiling occurs within the tubes. (Offic. Gaz.)

44115 IN-LINE VACUUM-DISTILLATION SODIUM SAMPLER. Olson, W. H. (Argonne National Lab., Idaho Falls, Idaho). Nucl. Technol.; 12: No. 1, 7-12(Sep 1971).

A prototype of an in-line, vacuum-distillation Na sampler has been tested in the nonradioactive secondary Na system at EBR-2. A 125g sample of Na is distilled in approximately 3 hours at an absolute pressure of 5μ and a temperature range of 675° to 700°F. Sample size is reproduced to better than 1%. The sampler is used to determine nonvolatile trace-metal and Na-compound concentrations in the ppb-ppm range. Results of tests with the prototype are being used to design a model for installation in the radioactive EBR-2 primary Na system. 4 references. (auth)

44116 RELIABILITY OF FLUENCE-EMBRITTLEMENT PROJECTIONS FOR PRESSURE VESSEL SURVEILLANCE ANALYSES. Serpan, C. Z. Jr. (Naval Research Lab., Washington, D. C.). Nucl. Technol.; 12: No. 1, 108-18(Sep 1971).

A simulated vessel wall environment was constructed that provided for measurements of steel embrittlement increase and neutron flux detector activation at two typical surveillance-program locations as well as at five additional locations through the thickness of an eight-inch thick steel "vessel wall." Neutron spectra for these locations were calculated using one transport and two diffusion theory reactor physics spectrum codes plus a multiple-foil spectrum analysis code. The measured increases in steel transition temperature from the experimental locations revealed the expected gradient of highest embrittlement near the core to least embrittlement at the outer edge of the simulated vessel. Good agreement with published trends was observed. Comparisons of the code calculations with measurements of the decrease in fluence level between locations, however, were favorable only over the shortest distances. Neutron fluences for the critically important region between fuel core and pressure vessel inner edge were significantly higher from a multiple-foil spectrum analysis code than from transport and diffusion codes when based on comparisons of spectrally-adjusted iron activation measurements. This evidence of the possibility that the real fluence values in the pressure vessel wall environment are higher than produced by common measurement techniques suggests the need for reevaluation of current surveillance data, improvements in reactor physics codes and continuing assessments of measured vs calculated surveillance-fluence data. 18 references. (auth)

44117 NEUTRON DOSIMETRY FOR REACTOR PRESSURE VESSEL APPLICATIONS. Serpan, C. Z. Jr. (Naval Research Lab., Washington, D. C.); Morgan, W. C. ASTM (Amer. Soc. Test. Mater.) Spec. Tech. Publ.; No. 484, 3-19(1970).

From Symposium on irradiation effects on structural alloys for nuclear reactor applications; Niagara Falls, Canada (Jun-Jul 1970). See ASTM-STP-484; CONF-700630.

The neutron dosimetry analysis effort discussed is aimed solely at obtaining the most accurate projections of neutron fluence and future radiation embrittlement in the pressure vessel of an oper-

XUM

ating commercial power reactor. The mechanical property changes in materials for reactor pressure vessel applications are caused by neutron/atomic lattice interactions that are highly sensitive to material composition, irradiation temperature, and population and energy of the damage causing neutrons. Of these, the neutron fluence and spectra are most difficult to define accurately for a given irradiation condition since neither can be measured directly. Nevertheless, if radiation induced changes are to be understood and subsequently used as a basis for projecting changes in real reactor components, the neutron dosimetry analysis must be as precise as possible; the ultimate results of any such projections are highly dependent upon the accuracy of the neutron spectrum and neutron fluence used as input. Improvements in both of these areas, as well as in standardization of approaches, are needed for accurate projection of radiation induced changes in reactor pressure vessels. The current status of neutron dosimetry in power reactors is reviewed, and guidelines are provided for improving future dosimetry of reactor pressure vessel surveillance programs. 30 references. (auth)

Fuels

Refer also to abstract 42882.

44118 (BMI-1905) PROGRESS ON DEVELOPMENT OF FUELS AND TECHNOLOGY FOR ADVANCED REACTORS DURING JANUARY-MARCH 1971. Quarterly Report. Keller, Donald L. (Battelle Memorial Inst., Columbus, Ohio). Apr 1971. Contract W-7405-eng-92. 108p. Dep. NTIS.

EXPERIMENTAL BREEDER REACTOR-II—fuel pins for, fabrication and irradiation testing of plutonium nitride-uranium nitride
LIQUID METAL FAST BREEDER REACTOR—fuels for, development of plutonium nitride-uranium nitride, (E)
—fuels for, high temperature irradiation performance of, (E/T)
—fuels for, effects of fission process on creep of, (E/T)
NITROGEN—diffusion in plutonium nitride-uranium nitride fuels, self, (E)
PLUTONIUM NITRIDES—PuN-UN, self-diffusion of nitrogen in, (E)
—PuN-UN, fabrication of fuel pins of
PLUTONIUM OXIDES PuO_2—PuO_2-UO_2, creep of, effects of fission process on, (E/T)
RADIATION TARGET CANS—fabrication of fuel irradiation capsules for EBR-2
REACTOR FUEL ELEMENTS—performance of stainless steel clad plutonium nitride-uranium nitride, during transient irradiation, (T)
—development of sodium-bonded stainless steel clad plutonium nitride-uranium nitride, (E)
REACTOR FUELS—radiation effects on performance of fast, at high temperature, (E/T)
—fission gas diffusion and bubble growth in, (T)
—creep of fast, effects of fission process on, (E/T)
REACTOR SAFETY EXPERIMENTS—fuel element irradiation in TREAT, analysis of stainless steel clad plutonium nitride-uranium nitride, (T)
URANIUM CARBIDES—radiation effects on high temperature swelling, fission gas release, and microstructure of, (E/T)
URANIUM NITRIDES—PuN-UN, irradiation testing of fuels of
URANIUM OXIDES UO_2—radiation effects on high temperature swelling, fission gas release, and microstructure of, (E/T)
—fission gas diffusion and bubble growth in, (T)
—stoichiometry control of, (E)
—creep of, effects of fission process on, (E/T) (H.D.R.)

44119 (EURFNR-923) EXPERIMENTAL INVESTIGATION OF LOOP CAUSED INFLUENCES ON PARALLEL FLOW-INDUCED VIBRATION OF FUEL PINS. Appelt, K. D.; Kadlec, J.; Krueger, W.; Ohlmer, E.; Schwemmle, R. (Kernforschungszentrum, Karlsruhe (West Germany). Institut fuer Reaktorentwicklung). Mar 1971. 25p. (KFK-1385; EUR-4574). Dep. NTIS (U. S. Sales Only).

Work performed under United States-Euratom Fast Reactor Exchange Program.

The influence of the test loop on parallel flow-induced vibration of fuel pins of the Na-1 fast reactor design was investigated. The experiments were performed with the same subassembly mock-up, mounted in the test section of four different flow loops with several modifications. Experimental results are presented in the form of diagrams of normalized rms-values of pressure fluctuations and vibration strains, plotted over the Reynolds number. The structure of pressure fluctuations and vibration strains is illustrated in several typical spectral density plots. 5 references. (auth)

44120 (GEAP-10355) DESIGN AND FABRICATION OF SPECIAL ASSEMBLY SA-1. Mergerth, F. H. (comp.) (General Electric Co., San Jose, Calif. Reactor Fuels and Reprocessing Dept.). Apr 1971. Contract AT(04-3)-189. 64p. Dep. NTIS.

Assembly SA-1 consisted of two 7 by 7 array subassemblies stacked one on top of the other in a channel of standard dimensions for the Dresden Reactor. The fuel rods consisted of sintered UO_2 pellets clad with annealed Zircaloy-2 tubing. The seamless tubing was fabricated by the cold drawing process. The cylindrical pellets were made from ceramic grade UO_2 powder produced from UF_6 by the ammonium diuranate method. The ends of the tubes were sealed with Zircaloy-2 plugs. Nearly 400 fuel rods of the above description were assembled into 4 by 4 array bundles and irradiated in the VBWR . At the conclusion of the VBWR operation, 98 rods were selected from this group for further irradiation in Assembly SA-1. In the rod selection process, burnup, residual fissile content, post-VBWR-irradiation ultrasonic testing results, severity of fretting wear, and general visual appearance were taken into account. The rod-average burnups ranged from 1.3×10^{20} to 2.6×10^{20} fissions/cm^3 (4800 to 9500 MWd/tU) and had a mean value of 1.9×10^{20} fissions/cm^3 (7100 MWd/tU). Some of the rods had operated at peak heat fluxes up to about 140 W/cm^2 (440,000 Btu/h-ft^2 or 14 kW/ft) in the VBWR. The 98 fuel rods were inserted into two specially fabricated stainless steel subassembly structures and transported to Dresden. Assembly of SA-1 was completed by loading the two bundles into a special stainless steel channel structure at the reactor site. (auth)

44121 (HEDL-SA-89) THERMAL PERFORMANCE LIMITS FOR FAST REACTOR OXIDE FUELS. Christensen, J. A. (Hanford Engineering Development Lab., Richland, Wash.). Apr 1971. Contract AT(45-1)-2170. 19p. (CONF-710414-7). Dep. NTIS.

From Conference on fast reactor fuel element technology; New Orleans, La. (13 Apr 1971).

A net reduction of nearly 30% in fuel pin linear heat rating must be applied in going from light water reactor (LWR) to liquid metal fast breeder reactor (LMFBR) applications. This reflects increased power densities, burnups, and ambient temperatures and effects of adding large fractions of PuO_2 to UO_2-base fuels. Over the past five years progress in understanding these effects led to a monatonic decrease in allowable fuel heat rating. Although first generation LMFBR designs show oxides to be adequate fuels, they contain little margin for increasing heat ratings above minimum required values. Reassessment of limit criteria and more sophisticated systems approaches to fuel pin design will help in overcoming further performance constraints which may arise in the future. Beyond these measures, modifications in fuel pellet design hold promise for achieving the higher ratings required for advanced LMFBR's. (auth)

44122 (N-71-17463) SOME CHARACTERISTICS OF A BOILING-WATER-COOLED VAPOR TRANSPORT FUEL PIN. McConaghy, James R, Jr. (National Aeronautics and Space Administration, Cleveland, Ohio. Lewis Research Center). Feb 1971. 28p. (NASA-TN-D-6162; E-5675). NTIS.

The behavior of a boiling-water-cooled vapor transport fuel pin is studied with the aid of a computer code. Pin behavior is investigated at high power output in the region of the boiling burnout point. A comparison is made that shows that much higher power densities can be obtained from a vapor transport fuel pin than from a conventional solid fuel pin design at pin diameters above 1 centimeter. (auth) (STAR)

44123 (ORNL-TM-3385) OBSERVATIONS OF FUEL-CLADDING CHEMICAL INTERACTIONS AS APPLIED TO GCBR FUEL RODS. Fitts, R. B.; Long, E. L. Jr.; Leitnaker, J. M. (Oak Ridge National Lab., Tenn.). Jul 1971. Contract W-7405-eng-26. 34p. (CONF-710414-9). Dep. NTIS.

From Conference on fast reactor fuel element technology; New Orleans, La. (13 Apr 1971).

Chemical interactions between fuel and cladding may be a major limitation to oxide-fueled fast breeder reactors. This limitation is especially important for long-term gas-cooled fast breeder reactor (GCBR) applications because of a strong economic incentive to operate at higher cladding temperatures. Irradiation tests of $(U,Pu)O_2$ fuel pins clad in Hastelloy X and Types 304 and 316 stainless steel show that the Hastelloy X cladding may be sufficiently compatible with mixed oxide fuels at 50 to 100°C higher. Out-of-reactor oxidation studies on Type 316 stainless steel, along with published information on oxidation of steels and in-reactor "fuel-cladding compatibility," are combined with a thermodynamic

analysis of postulated reactions to yield the following conclusion. Most observations of fuel-cladding chemical interaction appear to be the result of simple oxidation of the cladding followed in some areas by mechanical or liquid-phase transport of the outermost oxide layer onto the fuel, where it is reduced. This conclusion indicates that, although Type 316 stainless steel will be satisfactory for early GCBR application, either a more detailed understanding of the reaction involved is needed or alloys that are more oxidation resistant must be proven as cladding materials. 29 references. (auth)

44124 (ORNL-TM-3387) IN-REACTOR RESTRUCTURING TEMPERATURES AND KINETICS FOR $(U,Pu)O_2$. Olsen, A. R.; Fitts, R. B.; Lackey, W. J. (Oak Ridge National Lab., Tenn.). Jul 1971. Contract W-7405-eng-26. 32p. (CONF-710414-10). Dep. NTIS.

From Conference on fast reactor fuel element technology; New Orleans, La. (13 Apr 1971).

Data from a number of thermal flux irradiation tests of stainless-steel-clad $(U,Pu)O_2$ fuels were analyzed in terms of proposed mechanisms of fuel restructuring and actinide redistribution. The data indicate that columnar grain growth is the result of a vaporization-condensation process in fuels operating above about 1700°C. The columnar structure is not fully developed in fuels with a center temperature of 2000°C even after 28 days of operation, but the rate of restructuring increases with increasing temperature. Sintering and equiaxed grain growth processes are slower and therefore of secondary importance in early-life restructuring. A model is postulated in which the vaporization-condensation process can account for observed actinide concentration variations with either uranium or plutonium depletion in the highest temperature regions, depending on the operating temperatures and probably on the oxygen activity in the gas phase over the fuel. 27 references. (auth)

44125 (ORNL-TM-3427) FUEL ELEMENT DEVELOPMENT FOR THE GAS-COOLED FAST BREEDER REACTOR. PART I. SEALED FUEL ROD DESIGN. Washburn, T. N.; Fitts, R. B.; Conlin, J. A. (Oak Ridge National Lab., Tenn.). Jun 1971. Contract W-7405-eng-26. 18p. (CONF-710606-5). Dep. NTIS.

From 17th annual meeting of the American Nuclear Society; Boston, Mass. (13 Jun 1971).

Thermal flux irradiation tests were conducted in cooperation with Gulf General Atomic to evaluate the performance of sealed fuel pins designed for the Gas-Cooled Breeder Reactor, which has a coolant pressure of about 1250 psi. Three design concepts were tested: fuel supported, in which the thin cladding collapses onto the fuel on reaching temperature; fuel-cladding-interacting, in which the cladding experiences uniform creep and receives some support from the fuel; and prepressurized or free standing, in which the internal pressurization of the fuel pin minimizes or prevents creep of the cladding. Sixteen fuel pins were tested at cladding temperatures of 650 to 840°C, linear heat rates of 7 to 22 kW/ft, and fuel burnups to 60,000 MWd/metric ton. Ten fuel pins performed satisfactorily, but six developed unacceptable ovality. The fuel-supported pin was unacceptable because severe ovality developed during testing. Both the fuel-cladding-interacting and/or free standing pins performed satisfactorily at cladding temperatures below 800°C and cladding stresses (due to external pressure) below 12,000 psi. However, the results suggest that fuel-cladding chemical interactions and the need for reliable dimensional stability will place a practical limit of 700 to 750°C on the Hastelloy X cladding temperature. A fast flux test in EBR-II contains seven $(U,Pu)O_2$ fuel pins with Type 316 stainless steel cladding at 600 to 800°C. (auth)

44126 (WERL-ELPLA-1) FUEL ROD DEFORMATIONS: A TIME DEPENDENT FINITE ELEMENT ANALYSIS ON AXISYMMETRIC FUEL RODS, INCLUDING PELLET END EFFECTS (LWBR DEVELOPMENT PROGRAM). Visser, C.; VanBuren, W.; Wilson, W. K.; Gabrielse, S. E. (Westinghouse Research Labs., Pittsburgh, Pa.). Aug 1970. Contract AT(11-1)-Gen-14. 273p. Dep. NTIS.

For Bettis Atomic Power Lab., Pittsburgh, Pa.

The deformations of a fuel rod are very complex functions of time, temperature, etc. These deformations are in general three dimensional. At present, no exact analytical methods to predict these deformations are available. An approximate numerical method and computer program for the analysis of an axisymmetric model of the fuel element, which includes pellet end effects, are described. (auth)

Operation and Economics

44127 (CONF-700903-17) SENSITIVITY OF URANIUM AND SEPARATIVE WORK REQUIREMENTS TO VARIATIONS IN REACTOR PROGRAMMES, REACTOR DATA AND LOAD CHARACTERISTICS. Iliffe, C. E.; Linde, S.; Margen, P. H.; Scuricini, G. B.; Searby, P. J.; Wiechers, W. K. (Swedish Nuclear Industry Group, Stockholm). May 1970. 45p. Dep. NTIS (U. S. Sales Only).

From 4. Foratom congress on industrial aspects of the nuclear fuel cycle in Europe; Stockholm, Sweden (21 Sep 1970).

The sensitivity of uranium and separative work requirements to variations is examined. Calculations on the effect of allocating the nuclear load to stations in order of merit, the plant having lowest running cost being allocated the base load, were performed using a Swedish computer code assisted by a British program (DISCOUNT). A comparison is made with runs using an Italian code. A check was made on the effects of limiting station lifetimes to 30 years. The reasons for certain unexpected results in an earlier ENEA report, in particular the non-linear effect of changing the rate of load growth are illustrated. Allocation of the base load to fast breeders reduces the penetration of the fast breeders into the system in all cases largely due to the adverse effect which the greater out-of-pile Pu inventories for fast breeders at the higher load factor have on the rate of possible introduction of this reactor on the system. The uranium requirements are nevertheless reduced by the allocation of the base load to fast breeders due to the influence of the reduced load factor for the converters on these requirements. The fractional annual growth rate of the nuclear load has a strong and nonlinear influence on the reduction in uranium and separative work requirements achievable by the introduction of fast breeders, being particularly large when the fractional growth rate approaches the inverse doubling time of the fast breeders. An increasing incentive to develop high gain breeders if the nuclear growth rate exceeds current expectations and an influence of the expected saturation in the nuclear load growth rate on possible breeder penetration and uranium requirements are illustrated. Plant life limitations were not found to have a strong influence on the integrated uranium or separative work requirements during the 40 year period studied, though the influence becomes noticeable for relatively low nuclear growth rates, when reduced plant life increases fast breeder penetration and hence reduces uranium requirements. Certain of the runs made for this study were repeated by several of the National computer programs to check the agreement of different programs, and acceptable degree of agreement was found This facilitates the discussion and comparisons of results obtained by different establishments. (Sweden)

44128 (CONF-710315-20) SEFOR OPERATING EXPERIENCE. Arterburn, J. O.; Billuris, G.; Kruger, G. B. (American Society of Mechanical Engineers, New York). [1970]. Contract AT(04-3)-540. 8p. (71-NE-7). Dep. NTIS. ASME $2.00.

From Conference on fast reactors; Palo Alto, Calif. (7 Mar 1971).

The SEFOR program objectives and experimental results are given. Operating experience and information gained during preoperational testing through rise to power operation are presented. Problems encountered during early operational phase are discussed as well as results from operation of systems and components where good performance has been achieved. Plant availability data along with statistical information covering specific plant components and systems are given, and the applicability of SEFOR experience to commercial LMFBR plants is presented. 8 references. (auth)

44129 (EUR-4357) BISMUTH-IMPREGNATED GRAPHITE REFLECTOR IN A HEAVY WATER MODERATED REACTOR: AN EVALUATION. Lanza, F. (European Communities, Brussels (Belgium). Commission). 1970. 22p. NTIS (U. S. Sales Only).

The use of a bismuth-impregnated graphite reflector in a heavy-water-moderated reactor is discussed. The effect of stored energy and the importance of the polonium release in the heavy water are evaluated. An economical evaluation based on a 250 MW(e) Orgel Type Reactor is presented. The use of such a reflector allows a saving of about 1 million dollars and as a consequence a decrease in the cost of the KWh of 0.8%. (auth) (EURATOM)

44130 REACTOR FUEL MANAGEMENT OPTIMIZATION IN A DYNAMIC ENVIRONMENT. Elias, D. (Atomic Energy Commission, Washington, D. C.); Munno, F. J. Nucl. Technol.; 12: No. 1, 46-55(Sep 1971).

The computational system, 2DBCOST, efficiently determines optimum fast reactor fuel management strategies. 2DBCOST, including the associated optimization technique utilized, provides a basis upon which to study the impact of variables such as fabrication, reprocessing, shipping, interest, fuel handling, material costs, inventory lead times and post irradiation lag times on reactor fuel costs and subsequently determine the lowest cost operating policy. The computational system will adjust an LMFBR fuel

XUM

management policy to meet changing economic or market place conditions. Trial use has shown that the code will rapidly determine an optimum fast reactor blanket fuel management scheme for the cases studied. The impact of both blanket radial out-in subassembly movement and moderator seeding was investigated. Cost penalties associated with moving six subassemblies per cycle less than the optimum will approach three million dollars over a 10-year period and similar savings are demonstrated with respect to moderator seeding. The objective function is shown to be unimodal. 33 references. (auth)

44131 GAS-COOLED FAST BREEDER REACTOR FUEL ROD DESIGN CONSIDERATIONS. Thompson, W. I. (Gulf General Atomic Co., San Diego, Calif.). Nucl. Technol.; 12: No. 1, 63-8(Sep 1971).

The Gas-Cooled Fast Breeder Reactor (GCFR) fuel rod is presently designed within the same conservative limitations adopted for the LMFBR project. Since fuel rod irradiation experience is accumulating, and fuel rod mathematical modeling is becoming more reliable it is interesting to consider what improvement in power plant economics can be obtained by designing with less conservatism. Economic studies described show that savings of over 20% in fuel cycle cost and 10% in doubling time might be achieved in this way. Increasing the rod linear heating rate reduces the fuel cycle cost. The use of thinner cladding and increased fuel density lead to reduced inventory and doubling times. (auth)

Safety and Siting

Refer also to abstract 41833.

44132 (AI-AEC-12992) LMFBR SAFETY PROGRAMS. Quarterly Technical Progress Report, January-March 1971. (Atomics International, Canoga Park, Calif.). 31 May 1971. Contract AT-(04-3)-701. 53p. Dep. NTIS.

FAST FLUX TEST FACILITY — heat transfer system cell for, pressure rise during pipe rupture in, (T)
LIQUID METAL FAST BREEDER REACTOR — safety programs during January to March 1971
— coolant combustion accidents in, release and transport of aerosols and energy from sodium, (E/T)
— kinetics of, effects of sodium coolant boiling on, (E/T)
REACTOR SAFETY — accident analysis for liquid metal cooled fast, review of
SODIUM — combustion in liquid metal cooled reactor accidents, release and transport of aerosols and energy from, (E/T)
— boiling in liquid metal cooled reactors, initiation and thermal hydraulics aspects of, (E/T)
URANIUM OXIDES UO_2 — vaporization in sodium cooled reactor accidents, production and behavior of aerosols from, (E/T) (H.D.R.)

44133 (BNWL-1524) COOLANT BLOWDOWN STUDIES OF A REACTOR SIMULATOR VESSEL CONTAINING A SIMULATED REACTOR CORE. Allemann, R. T.; Gustafson, J. C.; Neuls, A. S.; Townsend, W. C.; Wilburn, N. P.; Witherspoon, M. E. (Battelle-Northwest, Richland, Wash. Pacific Northwest Lab.). Jun 1971. Contract AT(45-1)-1830. 94p. Dep. NTIS.

Blowdown experiments were made with a 150 ft^3 vessel containing a simulated reactor core consisting of 4' long tubes. High pressure water (up to 2100 psi, 500°F) was exhausted suddenly from the annular zone of the vessel through orifices of 1.69, 3.44, and 5.2" diameter. Temperature, pressure liquid level, pressure differential, and core movement were measured during the transient fluid flow period and much of the data is given. The forces measured during subcooled decompression were less than predicted, liquid remaining was less than after blowdown without a core structure although pressure histories were about the same. Development of a differential-pressure transducer is described. 10 references. (auth)

44134 (BNWL-1582) LEAKAGE OF FISSION PRODUCTS FROM ARTIFICIAL LEAKS IN THE CONTAINMENT SYSTEMS EXPERIMENT. Witherspoon, M. E.; Postma, A. K. (Battelle-Northwest, Richland, Wash. Pacific Northwest Lab.). Jun 1971. Contract AT(45-1)-1830. 51p. Dep. NTIS.

Decontamination of fission products in containment vessel leak paths was measured as part of the Containment Systems Experiment (CSE) program. Most of the leak paths were artificial. Use of artificial leak paths was required because natural leaks identified during air pressure tests plugged when steam was fed to the containment vessel. Both iodine and cesium were retained to an appreciable extent within the leak path. Collection of leaked iodine for 120 minutes following its release to the containment vessel atmosphere gave decontamination factors of 3.1 and 4.0 for leakage through stainless steel needle valves. For a natural leak past a butterfly valve, a decontamination factor of 34 was observed for a collection period of 24 hours. Less than 5% of iodine contained in leaked liquid became airborne when evaporated to dryness. 12 references. (auth)

44135 (CEA-R-4136) CALCULATION OF THE RADIOLOGICAL RISKS ARISING FROM A REACTOR ACCIDENT. Bessis, Joseph (Commissariat a l'Energie Atomique, Saclay (France). Centre d'Etudes Nucleaires). Mar 1971. 70p. (In French). Dep. NTIS (U. S. Sales Only).

The calculations and formulas used in the computer program PILAX are presented. This program assesses the radiological risks associated with an accident, e.g. dose equivalent (in Rems) received by the human body as a result of: irradiation and contamination inside the reactor enclosure; irradiation and contamination due to the plume rising from the chimney stack (semi-infinite cloud approach); irradiation from the building; irradiation from ground contaminated by the plume. The formation of radioelements by radioactive decay which occurs along the release path, especially after the air filters, is rigorously formulated (under certain physical assumptions). (auth) (France)

44136 (CONF-700224-, Paper 1) SAFETY ASPECTS AND FUTURE ROLE OF ENGINEERING INSPECTION OF NUCLEAR POWER REACTOR COMPONENTS. Latzko, D. G. H. (Technische Hogeschool, Delft (Netherlands)). 13p.

From International symposium on non-destructive testing of nuclear power reactor components; Rotterdam, The Netherlands (26 Feb 1970).

In Proceedings of the international symposium on non-destructive testing of nuclear power reactor components (1970).

Nondestructive inspection techniques in nuclear power engineering are discussed. Aspects of the techniques examined include: their importance from the standpoint of safety; the economics of their application; their effects on plant capital cost; and future trends in reactor applications. (H.D.R.)

44137 (CONF-700224-, Paper 3) DETECTION OF INCIPIENT FAILURE IN PRESSURE VESSELS BY STRESS WAVE EMISSION. Green, Allen T.; Hartbower, Carl E. (Aerojet-General Corp., Sacramento, Calif.). 33p.

From International symposium on non-destructive testing of nuclear power reactor components; Rotterdam, The Netherlands (26 Feb 1970).

In Proceedings of the international symposium on non-destructive testing of nuclear power reactor components (1970).

Progress in the development of stress-wave emission, or acoustic, techniques for in-place, continuous monitoring for incipient failure detection in reactor pressure vessels is surveyed. Operational systems that have been developed and utilized on pressure vessel systems are described and their reliability and availability are discussed. 27 references. (H.D.R.)

44138 (CONF-710431-1) THERMAL PLUME MEASUREMENTS. Romberg, Gerald P.; Prepejchal, William; Nelson, Donald M. (Argonne National Lab., Ill.). [1971]. 34p. Dep. NTIS.

From fourteenth conference on Great Lakes research; Toronto, Ontario, Canada (19 Apr 1971).

Temperature survey work off Commonwealth Edison's Waukegan electric plant on eight days during the summer of 1970 provide data for the construction of 17 separate plumes. On the average, 1000 temperature values collected over a 70 minute period are used to define the isotherms for each plume. Values of surface area, volume, and heat content are given for various temperature ranges and depths. Generally the largest fraction of the plume is contained in the upper 0.9 meters of water and in water less than 3°C above the defined ambient. Construction of a composite surface plume show the maximum areas and distances from the discharge that were ever observed to be affected by water a given temperature above the defined ambient temperature. (auth)

44139 (HEDL-SA-169) DESIGN CONSIDERATIONS OF FFTF SAFETY. Fox, P. F. (Westinghouse Electric Corp., Madison, Pa. Advanced Reactors Div.); Peterson, R. E. (WADCO Corp., Richland, Wash.). Mar 1971. 34p. (CONF-710315-22). Dep. NTIS.

From Conference on fast reactors; Palo Alto, Calif. (7 Mar 1971).

The Fast Flux Test Facility (FFTF) is an AEC Reactor to be constructed on the Hanford Reservation in Washington State. Designs as described are being translated into hardware. The purpose of the facility is to provide a "test bed" for the National LMFBR Program. High neutron flux is required to test fuel and in-core components; in-core closed and open test loops are being

provided for a total neutron flux of a level up to 10^{16}. Plant components and materials that will provide valuable experience in design, safety, construction and operation for demonstration plants are described. (auth)

44140 (NEDO-10329(Suppl.1)) LOSS-OF-COOLANT ACCIDENT AND EMERGENCY CORE COOLING MODELS FOR GENERAL ELECTRIC BOILING WATER REACTORS. Slifer, B. C.; Rogers, A. E. (General Electric Co., San Jose, Calif. Atomic Power Equipment Dept.). Apr 1971. 22p.

The effects of core spray cooling systems on peak cladding temperatures following loss of coolant accidents are analyzed. The Browns Ferry plant was used as the base case in the model evaluations. (H.D.R.)

44141 (ORNL-NSIC-86) INDEX TO NUCLEAR SAFETY, A Technical Progress Review by Chronology, Permuted Title, and Author. Vol. 1, No. 1 through Vol. 11, No. 6. Blakely, J. P.; Klein, Ann (Oak Ridge National Lab., Tenn.). Jul 1971. Contract W-7405-eng-26. 112p. Dep. NTIS.

44142 (RDT-C-16-1-T) SUPPLEMENTARY CRITERIA AND REQUIREMENTS FOR RDT REACTOR PLANT PROTECTION SYSTEMS. (Division of Reactor Development and Technology (AEC), Washington, D. C.). Dec 1969. 39p. RSO.

General criteria and requirements are presented for the design, fabrication and assembly, quality assurance, installation, testing, monitoring, calibration, surveillance, and modification of reactor and critical assembly plant protection systems. These include the system functional requirements for the instruments, logic, and actuators. (auth)

44143 (SGAE-RT-39/1971) ENERGY GENERATION AND THE ENVIRONMENT. Gruemm, H. (Oesterreichische Studiengesellschaft fuer Atomenergie G.m.b.H., Seibersdorf. Institut fuer Reaktortechnik). Mar 1971. 51p. (In German). Dep. NTIS (U. S. Sales Only).

Effects on the environment are compared for power plants using coal, oil, and nuclear energy. The comparison shows that nuclear energy affects the environment to a lesser degree than any other fuel. The study emphasizes the need for international cooperation with respect to environmental problems. Suggestions for large scale research on an international basis are outlined. 38 references. (H.B.G.)

44144 SAFETY AND RELIABILITY IN NUCLEAR POWER STATIONS. Takekoshi, Tadasu (Power Reactor and Nuclear Fuel Development Corp., Tokyo). FAPIG (Tokyo): No. 59, 146-54(Nov 1970). (In Japanese).

The safety evaluation of a nuclear power plant with the reliability of safety facilities is considered by means of a formula "risk = $\Sigma P_i H_i$," where H_i is degree of disaster of ith matter and P_i is probability of its occurrence. Then, trends of the safety evaluation with the reliability of safety facilities in the U.K., Canada, and the U.S. are reviewed. Finally, trial estimation of the reliability of facilities in the nuclear power plant is presented. (Japan)

44145 STRATEGIES FOR A NATIONAL NUCLEAR ENERGY PROGRAM. Starr, Chauncey; Smith, Craig B. (Univ. of California, Los Angeles). pp 1072-80 of Proceedings of the Fourth Intersociety Energy Conversion Engineering Conference, September 22-26, 1969, Washington, D. C. New York; American Inst. of Chemical Engineers (1969).

From fourth intersociety energy conversion engineering conference; Washington, D. C. (21 Sep 1969). See CONF-690905.

Nuclear energy resources can be employed in many ways, depending on national objectives. Using the total cost of national nuclear options as a criterion, several important conclusions can be drawn. First, the economic forces arising from increasing ore costs will prevent the indefinite use of light-water reactors alone, or thorium-cycle reactors, to meet nuclear power needs. Thus the fast breeder reactor is essential. If the fast breeder reactor development is delayed beyond the next two decades, then the thorium-cycle or natural uranium heavy-water reactor could economically "buy time" for another decade of fast breeder development. The near-term development of a successful fast breeder reactor with a doubling time of 7 years (as opposed to the most modest near-term design goal of a greater than 10 year doubling time) could lead to cumulative national economies in ore costs of tens of billion dollars. A doubling time less than the present installed electrical capacity doubling time of 10 years has the added advantage that conversion to an "all breeder reactor" economy would eventually be possible. (auth)

44146 NUCLEAR POWER GROWS UP. Economist (London); 239: 62-3(17 Apr 1971).

The changes brought about in world power generating buying and selling circles by Middle East Oil price increases, which for the first time gave nuclear power the edge over oil, are discussed. The differences in this field between the U.K. and the rest of the world, in particular the difficulties engendered by the AGR hold ups, are examined. Finally, a plea is given to press on with fusion reactor development since oil and coal will not be able to keep up with the increasing demands for electricity, the fusion reactor would be inherently safer than fission reactors and no radioactive waste is produced. (UK)

44147 COMPARISON OF THE VARIOUS POTENTIAL SITES FOR A NUCLEAR POWER STATION NEAR VIENNA FROM THE POINT OF VIEW OF ENVIRONMENTAL HAZARDS. Hoertner, H. (Technische Univ., Munich). Elektrotech. Maschinenbau; 87: No. 7, 341-3(Jul 1970). (In German).

The radiation dose to the thyroid glands of human populations from the potential release of radioactive iodine isotopes from nuclear power reactor accidents constitutes an essential criterion in the comparison of potential power plant locations. Since ^{131}I plays the most important role among the iodine isotopes, the various potential sites for a nuclear power station in the surroundings of Vienna were compared under this aspect. (INIS)

Power Conversion Systems

44148 (CONF-700224-, Paper 4) ULTRASONIC AND OTHER NON-DESTRUCTIVE TESTING METHODS FOR TUBE JOINTS USED IN HEAT EXCHANGERS. de Raad, J. A. (Roentgen Technische Dienst N. V.; Rotterdam (Netherlands)). 18p.

From International symposium on non-destructive testing of nuclear power reactor components; Rotterdam, The Netherlands (26 Feb 1970).

In Proceedings of the international symposium on non-destructive testing of nuclear power reactor components (1970).

Two methods for joining small tubes to the tube plate of a sodium heated steam generator were evaluated by nondestructive testing methods. A specially constructed x-ray tube was found to be better for inspection of internal bore welds. Ultrasonic techniques were found to be satisfactory for inspection of brazed joints. 13 references. (H.D.R.)

Research and Test Reactors

Refer also to abstracts 42048, 42178, 42206, 42816, 43775, 44096, 44103, and 44142.

44149 (AE-425) STUDY OF MATERIAL BUCKLING IN URANIUM-LOADED ASSEMBLIES OF THE FAST REACTOR FRO. Hakansson, R.; Tiren, L. I. (Aktiebolaget Atomenergi, Studsvik (Sweden)). May 1971. 32p. Dep. NTIS (U. S. Sales Only).

Values of material buckling were deduced from measured reaction rate distributions in FRO cores 1-9. The distributions were measured by means of fission chambers and foils with different energy responses. The results were analyzed for systematic errors by comparing values obtained with different detectors and with different reflector materials (copper and uranium). The systematic errors due to spectral mismatch near the reflector were studied quantitatively by numerical experiments which yield correction factors to the experimental data. A simple correction for heterogeneity was also applied. The resulting values have an estimated standard error of about $\Delta B^2 = \pm 2.4\ m^{-2}$, which is adequate for a comparison with theory. The experimental data were compared with theoretical bucklings obtained with the SPENG program. Values of reflector saving were also deduced. For the standard copper reflector a value of 11.0 ± 0.5 cm was obtained as an average for all assemblies. (auth) (Sweden)

44150 (ANL-7781) ACTIVATION-RATE MEASUREMENTS IN THE ZPR-3 MOCKUP CRITICAL EXPERIMENTS. PART I. MEASUREMENTS OF FOIL-ACTIVATION RATES AND FISSION YIELDS IN ASSEMBLY 60 OF ZPR-3: MOCKUP OF EBR-II WITH A URANIUM BLANKET. Dudey, N. D.; Heinrich, R. R.; Popek, R. J.; Larsen, R. P.; Oldham, R. D. (Argonne National Lab., Ill.). Apr 1971. Contract W-31-109-eng-38. 94p. Dep. NTIS.

Activation-rate measurements conducted in the ZPR-3 critical facility in mockup experiments designed to simulate various configurations of EBR-II are discussed. A complete description of the activation-rate measurements conducted in Assembly 60 of ZPR-3 is presented. The study consisted of two experiments de-

XUM

signed for different purposes. The first experiment was designed for dosimetry purposes to provide data necessary for characterizing the irradiation environment by means of activation-rate measurements. The second experiment was designed to provide data from which fast-neutron fission yields of various fission products could be established. Both experiments involved irradiations of foils near the center of the reactor core, near the core-blanket interface, and within the radial blanket. The reaction-rate data are presented, intercompared, and also compared with the results from a third activation-rate experiment conducted by an independent group. 17 references. (auth)

44151 (DOCKET-50231-88) SOUTHWEST EXPERIMENTAL FAST OXIDE REACTOR. Results of the Balanced Oscillator Experiments for Core I. (General Electric Co., Sunnyvale, Calif. Breeder Reactor Development Operation). 14 Jul 1971. 42p. Dep. NTIS.

The Southwest Experimental Fast Oxide Reactor (SEFOR) is a fast spectrum reactor fueled with mixed PuO_2-UO_2 and cooled with sodium. The reactor was designed to enable the determination of the Doppler coefficient at fuel temperatures up to the vicinity of fuel melting and an experimental program was planned that includes a series of tests at low power, proceeds through static and oscillator tests at various power levels up to full power (20 MW(t)), and culminates in a series of sub-prompt and super-prompt critical transients. The results of balanced oscillator experiments which were performed at operating conditions similar to those used for the conventional oscillator tests and which provide additional information about feedback reactivity effects are described. 7 references. (auth)

44152 (DOCKET-50231-89) SOUTHWEST EXPERIMENTAL FAST OXIDE REACTOR. Results of the Familiarization and Sub-Prompt Critical Transient Tests for Core I. (General Electric Co., Sunnyvale, Calif. Breeder Reactor Development Operation). 16 Jul 1971. 72p. Dep. NTIS.

The Southwest Experimental Fast Oxide Reactor (SEFOR) is a fast spectrum reactor fueled with mixed PuO_2-UO_2 and cooled with sodium. The reactor was designed to enable the determination of the Doppler coefficient at fuel temperatures up to the vicinity of fuel melting and an experimental program was planned that includes a series of tests at low power, proceeds through static and oscillator tests at various power levels up to full power (20 MW(t)), and culminates in a series of sub-prompt and super-prompt critical transients. The results of the familiarization and sub-prompt critical transient tests on Core I are presented. (7 references) (auth)

44153 (DOCKET-50231-90) SOUTHWEST EXPERIMENTAL FAST OXIDE REACTOR. Description of Overall Follow-On Program. (General Electric Co., Sunnyvale, Calif. Breeder Reactor Development Operation). 19 Jul 1971. 16p. Dep. NTIS.

44154 (EUR-4362) COMPARATIVE ANALYSIS OF CRITICAL AND EXPONENTIAL EXPERIMENTS BY HETEROGENEOUS METHODS. Casini, G.; Paillon, M. (European Communities, Brussels (Belgium). Commission). 1970. 19p. NTIS (U. S. Sales Only).

A comparative analysis between critical and exponential experiments carried-out in the Ispra heavy water facilities ECO and EXPO is presented. In the measurements, the test fuel elements were clusters of natural uranium metal and carbide with seventeen and nineteen rods per bundle, cooled by an organic liquid. A two-dimensional heterogeneous method was used for the analysis of the experiments. The results indicate a satisfactory agreement (± 0.2 m^{-2} in the material buckling) between critical substitution, exponential substitution and progressive loading measurements. However, in the case of exponential experiments, a discrepancy appeared in comparison with critical flux mapping. (auth) (EURATOM)

44155 (INR-1295) ^{131}I CONTENT IN PRIMARY COOLANT WATER AND IN THE AIR UNDER EWA-10 REACTOR TOP COVERS. Kostyrko, Andrzej (Institute of Nuclear Research, Warsaw (Poland)). 1971. 12p. (In Polish). Dep. NTIS (U. S. Sales Only).

The methods and results of ^{131}I-determinations in the primary coolant water and in the air passing under EWA-10-reactor top-covers are presented. The concentration of ^{131}I in water and in the air ranged respectively from 200 to 900 pCi cm^{-3} and from 0.2 to 2 pCi cm^{-3}. (8 references) (auth)

44156 (JINR-P3-5754) DEVELOPMENT AND APPLICATION OF PULSED FAST REACTORS IBR FOR SCIENTIFIC RESEARCHES. Frank, I. M. (Joint Inst. for Nuclear Research, Dubna (USSR). Lab. of Neutron Physics). 1971. 86p. (In Russian). Dep. NTIS (U. S. Sales Only).

The pulsed fast reactor IBR is described and its main characteristics are given. Basic research, performed in the Neutron Physics Laboratory of the Joint Institute for Nuclear Research during the period of working with pulsed fast reactor IBR, is briefly described. 51 references. (auth)

44157 (LA-4671) EARLY HISTORY OF CRITICALITY SAFETY. Reider, Roy (Los Alamos Scientific Lab., N. Mex.). May 1971. Contract W-7405-eng-36. 7p. Dep. NTIS.

Four of the earliest critical assemblies involving enriched ^{235}U are described. The safety procedures employed for them are discussed in detail. The Water Boiler. A uranyl sulphate solution was remotely air-pumped from an ever-safe vessel into the reactor sphere above. The Dragon Experiment. The reactor was constructed so that a slug dropped through an assembly (both of active material) gave a divergent chain reaction lasting for $^{1}/_{100}$ sec and supported by prompt neutrons alone. An ingenious mechanical structure with multiple safety devices and interlocks gave a high degree of safety to the experiment. The "Drop-Leaf" Assembly. A hydrogenous reflector in the form of paraffin slabs was stacked around an enriched uranium assembly; part of the reflector was built upon a hinged leaf supported by a prop that could be displaced electrically or by hand, using a long cord. The Movable-Table Assembly. A critical assembly was divided between a stationary table and a movable table that could be remotely manipulated to achieve criticality. Several independent safety devices could disassemble the active material in case of high radiation or utility failure. Conclusions are drawn from comparison of these well-planned experiments with the early hand-assembly accidents. (auth)

44158 (LB/G-2929) INSTALLATION OF A BEAM FACILITY ON THE TRITON REACTOR. INDUSTRIAL APPLICATIONS OF NEUTRON RADIOGRAPHY (OF INACTIVE SAMPLES). Farny, G.; Laporte, A. Translated by W. G. Stripp (Atomic Energy Research Establishment, Harwell (England)), from report CEA-N-1135. 9p. Dep. NTIS (U. S. Sales Only).

The installation of a neutron beam facility in the Triton Reactor for use in radiography of industrial samples is described. The layout of the radial axial channel, the basic neutron and gamma fluxes produced, and applications of the facility are presented. (H.D.R.)

44159 (ORNL-4621) HFIR CORE NUCLEAR DESIGN. Cheverton, R. D.; Sims, T. M. (Oak Ridge National Lab., Tenn.). Jul 1971. Contract W-7405-eng-26. 193p. Dep. NTIS.

The High-Flux Isotope Reactor is a flux-trap reactor containing Al-clad fully enriched fuel plates and light-water coolant and moderator. At its maximum steady-state power level of 100 MW the peak thermal-neutron flux in the flux trap is 5.5×10^{15} neutrons/$cm^2 \cdot$ sec. It is in the trap region that ^{242}Pu and heavier recycle material is irradiated to produce ^{252}Cf and lighter transplutonium isotopes. Numerous other experimental facilities are available and are presently being used for experiments requiring strong beam currents and high nonthermal fluxes. The peak total nonthermal flux in the reactor is 4.0×10^{15} neutrons/$cm^2 \cdot$ sec. In the process of designing the very high-performance HFIR core, several critical experiments and numerous other experiments pertaining to heat removal and structural integrity were conducted to insure satisfactory operation. Since the time that full power was first achieved (September 1966) 54 core loadings (as of October 1970) have been used with no fuel element damage or other serious problems. The fuel-cycle time at full power is 23 days (somewhat greater than was expected), and preliminary measurements indicate that the neutron fluxes over most of the core are essentially the same as predicted. Modified core loadings for achieving longer fuel cycles were investigated, and it appears that within the limitations imposed by fabrication and performance restrictions, 50% longer cycles could probably be obtained. 50 references. (auth)

44160 (ORNL-TM-3481) OAK RIDGE RESEARCH REACTOR QUARTERLY REPORT JANUARY, FEBRUARY, AND MARCH OF 1971. Hurt III, S. S.; Tabor, W. H. (Oak Ridge National Lab., Tenn.). 16 Jun 1971. 47p. Dep. NTIS.

The ORR operated 87.4% of the time during January, February, and March of 1971. The average power level was 29.9 MW, while 2,355 MWd of energy were produced. The average fuel burnup (decrease of ^{235}U) of the 28 fuel elements declared spent was 53%, while that for the four shim rods was 67.9%. Shipment of fuel to the ORR from the Nuclear Engineering Test Reactor at Wright-Patterson Air Force Base was begun. Twenty-four of a total of 90 elements were received and placed in storage to await modification for use at ORNL. Reactor shutdowns were limited to eight, seven of which were scheduled. Two end-of-cycle shutdowns ac-

counted for 92% of the total downtime, while the unscheduled downtime was only 0.067 hours. Temperature sensing elements (thermohms) for the Δt and exit temperature instrument channels were replaced as a preventive maintenance measure. Shim-rod-worth measurements and a core flux map were made in January, following changes in the core configuration, i.e., the replacement of fuel with beryllium in core positions C-8 and E-8. (auth)

44161 (WANL-TME-1895) DETERMINATION OF THE SHIELDING REQUIREMENTS FOR THE NPTR FUEL HANDLING SYSTEM. Ravets, J. M.; Stefanko, J. S. (Westinghouse Electric Corp., Pittsburgh, Pa. Astronuclear Lab.). Jan 1969. Contract BDR-362. 60p. Dep. NTIS.

The results of a study performed to determine the shielding requirements and access time limitations for the Nuclear Proof Test Reactor (NPTR) fuel handling system are presented. Three basic types of fuel handling operations were analyzed: manned access into the reactor cell onto a platform above the core for refueling operations; handling of driver fuel assemblies; and handling of change-out fuel pins during exchanging operations. Both gamma and neutron source activities were calculated for these operations as a function of time for various conditions. The NPTR core configuration represents the ninety-one assembly vertical FTR (Fast Test Reactor) core as of November, 1968. Fuel compositions were used which represent the most radioactive fuel envisioned for NPTR use. Dose rates were calculated and are presented for a number of detector points around each source configuration for a variety of shielding conditions. 11 references. (auth)

44162 NUCLEAR SAFETY EXPERIMENTAL PROGRAM WITH PULSE REACTOR. Ishikawa, Michio (Japan Atomic Energy Research Inst., Tokai). Genshiryoku Kogyo; 17: No. 2, 37-44(Feb 1971). (In Japanese).

Reactivity accidents and fuel destruction experiments carried out are reviewed; for the destruction behavior of light water reactor fuel, experiments with SPERT-Capsule Driver Core and Transient Reactor Experiment are described in detail. Then, NSRR (Nuclear Safety Research Reactor) program in Japan is described. This projected NSRR is an alteration of TRIGA-Annular Core Pulse Reactor. An experimental hole, hexagonal in cross section, runs vertically through the center of the reactor core, and in the core, fuel rods of mixed U and ZrH are arranged in cylindrical form. The reactor core is located in a water pool. Pulse power is obtained by rapid withdrawal of three transient rods; the maximum power is about 20,000 MW with reactor period of 1.3 ms. Self reactivity control of the core is by hardening of neutron spectra and Doppler effect. Purpose of the NSRR is to study safety of both light water and fast reactors. (Japan)

44163 EXPERIMENTAL DETERMINATION OF THE PERTURBATION DENOMINATOR IN FAST CRITICAL ASSEMBLIES. Redman, W. C.; Bretscher, M. M. (Argonne National Lab., Ill.). Nucl. Sci. Eng.; 44: No. 3, 450-3(Jun 1971).

A by-product of the measurement of capture-to-fission ratio by the reactivity-reaction rate method is the data necessary to provide several experimental determinations of the denominator of the expression given by perturbation theory for the reactivity of a sample. Such experimental determinations of the perturbation denominator would be useful for guidance in the selection of consistent combinations of cross-section sets and computational models. The apparent reactivity of a calibrated ^{252}Cf spontaneous fission source has been used to provide an experimentally based value of this quantity. In the measurements reported, absorbing and fissile samples also were used to provide independent determinations of the perturbation denominator for three fast criticals, ZPR-9 Assemblies 24 and 25, and ZPR-3 Assembly 57. 16 references. (auth)

44164 CALCULATIONS CONCERNING SOME ACTIVATION DOPPLER EXPERIMENTS IN FRO. Haeggblom, H. (Aktiebolaget Atomenergi, Studsvik, Sweden). J. Nucl. Energy; 25: 53-66 (Feb 1971).

A series of calculations were performed on some of the Doppler experiments carried out in the zero power fast reactor FRO. Some of the calculations were made at the Atomic Energy Establishment in Winfrith using the computer programs SDR and MURAL for producing group cross-sections and the Winfrith DSN-program for obtaining the final spectrum and reaction rates. The calculations in Sweden were done using the programs DORIX-2 and SPENG. These programs involve much coarser approximations than the Winfrith SDR program and their combined computing times are accordingly much shorter. The ^{238}U activation Doppler experiments in cores 5 and 8 and the ^{239}Pu fission activation effect in core 5/PuA were investigated. The results using the methods developed in Winfrith and at ABAE, Sweden, turned out to be of the same order of accuracy, compared with the experiments. Evidence was given that especially the plutonium Doppler effect is strongly dependent upon the resonance parameters. (auth) (UK)

44165 INVESTIGATION OF FAST-REACTOR FUEL TESTING IN A THERMAL REACTOR CORE. Carter, J. C.; Greenspan, J. C. (Argonne National Lab., Ill.). Nucl. Technol.; 12: No. 1, 36-45(Sep 1971).

The feasibility of testing fast-reactor fuel elements in the core of a thermal reactor is investigated. A fast-reactor environment is approximated by placing an assembly of fast-reactor fuel elements surrounded by a neutron filter in the core of a large thermal reactor. The scope of tests which can be performed in currently available thermal reactors is explored, and the effects of such parameters as the number of elements in a test assembly, the enrichment of each element, and the characteristics of neutron filters are investigated. The scoping calculations are based on a heterogeneous arrangement of fuel elements of a type currently being considered for use in large fast reactors. Hypothetical accidents resulting from the disintegration of the filter and/or loss of the sodium coolant are analyzed for the purpose of determining the period of time from the initiation of the accident to the loss of structural integrity of the fuel elements. Useful information pertaining to the operating characteristics and safety aspects of various fast-reactor fuel elements can be obtained from this method of testing. 11 references. (auth)

44166 DISSOCIATION KINETICS AND CRITICAL CONCENTRATION OF THE PEROXIDES ($H_2O_2 + UO_4$) IN THE FUEL SOLUTIONS OF AN AQUEOUS-HOMOGENEOUS NUCLEAR REACTOR. Ehn, E.; Tamberg, T. (Hahn-Meitner-Institut, Berlin). Z. Naturforsch.; 25a: 1670-4(Nov 1970). (In German).

For the fuel solution of the Berlin Nuclear Reactor the maximum stationary power density was determined at 40, 60, and 80°C without precipitation of UO_4. In addition, the rate constant of the peroxide reaction was determined in its relation to temperature. The highest possible peroxide concentration that will not precipitate UO_4 was calculated. Experimental studies of UO_4 precipitation and solution showed that the two processes were strongly inhibited and, therefore, associated with over- and undersaturation. (tr-auth)

44167 NEUTRON FLUENCE LIMIT DETERMINATIONS FOR SOME FAST FLUX TEST FACILITY COMPONENTS. Moen, R. A. (Battelle-Northwest, Richland, Wash.); Tobin, J. C.; Thomas, K. C. Contract AT(45-1)-1830. ASTM (Amer. Soc. Test. Mater.) Spec. Tech. Publ.; No. 484, 409-18(1970).

From Symposium on irradiation effects on structural alloys for nuclear reactor applications; Niagara Falls, Canada (Jun-Jul 1970). See ASTM-STP-484; CONF-700630.

The analytical procedures that have been developed at Battelle-Northwest Laboratory (BNWL) and Westinghouse Advanced Reactors Division (ARD) to determine neutron fluence limits for certain components of the Fast Flux Test Facility (FFTF), namely the core barrel, core support structure, and the reactor vessel, are described. 13 references. (auth)

Rocket and Space Reactors

Refer also to abstract 41995.

44168 (N-71-17933) TRANSFER FUNCTION DETERMINATION OF THE PRIMARY LOOP OF A CONCEPTUAL NUCLEAR BRAYTON SPACE POWER PLANT. Petrik, Edward J.; Kieffer, Arthur W. (National Aeronautics and Space Administration, Cleveland, Ohio. Lewis Research Center). Mar 1971. 45p. (NASA-TM-X-2193; E-5830). NTIS.

The primary loop of a conceptual nuclear Brayton space powerplant was described by a set of nonlinear differential equations. The equations were simplified and linearized. A phase variable technique was used to determine the transfer functions for small step input disturbances in each of the following: (1) reactivity, (2) Li flow rate in primary loop, and (3) Ar flow rate in power conversion loop. The time response obtained from the transfer functions for the three input disturbances agrees with the time response obtained from the original nonlinear differential equations. (auth) (STAR)

44169 THERMIONIC REACTOR CONCEPTS. Price, L. K. (Atomic Energy Commission, Washington, D. C.). pp 122-30 of Proceedings of the Fourth Intersociety Energy Conversion Engineering Conference, September 22-26, 1969, Washington, D. C. New York; American Inst. of Chemical Engineers (1969).

From fourth intersociety energy conversion engineering conference: Washington, D. C. (21 Sep 1969). See CONF-690905.

The various thermionic reactor concepts that have been examined in the United States are reviewed and discussed. The technical strengths and weaknesses of each concept are summarized;

XUM

approximate weights are presented for comparisons at various power levels; and the status of the reactor development program is discussed. 11 references. (auth)

44170 THERMIONIC FUEL ELEMENT DEVELOPMENT. Beard, D. S. (Atomic Energy Commission, Washington, D. C.). pp 131-6 of Proceedings of the Fourth Intersociety Energy Conversion Engineering Conference, September 22–26, 1969, Washington, D. C. New York; American Inst. of Chemical Engineers (1969).

From fourth intersociety energy conversion engineering conference; Washington, D. C. (21 Sep 1969). See CONF-690905.

Thermionic reactors are being developed for auxiliary power and electric propulsion applications. The status of thermionic converter development in the United States is reviewed with emphasis on thermionic fuel elements associated with in-pile thermionic reactor concepts. Thermionic converter designs and testing results are summarized and projected advances in thermionic converter developments are discussed. (auth)

44171 25-kWe REACTOR–THERMOELECTRIC POWER SYSTEM FOR MANNED ORBITING SPACE STATIONS. Gylfe, J. D. (Atomics International, Canoga Park, Calif.); Johnson, R. A.; DuVal, R. A.; Brantley, L. W. pp 308-20 of Proceedings of the Fourth Intersociety Energy Conversion Engineering Conference, September 22–26, 1969, Washington, D. C. New York; American Inst. of Chemical Engineers (1969).

From fourth intersociety energy conversion engineering conference; Washington, D. C. (21 Sep 1969). See CONF-690905.

A 25 kW(e) nuclear reactor-thermoelectric power system under design for potential use with NASA's space station in the mid-1970's is described. The integration of the system with the station is also covered. (auth)

44172 PRESENT STATUS OF DEVELOPMENT OF THERMIONIC DIODES AND THERMIONIC REACTORS IN THE FEDERAL REPUBLIC OF GERMANY. Einfeld, Klaus (Interatom, Bensberg, Ger.). pp 370-82 of Proceedings of the Fourth Intersociety Energy Conversion Engineering Conference, September 22–26, 1969, Washington, D. C. New York; American Inst. of Chemical Engineers (1969).

From fourth intersociety energy conversion engineering conference; Washington, D. C. (21 Sep 1969). See CONF-690905.

Work in the field of thermionics and reactors using thermionic diodes for energy conversion outside or inside the reactor core is being carried out at several research institutes and industrial companies in the FRG. Besides basic research work, out-of-core and in-core experiments have been performed with cylindrical diodes, which resulted in operating times of 14,000 hours and 3750 hours respectively. Extensive studies of different thermionic reactor systems have led to the initiation of the terrestrial version of the thermal in-core thermionic reactor project (ITR). The ITR reactor is characterized by 19 thermionic fuel elements in a yttrium hydride matrix surrounded by a fueled metal hydride driver and a Be reflector zone, sodium cooling, and an electric output power of 20 kWe. Studies and development work on a flight version of the ITR are in progress. Special versions of heat pipe cooling systems are under investigation. Applications are envisaged in the fields of direct TV broadcasting satellites and electrical propulsion systems. 22 references. (auth)

44173 STUDY OF A 300-kWe RANKINE CYCLE ADVANCED NUCLEAR–ELECTRIC SPACE POWER SYSTEM. Heller, J. A.; Moss, T. A.; Barna, G. J. (Lewis Research Center, Cleveland). pp 465-83 of Proceedings of the Fourth Intersociety Energy Conversion Engineering Conference, September 22–26, 1969, Washington, D. C. New York; American Inst. of Chemical Engineering (1969).

From fourth intersociety energy conversion engineering conference; Washington, D. C. (21 Sep 1969). See CONF-690905.

A system analysis is presented for a nominal 300 kW(e) potassium system employing a lithium cooled fast reactor and 2100°F turbine inlet. Trends in performance and weight are discussed for variations in design parameters. Performance and design of major components are reviewed, including material considerations. A typical conceptual system layout is shown. 19 references. (auth)

44174 UNIQUE PRODUCTION PROBLEMS ENCOUNTERED IN DEVELOPMENT OF NERVA SPACE ENGINE. Slivka, William R. (Space Nuclear Propulsion Office, Washington, D. C.). SAE (Soc. Automot. Eng.) J.; 78: 22-7(Oct 1970).

Nozzle and fuel element fabrication techniques used to overcome some complex manufacturing problems for the NERVA space engine are described. Problems encountered with the large Hastelloy X U-tube rocket nozzle included (1) the manufacture of large forgings possessing nearly isotropic properties, (2) the design and fabrication of a U-tube nozzle construction, (3) brazing of the U-tubes to the shell, and (4) development of special NDT techniques. The forgings techniques are described, together with the use of electrical discharge machining to obtain grooves in the nozzle. The fuel elements of the core consist of long hexagonal modules made of graphite-based material, with many axial channels for propellant ducting. The fabrication process used in manufacturing these elements is described schematically, with emphasis on the coating process utilized. (IAA)

Process Heat and Desalination Reactors

44175 ROLE OF NUCLEAR POWERED ENERGY CENTERS IN DEVELOPING ECONOMIES. Holmes, J. M. (Oak Ridge National Lab., Tenn.). pp 171-5 of Proceedings of the Fourth Intersociety Energy Conversion Engineering Conference, September 22–26, 1969, Washington, D. C. New York; American Inst. of Chemical Engineers (1969).

From fourth intersociety energy conversion engineering conference; Washington, D. C. (21 Sep 1969). See CONF-690905.

Large dual-purpose nuclear reactors could serve as the energy sources for agro-industrial complexes which would provide low-cost desalted water for agriculture and power for industry. The economic advantages that would accrue to such a complex include the sharing of common facilities, the economies of scale from large-size components, and cost savings provided by the internal transfer of by-products between processes. In some developing countries nuclear energy centers could provide irrigation water for reclaiming arid coastal regions as an avenue toward increasing world food production. Low-cost power could substitute for scarce raw materials (e.g., sulfur, hydrocarbons, coke) in the production of fertilizers and metallurgical products; the evaporator effluent could serve as a source of raw materials for salt and magnesium production. Products that have been considered for the agricultural portion of the complex include grains, vegetables, oil sources, fruits, and fibers. The allowable water costs for agricultural activities vary with the type of crop. Livestock, poultry, and fish culture are also being studied. Power-intensive applications that appear promising include nitrogenous fertilizers from electrolytic hydrogen, electric-furnace phosphorus, aluminum, magnesium, electric-furnace pig iron and steel, chlorine and caustic, and arc-process acetylene. Regions currently being studied as possible sites for agro-industrial sites include the Middle East, Puerto Rico, and sections of India. 13 references. (auth)

Marine and Portable Power Reactors

44176 (AD–715850) SM-1 CORE III 3.5 MWYR CORE PHYSICS REPORT. Final Report. Henry III, Charles D. (Army Engineer Reactors Group, Fort Belvoir, Va. Engineering Div.). 15 Nov 1970. 87p. (ED–7008). NTIS.

The conduct and results of the 3.5 MWYR core physics tests on SM-1 core 3 are discussed. The results are evaluated and compared with previous results where possible. The results are used to check the present behavior of the core, as compared to the predicted behavior. Various figures and tables are used to illustrate the measured results. (auth) (USGRDR)

44177 (NP–18908) REPORT ON THE NUCLEAR SHIP STUDY. (Department of Trade and Industry, London (England)). 1971. 112p. Dep. NTIS (U. S. Sales Only). UK 70p.

It is considered that the cost of transporting a standard container or a ton of oil during the early 1980s by a nuclear-powered ship would be 24 to 40% higher than by a conventionally-powered ship, leaving aside any allowance for investment grants and low interest loans. If investment grants and low interest loans at 1969 rates are assumed the costs of the nuclear ship would still be 18 to 35% higher. If only low interest loan facilities were available, the nuclear ship would be 22 to 40% more expensive. In each case, the difference is likely to be nearer the higher figure. These calculations were made on the assumption that; there will be significant improvements on current reactor performance, the present best performance of oil-burning ships will become the norm, the development costs of nuclear ships would be written off over ten years and a production of 120 ships and oil prices will remain at 1969 levels or fall by 1% per year in real terms. A subsidy of 30 to 50%, equivalent to the cost of the reactor would be required to make freight costs competitive

over the first 120 nuclear ships. Thereafter, the necessary subsidy would be only slightly smaller. Nuclear propulsion for merchant ships could become competitive, if the price of fuel oil rises by some 70 to 200% in real terms or if there is a dramatic improvement in the performance of nuclear reactors for use at sea, leading to a reduction of at least 50% both in the capital cost of reactors and in nuclear fuel. These conclusions are not materially changed by making comparisons between fleets of ships rather than individual ships. Neither are they expected to be significantly changed by complex and expensive design studies. (UK)

44178 (RCN–139) 120,000 SHP NUCLEAR SHIP PROPULSION STUDY. van den Bergh, J. W. H.; Bodewes, T. J. J.; Bonsel, W. G.; (and others) (Reactor Centrum Nederland, Petten). 1971. 105p. Dep. NTIS (U. S. Sales Only).

The design of a large container ship with a length of 900 feet is used in the Netherlands to study the implication of applying nuclear propulsion to merchant ships. Two different types of PWR reactor plants, the loop type reactor and the integral type reactor, have been designed in some detail for this purpose. Both reactor plants fit in the space required for the conventional boilers for a same size of plant, in front of the main engine room. The safety aspects, comprising containment vessel, collision barriers, and foundation separate from the double bottom, are discussed. The weight of the ship with the nuclear plant is calculated to be about 2400 tons more than the conventional ship. In order to satisfy two compartments standards, about 3000 tons more permanent ballast is required. This total of about 5400 tons extra weight is of the same order as the weight of the fuel supply for the conventional ship. (auth)

44179 ZIRCONIUM HYDRIDE REACTOR–ORGANIC RANKINE POWER SYSTEMS. VanOsdol, J. H. (Atomics International, Canoga Park, Calif.); Wilson, R. F.; Niggemann, R. E. pp 456-64 of Proceedings of the Fourth Intersociety Energy Conversion Engineering Conference, September 22–26, 1969, Washington, D. C. New York; American Inst. of Chemical Engineers (1969).

From fourth intersociety energy conversion engineering conference; Washington, D. C. (21 Sep 1969). See CONF-690905.

Various ZrH reactor-organic Rankine power systems, in the 50 to 500 kW(e) power range, designed for various terrestrial and marine applications are described. System performance, size, weight, operational characteristics, and cost estimates are presented. Present ZrH reactor and organic Rankine PCS technology are briefly reviewed and potential applications are discussed. (auth)

44180 ECONOMIC SELECTION OF UNDERSEA POWERPLANTS. Edwards, Russell N.; Cohen, Michael E.; Hill, James A. (General Electric Co., Philadelphia). pp 692-8 of Proceedings of the Fourth Intersociety Energy Conversion Engineering Conference, September 22–26, 1969, Washington, D. C. New York; American Inst. of Chemical Engineers (1969).

From fourth intersociety energy conversion engineering conference; Washington, D. C. (21 Sep 1969). See CONF-690905.

Selection of powerplants for challenging environments such as space and the deep ocean has commonly been on the basis of such performance criteria as specific weight of the system in #/KW. In the sea, cost effective performance is essential to the commercial goals of the near future. The establishment of powerplant criteria based on lifetime operating cost is discussed. Besides the development and production cost of the powerplant, the cost of its support and containment systems is calculated and summed with the maintenance and replenishment costs needed to maintain dependable system operation. A comparison is made between power supplied by cable from shore; closed cycle chemical systems, such as batteries and fuel cells; open cycle umbilically connected tethered buoy powerplants, and nuclear powerplants. It is shown that costs of tens to hundreds of $/KWH are to be expected with small and/or short lived powerplants and that levels of thousands of kilowatt years total mission energy are needed to approach familiar commercial power rates. The application of the open cycle tethered buoy powerplant is shown to be favorable in a surprisingly large fraction of the spectrum, for fixed station and low speed submersible applications. Cable drag limits the application if higher speed vehicles are needed. Nuclear systems are cost effective only when mission energy requirements exceed several thousand kilowatt years, or where covert or high speed vehicle operation is demanded. The storable fuel cell powerplant is more effective than all but the longest lived radioisotope power systems. 9 references. (auth)

Reactor Theory

44181 (EACRP-A–135) MODULAR CODING SYSTEM FOR REACTOR CALCULATIONS. Symposium Held in Ispra, December 1–3, 1970. Newsletter Bulletin No, 11, March 1971. (ENEA Computer Programme Library, Ispra (Italy)). 100p. (CONF-701213).

Included are 10 papers on the development and application of modular code systems for reactor physics calculations. A separate abstract was prepared for each of the papers. (H.D.R.)

For abstracts of individual papers see: 44098, 44107, 44182–44188, and 44193.

44182 (EACRP-A–135, pp 5-10) CODNUC: A MODULAR SYSTEM FOR REACTOR CALCULATIONS. Bayard, J. P. (Commissariat a l'Energie Atomique, Saclay (France). Centre d'Etudes Nucleaires).

In Modular coding system for reactor calculations.

The CODNUC system for reactor calculations was written to provide flexibility in use and in the modification of its parts. It was written in FORTRAN IV for the IBM 360 series. The basic characteristics and state of development of the system are described. (H.D.R.)

44183 (EACRP-A–135), pp 11-14) THE PROGRESS OF MODULAR CODE DEVELOPMENT IN THE U.K.A.E.A. Brissenden, R. J. (Atomic Energy Establishment, Winfrith (England)).

In Modular coding system for reactor calculations.

Four schemes for modular code development for reactor calculations are briefly described and compared. (H.D.R.)

44184 (EACRP-A–135, pp 38-49) PROPOSAL FOR A GENERALISED FORMAT FOR THE LAYOUT OF DATA IN PERIPHERAL STORAGE. Enderby, J. A. (United Kingdom Atomic Energy Authority, Risley (England). [Reactor Group]).

In Modular coding system for reactor calculations.

The problem is considered of specifying the layout of data on peripheral storage (disc or tape backing store) to serve as an interface between two or more programs, which apart from the use of such common data sets are completely independent of one another. It represents an attempt to generalize the ideas behind existing practical data interface and library formats to produce a specification which would be of quite general applicability. (auth)

44185 (EACRP-A–135, pp 50-9) MODULAR CODING FOR REACTOR CALCULATIONS IN THE UNITED STATES. Butler, D. K. (Argonne National Lab., Ill.).

In Modular coding system for reactor calculations.

The trend in U. S. reactor physics calculations towards the development of modular systems that are less dependent on computer make and configuration is examined. Some of the fundamental characteristics of computer software and hardware are examined, and some of the major modular systems under development are described. (H.D.R.)

44186 (EACRP-A–135, pp 60-2) MODULAR CODING SYSTEMS. Merkwitz, J. (Kernforschungszentrum, Karlsruhe (West Germany)).

In Modular coding system for reactor calculations.

Some comments are presented on the overall philosophy of modular systems for reactor calculations. The question of how modular systems should be structured is examined, and it is pointed out that modular systems must be formulated as the result of close cooperation between the users of the systems and those who design and implement the systems. (H.D.R.)

44187 (EACRP-A–135, pp 63-8) CARONTE: THE EURATOM MODULAR CALCULATIONAL SYSTEM. Mongini-Tamagnini, C. (European Atomic Energy Community, Ispra (Italy). Joint Nuclear Research Center).

In Modular coding system for reactor calculations.

The organization and preparation of the CARONTE system and its operation and application for calculations in the nuclear field are described. (H.D.R.)

44188 (EACRP-A–135, pp 69-86) ACTIVITIES ON MODULAR CODE SYSTEMS IN JAPAN. Katsuragi, S.; Kuroi, H. (Japan Atomic Energy Research Inst., Tokai. Tokai Research Establishment); Arai, K. (Hitachi, Ltd., [Tokyo] (Japan)).

In Modular coding system for reactor calculations.

The status of the NCCS and DOYC-1 modular systems for reactor physics calculations is reported, and development work on the JFRIC and JCOMPACT systems is described. A supporting system, the MCS editor, is described. 9 references. (H.D.R.)

44189 (Y-DR–63) GUIDANCE IN NUCLEAR CRITICALITY SAFETY. Thomas, J. T. (Union Carbide Corp., Oak Ridge, Tenn. Y-12 Plant). 28 May 1971. Contract W-7405-eng-26. 28p. (CONF-710606–4). Dep. NTIS.

From seventeenth annual meeting of the American Nuclear Society; Boston, Mass. (13 Jun 1971).

XUM

The introduction of a relation between unit mass and array reactivity in Monte Carlo calculations of the criticality of subcritical spherical components arranged in reflected cubic arrays is examined. Reference systems are used to investigate: the effect on array k_{eff} of changes in unit, cell, and array shape; the substitution of concrete for water as a reflector; the degree of coupling between arrays separated and reflected by concrete of uniform thickness; and the degree of coupling between concrete-reflected arrays as a function of their separation. (H.D.R.)

Kinetics

44190 (ANL–7710) APPLIED PHYSICS DIVISION ANNUAL REPORT, JULY 1, 1969–JUNE 30, 1970. (Argonne National Lab., Ill.). Jan 1971. Contract W-31-109-eng-38. 468p. Dep. NTIS.

Physics programs at the Argonne National Laboratory are reviewed under the following broad topics: fission properties and cross section data; fast reactor physics; experimental techniques and facilities; and reactor computation methods and theory. Separate abstracts are presented for each of the 4 sections included. (D.C.C.)

For abstracts of individual sections see: 42048, 43884, 44096, and 44191.

44191 (ANL–7710, pp 365-463) REACTOR COMPUTATION METHODS AND THEORY. (Argonne National Lab., Ill.).

To a large degree, the quality of reactor design and performance depends upon the quality of the conceptual models and their portrayal in accurate mathematical representation, and upon the quality and efficiency of computational methods. A priori, the continuous development and refinement of theory and computational methods leads to the design of more dependable, safer, and better performing reactors. The studies undertaken to provide accurate data for reactor design are described. (auth)

44192 (CEA-N–1367) PROGRAM FOR THE OPTIMAL REACTIVITY PROFILES IN ONE-DIMENSION CYLINDRICAL REACTORS (REPO). Edery, David (Commissariat a l'Energie Atomique, Saclay (France). Centre d'Etudes Nucleaires). Mar 1971. 51p. (In French). Dep. NTIS (U. S. Sales Only).

The code described treats the problem of the determination of the optimal distribution of reactivity in a reactor. The search for the optimal distribution is based on a stationary condition established using perturbation theory. Numerical results are presented for a two-group diffusion model in a one-dimensional cylindrical geometry. The diffusion equations are solved by a unique numerical method. 8 references. (auth) (France)

44193 (EACRP-A–135, pp 21-9) THERMAL REACTORS. Askew, J. R. (Atomic Energy Establishment, Winfrith (England)).

In Modular coding system for reactor calculations.

The WIMS "E" scheme of programs for neutronics design calculations relative to reactor core performance is described. The logic of the scheme is applicable to both fast and thermal reactor problems. (H.D.R.)

44194 (FEI–213) RESULTS OF THE CALCULATION FOR A STANDARD FAST REACTOR. Abagyan, L. P.; Petrova, L. V. (Gosudarstvennyi Komitet po Ispol'zovaniyu Atomnoi Energii SSSR, Obninsk. Fiziko-Energeticheskii Institut). 1970. 14p. (In Russian). Dep. NTIS (U. S. Sales Only).

A "standard" fast reactor is here understood to be a simple, spherical model of a fast reactor containing uranium oxide–plutonium fuel and a sodium coolant. Given a specified composition of the reactor (^{239}Pu, ^{238}U, with Ni, Fe, Cr, Na, O also present), and given a particular set of dimensions, calculations were performed to obtain the critical mass, the neutron spectrum, the neutron balance, and the breeding of Pu. (K.S.W.)

44195 (IAE–2010) DEMETRA PROGRAM SET FOR CALCULATING PROBLEMS OF NEUTRON THERMALIZATION IN THE ONE-DIMENSIONAL CELL OF A HETEROGENEOUS REACTOR BY THE QUASI-DIFFUSION METHOD. Trukhanov, G. Ya. (Institut Atomnoi Energii, Moscow (USSR)). 1970. 132p. (In Russian). Dep. NTIS (U. S. Sales Only).

The quasi-diffusion method of solving the multivelocity kinetic equation of neutron transport is discussed. The DEMETRA program set is described. This set of programs makes it possible to use the quasi-diffusion method to solve thermalization problems in the one-dimensional multizone cell of a heterogeneous reactor. 9 references. (JPRS)

44196 (LA-tr–71-44) KINETICS OF A FAST PULSED REACTOR IN A PERIODIC OR QUASI-PERIODIC STATE. Trombetti, T. (Comitato Nazionale per l'Energia Nucleare, Rome (Italy)). Translated by C. DePoorter (Los Alamos Scientific Lab., N. Mex.), from report RT/ING–(68)16. 23p. Dep. NTIS.

A kinetic study of a fast pulsed reactor is performed in the case that the reactivity is a periodic function of time and the flux has reached an asymptotic quasi-periodic behavior. The study is carried out in both cases of constant and non constant delayed neutron source. An evaluation of the conditions for the operation of the control system is given. Numerical results obtained by a computer code are also listed. (auth)

44197 NONLINEAR REACTOR STATICS. Dean, Edward Thomas. Berkeley, Calif.; Univ. of California (1970). 140p. University Microfilms Order No. 71-9789.

Thesis.

A model of the steady-state neutron distribution is proposed for reactors containing the feedback effects of temperature, xenon-poisoning, and void production in the coolant. The governing equation of this model is a nonlinear eigenvalue problem, that is, a second-order elliptic partial differential equation which is nonlinear in the dependent variable, with an eigenvalue. A method which was first proposed by Hammerstein is used to determine the "branching" of solutions, that is, the splitting off of multiple solutions from a known solution. A bound on the spectrum is obtained, thereby giving a good estimate of the eigenvalue at which branching occurs. A stability analysis of the related time-dependent problem indicates which solution is physically observed. An iterative method, first developed by Shampine, is applied to this problem; the iterative procedure is capable of providing convergence to both the least and greatest solution, depending on the starting function. Error bounds are developed. The analysis is applied to three reactor models: (1) fast breeder reactor with large positive void reactivity and a source; (2) water-cooled reactor with large negative temperature reactivity; (3) reactor with large positive power coefficient and xenon-poisoning feedback. (Diss. Abstr. Int., B)

44198 PROMPT NEUTRON DECAY CONSTANTS IN A REFLECTED FAST BURST REACTOR. Price, Charles Clayton. Albuquerque, N. M.; Univ. of New Mexico (1970). 197p. University Microfilms Order No. 71-9321.

Thesis.

A mathematical model describing the kinetic response of a reflected fast burst reactor is developed using point reactor theory. The equations of the model are used to derive a reflected inhour relationship and a two region Rossi-alpha equation. The model is investigated for three reactor-reflector configurations; the bare reactor, the reactor with a radially symmetric steel reflector, and a reactor with a radially symmetric polyethylene reflector. The investigation includes the results of a calculational study using Monte-Carlo techniques and an experimental program using Rossi-alpha, pulsed neutron, and reactor burst techniques on the Sandia Pulsed Reactor SPR II. A Type I (all counts and all times) multichannel time analyzer, which was designed and built to carry out the Rossi-alpha experiments, is described. Results of a supplementary experiment show the biasing of the prompt neutron decay constant when measured with a Type III (count-to-count) multichannel time analyzer. Rossi-alpha measurements at subprompt critical reactivities are used with limited success to predict reflector effects on the super prompt critical behavior of a fast burst reactor. (Diss. Abstr. Int., B)

44199 MAXIMUM LIKELIHOOD AND OTHER METHODS FOR THE ANALYSIS OF REACTOR NOISE. Szeless, Andreas. Berkeley, Calif.; Univ. of California (1970). 206p. University Microfilms Order No. 71-9934.

Thesis.

The main part of the study deals with the measurement and analysis of reactor neutron noise probability distributions. The distribution parameters are related to important reactor dynamic quantities. Accurate knowledge of the distribution parameters is desirable. Under certain conditions the negative binomial distribution is a very good approximation to the true probability distribution of the neutron fluctuations. For the estimation of the parameters of the negative binomial distribution the principle of maximum likelihood is used. It is compared with the usual moments estimation method. The maximum likelihood method fits the predicted probability profiles to the measured data best. Moreover, the principle of maximum likelihood is applied to a different problem, namely to the optimization of experiments designed to measure exponential decay constants. The criterion for optimality is, in this problem, the minimization of the error in the decay constant. Results are obtained for the optimum activation and counting time in multi-cycle activation experiments for a wide range of given experiment time and given ratio of background count rate to

saturation activity. Besides the use of negative binomial distributions in prompt neutron kinetics a new and entirely rigorous method to calculate neutron noise probability distributions from the Pál–Mogilner–Zolotukhin–Bell generating function is introduced. For a wide range of values to the four parameters of this generating function exact noise probability distributions are calculated and compared with the approximate and measured distributions. Furthermore, a nonlinear least squares technique is used to fit the Pál–Mogilner–Zolotukhin–Bell probability generating function to measured reactor noise data. The advantages and limitations of this method are discussed. Finally, the effects of delayed neutrons in the analysis of reactor noise are considered. An expression for the subcritical reactivity of a steady reactor is obtained in terms of measurable noise quantities. (Diss. Abstr. Int., B)

44200 SOME IMPROVEMENTS IN VARIATIONAL FLUX SYNTHESIS METHODS. Woodruff, William Lee. College Station, Tex.; Texas A and M Univ. (1970). 226p. University Microfilms Order No. 71-8926.

Thesis.

A variational synthesis model is proposed for combined space-time flux synthesis with discontinuities allowed in both space and time. Modifications are proposed which eliminate the anomalies noted in existing models at spatial and temporal interfaces of discontinuity. Three types of functions are proposed based on a consistent application of the semi-direct method of the calculus of variations. No difficulties exist for integrations across the points of discontinuity. The equivalence of these three forms for a given choice of the trial-weight function expansions is demonstrated. The Euler–Lagrange equations obtained are in analytic form and are the same for each case. The resulting synthesis model includes the proper asymmetric weighting of the temporal interfaces for initial-final value problems and provides two choices of mixed weighting of the spatial interface conditions. The model also provides variationally imposed boundary and initial-final value conditions and includes delayed neutron contributions. A simple finite difference representation is chosen for test purposes. Numerical results are reported for a 2 group, 2D, time dependent problem and a comparison made with the TWIGL code. Some observations on the choice of spatial interface weighting are also included. (Diss. Abstr. Int., B)

44201 SPACE TIME DEPENDENT REACTOR KINETICS IN A SMALL BERYLLIUM REFLECTED RESEARCH REACTOR. Cox, Edwin Lynn. Columbia, Mo.; Univ. of Missouri (1970). 173p. University Microfilms Order No. 71-8307.

Thesis.

The spatial dependence of the nuclear kinetic characteristics of the small doubly reflected nuclear reactor is examined. A short review of present techniques used to solve the time and space dependent neutron diffusion equations is followed by the results of studies using the digital computer. Experimental data are presented which result from rod drop experiments conducted on the University of Missouri Research Reactor. The result is the observation of kinetic response in the central reflector, "flux trap," of the reactor. This response is characterized by a rapid fall in flux level followed by a subsequent increase of approximately one half decade. This flux "dip" is not seen in regions of the reactor other than the flux trap. The work also shows that the kinetic behavior is very spatially dependent in this small reactor and point reactor kinetics fail to predict the experimental response. The diffusion codes TWIGL and VARI-QUIR fail to accurately predict the kinetic response in regions of the reactor close to the core. The results substantiate those from oscillator and noise experiments that popular mathematical models describing the time dependent neutron diffusion equations in a multiplying medium do not accurately predict the behavior of the University of Missouri Research Reactor. (Diss. Abstr. Int., B)

44202 ADJOINT SPECTRA FOR CALCULATING THERMAL GROUP CONSTANTS. Selengut, D. S. (Knolls Atomic Power Lab., Schenectady, N. Y.). Nucl. Sci. Eng.; 44: No. 3, 447–9 (Jun 1971).

Design procedures for high-depletion power reactors require thermal group constants for a large number of core regions throughout the reactor lifetime. The selection of adjoint trial spectra to be used for calculating the thermal group constants is examined. (H.D.R.)

Experimental Applications

44203 (INR-P-1266) STUDIES OF EPITHERMAL CELL PARAMETERS IN THE REACTOR LATTICES WITH MULTITUBE ENRICHED FUEL. Jozefowicz, E. T. (Institute of Nuclear Research, Warsaw (Poland)). 1971. 22p. Dep. NTIS (U. S. Sales Only).

The methods of measurement of epithermal cell parameters: epithermal-to-thermal fission ratio and resonance-to-thermal absorption ratio in ^{238}U in the reactor lattices with multitude enriched fuel are described. The interpretation of the experimental results in the frames of infinite multiplication factor is shown, and the simple methods of calculation of resonance escape probabilities in ^{235}U and ^{238}U with collision probability considerations taken into account in the cells with complicated structure are presented. The results for a few types of lattices are given and discussed: water moderated (WWR-SM normal and diluted), graphite and water moderated (ANNA with water), graphite moderated (ANNA without water) and beryllium and water moderated lattice (MR type). 10 references. (auth)

44204 INVESTIGATION OF THE SPATIALLY DEPENDENT REACTOR SOURCE TRANSFER FUNCTION WITH TEMPERATURE FEEDBACK. Bridges, Donald Norris. Atlanta; Georgia Inst. of Tech. (1970). 206p. University Microfilms Order No. 71-13,778.

Thesis.

An existing theoretical model, known as the complex source method and capable of predicting neutron flux response to a small periodic disturbance, was extended to include temperature feedback effects. Temperature feedback terms were included by relating reactor parameter changes to the fluctuating flux levels. This derivation was based on two-group diffusion theory and resulted in two sets of nonhomogeneous complex equations. These general equations were applied to a one-dimensional model of the GTRR and a computer program, SPARE, was developed for computing the source transfer function as a function of the reactor power level. The validity of the SPARE calculations was tested for both no feedback (zero-power) and temperature feedback (full-power) conditions. The results of the checks against the SPARE calculations were very good and served to validate the SPARE calculations. The experimental portion of the investigation involved the design and construction of an in-core pile oscillator. The pile oscillator was located in the center of the reactor since this arrangement permitted the experimental verification of a one-dimensional calculation. The pile oscillator employed a pseudo-random binary sequence for introducing flux disturbances with the desired frequency components. This approach offered the advantage of investigating a broad band of frequencies in a single experimental run. Measurements were made for several spatial detector locations within the reactor for zero-power and at-power (900 kW) conditions. The frequency range from 4×10^{-4} Hz to 8.5 Hz was investigated. Data were taken and stored on magnetic tape using a network of two PDP-8 computers and a magnetic tape unit. Data analysis was done using a Fast Fourier Transform program on a Univac 1108 computer. The results from the SPARE calculations and the experiments agreed quite closely. (Diss. Abstr. Int., B)

44205 DEVELOPMENT OF A FAST NEUTRON SPECTROMETER AND MEASUREMENT OF NEUTRON SPECTRA TRANSMITTED THROUGH IRON SLABS. Livengood, Charles David. Lafayette, Ind.; Purdue Univ. (1970). 329p. University Microfilms Order No. 71-9429.

Thesis.

The development of a 4π spectrometer for fast neutrons is described. Proton-recoil proportional counters and pulse-shape discrimination for elimination of gamma-ray induced events are used to give a spectrometer of good resolution and sensitivity. Two detectors were used for the measurements presented. One contained hydrogen and was used in the energy region from 20 keV to 250 keV while the other contained methane and was used from 200 keV to 1 MeV. The measurements presented are the neutron spectra from 23 keV to 1 MeV transmitted through 1- and 2-inch thicknesses of iron placed in the Purdue University Reactor I water pool adjacent to the reactor. Cross section resonances in iron, oxygen, and aluminum produced spectral details which are discussed. These include dips in the spectra corresponding to an oxygen resonance at 440 keV, an aluminum resonance at 36 keV, and an iron resonance at 28 keV. Also, inelastic scattering in the iron produced lower flux values at high energies behind 2 inches of iron than were observed behind 1 inch. (Diss. Abstr. Int., B)

Reactor Components, Fuels, and Accessories

Refer also to abstracts 41757, 41983, 42044, 42802, 42831, 42859, 42860, 42878, 42881, 42928, 42956, and 43010.

44206 (CEA-R-4181) CONTRIBUTION TO RESEARCH ON THE BEHAVIOR OF FISSION PRODUCTS IN NUCLEAR FUELS BY MEASUREMENT OF THE VAPOR PRESSURES OF THE CON-

XUM

STITUENTS OF $(UPu)O_2$ IRRADIATED IN A FAST NEUTRON FLUX. Halachmy, Matitiahu (Commissariat a l'Energie Atomique, Fontenay-aux-Roses (France). Centre d'Etudes Nucleaires). Apr 1971. 150p. (In French). Dep. NTIS (U. S. Sales Only).

Thesis. Submitted to Univ. of Paris, Orsay, France.

An apparatus to measure the vapor pressures of highly radioactive samples by Knudsen's method was designed and constructed. The fission products were classified on the basis of their oxidation potential compared to that of the matrix and the variation of the different phases of the fuel during irradiation was estimated. The development of a chemical compound simulating a fuel irradiated up to a burn-up of 6 atomic percent demonstrated that the chemical state and the distribution of the fission products agree with prediction. The vapor pressure measurements were carried out on a fuel sample of initial composition $(U_{0.75}Pu_{0.29})O_{1.986}$ after a 273-day irradiation in a fast neutron flux. The chemical and isotopic composition of fission and capture products and uranium and plutonium were calculated. The vapor pressure measurements were made between 1070 and 2320 deg K. The weights of the various elements deposited on a cooled target were determined by radiochemical analysis; counting and alpha spectrometry (Pu, Am, Cm), gamma spectrometry (Cs, Sb, Ce, Ru and Nb), beta counting (Sr). (auth)

44207 (KAE-68-46) IFA-30 FINAL REPORT. Olsson, T.; Junkrans, S. (Allmanna Svenska Electriska A. B., Vasteras, Institutt for Atomenergi, Halden (Norway)). 31 May 1968. 20p. Dep. NTIS (U. S. Sales Only).

The fuel bundle IFA-30, consisting of nine Zircaloy-2 canned UO_2 rods, was irradiated in Halden BWR. Total time at power was 5900 hours and the average burnup achieved was 5800 MWd/ton U. The behavior of the bundle was extremely good and no abnormal changes were detected. The post irradiation examination showed that the bundle was in excellent shape. Thus the suitability of the fuel bundle design and fabrication methods was verified. (auth)

44208 (KAE-68-81) THE IRRADIATION BEHAVIOUR OF THE SWEDISH TEST FUEL ASSEMBLY IFA-30. Junkrans, S. (Allmanna Svenska Electriska A. B., Vasteras). 4 Nov 1968. 15p. Dep. NTIS (U. S. Sales Only).

Addendum to report KAE-68-46.

Additional information to complement that included in report KAE-68-46 on the performance of fuel bundle IFA-30 is presented. IFA-30 consisted of 9 Zircaloy-2 clad uranium dioxide rods which were irradiated in the Halden Boiling Water Reactor to an average burnup of 5800 MWd/ton U. (H.D.R.)

44209 (RDT-C-15-2-T) WIDE-RANGE (10 DECADE) NEUTRON FLUX MONITORING CHANNEL. (Division of Reactor Development and Technology (AEC), Washington, D. C.). Feb 1971. 19p. RSO.

The basic requirements for the design, fabrication, testing, shipping, and quality assurance for a neutron monitoring channel capable of measuring ten decades of neutron flux using a single fixed position fission chamber are presented. The standard is applicable to neutron flux monitoring channels for thermal, fast, and some research reactors that have neutron flux changes of ten decades or less and when the normal operating period is not shorter than about ten seconds. (auth)

44210 (RDT-F-3-7-T) INSPECTION REQUIREMENTS FOR MATERIALS USED IN REACTOR COOLANT SYSTEM WEAR APPLICATIONS. (Division of Reactor Development and Technology (AEC), Washington, D. C.). 6 Oct 1967. 6p. RSO.

Nondestructive examination requirements (visual, liquid penetrant, radiographic and hardness determinations) and acceptance standards for wear applications within reactor coolant systems such as anti-friction bearings, valve seats, thrust and journal sleeve bearings, and similar applications are presented. These requirements apply to finished and semi-finished hard surfaces and surfaces of wrought, cold worked, and cast materials used in wear applications in components such as pumps, valves and control rod drive mechanisms. (auth)

44211 LIFTING MECHANISM AND REFUELING MACHINE. Paget, John A. (to United States Atomic Energy Commission). U. S. Patent 3,580,804. 25 May 1971. Filed 7 Mar 1969.

A composite lifting chain is formed with an interior, protected space for service lines such as electrical or pneumatic lines. To facilitate compact storage and winding of the composite chain, as within a limited storage space in a nuclear fuel handling machine, the composite chain is separated into first and second chains or portions which are wound on separate reeling mechanisms. Within the fuel handling machine, the composite chain may be bent and offset laterally by a chain displacement mechanism to align a grapple connected to its lower end with nuclear core elements or other device stored therein. (Offic. Gaz.)

44212 NUCLEAR REACTOR INSTALLATION. Nakagawa, Roy K.; Hubler, Peter; Isaac, Peter (to Atomic Energy of Canada Ltd.). U. S. Patent 3,567,580. 2 Mar 1971. Filed 15 Apr 1968.

Each fuel aggregate used for fuelling the reactor is divided into two portions between which a coupling is provided. During the procedures of loading and unloading such fuel aggregate into and from a selected reactor channel by means of a fuelling machine, the coupling is disengaged and the two portions are handled separately and sequentially. Locking means are provided for defining a predetermined position of the portion in the fuelling machine head such that proper engagement and disengagement of the coupling will be insured. This locking means includes a disc-shaped flange formed on that portion of the fuel aggregate, which is first inserted into and last withdrawn from the channel, and stop means mounted in the fuelling machine for engaging the flange in a pincer-like manner. (Offic. Gaz.)

44213 NUCLEAR REACTOR INSTALLATION. Isaac, Peter (to Atomic Energy of Canada Ltd.). U. S. Patent 3,567,578. 2 Mar 1971. Filed 15 Apr 1968.

A fuelling machine head comprises an end wall with a snout for connecting reactor fuel channels and replenishment fuel transfer channels, a skirt portion, and a turret rotatably mounted in the skirt portion for supporting a number of tubes and aligning them with the snout. The tubes serve snugly to receive used and fresh fuel strings and a plug closing the channels. A fluid pressure-tight seal is disposed between the turret and the end wall so that the space defined within the turret is small in comparison with the volume of the tubes. (Offic. Gaz.)

44214 NUCLEAR REACTOR INSTALLATION. Hubler, Peter; Nakagawa, Roy K. (to Atomic Energy of Canada Ltd.). U. S. Patent 3,567,579. 2 Mar 1971. Filed 15 Apr 1968.

Each fuel aggregate used for fueling the reactor is locked and sealed within its respective fuel channel by means of an end plug portion. For unlocking this portion, releasing the seal and displacing the fuel aggregate out of the channel, a mechanism is used which includes a casing for engaging the channel and two coaxial tubes for engaging the end plug portion. The two tubes are moved together along their longitudinal axis, relatively to the casing, and independently of this motion, the inner one of these tubes is moved along the same axis relatively to the outer tube. The end plug portion similarly comprises two coaxial tubular members, the outer one of which is provided with a set of captive balls and the inner one of which has a surface portion arranged to force these captive balls into a locking groove provided in the inner surface of the channel. The outer and inner tubes of the ram mechanism are similarly provided with a set of captive balls to lock the tubes to the outer and inner tubular members of the end plug portion respectively. The inner tube furthermore serves to displace the inner tubular member relatively to the outer tubular member to engage or disengage the captive balls of the end plug portion to or from the channel groove. The outer tube furthermore serves to actuate means for releasing the seal of the end plug portion. (Offic. Gaz.)

44215 NUCLEAR REACTOR INSTALLATION. Brooks, Gordon L. (to Atomic Energy of Canada Ltd.). U. S. Patent 3,567,577. 2 Mar 1971. Filed 15 Apr 1968.

For loading and unloading fuel aggregates into and from a plurality of vertically extending fuel channels of the reactor, the snout of a fuelling machine head is coaxially aligned with a selected such channel, vertically shifted towards the channel and clamped onto a projecting end thereof. To carry out the necessary motions, a carriage is vertically shiftably mounted on a horizontally movable vehicle and supports a suspension assembly in which the machine head is rotatably mounted about a horizontal axis. The suspension assembly includes four vertically suspended rods connecting the machine head to the carriage, each rod having a universal joint at both ends to permit free horizontal translation of the machine head relative to the carriage, thus compensating for minor misalignments between the snout and the selected channel. (Offic. Gaz.)

44216 NUCLEAR REACTOR INSTALLATION. Isaac, Peter (to Atomic Energy of Canada Ltd.). U. S. Patent 3,567,576. 2 Mar 1971. Filed 15 Apr 1968.

A T-coupling is provided between the fuel string and the closure plug assembly together forming a fuel aggregate for loading into each reactor fuel channel. A fuelling machine comprises a minimum of two barrels, one for receiving the fuel string and one for receiving the plug assembly, the barrels being disposed in a turret rotatable about an axis parallel to the barrels and the fuel channel. Intermediate engagement or disengagement of the cou-

pling when loading or unloading a fuel channel is made by rotating the turret. (Offic. Gaz.)

44217 PROSPECTS OF RADIOACTIVE MATERIALS AS FUTURE SOURCES OF FUEL AND POWER. Schejbal, C. (Inst. of Mining and Metallurgy, Ostrava, Czech.). Rudy (Prague); 17: No. 6, 157-61(Jun 1969). (In Czech).

Reasons are given for the future need for nuclear fuels as energy sources, and the possibilities of utilizing them are discussed. Conditions affecting the development of nuclear power in the world are shown in tables and graphs; estimates of uranium reserves and consumption are presented for some countries. (NSA of Czech.)

44218 FUEL RODS FOR NUCLEAR REACTORS. de Temple, Bernhard (to Gesellschaft fuer Kernforschung mbH). German Patent 1,295,710, 22 May 1969. Filed 18 Jul 1963. (In German).

Fuel rods with bulges for the alignment of the fuel element were developed. The bulges allow the rods to touch each other only at a point or in a line and therefore form a spacing lattice which permits the free flow of the coolant on all sides of the fuel rods. The bulges are formed of the cladding material. (J.S.R.)

44219 MATERIALS TECHNOLOGY. I. AN INTERAMERICAN APPROACH FOR THE SEVENTIES. Second Interamerican Conference, Mexico City, Mexico, August 24–27, 1970. New York; American Society of Mechanical Engineers (1970). 719p. $30.00. (CONF-700812).

Included are 71 papers on the field of processing of materials from the ore to the final product. A separate abstract was prepared for each of 19 papers on materials of interest in nuclear technology. (H.D.R.)

For abstracts of individual papers see: 41916–41919, 42028, 42029, 42827–42829, 42867–42869, 42950, 42951, 42976–42978, 43015, 44080.

XUM

GENERAL

44220 (ANCR–1004) NONRADIOACTIVE WASTE OIL DISPOSAL STUDY. Commander, J. C. (Idaho Nuclear Corp., Idaho Falls). Feb 1971. Contract AT(10-1)-1230. 53p. Dep. NTIS.

44221 (ANCR–1006) NONRADIOACTIVE WASTE SOLVENT DISPOSAL STUDY. Commander, J. C. (Idaho Nuclear Corp., Idaho Falls). Apr 1971. Contract AT(10-1)-1230. 36p. Dep. NTIS.

44222 (BDX–613–184) COMPARISON OF ORTHOGONAL CURVILINEAR COORDINATE SYSTEMS FOR MINIMUM ERROR. Final Report. Drake, S. R. (Bendix Corp., Kansas City, Mo.). Mar 1970. Contract AT(29-1)-613. 143p. Dep. NTIS.

44223 (BDX–613–269) CHEMICAL VAPOR DEPOSITION PROCESS EQUIPMENT. Progress through November 1970. Hale, G. J. (Bendix Corp., Kansas City, Mo.). May 1971. Contract AT(29-1)-613. 22p. Dep. NTIS.

44224 (BDX–613–274) DETERMINATION OF AVERAGE CYCLE TIME FOR AN AUTOMATED WAREHOUSE. Smith, Jerry C. (Bendix Corp., Kansas City, Mo.). Jun 1971. Contract AT(29-1)-613. 43p. Dep. NTIS.

44225 (BDX–613–326) FLATPACK INSTALLATION BY SINGLE-PROBE REFLOW SOLDERING. Final Report. Bowlen, D. W. (Bendix Corp., Kansas City, Mo.). May 1971. Contract AT(29-1)-613. 55p. Dep. NTIS.

44226 (BDX–613–327) COMPRESSION MOLDING OF LAMINATES. Quarterly Report, FY 70-4. Hishaw, R. J. (Bendix Corp., Kansas City, Mo.). May 1971. Contract AT(29-1)-613. 39p. Dep. NTIS.

44227 (BDX–613–330) FLOW SOLDERING AND SUPPORTING PROCESSES. Final Report. Moyle, Wm. F. (Bendix Corp., Kansas City, Mo.). May 1971. Contract AT(29-1)-613. 116p. Dep. NTIS.

44228 (BDX–613–355) MEASUREMENT METHOD FOR POLYSTYRENE. Final Report. Matzkanin, Ted (Bendix Corp., Kansas City, Mo.). Jun 1971. Contract AT(29-1)-613. 29p. Dep. NTIS.

44229 (BDX–613–366) FINE-EDGE BLANKING AND PIERCING. Final Report. Seese, H. J. (Bendix Corp., Kansas City, Mo.). Jun 1971. Contract AT(29-1)-613. 24p. Dep. NTIS.

44230 (BDX–613–369) THEORY AND OPERATION OF THE BENDIX MOLD HEATING AND COOLING EQUIPMENT. Floersch, R. H. (Bendix Corp., Kansas City, Mo.). Jun 1971. Contract AT(29-1)-613. 113p. Dep. NTIS.

44231 (BDX–613–395) PERCUSSIVE-ARC VERSUS PULSE-ARC WELDING. Hollar, D. L. (Bendix Corp., Kansas City, Mo.). May 1971. Contract AT(29-1)-613. 27p. Dep. NTIS.

44232 (BDX–613–404) QUALITY DIVISION QUARTERLY. (Bendix Corp., Kansas City, Mo.). May 1971. Contract AT-(29-1)-613. 289p. Dep. NTIS.

44233 (BDX–613–431) ELECTRONIC ENGINEERING QUARTERLY. (Bendix Corp., Kansas City, Mo.). Jun 1971. Contract AT(29-1)-613. 227p. Dep. NTIS.

44234 (BDX–613–443) SOLDER LEVELING OF PRINTED WIRING BOARDS. Mulholland, W. A. (Bendix Corp., Kansas City, Mo.). Jun 1971. Contract AT(29-1)-613. 38p. Dep. NTIS.
Reprint of report originally published in BDX–613–420.

44235 (BDX–613–454) ELECTROFORMED NICKEL MOLD INSERTS. Final Report. Robinson, R. D. (Bendix Corp., Kansas City, Mo.). Jul 1970. Contract AT(29-1)-613. 6p. Dep. NTIS.

44236 (BNWL–SA–3817) ROLE OF DESIGN IN CORROSION PREVENTION. Perrigo, Lyle D. (Battelle-Northwest, Richland, Wash. Pacific Northwest Lab.). [1971]. Contract AT-(45-1)-1830. 33p. (CONF-710504–2). Dep. NTIS.
From fifth annual western states corrosion seminar; San Dimas, Calif. (5 May 1971).

44237 (CALT–822–31) ELECTRICAL RESISTIVITY AND MAGNETIC SUSCEPTIBILITIES OF AMORPHOUS Cr–Ni–Pt–P ALLOYS. AEC Research and Development Report No. 26. Sinha, Ashok K. (California Inst. of Tech., Pasadena. W. M. Keck Lab. of Engineering Materials). Jun 1971. Contract AT(04-3)-822. 8p. Dep. NTIS.

44238 (CALT–822–32) MOESSBAUER EFFECT STUDY OF AMORPHOUS Fe–Pd–Si ALLOYS. Sharon, T. E.; Tsuei, C. C. (California Inst. of Tech., Pasadena. W. M. Keck Lab. of Engineering Materials). Jul 1971. Contract AT(04-3)-822. 12p. Dep. NTIS.

44239 (CGS–746–114) ALEUTIAN SEISMIC PROGRAM SEISMOLOGICAL BULLETIN, DECEMBER 1970. (National Ocean Survey, Rockville, Md.). Jun 1971. Contract AT-(29-2)-746. 72p. Dep. NTIS.

44240 (CONF-710515–1) CAN THE AEC COMPLEX REALLY EXCHANGE COMPUTER SYSTEMS AND PROGRAMS. Butler, Margaret K. (Argonne National Lab., Ill.). [1971]. 11p. Dep. NTIS.
From Atomic Energy Systems, Operations, and Programming Association; Gatlinburg, Tenn. (4 May 1971).

44241 (COO–1140–198) COMPUTER COLLECTION OF MASS SPECTROMETRIC IONIZATION EFFICIENCY CURVES. Conard, Bruce R.; Fast, Peter M.; Nordlund, David L.; Gilles, Paul W. (Kansas Univ., Lawrence. Dept. of Chemistry). 17 May 1971. 10p. (CONF-710704–3). Dep. NTIS.
From Conference on computers in chemical education and research; DeKalb, Ill. (19 Jul 1971).

44242 (COO–1147–35) LIMITATIONS IN APPLYING MASS SPECTROMETRY TO HIGH-TEMPERATURE EQUILIBRIUM STUDIES. Stafford, Fred E. (Northwestern Univ., Evanston, Ill.). [1971]. 27p. Dep. NTIS.

44243 (COO–1222–45) PRECISION FLOW-MONITORING SPECTROMETER WITH LOW NOISE AND HIGH STABILITY. Bidlingmeyer, Brian A.; Deming, Stanley N. (Purdue Univ., Lafayette, Ind. Dept. of Chemistry). [1970]. Contract AT(11-1)-1222. 13p. Dep. NTIS.

44244 (COO–1222–46) EFFECT OF LOADING ON SEPARATION EFFICIENCY USING STERIC EXCLUSION CHROMATOGRAPHY. Maldacker, T. A.; Rogers, L. B. (Purdue Univ., Lafayette, Ind. Dept. of Chemistry). [1970]. 19p. Dep. NTIS.

44245 (COO–1222–47) EFFECT OF AN ELECTRIC FIELD ON GAS CHROMATOGRAPHIC RETENTIONS BY LIQUID CRYSTALS. Taylor, Paul J.; Culp, Robert A.; Lochmueller, C. H.; Rogers, L. B. (Purdue Univ., Lafayette, Ind. Dept. of Chemistry); Barrall II, Edward M. (International Business Machines Corp., San Jose, Calif.). [1970]. Contract AT(11-1)-1222. 22p. Dep. NTIS.

44246 (COO–1222–48) STERIC-EXCLUSION CHROMATOGRAPHY AT PRESSURES UP TO 3500 KG/CM^2. Bidlingmeyer, B. A.; Rogers, L. B. (Purdue Univ., Lafayette, Ind. Dept. of Chemistry). [1971]. 9p. Dep. NTIS.

44247 (COO–1222–49) SPECIFICATION OF GAS CHROMATOGRAPHIC BEHAVIOR USING KOVATS INDICES AND ROHRSCHNEIDER CONSTANTS. Lorenz, L. J.; Rogers, L. B. (Purdue Univ., Lafayette, Ind. Dept. of Chemistry). [1970]. Contract AT(11-1)-1222. 43p. Dep. NTIS.

44248 (COO–1222–50) FUNDAMENTAL STUDIES ON SEPARATION PROCESSES. Technical Progress Report. Rogers, L. B. (Purdue Univ., Lafayette, Ind. Dept. of Chemistry). Jul 1971. Contract AT(11-1)-1222. 15p. Dep. NTIS.

44249 (COO–1313–27) PARTIAL PURIFICATION OF tRNA AND LEUCYL-tRNA SYNTHETASE FROM SUGAR BEET ROOT. Whitty, C. Dennis; Cherry, Joe H. (Purdue Univ., Lafayette, Ind. Dept. of Horticulture). [1970]. Contract AT(11-1)-1313. 18p. Dep. NTIS.

44250 (COO–1313–28) PROTEIN SYNTHESIS IN GERMINATING SEEDS. Cherry, Joe H.; Kanabus, Jan; Jachymczyk, Witold; Anderson, Marianne B. (Purdue Univ., Lafayette, Ind. Dept. of Horticulture). [1971]. 18p. Dep. NTIS.

44251 (COO–1559–7) FAUNISTIC STUDIES OF ARTHROPODS AT THE NATIONAL REACTOR TESTING STATION, IDAHO.

Allred, Dorald M. (Brigham Young Univ., Provo, Utah). 1970. Contract AT(11-1)-1559. 6p. Dep. NTIS.

44252 (COO-1599-33) COPRECIPITATION OF PHOSPHATE WITH CARBONATES IN A MARL LAKE. Otsuki, Akira; Wetzel, Robert G. (Michigan State Univ., Hickory Corners. W. K. Kellogg Biological Station). [1971]. Contract AT(11-1)-1599. 13p. Dep. NTIS.

44253 (COO-1630-26) THE METABOLISM OF RARE EARTHS FOLLOWING INHALATION: PATHOLOGICAL AND BIOCHEMICAL RESPONSE IN THE LUNG AND OTHER ORGANS. Technical Progress Report, September 16, 1970-September 15, 1971. Berke, Harry L. (Wayne State Univ., Detroit, Mich. Dept. of Occupational and Environmental Health). 15 Jun 1971. Contract AT(11-1)-1630. 34p. Dep. NTIS.

44254 (COO-1653-103) REGIONAL LUNG WATER: THE PRODUCTION OF LOCALIZED PULMONARY EDEMA IN THE DOG AND PRELIMINARY OBSERVATIONS USING ^{15}O-LABELED WATER, ^{131}I-IODOANTIPYRINE AND ^{113m}InDIUM LABELED TRANSFERRIN. (Washington Univ., Seattle. School of Medicine). [1971]. Contract AT(11-1)-1653. 7p. Dep. NTIS.

44255 (COO-2002-6) ENERGY BUDGET MODEL FOR WOODLAND STREAM ECOSYSTEMS. Cummins, Kenneth W. (Michigan State Univ., Hickory Corners. W. K. Kellogg Biological Station). [1971]. Contract AT(11-1)-2002. 5p. Dep. NTIS.

44256 (COO-2002-10) ENERGETICS OF NATURAL POPULATIONS OF FRESHWATER MACROCONSUMERS. Progress Report. Cummins, Kenneth W. (Michigan State Univ., Hickory Corners. W. K. Kellogg Biological Station). [1971]. Contract AT(11-1)-2002. 39p. Dep. NTIS.

44257 (COO-2121-3) CYTOGENETICS OF MONOSOMES IN ZEA MAYS. Technical Progress Report, October 1, 1970-September 31, 1971. Weber, David F. (Illinois State Univ., Normal. Dept. of Biological Sciences). Contract AT(11-1)-2121. 27p. Dep. NTIS.

44258 (CTC-INF-1030) EVALUATION OF THE IBM PROJECT MANAGEMENT SYSTEM/360, VERSION 3. Scott, P. E. (Union Carbide Corp., Oak Ridge, Tenn. Computing Technology Center). 15 Jun 1971. Contract W-7405-eng-26. 41p. Dep. NTIS.

44259 (HUX-2643-61) EARLY STEPS IN PROTEIN SYNTHESIS AND THEIR REGULATION: BACKGROUND STUDY RELATED TO THE BIOLOGICAL EFFECTS OF RADIATION. Progress Report, September 1, 1970-August 31, 1971. (Massachusetts General Hospital, Boston. John Collins Warren Labs.). Contract AT(30-1)-2643. 16p. Dep. NTIS.

44260 (IS-T-474) STABILITIES OF SOME RARE-EARTH MALONATO CHELATE SPECIES IN AQUEOUS AND METHYL ALCOHOL SOLUTION. Johnson, Douglas Kiester (Ames Lab., Iowa). Jul 1971. Contract W-7405-eng-82. 163p. Dep. NTIS. Thesis.

44261 (JUL-734-FF) PHONONS AND LIBRONS IN SOLID HYDROGEN AND DEUTERIUM. Mertens, Franz-Georg (Kernforschungsanlage, Juelich (West Germany). Institut fuer Festkoerperforschung). Feb 1971. 109p. Dep. NTIS (U. S. Sales Only). Thesis. Submitted to Technische Hochschule, Aachen, Ger.

44262 (K-1798(Pt.1)) INTERNAL RAREFIED GAS FLOWS WITH BACKSCATTERING. PART 1. THE BACKSCATTERING BOUNDARY CONDITION AND FREE MOLECULE FLOW IN A LONG CAPILLARY. Berman, A. S. (Oak Ridge Gaseous Diffusion Plant, Tenn.). 16 Jun 1971. Contract W-7405-eng-26. 18p. Dep. NTIS.

44263 (K-1798(Pt.4)) INTERNAL RAREFIED GAS FLOWS WITH BACKSCATTERING. PART 4. PLANE POISEUILLE FLOW WITH BACKSCATTERING. Berman, A. S. (Oak Ridge Gaseous Diffusion Plant, Tenn.). 16 Jun 1971. Contract W-7405-eng-26. 25p. Dep. NTIS.

44264 (K-1798(Pt.5)) INTERNAL RAREFIED GAS FLOWS WITH BACKSCATTERING. PART 5. FLOW IN CAPILLARIES AND ANNULI. Berman, A. S. (Oak Ridge Gaseous Diffusion Plant, Tenn.). 16 Jun 1971. Contract W-7405-eng-26. 22p. Dep. NTIS.

44265 (K-1799) HEAT EXCHANGER OPTIMIZATION CODE. Mott, J. E. (Union Carbide Corp., Oak Ridge, Tenn. Nuclear Div.). 12 Jul 1971. Contract W-7405-eng-26. 54p. Dep. NTIS.

44266 (KAPL-3482) ELECTRON MICROPROBE ANALYSIS OF THIN CORROSION FILMS. Merchant, R. W. (Knolls Atomic Power Lab., Schenectady, N. Y.). Jan 1969. Contract W-31-109-eng-52. 29p. Dep. NTIS.

44267 (LA-4249(Vol.2)) SURVEY OF TECHNIQUES EMPLOYED TO DEFINE AEROSOL RESPIRABLE DUST CONCENTRATION AND PARTICLE-SIZE CHARACTERISTICS. VOL. II. Ettinger, Harry J. (Los Alamos Scientific Lab., N. Mex.). Jun 1971. Contract W-7405-eng-36. 14p. Dep. NTIS.

44268 (MHSMP-71-28) TRANSITION METAL HE's. V. CAEP. Normal Process Development Endeavor No. 103, January-March 1971. Clink, G. L. (Mason and Hanger-Silas Mason Co., Inc., Amarillo, Tex.). Contract DA-11-173-AMC-487(A). 16p. Dep. NTIS.

44269 (NP-18843) GUIDELINES: BIOLOGICAL SURVEYS AT PROPOSED HEAT DISCHARGE SITES. Garton, Ronald R.; Harkins, Ralph D. (Pacific Northwest Water Lab., Corvallis, Oreg.). Apr 1970. 108p. GPO $1.00.

44270 (NYO-1371-64) GENETIC TRANSFORMATION IN HEMOPHILUS INFLUENZAE. Annual Progress Report, September 15, 1970-September 14, 1971. Herriott, Roger M. (Johns Hopkins Univ., Baltimore, Md. Dept. of Biochemistry). Contract AT(30-1)-1371. 18p. Dep. NTIS.

44271 (NYO-2504-59) PRESSURE DEPENDENCE OF THE ELASTIC CONSTANTS FOR SILVER FROM 77^{0}K TO 300^{0}K. Ho, Paul S.; Poirier, J. P.; Ruoff, Arthur L. (Cornell Univ., Ithaca, N. Y. Dept. of Materials Science and Engineering). [Jul 1969]. 19p. Dep. NTIS.

44272 (NYO-3590-7) PHYSIOPATHOLOGY OF BLOOD PLATELETS AND THE DEVELOPMENT OF PLATELET EXTRACTS AND SUBSTITUTES. Progress Report, August 1, 1970-July 31, 1971. Baldini, Mario G. (Brown Univ., Providence, R. I.). Contract AT(30-1)-3590. 26p. Dep. NTIS.

44273 (NYO-3699-56) VALIDITY OF THE BOLTZMANN EQUATION FOR SYSTEMS WITH BOTH ELECTRON-PHONON AND IMPURITY SCATTERING. Nickel, Bernie G.; Wilkins, John W. (Cornell Univ., Ithaca, N. Y. Lab. of Atomic and Solid State Physics). Jun 1971. 9p. Dep. NTIS.

44274 (NYO-3707-7) ROLE OF THE CARRIER IN ANTIBODY FORMATION. Progress Report, June 1, 1970-June 1, 1971. Plescia, Otto J. (Rutgers-The State Univ., New Brunswick, N. J. Inst. of Microbiology). Contract AT(30-1)-3707. 5p. Dep. NTIS.

44275 (NYO-4209) LOGICAL NETWORK COST AND ENTROPY. Cook, R. W.; Flynn, M. J. (Johns Hopkins Univ., Baltimore, Md.). Apr 1971. Contract AT(30-1)-4209. 13p. Dep. NTIS.

44276 (ORNL-4650) GEOMETRIC PROGRAMMING ALGORITHM. Westley, G. W. (Oak Ridge National Lab., Tenn.). Jul 1971. Contract W-7405-eng-26. 87p. Dep. NTIS.

44277 (ORNL-4683(Pt.1)) MOLECULAR ANATOMY (MAN) PROGRAM. Second Semiannual Progress Report, September 1, 1970-February 28, 1971. (Oak Ridge National Lab., Tenn.). Jul 1971. Contract W-7405-eng-26. 229p. Dep. NTIS.

44278 (ORNL-IBP-71-2) CODE FOR LINEAR MODELING OF AN ECOSYSTEM. Reeves III, Mark (Oak Ridge National Lab., Tenn.). Jul 1971. Contract W-7405-eng-26. 22p. Dep. NTIS.

44279 (ORNL-NSF-EP-3) THE ENVIRONMENT AND TECHNOLOGY ASSESSMENT. Progress Report, June-December 1970. (Oak Ridge National Lab., Tenn.). Feb 1971. Contract W-7405-eng-26. 251p. Dep. NTIS.

44280 (ORNL-NSIC-48) INFORMATION SCANNING AND PROCESSING AT THE NUCLEAR SAFETY INFORMATION CENTER. Parks, Celia; Julian, Carol (Oak Ridge National Lab., Tenn.). Jul 1971. Contract W-7405-eng-26. 57p. Dep. NTIS.

A detailed manual of the information specialist's duties at the Nuclear Safety Information Center is presented. Information specialists scan the literature for documents to be reviewed, procure the documents (books, journal articles, reports, etc.), keep the document location records, and return the documents to the plant library or other lender. These basic duties (selection and acquisition, cataloging, and general record-keeping) represent some of the key functions in the dissemination of information, and the procedures are designed to achieve the goal of error-free, economical operation. (auth)

XUM

44281 (ORNL-RMIC-11) RESEARCH MATERIALS INFORMATION CENTER BULLETIN AND STATUS REPORT. Connolly, T. F. (Oak Ridge National Lab., Tenn.). Apr 1971. Contract W-7405-eng-26. 42p. Dep. NTIS.

44282 (ORNL-TM-3408) NUMERICAL CALCULATION OF ELASTIC PROPERTIES FOR STRAIGHT DISLOCATIONS IN ANISOTROPIC CRYSTALS. Yoo, M. H.; Loh, B. T. M. (Oak Ridge National Lab., Tenn.). Jul 1971. Contract W-7405-eng-26. 58p. Dep. NTIS.

44283 (ORNL-TM-3477) ROOM TEMPERATURE MEASUREMENTS OF ELECTRICAL RESISTIVITY AND THERMAL CONDUCTIVITY OF VARIOUS GRAPHITES. McElroy, D. L.; Ewing, W. M.; Kollie, T. G.; Graves, R. S.; Steele, R. M. (Oak Ridge National Lab., Tenn.). Jul 1971. Contract W-7405-eng-26. 24p. Dep. NTIS.

44284 (ORNL-tr-2471) SOME PROPERTIES OF LITHIUM HYRRIDE WITH RESPECT TO ITS USE AS A ROCKET FUEL. PART I. THE DENSITY OF LiH GRAINS FORMED BY COMPRESSION OF LiH POWDER. Lo, R. E. Translated by R. Gregg Mansfield (Oak Ridge National Lab., Tenn.), from report DLR-FB-65-49. 17p. Dep. NTIS.

44285 (ORO-3082-6) ENZYMOLOGY AND REGULATION OF CYSTEINE METABOLISM IN MICROORGANISMS. Final Scientific Report, April 1, 1968-July 31, 1970. (Tennessee Univ., Knoxville). 18 Jun 1971. Contract AT(40-1)-3082. 26p. Dep. NTIS.

44286 (ORO-3091-21) DEFORMATION STUDIES OF SUPERLATTICE STRUCTURES. Final Report, March 1, 1963-August 31, 1970. Wert, James J. (Vanderbilt Univ., Nashville, Tenn.). 1 Jul 1971. Contract AT(40-1)-3091. 10p. Dep. NTIS.

44287 (RLO-2225-T-7-2) UPTAKE OF MOLYBDENUM, MARKED WITH ^{99}Mo, BY THE BIOTA OF FERN LAKE, WASHINGTON, IN A LABORATORY AND A FIELD EXPERIMENT. Short, Zella F.; Olson, P. R.; Palumbo, R. F.; Donaldson, J. R.; Lowman, F. G. (Washington Univ., Seattle. Coll. of Fisheries). [1971]. Contract AT(45-1)-2225. 43p. (CONF-710501-30). Dep. NTIS.
From third national symposium on radioecology; Oak Ridge, Tenn. (10 May 1971).

44288 (RLO-2227-T-8-1) METABOLISM OF ^{131}I IN TWO AMPHIBIAN SPECIES (TARICHA GRANULOSA AND RANA PIPIENS). Willis, David L.; Valett, Bryan B. (Oregon State Univ., Corvallis. Dept. of General Science). [1971]. 25p. (CONF-710501-27). Dep. NTIS.
From third national symposium on radioecology; Oak Ridge, Tenn. (10 May 1971).

44289 (SAN-651-129) BEARING INVESTIGATION. AEC ORGANIC RANKINE CYCLE TECHNOLOGY PROGRAM. Bland, T. J. (Sundstrand Aviation-[Rockford, Ill.]). [nd]. Contract AT(04-3)-651. 150p. Dep. NTIS.

44290 (SC-DR-68-814) SIDCAP REPORT NO. 4. SID CONTROLLER PROGRAM: A CDC 160A COMPUTER PROGRAM. Cover, Robert K. (Sandia Labs., Albuquerque, N. Mex.). May 1971. 86p. Dep. NTIS.

44291 (SC-RR-710301) ON ARTIFICIAL VISCOSITY. Roache, Patrick J. (Sandia Labs., Albuquerque, N. Mex.). Jul 1971. 26p. Dep. NTIS.

44292 (SRO-475-11) POWDER METALLURGY COMPACTION. Quarterly Progress Report, March 1, 1971-May 31, 1971. Schwartz, E. G.; Hornsby, James B.; Hammond, Riley G. Jr.; Ni, Tiee-Bor (South Carolina Univ., Columbia. Coll. of Engineering). Contract AT(38-1)-475. 6p. Dep. NTIS.

44293 (TID-25728) RESEARCH CONTRACTS IN THE LIFE SCIENCES. (Division of Biology and Medicine (AEC), Washington, D. C.). 1 Jul 1970. 87p. Dep. NTIS.
Research contracts in the field of life sciences administered by the AEC Division of Biology and Medicine during fiscal 1970 are listed alphabetically by research institution, alphabetically by states or foreign country, and are grouped according to the subject area investigated. The contract number, name of contractor (principal investigator), title of research study, and data on the cumulative amount and current level of AEC funding are included. The list includes all contracts that were active on June 30, 1970, and new contracts or contracts renewed through October 31, 1970. (C.H.)

44294 (TID-25739) IMAGE PROCESSING AND PATTERN RECOGNITION RESEARCH: ILLIAC III. Progress Report, April 19, 1971. (Illinois Univ., Urbana. Dept. of Computer Science). Contract AT(11-1)-2118. 23p. Dep. NTIS.

44295 (TID-25740) METHODOLOGY FOR OPTIMIZING POWER GENERATION-WATER DESALINATION SYSTEMS USING MATHEMATICAL PROGRAMMING DECOMPOSITION. Sea Water Conversion Lab. Report No. 71-2. Carasso, Meir (California Univ., Berkeley. Coll. of Engineering). Apr 1971. 90p.
Thesis.

44296 (TID-25742) CRYSTAL AND MOLECULAR STRUCTURES OF TRI-(p-FLUOROPHENYL)-AMINE AND TRI-(p-IODOPHENYL)-AMINE. Freeman, Gerald R. (North Texas Univ., Denton). Jan 1970. 128p. Dep. NTIS.
Thesis.

44297 (TID-25746) ELECTRON PARAMAGNETIC RESONANCE AND OPTICAL ABSORPTION STUDIES OF COLOR CENTERS AND IMPURITY IONS IN $KMgF_3$ AND MgF_2. Lewis, Joseph Thomas (Tennessee Univ., Knoxville). Jun 1971. 133p. Dep. NTIS.
Thesis.

44298 (TID-25758) PRELIMINARY VERSION OF RIPPLE SOFTWARE DESCRIPTIONS. Fortney, L. R.; Rose, C. M. (Duke Univ., Durham, N. C. Dept. of Physics). Jul 1971. Contract AT(40-1)-3065. 81p. Dep. NTIS.

44299 (UCID-30008) PIEGA: A NUMERICAL SOLUTION FOR DEFINITE INTEGRALS WITH OSCILLATING INTEGRANDS. Pexton, Robert L. (California Univ., Livermore. Lawrence Radiation Lab.). 1 Apr 1971. Contract W-7405-eng-48. 5p. Dep. NTIS.

44300 (UCID-30013(Pt.1)) TWO-DIMENSIONAL STRESS-INDUCED ADIABATIC FLOW. PART 1. MAIN CODE. Kransky, V.; Owens, J.; Cherry, J. T. (California Univ., Livermore. Lawrence Radiation Lab.). 1 Apr 1971. Contract W-7405-eng-48. 144p. Dep. NTIS.

44301 (UCID-30013(Pt.2)) TWO-DIMENSIONAL STRESS-INDUCED ADIABATIC FLOW. PART 2. GENERATOR CODE. Kransky, V.; Owens, J.; Cherry, J. T. (California Univ., Livermore. Lawrence Radiation Lab.). 1 Apr 1971. Contract W-7405-eng-48. 56p. Dep. NTIS.

44302 (UCID-30013(Pt.3)) TWO-DIMENSIONAL STRESS-INDUCED ADIABATIC FLOW. PART 3. U.N.C.L.E.: CODES OF TENSOR EXPLAINED. Kransky, V.; Owens, J.; Cherry, J. T. (California Univ., Livermore. Lawrence Radiation Lab.). 1 Apr 1971. Contract W-7405-eng-48. 41p. Dep. NTIS.

44303 (UCRL-51046) TWO-DIMENSIONAL FINITE FOURIER TRANSFORM TECHNIQUES. Brown, Norman J.; Weaver, H. Joseph Jr. (California Univ., Livermore. Lawrence Radiation Lab.). 30 Apr 1971. Contract W-7405-eng-48. 9p. Dep. NTIS.

44304 (UCRL-73046) CALORIMETRY DATA ACQUISITION AND CONTROL. English, J. C. (California Univ., Livermore. Lawrence Radiation Lab.). Feb 1971. 5p. (CONF-710514-1). Dep. NTIS.
From DECUS spring symposium; Atlanta, Ga. (13 May 1971).

44305 (UCRL-73104) LRL COMPUTER PROGRAM: MICROANALYSIS. Steele, Wayne J. (California Univ., Livermore. Lawrence Radiation Lab.). 12 May 1971. 25p. (CONF-710706-1). Dep. NTIS.
From 7th national conference on electron probe analysis; Pittsburgh, Pa. (28 Jul 1971).

44306 (UCRL-73161) CORRECTED FLUORESCENCE SPECTRA BY COMPUTER POSTPROCESSING. Mode, V. Alan; Sisson, David H.; Bailey, Carolyn A. (California Univ., Livermore. Lawrence Radiation Lab.). Apr 1971. 8p. (CONF-710704-1). Dep. NTIS.
From Conference on computers in chemical education and research; DeKalb, Ill. (19 Jul 1971).

44307 (UCRL-73184) WAVE PROPAGATION THEORY FOR ULTRASONIC TESTING. Nickerson, R. A. (California Univ.,

Livermore. Lawrence Radiation Lab.). 7 May 1971. 19p. (CONF-701050-1). Dep. NTIS.
From Ultrasonics symposium of the IEEE; San Francisco, Calif. (8 Oct 1970).

44308 (UCSD-34-P-127-10) AUTONOMOUS DEEP-SEA CINE SYSTEM. Shutts, Richard L.; Sessions, Meredith H. (Scripps Institution of Oceanography, La Jolla, Calif.). [1971]. Contract AT(11-1)-34. 5p. Dep. NTIS.

44309 (YALE-3227-77) ON THE USE OF PARAMETERS IN CRYSTAL FIELD THEORY AND RELATED CALCULATIONS. Wolf, W. P. (Yale Univ., New Haven, Conn.). [1970]. 11p. Dep. NTIS.

44310 BOOK OF SPLINES. Sard, Arthur; Weintraub, Sol. Wiley Series in Probability and Mathematical Statistics. New York; John Wiley and Sons, Inc. (1971). 824p. $22.50. (TID-25760).

XUM

CORPORATE AUTHOR INDEX

In the Corporate Author Index, technical report literature is indexed by the organization or institution responsible for issuing the report. Entries are given for all report literature and for published literature for which a corporate author approach is especially desirable, e.g., symposium and conference proceedings.

Each entry under a corporate author gives the publication title and the *NSA* volume and abstract numbers. Report numbers, where applicable, are given in parentheses at the end of the entry.

A

AEROJET-GENERAL CORP., SACRAMENTO, CALIF.
Detection of incipient failure in pressure vessels by stress wave emission, 25:44137 (CONF-700224-, Paper 3)
Fracture of structural metals as related to pressure-vessel integrity and in-service monitoring, 25:42840 (CONF-710512-4)

AEROSPACE CORP., EL SEGUNDO, CALIF.
Electrostatic vlf waves observed in polar magnetosphere, 25:43213 (AD-715898)
Measurement of the rf magnetic field distribution in a thermal induction plasma, 25:43338 (AD-715265)
Observation of autoionizing states in solar corona, 25:43065 (AD-715257)
Outer-zone electron precipitation, 25:43211 (AD-715266)
Prog. rpt. on low-energy proton damage to silicon/solar cells, 1/69--1/70, 25:42226 (AD-715261)
Turbulent loss of ring current protons, 25:43210 (AD-715260)
Volume ionization by means of laser radiation in a cesium plasma diode, 25:43181 (AD-715883)

AIR FORCE CAMBRIDGE RESEARCH LABS., L. G. HANSCOM FIELD, MASS.
Ionospheric model for Arctic, 25:43212 (AD-715893)

AIR FORCE WEAPONS LAB., KIRTLAND AFB, N. MEX.
Coupled electromagnetic and electron acoustic wave propagation in inhomogeneous lossy plasma layer, 25:43404 (AD-715910)

AIR LIQUIDE, SASSENAGE (FRANCE). CENTRE D'ETUDES CRYOGENIQUES.
Cooling of superconducting magnets, principles and uses, 25:43325 (CONF-700341-6)

AKADEMIYA NAUK SSSR, NOVOSIBIRSK. INSTITUT YADERNOI FIZIKI.
Studies of plasma turbulence by means of charged particle beam, 25:43339 (IYAF-7-70)

AKADEMIYA NAUK UKRAINSKOI SSR, KHARKOV. FIZIKO-TEKHNICHESKII INSTITUT.
Nonlinear stage of hydromagnetic current instability of plasma in a strong electrical field, 25:43386 (ORNL-tr-2434)

AKADEMIYA NAUK UKRAINSKOI SSR, KIEV. INSTITUT TEORETICHESKOI FIZIKI.
Asymptotic fields for the approximated, renormalized, two dimensional Yukawa model and :P(phi$_2$): model, 25:43667 (ITF-71-12-P)
Conformally plane cosmological solutions of the axial symmetry, 25:43085 (ITF-71-16-P)
Dual amplitude with Mandelstam analyticity, 25:43623 (ITF-71-28-E)
Problem of two-nucleon motion for Gauss potentials, 25:43638 (ITF-71-9-F)
Relativistic equations of motion without redundant components, 25:43654 (ITF-70-89-E)
Scaling, Pomeranchuk trajectory and J = 1 fixed poles in virtual Compton amplitude, 25:43584 (ITF-71-27-E)

AKTIEBOLAGET ATOMENERGI, STUDSVIK (SWEDEN).
Material buckling in U-loaded assemblies of fast reactor FRC, 25:44149 (AE-425)
Personnel dosimetry at AB Atomenergi during 1969, 25:42392 (AE-423)
Quantitative assay of ^{239}Pu and ^{240}Pu by neutron transmission measurements, 25:41750 (AE-416)

ALLMANNA SVENSKA ELECTRISKA A. B., VASTERAS.
IFA-30 final report, 25:44207 (KAE-68-46)
Irradiation behavior of fuel assembly IFA-30, 25:44208 (KAE-68-81)

AMERICAN ELECTRIC POWER SERVICE CORP., NEW YORK.
Donald C. Cook Nuclear Plant, Units 1 and 2. Benton Harbor Power Plant Limnological Studies. VII, 25:44058 (DOCKET-50315-41)
Donald C. Cook Nuclear Plant, Units 1 and 2. Benton Harbor Power Plant Limnological Studies. VI, 25:44055 (DOCKET-50315-38)
Donald C. Cook Nuclear Plant, Units 1 and 2. Lake Michigan environmental survey, 25:44057 (DOCKET-50315-40)
Donald C. Cook Nuclear Plant, Units 1 and 2. Underwater gamma radiation detection system, 25:44056 (DOCKET-50315-39)

AMERICAN SOCIETY OF MECHANICAL ENGINEERS, NEW YORK.
SEFOR operating experience, 25:44128 (CONF-710315-20)

AMES LAB., IOWA.
Anomalous elastic behavior of polycrystalline Nb_2Cs, 25:42585 (IS-T-446)
Creep stress distribution in long, cylindrical reactor pressure vessels, 25:42842 (CONF-710512-9)
Even-tempered atomic orbitals in quantum chemical ab initio calculations, 25:43160 (IS-T-456)
Stabilities of some rare-earth malonate chelate species in aqueous and methyl alcohol solution, 25:44260 (IS-T-474)
X-ray diffraction study of the yttria--hafnia system, 25:42883 (IS-T-425)

ARBETSGRUPP INOM INDUSTRI- OCH BYGGNADSBRUKS- OCH CIVILDEPARTEMENTEN (SWEDEN).
Reprocessing of nuclear fuel, 25:41896 (NP-18878)

ARGONNE NATIONAL LAB., ILL.
Activation-rate measurements in the ZPR-3 mockup critical experiments. Part I. Measurements of foil-activation rates and fission yields in Assembly 60 of ZPR-3: mockup of EBR-II with a uranium blanket, 25:44150 (ANL-7781)
Applied physics division annual report, July 1, 1969--June 30, 1970, 25:44190 (ANL-7710)
Can the AEC complex really exchange computer systems and programs, 25:44240 (CONF-710515-1)
Critical review of the energy released in nuclear fission, 25:43685 (ANL-7748)
Experimental techniques and facilities, 25:42048 (ANL-7710, pp 263-364)
Fast reactor physics, 25:44096 (ANL-7710, pp 53-262)
Fission properties and cross section data, 25:43884 (ANL-7710, pp 1-52)
Modular coding for reactor calculations in the United States, 25:44185 (EACRP-A-135, pp 50-9)
Reactor computation methods and theory, 25:44191 (ANL-7710, pp 365-463)
Solubility of helium and argon in liquid sodium, 25:41823 (ANL-7802)
Tentative design guide for calculating the vibration response of flexible cylindrical elements in axial flow, 25:41983 (ANL-ETD-71-7)
Thermal plume measurements, 25:44138 (CONF-710431-1)
U. S. experience with fast power reactors: EBR-II, 25:44085 (CONF-710427-1)

ARIZONA STATE UNIV., TEMPE. DEPT. OF CHEMISTRY.
Hydrothermal equilibria and crystal growth of rare earth oxides, hydroxides, hydroxynitrates, and hydroxycarbonates, 25:42934 (COO-1109-60)

ARIZONA UNIV., TUCSON. DEPT. OF NUCLEAR ENGINEERING.
Dynamics of a fast reactor with in-core thermionic converters. Fourth annual report, September 1, 1969--August 31, 1970, 25:44097 (COO-2109-5)
Multiple input-output feedback synthesis incorporating cross-coupling, 25:44104 (COO-2109-4)

ARIZONA UNIV., TUCSON. ENGINEERING EXPERIMENT STATION.
Effect of simulated fission products in interelectrode spacing of a thermionic diode, 25:43180 (AI-715805)

ARKANSAS POWER AND LIGHT CO., LITTLE ROCK.
Arkansas Nuclear One, Unit 2. Preliminary safety analysis report, Amendment 10, 25:44065 (DOCKET-50368-14)
Arkansas Nuclear One, Unit 2. Preliminary safety analysis report, amendment 11, 25:44066 (DOCKET-50368-15)

ARMY ELECTRONICS COMMAND, FORT MONMOUTH, N. J.
Studies of wavelike variations in the ionosphere, 25:43205 (AD-714993)

ARMY ELECTRONICS COMMAND, WHITE SANDS MISSILE RANGE, N. MEX. ATMOSPHERIC SCIENCES LAB.
Electrical strucutre of D and E region, 25:43208 (AD-714365)
ARMY ENGINEER REACTORS GROUP, FORT BELVOIR, VA. ENGINEERING DIV.
SM-1 core III 3.5 MWYR core physics report, 25:44176 (AD-715850)
ARNOLD ENGINEERING DEVELOPMENT CENTER, ARNOLD AIR FORCE STATION, TENN.
Ionizational and thermal nonequilibrium in MHD boundary layers, 25:43352 (AD-715272)
ARO, INC., ARNOLD AIR FORCE STATION, TENN.
Ionizational and thermal nonequilibrium in MHD boundary layers, 25:43352 (AD-715272)
ATLANTIC RICHFIELD HANFORD CO., RICHLAND, WASH.
Plutonium--uranium partitioning by a reflux extraction flowsheet, 25:41888 (ARH-SA-78)
Treatment of liquid wastes by evaporation to salt cakes, 25:41887 (ARH-SA-25)
ATOMIC ENERGY COMMISSION, WASHINGTON, D. C.
Environmental statement CANNIKIN, 25:42318 (TID-25735)
ATOMIC ENERGY ESTABLISHMENT, WINFRITH (ENGLAND).
Fast reactors: Flotran modular scheme, 25:44098 (EACRP-A-135, pp 30-7)
Progress of modular code development in the UKAEA, 25:44183 (EACRP-A-135, pp 11-14)
Shielding, 25:44107 (EACRP-A-135, pp 15-20)
Thermal reactors, 25:44193 (EACRP-A-135, pp 21-9)
ATOMIC ENERGY OF CANADA LTD., CHALK RIVER (ONTARIO). CHALK RIVER NUCLEAR LABS.
Prog. rpt. on chemistry and materials, 10--12/70, 25:41832 (AECL-3851)
Pulse radiolysis facilities at Chalk River, 25:41849 (AECL-3853)
ATOMIC ENERGY OF CANADA LTD., PINAWA (MANITOBA). WHITESHELL NUCLEAR RESEARCH ESTABLISHMENT.
Determination of sulfate in nitric acid--sulfuric acid mixtures, 25:41716 (AECL-3676)
Organic reactor coolant analysis: Canadian practice, 1970, 25:41713 (AECL-3672)
ATOMIC ENERGY RESEARCH ESTABLISHMENT, HARWELL (ENGLAND).
Comparison tests for extinguishing media on metal fires, 25:42837 (AERE-R-6745)
Note on the energy spread versus radial oscillation amplitude for the synchrocyclotron regenerative beam extractor, 25:43725 (AERE-R-6812)
ATOMIC WEAPONS RESEARCH ESTABLISHMENT, ALDERMASTON (ENGLAND).
Multi-element analysis of glass fragments by neutron activation and the application to forensic science, 25:41758 (AWRE-O-24/71)
ATOMIC WEAPONS TESTS SAFETY COMMITTEE, VICTORIA (AUSTRALIA).
Fallout over Australia from nuclear weapons tested by France in Polynesia, 5--8/70, 25:42367 (AWTSC-1)
ATOMICS INTERNATIONAL, CANOGA PARK, CALIF.
CLIP: a program to construct, update, and list the form of THREDES master data tape, 25:44095 (AI-CE-Memo-12)
Prog. rpt. on LMFBR physics programs, 1--3/71, 25:44094 (AI-AEC-12991)
Prog. rpt. on LMFBR safety programs, 1--3/71, 25:44132 (AI-AEC-12992)
ATOMICS INTERNATIONAL, CANOGA PARK, CALIF. LIQUID METAL ENGINEERING CENTER.
Liquid Metal Engineering Center (LMEC) semiannual technical progress report, July--December 1970, 25:42804 (LMEC-71-1)
AUSTRALIAN ATOMIC ENERGY COMMISSION RESEARCH ESTABLISHMENT, LUCAS HEIGHTS.
Precise determination of hydrogen in metals (with particular reference to zirconium) by the isotopic equilibration-mass spectrometry procedure, 25:41747 (AAEC/TM-588)
Preliminary ecological studies at Jervis Bay, 25:42314 (CONF-710511-3)
AVCO-EVERETT RESEARCH LAB., EVERETT, MASS.
Interaction of CTX wave with density fluctuations in an inhomogeneous magnetized plasma, 25:43402 (AD-715277)

B

BALTIMORE GAS AND ELECTRIC CO., MD.
Calvert Cliffs Nuclear Power Plant, Units 1 and 2. Preliminary safety analysis report, amendment 12 (includes final safety analysis report), 25:44059 (DOCKET-50317-26)
BATTELLE MEMORIAL INST., COLUMBUS, OHIO.
Mechanical-property data, 38-6-44 titanium alloy: aged forging, 25:42836 (AD-715877)
Prog. rpt. on development of fuels and technology for advanced reactors, 1--3/71, 25:44118 (BMI-1905)
BATTELLE-NORTHWEST, RICHLAND, WASH. PACIFIC NORTHWEST LAB.
Analysis of distributions produced by charged particles, 25:43414 (BNWL-SA-3705)
Coolant blowdown studies of a reactor simulator vessel containing a simulated reactor core, 25:44133 (BNWL-1524)
Development and design of an ultrasonic inspection system for radioactive waste containers, 25:42020 (BNWL-B-103)
Improved zirconium decontamination in Purex process, 25:41885 (BNWL-1573)
Leakage of fission products from artificial leaks in the Containment Systems Experiment, 25:44134 (BNWL-1582)
Multiple purpose use of thermal condenser discharges from large nuclear systems to supplement interregional water supply, 25:44083 (BNWL-SA-2738)
RACER: a computer program for calculating potential external dose from airborne fission products following postulated reactor accidents, 25:42393 (BNWL-B-65)
Role of design in corrosion prevention, 25:44236 (BNWL-SA-3817)
BENDIX CORP., KANSAS CITY, MO.
Comparison of orthogonal curvilinear coordinate systems for minimum error, 25:44222 (BDX-613-184)
Determination of average cycle time for an automated warehouse, 25:44224 (BDX-613-274)
Electroformed nickel mold inserts, 25:44235 (BDX-613-454)
Fine-edge blanking and piercing, 25:44229 (BDX-613-366)
Flatpack installation by single-probe reflow soldering, 25:44225 (BDX-613-326)
Flow soldering and supporting processes, 25:44227 (BDX-613-330)
Measurement method for polystyrene, 25:44228 (BDX-613-355)
Percussive-arc versus pulse-arc welding, 25:44231 (BDX-613-395)
Prog. rpt. of Quality Division, 5/71, 25:44232 (BDX-613-404)
Prog. rpt. on chemical vapor deposition process equipment, 11/70, 25:44223 (BDX-613-269)
Prog. rpt. on compression molding of laminates, FY 70-4, 25:44226 (BDX-613-327)
Prog. rpt. on electronic engineering, 6/71, 25:44233 (BDX-613-431)
Solder leveling of printed wiring boards, 25:44234 (BDX-613-443)
Theory and operation of Bendix mold heating and cooling equipment, 25:44230 (BDX-613-369)
BETTIS ATOMIC POWER LAB., PITTSBURGH, PA.
Computer utilization in nuclear reactor design, 25:44090 (WAPD-T-2358)
Fuel rod deformations: a time dependent finite element analysis on axisymmetric fuel rods, including pellet end effects (LWBR development program), 25:44126 (WERL-ELPLA-1)
Gas release from thoria-base oxide fuel pellets. (LWBR development program), 25:42958 (WAPD-TM-850)
BHABHA ATOMIC RESEARCH CENTRE, BOMBAY (INDIA).
Civil defence, an annotated bibliography 1960-1968, 25:42505 (BARC/BIB-1)
BOEING SCIENTIFIC RESEARCH LABS., SEATTLE, WASH.
Some algebraic solutions of the cyclotron resonance interaction, 25:43403 (AD-715636)
BRIGHAM YOUNG UNIV., PROVO, UTAH.
Faunistic studies of arthropods at National Reactor Testing Station, Idaho, 25:44251 (COO-1559-7)
BROOKHAVEN NATIONAL LAB., UPTON, N. Y.
Pion fluxes from 10-500 GeV proton synchrotrons, 25:43726 (BNL-15893)
Tabulated dose distribution data for gamma irradiator design, 25:41957 (BNL-50147(Rev.))
BROWN UNIV., PROVIDENCE, R. I.
Prog. rpt. on physiopathology of blood platelets, 8/70--7/71, 25:44272 (NYO-3590-7)
BROWN UNIV., PROVIDENCE, R. I. DEPT. OF PHYSICS.
Prog. rpt. on theoretical high-energy physics, 6/71, 25:43569 (NYO-2262-TA-245)
Triple Regge limits and duality sum rule, 25:43570 (NYO-2262-TA-247)
BUREAU OF LABOR STATISTICS, WASHINGTON, D. C.
Work injuries in atomic energy, 1968, 25:42498 (NP-18858)
BUREAU OF MINES, MORGANTOWN, W. VA. MORGANTOWN COAL RESEARCH CENTER.
Power required to circulate gas-solids suspensions, 25:41956 (BM-RI-7019)

C

CALIFORNIA INST. OF TECH., PASADENA.
Quantum numbers of cross-channel exchanges, 25:43565 (CALT-68-305)
CALIFORNIA INST. OF TECH., PASADENA. W. M. KECK LAB. OF ENGINEERING MATERIALS.
Electrical resistivity and magnetic susceptibilities of amorphous Cr--Ni--Pt--P alloys, 25:44237 (CALT-822-31)
Moessbauer effect study of amorphous Fe--Pd--Si alloys, 25:44238 (CALT-822-32)
CALIFORNIA UNIV., BERKELEY.
Table of hyperfine fields, 25:43469 (UCRL-20411)
CALIFORNIA UNIV., BERKELEY. COLL. OF ENGINEERING.
Methodology for optimizing power generation-water desalination systems using mathematical programing decomposition, 25:44295 (TID-25740)
CALIFORNIA UNIV., BERKELEY. LAWRENCE RADIATION LAB.
Ceramic science, 25:42957 (UCRL-20500, pp 147-73)
Chemistry, 25:41778 (UCRL-20500, pp 1-85)
Isospin purity and violations of mirror symmetry: the β-

XUM

delayed proton decay of ^{9}C, ^{13}C, ^{17}Ne, and ^{33}Ar, 25:43802 (UCRL-20480)
Metallurgy, 25:42886 (UCRL-20500, pp 86-146)
Monitoring of positively charged particles in the electron ring accelerator, 25:43734 (UCRL-20664)
Prog. rpt. on inorganic materials, annual, 1970, 25:41777 (UCRL-20500)
$\pi^+ + p \rightarrow \Delta^{++}(1236) + \pi^0$ AT 1.85 to 2.09 GeV: study of s- and t-channel effects, 25:43551 (UCR-34-P-107-B-108)
Solid state physics, 25:43470 (UCRL-20500, pp 175-204)
Study of $\pi^+p \rightarrow rho^+p$ at 1.85 to 2.09 GeV, 25:43552 (UCR-34-P-107-B-110)

CALIFORNIA UNIV., DAVIS.
Evidence for splitting in the Q region of $K^+\pi^+\pi^-$ mass, 25:43544 (COO-1428-275)
New evidence for splitting in the Q region of $K^+\pi^+\pi^-$ mass, 25:43543 (COO-1428-274)

CALIFORNIA UNIV., LIVERMORE. LAWRENCE RADIATION LAB.
Calorimetry data acquisition and control, 25:44304 (UCRL-73046)
Corrected fluorescence spectra by computer postprocessing, 25:44306 (UCRL-73161)
Livermore superconducting Levitron, 25:43399 (UCRL-73076)
LRL computer program: microanalysis, 25:44305 (UCRL-73104)
PIEGA: a numerical solution for definite integrals with oscillating integrands, 25:44299 (UCID-30008)
Pre-equilibrium decays of the compound nucleus, 25:43957 (UCRL-73152)
Two-dimensional finite Fourier transform techniques, 25:44303 (UCRL-51046)
Two-dimensional stress-induced adiabatic flow. I, 25:44300 (UCID-30013(Pt.1))
Two-dimensional stress-induced adiabatic flow. II, 25:44301 (UCID-30013(Pt.2))
Two-dimensional stress-induced adiabatic flow. III, 25:44302 (UCID-30013(Pt.3))
Wave propagation theory for ultrasonic testing, 25:44307 (UCRL-73184)

CALIFORNIA UNIV., LOS ANGELES. DEPT. OF PHYSICS.
Medium energy studies of the (p,p α) reaction on light nuclei, 25:43801 (UCLA-10-P-18-31)

CALIFORNIA UNIV., LOS ANGELES. INST. OF GEOPHYSICS AND PLANETARY PHYSICS.
Motion and structure of the magnetopause, 25:43220 (N-71-20853)

CALIFORNIA UNIV., LOS ANGELES. LAB. OF NUCLEAR MEDICINE AND RADIATION BIOLOGY.
Some physical and chemical characteristics of heated soils, 25:41926 (UCLA-12-819)

CALIFORNIA UNIV., LOS ANGELES. SCHOOL OF ENGINEERING AND APPLIED SCIENCE.
San Onofre Nuclear Generating Station vibration tests, 25:44079 (UCLA-ENG-7037)

CALIFORNIA UNIV., RIVERSIDE.
$\pi^+ + p \rightarrow \Delta^{++}(1236) + \pi^0$ AT 1.85 to 2.09 GeV: study of s- and t-channel effects, 25:43551 (UCR-34-P-107-B-108)
Reaction $\pi^+p \rightarrow rho^+p$ in C.M. energy region 1780 to 2140 MeV, 25:43553 (UCR-34-P-107-B-120)
Study of $\pi^+p \rightarrow rho^+p$ at 1.85 to 2.09 GeV, 25:43552 (UCR-34-P-107-B-110)

CALIFORNIA UNIV., RIVERSIDE. DEPT. OF PHYSICS.
Are there two A_2 mesons, 25:43624 (UCR-34-P-107-B-112)
Duality for inelastic anti KN scattering at intermediate energies, 25:43642 (UCR-34-P-107-B-106)

CAROLINA POWER AND LIGHT CO., RALEIGH, N.C.
H. B. Robinson Unit No. 2. Clad failure on primary side of steam generators, 25:44018 (DOCKET-50261-64)
H. B. Robinson Unit No. 2. Failure of liquid radioactive waste evaporator to meet specifications, 25:44017 (DOCKET-50261-63)
H. B. Robinson Unit No. 2. Preoperational flow test on safety injection system, 25:44045 (DOCKET-50261-65)
H. B. Robinson Unit No. 2. Reply regarding operation of emergency diesel generators, 25:44046 (DOCKET-50261-66)

CESKOSLOVENSKA AKADEMIE VED, REZ. USTAV JADERNEHO VYZKUMU.
Experimental investigation of temperature fields in an annular sodium channel with excentrically mounted inner heating element (e = 0/1), 25:41984 (INIS-mf-26)

CHICAGO WESLEY MEMORIAL HOSPITAL, ILL. NUCLEAR MEDICINE LAB.
Correlation between brain tumor detectability on brain scan and protein levels of the spinal fluid, 25:42547 (ACRH-1000-248)

CINCINNATI GAS AND ELECTRIC CO., OHIO.
Wm. H. Zimmer Nuclear Power Station, Unit 1. Preliminary safety analysis report, Amendment 13, 25:44063 (DOCKET-50358-19)
Wm. H. Zimmer Nuclear Power Station, Unit 1. Preliminary safety analysis report, amendment 14, 25:44064 (DOCKET-50358-20)

COLUMBIA UNIV., NEW YORK. PLASMA LAB.
Numerical simulation of strong plasma shock waves produced in an electromagnetic shock tube, 25:43360 (CU-3954-9)

COLUMBUS AND SOUTHERN OHIO ELECTRIC CO., COLUMBUS, OHIO.
Wm. H. Zimmer Nuclear Power Station, Unit 1. Preliminary safety analysis report, Amendment 13, 25:44063 (DOCKET-50358-19)
Wm. H. Zimmer Nuclear Power Station, Unit 1. Preliminary safety analysis report, amendment 14, 25:44064 (DOCKET-50358-20)

COMITATO NAZIONALE PER L'ENERGIA NUCLEARE, FRASCATI (ITALY). LABORATORIO GAS IONIZZATI.
Contribution to the study of dense plasmas, 25:43381 (LGI-68/16)

COMITATO NAZIONALE PER L'ENERGIA NUCLEARE, ROME (ITALY).
Conference on late effects of radiation, Casaccia, Italy, 4/69, 25:42604
Electrochemical etching of damaged track detectors by H. V. pulse and sinusoidal waveforms, 25:42056 (RT/PROT-(71)1)
Kinetics of a fast pulsed reactor in a periodic or quasi-periodic state, 25:44196 (LA-tr-71-44)

COMMISSARIAT A L'ENERGIE ATOMIQUE, BRUYERES-LE-CHATEL (FRANCE). CENTRE D'ETUDES.
Distribution of radioactivity in the lava issuing from the cavity of a nuclear explosion, 25:41953 (CEA-R-4059)
Principle of standard samples realization in analytical chemistry; trace elements problems in Pu, 25:41718 (CEA-R-4106)
Radioactivity distribution in environment of a contained nuclear explosion. I, 25:41954 (CEA-R-4128(1))

COMMISSARIAT A L'ENERGIE ATOMIQUE, FONTENAY-AUX-ROSES (FRANCE). CENTRE D'ETUDES NUCLEAIRES.
Behavior of fission products in nuclear fuels, 25:44206 (CEA-R-4181)
Investigation of some nonlinear effects in extraction equipment using computer simulation, 25:41890 (CEA-N-1450)
Oxidation resistant zirconium alloys in carbon dioxide at high temperatures, 25:42803 (CEA-R-4103)
Parameter study for a transit time magnetic pumping experiment in a torus, 25:43332 (EUR-CEA-FC-595)
Rapid detection of beryllium, 25:41717 (CEA-N-1446)
Socio-psychological factors limiting the emission of radioactive effluents, 25:41948 (CEA-CONF-1733)

COMMISSARIAT A L'ENERGIE ATOMIQUE, GRENOBLE (FRANCE). CENTRE D'ETUDES NUCLEAIRES.
Multi micro beams for ion implantation, 25:43728 (CEA-CONF-1767)
Nucleon--nucleon interaction from 3 nucleon interaction D(n,nnp) at 14 MeV, 25:43533 (CEA-R-4150)

COMMISSARIAT A L'ENERGIE ATOMIQUE, PARIS (FRANCE).
SAPRISTI code: nuclear reactions between light nuclei, 25:43779 (CEA-N-1327)
SAPRISTI code: nuclear reactions between light nuclei, 25:43780 (CEA-N-1327(Vol.4))

COMMISSARIAT A L'ENERGIE ATOMIQUE, SACLAY (FRANCE). CENTRE D'ETUDES NUCLEAIRES.
Calculation of the radiological risks arising from a reactor accident, 25:44135 (CEA-R-4136)
CODNUC: modular system for reactor calculations, 25:44182 (EACRP-A-135, pp 5-10)
Prog. rpt. on physical chemistry, semiannual, 7--12/70, 25:41850 (CEA-N-1438)
Program for optimal reactivity profiles in one-dimension cylindrical reactors, 25:44192 (CEA-N-1367)
Study of structure of physisorbed phases by thermodynamic analysis of stepwise isotherms of Kr, Xe, Ar, and methane on cleavage face of halides having a layer-like structure, 25:41824 (CEA-R-4089)

COMMONWEALTH EDISON CO., CHICAGO, ILL.
Dresden Nuclear Power Station, Unit 2. Current plan for operation, 25:44010 (DOCKET-50237-185)
Dresden Nuclear Power Station, Unit 2. Primary containment local leak rates outside technical specifications limits, 25:44008 (DOCKET-50237-183)
Dresden Nuclear Power Station, Unit 3. Failure of High Pressure Coolant Injection System auto-isolation signal reset, 25:44015 (DOCKET-50249-81)
Dresden Nuclear Power Station, Unit 3. Failure of high pressure coolant injection turbine stop valve to reset, 25:44016 (DOCKET-50249-83)
Dresden Nuclear Power Station, Unit 3. Failure of steam admission control valves to open, 25:44014 (DOCKET-50249-80)
Dresden Nuclear Power Station, Unit 3. Level and temperature limits of primary containment suppression chamber exceeded, 25:44013 (DOCKET-50249-79)
Dresden Nuclear Power Station, Units 2 and 3. Additional information concerning special report No. 3, Unit 2; and special report No. 15, Unit 3, 25:44036 (DOCKET-50237-186)
Dresden Nuclear Power Station, Units 2 and 3. Failure of diesel generator to start, 25:44009 (DOCKET-50237-184)
Quad-Cities Station, Units 1 and 2. Preliminary safety analysis report, amendment 28 (includes additions and revisions to final safety analysis report), 25:44042 (DOCKET-50254-45)
Quad-Cities Station, Units 1 and 2. Preliminary safety analysis report, amendment 27 (includes additional information to final safety analysis report), 25:44041 (DOCKET-50254-44)

COMMONWEALTH SCIENTIFIC AND INDUSTRIAL RESEARCH ORGANIZATION, MELBOURNE (AUSTRALIA). DIV. OF CHEMICAL PHYSICS.
Prog. rpt. on chemical physics, annual, 1969--70, 25:43468 (NP-18657)
CONNECTICUT YANKEE ATOMIC POWER CO., HADDAM.
Connecticut Yankee Atomic Power Plant. Operation report No. 71-5, May 1971, 25:44006 (DOCKET-50213-115)
CONSOLIDATED EDISON CO. OF NEW YORK, INC., NEW YORK.
Indian Point Nuclear Generating Unit No. 3. Preliminary safety analysis report, Amendment 14 (includes report: effect of tornado missiles on stored spent fuel), 25:44052 (DOCKET-50286-37)
Indian Point Nuclear Generating Unit No. 3. Preliminary safety analysis report, Amendment 15 (includes final facility description and safety analysis report, Suppl. No. 1), 25:44053 (DOCKET-50286-38)
Indian Point Station, Unit No. 1. Analysis of make-up water 4 inch nozzle sleeve modified design, 25:44024 (DOCKET-50003-80)
Verplanck Nuclear Facility, Units 1 and 2. Preliminary safety analysis report, Amendment 1(Suppl.1-Pt.A): revised pages, 25:44060 (DOCKET-50342-7)
CONSUMERS POWER CO., JACKSON, MICH.
Big Rock Point Nuclear Plant. Final safety summary report, Suppl. (includes quality assurance program), 25:44030 (DOCKET-50155-84)
Palisades Plant. Palisades interim loss of coolant analysis, 25:44043 (DOCKET-50255-48)
CORNELL UNIV., ITHACA, N. Y. DEPT. OF MATERIALS SCIENCE AND ENGINEERING.
Pressure dependence of elastic constants for Ag from 77°K to 300°K, 25:44271 (NYO-2504-59)
CORNELL UNIV., ITHACA, N. Y. LAB. OF ATOMIC AND SOLID STATE PHYSICS.
Validity of the Boltzmann equation for systems with both electron--phonon and impurity scattering, 25:44273 (NYO-3699-56)
CORNELL UNIV., ITHACA, N. Y. MATERIALS SCIENCE CENTER.
Thermomagnetic effects in normal and superconducting indium and niobium, 25:43289 (NYO-2150-71)

D

DAIRYLAND POWER COOPERATIVE, LA CROSSE, WIS.
La Crosse Boiling Water Reactor monthly operating report for 4/71, 25:44020 (TID-25737)
La Crosse Boiling Water Reactor. Failure of reactor building main steam isolation valve to close, 25:44000 (DOCKET-1155-125)
La Crosse Boiling Water Reactor. Failure of reactor safety system pressure channel No. 1 to trip during the performance of a technical specification test, 25:43998 (DOCKET-1155-123)
La Crosse Boiling Water Reactor. Unplanned reactor shutdown caused by closure of the 1A forced circulation pump (FCP) discharge valve, 25:43999 (DOCKET-1155-124)
DANISH ATOMIC ENERGY COMMISSION, RISOE. RESEARCH ESTABLISHMENT.
Effects of ionizing radiation for extending storage life of onions, 25:42745 (RISO-238)
Prog. rpt. on electronics, semiannual, 4--9/70, 25:42206 (RISO-M-1357)
Prog. rpt. on physics, annual, 1--12/70, 25:43435 (RISO-237)
DAYTON POWER AND LIGHT CO., OHIO.
Wm. H. Zimmer Nuclear Power Station, Unit 1. Preliminary safety analysis report, Amendment 13, 25:44063 (DOCKET-50358-19)
Wm. H. Zimmer Nuclear Power Station, Unit 1. Preliminary safety analysis report, amendment 14, 25:44064 (DOCKET-50358-20)
DEPARTMENT OF ATOMIC ENERGY, BOMBAY (INDIA). PHYSICS COMMITTEE.
Conference on nuclear physics and solid state physics, Roorkee, 12/69, 25:43466 (CONF-691208-(Vol.3))
DEPARTMENT OF TRADE AND INDUSTRY, LONDON (ENGLAND).
Report on the nuclear ship study, 25:44177 (NP-18908)
DEUTSCHES ELEKTRONEN-SYNCHROTRON, HAMBURG (WEST GERMANY).
Electroproduction of pions beyond the resonance region and the pion form factor, 25:43583 (DESY-71/22)
Finite-energy sum rules and the reactions e e → e e epsilon (750), e e → e e f (1260), 25:43582 (DESY-71/20)
Inelastic electron--proton scattering in the region of the Δ (1236) resonance, 25:43527 (DESY-71/21)
Unitarized finite energy sum rules and their application to πN-charge exchange, 25:43637 (DESY-71/24)
DIVISION OF BIOLOGY AND MEDICINE (AEC), WASHINGTON, D. C.
Research contracts in the life sciences, 25:44293 (TID-25728)
DIVISION OF COMPLIANCE (AEC), GLEN ELLYN, ILL. REGION III.
Big Rock Point Nuclear Plant. Report of inspection, 25:44031 (DOCKET-50155-85)
Point Beach Nuclear Plant, Unit No. 2. Report of inspection, 25:44054 (DOCKET-50301-35)
DIVISION OF COMPLIANCE (AEC), WASHINGTON, D.C.
Indian Point Nuclear Generating Unit No. 2. AEC Regulatory Staff safety evaluation, Suppl. 2, 25:44039 (DOCKET-50247-46)
DIVISION OF OPERATIONS ANALYSIS AND FORECASTING (AEC), WASHINGTON, D. C.
Forecast of growth of nuclear power, 25:43994 (WASH-1139)
DIVISION OF RADIOLOGICAL AND ENVIRONMENTAL PROTECTION (AEC), WASHINGTON, D.C.
Quad-Cities Station, Units 1 and 2. Final detailed statement on environmental considerations, 25:44040 (DOCKET-50254-42)
DIVISION OF REACTOR DEVELOPMENT AND TECHNOLOGY (AEC), WASHINGTON, D. C.
Alloy steel bolting materials for high-temperature service, 25:42798 (RDT-M-6-3-T)
Alloy steel bolting materials for low-temperature service, 25:42797 (RDT-M-6-1-T)
Alloy steel forgings, 25:42775 (RDT-M-2-4-T)
Austenitic stainless steel castings for high-temperature service, 25:42789 (RDT-M-4-2-T)
Brazing filler metal, 25:42769 (RDT-M-1-9-T)
Calcium silicate block and pipe thermal insulation, 25:43014 (RDT-M-12-2-T)
Calibration system requirements, 25:42205 (RDT-F-3-2-T)
Carbon steel forgings, 25:42773 (RDT-M-2-1-T)
Carbon steel plates for pressure vessels for moderate and lower-temperature service, 25:42792 (RDT-M-5-2-T)
Carbon--steel castings suitable for fusion welding for high-temperature service, 25:42788 (RDT-M-4-1-T)
Ceramic electrical insulators, 25:42204 (RDT-C-18-1-T)
Chromium and chromium--nickel stainless steel plate, sheet, and strip, 25:42791 (RDT-M-5-1-T)
Chromium--molybdenum alloy steel plates, 25:42795 (RDT-M-5-5-T)
Class I valves for liquid metal service, 25:41965 (RDT-E-1-18-T)
Cleaning and cleanliness requirements for nuclear reactor components, 25:44089 (RDT-F-5-1-T)
Cobalt--chromium alloy castings, wear and corrosion resistant, 25:42790 (RDT-M-4-3-T)
Collapsible-rotor, roller-nut control rod drive mechanism for sodium service, 25:44105 (RDT-E-6-5-T)
Continuous identification marking of wrought metal products, 25:42762 (RDT-F-7-1-T)
Copper and copper alloy arc-welding electrodes, 25:42767 (RDT-M-1-7-T)
Copper and copper alloy welding rods, 25:42768 (RDT-M-1-8-T)
Corrosion resisting chromium and chromium-nickel steel covered welding electrodes, 25:41972 (RDT-M-1-1-T)
Determination of insulation compaction in ceramic insulated conductors, 25:42190 (RDT-C-2-1-T)
Electromagnetic pump for liquid metal service, 25:41967 (RDT-E-3-9-T)
Examination requirements and acceptance standards for seal membranes, 25:41974 (RDT-M-9-2-T)
Factory made wrought austenitic steel welding fittings, 25:42776 (RDT-M-2-5-T)
Freeze vent for sodium service, 25:41968 (RDT-E-4-13-T)
Guard vessel for primary sodium containing components, 25:41969 (RDT-E-10-2-T)
Impregnated asbestos packing material, 25:43012 (RDT-M-11-2-T)
Inductive level measurement sensor for use in liquid metal, 25:42192 (RDT-C-5-1-T)
Inspection requirements for materials used in reactor coolant system wear applications, 25:44210 (RDT-F-3-7-T)
Liquid metal pressure measurement system, flush-mounted, eddy current type, inductive, absolute or gage, 25:42195 (RDT-C-6-3-T)
Liquid sodium bearing film thickness, variable reluctance transducer, proximity measurement system, 25:42201 (RDT-C-8-2-T)
Longitudinal-wave ultrasonic examination of plain and clad steel plates, 25:42024 (RDT-F-3-5-T)
Low alloy steel covered arc-welding electrodes, 25:42765 (RDT-M-1-4-T)
Low carbon chromium steel bars, 25:42799 (RDT-M-7-1-T)
Low carbon chromium steel forgings, 25:42777 (RDT-M-2-6-T)
Manganese--molybdenum and manganese--molybdenum--nickel alloy steel plates, quenched and tempered, for pressure vessels, 25:42793 (RDT-M-5-3-T)
Mechanical locking devices, 25:41973 (RDT-M-6-2-T)
Mild steel covered arc-welding electrodes, 25:42764 (RDT-M-1-3-T)
Mild steel electrodes and welding rods for gas--metal--arc welding, 25:42766 (RDT-M-1-6-T)
Multipoint strip-chart recording potentiometer, 25:42203 (RDT-C-9-2-T)
NaK-transmission high-temperature pressure transmitter for liquid metal service, 25:42194 (RDT-C-6-1-T)
Nickel and nickel alloy covered welding electrodes, 25:42770 (RDT-M-1-10-T)
Nickel and nickel-alloy bare welding rods and electrodes, 25:42771 (RDT-M-1-11-T)
Nickel--chromium--iron alloy plate, sheet, and strip, 25:42794 (RDT-M-5-4-T)
Nondestructive examination, 25:42025 (RDT-F-3-6-T)
Nonmetallic seal materials, 25:41975 (RDT-M-11-1-T)
Orifice plate for orifice flange union, 25:41963 (RDT-C-4-1-T)
Preloading threaded fasteners and closures, 25:41971

XUM

(RDT-F-8-1-T)
Preparations for sealing, packaging, packing, and marking of components for shipment and storage, 25:41970 (RDT-F-7-2-T)
Quality assurance program requirements, 25:44088 (RDT-F-2-2-T)
Quality verification program requirements, 25:42022 (RDT-F-2-4-T)
Quenched and tempered vacuum treated carbon and alloy steel forgings for pressure vessels, 25:42778 (RDT-M-2-7-T)
Reactor grade sodium-purchase specifications, 25:42801 (RDT-M-13-1-T)
Requirements for nuclear components, 25:43993 (RDT-E-15-2-T)
Resistive level measurement sensor for use in liquid metal, 25:42193 (RDT-C-5-2-T)
Seamless and welded austenitic stainless steel pipe, 25:42784 (RDT-M-3-6-T)
Seamless annealed nickel--chromium--iron and nickel--iron--chromium alloy condenser and heat exchanger tubes, 25:42782 (RDT-M-3-4-T)
Seamless austenitic stainless steel pipe, 25:42781 (RDT-M-3-3-T)
Seamless carbon steel pipe for high-temperature service, 25:42779 (RDT-M-3-1-T)
Seamless ferritic alloy steel pipe, 25:42787 (RDT-M-3-12-T)
Single-point strip-chart recording potentiometer, 25:42202 (RDT-C-9-1-T)
Small permanent magnet flowmeter for liquid metal service, 25:42191 (RDT-C-4-5-T)
Small, Class II, liquid metal valves, 25:41966 (RDT-E-1-19-T)
Special requirements for metal products, 25:42817 (RDT-F-3-37-T)
Stainless and alloy steel seamless tubes, 25:42780 (RDT-M-3-2-T)
Stainless steel welding rods and bare electrodes, 25:42763 (RDT-M-1-2-T)
Steam generator for pressurized water reactors, 25:44081 (RDT-E-4-1-T)
Supplementary criteria and requirements for RDT reactor plant protection systems, 25:44142 (RDT-C-16-1-T)
Test requirements for thermal insulating materials for use on austenitic stainless steels, 25:43013 (RDT-M-12-1-T)
Thermocouple assembly, nuclear grade, Chromel-P vs Alumel, stainless steel sheathed, Mg oxide insulated, 25:42200 (RDT-C-7-6-T)
Thermocouple material, copper and Constantan, solid conductor, 25:42198 (RDT-C-7-3-T)
Thermocouple material, copper-Constantan, magnesium-oxide insulated and sheathed, 25:42199 (RDT-C-7-4-T)
Thermocouple material, iron and Constantan, solid conductor, 25:42196 (RDT-C-7-1-T)
Thermocouple material, iron-Constantan, magnesium-oxide insulated and sheathed, 25:42197 (RDT-C-7-2-T)
Ultrasonic examination of heavy steel forgings, 25:42761 (RDT-F-3-3-T)
Ultrasonic examination of metal pipe and tubing for longitudinal discontinuities, 25:42026 (RDT-F-3-8-T)
Ultrasonic shear-wave examination of plates, 25:42023 (RDT-F-3-4-T)
Venturi flow tube for liquid sodium, 25:41964 (RDT-C-4-4-T)
Welded austenitic stainless steel tubing, 25:42783 (RDT-M-3-5-T)
Welded large diameter stainless steel pipe, 25:42785 (RDT-M-3-7-T)
Welding qualifications, 25:42850 (RDT-F-6-5-T)
Welding, 25:42849 (RDT-F-6-1-T)
Wide-range (10 decade) neutron flux monitoring channel, 25:44209 (RDT-C-15-2-T)
Wrought seamless carbon steel welding fittings, 25:42774 (RDT-M-2-3-T)
Zirconium and zirconium alloy bare welding rods, 25:42772 (RDT-M-1-16-T)
Zirconium and zirconium alloy ingots, 25:42800 (RDT-M-10-1-T)
Zirconium and zirconium alloy plate, sheet, and strip, 25:42796 (RDT-M-5-6-T)
Zirconium and zirconium alloy tubes, 25:42786 (RDT-M-3-8-T)

DIVISION OF REACTOR LICENSING (AEC), WASHINGTON, D. C.
Palisades Plant. Safety evaluation, supplement No. 4, 25:44044 (DOCKET-50255-49)
Vermont Yankee Nuclear Power Station. Safety evaluation, supplement No. 1, 25:44050 (DOCKET-50271-57)

DOW CHEMICAL CO., GOLDEN, COLO. ROCKY FLATS DIV.
Drybox gloves: evaluation and procurement, 25:42039 (RFP-1286)
Mechanical properties of uranium-base niobium alloys, 25:42851 (RFP-1703)
Neutron radiography with a sealed-tube neutron generator and graphite moderated system, 25:42027 (RFP-1706)

DU PONT DE NEMOURS (E.I.) AND CO., AIKEN, S. C. SAVANNAH RIVER LAB.
Fire prevention and protection in hot cells and canyons, 25:42036 (DP-1242)

DUKE POWER CO., CHARLOTTE, N.C.
McGuire Nuclear Station, Units 1 and 2. Preliminary safety analysis report, Amendment 8, 25:44067 (DOCKET-50369-12)

DUKE UNIV., DURHAM, N.C. DEPT. OF PHYSICS.
Preliminary version of RIPPLE software descriptions, 25:44298 (TID-25758)

E

EG AND G, INC., SANTA BARBARA, CALIF.
Artemisia shrub size and radiation damage to Artemisia from local fallout from Project Schooner, 25:42717 (EGG-1183-2272)

EIDGENOESSISCHES INSTITUT FUER REAKTORFORSCHUNG, WUERENLINGEN (SWITZERLAND).
Integral transport equation in one-dimensional cylindrical geometry. II, 25:43771 (EIR-189)

ELECTRO-OPTICAL SYSTEMS, INC., PASADENA, CALIF.
Prog. rpt. on solar-wind mass spectrograph, final, 8/12/69--8/12/70, 25:43221 (N-71-21469)

ENEA COMPUTER PROGRAMME LIBRARY, ISPRA (ITALY).
Conference on modular coding system for reactor calculations, Ispra, 12/70, 25:44181 (EACRP-A-135)

EUROPEAN ATOMIC ENERGY COMMUNITY.
Parameter study for a transit time magnetic pumping experiment in a torus, 25:43332 (EUR-CEA-FC-595)
Spectrophotometric determination of traces of americium in plutonium oxide, 25:41721 (EUR-4352)

EUROPEAN ATOMIC ENERGY COMMUNITY, ISPRA (ITALY). JOINT NUCLEAR RESEARCH CENTER.
CARONTE: Euratom modular calculation system, 25:44187 (EACRP-A-135, pp 63-8)
"DDO" computer procedure for the inventory control of a supply of deuterium, 25:41960 (EUR-4512)
Determination of eigenvalues of Mathieu equation, 25:43505 (EUR-4349)

EUROPEAN ATOMIC ENERGY COMMUNITY, PETTEN (NETHERLANDS). JOINT NUCLEAR RESEARCH CENTER.
Indirect experimental determination of photopeak efficiencies of NaI(Tl) detectors for cylindrical gaseous sources, 25:42049 (EUR-4513)

EUROPEAN COMMUNITIES, BRUSSELS (BELGIUM). COMMISSION.
Bismuth-impregnated graphite reflector in a heavy water moderated reactor: an evaluation, 25:44129 (EUR-4357)
Comparative analysis of critical and exponential experiments by heterogeneous methods, 25:44154 (EUR-4362)
Orgel prototype preliminary design: fine flux distributions in the fuel element, 25:44099 (EUR-4364)
Orgel prototype preliminary design: reactivity coefficients, 25:44100 (EUR-4365)

EUROPEAN ORGANIZATION FOR NUCLEAR RESEARCH, GENEVA (SWITZERLAND).
Quantum numbers of cross-channel exchanges, 25:43565 (CALT-68-305)
Study of hybrid electromagnetic waves in cylindrical structures, 25:43405 (CERN-71-4)
Systematics of extra-nuclear hadron cascades in shields, 25:43613 (CERN-71-13)

F

FRANKFURT UNIV. (WEST GERMANY). INSTITUT FUER ANGEWANDTE PHYSIK.
New Monte Carlo technique for radiation transport problems; calculation of combined spatial, angular, and energy distributions of multiply scattered gamma rays, 25:43413 (BMBW-FBK-71-2)

FRANKLIN INST. RESEARCH LABS., PHILADELPHIA, PA.
Indian Point Station, Unit No. 1. Analysis of make-up water 4 inch nozzle sleeve modified design, 25:44024 (DOCKET-50003-80)

G

GCA CORP., BEDFORD, MASS. GCA TECHNOLOGY DIV.
Investigation of the D and E regions of the ionosphere, 25:43215 (N-71-17052)

GENERAL ELECTRIC CO., PHILADELPHIA, PA. MISSILE AND SPACE DIV.
Equilibrium composition and normal shock parameters for nitrogen up through double ionization, 25:43331 (AD-715615)

GENERAL ELECTRIC CO., PLEASANTON, CALIF. NUCLEONICS LAB.
Fission gas re-solution rates. Quarterly report No. 2, October 1--December 31, 1970, 25:42952 (GEAP-12188)
Fission gas re-solution rates. Quarterly report No. 3, January 1--March 31, 1971, 25:42953 (GEAP-12189)

GENERAL ELECTRIC CO., SAN JOSE, CALIF. ATOMIC POWER EQUIPMENT DEPT.
Failure behavior of flawed carbon steel pipes and fittings, 25:42845 (GEAP-10236)
Loss-of-coolant accident and emergency core cooling models for BWR, 25:44140 (NEDO-10329(Suppl.1))

GENERAL ELECTRIC CO., SAN JOSE, CALIF. REACTOR FUELS AND REPROCESSING DEPT.
Design and fabrication of special assembly SA-1, 25:44120 (GEAP-10355)

GENERAL ELECTRIC CO., SCHENECTADY, N. Y. RESEARCH AND DEVELOPMENT CENTER.
Apollo helmet dosimetry experiments, 25:42160 (N-71-14602)
GENERAL ELECTRIC CO., SUNNYVALE, CALIF. BREEDER REACTOR DEVELOPMENT OPERATION.
Prog. rpt. on Integrated Safeguards Experiment, 12/70--3/71, 25:42035 (GHC-68-6)
Southwest Experimental Fast Oxide Reactor. Description of overall Follow-On Program, 25:44153 (DOCKET-50231-90)
Southwest Experimental Fast Oxide Reactor. Results of the balanced oscillator experiments for Core I, 25:44151 (DOCKET-50231-88)
Southwest Experimental Fast Oxide Reactor. Results of the familiarization and sub-prompt critical transient tests for Core I, 25:44152 (DOCKET-50231-89)
GENEVA UNIV. (SWITZERLAND).
Contribution to the study of dense plasmas, 25:43381 (LGI-68/16)
GEOLOGICAL SURVEY, DENVER, COLO.
Tectonic setting of Amchitka Island, Alaska, 25:41927 (USGS-474-75(Rev.1))
GEOTECH, GARLAND, TEX.
Seismic analysis of Gasbuggy explosion an earthquake of similar magnitude and epicenter, 25:41952 (AD-838894)
GOSUDARSTVENNYI KOMITET PO ISPOL'ZOVANIYU ATOMNOI ENERGII SSSR, MOSCOW. INSTITUT TEORETICHESKOI I EKSPERIMENTAL'NOI FIZIKI.
Filtering of tracks measured on the SMP, 25:42135 (CERN-Trans-71-8)
GOSUDARSTVENNYI KOMITET PO ISPOL'ZOVANIYU ATOMNOI ENERGII SSSR, OBNINSK. FIZIKO-ENERGETICHESKII INSTITUT.
Liquid boron neutron detector for a time-of-flight spectrometer, 25:42104 (FEI-208)
Pumps for circulating liquid metals, 25:41958 (CONF-700307-8)
Results of the calculation for a standard fast reactor, 25:44194 (FEI-213)
GOSUDARSTVENNYI KOMITET PO ISPOL'ZOVANIYU ATOMNOI ENERGII SSSR, SERPUKHOV. INSTITUT FIZIKI VYSOKIKH ENERGII.
High intensity (10-16) GeV/c negative particle beam, 25:43729 (CERN-Trans-71-16)
GRENOBLE UNIV. (FRANCE).
Nucleon--nucleon interaction from 3 nucleon interaction D(n,nnp) at 14 MeV, 25:43533 (CEA-R-4150)

H

HAHN-MEITNER-INSTITUT FUER KERNFORSCHUNG, BERLIN (WEST GERMANY).
Modular programming system for programming experiments on PDP-9, 25:42181 (CERN-Trans-71-18)
HANFORD ENGINEERING DEVELOPMENT LAB., RICHLAND, WASH.
Fracture and tensile behavior of neutron-irradiated A533-B pressure vessel steel, 25:42901 (HEDL-TME-71-76)
Thermal performance limits for fast reactor oxide fuels, 25:44121 (HEDL-SA-89)
HARVARD UNIV., CAMBRIDGE, MASS. DIV. OF ENGINEERING AND APPLIED PHYSICS.
Radiation-enhanced creep, 25:42900 (AD-719905)
HELIOTEK, SYLMAR, CALIF.
Prog. rpt. on development of lithium-diffused radiation-resistant solar cells, 10/70, 25:42227 (N-71-12257)
HITACHI, LTD., TOKYO (JAPAN).
Activities on modular code systems in Japan, 25:44188 (EACRP-A-135, pp 69-86)

I

IDAHO NUCLEAR CORP., IDAHO FALLS.
Nonradioactive waste oil disposal study, 25:44220 (ANCR-1004)
Nonradioactive waste solvent disposal study, 25:44221 (ANCR-1006)
Third processing campaign in the Waste Calcining Facility, 25:41933 (IN-1474)
ILLINOIS STATE UNIV., NORMAL. DEPT. OF BIOLOGICAL SCIENCES.
Prog. rpt. on cytogenetics of monosomes in Zea mays, 10/70--9/71, 25:44257 (COO-2121-3)
ILLINOIS UNIV., URBANA. DEPT. OF COMPUTER SCIENCE.
Prog. rpt. on image processing and pattern recognition research: ILLIAC III, 4/71, 25:44294 (TID-25739)
ILLINOIS UNIV., URBANA. DEPT. OF PHYSICS.
Failure of S-channel helicity conservation in A_1-production, 25:43554 (COO-1195-204)
Some recent experimental results for A_1, A_2, Q, and L mesons, 25:43542 (COO-1195-215)
INDIAN INST. OF TECH., KANPUR. DEPT. OF PHYSICS.
Crossing and positivity properties of partial waves. a review, 25:43711 (SU-1206-243)
INDIANA-PURDUE UNIV., INDIANAPOLIS. DEPT. OF PHYSICS.
Final states with three charged particles and a visible anti K^0 from K-d interactions at 4.5 GeV/c, 25:43549 (COO-1428-286)
INSTITUT ATOMNOI ENERGII, MOSCOW (USSR).
DEMETRA program set for calculating problems of neutron thermalization in one-dimensional cell of heterogeneous reactor, 25:44195 (IAE-2010)
INSTITUT FUER PLASMAPHYSIK, G.M.B.H. GARCHING (WEST GERMANY).
Survey of studies of laser produced plasmas at the IPP Garching, 25:43380 (IPP-4/9)
INSTITUTE OF NUCLEAR PHYSICS, KRAKOW (POLAND).
Distorted Wave Born Approximation programmes for inelastic scattering of charged particles MIS-0, MIS-2, MIS-3, MIS-4, and MIS-5, 25:43954 (INP-746)
INSTITUTE OF NUCLEAR RESEARCH, WARSAW (POLAND).
(n,α) reactions on heavy nuclei induced by 14.2-MeV neutrons, 25:43886 (INR-1268)
^{131}I content in primary coolant water and in the air under EWA-1C reactor top covers, 25:44155 (INR-1295)
Circular polarization of gamma rays, 25:43831 (INR-1262)
Closed shells for very heavy nuclei, 25:43955 (INR-1270)
Laboratory mixer--settler extractor LMOM2, 25:41895 (INR-1309)
Nb_3Sn superconducting phase identification in Nb--Sn alloys by critical temperature measurement method, 25:43288 (INR-1294)
Optimum start-up of the fuel reprocessing industry, 25:41894 (INR-1297)
Possibility of existence of a new process at interactions with energies above 10^{12} eV, 25:43567 (INR-1280)
Studies of epithermal cell parameters in the reactor lattices with multitube enriched fuel, 25:44203 (INR-P-1266)
INSTITUTE OF RADIATION PHYSICS, HELSINKI (FINLAND).
Elimination rate and radiation exposure following ingestion of ^{222}Rn rich water, 25:42247 (SFL-A-16)
INSTITUTO POLITECNICO NACIONAL, MEXICO CITY. ESCUELA SUPERIOR DE FISICA Y MATEMATICAS.
Conductivity at high frequencies of a completely ionized plasma with ion--ion correlations, 25:43363 (NP-18805)
Scattering length of the n--n reaction, 25:43534 (NP-18814)
INSTITUTT FOR ATOMENERGI, HALDEN (NORWAY).
IFA-30 final report, 25:44207 (KAE-68-46)
INTERNATIONAL ATOMIC ENERGY AGENCY, VIENNA (AUSTRIA).
Conference on biochemical indicators of radiation injury in man, Paris, 6/70, 25:42395 (STI/PUB-280)
Conference on nuclear techniques for mineral exploration and exploitation, Krakow, 12/69, 25:41941 (STI/PUB-279)
Radurization of scampi, shrimp, and cod, 25:42746 (STI/DOC-10/124)
INTERNATIONAL BUSINESS MACHINES CORP., SAN JOSE, CALIF.
Effect of an electric field on gas chromatographic retentions by liquid crystals, 25:44245 (COO-1222-47)
IOWA-ILLINOIS GAS AND ELECTRIC CO., DAVENPORT, IOWA.
Quad-Cities Station, Units 1 and 2. Preliminary safety analysis report, amendment 28 (includes additions and revisions to final safety analysis report), 25:44042 (DOCKET-50254-45)
Quad-Cities Station, Units 1 and 2. Preliminary safety analysis report, amendment 27 (includes additional information to final safety analysis report), 25:44041 (DOCKET-50254-44)
IOWA UNIV., IOWA CITY. DEPT. OF PHYSICS AND ASTRONOMY.
Distribution of plasmas and electric fields over auroral zones and polar caps, 25:43219 (N-71-20708)
Double probe measurements of dc electric fields with Injun 5 satellite, 25:43216 (N-71-18405)
ISRAEL ATOMIC ENERGY COMMISSION, TEL AVIV.
Prog. rpt., annual, 1--12/69, 25:41833 (IA-1218)
ISTITUTO NAZIONALE DI FISICA NUCLEARE, NAPLES (ITALY).
Inequalities for the pion--nucleon partial waves, 25:43641 (SU-1206-249)

J

JAPAN ATOMIC ENERGY RESEARCH INST., TAKASAKI. TAKASAKI RADIATION CHEMISTRY RESEARCH ESTABLISHMENT.
Chemical reactions by reactor radiation, 25:41851 (JAERI-13780)
JAPAN ATOMIC ENERGY RESEARCH INST., TOKAI.
Application test for radioisotopes developed in fiscal years of 1965, 66, and 67, 25:41990 (JAERI-13617)
Characteristics of proton recoil proportional counter GD-A for neutron and γ-ray, 25:42106 (JAERI-13580)
Determination of radioactive impurities in ^{45}Ca sample produced by (n,γ) reaction, 25:41878 (JAERI-13579)
Effect of neutron irradiation on precipitation-hardening of Al--3.8 percent Cu alloy, 25:42902 (JAERI-13692)
Electron microscope observation of the zirconium hydride, 25:42981 (JAERI-13635)
Evaluation of stainless steel pipe for cladding material of fast reactor, 25:42846 (JAERI-13578)
Full energy peak efficiency of NaI crystal, 25:42050 (JAERI-13546)
Inorganic ion exchanger, 25:41879 (JAERI-13726)
JAERI nuclear instrument module system, 25:42186 (JAERI-13768)
JAERI Nuclear Instrument module system. 5, 25:42185 (JAERI-13605)
JAERI pulsed type neutron spectrometer, 25:42107 (JAERI-13771)
Physical properties of carbide fuels and their evaluation, 25:42956 (JAERI-13517)
Power increasing plan of JAERI Linac, 25:43730 (JAERI-

XUM

13567)
Recrystallization of V--20 wt percent Ti alloy, 25:42884 (JAERI-13731)
Recrystallization of Zr--2.5 wt percent Nb alloy, 25:42885 (JAERI-13764)
Review of phase relations and structures of NaCl type compounds in the system U--Pu--C--N, 25:42982 (JAERI-13650)
RI liquid wastes carried from Japan Radioisotope Association to JAERI, 25:42037 (JAERI-13666)
Some cautionary problems of fluorometric determination of uranium, 25:41722 (JAERI-13622)
Studies on fundamental properties of alumina adsorbent for radioisotope production, 25:41991 (JAERI-13778)
Technique for determining activity and size distribution of β emitting particles by autoradiography, 25:42051 (JAERI-13718)
Theories and their applications of electromagnetic method in liquid flow rate-measurement, 25:42184 (JAERI-13536)

JAPAN ATOMIC ENERGY RESEARCH INST., TOKAI. TOKAI RESEARCH ESTABLISHMENT.
Activities on modular code systems in Japan, 25:44188 (EACRP-A-135, pp 69-86)
Gamma-ray discriminating system for a proton-recoil counter, 25:42105 (JAERI-13561)
Impurities in radioisotopes produced by (n,γ) reaction, 25:41877 (JAERI-13545)

JAPAN ATOMIC ENERGY RESEARCH INST., TOKYO.
Counting channel for use with gas flow proportional counter, 25:42052 (JAERI-13725)

JERSEY CENTRAL POWER AND LIGHT CO., MORRISTOWN, N. J.
Oyster Creek Nuclear Power Plant, Unit No. 1. Surveillance testing failures, 25:44007 (DOCKET-50219-142)

JET PROPULSION LAB., PASADENA, CALIF.
Thermoelectric generators for deep space application, 25:43184 (N-71-16776)

JOHNS HOPKINS UNIV., BALTIMORE, MD.
Logical network cost and entropy, 25:44275 (NYO-4209)

JOHNS HOPKINS UNIV., BALTIMORE, MD. DEPT. OF BIOCHEMISTRY.
Prog. rpt. on genetic transformation in Hemophilus influenzae, annual, 9/15/70--9/14/71, 25:44270 (NYO-1371-64)

JOINT INST. FOR NUCLEAR RESEARCH, DUBNA (USSR).
Acceleration and extraction of deuterons from JINR proton synchrotron, 25:43727 (BNL-tr-431)
Some specific features of the cold cathode operating at low pressures, 25:43346 (JINR-P9-5753)

JOINT INST. FOR NUCLEAR RESEARCH, DUBNA (USSR). LAB. OF COMPUTING TECHNIQUES AND AUTOMATION.
Ion--sound turbulence in dense plasma, 25:43406 (JINR-P9-5846)

JOINT INST. FOR NUCLEAR RESEARCH, DUBNA (USSR). LAB. OF HIGH ENERGY.
Characteristics of coherent interactions at 17 and 45 GeV, 25:43646 (JINR-P1-5775)
Interference at intersection of levels, 25:43506 (JINR-P4-5786)
Thermodynamical description of momentum distributions of pions in π⁻p interactions at p = 4 GeV/c, 25:43639 (JINR-P1-5849)

JOINT INST. FOR NUCLEAR RESEARCH, DUBNA (USSR). LAB. OF NEUTRON PHYSICS.
Development and application of pulsed fast reactors IBR for scientific researches, 25:44156 (JINR-P3-5754)

JOINT INST. FOR NUCLEAR RESEARCH, DUBNA (USSR). LAB. OF NUCLEAR PROBLEMS.
α decay of neutron-deficient radon isotopes, 25:43887 (JINR-P6-5791)
Methods of detecting particle tracks in liquid and solid media, 25:42053 (JINR-P13-5782)
Time properties of a spark chamber filled with helium and helium--hydrogen mixture, 25:42136 (JINR-P13-5828)

JOINT INST. FOR NUCLEAR RESEARCH, DUBNA (USSR). LAB. OF NUCLEAR REACTIONS.
Nanosecond lifetime measurements of excited nuclear states at heavy ion cyclotron, U-300, 25:42187 (JINR-P13-5801)
Sources of multicharged ions, 25:43731 (JINR-P7-5177)

JOINT INST. FOR NUCLEAR RESEARCH, DUBNA (USSR). LAB. OF THEORETICAL PHYSICS.
Application of Pade approximation to problem bound states in quasipotential approach, 25:43568 (JINR-P2-5765)
Model of the multiple particle production, 25:43614 (JINR-P2-5829)

K

KANSAS UNIV., LAWRENCE. DEPT. OF CHEMISTRY.
Computer collection of mass spectrometric ionization efficiency curves, 25:44241 (COO-1140-198)
Computer control of a high-temperature quadrupole mass spectrometer, 25:42182 (COO-1140-194)

KERNFORSCHUNGSANLAGE, JUELICH (WEST GERMANY).
Dielectric waveguides and aerials for 2 mm microwave interferometers with high spatial resolution for plasma density measurements, 25:42183 (CTO-756)

KERNFORSCHUNGSANLAGE, JUELICH (WEST GERMANY). INSTITUT FUER FESTKOERPERFORSCHUNG.
Phonons and librons in solid hydrogen and deuterium, 25:44261 (JUL-734-FF)

KERNFORSCHUNGSANLAGE, JUELICH (WEST GERMANY). INSTITUT FUER REAKTORWERKSTOFFE.
Formation of U_2C_3 by decomposition of uranium dicarbide, 25:42936 (JUL-728-RW)

KERNFORSCHUNGSANLAGE, JUELICH (WEST GERMANY). INSTITUT FUER TECHNISCHE PHYSIK.
Applied magnetohydrodynamics. VII, 25:43182 (JUL-742-TP)

KERNFORSCHUNGSANLAGE, JUELICH (WEST GERMANY). ZENTRALINSTITUT FUER ANGEWANDTE MATHEMATIK.
Investigation of the problem of characteristic value and nonnegative solution of a general stationary transport equation, 25:43415 (JUL-711-MA)

KERNFORSCHUNGSZENTRUM, KARLSRUHE (WEST GERMANY).
Modular coding systems, 25:44186 (EACRP-A-135, pp 60-2)

KERNFORSCHUNGSZENTRUM, KARLSRUHE (WEST GERMANY). INSTITUT FUER MATERIAL UND FESTKOERPERFORSCHUNG.
Room temperature mechanical properties and precipitation behavior of steel Incoloy and Inconel after annealing in contact with UC, 25:42844 (EURFNR-922)
Separation of vanadium on UC_2 spheres from the gaseous phase, 25:42935 (EURFNR-859)

KERNFORSCHUNGSZENTRUM, KARLSRUHE (WEST GERMANY). INSTITUT FUER RADIOCHEMIE.
Phase equilibria in the systems ThC_2--UO/sub 2+x/, CeO_2--UO/sub 2+x/, and NpO_2--UC/sub 2+x/, 25:42984 (ORNL-tr-2483)
Preparation and separation of carrier-free ^{131}Cs from irradiated $BaCO_3$, 25:41876 (CONF-680986-2)

KERNFORSCHUNGSZENTRUM, KARLSRUHE (WEST GERMANY). INSTITUT FUER REAKTORENTWICKLUNG.
Experimental investigation of loop caused influences on parallel flow-induced vibration of fuel pins, 25:44119 (EURFNR-923)
In-pile equipment for strain measurements on nuclear fuels and structural materials, 25:44086 (EURFNR-853)
Studies on wear and frictional behavior between fuel rod bundles and spacer grids in sodium, 25:44087 (EURFNR-854)

KERNFORSCHUNGSZENTRUM, KARLSRUHE (WEST GERMANY). ZYKLOTRON-LABORATORIUM.
Measured differential cross sections for elastic and inelastic scattering of 104-MeV α particles, 25:43832 (NP-18920)

KNOLLS ATOMIC POWER LAB., SCHENECTADY, N. Y.
Electron microprobe analysis of thin corrosion films, 25:44266 (KAPL-3482)

L

LABORATOIRE CENTRAL DE L'ARMEMENT, ARCUEIL (FRANCE).
Mathematical method for the computer processing of dosimetric films, 25:42161 (NP-18892)
Shielding thickness required to reduce neutron flux or dose rate, 25:43416 (NP-18863)

LOS ALAMOS SCIENTIFIC LAB., N. MEX.
DCHAIN: PDP-9/PDP-15 computer program for radioactive decay and capture chain calculations, 25:43889 (LA-4708)
Early history of criticality safety, 25:44157 (LA-4671)
Fabrication of CWR gamma shield assemblies, 25:42816 (LA-4644)
Fission fragment angular distributions for ^{230}Th, ^{232}Th, ^{231}Pa, and ^{239}Pu, 25:43888 (LA-4648)
Radiolysis of mixtures of carbon dioxide and hydrogen, 25:41852 (LA-4657)
Segregation of impurities on surfaces of thorium: thermodynamics and kinetics, 25:41825 (LA-DC-12348)
Survey of techniques employed to define aerosol respirable dust concentration and particle-size characteristics. Vol. II, 25:44267 (LA-4249(Vol.2))
Vela V and VI solar x-ray atlas. V, 25:43066 (LA-4454(Vol.5))

LOUISIANA POWER AND LIGHT CO., NEW ORLEANS.
Waterford Steam Electric Station, Units 3 and 4. Preliminary safety analysis report, amendment 3, 25:44070 (DOCKET-50382-7)

LYON UNIV. (FRANCE). INSTITUT DE PHYSIQUE NUCLEAIRE.
Reconstruction of amplitudes for pion--nucleon scattering from experimental data, 25:43640 (LYCEN-7110)

M

MARYLAND UNIV., COLLEGE PARK. DEPT. OF PHYSICS AND ASTRONOMY.
Bethe Goldstone equation in finite nuclei, 25:43956 (ORO-3765-30)

MASON AND HANGER-SILAS MASON CO., INC., AMARILLO, TEX.
Transition metal HE's. V, 25:44268 (MHSMP-71-28)

MASSACHUSETTS GENERAL HOSPITAL, BOSTON. JOHN COLLINS WARREN LABS.
Prog. rpt. on early steps in protein synthesis and their regulation, 9/70--8/71, 25:44259 (HUX-2643-61)

MASSACHUSETTS INST. OF TECH., CAMBRIDGE. DEPT. OF METALLURGY AND MATERIALS SCIENCE.
Basic research in crystalline and noncrystalline ceramic systems. Annual report, 25:42983 (MIT-3773-103)

MICHIGAN STATE UNIV., EAST LANSING. DEPT. OF BOTANY AND PLANT PATHOLOGY.
Effects of beta radiation from simulated fallout on the reproductive potential of a dominant plant species in a natural community, 25:42718 (ORO-3299-110)
MICHIGAN STATE UNIV., HICKORY CORNERS. W. K. KELLOGG BIOLOGICAL STATION.
Coprecipitation of phosphate with carbonates in a marl lake, 25:44252 (COO-1599-33)
Energy budget model for woodland stream ecosystems, 25:44255 (COO-2002-6)
Prog. rpt. on energetics of natural populations of freshwater macroconsumers, 1971, 25:44256 (COO-2002-10)
MICHIGAN UNIV., ANN ARBOR. DEPT. OF PATHOLOGY.
Prog. rpt. on effects of radiation and other factors on developing form and function of nervous system, comprehensive review, 1962--1971, 25:42615 (COO-1201-30)
MILLSTONE POINT CO., HARTFORD, CONN.
Millstone Nuclear Power Station, Unit 1. Generator load rejects on June 24-25, 1971, 25:44012 (DOCKET-50245-85)
MINNESOTA UNIV., MINNEAPOLIS.
Prog. rpt. on genetic control of physiological processes in higher plants, final, 1961--70, 25:42322 (COO-1097-46)
MONTREAL UNIV. (QUEBEC). LABORATOIRE DE PHYSIQUE NUCLEAIRE.
Geometrical correction factors for angular correlation measurements with Ge(Li) detectors, 25:42054 (LPN-UM-53)

N

NAGOYA UNIV. (JAPAN). INST. OF PLASMA PHYSICS.
Effect of working on change of permeability (μ) of austenitic stainless steels, 25:43467 (IPPJ-DT-20)
NAPLES UNIV. (ITALY). ISTITUTO DI FISICA TEORICA.
Inequalities for the pion--nucleon partial waves, 25:43541 (SJ-1206-249)
NATIONAL AERONAUTICS AND SPACE ADMINISTRATION, CLEVELAND, OHIO. LEWIS RESEARCH CENTER.
Effect of reactor irradiation on properties of a nongalling alloy, 25:42903 (N-71-14045)
Electrical performance of three solar thermoelectric test sections, 25:43185 (N-71-17252)
Evaluation of linear polyethylene and fiber glass reinforced epoxy for use as irradiation capsules, 25:43011 (N-71-16499)
Hot electrode drops in an unseeded supersonic argon magnetohydrodynamic generator, 25:43183 (N-71-15856)
Performance of ceramic insulator seals at high neutron and gamma fluence levels, 25:42228 (N-71-17325)
Some characteristics of a boiling-water-cooled vapor transport fuel pin, 25:44122 (N-71-17463)
Transfer function determination of primary loop of a conceptual nuclear Brayton space power plant, 25:44168 (N-71-17933)
NATIONAL AERONAUTICS AND SPACE ADMINISTRATION, GREENBELT, MD. GODDARD SPACE FLIGHT CENTER.
Average energies of ground and singly and doubly excited configurations in highly ionized atoms, 25:43069 (N-71-20535)
Ion-current response of Langmuir probes in presence of ion--atom collisions, 25:43340 (N-71-17594)
Topics in solar cosmic ray and x-ray production, 25:43057 (N-71-16749)
U-type solar radio burst originating in the outer corona, 25:43070 (N-71-21564)
NATIONAL AERONAUTICS AND SPACE ADMINISTRATION, HUNTSVILLE, ALA. GEORGE C. MARSHALL SPACE FLIGHT CENTER.
Contributions to x-ray physics in space, 25:43079 (N-71-20472)
Three investigations of the interstellar medium, 25:43080 (N-71-21563)
NATIONAL AERONAUTICS AND SPACE ADMINISTRATION, LANGLEY STATION, VA. LANGLEY RESEARCH CENTER.
Effect of radiation on cerium-doped solar-cell cover glass, 25:43008 (N-71-12278)
NATIONAL AERONAUTICS AND SPACE ADMINISTRATION, MOFFETT FIELD, CALIF. AMES RESEARCH CENTER.
Extension of Frost's mixture rule to include effects of multiple ionization on electrical conductivity, 25:43352 (N-71-18715)
Hypervelocity oxidation tests of thoria dispersed nickel--chromium alloys, 25:42805 (N-71-20390)
NATIONAL BUREAU OF STANDARDS, WASHINGTON, D. C.
High-dispersion spectral analysis of Ba II star HD 204075, 25:43019 (NBS-MON-119)
Index of U. S. voluntary engineering standards, 25:41961 (NBS-SPEC. PUBL-329)
Selected values of chemical thermodynamic properties, 25:41625 (NBS-TN-270-5)
NATIONAL INST. FOR METALLURGY, JOHANNESBURG (SOUTH AFRICA).
Determination of acid-soluble, acid-insoluble, and total uranium in silicate ores, 25:41723 (NIM-1077)
NATIONAL OCEAN SURVEY, ROCKVILLE, MD.
Aleutian seismic program seismological bulletin, 12/70, 25:44239 (CGS-746-114)
NAVAL RESEARCH LAB., WASHINGTON, D. C.
Analysis of radiation-induced embrittlement gradients on fracture characteristics of thick-walled pressure vessel steels, 25:42841 (CONF-710512-8)
NEBRASKA UNIV., LINCOLN. DEPT. OF FOOD SCIENCE AND TECHNOLOGY.
Prog. rpt. on study of control of public health problems using irradiation, annual, 5/69--4/70, 25:42744 (COO-2038-2)
NEDERLANDS ATOOMFORUM, THE HAGUE.
Conference on non-destructive testing of nuclear power reactor components, Rotterdam, 2/70, 25:44084 (CONF-700224)
NEVADA OPERATIONS OFFICE (AEC), LAS VEGAS. OFFICE OF EFFECTS EVALUATION.
Bibliography on seismology, aftershocks, and related phenomena associated with underground nuclear explosions, 25:41951 (NVO-87)
NEW HAMPSHIRE UNIV., DURHAM.
$\pi^+ + p \rightarrow \Delta^{++}(1236) + \pi^0$ AT 1.85 to 2.09 GeV: study of s- and t-channel effects, 25:43551 (UCR-34-P-107-B-108)
NEW SOUTH WALES UNIV., KENSINGTON (AUSTRALIA).
Prog. rpt. on radiation health and safety, annual, 12/31/70, 25:42369 (NP-18905)
NEW YORK UNIV., N. Y. INST. OF ENVIRONMENTAL MEDICINE.
Prog. rpt. on radioactivity studies. I, annual, 9/69--8/70, 25:42245 (NYO-3086-10(Vol.1))
Prog. rpt. on spatial distribution of radon daughter and ^{239}Pu alpha lung dose based on experimental energy absorption measurements, 12/70--6/71, 25:42354 (NYU-4256-1)
NIAGARA MOHAWK POWER CORP., SYRACUSE, N. Y.
Nine Mile Point Nuclear Station, Unit No. 1. Technical specifications and bases for operation at 1850 thermal megawatts, 25:44035 (DOCKET-50220-65)
NORTH CAROLINA STATE UNIV., RALEIGH. DEPT. OF MECHANICAL AND AEROSPACE ENGINEERING.
Nonequilibrium plasma boundary layer over a cathode, 25:43361 (N-71-12679)
NORTH CAROLINA UNIV., CHAPEL HILL.
Prog. rpt. on effects of ionizing radiation on plant species, populations and ecosystems, 9/70--8/71, 25:42316 (ORO-3299-107)
NORTH CAROLINA UNIV., CHAPEL HILL. DEPT. OF BOTANY.
Effects of beta radiation from simulated fallout on the reproductive potential of a dominant plant species in a natural community, 25:42718 (ORO-3299-110)
NORTH TEXAS STATE UNIV., DENTON.
Crystal and molecular structures of tri-(p-fluorophenyl)-amine and tri-(p-iodophenyl)-amine, 25:44256 (TID-25742)
NORTHERN STATES POWER CO., MINNEAPOLIS, MINN.
Monticello Nuclear Generating Plant, Unit 1. Report of occurrences, 25:44019 (DOCKET-50263-75)
NORTHWESTERN UNIV., EVANSTON, ILL.
Limitations in applying mass spectrometry to high-temperature equilibrium studies, 25:44242 (COO-1147-35)
NUCLEAR FUEL SERVICES, INC., WEST VALLEY, N.Y.
West Valley Reprocessing Plant. Proposed change in technical specifications for Operating License CSF-1, 25:41891 (DOCKET-50201-74)

O

OAK RIDGE ASSOCIATED UNIVERSITIES, INC., TENN. MEDICAL DIV.
Prog. rpt., annual, 1970, 25:42549 (ORAU-112)
Radiation effects and related topics, 25:42586 (ORAU-113, pp 4-77)
Research in nuclear medicine, 25:42587 (ORAU-113, pp 78-133)
OAK RIDGE GASEOUS DIFFUSION PLANT, TENN.
Internal rarefied gas flows with backscattering. I, 25:44262 (K-1798(Pt.1))
Internal rarefied gas flows with backscattering. IV, 25:44263 (K-1798(Pt.4))
Internal rarefied gas flows with backscattering. V, 25:44264 (K-1798(Pt.5))
OAK RIDGE NATIONAL LAB., TENN.
/sup 99m/Tc and gallium in medicine, 25:42550 (ORNL-TM-2091(Suppl.2))
Analytical basis for notch sharpening by fatigue, 25:42843 (CONF-710512-10)
Biological concentration and turnover of radionuclides in food chains: a bibliography, 25:42315 (ORNL-NSIC-65)
Blascon: an exploding pellet fusion reactor, 25:43358 (ORNL-TM-3231)
Calibration of Bonner ball neutron detectors used at Tower Shielding Facility, 25:42055 (ORNL-TM-3465)
Code for linear modeling of an ecosystem, 25:44278 (ORNL-IBP-71-2)
Differential cross sections at forward angles for hydrogen and helium particles from 62-MeV protons incident on ^{60}Ni, 25:43833 (ORNL-4698)
Discussion of SwRI model parametric tests, 25:42848 (ORNL-TM-3313)
Effect of fillets on stress concentrations in cylindrical

XUM

shells with step changes in outside diameter, 25:41959 (CONF-710512-15)
Effect of heat treatment and impurities on the current density of transition metal superconductors, 25:43290 (ORNL-4703)
Engineering-scale demonstration of the sol-gel process: preparation of 100 kg of ThO_2-UO_2 microspheres at the rate of 10 kg/day, 25:42937 (ORNL-4544)
Experimental and finite element stress analysis of a thin-shell cylinder-to-cylinder model, 25:42839 (CONF-710512-3)
Fuel element development for the Gas-Cooled Fast Breeder Reactor. Part I. Sealed fuel rod design, 25:44125 (ORNL-TM-3427)
Geometric programming algorithm, 25:44276 (ORNL-4650)
HFIR core nuclear design, 25:44159 (ORNL-4621)
In-reactor restructuring temperatures and kinetics for $(U,Pu)O_2$, 25:44124 (ORNL-TM-3397)
Index to nuclear safety, 25:44141 (ORNL-NSIC-86)
Information scanning and processing at NSIC, 25:44280 (ORNL-NSIC-48)
Interpretations of the drop weight test in terms of strain tolerance (gross strain) and fracture mechanics, 25:42847 (ORNL-TM-3247)
Kinetic models for the synthesis of (U,Pu)O/sub 2-y/ by hydrogen-reduction and carbothermic techniques, 25:41779 (ORNL-TM-3358)
Neutron energy-dependent capture gamma-ray yields in tantalum and tungsten, 25:43890 (ORNL-TM-3436)
Numerical calculation of elastic properties for straight dislocations in anisotropic crystals, 25:44282 (ORNL-TM-3408)
Observations of fuel-cladding chemical interactions as applied to GCBR fuel rods, 25:44123 (ORNL-TM-3385)
ORTHIS, ORTHAT: two computer programs for solving two-dimensional steady-state and transient heat conduction problems, 25:41985 (ORNL-TM-3324)
Performance characteristics of a short reentry tube steam generator at low steam output, 25:41962 (ORNL-TM-3236)
Preparation of data sets in ENDF format for Na, Mg, Cl, and K for use in shielding calculations, 25:43420 (ORNL-TM-3429)
Prog. rpt. on civil defense research project, 3/69--3/70, 25:42506 (ORNL-4556(Pt.1))
Prog. rpt. on environment and technology assessment, 6--12/70, 25:44279 (ORNL-NSF-EP-3)
Prog. rpt. on isotopic power fuels, 3/31/71, 25:41993 (ORNL-4692)
Prog. rpt. on molecular anatomy program, semiannual, 9/70--2/71, 25:44277 (ORNL-4683(Pt.1))
Prog. rpt. on Oak Ridge Research Reactor, 1--3/71, 25:44160 (ORNL-TM-3481)
Recent developments in the shielding of neutron sources, 25:43418 (ORNL-RSIC-32)
Review of ORNL electromagnetic separations program, 1968--69, 25:41992 (ORNL-4540)
RMIC bulletin and status report, 25:44281 (ORNL-RMIC-11)
Room temperature measurements of electrical resistivity and thermal conductivity of various graphites, 25:44283 (ORNL-TM-3477)
Study of the overlap conditions required in sequential discrete ordinates transport calculations for a 14-MeV neutron source in a 5000-m radius cylinder of air, 25:43419 (ORNL-TM-3269)
Thermal analysis of national radioactive waste repository: brief summary of results obtained through April 1971, 25:42038 (ORNL-TM-3426)

OESTERREICHISCHE STUDIENGESELLSCHAFT FUER ATOMENERGIE G.M.B.H., SEIBERSDORF. INSTITUT FUER REAKTORTECHNIK.
Energy generation and the environment, 25:44143 (SGAE-RT-39/1971)

OHIO STATE UNIV., COLUMBUS. DEPT. OF METALLURGICAL ENGINEERING.
Prog. rpt. on mechanisms of stress corrosion cracking in iron--nickel--chromium alloy system in chloride environments, 4--6/70, 25:42760 (COO-2069-7)

OHIO STATE UNIV. RESEARCH FOUNDATION, COLUMBUS.
Prog. rpt. on high energy physics studies, Pt. I and II, 7/1/71, 25:43566 (COO-1545-99)

OREGON STATE UNIV., CORVALLIS. DEPT. OF GENERAL SCIENCE.
Metabolism of ^{131}I in two amphibian species (Taricha granulosa and Rana pipiens), 25:44288 (RLO-2227-T-8-1)

OSAKA UNIV. (JAPAN). LAB. OF NUCLEAR STUDIES.
Annual report, 1--12/70, 25:43732 (OU-LNS-71-2)

P

PACIFIC GAS AND ELECTRIC CO., SAN FRANCISCO, CALIF.
Humboldt Bay Power Plant, Unit No. 3. Annual average offsite exposures below limits defined in 10 CFR 20, 25:44003 (DOCKET-50133-58)
Humboldt Bay Power Plant, Unit No. 3. Final safety analysis report, Suppl, 25:44026 (DOCKET-50133-59)

PACIFIC NORTHWEST RESEARCH FOUNDATION, SEATTLE, WASH.
Prog. rpt. on effects of ionizing radiation on the testicular function of man, annual, 8/70--7/71, 25:42674 (RLO-1780-32)

PACIFIC NORTHWEST WATER LAB., CORVALLIS, OREG.
Guidelines: biological surveys at proposed heat discharge sites, 25:44269 (NP-18643)

PANAMETRICS, INC., WALTHAM, MASS.
Prog. rpt. on ultrasonic thermometry in LMFBR systems, 3/69, 25:42189 (NYO-3905-6)

PARIS UNIV. (FRANCE).
Oxidation resistant zirconium alloys in carbon dioxide at high temperatures, 25:42803 (CEA-R-4103)

PARIS UNIV., ORSAY (FRANCE).
Behavior of fission products in nuclear fuels, 25:44206 (CEA-R-4181)
Study of structure of physisorbed phases by thermodynamic analysis of stepwise isotherms of Kr, Xe, Ar, and methane on cleavage face of halides having a layer-like structure, 25:41824 (CEA-R-4089)

PARIS UNIV., ORSAY (FRANCE). FACULTE DES SCIENCES.
Reaction (p,px) with light nuclei at 156 MeV, 25:43800 (NP-18880)

PARIS UNIV., ORSAY (FRANCE). LABORATOIRE DE L'ACCELERATEUR LINEAIRE.
Backward electron deuteron scattering below 280 MeV, 25:43528 (LAL-1250)

PENNSYLVANIA STATE UNIV., UNIVERSITY PARK. DEPT. OF BIOPHYSICS.
Action of ionizing radiation on sensitive strains of Escherichia coli B, 25:42728 (NYO-2804-39)
Action of ionizing radiation on the molecular biology of E. coli, 25:42727 (NYO-2804-38)
Effects of ionizing radiation on capacity of Escherichia coli to support bacteriophage growth, 25:42730 (NYO-2804-41)
Strain of Escherichia coli resistant to DNA degradation induced by ionizing radiation, 25:42729 (NYO-2804-40)
Sucrose gradient analysis of DNA in irradiated cells of PHH1, 25:42731 (NYO-2804-42)

PENNSYLVANIA STATE UNIV., UNIVERSITY PARK. MATERIALS RESEARCH LAB.
Prog. rpt. on role of trapping processes in solid state radiation dosimetry, final, 5/71, 25:42162 (NYO-3409-10)

PHILADELPHIA ELECTRIC CO., PA.
Limerick Generating Station, Units 1 and 2. Preliminary safety analysis report, amendment 9, 25:44061 (DOCKET-50352-15)
Peach Bottom Atomic Power Station, Unit 1. Emergency rod batteries: status report, 25:44032 (DOCKET-50171-89)
Peach Bottom Atomic Power Station, Unit 1. Monthly operations report No. 63, May 1971, 25:44004 (DOCKET-50171-90)
Peach Bottom Atomic Power Station, Unit 1. Thermally released shutdown absorber rods, 25:44033 (DOCKET-50171-91)

PHYSICS INTERNATIONAL CO., SAN LEANDRO, CALIF.
Theoretical ground motion predictions supporting HEST program, 25:41950 (AD-718388)

PITTSBURGH UNIV., PA. DEPT. OF PHYSICS.
Exact screened calculations of atomic-field pair production and low energy screening, 25:43417 (NYO-3829-71)
Mass spectrometer observation of NO in auroral arc, 25:43218 (N-71-18997)

PITTSBURGH UNIV., PA. SPACE RESEARCH COORDINATION CENTER.
Differential electron flux as determined by aurcral observations of N_2^+ and N_2^+ systems, 25:43214 (N-71-16589)

POWER REACTOR DEVELOPMENT CO., DETROIT, MICH.
Enrico Fermi Atomic Power Plant, Unit 1. [Operations] report, February 1971, 25:44001 (DOCKET-50016-121)
Enrico Fermi Atomic Power Plant, Unit 1. [Operations] report, March 1971, 25:44002 (DOCKET-50016-122)

PRINCETON UNIV., N. J. GUGGENHEIM LABS. FOR THE AEROSPACE PROPULSION SCIENCES.
Cathode region of a quasi-steady magnetoplasmadynamic arcjet. VIII, 25:43353 (N-71-19984)

PRINCETON UNIV., N. J. PLASMA PHYSICS LAB.
Broadband power density monitor for pulsed microwave sources, 25:42188 (MATT-845)
Consideration of power requirement in fusion feasibility experiment, 25:43333 (MATT-803)
Large superconducting magnet designs for fusion reactors, 25:43397 (MATT-848)
Steam conditions in a catalyzed D reactor, 25:43396 (MATT-804)

PUBLIC SERVICE CO. OF COLORADO, DENVER.
Fort St. Vrain Nuclear Generating Station, [Unit 1]. Preliminary safety analysis report, amendment 22 (includes additions and revisions to final safety analysis report), 25:44047 (DOCKET-50267-32)

PUBLIC SERVICE ELECTRIC AND GAS CO., NEWARK, N.J.
Newbold Island Nuclear Generating Station, Units 1 and 2. Preliminary safety analysis report, Amendment 8, 25:44062 (DOCKET-50354-15)

PUERTO RICO NUCLEAR CENTER, MAYAGUEZ.
Program for Fasciola hepatica in Puerto Rico, 1/70--4/71, 25:42246 (PRNC-148)
The Rain Forest Project. Annual report, 25:42317 (PRNC-147)

PUERTO RICO WATER RESOURCES AUTHORITY, SAN JUAN.
Aguirre Nuclear Plant, Unit No. 1. Criteria previously adopted are responsive to General Design Criterion 2, 25:44068 (DOCKET-50376-16)
Aguirre Nuclear Plant, Unit No. 1. Preliminary facility description and safety analysis report, Amendment 7,

25:44069 (DOCKET-50376-18)
PURDUE UNIV., LAFAYETTE, IND.
Coherent production of high mass meson states in π⁺d collisions at 13 GeV/c, 25:43550 (COO-1428-290)
Evidence for a Kπ resonance near 1750 MeV/c², 25:43546 (COO-1428-279)
Evidence for splitting in the Q region of K⁺π⁺π⁻ mass, 25:43544 (COO-1428-275)
K* (890) production in the charge exchange reaction K⁺n → K⁺π⁻ at 9.1 GeV, 25:43547 (COO-1428-281)
K* (890) production in the charge exchange reaction K⁺n → K⁺π⁻p at 9 GeV/c, 25:43548 (COO-1428-283)
New evidence for splitting in the Q region of K⁺π⁺π⁻ mass, 25:43543 (COO-1428-274)
R region in 13 GeV/c π⁺ nucleon interactions, 25:43545 (COO-1428-277)
PURDUE UNIV., LAFAYETTE, IND. DEPT. OF CHEMISTRY.
Effect of an electric field on gas chromatographic retentions by liquid crystals, 25:44245 (COO-1222-47)
Effect of loading on separation efficiency using steric exclusion chromatography, 25:44244 (COO-1222-46)
Precision flow-monitoring spectrometer with low noise and high stability, 25:44243 (COO-1222-45)
Prog. rpt. on fundamental studies on separation processes, annual, 7/71, 25:44248 (COO-1222-50)
Specification of gas chromatographic behavior using Kovats indices and Rohrschneider constants, 25:44247 (COO-1222-49)
Steric-exclusion chromatography at pressures up to 3500 kg/cm², 25:44246 (COO-1222-48)
PURDUE UNIV., LAFAYETTE, IND. DEPT. OF HORTICULTURE.
Effects of gamma-irradiation on DNA transcription and RNA translation in plants, 25:42716 (COO-1313-29)
Partial purification of tRNA and leucyl-tRNA synthetase from sugar beet root, 25:44249 (COO-1313-27)
Protein synthesis in germinating seeds, 25:44250 (COO-1313-28)
PURDUE UNIV., LAFAYETTE, IND. DEPT. OF PHYSICS.
Final states with three charged particles and a visible anti K⁰ from K⁻d interactions at 4.5 GeV/c, 25:43549 (COO-1428-286)

Q

QUEEN'S UNIV., BELFAST (NORTHERN IRELAND). DEPT. OF APPLIED MATHEMATICS AND THEORETICAL PHYSICS.
Physics of upper atmosphere, 25:43207 (AD-706130)
QUEEN'S UNIV., KINGSTON (ONTARIO).
Abstracts of papers to be presented at fifteenth Canadian high polymer forum, Kingston, Ontario, Canada, 9/69, 25:41842 (CONF-690977-(Absts.))

R

REACTOR CENTRUM NEDERLAND, PETTEN.
120,000 shp nuclear ship propulsion study, 25:44178 (RCN-139)
RENSSELAER POLYTECHNIC INST., TROY, N. Y.
Prog. rpt. on Linear Accelerator Project, 10--12/70, 25:43834 (RPI-328-209)
RENSSELAER POLYTECHNIC INST., TROY, N.Y. PLASMA DYNAMICS LAB.
Prog. rpt. on instabilities and turbulence in highly ionized plasmas in a magnetic field, semiannual, 3--8/70, 25:43385 (N-71-12892)
ROCHESTER GAS AND ELECTRIC CORP., N. Y.
Robert Emmett Ginna Nuclear Power Plant, Unit No. 1. Citation alleging noncompliance with action of the technical specifications, 25:44038 (DOCKET-50244-74)
Robert Emmett Ginna Nuclear Power Plant, Unit No. 1. Failure of main steam isolation valve to close, 25:44011 (DOCKET-50244-73)
Robert Emmett Ginna Nuclear Power Plant, Unit No. 1. Final facility description and safety analysis report, Suppl. 14, 25:44037 (DOCKET-50244-72)
ROCHESTER UNIV., N. Y. DEPT. OF PHYSICS AND ASTRONOMY.
Single-particle distributions of π-mesons produced in π⁺p, K⁺p, pp, and π⁻p collisions at high energies, 25:43554 (UR-875-340)
ROCHESTER UNIV., N. Y. DEPT. OF RADIATION BIOLOGY AND BIOPHYSICS.
Effects of epsilon-amino-n-caproic acid on radiation-induced increase in capillary permeability and subsequent pathology in skin, 25:42617 (UR-49-1462)
ROENTGEN TECHNISCHE DIENST N. V., ROTTERDAM (NETHERLANDS).
Conference on non-destructive testing of nuclear power reactor components, Rotterdam, 2/70, 25:44084 (CONF-700224)
Radiographic capacities of the RTD-LINAC 8 MeV linear accelerator, 25:44113 (CONF-700224-, Paper 8)
Ultrasonic and other non-destructive testing methods for tube joints used in heat exchangers, 25:44148 (CONF-700224-, Paper 4)
Ultrasonic inspection of welds in nuclear reactor pressure vessels, 25:44111 (CONF-700224-, Paper 6)
ROTTERDAMSCHE DROOGDOK MAATSCHAPPIJ N.V. (NETHERLANDS).
Conference on non-destructive testing of nuclear power reactor components, Rotterdam, 2/70, 25:44084 (CONF-700224)
Influence of engineering inspection standards on the manufacture of nuclear reactor pressure vessels, 25:44110 (CONF-700224-, Paper 5)
ROYAL ARMAMENT RESEARCH AND DEVELOPMENT ESTABLISHMENT, FORT HALSTEAD (ENGLAND).
Radiographic examination of heavy-wall pressure vessels: choice of source of radiation, 25:44112 (CONF-700224-, Paper 7)
RURAL COOPERATIVE POWER ASSOCIATION, ELK RIVER, MINN.
Elk River Reactor. Revised technical specifications (dismantling and maintenance), 25:44023 (DOCKET-1151-44)
RUTGERS - THE STATE UNIV., NEW BRUNSWICK, N. J. INST. OF MICROBIOLOGY.
Prog. rpt. on role of the carrier in antibody formation, annual, 6/70--6/71, 25:44274 (NYC-3707-7)

S

SAN DIEGO GAS AND ELECTRIC CO., CALIF.
San Onofre Nuclear Generating Station, Unit 1. Semiannual operating report No. 8, January 1--June 30, 1971, 25:44005 (DOCKET-50206-114)
SANDIA LABS., ALBUQUERQUE, N. MEX.
On artificial viscosity, 25:44291 (SC-RR-710301)
SID controller program: CDC 160A computer program, 25:44290 (SC-DR-68-814)
SAXTON NUCLEAR EXPERIMENTAL CORP., PA.
Saxton Reactor. License No. DPR-4; technical specifications change request No. 48, 25:44029 (DOCKET-50146-85)
Saxton Reactor. License No. DPR-4; technical specifications change request No. 47, 25:44028 (DOCKET-50146-84)
Saxton Reactor. Quality assurance program, 25:44027 (DOCKET-50146-82)
SCRIPPS INSTITUTION OF OCEANOGRAPHY, LA JOLLA, CALIF.
Autonomous deep-sea cine system, 25:44308 (UCSD-34-P-127-10)
SMITHSONIAN ASTROPHYSICAL OBSERVATORY, CAMBRIDGE, MASS.
Abundance analysis of stars in spectral range B5 through G2, 25:43018 (N-71-19301)
SOCIETE BELGE POUR NUCLEAIRE, BRUSSELS.
Study of head-end problem in nuclear fuel reprocessing, 25:41892 (EUR-4353)
SOCIETY FOR ANALYTICAL CHEMISTS OF PITTSBURGH, PA.
Conference (Pittsburgh) on analytical chemistry and applied spectroscopy, Cleveland, Ohio, 2/28--3/5/71, 25:41720 (CONF-710207-(Absts.))
Conference on analytical chemistry and applied spectroscopy, Cleveland, Ohio, 3/70, 25:41719 (CONF-700303-(Absts.))
SOUTH CAROLINA ELECTRIC AND GAS CO., COLUMBIA.
Virgil C. Summer Nuclear Station, Unit 1. Application for license, 25:44071 (DOCKET-50395-1)
Virgil C. Summer Nuclear Station, Unit 1. Environmental report, 25:44072 (DOCKET-50395-2)
Virgil C. Summer Nuclear Station, Unit 1. Preliminary safety analysis report, Vol. 3, 25:44075 (DOCKET-50395-5)
Virgil C. Summer Nuclear Station, Unit 1. Preliminary safety analysis report, Vol. 2, 25:44074 (DOCKET-50395-4)
Virgil C. Summer Nuclear Station, Unit 1. Preliminary safety analysis report, Vol. 6, 25:44078 (DOCKET-50395-8)
Virgil C. Summer Nuclear Station, Unit 1. Preliminary safety analysis report, Vol. 1, 25:44073 (DOCKET-50395-3)
Virgil C. Summer Nuclear Station, Unit 1. Preliminary safety analysis report, Vol. 5, 25:44077 (DOCKET-50395-7)
Virgil C. Summer Nuclear Station, Unit 1. Preliminary safety analysis report, Vol. 4, 25:44076 (DOCKET-50395-6)
SOUTH CAROLINA UNIV., COLUMBIA. COLL. OF ENGINEERING.
Prog. rpt. on powder metallurgy compaction, 3/71--5/71, 25:44292 (SRO-475-11)
SOUTHERN CALIFORNIA EDISON CO., LOS ANGELES.
San Onofre Nuclear Generating Station, Unit 1. Provisional operating license No. DPR-13, amendment 24. Quality assurance program, 25:44034 (DOCKET-50206-115)
San Onofre Nuclear Generating Station, Unit 1. Semiannual operating report No. 8, January 1--June 30, 1971, 25:44005 (DOCKET-50206-114)
SOUTHWEST RESEARCH INST., SAN ANTONIO, TEX.
In-service inspection of nuclear plants, 25:44109 (CONF-700224-, Paper 2)
Ultrasonic inspection of selected welds in stainless steel primary steam piping in Elk River Power Plant, 6/66, 25:44082 (SWRI-1228-9-10)
SOUTHWEST RESEARCH INST., SAN ANTONIO, TEX. DEPT. OF MATERIALS ENGINEERING.
Investigation of cracking in nuclear reactor primary piping system, 25:42838 (CONF-710512-1)
SOUTHWESTERN RADIOLOGICAL HEALTH LAB., LAS VEGAS, NEV.
¹³¹I transport through the air--forage--cow--milk system using an aerosol mist (Project Rainout), 25:42370 (SWRHL-43-r)
SPACE DISTURBANCES LAB., BOULDER, COLO.
High-altitude nuclear detection studies. I, 25:41932

(AD-719619)
High-altitude nuclear detection studies. II, 25:41933 (AD-719620)
SPECTROSCOPY SOCIETY OF PITTSBURGH, PA.
Conference (Pittsburgh) on analytical chemistry and applied spectroscopy, Cleveland, Ohio, 2/28--3/5/71, 25:41720 (CONF-710207-(Absts.))
Conference on analytical chemistry and applied spectroscopy, Cleveland, Ohio, 3/70, 25:41719 (CONF-700303-(Absts.))
STANFORD UNIV., CALIF. INST. FOR PLASMA RESEARCH.
Structure of the chromosphere--corona transition region, 25:43068 (N-71-19294)
Three-wave interaction in a beam--plasma system, 25:43407 (N-71-18696)
STANFORD UNIV., CALIF. RADIOSCIENCE LAB.
Polar substorm related traveling ionospheric disturbances based on columnar electron content measurements, 25:43217 (N-71-18502)
SUNDSTRAND AVIATION-ROCKFORD, ILL.
Bearing Investigation, 25:44289 (SAN-651-129)
SWEDISH NUCLEAR INDUSTRY GROUP, STOCKHOLM.
Sensitivity of uranium and separative work requirements to variations in reactor programs, 25:44127 (CONF-700903-17)
SYRACUSE UNIV., N. Y. DEPT. OF PHYSICS.
Crossing and positivity properties of partial waves. a review, 25:43711 (SU-1206-243)
Inelastic Compton scattering inequalities in quark-Parton model, 25:43586 (SU-1206-250)
Inequalities for the pion--nucleon partial waves, 25:43641 (SU-1206-249)
Note on the most probable number of partons in parton models, 25:43585 (SU-1206-246)

T

TECHNISCHE HOCHSCHULE, AACHEN (WEST GERMANY).
Phonons and librons in solid hydrogen and deuterium, 25:44251 (JUL-734-FF)
TECHNISCHE HOCHSCHULE, AACHEN (WEST GERMANY). PHYSIKALISCHES INSTITUT (III).
Possibility of CPT violation in neutral kaon decay, 25:43656 (PITHA-44)
TECHNISCHE HOGESCHOOL, DELFT (NETHERLANDS).
Safety aspects and future role of engineering inspection of nuclear power reactor components, 25:44136 (CONF-700224-, Paper 1)
TENNESSEE UNIV., KNOXVILLE.
Electron paramagnetic resonance and optical absorption studies of color centers and impurity ions in CaF_2 and MgF_2, 25:44297 (TID-25746)
Prog. rpt. on enzymology and regulation of cysteine metabolism in microorganisms, final, 4/68--7/70, 25:44285 (ORO-3082-6)
TEXAS UNIV., AUSTIN.
More simulated extensive air showers with a medium-strong interaction, 25:43647 (ORO-3992-61)
TUEBINGEN UNIV. (WEST GERMANY). INSTITUT FUER THEORETISCHE PHYSIK.
Monte Carlo Model for linear parameter variation, 25:43504 (BMBW-FBK-70-32)

U

UNION CARBIDE CORP., OAK RIDGE, TENN. COMPUTING TECHNOLOGY CENTER.
Evaluation of IBM Project Management System/360, Version 3, 25:44258 (CTC-INF-1030)
UNION CARBIDE CORP., OAK RIDGE, TENN. NUCLEAR DIV.
Heat exchanger optimization code, 25:44265 (K-1799)
UNION CARBIDE CORP., OAK RIDGE, TENN. Y-12 PLANT.
Guidance in nuclear criticality safety, 25:44189 (Y-DR-63)
Iron--nickel--tungsten phase diagram, 25:42887 (Y-1785)
UNITED KINGDOM ATOMIC ENERGY AUTHORITY, RISLEY (ENGLAND). REACTOR GROUP.
Calculations for a large fast reactor, 25:44101 (TRG-Report-2133)
Proposal for a generalised format for the layout of data in peripheral storage, 25:44184 (EACRP-A-135, pp 38-49)
UNITED KINGDOM ATOMIC ENERGY AUTHORITY, SELLAFIELD (ENGLAND). REACTOR GROUP.
Trapping of methyl iodide at high pressure and high temperature, 25:41898 (TRG-Report-2135)
UNITED NUCLEAR CORP., ELMSFORD, N. Y. RESEARCH AND ENGINEERING CENTER.
Prog. rpt. on continuous electrochemical meter for measurement of hydrogen in sodium, Phase II, 10--12/69, 25:42207 (UNC-5258)
UNITED STATES-EURATOM FAST REACTOR EXCHANGE PROGRAM.
Experimental investigation of loop caused influences on parallel flow-induced vibration of fuel pins, 25:44119 (EURFNR-923)
In-pile equipment for strain measurements on nuclear fuels and structural materials, 25:44086 (EURFNR-853)
Room temperature mechanical properties and precipitation behavior of steel Incoloy and Inconel after annealing in contact with UC, 25:42844 (EURFNR-922)
Separation of vanadium on UO_2 spheres from the gaseous phase, 25:42935 (EURFNR-859)
UNIVERSIDAD NACIONAL AUTONOMA DE MEXICO, MEXICO CITY. FACULTAD DE CIENCIAS.
New classical field theory, 25:43665 (NP-18831)
Radiolysis of petroleum products: residue after distillation, 25:41853 (NP-18817)
UPPSALA UNIV. (SWEDEN). INST. OF PHYSICS.
Iterative computer method for correction of spectral data, 25:42108 (UUIP-701)
Reduction of background in NaI(Tl) scintillation spectrometer by use of Geiger anticoincidence and massive shielding, 25:42109 (UUIP-737)

V

VANDERBILT UNIV., NASHVILLE, TENN.
Prog. rpt. on deformation studies of superlattice structures, final, 3/63--8/70, 25:44286 (ORO-3091-21)
VANDERBILT UNIV., NASHVILLE, TENN. SCHOOL OF MEDICINE.
Potential use of fluorescent scanning for brain tumor identification, 25:42548 (CONF-710204-4)
VERMONT YANKEE NUCLEAR POWER CORP., RUTLAND.
Vermont Yankee Nuclear Power Station. Conformance of BWR ECCS to AEC interim acceptance criteria for light water reactors, 25:44048 (DOCKET-50271-55)
Vermont Yankee Nuclear Power Station. Preliminary safety analysis report, amendment 28 (includes additions and revisions to final safety analysis report), 25:44049 (DOCKET-50271-56)
VIRGINIA ELECTRIC AND POWER CO., RICHMOND.
Surry Power Station, Units 1 and 2. Preliminary safety analysis report, Amendment 23, 25:44051 (DOCKET-50280-43)

W

WADCO CORP., RICHLAND, WASH.
Design considerations of FFTF safety, 25:44139 (HEDL-SA-169)
Dissolution of unirradiated mechanically blended mixed oxide fast reactor fuel, 25:42954 (HEDL-SA-131)
WAIKATO UNIV., HAMILTON (NEW ZEALAND). DEPT. OF PHYSICS.
Note on the most probable number of partons in parton models, 25:43585 (SU-1206-246)
WASHINGTON UNIV., SEATTLE.
Prog. rpt. on photobiology and photochemistry of ribonucleic acids, 1--12/70, 25:42257 (RLO-2225-T-15-3)
WASHINGTON UNIV., SEATTLE. COLL. OF FISHERIES.
Prog. rpt. on low level chronic irradiation of salmon, annual, 6/24/71, 25:42516 (RLO-2225-T-2-2)
Uptake of molybdenum, marked with ^{99}Mo, by biota of Fern Lake, Washington, 25:44287 (RLO-2225-T-7-2)
WASHINGTON UNIV., SEATTLE. SCHOOL OF MEDICINE.
Regional lung water: production of localized pulmonary edema in dog, 25:44254 (COO-1653-103)
WAYNE STATE UNIV., DETROIT, MICH. DEPT. OF OCCUPATIONAL AND ENVIRONMENTAL HEALTH.
Prog. rpt. on metabolism of rare earths following inhalation, annual, 9/16/70--9/15/71, 25:44253 (COO-1630-26)
WEST VIRGINIA UNIV., MORGANTOWN. ENGINEERING EXPERIMENT STATION.
Prog. rpt. on preparation of wood--plastic combinations using gamma radiation to induce polymerization, final, 11/61--6/68, 25:41843 (ORO-2945-10)
WESTINGHOUSE ELECTRIC CORP., MADISON, PA. ADVANCED REACTORS DIV.
Design considerations of FFTF safety, 25:44139 (HEDL-SA-169)
WESTINGHOUSE ELECTRIC CORP., PITTSBURGH, PA. ASTRONUCLEAR LAB.
Determination of shielding requirements for NPTR fuel handling system, 25:44161 (WANL-TME-1895)
WESTINGHOUSE ELECTRIC CORP., PITTSBURGH, PA. NUCLEAR ENERGY SYSTEMS DIV.
Indian Point Nuclear Generating Unit No. 3. Preliminary safety analysis report, Amendment 14 (includes report: effect of tornado missiles on stored spent fuel), 25:44052 (DOCKET-50286-37)
WESTINGHOUSE RESEARCH LABS., PITTSBURGH, PA.
Fracture mechanics and nondestructive testing of brittle materials, 25:42021 (CONF-710512-2)
Fuel rod deformations: a time dependent finite element analysis on axisymmetric fuel rods, including pellet end effects (LWBR development program), 25:44126 (WERL-ELPLA-1)
WISCONSIN UNIV., MADISON.
Genetic effects of irradiation in the rat, 25:42321 (COO-697-23)

Y

YALE UNIV., NEW HAVEN, CONN.
Anisotropic interactions between magnetic ions, 25:43471 (YALE-3227-71)
Radio frequency measurements of interactions in magnetic

insulators, 25:43472 (YALE-3227-74)
Use of parameters in crystal field theory and related calculations, 25:44309 (YALE-3227-77)

YANKEE ATOMIC ELECTRIC CO., WESTBORO, MASS.
Yankee Nuclear Power Station. Quality assurance program, 25:44025 (DOCKET-50029-152)

Z

ZENTRALSTELLE FUER ATOMKERNENERGIE-DOKUMENTATION, FRANKFURT AM MAIN (WEST GERMANY).
Surface and vacuum physics index, Vol. 6, No. 5, 1971, 25:43111

XUM

PERSONAL AUTHOR INDEX

Authors' names are indexed in the form appearing in the abstracted publication. Each entry under an author's name gives the publication title and the *NSA* volume and abstract numbers. Report numbers, where applicable, are given in parentheses at the end of the entry.

Because of problems involved in the mechanical preparation of this index, all accent marks are omitted. The following changes in spelling have been introduced to reduce some of the confusion which might result from omitting the accents:

Germanic	ä	appears as ae
Germanic	ö	oe
Germanic	ü	ue
Scandinavian	ø	oe

A

AACH, Richard D., Detection of Australia antigen by radioimmunoassay, 25:42308
ABAGYAN, L. P., Results of the calculation for a standard fast reactor, 25:44194 (FEI-213)
ABBATT, J. D., Cytogenetic indicators of radiation (and other) damage--calibration: present and future practical applications, 25:42405
ABBOTT, Lorraine S., Study of the overlap conditions required in sequential discrete ordinates transport calculations for a 14-MeV neutron source in a 5000-m radius cylinder of air, 25:43419 (ORNL-TM-3269)
ABDURAZAKOV, A. A., Beta-spectrographs with permanent magnets, 25:42110
ABE, K., Portevin--Le Chatelier effect in V, 25:43486
ABE, Ryuji, Electron spin resonance of γ-irradiated triglycine selenate, 25:41854
ABOUAF, R., Auger transition and supplementary electron ejection in ionization of Al, 25:43102
ABRAHAMSON, Adolf A., Onset of atomic-subshell filling in ordinary and superheavy elements, 25:43166
ABRAHAMSON, S., Induction of translocations in mature Drosophila oocytes over a dose range of 10 to 500 roentgens of x rays (stage-14 oocyte/radiation damage), 25:42333
ABRAO, Alcidio, Ion-exchange pilot plant for the preparation of nuclear pure uranium compounds, 25:41919
ABROSIMOV, N. K., Extraction of the proton beam of the 1-GeV synchrocyclotron, 25:43752
ABSOLONOVA, O., Serum lysozyme, trypsin inhibitors, and leucocytes number level after x-ray irradiation of rabbits, 25:42543
ACCAD, Y., S and P states of the isoelectronic sequence up to Z = 10, 25:43115
ACHE, Hans J., Interactions of positrons with defects in sodium chloride crystals, 25:43453
ACKERMANN, H., Relaxation phenomena and NMR of ^{115}In, 25:43894
ADAMS, G. E., Pulse radiolysis, 25:41862
ADAMS, G. W., Measurement of the effective electron loss rates in the D region during polar cap absorption events, 25:43255
ADAMS, W. H., Perturbation theory for configuration-interaction wave functions, 25:43161
ADEEV, G. D., Parametric method for calculating Coulomb energy of certain shapes of fissionable nuclei, 25:43952 (BNL-tr-424)
ADOLPH, J. B., Photoluminescence in GaP resulting from nitrogen ion implantation, 25:43462
AGRANAT, V. Z., Permissible levels of irradiation of the organism in radioisotope diagnosis, 25:42552
AHARONY, Amnon, Damped degenerate-level ston, 25:43513
AHLEN, M. C., Determination of mass of ^{87}Y, 25:43836
AHLERS, Guenter, Depression of superfluid transition temperature in ^{4}He by heat current, 25:43286
AHMED, N., Scattering of fast neutrons of ^{238}U, 25:43898
AHN, Kyung Ja., Effects of x irradiation on HeLa cells, 25:42295
AHNSTROEM, G., Effect of hydration on the decay of radiation-induced radicals and oxygen-sensitive centers in barley seeds, 25:42296
AKABOSHI, Sanya, Mode of radioprotective action of aminothiols in HeLa S_3 cells, 25:42514
AKAISHI, Jun, Some cautionary problems of fluorometric determination of uranium, 25:41722 (JAERI-13622)
AKASOFU, S.-I., Magnetospheric substorm observations near the neutral sheet, 25:43255
AKATKIN, O. A., Organization of physico-technical laboratory of Krasnodar dispensary, 25:42500
AKATKINA, N. V., Organization of physico-technical laboratory of Krasnodar dispensary, 25:42500
AKERLOF, C. W., Largle-angle differential cross section for K$^+$p elastic scattering at 4.0 and 5.0 GeV/c, 25:43559
AKHTAR, A., Plastic deformation of zirconium single crystals, 25:42856
AKIBA, Kenichi, Effect of solvents on the adduct formation of uranyl thenoyltrifluoroacetonate with tributyl phosphate, 25:41784
AKOPYAN, S. A., Bioelectrical activity of cerebral structures of the rabbit resulting from the combined action of radial acceleration and irradiation, 25:42653
ALADATOV, A. G., Ultrastructure of fibrin in acute radiation sickness, 25:42540
ALARCON-SEGOVIA, Donato, Radioisotopic evaluation of salivary gland dysfunction in Sjoegren's syndrome, 25:42566
ALDERSON, M. R., Long term follow-up of patients with menorrhagia treated by irradiation, 25:42702
ALDERSON, P. R., Lifetimes and decays of energy levels in ^{30}Si and ^{30}P, 25:43879
ALEFELD, G., Reversed isotope dependence for hydrogen diffusion in palladium, 25:41816
ALEKSEEVSKII, N. E., Superconductivity of cold-deposited beryllium films, 25:43303
ALESSANDRINI, V., Operator approach to dual multiparticle theory, 25:43578
ALEXA, J., Ion exchange chromatography of rare earths in aqueous organic media. VIII, 25:41910
ALEXANDER, Joseph K., Gum nebula, 25:43034
ALEXANDER, K. F., Determination of the activation cross-section of short lived nuclear isomers for thermal neutrons, 25:43891 (RFP-Trans-78)
ALEXEFF, I., Simulation of pseudowaves and of plasma sheath formation about a grid, 25:43369
ALFORD, W. P., Proton states in ^{173}Lu, ^{175}Lu, and ^{177}Lu, 25:43942
ALIKHANYAN, S., Applied aspects of microbial genetics, 25:42349
ALLAART, K., Comparison between BCS and FBCS formalisms as approximations to low-seniority shell model, 25:43985
ALLADINE, F., Gamma ray sterilisation of homograft valves, 25:42758
ALLEGRINI, M., Bone deposition of ^{210}Pb(^{210}Po) and ^{90}Sr, 25:42382
ALLEMANN, R. T., Coolant blowdown studies of a reactor simulator vessel containing a simulated reactor core, 25:44133 (BNWL-1524)
ALLISON, Robert W. Jr., Method for producing a chromium activated aluminum oxide scintillator, 25:42086
ALLRED, Dorald M., Faunistic studies of arthropods at National Reactor Testing Station, Idaho, 25:44251 (COO-1559-7)
ALMAZOV, A. V., Increasing the energy of an electrostatic accelerator, 25:43756
ALTER, Harvey J., Frequency of antibody to hepatitis-associated antigen as measured by a new radioimmunoassay technique, 25:42305
ALTMAN, K. I., Criteria for the evaluation and selection of radiation-induced metabolic changes as biochemical indicators of radiation damage, 25:42400
ALTYNTSEV, A. T., Thermal explosion induced in a collisionless plasma by a relativistic electron beam, 25:43372
ALVARADO, Fray de Landa Castillo, Conductivity at high frequencies of a completely ionized plasma with ion--ion correlations, 25:43363 (NP-18805)
ALYAMOVSKII, S. I., Nature of the bond and electrical conductivity of cubic zirconium carbides and oxycarbides, 25:43491
Possibility of the existence of stable zirconium

monoxide, 25:42987
AMADO, R. D., Equivalence of ^{3}He-t and d-α cluster description of ^{6}Li, 25:43825
AMAEV, A. D., Results of loop tests on Zr-clad experimental fuel rods in the Mr reactor, 25:43010
AMANN, J. F., Isospin splitting of the giant dipole resonance in ^{60}Ni, 25:43867
AMANO, Hiroshi, Determination of radioactive impurities in ^{48}Ca sample produced by (n,γ) reaction, 25:41878 (JAERI-13579)
Impurities in radioisotopes produced by (n,γ) reaction, 25:41877 (JAERI-13545)
Inorganic ion exchanger, 25:41879 (JAERI-13726)
Studies on fundamental properties of alumina adsorbent for radioisotope production, 25:41991 (JAERI-13778)
AMATI, D., Operator approach to dual multiparticle theory, 25:43578
AMIEL, Saadia, Analytical significance of peaks and peak ratios in x-ray fluorescence analysis using a high resolution semiconductor detector. Analysis of uranium solutions by x-ray spectrometry, 25:41733
AMMANN, A. C., Final states with three charged particles and a visible anti K^{0} from K^{-}d interactions at 4.5 GeV/c, 25:43549 (COO-1428-286)
ANAGNOSTIS, C. C., Prog. rpt. on study of control of public health problems using irradiation, annual, 5/69--4/70, 25:42744 (COO-2038-2)
ANANTHARAMAN, T. R., X-ray study of cold-work and recovery in tungsten, 25:42870
ANDERSEN, A. J., Uptake and distribution of strontium in oat as influenced by the time of supply, 25:42261
ANDERSEN, S. Ry., Radiotherapy of eye diseases, 25:42596
ANDERSON, E. M., Influence of the valence-shell structure on the internal conversion coefficients of γ-radiation and on the electron density near the nucleus, 25:43953 (BNL-tr-427)
ANDERSON, James G., Measurement of OH resonance fluorescence, 25:43252
ANDERSON, James L., Cosmological constant and fundamental length, 25:43087
ANDERSON, Larry B., Sulfur dioxide measurement system, 25:41759
ANDERSON, Larry G., Xerostomia in Sjoegren's syndrome. Evaluation by sequential salivary scintigraphy, 25:42571
ANDERSON, Marianne B., Protein synthesis in germinating seeds, 25:44250 (COO-1313-28)
ANDERSON, R. Ernest, Tectonic setting of Amchitka Island, Alaska, 25:41927 (USGS-474-75(Rev.1))
ANDO, Kozo, System for determination of time-varying spectral line profiles, 25:43343
ANDREEV, I. F., Phase equilibria in the high-alumina region of the system Al_2O_3--Nb_2O_5, 25:42985
ANDREEV, S. V., Absorbed doses during radon inhalation procedures, 25:42248
ANDREEVA, O. S., Problems of radiation safety and efficacy of preventive measures in work with U enriched with ^{235}U isotope, 25:42379
ANDREJTSCHEFF, W., Lifetimes of excited states in 89-neutron nucleus ^{151}Sm, 25:43937
ANDREWS, J. T., Differences between lesions in cerebral scanning, 25:42577
Optimum measurement of ^{75}Se for pancreas scanning, 25:42578
ANDRIANOV, V. T., Radiobiophysics of the nucleoproteins, 25:42274
ANTIPOV, V. S., Determination of O and N in metals using fluxes enriched with ^{18}O and ^{15}N isotopes, 25:41748
ANTOKU, Shigetoshi, Characteristics of linear accelerator at Hiroshima University, 25:43754
ANTOLKOVICH, B., Inelastic interaction of neutrons with H and deuterium, 25:43550
ANTONI, F., Some problems on the evaluation of biochemical indicators of radiation injury, 25:42407
ANTONUCCI, L., Health physics experiences in ENEL nuclear electric centers, 25:42478
Internal contamination in vicinity of nuclear electric center at Garigliano, 25:42435
Whole-body counter at nuclear electric center at Garigliano, 25:42081
ANTYUKHOV, V. A., Pulse pile-up monitor for a precision pulse-height spectrometer with RC filters, 25:42216
ANUFRIEVA, T. A., Influence of solar activity on the post-sunset peak of heights of the equatorial F region, 25:43228
ANWAR, Mahmood, Radiation-sterilization of the Mediterranean fruit fly (Diptera: tephritidae): Comparison of spermatogenesis in flies treated as pupae or adults, 25:42751
AOKI, Takayoshi, Quasi-K quantum number in ^{152}Gd, 25:43939
APPELT, K. D., Experimental investigation of loop caused influences on parallel flow-induced vibration of fuel pins, 25:44119 (EURFNR-923)
APPLEQUIST, Jon, Conformation of poly-β-alanine in aqueous solution from proton magnetic resonance and deuterium exchange studies, 25:41807
APPLETON, B. R., Energy-loss spectra of channeled iodine and oxygen ions in gold, 25:43454
APT, K. E., Three-quasiparticle $^{15}/_{2}^{-}$ isomer in ^{127}Sb, 25:43928
ARAI, K., Activities on modular code systems in Japan, 25:44188 (EACRP-A-135, pp 59-86)
ARAI, Tatsuo, Radiotherapy of cancer of uterine cervix, 25:42595
ARAPAKI-STRAPELIAS, M., Behavior of protactinium(V) on an indicator scale, 25:41786
ARAS, Namik K., Levels in ^{101}Ru populated by decay of ^{101}Tc, 25:43899
ARATONO, Yasuyuki, Fractional extraction of Zr, Nb, and Np with tri-n-butyl phosphate, 25:41901
ARENDT, P. R., Ionosphere-gravity wave interactions during the March 7, 1970, solar eclipse, 25:43270
Studies of wavelike variations in the ionosphere, 25:43209 (AD-714993)
ARENS, J. F., Position of the plasmapause during a storntime increase in trapped position of the plasmapause during a stormtime increase in trapped energetic (E > 280 keV) electrons, 25:43264
ARGENTIERO, P. D., Single spacecraft method of estimating shock normals, 25:43235
ARIENT, M., Some biochemical changes in body fluids as indicators of radiation damage, 25:42402
ARIMA, A., Structure of ^{12}C, 25:43827
ARISTARKHOV, N. N., Pumps for circulating liquid metals, 25:41958 (CONF-700307-8)
ARIZAN, D., Action of gamma rays on bacteria used as sanitary indicators, 25:42743
ARKHIPOVA, L. D., Comparative radiosensitivity of ascites ovarian tumors and ascites lymphosarcoma of rats, 25:42637
ARKLES, L. B., Optimum measurement of ^{75}Se for pancreas scanning, 25:42578
ARMSTRONG, T. P., Statistical study of solar protons, alpha particles, and Z greater than or equal to 3 nuclei in 1967--1968, 25:43231
ARNDT, Kenneth A., Local recurrence of generalized herpes zoster following x irradiation, 25:42689
ARNDT, Richard A., Analyses of elastic proton-alpha scattering, 25:43781
Comparison of Princeton--Pennsylvania n--p scattering data by phase-shift analyses, 25:43538
ARNOLD, H., Simple beam scanning methods for low currents, 25:42098
ARP, H. C., Photometric study of metal-rich globular cluster M71, 25:43035
ARSENIN, V. V., Possibility of suppressing screw modes of hydromagnetic instability of plasma column carrying current, 25:43384 (CTO-759)
ARTERBURN, J. O., SEFOR operating experience, 25:44128 (CONF-710315-20)
ARTHUR, Jett C. Jr., ESR study of intramolecular energy transfer in the radiolysis of cellulose thenoates, 25:41836
ARUTYUNYAN, R. K., Hematological and electrocardiographical changes during radiation sickness, 25:42660
ASAKURA, Hideo, Five cases suspected of radiation myelitis, 25:42700
Radioprotective effects of adenosine derivatives, 25:42516
ASBRIDGE, J. R., Time variations of the magnetotail plasma sheet, 25:43240
ASCOLI, G., Failure of S-channel helicity conservation in A_1^- production, 25:43664 (COO-1195-204)
ASHBY, M. F., Radiation-enhanced creep, 25:42900 (AD-719905)
ASHKENAZI, A., Prevention of tumor growth by immunizing hamsters with x-irradiated, SV_{40}-transformed cells, 25:42305
ASKEW, J. R., Thermal reactors, 25:44193 (EACRP-A-135, pp 21-9)
ASPINALL, J. A., Digital subtraction technique for dual isotope scintigraphy, 25:42059
ATANASOV, A., Application of Pade approximation to problem bound states in quasipotential approach, 25:43568 (JINR-P2-5765)
ATKINS, H. L., Visualization of the human spleen with /sup 99m/Tc-labeled red blood cells, 25:42235
ATKINSON, H. H., Applications of cryogenics to high energy nuclear physics, 25:43735
ATTALLA, Albert, Lithium isotopic analysis by nuclear magnetic resonance spectrometry, 25:41724
AUBERSON, G., Violation of Pomeranchuk theorem and zeros of scattering amplitudes, 25:43576
AUBRY, Michel P., Magnetotail changes in relation to the solar-wind magnetic field and magnetospheric substorms, 25:43239
Motion and structure of the magnetopause, 25:43220 (N-71-20853)
AUCHAPT, Jacqueline, Process for decontaminating radioactive effluents, 25:41911
AUDIDIERE, Pierre, Distribution of radioactivity in the lava issuing from the cavity of a nuclear explosion, 25:41953 (CEA-R-4099)
Radioactivity distribution in environment of a contained nuclear explosion. I, 25:41954 (CEA-R-4128(1))
AURILIA, Antonio, Self-consistency in the theory of quantized fields, 25:43688
AUSBAND, John R., Radioisotope scanning for parotid oncocytoma, 25:42572
AUSLOOS, P., Solid phase photolysis and radiolysis of ethylene at 20 to 77 K, 25:41875
AUST, J. C., In vitro detection of cytotoxic cellular immunity against tumor-specific antigens by a

XUM

radioisotopic technique, 25:42309
AUVIL, P. R., Threshold zeros and the N/D method in Yukawa-potential scattering, 25:43713
AVAKYAN, K. M., Study of a streamer chamber containing xenon, 25:42149
AVAKYAN, V. A., Mutagenesis of hybrids of wheat. II, 25:42360
AVANESSOFF, M., C--H valence vibrations in hydrocarbons and butyl halides, 25:41821
Fundamental and harmonic C--H/C--D valence vibrations of halogen derivatives of methane and of deuteriomethane, 25:41822
AVGUSTINIK, A. I., Structure of alloys in system Ta--C--Re, 25:42992
AVISHAI, Y., Three-body problems in the Amado model, 25:43716
AZAD, Ahmed A., Dark repair of uv-irradiated haploid Saccharomyces carlsbergensis, 25:42725
AZATYAN, R. A., Combined effect of nitrogen yperite and gamma radiation on seeds of Crepis capillaris L, 25:42359
AZIMOV, S. A., Characteristics of coherent interactions at 17 and 45 GeV, 25:43545 (JINR-P1-5775)
AZIZBEKYAN, R. R., Repair of uv-induced mutations in phage T4, 25:42339
AZMAN, A., Vibrational normal coordinate analysis of H(D)NCO and H(D)NCS, 25:41791

B

BABA, Sumiko, Full energy peak efficiency of NaI crystal, 25:42050 (JAERI-13545)
BABAYAN, Kh. P., Description of an ionization calorimeter supplemented with proportional counters, 25:42140
BABISKIN, J., Influence of additions of a third element on the critical magnetic field of titanium--niobium alloys, 25:43309
BABU, R., Impedances of warm plasmas near the lower hybrid resonance, 25:43375
BACHELIER, Daniel, Reaction (p,px) with light nuclei at 156 MeV, 25:43800 (NP-18880)
BADEWITZ, R. C., Coherent production of high mass meson states in π^+d collisions at 13 GeV/c, 25:43550 (COO-1428-290)
R region in 13 GeV/c π^+ nucleon interactions, 25:43545 (COO-1428-277)
BADHWAR, G. D., Charged-particle observations from OSO 3, 25:43178
BAECKLIN, A., Levels in ^{191}Ir, 25:43902
BAER, H. W., New 0^+ states in ^{50}Cr, 25:43849
BAEZ, Juan N., Nondestructive testing as a factor of technical and industrial development, 25:42028
BAGGALEY, W. J., Solar cycle variation in daytime ionospheric E/sub s/ parameters in South Pacific area, 25:43255
BAGLAN, R. J., Evidence for doorway states in ^{207}Pb, ^{208}Pb, and ^{57}Fe from threshold photoneutron cross-sections measurements, 25:43929
BAGRETSOV, N. F., Physicochemical conditions for burial of radioactive waste, 25:41925 (CEA-tr-R-1979)
BAHNG, J. D. R., Rapid variations in spectrum of zeta Tauri, 25:43041
BAILEY, C. A., Advanced cryogenics, 25:43326
BAILEY, Carolyn A., Corrected fluorescence spectra by computer postprocessing, 25:44306 (UCRL-73161)
BAILEY, D. C., Lifetimes and decays of energy levels in ^{30}Si and ^{30}P, 25:43879
BAILEY, S. M., Selected values of chemical thermodynamic properties, 25:41825 (NBS-TN-270-5)
BAILLY, H., Zirconium--copper alloys used in fuel element cladding for gas-cooled heavy-water reactors, 25:42881
BAISOGOLOV, G. D., Radiation sickness in man, 25:42542
BAKER, A. R., Calculations for a large fast reactor, 25:44101 (TRG-Report-2133)
BAKER, A. T. J., Damage-sensitive cathodoluminescence of zinc telluride, 25:43450
BAKER, T. G., Radiosensitivity of mammalian oocytes with particular reference to the human female, 25:42697
BAKHANOVICH, U. I., Comparative evaluation of the effects of uranium nitrate and radioactive iodine on auto-antibody formation, 25:42645
BAKLAVADZHYAN, O. G., Bioelectrical activity of cerebral structures of the rabbit resulting from the combined action of radial acceleration and irradiation, 25:42653
BALACHANDRAN, A. P., Crossing and positivity properties of partial waves. a review, 25:43711 (SU-1206-243)
Inequalities for the pion--nucleon partial waves, 25:43641 (SU-1205-249)
Inequalities for the $\pi\pi$ partial waves from the properties of a class of orthogonal polynomials, 25:43633
Inequalities for the s- and p-wave $\pi\pi$ partial-wave amplitudes, 25:43626
BALAKRISHNAN, A. V., Conference on optimization, Nice, 6--7/69, 25:43525
BALARD, Francois, Distribution of radioactivity in the lava issuing from the cavity of a nuclear explosion, 25:41953 (CEA-R-4099)
Radioactivity distribution in environment of a contained nuclear explosion. I, 25:41954 (CEA-R-4128(1))
BALAZS, E., Collective vibrations of the statistical nuclear model, 25:43910
BALBAKOV, Dzh, Radiation-induced changes in the electrical properties of LiF monocrystals alloyed with Na, 25:43445
BALDIN, A. M., Acceleration and extraction of deuterons from JINR proton synchrotron, 25:43727 (BNL-tr-431)
BALDIN, S. A., Use of an x-ray analyzer with a semiconductor detector for elemental analysis, 25:42217
BALDINI, Mario G., Prog. rpt. on physiopathology of blood platelets, 8/70--7/71, 25:44272 (NYO-3590-7)
BALDWIN, Barrett, Ablation and breakup of large meteoroids during atmospheric entry, 25:43263
BALDWIN, N. L., Head-end separation of BISO-coated fissile and fertile particles for high-temperature gas-cooled reactors, 25:41907
Head-end separation of TRISO-coated fissile and fertile particles for high-temperature gas-cooled reactors, 25:41906
BALESTIC, Francis, Radiochemical adhesion process, 25:41846
BALIAN, Roger, Statistical quasiparticles, effective Green's functions, and Landau descriptions of quantum liquids. I. Impurity systems at equilibrium, 25:43511
BALLANCE, P. E., Use of Cherenkov inserts for counting high energy β and γ contamination samples, 25:42082
BALMUKHANOV, S. B., Comparative radiosensitivity of ascites ovarian tumors and ascites lymphosarcoma of rats, 25:42637
BALUDA, V. P., Ultrastructure of fibrin in acute radiation sickness, 25:42540
BALUKOVA, V. D., Physicochemical conditions for burial of radioactive waste, 25:41925 (CEA-tr-R-1979)
BAMBUROV, V. G., Stabilities of solid solutions of system EuO--CaO when heated in air, 25:42954
BAME, S. J., Time variations of the magnetotail plasma sheet, 25:43240
BAM-ZELIKOVICH, G. M., Acceleration of conducting gas in strong nonstationary electromagnetic fields, 25:43195
BANDER, Myron, Time-longitudinal dilations and scaling behavior of high-energy collisions, 25:43575
BANERJEE, Manoj K., Bethe Goldstone equation in finite nuclei, 25:43956 (ORO-3765-30)
BANERJEE, S. N., Separable approximation to two-body t-matrix, 25:43980
BANKERT, L., Uptake of ^{144}Ce, ^{147}Pm, and ^{238}Pu by oat plants from soils, 25:42250
BANKS, C. V., Determination of uranyl and thorium(IV) by gas chromatography of volatile mixed-ligand complexes, 25:41725
BANKS, P. M., Interplanetary hydrogen and helium from cosmic dust and the solar wind, 25:43176
BANNAYAN, George A., Effect of irradiation on the maturation of Wilms' tumor, 25:42592
BAPTISTA, A. M., Quantitative gammagraphy of thyroid gland with /sup 99m/Tc and ^{131}I, 25:42569
BAQUE, P., Zirconium alloys used in carbon dioxide at high temperatures, 25:42812
BARABASH, L. S., Circuit parameters of a spark chamber with a decoupled high-voltage electrode, 25:42150
BARAN, Elena, Some hematologic changes due to ionizing radiations, 25:42600
BARAN, Traian, Some hematologic changes due to ionizing radiations, 25:42600
BARANGER, Michel, Folded diagrams, 25:43519
BARATTA, Edmond J., Separation of calcium--strontium investigated by the use of tracers, 25:41715
BARBIER, M., Systematics of extra-nuclear hadron cascades in shields, 25:43613 (CERN-71-13)
BARD, J. J., Detection of hyperfixing zones by means of a positron camera type positron. III, 25:42565
BARDEEN, James M., Reexamination of the post-Newtonian Maclaurin spheroids, 25:43093
Relativistic disks. I. Uniform rotation, 25:43092
BARDIN, D. Yu., Determination of the mass of the muonic neutrino in radiative pion decays, 25:43609
BARGAINNIER, Roger B., Forging of powder metallurgy preforms, 25:42829
BARKAT, Zalman, Thermonuclear detonations in evolved stellar cores, 25:43033
BARKER, F. C., States of ^{8}Be from analysis of ^{7}Li(p,α)^{4}He reaction data, 25:43829
BARNA, G. J., 300-kWe Rankine cycle advanced nuclear--electric space power system, 25:44173
BARNES, C. A., Chromosome aberration following radiophosphorus treatment of polycythaemia, 25:42713
BARNES, P. D., Effect of multipole pairing and particle-hole fields in particle-vibration coupling of ^{209}Pb. II, 25:43923
BARNETT, W. E., Mutagen specificity in Neurospora crassa, 25:42352
BARNHART, H. M., Low dose gamma irradiation of bovine metmyoglobin, 25:42756
BAROCH, C. J., Effect of irradiation on the mechanical properties of 19-9DL alloy, 25:42923
Effects of irradiation on the tensile properties of Zircaloy 2 and 4 and borated stainless steel, 25:42911
BARR, R. E., Intestinal enzyme activities following whole-body irradiation in hamsters, 25:42301
BARRALL II, Edward M., Effect of an electric field on gas

chromatographic retentions by liquid crystals, 25:44245 (COO-1222-47)
BARRERA, R., Volatile radiolytic compounds in irradiated fish, 25:42753
BARRETTE, J., Geometrical correction factors for angular correlation measurements with Ge(Li) detectors, 25:42054 (LPN-JM-53)
BARRY, P. J., Dose commitment, 25:42434
BARSUKOVA, K. V., Continuous isolation of isotopically pure ^{249}Cf from ^{249}Bk, 25:41882
BARTASIUS, J., Secondary-electron emission produced by relativistic primary electrons in strong electric fields, 25:43101 (SCL-T-59-256)
BARTEL, W., Inelastic electron--proton scattering in the region of the Δ (1236) resonance, 25:43527 (DESY-71/21)
BARTH, Delbert S., ^{131}I transport through the air--forage--cow--milk system using an aerosol mist (Project Rainout), 25:42370 (SWRHL-43-r)
BARTKE, Jerzy, Collective acceleration of particles, 25:43739
BARTON, H. R. Jr., Coherent production of high mass meson states in π^+d collisions at 13 GeV/c, 25:43550 (COO-1428-290)
R region in 13 GeV/c π^+ nucleon interactions, 25:43545 (COO-1428-277)
BARTON, P. J., Structure and tensile properties of AISI Type 315 steel, 25:42919
BARUA, A. K., Angular distribution of H^+ or D^+ from electron impact dissociation of HD^+ ion, 25:43152
BARYSHEVSKII, V. G., Interference at intersection of levels, 25:43505 (JINR-P4-5786)
BASARGIN, Yu. G., Longitudinal second-order abberrations in symmetric deflecting magneto-optical systems, 25:43763
BASHANDY, E., Level structure of ^{143}Pr from γ decay, 25:43921
BASSANI, B., Late somatic effects in syngeneic radiation chimaeras. I, 25:42655
BASSE-CATHALINAT, B., Positron camera in hospital practice, 25:42564
BATES, David R., Physics of upper atmosphere, 25:43207 (AD-706130)
BATIKYAN, G. G., Chromosomal breaks induced by x radiation in seeds, 25:42356
BATOLIN, N. A., Electrical properties of liquid V_2O_5, 25:42969
BAUER, A. A., Influence of irradiation temperature on the tensile properties of stainless steel, 25:42912
BAUER, Theodore Henry, Dynamical effects of instability in rho^0 meson photoproduction and elastic scattering, 25:43604
BAUSH, P. J., Radiolytic decomposition of solid oxalic acid, 25:41859
BAUMHACKER, H., Survey of studies of laser produced plasmas at the IPP Garching, 25:43380 (IPP-4/9)
BAXTER, Philip, Pollution in our environment, 25:42383
BAYARD, J. P., CODNJC: modular system for reactor calculations, 25:44182 (EACRP-A-135, pp 5-10)
BEACHLEY, M. C., Combination of preoperative irradiation and surgery in the treatment of cancer of the oropharynx, hypopharynx, and larynx, 25:42588
BEALL, Sam E. Jr., How to make a profit on waste heat, 25:44022
BEARD, D. S., Thermionic fuel element development, 25:44170
BEARSE, R. C., Determination of mass of ^{87}Y, 25:43836
BEASLEY, T. M., Silver-108m in biota sediments at Bikini and Eniwetok Atolls, 25:42377
BEATTIE, W. H., Radiolysis of mixtures of carbon dioxide and hydrogen, 25:41852 (LA-4557)
BEATY, Earl C., Sunlight photodetachment of O_3^-, 25:43257
BECCHETTI, F. D., Coulomb displacement energies for 1f-2p shell nuclei, 25:43883
BECK, C., Positron camera in hospital practice, 25:42564
BECKERMAN, Martin, Currents describing system of interacting pseudoscalar mesons and baryons, 25:43622
BECKSTRAND, Dale Ferrin, Reactions ^{40}K(n,γ)^{41}K and ^{39}K(t,p)^{41}K, 25:43845
BEDFORD, R. G., Crystal structure of YbPt, 25:42892
BEECHEY, C. V., Evidence against a cytogenetically radioresistant spermatogonial population in male mice, 25:42355
BEESTON, J. M., Axial fatigue of irradiated stainless steels tested at elevated temperatures, 25:42921
Effect of hydrogen on the ductile properties of irradiated pressure vessel steels, 25:42871
BEIGHTLER, C. S., Optimization of nuclear materials safeguards sampling systems by dynamic programming, 25:42045
BEKEFI, G., Radiation temperature of a bounded nonthermal plasma. II, 25:43354
Radiation temperature of a bounded nonthermal plasma. I, 25:43371
BEL, L., Origins of Schwarzschild and Curzon static solutions, 25:43597
BELL, M. B., Observations of extragalactic radio sources at centimeter wavelengths, 25:43052
BELL, W. A., Review of ORNL electromagnetic separations program, 1958--59, 25:41992 (ORNL-4640)
BELL, W. K., Tables of single-particle reduced matrix elements of spherical tensors, 25:43982
BELLOBONO, I. R., Spontaneous dissolution of metals in aqueous electrolytes. I. Kinetic isotope effects in the reaction of iron with hydrochloric acid, 25:41808
BELOUS, V. A., Corrosion and electrochemical behavior of zirconium alloy, 25:42814
BENDA, K., Oxidation of Zr--0.8 percent Cu--0.8 percent Mo alloy in carbon dioxide, 25:42809
BENDALL, D. E., Shielding, 25:44107 (EACRP-A-135, pp 15-20)
BENDIXSEN, C. L., Third processing campaign in the Waste Calcining Facility, 25:41893 (IN-1474)
BENETATA, Gr., Activity of pyrophosphatase and catalase after long irradiation with small doses of ^{60}Co, 25:42277
BENNETT, A. B., Nuclear electric power sources for biomedical application, 25:41996
BENSA, R., Fluorinated polymers and nuclear industry, 25:43016
BENSCH, Friedrich, Neutron physics practices. I, 25:43775
BENSINGER, James Robert, Reaction $\pi^+ + n \rightarrow p + \gamma$ rays at 2.15 GeV/c, 25:43562
BENSON, Royal H., Liquid scintillation counting composition and process, 25:42072
Liquid scintillator compositions for counting thermal neutrons, 25:42069
Method of treating a liquid scintillator composition, 25:42071
BENZ, K. W., Delayed fluorescence and phosphorescence in pure naphthalene crystals, 25:41813
BERAN, J., Corrosion of Zr alloys in water, 25:42807
BERESTETSKII, V. B., Relativistic quantum theory, 25:43086
BERGE, Ph., Corrosion of Zr alloys in heavy water under pressure and in superheated steam, 25:42815
BERGHEANU, S., Prevention of intestinal absorption of radiocesium and radiostrontium with the help of indigenous ionic resins, 25:42263
BERGMANIS, I. A., Determination of radiation dose to children during x-ray diagnostic procedures, 25:42412
BERGMANN, Peter G., Cosmology as a science, 25:43098
BERK, H. L., Straight-line orbit approximation in periodic systems, 25:43373
BERKARDA, B., Thrombelastography of antifibrinolytica before and after irradiation with gamma rays, 25:42293
BERKE, Harry L., Prog. rpt. on metabolism of rare earths following inhalation, annual, 9/16/70--9/15/71, 25:44253 (COO-1630-26)
BERLAND, R. F., CLIP: a program to construct, update, and list the form of THREDES master data tape, 25:44095 (AI-CE-Memo-12)
BERMAN, A. S., Internal rarefied gas flows with backscattering. IV, 25:44263 (K-1798(Pt.4))
Internal rarefied gas flows with backscattering. V, 25:44264 (K-1798(Pt.5))
Internal rarefied gas flows with backscattering. I, 25:44262 (K-1798(Pt.1))
BERMAN, B. L., Evidence for doorway states in ^{207}Pb, ^{208}Pb, and ^{57}Fe from threshold photoneutron cross-sections measurements, 25:43929
BERNAGE, P., Emission spectrum of Th in 5400 to 6400 cm^{-1} region, 25:43113
BERNEY, A., Measurement of ion temperature in plasma by multichannel Fabry--Perot interferometer, 25:43341
BERNGRUBER, Walter, Excited state and cyclobutadiene intermediates in the radiation chemistry of alkynes. γ radiolysis of 2-butyne, 25:41867
BERNHEIMER, Harriet P., Synergism in immunosuppression. I. Effect of methylprednisolone, azathioprine, chlorambucil, and radiation on tetanus antitoxin production, 25:42672
BERNOW, S., Isotope shift in muonic x-rays in the tin region, 25:43904
Resonance process and intensity anomaly in muonic ^{127}I, 25:43949
BERNSTEIN, Richard B., Collision time-delay functions and quasi-bound level properties of $H_2(X^1\Sigma/\text{sub } g/^+)$, 25:43124
BERRY, Edwin X., Modification of atmospheric tritium and water vapor by Lake Tahoe, 25:41938
BERRY, J. L., Zirconium alloys used in carbon dioxide at high temperatures, 25:42812
BERRY, R. S., Crossed-molecular-beam study of collision-induced dissociation of alkali halides, 25:43131
BERTAUD, J., Problems posed by radiodermatitis, 25:42544
BERTRAND, F. E., Differential cross sections at forward angles for hydrogen and helium particles from 62-MeV protons incident on ^{60}Ni, 25:43833 (ORNL-4698)
BES, D. R., Effect of multipole pairing and particle-hole fields in particle-vibration coupling of ^{209}Pb. I, 25:43974
Effective operators and the analysis of single-nucleon transfer reactions on closed-shell nuclei, 25:43976
BESPROZVANNAYA, A. S., Geomagnetic control of the geographic distribution of noon ionization of F2 layer, 25:43227
BESSIS, Joseph, Calculation of the radiological risks arising from a reactor accident, 25:44135 (CEA-R-4136)
BESWICK, C. K., Contribution to geobotanical and geochemical prospecting for gold by activation analysis, 25:41770
BETER, E. V., Characteristics of coherent interactions at 17 and 45 GeV, 25:43646 (JINR-P1-5775)

XUM

BETTERTON, J. O. Jr., Effect of heat treatment and impurities on the current density of transition metal superconductors, 25:43290 (ORNL-4703)

BETZ, E. H., Effect of normal and irradiated marrow grafts on the hemopoietic recovery after a sublethal irradiation, 25:42544

BEUERMANN, Klaus P., Secondary electrons and photons in the upper atmosphere, 25:43235

BEUS, M., Rearrangement--fragmentation in aromatic nitration, 25:41318

BEX, Guy, Radiochemical adhesion process, 25:41845

BEYER, G. H., Metals purification by solvent extraction, 25:41917

BEZDEK, H. F., Lattice-dynamical calculations for zinc and beryllium, 25:43478

BEZVERKHOV, B. M., Universal apparatus for measuring the parameters of strong ion beams, 25:43746

BHATNAGAR, A. S., Radon measurement in soil in the exploration for U in India, 25:41945

Status of nuclear methods in the program for mineral resources development in India, 25:41947

BHATT, K. H., Structure of ^{44}Ti and the role of single-particle energies, 25:43965

BIANU-MOREA, M., Mutants of cotyledons induced by γ irradiation in Arabidopsis thaliana, 25:42358

BICHIASHVILI, A. D., Evaluation of the contribution of excitation to the formation of free radicals in the radiolysis of alkanes, 25:41859

BICHSEL, Hans, Visual phenomena noted by human subjects on exposure to neutrons of energies less than 25 million electron volts, 25:42588

BIDLINGMEYER, B. A., Steric-exclusion chromatography at pressures up to 3500 kg/cm², 25:44246 (COO-1222-48)

BIDLINGMEYER, Brian A., Precision flow-monitoring spectrometer with low noise and high stability, 25:44243 (COO-1222-45)

BIEGER, W., Investigation of an inductive plasma accelerator for propulsion purposes, 25:43351

BIFANO, William J., Electrical performance of three solar thermoelectric test sections, 25:43185 (N-71-17252)

BILAL, B. A., Continuous separation of uranium and plutonium with the help of countercurrent ion migration, 25:41908

BILLURIS, G., SEFOR operating experience, 25:44128 (CONF-710315-20)

BINGHAM, Hans Gabers Jr., Elastic scattering of deuterons and alpha particles by ^{6}Li and ^{7}Li, 25:43810

BIRGE, R. W., $\pi^+ + p \rightarrow \Delta^{++}$ (1235) + π^0 AT 1.85 to 2.09 GeV: study of s- and t-channel effects, 25:43551 (UCR-34-P-107-8-108)

Study of $\pi^+ p \rightarrow$ rho$^+ p$ at 1.85 to 2.09 GeV, 25:43552 (UCR-34-P-107-8-110)

BIRYUKOV, N. S., Decreasing ion cluster repetition frequency in an FEI cyclotron, 25:43742

BIRZU, I., Mechanisms of chemical radioprotection, 25:42523

BIS, Jiri, Rated parameters at power station A-1, 25:44021

BISSINGER, G. A., Mass and half-life of ^{36}K, 25:43875

BISTER, M., Use of magnetic sector fields with cylindrical symmetry as one-gap broad-range spectrographs, 25:42221

BLACK, Stuart C., ^{131}I transport through the air--forage--cow--milk system using an aerosol mist (Project Rainout), 25:42370 (SWRHL-43-r)

BLACKMON, Maurice L., Inequalities for the s- and p-wave $\pi\pi$ partial-wave amplitudes, 25:43526

BLAND, William H., Nuclear medicine. Second edition, 25:42582

BLAINE, R. A., CLIP: a program to construct, update, and list the form of THREDES master data tape, 25:44095 (AI-CE-Memo-12)

BLAKE, R. L., Resolved structure in Fe Kα x rays produced by 30-MeV ions, 25:43110

BLAKELY, J. P., Index to nuclear safety, 25:44141 (ORNL-NSIC-86)

BLAMONT, J. E., Monitoring of the Lyman alpha emission line of the Sun during the year 1969, 25:43075

BLANARIU, D., Forbush microdecreases in the cosmic-ray intensity, 25:43172

BLANCHET, J., Corrosion of Zr alloys in water and steam, 25:42810

BLAND, T. J., Bearing Investigation, 25:44289 (SAN-651-129)

BLANK, A. B., Polyhydroxy flavones as extraction reagents, 25:41738

BLANN, M., Decay of ^{109}Cd and levels of ^{109}Ag, 25:43945

Decay of /sup 96 95m/Rh and levels of ^{96}Ru, 25:43943

BLANQUET, P., Positron camera in hospital practice, 25:42564

Use of a new vector in the diagnosis of melanomas, 25:42563

BLANUSA, Maja, Comparative strontium and calcium metabolism in lactation, 25:42255

BLASEWITZ, Albert G., Status of the waste solidification demonstration program, 25:41905

BLATT, S. L., Isospin splitting of the giant dipole resonance in ^{60}Ni, 25:43867

BLEICHRODT, J. F., Infection of spheroplasts of Pseudomonas with DNA of bacteriophage PM2, 25:42273

BLOCKER, N. K., Vela V and VI solar x-ray atlas. V, 25:43066 (LA-4454(Vol.5))

BLOCKI, J., Closed shells for very heavy nuclei, 25:43936

Closed shells for very heavy nuclei, 25:43955 (IVR-1270)

BLOK, H., Unified-model calculations in some Zr isotopes, 25:43938

BLOK, J., Beta--gamma circular polarization correlation measurements on the decays of ^{203}Hg, ^{199}Au, and ^{141}Ce, 25:43941

BLOOM, E. E., Effect of fast neutron irradiation on the creep rupture properties of Type 304 stainless steel, 25:42922

BLOOM, H. J. G., Concepts in natural history and treatment of medulloblastoma in children, 25:42593

BOASE, D. G., Determination of sulfate in nitric acid--sulfuric acid mixtures, 25:41716 (AECL-3676)

BOBLETER, O., Quantitative analysis by sorption on ion exchangers, 25:41742

BODAK, O. I., System yttrium--chromium--silicon, 25:42993

BODEWES, T. J., 120,000 shp nuclear ship propulsion study, 25:44178 (RCN-139)

BODIZS, Denes, Increase of gamma radiation with neutral flux around 1-MV Van de Graaff accelerator, 25:43769

BODMER, A. R., ΛN--ΣN coupling for ΛN scattering and for Λ-particle binding in nuclear matter, 25:43648

BOEHLAND, Heinz, Phenoxides of the triad elements, 25:41780 (SC-T-713038)

BOEHM, H., Influence of neutron irradiation on the creep rupture properties of a 16Cr--13Ni steel, 25:42924

BOEKER, E., Comparison between BCS and FBCS formalisms as approximations to low-seniority shell model, 25:43985

BOESGAARD, Ann Merchant, Lithium content of Capella, 25:43036

BOFFI, S., Coherence properties of thermal neutron beam, 25:43777

BOGANOV, A. G., Reduction cycle $MO_2 + M_2O_3$ for Ce, Pr, and Tb oxides, 25:42968

BOGDANOV, V. A., Method for activating chromed surfaces for radioindicator investigation of their wear (exchange experience), 25:42018

BOHIGAS, O., Spacing and individual eigenvalue distributions of two-body random Hamiltonians, 25:43968

BOHUN, A., Physics of exoelectron emission on ionic crystals, 25:43489

BOLAND, Joseph F., Mechanical properties of uranium-base niobium alloys, 25:42851 (RFP-1703)

BOLDESCU, Gabriela, Hemorrhagic syndrome in radiation sickness. II, 25:42537

BOLOTICH, E. G., Production of zirconium dioxide from baddeleyite concentrate, 25:42942

BOLOTIN, A. B., Ecitation of the aromatic molecules by electron impact. I, 25:43127 (BNL-tr-429)

BOLT, S. E., Experimental and finite element stress analysis of a thin-shell cylinder-to-cylinder model, 25:42839 (CONF-710512-3)

BONANOS, P., Steam conditions in a catalyzed D reactor, 25:43396 (MATT-804)

BOND, Howard E., Optically variable radio source PKS 1514-24 = AP Librae, 25:43082

BOND, V. P., Counter telescope measurements of a beam of negative π mesons, 25:42141

BOND, W. D., Engineering-scale demonstration of the sol-gel process: preparation of 100 kg of ThO_2-UO_2 microspheres at the rate of 10 kg/day, 25:42937 (ORNL-4544)

BONDAR, I. A., Phase equilibria in the system Er_2O_3--GeO_2, 25:42988

Three cross sections in system CaO--Nd_2O_3--Al_2O_3, 25:42995

BONDARENKO, L. N., Angular correlation between neutron spin and electron momentum in decay of polarized neutrons, 25:43532

BONDARENKO, N. P., Conformally plane cosmological solutions of the axial symmetry, 25:43085 (ITF-71-16-P)

BONDERUP, E., Stopping power and energy straggling for swift protons, 25:43432

BONE, Larry I., Gas-phase acidities of alcohols, 25:41871

BONNOR, W. B., Spherically symmetric radiation of charge in Einstein--Maxwell theory, 25:43710

BONSEL, W. G., 120,000 shp nuclear ship propulsion study, 25:44178 (RCN-139)

BOOS, A. H., Diffusion effects during determination of ranges of recoil atoms in gases, 25:41885

BORBELY, I., Application of the nonrelativistic peripheral model to reactions between light particles, 25:43966

BORCHERT, I., Decay of ^{77}Kr, 25:43843

BORENE, Jacques, Crystal structure of curienite, $Pb(UO_2)_2(VO_4)_2 \cdot 5H_2O$, 25:43000

BORGES, M. Aranha, Dose analysis in radiotherapy, 25:42415

BORIE, E., Radiative corrections in ee'N coincidence experiments, 25:43979

BORMAN, V. D., Certain dispersion effects in molecular gases in parallel constant and alternating magnetic fields, 25:43516

BORNEMISZA-PAUPERTL, P., Experiences concerning the possibilities of low level measurements in the ATOMKI, 25:42111

BORONOW, Richard C., Comparison of two radiation therapy-treatment plans for carcinoma of the cervix. I. Personnel radiation exposure, 25:42432

BORST, W. L., Mass spectrometer observation of NO in auroral arc, 25:43218 (N-71-18997)

BORUKHOVICH, A. S., Nature of the bond and electrical conductivity of cubic zirconium carbides and

oxycarbides, 25:43491
BOSE, S. K., Space--time symmetries and the spontaneous breakdown of dilation invariance, 25:43679
BOSHARD, J. P., Inherent dosimeter for irradiated foods: papayas, 25:42438
BOSSHARD, Ch., Quantitative analysis of gas chromatograms of partially separated material mixtures, 25:41746
BOTTCHER, C., Simple model for scattering of electrons by a rotating dipole, 25:43130
BOTTURI, M., Dose distributions around linear ^{192}Ir sources, 25:42423
Dosimetry of high energy electron beams, 25:42157
Protective considerations in use of ^{192}Ir for radiotherapy, 25:42477
BOUCHEY, G. D., Optimization of nuclear materials safeguards sampling systems by dynamic programming, 25:42045
BOUCKAERT, A., Bromine metabolism after lethal x-ray irradiation of the abdomen in rats, 25:42282
BOUTET, J., Levels of ^{159}Dy obtained by decay of ^{159}Ho, 25:43944
BOUVENG, R., Excretion of deoxyribosyl compounds in urine from rats and mice after irradiation, 25:42622
BOVARD, P., Socio-psychological factors limiting the emission of radioactive effluents, 25:41948 (CEA-CONF-1733)
BOVARD, Pierre, Nuclear pollution, 25:42410
BOWLEN, D. W., Flatpack installation by single-pass reflow soldering, 25:44225 (BDX-613-326)
BOWMAN, C. D., Evidence for doorway states in ^{207}Pb, ^{208}Pb, and ^{57}Fe from threshold photoneutron cross-sections measurements, 25:43929
BOYADZHIEV, A., Strontium-90 and ^{137}Cs in some Bulgarian foodstuffs, 25:42381
BOYADZHYAN, N. G., Description of an ionization calorimeter supplemented with proportional counters, 25:42140
BOYD, A. W., Radiolysis of hydrogen sulfide at very high dose rates. The effect of SF_6, 25:41860
BOYLE, William R., Prog. rpt. on preparation of wood--plastic combinations using gamma radiation to induce polymerization, final, 11/61--6/68, 25:41843 (ORO-2945-10)
BOYNE, P. J., Neutron radiography of osseous tumours, 25:42575
BOZDUGANOV, Athanas, New potentialities of combination of radioprotection and cyclophosphamide, 25:42518
BOZOKY, Laszlo, New research opportunities with 25-MeV betatron, 25:43758
BRACK, K., Thermal spiking in high-energy bombarded silicon, 25:43455
BRADEN, C. H., Gamma--γ directional correlations in the decay of ^{125}Sb. II, 25:43927
BRADLEY, R. A., Kinetic models for the synthesis of (U,Pu)O/sub 2-y/ by hydrogen-reduction and carbothermic techniques, 25:41779 (ORNL-TM-3358)
BRADU, E.-B., Forbush microdecreases in the cosmic-ray intensity, 25:43172
BRADY, T., Hall--Post lower bound calculations for the three-nucleon system, 25:43983
BRAEUER, N., Magnetic moments of isomeric levels in the Br isotopes, 25:43841
BRAGG, P. D., Effect of near-ultraviolet light on respiratory chain of E. coli, 25:42732
BRAMATI, L., Health physics experiences in ENEL nuclear electric centers, 25:42478
BRAMBILLA, M., Parameter study for a transit time magnetic pumping experiment in a torus, 25:43332 (EUR-CEA-FC-595)
BRANDSTAEDTER, O., Variation of nonlinear parameters to compute decay-constants and their standard deviation, 25:43521
BRANDT, D., Second sound reflection on liquid He II surface, 25:43279
BRANDT, John C., Gum nebula, 25:43034
BRANKOWSKI, Jerzy, Vinca Nova: automatic unit for neutron spectrometer control, 25:42114
BRANNON, P. J., Molecular oxygen density measurements from 80 to 140 kilometers, 25:43251
BRANTLEY, L. W., 25-kWe reactor--thermoelectric power system for space stations, 25:44171
BRANUM, David R., Livermore superconducting Levitron, 25:43399 (UCRL-73076)
BRASHEAR, Richard E., Use and interpretation of the lung scan, 25:42583
BRASSARD, C., Fast counting with NaI spectrometers, 25:42127
BRAST, Neil, Alterations in serum thyrotropin (TSH) and thyroid function following radiotherapy in patients with malignant lymphoma, 25:42695
BRATU, Elisabeta, Experimental studies on tooth eruption, 25:42638
BRAUER, G., Mixed crystal phases in system ThO_2--PrO/sub x/, 25:42996
BRAUN, Hildegard, Chemical protection and cell structure, 25:42520
BRAUN, L. D., Observations of extragalactic radio sources at centimeter wavelengths, 25:43062
BRCIC, B. S., Phase relationships and crystal chemistry in systems US--CaS, US--SrS, and US--BaS, 25:43002
BREHM, R. L., Dynamics of a fast reactor with in-core thermionic converters. Fourth annual report, September 1, 1969--August 31, 1970, 25:44097 (COO-2109-5)
BREIT, G., ^{1}H(n,n)^{1}H scattering observables required for high-precision fast-neutron measurements, 25:43798
BREKHOVSKIKH, S. M., Valence state of tin and the structure of radiation defects in silicate glasses containing tin, 25:43009
BREN, J., Structure and phases of Zr alloys with Cu and Mo, 25:42898
BRENDEL, Martin, Different photodynamic action of proflavine and methylene blue on bacteriophage. I, 25:42734
BRENT, T. P., Deoxyribonuclease activity of HeLa cells specific for uv-irradiated DNA, 25:42272
BRET, Antoine, Light conductors, 25:42230
BRETSCHER, M. M., Experimental determination of the perturbation denominator in fast critical assemblies, 25:44163
BREUER, F., Bone deposition of ^{210}Pb(^{210}Po) and ^{90}Sr, 25:42382
BREUNLICH, W. H., Statistical calculation of the density of doorway states and on the problems of their experimental detection, 25:43991
BREUS, T. K., Interrelation between electron and ion temperature, 25:43229
BREWER, George R., Acceleration system for implanting ions in specimen, 25:43740
BRICARD, Jean, Existence of small negative radioactive ions coming from a ^{228}Th source, 25:43100
BRICE, Neil, Harnessing the energy in the radiation belts, 25:43271
BRIDGES, Donald Norris, Investigation of the spatially dependent reactor source transfer function with temperature feedback, 25:44204
BRIGGS, Michael H., Chemical composition of the solar system, 25:43078
BRILL, A. B., Potential use of fluorescent scanning for brain tumor identification, 25:42548 (CONF-710204-4)
BRINKMAN, C. R., Axial fatigue of irradiated stainless steels tested at elevated temperatures, 25:42921
Effect of hydrogen on the ductile properties of irradiated pressure vessel steels, 25:42871
BRINKMANN, H. F., Determination of the activation cross-section of short lived nuclear isomers for thermal neutrons, 25:43891 (RFP-Trans-78)
BRISSENDEN, R. J., Fast reactors: Flotran modular scheme, 25:44098 (EACRP-A-135, pp 30-7)
Progress of modular code development in the UKAEA, 25:44183 (EACRP-A-135, pp 11-14)
BROCKMAN, H. E., Mutagen specificity in Neurospora crassa, 25:42352
BROCKWAY, D. V., Failure of S-channel helicity conservation in A_1^- production, 25:43654 (COO-1195-204)
BRODINE, John Charles, Electromagnetic final-state interaction corrections to some semileptonic weak interactions with reference to tests of time-reversal invariance, 25:43660
BRODSKII, A. M., Photoproduction of electrons in strong electromagnetic field, 25:43606
BRODSKY, M. B., 5f magnetism in palladium--actinide solid solutions, 25:43488
BRODERSE, J. J., Survival of colony-forming units in mouse bone marrow after in vivo irradiation with D--T neutrons, x-, and gamma radiation, 25:42601
BROGLIA, R. A., Effect of multipole pairing and particle-hole fields in particle-vibration coupling of ^{209}Pb. I, 25:43974
Effective operators and the analysis of single-nucleon transfer reactions on closed-shell nuclei, 25:43976
BROKLOFF, Robert W., Method for producing a chromium activated aluminum oxide scintillator, 25:42086
BRONSON, J. D., 192-detector system for study of 3-body reactions, 25:42124
BROOKE, N. M., Multi-element analysis of glass fragments by neutron activation and the application to forensic science, 25:41758 (AWRE-O-24/71)
BROOKS, Gordon L., Nuclear reactor installation, 25:44215
BROSTE, W. B., Reaction D(d,n)^{3}He at 0° with polarized beam, 25:43789
BROWN, Donald W., Computer processing of scans using Fourier and other transformations, 25:42557
BROWN, K. S., Rearrangement--fragmentation in aromatic nitration, 25:41818
BROWN, Leonard Carlton, Utilizing penetrating radiation, 25:42180
BROWN, Norman J., Two-dimensional finite Fourier transform techniques, 25:44303 (UCRL-51046)
BROWN, William J., Brayton-B power systems: a progress report, 25:42008
BROYLES, Morris, Television contribution to genetically significant radiation dose of population, 25:42366
BRUES, Austin M., Radiation thresholds, 25:42694
BRUNS, L. E., Plutonium--uranium partitioning by a reflux extraction flowsheet, 25:41888 (ARH-SA-78)
BRYANT, F. J., Damage-sensitive cathodoluminescence of zinc telluride, 25:43460
BUBB, I. F., Gamma rays following decay of ^{85}Sr and /sup 85m/Sr, 25:43877
BUCHHOLZ, F. I., Second sound reflection on liquid He II surface, 25:43279
BUCHIN, V. A., Joule dissipation in motion of fluid with variable conductivity in nonhomogeneous magnetic field,

XUM

25:43193
BUCHLER, Jean-Robert, Thermonuclear detonations in evolved stellar cores, 25:43033
BUCKEY, Charles R., Acceleration system for implanting ions in specimen, 25:43740
BUDDE, William L., Nucleophilic substitution at tetrahedral boron. Trimethyl- and triethylamine--borane substrates, 25:41802
Nucleophilic substitution at tetrahedral boron. Trimethylamine--alkyl- and -arylborane substrates, 25:41803
BUDINGER, Thomas F., Visual phenomena noted by human subjects on exposure to neutrons of energies less than 25 million electron volts, 25:42688
BUDNEV, V. M., Electromagnetic contributions to the total cross section of hadron scattering, 25:43616
BUECHL, K., Survey of studies of laser produced plasmas at the IPP Garching, 25:43380 (IPP-4/9)
BUERGER, K. H. Jr., Low-lying levels of ^{40}Ar, 25:43872
BUESSER, F.-W., Inelastic electron--proton scattering in the region of the Δ (1236) resonance, 25:43527 (DESY-71/21)
BUETTGENBACH, S., Hyperfine structure measurements in ground states of ^{181}Ta, 25:43121
BUFFEREAU, Michel, Principle of standard samples realization in analytical chemistry: trace elements problems in Pu, 25:41718 (CEA-R-4106)
BUGRII, A. I., Dual amplitude with Mandelstam analyticity, 25:43623 (ITF-71-28-E)
BUHL, A. R., Effect of gamma radiation on LMFBR subcriticality measurements using noise analysis, 25:44103
BUIJS, Hendricus Leonardus, Field-induced spectrum of hydrogen at high resolution, 25:43120
BUIJS, K., Spectrophotometric determination of traces of americium in plutonium oxide, 25:41721 (EUR-4352)
BUKAT, Andrzej, Nb_3Sn superconducting phase identification in Nb--Sn alloys by critical temperature measurement method, 25:43288 (INR-1294)
BULATOV, B. P., Some regularities of forming gamma radiation dose fields in shielding structures and shelters, 25:43428
BULGAKOV, Yu. V., Distribution of radiation defects in silicon irradiated with fast charged particles, 25:43463
BULL, H. G., Effects of α-deuterium substitution, polar substituents, temperature, and salts on the kinetics of hydrolysis of acetals and ortho esters, 25:41900
BULLOUGH, R., Mechanism and kinetics of void growth during neutron irradiation, 25:42915
BULLOUGH, R. K., Generalized nonrelativistic Lamb-shift theory, 25:43171
BUNDE, G. W., Performance of pressure-contacted lead-telluride thermoelectric generators, 25:42001
BUNTO, T. V., Healing of radiation ulcers of skin under the influence of metacyl and dibunol (experimental research), 25:42541
BURCH, D., Resolved structure in Fe Kα x rays produced by 30-MeV ions, 25:43110
BURDANINA, N. A., Dielectric properties of γ-irradiated crystals of KH_2PO_4, 25:43443
BURDE, J., Isobaric analogue resonances in ^{127}I, ^{125}I, and ^{123}I, 25:43933
BURGESS, D. A., Variable delay gate generator for two-channel counting systems, 25:42063
BURGHARD, H. C. Jr., Investigation of cracking in nuclear reactor primary piping system, 25:42838 (CONF-710512-1)
BURKE, D. G., Proton states in ^{173}Lu, ^{175}Lu, and ^{177}Lu, 25:43942
BURKHANOV, G. S., Ternary system molybdenum--iron--carbon, 25:42889
BURKHART, Andre, Device with a large dynamic range for measuring direct currents and voltages, 25:42208
BURLAGA, Leonard F., Nature and origin of directional discontinuities in the solar wind, 25:43237
BURMAN, R., Radiation damping of electromagnetic waves in plasmas, 25:43403
BURT, David H., Deoxyribonuclease activity of HeLa cells specific for uv-irradiated DNA, 25:42272
BUSBY, M. R., Classical model for gas--surface interaction, 25:43104
BUSBY, Nancy, Segregation following interchange induced by irradiating mature oocytes of Drosophila melanogaster, 25:42276
BUSCA, G., Indirect experimental determination of photopeak efficiencies of NaI(Tl) detectors for cylindrical gaseous sources, 25:42049 (EUR-4513)
BUSCHOW, K. H. J., Lattice constants and Curie temperatures of Th--Co compounds, 25:43485
BUSELLI, G., Weak x-ray sources in the southern hemisphere, 25:43057
BUSSE, C. A., Heat pipe thermionic converter research in Europe, 25:41975
BUSSIERE, P., Radioactivation of Pt by thermal neutrons and half-life of /sup 195m/Pt, 25:41920
BUTCHER, J. W., Influence of silicon and other elements in controlling interparticle friction and sintering of beryllium powder, 25:42826
BUTLER, D. K., Modular coding for reactor calculations in the United States, 25:44185 (EACRP-A-135, pp 50-9)
BUTLER, H. E., Conference on ultraviolet stellar spectra and related ground-based observations, Lunteren, Netherlands, 6/69, 25:43031
BUTLER, Margaret K., Can the AEC complex really exchange computer systems and programs, 25:44240 (CONF-710515-1)
BYERLY, Radford Jr., Sunlight photodetachment of O_3^-, 25:43257
BYKHOVSKII, A. V., Problems of protection from ionizing radiations in radiation chemistry, 25:42448

C

CABASSON, G. B., Problems posed by radiodermatitis, 25:42544
CACHARD, A., Analysis of silicon oxide films by (d,p) reactions and infrared spectrophotometry, 25:42999
CACHIN, Y., Mandibular osteoradionecrosis, 25:42543
CADET, J., Gamma irradiation of thymine in deaerated aqueous solution, 25:41874
CAFASSO, F. A., Solubility of helium and argon in liquid sodium, 25:41823 (ANL-7802)
CAGLIOTI, G., Coherence properties of thermal neutron beam, 25:43777
CAGNETTI, P., Categories of stability for regions of Italy, 25:41936
Dose-evaluation in carriage of γ-emitting materials in ships, 25:42043
Transport of radioactive materials on railroad car ferries, 25:42042
CAIRNS, William L., Photochemical degradation of flavins. VI. A new photoproduct and its use in studying the photolytic mechanism, 25:41788
CALLONNEC, Jean-Pierre, Mathematical method for the computer processing of dosimetric films, 25:42161 (NP-18892)
CALMET, J., Sixth-order radiative corrections to the anomalous magnetic moment of the electron, 25:43594
CAMERON, John R., Exposure rates from diagnostic x ray units, 25:42431
CAMPBELL, C. S., Effects of alloying and irradiation on the oxidation behaviour of zirconium alloys, 25:42927
CAMPBELL, J. A., More simulated extensive air showers with a medium-strong interaction, 25:43647 (ORO-3992-61)
CAMPBELL, John W. E., Method of operating liquid metal cooled nuclear reactor, 25:44114
CANTONI, Dennis A., Computer studies of 2- to 10-kW Brayton cycle space power system, 25:42009
CANTOR, Arnold J., Chiral SU(3) + SU(3) and the decay eta + 3π. II, 25:43658
Chiral SU(3) X SU(3) and the decay eta + 3π. I, 25:43659
CAPALNA, S., Activity of pyrophosphatase and catalase after long irradiation with small doses of ^{60}Co, 25:42277
CAPOCCHI, J. D. T., Sintering of uranium dioxide, 25:42950
CAPPS, Richard H., Mathematical quarks from a bootstrap principle, 25:43650
CARASSO, Meir, Metodology for optimizing power generation-water desalination systems using mathematical programing decomposition, 25:44295 (TID-25740)
CARGILLE, Charles M., Radioimmunoassay: a simplified procedure for dose interpolation, 25:42236
CARLSON, Donald E., Effect of acute radiation exposure rates on formation of hemagglutinating antibody in mice, 25:42307
CARLSON, R. R., Yield curves for Li + Li and Li + Be nuclear reactions, 25:43822
CARLSSON, G. A., Criticism of existing tabulations of mass energy transfer and mass energy absorption coefficients, 25:43434
CARLSSON, J., Personnel dosimetry at AB Atomenergi during 1969, 25:42392 (AE-423)
CARLTON, Robert Freeman, Reaction $^3He(d,p)^4He$, 25:43793
CARMONY, D. D., Evidence for a Kπ resonance near 1750 MeV/c^2, 25:43546 (COO-1428-279)
Evidence for splitting in the Q region of $K^+\pi^+\pi^-$ mass, 25:43544 (COO-1428-275)
Final states with three charged particles and a visible anti K^0 from K-d interactions at 4.5 GeV/c, 25:43549 (COO-1428-286)
K* (890) production in the charge exchange reaction K+n → K+π-p at 9 GeV/c, 25:43548 (COO-1428-283)
K* (890) production in the charge exchange reaction K+n → K+π- at 9.1 GeV, 25:43547 (COO-1428-281)
New evidence for splitting in the Q region of $K^+\pi^+\pi^-$ mass, 25:43543 (COO-1428-274)
CARNEVALE, E. H., Prog. rpt. on ultrasonic thermometry in LMFBR systems, 3/69, 25:42199 (NYO-3906-6)
CARPENTER, D. L., Position of the plasmapause during a stormtime increase in trapped position of the plasmapause during a stormtime increase in trapped energetic (E > 280 keV) electrons, 25:43264
CARR, Barney J., dc operated positive ion accelerator and neutron generator having an externally available ground potential target, 25:43778
CARRERA, M. A., Effects of actinomycin D on endogenous erythropoietic recovery of irradiated mice, 25:42673
CARROLL, Daniel E., Mass attenuation coefficients for plastic Pilot-B scintillator, 25:42064
CARROLL, James Patrick, Optical model for high energy scattering at all angles, 25:43571

CARTER, B., Causal sure in space--time, 25:43699
CARTER, J. C., Investigation of fast-reactor fuel testing in a thermal reactor core, 25:44165
CARTWRIGHT, D. C., Importance of polarization for electron scattering in the intermediate-energy region, 25:43138
CASA, Anna F., Nuclear pacemakers and production of ^{238}Pu sources, 25:42012
CASE, W., Inequalities for the pion--nucleon partial waves, 25:43641 (SU-1205-249)
CASINI, S., Comparative analysis of critical and exponential experiments by heterogeneous methods, 25:44154 (EUR-4352)
CASTALDELLI, L., Precipitation and influence of hydrides in zirconium alloys, 25:42855
CASTLES, Jeffrey R., Computer control of a high-temperature quadrupole mass spectrometer, 25:42182 (COO-1140-194)
CATALANO, E., Crystal structure of YbPt, 25:42892
CATALANO, S., Light curve and apsidal motion of AR Cas, 25:43046
CAUDREY, P. J., Generalized nonrelativistic Lamb-shift theory, 25:43171
CAUFFMANN, David P., Double probe measurements of ionospheric electric fields with Injun 5 satellite, 25:43216 (V-71-18405)
CAVAJ, Camillo, History of relativity, 25:43690
CAVIGNEAUX, A., Problems posed by radiodermatitis, 25:42544
CAZAUSSUS, A., Behavior of protactinium(V) on an indicator scale, 25:41785
CELEDA, J., Extraction of metals by amines. II, 25:41900
CENTOLANZI, Frank J., Hypervelocity oxidation tests of thoria dispersed nickel--chromium alloys, 25:42805 (N-71-20390)
CERRAI, E., Distribution of radioactivity in sediment from Ligurian Sea, 25:41949
CESARSKY, Diego A., Detection of H137α recombination-line emission from an H I region in direction of NGC 2024, 25:43050
CESBRON, Fabien, Crystal structure of curienite, $Pb(UO_2)_2(VO_4)_2.5H_2O$, 25:43000
CHADDHA, S. K., Radiation hazards and protection in dental radiography, 25:42484
CHAISSON, Eric J., Detection of an unidentified emission feature in microwave spectrum of W3, 25:43054
CHAKHLOV, V. L., Electromagnet of a transportable betatron, 25:43741
CHALABREYSEE, J., Study and results of examination made as a result of an inhalation of so-called soluble compounds of natural uranium. I, 25:42244 (GAT-Z-5047)
CHALMERS, David J., Reaction of p-phenylenebisdiazonium ion with alcohols, 25:41805
CHAMBERLAND, B. L., Hydrothermal synthesis of V_2O/sub 4-x/F/sub x/ derivatives, 25:42943
CHAMBERS, D. L., Radiation-sterilization of the Mediterranean fruit fly (Diptera: tephritidae): Comparison of spermatogenesis in flies treated as pupae or adults, 25:42751
CHAMBERS, W. H., Vela V and VI solar x-ray atlas. V, 25:43066 (LA-4454(Vol.5))
CHAN, B. W. B., Changes in proliferative activity of marrow leukemic cells during and after extracorporeal irradiation of blood, 25:42690
CHAN, Tsan Ung, $^6Li(\alpha,2\alpha)$ reaction as a test of the existence of α particles in ^6Li, 25:43803
CHANDRA, R., Positron annihilation in some transition and alkaline earth oxides, 25:43482
CHANDRASEKHAR, S., Post-Newtonian effects of general relativity on the equilibrium of uniformly rotating bodies. VI, 25:43090
Post-Newtonian effects of general relativity on the equilibrium of uniformly rotating bodies. V, 25:43091
CHANDRASEKHARAN, E. S., Radiochemical purification and continuous milking of ^{144}Pr from ^{144}Ce, 25:41883
CHANG, C. S., Quantum electrodynamical theory of atoms interacting with high-intensity radiation fields, 25:43170
Resonant interaction between two neutral atoms, 25:43169
CHANG, F. C., Discussion of a particular form of cluster wave functions, 25:43860
CHANG, Luke L. Y., Phase relations in the system PbO--WO_3, 25:43006
CHANG, Seung Han, Radioprotective effect of methylene blue. I, 25:42284
Serum of rats exposed to x rays, 25:42283
CHAPMAN, I. V., Labilization of hydrolytic enzymes in liver and spleen cells following whole-body x-irradiation of rats, 25:42528
CHARNODOLYA, Galina, Laboratory mixer--settler extractor LMOM2, 25:41895 (INR-1309)
CHATWIN, Robert Antony, Theory of pion interactions with atomic nuclei and of heavy ion scattering, 25:43978
CHAUHAN, S. D., Half-life measurements of 86.6-keV level in ^{233}Pa and 59.6-keV level in ^{237}Np, 25:43895
CHEISHVILI, O. D., Fluctuation conductivity of tunnel junctions, 25:43307
CHEN, I-wen, Cytologic-biochemical radiation dosimeters in man, 25:42406
CHEN, M. S., Single-particle distributions of π-mesons produced in π^+p, K^+p, pp, and π^-p collisions at high energies, 25:43554 (UR-875-340)
CHEN, M. Y., Resonance process and intensity anomaly in muonic ^{127}I, 25:43949
CHEN, S. S., Tentative design guide for calculating the vibration response of flexible cylindrical elements in axial flow, 25:41983 (ANL-ETD-71-7)
CHENG, Dah Yu., Converging-barrel plasma accelerator, 25:43350
CHENG, S. C., Isotone shift in muonic x-rays in the tin region, 25:43904
CHERDANTSEV, P. A., Parametric method for calculating Coulomb energy of certain shapes of fissionable nuclei, 25:43952 (BNL-tr-424)
CHEREJI, I., Studies on environmental radioactivity at Cluj Branch of Inst. of Atomic Physics during 1964 to 1968, 25:41928
CHERNENKO, L. P., Time properties of a spark chamber filled with helium and helium--hydrogen mixture, 25:42136 (JINR-P13-5828)
CHERNOV, A. S., Electromagnetic form factor for the pion in the dual resonant model, 25:43593
CHERNOV, G. M., Characteristics of coherent interactions at 17 and 45 GeV, 25:43646 (JINR-P1-5775)
CHERNOV, N. N., Extraction of the proton beam of the 1-GeV synchrocyclotron, 25:43762
CHERNYSHOVA, T. A., Examination of welded joints of Mo alloy TZM-2A, 25:42874
CHERRY, J. T., Two-dimensional stress-induced adiabatic flow. II, 25:44301 (UCID-30013(Pt.2))
Two-dimensional stress-induced adiabatic flow. III, 25:44302 (UCID-30013(Pt.3))
Two-dimensional stress-induced adiabatic flow. I, 25:44300 (UCID-30013(Pt.1))
CHERRY, Joe H., Effects of gamma-irradiation on DNA transcription and RNA translation in plants, 25:42716 (COO-1313-29)
Partial purification of tRNA and leucyl-tRNA synthetase from sugar beet root, 25:44249 (COO-1313-27)
Protein synthesis in germinating seeds, 25:44250 (COO-1313-28)
CHESTER, Marvin, Dissipation in He superflow, 25:43283
CHEUNG, T. H., Density fluctuations in an interacting Bose gas, 25:43522
CHEVERTON, R. D., HFIR core nuclear design, 25:44159 (ORNL-4621)
Thermal analysis of national radioactive waste repository: brief summary of results obtained through April 1971, 25:42038 (ORNL-TM-3426)
CHIKALLA, T. D., Crystal structure of promethium, 25:42893
CHILOSI, G., Levels in ^{101}Ru populated by decay of ^{101}Tc, 25:43899
CHIMONAS G., Enhancement of sporadic E by horizontal transport within the layer, 25:43255
CHIRIBOGA, Jorge, Program for Fasciola hepatica in Puerto Rico, 1/70--4/71, 25:42245 (PRNC-148)
CHISLEAG, Gheorghe, Some hematologic changes due to ionizing radiations, 25:42600
CHISTOV, E. D., Problems of protection from ionizing radiations in radiation chemistry, 25:42448
Radiation safety in design and operation of powerful β-installations, 25:42016
CHIU, Charles B., Baryon annihilation and exotic exchange, 25:43632
CHIU, Y. T., Arbitrary amplitude magneto-acoustic waves under gravity: an exact solution, 25:43073
CHIWAKI, Mitsukuni, Absolute measurement of Linac x-ray energy fluence, 25:43750
Radiation damage of MOS FETs by x-ray and electron irradiations, 25:42233
CHLEBOWSKA, D., Effect of the tau-t--A cluster structure of /sub Λ/Li + ^4He + ^3He + π^- decay, 25:43608
CHMELO, P., Contribution to the study of structures and phases of zirconium alloys, 25:42897
CHO, Boong Y., Sulfur dioxide measurement system, 25:41759
CHO, Dong Won, Multiple quark scattering analysis and its application to the hadron charge exchange scattering processes, 25:43615
CHOONG, Philip T., Subliming nuclear microthruster and its space applications, 25:42017
CHOUINARD, M. P., Positron annihilation in rare earth hydrides, 25:43126
CHOU KUO-CH'ENG, Motion of charged particles in magnetic fields with model experiments, 25:43507 (JPRS-52839, pp 3-16)
CHOWDHURY, A. Roy, Unitary symmetry and duality in meson--meson scattering, 25:43627
CHRISTENSEN, D., Theoretical ground motion predictions supporting HEST program, 25:41950 (AD-718388)
CHRISTENSEN, Hilbert, Radiation chemical studies of water and aqueous solutions of aromatic compounds, 25:41858
CHRISTENSEN, J. A., Thermal performance limits for fast reactor oxide fuels, 25:44121 (HEDL-SA-89)
CHRISTIANSEN, P. J., Nonlinear electron--wave interaction at Doppler-shifted cyclotron frequency, 25:43412
CHRISTOPOULOS, C., Nonlinear electron--wave interaction at Doppler-shifted cyclotron frequency, 25:43412
CHU, Sou-yie, Derivatives of 2-alkoxyiminomercaptans as radioprotective agents, 25:42532
CHUBAROV, L. B., Radiation-induced changes in the electrical properties of LiF monocrystals alloyed with Na, 25:43445
CHUITON, Genevieve, Rapid detection of beryllium, 25:41717 (CEA-N-1446)

CHUKHLANTSEV, V. G., Influence of some salts on the double decomposition of zircon with calcium carbonate, 25:42572
CHUMAKOV, V. V., Content of ^{137}Cs in population of Soviet Union, 25:42375
CHUMIN, V. G., α decay of neutron-deficient radon isotopes, 25:43887 (JINR-P6-5791)
CHURNEY, K. L., Selected values of chemical thermodynamic properties, 25:41826 (NBS-TN-270-5)
CHUTE, J. H., Alpha-activity of western Australian soils and wheats, 25:42427
CIGNA, A., Problems of the radiocontamination of man, 25:42375
CIONTESCU, Lelia, Effect of ionizing radiations on complex lipids of brain and protective effect of cysteine. II, 25:42520
CIRSTOIU, I., Prevention of intestinal absorption of radiocesium and radiostrontium with the help of indigenous ionic resins, 25:42263
CITROLO, J. C., Steam conditions in a catalyzed D reactor, 25:43395 (MATT-804)
CIUCA, M., Action of gamma radiation on enterococcal bacteriophage 341, 25:42740
CLAESSON, Mogens Helweg, Autoradiographic study of lymphoid cell decay, 25:42240
CLAIBORNE, H. Clyde, Recent developments in the shielding of neutron sources, 25:43418 (ORNL-RSIC-32)
CLANCY, M. C., Weak x-ray sources in the southern hemisphere, 25:43057
CLAPP, R. A., Alpha-activity of Western Australian soils and wheats, 25:42427
CLARK, W. G. Jr., Fracture mechanics and nondestructive testing of brittle materials, 25:42021 (CONF-710512-2)
CLAVELLI, L., New dual N-point functions, 25:43714
CLAYTON, C. G., Applications of radioisotope x-ray fluorescence analysers in metalliferous mineral exploration and in mining, 25:41739
Use of nuclear techniques in on-stream analysis in mineral processing plants, 25:41740
CLEMENT, C., Radioinduced sarcomas, 25:42705
CLEMENTE, G., Problems involved in assessing late effects of radiation in man, 25:42714
CLEMENTS, Richard G., The Rain Forest Project. Annual report, 25:42317 (PRNC-147)
CLINE, Thomas L., Topics in solar cosmic ray and x-ray production, 25:43067 (N-71-16749)
CLINK, G. L., Transition metal HE's. V, 25:44268 (MHSMP-71-28)
CLODE, W. H., Quantitative gammagraphy of thyroid gland with /sup 99m/Tc and ^{131}I, 25:42569
CLOPP, H. W., Evidence for a Kπ resonance near 1750 MeV/c^2, 25:43545 (COO-1428-279)
Evidence for splitting in the Q region of $K^+\pi^+\pi^-$ mass, 25:43544 (COO-1428-275)
K^*(890) production in the charge exchange reaction $K^+n \rightarrow K^+\pi^-p$ at 9 GeV/c, 25:43548 (COO-1428-283)
K^*(890) production in the charge exchange reaction $K^+n \rightarrow K^+\pi^-$ at 9.1 GeV, 25:43547 (COO-1428-281)
New evidence for splitting in the Q region of $K^+\pi^+\pi^-$ mass, 25:43543 (COO-1428-274)
COATES, N. H., Power required to circulate gas-solids suspensions, 25:41956 (BM-RI-7019)
COBB, William Ronald, Application of variational synthesis to solutions of multidimensional neutron transport problems, 25:43772
COBLE, R. L., Basic research in crystalline and noncrystalline ceramic systems. Annual report, 25:42983 (MIT-3773-103)
COGGI, J. V., Electrical/thermal integration of dynamic power and life-support systems for manned spacecraft, 25:42065
COHEN, E. L., Accurate and rapid measurement of plasma renin activity by radioimmunoassay. Results in normal and hypertensive people, 25:42238
COHEN, M., Attenuation of x rays in the human body, 25:42430
COHEN, Michael E., Economic selection of undersea powerplants, 25:44180
COHEN, Norman, Prog. rpt. on radioactivity studies. I, annual, 9/69--8/70, 25:42245 (NYO-3086-10(Vol.1))
COLE, L. J., Biochemical and radiobiological factors in the early detection of radiation injury in mammals, 25:42404
COLEMAN, Charles, Selective stripping of plutonium from organic extracts, 25:41912
COLEMAN, R. F., Multi-element analysis of glass fragments by neutron activation and the application to forensic science, 25:41758 (AWRE-U-24/71)
COLEMAN, Thomas Patrick, Model analyses of elementary particle scattering amplitudes, 25:43580
COLLINSON, C. D., Conservation laws in general relativity, 25:43704
COMFORT, J. R., Anomaly in angular distributions for (^3He,t) reactions, 25:43848
COMMANDER, J. C., Nonradioactive waste oil disposal study, 25:44220 (ANCR-1004)
Nonradioactive waste solvent disposal study, 25:44221 (ANCR-1005)
COMSTOCK, G. M., Apollo helmet dosimetry experiments, 25:42150 (N-71-14502)
CONARD, Bruce R., Computer collection of mass spectrometric ionization efficiency curves, 25:44241 (COO-1140-198)
CONLIN, J. A., Fuel element development for the Gas-Cooled Fast Breeder Reactor. Part I. Sealed fuel rod design, 25:44125 (ORNL-TM-3427)
CONN, J. W., Accurate and rapid measurement of plasma renin activity by radioimmunoassay. Results in normal and hypertensive people, 25:42238
CONNOLLY, T. F., RMIC bulletin and status report, 25:44281 (ORNL-RMIC-11)
CONSTANTINESCO, S. P., Action of gamma radiation on enterococcal bacteriophage 341, 25:42740
CONTANT, R. B., Radiogenetic effects of gamma- and fast neutron irradiation on different ontogenetic stages of the tomato, 25:42364
CONTENSCU, M., Conference on optimization, Nice, 6--7/65, 25:43526
CONVENTI, L., Differential sensitivity to uv-irradiation of virus and cell genome expression in SV40 transformed cells, 25:42733
CONWAY, James J., Radionuclide evaluation of the candy-walker malformation and congenital arachnoic cyst of the posterior fossa, 25:42568
COOK, David J., Scintiphotography and rectilinear scanning of lung using /sup 99m/Tc-MAFH (macroaggregated ferrous hydroxide), 25:42579
COOK, E. B. T., Determination of acid-soluble, acid-insoluble, and total uranium in silicate ores, 25:41723 (NIM-1077)
COOK, G. B., Contribution to geobotanical and geochemical prospecting for gold by activation analysis, 25:41770
Determination of trace amounts of gold in natural waters by non-destructive activation analysis using preconcentration before irradiation, 25:41771
COOK, R. W., Logical network cost and entropy, 25:44275 (NYO-4209)
COON, D. D., Asympotic behavior and the possibility of duality without ghosts in Feynman-diagram models, 25:43634
COOPER, J. A., Figure-of-merit measurements for Ge(Li) detectors, 25:42126
COOPER, J. W., Raising of discrete levels into the far continuum, 25:43112
COOPER, John A., Radioanalytical applications of gamma--gamma coincidence techniques with lithium-drifted germanium detectors, 25:42113
COOPER, M. H., Measurement of cesium sorption isotherms in liquid sodium, 25:42863
COPPOLA, M., Scattering of fast neutrons of ^{238}U, 25:43858
CORDARO, Matthew C., Investigation of electron transport utilizing the phase--space time evolution method, 25:43424
CORDES, E. H., Effects of α-deuterium substitution, polar substituents, temperature, and salts on the kinetics of hydrolysis of acetals and ortho esters, 25:41800
CORDS, D., Evidence for a Kπ resonance near 1750 MeV/c^2, 25:43546 (COO-1428-279)
Evidence for splitting in the Q region of $K^+\pi^+\pi^-$ mass, 25:43544 (COO-1428-275)
K^*(890) production in the charge exchange reaction $K^+n \rightarrow K^+\pi^-$ at 9.1 GeV, 25:43547 (COO-1428-281)
K^*(890) production in the charge exchange reaction $K^+n \rightarrow K^+\pi^-p$ at 9 GeV/c, 25:43548 (COO-1428-283)
New evidence for splitting in the Q region of $K^+\pi^+\pi^-$ mass, 25:43543 (COO-1428-274)
CORIOU, H., Corrosion of Zr alloys in water and steam, 25:42810
CORNELL, F. N., Differences between lesions in cerebral scanning, 25:42577
CORNWALL, John M., Turbulent loss of ring current protons, 25:43210 (AD-715260)
Unified theory of SAR arc formation at the plasmapause, 25:43242
CORONITI, F. V., Turbulent loss of ring current protons, 25:43210 (AD-715260)
Unified theory of SAR arc formation at the plasmapause, 25:43242
CORUM, J. M., Effect of fillets on stress concentrations in cylindrical shells with step changes in outside diameter, 25:41959 (CONF-710512-15)
Experimental and finite element stress analysis of a thin-shell cylinder-to-cylinder model, 25:42835 (CONF-710512-3)
COSGROVE, G. E., Life shortening and cause of death in irradiated germfree mice, 25:42663
COSTA, E. C., Experimental approach to the optimization of solvent extraction processes, 25:41916
COTT, Donald W., Ionizational and thermal nonequilibrium in MHD boundary layers, 25:43352 (AI-715272)
COTTERELL, K., Estimation of U distribution in MTR fuel plates, 25:42178
COUPLAND, J. R., Production of high current, high quality beams of ions, and neutral particles, 25:43401
COVELLI, V., Late somatic effects in syngeneic radiation chimeras. I, 25:42666
COVER, Robert K., SID controller program: CDC 1604 computer program, 25:44290 (SC-IR-68-814)
COWAN, Robert J., Radioisotope scanning for parotid oncocytoma, 25:42572
COX, Edwin Lynn, Space time dependent reactor kinetics in a small beryllium reflected research reactor, 25:44201
CRAIG, T., Studies of thermally-activated deformation in zirconium, 25:42877

CRANSTON, F. P., Thermal neutron capture cross sections in calcium, 25:43835
CRASEMANN, Bernd, Internal ionization of the K shell, 25:43575
CREAN, Peter Aidan, Experimental study of low-energy pion--nucleon charge--exchange scattering and threshold neutral pion production, 25:43564
CRENNELL, David J., K+ forward scattering from the reaction π-p → K+Σ(1375)- at 4.5 and 6 GeV/c, 25:43558
CREWTHER, R. J., Spontaneous breakdown of conformal and chiral invariance, 25:43662
CRIMMINS, P. P., Fracture of structural metals as related to pressure-vessel integrity and in-service monitoring, 25:42840 (CONF-710512-4)
CRISLER, D. F., Method for absolute calibration of Ge(Li) detectors using effective interaction depth, 25:42125
CRITTENDEN, E. C. Jr., Superconducting thin-film detector of nuclear particles, 25:42080
CROIZAT, Helene, Hematological effects of partial body irradiation: clinical and experimental data, 25:42595
CROSS, James Burke, Electron capture decay schemes of ^{203}Bi and ^{204}Bi, 25:43906
CROSSLEY, D. A. Jr., Feeding by caeculid mites on fungus demonstrated with radioactive tracers, 25:42242
CRUVER, J. E., ISOTEC thermoelectric generator for space power, 25:42006
CSIKOR, F., $A_{1\pi} + A_{1\pi}$ amplitudes in the Veneziano model, 25:43529
CSRMELY, E., Enzyme activity in irradiated skin, 25:42286
CSUPKA, St., Estimation of future radiostrontium level in the system fallout, fodder plant, milk, 25:42378
CUDERMAN, J. F., Electron multiplier detection of fast potassium atom beams, 25:42079
CUEILLERON, J., New method for preparing metal borides, 25:42944
CUJEC, B., Study of ^{61}Cu nucleus by ^{58}Ni(α,pγ)^{61}Cu reaction, 25:43839
CULP, Robert A., Effect of an electric field on gas chromatographic retentions by liquid crystals, 25:44245 (COO-1222-47)
CUMMINGS, S. L., Uptake of ^{144}Ce, ^{147}Pm, and ^{238}Pu by oat plants from soils, 25:42260
CUMMINS, Kenneth W., Energy budget model for woodland stream ecosystems, 25:44255 (COO-2002-6)
Prog. rpt. on energetics of natural populations of freshwater macroconsumers, 1971, 25:44256 (COO-2002-10)
CUNDALL, R. B., Pulse radiolysis, 25:41862
CURTIS, Howard J., Life-span of dividing mammalian cells in vivo, 25:42656
CUTCUDACHE, Caliopi, Hemorrhagic syndrome in radiation sickness. II, 25:42537

D

DA COSTA, Jose Ribeiro, Heavy concretes for gamma radiation protection, 25:42976
DADDI, L., Dosimetry of mixed gamma-neutron radiation, 25:42159
DAGBJARTSSON, B., Radurization of scampi, shrimp, and cod, 25:42745 (STI/DOC-10/124)
DAHL, R. E. Jr., Neutron dosimetry for fast reactor applications, 25:44102
DAION, M. I., Effect of a magnetic field on the accuracy with which particle momentum is determined in a streamer or spark chamber, 25:42148
DALE, L. S., Precise determination of hydrogen in metals (with particular reference to zirconium) by the isotopic equilibration-mass spectrometry procedure, 25:41747 (AAEC/TM-588)
DALMASTRI, B., Control rod fabrication experiments, 25:42822
DALTON, H., Purification and some properties of molybdoferredoxin, a component of nitrogenase from Clostridium pasteurianum, 25:41811
DALY, Norman Richard, Energy selective ion beam intensity measuring apparatus and method utilizing a scintillator to detect electrons generated by the beam, 25:42224
DALY, Thomas E., Preventive oral care for the irradiated cancer patient, 25:42471
DANG, G. Do., Self-consistent theory of nuclear spectra: the pairing-plus-quadrupole interation model applied to the tin isotopes, 25:43925
D'ANGELO, V., Dosimetry of mixed gamma-neutron radiation, 25:42159
D'ANGIO, Giulio J., Effect of irradiation on the maturation of Wilms' tumor, 25:42592
D'ARCA SIMONETTI, A., Bone deposition of ^{210}Pb(^{210}Po) and ^{90}Sr, 25:42382
DARDEN, S. E., Cross-section and polarization measurements for the ^{3}H(^{3}He,n)^{5}Li reaction, 25:43796
Narrow state at 23.9 MeV, 25:43782
DARINSKII, B. M., Dielectric properties of γ-irradiated crystals of KH_2PO_4, 25:43443
DA ROCHA, A. F. Goncalves, Dose analysis in radiotherapy, 25:42415
DARRAH, James G., Process for fabrication of stoichiometric uranium monocarbide, 25:42939
DARRAS, R., Zirconium alloys used in carbon dioxide at high temperatures, 25:42812
DARRAS, Raymond, Oxidation resistant zirconium alloys in carbon dioxide at high temperatures, 25:42802 (CEA-R-4103)
DAS GUPTA, S., Truncation of rotational states in the shell model, 25:43828
DA SILVA, M. F., States of ^{23}Na below 5.4 MeV, 25:43880
DASTIDAR, T. K. Rai, Angular distribution of H+ or D+ from electron impact dissociation of HI+ ion, 25:43152
DATZ, Sheldon, Energy-loss spectra of channeled iodine and oxygen ions in gold, 25:43454
DAUTOV, L. M., Effective nuclear charges in many-electron atoms, 25:43162
DAVIDOVICH, R. L., Outer-sphere interaction in $M_3LO_2F_8$ complexes, 25:41828
DAVIES, D. Elrug, Residual electrically active defects after lattice reordering in ion-implanted silicon, 25:43439
DAVIES, P. G., Radiometer studies of atmospheric attenuation of solar emission at 19 GHz, 25:43071
DAVIS, M. J., Polar substorms as the source of large-scale traveling ionospheric disturbances, 25:42250
DAVIS, Michael J., Polar substorm related traveling ionospheric disturbances based on columnar electron content measurements, 25:43217 (N-71-18502)
DAVIS, Monte V., Effect of simulated fission products in interelectrode spacing of a thermionic diode, 25:43180 (AD-715809)
DAVISON, P. J. N., Weak x-ray sources in the southern hemisphere, 25:43057
DAY, John R., Mathematical model of the Arc Pioneer 6/7 plasma probe, 25:42209
DAYASHANKAR, Neutron dose distributions for ^{252}Cf sources, 25:42445
DAYRAS, R., Study of ^{61}Cu nucleus by ^{58}Ni(α,pγ)^{61}Cu reaction, 25:43839
DEACON, J. A., Growth and properties of single crystal LaB_6, 25:42947
DEAN, Edward Thomas, Nonlinear reactor statics, 25:44157
DEANOVIC, Z., Early post-irradiation changes in the metabolism of biogenic amines, 25:42626
DE ARAUJO, J. A., Ion-exchange pilot plant for the preparation of nuclear pure uranium compounds, 25:41919
DE BROGLIE, Louis, Reinterpretation of wave mechanics, 25:43691
DEBRUNNER, H., Calculation of the multiplicity yield function of the IGY neutron monitor, 25:43175
DECONNINCK, G., ^{6}Li(α,2α) reaction as a test of the existence of α particles in ^{6}Li, 25:43803
DECOSTER, Alain, Central potential from a variational polarized-orbital method, 25:43148
DECOURTYE, L., New types of dahlia by induced mutations, 25:42327
DE CRESCENTI, Michael A., Process for fabrication of stoichiometric uranium mononcarbide, 25:42929
DECRESSIN, A., Orgel prototype preliminary design: fine flux distributions in the fuel element, 25:44059 (EUR-4364)
Orgel prototype preliminary design: reactivity coefficients, 25:44100 (EUR-4365)
DEDEK, W., Radioisotopes in pesticide research. IV and V, 25:42239
DE DOMINICIS, Cyrano, Statistical quasiparticles, effective Green's functions, and Landau descriptions of quantum liquids. I. Impurity systems at equilibrium, 25:43511
DEEV, L. I., Oxidation-reduction potential in tissues exposed to radioprotective agents, 25:42511
DE FRANCESCHI, L., Efficiency of scintillation crystals in medium contaminated by γ-emitters, 25:42096
DEGENHARDT, K. H., Modular programming system for programming experiments on PDP-9, 25:42181 (CERN-Trans-71-18)
DE GEOFFROY, J., Probabilistic appraisal of mineral resources in a portion of the Grenville Province of the Canadian Shield, 25:41944
DEHMER, J. L., Raising of discrete levels into the far continuum, 25:43112
DEHNHARD, D., Coulomb displacement energies for 1f-2p shell nuclei, 25:43883
DE JONG, S., Precise determination of hydrogen in metals (with particular reference to zirconium) by the isotopic equilibration-mass spectrometry procedure, 25:41747 (AAEC/TM-588)
DEJU, Raul A., Chemical extraction of low-grade resources, 25:41918
DEKANENKO, V. M., Formation of subcxides in the system niobium--oxygen, 25:42990
DELAFOSSE, J., Influence of Si on Zircaloy-2 and Zircaloy-4 alloys, 25:42876
Studies of the influence of N on alloys of Zr--Cr--Fe type, 25:42875
DE LEON, Delfin D., Program for Fascicle hepatica in Puerto Rico, 1/70--4/71, 25:42246 (PRNC-148)
DELLA SELVA, A., Inequalities for the pion--nucleon partial waves, 25:43641 (SU-1206-249)
DELPECH, Andre, Method and apparatus for the continuous precipitation of uranium, 25:41782
DELPLACE, Y., Problems posed by radiodermatitis, 25:42544
DELREZ, M., Effect of normal and irradiated marrow grafts on the hemopoietic recovery after a sublethal irradiation, 25:42644

XUM

DELSARTE, G., Determination by channelography of orientation of microcrystals, 25:43454
DEL VAL COB, M., Use of nuclear techniques in Spain's program for the development of mineral resources, 25:41945
DEMARS, H., Structure of Zr--Cr alloys, 25:42879
DEMARTHE, Jean-Michel, Investigation of some nonlinear effects in extraction equipment using computer simulation, 25:41890 (CEA-N-1450)
DEMIDOV, A. M., Gamma-ray spectrum from reaction (n,γ) on ^{150}Sm and ^{151}Sm samples, 25:43892
DEMING, Stanley N., Precision flow-monitoring spectrometer with low noise and high stability, 25:44243 (CDD-1222-45)
DEMOKAN, O., Mechanism causing nonlinear behavior in Tonks--Dattner resonance experiments, 25:43411
DEMONCY, Philippe, Combinations between U chalcogenides UX and U_2X_3 (X = S, Se, Te), and sulfides, selenides, and tellurides of lanthanides, Y, and Sc, 25:43001
DEMOS, Joslyn R., Bethe Goldstone equation in finite nuclei, 25:43955 (ORO-3765-30)
DEMUYNCK, J., Decay of /sup 81g/Se and /sup 81m/Se, 25:43844
DENAVIT, J., Comparison of numerical solutions of the Vlasov equation, 25:43358
DENINGER, Wolfgang, Process of producing moulded masses and coated substrates, 25:41847
DENISOVA, E. A., Variants of the syndrome of neurovascular dystonia in chronic radiation effect, 25:42676
DE PALMAS, Henri, Study of 3 ^{1}P--2 ^{1}S line of He excited by H ion beam, 25:43129
DE PANFILIS, G., Enzyme activity in irradiated skin, 25:42286
DER, R. C., Production of carbon K x rays by heavy-ion bombardment, 25:43107
DE RAAD, J. A., Ultrasonic and other non-destructive testing methods for tube joints used in heat exchangers, 25:44148 (CONF-700224-, Paper 4)
DERBENEV, Ya. S., Dynamics of particle polarization near spin resonances, 25:43770
DERBY, R. W., Interpretations of the drop weight test in terms of strain tolerance (gross strain) and fracture mechanics, 25:42347 (ORNL-TM-3247)
DEREBCHINSKII, A. I., Telescope of spark chambers with a magnetic spectrometer for polarization experiments, 25:42145
DERGUNOV, I. D., Behavior of fission products in soils of Uzbekistan, 25:42319
DERGUNOVA, V. S., Characteristics of porous graphite impregnated with fused zirconium, 25:42948
DE RIDDER, L., Organotypical culture of irradiated and non-irradiated chick mesonephros, 25:42643
DE SANCTIS, C., Effect of ionizing radiations on lymphocytes from adults and newborn infants, cultured in vitro in presence of phytohemagglutinin, 25:42602
DESARMOT, G., Determination by channelography of orientation of microcrystals, 25:43464
DESER, S., Self-coupled scalar gravitation, 25:43705
DE SERRES, F. J., Genetic alteration at molecular level of ultraviolet light-induced ad-3B mutants in Neurospora crassa, 25:42341
Mutagen specificity in Neurospora crassa, 25:42352
DESTEESE, J. G., Nuclear electric power sources for biomedical application, 25:41996
DE STERKE, A., Ultrasonic inspection of welds in nuclear reactor pressure vessels, 25:44111 (CONF-700224-, Paper 5)
DE STIGTER, J., System for digitalization of fast non-recurrent analogue signals, 25:42220
DETAR, Carleton Edward, Momentum spectrum of hadronic secondaries in the multiperipheral model, 25:43620
DE TEMPLE, Bernhard, Fuel rods for nuclear reactors, 25:44218
DETKO, J. F., Dual chamber vacuum cryostat for germanium lithium drifted diodes, 25:42132
DE TOMBOLESI, R. A. P., Effects of actinomycin D on endogenous erythropoietic recovery of irradiated mice, 25:42673
DE VERNEJOUL, P., External measurements of pulmonary pressures by means of radioisotopic dilution curves, 25:42554
DE VEUBEKE, B. F., Conference on optimization, Nice, 6--7/69, 25:43525
DE VILLEPIN, J., Vibrational spectra of and isotope effect in hydrogen bonded potassium hydrogen oxalate, 25:41790
DEVIN, B., French thermionic program and accomplishments, 25:41997
DEVREUX, M., Radiogenetic effects of gamma- and fast neutron irradiation on different ontogenetic stages of the tomato, 25:42354
DEWEY, C. Forbes Jr., Volume ionization by means of laser radiation in a cesium plasma diode, 25:43181 (AD-715883)
DE YOUNG, D. S., Dynamics of extended extragalactic radio sources, 25:43059
DHAR, S. K., Solubility of helium and argon in liquid sodium, 25:41823 (ANL-7802)
DIAMOND, H., g/sub J/ value for the atomic ground state of fermium, 25:43118
DIAMOND, R. M., High-spin isomer in ^{211}At, 25:43912
DIAMOND, S. D., Organic Rankine cycle for manned space applications, 25:42003
DIEHL, J. F., Preparation and properties of antimony(V) aquoxide, 25:41760
DIENER, E. M., Isospin splitting of the giant dipole resonance in ^{60}Ni, 25:43857
DIENER, Edward Moses, Giant dipole resonances in ^{40}Ca, ^{42}Ca, and ^{60}Ni, 25:43853
DIENER, Gerhard, Kinetic theory of fully ionized plasmas. I, 25:43376
DIENSTBIER, Z., Some biochemical changes in body fluids as indicators of radiation damage, 25:42402
DIESTLER, D. J., Transition probabilities for atom--atomic-oscillator collisions, 25:43146
DIETZSCH, O., Reaction ^{142}Nd(d,t)^{141}Nd, 25:43900
DI LORETO, A., Authorization of nuclear installations, 25:41979
DIMARCO, Giorgio, Radiation effects on allosteric enzyme, 25:42291
DI MATTEO, J., External measurements of pulmonary pressures by means of radioisotopic dilution curves, 25:42554
DINCLER, G., Quantitative analysis by sorption on ion exchangers, 25:41742
DIRIAN, Gregoire, Purifying gases containing oxidizable impurities, 25:41914
DISVETOVA, V. V., Healing of radiation ulcers of skin under the influence of metacyl and dibunol (experimental research), 25:42541
DITU, S., Late functional changes in irradiated rats, 25:42668
DIX, W.-R., Inelastic electron--proton scattering in the region of the Δ (1236) resonance, 25:43527 (DESY-71/21)
DMITRIEV, V. M., Behavior of superconductive thin-film bridges in SHF fields, 25:43298
DOBRESCU, G., Radioinduced sarcomas, 25:42705
DOBRETSOVA, I. N., Radiation yield of Mn^{+3} in dosimetric glasses, 25:42163
DOBRETSOVA, K. V., Systems of proper motions of stars of PZT program, 25:43029
DOHERTY, R. H., High-altitude nuclear detection studies. II, 25:41933 (AD-719620)
DOHERTY, Robert H., Observations suggesting particle precipitation at latitudes below 40°N, 25:43223
DOINIKOV, N. I., Shaping of magnetic fields in cylindrical cavities, 25:43330
DOLBILOV, G. V., Some specific features of the cold cathode operating at low pressures, 25:43346 (JINR-P9-5753)
DOLLFUS, M. A., Epithelioma developing on an angioma treated with Curietherapy, 25:42686
DOLPHIN, G. W., Biological problems in radiological protection of workers exposed to ^{239}Pu, 25:42488
DOMBROVSKII, V. A., Observations of the variability of the polarization of radiation of the high luminosity red variables, 25:43024
DOMINGUEZ, Arnulfo Zepeda, Production of W mesons in charged lepton--pion collisions, 25:43603
DONAHUE, T. M., Differential electron flux as determined by auroral observations of N_2^+ and N_2^+ systems, 25:43214 (N-71-16589)
Mass spectrometer observation of NO in auroral arc, 25:43218 (N-71-18997)
DONALDSON, J. R., Uptake of molybdenum, marked with ^{99}Mo, by biota of Fern Lake, Washington, 25:44287 (RLO-2225-T-7-2)
DONALDSON, Lauren R., Prog. rpt. on low level chronic irradiation of salmon, annual, 6/24/71, 25:42616 (RLO-2225-T-2-2)
DONDE, A. L., Cryostat for a Ge(Li) detector, 25:42084
DONNE, M. Dalle, Considerations on PyC and SiC coated oxide particles for gas cooled fast reactor application, 25:42963
DONOGHUE, T. R., Narrow state at 23.9 MeV, 25:43782
DOOLEY, R. B., Oxidation of tantalum--niobium, 25:42806
DORE, Earl K., Primary congenital lymphedema in infancy evaluated by isotope lymphangiography, 25:42559
DORIKENS, M., Decay of /sup 81g/Se and /sup 81m/Se, 25:43844
DORIKENS-VANPRAET, L., Decay of /sup 81g/Se and /sup 81m/Se, 25:43844
DORON, T. A., Decay of ^{104}Cd and levels of ^{104}Ag, 25:43945
Decay of /sup 96 95m/Rh and levels of ^{96}Ru, 25:43943
DORONIN, N. A., Production of high-quality zirconium concentrate, 25:42825
DOUDNEY, C. O., Deoxyribonucleic acid replication in uv-damaged bacteria revisited, 25:42290
DOUGLAS, Richard L., ^{131}I transport through the air--forage--cow--milk system using an aerosol mist (Project Rainout), 25:42370 (SWRHL-43-r)
DOUGLASS, Kenneth H., Applications of coherent state representation in theory of magnetism. I. The Heisenberg model, 25:43512
DOUZON, Jean, Detecting gamma radiation from drilled geological formations, 25:42117
DRAGO, A., Indirect experimental determination of photopeak efficiencies of NaI(Tl) detectors for cylindrical gaseous sources, 25:42049 (EUR-4513)
DRAGOUN, O., Contribution of outer atomic shells to total internal conversion coefficients, 25:43931
DRAGUN, O., Reaction (d,^{6}Li), 25:43987
DRAKE, S. R., Comparison of orthogonal curvilinear coordinate systems for minimum error, 25:44222 (BDX-

613-184)
DRANE, Joe B., Preventive oral care for the irradiated cancer patient, 25:42471
DRANOVA, Zh. I., Crowdion mechanism of plastic deformation, 25:43484
DRAPER, Douglas O., Open-field behavior and heart rate in prenatally x-irradiated rats, 25:42640
DRECHSEL, D., Radiative corrections in ee'N coincidence experiments, 25:43979
DREISS, Gerard J., Self-consistent theory of nuclear spectra: the pairing-plus-quadrupole interation model applied to the tin isotopes, 25:43925
DREIZLER, R. M., Self-consistent theory of nuclear spectra: the pairing-plus-quadrupole interation model applied to the tin isotopes, 25:43925
DREWRY, George E., The Rain Forest Project. Annual report, 25:42317 (PRNC-147)
DRICHKO, V. F., Age-specific peculiarities of ^{137}Cs elimination from human organism, 25:42250
DROPESKY, B. J., Decay of ^{126}Sn and of 19-min and 12.4-day isomers of ^{126}Sb, 25:43924
DRYANOVSKA, O. A., Ratio of sexes in F_1 after irradiation of female and male imagos of Sitotroga cerealella, 25:42610
DUBBERS, D., Relaxation phenomena and NMR of ^{116}In, 25:43894
DUBBERS, F., Lifetimes of excited states in 89-neutron nucleus ^{151}Sm, 25:43937
DUBININ, N. P., Dose-dependent frequency of encircled ring chromosomes, 25:42351
DUCASSOU, D., Positron camera in hospital practice, 25:42564
DUDEY, N. D., Activation-rate measurements in the ZPR-3 mockup critical experiments. Part I. Measurements of foil-activation rates and fission yields in Assembly 60 of ZPR-3: mockup of EBR-II with a uranium blanket, 25:44150 (ANL-7791)
DUER, Wayne Carlton, Thermochemical hydrogen--deuterium isotope effects, 25:41794
DUFFY, Thomas J., Livermore superconducting Levitron, 25:43399 (UCRL-73075)
DUINKER, P., Bubble density measurements with HPD 2 at CERN, 25:42153
DUL'KIN, I. N., Heat transfer with water and Freon-113 boiling on nonisothermal surface, 25:41989
DULL, Dennis L., Titanium--Be composites produced by the co-extrusion of powders, 25:42869
DUNAWAY, P. B., Biological concentration and turnover of radionuclides in food chains: a bibliography, 25:42315 (ORNL-NSIC-89)
DUNJIC, A., Late functional changes in irradiated rats, 25:42668
DUNSTER, H. J., Quality Factor: a sound concept, 25:42441
DUPOUY, Jean-Pierre, Distribution of radioactivity in the lava issuing from the cavity of a nuclear explosion, 25:41953 (CEA-R-4099)
Radioactivity distribution in environment of a contained nuclear explosion. I, 25:41954 (CEA-R-4128(1))
DUPUY, C. H. S., Analysis of silicon oxide films by (d,p) reactions and infrared spectrophotometry, 25:42999
DUPUY, J. C., Positron camera in hospital practice, 25:42554
DURDYMURADOVA, R., Magneto-electric properties of Ni--Mo alloys, 25:43475
DURFEE, R. C., ORTHIS, ORTHAT: two computer programs for solving two-dimensional steady-state and transient heat conduction problems, 25:41985 (ORNL-TM-3324)
DUSHUTIN, N. K., Model of the multiple particle production, 25:43614 (JINR-P2-5829)
DUSI, U., Radio-induced cardiopathy, 25:42704
DUSSEL, G. G., Reaction (d,^{6}Li), 25:43987
DUTTA, A. K., Probable significance of excitation quantum numbers in nuclei, 25:43958
DUTTON, J. W. R., Some analytical aspects of radioactive effluent disposal, 25:42380
DUVAL, R. A., 25-kWe reactor--thermoelectric power system for space stations, 25:44171
DUVAL, Xavier, Comparison of the catalytic effects of various metals in the graphite--oxygen and graphite--nitrous oxide reactions, 25:42931
Kinetics of graphite oxidation in N_2O, 25:42932
DWORETSKY, Michael M., Radio sources: 3.3-mm flux and variability measurements, 25:43060
DY, K. S., Measurement of the superconducting energy gap and Fermi velocity in single-crystal lead films by electron tunneling, 25:43312
D'YACHENKO, A. M., Crowdion mechanism of plastic deformation, 25:43484
DYBAN, Yu. P., Kinetics of solid-phase synthesis of zircon during sintering under pressure, 25:42940
DYBWAD, Jens Peter, Radiation effects on silicates, 25:43445
DYSON, P. L., Significance of electrostatic probe observations of electron density irregularities, 25:43258
DZHALAGANIYA, T. R., Brueckner--Hartree--Fock theory for the ^{4}He nucleus, 25:43785
DZUBAY, T. G., Coulomb displacement energies for 1f-2p shell nuclei, 25:43883
DZYUBENKO, I. I., Content of ^{137}Cs in population of Soviet

E

EACHUS, W. James, Solvable model in quantum field theory, 25:43668
EASSA, Eassa-Delmy M., Effects of epsilon-amino-n-caproic acid on radiation-induced increase in capillary permeability and subsequent pathology in skin, 25:42617 (UR-49-1462)
EAST, Larry V., DCHAIN: PDP-9/PDP-15 computer program for radioactive decay and capture chain calculations, 25:43889 (LA-4708)
EASTMAN, Michael P., ^{17}O NMR studies of uranium oxides, 25:43497
EASTON, D. S., Effect of heat treatment and impurities on the current density of transition metal superconductors, 25:43290 (ORNL-4703)
EBERSOLDT, Franz, Investigation of the problem of characteristic value and nonnegative solution of a general stationary transport equation, 25:43415 (JUL-711-MA)
EBERT, D., Transformation of stable elementary particles on Regge trajectories by means of field-theoretical boundary transitions, 25:43572
ECKELMAN, W., Visualization of the human spleen with /sup 99m/Tc-labeled red blood cells, 25:42235
ECKERT, Hans U., Measurement of the rf magnetic field distribution in a thermal induction plasma, 25:43338 (AD-715265)
ECKMANN, W., Uranium prospection of the Eisenwerkgesellschaft Maximilianshuette in Nordostbayern, 25:41942
ECKSTEIN, Ralph R., Lithium isotopic analysis by nuclear magnetic resonance spectrometry, 25:41724
ECOCHARD, R. M., Radiogenetic effects of gamma- and fast neutron irradiation on different ontogenetic stages of the tomato, 25:42364
EDELSTEIN, R. M., Duality in the triple Regge limit, 25:43649
EDERY, David, Program for optimal reactivity profiles in one-dimension cylindrical reactors, 25:44192 (CEA-N-1367)
EDWARDS, Russell N., Economic selection of undersea powerplants, 25:44180
EDWARDS, Steve, Optical model analysis of $^9Be(p,p_0)^9Be$ cross sections, 25:43804
EDWARDS, V. R. W., Evidence for a real Saxon Woods derivative term in the proton optical potential, 25:43967
EERING, J. Th., Radiographic capacities of the RTD-LINAC 8 MeV linear accelerator, 25:44113 (CONF-700224-, Paper 8)
EERNISSE, E. P., Sensitive technique for studying ion-implantation damage, 25:43441
EFIMOV, M. L., Comparative radiosensitivity of ascites ovarian tumors and ascites lymphosarcoma of rats, 25:42637
Content of protein SH-group in tumors of different radiosensitivity in norm and after irradiation, 25:42618
EGAMI, Nobuo, Mortality of fish under continuous irradiation conditions, 25:42634
EGAWA, Jun, Five cases suspected of radiation myelitis, 25:42700
EGIAZAROV, B. G., Use of an x-ray analyzer with a semiconductor detector for elemental analysis, 25:42217
EGOROV, O. K., Effect of a magnetic field on the accuracy with which particle momentum is determined in a streamer or spark chamber, 25:42148
EHN, E., Dissociation and critical concentration of peroxides (H_2O_2 + UO_4) in fuel solutions, 25:44166
EHRLICH, K., Influence of neutron irradiation on the creep rupture properties of a 16Cr--13Ni steel, 25:42924
EICHLER, Eugene, New observations in the A = 49 decay chain; levels in ^{49}Sc and ^{49}Ti, 25:43873
EIDMANN, K., Survey of studies of laser produced plasmas at the IPP Garching, 25:43380 (IPP-4/9)
EINFELD, Klaus, Thermionic diodes and thermionic reactors in the Federal Republic of Germany, 25:44172
EISEN, F. H., Oscillation frequencies of protons in planar channels of silicon, 25:43455
EISENBUD, Merril, Prog. rpt. on radioactivity studies. I, annual, 9/69--8/70, 25:42245 (NYO-3085-10(Vol.1))
EISENSTEIN, L., Failure of S-channel helicity conservation in A_1^- production, 25:43654 (COO-1195-204)
EISENZIMMER, M., Determination of sulfate in nitric acid--sulfuric acid mixtures, 25:41716 (AECL-3676)
EISMONT, O. A., Raleigh--Taylor instability in magnetohydrodynamics in galvanic approximation, 25:43204
EKBOTE, D. D., Structure of the plasma boundary layer at a conducting sphere, 25:43356
EKSTIG, B., Iterative computer method for correction of spectral data, 25:42108 (UUIP-701)
ELAM, LeRoy Harry, Neonatal cranial irradiation and its delayed effects on learning, 25:42655
ELBAKYAN, S. S., Problem of transition radiation for a plasma plate, 25:43367
ELDRIDGE, H. B., Method for absolute calibration of Ge(Li) detectors using effective interaction depth, 25:42125

XUM

ELDYSHEV, Yu. N., Forced level shifts and energy renormalization, 25:43518
ELIAS, D., Reactor fuel management optimization in a dynamic environment, 25:44130
ELIAVA, A. T., Brueckner--Hartree--Fock theory for the ^{4}He nucleus, 25:43785
ELISEEV, V. A., Extraction of the proton beam of the 1-GeV synchrocyclotron, 25:43752
ELKINS, Ralph Leroy Jr., Effects of limbic lesions on irradiation contingent saccharin preference shifts, 25:42647
ELLINGBOE, Albert H., Somatic recombination in common-AB diploid of Schizophyllum commune, 25:42336
ELLIS, Walton P., Segregation of impurities on surfaces of thorium: thermodynamics and kinetics, 25:41825 (LA-DC-12348)
ELMS, R. V. Jr., Radioisotope thermal energy sources for space station life-support systems, 25:42004
EL-NADI, M., Cluster transfer reactions at low energies, 25:43964
Finite-range Coulomb stripping in (t,p) and (^{3}He,n) reactions, 25:43955
ELOFF, Cynthia, Distribution coefficients and cation exchange behavior of elements in hydrochloric acid--acetone, 25:41899
ELTRINGHAM, James R., Alterations in serum thyrotropin (TSH) and thyroid function following radiotherapy in patients with malignant lymphoma, 25:42695
ELYUTIN, V. P., Characteristics of porous graphite impregnated with fused zirconium, 25:42948
EMMEL, R. H., Manifestation of autoionizing states in the ionization of krypton by electron impact, 25:43154
EMRICK, Donald D., Treatment of polypeptide-containing hydrophilic polymeric capsule wall material with uranium and vanadium compounds, 25:41781
ENDERBY, J. A., Proposal for a generalised format for the layout of data in peripheral storage, 25:44184 (EACRP-A-135, pp 38-49)
ENDO, Kouichi, Investigation of radiation hazard in x-ray workers, 25:42495
ENEROTH, C. M., Effect of irradiation in high doses on parotid glands, 25:42599
ENGELBERTINK, G. A. P., Lifetime of the $^{1}/_{2}^{-}$ 2791-keV ^{21}Ne level, 25:43870
ENGELMANN, J., Penetration of solar protons over the polar cap during the February 25, 1969, event, 25:43232
ENGELS, A. C., Survival of colony-forming units in mouse bone marrow after in vivo irradiation with D--T neutrons, x-, and gamma radiation, 25:42601
ENGLER, A., Isobaric analogue resonances in ^{127}I, ^{125}I, and ^{123}I, 25:43933
ENGLISH, J. C., Calorimetry data acquisition and control, 25:44304 (UCRL-73045)
ENKOVSKII, L. L., Dual amplitude with Mandelstam analyticity, 25:43523 (ITF-71-28-E)
ENOT, K. Jean, Scintiphotographic evaluation of response of brain neoplasms to systemic chemotherapy, 25:42556
ENSTROM, James E., Solution of Thomas--Fermi model with quantum corrections, 25:43157
ENSTROM, James Eugene, Measurement of two photon decay of K/sub L/^{0} meson, 25:43531
EPHERRE, M., Excitation functions of ^{7}Be and ^{11}C produced in N by low-energy protons, 25:43818
EPPLEY, Richard Earl, Neutron-deficient, odd-mass rare earths near N = 82 closed shell, 25:43909
EPSTEIN, Eugene E., Radio sources: 3.3-mm flux and variability measurements, 25:43060
EPSTEIN, H. T., X-ray study of competence development in Bacillus subtilis, 25:42735
ERDMANN, Ute, Film dosimetry of high-energy rays. IV, 25:42396
ERDOS, P., Electronic energy levels of U^{4+} and U^{3+} in UO_2 and UI_3 crystals, 25:43499
EREMENKO, E. V., High intensity (10-16) GeV/c negative particle beam, 25:43729 (CERN-Trans-71-16)
ERNST, D. M., Heat pipe development for thermionic applications, 25:41977
ERNST, W. P., Broadband power density monitor for pulsed microwave sources, 25:42189 (MATT-845)
ERDZOLIMSKII, B. F., Angular correlation between neutron spin and electron momentum in decay of polarized neutrons, 25:43532
ERSHOV, E. B., Dose distribution in skin contaminated with radioactive substances, 25:42257
ESCH, E. L., Neutrographic hydrogen determination in zirconium alloys, 25:41755
ESCHER, John Stuart, Magnetic flux flow and fluctuation effects in thin film superconductors, 25:43322
ES'KOV, A. G., Thermal explosion induced in a collisionless plasma by a relativistic electron beam, 25:43372
ESTABROOK, F. B., Hamiltonian cosmology, 25:43095
ESTABROOK, K., Simulation of pseudowaves and of plasma sheath formation about a grid, 25:43369
ESTBERG, Gustaf, Role of hydride embrittlement in failure of a Zy-2 clad fuel element, 25:42882
ESTERL, John Edward, Isospin purity and violations of mirror symmetry: the β-delayed proton decay of ^{9}C, ^{13}O, ^{17}Ne, and ^{33}Ar, 25:43802 (UCRL-20480)
ETOH, Hisami, Mortality of fish under continuous irradiation conditions, 25:42634
ETOURNEAU, J., Nonstoichiometric hexaboride of thorium Th/sub 1-x/B$_{6}$, 25:43003
ETTENHUBER, E., Accumulation of radionuclides by fishes, 25:42249
ETTINGER, Harry J., Survey of techniques employed to define aerosol respirable dust concentration and particle-size characteristics. Vol. II, 25:44267 (LA-4249(Vol.2))
EULDERINK, F., Combination of radiation and chronic physical trauma in carcinogenesis of the enamel organ in mice, 25:42670
EVANS, E. P., Evidence against a cytogenetically radioresistant spermatogonial population in male mice, 25:42355
EVANS, J. V., Observation of F-region vertical velocities at Millstone Hill. I. Evidence for drifts due to expansion, contraction, and winds, 25:43224
EVANS, L., X-ray detector for dynamic diffraction studies, 25:42210
EVANS, R. K., Advanced power systems, 25:43186
Advanced power systems, 25:43276
EVANS, W. H., Selected values of chemical thermodynamic properties, 25:41826 (NBS-TN-270-5)
EVENSON, Alan, Depression of superfluid transition temperature in ^{4}He by heat current, 25:43286
EVSEENKO, A. K., Semiautomatic television device for measuring ionization losses, 25:42142
EVTUSHOK, T. M., Interaction of carbon with boride coatings on high-melting metals, 25:42854
EWING, W. M., Room temperature measurements of electrical resistivity and thermal conductivity of various graphites, 25:44283 (ORNL-TM-3477)
EYRING, LeRoy, Hydrothermal equilibria and crystal growth of rare earth oxides, hydroxides, hydroxynitrates, and hydroxycarbonates, 25:42934 (COO-1109-60)

F

FABRE, F., Uv-supersensitive mutant in yeast Schizosaccharomyces pombe, 25:42337
FABRIKANT, Jacob I., Cell population kinetics in thymus lymphocytes under continuous irradiation, 25:42631
FAES, M. G., Electromyographic examination of striated muscle in guinea pig after ^{60}Co irradiation, 25:42652
FAGAN, A. Wayne, Allotropes of carbon (amorphous, graphite, diamond) as engineering materials, 25:42977
FAINBERG, Joseph, U-type solar radio burst originating in the outer corona, 25:43070 (N-71-21564)
FAISAL, F. H. M., Vibrorotational excitations of H_2^+ by e^+ impact. I, 25:43141
FAISSNER, H., Possibility of CPT violation in neutral kaon decay, 25:43656 (PITHA-44)
FAM, S., Prog. rpt. on ultrasonic thermometry in LMFBR systems, 3/69, 25:42189 (NYO-3906-6)
FANGMAN, Walton L., X-irradiation sensitivity in E. coli, 25:42331
FANO, U., Raising of discrete levels into the far continuum, 25:43112
FARMER, F. T., Positioning of film badges, 25:42442
FARNY, G., Installation of beam facility on triton reactor, 25:44158 (LB/G-2929)
FARULLA, A., Internal contamination in vicinity of nuclear electric center at Garigliano, 25:42435
Whole-body counter at nuclear electric center at Garigliano, 25:42081
FAST, Peter M., Computer collection of mass spectrometric ionization efficiency curves, 25:44241 (COO-1140-198)
Computer control of a high-temperature quadrupole mass spectrometer, 25:42182 (COO-1140-194)
FASTOVSKII, V. G., Heat transfer with water and Freon-113 boiling on nonisothermal surface, 25:41989
FAVARO, L., New double-tracer technique in the diagnosis of liver neoplasia, 25:42580
FAVRO, L. D., Cross-section enhancement by scattering with correlated nonstationary states, 25:43105
Energy transfer via scattering of a coherent modulated electron beam, 25:43106
FAWWAZ, Rashid Adib, Preparation and evaluation of various radioactive metalloporphyrins for selective lymphatic ablation, 25:42312
FEDER, H. M., Solubility of helium and argon in liquid sodium, 25:41823 (ANL-7802)
FEDORCHENKO, V. D., Asymmetry of the combination-frequency spectrum in a plasma, 25:43410
FEDORENKO, N. V., Electron capture and loss by atoms, protons, and negative hydrogen ions in collisions, 25:43149
FEDOROV, F. I., Partial wave analysis on the basis of complex vector parametrization, 25:43720
FEDOROV, N. F., Phase equilibria in the high-alumina region of the system Al_2O_3--Nb_2O_5, 25:42985
FEDOROVA, T. A., Post-radiational changes in DNA metabolism as indicators of radiation injury, 25:42403
FEDOTOV, L. N., Superconducting alloy, 25:43318
FEHLAU, P. E., Vela V and VI solar x-ray atlas. V, 25:43066 (LA-4454(Vol.5))
FEICHT, E. J., Direct measurement of (n,2n) cross section of ^{93}Nb, 25:43897
FEIGENBAUM, Joel, PCAC and rho contribution to error in Goldberger--Treiman relation, 25:43511
FEL'DGUN, L. I., Mechanism of the phase transition in boron nitride, 25:42994
FELDMAN, David, Prog. rpt. on theoretical high-energy

physics, 6/71, 25:43559 (NYO-2262-TA-245)
FELNER, I., Rare-earth silicides and germanides of Mn_5Si_3 type substituted by europium, 25:42895
FELS, Margaret Fulton, Calculation of energies and widths of compound-state resonances in elastic scattering: stabilization method, 25:43147
FELST, R., Inelastic electron--proton scattering in the region of the Δ (1236) resonance, 25:43527 (DESY-71/21)
FENNELL, J. F., Asymmetric access of energetic solar protons to the Earth's north and south polar caps, 25:43233
FERENCZ, A., Some problems on the evaluation of biochemical indicators of radiation injury, 25:42407
FERR, D. A., Dynamics of a fast reactor with in-core thermionic converters. Fourth annual report, September 1, 1969--August 31, 1970, 25:44097 (COO-2109-5)
FERR, David A., Multiple input-output feedback synthesis incorporating cross-coupling, 25:44104 (COO-2109-4)
FERRI, G. G., Radio-induced cardiopathy, 25:42704
FERRO-LUZZI, M., Duality for inelastic anti KN scattering at intermediate energies, 25:43642 (UCR-34-P-107-8-136)
FETTER, Alexander L., Impurities in an imperfect Bose gas. I. The condensate, 25:43273
FETTWEIS, P., Levels in ^{101}Ru populated by decay of ^{101}Tc, 25:43899
FEUER, P., Transition probabilities for atom--atomic-oscillator collisions, 25:43145
FIEDLER, O., Use of a controlled-grid multiplier for fluorescence investigations in the nano- and subnanosecond region, 25:43452
FIELD, D. R., Performance of pressure-contacted lead-telluride thermoelectric generators, 25:42001
FIKHTENGOL'TS, I. G., Gravitational potential tensor and equations of motion in relativistic mechanics, 25:43709
FILE, J., Large superconducting magnet designs for fusion reactors, 25:43397 (MATT-848)
FILIP, R., Properties of Zr--Cu--Mo alloys, 25:42878
FILIPPOVICH, I. V., Effect of modifying factors on radiosensitive biochemical reactions, 25:42625
FINEGOLD, Leonard, Lattice-dynamical calculations for zinc and beryllium, 25:43478
FINKELSTEIN, David, Cosmological constant and fundamental length, 25:43087
FINNEY, B. C., Engineering-scale demonstration of the sol-gel process: preparation of 100 kg of ThO_2-UO_2 microspheres at the rate of 10 kg/day, 25:42937 (ORNL-4544)
FIORENTINO, F., Health physics experiences in ENEL nuclear electric centers, 25:42478
FIRKOWSKI, Ryszard, Spark chamber as an element of the hodoscopic detector of extensive air showers, 25:42158
FISCHER, James J., Mathematical simulation of radiation therapy of solid tumors. I, 25:42437
FISHER, Gerald Allen, Radiative proton capture studies in giant resonance region of lower l/sub p/ shell nuclei, 25:43813
FISHER, William D., Membrane association of conjugally transferred deoxyribonucleic acid in Escherichia coli minicells, 25:42735
FISHMAN, L. Ya., Calculation of the sensitivity function of a detecting system with a multichannel ring collimator, 25:42089
FITTS, R. B., Fuel element development for the Gas-Cooled Fast Breeder Reactor. Part I. Sealed fuel rod design, 25:44125 (ORNL-TM-3427)
In-reactor restructuring temperatures and kinetics for $(U,Pu)O_2$, 25:44124 (ORNL-TM-3397)
Observations of fuel-cladding chemical interactions as applied to GCBR fuel rods, 25:44123 (ORNL-TM-3385)
FIZZOTTI, C., Control rod fabrication experiments, 25:42822
Precipitation and influence of hydrides in zirconium alloys, 25:42955
FLECK, Carl M., Neutron physics practices. I, 25:43775
FLEISCHER, R. L., Apollo helmet dosimetry experiments, 25:42160 (N-71-14502)
FLEMMING, Kurt, Radiation protection of non-specific body defence: reticuloendothelial system and adrenal cortex, 25:42513
FLIEDNER, T. M., Effect of tritiated thymidine on the oocytes of foetal rats following maternal infusion in pregnancy, 25:42550
FLIPOT, A. J., Importance of stearates in the fabrication of UO_2 and $(U,Pu)O_2$ pellets, 25:42949
FLOERSCH, R. H., Theory and operation of Bendix mold heating and cooling equipment, 25:44230 (BDX-613-369)
FLOM, Richard, Correlation between brain tumor detectability on brain scan and protein levels of the spinal fluid, 25:42547 (ACRH-1000-248)
FLORES, J., Spacing and individual eigenvalue distributions of two-body random Hamiltonians, 25:43968
FLUECKIGER, E., Calculation of the multiplicity yield function of the IGY neutron monitor, 25:43175
FLYNN, E. R., Effect of multipole pairing and particle-hole fields in particle-vibration coupling of ^{209}Pb. II, 25:43923
FLYNN, M. J., Logical network cost and entropy, 25:44275 (NYO-4209)
FOCKE, B., Magnetic moments of isomeric levels in the Br isotopes, 25:43841
FOGARTY, William G., Radio sources: 3.3-mm flux and variability measurements, 25:43060
FOGEL, R. P., ^{7}Li(p,n)^{7}Be neutron polarization measurements for E/sub p/ = 3.0 to 5.5 MeV, 25:43805
FOMALONT, E. B., Two-dimensional structures of 76 extragalactic radio sources at 1425 MHz, 25:43061
FOMENKO, L. A., Regeneration of γ-radiation-induced single ruptures of DNA strands by polynucleotide ligases in vitro, 25:42268
FOMINA, Z. S., Changes of the testes of irradiated mice in bone marrow transplantation, 25:42304
FORD III, W. E., Neutron energy-dependent capture gamma-ray yields in tantalum and tungsten, 25:43890 (ORNL-TM-3436)
FORGACS, R. L., Fast switching pulsed neutron polarization inverter, 25:43776
FORMAN, L., Evidence for violation of Porter--Thomas postulate in ^{232}Th, 25:43911
FORREST, D. L., Compact ^{60}Co kernel for space power, 25:42000
FORTNER, R. J., Production of carbon K x rays by heavy-ion bombardment, 25:43107
FORTNEY, L. R., Preliminary version of RIPPLE software descriptions, 25:44298 (TID-25758)
FORTUNE, H. T., ^{6}Li + ^{6}Li scattering at E = 5 to 7 MeV, 25:43816
T = 1 states in the A = 12 system, 25:43819
FORTY, A. J., Faraday cup LEED apparatus for investigating inelastically scattered or photoemitted electrons, 25:43474
FOSTER, B. E., X-ray attenuation scanning of nuclear fuel plates, 25:42031
FOSTER, J. L. Jr., Reaction ^{142}Nd(d,t)^{141}Nd, 25:43900
FOULQUIER, H., Structures of Zr alloys in heavy-water reactors, 25:42929
FOURNIER, Jacques, Measuring activity of radioisotopes in gas, 25:41753
FOWLER, J. F., Time-dose relations in radiotherapy, 25:42414
FOWLER, T. W., Iodine-131 discharges from an operating boiling water reactor nuclear power station, 25:42388
FOX, B. W., Toxicity of tritiated thymidine in P388F lymphoma cells. I, 25:42251
FOX, F. K., SNAP-21 10-watt thermoelectric power system, 25:41998
FOX, J. A., Recalculation of the crossed-graph contribution to the fourth-order Lamb shift, 25:43687
FOX, Margaret, Toxicity of tritiated thymidine in P388F lymphoma cells. I, 25:42251
FOX, P. F., Design considerations of FFTF safety, 25:44139 (HEDL-SA-169)
FOYT, D. C., Spin-free quantum chemistry. X, 25:43164
FRAAS, A. P., Blascon: an exploding pellet fusion reactor, 25:43398 (ORNL-TM-3231)
FRADKIN, D. M., Energy transfer via scattering of a coherent modulated electron beam, 25:43106
FRALICK, Joe A., Membrane association of conjugally transferred deoxyribonucleic acid in Escherichia coli minicells, 25:42735
FRANCA, J. M. Jr., Ion-exchange pilot plant for the preparation of nuclear pure uranium compounds, 25:41919
FRANCESCHINI, P., Effect of ionizing radiations on lymphocytes from adults and newborn infants, cultured in vitro in presence of phytohemagglutinin, 25:42602
FRANK, I. M., Development and application of pulsed fast reactors IBR for scientific researches, 25:44156 (JINR-P3-5754)
FRANK, L A., Distribution of plasmas and electric fields over auroral zones and polar caps, 25:43219 (N-71-20708)
FRANK, Richard B., Programming apparatus for an automatic liquid scintillation counting system, 25:42058
FRANKE, W.-G., Suitability of technetium-labeled erythrocytes for the examinations of the splenic function, 25:42570
FRANKLIN, D. G., Considerations of metal swelling and related phenomena caused by fast neutron irradiation, 25:42918
FRANKOVSKI, V., Optimum start-up of the fuel reprocessing industry, 25:41894 (INR-1297)
FRANZEL, Ruediger, Experiments on toroidal confinement of high-beta plasmas with helical multipole fields, 25:43336
FRED, M. S., g/sub J/ value for the atomic ground state of fermium, 25:43118
FREEDMAN, M. S., Ionization (shakeoff) accompanying K-shell internal conversion, 25:43871
Outer-shell internal conversion of the 14.4-keV transition in ^{57}Fe, 25:43865
FREEMAN, Gerald R., Crystal and molecular structures of tri-(p-fluorophenyl)-amine and tri-(p-iodophenyl)-amine, 25:44296 (TID-25742)
FREEMAN, John P., Configurational stabilities of strained α-sulfonyl carbanions. Kinetics of base-catalyzed racemization and deuterium exchange of representative thiete and thietane dioxides, 25:41805
FREEMAN, N. J., Decay of ^{126}Sn and of 19-min and 12.4-day isomers of ^{126}Sb, 25:43924

FREESTONE, R. M. Jr., Calibration of Bonner ball neutron detectors used at Tower Shielding Facility, 25:42055 (ORNL-TM-3455)
FREIDBERG, Errol C., Dark repair of ultraviolet-irradiated deoxyribonucleic acid by bacteriophage T4: purification and characterization of a dimer-specific phage-induced endonuclease, 25:42269
FRENKEL, J. M., Deformation and cracking in Zr--Cu cladding in carbon dioxide, 25:42928
FREVERT, L., Modular programming system for programming experiments on PDP-9, 25:42181 (CERN-Trans-71-18)
FRIEDMAN, Eli A., Synergism in immunosuppression. I. Effect of methylprednisolone, azathioprine, chlorambucil, and radiation on tetanus antitoxin production, 25:42572
FRIEDMAN, Herbert W., Collisionless shocks in plasmas, 25:43347
FRIESENHAHN, S. J., Light collection from large cylindrical scintillators, 25:42055
FRINDEL, Emilia, Hematological effects of partial body irradiation: clinical and experimental data, 25:42599
FROEHLICH, H., Superconductivity, lattice stability, and phonon frequencies, 25:43296
FROMM, Eckehard, Simultaneous oxide evaporation and thermal diffusion in tantalum--oxygen solid solutions, 25:42975
Some theoretical aspects of thermal diffusion in interstitial solid solutions, 25:42865
Thermal diffusion of O in Ta--O and Nb--O solid solutions, 25:42864
FRYE, E. R., Carbon--carbon materials for ablative environments, 25:42971
FRYER, B. C., Radioisotope-energized Stirling engine for spacecraft auxiliary electric power, 25:42010
FU, C. C., Shell-model calculations for ^{51}V and ^{52}Cr, 25:43862
FU, C. Y., Neutron energy-dependent capture gamma-ray yields in tantalum and tungsten, 25:43890 (ORNL-TM-3436)
FUEKI, Kenji, Effect of phase on excitation transfer in the radiolysis of isobutane, 25:41864
Role of reaction sites in the radiolysis of solid succinic acid, 25:41855
FUJIKAWA, Kazuo, Study of the self-coupling of weak lepton currents at high energies, 25:43612
FUJIMOTO, F., Effects of crystal surface and imperfections on channeling phenomena of protons, 25:43461
FUJIMURA, T., Embrittlement of pressure vessel steels irradiated in JPDR, 25:42905
FUJINAGA, Yutaka, Cases of atomic bomb radiation cataract in the last 10 years, 25:42546
FUJITA, Minoru, Monitoring for internal exposure. I, 25:42481
FUJITANI, Yoshiteru, Role of reaction sites in the radiolysis of solid succinic acid, 25:41865
FUJIWAKA, Setsuya, Effect of working on change of permeability (μ) of austenitic stainless steels, 25:43467 (IPPJ-DT-20)
FUJIWARA, Noboru, Heavy particle identification with TOF method in nuclear reactions, 25:42066
FUKAI, J., Plasmons and the linear and nonlinear two-stream instabilities, 25:43387
FUKUZAWA, F., High-energy humps in spectra of backscattered protons from Si, 25:43459
FULLER, J. C., Vela V and VI solar x-ray atlas. V, 25:43066 (LA-4454(Vol.5))
FULLERTON, D. C., Application of the statistical phase-space theory to the reactions of rare gas ions with nitrogen molecules, 25:43159
Statistical phase-space model of collision-induced dissociation of excited O_2^+ and NO^+ ions, 25:43158
FUNG, P. C. W., Structure of the chromosphere--corona transition region, 25:43068 (N-71-19294)
FUNG, S. Y., $\pi^+ + p \rightarrow \Delta^{++}$ (1236) + π^0 AT 1.85 to 2.09 GeV: study of s- and t-channel effects, 25:43551 (UCR-34-P-107-B-108)
Study of $\pi^+p \rightarrow rho^+p$ at 1.85 to 2.09 GeV, 25:43552 (UCR-34-P-107-B-110)
FURCHTGOTT, Ernest, Open-field behavior and heart rate in prenatally x-irradiated rats, 25:42640
FURICH, M., Inelastic interaction of neutrons with H and deuterium, 25:43550
FURNICA, M., Sensitization of living organisms by chemical agents towards the activity of radiations and cytostatics. I, 25:42535
FURUNO, Ikuko, Metabolism of Ehrlich ascites tumor cells under anoxia, 25:42532
FUSHCHICH, V. I., Relativistic equations of motion without redundant components, 25:43654 (ITF-70-89-E)
FYURS, G. P., Diffusion of plasma in a toroidal stellarator, 25:43374

G

GABRIELSE, S. E., Fuel rod deformations: a time dependent finite element analysis on axisymmetric fuel rods, including pellet end effects (LMBR development program), 25:44125 (WERL-ELPLA-1)
GADZHKOV, V., Processing of spectra from Ge--Li detectors on digital computers (KATOK program), 25:42115
GAEUMANN, T., C--H valence vibrations in hydrocarbons and butyl halides, 25:41821
Fundamental and harmonic C--H/C--D valence vibrations of halogen derivatives of methane and of deuteriomethane, 25:41822
Quantitative analysis of gas chromatograms of partially separated material mixtures, 25:41745
GAINES, E. E., Solar particle cutoffs as observed at low altitudes, 25:43234
GAL, O., Radiolytic decomposition of solid oxalic acid, 25:41868
GALANTER, L., Tabulated dose distribution data for gamma irradiator design, 25:41957 (BNL-50147(Rev.))
GALEEV, A. A., Diffusion of plasma in a toroidal stellarator, 25:43374
GALIMOV, D. G., Radiation yield of Mn^{+3} in dosimetric glasses, 25:42163
GALKIN, Yu. M., Influence of some salts on the double decomposition of zircon with calcium carbonate, 25:42972
GALLI, Alicia J. Couto, General properties of dual models: conformal invariance, 25:43555
GALLI, Eduardo Jorge, Topics in dual resonance models, 25:43619
GALLMANN, A., Levels of ^{36}S from $^{34}S(t,p)^{36}S$, 25:43869
GAMKRELIDZE, L. M., Effect of ionizing radiation on the quantitative content of carbohydrates in wheat radicles, 25:42721
GANEA, A., Sensitization of living organisms by chemical agents towards the activity of radiations and cytostatics. I, 25:42535
GANICHOT, D., Backward electron deuteron scattering below 280 MeV, 25:43528 (LAL-1250)
GANLEY, T., Enhancement of CO_2 laser power and efficiency by neutron irradiation, 25:42229
GARDINER, C. W., Note on the most probable number of partons in parton models, 25:43585 (SU-1206-246)
GARDNER-THORPE, Christopher, Chloroma following irradiation in ankylosing spondylitis, 25:42709
GARDZEI, G. M., Radiation resistance of hybrid plants, 25:42722
GARDZEI, I. A., Radiation resistance of hybrid plants, 25:42722
GARFINKEL, A. F., Evidence for splitting in the Q region of $K^+\pi^+\pi^-$ mass, 25:43544 (COO-1428-275)
Final states with three charged particles and a visible anti K^0 from K-d interactions at 4.5 GeV/c, 25:43549 (COO-1428-286)
New evidence for splitting in the Q region of $K^+\pi^+\pi^-$ mass, 25:43543 (COO-1428-274)
GARG, J. B., Neutron resonance spectroscopy. VII, 25:43874
GARG, J. C., Positron annihilation in some transition and alkaline earth oxides, 25:43482
GARG, R. K., Half-life measurements of 86.6-keV level in ^{233}Pa and 59.6-keV level in ^{237}Np, 25:43895
GARR, K. R., Effects of helium on the high-temperature ductility of Sandvik 12R72HV and Inco IN-744X, 25:42872
GARTNER, Leslie Paul, Aging and ionizing radiation, 25:42612
GARTON, Ronald R., Guidelines: biological surveys at proposed heat discharge sites, 25:44259 (NP-18843)
GARZA, Luis Rene, Radioisotopic evaluation of salivary gland dysfunction in Sjoegren's syndrome, 25:42566
GASCO, L., Volatile radiolytic compounds in irradiated fish, 25:42753
GASSMANN, G. J., Ionospheric model for Arctic, 25:43212 (AD-715893)
GATES, Gary F., Primary congenital lymphedema in infancy evaluated by isotope lymphangiography, 25:42559
GAUDIER, Jean-Francois, Process for decontaminating radioactive effluents, 25:41911
GAVLOVSKA, Vatslava, Laboratory mixer--settler extractor LMOM2, 25:41895 (INR-1309)
GAWIN, J., Possibility of existence of a new process at interactions with energies above 10^{12} eV, 25:43567 (INR-1280)
GAZIEV, A. I., Regeneration of γ-radiation-induced single ruptures of DNA strands by polynucleotide ligases in vitro, 25:42268
GEIGER, A. L., Measurement of the superconducting energy gap and Fermi velocity in single-crystal lead films by electron tunneling, 25:43312
GEISSLER, Erhard, Differences in host controlled reactivation of lambdoid and T phages, 25:42738
GEL'BSHTEIN, M. I., Morphological changes of thyroid cancer in telegammatherapy, 25:42679
GEL'D, P. V., Nature of the bond and electrical conductivity of cubic zirconium carbides and oxycarbides, 25:43491
Possibility of the existence of stable zirconium monoxide, 25:42987
GELFAND, Michael, Synergism in immunosuppression. I. Effect of methylprednisolone, azathioprine, chlorambucil, and radiation on tetanus antitoxin production, 25:42672
GENGOZIAN, Nazareth, Effect of acute radiation exposure rates on formation of hemagglutinating antibody in mice, 25:42307
GENTY, Claude, Principle of standard samples realization in analytical chemistry: trace elements problems in Pu,

25:41718 (CEA-R-4105)
GEORGI, Heinz W., Radiation detection system with automatic sample counting rate determination, 25:42103
GEORGIEV, Z., Changes in pea varieties as affected by gamma rays, 25:42329
GEORGIEVA-TODOROVA, Iordanka, X-rays influence on chromosome aberrations in H. annuus, 25:42361
GERASIMOV, V. V., Corrosion and electrochemical behavior of zirconium alloy, 25:42814
Thermal denaturation of ribonuclease dissolved in heavy water, 25:41793
GERBER, G. B., Influence of selection, non-uniform cell population, and repair on dose-effect curves of genetic effects, 25:42353
Mechanism of excess excretion of nucleic-acid and NAD metabolites after irradiation, 25:42623
Thoughts concerning the further development of biochemical indicators, 25:42685
GERESHTY, Anna M., Determination of acid-soluble, acid-insoluble, and total uranium in silicate ores, 25:41723 (NIM-1077)
GERSCH, H. A., High-energy neutron scattering from liquid helium in the impulse approximation, 25:43278
GETASHVILI, G. R., Thermal denaturation of ribonuclease dissolved in heavy water, 25:41793
GFIRTNER, H., Angular correlation studies on the 326- and 177-keV cascade in ^{131}Xe, 25:43896
GHEORGHE, N., Biochemical disequilibria induced in brain of rat by irradiation and protective effect of cysteine. I, 25:42619
Effect of ionizing radiations on complex lipids of brain and protective effect of cysteine. II, 25:42620
Prevention of intestinal absorption of radiocesium and radiostrontium with the help of indigenous ionic resins, 25:42253
GHIZARI, Eugenia, Activity of pyrophosphatase and catalase after long irradiation with small doses of ^{60}Co, 25:42277
GHOSH, Aparna, Fermi surface and energy bands of lanthanum, 25:43500
GHOSH, S., Observation of damage regions produced in silicon solar cells by neutron irradiation, 25:42232
GIACCONI, R., Discovery of periodic x-ray pulsations in Centaurus X-3 from Jhuru, 25:43055
GIBBONS, J. R. P., Gamma ray sterilisation of homograft valves, 25:42759
GIBERTINI, Giancarlo, Effect of x rays on the mouse thymus gland, 25:42297
GIBSON, W. M., Charged-particle radiation damage observed as dimpling of thin silicon targets, 25:43438
GIEBEL, Ray E., Drybox gloves: evaluation and procurement, 25:42039 (RFP-1295)
GIEDD, Ronald Elroy, Thermal conductivities of normal and superconducting indium--lead alloys at low temperatures, 25:43324
GIESE, Joern, Iodine-125-labelling of angiotensin I and II, 25:42241
GIESSNER, B. G., Manifestation of autoionizing states in the ionization of krypton by electron impact, 25:43154
GIFFON, M., Reconstruction of amplitudes for pion--nucleon scattering from experimental data, 25:43640 (LYCEN-7110)
GILES, M. S., Preliminary ecological studies at Jervis Bay, 25:42314 (CONF-710511-3)
GILISSEN, R., Importance of stearates in the fabrication of UO_2 and $(U,Pu)O_2$ pellets, 25:42949
GILLES, Paul W., Computer collection of mass spectrometric ionization efficiency curves, 25:44241 (COO-1140-198)
Computer control of a high-temperature quadrupole mass spectrometer, 25:42182 (COO-1140-194)
GILLY, C., In vitro study of effect of γ rays on human chromosomes, 25:42365
GILMAN, J. J., Lithium dihydrogen fluoride: an approach to metallic hydrogen, 25:43475
GILYAZUTDINOV, I. A., Effectiveness of scanning bone tumors with ^{85}Sr and /sup 87m/Sr, 25:42562
GIMBERT, J.-L., Effects of pulmonary lavage on the retention of particles of plutonium oxide, 25:42368 (LF-tr-53)
GINDLER, J. E., Critical review of the energy released in nuclear fission, 25:43985 (ANL-7748)
GINOZA, William, Effects of ionizing radiation on capacity of Escherichia coli to support bacteriophage growth, 25:42730 (NYO-2904-41)
GINSBURG, A., Isobaric analogue resonances in ^{127}I, ^{125}I, and ^{123}I, 25:43933
GINZBURG, I. F., Electromagnetic contributions to the total cross section of hadron scattering, 25:43616
GIORNI, A., ^{6}Li(α,2α) reaction as a test of the existence of α particles in ^{6}Li, 25:43803
GIRARDEAU, M. D., ODLRO and momentum distribution of electron pairs in superconductors, 25:43317
GIRAUD, B., Truncation of rotational states in the shell model, 25:43828
GIRSIG, F., Variation of nonlinear parameters to compute decay-constants and their standard deviation, 25:43521
GIUDICI, G., Categories of stability for regions of Italy, 25:41936
GIUFFRE, S., Parameter study for a transit time magnetic pumping experiment in a torus, 25:43332 (EUR-CEA-FC-595)
GIVORD, J. P., Structure of Zr--Cr alloys, 25:42879
GLADUN, A. D., Hydrodynamic stability of electron streams in vacuum, 25:43756
GLADYSHEVSKII, E. I., System yttrium--chromium--silicon, 25:42993
Systems Y--Al--Si (Ge,Sb), 25:42891
GLASS, N. W., Evidence for violation of Porter--Thomas postulate in ^{232}Th, 25:43911
GLATSTEIN, Eli, Alterations in serum thyrotropin (TSH) and thyroid function following radiotherapy in patients with malignant lymphoma, 25:42695
GLATZ, J., Measurement of nuclear half-lives up to 100 s by the delayed coincidence method, 25:42222
GLAVANAKOVA, S. I., Ratio of sexes in F_1 after irradiation of female and male imagos of Sitotraga cerealella, 25:42610
GLEIZER, Yu. Ya., Effectiveness of scanning bone tumors with ^{85}Sr and /sup 87m/Sr, 25:42562
GLEMBOTSKII, Ya. L., Genetic effects of chronic γ-irradiation of Drosophila melanogaster males, 25:42350
GLENDENNING, Norman K., Study of inelastic processes on (d,p) reactions in deformed nuclei, 25:43984
GLICKSON, J. D., Conformation of poly-β-alanine in aqueous solution from proton magnetic resonance and deuterium exchange studies, 25:41807
GLODEN, R. F., Determination of eigenvalues of Mathieu equation, 25:43505 (EUR-4349)
GLOTIN, Ph., Multi micro beams for ion implantation, 25:43728 (CEA-CONF-1767)
GLOWACKI, Jerzy, Spark chamber as an element of the hodoscopic detector of extensive air showers, 25:42158
GODFREY, T. G., Sintering of UN as a function of temperature and N_2 pressure, 25:42979
GODFREY, W. L., Treatment of liquid wastes by evaporation to salt cakes, 25:41887 (ARH-SA-25)
GOEBEL, J., Monitoring of positively charged particles in the electron ring accelerator, 25:43734 (UCRL-20664)
GOERNER, W., Burn-out of cadmium shields, 25:43422 (ORNL-tr-2488)
GOETZMANN, O., Room temperature mechanical properties and precipitation behavior of steel Incoloy and Inconel after annealing in contact with UC, 25:42844 (EURFNR-922)
GOFFMANN, Pshemyslav M., Laboratory mixer--settler extractor LMOM2, 25:41895 (INR-1309)
GOLDBERG, D. M., Alkaline ribonuclease activity in response to therapeutic radiation in the human female, 25:42683
GOLDSWORTHY, W. W., Digital nuclear spectrometer, 25:42121
GOL'FAND, Yu. A., Extension of algebra of Poincare group generators and violation of P invariance, 25:43676
GOLIC, L., Phase relationships and crystal chemistry in systems US--CaS, US--SrS, and US--BaS, 25:43002
GOLLIN, Frank F., Pre-irradiation 5-fluorouracil infusion in advanced head and neck carcinomas, 25:42589
GOLOVKOV, N. A., α decay of neutron-deficient radon isotopes, 25:43887 (JINR-P6-5791)
GOLOVNYA, N. I., High intensity (10-16) GeV/c negative particle beam, 25:43729 (CERN-Trans-71-16)
GOLOWICH, E., Current algebra and the trace of the energy--momentum tensor, 25:43630
GOLUBENTSEV, D. A., Effect of ionizing radiation on the excretion of radioprotectors in rats' urine, 25:42671
GOLUBEV, B. P., Dosimetry and protection against ionizing radiation, 25:42425
GONCHAR, V. Yu., Instrument for measuring and monitoring the energies of particles accelerated in a cyclotron, 25:43743
GONCHARENKO, I. I., Superconductive shielded magnetic lens, 25:43748
GONCHAROV, E. G., Phase diagram of the system Cd--As, 25:42989
GONCHAROV, V. V., Results of loop tests on Zr-clad experimental fuel rods in the Mr reactor, 25:43010
GONDRAND, Jean-Claude, Nucleon--nucleon interaction from 3 nucleon interaction D(n,nnp) at 14 MeV, 25:43533 (CEA-R-4150)
GONNIN, Rene, Measuring activity of radioisotopes in gas, 25:41753
GONZALEZ-JIMENEZ, Yolanda, Radioisotopic evaluation of salivary gland dysfunction in Sjoegren's syndrome, 25:42566
GOODE, G. C., Multi-element analysis of glass fragments by neutron activation and the application to forensic science, 25:41758 (AWRE-O-24/71)
GOODMAN, L. S., g/sub J/ value for the atomic ground state of fermium, 25:43118
GOODMAN, S. E., Mechanism for normal-fluid critical velocity in He II, 25:43275
GOPALAKRISHNAN, S. S., Investigation on ^{210}Pb concentrations in various regions of India, 25:42387
GORBARENKO, N. I., Variants of the syndrome of neurovascular dystonia in chronic radiation effect, 25:42676
GORDEN, R. Jr., Solid phase photolysis and radiolysis of ethylene at 20 to 77 K, 25:41875
GORDON, Howard A., K^+ forward scattering from the reaction $\pi^-p \rightarrow K^+\Sigma(1375)^-$ at 4.5 and 6 GeV/c, 25:43558
GORDON, Milton P., Prog. rpt. on photobiology and photochemistry of ribonucleic acids, 1--12/70, 25:42267 (RLO-2225-T-15-3)
GORDON, Sheffield, Pulse radiolysis of ammonia gas. II. Rate of disappearance of the $NH_2(X^2B_1)$ radical,

XUM

25:41869
GORMAN, F. J. Jr., Studies of wavelike variations in the ionosphere, 25:43209 (AD-714993)
GORNAK, K. A., Activity of redox enzymes in the liver in internal use of radon water, 25:42279
GORSHKOV, V. G., Interference between Coulomb and strong interactions at high energies, 25:43607
GORSKI, L., Solid-state detectors and electronics in gamma and x-ray spectrometry, 25:42133
GORYACHEV, I. V., Protection from penetrating radiation of a nuclear explosion, 25:42034 (JPRS-53498)
GOSWAMI, D. N., Inelastic Compton scattering inequalities in quark-Parton model, 25:43586 (SU-1206-250)
GOTTSCHALK, Alexander, Correlation between brain tumor detectability on brain scan and protein levels of the spinal fluid, 25:42547 (ACRH-1000-248)
GOULD, Harvey, Order-parameter fluctuations in a weakly interacting Bose gas near the superfluid transition, 25:43284
GOULD, R. J., Deviation from a Maxwellian velocity distribution in low-density plasmas, 25:43023
GOUNARIS, G. J., Veneziano model consistent with the Yang--Mills coupling of vector-meson fields, 25:43631
GOYAL, R., Effect of coherence on intensity-dependent frequency shift in Compton scattering, 25:43590
GRACHEV, M. I., High intensity (10-16) GeV/c negative particle beam, 25:43729 (CERN-Trans-71-16)
GRAF, W., Polytetrafluoroethylene: dosimeter for gamma dose measurements in about 10^{11} rad, 25:42170
GRAFSTROEM, P., Total absorption of 100 MeV protons with a Ge(Li) detector, 25:42128
GRAHAM, L. S., Determination of in vivo persistence of tantalum dust following bronchography using reactor-activated tantalum and total body counting, 25:42558
GRALL, L., Corrosion of Zr alloys in water and steam, 25:42810
GRASS, F., Quantitative determination of rare earths in meteorites by means of high voltage electrophoresis, 25:41776
Variation of nonlinear parameters to compute decay-constants and their standard deviation, 25:43521
GRATE, Helen E., X-ray and alkylating agents alter differentiation of surviving hematopoietic stem cells, 25:42651
GRAUL, E. H., Chemical radioprotection with N- and S-containing polymers, 25:42517
GRAVES, R. S., Room temperature measurements of electrical resistivity and thermal conductivity of various graphites, 25:44283 (ORNL-TM-3477)
GREEN, Allen T., Detection of incipient failure in pressure vessels by stress wave emission, 25:44137 (CONF-700224-, Paper 3)
Stress wave emission and fracture of prestressed concrete reactor vessel materials, 25:43015
GREEN, Thomas A., Euler--Lagrange optimization of plane-wave factors, 25:43144
GREENE, D. G. S., Polarization of the free--free bremsstrahlung in an anisotropic hot-electron plasma, 25:43357
GREENFIELD, H. H., Radioisotope thermal energy sources for space station life-support systems, 25:42004
GREENSPAN, J. C., Investigation of fast-reactor fuel testing in a thermal reactor core, 25:44165
GREENSPOON, S., Superconducting proximity effects by Josephson tunneling, 25:43308
GREENSTREET, W. L., Effect of fillets on stress concentrations in cylindrical shells with step changes in outside diameter, 25:41959 (CONF-710512-15)
Experimental and finite element stress analysis of a thin-shell cylinder-to-cylinder model, 25:42839 (CONF-710512-3)
GREENWALD, R. A., Dispersal of a localized density fluctuation in a uniform magnetoplasma, 25:43370
GREENWOOD, R. C., Coriolis coupling in doubly odd deformed nuclei, 25:43934
Level structure of ^{182}Ta, 25:43935
GREINER, Walter, Influence of nuclear forces on Coulomb fission, 25:43970
Stability of superheavy nuclei against fission, alpha decay, and electron capture, 25:43919
GRIDER, E. E., Form rolling complex close tolerance shapes, 25:42827
GRIDNEV, N. P., Group properties of MHD equations and their invariant solution, 25:43194
GRIENEISEN, Andre, Multistage process for extracting U and Pu with solvent comprising tributylphosphate, 25:41902
GRIFFIN, Allan, Density fluctuations in an interacting Bose gas, 25:43522
GRIGORENKO, L. P., Effect of direct current and x radiation on bone marrow cells, reticuloendothelial cells, and radiosensitivity of rats, 25:42530
GRIGORESCU, St., Mechanisms of chemical radioprotection, 25:42523
GRIGOR'EV, R. V., Changes in energy spectrum of capture centers (traps) in electron-bombarded CdS crystals, 25:43437
GRIGORYAN, S. S., Bioelectrical activity of cerebral structures of the rabbit resulting from the combined action of radial acceleration and irradiation, 25:42653
GRIM, C. E., Accurate and rapid measurement of plasma renin activity by radioimmunoassay. Results in normal and hypertensive people, 25:42238
GRIMES, S. M., Pre-equilibrium decays of the compound nucleus, 25:43957 (UCRL-73152)
GRIMES, Warren R., Method for separating U, Pa, and rare earth fission products from spent molten fluoride salts reactor fuels, 25:41903
GRIMSRUD, Eric Paul, Chlorine kinetic isotope effects in nucleophilic displacement reactions, 25:41795
GRIPSHOVER, Paul J., Comparison of conventional and hydrostatic pressing of metal powders, 25:42828
GRISHAM, Joe W., Detection of Australia antigen by radioimmunoassay, 25:42308
GRISHANOVA, S. I., Calculation of electroexcitation of C in the region of giant resonance, 25:43824
GRISHCHENKO, A. L., Relativistic equations of motion without redundant components, 25:43654 (ITF-70-89-E)
GRISHIN, V. G., Characteristics of coherent interactions at 17 and 45 GeV, 25:43645 (JINR-P1-5775)
Thermodynamical description of momentum distributions of pions in π-p interactions at p = 4 GeV/c, 25:43639 (JINR-P1-5849)
GRISHIN, V. K., Monoenergetic nature and stability of the beam current in linear induction accelerators, 25:43745
GRISS, Martin L., Inequalities on double partial-wave amplitudes from positivity, analyticity, and crossing symmetry, 25:43625
GRIVU, Ov., Experimental studies on tooth eruption, 25:42638
GRODNIK, Jesse, Functional-equation approach to canonical theories, 25:43678
GROMOV, K. Ya., Beta-spectrographs with permanent magnets, 25:42110
GROMOVOA, A. I., Corrosion and electrochemical behavior of zirconium alloy, 25:42814
GROSHEV, L. V., Gamma-ray spectrum from reaction (n,γ) on ^{150}Sm and ^{151}Sm samples, 25:43892
GROSS, E. F., Annihilation of excitons and exciton--phonon interaction, 25:43502
GROSS, Eugene P., Point transform theory of liquid helium, 25:43274
GROSS, Franz, Thermionic converter with concentric collector and emitter, 25:43189
GROSS, Julian, Induction of prophage lambda in mutant of E. coli, 25:42340
GROSSETETE, B., Backward electron deuteron scattering below 280 MeV, 25:43528 (LAL-1250)
GROSSMANN, H., Etiologic relation between radiation castration and malignant gynecologic neoplasms, 25:42675
GROSZ, Fred A., Some studies involving the determination of molybdenum by atomic absorption spectroscopy, 25:41728
GROUARD, Jean-Pierre, Study of 3 ^{1}P--2 ^{1}S line of He excited by H ion beam, 25:43129
GRUBER, E., Activation analytical studies of standardized Fe alloys. I, 25:41774
GRUDEN, Nevenka, Effect of alginates from algae on Sr transport through rat's duodenum, 25:42254
GRUDINKINA, N. P., Determination of the isotopic composition of tin and indium, 25:41727
Determination of the isotopic composition of cadmium, 25:41731
GRUEFF, Gavril, Flux density measurements of optically identified B2 radio sources at 5 GHz, 25:43063
GRUEMM, H., Energy generation and the environment, 25:44143 (SGAE-RT-39/1971)
GRUMANN, Jens, Stability of superheavy nuclei against fission, alpha decay, and electron capture, 25:43919
GSCHNEIDER, K. A. Jr., Preparation of lanthanide single crystals: Pr, Nd, and Lu, 25:42834
GUBATOVA, D. Ya., Determination of radiation dose to children during x-ray diagnostic procedures, 25:42412
GUBRIENKO, K. I., High intensity (10-16) GeV/c negative particle beam, 25:43729 (CERN-Trans-71-16)
GUDDEN, H., Uranium prospection of the Eisenwerkgesellschaft Maximilianshuette in Nordostbayern, 25:41942
GUENDEL, H., Partition function and effective ionization potential of an atom in a plasma. I, 25:43364
GUERNET, G., Multi micro beams for ion implantation, 25:43728 (CEA-CONF-1767)
GUERY, Marcel, Method for determining the concentration of a highly active element by α spectrometry of a thick radiation source and corresponding device, 25:42118
Small fission chamber, of pulse type, operating at high temperature, 25:42050
GUES, J., Beta--gamma circular polarization correlation measurements on the decays of ^{203}Hg, ^{199}Au, and ^{141}Ce, 25:43941
GUILLOT, Francois, Device with a large dynamic range for measuring direct currents and voltages, 25:42208
GUKOV, D. Ya., Phase diagram of the system Cd--As, 25:42989
GULAMOV, K. G., Characteristics of coherent interactions at 17 and 45 GeV, 25:43646 (JINR-P1-5775)
GULICK, J. M., Magnetic susceptibility of uranium monophosphide, 25:43495
GULLIFOR, P., Induction of translocations in mature Drosophila oocytes over a dose range of 10 to 500 roentgens of x rays (stage-14 oocyte/radiation damage), 25:42333

SULYAKIN, I. V., Behavior of fission products in soils of Uzbekistan, 25:42319
SULYAMOV, U. G., Characteristics of coherent interactions at 17 and 45 GeV, 25:43546 (JINR-P1-5775)
SUPPY, J. S., Dynamics of a fast reactor with in-core thermionic converters. Fourth annual report, September 1, 1969--August 31, 1970, 25:44097 (COO-2109-5)
SUPTA, Ashok Kumar, Superconducting state parameters for nontransition metals, 25:43305
SUPTA, R. K., X-ray study of cold-work and recovery in tungsten, 25:42870
SUPTA, R. P., Generalized susceptibility function for rare earths and thorium and their alloys, 25:43477
SUPTA, S. L., Half-life measurements of 86.6-keV level in ^{233}Pa and 59.5-keV level in ^{237}Np, 25:43895
SURALNIK, S. S., Two-loop approximations to propagators in the sigma model, 25:43584
SUREVICH, Yu. Ya., Photoproduction of electrons in strong electromagnetic field, 25:43606
SURNETT, D. A., Distribution of plasmas and electric fields over auroral zones and polar caps, 25:43219 (N-71-20705)
SURNETT, Donald A., Double probe measurements of dc electric fields with Injun 5 satellite, 25:43216 (N-71-18405)
SURSKY, H., Discovery of periodic x-ray pulsations in Centaurus X-3 from Jhuru, 25:43055
Strong x-ray source in Coma cluster observed by Jhuru, 25:43056
SURVICH, O. S., High-temperature materials, 25:42853
SUSEINOV, V. K., Study of complex formation between zirconium and certain organic reagents, 25:41737
SUS'KOVA, A. K., Radiation sickness in man, 25:42542
SUSS, Stephen B., Local recurrence of generalized herpes zoster following x irradiation, 25:42689
SUSTAFSON, D. R., Positron annihilation in rare earth hydrides, 25:43125
SUSTAFSON, J. C., Coolant blowdown studies of a reactor simulator vessel containing a simulated reactor core, 25:44133 (BNWL-1524)
SUTAY, L. J., Final states with three charged particles and a visible anti K^0 from K$^-$d interactions at 4.5 GeV/c, 25:43549 (COO-1428-286)
SUTKEVICH, S. M., Properties of FEU-79 photomultipliers used as photon counters in astronomical observations, 25:42068
SUZHOVSKII, B. Ya., Excitation mechanism of the isobaric analog states from analysis of resonance (p,n) reactions, 25:43893
SWALTNEY, R. C., Effect of fillets on stress concentrations in cylindrical shells with step changes in outside diameter, 25:41959 (CONF-710512-15)
Experimental and finite element stress analysis of a thin-shell cylinder-to-cylinder model, 25:42839 (CONF-710512-3)
SYLPE, J. D., 25-kWe reactor--thermoelectric power system for space stations, 25:44171

H

HA, Doo Bong, Effects of x irradiation on HeLa cells, 25:42295
HAAS, R. J., Effect of tritiated thymidine on the oocytes of foetal rats following maternal infusion in pregnancy, 25:42550
HABER, I., Electromagnetic and finite β/sub e/ effects on counterstreaming ion instability, 25:43394
HABS, D., Measured differential cross sections for elastic and inelastic scattering of 104-MeV α particles, 25:43832 (NP-18923)
HACKENBROICH, H. H., Two-channel calculation for elastic α-α scattering, 25:43784
HADZI, D., Vibrational normal coordinate analysis of H(D)NCO and H(D)NCS, 25:41791
HAEBERLI, Willy, Method for producing ions utilizing a charge-transfer collision, 25:43135
HAEGGBLOM, H., Activation Doppler experiments in FRO, 25:44164
HAEGI, Marcel, Contribution to the study of dense plasmas, 25:43381 (LGI-68/16)
HAENSSEN, H., Mean neutron energy from D(d,n)^{3}He reaction, 25:43790
HAERENDEL, Gerhard, Striations in ionospheric ion clouds. I, 25:43252
HAERING, M., Direct measurement of (n,2n) cross section of ^{93}Nb, 25:43897
HAGBERG, E., Total absorption of 100 MeV protons with a Ge(Li) detector, 25:42128
HAGEMANN, U., Nanosecond lifetime measurements of excited nuclear states at heavy ion cyclotron, U-300, 25:42187 (JINR-P13-5801)
HAGIE, L. T., Prog. rpt. on Integrated Safeguards Experiment, 12/70--3/71, 25:42035 (BMI-68-6)
HAHN, Henry, Development of ceramic fiber reinforced metals, 25:42978
HAJJ, Jack Philip, Particles of arbitrary mass and spin, 25:43572
HAKANSSON, R., Material buckling in U-loaded assemblies of fast reactor FRO, 25:44149 (AE-425)
HALACHMY, Matitiahu, Behavior of fission products in nuclear fuels, 25:44205 (CEA-R-4191)
HALASZ, A., Spectrophotometric determination of molybdenum with phenyl-fluorone, 25:41726
HALE, G. J., Prog. rpt. on chemical vapor deposition process equipment, 11/70, 25:44223 (BDX-613-269)
HALES, M. P., Third processing campaign in the Waste Calcining Facility, 25:41593 (IN-1474)
HALEY, F. A., Irradiation effects at cryogenic temperature on tensile properties of titanium and titanium-base alloys, 25:42926
HALIMI, Epithelioma developing on an angioma treated with Curietherapy, 25:42686
HALLEY, J. Woods, NMR experiment to observe spin waves in solutions of ^{3}He in ^{4}He and in pure ^{3}He, 25:43280
HALMSHAW, R., Radiographic examination of heavy-wall pressure vessels: choice of source of radiation, 25:44112 (CONF-700224-, Paper 7)
HALOW, I., Selected values of chemical thermodynamic properties, 25:41826 (NBS-TN-270-5)
HALPERN, L., Self-coupled scalar gravitation, 25:43705
HALPERN, M. B., Persistence of the photon in conformal-dual models, 25:43618
HALZEN, F., Quantum numbers of cross-channel exchanges, 25:43565 (CALT-68-305)
HAMAGUCHI, Yoshikazu, JAERI pulsed type neutron spectrometer, 25:42107 (JAERI-13771)
HAMEED, S., Perturbation calculation of atomic polarizabilities, 25:43117
HAMMOND, A. D., Calculations for a large fast reactor, 25:44101 (TRG-Report-2133)
HAMMOND, Riley G. Jr., Prog. rpt. on powder metallurgy compaction, 3/71--5/71, 25:44292 (SRO-475-11)
HAN, K. S., Largle-angle differential cross section for K$^+$p elastic scattering at 4.0 and 5.0 GeV/c, 25:43559
HANDEL, Stanley F., Scintiphotographic evaluation of response of brain neoplasms to systemic chemotherapy, 25:42556
HANEVELD, A. J. Klein, Erbium diselenide, 25:43004
HANKS, G. S., Fabrication of OWR gamma shield assemblies, 25:42816 (LA-4644)
HANNA, S. S., Lifetime of the first excited state of ^{11}Be, 25:43820
HANNAH, R. G., Development of an advanced space radiation system, 25:41978
HANNAN, M. A., Dark repair of uv-irradiated haploid Saccharomyces carlsbergensis, 25:42725
HANNESSON, G., Radurization of scampi, shrimp, and cod, 25:42746 (STI/DOC-10/124)
HANSEN, John, Field determination of uranium and thorium by gamma-ray spectrometry, exemplified by measurements in the Ilimaussaq alkaline intrusion, south Greenland, 25:41943
HANSEN, M. F., Effect of gamma radiation on Histomonas meleagridis, 25:42508
HANSEN, Niels Ebbe, Radiation induced changes in red cell filterability, 25:42706
HANSEN, W. L., High-purity germanium crystal growing, 25:42130
HANSON, B. D., Low-temperature heat capacities of transition metal borides, 25:42974
HANZ, George J., Programming apparatus for an automatic liquid scintillation counting system, 25:42058
HAOT, J., Effect of normal and irradiated marrow grafts on the hemopoietic recovery after a sublethal irradiation, 25:42644
HAQUE, A. K. M. M., Calibration of Ge(Li) detectors for level structure study in proton and neutron capture reactions, 25:42129
HARARI, Haim, Elastic hadronic processes, duality, and absorption, 25:43617
HARBINSON, E. N., Effects of irradiation on the tensile properties of Zircaloy 2 and 4 and borated stainless steel, 25:42911
HARBOTTLE, J. E., Temperature and neutron dose dependence of irradiation growth in Zircaloy 2, 25:42915
HARDIN, Virgil M., Liver and spleen scintigraphy in staging Hodgkin's disease, 25:42585
HARDY, D. G., Effect of neutron irradiation on the mechanical properties of zirconium alloy fuel cladding in uniaxial and biaxial tests, 25:42913
HARKINS, Ralph D., Guidelines: biological surveys at proposed heat discharge sites, 25:44259 (NP-18843)
HARKNESS, S. D., Considerations of metal swelling and related phenomena caused by fast neutron irradiation, 25:42918
HARMS, D., Inelastic electron--proton scattering in the region of the Δ (1235) resonance, 25:43527 (DESY-71/21)
HARMS, E., Hall--Post lower bound calculations for the three-nucleon system, 25:43983
HARMUT, Magda, Comparative strontium and calcium metabolism in lactation, 25:42255
HARRIS, E. G., Plasmons and the linear and nonlinear two-stream instabilities, 25:43387
HARRIS, John W., Radiobiological and biochemical studies of thiophosphate radioprotective compounds related to cysteamine, 25:42525
HARRIS, L. A., Saturation in continuous channel electron multipliers, 25:42057
HARRIS, W. R., Levels of ^{36}S from ^{34}S(t,p)^{36}S, 25:43869
Lifetime of the first excited state of ^{11}Be, 25:43820

XUM

HART, H. R. Jr., Apollo helmet dosimetry experiments, 25:42160 (N-71-14502)
HARTBLOWER, C. E., Fracture of structural metals as related to pressure-vessel integrity and in-service monitoring, 25:42840 (CONF-710512-4)
HARTBOWER, Carl E., Detection of incipient failure in pressure vessels by stress wave emission, 25:44137 (CONF-700224-, Paper 3)
HARTLE, James B., Long-range neutrino forces exerted by Kerr black holes, 25:43032
HARTWICK, F. D. A., Photometric study of metal-rich globular cluster M71, 25:43035
HARTWIG, H., Dielectric waveguides and serials for 2 mm microwave interferometers with high spatial resolution for plasma density measurements, 25:42183 (CTJ-756)
HARWIG, B., Dual-motion Moessbauer absorber system, 25:42120
HASCHKE, John M., Hydrothermal equilibria and crystal growth of rare earth oxides, hydroxides, hydroxynitrates, and hydroxycarbonates, 25:42934 (COO-1109-60)
HASIGUTI, R. R., Neutron irradiation effects on iron containing aluminum and nitrogen, 25:42908
HASINOFF, Michael David, Study of the isospin splitting of dipole excitations in intermediate mass nuclei, 25:43950
HASKETT, James Albert, Lifetimes of some nuclear states in ^{24}Mg, ^{26}Mg, ^{27}Al, and ^{28}Si, 25:43854
HASLETT, J. C., Measurement of the effective electron loss rates in the D region during polar cap absorption events, 25:43255
HASSE, Robert A., Effect of reactor irradiation on properties of a nongalling alloy, 25:42903 (N-71-14040)
HASTY, R. A., Gas chromatographic method for the microdetermination of iodine, 25:41745
HAUG, R. M., Some physical and chemical characteristics of heated soils, 25:41925 (UCLA-12-819)
HAUSER, G., Measured differential cross sections for elastic and inelastic scattering of 104-MeV α particles, 25:43832 (NP-18920)
HAUSER, W., Visualization of the human spleen with /sup 99m/Tc-labeled red blood cells, 25:42235
HAVENS, W. W. Jr., Neutron resonance spectroscopy. VII, 25:43874
HAWKINS, S. W., Stable and generic properties in general relativity, 25:43696
HAWS, C. C., Engineering-scale demonstration of the sol-gel process: preparation of 100 kg of ThO_2-UO_2 microspheres at the rate of 10 kg/day, 25:42937 (ORNL-4544)
HAWTHORNE, J. R., Analysis of radiation-induced embrittlement gradients on fracture characteristics of thick-walled pressure vessel steels, 25:42841 (CONF-710512-8)
Improved radiation embrittlement resistance of A533B steel, 25:42907
HAWTHORNE, M. Frederick, Nucleophilic substitution at tetrahedral boron. Trimethyl- and triethylamine--borane substrates, 25:41802
Nucleophilic substitution at tetrahedral boron. Trimethylamine--alkyl- and -arylborane substrates, 25:41803
Nucleophilic substitution at tetrahedral boron. Methylamine--diarylborane substrates, 25:41804
HAYASHI, M., Total absorption type lead glass Cherenkov counter with high resolution, 25:42154
HAYASHI, Takeo, Beta decay to second 2$^+$ excited state of ^{122}Te, 25:43947
HAYASHI, Toshikazu, Theories and their applications of electromagnetic method in liquid flow rate-measurement, 25:42184 (JAERI-13536)
HAYDT, H. M., Sintering of uranium dioxide, 25:42950
HAYGOOD, J. D., Classical model for gas--surface interaction, 25:43104
HAYHOE, F. G. J., Changes in proliferative activity of marrow leukemic cells during and after extracorporeal irradiation of blood, 25:42590
HAYN, Carl H., Mass attenuation coefficients for plastic Pilot-B scintillator, 25:42054
HAYNES, Gilbert A., Effect of radiation on cerium-doped solar-cell cover glass, 25:43008 (N-71-12278)
HAYTINK, B., Orgel prototype preliminary design: reactivity coefficients, 25:44100 (EUR-4365)
Orgel prototype preliminary design: fine flux distributions in the fuel element, 25:44099 (EUR-4364)
HAZI, Andrew U., Calculation of energies and widths of compound-state resonances in elastic scattering: stabilization method, 25:43147
HEACOCK, R. R., Spatial and temporal relations between Pi bursts and IPDP micropulsation events, 25:43247
HEAD, David Alan, Solvated electron yield in the radiolysis of formamide, 25:41863
HEBERLEIN, Fermin Viniegra, New classical field theory, 25:43665 (NP-18831)
HECHT, F., Neutron activation analytical determination of a number of trace elements in meteoritic phases, 25:41773
HECHT, Harry G., ^{17}O NMR studies of uranium oxides, 25:43497
HED, A. Z., Oxidation of Ni--20 wt. percent Cr--2ThO_2, 25:42930
HEDIN, G., Levels in ^{191}Ir, 25:43902
HEHN, Gerfried, Radiation field of the reactor, 25:44108
HEIDAM, N. Z., Microwave-phonon-induced extra currents in superconductive tunneling, 25:43316
HEINRICH, R. R., Activation-rate measurements in the ZPR-3 mockup critical experiments. Part I. Measurements of foil-activation rates and fission yields in Assembly 60 of ZPR-3: mockup of EBR-II with a uranium blanket, 25:44150 (ANL-7781)
HEISLER, A. G., Chemical radioprotection with N- and S-containing polymers, 25:42517
HEISS, P., Two-channel calculation for elastic α--α scattering, 25:43784
HEITMANN, D., Investigation of Cherenkov radiation by 50 keV electrons in thin silicon foils, 25:43429
HELD, E. E., Silver-108m in biota sediments at Bikini and Eniwetok Atolls, 25:42377
HELLER, Carl G., Prog. rpt. on effects of ionizing radiation on the testicular function of man, annual, 8/70--7/71, 25:42674 (RLO-1780-32)
HELLER, J. A., 300-kWe Rankine cycle advanced nuclear--electric space power system, 25:44173
HELLER, W., Influence of additions of a third element on the critical magnetic field of titanium--niobium alloys, 25:43309
HELLMAN, Samuel, X-ray and alkylating agents alter differentiation of surviving hematopoietic stem cells, 25:42661
HELMER, R. G., Coriolis coupling in doubly odd deformed nuclei, 25:43934
Level structure of ^{182}Ta, 25:43935
HELMREICH, D., Influence of vacancies and impurities on order--disorder transition in hexagonal ice Ih, 25:41812
HELMS, H. A., Beta--gamma circular polarization correlation measurements on the decays of ^{203}Hg, ^{199}Au, and ^{141}Ce, 25:43941
HENDRICKSON, M. M., RACER: a computer program for calculating potential external dose from airborne fission products following postulated reactor accidents, 25:42393 (BNWL-B-69)
HENISCH, H. K., Prog. rpt. on role of trapping processes in solid state radiation dosimetry, final, 5/71, 25:42162 (NYO-3409-10)
HENKEL, Raymond Paul, Superfluid density of He II in restricted geometries, 25:43287
HENNIG, K., Diagnostic findings in hypoplasia of the pulmonary artery, 25:42551
Suitability of technetium-labeled erythrocytes for the examinations of the splenic function, 25:42570
HENRIKSON, C. O., Effect of irradiation in high doses on parotid glands, 25:42699
HENRY, K. M., Calibration of Bonner ball neutron detectors used at Tower Shielding Facility, 25:42055 (ORNL-TM-3465)
HENRY III, Charles D., SM-1 core III 3.5 MWYR core physics report, 25:44176 (AD-715850)
HERMANN, F., Neutron activation analytical determination of a number of trace elements in meteoritic phases, 25:41773
HERMANS, Marie E. A., Method of preparing a stable mixed sol of hexavalent uranium and tetravalent thorium by peptization, 25:42945
HERRIOTT, Roger M., Prog. rpt. on genetic transformation in Hemophilus influenzae, annual, 9/15/70--9/14/71, 25:44270 (NYO-1371-64)
HERRMANN, G., Diffusion effects during determination of ranges of recoil atoms in gases, 25:41885
HERRMANN, H., Residual β activity and γ-spectrometric determinations in bees and honeys, 25:42374
HESSE, K., Superconducting particle detectors, 25:42097
HEUSCH, B., Study of ^{61}Cu nucleus by ^{58}Ni(α,pγ)^{61}Cu reaction, 25:43839
HEYDE, K., Shell-model calculations on the N = 82 odd-proton nuclei. II, 25:43989
HEYER, Herbert, Duality. Local compact groups, 25:43721
HIBBERT, F., Proton transfer from cyanocarbon acids. III. Primary and solvent kinetic isotope effects in the ionization of malononitriles, 25:41799
Proton transfer from cyanocarbon acids. II. General-base-catalyzed detritiation and bromination of malononitriles. Rates of the reverse reactions, 25:41798
HICKMAN, Bernard T., Comparison of two radiation therapy-treatment plans for carcinoma of the cervix. I. Personnel radiation exposure, 25:42432
HICKMAN, J. A., New technique for quantitative estimation of fibrinolysis using in vivo [^{125}I]fibrinogen, 25:42243
HICKS, Samuel P., Prog. rpt. on effects of radiation and other factors on developing form and function of nervous system, comprehensive review, 1962--1971, 25:42615 (COO-1201-30)
HIDDLESTON, Hoyt Rodney, Isobaric analog resonances in proton elastic and inelastic scattering from ^{130}Te, 25:43918
HIGASHI, Aritsune, Monitoring for internal exposure. III, 25:42479
HIGGINS, G. T., Studies of thermally-activated deformation in zirconium, 25:42877
HIGGINS, P. R. B., Structure and tensile properties of AISI Type 316 steel, 25:42919

HILL, A. J., Fire prevention and protection in hot cells and canyons, 25:42035 (DP-1242)
HILL, James A., Economic selection of undersea powerplants, 25:44180
HILLOVA, J., Determination of ^{90}Sr in milk and cottage cheese, 25:42395
HINES, Norman Leroy, Potential radioprotective agents, 25:42531
HINK, W., K-shell-fluorescence yield for carbon and other light elements, 25:43108
HINOJOSA, Oscar, ESR study of intramolecular energy transfer in the radiolysis of cellulose thenoates, 25:41836
HIRAKI, Akio, Permanent defects in electron bombarded n-type germanium, 25:43444
HIRANO, Katsuhiko, Radiolysis of 2,2'-azo-bis-isobutyronitrile in benzene solution. II, 25:41872
HIRAYAMA, Shoichi, Experimental fast reactor Joyo. Outline of Joyo, 25:44091
HIRD, Kathryn, Strain of Escherichia coli resistant to DNA degradation induced by ionizing radiation, 25:42729 (NYO-2804-40)
HIRSCHHORN, Joel S., Forging of powder metallurgy preforms, 25:42829
HIRSZOWSKI, Julien, Study of 3 ^1P--2 ^1S line of He excited by H ion beam, 25:43129
HISCOCKS, S. E. R., Growth and properties of single crystal LaB_6, 25:42947
HISHAW, R. J., Prog. rpt. on compression molding of laminates, FY 70-4, 25:44226 (BDX-613-327)
HO, H. S., Some algebraic solutions of the cyclotron resonance interaction, 25:43403 (AD-715636)
HO, Paul S., Pressure dependence of elastic constants for Ag from 77°K to 300°K, 25:44271 (NYO-2504-59)
HOCQUENGHEM, J. C., Truncation of rotational states in the shell model, 25:43828
HO DAC THANG, Fundamental and harmonic C--H/C--D valence vibrations of halogen derivatives of methane and of deuteriomethane, 25:41822
HODUL, P., Structure and phases of Zr alloys with Cu and Mo, 25:42898
HOEGLUND, A., Absolute transition rates in ^{182}W, 25:43903
HOERTNER, H., Potential sites for nuclear power station near Vienna, 25:44147
HOFFER, Paul B., Correlation between brain tumor detectability on brain scan and protein levels of the spinal fluid, 25:42547 (ACRH-1000-248)
HOFFMAN, J. M., Molecular oxygen density measurements from 80 to 140 kilometers, 25:43261
HOFFMANN, Gudrun, Measured differential cross sections for elastic and inelastic scattering of 104-MeV α particles, 25:43932 (NP-18920)
HOLCOMB, R. S., Performance characteristics of a short reentry tube steam generator at low steam output, 25:41962 (ORNL-TM-3236)
HOLLAND, P., Effects of x irradiation on various enzymic functions of NADP+-linked isocitrate dehydrogenase, 25:42299
HOLLAND, R. F., Evidence for splitting in the Q region of $K^+\pi^+\pi^-$ mass, 25:43544 (COO-1428-275)
New evidence for splitting in the Q region of $K^+\pi^+\pi^-$ mass, 25:43543 (COO-1428-274)
HOLLANDER, C. F., Pathology of the late syndrome in mice lethally irradiated and treated with isologous bone marrow transplantation, 25:42665
HOLLAR, D. L., Percussive-arc versus pulse-arc welding, 25:44231 (BDX-613-395)
HOLLAS, C. L., Reaction $^{36}Ar(d,p)^{37}Ar$, 25:43868
HOLM, Hartmut, Influence of nuclear forces on Coulomb fission, 25:43970
HOLMES, D. E., Inherent dosimeter for irradiated foods: papayas, 25:42433
HOLMES, H. L., Chromosome aberration following radiophosphorus treatment of polycythaemia, 25:42713
HOLMES, Howard, Feasibility of cytogenetic assay in radiophosphorus dose assessment, 25:42399
HOLMES, J. M., Role of nuclear powered energy centers in developing economies, 25:44175
HOLZAPFEL, Christian, Applied magnetohydrodynamics. VII, 25:43182 (JUL-742-TP)
HOMMA, S., Total absorption type lead glass Cherenkov counter with high resolution, 25:42154
HONES, E. W. Jr., Time variations of the magnetotail plasma sheet, 25:43240
HONTZEAS, S., Unified-model calculations in some Zr isotopes, 25:43938
HOPEWELL, J. W., Influence of hypertension on latent cerebral irradiation damage, 25:42667
HOPKINS, J. C., $^1H(n,n)^1H$ scattering observables required for high-precision fast-neutron measurements, 25:43798
HOPMAN, H. J., Three-wave interaction in a beam--plasma system, 25:43407 (N-71-18696)
HORA, H., Survey of studies of laser produced plasmas at the IPP Garching, 25:43380 (IPP-4/9)
HORAN, Paul, Strain of Escherichia coli resistant to DNA degradation induced by ionizing radiation, 25:42729 (NYO-2804-40)
Sucrose gradient analysis of DNA in irradiated cells of P4H1, 25:42731 (NYO-2804-42)
HORM, I. E., Improved method for americium analysis in urine, 25:41756
HORNBACK, C. E., High-altitude nuclear detection studies. II, 25:41933 (AD-719620)
High-altitude nuclear detection studies. I, 25:41932 (AD-719619)
HORNSBY, James B., Prog. rpt. on powder metallurgy compaction, 3/71--5/71, 25:44292 (SRO-475-11)
HORNSEY, Shirley, Animal survival and cell survival seen in dose rate effects on mouse intestinal damage, 25:42633
HORRELL, D. R., Radiolysis of liquid 1,1,2-trichlorotrifluoroethane, 25:41870
HORSKY, J., Autoradiographic localization of radioactivity in female rat neocortex after injection of tritiated estradiol, 25:42258
HORTACSU, Amable Dorotan, Diluent effects on diffusion for the system uranyl nitrate--tributyl phosphate--n-heptane, 25:41829
HORUBALA, Zenon, Nb_3Sn superconducting phase identification in Nb--Sn alloys by critical temperature measurement method, 25:43288 (INR-1294)
HOSBONS, R. R., Effect of fast neutron irradiation on the mechanical properties of some quenched and tempered steels, 25:42909
HOSHI, Yoshio, Study of the relations between glutathione and x-ray cataract, 25:42539
HOSHINO, Kiyoshi, Radiation effect on prenatal development, 25:42629
Species differences of the effects of x-irradiation upon the rat and mouse embryo, 25:42539
HOSONO, Kazuhiko, Broad energy protons from the reaction $^{12}C + d \rightarrow p + {}^{13}C$ (7.64 MeV and 8.33 MeV), 25:43814
HOUDART, R., Emission spectrum of Th in 5400 to 6400 cm^{-1} region, 25:43113
HOUZIAUX, L., Conference on ultraviolet stellar spectra and related ground-based observations, Lunteren, Netherlands, 6/69, 25:43031
HRABOVCOVA, Alojzia, Methods of determination of fast-neutron spectra from threshold--foil activation data, 25:42100
HSU, C. N., ^{90}Sr and ^{137}Cs levels in the diet of children on a school lunch program, 25:42422
HSUAN, H. C. S., Mechanism causing nonlinear behavior in Tonks--Dattner resonance experiments, 25:43411
HSUE, Chen-shiung, Functional integral formulation of dual resonance amplitudes, 25:43722
HSU JUNG-LAN, Motion of charged particles in magnetic fields with model experiments, 25:43507 (JPRS-52839, pp 3-16)
HU, Chi-yu, Binding energy of the triton with the Hamada--Johnston potential, 25:43795
HUBBARD, L. B., One-particle, j-j coefficients of fractional parentage in the isospin representation for n less than or equal to 5 in the j = 7/2 shell, 25:43981
HUBLER, Peter, Nuclear reactor installation, 25:44212
Nuclear reactor installation, 25:44214
HUBY, R., Spectroscopy of unbound levels with aid of Weinberg's quasiparticles, 25:43988
HUCHITAL, G., Prog. rpt. on instabilities and turbulence in highly ionized plasmas in a magnetic field, semiannual, 3--8/70, 25:43385 (N-71-12892)
HUEBENER, R. P., Rectification effect in thin-film superconductors in small, oscillatory magnetic fields, 25:43304
HUEBNER, H., Modification of the intensity of optical spectra of organic dyes through deuterium labeling, 25:41815
HUETTENRAUCH, R., Effect of high-energy radiation on the hydrolytic resistance of glass containers, 25:42754
HUG, Otto, Conference on biological aspects of radiation protection, Kyoto, 10/69, 25:42512
Radiation risk and protection, 25:42680
HUGHES, H. G., Stabilization of poliovirus to ^{32}P decay, 25:42741
HUGHES, V. W., Precise measurement of 2^3P_0--2^3P_1 fine-structure interval of He, 25:43122
HULET, E. K., Symmetric fission observed in thermal-neutron-induced and spontaneous fission of ^{257}Fm, 25:43920
HULL, J. L., Calibration of Bonner ball neutron detectors used at Tower Shielding Facility, 25:42055 (ORNL-TM-3465)
HUNSTEIN, W., Life span and tumor incidence in rats subjected to severe stress before whole body x-irradiation, 25:42669
HUNT, J. C. R., Magnetohydrodynamics at high Hartmann number, 25:43197
HUNTER, C. W., Fracture and tensile behavior of neutron-irradiated A533-B pressure vessel steel, 25:42901 (HEDL-TME-71-76)
HUNTER, R., Systematics of extra-nuclear hadron cascades in shields, 25:43613 (CERN-71-13)
HURT III, S. S., Prog. rpt. on Oak Ridge Research Reactor, 1--3/71, 25:44160 (ORNL-TM-3481)
HUSAIN, W., Separation of metal ions on inorganic ion-exchange papers, 25:41909
HUVOS, Andrew G., Effect of irradiation on the maturation of Wilms' tumor, 25:42592
HVELPLUND, P., Stopping power and energy straggling for swift protons, 25:43432
HWA, Rudolph C., Baryon annihilation and exotic exchange, 25:43632
HYNDS, R. J., Penetration of solar protons over the polar

XUM

cap during the February 25, 1969, event, 25:43232
HYDDO-TASUCHI, Yasuko, Mortality of fish under continuous irradiation conditions, 25:42634

I

IANCU, I., Radioinduced sarcomas, 25:42705
IBANEZ, P., San Onofre Nuclear Generating Station vibration tests, 25:44079 (UCLA-ENG-7037)
IBRAGIMOV, A. P., Effect of gamma-radiation on properties of extracted cottonseed oil for preparation of K-5 drying oil, 25:41839
ICE, Rodney D., Establishment of a university radiation safety office, 25:42503
ICHIMORI, Toshiro, Characteristics of proton recoil proportional counter GD-A for neutron and γ-ray, 25:42106 (JAERI-13580)
Gamma-ray discriminating system for a proton-recoil counter, 25:42105 (JAERI-13551)
IGATA, N., Neutron irradiation effects on iron containing aluminum and nitrogen, 25:42908
IGNAT'EV, O. M., Tunneling conductance anomaly and switching effect for normal MIM structures, 25:42219
IGNAT'EVA, N. I., Stabilities of solid solutions of system Eu_2O--CaO when heated in air, 25:42964
IGNATOV, D. V., Examination of welded joints of Mo alloy TZM-2A, 25:42874
IGO, G., Effect of multipole pairing and particle-hole fields in particle-vibration coupling of ^{209}Pb. II, 25:43923
IKEZOE, Yasumasa, Chemical reactions by reactor radiation, 25:41851 (JAERI-13790)
IKUTA, A., Experimental approach to the optimization of solvent extraction processes, 25:41916
ILBERY, P. L. T., Chromosone aberration following radiophosphorus treatment of polycythaemia, 25:42713
ILBERY, Peter, Feasibility of cytogenetic assay in radiophosphorus dose assessment, 25:42399
ILIFFE, C. E., Sensitivity of uranium and separative work requirements to variations in reactor programs, 25:44127 (CONF-700903-17)
ILYUKHIN, A. S., Corrosion and electrochemical behavior of zirconium alloy, 25:42814
IMAMOTO, K., Medical aspect of chronic hypoxia in radiation exposed glomerulus in hamsters treated with injected ozone gas, 25:42636
IMAMURA, Rikizo, Manufacture of DP pulps by irradiation. I, 25:41873
IMANGALIEVA, N. T., Content of protein SH-group in tumors of different radiosensitivity in norm and after irradiation, 25:42518
IMHOF, W. L., Solar particle cutoffs as observed at low altitudes, 25:43234
IMOTO, Shosuke, Thermodynamic calculations on quinary system U--Pu--C--O--N, 25:42998
INANO, Hiroshi, Steroid 7α-hydroxylase of rat testes, 25:42621
INOSAMOV, Sh. V., Thermodynamical description of momentum distributions of pions in π⁻p interactions at p = 4 GeV/c, 25:43639 (JINR-P1-5849)
INOUE, H., Influence of fibrous aluminium nitride on strength of sintered AlN--Y_2O_3, 25:42959
IOANNESYANTS, L. M., Use of an x-ray analyzer with a semiconductor detector for elemental analysis, 25:42217
IOVLEV, B. V., Alteration of the bioelectric activity of the brain in patients with arachnoiditis under the influence of radiation treatment, 25:42678
IRELAND, D. R., Radiation effects on the metallurgical fracture parameters and fracture toughness of pressure vessel steels, 25:42905
IROSHNIKOV, G. S., Electromagnetic form factor for the pion in the dual resonant model, 25:43593
ISAAC, Peter, Nuclear reactor installation, 25:44216
Nuclear reactor installation, 25:44213
Nuclear reactor installation, 25:44212
ISABELLE, D. B., Backward electron deuteron scattering below 280 MeV, 25:43528 (LAL-1250)
Detection of hyperfixing zones by means of a positron camera type positron. III, 25:42565
ISHIHARA, M., Lifetime measurements on E2 isomers in N = 48 nuclei, 25:43847
ISHIHARA, Toyohide, Environmental radiation monitoring system, 25:42094
ISHII, K., Lifetime measurements on E2 isomers in N = 48 nuclei, 25:43847
ISHII, Kameo, Quasi-K quantum number in ^{152}Gd, 25:43939
ISHIKAWA, Michio, Nuclear safety experimental program with pulse reactor, 25:44152
ISHIMORI, Tatsujiro, Infrared spectra of pentacyanonitrosylmanganese (^{14}NO and ^{15}NO) complexes, 25:41795
ISHIMORI, Tomitaro, Fractional extraction of Zr, Nb, and Np with tri-n-butyl phosphate, 25:41901
ISHIZAKA, Masatsuna, Investigation of radiation hazard in x-ray workers, 25:42485
ISHUTINOVA, L. N., Energies of mixing in systems containing germanium and silicon with elements of groups III and V, 25:42970
ISLAM, Fakhrul, Mutagenic effect of irradiated media on E. coli, 25:42755
ISMAILOV, B. I., Comparative radiosensitivity of ascites ovarian tumors and ascites lymphosarcoma of rats, 25:42637
Content of protein SH-group in tumors of different radiosensitivity in norm and after irradiation, 25:42618
ITO, Katsukiyo, Gamma-induced polymerization of fluorine-containing pentadiene, 25:41848
ITOH, Junkichi, NMR and relaxation of ^{163}Dy in Dy metal at low temperature, 25:43498
IVANITSKAYA, V. I., Indexes of remote sequelae of radiotherapy of breast cancer, 25:42270
IVANOV, E. G., Results of loop tests on Zr-clad experimental fuel rods in the Mr reactor, 25:43010
IVANOV, G. N., Instrument for measuring and monitoring the energies of particles accelerated in a cyclotron, 25:43743
IVANOV, R. B., α decay of neutron-deficient radon isotopes, 25:43887 (JINR-P6-5791)
IVAN'SHIN, Yu. I., Time properties of a spark chamber filled with helium and helium--hydrogen mixture, 25:42136 (JINR-P13-5828)
IVERSEN, Kay, Determination of uranyl and thorium(IV) by gas chromatography of volatile mixed-ligand complexes, 25:41725
IWASAKI, Machio, Electron spin resonance evidence for positive holes produced in irradiated single crystals of carboxylic acids, 25:41841
IZUTSU, Norihiko, Heavy particle identification with TOF method in nuclear reactions, 25:42066

J

JABLON, C., Radial dependence of trapped-particle instabilities, 25:43391
JACCHIA, L. G., Semiannual variation in the heterosphere: a reappraisal, 25:43258
JACHYMCZYK, Witold, Protein synthesis in germinating seeds, 25:44250 (COO-1313-28)
JACKSON, A. D., Triton calculations in a harmonic oscillator basis with realistic potentials, 25:43792
JACKSON, Herbert L., Mathematics of radiology and nuclear medicine, 25:42433
JACKSON, Ross J., Mechanical properties of uranium-base niobium alloys, 25:42851 (RFP-1703)
JACKSON, S. M., Long term follow-up of patients with menorrhagia treated by irradiation, 25:42702
JACOBS, Mathew A., Ghost-eliminating modifications in multipion amplitudes, 25:43528
JAFFE, A. A., Mass and half-life of ^{36}K, 25:43875
JAFFE-BRACHET, A., Protection of irradiated lambda phage by methylated proflavine, 25:42737
JAGARLAMOODY, S. M., In vitro detection of cytotoxic cellular immunity against tumor-specific antigens by a radioisotopic technique, 25:42309
JAHN, R. G., Cathode region of a quasi-steady magnetoplasmadynamic arcjet. VIII, 25:43353 (N-71-19984)
JAIN, M. C., Perpendicular field superconducting proximity effect in Cu/Pb/Cu sandwiches, 25:43315
JAIN, M. K., Heat transfer in MHD Couette flow as affected by wall electrical conductances and suction, 25:43198
JAKOBSSON, P. Aa., Effect of irradiation in high doses on parotid glands, 25:42699
JAMMET, H., Value of biochemical indicators, 25:42408
JANCSO, G., Thermodynamical description of momentum distributions of pions in π⁻p interactions at p = 4 GeV/c, 25:43639 (JINR-P1-5849)
JANOS, S., Slope change in temperature dependence of electrical resistivity of thulium near 22 K, 25:43487
JARMER, J. J., Method for absolute calibration of Ge(Li) detectors using effective interaction depth, 25:42125
JASKE, R. T., Multiple purpose use of thermal condenser discharges from large nuclear systems to supplement interregional water supply, 25:44083 (BNWL-SA-2738)
JASKOLA, M., (n,α) reactions on heavy nuclei induced by 14.2-MeV neutrons, 25:43886 (INR-1259)
JASSBY, Daniel Lewis, Transverse velocity shear instabilities in a magnetoplasma column, 25:43395
JATCZAK, J., Detection of high-energy neutrinos, 25:43174
JATCZAK, Jerzy, Effect of the radius of the apparatus on the mean distance of shower axis from its center, 25:42157
JAY, B., Scattering of fast neutrons of ^{238}U, 25:43898
JAYARMAN, S., Intercomparisons of absorbed dose in ^{60}Co teletherapy using mailed LiF dosimeters. II, 25:42172
JAYSON, G. G., Pulse- and x-radiolysis of 2-mercaptoethanol in aqueous solution, 25:42294
JEAN, A. G., High-altitude nuclear detection studies. II, 25:41933 (AD-719620)
JEDRZEJEC, Henryk, Nb_3Sn superconducting phase identification in Nb--Sn alloys by critical temperature measurement method, 25:43288 (INR-1294)
JEFFERTS, K. B., Discovery of interstellar silicon monoxide, 25:43052
JELLINEK, F., Erbium diselenide, 25:43004
JELTSCH, E., Polytetrafluoroethylene: dosimeter for gamma dose measurements in about 10^{11} rad, 25:42170
JEN, Chian-li, Triple Regge limits and duality sum rule,

25:43570 (NYO-2252-TA-247)
JENNINGS, W. C., Prog. rpt. on instabilities and turbulence in highly ionized plasmas in a magnetic field, semiannual, 3--8/70, 25:43385 (N-71-12892)
JERABEK, J., Personal monitoring of workers during the translocation of a ^{90}Sr--^{90}Y beta source by aid of TLD, 25:42444
JERNIGAN, T., Effect of a toroidal field on plasma transport in a magnetically perturbed multipole, 25:43335
JEYAPANDIAN, S., Generalized mean square amplitudes of vibration for substituted ethylene: vinylidene halides and their deuterates, 25:41814
JOCKEY, P., Effects of pulmonary lavage on the retention of particles of plutonium oxide, 25:42368 (LF-tr-53)
JOERGENSEN, Mogens, Iodine-125-labelling of angiotensin I and II, 25:42241
JOHANSSON, Erik, Quantitative assay of ^{239}Pu and ^{240}Pu by neutron transmission measurements, 25:41750 (AE-416)
JOHANSSON, K. A., Collimator and scattering foil for 10 to 20 MeV electrons, 25:43767
JOHN, W., Symmetric fission observed in thermal-neutron-induced and spontaneous fission of ^{257}Fm, 25:43920
JOHNSON, Bruce M., Process for fabrication of stoichiometric uranium monocarbide, 25:42939
JOHNSON, C. E., Precise measurement of $^3P_0$--$^3P_1$ fine-structure interval of He, 25:43122
JOHNSON, Dennis Ray, Mechanism and applications of nuclear track formation in polymers, 25:42070
JOHNSON, Douglas Kiester, Stabilities of some rare-earth malonato chelate species in aqueous and methyl alcohol solution, 25:44250 (IS-T-474)
JOHNSON, Hugh M., Radiofrequency observations of symmetric nebulae around Wolf--Rayet stars and O7f star, 25:43044
JOHNSON, James Russel, Neutral pion and eta photoproduction from hydrogen at high energies, 25:43529
JOHNSON, Mikkel B., Folded diagrams, 25:43519
JOHNSON, Quintin, Crystal structure of YbPt, 25:42892
X-ray detector for dynamic diffraction studies, 25:42210
JOHNSON, R. A., 25-kWe reactor--thermoelectric power system for space stations, 25:44171
JOHNSON, Robert O., Pre-irradiation 5-fluorouracil infusion in advanced head and neck carcinomas, 25:42589
JOHNSON, Shirley, Use of Cherenkov inserts for counting high energy β and γ contamination samples, 25:42082
JOHNSON, W. C., Observations of auroral hiss, 25:43246
JOHNSTON, Gerald S., Liver and spleen scintigraphy in staging Hodgkin's disease, 25:42585
JOHNSTON, K. J., Observations of 1.35-centimeter H_2O emission in southern hemisphere, 25:43051
JOHNSTON, R. E., Potential use of fluorescent scanning for brain tumor identification, 25:42548 (CONF-710204-4)
JOHRI, K. N., Quercetin as a spray reagent in inorganic thin-layer chromatography and evaluation of the chromatographed species by ring colorimetry, 25:41743
JOKEL, Jozef, Radiation unit RCH-gamma-30, 25:42015
JONES, G. D., Optical-model analysis of 38 MeV ^3He elastic scattering, 25:43878
JONES, K. W., Lifetime of the $^1/_2^-$ 2791-keV ^{21}Ne level, 25:43870
JONES, Stanley Tanner, Multiperipheral models in high energy scattering, 25:43602
JONES, W. D., Simulation of pseudowaves and of plasma sheath formation about a grid, 25:43369
JOSEPH, J., Reconstruction of amplitudes for pion--nucleon scattering from experimental data, 25:43640 (LYCEN-7110)
JOSHI, L. U., Investigation on ^{210}Pb concentrations in various regions of India, 25:42387
JOSHI, S. V., Monolayer studies with γ-irradiated poly-L-serine, 25:41834
JOSLIN, David E., Prog. rpt. on low-energy proton damage to silicon/solar cells, 1/69--1/70, 25:42226 (AD-715261)
JOST, E., Inherited sterility for control of harmful insects. I, 25:42335
JOVIC, B., Heat and mass transfer in turbulent boundary layers. II, 25:41988
Heat and mass transfer in turbulent boundary layers. I, 25:41987
JOZEFOWICZ, E. T., Studies of epithermal cell parameters in the reactor lattices with multitube enriched fuel, 25:44203 (INR-P-1266)
JUCKER, C., Dose distributions around linear ^{192}Ir sources, 25:42428
JULIAN, Carol, Information scanning and processing at NSIC, 25:44280 (ORNL-NSIC-48)
JUN, C. K., Thermal expansion of niobium carbide, hafnium carbide, and tantalum carbide at high temperatures, 25:42965
JUNKRANS, S., IFA-30 final report, 25:44207 (KAE-68-46)
Irradiation behavior of fuel assembly IFA-30, 25:44208 (KAE-68-81)
JYO, A., Oxidation of Am(III) with ammonium peroxydisulphate, 25:41785

K

KADAR, Imre, Time-to-amplitude converter, 25:42213
KADLEC, J., Experimental investigation of loop caused influences on parallel flow-induced vibration of fuel pins, 25:44119 (EURFNR-923)
KAERCHER, K. H., Enzymological examinations: an indication of radiation effects in experiments and clinical practice, 25:42409
KAHLOS, H., Elimination rate and radiation exposure following ingestion of ^{222}Rn rich water, 25:42247 (SFL-A-16)
KAISER, Gerald Yurek, Application of continuous moment sum rules to πN scattering, 25:43636
KAJIURA, N., Total absorption type lead glass Cherenkov counter with high resolution, 25:42154
KAKIGI, Shigeru, Broad energy protons from the reaction ^{12}C + d → p + ^{13}C (7.64 MeV and 8.33 MeV), 25:43814
KAKIHANA, Hidetake, Isotope effect and isotope separation, 25:41897 (ORNL-tr-2512)
KAKU, Michio, Unitarization of the dual-resonance amplitude, 25:43718
Unitarization of the dual-resonance amplitude. III, 25:43717
Unitarization of the dual-resonance amplitude. II, 25:43719
KALININ, Yu. G., Asymmetry of distribution of turbulent electric fields in direct-discharge plasma, 25:43344
KALKANOVA, E. V., Ratio of sexes in F_1 after irradiation of female and male imagos of Sitotroga cerealella, 25:42610
KALMUS, G. E., $\pi^+ + p \rightarrow \Delta^{++}(1236) + \pi^0$ AT 1.85 to 2.09 GeV: study of s- and t-channel effects, 25:43551 (UCR-34-P-107-B-108)
Study of $\pi^+p \rightarrow rho^+p$ at 1.85 to 2.09 GeV, 25:43552 (UCR-34-P-107-B-110)
KALMYKOV, A. A., Plasma acceleration in a pulsed coaxial accelerator, 25:43358
KALNAY, A. J., Lorentz-invariant localization for elementary systems. IV, 25:43577
KAMATA, Kohji, Effect of plastic deformation on crystal current density in Pb--In crystal, 25:43300
KAMEYAMA, Yoshiro, Radiation effect on prenatal development, 25:42629
Species differences of the effects of x-irradiation upon the rat and mouse embryo, 25:42639
KAMMERUD, Ronald Claire, Large angle proton--proton elastic scattering at intermediate momenta, 25:43539
KAMSHILOVA, E. M., Genetic effects of chronic γ-irradiation of Drosophila melanogaster males, 25:42350
KAMYSHEVA, L. N., Dielectric properties of γ-irradiated crystals of KH_2PO_4, 25:43443
KANABUS, Jan, Protein synthesis in germinating seeds, 25:44250 (COO-1313-28)
KANASHIN, Yu. P., Polarization of a zinc cathode during thorium precipitation from molten halide salts, 25:42821
KANAYA, T., Oxidation of Am(III) with ammonium peroxydisulphate, 25:41785
KANG, Kyungsik, Triple Regge limits and duality sum rule, 25:43570 (NYO-2262-TA-247)
KANG, Yung Sun, Effects of x irradiation on HeLa cells, 25:42295
KANGILASKI, M., Influence of irradiation temperature on the tensile properties of stainless steel, 25:42912
KANIJ, Johannes B. W., Method of preparing a stable mixed sol of hexavalent uranium and tetravalent thorium by peptization, 25:42945
KANO, L. M., Resistive phenomena in the intermediate state, 25:43299
KANTER, H., Response of superconducting point contacts to high-frequency radiation, 25:43297
KANTOR, M. M., Examination of welded joints of Mo alloy TZM-2A, 25:42874
KAPLAN, Henry S., Repair of x-radioinduced DNA strand breaks in vivo, 25:42326
KAPLON, M. F., Charged-particle observations from OSO 3, 25:43178
KAPOOR, M. L., Response of some varieties of hexaploid wheat and a two-rowed barley variety to chronic gamma-irradiation, 25:42724
KAPP, Daniel Stuart, Production and repair of x-ray induced strand breaks in DNA, 25:42357
KARABOVA, M., Measurement of small angles of scattered particles in a photographic emulsion, 25:42139
KARASHOKOV, K. E., Structure of electron beams, 25:43736
KARDASHEV, N. S., Study of the structure of radio sources, 25:43064
KARLE, Hans, Radiation induced changes in red cell filterability, 25:42705
KARPOV, A. V., Pumps for circulating liquid metals, 25:41958 (CONF-700307-8)
KARR, M. H., Multiple purpose use of thermal condenser discharges from large nuclear systems to supplement interregional water supply, 25:44083 (BNWL-SA-2738)
KARZHAVIN, Yu. A., New method of taking information from spark chambers, 25:42147
KASABOV, L. L., Chromosomal disturbances following x-ray examinations, 25:42362
KASCHE, Volker, Specific protein--protein interaction and its application in studies on radiation-induced protein modification, 25:42303
KASEMSANTA, S. P., Use of monoenergetic x-ray sources in x-ray fluorescence analysis, 25:41741
KASHEF, Bayestah Ghaffary, Λ--d scattering as probe of the Λ--N core potential, 25:43651

XUM

KASHUKEEV, N. T., Mechanical generator for ultracold neutrons, 25:43774
KASHY, E., Precision mass measurement of ^{9}C, ^{13}O, and ^{21}Mg, 25:43823
KASPARYAN, R. M., Phase equilibria in the high-alumina region of the system Al_2O_3--Nb_2O_5, 25:42985
KAST, J. W., Isotone shift in muonic x-rays in the tin region, 25:43904
KASTENBAUM, Marvin A., Credibility and inference in experimentation, 25:42715
KASTNER, Sidney O., Average energies of ground and singly and doubly excited configurations in highly ionized atoms, 25:43059 (N-71-20535)
KATAEV, R. S., Ternary system molybdenum--iron--carbon, 25:42889
KATANO, Yoshio, Electron microscope observation of the zirconium hydride, 25:42981 (JAERI-13635)
KATO, Mitsuaki, Fundamental investigations on solidification structure in weld metal, 25:42820
KATO, Ryuhei, Bubble nucleation induced in liquid films by irradiation, 25:41935
KATO, Toyoaki, Photon-activation analysis for zirconium with molybdenum used as the internal-reference element, 25:41764
KATSURA, Masahiro, Report on the uranium--nitrogen system, 25:42965
KATSURAGI, S., Activities on modular code systems in Japan, 25:44168 (EACRP-A-135, pp 69-86)
KATZIN, J. C., Equal-time commutators of T/sup ij/, 25:43685
KAUDEWITZ, F., Respiration deficient mutants of Schizosaccharomyces pombe I, 25:42338
KAVANAGH, T. M., Production of carbon K x rays by heavy-ion bombardment, 25:43107
KAWAI, Hisao, Effect of plastic deformation on crystal current density in Pb--In crystal, 25:43300
KAWAKAMI, H., Lifetime measurements on E2 isomers in N = 48 nuclei, 25:43847
KAWASAKI, Masayuki, Embrittlement of pressure vessel steels irradiated in JPDR, 25:42906
KAWASAKI, Minoru, Embrittlement of pressure vessel steels irradiated in JPDR, 25:42906
KAWASAKI, Satoru, Evaluation of stainless steel pips for cladding material of fast reactor, 25:42846 (JAERI-13578)
KAYUSHIN, L. P., Investigation of paramagnetic centers of irradiated proteins, 25:42275
KAZANJIAN, A. R., Radiolysis of liquid 1,1,2-trichlorotrifluoroethane, 25:41870
KAZUSA, Chudo, Characteristics of linear accelerator at Hiroshima University, 25:43754
KEARNS, K. D., Dynamics of a fast reactor with in-core thermionic converters. Fourth annual report, September 1, 1969--August 31, 1970, 25:44097 (COO-2109-5)
KEEFER, D. W., Void formation in proton irradiated stainless steel, 25:42917
KELLER, Donald L., Prog. rpt. on development of fuels and technology for advanced reactors, 1--3/71, 25:44118 (BMI-1905)
KELLOGG, E., Discovery of periodic x-ray pulsations in Centaurus X-3 from Uhuru, 25:43055
Strong x-ray source in Coma cluster observed by Uhuru, 25:43056
KELMAN, D. M., Form rolling complex close tolerance shapes, 25:42827
KEMPER, K. W., Spin of the 937-keV level in ^{54}Co, 25:43863
KEMPLAY, J. R., Digital subtraction technique for dual isotope scintigraphy, 25:42059
KENDALL, E. George, Titanium--Be composites produced by the co-extrusion of powders, 25:42869
KENDALL, J. M., Dynamics of a fast reactor with in-core thermionic converters. Fourth annual report, September 1, 1969--August 31, 1970, 25:44097 (COO-2109-5)
KENDRICK, N. S., Gamma--γ directional correlations in the decay of ^{125}Sb. II, 25:43927
KENESHEA, T. J., Electron loss during a nighttime PCA event, 25:43259
KENNEDY, D. I., Photoluminescence in GaP resulting from nitrogen ion implantation, 25:43462
KENNEL, C. F., Relativistic electron precipitation during magnetic storm main phase, 25:43243
KEREIAKES, J. G., Cytologic-biochemical radiation dosimeters in man, 25:42405
KERN, B. D., Low-lying levels of ^{40}Ar, 25:43872
KERNAN, A., Duality for inelastic anti KN scattering at intermediate energies, 25:43642 (UCR-34-P-107-B-106)
$\pi^+ + p \rightarrow \Delta^{++}(1235) + \pi^0$ AT 1.85 to 2.09 GeV: study of s- and t-channel effects, 25:43551 (UCR-34-P-107-B-108)
Study of $\pi^+p \rightarrow rho^+p$ at 1.85 to 2.09 GeV, 25:43552 (UCR-34-P-107-B-110)
KERR, Carolyn M. L., Supramolecular bonding orbitals from molecular antibonding orbitals, 25:41855
KERSHAW, John P., Development of ceramic fiber reinforced metals, 25:42979
KER-TEVA, A., Strontium-90 and ^{137}Cs in some Bulgarian foodstuffs, 25:42381
KESLEV, D., Strontium-90 and ^{137}Cs in some Bulgarian foodstuffs, 25:42381
KEYEUX, A., Late functional changes in irradiated rats, 25:42668
KHACHATRYAN, B. V., Problem of transition radiation for a plasma plate, 25:43367
KHACHATURYAN, M. N., New method of taking information from spark chambers, 25:42147
KHAIKOVICH, I. M., Gamma distribution in medium of arbitrary elemental composition, 25:43426
KHAIKOVSKII, A. A., Corrosion and mechanical properties of Zr alloys in CO_2, 25:42813
KHAKIMOV, F. Kh., Ion--sound turbulence in dense plasma, 25:43406 (JINR-P9-5846)
KHAN, F., Separation of metal ions on inorganic ion-exchange papers, 25:41909
KHAN, J. M., Production of carbon K x rays by heavy-ion bombardment, 25:43107
KHAN, S. U., Mutagenic effect of irradiated media on E. coli, 25:42755
KHANONKIND, M. A., Influence of the valence-shell structure on the internal conversion coefficients of γ-radiation and on the electron density near the nucleus, 25:43953 (BNL-tr-427)
KHIZHNYAK, N. A., Stability of an incompressible equilibrium plasma ellipsoid, 25:43392
KHODADAD, Parviz, Combinations between U chalcogenides UX and U_3X_4 (X = S, Se, Te), and sulfides, selenides, and tellurides of lanthanides, Y, and Sc, 25:43001
KHODYREV, Yu. S., High intensity (10-16) GeV/c negative particle beam, 25:43729 (CERN-Trans-71-16)
KHRISTENKO, E. V., Behavior of superconductive thin-film bridges in SHF fields, 25:43298
KHRISTIANOV, V. K., On radon content in the waters of the upper volga, 25:41929
KHRYLIN, B. A., Calculations of hypernuclei by means of K-harmonics method, 25:43652
KHUSIDMAN, M. B., Mechanism of the phase transition in boron nitride, 25:42994
KIBARSKA, T., Biochemical activity of anastomose Aspergillus niger strains influenced by x rays, 25:42363
KIDO, Yasumasa, Protection standards on radioactive contamination of food and drinking water in Japan, 25:42482
KIEFFER, Arthur W., Transfer function determination of primary loop of a conceptual nuclear Brayton space power plant, 25:44168 (N-71-17933)
KIEFFER, Stephen A., Scinticisternography in individuals without known neurological disease, 25:42567
KIESL, W., Neutron activation analytical determination of a number of trace elements in meteoritic phases, 25:41773
KIESLICH, Klaus, Preparation and ultraviolet light-induced transformation of an antifungal mixture of heptaene antibiotics of Streptomyces surinam, 25:42302
KIIBUS, A., Computer processing of cerebral scintillation camera studies, 25:42090
KIKUCHI, Takeo, Physical properties of carbide fuels and their evaluation, 25:42955 (JAERI-13517)
KILBEY, B. J., Genetic alteration at molecular level of ultraviolet light-induced ad-3B mutants in Neurospora crassa, 25:42341
KIM, M. V., Electromagnet of a transportable betatron, 25:43741
KING, John J., Dark repair of ultraviolet-irradiated deoxyribonucleic acid by bacteriophage T4: purification and characterization of a dimer-specific phage-induced endonuclease, 25:42269
KINGERY, W. D., Basic research in crystalline and noncrystalline ceramic systems. Annual report, 25:42983 (MIT-3773-103)
KINOSHITA, T., Violation of Pomeranchuk theorem and zeros of scattering amplitudes, 25:43575
KINSEY, R. R., Single-particle distributions of π-mesons produced in π^+p, K^+p, pp, and π^-p collisions at high energies, 25:43554 (UR-875-340)
KIPARISOV, S. S., Nitrogen diffusion in zirconium, 25:42967
KIRBY, R. S., Fabrication of OWR gamma shield assemblies, 25:42816 (LA-4644)
KIRCH, Dennis L., Computer processing of scans using Fourier and other transformations, 25:42557
KIREIKO, P. A., Compensation of the stray field of magnetic deflectors, 25:43744
KIRKMAN, M. J., Treatment of liquid wastes by evaporation to salt cakes, 25:41887 (ARH-SA-25)
KIRSHBAUM, Jack D., Study of aplastic anemia in an autopsy series with special reference to atomic bomb survivors in Hiroshima and Nagasaki, 25:42698
KIRSTEN, T., Detection of double beta decay, 25:43932
KISELEVA, E. S., Morphological changes of thyroid cancer in telegammatherapy, 25:42579
KISHINEVSKII, L. M., Characteristic energy losses in Ne^+--Ne collisions, 25:43150
KITAEV, V. Ya., Liquid boron neutron detector for a time-of-flight spectrometer, 25:42104 (FEI-208)
KITTL, R., Quantitative determination of rare earths in meteorites by means of high voltage electrophoresis, 25:41776
KITTRELL, Bill J., Radioisotope scanning for parotid oncocytoma, 25:42572
KIVELSON, Margaret G., Motion and structure of the magnetopause, 25:43220 (N-71-20853)

KLAGES, H. D., Time shaping of beam pulses from the Hamburg isochronous cyclotron by different central diaphragms, 25:43760
KLAPDOR, H. V., Hindrance of M1 transitions from analog to antianalog states in f-p shell nuclei, 25:43850
KLATT, H.-H., Reversed isotope dependence for hydrogen diffusion in palladium, 25:41816
KLEEFELDT, K., Studies on wear and frictional behavior between fuel rod bundles and spacer grids in sodium, 25:44087 (EURFNR-954)
KLEIN, Abraham, Self-consistent theory of nuclear spectra: the pairing-plus-quadrupole interation model applied to the tin isotopes, 25:43925
KLEIN, Ann, Index to nuclear safety, 25:44141 (ORNL-NSIC-56)
KLEIN, D. J., Spin-free quantum chemistry. IX, 25:43163
Spin-free quantum chemistry. X, 25:43164
KLEMOLA, A. R., Determination of correction to precession from stellar proper motions, 25:43048
KLENK, R., Variation of nonlinear parameters to compute decay-constants and their standard deviation, 25:43521
KLEPPER, H. H., Neutrographic hydrogen determination in zirconium alloys, 25:41755
KLEWE-NEBENIUS, H., Measured differential cross sections for elastic and inelastic scattering of 104-MeV α particles, 25:43932 (NP-18920)
KLOPCIC, J. T., Cross-section and polarization measurements for the $^{3}H(^{3}He,n)^{5}Li$ reaction, 25:43796
KLOPPER, J. F., Visualization of the human spleen with /sup 99m/Tc-labeled red blood cells, 25:42235
KLUGER, F., Neutron activation analytical determination of a number of trace elements in meteoritic phases, 25:41773
KLYKOV, O. V., Dose distribution in skin contaminated with radioactive substances, 25:42257
KNAPIK, Jerzy, Spark chamber as an element of the hodoscopic detector of extensive air showers, 25:42158
KNAPP, D. E., Nuclear electric power sources for biomedical application, 25:41996
KNIGHT, R. W., X-ray attenuation scanning of nuclear fuel plates, 25:42031
KNITTER, H.-H., Scattering of fast neutrons of ^{238}U, 25:43898
KNIZHNIKOV, V. A., Permissible levels of irradiation of the organism in radioisotope diagnosis, 25:42552
KNOWLES, Forrest E. Jr., Separation of calcium--strontium investigated by the use of tracers, 25:41715
KNOWLES, S. H., Observations of 1.35-centimeter H_2O emission in southern hemisphere, 25:43051
KO, Winston, Symmetric π⁻ production from K⁺ + p + π⁻ + anything at 12 GeV/c, 25:43557
KOBAYASHI, R. M., Radiation-sterilization of the Mediterranean fruit fly (Diptera: tephritidae): Comparison of spermatogenesis in flies treated as pupae or adults, 25:42751
KOBAYASHI, Shun-ichi, NMR and relaxation of ^{163}Dy in Dy metal at low temperature, 25:43498
KOBOS, Andrzej, Distorted Wave Born Approximation programmes for inelastic scattering of charged particles MIS-0, MIS-2, MIS-3, MIS-4, and MIS-5, 25:43954 (INP-745)
KOBUSHKIN, A. P., Dual amplitude for processes with participation of photons, 25:43592
KOBYLINSKII, N. A., Dual amplitude with Mandelstam analyticity, 25:43523 (ITF-71-28-E)
KOCH, L. J., U. S. experience with fast power reactors: EBR-II, 25:44085 (CONF-710427-1)
KOCHER, David Charles, Vector analyzing power and cross section for (d,p) stripping reactions on intermediate weight nuclei, 25:43845
KOCI, J., Personal monitoring of workers during the translocation of a ^{90}Sr--^{90}Y beta source by all of TLD, 25:42444
KODAMA, Takeshi, Beta-stability line and liquid-drop mass formulas, 25:43915
KOEHLER, H. S., Energy spectra of single-particle states in nuclei, 25:43825
KOEHLER, Helmut, Phenoxides of the triad elements, 25:41780 (SC-T-713038)
KOEHLER, K., Effects of α-deuterium substitution, polar substituents, temperature, and salts on the kinetics of hydrolysis of acetals and ortho esters, 25:41800
KOELMARK, H. G., Mutagen specificity in Neurospora crassa, 25:42352
KOEN, B. V., Optimization of nuclear materials safeguards sampling systems by dynamic programming, 25:42045
KOEPP, G., Possibility of CPT violation in neutral kaon decay, 25:43656 (PITHA-44)
KOERNER, O., Prevention of intestinal absorption of radiocesium and radiostrontium with the help of indigenous ionic resins, 25:42263
KOGA, Taeko, Radiation hazard control system, 25:42480
KOGAMI, Shinichi, Balloon-borne instrument for low-energy primary cosmic-ray measurements, 25:42159
KOH, Byung Joon, Application of optimum control to 600 MWe pressurized water reactor, 25:44106
KOIDAN, V. S., Studies of plasma turbulence by means of charged particle beam, 25:43339 (IYAF-7-70)
KOKOULIN, R. P., Filtering of tracks measured on the SMP, 25:42135 (CERN-Trans-71-8)
KOLACHKOVSKI, A., α decay of neutron-deficient radon isotopes, 25:43887 (JINR-P6-5791)
KOLAR, D., Phase relationships and crystal chemistry in systems US--CaS, US--SrS, and US--BaS, 25:43002
KOLB, W., Seasonal variations of concentration of ^{7}Be, ^{54}Mn and their decay products in ground-level air, 25:41934
KOLENKOVA, M. A., Production of zirconium dioxide from baddeleyite concentrate, 25:42942
KOLK, B., Dual-motion Moessbauer absorber system, 25:42120
KOLLIE, T. G., Room temperature measurements of electrical resistivity and thermal conductivity of various graphites, 25:44283 (ORNL-TM-3477)
KOLLMER, W. E., Increased elimination of radiostrontium during lactation, in relation to age of animals, 25:42252
KOLOMENSKAYA, T. I., Distribution of radiation defects in silicon irradiated with fast charged particles, 25:43463
KOMAC, M., Phase relationships and crystal chemistry in systems US--CaS, US--SrS, and US--BaS, 25:43002
KOMAKI, K., Effects of crystal surface and imperfections on channeling phenomena of protons, 25:43461
KOMAROV, O. K., Production of high-quality zirconium concentrate, 25:42825
KOMAROV, V. L., Ion-beam apparatus, 25:43747
KOMEYA, K., Influence of fibrous aluminium nitride on strength of sintered AlN--Y_2O_3, 25:42959
KONDO, T., Total absorption type lead glass Cherenkov counter with high resolution, 25:42154
KONDRATENKO, A. M., Dynamics of particle polarization near spin resonances, 25:43770
KONDRATEV, Yu. S., 5-BU sensitization to uv-induced killing and mutability in hcr⁺ and hcr⁻ strains of Escherichia coli, 25:42345
KONIJN, J., Intensities of γ-rays in the ^{57}Co decay, 25:43882
KONISHI, Takao, Effects of fabrication conditions on mechanical properties of Zircaloy tubes, 25:42860
KONISHI, Teruaki, Nuclear excitation by the bound muon, 25:43913
KONISHI, Yozo, Pionic complex level shifts and optical potential parameters in terms of the π--N scattering length, 25:43806
KONOVALOV, O. G., Telescope of spark chambers with a magnetic spectrometer for polarization experiments, 25:42146
KONSHIN, V. M., Properties of FEU-79 photomultipliers used as photon counters in astronomical observations, 25:42068
KONSTANTINOV, D. I., Optimizing the parameters of radiometric equipment when determining low levels of radiation, 25:42102
KONSTANTINOVA, Bl. P., Chromosomal disturbances following x-ray examinations, 25:42362
KOOISTRA, L. F., Interpretations of the drop weight test in terms of strain tolerance (gross strain) and fracture mechanics, 25:42847 (ORNL-TM-3247)
KOONS, Harry C., Electrostatic vlf waves observed in polar magnetosphere, 25:43213 (AD-715898)
Outer-zone electron precipitation, 25:43211 (AD-715266)
KOOPMAN, David W., Langmuir probe and microwave measurements of streaming plasmas, 25:43342
KOPECKY, A., Radiolysis of fats, 25:41861
KOPETSKII, Ch. V., Effect of carbon on the mechanical properties and structure of molybdenum crystals, 25:42899
KORBEL, Kazimierz, Semiconductor system for analog processing of radiometric signals for determination of Ca, 25:42175
KORCHUGANOV, B. N., On radon content in the waters of the upper volga, 25:41929
KORENKOV, I. P., Study of ^{210}Po content in environment and human body, 25:42429
KORGAONKAR, K. S., Monolayer studies with γ-irradiated poly-L-serine, 25:41834
KORNBLIT, Avinoam, Depression of superfluid transition temperature in ^{4}He by heat current, 25:43286
KORNILOV, I. I., Metal suboxides, 25:42991
KOROBEINIKOV, V. P., Gas dynamics of explosions, 25:43348
KOROES, E., Iodine-catalyzed iodine exchange reactions, 25:41817
KOROP, E. D., Acceleration of ions of cathode material in vacuum breakdown, 25:43383
KORSHAKOV, N. G., Kinetic description of plasma configurations, 25:43378
KORSUNSKII, M. I., Electrostatic spectrometer for beams of charged particles, 25:42215
Ion-optical properties of an electrostatic charged-particle energy analyzer, 25:43761
KORZUNOVA, R. A., Study of ^{210}Po content in environment and human body, 25:42429
KOSANKE, H. D., Neutrographic hydrogen determination in zirconium alloys, 25:41755
KOSS, Peter, Influence of neutron irradiation on the graphitization of unalloyed and alloyed malleable cast iron, 25:42904
KOSSIONIDES, S., States of ^{23}Na below 5.4 MeV, 25:43880
KOSTER, Thomas A., Table of hyperfine fields, 25:43469 (UCRL-20411)
KOSTEROVA, N. V., Structure of alloys in system Ta--C--Re, 25:42992
KOSTIAL, Krista, Comparative strontium and calcium metabolism in lactation, 25:42255

XUM

Effect of alginates from algae on Sr transport through rat's duodenum, 25:42254
KOSTIKOV, V. I., Characteristics of porous graphite impregnated with fused zirconium, 25:42948
Spreading of zirconium between parallel graphite plates, 25:42832
KOSTIN, V. I., Outer-sphere interaction in $M_3UO_2F_5$ complexes, 25:41828
KOSTYLEV, V. A., Calculation of the sensitivity function of a detecting system with a multichannel ring collimator, 25:42089
Determination of the optimal canal of registration of gamma-radiation in radioisotope diagnosis, 25:42397
KOSTYRKO, Andrzej, ^{131}I content in primary coolant water and in the air under EWA-10 reactor top covers, 25:44155 (INR-1295)
KOTOV, V. I., High intensity (10-16) GeV/c negative particle beam, 25:43729 (CERN-Trans-71-16)
KOTYZA, Vojtech, Rated parameters at power station A-1, 25:44021
KOVACS, V., Metabolism of ^{35}S-selenomethionine in rats. II, 25:42254
Sulfur-35-methionine and ^{75}Se-selenomethionine metabolism in rats. III, 25:42255
KOVAL'SKII, V. V., Role of microorganisms in biogenic migration of U, 25:42256
KOVTUN, R. I., Nonlinear interaction of electron beams with plasma, 25:43355
KOZLOVA, M. V., Study of ^{210}Po content in environment and human body, 25:42429
KOZYCZKOWSKI, J., Absolute transition rates in ^{182}W, 25:43903
KPONOU, A., Precise measurement of 2^3P_0--2^3P_1 fine-structure interval of He, 25:43122
KRAMAR, Jaroslav, Use of ion sputtering in making electrodes for thermionic energy converters, 25:43187
KRAMER, D., Effects of helium on the high-temperature ductility of Sandvik 12R72HV and Inco IN-744X, 25:42872
Void formation in proton irradiated stainless steel, 25:42917
KRAMER, William Robert, Interaction of a streaming plasma with a magnetic mirror, 25:43359
KRANSKY, V., Two-dimensional stress-induced adiabatic flow. II, 25:44301 (JCID-30013(Pt.2))
Two-dimensional stress-induced adiabatic flow. III, 25:44302 (UCID-30013(Pt.3))
Two-dimensional stress-induced adiabatic flow. I, 25:44300 (UCID-30013(Pt.1))
KRAPF, Rudolf, Thermionic converter with concentric collector and emitter, 25:43189
KRASNOV, N. N., Decreasing ion cluster repetition frequency in an FEI cyclotron, 25:43742
KRASZNOVSZKY, Sandor, Determination of spin parity by means of multipole moments, 25:43591
KRAUSE, H., Time shaping of beam pulses from the Hamburg isochronous cyclotron by different central diaphragms, 25:43760
KRAUSHAAR, J. J., New 0^+ states in ^{50}Cr, 25:43849
KREBES, E. S., Conjugate variables in two-body collisions, 25:43724
KREE, P., Conference on optimization, Nice, 6--7/69, 25:43525
KREGAR, M., Lifetimes of ^{39}K excited states, 25:43861
KREHBIEL, H., Inelastic electron--proton scattering in the region of the Δ (1236) resonance, 25:43527 (DESY-71/21)
KREISEL, W., Angular correlation studies on the 325- and 177-keV cascade in ^{131}Xe, 25:43896
KREUTZ, E. W., Effects of x radiation on MOS devices at 79K, 25:42234
KRIEGER, H. L., Iodine-131 discharges from an operating boiling water reactor nuclear power station, 25:42388
KRIMIGIS, S. M., Statistical study of solar protons, alpha particles, and Z greater than or equal to 3 nuclei in 1967--1968, 25:43231
KRISCH, O., Quenching of luminescence of organic crystals by x rays, 25:41840
KRISHNAMURTHY, K., Tabulated dose distribution data for gamma irradiator design, 25:41957 (BNL-50147(Rev.))
KRISS, Joseph P., Alterations in serum thyrotropin (TSH) and thyroid function following radiotherapy in patients with malignant lymphoma, 25:42695
KRISYUK, E. M., Content of ^{137}Cs in population of Soviet Union, 25:42375
KROEGER, Erich W., Electrical performance of three solar thermoelectric test sections, 25:43185 (N-71-17252)
KROGULSKI, T., Closed shells for very heavy nuclei, 25:43936
Closed shells for very heavy nuclei, 25:43955 (INR-1270)
KROH, J., Influence of γ irradiation of wheat seeds on ascorbic acid content of plant, 25:42726
KRUEGER, W., Experimental investigation of loop caused influences on parallel flow-induced vibration of fuel pins, 25:44119 (EURFNR-923)
KRUGER, J. B., SEFOR operating experience, 25:44128 (CONF-710315-20)
KRUSE, T., Elastic and inelastic proton scattering from heavy collective nuclei, 25:43901
KRUSE, U. E., Some recent experimental results for A_1, A_3, Q, and L mesons, 25:43542 (COO-1195-215)
KRUSZEWSKI, A., Wavelength dependence of polarization. XXIV. Infrared objects, 25:43042
KRYLOV, S. A., Effect of a magnetic field on the accuracy with which particle momentum is determined in a streamer or spark chamber, 25:42148
KRYSHKIN, V. I., Mean free path of the π^0 meson in nuclear matter, 25:43595
KRZYWOBLOCKI, M. Z. E., Equations of motion of plasma in axially symmetric coordinate system, 25:43366
KUBO, Soto-o, Infrared spectra of pentacyanonitrosylmanganese (^{14}NO and ^{15}NO) complexes, 25:41796
KUBOTA, Masumitsu, Impurities in radioisotopes produced by (n,γ) reaction, 25:41877 (JAERI-13545)
KUCHMA, A. S., Hyperfine magnetic field for ^{119}Sn impurity atoms in ferromagnetic terbium, 25:43494
KUDRYAVTSEV, V. A., Physical states on daughter trajectories in dual amplitude under condition α(0) = 1, 25:43712
KUEPPERS, G., Mercier's criterion for class of MHD equilibria, 25:43205
KUERZINGER, Klaus, Temperature-dependence of radiosensitivity in the dry state. II, 25:42288
KUHLMANN, P. E., Inelastic electron--proton scattering in the region of the Δ (1236) resonance, 25:43527 (DESY-71/21)
KUHN, H. G., Isotope shifts and hyperfine structure in the atomic spectrum of platinum, 25:41819
KUKHTEVICH, V. I., Protection from penetrating radiation of a nuclear explosion, 25:42034 (JPRS-53498)
KUKULIN, V. I., Shell interpretation of the separable interactions between lightest nuclei, 25:43786
KULAGIN, D. I., Space--time variations in radioactivity for surface layers of air in Tashkent, 25:41939
KULCINSKI, G. L., Use of heavy ions from a tandem accelerator to simulate high fluence, fast neutron damage in metals, 25:43758
KULESZA, J., Influence of γ irradiation of wheat seeds on ascorbic acid content of plant, 25:42726
KUL'KINA, L. P., Economical source for multiply-charged calcium and zinc ions, 25:43765
KULLECK, James Gerard, Neutron particle hole structure in ^{208}Pb through isobaric analog resonances, 25:43907
KUMAKHOV, M. A., Distribution of radiation defects in silicon irradiated with fast charged particles, 25:43463
KUMAR, N., States of ^8Be from analysis of $^7Li(p,\alpha)^4He$ reaction data, 25:43829
KUMAR, Santosh, Fermi surface and energy bands of lanthanum, 25:43500
KUMATORI, Toshiyuki, Hematological effects on heavily irradiated Japanese fishermen, 25:42681
KUNZ, Louis W., Superconducting energy gap in Pb, 25:43311
KUNZ, W. E., Vela V and VI solar x-ray atlas. V, 25:43066 (LA-4454(Vol.5))
KUNZLE-LUTZ, M., Effects of pulmonary lavage on the retention of particles of plutonium oxide, 25:42368 (LF-tr-53)
KUO, P. K., Cross-section enhancement by scattering with correlated nonstationary states, 25:43105
Energy transfer via scattering of a coherent modulated electron beam, 25:43105
KURAEV, E. A., Cross sections for production of e^+e^- pairs in collisions of heavy charged particles, 25:43598
Interference between Coulomb and strong interactions at high energies, 25:43607
KURI, Zen-ichiro, Effect of phase on excitation transfer in the radiolysis of isobutane, 25:41854
Role of reaction sites in the radiolysis of solid succinic acid, 25:41865
KURLANDZKI, J., Relativistic invariance and causality in the theory of continuous media, 25:43693
KURODA, P. K., Decay of ^{78}As, 25:43881
KUROI, H., Activities on modular code systems in Japan, 25:44188 (EACRP-A-135, pp 59-86)
KURZWEG, Lutz, Excitation of 3914-A N_2^+ radiation in collisions of heavy ions with N_2 and fine structure effects in Ly-α, 25:43151
KUSUMEGI, Asao, Absolute calibration of bremsstrahlung beam monitors, 25:42083
KUTNER, M., Discovery of interstellar silicon monoxide, 25:43052
KUZ'MIN, I. I., Radiation physics of ferroelectrics of barium titanate type, 25:43442
KUZNETSOV, V. I., Economical source for multiply-charged calcium and zinc ions, 25:43765
KUZNETSOVA, A. S., Influence of deformation rate on deformability of Mo--0.5 percent Ti alloy, 25:42833
KUZNETSOVA, L. M., Shell interpretation of the separable interactions between lightest nuclei, 25:43786
KWEI, G. H., Variable delay gate generator for two-channel counting systems, 25:42063
KYUTOV, D. D., Studies of plasma turbulence by means of charged particle beam, 25:43339 (IYAF-7-70)

L

LAASPERE, T., Observations of auroral hiss, 25:43246
LACKEY, M. E., Performance characteristics of a short reentry tube steam generator at low steam output, 25:41962 (ORNL-TM-3236)

LACKEY, W. J., In-reactor restructuring temperatures and kinetics for (U,Pu)O2, 25:44124 (ORNL-TM-3387)
LACKI, Eugeniusz, Semiconductor system for analog processing of radiometric signals for determination of Ca, 25:42175
LADU, M., Radioprotection at the electrosynchrotron at Frascati, 25:43738
LAGUARDA-FIGUERAS, A., Recovery effect of serotonin-creatinine sulfate complex on x-irradiated planarians, 25:42527
LAHET, G., New method for preparing metal borides, 25:42944
LAI, Kuan-wu, K+ forward scattering from the reaction π-p → K+Σ(1375)- at 4.5 and 5 GeV/c, 25:43558
LAKATOS, T., Silicon semiconductor spectrometer, 25:42112
LAL, S., Nuclear interaction of cosmic-ray pions and nucleons of energies > 20 GeV. I, 25:43540
LALOR, Eamon, New model for the interaction between a moving charged particle and a dielectric, and the Cherenkov effect, 25:43588
LALOR, Fergus J., Nucleophilic substitution at tetrahedral boron. Methylamine--diarylborane substrates, 25:41804
LAMB, Eugene, Prog. rpt. on isotopic power fuels, 3/31/71, 25:41993 (ORNL-4692)
LAMBERS, Rolf, Film dosimetry of high-energy rays. IV, 25:42396
LAMOUREUX, G., Geometrical correction factors for angular correlation measurements with Ge(Li) detectors, 25:42054 (LPN-UM-53)
LANDBERG, Torsten, Mantle treatment of Hodgkin's disease with ^{60}Co, 25:42594
LANDE, Larry C., Seismic analysis of Gasbuggy explosion an earthquake of similar magnitude and epicenter, 25:41952 (AD-838894)
LANDER, Harry, Scintiphotography and rectilinear scanning of lung using /sup 99m/Tc-MAFH (macroaggregated ferrous hydroxide), 25:42579
LANDER, Jerrold J., Frequency of antibody to hepatitis-associated antigen as measured by a new radioimmunoassay technique, 25:42306
LANDER, R. L., Evidence for splitting in the Q region of K+π+π- mass, 25:43544 (COO-1428-275)
New evidence for splitting in the Q region of K+π+π- mass, 25:43543 (COO-1428-274)
LANDER, Richard L., Symmetric π- production from K+ + p → π- + anything at 12 GeV/c, 25:43557
LANE, Richard A., Color television survey in Pennsylvania, 25:42501
LANGE, R., Theoretical ground motion predictions supporting HEST program, 25:41950 (AD-718388)
LANGEL, Robert A., Asymmetric ring current at twilight local time, 25:43241
LANGER, S., Dead-end separation of BISO-coated fissile and fertile particles for high-temperature gas-cooled reactors, 25:41907
Dead-end separation of TRISO-coated fissile and fertile particles for high-temperature gas-cooled reactors, 25:41906
LANGFORD, W. J., Metallurgical properties of cold-worked Zircaloy 2 pressure tubes, 25:42914
LANGHOFF, P. W., Schroedinger particle in a gravitational well, 25:43517
LANGKAU, R., Time shaping of beam pulses from the Hamburg isochronous cyclotron by different central diaphragms, 25:43760
LANGLANDS, A. O., Urinary excretion of β-aminoisobutyric acid after exposure to radiation, 25:42684
LANGMEAD, W. A., Positioning of film badges, 25:42442
LANKFORD, John C., Modification by acridine analogs of the survival of ultraviolet irradiated Escherichia coli B, 25:42533
LANTIN, B., New types of dahlia by induced mutations, 25:42327
LANZA, F., Bismuth-impregnated graphite reflector in a heavy water moderated reactor: an evaluation, 25:44129 (EUR-4357)
LANZOLA, E., Bone deposition of ^{210}Pb(^{210}Po) and ^{90}Sr, 25:42382
Results of 3 years (1964--1965) of measuring radioactivity of foods sampled in city and province of Pavia, 25:42389
LAPINS, K. O., Mutants of golden delicious apple induced by ionizing radiation, 25:42324
LA PLACA, S., Nonstoichiometric hexaboride of thorium Th/sub 1-x/B$_6$, 25:43003
LAPORTE, A., Installation of beam facility on triton reactor, 25:44158 (LB/G-2929)
LAPPENBUSCH, William L., Mechanism of radioprotective action of dimethyl sulfoxide, 25:42524
LARHER, Yves, Study of structure of physisorbed phases by thermodynamic analysis of stepwise isotherms of Kr, Xe, Ar, and methane on cleavage face of halides having a layer-like structure, 25:41824 (CEA-R-4089)
LARICHEV, A. V., Problems of protection from ionizing radiations in radiation chemistry, 25:42448
LAROZE, L., Hall--Post lower bound calculations for the three-nucleon system, 25:43983
LARSEN, Joergen Hannover, Effect of transplanted lymphoid cells, irradiation, and drug therapy on permanent immunologic tolerance, 25:42313
LARSEN, R. P., Activation-rate measurements in the ZPR-3 mockup critical experiments. Part I. Measurements of foil-activation rates and fission yields in Assembly 60 of ZPR-3: mockup of EBR-II with a uranium blanket, 25:44150 (ANL-7781)
LASLEY, Eric, Current algebra and the trace of the energy--momentum tensor, 25:43630
LATYSHEV, I. N., Empirical study of the pulsations of the upper layers of cepheids, 25:43025
Star streams in the solar neighborhood, 25:43027
LATZKO, D. G. H., Safety aspects and future role of engineering inspection of nuclear power reactor components, 25:44135 (CONF-700224-, Paper 1)
LAUTZENHEISER, C. E., Ultrasonic inspection of selected welds in stainless steel primary steam piping in Elk River Power Plant, 5/66, 25:44082 (SWRI-1228-9-10)
LAUTZENHEISER, Clarence E., Development of an inspection system for the Atucha nuclear reactor, 25:44080
LAVAL, G., Radial dependence of trapped-particle instabilities, 25:43391
LAVAN, M. J., Effect of approximate wave functions in composite-particle scattering, 25:43971
LAVEN, H., Inherited semisterility for control of harmful insects. I, 25:42335
LAVIGNE, Robert J., The Rain Forest Project. Annual report, 25:42317 (PRNC-147)
LAVOLLEE, Philippe, Radioactivity distribution in environment of a contained nuclear explosion. I, 25:41954 (CEA-R-4128(1))
LAVRENT'EV, I. V., Boundary problem on the distribution of electric fields along the channel with side bars, 25:43202
LAVROV, V. P., Electrostatic spectrometer for beams of charged particles, 25:42215
Ion-optical properties of an electrostatic charged-particle energy analyzer, 25:43761
LAWRENCE, George P., Reaction D(d,n)^{3}He at 0° with polarized beam, 25:43789
LAWRENCE, J. K., Focusing of gravitational radiation by the galactic core, 25:43700
LAZURIK-EL'TSUFIN, V. T., Cross sections for production of e+e- pairs in collisions of heavy charged particles, 25:43598
LEACH, C. E., Radioisotope-energized Stirling engine for spacecraft auxiliary electric power, 25:42010
LEAHY, J., Theoretical ground motion predictions supporting HEST program, 25:41950 (AD-718388)
LEBEDEV, V. A., Polarization of a zinc cathode during thorium precipitation from molten halide salts, 25:42821
LE BELLAC, M., Operator approach to dual multiparticle theory, 25:43578
LEBER, Robert L., Livermore superconducting Levitron, 25:43399 (UCRL-73076)
LE-CHI-NIEM, Two-channel calculation for elastic α--α scattering, 25:43784
LE COULTRE, Pierre, Ratio of neutral-to-charged hadrons in cosmic radiation at an atmospheric depth of 976 g c, 25:43621
LEE, H. K., Elastic and inelastic pion-^{12}C scattering at intermediate energies, 25:43830
LEE, W. Y., Resonance process and intensity anomaly in muonic ^{127}I, 25:43949
LEE, Y. T., Crossed-molecular-beam study of collision-induced dissociation of alkali halides, 25:43131
LEE-WHITING, G. E., Semi-analytical calculations for circular quadrupoles, 25:43757
LEFEBURE, Patrice, Study of 3 ^{1}P--2 ^{1}S line of He excited by H ion beam, 25:43129
LEFEVRE, Ultrahigh vacuum metrology, 25:42047
LE FLEM, J., Three cross sections in system CaO--Nd_2O_3--Al_2O_3, 25:42995
LEHMANN, B., Magnetic moments of isomeric levels in the Br isotopes, 25:43841
LEHOTAI, Lajos, Effect of whole-body x-radiation on the lipolytic activity of rat heart extracts, 25:42281
LEIGH, B., Induction by x-rays of double mosaics involving Y-chromosome, 25:42344
Interaction of chromosome breaks in spermatids and spermatocytes of Drosophila melanogaster, 25:42354
LEIGH, J. R., High-spin isomer in ^{211}At, 25:43912
LEIMAN, V. G., Hydrodynamic stability of electron streams in vacuum, 25:43756
LEITNAKER, J. M., Observations of fuel-cladding chemical interactions as applied to GCBR fuel rods, 25:44123 (ORNL-TM-3385)
LEITNER, Zbynek, Rated parameters at power station A-1, 25:44021
LELIEVELD, P., Survival of colony-forming units in mouse bone marrow after in vivo irradiation with D--T neutrons, x-, and gamma radiation, 25:42601
LEMAIRE, J., Simple model for an ion exosphere in an open magnetic field, 25:43222
LENZI, Giuseppe, Characteristics of the land surrounding CSN with reference to safety and medical protection, 25:41930
LEON, B., Magnetic characteristics of aluminum-rich ternary laves phases containing rare earths, nickel, and aluminum, 25:43480
LEON, M., X-ray yields in muonic hydrogen, 25:43125
LEONARD, A., Influence of selection, non-uniform cell population, and repair on dose-effect curves of genetic

XUM

effects, 25:42353
LEONARD, Albert Clark, Heat transfer from horizontal wires to He II at high heat-flux values, 25:43282
LEONARD, J. A., SNAP-27 program review, 25:41999
LEONOV, V. F., Gamma-ray spectrum from reaction (n,γ) on ^{150}Sm and ^{151}Sm samples, 25:43892
LEPINSKIKH, B. M., Electrical properties of liquid V_2O_5, 25:42969
LEPPER, R., Active radiation shield for cylindrically shaped vehicles, 25:43425
LEPPING, R. P., Single spacecraft method of estimating shock normals, 25:43235
LERCH, R. E., Dissolution of unirradiated mechanically blended mixed oxide fast reactor fuel, 25:42954 (HEDL-SA-131)
LERFALD, G. M., High-altitude nuclear detection studies. II, 25:41933 (AD-719520)
LE ROY, Robert J., Collision time-delay functions and quasi-bound level properties of $H_2(X^1\Sigma/sub\ g/^+)$, 25:43124
Eigenvalues and expectation values for levels of ground-state H_2, HD, and D_2, 25:43123
LETUNOVA, S. V., Role of microorganisms in biogenic migration of U, 25:42255
LEUNG, Man-chiu, Stochastic processes and thermal fluctuations in superconductors, 25:43320
LEVAKOV, E. N., Influence of some salts on the double decomposition of zircon with calcium carbonate, 25:42972
LEVI, H. W., Isotopic exchange between glasses and nonaqueous liquids, 25:41810
LEVIN, A. Ya., Characteristics of coherent interactions at 17 and 45 GeV, 25:43645 (JINR-P1-5775)
LEVIN, E. M., Determination of the isotopic composition of tin and indium, 25:41727
Physical states on daughter trajectories in dual amplitude under condition $\alpha(0) = 1$, 25:43712
LEVINE, S. H., Active radiation shield for cylindrically shaped vehicles, 25:43425
LEVINGER, J. S., Hall--Post lower bound calculations for the three-nucleon system, 25:43983
LEVINSKII, Yu. V., Nitrogen diffusion in zirconium, 25:42967
Synthesis and properties of molybdenum borocarbide, 25:42941
LEVITT, S. H., Combination of preoperative irradiation and surgery in the treatment of cancer of the oropharynx, hypopharynx, and larynx, 25:42588
LEWIS, Edward S., Reaction of p-phenylenebisdiazonium ion with alcohols, 25:41805
LEWIS, Joseph Thomas, Electron paramagnetic resonance and optical absorption studies of color centers and impurity ions in $KMgF_3$ and MgF_2, 25:44297 (TID-25746)
LEWIS, L. D., High-altitude nuclear detection studies. II, 25:41933 (AD-719520)
LEWIS, S. A., Precise measurement of 2^3P_0--2^3P_1 fine-structure interval of He, 25:43122
LEWIS, W. Burton, ^{17}O NMR studies of uranium oxides, 25:43497
LI, Che-yu, Considerations of metal swelling and related phenomena caused by fast neutron irradiation, 25:42918
LIEBSCHER, D.-E., Gravitation theory as theory of non-Lorentzian transformations of systems of reference, 25:43708
LIEBSCHER, Kurt, Comparison of physical evidence by means of trace element analysis, 25:41775
LIEMOHN, H. B., Some algebraic solutions of the cyclotron resonance interaction, 25:43403 (AD-715636)
LIFSHITZ, E. M., Relativistic quantum theory, 25:43086
LIFTON, Judith F., Fate of ^{13}N formed by $^{12}C(d,n)^{13}N$ reaction in inorganic carbides, 25:41886
LIGHTNER, G. S., Mass and charge dependent ion discrimination in a linear pulsed time-of-flight mass spectrometer, 25:42211
Multiple ionization of Ne, Ar, and Kr by x rays, 25:43142
LIGOU, J., Integral transport equation in one-dimensional cylindrical geometry. II, 25:43771 (EIR-189)
LIKHTMAN, E. P., Extension of algebra of Poincare group generators and violation of P invariance, 25:43676
LILLEY, J. S., Real part of the alpha-nucleus potential, 25:43973
LIM, T. K., Exactly soluble quantum-mechanical three-body problem, 25:43509
LIMA, F. W., Retention of Ta by hydrated Sb(V) oxide in strongly acid media, 25:41922
LIN, Chia-shi, Non-destructive determination of reactor fuel element burnup by measurement of fission neutrons, 25:41757
LIN, Jung, Study of neutron continuum from interaction of ^{7}Li with ^{3}He, 25:43788
LIN, Sin-shong, Simple positioner for quadrupole mass spectrometer, 25:42212
LIN, Tsing-ko., Inorganic yields of ^{38}Cl in Szilard--Chalmers reactions of α-, β-, γ-, and delta-benzene hexachlorides, 25:41884
LIN, Y. C., Energy spectra of single-particle states in nuclei, 25:43825
LINDE, S., Sensitivity of uranium and separative work requirements to variations in reactor programs, 25:44127 (CONF-700903-17)
LINDELL, Bo., Professional responsibilities of the health physicist in relation to the medical profession, 25:42711
LINDEMER, T. B., Kinetic models for the synthesis of (U,Pu)O/sub 2-y/ by hydrogen-reduction and carbothermic techniques, 25:41779 (ORNL-TM-3358)
LINDGARD, Per-Anker, Prog. rpt. on physics, annual, 1--12/70, 25:43435 (RISO-237)
LINDSKOUG, B., Collimator and scattering foil for 10 to 20 MeV electrons, 25:43767
LINGEMAN, E. W. A., Intensities of γ-rays in the ^{57}Co decay, 25:43882
LINK, C. H. Jr., Classical model for gas--surface interaction, 25:43104
LINSON, Lewis M., Collisionless shocks in plasmas, 25:43347
LION, Philippe, Process for decontaminating radioactive waters, 25:42384
LIONS, J. L., Conference on optimization, Nice, 6--7/69, 25:43526
LIPATOV, L. N., Interference between Coulomb and strong interactions at high energies, 25:43607
LISLE, J. C., States of ^{23}Na below 5.4 MeV, 25:43880
LISTENGARTEN, M. A., Influence of the valence-shell structure on the internal conversion coefficients of γ-radiation and on the electron density near the nucleus, 25:43953 (BNL-tr-427)
LITTBRAND, Bo, Chemical protection of the recovery process, 25:42521
LITTLE, C., Effects of x irradiation on various enzymic functions of NADP+-linked isocitrate dehydrogenase, 25:42299
LITTLE, Paul Edward, Directional correlation and decay scheme studies of ^{178}Hf and ^{156}Gd, 25:43917
LIU, Ching Lung, Transfer of immunity to Hymenolepis nana in mice with spleen cells or spleen cell fractions, 25:42311
LIU, S. H., Generalized susceptibility function for rare earths and thorium and their alloys, 25:43477
LIVENGOOD, Charles David, Development of a fast neutron spectrometer and measurement of neutron spectra transmitted through iron slabs, 25:44205
LIVERSAGE, W. E., Critical look at RET, 25:42413
Nominal standard dose and the RET, 25:42446
LLOYD, Christopher George, Handling facilities and methods, 25:42044
LO, R. E., Properties of lithium with respect to its use as a rocket fuel. I, 25:44284 (ORNL-tr-2471)
LOBANKOV, V. V., Synthesis and properties of molybdenum borocarbide, 25:42941
LOBANOV, E. M., Radiation-induced changes in the electrical properties of LiF monocrystals alloyed with Na, 25:43445
LOCHMUELLER, C. H., Effect of an electric field on gas chromatographic retentions by liquid crystals, 25:44245 (COO-1222-47)
LODHI, M. A. K., Residual potential and nucleon correlation in the shell model. I, 25:43815
LOEBNER, K. E. G., Measurement of nuclear half-lives up to 100 s by the delayed coincidence method, 25:42222
LOEFFLER, F. J., Evidence for splitting in the Q region of $K^+\pi^+\pi^-$ mass, 25:43544 (COO-1428-275)
New evidence for splitting in the Q region of $K^+\pi^+\pi^-$ mass, 25:43543 (COO-1428-274)
LOEHBERG, R., Influence of additions of a third element on the critical magnetic field of titanium--niobium alloys, 25:43309
LOEHKEN, R., Measured differential cross sections for elastic and inelastic scattering of 104-MeV α particles, 25:43832 (NP-18920)
LOEVBORG, Leif, Field determination of uranium and thorium by gamma-ray spectrometry, exemplified by measurements in the Ilimaussaq alkaline intrusion, south Greenland, 25:41943
LOGINOV, A. S., Scanning of the liver in the diagnosis of chronic hepatitis and cirrhosis, 25:42553
LOGINOV, V. S., Electromagnet of a transportable betatron, 25:43741
LOH, B. T. M., Numerical calculation of elastic properties for straight dislocations in anisotropic crystals, 25:44282 (ORNL-TM-3408)
LOHNERT, Wolfgang, Simultaneous oxide evaporation and thermal diffusion in tantalum--oxygen solid solutions, 25:42975
Some theoretical aspects of thermal diffusion in interstitial solid solutions, 25:42865
Thermal diffusion of O in Ta--O and Nb--O solid solutions, 25:42864
LOHSE, G. E., Third processing campaign in the Waste Calcining Facility, 25:41893 (IN-1474)
LOKEN, Merle K., Scinticisternography in individuals without known neurological disease, 25:42567
LOMBERSKA, L., Thermal stability and its relation to scintillation detector parameters with domestic NaI(Tl) crystals 40 x 40 mm and photomultipliers 61 PK 413 through 415 at elevated temperatures, 25:42092
LONG, A. B., Plutonium inhalation: the burden of negligible consequence, 25:42508
LONG, E. L. Jr., Observations of fuel-cladding chemical interactions as applied to GCBR fuel rods, 25:44123 (ORNL-TM-3385)
LONG, F. A., Proton transfer from cyanocarbon acids. III.

Primary and solvent kinetic isotope effects in the ionization of malononitriles, 25:41799
Proton transfer from cyanocarbon acids. II. General-base-catalyzed detritiation and bromination of malononitriles. Rates of the reverse reactions, 25:41798
LONGEQUENE, J. P., ^{6}Li(α,2α) reaction as a test of the existence of α particles in ^{6}Li, 25:43803
LONGO, Stephen A., New improved generator applied to conformal Lagrangians, 25:43677
LONNGREN, K. E., Mechanism causing nonlinear behavior in Tonks--Dattner resonance experiments, 25:43411
LOOS, Wesley E., Prog. rpt. on preparation of wood--plastic combinations using gamma radiation to induce polymerization, final, 11/61--6/68, 25:41843 (ORO-2945-10)
LOPEZ GONZALEZ, J. M., Clinical and experimental tests using irradiation, 25:42597
LOPRIENO, Nicola, Effect of caffeine on mutation and recombination in Schizosaccharomyces pombe, 25:42332
LOREL, Roland, Manufacturing of vapor deposited refractory materials, 25:42823
LORENZ, L. J., Specification of gas chromatographic behavior using Kovats indices and Rohrschneider constants, 25:44247 (COO-1222-49)
LORIERS, N., Zirconium alloys used in carbon dioxide at high temperatures, 25:42812
LORIERS, Henri, Process to obtain oxide layers on Zr, Hf, and their alloys, 25:42819
LOSS, F. J., Analysis of radiation-induced embrittlement gradients on fracture characteristics of thick-walled pressure vessel steels, 25:42841 (CONF-710512-8)
LOSSING, F. P., Manifestation of autoionizing states in the ionization of krypton by electron impact, 25:43154
LO TENERO, B., Control rod fabrication experiments, 25:42822
LOUGHEED, R. W., Symmetric fission observed in thermal-neutron-induced and spontaneous fission of ^{257}Fm, 25:43920
LOUIS, Serge, Magnetic cutoff variations during the main phase of a geomagnetic storm, 25:43179
LOVE, L. O., Review of ORNL electromagnetic separations program, 1958--69, 25:41992 (ORNL-4640)
LOVE, W. G., Nucleon--nucleon spin-orbit interaction in the inelastic excitation of high spin states in ^{90}Zr, 25:43915
LOWE, A. L. Jr., Effect of irradiation on the mechanical properties of 19-9DL alloy, 25:42923
LOWMAN, F. G., Uptake of molybdenum, marked with ^{99}Mo, by biota of Fern Lake, Washington, 25:44287 (RLO-2225-T-7-2)
LU, P., Fractional-order Bessel function approximations to both attractive and repulsive Coulomb scattering, 25:43132
LU, Winston Wen-deh, Neutron activation cross sections of medium-Z nuclei at 14.4 MeV, 25:43951
LUALDI, M., Radioisotope investigation of lymph system function and morphology, 25:42581
LUCAS, H. J., Power required to circulate gas-solids suspensions, 25:41956 (BM-RI-7019)
LUCCI, F., Radioprotection at the electrosynchrotron at Frascati, 25:43738
LUCY, L. B., Spectroscopic binaries with circular orbits, 25:43047
LUKIERSKI, J., Lee model with V particle having continuous mass spectrum and energy-conserving V--NTHETA vertex, 25:43671
LUK'YANOV, G. A., Steady supersonic source of nonequilibrium plasma, 25:43192
LUNDIN, Carl D., Welding defects, their origin and effect, 25:42867
LUNNEY, A. J., Comparison tests for extinguishing media on metal fires, 25:42837 (AERE-R-5745)
LUPAKOV, I. S., Corrosion of Zr and its alloys, 25:42811
LUR'E, K. A., Optimum magnetic field distribution along the channel of an MHD generator, 25:43190
LUTZE, W., Isotopic exchange between glasses and nonaqueous liquids, 25:41810
L'VOV, A. N., Cryostat for a Ge(Li) detector, 25:42084
L'VOV, K. M., Investigation of paramagnetic centers of irradiated proteins, 25:42275
LYASH, A. V., Ecitation of the aromatic molecules by electron impact. I, 25:43127 (BNL-tr-429)
LYASS, F. M., Permissible levels of irradiation of the organism in radioisotope diagnosis, 25:42552
LYKKEN, G. I., Measurement of the superconducting energy gap and Fermi velocity in single-crystal lead films by electron tunneling, 25:43312
LYKOV, A. V., Conference on heat and mass transfer, Minsk, 5/68. II, 25:41986
LYLE, F. F. Jr., Investigation of cracking in nuclear reactor primary piping system, 25:42838 (CONF-710512-1)
LYNN, K. R., Effects of γ-radiation on dilute solutions of trypsin, 25:42271
LYNNWORTH, L. C., Prog. rpt. on ultrasonic thermometry in LMFBR systems, 3/59, 25:42189 (NYO-3906-6)
LYSENKO, O. E., Stability of an incompressible equilibrium plasma ellipsoid, 25:43392
LYUBOMIROV, A. M., Spectral-angular characteristics of an electron beam in irradiation of a tissue-equivalent medium, 25:43421 (ORNL-tr-2476)
LYUBUTIN, I. S., Gradient-free oven for examining the Moessbauer effect, 25:42115

M

MA, B. M., Creep stress distribution in long, cylindrical reactor pressure vessels, 25:42842 (CONF-710512-9)
MA, Chin W., Negative-parity states in ^{209}Pb, 25:43926
MA, T. S., Microdetermination of tellurium and organo--tellurium compounds, 25:41744
MACCALLUM, M. A. H., Pulsating universe of Sengupta, 25:43097
MACKINTOSH, Raymond S., Study of inelastic processes on (d,p) reactions in deformed nuclei, 25:43984
MADANSKY, L., Boron-13 nuclear magnetic dipole moment, 25:43817
MADELAINE, Guy J., Existence of small negative radioactive ions coming from a ^{228}Th source, 25:43100
MADELUNG, O., Advances in solid state physics, 25:43483
MADJAR, A. Vidal, Monitoring of the Lyman alpha emission line of the Sun during the year 1959, 25:43075
MADSEN, Stig Nistrup, Liver damage following colloidal thorium dioxide, 25:42708
MAERKER, R. E., Calibration of Bonner ball neutron detectors used at Tower Shielding Facility, 25:42055 (ORNL-TM-3465)
MAFFI, A., Dosimetry of high energy electron beams, 25:42169
MAGARIK, K. N., Method for activating chromed surfaces for radioindicator investigation of their wear (exchange experience), 25:42018
MAGNE, Pierre, Comparison of the catalytic effects of various metals in the graphite--oxygen and graphite--nitrous oxide reactions, 25:42931
Kinetics of graphite oxidation in N_2O, 25:42932
MAGONOV, G. M., Semiautomatic television device for measuring ionization losses, 25:42142
MAHAJAN, K. K., Ionospheric estimates of atomic oxygen concentration from charged particle measurements, 25:43260
MAHANTI, D., Effect of tensor forces on charge form factor of α-particle, 25:43783
MAHNIG, M., Low-temperature heat capacities of transition metal borides, 25:42974
MAIER, K. H., High-spin isomer in ^{211}At, 25:43912
MAILLARD, J. P., ^{6}Li(α,2α) reaction as a test of the existence of α particles in ^{6}Li, 25:43803
MAISTERRENA, Jorge, Radioisotopic evaluation of salivary gland dysfunction in Sjoegren's syndrome, 25:42566
MAJKAROV, S., Radioactive needle with linear activity increasing gradually towards the ends, 25:42590
MAJOUBE, Michel, Fractionating of ^{18}O between ice and water vapor, 25:41921
MAJUMDAR, D. P., Inelastic Compton scattering inequalities in quark-Parton model, 25:43586 (SU-1206-250)
Note on the most probable number of partons in parton models, 25:43585 (SU-1206-246)
MAKHAN'KOV, V. G., Ion--sound turbulence in dense plasma, 25:43406 (JINR-P9-5846)
MAKOFSKE, W., Elastic and inelastic proton scattering from heavy collective nuclei, 25:43901
MAKSIMENKO, V. N., Saturation for interaction with a hard core, 25:43787
MALDACKER, T. A., Effect of loading on separation efficiency using steric exclusion chromatography, 25:44244 (COO-1222-46)
MALDONADO, Javier Flores, Scattering length of the n--n reaction, 25:43534 (NP-18814)
MALENCHANKA, A. F., Comparative evaluation of the effects of uranium nitrate and radioactive iodine on auto-antibody formation, 25:42545
MALLING, H. V., Genetic alteration at molecular level of ultraviolet light-induced ad-3B mutants in Neurospora crassa, 25:42341
MALMSKOG, S. G., Absolute transition rates in ^{182}W, 25:43903
Levels in ^{191}Ir, 25:43902
MALOSSI, S., Health physics experiences in ENEL nuclear electric centers, 25:42478
MALOV, G., Isotopic exchange between glasses and nonaqueous liquids, 25:41810
MAL'TSEV, V. M., Model of the multiple particle production, 25:43614 (JINR-P2-5829)
MAL'TSEVA, L. F., High-temperature materials, 25:42853
MALWAD, N. M., Civil defence, an annotated bibliography 1960-1968, 25:42505 (BARC/BIB-1)
MALY, Vl., Subcutaneous induration following telecobalt therapy, 25:42687
MAMIDZHANYAN, E. A., Description of an ionization calorimeter supplemented with proportional counters, 25:42140
MAMIN, E. B., Radiation safety in design and operation of powerful β-installations, 25:42016
MANCHESTER, R. N., Properties of PSR 0525 + 21, 25:43053
MANDEL, Heinrich, Process for the production of deuterium-enriched water, 25:41904
MANDULA, J., Quantum numbers of cross-channel exchanges, 25:43565 (CALT-68-305)
MANI, G. S., Spin assignments to excited states of ^{58}Fe, 25:43840

XUM

MANN, A., Theory of superfluidity, 25:43285
MANNING, J. J., Calibration of Bonner ball neutron detectors used at Tower Shielding Facility, 25:42055 (ORNL-TM-3455)
MANNING, William Roger, Anomalous elastic behavior of polycrystalline Nb_2O_5, 25:42955 (IS-T-446)
MANTENIEKS, Maris A., Hot electrode drops in an unseeded supersonic argon magnetohydrodynamic generator, 25:43183 (N-71-15855)
MAQUEDA, E., Reaction (d,^{6}Li), 25:43987
MARAFANTE, E., Metabolism of p-nitrophenol in whole-body irradiated rats, 25:42289
MARAN, Stephen P., Gum nebula, 25:43034
MARCHESE, G. S., Effect of ionizing radiations on lymphocytes from adults and newborn infants, cultured in vitro in presence of phytohemagglutinin, 25:42602
MARCHESELLI, W., Enzyme activity in irradiated skin, 25:42285
MARCHETTI, R., Results of 3 years (1964--1966) of measuring radioactivity of foods sampled in city and province of Pavia, 25:42389
MARDON, Yves, Radiochemical adhesion process, 25:41846
MAREEL, M., Organotypical culture of irradiated and non-irradiated chick mesonephros, 25:42643
MARELIUS, A., Absolute transition rates in ^{182}W, 25:43903
MARSEN, P. H., Sensitivity of uranium and separative work requirements to variations in reactor programs, 25:44127 (CONF-700903-17)
MARIANI, A., Problems of the radiocontamination of man, 25:42375
MARINOVA, Ts. S., Beryllium adsorption on tungsten, 25:43473
MARIS, Georgeta, Aspects of north--south asymmetry of chromospheric eruptions in correlation with geophysical phenomena, 25:43072
MARKOV, K. P., Use of photographic films for individual radiometry of the daughter products of radon, 25:42171
MARKOVA, M., Experimental J intoxication, 25:42510
MARKOVIC, P. D., Interaction of a helium plasma with an inhomogeneous transverse magnetic field, 25:43355
MARLOWE, M. O., Fission gas re-solution rates. Quarterly report No. 2, October 1--December 31, 1970, 25:42952 (GEAP-12188)
Fission gas re-solution rates. Quarterly report No. 3, January 1--March 31, 1971, 25:42953 (GEAP-12189)
MARLOWE, O. J., Computer utilization in nuclear reactor design, 25:44090 (AAPD-T-2358)
MARMER, E. N., High-temperature materials, 25:42853
MARMET, P., Natural line shapes resolved in ionization yield of He^+, 25:43139
MAROCHNIK, L. S., Spiral structure of galaxies, 25:43081
MARQUIARDT, E., Zirconium--niobium alloy weldments, 25:42831
MARSDEN, Howard, Effects of ionizing radiation on capacity of Escherichia coli to support bacteriophage growth, 25:42730 (NYO-2804-41)
MARSEL, J., Determination of B in nuclear materials by isotope dilution technique. I, 25:41749
MARTELLI, G. E. G., Nonlinear electron--wave interaction at Doppler-shifted cyclotron frequency, 25:43412
MARTENS, Uta, Measured differential cross sections for elastic and inelastic scattering of 104-MeV α particles, 25:43332 (NP-18920)
MARTIN, A., Violation of Pomeranchuk theorem and zeros of scattering amplitudes, 25:43576
MARTIN, K., Primary high-dosage ^{60}Co irradiation in advanced uterine cervix and vaginal cancer, 25:42598
MARTINELLI, Pierre, Chemical analysis from absorption measurements on Compton scattered radiation, 25:41752
MARTIROSYAN, S. N., Chromosomal breaks induced by x radiation in seeds, 25:42356
MARUYAMA, M., Intermediate structure near an isobaric analog resonance, 25:43851
MASON, Edward A., Subliming nuclear microthruster and its space applications, 25:42017
MASOUREDIS, S. P., Radioisotopes as applied to diagnostic hematology, 25:42573
MASTHOFF, Rolf, Phenoxides of the triad elements, 25:41780 (SC-T-713038)
MASTINU, G. G., Italian atmospheric radioactivity surveillance network, 25:41937
MATERSON, Barry J., Measurement of glomerular filtration rate, 25:42574
MATESE, John J., Choosing pseudostates in the close-coupling formalism for the electron--atomic-hydrogen system, 25:43140
MATEVOSYAN, E. M., Study of a streamer chamber containing xenon, 25:42149
MATSEN, F. A., Spin-free quantum chemistry. IX, 25:43163
Spin-free quantum chemistry. X, 25:43164
MATSUDA, Fukuhisa, Fundamental investigations on solidification structure in weld metal, 25:42820
MATSUDA, Katsuhiko, Effects of fabrication conditions on mechanical properties of Zircaloy tubes, 25:42860
MATSUDA, Tatsuo, Gamma-induced polymerization of fluorine-containing pentadiene, 25:41848
MATSUDAIRA, Hiromichi, Metabolism of Ehrlich ascites tumor cells under anoxia, 25:42632
MATSUI, Hiroshi, Technique for determining activity and size distribution of β emitting particles by autoradiography, 25:42051 (JAERI-13718)
MATSUI, Sumio, Experimental studies on change of maxillo-oral lymphatic system after telecobalt irradiation on the neck. II, 25:42652
MATSUKI, S., Method for preparing thin films of deuterated polyethylene, 25:43759
MATSUO, Takeshi, Study of aplastic anemia in an autopsy series with special reference to atomic bomb survivors in Hiroshima and Nagasaki, 25:42698
MATSUTSIN, A. A., Outer-sphere interaction in $M_3UO_2F_5$ complexes, 25:41828
MATSUURA, Niro, Formation of hypophosphate in the radiolysis of phosphite solution, 25:41866
MATTEI, Giulio, Propagation of MFD waves in a heat-conducting compressible fluid in presence of Hall effect, 25:43200
MATTHIESEN, R. B., San Onofre Nuclear Generating Station vibration tests, 25:44079 (JCLA-ENG-7037)
MATUS, L., Determination of MI-1305 mass spectrometer D/H ratio by using modulated accelerating voltage, 25:41729
MATVEENKO, I. I., Nature of the bond and electrical conductivity of cubic zirconium carbides and oxycarbides, 25:43491
MATVEENKO, L. I., Study of the structure of radio sources, 25:43064
MATVEENKO, O. G., Universal apparatus for measuring the parameters of strong ion beams, 25:43746
MATVEEV, V. V., Optimizing the parameters of radiometric equipment when determining low levels of radiation, 25:42102
Radiometric and radiation monitoring equipment of the near future, 25:42101
MATVEEVA, E. N., Effect of ultraviolet radiation on plastic scintillators with p-terphenyl, 25:42231
MAT'YAZH, V. A., Influence of deformation rate on deformability of Mo--0.5 percent Ti alloy, 25:42833
MATYUSHIN, A. T., New method of taking information from spark chambers, 25:42147
MATYUSHIN, V. T., New method of taking information from spark chambers, 25:42147
MATZKANIN, Ted, Measurement method for polystyrene, 25:44228 (BDX-613-355)
MATZNER, R. A., Perturbations in anisotropic Euclidean-homogeneous cosmologies, 25:43096
MAURER, Richard Hornsby, Divergence conditions and PCAC relations in perturbation theory, 25:43689
MAURICE, M. J., Spectrophotometric determination of traces of americium in plutonium oxide, 25:41721 (EUR-4352)
MAXCY, R. B., Prog. rpt. on study of control of public health problems using irradiation, annual, 5/69--4/70, 25:42744 (COO-2038-2)
MAXWELL, D., Theoretical ground motion predictions supporting HEST program, 25:41950 (AD-718388)
MAYER, I., Rare-earth silicides and germanides of Mn_5Si_3 type substituted by europium, 25:42895
MAZE, R., Possibility of existence of a new process at interactions with energies above 10^{12} eV, 25:43567 (INR-1280)
MAZZA, F., Spontaneous dissolution of metals in aqueous electrolytes. I. Kinetic isotope effects in the reaction of iron with hydrochloric acid, 25:41808
MCADAMS, Mary Jane, Gas-phase acidities of alcohols, 25:41871
MCCARTHY, S. L., Sensitivity of transition temperature to residual stress in high-T/sub c/ compounds, 25:43302
MCCARTOR, G. D., Calculation of ionization amplitudes by the complex-energy method, 25:43145
MCCASLIN, J. B., Monitoring of positively charged particles in the electron ring accelerator, 25:43734 (UCRL-20664)
MCCAULEY, D. G., Optimization technique applied to experiments measuring reaction gamma-ray angular distributions, 25:42223
MCCLURE, J. P., Equatorial ion temperature, 25:43251
MCCONAGHY, James R. Jr., Some characteristics of a boiling-water-cooled vapor transport fuel pin, 25:44122 (N-71-17463)
MCCORMICK, J. Frank, Effects of beta radiation from simulated fallout on the reproductive potential of a dominant plant species in a natural community, 25:42718 (ORO-3299-110)
Prog. rpt. on effects of ionizing radiation on plant species, populations and ecosystems, 9/70--8/71, 25:42316 (ORO-3299-107)
MCCOY, John J., Process and apparatus for producing UO_2 powder, 25:42938
MCCREERY, Paul N., Lot control in the production of uranium fuel cores, 25:42835
MCCULLOUGH, Edwin C., Exposure rates from diagnostic x ray units, 25:42431
MCDANIEL, C. L., Phase relations in the SrO--IrO_2--Ir system in air, 25:43005
MCDONALD, A., Superconvergence and algebraic realizations of chiral symmetry, 25:43651
MCELROY, D. L., Room temperature measurements of electrical resistivity and thermal conductivity of various graphites, 25:44283 (ORNL-TM-3477)
MCELROY, J., Inelastic electron--proton scattering in the region of the Δ (1236) resonance, 25:43527 (DESY-71/21)
MCELROY, Jack L., Status of the waste solidification demonstration program, 25:41905

MCELROY, W. N., Neutron dosimetry for fast reactor applications, 25:44102
MCGLINN, W. D., Space--time symmetries and the spontaneous breakdown of dilation invariance, 25:43679
MCGRORY, J. B., Structure of ^{44}Ti and the role of single-particle energies, 25:43866
MCHARDY-YOUNG, Stuart, Alterations in serum thyrotropin (TSH) and thyroid function following radiotherapy in patients with malignant lymphoma, 25:42695
MCINTYRE, J. A., 192-detector system for study of 3-body reactions, 25:42124
MCKAY, James Brian, Study of synthetic inorganic ion exchange materials including two applications of ammonium molybdophosphate ion exchanger, 25:41751
MCKHANN, C. F., In vitro detection of cytotoxic cellular immunity against tumor-specific antigens by a radioisotopic technique, 25:42309
MCKIBBEN, Joseph L., Reaction D(d,n)^{3}He at 0° with polarized beam, 25:43789
MCKINLEY, William A., Hellmann--Feynman theorems in classical and quantum mechanics, 25:43510
MCMANUS, H., Elastic and inelastic pion-^{12}C scattering at intermediate energies, 25:43830
MCPHERRON, Robert L., Magnetotail changes in relation to the solar-wind magnetic field and magnetospheric substorms, 25:43239
MCPHERSON, Donald A., Electrostatic vlf waves observed in polar magnetosphere, 25:43213 (AD-715898)
Outer-zone electron precipitation, 25:43211 (AD-715266)
MEADE, D. M., Effect of a toroidal field on plasma transport in a magnetically perturbed multipole, 25:43335
MEBONIYA, J. V., Brueckner--Hartree--Fock theory for the ^{4}He nucleus, 25:43785
MECHER, E., Experimental studies on tooth eruption, 25:42638
MEEK, R. L., Charged-particle radiation damage observed as dimpling of thin silicon targets, 25:43438
MEGILL, L. R., Measurement of the effective electron loss rates in the D region during polar cap absorption events, 25:43255
MEGRUE, G. H., Distribution and origin of He, Ne, and Ar isotopes in Apollo 12 samples, 25:43099
MEHRA, Harish C., Quercetin as a spray reagent in inorganic thin-layer chromatography and evaluation of the chromatographed species by ring colorimetry, 25:41743
MEHROTRA, K. N., Vibration spectra and Debye temperatures of some transition metals, 25:43490
MEHTANI, U., $\pi^+ + p \to \Delta^{++}(1236) + \pi^0$ AT 1.85 to 2.09 GeV: study of s- and t-channel effects, 25:43551 (UCR-34-P-107-B-108)
Study of $\pi^+p \to rho^+p$ at 1.85 to 2.09 GeV, 25:43552 (UCR-34-P-107-B-110)
MEIER, R. R., Observation of the O I 1304-A airglow from OGO 4, 25:43259
MEIJER, Albertus Cornelis, Neutron spectrometer employing two semiconductor counters in combination with a coincidence circuit for eliminating background, 25:42134
MEISEL, G., Hyperfine structure measurements in ground states of ^{181}Ta, 25:43121
MEISELS, G. G., Manifestation of autoionizing states in the ionization of krypton by electron impact, 25:43154
MELDOLESI, U., New double-tracer technique in the diagnosis of liver neoplasia, 25:42580
Relationship between signal and body background in external measurement of radioactivity, 25:42423
MELITAURI, T. G., Thermal denaturation of ribonuclease dissolved in heavy water, 25:41793
MEL'NIKOV, O. A., Systems of Frauhofer wavelengths in solar spectra, 25:43074
MELONI, C., Results of 3 years (1964--1966) of measuring radioactivity of foods sampled in city and province of Pavia, 25:42389
MELONI, G. A., Differential sensitivity to uv-irradiation of virus and cell genome expression in SV40 transformed cells, 25:42733
MENDE, F. F., Behavior of superconductive thin-film bridges in SHF fields, 25:43298
MENDELSSOHN, K., Superconductivity and superconducting devices, 25:43301
MENG, C.-I., Magnetospheric substorm observations near the neutral sheet, 25:43255
MENNICKE, H., Survey of studies of laser produced plasmas at the IPP Garching, 25:43380 (IPP-4/9)
MERCHANT, R. W., Electron microprobe analysis of thin corrosion films, 25:44255 (KAPL-3482)
MERCHANT, Virginia A., Feeding by caeculid mites on fungus demonstrated with radioactive tracers, 25:42242
MERCK, W. F. H., Boundary-layer development in an MHD duct, 25:43201
MERGERTH, F. H., Design and fabrication of special assembly SA-1, 25:44120 (GEAP-10355)
MERIAKRI, V. V., Device for diagnostics of plasma, 25:43345
MERKINA, T. N., Effect of ionizing radiation on the excretion of radioprotectors in rats' urine, 25:42671
MERKLE, J. G., Analytical basis for notch sharpening by fatigue, 25:42843 (CONF-710512-10)
Interpretations of the drop weight test in terms of strain tolerance (gross strain) and fracture mechanics, 25:42847 (ORNL-TM-3247)
MERKULOV, A. G., Kinetics of solid-phase synthesis of zircon during sintering under pressure, 25:42940
MERKWITZ, J., Modular coding systems, 25:44186 (EACRP-A-135, pp 60-2)
MERTENS, Franz-Georg, Phonons and librons in solid hydrogen and deuterium, 25:44261 (JUL-734-FF)
MERTENS, J., Relaxation phenomena and NMR of ^{115}In, 25:43894
MESHKOV, N., Mixing of collective states in an exactly soluble three-level model, 25:43972
METALLI, P., Late somatic effects in syngeneic radiation chimaeras. I, 25:42655
METIVIER, H., Effects of pulmonary lavage on the retention of particles of plutonium oxide, 25:42368 (LF-tr-53)
METSCHER, K., Continuous separation of uranium and plutonium with the help of countercurrent ion migration, 25:41908
METZLER, David E., Photochemical degradation of flavins. VI. A new photoproduct and its use in studying the photolytic mechanism, 25:41788
METZNER, Wolfgang, Process of producing moulded masses and coated substrates, 25:41847
MEWISSEN, D. J., Comparative late effects in mice following fast neutron external irradiation versus tritiated thymidine internal irradiation, 25:42664
MEWISSEN, Dieudonne J., Comparative late effects in mice following fast neutron or ^{60}Co irradiation, 25:42630
MEYER, D. I., Largle-angle differential cross section for K$^+$p elastic scattering at 4.0 and 5.0 GeV/c, 25:43559
MEYER, J., Inelastic electron--proton scattering in the region of the Δ (1235) resonance, 25:43527 (DESY-71/21)
Reconstruction of amplitudes for pion--nucleon scattering from experimental data, 25:43540 (LYCEN-7110)
MEYER, S. L., Muon capture in ^{6}Li in the ditriton channel, 25:43821
MEYER-SCHUETZMEISTER, L., Isospin nonconservation in reaction ^{12}C(d,α_2)^{10}B(1.74,T = 1), 25:43811
MEYNIEL, G., Detection of hyperfixing zones by means of a positron camera type positron. III, 25:42565
MEZZADRI, M. G., Distribution of radioactivity in sediment from Ligurian Sea, 25:41949
MICHAEL, W., $\pi^+ + p \to \Delta^{++}(1236) + \pi^0$ AT 1.85 to 2.09 GeV: study of s- and t-channel effects, 25:43551 (UCR-34-P-107-B-108)
Study of $\pi^+p \to rho^+p$ at 1.85 to 2.09 GeV, 25:43552 (UCR-34-P-107-B-110)
MIGLIACCIO, P. A., Problems of the radiocontamination of man, 25:42375
MIHAILOV, M., Radioactive needle with linear activity increasing gradually towards the ends, 25:42590
MIHALCEANU, I., Experimental studies on tooth eruption, 25:42638
MIKADO, Tomohisa, 33 MeV ETL electron linear accelerator, 25:43752
Absolute measurement of Linac x-ray energy fluence, 25:43750
Beam transport system of ETL Linac, 25:43764
Dependence of electron bremsstrahlung generation on target thickness and forward angle, 25:43751
Energy calibration of Linac analyzing system by means of photonuclear reaction, 25:43749
Ionization chamber response for pulsed radiation and the drift velocity distribution of filling gas, 25:42088
MIKADO, Tomoshisa, Reconstruction and performance of ETL electron linear accelerator, 25:43755
MIKHAILOV, N. N., Superconducting alloy, 25:43318
MIKHAILOV, V. A., Measurements in beams of fast electrons, 25:42411
MIKHAILOV, V. S., Thermal denaturation of ribonuclease dissolved in heavy water, 25:41793
MIKHAILOVSKII, I. M., Crowdion mechanism of plastic deformation, 25:43484
MIKHEEV, V. P., Filtering of tracks measured on the SMP, 25:42135 (CERN-Trans-71-8)
MIKHNEVICH, V. I., Production of zirconium dioxide from baddeleyite concentrate, 25:42942
MIKI, Eiichi, Infrared spectra of pentacyanonitrosylmanganese (^{14}NO and ^{15}NO) complexes, 25:41796
MIKI, Ryota, Radiation hazard control system, 25:42480
MIKSOVSKY, M., Determination of strontium in silicates, carbonates, and sulfates by atomic absorption spectroscopy, 25:41735
MILASIN, N. Lj., Correlation between the mechanical properties and microstructure of irradiated iron and low-carbon steel, 25:42925
MILEY, G. H., Enhancement of CO_2 laser power and efficiency by neutron irradiation, 25:42229
MILKEY, R. W., Vela V and VI solar x-ray atlas. V, 25:43066 (LA-4454(Vol.5))
MILLER, D. H., Coherent production of high mass meson states in π^+d collisions at 13 GeV/c, 25:43550 (COO-1428-290)
Final states with three charged particles and a visible anti K^0 from K$^-$d interactions at 4.5 GeV/c, 25:43549 (COO-1428-286)
R region in 13 GeV/c π^+ nucleon interactions, 25:43545 (COO-1428-277)
MILLER, Lois A., Results of radiation safety surveys of x-ray facilities within the Bureau of Prisons and Federal

Health Programs Service, 25:42502
MILLER, O. A., Radiolysis of hydrogen sulfide at very high dose rates. The effect of SF_6, 25:41860
MILLER, Robert Alan, Numerical study of Regge cuts due to absorption in neutral pion photoproduction, 25:43601
MILLER, William H., Classical S matrix for rotational excitation: quenching of quantum effects in molecular collisions, 25:43155
MILLIVOJEVIC, D., Determination of B in nuclear materials by isotope dilution technique. I, 25:41749
MILLS, Dallice I., Somatic recombination in common-AB diploid of Schizophyllum commune, 25:42336
MILLS, R. G., Large superconducting magnet designs for fusion reactors, 25:43397 (MATT-848)
MILLS, Robert, Propagator gauge transformations for non-Abelian gauge fields, 25:43680
MILOSAVLJEVIC, D., Electron beam welding of Zy-2, 25:42830
MILOSEVIC, V., Toxicity and analgesic activity by gamma rays, 25:42752
MILYANICH, D., Inelastic interaction of neutrons with H and deuterium, 25:43550
MINAKATA, Kayoko, Electron spin resonance evidence for positive holes produced in irradiated single crystals of carboxylic acids, 25:41841
MINGAY, D. W., Intermediate structure near an isobaric analog resonance, 25:43851
MINTI, Hari, Programming attempts of the orbital element determinations for the eclipsing variable stars, 25:43020
MIRANSKII, V. A., Scaling, Pomeranchuk trajectory and J = 1 fixed poles in virtual Compton amplitude, 25:43584 (ITF-71-27-E)
MIRENSKAYA, I. I., Polyhydroxy flavones as extraction reagents, 25:41738
MIRZAKARIMOV, R. M., Effect of gamma-radiation on properties of extracted cottonseed oil for preparation of K-S drying oil, 25:41839
MISHELOFF, Michael Norman, Triple-Regge vertex, 25:43723
MISHIMA, Yasushi, Apparatus for continuous observation of cosmic ray intensity at a shallow underground station, 25:42152
MISHKIN, Fred S., Use and interpretation of the lung scan, 25:42583
MITCHELL, Arthur, X-ray detector for dynamic diffraction studies, 25:42210
MITCHELL, E. W., Measurement of the superconducting energy gap and Fermi velocity in single-crystal lead films by electron tunneling, 25:43312
MITCHELL, I. V., Depth distribution of implanted J in GaP, 25:43447
MITRA, Jaganmay, Relative radio-sensitivity of different cell-types in Hydra, 25:42613
MITSEL'MAKHER, G. V., Determination of the mass of the muonic neutrino in radiative pion decays, 25:43609
MITTENDORF, Richard J., Evaluation of linear polyethylene and fiber glass reinforced epoxy for use as irradiation capsules, 25:43011 (N-71-15439)
MITTER, Werner, Influence of neutron irradiation on the graphitization of unalloyed and alloyed malleable cast iron, 25:42904
MIX, Michael Cary, Effects of ionizing radiation on oyster, 25:42607
MIYACHI, Takashi, Absolute calibration of bremsstrahlung beam monitors, 25:42083
MIYAGAWA, Tadayoshi, Apparatus for continuous observation of cosmic ray intensity at a shallow underground station, 25:42152
MIYAZAKI, Tadakuni, Apparatus for continuous observation of cosmic ray intensity at a shallow underground station, 25:42152
MIYAZAKI, Tetsuo, Effect of phase on excitation transfer in the radiolysis of isobutane, 25:41864
Role of reaction sites in the radiolysis of solid succinic acid, 25:41865
MIZUHO, Mitsuru, Counting channel for use with gas flow proportional counter, 25:42052 (JAERI-13725)
MIZUMACHI, Kunihiko, Infrared spectra of pentacyanonitrosylmanganese (^{14}NO and ^{15}NO) complexes, 25:41795
MIZUMOTO, Yoshihiko, Radiation hazard control system, 25:42480
MLYNEK, R., Slope change in temperature dependence of electrical resistivity of thulium near 22 K, 25:43487
MO, J. N., Study of ^{61}Cu nucleus by ^{58}Ni(α,pγ)^{61}Cu reaction, 25:43839
MOAK, C. D., Energy-loss spectra of channeled iodine and oxygen ions in gold, 25:43454
MOBERG, A., Radiotherapy of intracerebral astrocytomas, 25:42701
MOCKER, M., Method of normal modes for Vlasov--BGK equations, 25:43377
MODE, V. Alan, Corrected fluorescence spectra by computer postprocessing, 25:44306 (UCRL-73161)
MOELLER, H. Bjerrum, Prog. rpt. on physics, annual, 1--12/70, 25:43435 (RISO-237)
MOEN, R. A., Neutron fluence limit determinations for some FFTF components, 25:44157
MOHR, Peter Conrad, Channelization of liability with special regard for atomic law, 25:42507
MOISEEV, N. N., Conference on optimization, Nice, 6--7/69, 25:43525
MOLCHANOVA, E. I., Radioresistance of E. coli K-12, 25:42330
MOLDAN, B., Determination of strontium in silicates, carbonates, and sulfates by atomic absorption spectroscopy, 25:41735
MOLDOVANU, A., Forbush microdecreases in the cosmic-ray intensity, 25:43172
MOLE, R. H., Late effects of exposure to ionizing radiation, 25:42605
Radiation effects in man: current views and prospects, 25:42712
MOLIBE, D., Effects of pulmonary lavage on the retention of particles of plutonium oxide, 25:42368 (LF-tr-53)
MOMBELLI, L., New double-tracer technique in the diagnosis of liver neoplasia, 25:42580
MONAHAN, J. E., Isospin nonconservation in reaction ^{12}C(d,α_2)^{10}B(1.74,T = 1), 25:43811
T = 1 states in the A = 12 system, 25:43819
MONARO, S., Geometrical correction factors for angular correlation measurements with Ge(Li) detectors, 25:42054 (LPN-UM-53)
MONEY, J. N., Calibration of Bonner ball neutron detectors used at Tower Shielding Facility, 25:42055 (ORNL-TM-3465)
MONGINI-TAMAGNINI, C., CARONTE: Euratom modular calculation system, 25:44187 (EACRP-A-135, pp 63-8)
MONK, Marilyn, Induction of prophage lambda in mutant of E. coli, 25:42340
MONNET, A., Fluorinated polymers and nuclear industry, 25:43016
MONROE, S. E., Radioimmunoassay for rhesus monkey luteinizing hormone (LH) with anti-ovine LH serum and ovine LH-^{131}I, 25:42237
MONTGOMERY, John W., Radio sources: 3.3-mm flux and variability measurements, 25:43060
MONTI-BRAGADIN, C., Differential sensitivity to uv-irradiation of virus and cell genome expression in SV40 transformed cells, 25:42733
MONTOUR, James L., Abscopal radiation damage to chick thymus and bursa of fabricius, 25:42658
MOORE, Craig Damon, Strange particle production in π^+ deuteron interactions at 2.05, 2.19, and 2.35 GeV/c, 25:43561
MOORE, R. L., Structure of the chromosphere--corona transition region, 25:43058 (N-71-19294)
MOORE, W. H. Jr., Counter telescope measurements of a beam of negative π mesons, 25:42141
MORAN, T. F., Application of the statistical phase-space theory to the reactions of rare gas ions with nitrogen molecules, 25:43159
Statistical phase-space model of collision-induced dissociation of excited O_2^+ and NO^+ ions, 25:43158
MORCOS, N. A., Decay of ^{78}As, 25:43881
MORDIKHOVICH, V. V., Effect of ionizing radiation on the excretion of radioprotectors in rats' urine, 25:42671
MORETTI, J. L., Use of a new vector in the diagnosis of melanomas, 25:42563
MORETTO, L. G., Pairing correlation in excited nuclei with non-zero angular momentum, 25:43959
MORFILL, G., Penetration of solar protons over the polar cap during the February 25, 1969, event, 25:43232
MORGAN, W. C., Neutron dosimetry for reactor pressure vessel applications, 25:44117
MORGANSTERN, R. E., Brans--Dicke theory under a transformation of units and the three tests, 25:43702
MORI, Kazuo, System for determination of time-varying spectral line profiles, 25:43343
MORISHIMA, Hiroshige, Radiation hazard control system, 25:42480
MORLEY, J. Barrie, Differences between lesions in cerebral scanning, 25:42577
MOROVIC, Tihomir, Stability of superheavy nuclei against fission, alpha decay, and electron capture, 25:43919
MOROZ, V. D., Behavior of fission products in soils of Uzbekistan, 25:42319
MOROZOVA, I. K., Corrosion and electrochemical behavior of zirconium alloy, 25:42814
MOROZUMI, S., Portevin--Le Chatelier effect in V, 25:43486
MORRAL, F. R., Developing metal: cobalt, 25:42868
MORRIS, C. L., ^{7}Li(p,n)^{7}Be neutron polarization measurements for E/sub p/ = 3.0 to 5.5 MeV, 25:43805
MORRIS, J. A., Purification and some properties of molybdoferredoxin, a component of nitrogenase from Clostridium pasteurianum, 25:41811
MORRIS, T. W., Single-particle distributions of π-mesons produced in π^+p, K$^+$p, pp, and π^-p collisions at high energies, 25:43554 (UR-875-340)
MORRISON, G. C., ^{6}Li + ^{6}Li scattering at E = 5 to 7 MeV, 25:43816
MORRISON, George H., Evaluation of lunar elemental analyses, 25:41714
MORRISON, J. C., Many-body calculations for the heavy atoms, 25:43116
MORTENSON, L. E., Purification and some properties of molybdoferredoxin, a component of nitrogenase from Clostridium pasteurianum, 25:41811
MORY, J., Determination by channelography of orientation of microcrystals, 25:43464
MOSKALEV, Y. I., Biological action of ^{237}Np nitrate, 25:42253
MOSS, Harold M., Radiation-induced hydrogen transfer in nucleic acids, proteins, and related substances:

effects of temperature and scavengers, 25:41837
MOSS, T. A., 300-kWe Rankine cycle advanced nuclear--electric space power system, 25:44173
MOSTOVOI, Yu. A., Angular correlation between neutron spin and electron momentum in decay of polarized neutrons, 25:43532
MOTOHASHI, Haruhiko, JAERI pulsed type neutron spectrometer, 25:42107 (JAERI-13771)
MOTT, J. E., Heat exchanger optimization code, 25:44265 (K-1799)
MOULTON, David M., Method for separating U, Pa, and rare earth fission products from spent molten fluoride salts reactor fuels, 25:41903
MOULTON, W. G., Magnetic susceptibility of uranium monophosphide, 25:43495
MOURIQUAND, C., In vitro study of effect of γ rays on human chromosomes, 25:42365
MOUTAFTCHIEV, K., Radioactive needle with linear activity increasing gradually towards the ends, 25:42590
MOYLE, Wm. F., Flow soldering and supporting processes, 25:44227 (BDX-613-333)
MRKOUS, P., Oxidation of Zr--0.3 percent Cu--0.8 percent Mo alloy in carbon dioxide, 25:42809
MRNKA, Miroslav, Extraction of metals by amines. II, 25:41900
MUCKENTHALER, F. J., Calibration of Bonner ball neutron detectors used at Tower Shielding Facility, 25:42055 (ORNL-TM-3455)
MUELLER, A., Superconducting regions of A15 phase in Nb--Al--Ge, 25:43319
Superconductivity and range of existence of the A 15 phase in the system Nb--Al--Ge, 25:43291 (ORNL-tr-2461)
MUELLER, F. H., Chemical radioprotection with N- and S-containing polymers, 25:42517
MUHAMMED, Amir, Mutagenic effect of irradiated media on E. coli, 25:42755
MUIR, D. W., Fission fragment angular distributions for ^{230}Th, ^{232}Th, ^{231}Pa, and ^{239}Pu, 25:43888 (LA-4648)
MULAC, W., Pulse radiolysis of ammonia gas. II. Rate of disappearance of the $NH_2(X^2B_1)$ radical, 25:41869
MULHOLLAND, W. A., Solder leveling of printed wiring boards, 25:44234 (BDX-613-443)
MULSER, P., Survey of studies of laser produced plasmas at the IPP Garching, 25:43380 (IPP-4/9)
MUMINOVA, S. N., Effect of gamma-radiation on properties of extracted cottonseed oil for preparation of K-5 drying oil, 25:41839
MUNIM, A. V., Effects of irradiation on the tensile properties of Zircaloy 2 and 4 and borated stainless steel, 25:42911
MUNIR, M., Mutagenic effect of irradiated media on E. coli, 25:42755
MUNNO, F. J., Reactor fuel management optimization in a dynamic environment, 25:44130
MUNTEANU, G., Radiation measurements in Brasov during period 8/51--8/53, 25:42424
MURADOV, A., Approximate picture of the distribution of plasma drift in the F2 region, 25:43225
MURAKAMI, Akio, Comparison of stage sensitivity to x rays during meiosis in egg of silkworm, Bombyx mori, 25:42609
MURAKAMI, Kazuaki, Apparatus for continuous observation of cosmic ray intensity at a shallow underground station, 25:42152
MURAKAMI, Ujihiro, Radiation effect on prenatal development, 25:42529
Species differences of the effects of x-irradiation upon the rat and mouse embryo, 25:42639
MURAMATSU, Hiroshige, Gamma-induced polymerization of fluorine-containing pentadiene, 25:41848
MURATA, Tomomi, Effect of neutron irradiation on precipitation-hardening of Al--3.8 percent Cu alloy, 25:42902 (JAERI-13692)
MURATOV, V. I., Asymmetry of the combination-frequency spectrum in a plasma, 25:43410
MURAV'EV, V. N., Effect of petroleum growth substance on the healing of radiation wounds of the skin, 25:42539
MURAV'EVA, A. A., System γ--Al--Si (Ge,Sb), 25:42891
MURSOCI, P., Low radiation doses and control of metabolic pathways, 25:42505
MURPHY, Frederick V., Photons as hadrons, 25:43597
MURPHY, Peter G., Effects of beta radiation from simulated fallout on the reproductive potential of a dominant plant species in a natural community, 25:42718 (ORO-3299-110)
MURPHY, Peter George, Ecological effects of acute beta irradiation from simulated fallout particles upon a natural plant community, 25:42320
MURRAY, S., Strong x-ray source in Coma cluster observed by Uhuru, 25:43055
MURRI, Richard, Neutron radiography with a sealed-tube neutron generator and graphite moderated system, 25:42027 (RFP-1705)
MURTY, V. S., ESR absorption of x-irradiated $NaClO_2$ crystal, 25:43451
MUSACCHIA, X. J., Intestinal enzyme activities following whole-body irradiation in hamsters, 25:42301
MUSIKHIN, V. I., Electrical properties of liquid V_2O_5, 25:42959
MUSTAFA, Mohammed Rafti, ESR of x- and γ-irradiated potassium difluoromalonate, 25:41838
MUSTAFIN, K. S., Effect of solar overheating on cardiovascular system during radiation sickness, 25:42651
MUSTEA, I., Effect of some radioprotective substances on the redox equilibrium in the spleen, 25:42526
MUSUMECI, L., Dosimetry of mixed gamma-neutron radiation, 25:42168
MUTHUKRISHNAN, R., Effective s-wave interaction in finite nuclei, 25:43959
MUXART, R., Behavior of protactinium(V) on an indicator scale, 25:41786
MUZAFEROVA, R. Sh., Effects of γ-radiation doses on size of saffron pollen, 25:42720
MYASOEDOV, B. F., Continuous isolation of isotopically pure ^{249}Cf from ^{249}Bk, 25:41882
MYHRE, P. C., Rearrangement--fragmentation in aromatic nitration, 25:41818
MYNATT, F. R., Study of the overlap conditions required in sequential discrete ordinates transport calculations for a 14-MeV neutron source in a 5000-m radius cylinder of air, 25:43419 (ORNL-TM-3269)
MYNTSOV, F. F., Increasing the energy of an electrostatic accelerator, 25:43766

N

NAGAOKA, Yukio, RI liquid wastes carried from Japan Radioisotope Association to JAERI, 25:42037 (JAERI-13666)
NAGARAJAN, P. S., Neutron dose distributions for ^{252}Cf sources, 25:42445
NAGASAKI, Ryukichi, Effect of neutron irradiation on precipitation-hardening of Al--3.8 percent Cu alloy, 25:42902 (JAERI-13692)
Evaluation of stainless steel pipe for cladding material of fast reactor, 25:42846 (JAERI-13578)
Recrystallization of V--20 wt percent Ti alloy, 25:42884 (JAERI-13731)
Recrystallization of Zr--2.5 wt percent Nb alloy, 25:42885 (JAERI-13764)
NAGATANI, K., Lifetime of the first excited state of ^{11}Be, 25:43820
NAGY, J., Silicon semiconductor spectrometer, 25:42112
NAIR, Chitra, Structural and high temperature magnetic studies of systems $PrMn_2$--$GdMn_2$ and $PrMn_2$--$TbMn_2$, 25:42894
NAKAGAWA, Roy K., Nuclear reactor installation, 25:44214
Nuclear reactor installation, 25:44212
NAKAHIRA, Mitsuoki, Superstructure of VO/sub x/ in the range x = 1.15 to 1.25, and its stability, 25:43007
NAKAMURA, Haruto, Studies on fundamental properties of alumina adsorbent for radioisotope production, 25:41991 (JAERI-13778)
NAKAMURA, Hitoshi, Broad energy protons from the reaction ^{12}C + d → p + ^{13}C (7.64 MeV and 8.33 MeV), 25:43814
NAKANISHI, Noboru, Complex-ghost relativistic field theory, 25:43686
NAKAYAMA, H., Effects of crystal surface and imperfections on channeling phenomena of protons, 25:43461
NALIVAIKO, G. A., Ion-beam apparatus, 25:43747
NAM, Sang Yul, Radioprotective effect of methylene blue. I, 25:42284
Radioprotective effect of methylene blue in mice and rats, 25:42515
Serum of rats exposed to x rays, 25:42283
NAMATAME, H., Embrittlement of pressure vessel steels irradiated in JPDR, 25:42905
NANGIA, P., Pulse radiolysis of ammonia gas. II. Rate of disappearance of the $NH_2(X^2B_1)$ radical, 25:41869
NAQVI, S. I. H., Gamma rays following decay of ^{85}Sr and /sup 85m/Sr, 25:43877
NARCISI, R. S., Electron loss during a nighttime PCA event, 25:43269
NARITA, Masakuni, Feedback-type detection system for pulsed radiation measurement, 25:42087
NARITA, Nobuo, Balloon-borne instrument for low-energy primary cosmic-ray measurements, 25:42159
Isotopic composition of low-energy helium nuclei in primary cosmic rays, 25:43173
NARKEVICH, B. Ya., Calculation of the sensitivity function of a detecting system with a multichannel ring collimator, 25:42089
Determination of the optimal canal of registration of gamma-radiation in radioisotope diagnosis, 25:42397
NARO, G., Internal contamination in vicinity of nuclear electric center at Garigliano, 25:42435
Whole-body counter at nuclear electric center at Garigliano, 25:42081
NARUMI, Hajime, Nuclear excitation by the bound muon, 25:43913
Pionic complex level shifts and optical potential parameters in terms of the π--N scattering length, 25:43806
NARUSHIMA, Katsuya, Absolute calibration of bremsstrahlung beam monitors, 25:42083
NASLAIN, R., Nonstoichiometric hexaboride of thorium Th/sub 1-x/B_6, 25:43003
NATARAJAN, A. T., Response of some varieties of hexaploid wheat and a two-rowed barley variety to chronic gamma-irradiation, 25:42724

XUM

NATH, N., Analysis of $^{127}I(n,n'\gamma)$ reaction data, 25:43914
NATHER, Roy E., Radiation detection system with automatic sample counting rate determination, 25:42103
NEBENZAHL, I., Charge-exchange calculations with Hartree wave functions, 25:43157
NEDELCU, C., Mechanisms of chemical radioprotection, 25:42523
NEDVIDEK, A., Health education in Czechoslovak uranium industry, 25:42504
NEELY, H. H., Void formation in proton irradiated stainless steel, 25:42917
NEELY, Orville, Television contribution to genetically significant radiation dose of population, 25:42366
NEIRINCKX, R. D., Production of Fe-free and carrier-free ^{67}Ga, 25:41881
NELLIS, W. J., 5f magnetism in palladium--actinide solid solutions, 25:43488
NELSON, D. J., Biological concentration and turnover of radionuclides in food chains: a bibliography, 25:42315 (ORNL-NSIC-89)
NELSON, Donald M., Thermal plume measurements, 25:44138 (CONF-710431-1)
NELSON, J. W., Spin of the 937-keV level in ^{56}Co, 25:43863
NELSON, Paul Jr., Internal values in particle transport by the method of invariant imbedding, 25:43430
NEMANIC, E. B., Threshold zeros and the N/D method in Yukawa-potential scattering, 25:43713
NEMEC, R., Rats fed unsaturated fatty acid following x irradiation, 25:42298
NEMIRO, E. A., Determination of radiation dose to children during x-ray diagnostic procedures, 25:42412
NEMTSEVA, L. S., Dose-dependent frequency of encircled ring chromosomes, 25:42351
NEOPHYTOU, Michael, Chlorons following irradiation in ankylosing spondylitis, 25:42709
NESMEYANOV, V. S., Electrophysical properties and chemical bond types in compounds of beryllium with boron and carbon, 25:42997
Mechanism of the phase transition in boron nitride, 25:42994
NESS, N. F., Asymmetric access of energetic solar protons to the Earth's north and south polar caps, 25:43233
NESTEROV, M. M., Interference between Coulomb and strong interactions at high energies, 25:43607
NESTOR, C. W. Jr., ORTHIS, ORTHAT: two computer programs for solving two-dimensional steady-state and transient heat conduction problems, 25:41985 (ORNL-TM-3324)
NEUBERT, W., Nanosecond lifetime measurements of excited nuclear states at heavy ion cyclotron, U-300, 25:42187 (JINR-P13-5801)
NEUDACHIN, V. G., Shell interpretation of the separable interactions between lightest nuclei, 25:43786
NEUGEBAUER, M., Correlated observations of electrons and magnetic fields at the Earth's bow shock, 25:43238
NEULS, A. S., Coolant blowdown studies of a reactor simulator vessel containing a simulated reactor core, 25:44133 (BNWL-1524)
NEWPORT, R. W., Applications of cryogenics to nuclear physics, 25:42137
NEWTON, T. W., Kinetics of the reaction between uranium(III) and $Co(NH_3)_5(H_2O)^{3+}$ in aqueous perchlorate solutions, 25:41783
NI, Tiee-Bor, Prog. rpt. on powder metallurgy compaction, 3/71--5/71, 25:44292 (SRO-475-11)
NIAY, P., Emission spectrum of Th in 5400 to 6400 cm^{-1} region, 25:43113
NICHINI, F. M., Beryllium window tubes for mammographic examinations, 25:42545
NICHKOV, I. F., Polarization of a zinc cathode during thorium precipitation from molten halide salts, 25:42821
NICHOLAS, J. Blair, Interactions of positrons with defects in sodium chloride crystals, 25:43453
NICKEL, Bernie G., Validity of the Boltzmann equation for systems with both electron--phonon and impurity scattering, 25:44273 (NYO-3699-56)
NICKERSON, R. A., Wave propagation theory for ultrasonic testing, 25:44307 (UCRL-73184)
NIELSEN, H. L., Perturbed β-vibrational bands in ^{152}Sm, ^{154}Gd, and ^{156}Gd, 25:43940
NIELSEN, Meta Damkjaer, Iodine-125-labelling of angiotensin I and II, 25:42241
NIENDORF, L. R., SNAP-21 10-watt thermoelectric power system, 25:41993
NIEPORENT, Richard Joel, Study of proton--proton interactions at 25 GeV/c in four-prong final state, 25:43535
NIEWODNICZANSKA-ZAWADZKA, J., Macroscopic quantum interference effects in superconducting slug-type junctions, 25:43293
NIEWOLAK, S., Influence of gamma irradiation on milk microflora, 25:42742
NIGGEMANN, R. E., Zirconium hydride reactor--organic Rankine power systems, 25:44179
NIGMANOV, T. S., System of proportional wire chambers on-line with a computer, 25:42156
NIKANOROV, V. I., Methods of detecting particle tracks in liquid and solid media, 25:42053 (JINR-P13-5782)
NIKITIN, A. A., Spectra of nonstationary stars, 25:43030
NIKITIN, A. G., Relativistic equations of motion without redundant components, 25:43654 (ITF-70-89-E)
NIKITIN, E. E., Excitation transfer in collisions of highly excited alkali atoms, 25:43133
NIKITINA, G. V., Energies of mixing in systems containing germanium and silicon with elements of groups III and V, 25:42970
NIKODEMOVA, Denisa, Methods of determination of fast-neutron spectra from threshold--foil activation data, 25:42100
NIKOLAEV, B. I., Certain dispersion effects in molecular gases in parallel constant and alternating magnetic fields, 25:43516
NIKOLAEV, G. I., Determination of O and N in metals using fluxes enriched with ^{18}O and ^{15}N isotopes, 25:41748
NIKOLOVA, M., Strontium-90 and ^{137}Cs in some Bulgarian foodstuffs, 25:42381
NIKULIN, M. G., Stabilization of plasma filaments with variable current by quadrupole magnetic field, 25:43389
NIKULIN, M. P., Pumps for circulating liquid metals, 25:41958 (CONF-700307-8)
NILSSON, Agnar, Pathologic effects of different doses of radiostrontium in mice. Development and incidence of leukaemia, 25:42654
NILSSON, Oe., Pressure dependence of gain and background for parallel plate channel multipliers, 25:42099
NISHIIKE, U., Neutron irradiation effects on iron containing aluminum and nitrogen, 25:42908
NISHIOKA, I., Sintering of uranium dioxide, 25:42950
NISHITA, H., Some physical and chemical characteristics of heated soils, 25:41926 (UCLA-12-819)
NISHIYAMA, K., Magnetic moments of isomeric levels in the Br isotopes, 25:43841
NISWENDER, G. D., Radioimmunoassay for rhesus monkey luteinizing hormone (LH) with anti-ovine LH serum and ovine LH-^{131}I, 25:42237
NITZSCHE, M., Mean neutron energy from $D(d,n)^3He$ reaction, 25:43790
NOBLE, J. V., Equivalence of ^3He-t and d-α cluster description of ^6Li, 25:43825
NOCERA, F., Authorization of nuclear installations, 25:41979
Use of radioisotopes in industrial plants: observations on authorizations, 25:42013
NODA, Hiroji, 13 MeV linear accelerator at Kurume University, 25:43753
NOGA, Milan, Algebraic structure of pion--hadron transition amplitudes and hadron mass spectra, 25:43635
NOMURA, Koichi, Study of photon activation analysis, 25:41766
NOON, J. H., Prog. rpt. on instabilities and turbulence in highly ionized plasmas in a magnetic field, semiannual, 3--8/70, 25:43385 (N-71-12892)
NOOTHOUT, Arend J., Method of preparing a stable mixed sol of hexavalent uranium and tetravalent thorium by peptization, 25:42945
NORDLUND, David L., Computer collection of mass spectrometric ionization efficiency curves, 25:44241 (COO-1140-198)
NORSEEV, Yu. V., α decay of neutron-deficient radon isotopes, 25:43887 (JINR-P6-5791)
NOVAK, A., Vibrational spectra of and isotope effect in hydrogen bonded potassium hydrogen oxalate, 25:41790
NOVAK, D., Silicon semiconductor spectrometer, 25:42112
NOVAKOVA, E., Strontium-90 and ^{137}Cs in some Bulgarian foodstuffs, 25:42381
NOVIKOV, B. V., Changes in energy spectrum of capture centers (traps) in electron-bombarded CdS crystals, 25:43437
NOVIKOV, I. D., Does a vacuum gravitate, 25:43089
NOVIKOV, I. I., Ternary system molybdenum--titanium--carbon, 25:42890
NOVIKOV, Yu. V., Study of ^{210}Po content in environment and human body, 25:42429
NOVOTNY, J., Personal monitoring of workers during the translocation of a ^{90}Sr--^{90}Y beta source by aid of TLD, 25:42444
NURDIN, Guy, Shielding thickness required to reduce neutron flux or dose rate, 25:43416 (NP-18863)
NUTBROWN, D. A., Simple derivation of seagull terms for propagator functions, 25:43681
NUTTALL, J., Calculation of ionization amplitudes by the complex-energy method, 25:43145

O

OADES, G. C., Coulomb corrections to low energy elastic and charge exchange πN scattering, 25:43599
Mass differences as additional electromagnetic corrections in low-energy elastic and charge-exchange πN scattering, 25:43645
OBERMAN, C., Noise broadening of trapped-particle echoes, 25:43409
OBEROI, R. S., Choosing pseudostates in the close-coupling formalism for the electron--atomic-hydrogen system, 25:43140
OBRADOVIC, M., Vibrational normal coordinate analysis of H(D)NCO and H(D)NCS, 25:41791
OBST, B., Anisotropy in cubic superconductors. II, 25:43294
Anisotropy in cubic superconductors. I, 25:43295
OBU, Makoto, Characteristics of proton recoil proportional

counter GD-A for neutron and γ-ray, 25:42106 (JAERI-13580)
Gamma-ray discriminating system for a proton-recoil counter, 25:42105 (JAERI-13561)
OEHME, Reinhard, Complex negative-signature trajectories and the Pomeranchuk theorem, 25:43715
OESTERREICHER, Hans, Structural and high temperature magnetic studies of systems $PrMn_2$--$GdMn_2$ and $PrMn_2$--$TbMn_2$, 25:42834
OESTGAARD, E., Liquid ^{4}He. II, 25:43277
OESTLUND, A. Goete, Modification of atmospheric tritium and water vapor by Lake Tahoe, 25:41938
OESTMAN, B., Rearrangement--fragmentation in aromatic nitration, 25:41919
OETTINGER, Peter E., Volume ionization by means of laser radiation in a cesium plasma diode, 25:43181 (AD-715883)
OGATA, H., Elastic and inelastic proton scattering from heavy collective nuclei, 25:43901
OGAWA, Hideyuki, Genetic locations of uvrD and pol genes of E. coli, 25:42329
OGAWA, M., Medical aspect of chronic hypoxia in radiation exposed glomerulus in hamsters treated with injected ozone gas, 25:42536
OGAWA, Yutaka, Recrystallization of V--20 wt percent Ti alloy, 25:42884 (JAERI-13731)
Recrystallization of Zr--2.5 wt percent Nb alloy, 25:42885 (JAERI-13754)
OGAWA, Yutakai, Electron microscope observation of the zirconium hydride, 25:42981 (JAERI-13635)
OGORODNIKOV, K. F., Star streams in the solar neighborhood, 25:43027
OGRZEVAL'SKII, Z., Determination of γ-ray energy in a xenon bubble chamber, 25:42144
OGURA, Koichi, Balloon-borne instrument for low-energy primary cosmic-ray measurements, 25:42159
O'HANLON, John David, Static solutions of the combined Dirac--electromagnetic--gravitational field equations, 25:43703
OHINATA, K., Radiation-sterilization of the Mediterranean fruit fly (Diptera: tephritidae): Comparison of spermatogenesis in flies treated as pupae or adults, 25:42751
OHLMER, E., Experimental investigation of loop caused influences on parallel flow-induced vibration of fuel pins, 25:44119 (EURFNR-923)
OHLSEN, Gerald G., Reaction D(d,n)^{3}He at 0° with polarized beam, 25:43789
OHSAWA, Takao, Heavy particle identification with TOF method in nuclear reactions, 25:42066
OHYOSHI, A., Oxidation of As(III) with ammonium peroxydisulphate, 25:41785
OKA, Yoshinaga, Photon-activation analysis for zirconium with molybdenum used as the internal-reference element, 25:41764
OKADA, Shigefumi, Cysteamine and radiation-induced single strand breaks of DNA, 25:42522
OKADA, Touichi, Effect of plastic deformation on crystal current density in Pb--In crystal, 25:43300
OKAMOTO, Kosuke, System for determination of time-varying spectral line profiles, 25:43343
OKAZAKI, Kiyohiko, System for determination of time-varying spectral line profiles, 25:43343
O'KELLEY, G. Davis, Levels in ^{101}Ru populated by decay of ^{101}Tc, 25:43899
OKUNO, Hisateru, Infrared spectra of pentacyanonitrosylmanganese (^{14}NO and ^{15}NO) complexes, 25:41795
OLDHAM, R. D., Activation-rate measurements in the ZPR-3 mockup critical experiments. Part I. Measurements of foil-activation rates and fission yields in Assembly 60 of ZPR-3: mockup of EBR-II with a uranium blanket, 25:44150 (ANL-7751)
OLEJARCZYK, Wiktor, Vinca Nova: automatic unit for neutron spectrometer control, 25:42114
OLEJNICZAK, Wieslaw, Spark chamber as an element of the hodoscopic detector of extensive air showers, 25:42158
OLIVE, D., Operator approach to dual multiparticle theory, 25:43578
OLIVIER, P., Corrosion of Zr alloys in water and steam, 25:42810
OLNESS, J. W., Levels of ^{36}S from ^{34}S(t,p)^{36}S, 25:43869
Lifetime of the $^1/_2^-$ 2791-keV ^{21}Ne level, 25:43870
Lifetime of the first excited state of ^{11}Be, 25:43820
OLSEN, A. R., In-reactor restructuring temperatures and kinetics for $(U,Pu)O_2$, 25:44124 (ORNL-TM-3387)
OLSON, J. V., Correlated observations of electrons and magnetic fields at the Earth's bow shock, 25:43238
OLSON, Karin Emily, Effects of x-radiation on the cerebellar granule cell and the resultant effects on some vestibular and spinal reflexes, 25:42657
OLSON, P. R., Uptake of molybdenum, marked with ^{99m}Tc, by biota of Fern Lake, Washington, 25:44287 (RLO-2225-T-7-2)
OLSON, W. H., In-line vacuum-distillation sodium sampler, 25:44115
OLSSON, T., IFA-30 final report, 25:44207 (KAE-68-46)
OMEL'CHENKO, B. D., Power supply system for the 100-cm liquid hydrogen bubble chamber electromagnet, 25:42143
O'NEIL, R. A., Proton states in ^{173}Lu, ^{175}Lu, and ^{177}Lu, 25:43942
OPAUSZKI, J., Determination of MI-1305 mass spectrometer D/H ratio by using modulated accelerating voltage, 25:41729
ORBAN, M., Iodine-catalyzed iodine exchange reactions, 25:41817
ORDAN'YAN, S. S., Structure of alloys in system Ta--C--Re, 25:42992
ORDWAY III, Frederick I., Advances in space science and technology. IX, 25:43077
OREL, B., Vibrational normal coordinate analysis of H(D)NCO and H(D)NCS, 25:41791
ORLOV, N. F., Radiation yield of Mn^{+3} in dosimetric glasses, 25:42163
ORLOVA, K. B., Determination of O and N in metals using fluxes enriched with ^{18}O and ^{15}N isotopes, 25:41748
ORTH, C. J., Decay of ^{126}Sn and of 19-min and 12.4-day isomers of ^{126}Sb, 25:43924
ORTIZ, J. J., Effects of α-deuterium substitution, polar substituents, temperature, and salts on the kinetics of hydrolysis of acetals and ortho esters, 25:41800
ORZHEKHOVSKII, V. L., Effect of carbon on the mechanical properties and structure of molybdenum crystals, 25:42899
OSAKIEWICZ, W., (n,α) reactions on heavy nuclei induced by 14.2-MeV neutrons, 25:43886 (INR-1259)
OSANOV, D. P., Dose distribution in skin contaminated with radioactive substances, 25:42257
OSMAN, A., Cluster transfer reactions at low energies, 25:43964
Finite-range Coulomb stripping in (t,p) and (^{3}He,n) reactions, 25:43965
OSTROVERKHOV, N. T., Structure of electron beams, 25:43736
OTANI, Shiro, Characteristics of linear accelerator at Hiroshima University, 25:43754
OTSUKA, Haruki, Metabolism of Ehrlich ascites tumor cells under anoxia, 25:42532
OTSUKI, Akira, Coprecipitation of phosphate with carbonates in a marl lake, 25:44252 (COO-1599-33)
OTT, E., Theory of triggered vlf emissions, 25:43245
OVAKIMOV, V. G., Genetic effects of chronic γ-irradiation of Drosophila melanogaster males, 25:42350
OVSOV, Yu. V., Semiautomatic television device for measuring ionization losses, 25:42142
OWENS, J., Two-dimensional stress-induced adiabatic flow. II, 25:44301 (UCID-30013(Pt.2))
Two-dimensional stress-induced adiabatic flow. III, 25:44302 (UCID-30013(Pt.3))
Two-dimensional stress-induced adiabatic flow. I, 25:44300 (UCID-30013(Pt.1))
OZAWA, Yasutomo, Feedback-type detection system for pulsed radiation measurement, 25:42087
OZHIGOV, L. S., Thermal expansion of a copper--tungsten composite, 25:42873
OZIEWICZ, M., Lee model with V particle having continuous mass spectrum and energy-conserving V--NTHETA vertex, 25:43671

P

PACE III, J. V., Study of the overlap conditions required in sequential discrete ordinates transport calculations for a 14-MeV neutron source in a 5000-m radius cylinder of air, 25:43419 (ORNL-TM-3269)
PACELLI, M., Risks from small doses of radiations, 25:42703
PACHNER, J., Singularities in general relativity, 25:43695
PADEH, B., Effect of chemical protection against radiation as indicated by the chromosome aberrations in the bone marrow of mice after exposure to x radiation, 25:42534
PADMORE, Timothy C., Impurities in an imperfect Bose gas. I. The condensate, 25:43273
PAETZGEN SCHIECK, H., Narrow state at 23.9 MeV, 25:43782
PAGANO, Roberto, Gas scintillator as a kinetic energy spectrometer for fission fragments, 25:42076
PAGET, John A., Lifting mechanism and refueling machine, 25:44211
PAGGI, A., Radioprotection and nuclear design, 25:42041
PAGLIARI, M., Mechanical turbulence under conditions of thermal inversion, 25:41935
PAGNI, F., Efficiency of scintillation crystals in medium contaminated by γ-emitters, 25:42095
PAGNIA, H., Effects of x radiation on MOS devices at 79K, 25:42234
PAILLON, M., Comparative analysis of critical and exponential experiments by heterogeneous methods, 25:44154 (EUR-4362)
PAKHOMOV, V. P., Systems of Fraunhofer wavelengths in solar spectra, 25:43074
PAKHOMOVA, N. V., Phase diagram of the system Cd--As, 25:42989
PALER, K., Coherent production of high mass meson states in π^+d collisions at 13 GeV/c, 25:43550 (COO-1428-290)
Final states with three charged particles and a visible anti K^0 from K-d interactions at 4.5 GeV/c, 25:43549 (COO-1428-286)
R region in 13 GeV/c π^+ nucleon interactions, 25:43545 (COO-1428-277)
PALFREY, T. R. Jr., Coherent production of high mass meson states in π^+d collisions at 13 GeV/c, 25:43550 (COO-1428-290)
R region in 13 GeV/c π^+ nucleon interactions, 25:43545

XUM

(COO-1428-277)
PALLMER, P. G., Crystal structure of promethium, 25:42893
PALMS, J. M., Si(Li) spectrometers for electrons and low-energy photons, 25:42123
PALUMBO, R. F., Uptake of molybdenum, marked with ^{99m}Mo, by biota of Fern Lake, Washington, 25:44287 (RLO-2225-T-7-2)
PANA, I., Low radiation doses and control of metabolic pathways, 25:42506
PANASENKOV, A. A., Fast hydrogen-atom injector. II, 25:43109
PANOV, A. G., Action of fast neutrons on the nervous system, 25:42541
PAPADOPOULOS, K., Electromagnetic and finite B/sub z/ effects on counterstreaming ion instability, 25:43394
PAPEZOVA, A., Radioactive strontium in milk in Czechoslovakia, 25:42395
PAQUET, C., Natural line shapes resolved in ionization yield of He^+, 25:43139
PAQUETTE, Leo A., Configurational stabilities of strained α-sulfonyl carbanions. Kinetics of base-catalyzed racemization and deuterium exchange of representative thiete and thietane dioxides, 25:41805
PAQUIN, Michael L., Multi-foil thermal insulation development program, 25:42952
PARADELLIS, Th., Unified-model calculations in some Zr isotopes, 25:43938
PARCHEV, N., Biochemical activity of anastomose Aspergillus niger strains influenced by x rays, 25:42363
PARD, A. G., Effects of helium on the high-temperature ductility of Sandvik 12R72HV and Inco IN-744X, 25:42872
Void formation in proton irradiated stainless steel, 25:42917
PARFENOV, B. G., Corrosion of Zr and its alloys, 25:42811
PARFENOVA, V. I., Hyperfine magnetic field for ^{119}Sn impurity atoms in ferromagnetic terbium, 25:43494
PARIBOK, V. P., Recognition of pyrimidine dimers in DNA by incision enzyme from Micrococcus lysodeikticus, 25:42285
PARIS, J. M., Formation of carbonitrides and oxycarbonitrides of niobium crystallizing in the cubic system, 25:42945
PARIS, P., Levels of ^{159}Dy obtained by decay of ^{159}Ho, 25:43944
PARIS, R. A., New method for preparing metal borides, 25:42944
PARISH, Leslie Joe, Isobaric spin splitting of single nucleon states in ^{89}Y and particle-hole excitations of core, 25:43859
PARK, C. G., Position of the plasmapause during a stormtime increase in trapped position of the plasmapause during a stormtime increase in trapped energetic (E > 280 keV) electrons, 25:43254
PARK, Chung G., Westward electric fields as the cause of nighttime enhancements in electron concentrations in midlatitude F region, 25:43253
PARK, James L., Concept of transition in quantum mechanics, 25:43525
PARKER, Charles W., Detection of Australia antigen by radioimmunoassay, 25:42308
PARKER, V. B., Selected values of chemical thermodynamic properties, 25:41826 (NBS-TN-270-5)
PARKHOMENKO, G. M., Problems of radiation safety and efficacy of preventive measures in work with U enriched with ^{235}U isotope, 25:42379
PARKS, Celia, Information scanning and processing at NSIC, 25:44280 (ORNL-NSIC-48)
PARPALA, V., Radiation measurements in Brasov during period 8/61--8/68, 25:42424
PARRA GIL, F., Determination of environmental radioactivity, 25:41940
PARSHIKOV, V. G., Ternary system molybdenum--titanium--carbon, 25:42890
PARSONS, N. R., Pulsating auroral patches exhibiting sudden intensity-dependent spatial expansion, 25:43249
PARSONS, Sidney B., Temperature and gravity variations of the classical Cepheid beta Doradus, 25:43045
PASCHKE, H., K-shell-fluorescence yield for carbon and other light elements, 25:43108
PASHEV, I., Biochemical activity of anastomose Aspergillus niger strains influenced by x rays, 25:42363
PASHITSKII, E. A., Plasma waves and superconductivity in quanting semiconductor films and lamellar media, 25:43314
PASHKOVSKII, A. I., Effect of carbon on the mechanical properties and structure of molybdenum crystals, 25:42899
PASTERNACK, Bernard, Prog. rpt. on spatial distribution of radon daughter and ^{239}Pu alpha lung dose based on experimental energy absorption measurements, 12/70--6/71, 25:42394 (NYU-4255-1)
PASTUKHOV, E. A., Electrical properties of liquid V_2O_5, 25:42959
PASYUK, A. S., Economical source for multiply-charged calcium and zinc ions, 25:43765
Sources of multicharged ions, 25:43731 (JINR-P7-5177)
PATER, Maximilian, Igniting aid for high-efficiency plasma producers, 25:43382
PATET, J., In vitro study of effect of γ rays on human chromosomes, 25:42365
PATHEIGER, Manfred, Process of producing moulded masses and coated substrates, 25:41847
PATRICK, Richard M., Collisionless shocks in plasmas, 25:43347
PATRONIS, E. T. Jr., Gamma--γ directional correlations in the decay of ^{125}Sb. II, 25:43927
PATTERSON, H. W., Monitoring of positively charged particles in the electron ring accelerator, 25:43734 (UCRL-20664)
PATTERSON, H. Wade, What quality factor, 25:42443
PATTERSON, James D., Introduction to the theory of solid state physics, 25:43503
PATTON, James A., Potential use of fluorescent scanning for brain tumor identification, 25:42548 (CONF-710204-4)
PAUL, J. M., Rate of energy loss and intrinsic resolution of silicon detectors, 25:42155
PAUL, P., Isospin splitting of the giant dipole resonance in ^{60}Ni, 25:43867
PAUL, Robert, Phase equilibria in the systems ThO_2--UO/sub 2+x/, CeO_2--UO/sub 2+x/, and NpO_2--UO/sub 2+x/, 25:42984 (ORNL-tr-2483)
PAULIN, A., Effects of gamma radiation on the refrigeration storage of golden delicious apples, 25:42748
PAULSEN, A. D., Glass ampoule sealer, 25:42046
PAVLOVIC, M., Modulus of elasticity for Zircaloy-2 as function of temperature, 25:42880
PAWLICKI, Anthony Joseph, Backward eta meson production at 5.9 GeV/c, 25:43563
PAXSON, Tina, Nucleophilic substitution at tetrahedral boron. Methylamine--diaryiborane substrates, 25:41804
PAYNE, G. L., Effect of approximate wave functions in composite-particle scattering, 25:43971
PAYNE, P. A., Prog. rpt. on development of lithium-diffused radiation-resistant solar cells, 10/70, 25:42227 (N-71-12257)
PAZITNY, J., Contribution to the study of structures and phases of zirconium alloys, 25:42897
PEARLSTEIN, L. D., Straight-line orbit approximation in periodic systems, 25:43373
PECKHAM, W. D., Radioimmunoassay for rhesus monkey luteinizing hormone (LH) with anti-ovine LH serum and ovine LH-^{131}I, 25:42237
PECUL, K., Split Hamiltonian matrix method and interaction between two H atoms, 25:43155
PEDCHENKO, V. I., Study of ^{210}Po content in environment and human body, 25:42429
PEDRINAZZI, G., Dose distributions around linear ^{192}Ir sources, 25:42428
Dosimetry of high energy electron beams, 25:42167
Protective considerations in use of ^{192}Ir for radiotherapy, 25:42477
PEELLE, R. W., Differential cross sections at forward angles for hydrogen and helium particles from 62-MeV protons incident on ^{60}Ni, 25:43833 (ORNL-4698)
PEERCY, P. S., Raman scattering of ion-implanted GaAs, 25:43440
PEET, Frederick Gordon, Cross sections for the gravitational scattering of massless particles, 25:43706
PEKERIS, C. L., S and P states of He isoelectronic sequence up to Z = 10, 25:43115
PELET, Regis, Detecting gamma radiation from drilled geological formations, 25:42117
PELLAT, R., Radial dependence of trapped-particle instabilities, 25:43391
PELLETT, D. E., Evidance for splitting in the Q region of $K^+\pi^+\pi^-$ mass, 25:43544 (COO-1428-275)
New evidence for splitting in the Q region of $K^+\pi^+\pi^-$ mass, 25:43543 (COO-1428-274)
PELLICCIONI, M., Radioprotection at the electrosynchrotron at Frascati, 25:43738
PELRAS, M., Corrosion of Zr alloys in water and steam, 25:42810
PENN, A. W., Isotopic power sources, 25:42014
PENNY, S. K., Preparation of data sets in ENDF format for Na, Mg, Cl, and K for use in shielding calculations, 25:43420 (ORNL-TM-3429)
PENZIAS, A. A., Discovery of interstellar silicon monoxide, 25:43052
Origin of reported millimeter continuum in IRC + 10216, 25:43040
PERALTA, Jose Antonio, Radiolysis of petroleum products: residue after distillation, 25:41853 (NP-18817)
PERAZZO, R. P. J., Reaction (d,^{6}Li), 25:43987
PERDOMO, A., Application of the sterile-insect-release technique in Mediterranean fruit fly suppression, 25:42750
PERKINS, H. S., Rectification effect in thin-film superconductors in small, oscillatory magnetic fields, 25:43304
PERKINS, J. F., Variational-bound methods for auto-ionization states. II, 25:43168
PERKO, T. E., Perturbations in anisotropic Euclidean-homogeneous cosmologies, 25:43096
PERL, Martin L., How does the muon differ from the electron, 25:43591
PERMOGOROV, S. A., Annihilation of excitons and exciton--phonon interaction, 25:43502
PERRIGO, Lyle D., Role of design in corrosion prevention, 25:44236 (BNWL-SA-3817)
PERRIN, Alfred J., Method of operating liquid metal cooled

nuclear reactor, 25:44114
PERRIN, R. C., Mechanism and kinetics of void growth during neutron irradiation, 25:42916
PERROTTET, M., Sixth-order radiative corrections to the anomalous magnetic moment of the electron, 25:43594
PERSHINA, Z. G., Radioresistance of E. coli K-12, 25:42330
PESCHKA, W., Energy for spaceflight in the future, 25:43191
PESHEKHONOV, V. D., System of proportional wire chambers on-line with a computer, 25:42156
PETERMAN, B., Vibrational normal coordinate analysis of H(D)NCO and H(D)NCS, 25:41791
PETERS, J. T., Development of an advanced space radiation system, 25:41978
PETERS, Martin C., Method of operating liquid metal cooled nuclear reactor, 25:44114
PETERSON, A. R., Toxicity of tritiated thymidine in P388F lymphoma cells. I, 25:42251
PETERSON, D. T., Preparation of high purity thorium and thorium single crystals, 25:42824
PETERSON, R. E., Design considerations of FFTF safety, 25:44139 (HEDL-SA-159)
PETEU, G. I., Nuclear methods for prospecting and exploiting non-petroleum mineral resources, 25:41931
PETKOV, V., Changes in pea varieties as affected by gamma rays, 25:42329
PETRANOVIC, Drago, Phage-induced radioresistance of lysogenic bacteria, 25:42529
PETRASCU, M., Intermediate structure near an isobaric analog resonance, 25:43851
PETRIK, Edward J., Transfer function determination of primary loop of a conceptual nuclear Brayton space power plant, 25:44158 (N-71-17933)
PETRILAK, Michael Jr., Energy partition of heavy ions of intermediate energies in silicon surface-barrier detectors, 25:42061
PETROSYAN, R. A., Effect of direct current and x radiation on bone marrow cells, reticuloendothelial cells, and radiosensitivity of rats, 25:42530
PETROV, N. M., Problem of two-nucleon motion for Gauss potentials, 25:43538 (ITF-71-9-P)
PETROV, R. V., Radiation immunology and transplantation, 25:42310
PETROVA, L. V., Results of the calculation for a standard fast reactor, 25:44194 (FEI-213)
PETROVA, M. A., Phase equilibria in the system Er_2O_3--GeO_2, 25:42988
PETROVA, O. P., Scanning of the liver in the diagnosis of chronic hepatitis and cirrhosis, 25:42553
PETROVICH, I. K., Biological action of ^{237}Np nitrate, 25:42253
PETROVICI, A., Action of gamma radiation on enterococcal bacteriophage 341, 25:42740
PETRUNINA, A. N., Crystallization of Ni--Ta and Ni-Nb alloys at superhigh rates of cooling, 25:42888
PETSCHEK, Harry E., Collisionless shocks in plasmas, 25:43347
PEVZNER, M. G., Determination of the isotopic composition of cadmium, 25:41731
Determination of the isotopic composition of tin and indium, 25:41727
PEXTON, Robert L., PIEGA: a numerical solution for definite integrals with oscillating integrands, 25:44299 (UCID-30009)
PFALZNER, Paul M., Interconparisons of absorbed dose in ^{60}Co teletherapy using mailed LiF dosimeters. II, 25:42172
PFANNHAUSER, W., Separation of U(VI) by extraction chromatography, 25:41924
PFIRSCH, D., Survey of studies of laser produced plasmas at the IPP Garching, 25:43380 (IPP-4/9)
PHILIP, A. G. Davis, Hβ photometry of A-type stars near the North Galactic Pole, 25:43043
PHILLIPS, G. O., Radiolytic decomposition of solid oxalic acid, 25:41859
PHILLIPS, H. R., Head-end separation of BISO-coated fissile and fertile particles for high-temperature gas-cooled reactors, 25:41907
Head-end separation of TRISO-coated fissile and fertile particles for high-temperature gas-cooled reactors, 25:41906
PHILLIPS, Ralph, Energy decay for the neutrino equation in the exterior of a torus, 25:43610
PHILLIPS, Theodore L., Radiobiological and biochemical studies of thiophosphate radioprotective compounds related to cysteamine, 25:42525
PHONDKE, G. P., Low dose effects of x-rays on electrophoretic mobility of human erythrocytes, 25:42682
PICHANICK, F. M. J., Precise measurement of 2^3P_0--2^3P_1 fine-structure interval of He, 25:43122
PIEKOS, Boleslaw, Effect of x irradiation on tooth primordia in the golden hamster in early stages of development, 25:42549
PIETSCH, Anthony, Closed Brayton cycle power system applications, 25:42007
PIETTE, L. H., Inherent dosimeter for irradiated foods: papayas, 25:42439
PIHL, Alexander, Radiation effects on allosteric enzyme, 25:42291
PIL, B. N., Alteration of the bioelectric activity of the brain in patients with arachnoiditis under the influence of radiation treatment, 25:42678
PINEO, Evans William Fletcher, Average neutron total cross sections and the optical model, 25:43908
PINKSTON, William T., Negative-parity states in ^{208}Pb, 25:43926
PINSKY, Steven M., Correlation between brain tumor detectability on brain scan and protein levels of the spinal fluid, 25:42547 (ACRH-1000-248)
PINTER, Gyorgy, Determination of spin parity by means of multipole moments, 25:43581
PIRINGER, O., Quantitative analysis of gas chromatograms of partially separated material mixtures, 25:41746
PISAREV, A. F., Methods of detecting particle tracks in liquid and solid media, 25:42053 (JINR-P13-5782)
PISAREVSKII, A. N., Radiobiophysics of the nucleoproteins, 25:42274
PITAEVSKII, L. P., Relativistic quantum theory, 25:43086
PITROLO, A. A., SNAP-27 program review, 25:41999
PIVOT, J., Analysis of silicon oxide films by (d,p) reactions and infrared spectrophotometry, 25:42999
PLACE, R. L., Low-lying levels of ^{40}Ar, 25:43872
PLAJNER, Z., Contribution of outer atomic shells to total internal conversion coefficients, 25:43931
PLECEAS, M., Action of gamma radiation on enterococcal bacteriophage 341, 25:42740
Action of gamma rays on bacteria used as sanitary indicators, 25:42743
PLECEAS, Paula, Action of gamma radiation on enterococcal bacteriophage 341, 25:42740
PLENDL, H. S., Spin of the 937-keV level in ^{56}Co, 25:43863
PLESCIA, Otto J., Prog. rpt. on role of the carrier in antibody formation, annual, 5/70--5/71, 25:44274 (NYO-3707-7)
PLESHIVTSEV, N. V., Universal apparatus for measuring the paraneters of strong ion beams, 25:43746
PLETCHER, T. C., Effects of α-deuterium substitution, polar substituents, temperature, and salts on the kinetics of hydrolysis of acetals and ortho esters, 25:41800
PLYUTTO, A. A., Acceleration of ions of cathode material in vacuum breakdown, 25:43383
POCHINAILO, Andzhei, Laboratory mixer--settler extractor LMOM2, 25:41895 (INR-1309)
PODGORETSKII, M. I., Interference at intersection of levels, 25:43506 (JINR-P4-5785)
POE, N., Determination of in vivo persistence of tantalum dust following bronchography using reactor-activated tantalum and total body counting, 25:42558
POE, R. T., Are there two A_2 mesons, 25:43624 (UCR-34-P-107-B-112)
Duality for inelastic anti KN scattering at intermediate energies, 25:43642 (UCR-34-P-107-B-106)
Study of $\pi^+p \to rho^+p$ at 1.85 to 2.09 GeV, 25:43552 (UCR-34-P-107-B-110)
POEYDOMENGE, P., Influence of Si on Zircaloy-2 and Zircaloy-4 alloys, 25:42875
Studies of the influence of N on alloys of Zr--Cr--Fe type, 25:42875
POGOSOV, V. Z., Repair of uv-induced mutations in phage T4, 25:42339
POIRIER, J. P., Pressure dependence of elastic constants for Ag from 77°K to 300°K, 25:44271 (NYO-2504-59)
POKAZAN'EV, V. G., Nuclear gamma-acoustic resonance, 25:43493
POKORNY, G. J., Glass ampoule sealer, 25:42046
POLIAKOV, V. M., Theory of the undisturbed F2 layer, 25:43230
POLLANZ, Herwig, Sintering Fe--Mo and Fe--Cr, 25:42818
POLLARD, Ernest C., Action of ionizing radiation on sensitive strains of Escherichia coli B, 25:42728 (NYO-2804-39)
Action of ionizing radiation on the molecular biology of E. coli, 25:42727 (NYO-2804-38)
Effects of ionizing radiation on capacity of Escherichia coli to support bacteriophage growth, 25:42730 (NYO-2804-41)
Strain of Escherichia coli resistant to DNA degradation induced by ionizing radiation, 25:42729 (NYO-2804-40)
Sucrose gradient analysis of DNA in irradiated cells of PHR1, 25:42731 (NYO-2804-42)
POLYAK, K., Spectrophotometric determination of molybdenum with phenyl-fluorone, 25:41726
POLYAKOVA, T. A., Observations of the variability of the polarization of radiation of the high luminosity red variables, 25:43024
PONOMARENKO, A. G., Studies of plasma turbulence by means of charged particle beam, 25:43339 (IYAF-7-70)
PONOMAREV, Yu. T., Ultrastructure of fibrin in acute radiation sickness, 25:42540
POPA, Rodica, Hemorrhagic syndrome in radiation sickness. II, 25:42537
POPEK, R. J., Activation-rate measurements in the ZPR-3 mockup critical experiments. Part I. Measurements of foil-activation rates and fission yields in Assembly 60 of ZPR-3: mockup of EBR-II with a uranium blanket, 25:44150 (ANL-7781)
POPOV, D. K., Age-specific peculiarities of ^{137}Cs elimination from human organism, 25:42250
POPOV, V. K., Structure of electron beams, 25:43736
PORT, H., Delayed fluorescence and phosphorescence in pure naphthalene crystals, 25:41813
PORTER, E. D., Comparative radiomimetic effect of emulsin,

XUM

cycasin, methylazoxymethanol, and x rays in Zamia integrifolia, 25:42334
PORTER, F. T., Ionization (shakeoff) accompanying K-shell internal conversion, 25:43871
Outer-shell internal conversion of the 14.4-keV transition in ^{57}Fe, 25:43855
POSHYUNAITE, N. P., Excitation of the aromatic molecules by electron impact. I, 25:43127 (BNL-tr-429)
POSPISIL, J., Autoradiographic localization of radioactivity in female rat neocortex after injection of tritiated estradiol, 25:42258
Some biochemical changes in body fluids as indicators of radiation damage, 25:42402
POSTMA, A. K., Leakage of fission products from artificial leaks in the Containment Systems Experiment, 25:44134 (BNWL-1582)
POTASHOV, A. G., Mean free path of the π^0 meson in nuclear matter, 25:43595
POTTER, R. A., Sintering of UN as a function of temperature and N_2 pressure, 25:42979
POTUPA, A. S., Idealized measurements in quantum field theory, 25:43592
POWELL, Malcolm R., Scintiphotographic evaluation of response of brain neoplasms to systemic chemotherapy, 25:42556
POWELL, Royal Edward, Energy selective ion beam intensity measuring apparatus and method utilizing a scintillator to detect electrons generated by the beam, 25:42224
POZDNEEV, D. B., Spectral-angular characteristics of an electron beam in irradiation of a tissue-equivalent medium, 25:43421 (ORNL-tr-2476)
PRAKASH, H., Effect of coherence on intensity-dependent frequency shift in Compton scattering, 25:43590
PRANEVICIUS, O., Secondary-electron emission produced by relativistic primary electrons in strong electric fields, 25:43101 (SCL-T-69-256)
PRASAD, Y. V. R. K., Evaluation of rate-controlling obstacles for low-temperature deformation of zirconium, 25:42852
PRATT, R. H., Exact screened calculations of atomic-field pair production and low energy screening, 25:43417 (NYO-3829-71)
PREEDOM, B. M., Precision mass measurement of ^{9}C, ^{13}O, and ^{21}Mg, 25:43823
PRENTICE, Walter B., Scinticisternography in individuals without known neurological disease, 25:42567
PREPEJCHAL, William, Thermal plume measurements, 25:44138 (CONF-710431-1)
PRESL, J., Autoradiographic localization of radioactivity in female rat neocortex after injection of tritiated estradiol, 25:42258
PRESNYAKOV, L. P., Possibility of producing inverted population in atomic beams by charge exchange of protons with atoms, 25:43103
PRICE, Charles Clayton, Prompt neutron decay constants in a reflected fast burst reactor, 25:44198
PRICE, L. K., Thermionic reactor concepts, 25:44159
PRILEPSKII, V. N., Enthalpy and heat capacity of EuB_6, NdB_6, and SmB_6, 25:42951
PRIMACK, Joel Robert, Asymptotic behavior of the elastic form factor in field theory, 25:43587
PRINZ, D. K., Observation of the O I 1304-A airglow from OGO 4, 25:43259
PRIOR, R. M., Narrow state at 23.9 MeV, 25:43782
PROKOFEV, O. N., Content of ^{137}Cs in population of Soviet Union, 25:42375
PROPST, R. C., Conducting glass electrode in a thin-layer electrochemical cell with application to the analysis of neptunium, 25:41732
PROSSER, R. A., Protection against intense light. I. Discussion of the usual mechanisms of energy dissipation, 25:41827
PROTASOV, V. P., Filtering of tracks measured on the SMP, 25:42135 (CERN-Trans-71-8)
PSHESTANCHIK, V. R., Phase diagram of the system Cd--As, 25:42989
PUCKETT, O. H., Si(Li) spectrometers for electrons and low-energy photons, 25:42123
PUEHLHOFER, F., High-spin isomer in ^{211}At, 25:43912
PUESCHEL, Sonia M. P., Retention of Ta by hydrated Sb(V) oxide in strongly acid media, 25:41922
PUGACHEVICH, V. P., System of proportional wire chambers on-line with a computer, 25:42156
PULATOVA, M. K., Investigation of paramagnetic centers of irradiated proteins, 25:42275
PULLMANN, Michal, Radiation unit RCH-gamma-30, 25:42015
PUNG, Tong-chuin, Photon-activation analysis for zirconium with molybdenum used as the internal-reference element, 25:41764
Study of photon activation analysis, 25:41766
PUNSOR, E., Spectrophotometric determination of molybdenum with phenyl-fluorone, 25:41726
PURCELL, Robert H., Frequency of antibody to hepatitis-associated antigen as measured by a new radioimmunoassay technique, 25:42306
PURICELLI, G., Radioisotope investigation of lymph system function and morphology, 25:42581
PURKAYASTHA, Gita, Separable approximation to two-body t-matrix, 25:43980
PUSTOVALOV, V. V., Absorption of light by an inhomogeneous laser plasma, 25:43400
PUT, L. W., Optical-model analysis of 38 MeV ^{3}He elastic scattering, 25:43878
PUZAK, P. P., Analysis of radiation-induced embrittlement gradients on fracture characteristics of thick-walled pressure vessel steels, 25:42841 (CONF-710512-8)
PYSHNENKO, V. N., Catalogue of right ascensions of 231 pairs of stars, 25:43028

Q

QUAGLIA, L., Behavior of surface carbon during its determination by nuclear reactions, 25:41765
QUEMENER, J. J., Natural line shapes resolved in ionization yield of He$^+$, 25:43139
QUERCIGH, E., Bubble density measurements with HPD 2 at CERN, 25:42153
QUINN, James R., Medium energy studies of the (p,p α) reaction on light nuclei, 25:43801 (UCLA-10-P-18-31)
QUINN III, James L., Correlation between brain tumor detectability on brain scan and protein levels of the spinal fluid, 25:42547 (ACRH-1000-248)
QUINTANA, Victor, Genetic collapse of insect populations. I. Extinction of inbred and outbred lines in laboratory populations of the sugarcane borer, 25:42611
QUIRK, J. P., Alpha-activity of Western Australian soils and wheats, 25:42427
QURESHI, M., Separation of metal ions on inorganic ion-exchange papers, 25:41909

R

RABINOVITCH, B. S., Intramolecular energy relaxation. Nonrandom decomposition of hexafluorobicyclopropyl, 25:41809
RACHOWSKI, Jan, Spark chamber as an element of the hodoscopic detector of extensive air showers, 25:42158
RADMAN, M., Target size of DNA in ultraviolet irradiation, 25:42300
RADOVIC, G., Toxicity and analgesic activity by gamma rays, 25:42752
RADZYUK, K. A., Comparative evaluation of the effects of uranium nitrate and radioactive iodine on auto-antibody formation, 25:42645
RAFALSKI, A. L., Annealing kinetics of shock hardened plutonium--1 wt. percent gallium, 25:42857
RAFFENETTI, Richard Charles, Even-tempered atomic orbitals in quantum chemical ab initio calculations, 25:43160 (IS-T-456)
RAGHAVAN, R., Nuclear interaction of cosmic-ray pions and nucleons of energies > 20 GeV. I, 25:43540
RAGSDALE, H. L., Artemisia shrub size and radiation damage to Artemisia from local fallout from Project Schooner, 25:42717 (EGG-1183-2272)
RAIMBAULT, P. A., Polarization of the free--free bremsstrahlung in an anisotropic hot-electron plasma, 25:43357
RAINWATER, J., Neutron resonance spectroscopy. VII, 25:43874
RAJ, R., Shell-model calculations for ^{51}V and ^{52}Cr, 25:43862
RAJCHERT, A., Influence of γ irradiation of wheat seeds on ascorbic acid content of plant, 25:42726
RAJNAK, K., Many-body calculations for the heavy atoms, 25:43116
RAJPUT, J. S., Superconducting state parameters for nontransition metals, 25:43305
RAKOVA, V. A., Dose distribution in skin contaminated with radioactive substances, 25:42257
RAKOW, Adalbert, Standard ionic dose in compact and liquid media during x-ray and gamma irradiation, 25:42091
RAKUSHINA, N. I., Heat transfer with water and Freon-113 boiling on nonisothermal surface, 25:41989
RAMADORAI, Gopalan, Kinetics of molybdenum dioxide oxidation, 25:42933
RAMAN, Subramanian, New observations in the A = 49 decay chain; levels in ^{49}Sc and ^{49}Ti, 25:43873
RAMASASTRY, C., ESR absorption of x-irradiated $NaClO_2$ crystal, 25:43451
RAMIG, Alexander Jr., Reactivity ratios and microstructure for the radiation induced copolymers of styrene and methyl methacrylate, 25:41845
RAM MOHAN, L. R., Superconvergence and algebraic realizations of chiral symmetry, 25:43661
RANGAN, L. K., Evidence for splitting in the Q region of $K^+\pi^+\pi^-$ mass, 25:43544 (COO-1428-275)
New evidence for splitting in the Q region of $K^+\pi^+\pi^-$ mass, 25:43543 (COO-1428-274)
RANGARAJAN, C., Investigation on ^{210}Pb concentrations in various regions of India, 25:42387
RANGASWAMY, T. N., Nuclear interaction of cosmic-ray pions and nucleons of energies > 20 GeV. I, 25:43540
RANGASWAMY, Thambu Narayanaiyengar, Study of dipions in mass range 400 to 1000 MeV produced in π-p collisions, 25:43555
RAO, D. M., Induction of chlorophyll mutations by D_2O in Oryza sativa L, 25:42346
RAO, P. Venugopala, Si(Li) spectrometers for electrons and low-energy photons, 25:42123
RAO, S. V. Seshagiri, Heat transfer in MHD Couette flow as

affected by wall electrical conductances and suction, 25:43198
RAO, V. U. S., Magnetic characteristics of aluminum-rich ternary laves phases containing rare earths, nickel, and aluminum, 25:43480
RAPPOPORT, I. A., Effect of petroleum growth substance on the healing of radiation wounds of the skin, 25:42539
RASCHE, G., Coulomb corrections to low energy elastic and charge exchange πN scattering, 25:43599
Mass differences as additional electromagnetic corrections in low-energy elastic and charge-exchange πN scattering, 25:43545
RASMUSSEN, Darrell C., Seismic analysis of Gasbuggy explosion an earthquake of similar magnitude and epicenter, 25:41952 (AD-838894)
RASMUSSEN, V. K., Lifetimes and other properties of some levels in ^{23}Na, 25:43838
RASPOPIN, S. P., Polarization of a zinc cathode during thorium precipitation from molten halide salts, 25:42821
RASSOW, Juergen, Film dosimetry of high-energy rays. IV, 25:42395
RATYNSKI, W., Circular polarization of gamma rays, 25:43831 (INR-1252)
RAVETS, J. M., Determination of shielding requirements for NPTR fuel handling system, 25:44161 (WANL-TME-1895)
RAWLS, John M., Singularity structure of equal-time commutators, 25:43582
RAYMOND, David James, CP violating decay of neutral kaon into two neutral pions, 25:43657
RAYMOND, Louis, Titanium--Be composites produced by the co-extrusion of powders, 25:42359
RAZAVY, M., Conjugate variables in two-body collisions, 25:43724
RAZBIRIN, B. S., Annihilation of excitons and exciton--phonon interaction, 25:43502
RAZGULYAEV, I. I., Ion-beam apparatus, 25:43747
REAGAN, J. B., Solar particle cutoffs as observed at low altitudes, 25:43234
REALINI, G. C., Orgel prototype preliminary design: reactivity coefficients, 25:44100 (EUR-4365)
Orgel prototype preliminary design: fine flux distributions in the fuel element, 25:44099 (EUR-4364)
REARWIN, Stephen, Rocket measurements of low-energy auroral electrons, 25:43248
REBEL, H., Hexadecapole moments of ^{20}Ne and ^{28}Si from scattering of 104-MeV α particles, 25:43876
Measured differential cross sections for elastic and inelastic scattering of 104-MeV α particles, 25:43832 (NP-18920)
REDDY, G. M., Induction of chlorophyll mutations by D_2O in Oryza sativa L, 25:42345
REDDY, T. P., Induction of chlorophyll mutations by D_2O in Oryza sativa L, 25:42345
REDEKER, Maynard S., Antiproton--deuteron annihilations into kaons and pions at 2.2 GeV/c, 25:43536
RED'KIN, V. S., Electrostatic spectrometer for beams of charged particles, 25:42215
Ion-optical properties of an electrostatic charged-particle energy analyzer, 25:43761
REDMAN, W. C., Experimental determination of the perturbation denominator in fast critical assemblies, 25:44163
REECE, R. R., Determination of mass of ^{87}Y, 25:43836
REEVES III, Mark, Code for linear modeling of an ecosystem, 25:44278 (ORNL-IBP-71-2)
REICH, C. W., Coriolis coupling in doubly odd deformed nuclei, 25:43934
Level structure of ^{182}Ta, 25:43935
REICHLE, D. E., Biological concentration and turnover of radionuclides in food chains: a bibliography, 25:42315 (ORNL-NSIC-89)
REICHSTEIN, I., Study of p + ^{3}He and n + ^{3}H systems with the resonating-group method, 25:43797
REIDER, Roy, Early history of criticality safety, 25:44157 (LA-4671)
REINCKE, U., Life span and tumor incidence in rats subjected to severe stress before whole body x-irradiation, 25:42559
REITAN, A., Three-neutron resonance in the reaction ^{3}He(π$^-$,π$^+$)3n, 25:43791
REMINI, W., SNAP-27 program review, 25:41999
RENGAN, K., Radiochemical purification and continuous milking of ^{144}Pr from ^{144}Ce, 25:41883
RETNAKARAN, Arthur, Method for determining sperm precedence in insects, 25:42259
REVESZ, Laszlo, Chemical protection of the recovery process, 25:42521
REYNOLDS, M. B., Failure behavior of flawed carbon steel pipes and fittings, 25:42845 (GEAP-10236)
RHEE, S. K., Wetting of ceramics by liquid metals, 25:42980
RHOADS, W. A., Artemisia shrub size and radiation damage to Artemisia from local fallout from Project Schooner, 25:42717 (EGG-1183-2272)
RHODE, R. H., Application of the sterile-insect-release technique in Mediterranean fruit fly suppression, 25:42750
RHODES, C. G., Effects of helium on the high-temperature ductility of Sandvik 12R72HV and Inco IN-744X, 25:42872
RICE, J. K., Importance of polarization for electron scattering in the intermediate-energy region, 25:43138
RICHARD, J. J., Determination of uranyl and thorium(IV) by gas chromatography of volatile mixed-ligand complexes, 25:41725
RICHARD, Patrick, Resolved structure in Fe Kα x rays produced by 30-MeV ions, 25:43110
RICHARDS, P., Visualization of the human spleen with /sup 99m/Tc-labeled red blood cells, 25:42235
RICHER, Harvey B., Some intrinsic properties of carbon stars, 25:43037
RICHTER, A., Anomaly in angular distributions for (^{3}He,t) reactions, 25:43848
Isospin nonconservation in reaction ^{12}C(d,α_2)^{10}B(1.74,T = 1), 25:43811
RICHTER, F., Investigation of an inductive plasma accelerator for propulsion purposes, 25:43351
RIDINGS, G. Ray, Renal adenocarcinoma: regression of pulmonary metastases following irradiation of primary tumor, 25:42591
RIDLEY, B. W., New 0$^+$ states in ^{50}Cr, 25:43849
Optical-model analysis of 38 MeV ^{3}He elastic scattering, 25:43878
RIEGEL, D., Magnetic moments of isomeric levels in the Br isotopes, 25:43841
RIEGEL, Robert L., Drybox gloves: evaluation and procurement, 25:42039 (RFP-1285)
RIESZ, Peter, Radiation-induced hydrogen transfer in nucleic acids, proteins, and related substances: effects of temperature and scavengers, 25:41837
RIHAN, T. H., Cluster transfer reactions at low energies, 25:43964
Finite-range Coulomb stripping in (t,p) and (^{3}He,n) reactions, 25:43965
RILEY, Merle E., Euler--Lagrange optimization of plane-wave factors, 25:43144
RILEY, P. J., Reaction ^{36}Ar(d,p)^{37}Ar, 25:43868
RINEISKII, A. A., Pumps for circulating liquid metals, 25:41958 (CONF-700307-8)
RINGOT, C., Zirconium--copper alloys used in fuel element cladding for gas-cooled heavy-water reactors, 25:42881
RINGSDORF, H., Chemical radioprotection with N- and S-containing polymers, 25:42517
RIPKA, G., Hartree--Fock calculations of light deformed nuclei, 25:43986
RISSER, Thomas Bard, Neutral decays of eta^0 meson, 25:43530
RITCHIE, Lawrence S., Program for Fasciola hepatica in Puerto Rico, 1/70--4/71, 25:42246 (PRNC-148)
RITTENBERG, V., Duality in the triple Regge limit, 25:43649
RIZAEV, N. U., Effect of gamma-radiation on properties of extracted cottonseed oil for preparation of K-5 drying oil, 25:41839
RIZZO, F. X., Tabulated dose distribution data for gamma irradiator design, 25:41957 (BNL-50147(Rev.))
RO, Seung Gy., Determining dead times of a GM detector, 25:42095
ROACHE, Patrick J., On artificial viscosity, 25:44291 (SC-RR-710301)
ROBERTSON, J. S., Counter telescope measurements of a beam of negative π mesons, 25:42141
ROBERTSON, R. E., Sulfonyl chloride kinetics. III, 25:41792
ROBINSON, G. C., Discussion of SwRI model parametric tests, 25:42848 (ORNL-TM-3313)
ROBINSON, J. A., Determination of mass of ^{87}Y, 25:43836
ROBINSON, J. C., Void formation in proton irradiated stainless steel, 25:42917
ROBINSON, Mark T., Deduction of interaction potentials from planar-channeling experiments, 25:43456
Energy-loss spectra of channeled iodine and oxygen ions in gold, 25:43454
Oscillation frequencies of protons in planar channels of silicon, 25:43455
ROBINSON, R. D., Electroformed nickel mold inserts, 25:44235 (BDX-613-454)
ROCCELLA, M., Radioprotection at the electrosynchrotron at Frascati, 25:43738
ROCK, B. J., SNAP-27 program review, 25:41999
ROCKMORE, Ronald, Multiple production of massless pions as a consistency test in the algebraic realization of chiral symmetry, 25:43663
RODONO, M., Light curve and apsidal motion of AR Cas, 25:43046
RODRIGUEZ-GONZALEZ, Federico Angel, Application of neutron activation analysis to the study of interstitial solid solution of oxygen in niobium and in niobium--titanium alloys, 25:41761
ROESCH, W. C., Analysis of distributions produced by charged particles, 25:43414 (BNWL-SA-3705)
ROGER, J. A., Analysis of silicon oxide films by (d,p) reactions and infrared spectrophotometry, 25:42999
ROGERS, A. E., Loss-of-coolant accident and emergency core cooling models for BWR, 25:44140 (NEDO-10329(Suppl.1))
ROGERS, Alan E. E., Quasars revisited: rapid time variations observed via very-long-baseline interferometry, 25:43049
ROGERS, L. B., Effect of an electric field on gas chromatographic retentions by liquid crystals, 25:44245 (COO-1222-47)
Effect of loading on separation efficiency using steric

exclusion chromatography, 25:44244 (COO-1222-46)
Prog. rpt. on fundamental studies on separation processes, annual, 7/71, 25:44248 (COO-1222-50)
Specification of gas chromatographic behavior using Kovats indices and Rohrschneider constants, 25:44247 (COO-1222-49)
Steric-exclusion chromatography at pressures up to 3500 kg/cm², 25:44246 (COO-1222-48)
ROGOZIN, A. I., Studies of plasma turbulence by means of charged particle beam, 25:43339 (IYAF-7-70)
ROGULA, D., Relativistic invariance and causality in the theory of continuous media, 25:43693
ROHAL, Robert G., Performance of ceramic insulator seals at high neutron and gamma fluence levels, 25:42228 (N-71-17325)
ROLNICK, William B., Equal-time commutators of T/sup ij/, 25:43685
ROMANENKO, V. N., Energies of mixing in systems containing germanium and silicon with elements of groups III and V, 25:42970
ROMANOV, Yu. A., Plasma waves and superconductivity in quanting semiconductor films and lamellar media, 25:43314
ROMANTSEV, E. F., Effect of modifying factors on radiosensitive biochemical reactions, 25:42625
ROMBERG, Gerald P., Thermal plume measurements, 25:44138 (CONF-710431-1)
RONDARI, G., Relationship between signal and body background in external measurement of radioactivity, 25:42423
ROOSILD, S., Residual electrically active defects after lattice reordering in ion-implanted silicon, 25:43439
ROPER, L. David, Analyses of elastic proton-alpha scattering, 25:43781
Comparison of Princeton--Pennsylvania n--p scattering data by phase-shift analyses, 25:43538
ROSE, C. M., Preliminary version of RIPPLE software descriptions, 25:44298 (TID-25758)
ROSE-INNES, A. C., Macroscopic quantum interference effects in superconducting slug-type junctions, 25:43293
ROSENBERG, Gary L., Local recurrence of generalized herpes zoster following x irradiation, 25:42689
ROSENBLUTH, M., Finite-β stabilization of the collisionless trapped-particle instability, 25:43388
ROSENECKER, C. N., Power required to circulate gas-solids suspensions, 25:41956 (BM-RI-7019)
ROSINI, E., Categories of stability for regions of Italy, 25:41935
ROSS, William Alexander, Theoretical study of pion nucleon interactions, 25:43543
ROSSALL, B., Sulfonyl chloride kinetics. III, 25:41792
ROSSELLE, N., Electronyographic examination of striated muscle in guinea pig after ^{60}Co irradiation, 25:42652
ROSSOW, Terry L., Livermore superconducting Levitron, 25:43399 (UCRL-73075)
ROST, E., Shapes of angular distributions of (³He,t) and (p,n) transitions to 0⁺ antianalog states, 25:43842
ROTE, D. M., AN--EN coupling for AN scattering and for Λ-particle binding in nuclear matter, 25:43648
ROTSEY, W. B., Stress relaxation in beryllia, 25:42973
ROUBIN, M., Formation of carbonitrides and oxycarbonitrides of niobium crystallizing in the cubic system, 25:42946
ROUKLOVE, P., Thermoelectric generators for deep space application, 25:43184 (N-71-16776)
ROUKLOVE, Peter, Performance and life testing of thermoelectric generators, 25:42002
ROUND, K. J., Nuclear power source, 25:42019
ROUSSIN, R. W., Preparation of data sets in ENDF format for Na, Mg, Cl, and K for use in shielding calculations, 25:43420 (ORNL-TM-3429)
ROUTTI, Jorma T., What quality factor, 25:42443
ROUX, D. P., Effect of gamma radiation on LMFBR subcriticality measurements using noise analysis, 25:44103
ROUYER, Hubert, Investigation of some nonlinear effects in extraction equipment using computer simulation, 25:41890 (CEA-N-1450)
ROY, B. Barman, Shell-model calculations for ^{51}V and ^{52}Cr, 25:43862
ROY, T., Unitary symmetry and duality in meson--meson scattering, 25:43627
ROYZEN, L. I., Heat transfer with water and Freon-113 boiling on nonisothermal surface, 25:41989
RUBINSTEIN, H. R., Duality in the triple Regge limit, 25:43649
RUCH, Robert B., Electrical performance of three solar thermoelectric test sections, 25:43185 (N-71-17252)
RUD, Niels, Perturbed β-vibrational bands in ^{152}Sm, ^{154}Gd, and ^{156}Gd, 25:43940
RUDENCHENKO, E. V., Semiautomatic television device for measuring ionization losses, 25:42142
RUDENKO, V. S., Reduction cycle MO_2 + M_2O_3 for Ce, Pr, and Tb oxides, 25:42958
RUDMIN, J., Effect of a toroidal field on plasma transport in a magnetically perturbed multipole, 25:43335
RUDNITSKAYA, E. I., Biological action of ^{237}Np nitrate, 25:42253
RUDOLPH, Hans, Process of producing moulded masses and coated substrates, 25:41847
RUDRA, P., Electronic energy levels of U⁴⁺ and U³⁺ in UO_2 and UI_3 crystals, 25:43499
RUEDL, E., Quantitative transmission electron microscopy of bubbles in Al and Al--Al_2O_3 alloys, 25:42896
RUEHLE, W., Compact ^{60}Co kernel for space power, 25:42000
RUETHER, W., Chemical radioprotection with N- and S-containing polymers, 25:42517
RUFF, M. D., Effect of gamma radiation on Histomonas meleagridis, 25:42608
RUGGE, Hugo R., Observation of autoionizing states in solar corona, 25:43065 (AD-715257)
RUGH, Roberts, Immediate and delayed effects of 1000 R x-rays on the rodent testis, 25:42659
RUKHADZE, A. A., Nonlinear interaction of electron beams with plasma, 25:43365
RUOFF, Arthur L., Pressure dependence of elastic constants for Ag from 77°K to 300°K, 25:44271 (NYO-2504-59)
RUSSEL, Marjorie, X-irradiation sensitivity in E. coli, 25:42331
RUSSELL, C. T., Correlated observations of electrons and magnetic fields at the Earth's bow shock, 25:43238
RUSSELL, Christopher T., Motion and structure of the magnetopause, 25:43220 (N-71-20853)
RUSTGI, M. L., Shell-model calculations for ^{51}V and ^{52}Cr, 25:43862
RUTKEVICH, B. N., Asymmetry of the combination-frequency spectrum in a plasma, 25:43410
RYABOV, G. A., Extraction of the proton beam of the 1-GeV synchrocyclotron, 25:43762
RYABOV, N. V., Use of photographic films for individual radiometry of the daughter products of radon, 25:42171
RYBACHUK, N. T., Production of zirconium dioxide from baddeleyite concentrate, 25:42942
RYBIN, S. N., Instrument for measuring and monitoring the energies of particles accelerated in a cyclotron, 25:43743
RYERSON, Thomas W., Computer processing of scans using Fourier and other transformations, 25:42557
RYNBRANDT, J. D., Intramolecular energy relaxation. Nonrandom decomposition of hexafluorobicyclopropyl, 25:41809
RYUMSHINA, T. A., Activity of redox enzymes in the liver in internal use of radon water, 25:42279
RZEWUSKI, J., Some estimates for generating functionals with an application to quantum field theory, 25:43670
RZHEVSKII, V. E., Determination of the optimal canal of registration of gamma-radiation in radioisotope diagnosis, 25:42397

S

SAAD, Masoud, Influence of chemical binding on the neutron cross section in some uranium compounds, 25:43930
SABATO, Jorge A., Nondestructive testing as a factor of technical and industrial development, 25:42028
SABAU, C., Quantitative analysis by sorption on ion exchangers, 25:41742
SABOL, E., Induction of translocations in mature Drosophila oocytes over a dose range of 10 to 500 roentgens of x rays (stage-14 oocyte/radiation damage), 25:42333
SADARANGANI, S. H., Low dose effects of x-rays on electrophoretic mobility of human erythrocytes, 25:42682
SAEKI, Masanobu, Superstructure of VO/sub x/ in the range x = 1.15 to 1.25, and its stability, 25:43007
SAENGER, E. L., Cytologic-biochemical radiation dosimeters in man, 25:42406
SAENKO, A. S., Heterogeneity of liver nuclear RNA of irradiated rats, 25:42280
SAFI, N., Use of a new vector in the diagnosis of melanomas, 25:42563
SAFRANY, David R., Some comments on the possibility of thermodynamically equilibrating waste organic materials with nuclear devices, 25:41955
SAGDEEV, R. Z., Diffusion of plasma in a toroidal stellarator, 25:43374
SAHA, N. K., Half-life measurements of 85.5-keV level in ^{233}Pa and 59.6-keV level in ^{237}Np, 25:43895
SAHNI, V. C., Method of constructing irreducible multiplier representations, 25:43501
SAITO, S., Inequalities for the pion--nucleon partial waves, 25:43641 (SU-1206-249)
SAITO, Tatsuya, Study of photon activation analysis, 25:41766
SAKAI, M., Lifetime measurements on E2 isomers in N = 48 nuclei, 25:43847
SAKAI, Mitsuo, Quasi-K quantum number in ^{152}Gd, 25:43939
SAKAI, Takasuke, Balloon-borne instrument for low-energy primary cosmic-ray measurements, 25:42159
Isotopic composition of low-energy helium nuclei in primary cosmic rays, 25:43173
SALIBEKOV, S. E., Synthesis and properties of molybdenum borocarbide, 25:42941
SALMAN-ZADE, R. Kh., Systems of Frauhofer wavelengths in solar spectra, 25:43074
SALVADORI, G., Demonstration of intermediates in the hydrolysis of 4-ethoxypyrylium salts, 25:41789
SALZBERG, J. B., Gamma--γ directional correlations in the decay of ^{125}Sb. II, 25:43927
SALZMANN, H., Survey of studies of laser produced plasmas at the IPP Garching, 25:43380 (IPP-4/9)
SAMOILENKO, I. I., Radioresistance of E. coli K-12, 25:42330

SAMPSON, W. B., Superconducting properties of multifilamentary V_3Ga wires, 25:43292
SAMSONOV, G. V., Electrophysical properties and chemical bond types in compounds of beryllium with boron and carbon, 25:42997
Interaction of carbon with boride coatings on high-melting metals, 25:42854
Mechanism of the phase transition in boron nitride, 25:42994
SAMUELS, G., How to make a profit on waste heat, 25:44022
SANG, James B., Medical aspect of chronic hypoxia in radiation exposed glomerulus in hamsters treated with injected ozone gas, 25:42636
SANKEY, R. R., Spin of the 937-keV level in ^{56}Co, 25:43863
SANNER, T., Effect of hydration on the decay of radiation-induced radicals and oxygen-sensitive centers in barley seeds, 25:42295
SANNER, Tore, Radiation effects on allosteric enzyme, 25:42291
SANO, Naokatsu, NMR and relaxation of ^{163}Dy in Dy metal at low temperature, 25:43498
SANO, Tadao, Report on the uranium--nitrogen system, 25:42965
SANTHOLZER, Vilem, Determination of ^{90}Sr and ^{89}Sr, 25:41754
SANTINI, R., Enzyme activity in irradiated skin, 25:42286
SANTOS, G. G. Jr., Gold provinces in the Philippines defined by activation analysis, 25:41772
SARAF, B. L., Positron annihilation in some transition and alkaline earth oxides, 25:43482
SARANTSEV, V. P., Some specific features of the cold cathode operating at low pressures, 25:43346 (JINR-P9-5753)
SARASON, Leonard, Energy decay for the neutrino equation in the exterior of a torus, 25:43510
SARD, Arthur, Book of splines, 25:44310
SARGA, Tadeusz, Vinca Nova: automatic unit for neutron spectrometer control, 25:42114
SARGENT, G. A., Observation of damage regions produced in silicon solar cells by neutron irradiation, 25:42232
SARIS, F. W., Cross sections for Ar L--shell x-ray emission in collisions, 25:43134
SASAKI, Masao S., Radiation-induced chromosome aberrations in lymphocytes: possible biological dosimeter in man, 25:42398
SASTRY, D. H., Evaluation of rate-controlling obstacles for low-temperature deformation of zirconium, 25:42852
SASTRY, E. V. R., Impurity-controlled processes in production of F centers in alkali halides, 25:43450
SASTRY, S. B. S., ESR absorption of x-irradiated $NaClO_2$ crystal, 25:43451
SATCHLER, G. R., Tables of single-particle reduced matrix elements of spherical tensors, 25:43982
SATO, Fumiko, Mode of radioprotective action of aminothiols in HeLa S_3 cells, 25:42514
SATO, Isamu, Absolute calibration of bremsstrahlung beam monitors, 25:42933
SATO, Kazuo, Study of aplastic anemia in an autopsy series with special reference to atomic bomb survivors in Hiroshima and Nagasaki, 25:42698
SATO, M., Nonlinear stabilization of ionization waves, 25:43393
SATO, Nobuyoshi, Study of photon activation analysis, 25:41765
SATTERLEE, L. D., Low dose gamma irradiation of bovine metmyoglobin, 25:42755
SAUER, Jon Robert, Compton back-scattered high-energy photon beam, 25:43737
SAVARI RAJ, G. A., Generalized mean square amplitudes of vibration for substituted ethylene: vinylidene halides and their deuterates, 25:41814
SAVCHENKO, B. I., Thermal expansion of a copper--tungsten composite, 25:42873
SAVITSKII, E. M., Ternary system molybdenum--iron--carbon, 25:42889
SAWADA, S., Cysteamine and radiation-induced single strand breaks of DNA, 25:42522
SAYEED, M. M., Intestinal enzyme activities following whole-body irradiation in hamsters, 25:42301
SAYLOR, D. P., 192-detector system for study of 3-body reactions, 25:42124
SCANLAN, R. M., In situ field ion microscope study of irradiated W. II, 25:43458
In situ field ion microscope study of irradiated W. I, 25:43457
SCARBROUGH, J. O., Effect of heat treatment and impurities on the current density of transition metal superconductors, 25:43290 (ORNL-4703)
SCARO, J. L., Effects of actinomycin D on endogenous erythropoietic recovery of irradiated mice, 25:42673
SCARPA, Giorgio, Dosimetry of a ^{210}Po α source, 25:42436
SCHAEFFER, R., Shapes of angular distributions of (^3He,t) and (p,n) transitions to 0^+ antianalog states, 25:43842
SCHALK, T. L., Study of $\pi^+p \to rho^+p$ at 1.85 to 2.09 GeV, 25:43552 (UCR-34-P-107-B-110)
SCHALL, Gerald L., Xerostomia in Sjoegren's syndrome. Evaluation by sequential salivary scintigraphy, 25:42571
SCHARMANN, A., Influence of electric fields on scintillation process in CsI(Tl), 25:43448
SCHATZ, G., Measured differential cross sections for elastic and inelastic scattering of 104-MeV α particles, 25:43832 (NP-18920)
SCHAWOHL, P., Diagnostic findings in hypoplasia of the pulmonary artery, 25:42551
SCHEID, W., Achromatic lesions induced by x-rays in chromosomes of Vicia faba, 25:42343
SCHEJBAL, C., Prospects of radioactive materials as future sources of fuel and power, 25:44217
SCHELBERG, A. D., Evidence for violation of Porter--Thomas postulate in ^{232}Th, 25:43911
SCHEPPELE, Stuart E., β-secondary deuterium isotope effects as a measure of charge localization in carbonium ion reactions, 25:41820
SCHERER, M., Simple model for an ion exosphere in an open magnetic field, 25:43222
SCHIEFELBEIN, G. F., Dissolution of unirradiated mechanically blended mixed oxide fast reactor fuel, 25:42954 (HEDL-SA-131)
SCHIFF, B., S and P states of He isoelectronic sequence up to Z = 10, 25:43115
SCHIFFER, J. P., Anomaly in angular distributions for (^3He,t) reactions, 25:43848
SCHILLER, P., Contribution to geobotanical and geochemical prospecting for gold by activation analysis, 25:41770
Determination of trace amounts of gold in natural waters by non-destructive activation analysis using preconcentration before irradiation, 25:41771
SCHILLING, K.-D., Lifetimes of excited states in 89-neutron nucleus ^{151}Sm, 25:43937
SCHLUETER, H., Impedances of warm plasmas near the lower hybrid resonance, 25:43375
SCHMEIL, Franz, Phenoxides of the triad elements, 25:41780 (SC-T-713038)
SCHMID, E. R., Separation of U(VI) by extraction chromatography, 25:41924
SCHMID, E. W., Monte Carlo Model for linear parameter variation, 25:43504 (BMBW-FBK-70-32)
SCHMIDT, B. G., New definition of singular points in general relativity, 25:43698
SCHMIDT, F. A., Preparation of high purity thorium and thorium single crystals, 25:42824
SCHMIDT, R., Modification of dissipative terms in equations of helium II, 25:43281
SCHMIDT, Winfried, Electroproduction of pions beyond the resonance region and the pion form factor, 25:43583 (DESY-71/22)
SCHMITTER, E. F., Comparative study of radio and optical photometry of several H II regions, 25:43059
SCHMUTZLER, F., Contribution of outer atomic shells to total internal conversion coefficients, 25:43931
SCHNATZ, Thomas Wilbur, Vector equations of transfer with plane and spherical symmetry, 25:43423
SCHNEIDER, Felix H., Formation of U_2C_3 by decomposition of uranium dicarbide, 25:42935 (JUL-728-RW)
SCHNEIDER, H., Separation of vanadium on UO_2 spheres from the gaseous phase, 25:42935 (EURFNR-859)
SCHNEIDER, Kenneth J., Status of the waste solidification demonstration program, 25:41905
SCHNEIDER, S. J., Phase relations in the SrO--IrO_2--Ir system in air, 25:43005
SCHNEIDER, Stephen Henry, Numerical simulation of strong plasma shock waves produced in an electromagnetic shock tube, 25:43360 (CU-3954-9)
SCHOCKEN, Klaus, Contributions to x-ray physics in space, 25:43079 (N-71-20472)
Three investigations of the interstellar medium, 25:43080 (N-71-21563)
SCHOENWALD, D., Separation of vanadium on UO_2 spheres from the gaseous phase, 25:42935 (EURFNR-859)
SCHOONOVER, Donald Roy, Absolute excitation cross sections of He^+ in 20 to 100 keV He^+--He collisions, 25:43128
SCHOTT, L., Structure of the plasma boundary layer at a conducting sphere, 25:43356
SCHREIBER, B., Distribution of radioactivity in sediment from Ligurian Sea, 25:41949
SCHREIBER, William Michael, Neutrino pair production by photons, 25:43605
SCHREIER, E., Discovery of periodic x-ray pulsations in Centaurus X-3 from Uhuru, 25:43055
SCHREMPP, F., Finite-energy sum rules and the reactions e e + e e epsilon (750), e e + e e f (1260), 25:43582 (DESY-71/20)
Unitarized finite energy sum rules and their application to πN-charge exchange, 25:43637 (DESY-71/24)
SCHREMPP-OTTO, B., Finite-energy sum rules and the reactions e e + e e epsilon (750), e e + e e f (1260), 25:43582 (DESY-71/20)
SCHROETER, J., Propositions in quantum mechanics, 25:43514
SCHUEPBACH, M., Isolation and genetic classification of uv-sensitive mutants of Schizosaccharomyces pombe, 25:42723
SCHUEPBACH, Martin, Effect of caffeine on mutation and recombination in Schizosaccharomyces pombe, 25:42332
SCHULZ, G. J., Effect of rotational excitation on dissociative electron attachement in H_2, 25:43155
SCHULZE, W., Nanosecond lifetime measurements of excited nuclear states at heavy ion cyclotron, U-300, 25:42187 (JINR-P13-5801)
SCHUMACHER, G., Considerations on PyC and SiC coated oxide particles for gas cooled fast reactor application, 25:42963

XUM

SCHUMM, R. H., Selected values of chemical thermodynamic properties, 25:41825 (NBS-TN-270-5)
SCHWARTZ, E. G., Prog. rpt. on powder metallurgy compaction, 3/71--5/71, 25:44292 (SRD-475-11)
SCHWEIMER, G. W., Hexadecapole moments of ^{20}Ne and ^{28}Si from scattering of 104-MeV α particles, 25:43876
Measured differential cross sections for elastic and inelastic scattering of 104-MeV α particles, 25:43882 (NP-18920)
SCHWEITZER, A. L. M., "DDD" computer procedure for the inventory control of a supply of deuterium, 25:41960 (EUR-4512)
SCHWEMMLE, R., Experimental investigation of loop caused influences on parallel flow-induced vibration of fuel pins, 25:44119 (EURFNR-923)
SCHWEYEN, R. J., Respiration deficient mutants of Schizosaccharomyces pombe I, 25:42338
SCHWUTTKE, G. H., Thermal spiking in high-energy bombarded silicon, 25:43455
SCIELZO, G., Dose distributions around linear ^{192}Ir sources, 25:42423
Dosimetry of high energy electron beams, 25:42167
Protective considerations in use of ^{192}Ir for radiotherapy, 25:42477
SCIESINSKA, Ewa, Accuracy of the neutron method of moisture measurement, 25:42177
SCIESINSKI, Jan, Vinca Nova: automatic unit for neutron spectrometer control, 25:42114
SCOPPA, P., Metabolism of p-nitrophenol in whole-body irradiated rats, 25:42289
SCOTT, F. R., Interaction of a helium plasma with an inhomogeneous transverse magnetic field, 25:43355
SCOTT, Melvin R., Internal values in particle transport by the method of invariant imbedding, 25:43430
SCOTT, P. E., Evaluation of IBM Project Management System/360, Version 3, 25:44259 (CTC-INF-1030)
SCOTT, V. D., Influence of silicon and other elements in controlling interparticle friction and sintering of beryllium powder, 25:42826
SCOURFIELD, M. W. J., Pulsating auroral patches exhibiting sudden intensity-dependent spatial expansion, 25:43249
SCURICINI, G. B., Sensitivity of uranium and separative work requirements to variations in reactor programs, 25:44127 (CONF-700903-17)
SEABRON, LaVert C., Results of radiation safety surveys of x-ray facilities within the Bureau of Prisons and Federal Health Programs Service, 25:42502
SEAH, M. P., Faraday cup LEED apparatus for investigating inelastically scattered or photoemitted electrons, 25:43474
SEALS, Robert Kincaid Jr., Nonequilibrium plasma boundary layer over a cathode, 25:43361 (N-71-12679)
SEAMAN, G. G., Lifetimes of ^{39}K excited states, 25:43861
SEAQUIST, E. R., Observations of extragalactic radio sources at centimeter wavelengths, 25:43062
SEARBY, P. J., Sensitivity of uranium and separative work requirements to variations in reactor programs, 25:44127 (CONF-700903-17)
SEARLE, A. G., Evidence against a cytogenetically radioresistant spermatogonial population in male mice, 25:42355
SEBALD-ALTHAUS, M., Respiration deficient mutants of Schizosaccharomyces pombe I, 25:42338
SEBRANT, Yu. V., Biological effects of external beta irradiation, 25:42545
SEDDON, W. A., Pulse radiolysis facilities at Chalk River, 25:41849 (AECL-3853)
SEDIGHI, N., Isotopic exchange between glasses and nonaqueous liquids, 25:41810
SEESE, H. J., Fine-edge blanking and piercing, 25:44229 (BDX-613-365)
SEGEL, R. E., T = 1 states in the A = 12 system, 25:43819
SEIDE, C., Excitation functions of ^{7}Be and ^{11}C produced in N by low-energy protons, 25:43818
SEIDMAN, D. N., In situ field ion microscope study of irradiated W. I, 25:43457
In situ field ion microscope study of irradiated W. II, 25:43458
SEKI, Ryoichi, Boundary conditions for an infinite square-well potential in quantum mechanics, 25:43508
SEL'DYAKOV, Yu. P., Use of an x-ray analyzer with a semiconductor detector for elemental analysis, 25:42217
SELENGUT, D. S., Adjoint spectra for calculating thermal group constants, 25:44202
SELEZNEV, V. S., High intensity (10-16) GeV/c negative particle beam, 25:43729 (CERN-Trans-71-16)
SELIVANOV, G. I., Methods of detecting particle tracks in liquid and solid media, 25:42053 (JINR-P13-5792)
SELKIRK, E. B., Pulse radiolysis facilities at Chalk River, 25:41849 (AECL-3853)
SELLSCHOP, J. P. F., Charged-particle radiation damage observed as dimpling of thin silicon targets, 25:43438
SEMASHKO, N. N., Fast hydrogen-atom injector. II, 25:43109
SEMENOV, B. Yu., Pulse pile-up monitor for a precision pulse-height spectrometer with RC filters, 25:42216
SEMENOV, V. D., Indexes of remote sequelae of radiotherapy of breast cancer, 25:42270
SEMENOVA, I. P., Courses in channels upon the small parameter of interaction, 25:43203
SEMPREBON, L. C., Observations of auroral hiss, 25:43246
SEMWAL, B. S., Vibration spectra and Debye temperatures of some transition metals, 25:43490
SEN, S., Reaction ^{36}Ar(d,p)^{37}Ar, 25:43858
SENDA, Tomio, Fundamental investigations on solidification structure in weld metal, 25:42820
SEPHTON, R. G., Differences between lesions in cerebral scanning, 25:42577
SERGIENKO, V. I., Outer-sphere interaction in $M_3UO_2F_5$ complexes, 25:41828
SERIZAWA, Masahiko, Technique for determining activity and size distribution of β emitting particles by autoradiography, 25:42051 (JAERI-13718)
SEROV, Yu. A., Increasing the energy of an electrostatic accelerator, 25:43766
SERPAN, C. Z. Jr., Analysis of radiation-induced embrittlement gradients on fracture characteristics of thick-walled pressure vessel steels, 25:42841 (CONF-710512-8)
Neutron dosimetry for reactor pressure vessel applications, 25:44117
Reliability of fluence-embrittlement projections for pressure vessel surveillance analyses, 25:44116
SERYAKOV, V. N., Oxidation-reduction potential in tissues exposed to radioprotective agents, 25:42511
SESSELMANN, I., Influence of vacancies and impurities on order--disorder transition in hexagonal ice Ih, 25:41812
SESSIONS, Meredith H., Autonomous deep-sea cine system, 25:44308 (UCSD-34-P-127-10)
SESSLER, G. M., Charging of polymer foils with monoenergetic low-energy electron beams, 25:43436
SEXTON, James H., Livermore superconducting Levitron, 25:43399 (UCRL-73076)
SHADMI, Yehuda, Average energies of ground and singly and doubly excited configurations in highly ionized atoms, 25:43069 (N-71-20535)
SHAFFER, James H., Method for separating U, Pa, and rare earth fission products from spent molten fluoride salts reactor fuels, 25:41903
SHAFFER, P. T. B., Thermal expansion of niobium carbide, hafnium carbide, and tantalum carbide at high temperatures, 25:42966
SHAFRANOV, M. D., Effect of ultraviolet radiation on plastic scintillators with p-terphenyl, 25:42231
SHAFROTH, S. M., Mass and half-life of ^{36}K, 25:43875
SHALPYKOV, A. Sh., Radiation-induced changes in the electrical properties of LiF monocrystals alloyed with Na, 25:43445
SHANTYR, V. I., Problems in experimental and clinical radiology, 25:42292
SHAPIRO, E. L., Content of ^{137}Cs in population of Soviet Union, 25:42376
SHAPIRO, Irwin I., Quasars revisited: rapid time variations observed via very-long-baseline interferometry, 25:43049
SHAPIRO, N. L., Internal-conversion electrons emitted by different elements in fission of ^{252}Cf, 25:43922
SHAPIRO, V. S., Influence of solar activity on the post-sunset peak of heights of the equatorial F region, 25:43228
SHAPKIN, V. V., Asymmetry of distribution of turbulent electric fields in direct-discharge plasma, 25:43344
SHARMA, B. K., Positron annihilation in some transition and alkaline earth oxides, 25:43482
SHARMA, D., Decay and thermoluminescence of ZrS:Zr phosphors, 25:42062
SHARMA, H. C., Analysis of ^{127}I(n,n'γ) reaction data, 25:43914
SHARMA, P. K., Vibration spectra and Debye temperatures of some transition metals, 25:43490
SHARON, T. E., Moessbauer effect study of amorphous Fe--Pd--Si alloys, 25:44238 (CALT-322-32)
SHARPEY-SCHAFER, J. F., Lifetimes and decays of energy levels in ^{30}Si and ^{30}P, 25:43879
SHEA, D. W. J., Dispersal of a localized density fluctuation in a uniform magnetoplasma, 25:43370
SHEA, K. G., Radiation for fresher food, 25:42747
SHEAFFER, Yvonne, Ablation and breakup of large meteoroids during atmospheric entry, 25:43263
SHEFFIELD, G. V., Large superconducting magnet designs for fusion reactors, 25:43397 (MATT-848)
SHEFSIEK, P. K., Heat pipe development for thermionic applications, 25:41977
SHELEST, V. P., Scaling, Pomeranchuk trajectory and J = 1 fixed poles in virtual Compton amplitude, 25:43584 (ITF-71-27-E)
SHEMANSKY, D. E., Differential electron flux as determined by auroral observations of N_2^+ and N_2^+ systems, 25:43214 (N-71-16589)
SHEN, B. C., Are there two A_2 mesons, 25:43624 (UCR-34-P-107-8-112)
Duality for inelastic anti KN scattering at intermediate energies, 25:43642 (UCR-34-P-107-8-105)
Study of $\pi^+p \to rho^+p$ at 1.85 to 2.09 GeV, 25:43552 (UCR-34-P-107-8-110)
SHEN, Pu, Triple Regge limits and duality sum rule, 25:43570 (NYO-2252-TA-247)
SHENBERG, Cesia, Analytical significance of peaks and peak ratios in x-ray fluorescence analysis using a high resolution semiconductor detector. Analysis of uranium solutions by x-ray spectrometry, 25:41733

SHEPARD, H. K., Duality for inelastic anti ν_N scattering at intermediate energies, 25:43542 (UCR-34-P-107-B-106)
SHEPARD, J. R., New 0^+ states in ^{50}Cr, 25:43849
SHEPLEY, L. C., Perturbations in anisotropic Euclidean-homogeneous cosmologies, 25:43096
SHERCLIFF, J. A., Magnetohydrodynamics at high Hartmann number, 25:43197
SHERIDAN, William, Lifetime reproductive capacity in offspring of an irradiated mouse population, 25:42342
SHERMAN, M. P., Equilibrium composition and normal shock parameters for nitrogen up through double ionization, 25:43331 (AD-715515)
SHERSTYUK, A. I., Generalized Coulomb Green function for bound states of non-relativistic Schroedinger equation, 25:43675
SHESTAKOVA, T. V., Changes in energy spectrum of capture centers (traps) in electron-bombarded CdS crystals, 25:43437
SHEVCHUK, B. A., Plasma acceleration in a pulsed coaxial accelerator, 25:43358
SHEVEL'KO, V. P., Possibility of producing inverted population in atomic beams by charge exchange of protons with atoms, 25:43103
SHIELDS, Bernard, Dose commitment, 25:42434
SHIKITA, Mikio, Mode of radioprotective action of aminothiols in HeLa S_3 cells, 25:42514
SHILIN, G. F., Electromagnet of a transportable betatron, 25:43741
SHIMIZU, Mikio, Interaction of solar wind and planetary atmospheres, 25:43272
SHIMOJIMA, Hikaru, Inorganic yields of ^{38}Cl in Szilard--Chalmers reactions of α-, β-, γ-, and delta-benzene hexachlorides, 25:41884
SHIN, Jae In, Application of optimum control to 600 MWe pressurized water reactor, 25:44106
SHIN, Y. M., Coincidence system for electrodisintegration studies, 25:42131
SHINBROT, C. H., Electrical/thermal integration of dynamic power and life-support systems for manned spacecraft, 25:42005
SHINOHARA, T., Oxidation of Am(III) with ammonium peroxydisulphate, 25:41785
SHIRLEY, David A., Table of hyperfine fields, 25:43469 (UCRL-20411)
SHOKET, J. L., Polarization of the free--free bremsstrahlung in an anisotropic hot-electron plasma, 25:43357
SHOLIN, G. V., Asymmetry of distribution of turbulent electric fields in direct-discharge plasma, 25:43344
SHORIN, K. N., Compensation of the stray field of magnetic deflectors, 25:43744
SHORSHOROV, M. Kh., Examination of welded joints of Mo alloy TZM-2A, 25:42874
SHORT, Zella F., Uptake of molybdenum, marked with ^{99}Mo, by biota of Fern Lake, Washington, 25:44287 (RLO-2225-T-7-2)
SHOTWELL, Robert L., Analyses of elastic proton-alpha scattering, 25:43781
SHOUP, Robert Lynn, Study of electromagnetic transitions in ^{55}Co nucleus, 25:43858
SHPINEL, V. S., Hyperfine magnetic field for ^{119}Sn impurity atoms in ferromagnetic terbium, 25:43494
SHUKMAN, V. A., Resistive phenomena in the intermediate state, 25:43299
SHUKLA, J. P., Radiochemical purification and continuous milking of ^{144}Pr from ^{144}Ce, 25:41883
SHULL, Fred W. Jr., Membrane association of conjugally transferred deoxyribonucleic acid in Escherichia coli minicells, 25:42735
SHULOV, O. S., Properties of FEU-79 photomultipliers used as photon counters in astronomical observations, 25:42068
SHULTS, Gary W., Process for radiation sterlizing a packaged precooked meat and gravy product, 25:42759
SHUMEIKO, N. M., Determination of the mass of the muonic neutrino in radiative pion decays, 25:43609
SHUMENKO, V. N., Production of zirconium dioxide from baddeleyite concentrate, 25:42942
SHUTTS, Richard L., Autonomous deep-sea cine system, 25:44308 (UCSD-34-P-127-10)
SHVEIKIN, G. P., Possibility of the existence of stable zirconium monoxide, 25:42987
SIDORENKO, I. S., Superconductive shielded magnetic lens, 25:43748
SIECK, R. F., Determination of uranyl and thorium(IV) by gas chromatography of volatile mixed-ligand complexes, 25:41725
SIEGEL, Armand, Distinguishable equivalent particles with symmetrized wave functions, 25:43524
SIEGEL, E. J., Kilocycle acoustic emission during creep in Pb, Al, and Cd. II, 25:42851
Kilocycle acoustic emission during creep in Pb, Al, and Cd. I, 25:42852
SIEMSSEN, R. H., ^6Li + ^6Li scattering at E = 5 to 7 MeV, 25:43815
SIEWERT, Gerhard, Preparation and ultraviolet light-induced transformation of an antifungal mixture of heptaene antibiotics of Streptomyces surinam, 25:42302
SIGEL, R., Survey of studies of laser produced plasmas at the IPP Garching, 25:43380 (IPP-4/9)
SIL, N. C., Separable approximation to two-body t-matrix, 25:43980
SILAR, J., Thermal stability and its relation to scintillation detector parameters with domestic NaI(Tl) crystals 40 x 40 mm and photomultipliers 61 PK 413 through 415 at elevated temperatures, 25:42092
SILBERSTEIN, E. B., Cytologic-biochemical radiation dosimeters in man, 25:42405
SILFVERSKIOELD, B. P., Computer processing of cerebral scintillation camera studies, 25:42090
SILINI, G., Late somatic effects in syngeneic radiation chimaeras. I, 25:42666
SILVER, G. L., Potential-pH diagram for Pu, 25:41831
SILVERSTEIN, Calvin C., Surface heat flux for incipient boiling in liquid metal heat pipes, 25:41982
SIMIC, G., Modulus of elasticity for Zircaloy-2 as function of temperature, 25:42880
SIMMONS, J. E., Reaction $D(d,n)^3He$ at 0^o with polarized beam, 25:43789
SIMMS, P. C., Beta--gamma circular-polarization correlation and nuclear matrix elements of ^{76}As, 25:43864
SIMON, J., Application of the sterile-insect-release technique in Mediterranean fruit fly suppression, 25:42750
SIMON, Y., dc transport properties in Type-II superconductor, 25:43323
SIMONOV, B. L., Determination of the optimal canal of registration of gamma-radiation in radioisotope diagnosis, 25:42397
SIMON-VERMOT, A., Effects of pulmonary lavage on the retention of particles of plutonium oxide, 25:42368 (LF-tr-53)
SIMS, T. M., HFIR core nuclear design, 25:44159 (ORNL-4621)
SINGH, Amar, Decay and thermoluminescence of ZrS:Zr phosphors, 25:42062
SINGH, R. P., Shell-model calculations for ^{51}V and ^{52}Cr, 25:43862
SINGH, Sujan, ESR study of intramolecular energy transfer in the radiolysis of cellulose thenoates, 25:41836
SINGH, Udai, Radiation-induced hooded eye mutants in potato, 25:42323
SINGHAL, N. C., Radiation hazards and protection in dental radiography, 25:42484
SINGHAL, Ravi Prakash, Elastic scattering of electrons from the oxygen isotopes, 25:43807
SINGLETARY, V. A., Preparation of data sets in ENDF format for Na, Mg, Cl, and K for use in shielding calculations, 25:43420 (ORNL-TM-3429)
SINHA, Ashok K., Electrical resistivity and magnetic susceptibilities of amorphous Cr--Ni--Pt--P alloys, 25:44237 (CALT-822-31)
SINHA, B. C., Evidence for a real Saxon Woods derivative term in the proton optical potential, 25:43967
SINHA, S. K., Generalized susceptibility function for rare earths and thorium and their alloys, 25:43477
SINITSYNA, A. P., Measurements in beams of fast electrons, 25:42411
SISAK, St., Radiation measurements in Brasov during period 8/61--8/68, 25:42424
SISHODIA, Y. S., Positron annihilation in some transition and alkaline earth oxides, 25:43482
SISSON, David H., Corrected fluorescence spectra by computer postprocessing, 25:44306 (UCRL-73161)
SITES, James R., ^{54}Mn in Fe for ultralow-temperature thermometry, 25:43329
SIZONENKO, V. L., Nonlinear stage of hydromagnetic current instability of plasma in a strong electrical field, 25:43386 (ORNL-tr-2434)
SIZOVA, L. N., Dielectric properties of γ-irradiated crystals of KH_2PO_4, 25:43443
SKALKA, M., Some aspects on the degradation of macromolecules in lymphoid and haemopoietic tissues of irradiated animals, 25:42624
SKAREDOFF, L., Immediate and delayed effects of 1000 R x-rays on the rodent testis, 25:42659
SKARIC, V., Effect of alginates from algae on Sr transport through rat's duodenum, 25:42254
SKAVRONSKAYA, A. G., 5-BU sensitization to uv-induced killing and mutability in hcr^+ and hcr^- strains of Escherichia coli, 25:42345
SKEEN, David Roy, Numerical solutions of the neutron transport equation, 25:43773
SKJELTORP, Arne T., Radio frequency measurements of interactions in magnetic insulators, 25:43472 (YALE-3227-74)
SKOBELKIN, V. I., Propagation of the phase surface in superconducting thin films, 25:43313
SKOPIK, D. M., Coincidence system for electrodisintegration studies, 25:42131
SKOROMNYI, G. M., Superconductive shielded magnetic lens, 25:43748
SKORYUPIN, V. A., Asymmetry of distribution of turbulent electric fields in direct-discharge plasma, 25:43344
SKOU, J. P., Effects of ionizing radiation for extending storage life of onions, 25:42745 (RISO-238)
SKOVLI, Gunnar, Polar ionosphere and magnetospheric processes, 25:43226
SKRINSKII, A. N., Dynamics of particle polarization near spin resonances, 25:43770

SKRIPKO, N. S., Properties of FEU-79 photomultipliers used as photon counters in astronomical observations, 25:42058
SLATER, J. E., Prog. rpt. on mechanisms of stress corrosion cracking in iron--nickel--chromium alloy system in chloride environments, 4--6/70, 25:42750 (COO-2069-7)
SLATTERY, William J., Index of U. S. voluntary engineering standards, 25:41961 (NBS-SPEC. PUBL-329)
SLIFER, B. C., Loss-of-coolant accident and emergency core cooling models for BWR, 25:44140 (NEDO-10329(Suppl.1))
SLINKMAN, Roger, Television contribution to genetically significant radiation dose of population, 25:42366
SLIVKA, William R., Unique production problems encountered in development of NERVA space engine, 25:44174
SLOAN, I. H., Phase parameters for nucleon--deuteron scattering, 25:43799
SLOAN, M. L., Finite-B stabilization of the collisionless trapped-particle instability, 25:43368
SMID, R. J., Gas release from thoria-base oxide fuel pellets. (LWBR development program), 25:42958 (WAPD-TM-850)
SMIRNOV, B. M., Atomic collisions and elementary processes in plasma, 25:43349
SMITH, A. J., Comparison tests for extinguishing media on metal fires, 25:42837 (AERE-R-5745)
SMITH, A. R., Monitoring of positively charged particles in the electron ring accelerator, 25:43734 (UCRL-20664)
SMITH, A. R. B., Reduction of dosage in x rays of the pelvis, 25:42447
SMITH, C. B., San Onofre Nuclear Generating Station vibration tests, 25:44079 (UCLA-ENG-7037)
SMITH, Craig B., Strategies for a national nuclear energy program, 25:44145
SMITH, D. R., Electron spin resonance studies of radiolysis of aliphatic amines at 77°K, 25:41857
  Electron spin resonance studies of the radiolysis of aliphatic amines adsorbed on silica gel, 25:41856
SMITH, H., Urinary excretion of β-aminoisobutyric acid after exposure to radiation, 25:42684
SMITH, H. A., ^{54}Mn in Fe for ultralow-temperature thermometry, 25:43329
  Beta--gamma circular-polarization correlation and nuclear matrix elements of ^{76}As, 25:43864
SMITH, H. J. T., Superconducting proximity effects by Josephson tunneling, 25:43308
SMITH, J. R., ^{7}Li(p,n)^{7}Be neutron polarization measurements for E/sub p/ = 3.0 to 5.5 MeV, 25:43805
SMITH, Jerry C., Determination of average cycle time for an automated warehouse, 25:44224 (BDX-613-274)
SMITH, Kendric C., Repair of x-radioinduced DNA strand breaks in vivo, 25:42326
SMITH, L. G., Investigation of the D and E regions of the ionosphere, 25:43215 (N-71-17052)
SMITH, M. W., Systematic trends of atomic oscillator strengths along isoelectronic sequences, 25:43114
SMITH, Phil N., High-energy neutron scattering from liquid helium in the impulse approximation, 25:43278
SMITH, Roger L., Performance of ceramic insulator seals at high neutron and gamma fluence levels, 25:42228 (N-71-17325)
SMITH, Zdenka K., Mathematical model of the Arc Pioneer 6/7 plasma probe, 25:42209
SMITHERMAN, Thomas C., Radiation-induced hydrogen transfer in nucleic acids, proteins, and related substances: effects of temperature and scavengers, 25:41837
SMOLDERS, A., Importance of stearates in the fabrication of UO_2 and (U,Pu)O_2 pellets, 25:42949
SNYDER, Richard E., Decay scheme of /sup 121m/Sn and Moessbauer effect in ^{121}Sb, 25:43905
SNYDER, S. D., X-ray attenuation scanning of nuclear fuel plates, 25:42031
SOBELS, F. H., Induction by x-rays of double mosaics involving Y-chromosome, 25:42344
SOBER, Arthur J., Local recurrence of generalized herpes zoster following x irradiation, 25:42689
SOBICZEWSKI, A., Closed shells for very heavy nuclei, 25:43936
  Closed shells for very heavy nuclei, 25:43955 (INR-1270)
SOBOLEV, A. S., System yttrium--chromium--silicon, 25:42993
SOEDERBORG, B., Computer processing of cerebral scintillation camera studies, 25:42090
SOERBO, B., Excretion of deoxyribosyl compounds in urine from rats and mice after irradiation, 25:42622
SOERENSEN, Poul, Field determination of uranium and thorium by gamma-ray spectrometry, exemplified by measurements in the Ilimaussaq alkaline intrusion, south Greenland, 25:41943
SOEVENYI, Erwin, Effect of whole-body x-radiation on the lipolytic activity of rat heart extracts, 25:42281
SOGRISHIN, Yu. P., Influence of deformation rate on deformability of Mo--0.5 percent Ti alloy, 25:42833
SOICHER, H., Studies of wavelike variations in the ionosphere, 25:43209 (AD-714993)
SOKOLOV, V. I., Superconducting alloy, 25:43318
SOKOLOVSKII, L. L., Gamma-ray spectrum from reaction (n,γ) on ^{150}Sm and ^{151}Sm samples, 25:43892
SOLENTE, P., Cooling of superconducting magnets, principles and uses, 25:43325 (CONF-700341-6)
SOLL, Helen Jean Newman, T4 DNA replication and repair, 25:42297
SOLNYSHKOV, A. I., Ion-beam apparatus, 25:43747
SOLOMON, P. M., Origin of reported millimeter continuum in IRC + 10216, 25:43040
SOLOV'EV, S. P., Radiation physics of ferroelectrics of barium titanate type, 25:43442
SOMBERG, H., Prog. rpt. on development of lithium-diffused radiation-resistant solar cells, 10/70, 25:42227 (N-71-12257)
SOMOGYI, G., Alpha radiography with plastic track detectors, 25:42093
SONCK, W., Electromyographic examination of striated muscle in guinea pig after ^{60}Co irradiation, 25:42652
SONE, K., High-energy humps in spectra of backscattered protons from Si, 25:43459
SONEZAKI, Shozo, Therapeutic effect of glutathione on impaired leucopoiesis of irradiated bone marrow, 25:42536
SONI, R. N., Composition and stability of complex between uranyl ions and 2,4-dihydroxybenzoic acid in aqueous medium, 25:41830
SONNEN, C., Corrosion of Zr alloys in heavy water under pressure and in superheated steam, 25:42815
SORANTIN, H., Activation analytical studies of standardized Fe alloys. I, 25:41774
SOSNOVSKAYA, F. M., Bioelectric potentials of the brain in persons subjected to single whole-body and local irradiation, 25:42677
SOUTHALL, Hugh L., Coupled electromagnetic and electron acoustic wave propagation in inhomogeneous lossy plasma layer, 25:43404 (AD-715910)
SPADONI, M. A., Problems of the radiocontamination of man, 25:42375
SPALDING, D., Reaction ^{142}Nd(d,t)^{141}Nd, 25:43900
SPARKS, R. J., Coincidence studies of ^{52}Cr(p,γ)^{53}Mn reaction, 25:43837
SPASIC, Z., Modulus of elasticity for Zircaloy-2 as function of temperature, 25:42880
SPECHT, J., Hexadecapole moments of ^{20}Ne and ^{28}Si from scattering of 104-MeV α particles, 25:43876
  Measured differential cross sections for elastic and inelastic scattering of 104-MeV α particles, 25:43832 (NP-18920)
SPEIRS, K. K., Composite materials, 25:42951
SPENCE, D., Effect of rotational excitation on dissociative electron attachement in H_2, 25:43155
SPENCER, L. V., Energy deposition in cavities, 25:42166
SPENCER, Neal R., Sterilization of insect diet by gamma irradiation, 25:42749
SPENCER, Winthrop W., Strict compliance to product quality standards, 25:42032
SPIEL, Donald E., Superconducting thin-film detector of nuclear particles, 25:42090
SPIRIDON, M., Sensitization of living organisms by chemical agents towards the activity of radiations and cytostatics. I, 25:42535
SPITKOVSKII, D. M., Radiobiophysics of the nucleoproteins, 25:42274
SPITSYN, V. I., Physicochemical conditions for burial of radioactive waste, 25:41925 (CEA-tr-R-1979)
SPREAFICO, G. L., Radioisotope investigation of lymph system function and morphology, 25:42581
SPRETNAK, J. W., Influence of irradiation temperature on the tensile properties of stainless steel, 25:42912
SPROTT, J. C., Electron cyclotron heating in toroidal octupoles, 25:43334
SPURNY, Z., Personal monitoring of workers during the translocation of a ^{90}Sr--^{90}Y beta source by aid of TLD, 25:42444
SRAMEK, R. A., Measurement of gravitational deflection of microwave radiation near the Sun, October 1970, 25:43094
SREENIVASAN, A., Food preservation by irradiation, 25:42757
SRINIVASAN, T. M., Impurity-controlled processes in production of F centers in alkali halides, 25:43450
SRIVASTAVA, B. K., Effect of tensor forces on charge form factor of α-particle, 25:43783
SRIVASTAVA, D. S., Alpha radiography with plastic track detectors, 25:42093
SRIVASTAVA, Pratap Narain, Histopathological action of serotonin on certain tissues in mice, 25:42519
STACEY, Virginia, Isotope shifts and hyperfine structure in the atomic spectrum of platinum, 25:41819
STACY, Denzil Wayne, X-ray diffraction study of the yttria--hafnia system, 25:42883 (IS-T-425)
STAEHLE, R. W., Prog. rpt. on mechanisms of stress corrosion cracking in iron--nickel--chromium alloy system in chloride environments, 4--5/70, 25:42760 (COO-2069-7)
STAFFORD, Fred E., Limitations in applying mass spectrometry to high-temperature equilibrium studies, 25:44242 (COO-1147-35)
STAIF, M., Oxidation of Zr--0.8 percent Cu--0.8 percent Mo alloy in carbon dioxide, 25:42809
  Properties of Zr--Cu--Mo alloys, 25:42878
STAMM, H., Clinical and experimental tests using irradiation, 25:42597
  Thrombelastography of antifibrinolytica before and after irradiation with gamma rays, 25:42293
STAMPA, A., Investigation of an inductive plasma accelerator for propulsion purposes, 25:43351
STANTON, H. E., g/sub J/ value for the atomic ground state

of fermium, 25:43118
STANTON, Leonard, Basic medical radiation physics, 25:42555
STAPP, Henry P., Inclusive cross sections are discontinuities, 25:43574
STARACE, A. F., Raising of discrete levels into the far continuum, 25:43112
STARR, Chauncey, Strategies for a national nuclear energy program, 25:44145
STARUSZKIEWICZ, A., Consistent relativistic mechanics of point particles, 25:43573
STARY, F., Lifetimes of excited states in 89-neutron nucleus ^{151}Sm, 25:43937
Nanosecond lifetime measurements of excited nuclear states at heavy ion cyclotron, U-300, 25:42187 (JINR-P13-5801)
STAS, K. N., Use of photographic films for individual radiometry of the daughter products of radon, 25:42171
STAUFFER, H. M., Beryllium window tubes for mammographic examinations, 25:42545
STAUTBERG, M. M., Anomaly in angular distributions for (^{3}He,t) reactions, 25:43848
STECHER, Theodore P., Gum nebula, 25:43034
STECKEL, R. J., Determination of in vivo persistence of tantalum dust following bronchography using reactor-activated tantalum and total body counting, 25:42558
STEEGER, E. J., ISOTEC thermoelectric generator for space power, 25:42005
STEELE, L. E., Structure and composition effects on irradiation sensitivity of pressure vessel steels, 25:42910
STEELE, R. M., Room temperature measurements of electrical resistivity and thermal conductivity of various graphites, 25:44283 (ORNL-TM-3477)
STEELE, Wayne J., LRL computer program: microanalysis, 25:44305 (UCRL-73104)
STEFAN, Maria, Activity of pyrophosphatase and catalase after long irradiation with small doses of ^{60}Co, 25:42277
Modifications of the synthesis of the hepatic catalase in mice exposed to the effect of ionizing radiation, 25:42278
STEFANKO, J. S., Determination of shielding requirements for NPTR fuel handling system, 25:44161 (WANL-TME-1895)
STEFANOVIC, J., Serum lysozyme, trypsin inhibitors, and leucocytes number level after x-ray irradiation of rabbits, 25:42549
STEFANOVIC, V. M., Correlation between the mechanical properties and microstructure of irradiated iron and low-carbon steel, 25:42925
STEINFEST, H., New Monte Carlo technique for radiation transport problems; calculation of combined spatial, angular, and energy distributions of multiply scattered gamma rays, 25:43413 (BMBW-FBK-71-2)
STEINLE, P., Quantum electrodynamical theory of atoms interacting with high-intensity radiation fields, 25:43170
Resonant interaction between two neutral atoms, 25:43169
STEMPLE, Ruth M., /sup 99m/Tc and gallium in medicine, 25:42550 (ORNL-TM-2091(Suppl.2))
STENBERG, Allan, Reduction of background in NaI(Tl) scintillation spectrometer by use of Geiger anticoincidence and massive shielding, 25:42109 (UUIP-737)
STENBERG, B., Radiotherapy of intracerebral astrocytomas, 25:42701
STEPANEK, J., Subcutaneous induration following telecobalt therapy, 25:42587
STEPANOV, A. M., Some aspects of the construction of the 2-m liquid-hydrogen bubble chamber, 25:42145
STEPANOV, K. N., Nonlinear stage of hydromagnetic current instability of plasma in a strong electrical field, 25:43386 (ORNL-tr-2434)
STEPANYAN, E. D., Effect of direct current and x radiation on bone marrow cells, reticuloendothelial cells, and radiosensitivity of rats, 25:42530
STEPHAN, Craig Hamman, Thermomagnetic effects in normal and superconducting indium and niobium, 25:43289 (NYO-2150-71)
STEPHAS, Paul, Internal ionization of the K shell, 25:43975
STEPHENSON, R. L., Comparative creep-rupture properties of tungsten--25 percent rhenium consolidated by arc-melting and powder-metallurgy techniques, 25:42866
STERLIGOV, A. G., Mean free path of the π^0 meson in nuclear matter, 25:43595
STESHENKO, A. I., Saturation for interaction with a hard core, 25:43787
STEVEN, L. W., Differences between lesions in cerebral scanning, 25:42577
Optimum measurement of ^{75}Se for pancreas scanning, 25:42578
STEVENS, R., Temperature dependence of fracture effects in self-bonded SiC, 25:42950
STEWART, A., Prenatal radiation exposure and childhood cancer, 25:42595
STEWART, R. B., Organic reactor coolant analysis: Canadian practice, 1970, 25:41713 (AECL-3672)
STEYERT, W. A., ^{54}Mn in Fe for ultralow-temperature thermometry, 25:43329
STIEGLER, J. O., Effect of fast neutron irradiation on the creep rupture properties of Type 304 stainless steel, 25:42922
STIEGLITZ, Richard Gwydir, keV neutron capture and transmission measurements on ^{50}Cr, ^{52}Cr, ^{53}Cr, ^{54}Cr, ^{60}Ni, and V, 25:43857
STIGALL, G. E., Iodine-131 discharges from an operating boiling water reactor nuclear power station, 25:42388
STIRLING, D. A., Pulse- and x-radiolysis of 2-mercaptoethanol in aqueous solution, 25:42294
STOERMER, Olaf, Shear in a perturbed Friedmann universe, 25:43088
STOFEL, Edwin J., Prog. rpt. on low-energy proton damage to silicon/solar cells, 1/69--1/70, 25:42226 (AD-715261)
STOICHEVA, T. A., Some regularities of forming gamma radiation dose fields in shielding structures and shelters, 25:43428
STOJANOV, Milan, Tritium content in urine of neutron generator operators, 25:42390
STOLETOVA, I. M., Effect of ultraviolet radiation on plastic scintillators with p-terphenyl, 25:42231
STOLTZFUS, J. C., Isospin nonconservation in reaction ^{12}C(d,α_2)^{10}B(1.74,T = 1), 25:43811
STONE, E. J., Excitation of the O I(^{3}S) and N I(^{4}P) resonance states by electron impact on O and N, 25:43143
STONE, R. G., U-type solar radio burst originating in the outer corona, 25:43070 (N-71-21564)
STRANKS, D. R., Effect of pressure on the kinetics of the exchange of ^{18}O between hexaaquochromium(III) ion and solvent water. Evidence for an associative interchange mechanism, 25:41797
STRATTON, Lewis P., Membrane association of conjugally transferred deoxyribonucleic acid in Escherichia coli minicells, 25:42735
STREFFER, C., Biochemical post-irradiation changes and radiation indicators, 25:42401
STRELOW, F. W. E., Distribution coefficients and cation exchange behavior of elements in hydrochloric acid--acetone, 25:41899
STRENGE, D. L., RACER: a computer program for calculating potential external dose from airborne fission products following postulated reactor accidents, 25:42393 (BNWL-B-69)
STRINGER, J., Oxidation of tantalum--niobium, 25:42806
STRINGER, Thomas Arthur, Single- and double-pion production in proton--antiproton non-annihilations at 2.2 GeV/c, 25:43537
STROGONOV, Yu. D., Nitrogen diffusion in zirconium, 25:42967
STROM, Stephen E., Abundance analysis of stars in spectral range B5 through G2, 25:43018 (N-71-19301)
STRUETER, Horst-Dieter, Film dosimetry of high-energy rays. IV, 25:42396
STUDENA, Olga, Tritium content in urine of neutron generator operators, 25:42390
STUMPF, W. E., Room temperature mechanical properties and precipitation behavior of steel Incoloy and Inconel after annealing in contact with UC, 25:42844 (EURFNR-922)
STUTZ, E., Life span and tumor incidence in rats subjected to severe stress before whole body x-irradiation, 25:42669
STYRIS, D. L., In situ field ion microscope study of irradiated W. I, 25:43457
In situ field ion microscope study of irradiated W. II, 25:43458
SU, Ching-shen, Range of fission fragments in air determined by fission-track detector, 25:43427
SUCHKOV, A. A., Spiral structure of galaxies, 25:43081
SUDAKOVA, V. D., Effect of petroleum growth substance on the healing of radiation wounds of the skin, 25:42539
SUDAN, R. N., Theory of triggered vlf emissions, 25:43245
SUENAGA, M., Superconducting properties of multifilamentary V_3Ga wires, 25:43292
SUGAHARA, Tsutomu, Conference on biological aspects of radiation protection, Kyoto, 10/69, 25:42512
SUGAR, J., Raising of discrete levels into the far continuum, 25:43112
SUGATA, Eizi, Displacement energy of W atoms by irradiating FIM specimen, 25:43449
SUGAWARA, T., Kondo effect in single crystals of dilute Y--Ce alloys, 25:43479
SUGIYAMA, Suguru, Average energies of back scattered x-rays from Pb, Cu, and Duralumin, 25:43431
Beam transport system of ETL Linac, 25:43764
Construction and performance of a current spark chamber, 25:42151
Mean mass stopping power ratios for γ- and x-rays for use with cavity ionization chamber, 25:42085
SUITA, Tokuo, Effect of plastic deformation on crystal current density in Pb--In crystal, 25:43300
SULC, J., Corrosion of Zr alloys in water, 25:42807
SULC, V., Experimental investigation of temperature fields in an annular sodium channel with excentrically mounted inner heating element (e = 0/1), 25:41984 (INIS-mf-26)
SULLIVAN III, W. T., Observations of 1.35-centimeter H_2O emission in southern hemisphere, 25:43051
SUMARUKOV, G. V., Oxidation equilibrium and radiosensitivity of organisms, 25:42528
SUMBAEV, A. P., Some specific features of the cold cathode operating at low pressures, 25:43346 (JINR-P9-5753)

XUM

SUMM, B. D., Spreading of zirconium between parallel graphite plates, 25:42832
SUNAYASHIKI, Tadashi, Characteristics of linear accelerator at Hiroshima University, 25:43754
SUNDARAM, K., Low dose effects of x-rays on electrophoretic mobility of human erythrocytes, 25:42682
SUNDQVIST, B., Total absorption of 100 MeV protons with a Ge(Li) detector, 25:42128
SUOMELA, M., Elimination rate and radiation exposure following ingestion of ^{222}Rn rich water, 25:42247 (SFL-A-16)
SUSANNA, A., Dose-evaluation in carriage of γ-emitting materials in ships, 25:42043
Transport of radioactive materials on railroad car ferries, 25:42042
SUZUKI, Ikuo, Electron spin resonance of γ-irradiated triglycine selenate, 25:41854
SUZUKI, K., Embrittlement of pressure vessel steels irradiated in JPDR, 25:42905
SUZUKI, Nobuo, Effect of solvents on the adduct formation of uranyl thenoyltrifluoroacetonate with tributyl phosphate, 25:41784
SVAHN-TAPPER, Gudrun, Mantle treatment of Hodgkin's disease with ^{60}Co, 25:42594
SWADDLE, T. W., Effect of pressure on the kinetics of the exchange of ^{18}O between hexaaquochromium(III) ion and solvent water. Evidence for an associative interchange mechanism, 25:41797
SWALLOW, A. J., Pulse- and x-radiolysis of 2-mercaptoethanol in aqueous solution, 25:42294
SWANSON, J. L., Improved zirconium decontamination in Purex process, 25:41883 (BNWL-1573)
SWEENEY, M. A., Spectroscopic binaries with circular orbits, 25:43047
SWEENEY, Ronald E., Asymmetric ring current at twilight local time, 25:43241
SWIDER, W., Electron loss during a nighttime PCA event, 25:43269
SWINSON, Derek B., Solar modulation origin of sidereal cosmic-ray anisotropies, 25:43177
SZABO, A., Studies on environmental radioactivity at Cluj Branch of Inst. of Atomic Physics during 1964 to 1968, 25:41928
SZABO, Imre, Radio-mercury diagnosis of the tumor, 25:42575
SZABO, L. D., Some problems on the evaluation of biochemical indicators of radiation injury, 25:42407
SZABO, Rezso, Effect of whole-body x-radiation on the lipolytic activity of rat heart extracts, 25:42281
SZELESS, Andreas, Maximum likelihood and other methods for the analysis of reactor noise, 25:44199
SZIRMAI, E., Clinical and experimental tests using irradiation, 25:42597
Thrombelastography of antifibrinolytics before and after irradiation with gamma rays, 25:42293
SZIRTES, L., Use of zirconium tellurate in ion exchange separation technique, 25:41915
SZOEGHY, I. M., Study of ^{61}Cu nucleus by $^{58}Ni(\alpha,p\gamma)^{61}Cu$ reaction, 25:43839
SZUSZCZEWICZ, Edward P., Ion-current response of Langmuir probes in presence of ion--atom collisions, 25:43340 (N-71-17594)
SZYMANSKI, Z., Closed shells for very heavy nuclei, 25:43936
Closed shells for very heavy nuclei, 25:43955 (INR-1270)

T

TABOR, W. H., Prog. rpt. on Oak Ridge Research Reactor, 1--3/71, 25:44150 (ORNL-TM-3481)
TACHIMORI, Shoichi, Inorganic ion exchanger, 25:41879 (JAERI-13725)
TACKER, R. Stephen, Open-field behavior and heart rate in prenatally x-irradiated rats, 25:42640
TAGAWA, Hiroaki, Review of phase relations and structures of NaCl type compounds in the system U--Pu--C--N, 25:42982 (JAERI-13650)
TAIT, R. D., Allotropes of carbon (amorphous, graphite, diamond) as engineering materials, 25:42977
TAKAHASHI, Satoko, Determination of radioactive impurities in ^{45}Ca sample produced by (n,γ) reaction, 25:41878 (JAERI-13579)
TAKEKOSHI, Tadasu, Safety and reliability in nuclear power stations, 25:44144
TAKENAKA, Eiichi, Five cases suspected of radiation myelitis, 25:42700
TAKESHITA, Kenji, Characteristics of linear accelerator at Hiroshima University, 25:43754
TAKETA, S. Tom, Relationship between metabolism and radiosensitivity, 25:42535
TAKETATSU, Tomitsugu, Spectrophotometric study and analytical application of rare-earth tiron complexes. II, 25:41730
TAKIGAWA, N., Structure of ^{12}C, 25:43827
TAMAI, Eiji, Balloon-borne instrument for low-energy primary cosmic-ray measurements, 25:42159
Isotopic composition of low-energy helium nuclei in primary cosmic rays, 25:43173
TAMAKI, Shozo, Displacement energy of W atoms by irradiating FIM specimen, 25:43449
TAMAOKI, Bun-ichi, Steroid 7α-hydroxylase of rat testes, 25:42621
TAMBERG, T., Dissociation and critical concentration of peroxides (H_2O_2 + UO_4) in fuel solutions, 25:44166
TAMBLING, Thomas N., Performance of ceramic insulator seals at high neutron and gamma fluence levels, 25:42228 (N-71-17325)
TAN, Chung-I, Triple Regge limits and duality sum rule, 25:43570 (NYO-2262-TA-247)
TAN, H.-T., NMR experiment to observe spin waves in solutions of ^3He in ^4He and in pure ^3He, 25:43280
TANAKA, Kichizo, Full energy peak efficiency of NaI crystal, 25:42050 (JAERI-13546)
TANANBAUM, H., Discovery of periodic x-ray pulsations in Centaurus X-3 from Uhuru, 25:43055
TANASE, Ioana, Biochemical disequilibria induced in brain of rat by irradiation and protective effect of cysteine. I, 25:42619
Effect of ionizing radiations on complex lipids of brain and protective effect of cysteine. II, 25:42620
TANASIJEVIC, D., Toxicity and analgesic activity by gamma rays, 25:42752
TANG, Y. C., Study of p + ^3He and n + ^3H systems with the resonating-group method, 25:43797
TANIDA, Hiroaki, Feedback-type detection system for pulsed radiation measurement, 25:42087
TANIDA, Hiroshi, Secondary β-deuterium effects on the rates of solvolyses of benzonorbornen-2(exo)- and -2(endo)-yl p-bromobenzenesulfonates, 25:41801
TAPPHORN, R. M., Lifetimes of ^{39}K excited states, 25:43861
TAPPHORN, Ralph M., Lifetime measurements of excited states in ^{39}K, 25:43856
TARASOV, A. V., Double charge exchange on light nuclei, 25:43962
TARATUKHIN, V. R., Effect of petroleum growth substance on the healing of radiation wounds of the skin, 25:42539
TARENKOV, V. Yu., Tunneling conductance anomaly and switching effect for normal MIM structures, 25:42219
TASSI PELATI, L., Distribution of radioactivity in sediment from Ligurian Sea, 25:41949
TASSO, H., Mercier's criterion for class of MHD equilibria, 25:43206
TASSOUL, Jean-Louis, Nonlinear pulsations and stability of rapidly rotating columns, 25:43022
TATAEV, O. A., Study of complex formation between zirconium and certain organic reagents, 25:41737
TAWARA, Hiroyuki, Electron stripping of ground- and metastable-state He atoms in He, Ne, and Ar, 25:43153
TAYLOR, A. M., Organic Rankine cycle for manned space applications, 25:42003
TAYLOR, Clyde E., Livermore superconducting Levitron, 25:43399 (UCRL-73076)
TAYLOR, G. R., Measurement of cesium sorption isotherms in liquid sodium, 25:42863
TAYLOR, Lauriston S., Radiation protection standards, 25:42452
Radiation protection trends in the United States, 25:42487
TAYLOR, Lawnie, Prog. rpt. on solar-wind mass spectrograph, final, 8/12/69--8/12/70, 25:43221 (N-71-21469)
TAYLOR, Paul J., Effect of an electric field on gas chromatographic retentions by liquid crystals, 25:44245 (COO-1222-47)
TAYLOR, R., Trapping of methyl iodide at high pressure and high temperature, 25:41898 (TRG-Report-2135)
TAZIMA, Yataro, Problems of protection against the genetic effect of radiation, 25:42325
TEAS, H. J., Comparative radiomimetic effect of emulsin, cycasin, methylazoxymethanol, and x rays in Zamia integrifolia, 25:42334
TEBES, J., Coherent production of high mass meson states in π^+d collisions at 13 GeV/c, 25:43550 (COO-1428-290)
R region in 13 GeV/c π^+ nucleon interactions, 25:43545 (COO-1428-277)
TECH, Jack L., High-dispersion spectral analysis of Be II star HD 204075, 25:43019 (NBS-MON-119)
TEGHTSOONIAN, A., Plastic deformation of zirconium single crystals, 25:42856
TELBISZ, Ferenc, Determination of spin parity by means of multipole moments, 25:43581
TEMMER, G. M., Intermediate structure near an isobaric analog resonance, 25:43851
TENNERY, V. J., Sintering of UN as a function of temperature and N_2 pressure, 25:42979
TEOULE, R., Gamma irradiation of thymine in deaerated aqueous solution, 25:41874
TERAMOTO, M., High-energy humps in spectra of backscattered protons from Si, 25:43459
TERENT'EV, M. V., Reaction of production of two slow pions in ee and ep collisions, 25:43596
TERMAN, A. B., Radiation safety in design and operation of powerful β-installations, 25:42016
TERRELL, Robert Edward, Baryon exchange processes in three and four prong events from positive pions incident on deuterium at moments of 1.83, 2.01, 2.14, and 2.33 GeV/c, 25:43556
TERSHAK, D. R., Stabilization of poliovirus to ^{32}P decay, 25:42741
TETELMAN, A. S., Radiation effects on the metallurgical fracture parameters and fracture toughness of pressure vessel steels, 25:42905
TEW, R. H., In vitro detection of cytotoxic cellular

immunity against tumor-specific antigens by a radioisotopic technique, 25:42309
THADDEUS, P., Discovery of interstellar silicon monoxide, 25:43052
THAKUR, R. K., Deviation from a Maxwellian velocity distribution in low-density plasmas, 25:43023
THEISS, Erika, Experimental studies on tooth eruption, 25:42639
THEVENOT, F., New method for preparing metal borides, 25:42944
THEYSE, F. H., Ultracentrifuge separation of heavy isotopes, 25:41994
THIERFELDER, Charles, Television contribution to genetically significant radiation dose of population, 25:42365
THOMAS, E., Diagnostic findings in hypoplasia of the pulmonary artery, 25:42551
THOMAS, J. T., Guidance in nuclear criticality safety, 25:44189 (Y-DR-53)
THOMAS, K. C., Neutron fluence limit determinations for some FFTF components, 25:44157
THOMAS, R. M., Weak x-ray sources in the southern hemisphere, 25:43057
THOMAS, Ralph H., What quality factor, 25:42443
THOMAS, Ronald L., Computer studies of 2- to 10-kW Brayton cycle space power system, 25:42009
THOMI, P. A., Integral transport equation in one-dimensional cylindrical geometry. II, 25:43771 (EIR-189)
THOMPSON, C. J., Computer techniques in neutron activation analysis, 25:41759
THOMPSON, D. R., Study of p + ^{3}He and n + ^{3}H systems with the resonating-group method, 25:43797
THOMPSON, E., Production of high current, high quality beams of ions, and neutral particles, 25:43401
THOMPSON, W. I., Gas-cooled fast breeder reactor fuel rod design considerations, 25:44131
THOMPSON, William J., Optical model analysis of ^{9}Be(p,p$_0$)^{9}Be cross sections, 25:43804
THOMSON, R. G., Determination of sulfate in nitric acid--sulfuric acid mixtures, 25:41716 (AECL-3676)
THONTADARYA, S. R., Comparison of mass absorption coefficients of positive and negative beta particles in aluminum and tin, 25:43433
THOREL, P., dc transport properties in Type-II superconductor, 25:43323
THORNE, R. M., Relativistic electron precipitation during magnetic storm main phase, 25:43243
Unified theory of SAR arc formation at the plasmapause, 25:43242
THORNE, Richard M., Turbulent loss of ring current protons, 25:43210 (AD-715250)
THORNTON, S. T., ^{7}Li(p,n)^{7}Be neutron polarization measurements for E/sub p/ = 3.0 to 5.5 MeV, 25:43805
THORP, J. W., Monkey performance after partial body irradiation, 25:42542
THUEMMLER, Fritz, Sintering Fe--Mo and Fe--Cr, 25:42818
TIFFT, Linda E., Hβ photometry of A-type stars near the North Galactic Pole, 25:43043
TILBERG, Anna, Action of ionizing radiation on sensitive strains of Escherichia coli B, 25:42728 (NYO-2804-39)
TILLEY, D. R., Perpendicular field superconducting proximity effect in Cu/Pb/Cu sandwiches, 25:43315
TILLEY, John, Life-span of dividing mammalian cells in vivo, 25:42555
TIMOFEEV, A. D., Plasma acceleration in a pulsed coaxial accelerator, 25:43358
TIMOFEEV, V. A., Enthalpy and heat capacity of EuB_6, NdB_6, and SmB_6, 25:42951
TIMOFEEVA, E. N., Enthalpy and heat capacity of EuB_6, NdB_6, and SmB_6, 25:42951
TIMOFTE, D., Radioinduced sarcomas, 25:42705
TINTI, F., Precipitation and influence of hydrides in zirconium alloys, 25:42855
TIREN, L. I., Material buckling in U-loaded assemblies of fast reactor FRO, 25:44149 (AE-425)
TISLJAR-LENTULIS, G. M., Counter telescope measurements of a beam of negative π mesons, 25:42141
TISSIER, Jean-Claude, Process to obtain oxide layers on Zr, Hf, and their alloys, 25:42819
TITARENKO, N. N., Calculation of electroexcitation of C in the region of giant resonance, 25:43824
TITHERIDGE, J. E., Faraday rotation of satellite signals across the transverse region, 25:43254
TITOV, A. V., Effect of ionizing radiation on the excretion of radioprotectors in rats' urine, 25:42671
TIWARI, N. P., Prog. rpt. on study of control of public health problems using irradiation, annual, 5/69--4/70, 25:42744 (COO-2038-2)
TKHAREV, E. E., Partial wave analysis on the basis of complex vector parametrization, 25:43720
TOBIAS, Cornelius A., Visual phenomena noted by human subjects on exposure to neutrons of energies less than 25 million electron volts, 25:42688
TOBIN, J. C., Neutron fluence limit determinations for some FFTF components, 25:44157
TODORAN, Ioan, Period determination of variable star DP Aquarii, 25:43021
TOEROEK, G., Preparation and properties of antimony(V) aquoxide, 25:41750
TOKHIYAN, S. R., Hematological and electrocardiographical changes during radiation sickness, 25:42660
TOKUNAGA, Okihiro, Chemical reactions by reactor radiation, 25:41851 (JAERI-13780)
TOLMIE, R. W., Mobile equipment for combined neutron activation and x-ray fluorescence analysis, 25:41768
TOLSTOPYATENKO, L. I., X-ray spectrographic determination of tellurium and platinum, 25:41736
TOMA, K., Portevin--Le Chatelier effect in V, 25:43486
TOMASH, P., Inelastic interaction of neutrons with H and deuterium, 25:43560
TOMASSI, G., Problems of the radiocontamination of man, 25:42375
TOMILIN, M. V., Recognition of pyrimidine dimers in DNA by incision enzyme from Micrococcus lysodeikticus, 25:42285
TOMIMASU, Takio, 33 MeV ETL electron linear accelerator, 25:43752
Absolute measurement of Linac x-ray energy fluence, 25:43750
Average energies of back scattered x-rays from Pb, Cu, and Duralumin, 25:43431
Beam transport system of ETL Linac, 25:43764
Construction and performance of a current spark chamber, 25:42151
Dependence of electron bremsstrahlung generation on target thickness and forward angle, 25:43751
Energy calibration of Linac analyzing system by means of photonuclear reaction, 25:43749
Ionization chamber response for pulsed radiation and the drift velocity distribution of filling gas, 25:42088
Mean mass stopping power ratios for γ- and x-rays for use with cavity ionization chamber, 25:42085
Radiation damage of MOS FETs by x-ray and electron irradiations, 25:42233
Reconstruction and performance of ETL electron linear accelerator, 25:43755
TOMMASINO, L., Electrochemical etching of damaged track detectors by H. V. pulse and sinusoidal waveforms, 25:42056 (RT/PROT-(71)1)
TONAPETYAN, S. G., Telescope of spark chambers with a magnetic spectrometer for polarization experiments, 25:42146
TONNIES, J. J., Preparation of lanthanide single crystals: Pr, Nd, and Lu, 25:42834
TOPCHIEVA, A., Changes in pea varieties as affected by gamma rays, 25:42329
TORIYAMA, Kazumi, Electron spin resonance evidence for positive holes produced in irradiated single crystals of carboxylic acids, 25:41841
TOROPOV, N. A., Phase equilibria in the high-alumina region of the system Al_2O_3--Nb_2O_5, 25:42985
TORRES, J. P., Levels of ^{159}Dy obtained by decay of ^{159}Ho, 25:43944
TORRES, Josefa, Genetic collapse of insect populations. I. Extinction of inbred and outbred lines in laboratory populations of the sugarcane borer, 25:42611
TORRES, P. L., Lorentz-invariant localization for elementary systems. IV, 25:43577
TOSI, G., Dose distributions around linear ^{192}Ir sources, 25:42428
Dosimetry of high energy electron beams, 25:42167
Dosimetry of high energy electron beams, 25:42169
Protective considerations in use of ^{192}Ir for radiotherapy, 25:42477
TOTH, G., Large scale production of carrier-free ^{131}I, 25:41880
TOTH, Louis E., Low-temperature heat capacities of transition metal borides, 25:42974
TOTH-ALLEN, Jean Elizabeth, Distribution and histopathological effects of cis-platinum(II)diamminodichloride on nontumored and tumored (sarcoma 180) Swiss white mice, 25:41762
TOUFAR, Pavel, Rated parameters at power station A-1, 25:44021
TOUHILL, C. J., Multiple purpose use of thermal condenser discharges from large nuclear systems to supplement interregional water supply, 25:44083 (BNWL-SA-2738)
TOWN, Christopher D., Repair of x-radioinduced DNA strand breaks in vivo, 25:42326
TOWNSEND, W. C., Coolant blowdown studies of a reactor simulator vessel containing a simulated reactor core, 25:44133 (BNWL-1524)
TRADOWSKY, K., CAMAC: a system of computer-directed electronics, 25:42218
TRAJMAR, S., Importance of polarization for electron scattering in the intermediate-energy region, 25:43138
TRAUNFELDER, H., Influence of electric fields on scintillation process in CsI(Tl), 25:43448
TRAUT, H., Achromatic lesions induced by x-rays in chromosomes of Vicia faba, 25:42343
TRAUZEDDEL, R., Modification of the intensity of optical spectra of organic dyes through deuterium labeling, 25:41815
TREDER, H.-J., Gravitation theory as theory of non-Lorentzian transformations of systems of reference, 25:43708
Helmholtz and relativistic electrodynamics, 25:43666
Velocity of light in Newton and Einstein gravitational theories, 25:43694
TREDER, Hans-J., Global and local principles of relativity, 25:43707

XUM

TRENTELMAN, G. F., Precision mass measurement of ^{9}C, ^{13}O, and ^{21}Mg, 25:43823
TRENTELMAN, George Frederick, Experimental test of the isobaric multiplet mass equation, 25:43808
TRET'YAKOV, Yu. P., Economical source for multiply-charged calcium and zinc ions, 25:43765
TRSOVCEVIC, Zeljko, Phage-induced radioresistance of lysogenic bacteria, 25:42529
TRIPATHI, Ram Kishore, Brueckner calculations for light nuclei, 25:43794
TRIULZI, C., Distribution of radioactivity in sediment from Ligurian Sea, 25:41949
TROFIMOV, V. M., Radiation yield of Mn^{+3} in dosimetric glasses, 25:42153
TROMBETTI, T., Kinetics of a fast pulsed reactor in a periodic or quasi-periodic state, 25:44196 (LA-tr-71-44)
TROY, B. E. Jr., Equatorial ion temperature, 25:43251
TROYAN, V. I., Certain dispersion effects in molecular gases in parallel constant and alternating magnetic fields, 25:43515
TRUBITSYN, A. V., Behavior of superconductive thin-film bridges in SHF fields, 25:43298
TRUBITSYN, A. Ya., Enthalpy and heat capacity of EuB_6, NdB_6, and SmB_6, 25:42951
TRUE, William W., Negative-parity states in ^{208}Pb, 25:43926
TRUHLAR, D. G., Importance of polarization for electron scattering in the intermediate-energy region, 25:43138
TRUKHANOV, G. Ya., DEMETRA program set for calculating problems of neutron thermalization in one-dimensional cell of heterogeneous reactor, 25:44195 (IAE-2010)
TRUSCELLO, V., Thermoelectric generators for deep space application, 25:43184 (N-71-16776)
TRUSCELLO, Vincent, Performance and life testing of thermoelectric generators, 25:42002
TRYKOV, L. A., Protection from penetrating radiation of a nuclear explosion, 25:42034 (JPRS-53498)
TSAI, Hui-tuh, Study of photon activation analysis, 25:41766
TSAI, Jensan, Non-destructive determination of reactor fuel element burnup by measurement of fission neutrons, 25:41757
TSEBRO, V. I., Superconductivity of cold-deposited beryllium films, 25:43303
TSENG, H. K., Exact screened calculations of atomic-field pair production and low energy screening, 25:43417 (NYO-3829-71)
TSEPAKIN, S. G., Ion-beam apparatus, 25:43747
TSEREN, Ch., Double charge exchange on light nuclei, 25:43962
TSINOBER, A. B., Magnetohydrodynamic flow around bodies, 25:43199
TSUCHIYA, Yoshio, 33 MeV ETL electron linear accelerator, 25:43752
Absolute measurement of Linac x-ray energy fluence, 25:43750
Beam transport system of ETL Linac, 25:43764
Dependence of electron bremsstrahlung generation on target thickness and forward angle, 25:43751
Energy calibration of Linac analyzing system by means of photonuclear reaction, 25:43749
Ionization chamber response for pulsed radiation and the drift velocity distribution of filling gas, 25:42088
Reconstruction and performance of ETL electron linear accelerator, 25:43755
TSUEI, C. C., Moessbauer effect study of amorphous Fe--Pd--Si alloys, 25:44238 (CALT-922-32)
TSUPRUN, L. I., Corrosion and mechanical properties of Zr alloys in CO_2, 25:42813
TSUSHIMA, Tadahiko, Secondary β-deuterium effects on the rates of solvolyses of benzonorbornen-2(exo)- and -2(endo)-yl p-bromobenzenesulfonates, 25:41801
TSUYA, Akira, Nervous system and radiation, 25:42710
TUAN, Debbie Fu-tai, Interchange theorems for triple perturbation theory, 25:43520
TUBIANA, Maurice, Hematological effects of partial body irradiation: clinical and experimental data, 25:42599
TUCEK, J., Measurement of small angles of scattered particles in a photographic emulsion, 25:42139
TUCKER, Wallace H., Blast-wave model for Vela X supernova remnant and origin of Gum Nebula, 25:43039
TUCZEK, H., Investigation of an inductive plasma accelerator for propulsion purposes, 25:43351
TULLY, F. P., Crossed-molecular-beam study of collision-induced dissociation of alkali halides, 25:43131
TUMANYAN, M. A., Radioresistance of E. coli K-12, 25:42330
TUMOSA, Charles S., Interactions of positrons with defects in sodium chloride crystals, 25:43453
TURALA, M., System of proportional wire chambers on-line with a computer, 25:42156
TURCHI, L., Dosimetry of high energy electron beams, 25:42169
TURCHI, Peter J., Cathode region of a quasi-steady magnetoplasmadynamic arcjet. VIII, 25:43353 (N-71-19984)
TURJAK-ZEBIC, V., Effect of alginates from algae on Sr transport through rat's duodenum, 25:42254
TURKIEWICZ, J., (n,α) reactions on heavy nuclei induced by 14.2-MeV neutrons, 25:43886 (INR-1268)
TURNER, W. D., Thermal analysis of national radioactive waste repository: brief summary of results obtained through April 1971, 25:42038 (ORNL-TM-3426)
TYMOW, B. S., Pumps for circulating liquid metals, 25:41958 (CONF-700307-8)
TYUL'KIN, V. A., Valence state of tin and the structure of radiation defects in silicate glasses containing tin, 25:43009
TYZACK, C., Effects of alloying and irradiation on the oxidation behaviour of zirconium alloys, 25:42927

U

UCHIDA, Kunao, Radiation hazard control system, 25:42480
UDAGAWA, T., Higher multipole deformation of pairing density in deformed nuclei and their effects on (p,t) and (t,p) reactions, 25:43977
UDALOV, Yu. P., Three cross sections in system CaO--Nd_2O_3--Al_2O_3, 25:42995
UENO, Kaoru, Fractional extraction of Zr, Nb, and Np with tri-n-butyl phosphate, 25:41901
UENO, Takeo, Manufacture of DP pulps by irradiation. I, 25:41873
UGAI, Ya. A., Phase diagram of the system Cd--As, 25:42989
UKIGAYA, Fumio, Apparatus for continuous observation of cosmic ray intensity at a shallow underground station, 25:42152
ULITOVSKAYA, I. I., Action of fast neutrons on the nervous system, 25:42641
ULITOVSKII, D. A., Action of fast neutrons on the nervous system, 25:42541
ULIU, F. S., Lehmann--Symanzik--Zimmermann formalism in the (n,2) sector of the Lee model, 25:43673
ULLMAIER, Hans, Influence of point defects on magnetic properties of Type II superconductors, 25:43310
ULWICK, J. C., Electron loss during a nighttime PCA event, 25:43269
UMAKANTHA, N., Comparison of mass absorption coefficients of positive and negative beta particles in aluminum and tin, 25:43433
UMAROV, G. Ya., Beta-spectrographs with permanent magnets, 25:42110
UMBARGER, C. J., Determination of mass of ^{97}Y, 25:43836
UNIK, J. P., Critical review of the energy released in nuclear fission, 25:43885 (ANL-7748)
UNWIN, D. D., Radiation protection in a veterinary practice, 25:42485
UPADHYAYA, U. N., Low temperature properties of dilute superconducting alloys, 25:43306
UPHAM, T., Determination of in vivo persistence of tantalum dust following bronchography using reactor-activated tantalum and total body counting, 25:42558
URAKUBO, Goro, Protection standards on radioactive contamination of food and drinking water in Japan, 25:42482
URAY, Z., Effect of some radioprotective substances on the redox equilibrium in the spleen, 25:42526
URIN, M. G., Excitation mechanism of the isobaric analog states from analysis of resonance (p,n) reactions, 25:43893
URONE, P. P., Optical-model analysis of 38 MeV ^{3}He elastic scattering, 25:43878
USOV, Yu. P., Mean free path of the π^0 meson in nuclear matter, 25:43595

V

VACHASPATI, Effect of coherence on intensity-dependent frequency shift in Compton scattering, 25:43590
VACHERON, A., External measurements of pulmonary pressures by means of radioisotopic dilution curves, 25:42554
VAELIVAARA, K. G., Absolute transition rates in ^{182}W, 25:43903
VAGANOV, R. B., Device for diagnostics of plasma, 25:43345
VAGHIN, V., Study of hybrid electromagnetic waves in cylindrical structures, 25:43405 (CERN-71-4)
VAIDYA, P. C., Spherically symmetric radiation of charge in Einstein--Maxwell theory, 25:43710
VAKAET, L., Organotypical culture of irradiated and non-irradiated chick mesonephros, 25:42643
VALENTINE, D. A., Charged-particle observations from OSO 3, 25:43178
VALETT, Bryan B., Metabolism of ^{131}I in two amphibian species (Taricha granulosa and Rana pipiens), 25:44288 (RLO-2227-T-8-1)
VALKOVICH, V., Inelastic interaction of neutrons with H and deuterium, 25:43560
VALODZIN, U. G., Radiation resistance of hybrid plants, 25:42722
VAMPOLA, A. L., Electron pitch angle scattering in the outer zone during magnetically disturbed times, 25:43267
VAMPOLA, Alfred L., Outer-zone electron precipitation, 25:43211 (AD-715266)
VAN ALLEN, J. A., Asymmetric access of energetic solar protons to the Earth's north and south polar caps, 25:43233
VAN BEKKUM, D. W., Pathology of the late syndrome in mice lethally irradiated and treated with isologous bone marrow transplantation, 25:42665
VAN BREE, R., Intermediate structure near an isobaric

analog resonance, 25:43851
VAN BRUNT, R. J., Mass and charge dependent ion discrimination in a linear pulsed time-of-flight mass spectrometer, 25:42211
Multiple ionization of Ne, Ar, and Kr by x rays, 25:43142
VANBUREN, W., Fuel rod deformations: a time dependent finite element analysis on axisymmetric fuel rods, including pellet end effects (LWBR development program), 25:44126 (WERL-ELPLA-1)
VAN DEN BERGH, J. W. H., 120,000 shp nuclear ship propulsion study, 25:44178 (RCN-139)
VANDENBROUCK, C., Mandibular osteoradionecrosis, 25:42543
VAN DE REIT, William G., Incorporation of tritium into mouse tissues after oral administration of tritiated thymidine, 25:42252
VAN DER GOOT, A. S., Lattice constants and Curie temperatures of Th--Co compounds, 25:43485
VAN DER LINDE, A., Corrosion of Zr alloy samples in 340°C circulating water, 25:42808
VAN DER MERWE, M. J., Production of Fe-free and carrier-free ^{67}Ga, 25:41391
VAN DER PLAS, Theo, Method of preparing a stable mixed sol of hexavalent uranium and tetravalent thorium by peptization, 25:42345
VAN DER SCHANS, G. P., Infection of spheroplasts of Pseudomonas with DNA of bacteriophage PM2, 25:42273
VANDOR, Ferenc, Radio-mercury diagnosis of the tumor, 25:42575
VAN DYKE, Milton, Annual review of fluid mechanics. III, 25:43195
VAN HOVE, L., Particle production in high energy hadron collisions, 25:43579
VAN INGEN, A. M., System for digitalization of fast non-recurrent analogue signals, 25:42220
VAN KOTE, Francis, Distribution of radioactivity in the lava issuing from the cavity of a nuclear explosion, 25:41953 (CEA-R-4099)
Radioactivity distribution in environment of a contained nuclear explosion. I, 25:41954 (CEA-R-4128(1))
VANLEUGENHAGHE, C., Corrosion of Zr alloys in heavy water under pressure and in superheated steam, 25:42815
VANOSDOL, J. H., Zirconium hydride reactor--organic Rankine power systems, 25:44179
VAN RAMELE, H. J. F., System for digitalization of fast non-recurrent analogue signals, 25:42220
VAN RIJ, Willem Idaniel, Deformed spin--orbit potential in nuclear scattering and structure, 25:43963
VAN ROOIJEN, J. J., Beta--gamma circular polarization correlation measurements on the decays of ^{203}Hg, ^{199}Au, and ^{141}Ce, 25:43941
VAN STEENIS, H., Radiosensitivity of chromosomes of rat kangaroo cells in vitro, 25:42348
VAN VEEN, M. C., Influence of engineering inspection standards on the manufacture of nuclear reactor pressure vessels, 25:44110 (CONF-700224-, Paper 5)
VAN ZYL, C. R., Distribution coefficients and cation exchange behavior of elements in hydrochloric acid--acetone, 25:41999
VARGA, D., Silicon semiconductor spectrometer, 25:42112
VARICH, N. I., Crystallization of Ni--Ta and Ni-Nb alloys at superhigh rates of cooling, 25:42888
VARTERESZ, V., Some problems on the evaluation of biochemical indicators of radiation injury, 25:42407
VASHAKIDZE, I. Sh., Brueckner--Hartree--Fock theory for the ^{4}He nucleus, 25:43785
VASHOLZ, David Paul, Baryon currents and fields, 25:43644
VASILEV, P. N., Healing of radiation ulcers of skin under the influence of metacyl and dibunol (experimental research), 25:42541
VASIL'EV, V. F., Boundary problem on the distribution of electric fields along the channel with side bars, 25:43202
VASILEVSKIS, S., Determination of correction to precession from stellar proper motions, 25:43048
Expansion of the Orion-Nebula cluster, 25:43038
VASILIK, Dennis, Neutron radiography with a sealed-tube neutron generator and graphite moderated system, 25:42027 (RFP-1705)
VASIL'TSOV, V. V., Description of an ionization calorimeter supplemented with proportional counters, 25:42140
VASU, K. I., Evaluation of rate-controlling obstacles for low-temperature deformation of zirconium, 25:42852
VATNITSKII, S. M., Measurements in beams of fast electrons, 25:42411
VAVILOVA, V. V., Formation of suboxides in the system niobium--oxygen, 25:42990
VEGHTE, Richard Clark, Radiative corrections for muon decay in an intermediate vector boson theory, 25:43600
VELECKIS, E., Solubility of helium and argon in liquid sodium, 25:41823 (ANL-7802)
VELKOBORSKY, J., Properties of Zr--Cu--Mo alloys, 25:42878
VENINGA, T. S., Significance of biogenic amines as radioindicators in experimental animals with reference to man, 25:42527
VENKATARAMAN, G., Method of constructing irreducible multiplier representations, 25:43501
Neutron dose distributions for ^{252}Cf sources, 25:42445
VERDEYEN, J. T., Enhancement of CO_2 laser power and efficiency by neutron irradiation, 25:42229
VERIN, Ph., Use of a new vector in the diagnosis of melanomas, 25:42563
VERKHOVODOV, P. A., X-ray spectrographic determination of tellurium and platinum, 25:41736
VERNON, F. L. Jr., Response of superconducting point contacts to high-frequency radiation, 25:43297
VESELOVSKII, I. S., Exact solutions for a tenuous plasma in a magnetic field, 25:43379
VESTERMARK, A., Isotope separation of radioactive sodium isotopes by isotachophoresis, 25:41923
VIACLOVSKY, S. A., Ultrasonic inspection of selected welds in stainless steel primary steam piping in Elk River Power Plant, 6/66, 25:44082 (SWRI-1228-9-10)
VICTOR, A. H., Distribution coefficients and cation exchange behavior of elements in hydrochloric acid--acetone, 25:41899
VIDAL, H., Zirconium--copper alloys used in fuel element cladding for gas-cooled heavy-water reactors, 25:42881
VIEGAS, John R., Extension of Frost's mixture rule to include effects of multiple ionization on electrical conductivity, 25:43362 (N-71-18715)
VIGILEVA, E. S., Phase diagram of the system Pr--Te, 25:42986
VILLAIN, Paul, Measuring activity of radioisotopes in gas, 25:41753
VILLALOBOS-PIETRINI, R., Recovery effect of serotonin-creatinine sulfate complex on x-irradiated planarians, 25:42527
VINCENT, C. M., T = 1 states in the A = 12 system, 25:43819
VINCENTI, Walter G., Annual review of fluid mechanics. III, 25:43196
VINOGRADOV, A. V., Absorption of light by an inhomogeneous laser plasma, 25:43400
VINOGRADOV, V. M., Three-dimensional covariant formulation of two-body problem in quantum field theory, 25:43674
VISFELDT, Jakob, Limitations of chromosome analysis for biological dosimetry, 25:42707
VISHNEVETSKAYA, E. M., Indexes of remote sequelae of radiotherapy of breast cancer, 25:42270
VISHNYAKOV, Yu. S., Gradient-free oven for examining the Moessbauer effect, 25:42115
VISSER, C., Fuel rod deformations: a time dependent finite element analysis on axisymmetric fuel rods, including pellet end effects (LWBR development program), 25:44126 (WERL-ELPLA-1)
VITEZ, Andre, Device with a large dynamic range for measuring direct currents and voltages, 25:42208
VITOL, E. N., Determination of O and N in metals using fluxes enriched with ^{18}O and ^{15}N isotopes, 25:41748
VITORSKII, Ya. M., Influence of deformation rate on deformability of Mo--0.5 percent Ti alloy, 25:42833
VITOUX, Dominique, Coulomb excitation of first excited state of ^{24}Mg, 25:43852
VOELK, Heinrich J., Striations in ionospheric ion clouds. I, 25:43252
VOELKL, J., Reversed isotope dependence for hydrogen diffusion in palladium, 25:41815
VOIGTLANDER, J., Induction of translocations in mature Drosophila oocytes over a dose range of 10 to 500 roentgens of x rays (stage-14 oocyte/radiation damage), 25:42333
VOJTA, G., Method of normal modes for Vlasov--BGK equations, 25:43377
VOLCHENKOV, V. A., Extraction of the proton beam of the 1-GeV synchrocyclotron, 25:43762
VOLCK, Erling, Liver damage following colloidal thorium dioxide, 25:42708
VOLKOV, R. A., Propagation of the phase surface in superconducting thin films, 25:43313
VONACH, H., Direct measurement of (n,2n) cross section of ^{93}Nb, 25:43897
VON BLANCKENHAGEN, P., Relaxation phenomena and NMR of ^{116}In, 25:43894
VON EHRENSTEIN, D., Isospin nonconservation in reaction $^{12}C(d,\alpha_2)^{10}B(1.74,T = 1)$, 25:43811
VONSOVICH, Stanislav, Laboratory mixer--settler extractor LMOM2, 25:41895 (INR-1309)
VOROB'EV, E. D., Sources of multicharged ions, 25:43731 (JINR-P7-5177)
VOROBEVA, Z. V., Study of absorption of gases in lungs with ^{133}Xe, 25:42561

W

WADACHI, Yoshiki, RI liquid wastes carried from Japan Radioisotope Association to JAERI, 25:42037 (JAERI-13666)
WADEKAMPER, D. C., Prog. rpt. on Integrated Safeguards Experiment, 12/70--3/71, 25:42035 (BHO-68-6)
WAGMAN, D. D., Selected values of chemical thermodynamic properties, 25:41826 (NBS-TN-270-5)
WAGNER, C. E., Electromagnetic and finite β/sub e/ effects on counterstreaming ion instability, 25:43394
WAGNER, F. Jr., Ionization (shakeoff) accompanying K-shell internal conversion, 25:43871
WAGONER, Robert V., Relativistic disks. I. Uniform rotation, 25:43092
WAHLBERG, T., Personnel dosimetry at AB Atomenergi during 1969, 25:42392 (AE-423)
WAHLQUIST, H. D., Hamiltonian cosmology, 25:43095
WAIDELICH, W., Effects of x radiation on MOS devices at

XUM

79K, 25:42234
WAIT, G. D., Coincidence system for electrodisintegration studies, 25:42131
WAJSFELNER, Rene, Existence of small negative radioactive ions coming from a ^{228}Th source, 25:43100
WAKATSUKI, T., Low-lying levels of ^{40}Ar, 25:43872
WAKAYAMA, Terunobu, Effect of phase on excitation transfer in the radiolysis of isobutane, 25:41864
Role of reaction sites in the radiolysis of solid succinic acid, 25:41865
WAKUTA, Yoshihisa, Fission of U and Th by gamma rays from 200 to 1150 MeV, 25:43946
WALBURG, H. E. Jr., Life shortening and cause of death in irradiated germfree mice, 25:42663
WALIGORSKI, Michal, Spark chambers in high energy physics. III, 25:42138
WALKER, Arthur B. C. Jr., Observation of autoionizing states in solar corona, 25:43065 (AD-715287)
WALKER, D. G., Stress relaxation in beryllia, 25:42973
WALKER, David W., Genetic collapse of insect populations. I. Extinction of inbred and outbred lines in laboratory populations of the sugarcane borer, 25:42611
WALKER, E. Dean, Krypton-85 principles of application in materials surface studies, 25:42029
WALKER, James D., Excitation of atomic hydrogen, 25:43137
WALKER, John Scott, Three-dimensional MHD flow in diverging rectangular ducts, 25:43205
WALLACE, W. E., Magnetic characteristics of aluminum-rich ternary laves phases containing rare earths, nickel, and aluminum, 25:43480
WALLWORK, G. R., Oxidation of Ni--20 wt. percent Cr--2ThO_2, 25:42930
WALMSLEY, Donald E., Nucleophilic substitution at tetrahedral boron. Trimethylamine--alkyl- and -aryiborane substrates, 25:41803
WALRAVEN, R. L., Optinization technique applied to experiments measuring reaction gamma-ray angular distributions, 25:42223
WALSH, T. F., Finite-energy sum rules and the reactions e e + e e epsilon (750), e e + e e f (1260), 25:43582 (DESY-71/20)
WALTERS, E. A., Proton transfer from cyanocarbon acids. II. General-base-catalyzed detritiation and bromination of malononitriles. Rates of the reverse reactions, 25:41798
WALTERS, L. J. Jr., Gold provinces in the Philippines defined by activation analysis, 25:41772
Neutron activation analysis of sediments for halogens using Szilard--Chalmers reactions, 25:41763
WAMBSGANSS, M. W., Tentative design guide for calculating the vibration response of flexible cylindrical elements in axial flow, 25:41983 (ANL-ETD-71-7)
WANG, C. L., Pion fluxes from 10-500 GeV proton synchrotrons, 25:43726 (BNL-15893)
WANG, G. S. C., San Onofre Nuclear Generating Station vibration tests, 25:44079 (UCLA-ENG-7037)
WANG, P. K. C., Optinization problems in thermonuclear plasma confinement, 25:43337
WARBURTON, E. K., Lifetime of the $^1/_2^-$ 2791-keV ^{21}Ne level, 25:43870
WARD, M. A., Purification and some properties of molybdoferredoxin, a component of nitrogenase from Clostridium pasteurianum, 25:41811
WARD, T. E., Decay of ^{78}As, 25:43881
WARDMAN, P., Electron spin resonance studies of radiolysis of aliphatic amines at 77°K, 25:41857
Electron spin resonance studies of the radiolysis of aliphatic amines adsorbed on silica gel, 25:41856
WARE, A. A., Toroidal contributions to the shear and the kink instability in the Tokamak and screw pinch, 25:43390
WARNER, John W., Extraordinary red object in Sagittarius, 25:43084
WAROQUIER, M., Shell-model calculations on the N = 82 odd-proton nuclei. II, 25:43989
WARREN, J. H., Evidence for violation of Porter--Thomas postulate in ^{232}Th, 25:43911
WARREN, William W. Jr., Nuclear quadrupolar relaxation in solid and liquid $AuGa_2$, $Au_{0.95}Pd_{0.05}Ga_2$, and $AuIn_2$, 25:43495
WARZEE, M., Corrosion of Zr alloys in heavy water under pressure and in superheated steam, 25:42815
WASHBURN, T. N., Fuel element development for the Gas-Cooled Fast Breeder Reactor. Part I. Sealed fuel rod design, 25:44125 (ORNL-TM-3427)
WASSIL, G. N., Form rolling complex close tolerance shapes, 25:42827
WASSILEW, C., Influence of neutron irradiation on the creep rupture properties of a 16Cr--13Ni steel, 25:42924
WASSILOPULOS, Miltiades, Preparation and separation of carrier-free ^{131}Cs from irradiated $BaCO_3$, 25:41876 (CONF-530986-2)
WATANABE, Hiroshi, Beam transport system of ETL Linac, 25:43754
Reconstruction and performance of ETL electron linear accelerator, 25:43755
WATANABE, K., Neutron irradiation effects on iron containing aluminum and nitrogen, 25:42908
WATANABE, Shin-ichi, Absolute calibration of bremsstrahlung beam monitors, 25:42083
WATARI, Tsutomu, Five cases suspected of radiation myelitis, 25:42700
WATSON, E. C., FACER: a computer program for calculating potential external dose from airborne fission products following postulated reactor accidents, 25:42258 (BNWL-B-69)
WDOWCZYK, J., Possibility of existence of a new process at interactions with energies above 10^{12} eV, 25:42567 (INR-1280)
WEAVER, Boyd S., Selective stripping of plutonium from organic extracts, 25:41912
WEAVER, C. Kenneth, Radioimmunoassay: a simplified procedure for dose interpolation, 25:42236
WEAVER, H. Joseph Jr., Two-dimensional finite Fourier transform techniques, 25:44303 (UCRL-51046)
WEBB, Willis L., Electrical structure of D and E region, 25:43208 (AD-714365)
WEBER, David F., Prog. rpt. on cytogenetics of monosomes in Zea mays, 10/70--9/71, 25:44257 (COO-2121-3)
WEBER, G., Behavior of surface carbon during its determination by nuclear reactions, 25:41765
Inelastic electron--proton scattering in the region of the Δ (1236) resonance, 25:43527 (DESY-71/21)
WEBER, R., Orthogonality relations of many time generating functionals of harmonic oscillators, 25:43665
WECKERING, Rudolf, Space structure of energetically excited atomic nuclei, 25:43990
WEHAUSEN, J. V., Annual review of fluid mechanics. III, 25:43196
WEHRING, B. W., Internal-conversion electrons emitted by different elements in fission of ^{252}Cf, 25:43922
WEHRMANN, R. F., Allotropes of carbon (amorphous, graphite, diamond) as engineering materials, 25:42977
WEICK, Dietrich, Spectral intensity distribution of Compton radiation by Thomas--Fermi model, 25:43515
WEINSTEIN, Martin, Composite materials, 25:42951
WEINTRAUB, Sol, Book of splines, 25:44310
WEISS, Peter, Experimental and clinical studies of tissue damage in combination neck dissection and radiotherapy, 25:42603
WEISZ, M., Deformation and cracking in Zr--Cu cladding in carbon dioxide, 25:42928
WELCH, Dennis, Radionuclide evaluation of the dandy-walker malformation and congenital arachnoid cyst of the posterior fossa, 25:42568
WELCH, Michael J., Fate of ^{13}N formed by $^{12}C(d,n)^{13}N$ reaction in inorganic carbides, 25:41886
WELIACHEW, L., Detection of interstellar OH in two external galaxies, 25:43083
WENG, P. S., ^{90}Sr and ^{137}Cs levels in the diet of children on a school lunch program, 25:42422
WERBY, Michael F., Optical model analysis of $^9Be(p,p_0)^9Be$ cross sections, 25:43804
WERNICK, J. H., Nuclear quadrupolar relaxation in solid and liquid $AuGa_2$, $Au_{0.95}Pd_{0.05}Ga_2$, and $AuIn_2$, 25:43495
WERT, James J., Prog. rpt. on deformation studies of superlattice structures, final, 3/63--8/70, 25:44266 (CRG-3091-21)
WESOLOWSKI, J. J., Symmetric fission observed in thermal-neutron-induced and spontaneous fission of ^{257}Fm, 25:43920
WEST, D., Note on the energy spread versus radial oscillation amplitude for the synchrocyclotron regenerative beam extractor, 25:43725 (AERE-R-6812)
WEST, J. E., Charging of polymer foils with monoenergetic low-energy electron beams, 25:43436
WESTENHOLZ, C. v., Magnetic monopoles and quarks, 25:43565
WESTERLUND-HELMERSON, Ulla, Determination of iodine and fluorine in selenium, 25:41734
WESTLEY, G. W., Geometric programming algorithm, 25:44276 (ORNL-4650)
WETZEL, Robert G., Coprecipitation of phosphate with carbonates in a marl lake, 25:44252 (COO-1599-33)
WEYERMANS, J. F., Infection of spheroplasts of Pseudomonas with DNA of bacteriophage PM2, 25:42273
WEYERS, J., Quantum numbers of cross-channel exchanges, 25:43565 (CALT-68-305)
WEYL, Guy M., Interaction of OTX wave with density fluctuations in an inhomogeneous magnetized plasma, 25:43402 (AD-715277)
WHEELER, J. Craig, Thermonuclear detonations in evolved stellar cores, 25:43033
WHELAN, E. D. P., Effect of gamma radiation on seedling emergence of Cucumis sativus, 25:42719
WHIPPLE, E. C., Measurement of the effective electron loss rates in the D region during polar cap absorption events, 25:43256
WHISNANT, David Melvin, Dispersion dipole between S-state atoms, 25:43136
WHITE, D. H., Thermal neutron capture cross sections in calcium, 25:43835
WHITE, J. E., Neutron energy-dependent capture gamma-ray yields in tantalum and tungsten, 25:43890 (ORNL-TM-3436)
WHITE, James D., Kinetics of the reaction between uranium(III) and $Co(NH_3)_5(H_2O)^{3+}$ in aqueous perchlorate solutions, 25:41783
WHITEHEAD, W. D., Mass and charge dependent ion discrimination in a linear pulsed time-of-flight mass spectrometer, 25:42211
Multiple ionization of Ne, Ar, and Kr by x rays, 25:43142

WHITEN, Morris Lewis, Experimental inelastic scattering of 61 MeV protons from ^{89}Y and ^{90}Zr, 25:43855
WHITNEY, Alan R., Quasars revisited: rapid time variations observed via very-long-baseline interferometry, 25:43049
WHITTEMORE, W. L., Neutron radiography of osseous tumours, 25:42575
WHITTEN, David G., Excited state and cyclobutadiene intermediates in the radiation chemistry of alkynes. γ radiolysis of 2-butyne, 25:41867
WHITTON, J. L., Depth distribution of implanted O in GaP, 25:43447
WHITTY, C. Dennis, Partial purification of tRNA and leucyl-tRNA synthetase from sugar beet root, 25:44249 (CDD-1313-27)
WICKLUND, Arthur Barry, Meson spectrum in reaction PP → d MM, 25:43541
WIDNER, M., Simulation of pseudowaves and of plasma sheath formation about a grid, 25:43369
WIECHERS, W. K., Sensitivity of uranium and separative work requirements to variations in reactor programs, 25:44127 (CONF-700903-17)
WIECHERT, H., Second sound reflection on liquid He II surface, 25:43279
WIEDEMANN, B., Isotope separation of radioactive sodium isotopes by isotachophoresis, 25:41923
WIENKE, B. R., Muon capture in ^6Li in the ditriton channel, 25:43821
WIESE, W. L., Systematic trends of atomic oscillator strengths along isoelectronic sequences, 25:43114
WIGNALL, T. K., Probabilistic appraisal of mineral resources in a portion of the Grenville Province of the Canadian Shield, 25:41944
WILBURN, N. P., Coolant blowdown studies of a reactor simulator vessel containing a simulated reactor core, 25:44133 (BNWL-1524)
WILHELM, Mari S., Low dose gamma irradiation of bovine metmyoglobin, 25:42755
WILKINS, John W., Validity of the Boltzmann equation for systems with both electron--phonon and impurity scattering, 25:44273 (NYO-3699-56)
WILKINSON, D. H., Finite nuclear size and radiative corrections in the construction and assessment of Kurie plots for allowed beta-decay, 25:43992
WILL, H., In-pile equipment for strain measurements on nuclear fuels and structural materials, 25:44086 (EURFNR-853)
WILL, Wolfram, Standard ionic dose in compact and liquid media during x-ray and gamma irradiation, 25:42091
WILLAREDT, B., Mixed crystal phases in system ThO_2--PrO/sub x/, 25:42396
WILLIAMS, A., Demonstration of intermediates in the hydrolysis of 4-ethoxypyrylium salts, 25:41789
Hydrolysis of pyrylium salts. Kinetic evidence for hemiacetal intermediates, 25:41787
WILLIAMS, D. J., Position of the plasmapause during a stormtime increase in trapped position of the plasmapause during a stormtime increase in trapped energetic (E > 280 keV) electrons, 25:43264
WILLIAMS, D. R., Dissipation in He superflow, 25:43283
WILLIAMS, E. A., Noise broadening of trapped-particle echoes, 25:43409
WILLIAMS, Ffrancon, Supramolecular bonding orbitals from molecular antibonding orbitals, 25:41855
WILLIAMS, J. A., Fracture and tensile behavior of neutron-irradiated A533-B pressure vessel steel, 25:42901 (HEDL-TME-71-76)
WILLIAMS, R. L. Jr., Boron-13 nuclear magnetic dipole moment, 25:43817
WILLIAMSON, Y., $\pi^+ + p \rightarrow \Delta^{++}$ (1236) + π^0 AT 1.85 to 2.09 GeV: study of s- and t-channel effects, 25:43551 (UCR-34-P-107-B-108)
Study of $\pi^+p \rightarrow rho^+p$ at 1.85 to 2.09 GeV, 25:43552 (UCR-34-P-107-B-110)
WILLIAMSON, Yvonne, Reaction $\pi^+p \rightarrow rho^+p$ in C.M. energy region 1780 to 2140 MeV, 25:43553 (UCR-34-P-107-B-120)
WILLIS, C., Pulse radiolysis facilities at Chalk River, 25:41849 (AECL-3853)
Radiolysis of hydrogen sulfide at very high dose rates. The effect of SF_6, 25:41850
WILLIS, David L., Metabolism of ^{131}I in two amphibian species (Taricha granulosa and Rana pipiens), 25:44288 (RLO-2227-T-8-1)
WILLNER, O., Use of statistical tolerance limits in the nuclear industry, 25:42033
WILLSON, R. L., Pulse radiolysis, 25:41862
WILLSON, Richard C., Active cavity radiometric scale, international pyrheliometric scale, and solar constant, 25:43075
WILSKY, K., Perturbed β-vibrational bands in ^{152}Sm, ^{154}Gd, and ^{156}Gd, 25:43940
WILSON, A. J. C., Some statistical considerations in the location of Moessbauer lines, 25:42122
WILSON, Charles B., Scintiphotographic evaluation of response of brain neoplasms to systemic chemotherapy, 25:42556
WILSON, R. F., Zirconium hydride reactor--organic Rankine power systems, 25:44179
WILSON, R. W., Discovery of interstellar silicon monoxide, 25:43052
WILSON, W. K., Fuel rod deformations: a time dependent finite element analysis on axisymmetric fuel rods, including pellet end effects (LWBR development program), 25:44126 (WERL-ELPLA-1)
WINCHESTER, J. W., Activation analysis in mineral prospecting, 25:41767
Neutron activation analysis of sediments for halogens using Szilard--Chalmers reactions, 25:41763
WING, Robert F., Extraordinary red object in Sagittarius, 25:43084
WINKLER, P., Determination of hexadecapole transition moments by Coulomb excitation, 25:43948
WINNACKER, A., Relaxation phenomena and NMR of ^{115}In, 25:43894
WINSLOW, F. R., Iron--nickel--tungsten phase diagram, 25:42887 (Y-1785)
WINSTON, Anthony, Prog. rpt. on preparation of wood--plastic combinations using gamma radiation to induce polymerization, final, 11/51--6/58, 25:41843 (ORO-2945-10)
WINTERBON, K. B., Depth distribution of implanted O in GaP, 25:43447
WITHERSPOON, M. E., Coolant blowdown studies of a reactor simulator vessel containing a simulated reactor core, 25:44133 (BNWL-1524)
Leakage of fission products from artificial leaks in the Containment Systems Experiment, 25:44134 (BNWL-1582)
WITKOWSKI, S., Survey of studies of laser produced plasmas at the IPP Garching, 25:43390 (IPP-4/9)
WOLETZ, W., Modular programming system for programming experiments on PDP-9, 25:42181 (CERN-Trans-71-18)
WOLF, Emil, New model for the interaction between a moving charged particle and a dielectric, and the Cherenkov effect, 25:43588
WOLF, H. C., Delayed fluorescence and phosphorescence in pure naphthalene crystals, 25:41813
WOLF, K., Respiration deficient mutants of Schizosaccharomyces pombe I, 25:42338
WOLF, Robert O., Xerostomia in Sjoegren's syndrome. Evaluation by sequential salivary scintigraphy, 25:42571
WOLF, W. P., Anisotropic interactions between magnetic ions, 25:43471 (YALE-3227-71)
Use of parameters in crystal field theory and related calculations, 25:44309 (YALE-3227-77)
WOLFF, C., In vitro study of effect of γ rays on human chromosones, 25:42365
WOLFF, John M., Scinticisternography in individuals without known neurological disease, 25:42567
WOLFSON, J. L., Gamma rays following decay of ^{85}Sr and /sup 85m/Sr, 25:43877
WOLLENBERG, Harold, Field determination of uranium and thorium by gamma-ray spectrometry, exemplified by measurements in the Ilimaussaq alkaline intrusion, south Greenland, 25:41943
WOLLENWEBER, G., Reversed isotope dependence for hydrogen diffusion in palladium, 25:41816
WOLLER, P., Suitability of technetium-labeled erythrocytes for the examinations of the splenic function, 25:42570
WONG, T. F., Two-loop approximations to propagators in the sigma model, 25:43684
WONG, Victor K., Order-parameter fluctuations in a weakly interacting Bose gas near the superfluid transition, 25:43284
WOOD, B. R. A., Stress relaxation in beryllia, 25:42973
WOOD, G. A., Multi-element analysis of glass fragments by neutron activation and the application to forensic science, 25:41758 (AWRE-O-24/71)
WOOD, M. F., Helium-3 dilution refrigerator, 25:43327
Superconductive magnets, 25:43328
WOOD, R. E., Si(Li) spectrometers for electrons and low-energy photons, 25:42123
WOODBURN, Charles R., Radioactive force indicating device, 25:42179
WOODHEAD, D. S., Biological effects of radioactive waste, 25:42373
WOODRUFF, William Lee, Some improvements in variational flux synthesis methods, 25:44200
WOODYARD, John R., Method for producing a chromium activated aluminum oxide scintillator, 25:42086
WOOLF, N. J., Origin of reported millimeter continuum in IRC + 10216, 25:43040
WORTMAN, Oscar, Development of an inspection system for the Atucha nuclear reactor, 25:44080
WOTTON, B. L., Effect of fast neutron irradiation on the mechanical properties of some quenched and tempered steels, 25:42909
WRENN, McDonald E., Prog. rpt. on radioactivity studies. I, annual, 9/69--8/70, 25:42245 (NYO-3086-10(Vol.1))
WRIGHT, B. L., Radiation temperature of a bounded nonthermal plasma. II, 25:43354
Radiation temperature of a bounded nonthermal plasma. I, 25:43371
WRIGHT, D. J., Beryllium window tubes for mammographic examinations, 25:42545
WRIGHT, E. A., Influence of hypertension on latent cerebral irradiation damage, 25:42557
WRIGHT, J. B., Preparation of data sets in ENDF format for Na, Mg, Cl, and K for use in shielding calculations, 25:43420 (ORNL-TM-3429)
WU, C. S., Magnetic drift wave instabilities in plasmas with temperature gradient, 25:43244
WU, Wei-kuo, Range of fission fragments in air determined

XUM

by fission-track detector, 25:43427
WULLAERT, R. A., Influence of irradiation temperature on the tensile properties of stainless steel, 25:42912
Radiation effects on the metallurgical fracture parameters and fracture toughness of pressure vessel steels, 25:42905
WYART, Jean-Francois, Identification of configurations in spectrum of Dy II, 25:43119
WYBORNY, H. W., Yield curves for Li + Li and Li + Be nuclear reactions, 25:43822
WYCKOFF, H. O., Comments on radiation quantities and their significance in health physics. I and II, 25:42440
WYLD, H. W. Jr., Numerical studies of the Bethe--Salpeter equation and the multiperipheral integral equation of Amati, Bertocchi, Fubini, Stanghellini, and Tonin, 25:43683
WYLIE, Robert D., Development of an inspection system for the Atucha nuclear reactor, 25:44080
In-service inspection of nuclear plants, 25:44109 (CONF-700224-, Paper 2)
WYLY, L. D., Gamma--γ directional correlations in the decay of ^{125}Sb. II, 25:43927
WYMAN, M. E., Internal-conversion electrons emitted by different elements in fission of ^{252}Cf, 25:43922
WYVRATT, Matthew J., Configurational stabilities of strained α-sulfonyl carbanions. Kinetics of base-catalyzed racemization and deuterium exchange of representative thiete and thietane dioxides, 25:41860

Y

YABE, Akira, Monitoring for internal exposure. II, 25:42439
Some cautionary problems of fluorometric determination of uranium, 25:41722 (JAERI-13522)
YADAV, H. L., Effect of tensor forces on charge form factor of α-particle, 25:43793
YAGER, P. M., Evidence for splitting in the Q region of $K^+\pi^+\pi^-$ mass, 25:43544 (COO-1428-275)
New evidence for splitting in the Q region of $K^+\pi^+\pi^-$ mass, 25:43543 (COO-1428-274)
YAGI, E., Neutron irradiation effects on iron containing aluminum and nitrogen, 25:42908
YAKOVENKO, E. I., Polyhydroxy flavones as extraction reagents, 25:41738
YAKOVLEVA, S. S., Comparative radiosensitivity of ascites ovarian tumors and ascites lymphosarcoma of rats, 25:42637
YAKOVLEVA, V. A., Observations of the variability of the polarization of radiation of the high luminosity red variables, 25:43024
Polarimetric study of nebula near FU Ori, 25:43025
YAKUBENKO, A. E., Courses in channels upon the small parameter of interaction, 25:43203
YAKYMIV, Ya. M., Asymptotic fields for the approximated, renormalized, two dimensional Yukawa model and :P(phi$_2$): model, 25:43567 (ITF-71-12-P)
YALCIN, C., Charge-dependent effects and low-energy nucleon--nucleon scattering, 25:43960
YAMADA, S., Total absorption type lead glass Cherenkov counter with high resolution, 25:42154
YAMADA, Shigeru, Beta decay to second 2^+ excited state of ^{122}Te, 25:43947
YAMADA, Takahisa, Effect of phase on excitation transfer in the radiolysis of isobutane, 25:41864
YAMASHITA, S., Method for preparing thin films of deuterated polyethylene, 25:43759
YAMAUCHI, Taeko, Spectrophotometric study and analytical application of rare-earth tiron complexes. II, 25:41730
YAMAZAKI, L., Semi-analytical calculations for circular quadrupoles, 25:43757
YANG, Kyun Rin, Fallout radioactivity in Korean foodstuffs. IV, 25:42372
YANG, Teh-li, Fast neutron spectrum outside beam port by ^{6}Li semiconductor spectrometer, 25:42119
YAO, Kenneth T. S., Haploid cells in rat kangaroo corneal endothelium cultures and x-ray-induced chromosome aberrations, 25:42347
YAREMBASH, E. I., Phase diagram of the system Pr--Te, 25:42985
YAROVITSYN, V. V., Pumps for circulating liquid metals, 25:41958 (CONF-700307-8)
YARUSHKIN, Yu. P., Electromagnet of a transportable betatron, 25:43741
YARZAGARAY, Luis, Radionuclide evaluation of the dandy-walker malformation and congenital arachnoid cyst of the posterior fossa, 25:42568
YASUE, M., Method for preparing thin films of deuterated polyethylene, 25:43759
YASUE, Masaharu, Heavy particle identification with TOF method in nuclear reactions, 25:42066
YEN, Chen-shyong, Fast neutron spectrum outside beam port by ^{6}Li semiconductor spectrometer, 25:42119
YEN, W. L., Final states with three charged particles and a visible anti K^0 from K-d interactions at 4.5 GeV/c, 25:43549 (COO-1428-286)
YIELDING, K. Lemone, Modification by acridine analogs of the survival of ultraviolet irradiated Escherichia coli B, 25:42533
YODZIS, P., Some general relations in relativistic magnetohydrodynamics, 25:43701
YOO, M. H., Numerical calculation of elastic properties for straight dislocations in anisotropic crystals, 25:44282 (ORNL-TM-3408)
YOSHIDA, S., Kondo effect in single crystals of dilute Y--Ce alloys, 25:43479
YOSHIKAWA, N., Lifetime measurements on E2 isomers in N = 48 nuclei, 25:43847
YOSHIKAWA, S., Consideration of power requirement in fusion feasibility experiment, 25:43333 (MATT-803)
YOSHINAGA, H., Portevin--Le Chatelier effect in V, 25:43486
YOST, K. J., Neutron energy-dependent capture gamma-ray yields in tantalum and tungsten, 25:43890 (ORNL-TM-3436)
YOUNG, M. J., Pulse radiolysis facilities at Chalk River, 25:41849 (AECL-3853)
YOUNG, R. W., Monkey performance after partial body irradiation, 25:42642
YOUNGER, C. L., Irradiation effects at cryogenic temperature on tensile properties of titanium and titanium-base alloys, 25:42926
YOUNT, David E., Photons as hadrons, 25:43597
YU, Loh-ping, Unitarization of the dual-resonance amplitude. III, 25:43717
Unitarization of the dual-resonance amplitude, 25:43718
Unitarization of the dual-resonance amplitude. II, 25:43719
YUDIN, D. M., Radiation yield of Mn^{+3} in dosimetric glasses, 25:42163
YUILLE, W. D., Trapping of methyl iodide at high pressure and high temperature, 25:41998 (TRG-Report-2135)
YULDASHEV, B. S., Thermodynamical description of momentum distributions of pions in π-p interactions at p = 4 GeV/c, 25:43639 (JINR-P1-5849)
YURGELAITITE, K.-N. V., Dose-dependent frequency of encircled ring chromosomes, 25:42351
YUZVUK, Yu. A., Optimizing the parameters of radiometric equipment when determining low levels of radiation, 25:42102

Z

ZAICHIK, V. E., Distribution of radionuclide in the skin resulting from surface contamination by ^{89}Sr, 25:42371
ZAIMIDOROGA, O. A., Time properties of a spark chamber filled with helium and helium--hydrogen mixture, 25:42136 (JINR-P13-5828)
ZAIMOVSKII, A. S., Corrosion and mechanical properties of Zr alloys in CO_2, 25:42813
ZAINULIN, Yu. G., Nature of the bond and electrical conductivity of cubic zirconium carbides and oxycarbides, 25:43491
Possibility of the existence of stable zirconium monoxide, 25:42987
ZAITSEVA, K. K., Changes of the testes of irradiated mice in bone marrow transplantation, 25:42304
ZAJIC, V., Corrosion of Zr alloys in water, 25:42807
ZAKHAROV, A. M., Ternary system molybdenum--iron--carbon, 25:42889
Ternary system molybdenum--titanium--carbon, 25:42890
ZAKHARYAN, E. G., Effect of direct current and x radiation on bone marrow cells, reticuloendothelial cells, and radiosensitivity of rats, 25:42530
ZAKRZHEVSKAYA, D. T., Regeneration of γ-radiation-induced single ruptures of DNA strands by polynucleotide ligases in vitro, 25:42268
ZALESKI, Tadeusz, Vinca Nova: automatic unit for neutron spectrometer control, 25:42114
ZALIKIN, G. A., Biological action of ^{237}Np nitrate, 25:42253
ZALLY, George Daniel, Fluctuation contributions to the heat capacity of superconducting thin films, 25:43321
ZANDER, Arlen Ray, Reactions ^{7}Li(d,t)^{6}Li and ^{7}Li(h,α)^{6}Li, 25:43809
ZANETTI, P., Effect of ionizing radiations on lymphocytes from adults and newborn infants, cultured in vitro in presence of phytohemagglutinin, 25:42502
ZANEVSKII, Yu. V., System of proportional wire chambers on-line with a computer, 25:42156
ZARECHNYUK, O. S., Systems Y--Al--Si (Ge,Sb), 25:42891
ZAREMBA, Loren Andrew, Proton capture by ^{17}O, 25:43812
ZARETSKAYA, Yu. M., Radiation immunology and transplantation, 25:42310
ZARETSKII, D. F., Excitation mechanism of the isobaric analog states from analysis of resonance (p,n) reactions, 25:43893
ZASHKVARA, V. V., Electrostatic spectrometer for beams of charged particles, 25:42215
Ion-optical properties of an electrostatic charged-particle energy analyzer, 25:43761
ZAVOISKII, E. K., Asymmetry of distribution of turbulent electric fields in direct-discharge plasma, 25:43344
ZEH, H. D., Interpretation of measurement in quantum theory, 25:43523
ZELENSKAYA, N. S., Effect of tetragonal graph in heavy ion stripping (pick-up) reactions, 25:43961
ZEMBEKOV, A. A., Excitation transfer in collisions of highly excited alkali atoms, 25:43133
ZEMLO, L., (n,α) reactions on heavy nuclei induced by 14.2-

MeV neutrons, 25:43985 (INR-1258)
ZERMIZOGLOU, Roger, Purifying gases containing oxidizable impurities, 25:41914
ZERWAS, P., Possibility of CPT violation in neutral kaon decay, 25:43655 (PITHA-44)
ZGASA, Vera, Phage-induced radioresistance of lysogenic bacteria, 25:42529
ZHARKOV, Yu. A., Heterogeneity of liver nuclear RNA of irradiated rats, 25:42280
ZHELTONOG, K. S., Instrument for measuring and monitoring the energies of particles accelerated in a cyclotron, 25:43743
ZHULANOVA, Z. I., Effect of modifying factors on radiosensitive biochemical reactions, 25:42625
ZHUNKOVSKII, G. L., Interaction of carbon with boride coatings on high-melting metals, 25:42854
ZHURAVLEV, B. V., Decreasing ion cluster repetition frequency in an FEI cyclotron, 25:43742
ZHURKOV, O. K., Dielectric properties of γ-irradiated crystals of KH_2PO_4, 25:43443
ZICHA, B., Some biochemical changes in body fluids as indicators of radiation damage, 25:42402
ZIEGER, K., Distribution in separation tubes. I, 25:42011
ZIMBERG, Y., Combination of preoperative irradiation and surgery in the treatment of cancer of the oropharynx, hypopharynx, and larynx, 25:42588
ZIMIN, E. P., Raleigh--Taylor instability in magnetohydrodynamics in galvanic approximation, 25:43204
ZINOV'EV, G. M., Scaling, Pomeranchuk trajectory and J = 1 fixed poles in virtual Compton amplitude, 25:43584 (ITF-71-27-E)
ZIPE, E. C., Mass spectrometer observation of NO in auroral arc, 25:43218 (N-71-18997)
ZIPF, E. C., Differential electron flux as determined by auroral observations of N_2^+ and N_2^+ systems, 25:43214 (N-71-16589)
Excitation of the O I(^3S) and N I(^4P) resonance states by electron impact on O and N, 25:43143
ZIV, E. F., Production of high-quality zirconium concentrate, 25:42825
ZOELLNER, W. G., Microdetermination of tellurium and organo--tellurium compounds, 25:41744
ZOFKA, J., Hartree--Fock calculations of light deformed nuclei, 25:43986
ZOLLMAN, Dean Alvin, Non-relativistic hard pion production and the two nucleon interaction, 25:43653
ZOLOTOVITSKAYA, E. S., Polyhydroxy flavones as extraction reagents, 25:41738
ZOLOTOVSKII, O. A., Thermal explosion induced in a collisionless plasma by a relativistic electron beam, 25:43372
ZSINKA, L., Use of zirconium tellurate in ion exchange separation technique, 25:41915
ZUBENKO, Yu. V., Beryllium adsorption on tungsten, 25:43473
ZUBOVSKII, G. A., Effectiveness of scanning bone tumors with ^{85}Sr and /sup 87m/Sr, 25:42562
ZUCCARO LABELLARTE, G., Italian atmospheric radioactivity surveillance network, 25:41937
ZVENIGORODSKII, A. G., Excitation mechanism of the isobaric analog states from analysis of resonance (p,n) reactions, 25:43893
ZWEIG, G., Quantum numbers of cross-channel exchanges, 25:43565 (CALT-68-305)

XUM

SUBJECT INDEX

Cross references are included in cumulative subject indexes and in *Subject Headings Used by the USAEC Division of Technical Information* (USAEC report TID-5001).

The reader is also referred to *Guide to Abstracting and Indexing for Nuclear Science Abstracts* (USAEC report TID-4576).

Most headings in the subject index are specific materials, things, and processes. The headings are followed by modifiers that describe the properties of, or processes applied to, the headings.

All index entries cite *NSA* volume and abstract numbers; volume number precedes the colon and the abstract number follows it. The designation (R) following the abstract number indicates a progress report; (P) indicates a patent; and (T) indicates a translation. Abstracts for reports other than progress reports carry no letter designation. Report numbers, where applicable, are included in parentheses after the abstract number of the citation. Published literature (journal article or book) can be identified by the absence of a report number.

Ideas presented in the original literature, rather than key words, have been indexed. The indexers have selected what seemed the most probable and logical place to look for typical information. Since it is not always possible to anticipate where a user would look for information, the cumulative indexes include numerous cross references. Consideration of synonymous or closely related terms will prove valuable.

Information is indexed for the greatest use to the greatest number of users. This requires that a topic be indexed to headings that most specifically describe it and not ordinarily to the headings that describe its ultimate use or to the general class headings that include the specific headings. For example, information on boiler design for the Fermi Fast Breeder Reactor would be indexed under the headings BOILERS and FERMI FAST BREEDER REACTOR but not necessarily under the headings REACTORS, FAST or REACTORS, BREEDER.

General or broad headings are reserved for general summaries, reviews, comprehensive reports, and similar literature.

Subject Heading Styles

Generally, the direct form of subject entry is used rather than inverted headings; e.g., AMINO ACIDS rather than ACIDS, AMINO; HELIUM ISOTOPES He-4 rather than HELIUM—ISOTOPES He-4 or HELIUM—He-4 ISOTOPES. Note, however, that in some cases parenthetic modifying terms or inverted headings such as NEUTRONS, FAST, are used where the alphabetical arrangement of a direct entry would cause information to be scattered. In addition, organic compounds are usually entered in the index in the inverted form to facilitate grouping like or related compounds with the parent compounds; e.g., BENZENE, BROMO- rather than BROMOBENZENE. In general, the nomenclature used is that of the subject indexes to *Chemical Abstracts*.

Alphabetization

Subject headings are alphabetized word by word. Parenthetic qualifiers, numbers, and Greek letters within subject headings are disregarded in alphabetizing unless there are two or more headings that are otherwise identical, in which case the qualifier, numerical progression, or spelled names for the Greek letters determine the order.

Examples:

M-Capture
  see ELECTRON CAPTURE
MAGNESIUM
MAGNESIUM ALLOYS AND SYSTEMS
MANGANESE FLUORIDES
MANGANESE FLUORIDES MnF_2
MESONS
MESONS (π)
MESONS (ρ)
1-PENTANOL
2-PENTANOL

Modifying Phrases

The modifiers appearing under a subject heading are written specifically to show the relation between the item being indexed and the heading. The modifier therefore contains a maximum of useful information. Although the modifier begins with the word judged to be of greatest use to the greatest number of users, there is still need for the searcher to consider all modifiers under the heading(s) of interest.

Modifiers usually form meaningful phrases when combined with the subject heading. Some are intended to be read following the subject heading, e.g., the entry HYDROGEN—sorption by charcoal should be read "hydrogen sorption by charcoal." As a result of placing the important word first, however, many modifiers must be rearranged for smooth reading, e.g., FORMALDEHYDE—yields in radiolysis of ethyl ether, effects of deuterium on, should be read "effects of deuterium on formaldehyde yields in radiolysis of ethyl ether" and URANIUM—crystal structure of, effect of cooling rate on allotropic transformations in, should be read "effect of cooling rate on allotropic transformations in crystal structure of uranium."

Special characters are added to modifiers in the fields of physics and reactor technology; if the modifier does not establish the experimental or theoretical character of a reference, a symbol (E), (T), or (E/T) is placed immediately after the modifying phrase and before the abstract number.

Physical States and Configurations of Materials

The specific physical state, if other than normal, or the geometric configuration of the material is included in the modifying phrase; e.g., information on liquid metals is indexed under the specific metal with "liquid" in the modifier and carbon crucibles is indexed under CARBON with "crucibles" appropriately placed in the modifier. The information on carbon crucibles is also indexed under CRUCIBLES.

Nomenclature of Inorganic Compounds

Inorganic compounds are indexed to subject headings in the direct form. Cations are listed in the order of increasing valence for polycationic salts of varying valence and in alphabetic order for polycationic salts in which all cations have the same valence; e.g., SODIUM ALUMINUM SILICATES and POTASSIUM SODIUM SULFATES. If more than one anionic species is presented in a compound, the anions are arranged alphabetically, e.g., BERYLLIUM FLUORIDE HYDROXIDES.

Nomenclature of Organic Compounds

Organic compounds are indexed by subject headings based on the indexes to *Chemical Abstracts* except in the area of enzymes, in which specific enzymes, named according to the 1964 recommendations of the International Union of Biochemistry, are used. In many cases nonproprietary names for drugs are used as subject headings, and cross references are made from the systematic chemical names. Subject headings for hormones appear in the inverted style at HORMONES.

Nomenclature of Life Sciences

Subject headings for plants are names of phyla with one exception: members of the Phylum Tracheophyta are indexed under class or subclass names. Scientific names (genus and species) are used as the initial, or file, word in the modifying phrase. Scientific names are omitted only when the name is not available in the literature or cannot be found in available references.

Subject headings for animals are the names of phyla with the following exceptions: (1) members of Phylum Arthropoda and Phylum Chordata are indexed under appropriate class name, and (2) common names are used for members of Class Mammalia.

Subject headings are entered for various classes of commodities, and specific products are identified in the file-word position of the modifier. In the following examples, approved subject headings are capitalized and typical modifier file words are listed in lower case.

Example 1	Example 2
CEREALS	MEATS
bread	beef
flour	fish
oats	mutton
rice	pork
rye	poultry
wheat	seafood

Diseases, pathological conditions, and in vitro studies of atypical cells and tissues are indexed under subject headings for the organism affected, under the appropriate anatomical structure of physiological phenomenon affected, and under the appropriate disease heading. Subject headings for diseases (defined as any deviation from the norm) are DISEASES; DISEASES, INFECTIOUS; DISEASES, NEOPLASTIC; DISEASES, PHYSIOLOGICAL; DISEASES, PLANT; and DISEASES, TRAUMATIC.

Diseases of mixed etiology are treated in the following manner: neoplastic diseases that are also classified as infectious or physiological are indexed under DISEASES, NEOPLASTIC; diseases in which a microorganism is the etiologic agent are classified under DISEASES, INFECTIOUS; physiological anomalies that are neither neoplastic nor infectious are indexed under DISEASES, PHYSIOLOGICAL; the acute radiation syndrome, nonspecific radiation injuries, trauma, and wounds or incisions inflicted mechanically are indexed under DISEASES, TRAUMATIC.

Specific diseases or pathological conditions are named in the file-word position of the modifier, in the author's terminology, and are set off from the remainder of the modifier by commas. Neoplasms are designated as benign or malignant in the file-word position when more specific information is not available.

Multicomponent Alloys and Other Systems

Multicomponent alloys and systems, except well-known trade names, are indexed under a subject heading for each component in the form "element systems" for nonmetals or "element alloys and systems" for metals. The modifier begins with element symbols for each component arranged alphabetically. In addition, if significance is placed on the base metal of the alloy, this is indicated by adding "-base" to the element symbol.

Example: A 1.5C, 12Cr, 0.25V, 0.8Mo, bal Fe alloy is indexed as

```
CARBON SYSTEMS
  C--Cr--Fe-base--Mo--V, ...
CHROMIUM ALLOYS AND SYSTEMS
  C--Cr--Fe-base--Mo--V,...
IRON ALLOYS AND SYSTEMS
  C--Cr--Fe-base--Mo--V, ...
MOLYBDENUM ALLOYS AND SYSTEMS
  C--Cr--Fe-base--Mo--V, ...
VANADIUM ALLOYS AND SYSTEMS
  C--Cr--Fe-base--Mo--V, ...
```

Well-known alloys, such as ZIRCALOY-2, are indexed under the trade name; cross references from each component of the alloy to the trade name appear in cumulative indexes.

Multicomponent systems in which nonmetallic elements are present in large percentage and which are commonly referred to as systems or mixtures are indexed in a manner similar to alloys.

Example: A tungsten–silicon preparation is indexed as

```
TUNGSTEN ALLOYS AND SYSTEMS
  Si--W, ...
SILICON SYSTEMS
  Si--W, ...
```

Multicompound systems and mixtures of inorganic compounds are indexed under the subject heading for each component compound; the modifiers begin with an alphabetical listing of compound formulas.

Example: A lead titanate–lead zirconate mixture is indexed as

```
LEAD TITANATES
  PbTiO3--PbZrO3
LEAD ZIRCONATES
  PbTiO3--PbZrO3
```

XUM

A mixed system of compounds and elements is indexed by a combined form of the preceding conventions; e.g., a dispersion of copper and alumina would be indexed as

ALUMINUM OXIDES
  Al_2O_3--Cu, ...
COPPER ALLOYS AND SYSTEMS
  Al_2O_3--Cu, ...

Mixtures of organic compounds are indexed under subject headings for each component of the mixture; the modifiers begin with an alphabetical listing of compound names.

Example:

ACETIC ACID
  acetic acid--BF_3, ...
BORON FLUORIDES
  acetic acid--BF_3, ...

Example:

BENZENE, CHLORO-
  bromophenol--chlorobenzene, ...
PHENOL, BROMO-
  bromophenol--chlorobenzene, ...

If modifiers for alloys and systems are included with other modifiers under the same subject heading, they are filed last.

Example:

CARBON SYSTEMS
  deposition on nuclear fuel particles
  molecular structure of
  neutron total cross section for
  sorptive properties for xenon
  Young's modulus for
  Al--C--Cr, superconductivity in
  B--C, phase studies for
  C--U--Zr, fabrication and physical properties of

Nomenclature of High Energy Physics

Information on particle-particle events is indexed under subject headings for the specific particles involved. The modifier file word *interactions* is followed by the specific interaction written in symbolic form. Particle nomenclature and symbols follow that of Rosenfeld, et al. *Data on Particles and Resonant States,* UCRL-8030 (latest revision). For consistency the incident particle is always written first. The mass (in MeV) of a resonance state is included in parentheses after the symbol to avoid ambiguity. Hyperfragments are indicated in modifiers as in the following examples: Λ-He^5, Σ-H^3, $\Lambda\Lambda$-Be^{10}. The superscript on the right indicates the total number of baryons in the composite system.

Examples:

MESONS (π^-)
  interactions $\pi^- + p \rightarrow \Lambda + K^+ + \pi^-$ at 6 GeV/c in hydrogen bubble chamber, $\Lambda K(1700)$ enhancement in, (E)
BARYONS, RESONANCE (N*)
  production of $\Delta^{++}(1236)$ and $\Delta^0(1236)$ from $K^- + p \rightarrow K^- + p + \pi^+ + \pi^-$ interactions at 2.63 and 2.70 GeV/c, (E)
HYPERFRAGMENTS
  binding energy of $\Lambda\Lambda$-He^6, three-body α--Λ--Λ model for

Subject headings are also provided for specific models and theories.

Examples:

ELEMENTARY PARTICLE MODELS (TRIPLET)
  hadron total cross sections in quark, numerical analysis of
CURRENT ALGEBRA
  PCAC hypothesis for A_1 and rho dominance in $\pi \rightarrow e + \nu + \gamma$ decay
REGGE POLE THEORY
  predictions for polarization in $K^- + p \rightarrow$ anti $K^0 + n$, $\pi^- + p \rightarrow \pi^0 + n$, and $\pi^- + p \rightarrow$ eta + n interactions at high energies
SYMMETRY GROUPS
  SU(2) × SU(4) intermediate-coupling model for nucleon and hyperon isobars

Nomenclature of Reactor Technology

Subject headings for reactors are of three types:

(1) Specific reactors, e.g., ARGONNE RESEARCH REACTOR, SAXTON POWER REACTOR

(2) Reactors having a common physics or engineering characteristic, e.g., REACTORS, FAST; REACTORS, ORGANIC-COOLED; REACTORS, PRESSURIZED-WATER

(3) Reactors having a common purpose, e.g., REACTORS, POWER; REACTORS, RESEARCH

Information on specific reactors, type (1), is indexed under the one specific subject heading. Information on classes or types of reactors, types (2) (characteristics) and (3) (purpose), is indexed under all applicable headings. For example, information on a heavy-water-moderated organic-cooled power reactor is indexed under REACTORS, HEAVY WATER-MODERATED; REACTORS, ORGANIC-COOLED; and REACTORS, POWER.

Subject headings exist for selected reactor components, e.g., REACTOR FUEL ELEMENTS. When applicable, headings for components are indexed even though they may have been included in a modifier under a type (1) or (2) heading. The materials in reactor components are indexed when the information is peculiar to the material.

Modifier file words under reactor headings are of two primary types: one type expresses reactor characteristics, e.g., reactivity; the other, components, e.g., control rod. If no subject heading appears for a reactor component, the heading REACTORS is used, and the component is used as the modifier file word.

A

ACCELERATOR TUBES
current loading of 1-MV Van de Graaff, effects of neutral component of ion beam on, 25:43769
ACCELERATORS
beam analyzers and handling systems for, development of cryogenic, 25:43735
beam extraction from cyclic, compensation of stray field of magnetic deflectors for, 25:43744
description for fabrication of integrated circuits by ion implantation, 25:43729 (CEA-CONF-1767)
description of 20- to 200-keV, for ion implantation in semiconductors, 25:43747
design of electrostatic, for ion implantation into semiconductors, 25:43740(P)
development of superconducting, 25:43735
operating principles of collective, 25:43739
radiation monitoring of environment of, methods for, 25:42443
ACCIDENTS
handling procedures for radiation exposure and radioactive contamination, health physics and medical, 25:42391
radiation, legal responsibility in, in Germany, 25:42507
ACETAMIDE, 2-IODO-
effects on duodenum crypt cells in mice pretreated with radioprotective thiols, 25:42520
ACETIC ACID, [(CARBOXYMETHYLIMINO)BIS(ETHYLENENITRILO)]TETRA-
preparation of ytterbium-169-labeled, method for, 25:41833(R) (IA-1218)
ACETIC ACID, IODO-
effects on duodenum crypt cells in mice pretreated with radioprotective thiols, 25:42520
toxicity in rats, effects of cysteine on in vitro and in vivo, 25:42523
ACETIC ACID, TRIFLUORO-
copper salt, ESR of, 25:41838
zinc salt, complexes with copper, ESR of, 25:41838
ACETIC ACID, VINYL ESTER
radioinduced polymerization in wood, γ, 25:41843(R) (ORO-2945-10)
ACETONE
effects on yields of nitrogen from radiolysis of 2,2'-azobis[2-methylpropionitrile]--benzene, 25:41872
solution heat of, effects of deuterium on, 25:41794
ACETOPHENONE
effects on yields of nitrogen from radiolysis of 2,2-azobis[2-methylpropionitrile]--benzene, 25:41872
ACID PHOSPHATASE
radiation effects on distribution of, in rat liver and spleen, whole-body x, 25:42528
radiation effects on mouse thymus gland, whole-body x, 25:42287
ACRIDINE
effects of analogs of, on survival of uv-irradiated Escherichia coli, 25:42533
ACRIDINE, 3,6-DIAMINO-
effects on sensitivity of Serratiaphage kappa to uv radiation, 25:42734
radioprotective effects of methylated, on lambda phage, uv, 25:42737
ACRYLAMIDE
radioinduced polymerization of solid, at 77°K, ESR and NMR studies on radicals produced by γ, 25:41850(R) (CEA-N-1438)
ACRYLIC ACID
radioinduced polymerization of solid, at 77°K, ESR and NMR studies on radicals produced by γ, 25:41850(R) (CEA-N-1438)
ACRYLIC ACID, ESTERS
radioinduced polymerization in wood, γ, 25:41843(R) (ORO-2945-10)
ACRYLONITRILE
acrylonitrile--styrene, radioinduced polymerization in wood, γ, 25:41843(R) (ORO-2945-10)
ACTINIDE ALLOYS AND SYSTEMS
properties of, prediction of, 25:41778 (UCRL-20500, pp 1-85)
ACTINIDES
electronic states of gaseous atoms of, 25:41778 (UCRL-20500, pp 1-85)
ACTINIUM ISOTOPES Ac-227
properties for use as heat source for thermoelectric generators, 25:42014
ACTIVATION ANALYSIS
book: Neutron Physics Practices. Volume I. Physics and Technology of Activation Probes, 25:43775
computer techniques in neutron, review on, 25:41769
equipment for neutron, for mineral prospecting, design of mobile, 25:41758
sodium removal from samples in, 25:41760
uses in forensic science, reliability of evidence obtained by neutron, 25:41775
uses in mineral exploratio and exploitation, conference on, Krakow, Dec. 9 to 12, 1969, 25:41941 (STI/PUB-279)
uses of neutron, for mineral prospecting, review on, 25:41767
uses of neutron, in on-stream analysis in mineral processing plants, review on, 25:41740
ADENOSINE
radioprotective effects of derivatives of, on mice, lethal, γ, 25:42516
ADENOSINE 5'-TRIPHOSPHATE
effects on rejoining of x-radioinduced breaks in DNA of Ehrlich ascites tumor cells, 25:42632
ADHESION
radiochemical processes of, 25:41845(P)
ADRENAL GLANDS
effects of serotonin on mouse, 25:42519
radiation effects on mouse, protective effects of cysteamine, lipopolysaccharide, and serotonin against x, 25:42513
ADSORBENTS
properties for radioisotopes in liquid waste disposal, 25:41833(R) (IA-1218)
AEROSOLS
beta activity of, autoradiographic method for measuring, 25:42051 (JAERI-13718)
sampling at government installations in USA, survey of methods for, 25:44257 (LA-4249(Vol.2))
size distribution of beta emitting, autoradiographic method for measuring, 25:42051 (JAERI-13718)
AET
effects on redox potential of spleen, 25:42526
radioprotective effects of, on rat tissues, combined hypoxia and, 25:42511
radioprotective effects on rat tissues and organs, mechanism of in vitro and in vivo, 25:42523
AGE
effects on cesium-137 elimination from human organism, 25:42250
effects on strontium-85 retention in lactating and nonlactating rats, 25:42252
AGING
radioinduced in man, 25:42712
AGRICULTURE
irrigation in, use of reactor heated effluents for, 25:44083 (BNWL-SA-2738)
research programs of AEC during 1970 on, 25:44293 (TID-25728)
AGUIRRE POWER REACTOR, UNIT 1
site for, geological data for, 25:44059 (DOCKET-50376-18)
site for, possibility of tornadoes at, 25:44068 (DOCKET-50376-16)
AIR
analysis for beryllium, rapid colorimetric method for, 25:41717 (CEA-N-1446)
effects on yields of cresol isomers from electron or γ radiolysis of toluene--water systems, 25:41858
electric conductivity at 3000 to 28,000°K, effects of multiple ionization on, (T), 25:43362 (N-71-18715)
fission fragment range in, determined by fission-track detector, (E/T), 25:43427
mass stopping for gamma and x rays, calculation of mean, 25:42085
neutron transport calcultions for 14-MeV source in 5000-m radius cylinder of, overlap conditions for sequential discrete ordinates, 25:43419 (ORNL-TM-3269)
proton energy straggling and stopping at 100 to 500 keV in, (E/T), 25:43432
AIRCRAFT
radioactive materials shipment in cargo and passenger, regulation of International Air Transport Association governing, 25:42456
AIRGLOW
Doppler profiles of 5577-A, (T), 25:43207 (AD-706130)
oxygen 1304-A emission in day, OGO-4 temporal and morphological observations of atomic, (E), 25:43259
ALANINE
polymers, radioinduced hydrogen transfer in, effects of temperature and scavengers on γ, 25:41837
ALANINE AMINOTRANSFERASE
radiation effects on activity of, in rat serum, effects of unsaturated fatty acid content of diet on whole-body x, 25:42298
β-ALANINE, 2-METHYL-
radiation effects on excretion of, in human urine, x, 25:42684
radiation effects on metabolism of, in mice and rats, mechanisms for, 25:42623
ALASKA
ecosystems of Amchitka Island, use of Milrow data in prediction of effects of Cannikin underground nuclear test on marine and terrestrial, 25:42318 (TID-25735)
tectonic setting of Amchitka Island, 25:41927 (USGS-474-75(Rev.1))
ALBUMINS
radiation effects on distribution and exretion of iodine-131-labeled, in rats as indicator of radiation injury, whole-body γ, 25:42407
ALCOHOLS
radiolysis of mixtures of, ion--solvent interactions in x, 25:41871
ALEUTIAN ISLANDS
seismological bulletin for, December, 1970, 25:44239 (CGS-746-114)
ALGAE
effects of alginates from, on strontium-85 sorption

XUM

through intestine of rats, 25:42254
ALGINIC ACID
effects on strontium-85 sorption through intestine of rats, 25:42254
ALGORITHMS
development of geometric programming, 25:44276 (ORNL-4650)
ALKALI METAL HALIDES
exoelectron emission from ionic, (E), 25:43489
thorium precipitation from molten, effects of polarization on, 25:42821
ALKALINE PHOSPHATASE
radiation effects on activity in hamster intestine, whole-body γ, 25:42301
ALKANES
radiolysis in adamantane matrix, ESR studies on, 25:41832(R) (AECL-3851)
radiolysis of, effects of electronic excitation of molecules on yields of free radicals from, 25:41859
ALKENES
radiolysis in adamantane matrix, ESR studies on, 25:41832(R) (AECL-3851)
ALLOYS
fabrication of close tolerance shapes in most wrought, by form rolling, 25:42827
radioinduced swelling in, discussion of, 25:42920
ALPHA CROSS SECTIONS
measurements of elastic and inelastic scattering differential, for A = 5 to 209 nuclei at 104 MeV, (E), 25:43832 (NP-19920)
ALPHA DECAY
half-life for, delayed-coincidence method for measurement of, 25:42222
ALPHA PARTICLES
alpha elastic scattering by, two-channel calculation using soft-core potential, (T), 25:43784
cutoffs of 7 to 22 MeV solar, low-altitude observations of, (E), 25:43234
detection of cosmic-ray, design of balloon-borne counter telescope for, 25:42159
dose distribution in skin following penetration of surface contaminants, 25:42257
dosimetry in bronchial epithelium following inhalation of polonium-214, polonium-218, or plutonium-239, methods for, 25:42394(R) (NYU-4256-1)
effects on silicon at 25 MeV, distribution of defects induced in, (E), 25:43463
effects on thallium-activated cesium iodide crystals, influence of electric field on luminescent, (E), 25:43448
energy loss in tissue-equivalent polycarbonate and gases, methods of measurement of, 25:42394(R) (NYU-4256-1)
energy spectra of solar, Explorer-35 data from July 20, 1967 to May 14, 1968 of, (E), 25:43231
monitoring in lava from nuclear explosion cavity, 25:41953 (CEA-R-4099)
reactions (α,2α) with lithium-6 at 37.5 and 43.5 MeV, plane-wave impulse-approximation analysis of angular distributions from, (E/T), 25:43803
reactions (α,nγ) and (α,pγ) with aluminum-27 at 5 to 8 MeV, γ spectra from, (E), 25:43879
reactions (α,pγ) with nickel-58 at 10 MeV, γ spectra and p-γ angular correlations for, (E), 25:43839
reactions (α,t) with ytterbium-172, -174, and -176 at 30 MeV, triton spectra from, (E), 25:43942
scattering by A = 5 to 209 nuclei at 104 MeV, differential cross sections for elastic and inelastic, (E), 25:43832 (NP-19920)
scattering by aluminum-27, magnesium-24, magnesium-26, and silicon-28 at 22 MeV, α--γ coincidence spectra from inelastic, (E), 25:43854
scattering by lithium-6 and -7 at 12 to 18 MeV, optical-model analysis of elastic, (E/T), 25:43810
scattering by neon-20 and silicon-28 at 104 MeV, quadrupole and hexadecapole deformation parameters from coupled-channels analysis of differential cross sections for inelastic, (E/T), 25:43876
scattering by nuclei, real part of alpha--nucleus potential in region of nuclear surface, (T), 25:43973
scattering by yttrium-89 at 26 MeV, inelastic, (E), 25:43859
ALPHA SOURCES
dosimetry of flat circular polonium-210, in biological material, comparison of extrapolation ionization chamber and surface-barrier semiconductor detectors for, 25:42436
ALPHA SPECTROMETERS
design for determination of plutonium in plutonium--uranium alloys, 25:42118(P)
ALUMEL COUPLES
Alumel/Chromel-P, standard for magnesium oxide-insulated and stainless steel sheathed, 25:42200 (RDT-C-7-6-T)
ALUMINUM
beta-particle mass absorption coefficients of, negative and positive, 25:43433
bonding to lead for use as gamma shields for Omega West Reactor, 25:42815 (LA-4544)
creep of polycrystalline, kilocycle acoustic emission during, (E), 25:42862
determination in aluminum--silicon--uranium alloys by atomic absorption spectrometry, 25:41832(R) (AECL-3851)
effects on determination of strontium in carbonates, silicates, and sulfates by atomic absorption spectroscopy, 25:41735
effects on microstructure of fast neutron irradiated iron, 25:42908
effects on positron lifetimes and intensities in sodium chloride crystals, 25:43453
effects on superconducting critical field of niobium--titanium alloy wires, 25:43309
electron reactions up to 2000 eV with, Auger transitions and supplementary electron ejection in ionization by, (E), 25:43102
electron reactions with foils at 5 to 10 MeV, influence of electric field on secondary electron emission from, (E), 25:43101(T) (SCL-T-69-256)
electron transport through semi-infinite slab of, analysis using phase-space time-evolution method, (T), 25:43424
helium bubble density and size distribution in irradiated and annealed foils of, transmission electron microscopy of, 25:42896
mass stopping for gamma and x rays, calculation of mean, 25:42085
response mechanisms at high strain rates, analysis of, 25:42886 (UCRL-20500, pp 86-146)
separation from acetone--hydrochloric acid solutions by ion exchange using Bio-Rad, distribution coefficients for, 25:41899
separation from other metals using inorganic ion exchange papers, 25:41909
shielding properties against x radiation, 25:42447
superconducting parameter calculations, 25:43305
weld solidification in, structures and mechanism of, 25:42820
welding of, pulse-arc, 25:44233(R) (BDX-613-431)
ALUMINUM ALLOYS AND SYSTEMS
fatigue crack propagation in, model for, 25:42886 (UCRL-20500, pp 86-146)
Ag--Al-base, crystal stacking faults in, high-voltage imaging of, 25:42886 (UCRL-20500, pp 86-146)
Al--Al_2O_3, helium bubble density and size distribution in irradiated and annealed foils of, transmission electron microscopy of, 25:42895
Al--Cr--Fe-base, properties for use in high-temperature strain gages, 25:42804(R) (LMEC-71-1)
Al--Cr--Fe-base--Y, properties for use in high-temperature strain gages, 25:42804(R) (LMEC-71-1)
Al--Cr--Mo--Ti-base--V--Zr, mechanical properties of, 25:42836 (AD-715877)
Al--Cu, aging processes in, effects of trace metals on precipitation from, 25:42885 (UCRL-20500, pp 86-146)
Al--Cu, superconducting transition temperature in high T/sub c/ intermetallic $CuAl_2$, sensitivity to residual stress of, (E), 25:43302
Al--Er--Ni, magnetic properties of $ErAl_{2-x}Ni_x$, 25:43480
Al--Fe-base, microstructure of alpha-phase, in K-state, 25:42886 (UCRL-20500, pp 86-146)
Al--Gd--Ni, magnetic properties of $GdAl_{2-x}Ni_x$, 25:43480
Al--Ge, mixing in liquid and solid phases of, energy of, 25:42970
Al--Ge--Nb, superconductivity and range of existence of A15 phase in, (E), 25:43291(T) (ORNL-tr-2461)
Al--Ge--Y, phase diagram at 500°C, isothermal, 25:42891
Al--Ho--Ni, magnetic properties of $HoAl_{2-x}Ni_x$, 25:43480
Al--Mg--Zn, corrosion of age-hardened, by aqueous sodium chloride, stress, 25:42885 (UCRL-20500, pp 86-146)
Al--Mo--Ti-base--V, radiation effects on tensile properties of, at 17°K, fast neutron, 25:42926
Al--Ni--Tb, magnetic properties of $TbAl_{2-x}Ni_x$, 25:43480
Al--Sb--Y, phase diagram at 500°C, isothermal, 25:42891
Al--Si, mixing in liquid and solid phases of, energy of, 25:42970
Al--Si--U, analysis for aluminum by atomic absorption spectroscopy, 25:41832(R) (AECL-3851)
Al--Si--Y, phase diagram at 500°C, isothermal, 25:42891
Al--Sn--Ti-base, radiation effects on tensile properties of, at 17°K, fast neutron, 25:42926
Al--Ti-base--V, radiation effects on tensile properties of, at 17°K, fast neutron, 25:42926
Al--V, preparation of superconducting V_3Al intermetallic phase in, 25:42886 (UCRL-20500, pp 86-146)
Al--Zr-base, precipitation in, effects of vacancies on, 25:41832(R) (AECL-3851)
Al-base--Cu, radiation effects on precipitation hardening of, pile neutron, 25:42902 (JAERI-13692)
ALUMINUM CARBIDES
radiation effects on, reactions of recoil nitrogen-13 from deuteron, 25:41886
ALUMINUM COUPLES
Al/U, corrosion of, effects of capacitance discharge and frequency on galvanic, 25:41833(R) (IA-1218)
ALUMINUM IONS
reactions with argon at 30 to 130 keV, cross sections for argon L-shell x-ray emission in, (E), 25:43134
reactions with nitrogen molecules at 30 keV to 2 MeV, cross sections for excitation of N_2^+ 3914-A radiation in, (E), 25:43151

spectral levels in solar corona, autoionizing, (E), 25:43065 (AD-715257)
ALUMINUM ISOTOPES Al-27
alpha inelastic scattering at 22 MeV, α--γ coincidence spectra from, (E), 25:43854
alpha reactions (α,nγ) and (α,pγ) at 5 to 8 MeV, γ spectra from, (E), 25:43879
energy levels at 3.95 MeV from photon resonance scattering, width for, (E), 25:43838
energy levels from alpha inelastic scattering, lifetimes of, (E), 25:43854
helium-3 reactions (He-3,p) at 5 MeV, analysis including Coulomb distortion and finite-range effects, (T), 25:43964
photon elastic and inelastic scattering at 2 to 4 MeV, spectra from, (E), 25:43838
ALUMINUM ISOTOPES Al-28
energy levels from aluminum-27 neutron capture, spin--parity assignments for, (E), 25:43831 (INR-1262)
ALUMINUM NITRIDES
AlN--Y_2O_3, mechanical properties of sintered fiber-reinforced composites of, 25:42959
AlN--Y_2O_3, microstructure of sintered fiber-reinforced composites of, 25:42959
ALUMINUM OXIDES
book: High-Temperature Materials, 25:42853
preparation of high-purity, by thermal dissociation of chloride in sprays, 25:41833(R) (IA-1218)
properties for use as absorbent in radioisotope production, 25:41991 (JAERI-13778)
sorptive properties for cesium at 300 to 1000°F, tracer studies on, 25:42853
Al_2O_3--CaO--Nd_2O_3, phase diagrams of, 25:42995
Al_2O_3--glass, tensile properties of composites of, effects of internal strains on, 25:42957 (UCRL-20500, pp 147-73)
Al_2O_3--Nb_2O_5, phase studies of, 25:42985
Al_2O_3--SiO_2, phase studies of, 25:42957 (UCRL-20500, pp 147-73)
Al--Al_2O_3, helium bubble density and size distribution in irradiated and annealed foils of, transmission electron microscopy of, 25:42895
AMERICIUM
determination in plutonium oxide, spectrophotometric, 25:41721 (EJR-4352)
reactions of trivalent, with ammonium peroxydisulfate, effects of silver ions on, kinetic studies on, 25:41785
stability of pentavalent and hexavalent, in phosphoric acid solutions, 25:41833(R) (IA-1218)
AMERICIUM ISOTOPES Am-241
alpha decay of, α-γ delayed coincidence spectra from, (E), 25:43895
determination in urine by precipitation, ion exchange, electroplating, and α counting, 25:41756
distribution in skin following surface contamination, kinetics of, 25:42257
toxicity to rats in comparison to neptunium-237, 25:42253
uptake by bones in animals and man, induction of neoplasms and radiation injuries following, 25:42472
AMINES
crystal and molecular structures of arylamines, 25:44296 (TID-25742)
radiolysis of, ESR studies on, 25:41832(R) (AECL-3851)
AMINO ACIDS
book: Investigation of the Paramagnetic Centers of Irradiated Proteins, 25:42275
AMMETERS
design for measuring dc down to 10^{-14} A, 25:42208(P)
AMMONIA
complexes with cobalt, reactions of hydrated, with trivalent uranium in aqueous perchlorate solutions, 25:41783
radiolysis of, electron pulse, 25:41832(R) (AECL-3851)
radiolysis of, rate of disappearance of NH_2 and NH radicals from electron pulse, 25:41869
NH_3--N_2O, radiolysis of, γ and neutron, 25:41851 (JAERI-13780)
AMMONIUM HYDROXIDES
corrosive effects of dilute solutions of, on niobium--zirconium-base alloys at 300°C, 25:42814
AMMONIUM MOLYBDOPHOSPHATES
sorptive properties for radiocesium, 25:41751
AMMONIUM NITRATES
corrosive effects on zirconium alloys, 25:41832(R) (AECL-3851)
effects of methanol solutions of, on dissolution of niobium, tantalum, and tungsten by anodic polarization, 25:41833(R) (IA-1218)
AMMONIUM PEROXYDISULFATES
reactions with americium(III), effects of silver ions on, kinetic studies on, 25:41785
AMMONIUM URANATES
analysis for boron by isotope dilution method, 25:41749
preparation of pure, 25:41919
AMPHIBIA
Eleutherodactylus sp., radioisotope uptake by, in rain forest in Puerto Rico, 25:42317(R) (PRNC-147)
role in ecology of rain forest in Puerto Rico, 25:42317(R) (PRNC-147)
AMPLIFIERS
specifications for JAERI modular, 25:42185 (JAERI-13605)
B-AMYLASE
radiation effects on human salivary, as indicator of radiation injury, 25:42405
ANALYTICAL CHEMISTRY
conference on, Pittsburgh, Cleveland, Ohio, Feb. 28 to March 5, 1971, abstracts, 25:41720 (CONF-710207-(Absts.))
conference on, Pittsburgh, Cleveland, Ohio, March 1-6, 1970, abstracts, 25:41719 (CONF-700303-(Absts.))
research progress on, 25:41832(R) (AECL-3851)
ANAPHYLAXIS
book: Radiation Immunology and Transplantation, 25:42310
5B-ANDROSTANE-17-ONE, 3α-HYDROXY-
effects on irradiated human bone marrow cells as indicator of radiation injury, 25:42406
ANGIOSPERMIDAE
Allium cepa, radiation effects on root tip chromosomes of, in comparison to cycasin, emulsin, and methylazoxymethanol, aberrant x, 25:42334
Arabidopsis thaliana, radioinduced mutations for chlorophyll in, effects of dose and seed exposure on γ, 25:42358
Artemisia tridentata, radiation effects on survival of, effects of size at exposure on fallout beta and gamma, 25:42717 (EGG-1183-2272)
Avena sativa, radioisotope uptake from soils by, effects of fertilizers on cerium-144, plutonium-238, and promethium-147, 25:42260
Avena sativa, strontium-90 deposition in, effects of time of sorption from nutrient solution on site of, 25:42261
Beta sp., radiation effects on DNA transcription and RNA translation in, γ, 25:42716(R) (COO-1313-29)
Crepis capillaris, radioinduced chromosome aberrations in dry seeds of, effects of nitrogen mustard on γ, 25:42359
Crepis capillaris, radioinduced chromosome aberrations in, effects of DNA on recovery from x, 25:42356
Crepis capillaris, radioinduced chromosome aberrations in, effects of dose on γ, 25:42351
Crocus sativus, radiation effects on flower and pollen size of, effects of dose on γ, 25:42720
Cucumis sativus, radiation effects on seed emergence in, effects of dose on γ, 25:42719
Dahlia variabilis, radioinduced mutations in, for flower color, 25:42327
Glycine max, strontium-89 accumulation by, effects of environment and genotype on, 25:42322(R) (COO-1097-46)
Glycine max, strontium-90 accumulation by, effects of environment and genotype on, 25:42322(R) (COO-1097-46)
Helianthus annuus, radioinduced chromosome aberrations in roots of, effects of seed-exposure dose on x, 25:42361
Hordeum distichum, radiation effects on differential stage-sensitivity of, chronic-exposure γ, 25:42724
Hordeum vulgare, radiation effects on germination of seeds of, effects of oxygen and water on, 25:42296
Hordeum vulgare, strontium-89 accumulation by, effects of environment and genotype on, 25:42322(R) (COO-1097-46)
Hordeum vulgare, strontium-90 accumulation by, effects of environment and genotype on, 25:42322(R) (COO-1097-46)
Lycopersicum sp., radioinduced mutations in, fast neutron and γ, 25:42364
Oryza sativa, chlorophyll mutation frequency and growth following treatment of seeds with D_2O, effects of ethyl methanesulfonate on, 25:42346
Pisum sp., radioinduced chromosome aberrations in relation between radiation effects on biochemistry and morphology and γ, 25:42329
Pyrus sp., radioinduced mutations in dormant scions of, γ, 25:42324
Solanum sp., radioinduced mutations for hooded eyes in, γ, 25:42323
Triticum aestivum, radiation effects on gross morphology of, chronic-exposure γ, 25:42724
Triticum aestivum, strontium-89 accumulation by, effects of environment and genotype on, 25:42322(R) (COO-1097-46)
Triticum aestivum, strontium-90 accumulation by, effects of environment and genotype on, 25:42322(R) (COO-1097-46)
Triticum sp., radiation effects on ascorbic acid content following seed exposure, effects of dose on γ, 25:42726
Triticum sp., radiation effects on carbohydrate content in durum and soft, x, 25:42721
Triticum sp., radioactivity monitoring in Western Australia, natural α, 25:42427
Triticum sp., radioinduced mutations in, sensitivity of hybrids following x, 25:42350
Vicia faba, radioinduced chromosome aberrations in, use of protein-specific dyes to visualize x, 25:42343
Viguiera porteri, radiation effects on reproductive potential under field conditions, acute simulated-fallout beta, 25:42718 (ORO-3299-110)
Viguiera porteri, radiation effects on terminal buds of, simulated fallout yttrium-90, 25:42320
Zea mays, monosome cytogenetics in, 25:44257(R) (COO-2121-3)
Zea mays, radioinduced cytogenetic damage to, comparison of recovery of hybrid and parent strains from,

XUM

25:42722
ANGIOTENSINS
preparation of iodine-125 labeled, method for, 25:42241
radioimmunoassay in human plasma, method for, 25:42238
ANIMAL FEEDS
analysis for trace amounts of lithium and rubidium in alfalfa, spectrochemical, 25:41833(R) (IA-1218)
ANIMALS
book: Oxidation Equilibrium and the Radiosensitivity of Organisms, 25:42528
book: The Biological Effects of External β Irradiation, 25:42646
radiation dose to marine, following discharge of radioactive wastes into seawater, 25:42373
radiation effects on DNA metabolism in, dosimetry using, 25:42403
radiation effects on metabolism of biogenic amines in, as indicators of radiation injury, x, 25:42627
radiation effects on, latent, 25:42604
radiation effects on, relation of recommendations for human protection to, 25:42505
radioisotope accumulation by fish, invertebrates, and mammals, bibliography on, 25:42315 (ORNL-NSIC-89)
radioisotope sorption by intestines of, use of ion exchange resins for prevention of, 25:42263
silver-108m content of, at Bikini and Eniwetok atolls following nuclear testing during 1958, 25:42377
ANTARCTIC REGION
proton penetration to polar caps during Jan. 24, 1969 event, asymmetric access of solar, (E), 25:43233
ANTHRACENE
effects on yields of nitrogen from radiolysis of 2,2'-azobis[2-methylpropionitrile]--benzene, 25:41872
fluorescence excited by fast electrons, rise and decay times of, 25:43452
anthracene--2,3-dimethylnaphthalene, radioinduced quenching of luminescence of crystals of, x, 25:41840
anthracene--naphthacene, radioinduced quenching of luminescence of crystals of, x, 25:41840
ANTIBIOTICS
radioinduced transformation in mixture of Streptomyces surinam heptaene, uv, 25:42302
ANTIBODIES
book: Radiation Immunology and Transplantation, 25:42310
detection of Australia, using double-antibody radioimmunoassay, 25:42308
formation in response to antigen, reaction mechanisms for, 25:44274(R) (NYO-3707-7)
radiation effects on formation of, comparison of iodine-131 and uranium nitrate, 25:42645
radiation effects on production of tetanus, in mice, combined effects of drugs and γ, 25:42672
ANTIGENS
book: Radiation Immunology and Transplantation, 25:42310
detection of Australia, using double-antibody radioimmunoassay, 25:42308
ANTIMONY
determination in iron and steel standards by neutron activation and γ spectrometry, 25:41774
determination in minerals from Luzon, Philippines, by neutron activation, 25:41772
determination of trace amounts of, in meteorites by neutron activation and γ spectrometry, 25:41773
separation from acetone--hydrochloric acid solutions by ion exchange using Bio-Rad, distribution coefficients for, 25:41899
separation from aqueous solutions by ion exchange on zirconium tellurate, tracer studies on, 25:41915
separation from other metals using inorganic ion exchange papers, 25:41909
ANTIMONY ALLOYS AND SYSTEMS
Al--Sb--Y, phase diagram at 500°C, isothermal, 25:42891
Bi--Sb, superconducting thin films of, fluctuation contributions to thermal capacity of, 25:43321
Ce--Sb, magnetic structure in strong magnetic fields, 25:43435(R) (RISO-237)
Ge--Sb, mixing in liquid and solid phases of, energy of, 25:42970
Sb--Si, mixing in liquid and solid phases of, energy of, 25:42970
ANTIMONY ISOTOPES Sb-121
energy levels from tin-121 decay, spin--parity assignments and quadrupole moments of, (E), 25:43905
energy-level transitions from tin-121 decay, internal conversion coefficients for, (E), 25:43905
ANTIMONY ISOTOPES Sb-122
beta decay of, β-γ angular correlations from first forbidden, (E), 25:43947
ANTIMONY ISOTOPES Sb-125
beta decay of, γ--γ angular correlations in, (E), 25:43927
content in ground-level atmosphere of Brunswick, West Germany, effects of seasonal variations on, 25:41934
ANTIMONY ISOTOPES Sb-126
beta decay of, decay energy, Fermi-Kurie plots, log-ft values, and gamma spectra from, (E), 25:43924
energy levels from tin-125 beta decay, lifetimes and spin--parity assignments for, (E), 25:43924
energy-level transitions from tin-126 beta decay, branching ratios, intensities, and multipolarities for, (E), 25:43924
ANTIMONY ISOTOPES Sb-127
energy level at 1920 keV from tin-127 beta decay, lifetime and spin--parity assignments for isomeric, (E), 25:43928
isomeric transition in, half-life for, (E), 25:43928
ANTIMONY OXIDES
preparation of hydrates of, for sorption of sodium, 25:41760
sorptive properties of hydrated, for tantalum, 25:41922
ARACHNICIDES
research on, review of radioisotopes in, 25:42239
ARCHAEOLOGICAL SPECIMENS
analysis of jar handle, for minor and trace elements, spectrochemical, 25:41833(R) (IA-1218)
ARCTIC REGION
charged-particle distribution at low-altitude polar caps, relation with simultaneous dc electric fields, (E), 25:43219 (N-71-20708)
model of ionospheric, (E), 25:43212 (AD-715893)
proton penetration to polar caps during Jan. 24, 1969 event, asymmetric access of solar, (E), 25:43233
review papers from NATO Advanced Study Institute on Polar Ionosphere and Magnetospheric Processes, Apr. 9-18, 1969, 25:43226
ARGON
effects on self radiolysis of carbon dioxide--tritium systems, 25:41852 (LA-4657)
helium-atom reactions at 13 to 50 keV with, cross sections for one-electron loss in, (E), 25:43153
ion reactions at 30 to 130 keV with, cross sections for argon L-shell x-ray emission in, (E), 25:43134
nitrogen-oxide-ion (NO^+) reactions with, statistical phase-space model of dissociation in, 25:43158
oxygen-ion (O_2^+) reactions with, statistical phase-space model of dissociation in, 25:43158
photon reactions at 0.28 to 8.03 keV with, relative abundances of multiply charged ions produced by, (E), 25:43142
plasma of, radiative temperature of bounded nonthermal, (E), 25:43354
proton energy straggling and stopping at 100 to 500 keV in, (E/T), 25:43432
solubility in liquid sodium, effects of pressure and temperature on, 25:41823 (ANL-7802)
sorption by surfaces of cadmium chloride and nickel chloride, thermodynamic studies on stepwise isotherms for, 25:41824 (CEA-R-4089)
ARGON IONS
effects of implanted, on stripping rates of tantalum oxide films, 25:41832(R) (AECL-3851)
implantation in silicon at 220 keV, measurements of stresses induced by damage from, 25:43441
implantation in silicon at 300, 400, and 500 keV, technique for, 25:41832(R) (AECL-3851)
reactions with carbon at 20 keV to 1.5 MeV, cross sections for K x-ray production in, (E), 25:43107
reactions with nitrogen molecules at 0.05 to 200 eV, application of statistical phase-space theory to molecular and dissociative charge exchange in, 25:43159
ARGON ISOTOPES
distribution and origin of, in Apollo 12 samples, (E), 25:43099
ARGON ISOTOPES Ar-33
beta decay of, branching ratios, half-life, and log-ft values for, (E), 25:43802 (JCRL-20480)
ARGON ISOTOPES Ar-36
deuteron elastic scattering at 9.162 MeV, optical-model analysis of, (E), 25:43868
deuteron reactions (d,p) at 9.162 MeV, l-transfer values from DWBA analysis of differential cross sections and spectra from, (E), 25:43868
photon reactions (p,n) at 13.86 to 14.14 MeV, excitation function, Q values, and threshold energy for, (E), 25:43875
proton elastic scattering at 8.980 MeV, optical-model analysis of, (E), 25:43868
ARGON ISOTOPES Ar-37
energy levels from argon-36 (d,p) reactions, spectroscopic factors and spin--parity assignments for, (E), 25:43868
ARGON ISOTOPES Ar-40
alpha elastic scattering at 104 MeV, differential cross sections for, (E), 25:43832 (NP-18920)
energy levels from proton inelastic scattering, spin--parity assignments for, (E), 25:43872
energy-level transitions from proton inelastic scattering, branching and mixing ratios, multipolarities, and strengths for, (E), 25:43872
helium-3 reactions (He-3,t) with, form factors and distorted waves from DWBA analysis of, (T), 25:43842
proton inelastic scattering at 4.7 to 5.8 MeV, angular correlations, excitation functions, and spectra from, (E), 25:43872
ARGONNE BIOLOGICAL RESEARCH REACTOR
gamma spectra measurements for, Compton recoil spectroscopy methods for, 25:42048 (ANL-7710, pp 263-364)
neutron spectra measurements for, use of proton-recoil proportional detectors for, 25:42048 (ANL-7710, pp 263-364)

ARKANSAS NUCLEAR ONE POWER REACTOR, UNIT 2
design parameters of, revised and additional data on, 25:44065 (DOCKET-50368-14)
design parameters of, revised and additional data on, 25:44066 (DOCKET-50368-15)
operations aspects of, revised and additional data on, 25:44065 (DOCKET-50368-14)
operations aspects of, revised and additional data on, 25:44066 (DOCKET-50368-15)
personnel for, qualifications of, 25:44066 (DOCKET-50368-15)
quality assurance program for, 25:44066 (DOCKET-50368-15)
site for, hydrological data for, 25:44066 (DOCKET-50368-15)
ARMY REACTORS (SM-1)
physics parameters of core 3 for, evaluation of 3.5 MWYR, (E), 25:44175 (AD-715950)
ARSENIC
determination in iron standards by neutron activation and spectrometry, 25:41774
determination in minerals from Luzon, Philippines, by neutron activation, 25:41772
determination of trace amounts of, in meteorites by neutron activation and γ spectrometry, 25:41773
separation from acetone--hydrochloric acid solutions by ion exchange using Bio-Rad, distribution coefficients for, 25:41999
separation from aqueous solutions by ion exchange on zirconium tellurate, tracer studies on, 25:41915
separation from other metals using inorganic ion exchange papers, 25:41909
ARSENIC ISOTOPES As-71
energy level at 5.07 MeV from proton resonances in germanium-70, resonance parameters and spectroscopic factor for isobaric analog, (E), 25:43851
ARSENIC ISOTOPES As-75
neutron inelastic scattering up to 1.5 MeV, γ spectra from, 25:43884 (ANL-7710, pp 1-52)
neutron total cross section at 100 to 650 keV, optical model analysis of average, (E/T), 25:43908
ARSENIC ISOTOPES As-75
beta decay of, β--γ circular-polarization correlation and nuclear matrix elements for, (E/T), 25:43864
ARSENIC ISOTOPES As-79
beta decay of, Q-value and β and γ singles and coincidence spectra from, (E), 25:43881
ARSENIC SYSTEMS
As--Cd, phase studies of, partial, 25:42989
ARSINE
effects of alkyl-substituted, on electron-induced copolymerization of monomeric unsaturated compounds and unsaturated polyesters, 25:41847(P)
ARTHROPODA
Caeculus sp., feeding habits of, cesium-134 tracer study of, 25:42242
ASCORBIC ACID
radiation effects on content of, in wheat following seed exposure, effects of dose on γ, 25:42726
ASPARTATE AMINOTRANSFERASE
radiation effects on activity of, in rat serum, effects of unsaturated fatty acid content of diet on whole-body x, 25:42298
ASPARTATE KINASE
aspartate kinase--homoserine dehydrogenase, radiation effects on inactivation of threonine-sensitive, from E. coli, mechanism of x, 25:42291
ASTATINE ISOTOPES At-211
energy levels from heavy-ion reactions, shell-model analysis of g factors and spin--parity assignments for, (E), 25:43912
energy-level transitions from heavy-ion reactions, internal conversion coefficients, multipolarities, and probabilities for E3, (E), 25:43912
isomeric transition in, half-life and multipolarity of, (E), 25:43912
ASTRON DEVICE
plasma confinement in toroidal, prospects for, 25:43333 (MATT-803)
ASTRONAUTS
radiation dosimetry of Apollo, Lexan polycarbonate helmets as track detectors for, 25:42150 (N-71-14602)
ATMOSPHERE
density variations in heterosphere, effect of altitude and temperature variations on semiannual, (E/T), 25:43258
fallout content in, over Israel, 1968 and 1969, 25:41833(R) (IA-1218)
fallout detection in high-altitude, design and operation of HANDS system for, 25:41932 (AD-719619)
fallout detection in high-altitude, evaluation of HANDS program for, 25:41933 (AD-719620)
heating by solar uv radiation, effects on diurnal variation of density and temperature, (T), 25:43207 (AD-706130)
interaction of neutral, with ionospheric plasma, (T), 25:43225
meteoroid ablation and breakup during passage through, model for large, (E/T), 25:43263
particle dispersion in, method for rapid estimation of, 25:41833(R) (IA-1218)
particle production and propagation in upper, secondary negatrons, positrons, and photons, (E/T), 25:43235
plutonium oxide content of, recommended decrease in maximum permissible, 25:42508
radiation monitoring of work area, ICRP recommendations on, 25:42474
radio-emission attenuation at 19 GHz, solar, (E), 25:43071
radioactivity in Tashkent ground-level, space--time variations in, 25:41939
radioactivity monitoring in Ecuador, 1965 to 1967, 25:41940
radioactivity monitoring in Italian, statistical considerations in surveillance network for, 25:41937
radioactivity monitoring in surface, of Canada, Central and South America, and USA during November 1970, gross β, 25:42426
radioactivity monitoring in surface, of Canada, Central and South America, and USA during October 1970, gross β, 25:42418
radioisotope content following reactor accidents, computer method for calculation of, 25:42393 (BNWL-B-69)
radioisotope content of ground-level, in Brunswick, West Germany, effects of seasonal variations on, 25:41934
radioisotope content of particulates in surface, of USA during 1970, 25:42426
stability of lower layers of Italian, Pasquill's criteria for calculation of frequency of, 25:41936
tritium content of, over Lake Tahoe, Nevada, 25:41938
turbulence in, effects of thermal inversions on mechanical, 25:41935
uranium-235 contamination of uranium enrichment plant, methods for protection of personnel against, 25:42379
water vapor content of, over Lake Tahoe, Nevada, 25:41938
ATMOSPHERIC PRECIPITATION
fallout content in, over Israel, 1968 and 1969, 25:41833(R) (IA-1218)
radioactivity monitoring in Canada and USA during November 1970, gross β, 25:42426
radioactivity monitoring in Canada and USA during October 1970, gross β, 25:42418
ATOMIC BEAMS
reactions of, research progress on, 25:41778 (UCRL-20500, pp 1-85)
ATOMIC ENERGY
injuries in privately owned and operated establishments using, in USA during 1968, 25:42498 (NP-18858)
ATOMIC ENERGY COMMISSION (USA)
computer system and programs of, exchange of, 25:44240 (CONF-710515-1)
research contracts in life sciences administered during 1970 by Division of Biology and Medicine, 25:44293 (TID-25728)
ATOMIC ENERGY, LEGAL ASPECTS
amendment to Italian Act 1860 on sale, shipping, and storage of radioactive materials, 25:42040
authorization for construction of Italian nuclear facilities, review of procedures for, 25:41979
laws governing compensation of personnel for occupational radiodermatitis in France, 25:42544
laws governing responsibility in radiation accidents in Germany, 25:42507
legislation on calibration and dosimetry of radioactivity in Italy, enforcement of, 25:42509
regulations for personnel in industries using sealed radiation sources and x-ray generators in Great Britain, 1969, 25:42469
regulations for radioactive materials transport on roads in Great Britain, 1970, 25:42451
regulations governing authorization and use of radioisotopes in Italian industry, 25:42013
regulations on sealed radiation sources in industry in Great Britain, 1968, 25:42458
statute for shipping radioactive materials on roads in Great Britain, 1970, 25:42450
ATOMIC MODELS
quantum corrections to Thomas--Fermi, 25:43167
Thomas--Fermi, spectral intensity distribution of Compton radiation by use of, 25:43515
ATOMIC PHYSICS
bibliography on surface and vacuum physics, 25:43111
book: Atomic Collisions and Elementary Processes in Plasma (in Russian), 25:43349
unit of fundamental length in, relation to undetermined cosmological length in relativity, 25:43087
ATOMIC STRUCTURE
shell interactions in, aggregate theory of, 25:43163
spin Hamiltonian for coarse structure states, effective, 25:43164
subshell filling in ordinary and superheavy elements, atomic number for onset of, (T), 25:43166
ATOMS
decay of, interference at intersection of levels, (T), 25:43506 (JINR-P4-5786)
detection of fast potassium, sensitivity of electron multiplier tubes for, 25:42079
electron scattering at low energies by hydrogenic, central-potential form for, (T), 25:43148
energy levels of highly ionized, average, (T), 25:43069 (N-71-20535)

energy levels of three-electron, variational methods for calculating bounds of autoionizing, 25:43168
interaction between two, quantum electrodynamical study of, 25:43159
interaction of (N+1)-state, with thermal bath of bosons, damping of, (T), 25:43513
interactions between pairs of, long-range, (T), 25:43207 (AD-706130)
interactions between, aggregate theory of, 25:43163
interactions between, split Hamiltonian matrix method for calculating energies of, 25:43165
interactions with high-intensity radiation fields, quantum electrodynamical theory of, 25:43170
interactions with radiation fields, generalized nonrelativistic Lamb-shift theory for, 25:43171
ion reactions with, calculation of symmetric charge-exchange cross sections for, using Hartree--Fock--Slater wave functions, 25:43157
ionization potential in plasma, partition function for, (T), 25:43354
nuclear charges in many-electron, effective, (T), 25:43162
polarizability of, perturbation calculation of correlation corrections to, 25:43117
polarization of closed-shell core by outer electron, (T), 25:43207 (AD-705130)
positron scattering at low energies by hydrogenic, central-potential form for, (T), 25:43148
proton reactions with, inverted-population production by charge exchange from, (T), 25:43103
reactions with atomic oscillators, quantum mechanical transition probabilities for, (T), 25:43146
reactions with atoms, dipole moment induced in, (T), 25:43136
reactions with diatomic molecules, quenching of quantum effects in classical S-matrix approach to, 25:43156
reactions with surfaces, classical model for, 25:43104
scattering by atoms, Euler--Lagrange optimization of plane-wave factors in, (T), 25:43144
valence shells of, effects on internal conversion and inner-electron density of, (T), 25:43953(T) (BNL-tr-427)
wave functions for, even-tempered atomic orbitals as bases for, (T), 25:43150 (IS-T-456)
wave functions for, perturbation theory for configuration-interaction, 25:43161

ATPase
radiation effects on activity of, in hamster intestine, whole-body γ, 25:42301

ATUCHA POWER REACTOR
cooling system for, program for in-service ultrasonic inspection of, 25:44080

AURORAE
nitrogen oxide NO abundance in arc, mass-spectrometer observations of, (E), 25:43218 (N-71-18997)
oxygen abundance in arc, mass-spectrometer observations of molecular, (E), 25:43219 (N-71-18997)
pulsating patches in, sudden intensity-dependent spatial expansion of, (E), 25:43249
stable red arc formation at 300 to 700 km at plasmapause, ring-current heat source for, (T), 25:43242

AURORAL ZONE
charged-particle distribution at low altitude, relation of simultaneous dc electric fields with, (E), 25:43219 (N-71-20708)
electric fields in, latitude-dependent east--west convection reversals in dc, (E), 25:43216 (N-71-18405)
electron fluxes at 50 to 120° pitch angles, 1- to 30-keV, (E), 25:43248
electron precipitation in, correlation pulsating patches with, (E), 25:43249
model of, ionospheric night-E and sporadic E, (E), 25:43212 (AD-715393)
nitrogen-ion emission in, differential electron-flux determination from N^{2+} and N_2^+, (E), 25:43214 (N-71-16589)
proton enhancements during Feb. 25, 1969 event in, mechanism of, (E/T), 25:43232

AUSTRALIA
code of practice for radiation protection of personnel during sealed gamma source industrial radiography, 25:42490
ecology of Jervis Bay, marine, 25:42314 (CONF-710511-3)
handling radioactive cadavers in, code of practice for, 25:42497
procedures for care of personnel following accidents resulting in radiation exposure or contamination with radioactive materials, 25:42391
radiation dose to man in, following nuclear weapons testing in Polynesia during 1970, 25:42367 (AWTSC-1)
radiation monitoring programs at New South Wales University during 1970, 25:42369(R) (NP-18905)
radiation protection code of practice for children during school demonstrations using ionizing radiations, 25:42489
radiation protection code of practice for dental radiography, 25:42496
radiation protection code of practice for medical personnel using sealed radiation sources for therapy, 25:42492
radiation protection code of practice for sealed radiation source therapy, 25:42491
radiation protection standards for medical personnel and patients during diagnostic radiography, 25:42493
radiation protection standards for personnel in nuclear industry and research in, 1957 revision of, 25:42495
radiation protection standards for shipping radioisotopes by mail in, 25:42494
radioactivity monitoring in soils and wheat in Western, natural α, 25:42427
recommendations for shipment of radioactive materials by sea, 25:42449

AUTORADIOGRAPHY
method for measuring activity and size distribution of beta emitting particles, 25:42051 (JAERI-13718)
method for tritiated Zircaloy-2, 25:41832(R) (AECL-3851)

AVES
Gallus sp., radiation effects on organized structures and interstitial cell compartment of mesonephros of embryos of, effects of dose on, 25:42543
Gallus sp., radioinduced injuries of lymphatic tissues in, x, 25:42658

AZATHIOPRINE
effects on tetanus antitoxin production in mice, combined effects of γ radiation and, 25:42672

B

BABOONS
lead-210 metabolism in, following injection, tracer study of, 25:42245(R) (NYO-3086-10(Vol.1))

BACKGROUND RADIATION
measurement of, effects of shielding and source--detector distance on low-level, 25:42111

BACTERIOPHAGES
341, radioinduced inactivation of enterococcal, dose dependence of γ, 25:42740
effects on γ radiosensitivity of lysogenic bacterial host following heat treatment, 25:42529
lambda, radioprotective effects of methylated proflavine on, uv, 25:42737
lambda+, radiosensitivity of, effects of DNA content on uv, 25:42300
lambda62, radiosensitivity of, effects of DNA content on uv, 25:42300
PM2, radiation effects on DNA of, for use in infecting spheroplasts of Pseudomonas, γ, 25:42273
prophage lambda, radiation effects on induction of, in Escherichia coli mutants, 25:42340
radiation effects on lambdoid and T, host controlled reactivation following uv, 25:42738
Serratiaphage kappa, radioinduced inactivation of, sensitizing effects of methylene blue and proflavine on uv, 25:42734
T_4, effects on endonuclease induction by infection of E. coli cells, 25:42269
T1, radiosensitivity of, model for effects of temperature on proton, 25:42288
T4, growth on Escherichia coli, reaction mechanisms in radioinduced loss of capacity for, 25:42730 (NYO-2804-41)
T4, radioinduced breaks in DNA of, repair of uv, 25:42297
T4, radioinduced mutations in, effects of mutator alleles on repair of uv, 25:42339

BADDELEYITES
zirconium dioxide production from concentrates of, 25:42942

BARBITAL
effects on eruption of teeth of rats following prenatal exposure, 25:42638

BARITE CONCRETES
properties for use as shielding for gamma radiation protection, mechanical and physical, 25:42976
barite concrete--limonite concrete, properties for use as shielding for gamma radiation protection, mechanical and physical, 25:42976

BARIUM
effects on F-center growth curves in x-irradiated potassium chloride crystals, (E), 25:43450
effects on graphite--nitrous oxide and graphite--oxygen reactions, catalytic, 25:42931
separation from acetone--hydrochloric acid solutions by ion exchange using Bio-Rad, distribution coefficients for, 25:41899
separation from aqueous solutions by ion exchange on zirconium tellurate, tracer studies on, 25:41915
separation from other metals using inorganic ion exchange papers, 25:41909

BARIUM CARBONATES
separation of cesium-131 from neutron-irradiated, by solvent extraction, 25:41876 (CONF-680986-2)

BARIUM IONS
reactions with nitrogen molecules at 30 keV to 2 MeV, cross sections for excitation of N_2^+ 3914-A radiation in, (E), 25:43151

BARIUM ISOTOPES Ba-130
neutron reactions with, in barium carbonate, production of cesium-131 by, 25:41875 (CONF-680986-2)

BARIUM ISOTOPES Ba-137
energy-level transitions from cesium-137 beta decay, ionization (shakeoff) accompanying internal-conversion,

(E), 25:43871
separation of metastable, from cesium-137 by ion exchange using cesium-containing ammonium molybdophosphate, 25:41751
BARIUM ISOTOPES Ba-140
metabolism and tissue distribution following intake by man, 25:42457
BARIUM SULFIDES
BaS--US, phase studies of, 25:43002
BARIUM TITANATES
radiation effects on ferroelectric crystals of, 25:43442
BARYONS
exchange in backward $\pi^+ + n \rightarrow \pi^+ + \pi^- + p$ and $\pi^+ + p \rightarrow p + \pi^+ + \pi^- + \pi^0$ interactions at 1.83 to 2.33 GeV/c in deuterium bubble chamber, (E), 25:43556
interactions with antibaryons, exotic trajectory exchange with four-quark content in, 25:43632
interactions with baryons, mathematical quarks from bootstrap model of, 25:43650
mass differences of, model for relations among electromagnetic, (T), 25:43644
models with fields and currents for, (T), 25:43644
parity and spin of, multipole moments for determination of, (T), 25:43581
symmetry for, two-point functions of currents in formulation of asymptotic chiral, (T), 25:43644
theory for system of interacting pseudoscalar mesons and, currents in, (T), 25:43522
BARYONS (ANTIPARTICLES)
interactions with baryons, exotic trajectory exchange with four-quark content in, 25:43632
BARYONS, RESONANCE (N*)
mass and width of $\Delta^{++}(1200)$ and $\Delta^{--}(1200)$ in anti $p + p \rightarrow$ anti $p + p + \pi^+ + \pi^-$ interactions at 2.2 GeV/c in bubble chamber, (E), 25:43537
mass and width of $p\pi^+\pi^-(1426)$ and $p\pi^+\pi^-(1692)$ in $p + p \rightarrow p + p + \pi^+ + \pi^-$ interactions at 25 GeV/c in hydrogen bubble chamber, (E), 25:43535
production in $K^- + n$ interactions at 4.48 GeV/c in deuterium bubble chamber, (E), 25:43549 (CDD-1428-286)
production of A(1235) in anti $p + p \rightarrow$ anti $p + p + \pi^0$ interactions at 2.2 GeV/c in bubble chamber, (E), 25:43537
production of Δ^{++}, $p\pi^+\pi^-(1426)$ and $p\pi^+\pi^-(1692)$ in $p + p \rightarrow p + p + \pi^+ + \pi^-$ interactions at 25 GeV/c in hydrogen bubble chamber, (E), 25:43535
production of $\Delta^{++}(1200)$ and $\Delta^{--}(1200)$ production in anti $p + p \rightarrow$ anti $p + p + \pi^+ + \pi^-$ interactions at 2.2 GeV/c in bubble chamber, (E), 25:43537
production of $\Delta^{++}(1236)$ and $\Delta^{+}(1236)$ in $\pi^+ + p \rightarrow \pi^+ + \pi^0 + p$ interactions at 1.85 to 2.09 GeV in hydrogen bubble chamber, cross sections for, (E), 25:43552 (UCR-34-P-107-8-110)
production of $\Delta^{++}(1236)$ in $\pi^+ + p \rightarrow \Delta^{++} + \pi^0$ interactions at 1.1 to 1.95 GeV/c in hydrogen bubble chamber, (E), 25:43551 (UCR-34-P-107-8-108)
production of $n\pi^-$ system in anti $p + p \rightarrow$ anti $p + n + \pi^-$ interactions at 2.2 GeV/c in bubble chamber, forward, (E), 25:43537
production of $p\pi^+$ and $p\pi^-$ in $p + p \rightarrow p + n + 2\pi^+ + \pi^-$ interactions at 25 GeV/c in hydrogen bubble chamber, (E), 25:43535
BARYONS, RESONANCE (Y*)
decay of $\Sigma(1385)$, $\Lambda(1405)$, and $\Lambda(1520)$ in deuterium bubble chamber, angular correlations for, (E), 25:43561
production of $\Sigma(1385)$, $\Lambda(1405)$, and $\Lambda(1520)$ in $\pi^+ + d$ interactions at 2.05 to 2.35 GeV/c in deuterium bubble chamber, (E), 25:43561
production of $\Sigma(1765)$ in $K^- + n \rightarrow p + 2\pi^- +$ anti Σ^0 and $K^- + n \rightarrow \pi^+ + 2\pi^- +$ anti $K^0 + n$ interactions at 4.48 GeV/c in deuterium bubble chamber, (E), 25:43549 (CDD-1428-286)
production of $\Sigma^-(1385)$ in $\pi^- + p \rightarrow K^+ + \Sigma^-(1385)$ interactions at 4.5 and 5 GeV/c, mechanism for, (E/T), 25:43558
BATS
chromosomes of Phyllostomatidae, karyotypic studies on, 25:42317(R) (PRNC-147)
BEARINGS
development and performance of 12-pocket hydrostatic, for sodium pumps, 25:41958(T) (CONF-700307-8)
BEHAVIOR
radiation effects on rat learning, following head-exposure, x, 25:42555
radiation effects on rat open field, effects of loss and prenatal exposure on x, 25:42640
radiation effects on rat saccharin-avoidance, effects of amygdala, olfactory bulb, and septal lesions on x, 25:42647
BELGIUM
nuclear power industry activities in, review of, 25:44092
BENTONITES
effectiveness for removal of radioisotopes from water supplies, 25:42334(P)
BENZENE
2,2'-azobis[2-methylpropionitrile]--benzene, radiolysis of, effects of additives on yields of nitrogen from electron pulse, 25:41872
benzene--d_2O, radiolysis at 150 to 200°C, effects of iron(II), iron(III), and oxygen on yields of phenols from electron or γ, 25:41858
BENZENE, ALKYL-
radiolysis of, effects of electronic excitation of molecules on yields of free radicals from, 25:41859
BENZENE, CHLORO-
radiolysis of cyclohexane solutions of, mechanism of negative ion formation in, 25:41833(R) (IA-1218)
BENZENE, HEXACHLORO-
radiation effects on, effects of structural isomerism on Szilard--Chalmers reactions of chlorine-38 recoils from neutron, 25:41884
BENZENE, IODO-
photoinduced isotopic exchange between iodine and, mechanism of uv, 25:41833(R) (IA-1218)
BENZOIC ACID, p-(HYDROXYMERCURI)-
radiosensitizing effects on DNA in tissues of rats, 25:42535
BENZO[b]NAPHTHO[2,3-d]FURAN
benzo[b]naphtho[2,3-d]furan--naphthacene, radioinduced quenching of luminescence of crystals of, x, 25:41840
BENZOPHENONE
effects on yields of nitrogen from radiolysis of 2,2'-azobis[2-methylpropionitrile]--benzene, 25:41872
BERKELIUM
separation from californium by oxidation and sorption on zirconium phosphate silicate, 25:41882
BERKELIUM ISOTOPES Bk-249
beta decay of, production of californium-249 in, 25:41882
BERYLLIUM
compaction of powdered, model for effects of silicon on, 25:42826
determination in air, rapid colorimetric method for, 25:41717 (CEA-N-1446)
lattice-dynamical calculations for, 25:43478
polarizability of atomic, perturbation calculation of, 25:43117
proton reactions at 10 to 500 GeV, meson (π^-) fluxes from, (T), 25:43726 (BNL-15893)
separation from acetone--hydrochloric acid solutions by ion exchange using Bio-Rad, distribution coefficients for, 25:41899
separation from other metals using inorganic ion exchange papers, 25:41909
superconducting parameter calculations, 25:43305
superconductivity of cold-deposited films of, (E/T), 25:43303
thermionic emission of films of, adsorbed on tungsten single crystals, 25:43473
BERYLLIUM ALLOYS AND SYSTEMS
Be--Ti, fabrication and properties of co-extruded powder composites of, 25:42869
BERYLLIUM BORIDES
crystal structure of, effects of boron content on, 25:42997
properties of, relations with bonding and boron content, electric, mechanical, and physical, 25:42997
BERYLLIUM BOROCARBIDES
crystal structure of, effects of boron content on, 25:42997
properties of, relations with bonding and boron content, electric, mechanical, and physical, 25:42997
BERYLLIUM ISOTOPES Be-7
content in ground-level atmosphere of Brunswick, West Germany, effects of seasonal variations on, 25:41934
BERYLLIUM ISOTOPES Be-8
energy levels from lithium-7 (p,γ) reactions, giant resonance, (E), 25:43813
energy levels from resonances in lithium-7 (p,α) reactions, properties of, (E/T), 25:43829
BERYLLIUM ISOTOPES Be-9
alpha elastic scattering at 104 MeV, differential cross sections for, (E), 25:43832 (NP-18920)
helium-3 reactions (He-3,Li-6) with, analysis using tetragonal graphs, (T), 25:43961
helium-3 reactions (He-3,n) at 2.1 MeV, analysis including Coulomb distortion and finite-range effects, (T), 25:43965
lithium-6 reactions (Li-6,α), (Li-6,d), (Li-6,p), and (Li-6,t) at 4 to 14 MeV, cross sections for, (E), 25:43822
lithium-7 reactions (Li-7,α) and (Li-7,t) at 4 to 14 MeV, excitation functions for, (E), 25:43822
lithium-7 reactions (Li-7,d) and (Li-7,p) at 4 to 14 MeV, cross sections for, (E), 25:43822
proton elastic scattering at 5 to 30 MeV, optical model analysis of, (T), 25:43804
proton reactions (p,γ) in giant resonance region, γ yields and angular distributions for, (E), 25:43813
proton reactions (p,pα) at 25.0 to 46.8 MeV, coplanar angular and energy correlations and spectra from, (E/T), 25:43801 (UCLA-10-P-18-31)
BERYLLIUM ISOTOPES Be-11
energy level at 319.8 keV from beryllium-9 (t,p) reactions, lifetime of, (E), 25:43820
energy-level transitions from beryllium-9 (t,p) reactions, rates for E1, (E), 25:43820
BERYLLIUM OXIDES
book: High-Temperature Materials, 25:42853
positron annihilation in, angular correlation of, 25:43482

stress relaxation at 850 to 1240°C, 25:42973
BETA DECAY
half-life for, delayed-coincidence method for measurement of, 25:42222
internal ionization of K shell during, probability for, (T), 25:43975
Kurie plots for allowed, effects of finite nuclear size and radiative corrections in analysis of, (T), 25:43992
search for double, (E), 25:43932
BETA PARTICLES
absorption in aluminum and tin of negative and positive, coefficients of mass, 25:43433
book: The Biological Effects of External β Irradiation, 25:42645
detection of high-energy, use of Cherenkov inserts in, 25:42092
dose distribution around implanted iridium-192 sources, mathematical models for, 25:42428
dose distribution in skin following penetration of surface contaminants, 25:42257
dose to adult human bones, method for estimating, 25:42434
dosimetry in patients following administration of therapeutic doses of phosphorous-32, evaluation of chromosome aberrations in cultured hematopoietic cells for, 25:42713
effects of simulated fallout, on natural ecosystem, 25:42315(R) (ORO-3299-107)
effects on blood coagulation in dogs, effects of dose on, 25:42600
effects on blood of myeloid leukemia patients, proliferation of bone marrow cells following extracorporeal exposure, 25:42690
effects on human chromosomes, limitations of dosimetric uses of aberrant internal therapeutic, 25:42707
effects on metabolism in granite outcrop ecosystems following exposure to simulated fallout particles coated with yttrium-90, 25:42320
effects on reproductive potential of asters in natural ecosystems following acute exposure to simulated fallout, 25:42718 (ORO-3299-110)
effects on reproductive potential of dominant plant species in natural ecosystem, 25:42316(R) (ORO-3299-107)
effects on skin, effectiveness of petroleum growth substance for treatment of, 25:42539
effects on survival of desert shrubs at Nevada Test Site, effects of dose on, 25:42717 (EGG-1183-2272)
effects on survival of rats, protective effects of cyclophosphamide against, 25:42518
effects on thallium-activated cesium iodide crystals, influence of electric field on luminescent, (E), 25:43448
monitoring in lava from nuclear explosion cavity, 25:41953 (CEA-R-4099)
BETA SOURCES
activity in bees and honey in Germany, measurement of fallout, 25:42374
shielding for high-intensity, parameters for, 25:42016
transport of strontium-90--yttrium-90, use of thermoluminescent dosimeters for monitoring radiation dose to personnel during, 25:42444
use for therapy, radiation protection code for, 25:42491
use for therapy, radiation protection code for medical personnel during, 25:42492
BETA SPECTROMETERS
book: Beta Spectrographs with Permanent Magnets, 25:42110
description of cryostat, electronics, and vacuum system for silicon semiconductor, 25:42112
design from lithium-drifted silicon photon spectrometer, 25:42123
BETATRONS
description of Budapest 25-MeV, for therapy and medical research, 25:43758
magnet for transportable, 25:43741
BIBLIOGRAPHIES
on civil defense, 25:42505 (BARC/BIB-1)
on inorganic ion exchangers, 25:41879 (JAERI-13726)
on radioisotope transport through food chains and accumulation by fish, invertebrates, and mammals, 25:42315 (ORNL-NSIC-89)
on scintigraphy using gallium-67, gallium-68, or technetium-99m, 25:42550 (ORNL-TM-2091(Suppl.2))
on seismology, aftershocks, and related phenomena associated with underground nuclear explosions, 25:41951 (NVO-87)
on surface and vacuum physics, 25:43111
BIG ROCK POINT POWER REACTOR
control rod drive for, inspection of malfunction of, 25:44031 (DOCKET-50155-85)
quality assurance program for, 25:44030 (DOCKET-50155-84)
radioactive effluents from, inspection of, 25:44031 (DOCKET-50155-85)
BIKINI ATOLL
silver-108m content of animals, plants, and sediments at, following nuclear testing during 1958, 25:42377
BIOLOGICAL MATERIALS
analysis for uranium, uv fluorescence method for, 25:42246(T) (GAT-Z-5047)
electron diffraction patterns of, fading mechanisms in illuminated, 25:42886 (UCRL-20500, pp 86-146)
polonium-210 α dosimetry in, comparison of extrapolation ionization chamber and surface-barrier semiconductor detectors for, 25:42436
BIOLOGICAL MODELS
development for estimation of strontium-90 transport through vegetation--cattle--milk--man food chain, 25:42378
development for internal dose distribution around implanted beta-gamma sources, 25:42428
development for radiation dosimetry in therapy of solid tumors, 25:42437
use for kinetic studies of radioisotope distribution in human tissues, 25:42467
BIOLOGICAL STRESS
effects on life span and tumor incidence in whole-body x-irradiated rats, 25:42669
BIOPHYSICS
book: Radiobiophysics of the Nucleoproteins, 25:42274
BIOTITES
radiation effects on infrared spectrum of, 5-keV proton, deuteron, helium-ion, and nitrogen-ion, 25:43446
BISMUTH
separation from acetone--hydrochloric acid solutions by ion exchange using Bio-Rad, distribution coefficients for, 25:41899
separation from other metals using inorganic ion exchange papers, 25:41909
solvent properties of molten, for fission products, protactinium, and uranium from spent molten salt reactor fuels, 25:41903(P)
BISMUTH ALLOYS AND SYSTEMS
Bi--Sb, superconducting thin films of, fluctuation contributions to thermal capacity of, 25:43321
BISMUTH ISOTOPES Bi-203
electron-capture decay of, γ singles and coincidence spectra from, (E), 25:43906
BISMUTH ISOTOPES Bi-204
electron-capture decay of, γ singles and coincidence spectra from, (E), 25:43906
BISMUTH ISOTOPES Bi-209
alpha elastic scattering at 104 MeV, differential cross sections for, (E), 25:43832 (NP-18920)
energy levels from gamma resonance scattering, spin-parity assignments for, (E), 25:41833(R) (IA-1218)
energy levels from lead-208 proton resonances, isobaric analog, (E), 25:43907
BISMUTH ISOTOPES Bi-214
content in rat organs and tissues following inhalation of radon-222, 25:42248
BISMUTH URANATES
covalency in $BiUO_4$, oxygen-17 NMR study of, 25:43497
BLACK HOLES
neutrino force of Kerr, long-range, 25:43032
BLOOD
analysis for platinum from non-tumored and tumored Swiss white mice by neutron activation, radiochemical separation, and γ spectrometry, 25:41762
fibrinolytic activity of human, iodine-125 tracer method for measurement of, 25:42243
formation in man, review of tracer studies on, 25:42573
parameter variations in rabbit, during radiation sickness induced following destruction of hypothalamus, 25:42660
radiation effects on coagulation of dog, effects of dose on β and γ, 25:42600
radiation effects on coagulation of human, as biological dosimeter, 25:42600
radiation effects on distribution of iodine-131-labeled albumin in rat, as indicator of radiation injury, whole-body γ, 25:42407
radiation effects on, of myeloid leukemia patients, proliferation of bone marrow cells following extracorporeal exposure beta, 25:42690
radiation monitoring of human, at JAERI, dose calculations from, 25:42439
radioinduced diseases of rat, neptunium-237, 25:42253
BLOOD CELLS
radiation effects on deoxyribonucleoprotein in animal, mechanisms for, 25:42624
radiation effects on, in medical personnel, x, 25:42600
BLOOD PLATELETS
physiopathology of, research progress on, 25:44272(R) (NYO-3590-7)
radiation effects on survival of, in peripheral blood of man, γ, 25:42586 (ORAU-113, pp 4-77)
BLOOD PRESSURE
measurement in human lungs, radioisotope scanning method for, 25:42554
BLOOD SERUM
radiation effects on content of proteins, immunoglobulins, and transferrin of human, low-dose whole-body γ, 25:42586 (ORAU-113, pp 4-77)
radiation effects on content of sulfhydryl groups in human, following post-surgical therapy of mammary cancer, 25:42270
radiation effects on leukocyte count, lysozyme activity, and trypsin inhibitors in rabbit, effects of dose on whole-body x, 25:42548

BLOOD VESSELS
radiation effects on human, methods for studying dystonic, 25:42575
radiation effects on, in rat brain, effects of hypertension on x, 25:42667
BODY FLUIDS
radiation effects on biochemistry of, as indicator of radiation injuries, review on, 25:42402
BOHUNICE POWER REACTOR, UNIT 1
operating parameters of, computer program for analysis of, 25:44021
BOILERS
construction of reactor, standards for, 25:43993 (RDT-E-15-2-T)
operation of sodium-heated prototype, under simulated LMFBR conditions, 25:42804(R) (LMEC-71-1)
performance of short reentry tube steam, for use in radioisotope power plant, effects of configuration, flow rate, and pressure on, 25:41962 (JRNL-TM-3236)
performance of sodium-heated, in large component test facility, evaluation of, 25:42804(R) (LMEC-71-1)
standards for steam generators for pressurized water power reactors, 25:44081 (RDT-E-4-1-T)
BOLTS AND NUTS
standard for alloy steel, for low-temperature service, 25:42797 (RDT-M-5-1-T)
BONE MARROW
effects of irradiated and unirradiated transplants of, on hematopoiesis in x-irradiated mice, 25:42644
radiation effects on survival of colony-forming units in mouse, RBE for γ, neutron, and x, 25:42601
radioinduced chromosome aberrations in mouse and rat, effects of age on x, 25:42556
radioinduced chromosome aberrations in, in Japanese fishermen, latent fallout, 25:42681
radioprotective effects of transplants of, on mouse testes, γ, 25:42304
radiosensitivity of animal and human, 25:42472
transplantation in lethally x-irradiated mice, incidence of late radiation fibrosis following, 25:42665
BONES
radiation dose to adult human, method for estimating strontium-90 β, 25:42434
radiodiagnosis of tumors in, comparison of strontium-85, metastable strontium-87, and x-radiography for, 25:42552
radioinduced injuries and neoplasms in animal and human, following deposition of americium-241, phosphorus-32, plutonium-239, radium-225, radium-228, strontium-90, thorium-228, or yttrium-90, 25:42472
radioisotope deposition in, of cattle in Italy during 1962 to 1968, polonium-210 and strontium-90, 25:42382
radiosensitivity of animal and human, 25:42472
scintigraphy using fluorine-18 and positron camera, 25:42564
BORON
determination in nuclear materials by isotope dilution method, 25:41749
properties for use as corrosion-resistant coating on molybdenum, niobium, tantalum, and tungsten, 25:42854
reactivity worth in fast reactor spectra, specific, (E/T), 25:44094(R) (AI-AEC-12991)
BORON CARBIDES
fabrication of reactor control rods of, methods for, 25:42822
BORON IONS
spectra of B^{2+}, isotope shift in, 25:43207 (AD-706130)
BORON ISOTOPES B-9
proton decay of, proton spectra from beta-delayed, (E), 25:43802 (UCRL-20490)
BORON ISOTOPES B-10
energy levels from beryllium-9 (p,γ) reactions, giant resonance, (E), 25:43813
neutron reactions (n,α), use to enhance carbon-dioxide laser performance, 25:42229
radiation effects on performance of in-pile neutron detectors of, γ, (T), 25:44103
reactivity worth in fast reactor spectra, specific, (E/T), 25:44094(R) (AI-AEC-12991)
BORON ISOTOPES B-12
energy levels of, analysis of T = 1 isobaric analog, (T), 25:43819
BORON ISOTOPES B-13
nuclear magnetic dipole moment, Knight shifts, and effective g factors for, recoiling into gold, palladium, and platinum, (E), 25:43817
BORON NITRIDES
phase transition in, mechanism for α--β, 25:42994
BORSSELE POWER REACTOR
design parameters of, 25:43937
BOSONS
atom interaction with thermal bath of, damping of (N+1)-state, (T), 25:43513
bound states of system of two spinless, in quasipotential approach, Pade approximation for, (T), 25:43568 (JINR-P2-5765)
excitations of system of interacting, point-transformations method for microscopically based theory of, 25:43274
impurities in imperfect Bose gas, condensate energy from, (T), 25:43273
interactions of spinless, at high energies and all angles, optical model for, (T), 25:43571
interactions with spin-$^1/_2$ fermions at high energies and all angles, optical model for, (T), 25:43571
order-parameter fluctuations in weakly interacting gas of, near superfluid transition, (T), 25:43284
BOSONS, INTERMEDIATE-VECTOR
production of W^- in $e + \nu \rightarrow W^- + \nu + \nu$ interactions at 30 to 300 GeV, total cross sections for, (T), 25:43603
theory for radiative corrections to spectrum for μ beta decay, (T), 25:43600
BRAIN
destruction of rear hypothalamus in rabbit, changes in nature of radiation sickness following, 25:42660
radiation effects on bioelectric activity in human, electroencephalographic studies on local and whole-body, 25:42677
radiation effects on bioelectrical activity in human, following therapy for arachnoiditis, 25:42678
radiation effects on bioelectrical activity of rabbit, effects of radial acceleration on sublethal x, 25:42653
radiation effects on cerebellar granule cell of cat, vestibular and spinal reflexes following x, 25:42657
radiation effects on cerebellum of rat, comparison of ablation and, 25:42515(R) (COO-1201-30)
radiation effects on human, following therapy of intracerebral astrocytomas, 25:42701
radiation effects on metabolic equilibrium in rat, protective effects of cysteine against x, 25:42619
radiation effects on rat, effects of dose and hypertension on x, 25:42667
radioinduced malformations in mouse and rat embryo, x, 25:42629
scanning for lesion differentiation in, effectiveness of metastable indium-113 and metastable technetium-99 for, 25:42577
scanning for tumor diagnosis in, effectiveness of metastable technetium-99-labeled pertechnetate for, 25:42547 (ACRH-1000-248)
scanning for tumor localization, potential use of fluorescence radiation method for, 25:42548 (CONF-710204-4)
scanning of young human, for differential diagnosis of congenital arachnoid cysts and Dandy-Walker cysts, use of iodine-131-labeled human serum albumin for, 25:42568
scanning tumors of human, for evaluation of response to drug therapy, 25:42556
scintigraphy using sodium-22 and positron camera for localization of tumors, 25:42565
tritium-labeled estradiol autoradiographic localization in rat, 25:42258
BRAZING
standard for filler metal for, 25:42759 (RDT-M-1-9-T)
BREMSSTRAHLUNG
dosimetry of, energy and phantom depth dependence of film sensitivity for 43 MV, 25:42396
effects on leukocytes in man and mice, partial-body, 25:42599
emission from anisotropic hot-electron plasma in mirror machines, 25:43357
monitoring of 302- to 1102-MeV, calibration of ionization chambers and quantameters for, 25:42083
production of, effects of target thickness and forward angle on electron, 25:43751
reactions (γ,f) with thorium-232 and uranium-238 at 200 to 1150 MeV, cross sections and fragment energy and angular distributions for, (E), 25:43946
reactions (γ,n) with chromium-53 and iron-57 at 11.5 MeV endpoint energy, neutron energy spectra from, (E), 25:43929
reactions (γ,n) with lead-207 and -208 at 9.8 MeV endpoint energy, neutron energy spectra from, (E), 25:43929
reactions (γ,n) with lead-207 at 8.4 MeV endpoint energy, neutron energy spectra from, (E), 25:43929
reactions with molybdenum and zirconium isotopes at 20 to 60 MeV, 25:41764
scattering by aluminum-27 and sodium-23 at 2 to 4 MeV, spectra from elastic and inelastic, (E), 25:43838
BRITTANY POWER REACTOR (EL-4)
pressure tubes for, properties of Zircaloy-2 and copper--molybdenum--zirconium alloys for, 25:42929
BROMINE
determination in sedimentary minerals by Szilard--Chalmers reactions following neutron activation, 25:41763
determination in selenium by melting with sodium hydroxide and x-ray fluorescence, 25:41734
separation from fission products by selective negative surface ionization, 25:41833(R) (IA-1218)
BROMINE ISOTOPES
yields from thermal neutron fission of uranium-235, 25:41833(R) (IA-1218)
yields in uranium-235 thermal neutron fission, (E), 25:41833(R) (IA-1218)
BROMINE ISOTOPES Br-77
energy-level scheme from krypton-77 decay, (E), 25:43843
BROMINE ISOTOPES Br-78
nuclear magnetic moment of isomeric, (E), 25:43841

XUM

BROMINE ISOTOPES Br-80
reactions of recoil atoms of, with bromomethane, effects of energy on, 25:41833(R) (IA-1218)
BROMINE ISOTOPES Br-81
energy-level scheme from selenium-81 decay, (E), 25:43844
nuclear magnetic moment of isomeric, (E), 25:43841
BROMINE ISOTOPES Br-82
radiation effects on metabolism of, in rats, x, 25:42282
reactions of recoil atoms of, with bromomethane, effects of energy on, 25:41833(R) (IA-1218)
BUBBLES
radioinduced nucleation in thin liquid films, 25:41835
BUILDING MATERIALS
technology of, second inter-American conference on, 25:44219
BULGARIA
radioisotope content of dairy products, fruits, and vegetables during 1965, 25:42391
BUTANE, 1,2:3,4-DIEPOXY-
effects on Neurospora, specificity of mutagenic, 25:42352
2,3-BUTANEDIONE
effects on yields of nitrogen from radiolysis of 2,2'-azobis[2-methylpropionitrile]--benzene, 25:41872
1,3-BUTANEDIONE, 4,4,4-TRIFLUORO-1-(2-THIENYL)-
complexes with uranyl ions, adduct formation with TBP, effects of solvents on, 25:41754
1-BUTANOL, 3-METHYL-
solvent properties for metal complexes with morin, 25:41738
BUTYLAMINE
radiolysis of, adsorbed on silica gel at 77°K, ESR studies on trapped radicals produced by γ, 25:41856
tert-BUTYLAMINE
radiolysis at 77°K, ESR studies on trapped radicals produced by γ, 25:41857
2-BUTYNE
radiolysis of, excited states and cyclobutadiene intermediate in γ, 25:41867

C

CADAVERS
handling of radioactive, ICRP recommendations for radiation protection during, 25:42476
handling radioactive, Australian code of practice for, 25:42497
CADMIUM
analysis of, mass spectrometric method for isotopic, 25:41731
creep of polycrystalline, kilocycle acoustic emission during, (E), 25:42852
determination in minerals from Luzon, Philippines, by neutron activation, 25:41772
determination of trace amounts of, in zinc, spectrochemical, 25:41833(R) (IA-1218)
effects on F-center growth curves in x-irradiated potassium chloride crystals, (E), 25:43450
effects on graphite--nitrous oxide and graphite--oxygen reactions, catalytic, 25:42931
radiation effects on thin shields of, thermal neutron, 25:43422(T) (ORNL-tr-2488)
separation from acetone--hydrochloric acid solutions by ion exchange using Bio-Rad, distribution coefficients for, 25:41899
separation from aqueous solutions by ion exchange on zirconium tellurate, tracer studies on, 25:41915
separation from other metals using inorganic ion exchange papers, 25:41909
CADMIUM ALLOYS AND SYSTEMS
Ag--Cd--In, fabrication of reactor control rods of, methods for, 25:42822
As--Cd, phase studies of, partial, 25:42989
CADMIUM BROMIDES
sorptive properties of surfaces of, for krypton, thermodynamic studies on stepwise isotherms for, 25:41824 (CEA-R-4089)
CADMIUM CHLORIDES
sorptive properties of surfaces of, for argon, krypton, and xenon, thermodynamic studies on stepwise isotherms for, 25:41824 (CEA-R-4089)
CADMIUM IODIDES
sorptive properties of surfaces of, for krypton, thermodynamic studies on stepwise isotherms for, 25:41824 (CEA-R-4089)
CADMIUM ISOTOPES
determination in cadmium samples, mass spectrometric, 25:41731
CADMIUM ISOTOPES Cd-104
electron-capture decay of, γ spectra from, (E), 25:43945
CADMIUM ISOTOPES Cd-112
energy levels from photoexcitation, spin-parity assignments for, (E), 25:41833(R) (IA-1218)
CADMIUM ISOTOPES Cd-114
nuclear charge distribution of, determination from μ-mesic x-ray spectra, 25:43904
x-ray spectra of μ-mesic atoms of, (E), 25:43904
CADMIUM PERCHLORATES
complexes with ethylenediamine, explosive characteristics of, 25:44258 (MHSMP-71-28)
CADMIUM SULFIDES
radiation effects on capture center energy spectra in crystals of, 3-keV electron, 25:43437
vaporization rates of, effects of crystal orientation on, 25:42957 (UCRL-20500, pp 147-73)
CAFFEINE
effects on mutations and meiotic recombinations induced in yeasts by N-nitroso-N-methyl-N'-nitrosoguanidine and uv radiation, 25:42332
CALCIUM
determination during cement feeding, radiometric system for, 25:42175
distribution in barley, soybeans, and wheat during development, 25:42322(R) (COO-1097-46)
effects on oxidation resistance of zirconium alloys in carbon dioxide at high temperatures, 25:42803 (CEA-R-4103)
energy loss at 10 MeV to 100 GeV in silicon, calculations of most probable, (T), 25:42155
neutron capture by, cross section for thermal, (E), 25:43835
separation from acetone--hydrochloric acid solutions by ion exchange using Bio-Rad, distribution coefficients for, 25:41699
separation from aqueous solutions by ion exchange on zirconium tellurate, tracer studies on, 25:41915
separation from strontium using nitric acid, tracer studies on, 25:41715
superconducting parameter calculations, 25:43305
CALCIUM CARBIDES
radiation effects on, reactions of recoil nitrogen-13 from deuteron, 25:41885
CALCIUM CARBONATES
analysis for impurities by neutron activation, 25:41878 (JAERI-13579)
reactions with zirconium silicate during sintering at 1150 to 1300°C, effects of salt additions on, 25:42972
CALCIUM FLUORIDES
analysis for yttrium by x-ray fluorescence spectroscopy, 25:41832(R) (AECL-3851)
diffusion of calcium in CaF_2, 25:41832(R) (AECL-3851)
radioprotective effects of, on uranium mining personnel, animal experiments on, 25:42510
CALCIUM IONS
production of multiply-charged, for acceleration in cyclotron, ion source for, 25:43755
CALCIUM ISOTOPES
calcium--scandium Coulomb displacement energies, (E), 25:43883
CALCIUM ISOTOPES Ca-40
alpha elastic scattering at 104 MeV, differential cross sections for, (E), 25:43832 (NP-18920)
binding energy of, variational calculation using hard-core potential, 25:43787
deuteron reactions (d,p) at 5 to 12 MeV, cross section and vector analyzing power for, (E), 25:43846
energy levels from potassium-39 (p,γ) reactions, giant resonance, (E), 25:43853
energy levels of, self-consistent analysis of single-particle, (T), 25:43826
neutron capture by, cross section for thermal, (E), 25:43835
oxygen-16 elastic scattering by, analysis using absorptive optical potential, (T), 25:43978
CALCIUM ISOTOPES Ca-41
energy levels from calcium-40 (d,p) reactions, spectroscopic factors and spin assignments for, (E), 25:43846
separation from other isotopes during 1968 and 1969, review of ORNL program for, 25:41992 (ORNL-4640)
CALCIUM ISOTOPES Ca-42
energy levels from potassium-41 (p,γ) reactions, giant resonance, (E), 25:43853
helium-3 reactions (He-3,t) at 24.6 MeV, triton spectra from, (E), 25:43883
neutron capture by, cross section for thermal, (E), 25:43835
CALCIUM ISOTOPES Ca-43
helium-3 reactions (He-3,t) at 24.6 MeV, triton spectra from, (E), 25:43883
neutron capture by, cross section for thermal, (E), 25:43835
CALCIUM ISOTOPES Ca-44
energy levels of, effects of single-particle energies on shell-model calculations of, (T), 25:43866
helium-3 reactions (He-3,t) at 24.6 MeV, triton spectra from, (E), 25:43883
neutron capture by, cross section for thermal, (E), 25:43835
CALCIUM ISOTOPES Ca-45
metabolism and tissue distribution following intake by man, 25:42467
production by neutron irradiation of calcium carbonate, estimation of impurities formed in, 25:41878 (JAERI-13579)
CALCIUM ISOTOPES Ca-46
helium-3 reactions (He-3,t) at 24.6 MeV, triton spectra from, (E), 25:43883
neutron capture by, cross section for thermal, (E), 25:43835

CALCIUM ISOTOPES Ca-47
metabolism in rats in comparison to strontium-85, effects of lactation on, 25:42255
CALCIUM ISOTOPES Ca-48
energy levels of, self-consistent analysis of single-particle, (T), 25:43825
helium-3 reactions (He-3,t) at 23 MeV, distorted-wave analysis of angular distributions from, (T), 25:43848
helium-3 reactions (He-3,t) at 24.6 MeV, triton spectra from, (E), 25:43883
neutron capture by, cross section for thermal, (E), 25:43835
CALCIUM ISOTOPES Ca-49
beta decay of, gamma spectra from, (E), 25:43873
CALCIUM OXIDES
effects on electric properties of fused vanadium pentoxide at 600 to 1200°C, 25:42969
Al_2O_3--CaO--Nd_2O_3, phase diagrams of, 25:42995
CaO--EuO, stability of solid solutions of, effects of heating at 20 to 900°C on, 25:42964
CALCIUM SILICATES
standard for block and pipe thermal insulation of, 25:43014 (RDT-M-12-2-T)
CALCIUM SULFIDES
CaS--US, crystal structure of $CaUS_2$, 25:43002
CaS--US, phase diagram of, 25:43002
CALIFORNIA
radioactivity monitoring in environment of AEC installation in, during 1970, 25:42416
CALIFORNIUM
separation of berkelium from, by oxidation and sorption on zirconium phosphate silicate, 25:41882
CALIFORNIUM ISOTOPES Cf-249
preparation of isotopically pure, from berkelium-249, continuous, 25:41882
CALIFORNIUM ISOTOPES Cf-252
fission of, conversion-electron and x-ray coincidence spectra from spontaneous, (E), 25:43922
neutron dosimetry method for line-source of, in tissue-equivalent material, 25:42445
neutron fission yield measurements using manganese bath, leakage correction factor for, 25:42048 (ANL-7710, pp 263-364)
CALORIMETRY
data acquisition and control in, 25:44304 (UCRL-73046)
CALVERT CLIFFS POWER REACTOR, UNIT 1
containment structure for, safety analysis of misplaced vertical tendons in prestressed concrete, 25:44059 (DOCKET-50317-25)
CALVERT CLIFFS POWER REACTOR, UNIT 2
containment structure for, safety analysis of misplaced vertical tendons in prestressed concrete, 25:44059 (DOCKET-50317-25)
CANADA
fallout content of milk in, during 1970, 25:42417
radioactivity monitoring in atmospheric precipitation and surface atmosphere during November 1970, gross B, 25:42425
radioactivity monitoring in atmospheric precipitation and surface atmosphere during October 1970, gross B, 25:42418
radioisotope content of milk in, during November 1970, 25:42421
CANADIAN SHIELD
mineral resources in portion of Grenville Province of, probabilistic appraisal of, 25:41944
CAPILLARIES
radiation effects on permeability of rabbit skin, effects of 6-aminohexanoic acid on x, 25:42617 (UR-49-1462)
CARBIDES
book: High-Temperature Materials, 25:42853
CARBOHYDRATES
fermentation by γ-radioinduced mutants of Escherichia coli, 25:42330
radiation effects on accumulation of, in durum and soft wheat, x, 25:42721
CARBON
cosmic meson (π) reactions above 20 GeV, fluctuations in angular distributions of secondary particles from, (E), 25:43540
cosmic nucleon reactions above 20 GeV, fluctuations in angular distributions of secondary particles from, (E), 25:43540
determination on metal surfaces by methods using nuclear reactions, 25:41765
effects on hydrogen release from sintered thorium dioxide and thorium dioxide--uranium dioxide pellets at 800 to 2000°C, 25:42958 (WAPD-TM-850)
effects on properties of molybdenum crystals, 25:42899
electron reactions at 2 to 30 keV with, K-shell-fluorescence yield from, (E), 25:43108
energy levels from electroexcitation, coupled-channel calculation of giant resonance, (E), 25:43824
energy loss at 10 MeV to 100 GeV in silicon, calculations of most probable, (T), 25:42155
fabrication and testing of composites of, for use in ablative environments, 25:42971
ion reactions at 20 keV to 1.5 MeV with, cross sections for K x-ray production in, (E), 25:43107
mass stopping for gamma and x rays, calculation of mean, 25:42085
neutron inelastic scattering up to 1.5 MeV, γ spectra from, 25:43884 (ANL-7710, pp 1-52)
properties of amorphous, for use as engineering and structural material, review of, 25:42977
reactions with boride-coated molybdenum, niobium, tantalum, and tungsten, effects of temperature on, 25:42854
CARBON DIOXIDES
corrosive effects on copper--molybdenum--zirconium-base alloys at 450 to 500°C, 25:42813
corrosive effects on copper--molybdenum--zirconium-base alloys at 400 to 700°C, 25:42809
corrosive effects on copper--zirconium-base alloys at high temperatures, effects of copper content on, 25:42812
corrosive effects on zirconium alloys at high temperatures, 25:42803 (CEA-R-4103)
effects on cracking and deformation of copper--zirconium-base alloys at 600°C, 25:42928
radiolysis of, electron pulse, 25:41832(R) (AECL-3851)
yields from electron pulse radiolysis of oxalic acid, kinetics of production of, 25:41850(R) (CEA-N-1438)
CO_2--N, glass bead suspension in, power requirements for circulation of, 25:41956 (BM-RI-7019)
CO_2--T, radiolysis of, kinetics and G values of self, 25:41852 (LA-4657)
CARBON IONS
implantation in silicon junctions at 2 MeV, residual electrically active defects after lattice-reordering annealing of, 25:43439
reactions with argon at 30 to 130 keV, cross sections for argon L-shell x-ray emission in, (E), 25:43134
reactions with carbon at 20 keV to 1.5 MeV, cross sections for K x-ray production in, (E), 25:43107
CARBON ISOTOPES C-9
beta decay of, half-life for, (E), 25:43802 (UCRL-20480)
mass excess from (Be-3,He-6) reactions, (E), 25:43823
nuclear mass excess of, comparison with calculations using isobaric multiplet mass equation, (E), 25:43808
CARBON ISOTOPES C-12
alpha elastic and inelastic scattering at 104 MeV, differential cross sections for, (E), 25:43832 (NP-18920)
burning in evolved stellar cores, explosive, (T), 25:43033
deuteron reactions (d,α) at 14 to 17 MeV, angular distributions and excitation function for isospin-forbidden, (E), 25:43811
deuteron reactions (d,p) at 14.60 MeV, phase-shift analysis of energy spectra from, (E), 25:43814
electron quasi-elastic scattering with proton emission, radiative corrections in, 25:43979
energy levels of, analysis of T = 1 isobaric analog, (T), 25:43819
energy levels of, calculation using Heitler-London cluster model, (T), 25:43827
energy levels of, cluster-model extension of rotational, (T), 25:43828
energy-level transitions and optical potential parameters in pionic, πN scattering lengths for, 25:43806
helium-3 reactions (He-3,He-6) at 68 MeV, angular distribution, Q values, and spectra from, (E), 25:43823
helium-3 reactions (He-3,He-6) at 68 to 70 MeV, Q-value for, (E), 25:43808
meson (π) elastic and inelastic scattering at intermediate energies, DWIA analysis using diffraction approximation and modified distorted-wave code, (T), 25:43830
proton reactions (p,pd) at 1555 MeV, angular correlations and spectra from, (E), 25:43800 (NP-18880)
CARBON ISOTOPES C-14
metabolism and tissue distribution in man following uptake from carbon dioxide, 25:42467
radiation effects on excretion of albumin-incorporated, in rat urine as indicator of radiation injury, whole-body γ, 25:42407
use as tracer for studying sperm precedence in spruce budworms, 25:42259
CARBON SYSTEMS
C--Cr--Fe-base, radiation effects on graphitization of malleable cast, fast neutron, 25:42904
C--Fe--Mo-base, phase diagrams at 1200 and 1800°C, isothermal, 25:42889
C--Fe--Mo-base, properties of, mechanical and physical, 25:42889
C--Fe--Ni--V, crystal twinning in bulk and thin-foil, structure of transformation-type, 25:42886 (UCRL-20500, pp 86-146)
C--Fe-base--Mn, radiation effects on graphitization of malleable cast, fast neutron, 25:42904
C--Mn--Ni--steel, mechanical properties of tempered, relations with structure, 25:42886 (UCRL-20500, pp 86-146)
C--Mo-base--Ti, phase diagrams at 1200 to 2100°C, isothermal, 25:42890
C--N--Nb, preparation of cubic carbonitrides, 25:42946
C--N--Nb--O, preparation of cubic oxycarbonitrides, 25:42946
C--N--O--Pu--U, thermodynamic properties and stoichiometry of, 25:42998
C--N--Pu--U, phase studies and structures of, review on,

XUM

25:42982 (JAERI-13650)
C--Re--Ta, phase diagram at 2100°C, isothermal, 25:42952
C--steel, failure of flawed pipes and fittings of, method for prediction of, 25:42845 (GEAP-10236)
C--steel, standard for castings of, for fusion welding for high-temperature service, 25:42788 (RDT-M-4-1-T)
C--steel, standard for forgings of, 25:42773 (RDT-M-2-1-T)
C--steel, standard for quenched and tempered vacuum-treated forgings of, for pressure vessels, 25:42778 (RDT-M-2-7-T)
C--steel, standard for seamless pipes of, for high-temperature service, 25:42779 (RDT-M-3-1-T)
C--steel, standard for seamless welding fittings of, 25:42774 (RDT-M-2-3-T)
C--steel, weld solidification in, structures and mechanism of, 25:42820

CARBON TETRACHLORIDE
effects on formation of butyl radicals and hydrogen in γ radiolysis of 2-methylpropane, 25:41864

CARBONATES
analysis for strontium by atomic absorption spectroscopy, effects of aluminum and titanium on, 25:41735
polymers, alpha energy losses in tissue-equivalent, 25:42394(R) (NYU-4256-1)

CARDIAC PACEMAKERS
description of radioisotope-fueled, 25:42014
development of plutonium-238-fueled, review of programs for, 25:42012

CASCADE SHOWERS
production of extra-nuclear hadron, in shields, model for systematics in, (T), 25:43613 (CERN-71-13)

CAST IRON
radiation effects on graphitization of unannealed malleable, fast neutron, 25:42904

CATALASE
radiation effects on activity in blood of rats, continuous whole-body γ, 25:42277
radiation effects on synthesis of mouse liver, x, 25:42278

CATHODES
ion emission in vacuum breakdown, (E), 25:43383

CATS
radiation effects on vestibular and spinal reflexes of, following cerebellar granule cell exposure, 25:42657

CATTLE
radioisotope deposition in bones of, in Italy during 1962 to 1968, polonium-210 and strontium-90, 25:42382
vaccination against fascioliasis using irradiated metacercariae, 25:42245(R) (PRNC-148)

CAVITIES
radioactivity distribution in contained nuclear explosion, at high pressures and temperatures, method for calculation of, 25:41954 (CEA-R-4128(1))

CELLS
injection of spleen, from immunized donor mice into pre-irradiated recipient mice for transfer of immunity to Hymenoplepis nana, 25:42311
radiation effects on differentiation of surviving mouse stem, comparison of effects of alkylating agents and x, 25:42651
radiation effects on malignant and normal mouse tumor, protective effects of thiophosphate compounds against x, 25:42525
radiation effects on mitosis in rat bone marrow, protective effects of direct electric current against x, 25:42530
radiation effects on morphology and maturation time of primary and metastatic, of Wilms' tumors in human children, 25:42592
radiation effects on phagocytic activity of rat reticuloendothelial, protective effects of direct electric current against x, 25:42530
radiation effects on production of SV40 virus by PM3, after fusion with AGMK, effects of dose on uv, 25:42733
radiation effects on proliferation of bone marrow, in myeloid leukemia patients following extracorporeal exposure of blood, beta, 25:42690
radiation effects on SV-40 transformed, for immunization of hamsters against tumors, x, 25:42305
radiation effects on ultrastructure of Drosophila midgut, γ, 25:42612
radiation effects on, in digestive tubules and gonads of oysters, mechanisms of repopulation following, 25:42607
radiation effects on, metabolic control model for low-dose, 25:42606
radioinduced chromosome aberrations in non-uniform populations of, effects of selection and repair on dose-effect curves for, 25:42353
radioinduced injuries in living, molecular mechanisms for, 25:42727 (NYO-2804-38)
radiosensitivity of types of Hydra, x, 25:42613
tritium-labeled thymidine incorporation into DNA of lymphoma, survival following, 25:42251
use of tritium-labeled tumor, for evaluating cellular immune response against tumor-specific antigens, 25:42309

CELLS, CULTURED
decay of mouse lymphoid, nigrosin dye exclusion and tritium-labeled thymidne autoradiographic method for studying, 25:42240
radiation effects on Chinese hamster, mechanism of protective effects of cysteamine on combined anoxia or oxygen and x, 25:42521
radiation effects on count of haploid cells and incidence of chromosome aberrations in mammalian, effects of dose on x, 25:42347
radiation effects on DNA in mammalian, protective effects of cystamine or cysteamine against x, 25:42522
radioinduced aberrations of chromosomes in human, effects of dose on γ, 25:42365
radioinduced breaks in DNA in Ehrlich ascites tumor, effects of ATP production on rejoining of x, 25:42632
radiosensitivity of chromosomes in synchronized and unsynchronized rat kangaroo, comparison of x, 25:42348

CELLS, HeLa
effects on radiosensitivity of poliovirus to phosphorus-32 decay, 25:42741
radiation effects on oxygen consumption and lysine uptake of, effects of metabolic inhibitors on x, 25:42295
radiation effects on, mechanism of protective effects of MEA and MEG and its derivatives against x, 25:42514

CELLULOSE
2-thiophenecarboxylate, radiolysis of, ESR studies on intramolecular energy transfers from γ, 25:41836
radiation effects on, protective effects of thiophene groups against γ, 25:41835
radiolysis of, comparison of electron and γ, 25:41873
radiolysis of, ESR studies on intramolecular energy transfers from γ, 25:41836

CEMENTS
production of, radiometric system for determination of calcium during, 25:42175

CENTRAL AMERICA
fallout content of milk in, during 1970, 25:42417
radioactivity monitoring in surface atmosphere during November 1970, gross β, 25:42426
radioactivity monitoring in surface atmosphere during October 1970, gross β, 25:42418
radioisotope content of milk in, during November 1970, 25:42421

CERAMIC MATERIALS
crystal structure and microstructure of crystalline and noncrystalline, research program on, 25:42983(R) (MIT-3773-103)
preparation and properties of crystalline and noncrystalline, research program on, 25:42983(R) (MIT-3773-103)
research progress on, 25:41777(R) (UCRL-20500)
wetting by liquid metals, mechanisms of, 25:42980
ceramics--metals, preparation and properties of fiber-reinforced composites of, review of, 25:42978

CEREALS
bread, radiation processing of, shelf life following, 25:41833(R) (IA-1218)
maize, cesium-137 and strontium-90 content of, in Bulgaria during 1965, 25:42381
rice, cesium-137 and strontium-90 content of, in Bulgaria during 1965, 25:42381
wheat, cesium-137 and strontium-90 content of, in Bulgaria during 1965, 25:42381
wheat, distribution in USA, civil defense planning for, 25:42506(R) (ORNL-4566(Pt.1))

CEREBROSIDES
radiation effects on rat brain, protective effects of cysteine against x, 25:42620

CEREBROSPINAL FLUID
analysis for proteins, effectiveness of brain tumor diagnosis by, 25:42547 (ACRH-1000-248)
scanning flow patterns in normal human, use of metastable technetium-99-labeled human serum albumin for, 25:42567

CERIUM
determination following separation from other metal ions by thin-layer chromatography using quercetin, colorimetric, 25:41743
determination in meteorites by neutron activation and high-voltage electrophoresis, 25:41776
effects on radiation resistance of solar cell cover glass, 25:43008 (N-71-12278)
neutron total cross section at 100 to 550 keV, optical model analysis of average, (E/T), 25:43908
separation from acetone--hydrochloric acid solutions by ion exchange using Bio-Rad, distribution coefficients for, 25:41899
separation from ores, leaching methods for, 25:41918
separation from praseodymium by adsorption process using manganese oxide, 25:41883
separation from radioactive waste using oxidizing agent and manganese, 25:41911(P)
thermal capacity at low temperatures, 25:41778 (UCRL-20500, pp 1-85)

CERIUM ALLOYS AND SYSTEMS
Ce--Eu--Ge, structure of Ce/sub 5-x/Eu/sub x/Ge$_3$, 25:42895
Ce--Y-base, electric conductivity and magnetic susceptibility of single crystals of, Kondo and crystal-field effects on, 25:43479

CERIUM ISOTOPES Ce-141
beta decay of, β-γ circular polarization correlation for, (E), 25:43941

CERIUM ISOTOPES Ce-143
beta decay of, gamma and internal-conversion spectra from, (E), 25:43921
CERIUM ISOTOPES Ce-144
metabolism and tissue distribution following intake by man, 25:42457
properties for use as heat source for thermoelectric generators, 25:42014
sorption by gastrointestinal tract of suckling mice, 25:41833(R) (IA-1218)
sorption by sierozem soils, 25:42319
uptake by aquatic plants, 25:41833(R) (IA-1218)
uptake by oat plants from soils, effects of fertilizers on, 25:42260
CERIUM OXIDES
analysis for impurities, cathode region method for spectrochemical, 25:41833(R) (IA-1218)
reduction by heating, stability of compounds formed during, 25:42959
CESIUM
cesium-ion reactions with, charge-exchange cross sections for, (T), 25:43157
determination following separation by ion exchange, break-through and standard curves for, 25:41742
proton reactions at 1 to 40 keV with, charge-exchange cross section from, (E/T), 25:43103
reactions between ground-state and highly excited atoms of, excitation transfer in, (T), 25:43133
separation from acetone--hydrochloric acid solutions by ion exchange using Bio-Rad, distribution coefficients for, 25:41899
separation from aqueous solutions by ion exchange on zirconium tellurate, tracer studies on, 25:41915
separation from radioactive waste using oxidizing agent and manganese, 25:41911(P)
sorption by aluminum oxide at 300 to 1000°F, tracer studies on, 25:42863
sorption by as-received and polished stainless steel at 300 to 1000°F, tracer studies on, 25:42863
sorption by oxidized zirconium surfaces at 300 to 1000°F, tracer study on, 25:42863
sorption by polished nickel at 300 to 1000°F, tracer studies on, 25:42863
sorption by soils around Casaccia, Italy, 25:41930
CESIUM ALLOYS AND SYSTEMS
Ce--Sb, magnetic structure in strong magnetic fields, 25:43435(R) (RISO-237)
CESIUM BROMIDES
xenon-atom reactions with, crossed-beam study of dissociation in, 25:43131
CESIUM IODIDES
neutron total cross section at 100 to 650 keV, optical model analysis of average, (E/T), 25:43908
radioluminescence of thallium-activated crystals of, effects of electric field on α, β, γ, and uv, (E), 25:43448
xenon-atom reactions with, crossed-beam study of dissociation in, 25:43131
CESIUM IONS
reactions with cesium, charge-exchange cross sections for, (T), 25:43157
CESIUM ISOTOPES
determination of radioactive, in milk by ion exchange using ammonium molybdophosphate and counting, 25:41751
CESIUM ISOTOPES Cs-131
production of carrier-free, by neutron irradiation of barium carbonate and solvent extraction, 25:41876 (CONF-680985-2)
CESIUM ISOTOPES Cs-134
sorption by animal intestines, use of ion exchange resins for prevention of, 25:42263
uptake by frogs in rain forest in Puerto Rico, 25:42317(R) (PRNC-147)
use of fungus-incorporated, to determine feeding habits of Caeculid mites, 25:42242
CESIUM ISOTOPES Cs-137
beta decay of, ionization (shakeoff) in conversion-electron spectra from, (E), 25:43871
content in food in Israel, 25:41833(R) (IA-1218)
content in food in Pavia, Italy, 1964 to 1966, 25:42389
content in ground-level atmosphere of Brunswick, West Germany, effects of seasonal variations on, 25:41934
content in human diet and urine in Italy, effects of age on, 25:42375
content of dairy products, fruits, and vegetables in Bulgaria during 1965, 25:42391
content of diet of adults and children in Formosa, comparison of, 25:42422
content of human population in Soviet Union during 1966 to 1968, calculation of genetic dose from, 25:42376
content of institutional diets in USA during 1970, 25:42417
content of milk in Canada, Central and South America, and USA during November 1970, 25:42421
content of milk in Canada, Central and South America, and USA during 1970, 25:42417
content relative to strontium-90 in atmosphere and precipitation in Israel, 1958 and 1969, 25:41833(R) (IA-1218)
distribution in skin following surface contamination, kinetics of, 25:42257
dose distribution from plaque-type gamma source of, data tabulations on, 25:41957 (BNL-50147(Rev.))
elimination from human organism, effects of age on, 25:42250
leachability and volume strength of liquid, for incorporation in concrete mixtures, 25:41833(R) (IA-1218)
metabolism and tissue distribution following intake by man, 25:42467
properties for use as heat source for thermoelectric generators, 25:42014
separation of barium-137m from, by ion exchange using cesium-containing ammonium molybdophosphate, 25:41751
sorption by sierozem soils, 25:42319
uptake by aquatic plants, 25:41833(R) (IA-1218)
uptake by frogs and lizards from labeled trees, 25:42317(R) (PRNC-147)
use as tracer in cesium sorption studies, 25:42863
CHALCOPYRITES
analysis of Luzon, Philippines, for trace elements by neutron activation, 25:41772
CHARCOAL
sorptive properties for methyl iodide containing fissio product iodine in carbon dioxide--carbon monoxide--methane system, 25:41898 (IRG-Report-2135)
CHARGED-PARTICLE BEAMS
deflection of, longitudinal second-order aberrations in magnetic systems for, 25:43763
interactions with turbulent plasma, diagnostic use of, 25:43335 (IYAF-7-70)
monitoring of position, intensity, and energy distribution of low-intensity, method for, 25:42098
CHARGED PARTICLES
channeling images of microcrystals, use for orientation determination, (e), 25:43464
detection of heavy, development of high-rate time-of-flight system for, 25:42055
detection of highly ionizing, design of position-sensitive superconducting detectors for, 25:42097
distribution at low-altitude auroral zones and polar caps, relation with simultaneous dc electric fields, (E), 25:43219 (N-71-20708)
field equations for charged spin-$^1/_2$ matter, static solutions for combined Dirac--electromagnetic--gravitational, (T), 25:43703
interactions at high energies and fixed transferred momenta, validity of Bethe formula for relative phase shifts of Coulomb and hadron parts of amplitudes for, (T), 25:43607
interactions at high energies, asymptotic cross sections for e^+--e^- production in, 25:43598
interactions of moving, with infinite dielectric, model for, 25:43588
interactions of point, relativistic mechanics of, 25:43573
interactions with thin materials, analysis of distributions from, (T), 25:43414 (BNWL-SA-3705)
motion in electromagnetic fields, (T), 25:43507(T) (JPRS-52839, pp 3-16)
polarization near spin resonances in storage rings, dynamics of, (T), 25:43770
precipitation at latitudes below 40°N, if D-region pulse-reflection method for detection of, (E/T), 25:43223
slowdown in gases, atom or molecule excitation energy relevant to, (T), 25:43207 (AD-705130)
CHEMISTRY
research progress on, 25:41778 (UCRL-20500, pp 1-85)
CHLORAMBUCIL
effects on tetanus antitoxin production in mice, combined effects of γ radiation and, 25:42572
CHLORINE
determination in sedimentary minerals by Szilard--Chalmers reactions following neutron activation, 25:41763
CHLORINE IONS
reactions with argon at 30 to 130 keV, cross sections for argon L-shell x-ray emission in, (E), 25:43134
CHLORINE ISOTOPES
effects on nucleophilic displacement reactions of p-substituted benzyl chlorides, 25:41795
CHLORINE ISOTOPES Cl-33
energy levels from argon-33 beta decay, (E), 25:43802 (UCRL-20480)
proton decay of, branching ratios and gamma and proton spectra from beta-delayed, (E), 25:43802 (UCRL-20480)
CHLORINE ISOTOPES Cl-36
metabolism and tissue distribution following intake by man, 25:42467
CHLORINE ISOTOPES Cl-38
reactions of recoil atoms of, with chloromethane, effects of scavengers on yields from, 25:41833(R) (IA-1218)
reactions of recoil, from neutron irradiation of α-, β-, γ-, and delta-benzene hexachloride, 25:41884
CHLOROFORM
solution heat of, effects of deuterium on, 25:41794
CHOLINE, ACETYL-
radiation effects on metabolism of, in animals and man as indicators of radiation injury, x, 25:42626
CHROMATOGRAPHY
efficiency of steric exclusion, effect of loading on separation, 25:44244 (COO-1222-46)
performance of steric-exclusion, at high pressure,

25:44245 (COO-1222-48)
research progress on high-pressure liquid, 25:44248(R) (COO-1222-50)
solvent distribution in ion exchanger in mixed media, 25:41910
CHROMEL COUPLES
Alumel/Chromel-P, standard for magnesium oxide-insulated and stainless steel sheathed, 25:42200 (RDT-C-7-6-T)
CHROMIUM
determination of trace amounts of, in meteorites by neutron activation and γ spectrometry, 25:41773
effects on graphite--nitrous oxide and graphite--oxygen reactions, catalytic, 25:42931
effects on oxidation resistance of zirconium alloys in carbon dioxide at high temperatures, 25:42803 (CEA-R-4103)
effects on superconducting critical field of niobium--titanium alloy wires, 25:43309
lattice vibrational spectra and thermal capacities of, calculations, 25:43490
separation from acetone--hydrochloric acid solutions by ion exchange using Bio-Rad, distribution coefficients for, 25:41899
surface structure of, low-energy electron diffraction studies on, 25:41778 (UCRL-20500, pp 1-85)
wear of rubbing surfaces of, selenium-75 tracer studies of, 25:42018
CHROMIUM ALLOYS AND SYSTEMS
mechanical properties of sintered intermetallic compounds of, 25:42818
Al--Cr--Fe-base, properties for use in high-temperature strain gages, 25:42804(R) (LMEC-71-1)
Al--Cr--Fe-base--Y, properties for use in high-temperature strain gages, 25:42804(R) (LMEC-71-1)
Al--Cr--Mo--Ti-base--V--Zr, mechanical properties of, 25:42835 (AD-715877)
C--Cr--Fe-base, radiation effects on graphitization of malleable cast, fast neutron, 25:42904
Co--Cr, standard for wear- and corrosion-resistant castings of, 25:42790 (RDT-M-4-3-T)
Co-base--Cr, oxidation at 900 to 1200°C, comparison with TD-nickel chromium, 25:42930
Cr--Cu, thermal capacity at low temperatures, 25:41778 (UCRL-20500, pp 1-85)
Cr--Cu--Fe--Mo--Nb--V--Zr-base, corrosion resistance of, 25:42811
Cr--Fe, sintering of intermetallic compounds of, kinetics of, 25:42818
Cr--Fe--Ni, corrosion cracking in, containing trace chlorides, studies on mechanism of stress, 25:42760(R) (COO-2059-7)
Cr--Fe--Ni, standard for plates, sheets, and strips of, 25:42794 (RDT-M-5-4-T)
Cr--Fe--Sn--Zr-base, properties for use in water-cooled reactors, 25:42975
Cr--Fe--Zr-base, corrosion by steam and water at 300 to 400°C, kinetics of, 25:42815
Cr--Fe-base--Mn--Mo--Ni, ductility of irradiated Sandvik 12R72HV, at 500 to 800°C, effects of injected helium on, 25:42872
Cr--Fe-base--Ni, ductility of irradiated Inco IN-744X, at 500 to 800°C, effects of injected helium on, 25:42872
Cr--Mo--steel, corrosion by sodium--water reaction products at 600°F, 25:42804(R) (LMEC-71-1)
Cr--Mo--steel, standard for plates of, 25:42795 (RDT-M-5-5-T)
Cr--Ni--P--Pt, electric conductivity and magnetic susceptibilities of amorphous, 25:44237 (CALT-822-31)
Cr--Ni--stainless steel, standard for pipes of, 25:42785 (RDT-M-3-7-T)
Cr--Ni--stainless steel, standard for plates, sheets, and strips of, 25:42791 (RDT-M-5-1-T)
Cr--Ni-base, oxidation at 900 to 1200°C, comparison with TD-nickel chromium, 25:42930
Cr--O--Zr-base, properties of dilute, effects of chromium and oxygen contents on mechanical and structural, 25:42879
Cr--Si--Y, phase diagram at 800°C, isothermal, 25:42993
Cr--stainless steel, standard for plates, sheets, and strips of, 25:42791 (RDT-M-5-1-T)
CHROMIUM BORIDES
preparation of, method for, 25:42944
thermal capacity of, low-temperature, 25:42974
CrB--VB, thermal capacity of, low-temperature, 25:42974
CHROMIUM ISOTOPES
chromium--manganese Coulomb displacement energies, (E), 25:43883
chromium--vanadium Coulomb displacement energies, (E), 25:43883
CHROMIUM ISOTOPES Cr-50
energy levels from chromium-52 (p,t) reactions, spin--parity assignments and transition strengths for, (E), 25:43849
helium-3 reactions (He-3,t) at 24.6 MeV, triton spectra from, (E), 25:43883
neutron capture at 0.1 to 200 keV, cross sections for, (E), 25:43857
neutron transmission measurements up to 300 keV, (E), 25:43857
CHROMIUM ISOTOPES Cr-51
content of Columbia River during 1968 to 1969, 25:42419
CHROMIUM ISOTOPES Cr-52
deuteron reactions (d,p) at 5 to 12 MeV, cross section and vector analyzing power for, (E), 25:43846
energy levels from vanadium-51 (He-3,d) reactions, shell-model calculations of spectroscopic factors for, (T), 25:43862
energy levels of, shell-model calculation of, (T), 25:43862
helium-3 reactions (He-3,t) at 24.6 MeV, triton spectra from, (E), 25:43883
neutron capture at 0.1 to 200 keV, cross sections for, (E), 25:43857
neutron transmission measurements up to 300 keV, (E), 25:43857
proton reactions (p,γ) at 1 to 1.6 MeV, γ-γ coincidence spectra from, (E), 25:43837
proton reactions (p,t) at 27 MeV, DWBA analysis of differential cross sections for, (E), 25:43849
CHROMIUM ISOTOPES Cr-53
deuteron reactions (d,p) at 5 to 12 MeV, cross section and vector analyzing power for, (E), 25:43846
energy levels from chromium-52 (d,p) reactions, spectroscopic factors and spin assignments for, (E), 25:43846
helium-3 reactions (He-3,t) at 24.6 MeV, triton spectra from, (E), 25:43883
neutron capture at 0.1 to 200 keV, cross sections for, (E), 25.43857
neutron transmission measurements up to 300 keV, (E), 25:43857
photon reactions (γ,n) at 11.5 MeV endpoint energy, neutron energy spectra from, (E), 25:43929
CHROMIUM ISOTOPES Cr-54
helium-3 reactions (He-3,t) at 24.6 MeV, triton spectra from, (E), 25:43883
neutron capture at 0.1 to 200 keV, cross sections for, (E), 25:43857
neutron transmission measurements up to 300 keV, (E), 25:43857
CHROMOSOMES
radioinduced aberrations in bone marrow and leukocytes in Japanese fishermen, latent fallout, 25:42681
radioinduced aberrations in Crepis capillaris dry seeds, effects of nitrogen mustard on γ, 25:42359
radioinduced aberrations in human cells, in vivo and in vitro, 25:42691
radioinduced aberrations in human, as indicators of radiation dose or injury, 25:42405
radioinduced aberrations in human, as indicators of radiation dose, 25:42405
radioinduced aberrations in, in human lymphocytes as biological dosimeter, β, 25:42399
radioinduced aberrations in, in human lymphocytes as biological dosimeter, 25:42398
radioinduced aberrations of Crepis capillaris, effects of DNA on recovery from x, 25:42356
radioinduced aberrations of cultured human cell, effects of dose on γ, 25:42355
radioinduced aberrations of cultured mammalian cell, effects of dose on x, 25:42347
radioinduced aberrations of in Crepis capillaris, effects of dose on cesium-137 γ, 25:42351
radioinduced aberrations of male fruit fly Y, segregation of rearrangements following x, 25:42344
radioinduced aberrations of mouse and rat bone marrow, effects of age on x, 25:42656
radioinduced aberrations of mouse bone marrow cell, protective effects of cysteine derivatives against whole-body x, 25:42534
radioinduced aberrations of Pisum arvense and P. sativum, relation between radiation effects on biochemistry and morphology and γ, 25:42329
radioinduced aberrations of sunflower root, effects of seed-exposure dose on x, 25:42361
radioinduced aberrations of Vicia faba, use of protein-specific dyes to visualize x, 25:42343
radioinduced aberrations of, in cultured bone marrow cells and leukocytes from patients with polycythemia treated with phosphorus-32, 25:42713
radioinduced aberrations of, in human blood, comparison of chronic external and therapeutic internal, 25:42707
radioinduced aberrations of, in newborn child following radiography, x, 25:42362
radioinduced aberrations of, in non-uniform populations of cells, effects of repair and selection on dose-effect curves for, 25:42353
radioinduced translocations in Drosophila oocyte, effects of dose on frequency of x, 25:42333
radioinduced translocations in Drosophila, following exposure of male pupae, x, 25:42354
radioinduced translocations in mosquitoe, effects of dose on semisterility-producing x, 25:42335
radiosensitivity of rat kangaroo, in synchronized and unsynchronized cultures, comparison of x, 25:42348
segregation following interchange in x-irradiated mature oocytes of Drosophila, 25:42276
CHROMOSPHERE
eruptions in, north--south asymmetry of, (E/T), 25:43072
structure of transition region with corona, (T), 25:43068 (N-71-19294)
CIRCUITS
design of fast digitizing, for data acquisition in fast

single-shot experiments, 25:42220
fabrication of integrated, by ion implantation, accelerator for, 25:43728 (CEA-CONF-1767)
fabrication of printed, by single-probe reflow soldering, 25:44225 (BDX-513-325)
fabrication of printed, evaluation of solder leveling process for use in, 25:44234 (BDX-613-443)
fabrication of printed, use of flow-soldering method in, 25:44227 (BDX-513-330)
CIRCULATORY SYSTEM
radiation effects on rabbit, effects of solar exposure on x, 25:42651
CIVILIAN DEFENSE
bibliography on, 25:42505 (BARC/BIB-1)
programs in USA for, during 1971, 25:42506(R) (ORNL-4566(Pt.1))
research programs of AEC during 1970 on, 25:44293 (TID-25728)
CLAYS
analysis for halogens by Szilard--Chalmers reactions following neutron activation, 25:41763
CLEANING
requirements of reactor components, standards for, 25:44089 (RDT-F-5-1-T)
CNIDARIA
Hydra sp., radiosensitivity of types of cells of, comparison of x, 25:42513
COAL
prospecting for, review on nuclear borehole methods for, 25:41931
COATINGS
effects of oxide, on performance of multi-foil thermal insulation, 25:42962
thickness measurements of, beta backscatter gage for, 25:42173(P)
COBALT
complexes with ammonia, reactions of hydrated, with trivalent uranium in aqueous perchlorate solutions, 25:41783
effects on F-center growth curves in x-irradiated potassium chloride crystals, (E), 25:43450
hyperfine fields for substitutional impurities in, tables of, 25:43459 (UCRL-20411)
production and consumption of, worldwide, 25:42868
properties and uses of, review of, 25:42868
separation from acetone--hydrochloric acid solutions by ion exchange using Bio-Rad, distribution coefficients for, 25:41899
separation from aqueous solutions by ion exchange on zirconium tellurate, tracer studies on, 25:41915
separation from other metals using inorganic ion exchange papers, 25:41909
COBALT ALLOYS AND SYSTEMS
properties and uses of, review of, 25:42868
Co--Cr, standard for wear- and corrosion-resistant castings of, 25:42790 (RDT-M-4-3-T)
Co--Th, structure and Curie temperature of $ThCo_5$, effects of stoichiometry on, (E), 25:43485
Co-base--Cr, oxidation at 900 to 1200°C, comparison with TD-nickel chromium, 25:42930
COBALT BORIDES
preparation of, method for, 25:42944
CoB--FeB, thermal capacity of, low-temperature, 25:42974
COBALT CHLORIDES
sorptive properties of surfaces of, for krypton, thermodynamic studies on stepwise isotherms for, 25:41824 (CEA-R-4099)
COBALT FERRATES
defects in thin films of, relations with etching and electron microscopic field exposure, 25:42886 (UCRL-20500, pp 86-146)
COBALT ISOTOPES
cobalt--iron Coulomb displacement energies, (E), 25:43883
cobalt--nickel Coulomb displacement energies, (E), 25:43883
COBALT ISOTOPES Co-54
energy level at 937 keV from iron-54 (p,nγ) reactions, spin assignments for, (E), 25:43863
COBALT ISOTOPES Co-55
energy-level scheme from iron-54 (He-3,d) reactions, (E), 25:43858
COBALT ISOTOPES Co-57
beta decay of, chemical effects on conversion-electron spectra from, (E), 25:43865
electron-capture decay of, gamma energies and intensities from, (E), 25:43882
electron-capture decay of, ionization (shakeoff) in conversion-electron spectra from, (E), 25:43871
energy-level transitions from iron-56 (p,γ) reactions, strengths for M1, (E), 25:43850
COBALT ISOTOPES Co-59
helium-3 reactions (He-3,t) at 24.6 MeV, triton spectra from, (E), 25:43883
proton reactions (p,γ) at 4.40 to 13.60 MeV, angular distributions, excitation functions, and spectra from, (E/T), 25:43867
proton reactions (p,γ) in giant resonance region, angular distributions and cross sections for, (E), 25:43853
COBALT ISOTOPES Co-60
description of 7730 Ci gamma sources of, 25:42015
development of kernel-cluster heat sources of, for space power systems, 25:42000
dose distribution from plaque-type gamma source of, data tabulations on, 25:41957 (BNL-50147(Rev.))
metabolism and tissue distribution following intake by man, 25:42467
properties for use as heat source for thermoelectric generators, 25:42014
COBALT OXIDES
chemical activity in sodium silicate at 700 to 1100°C, 25:42957 (UCRL-20500, pp 147-73)
COENZYME Q
effects on reactivation of respiratory chain in uv-irradiated Escherichia coli, 25:42732
COINCIDENCE CIRCUITS
design of low-accidentals, for measurement of (e,e'p) reactions with light nuclei, 25:42131
COINCIDENCE MEASUREMENTS
method for measuring nuclear half-lives up to 100 sec by delayed-, using on-line computers, 25:42222
COLLIMATORS
design for electron beams at 10 to 20 MeV, 25:43767
COLLISION PROCESSES
ionization amplitudes in, calculation by complex-energy method, 25:43145
COLUMBIA RIVER
radioactivity monitoring during 1968 and 1969, β and γ, 25:42419
radioisotope content of, during 1968 to 1969, chromium-51, phosphorus-32, and zinc-65, 25:42419
COMMUNICATION SYSTEMS
uses of audiovisual, in scientific information dissemination, 25:41833(R) (IA-1218)
COMPOSITE MATERIALS
preparation and properties of ceramic fiber-reinforced metal, review of, 25:42978
production of clad-metal, diffusion coated metals, and fiber-reinforced, review of technologies for, 25:42951
COMPTON EFFECT
frequency shifts in, effects of coherence on intensity-dependent, (T), 25:43590
spectral intensity distribution in, by Thomas--Fermi model, 25:43515
COMPUTER PROGRAMS
CLIP, for manipulation of THREDES code for thermal reactor physics calculations, 25:44095 (AI-CE-Memo-12)
DCHAIN, for calculating time-dependent populations of radioactive decay and neutron capture chains, in FORTRAN IV for DEC PDP-9 or PDP-15, 25:43889 (LA-4708)
DDO, for inventory control of deuterium, 25:41960 (EUR-4512)
DEMETRA, for neutron thermalization calculations in one-dimensional heterogeneous reactor cells, 25:44195 (IAE-2010)
ENDF/B format for sodium, magnesium, chlorine, and potassium for shielding calculations, preparation of data sets in, 25:43420 (ORNL-TM-3429)
for analysis of particle tracks measured in SMP, 25:42135(T) (CERN-Trans-71-8)
for simulation of average cycle time for high density automated warehouse, 25:44224 (BDX-613-274)
for time dependent finite element analysis of reactor fuel rod deformations, FORTRAN IV for CDC 6600, 25:44126 (WERL-ELPLA-1)
KATOK, for processing spectra from lithium-drifted germanium gamma spectrometers, for Minsk-2, 25:42116
MICROANALYSIS, for converting electron-beam microprobe analyzer data into element concentrations in weight percent and atomic percent, 25:44305 (UCRL-73104)
MIS-0, for DWBA calculations of l = 0 inelastic scattering differential cross sections for charged particles, in MAT-4 for MINSK-22, 25:43954 (INP-746)
MIS-2, for DWBA calculations of l = 2 inelastic scattering differential cross sections for charged particles, in MAT-4 for MINSK-22, 25:43954 (INP-746)
MIS-3, for DWBA calculations of l = 3 inelastic scattering differential cross sections for charged particles, in MAT-4 for MINSK-22, 25:43954 (INP-746)
MIS-4, for DWBA calculations of l = 4 inelastic scattering differential cross sections for charged particles, in MAT-4 for MINSK-22, 25:43954 (INP-746)
MIS-5, for DWBA calculations of l = 5 inelastic scattering differential cross sections for charged particles, in MAT-4 for MINSK-22, 25:43954 (INP-746)
ORTHAT and ORTHIS, for solution of steady-state and transient heat transfer problems in two-dimensional geometries, FORTRAN IV for IBM 360, 25:41985 (ORNL-TM-3324)
PIEGA, numerical solution for definite integrals with oscillating integrands, 25:44299 (UCID-30008)
PMS/360 for project management, 25:44258 (CTC-INF-1030)
RACER, for calculation of external radiation dose to human population from airborne radioisotopes released during reactor accidents, Univac 1108, 25:42393 (BNWL-B-69)
RIPPLE, for film transport, 25:44298 (TID-25758)
SHADOK, for solution of integral neutron transport equation by three-term polynomial approximation, for CDC 6500, 25:43771 (EIR-189)
SID, for photograph digitizing using CDC 6600, 25:44290 (SC-DR-68-814)

XUM

COMPUTERS
electronics for, CAMAC standard, 25:42218
image processing and pattern recognition research: ILLIAC III, 25:44294(R) (TID-25739)
performance for calculating integral dose to man during therapy, 25:42415
requirements for digital, for use in reactor design, 25:44090 (WAPD-T-2358)
research progress at Johns Hopkins University, 25:44275 (NYO-4209)

CONCRETES
failure of reactor pressure vessels of prestressed, stress-wave emissions for detection of, 25:43015
radioisotope incorporation in, leachability and volume strength for liquid, 25:41933(R) (IA-1218)

CONDENSERS
standard for seamless annealed nickel--chromium--iron alloy tubes for, 25:42782 (RDT-M-3-4-T)

CONNECTICUT YANKEE POWER REACTOR
operations history for May 1971, 25:44006 (DOCKET-50213-115)

CONNECTORS (ELECTRIC)
specifications for coaxial high-voltage, ANSI N42.4-1971 standard for, 25:42214

CONSTANTAN COUPLES
Constantan/Cu, standard for magnesium oxide-insulated and stainless-steel sheathed, 25:42199 (RDT-C-7-4-T)
Constantan/Cu, standard for solid conductor thermocouples, 25:42198 (RDT-C-7-3-T)
Constantan/Fe, standard for, 25:42196 (RDT-C-7-1-T)
Constantan/Fe, standard for magnesium oxide-insulated and sheathed thermocouple, 25:42197 (RDT-C-7-2-T)

CONTAINMENT SYSTEMS EXPERIMENT
fission product holdup in leak paths in, decontamination factors for, (E), 25:44134 (BNWL-1582)

COPPER
complexes with zinc trifluoroacetate, ESR of, 25:41838
determination in minerals from Luzon, Philippines, by neutron activation, 25:41772
determination of trace amounts of, in zinc, spectrochemical, 25:41833(R) (IA-1218)
diffusion in praseodymium, mechanism of, 25:41833(R) (IA-1218)
dislocation slip band growth in monocrystalline, electron microscopic study of, 25:42886 (UCRL-20500, pp 86-146)
effects on oxidation resistance of zirconium alloys in carbon dioxide at high temperatures, 25:42803 (CEA-R-4103)
effects on superconducting critical field of niobium--titanium alloy wires, 25:43309
mass stopping for gamma and x rays, calculation of mean, 25:42085
neutron inelastic scattering up to 1.5 MeV, γ spectra from, 25:43884 (ANL-7710, pp 1-52)
neutron total cross section up to 1.5 MeV, (E), 25:43884 (ANL-7710, pp 1-52)
separation from acetone--hydrochloric acid solutions by ion exchange using Bio-Rad, distribution coefficients for, 25:41899
separation from aqueous solutions by ion exchange on zirconium tellurate, tracer studies on, 25:41915
separation from ores, leaching methods for, 25:41918
standard for welding rods of, 25:42768 (RDT-M-1-8-T)
superconducting proximity effect in Cu/Pb/Cu sandwiches, acoustic surface wave study of perpendicular field, 25:43315
weld solidification in, structures and mechanism of, 25:42829
x-ray backscattering at 11.3 to 23.2 MeV, (E), 25:43431

COPPER ALLOYS AND SYSTEMS
standard for welding rods of, 25:42768 (RDT-M-1-8-T)
Al--Cu, aging processes in, effects of trace metals on precipitation from, 25:42886 (UCRL-20500, pp 86-146)
Al--Cu, superconducting transition temperature in high T/sub c/ intermetallic $CuAl_2$, sensitivity to residual stress of, (E), 25:43302
Al-base--Cu, radiation effects on precipitation hardening of, pile neutron, 25:42902 (JAERI-13692)
Au--Cu, analysis by electron-beam microprobe method, computer program for processing of data from, 25:44305 (UCRL-73104)
Cr--Cu, thermal capacity at low temperatures, 25:41778 (UCRL-20500, pp 1-85)
Cr--Cu--Fe--Mo--Nb--V--Zr-base, corrosion resistance of, 25:42811
Cu--Fe, thermal capacity at low temperatures, 25:41778 (UCRL-20500, pp 1-85)
Cu--Fe--Ni, phase decomposition in, kinetics of spinodal, 25:42886 (UCRL-20500, pp 86-146)
Cu--Fe--Zr-base, oxidation by steam at 500°C, effects of crystal structure and impurities on, 25:42810
Cu--Mo--Zr-base, corrosion by carbon dioxide at 400 to 700°C, 25:42809
Cu--Mo--Zr-base, corrosion by carbon dioxide at 450 to 500°C, 25:42813
Cu--Mo--Zr-base, microstructure of phases in, 25:42898
Cu--Mo--Zr-base, phase studies of, 25:42897
Cu--Mo--Zr-base, properties for use in carbon dioxide-cooled reactors, 25:42878
Cu--Mo--Zr-base, radiation effects on mechanical properties of, relations of annealing with fast neutron, 25:42813
Cu--Mo--Zr-base, radiation effects on properties of, for use in EI-4 pressure tubes, neutron, 25:42929
Cu--Pt, deformation studies of, 25:44286(R) (ORO-3091-21)
Cu--W, thermal expansion of composites of, incorporating tungsten wire, 25:42873
Cu--Zr-base, cracking and deformation in fuel cladding of, effects of carbon dioxide at 600°C on, 25:42928
Cu--Zr-base, oxidation by carbon dioxide at high temperatures, effects of copper content on, 25:42812
Cu--Zr-base, properties for use as fuel cladding in carbon dioxide-cooled reactors, 25:42861
Cu--Zr-base, radiation effects on fuel cladding of, in-pile, 25:42881

COPPER COUPLES
Constantan/Cu, standard for magnesium oxide-insulated and stainless-steel sheathed, 25:42199 (RDT-C-7-4-T)
Constantan/Cu, standard for solid conductor thermocouples, 25:42198 (RDT-C-7-3-T)

COPPER IONS
reactions with argon at 30 to 130 keV, cross sections for argon L-shell x-ray emission in, (E), 25:43134

COPPER ISOTOPES
copper--nickel Coulomb displacement energies, (E), 25:43883
copper--zinc Coulomb displacement energies, (E), 25:43883
separation of, evaluation of methods for, 25:41897(T) (ORNL-tr-2512)

COPPER ISOTOPES Cu-61
energy levels from nickel-58 (α,pγ) reactions, spin-parity assignments for, (E), 25:43839
energy-level transitions from nickel-58 (α,pγ) reactions, γ-mixing and branching ratios for, (E), 25:43839

COPPER ISOTOPES Cu-63
helium-3 reactions (He-3,t) at 24.6 MeV, triton spectra from, (E), 25:43883

COPPER ISOTOPES Cu-64
testing of, produced in Japan, application, 25:41990 (JAERI-13617)
use of erythrocyte-incorporated, for scintigraphy of human spleen, 25:42564

COPPER ISOTOPES Cu-65
helium-3 reactions (He-3,t) at 24.6 MeV, triton spectra from, (E), 25:43883

COPPER SULFATES
physical properties of sulfuric acid solutions of, 25:41778 (UCRL-20500, pp 1-85)

CORROSION
prevention of, role of design in, 25:44236 (BNWL-SA-3817)

CORROSION FILMS
analysis of thin, electron microprobe, 25:44266 (KAPL-3482)

CORROSION INHIBITORS
effects on corrosion of Zircaloy-2 and Zircaloy-4, 25:42808

CORROSION LOOPS
maintenance and operation of large component, for testing FFTF and LMFBR materials, 25:42804(R) (LMEC-71-1)

COSMIC PARTICLES
charged-particle components of primary, rigidity spectrum of helium, medium and heavy nuclei, (E), 25:43178
detection of low-energy primary, design of balloon-borne counter telescope for, 25:42159
energy spectra of primary protons, calculation of neutron monitor multiplicity yield function from, 25:43175
flux estimates for neutron, in lunar materials, 25:41833(R) (IA-1218)
geomagnetic-cutoff variations during geomagnetic-storm main phase, (E), 25:43179
helium and hydrogen from solar-wind gas-saturated, inner solar system, (E/T), 25:43176
interactions above 10^{12} eV, production of massive particle in new process in, (T), 25:43567 (INR-1280)
reactions of mesons (π) and nucleons with carbon above 20 GeV, fluctuations in angular distributions of secondary particles from, (E), 25:43540

COSMIC RADIATION
hadron flux at atmospheric depth of 976 gcm^{-2}, above 12 GeV in, spark chamber study of ratio of neutral to charged, (E), 25:43621
helium isotopes in primary, (E), 25:43173
intensity variations of sidereal diurnal anisotropic, solar modulation mechanism of, (T), 25:43177
meson (π) flux at atmospheric depth of 976 gcm^{-2} at 12 to 15 GeV in, spark chamber study of ratio to nucleons for, (E), 25:43621
neutrino production in the atmosphere, (T), 25:43174
nucleon flux at atmospheric depth of 976 gcm^{-2} at 12 to 15 GeV in, spark chamber study of ratio to nucleons for, (E), 25:43621
production and propagation in upper atmosphere, secondary negatrons and positrons, (E/T), 25:43235

COSMIC RADIO SOURCES
flux densities at 90 GHz, (E), 25:43060
flux densities of 101 extragalactic, (E), 25:43062
flux densities of optically identified B2, at 5 GHz, (E), 25:43063
identification of PKS 1514-24 with AP Librae, (E), 25:43082

propagation of extended, into intergalactic medium, (T), 25:43058
silicon monoxide in Sgr B2, detection of, (E), 25:43052
spectra of 101 extragalactic, (E), 25:43062
structures of 75 extragalactic, two-dimensional, (E), 25:43061
COSMIC RAY TELESCOPES
description of underground scintillation, 25:42152
design of balloon-borne, for alpha particles and protons, 25:42159
COSMIC SHOWERS
detection of EAS, spark chamber hodoscope for, 25:42158
detection of, geometrical considerations of hodoscopes for, 25:42157
simulation of EAS, with medium-strong interaction, (T), 25:43647 (ORO-3992-61)
COSMIC X-RAY SOURCES
Ara X-1, flux and energy spectra of, (E), 25:43057
Cen X-1, discovery of periodic x-ray pulsations in emission of, (E), 25:43055
Cen X-2, flux from, (E), 25:43057
luminosity of, in Coma cluster, (E), 25:43056
Lup X-1, flux from, (E), 25:43057
Nor X-1, flux from, (E), 25:43057
Nor X-2, flux from, (E), 25:43057
radiation mechanisms for, (T), 25:43079 (N-71-20472)
Sco X-4, flux from, (E), 25:43057
spectra of, in Coma cluster, (E), 25:43056
COSMOLOGY
constant of, (T), 25:43087
Hamiltonian for Bianchi Type VIII and IX vacuum, (T), 25:43095
models of, Friedmann--Lemaitre, 25:43085 (ITF-71-16-P)
perturbations in anisotropic Euclidean homogeneous, (T), 25:43095
theory as empirical science, (T), 25:43098
theory for, general relations in relativistic MHD for, 25:43701
COULOMETRY
cell for, conducting glass electrode in thin-layer electrochemical, 25:41732
CRAB NEBULA
radio map of, (E), 25:43064
CREEP
acoustic emission during, theory of, 25:42861
CRITICAL ASSEMBLIES
criticality of plutonium oxide (PuO_2)--uranium oxide (UO_2) fueled ZPPR and ZPR-9, (E), 25:44096 (ANL-7710, pp 53-252)
design parameters for ZPR-6 Variable Temperature Rodded Zone, 25:44096 (ANL-7710, pp 53-262)
Doppler effects measurements in FRO, foil activation, (E/T), 25:44154
fission rate distribution measurements in, non-perturbing fission counter for, 25:42048 (ANL-7710, pp 263-364)
fuel handling system for NPTR, shielding requirements for, (T), 25:44151 (WANL-TME-1995)
gamma dose distribution in, thermoluminescent dosimetry methods for, 25:42048 (ANL-7710, pp 263-364)
kinetics of fast, (T), 25:44096 (ANL-7710, pp 53-262)
neutron activation-rate measurements in ZPR-3 mockup of EBR-II cores, 25:44150 (ANL-7781)
neutron buckling in FRO uranium-loaded fast assemblies, material, (E/T), 25:44149 (AE-425)
physics measurements for uranium fueled ZPR-9 Assembly 25, (E), 25:44096 (ANL-7710, pp 53-262)
physics measurements for uranium oxide (UO_2) fueled ZPR-6 Assembly 6, (E), 25:44096 (ANL-7710, pp 53-262)
physics measurements for ZPPR and ZPR-9 Assembly 26, for FTR-3 reference core, (E), 25:44096 (ANL-7710, pp 53-262)
physics measurements for ZPPR Assembly 2 benchmark core, (E), 25:44096 (ANL-7710, pp 53-262)
physics measurements for ZPR-3 Assemblies 60, 61, and 62, (E), 25:44096 (ANL-7710, pp 53-262)
physics measurements for ZPR-3, (E), 25:44096 (ANL-7710, pp 53-262)
protection systems for, standards for, 25:44142 (RDT-C-16-1-T)
reactivity for ZPPR, data acquisition systems for measurement of, 25:42048 (ANL-7710, pp 263-364)
reactivity worths in ZPR-3 and ZPR-9, perturbation denominator for, (E/T), 25:44163
safety of original uranium-235 fueled, history of, 25:44157 (LA-4671)
CRITICALITY
measurement of plutonium oxide (PuO_2)--uranium oxide (UO_2) two zone core, (E), 25:44096 (ANL-7710, pp 53-262)
reactivity of subcritical spherical components in reflected cubic arrays, relation of unit mass to, (T), 25:44189 (Y-DR-53)
CROSS SECTIONS
pair production, for photons at 1.073 to 2.615 MeV, (T), 25:43417 (NYO-3923-71)
CRYOGENICS
book: Advanced Cryogenics, 25:43326
developments in, for accelerator physics, 25:43735
CRYOSTATS
description for lithium-drifted germanium detector, 25:42084
CRYSTAL STRUCTURE
parameter approach to crystal field problems, 25:44309 (YALE-3227-77)
CRYSTALS
book: Introduction to the Theory of Solid State Physics, 25:43503
chromatographic retentions by liquid, effect of electric field on gas, 25:44245 (COO-1222-47)
creep of, acoustic emission during, (T), 25:42861
elastic properties for straight dislocations in anisotropic, numerical calculation of, 25:44282 (ORNL-TM-3408)
exciton annihilation in, (T), 25:43502
exciton--phonon interactions in, annihilation of, (T), 25:43502
exoelectron emission from ionic, (E), 25:43489
ion channeling in, interaction potentials from planar-channeling experiments, (T), 25:43456
magnetic ion spin--spin anisotropic interactions in, (T), 25:43471 (YALE-3227-71)
orientation determination by channeling images from micro-, (e), 25:43454
CULTURE MEDIA
radiation effects on DeVolt, used to grow Histomonas meleagridis, γ, 25:42608
radiation effects on minimal and nutrient, used to grow Escherichia coli, γ, 25:42755
radiosterilization of insect larvae, effects of dose on γ, 25:42749
CURIUM ISOTOPES Cm-242
properties for use as heat source for subliming microthruster for space propulsion, 25:42017
properties for use as heat source for thermoelectric generators, 25:42014
CURIUM ISOTOPES Cm-244
performance of heat source of, thermal, 25:41993(R) (ORNL-4692)
properties for use as heat source for subliming microthruster for space propulsion, 25:42017
properties for use as heat source for thermoelectric generators, 25:42014
CURIUM ISOTOPES Cm-245
separation from other isotopes during 1958 and 1969, review of ORNL program for, 25:41992 (ORNL-4640)
CURIUM ISOTOPES Cm-246
separation from other isotopes during 1958 and 1969, review of ORNL program for, 25:41992 (ORNL-4640)
CURIUM ISOTOPES Cm-248
separation from other isotopes during 1958 and 1969, review of ORNL program for, 25:41992 (ORNL-4640)
CURIUM OXIDES
solubility of pellets and powders of curium-244-enriched, in distilled water and seawater, 25:41993(R) (ORNL-4692)
CURRENT ALGEBRA
currents for system of interacting pseudoscalar mesons and baryons, 25:43622
CVC hypothesis in perturbation theory in, sigma model for, 25:43689
PCAC hypothesis in perturbation theory in, sigma model for divergence conditions in, 25:43589
SU(2) X SU(2), hadronic energy--momentum tensor for meson interactions in, 25:43630
SU(3) X SU(3), hadronic energy--momentum tensor for meson interactions in, 25:43630
SU(3) X SU(3), nonlinear Lagrangian calculation of eta + 3π decay in chiral, 25:43658
SU(3) X SU(3), nonlinear Lagrangian calculation of eta + 3π decay in chiral, 25:43659
CYCLOHEXANE, UNDECAFLUORO(TRIFLUOROMETHYL)-
radiolysis of solid, at 77°K, ESR and NMR studies on radicals produced by γ, 25:41850(R) (CEA-N-1438)
CYCLOPHOSPHAMIDE
effects on differentiation of surviving stem cells in mice, comparison of x radiation and, 25:42661
radioprotective effects of, on survival of guinea pigs, mice, and rats, whole-body x, 25:42518
CYCLOTRONS
beam energy monitor for, 25:43743
beam pulses of Hamburg isochronous, use of central diaphragms for time shaping of, 25:43760
beam pulsing from, using deflection plate, 25:43742
development and operation of Osaka Univ., 1970, 25:43732(R) (OU-LNS-71-2)
ion source for, multiply-charged calcium and zinc, 25:43765
research at Osaka Univ., 1970, 25:43732(R) (OU-LNS-71-2)
CYLINDERS
neutron transport in, computer program for solution of integral equation for, (T), 25:43771 (EIR-189)
stress analysis of thin-shell cylinder-to-cylinder model, comparison of experimental and finite element methods for, 25:42839 (CONF-710512-3)
CYSTAMINE
effects on content of non-protein thiols in urine of irradiated rats, 25:42671
radioprotective effects on coagulation and fibrinolysis of rat blood, x, 25:42537
radioprotective effects on DNA in mammalian cultured cells, x, 25:42522
toxicity to x-irradiated mammalian cultured cells, 25:42522

XUM

CYSTEAMINE
effects on Chinese hamster cells x-irradiated with or without oxygen, mechanism of, 25:42521
effects on ultrastructure of crypt cells in mouse duodenum, effects of thiol-blocking agents on, 25:42520
effects on urinary excretion of nucleic acid metabolites from γ-irradiated rats, mechanism of, 25:42625
radiation effects on excretion of, in rat urine, whole-body, 25:42671
radioprotective effects of, on HeLa cells, mechanism of x, 25:42514
radioprotective effects of, on mouse adrenal cortex and reticulo-endothelial systems, comparison of lipopolysaccharide and serotonin with x, 25:42513
radioprotective effects of, on rat tissues, combined hypoxia and, 25:42511
radioprotective effects on DNA in mammalian cultured cells, x, 25:42522
radioprotective effects on rat eyes, x, 25:42538
radiosensitizing effects on lipolytic activity of rat heart tissues, x, 25:42281
toxicity to x-irradiated mammalian cultured cells, 25:42522
CYSTEINE
effects on monoiodoacetic acid toxicity in rats, in vitro and in vivo inhibitory, 25:42523
effects on ultrastructure of crypt cells in mouse duodenum, effects of thiol-blocking agents on, 25:42520
metabolism in microorganisms, enzymology and regulation of, 25:44285(R) (ORO-3092-5)
radiation effects of content of sulfur-35-labeled, in rat organ proteins, x, 25:42265
radioprotective effects against damage to cerebrosides and phospholipids in rat brain, x, 25:42620
radioprotective effects against metabolic disequilibria in rat brain, x, 25:42519
radioprotective effects of derivatives of, on chromosomes in bone marrow cells of mice, x, 25:42534
radioprotective effects on rat tissues and organs, mechanism of in vitro and in vivo, 25:42523
CYSTINE
radiation effects of content of sulfur-35-labeled, in rat organ proteins, x, 25:42265
CYTIDINE, 2'-DEOXY-
radiation effects on metabolism of, in mice and rats, mechanisms for, 25:42523
CYTOCHROME OXIDASE
radiation effects on activity of human skin, x, 25:42286
CZECHOSLOVAKIA
strontium-90 content of milk in, during 1963 to 1966, 25:42385

D

DACTINOMYCIN
effects on erythropoietic recovery in spleen of partial-body x-irradiation mice, 25:42673
DAIRY PRODUCTS
butter, cesium-137 and strontium-90 content of, in Bulgaria during 1965, 25:42381
cottage cheese, strontium-90 content in, in Czechoslovakia during 1965 to 1968, 25:42386
milk, cesium-137 and strontium-90 content of, in Bulgaria during 1965, 25:42381
DATA ACQUISITION SYSTEMS
circuits for, design of fast digitizing, 25:42220
description of PDP-9 computer-based, for nuclear physics experiments, 25:42181(T) (CERN-Trans-71-18)
DATA PROCESSING SYSTEMS
description of PDP-9 computer-based, for nuclear physics experiments, 25:42181(T) (CERN-Trans-71-18)
development of computer, for clinical diagnostic studies using radioisotopes, 25:42549(R) (ORAU-113)
radioisotope scan resolution enhancement using, 25:42557
use for radiation dose interpolation during radioimmunoassay, 25:42236
DATA RECORDING SYSTEMS
development for computing effects of whole-body irradiation on man, 25:42549(R) (ORAU-113)
specifications for multipoint strip-chart recording potentiometer, standard for, 25:42203 (RDT-C-9-2-T)
specifications for single-point strip-chart recording potentiometer, standard for, 25:42202 (RDT-C-9-1-T)
DATA TABULATIONS
coefficients of fractional parentage for lower portion of j = 7/2 shell, (T), 25:43981
cross sections and polarizations for neutron elastic scattering by hydrogen at 0.1 to 30.0 MeV, total and differential, (T), 25:43798
differential cross sections for alpha elastic and inelastic scattering by A = 6 to 209 nuclei at 104 MeV, (E), 25:43832 (NP-18920)
internal conversion coefficients for outer shells and ratios to inner shells for Z = 37 to 100 nuclei for transition energies of 50 to 500 keV, (T), 25:43931
matrix elements of spherical tensors, calculations of single-particle reduced, (T), 25:43982
on hyperfine fields for substitutional impurities in cobalt, gadolinium, iron, and nickel, table of, 25:43469 (UCRL-20411)
DENSIMETERS
development of radiometric, for quantitative estimation of uranium distribution in MTR fuel plates, 25:42178
DEOXYRIBONUCLEASE
activity specific for uv-irradiated DNA in HeLa cells, 25:42272
DESALTING
systems for, mathematical programming for optimizing power generation in combination with, 25:44295 (TID-25740)
DEUTERIUM
determination in water by mass or ir spectrometry, 25:41832(R) (AECL-3851)
determination of hydrocarbon-incorporated, by gas chromatography, 25:41746
determination relative to hydrogen in water, mass spectroscopic, 25:41729
deuteron reactions (d,n) at 4.1 to 15.1 MeV, neutron polarization from, (E), 25:43789
deuteron reactions (d,n) with thick targets of, calculation of mean neutron energy for, (T), 25:43790
deuteron reactions (d,p) at 8.1 to 83 MeV, nonrelativistic peripheral-model calculations of angular distributions from, (T), 25:43966
diffusion in palladium at -60 to 200°C, comparison with hydrogen, 25:41816
effects of alpha, on kinetics of hydrolysis of acetals and ortho esters, 25:41800
effects of secondary beta-, on rates of solvolysis of benzonorbornen-2(exo)- and -2(endo)-yl p-bromobenzenesulfonates, 25:41801
effects on bromination of malonitrile, rates of reverse reactions, 25:41798
effects on carbon--hydrogen valence vibrations in hydrocarbons and butyl halides, 25:41821
effects on crystal structure of potassium acid oxalate, ir and Raman studies on, 25:41790
effects on dissolution of iron in hydrochloric acid solutions, 25:41808
effects on elastic constants and order--disorder transitions in ice, 25:41812
effects on fundamental and harmonic carbon--hydrogen valence vibrations of methyl halides, 25:41822
effects on hydrolysis of 4-ethoxypyrylium salts, 25:41789
effects on hydrolysis of pyrylium salts, 25:41787
effects on ionization of malononitriles, kinetic, 25:41799
effects on mean square amplitudes of vibration of vinylidene halides, 25:41814
effects on molybdoferredoxin sedimentation in water, 25:41811
effects on nonrandom decomposition of hexafluorobicyclopropyl, 25:41809
effects on nucleophilic substitution at tetrahedral boron, secondary kinetic, 25:41803
effects on nucleophilic substitution at tetrahedral boron, secondary kinetic, 25:41804
effects on nucleophilic substitution at tetrahedral boron, secondary kinetic, 25:41802
effects on optical spectra of organic dyes, 25:41815
effects on phosphorescence of pure naphthalene crystals at 300 to 50°K, 25:41813
effects on reactions of phenylenebisdiazonium ion with alcohols, 25:41806
effects on rearrangement and fragmentation in aromatic nitration, 25:41818
effects on solution heat of acetone, chloroform, ethanol, methanol, and water, 25:41794
effects on solvolysis of secondary and tertiary norborn-2-yl derivatives, β-secondary, 25:41820
effects on substituted benzenesulfonyl chloride solvolyses, kinetic solvent, 25:41792
effects on thermal denaturation of ribonuclease in water, 25:41793
effects on uv photolysis of riboflavin, 25:41788
effects on vibrational normal coordinate analysis of isocyanate and thioisocynate, 25:41791
energy levels of molecular, eigenvalues and expectation values for bound and quasi-bound ground-state, (T), 25:43123
exchange between heavy water and ribonuclease, 25:41793
exchange between hydrogen and water-d or methylamines, 25:41832(R) (AECL-3851)
exchange between poly-β-alanine and heavy water, 25:41807
exchange between thiete dioxide or cyclic sulfone and alcohols, 25:41805
inventory control of, computer program for, 25:41960 (EUR-4512)
lattice dynamics of solid ortho-, phonon dispersion curves for, 25:43435(R) (RISO-237)
lattice structure of solid, phonons and librons in, (T), 25:44261 (JUL-734-FF)
neutron reactions (n,nnp) at 14 MeV, spectrometer study of cross sections and spectra for n + p final-state interactions in, (E), 25:43533 (CEA-R-4150)
plasma of, production by laser irradiation of solid target, 25:43380 (IPP-4/9)
proton reactions (p,d) at 3.0 to 46.3 MeV,

nonrelativistic peripheral-model calculations of angular distributions from, (T), 25:43966
separation from hydrogen, electrochemical, 25:41832(R) (AECL-3851)
DEUTERIUM HYDRIDES
electron reactions with ions of, angular distribution of deuterons or protons from dissociation in, (T), 25:43152
energy levels of, eigenvalues and expectation values for bound and quasi-bound ground-state, (T), 25:43123
DEUTERIUM SYSTEMS
D--T, laser beam explosion of solid pellets, fusion reactions in, 25:43398 (ORNL-TM-3231)
DEUTERONS
effects on carbides, reactions of recoil nitrogen-13 from, 25:41886
effects on infrared spectra of silicates at 5 keV, 25:43445
effects on silicon at 12 MeV, distribution of defects induced in, (E), 25:43453
form factor from backward e + d → e + d interactions at 70 to 280 MeV, magnetic, (E), 25:43528 (LAL-1250)
interactions anti p + d at 2.2 GeV/c in deuterium bubble chamber, partial cross sections and K(890), Kanti K, KKπ, Kππ, and K*anti K* production in 2K, 4K, 2Kπ, and 2K2π final states in, (E), 25:43535
interactions d + ³He, shell interpretation of separable potentials for, (T), 25:43786
interactions e + d → e + d at 70 to 280 MeV, cross sections and deuteron magnetic form factor from backward, (E), 25:43528 (LAL-1250)
interactions e + d → e + p + n at 70 to 280 MeV, cross sections for backward, (E), 25:43528 (LAL-1250)
interactions K⁺ + d → K⁺ + π⁺ + π⁻ + d(n + p) at 9 GeV/c in deuterium bubble chamber, K(1243) and K(1344) production in Q region of K⁺π⁺π⁻ mass spectrum and K(890) production in, (E), 25:43544 (CDD-1428-275)
interactions K⁺ + d → K⁺ + π⁺ + π⁻ + d(p + n) at 9.04 GeV/c, K(1243) and K(1344) production in Q region and K(890) production in, (E), 25:43543 (CDD-1428-274)
interactions Λ + d at 100 to 300 MeV/c, probe of Λ--N core potential from cross sections for, (T), 25:43651
interactions n + d → n + p + n + γ, cross sections and spectra from, (E), 25:43560
interactions N + d below 40 MeV, phase shifts and inelastic scattering parameters for, (T), 25:43799
interactions π⁺ + d → d + 2π⁺ + π⁻ at 13 GeV/c in deuterium bubble chamber, production of A_3(1680) in 3π system in, (E), 25:43550 (CDD-1428-290)
interactions π⁺ + d → d + 3π⁺ + 2π⁻ at 13 GeV/c in deuterium bubble chamber, Sπ(1900) enhancement in, (E), 25:43550 (CDD-1428-290)
interactions π⁺ + d at 13 GeV/c in bubble chamber, production of A_3(1640), f⁰, rho, and 2π and 4π even-G-parity states in R region in, (E), 25:43545 (CDD-1428-277)
interactions π⁺ + d at 2.05 to 2.35 GeV/c in deuterium bubble chamber, strange particle and resonance production, cross sections, angular distributions, and polarization in, (E), 25:43561
production in p + p → d + MM interactions at 3.8 to 6.3 GeV, wire-chamber spectrometer study of differential cross sections for, (E), 25:43541
reactions (d,α) with carbon-12 at 14 to 17 MeV, angular distributions and excitation functions for isospin-forbidden, (E), 25:43811
reactions (d,Li-6) with nuclei, analysis of features of, (T), 25:43987
reactions (d,n) with deuterium at 4.1 to 15.1 MeV, neutron polarization from, (E), 25:43789
reactions (d,n) with thick targets of deuterium, calculation of mean neutron energy for, (T), 25:43790
reactions (d,p) with A = 28 to 119 nuclei at 5 to 12 MeV, cross sections and vector analyzing powers for, (E), 25:43846
reactions (d,p) with argon-36 at 9.162 MeV, l-transfer values from DWBA analysis of differential cross sections and spectra from, (E), 25:43868
reactions (d,p) with carbon-12 at 14.60 MeV, phase-shift analysis of energy spectra from, (E), 25:43814
reactions (d,p) with deformed nuclei, inelastic processes in, (T), 25:43984
reactions (d,p) with deuterium at 8.1 to 83 MeV, nonrelativistic peripheral-model calculations of angular distributions from, (T), 25:43966
reactions (d,p) with helium-3 at 250 to 650 keV, angular distribution and absolute cross section fr, (E), 25:43793
reactions (d,p) with zirconium-90 at 3 MeV, analysis including Coulomb distortion and finite-range effects, (T), 25:43964
reactions (d,t) with lithium-7 at 10 to 12 MeV, angular distributions for, (E), 25:43809
reactions (d,t) with neodymium-142 at 17 MeV, DWBA analysis of angular distributions for, (E), 25:43900
scattering by argon-36 at 9.152 MeV, optical-model analysis of elastic, (E), 25:43868
scattering by lithium-6 at 8 MeV, optical-model analysis of elastic, (E/T), 25:43810
scattering by lithium-7 at 10 to 12 MeV, angular distributions for elastic, (E), 25:43809
DIAMONDS
properties for use as engineering and structural material, review of, 25:42977
DIELECTRICS
book: Introduction to the Theory of Solid State Physics, 25:43503
charged-particle interaction with, model for moving, 25:43588
DIET
fallout content of institutional, in USA during 1970, 25:42417
radioisotope content of Formosan, comparison of cesium-137 and strontium-90, 25:42422
radioisotope content of human, in Italy, 25:42375
DIMETHYLAMINE
radiolysis of, adsorbed on silica gel at 77°K, ESR studies on trapped radicals produced by γ, 25:41856
DIRECT ENERGY CONVERSION DEVICES
survey of, 25:43186
DISEASES
radiodiagnosis of hematological, review on tracer methods for, 25:42573
DISEASES, INFECTIOUS
hepatitis, frequency of anti-hepatitis-associated antigen in men with, use of radioimmunoassay for measuring, 25:42306
hepatitis, radiodiagnosis of human, effectiveness of gold-198 liver scanning for, 25:42553
hepatitis, radiotherapy of human, 25:42597
herpes zoster, radioinduced, in leukemic men following therapy, recurrent x, 25:42589
pericarditis, radioinduced, following therapy for neoplasms of thoracic organs, 25:42704
radiotherapy of human eye, principles and indications for, 25:42596
DISEASES, NEOPLASTIC
adenocarcinomas, radiotherapy of human kidney, regression of lung metastases following γ, 25:42591
astrocytomas, radiotherapy of human intracerebral, estimation of hazards to brain following, 25:42701
cancer, radiotherapy of human gynecological, effectiveness of γ, 25:42599
cancer, radiotherapy of human, ribonuclease activity in urine and vaginal fluid following radium, 25:42683
carcinomas, incidence in children in relation to prenatal x-ray exposure in England and Wales during 1968, 25:42696
carcinomas, radioinduced, in enamel organ in mice, combined effects of physical trauma and x, 25:42670
carcinomas, radiotherapy of cervical, comparison of radiation dose to medical personnel under two different treatment plans for interstitial, 25:42432
carcinomas, radiotherapy of human head and neck, additive effects of 5-fluorouracil infusion on gamma and x, 25:42589
carcinomas, radiotherapy of human head and neck, condition of salivary glands following, 25:42699
carcinomas, radiotherapy of human larynx and pharynx, effectiveness of preoperative gamma and x, 25:42588
carcinomas, radiotherapy of human uterine cervical, effectiveness of combined radium-226 implant and external gamma, 25:42595
carcinomas, radiotherapy of mammary, content of sulfhydryl groups in serum following, 25:42270
epitheliomas, radioinduced, in human skin 33 years following therapy with radium-226 applicator, γ, 25:42686
Hodgkin's disease, radiodiagnosis by scintigraphy of human liver and spleen using technetium-99m-labeled sulfur colloid, 25:42585
Hodgkin's disease, radiotherapy of human, dosimetry during mantle technique for γ, 25:42594
leukemia, radioinduced, in man following therapy for menorrhagia, statistical study of long-term x, 25:42702
leukemia, radioinduced, in man, effects of dose and dose rate on, 25:42712
leukemia, radioinduced, in mice following exposure to strontium-90, relation between dose and incidence of, 25:42654
leukemia, radiotherapy of herpes zoster and lymphatic, in man, recurrence of herpetic lesions following x, 25:42689
leukemia, radiotherapy of human chronic granulocytic and lymphocytic, effectiveness of whole-body low-dose-rate low-dose γ, 25:42585 (ORAU-113, pp 4-77)
leukemia, therapeutic effects of allogenic bone marrow transplants on acute human, following administration of antilymphocyte globulin and whole-body gamma irradiation, 25:42586 (ORAU-113, pp 4-77)
lymphomas, radiotherapy of human, content of serum thyrotropin and thyroid function following x, 25:42695
lymphosarcoma, radiosensitivity of ascites Pliss', in rats in comparison with ascites ovarian tumors, x, 25:42637
lymphosarcomas, radiotherapy of human, effectiveness of whole-body low-dose-rate low-dose γ, 25:42586 (ORAU-113, pp 4-77)
malignant, radiodiagnosis of human brain, comparison of accuracy of spinal fluid protein measurements with technetium-99m-labeled pertechnetate, 25:42547 (ACRH-1000-248)

XUM

malignant, radioinduced breast and pelvic, in man following therapy for menorrhagia, statistical study of long-term x, 25:42702
malignant, radioinduced, in bones of animals and man following radioisotope uptake, 25:42472
malignant, radioinduced, in man, effects of dose and dose rate on, 25:42712
malignant, radioinduced, in man, threshold concept for, 25:42694
malignant, radioinduced, in women following castration, 25:42675
malignant, radioisotope scanning of, for evaluation of effectiveness of drug therapy, 25:42556
malignant, radiotherapy of human head and neck, methods for prevention of bone necrosis and tooth decay following, 25:42471
malignant, radiotherapy of human head and neck, occurrence of myelitis following, 25:42700
malignant, radiotherapy of, mathematical model for dosimetry in, 25:42437
medulloblastomas, radiotherapy in children, dose fractionation schedules for post-surgical, 25:42593
melanomas, radiodiagnosis of human eye, use of iodine-131-labeled iodoquine scanning for, 25:42563
metastases, radiation effects on spontaneous regression of human lung, following therapy for renal adenocarcinoma, γ, 25:42591
model for etiology of, based on similarity in molecular constituents and behavioral properties of early fetal cells and neoplastic cells, 25:44277(R) (ORNL-4693(Pt.1))
oncocytomas, radiodiagnosis of parotid, use of metastable technetium-99 scanning for, 25:42572
radiodiagnosis of human liver, double-tracer method using gold-198, and selenium-75 for, 25:42580
radiodiagnosis of human lymphatic, scintiscanning method for, 25:42581
radioinduced, in animals and man, review on relation of, 25:42605
radiotherapy of thoracic, injuries to heart following, 25:42704
sarcomas, occurrence of granulocytic, in human patient following therapy of ankylosing spondylitis, γ, 25:42709
sarcomas, radioinduced, in man following therapy, measures for prevention and treatment of, 25:42705
tumors, localization of bone, in biopsy samples using neutron radiography, 25:42575
tumors, phosphorus-32 uptake by nucleic acids in human, effects of cytotoxic agents on, 25:41833(R) (IA-1218)
tumors, radiation effects on incidence of, in mice, comparison of β, γ, and fast neutron, 25:42664
tumors, radiodiagnosis of bone, comparison of strontium-85, metastable strontium-87, and x-radiography for, 25:42562
tumors, radiodiagnosis of human brain, use of sodium-22 and positron camera for, 25:42565
tumors, radiodiagnosis of human genital, scintiscanning method for, 25:42581
tumors, radiodiagnosis of mammary, oral, and pharyngeal, comparison of mercury-197- and mercury-203-labeled chlomerodrin and mercuric chloride for, 25:42576
tumors, radioinduced, in human liver following intravascular injection of Thorotrast, latent α and γ, 25:42708
tumors, radioinduced, in mice, comparison of latent external fast neutron or γ and internal tritiated thymidine, 25:42630
tumors, radioinduced, in rats, effects of stress on x, 25:42669
tumors, radiosensitivity of ascites ovarian, in rats in comparison with ascites Pliss' lymphosarcoma, x, 25:42637
tumors, radiosensitivity of human, evaluation of enzyme activity following therapy as indicator of, 25:42409
tumors, radiosensitivity of rat C-45 and ISP, in relation to protein sulfhydryl group, 25:42618
tumors, radiotherapy of human eye, principles and indications for, 25:42596
tumors, radiotherapy of human thyroid, morphological structure following γ, 25:42679
tumors, radiotherapy of primary and metastatic Wilms', in human children, cell morphology and maturation time following, 25:42592

DISEASES, PHYSIOLOGICAL

anemia, radiation effects on incidence of late aplastic, in atomic bomb survivors, 25:42698
anemia, radiodiagnosis using iron-59 and whole-body counting, 25:41933(R) (IA-1218)
anemia, radiotherapy of human secondary, 25:42597
arachnoiditis, radiotherapy of human, bioelectrical activity of brain following, 25:42678
arteriosclerosis, radioinduced, in man following therapy for menorrhagia, statistical study of long-term x, 25:42702
caries, radioinduced human dental, following therapy of head and neck cancers, methods for prevention of, 25:42471
cataracts, radioinduced in human eyes, 25:42712
cataracts, radioinduced, in man exposed to atomic bomb on Hiroshima, occurrence and pathology of latent, 25:42545
cataracts, radioinduced, in rat eyes, protective effects of cysteamine and glutathione against x, 25:42538
cirrhosis, radiodiagnosis of human, effectiveness of gold-198 liver scanning for, 25:42553
cirrhosis, radioinduced, in human liver following intravascular injection of Thorotrast, latent α and γ, 25:42708
congenital lymphedema, radiodiagnosis in human infants using gold-198 scanning, 25:42559
dysplasia, radiodiagnosis of human bronchopulmonary, effectiveness of perfusion and ventilation scintigraphy for, 25:42551
edema, production of localized pulmonary, in dog, oxygen-15-labeled water, iodine-131-labeled iodoantipyrine, and indium-113m-labeled transferrin studies of, 25:44254 (COO-1653-103)
fibrosis, radioinduced subcutaneous, in man following telecobalt therapy, 25:42687
fibrosis, radioinduced, in mice treated with isologous bone marrow transplants, x, 25:42665
hydrothorax, incidence in x-irradiated thymectomized mice treated with isologous bone marrow transplants, 25:42665
jaundice, radiodiagnosis of human, using iodine-131-incorporated Rose Bengal, 25:41833(R) (IA-1218)
myelitis, radioinduced in man following therapy of neoplasms of head and neck, 25:42700
myocardiopathy, radioinduced, following therapy for neoplasms of thoracic organs, 25:42704
osteonecrosis, radioinduced mandibular, clinical description, pathological anatomy, and treatment of, 25:42543
osteonecrosis, radioinduced, in man following therapy of head and neck cancers, methods for prevention of, 25:42471
polycythemia, radiotherapy of human, effectiveness of whole-body low-dose-rate low-dose γ, 25:42586 (ORAU-113, pp 4-77)
polycythemia, radiotherapy using interstitial phosphorus-32, occurrence of chromosome aberrations in hematopoietic cells cultured following, 25:42713
ulcers, radioinduced rat skin, effectiveness of dibunol and metacil for treatment of x, 25:42541

DISEASES, TRAUMATIC

radiation injuries, conference on biochemical indicators for human, 25:42395 (STI/PUB-280)
radiation injuries, indicators for human and rat, evaluation of blood and bone marrow lymphocytes and DNA synthesis as, 25:42404
radiation injuries, indicators for human, use of radioinduced chromosome aberrations as, 25:42405
radiation injuries, indicators for mammalian and human, review on use of biochemical changes as, 25:42401
radiation injuries, indicators for, evaluation of radiation effects on DNA metabolism for use as, 25:42403
radiation injuries, indicators of human, development of biochemical, 25:42685
radiation injuries, treatment of rat skin ulcer, effectiveness of dibunol and metacil for, 25:42541
radiation injuries, treatment of skin, effectiveness of petroleum growth substance for β, 25:42539
radiation sickness, induction in rabbits following destruction of hypothalamus, changes in blood parameters during, 25:42660
radiation sickness, pathology and therapy in man, review on, 25:42542
radiation sickness, time sequence of anorexia, nausea, and vomiting in human, 25:42586 (ORAU-113, pp 4-77)
radiation sickness, treatment in rats using blood factor XIII transfusions from healthy animals, 25:42540
radiation sickness, ultrastructure of fibrin in rats with, effects of transfusion of blood factor XIII from healthy animals on, 25:42540
radiodermatitis, induction in human skin following diagnostic radiography using Be-window x-ray tube without filtration, 25:42545
radiodermatitis, occurrence, treatment, and insurance compensation of personnel for, in France, 25:42544

DISPERSION RELATIONS

production of ν--anti ν pairs in γ + γ + ν + anti ν interactions, cross sections and black-body neutrino luminosity for, 25:43605

DISPLACEMENT GAGES

design and testing for use in liquid sodium, standard for, 25:42201 (RDT-C-8-2-T)

DISULFIDES

radiolysis of n-alkyl, effects of electronic excitation of molecules on yields of free radicals from, 25:41859

DNA NUCLEOTIDYLTRANSFERASE

role in repair of x-radioinduced single-strand breaks in DNA of Escherichia coli mutants, 25:42326

DOGS

radiation effects on biochemistry of body fluids in, as indicator of radiation injuries, review on, 25:42402
radiation effects on blood coagulation in, effects of dose on β and γ, 25:42600
radiation effects on immune response to tissue transplants, effectiveness of metalloporphyrins as carriers for selective palladium-190 β, 25:42312
radioinduced ablation of lymph nodes in, effectiveness of

metalloporphyrin-incorporated palladium-109 for selective 8, 25:42312
radioinduced fibrosis and degeneration of cervical lymph nodes in, following neck exposure, γ, 25:42662
DONALD C. COOK POWER REACTOR, UNIT 1
effluents from, distribution in Lake Michigan of chemical and radioactive, 25:44057 (DOCKET-50315-40)
effluents from, effects on ecosystems of radioactive and thermal, 25:44058 (DOCKET-50315-41)
effluents from, effects on ecosystems of radioactive and thermal, 25:44055 (DOCKET-50315-38)
radioactive effluents from, monitoring of, 25:44056 (DOCKET-50315-39)
site for, environmental radiation survey for, 25:44057 (DOCKET-50315-40)
site for, limnological studies for, 25:44058 (DOCKET-50315-41)
site for, limnological studies for, 25:44055 (DOCKET-50315-38)
site for, underwater γ radiation detection system for environmental monitoring of, 25:44056 (DOCKET-50315-39)
DONALD C. COOK POWER REACTOR, UNIT 2
effluents from, distribution in Lake Michigan of chemical and radioactive, 25:44057 (DOCKET-50315-40)
effluents from, effects on ecosystems of radioactive and thermal, 25:44055 (DOCKET-50315-38)
effluents from, effects on ecosystems of radioactive and thermal, 25:44058 (DOCKET-50315-41)
radioactive effluents from, monitoring of, 25:44056 (DOCKET-50315-39)
site for, environmental radiation survey for, 25:44057 (DOCKET-50315-40)
site for, limnological studies for, 25:44058 (DOCKET-50315-41)
site for, limnological studies for, 25:44055 (DOCKET-50315-38)
site for, underwater γ radiation detection system for environmental monitoring of, 25:44056 (DOCKET-50315-39)
DRESDEN POWER REACTOR, UNIT 2
containment system for, excessive leak rates from primary, 25:44008 (DOCKET-50237-183)
cooling system for, possible fuel element damage and release rates from missing purge dam hardware in, 25:44036 (DOCKET-50237-186)
diesel generator for, failure to start of, 25:44009 (DOCKET-50237-184)
operations aspects for, proposed, 25:44010 (DOCKET-50237-185)
radioactive waste system for, process flow diagram for liquid, 25:44036 (DOCKET-50237-186)
DRESDEN POWER REACTOR, UNIT 3
containment structure for, incident of exceeding water level and temperature limits of suppression chamber, 25:44013 (DOCKET-50249-79)
cooling system for, possible fuel element damage and release rates from missing purge dam hardware in, 25:44036 (DOCKET-50237-186)
diesel generator for, failure to start of, 25:44009 (DOCKET-50237-184)
emergency core cooling system for, failure of auto-isolation signal reset for high pressure, 25:44015 (DOCKET-50249-81)
emergency core cooling system for, failure of high pressure coolant injection turbine stop valve to reset during startup test for, 25:44016 (DOCKET-50249-83)
emergency core cooling system for, failure of steam admission control valves for high pressure, 25:44014 (DOCKET-50249-80)
radioactive waste system for, process flow diagram for liquid, 25:44036 (DOCKET-50237-186)
DURALUMIN
x-ray backscattering at 11.3 to 23.2 MeV, (E), 25:43431
DUSTS
effects of interplanetary, on solar wind, origin of ^4H and ^3He from deionizing, (E/T), 25:43176
DYSPROSIUM
determination in meteorites by neutron activation and high-voltage electrophoresis, 25:41776
determination of trace amounts of, in yttrium oxide by activation methods, 25:41877 (JAERI-13545)
magnetic susceptibility of, generalized function for, (T), 25:43477
neutron total cross section at 100 to 650 keV, optical model analysis of average, (E/T), 25:43908
nuclear spin--lattice and spin--spin relaxations in, low-temperature NMR study of, 25:43498
DYSPROSIUM IONS
spectra of Dy II, identification of configurations in, 25:43119
DYSPROSIUM ISOTOPES Dy-159
energy levels from holmium-159, spin-parity assignments for, (E), 25:43944
energy-level transitions from holmium-159 decay, conversion coefficients and multipolarities for, (E), 25:43944
DYSPROSIUM ISOTOPES Dy-160
neutron reactions (n,α) at 14.2 MeV, level-density parameters and spectra from, (E), 25:43886 (INR-1268)
DYSPROSIUM ISOTOPES Dy-161
neutron reactions (n,α) at 14.2 MeV, level-density parameters and spectra from, (E), 25:43886 (INR-1268)
DYSPROSIUM ISOTOPES Dy-163
neutron reactions (n,α) at 14.2 MeV, level-density parameters and spectra from, (E), 25:43886 (INR-1268)
nuclear magnetic resonance in ferromagnetic dysprosium metal at low temperatures, 25:43498
DYSPROSIUM ISOTOPES Dy-164
neutron reactions (n,α) at 14.2 MeV, level-density parameters and spectra from, (E), 25:43886 (INR-1268)
DYSPROSIUM OXIDES
analysis for impurities, cathode region method for spectrochemical, 25:41833(R) (IA-1218)

E

EARTHQUAKES
effects on power reactor cooling system and buildings, 25:44079 (UCLA-ENG-7037)
seismic waves from, and Project Gasbuggy underground nuclear explosion, comparison of travel times for, 25:41952 (AD-838694)
ECOLOGY
research programs of AEC during 1970 on, 25:44293 (TID-25728)
ECOSYSTEMS
energetics of stream, 25:44255(R) (COO-2002-10)
energy budget model for woodland stream, 25:44255 (COO-2002-6)
modeling of, code for linear, 25:44278 (ORNL-IBP-71-2)
nuclear test effects on Amchitka Island marine and terrestrial, use of Milrow data in predictions of Cannikin, 25:42318 (TID-25735)
radiation dose to organisms in marine, following discharge of radioactive wastes into seawater, 25:42373
radiation effects on desert shrub, high-level local fallout, 25:42717 (EGG-1183-2272)
radiation effects on growth and survival of plant species in natural, beta and gamma, 25:42315(R) (ORO-3299-107)
radiation effects on metabolism in granite outcrop, following exposure to simulated fallout particles coated with yttrium-90, 25:42320
radiation effects on rain forest, in Puerto Rico, 25:42317(R) (PRNC-147)
radiation effects on reproductive potential of dominant plant species of granite outcrop, acute simulated fallout β, 25:42718 (ORO-3299-110)
survey of marine, Jervis Bay, Australia, nuclear power plant site, 25:42314 (CONF-710511-3)
ECUADOR
radioactivity monitoring in atmosphere and milk of, 1966 to 1967, 25:41940
EGGS
effects of powdered shells of, combined with radioprotective substances on reduction of radiation hazards to uranium mining personnel, 25:42510
radiation effects on development and survival of Chinook salmon, effects of dose and dose-rate on γ, 25:42616(R) (RLO-2225-T-2-2)
radiation effects on hatchability of silkworm, x, 25:42609
ELECTRIC ARCS
performance for production of multicharged ions, 25:43731 (JINR-P7-5177)
plasma properties near cathode region of MPD, (E), 25:43353 (N-71-19984)
ELECTRIC CHARGES
radiation of, solutions of Einstein--Maxwell equations for spherically symmetric, (T), 25:43710
ELECTRIC CONDUCTORS
insulators for, standard for determination of compaction in ceramic, 25:42190 (RDT-C-2-1-T)
ELECTRIC CURRENTS
effects on x radiosensitivity of rats, 25:42530
radioprotective effects of direct, on mitotic activity of bone marrow cells and phagocytic activity of reticuloendothelial cells in rats, x, 25:42530
ELECTRIC DISCHARGE
design for high efficiency plasma production, 25:43382(P)
ion emission from cathodes in vacuum breakdown, (E), 25:43383
plasma boundary layer over cathode in, nonequilibrium, (T), 25:43361 (N-71-12579)
plasma diagnostics in, turbulent electric field measurement using Stark profiles, (E), 25:43344
properties of cold cathode, at low pressures, 25:43346 (JINR-P9-5753)
striations in column, nonlinear stabilization of, (E), 25:43393
ELECTRIC FIELDS
characteristics of ionospheric broad-band frequency, (E/T), 25:43246
convection in auroral zone and at 1500 km, double-probe measurements of dc, (E), 25:43216 (N-71-18405)
distribution at low-altitude auroral zones and polar caps, relation with simultaneous charged-particle distribution, (E), 25:43219 (N-71-20708)
effect on F-region ion-drift vertical velocity, (E/T), 25:43224

XUM

effects of substorm-associated, on enhancements in electron concentrations in midlatitude nighttime F region, (E/T), 25:43253
ELECTRIC INSULATORS
compaction in ceramic insulated conductors, standard for determination of, 25:42190 (RDT-C-2-1-T)
specifications for ceramic, for high-temperature instrument use, standard for, 25:42204 (RDT-C-18-1-T)
ELECTRIC PROBES
performance of Langmuir, for diagnostics of laser-produced plasmas, (E), 25:43342
response of Langmuir, effects of ion--atom collisions on, (E), 25:43340 (N-71-17594)
ELECTROCHEMISTRY
interfacial phenomena in, optical studies on, 25:41778 (UCRL-20500, pp 1-85)
research progress on, 25:41778 (UCRL-20500, pp 1-85)
ELECTRODES
standard for copper and copper alloy arc-welding, 25:42767 (RDT-M-1-7-T)
standard for corrosion resistant chromium and chromium--nickel steel-covered welding, 25:41972 (RDT-M-1-1-T)
standard for low alloy steel covered arc-welding, 25:42765 (RDT-M-1-4-T)
standard for mild steel covered arc-welding, 25:42764 (RDT-M-1-3-T)
standard for mild steel, for gas--metal--arc welding, 25:42766 (RDT-M-1-6-T)
standard for nickel and nickel alloy bare welding, 25:42771 (RDT-M-1-11-T)
standard for nickel and nickel alloy covered welding, 25:42770 (RDT-M-1-10-T)
standard for stainless steel bare, 25:42763 (RDT-M-1-2-T)
ELECTRODYNAMICS
potentials in relativistic, Helmholtz, 25:43666
ELECTROLYTES
radiation effects on rat serum, protective effects of methylene blue against x, 25:42283
ELECTROLYTIC CELLS
development for continuous measurement of hydrogen in liquid sodium, 25:42207(R) (UNC-5258)
mass transfer studies in, 25:41778 (UCRL-20500, pp 1-85)
ELECTROMAGNETIC FIELDS
charged particle motion in, (T), 25:43507(T) (JPRS-52839, pp 3-16)
Einstein--Maxwell equations for spherically symmetric charge radiation, solutions of, (T), 25:43710
electron production in γ + N interactions in strong, final-state interaction for, (T), 25:43606
equations for charged spin-$^1/_2$ matter, static solutions for combined Dirac--electromagnetic--gravitational, (T), 25:43703
protection of personnel against high-energy, methods for, 25:42464
ELECTROMAGNETIC LENSES
design of circular quadrupole, for beam transport, 25:43757
design of superconducting shielded, 25:43748
ELECTROMAGNETIC PUMPS
performance requirements of liquid sodium, for reactors, comparison with mechanical pumps, 25:41958(T) (CONF-700307-8)
standard for liquid metal service, 25:41967 (RDT-E-3-9-T)
ELECTROMAGNETIC SEPARATION
contamination control in isotopic, review of methods for, 25:41992 (ORNL-4540)
equipment for isotope, development of two-stage, 25:41992 (ORNL-4540)
ELECTROMAGNETIC WAVES
characteristics of ionospheric broad-band frequency, (E/T), 25:43246
coupling with electron acoustic waves in inhomogeneous lossy plasma, (T), 25:43404 (AD-715910)
damping in plasmas, Landau, (T), 25:43408
effects of pulsed, on performance of electrical and electronic components of civil defense communication and power systems, 25:42506(R) (ORNL-4566(Pt.1))
interactions with density fluctuations in inhomogeneous magnetized plasma, (E), 25:43402 (AD-715277)
interactions with nonthermal plasmas, cyclotron resonance, (T), 25:43403 (AD-715636)
propagation in plasma-filled cylindrical waveguides, hybrid, (E/T), 25:43405 (CERN-71-4)
ELECTRON BEAMS
collimator and scattering foil for 10- to 20-MeV, 25:43767
current density distribution of, study of, 25:43736
dosimetry at 12 to 32 MeV, performance of glass photoluminescent dosimeters for, 25:42169
dosimetry of intense, at 5 to 43 MeV, sensitivity of thermoluminescent dosimeters for, 25:42167
interaction with collisionless plasma discharge, thermal explosion from, (E/T), 25:43372
interactions with plasma, finite amplitude electrostatic waves from nonlinear, (T), 25:43365
interactions with plasma, three-wave interactions from, (T), 25:43407 (N-71-18696)
production in cold cathode discharges at low pressures, 25:43346 (JINR-P9-5753)
scattering of coherent modulated, energy transfer from inelastic, 25:43106
stability in vacuum, hydrodynamic, 25:43756
ELECTRON CAPTURE
internal ionization of K shell during, probability for, (T), 25:43575
ELECTRON-DIFFRACTION ANALYSIS
apparatus for measuring inelastically scattered or photoemitted electrons in low-energy, Faraday-cup, 25:43474
research progress in, annual report, 1969--70 on, 25:43468 (NP-18657)
ELECTRON MICROSCOPES
resolution of, techniques for improvement of, 25:41832(R) (AECL-3851)
ELECTRON MICROSCOPY
method for measuring disappearance voltages of second-order reflections, 25:42886 (UCRL-20500, pp 86-146)
research progress in, annual report, 1969--70 on, 25:43468 (NP-18657)
ELECTRON MULTIPLIER TUBES
count rate of parallel-plate channel pressure dependence of spontaneous, 25:42099
gain in continuous channel, calculation of steady-state current, 25:42067
gain of parallel-plate channel, pressure deperdence of, 25:42099
sensitivity for detection of potassium atoms at 5 to 500 eV, 25:42079
ELECTRON PAIRS
production in charged particle interactions at high energies, asymptotic cross sections for, 25:43598
ELECTRON-RING ACCELERATORS
beam monitoring in, methods for positive charged-particle, 25:43734 (UCRL-20664)
development of, review on, 25:43739
ELECTRONIC EQUIPMENT
malfunctions in complex, diagnosis of, 25:44233(R) (BDX-613-431)
standard for, CAMAC, 25:42218
ELECTRONS
acceleration of solar, (E/T), 25:43067 (N-71-16749)
correlation with magnetic fields at magnetospheric bow shock, 100- and 200-eV, (E), 25:43238
density at 60 to 120° pitch angles in auroral zone, 1- to 30-keV, (E), 25:43248
detection of 200- to 900-MeV, calibration of high-resolution lead-glass Cherenkov detector for, 25:42154
dosimetry of 23-MeV, comparison of ionization chamber and photographic film methods for, 25:42411
dosimetry of 5- to 43-MeV betatron, energy and phantom-depth dependence of film sensitivity for, 25:42396
effects of fast, on ferroelectric crystals, 25:43442
effects of pulsed, on 2,2'-azobis[2-methylpropionitrile]--benzene, effects of additives on yields of nitrogen from, 25:41872
effects of pulsed, on ammonia, carbon dioxide, hydrogen sulfide, and nitrous oxide, 25:41832(R) (AECL-3851)
effects of pulsed, on ammonia, rate of disappearance of NH_2 and NH radicals from, 25:41869
effects of pulsed, on aqueous 2-mercaptoethanol solutions, 25:42294
effects of pulsed, on aqueous solutions of potassium periodate, 25:41850(R) (CEA-N-1438)
effects of pulsed, on nitrogen, 25:41850(R) (CEA-N-1438)
effects of pulsed, on oxalic acid, kinetics of production of carbon dioxide, hydrogen, and hydrogen peroxide from, 25:41850(R) (CEA-N-1438)
effects of pulsed, on water and aqueous solutions of aromatic compounds, 25:41858
effects of pulsed, on water--heavy water systems, 25:41832(R) (AECL-3851)
effects on capture center energy spectra of cadmium sulfide crystals at 3 keV, 25:43437
effects on cathodoluminescence of zinc telluride at 100 to 400 keV, (E), 25:43460
effects on cellulose, 25:41873
effects on hydrogen sulfide, effects of sulfur hexafluoride on hydrogen yields from, 25:41860
effects on man, development of necrosis following combined neck dissection and therapeutic, 25:42603
effects on mice, relation of survival of jejunum stem cells to dose dependent, 25:42633
effects on MOSFET transistors, 25:42233
effects on n-type germanium, model of permanent defects induced in, (T), 25:43444
effects on petroleum residues after distillation, yields of light hydrocarbons from, 25:41853 (NP-18817)
effects on polymer foils at 10 to 40 keV, charge trapping, 25:43436
effects on polymerization of monomeric unsaturated compounds and unsaturated polyesters, effects of alkyl arsines, phosphines, and stibines on, 25:41847(P)
effects on polymerization of vinyl monomers in wood, 25:41843(R) (ORO-2945-10)
effects on precipitation of silicon in electron microscopic fields, 25:42886 (UCRL-20500, pp 86-146)
effects on solar cell cover glass of protons and 1-MeV, effects of cerium doping on, 25:43008 (N-71-12278)
emission of exo-, from alkali halide crystals, (E), 25:43489
emission of secondary, from aluminum foils, influence of

electric field on, (E), 25:43101(T) (SCL-T-69-256)
interactions e + d + e + d at 70 to 280 MeV, cross sections and deuteron magnetic form factor from backward, (E), 25:43528 (LAL-1250)
interactions e + d + e + p + n at 70 to 280 MeV, cross sections for backward, (E), 25:43528 (LAL-1250)
interactions e + e + e + e + epsilon(750)(f(1260)), finite-energy sum rules for $\gamma + \pi^0 + \gamma + \pi^0$ interactions for epsilon$\gamma\gamma$ and f$\gamma\gamma$ coupling constants, radiative widths, and cross sections for, (T), 25:43582 (DESY-71/20)
interactions e + N + e + N, scaling, Pomeranchuk trajectory, and J = 1 fixed poles from finite-energy sum rule analysis of virtual Compton, (T), 25:43584 (ITF-71-27-E)
interactions e + N beyond resonance region, model with π form factor for π production in, (E/T), 25:43583 (DESY-71/22)
interactions e + p + e + p at 70 to 280 MeV, cross sections and proton magnetic form factor from backward, (E), 25:43528 (LAL-1250)
interactions e + p at 150 GeV, self-coupling of weak lepton currents in, (T), 25:43612
interactions e + p at high energies, multiperipheral model for form factor for inelastic, (T), 25:43602
interactions e + p near Δ(1236), spectrometer study of cross sections for inelastic, (E), 25:43527 (DESY-71/21)
interactions e + p, amplitude for production of two soft π in, 25:43596
interactions e + p, most probable number of partons in parton models for inelastic, (T), 25:43585 (SU-1206-246)
interactions e + π + W^- + ν + π at 30 to 300 GeV, total cross sections for, (T), 25:43603
interactions $e^+ + e^-$, amplitude for production of two soft π in, 25:43596
interactions γ + e, effects of coherence on intensity-dependent frequency shift in Compton, 25:43590
interactions γ + e, quark--parton model for inequalities for structure functions of inelastic Compton, (T), 25:43586 (SU-1206-250)
magnetic moments of, sixth-order radiative corrections to anomalous, 25:43594
photon reactions with, forced level shifts and energy renormalization in, (T), 25:43518
precipitation during magnetic-storm main phase from minimum and maximum L shells intersected by stormtime plasmapause, (T), 25:43243
production and propagation in upper atmosphere, secondary negatrons and positrons, (E/T), 25:43235
production in γ + N interactions in strong electromagnetic field, final-state interaction for, (T), 25:43606
production in $K_2^0 + \pi + e + \nu$ decay, time reversal invariance test in Coulomb final-state interaction corrections for charge asymmetry in, (T), 25:43660
properties of, comparison with muons, 25:43591
protection of personnel against high-energy, methods for, 25:42464
reactions (e,e'p) with light nuclei, low-accidentals coincidence system for measuring, 25:42131
reactions (e,pt) with helium-4 at 50 and 100 MeV, coincidence spectra from, (E), 25:42131
reactions with aluminum foils at 6 to 10 MeV, influence of electric field on secondary electron emission from, (E), 25:43101(T) (SCL-T-69-256)
reactions with aluminum up to 2000 eV, Auger transitions and supplementary electron ejection in ionization by, (E), 25:43102
reactions with carbon at 2 to 30 keV, K-shell-fluorescence yield from, (E), 25:43108
reactions with deuterium hydride ions, angular distribution of deuterons or protons from dissociation in, (T), 25:43152
reactions with helium, line shapes of He^- states and autoionizing states in ionization curve for, (E), 25:43139
reactions with hydrogen atoms at 100 to 450 eV, Balmer optical excitation cross sections for, (E), 25:43137
reactions with hydrogen atoms, complex-energy calculation of ionization amplitudes for, 25:43145
reactions with hydrogen molecules at gas temperatures of 300 to 1300°K, cross sections for dissociative electron attachment in, (E), 25:43155
reactions with iron-55 at 150 GeV, self-coupling of weak lepton currents in anti ν + ν pair production in, (T), 25:43612
reactions with krypton, autoionizing states produced by, (E), 25:43154
reactions with naphthacene and pyrene at 50 eV to 10 keV, cross sections for excitation in, (T), 25:43127(T) (BNL-tr-429)
reactions with nitrogen and oxygen atoms up to 150 eV, cross sections for excitation of resonance states in, (E), 25:43143
reactions with silicon foils, transition radiation from 50-keV, (E/T), 25:43429
reactions with water as tissue-equivalent medium, spectral-angular characteristics of, (T), 25:43421(T) (ORNL-tr-2476)
scattering by atoms at low energies, central-potential form for, (T), 25:43148
scattering by carbon-12 with proton emission, radiative corrections in quasi-elastic, 25:43979
scattering by helium and hydrogen molecules at 34 to 100 eV, polarization effects on angular dependence of, (T), 25:43138
scattering by hydrogen atom, pseudostates in close-coupling formalism for, (T), 25:43140
scattering by nuclei with nucleon emission, radiative corrections in quasi-elastic, 25:43979
scattering by rotating dipoles, model for, 25:43130
shielding of cylindrical space vehicles against, design of magnetic shield for, 25:43425
theory of Kikuchi, dynamic, 25:42886 (UCRL-20500, pp 86-146)
transport through aluminum, analysis using phase-space time-evolution method, (T), 25:43424
yields of solvated, from γ radiolysis of formamide, effects of nitrous oxide on, 25:41863

ELECTROSTATIC ANALYZERS
design of cylindrical-mirror type, 25:42215
ion-optical properties of cylindrical, with ring-axis focusing, 25:43761
response of quadrispherical ARC Pioneer 6/7 plasma probe, mathematical model of, 25:42209

ELECTROSTATIC FIELDS
emission of vlf waves in south polar magnetosphere at 2500 to 4500 km, (E), 25:43213 (AD-715898)

ELECTROSTATIC GENERATORS
design modification using charge exchange for increasing beam energy from 10.5 to 14 MeV, 25:43766

ELEMENTARY PARTICLE MODELS
dual oscillator, conformal invariance for, 25:43655
dual oscillator, hadron total widths on leading Regge trajectory in, 25:43619
dual resonance, unitarization of amplitude in, 25:43719
dual resonance, unitarization of amplitude in, 25:43718
dual resonance, unitarization of amplitudes in, 25:43717
dual, group-theory approach to π N-point amplitudes on, 25:43714
Fermi--Yang, baryon currents in, 25:43644
Feynman diagram, elastic scattering of spinless particles in ghost-free dual, 25:43634
Lee, continuous mass spectrum of V particle and energy-conserving V--NTHETA vertex in, 25:43671
Lee, LSZ formalism in (n,2) sector of, 25:43673
multi-particle dual, operatorial approach for analysis of, 25:43578
multiperipheral, form factor for inelastic e + p interactions in, 25:43602
multiperipheral, momentum spectrum of hadronic secondaries in two-body strong interactions at high energies in, 25:43620
optical, interactions at high energies and all angles in, 25:43571
optical, interactions π + N at high energies and all angles in, 25:43571
parton, dual amplitude for $\gamma + \pi + 2\pi$ interactions in, 25:43592
parton, most probable number of partons for inelastic e + p interactions in, 25:43585 (SU-1206-246)
quark--parton, inequalities for structure functions of inelastic γ + e Compton interactions in, 25:43586 (SU-1206-250)
sigma, divergence conditions in PCAC and CVC hypotheses in perturbation theory in, 25:43689
sigma, two-loop approximations to propagators in, 25:43684
Veneziano, consistency with Yang--Mills coupling of vector meson fields, 25:43631
Veneziano, functional formulation of N-particle amplitudes in, 25:43722
Veneziano, π electromagnetic form factor in, 25:43593
Veneziano, spin-1 zero-mass photon in conformal, 25:43618

ELEMENTARY PARTICLE MODELS (BOOTSTRAP)
baryon--baryon interactions in quark-, 25:43650

ELEMENTARY PARTICLE MODELS (TRIPLET)
baryon currents in quark, 25:43644
baryon--baryon interactions in bootstrap--quark, 25:43650
interactions γ + e in quark--parton, inequalities for structure functions of inelastic Compton, 25:43586 (SU-1206-250)
magnetic monopoles in, 25:43589

ELEMENTARY PARTICLES
angular momentum of free arbitrary-mass and -spin, (T), 25:43572
bound states of system of two spinless, in quasipotential approach, Pade approximation for, (T), 25:43568 (JINR-P2-5765)
decay of multiplet via interaction with meson bath, (T), 25:43513
interactions above 10^{12} eV, production of massive particle in new process in, (T), 25:43567 (INR-1280)
interactions at high energies, catalog for quantum numbers of crossed-channel exchanges in, (T), 25:43565 (CALT-68-305)
interactions at high energies, cut discontinuities for cross sections of inclusive, 25:43574
interactions at high energies, model analysis of

XUM

amplitudes for, (T), 25:43580
interactions at high energies, time-longitudinal dilations and scaling behavior of, 25:43575
interactions at high energies, violation of Pomeranchuk theorem and zeros of amplitudes for, 25:43576
interactions of massless, with massless particles, cross sections for gravitational, (T), 25:43706
interactions of, complex negative-signature trajectories for violation of Pomeranchuk theorem in, 25:43715
interactions of, review of crossing and positivity properties of partial waves for amplitudes of, (T), 25:43711 (SJ-1205-243)
localization for relativistic zero- and nonzero-mass, Lorentz-invariant, 25:43577
motion of arbitrary-spin, Poincare group for relativistic equations without redundant components for free, (T), 25:43654 (ITF-70-99-E)
multipole states of free arbitrary-mass and -spin, (T), 25:43572
parity and spin of, multipole moments for determination of, (T), 25:43581
production in hadron interactions at high energies, review of multiple, (E/T), 25:43579
production in high-energy interactions, model for multiple, (T), 25:43614 (JINR-P2-5829)
production of massive, in new process in interactions above 10^{12} eV, (T), 25:43557 (INR-1280)
research at Brown Univ., Sept. 1970 to June 1971, (T), 25:43569(R) (NYO-2252-TA-245)
research at Ohio State Univ., June 1970 to June 1971, (E/T), 25:43565(R) (COO-1545-99)
strong interactions at high energies, multiperipheral model for momentum spectrum of hadronic secondaries in two-body, (T), 25:43520
strong interactions of, duality and absorption in qualitative model for amplitudes of two-body elastic, (T), 25:43517
strong interactions of, duality relations with chiral symmetry breaking for, (T), 25:43619
strong interactions of, multiple quark scattering analysis for charge exchange, (T), 25:43615

ELEMENTARY PARTICLES (TRIPLET)
multiple quark scattering analysis for charge exchange in strong interactions, (T), 25:43615

ELEMENTS
abundance of 37, in atmosphere of HD 204075, (E), 25:43019 (NBS-MON-119)
atomic oscillator strengths along isoelectronic sequences, (E/T), 25:43114
determination in lunar materials, review of methods for, 25:41714
determination of trace amounts of, in plutonium, development of reference standards for, 25:41718 (CEA-R-4106)
subshell filling in ordinary and superheavy, atomic number for onset of, (T), 25:43166

ELK RIVER POWER REACTOR
dismantling of, revised technical specifications for, 25:44023 (DOCKET-1151-44)
maintenance for, revised technical specifications for, 25:44023 (DOCKET-1151-44)
steam system piping for, ultrasonic inspection of welds in, 25:44082 (SWRI-1228-9-10)

EMBRYOS
radiation effects on development and survival of rat, x, 25:42321 (COO-597-23)
radiation effects on development of teeth in hamster, x, 25:42649
radioinduced malformations in central nervous system in human, 25:42529
radiosensitivity of mouse and rat, comparison of x, 25:42639
radiosensitivity of mouse and rat, comparison of x, 25:42629
radiosensitivity of organized structures and interstitial cell compartment in mesonephros of chick, 25:42643

ENERGY
conference on equipment and methods for conversion of, Washington, D.C., Sept. 22 to 26, 1969, 25:41995

ENGINEERING
standards in, index of U.S, 25:41961 (NBS-SPEC. PUBL-329)

ENIWETOK ATOLL
silver-108m content of aninals, plants, and sediments at, following nuclear testing during 1958, 25:42377

ENVIRONMENT
fallout monitoring in, estimates of radiation dose to human populations from 1969, 25:42691
polonium-210 content of, in Soviet Union, 25:42429
quality of, NSF-CRNL program on assessment of technology and, 25:44279(R) (ORNL-NSF-EP-3)
radiation monitoring of, recommendations of ICRP for, 25:42465
radioactive contamination of human, contribution of nuclear power plant operation to, 25:42383
radioactive contamination of, relation of radiation dose received by human populations to, 25:42693
radioactive contamination of, relation of radiaton dose to human populations to, 25:42692
radioactivity monitoring in, Brasov, Romania during 1961 to 1968, 25:42424

ENZYMES
induction of dimer-specific endonuclease, by T_4 phage, purification and characterization following, 25:42269
radiolysis of, reactions of free radicals in pulse, 25:41862

EPITHELIUM
radiation dose to bronchial, following inhalation of polonium-214, polonium-216, or plutonium-239, methods for calculation of α, 25:42394(R) (NYO-4256-1)

EPOXY RESINS
performance of fiber glass-reinforced, as irradiation capsule, 25:43011 (N-71-18499)
radiation effects on adhesive properties of radiosensitive-monomer-modified, 25:41846(P)

EQUIPMENT AND PROCEDURES
design and construction of precision measuring machines, evaluation of curvilinear coordinate system for use in, 25:44222 (BDX-613-184)

ERBIUM
determination in meteorites by neutron activation and high-voltage electrophoresis, 25:41775
magnetic susceptibility of, generalized function for, (T), 25:43477
properties of monocrystals of, at low temperatures, elastic and magnetoelastic, 25:41833(R) (IA-1218)

ERBIUM ALLOYS AND SYSTEMS
Al--Er--Ni, magnetic properties of ErAl/sub 2-x/Ni/sub x/, 25:43480

ERBIUM HYDRIDES
electron band structure of, 25:43126
positron annihilation in, angular correlation of radiation from, (E), 25:43126

ERBIUM ISOTOPES Er-166
neutron capture by, cross sections and gamma spectra from thermal, (E), 25:43891(T) (RFP-Trans-78)
neutron reactions (n,α) at 14.2 MeV, level-density parameters and spectra from, (E), 25:43886 (INR-1268)

ERBIUM ISOTOPES Er-167
energy level at 208 keV from erbium-166 neutron capture, spin assignment for isomeric, (E), 25:43891(T) (RFP-Trans-78)
isomeric transition in, half-life, internal conversion coefficients, and gamma spectra from, (E), 25:43891(T) (RFP-Trans-78)

ERBIUM ISOTOPES Er-168
neutron reactions (n,α) at 14.2 MeV, level-density parameters and spectra from, (E), 25:43886 (INR-1268)

ERBIUM OXIDES
Er_2O_3--GeO_2, phase studies of, 25:42988

ERBIUM SELENIDES
crystal structure of β-$ErSe_2$, 25:43004

ERYTHROCYTES
effectiveness of technetium-99m-labeled, in spleen function studies, 25:42570
labeling with technetium-99m, 25:42235
radiation effects on electrophoretic mobility of human, combined effects of neuraminidase or potassium permanganate and low-dose x, 25:42682
radiation effects on filterability of human, in vitro γ, 25:42706

ERYTHROPOIESIS
radiation effects on, in mouse spleen, effects of actinomycin D on recovery from partial-body x, 25:42673

ESTERS
polymers, radioinduced polymerization with unsaturated monomers, 25:41847(P)

ETHANE
ethane--N_2O, radiolysis of, γ and neutron, 25:41851 (JAERI-13780)

ETHANE, PENTACHLORO-
radiolysis of cyclohexane solutions of, at 50 to 200°C, mechanism of γ, 25:41833(R) (IA-1218)

ETHANE, 1,1,2,2-TETRACHLORO-
radiolysis of cyclohexane solutions of, at 150 to 230°C, mechanism of γ, 25:41833(R) (IA-1218)

ETHANE, TRICHLOROTRIFLUORO-
heat transfer modes for boiling, on nonisothermal surface, (T), 25:41989
radiolysis of liquid, identification of types of bond scission in γ, 25:41870

ETHANOL
solution heat of, effects of deuterium on, 25:41794
ethanol--methanol, radiolysis of, ion--solvent interactions in x, 25:41871

ETHANOL, 2-MERCAPTO-
radiolysis of aqueous solutions of, pulsed electron and x, 25:42294

ETHYLAMINE
radiolysis at 77°K, ESR studies on trapped radicals produced by γ, 25:41857
radiolysis of, adsorbed on silica gel at 77°K, ESR studies on trapped radicals produced by γ, 25:41856

ETHYLENE
photolysis of films of, at 20 to 77°K, yields from, 25:41875
radiolysis of films of, at 20 to 77°K, yields from γ, 25:41875
ethylene--N_2O, radiolysis of, γ and neutron, 25:41851 (JAERI-13780)

ETHYLENE, CHLORO-
radioinduced polymerization in wood, γ, 25:41843(R)

(ORO-2945-10)
ETHYLENE, CHLORO-, POLYMERS
properties for thermal protection following nuclear explosions, 25:41827
ETHYLENE, CHLOROTRIFLUORO-, POLYMERS
properties for thermal protection following nuclear explosions, 25:41827
ETHYLENE, DIFLUORO-, POLYMERS
properties for thermal protection following nuclear explosions, 25:41827
ETHYLENE, FLUORO-, POLYMERS
properties for thermal protection following nuclear explosions, 25:41827
ETHYLENE POLYMERS
meson (π^+) and (π^-) absorption at 70 MeV, ionization curves for, (E), 25:42141
performance of linear, as irradiation capsule, 25:43011 (N-71-16499)
preparation of thin deuterated targets of, 25:43759
proton absorption at 150 MeV, ionization curves for, (E), 25:42141
ETHYLENE, TETRAFLUORO-, POLYMERS
properties for thermal protection following nuclear explosions, 25:41827
radioinduced charging of foils of, low-energy electron, 25:43436
ETHYLENE, TRIFLUORO-, POLYMERS
properties for thermal protection following nuclear explosions, 25:41827
EUMYCOTA
Actinomyces sp., radioinduced mutations in, for improved yield of antibiotics, fast neutron, uv, and x, 25:42349
Aspergillus niger, radioinduced mutations in, x, 25:42363
distribution of aquatic, in Puerto Rico, 25:42317(R) (PRNC-147)
Neurospora crassa, radioinduced mutations in, identification of base-pair alterations following uv, 25:42341
Neurospora crassa, radioinduced mutations in, specificity of uv and x, 25:42352
Penicillium digitatum, radiation effects on incubation period for, in grapefruit and oranges, γ, 25:41833(R) (IA-1218)
Penicillium italicum, radiation effects on incubation period for, in grapefruit and oranges, γ, 25:41833(R) (IA-1218)
Saccharomyces carlsbergensis, radioinduced lesions in, effects of delayed plating, media, and temperature on dark repair of uv, 25:42725
Schizophyllum commune, radiation effects on crossing over in recombinants of, uv, 25:42336
Schizosaccharomyces pombe, isolation and genetic classification of uv-radiosensitive mutants of, 25:42723
Schizosaccharomyces pombe, radioinduced meiotic recombination in, effects of caffeine on combined effects of N-nitroso-N-methyl-N'-nitrosoguanidine and uv, 25:42332
Schizosaccharomyces pombe, radioinduced mutations in, effects of caffeine on combined effects of N-nitroso-N-methyl-N'-nitrosoguanidine and uv, 25:42332
Schizosaccharomyces pombe, radioinduced respiration deficient mutants of, activity of respiratory enzymes in uv, 25:42338
Schizosaccharomyces pombe, radioinduced supersensitive mutants in, pathways for repair of uv, 25:42337
use of cesium-134-labeled, to study feeding habits of Caeculid mites, 25:42242
yeasts, radiation effects on sterilization of, in milk, effects of dose on γ, 25:42742
EUROPIUM
determination in meteorites by neutron activation and high-voltage electrophoresis, 25:41776
determination of trace amounts of, in samarium oxide by activation methods, 25:41877 (JAERI-13545)
determination using Tiron, spectrophotometric, 25:41730
magnetic structure in strong magnetic fields, 25:43435(R) (RISO-237)
radiolysis of aqueous solutions of, spectral studies on pulse, 25:41833(R) (IA-1218)
reactivity worth in fast reactor spectra, specific, (E/T), 25:44094(R) (AI-AEC-12991)
separation from aqueous solutions by ion exchange on zirconium tellurate, tracer studies on, 25:41915
separation from yttrium by elution chromatography, 25:41910
EUROPIUM ALLOYS AND SYSTEMS
Ce--Eu--Ge, structure of Ce/sub 5-x/Eu/sub x/Ge$_3$, 25:42895
Eu--Gd--Ge, structure of Gd/sub 5-x/Eu/sub x/Ge$_3$, 25:42895
Eu--Gd--Si, structure of Gd/sub 5-x/Eu/sub x/Si$_3$, Moessbauer study of, 25:42895
Eu--Ge--Pr, structure of Pr/sub 5-x/Eu/sub x/Ge$_3$, 25:42895
EUROPIUM BORIDES
enthalpy and heat capacity of EuB$_6$, 25:42961
EUROPIUM ISOTOPES Eu-145
energy-level scheme from gadolinium-145 decay, (E), 25:43909
EUROPIUM ISOTOPES Eu-149
energy-level scheme from gadolinium-149 decay, (E), 25:43909
EUROPIUM ISOTOPES Eu-152
beta and electron-capture decay of, γ spectra and γ-γ angular correlations from, (E), 25:43940
beta decay of, γ spectra and log ft value for, (E), 25:43939
EUROPIUM ISOTOPES Eu-154
beta decay of, γ and conversion electron spectra and γ-γ angular correlations from, (E), 25:43940
EUROPIUM ISOTOPES Eu-156
beta decay of, γ spectra from, (E), 25:43940
beta decay of, γ--γ angular correlations from, (E), 25:43917
EUROPIUM OXIDES
analysis for impurities, cathode region method for spectrochemical, 25:41833(R) (IA-1218)
CaO--Eu$_2$O$_3$, stability of solid solutions of, effects of heating at 20 to 900°C on, 25:42954
EXOSPHERE
model for ion, in open magnetic fields, 25:43222
EXPERIMENTAL BREEDER REACTOR-II
coolant sampling equipment for, development of in-line vacuum-distillation liquid sodium, 25:44115
design parameters of, 25:44085 (CONF-710427-1)
energy release in, dependence on captured-neutron energy of total, (T), 25:43885 (ANL-7748)
fuel pins for, fabrication and irradiation testing of plutonium nitride--uranium nitride, 25:44118(R) (BMI-1905)
neutron irradiation environment in, activation-rate measurements in ZPR-3 mockup of, 25:44150 (ANL-7781)
operation of, summary of, 25:44085 (CONF-710427-1)
EXPLOSIONS
blast wave propagation from, (T), 25:43348
effects of simple-array chemical, on ground motion, calculations for predicting, 25:41950 (AD-718388)
EXPONENTIAL PILES
exponential measurements on uranium fuel element clusters in EXPO, comparison of critical measurements with, 25:44154 (EUR-4362)
EYES
radiation effects on visual function of rat, following exposure of retina, 25:42515(R) (COO-1201-30)
radioinduced cataracts in rat, protective effects of cysteamine and glutathione against x, 25:42538
radioinduced cataracts in, of Hiroshima atomic bomb survivors, pathology of latent, 25:42546
radioinduced malformations in mouse and rat embryo, x, 25:42629
radioinduced visual phenomena in human, following exposure to neutron energies up to 25 MeV, 25:42688
radiosensitivity of human, 25:42712
radiotherapy of diseases of human, principles and indications for, 25:42596
scanning for diagnosis of melanomas in, use of iodine-131-labeled iodoquine for, 25:42563

F

FALLOUT
content in bees and honey in Germany, 25:42374
detection at high altitudes, design and operation of HANDS system for, 25:41932 (AD-719619)
detection at high altitudes, evaluation of HANDS program for, 25:41933 (AD-719620)
effects on blood picture and spermatozoa in Japanese fishermen, latent, 25:42681
effects on man in Australia following weapons testing in Polynesia during 1970, 25:42367 (AWTSC-1)
effects on strontium-90 content in milk in Korea from 1965 through 1968, 25:42372
monitoring of local, from Project Schooner at Nevada Test Site, 25:42717 (EGG-1183-2272)
radiation dose to human populations from, 25:42692
radiation dose to human populations from, 25:42693
radiation dose to human populations from, estimates for 1969, 25:42691
FAST FLUX TEST FACILITY
design of, safety considerations in, 25:44139 (HEDL-SA-169)
heat transfer system cell for, pressure rise during pipe rupture in, (T), 25:44132 (AI-AEC-12992)
physics measurements for, ZPPR and ZPR-9 criticality studies for, (E), 25:44096 (ANL-7710, pp 53-262)
FAST TEST REACTOR
core structures for, neutron flux limits for, 25:44167
physics measurements for, ZPPR and ZPR-9 criticality studies for, (E), 25:44096 (ANL-7710, pp 53-262)
pressure vessel for, neutron flux limits for, 25:44167
subcriticality measurements by noise analysis in, effects of γ radiation on detector performance in, (T), 25:44103
FASTENERS
standard for mechanical locking devices, 25:41973 (RDT-M-6-2-T)
standard for preloading threaded, 25:41971 (RDT-F-8-1-T)

XUM

FATS
radiolysis of, review on mechanism of, 25:41861
FATTY ACIDS
effects of unsaturated, in diet of whole-body x-irradiated rats on activity of serum aminotransferases, 25:42298
FECES
radiation monitoring of human, at JAERI, dose calculations from, 25:42439
FEDERAL REPUBLIC OF GERMANY
radiation accidents in, laws governing responsibility in, 25:42507
uranium ore prospecting in, 25:41942
FERMI FAST BREEDER REACTOR
operations history for February 1971, 25:44001 (DOCKET-50016-121)
operations history for March 1971, 25:44002 (DOCKET-50016-122)
FERMIONS
decay of, multipole moments for determination of parity and spin in, (T), 25:43581
field equations for charged spin-$^1/_2$ matter, static solutions for combined Dirac--electromagnetic--gravitational, (T), 25:43703
interactions with spin-0 bosons at high energies and all angles, optical model for, (T), 25:43571
parity and spin of, multipole moments for determination of, (T), 25:43581
FERMIUM
energy levels of, g/sub J/ value for ground state, (E/T), 25:43118
FERMIUM ISOTOPES Fm-257
fission of, mass and kinetic-energy distributions and cross sections for spontaneous and thermal-neutron, (E), 25:43920
neutron fission of, mass and kinetic-energy distributions and cross sections for thermal, (E), 25:43920
FERTILIZERS
effects on radioisotope uptake from soils by oat plants, 25:42260
FETUSES
radioinduced malformations in mouse and rat, comparison of x, 25:42639
FIBRIN
ultrastructure in rats with acute radiation sickness, effects of transfusion of blood factor XIII from healthy animals on, 25:42540
FIELD EMISSION MICROSCOPES
design of atom probe-type, 25:42986 (UCRL-20500, pp 86-146)
FIELD EMISSION MICROSCOPY
atomic displacement energy measurement for tungsten tips in, 25:43449
FIELD THEORY
field equations for charged spin-$^1/_2$ matter in, static solutions for combined Dirac--gravitational--electromagnetic, (T), 25:43703
formulation of Lorentz-invariant, in Minkowski space--time, 25:43655 (NP-18831)
pulsating Universe, Sengupta's, (T), 25:43097
FILMS
conference on magnetic thin, fourth international, Prague, 9/70, 25:43492
mounting of thin, for channeling studies, technique for, 25:41832(R) (AECL-3851)
radioinduced rupture of thin liquid, bubble nucleation model of, 25:41835
FIRE EXTINGUISHING AGENTS
performance for fire protection in canyons and hot cells, 25:42036 (DP-1242)
FIRES
prevention and protection in canyons and hot cells, performance of detectors and extinguishing agents for, 25:42036 (DP-1242)
radiation hazards from, involving radioactive materials, 25:42499
FISSION
Coulomb energy in, calculation using modified liquid-drop model, (T), 25:43952(T) (BNL-tr-424)
theory of Coulomb, effects of nuclear forces on cross sections in, (T), 25:43970
FISSION FRAGMENTS
energy distribution measurements using silicon detectors, 25:42048 (ANL-7710, pp 253-364)
energy spectra of, carbon tetrafluoride gas scintillation detector for measurement of, 25:42076
energy-level transitions in, conversion-electron and x-ray energies from, (E), 25:43922
range in air determined by fission-track detector, (E/T), 25:43427
FISSION PRODUCTS
distribution in contained nuclear explosion cavity, 25:41954 (CEA-R-4128(1))
energy-level transitions in, conversion-electron and x-ray energies from, (E), 25:43922
holdup in reactor containment vessel leak paths, decontamination factors for, (E), 25:44134 (BNWL-1582)
ranges in gases, effects of diffusion on, 25:41885
separation from neptunium, niobium, uranium, and zirconium by solvent extraction using tributyl phosphate, 25:41901
separation from spent molten salt reactor fuels by selective reduction and extraction using molten bismuth, 25:41903(P)
separation of bromine and iodine from, by selective negative surface ionization, 25:41833(R) (IA-1218)
separation of hexavalent uranium from nitric acid solutions of, by extraction chromatography using bis(2-ethylhexyl) phosphate, 25:41924
solubility in irradiated oxide fuels, research program on, 25:42953(R) (GEAP-12189)
solubility in irradiated oxide fuels, research program on kinetics of, 25:42952(R) (GEAP-12188)
sorption by impregnated charcoal in carbon dioxide--carbon monoxide--methane system, 25:41898 (TRG-Report-2135)
vapor pressures over irradiated uranium oxide (UO_2)--plutonium oxide (PuO_2) fuels, (E/T), 25:44206 (CEA-R-4181)
FISSIONABLE MATERIAL
shipping in cargo and passenger aircraft, international regulations governing, 25:42456
shipping in cargo and passenger aircraft, international regulations governing, 25:42457
FLANGES
standard for orifice plates for use with orifice, 25:41963 (RDT-C-4-1-T)
FLORIDA
radioactivity monitoring in environment of AEC installation in, during 1970, 25:42416
FLOWMETERS
design and testing of permanent magnet, for liquid metals, standard for, 25:42191 (RDT-C-4-5-T)
development of liquid metal, based on electromagnetic method, 25:42184 (JAERI-13536)
FLUID FLOW
book: Annual Review of Fluid Mechanics, Vol. 3, 25:43196
book: Magnetohydrodynamic Flow Around Bodies, 25:43199
calculation in capillaries and annuli, 25:44264 (K-1796(Pt.5))
computer code for two-dimensional stress-induced adiabatic, 25:44300 (UCID-30013(Pt.1))
computer code, TENSOR generator, for two dimensional stress-induced adiabatic flow, 25:44301 (UCID-30013(Pt.2))
computer code, UNCLE, for two-dimensional stress-induced adiabatic, 25:44302 (UCID-30013(Pt.3))
effects of axial, on vibration response of flexible cylindrical elements, design guide for calculation of, 25:41983 (ANL-BID-71-7)
electrohydrodynamic, in channels with small interaction parameters, (T), 25:43203
equations for, artificial viscosity terms in, 25:44291 (SC-RR-710301)
magnetohydrodynamic Couette, effect on heat transfer of wall electrical conductances and suction in, (T), 25:43198
magnetohydrodynamic, at high Hartmann number, (T), 25:43197
magnetohydrodynamic, boundary layer development in ducts, (T), 25:43201
magnetohydrodynamic, electric field distribution in channels with conducting walls, longitudinal boundary problems in, (T), 25:43202
magnetohydrodynamic, equations and invariant solution for, group properties of, (T), 25:43194
magnetohydrodynamic, Joule dissipation with variable conductivity in, (T), 25:43193
magnetohydrodynamic, MFD wave propagation in heat-conducting compressible, in presence of Hall effect, (T), 25:43200
magnetohydrodynamic, Rayleigh--Taylor instability in, galvanic approximation for, 25:43204
mass transfer in, 25:41778 (UCRL-20500, pp 1-85)
FLUIDS
emission of charged null, from spherically symmetric body, solutions of Einstein--Maxwell equations for, (T), 25:43710
FLUORESCENCE
measurement of rise and decay times in nanosecond region, apparatus for, 25:43452
FLUORIDES
molecular structure of high-valence fluorocations in, 25:41778 (UCRL-20500, pp 1-85)
FLUORINE
determination in selenium by melting with sodium hydroxide and potentiometry using ion-selective electrode, 25:41734
determination in Zircaloy by proton (p,$\alpha\gamma$) reactions using 1.188-MeV resonance, 25:41832(R) (AECL-3851)
FLUORINE ISOTOPES F-17
energy levels from neon-17 beta decay, (E), 25:43802 (UCRL-20480)
proton decay of, branching ratios and proton spectra from beta-delayed, (E), 25:43802 (UCRL-20480)
FLUORINE ISOTOPES F-18
energy levels from oxygen-17 (p,γ) reactions, spin--parity assignments for, 25:43812
energy levels of, calculation using approximation to Bethe--Goldstone equation, 25:43956 (ORO-3765-30)
separation from irradiated lithium carbonate, method for, 25:41833(R) (IA-1218)
testing of, produced in Japan, application, 25:41990

(JAERI-13617)
use for scintigraphy of human bones, 25:42564
FOILS
radioinduced charging of polymer, 10- to 40-keV electron, 25:43436
FONTENAY-AUX-ROSES REACTORS (TRITON)
neutron beam facility in, industrial radiography applications of, 25:44158(T) (LB/G-2929)
FOOD
radiation processing of, 19 nation survey research programs on, 25:42747
radiation processing of, research programs of AEC during 1970 on, 25:44293 (TID-25729)
radioactive materials content in, status of Japan standards for maximum permissible, 25:42482
radioactivity of honey in Germany, measurement of fallout β and γ, 25:42374
radioisotope content in Israel, 25:41833(R) (IA-1218)
radioisotope content of, in Pavia, Italy, 25:42389
radiopreservation of, in India, review on γ, 25:42757
FOOD CHAINS
iodine-131 transport through forage--cow--milk--man, following aerosol mist injection into atmosphere, 25:42370 (SWRHL-43-r)
radioisotope transport through, bibliography on, 25:42315 (ORNL-NSIC-89)
strontium-90 transport through vegetation--cattle--milk--man, biological models for, 25:42378
FORBUSH DECREASES
effect of short-lived, on daily variation of cosmic-ray intensity, (E), 25:43172
FORENSIC SCIENCE
activation analysis in, reliability of evidence obtained by neutron, 25:41775
FORESTS
radiation effects on ecosystems of, in Puerto Rico, 25:42317(R) (PRNC-147)
FORMAMIDE
radiolysis of, yields of solvated electrons from γ, 25:41863
FORMIC ACID
reactions with uranyl nitrates, apparatus for continuous precipitation of uranyl formates from, 25:41792(P)
FORMOSA
radioisotope content of diet of adults and children in, comparison of cesium-137 and strontium-90, 25:42422
FORT ST. VRAIN POWER REACTOR, UNIT 1
design parameters of, revised and additional data on, 25:44047 (DOCKET-50267-32)
operations aspects of, revised and additional data on, 25:44047 (DOCKET-50267-32)
site for, environmental radiation survey during January to March 1971, 25:44047 (DOCKET-50267-32)
thermal effluents from, economics of food production enclosure heating by, 25:44022
FOURIER TRANSFORMS
techniques for two-dimensional finite, 25:44303 (UCRL-51046)
FRANCE
compensation of personnel for occupational radiodermatitis in, Social Security coverage for, 25:42544
FREE RADICALS
book: Investigation of the Paramagnetic Centers of Irradiated Proteins, 25:42275
radioinduced in barley seeds, effects of hydration on decay of, 25:42296
radioinduced in papaya seed for use as γ dosimeter, 25:42438
radioinduced, in aliphatic amines adsorbed on silica gel at 77°K, ESR studies on γ, 25:41856
radioinduced, in aliphatic amines at 77°K, ESR studies on γ, 25:41857
reactions in pulse radiolysis of enzymes, 25:41862
yields from radiolysis of alkanes, effects of electronic excitation of molecules on, 25:41859
FRUITS
apples, cesium-137 and strontium-90 content of, in Bulgaria during 1965, 25:42381
apples, radiation effects on refrigeration storage of, in presence of nitrogen, γ, 25:42748
grapefruit, radiation effects on ethylene production, phenylalanine ammonia-lyase activity, and protein synthesis in peel of, γ, 25:41833(R) (IA-1218)
grapefruit, radiation effects on fungal decay and peel rot on, effects of heat treatment and waxing on, 25:41833(R) (IA-1218)
grapefruit, radiation effects on storage life of, inoculated with Penicillium digitatum and Penicillium italicum, combined heat and γ, 25:41833(R) (IA-1218)
grapes, cesium-137 and strontium-90 content of, in Bulgaria during 1965, 25:42381
oranges, radiation effects on fungal decay and peel rot on, effects of heat treatment and waxing on, 25:41833(R) (IA-1218)
oranges, radiation effects on storage life of, inoculated with Penicillium digitatum and Penicillium italicum, combined heat and γ, 25:41833(R) (IA-1218)
papayas, radiation processing of, use of free radical formation in seed for dosimetry during gamma, 25:42438
pears, cesium-137 and strontium-90 content of, in Bulgaria during 1965, 25:42381
pears, radiation effects on post-harvest ripening of avocado, 25:41833(R) (IA-1218)
plums, cesium-137 and strontium-90 content of, in Bulgaria during 1965, 25:42381
FUEL CAPSULES
development for SNAP-21, 25:41998
FUMARIC ACID
potassium salt, radiation effects on monocrystals of, ESR studies on positive holes from, 25:41841
FUNGICIDES
research on, review of radioisotopes in, 25:42239
FURNACES
design and performance of Chouca, in high radiation environments, 25:41980
design for destruction of graphite-coated uranium dioxide microspheres using replaceable combustion tube, 25:41832(R) (AECL-3851)
FUSED SALTS
corrosive effects of chloride--nitrate, on zirconium alloys, 25:41832(R) (AECL-3851)

G

GADOLINIUM
hyperfine fields for substitutional impurities in, tables of, 25:43469 (UCRL-20411)
magnetic susceptibility of, generalized function for, (T), 25:43477
neutron total cross section at 100 to 550 keV, optical model analysis of average, (E/T), 25:43908
spectra of singly ionized, 25:41833(R) (IA-1218)
GADOLINIUM ALLOYS AND SYSTEMS
Al--Gd--Ni, magnetic properties of GdAl/sub 2-x/Ni/sub x/, 25:43480
Eu--Gd--Ge, structure of Gs/sub 5-x/Eu/sub x/Ge_3, 25:42895
Eu--Gd--Si, structure of Gd/sub 5-x/Eu/sub x/Si_3, Moessbauer study of, 25:42895
Gd--Mn--Pr, magnetic properties of Pr/sub x/Gd/sub 1-x/Mn_2, high-temperature, 25:42894
Gd--Mn--Pr, structure of Pr/sub x/Gd/sub 1-x/Mn_2, 25:42894
Gd--Sn, hyperfine magnetic fields for Sn impurity atoms from tin-119 Moessbauer effect, (E), 25:43494
GADOLINIUM HYDRIDES
electron band structure of, 25:43125
positron annihilation in, angular correlation of radiation from, (E), 25:43126
GADOLINIUM HYDROXIDES
magnetic specific-heat study of interactions in, 25:43472 (YALE-3227-74)
GADOLINIUM ISOTOPES Gd-145
beta and electron-capture decay scheme of ground-state and isomeric, (E), 25:43909
GADOLINIUM ISOTOPES Gd-149
electron-capture decay scheme, (E), 25:43909
GADOLINIUM ISOTOPES Gd-152
energy levels from europium-152 decay, quasi-K quantum numbers for, (E), 25:43939
GADOLINIUM ISOTOPES Gd-153
use as gamma source for excitation of fluorescence radiation in tracer dose of bismuth for localization of brain tumors by external scanning, 25:42548 (CONF-710204-4)
GADOLINIUM ISOTOPES Gd-154
energy levels from europium-154 decay, transition probabilities and band-mixing parameters for, (E), 25:43940
energy-level transitions from europium-154 decay, conversion coefficients and γ-mixing ratios for, (E), 25:43940
GADOLINIUM ISOTOPES Gd-156
energy levels from europium-156 decay, transition probabilities and band-mixing parameters for, (E), 25:43940
energy-level scheme from europium-156 decay, (E), 25:43917
GADOLINIUM OXIDES
analysis for impurities, cathode region method for spectrochemical, 25:41833(R) (IA-1218)
GALAXIES
formation of, effect of anisotropy in, (T), 25:43096
hydroxyl in NGC 253 and M82, detection of interstellar, (E), 25:43083
motions of, determination of correction to precession from proper, (T), 25:43048
radio map of Andromeda, (E), 25:43064
structure of, formation and stability of spiral, (T), 25:43081
x-ray source in Coma cluster of, detection of, (E), 25:43056
GALLIUM
effects on superconducting critical field of niobium--titanium alloy wires, 25:43309
separation from acetone--hydrochloric acid solutions by ion exchange using Bio-Rad, distribution coefficients for, 25:41899
separation from aqueous solutions by ion exchange on zirconium tellurate, tracer studies on, 25:41915
separation from other metals using inorganic ion exchange

XUM

papers, 25:41909
GALLIUM ALLOYS AND SYSTEMS
Au--Ga, nuclear quadrupolar relaxation rates in $AuGa_2$, effects of melting on, 25:43496
Au--Ga--Pd, nuclear quadrupolar relaxation rates in $Au_{0.90}Pd_{0.05}Ga_2$, effects of melting on, 25:43496
Ga--Ge, mixing in liquid and solid phases of, energy of, 25:42970
Ga--Pu-base, annealing of shock-hardened, kinetics of, 25:42857
Ga--Si, mixing in liquid and solid phases of, energy of, 25:42970
Ga--V, superconducting properties of V_3Ga wires in copper--gallium matrix, effects of reaction and heat treatment on, 25:43292
GALLIUM ARSENIDES
ion-implantation effects on phonon modes of Raman spectra of, 400-keV xenon, 25:43440
radiation effects on structure of, 1.5-MeV electron, 25:41832(R) (AECL-3851)
radiation effects on, infrared absorption spectra of electron- and neutron-, (E), 25:41832(R) (AECL-3851)
vaporization of single crystals of, 25:41778 (UCRL-20500, pp 1-85)
GALLIUM ISOTOPES
gallium--zinc Coulomb displacement energies, (E), 25:43883
GALLIUM ISOTOPES Ga-67
effectiveness for scanning human lymph system for localization of neoplasms, 25:42549(R) (ORAU-113)
production of carrier-free and iron-free, by ion-exchange separation from deuteron-irradiated zinc, 25:41881
radiation dose to human adrenal glands, bone marrow, kidneys, liver, and spleen from tracer dose of, 25:42549(R) (ORAU-113)
uptake by neoplastic and normal tissues in man, mice, hamsters, and rats, 25:42549(R) (ORAU-113)
use in medicine, bibliography on, 25:42550 (ORNL-TM-2091(Suppl.2))
GALLIUM ISOTOPES Ga-68
use in medicine, bibliography on, 25:42550 (ORNL-TM-2091(Suppl.2))
GALLIUM ISOTOPES Ga-70
energy levels from gallium-69 neutron capture, spin--parity assignments for, (E), 25:43831 (INR-1262)
GALLIUM ISOTOPES Ga-71
neutron capture by, cross sections and gamma spectra from thermal, (E), 25:43891(T) (RFP-Trans-78)
GALLIUM ISOTOPES Ga-72
energy level from gallium-71 neutron capture, spin--parity assignment for isomeric, (E), 25:43891(T) (RFP-Trans-78)
energy levels from gallium-71 neutron capture, spin--parity assignments for, (E), 25:43831 (INR-1262)
isomeric transition in, half-life and gamma spectra from, (E), 25:43891(T) (RFP-Trans-78)
GALLIUM PHOSPHIDES
nitrogen-ion implantation in crystals of, photoluminescence spectrum of, (E), 25:43462
oxygen-ion implants in, depth distributions and annealing of 20- to 60-keV, 25:43447
GAMETES
radiation effects on tomato, mutagenic fast neutron and γ, 25:42364
GAMMA CAMERAS
performance for scintigraphy of blood perfusion in lungs using metastable technetium-99-labeled iron hydroxide macroaggregates, 25:42579
GAMMA DECAY
half-life for, delayed-coincidence method for measurement of, 25:42222
GAMMA RADIATION
acoustic resonance absorption in nuclei, (T), 25:43493
angular distributions of, techniques for optimization of measurement of, 25:42223
attenuation by Pilot-B plastic scintillator at 0.36 to 1.33 MeV, coefficients of mass, 25:42054
book: Investigation of the Paramagnetic Centers of Irradiated Proteins, 25:42275
detection from nucleon capture reactions at 100 keV to 12 MeV, calibration and performance of lithium-drifted germanium detectors for, 25:42129
detection of high-energy, use of Cherenkov inserts in, 25:42082
detection of, full energy peak efficiency of thallium-activated sodium iodide detector for, 25:42050 (JAERI-13546)
distribution in medium of arbitrary elemental composition, (T), 25:43426
dose distribution around implanted iridium-192 sources, mathematical models for, 25:42428
dose fields in shielding structures and shelters, (T), 25:43428
dose to human population in Soviet Union during 1966 to 1968 from fallout cesium-137, calculation of, 25:42376
dose to other patients and personnel from implanted iridium-192 source, methods for protection against, 25:42477
dose to personnel at JAERI, use of whole-body counting and sample analysis for calculating internal, 25:42439
dose to uranium enrichment personnel from uranium-235-contaminated air, methods for protection against, 25:42379
dosimetry during mantle treatment of Hodgkin's disease, methods for, 25:42594
dosimetry in human organ phantoms containing radioisotopes, role of body background in external, 25:42423
dosimetry in mixed fast neutron field, double ionization detector for, 25:42168
dosimetry in processing papayas, use of free radical formation in seed for, 25:42438
dosimetry of, energy and phantom-depth dependence of film sensitivity for, 25:42396
effectiveness for preoperative treatment of carcinomas of larynx and pharynx, effects of dose and dose fractionation on, 25:42588
effectiveness for sterilization of culture media for insect larvae, 25:42749
effectiveness for therapy of carcinomas of head and neck, additive effects of 5-fluorouracil infusion on, 25:42589
effectiveness of combined radium-226 implant and external beam, for treatment of uterine cervix carcinomas, 25:42595
effects in combination with nitrogen mustard on chromosomes in dry seeds of Crepis capillaris, aberrant, 25:42359
effects on 2-butyne, excited states and cyclobutadiene intermediates from, 25:41867
effects on 2-methylpropane, effects of phase on exciton transfer to carbon tetrachloride from, 25:41864
effects on activity and isoenzyme patterns of lactate dehydrogenase in organs and serum of rats, protective effects of methylene blue against, 25:42284
effects on activity of intestinal phosphatases in hamsters, cobalt-60 whole-body exposure, 25:42301
effects on adult and pupal male Med flies, comparison of sterilizing, 25:42751
effects on aliphatic amines adsorbed on silica gel at 77°K, ESR studies on trapped radicals produced by, 25:41856
effects on aliphatic amines at 77°K, ESR studies on trapped radicals produced by, 25:41857
effects on analgesic activity and toxicity of morphine solutions, effects of concentration on, 25:42752
effects on anhydrous, freeze-dried, and dihydrate solid oxalic acid, 25:41858
effects on antifibrinolytic activity of 6-aminohexanoic acid in blood of patients with carcinomas, 25:42293
effects on apples, mutagenic γ, 25:42324
effects on aqueous solutions of metals, hydrogen yields from, 25:41833(R) (IA-1218)
effects on aqueous solutions of sodium acid phosphites, kinetics of production of atomic hydrogen from, 25:41850(R) (CEA-N-1438)
effects on ascorbic acid content of wheat following seed exposure, effects of dose on, 25:42725
effects on bacteria for use as sanitary indicators, 25:42743
effects on bacteriophage 341, effects of dose on inactivating, 25:42740
effects on behavior of monkeys, effects of dose and partial shielding on, 25:42642
effects on biochemistry and morphology of Pisum arvense and P. sativum, in relation to effects on chromosomes, 25:42329
effects on blood coagulation in dogs, effects of dose on, 25:42600
effects on capacity of Escherichia coli to support bacteriophage growth, relation of dose to, 25:42730 (NYO-2804-41)
effects on carbon-14-labeled orotic acid or iodine-131-labeled albumin activity in rats as indicators of radiation injury, 25:42407
effects on catalase activity in blood and pyrophosphatase activity in brain and liver of rats following continuous whole-body exposure, 25:42277
effects on cell population kinetics in mouse thymus gland, chronic whole-body, 25:42631
effects on cellulose, 25:41873
effects on cellulose and cellulose 2-thiophenecarboxylate, ESR studies on intramolecular energy transfers from, 25:41836
effects on ceramic insulator seals at high fluence levels, 25:42228 (N-71-17325)
effects on cervical lymph nodes in dogs following neck exposure, effects of dose on pathological, 25:42662
effects on chemical composition of hemoglobin in mice following chronic whole-body exposure, effects of dose rate on, 25:42586 (ORAU-113, pp 4-77)
effects on chromosomes in cultured human cells, effects of dose on aberrant, 25:42365
effects on chromosomes of Crepis capillaris, effects of dose on aberrant, 25:42351
effects on chronic leukemia, lymphosarcoma, and polycythemia in man, effects of dose rate and total dose on therapeutic, 25:42586 (ORAU-113, pp 4-77)
effects on content of proteins, immunoglobulins, and transferrin in blood serum of man following low-dose whole-body exposure, 25:42586 (ORAU-113, pp 4-77)
effects on crystal structure of tin-containing glass, 25:43009

effects on culture media used to grow Escherichia coli, 25:42755
effects on development and survival of Chinook salmon following chronic exposure as eggs and alevins, effects of dose and dose rate on, 25:42616(R) (RLO-2225-T-2-2)
effects on development of subcutaneous indurations, therapeutic, 25:42587
effects on dielectric properties of potassium dihydrogen phosphate crystals, 25:43443
effects on dilute solutions of trypsin, 25:42271
effects on diseases in man, therapeutic, 25:42597
effects on DNA degradation in Escherichia coli, effects of dose and genetic strain on, 25:42731 (NYO-2804-42)
effects on DNA degradation in Escherichia coli, effects of dose and genetic strain on, 25:42729 (NYO-2804-40)
effects on DNA in Escherichia coli, effects of anoxia and genetic strain on, 25:42728 (NYO-2804-39)
effects on DNA in Escherichia coli, mechanisms for repair of, 25:42727 (NYO-2804-38)
effects on DNA of PM2 bacteriophage for use in infecting spheroplasts of Pseudomonas, 25:42273
effects on DNA strand breaks, regeneration by polynucleotide ligases in vitro following, 25:42268
effects on DNA transcription and RNA translation in plants, 25:42715(R) (COO-1313-29)
effects on electromyogram of guinea pig muscle, effects of dose on, 25:42552
effects on ethylene at 20 to 770K, 25:41875
effects on ethylene production, phenylalanine ammonia-lyase activity, and protein synthesis in grapefruit peel, 25:41833(R) (IA-1218)
effects on excretion of nucleic acid metabolites in rat urine, mechanism of effects of cysteamine on, 25:42625
effects on female and male grain moths in relation to percent flying-off and sex ratios among progeny, comparison of sub-sterilizing,, 25:42610
effects on ferroelectric crystals, 25:43442
effects on filterability of human erythrocytes, in vitro, 25:42706
effects on formamide, yields of solvated electrons from, 25:41863
effects on goldfish and Oryzias latipes, comparison of repeated high-dose x and chronic low-dose, 25:42634
effects on gross morphology of wheat and differential stage-sensitivity of barley following chronic exposure, 25:42724
effects on growth of pine seedlings and trees, effects of ozone on, 25:42316(R) (ORO-3299-107)
effects on growth of plants in rain forest in Puerto Rico, 25:42317(R) (PRNC-147)
effects on hemagglutinin formation in mice, exposure rate dependence of, 25:42307
effects on heterogeneity of nuclear RNA in liver of rats following whole-body exposure, 25:42280
effects on homograft heart valves for use in man, 25:42758
effects on human gynecological cancer, complications in adjacent organs following therapeutic, 25:42598
effects on human renal adenocarcinoma, spontaneous regression of lung metastases following therapeutic, 25:42591
effects on human skin, latent carcinogenic, 25:42686
effects on hydrogen transfer yields in dry salmon sperm DNA, D-glucose, ribonuclease, and poly-DL-alanine, 25:41837
effects on hydrolytic resistance of glass ampules, high dose sterilizing, 25:42754
effects on immune reactions to allogenic bone marrow transplants in acute leukemia patient, additive effects of antilymphocyte globulin on, 25:42586 (ORAU-113, pp 4-77)
effects on in vitro growth of Histomonas meleagridis, effects of dose on, 25:42608
effects on leukopoiesis in bone marrow of rabbits, protective effects of glutathione against, 25:42536
effects on life span and ultrastructure of midgut cells of Drosophila, 25:42612
effects on liquid trichlorotrifluoroethane, identification of types of bond scission in, 25:41870
effects on lysogenic bacteria, effects of induction of infecting bacteriophage on, 25:42529
effects on man following therapy, carcinogenic, 25:42709
effects on Micrococcus glutamicus, review of mutagenic, 25:42349
effects on microorganisms in milk, effects of dose on sterilizing, 25:42742
effects on morphology of human thyroid cancer following therapy, effects of tumor type on, 25:42679
effects on mouse testes, effects of bone marrow transplants on lethal whole-body, 25:42304
effects on myoglobin in beef, low-dose cobalt-60, 25:42756
effects on N-(N-glycyl)glycine selenate single crystals, ESR and ir spectra of radicals induced in, 25:41854
effects on nitrous oxide and its systems with ammonia, ethylene, and ethane, 25:41851 (JAERI-13780)
effects on organoleptic properties of apples, effects of nitrogen on, 25:42748
effects on pentachloroethane and tetrachloroethane in cyclohexane solutions, mechanism of, 25:41833(R) (IA-1218)
effects on performance of in-pile neutron detectors, (T), 25:44103
effects on phosphite solutions, yields of hypophosphate and phosphate from, 25:41955
effects on poly-L-serine, monolayer studies of, 25:41834
effects on polymerization of 3,4,5,5,5-pentafluoro-2-methyl-1,3-pentadiene and 3,4,5,5,5-pentafluoro-1,3-pentadiene, 25:41848
effects on polymerization of methyl methacrylate--styrene, effects of temperature on microstructure of polymers from, 25:41845
effects on polymerization of solid acrylamide and acrylic acid at 770K, ESR and NMR studies on radicals produced by, 25:41850(R) (CEA-N-1438)
effects on polymerization of vinyl monomers in wood, 25:41843(R) (ORO-2945-10)
effects on positron lifetimes and intensities in sodium chloride crystals, 25:43453
effects on potatoes, mutagenic, 25:42323
effects on preservation of food in India, review on, 25:42757
effects on properties of cottonseed oil, 25:41839
effects on reproductive capacity of Mediterranean fruit flies in Nicaragua, 25:42750
effects on respiratory function in man, additive effects of exercise on low-dose whole-body exposure, 25:42586 (ORAU-113, pp 4-77)
effects on saffron flower and pollen size, effects of dose on, 25:42720
effects on seed emergence in cucumbers, effects of dose on, 25:42719
effects on seeds of Arabidopsis, effects of dose on chlorophyll mutagenic, 25:42358
effects on single crystals of dipotassium difluoromalonate, ESR studies on, 25:41838
effects on solid succinic acid, role of reaction sites in, 25:41865
effects on sperm precedence in spruce budworms, 25:42259
effects on spermatogonia of Drosophila, comparison of effects of acute, chronic, and split-dose techniques on cobalt-60 low-dose mutagenic, 25:42350
effects on storage life and wholesome of cod fillets, lobster tails, and shrimp, 25:42746 (STI/DOC-10/124)
effects on storage life and wholesomeness of beef and pork, 25:42744(R) (COO-2038-2)
effects on storage life of grapefruit and oranges inoculated with Penicillium digitatum and Penicillium italicum, combined with effects of heat, 25:41833(R) (IA-1218)
effects on sulfuryl chloride, ESR spectra of radical anion from, 25:41855
effects on survival of blood platelets and leukocytes in peripheral blood of man, low-dose-rate low-dose, 25:42586 (ORAU-113, pp 4-77)
effects on survival of colony-forming units in mouse bone marrow, comparison of RBE for neutron x, and, 25:42601
effects on survival of desert shrubs at Nevada Test Site, effects of dose on, 25:42717 (EGG-1183-2272)
effects on survival of inbred and outbred lines of laboratory populations of sugarcane borers, 25:42611
effects on survival of mice and rats, protective effects of methylene blue against whole-body, 25:42515
effects on survival of mice, protective effects of adenosine derivatives against, 25:42516
effects on survival of pathogenic bacteria on beef and pork, effects of dose on, 25:42744(R) (COO-2038-2)
effects on synthesis of DNA and RNA in Escherichia coli, effects of dose and genetic strain on, 25:42729 (NYO-2804-40)
effects on tetanus antitoxin production in mice, combined effects of drugs and, 25:42672
effects on thallium-activated cesium iodide crystals, influence of electric field on luminescent, (E), 25:43448
effects on thymine in deaerated aqueous solutions, 25:41874
effects on thymine-dependent strain of Escherichia coli, 25:42330
effects on tomato gametes, pollen, and seed, mutagenic, 25:42364
effects on tumor incidence in mice, comparison of latent internal tritiated thymidine and external, 25:42630
effects on tumor incidence in mice, effects of dose on, 25:42664
effects on undecafluoro(trifluoromethyl)cyclohexane at 770K, ESR and NMR studies on radicals produced by, 25:41850(R) (CEA-N-1438)
effects on volatile compound production in fish tissues, 25:42753
effects on water and aqueous solutions of aromatic compounds, 25:41858
scattering, calculation of combined spatial, angular, and energy distributions of multiple, (T), 25:43413 (BMBW-FBK-71-2)
yields from neutron capture by tantalum-181 and natural tungsten at thermal energies to 907 keV, (T), 25:43890 (ORNL-TM-3436)

GAMMA SOURCES
activity in bees and honey in Germany, measurement of fallout, 25:42374
calibration of cobalt-60, for therapy, international comparison of dosimeters for, 25:42172

XUM

determination in gases by chromatography and counting, 25:41753(P)
determination in organic coolant, 25:41832(R) (AECL-3851)
radiation protection code for sealed, in industrial radiography, 25:42490
use for industrial radiography, ILO safety manual for, 25:42461
use for therapy, radiation protection code for, 25:42491
use for therapy, radiation protection code for medical personnel during, 25:42492

GAMMA SPECTROMETERS
background reduction in thallium-acivated sodium iodide, using anticoincidence circuits and massive shielding, 25:42109 (UUIP-737)
calibration of lithium-drifted germanium, method for absolute, 25:42125
circuits for thallium-activated sodium iodide, design of high-count-rate, 25:42127
design for well logging, 25:42117(P)
efficiency of lithium-drifted silicon, at 5 to 170 keV, photopeak, 25:42123
performance for scintillation scanning of selenium-75 in pancreas, 25:42578
performance of coincident lithium-drifted germanium, for radioisotope determination, 25:42113
sensitivities of lithium-drifted germanium, figure-of-merit measurements of, 25:42126
spectra from lithium-drifted germanium, computer program for processing, 25:42116
time resolution of lithium-drifted germanium, for (n,n'γ) experiments, 25:42048 (ANL-7710, pp 263-364)

GAMMA SPECTROSCOPY
developments in, review of, 25:42133

GARNETS
radiation effects on infrared spectrum of, 5-keV proton, deuteron, helium-ion, and nitrogen-ion, 25:43446

GAS CHROMATOGRAPHY
errors in, using Kovats indices, 25:44247 (COO-1222-49)
research progress on high precision, 25:44248(R) (COO-1222-50)

GAS FLOW
calculation of plane Poiseuille, with backscattering, 25:44263 (K-1799(Pt.4))
magnetohydrodynamic, acceleration in strong nonstationary electromagnetic fields, (T), 25:43195
magnetohydrodynamic, steady supersonic source of nonequilibrium plasma for, (T), 25:43192
reduction of free molecule, through long capillary, boundary condition for, 25:44262 (K-1798(Pt.1))

GASES
alpha energy losses in tissue-equivalent, methods of, 25:42394(R) (NYO-4255-1)
analysis for gamma sources by chromatography and counting, 25:41753(P)
density fluuctuations in interacting Bose, (T), 25:43522
dilution factor for, discharged in specially ventilated atmosphere, method for measuring, 25:41833(R) (IA-1218)
dispersion effects in molecular, in parallel constant and alternating magnetic fields, (T), 25:43516
exchange in human lungs, use of xenon-133 in studies of, 25:42561
hydrogen-atom and -ion (H^-) reactions up to 20 MeV with, review of cross sections for electron capture and loss in, (E), 25:43149
Landau description of quantum, (T), 25:43511
pressure measurement of radioactive, device for, 25:42179(P)
proton reactions up to 20 MeV with, review of cross sections for electron capture in, (E), 25:43149
reactions with surfaces, classical model for, 25:43104
theory for gas dynamics of explosions, 25:43348

GASTROINTESTINAL TRACT
cerium-144 sorption by suckling mouse, 25:41833(R) (IA-1218)

GATING SYSTEMS
design for pulse-height spectrometer for reducing pile-up errors, 25:42215
design of variable-delay, for two-channel counting systems, 25:42053

GENES
effects of location of, on uv radiosensitivity of Escherichia coli mutants, 25:42328
effects of mutator alleles of, on repair of uv-radioinduced mutations in phage T4, 25:42339
effects on reactivation of uv-irradiated phages, 25:42738

GENETIC STRAIN
effects on accumulation of strontium-89 and -90 in barley, soybeans, and wheat, 25:42322(R) (COO-1097-46)

GENETICS
radiation effects on human, conference on, 25:42512

GEOMAGNETIC FIELDS
disturbances of, relation to chromospheric eruptions, (E/T), 25:43072
effect on control of geographic distribution of ionospheric F2 noon ionization, (E/T), 25:43227
perturbations of, effect of Forbush microdecreases on, (E), 25:43172
pulsations in, spatial and temporal relations between Pi bursts and IPDP micro-, (T), 25:43247

GERMANIUM
analysis of detector-grade monocrystals of, for trace impurities, 25:41832(R) (AECL-3851)
effects on superconducting critical field of niobium--titanium alloy wires, 25:43309
preparation of high-purity, methods for, 25:42130
radiation damage in n-type, model of permanent defects induced in low-temperature electron, (T), 25:43444
separation from other metals using inorganic ion exchange papers, 25:41909

GERMANIUM ALLOYS AND SYSTEMS
Al--Ge, mixing in liquid and solid phases of, energy of, 25:42970
Al--Ge--Nb, superconducting and existence region of A15 phase of, (E/T), 25:43319
Al--Ge--Nb, superconductivity and range of existence of A15 phase in, (E), 25:43291(T) (ORNL-tr-2461)
Al--Ge--Y, phase diagram at 500°C, isothermal, 25:42891
Ce--Eu--Ge, structure of Ce/sub 5-x/Eu/sub x/Ge_3, 25:42895
Eu--Gd--Ge, structure of Gs/sub 5-x/Eu/sub x/Ge_3, 25:42895
Eu--Ge--Pr, structure of Pr/sub 5-x/Eu/sub x/Ge_3, 25:42895
Ga--Ge, mixing in liquid and solid phases of, energy of, 25:42970
Ge--In, mixing in liquid and solid phases of, energy of, 25:42970
Ge--Sb, mixing in liquid and solid phases of, energy of, 25:42970

GERMANIUM ISOTOPES Ge-70
neutron capture by, cross sections and gamma spectra from thermal, (E), 25:43891(T) (RFP-Trans-78)
proton elastic and inelastic scattering at 2.7 to 7.4 MeV, excitation functions for, (E), 25:43851

GERMANIUM ISOTOPES Ge-71
energy level at 198 keV from germanium-70 neutron capture, spin assignment for isomeric, (E), 25:43891(T) (RFP-Trans-78)
isomeric transition in, half-life, internal conversion coefficients, and gamma spectra from, (E), 25:43891(T) (RFP-Trans-78)

GERMANIUM ISOTOPES Ge-74
energy-level scheme from photoexcitation, (E), 25:41833(R) (IA-1218)

GERMANIUM OXIDES
Er_2O_3--GeO_2, phase studies of, 25:42988

GERMYL GROUP
chemical properties of, 25:41778 (UCRL-20500, pp 1-85)

GLASS
analysis for elements by neutron activation in forensic science uses, 25:41758 (AWRE-O-24/71)
mechanical properties of, effects of water content on, 25:42957 (UCRL-20500, pp 147-73)
radiation effects on crystal structure of tin-containing, gamma, 25:43009
radiation effects on quality of clinical ampules of, high dose γ, 25:42754
radiation resistance of solar cell cover, effects of cerium on space electron--proton, 25:43008 (N-71-12278)
sealing of ampules of, containing radioactive material, equipment and method for semiautomatic flameless, 25:42046
sodium self-diffusion coefficients in sodium calcium silicate and sodium aluminum phosphate, heterogeneous isotopic exchange measurements of, 25:41810
suspension of beads of, in carbon dioxide--nitrogen, power requirements for circulation of, 25:41956 (BM-RI-7015)
Al_2O_3--glass, tensile properties of composites of, effects of internal strains on, 25:42957 (UCRL-20500, pp 147-73)

GLOVE BOXES
gloves for, criteria for evaluation and testing of, 25:42039 (RFP-1286)

GLUCOSE
effects on redox potential of spleen, 25:42526
radiation effects on content of, in rat blood, protective effects of methylene blue against x, 25:42283
radioinduced hydrogen transfer in, effects of temperature and scavengers on yields from γ, 25:41837

β-GLUCOSIDASE
radiomimetic effects on root tip chromosomes of onion and Zamia in comparison to cycasin and methylazoxymethanol, 25:42334

β-GLUCURONIDASE
radiation effects on distribution of, in rat liver and spleen, whole-body x, 25:42528

GLUTATHIONE
radioprotective effects on rat eyes, x, 25:42538

GLYCINE, N-(N-GLYCYLGLYCYL)-
selenate, radioinduced radicals in single crystals of, ESR and ir spectra of γ, 25:41854

GLYCOGEN
radiation effects on content of, in rat liver, protective effects of methylene blue against x, 25:42283

GOLD
determination in geological samples by neutron activation, 25:41770

determination in minerals from Luzon, Philippines, by neutron activation, 25:41772
determination in natural waters by sorption on lead sulfide and neutron activation, 25:41771
determination of trace amounts of, in meteorites by neutron activation and γ spectrometry, 25:41773
ion channeling in, interaction potentials of helium, oxygen, and iodine, (T), 25:43456
ion energy-loss spectra in (111) and (100) channels of, oxygen and iodine, 25:43454
separation from acetone--hydrochloric acid solutions by ion exchange using Bio-Rad, distribution coefficients for, 25:41899
separation from aqueous solutions by ion exchange on zirconium tellurate, tracer studies on, 25:41915
separation from other metals using inorganic ion exchange papers, 25:41909
separation of radioactive platinum isotopes from neutron-irradiated, by paper chromatography, 25:41920

GOLD ALLOYS AND SYSTEMS
Au--Ga, nuclear quadrupolar relaxation rates in $AuGa_2$, effects of melting on, 25:43496
Au--Ga--Pd, nuclear quadrupolar relaxation rates in $Au_{0.95}Pd_{0.05}Ga_2$, effects of melting on, 25:43496
Au--In, nuclear quadrupolar relaxation rates in $AuIn_2$, effects of melting on, 25:43496
Au--Cu, analysis by electron-beam microprobe method, computer program for processing of data from, 25:44305 (UCRL-73104)

GOLD ISOTOPES Au-199
effectiveness for diagnosis of cirrhosis of liver and hepatitis, 25:42553
gamma spectra of, for accuracy in diagnosis, phantom measurements on, 25:42397
metabolism and tissue distribution following intake by man, 25:42457
use for scanning lymph system in human infants for evaluation of primary congenital lymphedema, 25:42559
use with selenium-75 for liver scanning, method for, 25:42580

GOLD ISOTOPES Au-199
beta decay of, β-γ circular polarization correlation for, (E), 25:43941

GONADS
radiation dose to, of workers during transport of strontium-90--yttrium-90 source, thermoluminescent dosimetric monitoring of β, 25:42444
radiosensitivity of tissues of human and monkeys, 25:42586 (ORAU-113, pp 4-77)

GRAPHITE
book: High-Temperature Materials, 25:42853
coating with liquid zirconium, kinetics of spread, 25:42832
desorption of chemisorbed oxygen from surfaces of, mechanism of, 25:41850(R) (CEA-N-1438)
electrical conductivity and thermal conductivity of, room temperature measurements of, 25:44283 (ORNL-TM-3477)
evaluation of bismuth impregnated, for reactor reflectors, 25:44129 (EUR-4357)
fabrication and testing of composites of, for use in ablative environments, 25:42971
neutron slowing down density distribution in, evaluation of ENDF/B data for, (E/T), 25:44094(R) (AI-AEC-12991)
oxidation by nitrous oxide, kinetics of, 25:42932
oxidation by oxygen, kinetics of, 25:42932
preparation and properties of zirconium-impregnated, at 1860 to 2550°C, 25:42948
properties for use as engineering and structural material, review of, 25:42977
reactions with nitrous oxide, catalytic effects of barium, cadmium, chromium, lead, and uranium on, 25:42931
reactions with oxygen, catalytic effects of barium, cadmium, chromium, lead and uranium on, 25:42931
reactions with oxygen, kinetics of, 25:41778 (UCRL-20500, pp 1-85)

GRAVITATION
field equation in Brans--Dicke theory, units transformations for, 25:43702
field equations for charged spin-$^1/_2$ matter in, static solutions for combined Dirac--electromagnetic--gravitational, (T), 25:43703
interactions of massless particles with massless particles, cross sections for, (T), 25:43706
metric space in, origins of Schwarzschild and Curzon static solutions for, 25:43697
repulsion property of interstellar space, (T), 25:43089
Schroedinger particle scattering from barriers of, (T), 25:43517
space--time in, causal structure in, 25:43699
theories of, velocity of light in Einstein and Newton, 25:43694
theory for, equations of motion in relativistic mechanics from potential tensor in, 25:43709
theory of self-coupled scalar, 25:43705
theory of, non-Lorentzian transformations of systems of reference in, 25:43708

GRAVITATIONAL COLLAPSE
theory for, general relations in relativistic MHD for, 25:43701

GRAVITATIONAL FIELDS
deflection of microwaves by solar, (E), 25:43094

GRAVITATIONAL RADIATION
focusing by galactic core, 25:43700

GRAVITY WAVES
interaction with ionosphere during Mar. 7, 1970 solar eclipse, (E/T), 25:43270
production in atmosphere, effect on sporadic-E enhancement, (E/T), 25:43255

GREAT BRITAIN
radiation protection regulations for transportation personnel handling radioactive materials, 1970, 25:42451
radioactive materials shipment on roads in, 1970 statute on, 25:42450
regulations for radiation protection of industrial personnel using sealed radiation sources and x radiation, 25:42469
regulations for radiation protection of industrial personnel using unsealed radioactive materials, 25:42468

GROUND
motion from detonation of simple-arrayed chemical explosives in alluvium, limestone-shale, and granite, calculations for predicting, 25:41950 (AD-718388)

GROUP THEORY
book: Duality. Local Compact Groups, 25:43721
conformal invariance for dual oscillator model, 25:43655
Poincare group algebra for quantum field theory, extension of, 25:43576
Poincare group for relativistic equations without redundant components for free motion of arbitrary-spin particles and antiparticles, 25:43654 (ITF-70-89-E)

GUANIDINE, 2-MERCAPTOETHYL-
radioprotective effects of derivatives of, on HeLa cells, x, 25:42514
radioprotective effects of, on HeLa cells, mechanism of x, 25:42514

GUANIDINE, 1-METHYL-3-NITRO-1-NITROSO-
effects on yeasts, effects of caffeine on mutagenic, 25:42332

GUINEA PIGS
radiation effects on electromyogram of muscles of, effects of dose on γ, 25:42552
radiation effects on survival of, protective effects of cyclophosphamide against whole-body x, 25:42518

GYMNOSPERMIDAE
Pinus sp., radiation effects on growth of, effects of ozone on gamma, 25:42316(R) (ORO-3299-107)
Zamia intergrifolia, radiation effects on root tip chromosomes of, in comparison to cycasin, emulsin, and methylazoxymethanol, aberrant x, 25:42334

H

H.B. ROBINSON POWER REACTOR, UNIT 2
boilers for, cladding failure on primary side of, 25:44016 (DOCKET-50261-54)
emergency core cooling system for, preoperational flow test for, 25:44045 (DOCKET-50261-65)
emergency diesel generators for, design parameters and operations aspects of, 25:44046 (DOCKET-50261-66)
radioactive waste evaporator for, inadequate performance of liquid, 25:44017 (DOCKET-50261-63)

HI REGIONS
radio recombination line H137α in, in direction of NGC 2024, detection of, (E), 25:43050

HII REGIONS
optical depth of several, (E), 25:43059
photometry of, radio and optical, (E), 25:43059
spectral emission feature in W3, detection of, (E), 25:43054

HADRONS
flux in cosmic radiation at atmospheric depth of 976 gcm^{-2} above 12 GeV, spark chamber study of ratio of neutron to charged, (E), 25:43621
interactions at high energies, review of multiparticle production in, (E/T), 25:43579
interactions of, electromagnetic contributions to total cross sections for, 25:43616
interactions of, two-Reggeon-particle and triple-Reggeon couplings from duality sum rule from di-triple Regge limits in inclusive, (T), 25:43570 (NYO-2262-TA-247)
interactions with hadrons at high energies, multiperipheral model for momentum spectrum of hadronic secondaries in two-body, (T), 25:43620
interactions with hadrons, duality and absorption in qualitative model for amplitudes of two-body elastic, (T), 25:43617
interactions with hadrons, duality relations with chiral symmetry breaking for, (T), 25:43619
interactions with hadrons, multiple quark scattering analysis for charge exchange, (T), 25:43615
interactions with photons at high energies, vector-dominance model of, 25:43597
mass spectra from ω decay, SO(4,3) group for, 25:43635
production in two-body strong interactions at high energies, multiperipheral model for momentum spectrum for, 25:43620
widths on leading Regge trajectory, dual oscillator model for total, (T), 25:43619

HAFNIUM
analysis for hydrogen by isotopic equilibration mass spectrometry, 25:41747 (AAEC/TM-588)
chemical thermodynamic properties of, selected values of, 25:41826 (NBS-TN-270-5)
coating with oxide films by heating in carbon dioxide atmosphere, 25:42819(P)
compounds, thermodynamic properties of, tables of, 25:41825 (NBS-TN-270-5)
determination in titanium by neutron activation, 25:41761
separation from acetone--hydrochloric acid solutions by ion exchange using Bio-Rad, distribution coefficients for, 25:41899
separation from zirconium by solvent extraction, 25:41917
HAFNIUM ALLOYS AND SYSTEMS
coating with oxide films by heating in carbon dioxide atmosphere, 25:42819(P)
Hf--Nb, superconducting critical current density of, effect of heat treatment and impurities on, 25:43290 (ORNL-4703)
HAFNIUM CARBIDES
thermal expansion to 2500°C, 25:42966
HAFNIUM ISOTOPES Hf-177
isomeric transitions in, lifetime of, (E), 25:42222
HAFNIUM ISOTOPES Hf-179
energy-level scheme from tantalum-178 decay, (E), 25:43917
HAFNIUM ISOTOPES Hf-182
beta decay of, γ singles and coincidence spectra from, (E), 25:43935
HAFNIUM OXIDES
HfO_2--Y_2O_3, phase diagrams of, 25:42883 (IS-T-425)
HALDEN BOILING REACTOR
fuel elements for, cladding failure mechanisms for, 25:42882
fuel elements in, irradiation testing of IFA-30, 25:44208 (KAE-69-31)
fuel elements in, irradiation testing of IFA-30, 25:44207 (KAE-69-45)
HALOCARBONS
ionization on graphite and thoriated tungsten, 25:41778 (UCRL-20500, pp 1-85)
HAMSTERS
immunization against tumors using x-irradiated SV-40 transformed kidney cells, 25:42305
radiation effects on activity of intestinal phosphatases in, whole-body γ, 25:42301
radiation effects on glomerulus enlargement in kidneys of, combined effects of chronic hypoxia and ozone injections on, 25:42636
radiation effects on teeth of, in utero x, 25:42649
HANDLING AND STORAGE
regulations for radioactive materials, in aircraft, 25:42455
regulations for radioactive materials, in aircraft, 25:42457
standards for preparing components for, 25:41970 (RDT-F-7-2-T)
HANDS
radiation dose to, of workers during transport of strontium-90--yttrium-90 source, thermoluminescent dosimetric monitoring of β, 25:42444
HASTELLOY X
chemical reactions with plutonium oxide (PuO_2)--uranium oxide (UO_2) fuels, effects of gas cooled fast breeder reactor conditions on, (E/T), 25:44123 (ORNL-TM-3385)
HEAD
radiation dose to, of workers during transport of strontium-90--yttrium-90 source, thermoluminescent dosimetric monitoring of β, 25:42444
radiotherapy of carcinomas of, additive effects of 5-fluorouracil infusion on gamma and x, 25:42589
HEALTH PHYSICS
development of Temple University office of, criteria for, 25:42503
experiences at nuclear power centers in Italy, 25:42478
procedures for handling accidents resulting in radiation exposure or contamination of personnel, 25:42391
HEART
radiation effects on beat rate of rat, effects of dose and prenatal exposure on x, 25:42640
radiation effects on lipolytic activity in rat, in relation to heparin content, sensitizing effects of cysteamine on x, 25:42281
radioinduced injuries in human, following therapy for neoplasms of thoracic organ, 25:42704
HEAT EXCHANGERS
optimization code for, 25:44265 (K-1799)
performance of large component test facility sodium, evaluation of, 25:42804(R) (LMEC-71-1)
standard for seamless annealed nickel--chromium--iron alloy tubes for, 25:42782 (RDT-M-3-4-T)
tube joints for sodium heated, x-ray and ultrasonic methods for inspection of, 25:44148 (CONF-700224-, Paper 4)
HEAT PIPES
boiling in liquid metal, method for calculating surface heat flux for incipient, 25:41982
design and performance of multiple, in radiator system for cooling thermoelectric generators, 25:41978
design and performance of, western European research programs on, 25:41976
performance for cooling or heating thermionic converters, western European research programs on, 25:41976
performance of lithium, for heating thermionic converters, (E), 25:41977
performance of potassium and sodium, for cooling thermionic converters, (E), 25:41977
use for dissipating excess heat in thermoelectric generators, evaluation of, 25:42002
HEAT-RESISTING ALLOYS AND METALS
deposition on substrates, method for vapor, 25:42823
properties of, chemical, electric, electronic, mechanical, optical, thermal, vacuum, 25:42853
HEAT SOURCES
development of radioisotope, ORNL program for, 25:41993(R) (ORNL-4592)
performance of spherical radioisotope, in ISOTEC thermoelectric generator for space power systems, 25:42006
thermal insulation for, program for development of multi-foil, 25:42962
HEAT TRANSFER
book: Heat and Mass Transfer in Turbulent Boundary Layers. Vol. II, 25:41988
book: Heat and Mass Transfer in Turbulent Boundary Layers. Vol. I, 25:41987
book: Heat and Mass Transfer. Vol. II. (In Russian), 25:41986
calculation of steady-state and transient, in two-dimensional geometries, computer program for, 25:41985 (ORNL-TM-3324)
calculation of surface, for incipient boiling in liquid metal heat pipes, method for, 25:41982
HEAT TRANSFER SYSTEMS
standard for welding, examining, and testing of liquid metal, 25:42849 (RDT-F-6-1-T)
HEATED EFFLUENTS
effects on ecology of aquatic animals and plants, guidelines for presite survey for establishment of, 25:44269 (NP-18843)
thermal plume physical characteristics from Lake Michigan power plants, (E), 25:44138 (CONF-710431-1)
use of warm water from power reactors for food production, economics of, 25:44022
uses of nuclear power plant, to supplement water supplies by regional canal systems, 25:44083 (BNWL-SA-2738)
HEAVY WATER ORGANIC-COOLED REACTOR
physics calculations for, CLIP code for manipulation of THREDES code for, 25:44095 (AI-CE-Memo-12)
HELIUM
abundance in inner solar system, from solar-wind gas-saturated cosmic dusts, (E/T), 25:43176
abundance in upper atmosphere, theoretical studies of, 25:43207 (AD-706130)
density and size distribution of bubbles of, in irradiated and annealed foils of aluminum and aluminum--aluminum oxide, transmission electron microscopy of, 25:42896
effects on ductility of irradiated chromium--iron--manganese--molybdenum--nickel and chromium--iron--nickel alloys at 500 to 800°C, 25:42872
effects on self radiolysis of carbon dioxide--tritium systems, 25:41852 (LA-4657)
electron reactions with, line shapes of He^- states and autoionizing states in ionization curve for, (E), 25:43139
electron scattering at 34 to 100 eV by, polarization effects on angular dependence of, (T), 25:43138
energy levels of, atomic-beam magnetic-resonance measurement of 2^3P_0--2^3P_1 fine-structure interval, 25:43122
energy levels of, calculation of S and P states, 25:43115
energy loss at 10 MeV to 100 GeV in silicon, calculations of most probable, (T), 25:42155
helium-ion reactions at 20 to 100 keV with, absolute excitation cross sections for, (E), 25:43128
helium-ion reactions with, charge-exchange cross sections for, (T), 25:43157
hydrogen-ion (H_2^+) reactions at 15 to 40 keV with, polarization of helium 3^1P--2^1S line excited by, (E), 25:43129
plasma of, interactions with inhomogeneous transverse magnetic fields, (E), 25:43355
plasma of, ion temperature measurement using multi-channel Fabry--Perot interferometer, 25:43341
plasma of, multichannel system for determination of time-varying spectral line profiles from, 25:43343
polarizability of atomic, perturbation calculation of, 25:43117
proton energy straggling and stopping at 100 to 500 keV in, (E/T), 25:43432
proton reactions at 15 to 40 keV with, polarization of helium 3^1P--2^1S line excited by, (E), 25:43129
reactions with argon, helium, and neon at 13 to 50 keV of ground-state and metastable atoms of, cross sections for one-electron loss in, (E), 25:43153
reactions with helium and hydrogen atoms, dipole moment induced in, (T), 25:43136
rigidity spectrum of nuclei of, in primary cosmic

radiation, (E), 25:43178
solubility in liquid sodium, effects of pressure and temperature on, 25:41823 (ANL-7802)
HELIUM IONS
channeling in sodium chloride at 1 MeV, (E), 25:41832(R) (AECL-3851)
effects on infrared spectra of silicates at 5 keV, 25:43446
effects on thin silicon crystals at 1.8 MeV, dimpling induced in, (E), 25:43438
energy levels of He^-, from electron reactions with helium, (E), 25:43139
implantation in silicon at 220 keV, measurements of stresses induced by damage from, 25:43441
reactions with argon at 30 to 130 keV, cross sections for argon L-shell x-ray emission in, (E), 25:43134
reactions with helium atoms at 20 to 100 keV, absolute excitation cross sections for, (E), 25:43128
reactions with helium, charge-exchange cross sections for, (T), 25:43157
reactions with nitrogen molecules at 0.05 to 200 eV, application of statistical phase-space theory to molecular and dissociative charge exchange in, 25:43159
HELIUM ISOTOPES
distribution and origin of, in Apollo 12 samples, (E), 25:43099
HELIUM ISOTOPES He-3
abundance of nuclei of, in primary cosmic radiation, (E), 25:43173
body form factors for, resonating-group calculation of, (T), 25:43797
deuteron reactions (d,p) at 250 to 850 keV, angular distribution and absolute cross section for, (E), 25:43793
interactions ^4He + ^3He, shell interpretation of separable potentials for, (E), 25:43786
meson reactions (π^-,π^+) at 140 MeV, differential cross sections for three-neutron resonance in, (T), 25:43751
proton elastic scattering at 0.5 to 40.0 MeV, phase-shift analysis using resonating-group method of, (T), 25:43797
proton elastic scattering at 1.51 to 23.25 MeV, resonating-group calculations of differential cross sections for, (T), 25:43797
radiation effects on performance of in-pile neutron detectors of, γ, (T), 25:44103
reactions (He-3,α) with lithium-7 at 16 to 18 MeV, angular distributions for, (E), 25:43809
reactions (He-3,d) with ytterbium-172, -174, and -176 at 28 MeV, deuteron spectra and angular distributions for, (E), 25:43942
reactions (He-3,dγ) with iron-54, d--γ coincidence spectra from, (E), 25:43858
reactions (He-3,He-5) with carbon-12, magnesium-24, and oxygen-16 at 68 MeV, Q values and spectra from, (E), 25:43823
reactions (He-3,He-5) with carbon-12, magnesium-24, and oxygen-16 at 68 to 70 MeV, Q-values for, (E), 25:43808
reactions (He-3,Li-5) with beryllium-9, analysis using tetragonal graphs, (T), 25:43961
reactions (He-3,n) with tritium at 0.7 to 3.8 MeV, DWBA analysis of differential cross sections, excitation functions, polarizations, and spectra from, (E), 25:43796
reactions (He-3,np) with tritium at 2.7 and 3.55 MeV, differential cross sections for, (E), 25:43796
reactions (He-3,p) with aluminum-27 at 5 MeV, analysis including Coulomb distortion and finite-range effects, (T), 25:43964
reactions (He-3,t) with A = 42 through 68 nuclei at 24.6 MeV, triton spectra from, (E), 25:43883
reactions (He-3,t) with argon-40, form factors and distorted waves from DWBA analysis of, (T), 25:43842
reactions (He-3,t) with calcium-48 and strontium-88 at 23 MeV, distorted-wave analysis of angular distributions from, (T), 25:43848
reactions (He-3,t) with zirconium-90 and -96 at 21 MeV, distorted-wave analysis of angular distributions from, (T), 25:43848
reactions with lithium-7 at 1 to 2 MeV, analysis of neutron continuum from, (E), 25:43788
scattering by iron-58, titanium-48, and zirconium-90 at 37.7 MeV, optical-model analysis of elastic, (E/T), 25:43878
scattering by nickel-58 at 36.8 to 38.1 MeV, optical-model analysis of elastic, (E/T), 25:43878
spin waves in pure, possible NMR experiment on, (T), 25:43280
He-3--He-4, spin waves in solutions of, possible NMR experiment on, (T), 25:43280
HELIUM ISOTOPES He-4
abundance of nuclei of, in primary cosmic radiation, (E), 25:43173
binding energy of, calculation using Brueckner theory with realistic potentials, (T), 25:43794
binding energy of, variational calculation using hard-core potential, 25:43787
Brueckner--Hartree--Fock calculations for, 25:43785
critical velocity of normal fluid in liquid II, mechanism for, (T), 25:43275
electron reactions (e,pt) at 50 and 100 MeV, coincidence spectra from, (E), 25:42131
heat transfer from horizontal wires to liquid II at high heat-flux values, (E), 25:43282
helium atoms in, off-diagonal long-range order and momentum distribution of, (T), 25:43317
helium-3 impurities in liquid II, (T), 25:43273
interactions ^4He + ^3He, shell interpretation of separable potentials for, (E), 25:43786
interactions ^4He + ^4He, shell interpretation of separable potentials for, (T), 25:43786
interactions d + ^4He, shell interpretation of separable potentials for, (T), 25:43786
interactions t + ^4He, shell interpretation of separable potentials for, (T), 25:43786
neutron scattering from superfluid, in impulse approximation, (T), 25:43278
nuclear charge form factor of, effect of tensor forces on, (T), 25:43783
phonon dispersion in liquid, calorimetric evidence for, 25:41778 (UCRL-20500, pp 1-85)
proton elastic scattering at 1 to 23 MeV, phase-shift analysis for, (T), 25:43781
second sound reflection by liquid II surface, (E), 25:43279
superfluid density of liquid II in restricted geometries, (E/T), 25:43287
superfluid flow in, dissipation in, (E), 25:43283
superfluid transition temperature in, depression by heat current of, 25:43286
theory of superfluid, point transform, 25:43274
thermohydrodynamic equations of liquid II, modification of dissipative terms in, (T), 25:43281
three-body correlations in liquid II, contribution to binding energy and depletion of, (T), 25:43277
vortex ring dynamics in superfluid, effect of ion drag on quantized, 25:43276
he-3--He-4, spin waves in solutions of, possible NMR experiment on, (T), 25:43280
HEMAGGLUTININS
radiation effects on formation of, in mice, exposure rate dependence of γ, 25:42307
HEMATOPORPHYRIN
effectiveness as carrier for palladium-109 for selective ablation of lymph nodes in dogs, 25:42312
HEMOGLOBIN
radioinduced changes in chemical composition of mouse, effects of dose rate on chronic whole-body γ, 25:42586 (ORAU-113, pp 4-77)
HEPARIN
effects on lipolytic activity in x-irradiated rat heart tissues, 25:42281
HEPTANE
heptane--TBP--$UO_2(NO_3)_2$, diffusion studies on, 25:41829
HEPTATHIAZOCINE
reactions with hydroxides, halides, and borohydrides, 25:41778 (UCRL-20500, pp 1-85)
HERBICIDES
research on, review of radioisotopes in, 25:42239
HEXANOIC ACID, 6-AMINO-
effects on x-radioinduced increase in capillary permeability in rabbit skin, 25:42617 (UR-49-1462)
radiation effects on antifibrinolytic activity of, in blood of patients with carcinomas, γ, 25:42293
HIGH-ENERGY PHYSICS
research at Brown Univ., Sept. 1970 to June 1971, (T), 25:43569(R) (NYO-2252-TA-245)
research at Ohio State Univ., June 1970 to June 1971, (E/T), 25:43566(R) (COO-1545-99)
HIROSHIMA
atomic bombing of, radiation effects on incidence of late aplastic anemia in survivors of, 25:42698
atomic bombing of, radioinduced cataracts in survivors of, occurrence and pathology of latent, 25:42546
HISTAMINE
radiation effects on metabolism of, in animals and man as indicators of radiation injury, x, 25:42626
radiation effects on metabolism of, in animals as indicator of radiation injury, x, 25:42627
HODOSCOPES
design of spark chamber, for extensive air showers, 25:42158
development of fast neutron, 25:42048 (ANL-7710, pp 263-364)
geometrical considerations for detecting cosmic ray showers, 25:42157
HOLMIUM
determination in meteorites by neutron activation and high-voltage electrophoresis, 25:41776
properties of monocrystals of, at low temperatures, elastic and magnetoelastic, 25:41833(R) (IA-1218)
HOLMIUM ALLOYS AND SYSTEMS
Al--Ho--Ni, magnetic properties of $HoAl_{2-x}Ni_x$, 25:43480
HOLMIUM HYDRIDES
electron band structure of, 25:43125
positron annihilation in, angular correlation of radiation from, (E), 25:43126
HOLMIUM ISOTOPES Ho-158
decay scheme for, 25:42110
HOLMIUM ISOTOPES Ho-159
decay scheme for, 25:42110

XUM

electron-capture decay of, γ singles and coincidence spectra and conversion electron intensities from, (E), 25:43944
HOLMIUM ISOTOPES Ho-165
neutron capture by, resonance spin assignments for, (E), 25:43884 (ANL-7710, pp 1-52)
neutron total cross section at 100 to 650 keV, optical model analysis of average, (E/T), 25:43908
proton elastic and inelastic scattering at 16 MeV, differential cross sections for, (E), 25:43901
HOLMIUM OXIDES
analysis form impurities, cathode region method for spectrochemical, 25:41833(R) (IA-1218)
HOMOSERINE DEHYDROGENASE
aspartate kinase--homoserine dehydrogenase, radiation effects on inactivation of threonine-sensitive, from E. coli, mechanism of x, 25:42291
HORMONES, ADRENAL
epinephrine, radiation effects on metabolism of, in animals as indicator of radiation injury, x, 25:42626
epinephrine, radioprotective effects on rat tissues and organs, mechanism of in vitro and in vivo, 25:42523
hydrocortisone, effects on eruption of teeth of rats following prenatal exposure, 25:42638
norepinephrine, radiation effects on metabolism of, in animals as indicator of radiation injury, x, 25:42626
HORMONES, PITUITARY
luteinizing hormone, radioimmunoassay in serum of monkeys, method for, 25:42237
thyrotropin, radiation effects on content of human serum following therapy of lymphomas, x, 25:42695
HORMONES, THYROID
radiation effects on formation of antibodies against, comparison of iodine-131 and uranium nitrate, 25:42645
thyroxine, effects on eruption of teeth of rats following prenatal exposure, 25:42638
HOSPITALS
radiation protection for patients and personnel of, ICRP recommendations on, 25:42476
HOT CELLS
fire prevention and protection in, performance of detectors and extinguishing agents for, 25:42036 (DP-1242)
HUMBOLDT BAY POWER REACTOR
quality assurance program for, 25:44026 (DOCKET-50133-59)
radioactive effluents from, clarification of annual average offsite exposures from, 25:44003 (DOCKET-50133-58)
HYDRAZINE
effects of derivatives of, on redox potential of spleen, 25:42526
HYDROCARBONS
spectra of, effects of pressure on ir, 25:41778 (UCRL-20500, pp 1-85)
yields of light, from radiolysis of petroleum residues after distillation, 25:41853 (NP-18817)
HYDROGEN
abundance in inner solar system, from solar-wind gas-saturated cosmic dusts, (E/T), 25:43176
abundance in upper atmosphere, theoretical studies of, 25:43207 (AD-706130)
determination in metals by isotopic equilibration mass spectrometry, 25:41747 (AAEC/TM-588)
determination in Zircaloy fuel cladding by neutron radiography, qualitative and quantitative, 25:41755
determination relative to tritium in water, mass spectroscopic, 25:41729
diffusion from sintered thorium dioxide and thorium dioxide--uranium dioxide pellets at 800 to 2000°C, effects of carbon content on, 25:42958 (WAPD-TM-850)
diffusion in palladium at -60 to 200°C, comparison with deuterium, 25:41815
effects on brittleness of TRIP steel, 25:42886 (UCRL-20500, pp 85-145)
effects on mechanical properties of irradiated Types A302B, A542, and HY-80 steels, 25:42871
electron reactions at 100 to 450 eV with atomic, Balmer optical excitation cross sections for, (E), 25:43137
electron reactions with atomic, complex-energy calculation of ionization amplitudes for, 25:43145
electron reactions with molecular, at gas temperatures of 300 to 1300°K, cross sections for dissociative electron attachment in, (E), 25:43155
electron scattering at 34 to 100 eV by molecular, polarization effects on angular dependence of, (T), 25:43138
electron scattering by atomic, pseudostates in close-coupling formalism for, (T), 25:43140
energy levels of molecular, eigenvalues and expectation values for bound and quasi-bound ground-state, (T), 25:43123
energy levels of molecular, lifetimes of quasi-bound rotational--vibrational, (T), 25:43124
interaction between three atoms of, long-range, (T), 25:43207 (AD-706130)
interactions between two atoms of, energies of, (T), 25:43165
Lamb shift in, crossed-graph contribution to fourth-order, 25:43687
lattice structure of solid, phonons and librons in, (T), 25:44261 (JUL-734-FF)
metallic state of, structure and stability of lithium dihydrogen fluoride as form of, 25:43475
monitoring in liquid sodium, electrochemical meter for continuous, 25:42207(R) (UNC-5258)
neutron elastic scattering at 0.1 to 30.0 MeV, total and differential cross sections and polarizations for, (T), 25:43798
physical state of interstellar clouds of, (T), 25:43080 (N-71-21563)
plasma of, production by laser irradiation of solid target, 25:43380 (IPP-4/9)
production and properties of atomic beams of, at 15 to 30 keV, 25:43109
production from organic waste materials using heat from contained underground nuclear explosion, feasibility study of, 25:41955
proton energy straggling and stopping at 100 to 500 keV in, (E/T), 25:43432
reactions between atoms of, resonance energies and widths in, (T), 25:43124
reactions with gases up to 20 MeV of atomic, review of cross sections for electron capture and loss in, (E), 25:43145
reactions with helium of atomic, dipole moment induced in, (T), 25:43136
separation from deuterium, electrochemical, 25:41832(R) (AECL-3851)
spectra of, beam--foil measurements of fine structure in Lyman-α, 25:43151
spectra of, field induced absorption, 25:43120
spectra of, Lyman-α emission line of whole solar disk during 1969, (E), 25:43075
x-ray yields of μ-mesic, as functions of density, (T), 25:43125
yields from electron pulse radiolysis of oxalic acid, kinetics of production of, 25:41850(R) (CEA-N-1438)
yields from electron radiolysis of hydrogen sulfide, effects of sulfur hexafluoride on, 25:41860
yields from γ radiolysis of aqueous solutions of metals, 25:41833(R) (IA-1218)
yields of atomic, from γ radiolysis of aqueous solutions of sodium acid phosphite, kinetics of production of, 25:41850(R) (CEA-N-1438)
HYDROGEN IONS
abundance in HI region in direction of NGC 2024, (E), 25:43050
HYDROGEN IONS (H^-)
photon reactions with, cross sections for electron detachment in, (T), 25:43140
reactions with gases up to 20 MeV, review of cross sections for electron loss in, (E), 25:43149
HYDROGEN IONS (H_2^+)
positron reactions with, vibrorotational excitation in, (T), 25:43141
reactions with helium at 15 to 40 keV, polarization of helium 3^1P--2^1S line excited by, (E), 25:43129
reactions with nitrogen molecules at 30 keV to 2 MeV, cross sections for excitation of N_2^+ 3914-A radiation in, (E), 25:43151
HYDROGEN PEROXIDES
reactions with uranyl sulfates in reactor aqueous fuel solutions, (E), 25:44166
yields from electron pulse radiolysis of oxalic acid, kinetics of production of, 25:41850(R) (CEA-N-1438)
HYDROGEN SULFIDES
radiolysis at high dose rates, effects of sulfur hexafluoride on hydrogen yields from electron, 25:41860
radiolysis of, electron pulse, 25:41832(R) (AECL-3851)
HYDROQUINONE, 2,5-DI-tert-BUTYL-
reactions with bis(2-ethylhexyl) phosphate extracts of plutonium and fission products for plutonium reduction, 25:41912(P)
HYDROURACIL, 6-HYDROXY-5-METHYL-
yields of cis- and trans-, from γ radiolysis of thymine in deaerated solutions, 25:41874
HYDROXYL (HO)
content at 50 to 85 km in mesosphere, altitude-dependent upper limit of, (E/T), 25:43262
detection of interstellar, in external galaxies, (E), 25:43083
radio emission from water in southern hemisphere regions containing, (E), 25:43051
HYPERFINE STRUCTURE
tables of hyperfine fields for substitutional impurities in cobalt, gadolinium, iron, and nickel, 25:43469 (UCRL-20411)
HYPERFRAGMENTS
decay $^{\Lambda}Li^7 \rightarrow {}^6He + {}^3He + \pi$, effects of ^3He--t--Λ cluster structure of $^{\Lambda}Li^7$ on angular and energy distributions from, (T), 25:43608
hyperon (Λ) binding energy in $^{\Lambda}He^4$ and $^{\Lambda}He^5$, K-harmonics method for ΛN potential for, (T), 25:43652
HYPERONS (Λ)
binding energy in $^{\Lambda}He^4$ and $^{\Lambda}He^5$, K-harmonics method for ΛN potential for, (T), 25:43652
binding energy in nuclear matter, ΛN coupling to virtual ΣN channel effects on, (T), 25:43648
coupling of ΛN to virtual ΣN for Λ + N scattering and Λ binding in nuclear matter, (T), 25:43648
interactions Λ + d at 100 to 300 MeV/c, probe of Λ--N

core potential from cross sections for, (T), 25:43651
interactions Λ + N at low energies, ΛN coupling to virtual ΣN channel effects on, (T), 25:43648
interactions Λ + N, cross sections of Λ + d interactions at 100 to 300 MeV/c as probe of core potential for, (T), 25:43651
HYPERONS (Σ)
coupling of virtual ΣN to ΛN for Λ + N scattering and Λ binding in nuclear matter, (T), 25:43648
HYPOXIA
effects on x radiosensitivity of rat tissues in combination with AET, MEA, or serotonin, 25:42511

I

ICE
oxygen-18 fractionation between water vapor and, 25:41921
ICE-d_2
elastic constants and order--disorder transitions in, effects of hydrofluoric acid doping on, 25:41812
ICELAND
economic impact of exportation of radiation-processed cod fish, lobster tails, and shrimp on, 25:42746 (STI/DOC-10/124)
IMMUNE REACTIONS
book: Radiation Immunology and Transplantation, 25:42310
evaluation of cellular, against tumor-specific antigens using tumor cells labeled with tritiated thymidine, 25:42309
radiation effects on bacteriophage 341, effects of dose on γ, 25:42740
radiation effects on, in dogs to tissue transplants, effectiveness of metalloporphyrins as carriers for selective palladium-109 β, 25:42312
radiation effects on, in leukemia patients treated with allogenic bone marrow transplants, additive effects of antilymphocyte globulin on γ, 25:42586 (ORAU-113, pp 4-77)
radiation effects on, in mice, combined effects of drugs and sublethal γ, 25:42572
radiation effects on, of mice to virus, x, 25:42313
IMMUNITY
book: Radiation Immunology and Transplantation, 25:42310
transfer to Hymenolepis nana by injection of spleen cells from immunized donor mice into pre-irradiated recipient mice, 25:42311
INCOLOY 800
annealing in uranium monocarbide powder, precipitation behavior after, 25:42844 (EURFNR-922)
mechanical properties of, effects of annealing in uranium monocarbide powder on, 25:42844 (EURFNR-922)
INCONEL X750
weld defects in, origin and effects of, 25:42867
INCONEL 600
weld defects in, origin and effects of, 25:42867
INCONEL 718
annealing in uranium monocarbide powder, precipitation behavior after, 25:42844 (EURFNR-922)
friction and wear of, sliding against similar material in liquid sodium, 25:42804(R) (LMEC-71-1)
mechanical properties of, effects of annealing in uranium monocarbide powder on, 25:42844 (EURFNR-922)
INDIA
mineral prospecting in, status of nuclear methods for, 25:41947
radiation levels in, seasonal variations in natural background, 25:42387
uranium prospecting in, use of radon content of soils for, 25:41945
INDIAN POINT POWER REACTOR, UNIT 1
cooling system for, design modifications for 4 inch nozzle sleeve for primary make-up water line of, 25:44024 (DOCKET-50003-80)
INDIAN POINT POWER REACTOR, UNIT 2
safety evaluation of, AEC Regulatory Staff, 25:44039 (DOCKET-50247-46)
INDIAN POINT POWER REACTOR, UNIT 3
design parameters of, revised and additional data on, 25:44053 (DOCKET-50286-38)
fuel storage pool for, effects of tornado driven missiles on, 25:44052 (DOCKET-50286-37)
operations aspects of, revised and additional data on, 25:44053 (DOCKET-50286-38)
site for, meteorological data for, 25:44053 (DOCKET-50286-38)
INDIUM
analysis by mass spectrography, isotopic, 25:41727
compounds, indium-115 relaxation rates and NMR in, 25:43894
deformation at 4°K, recovery after, 25:41832(R) (AECL-3851)
determination of trace amounts of, in meteorites by neutron activation and γ spectrometry, 25:41773
effects on superconducting critical field of niobium--titanium alloy wires, 25:43309
properties of superconducting films of, for radiation detection, 25:42080
separation from acetone--hydrochloric acid solutions by ion exchange using Bio-Rad, distribution coefficients for, 25:41899
separation from aqueous solutions by ion exchange on zirconium tellurate, tracer studies on, 25:41915
separation from other metals using inorganic ion exchange papers, 25:41909
superconducting parameter calculations, 25:43305
thermomagnetic effects in normal and superconducting, 25:43289 (NYO-2150-71)
INDIUM ALLOYS AND SYSTEMS
Au--In, nuclear quadrupolar relaxation rates in $AuIn_2$, effects of melting on, 25:43496
Ag--Cd--In, fabrication of reactor control rods of, methods for, 25:42822
Ge--In, mixing in liquid and solid phases of, energy of, 25:42970
In--Pb, thermal conductivities at low temperatures of normal and superconducting, 25:43324
In--Pb-base, magnetic anisotropy in superconducting, with Ginzburg--Landau parameter greater than 2-/super $1/2$/, (E/T), 25:43294
In--Pb-base, superconducting critical current in single crystals of, effects of plastic deformation on, 25:43300
INDIUM ISOTOPES In-113
determination in presence of indium-115 by mass spectrography, 25:41727
effectiveness of metastable, for brain scanning for lesion differentiation, 25:42577
separation of enriched tin-112 from exhausted generators of metastable, electrolytic method for, 25:41833(R) (IA-1218)
INDIUM ISOTOPES In-114
beta and electron-capture decay of, half-life for, (E), 25:42222
INDIUM ISOTOPES In-115
determination in presence of indium-113 by mass spectrography, 25:41727
neutron capture by, cross sections and gamma spectra from thermal, (E), 25:43891(T) (RFP-Trans-78)
nuclear charge distribution of, determination from μ-mesic x-ray spectra, 25:43904
x-ray spectra of μ-mesic atoms of, (E), 25:43904
INDIUM ISOTOPES In-116
energy level at 230 keV from indium-115 neutron capture, spin assignment for isomeric, (E), 25:43891(T) (RFP-Trans-78)
isomeric transition in, half-life, internal conversion coefficients, and gamma spectra from, (E), 25:43891(T) (RFP-Trans-78)
nuclear electric and magnetic moments of, determination from NMR spectra and relaxation rates, (E), 25:43894
INDOLE-3-ACETIC ACID, 5-HYDROXY-
radiation effects on metabolism of, in animals and man as indicators of radiation injury, x, 25:42626
radiation effects on metabolism of, in animals as indicator of radiation injury, x, 25:42627
INDUSTRIAL MANAGEMENT
personnel injuries in privately owned and operated establishment using atomic energy in USA during 1968, 25:42498 (NP-18858)
INFORMATION CENTERS
bulletin and status report of Research Materials, 25:44281 (ORNL-RMIC-11)
information scanning and processing at Nuclear Safety, 25:44280 (ORNL-NSIC-48)
INFORMATION RETRIEVAL SYSTEMS
audiovisual communication methods for, 25:41833(R) (IA-1218)
INORGANIC COMPOUNDS
research progress on, 25:41777(R) (UCRL-20500)
INORGANIC PYROPHOSPHATASE
radiation effects on activity in rat brain and liver, continuous whole-body γ, 25:42277
INSECTA
ants, ecology in rain forest in Puerto Rico, 25:42317(R) (PRNC-147)
Apis sp., radioactivity in, measurement of fallout β and γ, 25:42374
Bombyx mori, radiosensitivity of oocytes of, effects of meiotic stage on x, 25:42609
Callosobruchus maculatus, radiation effects on emergence of adult, from infested grains, 25:41833(R) (IA-1218)
Ceratitis capitata, radiosterilization in Nicaragua using sterile release technique, 25:42750
Ceratitis capitata, radiosterilization of male, comparison of effectiveness of adult and pupal exposure for γ, 25:42751
Choristoneura fumiferana, sperm precedence in, carbon-14 and tritium tracer studies on, 25:42259
Culex pipiens, radioinduced chromosome translocations resulting in semisterility of, effects of dose on x, 25:42335
Diatraea saccharalis, radiation effects on survival of inbred and outbred lines of laboratory populations of, γ, 25:42611
Drosophila melanogaster, radiation effects on life span and ultrastructure of midgut cells of, γ, 25:42612
Drosophila melanogaster, radioinduced chromosome translocations in, following exposure of male pupae, x, 25:42354
Drosophila melanogaster, radioinduced interchanges in mature oocytes of, segregation of chromosomes following

XUM

x, 25:42276
Drosophila melanogaster, radioinduced mutations in spermatogonia of, comparison of effects of acute, chronic, and split-dose exposure on low-dose γ, 25:42350
Drosophila melanogaster, radioinduced Y chromosome aberrations in male, segregation of rearrangements following x, 25:42344
Drosophila sp., radioinduced chromosome translocations in oocytes of, effects of dose on frequency of x, 25:42333
Sitotraga cerealella, radiation effects on female and male, in relation to percent flying-off and sex ratios among progeny, comparison of sub-sterilizing γ, 25:42610
Trichoplusia ni, radiosterilization of culture media for larvae of, effects of dose on γ, 25:42749
INSECTICIDES
research on, review of radioisotopes in, 25:42239
INSTRUMENTS
calibration of, standard for, 25:42205 (RDT-F-3-2-T)
description of JAERI modular, 25:42186 (JAERI-13768)
development at Risoe, April 1--Sept. 30, 1970, 25:42205(R) (RISO-M-1357)
development in Israel, 1959, 25:41833(R) (IA-1218)
specifications for JAERI modular, 25:42185 (JAERI-13605)
INTERFEROMETERS
design of microwave, for plasma density measurements, 25:42183(T) (CTC-756)
performance of multi-channel Fabry--Perot, for plasma ion temperature measurement, 25:43341
INTERNAL CONVERSION
coefficients for outer shells and ratios to inner shells for Z = 37 to 100 nuclei for transition energies of 50 to 500 keV, tables of, (T), 25:43931
INTERSTELLAR MATERIAL
density of, cosmic-ray study of, (E), 25:43173
detection of silicon monoxide in, (E), 25:43052
distribution of, (T), 25:43080 (N-71-21563)
effects on Hα intensities of H II regions, (E), 25:43059
INTESTINES
effects of radioprotective thiols on ultrastructure of duodenum crypt cells in mice, effects of thiol-blocking compounds on, 25:42520
radiation effects on jejunum stem cells in mouse, relation of animal survival to dose dependent, 25:42633
radiation effects on phosphatase activity in hamster, whole-body γ, 25:42301
radioisotope sorption by animal, use of ion exchange resins for prevention of, 25:42263
INVARIANCE PRINCIPLES
chiral and conformal invariance, theory of spontaneous breakdown of, 25:43662
CP violation in rate for $K_2^0 \rightarrow 2\pi$ decay, (E), 25:43657
CPT violation in K^0 decays, (T), 25:43656 (PITHA-44)
time reversal invariance tests in electromagnetic final-state interaction contribution to triple-product correlation coefficient in energy-level transitions in nuclear beta decay, (T), 25:43660
time reversal tests in Coulomb final-state interaction corrections to $K_2^0 \rightarrow \pi + l + \nu$ and $K_2^0 \rightarrow \pi + \pi + l + \nu$ decays, (T), 25:43550
IODINE
determination by photon activation using cesium as internal standard, 25:41765
determination in sedimentary minerals by Szilard--Chalmers reactions following neutron activation, 25:41763
determination in selenium by melting with sodium hydroxide and potentiometry using ion-selective electrode, 25:41734
determination of trace amounts of, gas chromatographic method for, 25:41745
photoinduced isotopic exchange between iodobenzene and, mechanism of uv, 25:41833(R) (IA-1218)
separation from fission products by selective negative surface ionization, 25:41833(R) (IA-1218)
IODINE IONS
energy-loss spectra in gold (111) and (100) channels at 15 and 21.6 MeV, 25:43454
IODINE ISOTOPES
exchange between molecular iodine and organic iodides, iodine-catalyzed, 25:41817
yields from thermal neutron fission of uranium-235, 25:41833(R) (IA-1218)
yields in uranium-235 thermal neutron fission, (E), 25:41833(R) (IA-1218)
IODINE ISOTOPES I-123
energy levels from tellurium-122 proton resonances, widths, spin-parity assignments, and spectroscopic factors for, (E), 25:43933
IODINE ISOTOPES I-125
energy levels from tellurium-124 proton resonances, widths, spin-parity assignments, and spectroscopic factors for, (E), 25:43933
incorporation in angiotensins, method for, 25:42241
use for labeling hepatitis-associated antigen for radioimmunoassay, 25:42306
use in double-antibody radioimmunoassay for Australia antigen, 25:42308
IODINE ISOTOPES I-127
energy levels from neutron inelastic scattering, spin--parity assignments for, (T), 25:43914
energy levels from tellurium-126 proton resonances, widths, spin-parity assignments, and spectroscopic factors for, (E), 25:43933
neutron elastic scattering at 4.0 MeV, optical-model analysis of, (T), 25:43914
neutron inelastic scattering at 0.2 to 0.8 MeV, resonance-theory calculations of excitation functions for, (T), 25:43914
nuclear charge distribution of, determination from μ-mesic x-ray spectra, 25:43904
nuclear hyperfine structure constants of, M1 and E2, (E), 25:43949
x-ray spectra of μ-mesic atoms of, (E), 25:43904
x-ray spectra of μ-mesic, analysis of intensity anomalies using resonance process, (E/T), 25:43949
IODINE ISOTOPES I-131
beta decay of, γ-γ angular correlations from, (E), 25:43896
content in drinking water in USA, standards for maximum permissible, 25:42470
content in EWA reactor vessel air and coolant water, determination of, (E), 25:44155 (INR-1295)
content of milk in Canada, Central and South America, and USA during November 1970, 25:42421
content of milk in Canada, Central and South America, and USA during 1970, 25:42417
dose to human thyroid glands, evaluation of nuclear power reactor sites in relation to potential accidental, 25:44147
effectiveness for quantitative thyroid scanning in comparison to metastable technetium-99, 25:42569
effectiveness of human serum albumin-incorporated, for scanning brain of children for differential diagnosis of congenital arachnoid cysts and Dandy-Walker cysts, 25:42568
effectiveness of iodoquine-incorporated, for scanning human eyes for localization of melanomas, 25:42563
effectiveness of Rose Bengal-incorporated, for diagnosis of jaundice in man, 25:41833(R) (IA-1218)
effects on formation of antibodies against thyroid hormones, 25:42645
energy levels from tellurium-130 proton resonances, isobaric analog, (E), 25:43918
gamma spectra of, for accuracy in diagnosis, phantom measurements on, 25:42397
incorporation in iodoquinine, 25:42563
metabolism and tissue distribution following intake by man, 25:42467
metabolism in frogs and newts following injection, 25:44288 (RLO-2227-T-8-1)
production of carrier-free, by sorption on platinum black from acid solutions of neutron-irradiated magnesium tellurate, 25:41880
radiation effects on distribution and excretion of orotic acid-incorporated, in rats as indicator of radiation injury, whole-body γ, 25:42407
release to environment during operation of boiling water nuclear power plants, programs for monitoring, 25:42388
testing of, produced in Japan, application, 25:41990 (JAERI-13617)
transport through forage--cow--milk--man food chains following injection into atmosphere as aerosol mist, 25:42370 (SWRHL-43-r)
IODOQUINE
labeling with iodine-131, 25:42563
ION BEAMS
parameters of, magnetic analyzer system for measuring, 25:43746
production from cathode materials in vacuum breakdown, (E), 25:43383
production of high-current, performance of hot-cathode constricted-arc plasma sources for, 25:43401
production using charge exchange between atomic beams, 25:43135(P)
ION EXCHANGERS
bibliography on inorganic, 25:41879 (JAERI-13726)
ION SOURCES
description of heavy-ion, for simulating fast-neutron radiation damage, 25:43758
design of multiply-charged calcium and zinc, for cyclotron, 25:43765
design using charge exchange between atomic beams, 25:43135(P)
development of stabilized thermal, for mass spectrometers, 25:41833(R) (IA-1218)
performance of hot-cathode constricted-arc plasma, for high-current neutral and positive beams, 25:43401
performance of laser and discharge, for multicharged ions, 25:43731 (JINR-P7-5177)
IONOSPHERE
characteristics of broad-band frequency electric fields and electromagnetic waves in, (E/T), 25:43246
D region, characteristics from sounding rocket measurements, (E), 25:43215 (N-71-17052)
D region, electron temperature in, (T), 25:43207 (AD-706130)
D region, electron-loss rates during polar-cap absorption events, (E), 25:43256

D region, if pulse reflection from, relation with particle precipitation at latitudes below 40°N, (E/T), 25:43223
D region, model of electrical structure of, (E), 25:43208 (AD-714365)
density variations in heterosphere, effect of altitude and temperature variations on semiannual, (E/T), 25:43258
disturbances at 200 to 600 km in, polar-substorm-related traveling, (E), 25:43217 (N-71-18502)
disturbances in midlatitude, relation with polar substorms, large-scale traveling, (E/T), 25:43250
E region, characteristics from sounding rocket measurements, (E), 25:43215 (N-71-17052)
E region, model of Arctic, (E), 25:43212 (AD-715893)
E region, model of electrical structure of, (E), 25:43208 (AD-714355)
electron loss during 1968 nighttime PCA event, comparison with 1962 nuclear event, (E/T), 25:43269
electron-density irregularities in, ambient electron density-dependent occurrences of, (E/T), 25:43268
F region, electron density enhancements in midlatitude nighttime, from westward electric fields, (E/T), 25:43253
F region, height and equatorial-width variations of, effect of solar activity on annual post-sunset, (E/T), 25:43228
F region, ion-drift vertical velocity in, expansion-, contraction-, and wind-related, (E/T), 25:43224
F region, model of Arctic, (E), 25:43212 (AD-715893)
F1 layer, electron and ion temperature, correlation with electron density, (E/T), 25:43229
F2 layer, electron and ion temperature, correlation with electron density, (E/T), 25:43229
F2 layer, electron density in undisturbed, diurnal and seasonal, (T), 25:43230
F2 layer, ionization of noon, geomagnetic-controlled geographic distribution of, (E/T), 25:43227
F2 layer, plasma drifts in global, effect of upper atmospheric winds on, (T), 25:43225
gravity-wave interaction with, during Mar. 7, 1970 solar eclipse, (E/T), 25:43270
ion clouds in, mechanism of striated irregularities in, (E/T), 25:43252
ion temperature in equatorial nighttime, incoherent scatter and retarding-potential analyzer measurements at 400 to 650 km of, (E/T), 25:43251
nitrogen-ion emission in auroral, differential electron-flux determination from N^{2+} and N_2^+, (E), 25:43214 (N-71-16589)
noise origin at auroral latitudes, lower hybrid resonance, (E/T), 25:43246
oxygen density from 80 to 140 km in, molecular, (E/T), 25:43261
plasma interaction with neutral atmospheric motion, (T), 25:43225
proton enhancements during Feb. 25, 1969 event over polar cap, mechanism of, (E/T), 25:43232
proton penetration to polar caps during Jan. 24, 1969 event, asymmetric access of solar, (E), 25:43233
proton precipitation during 1968 nighttime PCA event, relation to electron loss estimates, (E/T), 25:43269
radio-wave propagation across transverse, Faraday rotation of, (T), 25:43254
review papers from NATO Advanced Study Institute on Polar Ionosphere and Magnetospheric Processes, Apr. 9-18, 1969, 25:43226
sporadic E, frequency characteristics during solar cycles in daytime, over South Pacific, (E), 25:43265
sporadic E, horizontal ionic convergence from atmospheric-produced gravity waves in, enhancement mechanism for, (E/T), 25:43255
sporadic E, model of Arctic, (E), 25:43212 (AD-715893)
stable red arc formation at 300 to 700 km at plasmapause, ring-current heat source for, (T), 25:43242
structure in bottomside, relation to spatial periodic electron density of periodic, (E), 25:43209 (AD-714993)

IONS
atomic oscillator strengths along isoelectronic sequences, (E/T), 25:43114
energies of helium-sequence, relativistic corrections to eigen-, (T), 25:43207 (AD-706130)
energies of lithium-sequence, correlation, (T), 25:43207 (AD-706130)
energy levels of two-electron up to Z = 10, calculation of S and P states, 25:43115
implantation in solid surfaces, review of improved methods for, 25:41992 (ORNL-4640)
implantation into semiconductors, design of electrostatic accelerators for, 25:43740(P)
nuclear charges in many-electron, effective, (T), 25:43162
reactions with atoms, calculation of symmetric charge-exchange cross sections for, using Hartree--Fock--Slater wave functions, 25:43157
wave functions for atomic and triatomic, even-tempered atomic orbitals as bases for, (T), 25:43160 (IS-T-456)

IRIDIUM
determination of trace amounts of, in meteorites by neutron activation and γ spectrometry, 25:41773
separation from aqueous solutions by ion exchange on zirconium tellurate, tracer studies on, 25:41915
separation from other metals using inorganic ion exchange papers, 25:41909
separation of radioactive platinum isotopes from neutron-irradiated, by paper chromatography, 25:41920

IRIDIUM ALLOYS AND SYSTEMS
Ir--IrO_2--SrO, phase studies of, 25:43005
Ir--Th, superconducting transition temperature in high T/sub c/ intermetallic $ThIr_2$, sensitivity to residual stress of, (E), 25:43302

IRIDIUM ISOTOPES Ir-191
energy levels from platinum-191 decay, spin-parity assignments for, (E), 25:43902
energy-level transitions from platinum-191 decay, multipolarities and internal conversion coefficients for, (E), 25:43902

IRIDIUM ISOTOPES Ir-192
testing of, produced in Japan, application, 25:41990 (JAERI-13617)
use for interstitial therapy, mathematical models for internal dose distribution during, 25:42428
use for interstitial therapy, methods for protection of other patients and personnel during, 25:42477

IRIDIUM OXIDES
Ir--IrO_2--SrO, phase studies of, 25:43005

IRON
analysis of standards of ductile, for antimony, arsenic, and vanadium by neutron activation and γ spectrometry, 25:41774
corrosion of stressed, at various potentials of magnesium chloride, scanning electron microscopic studies of, 25:42760(R) (COO-2069-7)
determination following separation from other metal ions by thin-layer chromatography using quercetin, colorimetric, 25:41743
determination in minerals from Luzon, Philippines, by neutron activation, 25:41772
effects of trivalent, on yields of cresol isomers from electron or γ radiolysis of toluene--water, 25:41858
effects on superconducting critical field of niobium--titanium alloy wires, 25:43309
effects on yields of phenol from electron or γ radiolysis of benzene--water systems, 25:41858
energy loss at 10 MeV to 100 GeV in silicon, calculations of most probable, (T), 25:42155
hyperfine fields for substitutional impurities in, tables of, 25:43469 (UCRL-20411)
neutron reactions at 200 eV to 200 keV with natural, R-matrix analysis of total cross sections for, (E/T), 25:43874
neutron transmission through, spectrometer for measurement of fast, (E), 25:44205
oxygen-ion (O^{5+}) reactions at 30 MeV with, resolved structure in Kα x rays produced by, (E), 25:43110
phase transitions of, 25:41778 (UCRL-20500, pp 1-85)
radiation effects on mechanical properties of, relations of microstructure with fast neutron, 25:42925
radiation effects on microstructure of, relations of aluminum and nitrogen on fast neutron, 25:42908
separation from acetone--hydrochloric acid solutions by ion exchange using Bio-Rad, distribution coefficients for, 25:41899
separation from aqueous solutions by ion exchange on zirconium tellurate, tracer studies on, 25:41915
separation from gallium-67 produced by deuteron irradiation of zinc by ion exchange, 25:41881
separation from other metals using inorganic ion exchange papers, 25:41909

IRON ALLOYS AND SYSTEMS
mechanical properties of sintered intermetallic compounds of, 25:42818
Al--Cr--Fe-base, properties for use in high-temperature strain gages, 25:42804(R) (LMEC-71-1)
Al--Cr--Fe-base--Y, properties for use in high-temperature strain gages, 25:42804(R) (LMEC-71-1)
Al--Fe-base, microstructure of alpha-phase, in K-state, 25:42886 (UCRL-20500, pp 86-146)
C--Cr--Fe-base, radiation effects on graphitization of malleable cast, fast neutron, 25:42904
C--Fe--Mo-base, phase diagrams at 1200 and 1800°C, isothermal, 25:42889
C--Fe--Mo-base, properties of, mechanical and physical, 25:42889
C--Fe--Ni--V, crystal twinning in bulk and thin-foil, structure of transformation-type, 25:42886 (UCRL-20500, pp 86-146)
C--Fe-base--Mn, radiation effects on graphitization of malleable cast, fast neutron, 25:42904
Cr--Cu--Fe--Mo--Nb--V--Zr-base, corrosion resistance of, 25:42811
Cr--Fe, sintering of intermetallic compounds of, kinetics of, 25:42818
Cr--Fe--Ni, corrosion cracking in, containing trace chlorides, studies on mechanism of stress, 25:42760(R) (COO-2069-7)
Cr--Fe--Ni, standard for plates, sheets, and strips of, 25:42794 (RDT-M-5-4-T)
Cr--Fe--Sn--Zr-base, properties for use in water-cooled reactors, 25:42875
Cr--Fe--Zr-base, corrosion by steam and water at 300 to 400°C, kinetics of, 25:42815

XUM

Cr--Fe-base--Mn--Mo--Ni, ductility of irradiated Sandvik 12R72HV, at 500 to 800°C, effects of injected helium on, 25:42872
Cr--Fe-base--Ni, ductility of irradiated Inco IN-744X, at 500 to 800°C, effects of injected helium on, 25:42872
Cu--Fe, thermal capacity at low temperatures, 25:41778 (UCRL-20500, pp 1-85)
Cu--Fe--Ni, phase decomposition in, kinetics of spinodal, 25:42886 (UCRL-20500, pp 86-146)
Cu--Fe--Zr-base, oxidation by steam at 500°C, effects of crystal structure and impurities on, 25:42810
Fe--Mo, mechanical properties of sintered intermetallic compounds of, 25:42818
Fe--Mo, sintering of intermetallic compounds of, kinetics of, 25:42818
Fe--Nb--Ta--Ti-base--Zr, description of superconducting, 25:43318(P)
Fe--Ni, crystal twinning in bulk and thin-foil, structure of transformation-type, 25:42886 (UCRL-20500, pp 86-146)
Fe--Ni, dissolution in sulfuric acid, effects of solution analysis versus direct current readout methods on results from potentiostatic, 25:42760(R) (COO-2069-7)
Fe--Ni--W, phase diagram of, at 800 to 1650°C, 25:42887 (Y-1785)
Fe--Ni--Zr, radiation effects on properties of fuel cladding of, in-pile, 25:43010
Fe--Np, magnetic properties of cubic Laves phase in intermetallic compound $NpFe_2$, Moessbauer studies on, 25:41833(R) (IA-1218)
Fe--Pd--Si, Moessbauer effect study of amorphous, 25:44238 (CALT-822-32)
Fe--Pu, magnetic properties of cubic Laves phase in intermetallic compound $PuFe_2$, Moessbauer studies on, 25:41833(R) (IA-1218)
Fe--U, magnetic properties of cubic Laves phase in intermetallic compound UFe_2, Moessbauer studies on, 25:41833(R) (IA-1218)
Fe-base--Mn--Ni--Ti, mechanical properties of, effects of aging on, 25:42886 (UCRL-20500, pp 86-146)
Fe-base--Ni--Ti, mechanical properties of, effects of aging on, 25:42886 (UCRL-20500, pp 86-146)
Fe-base--Ta, tensile properties of, effects of intermetallic compound formation on, 25:42886 (UCRL-20500, pp 85-145)

IRON BORIDES
preparation of, method for, 25:42944
thermal capacity of, low-temperature, 25:42974
CoB--FeB, thermal capacity of, low-temperature, 25:42974
FeB--MnB, thermal capacity of, low-temperature, 25:42974

IRON CHLORIDES
sorptive properties of surfaces of, for krypton and xenon, thermodynamic studies on stepwise isotherms for, 25:41824 (CEA-R-4089)

IRON COUPLES
Constantan/Fe, standard for, 25:42196 (RDT-C-7-1-T)
Constantan/Fe, standard for magnesium oxide-insulated and sheathed thermocouple, 25:42197 (RDT-C-7-2-T)

IRON FLUORIDES
energy levels in high-temperature vapors of, 25:42557 (UCRL-20500, pp 147-73)

IRON IONS
reactions with argon at 30 to 130 keV, cross sections for argon L-shell x-ray emission in, (E), 25:43134

IRON ISOTOPES
cobalt--iron Coulomb displacement energies, (E), 25:43883
iron--manganese Coulomb displacement energies, (E), 25:43883

IRON ISOTOPES Fe-54
deuteron reactions (d,p) at 5 to 12 MeV, cross section and vector analyzing power for, (E), 25:43846
energy levels from neutron reactions, resonance parameters for, (E/T), 25:43874
helium-3 reactions (He^3,dγ) with, d--γ coincidence spectra from, (E), 25:43858
helium-3 reactions (He^3,t) at 24.6 MeV, triton spectra from, (E), 25:43883
proton reactions (p,nγ) at 10 MeV, angular distributions and spectra from, (E), 25:43863

IRON ISOTOPES Fe-55
energy levels from iron-54 (d,p) reactions, spectroscopic factors and spin assignments for, (E), 25:43846

IRON ISOTOPES Fe-56
electron reactions at 150 GeV, self-coupling of weak lepton currents in anti ν + ν pair production in, (T), 25:43612
energy levels from neutron reactions, resonance parameters for, (E/T), 25:43874
helium-3 reactions (He^3,t) at 24.6 MeV, triton spectra from, (E), 25:43883
meson (μ) reactions at 150 GeV, self-coupling of weak lepton currents in anti ν + ν pair production in, (T), 25:43612
neutrino reactions at 10 GeV, self-coupling of weak lepton currents in μ^+--μ^- pair production in, (T), 25:43612

IRON ISOTOPES Fe-57
deuteron reactions (d,p) at 5 to 12 MeV, cross section and vector analyzing power for, (E), 25:43846
energy levels from lead-207 (γ,n) reactions, parameters for resonance, (E), 25:43929
energy levels from neutron reactions, resonance parameters for, (E/T), 25:43874
energy-level transitions from cobalt-57 beta decay, effects of chemical environment on internal conversion ratios for, (E), 25:43865
energy-level transitions from cobalt-57 electron-capture decay, total internal conversion coefficients for, (E), 25:43882
energy-level transitions from cobalt-57 electron-capture decay, ionization (shakeoff) accompanying internal-conversion, (E), 25:43871
gamma acoustic resonance signal, (T), 25:43493
helium-3 reactions (He^3,t) at 24.6 MeV, triton spectra from, (E), 25:43883
photon reactions (γ,n) at 11.5 MeV endpoint energy, neutron energy spectra from, (E), 25:43929

IRON ISOTOPES Fe-58
energy levels from proton inelastic scattering, spin-parity assignments and deformation parameters for, (E), 25:43840
helium-3 elastic scattering at 37.7 MeV, optical-model analysis of angular distributions for, (E/T), 25:42878
helium-3 reactions (He^3,t) at 24.6 MeV, triton spectra from, (E), 25:43883
proton inelastic scattering at 49.4 MeV, DWBA analysis of angular distributions for, (E), 25:43840

IRON ISOTOPES Fe-59
metabolism and tissue distribution following intake by man, 25:42467

IRON OXIDES FeO
chemical activity in sodium silicate at 700 to 1100°C, 25:42957 (UCRL-20500, pp 147-73)

IRRADIATION FACILITIES
description of cylindrical cobalt-60, 25:42015
furnace for, design and performance of Chouca, 25:41980
gamma sources for, data tabulations on dose distribution for cesium-137 and cobalt-60, 25:41957 (BNL-50147(Rev.))

ISOCITRATE DEHYDROGENASE
radiosensitivity of, role of sulfhydryl group destruction in x, 25:42299

ISOPROPYLAMINE
radiolysis at 77°K, ESR studies on trapped radicals produced by γ, 25:41857

ISOTOPE EFFECTS
research progress on isotope separation based on, 25:41897(T) (ORNL-tr-2512)

ISOTOPE EXCHANGE
technique for measuring self-diffusion coefficients in glasses, 25:41810

ISOTOPE SEPARATION METHODS
columns for, steady-state distribution of multicomponent isotopic mixtures in, 25:42011
development and efficiency improvement during 1968 and 1969, review of ORNL program for, 25:41992 (ORNL-4640)
efficiency of, equations for evaluation of, 25:41897(T) (ORNL-tr-2512)

ISOTOPES
deposition on solid surfaces, review of methods for, 25:41992 (ORNL-4640)
separation from multicomponent mixtures, column parameters for, 25:42011
separation of heavy, fundamental equations for physical principles of ultracentrifuge, 25:41994
separation of, development of electromagnetic sector-type equipment for, 25:41992 (ORNL-4640)

ITALY
atmospheric stability in, Pasquill's criteria for calculation of frequency of, 25:41936
health physics experiences and personnel protection standards at nuclear power centers in, 25:42478
radioactive contamination of population groups in, effects of physiological factors on, 25:42375
radioactivity calibration and dosimetry in, enforcement of legislation on, 25:42509
radioactivity monitoring in atmosphere of, surveillance network for, 25:41937
radioisotope content of food in Pavia, 25:42389
radioisotope deposition in bones of cattle in, during 1962 to 1968, polonium-210 and strontium-90, 25:42382

J

JAPAN
radiation protection programs at Atomic Energy Research Institute in, 25:42481
radiation protection programs at Atomic Energy Research Institute in, 25:42480
radiation protection programs for personnel performing diagnostic radiography in, evaluation of, 25:42486
radioactivity in food and water in, programs for establishing standards for maximum permissible concentrations of, 25:42482
radioisotope production and use in, 1965 to 1967, 25:41990 (JAERI-13617)

JAPANESE EXPERIMENTAL FAST REACTOR
construction of JOYO, summary of, 25:44091

JUPITER (PLANET)
radio source on, angular diameter of, (E), 25:43064

K

KAOLINITES
dehydroxylation reactions in compacted, 25:42957 (UCRL-20500, pp 147-73)
KIDNEYS
radiation effects on content of sulfur-containing amino acids in proteins in rat, 25:42265
radiation effects on glomerulus enlargement in hamster, combined effects of chronic hypoxia and ozone injections on, 25:42636
radiation effects on human, following therapy, evaluation of leucine aminopeptidase and malate dehydrogenase activity as indicator of, 25:42409
radiation effects on metabolism of selenium-75 and sulfur-35 in rat, x, 25:42264
radioinduced diseases of rat, neptunium-237, 25:42253
scanning of human, for measurement of glomeruli filtration rate, evaluation of radioisotope methods for, 25:42574
scanning of human, method for bloodstream background subtraction in, 25:41933(R) (IA-1218)
KRYPTON
electron reactions with, autoionizing states produced by, (E), 25:43154
photon reactions at 0.29 to 8.03 keV with, relative abundances of multiply charged ions produced by, (E), 25:43142
proton energy straggling and stopping at 100 to 500 keV in, (E/T), 25:43432
sorption by surfaces of cadmium, cobalt, iron, lead, and nickel halides, thermodynamic studies on stepwise isotherms for, 25:41824 (CEA-R-4089)
KRYPTON IONS
implantation in silicon at 220 keV, measurements of stresses induced by damage from, 25:43441
reactions with carbon at 20 keV to 1.5 MeV, cross sections for K x-ray production in, (E), 25:43107
reactions with nitrogen molecules at 0.05 to 200 eV, application of statistical phase-space theory to molecular and dissociative charge exchange in, 25:43159
reactions with nitrogen molecules at 30 keV to 2 MeV, cross sections for excitation of N_2^+ 3914-A radiation in, (E), 25:43151
KRYPTON ISOTOPES
yields from thermal neutron fission of uranium-235, 25:41833(R) (IA-1218)
yields in uranium-235 thermal neutron fission, (E), 25:41833(R) (IA-1218)
KRYPTON ISOTOPES Kr-77
beta and electron-capture decay of, γ singles and coincidence spectra from, (E), 25:43843
KRYPTON ISOTOPES Kr-85
determination of metastable, by chromatography and counting, 25:41753(P)
separation from other krypton isotopes, review of improved methods for, 25:41992 (ORNL-4640)
use as tracer for detection of microdefects in materials, 25:42029
KRYPTON ISOTOPES Kr-88
determination in gases by chromatography and counting, 25:41753(P)
KYANITES
radiation effects on infrared spectrum of, 5-keV proton, deuteron, helium-ion, and nitrogen-ion, 25:43446

L

LA CROSSE BOILING-WATER REACTOR
cooling system pump speed comparator of, unscheduled shutdown from failure of, 25:43999 (DOCKET-1155-124)
instrumentation of, performance test failure of safety system pressure channel, 25:43998 (DOCKET-1155-123)
operations history for April 1971, 25:44020(R) (TID-25737)
steam isolation valve for, failure of reactor building main, 25:44000 (DOCKET-1155-125)
LABORATORIES
operation of radiological, personnel training and radiation safety factors in, 25:42500
LACQUERS
decontamination of Italian, effects of time and atmosphere on, 25:42041
LACTATE DEHYDROGENASE
radiation effects on activity and isoenzyme patterns of, in organs and serum of rats, protective effects of methylene blue against γ, 25:42284
radiation effects on activity of, in man following therapy as indicator of cell damage, 25:42409
LACTATION
effects on calcium-47 and strontium-85 metabolism in rats, 25:42255
LAMINATES
molding of, compression, 25:44226(R) (BDX-613-327)
superconductivity in, plasma waves and, (T), 25:43314
LANTHANUM
determination in cast steel standards by neutron activation and γ spectrometry, 25:41774
determination in meteorites by neutron activation and high-voltage electrophoresis, 25:41776
electron band structure calculations, 25:43500
separation from acetone--hydrochloric acid solutions by ion exchange using Bio-Rad, distribution coefficients for, 25:41899
separation from aqueous solutions by ion exchange on zirconium tellurate, tracer studies on, 25:41915
LANTHANUM BORIDES
crystal lattice parameters of single crystals of LaB_6, 25:42947
growth of single crystals of LaB_6, 25:42947
properties of single crystals of LaB_6, mechanical and thermal, 25:42947
LANTHANUM FLUORIDES
preparation and stability of La_2F_6, 25:42957 (UCRL-20500, pp 147-73)
LANTHANUM ISOTOPES La-139
energy levels from gamma resonance scattering, spin-parity assignments for, (E), 25:41833(R) (IA-1218)
neutron reactions (r,α) at 14.2 MeV, level-density parameters and spectra from, (E), 25:43886 (INR-1268)
LANTHANUM OXIDES
analysis for impurities, cathode region method for spectrochemical, 25:41833(R) (IA-1218)
LARYNX
radiotherapy of carcinomas of, effectiveness of preoperative gamma and x, 25:42588
LASER RADIATION
absorption by inhomogeneous laser-produced plasma, (E/T), 25:43400
reactions with solid hydrogen and deuterium targets, plasma production from, (E/T), 25:43380 (IPP-4/9)
LASERS
performance for production of multicharged ions, 25:43731 (JINR-P7-5177)
radiation effects of boron-10 (n,α) reaction on power and efficiency of carbon-dioxide, 25:42229
use for exploding deuterium--tritium pellets, 25:43398 (ORNL-TM-3231)
LAVA
radioactivity distribution in granite, from nuclear explosion cavity, 25:41953 (CEA-R-4099)
LEAD
bonding to 6061-T6 aluminum plates for use as gamma shields for Omega West Reactor, 25:42816 (LA-4644)
creep of polycrystalline, kilocycle acoustic emission during, (E), 25:42862
deformation at low temperature, recovery of normal and superconducting, 25:41832(R) (AECL-3851)
determination of trace amounts of, in zinc, spectrochemical, 25:41833(R) (IA-1218)
effects on graphite--nitrous oxide and graphite--oxygen reactions, catalytic, 25:42931
magnetic structure of superconducting intermediate state of, (E/T), 25:43295
photon reactions at 1.1 GeV, nucleon distribution and π^0 mean free path in nuclei from π^0 production in, 25:43595
rectification effect in thin-film superconducting, in small, oscillatory magnetic fields, 25:43304
separation from acetone--hydrochloric acid solutions by ion exchange using Bio-Rad, distribution coefficients for, 25:41899
separation from other metals using inorganic ion exchange papers, 25:41909
strong interaction radius from π^0 photoproduction at 1.1 GeV, 25:43595
superconducting energy gap and Fermi velocity in single-crystal films of, electron tunneling measurement of, 25:43312
superconducting energy gap in, photoelectric observation of, 25:43311
superconducting parameter calculations, 25:43305
superconducting proximity effect in Cu/Pb/Cu sandwiches, acoustic surface wave study of perpendicular field, 25:43315
superconductive tunneling in diodes with tin and tin oxide, effects of 2.5-GHz longitudinal microwaves on currents in, (E), 25:43316
superconductive tunneling in Josephson junctions with copper and lead oxide, proximity effects in, 25:43308
x-ray backscattering at 11.3 to 23.2 MeV, (E), 25:43431
LEAD ALLOYS AND SYSTEMS
In--Pb, thermal conductivities at low temperatures of normal and superconducting, 25:43324
In--Pb-base, magnetic anisotropy in superconducting, with Ginzburg--Landau parameter greater than 2^{-}/super $1/2$, (E/T), 25:43294
In--Pb-base, superconducting critical current in single crystals of, effects of plastic deformation on, 25:43300
Pb-base--Tl, magnetic anisotropy in superconducting, with Ginzburg--Landau parameter greater than 2^{-}/super $1/2$, (E/T), 25:43294
Pb-base--Tl, magnetic structure of superconducting intermediate state of, (E/T), 25:43295
LEAD IODIDES
sorptive properties of surfaces of, for krypton and xenon, thermodynamic studies on stepwise isotherms for,

25:41824 (CEA-R-4099)
LEAD ISOTOPES Pb-203
energy-level scheme from bismuth-203 decay, (E), 25:43906
LEAD ISOTOPES Pb-204
energy-level scheme from bismuth-204 decay, (E), 25:43905
LEAD ISOTOPES Pb-207
energy levels from lead-207 (γ,n) reactions, parameters for resonance, (E), 25:43929
energy levels from lead-208 (p,d) reactions, calculations of amplitudes and spectroscopic factors using particle--vibration-coupling model, (T), 25:43976
isomeric transitions in, lifetime of, (E), 25:42222
photon reactions (γ,n) at 8.4 MeV endpoint energy, neutron energy spectra from, (E), 25:43929
photon reactions (γ,n) at 9.8 MeV endpoint energy, neutron energy spectra from, (E), 25:43929
triton elastic scattering at 20 MeV, optical-model analysis of, (E), 25:43923
triton reactions (t,p) at 20 MeV, distorted-wave analysis of differential cross sections and spectra from, (E/T), 25:43923
LEAD ISOTOPES Pb-208
alpha elastic scattering at 104 MeV, differential cross sections for, (E), 25:43832 (NP-18920)
energy levels from proton inelastic scattering, spin--parity assignments for neutron particle-hole, (E), 25:43907
energy levels of, TDA shell-model calculation of spectroscopic factors and wave functions for negative-parity, (T), 25:43926
photon reactions (γ,n) at 9.8 MeV endpoint energy, neutron energy spectra from, (E), 25:43929
proton elastic and inelastic scattering with isobaric analog excitation, excitation functions and angular distributions for, (E), 25:43907
LEAD ISOTOPES Pb-209
energy levels from lead-207 (t,p) reactions, spectroscopic factors and spin-parity assignments for, (E/T), 25:43923
energy levels from lead-208 (d,p) reactions, calculations of amplitudes and spectroscopic factors using particle--vibration-coupling model, (T), 25:43976
energy levels of, calculation using particle--vibration-coupling formalism for amplitudes and single-particle pickup spectroscopic factors for, (T), 25:43974
LEAD ISOTOPES Pb-210
content of atmosphere, rain, and soil in India, relation of seasonal variations in natural background radiation to, 25:42387
content of uranium mining personnel following inhalation of radon-222, tracer study in baboons on, 25:42245(R) (NYO-3086-10(Vol.1))
metabolism in baboons following injection, tracer study of, 25:42245(R) (NYO-3086-10(Vol.1))
LEAD ISOTOPES Pb-214
content in rat organs and tissues following inhalation of radon-222, 25:42248
LEAD OXIDES
PbO--WO_3, phase studies of, 25:43006
LEAD SULFIDES
sorptive properties for gold, 25:41771
LEAD TITANATE ZIRCONATES
properties of, ferroelectric and sintering, 25:42957 (UCRL-20500, pp 147-73)
LEAD TITANATES
radiation effects on ferroelectric crystals of, 25:43442
LEAD URANYL VANADATES
crystal structure of, 25:43000
LEAD ZIRCONATES
radiation effects on ferroelectric crystals of, 25:43442
LEAKS
detection in hermetically-sealed assemblies, 25:44233(R) (BDX-613-431)
LEUCINE AMINOPEPTIDASE
radiation effects on excretion of, in human urine following therapy as indicator of kidney damage, 25:42409
LEUKOCYTES
radiation effects on human and mouse, partial-body bremsstrahlung, 25:42599
radiation effects on rabbit serum count of, effects of dose on whole-body x, 25:42648
radiation effects on survival of, in peripheral blood of man, γ, 25:42585 (ORAU-113, pp 4-77)
radioinduced chromosome aberrations in, in Japanese fishermen, latent fallout, 25:42681
LEUKOPOIESIS
radiation effects on rabbit bone marrow, protective effects of glutathione against γ, 25:42536
LEVEL INDICATORS
design and testing of inductive, for liquid metals, standard for, 25:42192 (RDT-C-5-1-T)
design and testing of resistive, for liquid metals, standard for, 25:42193 (RDT-C-5-2-T)
LIGASES
effects of polynucleotide, on radioinduced DNA strand breaks, 25:42255
role in repair of uv-radioinduced breaks in DNA of T4 phage, 25:42297
LIGHT
transport of polarized, in half-space problems, (T), 25:43423
velocity in Einstein and Newton gravitational theories, 25:43694
LIGNITE DEPOSITS
prospecting in India, status of nuclear methods for, 25:41947
LIMERICK POWER REACTOR, UNIT 1
design parameters of, revised and additional data on, 25:44061 (DOCKET-50352-15)
operations aspects of, revised and additional data on, 25:44061 (DOCKET-50352-15)
LIMERICK POWER REACTOR, UNIT 2
design parameters of, revised and additional data on, 25:44061 (DOCKET-50352-15)
operations aspects of, revised and additional data on, 25:44061 (DOCKET-50352-15)
LIMONITE CONCRETES
properties for use as shielding for gamma radiation protection, mechanical and physical, 25:42976
barite concrete--limonite concrete, properties for use as shielding for gamma radiation protection, mechanical and physical, 25:42976
limonite concrete--zircon, properties for use as shielding for gamma radiation protection, mechanical and physical, 25:42976
LINEAR ACCELERATORS
beam analyzing system for ETL 33-MeV electron, method for calibration of, 25:43749
beam current stability of induction, 25:43745
beam transport system for ETL 33-MeV electron, 25:43764
description of ETL 33-MeV electron, 25:43752
description of Hiroshima Univ. variable-energy electron, for research and radiotherapy, 25:43754
design modification and performance of ETL 33-MeV electron, 25:43755
design modification proposal for JAERI 20-MeV electron, 25:43730 (JAERI-13567)
experimental facility for ETL 33-MeV electron, quantameter for x-ray energy fluence measurements at, 25:43750
experimental facility for ETL 33-MeV electron, x-ray target, 25:43751
operation and performance of Kerume Univ. 13-MeV, for radiotherapy, 25:43753
performance for radiographic inspection of steel plate, 25:44113 (CONF-700224-, Paper 8)
LINEAR ENERGY TRANSFER
relation to quality factor in radiation dosimetry, 25:42440
LIPOPOLYSACCHARIDES
radioprotective effects of, on mouse adrenal cortex and reticulo-endothelial systems, comparison of cysteamine and serotonin with x, 25:42513
LIQUID FLOW
magnetohydrodynamic three-dimensional, in diverging rectangular ducts under strong transverse magnetic fields, (T), 25:43205
LIQUID METAL FAST BREEDER REACTOR
coolant combustion accidents in, release and transport of aerosols and energy from sodium, (E/T), 25:44132 (AI-AEC-12992)
fuel cycle optimization for, 2DBCOST computational system for, 25:44130
fuel elements for, thermal performance limits for pin type, 25:44121 (HEDL-SA-89)
fuels for, development of plutonium nitride--uranium nitride, (E), 25:44118(R) (BMI-1905)
fuels for, effects of fission process on creep of, (E/T), 25:44118(R) (BMI-1905)
fuels for, high temperature irradiation performance of, (E/T), 25:44118(R) (BMI-1905)
instrumentation for, development of ultrasonic thermometry, 25:42189(R) (NYO-3906-5)
kinetics of 1000 MW(e), comparison of fuels and core sizes for, 25:44095 (ANL-7710, pp 53-262)
kinetics of, effects of refractory metal cladding on, 25:44096 (ANL-7710, pp 53-262)
kinetics of, effects of sodium coolant boiling on, (E/T), 25:44132 (AI-AEC-12992)
physics measurement programs during January to March 1971, 25:44094(R) (AI-AEC-12991)
physics measurements for, review of critical assemblies experimental programs for, (E), 25:44096 (ANL-7710, pp 53-262)
safety programs during January to March 1971, 25:44132 (AI-AEC-12992)
subcriticality measurements by noise analysis in, effects of γ radiation on detector performance in, (T), 25:44103
LIQUIDS
Landau description of quantum, (T), 25:43511
radioinduced rupture of thin films of, bubble nucleation model of, 25:41835
LITHIUM
abundance in α Aur, (E), 25:43036
compounds, analysis for lithium-6 and lithium-7 by thermal neutron activation, Cherenkov and proportional detector arrangement for, 25:41833(R) (IA-1218)
determination of trace amounts of, in alfalfa, spectrochemical, 25:41833(R) (IA-1218)

energy loss at 10 MeV to 100 GeV in silicon, calculations of most probable, (T), 25:42155
polarizability of atomic, perturbation calculation of, 25:43117
separation from acetone--hydrochloric acid solutions by ion exchange using Bio-Rad, distribution coefficients for, 25:41899
spectra of, isotope shift in, 25:43207 (AD-706130)
superconductivity of, search for, 25:41778 (UCRL-20500, pp 1-85)

LITHIUM ACID FLUORIDES
structure and stability of LiH_2F as metallic hydrogen form, 25:43475

LITHIUM CARBIDES
radiation effects on, reactions of recoil nitrogen-13 from deuteron, 25:41886

LITHIUM CARBONATES
separation of fluorine-18 from irradiated, method for, 25:41833(R) (IA-1218)

LITHIUM CHLORIDES
LiCl--$NaNO_3$, molal volumes for aqueous solutions of, 25:41833(R) (IA-1218)

LITHIUM FERRATES
properties of, effects of processing on magnetic and physical, 25:42957 (UCRL-20500, pp 147-73)

LITHIUM FLUORIDES
creep of monocrystalline, at high temperatures, 25:42957 (UCRL-20500, pp 147-73)
radiation effects on electric properties of sodium-doped monocrystals of, neutron, 25:43445

LITHIUM HYDRIDES
density of grains of, formed by compression of lithium hydride powder, 25:44284(T) (ORNL-tr-2471)

LITHIUM ISOTOPES
separation of, evaluation of methods for, 25:41897(T) (ORNL-tr-2512)

LITHIUM ISOTOPES Li-5
energy level at 15.5 MeV from resonances in helium-3 (d,p) reactions, Breit--Wigner resonance parameters for, (E/T), 25:43793

LITHIUM ISOTOPES Li-6
alpha elastic scattering at 104 MeV, differential cross sections for, (E), 25:43832 (NP-18920)
alpha elastic scattering at 12 to 18 MeV, optical-model analysis of, (E/T), 25:43810
alpha reactions (α,2α) at 37.5 and 43.5 MeV, plane-wave impulse-approximation analysis of angular distributions from, (E/T), 25:43803
cluster descriptions of, equivalence of d--α and He-3--t, (T), 25:43825
cluster structure of, from proton quasi-elastic scattering, (E), 25:43900 (NP-18880)
determination by nuclear magnetic resonance spectrometry, 25:41724
determination in lithium compounds by thermal neutron activation, Cherenkov and proportional detector arrangement for, 25:41833(R) (IA-1218)
determination of abundance of, relative to lithium-7, NMR method for, 25:41724
deuteron elastic scattering at 8 MeV, optical-model analysis of, (E/T), 25:43810
energy-level transitions in, calculations using correlated wave functions of E2, (T), 25:43815
lithium-6 elastic scattering at 5 to 17 MeV, optical-model and phase-shift analyses of angular distributions and excitation functions for, (E/T), 25:43816
lithium-6 reactions (Li-6,α), (Li-6,d), (Li-6,p), and (Li-6,t) at 4 to 14 MeV, cross sections for, (E), 25:43822
lithium-7 reactions (Li-7,α), (Li-7,d), and (Li-7,p) at 4 to 14 MeV, cross sections for, (E), 25:43822
lithium-7 reactions (Li-7,t) at 4 to 14 MeV, excitation functions for, (E), 25:43822
meson (μ^-) capture by, reaction rates and triton energy distributions from, (T), 25:43821
neutron total cross section up to 1.5 MeV, (E), 25:43884 (ANL-7710, pp 1-52)
nuclear wave functions for, correlated, (T), 25:43815
proton reactions (p,pd) and (p,p He-3) at 156 MeV, angular correlations in, (E), 25:43800 (NP-18880)
reactions (Li-6,α) and (Li-6,d) with lithium-7 at 4 to 14 MeV, excitation functions for, (E), 25:43822
reactions (Li-6,α), (Li-6,d), (Li-6,p), and (Li-6,t) with lithium-6 at 4 to 14 MeV, cross sections for, (E), 25:43822
reactions (Li-6,α), (Li-6,d), (Li-6,p), and (Li-6,t) with beryllium-9 at 4 to 14 MeV, cross sections for, (E), 25:43822
reactions (Li-6,p) and (Li-6,t) with lithium-7 at 4 to 14 MeV, cross sections for, (E), 25:43822
scattering by lithium-6 at 5 to 17 MeV, optical-model and phase-shift analyses of angular distributions and excitation functions for elastic, (E/T), 25:43816

LITHIUM ISOTOPES Li-7
alpha elastic scattering at 12 to 18 MeV, optical-model analysis of, (E/T), 25:43810
cluster structure of, from proton quasi-elastic scattering, (E), 25:43900 (NP-18880)
determination by nuclear magnetic resonance spectrometry, 25:41724
determination in lithium compounds by thermal neutron activation, Cherenkov and proportional detector arrangement for, 25:41833(R) (IA-1218)
determination of abundance of, relative to lithium-6, NMR method for, 25:41724
deuteron elastic scattering at 10 to 12 MeV, angular distributions for, (E), 25:43809
deuteron reactions (d,t) at 10 to 12 MeV, angular distributions for, (E), 25:43809
helium-3 reactions (He-3,α) at 16 to 18 MeV, angular distributions for, (E), 25:43809
helium-3 reactions at 1 to 2 MeV, analysis of neutron continuum from, (E), 25:43788
lithium-6 reactions (Li-6,α) and (Li-6,d) at 4 to 14 MeV, excitation functions for, (E), 25:43822
lithium-6 reactions (Li-6,p) and (Li-6,t) at 4 to 14 MeV, cross sections for, (E), 25:43822
lithium-7 reactions (Li-7,α) at 2 to 21 MeV, excitation functions for, (E), 25:43822
lithium-7 reactions (Li-7,d), (Li-7,p), and (Li-7,t) at 2 to 21 MeV, cross sections for, (E), 25:43822
proton reactions (p,α) up to 7 MeV, R-matrix analysis of, (E/T), 25:43829
proton reactions (p,γ) in giant resonance region, γ yields and angular distributions for, (E), 25:43813
proton reactions (p,n) at 3 to 5.5 MeV, angular distribution of neutron polarization in, (E), 25:43805
proton reactions (p,pt) at 156 MeV, angular correlations and spectra from, (E), 25:43800 (NP-18880)
reactions (Li-7,α) and (Li-7,t) with beryllium-9 at 4 to 14 MeV, excitation functions for, (E), 25:43822
reactions (Li-7,α) with lithium-7 at 2 to 21 MeV, excitation functions for, (E), 25:43822
reactions (Li-7,α), (Li-7,d), and (Li-7,p) with lithium-6 at 4 to 14 MeV, cross sections for, (E), 25:43822
reactions (Li-7,d) and (Li-7,p) with beryllium-9 at 4 to 14 MeV, cross sections for, (E), 25:43822
reactions (Li-7,d), (Li-7,p), and (Li-7,t) with lithium-7 at 2 to 21 MeV, cross sections for, (E), 25:43822
reactions (Li-7,t) with lithium-6 at 4 to 14 MeV, excitation functions for, (E), 25:43822

LIVER
effects of extract of, combined with radioprotective substances on reduction of radiation hazards to uranium mining personnel, 25:42510
effects of serotonin on mouse, 25:42519
radiation effects on activity of redox enzymes in, of rats following ingestion of radon-containing water, effects of dose on, 25:42279
radiation effects on content of sulfur-containing amino acids in proteins in rat, 25:42265
radiation effects on distribution of acid phosphatase and β-glucuronidase in rat, whole-body x, 25:42628
radiation effects on distribution of iodine-131-labeled albumin in rat, as indicator of radiation injury, whole-body γ, 25:42407
radiation effects on heterogeneity of nuclear RNA of rat, whole-body γ exposure, 25:42280
radiation effects on metabolism of selenium-75 and sulfur-35 in rat, x, 25:42254
radiation effects on oxidation-reduction potential in rat, protective effects of AET, MEA, or serotonin in combination with hypoxia against x, 25:42511
radioinduced diseases in human, following intravascular injection of Thorotrast, latent α and γ, 25:42708
radioinduced diseases of rat, neptunium-237, 25:42253
scanning of human, double-tracer method using gold-198 and selenium-75 for, 25:42580
scanning of human, for diagnosis of cirrhosis or hepatitis, effectiveness of gold-198, 25:42553
scintigraphy of human, using technetium-99m-labeled sulfur colloid for diagnosis of Hodgkin's disease, 25:42585

LOS ALAMOS OMEGA WEST REACTOR
gamma shields for, fabrication of layered aluminum--lead, 25:42816 (LA-4644)

LUMINESCENT MATERIALS
radiation protection guide for personnel using radiation-activated, ILO, 25:42462

LUNAR MATERIALS
analysis of, review of methods for, 25:41714
distribution and origin of helium, neon, and argon isotopes in Apollo 12 samples, (E), 25:43099
neutron flux estimates in, 25:41833(R) (IA-1218)
radiation effects on silicate, 5-keV D^+, H^+, He^+, and N_2^+, 25:43446

LUNGS
book: Use and Interpretation of the Lung Scan, 25:42583
gas exchange in human, use of xenon-133 in studies of, 25:42561
plutonium oxide burden in human, recommended decrease in maximum permissible, 25:42508
plutonium oxide removal from, effectiveness of saline lavage for, 25:42368(T) (LF-tr-53)
radiation effects on distribution of iodine-131-labeled albumin in rat, as indicator of radiation injury, whole-body γ, 25:42407
radioisotope scanning for measurement of blood pressure in, 25:42554
radiosensitivity of rat, effects of pneumothorax on, 25:41833(R) (IA-1218)
scintigraphy of blood perfusion in, using metastable technetium-99-labeled iron hydroxide macroaggregates

XUM

and gamma camera or rectilinear scanner, 25:42579
LUTETIUM
determination in meteorites by neutron activation and high-voltage electrophoresis, 25:41776
magnetic susceptibility of, generalized function for, (T), 25:43477
preparation of large single crystals of, 25:42834
separation from aqueous solutions by ion exchange on zirconium tellurate, tracer studies on, 25:41915
LUTETIUM ISOTOPES Lu-173
energy levels from (α,t) and (He-3,d) reactions, spectroscopic factors and spin-parity assignments for, (E), 25:43942
LUTETIUM ISOTOPES Lu-175
energy levels from (α,t) and (He-3,d) reactions, spectroscopic factors and spin-parity assignments for, (E), 25:43942
LUTETIUM ISOTOPES Lu-177
energy levels from (α,t) and (He-3,d) reactions, spectroscopic factors and spin-parity assignments for, (E), 25:43942
LUXEMBOURG
nuclear power industry activities in, review of, 25:44092
LYMPH NODES
radiation effects on deoxyribonucleoprotein in animal, mechanisms for, 25:42624
radioinduced ablation of dog, effectiveness of metalloporphyrin-incorporated palladium-109 for selective β, 25:42312
radioinduced fibrosis and degeneration of dog cervical, following neck exposure, γ, 25:42662
scanning of human iliac and inguinal, comparison of radiological lymphadenography and radioisotope, 25:42581
LYMPH SYSTEM
radioinduced injuries in tissues of chicken, x, 25:42658
scanning for localization of neoplasms in human, effectiveness of gallium-67 for, 25:42549(R) (ORAU-113)
scanning human infant, for evaluation of primary congenital lymphedema using gold-198, 25:42559
LYMPHOCYTES
radiation effects on cultured, from infant and adult man, effects of dose and phytohemagglutinin on, 25:42602
radiation effects on human peripheral blood, as indicators of radiation injury, 25:42404
radioinduced chromosome aberrations in human, as biological dosimeter, β, 25:42399
radioinduced chromosome aberrations in human, as biological dosimeter, 25:42398
radiosensitivity of dog bone marrow, as indicators of radiation injury, 25:42404
LYSINE
radiation effects on HeLa cell uptake of, effects of metabolic inhibitors on x, 25:42295
radioprotective effects of, on uranium mining personnel, animal experiments on, 25:42510
LYSOZYME
radiation effects on activity of, in rabbit serum, effects of dose on whole-body x, 25:42648

M

MC GUIRE POWER REACTOR, UNIT 1
design parameters of, revised and additional data on, 25:44067 (DOCKET-50369-12)
operations aspects of, revised and additional data on, 25:44067 (DOCKET-50369-12)
MC GUIRE POWER REACTOR, UNIT 2
design parameters of, revised and additional data on, 25:44067 (DOCKET-50369-12)
operations aspects of, revised and additional data on, 25:44067 (DOCKET-50369-12)
MACHINING
development of fine-edge blanking and piercing processes in, 25:44229 (BDX-613-366)
MAGNESIUM
combustion of, comparison of effectiveness of dry powders for extinguishing, 25:42837 (AERE-R-6745)
distribution in barley, soybeans, and wheat during development, 25:42322(R) (COO-1097-46)
polarizability of atomic, perturbation calculation of, 25:43117
separation from acetone--hydrochloric acid solutions by ion exchange using Bio-Rad, distribution coefficients for, 25:41899
separation from aqueous solutions by ion exchange on zirconium tellurate, tracer studies on, 25:41915
separation from other metals using inorganic ion exchange papers, 25:41909
superconductivity of, search for, 25:41778 (UCRL-20500, pp 1-85)
MAGNESIUM ALLOYS AND SYSTEMS
Al--Mg--Zn, corrosion of age-hardened, by aqueous sodium chloride, stress, 25:42886 (UCRL-20500, pp 86-146)
Mg--Zn, superconducting transition temperature in high T/sub c/ intermetallic $MgZn_2$, sensitivity to residual stress of, (E), 25:43302
MAGNESIUM FLUORIDES
color centers and impurity ions in, EPR and optical absorption studies of, 25:44297 (TID-25746)
MAGNESIUM IONS
spectral levels in solar corona, autoionizing, (E), 25:43065 (AD-715257)
MAGNESIUM ISOTOPES Mg-21
mass excess from (He-3,He-6) reactions, (E), 25:43823
nuclear mass excess of, comparison with calculations using isobaric multiplet mass equation, (E), 25:43808
MAGNESIUM ISOTOPES Mg-24
alpha inelastic scattering at 22 MeV, α--γ coincidence spectra from, (E), 25:43854
energy level from Coulomb excitation, reduced transition probability and quadrupole moment of first excited, (E), 25:43852
energy levels from alpha inelastic scattering, lifetimes of, (E), 25:43854
helium-3 reactions (He-3,He-6) at 68 MeV, Q values and spectra from, (E), 25:43823
helium-3 reactions (He-3,He-6) at 68 to 70 MeV, Q-value for, (E), 25:43808
triton reactions (t,αγ) at 4 to 4.5 MeV, α and γ spectra and α-γ angular correlations from, (E), 25:43880
MAGNESIUM ISOTOPES Mg-26
alpha elastic and inelastic scattering at 104 MeV, differential cross sections for, (E), 25:43832 (NP-18520)
alpha inelastic scattering at 22 MeV, α--γ coincidence spectra from, (E), 25:43854
energy levels from alpha inelastic scattering, lifetimes of, (E), 25:43854
MAGNESIUM ISOTOPES Mg-28
testing of, produced in Japan, application, 25:41990 (JAERI-13617)
MAGNESIUM NITRIDES
vaporization behavior of, model for, 25:42957 (UCRL-20500, pp 147-73)
MAGNESIUM OXIDES
book: High-Temperature Materials, 25:42853
deformation of polycrystalline, relations with microstructure, 25:42957 (UCRL-20500, pp 147-73)
diffusion in monocrystals of, 25:41832(R) (AECL-3851)
mechanical properties of, at high temperatures, 25:42957 (UCRL-20500, pp 147-73)
MAGNESIUM TELLURATES
radiation effects on, production of iodine-131 from neutron, 25:41880
MAGNET COILS
design of large superconducting, for fusion reactors, 25:43397 (MATT-848)
design of superconducting, to produce constant current density and produce desired field in cylindrical cavities, 25:43330
MAGNETIC ANALYZERS
aberrations in symmetric, longitudinal second-order, 25:43763
description for measuring parameters of strong ion beams, 25:43746
design of broad-range heavy-particle, 25:42221
design of energy-selective ion beam, 25:42224(P)
energy calibration for 30-MeV proton beams, 25:43823
MAGNETIC FIELDS
correlation with 100- and 200-eV electrons at magnetospheric bow shock, (E), 25:43238
coupling to central polar cap-field lines, relation of proton enhancements during Feb. 25, 1959 event to interplanetary, (E/T), 25:43232
effect of Mar. 27, 1968 reversal of interplanetary, on structure of magnetopause, (E), 25:43220 (N-71-20853)
effect on dispersion in molecular gases, parallel constant and alternating, (T), 25:43516
effect on sidereal diurnal cosmic-ray anisotropies, interplanetary, (T), 25:43177
plasma drift-wave instabilities in, temperature-gradient, (T), 25:43244
structure in cylindrical cavities, superconducting coil design for shaping desired, 25:43330
MAGNETIC MIRROR MACHINES
bremsstrahlung emission from anisotropic hot-electron plasma in, free--free, (E), 25:43357
MAGNETIC MIRRORS
charged-particle orbit approximation in periodic systems, straight-line, (T), 25:43373
plasma injection into, shock wave formation in, (E), 25:43359
MAGNETIC MONOPOLES
quark model with, 25:43589
MAGNETIC STORMS
activity of magnetospheric substorms, correlation with magnetotail configuration changes, (E/T), 25:43239
correlation of Mar. 13--15, 22--25, and 28--29, 1966, with asymmetric twilight ring current, (E), 25:43241
correlation of polar substorms with Pi bursts and IPDP micropulsations, (T), 25:43247
effect on energetic electron-flux variations near neutral sheet, magnetospheric, (E/T), 25:43266
effect on magnetic cutoff variations during main phase of, (E), 25:43179
effects of June 15, 1955, on plasmapause position, relation to trapped enhanced >280 keV electron flux, (E), 25:43264
effects on energetic electron fluxes in outer radiation

belts, (E/T), 25:43267
electron precipitation during main phase of, from minimum and maximum L shells intersected by stormtime plasmapause, (T), 25:43243
origin of polar substorms from large-scale traveling ionospheric disturbances, (E/T), 25:43250
relation to traveling ionospheric disturbances at 200 to 600 km, (E), 25:43217 (N-71-18502)
MAGNETISM
book: Introduction to the Theory of Solid State Physics, 25:43503
conference on magnetic thin films, fourth international, Prague, 9/70, 25:43492
theory of, Heisenberg model transformation in coherent state representation of, 25:43512
MAGNETOHYDRODYNAMIC GENERATORS
electrical and thermal measurements on unseeded supersonic argon, 25:43183 (N-71-15856)
electrical losses in, flow model studies of, (T), 25:43182 (JUL-742-TP)
magnetic field distribution along channel of, optimum, 25:43190
thermodynamic drive for, 25:43188(P)
MAGNETOHYDRODYNAMICS
book: Magnetohydrodynamic Flow Around Bodies, 25:43199
equilibria in, Mercier's criterion for class of, (T), 25:43206
MAGNETOPAUSE
structure of, phenomena following Mar. 27, 1968 interplanetary magnetic-field reversal, (E), 25:43220 (N-71-20853)
MAGNETOSPHERE
bow shock in, correlation of 100- and 200-eV electrons and magnetic fields at, (E), 25:43238
effect of protonospheric downward flux on nighttime F-region enhancement, (E/T), 25:43253
electron-flux variations in plasma sheet during March--April 1966 magnetospheric substorms, energetic, (E/T), 25:43266
electrostatic emissions at 2500 to 4500 km in south polar, vlf, (E), 25:43213 (AD-715898)
magnetic storms in, relation to magnetotail configuration changes, (E/T), 25:43239
plasma sheet in, energy conservation by cold plasma injection in, (T), 25:43271
radio-wave emission from whistler trains and man-made signals, triggered vlf discrete, (T), 25:43245
review papers from NATO Advanced Study Institute on Polar Ionosphere and Magnetospheric Processes, Apr. 9-18, 1969, 25:43226
MAGNETOTAIL
configuration changes of, relation to solar-wind magnetic field and magnetospheric substorms, (E/T), 25:43239
electron flux near neutral sheet in March--April 1966, during magnetospheric substorms, (E/T), 25:43266
plasma sheet time variations at 18 R/sub E/ from simultaneous satellite observations, (E), 25:43240
MAGNETS
cooling superconducting, 25:43325 (CONF-700341-6)
design for transportable betatron, 25:43741
design of circular quadrupole, for beam transport, 25:43757
power supply for 100-cm liquid hydrogen bubble chamber, 25:42143
review of superconducting, 25:43328
stray fields of magnetic deflector, for beam extraction from cyclic accelerators, compensation of, 25:43744
use of superconducting, in active shield for cylindrical space vehicles, 25:43425
MALATE DEHYDROGENASE
radiation effects on, in man following therapy as indicator of human kidney damage, 25:42409
MALEIMIDE, N-ETHYL-
effects on duodenum crypt cells in mice pretreated with radioprotective thiols, 25:42520
MALONIC ACID, DIFLUORO-
potassium salt, radiation effects on single crystals of, ESR studies on γ and x, 25:41838
MAMMALIA
radiation effects on biochemistry of, for use as indicator of injuries, review on, 25:42401
radiation effects on bones and bone marrow of, pathological external and internal exposure, 25:42472
radiosensitivity of oocytes of, effects of age, criteria for assessment, dose, species, and strain on, 25:42697
MAN
book: Radiation Sickness in Man, 25:42542
cesium-137 content of, in Soviet Union during 1966 to 1968, calculation of genetic dose from, 25:42376
cesium-137 elimination from, effects of age on, 25:42250
fibrinolytic activity of blood of, iodine-125 tracer method for measurement of, 25:42243
gallium-67 uptake by neoplastic and normal tissues of, 25:42549(R) (ORAU-113)
plutonium oxide burden in lungs of, recommended decrease in maximum permissible, 25:42508
plutonium oxide removal from lungs of, effectiveness of saline lavage for, 25:42368(T) (LF-tr-53)
polonium-210 content of tissues of, in Soviet Union, 25:42429
radiation attenuation in tissues of, effects of energy on x, 25:42430
radiation dose calculations for tissues in, following deposition of radioactive materials and radioisotopes, 25:42467
radiation dose distribution in tissues of, 25:42454
radiation dose limits for, relation of animal experimentation to, 25:42605
radiation dose to adrenal glands, bone marrow, kidneys, liver, and spleen of, following administration of tracer dose of gallium-67, 25:42549(R) (ORAU-113)
radiation dose to bones of adult, method for estimating strontium-90 β, 25:42434
radiation dose to children of, from different radiographic procedures, comparison of, 25:42412
radiation dose to children of, up to 18 years of age, maximum permissible, 25:42473
radiation dose to skin of, during diagnostic radiography, method for calculation of, 25:42431
radiation dose to thyroid and whole body of, in Australia during 1970, 25:42367 (AWTSC-1)
radiation dose to, estimates of 1969 fallout, 25:42651
radiation dose to, from ingested radon-222, 25:42247 (SFL-A-16)
radiation dose to, ICRP recommendations for maximum permissible, 25:42680
radiation dose to, methods for measurement of maximum permissible, 25:42454
radiation dose to, natural background and medical exposure, 25:42711
radiation effects on 2-methyl-β-alanine excretion in urine of, x, 25:42684
radiation effects on biochemistry of body fluids in, as indicator of radiation injuries, review on, 25:42402
radiation effects on biochemistry of, for use as indicator of injuries, review on, 25:42401
radiation effects on bioelectric activity in brain in, electroencephalographic studies on local and whole-body, 25:42677
radiation effects on bioelectric activity in brain in, following therapy for arachnoiditis, 25:42678
radiation effects on blood and urine biochemical constituents, cell populations, and chromosomes in, evaluation of dosimetric use of, 25:42406
radiation effects on blood coagulation in, as biological dosimeter, 25:42600
radiation effects on blood picture and spermatozoa in Japanese, latent fallout, 25:42681
radiation effects on bones and bone marrow of, pathological external and internal exposure, 25:42472
radiation effects on central nervous system during prenatal and postnatal development, effects of dose on pathological, 25:42710
radiation effects on content of proteins, immunoglobulins, and transferrin in blood serum of, γ, 25:42586 (ORAU-113, pp 4-77)
radiation effects on content of serum thyrotropin and thyroid function of, following therapy of lymphomas, x, 25:42695
radiation effects on cytochrome oxidase and monoamine oxidase activity in skin of, x, 25:42286
radiation effects on filterability of erythrocytes of, in vitro γ, 25:42706
radiation effects on incidence of cancer in children of, following prenatal exposure in England and Wales during 1968, 25:42696
radiation effects on incidence of late aplastic anemia in, surviving atomic bombing of Hiroshima and Nagasaki, 25:42698
radiation effects on metabolic changes in, for use as indicator of radiation injury, criteria for evaluating, 25:42400
radiation effects on metabolism of biogenic amines in, as indicators of radiation injury, x, 25:42626
radiation effects on morphology and maturation time of cells in primary and metastatic Wilms' tumor in children of, 25:42592
radiation effects on morphology of cells in testes of, effects of dose and post-exposure time on x, 25:42674(R) (RLO-1780-32)
radiation effects on morphology of thyroid cancer in, following therapy, effects of tumor type on γ, 25:42679
radiation effects on neurovascular system in, methods for studying dystonic, 25:42676
radiation effects on peripheral blood of, as indicators of radiation injury, 25:42404
radiation effects on proliferation of bone marrow cells of, following extracorporeal exposure of blood, beta, 25:42690
radiation effects on respiratory function in, additive effects of exercise on low-dose whole-body γ, 25:42586 (ORAU-113, pp 4-77)
radiation effects on ribonuclease activity in urine and vaginal fluid in, following therapy for cervical carcinomas, lymphomas, or tumors, 25:42683
radiation effects on salivary glands of, following therapy of head and neck tumors, 25:42699
radiation effects on survival of leukocytes and platelets in peripheral blood of, low-dose-rate low-dose whole-body γ, 25:42586 (ORAU-113, pp 4-77)
radiation effects on tubes and uterus in, following castration, carcinogenic, 25:42675

XUM

radiation effects on, conference on, 25:42512
radiation effects on, credibility of statistical inferences regarding low-dose, 25:42715
radiation effects on, development of recording system for data on whole-body, 25:42549(R) (ORAU-113)
radiation effects on, effectiveness of biochemical indicators for evaluating heterogenous, 25:42408
radiation effects on, effects of dose and dose rate on somatic, 25:42712
radiation effects on, effects of dose on genetic and somatic, 25:42692
radiation effects on, effects of dose on genetic and somatic, 25:42693
radiation effects on, effects of dose, dose rate, age, and sex on genetic and somatic x, 25:42453
radiation effects on, evaluation of enzyme activity as indicator of, 25:42409
radiation effects on, evaluation of genetic and somatic low-dose, 25:42475
radiation effects on, following therapy of menorrhagia, statistical study on long-term x, 25:42702
radiation effects on, genetic, 25:42711
radiation effects on, latent, 25:42604
radiation effects on, problems in correlating dose and late, 25:42714
radiation hazards to, analysis of calculations on low dose, 25:42703
radiation hazards to, during dental radiography, measures for protection against, 25:42484
radiation injuries in, conference on biochemical indicators of, 25:42395 (STI/PUB-280)
radiation injuries in, following therapy, 25:42597
radiation injuries to, development of biochemical indicators of, 25:42685
radiation protection code for, using sealed radiation sources for therapy, 25:42491
radiation protection during dental radiography, Australian code of practice for, 25:42496
radiation protection during diagnostic radiography, ICRP standards for, 25:42453
radiation protection of genetic system of, problems in, 25:42325
radiation protection of gonads in, use of aluminum filters during diagnostic radiography of pelvic area for x, 25:42447
radiation protection of, design of above-ground fallout shelters for, 25:42034(T) (JPRS-53498)
radiation protection of, recommendations of ICRP for external-source, 25:42455
radiation protection of, recommendations of ICRP for, 25:42465
radiation protection recommendations for, in hospitals, ICRP, 25:42476
radiation sickness pathology and therapy in, review of, 25:42542
radiation sickness pathology in, time sequence of anorexia, nausea, and vomiting in, 25:42586 (ORAU-113, pp 4-77)
radiodiagnosis of cirrhosis or hepatitis in, effectiveness of gold-198 liver scanning for, 25:42553
radioinduced aberrations of chromosomes in cultured cells from, effects of dose on γ, 25:42365
radioinduced cataracts of, exposed to atomic bomb at Hiroshima, occurrence and pathology of latent, 25:42546
radioinduced chromosome aberrations in lymphocytes in, as biological dosimeter, β, 25:42399
radioinduced chromosome aberrations in lymphocytes of, as biological dosimeter, 25:42398
radioinduced chromosome aberrations in newborn child of, following radiography, x, 25:42362
radioinduced chromosome aberrations in peripheral blood in, limitations of dosimetric uses of chronic external and therapeutic internal, 25:42707
radioinduced diseases in liver in, following intravascular injection of Thorotrast, latent α and γ, 25:42708
radioinduced epithelioma of, 33 years following skin exposure with radium-225 applicator, 25:42686
radioinduced granulocytic sarcoma in, following therapy of ankylosing spondylitis, γ, 25:42709
radioinduced herpetic lesions in leukemic, following therapy, recurrent x, 25:42689
radioinduced injuries in adult and developing nervous system of, 25:42591
radioinduced injuries to, following combined neck dissection and therapy, fast electron, 25:42603
radioinduced leukopenia in, partial-body bremsstrahlung, 25:42599
radioinduced malformations in central nervous system in embryos of, 25:42629
radioinduced malignant diseases in, threshold concept for, 25:42694
radioinduced myelitis in, following therapy of head and neck neoplasms, 25:42700
radioinduced sarcomas in, following therapy, measures for prevention of, 25:42705
radioinduced subcutaneous indurations in, following telecobalt therapy, 25:42687
radioinduced visual phenomena in, following exposure to neutron energies up to 25 MeV, 25:42688
radioisotope content of diet and urine of, in Italy, effects of age on, 25:42375
radioisotope content of diet of adult and young, in Formosa, comparison of cesium-137 and strontium-90, 25:42422
radioisotope hazards to, during diagnosis, establishment of permissible dose levels for minimizing, 25:42552
radioisotope scanning of lymph system in, method for, 25:42581
radiosensitivity of oocytes of, effects of age, criteria for assessment, and dose on, 25:42697
radiosensitivity of tissues of gonads in, 25:42586 (ORAU-113, pp 4-77)
radiosensitivity of various tissues of, 25:42454
radiotherapy of carcinomas of head and neck of, additive effects of 5-fluorouracil infusion on gamma and x, 25:42589
radiotherapy of carcinomas of larynx and pharynx in, effectiveness of preoperative gamma and x, 25:42588
radiotherapy of eye diseases in, principles and indications for, 25:42596
radiotherapy of gynecological cancer in, effectiveness of high-dose γ, 25:42598
radiotherapy of head and neck cancers in, methods for prevention of bone necrosis and tooth decay following, 25:42471
radiotherapy of Hodgkin's disease in, dosimetry during mantle technique for γ, 25:42594
radiotherapy of intracerebral astrocytomas of, estimation of hazards to brain following, 25:42701
radiotherapy of medulloblastomas in children of, dose fractionation schedules for post-surgical, 25:42592
radiotherapy of renal adenocarcinoma in, spontaneous regression of lung metastases following γ, 25:42591
radiotherapy of uterine cervix carcinomas in, effectiveness of combined radium-226 implant and external gamma, 25:42595
radon-222 excretion following ingestion in water, 25:42247 (SFL-A-16)
uranium hexafluoride inhalation by, uptake, excretion, and retention following, 25:42244(T) (CAT-Z-5047)

MANGANESE
determination in minerals from Luzon, Philippines, by neutron activation, 25:41772
effects on superconducting critical field of niobium--titanium alloy wires, 25:43309
separation from acetone--hydrochloric acid solutions by ion exchange using Bio-Rad, distribution coefficients for, 25:41899
separation from other metals using inorganic ion exchange papers, 25:41909

MANGANESE ALLOYS AND SYSTEMS
C--Fe-base--Mn, radiation effects on graphitization of malleable cast, fast neutron, 25:42904
C--Mn--Ni--steel, mechanical properties of tempered, relations with structure, 25:42886 (UCRL-20500, pp 86-146)
Cr--Fe-base--Mn--Mo--Ni, ductility of irradiated Sandvik 12R72HV, at 500 to 800°C, effects of injected helium on, 25:42872
Fe-base--Mn--Ni--Ti, mechanical properties of, effects of aging on, 25:42886 (UCRL-20500, pp 86-146)
Gd--Mn--Pr, magnetic properties of Pr/sub x/Gd/sub 1-x/Mn_2, high-temperature, 25:42894
Gd--Mn--Pr, structure of Pr/sub x/Gd/sub 1-x/Mn_2, 25:42894
Mn--Mo--Ni--steel, standard for plates of, for pressure vessels, 25:42793 (RDT-M-5-3-T)
Mn--Mo--steel, standard for plates of, for pressure vessels, 25:42793 (RDT-M-5-3-T)
Mn--Pr--Tb, magnetic properties of Pr/sub x/Tb/sub 1-x/Mn_2, high-temperature, 25:42894
Mn--Pr--Tb, structure of Pr/sub x/Tb/sub 1-x/Mn_2, 25:42894

MANGANESE BORIDES
FeB--MnB, thermal capacity of, low-temperature, 25:42974

MANGANESE CHLORIDES
sorptive properties of surfaces of, for krypton, thermodynamic studies on stepwise isotherms for, 25:41824 (CEA-R-4089)

MANGANESE IONS
radioinduced oxidation in dosimetric phosphate glass, yield of, 25:42163

MANGANESE ISOTOPES
chromium--manganese Coulomb displacement energies, (E), 25:43883
iron--manganese Coulomb displacement energies, (E), 25:43883

MANGANESE ISOTOPES Mn-51
energy-level transitions from chromium-50 (p,γ) reactions, strength for M1, (E), 25:43850

MANGANESE ISOTOPES Mn-53
energy-level transitions from chromium-52 (p,γ) reactions, branching ratios for, (E), 25:43837

MANGANESE ISOTOPES Mn-54
content in ground-level atmosphere of Brunswick, West Germany, effects of seasonal variations on, 25:41934
testing of, produced in Japan, application, 25:41990 (JAERI-13617)
uptake by frogs and lizards from labeled trees, 25:42317(R) (PRNC-147)
uptake by frogs in rain forest in Puerto Rico,

25:42317(R) (PRNC-147)
MANGANESE ISOTOPES Mn-55
helium-3 reactions (He-3,t) at 24.6 MeV, triton spectra from, (E), 25:43983
MANY BODY PROBLEM
Bethe--Goldstone equation in, methods for solution in finite nuclei, (T), 25:43956 (ORO-3765-30)
exactly soluble three-body problem in quantum mechanics, (T), 25:43509
folded diagrams for, derivation of, 25:43519
MARS (PLANET)
atmosphere of, meteoroid ablation and breakup during passage through, (E/T), 25:43263
atmosphere of, space-probe data of solar-wind interaction with, (E), 25:43272
MARTENSITE
morphology and substructure of, 25:42886 (UCRL-20500, pp 86-146)
MARYLAND
radiation monitoring near nuclear power station in, 25:42388
MASS LAW
derivation of gross, based on incompressible liquid-drop model, (T), 25:43916
testing of isobaric-multiplet, by measurement of T/sub z/ = 3/2 masses, (E), 25:43823
MASS SPECTROGRAPHY
ionization efficiency curves for, computer collection of, 25:44241 (COO-1140-198)
limitations in high-temperature equilibrium studies, 25:44242 (COO-1147-35)
research progress in, annual report, 1969--70 on, 25:43468 (NP-18557)
MASS SPECTROMETERS
control and data acquisition system for high-temperature quadrupole, computer, 25:42182 (COO-1140-194)
design and performance of magnetic double-focusing, for measuring solar wind mass/charge number composition, (E), 25:43221(R) (N-71-21459)
efficiency of linear pulsed time-of-flight, charge- and mass-dependent effects on, 25:42211
energy calibration for 30-MeV proton beams, 25:43823
ion source for, stabilized thermal, 25:41833(R) (IA-1218)
positioning of quadrupole, device for, 25:42212
MASS TRANSFER
book: Heat and Mass Transfer in Turbulent Boundary layers. Vol. I, 25:41987
book: Heat and Mass Transfer in Turbulent Boundary Layers. Vol. II, 25:41988
book: Heat and Mass Transfer. Vol. II. (In Russian), 25:41986
MATERIALS TESTING, NONDESTRUCTIVE
conference on equipment and procedures for reactor components, 25:44094 (CONF-700224)
development and research in methods for, Argentina center for, 25:42028
development of ultrasonic, for in-service inpile reactor components, 25:44080
method for testing of brittle materials, fracture mechanics development of, 25:42021 (CONF-710512-2)
methods for quality assurance, development, selection, and uses of, 25:42032
standard for, 25:42025 (RDT-F-3-6-T)
MATHEMATICAL PHYSICS
variation of nonlinear parameters for computing decay constants and standard deviation, 25:43521
MATHEMATICS
book: Mathematics of Radiology and Nuclear Medicine, 25:42433
irreducible multiplier representations in, method for constructing, 25:43501
Mathieu equation in, eigenvalues for, 25:43505 (EUR-4349)
MEATS
beef, radiation processing effects on desmination of myoglobin in, low-dose γ, 25:42756
beef, radiation processing effects on storage life and wholesomeness of, γ, 25:42744(R) (COO-2038-2)
beef, radiation processing of pre-cooked, and its gravy, method for, 25:42759(P)
fish, radiation processing of, volatile radiolytic compounds from γ, 25:42753
pork, radiation processing effects on storage life and wholesomeness of, γ, 25:42744(R) (COO-2038-2)
salvaging from lethally-irradiated live stock in post-attack environment, 25:42506(R) (ORNL-4566(Pt.1))
seafood, radiation processing of cod fillets, lobster tails, and shrimp for export from Iceland, 25:42746 (STI/DOC-10/124)
MECHANICS
equations of motion in relativistic, gravitational potential tensor for, 25:43709
formulation of statistical, solvable model in quantum field theory for Araki--Woods, 25:43668
Hellmann--Feynman theorems in classical, (T), 25:43510
MEDICAL PERSONNEL
radiation dose to, during interstitial therapy of carcinomas under two different treatment plans, 25:42432
radiation effects on blood cells in, x, 25:42600
radiation protection code for, using sealed radiation sources for therapy, 25:42492
radiation protection code for, using sealed radiation sources for therapy, 25:42491
radiation protection for dental radiography, Australian code of practice for, 25:42496
radiation protection of veterinary, code of practice for x, 25:42485
radiation protection of, ICRP recommendations for, 25:42476
radiation protection programs for diagnostic radiography, in Japan, evaluation of, 25:42486
MEDICAL SUPPLIES
radiosterilization of glass ampule, effectiveness of high dose γ, 25:42754
radiosterilization of homograft heart valves for use in man, effectiveness of γ, 25:42758
MEDICINE
book: Basic Medical Radiation Physics, 25:42555
book: Mathematics of Radiology and Nuclear Medicine, 25:42433
book: Nuclear Medicine, Second Edition, 25:42582
conference on nuclear, abstracts of, 25:42584
procedures for care of personnel following accidents resulting in radiation exposure or contamination by radioactive materials, 25:42391
radiation dose to human populations from nuclear, 25:42692
radiation dose to human populations from nuclear, 25:42693
radiation in, dose to man from, 25:42711
research programs at Oak Ridge Associated Universities on nuclear, 25:42587 (ORAU-113, pp 79-133)
research programs of AEC during 1970 on, 25:44293 (TID-25728)
tracer technique development for, abstracts of 300 papers on, 25:42560
MEIOSIS
effects of stage of, on x radiosensitivity of oocytes of silkworms, 25:42609
MEMBRANES
stability of elasto-plastic, effects of shock loading on, 25:42506(R) (ORNL-4566(Pt.1))
standard for seal, 25:41974 (RDT-M-9-2-T)
MERCAPTO GROUP
radiation effects on content of albumin and globulin fractions of, in human serum following post-surgical therapy of mammary cancer, 25:42270
radiation effects on content of, in rat cell proteins in relation to sensitivity of transplanted tumors, 25:42618
role in x radiosensitivity of isocitrate dehydrogenase in vitro, 25:42299
MERCHANT VESSELS
design of container, with 120,000 shp marine reactor, 25:44178 (RCN-139)
economic comparison of nuclear and conventional, 25:44177 (NP-18908)
MERCURY
determination of trace amounts of, in meteorites by neutron activation and γ spectrometry, 25:41773
mercury-ion reactions with, charge-exchange cross sections for, (T), 25:43157
neutron total cross section at 100 to 650 keV, optical model analysis of average, (E/T), 25:43908
separation from acetone--hydrochloric acid solutions by ion exchange using Bio-Rad, distribution coefficients for, 25:41899
separation from aqueous solutions by ion exchange on zirconium tellurate, tracer studies on, 25:41915
separation from reactor cooling gases by combustion on catalyst, 25:41914(P)
superconducting parameter calculations, 25:43305
MERCURY IONS
reactions with mercury, charge-exchange cross sections for, (T), 25:43157
MERCURY ISOTOPES Hg-197
effectiveness of mercuric chloride-incorporated, for diagnosis of mammary, oral, and pharyngeal tumors, 25:42576
MERCURY ISOTOPES Hg-203
beta decay of, β-γ circular polarization correlation for, (E), 25:43941
effectiveness of chlormerodrin-incorporated, for diagnosis of mammary, oral, and pharyngeal tumors, 25:42576
effectiveness of mercuric chloride-incorporated, for diagnosis of mammary, oral, and pharyngeal tumors, 25:42576
MESIC ATOMS
energy-level transitions and optical potential parameters in carbon-12 and oxygen-16 π-, πN scattering lengths for, 25:43806
x-ray yields from hydrogen μ-, as functions of density, 25:43125
MESONS
fields of massive, idealized measurements in quantum field theory for, (T), 25:43692
interactions of scalar, group-theory approach to N-point function for dual amplitudes for, 25:43714
interactions of spinless, at high energies and all angles, optical model for, (T), 25:43571

XUM

interactions with mesons, dual amplitudes with unitary symmetry for pseudoscalar, 25:43627
interactions with spin-1/2 fermions at high energies and all angles, optical model for, (T), 25:43571
theory for scalar, functional equations in lambda phi**4, 25:43678
theory for system of interacting baryons and pseudoscalar, currents in, (T), 25:43622

MESONS (eta)
decay eta' → 2γ in deuterium bubble chamber, branching ratio for, (E), 25:43562
decay eta → 3π, chiral SU(3) X S(3) algebra for nonlinear Lagrangian calculation of, 25:43658
decay eta → 3π, chiral SU(3) X SU(3) algebra for nonlinear Lagrangian calculation of, 25:43659
decay eta → 3π⁰ in deuterium bubble chamber, branching ratio for, (E), 25:43562
decay eta → π⁺ + π⁻ + γ, comparison of chiral Lagrangian model and Veneziano model of amplitudes for, 25:43631
decay eta⁰ → 2γ, spark chamber study of branching ratio for, (E), 25:43530
decay eta⁰ → 3π⁰, spark chamber study of branching ratio for, (E), 25:43530
decay eta⁰ → π⁰ + 2γ, spark chamber study of branching ratio for, (E), 25:43530
production in γ + p → eta + p interactions at 4 to 9 GeV, spectrometer study of energy dependence of cross sections for, (E), 25:43529
production in π⁻ + p → n + eta interactions at 5.9 GeV/c, spark chamber and scintillation counter study of differential and total cross sections for backward, (E), 25:43563
production of eta and eta' in π⁺ + n → p + mγ interactions at 2.15 GeV/c in deuterium bubble chamber, cross sections and angular distributions for, (E), 25:43562
production of eta⁰ in π⁺ + n → p + π⁺ + π⁻ + π⁰ backward interactions at 1.83 to 2.33 GeV/c in deuterium bubble chamber, (E), 25:43556

MESONS (f)
coupling constant for fγγ, finite-energy sum rules for γ + π⁰ → γ + π⁰ interactions for, (T), 25:43582 (DESY-71/20)
production in e + e → e + e + f(1260) interactions, radiative widths and cross sections for, (E), 25:43582 (DESY-71/20)
production of f⁰ in p + p → p + p + π⁺ + π⁻ interactions at 25 GeV/c in hydrogen bubble chamber, cross sections for, (E), 25:43535
production of f⁰ in π⁺ + d interactions at 13 GeV/c in bubble chamber, (E), 25:43545 (COO-1428-277)

MESONS (K)
energy loss at 10 MeV to 100 GeV in silicon, calculations of average and most probable, (T), 25:42155
interactions anti K + N → π + Σ(Λ) at 400 to 1200 MeV/c, test of duality predictions from partial-wave analysis of, (E/T), 25:43642 (UCR-34-P-107-B-106)

MESONS (K⁻)
interactions K⁻ + n → p + 2π⁻ + anti K⁰ + MM at 4.48 GeV/c in deuterium bubble chamber, cross sections and K(890) production in, (E), 25:43549 (COO-1428-286)
interactions K⁻ + n → p + 2π⁻ + anti K⁰ + π⁰ at 4.48 GeV/c in deuterium bubble chamber, K(890), Δ(1236), and N(1525) production and cross sections in, (E), 25:43549 (COO-1428-286)
interactions K⁻ + n → p + 2π⁻ + anti K⁰ at 4.48 GeV/c in deuterium bubble chamber, K(890), Δ(1236), N(1525), N(1688), and Σ(1765) production and cross sections in, (E), 25:43549 (COO-1428-286)
interactions K⁻ + n → π⁺ + 2π⁻ + anti K⁰ + n at 4.48 GeV/c in deuterium bubble chamber, K(890), Δ(1236), N(1525), and Σ(1765) production and cross sections in, (E), 25:43549 (COO-1428-286)

MESONS (K⁰)
decay K₂⁰ → 2γ spark chamber and scintillation counter study of branching ratios for, (E), 25:43531
decay K₂⁰ → 2π, CP violation in spark chamber study of rate for, (E), 25:43657
decay K₂⁰ → π + e + ν, time-reversal invariance test in Coulomb final-state interaction corrections to, (T), 25:43660
decay K₂⁰ → π + μ + ν, time reversal invariance test in Coulomb final-state interaction corrections to, (T), 25:43660
decay K₂⁰ → π + π + l + ν, time reversal invariance test in Coulomb final state interaction corrections to, (T), 25:43660
decay of, CPT violation in, (T), 25:43656 (PITHA-44)

MESONS (K⁺)
interactions K⁺ + n → p(n) + K⁺(K⁰) + π⁻(π⁺) at 9.0 GeV/c in deuterium bubble chamber, production of Kπ(1750) in, (E), 25:43546 (COO-1428-279)
interactions K⁺ + d → K⁺ + π⁺ + π⁻ + d(n + p) at 9 GeV/c in deuterium bubble chamber, K(1243) and K(1344) production in Q region of K⁺π⁺π⁻ mass spectrum and K(890) production in, (E), 25:43544 (COO-1428-275)
interactions K⁺ + d → K⁺ + π⁺ + π⁻ + d(p + n) at 9.04 GeV/c, K(1243) and K(1344) production in Q region and K(890) production in, (E), 25:43543 (COO-1428-274)
interactions K⁺ + n → K⁺ + π⁻ + p at 9 GeV/c in, deuterium bubble chamber, K(1420) production, and π exchange mechanism, energy dependence of cross sections, and density matrix elements for K(890) production in, (E), 25:43548 (COO-1428-283)
interactions K⁺ + n → K⁺ + π⁻ + p at 9.1 GeV in deuterium bubble chamber, cross sections, mass, and width for K(890) and K(1420) production and energy dependence of cross sections, density matrix elements, and π-exchange mechanism for K(890) production in, (E), 25:43547 (COO-1428-281)
interactions K⁺ + p → K⁺ + p at 4.0 and 5.0 GeV/c, differential cross sections for large-angle, (E), 25:43559
interactions K⁺ + p → π⁻ + particles at 12 GeV/c, symmetric π⁻ production in, (E), 25:43557
interactions K⁺ + p at 12.7 GeV/c in bubble chamber, factorization in inclusive processes from single-particle momentum distributions of π produced in, (E), 25:43554 (UR-875-340)

MESONS (μ)
decay of, intermediate vector boson theory for radiative corrections to spectrum of beta, (T), 25:43600
energy loss at 10 MeV to 100 GeV in silicon, calculations of average and most probable, (T), 25:42155
interactions μ + p at 150 GeV, self-coupling of weak lepton currents in anti ν--ν pair production in, (T), 25:43612
properties of, comparison with electrons, 25:43591
reactions with iron-56 at 150 GeV, self-coupling of weak lepton currents in anti ν--ν pair production in, (T), 25:43612

MESONS (μ⁻)
capture by hydrogen, K x-ray yields as functions of density, (T), 25:43125
capture by lithium-6, reaction rates and tritон energy distributions from, (T), 25:43821
production in K₂⁰ → π + μ + ν decay, time reversal invariance test in Coulomb final-state interaction corrections for charge asymmetry and polarization in, (T), 25:43660
production of μ⁺--μ⁻ pairs in ν + p interactions and ν reactions with iron-56 at 10 GeV, self-coupling of weak lepton currents in, (T), 25:43612

MESONS (μ⁺)
production in K₂⁰ → π + μ + ν decay, time reversal invariance test in Coulomb final-state interaction corrections for charge asymmetry and polarization in, (T), 25:43660
production of μ⁺--μ⁻ pairs in ν + p interactions and ν reactions with iron-56 at 10 GeV, self-coupling of weak lepton currents in, (T), 25:43612

MESONS (ω)
decay ω → 3π, comparison of chiral Lagrangian model and Veneziano model of amplitudes for, 25:43631
decay ω → 3π, multipole moments for determination of parity and spin from, (T), 25:43581
decay ω → γ + π⁰ in deuterium bubble chamber, branching ratio for, (E), 25:43562
parity and spin of, multipole moments for ω → 3π decay for determination of, (T), 25:43581
production in π⁺ + n → p + πγ at 2.15 GeV/c in deuterium bubble chamber, cross sections and angular distributions for, (E), 25:43562
production of ω⁰ in π⁺ + n → p + π⁺ + π⁻ + π⁰ backward interactions at 1.83 to 2.33 GeV/c in deuterium bubble chamber, (E), 25:43556

MESONS (π)
decay into hadrons, SU(4,3) group for hadron mass spectra and transition amplitude for, 25:43635
decay of, PCAC hypothesis for πrho contribution to error in Goldberger--Treiman relation for constant of, (T), 25:43611
energy loss at 10 MeV to 100 GeV in silicon, calculations of average and most probable, (T), 25:42155
exchange in K⁺ + n → K(890) + p interactions at 9 GeV/c in deuterium bubble chamber, (E), 25:43548 (COO-1428-283)
exchange in K⁺ + n → K(890) + p interactions at 9.1 GeV in deuterium bubble chamber, (E), 25:43547 (COO-1428-281)
flux in cosmic radiation at atmospheric depth of 976 gcm⁻² at 12 to 15 GeV, spark chamber study of ratio to nucleons for, (E), 25:43621
form factor from π production in e + N interactions beyond resonance region, model for, (E/T), 25:43583 (DESY-71/22)
form factor in dual resonance model, electromagnetic, 25:43593
interactions A_1 + π → A_1 + π in Veneziano model, amplitude for, 25:43629
interactions e + π → W^- + ν + π at 30 to 300 GeV, total cross sections for, (T), 25:43603
interactions γ + π → 2π, parton model for dual amplitude for, 25:43592
interactions of, ghost-eliminating modifications and factorization of amplitudes for, 25:43628
interactions π + N → 2π + N at low energies, final-state mass spectra relation with two-body forces for, (T), 25:43643
interactions π + N at 2.75 to 10 GeV/c, experimental data for reconstruction of energy and angular dependence of amplitudes in near forward, (E/T), 25:43640 (LYCEN-7110)

interactions π + N at high energies and all angles, optical model for, (T), 25:43571
interactions π + N, inequalities for partial waves for, (T), 25:43641 (SU-1206-249)
interactions π + N, Regge cuts for unitarized finite-energy sum rules for charge-exchange, (T), 25:43637 (DESY-71/24)
interactions π + π → π + π, dual crossing-symmetric amplitude with Mandelstam analyticity for, (T), 25:43623 (ITF-71-28-E)
interactions π + π in π⁺ + n → p + mγ interactions at 2.15 GeV/c in deuterium bubble chamber, 2π⁰ final state for s-wave, (E), 25:43562
interactions π + π in π⁻ + p → π⁻ + π⁺ + n interactions at 3 to 5 GeV/c, counter--spark chamber study of, (E), 25:43555
interactions π + π, dual amplitudes with unitary symmetry for, 25:43627
interactions π + π, Regge pole exchanges in continuous-moment sum rules for, (T), 25:43636
interactions π + π, review of crossing and positivity properties of s and p partial waves for amplitudes of, 25:43711 (SU-1206-243)
production in e + N interactions beyond resonance region, model with π form factor for, (E/T), 25:43583 (DESY-71/22)
production in K⁺ + p, π⁻ + p, π⁺ + p, and p + p interactions at 7.0 to 28.5 GeV/c in bubble chamber, factorization in inclusive processes from single-particle momentum distributions for, (E), 25:43554 (UR-875-340)
production in meson (π⁻) reactions with complex nuclei at 17 and 45 GeV, Deck model for diffraction coherent, (T), 25:43646 (JINR-P1-5775)
production in p + p → d + MM interactions at 3.8 to 6.3 GeV, wire-chamber spectrometer study of rate for, (E), 25:43541
production in π + N → 2π + N interactions at low energies, final-state mass spectra relation with two-body forces for, (T), 25:43643
production in π⁻ + p interactions at 4 GeV/c, thermodynamical description of momentum distributions for, (T), 25:43639 (JINR-P1-5849)
production of massless, consistency test in algebraic realization of chiral symmetry from multiple, 25:43663
production of single hard, in N + N nonrelativistic interactions, N + N interactions from, (T), 25:43653
production of soft, in e + e and e + p interactions amplitude for, 25:43596
reactions with carbon above 20 GeV, fluctuations in angular distributions of secondary particles from, (E), 25:43540
reactions with nuclei, theory of charge-exchange, 25:43978
scattering by carbon-12 at intermediate energies, DWIA analysis using diffraction approximation and modified distorted-wave code, (T), 25:43830

MESONS (π⁻)
absorption in polyethylene, at 70 MeV ionization curves for, (E), 25:42141
interactions π⁻ + p → 2π⁰ + n at 291 to 407 MeV, total cross sections for, (E), 25:43564
interactions π⁻ + p → A_1^- + p at 5 to 25 GeV/c in hydrogen bubble chamber, cross sections and failure of s-channel helicity conservation in, (E), 25:43664 (COO-1195-204)
interactions π⁻ + p → K⁺ + Σ⁻(1385) at 4.5 and 6 GeV/c, production mechanism for forward, (E/T), 25:43558
interactions π⁻ + p → n + eta at 5.9 GeV/c, spark chamber and scintillation counter study of differential and total cross sections for backward, (E), 25:43563
interactions π⁻ + p → π⁰ + n, multiple quark scattering analysis for polarization effect and energy and momentum transfer square dependencies of differential cross sections for, (E), 25:43615
interactions π⁻ + p → π⁰ + p at 150 to 600 MeV at 60 to 170°, scintillation counter study of differential cross sections for, (E), 25:43564
interactions π⁻ + p → π⁺ + 2π⁻ + p at 5 GeV/c, multi-Regge model for, (T), 25:43602
interactions π⁻ + p → π⁻ + p and π⁻ + p → π⁰ + n interactions at low energies, mass difference and Coulomb effects in, 25:43645
interactions π⁻ + p → π⁻ + p at 0.55 to 1.3 GeV/c, resonance and diffraction parameters in model for, (T), 25:43643
interactions π⁻ + p → π⁻ + π⁺ + n at 3 to 5 GeV/c, counter--spark chamber study of π + π interactions and ππ(645), ππ(936), and ππ(1029) enhancements in, (E), 25:43555
interactions π⁻ + p → π⁻ + X at 8 and 16 GeV/c, duality in triple Regge limit, (T), 25:43649
interactions π⁻ + p → π⁻(π⁰) + p(n) at low energies, Coulomb corrections for, (T), 25:43599
interactions π⁻ + p at 24.8 GeV/c in bubble chamber, factorization in inclusive processes from single-particle momentum distributions of π produced in, (E), 25:43554 (UR-875-340)
interactions π⁻ + p at 4 GeV/c, thermodynamical description of momentum distributions of π produced in, (T), 25:43639 (JINR-P1-5849)
production in K⁺ + p → π⁻ + particles at 12 GeV/c, symmetric, (E), 25:43557
production in proton reactions with beryllium at 10 to 500 GeV, estimation of flux of, (T), 25:43726 (BNL-15893)
production of π⁺--π⁻ pairs in nonresonant and rho⁰ production in γ reactions with nuclei at high energies, dynamical effects of instability in, (T), 25:43604
reactions (π⁻,π⁺) with helium-3 at 140 MeV, differential cross sections for three-neutron resonance in, (T), 25:43791
reactions with complex nuclei at 17 and 45 GeV, Deck model for diffraction coherent production of π in, (T), 25:43646 (JINR-P1-5775)

MESONS (π⁰)
interactions γ + π⁰ → γ + π⁰, coupling constants for fγγ and epsilonγγ from finite-energy sum rules for, (T), 25:43582 (DESY-71/20)
interactions π⁰ + π⁰ → π⁰ + π⁰, inequalities for s-wave and p-wave amplitudes for, 25:43626
interactions π⁰ + π⁰ → π⁺ + π⁻, inequalities for s-wave and p-wave amplitudes for, 25:43626
interactions π⁰ + π⁰, analyticity, crossing symmetry, and positivity constraints on partial-wave amplitudes for, 25:43625
interactions π⁰ + π⁰, inequalities on partial waves from orthogonal polynomials for, 25:43633
mean free path in nuclei from photoproduction on lead at 1.1 GeV, 25:43595
production in γ + N → π⁰ + N interactions, Regge cuts due to absorption in, (T), 25:43601
production in γ + p → π⁰ + p interactions at 4 to 18 GeV, spectrometer study of energy dependence of cross sections for, (E), 25:43529
production in photon reactions with lead at 1.1 GeV, nucleon distribution and π⁰ mean free path in nuclei from, 25:43595
production in π⁻ + p → 2π⁰ + n interactions at 291 to 407 MeV, total cross sections for, (E), 25:43564

MESONS (π⁺)
absorption in polyethylene, at 70 MeV ionization curves for, (E), 25:42141
decay π⁺ → μ⁺ + nu + γ, mass of nu from γ spectra in, 25:43609
interactions π⁺ + d → d + 2π⁺ + π⁻ at 13 GeV/c in deuterium bubble chamber, production of A_3(1600) in 3π system in, (E), 25:43550 (COO-1428-290)
interactions π⁺ + d → d + 3π⁺ + 2π⁻ at 13 GeV/c in deuterium bubble chamber, 5π(1900) enhancement in, (E), 25:43550 (COO-1428-290)
interactions π⁺ + d at 13 GeV/c in bubble chamber, production of A_3(1640), f⁰, rho, and 2π and 4π even-G-parity states in R region in, (E), 25:43545 (COO-1428-277)
interactions π⁺ + d at 2.05 to 2.35 GeV/c in deuterium bubble chamber, strange particle and resonance production, cross sections, angular distributions, and polarization in, (E), 25:43561
interactions π⁺ + n → p + mγ at 2.15 GeV/c in deuterium bubble chamber, 2π⁰ final state, eta, ω, and eta' production and s-wave π + π interactions in, (E), 25:43562
interactions π⁺ + n → p + π⁺ + π⁻ + π⁰ at 1.83 to 2.33 GeV/c in deuterium bubble chamber, baryon exchange and ω⁰, eta⁰, and π⁺π⁻π⁰(1050) production in, (E), 25:43556
interactions π⁺ + n → p + π⁺ + π⁻ at 1.83 to 2.33 GeV/c in deuterium bubble chamber, baryon exchange and rho⁰ production in backward, (E), 25:43556
interactions π⁺ + p → Δ⁺⁺(1236) + π⁰ at 1.1 to 1.95 GeV/c in hydrogen bubble chamber, s- and t-channel effects on angular distributions and differential cross sections for, (E), 25:43551 (UCR-34-P-107-B-108)
interactions π⁺ + p → π⁺ + p at low energies, Coulomb corrections for, (T), 25:43599
interactions π⁺ + p → π⁺ + π⁰ + p at 1.85 to 2.09 GeV in hydrogen bubble chamber, cross sections for Δ⁺⁺(1236) and Δ(1236) production in, (E), 25:43552 (UCR-34-P-107-B-110)
interactions π⁺ + p → rho⁺ + p at 1.780 to 2.140 MeV in hydrogen bubble chamber, differential cross sections, angular distributions, and density matrix elements of rho⁺ in, (E), 25:43553 (UCR-34-P-107-B-120)
interactions π⁺ + p → rho⁺ + p at 1.85 to 2.09 GeV in hydrogen bubble chamber, cross sections, angular distributions, and Dalitz plot for, (E), 25:43552 (UCR-34-P-107-B-110)
interactions π⁺ + p at 7.0 GeV/c in bubble chamber, factorization in inclusive processes from single-particle momentum distributions of π produced in, (E), 25:43554 (UR-875-340)
production of π⁺--π⁻ pairs in nonresonant and rho⁰ production in γ reactions with nuclei at high energies, dynamical effects of instability in, (T), 25:43604

MESONS (rho)
interactions rho⁰ + N → rho⁰ + N, dynamical effects of instability in, (T), 25:43604
production in γ + N → rho⁰ + N interactions, dynamical effects of instability in, (T), 25:43604
production in p + p → d + MM interactions at 3.8 to 6.3 GeV, wire-chamber spectrometer study of rate for, (E), 25:43541

XUM

production in π^+ + d interactions at 13 GeV/c in bubble chamber, (E), 25:43545 (COO-1428-277)
production in π^+ + p → Δ^{++}(1236) + π^0 interactions at 1.1 to 1.95 GeV/c in hydrogen bubble chamber, (E), 25:43551 (UCR-34-P-107-B-108)
production in π^+ + p → rho$^+$ + p interactions at 1.85 to 2.09 GeV in hydrogen bubble chamber, cross sections, angular distributions, and Dalitz plot for, (E), 25:43552 (UCR-34-P-107-B-110)
production in π^+ + p → rho$^+$ + p interactions at 1.780 to 2.140 MeV in hydrogen bubble chamber, differential cross sections, angular distributions, and density matrix elements for, (E), 25:43553 (UCR-34-P-107-B-120)
production of rho^0 in backward π^+ + n → p + π^+ + π^- interactions at 1.83 to 2.33 GeV/c in deuterium bubble chamber, angular distribution for, (E), 25:43556
production of rho^0 in photon reactions with nuclei at high energies, dynamical effects of instability in π^+--π^- pair production from, (T), 25:43604

MESONS (X^0)
decay X^0 → π^+ + π^- + γ, comparison of chiral Lagrangian model and Veneziano model of amplitudes for, 25:43631

MESONS, RESONANCE
coupling constant for epsilon$\gamma\gamma$, finite-energy sum rules for γ + π^0 → γ + π^0 interactions for, (T), 25:43582 (DESY-71/20)
decay A_1 → epsilon + π, current algebra prediction for width of, 25:43630
decay A_3(1600) → f^0(rho) + π^+ in deuterium bubble chamber, branching ratios for, (E), 25:43550 (COO-1428-290)
decay epsilon → π + π, current algebra prediction for width of, 25:43630
decay K(890) → K$^+$ + π^- in deuterium bubble chamber, asymmetry in angular distribution for, (E), 25:43548 (COO-1428-283)
decay K(890) → K$^+$ + π^- in deuterium bubble chamber, asymmetry in angular distribution for, (E), 25:43547 (COO-1428-281)
decay of K(890) and phi(1020) in deuterium bubble chamber, angular correlations for, (E), 25:43561
interactions A_1 + π → A_1 + π in Veneziano model, amplitude for, 25:43629
isospin of Kanti K enhancement in 4K, 2Kπ, and 2K2π final states in anti p + d and anti p + p interactions at 2.2 GeV/c in bubble chamber, (E), 25:43536
mass and width of (975) enhancement in p + p → d + MM interactions at 3.8 to 6.3 GeV, wire-chamber spectrometer study of, (E), 25:43541
mass and width of A_3(1640) in π^+ + d interactions at 13 GeV/c in bubble chamber, (E), 25:43545 (COO-1428-277)
mass and width of K(890) and K(1420) in K$^+$ + n → K$^+$ + π^- + p interactions at 9.1 GeV in deuterium bubble chamber, (E), 25:43547 (COO-1428-281)
mass and width of $\pi\pi$(645), $\pi\pi$(936), and $\pi\pi$(1029) enhancements in π^- + p → π^- + π^+ + n interactions at 3 to 5 GeV/c, counter--spark chamber study of, (E), 25:43555
mass structure of A_2(1300), model for two-meson, (T), 25:43580
parity and spin of A_3(1680) from decay in deuterium bubble chamber, (E), 25:43550 (COO-1428-290)
parity and spin of, multipole moments for determination of, (T), 25:43581
production and properties of A_1, A_3, Q, and L, review of, (E), 25:43542 (COO-1195-215)
production of (975) enhancement in p + p → d + MM interactions at 3.8 to 6.3 GeV, wire-chamber spectrometer study of, (E), 25:43541
production of 5π(1900) enhancement in π^+ + d → d + 3π^+ + 2π^- interactions at 13 GeV/c in deuterium bubble chamber, (E), 25:43550 (COO-1428-290)
production of A_1^- in π^- + p → A_1^- + p interactions at 5 to 25 GeV/c in hydrogen bubble chamber, cross sections and failure of s-channel helicity conservation in, (E), 25:43664 (COO-1195-204)
production of A_3(1600) in 3π system in π^+ + d → d + 2π^+ + π^- interactions at 13 GeV/c in deuterium bubble chamber, (E), 25:43550 (COO-1428-290)
production of A_3(1640) and 2π and 4π even-G-parity states in R region in π^+ + d interactions at 13 GeV/c in bubble chamber, (E), 25:43545 (COO-1428-277)
production of delta(963) in p + p → d + MM interactions at 3.8 to 6.3 GeV, wire-chamber spectrometer study of upper limits for, (E), 25:43541
production of epsilon(750) in e + e → e + e + epsilon(750) interactions, radiative widths and cross sections for, (E), 25:43582 (DESY-71/20)
production of K(1243) and K(1344) in Q region and K(890) in K$^+$ + d → K$^+$ + π^+ + π^- + d(p + n) interactions at 9.04 GeV/c, (E), 25:43543 (COO-1428-274)
production of K(1243) and K(1344) in Q region of K$^+\pi^+\pi^-$ mass spectrum and K(890) in K$^+$ + d → K$^+$ + π^+ + π^- + d(n + p) interactions at 9 GeV/c in deuterium bubble chamber, (E), 25:43544 (COO-1428-275)
production of K(1420) in K$^+$ + n → K$^+$ + π^- + p interactions at 9 GeV/c in deuterium bubble chamber, (E), 25:43548 (COO-1428-283)
production of K(890) and K(1420) in K$^+$ + n → K$^+$ + π^- + p interactions at 9.1 GeV in deuterium bubble chamber, cross sections, mass, and width for, (E), 25:43547 (COO-1428-281)
production of K(890) and phi(1020) in π^+ + d interactions at 2.05 to 2.35 GeV/c in deuterium bubble chamber, (E), 25:43561
production of K(890) in K$^+$ + n → K$^+$ + π^- + p interactions at 9.1 GeV in deuterium bubble chamber, energy dependence of cross sections, π-exchange mechanism, and density matrix elements for, (E), 25:43547 (COO-1428-281)
production of K(890) in K$^+$ + n → K$^+$ + π^- + p interactions at 9 GeV/c in deuterium bubble chamber, π exchange mechanism, energy dependence of cross sections, and density matrix elements for, (E), 25:43548 (COO-1428-283)
production of K(890) in K$^-$ + n interactions at 4.48 GeV/c in deuterium bubble chamber, (E), 25:43549 (COO-1428-286)
production of K(890), Kanti K, KKπ, K$\pi\pi$, and K*anti K* in 2K, 4K, 2Kπ, and 2K2π final states in anti p + d and anti p + p interactions at 2.2 GeV/c in bubble chamber, (E), 25:43536
production of Kπ(1750) in K$^+$ + n → p(n) + K$^+$(K^0) + π^-(π^+) at 9.0 GeV/c in deuterium bubble chamber, (E), 25:43546 (COO-1428-279)
production of $\pi^+\pi^-\pi^0$(1050) in π^+ + n → p + π^+ + π^- + π^0 backward interactions at 1.83 to 2.33 GeV/c in deuterium bubble chamber, (E), 25:43556
production of $\pi\pi$(645), $\pi\pi$(936), and $\pi\pi$(1029) enhancements in π^- + p → π^- + π^+ + n interactions at 3 to 5 GeV/c, counter--spark chamber study of, (E), 25:43555
properties of K(1243) and K(1344) in Q region of K$^+\pi^+\pi^-$ mass spectrum in K$^+$ + d → K$^+$ + π^+ + π^- + d(n + p) interactions at 9 GeV/c in deuterium bubble chamber, (E), 25:43544 (COO-1428-275)
splitting of A_2, model for, (T), 25:43624 (UCR-34-P-107-B-112)

MESOSPHERE
hydroxyl (OH) column density at 50 to 85 km in, altitude-dependent upper limit, (E/T), 25:43262

METABOLIC-INHIBITOR DRUGS
effects on oxygen consumption and lysine uptake by x-irradiated HeLa cells, 25:42295

METABOLISM
effects on x radiosensitivity of rats in relation to age and sex, 25:42635
radiation effects on control of pathways in, model for low-dose, 25:42606
radiation effects on human, for use as indicator of radiation injury, criteria for evaluating, 25:42400

METALLIC FOILS
performance of multi-layered oxide-coated, as thermal insulation for high- and low-temperature uses, 25:42962

METALLURGY
research progress on, 25:41777(R) (UCRL-20500)

METALS
abundance in globular cluster M71, (E), 25:43035
analysis for hydrogen by isotopic equilibration mass spectrometry, 25:41747 (AAEC/TM-588)
analysis for surface carbon by methods using nuclear reactions, 25:41765
analysis of refractory, for nitrogen and oxygen using fluxes enriched with nitrogen-15 and oxygen-18, isotope dilution, 25:41748
ceramic wetting by liquid, mechanisms of, 25:42980
complexes with morin, separation of, using isoamyl alcohol, 25:41738
determination using morin, extraction-photometric or extraction-fluorometric, 25:41738
electric conductivity of, validity of Boltzmann equation for systems with both electron-phonon and impurity scattering for calculating, 25:44273 (NYO-3699-56)
fabrication and testing of, for use in reactors, standard for, 25:42817 (RDT-F-3-37-T)
fabrication of close tolerance shapes in most wrought, by form rolling, 25:42827
flow rate measurements of liquid, theories of electromagnetic method for, 25:42184 (JAERI-13536)
flow rate of liquid, standard for design and testing of permanent magnet flowmeter for measuring, 25:42191 (RDT-C-4-5-T)
forging of powder metallurgy preforms of, in closed dies, review of methods for, 25:42829
level measurement of liquid, standard for design and testing of resistive sensor for, 25:42193 (RDT-C-5-2-T)
level measurement of liquid, standard for design and testing of inductive sensor for, 25:42192 (RDT-C-5-1-T)
plastic deformation in, at low temperatures, Crowdion mechanism of, (E/T), 25:43484
pressing of powdered, comparison of conventional and hydrostatic methods for, 25:42828
pressure gage for liquid metal, standard for design and testing of eddy current, 25:42195 (RDT-C-6-3-T)
pressure transmitters for liquid, standard for design and testing of, 25:42194 (RDT-C-6-1-T)
production of composites of clad- and diffusion coated, review of technologies for, 25:42951
radiation effects on, description of heavy-ion accelerators for simulating fast-neutron, 25:43758

radioinduced creep in, model for neutron, 25:42900 (AD-719935)
radioinduced swelling in, discussion of, 25:42920
radioinduced swelling in, review of model for fast neutron, 25:42918
standard for identification marking of products of, 25:42762 (RDT-F-7-1-T)
thermal capacities under high pressure, 25:41778 (UCRL-20500, pp 1-85)
ceramics--metals, preparation and properties of fiber-reinforced composites of, review of, 25:42978
METEORITES
analysis for rare earths by neutron activation and high-voltage electrophoresis, 25:41776
analysis for trace elements by neutron activation and γ spectrometry, 25:41773
composition of, chemical, (T), 25:43076
distribution and origin of helium, neon, and argon isotopes in, (E), 25:43099
METEOROIDS
ablation and breakup during passage through planetary atmosphere, large, (E/T), 25:43263
METHACRYLIC ACID, METHYL ESTER
radioinduced polymerization in wood, γ, 25:41843(R) (ORO-2945-10)
methyl methacrylate--styrene, radioinduced polymerization of, effects of temperature on microstructure of products from γ, 25:41845
METHANE
sorption by surfaces of nickel chloride, thermodynamic studies on stepwise isotherms for, 25:41824 (CEA-R-4089)
METHANE, BROMO-
reactions with bromine-80 and bromine-82 recoil atoms, effects of energy on, 25:41833(R) (IA-1218)
METHANE, CHLORO-
reactions with chlorine-38 recoil atoms, effects of scavengers on yields from, 25:41833(R) (IA-1218)
METHANE, IODO-
sorption by impregnated charcoal in carbon dioxide--carbon monoxide--methane system, 25:41898 (TRG-Report-2135)
METHANESULFONIC ACID, ETHYL ESTER
effects on chlorophyll mutation frequency and growth of rice seedlings following treatment of seeds with D_2O, 25:42345
effects on Neurospora, specificity of mutagenic, 25:42352
METHANOL
solution heat of, effects of deuterium on, 25:41794
ethanol--methanol, radiolysis of, ion--solvent interactions in x, 25:41871
METHIONINE
radiation effects of content of sulfur-35-labeled, in rat organ proteins, x, 25:42265
METHOXYAMINE
radiolysis at 77°K, ESR studies on trapped radicals produced by γ, 25:41857
METHYL SULFOXIDE
radioprotective effects of, in rats, mechanism of x, 25:42524
METHYLAMINE
radiolysis at 77°K, ESR studies on trapped radicals produced by γ, 25:41857
radiolysis of, adsorbed on silica gel at 77°K, ESR studies on trapped radicals produced by γ, 25:41856
METHYLENE BLUE
effects on uv radiosensitivity of Serratiaphage kappa, 25:42734
radioprotective effects of, on mice and rats, whole-body γ or x, 25:42515
radioprotective effects on blood glucose, liver glycogen, and serum electrolytes of rats, x, 25:42283
radioprotective effects on lactate dehydrogenase activity in rats, γ, 25:42284
METHYLPREDNISOLONE
effects on tetanus antitoxin production in mice, combined effects of γ radiation and, 25:42672
METROLOGY
theory of quantum, 25:43523
MICE
cerium-144 sorption by gastrointestinal tract of suckling, 25:41833(R) (IA-1218)
effects of radioprotective thiols on ultrastructure of duodenum crypt cells in, effects of thiol-blocking compounds on, 25:42520
effects of serotonin on adrenal glands, liver, ovaries, and thyroid glands in, 25:42519
lymphoid cell decay in mesenteric lymph node in, tritium autoradiography and nigrosin dye exclusion method for studying, 25:42240
radiation effects on acid phosphatase in thymus gland of, whole-body x, 25:42287
radiation effects on adrenal cortex and reticulo-endothelial system in, protective effects of cysteamine, lipopolysaccharide, and serotonin against x, 25:42513
radiation effects on carcinogenesis in enamel organ in, combined effects of physical trauma and x, 25:42670
radiation effects on cell population kinetics in thymus gland in, chronic whole-body, 25:42631
radiation effects on chemical composition of hemoglobin in, effects of dose rate on chronic whole-body, 25:42586 (ORAU-113, pp 4-77)
radiation effects on differentiation of surviving stem cells in, comparison between effects of alkylating agents and x, 25:42661
radiation effects on DNA in tissues of, following ingestion of tritium-labeled thymidine, β, 25:42262
radiation effects on excretion of deoxyribosyl compounds in urine of, as indicator of radiation injury, 25:42622
radiation effects on fertility in, following testicular exposure, x, 25:42659
radiation effects on hemagglutinin formation in, exposure rate dependence of γ, 25:42307
radiation effects on hematopoiesis in, effects of irradiated and unirradiated bone marrow transplants on x, 25:42644
radiation effects on immunological tolerance to virus, x, 25:42313
radiation effects on immunosuppression in, combined effects of drugs and γ, 25:42672
radiation effects on life span of germfree, effects of age and sex on x, 25:42663
radiation effects on metabolism of nicotinamide-adenine dinucleotide and nucleic acid metabolites in, mechanisms for, 25:42623
radiation effects on spermatogonia of, in relation to lifetime reproductive capacity of offspring, x, 25:42342
radiation effects on spleen stem cells in, effects of actinomycin D on erythropoietic recovery following partial-body x, 25:42673
radiation effects on survival of, long-term protective effects of N- and S-containing polymers against x, 25:42517
radiation effects on survival of, protective effects of adenosine derivatives against γ, 25:42516
radiation effects on survival of, protective effects of methylene blue against whole-body γ or x, 25:42515
radiation effects on survival of, protective effects of cyclophosphamide against lethal x, 25:42518
radiation effects on synthesis of liver catalase in, x, 25:42278
radiation effects on testes in, effects of bone marrow transplants on lethal whole-body γ, 25:42304
radiation effects on tumor incidence in, comparison of β, γ, and fast neutron, 25:42654
radiation effects on tumor incidence in, comparison of latent external fast neutron or γ and internal tritiated thymidine, 25:42630
radiation effects on, relation of survival of jejunum stem cells to dose dependent electron, 25:42633
radiation effects on, role of bone marrow transplants in long-term survival following x, 25:42666
radioinduced chromosome aberrations in bone marrow cells of, protective effects of cysteine derivatives against whole-body x, 25:42534
radioinduced chromosome translocations in spermatogonia of, in relation to radioresistant cell lines, fast neutron, 25:42355
radioinduced late syndrome in, following treatment with isologous bone marrow transplants, pathology of x, 25:42665
radioinduced leukemia in, following exposure to strontium-90, relation between dose and incidence of, 25:42654
radioinduced leukopenia in, partial-body bremsstrahlung, 25:42599
radioinduced malformations in central nervous system in embryos of, x, 25:42629
radioinduced malformations in fetuses of, in comparison to rats, x, 25:42639
radiosensitivity of bone marrow cells of, effects of age on x, 25:42656
tritium metabolism in tissues of, following ingestion of labeled thymidine, 25:42262
MICHIGAN, LAKE
thermal plumes in, physical characteristics of power plant, (E), 25:44138 (CONF-710431-1)
MICROORGANISMS
conference on, abstracts of papers presented at American Society for Microbiology Annual Meeting (1971), 25:42739
radioinduced mutations for improvement in practical applications of, review of fast neutron, uv, and x, 25:42349
uranium transport in lake silts by, 25:42256
MICROWAVE EQUIPMENT
design of interferometric, for plasma density measurements, 25:42183(T) (CTC-756)
MICROWAVES
detectors of, response of superconducting point-contact, (E/T), 25:43297
gravitational deflection in solar field, (E), 25:43094
interactions with plasma column, nonlinear behavior of Tonks--Dattner resonances in, (T), 25:43411
monitoring system for pulsed, broadband, 25:42188 (MATT-845)
performance for diagnostics of laser-produced plasmas, (E), 25:43342
use for plasma diagnostics, 25:43345(P)

XUM

MILK
analysis for radiocesium by ion exchange using ammonium molybdophosphate and counting, 25:41751
effects of products of, combined with radioprotective substances on reduction of radiation hazards to uranium mining personnel, 25:42510
fallout content of, in Canada, Central and South America, and USA during 1970, 25:42417
iodine-131 content of, following injection into atmosphere as aerosol mist, 25:42370 (SWRHL-43-r)
radioactivity monitoring in Ecuador, 1966 to 1967, 25:41940
radioisotope content in Korean, from 1965 through 1968, effects of fallout specific activity on, 25:42372
radioisotope content of, in Canada, Central and South America, and USA during November 1970, 25:42421
radioisotope content of, in Pavia, Italy, 25:42389
strontium-90 content in, in Czechoslovakia during 1965 to 1968, 25:42386
strontium-90 content of, in Czechoslovakia during 1963 to 1966, 25:42385

MILKY WAY
properties of extraordinary red object in Sagittarius, (E), 25:43084
x-ray background in, (T), 25:43079 (N-71-20472)

MILLSTONE POINT POWER REACTOR, UNIT 1
electric generator for, description of load trips for, 25:44012 (DOCKET-50245-85)

MINERAL RESOURCES
estimates of portion of Grenville Province of Canadian Shield, probabilistic, 25:41944

MINERALS
analysis for trace elements in prospecting, review on neutron activation methods for, 25:41767
analysis of sedimentary, for halogens by Szilard--Chalmers reactions following neutron activation, 25:41763
exploration for conference on nuclear techniques for, Krakow, Dec. 8 to 12, 1969, 25:41941 (STI/PUB-279)
exploration of, uses of radioisotope x-ray fluorescence analysis in, 25:41739
prospecting and on-stream analysis of, use of x-ray fluorescence analysis in, 25:41741
prospecting in Spain, review of nuclear methods for, 25:41946

MINING
hazards to Czechoslovakian personnel from uranium, health education for prevention of, 25:42504
hazards to personnel from uranium, ILO radiation protection manual for prevention of, 25:42463

MISCH METAL
combustion of, comparison of effectiveness of dry powders for extinguishing, 25:42837 (AERE-R-6745)

MITOCHONDRIA
effects of radioprotective thiols on, in duodenum crypt cells in mice, effects of thiol-blocking compounds on, 25:42520

MITOSIS
radiation effects on rat bone marrow cells, protective effects of direct electric current against x, 25:42530
radiation effects on, in gonads of oysters, effects of dose on, 25:42507
radioinduced delay in human lymphocyte, effects of age and phytohemagglutinin on, 25:42602

MIXER-SETTLERS
design and operation of, 25:41895 (INR-1309)
performance for separation of uranium from nitric acid solutions, comparison between computer-simulated and actual, 25:41890 (CEA-N-1450)

MOESSBAUER SPECTROMETERS
absorber system with two moving absorbers for measurement of recoilless fractions of quadrupole split sources, 25:42120
drive system for, 25:41833(R) (IA-1218)
oven for, design of gradient-free, 25:42115
spectral lines in, optimal determination of location of, 25:42122

MOISTURE GAGES
accuracy of neutron radiometric, 25:42177

MOLDS
temperature cycling of, operational theory of equipment used to control, 25:44230 (BDX-613-369)

MOLECULAR BEAMS
production of high-current, performance of hot-cathode constricted-arc plasma sources for, 25:43401
reactions of, research progress on, 25:41778 (UCRL-20500, pp 1-85)
scattering in correlated nonstationary states, cross section enhancement by, 25:43105

MOLECULES
atom reactions with diatomic, quenching of quantum effects in classical S-matrix approach to, 25:43156
electron scattering by polar, model for, 25:43130
interactions between, aggregate theory of, 25:43163
radiation effects on, relation between physiological state of living cells and, 25:42727 (NYO-2804-38)
wave functions for diatomic, even-tempered atomic orbitals as bases for, (T), 25:43160 (IS-T-456)

MOLLUSCA
Caracollus sp., radioisotope uptake by, in rain forest in Puerto Rico, 25:42317(R) (PRNC-147)
Crassostrea gigas, radiation effects on tissues and survival of, effects of dose on, 25:42607
Lymnaea sp., role as vector of Fasciola hapatica in Puerto Rico, 25:42246(R) (PRNC-148)

MOLYBDENUM
book: High-Temperature Materials, 25:42953
carburization of boride-coated, effects of temperature on, 25:42854
crystal structure of, effects of trace carbon on, 25:42899
determination following separation from other metal ions by thin-layer chromatography using quercetin, colorimetric, 25:41743
determination in aqueous solutions using 2,6,7-trihydroxy-9-phenyl-3H-xanthen-3-one or 2,6,7-trihydroxy-9-methyl-3H-xanthen-3-one, spectrophotometric, 25:41726
determination in steels by atomic absorption spectrometry, 25:41728
determination of trace amounts of, in meteorites by neutron activation and γ spectrometry, 25:41773
mechanical properties of crystalline, effects of trace carbon on, 25:42899
properties as internal reference in zirconium determination, 25:41764
separation from acetone--hydrochloric acid solutions by ion exchange using Bio-Rad, distribution coefficients for, 25:41699
separation from ores, leaching methods for, 25:41918
separation from other metals using inorganic ion exchange papers, 25:41909

MOLYBDENUM ALLOYS AND SYSTEMS
Al--Cr--Mo--Ti-base--V--Zr, mechanical properties of, 25:42836 (AD-715877)
Al--Mo--Ti-base--V, radiation effects on tensile properties of, at 17°K, fast neutron, 25:42926
C--Fe--Mo-base, phase diagrams at 1200 and 1800°C, isothermal, 25:42889
C--Fe--Mo-base, properties of, mechanical and physical, 25:42889
C--Mo-base--Ti, phase diagrams at 1200 to 2100°C, isothermal, 25:42890
Cr--Cu--Fe--Mo--Nb--V--Zr-base, corrosion resistance of, 25:42811
Cr--Fe-base--Mn--Mo--Ni, ductility of irradiated Sandvik 12R72HV, at 500 to 800°C, effects of injected helium on, 25:42872
Cr--Mo--steel, corrosion by sodium--water reaction products at 600°F, 25:42804(R) (LMEC-71-1)
Cr--Mo--steel, standard for plates of, 25:42795 (RDT-M-5-5-T)
Cu--Mo--Zr-base, corrosion by carbon dioxide at 400 to 700°C, 25:42809
Cu--Mo--Zr-base, corrosion by carbon dioxide at 450 to 500°C, 25:42813
Cu--Mo--Zr-base, microstructure of phases in, 25:42898
Cu--Mo--Zr-base, phase studies of, 25:42897
Cu--Mo--Zr-base, properties for use in carbon dioxide-cooled reactors, 25:42878
Cu--Mo--Zr-base, radiation effects on mechanical properties of, relations of annealing with fast neutron, 25:42813
Cu--Mo--Zr-base, radiation effects on properties of, for use in El-4 pressure tubes, neutron, 25:42929
Fe--Mo, mechanical properties of sintered intermetallic compounds of, 25:42818
Fe--Mo, sintering of intermetallic compounds of, kinetics of, 25:42818
Mn--Mo--Ni--steel, standard for plates of, for pressure vessels, 25:42793 (RDT-M-5-3-T)
Mn--Mo--steel, standard for plates of, for pressure vessels, 25:42793 (RDT-M-5-3-T)
Mo--Ni-base, crystal ordering in solid-solution, mechanisms of short-range, 25:42886 (UCRL-20500, pp 86-146)
Mo--Ni-base, electric and thermomagnetic properties of, 25:43476
Mo--Re, superconducting transition temperature in high T/sub c/ intermetallic $MoRe_3$, sensitivity to residual stress of, (E), 25:43302
Mo--ThO_2, permeability and porosity of cold-pressed and sintered pellets of, 25:41993(R) (ORNL-4692)
Mo-base--Re, deformation at low temperatures, effects of crystal orientation on plastic, 25:42886 (UCRL-20500, pp 86-146)
Mo-base--Ti, deformation behavior of, effects of deformation rates on, 25:42833
Mo-base--Ti, properties for use in turbine blades, 25:42833

MOLYBDENUM BORIDE CARBIDE
preparation of, method for, 25:42941
properties of, electric, mechanical, and thermal, 25:42941

MOLYBDENUM ISOTOPES
photon reactions at 20 to 60 MeV, 25:41764

MOLYBDENUM ISOTOPES Mo-90
energy levels from niobium-93 (p,4n) reactions, lifetimes for, (E), 25:43847
energy-level transitions from niobium-93 (p,4n) reactions, probability for E2, (E), 25:43847

MOLYBDENUM ISOTOPES Mo-94
energy levels from gamma resonance scattering, spin-

parity assignments for, (E), 25:41833(R) (IA-1218)
MOLYBDENUM ISOTOPES Mo-98
energy levels from gamma resonance scattering, spin-parity assignments for, (E), 25:41833(R) (IA-1218)
neutron elastic and inelastic scattering up to 1.5 MeV, cross sections for, (E), 25:43884 (ANL-7710, pp 1-52)
neutron total cross section up to 1.5 MeV, (E), 25:43884 (ANL-7710, pp 1-52)
MOLYBDENUM ISOTOPES Mo-99
uptake by animals and plants in lake ecosystem, tracer study on, 25:44297 (RLO-2225-T-7-2)
MOLYBDENUM OXIDES
oxidation of MoO_2, kinetics of, 25:42933
MONEL
weld solidification in, structures and mechanism of, 25:42820
MONKEYS
plutonium oxide removal from lungs of, effectiveness of saline lavage for, 25:42368(T) (LF-tr-83)
radiation effects on behavior of, effects of dose and partial shielding on mixed γ and neutron, 25:42642
radiosensitivity of tissues of gonads in, 25:42586 (GRAJ-113, pp 4-77)
MONOAMINE OXIDASE
radiation effects on activity of human skin, x, 25:42286
MONOMERS
radioinduced polymerization of unsaturated, with polyesters, 25:41847(P)
MONTE CARLO METHOD
model for linear parameter variation in, 25:43504 (BMBW-FBK-70-32)
MONTICELLO POWER REACTOR, UNIT 1
coolant temperature increase in, safety analysis of 115°F per hour, 25:44019 (DOCKET-50263-75)
protection system for, failure of high pressure scram switches for, 25:44019 (DOCKET-50263-75)
standby gas treatment system for, failure of air heater control circuit for, 25:44019 (DOCKET-50263-75)
MORIN
complexes with metals, separation of, using isoamyl alcohol, 25:41738
MORPHINE
radiation effects on analgesic activity and toxicity of solutions of, effects of concentration on γ, 25:42752
MUSCLES
cesium-137 metabolism in human, effects of fiber size on, 25:42250
radiation effects on distribution of iodine-131-labeled albumin in rat, as indicator of radiation injury, whole-body γ, 25:42407
radiation effects on electromyogram of guinea pig, effects of dose on, 25:42652
MUTATIONS
incidence in Escherichia coli grown on γ-irradiated culture media, 25:42755
induction in Neurospora crassa by chemicals and radiation, specificity of, 25:42252
induction in rice plants by D_2O following seed treatment, effects of ethyl methanesulfonate on, 25:42346
radioinduced dominant and recessive autosomal lethal and sex-linked recessive lethal, in rats following exposure of nine generations, x, 25:42321 (COO-697-23)
radioinduced respiration deficient, in Schizosaccharomyces pombe, uv, 25:42338
radioinduced supersensitive yeast, genetic analysis of uv, 25:42337
radioinduced, for fruit and tree improvement of apples, γ, 25:42324
radioinduced, in Arabidopsis for chlorophyll, effects of dose and seed exposure on γ, 25:42358
radioinduced, in Aspergillus niger, x, 25:42363
radioinduced, in dahlias for flower color, 25:42327
radioinduced, in Escherichia coli, effects of 5-bromouracil on sensitivity to uv, 25:42345
radioinduced, in microorganisms for improvement in practical applications, review of fast neutron, uv, and x, 25:42349
radioinduced, in Neurospora crassa, identification of base-pair alterations following uv, 25:42341
radioinduced, in phage T4, effects of mutator alleles on repair of uv, 25:42339
radioinduced, in potatoes for hooded eyes, γ, 25:42323
radioinduced, in rats following exposure of nine generations, effects of random and full-sib mating on x, 25:42321 (COO-697-23)
radioinduced, in spermatogonia of Drosophila, comparison of effects of acute, chronic, and split-dose exposure on low-dose γ, 25:42350
radioinduced, in thymine-dependent strains of Escherichia coli for Gram staining, capacity to ferment carbohydrates, immune reactions, and increased radioresistance, γ, 25:42330
radioinduced, in tomatoes, fast neutron and γ, 25:42364
radioinduced, in wheat, sensitivity of hybrids following x, 25:42365
radiosensitivity of Escherichia coli, in relation to x-radioinduced breaks in DNA, 25:42357
radiosensitivity of Escherichia coli, in relation to gene location, uv, 25:42328
MYOGLOBIN
radioinduced deamination of beef, low-dose γ, 25:42756

N

NAGASAKI
radiation effects on incidence of late aplastic anemia in atomic bomb survivors in, 25:42698
NAPHTHACENE
electron reactions at 50 eV to 10 keV with, cross sections for excitation in, (T), 25:43127(T) (BNL-tr-429)
anthracene--naphthacene, radiinduced quenching of luminescence of crystals of, x, 25:41840
benzo[b]naphtho[2,3-d]furan--naphthacene, radioinduced quenching of luminescence of crystals of, x, 25:41840
naphthacene--p-terphenyl, fluorescence excited by fast electrons, rise and decay times of, 25:43452
NAPHTHALENE
effects on yields of nitrogen from radiolysis of 2,2'-azobis[2-methylpropionitrile]--benzene, 25:41872
NAPHTHALENE, 2,3-DIMETHYL-
anthracene--2,3-dimethylnaphthalene, radiinduced quenching of luminescence of crystals of, x, 25:41840
NATIONAL ACCELERATOR LABORATORY SYNCHROTRON
meson (π⁻) fluxes available from, (T), 25:43726 (BNL-15893)
site survey for, geology and hydrology, 25:43733 (TID-25751)
NATIONAL REACTOR TESTING STATION
ecology of free-living and parasitic arthropods on mammalian, bird, and reptile hosts at, 25:44251 (COO-1559-7)
NATURAL BACKGROUND RADIATION
monitoring in soils and wheat in Western Australia, 25:42427
radiation dose to human population from, 25:42711
radiation dose to human populations from, 25:42693
radiation dose to human populations from, 25:42692
variations in India, relation of lead-210 content of atmosphere, rain, and soil to seasonal, 25:42387
NAVIGATIONAL INSTRUMENTS
design of radiation source--detector system for maintaining helicopter flight formations, 25:42186(P)
NEBULAE
electron temperatures in Gum, (e), 25:43034
origin of Gum, (T), 25:43039
parameters of Gum, (E), 25:43034
physical characteristics of, around Wolf--Rayet stars, (E), 25:43044
plasma electron velocity distribution in, deviation from Maxwellian, 25:43023
polarization of, near FU Ori, (E), 25:43025
properties of peculiar red, in Sagittarius, (E), 25:43084
NECK
radioinduced injuries to human, following combined surgery and therapy, fast electron, 25:42602
radiotherapy of carcinomas of, additive effects of 5-fluorouracil infusion on gamma and x, 25:42585
NEODYMIUM
magnetic structure in strong magnetic fields, 25:43435(R) (RISO-237)
magnetic susceptibility of, generalized function for, (T), 25:43477
neutron total cross section at 100 to 650 keV, optical model analysis of average, (E/T), 25:43908
preparation of large single crystals of, 25:42834
separation from aqueous solutions by ion exchange on zirconium tellurate, tracer studies on, 25:41915
NEODYMIUM BORIDES
enthalpy and heat capacity of NbB_4, 25:42961
NEODYMIUM ETHYL SULFATES
magnetic ac susceptibility study of relaxation processes in nonahydrate of, 25:43472 (YALE-3227-74)
NEODYMIUM ISOTOPES Nd-141
energy levels from neodymium-142 (d,t) reactions, spectroscopic factors and spin-parity assignments for, (E), 25:43900
NEODYMIUM ISOTOPES Nd-142
deuteron reactions (d,t) at 17 MeV, DWBA analysis of angular distributions for, (E), 25:43900
NEODYMIUM ISOTOPES Nd-144
neutron total cross section at 100 to 650 keV, optical model analysis of average, (E/T), 25:43908
NEODYMIUM ISOTOPES Nd-146
neutron total cross section at 100 to 650 keV, optical model analysis of average, (E/T), 25:43908
NEODYMIUM ISOTOPES Nd-148
neutron total cross section at 100 to 650 keV, optical model analysis of average, (E/T), 25:43908
reactions (he-148,f) with uranium-238, effects of nuclear forces on cross sections for Coulomb fission, (T), 25:43970
NEODYMIUM OXIDES
analysis for impurities, cathode region method for spectrochemical, 25:41833(R) (IA-1218)
preparation of crystals of, hydrothermal studies of equilibria with water in, 25:42934 (COO-1105-60)
Al_2O_3--CaO--Nd_2O_3, phase diagrams of, 25:42955
NEON
energy loss at 10 MeV to 100 GeV in silicon, calculations

XUM

of most probable, (T), 25:42155
helium-atom reactions at 13 to 50 keV with, cross sections for one-electron loss in, (E), 25:43153
neon-ion reactions with, characteristic energy losses from excitation and ionization in, (T), 25:43150
nitrogen-oxide-ion (NO^+) reactions with, statistical phase-space model of dissociation in, 25:43159
oxygen-ion (O_2^+) reactions with, statistical phase-space model of dissociation in, 25:43158
photon reactions at 0.28 to 8.03 keV with, relative abundances of multiply charged ions produced by, (E), 25:43142
polarizability of atomic, perturbation calculation of, 25:43117
proton energy straggling and stopping at 100 to 500 keV in, (E/T), 25:43432

NEON IONS
implantation in silicon at 220 keV, measurements of stresses induced by damage from, 25:43441
reactions with carbon at 20 keV to 1.5 MeV, cross sections for K x-ray production in, (E), 25:43107
reactions with neon, characteristic energy losses from excitation and ionization in, (T), 25:43150
reactions with nitrogen molecules at 0.05 to 200 eV, application of statistical phase-space theory to molecular and dissociative charge exchange in, 25:43159
reactions with nitrogen molecules at 30 keV to 2 MeV, cross sections for excitation of N_2^+ 3914-A radiation in, (E), 25:43151

NEON ISOTOPES
distribution and origin of, in Apollo 12 samples, (E), 25:43099

NEON ISOTOPES Ne-17
beta decay of, branching ratios, half-life, and log-ft values for, (E), 25:43802 (UCRL-20480)

NEON ISOTOPES Ne-20
alpha elastic and inelastic scattering at 104 MeV, differential cross sections for, (E), 25:43832 (NP-18920)
alpha inelastic scattering at 104 MeV, quadrupole and hexadecapole deformation parameters from coupled-channels analysis of differential cross sections for, (E/T), 25:43875
deformation parameters from alpha inelastic scattering, (E/T), 25:43875
energy levels of, effects of single-particle energies on shell-model calculations of, (T), 25:43866
energy levels of, interpretation of cluster wave functions for ground-state rotational, (T), 25:43860
energy-level transitions in, shell-model calculations of probabilities for E2, (T), 25:43866
proton reactions (p,pa) at 46.8 MeV, coplanar angular and energy correlations and spectra from, (E/T), 25:43801 (UCLA-10-P-18-31)

NEON ISOTOPES Ne-21
energy level at 2.791 MeV from helium-4 (O-18,n) reactions, lifetime for, (E), 25:43870
energy-level transitions from helium-4 (O-18,n) reactions, branching ratios, multipolarities, and strengths for, (E), 25:43870

NEON ISOTOPES Ne-22
alpha elastic and inelastic scattering at 104 MeV, differential cross sections for, (E), 25:43832 (NP-18920)

NEPTUNIUM
determination by coulometry, conducting glass electrode in thin-layer electrochemical cell for, 25:41732
separation from niobium, uranium, zirconium, and fission products by solvent extraction using tributyl phosphate, 25:41901

NEPTUNIUM ALLOYS AND SYSTEMS
Fe--Np, magnetic properties of cubic Laves phase in intermetallic compound $NpFe_2$, Moessbauer studies on, 25:41833(R) (IA-1218)
Np--Pd-base, magnetic properties at 2.5 to 300°K, (E/T), 25:43488

NEPTUNIUM IONS
valence of recoil atoms of, following α decay, Moessbauer studies on, 25:41833(R) (IA-1218)

NEPTUNIUM ISOTOPES Np-237
alpha decay of, α-γ delayed coincidence spectra from, (E), 25:43895
energy level at 59.5 keV from americium-241 decay, lifetime of, (E), 25:43895
separation from plutonium-238 by valence control, method for, 25:41833(R) (IA-1218)
toxicity to blood, kidneys, and liver of rats, effects of concentration on, 25:42253

NEPTUNIUM ISOTOPES Np-239
metabolism and tissue distribution following intake by man, 25:42457

NERVOUS SYSTEM
radiation effects on growth of corticospinal tract of rat, 25:42615(R) (COO-1201-30)
radiation effects on histology of rat, RBE for fast neutron, 25:42641
radiation effects on human, during prenatal and postnatal development, effects of dose on pathological, 25:42710
radiation effects on human, methods for studying dystonic, 25:42676
radiation effects on vestibular and spinal reflexes of cat, following exposure of cerebellum, x, 25:42657
radioinduced injuries in adult and developing human, 25:42691
radioinduced malformations in central, in human embryos, 25:42629

NETHERLANDS
nuclear power industry activities in, review of, 25:44092
power requirements of, summary of, 25:43997

NEURAMINIDASE
effects on electrophoretic mobility of x-irradiated human erythrocytes in relation to dose, 25:42682

NEUTRINOS
detection of high energy, (T), 25:43174
interactions $\nu + p$ at 10 GeV, self-coupling of weak lepton currents in $\mu^+ - \mu^-$ pair production from, (T), 25:43612
interactions of two- and four-component, with massless particles, cross sections for gravitational, (T), 25:43706
interactions of, energy decay for equation in exterior of torus for, (T), 25:43610
reactions with iron-56 at 10 GeV, self-coupling of weak lepton currents in $\mu^+ - \mu^-$ pair production in, (T), 25:43612

NEUTRINOS (ν/sub e/)
production of anti $\nu + \nu$ pairs in e + p interactions and electron reactions with iron-56 at 150 GeV, self-coupling of weak lepton currents in, (T), 25:43612
production of ν--anti ν pairs in $\gamma + \gamma \rightarrow \nu +$ anti ν interactions, dispersion relations for cross sections and black-body neutrino luminosity for, (T), 25:43605

NEUTRINOS (anti ν/sub e/)
production of anti $\nu + \nu$ pairs in e + p interactions and electron reactions with iron-56 at 150 GeV, self-coupling of weak lepton currents in, (T), 25:43612
production of ν--anti ν pairs in $\gamma + \gamma \rightarrow \nu +$ anti ν interactions, dispersion relations for cross sections and black-body neutrino luminosity for, (T), 25:43605

NEUTRINOS (ν/sub μ/)
mass from γ spectra in $\pi^+ \rightarrow \mu^+ + \nu + \gamma$ decay, 25:43609
production in anti ν--ν pairs in μ + p interactions and μ reactions with iron-56 at 150 GeV, self-coupling of weak lepton currents in, (T), 25:43612
production of ν--anti ν pairs in $\gamma + \gamma \rightarrow \nu +$ anti ν interactions, dispersion relations for cross sections and black-body neutrino luminosity for, (T), 25:43605

NEUTRINOS (anti ν/sub μ/)
production in anti ν--ν pairs in μ + p interactions and μ reactions with iron-56 at 150 GeV, self-coupling of weak lepton currents in, (T), 25:43612
production of ν--anti ν pairs in $\gamma + \gamma \rightarrow \nu +$ anti ν interactions, dispersion relations for cross sections and black-body neutrino luminosity for, (T), 25:43605

NEUTRON BEAMS
antibunching effects of Fermi--Dirac statistics on, possibility of observing, (T), 25:43777
monitoring of position, intensity, and energy distribution of low-intensity, method for, 25:42098
polarization of, review of methods for, 25:43831 (INR-1262)
production of preferentially oriented skin-polarized pulsed, fast switching circuits for, 25:43776

NEUTRON CROSS SECTIONS
calculation of total and differential, for elastic scattering by hydrogen at 0.1 to 30.0 MeV, (T), 25:43798
calculation of, revised MC² computer program for, 25:44191 (ANL-7710, pp 365-463)
calculations for fast assemblies, evaluation of ENDF/B data for, (E/T), 25:44094(R) (AI-AEC-12991)

NEUTRON SOURCES
beam buncher for Dynamitron, klystron, 25:42048 (ANL-7710, pp 263-364)
book: Neutron Physics Practices. Volume I. Physics and Technology of Activation Probes, 25:43775
description of Dynamitron, 25:42048 (ANL-7710, pp 263-364)
design and performance of mechanical, for cold neutrons, 25:43774
design of sealed tube accelerator--target, 25:43778(P)
neutron polarization from deuterium (d,n), (E), 25:43789
performance of sealed-tube graphite moderated, for radiography, 25:42027 (RFP-1705)
shielding, recent developments in, 25:43418 (ORNL-RSIC-32)

NEUTRON SPECTROMETERS
circuit for proton-recoil, performance of gamma discriminating, 25:42105 (JAERI-13561)
control system for triple-axis, 25:42114
design improvements to JAERI time-of-flight, 25:42107 (JAERI-13771)
design of liquid boron scintillation detector for time-of-flight thermal, 25:42104 (FEI-208)
design of proton-recoil, using hydrogen-rich foil and semiconductor telescope detector, 25:42134(P)
development of fast, for measurement of spectra transmitted through iron slabs, (E), 25:44205
development of proton-recoil proportional, 25:42106 (JAERI-13580)
development of proton-recoil proportional, 25:42048

(ANL-7710, pp 263-364)
performance of lithium-6 fluoride sandwich semiconductor, 25:42119
NEUTRON STARS
energy source for, uniformly rotating relativistic disks as, (T), 25:43092
relativistic effects in rapidly rotating, (t), 25:43093
NEUTRONS
attenuation by shielding, computation of thickness required for, 25:43415 (NP-18863)
capture by chromium isotopes, nickel-60, and vanadium at 0.1 to 200 keV, cross sections for, (E), 25:43857
capture by holmium-165, resonance spin assignments for, (E), 25:43884 (ANL-7710, pp 1-52)
capture by tantalum-181 and natural tungsten at thermal energies to 907 keV, gamma-ray yields from, (T), 25:43890 (ORNL-TM-3436)
decay of polarized, angular correlation between neutron spin and electron momentum in, 25:43532
detection of, calibration of Bonner ball boron trifluoride detectors for, 25:42055 (ORNL-TM-3465)
dosimetry techniques for fast reactors, 25:44102
effects of 25 MeV, on vision of man, 25:42698
effects on anhydrous, freeze-dried, and dihydrate solid oxalic acid, 25:41858
effects on α-, β-, γ-, delta-benzene hexachloride, yields of recoil chlorine-38 from, 25:41884
effects on behavior of monkeys, effects of dose and partial shielding on, 25:42542
effects on ceramic insulator seals at high fluence levels, 25:42228 (N-71-17325)
effects on creep in reactor materials, 25:42900 (AD-719935)
effects on electric properties of sodium-doped lithium fluoride monocrystals, 25:43445
effects on embrittlement of A302-B steel, (E/T), 25:44116
effects on embrittlement of pressure vessel steels, review of relations of composition and microstructure with, 25:42910
effects on mechanical properties of plutonium oxide (PuC_2)--uranium oxide (UO_2) fuel pins, 25:44125 (ORNL-TM-3427)
effects on nitrous oxide and its systems with ammonia, ethylene, and ethane, 25:41851 (JAERI-13780)
effects on power reactor steel pressure vessels, dosimetry techniques for, 25:44117
effects on properties of copper--molybdenum--zirconium-base pressure tubes, 25:42929
effects on silicon solar cells, 25:42232
effects on structural materials for reactors, 25:44093
effects on survival of colony-forming units in mouse bone marrow, RBE comparison with γ and x radition for, 25:42601
effects on swelling in Zircaloy-2, relations with dose and irradiation temperature, 25:42915
effects on thermally-activated deformation of zirconium and zirconium alloys, 25:42877
effects on void growth in stainless steel, model for kinetics and mechanism of, 25:42916
effects on zirconium and zirconium alloys, annealing of, 25:41832(R) (AECL-3851)
fluence in reactor steel pressure vessel walls, reliability of codes for calculation of, (E/T), 25:44116
flux distribution in reactors, nonlinear model of steady-state, 25:44197
flux limits for fast reactor core structures and pressure vessel, 25:44167
flux monitoring in reactors, standards for wide-range channels for, 25:44209 (RDT-C-15-2-T)
flux synthesis for reactor calculations, variational models for space-time, (T), 25:44191 (ANL-7710, pp 365-463)
interactions $K^+ + n \rightarrow p(n) + K^+(K^0) + \pi^-(\pi^+)$ at 9.0 GeV/c in deuterium bubble chamber, production of $K\pi(1750)$ in, (E), 25:43546 (COO-1428-279)
interactions $K^+ + n \rightarrow K^+ + \pi^- + p$ at 9 GeV/c in, deuterium bubble chamber, K(1420) production, and π exchange mechanism, energy dependence of cross sections, and density matrix elements for K(890) production in, (E), 25:43548 (COO-1428-283)
interactions $K^+ + n \rightarrow K^+ + \pi^- + p$ at 9.1 GeV in deuterium bubble chamber, cross sections, mass, and width for K(890) and K(1420) production and energy dependence of cross sections, density matrix elements, and π-exchange mechanism for K(890) production in, (E), 25:43547 (COO-1428-281)
interactions $K^- + n \rightarrow p + 2\pi^- +$ anti $K^0 +$ MM at 4.48 GeV/c in deuterium bubble chamber, cross sections and K(890) production in, (E), 25:43549 (COO-1428-286)
interactions $K^- + n \rightarrow p + 2\pi^- +$ anti $K^0 + \pi^0$ at 4.48 GeV/c in deuterium bubble chamber, K(890), Δ(1236), and N(1525) production and cross sections in, (E), 25:43549 (COO-1428-286)
interactions $K^- + n \rightarrow p + 2\pi^- +$ anti K^0 at 4.48 GeV/c in deuterium bubble chamber, K(890), Δ(1236), N(1525), N(1688), and Σ(1765) production and cross sections in, (E), 25:43549 (COO-1428-286)
interactions $K^- + n \rightarrow \pi^+ + 2\pi^- +$ anti $K^0 +$ MM at 4.48 GeV/c in deuterium bubble chamber, cross sections and K(890) production in, (E), 25:43549 (COO-1428-286)
interactions $K^- + n \rightarrow \pi^+ + 2\pi^- +$ anti $K^0 + n$ at 4.48 GeV/c in deuterium bubble chamber, K(890), Δ(1236), N(1525), and Σ(1765) production and cross sections in, (E), 25:43549 (COO-1428-286)
interactions n + n, test of symmetry of nuclear forces with respect to charge hypothesis from scattering length of, (E/T), 25:43534 (NP-18814)
interactions n + p at 210 to 330 MeV, phase shift analysis for, (E), 25:43538
interactions n + p in neutron reactions (n,nnp) with deuterium at 14 MeV, spectrometer study of cross sections and spectra for final-state, (E), 25:43533 (CEA-R-4150)
interactions n + p, multiple quark scattering analysis for energy and momentum transfer square dependencies of differential cross sections for charge exchange, (E), 25:43615
interactions $\pi^+ + n \rightarrow p +$ my at 2.15 GeV/c in deuterium bubble chamber, $2\pi^0$ final state, eta, ω, and eta' production and s-wave π + π interactions in, (E), 25:43562
interactions $\pi^+ + n \rightarrow p + \pi^+ + \pi^- + \pi^0$ at 1.83 to 2.33 GeV/c in deuterium bubble chamber, baryon exchange and ω^0, eta^0, and $\pi^+\pi^-\pi^0(1050)$ production in, (E), 25:43556
interactions $\pi^+ + n \rightarrow p + \pi^+ + \pi^-$ at 1.83 to 2.33 GeV/c in deuterium bubble chamber, baryon exchange and rho^0 production in backward, (E), 25:43555
protection of personnel against, with energies up to 1000 MeV, 25:42464
reactions (n,α) with boron-10, use to enhance laser performance, 25:42229
reactions (n,f) with plutonium, thorium, and uranium isotopes at thermal energies to 14 MeV, calculations of total energy released during, (T), 25:43885 (ANL-7748)
reactions with barium-130 in barium carbonate, production of cesium-131 by, 25:41876 (CONF-680986-2)
reactions with natural iron, nickel, and titanium at 200 eV to 200 keV, R-matrix analysis of total cross sections for, (E/T), 25:43874
reactions with nuclei, cross section measurements for, 25:43834(R) (RPI-328-209)
reactions with platinum, activation in, 25:41920
reactions with uranium carbides, uranium deuterides, uranium hydrides, and uranium dioxides at 0.02 to 0.50 eV, total cross sections for, (E), 25:43930
scattering by nuclei at resonance energies, analysis of unbound levels using method of Weinberg quasiparticles, (T), 25:43988
slowdown theory for fast reactor, derivation of elastic, (T), 25:44191 (ANL-7710, pp 365-463)
thermalization in one-dimensional heterogeneous reactors, DEMETRA code for quasi-diffusion method calculations of, 25:44195 (IAE-2010)
transmission in chromium isotopes, nickel-60, and vanadium up to 300 keV, 25:43857
transport calculations for 14-MeV source in 5000-m radius cylinder of air, overlap conditions for sequential discrete ordinates, 25:43419 (ORNL-TM-3269)
transport equation for, numerical solutions of, (T), 25:43773
transport in reactor materials, research on, 25:43834(R) (RPI-328-209)
transport of, application of variational synthesis to multidimensional, 25:43772
transport of, computer program for solution of integral equation for, (T), 25:43771 (EIR-189)
use in radiography, 25:42575
NEUTRONS, COLD
production of beams of, mechanical generator for, 25:43774
NEUTRONS, FAST
dosimetry in mixed gamma field, double ionization detector for, 25:42168
effects on chromosome translocations in spermatogonia of mice in relation to radioresistant cell lines, effects of dose fractionation on, 25:42355
effects on creep rupture properties and microstructure of Type 304 stainless steel at 600°C, 25:42922
effects on creep rupture properties of niobium-stabilized stainless steel, relations with heat treatments, cold work conditions, and irradiation temperature, 25:42924
effects on embrittlement of Type A533B steel, relations of control of residual element content on resistance to, 25:42907
effects on embrittlement of Types A302B, A-336, A533B, and A542 steels, evaluation of, 25:42906
effects on ferroelectric crystals, 25:43442
effects on fracture and tensile properties of Type A533B pressure vessel steel, 25:42901 (HEDL-TME-71-76)
effects on graphitization of malleable cast iron and cast iron alloys, 25:42904
effects on histology of rat nervous system, REE for, 25:42641
effects on mechanical properties of cold-worked Zircaloy-2 reactor pressure tubes, 25:42914
effects on mechanical properties of copper--molybdenum--zirconium-base alloys, relations with annealing, 25:42813
effects on mechanical properties of iron and low-carbon steel, relations with microstructure, 25:42925

XUM

effects on mechanical properties of niobium--zirconium alloy, Zircaloy-2, and Zircaloy-4 cladding at 20 and 300°C, relations with cold work, 25:42913
effects on mechanical properties of quenched and tempered steels, 25:42909
effects on mechanical properties of Type 19-9DL stainless steel at 55 to 413°C, 25:42923
effects on mechanical properties of Types A212B and A533B steel, 25:42905
effects on mechanical properties of Waukesha 88 at 355°K, 25:42903 (N-71-14040)
effects on metals at high fluence, heavy-ion accelerators for simulating, 25:43758
effects on Micrococcus glutamicus, review of mutagenic, 25:42349
effects on microorganisms, review of improvement in practical applications through mutagenic, 25:42349
effects on microstructure of iron, relations with aluminum and nitrogen, 25:42908
effects on swelling in metals, review of model for, 25:42918
effects on tensile properties of borated Type 304 stainless steel, Zircaloy-2, and Zircaloy-4 at 70 to 1600°F, 25:42911
effects on tensile properties of titanium and aluminum--molybdenum--titanium--vanadium, aluminum--tin--titanium, and aluminum--titanium--vanadium alloys at 17°K, 25:42926
effects on tensile properties of Type 347 stainless steel, relations with irradiation temperature, 25:42912
effects on tomato gametes, pollen, and seed, mutagenic, 25:42354
effects on tumor incidence in mice, comparison of latent internal tritiated thymidine and external, 25:42630
effects on tumor incidence in mice, effects of dose on whole-body, 25:42664
effects on uniaxial fatigue of Types 304, 304L, and 316 stainless steels at 400 to 700°C, 25:42921
effects on uranium oxide (UO_2)--plutonium oxide (UO_2), fission product vapor pressure from, (E/T), 25:44206 (CEA-R-4181)
interactions n + d → n + p + n + γ, cross sections and spectra from, (E), 25:43560
interactions n + p → n + p + γ, cross sections and spectra from, (E), 25:43560
reactions (n,2n) with niobium-93 at 14 MeV, cross section for, (E), 25:43897
reactions (n,α) with ten A = 122 to 169 nuclei at 14.2 MeV, level-density parameters and spectra from, (E), 25:43886 (INR-1268)
reactions (n,f) with plutonium-239, protactinium-231, and thorium-230 and -232 at 0.1 to 3.0 MeV, power-series fits to fragment angular distributions from, (T), 25:43888 (LA-4643)
reactions (n,f) with uranium-233 and -235 at 0.5 to 1.5 MeV, cross-section ratio for, (E), 25:43884 (ANL-7710, pp 1-52)
reactions (n,f) with uranium-238 at 1.5 to 5.5 MeV, neutron spectra and angular distributions for, (E), 25:43898
reactions with copper, lithium-6, molybdenum-98, palladium, plutonium-240, thorium-232, and titanium up to 1.5 MeV, total cross sections for, (E), 25:43884 (ANL-7710, pp 1-52)
reactions with medium-Z nuclei at 14.4 MeV, model analysis of activation cross sections for, (E/T), 25:43951
reactions with uranium-238 up to 10 MeV, optical-model analysis of total cross section for, (E/T), 25:43884 (ANL-7710, pp 1-52)
reactions with Z = 21 to 80 nuclei at 100 to 650 keV, optical model analysis of average total cross sections for, 25:43908
scattering by arsenic-75, carbon, copper, sodium-23 and uranium-238 up to 1.5 MeV, γ spectra from inelastic, (E), 25:43884 (ANL-7710, pp 1-52)
scattering by hydrogen at 0.1 to 30.0 MeV, total and differential cross sections and polarizations for elastic, (T), 25:43798
scattering by iodine-127 at 0.2 to 0.8 MeV, resonance-theory calculations of excitation functions for inelastic, (T), 25:43914
scattering by iodine-127 at 4.0 MeV, optical-model analysis of elastic, (T), 25:43914
scattering by molybdenum-98, plutonium-240, and titanium up to 1.5 MeV, cross sections for, (E), 25:43884 (ANL-7710, pp 1-52)
scattering by superfluid helium in impulse approximation, (T), 25:43278
scattering by tritium at 0.75 to 10.58 MeV, resonating-group calculations of differential cross sections for elastic, (T), 25:43797
scattering by tritium at 1 to 14 MeV, effects of approximate wave functions on phase-shift analysis of, (T), 25:43971
scattering by uranium-238 at 1.5 to 5.5 MeV, angular distributions for elastic and inelastic, (E), 25:43898
scattering by uranium-238 up to 10 MeV, optical-model analysis of, (E/T), 25:43884 (ANL-7710, pp 1-52)
scattering in cesium iodide, potassium chloride, and rubidium bromide at 100 to 650 keV, optical model analysis of average total cross section for, (E/T), 25:43908
spectra in uranium oxide (UC_2) core, (E), 25:44096 (ANL-7710, pp 53-262)
spectra measurements of, data processing methods for activation detectors for, 25:42100
spectra transmission through iron slabs, spectrometer for measurement of, (E), 25:44205
spectrum in plutonium oxide (PuC_2)--uranium oxide (UO_2) core, (E), 25:44096 (ANL-7710, pp 53-262)

NEUTRONS, FISSION
dosimetry method for californium-252 line-source, in tissue-equivalent material, 25:42445

NEUTRONS, INTERMEDIATE
capture by tantalum-181 at 2 keV, γ spectra from, (E), 25:43935
capture by thorium-232 at 20 to 30 keV, disagreement of cross sections with Porter--Thomas postulate, (E), 25:43911

NEUTRONS, PILE
effects on corrosion of zirconium alloys by water, 25:42927
effects on microstructure and tensile properties of solution-treated Type 316 stainless steel, relations of irradiation temperature with, 25:42919
effects on precipitation hardening of aluminum--copper alloys, 25:42902 (JAERI-13692)

NEUTRONS, PROMPT
decay constants in reflected fast burst reactors, model for calculation of, (E/T), 25:44198

NEUTRONS, THERMAL
capture by A = 23 to 174 nuclei, cross sections and spectra from, (E), 25:43891(T) (RFP-Trans-78)
capture by calcium-40, -42, -43, -44, -46, -48, and natural calcium, cross sections for, (E), 25:43835
capture by nuclei, analysis of gamma radiation from polarized, (T), 25:43831 (INR-1262)
capture by potassium-40, γ singles and coincidence spectra from, (E), 25:43845
capture by samarium-150 and -151, γ spectra from, (E), 25:43892
capture by tantalum-181, γ spectra from, (E), 25:43935
detection of, liquid scintillator composition for, 25:42069(P)
reactions (n,f) with fermium-257, mass and kinetic-energy distributions and cross sections for, (E), 25:43920
shielding by cadmium foils, burnout of, 25:43422(T) (ORNL-tr-2488)

NEVADA TEST SITE
desert shrub ecology in area of high-level fallout at, 25:42717 (EGG-1183-2272)

NEWBOLD ISLAND POWER REACTOR, UNIT 1
design parameters of, revised and additional data on, 25:44062 (DOCKET-50354-15)
operations aspects of, revised and additional data on, 25:44062 (DOCKET-50354-15)

NEWBOLD ISLAND POWER REACTOR, UNIT 2
design parameters of, revised and additional data on, 25:44062 (DOCKET-50354-15)
operations aspects of, revised and additional data on, 25:44062 (DOCKET-50354-15)

NICKEL
corrosion of stressed, at various potentials of magnesium chloride, scanning electron microscopic studies of, 25:42760(R) (COO-2069-7)
effects on oxidation resistance of zirconium alloys in carbon dioxide at high temperatures, 25:42803 (CEA-R-4103)
effects on superconducting critical field of niobium--titanium alloy wires, 25:43309
hyperfine fields for substitutional impurities in, tables of, 25:43469 (UCRL-20411)
neutron reactions at 200 eV to 200 keV with natural, R-matrix analysis of total cross sections for, (E/T), 25:43874
production of electroformed mold inserts of, 25:44235 (BDX-613-454)
separation from acetone--hydrochloric acid solutions by ion exchange using Bio-Rad, distribution coefficients for, 25:41899
separation from aqueous solutions by ion exchange on zirconium tellurate, tracer studies on, 25:41915
separation from ores, leaching methods for, 25:41918
separation from other metals using inorganic ion exchange papers, 25:41909
sorptive properties for cesium at 300 to 1000°F, tracer studies on, 25:42863
weld solidification in, structures and mechanism of, 25:42820

NICKEL 200
weld defects in, origin and effects of, 25:42867

NICKEL ALLOYS AND SYSTEMS
Al--Er--Ni, magnetic properties of $ErAl_{2-x}Ni_x$, 25:43480
Al--Gd--Ni, magnetic properties of $GdAl_{2-x}Ni_x$, 25:43480
Al--Ho--Ni, magnetic properties of $HoAl_{2-x}Ni_x$, 25:43480
Al--Ni--Tb, magnetic properties of $TbAl_{2-x}Ni_x$, 25:43480
C--Fe--Ni--V, crystal twinning in bulk and thin-foil,

structure of transformation-type, 25:42886 (UCRL-20500, pp 86-146)
C--Mn--Ni--steel, mechanical properties of tempered, relations with structure, 25:42886 (UCRL-20500, pp 86-146)
Cr--Fe--Ni, corrosion cracking in, containing trace chlorides, studies on mechanism of stress, 25:42760(R) (COO-2069-7)
Cr--Fe--Ni, standard for plates, sheets, and strips of, 25:42794 (RDT-M-5-4-T)
Cr--Fe-base--Mn--Mo--Ni, ductility of irradiated Sandvik 12R72HV, at 500 to 800°C, effects of injected helium on, 25:42872
Cr--Fe-base--Ni, ductility of irradiated Inco IN-744X, at 500 to 800°C, effects of injected helium on, 25:42872
Cr--Ni--P--Pt, electric conductivity and magnetic susceptibilities of amorphous, 25:44237 (CALT-822-31)
Cr--Ni--stainless steel, standard for pipes of, 25:42785 (RDT-M-3-7-T)
Cr--Ni--stainless steel, standard for plates, sheets, and strips of, 25:42791 (RDT-M-5-1-T)
Cr--Ni-base, oxidation at 900 to 1200°C, comparison with TD-nickel chromium, 25:42930
Cu--Fe--Ni, phase decomposition in, kinetics of spinodal, 25:42886 (UCRL-20500, pp 86-146)
Fe--Ni, crystal twinning in bulk and thin-foil, structure of transformation-type, 25:42886 (UCRL-20500, pp 86-146)
Fe--Ni, dissolution in sulfuric acid, effects of solution analysis versus direct current readout methods on results from potentiostatic, 25:42760(R) (COO-2069-7)
Fe--Ni--W, phase diagram of, at 800 to 1650°C, 25:42887 (Y-1785)
Fe--Ni--Zr, radiation effects on properties of fuel cladding of, in-pile, 25:43010
Fe-base--Mn--Ni--Ti, mechanical properties of, effects of aging on, 25:42886 (UCRL-20500, pp 86-146)
Fe-base--Ni--Ti, mechanical properties of, effects of aging on, 25:42886 (UCRL-20500, pp 86-146)
Mn--Mo--Ni--steel, standard for plates of, for pressure vessels, 25:42793 (RDT-M-5-3-T)
Mo--Ni-base, crystal ordering in solid-solution, mechanisms of short-range, 25:42886 (UCRL-20500, pp 86-146)
Mo--Ni-base, electric and thermomagnetic properties of, 25:43476
Nb--Ni-base, crystallization at cooling rates of 10^7 to 10^8 degrees/sec, 25:42888
Ni-base--Ta, crystallization at cooling rates of 10^7 to 10^8 degrees/sec, 25:42888

NICKEL BORIDES
preparation of, method for, 25:42944

NICKEL CHLORIDES
sorption of argon, krypton, methane, and xenon by surfaces of, thermodynamic studies on stepwise isotherms for, 25:41824 (CEA-R-4089)

NICKEL ISOTOPES
cobalt--nickel Coulomb displacement energies, (E), 25:43883
copper--nickel Coulomb displacement energies, (E), 25:43883

NICKEL ISOTOPES Ni-55
energy levels of, self-consistent analysis of single-particle, (T), 25:43825

NICKEL ISOTOPES Ni-58
alpha elastic and inelastic scattering at 104 MeV, differential cross sections for, (E), 25:43832 (NP-18920)
alpha reactions (α,pγ) at 10 MeV, γ spectra and p-γ angular correlations for, (E), 25:43839
energy levels from neutron reactions, resonance parameters for, (E/T), 25:43874
helium-3 elastic scattering at 36.8 to 38.1 MeV, optical-model analysis of angular distributions for, (E/T), 25:43878
helium-3 reactions (He-3,t) at 24.6 MeV, triton spectra from, (E), 25:43883

NICKEL ISOTOPES Ni-60
alpha elastic and inelastic scattering at 104 MeV, differential cross sections for, (E), 25:43832 (NP-18920)
energy levels from cobalt-59 (p,γ) reactions, giant resonance, (E), 25:43853
energy levels from cobalt-59 (p,γ) reactions, parameters for giant dipole resonance, (E/T), 25:43867
energy levels from neutron reactions, resonance parameters for, (E/T), 25:43874
helium-3 reactions (He-3,t) at 24.6 MeV, triton spectra from, (E), 25:43883
neutron capture at 0.1 to 200 keV, cross sections for, (E), 25:43857
neutron transmission measurements up to 300 keV, (E), 25:43857
proton reactions at 61.7 MeV, cross sections and spectra from, (E), 25:43833 (ORNL-4698)

NICKEL ISOTOPES Ni-61
helium-3 reactions (He-3,t) at 24.6 MeV, triton spectra from, (E), 25:43883

NICKEL ISOTOPES Ni-62
alpha elastic and inelastic scattering at 104 MeV, differential cross sections for, (E), 25:43832 (NP-18920)
energy levels from neutron reactions, resonance parameters for, (E/T), 25:43874
helium-3 reactions (He-3,t) at 24.6 MeV, triton spectra from, (E), 25:43883

NICKEL ISOTOPES Ni-64
alpha elastic and inelastic scattering at 104 MeV, differential cross sections for, (E), 25:43832 (NP-18920)
helium-3 reactions (He-3,t) at 24.6 MeV, triton spectra from, (E), 25:43883

NICKEL OXIDES
chemical activity in sodium silicate at 700 to 1100°C, 25:42957 (UCRL-20500, pp 147-73)
positron annihilation in, angular correlation and three-quantum yield of, 25:43482

NICOTINAMIDE-ADENINE DINUCLECTIDE
radiation effects on metabolism of nicotinamide-adenine dinucleotide and nucleic acid metabolites in, mechanisms for, 25:42623

NICOTINAMIDE, N-METHYL-
radiation effects on metabolism of, in mice and rats, mechanisms for, 25:42623

NICOTINIC ACID
radiation effects on metabolism of, in mice and rats, mechanisms for, 25:42623

NINE MILE POINT POWER REACTOR
technical specifications for 1850 MW(t) operation, 25:44035 (DOCKET-50220-65)

NIOBIUM
analysis for hydrogen by isotopic equilibration mass spectrometry, 25:41747 (AAEC/TM-588)
analysis for interstitial oxygen by neutron activation and γ spectrometry, 25:41761
book: High-Temperature Materials, 25:42853
carburization of boride-coated, effects of temperature on, 25:42854
chemical thermodynamic properties of, selected values of, 25:41826 (NBS-TN-270-5)
compounds, thermodynamic properties of, tables of, 25:41826 (NBS-TN-270-5)
diffusion of oxygen in, at 800 to 1500°C, effects of concentration on thermal, 25:42864
lattice vibrational spectra and thermal capacities of, calculations, 25:43490
separation from acetone--hydrochloric acid solutions by ion exchange using Bio-Rad, distribution coefficients for, 25:41899
separation from neptunium, uranium, zirconium, and fission products by solvent extraction using tributyl phosphate, 25:41901
separation from radioactive waste using oxidizing agent and manganese salt, 25:41911(P)
solubility in ammonium nitrate in methanol at room temperature by anodic polarization, 25:41833(R) (IA-1218)
superconductivity of, effects of interstitial oxygen on, 25:41761
thermomagnetic effects in normal and superconducting, 25:43289 (NYO-2150-71)
transport properties of superconducting, dc, (E), 25:43323
weld solidification in, structures and mechanism of, 25:42820

NIOBIUM ALLOYS AND SYSTEMS
Al--Ge--Nb, superconducting and existence region of A15 phase of, (E/T), 25:43319
Al--Ge--Nb, superconducting and existence region of A15 phase of, (E/T), 25:43319
Al--Ge--Nb, superconductivity and range of existence of A15 phase in, (E), 25:43291(T) (ORNL-tr-2461)
C--N--Nb, preparation of cubic carbonitrides, 25:42946
C--N--Nb--O, preparation of cubic oxycarbonitrides, 25:42946
Fe--Nb--Ta--Ti-base--Zr, description of superconducting, 25:43318(P)
Hf--Nb, superconducting critical current density of, effect of heat treatment and impurities on, 25:43290 (ORNL-4703)
Nb--Ni-base, crystallization at cooling rates of 10^7 to 10^8 degrees/sec, 25:42888
Nb--O, analysis for oxygen by neutron activation and γ spectrometry, 25:41761
Nb--O, phase studies of suboxides of, 25:42990
Nb--O--Ti, analysis for oxygen by neutron activation and γ spectrometry, 25:41761
Nb--Sn, superconducting phase identification in, critical temperature measurement method for intermetallic Nb_3Sn, 25:43288 (INR-1294)
Nb--Ta-base, oxidation of monocrystalline and polycrystalline, at 850 to 1050°C and 740 torr, 25:42806
Nb--Ti, analysis for interstitial oxygen by neutron activation and γ spectrometry, 25:41761
Nb--Ti, superconducting critical current density of, effect of heat treatment and impurities on, 25:43290 (ORNL-4703)
Nb--Ti, superconducting critical field of wires of, effects of additives on, 25:43309
Nb--Ti, superconductivity of, effects of interstitial oxygen on, 25:41761
Nb--Zr, radiation effects on properties of fuel cladding

XUM

of, in-pile, 25:43010
Nb--Zr, superconducting critical current density of, effect of heat treatment on impurities on, 25:43290 (ORNL-4703)
Nb--Zr-base, corrosion by aqueous solutions at 300°C, effects of pH on, 25:42814
Nb--Zr-base, corrosion by fused chloride--nitrate salts, stress, 25:41832(R) (AECL-3851)
Nb--Zr-base, corrosion rates in flowing water, polarization resistance method for measurement of, 25:42807
Nb--Zr-base, crystallization of, kinetics of, 25:42885 (JAERI-13764)
Nb--Zr-base, radiation effects on corrosion of, model for studies of in-pile, 25:42927
Nb--Zr-base, radiation effects on mechanical properties of cladding of, at 20 and 300°C, relations of cold work with fast neutron, 25:42913
Nb--Zr-base, welding of, optimum methods for, 25:42831
NIOBIUM BORIDES
thermal capacity of, low-temperature, 25:42974
NIOBIUM CARBIDES
thermal expansion to 2600°C, 25:42966
NIOBIUM ISOTOPES Nb-93
neutron reactions (n,2n) at 14 MeV, cross section for, (E), 25:43897
NIOBIUM ISOTOPES Nb-95
uptake by aquatic plants, 25:41833(R) (IA-1218)
NIOBIUM OXIDES
electric conductivity of, temperature dependence of, 25:43481
positron annihilation in, angular correlation and three-quantum yield of, 25:43482
Al_2O_3--Nb_2O_5, phase studies of, 25:42985
NbO_2--VO_2, electric conductivity of, temperature dependence of, 25:43481
NIOBIUM OXYBROMIDES
elastic properties of polycrystalline Nb_2O_5, effects of fabrication methods and temperature on, 25:42955 (IS-T-446)
NITRIC ACID
analysis for sulfates by ion exchange and titration, 25:41715 (AECL-3575)
corrosive effects of dilute solutions of, on niobium--zirconium-base alloys at 300°C, 25:42814
separation of uranium from solutions of, by solvent extraction using TBP, comparison between computer-simulated and actual performance of mixer-settlers for, 25:41890 (CEA-N-1450)
NITROGEN
determination in refractory metals using fluxes enriched with nitrogen-15, isotope dilution, 25:41748
determination simultaneously with oxygen in silicon nitride films by deuteron activation, 25:41832(R) (AECL-3851)
diffusion in α-zirconium solid solution and zirconium nitride at 1260 to 1720°C, 25:42967
diffusion in plutonium nitride--uranium nitride fuels, self, (E), 25:44118(R) (BMI-1905)
effects on microstructure of fast neutron irradiated iron, 25:42908
effects on organoleptic properties of γ-irradiated apples, 25:42748
effects on stabilization of uranium dicarbide fuel, 25:42936 (JUL-728-RW)
electron reactions up to 150 eV with atomic, cross sections for excitation of ^4P state in, (E), 25:43143
equilibrium composition and normal shock parameters for, through double ionization, 25:43331 (AD-715615)
ion reactions at 30 keV to 2 MeV with molecular, cross sections for excitation of N_2^+ 3914-A radiation in, (E), 25:43151
plasma of, ion temperature measurement using multi-channel Fabry--Perot interferometer, 25:43341
radiolysis of, emission stimulated by electron pulse, 25:41850(R) (CEA-N-1438)
rare-gas-ion reactions at 0.05 to 200 eV with molecular, application of statistical phase-space theory to molecular and dissociative charge exchange in, 25:43159
yields from radiolysis of 2,2'-azobis[2-methylpropionitrile]--benzene, 25:41872
NITROGEN IONS
emission in auroral ionosphere, differential electron-flux determination from N^{2+}, (E), 25:43214 (N-71-16589)
implantation in gallium phosphide crystals, photoluminescence spectrum of, (E), 25:43462
implantation in silicon at 2 MeV, thermal spiking in damage from, (E/T), 25:43465
NITROGEN IONS (N^+)
reactions with argon at 30 to 130 keV, cross sections for argon L-shell x-ray emission in, (E), 25:43134
reactions with carbon at 20 keV to 1.5 MeV, cross sections for K x-ray production in, (E), 25:43107
reactions with nitrogen molecules at 30 keV to 2 MeV, cross sections for excitation of N_2^+ 3914-A radiation in, (E), 25:43151
NITROGEN IONS (N_2^+)
effects on infrared spectra of silicates at 5 keV, 25:43446
emission in auroral ionosphere, differential electron-flux determination from, (E), 25:43214 (N-71-16589)
reactions with nitrogen molecules at 30 keV to 2 MeV, cross sections for excitation of N_2^+ 3914-A radiation in, (E), 25:43151
NITROGEN ISOTOPES
separation of, evaluation of methods for, 25:41897(T) (ORNL-tr-2512)
NITROGEN ISOTOPES N-13
energy levels from oxygen-13 beta decay, (E), 25:43802 (UCRL-20480)
proton decay of, proton spectra from beta-delayed, (E), 25:43802 (UCRL-20480)
reactions of recoil, in deuteron-irradiated carbides, 25:41886
NITROGEN ISOTOPES N-14
alpha elastic scattering at 104 MeV, differential cross sections for, (E), 25:43832 (NP-18920)
proton reactions (p,2α) at 13 to 42 MeV, excitation functions for, (E), 25:43818
proton reactions (p,α) at 5 to 24 MeV, excitation functions for, (E), 25:43818
triton reactions (t,p) at 1.8 MeV, analysis including Coulomb distortion and finite-range effects, (T), 25:43965
NITROGEN ISOTOPES N-15
effects on ir spectra of pentacyanonitrosylmanganese complexes, 25:41796
NITROGEN MUSTARDS
effects in combination with gamma radiation on chromosomes in dry seeds of Crepis capillaris, aberrant, 25:42359
effects on differentiation of surviving stem cells in mice in comparison to effects of x rays, 25:42661
NITROGEN OXIDES NO
abundance in auroral arc, mass-spectrometer observations of neutral and ionized, (E), 25:43218 (N-71-18997)
oxidation of, photochemical chain reactions in, 25:41778 (UCRL-20500, pp 1-85)
reactions with argon and neon atoms of excited ions of, statistical phase-space model of dissociation in, 25:43158
NITROGEN OXIDES N_2O
abundance in upper atmosphere, theoretical studies of, 25:43207 (AD-706130)
effects on formation of butyl radicals and hydrogen in γ radiolysis of 2-methylpropane, 25:41864
effects on yields of solvated electrons from γ radiolysis of formamide, 25:41863
radiolysis of, effects of pressure and temperature on yields of nitrogen from γ, 25:41851 (JAERI-13780)
radiolysis of, electron pulse, 25:41832(R) (AECL-3851)
reactions with graphite, catalytic effects of barium, cadmium, chromium, lead, and uranium on, 25:42931
reactions with graphite, kinetics of, 25:42932
ethane--N_2O, radiolysis of, γ and neutron, 25:41851 (JAERI-13780)
ethylene--N_2O, radiolysis of, γ and neutron, 25:41851 (JAERI-13780)
NH_3--N_2O, radiolysis of, γ and neutron, 25:41851 (JAERI-13780)
NITROGEN SYSTEMS
C--N--Nb, preparation of cubic carbonitrides, 25:42946
C--N--Nb--O, preparation of cubic oxycarbonitrides, 25:42946
C--N--O--Pu--U, thermodynamic properties and stoichiometry of, 25:42998
C--N--Pu--U, phase studies and structures of, review on, 25:42982 (JAERI-13650)
CO_2--N, glass bead suspension in, power requirements for circulation of, 25:41956 (BM-RI-7019)
NITROUS ACID
effects on Neurospora, specificity of mutagenic, 25:42352
NOVAE
spectra of, comparison with spectra of WR stars, (E/T), 25:43030
NUCLEAR ACOUSTIC RESONANCE
effects on gamma absorption and emission, (T), 25:43493
NUCLEAR AUXILIARY POWER SYSTEMS
cooling system of Brayton cycle space, transfer function of primary loop in, (T), 25:44168 (N-71-17933)
design parameters of 25 kW(e) thermoelectric reactor for manned space stations, 25:44171
design parameters of zirconium hydride reactors with organic Rankine power cycles, 25:44179
design studies of plutonium-238-fueled Stirling, for spacecraft auxiliary power system, 25:42010
development of Brayton-B, for space use with radioisotope, solar, or SNAP-8 reactor source, 25:42008
development of closed Brayton cycle, for use in lunar, space, terrestrial, and undersea environments, 25:42007
development of promethium-147-fueled Betacel, for biomedical applications, 25:41996
development of thermionic reactor concepts, review of U. S, 25:44169
development of thermionic reactors in Germany, review of, 25:44172
dynamics of Brayton cycle, for space power systems, analog computer simulation of, 25:42009

economics of radioisotopic and reactor, for undersea uses, 25:44180
evaluation of radioisotope-powered thermoelectric generators for deep space use, 25:43184 (N-71-16776)
fuel element development for thermionic reactors, review of U. S, 25:44170
heat sources for Ripple, evaluation of radioisotope, 25:42014
heat sources for space, development of cobalt-60 kernel-clustered, 25:42000
performance of 300 kW(e) lithium cooled fast reactor concept with potassium Rankine cycle, 25:44173
steam generator for radioisotope-fueled, performance of short reentry tube once-through, 25:41962 (ORNL-TM-3236)
NUCLEAR ELECTRIC MOMENTS
determination of E4 transition moments by Coulomb excitation, 25:43948
NUCLEAR EMULSIONS
particle tracks in, measurement of small angle scattering in, 25:42139
NUCLEAR EXPLOSIONS
thermal energy from, use of halogenated vinyl polymers for protection against, 25:41827
NUCLEAR EXPLOSIONS, ATMOSPHERIC
silver-108m content of animals, plants, and sediments at Bikini and Eniwetok atolls following, 25:42377
NUCLEAR EXPLOSIONS, UNDERGROUND
bibliography on seismology, aftershocks, and related phenomena associated with, 25:41951 (NVO-87)
effects of Cannikin, on ecology, geology, hydrology, and seismicity of Amchitka Island, Alaska, use of Milrow data in predictions of, 25:42318 (TID-25735)
performance in ore fracturing, 25:41918
radioactivity distribution in cavity from, theoretical studies of, 25:41954 (CEA-R-4128(1))
radioactivity distribution in lava from cavity of, 25:41953 (CEA-R-4099)
seismic waves from Project Gasbuggy, and an earthquake, comparison of travel times for, 25:41952 (AD-838894)
use of heat from contained, for producing hydrogen from organic waste materials, feasibility study of, 25:41955
NUCLEAR ISOMERS
lifetimes of, delayed-coincidence method for measurement of, 25:42222
NUCLEAR MATERIALS MANAGEMENT
safeguards system for, dynamic mathematical model for optimization of, 25:42045
NUCLEAR MATTER
hyperon (Λ) binding energy in, ΛN coupling to virtual ΣN channel effects on, (T), 25:43648
NUCLEAR MODELS
optical, evidence for real Saxon--Woods derivative term in proton elastic scattering, (T), 25:43967
shell, coefficients of fractional parentage for lower portion of j = 7/2 shell, (T), 25:43981
NUCLEAR PHYSICS
data fitting in, techniques for optimization of experiments for, 25:42223
research at Argonne National Laboratory during July 1969 to June 1970, 25:44190(R) (ANL-7710)
research at Osaka Univ., 1970, 25:43732(R) (OU-LNS-71-2)
NUCLEAR POWER PLANTS
components for, standard for fabrication and testing of metal products for, 25:42817 (RDT-F-3-37-T)
construction of, 1970 to 1985 forecast of worldwide, 25:43994 (WASH-1139)
development of, effects of petroleum costs on, 25:44146
development of, prospects for, 25:44217
effects on environment, 25:42383
environmental effects of, comparison with fossil fueled plants of, 25:44143 (SGAE-RT-39/1971)
hazards evaluation for, computer method for, 25:41833(R) (IA-1218)
health physics experiences and personnel protection standards at, in Italy, 25:42478
iodine-131 release to atmosphere during operation of, programs for monitoring, 25:42388
personnel access locks in, German standard for, 25:43996
siting in Vienna, effects of potential accidental iodine-131 dose to human thyroid glands on, 25:44147
thermal effluents from, economics of food production enclosure heating by, 25:44022
thermal effluents from, regional canal system concept for utilization of, 25:44083 (BNWL-SA-2738)
NUCLEAR REACTIONS
bibliography for light nuclei, (E), 25:43780 (CEA-N-1327(Vol.4))
bibliography for light nuclei, index to, 25:43779 (CEA-N-1327)
cluster transfer processes in, Coulomb distortion and finite-range effects on, (T), 25:43964
compound-nucleus decays in, review of pre-equilibrium, (E/T), 25:43957 (UCRL-73152)
effects of higher multipole deformation of the pairing density in deformed nuclei on (p,t) and (t,p), (T), 25:43977
measurement of three-body, design of 4π scintillation spectrometer for kinematically complete, 25:42124
particle identification in, development of high-rate time-of-flight system for, 25:42066
resonances in, statistical calculation of density of doorway-state, (T), 25:43991
theory of double charge exchange, on light nuclei, 25:43962
theory of multiparticle transfer, using tetragonal graphs, 25:43961
theory of two-nucleon stripping, including Coulomb distortion and finite-range effects, 25:43965
NUCLEAR REACTIONS (DIRECT)
angular distributions from (He-3,t), distorted-wave analysis of anomalies in, (T), 25:43848
angular distributions of (He-3,t) and (p,π) transitions to 0⁺ antianalog energy levels, analysis of shapes of, (T), 25:43842
calculation of single-nucleon-transfer, using particle--vibration-coupling model, (T), 25:43976
inelastic scattering differential cross sections for charged particles, computer programs for DWBA calculations of, (T), 25:43954 (INP-746)
nucleon scattering by light nuclei, effects of approximate wave functions on analysis of, (T), 25:43971
peripheral model of light-particle, nonrelativistic, (T), 25:43966
NUCLEAR STRUCTURE
calculations for N = 82 odd-proton nuclei using shell model and Tamm-Dancoff approximation, 25:43989
calculations using deformed spin-orbit potential, 25:43963
collective states in exactly soluble three-level model of, mixing of, (T), 25:43972
NUCLEAR THEORY
book: Space Structure of Energetically Excited Atomic Nuclei, 25:43990
comparison of BCS and fixed-particle-number BCS formalisms in, 25:43985
Hartree-Fock calculations for light deformed nuclei using density-dependent interactions, 25:43986
matrix elements of spherical tensors, tables of singles-particle reduced, 25:43982
nucleon-nucleon potentials in, separable approximation to T-matrix for short-range central local, 25:43980
three-nucleon system in, analysis of Hall-Post lower bound calculations for, 25:43983
two-body random Hamiltonians in, Monte Carlo calculations of spacing and individual eigenvalue distributions of, 25:43968
NUCLEI
alpha elastic scattering by, real part of alpha--nucleus potential in region of nuclear surface, (T), 25:43973
binding energies of spherical, calculations using s-wave separable interactions of, (T), 25:43959
Coulomb energy of fissioning, calculation using modified liquid-drop model, (T), 25:43952(T) (BNL-tr-424)
decay of, interference at intersection of levels, (T), 25:43506 (JINR-P4-5786)
deuteron reactions (d,Li-6) with, analysis of features of, (T), 25:43987
deuteron reactions (d,p) with deformed, inelastic processes in, (T), 25:43984
electron quasi-elastic scattering with nucleon emission, radiative corrections in, 25:43979
electron reactions (e,e'p) with light, low-accidentals coincidence system for measuring, 25:42131
energy levels and gaps of A = 200 to 600, calculations using Woods--Saxon potential, (T), 25:43955 (INR-1270)
energy levels from single-nucleon transfer reactions on closed-shell, calculations using particle--vibration-coupling model, (T), 25:43976
energy levels of heavy and superheavy, calculations using Woods-Saxon potential for single-particle, (T), 25:43936
energy levels of, apparatus for nanosecond-lifetime measurements at U-300 heavy-ion cyclotron, 25:42187 (JINR-P13-5801)
energy levels of, effect of multipole pairing and particle--hole fields in particle--vibration coupling in, (T), 25:43974
energy spectra of solar, Explorer-35 data from July 20, 1967 to May 14, 1968 of Z greater than or equal to 3, (E), 25:43231
energy-level transitions in beta decay of, time reversal invariance tests in electromagnetic final-state interaction contribution to triple-product correlation coefficient in, (T), 25:43660
energy-level transitions in, effects of valence shell structure on internal conversion, (T), 25:43953(T) (BNL-tr-427)
excitation quantum numbers in, effects on binding and excitation energies of, (T), 25:43958
forces in, scattering lengths of n + n interactions for test of hypothesis of symmetry with respect to charge for, (E/T), 25:43534 (NP-18814)
gamma acoustic resonance absorption in, (T), 25:43493
masses of odd-A, derivation of liquid-drop formula for, (T), 25:43516
meson (π) reactions with, theory of charge-exchange, 25:43978
meson (π⁻) reactions with complex, at 17 and 45 GeV, Deck model for diffraction coherent production of π in, (T), 25:43646 (JINR-P1-5775)

XUM

neutron capture by, analysis of gamma radiation from polarized, (T), 25:43831 (INR-1262)
neutron capture by, computer program for calculating time-dependent populations of isotopes in, (E), 25:43889 (LA-4703)
neutron reactions at 14.4 MeV with medium-Z, model analysis of activation cross sections for, (E/T), 25:43951
neutron resonance scattering by, analysis of unbound levels using method of Weinberg quasiparticles, (T), 25:43988
nuclear quadrupole moment of, effects of bound μ meson on, (T), 25:43913
nucleon elastic scattering by light, effects of approximate wave functions on analysis of, (T), 25:43971
pairing correlations in excited, with non-zero angular momentum, (T), 25:43969
photon reactions at high energies, dynamical effects of instability in nonresonant and rho^0 production in π^+--π^- pair production in, (T), 25:43604
proton elastic scattering at 20 to 61.4 MeV by A = 12 to 208, optical-model analysis with real Saxon--Woods derivative term, (T), 25:43967
proton reactions (p,n) with, effect of compound nucleus levels on isobaric analog resonances in, 25:43893
radii of spherical, calculations using s-wave separable interactions of, (T), 25:43959
rigidity spectrum in primary cosmic radiation, medium and heavy, (E), 25:43178

NUCLEIC ACID
radiation effects on excretion of metabolites of, in rat urine, mechanism of effects of cysteamine on γ, 25:42625
radiation effects on metabolism of, in mice and rats, mechanisms for, 25:42623
radioprotective effects on coagulation and fibrinolysis of rat blood, x, 25:42537

NUCLEIC ACID, DEOXYRIBO-
book: Radiobiophysics of the Nucleoproteins, 25:42274
DNAase activity specific for uv-irradiated, in HeLa cells, 25:42272
effects of content of, on uv-radiosensitivity bacteriophages lambda+ and lambda62, 25:42300
effects on recovery from chromosome damage in x-irradiated Crepis capillaris, 25:42356
radiation effects on E. coli, effects of dose and temperature on products from uv, 25:41833(R) (IA-1218)
radiation effects on membrane association of conjugally transferred, in Escherichia coli minicells, x, 25:42735
radiation effects on metabolism of, in animals as indicator of radiation injury, 25:42403
radiation effects on rat tissue, sensitizing effects of hydroxymercuribenzoic acid on, 25:42535
radiation effects on synthesis of, in Escherichia coli, effects of dose and genetic strain on γ, 25:42729 (NYO-2804-40)
radiation effects on synthesis of, in rat lymphocytes as indicator of dose, in vitro effects of phytohemagglutinin on, 25:42404
radiation effects on transcription of plant, γ, 25:42715(R) (COO-1313-29)
radiation effects on, effects of phage T$_4$ induced endonuclease on dark repair following uv, 25:42269
radiation effects on, in tissues of mice following ingestion of tritium-labeled thymidine, β, 25:42262
radioinduced breaks in Ehrlich ascites tumor cells, effects of ATP production on rejoining of x, 25:42632
radioinduced breaks in T4 phage, role of polynucleotide ligase in repair of uv, 25:42297
radioinduced degradation of Escherichia coli, effects of dose, genetic strain, and temperature on rate of repair of γ, 25:42731 (NYO-2804-42)
radioinduced degradation of Escherichia coli, effects of dose and genetic strain on γ, 25:42729 (NYO-2804-40)
radioinduced degradation of Escherichia coli, effects of anoxia and genetic strain on repair of γ, 25:42728 (NYO-2804-39)
radioinduced degradation of Escherichia coli, mechanisms for repair of γ, 25:42727 (NYO-2804-38)
radioinduced delay in replication of Escherichia coli, effects of dose on uv, 25:42290
radioinduced denaturation of, for use in infecting spheroplasts of Pseudomonas, γ, 25:42273
radioinduced hydrogen transfer in dry salmon sperm, effects of temperature and scavengers on yields from γ, 25:41837
radioinduced pyrimidine dimers in Bacillus subtilis, use of endonuclease from Micrococcus lysodeikticus for recognition of uv, 25:42285
radioinduced single strand breaks in cultured mammalian cell, protective effects of cystamine or cysteamine against x, 25:42522
radioinduced single-strand breaks in Escherichia coli mutant, role of DNA polymerase in repair of x, 25:42326
radioinduced single-strand breaks in Escherichia coli, relation between repair and lethality in x, 25:42357
radioinduced single-strand breaks in Escherichia coli mutant, repair of uv and x, 25:42331
radioinduced strand breaks in, regeneration by polynucleotide ligases in vitro following γ, 25:42268
tritium-labeled thymidine incorporation into lymphoma cell, effects of, on survival, 25:42251

NUCLEIC ACID, RIBO-
photolysis of, role in photoreactivation of dimers produced by uv, 25:42257(R) (RLO-2225-T-15-3)
purification of transfer and leucyl-transfer, synthetase from sugar beet root, partial, 25:44249 (COO-1313-27)
radiation effects on heterogeneity of rat liver, whole-body γ, 25:42280
radiation effects on polymerase activity in plant, γ, 25:42716(R) (COO-1313-29)
radiation effects on synthesis of, in Escherichia coli, effects of dose and genetic strain on γ, 25:42729 (NYO-2804-40)

NUCLEONS
coupling of ΛN to virtual ΣN for Λ + N scattering and Λ binding in nuclear matter, (T), 25:43648
flux in cosmic radiation at atmospheric depth of 976 gcm^{-2} at 12 to 15 GeV, spark chamber study of ratio to π for, (E), 25:43621
interactions anti K + N → π + Σ(Λ) at 400 to 1200 MeV/c, test of duality predictions from partial-wave analysis of, (E/T), 25:43642 (UCR-34-P-107-E-106)
interactions e + N → e + N, scaling, Pomeranchuk trajectory, and J = 1 fixed poles from finite-energy sum rule analysis of virtual Compton, (T), 25:43584 (ITF-71-27-E)
interactions e + N beyond resonance region, model with π form factor for π production in, (E/T), 25:43583 (DESY-71/22)
interactions γ + N → π^0 + N, Regge cuts due to absorption in, (T), 25:43601
interactions γ + N → rho^0 + N, dynamical effects of instability in, (T), 25:43604
interactions γ + N in strong electromagnetic field, final-state interaction for electron production in (T), 25:43606
interactions Λ + N at low energies, ΛN coupling to virtual ΣN channel effects on, (T), 25:43648
interactions Λ + N, cross sections of Λ + d interactions at 100 to 300 MeV/c as probe of core potential for, (T), 25:43651
interactions N + d below 40 MeV, phase shifts and inelastic scattering parameters for, (T), 25:43799
interactions N + N, charge-dependent effects in low-energy, 25:43960
interactions N + N, N + N interactions from single hard π production in nonrelativistic, (T), 25:43653
interactions N + N, single hard π production in N + N nonrelativistic interactions for, (T), 25:43653
interactions π + N → 2π + N at low energies, final-state mass spectra relation with two-body forces for, (T), 25:43643
interactions π + N at 2.75 to 10 GeV/c, experimental data for reconstruction of energy and angular dependence of amplitudes in near forward, (E/T), 25:43640 (LYCEN-7110)
interactions π + N at high energies and all angles, optical model for, (T), 25:43571
interactions π + N, inequalities for partial waves for, (T), 25:43641 (SU-1205-249)
interactions π + N, Regge cuts for unitarized finite-energy sum rules for charge-exchange, (T), 25:43637 (DESY-71/24)
interactions rho^0 + N → rho^0 + N, dynamical effects of instability in, (T), 25:43604
motion of two, Gauss potential approximation for, (T), 25:43638 (ITF-71-9-P)
reactions with carbon above 20 GeV, fluctuations in angular distributions of secondary particles from, (E), 25:43540
scattering by light nuclei, effects of approximate wave functions on analysis of elastic, (T), 25:43971

NUCLEOPROTEINS
radiation effects on, in unimal hematopoietic and lymphatic cells, mechanisms for, 25:42624

NUCLEOPROTEINS, DEOXYRIBO-
book: Radiobiophysics of the Nucleoproteins, 25:42274

O

OHIO
radioactivity monitoring in environment of Fernald Feed Materials Production Center in, during 1970, 25:42420

OILS
disposal of waste, 25:44220 (ANCR-1004)
radiation effects on properties of cottonseed, γ, 25:41839

OLFACTORY ORGANS
lesions in rat, effects on x-radioinduced saccharin-avoidance behavior of, 25:42647

OLIVINES
radiation effects on infrared spectrum of, 5-keV proton, deuteron, helium-ion, and nitrogen-ion, 25:43446

OOCYTES
radiation effects on rat fetus, following administration of tritium-labeled thymidine by maternal infusion during pregnancy, 25:42650
radioinduced chromosome translocations in Drosophila,

effects of dose on frequency of x, 25:42333
radioinduced interchanges in mature Drosophila, segregation of chromosomes following x, 25:42276
radiosensitivity of human and mammalian, factors affecting, 25:42597
radiosensitivity of silkworm, effects of meiotic stage on x, 25:42609
OPTICAL SYSTEMS
design of light conductors for use in neutron fields at high temperature, 25:42230(P)
ORES
fracturing by underground nuclear explosions, 25:41518
prospecting for, review on nuclear borehole methods for, 25:41531
ORGANIC COMPOUNDS, PHOSPHO-
uranyl nitrate transport through solvent membranes of, 25:41803(R) (IA-1218)
ORGANS
radiation dosimetry in human, containing radioisotopes, use of phantoms to determine role of body background in external γ, 25:42423
radiation injuries to human pelvic, following therapy for uterine and vaginal cancer, γ, 25:42598
radioisotope content in animal, effects of ion exchange resins on, 25:42263
radon daughter content in rat, following inhalation of radon-222, 25:42248
ORGEL REACTOR
fuel element cluster for, neutron flux and power distributions in prototype, 25:44099 (EUR-4364)
reactivity temperature coefficients for prototype core of, (T), 25:44100 (EUR-4365)
ORNL HIGH-FLUX ISOTOPE REACTOR
core for, design and physics parameters of, 25:44159 (ORNL-4621)
ORNL RESEARCH REACTOR
maintenance during January to March 1971, 25:44160(R) (ORNL-TM-3481)
operation during January to March 1971, 25:44160(R) (ORNL-TM-3481)
OROTIC ACID
radiation effects on excretion of carbon-14-labeled, in rat urine as indicator of radiation injury, whole-body γ, 25:42407
OSCILLATORS
design of tunnel-diode, for ac susceptibility measurements at radio frequencies, 25:43472 (YALE-3227-74)
OSMIUM
determination of trace amounts of, in meteorites by neutron activation and γ spectrometry, 25:41773
OSMIUM ISOTOPES Os-188
proton elastic and inelastic scattering at 16 MeV, differential cross sections for, (E), 25:43901
OSMIUM ISOTOPES Os-190
proton elastic and inelastic scattering at 16 MeV, differential cross sections for, (E), 25:43901
OSMIUM ISOTOPES Os-192
nuclear quadrupole moment of, effects of bound μ meson on, (T), 25:43913
proton elastic and inelastic scattering at 16 MeV, differential cross sections for, (E), 25:43901
OSTEICHTHYES
Carassius auratus, radiation effects on, comparison of chronic low-dose γ and repeated high-dose x, 25:42634
Onchorhynchus tshawytscha, radiation effects on development and survival of, following chronic exposure as eggs and alveins, low-dose γ, 25:42616(R) (RLO-2225-T-2-2)
Oryzias latipes, radiation effects on, comparison of chronic low-dose γ and repeated high-dose x, 25:42634
radioisotope content in, review on effects of environmental factors and type on, 25:42249
OVARIES
effects of serotonin on mouse, 25:42519
OVENS
design of gradient-free, for studying Moessbauer effect, 25:42115
OXALIC ACID
radiolysis of anhydrous, dihydrate, and freeze-dried solid, γ and neutron, 25:41868
radiolysis of, kinetics of production of carbon dioxide, hydrogen, and hydrogen peroxide from electron pulse, 25:41850(R) (CEA-N-1438)
OXAZOLE, 2,5-DIPHENYL-
effects on yields of nitrogen from radiolysis of 2,2'-azobis[2-methylpropionitrile]--benzene, 25:41872
OXIDATION
book: Oxidation Equilibrium and the Radiosensitivity of Organisms, 25:42528
OXIDES
deposition of films of, on hafnium, zirconium, and their alloys, method for, 25:42819(P)
diffusion and evaporation in oxygen--tantalum solid solutions at 1600 to 2000°C, simultaneous, 25:42975
OXIDOREDUCTASES
radiation effects on activity in liver of rats following ingestion of radon-containing water, effects of dose on, 25:42279
radiation effects on activity of 7α-hydroxylase, in rat testes, x, 25:42621
OXYGEN
abundance in auroral arc, mass-spectrometer observations of molecular, (E), 25:43218 (N-71-18597)
content at 80 to 140 km in ionosphere, molecular, (E/T), 25:43261
content of thermospheric atomic, relation with seasonal, diurnal, and solar-activity variations, (E/T), 25:43260
desorption from graphite surfaces in presence of hydrogen or nitrogen, 25:41850(R) (CEA-N-1438)
determination in niobium and niobium--titanium alloys by neutron activation and γ spectrometry, 25:41761
determination in refractory metals using fluxes enriched with oxygen-18, isotope dilution, 25:41748
determination simultaneously with nitrogen in silicon nitride films by deuteron activation, 25:41822(R) (AECL-3851)
diffusion in niobium and tantalum at 800 to 1500°C, effects of concentration on thermal, 25:42664
effects on yields of phenol from electron or γ radiolysis of benzene--water systems, 25:41858
electron reactions up to 150 eV with atomic, cross sections for excitation of ^3S state in, (E), 25:42142
emission in day airglow from atomic, OGO-4 temporal and morphological observations of 1304-A, (E), 25:42255
plasma of, ion temperature measurement using multi-channel Fabry--Perot interferometer, 25:42241
radiation effects on HeLa cell consumption of, effects of metabolic inhibitors on x, 25:42295
reactions of dry, with monocrystalline and polycrystalline niobium--tantalum alloys at 850 to 1050°C and 740 torr, oxidation, 25:42806
reactions with chromium--cobalt, chromium-nickel, and TD-nickel chromium alloys at 900 to 1200°C, oxidation, 25:42930
reactions with graphite, catalytic effects of barium, cadmium, chromium, lead, and uranium on, 25:42931
reactions with graphite, kinetics of, 25:42932
reactions with graphite, kinetics of, 25:41778 (UCRL-20500, pp 1-85)
OXYGEN IONS
energy-loss spectra in gold (111) and (100) channels at 10 MeV, 25:43454
implantations in gallium phosphide at 20 to 60 keV, depth distributions and annealing of, 25:43447
reactions with iron at 30 MeV of O^{5+}, resolved structure in Kα x rays produced by, (E), 25:43110
OXYGEN IONS (O^+)
reactions with argon at 30 to 130 keV, cross sections for argon L-shell x-ray emission in, (E), 25:42124
reactions with carbon at 20 keV to 1.5 MeV, cross sections for K x-ray production in, (E), 25:43107
reactions with nitrogen molecules at 30 keV to 2 MeV, cross sections for excitation of N_2^+ 3914-A radiation in, (E), 25:43151
OXYGEN IONS (O_2^+)
reactions with neon and argon atoms of excited, statistical phase-space model of dissociation in, 25:43158
OXYGEN IONS (O_3^-)
photodetachment rate of, approximate photon-energy dependence of cross section and sunlight, (E), 25:43257
OXYGEN ISOTOPES O-13
beta decay of, branching ratios, half-life, and log-ft values for, (E), 25:43802 (UCRL-20480)
mass excess from (He-3,He-6) reactions, (E), 25:43823
nuclear mass excess of, comparison with calculations using isobaric multiplet mass equation, (E), 25:43808
OXYGEN ISOTOPES O-16
alpha elastic scattering at 104 MeV, differential cross sections for, (E), 25:43832 (NP-18920)
binding energy of, calculation using Brueckner theory with realistic potentials, (T), 25:43794
binding energy of, variational calculation using hard-core potential, 25:43787
burning in evolved stellar cores, explosive, (T), 25:43033
energy levels of, self-consistent analysis of single-particle, (T), 25:43826
energy-level transitions and optical potential parameters in pionic, πN scattering lengths for, 25:43806
helium-3 reactions (He-3,He-6) at 68 MeV, Q values and spectra from, (E), 25:43823
helium-3 reactions (He-3,He-6) at 68 to 70 MeV, Q-value for, (E), 25:43808
nuclear electric charge radius of, determination from electron scattering, (E), 25:43807
oxygen-16 elastic scattering by, analysis using absorptive optical potential, (T), 25:43978
proton reactions (p,pα) at 46.8 MeV, coplanar angular and energy correlations and spectra from, (E/T), 25:42801 (UCLA-10-P-18-31)
scattering by calcium-40, analysis using absorptive optical model, (T), 25:43978
OXYGEN ISOTOPES O-17
nuclear electric charge radius of, determination from electron scattering, (E), 25:43807
nuclear magnetic resonance in uranic, potassium uranate, and bismuth uranate, 25:43497
proton reactions (p,α) and (p,γ) at 5.8 to 7.1 MeV, energy spectra and angular correlations and

XUM

distributions for, (E), 25:43812
OXYGEN ISOTOPES O-18
effects on hydrolysis of 4-ethoxypyrylium salts, 25:41789
exchange between hexaaquochromium ion and solvent water, effect of pressure on kinetics of, 25:41797
fractionation factors of, between ice and water vapor at 0 to 33.4°C, 25:41921
nuclear electric charge radius of, determination from electron scattering, (E), 25:43807
proton reactions (p,α), use to measure depth distribution of oxygen-ion implants in gallium phosphide, 25:43447
OXYGEN SYSTEMS
C--N--Nb--O, preparation of cubic oxycarbonitrides, 25:42946
C--N--O--Pu--U, thermodynamic properties and stoichiometry of, 25:42998
Cr--O--Zr-base, properties of dilute, effects of chromium and oxygen contents on mechanical and structural, 25:42879
Nb--O, analysis for oxygen by neutron activation and γ spectrometry, 25:41761
Nb--O, phase studies of suboxides of, 25:42990
Nb--O--Ti, analysis for oxygen by neutron activation and γ spectrometry, 25:41761
O--Ta, diffusion and evaporation of oxides in solid solutions of, at 1600 to 2000°C, simultaneous, 25:42975
O--Ta, phase diagram of, 25:41993(R) (ORNL-4692)
O--Ti, phase diagram of, 25:42991
O--Zr-base, deformation of dilute, mechanisms of thermally-activated, 25:42877
OYSTER CREEK POWER REACTOR, UNIT 1
containment system for, failure of absorption chamber spray header valve for, 25:44007 (DOCKET-50219-142)
containment system for, failure of isolation condenser time delay relay for, 25:44007 (DOCKET-50219-142)
containment system for, failure of standby gas treatment system train inlet valve for, 25:44007 (DOCKET-50219-142)
OZONE
effects on combined hypoxia and radioinduced glomerulus enlargement in hamster kidneys, 25:42636

P

PACKAGING
regulations for, and in shipment of radioactive materials in aircraft, 25:42456
regulations for, and in shipment of radioactive materials in aircraft, 25:42457
standards for radioisotopes transported by mail, 25:42494
PADUCAH AREA (Ky.)
radioactivity monitoring in environment of, during 1970, 25:42420
PAINTS
radiation protection guide for personnel using radiation-activated, ILO, 25:42462
PAIR PRODUCTION
cross sections for incident photons of 1.073 to 2.615 MeV, (T), 25:43417 (NYO-3829-71)
PALISADES POWER REACTOR
coolant loss accident in, safety analysis of, 25:44043 (DOCKET-50255-48)
emergency core cooling system for, performance requirements for, 25:44043 (DOCKET-50255-48)
safety evaluation of, Division of Reactor Licensing, 25:44044 (DOCKET-50255-49)
PALLADIUM
diffusion of deuterium and hydrogen in, at -60 to 200°C, comparison of, 25:41815
lattice vibrational spectra and thermal capacities of, calculations, 25:43490
neutron total cross section up to 1.5 MeV, (E), 25:43884 (ANL-7710, pp 1-52)
separation from acetone--hydrochloric acid solutions by ion exchange using Bio-Rad, distribution coefficients for, 25:41899
separation from aqueous solutions by ion exchange on zirconium tellurate, tracer studies on, 25:41915
separation from other metals using inorganic ion exchange papers, 25:41909
PALLADIUM ALLOYS AND SYSTEMS
Au--Ga--Pd, nuclear quadrupolar relaxation rates in $Au_{0.95}Pd_{0.05}Ga_2$, effects of melting on, 25:43496
Fe--Pd--Si, Moessbauer effect study of amorphous, 25:44238 (CALT-822-32)
Np--Pd-base, magnetic properties at 2.5 to 300°K, (E/T), 25:43488
Pd-base--Pu, magnetic properties at 2.5 to 300°K, (E/T), 25:43488
PALLADIUM ISOTOPES Pd-109
use of metalloporphyrin-incorporated, for selective ablation of lymph nodes in dogs, 25:42312
PANCREAS
scanning using selenium-75 and gamma spectrometer, 25:42578
PAROTID GLANDS
scanning of human, use of metastable technetium-99 for, 25:42572
PARTICLE TRACKS
analysis of bubble-chamber, performance of HPD 2 flying spot digitizer for, 25:42153
analysis of SMP, computer program for, 25:42135(T) (CERN-Trans-71-8)
measurement of ionization loss in bubble chamber, semiautomatic television device for, 25:42142
PARTICLES
interactions of point, relativistic mechanics of, 25:43573
PEACH BOTTOM POWER REACTOR, UNIT 1
emergency shutdown rods for, status report on batteries for, 25:44032 (DOCKET-50171-89)
operations history for May 1971, 25:44004 (DOCKET-50171-90)
shutdown rods for, safety analysis of temperature actuated, 25:44033 (DOCKET-50171-91)
PENNSYLVANIA
radiation hazards from color television sets in, during 1968 to 1970, survey of x, 25:42501
1,3-PENTADIENE, 2-METHYL-3,4,5,5,5-PENTAFLUORO-
radioinduced polymerization at -196 to 25°C, properties and structure of products of γ, 25:41848
1,3-PENTADIENE, 3,4,5,5,5-PENTAFLUORO-
radioinduced polymerization at -196 to 25°C, properties and structure of products of γ, 25:41848
PERSONNEL
hazards to Czechoslovakian uranium chemical plant and mining, health education for prevention of, 25:42504
injuries of atomic energy, in privately owned and operated establishment in USA during 1968, 25:42498 (NP-18858)
lead-210 uptake by uranium mining, following inhalation of radon-222, tracer study in baboons on, 25:42245(R) (NYO-3086-10(Vol.1))
medical care procedures for, following accidental exposure to external radiations, internal contamination, or skin contamination with radioactive materials, 25:42391
monitoring for internal exposure at JAERI, 25:42439
radiation dose to respiratory tract tissues of uranium mining, following inhalation of radon-222, method for calculation of α, 25:42394(R) (NYU-4256-1)
radiation dose to, during transport of strontium-90--yttrium-90 source, thermoluminescent dosimetric monitoring of β, 25:42444
radiation dose to, methods for determination of maximum permissible, 25:42454
radiation hazards to uranium mining, effects of foods and radioprotective substances on reduction of, 25:42510
radiation hazards to, from plutonium-239 in air, 25:42488
radiation monitoring of, ICRP recommendations on, 25:42474
radiation monitoring of, performance of photographic film dosimeters for, 25:42442
radiation monitoring programs for AB Atomenergi, Sweden, during 1969, 25:42392 (AE-423)
radiation protection manual for industrial, part 1 of ILO, 25:42458
radiation protection manual for industrial, part 2 of ILO, 25:42459
radiation protection manual for industrial, part 3 of ILO, 25:42460
radiation protection manual for industrial, part 4 of ILO, 25:42461
radiation protection manual for industrial, part 5 of ILO, 25:42462
radiation protection manual for radioactive ore mining and milling, part 6 of ILO, 25:42463
radiation protection methods for uranium enrichment, γ, 25:42379
radiation protection of, ICRP recommendations for high-energy electromagnetic, electron, neutron, and proton, 25:42464
radiation protection of, recommendations of ICRP for external-source, 25:42455
radiation protection of, recommendations of ICRP for, 25:42466
radiation protection recommendations for, ICRP, 25:42467
radiation protection regulations for transportation, carrying radioactive materials on roads in Great Britain, 25:42451
radiation protection standards for, at nuclear power centers in Italy, 25:42478
radioactive contamination of nuclear power plant, in Italy, results of whole-body counting methods for measurement of internal, 25:42435
radiodermatitis occurrence, treatment, and insurance compensation for, in France, 25:42544
training in radiological laboratory, organization of services for, 25:42500
tritium content in urine of, operating neutron generators, 25:42390
PERTURBATION THEORY
folded diagrams for, derivation of, 25:43519
interchange theorems for triple, 25:43520
PCAC and CVC hypotheses in, sigma model for divergence conditions in, 25:43689
shear in Friedmann Universe, (T), 25:43088

PESTICIDES
research on, review of radioisotopes in, 25:42239
PETROLEUM
effects of cost of Middle East, on development of nuclear power, 25:44145
prospecting in India, status of nuclear methods for, 25:41947
radiolysis of residues after distillation of, production of light hydrocarbons by electron, 25:41853 (WP-18817)
PHAGOCYTOSIS
radiation effects on rat reticuloendothelial cell, protective effects of direct electric current against x, 25:42530
PHANTOMS
radiation dose measurements in water, methods for Bremsstrahlung, electron, γ, and x, 25:42396
radiation dosimetry in human organ, containing radioisotopes, role of body background in external γ, 25:42423
radiation dosimetry in, for accuracy in diagnosis, statistical evaluation of γ, 25:42397
PHARMACEUTICALS
ointments, effectiveness of petroleum growth substance, for treatment of radiation injuries, 25:42539
PHARYNX
radiotherapy of carcinomas of, effectiveness of preoperative gamma and x, 25:42588
PHENOL, 2,6-DI-tert-BUTYL-4-METHYL-
effectiveness for treatment of x-radioinduced skin ulcers in rats, 25:42541
PHENOL, p-NITRO-
radiation effects on rat metabolism of, whole-body x, 25:42289
PHENOXIDES
preparation and reactions of triad element, 25:41780(T) (SC-T-713038)
PHOSPHATES
sodium self-diffusion coefficients in glasses of, 25:41810
PHOSPHINE
effects of alkyl-substituted, on electron-induced copolymerization of monomeric unsaturated compounds and unsaturated polyesters, 25:41847(P)
PHOSPHITES
radiolysis of solutions of, yields of hypophosphate and phosphate from γ, 25:41866
PHOSPHOLIPIDS
radiation effects on rat brain, protective effects of cysteine against x, 25:42620
PHOSPHORIC ACID
corrosive effects on zirconium alloys, 25:41832(R) (AECL-3851)
PHOSPHORIC ACID, BIS(2-ETHYLHEXYL) ESTER
solvent properties for hexavalent uranium in nitric acid solutions of fission products, 25:41924
PHOSPHORIC ACID, TRIBUTYL ESTER
adducts with uranyl thenoyltrifluoroacetone complexes, effects of solvents on formation of, 25:41784
solvent properties for neptunium, niobium, and zirconium, 25:41901
solvent properties for thorium, 25:41916
solvent properties for uranium, 25:41895 (INR-1309)
heptane--TBP--$UO_2(NO_3)_2$, diffusion studies on, 25:41829
PHOSPHOROTHIOIC ACID, S-(2-AMINOETHYL) ESTER
effects on content of non-protein thiols in urine of irradiated rats, 25:42671
sodium salt, radioprotective effects of, on mouse tumor cells, biochemical studies on x, 25:42525
PHOSPHOROTHIOIC ACID, S-2-(3-AMINOPROPYLAMINO)ETHYL ESTER
radioprotective effects of, on mouse tumor cells, biochemical studies on x, 25:42525
PHOSPHORS
luminescence and thermoluminescence of zirconium-activated strontium sulfide, kinetics of, 25:42062
PHOSPHORUS
distribution in barley, soybeans, and wheat during development, 25:42322(R) (COO-1097-46)
PHOSPHORUS ISOTOPES P-30
energy levels from aluminum-27 (α,n) reactions, lifetimes of, (E), 25:43879
PHOSPHORUS ISOTOPES P-32
content of Columbia River during 1968 to 1969, 25:42419
effects on chromosomes in human lymphocytes in relation to dose, aberrant, 25:42399
effects on poliovirus-infected Hela cells, radioresistance studies on, 25:42741
metabolism and tissue distribution following intake by man, 25:42467
separation of carrier-free, from irradiated sulfur by thermic oxidation, 25:41833(R) (IA-1218)
testing of, produced in Japan, application, 25:41990 (JAERI-13617)
uptake by bones in animals and man, induction of neoplasms and radiation injuries following, 25:42472
uptake by nucleic acids in human tumors, effects of cytotoxic agents on, 25:41833(R) (IA-1218)
use for therapy of polycythemia, occurrence of chromosome aberrations in cultured hematopoietic cells following, 25:42713
PHOSPHORUS SYSTEMS
Cr--Ni--P--Pt, electric conductivity and magnetic susceptibilities of amorphous, 25:44237 (CALT-822-31)
PHOTOMULTIPLIER TUBES
properties of FEU-79, for astronomical photon observations, 25:42068
thermal stability of, 25:42092
use of controlled-grid, for fluorescence time measurements in nanosecond region, 25:43452
PHOTON BEAMS
monitoring of 302- to 1102-MeV, calibration of ionization chambers and quantameters for, 25:42093
monitoring of position, intensity, and energy distribution of low-intensity, method for, 25:42098
theory for Compton backscattered high-energy, (T), 25:43737
use of Compton backscattered high-energy, as nondestructive probe for relativistic beam studies, 25:43737
PHOTONS
coupling constants for epsilon$\gamma\gamma$ and f$\gamma\gamma$, finite-energy sum rules for $\gamma + \pi^0 \rightarrow \gamma + \pi^0$ interactions for, (T), 25:43582 (DESY-71/20)
effects on ethylene at 20 to 77°K and 8.4 to 21.2 eV, 25:41875
interactions $\gamma + e$, effects of coherence on intensity-dependent frequency shift in Compton, 25:43590
interactions $\gamma + e$, quark--parton model for inequalities for structure functions of inelastic Compton, (T), 25:43586 (SU-1206-250)
interactions $\gamma + \gamma \rightarrow \nu +$ anti ν, dispersion relations for cross sections for ν--anti ν pair production and black-body neutrino luminosity in, (T), 25:43605
interactions $\gamma + N \rightarrow \pi^0 + N$, Regge cuts due to absorption in, (T), 25:43601
interactions $\gamma + N \rightarrow rho^0 + N$, dynamical effects of instability in, (T), 25:43604
interactions $\gamma + N$ in strong electromagnetic field, final-state interaction for electron production in (T), 25:43606
interactions $\gamma + p \rightarrow eta + p$ at 4 to 9 GeV, spectrometer study of energy dependence of cross sections for, (E), 25:43529
interactions $\gamma + p \rightarrow \pi^0 + p$ at 4 to 18 GeV, spectrometer study of energy dependence of cross sections for, (E), 25:43529
interactions $\gamma + \pi \rightarrow 2\pi$, parton model for dual amplitude for, 25:43592
interactions $\gamma + \pi^0 \rightarrow \gamma + \pi^0$, coupling constants for f$\gamma\gamma$ and epsilon$\gamma\gamma$ from finite-energy sum rules for, (T), 25:43582 (DESY-71/20)
interactions with hadrons at high energies, vector-dominance model of, 25:43597
interactions with massless particles, cross sections for gravitational, (T), 25:43706
mass energy transfer and mass energy absorption coefficients for, criticism of existing tabulations of, 25:43434
production and propagation in upper atmosphere, secondary, (E/T), 25:43235
reactions with electrons, forced level shifts and energy renormalization in, (T), 25:43518
reactions with lead at 1.1 GeV, nucleon distribution and π^0 mean free path in nuclei from π^0 production in, 25:43595
reactions with nuclei at high energies, dynamical effects of instability in nonresonant and rho^0 production in π^+--π^- pair production in, (T), 25:43604
PHYSICS
book: Basic Medical Radiation Physics, 25:42555
PHYTOHEMAGGLUTININ
effects on DNA synthesis in irradiated rat lymphocytes as indicator of dose, in vitro, 25:42404
effects on irradiated lymphocytes from infant and adult man, 25:42602
PINCH DEVICES
plasma instabilities in toroidal screw, shear and kink, (T), 25:43390
PIPE FITTINGS
failure of flawed ASTM A105B steel, hydrostatic testing of, 25:42845 (GEAP-10236)
PIPES
failure of flawed ASTM A105B steel, hydrostatic testing of, 25:42845 (GEAP-10236)
standard for ultrasonic testing for longitudinal discontinuities, 25:42026 (RDT-F-3-8-T)
welding of, design of remote automated welder for, 25:41981
PLANETARY NEBULAE
identification of NGC 7635 as, (E), 25:43044
PLANETS
composition of, chemical, (T), 25:43078
PLANTS
analysis for gold by neutron activation, 25:41770
population dynamics of Euterpe globosa and Viguiera porteri, in natural ecosystem, 25:42316(R) (ORO-3299-107)
radiation dose to marine, following discharge of radioactive wastes into seawater, 25:42373
radioisotope uptake by aquatic, comparison studies on, 25:41833(R) (IA-1218)
silver-108m content of, at Bikini and Eniwetok atolls following nuclear testing during 1958, 25:42377

XUM

PLANTS (INDUSTRIAL)
authorization for construction of Italian nuclear, review of Italian procedures for, 25:41979
PLASMA
book: Atomic Collisions and Elementary Processes in Plasma (in Russian), 25:43349
boundary layer over cathode, nonequilibrium, (T), 25:43361 (N-71-12579)
boundary layer structure at conducting sphere, (E), 25:43356
boundary layers of, transition radiation at vacuum, (T), 25:43367
boundary sheath in magnetic fields, kinetic theory of, 25:43378
boundary sheath near pulsed transparent grid, ion distribution function for, (T), 25:43369
charged-particle orbit approximation in periodic systems, straight-line, (T), 25:43373
conductivity of air, effects of multiple ionization on, (T), 25:43352 (N-71-18715)
conductivity of fully ionized, with ion--ion correlations, (T), 25:43363 (NP-18805)
conductivity of warm, near lower hybrid resonance, (T), 25:43375
confinement of high-beta, in toroidal geometries with helical multipole fields, (E), 25:43336
confinement of, optimization problems in, 25:43337
diagnostics of laser-produced, Langmuir probe and microwave, (E), 25:43342
diagnostics of turbulent electric fields in discharge, using polarization of Stark profiles, (E), 25:43344
diagnostics of turbulent, using charged particle beams, 25:43339 (IYAF-7-70)
diagnostics of, microwave interferometer for density, 25:42183(T) (CTC-756)
diagnostics of, microwave system for, 25:43345(P)
diagnostics of, multichannel system for determination of time-varying spectral line profiles, 25:43343
diagnostics using Langmuir probes, ion current response to ion--atom collisions, (E), 25:43340 (N-71-17594)
diagnostics using multi-channel Fabry--Perot interferometer, ion temperature, 25:43341
diffusion in magnetically perturbed multipoles, effect of toroidal field on, (E), 25:43335
diffusion in toroidal stellarator, (T), 25:43374
diffusion of localized density fluctuation in uniform magneto-, (T), 25:43370
drift-wave instabilities in magnetic fields of, with temperature gradient, (T), 25:43244
electron beam interaction with collisionless discharge, thermal explosion from, (E/T), 25:43372
electron beam interactions with, finite amplitude electrostatic waves from nonlinear, (T), 25:43365
electron beam interactions with, three-wave interactions from, (T), 25:43407 (N-71-18595)
electron velocity distribution in low density, deviation from Maxwellian, 25:43023
heating by transit time magnetic pumping, in torus, 25:43332 (EUR-CEA-FC-595)
heating in toroidal octupoles, electron cyclotron, (E), 25:43334
heating of, power requirements for various methods of, 25:43333 (MATT-803)
injection into magnetic mirrors, shock wave formation in, (E), 25:43359
interactions with inhomogeneous transverse magnetic fields, (E), 25:43355
interactions with magnetic fields, exact solutions for tenuous, (T), 25:43379
ion distribution function in sheath near pulsed transparent grid, (T), 25:43369
ionization potential of atoms in, partition function for, (T), 25:43364
kinetic theory of collisionless, Vlasov solutions for, 25:43368
kinetic theory of fully ionized, BBGKY hierarchy, 25:43375
kinetic theory of, method of normal modes for Vlasov--BGK equations, 25:43377
laser-beam absorption by inhomogeneous laser-produced, (E/T), 25:43400
motion of, theory for axially symmetric coordinate system, 25:43355
oscillations in, asymmetry of combination frequency spectrum of, 25:43410
plasmons in, linear and nonlinear two-stream instabilities from, (T), 25:43387
production by laser irradiation of solid hydrogen and deuterium, (E/T), 25:43380 (IPP-4/9)
production of dense, research on, (E/T), 25:43381 (LGI-68/16)
production of, igniting aid for high-efficiency, 25:43382(P)
properties near cathode region of MPD arc jet, (E), 25:43353 (N-71-19984)
radiations from anisotropic hot electron, polarization of free--free bremsstrahlung, (E), 25:43357
radiative temperature of bounded nonthermal, (E), 25:43354
radiative temperature of bounded nonthermal, (T), 25:43371
research on dense, (E/T), 25:43381 (LGI-68/16)
shock wave propagation in electromagnetic shock tubes, simulation of strong, (T), 25:43360 (CU-3954-9)
shock wave structure in magnetized, review of collisionless, (E/T), 25:43347
stability in strong electric fields, nonlinear stage of hydromagnetic current, (T), 25:43385(T) (ORNL-tr-2434)
stability in Toksmak and screw pinches, toroidal contributions to shear and kink instabilities, (T), 25:43390
stability in toroidal devices, radial dependence of trapped-particle, (T), 25:43391
stability of elliposoidal, in traveling electromagnetic fields, (t), 25:43392
stability of magnetized column, Kelvin--Helmholtz, (E/T), 25:43395
stability of, electromagnetic and finite β/sub e/ effects on counterstreaming ion, (T), 25:43394
stability of, plasmon theory for linear and nonlinear two-stream, (T), 25:43387
stabilization of collisionless trapped-particle instabilities in, finite-beta, (T), 25:43388
stabilization of filaments of, with variable current by quadrupole magnetic field, 25:43389
stabilization of screw instabilities in current-carrying, by feedback, (T), 25:43384(T) (CTC-759)
striations in column, nonlinear stabilization of, (E), 25:43393
turbulence in highly ionized magnetized, instabilities in, 25:43385(R) (N-71-12892)
wave coupling in inhomogeneous lossy, electromagnetic and electron acoustic, (T), 25:43404 (AD-715910)
wave damping in, electromagnetic, (T), 25:43408
wave echoes in, effect of noise broadening on trapped-particle, (T), 25:43409
wave excitation in beam--plasma system, finite amplitude electrostatic, (T), 25:43365
wave interactions in beam--plasma system, three-, (T), 25:43407 (N-71-18696)
wave interactions in, asymmetry of combination frequency spectrum of, 25:43410
wave interactions with density fluctuations in inhomogeneous magnetized, electromagnetic, (E), 25:43402 (AD-715277)
wave interactions with electrons in, at Doppler shifted cyclotron frequency, (E), 25:43412
wave interactions with magnetized, cyclotron resonance, (T), 25:43403 (AD-715636)
wave interactions with, nonlinear behavior of Tonks--Dattner resonances in, (T), 25:43411
wave propagation in cylindrical waveguides, hybrid electromagnetic, (E/T), 25:43405 (CERN-71-4)
wave propagation in dense, ion sound turbulence in, (T), 25:43406 (JINR-P9-5846)
wave propagation in, solutions for magneto-acoustic, under gravity, (T), 25:43073
PLASMA ACCELERATORS
boundary layers in, ionization and thermal nonequilibrium in, (E), 25:43352 (AD-715272)
design of converging-barrel, 25:43350(P)
performance of induction, for propulsion, 25:43351
performance of pulsed coaxial, jet kinetics in, (e), 25:43358
PLASMA JETS
diagnostics of laser-produced, Langmuir probe and microwave, (E), 25:43342
diagnostics of thermal, induction, rf magnetic field distribution, (E), 25:43338 (AD-715265)
kinetic theory in axially symmetric coordinate system, 25:43366
stability of, electromagnetic and finite β/sub e/ effects on counterstreaming ion, (T), 25:43394
PLASMAPAUSE
correlation with SAR arc latitudinal location, (T), 25:43242
location effect in low-latitude decrease of outer-zone electron precipitation, morning, (E/T), 25:43211 (AD-715266)
position during June 15, 1965 magnetic storm, relation to trapped enhanced >280 keV electron flux, (E), 25:43264
PLASTICS
stability of membranes of, effects of shock loading on, 25:42506(R) (ORNL-4566(Pt.1))
plastics--wood, properties of, produced by radioinduced polymerization, 25:41843(R) (ORO-2945-10)
PLATES
standard for ultrasonic shear-wave testing of, 25:42023 (RDT-F-3-4-T)
PLATINUM
atomic spectra of, isotope shifts and hyperfine structure in, 25:41819
determination by x ray spectrography, 25:41736
determination in blood and tissues of non-tumored and tumored Swiss white mice by neutron activation, radiochemical separation, and γ spectrometry, 25:41762
neutron reactions with, activation in, 25:41920
properties for use in pressure transducers, 25:42804(R) (LMEC-71-1)
separation from acetone--hydrochloric acid solutions by ion exchange using Bio-Rad, distribution coefficients for, 25:41899
separation from aqueous solutions by ion exchange on

zirconium tellurate, tracer studies on, 25:41915
separation from gold and iridium after neutron activation by paper chromatography, 25:41920
separation from other metals using inorganic ion exchange papers, 25:41909
sorptive properties for iodine-131 from acid solutions of neutron-irradiated magnesium tellurate, 25:41980
surface structures of chemisorbed aromatic molecules of, LEED studies on, 25:41778 (UCRL-20500, pp 1-85)

PLATINUM ALLOYS AND SYSTEMS
Cr--Ni--P--Pt, electric conductivity and magnetic susceptibilities of amorphous, 25:44237 (CALT-822-31)
Cu--Pt, deformation studies of, 25:44286(R) (ORO-3091-21)
Pt--Yb, crystal structure of YbPt, 25:42892
Pt-base--Rh--W, fabrication and properties of cladding of, 25:41993(R) (ORNL-4692)

PLATINUM ISOTOPES
effects on spectra of platinum, relative, 25:41819

PLATINUM ISOTOPES Pt-191
electron-capture decay of, γ singles and coincidence spectra and conversion electron spectra from, (E), 25:43902

PLATINUM ISOTOPES Pt-194
proton elastic and inelastic scattering at 16 MeV, differential cross sections for, (E), 25:43901

PLATINUM ISOTOPES Pt-198
proton elastic and inelastic scattering at 16 MeV, differential cross sections for, (E), 25:43901

PLATYHELMINTHES
Dugesia dorotocephala, radiation effects on survival of, protective effects of serotonin against x, 25:42527
Fasciola hepatica, control in cattle in Puerto Rico using irradiated metacercariae, 25:42246(R) (PRNC-148)
Hymenolepis nana, transfer of immunity to, by injection of spleen cells from immunized donor mice into pre-irradiated recipient mice, 25:42311

PLOWSHARE PROJECT
monitoring local fallout from Project Schooner at Nevada Test Site, 25:42717 (EGG-1183-2272)

PLUTONIUM
analysis for trace impurities, development of reference standards for, 25:41718 (CEA-R-4106)
determination in plutonium--uranium alloys by α spectrometry, 25:42118(P)
oxidation-reduction potential of, effects of pH on, 25:41831
separation from aqueous solutions from fuel reprocessing by multistage extraction using tributyl phosphate, 25:41902(P)
separation from organic solutions of bis(2-ethylhexyl) phosphate by reduction using dialkyl substituted hydroquinones, 25:41912(P)
separation from uranium by countercurrent ionophoresis, continuous, 25:41908
separation from uranium in fuel fabrication scrap, reflux extraction flowsheet using TBP for, 25:41888 (ARH-SA-78)

PLUTONIUM ALLOYS AND SYSTEMS
C--N--O--Pu--U, thermodynamic properties and stoichiometry of, 25:42998
C--N--Pu--U, phase studies and structures of, review on, 25:42982 (JAERI-13650)
Fe--Pu, magnetic properties of cubic Laves phase in intermetallic compound $PuFe_2$, Mossbauer studies on, 25:41833(R) (IA-1218)
Ga--Pu-base, annealing of shock-hardened, kinetics of, 25:42857
Pd-base--Pu, magnetic properties at 2.5 to 300°K, (E/T), 25:43488
Pu--U, analysis for plutonium by α spectrometry, 25:42118(P)

PLUTONIUM ISOTOPES Pu-238
content of airborne particulates in USA during 1970, 25:42426
production of heat sources of, for cardiac pacemakers, review of programs for, 25:42012
properties for use as heat source for subliming microthruster for space propulsion, 25:42017
properties for use as heat source for thermoelectric generators, 25:42014
separation from neptunium-237 by valence control, method for, 25:41833(R) (IA-1218)
separation from other isotopes during 1968 and 1969, review of ORNL, 25:41992 (ORNL-4640)
separation from other isotopes during 1968 and 1969, review of ORNL, 25:41992 (ORNL-4640)
uptake by oat plants from soils, effects of fertilizers on, 25:42260
use as heat source for organic Rankine cycle space power system, 25:42003
use as heat source in SNAP-27, review of program for, 25:41999

PLUTONIUM ISOTOPES Pu-239
content in laboratory air, maximum permissible, 25:42488
content of airborne particulates in USA during 1970, 25:42426
determination by neutron transmission measurements, 25:41750 (AE-416)
distribution in skin following surface contamination, kinetics of, 25:42257
inhalation of, alpha dosimetry in bronchial epithelium following, 25:42394(R) (NYJ-4256-1)
neutron capture-to-fission ratio in plutonium oxide (PuO_2)--uranium oxide (UO_2) core, (E), 25:44096 (ANL-7710, pp 53-262)
neutron fission at 0.1 to 3.0 MeV, power-series fits to fragment angular distributions from, (T), 25:43888 (LA-4648)
neutron fission cross section for, evaluation of ENDF/B data for microscopic, (E/T), 25:44094(R) (AI-AEC-12991)
neutron fission from thermal energies to 14 MeV, calculations of total energy released during, (T), 25:43885 (ANL-7748)
neutron fission of, central reaction ratio of uranium-235 fission to, (E/T), 25:44094(R) (AI-AEC-12991)
neutron fission rate in plutonium oxide (PuO_2)--uranium oxide (UO_2) two zone core, (E), 25:44096 (ANL-7710, pp 53-262)
neutron fission reaction rate in, Doppler effects on, (E/T), 25:44164
radiation hazards of airborne, to personnel, 25:42488
separation from other isotopes during 1968 and 1969, review of ORNL, 25:41992 (ORNL-4640)
toxicity to rats in comparison to neptunium-237, 25:42253
uptake by bones in animals and man, induction of neoplasms and radiation injuries following, 25:42472

PLUTONIUM ISOTOPES Pu-240
determination by neutron transmission measurements, 25:41750 (AE-416)
neutron elastic and inelastic scattering up to 1.5 MeV, cross sections for, (E), 25:43884 (ANL-7710, pp 1-52)
neutron fission from thermal energies to 14 MeV, calculations of total energy released during, (T), 25:43885 (ANL-7748)
neutron fission rate in plutonium oxide (PuO_2)--uranium oxide (UO_2) two zone core, (E), 25:44096 (ANL-7710, pp 53-262)
neutron total cross section up to 1.5 MeV, (E), 25:43884 (ANL-7710, pp 1-52)
separation from other isotopes during 1968 and 1969, review of ORNL, 25:41992 (ORNL-4640)

PLUTONIUM ISOTOPES Pu-241
metabolism and tissue distribution following intake by man, 25:42467
neutron fission from thermal energies to 14 MeV, calculations of total energy released during, (T), 25:43885 (ANL-7748)
separation from other isotopes during 1968 and 1969, review of ORNL, 25:41992 (ORNL-4640)

PLUTONIUM ISOTOPES Pu-242
neutron fission from thermal energies to 14 MeV, calculations of total energy released during, (T), 25:43885 (ANL-7748)
separation from other isotopes during 1968 and 1969, review of ORNL, 25:41992 (ORNL-4640)

PLUTONIUM ISOTOPES Pu-244
separation from other isotopes during 1968 and 1969, review of ORNL, 25:41992 (ORNL-4640)

PLUTONIUM NITRATES
analysis of aqueous solutions of, for sulfates by ion exchange and titration, 25:41716 (AECL-3676)
storage of solutions of, at West Valley Processing Plant, 25:41891 (DOCKET-50201-74)

PLUTONIUM NITRIDES
PuN--UN, fabrication of fuel pins of, 25:44118(R) (BMI-1905)
PuN--UN, irradiation testing of fuels of, 25:44118(R) (BMI-1905)
PuN--UN, self-diffusion of nitrogen in, (E), 25:44118(R) (BMI-1905)

PLUTONIUM OXIDES
analysis for americium, spectrophotometric, 25:41721 (EUR-4352)
removal from lungs following inhalation, effectiveness of saline lavage for, 25:42368(T) (LF-tr-53)

PLUTONIUM OXIDES PuO
PuO--UO, preparation of hypostoichiometric $(U,Pu)O_2$, by hydrogen reduction and carbothermic methods, 25:41779 (ORNL-TM-3358)

PLUTONIUM OXIDES PuO_2
content of air, recommended decrease in maximum permissible, 25:42508
inhalation by man, recommended decrease in maximum permissible lung burden following, 25:42508
PuO_2--UO_2, chemical reactions with Hastelloy X and stainless steels, effects of gas cooled fast breeder reactor conditions on, (E/T), 25:44123 (ORNL-TM-3385)
PuO_2--UO_2, creep of, effects of fission process on, (E/T), 25:44118(R) (BMI-1905)
PuO_2--UO_2, fabrication of pellets of, effects of stearate additives or lubricants on, 25:42949
PuO_2--UO_2, fission product vapor pressures over fast neutron irradiated, (E/T), 25:44206 (CEA-R-4181)
PuO_2--UO_2, radiation effects on mechanical properties of, neutron, 25:44125 (ORNL-TM-3427)
PuO_2--UO_2, restructuring temperatures and kinetics for fuels of, in-pile, (E/T), 25:44124 (ORNL-TM-3387)
PuO_2--UO_2, solubility of pellets of, statistical study of effects of fabrication variables on, 25:42954 (HEDL-SA-131)

XUM

POINT BEACH POWER REACTOR, UNIT 2
boiler for, inspection of repairs for, 25:44054 (DOCKET-50301-35)
testing program for, inspection of pre-operation, 25:44054 (DOCKET-50301-35)
POLLEN
radiation effects on size of saffron, effects of dose on γ, 25:42720
radiation effects on tomato, mutagenic fast neutron and γ, 25:42364
POLONIUM ISOTOPES Po-203
energy levels from radon-207 alpha decay, spin--parity assignments for, (E), 25:43887 (JINR-P6-5791)
POLONIUM ISOTOPES Po-204
energy levels from radon-208 alpha decay, spin--parity assignments for, (E), 25:43887 (JINR-P6-5791)
POLONIUM ISOTOPES Po-205
energy levels from radon-209 alpha decay, spin--parity assignments for, (E), 25:43887 (JINR-P6-5791)
POLONIUM ISOTOPES Po-206
energy levels from radon-210 alpha decay, spin--parity assignments for, (E), 25:43887 (JINR-P6-5791)
POLONIUM ISOTOPES Po-207
energy levels from radon-211 alpha decay, spin--parity assignments for, (E), 25:43887 (JINR-P6-5791)
POLONIUM ISOTOPES Po-208
energy levels from radon-212 alpha decay, spin--parity assignments for, (E), 25:43887 (JINR-P6-5791)
POLONIUM ISOTOPES Po-210
content of environment and human tissues in Soviet Union, 25:42429
deposition in bones of cattle in Italy during 1962 to 1968, 25:42382
metabolism and tissue distribution following intake by man, 25:42467
properties for use as heat source for subliming microthruster for space propulsion, 25:42017
properties for use as heat source for thermoelectric generators, 25:42014
POLONIUM ISOTOPES Po-214
inhalation of, alpha dosimetry in bronchial epithelium following, 25:42394(R) (NYJ-4256-1)
POLONIUM ISOTOPES Po-218
content in rat organs and tissues following inhalation of radon-222, 25:42248
inhalation of, alpha dosimetry in bronchial epithelium following, 25:42394(R) (NYJ-4256-1)
POLYMERIZATION
radioinduced, abstracts of conference papers on, 25:41842 (CONF-690977-(Absts.))
POLYMERS
conference on, Kingston, Ontario, Canada, Sept. 3 to 5, 1969, abstracts of papers at, 25:41842 (CONF-690977-(Absts.))
properties for use in nuclear industry, 25:43016
radiation effects on properties of, 25:43016
radioinduced production of, effects of alkyl arsines, phosphines, and stibines on, 25:41847(P)
radioprotective effects of N- and S-containing, on mice and rats, long-term x, 25:42517
reactions of uranyl and vanadyl ions with polypeptide-containing hydrophilic capsule wall material of, 25:41781(P)
POLYPHENYL SYSTEMS
analysis of hydrogenated, used for reactor cooling, 25:41713 (AECL-3672)
properties of hydrogenated, used for reactor cooling, 25:41713 (AECL-3672)
POPULATIONS
radiation action levels for, in vicinity of nuclear installations in Israel, 25:41833(R) (IA-1218)
radiation dose estimates for human, from fallout in environment during 1969, 25:42691
radiation dose to human, following release of radioisotopes to atmosphere during reactor accidents, computer methods for calculation of, 25:42393 (BNWL-B-69)
radiation dose to human, from television, annual x, 25:42366
radiation dose to human, sources of, 25:42692
radiation dose to human, sources of, 25:42693
radiation dose to thyroid glands of human, evaluation of nuclear power reactor sites in relation to potential accidental iodine-131, 25:44147
POSITRON CAMERAS
performance for scintigraphy of human bones using fluorine-18, 25:42564
performance for scintigraphy of human brain using sodium-22, 25:42565
performance for scintigraphy of human liver using copper-64-labeled erythrocytes, 25:42564
POSITRONS
annihilation in beryllia, nickel oxide, zirconia, and niobia, angular correlations and three-quantum yields of, 25:43482
annihilation in ytterbium under pressure, 25:41778 (UCRL-20500, pp 1-85)
interactions $e^+ + e^-$, amplitude for production of two soft ν in, 25:43596
lifetimes and intensities in sodium chloride crystals, effects of irradiation on, 25:43453
production and propagation in upper atmosphere, secondary negatrons and positrons, (E/T), 25:43235
production in $K_2^0 \rightarrow \pi + e + \nu$ decay, time reversal invariance test in Coulomb final-state interaction corrections for charge asymmetry in, (T), 25:43660
reactions with hydrogen ions (H_2^+), vibrorotational excitation in, (T), 25:43141
scattering by atoms at low energies, central-potential form for, (T), 25:43148
POTASH
prospecting for, review on nuclear borehole methods for, 25:41931
POTASSIUM
beams of atomic, sensitivity of electron multiplier tubes for detection of, 25:42079
content in human body, statistical survey for whole-body counting of, 25:41833(R) (IA-1218)
distribution in barley, soybeans, and wheat during development, 25:42322(R) (COO-1097-46)
potassium-ion reactions with, charge-exchange cross sections for, (T), 25:43157
separation from acetone--hydrochloric acid solutions by ion exchange using Bio-Rad, distribution coefficients for, 25:41899
separation from aqueous solutions by ion exchange on zirconium tellurate, tracer studies on, 25:41915
separation from ores, leaching methods for, 25:41918
superconducting parameter calculations, 25:43305
POTASSIUM ACID PHOSPHATES
radiation effects on dielectric properties of crystals of, gamma, 25:43443
POTASSIUM BOROHYDRIDES
hydrolysis of KB_3H_8 in hydrochloric acid, 25:41778 (UCRL-20500, pp 1-85)
POTASSIUM CHLORIDES
neutron total cross section at 100 to 650 keV, optical model analysis of average, (E/T), 25:43908
proton channeling at 1.5 MeV in crystals of, effects of surface and imperfections on, (E/T), 25:43461
radioinduced F centers in crystals of, effects of dopants on growth curves of x-, (E), 25:43450
POTASSIUM IONS
reactions with nitrogen molecules at 30 keV to 2 MeV, cross sections for excitation of N_2^+ 3914-A radiation in, (E), 25:43151
reactions with potassium, charge-exchange cross sections for, (T), 25:43157
POTASSIUM ISOTOPES K-36
beta decay of, half-life and log-ft values for, (E), 25:43875
mass excess from argon-36 (p,n) reactions, (E), 25:43875
POTASSIUM ISOTOPES K-39
energy levels from proton inelastic scattering, lifetimes for, (E), 25:43861
energy levels of, lifetimes and transition strengths for, (E), 25:43856
energy-level transitions from proton inelastic scattering, attenuation factors and mixing ratios for, (E), 25:43861
proton reactions (p,γ) in giant resonance region, angular distributions and cross sections for, (E), 25:43853
triton reactions (t,p) at 7.5 MeV, angular distributions for, (E), 25:43845
POTASSIUM ISOTOPES K-40
content in Romanian environment, method for measurement of, 25:41928
neutron capture by, γ singles and coincidence spectra from thermal, (E), 25:43845
uptake by aquatic plants, 25:41833(R) (IA-1218)
POTASSIUM ISOTOPES K-41
energy levels from potassium-39 (t,p) and potassium-40 (n,γ) reactions, spin--parity assignments for, (E), 25:43845
proton reactions (p,γ) in giant resonance region, angular distributions and cross sections for, (E), 25:43853
POTASSIUM MAGNESIUM FLUORIDES
color centers and impurity ions in, EPR and optical absorption studies of, 25:44297 (TID-25746)
POTASSIUM PERIODATES
radiolysis of aqueous solutions of, transitory species from electron pulse, 25:41850(R) (CEA-N-1438)
POTASSIUM PERMANGANATES
effects on electrophoretic mobility of x-irradiated human erythrocytes in relation to dose, 25:42682
POTASSIUM SODIUM NIOBATES
sintering behavior of, 25:42957 (UCRL-20500, pp 147-73)
POTASSIUM URANATES
covalency in KUO_3, oxygen-17 NMR study of, 25:43497
POWDER METALLURGY
method for forging of preforms in closed dies, review of, 25:42829
research progress on, 25:44292(R) (SRO-475-11)
POWDERS
properties of dry, for combating fires of magnesium, misch metal, sodium, uranium, comparison of effectiveness of, 25:42837 (AERE-R-6745)
POWER CYCLES
bearings for organic Rankine, 25:44289 (SAN-651-129)
electric--thermal integration of cobalt-60-fueled organic Rankine, in manned spacecraft environmental control and life support systems, 25:42005
evaluation of Brayton, for space power systems, 25:42008

evaluation of Brayton, for space power systems, analog computer studies for, 25:42009
evaluation of plutonium-238-fueled organic Rankine, or manned space station power system, (T), 25:42003
evaluation of plutonium-238-fueled Stirling, for spacecraft auxiliary power systems,, 25:42010
performance of closed Brayton, in power supply systems for lunar, space, terrestrial, and undersea environments, 25:42007
POWER PLANTS
economics of chemical and nuclear, for undersea uses, 25:44180
PRASEODYMIUM
determination in meteorites by neutron activation and high-voltage electrophoresis, 25:41776
diffusion of copper and zinc in, mechanism of, 25:41833(R) (IA-1218)
magnetic structure in strong magnetic fields, 25:43435(R) (RISO-237)
magnetic susceptibility of, generalized function for, (T), 25:43477
preparation of large single crystals of, 25:42834
separation from cerium by adsorption process using manganese oxide, 25:41883
PRASEODYMIUM ALLOYS AND SYSTEMS
Eu--Ge--Pr, structure of Pr/sub 5-x/Eu/sub x/Ge_3, 25:42895
Gd--Mn--Pr, magnetic properties of Pr/sub x/Gd/sub 1-x/Mn_2, high-temperature, 25:42894
Gd--Mn--Pr, structure of Pr/sub x/Gd/sub 1-x/Mn_2, 25:42894
Mn--Pr--Tb, magnetic properties of Pr/sub x/Tb/sub 1-x/Mn_2, high-temperature, 25:42894
Mn--Pr--Tb, structure of Pr/sub x/Tb/sub 1-x/Mn_2, 25:42894
Pr--Te, phase studies of, 25:42986
PRASEODYMIUM HYDROXIDES
preparation of crystals of, hydrothermal studies of equilibria with water in, 25:42934 (COO-1109-60)
PRASEODYMIUM HYDROXYCARBONATES
preparation of monocrystals of, hydrothermal studies of equilibria with water in, 25:42934 (COO-1109-60)
PRASEODYMIUM HYDROXYNITRATES
preparation of monocrystals of, hydrothermal studies of equilibria with water in, 25:42934 (COO-1109-60)
PRASEODYMIUM IONS
properties of Pr^{3+}, configuration-interaction corrections to Hartree--Fock calculations of, 25:43116
PRASEODYMIUM ISOTOPES Pr-141
proton reactions (p,γ) with, resonance in, (E), 25:43950
PRASEODYMIUM ISOTOPES Pr-143
energy levels from cerium-143 beta decay, spin--parity assignments for, (E), 25:43921
energy-level transitions from cerium-143 beta decay, internal conversion coefficients and multipolarities for, (E), 25:43921
PRASEODYMIUM ISOTOPES Pr-144
production of carrier-free, by milking from cerium-144 using manganese oxide column, 25:41883
PRASEODYMIUM OXIDES
analysis for impurities, cathode region method for spectrochemical, 25:41833(R) (IA-1218)
preparation of crystals of, hydrothermal studies of equilibria with water in, 25:42934 (COO-1109-60)
reduction by heating, stability of compounds formed during, 25:42968
PrO--ThO_2, phase relations and lattice parameters for, 25:42996
PRASEODYMIUM OXYCARBONATES
preparation of monocrystals of, hydrothermal studies of equilibria with water in, 25:42934 (COO-1109-60)
PREAMPLIFIERS
specifications for JAERI modular, 25:42185 (JAERI-13605)
PRESSURE GAGES
design and testing of eddy current liquid metal, standard for, 25:42195 (RDT-C-6-3-T)
design for radioactive gases, 25:42179(P)
PRESSURE TRANSMITTERS
design and testing of liquid metal, standard for, 25:42194 (RDT-C-6-1-T)
PRESSURE VESSELS
carbon and alloy steel forgings for, standard for quenched and tempered vacuum-treated, 25:42778 (RDT-M-2-7-T)
construction of reactor, standards for, 25:43993 (RDT-E-15-2-T)
creep stress distribution in long cylindrical reactor, analysis of, 25:42842 (CONF-710512-9)
fabrication of reactor, effects of inspection standards on, 25:44110 (CONF-700224-, Paper 5)
failure of reactor, stress wave emission techniques for detection of incipient, 25:44137 (CONF-700224-, Paper 3)
fracture behavior of thick-walled steel, effects of radioinduced toughness gradient on, 25:42841 (CONF-710512-8)
inspection of reactor, equipment for radiographic, 25:44112 (CONF-700224-, Paper 7)
inspection of reactor, performance of linear accelerator for radiographic, 25:44113 (CONF-700224-, Paper 8)
inspection of steel, procedures for in-service ultrasonic, 25:44109 (CONF-700224-, Paper 2)
plates for, standard for carbon steel, 25:42792 (RDT-M-5-2-T)
plates for, standard for manganese--molybdenum--nickel alloy steel, 25:42793 (RDT-M-5-3-T)
radiation effects on steel, dosimetry techniques for neutron, 25:44117
surveillance program analyses for reactor steel, reliability of neutron fluence and embrittlement calculations in, (E/T), 25:44116
welding qualifications for, standard for, 25:42850 (RDT-F-6-5-T)
welds in reactor, system for automatic ultrasonic inspection of, 25:44111 (CONF-700224-, Paper 6)
PROMETHIUM
crystal structure of, 25:42893
hardness of, 25:42893
PROMETHIUM ISOTOPES Pm-141
energy-level scheme from samarium-141 decay, (E), 25:43909
PROMETHIUM ISOTOPES Pm-147
design of power source of, for high voltages and small currents, 25:42019(P)
uptake by oat plants from soils, effects of fertilizers on, 25:42260
use as power source in betavoltaic cells and thermionic converters for biomedical applications, 25:41996
PROMETHIUM ISOTOPES Pm-151
beta decay of, β-γ and γ-Ce delayed coincidence spectra from, (E), 25:43937
PROPANE, 2-METHYL-
radiolysis at 77 and 195°K, effects of phase on excitation transfer in γ, 25:41864
PROPIONITRILE, 2,2'-AZOBIS[2-METHYL-
2,2'-azobis[2-methylpropionitrile]--benzene, radiolysis of, effects of additives on yields of nitrogen from electron pulse, 25:41872
PROPYLAMINE
radiolysis of, adsorbed on silica gel at 77°K, ESR studies on trapped radicals produced by γ, 25:41856
PROSPECTING
conference on nuclear techniques for mineral, Krakow, Dec. 8 to 12, 1969, 25:41941 (STI/PUB-279)
PROTACTINIUM
existence of anionic, paper chromatographic, electrophoretic, and ion-exchange studies on, 25:41786
separation from spent molten salt reactor fuels by selective reduction and extraction using molten bismuth, 25:41903(P)
PROTACTINIUM ISOTOPES Pa-231
neutron fission at 0.1 to 3.0 MeV, power-series fits to fragment angular distributions from, (T), 25:43888 (LA-4648)
PROTACTINIUM ISOTOPES Pa-233
energy level at 86.6 keV from neptunium-237 decay, lifetime of, (E), 25:43895
PROTEINS
book: Investigation of the Paramagnetic Centers of Irradiated Proteins, 25:42275
determination in spinal fluid, effectiveness of brain tumor diagnosis by, 25:42547 (ACRH-1000-248)
radiation effects on composition of rat blood serum, following head exposure, x, 25:42655
radiation effects on content of sulfur-containing amino acids in rat organ, chromatographic study on x, 25:42265
radiation effects on sulfhydryl group in cell, in relation to sensitivity of transplanted tumors in rats, 25:42618
radiation effects on uptake of selenium-75 and sulfur-35 in rat organ, x, 25:42264
radioinduced modification of, use of specific protein--protein interactions in studies of, 25:42303
synthesis of, reaction mechanisms for, 25:44259(R) (HUX-2643-61)
PROTON BEAMS
interactions with turbulent plasma, diagnostic use of, 25:43339 (IYAF-7-70)
production and properties of 15- to 30-keV, 25:43109
PROTONS
absorption in polyethylene at 150 MeV, ionization curves for, (E), 25:42141
acceleration of solar, (E/T), 25:43067 (N-71-16749)
channeling in crystals at 1.5 MeV, effects of surface and imperfections on, (E/T), 25:43461
cutoffs of 1.4 to 46 MeV solar, low-altitude observations of, (E), 25:43234
detection of 20- to 100-MeV, characteristics of lithium-drifted germanium detectors for, 25:42128
detection of cosmic-ray, design of balloon-borne counter telescope for, 25:42159
effects of 30-MeV, on positron lifetimes and intensities in sodium chloride crystals, 25:43453
effects on activity of T1 bacteriophage, model for effects of temperature on, 25:42288
effects on infrared spectra of silicates at 5 keV, 25:43446
effects on silicon at 6.3 MeV, distribution of defects induced in, (E), 25:43463
effects on silicon solar cells below 2 MeV, 25:42226 (AD-715261)
effects on solar cell cover glass of electrons and 22-

XUM

MeV, effects of cerium doping on, 25:43008 (N-71-12278)
effects on void formation in Type 316 stainless steel at 500°C at 1.2 MeV, 25:42917
energy loss at 10 MeV to 100 GeV in silicon, calculations of average and most probable, (T), 25:42155
energy spectra from single-crystal silicon, high-energy humps in backscattered 0.5- and 1.0-MeV, (E), 25:43459
energy spectra of solar, Explorer-35 data from July 20, 1967 to May 14, 1968 of, (E), 25:43231
energy straggling in gases at 100 to 500 keV, (E/T), 25:43432
form factor from backward e + p → e + p interactions at 70 to 280 MeV, magnetic, (E), 25:43528 (LAL-1250)
form factor of, local relativistic quantum field theory for asymptotic behavior of elastic, (T), 25:43587
interactions anti p + p → anti p + n + π⁻ at 2.2 GeV/c in bubble chamber, cross sections and forward production of nπ⁻ system in, (E), 25:43537
interactions anti p + p → anti p + p + π⁰ at 2.2 GeV/c in bubble chamber, cross sections and Δ(1236) production in, (E), 25:43537
interactions anti p + p → p + anti p + π⁺ + π⁻ at 2.2 GeV/c in bubble chamber, cross sections and Δ⁺⁺(1200) and Δ⁻⁻(1200) production in, (E), 25:43537
interactions anti p + p at 2.2 GeV/c in hydrogen bubble chamber, partial cross sections and K(890), Kanti K, KKπ, Kππ, and K*anti K* production in 2K, 4K, 2Kπ, and 2K2π final states in, (E), 25:43536
interactions anti p + p, multiple quark scattering analysis for energy and momentum transfer square dependencies of differential cross sections for charge exchange, (E), 25:43615
interactions e + p → e + p at 70 to 280 MeV, cross sections and proton magnetic form factor from backward, (E), 25:43528 (LAL-1250)
interactions e + p at 150 GeV, self-coupling of weak lepton currents in, (T), 25:43612
interactions e + p at high energies, multiperipheral model for form factor for inelastic, (T), 25:43602
interactions e + p near Δ(1236), spectrometer study of cross sections for inelastic, (E), 25:43527 (DESY-71/21)
interactions e + p, amplitude for production of two soft π in, 25:43596
interactions e + p, most probable number of partons in parton models for inelastic, (T), 25:43585 (SU-1206-246)
interactions γ + p → eta + p at 4 to 9 GeV, spectrometer study of energy dependence of cross sections for, (E), 25:43529
interactions γ + p → π⁰ + p at 4 to 18 GeV, spectrometer study of energy dependence of cross sections for, (E), 25:43529
interactions K⁺ + p → K⁺ + p at 4.0 and 5.0 GeV/c, differential cross sections for large-angle, (E), 25:43559
interactions K⁺ + p → π⁻ + particles at 12 GeV/c, symmetric π⁻ production in, (E), 25:43557
interactions K⁺ + p at 12.7 GeV/c in bubble chamber, factorization in inclusive processes from single-particle momentum distributions of π produced in, (E), 25:43554 (UR-875-340)
interactions μ + p at 150 GeV, self-coupling of weak lepton currents in anti ν--ν pair production in, (T), 25:43612
interactions n + p → n + p + γ, cross sections and spectra from, (E), 25:43560
interactions n + p at 210 to 330 MeV, phase shift analysis for, (E), 25:43538
interactions n + p in neutron reactions (n,nnp) with deuterium at 14 MeV, spectrometer study of cross sections and spectra for final-state, (E), 25:43533 (CEA-R-4150)
interactions n + p, multiple quark scattering analysis for energy and momentum transfer square dependencies of differential cross sections for charge exchange, (E), 25:43615
interactions ν + p at 10 GeV, self-coupling of weak lepton currents in μ⁺--μ⁻ pair production from, (T), 25:43612
interactions p + p → 2p + π⁺ + π⁻ + π⁰ at 25 GeV/c in hydrogen bubble chamber, multiparticle final state production in, (E), 25:43535
interactions p + p → d + MM at 3.8 to 6.3 GeV, wire-chamber spectrometer study of differential cross sections for d and rates for π and rho production, (975) enhancement and delta(963) production in, (E), 25:43541
interactions p + p → p + n + 2π⁺ + π⁻ at 25 GeV/c in hydrogen bubble chamber, cross sections for pπ⁺ and pπ⁻ resonance production in, (E), 25:43535
interactions p + p → p + p + π⁺ + π⁻ at 25 GeV/c in hydrogen bubble chamber, Δ⁺⁺, f⁰, pπ⁺π⁻(1426), and pπ⁺π⁻(1692) production in, (E), 25:43535
interactions p + p → p + p at 1.5 to 5.5 GeV/c at 30 to 90°, spark chamber and scintillation counter study of differential cross sections and angular distributions for, (E), 25:43539
interactions p + p → p + π⁻ + Δ⁺⁺ at 22 GeV/c, double Regge pole models for, (T), 25:43580
interactions p + p → p + X at 6.2 to 29.7 GeV/c, duality in triple Regge limit, (T), 25:43649
interactions p + p at 28.5 GeV/c in bubble chamber, factorization in inclusive processes from single-particle momentum distributions of π produced in, (E), 25:43554 (UR-875-340)
interactions π⁻ + p → 2π⁰ + n at 291 to 407 MeV, total cross sections for, (E), 25:43564
interactions π⁻ + p → A₁⁻ + p at 5 to 25 GeV/c in hydrogen bubble chamber, cross sections and failure of s-channel helicity conservation in, (E), 25:43664 (CGO-1195-204)
interactions π⁺ + p → Δ⁺⁺(1236) + π⁰ at 1.1 to 1.95 GeV/c in hydrogen bubble chamber, s- and t-channel effects on angular distributions and differential cross sections for, (E), 25:43551 (UCR-34-P-107-B-108)
interactions π⁻ + p → K⁺ + Σ⁻(1385) at 4.5 and 6 GeV/c, production mechanism for forward, (E/T), 25:43558
interactions π⁻ + p → n + eta at 5.9 GeV/c, spark chamber and scintillation counter study of differential and total cross sections for backward, (E), 25:43563
interactions π⁻ + p → π⁰ + n, multiple quark scattering analysis for polarization effect and energy and momentum transfer square dependencies of differential cross sections for, (E), 25:43615
interactions π⁻ + p → π⁰ + p at 150 to 600 MeV at 60 to 170°, scintillation counter study of differential cross sections for, (E), 25:43564
interactions π⁻ + p → π⁺ + 2π⁻ + p at 5 GeV/c, multi-Regge model for, (T), 25:43602
interactions π⁻ + p → π⁻ + p and π⁻ + p → π⁰ + n interactions at low energies, mass difference and Coulomb effects in, 25:43645
interactions π⁻ + p → π⁻ + p at 0.55 to 1.3 GeV/c, resonance and diffraction parameters in model for, (T), 25:43643
interactions π⁺ + p → π⁺ + p at low energies, Coulomb corrections for, (T), 25:43599
interactions π⁺ + p → π⁺ + π⁰ + p at 1.85 to 2.09 GeV in hydrogen bubble chamber, cross sections for Δ⁺⁺(1236) and Δ(1236) production in, (E), 25:43552 (UCR-34-P-107-B-110)
interactions π⁻ + p → π⁻ + π⁺ + n at 3 to 5 GeV/c, counter--spark chamber study of π + π interactions and ππ(645), ππ(936), and ππ(1029) enhancements in, (E), 25:43555
interactions π⁻ + p → π⁻ + X at 8 and 16 GeV/c, duality in triple Regge limit, (T), 25:43649
interactions π⁻ + p → π⁻(π⁰) + p(n) at low energies, Coulomb corrections for, (T), 25:43599
interactions π⁺ + p → rho⁺ + p at 1.780 to 2.140 MeV in hydrogen bubble chamber, differential cross sections, angular distributions, and density matrix elements of rho⁺ in, (E), 25:43553 (UCR-34-P-107-B-120)
interactions π⁺ + p → rho⁺ + p at 1.85 to 2.09 GeV in hydrogen bubble chamber, cross sections, angular distributions, and Dalitz plot for, (E), 25:43552 (UCR-34-P-107-B-110)
interactions π⁻ + p at 24.8 GeV/c in bubble chamber, factorization in inclusive processes from single-particle momentum distributions of π produced in, (E), 25:43554 (UR-875-340)
interactions π⁻ + p at 4 GeV/c, thermodynamical description of momentum distributions of π produced in, (T), 25:43639 (JINR-P1-5849)
interactions π⁺ + p at 7.0 GeV/c in bubble chamber, factorization in inclusive processes from single-particle momentum distributions of π produced in, (E), 25:43554 (UR-875-340)
polarization measurements from high-energy photon reactions with nuclei, spark chamber telescope with magnetic spectrometer for, 25:42146
protection of personnel against, methods for, 25:42464
reactions (p,2α) with nitrogen-14 at 13 to 42 MeV, excitation functions for, (E), 25:43818
reactions (p,α) and (p,γ) with oxygen-17 at 5.8 to 7.1 MeV, energy spectra and angular correlations and distributions for, (E), 25:43812
reactions (p,α) with lithium-7 up to 7 MeV, R-matrix analysis of, (E/T), 25:43829
reactions (p,α) with nitrogen-14 at 5 to 24 MeV, excitation functions for, (E), 25:43818
reactions (p,α) with oxygen-18, use to measure depth distribution of oxygen-ion implants in gallium phosphide, 25:43447
reactions (p,d) with deuterium at 3.0 to 46.3 MeV, nonrelativistic peripheral-model calculations of angular distributions from, (T), 25:43966
reactions (p,γ) with beryllium-9 and lithium-7 in giant resonance region, γ yields and angular distributions for, (E), 25:43813
reactions (p,γ) with chromium-52 at 1 to 1.6 MeV, γ-γ coincidence spectra from, 25:43837
reactions (p,γ) with cobalt-59 at 4.40 to 13.60 MeV, angular distributions, excitation functions, and spectra from, (E/T), 25:43867
reactions (p,γ) with cobalt-59, potassium-39, and potassium-41 in giant resonance region, angular distributions and cross sections for, (E), 25:43853
reactions (p,γ) with praseodymium-141, resonances in, (E), 25:43950
reactions (p,γ) with strontium-86 at 2.917 MeV, Q-value

for, (E), 25:43836
reactions (p,n) with argon-36 at 13.86 to 14.14 MeV, excitation functions for, (E), 25:43875
reactions (p,n) with lithium-7 at 3 to 5.5 MeV, angular distribution of neutron polarization in, (E), 25:43805
reactions (p,n) with nuclei, effect of compound nucleus levels on isobaric analog resonances in, 25:43893
reactions (p,n) with strontium-87 at 3 to 3.1 MeV, cross section and Q-value for, (E), 25:43836
reactions (p,nγ) with iron-54 at 10 MeV, angular distributions and spectra from, (E), 25:43863
reactions (p,pα) with beryllium-9 at 26.0 to 46.8 MeV, coplanar angular and energy correlations and spectra from, (E/T), 25:43801 (UCLA-10-P-18-31)
reactions (p,pα) with neon-20 and oxygen-16 at 46.8 MeV, coplanar angular and energy correlations and spectra from, (E/T), 25:43801 (UCLA-10-P-18-31)
reactions (p,pd) and (p,p He-3) with lithium-6 at 156 MeV, angular correlations in, (E), 25:43800 (NP-18880)
reactions (p,pd) with carbon-12 at 156 MeV, angular correlations and spectra from, (E), 25:43800 (NP-18880)
reactions (p,pt) with lithium-7 at 156 MeV, angular correlations and spectra from, (E), 25:43800 (NP-18880)
reactions (p,t) with chromium-52 at 27 MeV, DWBA analysis of differential cross sections for, (E), 25:43849
reactions (p,t) with deformed nuclei, effects of higher multipole deformation of the pairing density on, (T), 25:43977
reactions with atoms, inverted-population production by charge exchange from, (T), 25:43103
reactions with beryllium at 10 to 500 GeV, meson (π^-) fluxes from, (T), 25:43726 (BNL-15893)
reactions with cesium atomic beams at 1 to 40 keV, charge-exchange cross section from, (E/T), 25:43103
reactions with gases up to 20 MeV, review of cross sections for electron capture in, (E), 25:43149
reactions with helium at 15 to 40 keV, polarization of helium 3^1P--2^1S line excited by, (E), 25:43129
reactions with nickel-60 at 61.7 MeV, cross sections and spectra from, (E), 25:43833 (ORNL-4698)
scattering by A = 12 to 208 nuclei at 20 to 61.4 MeV, optical-model analysis with real Saxon--Woods derivative term of elastic, (T), 25:43967
scattering by A = 148 through 198 nuclei at 16 MeV, differential cross sections for elastic and inelastic, (E), 25:43901
scattering by argon-36 at 8.980 MeV, optical-model analysis of elastic, (E), 25:43868
scattering by argon-40 at 4.7 to 5.8 MeV, angular correlations, excitation functions, and spectra from inelastic, (E), 25:43872
scattering by beryllium-9 at 6 to 30 MeV, optical model analysis of elastic, (T), 25:43804
scattering by germanium-70 at 2.7 to 7.4 MeV, excitation functions for elastic and inelastic, (E), 25:43851
scattering by helium-3 at 0.5 to 40.0 MeV, phase-shift analysis using resonating-group method of elastic, (T), 25:43797
scattering by helium-3 at 1.51 to 23.25 MeV, resonating-group calculations of differential cross sections for elastic, (T), 25:43797
scattering by helium-4 at 1 to 23 MeV, phase-shift analysis of elastic, (T), 25:43781
scattering by iron-58 at 49.4 MeV, DWBA analysis of angular distributions for inelastic, (E), 25:43840
scattering by lead-208 with isobaric analog excitation, angular distributions and excitation functions for elastic and inelastic, (E), 25:43907
scattering by tellurium-122, -124, and -126 at 6.7 to 12.5 MeV, proton spectra and angular distributions for, (E), 25:43933
scattering by tellurium-130, angular distributions and excitation functions for elastic and inelastic, (E), 25:43918
scattering by tritium at 5.35 to 5.65 MeV, search for helium-4 resonance in excitation function for elastic, (E), 25:43782
scattering by yttrium-89 and zirconium-90 at 61.2 MeV, microscopic-model analyses of inelastic, (E/T), 25:43855
scattering by zirconium-90 at 61.2 MeV, calculations using Gaussian potential of differential cross sections for high-spin states in inelastic, (T), 25:43915
stopping in gases at 100 to 500 keV, (E), 25:43432
stopping power in silicon planar channels of 0.4-MeV, effects of oscillation frequency on, 25:43455

PROTONS (anti p)
interactions anti p + d at 2.2 GeV/c in deuterium bubble chamber, partial cross sections and K(890), Kanti K, KKπ, Kππ, and K*anti K* production in 2K, 4K, 2Kπ, and 2K2π final states in, (E), 25:43536
interactions anti p + p + anti p + n + π^- at 2.2 GeV/c in bubble chamber, cross sections and forward production of $n\pi^-$ system in, (E), 25:43537
interactions anti p + p + anti p + p + π^0 at 2.2 GeV/c in bubble chamber, cross sections and Δ(1236) production in, (E), 25:43537
interactions anti p + p + p + anti p + π^+ + π^- at 2.2 GeV/c in bubble chamber, cross sections and Δ++(1200) and Δ--(1200) production in, (E), 25:43537
interactions anti p + p at 2.2 GeV/c in hydrogen bubble chamber, partial cross sections and K(890), Kanti K, KKπ, Kππ, and K*anti K* production in 2K, 4K, 2Kπ, and 2K2π final states in, (E), 25:43536
interactions anti p + p, multiple quark scattering analysis for energy and momentum transfer square dependencies of differential cross sections for charge exchange, (E), 25:43615

PROTOPORPHYRINS
effectiveness as carrier for palladium-109 for selective ablation of lymph nodes in dogs, 25:42312

PROTOZOA
Histomonas meleagridis, radiation effects on in vitro growth of, effects of dose on γ, 25:42608

PUERTO RICO
program for control of fascioliasis using irradiated metacercariae, 25:42246(R) (PRNC-148)
radiation effects on ecology of rain forest of, 25:42317(R) (PRNC-147)

PULSARS
activity of Vela X, 25:43039
PSR 0525 + 12, dispersion and rotation, pulse profiles, and polarization of, (E), 25:43053
radiation mechanisms for, (T), 25:43079 (N-71-20472)
theory for, general relations in relativistic MHD for, 25:43701

PULSE ANALYZERS
pulse pile-up monitor for, 25:42216

PULSE CONVERTERS
design and performance of time-to-amplitude, 25:42213
design of analog-to-digital, for microsecond signals, 25:42220
design of on-line dead-time-free time-to-pulse height, for measurement of nuclear half-lives up to 100 sec by delayed-coincidence method, 25:42222
specifications for JAERI modular risetime-to-height, 25:42185 (JAERI-13605)

PULSE DISCRIMINATORS
performance for proton-recoil neutron spectrometer, for gamma discrimination, 25:42105 (JAERI-13561)
specifications for JAERI modular, 25:42185 (JAERI-13605)

PULSE GENERATORS (ELECTRONICS)
development of programmed, for NMR measurements, 25:41833(R) (IA-1218)

PUMPS
maintenance and operation of liquid sodium, in LMFBR components test loop, 25:42804(R) (LMEC-71-1)
packings for, standard for coil and ring braided asbestos, 25:43012 (RDT-M-11-2-T)

PUMPS (LIQUID METAL)
bearings for sodium, development and performance of 12-pocket hydrostatic, 25:41958(T) (CONF-700307-8)
performance requirements of mechanical sodium, for reactors, comparison with electromagnetic pumps, 25:41958(T) (CONF-700307-8)

PUREX PROCESS
zirconium decontamination efficiencies in, effects of fluoride in feed solutions on, 25:41889 (BNWL-1573)

PURINE, 2-AMINO-
effects on Neurospora, specificity of mutagenic, 25:42352

PYRENE
electron reactions at 50 eV to 10 keV with, cross sections for excitation in, (T), 25:43127(T) (BNL-tr-429)

3,4-PYRIDINEDIMETHANOL, 5-MERCAPTO-6-METHYL-
effects on ultrastructure of crypt cells in mouse duodenum, effects of thiol-blocking agents on, 25:42520

2-PYRIDONE
radiation effects on metabolism of, in mice and rats, mechanisms for, 25:42623

PYRITES
analysis of Luzon, Philippines, for trace elements by neutron activation, 25:41772

PYROCATECHOL
radiation effects on metabolism of amine derivatives of, in rabbits as indicator of radiation injury, x, 25:42627

Q

QUAD CITIES POWER REACTOR, UNIT 1
cooling systems for, pipe whip protection requirements for, 25:44041 (DOCKET-50254-44)
effluents from, effects on environment of chemical, radioactive, and thermal, 25:44040 (DOCKET-50254-42)
emergency core cooling system for, performance characteristics of, 25:44042 (DOCKET-50254-45)
emergency core cooling system for, performance requirements for, 25:44041 (DOCKET-50254-44)
fuel casks for, safety aspects of drop accident for, 25:44041 (DOCKET-50254-44)

QUAD CITIES POWER REACTOR, UNIT 2
cooling systems for, pipe whip protection requirements for, 25:44041 (DOCKET-50254-44)
effluents from, effects on environment of chemical, radioactive, and thermal, 25:44040 (DOCKET-50254-42)
emergency core cooling system for, performance characteristics of, 25:44042 (DOCKET-50254-45)

XUM

emergency core cooling system for, performance requirements for, 25:44041 (DOCKET-50254-44)
fuel casks for, safety aspects of drop accident for, 25:44041 (DOCKET-50254-44)
QUALITY CONTROL
conference on methods and uses for, Los Angeles, Calif., May 5 to 7, 1959, 25:42030
methods for assuring, during production of commercial, industrial, and military equipment, use of nondestructive materials testing techniques in, 25:42032
methods for fuel element fabrication, use of statistical tolerance limits in, 25:42033
standard for items or services purchased for nuclear reactor, test facility, and engineering development applications, 25:42022 (RDT-F-2-4-T)
QUANTUM ELECTRODYNAMICS
book: Relativistic Quantum Theory. Vol. 4, 25:43086
Lamb shift in, crossed-graph contribution to fourth-order, 25:43697
QUANTUM FIELD THEORY
Bethe--Salpeter equation with scalar couplings in, numerical calculations of Regge poles from, 25:43683
commutation relations for variations of canonical momants in, equal-time, 25:43685
commutators in, singularity structure of equal-time, 25:43682
dilation invariance breakdown and space-time symmetries for, 25:43679
dynamics relations with physical states in, self-consistency in, 25:43688
functional equations in lambda phi⁴ theory of scalar mesons in, 25:43678
harmonic oscillators in, orthogonality relations of many time generating functionals, 25:43669
Hilbert space for physical states in, self-consistency in method for constructing, 25:43688
Lagrangians in, improved generator for conformal, 25:43677
LSZ formalism in (n,2) sector of Lee model, 25:43673
measurements for massive meson fields in, idealized, 25:43692
meson fields in, idealized measurements for massive, 25:43692
model in, solvable, 25:43668
P(phi_2) model in, asymptotic fields for approximate renormalized, (T), 25:43667 (ITF-71-12-P)
propagator functions in, derivation of Lehmann--Kaellen representation for, 25:43681
propagator gauge transformations for non-Abelian gauge fields in, 25:43680
proton elastic form factor in local relativistic, asymptotic behavior of, 25:43587
S-matrix elements in, generating functionals for, 25:43670
self-consistency in, 25:43688
sigma model in, two-loop approximations to propagations in, 25:43684
symmetries in, extension of Poincare group algebra and P violation for higher, 25:43676
two-body problem in three-dimensional formulation of, relativistic, 25:43674
validity of complex-ghost relativistic, 25:43686
Yukawa model in, asymptotic fields for approximate renormalized two-dimensional, (T), 25:43667 (ITF-71-12-P)
QUANTUM MECHANICS
boundary conditions for an infinite square-well potential in, (T), 25:43503
coherent state representation in theory of magnetism, Heisenberg model for, 25:43512
conjugate variables in two-body collisions, 25:43724
effective spin Hamiltonian for coarse structure states in, 25:43154
functional equations for anharmonic oscillator in, 25:43678
Hellmann--Feynman theorems in, (T), 25:43510
impurity systems at equilibrium in, statistical quasiparticles, effective Green's functions, and Landau descriptions of quantum liquids in, 25:43511
localization for elementary systems in relativistic, 25:43577
measurement in, 25:43523
particles with symmetrized wave functions in, distinguishable equivalent, 25:43524
propositions in, interpretation of, 25:43514
Schroedinger equation in, Coulomb Green function for bound states of nonrelativistic, 25:43675
Schroedinger particle in a gravitational well, (T), 25:43517
three-body problem in, exactly soluble, (T), 25:43509
transition in, concept of, 25:43525
wave and particle coexistence in relativistic, 25:43691
QUASARS
energy source for, uniformly rotating relativistic disks as, (T), 25:43092
magnitude--redshift relation for, (T), 25:43089
microwave radiation from 3C 279, gravitational deflection near Sun, (E), 25:43094
structure of 3C 279 and 3C 273, rapid variations of, (E), 25:43049

R

RABBITS
radiation effects on bioelectrical activity in brain of, effects of radial acceleration on sublethal x, 25:42653
radiation effects on leukocyte count, lysozyme activity, and trypsin inhibitors in serum of, effects of dose on whole-body x, 25:42548
radiation effects on leukopoiesis in bone marrow of, protective effects of glutathione against γ, 25:42536
radiation sickness following destruction of hypothalamus in, changes in blood parameters during, 25:42660
radiation sickness in, effects of solar exposure on cardiovascular system during x, 25:42551
radioinduced increase in capillary permeability in skin of, effects of 6-aminohexanoic acid on x, 25:42617 (UR-49-1462)
radioinduced injuries to neck tissues in, following surgery and therapy, 25:42603
RADIATION
book: Radiation Immunology and Transplantation, 25:42310
dose calculations following reactor accidents, PILAX code for, 25:44135 (CEA-R-4136)
dose distribution in human tissues, 25:42454
dose to human populations following release of radioisotopes to atmosphere during reactor accidents, computer method for calculation of, 25:42393 (BNWL-B-65)
dose to human populations from fallout during 1969, estimates of, 25:42691
dose to man during therapy, computer method for calculating integral, 25:42415
dose to man, natural background and medical exposure, 25:42711
dose to medical personnel during interstitial therapy of cervical carcinomas under two different treatment plans, comparison of, 25:42432
dosimetry for therapy, evaluation of Roentgen equivalent therapeutic (ret) units for expression of nominal standard dose (NSD) in, 25:42446
dosimetry for therapy, mathematical model for, 25:42437
dosimetry for therapy, use of roentgen equivalent therapeutic (ret) units for, 25:42413
dosimetry for therapy, use of roentgen equivalent therapeutic (ret) units for calculations of dose fractionation schedules for, 25:42414
effects of pulsed, on aqueous solutions of europium, samarium, terbium, and ytterbium, spectral studies on, 25:41833(R) (IA-1218)
effects on activity of redox enzyme activity in rat liver following ingestion of radon-containing water, 25:42279
effects on adhesive properties of modified resins, 25:41846(P)
effects on aging, genetics, and neoplasms in animals and man, review on relation of, 25:42605
effects on animals and man, latent, 25:42604
effects on barley seed, effects of hydration on decay of free radicals induced by, 25:42296
effects on biochemistry of body fluids in dogs, man, and rats as indicator of radiation injuries, review on, 25:42402
effects on bioelectric activity in human brain following therapy for arachnoiditis, 25:42678
effects on bioelectric activity in human brain, electroencephalographic studies on local and whole-body, 25:42677
effects on Callosobruchus maculatus emergence as adult from infested grains, 25:41833(R) (IA-1218)
effects on chlorobenzene in cyclohexane solutions, mechanism of negative ion formation in, 25:41833(R) (IA-1218)
effects on content of sulfhydryl groups in serum following use for post-surgical therapy of human mammary cancer, 25:42270
effects on control of metabolic pathways, model for role of enzymes in, 25:42606
effects on cultured lymphocytes from infant and adult man, effects of dose and phytohemagglutinin on, 25:42602
effects on curing of urethan coatings, 25:41844(P)
effects on deoxyribonucleoprotein in animal hematopoietic and lymphatic cells, mechanisms for, 25:42624
effects on development of central nervous system in human embryos, aberrant, 25:42629
effects on development of nervous system of rats in comparison to effects of ablation, 25:42615(R) (COO-1201-30)
effects on DNA in tissues of rats, sensitizing effects of hydroxymercuribenzoic acid on, 25:42535
effects on excretion of deoxyribosyl compounds in mouse and rat urine as indicator of radiation injury, 25:42622
effects on excretion of MEA in rat urine, whole-body, 25:42671
effects on flower color of dahlias, mutagenic, 25:42327
effects on fungal decay and peel rot on grapefruit and

oranges, effects of heat treatment and waxing on, 25:41833(R) (IA-1218)
effects on germination of barley seeds, effects of oxygen and water on, 25:42295
effects on glomerulus enlargement in hamster kidneys, combined effects of chronic hypoxia and ozone injections on, 25:42636
effects on heart following therapy for neoplasms of thoracic organs, 25:42704
effects on human adult and developing nervous system, 25:42691
effects on human and animal bones and bone marrow, external and internal exposure, 25:42472
effects on human and mammalian oocytes, factors affecting sensitivity to lethal and mutagenic, 25:42697
effects on human cells, aberrant, 25:42691
effects on human central nervous system during prenatal and postnatal development, effects of dose on pathological, 25:42710
effects on human chromosomes as indicator of radiation dose or injury, aberrant, 25:42405
effects on human chromosomes, limitations of dosimetric uses of aberrant external, 25:42707
effects on human eyes, latent pathological, 25:42546
effects on human genetics, problems in protection against, 25:42325
effects on human neurovascular system, methods for studying dystonic, 25:42676
effects on human salivary glands following therapy of head and neck tumors, high-dose exposure, 25:42699
effects on human tissues, variations in pathological, 25:42454
effects on hybrid and parent strains of maize, comparison of recovery from, 25:42722
effects on incidence of aplastic anemia in atomic bomb survivors, late, 25:42698
effects on life span of rats, tracer studies on role of physiological functions in, 25:42668
effects on living cells, molecular mechanisms for, 25:42727 (NYO-2804-38)
effects on man, credibility of statistical inferences regarding low-dose, 25:42715
effects on man, development of biochemical indicators of, 25:42685
effects on man, effects of dose on genetic and somatic, 25:42693
effects on man, effects of dose on genetic and somatic, 25:42692
effects on man, ICRP evaluation of genetic and somatic low-dose, 25:42475
effects on man, problems in correlating dose with late, 25:42714
effects on man, somatic, 25:42712
effects on man, threshold concept for carcinogenic, 25:42694
effects on manganese (II) ions in dosimetric phosphate glass, oxidative, 25:42153
effects on metabolism of nicotinamide-adenine dinucleotide and nucleic acid metabolites in mice and rats, mechanisms for, 25:42623
effects on metacercariae of Fasciola hepatica for use as vaccine, 25:42246(R) (PRNC-148)
effects on monocrystals of carboxylic acids, ESR studies on positive holes from, 25:41841
effects on morphology and maturation time of cells in primary and metastatic Wilms' tumor in children, 25:42592
effects on non-uniform populations of cells, effects of repair and selection on dose--effect curves of genetic, 25:42353
effects on organized structures and interstitial cell compartment of mesonephros of chick embryo, effects of dose on, 25:42643
effects on post-harvest ripening of avocado pears, 25:41833(R) (IA-1218)
effects on pre-cooked meat and gravy product, sterilizing, 25:42759(P)
effects on proteins, use of specific protein--protein interactions in studies of, 25:42303
effects on rat tissues and organs, mechanism of protective effects of adrenalin, AET, and cysteine against in vitro and in vivo, 25:42523
effects on reducing sugar, total soluble solids, total sugar, and vitamin C content in potatoes during subsequent storage, 25:41833(R) (IA-1218)
effects on sarcoma incidence in man, therapeutic, 25:42705
effects on shelf life of bread, 25:41833(R) (IA-1218)
effects on sprout darkening of onions during subsequent storage, 25:41833(R) (IA-1218)
effects on sprouting and storage life of onions, effects of dose on, 25:42745 (RISO-238)
effects on sprouting in winter-harvested potatoes during subsequent storage, 25:41833(R) (IA-1218)
effects on storage life and wholesomeness of foods, research program on, 25:42747
effects on thin liquid films, bubble nucleation and rupture in, 25:41835
effects on tissues and survival of oysters, effects of dose on, 25:42607
effects on tubes and uterus in women following castration, carcinogenic, 25:42675
effects on tumors in human eyes, therapeutic, 25:42596
exposure to, health physics and medical procedures for handling accidental, 25:42391
hazards to man, analysis of calculations on low dose, 25:42703
measurement of deformed backscattered, effects of shielding and source--detector distance on low-level, 25:42111
monitoring methods for mixed, around accelerators, 25:42443
use for therapy of intracerebral astrocytomas, estimation of hazards to brain following, 25:42701
use for therapy of neoplasms of human head and neck, effects of dose on occurrence of myelitis following, 25:42700
use for treatment of medulloblastomas in children, dose fractionation schedules for post-surgical, 25:42593
uses in industry, effects on radiation dose to human populations, 25:42693
uses in industry, effects on radiation dose to human populations, 25:42592
RADIATION CHEMISTRY
biochemistry and enzyme studies by pulse radiolysis, 25:41862
book: Problems of Protection from Ionizing Radiations in Radiation Chemistry, 25:42448
equipment and facilities for pulse radiolysis studies at Chalk River, Canada, 25:41849 (AECL-3853)
RADIATION DETECTORS
circuits for, design of variable-delay gating, 25:42063
dead time corrections for counting rapidly decaying sources, 25:42048 (ANL-7710, pp 263-364)
design and operation of HANDS system, for detecting fallout at high altitudes, 25:41932 (AD-719619)
design for environmental monitoring, optimization of, 25:42094
design of baloon-borne counter-telescope, for detection of cosmic-ray alpha particles and protons, 25:42159
design of position-sensitive, based on superconducting indium strips, 25:42097
development of indium and tin superconducting films as, 25:42080
development of simple electrostatic, for monitoring gamma dose around home fallout shelters, 25:42506(R) (ORNL-4566(Pt.1))
development of, new concepts in, 25:42053 (JINR-P13-5782)
development of, review on, 25:42101
performance of HANDS system, for detecting fallout at high altitudes, 25:41933 (AD-719620)
sensitivity threshold for low-level counting, optimization of, 25:42102
use of portable, rules for, 25:42073
RADIATION DETECTORS, ACTIVATION
data processing methods for fast neutron spectra measurements, performance of, 25:42100
radiation efffects on performance of in-pile, γ, (T), 25:44103
RADIATION DETECTORS, BUBBLE CHAMBER
cryogenics for, developments in, 25:43735
description of ITEP 2-meter liquid hydrogen, 25:42145
developments in cryogenic, 25:42137
magnet power supply system for 100-cm liquid hydrogen, 25:42143
particle ionization loss in, semiautomatic television device for measuring, 25:42142
particle track analysis by integral cascade curves in xenon, for measuring gamma energy, 25:42144
particle tracks in, performance of HPD 2 flying spot digitizer for measurement of, 25:42153
RADIATION DETECTORS, CHEMICAL
description of dose indicator plastic, 25:42077(P)
description of dose indicator paint, 25:42078(P)
RADIATION DETECTORS, CHERENKOV
calibration of high-resolution lead-glass, for 200- to 900-MeV electrons, 25:42154
cryogenics for, developments in, 25:43735
design of inserts for, for elimination of count-rate variations due to pigments in radioactive solutions, 25:42082
performance for particle identification by using distinctive angles of light emission, 25:42141
resolution of total-absorption lead-glass, for 200- to 900-MeV electrons, 25:42154
RADIATION DETECTORS, DIELECTRIC TRACK
particle track etching in, electrochemical, 25:42056 (RT/PROT-(71)1)
particle track formation in plastic, mechanism and applications of, 25:42070
performance of Apollo astronaut helmets of Lexan polycarbonate, for dosimetry, 25:42160 (N-71-14602)
performance of plastic, for alpha radiography, 25:42093
RADIATION DETECTORS, FISSION CHAMBER
design of small, for operation at high temperature, 25:42060(P)
performance of non-perturbing, for fission rate distribution measurements in critical assemblies, 25:42048 (ANL-7710, pp 263-364)
RADIATION DETECTORS, GEIGER-MUELLER
dead time as function of count rate, method for determining, 25:42095

XUM

response of feedback-type, for pulsed radiation, (E/T), 25:42087
test procedure for, standard, 25:42057
RADIATION DETECTORS, IONIZATION CHAMBER
air equivalence of chamber materials of, pressure effects on, 25:42091
calibration for monitoring bremsstrahlung beams, constants and ion collection efficiencies for, 25:42083
calibration of Bonner ball boron trifluoride, for neutron detection, 25:42055 (ORNL-TM-3465)
calibration of, mean mass stopping power calculations for gamma and x rays for, 25:42085
cavity theory for energy deposition, Bragg--Gray, 25:42166
design and calibration of pair of, for dosimetry of mixed gamma radiation and fast neutrons, 25:42168
multiplicity yield function of IGY neutron monitor, (E), 25:43175
performance of extrapolation, for dosimetry of flat circular polonium-210 α source in biological material, 25:42436
performance of tissue-equivalent, for measurements of absorbed radiation dose, 25:42443
performance or dosimetry of 23-Mev electron beam, comparison of photographic film with, 25:42411
response to pulsed radiation, measurement of drift velocity distribution for filling gases for studying, 25:42088
use of condensor-type, for personnel monitoring, rules for, 25:42075
use of pocket electroscopes for personnel monitoring, rules for, 25:42074
RADIATION DETECTORS, PROPORTIONAL
circuits for multiwire on-line, block diagram for logic, 25:42156
design of multiwire on-line, for detection of high-energy particles, 25:42156
development of proton-recoil, for fast neutron spectroscopy, 25:42106 (JAERI-13580)
development of proton-recoil, for neutron spectroscopy, 25:42048 (ANL-7710, pp 263-364)
pulse readout circuit for gas flow, performance of voltage, 25:42052 (JAERI-13725)
RADIATION DETECTORS, SCINTILLATION
background due to chemiluminescence in liquid, treatment method for reducing, 25:42071(P)
circuits for thallium-activated sodium iodide, design of high-count-rate, 25:42127
design and construction of 192-element 4π, for study of three-body reactions, 25:42124
design of liquid boron, for time-of-flight thermal neutron spectroscopy, 25:42104 (FEI-208)
development of helium-3 gas, for time-of-flight neutron measurements, 25:42048 (ANL-7710, pp 263-364)
development of liquid, for aqueous samples, 25:42072(P)
development of liquid, for thermal neutrons, 25:42069(P)
efficiency of crystal, immersed in homogeneous medium contaminated by gamma emitters, (E/T), 25:42096
efficiency of thallium-activated sodium iodide, for cylindrical gaseous sources, photopeak, (E), 25:42049 (EUR-4513)
efficiency of thallium-activated sodium iodide, full energy peak, (E), 25:42050 (JAERI-13546)
light collection efficiency of large liquid, experimental and theoretical study of parameters affecting, 25:42065
linear absorption coefficients for photon interactions in, 25:42133
mass attenuation coefficients of Pilot-B plastic, for 0.36- to 1.33-MeV gamma rays, 25:42064
performance of carbon tetrafluoride gas, for kinetic energy measurements of fission fragments, (E/T), 25:42076
preparation of chromium-activated aluminum oxide, 25:42086(P)
radiation effects on plastic, ultraviolet, 25:42231
sample handling system for automatic liquid, programmed, 25:42058(P)
thermal stability of thallium-activated sodium iodide, 25:42092
RADIATION DETECTORS, SEMICONDUCTOR
design of telescope, used with hydrogen-rich foil for proton-recoil neutron spectroscopy, 25:42134(P)
development of high-rate time-of-flight, for detection of heavy charged particles produced in nuclear reactions, 25:42065
performance of surface-barrier, for dosimetry of flat circular polonium-210 α source in biological material, 25:42436
RADIATION DETECTORS, SEMICONDUCTOR (GERMANIUM)
calibration and performance of lithium-drifted, for detection of gamma radiation at 100 keV to 12 MeV from nucleon capture reactions, 25:42129
calibration of lithium-drifted, method for absolute, 25:42125
cryostat for lithium-drifted, 25:42084
cryostats for lithium-drifted, description of dual-chamber vacuum, 25:42132
efficiency calibration of lithium-drifted, 25:42048 (ANL-7710, pp 263-364)
efficiency of lithium-drifted, effects of source distance on, 25:42048 (ANL-7710, pp 263-364)
efficiency of lithium-drifted, for gamma and x radiation, 25:42133
energy resolution of lithium-drifted, for detection of 20- to 100-MeV protons, 25:42128
geometrical correction factors for angular correlation measurements with coaxial lithium-drifted, 25:42054 (LPN-UM-53)
linear absorption coefficients for photon interactions in, 25:42133
linearity of lithium-drifted, for detection of 20- to 100-MeV protons, 25:42128
preparation of high-purity germanium for, 25:42130
resolution of lithium-drifted, for gamma and x radiation, 25:42133
sensitivities for lithium-drifted, figure-of-merit measurements of, 25:42126
RADIATION DETECTORS, SEMICONDUCTOR (SILICON)
conversion of photon lithium-drifted, for electron spectroscopy, 25:42123
description of cryostat, electronics, and vacuum system for, for beta spectroscopy, 25:42112
development of sandwich, for simultaneous alpha and beta detection, 25:41833(R) (IA-1218)
efficiency of lithium-drifted, at 5 to 170 keV, determination of photopeak, 25:42123
efficiency of lithium-drifted, for gamma and x radiation, 25:42133
linear absorption coefficients for photon interactions in, 25:42133
performance for fission fragment energy distribution measurements, 25:42048 (ANL-7710, pp 263-364)
performance of lithium-6 fluoride sandwich, for fast neutron spectroscopy, 25:42119
pulse-height defect in surface-barrier, due to energy partition of heavy ions of intermediate energy, 25:42061
resolution for mesons, nuclei, and protons at 10 MeV to 100 GeV, 25:42155
RADIATION DETECTORS, SPARK CHAMBER
circuit parameters of, with decoupled high-voltage electrode, 25:42150
cryogenics for, developments in, 25:43735
description of magnetic telescope, for measuring proton polarization from high-energy photon reactions with nuclei, 25:42146
design and performance of current, 25:42151
design of hodoscope of, for extensive air showers, 25:42158
particle momentum measurements in streamer, effect of magnetic field on accuracy of, 25:42148
properties of streamer, containing xenon, 25:42149
readout methods for, filmless, 25:42138
readout system for, piezoelectric, 25:42147
time properties of helium and helium--hydrogen, 25:42136 (JINR-P13-5828)
RADIATION DOSE
calculations for human tissues following deposition of radioactive materials and radioisotopes, methods for, 25:42467
maximum permissible, for body parts of children up to 18 years of age, 25:42473
maximum permissible, for industrial personnel using sealed sources and x rays in Great Britain, 25:42469
maximum permissible, for man, ICRP methods for determination of, 25:42454
maximum permissible, for non-occupational and occupational exposure of man, basis of ICRP recommendations for, 25:42466
maximum permissible, for patients during diagnosis, criteria for, 25:42552
maximum permissible, for population groups, additivity of external and internal, 25:41833(R) (IA-1218)
maximum permissible, ILO recommendations for industrial personnel, 25:42460
maximum permissible, to man, ICRP recommendations for, 25:42680
RADIATION DOSIMETERS
activator-ion optimization for phosphate-glass, radiation yield study for manganese, 25:42153
design and performance for monitoring personnel in industry, 25:42460
development of new concepts in solid state, 25:42162(R) (NYO-3409-10)
performance of polytetrafluoroethylene, for gamma dosimetry at 10^{11} rad based on melting point and viscosity, 25:42170
standardization for gamma source calibration for therapy, international comparison for, 25:42172
RADIATION DOSIMETERS, BIOLOGICAL
development of biochemical indicators as, 25:42685
evaluation of biochemical changes in mammals and man for use as, review on, 25:42401
evaluation of biochemical indicators as, 25:42408
evaluation of chromosome aberrations in cultured hematopoietic cells as β, 25:42713
evaluation of chromosome aberrations in human lymphocytes as, 25:42399
evaluation of chromosome aberrations in human lymphocytes as, 25:42398
evaluation of enzyme activity as, 25:42409

evaluation of free radical formation in papaya seed as γ, 25:42438
evaluation of γ-radiation effects on labeled metabolic products in rats as, 25:42407
evaluation of radiation effects on biochemical activity of body fluids as, 25:42402
evaluation of radiation effects on blood and urine biochemical constituents, cell populations, and chromosomes in man as, 25:42406
evaluation of radiation effects on cells and DNA synthesis as, 25:42404
evaluation of radiation effects on DNA metabolism in animals as, 25:42403
evaluation of radiation effects on excretion of deoxyribosyl compounds in mouse and rat urine as, 25:42622
evaluation of radiation effects on human blood coagulation as, 25:42500
evaluation of radiation effects on metabolism of biogenic amines in animals as, 25:42526
evaluation of radiation effects on metabolism of biogenic amines in animals as, 25:42527
evaluation of radioinduced chromosome aberrations in man as, 25:42405
evaluation of radioinduced metabolic changes in man as, criteria for, 25:42400
evaluation of x-radiation effects on metabolism of biogenic amines in animals and man as, 25:42626
RADIATION DOSIMETERS, CALORIMETRIC
description of ionization, supplemented with proportional detectors, 25:42140
RADIATION DOSIMETERS, PHOTOGRAPHIC FILM
accuracy of readout services for, standard for, 25:42165
development for personnel monitoring of radon decay products, 25:42171
performance for dosimetry of 23-MeV electron beam, comparison of ionization chamber with, 25:42411
performance for personnel monitoring, effects of positioning on, 25:42442
processing of, mathematical method for computer, 25:42161 (NP-18892)
use for personnel monitoring, rules for, 25:42164
RADIATION DOSIMETERS, PHOTOLUMINESCENT
performance of glass, for dosimetry of electron beams at 12 to 32 MeV, 25:42169
RADIATION DOSIMETERS, THERMOLUMINESCENT
calibration and performance for dose distribution measurements in critical assemblies, 25:42048 (ANL-7710, pp 263-354)
performance for monitoring workers during transport of strontium-90--yttrium-90 β source, 25:42444
sensitivity of lithium fluoride, for dosimetry of intense electron beams at 5 to 43 MeV, 25:42167
RADIATION DOSIMETRY
book: Dosimetry and Protection Against Ionizing Radiation, 25:42425
methods for fast reactor, 25:44102
methods for neutron, for irradiation studies on power reactor steel pressure vessels, 25:44117
methods for personnel at AB Atomenergi, Sweden during 1969, 25:42392 (AE-423)
quality factor definitions for, 25:42441
quality factor definitions for, 25:42443
quantities in, definitions of dose equivalent, linear energy transfer, quality factor, and reference dose, 25:42440
research programs of AEC during 1970 on, 25:44293 (TID-25728)
RADIATION FILTERS
effectiveness for dose reduction during x radiography of pelvic region, 25:42447
RADIATION MONITORING
methods for external, at Atomic Energy Research Institute, Japan, 25:42480
methods for internal, of personnel at Atomic Energy Research Institute, Japan, 25:42481
principles for industrial, 25:42460
program at New South Wales University, Australia, during 1970, 25:42359(R) (NP-18905)
programs for liquid wastes discharged to environment in United Kingdom, 25:42390
programs for radiochemical processing plants, 25:42410
recommendations for environmental, ICRP, 25:42465
recommendations for work areas and personnel, ICRP, 25:42474
research programs of AEC during 1970 on, 25:44293 (TID-25728)
RADIATION PROTECTION
book: Dosimetry and Protection Against Ionizing Radiation, 25:42425
book: Problems of Protection from Ionizing Radiations in Radiation Chemistry, 25:42448
code for children in schools, 25:42489
code for medical personnel using sealed radiation sources for therapy, 25:42492
code for, during sealed gamma source industrial radiography, 25:42490
code for, during sealed source radiotherapy, 25:42491
fallout shelters for, design of above-ground, 25:42034(T) (JPRS-53498)
manual for personnel in industry, part 1 of International Labor Office (1960), 25:42458
manual for personnel in industry, part 2 of International Labor Office (1959), 25:42459
manual for personnel in industry, part 3 of International Labor Office (1963), 25:42450
manual for personnel in industry, part 4 of International Labor Office (1954), 25:42461
manual for personnel in industry, part 5 of International Labor Office (1964), 25:42462
manual for personnel in industry, part 6 of International Labor Office (1968), 25:42463
methods for operator and patient, during dental radiography, 25:42484
methods for patients and personnel in vicinity of implanted iridium-192 source, 25:42477
problems in genetic, in man, 25:42325
programs at Atomic Energy Research Institute, Japan, 25:42481
programs at Atomic Energy Research Institute, Japan, 25:42480
programs for diagnostic radiography personnel in Japan, evaluation of, 25:42485
programs for personnel at Tokai Nuclear Power Station, Japan, 25:42479
programs for personnel exposed to plutonium-239 in air, 25:42488
programs in Sweden, 25:42483
programs in USA for, 25:42487
radiation monitoring for, general principles of, 25:42474
recommendation on, ICRP, 25:42467
recommendations for external source, ICRP (1970), 25:42455
recommendations for hospital patients and personnel, ICRP (1965), 25:42476
recommendations for pupils in schools, ICRP, 25:42473
recommendations for shipping radioactive materials by sea, Australian, 25:42449
recommendations for veterinary surgeons, 25:42485
recommendations for, of personnel against high-energy electromagnetic radiations, electrons, neutrons, and protons, ICRP, 25:42464
regulations for personnel transporting radioactive materials on roads in Great Britain, 1970, 25:42451
regulations for shipment of radioactive materials by air, International Air Transport Association (1970), 25:42457
regulations for shipment of radioactive materials by air, International Air Transport Association (1970), 25:42456
regulations in Great Britain for industrial personnel using unsealed radioactive materials, 25:42468
regulations in Great Britain for industrial personnel using sealed radiation sources and x radiation, 25:42469
standards for human populations, review of background data for, 25:42693
standards for human populations, review of background data for, 25:42692
standards for human populations, review of background data for, 25:42691
standards for man during diagnostic radiography, ICRP, 25:42453
standards for man, ICRP (1969), 25:42454
standards for medical personnel and patients during diagnostic radiography, 25:42493
standards for personnel at nuclear power centers in Italy, 25:42478
standards for personnel, in nuclear industry and research in Australia, 25:42495
standards for shipping radioisotopes by mail in Australia, 25:42494
standards for, evolution of USA and international, 25:42452
standards for, summary of basic principles for ICRP, 25:42466
standards in USA for, trends in National Council on Radiation Protection (1957), 25:42487
RADIATION RATE METERS
design for count rate analysis, 25:42103(P)
RADIATION-SCATTERING ANALYSIS
development of, using Compton effect, 25:41752(P)
RADIATION SOURCES
handling in hospitals, ICRP recommendations for radiation protection in, 25:42476
shipment in cargo and passenger aircraft, international regulations governing, 25:42456
shipment in cargo and passenger aircraft, international regulations governing, 25:42457
RADIATION STANDARDS AND UNITS
definitions of dose equivalent, linear energy transfer, quality factor, and reference dose, ICRP and ICRU, 25:42440
definitions of quality factor, 25:42441
definitions of, for radiation protection program, 25:42460
evaluation of Roentgen equivalent therapeutic (ret) for expression of nominal standard dose (NSD) for therapy, 25:42446
evaluation of roentgen equivalent therapeutic (ret), for dosimetry for therapy, 25:42413
quality factor definitions, 25:42443

XUM

RADIATION TARGET CANS
design for creep measurements on fast reactor fuels and structural materials, 25:44086(T) (EURFNR-853)
fabrication of fuel irradiation capsules for EBR-2, 25:44118(R) (BMI-1905)
materials for, evaluation of fiber glass-reinforced epoxy and polyethylene, 25:43011 (N-71-16499)

RADIATION TARGETS
cryogenics for, development in, 25:43735
preparation of thin deuterated polyethylene, 25:43759

RADIATORS
fabrication and testing of multiple-heat pipe, for cooling thermoelectric converters in space power systems, 25:41978

RADIO GALAXIES
energy source for, uniformly rotating relativistic disks as, (T), 25:43092
identification of AP Librae with PKS 1514-24, (E), 25:43082
spectral shape of, relation to absolute power, (E), 25:43063

RADIO TELESCOPES
resolving power and principles of, (E), 25:43064

RADIO WAVES
attenuation of 19-GHz solar, in atmosphere, (E), 25:43071
emission of triggered vlf discrete, by whistler trains and man-made signals, (T), 25:43245
Faraday rotation of high-frequency, across ionospheric transverse region, (T), 25:43254
intensity of frequency-dependent auroral hiss, correlation with soft electron fluxes, (E/T), 25:43246
origin of, from Vela X, (T), 25:43039
reflection from D region, method for detection of charged-particle precipitation at latitudes below 40°N, (E/T), 25:43223

RADIOACTIVE CONTAMINATION
handling procedures for, health physics and medical, 25:42391
measurement of internal, in nuclear power plant personnel in Italy, results of whole-body counting methods for, 25:42435
regulations for maximum permissible surface, in industrial establishments in Great Britain, 25:42468
sources of environmental, comparison of natural and nuclear power plant, 25:42383

RADIOACTIVE MATERIALS
content of food and water in Japan, maximum permissible, 25:42482
glass ampules for, equipment and method for semiautomatic flameless sealing of, 25:42046
hazards from fires involving, 25:42499
sale, shipping, and storage of, amendment to Italian Act 1860 on, 25:42040
shipment by sea, recommendations for safety in, 25:42449
shipment in cargo and passenger aircraft, international regulations governing, 25:42456
shipment in cargo and passenger aircraft, international regulations governing, 25:42457
shipping by railroad car ferry, health and safety aspects of, 25:42042
shipping of gamma-emitting, method for calculation of safe distances in marine, 25:42043

RADIOACTIVE WASTE
containers for storage of, design and development of ultrasonic inspection system for, 25:42020 (BWWL-B-103)
decontamination of, using oxidizing agent and manganese salt, 25:41911(P)
disposal in geologic media, physicochemical conditions for, 25:41925(T) (CEA-tr-R-1979)
disposal in thick underground salt formations, thermal analysis of, 25:42038 (ORNL-TM-3426)
disposal into oceans, sociopsychological factors for limitation of, 25:41948 (CEA-CONF-1733)
disposal of liquid and solid hospital, ICRP recommendations on, 25:42476
disposal of liquid, from pot, spray, and phosphate glass solidification processes, 25:41905
effects on marine organisms following discharge into seawater, 25:42373
evaporation of liquid, to salt cakes, in-tank, 25:41887 (ARH-SA-25)
monitoring chemical processing plant, 25:42410
monitoring following discharge of liquid, programs in United Kingdom for, 25:42380
processing and disposal of liquid, in Japan, 25:42037 (JAERI-13666)
processing of fuel fabrication scrap, flow-sheet for plutonium partitioning from uranium in, 25:41888 (ARH-SA-78)
processing of, containing zirconium fluoride or aluminum nitrate at ICPP Waste Calcining Facility, 25:41893 (IN-1474)
separation of ruthenium from, by pH adjustment and treatment with zeolites, 25:41913(P)
solidification of high-level, by pot, spray, and phosphate glass processes, 25:41905
storage of high-level solid, effects of temperature, feed type, and activity on, 25:41905
treatment of liquid, effects of flocculents on decantation in, 25:41833(R) (IA-1218)

RADIOACTIVITY
calibration and dosimetry in Italy, enforcement of legislation on, 25:42509
decay constants for, variation of nonlinear parameters for computing, 25:43521
monitoring in atmosphere and milk in Ecuador, 1966 to 1967, 25:41940
monitoring in atmospheric precipitation and surface atmosphere in Canada and USA during November 1970, gross β, 25:42426
monitoring in atmospheric precipitation and surface atmosphere in Canada and USA during October 1970, gross β, 25:42418
monitoring in Columbia River during 1968 to 1969, β and γ, 25:42419
monitoring in environment of AEC installations in California and Florida during 1970, 25:42416
monitoring in environment of Fernald Feed Materials Production Center and Paducah Plant during 1970, 25:42420
monitoring in environment surrounding Brasov, Romania during 1961 to 1968, 25:42424
monitoring in Italian atmosphere, surveillance network for, 25:41937
monitoring in Romanian environment, equipment and methods for measurement of, 25:41928
monitoring in surface atmosphere of Central and South America during November 1970, gross β, 25:42426
monitoring in surface atmosphere of Central and South America during October 1970, gross β, 25:42418
monitoring in Tashkent ground-level atmosphere, 1966 to 1967, 25:41939
monitoring in Washington surface waters during 1968 to 1969, β, 25:42419

RADIOAPPLICATORS
design of radium-226, for therapy, 25:42590

RADIOBIOLOGY
book: Radiobiophysics of the Nucleoproteins, 25:42274
conference on, abstracts of, 25:42584
research programs of AEC during 1970 on, 25:44293 (TID-25728)

RADIOCHEMICAL PROCESSING PLANTS
costs for fuel reprocessing, optimization of, 25:41894 (INR-1297)
hazards to Czechoslovakian personnel from uranium, health education for prevention of, 25:42504
radiation monitoring programs for, 25:42410

RADIOELECTRIC CELLS
development of broadband, for power density monitoring of pulsed microwaves, 25:42188 (MATT-845)

RADIOGRAPHY, BIOMEDICAL
book: Mathematics of Radiology and Nuclear Medicine, 25:42433
dermatitis induction in diagnostic, using Be-window x-ray tube without filtration, 25:42545
doses to children from different x-ray procedures for, comparison of, 25:42412
effectiveness of neutron, for in vitro localization of bone tumor, 25:42575
equipment and facilities for, safety survey of federal, 25:42502
radiation dose to human population from diagnostic, 25:42711
radiation dose to human skin during diagnostic, method for calculation of, 25:42431
radiation dose to human tissues during, effects of energy on x, 25:42430
radiation protection code-of-practice for dental, Australia, 25:42496
radiation protection methods for medical personnel and patients during diagnostic, 25:42493
radiation protection of human gonads during pelvic, use of aluminum filters for, 25:42447
radiation protection of patients during diagnostic, ICRP standards for, 25:42453
radioopaque agent for respiratory tract, testing tantalum aerosols as, 25:42558
use of x, for diagnosis of bone tumors in comparison with strontium-85 and metastable strontium-87, 25:42562

RADIOGRAPHY, INDUSTRIAL
detectors for alpha, performance of plastic track, 25:42053
equipment for thermal neutron, performance of sealed-tube neutron generator and graphite moderated system, 25:42027 (RFP-1706)
method for detection of microdefects in materials using krypton-85 tracer, 25:42029
radiation protection code for, 25:42490
radiation protection manual for, ILO, 25:42461

RADIOIMMUNOASSAY
method for angiotensin I, in human plasma as assay for plasma renin activity, 25:42238
method for Australia antigen, double-antibody, 25:42308
method for luteinizing hormone, in serum of monkeys, 25:42237
method for measuring frequency of antibody to hepatitis-associated antigen using iodine-125, 25:42306
radiation dose interpolation for, use of computer calculations for, 25:42236

RADIOISOTOPE SCANNERS
development for dual isotope scintigraphy, using digital subtraction technique, 25:42059
performance of rectilinear, for metastable technetium-99-labeled iron hydroxide macroaggregate scanning of blood perfusion in lungs, 25:42579
sensitivity calculations for, using multichannel ring collimator, 25:42089
RADIOISOTOPE SCANNING
bibliography on gallium-67, gallium-68, or technetium-99m for, 25:42550 (ORNL-TM-2091(Suppl.2))
book: Problems in Experimental and Clinical Radiology, 25:42292
book: Use and Interpretation of the Lung Scan, 25:42583
data analysis for enhancement of scan resolution, methods for computer, 25:42557
development of new methods for, abstracts of 300 papers on, 25:42550
effectiveness for evaluation of response of human brain tumors to drug therapy, 25:42556
effectiveness for measurement of blood pressure in human lungs, 25:42554
effectiveness of perfusion and ventilation, for diagnosis of human bronchopulmonary dysplasia, 25:42551
evaluation for measurement of glomeruli filtration rate in human kidneys, 25:42574
method for diagnosis of liver neoplasia, gold-198 and selenium-75 double-tracer, 25:42580
method for study of lymph system function and morphology in man, 25:42581
methods for measurement of internal contamination of nuclear power plant personnel in Italy, results of, 25:42435
RADIOISOTOPES
bibliography on transport through food chains and concentration by fish, invertebrates, and mammals, 25:42315 (ORNL-NSIC-89)
book: Recommendations on the Use of Radioisotope Methods for Determining the Physico-mechanical Properties of Soils, 25:42175
content in fish, review on effects of environmental factors and species type on, 25:42249
decay chains of, computer program for calculating time-dependent populations of isotopes in, (E), 25:43889 (LA-4708)
determination of small amounts of, optimization of radiometric equipment for, 25:42102
determination of small amounts of, using lithium-drifted germanium spectrometers, 25:42048 (ANL-7710, pp 263-364)
determination of, coincident lithium-drifted germanium gamma spectrometers for, 25:42113
dispersion in atmosphere following reactor accidents, computer method for calculation of, 25:42393 (BNWL-B-69)
handling in hospitals, ICRP recommendations for radiation protection in, 25:42476
hazards to patients during diagnosis, establishment of permissible dose levels for minimizing, 25:42552
production of, properties of aluminum oxide for use as adsorbent in, 25:41991 (JAERI-13778)
production of, use of inorganic ion exchangers in, 25:41879 (JAERI-13726)
separation from water supplies, effectiveness of bentonites for, 25:42384(F)
shipment by mail in Australia, radiation protection standards for, 25:42494
shipment in cargo and passenger aircraft, international regulations governing, 25:42456
shipment in cargo and passenger aircraft, international regulations governing, 25:42457
sorption by inorganic sorbents in liquid waste disposal, 25:41833(R) (IA-1218)
testing of, produced in Japan in 1965 to 1967, application, 25:41990 (JAERI-13617)
toxicity for man, 25:42458
use as thermal energy sources for life support systems in space vehicles, evaluation of, 25:42004
use as tracers for determining nutrient cycling in rain forest in Puerto Rico, 25:42317(R) (PRNC-147)
use in pesticide research, review of, 25:42239
uses in Italian industry, legal aspects of, 25:42013
RADIOLOGY
book: Basic Medical Radiation Physics, 25:42555
book: Mathematics of Radiology and Nuclear Medicine, 25:42433
book: Problems in Experimental and Clinical Radiology, 25:42292
RADIOMETERS
performance of active cavity, for scalar radiant flux of sun, (E), 25:43075
RADIOMETRIC ANALYSIS
uses in mineral exploratio and exploitation, conference on, Krakow, Dec. 9 to 12, 1969, 25:41941 (STI/PUB-279)
RADIOMIMETIC SUBSTANCES
cycasin, effects on root tip chromosomes of onion and Zamia in comparison to β-glucosidase and methylazoxymethanol, 25:42334
methylazoxymethanol, effects on root tip chromosomes of onion and Zamia in comparison to β-glucosidase, cycasin, and x radiation, 25:42334
RADIOMETRIC TESTING
book: Recommendations on the Use of Radioisotope Methods for Determining the Physico-mechanical Properties of Soils, 25:42176
RADIOOPAQUE AGENTS
testing tantalum aerosols for use as, for respiratory tract radiography, 25:42558
RADIOPROTECTIVE COMPOUNDS
adenosine derivatives, effects on survival of γ-irradiated mice, 25:42516
book: Oxidation Equilibrium and the Radiosensitivity of Organisms, 25:42528
effects of N- and S-containing polymers on survival of x-irradiated mice and rats, 25:42517
effects on animals, conference on, 25:42512
effects on survival of β- and x-irradiated guinea pigs, mice, and rats, combined effects of cyclophosphamide and, 25:42518
preparation and effectiveness of O-alkyloximinomercaptans as, 25:42531
preparation and properties of 2-alkoxyiminomercaptans as, 25:42532
RADIOSENSITIVITY
book: Oxidation Equilibrium and the Radiosensitivity of Organisms, 25:42528
RADIOTHERAPY
dose units for, evaluation of ret, 25:42413
dose--time relations in, ret concepts for, 25:42414
radiation dose to human tissues during, effects of energy on x, 25:42430
radiation protection code for sealed beta and gamma source, 25:42492
radiation protection code for sealed source, 25:42491
research programs of AEC during 1970 on, 25:44293 (TID-25728)
research studies at Oak Ridge Associated Universities during 1970 on, 25:42587 (ORAU-113, pp 78-133)
treatment plans for interstitial cervical carcinoma, comparison of radiation dose to medical personnel under two different, 25:42432
RADIUM
abundance relative to radon in Russian rivers, 25:41929
content in Romanian environment, method for measurement of, 25:41928
effects on human cervical carcinomas, ribonuclease activity in urine and vaginal fluid following, 25:42683
RADIUM ISOTOPES Ra-226
content in drinking water in USA, standards for maximum permissible, 25:42470
distribution in Ligurian Sea sediments, measurement of vertical, 25:41949
effects on man, effects of dose on late, 25:42714
metabolism and tissue distribution following intake by man, 25:42467
uptake by bones in animals and man, induction of neoplasms and radiation injuries following, 25:42472
use in therapy, design of applicator for, 25:42590
RADIUM ISOTOPES Ra-228
uptake by bones in animals and man, induction of neoplasms and radiation injuries following, 25:42472
RADON
abundance relative to radium in Russian rivers, 25:41929
content in rat organs and tissues following inhalation of radon-222, 25:42248
content in Romanian environment, equipment for measurement of, 25:41928
effects on activity of redox enzymes in rat liver following ingestion in water, effects of dose on, 25:42279
measurement in Indian soils, use for uranium exploration, 25:41945
monitoring of decay products of, photographic film system for personnel, 25:42171
RADON ISOTOPES Rn-206
alpha decay of, branching ratios and hindrance factors for, (E), 25:43887 (JINR-P6-5791)
RADON ISOTOPES Rn-207
alpha decay of, branching ratios, half-lives, hindrance factors, and spectra from, (E), 25:43887 (JINR-P6-5791)
RADON ISOTOPES Rn-208
alpha decay of, branching ratios, half-lives, and hindrance factors for, (E), 25:43887 (JINR-P6-5791)
RADON ISOTOPES Rn-209
alpha decay of, branching ratios, half-lives, hindrance factors, and spectra from, (E), 25:43887 (JINR-P6-5791)
RADON ISOTOPES Rn-210
alpha decay of, branching ratios, half-lives, and hindrance factors for, (E), 25:43887 (JINR-P6-5791)
RADON ISOTOPES Rn-211
alpha decay of, branching ratios, half-lives, hindrance factors, and spectra from, (E), 25:43887 (JINR-P6-5791)
RADON ISOTOPES Rn-212
alpha decay of, branching ratios, half-lives, and hindrance factors for, (E), 25:43887 (JINR-P6-5791)
RADON ISOTOPES Rn-222
effects on organs and tissues in rats following inhalation, 25:42248
excretion by man following ingestion in water, 25:42247

XUM

(SFL-A-16)
inhalation by personnel in uranium mines, methods for alpha dosimetry in respiratory tract tissues following, 25:42394(R) (NYU-4256-1)
RARE EARTH ALLOYS AND SYSTEMS
properties of, prediction of, 25:41778 (UCRL-20500, pp 1-85)
rare earth--Th, magnetic susceptibility of, generalized functions for, (T), 25:43477
RARE EARTH CHALCOGENIDES
rare earth chalcogenides--uranium chalcogenides, phase studies of combinations of, 25:43001
RARE EARTH ISOTOPES
distribution in Ligurian Sea sediments, measurement of vertical, 25:41949
RARE EARTH OXIDES
H_2O--rare earth oxides, phase studies of, 25:42934 (COO-1109-60)
RARE EARTHS
complexes with substituted malonate ligands, stability in aqueous and methanol solutions, 25:44260 (IS-T-474)
determination by gamma scattering methods using americium-241 source, 25:41752(P)
metabolism following inhalation by dogs and rats, 25:44253(R) (COO-1530-25)
separation from uranium by precipitation using oxalic acid, 25:41919
spectra of, interpretation of discrete and continuum levels in absorption, (T), 25:43112
RARE GAS IONS
effects on tungsten tips in field-ion microscope, atomic displacement energy of, 25:43449
RARE GASES
chemistry of, 25:41778 (UCRL-20500, pp 1-85)
electronic states of gaseous atoms of, 25:41778 (UCRL-20500, pp 1-85)
ranges of fission product, in gases, effects of diffusion on, 25:41885
reactions between atoms of, dipole moment induced in, (T), 25:43136
RATS
fibrin ultrastructure in, with acute radiation sickness, effects of transfusion of blood factor XIII from healthy animals on, 25:42540
radiation effects on activity of redox enzymes in liver of, following ingestion of radon-containing water, effects of dose on, 25:42279
radiation effects on aminotransferase activity in serum of, effects of unsaturated fatty acid content of diet on whole-body x, 25:42298
radiation effects on biochemistry of body fluids in, as indicator of radiation injuries, review on, 25:42402
radiation effects on bromine-82 metabolism following exposure of abdomen, x, 25:42282
radiation effects on carbon-14-labeled orotic acid or iodine-131-labeled albumin activity in, as indicators of radiation injury, whole-body γ, 25:42407
radiation effects on catalase activity in blood and pyrophosphatase activity in brain and liver of, continuous whole-body γ, 25:42277
radiation effects on cerebral hemispheres in, effects of hypertension on latent x, 25:42667
radiation effects on cerebrosides and phospholipids in brain of, protective effects of cysteine against x, 25:42620
radiation effects on coagulation and fibrinolysis of blood of, protective effects of cystamine and bone marrow nucleic acids against x, 25:42537
radiation effects on content of sulfur-containing amino acids in organ proteins in, chromatographic study on x, 25:42265
radiation effects on development of nervous system of, in comparison to effects of ablation, 25:42615(R) (COO-1201-30)
radiation effects on distribution of acid phosphatase and β-glucuronidase in liver and spleen of, whole-body x, 25:42628
radiation effects on DNA in tissues of, sensitizing effects of hydroxymercuribenzoic acid on, 25:42535
radiation effects on DNA synthesis in lymphocytes of, as indicator of dose, in vitro effects of phytohemagglutinin on, 25:42404
radiation effects on excretion of deoxyribosyl compounds in urine of, as indicator of radiation injury, 25:42622
radiation effects on excretion of MEA in urine of, whole-body, 25:42671
radiation effects on excretion of nucleic acid metabolites in urine of, mechanism of effects of cysteamine on γ, 25:42625
radiation effects on eyes of, protective effects of cysteamine and glutathione against pathological x, 25:42538
radiation effects on fertility of, following exposure of nine generations, x, 25:42321 (COO-697-23)
radiation effects on heart rate and open field behavior of, effects of dose and prenatal exposure on x, 25:42640
radiation effects on heterogeneity of nuclear RNA in liver of, whole-body γ exposure, 25:42280
radiation effects on histology of nervous system of, RBE for fast neutron, 25:42641
radiation effects on learning following head exposure at one-day old, effects of dose on x, 25:42655
radiation effects on life span and tumor incidence in, effects of stress on x, 25:42669
radiation effects on life span of, tracer studies of role of physiological functions in, 25:42668
radiation effects on metabolic equilibrium in brain of, protective effects of cysteine against x, 25:42619
radiation effects on metabolism of nicotinamide-adenine dinucleotide and nucleic acid metabolites in, mechanisms for, 25:42623
radiation effects on metabolism of selenium-75 and sulfur-35 in organs of, x, 25:42264
radiation effects on mitosis in bone marrow cells and phagocytic activity of reticuloendothelial cells of, protective effects of direct electric current against x, 25:42530
radiation effects on oocytes of fetal, following maternal infusion of tritium-labeled thymidine during pregnancy, 25:42650
radiation effects on organs and tissues of, mechanism of protective effects of adrenalin, AET, and cysteine against in vitro and in vivo, 25:42523
radiation effects on oxidation-reduction potential in tissues of, protective effects of AET, MEA, or serotonin in combination with hypoxia against x, 25:42511
radiation effects on p-nitrophenol metabolism in, whole-body x, 25:42289
radiation effects on saccharin-avoidance behavior in, effects of amygdala, olfactory bulb, and septal lesions on x, 25:42647
radiation effects on survival of, long-term protective effects of N- and S-containing polymers against x, 25:42517
radiation effects on survival of, protective effects of cyclophosphamide against β and x, 25:42518
radiation effects on survival of, protective effects of methylene blue against whole-body γ or x, 25:42515
radiation effects on, mechanism of protective effects of dimethyl sulfoxide against x, 25:42524
radioinduced diseases in blood, kidneys, and liver of, neptunium-237, 25:42253
radioinduced malformations in central nervous system in embryos of, x, 25:42629
radioinduced malformations in fetuses of, in comparison to those of mice, x, 25:42639
radioinduced motor abnormalities of, following exposure of frontal region of brain, 25:42615(R) (COO-1201-30)
radioinduced mutations in, following exposure of nine generations, x, 25:42321 (COO-697-23)
radioinduced skin ulcers in, effectiveness of dibunol and metacil for treatment of x, 25:42541
radioisotope metabolism in, effects of lactation on, 25:42255
radiosensitivity of bone marrow cells of, effects of age on x, 25:42656
radiosensitivity of pulmonary tissue in, effects of pneumothorax on, 25:41833(R) (IA-1218)
radiosensitivity of transplanted tumors in, relation of protein sulfhydryl group to, 25:42618
radiosensitivity of, effects of direct electric current on x, 25:42530
radiosensitivity of, relation of age and sex to effects of metabolic activity on x, 25:42635
radon daughter content in organs and tissues in, following inhalation of radon-222, 25:42248
strontium-85 retention in, effects of age and lactation on, 25:42252
strontium-85 sorption by intestine of, effects of alginates from algae on, 25:42254
tritium-labeled estradiol autoradiographic localization in brain of, 25:42258
REACTIVITY
Doppler effect on plutonium oxide (PuO_2)--uranium oxide (UO_2) two zone core, (E), 25:44096 (ANL-7710, pp 53-262)
REACTOR CONTAINMENT STRUCTURES
fission product holdup in leak paths in, decontamination factors for, (E), 25:44134 (BNWL-1582)
REACTOR CONTROL ELEMENTS
drive system for, testing in sodium under LMFBR conditions, 25:42804(R) (LMEC-71-1)
drives for sodium cooled, standards for collapsible-rotor roller-nut, 25:44105 (RDT-E-6-5-T)
fabrication of, methods for, 25:42822
materials for fast, reactivity worths of, (E/T), 25:44094(R) (AI-AEC-12991)
vibration response of long flexible cylindrical, in axial flow, tentative design guide for calculation of, 25:41983 (ANL-ETD-71-7)
REACTOR CONTROL SYSTEMS
design of linear multivariable, feedback synthesis technique with multiple input-output cross coupling for, 25:44104 (COO-2109-4)
design of optimum, feedback of state variables through constant gain elements for, (T), 25:44106
instrumentation for, statistics of fluctuations in, 25:42048 (ANL-7710, pp 263-364)
REACTOR COOLANTS
analysis of organic, for gamma emitters, 25:41832(R)

(AECL-3851)
purification of gaseous, by combustion on catalyst, 25:41914(P)
REACTOR EXPERIMENTAL FACILITIES
book: Neutron Physics Practices. Volume I. Physics and Technology of Activation Probes, 25:43775
neutron radiography facility in TRITON, installation of industrial, 25:44158(T) (LB/G-2929)
REACTOR FUEL ELEMENTS
cladding for, data sheets on Zircaloy, 25:42859
cladding for, effects of fabrication methods on mechanical properties of Zircaloy, 25:42860
cladding for, optimum welding methods for niobium--zirconium alloy, 25:42831
configuration of cladding of, development for spacers of bulges in, 25:44218(P)
deformation of, computer program for time dependent finite element analysis of, 25:44126 (WERL-ELPLA-1)
design with coupling means between separable sections, 25:44212(P)
development of sodium-bonded stainless steel clad plutonium nitride--uranium nitride, (E), 25:44118(R) (BMI-1905)
development of thermionic, review of U. S, 25:44170
fabrication of Zircaloy-2 clad uranium oxide (UO_2), for high burnup irradiation testing in VBWR and Dresden, 25:44120 (GEAP-10355)
fabrication of, statistical tolerance limits for quality assurance during, 25:42033
fission product vapor pressures over fast neutron irradiated uranium oxide (UO_2)--plutonium oxide (PuO_2), (E/T), 25:44206 (CEA-R-4181)
handling of irradiated, design of equipment for, 25:42044(P)
identification markings on power, U.S. standard for, 25:43995
inspection of plate-type, for homogeneity, x-ray attenuation scanning method for, 25:42031
performance limits for liquid metal cooled pin type, thermal, 25:44121 (HEDL-SA-89)
performance of gas cooled fast, effects on fuel cycle costs of, (T), 25:44131
performance of stainless steel clad plutonium nitride--uranium nitride, during transient irradiation, (T), 25:44118(R) (BMI-1905)
power density of boiling water cooled vapor transport pin type, maximum, (T), 25:44122 (N-71-17463)
radiation effects on zirconium alloy-clad uranium dioxide, in-pile, 25:43010
radiation effects testing of Zircaloy-2 clad uranium oxide (UO_2), 25:44208 (KAE-68-81)
radiation effects testing of Zircaloy-2 clad uranium oxide (UO_2), 25:44207 (KAE-68-46)
radiation testing of plutonium oxide (PuO_2)--uranium oxide (UO_2) pin type, for gas cooled fast breeder reactors, 25:44125 (ORNL-TM-3427)
reprocessing of, head-end problems in, 25:41892 (EUR-4353)
spacer grids for sodium cooled, effects of wear and friction on, (E), 25:44087(T) (EURFNR-854)
spacers for, formation of bulges in cladding for, 25:44218(P)
testing of fast, use of thermal reactors for, (T), 25:44165
uranium distribution in MTR-type, radiometric quantitative estimation in, 25:42178
vibration of liquid metal cooled pin type, effects of test loop on parallel flow induced, 25:44119 (EURFNR-923)
vibration response of long flexible cylindrical, in axial flow, tentative design guide for calculation of, 25:41983 (ANL-ETD-71-7)
REACTOR FUELS
actinide redistribution in mixed oxide fast, temperature and kinetics for in-pile, 25:44124 (ORNL-TM-3387)
burnup analysis by measurement of fission neutrons, nondestructive, 25:41757
creep measurements on fast, irradiation capsule for in-pile, 25:44086(T) (EURFNR-853)
creep of fast, effects of fission process on, (E/T), 25:44118(R) (BMI-1905)
cycle of fast, 2DBCOST computational system for optimization of, 25:44130
fission gas diffusion and bubble growth in, (T), 25:44118(R) (BMI-1905)
fission gas re-solution rates in irradiated oxide, research progress in, 25:42952(R) (GEAP-12188)
fission gas re-solution rates in irradiated oxide, research progress on, 25:42953(R) (GEAP-12189)
production of, iot controls in, 25:42835
properties of carbide and nitride, for use in breeder reactors, 25:42956 (JAERI-13517)
radiation effects on performance of fast, at high temperature, (E/T), 25:44118(R) (BMI-1905)
reactions of mixed oxide fast, with cladding alloys, (E/T), 25:44123 (ORNL-TM-3385)
reprocessing of BISO-coated fissile and fertile, head-end, 25:41907
reprocessing of irradiated, multistage extraction process using tributyl phosphate for, 25:41902(P)
reprocessing of molten salt, by selective reduction and extraction using molten bismuth, 25:41903(P)
reprocessing of TRISO-coated ceramic, head-end separation of uranium-233 oxide and uranium-235 carbide particles in, 25:41906
reprocessing of Zircaloy-clad, zirconium decontamination in Zirflex and Purex processes in, 25:41889 (BNWL-1573)
reprocessing of, decontamination of waste solutions from, 25:41911(P)
reprocessing of, optimization of plants for, 25:41894 (INR-1297)
reprocessing of, Swedish plans and forecasts for, 25:41896 (NP-18878)
requirements for, 1970 to 1985 forecast of, 25:43994 (WASH-1139)
requirements in Europe during 1970 to 2010, effects of variations in reactor programs on, 25:44127 (CONF-700903-17)
reserves of, prediction of, 25:44217
restructuring of mixed oxide fast, temperatures and kinetics for in-pile, (E/T), 25:44124 (ORNL-TM-3387)
REACTOR LOADING MACHINES
design with ball-driven members for unlocking fuel channel seals, 25:44214(P)
design with means for handling fuel elements with separable sections, 25:44212(P)
design with means for minimizing volume of coolant water in machine head, 25:44213(P)
design with means for separately handling fuel string and closure plug assembly, 25:44216(P)
design with means to compensate for misalignments between machine head and fuel channel, 25:44215(P)
lifting chain for compact winding and storage in, 25:44211(P)
shielding requirements for critical assembly, 25:44161 (WANL-TME-1895)
REACTOR SAFETY
accident analysis for liquid metal cooled fast, review of, 25:44132 (AI-AEC-12992)
coolant loss accidents, effects on emergency core cooling on peak temperatures of fuel element cladding during, 25:44140 (NEDO-10329(Suppl.1))
coolant loss in pressurized and boiling water reactors, transient and dynamic pressures, temperatures, stresses, flow rates, and hydraulic forces from sudden, 25:44133 (BNWL-1524)
radiological risks following reactor accidents, PILAX code for calculation of, 25:44135 (CEA-R-4136)
technical progress review on, index to, 25:44141 (ORNL-NSIC-86)
REACTOR SAFETY EXPERIMENTS
design parameters of Japanese pulse reactor for, 25:44162
fuel element irradiation in TREAT, analysis of stainless steel clad plutonium nitride--uranium nitride, (T), 25:44118(R) (BMI-1905)
REACTORS
accidents in, computer method for calculation of radiation dose to human population following release of radioisotopes to atmosphere during, 25:42393 (BNWL-B-69)
components for, standard for fabrication and testing of metal products for, 25:42817 (RDT-F-3-37-T)
components for, standards for cleaning and cleanliness of, 25:44089 (RDT-F-5-1-T)
cooling systems for, inspection standards for materials subject to wear in, 25:44210 (RDT-F-3-7-T)
core design calculations for, WIMS E program modules for, 25:44193 (EACRP-A-135, pp 21-9)
core design for, adjoint trial spectra for calculating thermal group constants used in, 25:44202
design of, digital computer requirements for use in, 25:44090 (WAPD-T-2358)
development of, quality assurance program standards for, 25:44088 (RDT-F-2-2-T)
kinetics calculations for, space-time variational flux synthesis model for, 25:44200
kinetics equations for, analysis of multinode, (T), 25:44191 (ANL-7710, pp 365-463)
kinetics for, computer programs for, 25:44191 (ANL-7710, pp 365-463)
kinetics of beryllium reflected, space-time dependence of, (E/T), 25:44201
kinetics of, revisions in MC² computer program for, 25:44191 (ANL-7710, pp 365-463)
lattice parameters in multitube enriched uranium fueled, epithermal cell, (E/T), 25:44203 (INR-F-1266)
materials for, radiation effects on structural, 25:44093
neutron decay constants in reflected fast burst, model for prompt, (E/T), 25:44198
neutron flux distribution in, nonlinear model of steady-state, 25:44197
neutron flux monitoring channels for, standards for wide-range, 25:44209 (RDT-C-15-2-T)
neutron flux synthesis for, variational models for space-time, (T), 25:44191 (ANL-7710, pp 365-463)
noise probability distributions in, methods for calculation of, 25:44199
physics calculations for, CARCNTE modular coding system for, 25:44187 (EACRP-A-135, pp 63-8)
physics calculations for, conference on modular coding systems for, 25:44181 (EACRP-A-135)

XUM

physics calculations for, design of modular systems for, 25:44186 (EACRP-A-135, pp 60-2)
physics calculations for, development of CODNUC system for, 25:44182 (EACRP-A-135, pp 5-10)
physics calculations for, Japanese modular coding systems for, 25:44188 (EACRP-A-135, pp 69-86)
physics calculations for, modular code development for, 25:44183 (EACRP-A-135, pp 11-14)
physics calculations for, scheme for peripheral storage of data for, 25:44184 (EACRP-A-135, pp 38-49)
physics calculations for, U. S. modular coding systems for, 25:44185 (EACRP-A-135, pp 50-9)
pressure vessels for, effects of inspection standards on fabrication on, 25:44110 (CONF-700224-, Paper 5)
pressure vessels for, equipment for radiographic inspection of, 25:44112 (CONF-700224-, Paper 7)
pressure vessels for, performance of linear accelerator for radiographic inspection of, 25:44113 (CONF-700224-, Paper 8)
pressure vessels for, stress wave emission techniques for incipient failure detection in, 25:44137 (CONF-700224-, Paper 3)
pressure vessels for, system for automatic ultrasonic inspection of welds in, 25:44111 (CONF-700224-, Paper 6)
protection systems for, standards for, 25:44142 (RDT-C-16-1-T)
reactivity distribution in one-dimensional cylindrical, REPO code for optimal, 25:44192 (CEA-N-1367)
shielding calculations for, WSRPG modular programming system for, 25:44107 (EACRP-A-135, pp 15-20)
shielding for, neutron and γ-ray fields and heat balance for, (T), 25:44108
transfer function with temperature feedback, prediction of spatially dependent source, (E/T), 25:44204

REACTORS, BOILING
coolant blowdown in, transient and dynamic pressures, temperatures, stresses, flow rates, and hydraulic forces from, (E/T), 25:44133 (BNWL-1524)
emergency core cooling systems for, effects on fuel element cladding peak temperatures of, (T), 25:44140 (NEDO-10329, Suppl.1))
fuel pins for, maximum power density for vapor transport type, (T), 25:44122 (N-71-17463)
iodine-131 release to atmosphere during operation of, programs for monitoring, 25:42388

REACTORS, BREEDER
economics of gas cooled, effects of fuel element performance on, (T), 25:44131
fuel elements for gas cooled fast, radiation testing of plutonium oxide (PuO_2)--uranium oxide (UO_2) pin type, 25:44125 (ORNL-TM-3427)
fuels for gas cooled, chemical reactions of cladding with mixed oxide, (E/T), 25:44123 (ORNL-TM-3385)
fuels for, properties of carbide and nitride, 25:42956 (JAERI-13517)
operation in European nuclear power systems, effects on 1970 to 2010 uranium requirements of, 25:44127 (CONF-700903-17)
physics calculations for sodium cooled fast, comparison of international, 25:44101 (TRG-Report-2133)
stability of operating, effects of nuclear weapon shock waves on, 25:42506(R) (ORNL-4566(Pt.1))

REACTORS, FAST
Doppler coefficient measurements for, review and evaluation of, (E/T), 25:44094(R) (AI-AEC-12991)
dynamics of in-core thermionic concepts, (T), 25:44097(R) (COO-2109-5)
economics of gas cooled, effects of fuel element performance on, (T), 25:44131
fission product vapor pressure over irradiated fuel elements in, (E/T), 25:44206 (CEA-R-4181)
fuel cycle management procedures for, calculation of optimum, 25:44096 (ANL-7710, pp 53-262)
fuel cycle optimization for, 2DBCOST computational system for, 25:44130
fuel elements for gas cooled breeder, radiation testing of plutonium oxide (PuO_2)--uranium oxide (UO_2) pin type, 25:44125 (ORNL-TM-3427)
fuel elements for sodium cooled, friction and erosion between spacer grids and, (E), 25:44087(T) (EURFNR-854)
fuel elements for, use of thermal reactors for testing, (T), 25:44165
fuel pins for Na-1, effects of test loop on parallel flow induced vibration of, 25:44119 (EURFNR-923)
fuels for gas cooled, chemical reactions of cladding with mixed oxide, (E/T), 25:44123 (ORNL-TM-3385)
fuels for, irradiation capsule for in-pile creep measurements on, 25:44086(T) (EURFNR-853)
fuels for, temperatures and kinetics for restructuring of mixed oxide, (E/T), 25:44124 (ORNL-TM-3387)
kinetics for, research at Argonne National Laboratory during July 1969 to June 1970, 25:44190(R) (ANL-7710)
kinetics of pulsed, effects of periodic reactivity and quasi-periodic neutron flux conditions on, (T), 25:44196(T) (LA-tr-71-44)
neutron dosimetry techniques for, 25:44102
neutron slowdown theory for, derivation of elastic, (T), 25:44191 (ANL-7710, pp 365-463)
operation in European nuclear power systems, effects on 1970 to 2010 uranium requirements of, 25:44127 (CONF-700903-17)
physics calculations for sodium cooled uranium oxide (UO_2)--plutonium oxide (PuO_2) fueled, 25:44194 (FEI-213)
physics calculations for sodium cooled, comparison of international, 25:44101 (TRG-Report-2133)
physics calculations for, development of VIM computer program for, 25:44094(R) (AI-AEC-12991)
physics calculations for, Flotran modular scheme for, 25:44098 (EACRP-A-135, pp 30-7)
stability of operating, effects of nuclear weapon shock waves on, 25:42506(R) (ORNL-4566(Pt.1))
structural materials for, irradiation capsule for in-pile creep measurements on, 25:44086(T) (EURFNR-853)

REACTORS, GAS-COOLED
economics of fast, effects of fuel element performance on, (T), 25:44131
fuel cycle economics for high-temperature, role of reprocessing BISO-coated particles in, 25:41907
fuel elements for fast breeder, radiation testing of plutonium oxide (PuO_2)--uranium oxide (UO_2) pin type, 25:44125 (ORNL-TM-3427)
loading machine for, lifting chain for compact winding and storage in, 25:44211(P)

REACTORS, GERMANY
personnel access locks in, standard for, 25:43996

REACTORS, HEAVY WATER-MODERATED
loading machine for, with ball-driven members for unlocking fuel channel seals, 25:44214(P)
loading machine for, with means for separately handling fuel string and closure plug assembly, 25:44216(P)
loading machine for, with means for uncoupling and securing fuel elements with separable sections, 25:44212(P)
loading machine for, with means to compensate for misalignments between machine head and fuel channel, 25:44215(P)
reflectors for, evaluation of bismuth-impregnated graphite, (T), 25:44129 (EUR-4357)

REACTORS, HETEROGENEOUS
neutron thermalization in one-dimensional, DEMETRA code for quasi-diffusion method calculations of, 25:44195 (IAE-2010)

REACTORS, LIQUID METAL-COOLED
control rod drives for sodium cooled, standards for collapsible-rotor roller-nut, 25:44105 (RDT-E-6-5-T)
coolant sampling equipment for, development of in-line vacuum-distillation liquid sodium, 25:44115
cooling system for, recirculation loop for prevention of burnout in, 25:44114(P)
fuel elements for sodium cooled, friction and erosion between spacer grids and, (E), 25:44087(T) (EURFNR-854)
heat exchangers for, nondestructive testing methods for tube joints in, 25:44148 (CONF-700224-, Paper 4)
physics calculations for sodium cooled uranium oxide (UO_2)--plutonium oxide (PuO_2) fueled, 25:44194 (FEI-213)
physics calculations for sodium cooled, comparison of international, 25:44101 (TRG-Report-2133)

REACTORS, MARITIME
design for container ship with 120,000 shp, 25:44178 (RCN-139)
economics of, comparison of conventional ship propulsion to, 25:44177 (NP-18908)

REACTORS, POWER
construction of, economic and safety aspects of nondestructive testing in, 25:44136 (CONF-700224-, Paper 1)
cooling systems for, standards for construction of, 25:43993 (RDT-E-15-2-T)
development in Benelux countries, review of, 25:44092
development of U. S., economic strategies for, 25:44145
economics of dual purpose, in agro-industrial complexes, 25:44175
emergency core cooling systems for boiling water, effects on fuel element cladding peak temperatures of, (T), 25:44140 (NEDO-10329(Suppl.1))
fuel assemblies for, U.S. standard for identification markings on, 25:43995
pressure vessels for, dosimetry techniques for neutron radiation effects on steel, 25:44117
pressure vessels for, in-service ultrasonic inspection of steel, 25:44109 (CONF-700224-, Paper 2)
pressure vessels for, reliability of neutron fluence and embrittlement calculations for steel, (E/T), 25:44116
safety of, reliability estimate method for evaluation of, 25:44144
siting in Israel, inland and underground, 25:41833(R) (IA-1218)
thermal effluents from, physical characteristics of plume in Lake Michigan from, (E), 25:44138 (CONF-710431-1)

REACTORS, PRESSURIZED-WATER
control systems for, feedback of state variables through constant gain elements for design of optimum, (T), 25:44106
coolant blowdown in, transient and dynamic pressures, temperatures, stresses, flow rates, and hydraulic forces from, (E/T), 25:44133 (BNWL-1524)
steam generators for, standards for, 25:44081 (RDT-E-4-1-T)

REACTORS, PROCESS HEAT
economics of dual purpose, in agro-industrial complexes, 25:44175
REACTORS, RESEARCH
control system for DR-2, development of computer, 25:42205(R) (RISO-M-1357)
coolant for EWA, iodine-131 content in vessel air and, (E), 25:44155 (INR-1295)
critical measurements on uranium fuel element clusters in D2O, comparison of exponential measurements with, 25:44154 (EJR-4352)
design of conceptual Nuclear Safety Research Reactor (NSRR), 25:44162
development of IBR pulsed fast, 25:44156 (JINR-P3-5754)
fuel solutions for BER, dissociation kinetics and concentration of peroxides in, (E), 25:44166
use of IBR pulsed fast, 25:44156 (JINR-P3-5754)
REACTORS, THERMAL
fuel element testing in, simulation of fast reactor conditions for, (T), 25:44165
REACTORS, WATER-COOLED
coolant blowdown in, transient and dynamic pressures, temperatures, stresses, flow rates, and hydraulic forces from, (E/T), 25:44133 (BNWL-1524)
coolant systems for, standard for welding, examining, and testing components for, 25:42849 (RDT-F-6-1-T)
cooling systems for, standards for construction of, 25:43993 (RDT-E-15-2-T)
loading machine for, with means to minimize volume of water in machine head, 25:44213(P)
REFRIGERATION
description of helium-3-dilution, 25:43327
REGGE POLE THEORY
cuts due to absorption in $\gamma + N \to \pi^0 + N$ interactions in, 25:43601
cuts for unitarized finite-energy sum rules for charge-exchange $\pi + N$ interactions, 25:43637 (DESY-71/24)
daughter trajectory in generalized Veneziano model, ghost states on, 25:43712
double-Regge-pole model for $p + p \to p + \pi^+ + \Delta^{++}$ interactions at 22 GeV/c, 25:43580
dual amplitude with Mandelstam analyticity for $\pi + \pi \to \pi + \pi$ interactions, 25:43623 (ITF-71-28-E)
dual model in, operatorial approach for analysis of multi-particle, 25:43578
dual resonance amplitudes in, functional formulation of, 25:43722
duality in model for amplitudes of two-body elastic strong interactions in, 25:43617
duality predictions test in partial-wave analysis of anti $K + N \to \pi + \Sigma(\Lambda)$ interactions, 25:43642 (UCR-34-P-107-B-106)
duality relations with chiral symmetry breaking for strong interactions, 25:43619
duality sum rule for two-Reggeon-particle and triple-Reggeon couplings, di-triple Regge limits in inclusive hadron interactions for, 25:43570 (NYO-2262-TA-247)
elementary particle reggeization in, dynamic limit for, 25:43672
model for $\pi^- + p \to \pi^+ + 2\pi^- + p$ interactions at 5 GeV/c in, multi-Regge, 25:43592
pole exchanges in continuous-moment sum rules for $\pi + \pi$ interactions, 25:43636
Pomeranchuk trajectory for virtual Compton $e + N \to e + N$ interactions, finite-energy sum rule analysis for, 25:43584 (ITF-71-27-E)
Regge limits in inclusive hadron interactions, two-Reggeon-particle and triple Reggeon couplings from duality sum rule and Reggeon--Reggeon amplitude from di-triple, 25:43570 (NYO-2252-TA-247)
Regge vertex, amplitude for triple, 25:43723
Reggeon--Reggeon amplitude from di-triple Regge limits in inclusive hadronic interactions, 25:43570 (NYO-2262-TA-247)
Reggeon-particle and triple-Reggeon couplings from duality sum rule from di-triple Regge limits in inclusive hadron interactions, two, 25:43570 (NYO-2262-TA-247)
trajectories for amplitudes violating Pomeranchuk theorem, complex negative-signature, 25:43715
trajectories in, dual oscillator model for hadron total widths on leading, 25:43619
RELATIVE BIOLOGICAL EFFECTIVENESS
comparison of γ, neutron, and x radiation, for colony-forming units in mouse bone marrow, 25:42601
RELATIVITY THEORY
book: Relativistic Quantum Theory. Vol. 4, 25:43086
Cauchy problem in general, 25:43696
causality in general, stable, 25:43696
causality in theory of continuous media in special, invariance for, 25:43693
conservation laws in general, existence of preferred collineations for, 25:43704
corrections to Maclaurin spheroids, post-Newtonian, (T), 25:43093
cosmological constant and fundamental length, (T), 25:43087
effects on deformed figures of Jacobi ellipsoids, post-Newtonian, (T), 25:43090
effects on deformed figures of Maclaurin spheroids, post-Newtonian, (t), 25:43091
Einstein--Maxwell equations for spherically symmetric charge radiation, solutions of, 25:43710
field theory in Minkowski space--time in general, Lorentz-invariant, 25:43665 (NP-18831)
formulation of local and global principles in, 25:43707
gravitational deflection of microwaves in solar field, (E), 25:43094
Lorentz metrics in general, stable and generic properties of, 25:43696
magnetohydrodynamics in general, general relations for behavior of, 25:43701
metric space in general, origins of Schwarzschild and Curzon static solutions for, 25:43697
singularities in general, definition of, 25:43698
singularities in general, local observation of, 25:43695
space--time in general, causal structure in, 25:43695
structure and gravitational field of uniformly rotating disks in, (T), 25:43092
theory for special, historical review of, 25:43690
REMOTE-HANDLING EQUIPMENT
design for irradiated fuel elements, 25:42044(P)
REPTILIA
Anolis gundlachi, radioisotope uptake by, in rain forest in Puerto Rico, 25:42317(R) (PRNC-147)
REPUBLIC OF KOREA
radioisotope content of milk in, 1965 through 1968, effects of fallout specific activity on, 25:42372
RESINS
effects on intestinal sorption of cesium-134 and strontium-89 in animals, 25:42263
8-RESORCYLIC ACID
complexes with uranyl ions, spectral and thermodynamics studies on, 25:41830
RESPIRATORY SYSTEM
radiation dose to bronchial epithelium in, following inhalation of polonium-214, polonium-218, or plutonium-239, methods for calculation of α, 25:42394(R) (NYU-4256-1)
radiography of human, testing tantalum aerosols for use as radioopaque agent for, 25:42558
RETICULO-ENDOTHELIAL SYSTEM
radiation effects on mouse, protective effects of cysteamine, lipopolysaccharide, and serotonin against x, 25:42513
RHENIUM
book: High-Temperature Materials, 25:42853
determination following separation from other metal ions by thin-layer chromatography using quercetin, colorimetric, 25:41743
determination of trace amounts of, in meteorites by neutron activation and γ spectrometry, 25:41773
RHENIUM ALLOYS AND SYSTEMS
C--Re--Ta, phase diagram at 2100°C, isothermal, 25:42992
Mo--Re, superconducting transition temperature in high T/sub c/ intermetallic $MoRe_3$, sensitivity to residual stress of, (E), 25:43302
Mo-base--Re, deformation at low temperatures, effects of crystal orientation on plastic, 25:42886 (UCRL-20500, pp 86-146)
Re--W-base, creep rupture at 1650 and 2200°K, comparison of effects of consolidation by arc-melting and powder metallurgy methods on, 25:42866
RHENIUM OXIDES
properties and spectra of gaseous, 25:42957 (UCRL-20500, pp 147-73)
RHODIUM
separation from acetone--hydrochloric acid solutions by ion exchange using Bio-Rad, distribution coefficients for, 25:41899
RHODIUM ALLOYS AND SYSTEMS
Pt-base--Rh--W, fabrication and properties of cladding of, 25:41993(R) (ORNL-4692)
RHODIUM ISOTOPES Rh-96
beta decay of ground-state and isomeric, half-lives and γ spectra for, (E), 25:43943
RIBONUCLEASE
radiation effects on activity of, in human urine and vaginal fluid following therapy for cervical carcinomas, lymphomas, or tumors, 25:42683
radioinduced hydrogen transfer in, effects of temperature and scavengers on yields from γ, 25:41837
RIBOSE, DEOXY-
radiation effects on excretion of, in mouse and rat urine as indicator of radiation injury, 25:42622
RING CURRENT
analysis of asymmetric twilight, during Mar. 13--15, 22--25, and 28--29, 1966 magnetic storms, (E), 25:43241
effects on ion-cyclotron wave turbulence, SAR arc formation at plasmapause from, (T), 25:43242
proton loss during magnetic storms, mechanism of turbulent, (E/T), 25:43210 (AD-715260).
RIVERS
radium/radon content of Russian, 25:41929
ROBERT E. GINNA POWER REACTOR, UNIT 1
effluents from, measurements and monitoring procedures for radioactive and thermal, 25:44038 (DOCKET-50244-74)
quality assurance program for, 25:44037 (DOCKET-50244-72)
steam isolation valve for, failure of main, 25:44011 (DOCKET-50244-73)

XUM

ROCKET MOTORS
design study for radioisotope-heated subliming microthruster, 25:42017
ROCKET REACTORS (NERVA)
fuel elements for, problems in fabrication of, 25:44174
nozzles for, problems in fabrication of, 25:44174
ROCKS
analysis for gold by neutron activation, 25:41770
analysis for trace elements in prospecting, review on neutron activation methods for, 25:41767
analysis of sedimentary, for halogens by Szilard--Chalmers reactions following neutron activation, 25:41763
thorium content and distribution of alkaline, of Ilimaussaq intrusion, south Greenland, gamma spectrometry method for determination of, 25:41943
uranium content and distribution of alkaline, of Ilimaussaq intrusion, south Greenland, gamma spectrometry method for determination of, 25:41943
RODS
vibration response of long flexible cylindrical, in axial flow, tentative design guide for calculation of, 25:41983 (ANL-ETD-71-7)
ROLLING
method for form, for production of close tolerance shapes in most wrought metals and alloys, 25:42827
ROMANIA
radioactivity monitoring in environment surrounding Brasov, during 1961 to 1968, 25:42424
radioactivity monitoring of environment of, 1964 to 1968, 25:41928
RUBIDIUM
determination by photon activation using cesium or strontium as internal standards, 25:41766
determination of trace amounts of, in alfalfa, spectrochemical, 25:41833(R) (IA-1218)
separation from acetone--hydrochloric acid solutions by ion exchange using Bio-Rad, distribution coefficients for, 25:41899
separation from aqueous solutions by ion exchange on zirconium tellurate, tracer studies on, 25:41915
RUBIDIUM BROMIDES
neutron total cross section at 100 to 650 keV, optical model analysis of average, (E/T), 25:43908
RUBIDIUM IODIDES
xenon-atom reactions with, crossed-beam study of dissociation in, 25:43131
RUBIDIUM ISOTOPES Rb-95
metabolism and tissue distribution following intake by man, 25:42457
testing of, produced in Japan, application, 25:41990 (JAERI-13617)
uptake by frogs and lizards from labeled trees, 25:42317(R) (PRNC-147)
RUTHENIUM
determination of trace amounts of, in meteorites by neutron activation and γ spectrometry, 25:41773
separation from aqueous solutions by ion exchange on zirconium tellurate, tracer studies on, 25:41915
separation from other metals using inorganic ion exchange papers, 25:41909
separation from radioactive effluents by pH adjustment and treatment with zeolites, 25:41913(P)
separation from radioactive waste using oxidizing agent and manganese salt, 25:41911(P)
RUTHENIUM ISOTOPES Ru-96
energy levels from α inelastic scattering and rhodium-96 decay, (E), 25:43943
RUTHENIUM ISOTOPES Ru-101
energy levels from technetium-101 decay, spin-parity assignments for, (E), 25:43899
RUTHENIUM ISOTOPES Ru-106
leachability and volume strength of liquid, for incorporation in concrete mixtures, 25:41833(R) (IA-1218)

S

S-MATRIX
generating functionals for, estimates of, 25:43670
SAFETY
manual for radioactive materials industry, part 2 of ILO, 25:42459
survey of federal x-ray equipment and facilities, 25:42502
Temple University office of radiation, criteria for establishing, 25:42503
SALIVARY GLANDS
radiation effects on function and morphology of human, following therapy of head and neck tumors, 25:42699
scanning for function using metastable technetium-99, 25:42566
scanning of human, use of metastable technetium-99-labeled sodium pertechnetate for sequential, 25:42571
SALT DEPOSITS
radioactive waste disposal in, thermal analysis of Lyons, Kansas repository for, 25:42038 (ORNL-TM-3426)
SALTS
thermal decomposition of solutions of, in falling droplets, equipment and method for measuring, 25:41833(R) (IA-1218)
SAMARIUM
determination in meteorites by neutron activation and high-voltage electrophoresis, 25:41775
neutron total cross section at 100 to 650 keV, optical model analysis of average, (E/T), 25:43908
radiolysis of aqueous solutions of, spectral studies on pulse, 25:41833(R) (IA-1218)
separation from aqueous solutions by ion exchange on zirconium tellurate, tracer studies on, 25:41915
SAMARIUM BORIDES
enthalpy and heat capacity of SmB_6, 25:42961
SAMARIUM ISOTOPES Sm-141
decay of ground-state and isomeric, γ spectra and half-lives for, (E), 25:43909
SAMARIUM ISOTOPES Sm-148
proton elastic and inelastic scattering at 16 MeV, differential cross sections for, (E), 25:43901
SAMARIUM ISOTOPES Sm-149
neutron total cross section at 100 to 650 keV, optical model analysis of average, (E/T), 25:43908
SAMARIUM ISOTOPES Sm-150
energy levels from γ resonance scattering, total radiative widths for, (E), 25:41833(R) (IA-1218)
neutron caputre by, γ spectra from thermal, (E), 25:43892
proton elastic and inelastic scattering at 16 MeV, differential cross sections for, (E), 25:43901
SAMARIUM ISOTOPES Sm-151
energy levels from promethium-151 decay, lifetimes of, (E), 25:43937
energy levels of, determination of E4 transition moments by Coulomb excitation, 25:43948
energy-level scheme from samarium-150 thermal neutron capture, (E), 25:43892
neutron caputre by, γ spectra from thermal, (E), 25:43892
separation from other isotopes during 1968 and 1969, review of ORNL program for, 25:41992 (ORNL-4640)
SAMARIUM ISOTOPES Sm-152
energy levels from europium-152 decay, transition probabilities and band-mixing parameters for, (E), 25:43940
energy-level scheme from samarium-151 thermal neutron capture, (E), 25:43892
energy-level transitions from europium-152 decay, conversion coefficients and γ-mixing ratios for, (E), 25:43940
neutron total cross section at 100 to 650 keV, optical model analysis of average, (E/T), 25:43908
proton elastic and inelastic scattering at 16 MeV, differential cross sections for, (E), 25:43901
SAMARIUM ISOTOPES Sm-153
production by neutron capture reactions in samarium, impurities formed in, 25:41877 (JAERI-13545)
SAMARIUM ISOTOPES Sm-154
proton elastic and inelastic scattering at 16 MeV, differential cross sections for, (E), 25:43901
SAMARIUM OXIDES
analysis for impurities by activation methods, 25:41877 (JAERI-13545)
analysis for impurities, cathode region method for spectrochemical, 25:41833(R) (IA-1218)
SAMPLING
equipment for liquid sodium, development of in-line vacuum-distillation, 25:44115
method for reactor fuel elements, statistical tolerance limits for, 25:42033
system for safeguarding nuclear materials, dynamic mathematical model for optimization of, 25:42045
SAN ONOFRE POWER REACTOR, UNIT 1
buildings for, vibration tests for effects of earthquake motion on, 25:44079 (UCLA-ENG-7037)
cooling system for, vibration tests for effects of earthquake motion on, 25:44079 (UCLA-ENG-7037)
operations history for January to June 1971, 25:44005 (DOCKET-50206-114)
quality assurance program for, 25:44034 (DOCKET-50206-115)
SAXTON POWER REACTOR
fuel element assembly for, insertion of solid Zircaloy 4 rod in plutonium oxide (PuO_2)--uranium oxide (UO_2), 25:44028 (DOCKET-50146-84)
fuel rods for, revised technical specifications for Zircaloy 4 clad plutonium oxide (PuO_2)--uranium oxide (UO_2) pellet type, 25:44029 (DOCKET-50146-85)
quality assurance program for, 25:44027 (DOCKET-50146-82)
SCANDIUM
chemical thermodynamic properties of, selected values of, 25:41826 (NBS-TN-270-5)
compounds, thermodynamic properties of, tables of, 25:41826 (NBS-TN-270-5)
determination of trace amounts of, in meteorites by neutron activation and γ spectrometry, 25:41773
magnetic susceptibility of, generalized function for, (T), 25:43477
separation from acetone--hydrochloric acid solutions by ion exchange using Bio-Rad, distribution coefficients for, 25:41899
separation from aqueous solutions by ion exchange on

zirconium tellurate, tracer studies on, 25:41915
SCANDIUM ISOTOPES
calcium--scandium Coulomb displacement energies, (E), 25:43883
scandium--titanium Coulomb displacement energies, (E), 25:43883
SCANDIUM ISOTOPES Sc-45
helium-3 reactions (de-3,t) at 24.6 MeV, triton spectra from, (E), 25:43883
neutron total cross section at 100 to 650 keV, optical model analysis of average, (E/T), 25:43908
SCANDIUM ISOTOPES Sc-49
beta decay of, gamma spectra from, (E), 25:43873
energy levels from calcium-49 beta decay, mixing ratios and spin--parity assignments for, (E), 25:43873
SCATTERING
amplitudes in dual resonance model, planar N-loop, 25:43718
amplitudes in dual resonance model, unitarization of, 25:43717
amplitudes of three-particle, solution in Amado model for, 25:43716
amplitudes of, complex vector parametrization of Lorentz group for partial-wave analysis of, 25:43720
amplitudes of, functional formulation of dual resonance, 25:43722
amplitudes of, functional formulation of N-particle Veneziano and planar and nonplanar one-loop, 25:43722
amplitudes of, review of crossing and positivity properties of partial waves for, 25:43711 (SU-1206-243)
amplitudes of, triple Regge vertex from asymptotic form of, 25:43723
amplitudes on dual resonance model, nonplanar N-loop, 25:43719
compound-state resonances in elastic, stabilization method for calculation of energies and widths of, 25:43147
conjugate variables in two-body, 25:43724
cross sections for attractive and repulsive Coulomb, fractional-order Bessel-function approximations to, 25:43132
Feynman diagrams for elastic, asymptotic behavior and duality without ghosts in, 25:43634
Monte Carlo model for linear parameter variation, 25:43504 (BMBW-FBK-70-32)
potential, threshold zeros and N/D method in Yukawa, 25:43713
SCHIZOMYCOTA
Bacillus subtilis, radiation effects on competence development in, in relation to multi-target state of cells, 25:42736
Bacillus subtilis, radiation effects on production of pyrimidine dimers in DNA of, uv, 25:42285
Escherichia coli, growth, incidence of mutations, and survival of, grown on γ-irradiated culture media, 25:42755
Escherichia coli, radiation effects on capacity to support bacteriophage growth, γ, 25:42730 (NYO-2804-41)
Escherichia coli, radiation effects on DNA-membrane association in minicells of mutant strain of, x, 25:42735
Escherichia coli, radiation effects on mutants of, defective in DNA replication, uv and x, 25:42331
Escherichia coli, radiation effects on prophage lambda induction in mutants of, defective in initiation of DNA replication at high temperatures, 25:42340
Escherichia coli, radiation effects on respiration in, uv, 25:42732
Escherichia coli, radiation effects on survival of, effects of acridine analogs on uv, 25:42533
Escherichia coli, radiation effects on synthesis of DNA and RNA in, effects of dose and genetic strain on γ, 25:42729 (NYO-2804-40)
Escherichia coli, radioinduced breaks in DNA of, relation of lethality to x, 25:42357
Escherichia coli, radioinduced degradation of DNA in, effects of genetic strain on γ, 25:42729 (NYO-2804-40)
Escherichia coli, radioinduced delay in replication of DNA of, effects of dose on uv, 25:42290
Escherichia coli, radioinduced DNA strand breaks in, repair mechanisms for γ, 25:42727 (NYO-2804-39)
Escherichia coli, radioinduced DNA strand breaks in, effects of anoxia and genetic strain on γ, 25:42728 (NYO-2804-39)
Escherichia coli, radioinduced mutations in thymine-dependent strains of, γ, 25:42330
Escherichia coli, radioinduced mutations in, effects of 5-bromouracil on sensitivity to uv, 25:42345
Escherichia coli, radioinduced single-strand breaks in DNA of mutants of, role of DNA polymerase in repair of x, 25:42326
Escherichia coli, radioinduced strand breaks of DNA in, effects of genetic strain and temperature on repair rate of γ, 25:42731 (NYO-2804-42)
Escherichia coli, radiosensitivity of lysogenic, effects of induction of infecting bacteriophage on γ, 25:42529
Escherichia coli, radiosensitivity of mutants of, in relation to gene location, uv, 25:42328
Escherichia coli, radiosensitivity of, as sanitary indicator, γ, 25:42743
Micrococcus glutamicus, radicinduced mutations in, review of fast neutron, gamma, and uv, 25:42349
Micrococcus lysodeikticus, recognition of pyrimidine dimers in DNA by endonuclease from, 25:42285
Proteus vulgaris, radiosensitivity of, as sanitary indicator, γ, 25:42743
Pseudomonas sp., spheroplast infection using DNA from PM2 bacteriophage, 25:42273
radiation effects on sterilization of, in milk, effects of dose on γ, 25:42742
radiosterilization of pathogenic, on beef and pork, public health aspects of, 25:42744(R) (COO-2038-2)
Salmonella typhi, radiosensitivity of, as sanitary indicator, γ, 25:42743
Streptococcus faecalis, radiosensitivity of, as sanitary indicator, γ, 25:42743
SCINTILLATION CAMERAS
data processing for cerebral studies, on-line computer, 25:42090
SEALS AND GLANDS
radiation effects on ceramic insulator, high-fluence neutron and gamma, 25:42228 (N-71-17325)
standard for coil and ring braided asbestos packings for valve stems and pumps, 25:43012 (RDT-M-11-2-T)
standard for nonmetallic seal materials for use in nuclear power plant components, 25:41975 (RDT-M-11-1-T)
SEAS
marine life activity on floor of, autonomous deep-sea cine camera system for photographing, 25:44308 (UCSD-34-P-127-10)
SEAWATER
radioactive waste disposal in, effects on marine organisms of, 25:42373
solvent properties for curium-244-oxide pellets and powders, 25:41993(R) (ORNL-4692)
SEED
protein synthesis in germinating, 25:44250 (COO-1313-28)
radiation effects on emergence of cucumber, effects of dose on γ, 25:42719
radiation effects on germination of barley, effects of oxygen and water on, 25:42296
radiation effects on tomato, mutagenic fast neutron and γ, 25:42364
radioinduced chromosome aberrations in dry Crepis capillaris, effects of nitrogen mustard on γ, 25:42359
radioinduced free radical formation in papaya, use as γ dosimeter, 25:42438
SEIGNETTOELECTRIC MATERIALS
radiation effects on barium titanate-type crystals, 25:43442
SEISMIC WAVES
ground motion from simple-array chemical-explosion-generated, calculations for predicting, 25:41950 (AD-718388)
propagation from earthquakes and Project Gasbuggy underground nuclear explosion, comparison of, 25:41952 (AD-838894)
SELENIUM
analysis for halogens, evaluation of methods for, 25:41734
determination of trace amounts of, in meteorites by neutron activation and γ spectrometry, 25:41773
neutron total cross section at 100 to 650 keV, optical model analysis of average, (E/T), 25:43908
separation from acetone--hydrochloric acid solutions by ion exchange using Bio-Rad, distribution coefficients for, 25:41899
separation from aqueous solutions by ion exchange on zirconium tellurate, tracer studies on, 25:41915
separation from other metals using inorganic ion exchange papers, 25:41909
SELENIUM ISOTOPES Se-75
gamma spectra of, for accuracy in diagnosis, phantom measurements on, 25:42397
use as tracer to measure wear of chromium plated surfaces, 25:42018
use with gold-198 for liver scanning, method for, 25:42580
SELENIUM ISOTOPES Se-76
neutron capture by, cross sections from thermal, (E), 25:43891(T) (RFP-Trans-78)
SELENIUM ISOTOPES Se-77
energy level at 161 keV from selenium-76 neutron capture, spin assignment for isomeric, (E), 25:43891(T) (RFP-Trans-78)
isomeric transition in, half-life for, (E), 25:43891(T) (RFP-Trans-78)
SELENIUM ISOTOPES Se-78
energy levels from arsenic-78 decay, spin-parity assignments for, (E), 25:43881
SELENIUM ISOTOPES Se-80
energy levels from γ resonance scattering, total radiative widths for, (E), 25:41833(R) (IA-1218)
SELENIUM ISOTOPES Se-81
beta decay of ground-state and isomeric, γ spectra and half-lives for, (E), 25:43844
SELENIUM ISOTOPES Se-82
beta decay of, search for double, (E), 25:43932
SEMICONDUCTOR JUNCTIONS
tunneling conductance anomaly and switching effect in

XUM

normal metal/insulator/metal, 25:42219
SEMICONDUCTORS
book: Advances in Solid-State Physics (in German and English), 25:43483
book: Introduction to the Theory of Solid State Physics, 25:43503
ion implantation in, 20- to 200-keV accelerator for, 25:43747
ion implantation into, design of electrostatic accelerator for, 25:43740(P)
superconductivity in quantizing films of, plasma waves and, (T), 25:43314
tunneling junctions, conductance anomaly and switching effect in metal/insulator/metal, 25:42219
SERINE
polymers, radiation effects on film properties of, γ, 25:41834
SEROTONIN
effects on adrenal glands, liver, ovaries, and thyroid glands in mice, 25:42519
effects on excretion of non-protein thiols in rat urine, combined effects of radioprotectors and, 25:42671
radiation effects on metabolism of, in animals and man as indicators of radiation injury, x, 25:42626
radiation effects on metabolism of, in animals as indicator of radiation injury, x, 25:42627
radioprotective effects of, on mouse adrenal cortex and reticulo-endothelial system, comparison of cysteamine and lipopolysaccharide with x, 25:42513
radioprotective effects of, on rat tissues, combined hypoxia and, 25:42511
radioprotective effects on planarians, x, 25:42527
SERPUKHOV SYNCHROTRON
experimental facility for, high-intensity 10- to 16-GeV/c negative particle beam, 25:43729(T) (CERN-Trans-71-16)
SEWAGE
hydrogen production from organic solid, feasibility study of using heat from contained underground nuclear explosions for, 25:41955
SF MATERIALS ACCOUNTING
safeguards experiment for, development of data reduction and limit of error model for, 25:42035(R) (BHJ-68-6)
SHELLS (GEOMETRY)
stress concentrations in cylindrical, with step changes in outside diameter, finite element studies of effects of fillets on, 25:41959 (CONF-710512-15)
SHELTERS
cost factors for high-protective-factor civil defense, 25:42505(R) (ORNL-4566(Pt.1))
design features of high-protective-factor quickly-constructed, for use in rural areas, 25:42506(R) (ORNL-4566(Pt.1))
design of above-ground fallout, for radiation protection, 25:42034(T) (JPRS-53499)
gamma dose fields in shielding structures and, (T), 25:43428
SHIELDED CONTAINERS
regulations for radioactive material for shipping in aircraft, 25:42456
regulations for radioactive material, for shipping in aircraft, 25:42457
SHIELDING
burn-out of cadmium, in thermal neutron field, 25:43422(T) (ORNL-tr-2488)
calculations for high-intensity beta source, 25:42016
calculations for, preparation of data sets in ENDF/B format for sodium, magnesium, chlorine, and potassium for, 25:43420 (ORNL-TM-3429)
cascade shower production in, model for systematics of extra-nuclear hadron, (T), 25:43613 (CERN-71-13)
design of magnetic, for cylindrical space vehicles from electron, 25:43425
development of biological, for SNAP-21, 25:41998
development of neutron source, 25:43418 (ORNL-RSIC-32)
effectiveness of lead, for protection of patients and personnel from implanted iridium-192 source, 25:42477
gamma dose fields in structures and shelters, (T), 25:43428
neutron attenuation in, computation of thickness required for, 25:43415 (NP-18853)
optimization of reactor, neutron and γ-ray fields and heat balance calculations for, (T), 25:44108
standards for high-energy radiation generators, 25:42464
SHIPPING
radiation protection recommendations for radioactive materials, by sea, 25:42449
radiation protection standards for radioisotope, by mail in Australia, 25:42494
regulations for radioactive materials, by air, quick reference guide to 1970 International Air Transport Association, 25:42457
regulations for radioactive materials, International Air Transport Association (1970), 25:42456
statute for radioactive materials, on roads in Great Britain, 1970, 25:42450
SHOCK WAVES
effects of nuclear weapon, on stability of operating fast breeder reactors, 25:42506(R) (ORNL-4566(Pt.1))
model for Vela X featuring, (T), 25:43039
shock normals in interplanetary space, single spacecraft method for estimating, (E/T), 25:43236
simulation of strong, in electromagnetic shock tubes, (T), 25:43360 (CU-3954-9)
structure of collisionless, in magnetoplasmas, (E/T), 25:43347
theory for gas dynamics of explosions, 25:43348
SIALIC ACIDS
radiation effects on content of, on surface of human erythrocytes, in relation to electrophoretic mobility of cells, x, 25:42682
SILICATES
analysis for strontium by atomic absorption spectroscopy, effects of aluminum and titanium on, 25:41735
sodium self-diffusion coefficients in glasses of, 25:41810
SILICON
charged-particle energy loss at 10 MeV to 100 GeV in, (T), 25:42155
crack propagation in monocrystalline, kinetics of, 25:42886 (UCRL-20500, pp 86-145)
effects on compaction of beryllium powder, model for, 25:42826
effects on corrosion resistance and mechanical properties of Zircaloy-2 and -4, 25:42876
electron reactions with foils of, transition radiation from 50-keV, (E/T), 25:43429
ion implantation with 300-, 400-, and 500-keV Ar^+ ions, technique for, 25:41832(R) (AECL-3851)
ion-implantation damage in, interference fringes in x-ray topographs of 2-MeV nitrogen, (E/T), 25:43465
ion-implantation damage in, stress measurements on 220-keV rare-gas, 25:43441
precipitation of second phases in high-purity, mechanisms of, 25:42886 (UCRL-20500, pp 86-146)
proton channeling at 1.5 MeV in crystals of, effects of surface and imperfections on, (E/T), 25:43461
proton channeling in, interaction potentials of, (T), 25:43456
proton energy spectra from single-crystal, high-energy humps in backscattered 0.5- and 1.0-MeV, (E), 25:43459
proton stopping power in planar channels of, effects of oscillation frequency on, 25:43455
radioinduced defects in, distribution of proton, deuteron, and alpha-particle, (E), 25:43463
radioinduced dimpling of thin single crystals of, annealing of 1.8-MeV helium-ion, (E), 25:43438
radioinduced precipitation during electron microscopic studies of, electron, 25:42886 (UCRL-20500, pp 86-146)
SILICON CARBIDES
fracture effects in self-bonded, at 25 to 1100°C, 25:42960
properties for use as outer coating on pyrolytic carbon-coated oxide particles, effects of internal pressure on, 25:42963
SILICON IONS
spectral levels in solar corona, autoionizing, (E), 25:43065 (AD-715257)
SILICON ISOTOPES Si-28
alpha elastic and inelastic scattering at 104 MeV, differential cross sections for, (E), 25:43832 (NP-18920)
alpha inelastic scattering at 104 MeV, quadrupole and hexadecapole deformation parameters from coupled-channels analysis of differential cross sections for, (E/T), 25:43876
alpha inelastic scattering at 22 MeV, α--γ coincidence spectra from, (E), 25:43854
deformation parameters from alpha inelastic scattering, (E/T), 25:43876
deuteron reactions (d,p) at 5 to 12 MeV, cross section and vector analyzing power for, (E), 25:43846
energy level at 1.78 MeV from proton inelastic scattering, calculation using deformed spin-orbit potential, 25:43963
energy levels from alpha inelastic scattering, lifetimes of, (E), 25:43854
SILICON ISOTOPES Si-29
energy levels from silicon-28 (d,p) reactions, spectroscopic factors and spin assignments for, (E), 25:43846
SILICON ISOTOPES Si-30
energy levels from aluminum-27 (α,p) reactions, lifetimes of, (E), 25:43879
SILICON JUNCTIONS
ion-implantation damage in, residual electrically active defects after lattice-reordering annealing of 2-MeV carbon, 25:43439
radiation effects on solar cells of, neutron, 25:42232
SILICON NITRIDES
analysis of films of, for nitrogen and oxygen by deuteron activation, 25:41832(R) (AECL-3851)
SILICON OXIDES
bonding in evaporated SiO films, nuclear reaction studies of, 25:42999
density of fused, relations with water content, 25:42957 (UCRL-20500, pp 147-73)
effects of gels of, on γ radiolysis of aliphatic amines at 77°K, ESR studies on, 25:41856
radio emission from, in interstellar materials, (E), 25:43052
reactions with zirconium dioxide at 1400°C to prepare zirconium silicate, kinetics of solid-state, 25:42940
stoichiometry of evaporated SiO films, nuclear reaction

studies of, 25:42999
Al_2O_3--SiO_2, phase studies of, 25:42957 (UCRL-20500, pp 147-73)
SILICON SYSTEMS
Al--Si, mixing in liquid and solid phases of, energy of, 25:42970
Al--Si--U, analysis for aluminum by atomic absorption spectroscopy, 25:41832(R) (AECL-3851)
Al--Si--Y, phase diagram at 500°C, isothermal, 25:42891
Cr--Si--Y, phase diagram at 800°C, isothermal, 25:42993
Eu--Gd--Si, structure of Gd/sub 5-x/Eu/sub x/Si_3, Moessbauer study of, 25:42895
Fe--Pd--Si, Moessbauer effect study of amorphous, 25:44238 (CALT-822-32)
Ga--Si, mixing in liquid and solid phases of, energy of, 25:42970
Sb--Si, mixing in liquid and solid phases of, energy of, 25:42970
SILTS
analysis for gold by neutron activation, 25:41770
radioisotope distribution in Ligurian Sea, measurements of artificial and natural, 25:41949
silver-108m content of, at Bikini and Eniwetok atolls following nuclear testing during 1958, 25:42377
uranium transport in lake, by microorganisms, 25:42256
SILVER
determination of trace amounts of, in zinc, spectrochemical, 25:41833(R) (IA-1218)
effects on reactions of americium with ammonium peroxydisulfate, kinetic studies on, 25:41785
effects on superconducting critical field of niobium--titanium alloy wires, 25:43309
elastic constants for, from 77 to 300°K, pressure dependence of, 25:44271 (NYO-2504-59)
separation from aqueous solutions by ion exchange on zirconium tellurate, tracer studies on, 25:41915
separation from other metals using inorganic ion exchange papers, 25:41909
SILVER ALLOYS AND SYSTEMS
Ag--Al-base, crystal stacking faults in, high-voltage imaging of, 25:42886 (UCRL-20500, pp 86-146)
Ag--Cd--In, fabrication of reactor control rods of, methods for, 25:42822
SILVER ISOTOPES Ag-104
energy levels from cadmium-104 decay, (E), 25:43945
SILVER ISOTOPES Ag-108
activity ratio of metastable, to silver-110m in Pacific Ocean following nuclear testing during 1958, 25:42377
content of metastable, in animals, plants, and sediments at Bikini and Eniwetok atolls following nuclear testing during 1958, 25:42377
SILVER ISOTOPES Ag-110
activity ratio of metastable, to silver-108m in Pacific Ocean following nuclear testing during 1958, 25:42377
SINGLE CRYSTALS
molecular beam scattering from surfaces of, 25:41778 (UCRL-20500, pp 1-85)
SKIN
radiation dose distribution in structural layers of, following penetration of surface contaminants, α and β, 25:42257
radiation dose to human, during diagnostic radiography, 25:42431
radiation effects on capillary permeability in rabbit, x, 25:42617 (UR-49-1452)
radiation effects on cytochrome oxidase and monoamine oxidase activity in human, x, 25:42286
radiation injuries to, effectiveness of petroleum growth substance for treatment of β, 25:42539
radioisotope distribution kinetics in, following surface contamination, 25:42257
strontium-89 distribution in, following surface contamination, dose measurements on, 25:42371
SODIUM
boiling in liquid metal cooled reactors, initiation and thermal hydraulics aspects of, (E/T), 25:44132 (AI-AEC-12992)
boiling of liquid, in heat pipes, method for calculating surface heat flux for incipient, 25:41982
combustion in liquid metal cooled reactor accidents, release and transport of aerosols and energy from, (E/T), 25:44132 (AI-AEC-12992)
combustion of, comparison of effectiveness of dry powders for extinguishing, 25:42837 (AERE-R-6745)
diffusion in glasses, isotopic exchange measurements of self-, 25:41810
fluorescence of, quenching of, 25:41778 (UCRL-20500, pp 1-85)
hydrogen content in liquid, electrochemical meter for continuous measurement of, 25:42207(R) (UNC-5258)
impurities in liquid, development of in-line vacuum-distillation sampling equipment for detecting, 25:44115
impurities in liquid, in LMFBR test loops, monitoring and control of, 25:42804(R) (LMEC-71-1)
leakage from reactor coolant, standard for guard vessel for collecting, 25:41969 (RDT-E-10-2-T)
monitoring of vapors of, system based on atomic absorption of sodium light for, 25:42048 (ANL-7710, pp 263-364)
polarizability of atomic, perturbation calculation of, 25:43117
reactions with leaking steam or water in boilers, effects on steel tubes, 25:42804(R) (LMEC-71-1)
separation from acetone--hydrochloric acid solutions by ion exchange using Bio-Rad, distribution coefficients for, 25:41895
separation from aqueous solutions by ion exchange on zirconium tellurate, tracer studies on, 25:41915
separation from biological samples prior to activation analysis, 25:41760
solvent properties of liquid, for argon and helium, effects of pressure and temperature on, 25:41823 (ANL-7862)
standard for purchase specifications for reactor-grade, 25:42801 (RDT-M-13-1-T)
standard for venturi flow tube for liquid, 25:41964 (RDT-C-4-4-T)
superconducting parameter calculations, 25:43305
temperature distribution in flowing, in annular channels with excentrically mounted inner heating element, 25:41984 (INIS-mf-26)
SODIUM ACID PHOSPHITES
radiolysis of aqueous solutions of, effects of nitrates and nitrites on kinetics of production of atomic hydrogen from γ, 25:41850(R) (CEA-N-1438)
SODIUM CARBIDES
radiation effects on, reactions of recoil nitrogen-13 from deuteron, 25:41886
SODIUM CHLORATES
radiation effects on crystals of, ESR spectrum after 200°C thermal bleaching of x-, 25:43451
SODIUM CHLORIDES
corrosive effects of aqueous, on aluminum--magnesium--zinc alloys, 25:42886 (UCRL-20500, pp 86-146)
ion channeling in, 1-MeV He^+, (E), 25:41832(R) (AECL-3851)
radioinduced defects in single crystals of, interactions with positrons, 25:43453
stability of trimers and tetramers of, 25:42957 (UCRL-20500, pp 147-73)
SODIUM IODIDES
photodissociation of, quenching of excited sodium from, 25:41778 (UCRL-20500, pp 1-85)
SODIUM ISOTOPES
separation by isotachophoresis, 25:41923
SODIUM ISOTOPES Na-22
effects on isotachophoresis of sodium, 25:41923
metabolism and tissue distribution following intake by man, 25:42467
use for scintigraphy of human brain for localization of tumors, 25:42565
SODIUM ISOTOPES Na-23
energy levels from magnesium-24 (t,α) reactions, spin assignments for, (E), 25:43880
energy levels from photon resonance scattering, spin assignments and widths for, (E), 25:43838
energy-level transitions from magnesium-24 (t,α) reactions, branching and mixing ratios for, (E), 25:43880
neutron capture by, cross sections and gamma spectra from thermal, (E), 25:43891(T) (RFP-Trans-78)
neutron inelastic scattering up to 1.5 MeV, γ spectra from, 25:43884 (ANL-7710, pp 1-52)
photon elastic and inelastic scattering at 2 to 4 MeV, spectra from, (E), 25:43838
SODIUM ISOTOPES Na-24
effects on isotachophoresis of sodium, 25:41923
energy level at 472 keV from sodium-23 neutron capture, spin assignment for isomeric, (E), 25:43891(T) (RFP-Trans-78)
isomeric transition in, half-life and gamma spectra from, (E), 25:43891(T) (RFP-Trans-78)
SODIUM NITRATES
LiCl--$NaNO_3$, molal volumes for aqueous solutions of, 25:41833(R) (IA-1218)
SODIUM SILICATES
chemical activities of oxides of cobalt, iron, and nickel in, at 700 to 1100°C, 25:42957 (UCRL-20500, pp 147-73)
SOILS
book: Recommendations on the Use of Radioisotope Methods for Determining the Physico-mechanical Properties of Soils, 25:42176
carbonate--phosphate precipitation in marl lake, 25:44252 (CCO-1599-33)
physicochemical properties of, around CSN Casaccia, Italy, 25:41930
properties of heated, at 100 to 1000°C, chemical, electric, and physical, 25:41926 (UCLA-12-819)
radioactivity monitoring in Western Australia, natural α, 25:42427
radioisotope sorption by sierozem, cerium-144, cesium-137, and strontium-90, 25:42319
radioisotope uptake by oat plants from, effects of fertilizers on, 25:42260
radon content in Indian, use for uranium exploration, 25:41945
sorptive properties of Casaccia, Italy, for cesium and strontium, 25:41930
SOLAR CELLS
cover glass for, effects of cerium doping on improved radiation resistance of, 25:43008 (N-71-12278)
radiation effects on silicon, low-energy proton,

XUM

25:42226 (AD-715261)
radiation effects on silicon, neutron, 25:42232
radiation resistant lithium-diffused, development of, 25:42227(R) (N-71-12257)
SOLAR CORONA
ionizing states in, auto-, (E), 25:43065 (AD-715257)
structure of transition region with chromosphere, (T), 25:43068 (N-71-19294)
SOLAR FLARES
magneto-acoustic wave propagation in, exact solutions for, (T), 25:43073
proton penetration over polar cap during Feb. 25, 1969, satellite measurements of, (E), 25:43232
proton penetration to polar caps during Jan. 24, 1969 event, asymmetric access of, (E), 25:43233
radio map of, (E), 25:43064
SOLAR PARTICLES
energy spectra of protons, alpha particles, and Z greater than or equal to 3 nuclei, July 20, 1967 to May 14, 1968, (E), 25:43231
mass/charge number composition of, magnetic double-focusing mass spectrograph for measurement of, 25:43221(R) (N-71-21469)
production and acceleration of, (E/T), 25:43067 (N-71-16749)
SOLAR RADIATION
effect on sidereal diurnal cosmic-ray anisotropies, (T), 25:43177
radio emission at 19 GHz, atmospheric attenuation of, (E), 25:43071
SOLAR RADIO BURSTS
model for U-Type, (E), 25:43070 (N-71-21564)
observation of U-Type, at 0.7 to 5 MHz, (E), 25:43070 (N-71-21564)
SOLAR SPICULES
relation to structure of corona--chromosphere transition region, (T), 25:43068 (N-71-19294)
SOLAR SYSTEM
composition of, chemical, (T), 25:43078
precession in, corrections for, (T), 25:43048
SOLAR WIND
direction discontinuities from Dec. 18 to 25, 1965 in, nature and origin of, (E/T), 25:43237
helium and hydrogen abundance from cosmic dusts saturated with solar-wind gases, inner solar system, (E/T), 25:43176
implantation of helium, neon, and argon isotopes in lunar materials, (E), 25:43099
interaction with atmospheres of Venus and Mars, space-probe data of, (E), 25:43272
magnetic field of, relation to magnetotail configuration changes, (E/T), 25:43239
mass/charge number composition of, magnetic double-focusing mass spectrograph for measurement of, 25:43221(R) (N-71-21469)
proton enhancements during Feb. 25, 1969 event over polar cap, mechanism of, (E/T), 25:43232
proton penetration to polar caps during Jan. 24, 1969 event, asymmetric access of solar, (E), 25:43233
SOLID STATE PHYSICS
book: Advances in Solid-State Physics (in German and English), 25:43483
book: Introduction to the Theory of Solid State Physics, 25:43503
conference on nuclear physics and, Roorkee, India, 12/69, 25:43466 (CONF-691208-(Vol.3))
irreducible multiplier representations in, method for constructing, 25:43501
Mathieu equation in, eigenvalues for, 25:43505 (EUR-4349)
research summary for 1970 in, Inorganic Materials Research Div., UCRL, Berkeley, 25:43470 (UCRL-20500, pp 175-204)
SOLIDS
atom reactions with surfaces of, classical model for, 25:43104
plastic deformation in, at low temperatures, crowdion mechanism of, (E/T), 25:43484
SOLVENT EXTRACTION PROCESSES
optimization for purification of nuclear materials, 25:41916
SOLVENTS
disposal of waste, 25:44221 (ANCR-1006)
SOUND
emission during creep in aluminum, cadmium, and lead, (E), 25:42862
emission during creep, theory of, 25:42861
SOUTH AMERICA
fallout content of milk in, during 1970, 25:42417
radioactivity monitoring in surface atmosphere during November 1970, gross β, 25:42426
radioactivity monitoring in surface atmosphere during October 1970, gross β, 25:42418
radioisotope content of milk in, during November 1970, 25:42421
SOUTHWEST EXPERIMENTAL FAST OXIDE REACTOR
kinetics for, sub-prompt critical transient tests for Core 1, 25:44152 (DOCKET-50231-89)
operating experience with, summary of, 25:44128 (CONF-710315-20)
operations aspects of, follow-on program content and schedule for, 25:44153 (DOCKET-50231-90)
reactivity feedback effects in Core 1, balanced oscillator experiments for, 25:44151 (DOCKET-50231-88)
SOVIET UNION
cesium-137 content of human population in, during 1966 to 1968, calculation of genetic dose from, 25:42376
polonium-210 content of environment and human tissues in, 25:42429
SPACE
book: Advances in Space Science and Technology, Vol. 9, 25:43077
gravitation in interstellar, (T), 25:43089
shock normals in interplanetary, single spacecraft method for estimating, (E/T), 25:43236
x-ray attenuation in interstellar and intergalactic, (T), 25:43080 (N-71-21563)
SPACE FLIGHT
energy sources for future, 25:43191
SPACE VEHICLES
conference on prospect for use of orbital stations and space shuttles, Rome, Italy, 4/71, 25:43017
environment control within manned, electric--thermal integration of cobalt-60-fueled organic Rankine cycle power supply system in, 25:42005
life support system for manned, electric--thermal integration of cobalt-60-fueled organic Rankine cycle power supply system in, 25:42005
life support systems for, evaluation of radioisotope thermal energy sources for, 25:42004
power supplies for manned, computer analysis of plutonium-238-fueled organic Rankine cycle system for, 25:42003
power supply system for, development of ISOTEC thermoelectric generator for, 25:42006
power supply systems for, development of closed Brayton cycle, 25:42007
power system for manned space stations, design of 25 kW(e) thermoelectric reactor, 25:44171
power system for, design studies of plutonium-238-fueled Stirling engine for auxiliary, 25:42010
power systems for, analog computer simulation of dynamics of Brayton cycle, 25:42009
propulsion of, design study of radioisotope-heated subliming microthruster for, 25:42017
propulsion of, inductive plasma accelerator for, 25:43351
shielding against electrons of cylindrical, magnetic shield design for, 25:43425
SPAIN
uranium prospecting in, review of nuclear methods for, 25:41946
SPECTRA
atomic oscillator strengths along isoelectronic sequences, (E/T), 25:43114
SPECTROMETERS
design and performance of digital, for nuclear spectroscopy, 25:42121
design of electrostatic cylindrical mirror-type, 25:42215
design of superconducting, using kinetic inductance effects, 25:42097
design parameters for one-gap broad-range heavy-particle magnetic, with cylindrical symmetry, 25:42221
development of high-rate time-of-flight, for heavy particles produced in nuclear reactions, 25:42066
SPECTROPHOTOMETERS
corrected fluorescence spectra by computer postprocessing, 25:44306 (UCRL-73161)
design modification of Bausche and Lomb Spectronic 20, for monitoring chromatographic columns, 25:44243 (COO-1222-45)
SPECTROSCOPY
conference on, Pittsburgh, Cleveland, Ohio, Feb. 28 to March 5, 1971, abstracts, 25:41720 (CONF-710207-(Absts.))
conference on, Pittsburgh, Cleveland, Ohio, March 1-6, 1970, abstracts, 25:41719 (CONF-700303-(Absts.))
data correction for, iterative computer method for, 25:42108 (UUIP-701)
research progress in, annual report, 1969--70 on, 25:43468 (NP-18657)
SPERM
precedence determination in spruce budworms, using carbon-14 and tritium, 25:42259
SPERMATOGENESIS
radiation effects on, in Japanese fishermen, fallout, 25:42681
SPERMATOGONIA
radioinduced chromosome translocations in, of mice in relation to radioresistant cell lines, fast neutron, 25:42355
radioinduced mutations in Drosophila, comparison of effects of acute, chronic, and split-dose exposure on low-dose γ, 25:42350
SPHALERITES
analysis of Luzon, Philippines, for trace elements by neutron activation, 25:41772
SPHERES
neutron transport in, computer program for solution of integral equation for, (T), 25:43771 (EIR-189)
SPINELS
mechanical properties of freeze-dry prepared, 25:42957

(UCRL-20500, pp 147-73)
microstructure of freeze-dry prepared, 25:42957 (UCRL-20500, pp 147-73)
SPLEEN
function studies of, use of metastable technetium-99-labeled erythrocytes for, 25:42570
radiation effects on content of sulfur-containing amino acids in proteins in rat, 25:42265
radiation effects on distribution of acid phosphatase and β-glucuronidase in rat, whole-body x, 25:42628
radiation effects on distribution of iodine-131-labeled albumin in rat, as indicator of radiation injury, whole-body γ, 25:42407
radiation effects on metabolism of selenium-75 and sulfur-35 in rat, x, 25:42264
radiation effects on oxidation-reduction potential in rat, protective effects of AET, MEA, or serotonin in combination with hypoxia against x, 25:42511
radiation effects on stem cells in mouse, effects of actinomycin D on erythropoietic recovery following partial-body x, 25:42673
redox potential of, effects of radioprotective substances on, 25:42526
scintigraphy of human, using technetium-99m-labeled sulfur colloid for diagnosis of Hodgkin's disease, 25:42585
scintigraphy using copper-64-labeled erythrocytes and positron camera, 25:42564
STABLE ISOTOPES
separation at ORNL during 1968 and 1969, review of program for electromagnetic, 25:41992 (ORNL-4640)
STACK DISPOSAL
sulfur dioxide monitoring for, activation method for, 25:41759(P)
STAINLESS STEEL
chemical reactions of Type 304 and Type 316 with plutonium oxide (PuO_2)--uranium oxide (UO_2) fuels, effects of gas cooled fast breeder reactor conditions on, (E/T), 25:44123 (ORNL-TM-3385)
corrosion by chlorides in reactor steam generators, stress, 25:42804(R) (LMEC-71-1)
corrosion of stressed Type 304, at various potentials of magnesium chloride, scanning electron microscopic studies of, 25:42760(R) (COO-2069-7)
failure of reactor components of type 304, effects of corrosion and tensile stresses on, 25:42838 (CONF-710512-1)
friction and wear of Type 316, sliding against similar material in liquid sodium, 25:42804(R) (LMEC-71-1)
magnetic permeability of austenitic, effects of machining and working on, 25:43467 (IPPJ-LT-20)
mechanical properties of tubes of Type 316, effects of prolonged heating on, 25:42846 (JAERI-13578)
microstructure of tubes of Type 316, effects of prolonged heating on, 25:42846 (JAERI-13578)
radiation effects on creep rupture properties and microstructure of Type 304, at 600°C, fast neutron, 25:42922
radiation effects on creep rupture properties of niobium-stabilized, relations of heat treatments, cold work conditions, and irradiation temperature of fast neutron, 25:42924
radiation effects on mechanical properties of Type 19-9DL, at 55 to 413°C, fast neutron, 25:42923
radiation effects on microstructure and tensile properties of solution-treated Type 316, relations of irradiation temperature with pile neutron, 25:42919
radiation effects on tensile properties of borated Type 304, at 70 to 1450°F, fast neutron, 25:42911
radiation effects on tensile properties of Type 347, relations of irradiation temperature with fast neutron, 25:42912
radiation effects on uniaxial fatigue of Types 304, 304L, and 316, at 400 to 700°C, fast neutron, 25:42921
radiation effects on void growth in, model for kinetics and mechanism of neutron, 25:42916
radioinduced void formation in Type 316, at 500°C, 1.2-MeV proton, 25:42917
sorptive properties for cesium at 300 to 1000°F, tracer studies on, 25:42863
standard for bars of Types 403 and 410, 25:42799 (RDT-M-7-1-T)
standard for castings of, for high-temperature service, 25:42789 (RDT-M-4-2-T)
standard for forgings of Type 403, 25:42777 (RDT-M-2-6-T)
standard for seamless and welded pipes of austenitic, 25:42784 (RDT-M-3-6-T)
standard for seamless pipes of austenitic, 25:42781 (RDT-M-3-3-T)
standard for seamless tubes of, 25:42780 (RDT-M-3-2-T)
standard for welded tubes of austenitic, 25:42783 (RDT-M-3-5-T)
weld defects in Type 310, origin and effects of, 25:42867
weld solidification in, structures and mechanism of, 25:42820
Cr--Ni--stainless steel, standard for pipes of, 25:42785 (RDT-M-3-7-T)
Cr--Ni--stainless steel, standard for plates, sheets, and strips of, 25:42791 (RDT-M-5-1-T)
Cr--stainless steel, standard for plates, sheets, and strips of, 25:42791 (RDT-M-5-1-T)
STAINLESS STEEL COUPLES
stainless steel/U, corrosion of, effects of capacitance discharge and frequency on galvanic, 25:41833(R) (IA-1218)
STANDARDS
alloy steel bolting materials for high temperature service, modified ASTM A193, 25:42798 (RDT-M-6-3-T)
alloy steel bolting materials for low-temperature service, modified ASTM A320, 25:42797 (RDT-M-6-1-T)
analysis of iron and steel from National Bureau of Standards for trace elements by neutron activation and γ spectrometry, 25:41774
brazing filler metal, modified ASTM B260, 25:42769 (RDT-M-1-9-T)
calcium silicate block and pipe thermal insulation, ASTM C533 with additional requirements, 25:43014 (RDT-M-12-2-T)
calibration of instruments, 25:42205 (RDT-F-3-2-T)
carbon steel castings suitable for fusion welding for high-temperature service, modified ASTM A216, 25:42788 (RDT-M-4-1-T)
carbon steel forgings, modified ASTM A105, 25:42773 (RDT-M-2-1-T)
carbon steel pipe for high temperature service, modified ASTM A106, 25:42779 (RDT-M-3-1-T)
carbon steel plates for pressure vessels for moderate and lower-temperature service, modified ASTM A516, 25:42792 (RDT-M-5-2-T)
chromium and nickel--chromium stainless steel plate, sheet and strip, modified ASTM A240, 25:42791 (RDT-M-5-1-T)
chromium--cobalt alloy wear- and corrosion-resistant castings, 25:42790 (RDT-M-4-3-T)
chromium--iron--nickel alloy plates, sheets, and strips, modified ASTM B168, 25:42794 (RDT-M-5-4-T)
chromium--molybdenum alloy steel plates, modified ASTM A387, 25:42795 (RDT-M-5-5-T)
cleaning and cleanliness of reactor components, 25:44089 (RDT-F-5-1-T)
condensers and heat exchanger tubes, seamless annealed nickel--chromium--iron alloy, modified ASTM B163, 25:42782 (RDT-M-3-4-T)
construction of power reactor cooling system components, 25:43993 (RDT-E-15-2-T)
control rod drives for sodium service, 25:44105 (RDT-E-6-5-T)
copper and copper alloy arc-welding electrodes, modified ASTM B225, 25:42767 (RDT-M-1-7-T)
copper and copper alloy welding rods, modified ASTM B259, 25:42768 (RDT-M-1-8-T)
corrosion-resistant chromium and chromium--nickel steel-covered welding electrodes, modified ASTM A298, 25:41972 (RDT-M-1-1-T)
displacement gages for use in liquid sodium, standard for design and testing of, 25:42201 (RDT-C-8-2-T)
drinking water, in USA, Public Health Service Publication No. 956 (1962), 25:42470
electric connectors for nuclear instruments, coaxial high-voltage, ANSI N42.4-1971, 25:42214
electric insulators for high-temperature instrument use, ceramic, 25:42204 (RDT-C-18-1-T)
electromagnetic pump for liquid metal service, 25:41967 (RDT-E-3-9-T)
examination and acceptance requirements for seal membranes, 25:41974 (RDT-M-9-2-T)
factory-made wrought austenitic steel welding fittings, modified ASTM A403, 25:42776 (RDT-M-2-5-T)
film badge services, 25:42165
flowmeter for liquid metals, standard for permanent magnet, 25:42191 (RDT-C-4-5-T)
freeze vent for sodium service, 25:41968 (RDT-E-4-13-T)
fuel assembly identification markings, ANS 13.8, 25:43955
Geiger--Mueller detectors, ANSI N42.3 standard test procedure for, 25:42057
guard vessel for primary sodium-containing components, 25:41965 (RDT-E-10-2-T)
impregnated asbestos packing material, 25:43012 (RDT-M-11-2-T)
index of U.S. voluntary engineering, 25:41961 (NBS-SPEC. PUBL-329)
inspection of materials in reactor cooling system wear applications, 25:44210 (RDT-F-3-7-T)
insulation compaction in ceramic insulated conductors, determination of, 25:42190 (RDT-C-2-1-T)
level indicator for liquid metals, design and testing of inductive, 25:42192 (RDT-C-5-1-T)
level indicator for liquid metals, design and testing of resistive, 25:42193 (RDT-C-5-2-T)
liquid metal valves, small Class II, 25:41966 (RDT-E-1-19-T)
low alloy steel covered arc-welding electrodes, modified ASTM A316, 25:42765 (RDT-M-1-4-T)
manganese--molybdenum steel and manganese--molybdenum--nickel alloy steel plates for pressure vessels, modified ASTM A533, 25:42793 (RDT-M-5-3-T)
marking of wrought metal products, requirements for identification, 25:42762 (RDT-F-7-1-T)
mechanical locking devices for fasteners, 25:41973 (RDT-M-6-2-T)

XUM

mild steel covered arc-welding electrodes, modified ASTM A233, 25:42764 (RDT-M-1-3-T)
neutron flux monitoring channels in reactors, 25:44209 (RDT-C-15-2-T)
nickel and nickel alloy bare welding rods and electrodes, modified ASTM B304, 25:42771 (RDT-M-1-11-T)
nickel and nickel alloy covered welding electrodes, modified ASTM B295, 25:42770 (RDT-M-1-10-T)
nondestructive testing, 25:42025 (RDT-F-3-6-T)
nonmetallic seal materials for use in nuclear power plant components, 25:41975 (RDT-M-11-1-T)
orifice plate for orifice flange union, 25:41963 (RDT-C-4-1-T)
preloading threaded fasteners and closures, 25:41971 (RDT-F-8-1-T)
preparations for sealing, packaging, packing, and marking components for shipment and storage, 25:41970 (RDT-F-7-2-T)
pressure gages for liquid metal, standard for design and testing of eddy current, 25:42195 (RDT-C-6-3-T)
protection systems for reactors, 25:44142 (RDT-C-16-1-T)
quality assurance programs for reactor development projects, 25:44088 (RDT-F-2-2-T)
quality verification program requirements, 25:42022 (RDT-F-2-4-T)
quenched and tempered vacuum-treated carbon and alloy steel forgings for pressure vessels, modified ASTM A508, 25:42778 (RDT-M-2-7-T)
radiation protection for pupils in schools using ionizing radiations and radiation sources for demonstrations and experiments, ICRP (1968), 25:42473
radiation protection, basis of ICRP (1965), 25:42466
radiation protection, evolution of USA and international, 25:42452
radiation protection, for human populations, review of background data for, 25:42692
radiation protection, for human populations, review of background data for, 25:42693
radiation protection, for medical personnel and patients during use of sealed radiation sources for therapy, 25:42491
radiation protection, for medical personnel and patients during diagnostic radiography, 25:42493
radiation protection, for medical personnel using sealed radiation sources for therapy, 25:42492
radiation protection, for personnel in nuclear industry and research in Australia, 25:42495
radiation protection, for school children watching demonstrations using ionizing radiations, 25:42489
radiation protection, for sealed gamma source industrial radiography, 25:42490
radiation protection, for shipping radioisotopes by mail in Australia, 25:42494
reactor-grade sodium purchase specifications, 25:42801 (RDT-M-13-1-T)
recording potentiometer, multipoint strip-chart, 25:42203 (RDT-C-9-2-T)
recording potentiometer, single-point strip-chart, 25:42202 (RDT-C-9-1-T)
safety for x-ray diffraction and fluorescence analysis equipment, ANSI N43.2 1967, 25:42225
seamless and welded stainless steel pipe, modified ASTM A312, 25:42784 (RDT-M-3-6-T)
seamless austenitic stainless steel pipe, modified ASTM A376, 25:42781 (RDT-M-3-3-T)
seamless ferritic alloy steel pipe, modified ASTM A335, 25:42787 (RDT-M-3-12-T)
special requirements for metal products, July 1971, 25:42817 (RDT-F-3-37-T)
stainless and alloy steel seamless tubes, ASME SA-213 with additional requirements, 25:42780 (RDT-M-3-2-T)
stainless steel bars, Types 403 and 410, modified ASTM A276, 25:42799 (RDT-M-7-1-T)
stainless steel castings for high-temperature service, modified ASTM A351, 25:42789 (RDT-M-4-2-T)
stainless steel forgings, Type 403, modified ASTM A473, 25:42777 (RDT-M-2-6-T)
stainless steel welding rods and bare electrodes, ASME SFA-5.9 with additional requirements, 25:42763 (RDT-M-1-2-T)
steam generators for pressurized water reactors, 25:44081 (RDT-E-4-1-T)
steel electrodes and welding rods for gas--metal--arc welding, modified ASTM A559, 25:42766 (RDT-M-1-6-T)
steel forgings, modified ASTM A336, 25:42775 (RDT-M-2-4-T)
thermal insulating materials for use on stainless steel, 25:43013 (RDT-M-12-1-T)
thermocouple material, copper and Constantan, solid conductor, 25:42198 (RDT-C-7-3-T)
thermocouple material, magnesium oxide-insulated Constantan/Fe, 25:42197 (RDT-C-7-2-T)
thermocouple materials, solid conductor iron and Constantan, 25:42196 (RDT-C-7-1-T)
thermocouples of Alumel/Chromel-P, magnesium oxide insulated and stainless steel sheathed, 25:42200 (RDT-C-7-6-T)
thermocouples of Constantan/Cu, magnesium oxide-insulated and stainless steel sheathed, 25:42199 (RDT-C-7-4-T)
ultrasonic examination of heavy steel forgings, modified ASTM A388, 25:42761 (RDT-F-3-3-T)
ultrasonic examination of metal pipe and tubing for longitudinal discontinuities, modified ASTM E213, 25:42026 (RDT-F-3-8-T)
ultrasonic examination of plain and clad steel plates, modified ASTM A578, 25:42024 (RDT-F-3-5-T)
ultrasonic shear-wave examination of plates, modified ASTM A577, 25:42023 (RDT-F-3-4-T)
valves for liquid metal service, Class I, 25:41965 (RDT-E-1-18-T)
venturi flow tube for liquid sodium, 25:41964 (RDT-C-4-4-T)
welded austenitic stainless steel tubing, modified ASTM A249, 25:42783 (RDT-M-3-5-T)
welded large diameter chromium--nickel alloy steel pipe, modified ASTM A358, 25:42785 (RDT-M-3-7-T)
welding qualifications, supplement to ASME Boiler and Pressure Vessel Code Section IX, 25:42850 (RDT-F-6-5-T)
welding, examining, and testing of water-cooled reactor coolant systems and liquid metal heat transfer systems, 25:42849 (RDT-F-6-1-T)
wrought seamless carbon steel welding fittings, modified ASTM A234, 25:42774 (RDT-M-2-3-T)
zirconium and zirconium alloy bare welding rods, ASTM B351 with additional requirements, 25:42772 (RDT-M-1-16-T)
zirconium and zirconium alloy ingots, ASTM B350 with additional requirements, 25:42800 (RDT-M-10-1-T)
zirconium and zirconium alloy plate, sheet, and strip, ASTM B352 with additional requirements, 25:42796 (RDT-M-5-6-T)
zirconium and zirconium alloy tubes, ASTM B353 with additional requirements, 25:42786 (RDT-M-3-8-T)

STAR CLUSTERS
age of M71, (E), 25:43035
color--magnitude diagram for M71, (e), 25:43035
expansion of Orion Nebula, (E), 25:43038
metal abundance in M71, (E), 25:43035
star evolution in, (E), 25:43018 (N-71-19301)

STARS
abundance analysis of super-metal-rich k-giant, (E), 25:43018 (N-71-19301)
color--color diagram for carbon, (E), 25:43037
conference on uv stellar spectra and related ground-based observations, Lunteren, Netherlands, 6/69, 25:43031
distribution in solar neighborhood, (E/T), 25:43027
gravity variations in β Dor, surface, (E), 25:43045
light curve and apsidal motion of AR Cas, (E), 25:43046
lithium abundance in α Aur, (E), 25:43036
luminosity of carbon, (E), 25:43037
magnitude of β Dor, (E), 25:43045
motions of, determination of correction to precession from proper, (T), 25:43046
motions of, proper, (E/T), 25:43029
orbital elements of eclipsing variable, program for, (E), 25:43020
orbital elements of Z Vul, (E), 25:43020
orbits of spectroscopic binary, (E/T), 25:43047
period of DP Aquarii, (E), 25:43021
photometry in Hβ of A-Type, near North Galactic Pole, (E), 25:43043
photometry of blue-straggler, (T), 25:43018 (N-71-19301)
polarimetric obervations of 11 infrared, (E), 25:43042
polarization of high-luminosity red-variable, variation of, (E), 25:43024
pulsations of rapidly rotating, nonlinear, (T), 25:43022
pulsations of upper layers of Cepheid, (E/T), 25:43026
radio observations of nebulae around Wolf--Rayet and ED + 60°2522, (E), 25:43044
radius of β Dor, mean, (E), 25:43045
relativistic effects in rapidly rotating, (t), 25:43093
right ascensions of 231 pairs of, (E), 25:43028
spectra of IRC + 10206, origin of reported millimeter continuum in, (E), 25:43040
spectra of WR, (E/T), 25:43030
spectra of zeta Tauri, rapid variations in, (E), 25:43041
spectral analysis of HD 204075, (E), 25:43019 (NBS-MON-119)
spectral classification of carbon, (E), 25:43037
stability of rapidly rotating, (T), 25:43022
temperature of β Dor, effective, (E), 25:43045
thermonuclear detonations in evolved cores of, (T), 25:43033
ultraviolet spectra of, conference papers on, 25:43031

STATISTICS
book: A Book of Splines, 25:44310
formulation of statistical mechanics, solvable model in quantum field theory for Araki--Woods, 25:43668
role in determining sampling requirements for quality assurance during reactor fuel fabrication, 25:42033

STEAM
corrosive effects on copper--iron--zirconium-base alloys at 500°C, 25:42810
corrosive effects on Zircaloy and chromium--iron--zirconium-base alloys at 300 to 400°C, kinetics, 25:42815
reactions with leaking heated sodium in boilers, effects on steel tubes, 25:42804(R) (LMEC-71-1)

STEAM POWER PLANTS
environmental effects of fossil fueled, comparison with nuclear plants of, 25:44143 (SGAE-RT-39/1971)

STEARATES
effects on fabrication of plutonium dioxide--uranium dioxide and uranium dioxide pellets, 25:42949
STEEL
analysis for molybdenum by atomic absorption spectrometry, 25:41728
analysis of standards of cast, for antimony, lanthanum, and vanadium by neutron activation and γ spectrometry, 25:41774
annealing of Type 4988, in uranium monocarbide powder, precipitation behavior after, 25:42844 (EURFNR-922)
embrittlement of TRIP, mechanisms of hydrogen, 25:42886 (UCRL-20500, pp 86-146)
fracture behavior of thick-walled pressure vessel, effects of radioinduced toughness gradient on, 25:42841 (CONF-710512-8)
fracture mechanisms in metastable austenitic, under cyclic loading, 25:42886 (UCRL-20500, pp 86-146)
fracture of pressure vessel, use of elastic-wave emissions for in-service monitoring of, 25:42840 (CONF-710512-4)
fracture toughness of Type 1070, effects of second-phase morphology on, 25:42886 (UCRL-20500, pp 86-146)
mechanical properties of irradiated Types A302B, A542, and HY-80, effects of hydrogen on, 25:42871
mechanical properties of Type 4988, effects of annealing in uranium monocarbide powder on, 25:42844 (EURFNR-922)
notch sharpening of large fracture test specimen of A533B, effects of fatigue from local compressive stresses on, 25:42843 (CONF-710512-10)
preparation for incorporation of TRIP characteristics in, method for, 25:42886 (UCRL-20500, pp 86-146)
preparation of high-strength metastable, method for, 25:42886 (UCRL-20500, pp 86-146)
radiation effects on embrittlement of A302-B, neutron, (E/T), 25:44116
radiation effects on embrittlement of pressure vessel, review of relations of composition and microstructure with neutron, 25:42910
radiation effects on fracture and tensile properties of Type A533B pressure vessel, fast neutron, 25:42901 (HEDL-TME-71-76)
radiation effects on mechanical properties of low-carbon, relations of microstructure with fast neutron, 25:42925
radiation effects on mechanical properties of quenched and tempered, fast neutron, 25:42909
radiation effects on mechanical properties of Types A212B and A533B, fast neutron, 25:42905
radioinduced embrittlement of Type A533B, effects of control of residual element content on resistance to fast neutron, 25:42907
radioinduced embrittlement of Types A302B, A-336, A533B, and A542, evaluation of fast neutron, 25:42906
standard for boiling materials for high-temperature service, 25:42798 (RDT-M-6-3-T)
standard for factory-made wrought welding fittings of austenitic, 25:42776 (RDT-M-2-5-T)
standard for forgings of, 25:42775 (RDT-M-2-4-T)
standard for longitudinal-wave ultrasonic testing of plain and clad plates of, 25:42024 (RDT-F-3-5-T)
standard for plates of, for pressure vessels for moderate and lower-temperature service, 25:42792 (RDT-M-5-2-T)
standard for seamless tubes of, 25:42780 (RDT-M-3-2-T)
standard for ultrasonic testing of forgings of, 25:42761 (RDT-F-3-3-T)
strain tolerance of drop weight specimen of A533B, inelastic bending analysis for determination of, 25:42847 (ORNL-TM-3247)
tensile properties of thick-plate specimens of, effects of specimen geometry on testing of, 25:42848 (ORNL-TM-3313)
C--Mn--Ni--steel, mechanical properties of tempered, relations with structure, 25:42886 (UCRL-20500, pp 86-146)
C--steel, failure of flawed pipes and fittings of, method for prediction of, 25:42845 (GEAP-10236)
C--steel, standard for castings of, for fusion welding for high-temperature service, 25:42788 (RDT-M-4-1-T)
C--steel, standard for forgings of, 25:42773 (RDT-M-2-1-T)
C--steel, standard for quenched and tempered vacuum-treated forgings of, for pressure vessels, 25:42778 (RDT-M-2-7-T)
C--steel, standard for seamless pipes of, for high-temperature service, 25:42779 (RDT-M-3-1-T)
C--steel, standard for seamless welding fittings of, 25:42774 (RDT-M-2-3-T)
C--steel, weld solidification in, structures and mechanism of, 25:42820
Cr--Mo--steel, corrosion by sodium--water reaction products at 600°F, 25:42804(R) (LMEC-71-1)
Cr--Mo--steel, standard for plates of, 25:42795 (RDT-M-5-5-T)
Mn--Mo--Ni--steel, standard for plates of, for pressure vessels, 25:42793 (RDT-M-5-3-T)
Mn--Mo--steel, standard for plates of, for pressure vessels, 25:42793 (RDT-M-5-3-T)
STELLARATORS
plasma diffusion in toroidal, (T), 25:43374
plasma heating by transit time magnetic pumping, performance of, 25:43332 (EUR-CEA-FC-595)
STIBINE
effects of alkyl-substituted, on electron-induced copolymerization of monomeric unsaturated compounds and unsaturated polyesters, 25:41847(P)
STORAGE RINGS
particle polarization near spin resonances in, dynamics of, 25:43770
STRAIN GAGES
development for use in air or sodium at 1200°F, 25:42804(R) (LMEC-71-1)
STRANGE PARTICLES
production in π^+ + d interactions at 2.05 to 2.35 GeV/c in deuterium bubble chamber, cross sections, angular distributions, and polarization for, (E), 25:43561
STRONTIUM
determination following separation by ion exchange, break-through and standard curves for, 25:41742
determination in carbonates, silicates, and sulfates by atomic absorption spectroscopy, effects of aluminum and titanium on, 25:41735
separation from acetone--hydrochloric acid solutions by ion exchange using Bio-Rad, distribution coefficients for, 25:41899
separation from aqueous solutions by ion exchange on zirconium tellurate, tracer studies on, 25:41915
separation from calcium using nitric acid, tracer studies on, 25:41715
separation from other metals using inorganic ion exchange papers, 25:41909
separation from radioactive waste using oxidizing agent and manganese salt, 25:41911(P)
sorption by soils around Casaccia, Italy, 25:41930
STRONTIUM ISOTOPES Sr-85
electron-capture decay of ground-state and isomeric, γ singles and coincidence spectra and half-lives for, (E), 25:43877
metabolism and tissue distribution following intake by man, 25:42467
metabolism in rats in comparison to calcium-47, effects of lactation on, 25:42255
retention in rats, effects of age and lactation on, 25:42252
sorption through intestine of rat, effects of alginates from algae on, 25:42254
uptake by frogs and lizards from labeled trees, 25:42317(R) (PRNC-147)
uptake by frogs in rain forest in Puerto Rico, 25:42317(R) (PRNC-147)
use for diagnosis of bone tumors in comparison with metastable strontium-87 and x-radiography, 25:42562
STRONTIUM ISOTOPES Sr-86
energy levels from (p,pxn) reactions with natural strontium, lifetimes and spin--parity assignments for, (E), 25:43847
energy levels from γ resonance scattering, total radiative widths for, (E), 25:41833(R) (IA-1218)
energy-level transitions from (p,pxn) reactions with natural strontium, neutron polarization charge and probability for E2, (E), 25:43847
proton reactions (p,γ) at 2.917 MeV, Q-value for, (E), 25:43836
STRONTIUM ISOTOPES Sr-87
proton reactions (p,n) at 3 to 3.1 MeV, cross section and Q-value for, (E), 25:43836
use of metastable, for diagnosis of bone tumors in comparison with strontium-85 and x-radiography, 25:42562
STRONTIUM ISOTOPES Sr-88
energy levels from rubidium-87 proton resonances, isospin splitting of giant dipole, (E), 25:43950
helium-3 reactions (He-3,t) at 23 MeV, distorted-wave analysis of angular distributions from, (T), 25:43848
STRONTIUM ISOTOPES Sr-89
accumulation in barley, soybeans, and wheat, effects of genotype on, 25:42322(R) (COO-1097-46)
content in drinking water in USA, standards for maximum permissible, 25:42470
content of institutional diets in USA during 1970, 25:42417
determination of, effects of fractionation phenomena in beta spectrometric, 25:41754
distribution in barley, soybeans, and wheat during development, 25:42322(R) (COO-1097-46)
distribution in skin following surface contamination, methods for measuring, 25:42371
distribution in skin following surface contamination, kinetics of, 25:42257
metabolism and tissue distribution following intake by man, 25:42467
sorption by animal intestines, use of ion exchange resins for prevention of, 25:42263
STRONTIUM ISOTOPES Sr-90
accumulation in barley, soybeans, and wheat, effects of genotype on, 25:42322(R) (COO-1097-46)
content in cottage cheese and milk in Czechoslovakia during 1965 to 1968, 25:42386
content in drinking water in USA, standards for maximum permissible, 25:42470
content in food in Israel, 25:41833(R) (IA-1218)

XUM

content in food in Pavia, Italy, 1964 to 1966, 25:42389
content in human diet and urine in Italy, effects of age on, 25:42375
content in milk in Korea, effects of fallout specific activity on, 25:42372
content of dairy products, fruits, and vegetables in Bulgaria during 1965, 25:42381
content of diet of adults and children in Formosa, comparison of, 25:42422
content of institutional diets in USA during 1970, 25:42417
content of milk in Canada, Central and South America, and USA during 1970, 25:42417
content of milk in Canada, Central and South America, and USA during November 1970, 25:42421
content of milk in Czechoslovakia during 1963 to 1966, 25:42385
content relative to cesium-137 in atmosphere and precipitation in Israel, 1968 and 1969, 25:41833(R) (IA-1218)
deposition in bones of cattle in Italy during 1962 to 1968, 25:42382
deposition in developing parts of oat plants following sorption from nutrient solution, 25:42261
determination of, effects of fractionation phenomena in beta spectrometric, 25:41754
distribution in Ligurian Sea sediments, measurement of vertical, 25:41949
effects on mice, effects of dose on leukemogenic, 25:42654
leachability and volume strength of liquid, for incorporation in concrete mixtures, 25:41833(R) (IA-1218)
metabolism and tissue distribution following intake by man, 25:42467
properties for use as heat source for thermoelectric generators, 25:42014
sorption by sierozem soils, 25:42319
transport through vegetation--cattle--milk--man food chain, biological models for, 25:42378
uptake by bones in animals and man, induction of neoplasms and radiation injuries following, 25:42472
STRONTIUM OXIDES
Ir--IrO_2--SrO, phase studies of, 25:43005
STRONTIUM SULFIDES
luminescence and thermoluminescence of zirconium-activated phosphors of, kinetics of, 25:42062
SrS--US, crystal structure of $SrUS_2$, 25:43002
SrS--US, phase diagram of, 25:43002
STYRENE
radioinduced polymerization in wood, γ, 25:41843(R) (ORO-2945-10)
acrylonitrile--styrene, radioinduced polymerization in wood, γ, 25:41843(R) (ORO-2945-10)
methyl methacrylate--styrene, radioinduced polymerization of, effects of temperature on microstructure of products from γ, 25:41845
STYRENE POLYMERS
deformation during contact gaging, 25:44232(R) (BDX-613-404)
diameters of billets of, method for measurement of, 25:44228 (BDX-613-355)
SUCCINIC ACID
radiolysis of solid, role of reaction sites in yields of gaseous products from γ, 25:41865
SULFATES
analysis for strontium by atomic absorption spectroscopy, effects of aluminum and titanium on, 25:41735
determination in nitric acid and plutonium nitrate solutions by ion exchange and titration, 25:41716 (AECL-3676)
SULFITES
effects on redox potential of spleen, 25:42526
SULFUR
separation of carrier-free phosphorus-32 from irradiated, by thermic oxidation, 25:41833(R) (IA-1218)
SULFUR DIOXIDES
determination in stack gases, activation method for, 25:41759(P)
reactions with SO^- ions, method for measurement of rates of charge exchange in, 25:41833(R) (IA-1218)
SULFUR FLUORIDES
effects on formation of butyl radicals and hydrogen in γ radiolysis of 2-methylpropane, 25:41864
effects on hydrogen yields from electron radiolysis of hydrogen sulfide, 25:41860
SULFUR IONS
spectral levels in solar corona, autoionizing, (E), 25:43065 (AD-715257)
SULFUR ISOTOPES S-34
triton reactions (t,p) at 3.45 MeV, spectrum of internal pairs from, (E), 25:43869
triton reactions (t,pγ) at 3.12 MeV, angular correlations and spectra from, (E), 25:43869
SULFUR ISOTOPES S-35
metabolism and tissue distribution following intake by man, 25:42467
testing of, produced in Japan, application, 25:41990 (JAERI-13617)
SULFUR ISOTOPES S-36
energy levels from sulfur-34 (t,pγ) reactions, lifetimes and spin--parity assignments for, (E), 25:43869
energy-level transitions from sulfur-34 (t,pγ) reactions, branching and mixing ratios and multipolarities for, (E), 25:43869
SULFURYL CHLORIDE
radiolysis of, ESR studies on supramolecular bonding orbitals from molecular antibonding orbitals from γ, 25:41855
SUN
activity cycles, relation to daytime ionospheric sporadic-E parameters in South Pacific, (E), 25:43265
activity of, effect on annual post-sunset ionospheric F-region height and equatorial-width variations, (E/T), 25:43228
activity of, effect on ionospheric F-region electron density-dependent electron and ion temperatures, (E/T), 25:43229
activity variations of, relation with thermospheric atomic oxygen density, (E/T), 25:43260
composition of, chemical, (T), 25:43078
eclipse of Mar. 7, 1970, gravity-wave interaction with ionosphere during, (E/T), 25:43270
effects on cardiovascular system in x-irradiated rabbits, 25:42651
radiant flux of, radiometric scale for optical, (E), 25:43076
spectra of, differential line shifts in center and at limb in Fraunhofer, (E), 25:43074
spectral emission of disk of, monitoring during 1969 of Lyman-α line in, (E), 25:43075
star distribution in neighborhood of, (E/T), 25:43027
ultraviolet spectra of, conference papers on, 25:43031
x-ray emission from, Vela VI data for Sept. 1, 1970 to Jan. 1, 1971, (E), 25:43066 (LA-4454(Vol.5))
x-ray flux from quiet, (E), 25:43057
SUPERCONDUCTIVITY
review of, and applications, 25:43301
SUPERCONDUCTORS
critical current density enhancement for niobium alloys, 25:43290 (ORNL-4703)
electron pairs in, off-diagonal long-range order and momentum distribution of, (T), 25:43317
Josephson tunneling in SLUG-type junctions, quantum interference effects in, (E), 25:43293
lattice stability and phonon frequencies in, (T), 25:43296
magnetic flux flow and fluctuation effects in thin film, (E/T), 25:43322
magnetic impurity effects on energy gap and density of states in, (T), 25:43306
magnetic properties of Type-II, effect of point defects on, 25:43310
parameter calculation for nontransition metals, 25:43305
phase surface propagation in thin films, 25:43313
point contact response to high-frequency radiation, (E/T), 25:43297
preparation by co-condensation of component elements, 25:42886 (UCRL-20500, pp 86-146)
properties of niobium--aluminum--germanium, in A15 phase, (E), 25:43291(T) (ORNL-tr-2461)
proximity effects in Josephson tunneling junctions, (E), 25:43308
stochastic processes and thermal fluctuations in, (T), 25:43320
transition temperature of quantizing semiconductor films and lamellar media, (T), 25:43314
transition to intermediate state in, resistive phenomena in initial stage of, (E/T), 25:43299
tunneling in junctions of, fluctuation conductivity of electron, (T), 25:43307
SUPERFLUIDITY
theory of, 25:43285
transition in, order-parameter fluctuations in weakly interacting Bose gas near, 25:43284
SUPERNOVA REMNANTS
model for Vela X, blast wave, (T), 25:43039
SUPERNOVAE
energy source for, uniformly rotating relativistic disks as, (T), 25:43092
observations of Gum Nebula, possible, (E), 25:43034
thermonuclear detonations in evolved stellar cores, (T), 25:43033
SURFACE WATERS
radioactivity monitoring in, of Washington during 1968 to 1969, β, 25:42419
tritium content of Washington, during 1968 to 1969, 25:42419
SURFACES
bibliography on surface and vacuum physics, 25:43111
SURRY POWER REACTOR, UNIT 1
design parameters of, revised and additional data on, 25:44051 (DOCKET-50280-43)
engineered safeguards for, operation and testing of, 25:44051 (DOCKET-50280-43)
operations aspects of, revised and additional data on, 25:44051 (DOCKET-50280-43)
piping systems for, earthquake resistant design requirements for, 25:44051 (DOCKET-50280-43)
site for, meteorological data for, 25:44051 (DOCKET-50280-43)
structures for, earthquake resistant design requirements for, 25:44051 (DOCKET-50280-43)

SURRY POWER REACTOR, UNIT 2
design parameters of, revised and additional data on, 25:44051 (DOCKET-50280-43)
engineered safeguards for, operation and testing of, 25:44051 (DOCKET-50280-43)
operations aspects of, revised and additional data on, 25:44051 (DOCKET-50280-43)
piping systems for, earthquake resistant design requirements for, 25:44051 (DOCKET-50280-43)
site for, meteorological data for, 25:44051 (DOCKET-50280-43)
structures for, earthquake resistant design requirements for, 25:44051 (DOCKET-50280-43)
SWEDEN
radiation monitoring programs for personnel at AB Atomenergi during 1969, 25:42392 (AE-423)
radiation protection programs in, 25:42483
SWITCHES
response of superconducting point contacts to high-frequency radiation, (E/T), 25:43297
SYMMETRY GROUPS
algebraic realization of chiral, multiple production of massless π as test of, 25:43663
chiral breaking for strong interactions, duality relations with, 25:43619
chiral, superconvergence and algebraic realizations of, 25:43661
formulation of asymptotic chiral, for two-point functions of baryon currents, 25:43644
SO(4,3), for hadron mass spectra and transition amplitude for π decay, 25:43635
SU(2), interactions π + π in, dual amplitudes for, 25:43627
SYMMETRY GROUPS SU(3)
interactions π + π in, dual amplitudes for, 25:43627
SYNCHROCYCLOTRONS
beam extraction from USSR 1-GeV proton, 25:43762
beam extraction from, relation between radial oscillation amplitude and energy spread for regenerative, 25:43725 (AERE-R-6812)
SYNCHROTRON RADIATION
emission of, in Milky Way, (T), 25:43079 (N-71-20472)
SYNCHROTRONS
meson (π⁻) fluxes available from 10- to 500-GeV proton, (T), 25:43726 (BNL-15893)
operation and performance of JINR proton, for acceleration of deuterons to 11 GeV/c, 25:43727(T) (BNL-tr-431)
radiation protection at Frascati electron, following beam intensity increase, 25:43738
SYSTEMS FOR NUCLEAR AUXILIARY POWER (SNAP-11)
thermoelectric generators for, performance and life testing of, 25:42002
SYSTEMS FOR NUCLEAR AUXILIARY POWER (SNAP-19)
thermoelectric generators for, performance and life testing of, 25:42002
SYSTEMS FOR NUCLEAR AUXILIARY POWER (SNAP-21)
thermoelectric generator for, design and development of 10-W, 25:41998
SYSTEMS FOR NUCLEAR AUXILIARY POWER (SNAP-27)
development of plutonium-238-fueled, for powering lunar surface equipment, review of program for, 25:41999

T

TANTALUM
book: High-Temperature Materials, 25:42853
carburization of boride-coated, effects of temperature on, 25:42854
chemical thermodynamic properties of, selected values of, 25:41825 (NBS-TN-270-5)
compounds, thermodynamic properties of, tables of, 25:41825 (NBS-TN-270-5)
diffusion of oxygen in, at 800 to 1500°C, effects of concentration on thermal, 25:42864
lattice vibrational spectra and thermal capacities of, calculations, 25:43490
reactivity worth in fast reactor spectra, specific, (E/T), 25:44094(R) (AI-AEC-12991)
separation from aqueous acid solutions by retention on hydrated antimony oxide, 25:41922
solubility in ammonium nitrate in methanol at room temperature by anodic polarization, 25:41833(R) (IA-1218)
use of aerosols of, for use as radioopaque agents during radiography of respiratory tract, 25:42558
weld solidification in, structures and mechanism of, 25:42820
TANTALUM ALLOYS AND SYSTEMS
C--Re--Ta, phase diagram at 2100°C, isothermal, 25:42992
Fe--Nb--Ta--Ti-base--Zr, description of superconducting, 25:43318(P)
Fe-base--Ta, tensile properties of, effects of intermetallic compound formation on, 25:42886 (UCRL-20500, pp 86-146)
Nb--Ta-base, oxidation of monocrystalline and polycrystalline, at 850 to 1050°C and 740 torr, 25:42806
Ni-base--Ta, crystallization at cooling rates of 10^7 to 10^8 degrees/sec, 25:42888
O--Ta, diffusion and evaporation of oxides in solid solutions of, at 1600 to 2000°C, simultaneous, 25:42975
O--Ta, phase diagram of, 25:41993(R) (ORNL-4692)
Ta--Zr, superconducting critical current density of, at high fields, 25:43290 (ORNL-4703)
TANTALUM BORIDES
thermal capacity of, low-temperature, 25:42974
TANTALUM CARBIDES
thermal expansion to 2500°C, 25:42966
TANTALUM ISOTOPES Ta-178
beta and electron-capture decay of, γ--γ angular correlations from, (E), 25:43917
TANTALUM ISOTOPES Ta-181
hyperfine structure of, (E), 25:43121
neutron capture at thermal and 2 keV energies, γ spectra from, (E), 25:43935
neutron capture at thermal energies to 907 keV, gamma-ray yields from, (T), 25:43890 (ORNL-TM-3436)
neutron capture cross sections for, evaluation of data for calculation of, (T), 25:44094(R) (AI-AEC-12991)
TANTALUM ISOTOPES Ta-182
beta decay of, β--Ce and β--γ delayed coincidence spectra from, (E), 25:43903
energy levels of, Coriolis-mixing analysis of, (T), 25:43934
energy-level scheme for, (E), 25:43935
isomeric transition in, γ singles and coincidence spectra from, (E), 25:43935
TANTALUM ISOTOPES Ta-183
beta decay of, β--Ce and β--γ delayed coincidence spectra from, (E), 25:43903
TANTALUM OXIDES
removal from tantalum surfaces, effects of ion implantation on, 25:41832(R) (AECL-3851)
TD-NICKEL CHROMIUM
oxidation at 900 to 1200°C, comparison with chromium--cobalt and chromium--nickel alloys, 25:42930
oxidation resistance of, hypervelocity testing of, 25:42805 (N-71-20390)
TECHNETIUM
separation from aqueous solutions by ion exchange on zirconium tellurate, tracer studies on, 25:41915
TECHNETIUM ISOTOPES Tc-99
effectiveness of erythrocyte-incorporated metastable, in spleen function studies, 25:42570
effectiveness of metastable pertechnetate-incorporated, for scanning for diagnosis of brain tumors, 25:42547 (ACRH-1000-248)
effectiveness of metastable, for brain scanning for lesion differentiation, 25:42577
effectiveness of sulfur colloid-incorporated metastable, for scintigraphy of human liver and spleen for diagnosis of Hodgkin's disease, 25:42585
incorporation of metastable, in erythrocytes, 25:42235
use as gamma source for excitation of fluorescence radiation in tracer dose of bismuth for localization of brain tumors by external scanning, 25:42548 (CONF-710204-4)
use of human serum albumin-incorporated metastable, for scanning for cerebrospinal fluid flow patterns in normal man, 25:42567
use of iron hydroxide macroaggregate-incorporated metastable, for scintigraphy of blood perfusion in lungs, 25:42579
use of metastable, for quantitative thyroid scanning in comparison to iodine-131, 25:42569
use of metastable, for scanning of parotid gland for diagnosis of oncocytomas, 25:42572
use of metastable, in medicine, bibliography on, 25:42550 (ORNL-TM-2091(Suppl.2))
use of pertechnetate-incorporated metastable, for scanning human salivary glands for function, 25:42566
use of pertechnetate-incorporated metastable, for assessing clearance time in capillaries of rabbit skin, 25:42617 (UR-49-1462)
use of sodium pertechnetate-incorporated metastable, for sequential scanning of human salivary glands, 25:42571
TECHNETIUM ISOTOPES Tc-101
beta decay of, β and γ singles and coincidence spectra from, (E), 25:43859
TEETH
radiation effects on in utero hamster, x, 25:42649
radiography of human, hazards and protective measures during, 25:42484
radioinduced carcinomas in enamel organ in mouse incisor, effects of thread implantation on x, 25:42670
radioinduced delay in eruption of rat, effects of prenatal exposure on x, 25:42638
TELEVISION EQUIPMENT
radiation dose to man from, annual x, 25:42366
radiation hazards from color, in Pennsylvania during 1968 to 1970, survey of x, 25:42501
TELLURIUM
determination by x ray spectrography, 25:41736
determination of trace amounts of elemental or organo-, following sample digestion with nitric and sulfuric acids, spectrophotometric or titrimetric, 25:41744
separation from acetone--hydrochloric acid solutions by ion exchange using Bio-Rad, distribution coefficients for, 25:41899
separation from other metals using inorganic ion exchange

XUM

papers, 25:41909
TELLURIUM ISOTOPES Te-122
neutron reactions (n,α) at 14.2 MeV, level-density parameters and spectra from, (E), 25:43886 (INR-1268)
proton elastic and inelastic scattering at 6.7 to 12.5 MeV, proton spectra and angular distributions for, (E), 25:43933
TELLURIUM ISOTOPES Te-124
proton elastic and inelastic scattering at 6.7 to 12.5 MeV, proton spectra and angular distributions for, (E), 25:43933
TELLURIUM ISOTOPES Te-126
energy levels from antimony-126 beta decay, spin--parity assignments for, (E), 25:43924
energy levels from proton inelastic scattering, spin-parity assignments for, (E), 25:43933
energy-level transitions from antimony-126 beta decay, branching ratios, K-conversion coefficients, and multipolarities for, (E), 25:43924
nuclear charge distribution of, determination from μ-mesic x-ray spectra, 25:43904
proton elastic and inelastic scattering at 6.7 to 12.5 MeV, proton spectra and angular distributions for, (E), 25:43933
x-ray spectra of μ-mesic atoms of, (E), 25:43904
TELLURIUM ISOTOPES Te-130
beta decay of, search for double, (E), 25:43932
energy levels from γ resonance scattering, total radiative widths for, (E), 25:41833(R) (IA-1218)
energy levels from proton inelastic scattering, spin--parity assignments and spectroscopic factors for, (E), 25:43918
proton elastic and inelastic scattering by, angular distributions and excitation functions for, (E), 25:43918
TELLURIUM ISOTOPES Te-132
metabolism and tissue distribution following intake by man, 25:42467
TELLURIUM SYSTEMS
Pr--Te, phase studies of, 25:42986
TERBIUM
determination of trace amounts of, in yttrium oxide by activation methods, 25:41877 (JAERI-13545)
magnetic susceptibility of, generalized function for, (T), 25:43477
properties of monocrystals of, at low temperatures, elastic and magnetoelastic, 25:41833(R) (IA-1218)
radiolysis of aqueous solutions of, spectral studies on pulse, 25:41833(R) (IA-1218)
separation from aqueous solutions by ion exchange on zirconium tellurate, tracer studies on, 25:41915
TERBIUM ALLOYS AND SYSTEMS
Al--Ni--Tb, magnetic properties of TbAl/sub 2-x/Ni/sub x/, 25:43480
Mn--Pr--Tb, magnetic properties of Pr/sub x/Tb/sub 1-x/Mn_2, high-temperature, 25:42894
Mn--Pr--Tb, structure of Pr/sub x/Tb/sub 1-x/Mn_2, 25:42894
Sn--Tb, hyperfine magnetic fields for Sn impurity atoms from tin-119 Moessbauer effect, (E), 25:43494
TERBIUM HYDROXIDES
magnetic specific-heat study of interactions in, 25:43472 (YALE-3227-74)
TERBIUM ISOTOPES Tb-159
neutron reactions (n,α) at 14.2 MeV, level-density parameters and spectra from, (E), 25:43886 (INR-1268)
neutron total cross section at 100 to 650 keV, optical model analysis of average, (E/T), 25:43908
TERBIUM OXIDES
preparation of crystals of, hydrothermal studies of equilibria with water in, 25:42934 (COO-1109-60)
reduction by heating, stability of compounds formed during, 25:42968
TEREPHTHALIC ACID, POLYETHYLENE ESTERS
radioinduced charging of foils of, low-energy electron, 25:43436
p-TERPHENYL
fluorescence excited by fast electrons, rise and decay times of, 25:43452
naphthacene--p-terphenyl, fluorescence excited by fast electrons, rise and decay times of, 25:43452
TESTES
radiation effects on 7α-hydroxylase activity in rat, x, 25:42621
radiation effects on morphology of cells in human, effects of dose and post-irradiation time on x, 25:42674(R) (RLO-1780-32)
radiation effects on mouse, development following x, 25:42659
radiation effects on mouse, effects of bone marrow transplants on lethal whole-body γ, 25:42304
THALLIUM
separation from acetone--hydrochloric acid solutions by ion exchange using Bio-Rad, distribution coefficients for, 25:41899
separation from other metals using inorganic ion exchange papers, 25:41909
superconducting parameter calculations, 25:43305
THALLIUM ALLOYS AND SYSTEMS
Pb-base--Tl, magnetic anisotropy in superconducting, with Ginzburg--Landau parameter greater than 2-/super $1/_2$/, (E/T), 25:43294
Pb-base--Tl, magnetic structure of superconducting intermediate state of, (E/T), 25:43295
THERMAL INSULATION
development and testing of oxide-coated multi-foil, for use at high- or low-temperatures, 25:42962
development of evacuated multi-layer, for SNAP-21, 25:41998
standard for materials for use on stainless steel, 25:43013 (RDT-M-12-1-T)
THERMIONIC CONVERTERS
cooling and heating of, performance of heat pipes for, (E), 25:41977
cooling or heating of, western European research programs on heat pipes for, 25:41976
design and development of, review of French research program for, 25:41997
design of, with concentric collector and emitter, 25:43189(P)
development in Germany, review of, 25:44172
development of nuclear, for high-temperature operation, 25:43180 (AD-715809)
development of promethium-147-fueled isomite, for biomedical applications, 25:41996
electrode fabrication for, use of ion sputtering in, (E), 25:43187
ionization in cesium diode, by laser radiation, 25:42181 (AD-715883)
THERMOELECTRIC CONVERTERS
cooling of space power system, fabrication and testing of multiple-heat pipe radiator system for, 25:41978
design and development of radioisotope-fueled, for SNAP-21, 25:41998
design and operation of ISOTEC, for space power systems, 25:42006
evaluation of radioisotope-powered, for deep space use, 25:43184 (N-71-16776)
heat sources for, evaluation of radioisotope, 25:42014
performance characteristics of pressure-contacted lead--telluride, mathematical model for describing, 25:42001
performance testing of SNAP-11, SNAP-19, and heat-pipe-mounted, equipment, methods, and results for, 25:42002
performance testing of three planar sections of solar, 25:43185 (N-71-17252)
THERMOELECTRIC MATERIALS
performance of N- and P-type, in thermoelectric generators, (E/T), 25:42001
THERMOMETRY
development of instruments for ultrasonic, for LMFBR, 25:42189(R) (NYO-3906-6)
nuclear orientation studies for ultralow-temperature, using ^{54}Mn in Fe, 25:43329
THERMONUCLEAR REACTORS
design and operation of Livermore superconducting Levitron, 25:43399 (UCRL-73076)
development of deuterium--tritium exploding-pellet, by lasers, 25:43398 (ORNL-TM-3231)
magnet design for, large superconducting, 25:43397 (MATT-848)
plasma confinement in torus with helical multipole fields, high-beta, (E), 25:43336
plasma heating by transit time magnetic pumping in toroidal, 25:43332 (EUR-CEA-FC-595)
plasma heating in toroidal octupoles, electron cyclotron, (E), 25:43334
plasma instabilities in toroidal, radial dependence of trapped-particle, (T), 25:43391
plasma transport in magnetically perturbed multipoles, effect of toroidal field on, (E), 25:43335
power cycles for catalyzed deuterium-fueled, steam conditions in, (T), 25:43396 (MATT-804)
THERMOSPHERE
density variations in heterosphere, effect of altitude and temperature variations on semiannual, (E/T), 25:43258
electric-field noise at 1500 km over auroral-zone/polar-cap, irregular, (E), 25:43216 (N-71-18405)
electron and ion temperature at 500 to 1000 km in, correlation with electron density, (E/T), 25:43229
oxygen density in, relation of seasonal, diurnal, and solar-activity variations with atomic, (E/T), 25:43260
THICKNESS GAGES
design of beta backscatter, 25:42174(P)
design of beta backscatter, for coatings, 25:42173(P)
THIOLS
effects of amino-, on redox potential of spleen, 25:42526
preparation of 2-alkoxyimino-substituted, as potential radioprotective compounds, 25:42532
preparation of O-alkyloximino-substituted, as potential radioprotective compounds, 25:42531
radiolysis of n-alkyl, effects of electronic excitation of molecules on yields of free radicals from, 25:41859
radioprotective effectiveness of O-alkyloximino-substituted, 25:42531
THIOPHENE
radioprotective effects on cellulose, 25:41836
THIOPYRONINE
effects on lambdoid and T phages following photodynamic inactivation, sensitizing, 25:42738
THORAX
radiotherapy of neoplasms of, injuries to heart

following, 25:42704
THORIUM
content and distribution in Ilimaussaq alkaline intrusion, south Greenland, gamma spectrometry method for determination of, 25:41943
content in Romanian environment, method for measurement of, 25:41928
determination following complexation with butyl sulfoxide and 1,1,1,5,5,5-hexafluoro-2,4-pentanedione, gas chromatographic, 25:41725
determination following separation from other metal ions by thin-layer chromatography using quercetin, colorimetric, 25:41743
impurity segregation on surfaces of, thermodynamics and kinetics of, 25:41825 (LA-DC-12348)
magnetic susceptibility of, generalized function for, (T), 25:43477
metabolism and tissue distribution following intake by man, 25:42467
precipitation from molten halide salts, effects of polarization on, 25:42821
preparation of single crystals of ultrahigh purity, by repeated and prolonged heating, 25:42824
preparation of ultrahigh purity, by electrotransport, 25:42824
separation from acetone--hydrochloric acid solutions by ion exchange using Bio-Rad, distribution coefficients for, 25:41899
separation from nitric acid solutions by solvent extraction using TBP, optimization of, 25:41916
separation from ores, leaching methods for, 25:41918
separation from other metals using inorganic ion exchange papers, 25:41909
separation from uranium by precipitation using oxalic acid, 25:41919
spectra between 5400 and 6400 cm^{-1}, emission, (E), 25:43113
THORIUM ALLOYS AND SYSTEMS
Co--Th, structure and Curie temperature of $ThCo_5$, effects of stoichiometry on, (E), 25:43485
Ir--Th, superconducting transition temperature in high T/sub c/ intermetallic $ThIr_2$, sensitivity to residual stress of, (E), 25:43302
rare earth--Th, magnetic susceptibility of, generalized functions for, (T), 25:43477
THORIUM BORIDES
crystal structure of nonstoichiometric hexaboride, 25:43003
preparation of nonstoichiometric hexaboride, 25:43003
THORIUM DEPOSITS
prospecting in India, status of nuclear methods for, 25:41947
THORIUM ISOTOPES
distribution in Ligurian Sea sediments, measurement of vertical, 25:41949
THORIUM ISOTOPES Th-228
ion emission from, small negative radioactive, 25:43100
properties for use as heat source for thermoelectric generators, 25:42014
uptake by bones in animals and man, induction of neoplasms and radiation injuries following, 25:42472
THORIUM ISOTOPES Th-230
distribution in Ligurian Sea sediments, measurement of vertical, 25:41949
neutron fission at 0.1 to 3.0 MeV, power-series fits to fragment angular distributions from, (T), 25:43888 (LA-4648)
separation from other isotopes during 1968 and 1969, review of CRNL, 25:41992 (ORNL-4640)
THORIUM ISOTOPES Th-232
neutron capture at 20 to 30 keV, disagreement of cross sections with Porter--Thomas postulate, (E), 25:43911
neutron fission at 0.1 to 3.0 MeV, power-series fits to fragment angular distributions from, (T), 25:43888 (LA-4648)
neutron fission from thermal energies to 14 MeV, calculations of total energy released during, (T), 25:43885 (ANL-7748)
neutron total cross section up to 1.5 MeV, (E), 25:43884 (ANL-7710, pp 1-52)
photofission at 200 to 1150 MeV, cross section and fragment energy and angular distributions for, (E), 25:43946
uptake by aquatic plants, 25:41833(R) (IA-1218)
THORIUM OXIDES
book: High-Temperature Materials, 25:42853
effects on man, effects of dose on late, 25:42714
THORIUM OXIDES ThO_2
effects on human liver following intravascular injection, latent, 25:42708
fluorescence under uv light, 25:41832(R) (AECL-3851)
hydrogen release from sintered pellets of, at 1000 and 1600°C, effects of carbon content on, 25:42958 (WAPD-TM-850)
spectra of, effects of impurities on optical absorption, 25:41832(R) (AECL-3851)
thermoluminescence of, 25:41832(R) (AECL-3851)
Mo--ThO_2, permeability and porosity of cold-pressed and sintered pellets of, 25:41993(R) (ORNL-4692)
PrO--ThO_2, phase relations and lattice parameters for, 25:42956
ThO_2--UO_2, hydrogen release from sintered pellets of, at 800 to 2000°C, effects of carbon content on, 25:42958 (WAPD-TM-850)
ThO_2--UO_2, preparation of soln of, 25:42945(P)
ThO_2--UO_2, stability of sol-gel microspheres of, under oxidizing conditions in fluid bed, 25:41907
ThO_2--UO_2--U_3C_2, phase diagram at 1100 to 1550°C, 25:42984(T) (ORNL-tr-2483)
ThO_2-base--UC_2, preparation of microspheres of, engineering-scale demonstration of sol-gel process for, 25:42937 (ORNL-4544)
THULIUM
electric conductivity of, slope change in temperature dependence near 22°K, (E), 25:43487
separation from aqueous solutions by ion exchange on zirconium tellurate, tracer studies on, 25:41915
THULIUM ISOTOPES Tm-169
neutron reactions (n,α) at 14.2 MeV, level-density parameters and spectra from, (E), 25:43886 (INR-1268)
THULIUM OXIDES
Tm_2O_3--Yb_2O_3, preparation by coprecipitation method, 25:41993(R) (ORNL-4692)
THYMIDINE
effects of tritium-labeled, on oocytes of rat fetus following administration by maternal infusion during pregnancy, 25:42650
incorporation of tritium-labeled, into DNA of lymphoma cells, survival following, 25:42251
THYMINE
radiation effects on frozen solutions of, products from uv, 25:41833(R) (IA-1218)
radiolysis of deaerated aqueous solutions of, yields of cis- and trans-6-hydroxy-5-methylhydrouracil from γ, 25:41874
THYMUS GLAND
radiation effects on acid phosphatase in mouse, whole-body x, 25:42287
radiation effects on cell population kinetics in mouse, chronic whole-body, 25:42631
radioinduced injuries in tissues of chicken, x, 25:42658
THYROID GLAND
effects of serotonin on mouse, 25:42519
radiation dose to human, evaluation of nuclear power reactor sites in relation to potential accidental iodine-131, 25:44147
radiation dose to human, in Australia during 1970 from nuclear weapons test fallout, 25:42367 (AWTSC-1)
radiation effects on function of human, following therapy of lymphomas, x, 25:42695
radiation effects on morphology of cancer of human, following therapy, effects of tumor type on γ, 25:42679
scanning of human, comparison of iodine-131 and metastable technetium-99 for quantitative, 25:42569
TIMING CIRCUITS
design for measurement of nanosecond nuclear lifetimes, 25:42187 (JINR-P13-5801)
TIN
analysis by mass spectrography, isotopic, 25:41727
beta-particle mass absorption coefficients of, negative and positive, 25:43433
determination of trace amounts of, in meteorites by neutron activation and γ spectrometry, 25:41773
effects on superconducting critical field of niobium--titanium alloy wires, 25:43309
properties of superconducting films of, for radiation detection, 25:42080
rectification effect in thin-film superconducting, in small, oscillatory magnetic fields, 25:43304
separation from acetone--hydrochloric acid solutions by ion exchange using Bio-Rad, distribution coefficients for, 25:41899
separation from aqueous solutions by ion exchange on zirconium tellurate, tracer studies on, 25:41915
separation from other metals using inorganic ion exchange papers, 25:41909
superconducting behavior of thin-film bridges in shf fields, (E), 25:43298
superconducting parameter calculations, 25:43305
superconducting transition to intermediate state in cold-rolled foils and annealed plates of, resistive phenomena of, (E/T), 25:43299
superconductive tunneling in diodes with tin oxide and lead, effects of 2.5-GHz microwaves on currents in, (E), 25:43316
TIN ALLOYS AND SYSTEMS
Al--Sn--Ti-base, radiation effects on tensile properties of, at 17°K, fast neutron, 25:42926
Cr--Fe--Sn--Zr-base, properties for use in water-cooled reactors, 25:42875
Gd--Sn, hyperfine magnetic fields for Sn impurity atoms from tin-119 Moessbauer effect, (E), 25:43494
Nb--Sn, superconducting phase identification in, critical temperature measurement method for intermetallic Nb_3Sn, 25:43288 (INR-1294)
Sn--Tb, hyperfine magnetic fields for Sn impurity atoms from tin-119 Moessbauer effect, (E), 25:43494
Sn--Zr-base, properties for use as getter in vacuum containers, 25:42858(P)
TIN HYDRIDES
chemical properties of, 25:41778 (UCRL-20500, pp 1-85)

XUM

TIN ISOTOPES
determination in tin by mass spectrography, 25:41727
TIN ISOTOPES Sn-111
energy levels of, pairing-plus-quadrupole-interaction calculation of relative spectroscopic factors and spin--parity assignments for, (T), 25:43925
TIN ISOTOPES Sn-112
energy levels of, pairing-plus-quadrupole-interaction calculation of quadrupole moments of first 2+, (T), 25:43925
separation of enriched, from exhausted indium-113m generators, electrolytic method for, 25:41833(R) (IA-1218)
TIN ISOTOPES Sn-113
energy levels of, pairing-plus-quadrupole-interaction calculation of spin--parity assignments for, (T), 25:43925
TIN ISOTOPES Sn-114
energy levels of, pairing-plus-quadrupole-interaction calculation of quadrupole moments of first 2+, (T), 25:43925
TIN ISOTOPES Sn-115
energy levels of, pairing-plus-quadrupole-interaction calculation of relative spectroscopic factors and spin--parity assignments for, (T), 25:43925
TIN ISOTOPES Sn-116
energy levels of, pairing-plus-quadrupole-interaction calculation of quadrupole moments of first 2+, (T), 25:43925
nuclear charge distribution of, determination from μ-mesic x-ray spectra, 25:43904
x-ray spectra of μ-mesic atoms of, (E), 25:43904
TIN ISOTOPES Sn-117
deuteron reactions (d,p) at 5 to 12 MeV, cross section and vector analyzing power for, (E), 25:43846
energy levels of, pairing-plus-quadrupole-interaction calculation of spin--parity assignments for, (T), 25:43925
TIN ISOTOPES Sn-118
energy levels of, pairing-plus-quadrupole-interaction calculation of quadrupole moments of first 2+, (T), 25:43925
TIN ISOTOPES Sn-119
deuteron reactions (d,p) at 5 to 12 MeV, cross section and vector analyzing power for, (E), 25:43846
energy levels of, pairing-plus-quadrupole-interaction calculation of relative spectroscopic factors and spin--parity assignments for, (T), 25:43925
energy-level transitions in, effects of valence shell structure on internal conversion, (T), 25:43953(T) (BNL-tr-427)
hyperfine magnetic field for impurity, in Sn--Tb and Gd--Sn alloys by Moessbauer effect, (E), 25:43494
TIN ISOTOPES Sn-120
energy levels from γ resonance scattering, total radiative widths for, (E), 25:41833(R) (IA-1218)
energy levels of, pairing-plus-quadrupole-interaction calculation of quadrupole moments of first 2+, (T), 25:43925
TIN ISOTOPES Sn-121
beta decay of ground-state and isomeric, β and γ spectra from, (E), 25:43905
energy levels of, pairing-plus-quadrupole-interaction calculation of relative spectroscopic factors and spin--parity assignments for, (T), 25:43925
TIN ISOTOPES Sn-122
energy levels of, pairing-plus-quadrupole-interaction calculation of quadrupole moments of first 2+, (T), 25:43925
TIN ISOTOPES Sn-123
energy levels of, pairing-plus-quadrupole-interaction calculation of relative spectroscopic factors and spin--parity assignments for, (T), 25:43925
TIN ISOTOPES Sn-124
alpha elastic scattering at 104 MeV, differential cross sections for, (E), 25:43832 (NP-18920)
energy levels of, pairing-plus-quadrupole-interaction calculation of quadrupole moments of first 2+, (T), 25:43925
nuclear charge distribution of, determination from μ-mesic x-ray spectra, 25:43904
x-ray spectra of μ-mesic atoms of, (E), 25:43904
TIN ISOTOPES Sn-126
beta decay of, Fermi--Kurie plots, log-ft values, and conversion-electron and gamma spectra from, (E), 25:43924
TISSUES
analysis for platinum from non-tumored and tumored Swiss white mice by neutron activation, radiochemical separation, and γ spectrometry, 25:41762
neutron dose-rate distribution from implanted californium-252 line-source in, method for measurement of, 25:42445
radiation effects on oxidation-reduction potential in rat, protective effects of AET, MEA, or serotonin in combination with hypoxia against x, 25:42511
radon daughter content in rat, following inhalation of radon-222, 25:42248
TITANIUM
analysis for hafnium and zirconium by neutron activation, 25:41761
chemical thermodynamic properties of, selected values of, 25:41826 (NBS-TN-270-5)
compounds, thermodynamic properties of, tables of, 25:41826 (NBS-TN-270-5)
determination following separation from other metal ions by thin-layer chromatography using quercetin, colorimetric, 25:41743
effects on determination of strontium in carbonates, silicates, and sulfates by atomic absorption spectroscopy, 25:41735
neutron elastic and inelastic scattering up to 1.5 MeV, cross sections for, (E), 25:43884 (ANL-7710, pp 1-52)
neutron reactions at 200 eV to 200 keV with natural, R-matrix analysis of total cross sections for, (E/T), 25:43874
neutron total cross section up to 1.5 MeV, (E), 25:43884 (ANL-7710, pp 1-52)
radiation effects on tensile properties of, at 17°K, fast neutron, 25:42926
solvation of trivalent, oxygen-17 NMR studies on, 25:41778 (UCRL-20500, pp 1-85)
weld solidification in, structures and mechanism of, 25:42820
TITANIUM ALLOYS AND SYSTEMS
Al--Cr--Mo--Ti-base--V--Zr, mechanical properties of, 25:42836 (AD-715877)
Al--Mo--Ti-base--V, radiation effects on tensile properties of, at 17°K, fast neutron, 25:42926
Al--Sn--Ti-base, radiation effects on tensile properties of, at 17°K, fast neutron, 25:42926
Al--Ti-base--V, radiation effects on tensile properties of, at 17°K, fast neutron, 25:42926
Be--Ti, fabrication and properties of co-extruded powder composites of, 25:42869
C--Mo-base--Ti, phase diagrams at 1200 to 2100°C, isothermal, 25:42890
Fe--Nb--Ta--Ti-base--Zr, description of superconducting, 25:43318(P)
Fe-base--Mn--Ni--Ti, mechanical properties of, effects of aging on, 25:42886 (UCRL-20500, pp 86-146)
Fe-base--Ni--Ti, mechanical properties of, effects of aging on, 25:42886 (UCRL-20500, pp 86-146)
Mo-base--Ti, deformation behavior of, effects of deformation rates on, 25:42833
Mo-base--Ti, properties for use in turbine blades, 25:42833
Nb--O--Ti, analysis for oxygen by neutron activation and γ spectrometry, 25:41761
Nb--Ti, analysis for interstitial oxygen by neutron activation and γ spectrometry, 25:41761
Nb--Ti, superconducting critical current density of, effect of heat treatment and impurities on, 25:43290 (ORNL-4703)
Nb--Ti, superconducting critical field of wires of, effects of additives on, 25:43309
Nb--Ti, superconductivity of, effects of interstitial oxygen on, 25:41761
O--Ti, phase diagram of, 25:42991
Ti--V-base, crystallization of annealed and cold rolled, kinetics of, 25:42884 (JAERI-13731)
TITANIUM BORIDES
preparation of, method for, 25:42944
TITANIUM IONS
reactions with argon at 30 to 130 keV, cross sections for argon L-shell x-ray emission in, (E), 25:43134
TITANIUM ISOTOPES
scandium--titanium Coulomb displacement energies, (E), 25:43883
titanium--vanadium Coulomb displacement energies, (E), 25:43883
TITANIUM ISOTOPES Ti-44
energy levels of, effects of single-particle energies on shell-model calculations of, (T), 25:43866
energy-level transitions in, shell-model calculations of probabilities for E2, (T), 25:43866
TITANIUM ISOTOPES Ti-46
deuteron reactions (d,p) at 5 to 12 MeV, cross section and vector analyzing power for, (E), 25:43846
energy levels from neutron reactions, resonance parameters for, (E/T), 25:43874
helium-3 reactions (He-3,t) at 24.6 MeV, triton spectra from, (E), 25:43883
TITANIUM ISOTOPES Ti-47
energy levels from neutron reactions, resonance parameters for, (E/T), 25:43874
energy levels from titanium-46 (d,p) reactions, spectroscopic factors and spin assignments for, (E), 25:43846
helium-3 reactions (He-3,t) at 24.6 MeV, triton spectra from, (E), 25:43883
TITANIUM ISOTOPES Ti-48
deuteron reactions (d,p) at 5 to 12 MeV, cross section and vector analyzing power for, (E), 25:43846
energy levels from neutron reactions, resonance parameters for, (E/T), 25:43874
helium-3 elastic scattering at 37.7 MeV, optical-model analysis of angular distributions for, (E/T), 25:43878
helium-3 reactions (He-3,t) at 24.6 MeV, triton spectra from, (E), 25:43883
TITANIUM ISOTOPES Ti-49
energy levels from neutron reactions, resonance parameters for, (E/T), 25:43874

energy levels from scandium-49 beta decay, spin--parity assignments for, (E), 25:43873
energy levels from titanium-48 (d,p) reactions, spectroscopic factors and spin assignments for, (E), 25:43846
helium-3 reactions (He-3,t) at 24.6 MeV, triton spectra from, (E), 25:43883
TITANIUM ISOTOPES Ti-50
deuteron reactions (d,p) at 5 to 12 MeV, cross section and vector analyzing power for, (E), 25:43846
energy levels from neutron reactions, resonance parameters for, (E/T), 25:43874
energy levels of, shell-model calculation of, (T), 25:43862
helium-3 reactions (He-3,t) at 24.6 MeV, triton spectra from, (E), 25:43883
TITANIUM ISOTOPES Ti-51
energy levels from titanium-50 (d,p) reactions, spectroscopic factors and spin assignments for, (E), 25:43846
TITANIUM OXIDES
TiO_2--VO_2, electric conductivity of, temperature dependence of, 25:43481
TOKAI-MURA POWER REACTOR
radiation protection programs for personnel at, 25:42479
TOKAMAK DEVICES
plasma heating by transit time magnetic pumping, performance of, 25:43332 (EUR-CEA-FC-595)
plasma instabilities in, shear and kink, (T), 25:43390
TOLUENE
H_2O--toluene, radiolysis, effects of air and iron(III) on yields of cresol isomers from electron or γ, 25:41858
TONSILS
lesions in rat, effects on x-radioinduced saccharin-avoidance behavior of, 25:42647
TRACER TECHNIQUES
development for diagnosis of hematological diseases, review of, 25:42573
development for measurement of fibrinolytic activity of blood, 25:42243
development for medicine, abstracts of 300 papers on, 25:42560
method for measuring wear of chromium plated surfaces using selenium-75, 25:42018
radiation dose to human population from medical uses of radioisotope, 25:42711
research studies at Oak Ridge Associated Universities during 1970 on uses of radioisotope, for clinical diagnosis, 25:42587 (ORAU-113, pp 78-133)
TRANSACTINIDE ELEMENTS
alpha decay of, calculations of half-lives for, (T), 25:43919
decay of, calculations of half-lives for, (T), 25:43919
electron-capture decay of, calculations of half-lives for, (T), 25:43919
energy levels and gaps of very heavy, calculations using Woods--Saxon potential, (T), 25:43955 (INR-1270)
fission of, calculations of half-lives for spontaneous, (T), 25:43919
half-lives of A = 382 and 472, calculations using Woods--Saxon potential, (T), 25:43955 (INR-1270)
production of A = 382 and 392 doubly magic, (T), 25:43955 (INR-1270)
stability of, potential-energy surfaces from calculations of, (T), 25:43919
TRANSDUCERS
sensing elements for pressure, testing of platinum, 25:42804(R) (LMEC-71-1)
TRANSISTORS
radiation damage to MOSFET, electron and x, 25:42233
radiation effects on MOSFET, annealing of 79°K, 25:42234
TRANSITION METAL ALLOYS AND SYSTEMS
superconductivity of amorphous 4-d level, 25:42886 (UCRL-20500, pp 85-146)
TRANSITION METAL OXIDES
existence of binary and ternary suboxides of, review of, 25:42991
TRANSITION METALS
critical temperature of amorphous, model for, 25:42886 (UCRL-20500, pp 85-146)
diffusion in interstitial solid solutions of, theoretical models for thermal, 25:42865
hydrogen bonding in hydrates of, EPR studies on, 25:41778 (UCRL-20500, pp 1-85)
TRANSITION RADIATION
calculation at vacuum boundary of plasma plates, (T), 25:43367
emission patterns from 50-keV electrons traversing thin silicon foils, (E/T), 25:43429
TRANSPLANTS
book: Radiation Immunology and Transplantation, 25:42310
TRANSPORT THEORY
discrete ordinates calculations for 14-MeV neutron source in 5000-m radius cylinder of air, overlap conditions for sequential, 25:43419 (ORNL-TM-3269)
equations for transfer of polarized light in half-space albedo and Milne problems, vector, 25:43423
invariant imbedding method in particle, internal values in, 25:43430
Monte Carlo technique for radiation, new, 25:43413 (BMBW-FBK-71-2)
solutions for general, positive, 25:43415 (JUL-711-MA)
TRANSURANIUM ELEMENTS
internal conversion coefficients for outer shells and ratios to inner shells for Z < 101, 25:43931
TRIMETHYLAMINE
radiolysis of, adsorbed on silica gel at 77°K, ESR studies on trapped radicals produced by γ, 25:41856
TRIOCTYLAMINE
solvent properties for uranium as uranyl chloride in hydrochloric acid solutions, 25:41900
TRITIUM
autoradiographic localization of estradiol-incorporated, in brain of rats, 25:42258
binding energy of, calculation using Brueckner theory with realistic potentials, (T), 25:43794
body form factors for, resonating-group calculation of, (T), 25:43797
content in atmosphere over Lake Tahoe, Nevada, 25:41538
content in urine of neutron generator operators, 25:42390
content of Washington surface waters during 1968 to 1969, 25:42419
distribution in skin following surface contamination, kinetics of, 25:42257
effects on DNA in tissues of mice following ingestion of labeled thymidine, 25:42262
effects on tumor incidence in mice, comparison of latent fast neutron or γ and internal, 25:42630
effects on tumor incidence in mice, thymidine-incorporated, 25:42664
exchange reaction in general base-catalyzed detritiation of malonitriles, 25:41798
helium-3 reactions (He-3,n) at 0.7 to 3.8 MeV, DWBA analysis of differential cross sections, excitation functions, polarizations, and spectra from, (E), 25:43796
helium-3 reactions (He-3,np) at 2.7 and 3.55 MeV, differential cross sections for, (E), 25:43796
metabolism in tissues of mice following ingestion of labeled thymidine, 25:42262
neutron elastic scattering at 0.75 to 10.58 MeV, resonating-group calculations of differential cross sections for, (T), 25:43797
neutron elastic scattering at 1 to 14 MeV, effects of approximate wave functions on phase-shift analysis of, (T), 25:43571
proton elastic scattering at 5.35 to 5.65 MeV, search for helium-4 resonance in excitation function for, (E), 25:43782
use as tracer for determining sperm precedence in spruce budworms, 25:42259
use of thymidine-incorporated, for autoradiographic study of lymphoid cell decay in mouse mesenteric lymph node, method for, 25:42240
use of tumor cells with thymidine-incorporated, for evaluating cellular immune response against tumor-specific antigens, 25:42309
TRITIUM SYSTEMS
CO_2--T, radiolysis of, kinetics and G values of self, 25:41852 (LA-4657)
D--T, laser beam explosion of solid pellets, fusion reactions in, 25:43398 (ORNL-TM-3231)
TRITONS
binding energy of, calculations using Reid soft-core potential in harmonic oscillator basis, 25:43792
binding energy of, variational calculations using Hamada--Johnston potential, (T), 25:43795
interactions t + ^{4}He, shell interpretation of separable potentials for, (T), 25:43786
reactions (t,αγ) with magnesium-24 at 4 to 4.5 MeV, α and γ spectra and α-γ angular correlations from, (E), 25:43880
reactions (t,p) with deformed nuclei, effects of higher multipole deformation of the pairing density on, (T), 25:43977
reactions (t,p) with lead-207 at 20 MeV, distorted-wave analysis of differential cross sections and spectra from, (E/T), 25:43923
reactions (t,p) with nitrogen-14 at 1.5 MeV, analysis including Coulomb distortion and finite-range effects, (T), 25:43965
reactions (t,p) with potassium-39 at 7.5 MeV, angular distributions for, (E), 25:43845
reactions (t,p) with sulfur-34 at 3.45 MeV, spectrum of internal pairs from, (E), 25:43869
reactions (t,pγ) with sulfur-34 at 3.12 MeV, angular correlations and spectra from, (E), 25:43869
scattering by lead-207 at 20 MeV, optical-model analysis of elastic, (E), 25:43923
wave functions for, variational calculations using Hamada--Johnston potential, (T), 25:43795
wave functions of ground state of, S-state, (T), 25:43509
TRYPSIN
radiation effects on activity, tryptophan content, and difference spectra of, γ, 25:42271
TRYPTOPHAN
radiation effects on metabolism of, in mice and rats, mechanisms for, 25:42623
radioprotective effects of, on uranium mining personnel, animal experiments on, 25:42510

XUM

TUBES
joints for sodium heated heat exchangers, x-ray and ultrasonic methods for inspection of, 25:44148 (CONF-700224-, Paper 4)
standard for ultrasonic testing for longitudinal discontinuities, 25:42026 (RDT-F-3-8-T)
vibration response of long flexible cylindrical, in axial flow, tentative design guide for calculation of, 25:41983 (ANL-ETD-71-7)
TUNGSTEN
book: High-Temperature Materials, 25:42853
carburization of boride-coated, effects of temperature on, 25:42854
deposition of (110) layers of, method for vapor, 25:42823
determination following separation from other metal ions by thin-layer chromatography using quercetin, colorimetric, 25:41743
dislocation density in cold worked, effects of annealing at increasing temperatures on recovery of, 25:42870
fabrication of components of, research progress on chemical vapor deposition process equipment for, 25:44223(R) (BDX-613-269)
neutron capture at thermal energies to 907 keV by natural, gamma-ray yields from, (T), 25:43890 (ORNL-TM-3436)
plastic deformation in, at low temperatures, crowdion mechanism of, (E/T), 25:43484
radiation effects on mobility of single self-interstitial atoms of, in situ field-ion microscope study of 20-keV W^+, (T), 25:43458
radiation effects on mobility of single self-interstitial atoms of, in situ field ion microscope study of 20-keV W^+, (E), 25:43457
radioinduced displacement energy of atoms of, field-ion microscopic study of, 25:43449
separation from acetone--hydrochloric acid solutions by ion exchange using Bio-Rad, distribution coefficients for, 25:41899
separation from aqueous solutions by ion exchange on zirconium tellurate, tracer studies on, 25:41915
solubility in ammonium nitrate in methanol at room temperature by anodic polarization, 25:41833(R) (IA-1218)
thermal capacity at low temperatures, 25:41778 (UCRL-20500, pp 1-85)
thermionic emission by faces of single crystals of, effects of adsorbed beryllium films on, 25:43473
weld defects in, origin and effects of, 25:42867
TUNGSTEN ALLOYS AND SYSTEMS
Cu--W, thermal expansion of composites of, incorporating tungsten wire, 25:42873
Fe--Ni--W, phase diagram of, at 800 to 1650°C, 25:42887 (Y-1785)
Pt-base--Rh--W, fabrication and properties of cladding of, 25:41993(R) (ORNL-4692)
Re--W-base, creep rupture at 1650 and 2200°K, comparison of effects of consolidation by arc-melting and powder metallurgy methods on, 25:42866
TUNGSTEN IONS
effects of W^+ on tungsten at 20 keV, in situ field ion microscope studies of, (E), 25:43457
effects of W^+ on tungsten at 20 keV, in situ field ion microscope studies of, (T), 25:43458
TUNGSTEN ISOTOPES W-182
energy levels from tantalum-182 decay, lifetimes of, (E), 25:43903
proton elastic and inelastic scattering at 16 MeV, differential cross sections for, (E), 25:43901
TUNGSTEN ISOTOPES W-183
energy level at 453 keV from tantalum-183 decay, lifetime of, (E), 25:43903
energy levels from tungsten-182 neutron capture, spin--parity assignments for, (E), 25:43831 (INR-1262)
TUNGSTEN ISOTOPES W-184
energy levels from gamma resonance scattering, spin-parity assignments for, (E), 25:41833(R) (IA-1218)
energy levels from tungsten-183 neutron capture, spin--parity assignments for, (E), 25:43831 (INR-1262)
proton elastic and inelastic scattering at 16 MeV, differential cross sections for, (E), 25:43901
TUNGSTEN ISOTOPES W-186
energy levels from gamma resonance scattering, spin-parity assignments for, (E), 25:41833(R) (IA-1218)
proton elastic and inelastic scattering at 16 MeV, differential cross sections for, (E), 25:43901
TUNGSTEN ISOTOPES W-187
energy levels from tungsten-186 neutron capture, spin--parity assignments for, (E), 25:43831 (INR-1262)
TUNGSTEN OXIDES
PbO--WO_3, phase studies of, 25:43006
TZM (MOLYBDENUM ALLOY)
grain structure of welds of, inhibition of second phase formation in, 25:42874
weld defects in, origin and effects of, 25:42867

U

ULTRACENTRIFUGATION
method for separation of heavy isotopes, fundamental equations for physical principles of, 25:41994
ULTRASONIC TESTING
equipment for radioactive waste containers, design and development of, 25:42020 (BNWL-B-103)
wave propagation theory for, 25:44307 (UCRL-73184)
ULTRAVIOLET RADIATION
conference on uv stellar spectra and related ground-based observations, Lunteren, Netherlands, 6/69, 25:43031
effects on activity of bacteriophages, effects of DNA content on, 25:42300
effects on DNA of HeLa cells, DNA-ase activity specific for, 25:42272
effects on DNA of T4 bacteriophage, role of polynucleotide ligase in repair of, 25:42297
effects on DNA, effects of phage T_4 induced endonuclease on dark repair following, 25:42269
effects on E. coli DNA, effects of dose and temperature on products from, 25:41833(R) (IA-1218)
effects on Escherichia coli mutants defective in DNA replication, 25:42331
effects on Escherichia coli mutants in relation to gene location, 25:42328
effects on Escherichia coli, effects of 5-bromouracil on sensitivity to lethal and mutagenic, 25:42345
effects on Escherichia coli, effects of acridine analogs on lethal, 25:42533
effects on frequency of crossing over in recombinants of Schizophyllum commune, 25:42336
effects on frozen thymine solutions, products from, 25:41833(R) (IA-1218)
effects on haploid yeast cells, effects of delayed plating, media, and temperature on dark repair of, 25:42725
effects on incidence of respiration deficient mutants in Schizosaccharomyces pombe, 25:42338
effects on isotopic exchange between iodine and iodobenzene, mechanism of, 25:41833(R) (IA-1218)
effects on lambda bacteriophage, protective effects of methylated proflavine against, 25:42737
effects on lambdoid and T phages, host controlled reactivation following, 25:42738
effects on Micrococcus glutamicus, review of mutagenic, 25:42349
effects on microorganisms, review of improvement in practical applications through mutagenic, 25:42349
effects on mixture of heptaene antibiotics of Streptomyces surinam, 25:42302
effects on Neurospora crassa, identification of base-pair alterations following mutagenic, 25:42341
effects on Neurospora, specificity of mutagenic, 25:42352
effects on plastic scintillators with p-terphenyl, 25:42231
effects on production of pyrimidines dimers in DNA of Bacillus subtilis, 25:42285
effects on production of SV40 virus by PM3 cells after fusion with AGMK cells, 25:42733
effects on prophage lambda induction in Escherichia coli mutants defective in initiation of DNA replication at high temperatures, 25:42340
effects on replication delay in DNA of Escherichia coli, effects of dose on, 25:42290
effects on respiration in bacteria, inactivating, 25:42732
effects on riboflavin, 25:41788
effects on RNA in E. coli, potato virus, and tobacco mosaic virus, reactions of dimers produced by, 25:42267(R) (RLC-2225-T-15-3)
effects on Schizosaccharomyces pombe, isolation and classification of mutants for enhanced, 25:42723
effects on Serratiaphage kappa, sensitizing effects of methylene blue and proflavine on inactivating, 25:42734
effects on T4 phage, effects of mutator alleles on repair of mutagenic, 25:42339
effects on thallium-activated cesium iodide crystals, influence of electric field on luminescent, (E), 25:43448
effects on yeast, repair pathways of supersensitive mutagenic, 25:42337
effects on yeasts, effects of caffeine on mutagenic, 25:42332
stellar spectra in, conference at Lunterer, Netherlands, 6/69, (E), 25:43031
UNITED KINGDOM
radiation monitoring programs for liquid wastes discharged to environment in, 25:42380
UNITED STATES
civilian defense programs during 1971, 25:42506(R) (ORNL-4566(Pt.1))
fallout content of institutional diets in, during 1970, 25:42417
fallout content of milk in, during 1970, 25:42417
food distribution in, civil defense planning for, 25:42506(R) (ORNL-4566(Pt.1))
radiation protection programs in, 25:42487
radiation protection standards in, review of evolution of, 25:42452
radioactivity monitoring in atmospheric precipitation and surface atmosphere during November 1970, gross β, 25:42426

radioactivity monitoring in atmospheric precipitation and surface atmosphere during October 1970, gross β, 25:42418
radioisotope content of airborne particulates in, during 1970, 25:42426
radioisotope content of milk in, during November 1970, 25:42421
standards for drinking water in, Public Health Service Publication No. 956 (1962), 25:42470

UNIVERSE
pulsating, Sengupta's model for, (T), 25:43097
shear in perturbed Friedmann, (T), 25:43088

URACIL, 5-BROMO-
effects on uv-radiosensitivity of Escherichia coli, 25:42345

URACIL, 5-FLUORO-
effects on γ- and x- radiosensitivity of carcinomas in man, 25:42589

URACIL, 6-METHYL-2-THIO-
effectiveness for treatment of x-radioinduced skin ulcers in rats, 25:42541

URANIUM
combustion of, comparison of effectiveness of dry powders for extinguishing, 25:42837 (AERE-R-6745)
complexes with β-resorcylic acid, spectral and thermodynamic studies on, 25:41830
content and distribution in Ilimaussaq alkaline intrusion, south Greenland, gamma spectrometry method for determination of, 25:41943
determination by neutron activation and multiple γ ratio, 25:41833(R) (IA-1218)
determination following complexation with butyl sulfoxide and 1,1,1,5,5,5-hexafluoro-2,4-pentanedione, gas chromatographic, 25:41725
determination following separation from other metal ions by thin-layer chromatography using quercetin, colorimetric, 25:41743
determination in biological materials, uv fluorescence method for, 25:42244(T) (GAT-Z-5047)
determination in solutions by x-ray-fluorescence spectroscopy, 25:41733
determination in uranium nitrate solutions by x-ray fluorescence using lithium-drifted silicon detector, 25:41833(R) (IA-1218)
determination of acid-soluble, acid-insoluble, and total, in silicate ores, spectrophotometric, 25:41723 (NIM-1077)
determination of, evaluation of problems and sensitivity of fluorometric method for, 25:41722 (JAERI-13622)
effects on graphite--nitrous oxide and graphite--oxygen reactions, catalytic, 25:42931
hazards to Czechoslovakian chemical plant and mining personnel, health education for prevention of, 25:42504
hazards to mining personnel, use of foods and radioprotective substances for reducing, animal experiments on, 25:42510
metabolism and tissue distribution following intake by man, 25:42467
precipitation as uranyl formate, apparatus for continuous, 25:41782(P)
production of fuel cores of, lot controls in, 25:42835
purification by ion exchange, pilot plant for, 25:41919
reactions of trivalent, with hydrated cobalt complexes with ammonia in aqueous perchlorate solutions, 25:41783
reactions with uranium silicide, kinetics of transformation, 25:41833(R) (IA-1218)
requirements in Europe during 1970 to 2010, effects of variations in reactor programs on, 25:44127 (CONF-700903-17)
separation as uranyl nitrate from nitric acid solutions by solvent extraction using TBP and mixer-settler, 25:41895 (INR-1309)
separation from acetone--hydrochloric acid solutions by ion exchange using Bio-Rad, distribution coefficients for, 25:41899
separation from aqueous solutions as uranyl chloride by solvent extraction using trioctylamine, 25:41900
separation from aqueous solutions from fuel reprocessing by multistage extraction using tributyl phosphate, 25:41902(P)
separation from by-products in phosphoric acid production, leaching and precipitation and solvent extraction methods for, 25:41833(R) (IA-1218)
separation from neptunium, niobium, zirconium, and fission products by solvent extraction using tributyl phosphate, 25:41901
separation from nitric acid solutions by solvent extraction using TBP, comparison between computer-simulated and actual performance of mixer-settlers for, 25:41890 (CEA-N-1450)
separation from other metals using inorganic ion exchange papers, 25:41909
separation from plutonium by countercurrent ionophoresis, continuous, 25:41908
separation from plutonium in fuel fabrication scrap, reflex extraction flowsheet using TBP for, 25:41888 (ARH-SA-78)
separation from spent molten salt reactor fuels by selective reduction and extraction using molten bismuth, 25:41903(P)
separation of hexavalent, from nitric acid solutions of fission products by extraction chromatography using bis(2-ethylhexyl) phosphate, 25:41924
superconductivity in α-, at zero pressure, 25:41778 (UCRL-20500, pp 1-85)
transport by microorganisms in lake silts, 25:42256
uptake by aquatic plants, 25:41833(R) (IA-1218)

URANIUM ALLOYS AND SYSTEMS
Al--Si--U, analysis for aluminum by atomic absorption spectroscopy, 25:41832(R) (AECL-3851)
C--N--O--Pu--U, thermodynamic properties and stoichiometry of, 25:42998
C--N--Pu--U, phase studies and structures of, review on, 25:42982 (JAERI-13650)
Fe--U, magnetic properties of cubic Laves phase in intermetallic compound UFe_2, Moessbauer studies on, 25:41833(R) (IA-1218)
Pu--U, analysis for plutonium by α spectrometry, 25:42118(P)
U-base--Zr, mechanical properties of, data tabulation on, 25:42851 (RFP-1703)

URANIUM CARBIDES
decomposition of UC_2, formation of U_2C_3 by, 25:42936 (JUL-728-RW)
effects of annealing in powders of, on mechanical properties of Type 4988 steel, Incoloy 800 and Inconel 718, 25:42844 (EURFNR-922)
fabrication of stoichiometric monocarbide reactor fuels of, method for, 25:42939(P)
neutron reactions at 0.02 to 0.18 eV at 24 to 510°C, total cross sections for, (E), 25:43930
preparation of U_2C_3, by decomposition of UC_2, 25:42936 (JUL-728-RW)
radiation effects on high temperature swelling, fission gas release, and microstructure of, (E/T), 25:44118(R) (BMI-1905)

URANIUM CHALCOGENIDES
rare earth chalcogenides--uranium chalcogenides, phase studies of combinations of, 25:43001

URANIUM COUPLES
Al/U, corrosion of, effects of capacitance discharge and frequency on galvanic, 25:41833(R) (IA-1218)
stainless steel/U, corrosion of, effects of capacitance discharge and frequency on galvanic, 25:41833(R) (IA-1218)
U/Zr, corrosion of, effects of capacitance discharge and frequency on galvanic, 25:41833(R) (IA-1218)

URANIUM DEPOSITS
prospecting in Federal Republic of Germany, 25:41942
prospecting in India using radon content of soils, 25:41945
prospecting in India, status of nuclear methods for, 25:41947

URANIUM DEUTERIDES
neutron reactions at 0.06 to 0.5 eV, total cross sections for, (E), 25:43930

URANIUM FLUORIDES UF_6
inhalation of, uptake, excretion, and retention following, 25:42244(T) (GAT-Z-5047)

URANIUM HYDRIDES
neutron reactions at 0.03 to 0.48 eV, total cross sections for, (E), 25:43930
proton spin lattice relaxation time in, at 150 to 400°C, 25:41833(R) (IA-1218)

URANIUM IODIDES UI_3
uranium-ion energy levels in, calculations, 25:43499

URANIUM IONS
energy levels in uranium dioxide and triiodide, calculations, 25:43499

URANIUM ISOTOPES
distribution in Ligurian Sea sediments, measurement of vertical, 25:41949
separation of, evaluation of methods for, 25:41897(T) (ORNL-tr-2512)

URANIUM ISOTOPES U-232
properties for use as heat source for thermoelectric generators, 25:42014

URANIUM ISOTOPES U-233
metabolism and tissue distribution following intake by man, 25:42467
neutron capture-to-fission ratio in plutonium oxide (PuO_2)--uranium oxide (UO_2) core, (E), 25:44096 (ANL-7710, pp 53-262)
neutron fission at 0.5 to 1.5 MeV, cross-section ratio to uranium-235, (E), 25:43884 (ANL-7710, pp 1-52)
neutron fission from thermal energies to 14 MeV, calculations of total energy released during, (T), 25:43885 (ANL-7748)
separation from other isotopes during 1968 and 1969, review of ORNL program for, 25:41992 (ORNL-4640)
separation from TRISO-coated HTGR fuel, head-end, 25:41906

URANIUM ISOTOPES U-234
half-life of, 25:41832(R) (AECL-3851)
metabolism and tissue distribution following intake by man, 25:42467
separation from other isotopes during 1968 and 1969, review of ORNL program for, 25:41992 (ORNL-4640)

URANIUM ISOTOPES U-235
determination in fuels as measure of burnup, nondestructive, 25:41757

fission of, yields of krypton isotopes from thermal neutron, 25:41833(R) (IA-1218)
fission of, yields of short-lived bromine and iodine isotopes from thermal neutron, 25:41833(R) (IA-1218)
metabolism and tissue distribution following intake by man, 25:42467
neutron capture-to-fission ratio in plutonium oxide (PuO_2)--uranium oxide (UO_2) core, (E), 25:44096 (ANL-7710, pp 53-262)
neutron fission at 0.5 to 1.5 MeV, cross-section ratio to uranium-233, (E), 25:43884 (ANL-7710, pp 1-52)
neutron fission from thermal energies to 14 MeV, calculations of total energy released during, (T), 25:43885 (ANL-7748)
neutron fission of, central reaction ratios of plutonium-239 and uranium-238 fission and uranium-238 capture to, (E/T), 25:44094(R) (AI-AEC-12991)
neutron fission of, diffusion effects on ranges of products from, 25:41885
neutron fission of, independent yields of bromine, iodine, and krypton isotopes in thermal, (E), 25:41833(R) (IA-1218)
neutron fission rate in plutonium oxide (PuO_2)--uranium oxide (UO_2) two zone core, (E), 25:44096 (ANL-7710, pp 53-262)
neutron fission ratio in lattices with multitube enriched fuel, epithermal to thermal, (E/T), 25:44203 (INR-P-1266)
protection against airborne, in enrichment plants, 25:42379
radiation effects on performance of in-pile neutron detectors of, γ, (T), 25:44103
separation from other isotopes during 1968 and 1969, review of ORNL program for, 25:41992 (ORNL-4640)
separation from TRISO-coated HTGR fuel, head-end, 25:41906

URANIUM ISOTOPES U-238

Coulomb fission by neodymium-148 and xenon-132, effects of nuclear forces on cross sections for, (T), 25:43970
energy-level scheme from neutron inelastic scattering, (E), 25:43884 (ANL-7710, pp 1-52)
metabolism and tissue distribution following intake by man, 25:42467
neutron absorption ratio in lattices with multitube enriched fuel, resonance to thermal, (E/T), 25:44203 (INR-P-1266)
neutron capture by, central reaction ratio of uranium-235 fission to, (E/T), 25:44094(R) (AI-AEC-12991)
neutron capture reaction rate in, Doppler effects on, (E/T), 25:44164
neutron capture-to-fission ratio in plutonium oxide (PuO_2)--uranium oxide (UO_2) core, (E), 25:44096 (ANL-7710, pp 53-262)
neutron elastic and inelastic scattering at 1.5 to 5.5 MeV, angular distributions for, 25:43898
neutron elastic and inelastic scattering up to 10 MeV, optical-model analysis of, (E/T), 25:43884 (ANL-7710, pp 1-52)
neutron fission at 1.5 to 5.5 MeV, neutron spectra and angular distributions from, (E), 25:43898
neutron fission from thermal energies to 14 MeV, calculations of total energy released during, (T), 25:43885 (ANL-7748)
neutron fission of, central reaction ratio of uranium-235 fission to, (E/T), 25:44094(R) (AI-AEC-12991)
neutron fission rate in plutonium oxide (PuO_2)--uranium oxide (UO_2) two zone core, (E), 25:44096 (ANL-7710, pp 53-262)
neutron inelastic scattering up to 1.5 MeV, γ spectra from, 25:43884 (ANL-7710, pp 1-52)
neutron total cross section up to 10 MeV, optical-model analysis of, (E/T), 25:43884 (ANL-7710, pp 1-52)
photofission at 200 to 1150 MeV, cross section and fragment energy and angular distributions for, (E), 25:43946

URANIUM NITRATES

analysis for uranium by x-ray fluorescence using lithium-drifted silicon detector, 25:41833(R) (IA-1218)
effects on formation of antibodies against thyroid hormones, 25:42645

URANIUM NITRIDES

sintering of, effects of nitrogen pressure and temperature on, 25:42979
thermodynamic properties of, (T), 25:42965
PuN--UN, fabrication of fuel pins of, 25:44118(R) (BMI-1905)
PuN--UN, irradiation testing of fuels of, 25:44118(R) (BMI-1905)
PuN--UN, self-diffusion of nitrogen in, (E), 25:44118(R) (BMI-1905)

URANIUM ORES

analysis of silicate, for acid-soluble, acid-insoluble, and total uranium, spectrophotometric, 25:41723 (NIM-1077)
mining and milling of, radiation protection manual for personnel, 25:42463

URANIUM OXIDES UO

PuO--UO, preparation of hypostoichiometric $(U,Pu)O_{2-x}$ by hydrogen reduction and carbothermic methods, 25:41779 (ORNL-TM-3358)

URANIUM OXIDES UO_2

analysis for boron by isotope dilution method, 25:41749
coating of spheres of, with vanadium by fluidized bed reduction of vanadium chloride vapors, 25:42935(T) (EURFNR-859)
covalency in, oxygen-17 NMR study of, 25:43497
creep of, effects of fission process on, (E/T), 25:44118(R) (BMI-1905)
fabrication of pellets of, effects of stearate additives or lubricants on, 25:42949
fission gas diffusion and bubble growth in, (T), 25:44118(R) (BMI-1905)
microstructure of fission gas bubbles in, electron microscope studies of, 25:42953(R) (GEAP-12189)
neutron reactions at 0.03 to 0.12 eV, total cross sections for, (E), 25:43930
preparation and properties of sintered, correlation between, 25:41833(R) (IA-1218)
preparation of disk specimens of, abrasive blasting method for out-of-pile thinning, 25:42953(R) (GEAP-12189)
preparation of powdered, for use in reactor fuels, equipment and method for, 25:42938(P)
properties of pellets and powders of, effects of preparation method on chemical and physical, 25:42950
radiation effects on high temperature swelling, fission gas release, and microstructure of, (E/T), 25:44118(R) (BMI-1905)
radiation effects on Zircaloy-2 clad, in-pile, 25:44207 (KAE-68-46)
radiation effects on Zircaloy-2-clad, in-pile, 25:44208 (KAE-68-81)
radiation effects on zirconium alloy clad fuel elements of, in-pile, 25:43010
sintering of powders of, at 1400°C, effects of powder characteristics on, 25:42950
stoichiometry control of, (E), 25:44118(R) (BMI-1905)
uranium-ion energy levels in, calculations, 25:43499
vaporization in sodium cooled reactor accidents, production and behavior of aerosols from, (E/T), 25:44132 (AI-AEC-12992)
PuO_2--UO_2, chemical reactions with Hastelloy X and stainless steels, effects of gas cooled fast breeder reactor conditions on, (E/T), 25:44123 (ORNL-TM-3385)
PuO_2--UO_2, creep of, effects of fission process on, (E/T), 25:44118(R) (BMI-1905)
PuO_2--UO_2, fabrication of pellets of, effects of stearate additives or lubricants on, 25:42949
PuO_2--UO_2, fission product vapor pressures over fast neutron irradiated, (E/T), 25:44206 (CEA-R-4181)
PuO_2--UO_2, radiation effects on mechanical properties of, neutron, 25:44125 (ORNL-TM-3427)
PuO_2--UO_2, restructuring temperatures and kinetics for fuels of, in-pile, (E/T), 25:44124 (ORNL-TM-3387)
PuO_2--UO_2, solubility of pellets of, statistical study of effects of fabrication variables on, 25:42954 (HEDL-SA-131)
ThO_2--UO_2, hydrogen release from sintered pellets of, at 80C to 2000°C, effects of carbon content on, 25:42958 (WAPD-TM-850)
ThO_2--UO_2, preparation of sols of, 25:42945(P)
ThO_2--UO_2, stability of sol-gel microspheres of, under oxidizing conditions in fluid bed, 25:41907
ThO_2--UO_2--U_3C_2, phase diagram at 1100 to 1550°C, 25:42984(T) (ORNL-tr-2483)
ThO_2-base--UO_2, preparation of microspheres of, engineering-scale demonstration of sol-gel process for, 25:42937 (ORNL-4544)

URANIUM OXIDES U_3O_8

ThO_2--UO_2--U_3O_8, phase diagram at 1100 to 1550°C, 25:42984(T) (ORNL-tr-2483)

URANIUM PHENOXIDE

preparation and properties of, 25:41780(T) (SC-T-713038)

URANIUM PHOSPHIDES

magnetic susceptibility of UP from 1.3 to 300°K, (E), 25:43495

URANIUM SILICIDES

reactions with uranium, kinetics of transformation, 25:41833(R) (IA-1218)

URANIUM SULFIDES

crystalline lattice parameters of U_3S_4, 25:43001
BaS--US, phase studies of, 25:43002
CaS--US, crystal structure of $CaUS_2$, 25:43002
CaS--US, phase diagram of, 25:43002
SrS--US, crystal structure of $SrUS_2$, 25:43002
SrS--US, phase diagram of, 25:43002

URANYL CHLORIDES

solubility in trioctylamine, 25:41900

URANYL COMPOUNDS

complexes with thenoyltrifluoroacetone, adduct formation with TBP, effects of solvents on, 25:41784
reactions with polypeptide-containing hydrophilic polymeric capsule wall material, 25:41781(P)

URANYL FLUORIDES

spectra of complex, influence of outer sphere cations on ir, luminescence, and Raman, 25:41828

URANYL FORMATES

precipitation by reactions of formic acid with uranyl nitrate solution, apparatus for continuous, 25:41782(P)

URANYL NITRATES

analysis for boron by isotope dilution method, 25:41749
diffusion in phosphate ester solvent membranes,

coefficients for, 25:41833(R) (IA-1218)
preparation from sodium diuranate, 25:41919
reactions with formic acid, apparatus for continuous precipitation of uranyl formates from, 25:41782(P)
storage of solutions of depleted, at West Valley Processing Plant, 25:41891 (DOCKET-50201-74)
transport through alkyl or allyl phosphoric acid ester membranes, 25:41833(R) (IA-1218)
heptane--TBP--$UO_2(NO_3)_2$, diffusion studies on, 25:41829
URANYL SULFATES
reactions with hydrogen peroxide in reactor aqueous fuel solutions, (E), 25:44155
UREA, HYDROXY-
effects on repair of x-radioinduced breaks in DNA of Escherichia coli, 25:42357
URETHAN POLYMERS
radioinduced curing of coatings of, 25:41844(P)
URINE
analysis for americium-241 by precipitation, ion exchange, electroplating, and a counting, 25:41756
radiation effects on carbon-14-labeled orotic acid or iodine-131-labeled albumin excretion in rat, as indicators of radiation injury, whole-body γ, 25:42407
radiation effects on excretion of MEA in rat, whole-body, 25:42671
radiation effects on excretion of nucleic acid metabolites in rat, effects of cysteamine on, 25:42625
radiation monitoring of human, at JAERI, dose calculations from, 25:42439
radioisotope content of human, in Italy, 25:42375
tritium content in, of neutron generator operators, equations for calculating dose equivalents from, 25:42390
uranium excretion in human, following inhalation of uranium hexafluoride, 25:42244(T) (GAT-Z-5047)
UTERUS
radiation effects on human, following castration, carcinogenic, 25:42675
radiotherapy of cancer of human, effectiveness of high-dose γ, 25:42598

V

VACUUM
bibliography on surface and vacuum physics, 25:43111
VACUUM GAGES
description and calibration of, for ultrahigh vacuum metrology, 25:42047
VACUUM SYSTEMS
pressure measurements in ultrahigh, gage calibration for, 25:42047
VAGINA
radiotherapy of cancer of human, effectiveness of high-dose γ, 25:42598
VALVES
standard for class I, for liquid metal service, 25:41965 (RDT-E-1-18-T)
standard for freeze vent for sodium service, 25:41968 (RDT-E-4-13-T)
standard for small, Class II, liquid metal, 25:41966 (RDT-E-1-19-T)
VAN ALLEN RADIATION BELTS
electron pitch-angle scattering in outer, during magnetic storms, (E/T), 25:43267
electron precipitation from outer, knee occurrence in L-shell profile from, (E/T), 25:43211 (AD-715266)
energy conservation by cold plasma injection in, (T), 25:43271
VAN DE GRAAFF ACCELERATORS
accelerating tubes of 1-MV, effects of neutral component of ion beam on current loading of, 25:43769
description of heavy-ion, for simulating fast-neutron radiation damage, 25:43758
VANADIUM
analysis for hydrogen by isotopic equilibration mass spectrometry, 25:41747 (AAEC/TM-588)
chemical thermodynamic properties of, selected values of, 25:41826 (NBS-TN-270-5)
compounds, thermodynamic properties of, tables of, 25:41826 (NBS-TN-270-5)
deposition on uranium dioxide spheres by reduction of vanadium chloride vapors, 25:42935(T) (EURFNR-855)
determination following separation from other metal ions by thin-layer chromatography using quercetin, colorimetric, 25:41743
determination in iron and steel standards by neutron activation and γ spectrometry, 25:41774
hardness at 600 to 1000°C, 25:42884 (JAERI-13731)
neutron capture at 0.1 to 200 keV, cross sections for, (E), 25:43857
neutron transmission measurements up to 300 keV, (E), 25:43857
separation from acetone--hydrochloric acid solutions by ion exchange using Bio-Rad, distribution coefficients for, 25:41899
separation from other metals using inorganic ion exchange papers, 25:41909
surface structure of, low-energy electron diffraction studies on, 25:41778 (UCRL-20500, pp 1-85)
tensile properties of, Portevin--Le Chatelier effect on temperature and strain rate, (E), 25:43486
VANADIUM ALLOYS AND SYSTEMS
Al--Cr--Mo--Ti-base--V--Zr, mechanical properties of, 25:42836 (AD-715877)
Al--Mo--Ti-base--V, radiation effects on tensile properties of, at 17°K, fast neutron, 25:42926
Al--Ti-base--V, radiation effects on tensile properties of, at 17°K, fast neutron, 25:42926
Al--V, preparation of superconducting V_3Al intermetallic phase in, 25:42886 (UCRL-20500, pp 86-146)
C--Fe--Ni--V, crystal twinning in bulk and thin-foil, structure of transformation-type, 25:42886 (UCRL-20500, pp 86-146)
Cr--Cu--Fe--Mo--Nb--V--Zr-base, corrosion resistance of, 25:42811
Ga--V, superconducting properties of V_3Ga wires in copper--gallium matrix, effects of reaction and heat treatment on, 25:43292
Ti--V-base, crystallization of annealed and cold rolled, kinetics of, 25:42884 (JAERI-13731)
VANADIUM BORIDES
preparation of, method for, 25:42944
thermal capacity of, low-temperature, 25:42974
CrB--VB, thermal capacity of, low-temperature, 25:42974
VANADIUM ISOTOPES
chromium--vanadium Coulomb displacement energies, (E), 25:43883
titanium--vanadium Coulomb displacement energies, (E), 25:43883
VANADIUM ISOTOPES V-51
energy levels from titanium-50 (He-3,d) reactions, shell-model calculations of spectroscopic factors for, (T), 25:43862
energy levels of, shell-model calculation of magnetic dipole and electric quadrupole moments, spin--parity assignments, and wave functions for, (T), 25:43862
energy-level transitions in, shell-model calculations of probabilities for E2 and M1, (T), 25:43862
helium-3 reactions (He-3,t) at 24.6 MeV, triton spectra from, (E), 25:43883
VANADIUM OXIDES
electric conductivity of, effects of titania and niobia on temperature dependence of, 25:43481
electric properties of fused, at 600 to 1200°C, effects of calcium oxide addition and oxygen partial vapor pressure on, 25:42969
structure of VO/sub 1.15 to 1.25/, superstructure stability in, 25:43007
NbO_2--VO_2, electric conductivity of, temperature dependence of, 25:43481
TiO_2--VO_2, electric conductivity of, temperature dependence of, 25:43481
VANADIUM OXYFLUORIDES
crystal structure of, 25:42943
preparation of, method for, 25:42943
VANADYL COMPOUNDS
reactions with polypeptide-containing hydrophilic polymeric capsule wall material, 25:41781(P)
VEGETABLES
beans, cesium-137 and strontium-90 content of, in Bulgaria during 1965, 25:42381
cabbage, cesium-137 and strontium-90 content of, in Bulgaria during 1965, 25:42381
onions, cesium-137 and strontium-90 content of, in Bulgaria during 1965, 25:42381
onions, radiation effects on sprout darkening during subsequent storage, 25:41833(R) (IA-1218)
onions, radiation effects on sprouting and storage life of, effects of dose on, 25:42745 (RISO-238)
peppers, cesium-137 and strontium-90 content of, in Bulgaria during 1965, 25:42381
potatoes, cesium-137 and strontium-90 content of, in Bulgaria during 1965, 25:42381
potatoes, radiation effects on reducing sugar, total soluble solids, total sugar, and vitamin C content during subsequent storage, 25:41833(R) (IA-1218)
potatoes, radiation effects on sprouting of winter-harvested, during subsequent storage, 25:41833(R) (IA-1218)
tomatoes, cesium-137 and strontium-90 content of, in Bulgaria during 1965, 25:42381
VENUS (PLANET)
atmosphere of, space-probe data of solar-wind interaction with, (E), 25:43272
VERMONT YANKEE POWER REACTOR
emergency core cooling system for, AEC acceptance requirements for, 25:44048 (DOCKET-50271-55)
emergency core cooling system for, performance requirements for, 25:44049 (DOCKET-50271-56)
personnel for, qualifications of pre-operation and power operation testing, 25:44049 (DOCKET-50271-56)
safety evaluation of, Division of Reactor Licensing, 25:44050 (DOCKET-50271-57)
VERPLANCK POWER REACTOR, UNIT 1
design parameters of, revised and additional data on, 25:44060 (DOCKET-50342-7)
operations aspects of, revised and additional data on, 25:44060 (DOCKET-50342-7)
VERPLANCK POWER REACTOR, UNIT 2
design parameters of, revised and additional data on, 25:44060 (DOCKET-50342-7)
operations aspects of, revised and additional data on,

XUM

25:44060 (DOCKET-50342-7)
VESSELS
sealing of glass ampule-type, containing radioactive material, equipment and method for semiautomatic flameless, 25:42046
testing of radioactive waste storage, design and development of ultrasonic system for, 25:42020 (BNWL-B-103)
VINBLASTINE
effects on bone marrow cells of x-irradiated mice and rats, 25:42655
VIRGIL C. SUMMER POWER REACTOR, UNIT 1
auxiliary systems for, preliminary safety analysis of, 25:44077 (DOCKET-50395-7)
construction of, permit application for, 25:44071 (DOCKET-50395-1)
containment structures and systems for, preliminary safety analysis of, 25:44076 (DOCKET-50395-6)
control systems for, preliminary safety analysis of, 25:44076 (DOCKET-50395-6)
cooling system for, preliminary safety analysis of, 25:44075 (DOCKET-50395-5)
design parameters of, preliminary safety analysis of, 25:44073 (DOCKET-50395-3)
design parameters of, preliminary safety analysis of, 25:44075 (DOCKET-50395-5)
effluents from, effects on environment of chemical, radioactive, and thermal, 25:44072 (DOCKET-50395-2)
electrical systems for, preliminary safety analysis of, 25:44077 (DOCKET-50395-7)
engineered safeguards for, preliminary safety analysis of, 25:44076 (DOCKET-50395-6)
instrumentation for, preliminary safety analysis of, 25:44076 (DOCKET-50395-6)
operation of, license application for, 25:44071 (DOCKET-50395-1)
operations aspects of, preliminary safety analysis of, 25:44073 (DOCKET-50395-3)
operations aspects of, preliminary safety analysis of, 25:44077 (DOCKET-50395-7)
owners of, financial statements of, 25:44071 (DOCKET-50395-1)
radiation protection system for, preliminary safety analysis of, 25:44077 (DOCKET-50395-7)
radioactive waste disposal system for, preliminary safety analysis of, 25:44077 (DOCKET-50395-7)
safety analysis for, 25:44078 (DOCKET-50395-8)
site for, preliminary safety analysis of, 25:44074 (DOCKET-50395-4)
steam and power conversion systems for, preliminary safety analysis of, 25:44077 (DOCKET-50395-7)
technical specifications for, 25:44078 (DOCKET-50395-8)
testing programs for, preliminary safety analysis of, 25:44077 (DOCKET-50395-7)
VIRUSES
Hemophilus influenzae, genetic transformation in, research progress on, 25:44270(R) (NYO-1371-64)
lymphocytic choriomeningitis, radiation effects on immunological tolerance of mice to, x, 25:42313
radiosensitivity of polio, during infection of Hela cells, phosphorus-32 β, 25:42741
SV40, radiation effects on production of, by PM3 cells after fusion with AGMK cells, uv, 25:42733
VITAMIN A GROUP
effects on eruption of teeth of rats following prenatal exposure, 25:42638
VITAMIN B GROUP
nicotinamide, radiation effects on metabolism of, in mice and rats, mechanisms for, 25:42623
riboflavin, photolysis of, uv, 25:41788
VITAMINS
effects on reduction of radiation hazards to uranium mining personnel, combined effects of radioprotective substances and, 25:42510
VOLTMETERS
design of wide-range, for very low voltages, 25:42208(P)

W

WASHINGTON
radioactivity monitoring in surface waters of, during 1968 to 1969, β, 25:42419
tritium content of surface waters in, during 1968 to 1969, 25:42419
WATER
analysis for deuterium by ir or mass spectrometry, 25:41832(R) (AECL-3851)
analysis for gold by neutron activation, 25:41770
analysis for gold by sorption on lead sulfide and neutron activation, 25:41771
corrosive effects of neutral, on niobium--zirconium alloys at 300°C, 25:42814
corrosive effects on niobium--zirconium-base alloys, measurement by polarization resistance, 25:42807
corrosive effects on Zircaloy and chromium--iron--zirconium-base alloys at 300 to 400°C, kinetics, 25:42815
corrosive effects on Zircaloy at 340°C, effects of decontamination processing on, 25:42808
corrosive effects on zirconium alloys at high temperatures, relations with radiation dose, 25:42927
effects on self radiolysis of carbon dioxide--tritium systems, 25:41852 (LA-4657)
electron reactions with, spectral-angular characteristics in, (T), 25:43421(T) (ORNL-tr-2475)
exchange between hydrated cations and solvent, oxygen-17 NMR studies on, 25:41778 (UCRL-20500, pp 1-85)
heat transfer modes for boiling, on nonisothermal surface, (T), 25:41989
mass stopping for gamma and x rays, calculation of mean, 25:42085
neutron slowing down density distribution in, evaluation of ENDF/B data for, (E/T), 25:44094(R) (AI-AEC-12991)
radio emission from, in southern hemisphere OH regions, (E), 25:43051
reactions with leaking heated sodium in boilers, effects on steel tubes, 25:42804(R) (LMEC-71-1)
solution heat of, effects of deuterium on, 25:41794
solvent properties of distilled, for curium-244-oxide pellets and powders, 25:41993(R) (ORNL-4692)
benzene--H_2O, radiolysis at 150 to 200°C, effects of iron(II), iron(III), and oxygen on yields of phenols from electron or γ, 25:41858
D_2O--H_2O, radiolysis of, electron pulse, 25:41832(R) (AECL-3851)
H_2O--rare earth oxides, phase studies of, 25:42934 (COO-1109-60)
H_2O--toluene, radiolysis, effects of air and iron(III) on yields of cresol isomers from electron or γ, 25:41858
WATER-d
analysis for deuterium/hydrogen ratio, mass spectroscopic, 25:41729
WATER-d_2
effects on chlorophyll mutation frequency and growth of rice seedlings following seed treatment, effects of EMS on, 25:42346
effects on ionization of malononitrile, kinetic, 25:41799
neutron slowing down density distribution in, evaluation of ENDF/B data for, (E/T), 25:44094(R) (AI-AEC-12991)
production in cooling towers in series, 25:41904(P)
D_2O--H_2O, radiolysis of, electron pulse, 25:41832(R) (AECL-3851)
WATER-t_2
metabolism and tissue distribution following intake by man, 25:42467
WATER SUPPLIES
production of regional, by multiple purpose use of thermal effluent discharges from nuclear power plants, 25:44083 (BNWL-SA-2738)
radioactivity in, status of Japan standards for maximum permissible, 25:42482
radioisotope content of USA, standards on maximum permissible, 25:42470
radioisotope removal from, effectiveness of bentonites for cesium-137, ruthenium-106, and strontium-90, 25:42384(P)
radon-222 content in, whole-body counter measurements on radiation dose from, 25:42247 (SFL-A-16)
standards for drinking water, USA, 25:42470
WATER VAPOR
content in atmosphere over Lake Tahoe, Nevada, 25:41938
oxygen-18 fractionation between ice and, 25:41921
WATERFORD POWER REACTOR, UNIT 3
quality assurance requirements for, additional data on, 25:44070 (DOCKET-50382-7)
WATERFORD POWER REACTOR, UNIT 4
quality assurance requirements for, additional data on, 25:44070 (DOCKET-50382-7)
WAUKESHA 88
radiation effects on mechanical properties of, at 355°K, 25:42903 (N-71-14040)
WELDING
equipment for pipe, design of remote automated, 25:41981
evaluation of percussive-arc and pulse-arc, 25:44231 (BDX-613-395)
WELDING RODS
standard for gas--metal arc welding, 25:42766 (RDT-M-1-6-T)
standard for nickel and nickel alloy bare welding, 25:42771 (RDT-M-1-11-T)
standard for stainless steel, 25:42763 (RDT-M-1-2-T)
standards for copper and copper alloy, 25:42768 (RDT-M-1-8-T)
WELDS
inspection of steam pipe, use of ultrasonics for, 25:44082 (SWRI-1228-9-10)
inspection of, system for automatic ultrasonic, 25:44111 (CONF-700224-, Paper 6)
solidification structures and mechanism in metal, (E/T), 25:42820
standard for testing of fuel element cladding closure, 25:42025 (RDT-F-3-6-T)
WELL LOGGING
equipment for, gamma spectrometer, 25:42117(P)
methods for nonpetroleum mineral resources prospecting, review of nuclear, 25:41931
WEST VALLEY PROCESSING PLANT
plutonium nitrate receipt and storage at, proposed changes in technical specifications for, 25:41891 (DOCKET-50201-74)
uranyl nitrate receipt and storage at, proposed changes

in technical specifications for depleted, 25:41851 (DOCKET-50201-74)
WHISTLERS
interactions with electrons in plasma at Doppler shifted cyclotron frequency, (E), 25:43412
radio-wave emission from trains, triggered vlf discrete, (T), 25:43245
WHOLE-BODY COUNTERS
description of Garigliano, 25:42081
design of reduced-shield, for monitoring internal contamination, 25:41833(R) (IA-1218)
WILLIAM H. ZIMMER POWER REACTOR, UNIT 1
design parameters of, revised and additional data on, 25:44063 (DOCKET-50358-19)
design parameters of, revised and additional data on, 25:44064 (DOCKET-50358-20)
operations aspects of, revised and additional data on, 25:44063 (DOCKET-50358-19)
operations aspects of, revised and additional data on, 25:44064 (DOCKET-50358-20)
WIND
effect of neutral, on F-region ion-drift vertical velocity, (E/T), 25:43224
effect of upper atmospheric, on F2-layer plasma drifts, (T), 25:43225
WOOD
radioinduced polymerization of vinyl monomers in, research progress on electron or γ, 25:41843(R) (ORO-2945-10)
plastics--wood, properties of, produced by radioinduced polymerization, 25:41843(R) (ORO-2945-10)

X

X RADIATION
attenuation in interstellar and intergalactic space, (T), 25:43080 (N-71-21563)
cosmic background, origin and properties of, (T), 25:43079 (N-71-20472)
dose to children from different radiographic procedures, comparison of, 25:42412
dose to human gonads during diagnostic radiography of pelvic region, use of aluminum filters for reduction of, 25:42447
dose to human skin during diagnostic radiography, method for calculation of, 25:42431
dose to human tissues during diagnostic radiography and therapy, effects of energy on absorbed, 25:42430
dose to man from television, annual, 25:42366
dosimetry of, energy and phantom-depth dependence of film sensitivity for 60 to 300 kV, 25:42396
effectiveness for preoperative treatment of carcinomas of larynx and pharynx, effects of dose and dose fractionation on, 25:42588
effectiveness for therapy of carcinomas of head and neck, additive effects of 5-fluorouracil infusion on, 25:42589
effects on 2-methyl-β-alanine excretion in human urine, 25:42684
effects on 7α-hydroxylase activity in rat testes, 25:42621
effects on acid phosphatase in thymus gland of mice, whole-body exposure, 25:42287
effects on alcohol mixtures, ion--solvent interactions in, 25:41871
effects on aminotransferase activity in serum of rats, effects of unsaturated fatty acid content of diet on whole-body exposure, 25:42298
effects on aqueous solutions of 2-mercaptoethanol, lytic, 25:42294
effects on ascites ovarian tumors and ascites Pliss' lymphosarcoma in rats, comparison of, 25:42637
effects on Aspergillus niger, mutagenic, 25:42363
effects on avoidance behavior in rats, 25:42321 (COO-697-23)
effects on bioelectrical activity in brain of rabbits, effects of radial acceleration on sublethal, 25:42653
effects on blood cells in medical personnel, 25:42600
effects on blood glucose, serum electrolytes, and liver glycogen of rats, protective effects of methylene blue against, 25:42283
effects on bone marrow cells of mice and rats, effects of vinblastine on, 25:42656
effects on brain of rats, effects of hypertension on latent, 25:42667
effects on bromine-82 metabolism in rats following exposure of abdomen, 25:42282
effects on capillary permeability in rabbit skin, effects of 6-aminohexanoic acid on, 25:42617 (UR-49-1462)
effects on carbohydrate content in durum and soft wheat, 25:42721
effects on carcinogenesis in enamel organ in mice, combined effects of physical trauma and, 25:42670
effects on central nervous system in mouse and rat embryos, aberrant, 25:42629
effects on cerebrosides and phospholipids in rat brain, protective effects of cysteine against damaging, 25:42620
effects on Chinese hamster cells with and without oxygen, mechanism of protective effects of cysteamine on, 25:42521
effects on chromosomes in bone marrow cells of mice, protective effects of cysteine derivatives against aberrant whole-body exposure, 25:42534
effects on chromosomes in Crepis capillaris, effects of DNA on recovery from aberrant, 25:42356
effects on chromosomes of newborn child following radiography, aberrant, 25:42362
effects on chromosomes of synchronized and unsynchronized cultured rat kangaroo cells, comparison of aberrant, 25:42348
effects on chromosomes of Vicia faba, use of protein-specific dyes to visualize aberrant, 25:42343
effects on coagulation and fibrinolysis of rat blood, protective effects of cystamine and bone marrow nucleic acids against, 25:42537
effects on competence development in Bacillus subtilis in relation to multi-target state of cells, 25:42736
effects on content of serum thyrotropin and thyroid function of man following therapy of lymphomas, 25:42695
effects on content of sulfur-containing amino acids in organ proteins in rats, 25:42265
effects on count of haploid cells and incidence of chromosome aberrations in cultured mammalian cells, effects of dose on, 25:42347
effects on cytochrome oxidase and monoamine oxidase activity in human skin, 25:42285
effects on differentiation of surviving stem cells in mice in comparison to effects of alkylating agents, 25:42661
effects on diseases in man, therapeutic, 25:42597
effects on distribution of acid phosphatase and β-glucuronidase in rat liver and spleen, whole-body, 25:42628
effects on DNA in cultured mammalian cells, protective effects of cystamine or cysteamine against, 25:42522
effects on DNA in Ehrlich ascites tumor cells, effects of ATP production on rejoining of breaks following x, 25:42632
effects on DNA of Escherichia coli mutants, role of DNA polymerase in repair of single-strand break, 25:42326
effects on DNA of Escherichia coli, relation between lethality and repair of in vitro and in vivo single-strand breaks induced by, 25:42357
effects on doped potassium chloride crystals, growth curves of F centers induced in, (E), 25:43450
effects on electrophoretic mobility of human erythrocytes, combined effects of neuraminidase or potassium permanganate on low-dose, 25:42682
effects on eruption of teeth of rats following prenatal exposure, 25:42638
effects on Escherichia coli mutants defective in DNA replication, 25:42331
effects on eyes of rats, protective effects of cysteamine and glutathione against, 25:42538
effects on fertility in mice following testicular exposure, 25:42655
effects on fetuses of mice and rats, effects of species on, 25:42639
effects on frequency of chromosome translocations in oocytes of Drosophila, effects of dose on, 25:42333
effects on goldfish and Oryzias latipes, comparison of chronic low-dose γ and repeated high dose, 25:42634
effects on heart rate and open field behavior of rats, effects of dose and prenatal exposure on, 25:42640
effects on HeLa cells, mechanism of protective effects of MEA and MEG and its derivatives against, 25:42514
effects on hematopoiesis in mice, effects of irradiated and unirradiated bone marrow transplants on, 25:42644
effects on immunity of recipient mice to Hymenolepis nana following injection of spleen cells from immunized donor mice, 25:42311
effects on immunological tolerance of mice to virus, 25:42313
effects on in vitro activity of isocitrate dehydrogenase, role of sulfhydryl group destruction in, 25:42299
effects on inactivation of threonine-sensitive aspartate kinase--homoserine dehydrogenase from E. coli, 25:42291
effects on incidence of childhood cancer following prenatal exposure in England and Wales during 1968, 25:42696
effects on incidence of chromosome aberrations in roots of sunflowers, effects of seed-exposure dose on, 25:42361
effects on incidence of chromosome translocations resulting in sterility in mosquitoes, effects of dose on, 25:42335
effects on incidence of chromosome translocations in Drosophila following exposure of male pupae, 25:42354
effects on incidence of mutations in rats following exposure of nine generations, 25:42321 (COO-697-23)
effects on learning following exposure of head of one-day-old rats, 25:42655
effects on leukocyte count, lysozyme activity, and trypsin inhibitors in serum of rabbits, effects of dose on whole-body exposure, 25:42648
effects on life span and tumor incidence in rats, effects of stress on whole-body, 25:42669
effects on life span of mice, effects of microbial flora on whole-body, 25:42663

XUM

effects on lipolytic activity of rat heart tissues in relation to heparin content, sensitizing effects of cysteamine on, 25:42281
effects on luminescence of organic crystals, quenching, 25:41840
effects on lymphatic tissues in chickens, effects of dose on pathological, 25:42658
effects on man following therapy of menorrhagia, statistical study of long-term neoplastic and pathological, 25:42702
effects on man, effects of dose, dose rate, age, and sex on pathological, 25:42453
effects on mature Drosophila oocytes, segregation of chromosomes following, 25:42276
effects on membrane association of conjugally transferred DNA in Escherichia coli minicells, 25:42735
effects on metabolic equilibrium in rat brain, protective effects of cysteine against damaging, 25:42619
effects on metabolism of biogenic amines in animals as indicators of radiation injury, 25:42626
effects on metabolism of biogenic amines in rabbits as indicators of radiation injury, 25:42627
effects on metabolism of p-nitrophenol in rats, whole-body exposure, 25:42289
effects on metabolism of selenium-75 and sulfur-35 in rat organs, 25:42264
effects on mice treated with isologous bone marrow transplants, pathology of, 25:42665
effects on mice, protective effects of thiophosphate compounds against, 25:42525
effects on mice, role of bone marrow transplants in long-term survival following, 25:42666
effects on microorganisms, review of improvement in practical applications through mutagenic, 25:42345
effects on mitosis in bone marrow cells and phagocytic activity of reticuloendothelial cells in rats, protective effects of direct electric current against, 25:42530
effects on morphology of cells in human testes following local exposure, effects of dose on, 25:42674(R) (RLO-1780-32)
effects on MOS field-effect transistors at 79°K, annealing of, 25:42234
effects on MOSFET transistors, 25:42233
effects on mouse adrenal cortex and reticuloendothelial systems, protective effects of cysteamine, lipopolysaccharide, and serotonin against, 25:42513
effects on Neurospora, specificity of mutagenic, 25:42352
effects on oocytes of silkworms, effects of meiotic stage on, 25:42609
effects on oxidation-reduction potential in rat tissues, protective effects of AET or MEA in combination with hypoxia against, 25:42511
effects on oxygen consumption and lysine uptake of HeLa cells, effects of metabolic inhibitors on, 25:42295
effects on patient with leukemia and herpes zoster, recurrence of herpetic lesions following therapeutic, 25:42689
effects on positron lifetimes and intensities in sodium chloride crystals, 25:43453
effects on rabbit cardiovascular system, effects of solar exposure on whole-body, 25:42651
effects on rats in relation to age and sex, effects of metabolic activity on, 25:42635
effects on rats, mechanism of protective effects of dimethyl sulfoxide against, 25:42524
effects on rats, protective effects of direct electric current against lethal, 25:42530
effects on ribonuclease activity in human urine and vaginal fluid following therapy, 25:42683
effects on root tip chromosomes of onion and Zamia in comparison to cycasin, emulsin, and methylazoxymethanol, abberant, 25:42334
effects on saccharin-avoidance behavior in rats, effects of amygdala, olfactory bulb, and septal lesions on, 25:42647
effects on serotonin metabolism in cats as indicator of radiation injury, 25:42627
effects on single crystals of dipotassium difluoromalonate, ESR studies on, 25:41838
effects on sodium chlorate crystals, ESR spectrum after 200°C thermal bleaching of, 25:43451
effects on spermatogonia of mice in relation to lifetime reproductive capacity of offspring, 25:42342
effects on spleen stem cells in mice, effects of actinomycin D on erythropoietic recovery following partial-body, 25:42673
effects on survival of colony-forming units in mouse bone marrow, RBE comparison with D-T neutrons and γ radiation for, 25:42601
effects on survival of guinea pigs, mice, and rats, protective effects of cyclophosphamide against whole-body, 25:42518
effects on survival of mice and rats, long term protective effects of N- and S-containing polymers against, 25:42517
effects on survival of mice and rats, protective effects of methylene blue against whole-body, 25:42515
effects on survival of planarians, role of serotonin in recovery from, 25:42527
effects on SV-40 transformed kidney cells of hamsters used in immunization against tumors, 25:42305
effects on synthesis of liver catalase in mice, 25:42278
effects on teeth of hamsters in utero, 25:42649
effects on tumors in rats in relation to protein sulfhydryl group, methods for studying, 25:42618
effects on types of Hydra cells, 25:42613
effects on vestibular and spinal reflexes of cats following cerebellar granule cell, 25:42657
effects on wheat, sensitivity of induced hybrids following mutagenic, 25:42360
effects on Y chromosome in male fruit flies, segregation of rearrangements following aberrant, 25:42344
emission by color television sets in Pennsylvania during 1968 to 1970, survey of hazards from, 25:42501
emission from Sun, Vela VI data for Sept. 1, 1970 to Jan. 1, 1971, (E), 25:43066 (LA-4454(Vol.5))
energy fluence measurements of pulsed, quantameter for, 25:43750
hazards of diagnostic, methods for minimizing, 25:42493
origin of, from Vela X, (T), 25:43039
production of solar, (E/T), 25:43067 (N-71-16749)
properties of galactic, (T), 25:43079 (N-71-20472)
protection of human patients against, during diagnostic radiography, ICRP standards for, 25:42453
reactions with argon, krypton, and neon at 0.28 to 8.03 keV, relative abundances of multiply charged ions produced by, (E), 25:43142
scattering by copper, Duralumin, and lead at 11.3 to 23.2 MeV, back-, (E), 25:43431

X-RAY-ABSORPTION ANALYSIS
uses in on-stream analysis in mineral processing plants, review on, 25:41740

X-RAY-DIFFRACTION ANALYSIS
research progress in, annual report, 1969--70 on, 25:43468 (NP-18657)

X-RAY DIFFRACTOMETERS
design and operation of, safety standards for, 25:42225
design and performance of scintillation, for dynamic studies, 25:42210

X-RAY EQUIPMENT
hazards to veterinary surgeons using, code of practice for protection against, 25:42485
radiation safety for diffraction and fluorescence analysis, standards for, 25:42225
safety of Be-window tube without filtration for diagnostic radiography, evaluation of, 25:42545

X-RAY FLUORESCENCE ANALYSIS
equipment for mineral prospecting by, design of mobile, 25:41768
equipment for, safety standards for, 25:42225
equipment for, semiconductor x-ray spectrometer, 25:42217
uses in mineral prospecting and on-stream analysis, 25:41741
uses in on-stream analysis in mineral processing plants, review on, 25:41740
uses of radioisotope, in mineral exploration and mining, 25:41739

X-RAY SOURCES
design of monoenergetic radioisotope, for x-ray fluorescence analysis for mineral prospecting, 25:41741
use for industrial radiography, ILO safety manual for, 25:42461

X-RAY SPECTROMETERS
performance of semiconductor, for fluorescence analysis, 25:42217

X-RAY SPECTROSCOPY
developments in, review of, 25:42133

XENON
reactions with alkali metal halides, crossed-beam study of dissociation in, 25:43131
sorption by surfaces of cadmium chloride, iron chloride, lead chloride, and nickel chloride, thermodynamic studies on stepwise isotherms for, 25:41824 (CEA-R-4089)

XENON IONS
implantation in gallium arsenide at 400 keV, effects on phonon modes of Raman spectrum, 25:43440
implantation in silicon at 220 keV, measurements of stresses induced by damage from, 25:43441
reactions with carbon at 20 keV to 1.5 MeV, cross sections for K x-ray production in, (E), 25:43107
reactions with nitrogen molecules at 30 keV to 2 MeV, cross sections for excitation of N_2^+ 3914-A radiation in, (E), 25:43151

XENON ISOTOPES Xe-131
energy levels from iodine-131 decay, spin-parity assignments for, (E), 25:43896

XENON ISOTOPES Xe-132
reactions (Xe-132,f) with uranium-238, effects of nuclear forces on cross sections for Coulomb fission, (T), 25:43970

XENON ISOTOPES Xe-133
determination in gases by chromatography and counting, 25:41753(P)
use to study gas exchange in human lungs, 25:42561

XENON ISOTOPES Xe-135
determination in gases by chromatography and counting, 25:41753(P)

Y

YANKEE POWER REACTOR
quality assurance program for, 25:44025 (DOCKET-50029-152)
YTTERBIUM
determination in meteorites by neutron activation and high-voltage electrophoresis, 25:41776
positron annihilation in, under pressure, 25:41778 (UCRL-20500, pp 1-85)
radiolysis of aqueous solutions of, spectral studies on pulse, 25:41833(R) (IA-1218)
separation from acetone--hydrochloric acid solutions by ion exchange using Bio-Rad, distribution coefficients for, 25:41899
separation from aqueous solutions by ion exchange on zirconium tellurate, tracer studies on, 25:41915
YTTERBIUM ALLOYS AND SYSTEMS
Pt--Yb, crystal structure of YbPt, 25:42892
YTTERBIUM HYDRIDES
electron band structure of, 25:43126
positron annihilation in, angular correlation of radiation from, (E), 25:43126
YTTERBIUM ISOTOPES Yb-169
preparation of DTPA-incorporated, method for, 25:41833(R) (IA-1218)
YTTERBIUM ISOTOPES Yb-172
alpha reactions (α,t) at 30 MeV, triton spectra from, (E), 25:43942
helium-3 reactions (He-3,d) at 28 MeV, deuteron spectra and angular distributions for, (E), 25:43942
proton elastic and inelastic scattering at 16 MeV, differential cross sections for, (E), 25:43901
YTTERBIUM ISOTOPES Yb-174
alpha reactions (α,t) at 30 MeV, triton spectra from, (E), 25:43942
helium-3 reactions (He-3,d) at 28 MeV, deuteron spectra and angular distributions for, (E), 25:43942
neutron capture by, cross sections and gamma spectra from thermal, (E), 25:43891(T) (RFP-Trans-78)
proton elastic and inelastic scattering at 16 MeV, differential cross sections for, (E), 25:43901
YTTERBIUM ISOTOPES Yb-175
energy level at 513 keV from ytterbium-174 neutron capture, spin assignment for isomeric, (E), 25:43891(T) (RFP-Trans-78)
isomeric transition in, half-life and gamma spectra from, (E), 25:43891(T) (RFP-Trans-78)
YTTERBIUM ISOTOPES Yb-176
alpha reactions (α,t) at 30 MeV, triton spectra from, (E), 25:43942
helium-3 reactions (He-3,d) at 28 MeV, deuteron spectra and angular distributions for, (E), 25:43942
proton elastic and inelastic scattering at 16 MeV, differential cross sections for, (E), 25:43901
YTTERBIUM OXIDES
analysis for impurities, cathode region method for spectrochemical, 25:41833(R) (IA-1218)
Tm_2O_3--Yb_2O_3, preparation by coprecipitation method, 25:41993(R) (ORNL-4692)
YTTRIUM
chemical thermodynamic properties of, selected values of, 25:41826 (NBS-TN-270-5)
compounds, thermodynamic properties of, tables of, 25:41826 (NBS-TN-270-5)
determination in calcium fluoride by x-ray fluorescence spectrometry, 25:41832(R) (AECL-3851)
magnetic susceptibility of, generalized function for, (T), 25:43477
separation from acetone--hydrochloric acid solutions by ion exchange using Bio-Rad, distribution coefficients for, 25:41899
separation from aqueous solutions by ion exchange on zirconium tellurate, tracer studies on, 25:41915
separation from europium by elution chromatography, 25:41910
YTTRIUM ALLOYS AND SYSTEMS
Al--Cr--Fe-base--Y, properties for use in high-temperature strain gages, 25:42804(R) (LMEC-71-1)
Al--Ge--Y, phase diagram at 500°C, isothermal, 25:42891
Al--Sb--Y, phase diagram at 500°C, isothermal, 25:42891
Al--Si--Y, phase diagram at 500°C, isothermal, 25:42891
Ce--Y-base, electric conductivity and magnetic susceptibility of single crystals of, Kondo and crystal-field effects on, 25:43479
Cr--Si--Y, phase diagram at 800°C, isothermal, 25:42993
YTTRIUM ISOTOPES Y-87
nuclear mass excess of, (E), 25:43836
YTTRIUM ISOTOPES Y-89
alpha inelastic scattering at 26 MeV, (E), 25:43859
energy levels of, shell-model analyses of collective core, (E/T), 25:43859
proton inelastic scattering at 61.2 MeV, microscopic-model analyses of, (E/T), 25:43855
YTTRIUM ISOTOPES Y-90
content in milk in Korea, effects of fallout specific activity on, 25:42372
effects on metabolism in granite outcrop ecosystems, 25:42320
production by neutron capture reactions in yttrium, impurities formed in, 25:41877 (JAERI-13545)
uptake by bones in animals and man, induction of neoplasms and radiation injuries following, 25:42472
YTTRIUM OXIDES
analysis for impurities by activation methods, 25:41877 (JAERI-13545)
analysis for impurities, cathode region method for spectrochemical, 25:41833(R) (IA-1218)
AlN--Y_2O_3, mechanical properties of sintered fiber-reinforced composites of, 25:42959
AlN--Y_2O_3, microstructure of sintered fiber-reinforced composites of, 25:42959
HfO_2--Y_2O_3, phase diagrams of, 25:42883 (IS-T-425)

Z

ZINC
analysis for trace amounts of cadmium, copper, lead, and silver, spectrochemical, 25:41833(R) (IA-1218)
analysis of high-purity and pure, for trace amounts of impurities, indirect spectrochemical method for, 25:41833(R) (IA-1218)
determination in minerals from Luzon, Philippines, by neutron activation, 25:41772
determination of trace amounts of, in meteorites by neutron activation and γ spectrometry, 25:41773
diffusion in praseodymium, mechanism of, 25:41833(R) (IA-1218)
lattice-dynamical calculations for, 25:43478
neutron total cross section at 100 to 650 keV, optical model analysis of average, (E/T), 25:43908
separation from acetone--hydrochloric acid solutions by ion exchange using Bio-Rad, distribution coefficients for, 25:41899
separation from aqueous solutions by ion exchange on zirconium tellurate, tracer studies on, 25:41915
separation from other metals using inorganic ion exchange papers, 25:41909
separation of carrier-free and iron-free gallium-67 from deuteron-irradiated, by ion exchange, 25:41881
ZINC ALLOYS AND SYSTEMS
Al--Mg--Zn, corrosion of age-hardened, by aqueous sodium chloride, stress, 25:42886 (UCRL-20500, pp 86-146)
Mg--Zn, superconducting transition temperature in high T/sub c/ intermetallic $MgZn_2$, sensitivity to residual stress of, (E), 25:43302
ZINC IONS
production of multiply-charged, for acceleration in cyclotron, ion source for, 25:43765
ZINC ISOTOPES
copper--zinc Coulomb displacement energies, (E), 25:43883
gallium--zinc Coulomb displacement energies, (E), 25:43883
ZINC ISOTOPES Zn-64
helium-3 reactions (He-3,t) at 24.6 MeV, tritон spectra from, (E), 25:43883
ZINC ISOTOPES Zn-65
content of Columbia River during 1968 to 1969, 25:42419
uptake by frogs, lizards, and snails from labeled algae, bryophytes, and lichens, 25:42317(R) (PRNC-147)
ZINC ISOTOPES Zn-66
helium-3 reactions (He-3,t) at 24.6 MeV, tritон spectra from, (E), 25:43883
ZINC ISOTOPES Zn-67
helium-3 reactions (He-3,t) at 24.6 MeV, tritон spectra from, (E), 25:43883
ZINC ISOTOPES Zn-68
helium-3 reactions (He-3,t) at 24.6 MeV, tritон spectra from, (E), 25:43883
ZINC SULFIDES
sublimation of monocrystalline, kinetics of, 25:42957 (UCRL-20500, pp 147-73)
ZINC TELLURIDES
luminescent emission of damage-sensitive, 100- to 400-keV electron-bombarded lattice-defect-created, (E), 25:43460
ZIRCALOY
analysis for fluorine by proton (p,αγ) reactions using 1.188-MeV resonance, 25:41832(R) (AECL-3851)
analysis for hydrogen by isotopic equilibration mass spectrometry, 25:41747 (AAEC/TM-588)
analysis of fuel cladding of, for hydrogen by neutron radiography, qualitative and quantitative, 25:41755
mechanical properties of tubes of, effects of fabrication methods on, 25:42860
properties for use as fuel cladding, data sheets on, 25:42859
ZIRCALOY-2
corrosion by fused chloride--nitrate salts, stress, 25:41832(R) (AECL-3851)
corrosion by steam and water at 300 to 400°C, kinetics of, 25:42815
corrosion by water at 340°C, effects of decontamination processing on, 25:42808
crystal structure of oxide films on, 25:41832(R) (AECL-3851)
deformation of, mechanisms of thermally-activated, 25:42877
elastic properties at 27 to 400°C, 25:42880

XUM

failure of Halden Reactor fuel cladding of, mechanisms of, 25:42892
oxide film formation on, model for electric switching in anodic, 25:41832(R) (AECL-3851)
properties of, effects of silicon additions on corrosion and mechanical, 25:42876
radiation effects on corrosion of, model for studies of in-pile, 25:42927
radiation effects on mechanical properties of cladding of, at 20 to 300°C, relations of cold work with fast neutron, 25:42913
radiation effects on mechanical properties of cold-worked reactor pressure tubes of, fast neutron, 25:42914
radiation effects on properties of, for use in El-4 pressure tubes, 25:42929
radiation effects on tensile properties of, at 70 to 750°F, fast neutron, 25:42911
radioinduced swelling in, effects of dose and irradiation temperature on neutron, 25:42915
welding of, optimum parameters for electron beam, 25:42830
ZIRCALOY-4
corrosion by water at 340°C, effects of decontamination processing on, 25:42808
properties of, effects of silicon additions on corrosion and mechanical, 25:42876
radiation effects on mechanical properties of cladding of, at 20 to 300°C, relations of cold work with fast neutron, 25:42913
radiation effects on tensile properties of, at 900 to 1600°F, fast neutron, 25:42911
ZIRCONIUM
analysis for hydrogen by isotopic equilibration mass spectrometry, 25:41747 (AAEC/TM-588)
chemical thermodynamic properties of, selected values of, 25:41826 (NBS-TN-270-5)
coating with oxide films by heating in carbon dioxide atmosphere, 25:42819(P)
complexes with glycinecresol red, glycinethymol blue, 9-salicylfluorone, and p-dimethylaminophenylfluorone, preparation of, 25:41737
compounds, thermodynamic properties of, tables of, 25:41826 (NBS-TN-270-5)
corrosion of, effects of alloying additions and cold working on, 25:42811
deposition and spreading on graphite plates at 2060°C, kinetics of, 25:42832
determination by photon activation using molybdenum as internal standard, 25:41766
determination by photon activation using molybdenum as internal reference, 25:41764
determination following separation from other metal ions by thin-layer chromatography using quercetin, colorimetric, 25:41743
determination in titanium by neutron activation, 25:41761
determination using trihydroxyfluorones, spectrophotometric, 25:41737
diffusion of nitrogen in solid solution of α-, at 1260 to 1720°C, 25:42967
effects on superconducting critical field of niobium--titanium alloy wires, 25:43309
oxide film formation on, morphology of ammonium nitrate-induced, 25:41832(R) (AECL-3851)
oxide film formation on, morphology of phosphoric acid-induced, 25:41832(R) (AECL-3851)
plastic deformation of single crystals of, effects of crystal orientation on, 25:42856
plastic flow of alpha, rate-controlling mechanisms for low-temperature, 25:42852
purification of concentrates of, flow sheet for calcination method for, 25:42825
radiation effects on thermally-activated deformation of, neutron, 25:42877
radiation effects on, annealing of neutron, 25:41832(R) (AECL-3851)
separation from acetone--hydrochloric acid solutions by ion exchange using Bio-Rad, distribution coefficients for, 25:41899
separation from hafnium by solvent extraction, 25:41917
separation from neptunium, niobium, uranium, and fission products by solvent extraction using tributyl phosphate, 25:41901
separation from other metals using inorganic ion exchange papers, 25:41909
separation from radioactive waste using oxidizing agent and manganese salt, 25:41911(P)
separation from spent Zircaloy-clad fuels, effects of fluoride in feed solutions on Zirflex and Purex processes in, 25:41889 (BNWL-1573)
standard for ingots of, 25:42800 (RDT-M-10-1-T)
standard for plate, sheet, and strip, 25:42796 (RDT-M-5-6-T)
standard for welding rods of, 25:42772 (RDT-M-1-16-T)
standards for tubes of, 25:42786 (RDT-M-3-8-T)
weld solidification in, structures and mechanism of, 25:42820
ZIRCONIUM ALLOYS AND SYSTEMS
coating with oxide films by heating in carbon dioxide atmosphere, 25:42819(P)
conference on properties of, for use in nuclear reactors, Marianske Lazne, Czechoslovakia, Oct. 1 to 3, 1968, 25:42802
oxidation resistance of, in carbon dioxide at high temperatures, 25:42803 (CEA-R-4103)
radiation effects on, annealing of neutron, 25:41832(R) (AECL-3851)
standard for ingots of, 25:42800 (RDT-M-10-1-T)
standard for plate, sheet, and strip, 25:42796 (RDT-M-5-6-T)
standard for welding rods of, 25:42772 (RDT-M-1-16-T)
standards for tubes of, 25:42786 (RDT-M-3-8-T)
zirconium hydride precipitation in supersaturated, relations with mechanical properties, 25:42855
Al--Cr--Mo--Ti-base--V--Zr, mechanical properties of, 25:42836 (AD-715877)
Al--Zr-base, precipitation in, effects of vacancies on, 25:41832(R) (AECL-3851)
Cr--Cu--Fe--Mo--Nb--V--Zr-base, corrosion resistance of, 25:42811
Cr--Fe--Sn--Zr-base, properties for use in water-cooled reactors, 25:42875
Cr--Fe--Zr-base, corrosion by steam and water at 300 to 400°C, kinetics of, 25:42815
Cr--O--Zr-base, properties of dilute, effects of chromium and oxygen contents on mechanical and structural, 25:42879
Cu--Fe--Zr-base, oxidation by steam at 500°C, effects of crystal structure and impurities on, 25:42810
Cu--Mo--Zr-base, corrosion by carbon dioxide at 400 to 700°C, 25:42809
Cu--Mo--Zr-base, corrosion by carbon dioxide at 450 to 500°C, 25:42813
Cu--Mo--Zr-base, microstructure of phases in, 25:42898
Cu--Mo--Zr-base, phase studies of, 25:42897
Cu--Mo--Zr-base, properties for use in carbon dioxide-cooled reactors, 25:42878
Cu--Mo--Zr-base, radiation effects on mechanical properties of, relations of annealing with fast neutron, 25:42813
Cu--Mo--Zr-base, radiation effects on properties of, for use in El-4 pressure tubes, neutron, 25:42929
Cu--Zr-base, cracking and deformation in fuel cladding of, effects of carbon dioxide at 600°C on, 25:42928
Cu--Zr-base, oxidation by carbon dioxide at high temperatures, effects of copper content on, 25:42812
Cu--Zr-base, properties for use as fuel cladding in carbon dioxide-cooled reactors, 25:42881
Cu--Zr-base, radiation effects on fuel cladding of, in-pile, 25:42881
Fe--Nb--Ta--Ti-base--Zr, description of superconducting, 25:43318(P)
Fe--Ni--Zr, radiation effects on properties of fuel cladding of, in-pile, 25:43010
Nb--Zr, radiation effects on properties of fuel cladding of, in-pile, 25:43010
Nb--Zr, superconducting critical current density of, effect of heat treatment on impurities on, 25:43290 (ORNL-4703)
Nb--Zr-base, corrosion by aqueous solutions at 300°C, effects of pH on, 25:42814
Nb--Zr-base, corrosion by fused chloride--nitrate salts, stress, 25:41832(R) (AECL-3851)
Nb--Zr-base, corrosion rates in flowing water, polarization resistance method for measurement of, 25:42807
Nb--Zr-base, crystallization of, kinetics of, 25:42885 (JAERI-13764)
Nb--Zr-base, radiation effects on corrosion of, model for studies of in-pile, 25:42927
Nb--Zr-base, radiation effects on mechanical properties of cladding of, at 20 and 300°C, relations of cold work with fast neutron, 25:42913
Nb--Zr-base, welding of, optimum methods for, 25:42831
O--Zr-base, deformation of dilute, mechanisms of thermally-activated, 25:42877
Sn--Zr-base, properties for use as getter in vacuum containers, 25:42858(P)
Ta--Zr, superconducting critical current density of, at high fields, 25:43290 (ORNL-4703)
U-base--Zr, mechanical properties of, data tabulation on, 25:42851 (RFP-1703)
ZIRCONIUM CARBIDES
electric conductivity of, relations with stoichiometry, 25:43491
ZIRCONIUM COUPLES
U/Zr, corrosion of, effects of capacitance discharge and frequency on galvanic, 25:41833(R) (IA-1218)
ZIRCONIUM HYDRIDES
crystal structure of, electron microscopic studies of, 25:42981 (JAERI-13635)
precipitation in zirconium alloys, effects on mechanical properties, 25:42855
ZIRCONIUM ISOTOPES
photon reactions at 20 to 60 MeV, 25:41764
ZIRCONIUM ISOTOPES Zr-88
energy levels from yttrium-89 (p,2n) reactions, lifetimes for, (E), 25:43847
energy-level transitions from yttrium-89 (p,2n) reactions, probability for E2, (E), 25:43847
ZIRCONIUM ISOTOPES Zr-90
alpha elastic scattering at 104 MeV, differential cross sections for, (E), 25:43832 (NP-18920)

deuteron reactions (d,p) at 3 MeV, analysis including Coulomb distortion and finite-range effects, (T), 25:43964
energy levels from yttrium-89 proton resonances, isospin splitting of giant dipole, (E), 25:43950
energy levels of, statistical model calculation of vibrational, (T), 25:43910
helium-3 elastic scattering at 37.7 MeV, optical-model analysis of angular distributions for, (E/T), 25:43878
helium-3 reactions (He-3,t) at 21 MeV, distorted-wave analysis of angular distributions from, (T), 25:43848
proton inelastic scattering at 61.2 MeV, calculations using Gaussian potential of differential cross sections for high-spin states in, (T), 25:43915
proton inelastic scattering at 61.2 MeV, microscopic-model analyses of, (E/T), 25:43855
ZIRCONIUM ISOTOPES Zr-91
energy levels of, unified-model calculations for, (T), 25:43938
ZIRCONIUM ISOTOPES Zr-92
energy levels of, unified-model calculations for, (T), 25:43938
ZIRCONIUM ISOTOPES Zr-93
energy levels of, unified-model calculations for, (T), 25:43938
ZIRCONIUM ISOTOPES Zr-94
energy levels of, unified-model calculations for, (T), 25:43938
ZIRCONIUM ISOTOPES Zr-95
energy levels of, unified-model calculations for, (T), 25:43938
uptake by aquatic plants, 25:41833(R) (IA-1218)
ZIRCONIUM ISOTOPES Zr-96
helium-3 reactions (He-3,t) at 21 MeV, distorted-wave analysis of angular distributions from, (T), 25:43848
ZIRCONIUM NITRIDES
diffusion of nitrogen in, at 1260 to 1720°C, 25:42967
ZIRCONIUM OXIDES
book: High-Temperature Materials, 25:42853
electric conductivity of crystalline and powdered, 25:41832(R) (AECL-3851)
phase study search for ZrC and Zr_2O_3, 25:42987
positron annihilation in, angular correlation and three-quantum yield of, 25:43482
production from baddeleyite concentrate, 25:42942
sorptive properties for cesium at 300 to 1000°F, tracer studies on, 25:42863
reactions with silicon oxides at 1400°C to prepare zirconium silicate, kinetics of solid-state, 25:42940
ZIRCONIUM OXYCARBIDES
electric conductivity of, relations with stoichiometry, 25:43491
ZIRCONIUM SILICATES
preparation by reactions of silicon oxide with zirconium dioxide, 25:42940
reactions with calcium carbonate during sintering at 1150 to 1300°C, effects of salt additions on, 25:42972
ZIRCONIUM TELLURATES
sorptive properties for separation of ions, 25:41915
ZIRCONS
limonite concrete--zircon, properties for use as shielding for gamma radiation protection, mechanical and physical, 25:42976

XUM

REPORT NUMBER INDEX

Reports, conference papers and proceedings, numbered translations, and patents are included in this index. Each item is listed by report number; this is followed by the abstract number and a brief notation regarding public availability. The index entries show which reports are on file in the institutions listed on the back of the front cover (Dep.), which reports have been published in open-literature journals (journal citation), and which reports can be purchased (source and price). Whenever a report is identified by more than one number, the availability is given under the primary number, and a cross reference is given under the secondary report number.

The report number codes apply to USAEC reports unless designated otherwise. Non-USAEC reports are identified by parenthetical notes after the report codes; e.g., (non-AEC), (British), (Canadian), (French). The note (Misc.) identifies the codes used for both USAEC and non-USAEC reports. Patents are listed under the heading "PATENTS"; the country of origin is included in parentheses.

A comprehensive list of both USAEC and non-USAEC report codes is contained in the latest revision of TID-85, *Report Number Series Used by the Division of Technical Information in Cataloging Reports.* This information is also included in the Cumulative Report Number Index (issued annually).

Availability of USAEC Reports

All USAEC Reports abstracted in *Nuclear Science Abstracts* are available through one or more of the following sources:

(1) University and public libraries in the United States. A list of these organizations appears on the inside front cover of each issue of *NSA*.

(2) NCR Microcard Editions in Microcard and micronegative form. Orders and inquiries should be sent to: Order Processing Department, 365 South Oak Street, West Salem, Wisconsin 54669.

(3) National Technical Information Service, U. S. Department of Commerce, Springfield, Virginia 22151.

(4) Superintendent of Documents, U. S. Government Printing Office, Washington, D. C. 20402.

(5) National Cash Register Co., P. O. Box 3111, Oak Ridge, Tenn. 37830, in micronegative form. Purchase details available on request.

Availability of Non-USAEC Reports

U. S. Reports. Reports of U. S. Government agencies are available to the public from the National Technical Information Service (NTIS). If specific availability is not shown, inquiries may be directed to NTIS.

Non-U. S. Reports. Reports of atomic energy organizations of other countries are available from NTIS for U. S. sale only. Specific availability in the country of origin is shown, when known, at the report number entry. Otherwise, inquiries should be made to the organizations listed below:

AUSTRALIA

Australian Atomic Energy Commission Research Establishment. Available upon request from the Library, Australian Atomic Research Establishment, Private Mail Bag, Sutherland, New South Wales, Australia.

BELGIUM

Centre d'Étude de l'Energie Nucléaire. Available upon request to individuals and organizations from the Centre d'Etude de l'Energie Nucléaire (C.E.N.), Studiecentrum voor Kernenergie (S.C.K.), Technical Information Dept., MOL-DONK (Belgium).

CERN

CERN European Organization for Nuclear Research. Available without charge from CERN European Organization for Nuclear Research, Geneva 23, Switzerland. Copies are deposited in libraries throughout the world.

FRANCE

Commissariat à l'Energie Atomique. Inquiries for reports numbered 1-2199 should be addressed to Service Central de Documentation du C.E.A., Centre d'Etudes Nucléaires de Saclay, Boîte postale n° 2, 91. GIF-sur-YVETTE, FRANCE. Reports numbered 2200 and above are available from La Documentation Française, 31 quai Voltaire, 75, PARIS (7e), FRANCE.

Service Central de Protection contre les Rayonnements Ionisants. Copies are available from Ministère de la Santé Publique, Service Central de Protection contre les Rayonnements Ionisants, B.P. n° 78 Le Vesinet (France) Telex 25667.

GERMANY

Deutsches Elektronen-Synchrotron DESY. Copies are available from Deutsches Elektronen-Synchrotron DESY, Dokumentation, 2000 Hamburg 52, Notkestieg 1, Germany.

Gesellschaft für Kernforschung mbH (KFK). Copies are available from Gesellschaft für Kernforschung mbH, 75 Karlsruhe, Postfach 947, Germany. Copies are also deposited in many national nuclear centers in the world.

Kernforschungsanlage. Copies may be ordered from Zentralbibliothek der Kernforschungsanlage Jülich, Jülich, Bundesrepublik Deutschland.

Hahn-Meitner-Institute für Kernforschung. Available without charge from Hahn-Meitner-Institute für Kernforschung Ber-

lin, Bibliothek, Glienicker Strasse 100, 1 Berlin 39, Germany. Copies are deposited in many national nuclear centers in the world.

Johann-Wolfgang-Goethe Universität, Frankfurt Am Main, Institut für Kernphysik, (IKF). Copies are available from Gmelin Institut, 40–42 Varrentrappstrasse, Frankfurt (Main), West Germany.

ISRAEL

Israel Atomic Energy Commission. Available without charge from Israel Atomic Energy Commission, Soreq Nuclear Research Centre, Yavne, Israel.

ITALY

Centro Informazioni Studi Esperienze (CISE). For sale at CISE Press Office, Casella Postale 3986, Milano, Italy. Copies are deposited in the libraries of various nuclear centers in Italy and abroad.

Comitato Nazionale per l'Energia Nucleare. Copies are available from Comitato Nazionale per l'Energia Nucleare, Divisione Affari Internazionali e Studi Economici, Ufficio Pubblicazioni, Via Belisario, 15, Roma, Italy.

JAPAN

Japan Atomic Energy Research Institute (JAERI). Available from the Staff Supply Cooperative of Japan Atomic Energy Research Institute (JAERI), Tokai-mura, Naka-gun, Ibaraki-ken, Japan. Copies are deposited in depositories in Tokyo, Nagoya, and Osaka.

Nagoya University. Copies are available from Research Information Center, Institute of Plasma Physics, Nagoya University, Nagoya, Japan.

University of Tokyo. Available free of charge from Institute for Nuclear Study, University of Tokyo, Tanashi-Machi, Kitatama-gun, Tokyo, Japan.

NETHERLANDS

Reactor Centrum Nederland. For sale by Reactor Centrum Nederland, 112 Scheveningseweg, 's-Gravenhage, The Netherlands. Copies are deposited in university libraries in Holland and in many national nuclear centers in the world.

NEW ZEALAND

Institute of Nuclear Sciences. Copies are available from Librarian, N. Z. Institute of Nuclear Sciences, D.S.I.R., Private Bag, Lower Hutt, New Zealand. Copies are deposited in other countries.

PAKISTAN

Atomic Energy Center. Copies are available from Atomic Energy Center, P. O. Box 658, Lahore, (West Pakistan).

POLAND

Reports of the Polish nuclear institutes are published by the Nuclear Energy Information Center of the Government Commissioner for Use of Nuclear Energy. Copies are available free of charge from Nuclear Energy Information Center, Palace of Culture and Science, Warsaw, Poland.

SPAIN

Junta de Energia Nuclear. "JEN" reports are available without charge from Servicio de Documentation, Junta de Energia Nuclear, Ciudad Universitaria, Madrid (3), España.

SWITZERLAND

Eidgenössisches Institut für Reaktorforschung. "EIR" reports are available from Eidgenössisches Institut für Reaktorforschung, c/o Bibliothek, 5303 Würenlingen/Switzerland.

TURKEY

Turkish Atomic Energy Commission. Copies are available free of charge from T.A.E.C., Çekmece Nuclear Research Center, P. O. Box 1, Airport, Istanbul, Turkey.

Conferences

Published conference proceedings as well as individual unpublished papers from conferences are included in this index. A CONF number is assigned to the conference if published proceedings are received and also if only a single paper is received. The base number used is year-month-sequence. Thus, the number CONF-650101 indicates that the conference was held in 1965, in January, and that this was the first January 1965 conference so received. This number would be assigned to complete published proceedings. If individual papers are received, the base number is extended to include a paper number, e.g., CONF-650101-1. As additional papers are received, they will be assigned consecutive numbers in the series, CONF-650101-1, CONF-650101-2, etc. This numbering system ensures that all papers received from a conference will be associated with that conference in this index.

If published proceedings are received after the receipt of individual papers, the complete proceedings will be abstracted and the abstract number will appear in this index with the base CONF number.

Abbreviations Used in Availability Column

AECL — Reports of the Atomic Energy of Canada Limited are for sale by the Scientific Document Distribution Office, Atomic Energy of Canada Limited, Chalk River, Ontario, Canada.

CFSTI — See NTIS

DENM — Reports of the Atomic Energy Commission Research Establishment, Risö, are available on exchange from the Library, Danish Atomic Energy Commission, Risö, Roskilde, Denmark. Also for sale at the price shown from Jul. Gjellerup, Booksellers, 87 Sölvgade, Kobenhavn K., Denmark.
Reports of Danatom are available on loan from Research Establishment, Risö, Roskilde, Denmark. Copies are available from Danatom, Aurehojvej 2, Hellerup, Denmark.

Dep. — AEC reports so designated are maintained in the organizations listed on the inside front cover of *NSA*. Prior to July 1, 1965, reports were deposited either in printed copy form or in microform. After that time, all reports have been in the form of micronegatives.
Reports from other countries so designated are available in the United States at the organizations listed on the inside front cover of *NSA*.

XUM

DTIE — Available from the U. S. Atomic Energy Commission, Division of Technical Information Extension, P. O. Box 62, Oak Ridge, Tennessee 37830. (Conference papers are available on loan only.)

EM — Blueline prints of AEC engineering drawings are available from NTIS, U. S. Department of Commerce, Springfield, Virginia 22151. Current prices of the CAPE-packages may be obtained from this address. TID-4100, available from the Division of Technical Information Extension, P. O. Box 62, Oak Ridge, Tennessee 37830, contains information on all the CAPE-packages for sale.

EUR — For sale by Centrale de vente des publications des Communautés européennes 37, rue Glesener-Luxembourg.

GPO — For sale by the Superintendent of Documents, Government Printing Office, Washington, D. C. 20402.

IAEA — Available from the International Atomic Energy Agency, Vienna, Austria, and from its sales agencies in various countries throughout the world. A list of these agencies is found in each STI/DOC and STI/PUB publication.

LMEC — Available *only to requesters within the United States* from the Liquid Metal Engineering Center, P. O. Box 1449, Canoga Park, CA 91304

NORW — Reports from Forsvarets Forskningsinstitutt are available from Norwegian Defense Research Establishment, Library, P. O. Box 25, Kjeller, Norway.
"KR" reports are available on an exchange basis from the Library, Institutt for Atomenergi, Box 40, Kjeller, Norway.
Reports of the Norwegian Reactor School are available from the Library, Institutt for Atomenergi, P. O. Box 40, Kjeller, Norway.

NRC — For sale by the National Research Council of Canada, Ottawa, Ontario, Canada.

NTIS — For sale by the National Technical Information Service (NTIS), U. S. Department of Commerce, Springfield, Virginia 22151 at the following prices for eye legible copy:

1–300 pages	$3.00
301–600 pages	$6.00
601–900 pages	$9.00

Documents over 900 pages have special prices which may be obtained from NTIS. Microfiche copy of each separately bound document can be purchased for $0.95.
Reports issued by organizations outside the United States will be sold by NTIS *only to purchasers within the United States.*
Purchasers outside the United States may acquire such reports from the sources described elsewhere in these columns.

OECD — Available from O. E. C. D., Publications 2, rue, André-Pascal, 75 Paris 16^{e}, France, and from its sales agencies in various countries throughout the world. A list of these agencies is found in each OECD publication.

RSO — Available *only to requesters within the United States* from the Reactor Standards Office, Oak Ridge National Laboratory, P. O. Box X, Oak Ridge, TN 37830

SWED — "AE" reports are for sale from Aktiebolaget Atomenergi, Library Section, Box 43041, Stockholm 43, Sweden. Microcopy of these reports is available from the International Documentation Center, Turnba, Sweden.
Reports of the VDDIT-series may be obtained from Aktiebolaget Atomenergi, Information Office, Scientific and Technical Information, Box 43041, Stockholm 43, Sweden.
Other series are not generally available to the public. Organizations in the Atomic Energy field may obtain copies from Aktiebolaget Atomenergi.

UK — United Kingdom Atomic Energy Authority reports generally may be purchased from Her Majesty's Stationery Office, P. O. Box 569, London S.E.1. Copies of many UKAEA reports (particularly earlier ones) may be purchased in microcopy form from Micro Methods Ltd., East Ardsley, Wakefield, Yorkshire, England. Copies of UKAEA reports are deposited with the National Lending Library for Science and Technology and 10 public libraries in England; with the USAEC and (through USAEC) with NTIS; and in most national nuclear centers throughout the world. In the USA, UKAEA reports are available on a subscription basis, by subject category, from UNIPUB, Inc., P. O. Box 433, New York, NY 10016, USA; and from Pendragon House, Inc., 1093 Charter Avenue, Redwood City, CA 94063, USA.

UN — Mail orders should be directed to the Sales Section, Room 1059, United Nations Headquarters, New York, New York 10017.

ZAED — Available from Zentralstelle für Atomkernenergie Dokumentation, 6000 Frankfurt/Main 90, P. O. Box 901069, Westendstr. 21, West Germany

Report No.	Abstract No.	Availability
A-	(Misc.)	
3553	25-43352	See N-71-18715
AAEC/TM-	(Australian)	
588	25-41747	Dep. NTIS (U. S. Sales Only), 11p.
ACRH-		
1000-248	25-42547	Dep. NTIS, 11p.
AD-	(Misc.)	
706130	25-43207	NTIS, 18p.
714365	25-43208	NTIS, 28p.
714993	25-43209	NTIS, 24p.
715257	25-43055	NTIS, 33p.
715260	25-43210	NTIS, 38p.
715261	25-42226	NTIS, 37p.
715265	25-43338	NTIS, 26p.
715266	25-43211	NTIS, 32p.
715272	25-43352	NTIS, 71p.
715277	25-43402	NTIS, 17p.
715615	25-43331	NTIS, 36p.
715636	25-43403	NTIS, 40p.
715809	25-43180	NTIS, 24p.
715850	25-44176	NTIS, 87p.
715877	25-42836	NTIS, 9p.
715883	25-43181	NTIS, 43p.
715893	25-43212	NTIS, 17p.
715898	25-43213	NTIS, 37p.
715910	25-43404	NTIS, 171p.
718388	25-41950	NTIS, 85p.
719619	25-41932	
719620	25-41933	
719905	25-42900	NTIS, 16p.
838894	25-41952	NTIS, 55p.
AE-	(Non-AEC)	
416	25-41750	Dep. NTIS (U. S. Sales Only), 25p.
423	25-42392	Dep. NTIS (U. S. Sales Only), 10p.
425	25-44149	Dep. NTIS (U. S. Sales Only), 32p.
AEC-tr-		
7215	25-42614	Dep. NTIS
7225	25-42255	Dep. NTIS
AECL-	(Canadian)	
3572	25-41713	Dep. NTIS (U. S. Sales Only). AECL $1.00, 30p.
3576	25-41716	Dep. NTIS (U. S. Sales Only). AECL $0.50, 12p.
3839	25-43447	Can. J. Phys.; 49: No. 10, 1225-32(15 May 1971)
3848	25-41860	Can. J. Chem.; 49: 1677-81(15 May 1971)
3851	25-41832	Dep. NTIS (U. S. Sales Only). AECL $3.00, 143p.
3853	25-41849	Dep. NTIS (U. S. Sales Only). AECL $1.50, 66p.
3871	25-41855	Can. J. Chem.; 49: 1880-7(1 Jun 1971)
3872	25-41857	Can. J. Chem.; 49: 1869-79(1 Jun 1971)
AEDC-TR-	(Non-AEC)	
70-231	25-43352	See AD-715272
AERE-R-	(British)	
5745	25-42837	Dep. NTIS (U. S. Sales Only). UK 50p, 82p.
5912	25-43725	Dep. NTIS (U. S. Sales Only). UK 9p, 8p.
AERL-RR-		
361	25-43402	See AD-715277
AFCRL-	(Non-AEC)	
70-204	25-43207	See AD-706130
70-562	25-43212	See AD-715893
AFCRL-ERP-	(Non-AEC)	
332	25-43212	See AD-715893
AFWL-TR-	(Non-AEC)	
70-110	25-43404	See AD-715910
AI-AEC-		
12991	25-44094	Dep. NTIS, 30p.
12992	25-44132	Dep. NTIS, 53p.
AI-CE-Memo-		
12	25-44095	Dep. NTIS, 26p.
ANCR-		
1004	25-44220	Dep. NTIS, 53p.
1006	25-44221	Dep. NTIS, 36p.
ANL-		
7710	25-44190	Dep. NTIS, 468p.
7748	25-43885	Dep. NTIS, 54p.
7781	25-44150	Dep. NTIS, 94p.
7802	25-41823	Dep. NTIS, 10p.
ANL-ETD-		
71-7	25-41983	Dep. NTIS, 26p.
ARH-SA-		
25	25-41887	Dep. NTIS, 17p.
78	25-41888	Dep. NTIS, 17p.
ARO-PWT-TR-	(Non-AEC)	
70-155	25-43352	See AD-715272
ASTM-STP-	(Non-AEC)	
484	25-44093	Philadelphia; American Society for Testing and Materials (1970). 569p. $49.25
AWRE-O-	(British)	
24/71	25-41758	Dep. NTIS (U. S. Sales Only). UK 30p, 32p.
AWTSC-	(Australian)	
1	25-42367	Dep. NTIS (U. S. Sales Only), 40p.
BARC/BIB-	(Indian)	
1	25-42505	NTIS (U. S. Sales Only), 250p.
BDX-		
613-184	25-44222	Dep. NTIS, 143p.
613-269	25-44223	Dep. NTIS, 22p.
613-274	25-44224	Dep. NTIS, 43p.
613-326	25-44225	Dep. NTIS, 55p.
613-327	25-44226	Dep. NTIS, 39p.
613-330	25-44227	Dep. NTIS, 116p.
613-355	25-44228	Dep. NTIS, 29p.
613-366	25-44229	Dep. NTIS, 24p.
613-369	25-44230	Dep. NTIS, 113p.
613-395	25-44231	Dep. NTIS, 27p.
613-404	25-44232	Dep. NTIS, 289p.
613-431	25-44233	Dep. NTIS, 227p.
613-443	25-44234	Dep. NTIS, 38p.
613-454	25-44235	Dep. NTIS, 6p.
BHO-		
68-6	25-42035	Dep. NTIS, 19p.
BM-RI-	(Misc.)	
7019	25-41956	Dep. NTIS, 10p.
BMBW-FBK-	(West German)	
70-32	25-43504	Dep. NTIS (U. S. Sales Only), 26p.
71-2	25-43413	Dep. NTIS (U. S. Sales Only), 111p.
BMI-	(Misc.)	
1905	25-44118	Dep. NTIS, 108p.
BNL-		
15893	25-43726	Dep. NTIS, 26p.
50147(Rev.)	25-41957	Dep. NTIS, 66p.
BNL-tr-		
424	25-43952	Dep. NTIS
427	25-43953	Dep. NTIS
429	25-43127	Dep. NTIS
431	25-43727	Dep. NTIS
BNWL-		
1524	25-44133	Dep. NTIS, 94p.
1573	25-41889	Dep. NTIS, 22p.
1582	25-44134	Dep. NTIS, 51p.
BNWL-B-		
69	25-42393	Dep. NTIS, 78p.
103	25-42020	Dep. NTIS, 31p.
BNWL-SA-		
2738	25-44083	Dep. NTIS, 17p.
3705	25-43414	Dep. NTIS, 9p.
3817	25-44236	Dep. NTIS, 33p.
CALT-		
68-305	25-43565	Dep. NTIS, 11p.
822-31	25-44237	Dep. NTIS, 8p.
822-32	25-44238	Dep. NTIS, 12p.
CAPE-		
2086	25-41981	EP
CEA-CONF-	(French)	
1733	25-41948	Dep. NTIS (U. S. Sales Only), 7p.
1767	25-43728	Dep. NTIS (U. S. Sales Only), 10p.
CEA-N-	(French)	
1135	25-44158	For translation see LE/G-2929
1327	25-43779	Dep. NTIS (U. S. Sales Only), 64p.
1327(Vol.4)	25-43780	Dep. NTIS (U. S. Sales Only), 84p.
1367	25-44192	Dep. NTIS (U. S. Sales Only), 51p.
1438	25-41850	Dep. NTIS (U. S. Sales Only), 59p.
1446	25-41717	Dep. NTIS (U. S. Sales Only), 22p.
1450	25-41890	Dep. NTIS (U. S. Sales Only), 21p.
CEA-R-	(French)	

XUM

Report No.	Abstract No.	Availability
4089	25-41824	Dep. NTIS (U. S. Sales Only), 203p.
4099	25-41953	Dep. NTIS (U. S. Sales Only), 25p.
4103	25-42803	Dep. NTIS (U. S. Sales Only), 121p.
4106	25-41718	Dep. NTIS (U. S. Sales Only), 43p.
4128(1)	25-41954	Dep. NTIS (U. S. Sales Only), 47p.
4136	25-44135	Dep. NTIS (U. S. Sales Only), 70p.
4150	25-43533	Dep. NTIS (U. S. Sales Only), 74p.
4181	25-44206	Dep. NTIS (U. S. Sales Only), 150p.
CEA-tr-R-	(French)	
1979	25-41925	Dep. NTIS (U. S. Sales Only)
CENPD-	(Non-AEC)	
22	25-44043	See DOCKET-50255-48
CERN-	(European Organization for Nuclear Research)	
71-4	25-43405	Dep. NTIS (U. S. Sales Only), 132p.
71-13	25-43613	Dep. NTIS (U. S. Sales Only), 35p.
CERN-Trans-	(European Organization for Nuclear Research)	
71-8	25-42135	Dep. NTIS (U. S. Sales Only)
71-16	25-43729	Dep. NTIS (U. S. Sales Only)
71-18	25-42181	Dep. NTIS (U. S. Sales Only)
CGS-		
746-114	25-44239	Dep. NTIS, 72p.
CONF-680535-	(14th National Conference of the Italian Association for Health Physics and Protection from Radiation, Formia, Italy, May 29-31, 1968)	
3	25-41949	Minerva Fisiconucl.; 13: 1-19(Jan-Mar 1969)
5	25-41935	Minerva Fisiconucl.; 13: 46-60 (Jan-Mar 1969)
7	25-42043	Minerva Fisiconucl.; 13: 61-71(Jan-Mar 1969)
14	25-42169	Minerva Fisiconucl.; 13: 135-40(Apr-Jun 1969)
15	25-42168	Minerva Fisiconucl.; 13: 141-4(Apr-Jun 1969)
17	25-42013	Minerva Fisiconucl.; 13: 154-9(Apr-Jun 1969)
18	25-41979	Minerva Fisiconucl.; 13: 160-4(Apr-Jun 1969)
19	25-42096	Minerva Fisiconucl.; 13: 165-72(Apr-Jun 1969)
31	25-42478	Minerva Fisiconucl.; 14: 74-8(Apr-Jun 1970)
32	25-42081	Minerva Fisiconucl.; 14: 104-8(Jul-Sep 1970)
33	25-42435	Minerva Fisiconucl.; 14: 101-3 (Jul-Sep 1970)
CONF-680563-	(Conference on Heat and Mass Transfer, Minsk, U.S.S.R., May 14-18, 1968)	
	25-41985	Minsk; Institute of Heat and Mass Transfer (1969). 1074p
CONF-680985-	(Meeting on Preparative Radiochemistry Production of Radionuclides and Labelled Compounds, Lindau Im Bodensee, Germany, Sept. 5-6, 1968)	
2	25-41875	Dep. NTIS (U. S. Sales Only), 7p.
CONF-681086-	(Conference on the Use of Zirconium Alloys in Nuclear Reactors, Marianske Lazne, Czechoslovakia, Oct. 1-3, 1968)	
	25-42802	Plzen, Czech.; Skoda Works (1968). 512p
CONF-690414-	(1st European Symposium on Late Effects of Radiation, Rome, Italy, Apr. 22-23, 1969)	
	25-42504	Rome; Comitato Nazionale Energia Nucleare (1970). 215p
CONF-690524-	(23rd Annual Technical Conference of the American Society for Quality Control, Los Angeles, Calif., May 5-7, 1969)	
	25-42030	Milwaukee; American Society for Quality Control, Inc. (1969). 831p. $13.00
CONF-690659-	(Symposium on Ultraviolet Stellar and Related Ground-Based Observations, Lunteren, The Netherlands, June 24-27, 1969)	
	25-43031	New York; Springer-Verlag New York Inc. (1970). 373p. $19.80
CONF-690660-	(Symposium on Optimization, Nice, France, June 29-July 5, 1969)	
	25-43526	Berlin; Springer-Verlag (1970). 355p. $6.10
CONF-690819-	(66th National Meeting of the American Institute of Chemical Engineers, Portland, Ore., Aug. 24-27, 1969)	
3	25-41897	See ARH-SA-25
CONF-690905-	(4th Intersociety Energy Conversion Engineering Conference, Washington, D.C., Sept. 21-26, 1969)	

Report No.	Abstract No.	Availability
	25-41995	New York; American Institute of Chemical Engineers (1969). 1186p. $45.70
CONF-690929-	(15th National Congress of the Italian Association for Health Physics and Protection Against Radiation, Cagliari, Italy, Sept. 29-Oct. 3, 1969)	
4	25-43738	Minerva Fisiconucl.; 14: 1-6(Jan-Mar 1970)
6	25-41937	Minerva Fisiconucl.; 14: 17-23(Jan-Mar 1970)
8	25-42167	Minerva Fisiconucl.; 14: 65-9(Apr-Jun 1970)
9	25-42477	Minerva Fisiconucl.; 14: 70-3(Apr-Jun 1970)
11	25-41935	Minerva Fisiconucl.; 14: 120-3(Jul-Sep 1970)
13	25-42382	Minerva Fisiconucl.; 14: 132-6(Jul-Sep 1970)
CONF-690977-	(15th Canadian High Polymer Forum, Kingston, Ontario, Canada, Sept. 3-5, 1969)	
(Absts.)	25-41842	
CONF-690978-	(Radiobiological Conference, Tatranska Lomnica, Czechoslovakia, Sept. 30-Oct. 4, 1969)	
(Absts.)	25-42584	Kosice, Czech.; P. J. Safarik University ([1969]). 91p
CONF-691041-	(International Symposium on Biological Aspects of Radiation Protection, Kyoto, Japan, Oct. 13-15, 1969)	
	25-42512	Tokyo; Igaku Shoin Ltd. (1971). 279p. $18.00
CONF-691104-	(International Congress on the Diffusion of Fission Products, Saclay, France, Nov. 4-6, 1969)	
6	25-41898	See IRG-Report-2135
CONF-691208-	(Nuclear Physics and Solid State Physics Symposium, Roorkee, India, Dec. 28-31, 1969)	
(Vol.3)	25-43466	
CONF-691229-	(Panel on Nuclear Techniques and Mineral Resources in Developing Countries, Krakow, Poland, Dec. 8-12, 1969)	
	25-41941	See STI/PUB-279
CONF-700212-	(67th National Meeting of the American Institute of Chemical Engineers, Atlanta, Ga., Feb. 17, 1970)	
2	25-44083	See BNWL-SA-2738
CONF-700224-	(International Symposium on Non-Destructive Testing of Nuclear Power Reactor Components, Rotterdam, The Netherlands, Feb. 25-27, 1970)	
	25-44084	
CONF-700303-	(21st Conference on Analytical Chemistry and Applied Spectroscopy, Cleveland, Ohio, Mar. 1-6, 1970)	
(Absts.)	25-41719	
CONF-700307-	(Symposium on Progress in Sodium-Cooled Fast Reactor Engineering, Monaco, Mar. 23-27, 1970)	
8	25-41958	Dep. NTIS
CONF-700341-	(Panel on Superconductors, Paris, France, Mar. 17-18, 1970)	
6	25-43325	Dep. NTIS (U. S. Sales Only), 9p.
CONF-700443-	(AEC Computer Information Meeting, Washington, D.C., Apr. 30-May 1, 1970)	
1	25-44090	See WAPD-T-2358
CONF-700630-	(Symposium on Irradiation Effects on Structural Alloys for Nuclear Reactor Applications, Niagara Falls, Canada, June 29-July 1, 1970)	
	25-44093	Philadelphia; American Society for Testing and Materials (1970). 559p. $49.25
CONF-700650-	(Meeting on Biochemical Indicators of Radiation Injury in Man, Paris, France, June 22-26, 1970)	
	25-42395	See STI/PUB-280
CONF-700715-	(3rd International Symposium on Exoelectrons, Brunswick, West Germany, July 6-8, 1970)	
1	25-43489	PTB Mitt.; 80: 320-9(Oct 1970)
CONF-700806-	(15th International Conference on High Energy	

Report No.	Abstract No.	Availability
		Physics, Kiev, U.S.S.R., Aug. 26-Sept. 4, 1970)
51	25-43624	See UCR-34-P-107-B-112
52	25-43642	See UCR-34-P-107-B-106
53	25-43551	See UCR-34-P-107-B-108
54	25-43552	See UCR-34-P-107-B-110
CONF-700812-		(2nd Inter-American Conference on Materials Technology, Mexico City, Mex., Aug. 24-27, 1970)
	25-44219	New York; American Society of Mechanical Engineers (1970). 719p. $30.00
CONF-700903-		(4th Foratom Congress on Industrial Aspects of the Nuclear Fuel Cycle in Europe, Stockholm, Sweden, Sept. 21-23, 1970)
17	25-44127	Dep. NTIS (U. S. Sales Only), 45p.
CONF-700933-		(Conference on Hyperfine Interactions Detected by Nuclear Radiation, Rehovot and Jerusalem, Israel, Sept. 6-11, 1970)
5	25-43459	See UCRL-20411
CONF-700945-		(Conference on Ion Implantation, Reading, England, Sept. 7-9, 1970)
2	25-43728	See CEA-CONF-1767
CONF-700963-		(4th International Conference on Magnetic Thin Films, Prague, Czechoslovakia, Sept. 21-23, 1970)
	25-43492	Czech. J. Phys.; 21: No. 4-5, 329-587(1971)
CONF-701050-		(Ultrasonics Symposium of the IEEE, San Francisco, Calif., Oct. 8-9, 1970)
1	25-44307	See UCRL-73184
CONF-701127-		(Panel on Procedures for Establishing Limits for Radionuclides in the Sea, Vienna, Austria, Nov. 9-13, 1970)
1	25-41948	See CEA-CONF-1733
CONF-701129-		(56th Annual Meeting of the Radiological Society of America, Chicago, Ill., Nov. 29-Dec. 4, 1970)
2	25-42547	See ACRH-1000-248
CONF-701212-		(Symposium on Particles and Fields, Madras, India, Dec. 30, 1970-Jan. 4, 1971)
1	25-43711	See SU-1206-243
CONF-701213-		(Symposium on Modular Coding Systems for Reactor Calculations, Ispra, Italy, Dec. 1-3, 1970)
	25-44181	See EACRP-A-135
CONF-710204-		(Symposium on the Role of Semi-Conductor Detectors in the Future of Nuclear Medicine, Chicago, Ill., Feb. 12-13, 1971)
4	25-42549	Dep. NTIS, 31p.
CONF-710207-		(22nd Pittsburgh Conference on Analytical Chemistry and Applied Spectroscopy, Cleveland, Ohio, Feb. 28-Mar. 5, 1971)
(Absts.)	25-41720	
CONF-710315-		(Conference on Fast Reactors, Palo Alto, Calif., Mar. 7-10, 1971)
20	25-44128	Dep. NTIS. ASME $2.00
22	25-44139	See HEDL-SA-169
CONF-710316-		(Workshop on Particle Physics at Intermediate Energies, Pasadena, Calif., Mar. 29-30, 1971)
2	25-43565	See CALT-68-305
CONF-710413-		(American Physical Society Meeting, Washington, D.C., Apr. 26-29, 1971)
2	25-43957	See UCRL-73152
3	25-43553	See UCR-34-P-107-B-120
CONF-710414-		(Conference on Fast Reactor Fuel Element Technology, New Orleans, La., Apr. 13-15, 1971)
7	25-44121	See HEDL-SA-89
9	25-44123	See ORNL-TM-3385
10	25-44124	See ORNL-TM-3387
CONF-710415-		(73rd Annual Meeting of the American Ceramics Society, Chicago, Ill., Apr. 26-28, 1971)
2	25-41779	See ORNL-TM-3358
CONF-710417-		(International Solvent Extraction Conference, The Hague, Netherlands, Apr. 19-23, 1971)
3	25-41899	See ARH-SA-78
CONF-710418-		(4th Symposium of Engineering Problems of Fusion Research, Washington, D.C., Apr. 20-23, 1971)
13	25-43396	See MATT-804
14	25-43397	See MATT-848
15	25-43399	See UCRL-73076
17	25-42188	See MATT-845
CONF-710421-		(International Conference on Meson Resonances and Related Electromagnetic Phenomena, Bologna, Italy, Apr. 14-16, 1971)
2	25-43543	See COO-1428-274
3	25-43545	See COO-1428-277
CONF-710426-		(7th Annual Symposium on Vacuum Science, Albuquerque, N. Mex., Apr. 21-23, 1971)
1	25-41825	See LA-DC-12348
CONF-710427-		(American Power Conference, Chicago, Ill., Apr. 20-22, 1971)
1	25-44085	Dep. NTIS, 24p.
CONF-710430-		(11th International Technical and Scientific Conference on Space, Rome, Italy, Apr. 1-3, 1971)
	25-43017	Rome; XVIII Rassegna Internazionale Elettronica e Nucleare (1971). 375p
CONF-710431-		(14th Conference on Great Lakes Research, Toronto, Ontario, Canada, Apr. 19-21, 1971)
1	25-44138	Dep. NTIS, 34p.
CONF-710501-		(3rd National Symposium on Radioecology, Oak Ridge, Tenn., May 10-12, 1971)
22	25-42718	See ORO-3299-110
23	25-42717	See EGG-1183-2272
27	25-44288	See RLO-2227-T-8-1
30	25-44287	See RLO-2225-T-7-2
CONF-710504-		(5th Annual Western States Corrosion Seminar, San Dimas, Calif., May 5-7, 1971)
2	25-44236	See BNWL-SA-3817
CONF-710508-		(19th Annual Meeting of the Radiation Research Society, Boston, Mass., May 9-13, 1971)
1	25-43414	See BNWL-SA-3705
CONF-710511-		(43rd Congress of the Australian and New Zealand Association For the Advancement of Science, Brisbane, Australia, May 24-28, 1971)
3	25-42314	Dep. NTIS (U. S. Sales Only), 22p.
CONF-710512-		(1st National Congress on Pressure Vessels and Piping, San Francisco, Calif., May 10-12, 1971)
1	25-42838	
2	25-42021	ASME, New York $2.00
3	25-42839	ASME, New York $2.00
4	25-42840	ASME, New York $2.00
8	25-42841	ASME, New York $2.00
9	25-42842	ASME, New York $2.00
10	25-42843	ASME, New York $2.00
15	25-41959	Dep. NTIS, 7p.
CONF-710514-		(DECUS Spring Symposium, Atlanta, Ga., May 13-15, 1971)
1	25-44304	See UCRL-73046
CONF-710515-		(Atomic Energy Systems, Operations, and Programming Association, Gatlinburg, Tenn., May 4-5, 1971)
1	25-44240	Dep. NTIS, 11p.
CONF-710516-		(Bacteriological Proceedings, Minneapolis, Minn., May 2-7, 1971)
(Absts.)	25-42739	Washington, D. C.; American Society for Microbiology (1971). 283p
CONF-710605-		(18th Annual Meeting on Society of Nuclear Medicine, Los Angeles, Calif., June 28-July 2, 1971)
(Absts.)	25-42560	J. Nucl. Med.; 12: No. 6, 334-483(Jun 1971)
CONF-710606-		(17th Annual Meeting of The American Nuclear Society, Boston, Mass., June 13-17, 1971)
1	25-42954	See HEDL-SA-131
4	25-44189	See Y-DR-63
5	25-44125	See ORNL-TM-3427
CONF-710609-		(International Conference on Elementary Particles, Amsterdam, Netherlands, June 30-July 6, 1971)
1	25-43546	See COO-1428-279
2	25-43547	See COO-1428-281
3	25-43544	See COO-1428-275
5	25-43554	See UR-875-340
CONF-710704-		(Conference on Computers in Chemical Education and Research, DeKalb, Ill., July

XUM

Report No.	Abstract No.	Availability
	19-23, 1971)	
1	25-44335	See JCRL-73161
2	25-42192	See COO-1140-194
3	25-44241	See COO-1140-198
CONF-710706-	(6th National Conference on Electron Probe Analysis, Pittsburgh, Pa., July 28-30, 1971)	
1	25-44305	See JCRL-73104
COO-		
697-23	25-42321	Dep. NTIS, 23p.
1097-46	25-42322	Dep. NTIS, 19p.
1109-60	25-42934	Dep. NTIS, 39p.
1140-194	25-42182	Dep. NTIS, 8p.
1140-198	25-44241	Dep. NTIS, 10p.
1147-35	25-44242	Dep. NTIS, 27p.
1195-204	25-43664	Dep. NTIS, 11p.
1195-215	25-43542	Dep. NTIS, 18p.
1201-30	25-42615	Dep. NTIS, 21p.
1209-8	25-42608	Exp. Parasitol.; 28: 450-64(Dec 1970)
1222-45	25-44243	Dep. NTIS, 13p.
1222-46	25-44244	Dep. NTIS, 19p.
1222-47	25-44245	Dep. NTIS, 22p.
1222-48	25-44246	Dep. NTIS, 9p.
1222-49	25-44247	Dep. NTIS, 43p.
1222-50	25-44248	Dep. NTIS, 15p.
1265-96	25-43883	Nucl. Phys.; A168: No. 1, 151-76(1971)
1313-27	25-44249	Dep. NTIS, 18p.
1313-28	25-44250	Dep. NTIS, 18p.
1313-29	25-42716	Dep. NTIS, 14p.
1428-274	25-43543	Dep. NTIS, 3p.
1428-275	25-43544	Dep. NTIS, 10p.
1428-277	25-43545	Dep. NTIS, 9p.
1428-279	25-43546	Dep. NTIS, 6p.
1428-281	25-43547	Dep. NTIS, 14p.
1428-283	25-43548	Dep. NTIS, 11p.
1428-286	25-43549	Dep. NTIS, 40p.
1428-290	25-43550	Dep. NTIS, 11p.
1545-99	25-43566	Dep. NTIS, 34p.
1559-7	25-44251	Dep. NTIS, 6p.
1599-33	25-44252	Dep. NTIS, 13p.
1630-26	25-44253	Dep. NTIS, 34p.
1553-103	25-44254	Dep. NTIS, 7p.
2002-6	25-44255	Dep. NTIS, 5p.
2002-10	25-44256	Dep. NTIS, 39p.
2038-2	25-42744	Dep. NTIS, 38p.
2069-7	25-42760	Dep. NTIS, 66p.
2109-4	25-44104	Dep. NTIS, 187p.
2109-5	25-44097	Dep. NTIS, 14p.
2121-3	25-44257	Dep. NTIS, 27p.
CPT-	(Non-AEC)	
111	25-43647	See ORC-3992-61
CTC-		
40	25-43419	See ORNL-TM-3269
CTC-INF-		
1030	25-44258	Dep. NTIS, 41p.
CTO-	(Non-AEC)	
756	25-42183	Dep. NTIS (U. S. Sales Only)
759	25-43384	Dep. NTIS (U. S. Sales Only)
CU-	(Misc.)	
3954-9	25-43350	Dep. NTIS, 112p.
D-	(Misc.)	
1-82-1010	25-43403	See AD-715636
DASA-	(Misc.)	
2575	25-41950	See AD-718388
DESY-	(German)	
71/20	25-43592	Dep. NTIS (U. S. Sales Only), 9p.
71/21	25-43527	Dep. NTIS (U. S. Sales Only), 10p.
71/22	25-43583	Dep. NTIS (U. S. Sales Only), 25p.
71/24	25-43637	Dep. NTIS (U. S. Sales Only), 47p.
DLR-FB-	(German)	
55-49	25-44284	For translation see ORNL-tr-2471
DOCKET-1151-	(Elk River Reactor) (AEC)	
44	25-44023	Dep. NTIS, 12p.
DOCKET-1155-	(LaCrosse Boiling Water Reactor) (AEC)	
123	25-43998	Dep. NTIS, 4p.
124	25-43999	Dep. NTIS, 3p.
125	25-44000	Dep. NTIS, 5p.
DOCKET-50003-	(Indian Point Station; See Also DOCKET-50247, DOCKET-50286) (Non-AEC)	
80	25-44024	Dep. NTIS, 208p.
DOCKET-50016-	(Enrico Fermi Atomic Power Plant) (Non-AEC)	
121	25-44001	Dep. NTIS, 12p.
122	25-44002	Dep. NTIS, 13p.
DOCKET-50029-	(Yankee Atomic Electric Co.) (Non-AEC)	

Report No.	Abstract No.	Availability
152	25-44025	Dep. NTIS, 16p.
DOCKET-50133-	(Humboldt Bay Power Plant) (Non-AEC)	
58	25-44003	Dep. NTIS, 2p.
59	25-44026	Dep. NTIS, 10p.
DOCKET-50146-	(Saxton Nuclear Experimental Corporation) (Non-AEC)	
82	25-44027	Dep. NTIS, 4p.
84	25-44028	Dep. NTIS, 3p.
85	25-44029	Dep. NTIS, 3p.
DOCKET-50155-	(Big Rock Point Reactor) (Misc.)	
84	25-44030	Dep. NTIS, 5p.
85	25-44031	Dep. NTIS, 2p.
DOCKET-50171-	(Peach Bottom Atomic Power Station; See also DOCKET-50277 and DOCKET-50278) (Non-AEC)	
89	25-44032	Dep. NTIS, 5p.
90	25-44004	Dep. NTIS, 15p.
91	25-44033	Dep. NTIS, 3p.
DOCKET-50201-	(West Valley Reprocessing Plant--Formerly Spent Fuel Processing Plant) (Misc.)	
74	25-41891	Dep. NTIS, 2p.
DOCKET-50206-	(San Onofre Nuclear Generating Station) (Misc.)	
114	25-44005	Dep. NTIS, 7p.
115	25-44034	Dep. NTIS, 30p.
DOCKET-50213-	(Haddam Neck Plant, Unit 1) (Misc.)	
115	25-44006	Dep. NTIS, 22p.
DOCKET-50219-	(Oyster Creek Nuclear Power Plant) (Non-AEC)	
142	25-44007	Dep. NTIS, 4p.
DOCKET-50220-	(Nine Mile Point Nuclear Station) (Non-AEC)	
65	25-44035	Dep. NTIS, 142p.
DOCKET-50231-	(Southwest Experimental Fast Oxide Reactor) (Non-AEC)	
88	25-44151	Dep. NTIS, 42p.
89	25-44152	Dep. NTIS, 72p.
90	25-44153	Dep. NTIS, 16p.
DOCKET-50237-	(Dresden Nuclear Power Station, See also DOCKET-50249) (Non-AEC)	
183	25-44008	Dep. NTIS, 2p.
184	25-44009	Dep. NTIS, 2p.
185	25-44010	Dep. NTIS, 2p.
186	25-44036	Dep. NTIS, 5p.
DOCKET-50244-	(Robert Emmett Ginna Nuclear Power Plant, Formerly Brookwood Nuclear Station) (Non-AEC)	
72	25-44037	Dep. NTIS, 8p.
73	25-44011	Dep. NTIS, 2p.
74	25-44038	Dep. NTIS, 17p.
DOCKET-50245-	(Millstone Point Nuclear Power Station) (Non-AEC)	
85	25-44012	Dep. NTIS, 3p.
DOCKET-50247-	(Indian Point Nuclear Generating; See also DOCKET-50286) (Non-AEC)	
46	25-44039	Dep. NTIS, 14p.
DOCKET-50249-	(Dresden Nuclear Power Station; See also DOCKET-50237) (Non-AEC)	
78	25-44009	See DOCKET-50237-184
79	25-44013	Dep. NTIS, 2p.
80	25-44014	Dep. NTIS, 2p.
81	25-44015	Dep. NTIS, 2p.
82	25-44036	See DOCKET-50237-186
83	25-44016	Dep. NTIS, 3p.
DOCKET-50254-	(Quad-Cities Station; See also DOCKET-50265) (Non-AEC)	
42	25-44040	Dep. NTIS, 108p.
44	25-44041	Dep. NTIS, 41p.
45	25-44042	Dep. NTIS, 4p.
DOCKET-50255-	(Palisades Plant) (Non-AEC)	
48	25-44043	Dep. NTIS, 103p.
49	25-44044	Dep. NTIS, 18p.
DOCKET-50261-	(H. B. Robinson) (Non-AEC)	
63	25-44017	Dep. NTIS, 1p.
64	25-44018	Dep. NTIS, 1p.
65	25-44045	Dep. NTIS, 3p.
66	25-44046	Dep. NTIS, 23p.
DOCKET-50263-	(Monticello Nuclear Generating Plant) (Non-AEC)	
75	25-44019	Dep. NTIS, 8p.
DOCKET-50265-	(Quad-Cities Station; See also DOCKET-50254) (Non-AEC)	

Report No.	Abstract No.	Availability
38	25-44040	See DOCKET-50254-42
39	25-44041	See DOCKET-50254-44
40	25-44042	See DOCKET-50254-45
DOCKET-50267-	(Fort St. Vrain Nuclear Generating Station) (Non-AEC)	
32	25-44047	Dep. NTIS, 114p.
DOCKET-50271-	(Vermont Yankee Nuclear Power Station) (Non-AEC)	
55	25-44048	Dep. NTIS, 17p.
56	25-44049	Dep. NTIS, 48p.
57	25-44050	Dep. NTIS, 42p.
DOCKET-50280-	(Surry Power Station, See also DOCKET-50281) (Non-AEC)	
43	25-44051	Dep. NTIS, 169p.
DOCKET-50281-	(Surry Power Station, See also DOCKET-50280) (Non-AEC)	
42	25-44051	See DOCKET-50280-43
DOCKET-50286-	(Indian Point Nuclear Plant) (Non-AEC)	
37	25-44052	Dep. NTIS, 42p.
38	25-44053	Dep. NTIS, 170p.
DOCKET-50301-	(Point Beach Nuclear Plant) (Non-AEC)	
35	25-44054	Dep. NTIS, 2p.
DOCKET-50315-	(Donald C. Cook Nuclear Power Plant, See also DOCKET-50316) (Non-AEC)	
38	25-44055	Dep. NTIS, 86p.
39	25-44056	Dep. NTIS, 54p.
40	25-44057	Dep. NTIS, 119p.
41	25-44058	Dep. NTIS, 90p.
DOCKET-50316-	(Donald C. Cook Nuclear Power Plant, See also DOCKET-50315) (Non-AEC)	
38	25-44055	See DOCKET-50315-38
39	25-44056	See DOCKET-50315-39
40	25-44057	See DOCKET-50315-40
41	25-44058	See DOCKET-50315-41
DOCKET-50317-	(Calvert Cliffs Nuclear Power Plant, See also DOCKET-50318) (Non-AEC)	
25	25-44059	Dep. NTIS, 95p.
DOCKET-50318-	(Calvert Cliffs Nuclear Power Plant, See also DOCKET-50317) (Non-AEC)	
25	25-44059	See DOCKET-50317-25
DOCKET-50342-	(Consolidated Edison Company) (See also DOCKET-50343) (Non-AEC)	
7	25-44060	Dep. NTIS, 560p.
DOCKET-50343-	(Consolidated Edison Company) (See also DOCKET-50342) (Non-AEC)	
7	25-44060	See DOCKET-50342-7
DOCKET-50352-	(Limerick Generating Station) (See also DOCKET-50353) (Non-AEC)	
15	25-44061	Dep. NTIS, 411p.
DOCKET-50353-	(Limerick Generating Station) (See also DOCKET-50352) (Non-AEC)	
15	25-44061	See DOCKET-50352-15
DOCKET-50354-	(Newbold Island Nuclear Generating Station) (See also DOCKET-50355) (Non-AEC)	
15	25-44062	Dep. NTIS, 190p.
DOCKET-50355-	(Newbold Island Nuclear Generating Station) (See also DOCKET-50354) (Non-AEC)	
15	25-44062	See DOCKET-50354-15
DOCKET-50358-	(Wm. H. Zimmer Nuclear Power Station, Units 1 and 2) (See also DOCKET-50359) (Non-AEC)	
19	25-44063	Dep. NTIS, 207p.
20	25-44064	Dep. NTIS, 51p.
DOCKET-50368-	(Arkansas Nuclear One) (Non-AEC) (Unit 2)	
14	25-44065	Dep. NTIS, 43p.
15	25-44066	Dep. NTIS, 54p.
DOCKET-50369-	(McGuire Nuclear Station) (See also DOCKET-50370) (Non-AEC) (Units 1 and 2)	
12	25-44067	Dep. NTIS, 79p.
DOCKET-50370-	(McGuire Nuclear Station) (See also DOCKET-50369) (Non-AEC) (Units 1 and 2)	
11	25-44067	See DOCKET-50369-12
DOCKET-50376-	(Aguirre Nuclear Plant) (Non-AEC)	
16	25-44068	Dep. NTIS, 2p.
18	25-44069	Dep. NTIS, 81p.
DOCKET-50382-	(Louisiana Power and Light Plant) (Non-AEC) (See also DOCKET-50383)	
7	25-44070	Dep. NTIS, 8p.

Report No.	Abstract No.	Availability
DOCKET-50383-	(Louisiana Power and Light Plant) (Non-AEC) (See also DOCKET-50382)	
7	25-44070	See DOCKET-50382-7
DOCKET-50395-	(Virgil C. Summer Nuclear Station)(Non-AEC)	
1	25-44071	Dep. NTIS, 33p.
2	25-44072	Dep. NTIS, 186p.
3	25-44073	Dep. NTIS, 300p.
4	25-44074	Dep. NTIS, 379p.
5	25-44075	Dep. NTIS, 421p.
6	25-44076	Dep. NTIS, 749p.
7	25-44077	Dep. NTIS, 400p.
8	25-44078	Dep. NTIS, 514p.
DP-		
1242	25-42036	Dep. NTIS, 140p.
DPC-		
71-11	25-43998	See DOCKET-1155-123
71-12	25-43999	See DOCKET-1155-124
71-13	25-44000	See DOCKET-1155-125
851-26	25-44020	See TID-25737
E-	(Misc.)	
5675	25-44122	See N-71-17463
5683	25-42228	See N-71-17325
5704	25-42903	See N-71-14040
5830	25-44168	See N-71-17933
5925	25-43185	See N-71-17252
5926	25-43183	See N-71-15856
EACRP-A-	(European-American Committee on Reactor Physics)	
135	25-44181	
ECOM-	(Non-AEC)	
3332	25-43209	See AD-714993
5313	25-43208	See AD-714365
ED-	(Non-AEC)	
7008	25-44176	See AD-715850
EGG-		
1183-2272	25-42717	Dep. NTIS, 25p.
EIR-	(Swiss)	
189	25-43771	Dep. NTIS (U. S. Sales Only), 85p.
ENDF-		
151	25-43420	See ORNL-TM-3429
EOS-	(Non-AEC)	
4044	25-43221	See N-71-21469
ERL-		
188	25-41932	See AD-719619
188-2	25-41933	See AD-719620
EUR-	(European Atomic Energy Community)	
4349	25-43505	NTIS (U. S. Sales Only), 37p.
4352	25-41721	NTIS (U. S. Sales Only), 10p.
4353	25-41892	NTIS (U. S. Sales Only), 284p.
4357	25-44129	NTIS (U. S. Sales Only), 22p.
4362	25-44154	NTIS (U. S. Sales Only), 19p.
4364	25-44099	NTIS (U. S. Sales Only), 21p.
4365	25-44100	NTIS (U. S. Sales Only), 44p.
4512	25-41960	NTIS (U. S. Sales Only), 32p.
4513	25-42049	NTIS (U. S. Sales Only), 10p.
4574	25-44119	See EURFNR-923
EUR-CEA-FC-	(European Atomic Energy Community)	
595	25-43332	Dep. NTIS (U. S. Sales Only), 48p.
EURFNR-	(European Atomic Energy Community)	
853	25-44086	Dep. NTIS
854	25-44087	Dep. NTIS
859	25-42935	Dep. NTIS
922	25-42844	Dep. NTIS (U. S. Sales Only), 66p.
923	25-44119	Dep. NTIS (U. S. Sales Only), 25p.
FEI-	(Russian)	
208	25-42104	Dep. NTIS (U. S. Sales Only), 11p.
213	25-44194	Dep. NTIS (U. S. Sales Only), 14p.
GAT-Z-		
5047	25-42244	Dep. NTIS
GCA-TR-	(Misc.)	
70-11-N	25-43215	See N-71-17052
GEAP-	(Misc.)	
10236	25-42845	Dep. NTIS, 36p.
10355	25-44120	Dep. NTIS, 64p.
12114-6	25-42035	See BHO-68-6
12188	25-42952	Dep. NTIS, 5p.
12189	25-42953	Dep. NTIS, 7p.
HEDL-SA-		
89	25-44121	Dep. NTIS, 19p.
131	25-42954	Dep. NTIS, 22p.
169	25-44139	Dep. NTIS, 34p.

XUM

Report No.	Abstract No.	Availability
HEDL-TME-		
71-76	25-42901	Dep. NTIS, 49p.
HMI-B-	(German)	
96	25-42181	For translation see CERN-Trans-71-18
HUX-		
2643-61	25-44259	Dep. NTIS, 16p.
IA-	(Israel)	
1218	25-41833	Dep. NTIS (U. S. Sales Only), 268p.
IAE-	(Russian)	
2010	25-44195	Dep. NTIS (U. S. Sales Only), 132p.
IFVE-OP-	(Russian)	
70-28	25-43729	For translation see CERN-Trans-71-15
IN-		
1474	25-41893	Dep. NTIS, 50p.
INIS-mf-	(International Atomic Energy Agency)	
25	25-41934	NTIS (U. S. Sales Only), 23p.
INP-	(Polish)	
746	25-43954	Dep. NTIS (U. S. Sales Only), 49p.
INR-	(Non-AEC)	
1262	25-43931	Dep. NTIS (U. S. Sales Only), 85p.
1268	25-43885	Dep. NTIS (U. S. Sales Only), 10p.
1270	25-43955	Dep. NTIS (U. S. Sales Only), 36p.
1280	25-43567	Dep. NTIS (U. S. Sales Only), 15p.
1294	25-43288	Dep. NTIS (U. S. Sales Only), 22p.
1295	25-44155	Dep. NTIS (U. S. Sales Only), 12p.
1297	25-41894	Dep. NTIS (U. S. Sales Only), 14p.
1309	25-41895	Dep. NTIS (U. S. Sales Only), 26p.
INR-P-	(Polish)	
1266	25-44203	Dep. NTIS (U. S. Sales Only), 22p.
IPP-	(Non-AEC)	
4/9	25-43390	Dep. NTIS (U. S. Sales Only), 26p.
IPPJ-DT-	(Japanese)	
20	25-43457	Dep. NTIS (U. S. Sales Only), 27p.
IS-T-		
425	25-42983	Dep. NTIS, 94p.
446	25-42955	Dep. NTIS, 150p.
456	25-43150	Dep. NTIS, 291p.
474	25-44250	Dep. NTIS, 163p.
ITEF-	(Russian)	
734	25-42135	For translation see CERN-Trans-71-8
ITF-	(Russian)	
70-89-E	25-43654	Dep. NTIS (U. S. Sales Only), 27p.
71-9-P	25-43638	Dep. NTIS (U. S. Sales Only), 19p.
71-12-P	25-43667	Dep. NTIS (U. S. Sales Only), 22p.
71-16-P	25-43085	Dep. NTIS (U. S. Sales Only), 20p.
71-27-E	25-43584	Dep. NTIS (U. S. Sales Only), 7p.
71-28-E	25-43623	Dep. NTIS (U. S. Sales Only), 9p.
IYAF-	(Russian)	
7-70	25-43339	Dep. NTIS (U. S. Sales Only), 22p.
JAERI-	(Japanese)	
13517	25-42956	NTIS (U. S. Sales Only), 26p.
13536	25-42184	NTIS (U. S. Sales Only), 86p.
13545	25-41877	NTIS (U. S. Sales Only), 12p.
13546	25-42050	NTIS (U. S. Sales Only), 23p.
13561	25-42105	NTIS (U. S. Sales Only), 39p.
13567	25-43730	NTIS (U. S. Sales Only), 58p.
13578	25-42846	NTIS (U. S. Sales Only), 44p.
13579	25-41878	NTIS (U. S. Sales Only), 19p.
13580	25-42106	NTIS (U. S. Sales Only), 44p.
13605	25-42185	NTIS (U. S. Sales Only), 87p.
13617	25-41990	NTIS (U. S. Sales Only), 17p.
13622	25-41722	NTIS (U. S. Sales Only), 21p.
13635	25-42931	NTIS (U. S. Sales Only), 21p.
13650	25-42932	NTIS (U. S. Sales Only), 29p.
13666	25-42037	NTIS (U. S. Sales Only), 6p.
13692	25-42902	NTIS (U. S. Sales Only), 23p.
13718	25-42051	NTIS (U. S. Sales Only), 18p.
13725	25-42052	NTIS (U. S. Sales Only), 18p.
13726	25-41879	NTIS (U. S. Sales Only), 36p.
13731	25-42884	NTIS (U. S. Sales Only), 19p.
13764	25-42885	NTIS (U. S. Sales Only), 21p.
13768	25-42186	NTIS (U. S. Sales Only), 39p.
13771	25-42107	NTIS (U. S. Sales Only), 60p.
13778	25-41991	NTIS (U. S. Sales Only), 20p.
13780	25-41851	NTIS (U. S. Sales Only), 26p.
JINR-	(Russian)	
P1-5775	25-43646	Dep. NTIS (U. S. Sales Only), 16p.
P1-5849	25-43639	Dep. NTIS (U. S. Sales Only), 16p.
P2-5765	25-43568	Dep. NTIS (U. S. Sales Only), 13p.
P2-5829	25-43614	Dep. NTIS (U. S. Sales Only), 17p.
P3-5754	25-44156	Dep. NTIS (U. S. Sales Only), 86p.
P4-5786	25-43506	Dep. NTIS (U. S. Sales Only), 7p.
P6-5791	25-43887	Dep. NTIS (U. S. Sales Only), 21p.
P7-5177	25-43731	Dep. NTIS (U. S. Sales Only), 32p.
P9-5442	25-43727	For translation see BNL-tr-431
P9-5753	25-43346	Dep. NTIS (U. S. Sales Only), 24p.
P9-5846	25-43406	Dep. NTIS (U. S. Sales Only), 13p.
P13-5782	25-42053	Dep. NTIS (U. S. Sales Only), 14p.
P13-5801	25-42187	Dep. NTIS (U. S. Sales Only), 16p.
P13-5828	25-42136	Dep. NTIS (U. S. Sales Only), 13p.
JPL-TR-	(Non-AEC)	
32-1495	25-43184	See N-71-16776
JPRS-	(Non-AEC)	
53498	25-42034	NTIS
JUL-	(German)	
473-PP	25-42183	For translation see CTO-756
711-MA	25-43415	Dep. NTIS (U. S. Sales Only), 54p.
728-RW	25-42936	Dep. NTIS (U. S. Sales Only), 17p.
734-FF	25-44261	Dep. NTIS (U. S. Sales Only), 109p.
742-TP	25-43182	Dep. NTIS (U. S. Sales Only), 65p.
K-		
1798(Pt.1)	25-44262	Dep. NTIS, 18p.
1798(Pt.4)	25-44263	Dep. NTIS, 25p.
1798(Pt.5)	25-44264	Dep. NTIS, 22p.
1799	25-44265	Dep. NTIS, 54p.
KAE-	(Norwegian)	
68-46	25-44207	Dep. NTIS (U. S. Sales Only), 20p.
68-81	25-44208	Dep. NTIS (U. S. Sales Only), 15p.
KAPL-		
3482	25-44266	Dep. NTIS, 29p.
KFK-	(German)	
1281	25-44086	For translation see EURFNR-853
1290	25-44087	For translation see EURFNR-854
1292	25-42935	For translation see EURFNR-859
1297	25-42984	For translation see ORNL-tr-2483
1384	25-42844	See EURFNR-922
1385	25-44119	See EURFNR-923
KHFTI-	(Russian)	
70-45	25-43386	For translation see ORNL-tr-2434
L-	(Misc.)	
7323	25-43008	See N-71-12278
LA-		
4249(Vol.2)	25-44257	Dep. NTIS, 14p.
4454(Vol.5)	25-43066	Dep. NTIS, 124p.
4644	25-42816	Dep. NTIS, 12p.
4648	25-43888	Dep. NTIS, 10p.
4657	25-41852	Dep. NTIS, 14p.
4671	25-44157	Dep. NTIS, 7p.
4708	25-43889	Dep. NTIS, 10p.
LA-DC-		
12348	25-41825	Dep. NTIS, 7p.
LA-tr-		
71-44	25-44196	Dep. NTIS
LAL-	(French)	
1250	25-43528	Dep. NTIS (U. S. Sales Only), 35p.
LB/G-	(British)	
2929	25-44158	Dep. NTIS (U. S. Sales Only)
LF-tr-		
53	25-42368	Dep. NTIS
LGI-	(Italian)	
68/16	25-43381	Dep. CFSTI (U. S. Sales Only), 118p.
LMEC-		
71-1	25-42804	Dep. NTIS, 113p.
LPN-UM-	(Canadian)	
53	25-42054	Dep. NTIS (U. S. Sales Only), 41p.
LYCEN-	(French)	
7110	25-43640	Dep. NTIS (U. S. Sales Only), 22p.
MATT-		
803	25-43333	Dep. NTIS, 17p.
804	25-43396	Dep. NTIS, 10p.
845	25-42188	Dep. NTIS, 11p.
848	25-43397	Dep. NTIS, 8p.
MHSMP-		
71-28	25-44268	Dep. NTIS, 16p.
MIT-	(Misc.)	
3773-103	25-42983	Dep. NTIS, 44p.
N-	(Misc.)	

Report No.	Abstract No.	Availability
71-12257	25-42227	NTIS, 31p.
71-12278	25-43008	NTIS, 14p.
71-12679	25-43361	NTIS, 68p.
71-12892	25-43385	NTIS, 40p.
71-14040	25-42903	NTIS, 33p.
71-14602	25-42160	NTIS, 29p.
71-15856	25-43183	NTIS, 23p.
71-16499	25-43011	NTIS, 24p.
71-16589	25-43214	NTIS, 20p.
71-16749	25-43067	NTIS, 50p.
71-16776	25-43184	NTIS, 27p.
71-17052	25-43215	NTIS, 90p.
71-17252	25-43185	NTIS, 24p.
71-17325	25-42228	NTIS, 15p.
71-17463	25-44122	NTIS, 28p.
71-17594	25-43340	NTIS, 13p.
71-17933	25-44169	NTIS, 45p.
71-18405	25-43216	NTIS, 75p.
71-18502	25-43217	NTIS, 147p.
71-18696	25-43407	NTIS, 48p.
71-18715	25-43362	NTIS, 30p.
71-18997	25-43218	NTIS, 34p.
71-19294	25-43068	NTIS, 49p.
71-19301	25-43018	NTIS, 26p.
71-19984	25-43353	NTIS, 151p.
71-20390	25-42805	NTIS, 52p.
71-20472	25-43079	NTIS, 62p.
71-20535	25-43069	NTIS, 258p.
71-20708	25-43219	NTIS, 56p.
71-20853	25-43220	NTIS, 70p.
71-21469	25-43221	NTIS, 79p.
71-21563	25-43080	NTIS, 30p.
71-21564	25-43070	NTIS, 14p.
NASA-CR-	(Misc.)	
111514	25-43385	See N-71-12892
111581	25-42227	See N-71-12257
111611	25-43361	See N-71-12679
114804	25-42150	See N-71-14602
114948	25-43221	See N-71-21469
116240	25-43214	See N-71-16589
116246	25-43184	See N-71-16776
116441	25-43215	See N-71-17052
116783	25-43407	See N-71-18696
116784	25-43217	See N-71-18502
116791	25-43216	See N-71-18405
116862	25-43018	See N-71-19301
116872	25-43068	See N-71-19294
116877	25-43218	See N-71-18997
117040	25-43353	See N-71-19984
117403	25-43219	See N-71-20708
117741	25-43220	See N-71-20853
NASA-SP-	(Misc.)	
3056	25-43069	See N-71-20535
NASA-TM-X-	(Misc.)	
2144	25-42903	See N-71-14040
2175	25-43185	See N-71-17252
2180	25-42223	See N-71-17325
2193	25-44169	See N-71-17933
52957	25-43011	See N-71-16499
62015	25-42805	See N-71-20390
64571	25-43079	See N-71-20472
64577	25-43080	See N-71-21563
65439	25-43067	See N-71-16749
65445	25-43340	See N-71-17594
65484	25-43070	See N-71-21564
NASA-TN-D-	(Misc.)	
5977	25-43352	See N-71-18715
5024	25-43008	See N-71-12278
6162	25-44122	See N-71-17463
7041	25-43183	See N-71-15856
NBS-MON-	(Misc.)	
119	25-43019	GPO $3.25
NBS-SPEC. PUBL-	(Non-AEC)	
329	25-41961	GPO $9.00
NBS-TN-	(Misc.)	
270-5	25-41826	GPO $0.55
NEDO-	(Non-AEC)	
10329 (Suppl.1)	25-44140	
NIM-	(Non-AEC)	
1077	25-41723	Dep. NTIS (U. S. Sales Only), 7p.
NP-	(AEC File No. for Non-AEC Reports)	
13657	25-43469	Dep. NTIS (U. S. Sales Only), 52p.
18805	25-43363	Dep. NTIS (U. S. Sales Only), 64p.
18814	25-43534	Dep. NTIS (U. S. Sales Only), 52p.
18817	25-41853	Dep. NTIS (U. S. Sales Only), 51p.
18831	25-43665	Dep. NTIS (U. S. Sales Only), 29p.
18843	25-44269	GPO $1.00
18858	25-42498	
18863	25-43416	Dep. NTIS (U. S. Sales Only), 18p.
18878	25-41896	Dep. NTIS (U. S. Sales Only), 69p.
18880	25-43600	Dep. NTIS (U. S. Sales Only), 74p.
18892	25-42161	Dep. NTIS (U. S. Sales Only), 45p.
18905	25-42369	Dep. NTIS (U. S. Sales Only), 15p.
18908	25-44177	Dep. NTIS (U. S. Sales Only). UK 70p, 112p.
18920	25-43832	Dep. NTIS (U. S. Sales Only), 69p.
NVO-		
87	25-41951	Dep. NTIS, 36p.
NYO-		
1371-64	25-44270	Dep. NTIS, 18p.
2150-71	25-43289	Dep. NTIS, 109p.
2262-TA-245	25-43563	Dep. NTIS, 9p.
2262-TA-247	25-43570	Dep. NTIS, 11p.
2504-59	25-44271	Dep. NTIS, 19p.
2804-38	25-42727	Dep. NTIS, 37p.
2804-39	25-42728	Dep. NTIS, 48p.
2804-40	25-42729	Dep. NTIS, 21p.
2804-41	25-42730	Dep. NTIS, 33p.
2804-42	25-42731	Dep. NTIS, 9p.
3086-10 (Vol.1)	25-42245	Dep. NTIS, 235p.
3250-60	25-44006	See DOCKET-50213-115
3399-243	25-43711	See SU-1206-243
3399-246	25-43585	See SU-1206-246
3399-249	25-43641	See SU-1206-249
3399-250	25-43586	See SU-1206-250
3409-10	25-42162	Dep. NTIS, 40p.
3590-7	25-44272	Dep. NTIS, 26p.
3699-56	25-44273	Dep. NTIS, 9p.
3707-7	25-44274	Dep. NTIS, 5p.
3829-71	25-43417	Dep. NTIS, 38p.
3906-6	25-42189	Dep. NTIS, 8p.
4209	25-44275	Dep. NTIS, 13p.
NYU-		
4256-1	25-42394	Dep. NTIS, 152p.
ORAU-		
113	25-42549	Dep. NTIS, 216p.
ORNL-		
4544	25-42937	Dep. NTIS, 90p.
4566(Pt.1)	25-42506	Dep. NTIS, 100p.
4621	25-44159	Dep. NTIS, 193p.
4640	25-41992	Dep. NTIS, 65p.
4650	25-44276	Dep. NTIS, 87p.
4683(Pt.1)	25-44277	Dep. NTIS, 229p.
4692	25-41993	Dep. NTIS, 24p.
4698	25-43833	Dep. NTIS, 23p.
4703	25-43290	Dep. NTIS, 35p.
ORNL-IBP-		
71-2	25-44278	Dep. NTIS, 22p.
ORNL-NSF-EP-		
3	25-44279	Dep. NTIS, 251p.
ORNL-NSIC-		
48	25-44280	Dep. NTIS, 57p.
86	25-44141	Dep. NTIS, 112p.
89	25-42315	Dep. NTIS, 42p.
ORNL-RMIC-		
11	25-44281	Dep. NTIS, 42p.
ORNL-RSIC-		
32	25-43418	Dep. NTIS, 54p.
ORNL-TM-		
2091(Suppl. 2)	25-42550	Dep. NTIS, 29p.
2492	25-42315	See ORNL-NSIC-89
3231	25-43398	Dep. NTIS, 45p.
3236	25-41962	Dep. NTIS, 38p.
3247	25-42847	Dep. NTIS, 57p.
3269	25-43419	Dep. NTIS, 13p.
3313	25-42848	Dep. NTIS, 21p.
3324	25-41985	Dep. NTIS, 173p.
3358	25-41779	Dep. NTIS, 35p.
3385	25-44123	Dep. NTIS, 34p.
3387	25-44124	Dep. NTIS, 32p.
3408	25-44282	Dep. NTIS, 58p.
3426	25-42038	Dep. NTIS, 27p.
3427	25-44125	Dep. NTIS, 18p.
3429	25-43420	Dep. NTIS, 11p.
3436	25-43890	Dep. NTIS, 36p.
3465	25-42055	Dep. NTIS, 16p.
3477	25-44283	Dep. NTIS, 24p.
3481	25-44160	Dep. NTIS, 47p.
ORNL-tr-		
2434	25-43386	Dep. NTIS
2461	25-43291	Dep. NTIS
2471	25-44284	Dep. NTIS
2476	25-43421	Dep. NTIS
2483	25-42984	Dep. NTIS
2488	25-43422	Dep. NTIS

XUM

Report No.	Abstract No.	Availability
2512	25-41897	Dep. NTIS
ORO-		
2945-10	25-41843	Dep. NTIS, 249p.
2968-60	25-41855	J. Amer. Chem. Soc.; 93: No. 11, 2805-7(2 Jun 1971)
3082-6	25-44285	Dep. NTIS, 26p.
3091-21	25-44285	Dep. NTIS, 10p.
3299-107	25-42315	Dep. NTIS, 18p.
3299-110	25-42718	Dep. NTIS, 19p.
3755-30	25-43966	Dep. NTIS, 42p.
3992-61	25-43647	Dep. NTIS, 8p.
OU-LNS-	(Japanese)	
71-2	25-43732	Dep. NTIS (U. S. Sales Only), 49p.
PATENTS	(British)	
1,224,152	25-42958	
1,225,921	25-42044	
1,230,937	25-41782	
1,231,484	25-42173	
1,231,485	25-42174	
1,234,172	25-42078	
1,234,684	25-41844	
1,234,906	25-41904	
1,234,958	25-42230	
1,235,567	25-41913	
1,235,970	25-42077	
1,235,990	25-41947	
1,236,052	25-43188	
PATENTS	(Canadian)	
870,188	25-42019	
PATENTS	(French)	
1,597,725	25-42819	
1,602,171	25-42208	
2,029,146	25-42113	
2,029,939	25-41845	
2,031,672	25-42050	
2,031,748	25-42384	
2,031,844	25-41911	
2,034,347	25-41753	
2,036,754	25-42117	
2,038,559	25-41914	
2,038,755	25-41752	
PATENTS	(German)	
1,295,710	25-44213	
PATENTS	(Russian)	
204,393	25-43345	
243,841	25-43318	
PATENTS	(U. S.)	
3,523,765	25-41902	
3,567,576	25-44215	
3,567,577	25-44215	
3,567,578	25-44213	
3,567,579	25-44214	
3,567,580	25-44212	
3,568,781	25-44114	
3,569,757	25-43740	
3,571,596	25-42058	
3,573,067	25-42759	
3,573,217	25-42945	
3,573,218	25-42072	
3,573,219	25-42071	
3,573,220	25-42059	
3,576,758	25-41781	
3,577,026	25-43135	
3,577,225	25-41903	
3,578,406	25-41759	
3,578,610	25-42939	
3,578,960	25-42103	
3,578,991	25-43199	
3,579,027	25-43382	
3,579,028	25-43350	
3,579,270	25-42224	
3,579,311	25-42938	
3,580,705	25-41912	
3,580,804	25-44211	
3,580,822	25-42085	
3,581,090	25-42130	
3,581,091	25-42134	
3,581,093	25-43778	
3,584,217	25-42179	
PIFR-	(Non-AEC)	
52	25-41950	See AD-718388
PITHA-	(German)	
44	25-43656	Dep. NTIS (U. S. Sales Only), 19p.
PR-CMa-	(Canadian)	
15	25-41932	See AECL-3851
PRDC-EF-		
90	25-44001	See DOCKET-50016-121
91	25-44002	See DOCKET-50016-122
PRNC-		

Report No.	Abstract No.	Availability
147	25-42317	Dep. NTIS, 142p.
148	25-42246	Dep. NTIS, 18p.
R-	(Misc.)	
64-SD-68	25-43331	See AD-715615
RCN-	(Dutch)	
139	25-44178	Dep. NTIS (U. S. Sales Only), 105p.
RDT-C-		
2-1-T	25-42190	RSO
4-1-T	25-41963	RSO
4-4-T	25-41964	LMEC
4-5-T	25-42191	LMEC
5-1-T	25-42192	LMEC
5-2-T	25-42193	LMEC
6-1-T	25-42194	LMEC
6-3-T	25-42195	LMEC
7-1-T	25-42196	RSO
7-2-T	25-42197	RSO
7-3-T	25-42198	RSO
7-4-T	25-42199	RSO
7-6-T	25-42200	RSO
8-2-T	25-42201	LMEC
9-1-T	25-42202	RSO
9-2-T	25-42203	RSO
15-2-T	25-44209	RSO
16-1-T	25-44142	RSO
18-1-T	25-42204	LMEC
RDT-E-		
1-18-T	25-41965	LMEC
1-19-T	25-41966	LMEC
3-9-T	25-41967	LMEC
4-1-T	25-44081	RSO
4-13-T	25-41968	LMEC
6-5-T	25-44105	LMEC
10-2-T	25-41969	LMEC
15-2-T	25-43993	RSO
RDT-F-		
2-2-T	25-44088	RSO
2-4-T	25-42022	RSO
3-2-T	25-42205	RSO
3-3-T	25-42761	RSO
3-4-T	25-42023	RSO
3-5-T	25-42024	RSO
3-6-T	25-42025	RSO
3-7-T	25-44210	RSO
3-8-T	25-42026	RSO
3-37-T	25-42817	RSO
5-1-T	25-44089	RSO
6-1-T	25-42849	RSO
6-5-T	25-42850	RSO
7-1-T	25-42762	RSO
7-2-T	25-41970	RSO
8-1-T	25-41971	RSO
RDT-M-		
1-1-T	25-41972	RSO
1-2-T	25-42763	RSO
1-3-T	25-42764	RSO
1-4-T	25-42765	RSO
1-6-T	25-42766	RSO
1-7-T	25-42767	RSO
1-8-T	25-42768	RSO
1-9-T	25-42769	RSO
1-10-T	25-42770	RSO
1-11-T	25-42771	RSO
1-16-T	25-42772	RSO
2-1-T	25-42773	RSO
2-3-T	25-42774	RSO
2-4-T	25-42775	RSO
2-5-T	25-42776	RSO
2-6-T	25-42777	RSO
2-7-T	25-42778	RSO
3-1-T	25-42779	RSO
3-2-T	25-42780	RSO
3-3-T	25-42781	RSO
3-4-T	25-42782	RSO
3-5-T	25-42783	RSO
3-6-T	25-42784	RSO
3-7-T	25-42785	RSO
3-8-T	25-42786	RSO
3-12-T	25-42787	RSO
4-1-T	25-42788	RSO
4-2-T	25-42789	RSO
4-3-T	25-42790	RSO
5-1-T	25-42791	RSO
5-2-T	25-42792	RSO
5-3-T	25-42793	RSO
5-4-T	25-42794	RSO
5-5-T	25-42795	RSO
5-6-T	25-42796	RSO
6-1-T	25-42797	RSO
6-2-T	25-41973	RSO
6-3-T	25-42798	RSO
7-1-T	25-42799	RSO
9-2-T	25-41974	RSO

Report No.	Abstract No.	Availability
10-1-T	25-42800	RSO
11-1-T	25-41975	RSO
11-2-T	25-43012	RSO
12-1-T	25-43013	RSO
12-2-T	25-43014	RSO
13-1-T	25-42901	LMEC
RFP-		
1286	25-42039	Dep. NTIS, 30p.
1703	25-42951	Dep. NTIS, 32p.
1706	25-42027	Dep. NTIS, 25p.
RFP-Trans-		
79	25-43891	Dep. NTIS
RISO-	(Danish)	
237	25-43435	Dep. NTIS (U. S. Sales Only), 46p.
238	25-42745	Dep. NTIS (U. S. Sales Only), 46p.
RISO-M-	(Danish)	
1357	25-42206	Dep. NTIS (U. S. Sales Only), 28p.
RLO-		
1780-32	25-42674	Dep. NTIS, 67p.
2225-T-2-2	25-42616	Dep. NTIS, 19p.
2225-T-7-2	25-44287	Dep. NTIS, 43p.
2225-T-15-3	25-42267	Dep. NTIS, 8p.
2227-T-8-1	25-44288	Dep. NTIS, 25p.
RPI-	(Misc.)	
328-209	25-43834	Dep. NTIS, 47p.
RT/ING-	(Italian)	
(58)16	25-44195	For translation see LA-tr-71-44
RT/PROT-	(Italian)	
(70)4	25-42042	Minerva Fisiconucl.; 13: 145-53(Apr-Jun 1969)
(71)1	25-42055	Dep. NTIS (U. S. Sales Only), 18p.
(71)6	25-42375	Quad. Nutr.; No. 6, 397-408(1968)
S-	(Misc.)	
54-TP	25-42717	See EGG-1183-2272
SAMSO-TR-	(Non-AEC)	
70-47	25-42225	See AD-715261
70-391	25-43055	See AD-715257
70-393	25-43213	See AD-715898
70-395	25-43211	See AD-715266
70-396	25-43338	See AD-715265
70-397	25-43191	See AD-715883
70-406	25-43210	See AD-715260
SAN-		
651-129	25-44289	Dep. NTIS, 150p.
SC-DC-		
70-5157	25-42971	Nucl. Technol.; 12: No. 1, 93-107(Sep 1971)
SC-DR-		
58-814	25-44290	Dep. NTIS, 86p.
SC-RR-		
710301	25-44291	Dep. NTIS, 26p.
SC-T-		
713038	25-41780	Dep. NTIS
SCL-T-		
59-256	25-43101	Dep. NTIS
SDL-	(Non-AEC)	
18	25-41932	See AD-719619
18-2	25-41933	See AD-719620
SFL-A-	(Finnish)	
15	25-42247	Dep. NTIS (U. S. Sales Only), 51p.
SGAE-RT-	(Non-AEC)	
39/1971	25-44143	Dep. NTIS (U. S. Sales Only), 51p.
SRCC-	(Non-AEC)	
133	25-43218	See N-71-18997
146	25-43214	See N-71-16589
SRD-	(Misc.)	
475-11	25-44292	Dep. NTIS, 6p.
STI/DOC-	(International Atomic Energy Agency)	
10/124	25-42746	IAEA $3.00
STI/PUB-	(International Atomic Energy Agency)	
279	25-41941	IAEA $5.00
290	25-42395	IAEA $9.00
SU-	(Misc.)	
1206-243	25-43711	Dep. NTIS, 18p.
1206-246	25-43585	Dep. NTIS, 11p.
1206-249	25-43641	Dep. NTIS, 9p.
1206-250	25-43586	Dep. NTIS, 16p.
SU-IPR-		
377	25-43068	See N-71-19294
402	25-43407	See N-71-19596
SU-SEL-	(Misc.)	
70-51	25-43217	See N-71-18502
SWRHL-		
43-r	25-42370	Dep. NTIS, 38p.
SWRI-		
1228-9-10	25-44082	Dep. NTIS, 9p.
TID-		
25728	25-44293	Dep. NTIS, 87p.
25735	25-42318	Dep. NTIS, 111p.
25737	25-44020	Dep. NTIS, 30p.
25739	25-44294	Dep. NTIS, 23p.
25740	25-44295	
25742	25-44296	Dep. NTIS, 128p.
25746	25-44297	Dep. NTIS, 133p.
25751	25-43733	Dep. NTIS, 435p.
25758	25-44298	Dep. NTIS, 81p.
25760	25-44310	New York; John Wiley and Sons, Inc. (1971). 824p. $22.50
TR-	(Misc.)	
4	25-42900	See AD-719905
12	25-43217	See N-71-18502
59(6220-50)-6	25-43181	See AD-715883
59(6250-20)-8	25-42226	See AD-715261
59(6260-20)-10	25-43210	See AD-715260
59(9220-02)-2	25-43338	See AD-715265
59(9220-02)-4	25-43213	See AD-715898
59(9220-02)-5	25-43211	See AD-715266
59(9260-02)-2	25-43065	See AD-715257
68-15	25-41952	See AD-838894
70-2	25-43385	See N-71-12892
TRG-Report-	(British)	
2133	25-44101	Dep. NTIS (U. S. Sales Only). UK 70p, 105p.
2135	25-41898	Dep. NTIS (U. S. Sales Only), 13p.
UCID-		
30008	25-44299	Dep. NTIS, 5p.
30013(Pt.1)	25-44300	Dep. NTIS, 144p.
30013(Pt.2)	25-44301	Dep. NTIS, 56p.
30013(Pt.3)	25-44302	Dep. NTIS, 41p.
UCLA-		
10-P-18-31	25-43801	Dep. NTIS, 118p.
12-819	25-41926	Dep. NTIS, 31p.
UCLA-ENG-		
7037	25-44079	
UCR-		
34-P-107-B-106	25-43642	Dep. NTIS, 27p.
34-P-107-B-108	25-43551	Dep. NTIS, 20p.
34-P-107-B-110	25-43552	Dep. NTIS, 12p.
34-P-107-B-112	25-43624	Dep. NTIS, 13p.
34-P-107-B-120	25-43553	Dep. NTIS, 9p.
UCRL-		
20411	25-43469	Dep. NTIS, 17p.
20480	25-43802	Dep. NTIS, 111p.
20500	25-41777	Dep. NTIS, 254p.
20664	25-43734	Dep. NTIS, 11p.
51046	25-44303	Dep. NTIS, 9p.
73046	25-44304	Dep. NTIS, 5p.
73076	25-43399	Dep. NTIS, 18p.
73104	25-44305	Dep. NTIS, 25p.
73152	25-43957	Dep. NTIS, 36p.
73161	25-44306	Dep. NTIS, 8p.
73184	25-44307	Dep. NTIS, 19p.
UCSD-		
34-P-127-10	25-44308	Dep. NTIS, 5p.
UNC-	(Misc.)	
5258	25-42207	Dep. NTIS, 22p.
UR-		
49-1333	25-42400	pp 1-9 of Biochemical Indicators of Radiation Injury in Man. Vienna; International Atomic Energy

XUM

Report No.	Abstract No.	Availability Agency (1970)
49-1462	25-42617	Dep. NTIS, 199p.
875-340	25-43554	Dep. NTIS, 13p.
USGS-		
474-75(Rev. 1)	25-41927	Dep. NTIS, 46p.
UUIP-	(Swedish)	
731	25-42103	NTIS (U. S. Sales Only), 6p.
737	25-42109	Dep. NTIS (U. S. Sales Only), 31p.
WANL-TME-	(Non-AEC)	
1395	25-44151	Dep. NTIS, 50p.
WAPD-T-		
2358	25-44090	Dep. NTIS, 14p.
WAPD-TM-	(Misc.)	
850	25-42958	Dep. NTIS, 33p.
WASH-		
1139	25-43994	GPO $1.50

Report No.	Abstract No.	Availability
WCAP-	(Misc.)	
7572	25-44052	See DOCKET-50286-37
WERL-ELPLA-		
1	25-44126	Dep. NTIS, 273p.
X-	(Misc.)	
625-71-34	25-43340	See N-71-17594
661-71-33	25-43057	See N-71-15749
693-71-107	25-43070	See N-71-21564
Y-		
1785	25-42887	Dep. NTIS, 21p.
Y-DR-		
63	25-44189	Dep. NTIS, 28p.
YALE-		
3227-71	25-43471	Dep. NTIS, 28p.
3227-74	25-43472	Dep. NTIS, 308p.
3227-77	25-44309	Dep. NTIS, 11p.

☆U. S. GOVERNMENT PRINTING OFFICE: 1971—745-060/5

UNITED STATES ATOMIC ENERGY COMMISSION

NUCLEAR SCIENCE ABSTRACTS

Volume 25
Numbers 13-18

Abstracts 28912-44310

July-September
1971

Division of Technical Information

XUM

STAFF OF NUCLEAR SCIENCE ABSTRACTS

John W. Norris
Managing Editor

Donald D. Davis
Assistant Managing Editor

David E. Bost
Production Manager

Sidney F. Lanier
Subject Heading Specialist

J. Paul Meredith
Descriptive Cataloging Specialist

Frederick E. Marsh, Jr.
Computer Index Coordinator

Clara L. Fox
Corporate Author Specialist

Helen W. White
Report Number Specialist

Section Editors

Everett J. Hoffman
Chemistry

Robert C. Kelly
Engineering; Earth Sciences; Metals, Ceramics, and Other Materials

Lee M. Thompson
General Physics

Charles E. Stuber
High Energy Physics; Instrumentation

Donald D. Davis
Life Sciences

Lawrence T. Whitehead
Nuclear Physics

James M. Jacobs
Reactor Technology

Evaluators

Thomas S. Chapman
John H. Mitchell
Mary H. Newman
Polly C. Summers

Abstractors

F. S. Armstrong*
Ellis R. Bedford
Mary M. Brown
Jane G. Buchanan
D. Lamar Cason
Gloria M. Caton
David C. Cunningham
James R. Dulaney
Helga B. Gerstner
Mary C. Grissom
Phyllis C. Hansen
Carolyn D. Houston
Elaine E. Huber
Rose V. Jermain
W. Hugh Kinser, Jr.
Lisbeth C. Lieberman
Betty L. McDowell
Patricia B. McEwen
Fay M. Martin
William D. Matheny
Dora H. Moneyhun
Jean F. Peckham
Henry D. Raleigh
Mona H. Raridon
Julia S. Redford
Jessie W. Rushing
Robert W. Rutkowski
Francis L. Sachs
Lila B. Smith
Anne G. Ward
Helen L. Ward
Kenneth S. Warren
Milton O. Whitson
Juanita Wilson

*Atomic Energy of Canada, Ltd.

Charles R. Bruce
Publishing Coordinator

Communication concerning the editorial policy and content of *Nuclear Science Abstracts* should be addressed to the Managing Editor, *Nuclear Science Abstracts*, USAEC Division of Technical Information Extension, P. O. Box 62, Oak Ridge, Tennessee 37830.

Use of funds for printing this publication approved by the Director of the Bureau of the Budget, June 26, 1969.

XUM

UNITED STATES
ATOMIC ENERGY COMMISSION
P. O. BOX 62
OAK RIDGE, TENNESSEE 37830

OFFICIAL BUSINESS

POSTAGE AND FEES PAID
U. S. ATOMIC ENERGY COMMISSION

STAGE AND FEES PAID
/ERNMENT PRINTING OFFICE

U.S.MAIL

UNIVERSITY MICROFILMS
SERIAL PUBLICATIONS
300 NORTH ZEEB ROAD
ANN ARBOR MICHIGAN 48106

1

Announcing the publication of

Public Safety
& Underground Nuclear Detonations

Samuel Glasstone

June 1971

Introduction
Basic Principles of Nuclear Explosions
Underground Nuclear Explosions:
Local Events
Geology, Hydrology, and Safety of
Water Supplies
Ground Motion and the Response of
Structures
Seismology and Water Wave Phenomena
Meteorology and Radiation Predictions
The Radiological Safety Program
The Bioenvironmental Safety Program
Safety Controls for Nuclear Detonations
Nuclear Excavation Safety
References
Glossary
Index
(6 X 9; 286 pages; 109 illustrations)

Available for $3.00 as TID-25708 from
National Technical Information Service
U. S. Department of Commerce
Springfield, Virginia 22151

The United States program for testing nuclear explosive systems has two main objectives: first, to maintain the nation's security and, second, to develop peaceful applications of nuclear explosives for the benefit of all mankind.

To meet the national objective of developing nuclear explosives for peaceful applications, the Atomic Energy Commission in 1957 established the Plowshare Program. For such applications as stimulating the flow of natural gas and petroleum, mining and quarrying and other earth-moving projects, and cracking high-temperature rocks to utilize their natural geothermal energy, the Plowshare Program will require the design and testing of special nuclear explosives.

This book describes the comprehensive safety program carried out by the Atomic Energy Commission and the methods through which those responsible for ensuring safety in underground nuclear detonations implement their basic philosophy, which has been summarized as follows: A nuclear device can be detonated safely only when it is ascertained that the operation can be accomplished without injury to people and domestic animals, directly or indirectly, and without an unacceptable damage risk to ecological systems and to natural and man-made structures.

Published by the Atomic Energy Commission, the book was prepared through the coordinated effort of government agencies and contractors; the work of many competent scientists in a number of related disciplines is presented.

XUM